OBJAVLJENI NAUČNI RADOVI

Dr Milana Dimitrijevića
(prvi deo)

Priredili: Dr Milan Dimitrijević
Dr Slaviša Milisavljević

Beograd, 2013

A&A 469, 749–754 (2007)
DOI: 10.1051/0004-6361:20077206
© ESO 2007

Astronomy & Astrophysics

The influence of H_2^+- photo-dissociation and (H + H^+)- radiative collisions on the solar atmosphere opacity in UV and VUV regions

A. A. Mihajlov[1,3], Lj. M. Ignjatović[1,3], N. M. Sakan[1], and M. S. Dimitrijević[2,3]

[1] Institute of Physics, PO Box 57, 11001 Belgrade, Serbia
e-mail: ljuba@phy.bg.ac.yu
[2] Astronomical Observatory, Volgina 7, 11160 Belgrade 74, Serbia
[3] Isaac Newton Institute of Chile, Yugoslavia Branch

Received 31 January 2007 / Accepted 16 March 2007

ABSTRACT

Aims. To estimate the total contribution of the absorption processes $\epsilon_\lambda + H_2^+(X^2\Sigma_g^+) \Rightarrow H(1s) + H^+$ and $\epsilon_\lambda + H(1s) + H^+ \Rightarrow H^+ + H(1s)$ to the opacity of Solar atmosphere in UV and VUV region, and compare it with the contribution of other relevant radiative processes included in standard models.

Methods. The strict quantum-mechanical method was used for the determination of the average cross-section for the photo-dissociation of the molecular ion $H_2^+(X^2\Sigma_g^+)$; the previously developed quasi-static method was used for determination of the corresponding spectral coefficient which characterizes the absorption charge exchange in H(1s) + H^+ collisions.

Results. Spectral absorption coefficients characterizing the considered processes were calculated for the solar photosphere and lower chromosphere, within the 90 nm $\leq \lambda \leq$ 370 nm spectral range; the total contribution of the considered processes to the solar opacity was estimated and compared to relevant radiative processes included in standard Solar models.

Conclusions. In comparison with other absorption processes included in standard Solar models, the contribution of the considered processes in the UV and VUV regions is so important that they have to be taken into account in modeling the Solar photosphere and the lower chromosphere.

Key words. Sun: photosphere – Sun: UV radiation – atomic processes – molecular processes

1. Introduction

Opacities of the solar and other stellar atmospheres are naturally caused by a large number of radiative processes. Within development of more sophisticated stellar atmosphere models, we can further investigate known processes and include all processes not considered before.

The Mihajlov & Dimitrijević (1986) were considered absorption processes

$$\epsilon_\lambda + H_2^+ \Longrightarrow H + H^+, \tag{1a}$$

$$\epsilon_\lambda + H + H^+ \Longrightarrow H^+ + H, \tag{1b}$$

were considered, where H = H(1s), H_2^+ is the molecular ion in the electronic ground state $X^2\Sigma_g^+$, and ϵ_λ – energy of a photon with wavelength λ. The aim of this paper is to determine the relative importance of the processes of absorption charge exchange (1b), which were not taken into account before, with respect to the photo-dissociation processes (1a), which were already treated in the literature (Mihalas 1978). It was demonstrated that the absorption processes (1) in the optical part of spectra should be considered in the Solar photosphere and the lower chromosphere together, since in this case their influences on the opacity are similar. In subsequent papers (Mihajlov et al. 1993, 1994a), the absorption processes (1) were investigated in more detail and their contributions to the solar opacity were determined by using standard Solar atmosphere models (Vernazza et al. 1981; Maltby et al. 1986). Then, these contributions were compared with the contributions of other relevant radiative processes, namely

$$\epsilon_\lambda + \begin{cases} H^- \\ H + e' \end{cases} \Longrightarrow H + e'', \tag{2a}$$

$$\epsilon_\lambda + \begin{cases} H^*(n) \\ H^+ + e' \end{cases} \Longrightarrow H + e'', \tag{2b}$$

where H^- is a stable negative hydrogen ion, $H^*(n)$ – an excited hydrogen atom in a state with the principal quantum number $n > 1$, and e′ and e″ – a free electron with the corresponding energy.

In Mihajlov et al. (1993, 1994a) the part of the optical region 365 nm $\leq \lambda \leq$ 820 nm was taken into account. It was found that in this region the processes (1) give a contribution of 10–12% in comparison with processes (2). This fact alone demonstrated that considered ion-atom radiative processes must be taken into account for Solar atmosphere modeling. Later estimates showed however that the relative influence of the absorption processes (1) on the Solar atmosphere opacity should significantly increase at the transition from the considered wavelength region $\lambda \geq 365$ nm to the region $\lambda_b \lesssim \lambda < 365$ nm, where $\lambda_b \cong 91.1262$ nm is the wavelength that corresponds to the ionization threshold of the H(1s) atom. This requires detailed investigation of these processes within the short wavelength region, since the significant increase of their influence will make the considered processes particularly important for Solar atmosphere modeling, especially due to the observational possibilities provided by development of space astronomy in UV and VUV regions.

Article published by EDP Sciences and available at http://www.aanda.org or http://dx.doi.org/10.1051/0004-6361:20077206

In this paper the calculations of the spectral absorption coefficients, that characterize the processes (1) were performed in the region 90 nm $\leq \lambda \leq$ 370 nm. Calculations of the absorption coefficient were performed for the solar photosphere and lower chromosphere by means of a standard Solar atmosphere model (Model C, Vernazza et al. 1981), and the total contribution of the processes (1) to the solar opacity was estimated.

2. Theoretical remarks

The spectral coefficients. The absorption processes (1) separately are characterized here by partial spectral absorption coefficients $\kappa_{ia}^{(a)}(\lambda)$ and $\kappa_{ia}^{(b)}(\lambda)$ taken in the form

$$\kappa_{ia}^{(a)}(\lambda) = \sigma_{\rm phd}(\lambda, T) N(H_2^+), \tag{3}$$

$$\kappa_{ia}^{(b)}(\lambda) = K_{ia}^{(b)}(\lambda, T) N(H) N(H^+), \tag{4}$$

where T and $N(H)$, $N(H^+)$ and $N(H_2^+)$ are the temperature and the densities of H, H^+ and H_2^+ in the considered layer of the solar atmosphere, and $\sigma_{\rm phd}(\lambda, T)$ is the average cross-section for photo-dissociation of the molecular ion H_2^+. As in previous papers the partial spectral absorption coefficient $\kappa_{ia}^{(a)}(\lambda)$ will also be used in the form

$$\kappa_{ia}^{(a)}(\lambda) = K_{ia}^{(a)}(\lambda, T) N(H) N(H^+), \tag{5}$$

where the coefficient $K_{ia}^{(a)}(\lambda, T)$ is connected with $\sigma_{\rm phd}(\lambda, T)$ by the relations

$$K_{ia}^{(a)}(\lambda) = \sigma_{\rm phd}(\lambda, T) \cdot \chi^{-1}, \qquad \chi = \frac{N(H) N(H^+)}{N(H_2^+)}. \tag{6}$$

The total spectral absorption coefficient $\kappa_{ia}(\lambda)$, which characterizes the processes (1) together, can be taken in the form

$$\begin{aligned} \kappa_{ia}(\lambda) &= K_{ia}(\lambda, T) \cdot N(H) N(H^+), \\ K_{ia}(\lambda, T) &= K_{ia}^{(a)}(\lambda, T) + K_{ia}^{(b)}(\lambda, T). \end{aligned} \tag{7}$$

In accordance with the definition of the absorption coefficients $\kappa_{ia}^{(a,b)}(\lambda)$ and $\kappa_{ia}(\lambda)$, the coefficients $K_{ia}^{(a,b)}(\lambda, T)$ and $K_{ia}(\lambda, T)$ are given here in units [cm^5].

The methods of calculation. The photo-dissociation cross-section $\sigma_{\rm phd}(\lambda, T)$, as well as the coefficients $K_{ia}^{(a)}(\lambda, T)$ and $K_{ia}^{(b)}(\lambda, T)$, are determined within the approximation where the processes (1) are treated as the result of the radiative transitions between the ground and the first excited adiabatic electronic state of the molecular ion H_2^+ which are caused by the interaction of the electron component of the ion-atom system (H_2^+ or $H + H^+$) with the free electromagnetic field taken in the dipole approximation. The mentioned adiabatic electronic states, $X^2\Sigma_g^+$ and $A^2\Sigma_u^-$, are denoted here with $|1\rangle$ and $|2\rangle$ and the corresponding potential curves with $U_1(R)$ and $U_2(R)$, where R is the internuclear distance in the considered ion-atom system. These potential curves are shown in Fig. 1.

Apart from the potentials $U_1(R)$ and $U_2(R)$, for determination of $\sigma_{\rm phd}(\lambda, T)$ and $K_{ia}^{(b)}(\lambda, T)$ it is important to know the dipole matrix element $D_{12}(R)$ defined by relations

$$D_{12}(R) = |\mathbf{D}_{12}(\boldsymbol{R})|, \qquad \mathbf{D}_{12}(\boldsymbol{R}) = \langle 1|\mathbf{D}(\boldsymbol{R})|2\rangle, \tag{8}$$

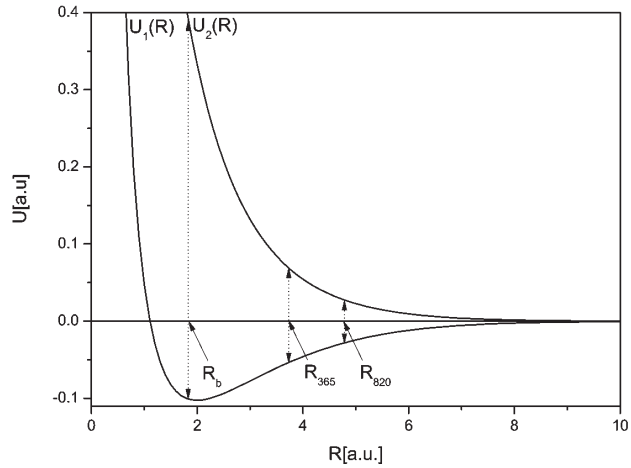

Fig. 1. The potential curves for the molecular ion H_2^+: $U_1(R)$ corresponds to the ground electronic state $X^2\Sigma_g^+$, and $U_2(R)$ – to the first excited electronic state $A^2\Sigma_u^+$.

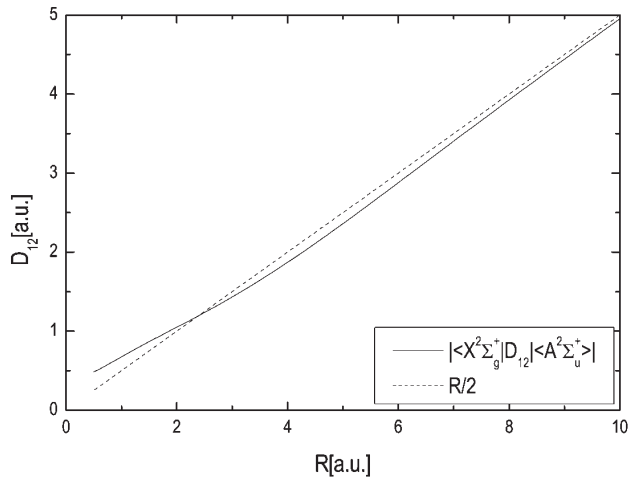

Fig. 2. The matrix element $D_{12}(R)$ for the transitions between the electronic states $X^2\Sigma_g^+$ and $A^2\Sigma_u^+$ of the ion H_2^+.

where $R = |\boldsymbol{R}|$ and $\mathbf{D}(\boldsymbol{R})$ is the operator of electron dipole momentum. Here it is assumed that the system $H + H^+$ or H_2^+ is considered within the center-of-mass reference frame, and the vector $\boldsymbol{R}$ determines the configuration of protons. The dipole matrix element $D_{12}(R)$ is shown in Fig. 2.

The described mechanism of the processes (1) causes absorption of the photon with energy ϵ_λ near the resonant point $R = R_\lambda$, where R_λ is the root of the equation

$$U_{12}(R) \equiv U_1(R) - U_2(R) = \epsilon_\lambda. \tag{9}$$

In Fig. 1 we show the resonant points $R = R_{365}$ and $R = R_{820}$ for absorption/emission of the photons with λ = 365 nm and λ = 820 nm, which are the lower and upper boundaries of region of R important for the part of spectra 365 nm $\leq \lambda \leq$ 820 nm examined in Mihajlov et al. (1993, 1994a). In the same figure the resonant point $R = R_b$ for absorption/emission of the photons with $\lambda = \lambda_b \cong 91.1262$ nm is shown.

One can see that the region of $R \gtrsim R_{365}$ is very far from the minimum of the potential curve $U_1(R)$. In Mihajlov et al. (1993, 1994a) it was possible to use the quasi-static method for the determination of spectral coefficients $K_{ia}^{(a,b)}(\lambda, T)$ and $K_{ia}(\lambda, T)$, which was developed in Mihajlov & Dimitrijević (1986) on the

basis of the semi-classical theory from Mihajlov & Popović (1981). Within this method it is assumed that not only the collisional system $H + H^+$, but the molecular ion H_2^+ also are treated in the semi-classical way.

The significant advantage of the quasi-static approach is that the corresponding coefficients $K_{ia}^{(a,b)}(\lambda, T)$ and $K_{ia}(\lambda, T)$ are given by simple analytical expressions. Such an approach, which was applied in Bates et al. (1953), works very well for the radiative ion-atom collision processes at thermal impact energies which can be described in the semi-classical way (see e.g. Boggess 1959; Mihajlov & Popović 1981; Lam & George 1982; Stancil 1994; Ermolaev et al. 1995; Lebedev & Presnyakov 2002). For these reasons the quasi-static method will be applied here to determine of the absorption coefficient $K_{ia}^{(b)}(\lambda, T)$. In accordance with Mihajlov et al. (1994a) this coefficient can be presented in the form

$$K_{ia}^{(b)}(\lambda, T) = 0.62 \times 10^{-42} \frac{C(R_\lambda)(R_\lambda/a_0)^4}{1 - a_0/R_\lambda} \times \exp\left[-\frac{U_1(R_\lambda)}{kT}\right] \cdot \frac{\Gamma\left(\frac{3}{2}; -\frac{U_1(R_\lambda)}{kT}\right)}{\Gamma\left(\frac{3}{2}\right)}, \quad (10)$$

where a_0 is the atomic unit of length, and the values of the coefficient $C(R_\lambda)$ for the considered region of λ are given in the Table 1, together with the values of the other parameters of the molecular ion H_2^+.

However, in the short-wave length region 92 nm $\lesssim \lambda <$ 365 nm, the relative contribution of the photo-dissociation processes (1a) significantly increases and the low-lying ro-vibrational states of molecular ion H_2^+ become especially important, which requires quantum-mechanical treatment of the internuclear motion. Consequently, for the spectral absorption coefficient $\kappa_{ia}^{(a)}(\lambda, T)$ expression (3) will be used, where the photo-dissociation cross-section $\sigma_{\rm phd}(\lambda, T)$ is determined in the quantum-mechanical way. In the general case this cross-section can be expressed by the relations

$$\sigma_{\rm phd}(\lambda, T) = Z^{-1} \cdot \sum_v \left[\sum_{{\rm odd}J} \frac{3}{2}(2J+1) e^{\frac{-E_{o,o}^{v,J}}{kT}} \cdot \sigma_{v,J}(\lambda) + \sum_{{\rm even}J} \frac{1}{2}(2J+1) e^{\frac{-E_{o,o}^{v,J}}{kT}} \cdot \sigma_{v,J}(\lambda)\right],$$

$$Z = \sum_v \left[\sum_{{\rm odd}J} \frac{3}{2}(2J+1) e^{\frac{-E_{o,o}^{v,J}}{kT}} + \sum_{{\rm even}J} \frac{1}{2}(2J+1) e^{\frac{-E_{o,o}^{v,J}}{kT}}\right], \quad (11)$$

$$E_{o,o}^{v,J} = E_{v,J} - E_{v=0,J=0}, \quad (12)$$

where v and J are respectively the vibrational and the rotational quantum number of the individual ro-vibrational states (v, J) of the molecular ion $H_2^+(X^2\Sigma_g^+)$, and $E_{v,J}$ are the corresponding energies. Let us draw attention to the fact that the structure of the expression (11) is a consequence of the consistent taking the proton spin into account (see e.g. Patch 1969; Stancil 1994). With $\sigma_{v,J}(\lambda)$ in that expression is denoted the partial photo-dissociation cross-section of H_2^+ in the ro-vibrational state (v, J) for the same λ, namely

$$\sigma_{v,J}(\lambda) = \frac{8\pi^3}{3\lambda}\left[\frac{J+1}{2J+1} \cdot |D_{E,J+1;v,J}|^2 + \frac{J}{2J+1} \cdot |D_{E,J-1;v,J}|^2\right], \quad (13)$$

Table 1. Parameters of molecular ion H_2^+.

λ [nm]	R_λ [AU]	$C(R_\lambda)$ [AU]	$U_1(R_\lambda)$ [AU]	$U_2(R_\lambda)$ [AU]
90	1.79	0.717	–0.1001	0.4060
100	1.94	0.744	–0.1024	0.3530
125	2.24	0.780	–0.1001	0.2643
150	2.49	0.802	–0.0941	0.2096
175	2.70	0.816	–0.0876	0.1727
200	2.89	0.827	–0.0815	0.1463
225	3.05	0.837	–0.0760	0.1265
250	3.19	0.845	–0.0710	0.1111
275	3.32	0.851	–0.0667	0.0990
300	3.44	0.857	–0.0628	0.0891
325	3.55	0.863	–0.0593	0.0809
350	3.65	0.868	–0.0561	0.0740
370	3.73	0.871	–0.0539	0.0692

where $D_{E,J+1;v,J}$ and $D_{E,J-1;v,J}$ are the radial matrix elements given by relations

$$D_{E,J;v,J'} = \langle \Psi_{2;E,J'}(R)|D_{12}(R)|\Psi_{1;v,J}(R)\rangle, \quad J = J \pm 1, \quad (14)$$

and $D_{12}(R)$ is defined by Eq. (8). Here, with $\Psi_{1;v,J}(R)$ and $\Psi_{2;E,J'}(R)$ the nuclear radial wave functions are denoted, which describe the bound state (v, J) in the potential $U_1(R)$ and the continual state (E, J') in the potential $U_2(R)$, where the energy E satisfies the condition

$$E - E_{v,J} = \varepsilon_\lambda. \quad (15)$$

The wave functions $\Psi_{1;v,J}(R)$ and $\Psi_{2;E,J'}(R)$ are determined by solving the radial Schrödinger equations with the potentials $U_1(R)$ and $U_2(R)$ under the usual normalization conditions

$$\int_0^\infty |\Psi_{n;v,J}(R)|^2 R^2 dR = 1,$$
$$\int_0^\infty \Psi^*_{n;E',J'}(R)\Psi_{n;E,J'}(R) R^2 dR = \delta(E' - E). \quad (16)$$

The potentials $U_1(R)$ and $U_2(R)$, as well as the dipole matrix element $D_{12}(R)$, were generated by means of the numerical procedure described in Ignjatović & Mihajlov (2005). The values of these quantities, shown in Figs. 1 and 2, agree with the values presented in Madsen & Peek (1971) and Ramaker & Peek (1973) with accuracy better than 0.1%.

The results of our calculations of the average photo-dissociation cross-section $\sigma_{\rm phd}(\lambda, T)$ are illustrated by Fig. 3. The curves in this figure show the behavior of $\sigma_{\rm phd}(\lambda, T)$ as a function of λ for some temperatures, namely T = 4200 K, 5040 K and 6300 K, which are relevant for the solar photosphere. These values of T are chosen because there are calculations of the average photo-dissociation cross-section in Stancil (1994), where the results were obtained with a expression equivalent to Eq. (11), and in Lebedev & Presnyakov (2002), where a simpler expression was used. Here we have in mind the expression obtained from Eq. (11) by replacing the factors 3/2 and 1/2 with 1, which corresponds to neglecting the proton spin. With both approaches one obtains very close results for the considered temperatures (see e.g. Patch 1969). Comparison of our results with the results from Stancil (1994) and Lebedev & Presnyakov (2002) shows that in the whole considered region 90 nm $\leq \lambda \leq$ 370 nm there is a very good agreement among all results mentioned. This fact justifies the applicability of the procedure used for the determination of $\sigma_{\rm phd}(\lambda, T)$ in all other calculations.

Table 2. The coefficient K_{ia} as a function of λ and T.

	K_{ia}[cm^5]					
λ[nm]	4000 K	4500 K	5000 K	6000 K	7000 K	8000 K
90	.262E-37	.111E-37	.553E-38	.196E-38	.932E-39	.533E-39
100	.413E-37	.170E-37	.838E-38	.289E-38	.135E-38	.760E-39
125	.586E-37	.245E-37	.122E-37	.427E-38	.202E-38	.115E-38
150	.539E-37	.236E-37	.122E-37	.454E-38	.224E-38	.132E-38
170	.457E-37	.209E-37	.112E-37	.439E-38	.225E-38	.136E-38
200	.344E-37	.168E-37	.946E-38	.400E-38	.217E-38	.137E-38
225	.273E-37	.140E-37	.817E-38	.366E-38	.207E-38	.135E-38
250	.220E-37	.118E-37	.713E-38	.337E-38	.197E-38	.132E-38
275	.181E-37	.101E-37	.628E-38	.311E-38	.188E-38	.129E-38
300	.152E-37	.874E-38	.561E-38	.289E-38	.180E-38	.126E-38
325	.130E-37	.769E-38	.506E-38	.271E-38	.173E-38	.124E-38
350	.113E-37	.688E-38	.463E-38	.256E-38	.168E-38	.122E-38
370	.102E-37	.635E-38	.434E-38	.246E-38	.164E-38	.121E-38

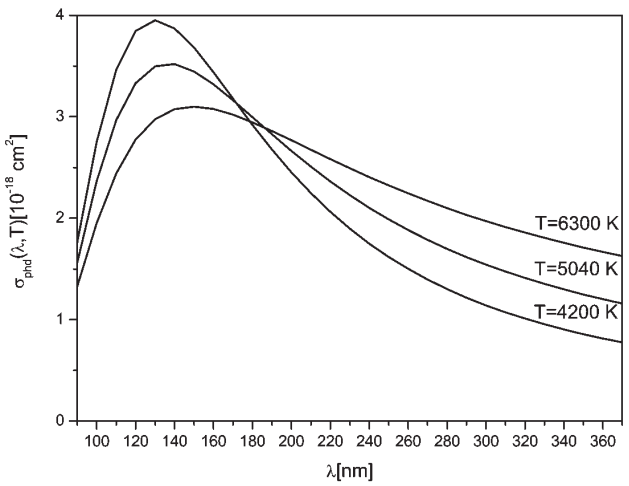

Fig. 3. The Behavior of average cross-section for the photo-dissociation of the ion H_2^+, as a function of λ and T.

Table 3. The branch coefficient $X^{(a)}$ which characterize the relative contribution of the process (1a).

	$X^{(a)}$					
λ [nm]	4000 K	4500 K	5000 K	6000 K	7000 K	8000 K
90	0.999	0.997	0.994	0.985	0.970	0.951
100	0.999	0.997	0.995	0.986	0.973	0.954
125	0.999	0.997	0.994	0.985	0.971	0.951
150	0.998	0.996	0.992	0.980	0.962	0.939
175	0.997	0.994	0.989	0.974	0.953	0.926
200	0.995	0.991	0.984	0.965	0.939	0.909
225	0.993	0.987	0.978	0.954	0.924	0.889
250	0.989	0.981	0.970	0.942	0.907	0.868
275	0.985	0.975	0.962	0.928	0.888	0.846
300	0.980	0.967	0.952	0.913	0.869	0.823
325	0.976	0.961	0.943	0.901	0.854	0.806
350	0.969	0.952	0.932	0.885	0.834	0.783
370	0.963	0.943	0.921	0.870	0.817	0.764

3. Results and discussion

Figure 3 shows that $\sigma_{\rm phd}(\lambda, T)$ in the region $\lambda < 365$ nm significantly increases with decreasing λ and becomes noticeably decreasing only in the region $\lambda < 100$ nm. Such a behavior of $\sigma_{\rm phd}(\lambda, T)$ causes the equal increasing of the partial spectral absorption coefficient $\kappa_{ia}^{(a)}(\lambda, T)$, for the same values of T, N(H) and $N(H^+)$, with the transition from the region $\lambda > 365$ nm into the region 100 nm $\lesssim \lambda < 365$ nm. At the same time the total spectral absorption coefficient $\kappa_{ia}(\lambda, T)$ has to significantly increase within the same region of λ. Since this fact has to reflect the spectral characteristics of the Solar photosphere and the lower chromosphere, the corresponding calculations are made here.

As the first step, the values of the total coefficient $K_{ia}(\lambda, T)$, defined by Eqs. (6) and (7), are calculated in the regions 90 nm $\leq \lambda \leq 370$ nm and 4000 K $\leq T \leq 8000$ K and presented in the Table 2. Here it was assumed that in Eq. (6) the quantity χ can be treated as in our previous papers (Mihajlov & Dimitrijević 1986; Mihajlov et al. 1993, 1994b), as a constant of dissociative-associative equilibrium for a given T.

The relative contribution of the processes (1) can be characterized by the branch coefficients

$$X^{(a)} = \frac{\kappa_{ia}^{(a)}(\lambda, T)}{\kappa_{ia}(\lambda, T)} = \frac{K_{ia}^{(a)}(\lambda, T)}{K_{ia}(\lambda, T)}, \qquad X^{(b)} = \frac{\kappa_{ia}^{(b)}(\lambda, T)}{\kappa_{ia}(\lambda, T)} \equiv 1 - X^{(a)}. \tag{17}$$

The values of the coefficient $X^{(a)}$ characterizing the photo-dissociation process (1a) are presented in Table 3 for the same regions λ and T. This table shows that in accordance with expectations the relative contribution of the photo-dissociation process (1a) significantly increases with decreasing of λ in the short-wave region.

As the second step, the values of the spectral absorption coefficient $\kappa_{ia}(\lambda, T)$, defined by Eq. (7), are determined as a function of altitude h taking N(H), $N(H^+)$ and T which corresponds to the standard model C from Vernazza et al. (1981). These values are presented in Table 4 for 92 nm $\leq \lambda \leq 350$ nm and -75 km $\leq h \leq$ 1065 km. Also, at the bottom of Table 4 are given the values of the corresponding spectral optical depth $\Delta\tau$ for the considered layer of the solar atmosphere. These values of $\Delta\tau$ show that the processes (1) cause a significant decrease (25–50%) of the radiation flux which comes from deeper layers of the Sun. So, only the considered layer gives a non-negligible contribution to the total absorption caused by processes (1) in the region $\lambda < 365$ nm.

Because of all the mentioned above factors it is especially important to compare the relative contribution of the

Table 4. The total spectral absorption coefficient $\kappa_{ia}(\lambda)$ for solar photosphere and lower chromosphere, calculated for the model C from Vernazza et al. (1981).

	κ_{ia}[cm^{-1}]						
h[km]	92 nm	100 nm	150 nm	200 nm	250 nm	300 nm	350 nm
1065	0.1978E-14	0.2649E-14	0.4165E-14	0.3676E-14	0.3077E-14	0.2625E-14	0.2309E-14
980	0.6984E-14	0.9370E-14	0.1462E-13	0.1275E-13	0.1056E-13	0.8937E-14	0.7811E-14
905	0.1396E-13	0.1879E-13	0.2900E-13	0.2480E-13	0.2021E-13	0.1689E-13	0.1461E-13
855	0.2222E-13	0.2995E-13	0.4589E-13	0.3876E-13	0.3127E-13	0.2592E-13	0.2228E-13
755	0.4808E-13	0.6526E-13	0.9725E-13	0.7827E-13	0.6071E-13	0.4878E-13	0.4087E-13
705	0.5655E-13	0.7715E-13	0.1126E-12	0.8738E-13	0.6577E-13	0.5160E-13	0.4242E-13
655	0.5718E-13	0.7855E-13	0.1115E-12	0.8243E-13	0.5958E-13	0.4527E-13	0.3627E-13
605	0.3793E-13	0.5252E-13	0.7218E-13	0.5041E-13	0.3473E-13	0.2541E-13	0.1974E-13
555	0.2703E-13	0.3763E-13	0.5060E-13	0.3398E-13	0.2266E-13	0.1615E-13	0.1229E-13
515	0.3019E-13	0.4212E-13	0.5622E-13	0.3727E-13	0.2457E-13	0.1736E-13	0.1312E-13
450	0.6696E-13	0.9325E-13	0.1252E-12	0.8393E-13	0.5586E-13	0.3975E-13	0.3022E-13
350	0.4487E-12	0.6205E-12	0.8571E-12	0.6038E-12	0.4191E-12	0.3084E-12	0.2408E-12
250	0.4546E-11	0.6237E-11	0.8897E-11	0.6633E-11	0.4829E-11	0.3689E-11	0.2969E-11
150	0.8262E-10	0.1123E-09	0.1660E-09	0.1317E-09	0.1010E-09	0.8043E-10	0.6690E-10
100	0.4018E-09	0.5435E-09	0.8211E-09	0.6768E-09	0.5350E-09	0.4365E-09	0.3703E-09
50	0.1913E-08	0.2570E-08	0.3989E-08	0.3445E-08	0.2831E-08	0.2381E-08	0.2070E-08
0	0.8309E-08	0.1106E-07	0.1779E-07	0.1630E-07	0.1411E-07	0.1231E-07	0.1105E-07
–25	0.1820E-07	0.2409E-07	0.3971E-07	0.3797E-07	0.3406E-07	0.3061E-07	0.2808E-07
–50	0.4090E-07	0.5372E-07	0.9132E-07	0.9188E-07	0.8596E-07	0.8019E-07	0.7570E-07
–75	0.7898E-07	0.1030E-06	0.1798E-06	0.1888E-06	0.1830E-06	0.1756E-06	0.1700E-06
$\Delta\tau$	0.29	0.38	0.64	0.64	0.60	0.56	0.53

processes (1) to the opacity of solar atmosphere, with the contribution of the other relevant absorption processes (2). The contribution of these processes will be characterized by the absorption coefficients $\kappa_{ea}(\lambda)$ and $\kappa_{ei}(\lambda)$, defined by relations

$$\kappa_{ea}(\lambda) = K_{ea}(\lambda, T) \cdot N_e \cdot N(H),$$
$$K_{ea}(\lambda, T) = \sigma^{(-)}_{phd}(\lambda) \cdot \chi^{-1}_{ea} + K^{(b)}_{ea}(\lambda, T), \tag{18}$$

$$\kappa_{ei}(\lambda) = K_{ei}(\lambda, T) \cdot N_e \cdot N(H^+),$$
$$K_{ei}(\lambda, T) = \sum_{n\geq 2} \sigma_n(\lambda) \cdot \frac{N(H^*(n))}{N(H)} \cdot \chi^{-1}_{ei} + K^{(b)}_{ei}(\lambda, T) \tag{19}$$

$$\chi_{ea} = \frac{N_e N(H)}{N(H^-)}, \qquad \chi_{ei} = \frac{N_e N(H^+)}{N(H)}, \tag{20}$$

where $\sigma^{(-)}_{phd}(\lambda)$ is the photo-dissociation cross-section of the negative ion H^-, $K^{(b)}_{ea}(\lambda, T)$ – the rate coefficient that describes absorption by (e + H)-collision systems, $\sigma_n(\lambda)$ – average photo-ionization cross-section for the excited atom $H^*(n)$, $K^{(b)}_{ei}(\lambda, T)$ – the rate coefficient that describes absorption by $(e + H^+)$-collision systems, and N_e, $N(H^-)$ and $N(H^*(n))$ – respectively the densities of free electrons, negative ions H^- and excited atom $H^*(n)$. The coefficients χ_{ea} and χ_{ei} are treated here as the constants of dissociative-associative and ionization-recombination equilibrium, respectively, for a given T.

The relative contributions of the processes (1) together, with respect to processes (2) separately, is described by the quantities F_{ea} and F_{ei} defined by relations

$$F_{ea} = \frac{\kappa_{ia}(\lambda)}{\kappa_{ea}(\lambda)} = \frac{K_{ia}(\lambda, T)}{K_{ea}(\lambda, T)} \cdot \frac{N(H^+)}{N_e}, \tag{21}$$

$$F_{ei} = \frac{\kappa_{ia}(\lambda)}{\kappa_{ei}(\lambda)} = \frac{K_{ia}(\lambda, T)}{K_{ei}(\lambda, T)} \cdot \frac{N(H)}{N_e}, \tag{22}$$

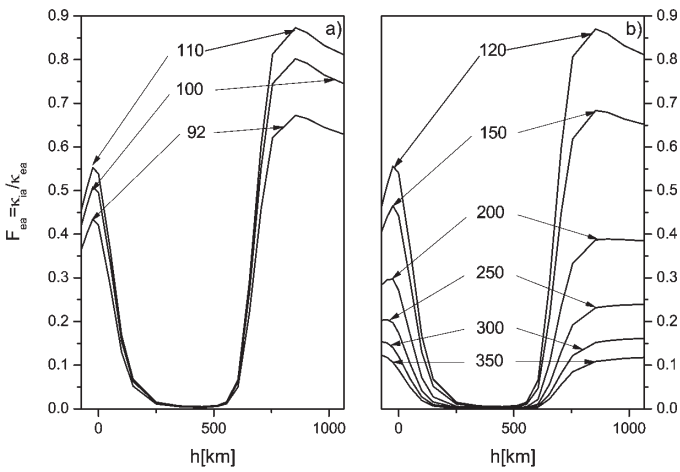

Fig. 4. Behavior of the quantity $F_{\kappa_{ea}} = \kappa_{ia}/\kappa_{ea}$ as a function of λ and h.

where the coefficients $K_{ea}(\lambda, T)$ and $K_{ei}(\lambda, T)$ are given by Eqs. (18)–(20). The values of the coefficient $K_{ea}(\lambda, T)$ are determined by means of data from Stilley & Callaway (1970) and Wishart (1979) for the emission processes inverse to the absorption processes (2a) and the principle of thermodynamic balance. In the case of the absorption processes (2b) the values of the coefficient $K_{ei}(\lambda, T)$ are determined by exact quantum-mechanical expressions for the ionization cross-section $\sigma_n(\lambda)$ and the quasi-classical expression for the coefficient $K^{(b)}_{ei}(\lambda, T)$ from Sobel'man (1979). In the calculations of $\kappa_{ea}(\lambda)$ and $\kappa_{ei}(\lambda)$ the densities N_e, $N(H)$ and $N(H^+)$, as well as the densities $N(H^*(n))$ with $2 \leq n \leq 8$, are taken from Vernazza et al. (1981), while the densities $N(H^*(n > 8))$ were determined by means of Boltzman's formula for given $N(H^*(n = 8))$ and T.

The results of the calculations of the ratios $F_{ea}(h)$ and $F_{ei}(h)$ for 92 nm $\leq \lambda \leq$ 350 nm are presented in Figs. 4 and 5. The first of these figures shows that in the significant part of the considered region of altitudes (−75 km $\leq h \leq$ 1065 km) the absorption

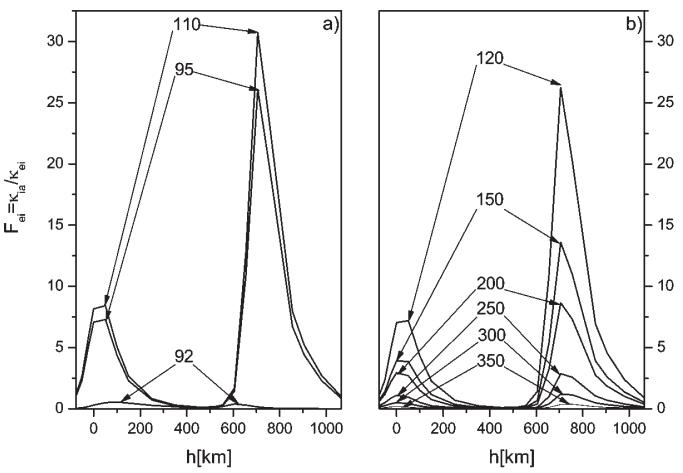

Fig. 5. Behavior of the quantity $F_{\kappa_{ei}} = \kappa_{ia}/\kappa_{ei}$ as a function of λ and h.

processes (1) together give the contribution which varies from about 10% to about 90% of the contribution of the absorption processes (2a), which are considered as the main absorption processes. In connection with the other known absorption processes (2b) Fig. 5 shows that in the considered region of altitude there are significant parts where the processes (1) completely dominate.

4. Conclusions

Spectral absorption coefficients $\kappa_{ia}(\lambda, T)$, defined by Eq. (7), characterizing the processes (1), were calculated for the Solar photosphere and the lower chromosphere within the 90 nm $\leq \lambda \leq$ 370 nm spectral range as functions of altitude h taking N(H), $N(H^+)$ and T corresponding to the standard model C from Vernazza et al. (1981). Also, the total contribution of the processes (1) to the solar opacity, and their relative contribution in comparison with the other relevant absorption processes (2), were determined. In significant parts of the considered layer (-75 km $\leq h \leq$ 1065 km) the total contribution of the processes (1) varies from about 10% to about 90% of the contribution of the absorption processes (2a), and it is completely dominant in comparison with absorption processes (2b). The results obtained demonstrate that, due to the investigated processes (1), the radiation flux that comes from deeper layers of Sun decreases significantly (25−50%). Consequently, the processes (1) have to be treated as a serious factor that influences the continuous part of the absorption spectra of the Solar atmosphere, particularly in UV and VUV regions, and changes accordingly the mechanism of UV and VUV radiative transfer. They influence indirectly and the plasma state within particular layers of the Solar atmosphere, which is formed in an interaction with electromagnetic radiation. Moreover, photo-dissociation of H_2^+ molecular ions, directly influences the kinetics inside the plasma. These facts also have implications in the corresponding equations of state. Due to all these reasons the processes (1) have to be consistently included in standard models of the solar atmosphere.

Acknowledgements. This work is a part of the projects "Radiation and transport properties of the non-ideal laboratory and ionospheric plasma" (Project number 141033) and "Influence of collisional processes on astrophysical plasma line shapes (Project number 146001) and was supported by the Ministry of Science and Environment Protection of Serbia.

References

Bates, D. R., Ledsham, K., & Stewart, A. L. 1953, Phil. Trans. Roy. Soc., 215
Boggess, A. 1959, Astrophys. J., 129, 432
Ermolaev, A. M., Mihajlov, A. A., Ignatović, L. M., & Dimitrijević, M. S. 1995, J. Phys. D, 28, 1047
Ignjatović, L., & Mihajlov, A. A. 2005, Phys. Rev. A, 72, 022715
Lam, K. S., & George, T. F. 1982, J. Chem. Phys., 76, 3396
Lebedev, V. S., & Presnyakov, L. P. 2002, J. Phys. B: At. Mol. Opt. Phys., 35, 4347
Madsen, M. M., & Peek, J. M. 1971, Atomic Data, 2, 171
Maltby, P., Avertt, E. H., Carlsson, M., et al. 1986, ApJ, 306, 284
Mihajlov, A. A., & Popović, M. P. 1981, Phys. Rev. A, 23, 1679
Mihajlov, A. A., & Dimitrijević, M. S. 1986, A&A, 155, 319
Mihajlov, A. A., Dimitrijević, M. S., & Ignjatović, L. M. 1993, A&A, 276, 187
Mihajlov, A., Dimitrijević, M., & Ignjatović, L. 1994a, A&A, 287, 1026
Mihajlov, A. A., Dimitrijević, M. S., Ignjatović, L. M., & Djurić, Z. 1994b, A&ASS, 103, 57
Mihalas, D. 1978, Stellar Atmospheres (San Francisco: W. H. Freeman)
Patch, R. W. 1969, J.Q.S.R.T, 9, 63
Ramaker, D. E., & Peek, J. M. 1973, Atomic Data, 5, 167
Sobel'man, I. I. 1979, Atomic Spectra and Radiative Transitions (Berlin: Springer Verlag)
Stancil, P. C. 1994, ApJ, 430, 360
Stilley, J. L., & Callaway, J. 1970, ApJ, 160, 245
Vernazza, J., Avrett, E., & Loser, R. 1981, ApJS, 45, 635
Wishart, A. W. 1979, MNRAS, 187, 59

A&A 471, 671–673 (2007)
DOI: 10.1051/0004-6361:20077517
© ESO 2007

Astronomy & Astrophysics

Influence of chemi-ionization and chemi-recombination processes on hydrogen line shapes in M dwarfs

A. A. Mihajlov[1,3], D. Jevremović[2], P. Hauschildt[4,5], M. S. Dimitrijević[2,3], Lj. M. Ignjatović[1,3], and F. Alard[6]

[1] Institute of Physics, PO Box 57, 11001 Belgrade, Serbia
e-mail: mihajlov@phy.bg.ac.yu
[2] Astronomical Observatory, Volgina 7, 11160 Belgrade 74, Serbia
[3] Isaac Newton Institute of Chile, Yugoslavia Branch
[4] Depart. of Phys. and Astronomy and Center for Simulat. Physics, University of Georgia, Athens, GA 30602, USA
[5] Hamburger Sternwarte, Universitaet Hamburg, Gojenbergsweg 112, 21029 Hamburg, Germany
[6] CRAL/ENS, 46 allée d'Italie, 69634 Lyon Cedex 07, France

Received 21 March 2007 / Accepted 20 May 2007

ABSTRACT

Aims. We study the influence of chemi-ionization in $H^*(n)$ + H(1s) collisions and inverse chemi-recombination processes on the population of higher levels and consequently on profiles of hydrogen lines in the atmospheres of late type (M) stars.
Methods. Modeling, using general stellar atmosphere code PHOENIX to reveal the importance of the inclusion of such processes.
Results. We demonstrate for the first time observationally detectable effects of these chemi-processes on stellar spectra.
Conclusions. It is very important to include chemi-ionization and chemi-recombination processes in modeling of atmospheres of late type stars, especially if one wants to use line profiles for diagnostics of stellar photospheres and lower chromospheres.

Key words. atomic processes – molecular processes – stars: atmosphere – line: formation – stars: chromospheres – stars: late-type

1. Introduction

We have demonstrated previously (Mihajlov et al. 1992; Mihajlov et al. 1996) the influence of a group of collisional chemi-ionization and chemi-recombination processes on the excited atom populations in hydrogen plasmas with ionization degree less than 10^{-3}. Here, we have considered namely the ionization processes

$$H^*(n) + H \Longrightarrow e + H_2^+, \tag{1a}$$

$$H^*(n) + H \Longrightarrow e + H + H^+ \tag{1b}$$

and the corresponding inverse recombination processes

$$e + H_2^+ \Longrightarrow H^*(n) + H, \tag{2a}$$

$$e + H + H^+ \Longrightarrow H^*(n) + H \tag{2b}$$

where H = H(1s), $H^*(n)$ – is the hydrogen atom in the excited state with the principal quantum number n, H_2^+ – the molecular ion in the ground electronic state, and e–a free electron. The results obtained were used as a basis to study the processes (1a)–(2b) in the weakly ionized layers of the Solar atmosphere (Mihajlov et al. 1997b) and atmospheres of cool stars (Mihajlov et al. 2003b). The efficiency of these processes was compared with the efficiency of the other relevant ionization and recombination processes, namely, with the electron-atom impact ionization, electron-electron-ion recombination, and electron-ion photo-recombination processes

$$e + H^*(n) \Longrightarrow e + e + H^+ \tag{3}$$

$$e + e + H^+ \Longrightarrow e + H^*(n) \tag{4}$$

$$e + H^+ \Longrightarrow \epsilon_\lambda + H^*(n) \tag{5}$$

where ϵ_λ denotes the energy of the emitted photon. The significant, and often dominant influence of the processes (1a)–(2b) on the populations of excited atom $H^*(n)$ with $n > 3$ in the Solar photosphere and lower chromosphere and in considered cool star atmospheres was demonstrated. Previous work has shown the importance of including the above-mentioned processes, given that population numbers can differ by up to 50% (Mihajlov et al. 2003b).

Investigation of these processes in stellar atmospheres was first reported in Mihajlov et al. (1994). Prior to this, they were mainly investigated for alkali-metal atoms under laboratory conditions. However, they are ab initio included in stellar atmosphere modeling only in Mihajlov et al. (2003). One of the aims of the present paper is to provide, together with that of Mihajlov et al. (2003), enough arguments that these processes are essential for the modeling of stellar photospheres and lower chromospheres for solar-like and cooler stars.

Moreover, in Mihajlov et al. (1997a) chemi-ionization and chemi-recombination processes similar to the processes (1a)–(2b), but in the helium case, were considered, and their influence on the excited atom populations in weakly-ionized helium plasma was demonstrated. Subsequently, the importance of such processes on the excited helium atom populations in atmospheres of some DB white dwarfs (Mihajlov et al. 2003a) was shown.

Since the previous results showed that the chemi-ionization and chemi-recombination processes change the population of excited states and the electron density as a function of optical depth in the photospheres and lower chromospheres of solar-like and cooler stars, we consider here the possible influences of the

Article published by EDP Sciences and available at http://www.aanda.org or http://dx.doi.org/10.1051/0004-6361:20077517

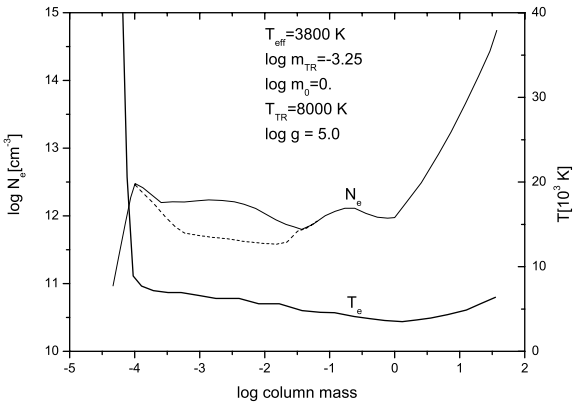

Fig. 1. Structure of model atmosphere – temperature T_e and electron density N_e vs. column mass. Solid line for N_e denotes electron density profile determined with inclusion of chemi-ionization and chemi-recombination processes (1a)–(2b), for all $n > 1$, and dashed one denotes the electron density profile determined without these processes.

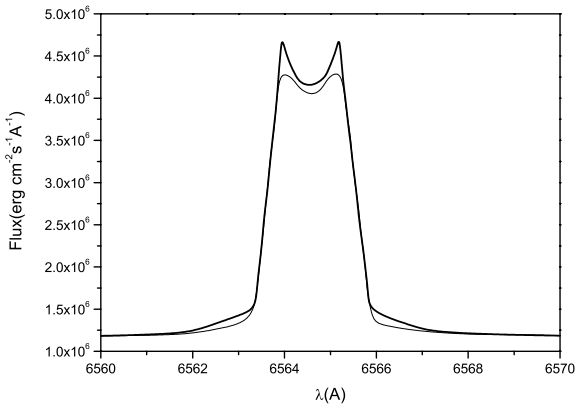

Fig. 2. Line profiles with (full) and without (thin) inclusion of chemi-ionization and chemi-recombination processes for H_α line from the atmosphere described in text and shown in Fig. 1.

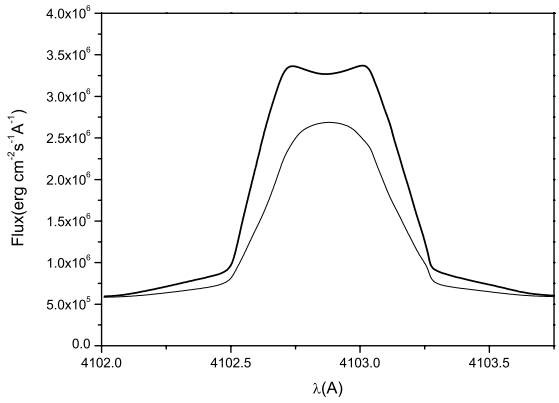

Fig. 3. As in Fig. 2 but for H_δ line.

processes (1a)–(2b) on the hydrogen spectral line shapes in non-LTE stellar atmospheres. The stellar atmosphere plasma similar to that examined in Mihajlov et al. (2003b), will be investigated applying similar methodology.

In the case of hydrogen, the method used is correct for $n \geq 5$, when the potential curves of the $H^*(n)$ + H system are above the potential curves of the $H^+ + H^-$ system. However the cross-points of the potential curves of the systems $H^*(n = 4)$ + H and $H^+ + H^-$, are so distant that their existence could be ignored so that the method used is applicable for $n \geq 4$. This question was examined in detail in Janev & Mihajlov (1979) and not considered again in subsequent works. Earlier (Mihajlov et al. 2003), we did not find the rate coefficients for $n = 2$ and 3, since they were not given in direct form in Janev et al. (1987). There, only the data which enable to derive the needed constants are present. So, in the present work we derived them using data from this reference. Also in Mihajlov et al. (2003) our principal aim was to demonstrate that the already-examined processes with $n \geq 4$ are significant for modeling.

Here we introduced in PHOENIX code collisional rates for $n = 2$ and 3 obtained on the basis of data from Janev et al. (1987), and thus the theory of processes (1a)–(2b) is completed here.

2. Results and discussion

We use the general stellar atmosphere code PHOENIX (Baron & Hauschildt 1998; Hauschildt et al. 1999; Short et al. 1999) for our modeling. This code has the advantage that apart for solving the atmospheric structure, it also calculates output spectra, so changes in population levels are reflected on line shapes. The procedure similar to that used in Mihajlov et al. (2003b) was applied, but for all $H^*(n)$ atom populations with $n > 1$. Rate coefficients are theoretically determined by means of the method developed in Mihajlov et al. (1992, 1996). This method is in principle the same as that developed for the chemi-ionization processes in the alkali-metal atom collisions, where it is confirmed many times by experiment (see e.g. Ignjatović & Mihajlov 2005). Basic atmosphere has an effective temperature of $T_{\rm eff} = 3800$ K, with chromosphere and transition region appearing at logarithm column mass of 0.04 and −4.0 respectively and temperature at the bottom of transition region fixed at 8000 K. This basic atmosphere is shown in Fig. 1. The solid line for N_e denotes the electron density profile determined with inclusion of chemi-ionization and chemi-recombination processes (1a)–(2b), for all $n > 1$, while the dashed line denotes the electron density profile determined without these processes. The hydrostatic equilibrium, the equations of state, and the non-LTE rate equations for H were iterated until changes in populations of levels of atomic hydrogen were less than 1%. We find that inclusion of the new chemi-processes (1a)–(2b) significantly affects the H energy level number densities in M dwarfs, as was found in Mihajlov (2003b) but without $n = 2$ and 3 level contribution. Also, the expected change of electron density N_e is confirmed, and found to be particularly important not only when processes (1a)–(2b) with $n > 3$ are included, but also the processes with $n = 2$ and 3. This is illustrated in Fig. 1. Such changes should also influence spectral line profiles.

In Figs. 2–5 we show the final line profiles of H_α, H_δ, H_ϵ Pa_ϵ with and without inclusion of new processes. Profiles we synthesized with PHOENIX code with Stark broadening calculated using tables from Vidal et al. (1971) for Stark broadening of hydrogen lines (linear Stark effect). The line intensity changes seen in Figs. 2–5 directly demonstrate the influence of the changes of $H^*(n)$ atom populations. Lineshape changes, especially in the wings, show the influence of the electron density change having direct influence on the Stark broadening of hydrogen lines. The particular significance of this result is that it is the first demonstration of the possibility of confirming the influence of chemi-ionization and chemi-recombination processes (1a)–(2b) by direct observations of stellar spectra.

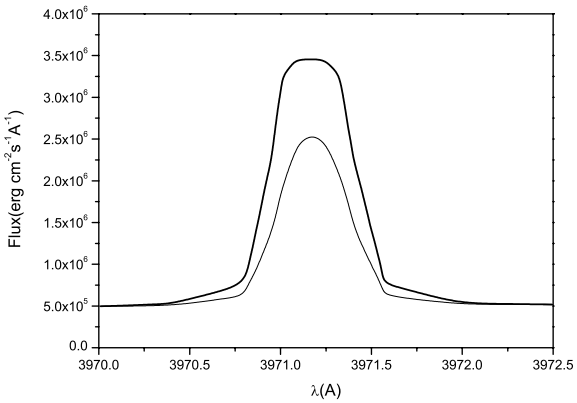

Fig. 4. As in Fig. 2 but for H_ϵ line.

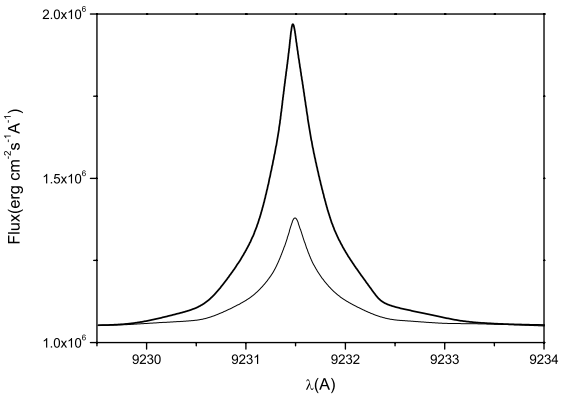

Fig. 5. As in Fig. 2 but for Pa_ϵ line.

The most important effect of electron density (N_e) changes must be on the thermalization depth of the line, and hence the brightness in the line core for a given temperature structure. With increased N_e, the rate of thermalizing collisions with electrons in the chromosphere will be higher, causing the line center radiative source function to be more closely coupled to the Planck function, hence making the lines righter (i.e. stronger) for a given model structure. This is very important because it systematically affects the diagnostic accuracy of the lines: without inclusion of chemi ionization/recombination processes (1a)−(2b), one would predict emission lines that are too weak from a given model, and, therefore, conclude that the atmospheric pressure is larger than it really is.

Consequently, we can conclude that this is the first demonstration of a significant and observable (measurable) change in line profiles, as a consequence of the influence of the considered processes. Thus it is very important to include chemi-ionization and chemi-recombination processes (1a)−(2b) in modeling of atmospheres of late-type stars, especially if one wants to use line profiles for diagnostics of stellar atmospheres. Moreover, it should be taken into account that within the effective temperature range 3000 K $< T_{\rm eff} <$ 6000 K, the relative influence of the processes (1a)−(2b) related to other relevant processes (3)−(5) can only increase with the increase of $T_{\rm eff}$, if the atmospheric composition remains similar to Solar composition. Consequently, for Solar photosphere and lower chromosphere, we should expect the more enhanced influence of the processes (1a)−(2b) than for the case considered here. It should be taken into account however, that within the region where the ionization degree is up to 10^{-3}, the concurrent processes increase with the increase in temperature, as do electron-atom and electron-ion, as well as radiative processes. So, while $T_{\rm eff}$ increases, but stays below or close to Solar, on the basis of previous results, (Mihajlov et al. 1997), the increase of the relative influence of chemi-ionization/recombination processes (1a)−(2b) on excited atom populations and electron densities is expected. Generally, according to our knowledge, further improvements to the used method will result in an increase in the influence of chemi-ionization-recombination processes.

Acknowledgements. This work is part of the projects *Radiation and transport properties of the non-ideal laboratory and ionospheric plasma* (Project number 141033) and *Influence of collisional processes on astrophysical plasma lineshapes* (Project number 146001) and was supported by the Ministry of Science and Environment Protection of Serbia. We are grateful to Ian Short for very useful suggestions and comments.

References

Baron, E., & Hauschildt, P. H. 1998, ApJ, 495, 370
Hauschildt, P. H., Allard, F., & Baron, E. 1999, ApJ, 512, 377
Ignjatović, Lj. M., & Mihajlov, A. A. 2005, Phys. Rev. A, 72, 022715
Janev, R. K., & Mihajlov, A. A. 1979, Phys. Rev. A, 20, 1890
Janev, R. K., Langer, W. D., Evans Jr., K., & Post Jr., D. E. 1987, Elementary Processes in Hydrogen-Helium Plasmas (Springer-Verlag)
Mihajlov, A. A., Ljepojević, N. N., & Dimitrijević, M. S. 1992, J. Phys. B, 25, 5121
Mihajlov, A. A., Dimitrijević, M. S., Ignjatović, Lj. M., & Djurić, Z. 1994, A&AS, 103, 57
Mihajlov, A. A., Dimitrijević, M. S., & Djurić, Z. 1996, Phys. Scr., 53, 159
Mihajlov, A. A., Dimitrijević, M. S., Djurić, Z., & Ljepojević, N. N. 1997a, Phys. Scr., 56, 631
Mihajlov, A. A., Ignjatović, L. M., Vasilijević, M. M., & Dimitrijević, M. S. 1997b, A&A, 324, 1206
Mihajlov, A. A., Ignjatović, L. M., Dimitrijević, M. S., & Djurić, Z. 2003a, ApJS, 147, 369
Mihajlov, A. A., Jevremović, D., Hauschildt, P., et al. 2003b, A&A, 403, 787
Short, C. I., Hauschildt, P. H., & Baron, E. 1999, ApJ, 525, 375
Vidal, C. R., Cooper, J., & Smith, E. W. 1971, J. Quant. Spectrosc. Radiative Transfer, 11, 263

A&A 552, A33 (2013)
DOI: 10.1051/0004-6361/201220699
© ESO 2013

Astronomy & Astrophysics

Excitation and deexcitation processes in atom-Rydberg atom collisions in helium-rich white dwarf atmospheres *(Research Note)*

V. A. Srećković[1,2], A. A. Mihajlov[1,2], Lj. M. Ignjatović[1,2], and M. S. Dimitrijević[3,2,4]

[1] University of Belgrade, Institute of physics, PO Box 57, 11001 Belgrade, Serbia
e-mail: vlada@ipb.ac.rs
[2] Institute Isaac Newton of Chile, Yugoslavia Branch, 11060 Belgrade, Serbia
[3] Astronomical Observatory, Volgina 7, 11060 Belgrade 74, Serbia
[4] Observatoire de Paris, 92195 Meudon Cedex, France

Received 6 November 2012 / Accepted 14 February 2013

ABSTRACT

We aim to show the importance of non-elastic excitation and deexcitation processes in $He^*(n) + He(1s^2)$ collisions with the principal quantum number $n \geq 3$ for helium-rich white dwarf atmospheres. We compare the efficiencies of these processes with those of the known non-elastic electron-$He^*(n)$ atom processes in the atmospheres of some DB white dwarfs. We show that in significant parts of the considered atmospheres, which contain weakly ionized layers (the ionization degree $\lesssim 10^{-3}$), the influence of the studied atom-Rydberg atom processes on excited helium atom populations is dominant or at least comparable to the influence of the concurrent electron-$He^*(n)$-atom processes.

Key words. atomic processes – astrochemistry – stars: atmospheres – white dwarfs

1. Introduction

We here continue our previous investigations of inelastic $A + A^*(n)$ atom-Rydberg atom collision processes (where the principal quantum number was $n \gg 1$ and A was the ground-state atom), which influence the excited atom populations in stellar atmospheres. We consider the processes that can be interpreted as resulting from a resonant energy exchange between the subsystem $A + A^+$, in which A^+ is the core of the Rydberg atom $A^*(n)$, and the outer electron of this atom. There are two groups of such processes. The first group involves the chemi-ionization processes (Janev & Mihajlov 1980; Mihajlov et al. 1996, 1997), which connect the block of atomic Rydberg states with the continuum. The second group comprises the so-called $(n - n')$-mixing processes within the above mentioned block of atomic Rydberg states (Mihajlov 1982; Mihajlov et al. 2004, 2008), i.e. the excitation and deexcitation processes that imply transitions between the Rydberg states with the principal quantum numbers n and $n' \neq n$.

The chemi-ionization processes in $A^*(n) + A$ collisions, together with their inverse processes, have been studied for both $A = H$ and $A = He$ cases, which are especially important for stellar atmospheres. Mihajlov et al. (2003, 2007) studied the influence of these processes on the excited hydrogen atom populations and the spectral line profiles in the atmosphere of an M red dwarf ($T_{eff} = 3800$ K) using the PHOENIX code. Mihajlov et al. (1997, 2011, 2003) studied the potential influence of these processes on the excited hydrogen and helium atom populations in the atmospheres of Sun and of some DB white dwarfs.

However, the possible influence of the $(n - n')$-mixing processes in $A^*(n) + A$ collisions on the excited-atom populations in stellar atmospheres has only been studied for the $A = H$ case in the context of the atmosphere of the Sun (Mihajlov et al. 2005). In the above mentioned studies concerning the solar atmosphere, the necessary calculations were performed within the corresponding non-local thermodynamic equilibrium (non-LTE) model proposed by Vernazza et al. (1981). The findings of these studies have shown that the efficiency of these processes in a major part of the solar photosphere is dominant with respect to the efficiency of the relevant concurrent excitation and deexcitation processes for $n = 4, 5$ and 6, and is comparable with them for $n = 7$ and 8. The above mentioned studies concluded that the excitation and deexcitation processes in $H^*(n) + H$ collisions should be included ab initio into future non-LTE models of the solar atmosphere. The importance and effects of the atom-Rydberg atom $(n-n')$-mixing processes have also been analyzed in Barklem (2007) and Mashonkina (2009).

We found no non-LTE models similar to that of Vernazza et al. (1981) for the Sun that would have provided all data necessary for calculations as in Mihajlov et al. (2005), in relation to the atmospheres of DB white dwarfs and other similar helium-rich stellar atmospheres. However, since the influence of strong electromagnetic emission is the same in helium-rich atmospheres as in the Sun, the distribution shape of the helium excited-atom population probably deviates considerably from the Boltzmann distribution. Taking this into account and because the data on the relative efficiencies of atom-Rydberg atom processes and the relevant concurrent processes would be useful for future non-LTE stellar-atmosphere models, the chemi-ionization processes in $He^*(n) + He$ collisions were studied in Mihajlov et al. (2003) in the context of DB white dwarf atmospheres, within the models proposed by Koester (1980). In the current

study, for the same reason and using the same models, the efficiencies of the excitation processes

$$\mathrm{He}^*(n) + \mathrm{He} = \begin{cases} \mathrm{He}^*(n' = n + p) + \mathrm{He}, \\ \mathrm{He} + \mathrm{He}^*(n' = n + p), \end{cases} \quad p \geq 1, \tag{1}$$

and the inverse deexcitation processes

$$\mathrm{He}^*(n) + \mathrm{He} = \begin{cases} \mathrm{He}^*(n' = n - p) + \mathrm{He}, \\ \mathrm{He} + \mathrm{He}^*(n' = n - p), \end{cases} \quad 0 < p \leq n - 3, \tag{2}$$

(where $n + p$ and $n - p$ are the principal quantum numbers of the final Rydberg states) are compared for $3 \leq n \leq 8$ with the efficiencies of the relevant concurrent processes. Here, we consider the well-known electron-excited-atom collision excitation/deexcitation processes

$$\mathrm{He}^*(n) + \vec{e} = \mathrm{He}^*(n \pm p) + \vec{e}', \tag{3}$$

where $\vec{e}$ and $\vec{e}'$ denote a free electron in the initial and final states, respectively. The necessary calculations were performed using the models in Koester (1980) for DB white dwarf atmospheres with $\log g = 8$ and $T_{\mathrm{eff}} = 12\,000$ K and $T_{\mathrm{eff}} = 14\,000$ K.

2. Theoretical remarks

As several of the above mentioned studies have reported, the same dipole resonant mechanism (DRM) causes the non-elastic $(n - n')$-mixing and chemi-ionization processes in $A^*(n) + A$ collisions. The DRM was also discussed in detail in Mihajlov et al. (2012). For the $(n - n')$-mixing processes (1) and (2), with $A = \mathrm{He}$, the DRM assumes that they occur in the region $R_{n;n\pm p} \ll r_n$, where R is the internuclear distance and $r_n \sim n^2$ is the characteristic radius of atom $\mathrm{He}^*(n)$, in the vicinity of the corresponding resonant points $R_{n;n\pm p}$. These parameters are found to be the roots of the equation $U_2(R) - U_1(R) = \varepsilon_{n\pm p} - \varepsilon_n$, where ε_n and $\varepsilon_{n\pm p}$ denote the energies of the Rydberg states $|n>$ and $|n \pm p>$ with the principal quantum numbers n and $n \pm p$; and $U_1(R)$ and $U_2(R)$ are the adiabatic energies of the electronic ground state $|1; R>$ and the first excited state $|2; R>$ of the molecular ion He_2^+. We took the potential curves $U_1(R)$ and $U_2(R)$ from Ignjatović et al. (2009) and following the foundational work of Janev & Mihajlov (1979), which focuses on the $(n - n')$-mixing processes, we assumed that the processes (1) and (2) are caused exclusively by the transitions $|n> \rightarrow |n+p>$ and $|n> \rightarrow |n-p>$ of the outer electron, which occur simultaneously with the transitions $|2; R> \rightarrow |1; R>$ and $|1; R> \rightarrow |2; R>$, respectively, in the subsystem $\mathrm{He}^+ + \mathrm{He}$, close to the resonant points $R_{n;n\pm p}$. This fact is responsible for the resonant character of the processes in (1) and (2).

For $A = \mathrm{H}$ only chemi-ionization processes with $n \geq 4$ and $(n-n')$-mixing processes with $\min(n, n') \geq 4$ can be described on the basis of the DRM, which caused by the existence of the stable negative ion H^-. In contrast, for $A = \mathrm{He}$, the excited helium state with $n = 3$ can be taken as the lower boundary of the block of Rydberg states. This was also used in Mihajlov et al. (2003), who focused on the chemi-ionization processes in DB white dwarf atmospheres.

The processes (1) and (2) are characterized by the excitation and deexcitation rate coefficients $K_{n;n+p}(T)$ and $K_{n;n-p}(T)$, where T is the local temperature of the atomic particles in the considered stellar atmosphere. In accordance with the aim of this work, these rate coefficients are defined as the quantities that determine the mean rates of transition (per single excited atom) caused by the processes (1) and (2) between whole shells with a given n and $n \pm p$. They are determined here using a method similar to that described in Mihajlov et al. (2008): the excitation rate coefficients $K_{n;n+p}(T)$ are calculated directly and numerically in the semi-classical way, while the deexcitation rate coefficients $K_{n;n-p}(T)$ are determined later according to the principle of thermodynamical balance. All necessary expressions are given in Mihajlov et al. (2008).

Table 1. Excitation rate coefficients $K_{3;3+p}(T)$ for $1 \leq p \leq 5$ in $[10^{-9}\ \mathrm{cm}^3\ \mathrm{s}^{-1}]$.

	T $[10^3$ K]						
p	5	6	8	10	12	16	20
1	1.418	1.723	2.187	2.514	2.753	3.074	3.277
2	0.197	0.271	0.401	0.504	0.585	0.701	0.778
3	0.062	0.091	0.146	0.192	0.230	0.286	0.324
4	0.028	0.042	0.071	0.096	0.117	0.148	0.170
5	0.015	0.023	0.040	0.055	0.068	0.088	0.102

For the DB white dwarf atmospheres considered here, the values of $K_{n;n+p}(T)$ and $K_{n;n-p}(T)$, which are used in Eqs. (1) and (2) for all necessary temperatures, can be calculated in principle by fitting the values of $K_{n;n+p}(T)$ presented in Table 2 of Mihajlov et al. (2008), but only for the region $4 \leq n \leq 8$. Bearing this in mind, Table 1 shows the values of the excitation rate coefficients $K_{3;n+p}(T)$ when $1 \leq p \leq 5$. These values, together with Table 1 in Mihajlov et al. (2008), enable the calculation of $K_{n;n+p}(T)$ and $K_{n;n-p}(T)$ for the entire block, $3 \leq n \leq 8$.

The concurrent electron-Rydberg atom processes (3) are characterized here by the rate coefficients $\alpha_{n;n\pm p}(T_{\mathrm{e}} = T)$, where T_{e} denotes the electron temperature, which in the general case is not equal to the atomic temperature. In the current study, the values of $\alpha_{n;n\pm p}(T)$ are determined from the corresponding expressions given in Vriens & Smeets (1980) and Johnson (1972). We note that ion-atom non elastic collisional processes, although they are also characterized by long-range interaction, cannot be concurrent. The reason is the huge difference in masses of electron and ion, which causes the impact ion-atom velocity to be several orders of magnitudes lower than electron-atom impact velocity.

To estimate the relative efficiency of processes (1) and (2) and the concurrent processes (3), it is sufficient to study the behavior of quantities $F_n^{(+)}$ and $F_n^{(-)}$ in the considered DB white dwarf atmospheres, which are given by the expressions

$$F_n^{(+)} = \frac{\sum_{p=1}^{5} K_{n,n+p} \cdot N(n) \cdot N(1)}{\sum_{p=1}^{5} \alpha_{n,n+p} \cdot N(n) \cdot N_{\mathrm{e}}} = \frac{\sum_{p=1}^{5} K_{n,n+p}}{\sum_{p=1}^{5} \alpha_{n,n+p}} \cdot \eta, \quad n \geq 3, \tag{4}$$

and

$$F_n^{(-)} = \frac{\sum_{p=1}^{n-3} K_{n,n-p} \cdot N(n) \cdot N(1)}{\sum_{p=1}^{n-3} \alpha_{n,n-p} \cdot N(n) \cdot N_{\mathrm{e}}} = \frac{\sum_{p=1}^{n-3} K_{n,n-p}}{\sum_{p=1}^{n-3} \alpha_{n,n-p}} \cdot \eta, \quad n \geq 4, \tag{5}$$

where $N(n)$, $N(1)$, and N_{e} are the local densities of all Rydberg helium atoms in the states with a given $n \geq 3$, of a helium atom in the ground state, and of free electrons, respectively; and the products $K_{n,n\pm p} \cdot N(n) \cdot N(1)$ and $\alpha_{n,n\pm p} \cdot N(n) \cdot N_{\mathrm{e}}$ are the partial atom- and electron-Rydberg atom excitation/deexcitation fluxes. The factor η is defined here by the relation

$$\eta \equiv N(1)/N_{\mathrm{e}} \cong (\text{ionization degree})^{-1}, \tag{6}$$

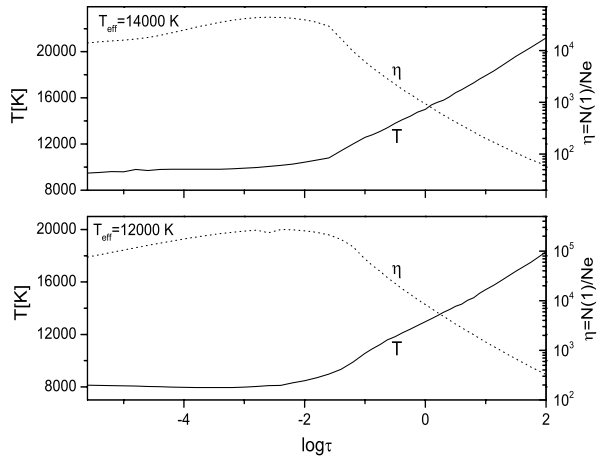

Fig. 1. Parameters (temperature T – full line and $\eta = N(1)/N_e$ – dotted) for DB white dwarf atmosphere models with $\log g = 8$ and $T_{\rm eff} = 12\,000$ K and $14\,000$ K from Koester (1980) as functions of $\log \tau$, where τ is the Rosseland optical depth.

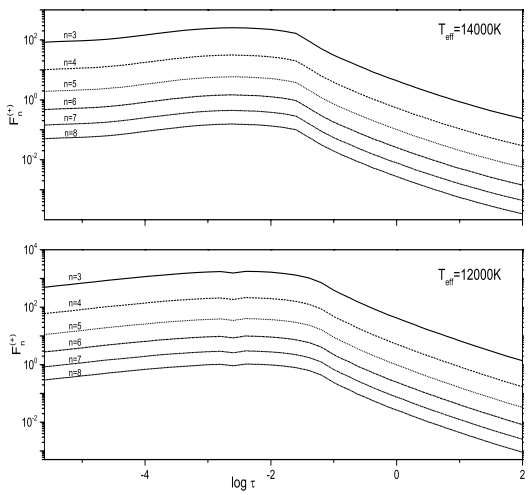

Fig. 2. Behavior of quantities $F_n^{(+)}$, given by Eq. (4) with $3 \le n \le 8$, on the basis of DB white dwarf atmosphere models from Koester (1980) for $\log g = 8$ and $T_{\rm eff} = 12\,000$ K and $14\,000$ K, as functions of $\log \tau$, where τ is the Rosseland optical depth.

and its behavior in the atmospheres of the considered DB white dwarfs (which is very important for the studied processes) is presented in Fig. 1.

3. Results and discussion

Figure 2 illustrates the behavior of the quantity $F_n^{(+)}$ with $3 \le n \le 8$ in the DB white dwarf atmospheres described by the models presented in Koester (1980), for $\log g = 8$ and $T_{\rm eff} = 12\,000$ K and $14\,000$ K. All results were obtained using the data from Koester (1980), and these quantities are presented as functions of $\log \tau$, where τ is the Rosseland optical depth. Figure 2 unambiguously shows that for DB white dwarf atmospheres with $T_{\rm eff} \lesssim 14\,000$ K, the excitation processes (1) in the lower part of the Rydberg block ($3 \le n \le 8$) must be taken into account as a new important factor that influences the helium Rydberg-state populations. Figure 2 shows that in the parts of the atmosphere where the ionization degree is $\lesssim 10^{-3}$, the processes (1) with $n = 3, 4$, and 5 are dominant with respect to the known concurrent processes (3); for $n = 6$ and 7 they are dominant in the parts where the ionization degree is $\lesssim 10^{-4}$; and in the remaining parts their efficiency is comparable with the efficiency of the processes (3). Even the efficiency of the processes (1) with $n = 8$ is close to, or at least comparable with, the efficiency of the processes (3) in the parts where the ionization degree is $< 10^{-4}$.

These facts are especially important for the considered DB white dwarf atmospheres, because for any temperature from the relevant temperature regions, the corresponding Boltzman distribution of the excited helium atom populations will have a distinct minimum (known as the "bottleneck") only in the region $3 \le n < 8$. Thus, it is correct to expect that even a considerable perturbation of the mentioned distribution would not result in a significant change in the position of this minimum. Hence, it follows that the excitation processes (1) should by all means be taken into account in any future non-LTE model of DB white dwarf atmospheres with similar parameters.

Examining the behavior of the quantities $F_n^{(-)}$ with $4 \le n \le 8$ in the same DB white dwarf atmospheres would lead to the same conclusions, including the necessity of introducing the deexcitation processes (2) into the mentioned models. For this reason, the efficiencies of the considered $(n - n')$-mixing processes are only illustrated in Fig. 2.

Finally, we emphasize that these results are relevant not only to the atmospheres of the DB white dwarfs mentioned here, but also to a considerably wider range of helium-rich stellar atmospheres. For instance, an entire array of white dwarfs of other types, as described in Wegner & Koester (1985), Dufour et al. (2006, 2007), have similar parameters. Consequently, processes (1) and (2) must be just as important as the concurrent processes (3). Overall, the findings suggest that the considered atom-Rydberg atom $(n - n')$-mixing processes (1) and (2) should be included ab initio in the modeling of the helium-rich white dwarf atmospheres.

Acknowledgements. The authors are grateful to the Ministry of Education, Science and Technological Development of the Republic of Serbia for the support of this work within the projects 176002, III4402.

References

Barklem, P. S. 2007, A&A, 466, 327
Dufour, P., Bergeron, P., Schmidt, G. D., et al. 2006, ApJ, 651, 1112
Dufour, P., Bergeron, P., Liebert, J., et al. 2007, ApJ, 663, 1291
Ignjatović, L. M., Mihajlov, A. A., Sakan, N. M., Dimitrijević, M. S., & Metropoulos, A. 2009, MNRAS, 396, 2201
Janev, R. K., & Mihajlov, A. A. 1979, Phys. Rev. A, 20, 1890
Janev, R. K., & Mihajlov, A. A. 1980, Phys. Rev. A, 21, 819
Johnson, L. C. 1972, ApJ, 174, 227
Koester, D. 1980, A&AS, 39, 401
Mashonkina, L. 2009, Phys. Scr. T, 134, 014004
Mihajlov, A. A. 1982, in Proceedings of international conference on plasma physics. G
Mihajlov, A. A., Dimitrijević, M. S., & Djurić, Z. 1996, Phys. Scri., 53, 159
Mihajlov, A. A., Ignjatović, L. M., Vasilijević, M. M., & Dimitrijević, M. S. 1997, A&A, 324, 1206
Mihajlov, A. A., Jevremović, D., Hauschildt, P., et al. 2003, A&A, 403, 787
Mihajlov, A. A., Ignjatović, L. M., Djurić, Z., & Ljepojević, N. N. 2004, J. Phys. B At. Mol. Phys., 37, 4493
Mihajlov, A. A., Ignjatović, L. M., & Dimitrijević, M. S. 2005, A&A, 437, 1023
Mihajlov, A. A., Jevremović, D., Hauschildt, P., et al. 2007, A&A, 471, 671
Mihajlov, A. A., Ignjatović, L. M., Srećković, V. A., & Djurić, Z. 2008, J. Quant. Spec. Radiat. Transf., 109, 853
Mihajlov, A. A., Ignjatović, L. M., Srećković, V. A., & Dimitrijević, M. S. 2011, ApJS, 193, 2
Mihajlov, A. A., Srećković, V. A., Ignjatović, L. M., & Klyucharev, A. N. 2012, J. Cluster Sci., 23, 47
Vernazza, J. E., Avrett, E. H., & Loeser, R. 1981, ApJS, 45, 635
Vriens, L., & Smeets, A. H. M. 1980, Phys. Rev. A, 22, 940
Wegner, G., & Koester, D. 1985, ApJ, 288, 746

1981A&A...102...93D

Astron. Astrophys. 102, 93–96 (1981)

ASTRONOMY AND ASTROPHYSICS

Semiempirical Stark Linewidths of Alkali Like Ions*

M. S. Dimitrijević and N. Konjević

Institute of Applied Physics, P.O. Box 58, YU-11071 Beograd, Yugoslavia

Received April 7, accepted June 15, 1981

Summary. In this paper we have tested the applicability of modified semi-empirical formula with newly proposed Gaunt factors for evaluation of Stark linewidths of alkali like ions. The comparison with experiments and other, already tested theoretical approaches indicates that these new Gaunt factors can be used successfully for Stark linewidth calculations.

Key words: atomic data – line broadening

Stark broadening data for the spectral lines of neutral and ionized atoms are the important quantities in astrophysics and plasma diagnostics. In astrophysics Stark broadening data are required for the evaluation of the physical conditions in the stellar atmospherae from the analysis of stellar spectra. This is, in particular, important method of diagnostics for the hot stars of O and B type and some white dwarfs, objects with atmospheric conditions giving rise to the Stark effect as a main collisional broadening mechanism. Further, Stark broadening data are also required for determination of the abundances of elements and for evaluations of the radiative transfer through the stellar interior. In the latter case a great number of Stark broadening data are often needed. For such, large scale calculations, high accuracy of these data is not so important. One requires only a reasonable accuracy for the large number of lines.

For evaluation of Stark linewidths and shifts of non-hydrogenic spectral lines of ionized atoms, various theoretical approaches have been used (see e.g. Griem, 1974). Most of these approaches require a considerable labour even for the evaluation of a single linewidth. Whenever a large number of theoretical data of the linewidths are required tedious calculations can be avoided if one uses simple, approximative formulae with good average accuracy.

In 1968 Griem suggested simple formula based upon Baranger's original formulation (Baranger, 1958), together with the use of semi-empirical effective Gaunt-factor approximation proposed by Seaton (1962) and Van Regemorter (1962). For singly ionized atoms semi-empirical formula agrees in average within 50% with the experiment (Griem, 1974). For multiply ionized atoms the agreement becomes worse and few attempts have been made to extend the applicability of this approach to higher ionization stages (Hey, 1977; Dimitrijević and Konjević, 1980; Hey and Breger, 1980).

Main limitation for the application of the semi-empirical formula for highly ionized atoms imposes the lack of the effective Gaunt factor values. Recently, for alkaline like ions an analytic expressions for effective Gaunt factor dependence upon the nuclear charge have been derived (Younger and Wiese, 1979) for $\Delta n=0$ transitions of alkali like ions. The aim of this work is to test the usefulness of these, new effective Gaunt factors for evaluation of the Stark widths of alkali like ions.

Theory

Within the impact approximation, Baranger (1958) derived a quantum-mechanical expression for the width of an isolated ion line:

$$W=N\left\{v\left[\sum_{i'}\sigma_{i'i}+\sum_{f'}\sigma_{f'f}\right]\right\}_{av}+W_{el'}, \tag{1}$$

where W is the full half-width (FWHM) in units of angular frequency and N is the electron concentration. The symbols $\sigma_{i'i}$ and $\sigma_{f'f}$ represent the inelastic cross sections for collisional transitions to i', f' from initial (i) and final (f) levels, respectively, of the optical transition. W_{el} is the line width induced by elastic collisions. The averaging in Eq. (1) has to be performed over the electron velocity (v) distribution.

Within the framework of the dipole approximation, one may use Bethe's (1930) relation

$$\sigma_{j'j}=\frac{8\pi}{3}\lambda\!\!\!^{-2}\boldsymbol{R}^2_{j'j}\frac{\pi}{\sqrt{3}}g \tag{2}$$

to evaluate inelastic cross sections. In this expression $\lambda\!\!\!^{-}=\hbar/mv$ is the reduced de Broglie wavelength of an electron and $\boldsymbol{R}^2_{j'j}$ (in units of the Bohr radius a_0) is the square of the coordinate operator matrix element summed over all components of the operator and the magnetic substates of total angular momentum J', and averaged over the magnetic substates of J.

For higher electron temperatures, Griem (1968) assumed that the contribution of elastic collisions to the line width [cf. Eq. (1)] can be neglected. The same author made an attempt to take elastic collisions into account at the low temperature limit by using the threshold value of the inelastic cross section below the threshold. The Stark line width can then be calculated from the well known

Send offprint requests to: M. S. Dimitrijević

* This work is partially supported by US National Bureau of Standards

© European Southern Observatory • Provided by the NASA Astrophysics Data System

1981A&A...102...93D

semi-empirical formula (Griem, 1968)

$$W=N\frac{8\pi}{3}\frac{\hbar^2}{m^2}\left(\frac{2m}{\pi kT}\right)^{1/2}\frac{\pi}{\sqrt{3}}\left[\sum_{i'}\boldsymbol{R}^2_{j'j}g\left(\frac{E}{\Delta E_{i'i}}\right)+\sum_{f'}\boldsymbol{R}^2_{f'f}g\left(\frac{E}{\Delta E_{f'f}}\right)\right]. \quad (3)$$

Here, $E=3kT/2$ is the energy of the perturbing electron and $\Delta E_{j'j}=|E_{j'}-E_j|$ is the energy difference between levels j and j': $g(x)=0.20$ for $x=2$ and $g(x)=0.24$, 0.33, 0.56, 0.98, and 1.33 for $x=3$, 5, 10, 30, and 100.

If one uses Eq. (3) to calculate Stark line widths, a lack of atomic data causes difficulties in the evaluation of the matrix elements. These difficulties are especially serious for multiply-ionized atoms for which, data for higher perturbing levels are sometimes completely missing in the literature. To overcome this problem and further improve semi-empirical theoretical approach we have separated the transitions with $\Delta n=0$ (Dimitrijević and Konjević, 1980). In this case, only two matrix elements are calculated: one for the transition array $l\to l+1(R^2_{l,l+1})$ and the other for $l\to l-1(R^2_{l,l-1})$. The same technique has been used by Griem (1974) with semi-classical formula for the evaluation of the linewidths of multiply charged ions.

For the transitions with $\Delta n=0$ effective Gaunt factor g is calculated from the following expression (Younger and Wiese, 1979)

$$\tilde{g}\cong\left(1-\frac{1}{Z_e}\right)\left(0.7+\frac{1}{n}\right)\left[0.6+0.25\ln\left(\frac{E}{\Delta E_{ij}}\right)\right], \quad (4)$$

where Z_e is the effective charge of the ion and n is the principal quantum number.

In case of $\Delta n\neq 0$ energy separation to the nearest perturbing level is taken as

$$\Delta E_{n,n+1}=\frac{2Z^2E_H}{n^{*3}}, \quad (5)$$

where n^* is the effective principal quantum number.

At higher electron temperatures Gaunt factor for the transitions $\Delta n\neq 0$ is derived from the GBKO high temperature limit (Griem et al., 1962)

$$g(T)=\frac{\sqrt{3}}{\pi}\left[\frac{1}{2}+\ln\left(\frac{n^*kT}{ZE_H}\right)\right]. \quad (6)$$

Equation (3) becomes now

$$W=N\frac{8\pi}{3}\frac{\hbar^2}{m^2}\left(\frac{2m}{\pi kT}\right)^{1/2}\frac{\pi}{\sqrt{3}}\left[\boldsymbol{R}^2_{l_i,l_i+1}\tilde{g}\left(\frac{E}{\Delta E_{l_i,l_i+1}}\right)+\boldsymbol{R}^2_{l_i,l_i-1}\tilde{g}\left(\frac{E}{\Delta E_{l_i,l_i-1}}\right)+\boldsymbol{R}^2_{l_f,l_f+1}\tilde{g}\left(\frac{E}{\Delta E_{l_f,l_f+1}}\right)+\boldsymbol{R}^2_{l_f,l_f-1}\tilde{g}\left(\frac{E}{\Delta E_{l_f,l_f-1}}\right)+\sum_{i'}(\boldsymbol{R}^2_{ii'})_{\Delta n\neq 0}\cdot g\left(\frac{3kTn_i^{*3}}{4Z^2E_H}\right)+\sum_{f'}(\boldsymbol{R}^2_{ff'})_{\Delta n\neq 0}g\left(\frac{3kTn_f^{*3}}{4Z^2E_H}\right)\right], \quad (7)$$

Relevant matrix elements can be calculated using Coulomb approximation of Bates and Damgaard (1949)

$$\boldsymbol{R}^2_{l,l'}\simeq\left(\frac{3n^*}{2Z}\right)^2\frac{\max(l,l')}{2l+1}[n^{*2}-\max^2(l,l')]\phi^2. \quad (8)$$

Here, ϕ represents the Bates-Damgaard factor.

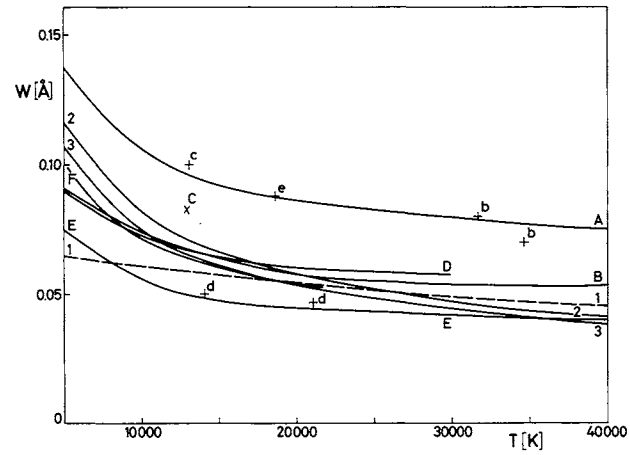

Fig. 1. Measured and calculated line widths for the resonance lines of Mg II 2802.7 Å and 2795.5 Å normalized to $N_e=10^{17}\,\mathrm{cm}^{-3}$, as a function of temperature. Curves: *1* modified semi-empirical formula, Eq. (7) with effective Gaunt factor from, Eq. (4), *2* modified semi-empirical formula, Eq. (7), *3* semi-empirical formula, Eq. (3), *B* and *F* semi-classical calculations by Chapelle and Sahal-Bréchot (1970) and Roberts and Barnard (1972) and *D* and *E* quantum mechanical calculations by Bely and Griem (1970) and Barnes (1971), respectively. Theoretical point: *C* semi-classical result by Fleurier et al. (1977). Experimental points: *b* Hadžiomerspahić et al. (1973), *c* Fleurier et al. (1977), *d* Roberts and Barnard (1972), and *e* Jones et al. (1972)

Since the comparison is being made with the semi-classical results of Jones et al. (1971) and Griem (1974) and these data do not contain the results for Sr II semi-classical calculations for this element were also performed, using computer code kindly supplied by Griem.

Results and Comparisons

The results of various theoretical approaches are compared with available experimental data in Figs. 1–5 for singly ionized earth alkaline metals. In these figures following notation of the curves is used:

1. modified semi-empirical formula, Eq. (7) with effective Gaunt factor from Eq. (4);
2. modified semi-empirical formula, Eq. (7), and
3. semi-empirical formula, Eq. (3).

A semi-classical results (Jones et al., 1971; Griem, 1974).

With other capital letters are designated various theoretical calculations while the experimental results are marked with small letters.

The ratio of measured w_m to calculated line widths for triply ionized carbon and silicon are given in Table 1. Here, the same notation as in Figs. 1–5 is used for theoretical results. Finally the results of the theoretical calculations for Si XII $2s^2S-2p^2P^0$ $\lambda=506.3$ Å line are given in Fig. 6.

The comparison of semi-empirical results with new values of effective Gaunt factor, Eq. (4) with other theoretical approaches and with the experiments, Figs. 1–5 and Table 1 show that the agreement with experiments is good with exception of some results which do not agree with any theoretical data (see in Fig. 5 results for Ba II $6s^2S_{1/2}-6p^2P^0_{3/2}$ $\lambda=4554.0$ Å); for triply ionized carbon and silicon the agreement with experiment is within 25% with exception of the transition $2s^2S-2p^2P^0$ where the discrepancy exceeds a factor of two; however, other theoretical approaches do

© European Southern Observatory • Provided by the NASA Astrophysics Data System

1981A&A...102...93D

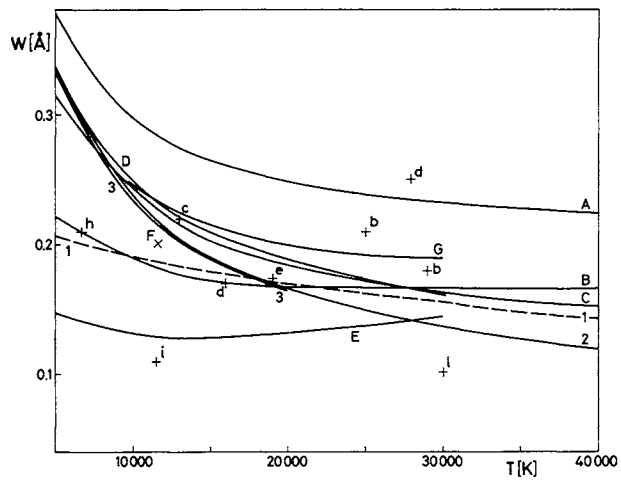

Fig. 2. Measured and calculated line widths for the resonance lines of Ca II 3933.7 Å and 3968.5 Å normalized to $N_e = 10^{17}\,\mathrm{cm}^{-3}$ as a function of temperature. The meaning of Curves *1–3* and *A* is described in the caption of Fig. 1. Curves: *B* Chapelle and Sahal-Bréchot (1970), *D* Roberts and Barnard (1972), *E* Kobzev (1971), and *G* Hildum and Cooper (1971) represent the results of semi-classical calculations as well as theoretical point *F* by Yukov (1972). Experimental points: *b* Hadžiomerspahić et al. (1973), *c* Fleurier et al. (1977), *d* Roberts and Barnard (1972), *e* Jones et al. (1972), *h* Baur and Cooper (1977), *i* Yamamoto (1966), *k* Hildum and Cooper (1971), and *l* Roberts and Eckerle (1967)

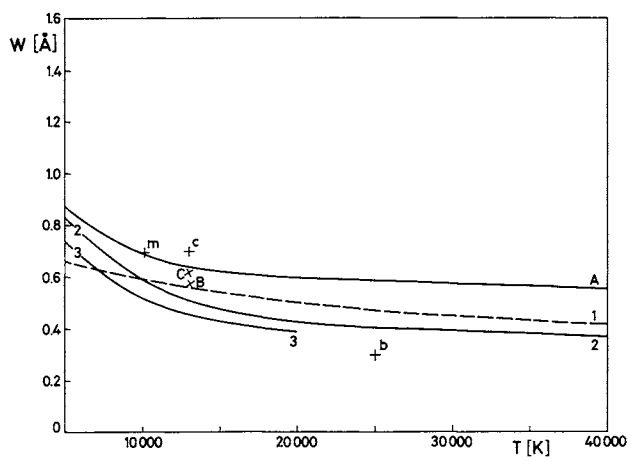

Fig. 3. Measured and calculated widths for Ca II lines 3706.3 Å and 3736.9 Å, (transition $4p^2P - 5s^2S$) normalized to $N_e = 10^{17}\,\mathrm{cm}^{-3}$ as a function of temperature. The meaning of Curves *1–3* and *A* is described in the caption of Fig. 1. Theoretical points *B* and *C* represent the results of semi-classical calculations by Sahal-Bréchot (1969) and Fleurier et al. (1977). Experimental points: *b* Hadžiomerspahić et al. (1973), *c* Fleurier et al. (1977), and *m* Hühn and Kusch (1973)

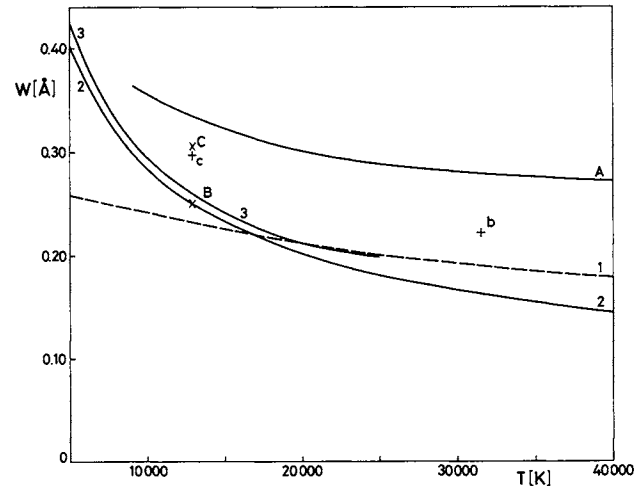

Fig. 4. Measured and calculated line widths for the resonance line of Sr II 4077.7 Å, (transition $5s^2S_{1/2} - 5p^2P^0_{3/2}$) normalized to $N_e = 10^{17}\,\mathrm{cm}^{-3}$ as a function of temperature. Meaning of Curves *1–3* and *A* is described in the caption of Fig. 1. Theoretical points *B* and *C* represent the results of semi-classical calculations by Sahal-Bréchot (1969) and Fleurier et al. (1977). Experimental points: *b* Hadžiomerspahić et al. (1973), and *c* Fleurier et al. (1977)

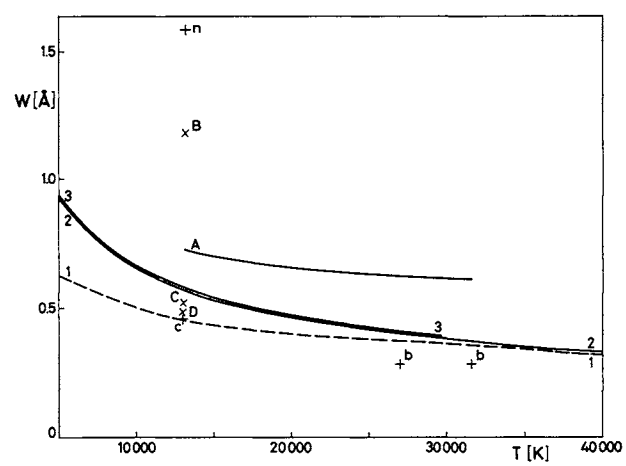

Fig. 5. Measured and calculated line widths for resonance line of Ba II 4554.0 Å (transition $6s^2S_{1/2} - 6p^2P^0_{3/2}$) normalized to $N_e = 10^{17}\,\mathrm{cm}^{-3}$ as a function of temperature. The meaning of Curves *1–3* and *A* is described in the caption of Fig. 1. Theoretical points: *B–D* semi-classical calculations, by Sahal-Bréchot (1969), Fleurier et al. (1977), and Cooper and Oertel (1967). Experimental points: *b* Hadžiomerspahić et al. (1977), *c* Fleurier et al. (1977), and *n* Jaeger (1969)

do not agree as well; the agreement with other, more sophisticated theoretical approaches is within the limits of their uncertainties; it is very encouraging good agreement with quantum mechanical results (see Figs. 1 and 2); since, to the authors knowledge, there is no experimentale data for Si XII $2s^2S - 2p^2P^0$ $\lambda = 506.3$ Å, only comparison with modified semi-empirical approach is being made; the discrepancy becomes large at high electron temperatures where Curve 3 shows different temperature trend.

Conclusions

On the basis of the comparisons with experimental as well as other theoretical results one can conclude that semi-empirical formula

© European Southern Observatory • Provided by the NASA Astrophysics Data System

1981A&A...102...93D

Table 1. Ratio of measured w_m and calculated linewidths of doubly-ionized atoms. Meaning of indexes 1 and 2 for theoretical data is the same as in Figs. 1–7. Theoretical results W_{RSS} and W_{SBS} are taken from Romanov et al. (1979) and Sahal-Bréchot and Segre (1971), respectively. Experimental results for C IV and Si IV are taken from Bogen (1972) and Platiša et al. (1977), respectively

Ion	Transition (mult.No)	T(K)	W_m(Å)	$\frac{W_m}{W_1}$	$\frac{W_m}{W_2}$	$\frac{W_m}{W_{RSS}}$	$\frac{W_m}{W_{SBS}}$
C IV	$2s^2S-2p^2P^o$ (14 UV)	58000	0,006	2,21	1,99	2,00	1,30*
	$3s^2S-3p^2P^o$ (1)	58000	0,4	1,02	1,01	1,00	-
Si IV	$4s^2S-4p^2P^o$ (1)	25600	0,22	0,76	0,57	-	
	$4p^2P^o-4d^2D$	25600	0,24	0,94	0,75	-	

*extrapolated value

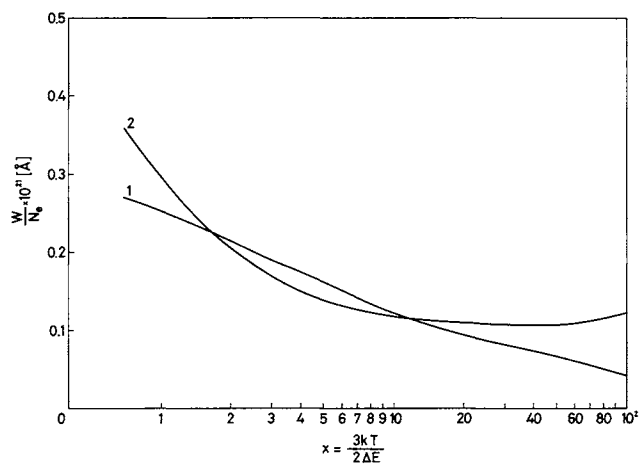

Fig. 6. Calculated line widths for resonance line of Si XII 506.3 Å (transition $2s^2S-2p^2P^0$) normalized to $N_e=10^{21}\,\mathrm{cm}^{-3}$ as a function of $3kT/\Delta E$ where ΔE is the energy separation to the nearest perturbing level. Meaning of Curves *1* and *2* is described in the caption of Fig. 1

with newly proposed Gaunt factors (Younger and Wiese, 1978) derived mainly from the comparison data on light elements (Be, Mg, Ca) can be used with the confidence for evaluation of Stark line widths of even heavy alkali like ions like Sr II and Ba II. This approach should be useful for evaluation of the line widths of multiply ionized atoms.

However, it should be pointed out that reliable experimental data for highly ionized atoms are needed to clarify the usefulness of various theoretical approaches.

Acknowledgement. The authors gratefully acknowledge the interest of Dr. W. L. Wiese in this work.

References

Baranger, M.: 1958, *Phys. Rev.* **112**, 855
Barnes, K.S., Peach, G.: 1970, *J. Phys.* B **3**, 350
Barnes, K.S.: 1971, *J. Phys.* B **4**, 1377
Bates, D.R., Damgaard, A.: 1949, *Phil. Trans. Roy. Soc. London* A **242**, 101
Baur, J.F., Cooper, J.: 1977, *J. Quant. Spectroscop. Radiat. Transfer* **17**, 311
Belly, O., Griem, H.R.: 1972, *Phys. Rev.* A **1**, 97
Bethe, H.A.: 1930, *Ann.* Physik **5**, 3251
Bogen, P.: 1972, *Z. Naturforsch.* **27** A, 210
Chapelle, J., Sahal-Bréchot, S.: 1970, *Astron. Astrophys.* **6**, 415
Cooper, J., Oertel, G.K.: 1967, *Phys. Rev. Letters* **18**, 985
Dimitrijević, M.S., Konjević, N.: 1980, *J. Quant. Spectroscop. Radiat. Transfer* **24**, 451
Fleurier, C., Sahal-Bréchot, S., Chapelle, J.: 1977, *J. Quant. Spectroscop. Radiat. Transfer* **17**, 595
Griem, H.R., Baranger, M., Kolb, A.C., Oertel, G.: 1962, *Phys. Rev.* **125**, 177
Griem, H.R.: 1968, *Phys. Rev.* **165**, 258
Griem, H.R.: 1974, Spectral line broadening by plasmas, McGraw-Hill, New York
Hadžiomerspahić, D., Platiša, M., Konjević, N., Popović, M.: 1973, *Z. Phys.* **262**, 169
Hey, J.D.: 1977, *J. Quant. Spectroscop. Radiat. Transfer* **18**, 649
Hey, J.D., Breger, P.: 1980, *J. Quant. Spectroscop. Radiat. Transfer* **24**, 349
Hildum, J.S., Cooper, J.: 1971, *Phys. Letters* A **36**, 153
Hühn, R., Kusch, H.J.: 1973, *Astron. Astrophys.* **28**, 159
Jaeger, H.: 1969, *Z. Phys.* **223**, 19
Jones, W.W., Benett, S.M., Griem, H.R.: 1971, Calculated Electron Impact Broadening Parameters for Isolated Spectral Lines from the Singly Charged Ions: Lithium through Calcium, Techn. Rep. No. 71–128, Univ. Maryland
Jones, W.W., Sanchez, A., Greig, J.R., Griem, H.R.: 1972, *Phys. Rev.* A **5**, 2318
Kobzev, G.A.: 1971, *Opt. Spectrosc.* (USSR) **30**, 106
Regemorter, V.: 1962, *Astrophys. J.* **136**, 906
Roberts, J., Eckerle, K.L.: 1967, *Phys. Rev.* **159**, 104
Roberts, D.E., Barnard, A.J.: 1972, *J. Quant. Spectroscop. Radiat. Transfer* **12**, 1205
Romanov, G.S., Stepanov, K.L., Sirkin, M.I.: 1979, *Opt. Spectrosc.* (USSR) **47**, 860
Sahal-Bréchot, S.: 1969, *Astron. Astrophys.* **2**, 322
Sahal-Bréchot, S., Segre, E.R.H.: 1971, *Astron. Astrophys.* **13**, 161
Sanchez, A., Blaha, M., Jones, W.W.: 1973, *Phys. Rev.* A **8**, 774
Seaton, M.J.: 1962, in *Atomic and Molecular Processes*, ed. by D.R. Bates, Academic Press, New York, Chap. 11
Yamamoto, M.: 1966, *Phys. Rev.* **146**, 137
Younger, S.M., Wiese, W.L.: 1979, *J. Quant. Spectroscop. Radiat. Transfer* **22**, 161
Yukov, E.A.: 1972, *Sov. Astron. J.* **15**, 867

© European Southern Observatory • Provided by the NASA Astrophysics Data System

1983A&A...123..249V

Astron. Astrophys. 123, 249–252 (1983)

ASTRONOMY AND ASTROPHYSICS

Half-widths of neutral fluorine spectral lines

V. Vujnović[1], Č. Vadla[1], V. Lokner[1], and M. S. Dimitrijević[2]

[1] Institute of Physics of the University, P.O.B. 304, YU-41001 Zagreb, Yugoslavia
[2] Institute of Applied Physics, P.O.B. 58, YU-11071 Belgrade, Yugoslavia

Received November 25, 1982; accepted March 14, 1983

Summary. The profiles of 29 fluorine spectral lines from seven transitions, emitted by a wall-stabilized arc, were measured, and the electron impact broadening half-widths of the transitions were calculated using the semiclassical perturbation approach. The plasma conditions were given by $T=14{,}000$ K and $N_e=10^{23}\,\mathrm{m}^{-3}$. A close agreement between the experimental results and the calculations was found, depending on the calibration of the electron concentration and on the evaluation approach.

Key words: atomic physics – line-widths – neutral fluorine – wall-stabilized arc

1. Introduction

The broadening of spectral lines of neutral fluorine has hardly been investigated. Theoretically it has been treated by Benett and Griem (1971), and the results were published in Griem's book (1974). The experiment by Konjević et al. (1972, 1976) produced values equal to 30–50% of the theoretical ones. However, another experiment (Purić et al., 1977) showed much better agreement. Both experiments were performed using transient plasmas. Konjević et al. (1972) used the low pressure arc (*Z*-pinch) observed axially, and Purić et al. (1977) *T*-tube plasma (measurements done in reflected shock-wave). The diagnoses of these plasmas were carried out in a similar manner, and the profiles were scanned shot-to-shot. One single data of F I spectral line is given by Schulz-Gulde and Wenzel (1980), obtained in the d.c. arc.

2. Experimental

We have observed the fluorine spectrum emitted by a normal pressure d.c. arc, stabilized by the walls. The plasma was a mixture of argon and fluorine, supplemented by a small amount of hydrogen in order to monitor electron concentration. All observations were conducted axially, using an 1-m normal incidence McPherson photoelectric monochromator. Fitted with 1200 grooves/mm grating, the monochromator had an instrumental half-width of 0.01 nm; this was measured by means of a laser line. The monochromator had a calibrated relative spectral response. The experimental apparatus was described in more detail by Lokner et al. (1983).

The electron concentration differed depending on the adopted H_β half-width calibration. The WKP calibration (Wiese et al., 1972) lead to the electron concentration within the range of 1.25–1.55 $10^{23}\,\mathrm{m}^{-3}$ [for the physical conditions found in our arc, the same range followed from the data given by Vidal et al. (1973)]. The KG calibration of Kepple and Griem (Griem, 1974) leads to the electron concentration within the range of 1.1–1.35 $10^{23}\,\mathrm{m}^{-3}$. The difference is sufficient to influence the agreement with the theoretical calculations. Error inherent in the electron concentration measurements amounts to 10%.

The temperature was measured by using the relative line intensities of the Ar I and Ar II lines and the electron concentration, and was found in the range of 13,500–14,000 K.

Analyses of the profiles were conducted using the straightforward procedure of Lokner and Movre (1980) designed for a class of the Voigt profiles the broadening parameter (the ratio of the Lorentz half-width and the Doppler constant) of which exceeds 1.4. In this procedure, an arbitrary estimate of the background level and the corresponding apparent half-width leads to the Lorentz component half-width. We found the observed profiles to be of the Voigt type. One example is shown in Fig. 1. All measured profiles had broadening parameter of about 4.

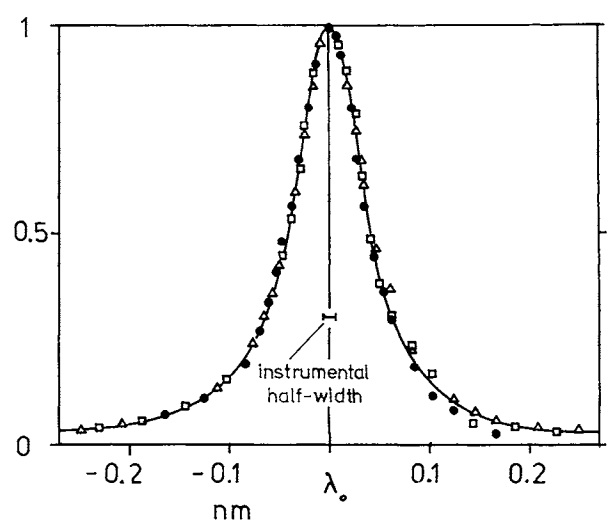

Fig. 1. Normalized profiles of three spectral lines of the multiplet 4, at $N_e=1.4\,10^{23}\,\mathrm{m}^{-3}$, and $T=13{,}800$ K: □ 760.7 nm, △ 775.4 nm, ● 780.0 nm. The total half-width is equal to 0.083 nm, the Lorentz half-width to 0.080, the thermal Doppler half-width to 0.015 nm, and the instrumental Gauss half-width to 0.01 nm. The Van der Waals broadening (Griem, 1964) was negligible (10^{-4} nm)

Send offprint requests to: V. Vujnović

© European Southern Observatory • Provided by the NASA Astrophysics Data System

1983A&A...123..249V

Table 1. Comparison of experimental, w_m, and theoretical full half-width, w_t. Maximum relative errors of experimental data are quoted. The electron density was measured in the range of (1.26–1.54) 10^{23} m^{-3} according to the WKP calibration, or in the range of (1.11–1.35) 10^{23} m^{-3} according to the KG calibration

Transition	Wavelength nm	Half-width				
		w_m/nm	w_m/nm		w_t/nm at 10^{23} m^{-3}, 14,000 K	
		Range measured	at 10^{23} m^{-3} for WKP calibration	at 10^{23} m^{-3} for KG calibration	This work	Griem (1974)
$3s^4P-3p^4P^0$	733.1	0.062–0.064	$0.043\pm15\%$	$0.050\pm15\%$	0.047	0.058
	739.8	0.064–0.070				
	742.5	0.052–0.058				
	748.2	0.052–0.068				
	755.2	0.054–0.064				
Multiplet 1	757.3	0.054–0.062				
$3s^4P-3p^4D^0$	670.8	0.054–0.056	$0.041^{+15\%}_{-20\%}$	$0.048^{+15\%}_{-20\%}$	0.049	0.056
	677.3	0.056				
	679.5	0.056–0.062				
	683.4	0.057–0.062				
	687.0	0.050				
	690.2	0.056–0.068				
Multiplet 2	690.9	0.058–0.062				
$3s^4P-3p^4S^0$	623.9	0.064–0.072	$0.047\pm8\%$	$0.053\pm8\%$	0.051	0.061
	634.8	0.066–0.072				
Multiplet 3	641.3	0.066–0.069				
$3s^2P-3p^2D^0$	760.7	0.078–0.089	$0.060\pm12\%$	$0.068\pm12\%$	0.065	0.076
	775.4	0.074–0.100				
Multiplet 4	780.0	0.078–0.092				
$3s^2P-3p^2S^0$ Multiplet 5	748.9	0.104	0.073	0.081	0.067	0.078
$3s^2P-3p^2P^0$	703.7	0.086–0.092	$0.062^{+15\%}_{-11\%}$	$0.069^{+15\%}_{-11\%}$	0.065	0.081
	712.7	0.084–0.088				
Multiplet 6	720.2	0.082–0.092				
$3s^4P-3p^2D^0$	656.9	0.058	$0.047\pm15\%$	$0.053\pm15\%$	0.051	–
	658.0	0.060				
	665.0	0.058–0.062				
	669.0	0.076				

For the analysis only optically thin lines were chosen. The choice was made by comparing the peak intensities with the peak intensity of the strong argon line at 763.5 nm which was saturated and eventually reached the black-body level. Selected were only spectral lines with peak intensities below 10% of the 763.5 peak intensity.

The measured Stark broadening half-widths are shown in Figs. 2 and 3, and in Table 1, together with the values linearly scaled to the electron concentration of 10^{23} m^{-3}. The interval of the electron concentrations was too small to allow observation of the regular changes of the profile width vs. the electron concentration. Maximum dispersion of the experimental data of 10–15% can be explained as a combined effect of the noise observed during the photoelectric registration, the arc emission instability, and of errors made during graphical evaluation of traces.

3. Theoretical

The basis for calculation was the Sahal-Bréchot computer code (1969a) which evaluated the electron impact broadening parameters of isolated spectral lines using the semiclassical perturbation approach. The relation for (full) half-width w which enters the computer code is

$$w=N\int_0^\infty vf(v)dv\left[\sum_{j\neq i}\sigma_{ij}(v)+\sum_{j'=f}\sigma_{fj'}(v)+\sigma_{el}\right].$$

The inelastic cross section $\sigma_{ij}(v)$ can be expressed by an integration over the impact parameter ϱ of the transition probability P_{ij} as

$$\sum_{j\neq i}\sigma_{ij}(v)=\tfrac{1}{2}\pi R_1^2+\int_{R_1}^{R_d}2\pi\varrho d\varrho\sum_{j\neq i}P_{ij}(\varrho,v),$$

© European Southern Observatory • Provided by the NASA Astrophysics Data System

1983A&A...123..249V

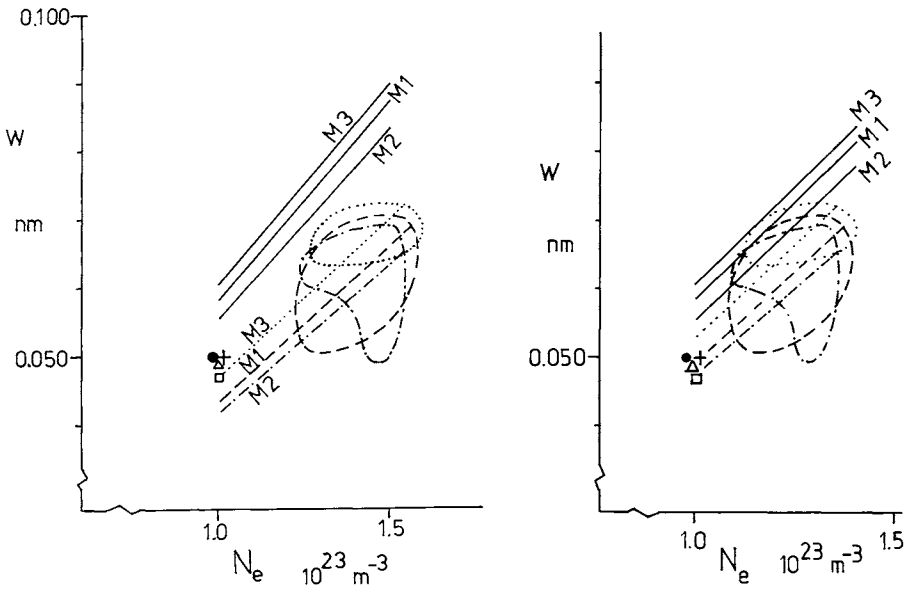

Fig. 2. a (left) Comparison of the observed and evaluated Stark full halfwidths. The closed curves delimit the field of the experimental points. In order to obtain experimental widths w_m quoted in Table 1, the average values of the measured half-widths are scaled down to the electron concentration of $10^{23}\,m^{-3}$ by linear extrapolation to zero half-width for zero electron concentration. Our calculations are shown for the electron concentration of $10^{23}\,m^{-3}$. ——— theoretical values according to Griem (1974); – – – multiplet 1 (6 spectral lines, 18 experimental points), □ our calculation; –·–·– multiplet 2 (8 spectral lines, 19 experimental points) △ our calculation; ····· multiplet 3 (8 spectral lines, 19 experimental points), ● our calculation; + 670.8 nm line, belonging to the multiplet 2, the line half-width obtained by Schulz-Gulde and Wenzel (1980). Scale of the electron concentration was obtained with WKP calibration **b** (right) The same as Fig. 2a, but the scale of the electron concentration was obtained with KG calibration

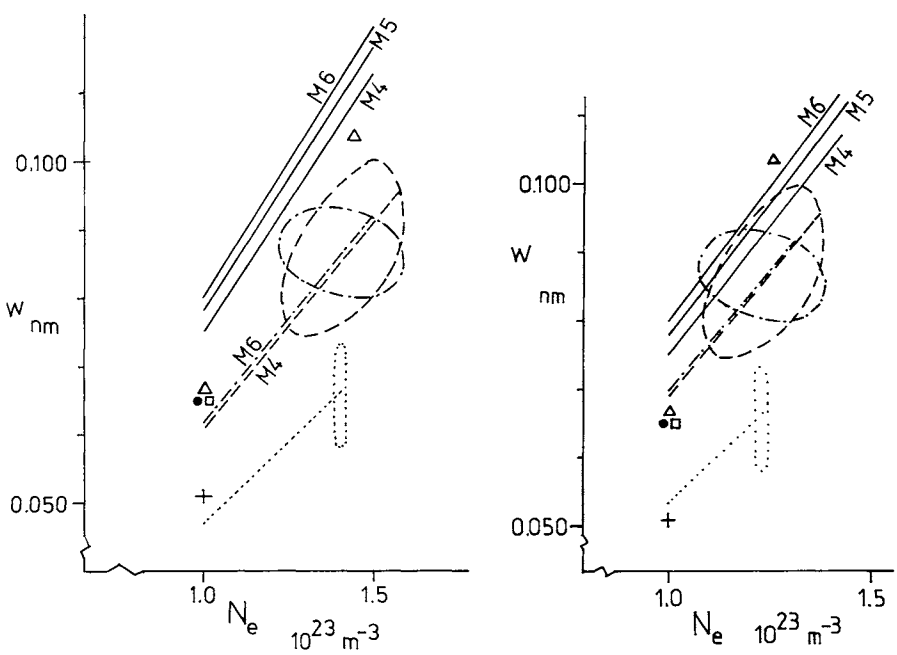

Fig. 3. a (left) The same as Fig. 2. ——— theoretical relation according to Griem (1974); – – – multiplet 4 (3 spectral lines, 12 experimental points), □ our calculation; △ experiment (1 spectral line and 1 point) and calculation for the multiplet 5; –·–·– multiplet 6 (3 spectral lines, 7 experimental points), ● our calculation; ····· transition $3s^4P-3p^2D^0$ (4 spectral lines and 6 experimental points), + our calculation. The scale of the electron concentration was obtained with WKP calibration
b (right) The same as Fig. 3a but the scale of the electron concentration was obtained with KG calibration

and the elastic cross section is given by

$$\sigma_{el}=2\pi R_2^2+\int_{R_2}^{R_d} 8\pi\varrho d\varrho \sin^2\delta,$$

$$\delta=(\phi_p^2+\phi_q^2)^{1/2},$$

$$\phi_p=\sum_{j\neq i}\phi_{ij}-\sum_{j'\neq f}\phi_{fj'}.$$

The phase shifts ϕ_p and ϕ_q, due respectively to the polarisation potential (r^{-4}) and to the quadrupolar potential (r^{-3}), are given by Sahal-Bréchot (1969a, Sect. 3, Chap. 2).

The cut-offs (R_1, R_2) as well as the symmetrization procedures in the inelastic cross sections have been described by Sahal-Bréchot (1969b, Sect. 1, Chap. 3). We also took into account the Debye shielding by introducing the Debye cut-off R_d as an upper cut-off in the integration procedure.

© European Southern Observatory • Provided by the NASA Astrophysics Data System

1983A&A...123..249V

The data for atomic energy levels necessary for these computations were taken from Bashkin and Stoner (1975). The required oscillator strengths were calculated in the Coulomb approximation using the method of Bates and Damgaard (1949) (see also Oertel and Shomo, 1968). An important parameter for the critical evaluation of the Stark broadening data is $\Delta S/S$ (see e.g. Jones, 1973). This parameter gives an indication of how much complete (with regard to the dipole matrix elements) a particular set of energy is.

The results of the calculation are for $N_e = 10^{23}\,\mathrm{m}^{-3}$ and $T = 14{,}000\,\mathrm{K}$ quoted in Table 1. Ion broadening was not taken into account since, according to the treatment given by Griem (1974), it is of the order of 1% of the electron impact broadening.

4. Conclusion

Comparison of the mean experimental values normalized to the electron concentration of $10^{23}\,\mathrm{m}^{-3}$ and calculated values, brings out a systematic behaviour and dependence on the electron concentration calibration. The normalized widths obtained with WKP calibration are in average smaller than our theoretical widths by 8–9% (excluding the multiplet 5 which has only one measured point), and smaller than the results of Benett and Griem (1971) by 24%. The difference decreases for the normalized widths obtained with KG calibration; then the values are in average 4% larger than our theoretical results, and 15% smaller than those of Benett and Griem (1971).

The result of Schulz-Gulde and Wenzel for the multiplet 2 agrees with our experimental results very well. They estimated the error to be $\pm 15\%$.

The two calculations, that of Benett and Griem (1971) and this described here, differ in several respects: we took into account symmetrization, while they did not; we did not use the one-electron approximation for the matrix element calculation, while they did; the cut-off criteria, and strong collision term differ in approach. Also, the used set of energy levels is more complete in our case, since we used the tables of Bashkin and Stoner (1975) including the paper of Hansen and Persson (1973) not available at the time of Benett and Griem's (1971) work.

Acknowledgements. This work was supported in part by the NBS, Washington, D.C., by the Self-Managed Community of Interest for Science of the SR of Croatia, and the Republican Community for Science of the SR of Serbia. We are indebted to S. Sahal-Bréchot for providing us with the computer code for the semi-classical calculations.

References

Bashkin, S., Stoner, J.O.: 1975, Atomic Energy Levels and Grotrian Diagrams, Vol. I, North-Holland and Elsevier P.C., Amsterdam, New York, Oxford

Bates, D.R., Damgaard, A.: 1949, *Phil. Trans. R. Soc. London Ser. A* **242**, 102

Benett, S.M., Griem, H.R.: 1971, Calculated Stark Broadening Parameters for Isolated Spectral Lines from the Atoms Helium through Calcium and Cesium, Techn. Rep. No. 71-097, Univ. Maryland

Griem, H.R.: 1964, Plasma Spectroscopy, McGraw-Hill, New York

Griem, H.R.: 1974, Spectral Line Broadening by Plasmas, Academic Press, New York

Hansen, J.E., Persson, W.: 1973, *Physica Scripta* **8**, 197

Jones, W.W.: 1973, *Phys. Rev.* A **7**, 1826

Konjević, N., Platiša, M., Popović, M.: 1972, *Z. Physik* **257**, 235

Konjević, N., Roberts, J.R.: 1976, *J. Phys. Chem. Data* **5**, 209

Lokner, V., Movre, M.: 1980, *Fizika* **12**, 61

Lokner, V., Vadla, Č., Vujnović, V.: 1983, *J. Quant. Spectrosc. Radiat. Transfer* (in press)

Oertel, G.K., Shomo, L.P.: 1968, *Astrophys. J. Suppl. Series* **16**, 175

Purić, J., Lakićević, I., Labat, J., Djeniže, S., Ćirković, Lj.: 1977, *Phys. Letters* A **63**, 243

Sahal-Bréchot, S.: 1969a, *Astron. Astrophys.* **1**, 91

Sahal-Bréchot, S.: 1969b, *Astron. Astrophys.* **2**, 322

Schulz-Gulde, E., Wenzel, A.: 1980, *J. Phys. B. Atom. Mol. Phys.* **13**, 3733

Vidal, C.R., Cooper, J., Smith, E.W.: 1973, *Astrophys. J. Suppl. Series* **25**, 37

Wiese, W.L., Kelleher, D.E., Paquette, D.R.: 1972, *Phys. Rev.* A **6**, 1132

© European Southern Observatory • Provided by the NASA Astrophysics Data System

1983A&A...127...68D

Astron. Astrophys. 127, 68–72 (1983)

ASTRONOMY AND ASTROPHYSICS

Stark broadening of Si II and Si III spectral lines

M. S. Dimitrijević

Institute of Physics; P.O. Box 57, YU-11001 Beograd, Yugoslavia

Received March 14, accepted June 21, 1983

Summary. Modified semiempirical and approximative semi-classical methods have been used for the calculation of recently measured Si II and Si III Stark line widths in order to test both methods, as well as the new experimental data (Kusch and Schröder, 1982).

Key words: plasma spectroscopy – silicon – line broadening

Introduction

Stark broadening parameters for silicon spectral lines are useful for a number of astrophysical problems. Reliable data are required for the evaluation of the physical conditions in the stellar plasma as well as for the opacity calculations, since the silicon takes the sixth place in the stellar abundance of elements (Unsöld, 1967). In spectra of hot stars of B and A type the Si II spectral lines are usually present. During the spectral investigation of some peculiar stars of types mentioned, especially the silicon Ap-stars, a large number of less intensive Si II and Si III lines is observed (Jaschek and Garcia, 1966; Hohlova and Ryabtchikova, 1970). Also, silicon lines are often among the principal impurity lines in the analysis of the plasma radiation during laboratory and nuclear fusion research.

For calculation of Stark broadening parameters one can use various more or less sophisticated theoretical approaches (see e.g. Griem, 1974). In particular cases e.g. when a large number of theoretical data are required, or there is not enough data for a reasonable set of perturbing energy levels, or when with the sophistication of calculations the relevant increase of accuracy is not satisfactory due to the complexity of investigated spectrum, simple approximative formulae with good average accuracy may be very useful.

The simple semi-empirical method (Griem, 1968) agrees in average within 50% with the experimental data for singly ionized atoms (Griem, 1974). For multiple ionized atoms the agreement becomes worse and few attempts have been made to extend the applicability of this approach to higher ionization stages (Hey, 1977; Dimitrijević and Konjević, 1980; 1981a; 1981b; Hey and Breger, 1980). For the modified semi-empirical formula (Dimitrijević and Konjević, 1980; 1981a) the average ratio of measured to calculated widths is 1.06 ± 0.31 for doubly- and 0.91 ± 0.42 for triple-charged ions (Dimitrijević and Konjević, 1980). It is interesting that the worse agreement between numerical and experimental values is just for Si III lines (the average ratio of measured to calculated line widths is only 0.67 for this case).

New experimental results for Stark broadening parameters for prominent Si II and Si III lines, have been published recently (Kusch and Schröder, 1982). A number of references concerning experimental and numerical determination of Si II and Si III Stark broadening parameters (Sahal-Bréchot, 1969; Yukov, 1972; Lesage et al. 1977; Hey, 1977c; Platiša et al., 1977; Dimitrijević and Konjević, 1980; 1981a) have not been taken into account in that paper and it is interesting to compare these new experimental data with previously published results. Also, the modified semi-empirical, and approximative semi-classical calculations of Stark widths for Si II and Si III lines have been performed in order to test both methods in the case of Si II and Si III lines, as well as the new experimental data.

Theory

Within the impact approximation Baranger (1958) has derived the quantum-mechanical expression for the width of an isolated ion line:

$$W = N\left\{v\left[\sum_{i'}\sigma_{i'i} + \sum_{f'}\sigma_{f'f}\right]\right\}_{av} + W_{el} \tag{1}$$

where W is the full half-width (FWHM) in units of angular frequency and N is the electron concentration. The symbols $\sigma_{i'i}$ and $\sigma_{f'f}$ represent the inelastic cross sections for collisional transitions to i', f' from initial (i) and final (f) levels, respectively, of the optically allowed transition. W_{el} is the line width induced by elastic collisions. The averaging in Eq. (1) has to be performed over the electron velocity (v) distribution.

Griem (1968) assumed that the contribution of elastic collisions to the line width can be neglected for higher electron temperatures. The same author made an attempt to take elastic collisions into account at the low temperature limit by using the threshold value of the inelastic cross section below the threshold. Within the framework of the dipole approximation, using Bethe's (1930) relation for cross sections together with semi-empirical effective Gaunt-factor approximation proposed by Seaton (1962) and Van Regemorter (1962), we can calculate Stark line width from the well known semi-empirical formula (Griem, 1968)

$$W = N\frac{8\pi}{3}\frac{\hbar^2}{m^2}\left(\frac{2m}{\pi kT}\right)^{1/2}\frac{\pi}{\sqrt{3}} \cdot\left[\sum_{i'}\boldsymbol{R}^2_{j'j}\,g\left(\frac{E}{\Delta E_{i'i}}\right) + \sum_{f'}\boldsymbol{R}^2_{f'f}\,g\left(\frac{E}{\Delta E_{f'f}}\right)\right]. \tag{2}$$

© European Southern Observatory • Provided by the NASA Astrophysics Data System

1983A&A...127...68D

In this expression $R^2_{j'j}$ (in units of the Bohr radius a_0^2) is the square of the coordinate operator matrix element summed over all components of the operator and the magnetic substates of total angular momentum J', and averaged over the magnetic substates of J; $E=3kT/2$ is the energy of the perturbing electron and $\Delta E_{j'j}=|E_{j'}-E_j|$ is the energy difference between levels j and j'. The semi-empirical effective Gaunt factor $g(x)=0.20$ for $x\leqq 2$ and $g(x)=0.24$, 0.33, 0.56, 0.98 and 1.33 for $x=3$, 5, 10, 30, and 100.

For singly ionized atoms semi-empirical formula agrees in average within 50% with the experiment (Griem, 1974). Griem (1974) suggested that this formula can be used for multiple ionized atoms as well, but with an uncertainty of $\pm 100\%$. However, the comparison with the experimental data for doubly- and triply-ionized atoms (Hey, 1976; 1977a; 1977b; Hey and Bryan, 1977; Bogen, 1972; Platiša et al., 1977; 1979) shows that the calculated values are systematically lower. This is an indication that the threshold value $g=0.2$ is rather small for multiple ionized atoms. For multiple ionized atoms it is also sometimes difficult to complete a reasonable set of atomic energy levels since data for higher perturbing levels are often missing in the literature.

To overcome these difficulties and further improve semi-empirical method one can separate transitions to the perturbing levels in three groups (Dimitrijević, and Konjević, 1980; 1981a): transitions with (i) $\Delta n=0$, $l\to l+1$; (ii) $\Delta n=0$, $l\to l-1$, (iii) $\Delta n\neq 0$ (as was used previously by Kobzev (1971) and Griem (1974) within the semi-classical method). Within each group of transitions, matrix elements are treated lumped together. For the transitions with the principal quantum number n unchanged, Bely (1966) found that near threshold values of g could be significantly larger than 0.2. A study of transitions of this type has been made by Blaha (1969) for 15 different isoelectronic sequences. He finds threshold values of g ranging from 0.31 to 0.96. Kobzev (1971) suggested an empirical value of $g=0.9-1.1/z$ at threshold, which is in agreement with the conclusion of Blaha (1969). We have adopted this suggestion calculating the Gaunt factor for higher electron energies from the following equation:

$$\tilde{g}(x)=0.7-1.1/z+g(x) \tag{3}$$

For transitions with $\Delta n\neq 0$, $g=0.2$ at threshold is retained and the energy separation to the nearest perturbing level is estimated from

$$\Delta E_{n,n+1}\approx 2Z^2E_H/n^{*3}, \tag{4}$$

where Z is the charge "seen" by the optical electron ($Z=1$ for neutrals, 2 for singly charged ions etc.) and n^* is the effective principal quantum number.

Equation (1) becomes now

$$\begin{aligned} W=N\frac{8\pi}{3}\frac{\hbar^2}{m^2}\left(\frac{2m}{\pi kT}\right)^{1/2}\frac{\pi}{\sqrt{3}}\Bigg[&\boldsymbol{R}^2_{l_i,l_i+1}\tilde{g}\left(\frac{E}{\Delta E_{l_i,l_i+1}}\right)\\ &+\boldsymbol{R}^2_{l_i,l_i-1}\tilde{g}\left(\frac{E}{\Delta E_{l_i,l_i-1}}\right)+\boldsymbol{R}^2_{l_f,l_f+1}\tilde{g}\left(\frac{E}{\Delta E_{l_f,l_f+1}}\right)\\ &+\boldsymbol{R}^2_{l_f,l_f-1}\tilde{g}\left(\frac{E}{\Delta E_{l_f,l_f-1}}\right)+\sum_{i'}(\boldsymbol{R}^2_{ii'})_{\Delta n\neq 0}g\left(\frac{3kTn_i^{*3}}{4Z^2E_H}\right)\\ &+\sum_{f'}(\boldsymbol{R}^2_{ff'})_{\Delta n\neq 0}g\left(\frac{3kTn_f^{*3}}{4Z^2E_H}\right)\Bigg]. \end{aligned} \tag{5}$$

Relevant matrix elements can be calculated using Coulomb approximation of Bates and Damgaard (1949)

$$\boldsymbol{R}^2_{l,l'}\simeq\left(\frac{3n^*}{2Z}\right)^2\frac{\max(l,l')}{2l+1}[n^{*2}-\max^2(l,l')]\phi^2 \tag{6}$$

$$\sum_{j'}(\boldsymbol{R}^2_{jj'})_{\Delta n\neq 0}\simeq\left(\frac{3n_j^*}{2Z}\right)^2\frac{1}{9}(n_j^{*2}+3l_j^2+3l_j+11),\qquad j=i,f. \tag{7}$$

Here, ϕ represents the Bates-Damgaard factor [tabulated e.g. in Oertel and Shomo's (1968) paper].

At higher electron temperatures (Say $3kT/2\Delta E>50$), all Gaunt factors are calculated in accordance to the GBKO (Griem et al., 1962) high temperature limit, viz.

$$\tilde{g}_{j'j}=g_{j'j}=\frac{\sqrt{3}}{\pi}\left[\frac{1}{2}+\ln\left(\frac{2ZkT}{n_j^{*2}\Delta E_{j'j}}\right)\right]. \tag{8}$$

Modified semi-empirical formula, Eq. (5), is very similar in form to the equation for isolated line widths of multiple-charged ions derived by Griem (1974) within the semi-classical-perturbation formalism and slightly modified recently (Dimitrijević and Konjević, 1980), i.e.

$$\begin{aligned} W=N\frac{8\pi}{3}\frac{\hbar^2}{m^2}\int_0^\infty\frac{f(v)}{v}dv\Bigg\{&\left[\left(\boldsymbol{R}^2\ln\frac{\varepsilon_{\max}}{\varepsilon_{\min}}\right)_{l_i,l_i+1}+\left(\boldsymbol{R}^2\ln\frac{\varepsilon_{\max}}{\varepsilon_{\min}}\right)_{l_i,l_i-1}\right.\\ &\left.+\left(\boldsymbol{R}^2\ln\frac{\varepsilon_{\max}}{\varepsilon_{\min}}\right)_{l_f,l_f+1}+\left(\boldsymbol{R}^2\ln\frac{\varepsilon_{\max}}{\varepsilon_{\min}}\right)_{l_f,l_f-1}\right]_{\Delta n=0}\\ &+\sum_{i'}(\boldsymbol{R}^2_{i'i})_{\Delta n=0}\left(\ln\frac{\varepsilon_{\max}}{\varepsilon_{\min}}\right)_{n_i,n_i+1}\\ &+\sum_{f'}(\boldsymbol{R}^2_{f'f})_{\Delta n=0}\left(\ln\frac{\varepsilon_{\max}}{\varepsilon_{\min}}\right)_{n_f,n_f+1}\Bigg\}+\mathrm{W}_{c'}, \end{aligned} \tag{9}$$

$$\left(\ln\frac{\varepsilon_{\max}}{\varepsilon_{\min}}\right)_{l,l'}=\ln\left\{1.4+\xi_{l,l'}^{-1}\left[1+\frac{mv^2n_l^{*2}}{2E_HZ(Z-1)}\right]^{-1}\right\},$$

$$\xi_{l,l'}=\frac{(Z-1)e^2\omega_c}{mv^3}, \tag{10}$$

$$\omega_c=\max\{|\omega_{l,l'}|,\omega_P,\omega_F,\Delta\omega_i\}.$$

Here, ε is the eccentricity of the hyperbolic perturber path, $\omega_{l,l'}$ is the frequency separation between, l,l' levels, $\omega_P=(4\pi Ne^2/m)^{1/2}$ is the plasma frequency, ω_F is the fine structure splitting, and $\Delta\omega_i$ is the ion splitting. Furthermore, since the $n\to n+1$ transitions dominate between all $n\neq 0$ contributions, one should take $\hbar\omega_c\approx 2Z^2E_H/n^{*-3}$.

In Eq. (9), W_c is the line width induced by strong collisions and higher multipole interactions, i.e.

$$W_c=2\pi N\left(\frac{2m}{\pi kT}\right)^{1/2}\left(\frac{\hbar}{mZ}\right)^2n_i^{*4}\left[1+\frac{kT}{E_H\left(1+\frac{kT}{E_H}+\frac{Z^2}{n_i^{*4}}\right)}\right]. \tag{11}$$

Comparisons with reliable experimental data for doubly-ionized atoms yield, as an average ratio of measured to calculated widths, 1.06 ± 0.31 for the modified semi-empirical and 0.96 ± 0.24 for the approximative semi-classical method (Dimitrijević and Konjević, 1980). For triply ionized atoms these ratios are 0.91 ± 0.42 and 1.08 ± 0.41 respectively.

Results and discussion

All atomic data needed for calculations were taken from Moore (1965). The Key data on all experiments discussed in this paper are systematized in Table 1. The results of various experimental

© European Southern Observatory • Provided by the NASA Astrophysics Data System

1983A&A...127...68D

Table 1. Key data on experiments

Ref.	Plasma source	Method of measurement		
		Electron density	Temperature	Spectrum
Miller (1968) Lesage and Miller (1975) Lesage et al. (1977)	Gas driven shock tube	H_β Stark width	Line reversal technique applied to H_α line, absolute intensity of NeI 5852 Å line and H_β	Photographicaly
Purić et al. (1974)	T-tube	Laser interferometry at 6328 Å	Boltzmann plot of ArII line intensities	Photoelectricaly, shot by shot
Platiša et al. 1977	Low pressure pulsed arc	Laser interferometry at 6328 Å	Boltzmann plot of ClIII line intensities	Photoelectricaly, shot by shot
Kusch and Schröder 1982.	Pulsed discharge	H_β Stark width	Ratio of the SiIII - line 3791 Å and the SiII-line 5979 Å	Photographicaly

Table 2. Experimental and theoretical Stark widths (FWHM) of Si II. Experimental data: W_M: Miller (1968); W_{LM}: Lesage and Miller (1975); W_{LSM}: Lesage et al. (1977); W_{KS}: Kusch and Schröder (1982). Theoretical data: W_{JBG}: Jones et al. (1971); W_{ASC}: Present approximative semiclassical calculations; W_{SB}: Sahal-Bréchot (1969); W_{CO}: Calculations of Bengston according to Cooper and Oertel (1967, 1969) given in Lesage et al. (1977); W_Y: Yukov (1972); W_{SEM}: Present calculations according to modified semi-empirical approach; W_{SE}: semi-empirical calculations (Hey, 1977c)

Ion	Transition multiplet	Wavelength	T(K)	Experimental data (Å)				Theoretical data (Å)						
				W_M	W_{LM}	W_{LSM}	W_{KS}	W_{JBG}	W_{ASC}	W_{SB}	W_{CO}	W_Y	W_{SEM}	W_{SE}
SiII	$4p^2P^o$-$4d^2D$ (5)	5041.03	10000	3.0	3.5	2.53		2.90	2.94	2.62	2.2	2.0	1.76	1.96
			23500				3.90	2.66	2.34				1.41	
		5056.31	10000	3.0	3.5	2.69		2.90	2.94	2.62	2.2	2.0	1.76	1.96
			23500				4.53	2.66	2.34				1.41	
SiII	$4p^2P^o$-$5s^2S$ (4)	5957.56	10000	2.4	3.3	2.78		2.58	3.86	2.83	2.5		2.60	2.55
			23500				3.69	2.30	3.14				2.02	
		5978.93	10000	2.4	3.3	2.75		2.58	3.86	2.83	2.5		2.60	2.55
			23500				4.08	2.30	3.14				2.02	
SiII	$4p^2P^o$-$6s^2S$ (6)	3339.82	23500				0.273	1.90	2.77				2.16	
		3333.14	23500				0.249	1.90	2.77				2.16	
SiII	$3d'^2D^o$-$4p'^2P$ (7.26)	4190.72	23500				0.435		0.528				0.280	
		4198.13	23500				0.446		0.528				0.280	
SiII	$3d'^4F^o$-$4p'^4D$ (7.33)	5688.81	23500				0.835		0.906				0.480	
		5701.37	23500				0.789		0.906				0.480	
		5706.37	23500				0.725		0.906				0.480	

and numerical data for Si II Stark line widths are compared in Table 1 with experimental data of Kusch and Schröder (1982). Experimental full Stark widths (FWHM) of Lesage et al., (1977) (W_{LSM}) are the final result of a series of measurements [Miller, 1968 (W_M); Lesage and Miller (1975) (W_{LM})] and they are systematically lower than the values of Kusch and Schröder (1982) (W_{KS}). The semiclassical half-halfwidths (HWHM) of Jones et al. (1971) (W_{JBG}) [given also in Griem's (1974) book] are erroneously interpreted as full-halfwidths (FWHM) in the paper of Kusch and Schröder (1982). We can see that particularly large difference (a factor of 7) between experimental semiclassical values exists for the multiplet 6, indicating possibly a typing error in the order of magnitude.

Present approximative semiclassical calculations according to Eq. 9 (W_{ASC}) and modified semiempirical calculations according to Eq. 5 (W_{SEM}) are compared in Table 2 with various semiclassical

© European Southern Observatory • Provided by the NASA Astrophysics Data System

1983A&A...127...68D

calculations and experimental results. If we compare present approximative calculations with experimental results of Lesage et al. (1977) and with other, more sophisticated semiclassical calculations, we can conclude, taking into account the simplicity of the approach, that both methods can be used for the estimate of the Stark widths in the case of transitions between configurations with the core ^1S (multiplets 4, 5, 6). In the case of transitions between configurations with the core ^3P (multiplets 7.26 and 7.33), we can see that a difference of the factor of 2 exists between approximate semiclassical and modified semi-empirical results, indicating that the semi-empirical Gaunt factors are too small in this case. One can notice that in all previously investigated cases (Dimitrijević and Konjević, 1980; 1981a; 1981b) the agreement of modified semi-empirical approach with reliable data was better. One must take into account that in present case perturbing energy level structure is complex. This is particularly case for 7.26 and 7.33 multiplets where the $3d'$ levels are the closest perturbing levels for the $4p'$ energy levels and where for $n=3$ only $3d'$ levels exist. If we analyse, as an example, the contribution of various processes to the Stark width according to the approximative semiclassical approach, we can see that usually dominant contribution to the width of no quenching collisions ($\Delta n=0$) is only 0.224 Å at 20,000 K for the multiplet 7.33. For the same multiplet, the contribution of inelastic collisions ($\Delta n \neq 0$) is 0.329 Å and the correction for strong collisions and higher order multipole interactions 0.400 Å, at the same conditions. From the above analysis one can conclude that the semi-empirical Gaunt factor is not sufficiently large to compensate for the strong collision and higher order multipole interaction yield to the width.

A part of the disagreement between experimental data and the modified semi-empirical approach for the 7.26 and 7.33 multiplets is due also to the failure of the Bates and Damgaard (1949) approach. Strong configuration interaction effects occur in the atomic structure for Si II: they perturb the dipole line strengths; especially in the cases for which an electron of the internal shell $3s^2$ is excited (cf. Nussbaumer, 1977). Finally, the upper levels of these multiplets are autoionization levels: the autoionization widths (w_a) can be large (cf. Artru et al., 1981), and must be added to the collisional width (w_c) before comparing to the experimental one, especially at low densities. For example the width of the line 4190.72 Å has been measured (Kusch and Schröder, 1982) at $N_e = 0.5-2\,10^{17}\,\mathrm{cm}^{-3}$. The collisional width is 0.218–0.870 Å and the autoionization width is 0.028 Å (Artru et al., 1981). Since the autoionization width does not depend on electron density, we can see that at $N_e = 10^{16}\,\mathrm{cm}^{-3}$, w_a has the same order of magnitude as w_c. It is interesting that in the Si II spectrum transitions exist with $w_a \gg w_c$ at $N_e = 10^{17}\,\mathrm{cm}^{-3}$ (e.g. for the level $4p'^2D$ the autoionization width is 150 meV and for $3d'^2F^0$, 409 meV; Artru et al., 1981). Also, autoionization widths within a multiplet may differ several times due to departure from LS coupling. This is an additional reason for eventual differences of experimental line widths within a multiplet.

Table 3. Experimental and theoretical Stark widths (FWHM) of Si III. Experimental data: W_{PDLC}: Purić et al. (1974); W_{PDKP}: Platiša et al. (1977); W_{KS}: Kusch and Schröder (1982). Theoretical data: W_{SEM}: Modified semi-empirical approach. Present calculations and results from Dimitrijević and Konjević (1980, 1981a). W_{SE}: Semi-empirical calculations according to Griem (1968). Results from Dimitrijević and Konjević (1980, 1981a). W_{ASC}: Approximative semi-classical approach. Present calculations and results from Dimitrijević and Konjević (1980, 1981a)

Ion	Transition (multiplet)	Wavelength	T(K)	Experimental data (Å)			Theoretical data (Å)		
				W_{PDLC}	W_{PDKP}	W_{KS}	W_{SEM}	W_{SE}	W_{ASC}
SiIII	$4s^3S-4p^3P^o$ (2)	4552.62	8700	0.48			0.778	0.469	0.636
			10600	0.42			0.704	0.424	0.588
			12800	0.40			0.641	0.386	0.548
			16400	0.38			0.566	0.341	0.503
			25600		0.310		0.453	0.272	0.437
		4567.82	8700	0.56			0.778	0.469	0.636
			25600		0.312		0.453	0.272	0.437
		4574.76	23500			3.056	0.469	0.283	0.447
			25600		0.303		0.453	0.272	0.437
SiIII	$4s^1S-4p^1P^o$ (4)	5739.73	23500			0.710	0.804	0.495	0.774
SiIII	$4p^3P^o-4d^3D$ (5)	3806.54	23500			0.472	0.512	0.343	0.562
		3796.11	23500			0.476	0.512	0.343	0.562
		3791.41	23500			0.376	0.512	0.343	0.562
			25600		0.352		0.490	0.338	0.548
SiIII	$4p^1P^o-4d^1D$ (7)	3590.47	23500			0.537	0.664	-	0.688
SiIII	$4p^3P^o-5s^3S$ (6)	3241.61	25600		0.321		0.522	0.316	0.526
		3233.95	25600		0.321		0.522	0.316	0.526
		3230.50	25600		0.314		0.522	0.316	0.526
SiIII	$4d^3D-5f^3F^o$ (8.06)	3486.91	12800	0.52			3.11*		2.64*

*The line is not isolated

© European Southern Observatory • Provided by the NASA Astrophysics Data System

1983A&A...127...68D

It will be very interesting to obtain reliable experimental data for multiplets 7.26 and 7.33 at various temperatures, since the complex perturbing energy levels structure provides the opportunity to test various approximations within the perturbation – semi-classical formalism.

The experimental and theoretical Stark widths for Si III lines are presented in Table 3. We can see that difference between the various data is within the tolerable limits in all cases with the exception of two values. One of them is the experimental Stark width of Kusch and Schröder for 4574.76 Å line (Mult. 2) approximatively one order of magnitude larger than other experimental and theoretical data (probably a typing error for the order of magnitude?). The other uncertain value is the Stark width for 3486.91 Å (Mult. 8.06) line (Purić et al., 1974). In this case, the perturbing level $5g^3G$ is so close to the $5f^3F^0$ energy level ($32\,\mathrm{cm}^{-1}$) that the considered line is not isolated at electron densities of experiment. If we compare the reliable data with calculated values we can se that an average ratio of measured and calculated widths is 0.71 for the modified semi-empirical 1.13 for the semi-empirical and 0.73 for the approximative semi-classical approach.

Acknowledgement. I am indebted to Dr. Sylvie Sahal-Bréchot for very illuminating discussion and for her interest to this work.

References

Artru, M.C., Jamar, C., Petrini, D., Praderie, F.: 1981, *Astron. Astrophys.* **96**, 380

Baranger, M.: 1958, *Phys. Rev.* **112**, 855

Bates, D.R., Damgaard, A.: 1949, *Phil. Trans. Roy. Soc. London* A **242**, 101

Bely, O.: 1966, *Proc. Phys. Soc.* **58**, 587

Bethe, H.A.: 1930, *Ann. Physik* **5**, 3251

Blaha, M.: 1969, *Astrophys. J.* **157**, 473

Bogen, P.: 1972, *Z. Naturforsch.* **27**a, 210

Cooper, J., Oertel, G.K.: 1967, *Phys. Rev. Letters* **18**, 985

Cooper, J., Oertel, G.K.: 1969, *Phys. Rev.* **180**, 286

Dimitrijević, M.S., Konjević, N.: 1980, *J. Quant. Spectroscop. Radiat. Transfer* **24**, 451

Dimitrijević, M.S., Konjević, N.: 1981a, in *Spectral Line Shapes*, ed. B. Wende, W. de Gruyter, Berlin, New York 211

Dimitrijević, M.S., Konjević, N.: 1981b, *Astron. Astrophys.* **102**, 93

Griem, H.R., Baranger, M., Kolb, A.C., Oertel, G.: 1962, *Phys. Rev.* **125**, 177

Griem, H.R.: 1968, *Phys. Rev.* **165**, 258

Griem, H.R.: 1974, Spectral Line Broadening by Plasmas, McGraw-Hill, New York

Hey, J.D.: 1976, *J. Quant. Spectroscop. Radiat. Transfer* **16**, 575

Hey, J.D.: 1977a, *J. Quant. Spectroscop. Radiat. Transfer* **17**, 729

Hey, J.D.: 1977b, *J. Quant. Spectroscop. Radiat. Transfer* **18**, 649

Hey, J.D.: 1977c, *J. Quant. Spectroscop. Radiat. Transfer* **18**, 425

Hey, J.D., Bryan, R.J.: 1977, *J. Quant. Spectroscop. Radiat. Transfer* **17**, 221

Hey, J.D., Breger, P.: 1980, *J. Quant. Spectroscop. Radiat. Transfer* **24**, 349

Hohlova, V.L., Ryabtchikova, T.A.: 1970, *Astrofizika* **6**, 227

Jaschek, M., Garcia, Z.L.: 1966, *Z. Astrophysik* **64**, 217

Jones, W.W., Benett, S.M., Griem, H.R.: 1971, Calculated Electron Impact Broadening Parameters for Isolated Spectral Lines from the Singly Charged Ions: Lithium through Calcium, Techn. Rep. No. 71-128, Univ. Maryland

Kobzev, G.A.: 1971, *Opt. Spectrosc.* (USSR) **30**, 106

Kusch, H.J., Schröder, K.: 1982, *Astron. Astrophys.* **116**, 255

Lesage, A., Miller, M.: 1975, *C.R.H. Acad. Sci.* B **280**, 645

Lesage, A., Sahal-Bréchot, S., Miller, M.H.: 1977, *Phys. Rev.* A **16**, 1617

Miller, M.H.: 1968, Thermally Insensitive Determinations of Transition Probabilities for C I, O I, Ne I, Al II, Si I, Si II, P I, P II, S I, S II, and Cl I, Techn. Note BN-550, Univ. of Maryland

Moore, C.E., 1965, Selected Tables of Atomic Spectra, Si II, Si III, Si IV, NSRDS-NBS 3, section 1, U.S. Govt. Printing Office, Washington D.C.

Nussbaumer, H.: 1977, *Astron. Astrophys.* **58**, 291

Oertel, G.K., Shomo, L.P.: 1968, *Astrophys. J. Suppl. Series* **16**, 175

Platiša, M., Dimitrijević, M., Popović, M., Konjević, N.: 1977, *J. Phys.* B **10**, 2997

Platiša, M., Dimitrijević, M., Popović, M., Konjević, N.: 1979, *J. Quant. Spectroscop. Radiat. Transfer* **22**, 333

Purić, J., Djeniže, S., Labat, J., Ćirković, Lj.: 1974, *Z. Physik* **267**, 71

Regemorter, H. Van: 1962, *Astrophys. J.* **136**, 906

Sahal-Bréchot, S.: 1969, *Astron. Astrophys.* **2**, 322

Seaton, M.J.: 1962 in *Atomic and Molecular Processes*, ed. by D.R. Bates, Academic Press, New York, Chap. 11

Unsöld, A.: 1967, Der Neue Kosmos, Springer, Berlin, Göttingen, Heidelberg

Yukov, E.A.: 1972, *Soviet. Astron. AJ* **15**, 867

© European Southern Observatory • Provided by the NASA Astrophysics Data System

1984A&A...131..327D

Astron. Astrophys. 131, 327–328 (1984)

ASTRONOMY AND ASTROPHYSICS

Electron impact line widths of the resonance lines of Be-like ions

M. S. Dimitrijević

Institute of Physics, P.O. Box 57, YU-11001 Belgrade, Yugoslavia

Received August 22, accepted October 3, 1983

Summary. Analytical expressions recently obtained for the collision strengths of resonant transitions of Be-like ions are used for the calculation of Stark broadening parameters.

Key words: Stark broadening – plasma spectroscopy – Be-like ions

Stellar and laboratory plasma diagnostic, atomic abundances, opacity calculations, all have led to a need for knowledge about Stark broadening data. For the calculation of Stark broadening parameters sophisticated quantum-mechanical and semiclassical methods (see e.g. Griem, 1974) exist, but they often require a considerable labour even for the evaluation of a single line width. Moreover, when there are not enough reliable atomic data for more involved calculations, or when quick estimate is needed, the approximate approaches may be very useful.

One such approximate method is the modified (Dimitrijević and Konjević, 1980, 1981) semi-empirical (Griem, 1968) formula suitable for singly as well as for multiply charged ion lines. Data recently obtained for the electron impact excitation collision strengths for $ns^2\ {}^1S$-$nsnp\,{}^1P^0$ resonance transitions in the Be isoelectronic sequence (Younger, 1980) may be easily incorporated in the approach mentioned above. These data were obtained in the distorted wave approximation, taking into account exchange effects, and using an approximate treatment of intrashell correlation effects in the target state. Using, for the Stark broadening calculations, Gaunt factors derived from the analytical expression for the collision strengths one can: (i) test the modified semi-empirical approach (ii) provide new Stark broadening data for Be-like resonance lines observed in the Solar spectrum (see e.g. Malinovsky, 1975; Loulergue and Nussbaumer, 1976), and (iii) demonstrate how the data on collision strengths can be used for the Stark broadening calculations within the mentioned method.

According to the modified semi-empirical method, the full Stark width (W) of an ionic line can be calculated from the following expression (Dimitrijević and Konjević, 1980):

$$W=N\frac{8\pi}{3}\frac{\hbar^2}{m^2}\left(\frac{2m}{\pi kT}\right)^{1/2}\frac{\pi}{\sqrt{3}}\left[\boldsymbol{R}^2_{l_i,l_i+1}\tilde{g}\left(\frac{E}{\Delta E_{l_i,l_i+1}}\right)+\boldsymbol{R}^2_{l_i,l_i-1}\tilde{g}\left(\frac{E}{\Delta E_{l_i,l_i-1}}\right)+\boldsymbol{R}^2_{l_f,l_f+1}\tilde{g}\left(\frac{E}{\Delta E_{l_f,l_f+1}}\right)+\boldsymbol{R}^2_{l_f,l_f-1}\tilde{g}\left(\frac{E}{\Delta E_{l_f,l_f-1}}\right)+\sum_{i'}(\boldsymbol{R}_{ii'})_{\Delta n\neq 0}g\left(\frac{3kTn_i^3}{4z^2E_H}\right)+\sum_{f'}(\boldsymbol{R}^2_{ff'})_{\Delta n\neq 0}g\left(\frac{3kTn_f^3}{4z^2E_H}\right)\right]. \quad (1)$$

Here, $E\approx 3kT/2$ is the energy of the perturbing electrons, $\Delta E_{jj'}=|E_{j'}-E_j|$ is the energy difference between the initial ($j=i$) or final ($j=f$) levels, and their perturbing levels ($j'=i',f'$) and n is the effective principal quantum number. The semi-empirical procedure for the calculation of electron impact widths accounts explicitly for interactions from "weak" collisions only (Griem, 1974). It is assumed (Griem, 1968) that the contribution of elastic collisions can be neglected for higher energies. The same author (Griem, 1968) made an attempt to take elastic collisions and resonance effects into account at the low energy limit by beginning the integration over the Maxwell distribution at zero velocity. Below the threshold velocity for a particular inelastic process the threshold value of the Gaunt factor is used. The effective semi-empirical Gaunt factor (Griem, 1968) is given by $g(x)=0.20$ for $x\leqq 2$ and $g(x)=0.24$, 0.33, 0.56, 0.98, and 1.33 for $x=3$, 5, 10, 30, and 100. For transitions with $\Delta n=0$, Dimitrijević and Konjević (1980) used the Gaunt factor $g(x)=0.7-1.1/z+g(x)$, where z is the charge "seen" by the optical electron ($z=2$ for singly-, 3 for doubly-charged ions etc.). At high temperatures, say $3kT/\Delta E>50$, all Gaunt factors in Eq. (1) are calculated in accordance with the GBKO high temperature limit (Griem et al., 1962), viz.

$$\tilde{g}_{jj'}=g_{jj'}=\frac{\sqrt{3}}{\pi}\left[\frac{1}{2}+\ln\left(\frac{2zkT}{n^2\Delta E_{jj'}}\right)\right]. \quad (2)$$

Relevant matrix elements are:

$$\boldsymbol{R}^2_{l,l'}\simeq\left(\frac{3n}{2z}\right)^2\frac{\max(l,l')}{2l+1}[n^2-\max^2(l,l')]\phi^2, \quad (3)$$

$$\sum_{j'}(\boldsymbol{R}^2_{jj'})_{\Delta n\neq 0}\simeq\left(\frac{3n_j}{2z}\right)^2\frac{1}{9}(n_j^2+3l_j^2+3l_j+11). \quad (4)$$

Here, ϕ represents the Bates and Damgaard (1949) factor, tabulated by Oertel and Shomo (1968). For the transitions of the type $s^2SL-s(S_c,L_c)pSL$, Eqs. (3) and (4) must be multiplied by a factor $2(2S_c+1)/(2S+1)$ (Shore and Menzel, 1965). Using the relation between the Gaunt factor and the collision (Ω) and line (S) strengths

$$g=\frac{3\sqrt{3}}{8\pi}\frac{\Omega}{S}, \quad (5)$$

and knowing the sum rule for all lines originating or ending in a term SL (Shore and Menzel, 1965), the four first terms in Eq. (1) become $\Omega/g_i+\Omega/g_f$. Here, the statistical weight g_j is equal to $(2L_j+1)\ (2S_j+1)$; $j=i,f$ and L_j and S_j are the total angular momentum quantum number and the total spin, respectively.

© European Southern Observatory • Provided by the NASA Astrophysics Data System

1984A&A...131..327D

Table 1. Stark line widths (FWHM) for C III and N IV resonance lines according to present (W) and the modified semi-empirical approach (W_{SEM}), at $N_e = 10^{18}$ cm^{-3}

Ion	Transition	T (K)	W (Å)	W_{SEM} (Å)
C III	$2s^2\,{}^1S - 2p^1P^0$	20,000	0.0174	0.0151
	$\lambda = 977$ Å	80,000	0.00872	0.00754
		320,000	0.00436	0.00377
N IV	$2s^2\,{}^1S - 2p^1P^0$	30,000	0.00534	0.00550
	$\lambda = 765.1$ Å	120,000	0.00267	0.00275
		480,000	0.00134	0.00137

Therefore, the Stark width for the resonance lines of the Be-like ions becomes

$$W = \pi N \left(\frac{\hbar}{m}\right)^2 \left(\frac{2m}{\pi k T}\right)^{1/2} \left[\frac{4\Omega}{3} + \frac{8\pi}{3\sqrt{3}} \sum_{i'} (\boldsymbol{R}_{ii'}^2)_{\Delta n \neq 0} \cdot g\left(\frac{3kTn_i^3}{4z^2 E_H}\right) + \frac{8\pi}{3\sqrt{3}} 4 \sum (\boldsymbol{R}_{ff'}^2)_{\Delta n \neq 0} g\left(\frac{3kTn_f^3}{4z^2 E_H}\right)\right]. \quad (6)$$

According to Younger (1980), the collision strength for the $2s^2\,{}^1S - 2s2p^1P^0$ transition along the Be-isoelectronic sequence may be expressed as:

$$\Omega = \alpha_1 + \frac{\alpha_2}{x} + \alpha_3 \ln(x),$$
$$x = \frac{E}{\Delta E_{jj'}},$$
$$\alpha_1 = 0.0348/Z + 65.9/Z^2 - 174/Z^3, \quad (7)$$
$$\alpha_2 = 3.37/Z + 45.7/Z^2 - 115/Z^3,$$
$$\alpha_3 = 0.897/Z + 38.1/Z^2 - 58.6/Z^3.$$

Here Z is the effective charge of the ion.

In order to take elastic collisions and resonance effects into account, the collision strength is extrapolated below the threshold for corresponding inelastic process; $\Omega = \alpha_1 + \alpha_2$ for $0 \leqq x \leqq 1$.

Semi-empirical Gaunt factors used here are based on the investigations of Seaton (1962), Regemorter (1962), Kobzev (1971), and Griem (1968). By examining the excitation of lithium-like ions by electron impacts, Bely (1966) has found that the threshold value of the Gaunt factor is larger than 0.2 for $2s - 2p$ transitions [for transitions with $\Delta n = 0$, the value $g = 0.9 - 1.1/z$ is used according to the suggestion of Kobzev (1971)], and smaller than 0.2 for $2s - np$, $n > 2$ transitions. Bely (1966) has found also that the function $g(x)$ is different for the cases $\Delta n = 0$ and $\Delta n \neq 0$. Relations given by Griem (1968), Kobzev (1971), and Younger (1980) are used here because they are given in simple, analytic form, valid for all lines under consideration. For a particular case, more involved calculations may be performed by deducing needed Gaunt factors from numerical data for corresponding cross sections or collision strengths [e.g. data of Malinovsky (1975) for collision strengths of some solar O V transitions] and also, by using data on the influence of resonances if such data exist [e.g. Malinovsky (1975) for O V].

As a numerical example, Stark width (FWHM) calculations [according to Eqs. (6) and (7)] for C III and N IV resonance lines are compared in Table 1 with the modified semi-empirical results [Eq. (1)]. This corresponds to the low temperature case ($E/\Delta E_{jj'} \lesssim 2$) and according to Eqs. (6) and (7) the line widths depend on T as $T^{-1/2}$. Therefore, widths for temperatures between values given in the Table can be obtained easily.

The agreement between the simple modified semi-empirical approach and the calculations with the more accurate collision strength values is very encouraging and it indicates that this simple method can be used with confidence. We can conclude also that the present approach [Eqs. (6) and (7)] is suitable for the calculation of electron impact contributions to the line width of multiply charged Be-like ions.

Acknowledgements. The author gratefully acknowledges the help of D. Grubor in this work.

References

Bates, D.R., Damgaard, A.: 1949, *Phil. Trans. Roy. Soc. London* A **242**, 101

Bely, O.: 1966, *Proc. Phys. Soc.* **88**, 587

Dimitrijević, M.S., Konjević, N.: 1980, *J. Quant. Spectroscopy Radiat. Transfer* **24**, 451

Dimitrijević, M.S., Konjević, N.: 1981, in *Spectral Line Shapes*, ed. B. Wende, de Gruyter, Berlin, New York, p. 211

Griem, H.R., Baranger, M., Kolb, A.C., Oertel, G.: 1962, *Phys. Rev.* **125**, 177

Griem, H.R.: 1968, *Phys. Rev.* **165**, 258

Griem, H.R.: 1974, Spectral Line Broadening by Plasmas, McGraw-Hill, New York

Kobzev, G.A.: 1971, *Opt. Spectrosc.* (USSR) **30**, 106

Loulergue, M., Nussbaumer, H.: 1976, *Astron. Astrophys.* **51**, 163

Malinovsky, M.: 1975, *Astron. Astrophys.* **43**, 101

Oertel, G.K., Shomo, L.P.: 1968, *Astrophys. J. Suppl.* **16**, 175

Regemorter, van, H.: 1962, *Astrophys. J.* **136**, 906

Seaton, M.J.: 1962, in Atomic and Molecular Processes, ed. D.R. Bates, Academic Press, New York, Chap. 11

Shore, B.W., Menzel, D.H.: 1965, *Astrophys. J. Suppl.* **12**, 187

Younger, S.M.: 1980, *J. Quant. Spectroscopy Radiat. Transfer* **23**, 489

© European Southern Observatory • Provided by the NASA Astrophysics Data System

1984A&A...136..289D

Astron. Astrophys. 136, 289–298 (1984)

ASTRONOMY AND ASTROPHYSICS

Stark broadening of neutral helium lines of astrophysical interest. Regularities within spectral series

M. S. Dimitrijević* and S. Sahal-Bréchot

Observatoire de Paris, F-92190 Meudon, France

Received September 30, 1983; accepted February 8, 1984

Summary. Following our earlier work, and using a semiclassical-perturbation formalism for the Stark broadening of atomic lines, we have calculated electron and proton impact line widths and shifts of 36 neutral He lines.

Stark broadening parameters were calculated for lines originating from upper energy levels with $4 \leqq n \leqq 10$, and for an electron density of $10^{13}\,\mathrm{cm}^{-3}$.

The comprehensive set of results obtained is used for the investigation of line-broadening parameter regularities within the spectral series.

Key words: Stark broadening – helium lines – line profiles

1. Introduction

Reliable Stark-broadening data for He lines are of interest for a number of astrophysical problems, particularly for evaluations of the physical conditions in the atmospheres of hot stars of types O and B and some white dwarfs, and for estimation of the radiative transfer through the stellar plasma. Recently, we have calculated (Dimitrijević and Sahal-Bréchot, 1984) electron and proton impact line widths and shifts of 56 neutral He lines in the ultraviolet, visible and infrared regions of the spectrum for an electron density $N_e = 10^{16}\,\mathrm{cm}^{-3}$. Here, we present electron and proton impact broadening parameters for 36 additional He I lines, originating from upper energy levels with $4 \leqq n \leqq 10$, and for $N_e = 10^{13}\,\mathrm{cm}^{-3}$, typical for stellar atmospheres. Those lines practically do not exist in available large scale Stark broadening calculations for He lines (Griem et al., 1962; Benett and Griem, 1971; Bassalo et al., 1982; Dimitrijević and Sahal-Bréchot, 1984).

The results obtained have also been used for following up our investigation of the behaviour of Stark broadening parameters within spectral series (Dimitrijević and Sahal-Bréchot, 1984). From general consideration of atomic energy structure and on the basis of experimental data for some Cs I and He lines, Wiese and Konjević (1982) have shown that for lines belonging to a particular spectral series, the electron impact width increases gradually with increasing principal quantum number of the upper state. On the basis of our previous calculations (Dimitrijević and Sahal-Bréchot, 1984) we have proved this statement convincingly for neutral He lines. We have investigated also the electron impact shift behaviour within a spectral series (Dimitrijević and Sahal-Bréchot, 1984) and the influence of atomic energy level structure (Dimitrijević, 1982; Dimitrijević and Sahal-Bréchot, 1984) on the Stark broadening parameter regularities. In the present paper, we extend our investigations on the basis of a new set of results for higher members of spectral series.

2. Theory

The basis for calculations is the computer code which evaluates electron and ion impact-broadening parameters of isolated spectral lines, using the semiclassical perturbation approach (Sahal-Bréchot, 1969a). The formulae which lead to the full halfwidth ($2W$) and the shift (d) are

$$2W = N \int_0^\infty v f(v) dv \left(\sum_{j \neq i} \sigma_{ij}(v) + \sum_{j' \neq f} \sigma_{fj'}(v) + \sigma_{\mathrm{el}} \right), \tag{1}$$

$$d = N \int_0^\infty v f(v) dv \int_{R_3}^{R_d} 2\pi \varrho d\varrho \sin 2\phi_p . \tag{2}$$

The inelastic cross section $\delta_{ij}(v)$ can be expressed by an integration over the impact parameter of the transition probability P_{ij} as

$$\sum_{j \neq i} \sigma_{ij}(v) = \tfrac{1}{2}\pi R_1^2 + \int_{R_1}^{R_d} 2\pi \varrho d\varrho \sum_{j \neq i} P_{ij}(\varrho, v), \tag{3}$$

the elastic cross section is given by

$$\sigma_{\mathrm{el}} = 2\pi R_2^2 + \int_{R_2}^{R_d} 8\pi \varrho d\varrho \sin^2 \delta , \tag{4}$$

$$\delta = (\phi_p^2 + \phi_q^2)^{1/2}, \qquad \phi_p = \sum_{j \neq i} \phi_{ij} - \sum_{j' \neq f} \phi_{fj'} . \tag{5}$$

Here, i and f denote, the initial and final levels and j, j' the corresponding perturbing levels, respectively. The phase shifts ϕ_p and ϕ_q, due respectively to the polarization ($\sim r^{-4}$) and to the quadrupole potential ($\sim r^{-3}$), are given by Sahal-Bréchot (1969a, Sect. 3, Chap. 2).

All the cutoffs (R_1, R_2, R_3), as well as the symmetrization procedures in the inelastic cross sections, are described by Sahal-Bréchot, 1969b, Sect. 1, Chap. 3). We recall here that we allow for Debye shielding by introducing the Debye cutoff R_d as an upper cutoff in the integration procedure.

It is not necessary to discuss uncertainties arising from all of the approximations involved in our calculations, since the criteria

Send offprint requests to: M. S. Dimitrijević, Beograd

* Permanent address: Institute of Physics, P.O. Box 57, YU-11001 Beograd, Yugoslavia

© European Southern Observatory • Provided by the NASA Astrophysics Data System

1984A&A...136..289D

Table 1. This table lists Stark-broadening parameters for He I resonance lines at an electron density of 10^{13} cm^{-3} and temperatures from 10,000 K to 200,000 K. Transitions and averaged wavelengths for the multiplet (in Å) are also given. Under $2W_e$ and $2W_p$ are given electron and proton impact full halfwidths, while d_e and d_p denote corresponding shifts. If we devide C by $2W_e$ we obtain an estimate for the maximum electron density for which the line may be treated as isolated and the tabulated values may be used. Asterisks denote cases when the frequency distance between the upper level and the nearest perturbing level is smaller than or equal to the electron plasma frequency. For these lines the behaviour of N_e deviates from linear (especially for the shift); for another electron density, the influence of Debye shielding must be taken into account (see, e.g., Ref. 8, Appendix IVa)

Transition	T	$2W_e$	d_e	$2W_p$	d_p
	(K)	(Å)			
$1s^2\,{}^1S-5p\,{}^1P^0$	10,000	0.754(−4)	− 0.246(−4)	0.299(−4)	−0.274(−4)
516.617 Å	20,000	0.688(−4)	− 0.184(−4)	0.338(−4)	−0.311(−4)
$C=6.45(+11)$	40,000	0.612(−4)	− 0.130(−4)	0.382(−4)	−0.354(−4)
	100,000	0.510(−4)	− 0.832(−5)	0.421(−4)	−0.432(−4)
	150,000	0.464(−4)	− 0.682(−5)	0.415(−4)	−0.476(−4)
	200,000	0.432(−4)	− 0.592(−5)	0.397(−4)	−0.501(−4)
$1s^2\,{}^1S-6p\,{}^1P^0$	10,000	0.174(−3)	− 0.477(−4)	0.715(−4)	−0.649(−4)
512.098 Å	20,000	0.158(−3)	− 0.325(−4)	0.813(−4)	−0.737(−4)
$C=3.72(+11)$	40,000	0.140(−3)	− 0.209(−4)	0.935(−4)	−0.841(−4)
	100,000	0.116(−3)	− 0.120(−4)	0.107(−3)	−0.103(−3)
	150,000	0.107(−3)	− 0.964(−5)	0.107(−3)	−0.114(−3)
	200,000	0.999(−4)	− 0.832(−5)	0.103(−3)	−0.121(−3)
$1s^2\,{}^1S-7p\,{}^1P^0$	10,000	0.642(−3)	0.212(−3)	0.974(−4)	−0.857(−4)
509.998 Å	20,000	0.670(−3)	0.275(−3)	0.114(−3)	−0.980(−4)
$C=2.35(+11)$	40,000	0.697(−3)	0.343(−3)	0.131(−3)	−0.115(−3)
	100,000	0.724(−3)	0.435(−3)	0.128(−3)	−0.143(−3)
	150,000	0.725(−3)	0.473(−3)	0.118(−3)	−0.138(−3)
	200,000	0.721(−3)	0.493(−3)	0.117(−3)	−0.134(−3)
$1s^2\,{}^1S-9p\,{}^1P^0$ *	10,000	2.88	0.	0.577(−1)	0.
507.718 Å	20,000	10.0	0.242(−3)	0.208	0.
$C=1.10(+11)$	40,000	18.6	2.58	0.240	0.
	100,000	26.3	12.6	2.29	0.173(−8)
	150,000	28.6	16.7	5.98	0.144(−1)
	200,000	30.2	19.5	6.44	0.370
$1s^2\,{}^1S-10p\,{}^1P^0$ *	10,000	3.03	0.	0.636(−1)	0.
507.058 Å	20,000	6.95	0.	0.259	0.
$C=8.15(+10)$	40,000	23.0	0.	0.152	0.
	100,000	88.4	0.	1.98	0.
	150,000	74.3	0.	5.07	0.
	200,000	173.	0.	3.12	0.

for their application are given in detail elsewhere (Sahal-Bréchot, 1969a). We recall however, the conditions of validity for the isolated line approximation. A line is isolated if nondegenerate energy levels broadened by collisions do not overlap. Denoting by $2W_i$ and $2W_f$ the corresponding level widths, we can express the specified conditions by

$$2W_i \leqq \omega_{ii'}, \quad 2W_f \leqq \omega_{ff'}, \tag{6}$$

where $\omega_{jj'}(j=i,f)$ is the distance to the corresponding nearest perturbing level. If $W<\omega_{jj'}$ [where W is the halfwidth of the line and $\omega_{jj'}$ is the energy distance to the nearest perturbing level, $\omega_{jj'}=\min(\omega_{ii'},\omega_{ff'})$], the line is isolated. By using Eq. (6), the validity condition for the isolated line approximation is given by

$$2W(\text{Å}) < C/10^{13},$$

where

$$C=10^5\lambda^2(\text{Å})\,[(E_j-E_{j'})\,(\text{cm}^{-1})] \tag{7}$$

if we want to ensure that the line is isolated. If halfwidths are available for the electron concentration $N=10^{13}$ cm^{-3}, then one has for the limiting concentration

$$N_l(\text{cm}^{-3})=\frac{C}{2W}(\text{in Å at } N=10^{13}\,\text{cm}^{-3}). \tag{8}$$

© European Southern Observatory • Provided by the NASA Astrophysics Data System

1984A&A...136..289D

For an electron concentration lower than N_l, the core of a line can be treated as isolated, even if weak forbidden components due to the failure of this approximation still appear in the wings.

Estimates of the validity conditions (Sahal-Bréchot, 1969a) show that the impact approximation may be applied for protons in stellar atmospheres $N \lesssim 10^{15}\,\mathrm{cm}^{-3}$). In the cases when protons are not the dominant ion perturbers or when the impact approximation is not valid, the ion broadening contribution may be estimated by using the quasistatic ion-broadening parameter introduced by Griem et al. (1962).

3. Results and discussion of regularities

Data for needed energy levels are taken from Martin (1973). The calculated values are divided into three parts. Our results for electron (W_e) and proton (W_p) impact full halfwidths and shifts (d_e and d_p, respectively) for He I resonance lines (which lie in the far ultraviolet) are shown in Table 1 for $N_e = 10^{13}\,\mathrm{cm}^{-3}$ and $T = 10{,}000$, 20,000, 40,000, 100,000, 150,000, and 200,000 K. According to the impact approximation and the isolated-line approximation the impact widths and shifts show linear behaviour in N_e if Debye shielding effects are negligible. An interpolation is necessary to obtain values for temperatures not listed in the table.

The results for lines between 2500 and 7000 Å are shown in Table 2 for a number of temperatures, while the results for lines with $\lambda > 7000$ Å are presented in Table 3 for $T = 2500$, 5000, 10,000, 20,000, 40,000, and 80,000 K. In Tables 1–3, we also give the parameter C (see Eq. (7), which can be used to estimate if a line is isolated for the needed electron density).

It was shown earlier (Wiese and Konjević, 1982; Dimitrijević and Sahal-Bréchot, 1984) that, for lines belonging to a spectral series, electron impact width increases gradually with increasing principal quantum number of the upper state, and that electron impact shift changes gradually (Dimitrijević and Sahal-Bréchot, 1984). We extend here this investigation using the present results for higher members of a series. It is also interesting to examine the behaviour of proton impact broadening parameters within a spectral series.

By inspecting energy separations between the upper level and the principal perturbing levels for $2s^1S - np^1P^0$ and $2p^1P^0 - nd^1D$ series (Figs. 1 and 2), we find that this separation decreases gradually. Thus, we expect a gradual change of the Stark broadening parameters.

The electron and proton impact full halfwidth (in angular frequency units) for the $2s^1S - np^1P^0$ series as a function of the principal quantum number of the upper level (n_i) are shown in Figs. 3 and 4. In both cases we can see a gradual increase of the line widths with the increases of the n_i. We can notice also that the influence of the temperature is remarkably greater for $n_i = 9$ and 10 electron and proton impact line widths than for $n_i < 9$ case. This effect can be explained by the influence of the Debye shielding. For

Table 2. Same as in Table 1 but for the He I lines in the range $2500 < \lambda\,(\text{Å}) < 7000$ and for temperatures from 5000 to 80,000 K

Transition	T	$2W_e$	d_e	$2W_p$	d_p
	(K)	(Å)			
$2s^1S - 5p^1P^0$	5,000	0.398(−2)	− 0.160(−2)	0.130(−2)	− 0.118(−2)
3613.64 Å	10,000	0.369(−2)	− 0.117(−2)	0.146(−2)	− 0.134(−2)
$C = 3.16(+13)$	20,000	0.337(−2)	− 0.893(−3)	0.166(−2)	− 0.152(−2)
	30,000	0.316(−2)	− 0.734(−3)	0.178(−2)	− 0.164(−2)
	40,000	0.301(−2)	− 0.638(−3)	0.187(−2)	− 0.173(−2)
	80,000	0.263(−2)	− 0.458(−3)	0.204(−2)	− 0.201(−2)
$2s^1S - 6p^1P^0$	5,000	0.843(−2)	− 0.305(−2)	0.287(−2)	− 0.258(−2)
3447.59 Å	10,000	0.790(−2)	− 0.216(−2)	0.324(−2)	− 0.294(−2)
$C = 1.69(+13)$	20,000	0.717(−2)	− 0.147(−2)	0.368(−2)	− 0.334(−2)
	30,000	0.668(−2)	− 0.113(−2)	0.400(−2)	− 0.360(−2)
	40,000	0.634(−2)	− 0.942(−3)	0.424(−2)	− 0.381(−2)
	80,000	0.553(−2)	− 0.616(−3)	0.475(−2)	− 0.444(−2)
$2s^1S - 7p^1P^0$	5,000	0.391(−1)	0.190(−1)	0.354(−2)	0.319(−2)
3354.55 Å	10,000	0.423(−1)	0.230(−1)	0.385(−2)	0.366(−2)
$C = 1.01(+13)$	20,000	0.458(−1)	0.273(−1)	0.404(−2)	0.411(−2)
	30,000	0.483(−1)	0.301(−1)	0.417(−2)	0.431(−2)
	40,000	0.502(−1)	0.323(−1)	0.431(−2)	0.443(−2)
	80,000	0.553(−1)	0.379(−1)	0.495(−2)	0.472(−2)
$2s^1S - 8p^1P^0$	5,000	2.57	1.84	0.659	0.178
3296.77 Å	10,000	2.88	2.29	0.819	0.413
$C = 6.49(+12)$	20,000	3.24	2.73	0.935	0.620
	30,000	3.47	2.99	1.00	0.732
	40,000	3.64	3.18	1.05	0.808
	80,000	4.12	3.65	1.18	0.985

© European Southern Observatory • Provided by the NASA Astrophysics Data System

1984A&A...136..289D

Table 2 (continued)

Transition	T	$2W_e$	d_e	$2W_p$	d_p
	(K)	(Å)			
$2s^1S-9p^1P^0$ *	5,000	30.0	0.	0.507	0.
3258.28 Å	10,000	135.	2.46	3.40	0.
$C=4.53(+12)$	20,000	195.	54.0	7.65	0.
	30,000	224.	93.8	8.02	0.
	40,000	240.	120.	26.5	0.726(−5)
	80,000	273.	179.	58.8	5.78
$2s^1S-10p^1P^0$*	5,000	56.9	0.	0.825	0.
3231.27 Å	10,000	176.	0	2.04	0.
$C=3.31(+12)$	20,000	268.	0.	8.01	0.
	30,000	677.	0.	8.26	0.
	40,000	0.100(+4)	0.	23.9	0.
	80,000	0.169(+4)	0.	51.8	0.
$2p^1P^0-4d^1D$	5,000	0.392(−2)	0.110(−2)	0.255(−2)	0.226(−2)
4921.93 Å	10,000	0.339(−2)	0.789(−3)	0.287(−2)	0.263(−2)
$C=1.32(+13)$	20,000	0.287(−2)	0.575(−3)	0.298(−2)	0.306(−2)
	30,000	0.258(−2)	0.471(−3)	0.287(−2)	0.329(−2)
	40,000	0.239(−2)	0.409(−3)	0.273(−2)	0.341(−2)
	80,000	0.198(−2)	0.291(−3)	0.217(−2)	0.352(−2)
$2p^1P^0-5d^1D$	5,000	0.999(−2)	0.248(−2)	0.630(−2)	0.546(−2)
4387.93 Å	10,000	0.861(−2)	0.184(−2)	0.716(−2)	0.639(−2)
$C=5.39(+12)$	20,000	0.725(−2)	0.135(−2)	0.763(−2)	0.751(−2)
	30,000	0.651(−2)	0.111(−2)	0.752(−2)	0.814(−2)
	40,000	0.601(−2)	0.963(−3)	0.725(−2)	0.851(−2)
	80,000	0.492(−2)	0.684(−3)	0.608(−2)	0.899(−2)
$2p^1P^0-6d^1D$	5,000	0.221(−1)	0.451(−2)	0.167(−1)	0.139(−1)
4143.76 Å	10,000	0.189(−1)	0.339(−2)	0.185(−1)	0.167(−1)
$C=2.82(+12)$	20,000	0.158(−1)	0.256(−2)	0.187(−1)	0.196(−1)
	30,000	0.141(−1)	0.213(−2)	0.176(−1)	0.210(−1)
	40,000	0.130(−1)	0.187(−2)	0.165(−1)	0.216(−1)
	80,000	0.106(−1)	0.136(−2)	0.130(−1)	0.218(−1)
$2p^1P^0-7d^1D$ *	5,000	0.734(−1)	0.378(−1)	0.317(−1)	0.255(−1)
4009.27 Å	10,000	0.723(−1)	0.404(−1)	0.360(−1)	0.307(−1)
$C=1.69(+12)$	20,000	0.723(−1)	0.439(−1)	0.388(−1)	0.365(−1)
	30,000	0.732(−1)	0.464(−1)	0.390(−1)	0.398(−1)
	40,000	0.744(−1)	0.485(−1)	0.385(−1)	0.418(−1)
	80,000	0.785(−1)	0.544(−1)	0.358(−1)	0.450(−1)
$2p^1P^0-8d^1D$ *	5,000	0.674	0.477	0.240	0.151
3926.53 Å	10,000	0.725	0.547	0.254	0.204
$C=9.71(+11)$	20,000	0.784	0.620	0.261	0.245
	30,000	0.826	0.666	0.266	0.263
	40,000	0.861	0.699	0.270	0.274
	80,000	0.971	0.788	0.287	0.299
$2p^1P^0-9d^1D$ *	5,000	80.2	0.122(−1)	0.692	0.
3871.79 Å	10,000	131.	20.7	6.05	0.
$C=7.80(+11)$	20,000	171.	72.4	5.97	0.
	30,000	188.	101.	27.4	0.174(−2)
	40,000	198.	121.	41.7	0.525
	80,000	224.	163.	58.9	15.6

© European Southern Observatory • Provided by the NASA Astrophysics Data System

1984A&A...136..289D

Table 2 (continued)

Transition	T (K)	$2W_e$ (Å)	d_e	$2W_p$	d_p
$2p^3P^0-10s^3S$ *	5,000	65.4	0.320	0.925	0.
3562.95 Å	10,000	91.6	21.8	2.25	0.
$C=6.74(+13)$	20,000	116.	55.0	10.1	0.105(−7)
	30,000	127.	72.8	25.9	0.703(−1)
	40,000	134.	84.6	28.0	1.73
	80,000	155.	111.	40.2	13.7
$2p^3P^0-4d^3D$	5,000	0.245(−2)	0.860(−4)	0.152(−2)	0.134(−2)
4471.5 Å	10,000	0.216(−2)	0.576(−4)	0.173(−2)	0.156(−2)
$C=1.48(+13)$	20,000	0.186(−2)	0.162(−4)	0.184(−2)	0.184(−2)
	30,000	0.171(−2)	0.158(−4)	0.175(−2)	0.201(−2)
	40,000	0.160(−2)	0.131(−4)	0.164(−2)	0.229(−2)
	80,000	0.137(−2)	0.818(−5)	0.117(−2)	0.212(−2)
$2p^3P^0-5d^3D$	5,000	0.667(−2)	0.350(−3)	0.404(−2)	0.351(−2)
4026.2 Å	10,000	0.585(−2)	0.233(−3)	0.462(−2)	0.409(−2)
$C=6.38(+12)$	20,000	0.501(−2)	0.169(−3)	0.499(−2)	0.483(−2)
	30,000	0.455(−2)	0.137(−3)	0.486(−2)	0.534(−2)
	40,000	0.424(−2)	0.119(−3)	0.459(−2)	0.555(−2)
	80,000	0.356(−2)	0.844(−4)	0.337(−2)	0.572(−2)
$2p^3P^0-6d^3D$	5,000	0.147(−1)	0.661(−3)	0.932(−2)	0.787(−2)
3819.6 Å	10,000	0.128(−1)	0.386(−3)	0.106(−1)	0.931(−2)
$C=3.38(+12)$	20,000	0.109(−1)	0.290(−3)	0.117(−1)	0.113(−1)
	30,000	0.988(−2)	0.274(−3)	0.109(−1)	0.122(−1)
	40,000	0.918(−2)	0.240(−3)	0.108(−1)	0.133(−1)
	80,000	0.764(−2)	0.175(−3)	0.823(−2)	0.133(−1)
$2p^3P^0-7d^3D$ *	5,000	0.338(−1)	0.668(−2)	0.226(−1)	0.182(−1)
3705.0 Å	10,000	0.314(−1)	0.720(−2)	0.254(−1)	0.221(−1)
$C=2.12(+12)$	20,000	0.290(−1)	0.813(−2)	0.259(−1)	0.265(−1)
	30,000	0.277(−1)	0.879(−2)	0.241(−1)	0.287(−1)
	40,000	0.267(−1)	0.933(−2)	0.220(−1)	0.298(−1)
	80,000	0.245(−1)	0.106(−1)	0.152(−1)	0.297(−1)
$2p^3P^0-8d^3D$ *	5,000	0.580	0.459	0.166	0.106
3634.2 Å	10,000	0.642	0.533	0.187	0.141
$C=1.31(+12)$	20,000	0.717	0.611	0.211	0.173
	30,000	0.770	0.660	0.226	0.192
	40,000	0.813	0.696	0.237	0.206
	80,000	0.944	0.789	0.265	0.239
$2p^3P^0-9d^3D$ *	5,000	4.14	2.45	0.947	0.186
3587.3 Å	10,000	4.54	3.03	1.21	0.547
$C=9.78(+11)$	20,000	4.99	3.60	1.40	0.877
	30,000	5.28	3.93	1.50	1.05
	40,000	5.50	4.17	1.58	1.17
	80,000	6.13	4.78	1.78	1.45
$2p^3P^0-10d^3D$ *	5,000	51.6	0.	1.37	0.
3554.4 Å	10,000	160.	0.195(−4)	2.42	0.
$C=6.99(+11)$	20,000	368.	29.6	4.71	0.
	30,000	467.	115.	8.07	0.
	40,000	520.	184.	29.4	0.
	80,000	614.	341.	118.	0.641(−1)

© European Southern Observatory • Provided by the NASA Astrophysics Data System

1984A&A...136..289D

Table 3. The same as in Table 1 but for infrared HeI lines with $\lambda > 7000$ Å and for temperatures from 2500 to 80,000 K

Transition	T	$2W_e$	d_e	$2W_p$	d_p
	(K)	(Å)			
$3s^1S-5p^1P^0$	2,500	0.393(−1)	−0.192(−1)	0.108(−1)	−0.962(−2)
11,013.1 Å	5,000	0.377(−1)	−0.159(−1)	0.121(−1)	−0.110(−1)
$C=2.93(+14)$	10,000	0.351(−1)	−0.120(−1)	0.136(−1)	−0.125(−1)
	20,000	0.323(−1)	−0.922(−2)	0.154(−1)	−0.142(−1)
	40,000	0.290(−1)	−0.663(−2)	0.174(−1)	−0.161(−1)
	80,000	0.256(−1)	−0.473(−1)	0.190(−1)	−0.187(−1)
$3s^1S-6p^1P^0$	2,500	0.692(−1)	−0.316(−1)	0.199(−1)	−0.173(−1)
9603.42 Å	5,000	0.657(−1)	−0.240(−1)	0.223(−1)	−0.200(−1)
$C=1.31(+14)$	10,000	0.616(−1)	−0.171(−1)	0.252(−1)	−0.228(−1)
	20,000	0.562(−1)	−0.119(−1)	0.286(−1)	−0.259(−1)
	40,000	0.498(−1)	−0.783(−2)	0.329(−1)	−0.296(−1)
	80,000	0.437(−1)	−0.524(−2)	0.369(−1)	−0.345(−1)
$3p^1P^0-4d^1D$	2,500	0.953	2.90	1.63	1.04
19,089.4 Å	5,000	0.570	2.33	1.84	1.38
$C=1.98(+14)$	10,000	0.258	1.82	2.07	1.70
	20,000	0.908(−1)	1.31	2.34	2.01
	40,000	0.499(−1)	0.930	2.66	2.33
	80,000	0.371(−1)	0.658	3.06	2.69
$3p^1P^0-5d^1D$	2,500	0.984(−1)	0.413(−3)	0.161(−2)	0.137(−3)
12,968.4 Å	5,000	0.893(−1)	0.422(−3)	0.161(−2)	0.151(−3)
$C=4.71(+13)$	10,000	0.782(−1)	0.405(−3)	0.158(−2)	0.158(−3)
	20,000	0.665(−1)	0.345(−3)	0.150(−2)	0.154(−3)
	40,000	0.555(−1)	0.266(−3)	0.133(−2)	0.140(−3)
	80,000	0.457(−1)	0.193(−3)	0.114(−2)	0.119(−3)
$3p^1P^0-6d^1D$	2,500	0.176	0.145(−3)	0.266(−2)	0.552(−4)
11,045.0 Å	5,000	0.157	0.137(−3)	0.266(−2)	0.590(−4)
$C=2.00(+13)$	10,000	0.136	0.124(−3)	0.266(−2)	0.592(−4)
	20,000	0.114	0.102(−3)	0.260(−2)	0.553(−4)
	40,000	0.942(−1)	0.778(−4)	0.243(−2)	0.483(−4)
	80,000	0.770(−1)	0.562(−4)	0.214(−2)	0.396(−4)
$3d^1D-4p^1P^0$	2,500	0.120	0.349(−3)	0.172(−2)	0.138(−3)
18,555.6 Å	5,000	0.990(−1)	0.317(−3)	0.170(−2)	0.147(−3)
$C=1.59(+15)$	10,000	0.808(−1)	0.276(−3)	0.164(−2)	0.146(−3)
	20,000	0.657(−1)	0.227(−3)	0.149(−2)	0.136(−3)
	40,000	0.534(−1)	0.176(−3)	0.129(−2)	0.117(−3)
	80,000	0.434(−1)	0.129(−3)	0.109(−2)	0.957(−4)
$3d^1D-5p^1P^0$	2,500	0.470(−1)	0.636(−4)	0.217(−2)	0.293(−4)
12,755.7 Å	5,000	0.479(−1)	0.543(−4)	0.217(−2)	0.295(−4)
$C=3.93(+14)$	10,000	0.463(−1)	0.445(−4)	0.216(−2)	0.277(−4)
	20,000	0.429(−1)	0.351(−4)	0.207(−2)	0.243(−4)
	40,000	0.386(−1)	0.264(−4)	0.188(−2)	0.200(−4)
	80,000	0.338(−1)	0.192(−4)	0.162(−2)	0.157(−4)
$3d^1D-4f^1F^0$ *	2,500	0.354(−1)	−0.489(−2)	0.225(−1)	−0.198(−1)
18,696.9 Å	5,000	0.298(−1)	−0.275(−2)	0.259(−1)	−0.229(−1)
$C=1.87(+14)$	10,000	0.246(−1)	−0.174(−2)	0.286(−1)	−0.279(−1)
	20,000	0.203(−1)	−0.957(−3)	0.281(−1)	−0.314(−1)
	40,000	0.173(−1)	−0.617(−3)	0.225(−1)	−0.341(−1)
	80,000	0.149(−1)	−0.402(−3)	0.144(−1)	−0.328(−1)

© European Southern Observatory • Provided by the NASA Astrophysics Data System

1984A&A...136..289D

Table 3 (continued)

Transition	T (K)	$2W_e$ (Å)	d_e	$2W_p$	d_p
$3d^1D-5f^1F^0$ *	2,500	0.104	−0.424(−2)	0.517(−1)	0.529(−1)
12,790.3 Å	5,000	0.870(−1)	−0.230(−2)	0.466(−1)	0.492(−1)
$C=8.83(+12)$	10,000	0.711(−1)	−0.102(−2)	0.367(−1)	0.392(−1)
	20,000	0.574(−1)	−0.276(−3)	0.357(−1)	0.199(−1)
	40,000	0.461(−1)	−0.482(−4)	0.269(−1)	0.658(−2)
	80,000	0.371(−1)	−0.425(−5)	0.156(−1)	−0.453(−2)
$3d^3D-4f^3F^0$ *	2,500	0.331(−1)	−0.506(−2)	0.188(−1)	−0.168(−1)
18,686.0 Å	5,000	0.282(−1)	−0.287(−2)	0.217(−1)	−0.192(−1)
$C=2.58(+14)$	10,000	0.235(−1)	−0.182(−2)	0.245(−1)	−0.224(−1)
	20,000	0.195(−1)	−0.102(−2)	0.254(−1)	−0.264(−1)
	40,000	0.167(−1)	−0.661(−3)	0.220(−1)	−0.297(−1)
	80,000	0.145(−1)	−0.432(−3)	0.150(−1)	−0.300(−1)
$3d^3D-5f^3F^0$ *	2,500	0.156(−1)	0.681(−3)	0.371(−3)	0.217(−3)
12,785.0 Å	5,000	0.233(−1)	0.709(−3)	0.372(−3)	0.243(−3)
$C=8.99(+12)$	10,000	0.111(−1)	0.708(−3)	0.359(−3)	0.262(−3)
	20,000	0.925(−2)	0.645(−3)	0.336(−3)	0.266(−3)
	40,000	0.784(−2)	0.520(−3)	0.319(−3)	0.251(−3)
	80,000	0.679(−2)	0.388(−3)	0.316(−3)	0.222(−3)

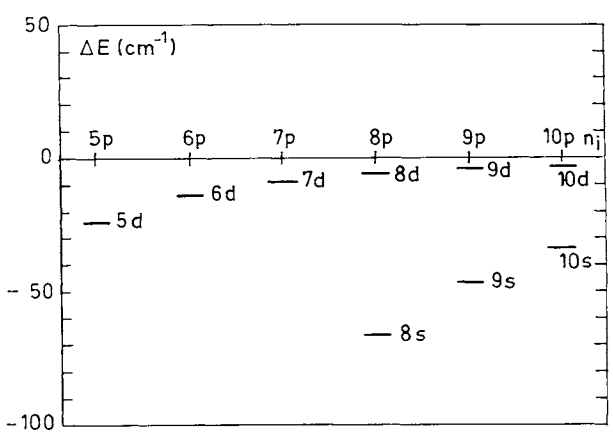

Fig. 1. Energy separations between the upper level and the principal perturbing levels for He I $2s^1S-np^1P^0$ lines

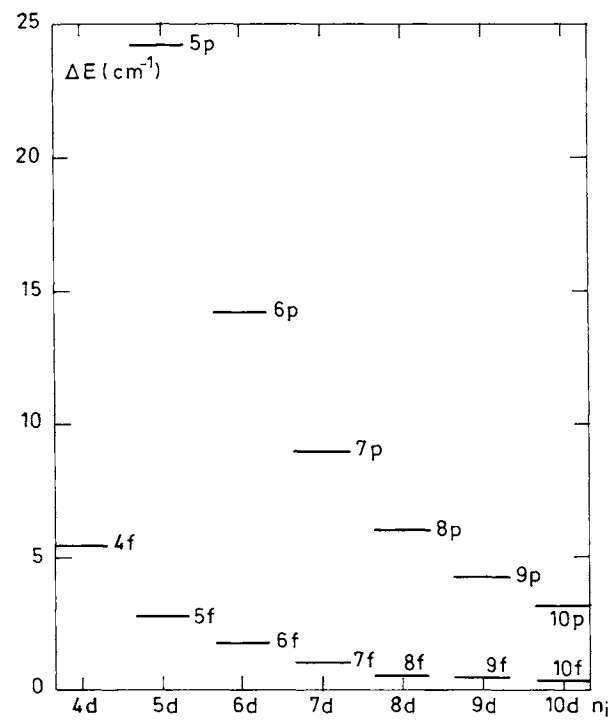

Fig. 2. Energy separations between the upper level and the principal perturbing levels for He I $2p^1P^0-nd^1D$ lines

$n_i=9$ and 10, R_D is smaller than R_1 for $T=5000$ K for the electron as well as for the proton case. In this case δ_{el} [see Eq. (4)] becomes equal to $\pi R_D^2/2$, i.e. proportional to T. As can be seen in Figs. 3 and 4, this temperature dependence is more pronounced for proton impact broadening, because the influence of elastic collisions is dominant in this case. This is an indication of the failure of the impact semi-classical approximation: collective effects and close interactions become predominant. A quantum non impact theory is then needed but further approximations may be done (cf. Peach, 1981).

Electron and proton impact shifts (in angular frequency units) for the $2s^1S-np^1P^0$ series are presented in Table 4. For $n_i=5$ and 6 shifts are negative (towards the blue) because the polarizability of the lower state ($2s^1S$) is larger than the polarizability of the upper state. This is partially due to the fact that the energy difference between the upper state and the most important perturbing states (see Fig. 1) is negative. But since the influence of the upper level increases with n_i, the shift becomes positive for $n_i>6$. When R_D is smaller than R_3 [see Eq. (2)] the shift is zero.

© European Southern Observatory • Provided by the NASA Astrophysics Data System

1984A&A...136..289D

Table 4. The electron- and proton-impact shifts for He I $2s^1S-np^1P^0$ lines as a function of n_i for $T=5000$ K and $T=80{,}000$ K at $N_e=10^{13}\,\mathrm{cm}^{-3}$

Transition	Electrons		Protons	
	$d(\mathrm{s}^{-1})$ at 5,000 K	$d(\mathrm{s}^{-1})$ at 80,000 K	$d(\mathrm{s}^{-1})$ at 5,000 K	$d(\mathrm{s}^{-1})$ at 80,000 K
$2s^1S-5p^1P^0$	−2.31(+9)	−6.59(+8)	−1.70(+9)	−2.90(+9)
$-6p^1P^0$	−4.83(+9)	−9.77(+8)	−4.09(+9)	−7.03(+9)
$-7p^1P^0$	+3.18(+10)	+6.34(+10)	+5.34(+9)	+7.90(+9)
$-8p^1P^0$	+3.19(+12)	+6.32(+12)	+3.08(+11)	+1.71(+12)
$-9p^1P^0$	0	+3.17(+14)	0	+1.03(+13)
$-10p^1P^0$	0	0	0	0

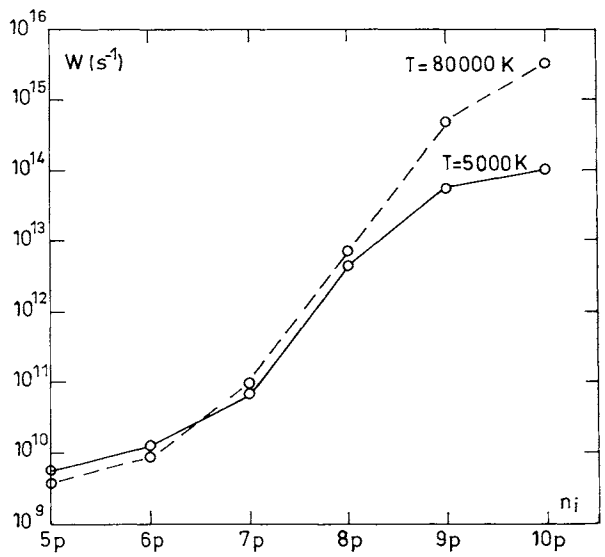

Fig. 3. The electron-impact halfwidth for He I $2s^1S-np^1P^0$ lines as a function of n_i for $T=5000$ and 80,000 K at $N_e=10^{13}\,\mathrm{cm}^{-3}$

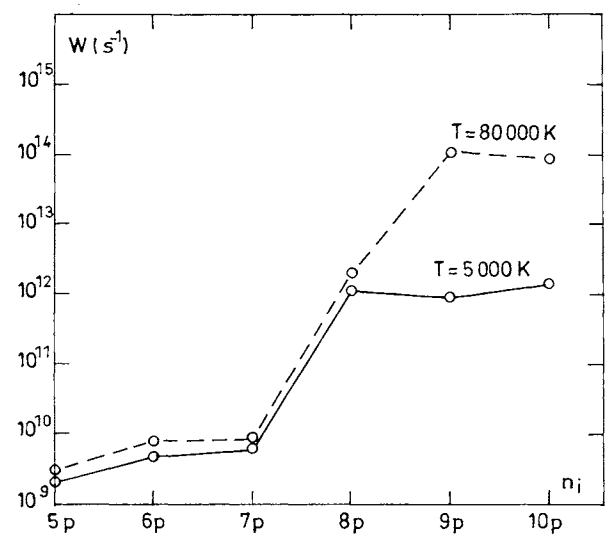

Fig. 4. The same title as in Fig. 3 applies but for the proton-impact halfwidth

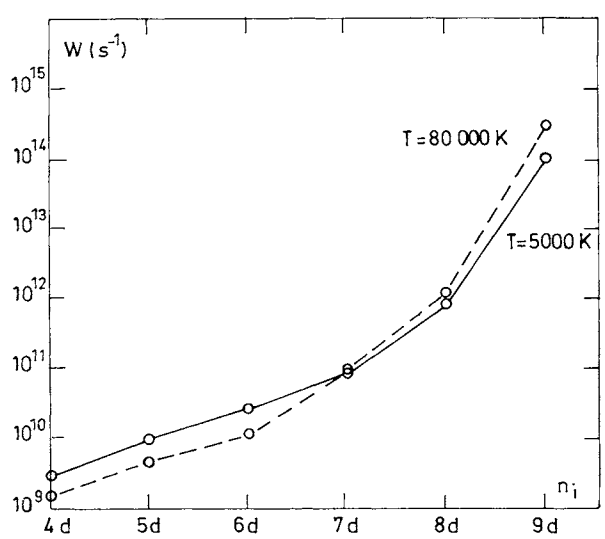

Fig. 5. The electron-impact halfwidth for He I $2p^1P^0-nd^1D$ lines as a function of n_i for $T=5000$ and 80,000 K at $N_e=10^{13}\,\mathrm{cm}^{-3}$

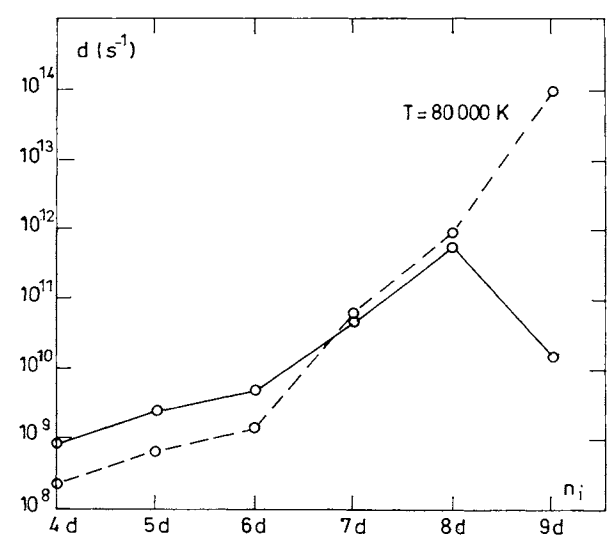

Fig. 6. The same title as in Fig. 5 applies but for the electron-impact shift

© European Southern Observatory • Provided by the NASA Astrophysics Data System

1984A&A...136..289D

Electron and proton impact widths and shifts for $2p\,^1P^0 - nd\,^1D$ lines are presented in Figs. 5–8. The gradual increase of the line widths and shifts appears clearly as well as the influence of the Debye shielding effect for $n_i=9$, $T=5000$ K. Now, we can ask ourselves why the Debye shielding effect is less pronounced in the $2p\,^1P^0-nd\,^1D$ than in the $2s\,^1S-np\,^1P^0$ case, in spite of the fact that nf levels are closer to $nd\,^1D^0$ levels, than nd to $np\,^1P^0$. By comparing the oscillator strengths for $d-f$ and $d-p$ transitions [e.g. $f\,(4p-4d)=0.0240$ and $f\,(4d-4f)=0.00253$ (Wiese et al., 1966)] we can see that the principal perturbing levels for $2p\,^1P^0 - nd\,^1D$ lines are $np\,^1P^0$ and not $nf\,^1F^0$ energy levels. Therefore the influence of $nf\,^1F^0$ levels on R_1, R_2 and R_3 [see Eqs. (1)–(4)] is not crucial and the influence of Debye shielding on the Stark broadening parameters (which depends on R_D-R_1, R_D-R_2 and R_D-R_3) is not so important as expected.

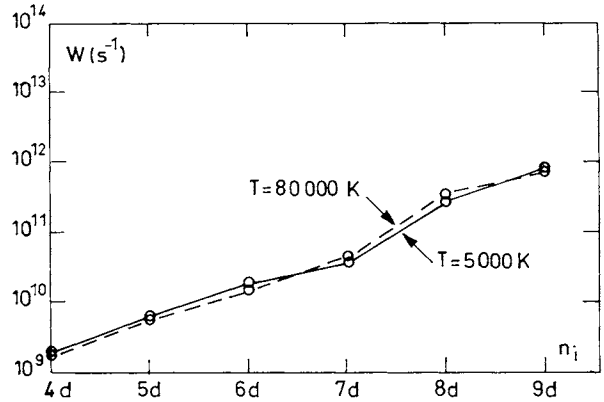

Fig. 7. The same title as in Fig. 5 applies but for the proton-impact halfwidth

4. Influence of Debye shielding

In order to investigate the influence of Debye shielding on the electron impact width and shift, we have calculated line widths and shifts for several lines as a function of electron density. The results are presented in Fig. 9 for $T=40{,}000$ K. We can see that the $1s^2\,^1S - 8p\,^1P^0$ line width depends linearly on electron density up to $N_e=10^{15}\,\mathrm{cm}^{-3}$. Then, due to the influence of Debye shielding, the dependence deviates from the linear one. For the following line in the series ($1s^2\,^1S-9p\,^1P^0$), the dependence on the electron density is linear only up to $N_e=10^{12}\,\mathrm{cm}^{-3}$, because the corresponding perturbing energy levels are closer to the upper energy level of the transition. We can see also that after $N_e=10^{10}\,\mathrm{cm}^{-3}$ the curve rises faster. This is the numerical consequence of the fact that we have two cutoffs in Eq. (1) [see also Eqs. (3) and (4)] for the halfwidths. The important quantities for an estimate of the influence of the Debye shielding, are the differences between R_D and R_1, R_2, and R_3. If these differences are small, the influence of Debye shielding is large. But in this case the exact values of cutoffs play a crucial rôle for the accuracy of the results obtained, and in different impact cutoff theories (e.g. Griem et al., 1962; Sahal-Bréchot, 1969a, b) cutoffs are determined in different manners. Thus we can have confidence in the results only if Debye shielding effects are small. The results obtained shot also that the sophistication of a theory with simple cutoffs, with introducing e.g. Debye-Hückel potential, is unnecessary, because if Debye shielding effects are important, lower cutoffs are the source of inaccuracy and, then it is better to use a convergent theory (e.g. Bassalo et al., 1982).

In Fig. 9, the shift for $1s^2\,^1S-8p\,^1P^0$ line is presented with a dotted line. We can see that the shift becomes zero when R_D is smaller than R_3.

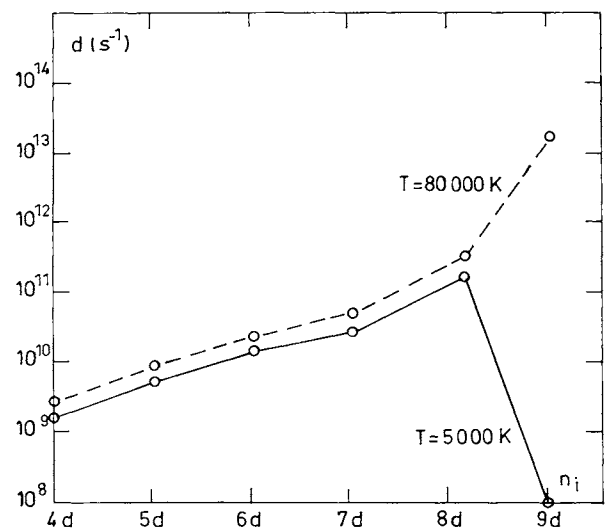

Fig. 8. The same title as in Fig. 5 applies but for the proton-impact shift

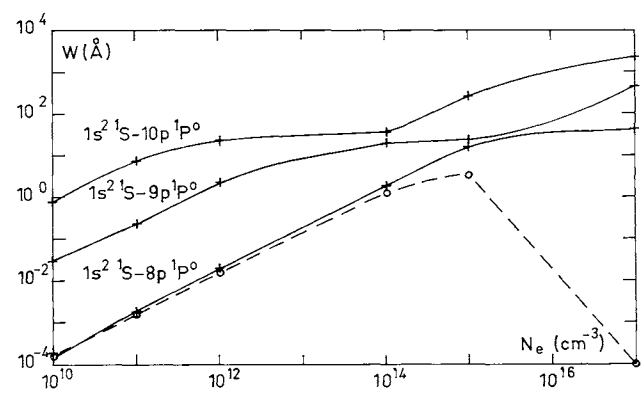

Fig. 9. Full halfwidth (——) and shift (- - -) for different series of He I spectral lines as a function of the electron density. $T=40{,}000$ K

5. Conclusion

Following up our earlier work (Dimitrijević and Sahal-Bréchot, 1983), we have calculated electron and proton impact line widths and shifts of 36 neutral He lines originating from upper energy levels with $4\leqq n\leqq 10$, for an electron density of $10^3\,\mathrm{cm}^{-3}$, typical for stellar atmospheres.

The results obtained have been used for the investigation of the behaviour of Stark broadening parameters within spectral series. Our results confirm the previous conclusions (Wiese and Konjević, 1982; Dimitrijević and Sahal-Bréchot, 1984) that for lines belonging to a spectral series, the electron impact width increases gradually with increasing principal quantum number of the upper state. We find that this conclusion applies also to proton-impact widths (the attractive Coulomb potential). For the shifts we find that the upper level contribution increases gradually within a spectral series if $R_D>R_3$. In the case $R_D<R_3$, the shift is zero. If the shift is negative (blue) for lower members of a series due to larger polarization of the lower level of the transitions, for higher

© European Southern Observatory • Provided by the NASA Astrophysics Data System

1984A&A...136..289D

members of the series it becomes positive (red) owing to the gradual increase of the upper level contribution.

If the influence of Debye shielding is large, impact theories with simple cutoffs become unreliable and it is better to use a convergent approach.

References

Bassalo, J.M., Cattani, M., Walder, V.S.: 1982, *J. Quant. Spectrosc. Radiative Transfer* **28**, 75

Benett, S.M., Griem, H.R.: 1971, Univ. Maryland, Technical Report No. 71-097, College Park, Maryland

Dimitrijević, M.S.: 1982, *Astron. Astrophys.* **112**, 251

Dimitrijević, M.S., Sahal-Bréchot, S.: 1984, *J. Quant. Spectrosc. Radiative Transfer* (in press)

Griem, H.R., Baranger, M., Kolb, A.C., Oertel, G.: 1962, *Phys. Rev.* **125**, 177

Martin, W.C.: 1973, *J. Phys. Chem. Ref. Data* **2**, 257

Peach, G.: 1981, *Adv. Phys.* **30**, 367

Sahal-Bréchot, S.: 1969a, *Astron. Astrophys.* **1**, 91

Sahal-Bréchot, S.: 1969b, *Astron. Astrophys.* **2**, 322

Wiese, W.L., Konjević, N.: 1982, *J. Quant. Spectrosc. Radiative Transfer* **28**, 185

Wiese, W.L., Smith, M.W., Glennon, B.M.: 1966, Atomic Transitions Probabilities, Vol. I, US Govt. Printing Office, Washington, D.C.

© European Southern Observatory • Provided by the NASA Astrophysics Data System

1985A&A...145..439D

Astron. Astrophys. 145, 439–442 (1985)

ASTRONOMY AND ASTROPHYSICS

Dependence of Stark widths and shifts on the ionization potential: $np^{k-1}(n+1)s-np^k$ resonance transitions

M. S. Dimitrijević[1,2]

[1] Astronomical Observatory, Volgina 7, YU-11050 Beograd, Yugoslavia
[2] Institute of Physics, P.O. Box 57, YU-11001 Beograd, Yugoslavia

Received July 26, accepted December 3, 1984

Summary. Simple relations between the Stark broadening parameters and the ionization potential are derived for $np^{k-1}(n+1)s-np^k$ resonance transitions of singly ionized emitters, using the semiclassical approach. The relations obtained are compared with those derived by Purić et al. (1980).

Key words: Stark broadening – line profiles

1. Introduction

A method for a simple estimate of Stark broadening parameters may be useful for a number of astrophysical (e.g. the radiative transfer through stellar plasma, evaluations of physical conditions in stellar atmospheres) and physical problems. Recently, such a method was proposed by Purić et al. (1980) (see also Lakićević and Purić, 1983 and references therein). They have found that the Stark width ω and the shift δ (in units of angular frequency) of spectral lines emitted by a non-hydrogenic atom (or ion) depend on the "effective ionization energy" $I(eV)=I_0-E_f$ (I_0 and E_f denote the ionization potential and the energy of the lower level, respectively, both counted from the ground level) in the general form of a power series:

$$\omega=\sum_n A'_n I^{-n} \quad \text{and} \quad \delta=\sum_n B'_n I^{-n}. \tag{1a, b}$$

After calculating coefficients in Eqs. (1) and averaging them over a number of elements, Purić et al. (1980) found that for particular plasma conditions $N_e=10^{17}\,\mathrm{cm}^{-3}$ and $T=20{,}000$ K, for the resonance lines of singly charged ions, half halfwidth w and shift d in wavelengths units can be expressed as

$$w\approx 2050\ I^{-4}(\text{Å}) \text{ and } d\approx 2050\ I^{-4}(\text{Å}), \tag{2a, b}$$

where I has to be taken in eV. Purić et al. (1980) confirmed Eqs. (2) empirically using all available experimental (in temperature range 9500–34,000 K) and theoretical data at 20,000 K. One of their conclusions was that "the Stark widths and shifts of singly charged ion resonances do not depend on the number of equivalent electrons". The trends obtained were used by Lakićević (1983) in calculating the Stark widths and shifts of neutral atom and singly charged ion resonance spectral lines. Recently, Dimitrijević and Konjević (1984) have demonstrated that Eqs. (1) can be expressed as

$$\omega=\sum_n A_n I_0^{-n} \quad \text{and} \quad \delta=\sum_n B_n I_0^{-n}. \tag{3a, b}$$

They draw attention also on the implicit dependence of the wavelength λ on the ionization potential I_0 and I, not taken into account by Purić et al. (1980).

Here, we want to study the relation between the Stark broadening parameters and the ionization potential for $np^{k-1}(n+1)s-np^k$ resonance transitions of singly ionized emitters and to check the conclusion by Purić et al. (1980) that the Stark widths and shifts of singly charged ion resonances do not depend on the number of equivalent electrons.

2. Theoretical formulae

According to the semi-empirical approach (Griem, 1968), the Stark line width in angular frequency units is given by

$$\omega=8\left(\frac{\pi}{3}\right)^{3/2}\frac{\hbar a_0}{m}N_e\left(\frac{E_H}{kT}\right)^{1/2}\sum_{i',f'}\left[\left|\left\langle i'\left|\frac{\boldsymbol{r}}{a_0}\right|i\right\rangle\right|^2 \cdot\bar{g}\left(\frac{\bar{E}}{|\Delta E_{i'i}|}\right)+\left|\left\langle f'\left|\frac{\boldsymbol{r}}{a_0}\right|f\right\rangle\right|^2\bar{g}\left(\frac{\bar{E}}{|\Delta E_{f'f}|}\right)\right], \tag{4}$$

where $\bar{g}$ is the effective Gaunt factor (Seaton, 1962; Van Regemorter, 1962). For $np^{k-1}(n+1)s-np^k$ transitions Eq. (4) is not applicable in this form due to the existence of equivalent electrons. If we take into account the influence of equivalent electrons and single out from the sum of matrix elements for the initial level (i), the matrix element corresponding to the $np^{k-1}(L_cS_c)\ (n+1)\ s(L'S)-np^k(LS)$ transition, Eq. (4) becomes

$$\omega=8\left(\frac{\pi}{3}\right)^{3/2}\frac{\hbar a_0}{m}N_e\left(\frac{E_H}{kT}\right)^{1/2}\left[\sum_{i'\neq f}\left|\left\langle i'\left|\frac{\boldsymbol{r}}{a_0}\right|i\right\rangle\right|^2 \cdot\bar{g}\left(\frac{\bar{E}}{|\Delta E_{i'i}|}\right)+k\langle p^k\{|p^{k-1}\rangle^2\left|\left\langle f\left|\frac{\boldsymbol{r}}{a_0}\right|i\right\rangle\right|^2\bar{g}\left(\frac{\bar{E}}{|\Delta E_{fi}|}\right)\right.$$
$$\left.+\sum_{L_c}\sum_{f'}k\langle p^k\{|p^{k-1}\rangle^2\left|\left\langle f'\left|\frac{\boldsymbol{r}}{a_0}\right|f\right\rangle\right|^2\bar{g}\left(\frac{\bar{E}}{|\Delta E_{f'f}|}\right)\right]. \tag{5}$$

Here, k is the number of equivalent electrons and $\langle p^k\{|p^{k-1}\rangle$ the coefficient of fractional parentage (Shore and Menzel, 1965).

At temperatures lower than or equal to 20,000 K, the successful approximation for the resonance transitions in consideration is the low temperature limit form of Eq. (5). In such a case we may replace the Gaunt factor by its threshold value $\bar{g}_{th}=0.2$, and

Send offprint requests to: M. S. Dimitrijević (Astronomical Observatory)

© European Southern Observatory • Provided by the NASA Astrophysics Data System

1985A&A...145..439D

perform the summation over states i' and f'. Now Eq. (5) becomes

$$\omega = 8\left(\frac{\pi}{3}\right)^{3/2}\frac{\hbar a_0}{m}N_e\left(\frac{E_H}{kT}\right)^{1/2}\left[\left\langle i\left|\left(\frac{r}{a_0}\right)^2\right|i\right\rangle \bar{g}_{th} + \sum_{L_c} k\langle p^k\{|p^{k-1}\rangle^2\left\langle f\left|\left(\frac{r}{a_0}\right)^2\right|f\right\rangle \bar{g}_{th} + \left|\left\langle i\left|\frac{r}{a_0}\right|f\right\rangle\right|^2 (k\langle p^k\{|p^{k-1}\rangle^2 - 1)\,\bar{g}_{th}\right], \tag{6}$$

where

$$\left\langle j\left|\left(\frac{r}{a_0}\right)^2\right|j\right\rangle = \frac{n_j^{*2}}{2Z^2}\,[5n_j^{*2}+1-3l_j(l_j+1)];\; j=i,\, f$$

and

$$\left|\left\langle i\left|\frac{r}{a_0}\right|f\right\rangle\right|^2 \approx \left(\frac{3\,n_i^*}{2\,Z}\right)^2 [n_i^{*2}-1]\,\phi^2$$

for $s-p$ transitions. Here, Z is the atomic charge "seen" by the optical electron and ϕ the Bates and Damgaard (1949) factor. For every particular L_c, the ionization energy needed in calculating the effective principal quantum number n^* is different, so that $\langle f|(r/a_0)^2|f\rangle$ depends on L_c.

Starting from Eq. (6) we can easily derive the following expression

$$\omega \approx \frac{AN_e}{T^{1/2}}\left[\frac{\alpha}{(I_0-E_i)^2} + \sum_{L_c}\frac{\beta}{(I_0+E_{L_c})^2} + \frac{\gamma}{I_0-E_i} - \sum_{L_c}\frac{\eta}{I_0+E_{L_c}}\right] \tag{7}$$

where I_0 is the ionization energy, E_i the energy of the $np^{k-1}(n+1)s$ level, E_{L_c} the parent term energy counted from the ground level of the next ionization stage and

$$A = \frac{4\pi^2}{3\sqrt{3}}\left(\frac{\hbar}{m}\right)^2\left(\frac{2m}{\pi k}\right)^{1/2}\bar{g}_{th}, \tag{8}$$

$$\alpha = \frac{E_H^2 Z^2}{2}\,[5+\tfrac{9}{2}\,(k\langle p^k\{|p^{k-1}\rangle^2-1)\,\overline{\phi^2}], \tag{9}$$

$$\beta = \frac{5\,E_H^2\,Z^2}{2}\,k\langle p^k\{|p^{k-1}\rangle^2, \tag{10}$$

$$\gamma = \frac{E_H}{2}\,[1-\tfrac{9}{2}\,(k\langle p^k\{|p^{k-1}\rangle^2-1)\,\overline{\phi^2}], \tag{11}$$

$$\eta = \frac{5\,E_H}{2}\,k\langle p^k\{|p^{k-1}\rangle^2. \tag{12}$$

We introduced here an averaged Bates and Damgaard factor $\overline{\phi^2}$ for a series of $np^{k-1}(n+1)s-np^k$ resonance lines with the same k and different n.

We demonstrate empirically here (see Figs. 1 and 2) that between the energy of the $np^{k-1}(n+1)s$ level $-E_i$ and I_0 there exists a relationship, which may be approximatively expressed as:

$$E_i = a + bI_0 \tag{13}$$

Coefficients a and b for $np^{k-1}(n+1)s-np^k$ resonance lines are given in Table 1. The average Bates and Damgaard coefficient $\overline{\phi^2}$ is so small in all considered cases that we can put $\overline{\phi^2}\approx 0$. This means that the third term in Eq. (6) is negligible.

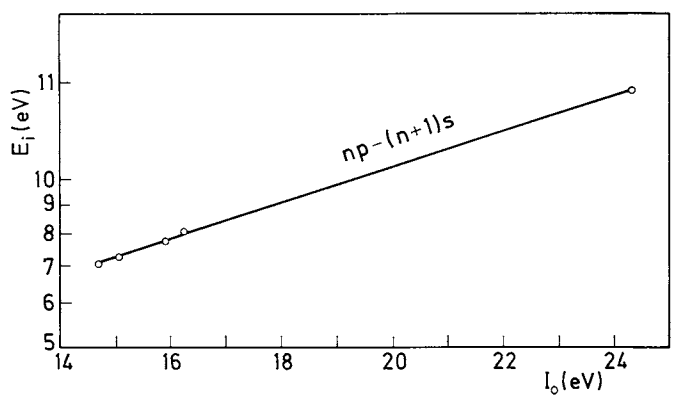

Fig. 1. The energy of $(n+1)s$ level (E_i) as a function of the ionization potential I_0, for $np-(n+1)s$ lines (Sn II, Pb II, Ge II, Si II, C II)

Table 1. a and b coefficients empirically obtained in relation $E_i = a + bI_0$ [Eq. (13)] for different numbers of equivalent electrons $-k$

k	a	b
1	−4.7696	0.7938
2	−4.2500	0.7652
3	−4.7924	0.7909
4	−4.9112	0.7891
5	−5.0737	0.8011
6	−5.3842	0.8104

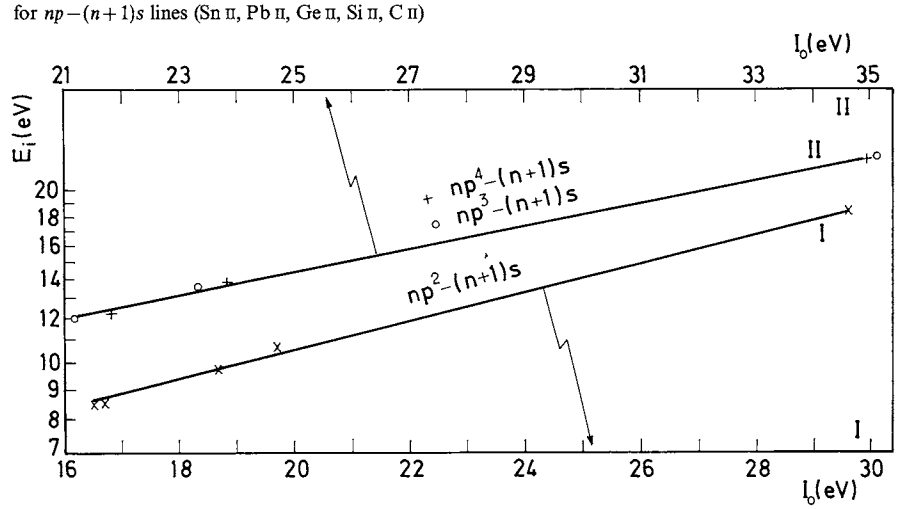

Fig. 2. The energy of $(n+1)s$ level (E_i) as a function of the ionization potential I_0, for $np^2-np(n+1)s$ (Sb II, Bi II, As II, P II, N II); $np^3-np^2(n+1)s$ (Se II, S II, O II); and $np^4-np^3(n+1)s$ lines (Br II, Cl II, F II)

© European Southern Observatory • Provided by the NASA Astrophysics Data System

1985A&A...145..439D

The Eq. (7) may be expressed now as a series in terms of I_0

$$\omega=\frac{AN_e}{T^{1/2}}\left\{\sum_{n=0}^{\infty}\frac{a^n}{(1-b)^{n+1}}I_0^{-(n+1)}\left[\frac{(n+1)\alpha}{(1-b)I_0}+\gamma\right]+\frac{\beta}{I_0^2}-\frac{\eta}{I_0}\right.$$
$$\left.+\sum_{L_c(E_{L_c}\neq 0)}\sum_{n=0}^{\infty}E_{L_c}^n(-1)^n I_0^{-(n+1)}\left[\frac{(n+1)\beta}{I_0}-\eta\right]\right\}$$
$$=\sum_{n=1}^{\infty}A_n(T,N_e,k)I_0^{-n}$$
$$A_n=\frac{AN_e}{T^{1/2}}\begin{cases}A_1'-5kE_H/2 & n=1\\ A_2'+5Z^2kE_H^2/2+\sum_{L_c(E_{L_c}\neq 0)}E_{L_c}\eta\,, & n=2\\ A_n'\,, & n\geq 3\end{cases}$$
$$A_n'=\frac{\gamma a^{n-1}+(n-1)\alpha a^{n-2}}{(1-b)^n}$$
$$+\sum_{L_c(E_{L_c}\neq 0)}E_{L_c}^{n-2}(-1)^n[(n-1)\beta+\eta E_{L_c}]\,.$$

If we want to obtain the half halfwidth (w) in wavelength units, the conversion factor is

$$\frac{\lambda^2}{2\pi c}\approx\frac{h^2C}{2\pi b^2 I_0^2}\left(1-\frac{2a}{bI_0}\right)=\frac{\varepsilon}{I_0^2}-\frac{\zeta}{I_0^3}\,. \tag{15}$$

Using Eq. (15), Eq. (14) may be expressed as

$$W=\sum_n B_n(N_e,T,k)I_0^{-n},\ n\geq 3\,, \tag{16}$$
$$B_n=A_{n-2}\varepsilon-A_{n-3}\zeta,\ n\geq 3,\ A_0=0\,.$$

If we want to make sure that the series given by Eqs. (14) and (16) are convergent, we may find the following relation

$$\left|\frac{A_{n+1}}{I_0A_n}\right|\approx\left|\frac{B_{n+1}}{I_0B_n}\right|\approx\left|\frac{a}{I_0(1-b)}\right|\ll 1\,. \tag{17}$$

Equation (17) is a strong limitation for the application of this method. In the case where $E_i\approx bI_0(|a|\ll|bI_0|)$ (In our case $I_0\gg 6.25$ eV, which is also a strong limitation) the series given by Eqs. (14) and (16) are convergent.

If we retain only the most important term in Eq. (16), we obtain the relation similar to that derived by Purić et al. (1980),

$$W\approx\frac{AN_e}{T^{1/2}}\frac{5E_H^2Z^2h^2C}{4\pi b^2}\left[(1-b)^{-2}+k+\frac{2ka}{Z^2E_H^2b(1-b)}\right]I_0^{-4}\,. \tag{18}$$

For $T=20{,}000$ K, $N_e=10^{17}\,\mathrm{cm}^{-3}$ and $k=1$, our result is $w(\text{Å})\approx 1655\,I_0^{-4}$ (where I_0 is expressed in eV), and for $k=6$, $w(\text{Å})\approx 1730\,I_0^{-4}$. Both results are relatively close to Eq. (2a) derived by Purić et al. (1980).

Within the semi-empirical approach the shift δ in the angular frequency units may be expressed as (Griem, 1968)

$$\delta=-8\left(\frac{\pi}{3}\right)^{3/2}\frac{\hbar a_0}{m}N_e\left(\frac{E_H}{kT}\right)^{1/2}\sum_{i'f'}\left[\frac{\Delta E_{i'i}}{|\Delta E_{i'i}|}\left|\left\langle i'\left|\frac{\boldsymbol{r}}{a_0}\right|i\right\rangle\right|^2\right.$$
$$\left.\cdot\,\bar{g}_{sh}\left(\frac{3kT}{2|\Delta E_{i'i}|}\right)-\frac{\Delta E_{f'f}}{|\Delta E_{f'f}|}\left|\left\langle f'\left|\frac{\boldsymbol{r}}{a_0}\right|f\right\rangle\right|^2\bar{g}_{sh}\left(\frac{3kT}{2|\Delta E_{f'f}|}\right)\right]. \tag{19}$$

Gaunt factors for width ($\bar{g}$) and shift ($\bar{g}_{sh}$) are related to each other by a Cauchy integral (dispersion) relation (Griem and Shen, 1962). At the threshold, $\bar{g}_{sh}\approx 0.2$ and values for other energies are given by Griem (1968).

For $np^{k-1}(n+1)s-np^k$ transitions, Eq. (19) becomes

$$\delta=-8\left(\frac{\pi}{3}\right)^{3/2}\frac{\hbar a_0}{m}N_e\left(\frac{E_H}{kT}\right)^{1/2}\left[\sum_{i'\neq f}\frac{\Delta E_{i'i}}{|\Delta E_{i'i}|}\right.$$
$$\cdot\left|\left\langle i'\left|\frac{\boldsymbol{r}}{a_0}\right|i\right\rangle\right|^2\bar{g}_{sh}\left(\frac{3kT}{2|\Delta E_{i'i}|}\right)+\frac{\Delta E_{if}}{|\Delta E_{if}|}k\langle p^k\{|p^{k-1}\rangle^2$$
$$\cdot\left|\left\langle f\left|\frac{\boldsymbol{r}}{a_0}\right|i\right\rangle\right|^2\bar{g}_{sh}\left(\frac{3kT}{2|\Delta E_{fi}|}\right)-\sum_{f'}\frac{\Delta E_{f'f}}{|\Delta E_{f'f}|}\sum_{L_c}$$
$$\left.\cdot\,k\langle p^k\{|p^{k-1}\rangle^2\left|\left\langle f'\left|\frac{\boldsymbol{r}}{a_0}\right|f\right\rangle\right|^2\bar{g}_{sh}\left(\frac{3kT}{2|\Delta E_{f'f}|}\right)\right]. \tag{20}$$

The low temperature limit form of Eq. (20) is

$$\delta=-\frac{AN_e}{T^{1/2}}\left[-\left|\left\langle i\left|\frac{\boldsymbol{r}}{a_0}\right|f\right\rangle\right|^2(k\langle p^k\{|p^{k-1}\rangle^2+1)\right.$$
$$\left.+\left\langle i\left|\left(\frac{\boldsymbol{r}}{a_0}\right)^2\right|i\right\rangle-\sum_{L_c}k\langle p^k\{|p^{k-1}\rangle^2\left\langle f\left|\left(\frac{\boldsymbol{r}}{a_0}\right)^2\right|f\right\rangle\right]. \tag{21}$$

In a similar way like for the width, Eq. (21) may be expressed as a series in terms of I_0.

$$\delta\approx-\frac{AN_e}{T^{1/2}}\left\{\sum_{n=0}^{\infty}\frac{a_n}{(1-b)^{n+1}}I_0^{-(n+1)}\frac{E_H}{2}\left[\frac{E_HZ^2(n+1)}{I_0(1-b)}+1\right]-\beta I_0^{-2}\right.$$
$$\left.+\eta I_0^{-1}-\sum_{L_c(E_{L_c}\neq 0)}\sum_{n=0}^{\infty}E_{L_c}^n(-1)^nI_0^{-(n+1)}\left[\frac{(n+1)\beta}{I_0}-\eta\right]\right\}$$
$$=-\sum_{n=1}^{\infty}C_n(T,N_e,k)I_0^{-n} \tag{22}$$

$$C_n=\frac{AN_e}{T^{1/2}}\begin{cases}C_1'+5E_Hk/2\,, & n=1\\ C_2'-5E_H^2Z^2k/2+\sum_{L_c(E_{L_c}\neq 0)}E_{L_c}\eta\,, & n=2\\ C_n'\,, & n\geq 3\end{cases} \tag{23}$$

$$C_n'=\frac{E_Ha^{n-1}/2+(n-1)5E_H^2Z^2a^{n-2}/2}{(1-b)^n}-$$
$$\sum_{L_c(E_{L_c}\neq 0)}E_{L_c}^{n-2}(-1)^n[(n-1)\beta-\eta E_{L_c}]\,.$$

Using Eq. (15), Eq. (21) may be expressed as

$$d=-\sum_n D_n(N_e,T,k)I_0^{-n},\quad n\geq 3 \tag{24}$$
$$D_n=C_{n-2}\varepsilon-C_{n-3}\zeta,\quad n\geq 3,\quad C_0=0\,.$$

In the case when $E_i\approx bI_0$, and if we retain only the most important term, Eq. (24) becomes

$$d\approx-\frac{AN_e}{T^{1/2}}\frac{5E_H^2Z^2h^2C}{4\pi b^2}\left[(1-b)^{-2}-k-\frac{2ka}{Z^2E_Hb(1-b)}\right]I_0^{-4} \tag{25}$$

For $T=20{,}000$ K, $N_e=10^{17}\,\mathrm{cm}^{-3}$ and $k=1$ our result is $|d|(\text{Å})=1665\,I_0^{-4}$ and for $k=6$, $|d|(\text{Å})=2001\,I_0^{-4}$, where I_0 is in eV. We can see that the difference between the case with six equivalent electrons and without equivalent electrons is 20% for the shift and 4.5% for the width. Since the process of averaging over a large number of lines (used by Purić et al., 1980) is apt to smooth out such differences, we can say that our results confirm the statement of Purić et al. (1980) that the influence of equivalent electrons is relatively small in the case of Stark widths of singly charged ion resonance lines.

We can also see that our analytical results differ only by 20% from the result obtained by Purić et al. (1980) (Eq. 2) as an average

© European Southern Observatory • Provided by the NASA Astrophysics Data System

1985A&A...145..439D

over a large number of different lines (For resonance lines $I = I_0$, so that our calculations may be compared with results of Purić et al., 1980).

3. Conclusion

The simple relations between the Stark broadening parameters and the ionization potential derived here for $np^{k-1}(n+1)s - np^k$ resonance transitions of singly charged ions, as well as those derived previously by Purić et al. (1980), may be useful in some cases to provide a rough estimate of Stark broadening parameters without more refined calculations. Our results confirm the main findings of Purić et al. (1980) (see also Dimitrijević and Konjević, 1984) and give a model how to find a similar relation for a different type of transition.

Besides the use of the ionization potential instead of "effective ionization energy" we took into account empirically and analytically the implicit dependence of wavelength on I_0. An important difference between our results and the work by Purić et al. (1980) is that we can obtain the sign of the shift properly, contrary to Purić et al. (1980) and Lakićević (1983) who were able to provide only the absolute value of the shift. We take into account also the variation of w and d with N_e and T while the relations of Purić et al. (1980) are obtained for $T = 20{,}000$ K and $N_e = 10^{17}$ cm^{-3}.

The extension of this method to the lines of elements with large atomic charge numbers Z (like e.g. for lantanides, radioactive elements and Z up to 89 in the article of Lakićević, 1983) must be checked additionally in order to see the effect of the complex structure of the radiator (see e.g. Dimitrijević and Konjević, 1983; Hey and Breger, 1980).

Acknowledgements. I am indebted to Dr. Nikola Konjević for numerous discussions and to the referee for useful suggestions.

References

Bates, D.R., Damgaard, A.: 1949, *Phil. Trans. Roy. Soc. London* (Ser. A) **242**, 101
Dimitrijević, M.S., Konjević, N.: 1983, *J. Quant. Spectrosc. Radiat. Transfer* **30**, 45
Dimitrijević, M.S., Konjević, N.: 1984, *Z. Naturforsch.* **39a**, 553
Griem, H.R.: 1968, *Phys. Rev.* **165**, 258
Griem, H.R., Shen, C.S.: 1962, *Phys. Rev.* **125**, 196
Hey, J.D., Breger, P.: 1980, *J. Quant. Spectrosc. Radiat. Transfer* **23**, 311
Lakićević, I.S.: 1983, *Astron. Astrophys.* **127**, 37
Lakićević, I.S., Purić, J.: 1983, in *Spectral Line Shapes II*, ed. K. Burnett, W. deGruyter, Berlin, 147
Purić, J., Lakićević, I., Glavonjić, V.: 1980, *Phys. Letters.* **76A**, 128
Seaton, M.J.: 1962, in *Atomic and Molecular Processes*, ed. D.R. Bates, Academic Press, New York, Chap. 11
Shore, B.W., Menzel, D.H.: 1965, *Astrophys. J. Suppl. Series* **12**, 187
Van Regenmorter, H.: 1962, *Astrophys. J.* **136**, 906

© European Southern Observatory • Provided by the NASA Astrophysics Data System

1986A&A...155..319M

Astron. Astrophys. 155, 319–322 (1986)

ASTRONOMY AND ASTROPHYSICS

Influence of ion-atom collisions on the absorption of radiation

A.A. Mihajlov[1,2] **and M.S. Dimitrijević**[1,2]

[1] Institute of Physics, P.O. Box 57, YU-11001 Beograd, Yugoslavia
[2] Astronomical Observatory, Volgina 7, YU-11050 Beograd, Yugoslavia

Received March 18, accepted July 1, 1985

Summary. It is shown that for the interpretation of the continuum absorption spectra, of A type stars, the processes $H_2^+ + \hbar\omega \rightarrow H + H^+$ and $H + H^+ + \hbar\omega \rightarrow H + H^+$ must be considered together since their contribution is comparable. The corresponding absorption coefficients are also determined.

Key words: radiation absorption – continuous spectrum – stellar spectrum – A type stars.

1. Introduction

The influence of the absorption from vibrational levels of H_2^+ having a non-LTE distribution on the solar opacity was studied by Tarafdar and Vardya (1975) (see also Krishna Swamy and Stecher, 1974) and was found insignificant at $\lambda = 2000$ Å However, it is well known that an important contribution to the continuum opacity of the A type s ar atmospheres (Mihalas, 1978) is given by the photodissociative process:

$$H_2^+ + \hbar\omega \rightarrow H + H^+ . \tag{1a}$$

Simultaneously with this process, the photon absorption by the ion-atom complexes must occur:

$$H + H^+ + \hbar\omega \rightarrow \begin{cases} H + H^+ \\ H^+ + H \end{cases} . \tag{1b}$$

We will assume that in the region of internuclear distances $R(\omega)$, where this process occurs, the ion-atom subsystem in the input channel is in the same electron state (Σ_g^+), as a molecular ion in the process (1a) and the absorption is connected with the transition of the subsystem to the same electron state (Σ_u^+) as in the case of process (1a).

The relation between process (1b) and process (1a) is as, e.g., the relation of the process of photon absorption for electron free-free transitions in the ion fields to that of atom photoionisation (i.e. to the corresponding bound-free transitions).

The contribution of process (1a) to the opacity depends on $N(H_2^+)$ and the contribution of process (lb) on $N(H) \cdot N(H^+)$, where N is the concentration. In A type stars atmospheres, $N(H_2^+) \sim N(H) \cdot N(H^+)$, where the coefficient of proportionality is a function of T and pressure. Processes (1a) and (1b) are apparent only when $N(H)$ and $N(H^+)$ are close or at least comparable, i.e. when the degree of hydrogen atom ionization is close to 0.5. That is characteristic for the atmospheres of A type stars, where it has been estimated that about 10% of the atmosphere opacity in the visible region is influenced by this process (1a) (Mihalas, 1978).

Recently (Mihajlov and Popović, 1981), the spectral coefficients for the process inverse to the process (1b) have been determined. The specific problem of the radiative association of H_2^+ was studied from the quantum-mechanics point of view by Ramaker and Peek (1976) and the corresponding transition operator can be found in the article by the same authors (Ramaker and Peek, 1972; 1973).

The aim of this paper is (i) to show that for the interpretation of the continuum absorption spectra of A type stars processes (1a) and (1b) must be considered together since their contribution is comparable and (ii) using the approach of Mihajlov and Popović (1981) and the principle of detailed balance to determine the corresponding absorption coefficients.

2. Theory and discussion

Let us consider the processes

$$H + H^+ \rightarrow \hbar\omega + H_2^+ , \tag{2a}$$

$$H + H^+ \rightarrow \hbar\omega + \begin{cases} H + H^+ \\ H^+ + H \end{cases} , \tag{2b}$$

where the photon emission is connected with the ion-atom subsystem transition from the electron state Σ_u^+ to the state Σ_g^+. Mihajlov and Popović (1981) have determined, using the semiclassical approximation, the spectral intensity (S) of the continuum electromagnetic radiation with any polarization (in the space angle 4π from the unit volume of the partially ionized gas at the temperature T and for a unitary atom and ion concentration), for the above mentioned processes. In such a way, the spectral intensities defined, caused by any of the processes (2a) and (2b) separately will be marked as $S_\omega^{(a)}(T)$ and $S_\omega^{(b)}(T)$, so that $S_\omega^{(ab)}(T) \equiv S_\omega^{(a)}(T) + S_\omega^{(b)}(T)$. The energy emitted Δq is $S_\omega N_H N_{H^+} \Delta\omega \Delta V \Delta t$ where $\Delta\omega$ is the spectral interval, V the volume and t the time. Using the results of Mihajlov and Popović (1981) appropriate for the case considered (i.e. Eqs. 23 with $P_{in} = 0.5$, $\gamma = 1/a_0$ and $\omega > \omega_c$) we have

$$S_\omega^{(ab)}(T) = \frac{2\pi e^2 a_0}{3c^3} \cdot R_\omega^4 \cdot \omega^3 \cdot \exp\left[-\frac{U_u(R_\omega)}{kT}\right], \tag{3a}$$

Send offprint requests to: A.A. Mihajlov (Institute of Physics)

© European Southern Observatory • Provided by the NASA Astrophysics Data System

1986A&A...155..319M

where R_ω is determined from (Mihajlov and Popović, 1981):

$$\hbar\omega = U_u(R_\omega) - U_g(R_\omega) \tag{3b}$$

assuming that the photon absorption occurs in the direct vicinity of the resonant internuclear distance R_ω. Here, $U_g(R_\omega)$ and $U_u(R_\omega)$ are the corresponding energies of the states.

In Eq. 3 the square of the corresponding dipole matrix element is approximated as $\sim e^2 R_\omega^2/4$ (for details see Appendix A in Mihajlov and Popović, 1981).

It could be shown that (Mihajlov and Janev, 1981)

$$S_\omega^{(a)}(T) = S_\omega^{(ab)}(T) \cdot \gamma\left(\frac{3}{2}, \frac{|U_g(R_\omega)|}{kT}\right) \Big/ \Gamma\left(\frac{3}{2}\right), \tag{4a}$$

$$S_\omega^{(b)}(T) = S_\omega^{(ab)}(T) \cdot \Gamma\left(\frac{3}{2}, \frac{|U_g(R_\omega)|}{kT}\right) \Big/ \Gamma\left(\frac{3}{2}\right), \tag{4b}$$

where $\Gamma(x)$, $\gamma(x, y)$ and $\Gamma(x, y)$ are complete and incomplete gamma functions (Abramowitz and Stegun, 1972). We should emphasize also that in plasma conditions the spontaneous electromagnetic radiation due to processes (2a) and (2b) is non-polarized and isotropic if macroscopic volume are considered.

We could now consider the processes of stimulated emission in a standard way (Heitler, 1954)

$$\hbar\omega + \mathrm{H} + \mathrm{H}^+ \to 2\hbar\omega + \mathrm{H}_2^+, \tag{5a}$$

$$\hbar\omega + \mathrm{H} + \mathrm{H}^+ \to 2\hbar\omega + \begin{cases} \mathrm{H} + \mathrm{H}^+ \\ \mathrm{H}^+ + \mathrm{H} \end{cases}, \tag{5b}$$

occuring in plasma conditions simultaneously with the processes (2a) and (2b). The group of processes (2) and (5) is opposite to the processes (1).

Now we will consider the partially ionized hydrogen gas in the state of the thermodynamic equilibrium. The equilibrium concentration will be denoted as N_T, the equilibrium volume spectral density of the electromagnetic field energy as $U_T(\omega)$, and the equilibrium photon distribution as $f_T(\omega)$, so that

$$U_T(\omega) = \frac{\hbar\omega^3}{\pi^2 c^3} \cdot f_T(\omega), \qquad f_T(\omega) = \left[\exp\left(\frac{\hbar\omega}{kT}\right) - 1\right]^{-1}. \tag{6}$$

The intensity of the spontaneous emission per unit volume in this case is $S_\omega^{(i)}(T) \cdot N(\mathrm{H}) \cdot N_T(\mathrm{H}^+)$, $i = a, b$. The dependence on photon polarization and eventual non-isotropy could be manifested in the processes (1) in a plasma in the case of macroscopic volumes without physically distinguishable directions, only through the photon distribution function over states with different wave vectors and polarizations. Taking this into account we will introduce the spectral coefficients of stimulated emission, and absorption in the form of $P_\omega^{(i)}(T) \cdot f_T(\omega)$ and $Q_\omega^{(i)} \cdot f_T(\omega)$, $i = a, b$. The corresponding balance equations are

$$[S_\omega^{(a)}(T) + P_\omega^{(a)}(T) \cdot f_T(\omega)] \cdot N(\mathrm{H}) N_T(\mathrm{H}^+) = Q_\omega^{(a)}(T) \cdot f_T(\omega) \cdot N_T(\mathrm{H}_2^+), \tag{7a}$$

$$[S_\omega^{(b)}(T) + P_\omega^{(b)}(T) \cdot f_T(\omega)] \cdot N(\mathrm{H}) \cdot N_T(\mathrm{H}^+) = Q_\omega^{(b)}(T) \cdot f_T(\omega) \cdot N(\mathrm{H}) \cdot N_T(\mathrm{H}^+). \tag{7b}$$

Repeating the procedure applied before (e.g. Heitler, 1954) we have

$$P_\omega^{(i)}(T) = S_\omega^{(i)}(T), \qquad i = a, b. \tag{8}$$

From (6–8) it follows that

$$Q_\omega^{(a)}(T) = S_\omega^{(a)}(T) \cdot \exp\left(\frac{\hbar\omega}{kT}\right) \cdot \chi_T, \tag{9a}$$

$$Q_\omega^{(b)}(T) = S_\omega^{(b)}(T) \cdot \exp\left(\frac{\hbar\omega}{kT}\right), \tag{9b}$$

where $\chi_T \equiv N(\mathrm{H}) \cdot N_T(\mathrm{H}^+)/N_T(\mathrm{H}_2^+)$, at fixed $N(\mathrm{H})$.

In order to determine the absorption spectral coefficients, we can use the relationship (Griem, 1964)

$$Q_\omega^{(i)}(T) \cdot f_T(\omega) = K_\omega^{(i)}(T) \cdot c \cdot U_T(\omega).$$

Using (3, 4 and 6) we have

$$\tilde{K}_\omega^{(a)}(T) = K_\omega^{(ab)}(T) \cdot X^{(a)}(\omega, T) \cdot \chi_T, \tag{10a}$$

$$K_\omega^{(b)}(T) = K_\omega^{(ab)}(T) \cdot X^{(b)}(\omega, T), \tag{10b}$$

$$K_\omega^{(ab)}(T) = 0.62\,10^{-42} \cdot (\mathrm{R}_\omega/a_0)^4 \cdot \exp\left[\frac{|U_g(R_\omega)|}{kT}\right] \cdot [\mathrm{cm}^5], \tag{10c}$$

$$X^{(a)}(\omega, T) = \gamma\left(\frac{3}{2}, \frac{|U_g(R_\omega)|}{kT}\right) \Big/ \Gamma\left(\frac{3}{2}\right),$$

$$X^{(b)}(\omega, T) = \Gamma\left(\frac{3}{2}, \frac{|U_g(R_\omega)|}{kT}\right) \Big/ \Gamma\left(\frac{3}{2}\right). \tag{10d}$$

Here, $\tilde{K}$ is normalized to $N(\mathrm{H}_2^+) = 1$ opposite to K normalized to $N(\mathrm{H}) = N(\mathrm{H}^+) = 1$. One can see that

$$\tilde{K}_\omega^{(a)}(T) \to K_\omega^{(a)}(T) \equiv \tilde{K}_\omega^{(a)}(T) \cdot \chi^{-1}(T),$$

where $\chi(T) \equiv N(\mathrm{H}) \cdot N(\mathrm{H}^+)/N(\mathrm{H}_2^+)$, at $N(\mathrm{H})$ previously fixed. Assuming the existence of dissociation-recombination equilibrium between H, H^+ and H_2^+ at given T (a realistic assumption for A type stars atmospheres), $\chi_T = \chi(T)$. Consequently $K_\omega^{(a)}(T)$ and $K_\omega^{(b)}(T)$ are given as

$$K_\omega^{(a)}(T) = K_\omega^{(ab)}(T) \cdot X^{(a)}(\omega, T), \tag{11a}$$

$$K_\omega^{(b)}(T) = K_\omega^{(ab)}(T) \cdot X^{(b)}(\omega, T), \tag{11b}$$

Now, $K_\omega^{(ab)}(T) \equiv K_\omega^{(a)}(T) + K_\omega^{(b)}(T)$ represents the total absorption coefficient for processes (1a) and (1b) together.

The results obtained make it possible to determine the corresponding spectral coefficients of the stimulated emission (negative absorption, the processes (5)) denoted here by Z. Since in the case of the thermodynamic equilibrium these coefficients are connected with $P_\omega^{(a,b)}(T) \cdot f_T(\omega)$ as the absorption coefficients with $Q_\omega^{(a,b)}(T) \cdot f_T(\omega)$, we have

$$Z_\omega^{(i)}(T) = Z_\omega^{(ab)}(T) \cdot X^{(i)}(\omega, T), \qquad i = a, b, \tag{12}$$

where

$$Z_\omega^{(ab)}(T) = K_\omega^{(ab)}(T) \cdot \exp\left(-\frac{\hbar\omega}{kT}\right). \tag{13}$$

Finally, we could determine the absolute coefficients of absorption, marked by *:

$$K_\omega^{*(i)} = K_\omega^{(i)}(T) - Z_\omega^{(i)}(T), \qquad i = a, b.$$

We have

$$K_\omega^{*(i)}(T) = K_\omega^{(i)}(T) \cdot \left[1 - \exp\left(-\frac{\hbar\omega}{kT}\right)\right]. \tag{14}$$

© European Southern Observatory • Provided by the NASA Astrophysics Data System

1986A&A...155..319M

The reduction of absorption occurs due to the simultaneous process of stimulated emission.

In order to determine spectral coefficients, one can first determine R_ω using Eq. (3b). Our analysis shows that for plasma conditions and λ-range considered here, one can use in (3b) asymptotic approximation (Herring, 1962; Smirnov, 1964) for $U_{g,u}(R)$:

$$U_{u,g}(R) = \pm 1.472 \cdot I_{\mathrm{H}} \cdot (R/a_0) \exp(-R/a_0) - \frac{\alpha e^2}{2R^4},$$

where α is the polarizability and I_{H}, H ionization energy. The values for R_ω are given in Table 1, and they differ up to 6% from the case when exact values for $U_{u,g}(R)$ (Bates et al., 1953) are used.

It is easy to show that

$$X^{(a)}(\omega, T) = \Phi(\sqrt{Z}) - \frac{2}{\sqrt{\pi}} Z \cdot \exp(-Z),$$

$$X^{(b)}(\omega, T) = 1 - \Phi(\sqrt{Z}) - \frac{2}{\sqrt{\pi}} Z \cdot \exp(-Z),$$

$$Z = -\frac{U_g(R_\omega)}{kT}.$$

where Φ is the error function (Abramowitz and Stegun, 1972).

The ratio $K_\omega^{(b)}(T)/K_\omega^{(ab)}(T)$ as a function of $\sqrt{Z}$ is presented in Table 2, while in Table 3, $\sqrt{Z}$ as a function of λ and T is given.

Table 1. The R_ω (a.u.) as a function of λ[Å]

λ[Å]	R_ω[a.u.]
3000	3.534
4000	3.927
5000	4.223
6000	4.459
7000	4.657
8000	4.826
9000	4.974
10000	5.106
11000	5.224
12000	5.331
13000	5.429
14000	5.520
15000	5.604
16000	5.683
17000	5.756
18000	5.825
19000	5.890
20000	5.952

Table 2. The $X^{(b)}(\omega, T) = K_\omega^{(b)}(T)/K_\omega^{(ab)}(T)$ as a function of $\sqrt{Z} = \left[-\frac{U_g(R_\omega)}{kT}\right]^{1/2}$

$\sqrt{Z}$	$X^{(b)}$
0.6	0.6795
0.7	0.6609
0.8	0.6390
0.9	0.6097
1.0	0.5724
1.1	0.5269
1.2	0.4747
1.3	0.4179
1.4	0.3592
1.5	0.3015
1.6	0.2470
1.7	0.1974
1.8	0.1541
1.9	0.1174
2.0	0.0874
2.2	0.0450
2.4	0.0212
2.6	0.0091
2.8	0.0036
3.0	0.0013

Table 3. The $\sqrt{Z} = \left[-\frac{U_g(R\omega)}{kT}\right]^{1/2}$ as a function of T[K] and λ[Å]

λ[Å] \ T[K]	4000	5000	6000	7000	8000	9000	10000	11000
3000	2.671	2.389	2.181	2.019	1.888	1.780	1.689	1.610
4000	2.290	2.048	1.869	1.731	1.619	1.526	1.448	1.381
5000	2.038	1.823	1.664	1.541	1.441	1.359	1.289	1.229
6000	1.856	1.660	1.516	1.403	1.313	1.238	1.174	1.119
7000	1.716	1.535	1.402	1.298	1.214	1.144	1.086	1.035
8000	1.605	1.435	1.310	1.213	1.135	1.070	1.015	0.968
9000	1.513	1.353	1.235	1.143	1.070	1.008	0.957	0.912
10000	1.435	1.284	1.172	1.085	1.015	0.957	0.908	0.865
12000	1.311	1.172	1.070	0.991	0.927	0.874	0.829	0.790
14000	1.215	1.087	0.992	0.918	0.859	0.810	0.768	0.733
16000	1.138	1.017	0.929	0.860	0.804	0.758	0.719	0.686
18000	1.074	0.961	0.877	0.812	0.759	0.716	0.679	0.648
20000	1.020	0.912	0.833	0.771	0.721	0.680	0.645	0.615

© European Southern Observatory • Provided by the NASA Astrophysics Data System

1986A&A...155..319M

Using Tables 1–3 we can determine quickly the spectral coefficients for stellar conditions. If for e.g. $\lambda = 5000$ Å and $T = 10000$ K (this is characteristic for A0 type stars) we find the corresponding $\sqrt{Z}$ in Table 3, we can see from Table 2 that the process $H + H^+ + \hbar\omega \rightarrow \begin{cases} H + H^+ \\ H^+ + H \end{cases}$ (usually neglected, Mihalas, 1978) contributes 41% to the $K_\omega^{(ab)}$. We can conclude that in investigations of the continuum in A star atmospheres, processes (1a) and (1b) must be treated together since their contributions are comparable. Moreover, process 1b becomes more significant than 1a in the infrared part of the spectrum.

References

Abramowitz, M., Stegun, I.: 1972, Handbook of Mathematical Functions, Dover, New York

Bates, D.R., Ledsham, K., Stewart, A.L.: 1953, *Phil. Trans. Roy. Soc, London* **246**, 215

Griem, H.R.: 1964, Plasma Spectroscopy, McGraw-Hill, New York

Heitler, W.: 1954, Quantum Theory of Radiation, Cavendon, Oxford

Herring, C.: 1962, *Rev. Mod. Phys.* **34**, 631

Krishna Swamy, K.S., Stecher, T.P.: 1974, *Astrophys. J. Letters* **194**, L153

Mihajlov, A.A., Janev, R.K.: 1981, *J. Phys. B* **14**, 1639

Mihajlov, A.A., Popović, M.M.: 1981, *Phys. Rev. A* **23** 1679

Mihalas, D.: 1978, Stellar Atmospheres, W.H. Freeman and Co., San Francisco, Chap. 4.4

Ramaker, D.E., Peek, J.M.: 1972, *J. Phys. B* **5**, 2175

Ramaker, D.E., Peek, J.M.: 1973, *Atomic Data* **5**, 167

Ramaker, D.E., Peek, J.M.: 1976, *Phys. Rev. A* **13**, 58

Smirnov, B.M.: 1964, ZhETF **47**, 518

Tarafdar, S.P., Vardya, M.S.: 1975, *Astrophys. J.* **201**, L99

© European Southern Observatory • Provided by the NASA Astrophysics Data System

1986A&A...163..297D

Astron. Astrophys. 163, 297–300 (1986)

ASTRONOMY AND ASTROPHYSICS

Simple formulae for estimating Stark widths and shifts of neutral atom lines

M. S. Dimitrijević[1] **and N. Konjević**[2]

[1] Astronomical Observatory, Volgina 7, YU-11050 Beograd, Yugoslavia
[2] Institute of Physics, P.O. Box 57, YU-11001 Beograd, Yugoslavia

Received October 18, 1985; accepted February 27, 1986

Summary. Formulae for estimating Stark widths and shifts of neutral atom lines, based on the simple method of Freudenstein and Cooper and the GBKO semiclassical theory, are presented. For the calculations, most of the available personal computers are sufficient. Obtained formulae have been applied to He I and Mg I lines and results are compared with calculations of Benett and Griem and values obtained according to the method of Freudenstein and Cooper.

Key words: line profiles

1. Introduction

Astrophysicists performing calculations of radiative transfer through stellar plasma or evaluation of physical conditions in stellar atmospheres often require Stark broadening data for a large number of transitions in many atoms. To obtain these data one can use, e.g., so called semiclassical or fully quantum mechanical theoretical approaches (see e.g. Griem, 1974) which both require elaborate calculations even for a single line. To overcome this problem Cowley (1971) offered a very simple approximative formula for evaluation of neutral line widths. Here, atomic structure is taken into account in the crudest possible way only through the effective principal quantum number of the upper level of the transition. As noted by Cowley (1971) this formula gives the wrong temperature dependence. Namely, calculated Stark widths vary as a function of $T^{-1/2}$ while the widths of neutral lines usually increase with temperature (see e.g. Griem, 1974). He therefore advocates using the value at $T=10^4$ K at all temperatures.

A simple formula for estimating Stark widths of neutral lines derived by Freudenstein and Cooper (1978) gives the correct trend of Stark width dependence upon electron temperature. Furthermore, this formula makes better allowance for atomic structure by taking into account the actual position of the closest interacting level to the upper energy level of the considered transition.

In this paper we report an approximate Stark broadening formula for even more sophisticated estimations of the line widths and extend its applicability to the evaluation of the shifts. These formulae require a complete set of interacting levels and as a consequence larger computation time per spectral line is needed. However, with most of the available personal computers this problem is marginal. The drawback for the application of these formulae may be the eventual lack of the complete set of perturbing energy levels for some transitions.

Send offprint requests to: M.S. Dimitrijević

2. Theory

The half-halfwidth (w) and shift (d) of a neutral atom spectral line broadened by electron-impacts (Griem et al., 1962) are given by

$$w+id=\frac{4\pi}{3}N_e\left(\frac{\hbar}{m}\right)^2\int\frac{dv}{v}f(v)\left\{\frac{3}{4}\left(\frac{mv}{\hbar}\right)^2\tilde{\varrho}^2_{\min}\right.$$
$$+\sum_{i'}\boldsymbol{R}^2_{ii'}\,[a_{ii'}(z^{\min}_{ii'})-i\,\varepsilon_{ii'}\,b_{ii'}(\tilde{z}^{\min}_{ii'})]$$
$$\left.+\sum_{f'}\boldsymbol{R}^2_{ff'}\,[a_{ff'}(z^{\min}_{ff'})+i\,\varepsilon_{ff'}\,b_{ff'}(\tilde{z}^{\min}_{ff'})]\right\}. \quad (1)$$

Here, $\boldsymbol{R}^2_{jj'}$ (in units of the Bohr radius a_0^2) is the square of the coordinate operator matrix element (summed over all components of the operator and over the magnetic substates of total momentum J' and averaged over the magnetic substates of J), N_e the electron density, $f(v)$ the Maxwellian distribution of the electron velocity (v), i,f denote the initial and final states and i',f' are the corresponding perturbing states within the dipole approximation. The quantity $\varepsilon_{jj'}$ determines the signs of individual contributions to the shift, viz.,

$$\varepsilon_{jj'}=(E_j-E_{j'})/|E_j-E_{j'}|$$

where E_j and $E_{j'}$ are the energies of the corresponding states. The minimum impact parameter $\varrho_{\min}$ allowed by the unitarity condition (Griem et al., 1962) is given by

$$\tilde{\varrho}^2_{\min}=\frac{2}{3}\left(\frac{\hbar}{mv}\right)^2\left|\sum_{i'}\boldsymbol{R}^2_{ii'}\,[A_{ii'}(z_{ii'})-i\,\varepsilon_{ii'}\,B_{ii'}(z_{ii'})]\right.$$
$$\left.+\sum_{f'}\boldsymbol{R}^2_{ff'}\,[A_{ff'}(z_{ff'})+i\,\varepsilon_{ff'}\,B_{ff'}(z_{ff'})]\right|, \quad (2)$$

where $a_{jj'}$, $b_{jj'}$, $A_{jj'}$ and $B_{jj'}$ are the GBKO (Griem et al., 1962; Griem, 1974) Stark broadening functions of the arguments $z_{jj'}$ and $\tilde{z}_{jj'}$,

$$z_{jj'}=\varrho\,(E_j-E_{j'})/\hbar v,\ \tilde{z}_{jj'}=0{,}75\,z_{jj'},$$

© European Southern Observatory • Provided by the NASA Astrophysics Data System

1986A&A...163..297D

and ϱ is the impact parameter. In the expression for $z_{jj'}^{\min}$, $\varrho_{\min}$ is used instead of ϱ. Further, we shall approximate the velocity average as $1/\bar{v} \sim (m/3kT)^{1/2}$, following the suggestion of Freudenstein and Cooper (1978), since $\langle 1/v \rangle = (2m/\pi kT)^{1/2}$ tends to weight low velocities, whereas the most important contribution to the width comes from small $z^{\min}$, corresponding to high velocities (Freudenstein and Cooper, 1978), due to the properties of the $a_{jj'}(z)$ function.

In order to simplify Eqs. (1) and (2) we introduce here the approximation

$$\left|\sum_{j'} \boldsymbol{R}_{jj'}^2 [A_{jj'} + \mathrm{i}\varepsilon_{jj'} B_{jj'}]\right| \approx \sum_{j'} \boldsymbol{R}_{jj'}^2 \left|[A_{jj'} + i\varepsilon_{jj'} B_{jj'}]\right|, \tag{3}$$

i.e. $\tilde{\varrho}_{\min}^2 \approx \sum_{j'} \varrho_{j'}^2$.

For a series of complex numbers z_j we have

$$\left|\sum_j z_j\right| \leqq \sum_j |z_j|,$$

where the sign of equality holds in the case where all z_j have equal arguments. This means that $A_{jj'} \gg B_{jj'}$ which is satisfied for close collisions, high velocities or close perturbing levels which usually give the principal contribution to the line broadening.

The overestimation of $z_{jj'}$ by approximation (3) may be partially compensated by assuming that $z_{jj'} \approx \varrho_{j'} \omega_{jj'}/v$, which lowers the $z_{jj'}$ values.

Define

$$\eta_{jj'} \equiv |E_j - E_{j'}|/3kT.$$

Then

$$w + id \approx \left(\frac{32}{27}\right)^{1/2} N_e \pi \left(\frac{\hbar a_0}{m}\right) \left(\frac{E_{\mathrm{H}}}{kT}\right)^{1/2} \left\{\sum_{i'} \boldsymbol{R}_{ii'}^2 [f_w(\eta_{ii'} \mathrm{R}_{ii'}) - i\varepsilon_{ii'} f_d(\eta_{ii'} \mathrm{R}_{ii'})] + \sum_{f'} \boldsymbol{R}_{ff'}^2 [f_w(\eta_{ff'} \boldsymbol{R}_{ff'}) + i\varepsilon_{ff'} f_d(\eta_{ff'} \boldsymbol{R}_{ff'})]\right\}, \tag{4}$$

where

$$f_w(\eta_{jj'} \boldsymbol{R}_{jj'}) = \tfrac{1}{2}[A^2(z_{jj'}^{\min}) + B^2(z_{jj'}^{\min})]^{1/2} + a(z_{jj'}^{\min}) \tag{5}$$

as suggested by Freudenstein and Cooper (1978) and

$$f_d(\eta_{jj'} \boldsymbol{R}_{jj'}) = b(\tilde{z}_{jj'}^{\min}), \tag{6}$$

To obtain $f_w(\eta_{jj'} \boldsymbol{R}_{jj'})$ and $f_d(\eta_{jj'} \boldsymbol{R}_{jj'})$ it is necessary only to solve the following equation

$$(z_{jj'}^{\min})^2 = \tfrac{2}{3}(\eta_{jj'} \boldsymbol{R}_{jj'})^2 [A^2(z_{jj'}^{\min}) + B^2(z_{jj'}^{\min})]^{1/2} \tag{7}$$

obtained from Eq. (2) and then to substitute the solution into Eqs. (5) and (6). Using asymptotic forms of GBKO Stark broadening functions, the following analytic expressions may be obtained. For $\eta R \gg 1$,

$$z_{jj'}^{\min} \approx [\pi(\eta_{jj'} \boldsymbol{R}_{jj'})^2/6]^{1/3}$$

and

$$f_w(\eta_{jj'} \boldsymbol{R}_{jj'}) \approx \tfrac{1}{2}[3\pi^2/32(\eta \boldsymbol{R}_{jj'})^2]^{1/3} \approx 0{,}487(\eta_{jj'} \boldsymbol{R}_{jj'})^{-2/3}$$

$$f_d(\eta_{jj'} \boldsymbol{R}_{jj'}) \approx 2\left(\frac{\pi}{6}\right)^{2/3} (\eta_{jj'} \boldsymbol{R}_{jj'})^{-2/3}$$

For $\eta R \ll 1$,

$$z_{jj'}^{\min} \approx (\tfrac{2}{3})^{1/2} \eta_{jj'} \boldsymbol{R}_{jj'}$$

$$f_w(\eta_{jj'} \boldsymbol{R}_{jj'}) \approx \ln(2.27/\eta_{jj'} \boldsymbol{R}_{jj'})$$

$$f_d(\eta_{jj'} \boldsymbol{R}_{jj'}) \approx \pi/2.$$

In Fig. 1, $f_w(\eta_{jj'} \boldsymbol{R}_{jj'})$ and $f_d(\eta_{jj'} \boldsymbol{R}_{jj'})$ are presented. Approximate fitted expressions for $f_w(\eta_{jj'} \boldsymbol{R}_{jj'})$ (Freudenstein and Cooper, 1978) and $f_d(\eta_{jj'} \boldsymbol{R}_{jj'})$ are

$$f_w(x) = e^{-1.33x} \ln\left(1 + \frac{2.27}{x}\right) + \frac{0.487x}{0.153 + x^{5/3}} + \frac{x}{7.93 + x^3}, \tag{8}$$

$$f_d(x) = 1.571\, e^{-2.482x} + \frac{1.295x}{0.415 + x^{5/3}} + \frac{0.713x}{8.139 + x^3}, \tag{9}$$

where $x = \eta_{jj'} \boldsymbol{R}_{jj'}$.

Using Eqs. (4), (8), and (9), electron-impact width and shift of neutral atom lines may be easily calculated.

One can remark here that the f_d/f_w ratio is not consistent with the well known adiabatic limit ($d/w = \sqrt{3}$). Namely, the GBKO (Griem et al., 1962) theory is fitted to the classical adiabatic limit using slightly modified unitary condition not used by Freudenstein and Cooper (1978). So we may choose it to be consistent either with Freudenstein and Cooper's (1978) results, Eqs. (8) and (9) derived in the present paper, or to obtain the classical adiabatic limit. Moreover, Dimitrijević and Grujić (1979) have demonstrated recently that the d/w ratio is strongly modified at the adiabatic limit if one takes into account the back reaction of the neutral emitter on a perturbing electron. However, if one wants it to be consistent with the classical adiabatic limit, one must use the unitary condition in the GBKO (Griem et al., 1962) form. Then Eqs. (5) and (7) become

$$f_w(x) = \tfrac{1}{2}(\tfrac{4}{3})^{3/2} [A^2(z_{jj'}^{\min}) + B^2(z_{jj'}^{\min})]^{1/2} + a(z_{jj'}^{\min}), \tag{5a}$$

$$(z_{jj'}^{\min})^2 = \tfrac{2}{3}(\tfrac{4}{3})^{3/2} x^2 [A^2(z_{jj'}^{\min}) + B^2(z_{jj'}^{\min})]^{1/2}. \tag{7a}$$

Using now Eqs. (4), (5a), and (7a) one can easily obtain shift and width in accordance with the classical adiabatic limit.

Another source of Stark broadening in stellar atmospheres are collisions with protons. We can estimate the correction to the Stark width due to the proton-impact contribution using the expression for the "quadrupole" ion-impact width (Griem, 1974) adapted for the case considered:

$$w(\text{Å}) = 0.4074\ 10^{-26} N_e(\mathrm{cm}^{-3})\ \lambda^2(\text{Å})\,(n_i^{*2} - n_f^{*2})^2/Z^2. \tag{10}$$

For typical stellar conditions ($N_e \sim 10^{13}\,\mathrm{cm}^{-3}$) the impact approximation is usually valid also for proton perturbers. The total Stark width is simply obtained by adding electron and proton impact widths.

In Eq. (10) $(Z-1)$ is the ionic charge and n_j^* the effective principal quantum number

$$n_j^{*2} = Z^2 \frac{E_{\mathrm{H}}}{E_\infty - E_j},$$

where E_{H} is the hydrogen ionization energy and E_∞ is the appropriate series limit.

When dipole interactions are more important, one can use the approximate formulae of Griem (1962) to calculate the full line width w_{tot} and shift d_{tot}

$$w_{\mathrm{tot}} \approx 2[1 + 1.75\,10^{-4} N_e^{1/4} A(1 - 0.068\, N_e^{1/6} T^{-1/2})]\,10^{-16} w N_e, \tag{11}$$

$$d_{\mathrm{tot}} \approx [d \pm 2.0\ 10^{-4} N_e^{1/4} A w(1 - 0.068\, N_e^{1/6} T^{-1/2})]\ 10^{-16} N_e, \tag{12}$$

© European Southern Observatory • Provided by the NASA Astrophysics Data System

1986A&A...163..297D

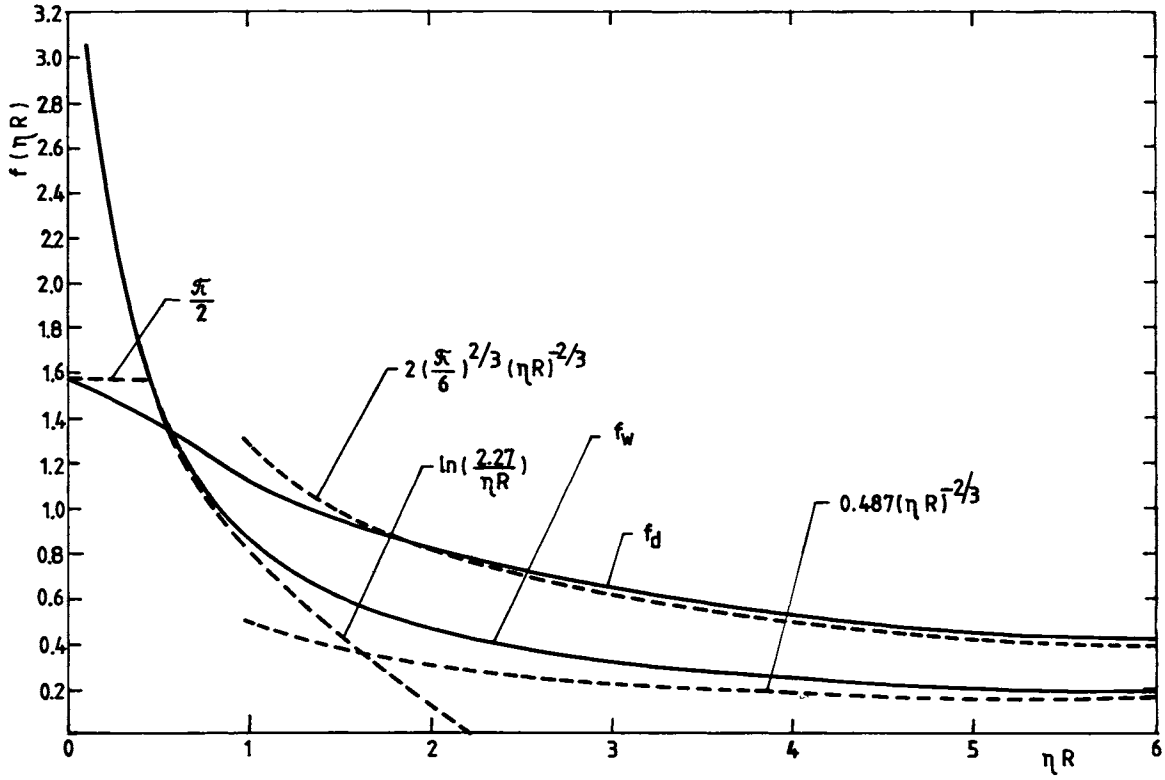

Fig. 1. A plot of the functions $f_w(\eta R)$ and $f_d(\eta R)$ as calculated from Eqs. (5) and (6) or (8) and (9) and their asymptotic limits

where w, d, and A are the electron impact half-halfwidth, shift and ion broadening parameter, respectively, all of them taken at $N_e = 10^{16}\,\mathrm{cm}^{-3}$ and at electron temperature T(K); N_e is the electron density (cm^{-3}) at which w_{tot} and d_{tot} are to be given. There are certain restrictions to the applicability of Eqs. (11) and (12), and they are:

$$B = 8.99\ 10^{-2} N_e^{1/6} T^{-1/2} \lesssim 0.8$$

$$0.05 \lesssim A \lesssim 0.5 .$$

Since we have already described the procedure for evaluating w and d, methods for the estimation of the ion broadening parameter A will be discussed here. Freudenstein and Cooper (1978) described the procedure for a crude estimation of A. However, in connection with the present work we would suggest a more sophisticated method described by Griem et al. (1962) and given also by Griem (1974, Eq. (224)). This method requires the evaluation of a number of matrix elements $\sum R_{ii'}^2$ and $\sum R_{ff'}^2$ which are also needed for the calculation of electron impact width and shift, see Eq. (4).

From Eqs. (4), (8), and (9) it is obvious that for reliable calculation of Stark widths and shifts one must use a sufficiently complete set of perturbing energy levels. Therefore, it is of importance to estimate completeness (with regard to dipole matrix elements) of perturbing levels taken for the evaluation of Stark broadening parameter. For this purpose Jones et al. in 1971 (see also Griem, 1974) introduced the parameter $\Delta S/S$ in the following way

$$\frac{\Delta S}{S} = \frac{\sum_{i'} R_{ii'}^2 + \sum_{f'} R_{ff'}^2 - R_{ii}^2 - R_{ff}^2}{R_{ii}^2 + R_{ff}^2},$$

where

$$R_{jj}^2 = \frac{n_j^{*2}}{2Z^2}\,[5n_j^{*2} + 1 - 3l_j(l_j+1)] .$$

If this parameter is close to zero, the set of energy levels used is sufficiently complete. Another indication of the importance of inclusion of a particular perturbing level is the ratio $f_{i'i}/|E_i - E_{i'}|$, where $f_{ii'}$ is the absorption oscillator strength.

Within the one-electron approximation (Griem, 1974), i.e. using only one energy level for each nl electron, with the other quantum numbers chosen as to select the dominant contributions, the dipole matrix element $R_{jj'}^2$ for the sum of all lines originating or ending in a term SL, is

$$R_{jj'}^2 = \frac{l_>}{2l'+1} R_{l'l}^2 .$$

Here, $l_>$ is the greater of l, l' and $R_{l,l'}^2$ is the radial factor (Shore and Menzel, 1965).

For complex atoms it is better (Dimitrijević, 1982) to take into account every particular component of the supermultiplet. In such a case one can use the expression

$$R_{jj'}^2 = \frac{l_> R_{\mathrm{mult}}^2 R_{l,l'}^2}{(2L+1)},$$

were R_{mult}^2 is the multiplet factor (Shore and Menzel, 1965).

If the energy difference between the perturbing and perturbed level is comparable to the Debye (plasma) frequency, we must take into account Debye shielding corrections (see e.g. Griem, 1974). In such a case it is better to check also whether the line is isolated or not (see e.g. Dimitrijević and Sahal-Bréchot, 1984).

© European Southern Observatory • Provided by the NASA Astrophysics Data System

1986A&A...163..297D

Table 1. Electron impact half-halfwidths w and shifts d in Angstrom units for He I and Mg I lines as a function of temperature (T): W_{DK} – present results; W_{BG} – semiclassical of Benett and Griem (1974); W_{FC} – present calculations according to Freudenstein and Cooper (1978). Electron density is 10^{16} cm^{-3}

T	W_{DK}	W_{BG}	W_{FC}	d_{DK}	d_{BG}
He I 4438 Å $2p\ ^1P^0$–$5s\ ^1S$					
5000	1.46	1.41	1.34	1.73	1.51
10000	1.77	1.57	1.64	1.49	1.43
20000	1.85	1.65	1.72	1.12	1.24
30000	1.79	–	1.66	0.924	–
40000	1.72	1.62	1.60	0.803	0.996
He I 6678 Å $2p\ ^1P^0 - 3d\ ^1D$					
5000	0.468	0.423	0.948	0.236	0.275
10000	0.428	0.386	0.825	0.181	0.233
20000	0.389	0.349	0.696	0.135	0.196
30000	0.364	–	0.623	0.111	–
40000	0.344	0.318	0.573	0.096	0.161
Mg I 3835 Å $3p\ ^3P^0$–$3d\ ^3D$					
5000	0.098	0.107	0.239	−0.0266	−0.0445
10000	0.087	0.0962	0.207	−0.0170	−0.0270
20000	0.076	0.0852	0.173	−0.0111	−0.0139
30000	0.070	–	0.155	−0.0089	–
40000	0.066	0.0752	0.142	−0.0078	−0.00512

3. Results and discussion

In Table 1 present results for half-halfwidths w_{DK} and shifts d_{DK} are compared with our width calculations according to the method of Freudenstein and Cooper (1978) w_{FC} and semiclassical results w_{BG} of Benett and Griem (1972), given also by Griem (1974).

In the case of the He I 4438 Å line, the one-level approximation used by Freudenstein and Cooper (1978) is well satisfied since the $5p$ energy level contribution is dominant and all results are mutually close. In the two other examples, for the He I $2p\,^1P^0 - 3d\,^1D$ and Mg I $3p\,^3P^0 - 3d\,^3D$ lines, we have no dominant perturbing level and our results are considerably closer to the semiclassical ones than to values calculated from the simple approximate formula (Freudenstein and Cooper, 1978).

We believe that the simple formulae presented here will be useful when astrophysicists or physicists require a number of reliable atom line widths and shifts influenced by the Stark effect.

References

Benett, S.M., Griem, H.R.: 1971, Calculated Stark Broadening Parameters for Isolated Spectral Lines from the Atoms Helium through Calcium and Cesium, Techn. Rep. No 71–097, Univ. Maryland

Cowley, C.R.: 1971, *Observatory* **91**, 139

Dimitrijević, M.S.: 1982, *Astron. Astrophys.* **112**, 251

Dimitrijević, M.S., Grujić, P.: 1979, *Z. Naturforsch.* **34a**, 1362

Dimitrijević, M.S., Sahal-Bréchot, S.: 1984, *Astron. Astrophys.* **136**, 289

Freudenstein, S.A., Cooper, J.: 1978, *Astrophys. J.* **224**, 1079

Griem, H.R.: 1962, *Phys. Rev.* **128**, 515

Griem, H.R.: 1974, Spectral Line Broadening by Plasmas, Academic Press, New York

Griem, H.R., Baranger, M., Kolb, A.C., Oertel, G.: 1962, *Phys. Rev.* **125**, 177

Jones, W.W., Benett, S.M., Griem, H.R.: 1971, Calculated Electron Impact Broadening Parameters for Isolated Spectral Lines from the Singly Charged Ions: Lithium through Calcium, Techn. Rep. No 71–128, Univ. Maryland

Shore, B.W., Menzel, D.H.: 1965, *Astrophys. J. Suppl. Series* **12**, 187

© European Southern Observatory • Provided by the NASA Astrophysics Data System

1987A&A...172..345D

Astron. Astrophys. 172, 345–349 (1987)

ASTRONOMY AND ASTROPHYSICS

Simple estimates for Stark broadening of ion lines in stellar plasmas

M. S. Dimitrijević [1] **and N. Konjević** [2]

[1] Astronomical Observatory, Volgina 7, YU-11050 Beograd, Yugoslavia
[2] Institute of Physics, YU-11001 Beograd, P. O. Box 57, Yugoslavia

Received April 15, accepted August 6, 1986

Summary. Simple analytical expressions for estimation of Stark widths and shifts of ionized atom lines have been derived from the low temperature limit of a modified semiempirical formula.

Key words: lines: profile – atomic and molecular data

1. Introduction

In stellar atmosphere calculations, collisional broadening parameters for a large number of lines of various elements are required and they are frequently unavailable [for critical reviews of available experimental data on Stark broadening of non-hydrogenic atom and ion lines see Konjević and Roberts (1976), Konjević and Wiese (1976), and Konjević et al. (1984a, b)]. Moreover in O and B stars and white dwarfs atmospheres the Stark effect is the main pressure broadening mechanism. Even in atmospheres of relatively cool stars, such as the Sun, where line broadening caused by collisions with neutral perturbers is dominant, for higher members of spectral series the Stark effect may compete with the neutral perturber interaction on the emitter (Vince et al., 1985a, b). For evaluation of Stark broadening parameters, one can use the so-called semi-classical approach or a fully quantum mechanical theoretical approach (see e.g. Griem, 1974 and references therein), which requires elaborate calculations even for a single line. For large-scale calculations, when high accuracy for each particular line is not required, simple approximations with good average accuracy are very useful. For neutral atom lines the simplified semi-classical method (Freudenstein and Cooper, 1978; Dimitrijević and Konjević, 1986) is very convenient, while for singly ionized atoms the semi-empirical method of Griem (1968) (see also Hey, 1977; Hey and Breger, 1982) is suggested. This method has been modified recently in order to avoid an extensive set of input atomic data and extended also to multiply charged ion line widths (Dimitrijević and Konjević, 1980, 1981) and shifts (Dimitrijević and Kršljanin, 1986). Tables of calculated Stark widths of prominent lines of some doubly and triply-charged ions are given by Dimitrijević and Konjević (1981). By inspecting these tables one can determine that for typical conditions in hot stars and white dwarfs atmospheres ($T \sim 10^4$ K) the threshold value of the required Gaunt factor may be aften used in the modified semi-empirical approach for most of the intense lines in doubly – and triply – charged ion spectra. When such a situation occurs, considerable simplification of the semi-empirical method occurs (Griem, 1968). The aim of this paper is to obtain in analytical form the low temperature limit of the modified semi-empirical formulae (Dimitrijević and Konjević, 1980; Dimitrijević and Kršljanin, 1986) which can be useful for simple estimates of Stark broadening parameters of singly and multiply charged ion lines in plasmas.

Send offprint requests to: M.S. Dimitrijević

2. Theory

Stark widths and shift of isolated ion lines can be calculated e.g. from the modified semi-empirical formula (Dimitrijević and Konjević, 1980), which for the full widths (in angular frequency units) has the following form:

$$
\begin{aligned}
w = N \frac{8\pi}{3} \frac{\hbar^2}{m^2} \left(\frac{2m}{\pi kT}\right)^{1/2} \frac{\pi}{\sqrt{3}} \Bigg[& \boldsymbol{R}^2_{l_i,l_i+1} \tilde{g}\left(\frac{E}{\Delta E_{l_i,l_i+1}}\right) \\
& + \boldsymbol{R}^2_{l_i,l_i-1} \tilde{g}\left(\frac{E}{\Delta E_{l_i,l_i-1}}\right) \\
& + \boldsymbol{R}^2_{l_f,l_f+1} \tilde{g}\left(\frac{E}{\Delta E_{l_f,l_f+1}}\right) + \boldsymbol{R}^2_{l_f,l_f-1} \tilde{g}\left(\frac{E}{\Delta E_{l_f,l_f-1}}\right) \\
& + \sum_{i'} (\boldsymbol{R}^2_{ii'})_{\Delta n \neq 0}\, g\left(\frac{3kTn_i^3}{4Z^2 E_H}\right) + \sum_{f'} (\boldsymbol{R}^2_{ff'})_{\Delta n \neq 0}\, g\left(\frac{3kTn_f^3}{4Z^2 E_H}\right) \Bigg] .
\end{aligned}
\tag{1}
$$

$$\boldsymbol{R}^2_{ll'} \cong \left(\frac{3n}{2Z}\right)^2 \frac{l_>}{2l+1} (n^2 - l_>^2)\, \phi^2$$

$$\sum_{j'} (\boldsymbol{R}^2_{jj'})_{\Delta n \neq 0} \cong \left(\frac{3n_j}{2Z}\right)^2 \frac{1}{9} (n_j^2 + 3l_j^2 + 3l_j + 11),$$

where N and T are the electron density and electron temperature respectively, $E = 3kT/2$ is the energy of perturbing electron, and $E_{jj'} = |E_{j'} - E_j|$ is the energy difference between levels j and j', $l_> = \max(l, l')$, $Z-1$ is the ionic charge ϕ is a tabulated correction factor (Bates and Damgaard, 1949; Oertel and Shomo, 1968) n is the effective principal quantum number while g (Griem, 1968) and $\tilde{g}$ (Dimitrijević and Konjević, 1980) are the effective Gaunt factors.

The comparison between experiments and the results obtained from Eq. (1) yields as an average ratio of measured to calculated widths of 1.06 ± 0.31 for doubly-, while for triply-ionized atoms this ratio is 0.92 ± 0.42 (Dimitrijević and Konjević, 1980).

When the nearest perturbing level is so far from E_j that $E/\Delta E \leqq 2$ is satisfied, Griem's semi-empirical formula may be considerably simplified (Griem, 1968).

© European Southern Observatory • Provided by the NASA Astrophysics Data System

1987A&A...172..345D

Table 1. Comparison of measured w_m and calculated Stark widths of doubly and triply ionized atoms. The values for the experimental widths w_m are normalized for electron density $N = 10^{17}$ cm^{-3}. The element, transition, multiplet number and electron temperature are given. Ratios of measured w_m to theoretical results are given in the following order: $w_{\mathrm{Eq.(1)}}$ modified semi-empirical formula Eq. (1) and $w_{\mathrm{Eq.(2)}}$ low temperature limit of same formula, Eq. (2). References: 1. Platiša et al. (1975a); 2. Purcell and Barnard (1984); 3. Platiša et al. (1975b); 4. Purić et al. (1974); 5. Platiša et al. (1977a); 6. Platiša et al. (1979); 7. Platiša et al. (1977b); 8. Platiša et al. (1975c); 9. Bogen (1972); 10. El-Farra and Hughes (1983)

Ion	Transition (mult. No.)	T(K)	w_m(Å) at 10^{17} cm^{-3}	$\frac{w_m}{w_{\mathrm{Eq.(1)}}}$	$\frac{w_m}{w_{\mathrm{Eq.(2)}}}$	Ref.
N III	$3s^2S-3p^2P^0$ (1)	24300	0.17	0.82	0.89	1
	$3p^2P^0-3d^2D$ (2)	24300	0.21	0.76	1.14	1
		36100	0.27	1.23	1.84	2
	$3s^4P^0-3p^4D$ (5)	24300	0.18	1.18	1.29	1
O III	$3s^3P^0-3p^3D$ (2)	25900	0.14	1.03	1.13	3
	$3s^3P^0-3p^3P$ (4)	25900	0.11	1.09	1.19	3
	$3p^3D-3d^3F^0$ (8)	25900	0.12	1.15	1.85	3
	$3p^3P-3d^3D^0$ (14)	25900	0.14	0.93	1.40	3
Si III	$4s^3S-4p^3P^0$ (2)	16400	0.38	0.67	0.57	4
		25600	0.31	0.68	0.58	5
S III	$3d^3P^0-4p^3P$ (2)	28500	0.15	1.16	1.40	6
	$3d^3D^0-4p^3P$ (8)	28500	0.17	0.96	1.12	6
	$4s^3P^0-4p^3D$ (4)	28500	0.25	0.88	0.79	6
	$4s^3P^0-4p^3P$ (5)	28500	0.20	0.86	0.77	6
	$4s^3P^0-4p^3S$ (6)	28500	0.18	0.84	0.76	6
	$4p^3D-4d^3F^0$ (15 UV)	28500	0.20	1.56	1.16	6
	$4p^3D-4d^3D^0$ (16 UV)	28500	0.20	1.64	1.20	6
	$4p^3P-4d^3D^0$ (18 UV)	28500	0.21	1.43	1.04	6
Cl III	$3d^4P-4p^4P^0$ (7)	24200	0.19	1.04	1.38	7
	$4s^4P-4p^4D^0$ (1)	24200	0.10	1.00	0.91	7
	$4s^4P-4p^4P^0$ (2)	24200	0.17	1.08	0.98	7
	$4s^4P-4p^4S^0$ (3)	24200	0.17	1.10	1.00	7
	$4s^2P-4p^2D^0$ (5)	24200	0.19	0.92	0.81	7
	$4s'^2D-4p'^2F^0$ (10)	24200	0.18	1.05	0.93	7
	$4s'^2D-4p'^2D^0$ (11)	24200	0.14	0.90	0.80	7
Ar III	$3d''^3P^0-4p''^3P$ (6)	21100	0.13	1.18	1.46	8
	$4s^5S^0-4p^5P$ (1)	21100	0.15	1.02	0.89	8
	$4s'^3D^0-4p'^3D$ (2)	21100	0.13	0.81	0.88	8
	$4s'^3D^0-4p'^3F$ (3)	21100	0.14	0.94	0.86	8
C IV	$2s^2S-2p^2P^0$ (1 UV)	58000	0.006	1.99	2.74	9
		53000	0.0027	1.09	1.18	10
Si IV	$4s^2S-4p^2P^0$ (1)	25600	0.22	0.57	0.52	5
S IV	$4s^2S-4p^2P^0$ (1)	28500	0.12	0.80	0.71	6
Ar IV	$4s^4P-4p^4D^0$ (4 UV)	20750	0.06	0.74	0.54	8
		22200	0.06	0.74	0.55	8
	$4s^4P-4p^4P^0$ (5 UV)	20750	0.06	0.76	0.55	8
		22200	0.06	0.79	0.57	8

© European Southern Observatory • Provided by the NASA Astrophysics Data System

1987A&A...172..345D

Here, we shall perform analogous simplification of the modified semi-empirical formula, Eq. (1), for all cases when $E/\Delta E \leqq 2$. Then $g=0.2$ and $\tilde{g}=0.9-1.1/Z$. Furthermore, one can put $\phi^2=1$ in Eq. (1) which is a reasonable assumption for $\Delta n=0$ (see e.g. Griem, 1974, p. 31), since exact values of ϕ^2 usually range between 0.8 and 1. If one performs the summation in Eq. (1) it is easy to obtain

$$w(\text{Å}) = 0.4430\ 10^{-8}\ \frac{\lambda^2(\text{cm})\,N(\text{cm}^{-3})}{T^{1/2}(\text{K})} \cdot \sum_{j=i,f}\left[\boldsymbol{R}_j^2 + \frac{\tilde{g}_{th}-g_{th}}{g_{th}}\left(\frac{3n_j}{2Z}\right)^2 (n_j^2-l_j^2-l_j-1)\right]$$

$$\boldsymbol{R}_j^2 = \sum_{j'} \boldsymbol{R}_{jj'}^2 .$$

Since the contribution to the total line width of the transitions with $\Delta n \neq 0$ does not exceed 25% and it is compensated by assuming $\phi^2=1$, we can neglect them and finally obtain

$$w(\text{Å}) = 2.2151\ 10^{-8}\ \frac{\lambda^2(\text{cm})\,N(\text{cm}^{-3})}{T^{1/2}(\text{K})} \cdot \left(0.9-\frac{1.1}{Z}\right) \sum_{j=i,f}\left(\frac{3n_j}{2Z}\right)^2 (n^2-l_j^2-l_j-1), \tag{2}$$

where n_i and n_f are the effective quantum numbers of the upper and lower energy levels of the transition.

Recently, a modified semi-empirical formula for the shift has also been reported (Dimitrijević and Kršljanin, 1986). Since we are interested in the low temperature limit, we shall, as in previous case, neglect the collisions with $\Delta n \neq 0$. Then the simplified version of the modified semi-empirical formula for the shift is

$$d = N\,\frac{4\pi}{3}\,\frac{\hbar^2}{m}\left(\frac{2m}{\pi kT}\right)^{1/2}\frac{\pi}{\sqrt{3}}\left[\boldsymbol{R}_{l_i,l_i+1}^2\,\tilde{g}_{sh}\left(\frac{E}{\Delta E_{l_i,l_i+1}}\right) - \boldsymbol{R}_{l_i,l_i-1}^2\,\tilde{g}_{sh}\left(\frac{E}{\Delta E_{l_i,l_i-1}}\right) - \boldsymbol{R}_{l_f,l_f+1}^2\,\tilde{g}_{sh}\left(\frac{E}{\Delta E_{l_f,l_f+1}}\right) + \boldsymbol{R}_{l_f,l_f-1}^2\,\tilde{g}_{sh}\left(\frac{E}{\Delta E_{l_f,l_f-1}}\right) + \sum_k \delta_k\right]. \tag{3}$$

The sum $\sum_k \delta_k$ is not equal to zero only if perturbing levels strongly violating the assumed approximations exist, i.e. if there are levels with $|\Delta E_{jj'}| \ll |\Delta E_{n,n+1}|$. The contribution of each such level should be calculated as

$$\delta_j = \pm\,\varepsilon_j(\boldsymbol{R}_{jj'}^2)\left[g_{sh}\left(\frac{E}{\Delta E_{j,j'}}\right) \pm g_{sh}\left(\frac{E}{\Delta E_{n_i,n_i+1}}\right)\right]$$

where the lower sign corresponds to $\Delta E_{jj'}<0$ and

$$\varepsilon_j = \begin{cases} +1, j=i \\ -1, j=f. \end{cases}$$

Taking into account that $\tilde{g}_{sh} \equiv \tilde{g}$ and g_{sh} near the threshold, and applying the same procedure as for the width, we obtain, for $E/\Delta E \leqq 2$

$$d \approx 1.1076\ 10^{-8}\ \frac{\lambda^2(\text{cm})\,N(\text{cm}^{-3})}{T^{1/2}(\text{K})}\left(0.9-\frac{1.1}{Z}\right)\frac{9}{4Z^2}\sum_{j=i,f}\frac{n_j^2\,\varepsilon_j}{2l_j+1} \cdot \left\{(l_j+1)\,[n_j^2-(l_j+1)^2]-l_j(n_j^2-l_j^2)\right\}. \tag{4}$$

If all levels $l_{i,f}\pm 1$ exist, an additional summation may be performed in Eq. (4) to obtain

$$d \approx 1.1076\ 10^{-8}\ \frac{\lambda^2(\text{cm})\,N(\text{cm}^{-3})}{T^{1/2}(\text{K})}\left(0.9-\frac{1.1}{Z}\right)\frac{9}{4Z^2} \cdot \sum_{j=i,f}\frac{n_j^2\,\varepsilon}{2l_j+1}\,(n_j^2-3l_j^2-3l_j-1). \tag{5}$$

3. Results and discussion

3.1. Widths

In order to test the equation obtained for the low temperature limit of the modified semi-empirical formula we compared first the results from Eq. (2) with the results of comprehensive width calculations for doubly and triply ionized atoms (Dimitrijević and Konjević, 1981) in which Eq. (1) is used. The discrepancy did not exceed ±30% on the average. Furthermore, in Table 1 comparison is made between the results from Eq. (1) and Eq. (2) for the experimental results obtained at electron temperatures when condition $E/\Delta E_{jj'} \leqq 2$ is satisfied. Experimental data in Table 1 are taken from Tables 1 and 2 of the paper by Dimitrijević and Konjević (1980), which have been further updated by new results.

Table 2. Comparison of experimental and theoretical Stark widths of analogous transitions of doubly ionized inert gases, multiplets $ns\,^3S^0-np\,^3P$: w_m – experimental data (Konjević and Pittman, 1984) and $w_{\text{Eq.(1)}}$ and $w_{\text{Eq.(2)}}$ calculated ones using Eqs. (1) and (2) respectively

Ion	Wavelength	Temperature	Full width in Å units at $N=10^{17}\,\text{cm}^{-3}$		
	(Å)	(K)	w_m	$w_{\text{Eq.(1)}}$	$w_{\text{Eq.(2)}}$
Ne III	2677.90	34000	0.063	0.052	0.049
	2678.64	34000	0.062	0.052	0.049
Ar III	3509.33	27500	0.160	0.153	0.174
	3514.18	27500	0.148	0.153	0.174
Kr III	3564.23	26000	0.160	0.168	0.194
Xe III	3780.98	27000	0.222	0.235	0.267

© European Southern Observatory • Provided by the NASA Astrophysics Data System

1987A&A...172..345D

From Table 1 the average ratio of experimental w_m and calculated values from Eq. (1) and (2) are 1.01 and 1.04, respectively. Finally, in Table 2 are given the results obtained from Eqs. (1) and (2) together with recently measured Stark widths (Konjević and Pittman, 1984) of analogous transitions of doubly ionized inert gases. Here, the condition $E/\Delta E_{jj'} \leqq 2$ is always satisfied and the agreement between two sets of calculated data is within $\pm 15\%$, while the discrepancy with the experiment does not exceed 21%. Therefore, on the basis of comparisons in Tables 1 and 2 we estimate that the results of Eq. (2) for widths of doubly- and triply-ionized atoms agree with experiment within $\pm 40\%$. The experimental results for higher ionization stages are not available for comparison.

3.2. Shifts

The possibilities of the theory and expected accuracy in the case of shifts are considerably smaller than for the line widths (see e.g. Dimitrijević et al., 1981; Griem, 1974). In Figs. 1–3 comparison is made between various experimental results for Be II $2s^2S-2p^2P^0$, Mg II $3p^2P^0-4s^2S$ and Ca II $4s^2S-4p^2P^0$ lines, calculations according to Eq. (4) and other theoretical calculations. On the basis of the comparison of data in Figs. 1–3 one can conclude that the agreement of the proposed simple method with experimental results is at least comparable with more elaborate approaches.

We believe that simple formulae, Eqs. (2) and (4), will be adequate when astrophysicists require a large number of ion line widths of doubly and triply charged ions due to the Stark broadening. The estimate requires only the knowledge of atomic data for ionization potentials, energy levels and orbital quantum numbers of the upper and lower level of the considered transition. However, before using Eqs. (2) and (4), the condition $E/\Delta E_{jj'} \leqq 2$ should be checked, and if this condition is not satisfied Eqs. (1) or (3) must be used.

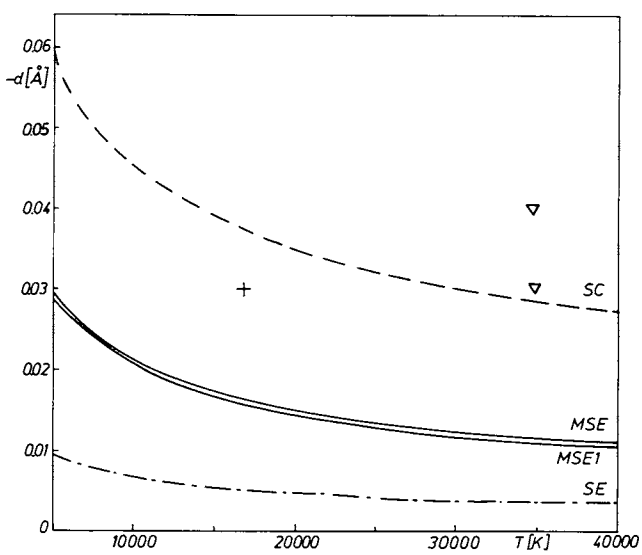

Fig. 1. Stark shifts for Be II $2s^2S-2p^2P^0$ multiplet. Calculations: MSE – modified semi-empirical (Dimitrijević and Kršljanin, 1986); MSE1 – present results; SE – semi-empirical according to Griem (1968); SC – semi-classical, Jones et al. (1971); QM – quantum mechanical, Barnes and Peach (1970). Experimental points: + – Purić and Konjević (1972); △ – Hadžiomerspahić et al. (1973); △ – Roberts and Barnard (1972); ○ – Fleurier et al. (1977); □ – Helbig and Kusch (1972)

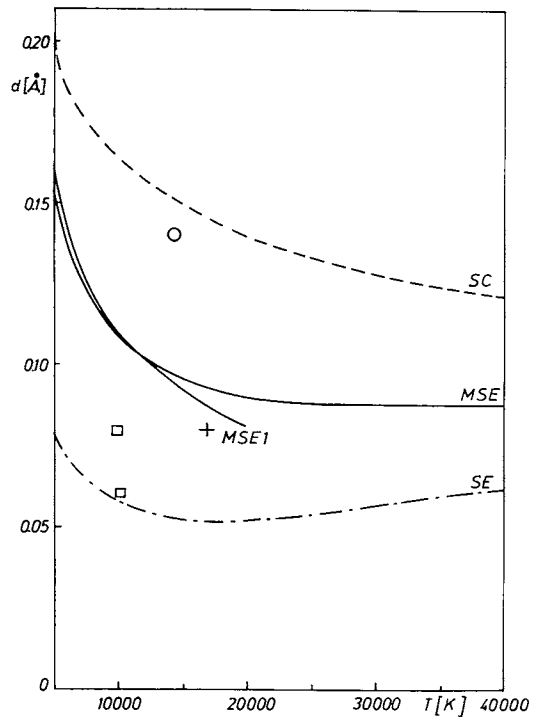

Fig. 2. Stark shifts for Mg II $3p^2P^0-4s^2S$ multiplet. Notation is the same as in Fig. 1

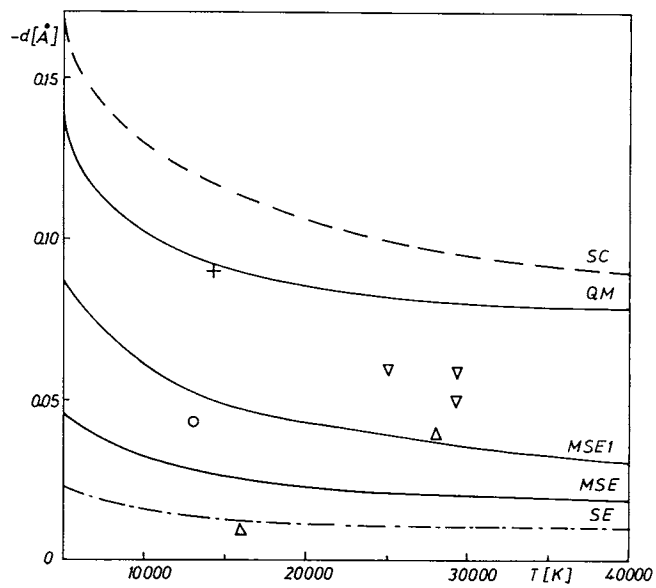

Fig. 3. Stark shifts for Ca II $4s^2S-4p^2P^0$ multiplet. Notation is the same as in Fig. 1

References

Barnes, K.S., Peach, G.: 1970, *J. Phys.* B**3**, 350

Bates, D.R., Damgaard, A.: 1949, *Phil. Trans. Roy. Soc. London* (Ser. A) **242**, 101

Bogen, P.: 1972, *Z. Naturforsch.* **27A**, 210

Dimitrijević, M.S., Feautrier, N., Sahal-Bréchot, S.: 1981, *J. Phys.* B**14**, 2559

© European Southern Observatory • Provided by the NASA Astrophysics Data System

1987A&A...172..345D

Dimitrijević, M.S., Konjević, N.: 1980, *J. Quant. Spectrosc. Radiat. Transfer* **24**, 451
Dimitrijević, M.S., Konjević, N.: 1981, in *Spectral Line Shapes*, ed. B. Wende, W. de Gruyter, Berlin, New York, p. 211
Dimitrijević, M.S., Konjević, N.: 1986, *Astron. Astrophys.* **163**, 297
Dimitrijević, M.S., Kršljanin, V.: 1986, *Astron. Astrophys.* **165**, 269
El-Farra, M.A., Hughes, T.P.: 1983, *J. Quant. Spectrosc. Radiat. Transfer* **30**, 335
Fleurier, C., Sahal-Bréchot, S., Chapelle, J.: 1977, *J. Quant. Spectrosc. Radiat. Transfer* **17**, 595
Freudenstein, S.A., Cooper, J.: 1978, *Astrophys. J.* **224**, 1079
Griem, H.R., Baranger, M., Kolb, A.C., Oertel, G.: 1962, *Phys. Rev.* **125**, 1977
Griem, H.R.: 1968, *Phys. Rev.* **165**, 258
Griem, H.R.: 1974, Spectral Line Broadening by Plasmas, McGraw-Hill, New York
Hadžiomerspahić, D., Platiša, M., Konjević, N., Popović, M.: 1973, *Z. Phys.* **262**, 169
Helbig, V., Kusch, H.J.: 1972, *Astron. Astrophys.* **20**, 299
Hey, J.D.: 1977, *J. Quant. Spectrosc. Radiat. Transfer* **17**, 729
Hey, J.D., Breger, P.: 1982, *S. Afr. J. Phys.* **5**, 111
Jones, W.W., Benett, S.M., Griem, H.R.: 1971, Tech. Rep. No. 71–128, Univ. Maryland
Konjević, N., Roberts, J.R.: 1976, *J. Phys. Chem. Ref. Data* **5**, 209
Konjević, N., Wiese, W.L.: 1976, *J. Phys. Chem. Ref. Data* **5**, 259
Konjević, N., Dimitrijević, M.S., Wiese, W.L.: 1984a, *J. Phys. Chem. Ref. Data* **13**, 619
Konjević, N., Dimitrijević, M.S., Wiese, W.L.: 1984b, *J. Phys. Chem. Ref. Data* **13**, 649
Konjević, N., Pittman, T.: 1984, XII Symposium on Physics of Ionized Gases, Šibenik, contributed papers, Institute of Physics, Beograd, p. 450
Oertel, G., Shomo, L.P.: 1968, *Astrophys. J. Suppl. Series* **16**, 187
Platiša, M., Popović, M., Konjević, N.: 1975a, *Astron. Astrophys.* **41**, 463
Platiša, M., Popović, M., Konjević, N.: 1975b, *Astron. Astrophys.* **45**, 325
Platiša, M., Popović, M., Dimitrijević, M., Konjević, N.: 1975c, *Z. Naturforsch.* **30A**, 212
Platiša, M., Dimitrijević, M., Popović, M., Konjević, N.: 1977a, *J. Phys.* B**10**, 2997
Platiša, M., Dimitrijević, M., Popović, M., Konjević, N.: 1977b, *Astron. Astrophys.* **54**, 837
Platiša, M., Popović, M., Dimitrijević, M., Konjević, N.: 1979, *J. Quant. Spectrosc. Radiat. Transfer* **22**, 333
Purcell, S.T., Barnard, A.J.: 1984, *J. Quant. Spectrosc. Radiat. Transfer* **32**, 205
Purić, J., Djeniže, S., Labat, J., Ćirković, Lj.: 1974, *Z. Phys.* **267**, 71
Purić, J., Konjević, N.: 1972, *Z. Phys.* **249**, 440
Roberts, D.E., Barnard, A.J.: 1972, *J. Quant. Spectrosc. Radiat. Transfer* **12**, 1205
Vince, I., Dimitrijević, M.S., Kršljanin, V.: 1985a, in *Spectral Line Shapes*, ed. F. Rostas, W. de Gruyter Berlin, New York, p. 649
Vince, I., Dimitrijević, M.S., Kršljanin, V.: 1985b, in *Progress in Stellar Spectral Line Formation Theory*, eds. J.E. Beckman, L. Crivelari, D. Raidel, Boston, p. 373

© European Southern Observatory • Provided by the NASA Astrophysics Data System

1988A&A...192..249L

Astron. Astrophys. 192, 249–254 (1988)

ASTRONOMY AND ASTROPHYSICS

Stark broadening of visible Si II lines in stellar atmospheres

T. Lanz [1], M.S. Dimitrijević [2], and M.-C. Artru [3]

[1] Institut d'Astronomie de l'Université de Lausanne, CH-1290 Chavannes-des-Bois, Switzerland
[2] Astronomical Observatory, Volgina 7, YU-11050 Beograd, Yugoslavia
[3] Observatoire de Paris, Section de Meudon, F-92195 Meudon, France

Received March 30, accepted August 12, 1987

Summary. The Stark broadening of visible Si II lines is studied and its consequence on the intensity of the stellar absorption is analyzed. A complete set of atomic data concerning the Stark widths, is elaborated for 19 multiplets of Si II of astrophysical importance. Previous available determinations are reviewed and new Stark widths are calculated by means of the semi-classical impact theory. The accuracy of different theoretical and empirical methods are discussed.

The new adopted Stark widths are applied, in several examples, to the analysis of stellar absorption lines. These widths are generally smaller than the previous theoretical estimates for the low-excitation transitions of Si II. But it leads to reduce only slightly (less than 10%) the equivalent widths, even with enhanced silicon. The only exception is the multiplet 1, whose equivalent width could be reduced from 10% to 35%. On the other hand, the influence of the large Stark widths obtained for the high-excitation multiplets, is shown to be critical for the abuncance analysis. The example of the 4d–8f transition, at 4201 Å, is detailed.

Radiative widths are also given for these 19 multiplets and could be as large as 40 times the classical damping. Such widths affect particularly the low-excitation transitions and increase the equivalent widths up to 30% with respect to those calculated with the classical value.

Key words: atomic and molecular data – lines: profile – stars: atmospheres

1. Introduction

Because of its large cosmic abundance, the silicon is of special importance in solar and stellar studies. For stars with effective temperature from 10000 to 20000 K (A 0 to B 3) the Si II spectrum is dominant, with strong lines in the visible, as well as in the ultraviolet where occur the resonance multiplets. Many silicon abundances were derived from visible Si II lines, by using the theoretical equivalent widths calculated in LTE by Mihalas for the two Si II multiplets at $\lambda\lambda$4128–4130 and λ4201 (Mihalas and Henshaw, 1966; Mégessier, 1971). The other strong multiplets commonly used are those at λ3856 (No. 1) and λ6347 (No. 2). These lines are also important in the NLTE investigation of the silicon absorption in hot stars (Kamp, 1978; Lennon et al., 1986). Meanwhile the wealth of good observations has increased and reliable equivalent widths for weaker lines become now accessible. In particular the Ap Si stars spectra reveal many Si II lines of high excitation, such as those of the 4d–nf series (e.g. λ4201, λ3955) which are very sensitive to the plasma broadening effects. Moreover the ultraviolet range is also observed at high resolution and leads to independant abundance determinations (Artru and Lanz, 1987) that are 2 to 5 times lower and must be reconcilied with the visible ones.

In order to further develop the study of the silicon abundance in the A and B stars, either normal or peculiar, it is necessary to insure the reliability of the basic atomic data needed. From a recent compilation of available oscillator strengths for Si II (Lanz and Artru, 1985) we have obtained a consistent set of gf data which can be used with confidence. It is also important to make a reliable estimation of the line-broadening mechanism in the stellar atmosphere, and especially the quadratic Stark effect on each considered line must be investigated. Some of these data already exist in the literature, but have not yet been systematically exploited in the astrophysical studies.

In this paper, we select the visible Si II multiplets which are currently present in stellar spectra, or likely to appear when silicon is enhanced. We first discuss for these lines the different broadening effects and their relative importance in the formation of stellar lines. We could point out that a precise determination of the quadratic Stark widths is essential for stellar spectra analyses. From a critical discussion of the Stark widths collected in published atomic studies, we retain the previous reliable data. Then we perform new theoretical calculations by means of the semi-classical perturbation impact theory (Sahal-Bréchot, 1969a, b, 1974), in order to provide a consistent set of Stark widths, with an evaluation of their accuracy. Finally we recalculate theoretical equivalent widths for a sample of significative Si II stellar lines, for different typical stellar atmospheres, in order to show how the equivalent width of stellar lines may be sensitve to the adopted Stark width, and to discuss the errors in abundance determinations that can be attributed to uncertainties on the Stark width data, especially for the highly-excited transitions.

2. The Stark widths of visible Si II lines

2.1. Broadening effects in the formation of stellar lines

Moore (1965) listes 69 Si II multiplets in the visible range, but we should consider here only those which are likely to be present in stellar spectra. Table 1 contains 19 such multiplets, with their

Send offprint requests to: T. Lanz

© European Southern Observatory • Provided by the NASA Astrophysics Data System

1988A&A...192..249L

Table 1. Selected visible Si II multiplets of astrophysical interest

Multiplet[a]	Wavelength[b]	Classification[a]	$\Delta\lambda_{rad}^{(c)}$
7	3210	4p $^2P^\circ$ – 5d ^2D	0.15
6	3340	4p $^2P^\circ$ – 6s ^2S	0.20
1	3856	3p^2 ^2D – 4p $^2P^\circ$	0.094
7.07	3955	4d ^2D – 9f $^2F^\circ$	0.93
3.01	4075	3d ^2D – 5p $^2P^\circ$	2.2
3	4131	3d ^2D – 4f $^2F^\circ$	2.5
7.26	4190	3d' $^2D^\circ$ – 4p' ^2P[d]	28.
7.06	4201	4d ^2D – 8f $^2F^\circ$	1.1
7.16	4377	4f $^2F^\circ$ – 9g ^2G	0.29
7.05	4621	4d ^2D – 7f $^2F^\circ$	1.3
7.15	4673	4f $^2F^\circ$ – 8g ^2G	0.34
5	5056	4p $^2P^\circ$ – 4d ^2D	1.6
7.14	5186	4f $^2F^\circ$ – 7g ^2G	0.43
23	5202	4p' ^4D – 4d' $^4F^\circ$	0.38
7.03	5467	4d ^2D – 6f $^2F^\circ$	1.9
4	5979	4p $^2P^\circ$ – 5s ^2S	2.2
7.13	6240	4f $^2F^\circ$ – 6g ^2G	0.65
2	6347	4s ^2S – 4p $^2P^\circ$	1.7
7.02	7850	4d ^2D – 5f $^2F^\circ$	3.9

[a] The multiplet number and the level designations are from Moore(1965).
[b] Air wavelength in Å is referred to the strongest line of the multiplet.
[c] Radiative widths (FWHM in mÅ).
[d] Autoionised level with $\Gamma_A = 0.02$ meV (Artru et al., 1981)

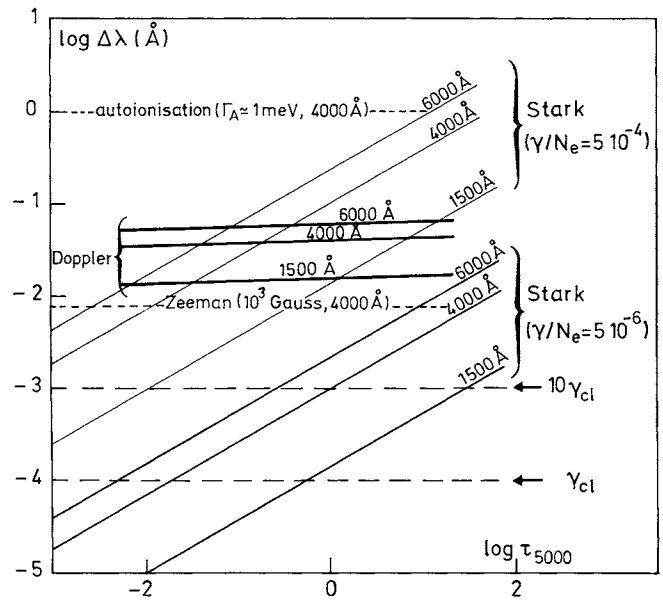

Fig. 1. Comparison between various line broadening effects at different depths of a stellar atmosphere with $T_{eff} = 13000$ K and $\log g = 4.2$, which is typical of late B-type stars

identification, totalizing 36 individual lines. For these Si II lines, besides the thermal Doppler effect, the profile is mainly influenced by the Stark broadening due to the interaction of the absorber with charged particles. The radiative damping is generally smaller than the pressure broadening in stellar photospheres. Autoionisation occurs only for the multiplet 7.26 (λ4190) according to Artru et al. (1981). The Zeeman effect becomes significant for magnetic fields larger than about 1 kG (see Fig. 1), and must be taken into account for most of the magnetic Ap Si stars. Its influence is not considered in the present work.

The radiative damping comes straight from the finite lifetime of the two levels of the transition. These lifetime measurements have been compiled (Lanz and Artru, 1985) or could be estimated from the transition probabilities of the decay multiplets. We give in Table 1 the radiative widths, which are up to 40 times greater than the classical damping.

The Stark width, mainly due to the electron collisions, can be assumed to be proportional to the electronic density N_e, in a wide range of plasma conditions. We will give it by the value of $2w = \Delta\lambda_S\, 10^{17}/N_e$, in unit of Å cm^3, $\Delta\lambda_S$ being the full width at half maximum (FWHM) of the Lorentz profile in wavelength. It can be given as γ_e/N_e, where γ_e is the width (FWHM) in unit of angular frequency (rad s^{-1}) directly related to the level widths. The conversion is: $(\gamma_e/N_e) = 188\,(2w/\lambda^2)$ with wavelengths in Å.

The equivalent width of stellar absorption lines strongly depends on the Stark effect in two cases: first if the Stark broadening $\Delta\lambda_S$ is larger than the Doppler width, $\Delta\lambda_D$, it contributes to desaturate the core of the line; second, in case of very strong lines beyond the saturation plateau, most of the absorbed energy lies in the wings of the Voigt profile which is determined by $\Delta\lambda_S$ only. Figure 1 compares the various broadening effects in a standard atmosphere model of a late B-type star. It shows how the Stark width $\Delta\lambda_S$ varies at different given wavelengths, for two typical values of the Stark broadening constant: the lower curves correspond to $(\gamma_e/N_e) = 5\,10^{-6}$ rad s^{-1}, which is a common value for a Si II line of low excitation, the upper ones correspond to 100 times this value, which may be the order of magnitude of the broadening for highly-excited levels, such as those of the nf or ng series (see the results below in Table 3). It can be seen that the values from 10^{-4} to 10^{-3} Å (1 to 10 times the classical damping) sometimes used for synthetic spectra are roughly correct to represent the Stark effect in the $\tau_{5000} = 1$ range for the low excitation visible lines, but it does not reproduce its real variation versus N_e along the atmosphere depth. On the contrary, it is underestimated by about two orders of magnitude in the case of high-excitation lines, which are more sensitive to the electric field fluctuations (Vince et al., 1985). In this case (for example the Si II lines at λ4201) the Stark width is comparable or even larger than the Doppler width around $\tau_{5000} = 1$, and the calculated values of the equivalent widths become very sensitive to the adopted Stark broadening as soon as the core begin to saturate. Then an accurate determination of the Stark width is essential, although it is more difficult to calculate it when it involves the high-excitation levels.

2.2. *Available data for the Stark widths of Si II*

The first extensive calculations of the Stark widths were given by Griem (1964), assuming straight trajectories for the perturbers. These results were applied to the stellar absorption by Mihalas and Henshaw (1966) who fitted them with a parametric relation. Further extended semi-classical calculations by Jones et al. (1971), also published in Griem (1974), were done with hyperbolic trajectories, and provided larger values, by about one order of magnitude, in better agreement with experimental results. Other theoretical results were obtained within the semi-classical perturbational formalism by Sahal-Bréchot (1969), Sahal-Bréchot and Segré (1971), in the UV range, and Lesage et al. (1977). Also Blaha applied the distorted-wave method (reported by Chiang and Griem, 1978), and Yukov (1972) and Dimitrijević (1983) used

© European Southern Observatory • Provided by the NASA Astrophysics Data System

1988A&A...192..249L

different simplified semi-classical approaches. Results obtained from different semi-empirical methods were also published for Si II (Griem, 1968; Hey, 1977; Dimitrijević, 1983). The available experimental determinations are based on various procedures which are summarized by Dimitrijević (1983, Table 1). The results are collected in the recent general compilations of Konjević and Wiese (1976) and Konjević et al.(1984). Most of these published data concern the Stark widths of the strongest visible multiplets (Nos 1–5), and are limited to a few plasma temperatures. In a later work, Lesage et al. (1983) give a thorough comparison of all Stark widths, calculated or measured, for each of these five multiplets.

From the previous compilations it appears that more than half of the multiplets selected in Table 1 have no published Stark width. Therefore we perform new calculations, as described in the next section, to evaluate the missing data. The widths with previous determinations are recalculated to insure the consistency of the new set of data, and to allow comparisons between the independant theoretical methods.

2.3. *New theoretical calculations of* Si II *Stark widths*

The semi-classical perturbation theory (SC) is extensively used to produce the Stark widths of the Si II multiplets selected in Table 1. We also apply the modified semi-empirical (MSE) approach in order to test this simple method which can easily provide many other Stark widths necessary in astrophysical studies. Both methods are briefly recalled below and their results are compared on several examples.

2.3.1. Semi-classical calculations

The semi-classical calculations [1] are done by applying the method developed by Sahal-Bréchot (1969a, b, 1974). In this formalism, the width of an electron impact broadened line is expressed as

$$2w = 2N_e \int v f(v)\, dv \left[\sum_{i' \neq i} \sigma_{ii'}(v) + \sum_{f' \neq f} \sigma_{ff'}(v) + (\sigma_{el} + W_R) \right]. \quad (1)$$

$f(v)$ is the maxwellian velocity distribution function for the electrons; the cross-sections indices i, f denote the initial or final atomic states, and i', f' their perturbing levels; the W_R term gives the contribution of the Feshbach resonances (Fleurier et al., 1977) to the elastic term. The inelastic cross-section $\sigma_{ii'}(v)$ is obtained by an integration over the the impact parameter ϱ of a sum of transition probabilities $P_{ii'}(\varrho, v)$.

$$\sum_{i' \neq i} \sigma_{ii'}(v) = \frac{1}{2} \pi R_1^2 + \int_{R_1}^{R_D} 2\pi \varrho\, d\varrho \sum_{i' \neq i} P_{ii'}(\varrho, v). \quad (2)$$

The elastic collision contribution is given by

$$\sigma_{el} = 2\pi R_2^2 + \int_{R_2}^{R_D} 8\pi \varrho\, d\varrho \sin^2 \delta \quad (3)$$

$$\delta = \sqrt{(\Phi_P^2 + \Phi_Q^2)}.$$

The phase shifts Φ_P and Φ_Q due respectively to the polarisation potential (r^{-4}) and to the quadrupolar potential (r^{-3}) part, are given by Sahal-Bréchot (1969a, Sect. 2.3). All the cut-offs R_1, R_2, R_D are detailed by Sahal-Bréchot (1969b, Sect. 3.1). The angular factors for complex configurations are introduced by Sahal-Bréchot (1974).

[1] The computations were performed at C.I.R.C.E. (Orsay)

The effect of Debye shielding, which affects the linear dependance of the Stark widths with increasing N_e (e.g. Dimitrijević and Sahal-Bréchot, 1984), is approximated only if it remains a small correction, by means of an upper cut-off at the Debye sphere radius. But the SC results are no more valid at too high density N_e, when the plasma frequency becomes larger than the typical distance between the upper level of the transition and the closest perturbing one. In Si II this limit varies from about $N_e = 10^{17}$ to $10^{16}\,\mathrm{cm}^{-3}$, for upper levels 6f to 9f respectively, and it is about ten times smaller for the ng series. The Debye shielding is reached before the degenerescence of any upper level considered here.

Input data for this code require the oscillator strengths of all allowed transitions between each level involved in the considered line, and the neighbouring perturbing levels. The oscillator strengths are taken in the compilation of Lanz and Artru (1985) if possible, or estimated by means of the Coulomb approximation. The Stark widths due to the collisions with the protons H^+ are also obtained by the SC method: they appear to contribute to about 10% to the total Stark broadening effect in the stellar conditions.

2.3.2. Semi-empirical calculations

The modified semi-empirical method developed by Dimitrijević and Konjević (1980) allows to greatly simplify the numerical application of Eq. 1, with a satisfactory degree of accuracy. This approach consists of introducing the Gaunt factors in the evaluation of the inelastic cross-sections and to approximate the elastic term by the threshold values of the inelastic cross-section. Detailed formulas are given by Dimitrijević and Konjević (1980, Eq. 7–10). They have been simplified again by Dimitrijević and Konjević (1987): their Eq. 2 is a direct expression of the half-width w, applicable when the thermal energy does not exceed the typical distance ΔE between one level of the transition and its closest perturber ($X = 3kT/2\Delta E \leqq 2$). It must be emphasized that this simple formula can apply to many astrophysical lines of low excitation. For the Si II transitions and the range of temperature considered here, the condition $X \leqq 2$ is not fullfilled. We calculated the MSE widths for the 4d–nf and 4f–ng series lines (mult. 7.02 to 7.07 and 7.13 to 7.16) in order to compare them with the results of the SC computation and to test their reliability, as discussed in the following section.

2.3.3 Comparisons of the results

Various comparisons between different sources of Stark widths for Si II, especially with experiments, have already been shown by Dimitrijević (1983) and by Lesage et al. (1983) who have plotted all the data available for the five strong multiplets Nos. 1–5. On these graphs (their Fig. 2) the overall scattering of the data amounts to typically 50%. It also appears that the semi-classical calculations of Lesage et al. (1977) who used the same code as us (Sect. 2.3.1) give the best general agreement with the experimental points. The code has been slightly modified since the work of Lesage et al. (1977). Moreover our new SC calculations take advantage of the improvement of oscillator strengths, so that our results generally lie closer to the experimental widths than those of Lesage et al. (1977). The previous theoretical widths of Jones et al. (1971) obtained by means of a different version of the semi-classical impact theory (Griem, 1974) are generally larger. From Dimitrijević (1983) it appears that the MSE widths for the multiplets No 4, 5 and 6 of Si II agree within about 10% with the more elaborate SC calculations.

For the transitions with higher excitation energy ($\geqq 12$ eV) there is no experimental check. Table 2 shows a comparison of the

© European Southern Observatory • Provided by the NASA Astrophysics Data System

1988A&A...192..249L

Table 2. Comparison between different sources of data for the Stark broadening of the 4d–*n*f and 4f–*n*g transitions in Si II at $T = 10\,000$ K

Multiplet	Transition	Wavelength (Å)	$2w^{(a)}$			
			SC theory[(b)]		MSE	Previous[(c)]
7.02	4d–5f	7850	20.0	15.1	20	10
7.03	4d–6f	5467	23.8	16.3	24	12
7.05	4d–7f	4621	35.4	23.3	35	18
7.06	4d–8f	4201		34.5	81	29
7.07	4d–9f	3956		52.6	131	47
7.13	4f–6g	6240		32.2	47	16
7.14	4f–7g	5186		53.1	74	24
7.15	4f–8g	4673		84.7	125	38
7.16	4f–9g	4377		131.	198	60

(a) The value of $2w = \Delta\lambda_S \cdot 10^{17}/N_e$ is given in Å·cm^3, $\Delta\lambda_S$ being the FWHM of the broadened line.
(b) The first column gives the data of Griem(1974), and the second our newly calculated SC values.
(c) Estimated values used by Kurucz(1979) (Eq. 11).
Mihalas and Henshaw(1966) used for the λ4201Å transition a much smaller value of 0.9, as a tentative guess. For each of the 4d–nf and 4f–ng series, an approximate value of 19.2 and 27.1 respectively can be deduced from the formula $w = 2050 \cdot I^{-4}$ (Lakićević 1983) where I is the ionisation energy (in eV units) of the initial state, 4d or 4f.

Table 3. Stark widths of the Si II multiplets[(a)]

Multiplet	Wavelength (Å)	$2\,w^{(b)}$				$2\,w'^{(c)}$
		5000 K	10000 K	20000 K	40000 K	
7	3210	2.68	2.22	1.97	1.90	0.36
6	3340	2.37	1.76	1.53	1.42	0.24
1	3856	0.82	0.56	0.42	0.33	0.05
7.07	3955	48.9	52.6	55.8	56.0	
3.01	4075	1.93	1.55	1.35	1.28	
3	4131	1.58	1.19	0.96	0.85	0.10
7.26	4190	0.67	0.51	0.40	0.34	
7.06	4201	32.3	34.5	36.5	36.8	
7.16	4377	141.	131.	119.	105.	
7.05	4621	22.8	23.3	24.0	24.0	
7.15	4673	91.9	84.7	76.6	68.1	
5	5056	2.84	2.24	1.95	1.79	0.29
7.14	5186	58.4	53.1	47.9	42.6	
23	5202	1.95	1.45	1.24	1.16	0.15
7.03	5467	16.4	16.3	16.4	16.5	
4	5979	3.94	2.78	2.27	2.00	0.23
7.13	6240	36.5	32.2	28.6	25.4	
2	6347	2.74	1.93	1.44	1.19	0.16
7.02	7850	16.2	15.1	14.7	14.4	

(a) All given widths are calculated by means of the semi-classical perturbation impact method (SC).
(b) The value of $2w = \Delta\lambda_S \cdot 10^{17}/N_e$ is given in Å·cm^3, $\Delta\lambda_S$ being the FWHM of the broadened line. The uncertainty is estimated to be lower than 20% for multiplet 1 to 7, but may be larger for the other ones.
(c) Extra line broadening due to H^+ collisions (in Å· cm^3).

available theoretical widths, including our SC and MSE results and also the previous empirical evaluations made for astrophysical applications, for the lines of the 4d–*n*f and 4f–*n*g series. For the 4d–*n*f lines, the semi-classical values of Griem (1974) are again larger (by a factor of about 1.5) than our new SC results which have been adopted hereafter. The MSE results are close to Griem's data for the lower terms of the series 4d–*n*f, but they become too large for high *n* values. In this case the MSE method is less reliable because the empirical Gaunt factor is determined on the basis of the low-excitation transitions. The last column of Table 2 shows that Kurucz and Peytremann (1975) have obtained a good estimate of these Si II Stark widths by mean of a very crude empirical formula.

It can be noticed that the core-excited transitions (for example $4\,p'\,^4D - 4\,d'\,^4F^0$ at λ 5202) have Stark broadenings comparable to the low-excitation multiplets in spite of their high excitation energies.

2.4 *Adopted Stark widths for* Si II

The data that we adopt are summarized in Table 3. The best accuracy is expected for the results of the semi-classical perturbation method which are now available for all the selected multiplets. The theoretical data are all obtained with the same code and provide a consistent set of reliable values. From the previous comparisons, the accuracy can be estimated to be better than about 20% for the SC widths of the transitions with lower excitation (mult. 1 to 7). However a greater uncertainty is expected for the higher members of the series lines which are much more broadened ($2\,w \gtrsim 50$ Å cm^3).

We also give in Table 3 the supplementary line broadening due to collisions with protons. As it contributes to about 10% to the total widths, we list for the considered temperature range a mean value of these extra widths which are proportional to the proton density. We forego giving this value for highly-excited multiplets, because the impact approximation is no more valid in this case for protons.

3. Influence of the Stark broadening on the theoretical widths of stellar Si II lines

3.1 *LTE equivalent widths*

To investigate the influence of Stark broadening, we compute theoretical equivalent widths for two temperatures ($T = 10\,000$ K, 15 000 K) which are typical of A and B-type stars. This is done with several silicon abundances (1, 10, and 100 times solar) to show differences occuring with saturation. But, on the other hand, we decide to hold constant the other parameters (atmosphere model, oscillator strengths, microturbulence) which affect the equivalent widths, because we want to point out only how large is the uncertainty on equivalent widths due to the choice of a given Stark width.

For the considered temperatures, we use Kurucz (1979) atmospheres models with solar metallicity. When the silicon abundance is 100 times solar, silicon becomes the most abundant element besides H and He. The plasma density is increased by about 7% (at H nucleus density constant), and thus affects the hydrostatic equilibrium. So we take the temperature vertical scale from the Kurucz models and then recompute the hydrostatic and ionisation equilibria to take in account the real contents in silicon. This modifies slightly the gas and electronic pressures[2]. The continuous opacities are calculated with an improved version of a code initiated at Geneva Observatory by Y. Chmielewski (Lanz, 1987). The equivalent widths are finally calculated assuming LTE in line formation, Voigt profile for the line absorption coeffi-

[2] We verified that the calculated equivalent widths are lower by several percents if this effect is neglected

© European Southern Observatory • Provided by the NASA Astrophysics Data System

1988A&A...192..249L

Table 4. Theoretical equivalent widths (in mÅ) for the strongest line of low-excitation Si II multiplets

Line (Mult.)	Silicon abundance[a]	Model (10000 K; 4.0) $W^{(b)}$	$W^{(b)}_{Gr74}$	$\delta W/W$	Model (15000 K; 4.0) $W^{(b)}$	$W^{(b)}_{Gr74}$	$\delta W/W$
3856 Å	$1\times\odot$	132	154	17%	116	127	9%
(1)	$10\times\odot$	300	388	29%	224	282	26%
	$100\times\odot$	862	1156	34%	602	803	33%
6347 Å	$1\times\odot$	115	116	1%	134	137	2%
(2)	$10\times\odot$	265	272	3%	321	331	3%
	$100\times\odot$	763	788	3%	929	965	4%
4131 Å	$1\times\odot$	118	120	2%	136	138	1%
(3)	$10\times\odot$	305	312	2%	348	356	2%
	$100\times\odot$	911	933	2%	1043	1068	2%
5979 Å	$1\times\odot$	39.4	39.0	-1%	68.5	67.9	-1%
(4)	$10\times\odot$	103	101	-2%	146	143	-2%
	$100\times\odot$	259	248	-4%	382	369	-3%
5056 Å	$1\times\odot$	85	88	3%	113	116	3%
(5)	$10\times\odot$	210	219	4%	269	281	4%
	$100\times\odot$	598	629	5%	783	823	5%

[a] The assumed solar abundance is $\log_{10}(Si/H) = -4.55$ (Grevesse, 1984)
[b] Stark widths from Table 3 and Griem(1974) respectively.

Table 5. Theoretical equivalent widths (in mÅ) for high-excitation Si II multiplets

Line (Mult.)	Silicon abundance[a]	Model (10000 K; 4.0) $W^{(b)}_{cl}$	$W^{(c)}_{Ku79}$	$W^{(c)}_{MSE}$	$W^{(c)}_{SC}$	$W^{(d)}_{other}$
4621 Å	$1\times\odot$	10.4	12.3	12.8	12.5	12.8
(7.05)	$10\times\odot$	46.4	73.6	84.4	77.9	84.4
4d–7f	$100\times\odot$	118.	269.	337.	293.	338.
4201 Å	$1\times\odot$	8.7	10.2	10.5	10.3	8.8
(7.06)	$10\times\odot$	41.2	71.2	84.2	73.7	43.7
4d–8f	$100\times\odot$	108.	294.	420.	315.	125.
3955 Å	$1\times\odot$	6.9	8.0	8.2	8.0	
(7.07)	$10\times\odot$	36.0	64.0	72.4	65.4	
4d–9f	$100\times\odot$	98.	310.	435.	326.	
		Model (15000 K; 4.0)				
4621 Å	$1\times\odot$	32.0	36.4	38.4	37.2	38.4
(7.05)	$10\times\odot$	105.	156.	184.	166.	183.
4d–7f	$100\times\odot$	188.	408.	519.	449.	517.
4201 Å	$1\times\odot$	22.1	25.2	26.3	25.4	22.3
(7.06)	$10\times\odot$	90.	142.	179.	149.	91.
4d–8f	$100\times\odot$	170.	421.	627.	456.	190.
3955 Å	$1\times\odot$	15.6	17.5	17.8	17.6	
(7.07)	$10\times\odot$	76.	124.	146.	127.	
4d–9f	$100\times\odot$	156.	437.	649.	465.	

[a] The assumed solar abundance is $\log_{10}(Si/H) = -4.55$ (Grevesse, 1984)
[b] The total width of the Lorentz profile is $10\cdot\gamma_{cl}$, as usually used to take into account the radiative damping and Stark broadening when accurate data are missing.
[c] Stark widths are from Kurucz(1979) estimation, or from MSE and SC methods respectively.
[d] Stark widths are from Griem(1974) (4621 Å) or from Mihalas and Henshaw(1966) (4201 Å).

cient, no variations of the continuous opacity over the wavelength range of the line and no microturbulence. Oscillator strengths are taken from Lanz and Artru (1985) and radiative widths are those given in Table 1.

In a few cases, we compare the results with those calculated with a second code independently written at Meudon Observatory (F. Praderie, private communication). It includes similar continuous opacity sources. A very good agreement is found between the results, discrepancies remaining between 0.5 and 1%. This gives a good confidence in the reliability of the obtained equivalent widths.

3.2. *Study of the low-excitation multiplets*

We present in Table 4 the theoretical equivalent widths obtained for the strongest line of the Si II visible multiplets Nos. 1–5 corresponding to excitation energy from 6.86 to 10.07 eV. Two different sets of semi-classical Stark widths are introduced: the ones that we adopt in Table 3, and the previous results given by Griem (1974) for comparison. These Stark widths differ by 10 to 50% depending on the multiplet and temperature (see Fig. 2, Lesage et al., 1983). It appears in Table 4 that they result in equivalent width which varies by 1 to 20% if the silicon abundance is solar and by 2 to 35% if it is 100 times enhanced. The worse discrepancy occurs for λ 3856 and results in an uncertainty of the order of 0.3 dex on the derived LTE abundance. In the other cases the abundance uncertainty due to the Stark width evaluation is lower than 0.05 dex.

The equivalent widths are also sensitive to the adopted radiative widths. They increase up to 30% with respect to the ones calculated with $\gamma_{rad} = \gamma_{cl}$. Finally we can point out that the new equivalent widths of the line at 4131 Å (mult. 3, often used in stellar abundances analyses) that we obtained with the adopted radiative and Stark data, are larger than those tabulated by Mihalas and Henshaw (1966) by about 30% to 50% when silicon is 10 to 100 times solar.

3.3. *The high-excitation multiplets of the 4d–nf series*

The three blue multiplets of the 4d–*n*f series (No. 7.05, 7.06, 7.07) are often observed as strongly enhanced in the spectra of the silicon rich Ap Si stars. The only quantitative analysis of the λ 4201 multiplet (No. 7.06) was performed by Mihalas and Henshaw (1966), who found LTE abundances greater by 0.4 dex on the average than those derived from the $\lambda\lambda$ 4128–31 multiplet. They attributed this excess to the uncertainty on the oscillator strength, obtained in the hydrogenic approximation, and to blending effects. But Table 2 shows that their Stark width was largely under-estimated. To point out the consequences of these large Stark widths, on the stellar spectra analyses, we calculate the equivalent widths of these three multiplets, by using successively the various Stark width estimates. Results are shown in Table 5, for models at $T_{eff} = 10\,000$ and $15\,000$ K. The Mihalas and Henshaw estimate gives similar equivalent widths to those calculated with the *standard* damping value (i.e. $10\,\gamma_{cl}$). But these equivalent widths are much lower (a factor of 2.5 to 3 with silicon 100 times solar) than those obtained with our new Stark data. The discrepancy also appears clearly on the curves-of-growth given in Fig. 2 for the λ 4201 multiplet at $T_{eff} = 10\,000$ K. For equivalent widths larger than 100 mÅ, as commonly observed in Ap Si stars, the abundance is overestimated by a factor of 6 (0.8 dex)! An analysis of the equivalent widths of these lines, with the use of the new SC Stark widths, is performed by Lanz (1987), who found then a good agreement between the abundances derived from both multiplets (λ 4131 and λ 4201). Similar differences could be pointed out for the other multiplets in the series.

4. Conclusions

The Stark broadening effect on visible lines of Si II have been studied, with an effort to compile and improve the previous

© European Southern Observatory • Provided by the NASA Astrophysics Data System

1988A&A...192..249L

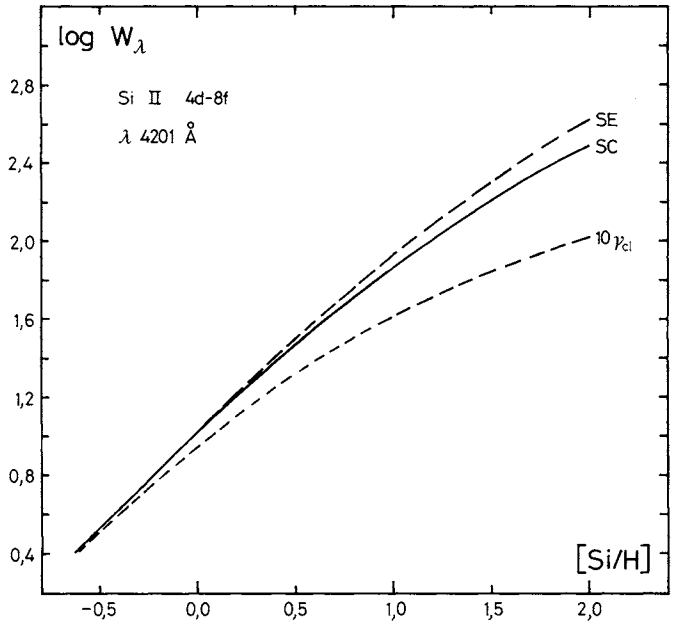

Fig. 2. Theoretical curves-of-growth of the λ4201 multiplet with different estimates of its Stark width ($10\,\gamma_{cl}$, SC and MSE) for $T = 10\,000$ K

available data. The semi-classical theoretical method is found to provide the more reliable results and has been applied to obtain the new Stark widths adopted here. A systematic comparison with the data from the modified semi-empirical method is discussed, as a test of the reliability of this method.

Then the influence of the Stark broadening on the intensity of the stellar absorption lines of Si II, is shown on two examples: in the cases of the low excitation multiplet (Nos. 1–5) the Stark effect is relatively small compared to other broadening causes (Doppler and possibly Zeeman effects) and the abundance analyses are only slightly dependant on the right choice of the Stark data; however the Stark broadening is dominant for the high-excitation transition, namely those of the 4d–*n*f or 4f–*n*g series, which is shown by our new theoretical curves-of-growth for the λ4201 line.

Now we have at our disposal for Si II a full set of oscillator strengths, radiative and Stark widths of similar accuracy for stellar abundance analyses. The uncertainty coming from this atomic data set on the stellar abundance is typically 0.1 dex.

Acknowledgements. We wish to thank S. Sahal-Bréchot for placing her code at our disposal. This work was partly supported by the Swiss National Foundation for Scientific Research.

References

Artru M.-C., Jamar C., Petrini D., Praderie F.: 1981, *Astron. Astrophys. Suppl. Ser.* **44**, 171
Artru M.-C., Lanz T.: 1987, *Astron. Astrophys.* **182**, 273
Chiang W.T., Griem H.R.: 1978, *Phys. Rev. A* **18**, 1169
Dimitrijević M.S.: 1983, *Astron. Astrophys.* **127**, 68
Dimitrijević M.S., Sahal-Bréchot S.: 1984, *Astron. Astrophys.* **136**, 289
Dimitrijević M.S., Konjević N.: 1980, *J. Quant. Spectrosc. Radiat. Transfer* **24**, 451
Dimitrijević M.S., Konjević N.: 1987, *Astron. Astrophys.* **172**, 345
Fleurier C., Chapelle J., Sahal-Bréchot S.: 1977, *J. Quant. Spectrosc. Radiat. Transfer* **17**, 595
Grevesse N.: 1984, *Physica Scripta* **T 8**, 145
Griem H.R.:1964, *Plasma Spectroscopy*, McGraw-Hill, New York
Griem H.R.: 1968, *Phys. Rev.* **165**, 258
Griem H.R.: 1974, *Spectral Line Broadening by Plasmas*, Academic Press, New York
Hey J.D.: 1977, *J. Quant. Spectrosc. Radiat. Transfer* **18**, 425
Jones W.W., Benett S.M., Griem H.R.: 1971, Techn. Rep. No 71–128, Univ. of Maryland
Kamp L.W.: 1978, *Astrophys. J. Suppl. Ser.* **36**, 143
Konjević N., Wiese W.L.: 1976, *J. Phys. Chem. Ref. Data* **5**, 259
Konjević N., Dimitrijević M.S., Wiese W.L.: 1984, *J. Phys. Chem. Ref. Data* **13**, 649
Kurucz R.L.: 1979, *Astrophys. J. Suppl. Ser.* **40**, 1
Kurucz R.L., Peytremann E.: 1975, *SAO Special Report* **362**
Lakićević I.S.: 1983, *Astron. Astrophys.* **127**, 37
Lanz T.: 1987, Ph. D. thesis, Geneva Observatory
Lanz T., Artru M.-C.: 1985, *Physica Scripta* **32**, 115
Lennon D.J., Lynas-Gray A.E., Brown P.J.F., Dufton P.L.: 1986, *Monthly Notices Roy. Astron. Soc.* **222**, 719
Lesage A., Sahal-Bréchot S., Miller M.H.: 1977, *Phys. Rev. A* **16**, 1617
Lesage A., Rathore B.A., Lakićević I S., Purić J.: 1983, *Phys. Rev. A.* **28**, 2264
Mégessier C.: 1971, *Astron. Astrophys.* **10**, 332
Mihalas D., Henshaw J.L.: 1966, *Astrophys. J.* **144**, 25
Moore C.E.: 1965, Selected Tables of Atomic Spectra, NSRDS-NBS 3, Sect. 1
Sahal-Bréchot S.: 1969a, *Astron. Astrophys.* **1**, 91
Sahal-Bréchot S.: 1969b, *Astron. Astrophys.* **2**, 322
Sahal-Bréchot S.: 1974, *Astron. Astrophys.* **35**, 319
Sahal-Bréchot S., Segré E.: 1971, *Highlights of Astronomy* **2**, ed. C. de Jager, p. 566
Vince I., Dimitrijević M.S., Kršljanin V.: 1985, *Progress in Stellar Spectral Line Formation Theory*, eds. Beckmann et al., p. 373
Yukov E.A.: 1972, *Sov. Astron.* **15**, 867

© European Southern Observatory • Provided by the NASA Astrophysics Data System

1988A&A...200..285V

Astron. Astrophys. 200, 285–290 (1988)

ASTRONOMY AND ASTROPHYSICS

Stark broadening along a homologous sequence of noble gas atomic lines in dense plasmas

Y. Vitel[1], M. Skowronek[1], M.S. Dimitrijević[2], and M.M. Popović[3]

[1] Laboratoire des Plasmas Denses, Tour 12 E5, Université P. et M. Curie, 4 Pl. Jussieu, F-75252 Paris Cedex 05, France
[2] Astronomical Observatory, Volgina 7, YU-11050 Beograd, Yugoslavia
[3] Institute of Physics, Maksima Gorkog 118, YU-11080 Beograd-Zemun, Yugoslavia

Received June 29, 1987; accepted February 2, 1988

Summary. We present experimental results on the broadening and shift of some rare gas atomic lines emitted by high electron density plasmas created in linear flashtubes. From a semi-empirical formula, we find a theoretical dependence of the Stark broadening parameters on the ionisation potential for lines broadened by electron impacts. Experimentally, a non-linear dependence is found between the Stark width w and shift d, and the electron density. At the lowest electron density, our values of w and d agree with other experimental determinations. We have observed a regularity of w and d for analogous lines of homologous atoms.

Key words: line profiles – Stark broadening

1. Introduction

Precise data about the Stark broadening of non-hydrogenic lines are of interest in the investigation of astrophysical and laboratory plasmas. For instance, the evaluation of the physical conditions in stellar atmospheres and also abundance determinations need the knowledge of the broadening parameters for a large number of elements.

The case of the noble gas atoms spectral lines as Ar I, Kr I, Xe I is of special interest for laboratory plasmas because they are carrier gases in numerous experiments.

a) Ar I. An extensive number of experimental data exists in the range of electron density: $6\,10^{15}\,\mathrm{cm}^{-3}-2\,10^{17}\,\mathrm{cm}^{-3}$. These data have been reviewed and selected by Konjević and Roberts (1976) and also by Konjević et al. (1984).

b) Kr I. Measurements were performed recently in the range of electron density: $1\,10^{16}\,\mathrm{cm}^{-3}-1.9\,10^{17}\,\mathrm{cm}^{-3}$ by the following experimental groups: Klein and Meiners (1977), Ernst et al. (1978), Baessler et al. (1979), Brandt et al. (1981, 1982). These data have been also reviewed by Konjević et al. (1984).

c) Xe I. Experimental data are available in the range: $2\,10^{16}\,\mathrm{cm}^{-3}-10^{17}\,\mathrm{cm}^{-3}$. These data have been critically reviewed by Konjević et al. (1984).

We will present in this paper the first experimental investigation on the Stark broadening parameters of Ar I, Kr I and Xe I lines at higher electron density i.e. in the range: $5.0\,10^{17}\,\mathrm{cm}^{-3}-1.6\,10^{18}\,\mathrm{cm}^{-3}$.

A recent theoretical analysis by Purić et al. (1977, 1978) and by Miller et al. (1980) has shown that there exist some systematic relations between the Stark widths of homologous resonance lines. An analysis of the Stark broadening is then performed along a homologous sequence, in order to extend the study of the regularities to higher energy levels and electron densities.

The first part of this paper is devoted to the theory, in order to estimate the dependence of the Stark parameters on the ionisation potential along a homologous sequence. In the second part, we describe shortly the experimental set-up allowing precise measurements of the plasma parameters. Then we present and discuss our experimental results on the line profiles, the linewidths and the lineshifts which are compared with other experimental values.

2. Theory

2.1. General formula

In order to evaluate the Stark broadening and shift of an atom spectral line, we start from the well known semiemperical formula for w and d in angular frequency units (Freudenstein and Cooper, 1978; Dimitrijević and Konjević, 1986):

$$w+id=(32/27)^{1/2}N_e\pi(\hbar a_0/m)(E_H/kT)^{1/2}$$
$$\{\Sigma_{i'}R^2_{ii'}[f_w(\eta_{ii'}R_{ii'})-i\varepsilon_{ii'}f_d(\eta_{ii'}R_{ii'})]$$
$$+\Sigma_{f'}R^2_{ff'}[f_w(\eta_{ff'}R_{ff'})+i\varepsilon_{ff'}f_d(\eta_{ff'}R_{ff'})]\}, \quad (1)$$

where all quantities are in the standard notation, i, f denote the initial and final states and i′, f′ the corresponding perturbing states within the dipole approximation.

The quantity $\varepsilon_{jj'}$ determines the sign of the individual contributions to the shift, viz.

$$\varepsilon_{jj'}=(E_j-E_{j'})/|E_j-E_{j'}|,$$

where E_j and $E_{j'}$ are the energies of the corresponding states, and

$$\eta_{jj'}=|E_j-E_{j'}|/3kT.$$

For the lines studied in our plasmas, the term ηR is widely greater than one. In this case, the functions $f_w(X)$ and $f_d(X)$

Send offprint requests to: Y. Vitel

© European Southern Observatory • Provided by the NASA Astrophysics Data System

1988A&A...200..285V

exhibit the asymptotic forms (2):

$$f_w(X) \approx 0.487 X^{-2/3} \text{ and } f_d(X) \approx 2(\pi/6)^{2/3} X^{-2/3}, \quad (2)$$

where $X = \eta R$.

The case $X \gg 1$, i.e. $nR \gg 1$ is of particular interest for astrophysical purposes, for low temperatures and for transitions between low lying energy levels. Starting from Eqs. (1) and (2), expressing the radial matrix elements R in the Coulomb approximation for electric dipole transitions (Griem, 1974), we can derive the following expression for w and d (in rd s^{-1}):

$$\begin{aligned} w + id \approx {} & A N_e T^{1/6} \{ \Sigma_{i'} |E_i - E_{i'}|^{-2/3} \Phi^{4/3}(I_0, E_i, E_{i'}) \\ & \times [[\max(l, l')/((2l+1)(I_0 - E_i))] [E_H/(I_0 - E_i) - \max^2(l, l')]]^{2/3} \\ & \times (0.487 - i\varepsilon_{jj'} 2(\pi/6)^{2/3}) + \Sigma_{f'} |E_f - E_{f'}|^{-2/3} \Phi^{4/3}(I_0, E_f, E_{f'}) \\ & \times [[\max(l, l')/((2l+1)(I_0 - E_f))] [E_H/(I_0 - E_f) - \max^2(l, l')]]^{2/3} \\ & \times (0.487 + i\varepsilon_{ff'} 2(\pi/6)^{2/3}) \}, \end{aligned} \quad (3)$$

with $A = \pi(ha_0/m)(2E_H)^{7/6} k^{1/6} \sqrt{3}\, 2^{7/6}$ and l, l' the orbital quantum numbers of the considered states. I_0 is the ionization energy; Φ is the Bates and Damgaard factor.

Besides these widths and shifts produced by electron impacts, we should take into account the influence of ion-broadening on the total width and shift. This influence can be estimated within the quasistatic approximation (Griem, 1974). In our experimental conditions, this correction is always less than 10%, so we can neglect it for the estimation of the Stark parameters.

Analysing Eq. (3) leads to the conclusion that a regular behaviour of the Stark broadening parameters may be expected within a series of homologous atoms provided that the ionisation potential varies more or less regularly from one atom to another and that the change in the level energy follows the change in ionization potential.

We notice nevertheless that, in the case of noble gas atoms, the dependence of Stark widths and shifts on the ionisation potential is not as simple as the case of ion lines (Purić et al., 1980; Dimitrijević and Konjević, 1986; Dimitrijević, 1985).

2.2. *Regularities within a sequence of homologous atoms*

Since the rare gases possess similar atomic structures, they should exhibit systematic trends for the Stark effect, for the same type of transition.

In the case of *ns-np'* transitions for rare gas atoms, the principal perturbing levels are $(n+1)s'$ and $n'd'$ with $n' = n$ for Ne I and $n' = n - 1$ for Ar I, Kr I and Xe I. In order to estimate roughly the variation of the Stark widths and shifts along such a homologous sequence, we may neglect the lower level contributions. Moreover, we will put $\Phi^{4/3} \approx 1$ in Eq. (3). For $\Delta n = 0$, the values of Φ^2 range usually between 0.8 and 1 (Griem, 1974), consequently $\Phi^{4/3}$ is in the range 0.86 to 1. Since the $(n+1)s'$ level is close to the np' level, then $\Phi^{4/3}$ is again close to 1. Moreover, in such a way, we compensate partially for the neglect of other perturbing levels.

With all these simplifying assumptions, Eq. (3) reduces to the following expression:

$$\begin{aligned} w + id \approx {} & A N_e T^{1/6} (0.487 - i1.299) \\ & \times \{ [(E_H - I_0 + E_i)/(3(I_0 - E_i)^2 (E_s - E_i))]^{2/3} \\ & + [2(E_H - 4I_0 + 4E_i)/(3(I_0 - E_i)^2 (E_d - E_i))]^{2/3} \}, \end{aligned} \quad (4)$$

where E_s and E_d are the energies of the $(n+1)s'$ and $n'd$ levels, respectively. A linear relation $E_j = a + bI_0$ may be found between the level energy and the ionisation potential for each interacting level along a homologous sequence, with a good regression coefficient. Using Eq. (4) and the linear relations, one can estimate the Stark broadening parameters for $ns - np'$ transitions of noble gas atoms, knowing only the ionisation potential I_0, the electron density N_e and the temperature T. One might notice that the dependence of w and d on I_0 is more complicated than in the case of resonance transitions of singly ionised emitters which were studied by Dimitrijević (1985).

3. Experimental set-up

In Fig. 1, the main parts of the experimental set-up are drawn schematically.

The plasmas are produced in linear flashtubes filled with a noble gas at an initial pressure in the range 50 torr to one atmosphere (7–100 kPa) (Markiewicz and Emmett, 1966). The inner diameter of our flashtubes is 6 mm and the distance between the electrodes is 150 mm.

The triggering of the discharge is performed by applying a 30 kV, 1 μs pulse on a separate external electrode. Then, a low current (600 mA) simmer is maintained during 120 ms in order to prepare an ionised channel centered on the tube axis and to avoid numerous perturbative phenomena due to interactions with the wall (Vitel et al., 1979; Vitel and Skowronek, 1987). The main electrical pulse, whose intensity is about 1 kA with a duration of 1 ms, is finally sent through the flashtube. The current on the plateau is constant within 1% and very reproducible from one shot to another. It is maintained a sufficiently long time (about 1 ms) in order to reach a stationary regime. During this stationary phase, a dense plasma is produced, which is homogeneous and reproducible.

A high-speed electronic camera is used to follow the filling of the tube by the plasma. Two spectrographs are used for the measurements of the emitted light: the first one having a low resolution, for the continuum, and the second one with a high spectral resolution, for the line profiles.

An optical multichannel analyser (OMA II) is used for the light detection, the calibration, and for the mathematical treatment of the spectrum.

4. Plasma diagnostics

The plasma parameters are determined at the moment of the best filling of the flashtube by the plasma column. Redundant measurements are performed in order to ensure a good confidence in the plasma parameters. The electron density profiles $N_e(r)$ are deduced from absolute continuum measurements and from laser interferometry. The temperature profiles $T_e(r)$ are obtained from the central intensity of optically thick lines, and from the thermodynamic equilibrium equations of the plasma (Drawin and Felenbok, 1965).

All the details concerning this determination of the plasma parameters are explained in previous papers (Vitel, 1987; Vitel and Skowronek, 1987). Finally, the relative precisions may be estimated at 5% for $N_e(r)$ and 3% for $T_e(r)$. Typical profiles are displayed in Fig. 2, which shows the flatness of these profiles.

© European Southern Observatory • Provided by the NASA Astrophysics Data System

1988A&A...200..285V

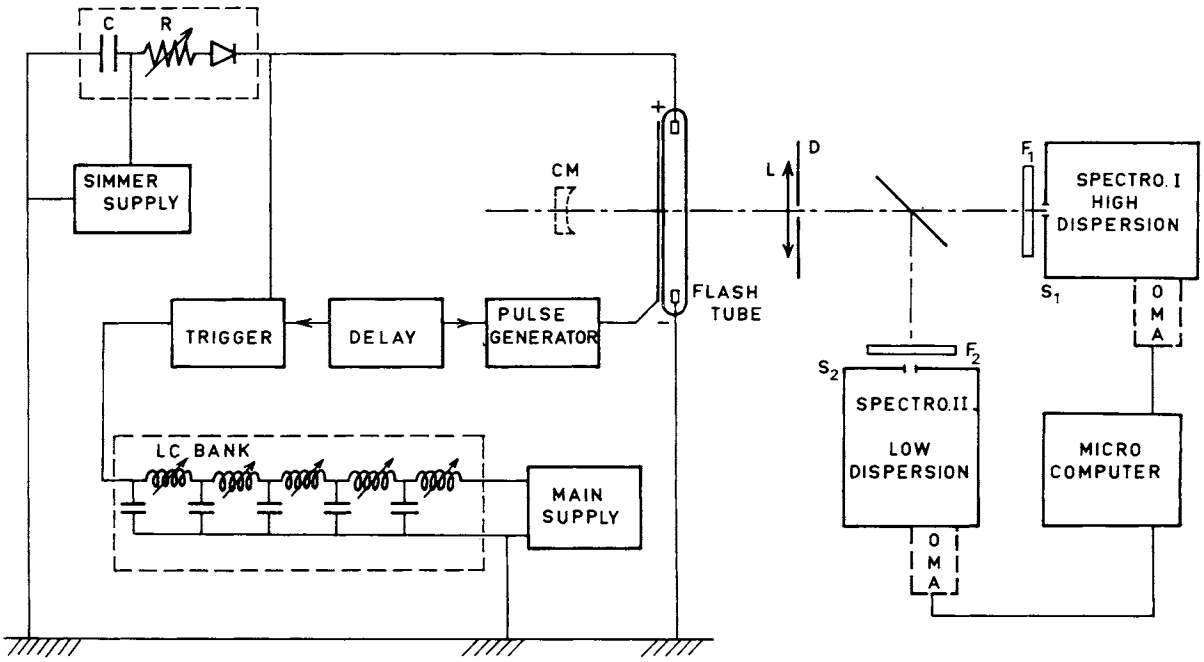

Fig. 1. Schematic representation of the experimental set-up

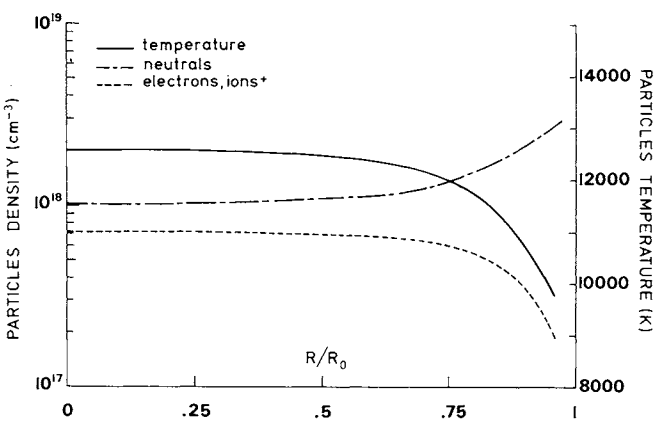

Fig. 2. Radial distribution in the plasma of electron density, neutral density and temperature for a flashtube filled with xenon at 200 torr (initial pressure) and a discharge current of 490 A

5. Measurement of the atomic linewidths and shifts

5.1. Experimental procedure

The experimental procedure is described in a previous paper (Vitel and Skowronek, 1987). The different lines are registered by means of the optical multichannel analyser in the best conditions for the plasma filling of the tubes. The precision of the wavelength scale is about 0.01 nm. The lines are selected in order to avoid any complicated mathematical treatment caused by the absorption or by a neighbouring perturbing line. The experimental profiles are fitted to a Lorentzian, taking into account the density and temperature profiles. Indeed, the other broadening mechanisms like the Doppler effect or the Van der Waals effect are negligible, in our case, compared with the Stark effect.

5.2. Results

The main results are summarised in Table 1.

5.3. Discussion

The dependence of the measured widths and shifts on the electron density shows a slight but significant departure from a linear variation.

This relative decrease of w and d versus N_e cannot be explained by the Debye shielding correction given by Griem (1974). The energy level differences between the higher level of the studied lines and their perturbing levels are equal or above 0.5 eV, to be compared with the plasmon energy close to 0.04 eV ($\cong h\nu_{pe}$, where ν_{pe} is the plasma frequency). In this case, the Debye shielding correction is negligible.

In our plasmas, at the higher electron densities, the Debye length is of the same order as the interparticle distance. So, the correlation effect between particles becomes important and the collisions cannot be treated as simple binary collisions. We think that this non linearity of w and d versus N_e could be interpreted as a correlation effect mainly on the weak collision terms in the line profile calculation and less on the strong collision term. Indeed, according to Cooper and Oertel (1969), we can estimate the range of the strong collision cutoff ρ_{min} as being:

$$n^2\lambda\!\!\!^{-} \geq \rho_{min} \geq n^2\lambda\!\!\!^{-}(kT/E_H)^{1/3},$$

where $\lambda\!\!\!^{-}$ is the De Broglie length divided by 2π, n is the principal quantum number of the upper level of the line and E_H the ionization energy of hydrogen.

In case of our higher electron density for each gas, we obtain:
for argon at $N_e = 1.0\,10^{18}\,\mathrm{cm}^{-3}$, $T_e = 18700$ K:
$35\,\text{Å} \geq \rho_{min} \geq 17\,\text{Å}$,
for krypton at $N_e = 1.62\,10^{18}\,\mathrm{cm}^{-3}$, $T_e = 15700$ K:
$59\,\text{Å} \geq \rho_{min} \geq 27\,\text{Å}$,

© European Southern Observatory • Provided by the NASA Astrophysics Data System

1988A&A...200..285V

Table 1. Variations of the full width and shift of the neutral spectral lines versus the electron density and temperature

Line	$N_e(0)$ (10^{17} cm^{-3})	$T_e(0)$ (K)	w (Å)	d (Å)
696.543 nm	6.0	16500	4.4	1.9
	6.2	17400	4.9	2.1
Ar I	7.3	17700	5.2	2.2
4s[3/2]° –	8.2	18000	5.7	2.3
4p′[1/2]	9.4	18500	5.9	2.6
	10.0	18700	6.5	2.6
578.092 nm	7.6	15500	4.8	1.9
	9.2	14900	5.4	2.0
Kr I	9.7	14300	5.6	2.1
5s[3/2]° –	12.3	16200	6.4	2.5
5p′[3/2]	12.4	15000	6.9	2.5
	15.8	17400	8.2	3.0
	16.2	15700	9.0	3.2
473.415 nm	4.7	14800	*	1.1
	9.0	13000	*	1.8
Xe I	9.8	13400	*	2.0
6s[3/2]° –	10.8	13500	*	2.1
6p′[3/2]	12.3	13900	*	2.3
	13.4	14300	*	2.6

(* = overlapping)

for xenon at $N_e = 1.34\,10^{18}$ cm^{-3}, $T_e = 14300$ K:
89 Å $\geq \rho_{min} \geq$ 40 Å.

These values give a number of electrons in the sphere of radius ρ_{min} in the range:
0.18–2 10^{-2} for argon
1.4–0.13 for krypton
3.9–0.36 for xenon.

So, especially for krypton and xenon, the effect of correlation must be also taken into account in the calculation of the strong collision term for the higher electron densities in our plasmas.

The collective behaviour of our weakly correlated plasmas requires a many-body theoretical approach (Kraeft et al., 1986; Hitzchke et al., 1986) which is not yet solved and remains an open question.

Then, for the main purpose of this work, the study of the regularities on the Stark effect in an homologous sequence of atoms, we must use only the values obtained at the lowest electron density where the semiclassical impact approximation seems still valid. In the next chapter, we shall show that, on the whole, these values agree with those from other experiments at lower electron density.

5.4. *Comparison with other experimental values*

5.4.1. Ar I case

In Table 2 are reported the values of the FWHM w and the shift d in Å units, measured on the line 696.5 nm (4s[3/2]° – 4p′[1/2]), by: (a) Popenoe and Shumaker (1965), (b) Evans and Tankin, 1967, (c) Chapelle et al. (1968), (d) Tonejć et al. (1972), and (e) our own values taken at the lowest electron density.

In the two last columns, are reported the normalised values at an electron density of 10^{17} cm^{-3} and a temperature of 10 000 K, deduced from the dependence of w and d versus N_e and T in Eq. (3):

$$w_N = w\,(10^{17}/N_e)(10^4/T)^{1/6} \quad \text{and} \quad d_N = d(10^{17}/N_e)(10^4/T)^{1/6}.$$

A good agreement is seen between the "normalised" w_N and d_N values, within 25%, except (a) which is for w_N within 50%. We may notice that the authors (a), however, have a significantly higher w_N at the lowest electron density.

5.4.2. Kr I case

In Table 3, we have reported the values obtained in the measurement of the line 587 nm (5s[3/2]° – 5p′[3/2]) by: (a) Klein and Meiners (1977), who have used a shock tube, (b) Brandt et al. (1981) and by us (c) with the same notation as before.

For w_N, our values are in good agreement with those of (b). But it seems that the value of w given by (a) is strongly overestimated. According to Brandt et al. (1981), this may be due to the neglect of the resonance broadening and to an insufficient correction of the optical thickness of the line. The shift value d given by (a) was estimated by Konjević et al. (1984) to be more precise than the width, it is in good agreement with our results.

5.4.3. Xe I case

In Table 4, are reported the measurements on the line 473.4 nm (6s[3/2]° – 6p′[3/2]) performed by: (a) Klein and Meiners (1977), (b) Truong-Bach et al. (1981) and by us (c) with the same notations as before.

We only report our shift measurements because that line is perturbed by two Xe I lines, 467.1 nm and 469.7 nm. Our shift

Table 2. Comparison of the values of the FWHM w and the shift d in Å units, measured on the line 696.5 nm (4s[3/2]° – 4p′[1/2]) of Ar I; for the meaning of (a)–(e) see text. w_N and d_N are the normalised values at an electron density of 10^{17} cm^{-13} and a temperature of 10 000 K

Authors	N_e (10^{17} cm^{-3})	T (10^4 K)	w (Å)	d (Å)	w_N (Å)	d_N (Å)
(a)	0.6	1.18	0.63	0.23	1.02	0.37
(b)	2	2	1.4	0.67	0.62	0.30
(c)	1.45	1.38	0.8	—	0.52	—
(d)	0.77	1.22	0.66	—	0.83	—
(e)	6	1.65	4.4	1.9	0.67	0.29

© European Southern Observatory • Provided by the NASA Astrophysics Data System

1988A&A...200..285V

value is in agreement with that of (a), but the difference with the value of (b) may be due to an unsufficient spectral resolution in their experiment for this line, as reported by Truong Bach et al. (1981).

5.5. *Trend to regularity within homologous sequence*

If the regularity of w and d should hold for analogous spectral lines of homologous atoms, the ratios of w_N and d_N (expressed in rd s^{-1}) divided by the "normalisation" factor NF, defined from Eq. (4):

$$NF = [(E_H - I_0 + E_i)/(3(I_0 - E_i)^2(E_s - E_i))]^{2/3} + [2(E_H - 4I_0 + 4E_i)/(3(I_0 - E_i)^2(E_d - E_i))]^{2/3}$$

would have to remain constant. These values are given in Table 5.

The regularity in the Stark broadening and shift of the investigated spectral lines originating from the same type of transition ($ns - np'$) is not well verified. But, knowing that the atomic spectra of the studied rare gases are very complicated, we think that the theoretical dependence found for the width and the shift of these lines on the ionization potential, gives a good enough approximation for their calculation (within 25%). This can be used for the evaluation of the Stark parameters w and d of an uninvestigated spectral line originating from the same type of transitions.

6. Conclusion

This work has permitted the extension of Stark broadening and shift of non resonance lines of homologous atoms with complex spectra to the case of dense plasmas. The Stark parameters measured exhibit a non-linear dependence on the electron density. This result can be interpreted as a particle correlation effect. The measurements of w and d done at the lowest electron density of our plasmas are in agreement with those of other experiments done at even lower electron densities. The regularity of these parameters in the case of non-resonance lines of homologous atoms is not pronounced. Nevertheless, the simplified theoretical

Table 3. Comparison of the values of the FWHM w and the shift d in Å unit, measured on the line 587.0 nm ($5s[3/2]^\circ - 5p'[3/2]$) of Kr I; for the meaning of (a)–(c) see text. w_N and d_N are the normalised values at an electron density of 10^{17} cm^{-3} and a temperature of 10 000 K

Authors	N_e (10^{17} cm^{-3})	T (10^4 K)	w (Å)	d (Å)	w_N (Å)	d_N (Å)
(a)	1.24	1.03	1.5	0.27	1.20	0.22
(b)	1.4	1.23	0.81	—	0.56	—
(c)	7.6	1.55	4.8	1.9	0.59	0.23

Table 4. Comparison of the values of the FWHM w and the shift d in Å units, measured on the line 473.4 nm ($6s[3/2]^\circ - 6p'[3/2]$) of Xe I; for the meaning of (a)–(c) see text. w_N and d_N are the normalised values at an electron density of 10^{17} cm^{-3} and a temperature of 10 000 K

Authors	N_e (10^{17} cm^{-3})	T (10^4 K)	w (Å)	d (Å)	w_N (Å)	d_N (Å)
(a)	1.14	0.9	1.62	0.32	1.45	0.29
(b)	1	1	1.14	0.14	1.14	0.14
(c)	4.7	1.48	—	1.1	—	0.22

Table 5. Values of the ratios of the normalised widths and shifts divided by normalisation factor NF for the spectral lines studied

Line	w_N (10^{11} rd s^{-1})	d_N (10^{11} rd s^{-1})	w_N/NF (10^{16})	d_N/NF (10^{16})
Ar I 696.5 nm	2.60	1.13	3.12	1.36
Kr I 587.0 nm	3.22	1.26	3.90	1.53
Xe I 473.4 nm	—	1.85	—	1.76

© European Southern Observatory • Provided by the NASA Astrophysics Data System

1988A&A...200..285V

expression of w and d obtained, which depends only on the ionization potential and plasma conditions, can be used to give an estimate.

Acknowledgements. This work has been supported by the Centre National de la Recherche Scientifique, France, by Electricité de France, Club Arc électrique, and by the French-Yugoslavian Program for cultural, scientific and technical Cooperation and Exchange.

References

Baessler, P., Obbarius, M.U., Schulz-Gulde, E.: 1979, *Physica* **96C**, 147
Brandt, T., Helbig, V., Nick, K.P.: 1981, *Spectral Line Shapes*, Vth Int. Conf. Berlin, F.R.G., 1980, W. de Gruyter, Berlin, p. 265
Brandt, T., Helbig, V., Nick, K.P.: 1982, *J. Phys. B: Atom. Mol. Phys.* **15**, 2139
Chapelle, J., Sy, A., Cabannes, F., Blandin, J.: 1968, *J. Quant. Spectrosc. Radiat. Transfer* **8**, 1201
Cooper, J., Oertel, G.K.: 1969, *Phys. Rev.* **180**, 286
Dimitrijević, M.S.: 1985, *Astron. Astrophys* **145**, 439
Dimitrijević, M.S., Konjević, N.: 1986, *Astron. Astrophys.* **163**, 297
Drawin, H.W., Felenbok, P.: 1965, Data for Plasmas in Local Thermodynamic Equilibrium, Gauthier-Villars, Paris
Ernst, W.E., Müller, B.H., Zaengel, T.H.: 1978, *Physica* **93C**, 414
Evans, D.L., Tankin, R.S.: 1967, *Phys. Fluids* **10**, 1137
Freudenstein, S.A., Cooper, J.: 1978, *Astrophys. J.* **224**, 1079
Griem, H.R.: 1974, Spectral Line Broadening by Plasmas, *Pure Appl. Phys.* **39**, Academic Press ed., New-York, p. 31
Hitzschke, L., Röpke, G., Seifert, T., Zimmermann, R.: 1986, *J. Phys. B: At. Mol. Phys.* **19**, 2443.
Klein, P., Meiners, D.: 1977, *J. Quant. Spectrosc. Radiat. Transfer* **17**, 1977
Konjević, N., Roberts, J.L.: 1976, *J. Phys. Chem. Ref. Data* **5**, 209
Konjević, N., Dimitrijević, M.S., Wiese, W.L.: 1984, *J. Phys. Chem. Ref. Data* **13**, 619
Kraeft, W.D., Kremp, D., Ebeling, W., Röpke, G.: 1986 *Quantum Statistics of Charged Particle Systems*, Chapt. 8, Plenum Press, New York, USA
Markiewicz, J.P., Emmett, J.L.: 1966, *IEEE J. Quantum Electron.* **QE-2**, No. 11, 707
Miller, M.H., Lesage, A., Purić, J.: 1980, *Astrophys. J.* **239**, 410
Popenoe, C.M., Shumaker, J.B.: 1965, *J. Res. Nat. Bur. Stand.* **A69**, 495
Purić, J., Labat, J., Cirković, Lj., Lakicević, I.S., Djenize, S.: 1977, *J. Phys. B: Atom. Mol. Phys.* **10**, 2375
Purić, J., Dimitrijević, M.S., Lakicević, I.S.: 1978, *Phys. Letters* **67A**, 189
Purić, J., Lakicević, I., Glavonjić, V.: 1980, *Phys. Letters* **76A**, 128
Tonejć, A.M., Acinger, K., Vujnović, V.: 1972, *J. Quant. Spectrosc. Radiat. Transfer* **12**, 305
Truong-Bach, Richou, J., Lesage, A., Müller, M.H.: 1981, *Phys. Rev.* **A24**, 2550
Vitel, Y.: 1987, *J. Phys. B: Atom. Mol. Phys.* **20**, 2327
Vitel, Y., Skowronek, M., Benisty, K., Popović, M.M.: 1979, *J. Phys. D: Appl. Phys.* **12**, 1125
Vitel, Y., Skowronek, M.: 1987, *J. Phys. B: Atom. Mol. Phys* **20**, 6477
Vitel, Y., Skowronek, M.: 1987, *Revue Phys. Appl.* **22**, 193

© European Southern Observatory • Provided by the NASA Astrophysics Data System

1989A&A...217..201D

Astron. Astrophys. 217, 201–203 (1989)

ASTRONOMY AND ASTROPHYSICS

Research Note

Estimates of Stark width along a homologous sequence

M.S. Dimitrijević [1] **and M.M. Popović** [2]

[1] Astronomical Observatory, Volgina 7, YU-11050 Beograd, Yugoslavia
[2] Institute of Physics, P.O. Box 57, YU-11001 Beograd, Yugoslavia

Received July 28, accepted November 15, 1988

Summary. A simple analytical expression for Stark widths as a function of the ionization potential suitable for critical evaluation of existing experiments and interpolation of new data along homologous ion sequences at low temperature limit, has been derived.

Key words: lines: profile-atomic and molecular data – Stark broadening

1. Introduction

Since for astrophysical purposes data for a large number of spectral lines for various elements and ionization stages are needed (e.g. in the opacity project 10^6–10^7 spectral lines are included (Pradham, 1987), methods for a simple estimate of Stark broadening parameters may be useful. Consequently, an effort to provide a simple method with a good average accuracy has been made (Griem, 1968; Hey and Bryan, 1977; Dimitrijević and Konjević, 1980, 1987; Lakićević, 1983; Dimitrijević, 1985, 1988; Seaton, 1987).

Another possibility for the critical estimation of experimental values and interpolation of new Stark broadening data is the investigation of regularities and systematic trends (e.g. Purić and Ćirković, 1973; Konjević and Dimitrijević, 1981; Wiese and Konjević, 1982; Dimitrijević and Truong Bach, 1986). For example, a systematic behaviour of Stark broadening parameters, such as gradual variations, are expected in the case of homologous atoms and ions, which exhibit similar atomic structures.

Recently, Vitel et al. (1988) demonstrated that in the case of noble gases one can find a normalization factor for analogous transitions which enables to interpolate along the homologous sequence. In this paper we demonstrate that such normalization is possible in the case of homologous ion lines and present a simple method suitable for critical evaluation of existing data and interpolation of new Stark widths along homologous sequences.

Send offprint requests to: M.S. Dimitrijević

2. Theory

At low temperatures, when the nearest perturbing level (j') is so far from the upper or lower energy level (j), that the condition

$$\frac{3kT}{2\,|E_{j'}-E_j|} \leqq 2 \tag{1}$$

is satisfied (E_j is the energy of the level j, and T the electron temperature), the modified semi-empirical formula (Dimitrijević and Konjević, 1980, 1981) may be considerably simplified (Dimitrijević and Konjević, 1987). The full Stark width (in angular frequency units) of an isolated line has now the following form

$$W(\text{Å}) = 2.2151\ 10^{-8}\,\frac{\lambda^2(\text{cm})\,N(\text{cm}^{-3})}{T^{1/2}(\text{K})}\left(0.9-\frac{1.1}{Z}\right) \times \sum_{j=i,f}\left(\frac{3n_j}{2Z}\right)^2 (n_j^2-l_j^2-l_j-1)\,, \tag{2}$$

where N is the electron density, $Z-1$ the ionic charge and n_j, l_j the effective principal and angular momentum quantum numbers for the level j, respectively. The case when Eq. (2) is valid is of particular interest for astrophysical purposes, low temperature plasma diagnostics, and for transitions between low lying levels.

In a number of papers (Purić et al., 1980; Lakićevic and Purić (and references therein), 1983; Dimitrijević and Konjević, 1984; Dimitrijević, 1985) has been demonstrated that Stark broadening parameters may be presented as a function of the ionization potential I_0. Representing the effective quantum number n as a function of the ionization energy I_0, Eq. (2) becomes

$$W(\text{Å}) = 1.7444\ 10^{-8}\,\frac{\lambda^2(\text{cm})\,N(\text{cm}^{-3})}{T^{1/2}(\text{K})} \cdot \sum_{j=i,f}\frac{E_\text{H}}{I_0-E_j}\left(\frac{4E_\text{H}}{I_0-E_j}-l_j^2-l_j-1\right), \tag{3}$$

where E_H is the ionization energy of hydrogen and E_i, E_f are energies of initial and final levels respectively. In some cases there exists a linear relationship between the analogous energy level E_j

© European Southern Observatory • Provided by the NASA Astrophysics Data System

1989A&A...217..201D

within a homologous sequence and I_0 (Dimitrijević, 1985; Vitel et al., 1988):

$$E_j = a_j + b_j I_0, \tag{4}$$

where the coefficients a_j, b_j may be determined empirically for the analogous energy levels within a homologous sequence. Now Eq. (3) becomes

$$W(\text{Å}) = 1.7444\ 10^{-8}\ \frac{\lambda^2(\text{cm})\ N(\text{cm}^{-3})}{T^{1/2}(\text{K})} \sum_{j=i,f} \frac{E_\text{H}}{I_0(1-b_j)-a_j} \times \left[\frac{4\,E_\text{H}}{I_0(1-b_j)-a_j} - l_j^2 - l_j - 1\right]. \tag{5}$$

From Eq. (5) follows that the full Stark widths for analogous transitions within homologous radiator spectra may be expressed as a function of the ionization potential I_0 and plasma condition parameters. Moreover, we can see that the sum on the right hand side of Eq. (5) may be used as a normalization factor for the critical examination of homologous experimental values devided by λ^2. If ratio of such values and the normalization factor is nearly constant within homologous sequence (at plasma conditions when the used assumptions are valid), we may expect that the available data set is consistent.

Table 1. Values of the coefficients for the linear relation $E_j = a + bI_0$. Here, E_j is the energy of the level j and I_0 is the ionization potential

E_j	a (cm^{-1})	b	Remarks
np^4P^0	−31477.7	0.83824	Ne II homologous sequence
np^4D^0	−29487.1	0.84120	For Ne II, $n=3$
ns^4P	−39149.4	0.77998	
ns^2S	−14018.7	0.69419	Be II homologous sequence For Be II, $n=3$

We may neglect the lower level contribution in the normalization factor, since this contribution is often negligible and moreover one may expect that the regular behaviour within the homolgous sequence is similar for both levels in most cases. The normalization factor is now

$$NF = \frac{E_\text{H}}{I_0(1-b_\text{i})-a_\text{i}} \left[\frac{4\,E_\text{H}}{I_0(1-b_\text{i})-a_\text{i}} - l_\text{i}^2 - l_\text{i} - 1\right]. \tag{6}$$

If we have Stark widths for several homologous transitions, we may interpolate a new value by calculating

$$W' = 1.7444\ 10^{-8}\ \frac{\lambda^2(\text{cm})\ N(\text{cm}^{-3})}{T^{1/2}(\text{K})}\ NF \tag{7}$$

and then, multiplying the obtained result with the averaged ratio of experimental and calculated values:

$$W = W'\ (W_\text{exp}/W')_\text{av}. \tag{8}$$

In such a way we also correct the neglecting of the lower level broadening contribution.

3. Numerical, examples and discussion

The proposed method is applied to the $np-(n+1)s$ transitions of the earth-alkali ions and to the $ns-np$ transitions of the noble gas ions. We found that the linear relation (Eq. 4) between the ionization potential and the energy levels of interest, exists for the case considered, and corresponding empirical coefficients a and b are given in the Table 1.

In the Table 2 we present critically selected experimental Stark widths, (mormalized at $N=10^{17}\,\text{cm}^{-3}$ and $T=10000\,\text{K}$ and devided by λ^2) compared with our estimates. We can see that the experimental widths devided by λ^2 and the normalization factor NF are nearly constant. Moreover, our estimates obtained using Eq. (8) are in good agreement with the experimental values.

Table 2. Normalized values of the experimental full halfwidths (W) at $N=10^{17}\,\text{cm}^{-3}$ and $T=10000\,\text{K}$, divided by λ^2, compared with simple theoretical estimates: (a) obtained using Eq. (7); b) results under (a), multiplied with the averaged ratio of experimental and theoretical data. Ratios of the normalized widths devided by the normalization factor NF are also given

Element	λ (Å)	$\frac{W}{\lambda^2}$ (10^{-8} Å^{-1}) Experimental	Theoretical a	Theoretical b	$W/\lambda^2 NF$ (10^{-8} Å^{-1})	Ref.
Mg II	2928.75	4.4	3.2	4.1	0.24	Fleurier et al. (1977)
		4.1	3.2	4.1	0.22	Helbig and Kusch (1972)
	2936.54	4.4	3.2	4.1	0.24	Fleurier et al. (1977)
		4.2	3.2	4.1	0.23	Helbig and Kusch (1972)
Ca II	3706.03	5.9	4.5	5.7	0.23	Fleurier et al. (1977)
		5.1	4.5	5.7	0.20	Hühn and Kusch (1973)
	3736.20	5.8	4.5	5.7	0.23	Fleurier et al. (1977)
		4.9	4.5	5.7	0.19	Hühn and Kusch (1973)
Ba II	4899.9	7.1	5.6	7.1	0.22	Jaeger (1969)
	4524.9	7.2	5.6	7.1	0.22	Jaeger (1969)

© European Southern Observatory • Provided by the NASA Astrophysics Data System

1989A&A...217..201D

Table 3. Low density case. Normalized values of the experimental full halfwidths (Vitel and Skowronek, 1987a, b), at $N = 10^{17}\,\mathrm{cm}^{-3}$, and $T = 10000\,\mathrm{K}$, devided by λ^2, compared with simple theoretical estimates: (a) obtained using Eq. (7); (b) results under (a), multiplied with the averaged ratio of experimental and theoretical data. Ratios of the normalized widths devided by the normalization factor NF are also given

Element	λ (Å)	$\frac{W}{\lambda^2}$ (10^{-8} Å^{-1})			$W/\lambda^2 NF$ (10^{-8} Å^{-1})
		Experimental	Theoretical		
			a	b	
Ar II	4806.02	1.5	1.0	1.4	0.26
	4847.87	1.5	1.0	1.4	0.25
	4348.06	1.9	1.1	1.6	0.30
Kr II	4355.48	1.7	1.3	1.9	0.23
	4658.87	1.7	1.2	1.7	0.25
	4739.00	1.7	1.2	1.7	0.25
Xe II	5292.22	1.9	1.4	2.0	0.24
	5339.38	2.0	1.4	2.0	0.24
	4844.33	2.0	1.6	2.3	0.22
	5419.15	2.3	1.6	2.3	0.25

Table 4. Same as in Table 3 but for high density case

Element	λ (Å)	$\frac{W}{\lambda^2}$ (10^{-8} Å^{-1})			$W/\lambda^2 NF$ (10^{-8} Å^{-1})
		Experimental	Theoretical		
			a	b	
Ar II	4806.02	1.3	1.0	1.2	0.23
	4847.87	1.3	1.0	1.2	0.22
	4348.06	1.6	1.1	1.3	0.24
Kr II	4355.48	1.4	1.3	1.6	0.19
	4658.87	1.4	1.2	1.4	0.21
	4739.00	1.4	1.2	1.4	0.20
Xe II	5292.22	1.6	1.4	1.7	0.19
	5339.38	1.6	1.4	1.7	0.20
	4844.33	1.8	1.6	1.9	0.20
	5419.15	1.8	1.6	1.9	0.20

In Tables 3 and 4, the values obtained using Eqs. (6)–(8) are compared with recently published experimental values (Vitel and Skowronek, 1987a, b) obtained at low (Tables 3) and high (Table 4) density. We can see that in both cases the experimental and theoretical values compare well and that the experimental values devided with the normalization factor are nearly constant in low density as well as in high density case. This demonstrates the regular behaviour of Stark widths within the homologous sequence examined. This regularity is conserved also in the high density case.

In all cases examined, a selfconsistent data set of homologous transitions is obtained. This indicates that the interpolation of new data (e.g. for Sr II from Table 2) may be successful.

Acknowledgements. We are indebted to Dr. Yves Vitel for very useful discussions. This work is partially financed by RZN of Serbia.

References

Dimitrijević, M.S.: 1985, *Astron. Astrophys.* **145**, 439
Dimitrijević, M.S.: 1988, *Astron. Astrophys. Suppl.* **76**, 53
Dimitrijević, M.S., Konjević, N.: 1980, *J. Quant. Spectrosc. Radiat. Transfer* **24**, 451
Dimitrijević, M.S., Konjević, N.: 1981, in *Spectral Line Shapes*, ed. B. Wende, de Gruyter, Berlin, New York, p. 211
Dimitrijević, M.S., Konjević, N.: 1984, *Z. Naturforsch.* **39a**, 553
Dimitrijević, M.S., Konjević, N.: 1987, *Astron. Astrophys.* **172**, 345
Dimitrijević, M.S., Truong-Bach: 1986, *Z. Naturforsch.* **41a**, 772
Fleurier, C., Sahal-Brechot, S., Chapelle, J.: 1977, *J. Quant. Spectrosc. Radiative Transfer* **17**, 595
Griem, H.R.: 1968, *Phys. Rev.* **165**, 258
Helbig, V., Kusch, H.J.: 1972, *Astron. Astrophys.* **20**, 299
Hey, J.D., Bryan, R.J.: 1977, *J. Quant. Spectrosc. Radiat. Transfer* **17**, 221
Hühn, R., Kusch, H.J.: 1973, *Astron. Astrophys.* **28**, 159
Jaeger, H.: 1969, *Z. Phys.* **223**, 19
Konjević, N., Dimitrijević, M.S.: 1981, in *Spectral Line Shapes*, ed. B. Wende, de Gruyter, Berlin, New York, p. 241
Konjević, N., Pittman, T.L.: 1987, *J. Quant. Radiat. Transfer* **37**, 311
Lakićević, I.S.: 1983, *Astron. Astrophys.* **127**, 37
Lakićević, I.S., Purić, J.: 1983, in *Spectral Line Shapes II*, ed. K. Burnett, de Gruyter, Berlin, New York, p. 147
Pradham, A.K.: 1987, Physica Scripta **35**, 840
Purić, J., Ćirković, L.: 1973, Proc. 11th Int. Conf. Phen. Ioniz. Gases, Prague, p. 398
Purić, J., Lakićević, I., Glavonjić, V.: 1980, *Phys. Lett.* **76A**, 128
Seaton, M.J.: 1987, *J. Phys. B* **20**, 6431
Vitel, Y., Skowronek, M.: 1987a, *J. Phys. B* **20**, 6477
Vitel, Y., Skowronek, M.: 1987b, *J. Phys. B.* **20**, 6493
Vitel, Y., Skowronek, M., Dimitrijević, M.S., Popović, M.M.: 1988, *Astron. Astrophys.* **200**, 285
Wiese, W.L., Konjević, N.: 1982, *J. Quant. Spectrosc. Radiat. Transfer* **28**, 185

© European Southern Observatory • Provided by the NASA Astrophysics Data System

1990A&A...236..261D

Astron. Astrophys. 236, 261–267 (1990)

ASTRONOMY AND ASTROPHYSICS

Regularities and similarities in the widths of spectral lines perturbed by neutral atoms

M.S. Dimitrijević[1] **and G. Peach**[2]

[1] Astronomical Observatory, Volgina 7, 11050 Belgrade, Yugoslavia
[2] Department of Physics and Astronomy, University College London, Gower Street, London WC1E 6BT, England

Received November 16, 1989; accepted February 19, 1990

Abstract. Regularities and similarities in the widths of spectral lines perturbed by neutral atoms have been studied in order to find out if they are apparent to such a degree that they can be used to obtain data by interpolation and hence provide a tool for the critical evaluation of new experimental results. Consideration of the structure of the emitting (or absorbing atom) indicates that similarities should exist for lines within a multiplet or supermultiplet. Line widths should also have a regular behaviour along a spectral series, for corresponding transitions in homologous emitters, and for isoelectronic sequences. The dependence of line widths on perturber properties such as polarisability has also been examined. Critically selected experiments on the non-resonant broadening of spectral lines have been examined and exceptions from expected regularities are discussed.

Key words: line broadening – atomic data

1. Introduction

The broadening of a line depends on both the dynamics of the individual emitter-perturber collisions and on the collective effect of all the perturbers interacting with the emitter. The relative importance of these factors depends on whether the perturber density is low or high. Line broadening depends also on the particle properties and consideration of the structure of the emitting (or absorbing atom) indicates that similarities should exist for lines within a multiplet or supermultiplet. Widths also depend on perturber properties such as polarisability and should have a regular behaviour along spectral series, for corresponding transitions in homologous emitters, and for isoelectronic sequences.

Regularities and systematic trends for the widths of isolated non-hydrogenic spectral lines in plasmas have been studied recently in a number of papers, see for example Wiese and Konjević, 1982; Dimitrijević, 1982; Konjević and Dimitrijević, 1981, and references therein. The aim of such studies is to find out if regularities and systematic trends can be used to predict line widths and to critically evaluate experimental data. In this article, we demonstrate that such regularities are also apparent in the case of non-resonant broadening of spectral lines by neutral atoms.

Send offprint requests to: M.S. Dimitrijević

2. Experiment and theory

2.1. The experimental data

In order to find out if regularities and similarities due to particle properties are apparent in the case of line broadening by non-resonant collisions with neutral atoms, we have analysed the experimental data selected by Allard and Kielkopf (1982). In this critical review, only data for states with effective principal quantum numbers less than five have been included. Moreover, only data of high photometric precision have been selected, that is no photographic measurements are listed; also only measurements for which instrumental effects and other possible sources of broadening have been subtracted are given. In our analysis, we list the individual references for all the data used.

2.2. The Van der Waals formula

For a pure Van der Waals interaction between emitter and perturber, the impact approximation to the line width, valid for low perturber density N, is given by

$$w(\text{theory}) = \pi N \bar{v} \left(\frac{3\pi C_6}{8\bar{v}}\right)^{2/5} \Gamma\left(\frac{3}{5}\right)\Gamma\left(\frac{9}{5}\right)\cos\left(\frac{\pi}{5}\right)\left(\frac{\pi}{4}\right)^{-1/5};$$

$$\bar{v} = \left(\frac{8kT}{\pi\mu}\right)^{1/2} = 3.950403257\, N \bar{v}^{3/5} C_6^{2/5} \tag{1}$$

where T is the temperature and w is the half-half width, see for example Eq. (3.34) of Peach (1981). The reduced mass of the emitter-perturber system is μ, C_6 is the Van der Waals constant, and k is the Boltzmann constant. Although it is well known that formula (1) can easily be in error by a factor of two in specific cases, it provides a simple expression that can be used as a convenient scaling function to help in the clarification of the trends in the spectral data. In the discussion that follows, we consider the ratio of w(experiment)/w(theory) as a function of

$$f(C_6, \mu, T) = C_6^{2/5}(T/\mu)^{3/10} \tag{2}$$

where all quantities are expressed in atomic units. A simple expression for C_6 can be obtained by averaging over the degenerate magnetic sublevels, see Al-Saqabi and Peach (1987), and so we approximate to C_6 by writing

$$C_6 = \alpha_d(\overline{r_i^2} - \overline{r_j^2}), \tag{3}$$

where α_d is the dipole polarisability and $\overline{r_i^2}$ and $\overline{r_j^2}$ are the mean

© European Southern Observatory • Provided by the NASA Astrophysics Data System

1990A&A...236..261D

Table 1. Effective principal quantum numbers for the atomic states

State	n^*	Reference	State	n^*	Reference
Li $(2s^2S_{1/2})$	1.588472	a	Ca $(4s4p\,^3P_0)$	1.792639	f
Li $(2p^2P_{1/2,3/2})$	1.959314		Ca $(4s4p\,^3P_1)$	1.794009	
			Ca $(4s4p\,^3P_2)$	1.796801	
Na $(3s^2S_{1/2})$	1.627094	b			
Na $(3p^2P_{1/2})$	2.116648		Ca $(4s3d\,^3D_3)$	1.947442	f
Na $(3p^2P_{3/2})$	2.117391		Ca $(4s3d\,^1D_2)$	1.999194	
K $(4s^2S_{1/2})$	1.770433	b	Ca $(4s3d\,^3D_1)$	1.796913	g
K $(4p^2P_{1/2})$	2.232133		Ca $(4s3d\,^3D_2)$	1.796546	
K $(4p^2P_{3/2})$	2.235064		Ca $(4s3d\,^3D_3)$	1.794372	
			Ca $(4s3d\,^1D_2)$	1.756670	
Rb $(5s^2S_{1/2})$	1.804762	c			
Rb $(5p^2P_{1/2})$	2.279883		Ca $(4s5s\,^3S_1)$	2.485287	f
Rb $(5p^2P_{3/2})$	2.292821				
			Ca $(4s5p\,^3P_2)$	2.935957	f
Cs $(6s^2S_{1/2})$	1.869248	d	Ca $(4s5p\,^1P_1)$	2.954171	
Cs $(6p^2P_{1/2})$	2.329152				
Cs $(6p^2P_{3/2})$	2.361719		Ca $(3d4p\,^3F_2)$	2.007644	f, g
Cs $(7p^2P_{1/2})$	3.373753		Ca $(3d4p\,^3F_3)$	2.010906	
Cs $(7p^2P_{3/2})$	3.405884		Ca $(3d4p\,^3F_4)$	2.011554	
Cs $(8p^2P_{1/2})$	4.388647		Ca $(3d4p\,^3D_1)$	2.105077	
Cs $(8p^2P_{3/2})$	4.420837		Ca $(3d4p\,^3D_2)$	2.103635	
			Ca $(3d4p\,^3D_3)$	2.105334	
Ca^+ $(4s^2S_{1/2})$	2.141068	e	Ca $(3d4p\,^1D_2)$	2.011525	
Ca^+ $(4p^2P_{1/2})$	2.494156		Ca $(3d4p\,^3P_1)$	2.155405	
Ca^+ $(4p^2P_{3/2})$	2.498105		Ca $(3d4p\,^1P_1)$	2.398002	

References: (a) Johansson (1959). (b) Risberg (1956). (c) Johansson (1961). (d) Kleiman (1962). (e) Edlén and Risberg (1956). (f) Risberg (1968). (g) n^* calculated using the series limit Ca^+(3d)

square radii of the upper and lower states i and j of the atomic transition. The mean square radii are estimated from the formula

$$\overline{r_k^2} = \frac{n_k^{*2}}{2z^2}[5n_k^{*2} + 1 - 3l(l+1)], \tag{4}$$

where n_k^* is the effective principal quantum number of the state k defined by

$$E_k = \frac{z^2}{2n_k^{*2}}. \tag{5}$$

In (5), E_k is the binding energy in atomic units of the electron active in the transition and z is the charge on the associated atomic core, i.e. $z=1$ for a neutral emitter, $z=2$ for a singly ionized emitter, etc. The atomic data used in this study are listed in Tables 1 and 2.

2.3. *Multiplets, supermultiplets and transition arrays*

Multiplets are the smallest distinct grouping of lines found in complex atomic spectra. The upper levels of the lines in the group may have different values of total angular momentum quantum number J_i, but all other quantum numbers are the same. Similarly, the lower levels of the lines differ from each other only in their total angular momentum quantum number J_f. The energy splitting of the groups of upper and lower levels is very small, and unless there are strong perturbations present that selectively affect the levels, the radial wave functions for levels within a group are virtually identical. This explains why in some of the theoretical approaches, calculations have been performed using single upper and lower levels placed at the centres of gravity of the groups of fine structure components. Thus, to a first

Table 2. Atomic masses and polarisabilities

Atom	Mass	Reference	α_d(a.u.)	Reference
Li	6.941	a		
Na	22.9898	a		
K	39.102	a		
Rb	85.4678	a		
Cs	132.905	a		
Ca	40.08	a		
He	4.0026	a	1.3834	b
Ne	20.179	a	2.669	c
Ar	39.948	a	11.080	d
Kr	83.80	a	16.734	d
Xe	131.30	a	27.292	d

References: (a) Allen (1973); atomic masses are on the scale $M(^{12}C) = 12.00$. (b) Thomas and Humberston (1972). (c) Saxon (1973). (d) Dalgarno and Kingston (1960)

© European Southern Observatory • Provided by the NASA Astrophysics Data System

1990A&A...236..261D

approximation, it is to be expected that the widths of all the components in the multiplet are the same (see for example Allard and Kielkopf, 1982 or Peach, 1981).

Supermultiplets are groups of multiplets where the groups of upper and lower levels respectively, all belong to the same configuration and have the same total spin angular momentum quantum number $S_i = S_f$. Transition arrays are a still larger grouping of lines in which the groups of upper and lower levels have the same configurations, but in which firstly the total spin is not necessarily the same for all the transitions and secondly, spin is not necessarily conserved for a particular transition. For these much more general groupings of lines, one expects that the line widths will be of roughly the same size if the long-range part of the emitter-perturber interaction is the dominant feature producing broadening of the lines.

3. Regularities and systematic trends

In order to highlight the regularities and systematic trends, all the line-width data considered are presented in Figs. 1–5 in the form of w(experiment)/w(theory) plotted as a function of $f(C_6, \mu, T)$ where w(theory) and $f(C_6, \mu, T)$ are defined in Eqs. (1) and (2).

3.1. *Multiplets in homologous atoms*

Experimental data for the half-half widths of the resonance transitions in homologous atoms perturbed by rare gases are listed in Table 3 and shown in Fig. 1. The figure clearly shows that the result of Bernabeu and Alvarez (1980) for the $6s^2S_{1/2} - 6p^2P_{3/2}$ transition in Cs I broadened by Xe is too large, as the deviation from the average is outside acceptable limits and there is no configuration-interaction effect in caesium that could selectively perturb this transition. The scatter in the data for helium and neon perturbers is the greatest, because the effect of the short-range part of the radiator-perturber interaction is dominant and this is not directly related to the Van der Waals interaction at all (cf. Al-Saqabi and Peach, 1987). Particularly interesting is the case of neon. If the line widths are considered to

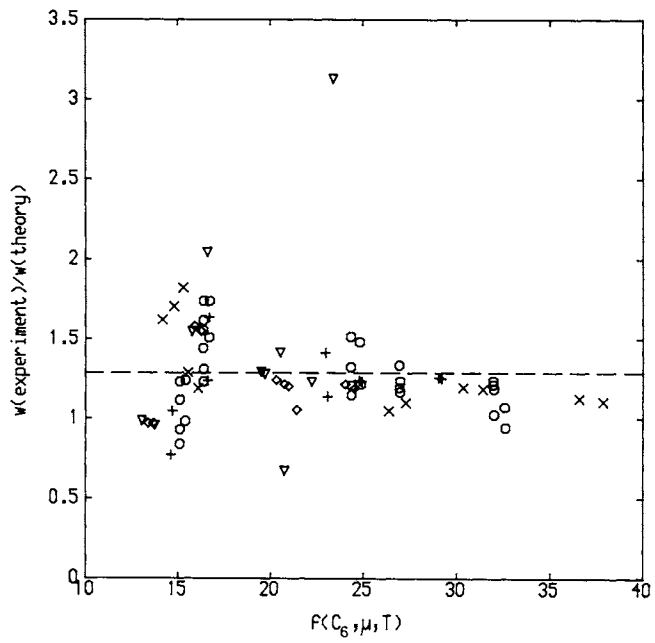

Fig. 1. The ratio w(experiment)/w(theory) as a function of $f(C_6, \mu, T)$ for resonance lines of homologous atoms; the experimental data are listed in Table 3. The lines of Li, Na, K, Rb and Cs are denoted by ×, ○, +, ◇ and ∇ respectively. The average vaue of the ratio is 1.285

Table 3. Half-half widths for resonance transitions in homologous atoms perturbed by He, Ne, Ar, Kr and Xe. The quantity tabulated is $w/(10^{-9}\,\mathrm{rad\,s^{-1}}\,N\,\mathrm{cm}^3)$

Transition	λ(Å)	T(K)	He	Ne	Ar	Kr	Xe	Reference
Li I $2s^2S_{1/2} - 2p^2P_{1/2,3/2}$		520	1.73					a
		600	1.90	1.51	2.08	2.73	3.10	b
	6707.8	673	2.10	1.44	2.26	2.80	3.15	c
Na I $3s^2S_{1/2} - 3p^2P_{1/2}$	5895.9	450	1.52					d
			1.78	1.40	2.78	2.42	2.92	e
			1.92	0.953	2.43	2.71	2.98	f
		480	1.90	1.14	2.77		2.63	g
Na I $3s^2S_{1/2} - 3p^2P_{3/2}$	5890.0	450	1.62					d
			2.15	1.27	2.11	2.37	2.47	e
			2.00	1.06	2.22	2.51	2.86	f
		480	2.19	1.44	2.27		2.32	g
K I $4s^2S_{1/2} - 4p^2P_{1/2}$	7699.0	410	1.55	0.85	2.45	2.31	2.75	b
K I $4s^2S_{1/2} - 4p^2P_{3/2}$	7664.9	410	2.06	1.16	1.98	2.31	2.75	b
Rb I $5s^2S_{1/2} - 5p^2P_{1/2}$	7947.6	320	1.9	0.98	1.9	1.9	2.2	h
Rb I $5s^2S_{1/2} - 5p^2P_{3/2}$	7800.3	320	1.9	1.0	1.9	1.7	2.2	h
Cs I $6s^2S_{1/2} - 6p^2P_{1/2}$	8943.5	295	1.84	0.969	1.90	1.90	2.06	i
Cs I $6s^2S_{1/2} - 6p^2P_{3/2}$	8521.1	295	2.56	0.990	2.19	1.05	5.52	i

References: (a) Smith and Collins (1976). (b) Lwin et al. (1977). (c) Gallagher (1975). (d) Deleage et al. (1973). (e) Chatham et al. (1980). (f) Kielkopf (1980). (g) McCartan and Farr (1976). (h) Ottinger et al. (1975). (i) Bernabeu and Alvarez (1980)

© European Southern Observatory • Provided by the NASA Astrophysics Data System

1990A&A...236..261D

be only a function of perturber polarisability, one obtains a pronounced irregular minimum for neon explained as 'expected on the basis of the Ramsauer-Townsend effect' by Kielkopf (1980). However, this anomaly disappears almost completely when the full dependence on all the physical parameters are taken into account as is done in Fig. 1.

3.2. Members of series of multiplets

Experimental data for the half-half widths for members of the series Cs $6s^2S-np^2P$; $n=6, 7, 8$ perturbed by rare gases are listed in Table 4 and shown in Fig. 2. There is a gradual increase in line width and a trend is evident. For every large values of n the line widths stop varying, and then comparison with w(theory) in Eq. (1) is meaningless because the long-range Van der Waals interactions are unimportant, see Allard and Kielkopf (1982).

3.3. Multiplets and supermultiplets in calcium

Experimental data for the half-half widths of multiplets and supermultiplets of neutral calcium perturbed by He, Ne and Ar are listed in Table 5 and shown Figs. 3 and 4. Despite the fact that

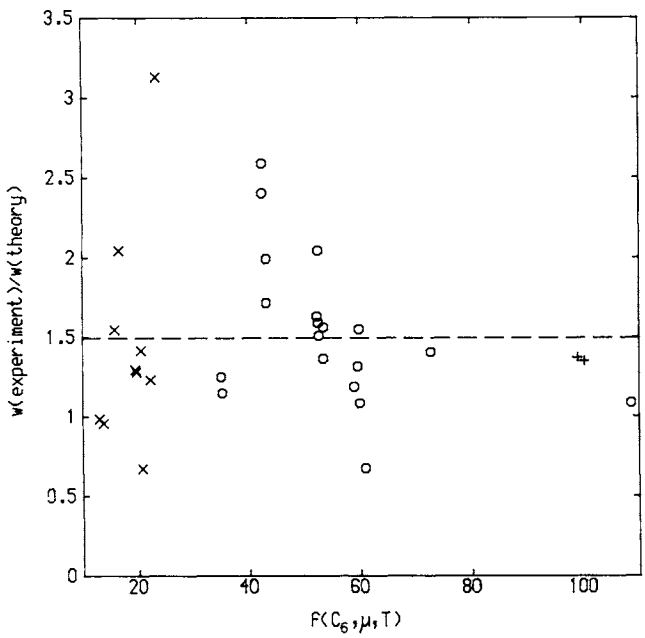

Fig. 2. The ratio w(experiment)/w(theory) as a function of $f(C_6, \mu, T)$ for the spectral series Cs $6s-np$; the experimental data are listed in Table 4. The lines with $n=6$, 7 and 8 are denoted by ×, ○ and + respectively. The average value of the ratio is 1.495

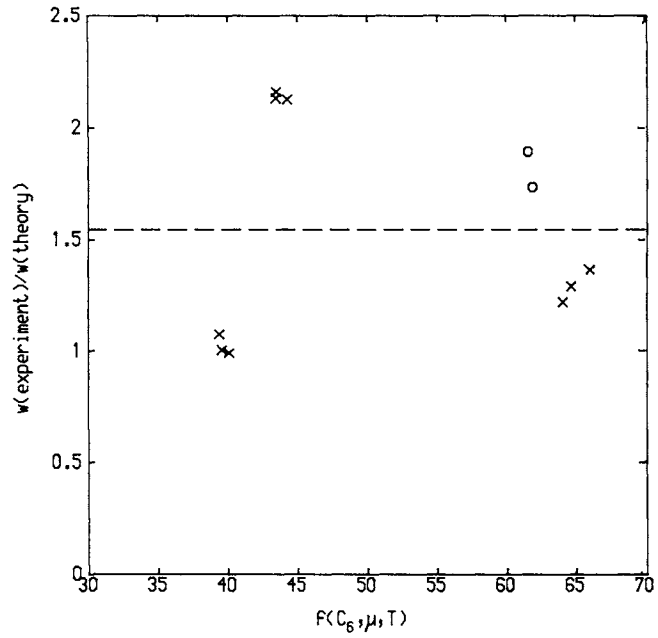

Fig. 3. The ratio w(experiment)/w(theory) as a function of $f(C_6, \mu, T)$ for supermultiplets Ca $4s4p-4s5s$ and Ca $4s3d-4s5p$; the experimental data are listed in Table 5. The lines are denoted by × and ○ respectively. The average value of the ratio is 1.545

Table 4. Half-half widths for members of a spectral series perturbed by He, Ne, Ar, Kr and Xe. The quantity tabulated is $w/(10^{-9}\,\mathrm{rad\,s^{-1}}\,N\,\mathrm{cm}^3)$

Transition	λ(Å)	T(K)	He	Ne	Ar	Kr	Xe	Reference
Cs I $6s^2S_{1/2}-6p^2P_{1/2}$	8943.5	295	1.84	0.969	1.90	1.90	2.06	a
Cs I $6s^2S_{1/2}-6p^2P_{3/2}$	8521.1	295	2.56	0.990	2.19	1.05	5.52	a
Cs I $6s^2S_{1/2}-7p^2P_{1/2}$	4593.2	380					5.27	b
		395		3.30	6.44		5.91	c
		400	7.7		8.1		7.0	d
		400	8.3		6.3			e
		4500		7.7	8.9			f
Cs I $6s^2S_{1/2}-7p^2P_{3/2}$	4555.3	380					4.90	b
		380		3.05	5.99			c
		400	5.6		6.3		3.1	d
		400	6.5		5.5			e
Cs I $6s^2S_{1/2}-8p^2P_{1/2}$	3888.6	450					10.23	b
Cs I $6s^2S_{1/2}-8p^2P_{3/2}$	3876.1	450					10.19	b

References: (a) Bernabeu and Alvarez (1980). (b) Kielkopf and Allard (1980). (c) Smith (1975). (d) Evdokimov (1968). (e) Rostas and Lemaire (1971). (f) Evans and Cooper (1972)

© European Southern Observatory • Provided by the NASA Astrophysics Data System

1990A&A...236..261D

Table 5. Half-half widths for members of supermultiplets perturbed by He, Ne and Ar. The quantity tabulated is $w/(10^{-9}\ \mathrm{rad\,s^{-1}}\ N\ \mathrm{cm}^3)$

Transition	λ(Å)	T(K)	He	Ne	Ar	Reference
Ca I $4s4p\,^3P_0-4s5s\,^3S_1$	6102.7	2080	7.1			a
		2300		3.0		a
		2700			6.8	a
Ca I $4s4p\,^3P_1-4s5s\,^3S_1$	6122.2	1970	7.1			a
		2210		3.0		a
		2530			6.3	a
Ca I $4s4p\,^3P_2-4s5s\,^3S_1$	6162.2	1970	7.0			a
		2180		3.2		a
		2460			5.9	a
Ca I $4s3d\,^3D_3-3d4p\,^3F_4$	6439.1	2500	3.1			b
Ca I $4s3d\,^3D_2-3d4p\,^3F_3$	6462.6	2500	3.3			b
Ca I $4s3d\,^3D_1-3d4p\,^3F_2$	6493.8	2500	3.0			b
Ca I $4s3d\,^3D_3-3d4p\,^3F_3$	6471.7	2500	3.1			b
Ca I $4s3d\,^3D_3-3d4p\,^3D_3$	5588.8	2500	3.7			b
Ca I $4s3d\,^3D_2-3d4p\,^3D_2$	5594.5	2500	3.5			b
Ca I $4s3d\,^3D_1-3d4p\,^3D_1$	5598.5	2500	3.4			b
Ca I $4s3d\,^3D_1-3d4p\,^1D_2$	6449.8	2500	3.6			b
Ca I $4s3d\,^1D_2-3d4p\,^1D_2$	7148.2	2500	3.2			b
Ca I $4s3d\,^3D_1-3d4p\,^3P_1$	5261.7	2500	6.0			b
Ca I $4s3d\,^1D_2-3d4p\,^1P_1$	5041.6	2500	12.8			b
Ca I $4s3d\,^3D_3-4s5p\,^3P_2$	6169.6	2500	8.8			b
Ca I $4s3d\,^1D_2-4s5p\,^1P_1$	6717.7	2500	8.1			b

References: (a) O'Neill and Smith (1980). (b) Smith and Raggett (1981)

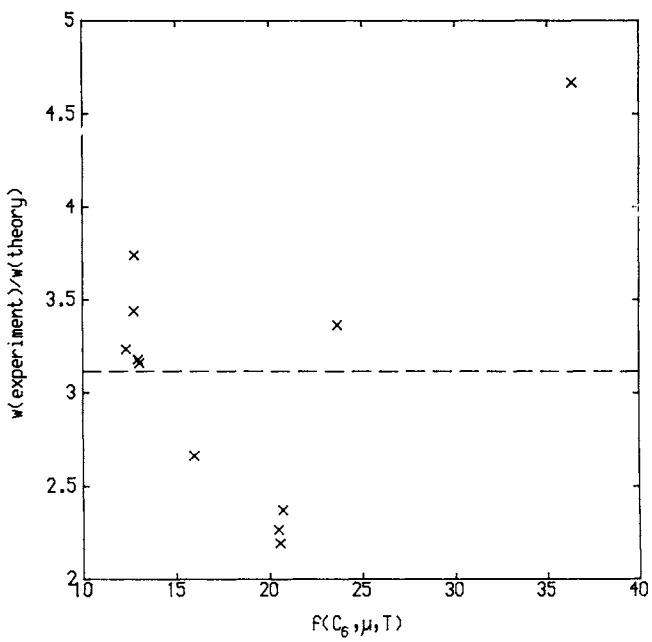

Fig. 4. The ratio w(experiment)/w(theory) as a function of $f(C_6, \mu, T)$ for supermultiplet Ca $4s3d-3d4p$; the experimental data are listed in Table 5. The average value of the ratio is 3.114

calcium has a very complicated structure in which there is considerable configuration interaction, the transitions for which the residual Ca^+ core is in its ground state, $4s^2S$, show a trend that is not very different to those shown in Figs. 1 and 2. The supermultiplet $4s3d-3d4p$ comprises a group of transitions in which the residual Ca^+ core is in its first excited state, $3d^2D$, and again a general trend is evident although the average value of w(experiment)/w(theory) is about twice the value found previously. The scatter in the data is quite large because the configurations $3d4p$ and $4snp$; $n=4, 5, 6$ are strongly mixed, see Smith and Raggett (1981).

3.4. *Multiplets in isoelectronic sequences*

Experimental data for the half-half widths of the resonance transitions in the potassium isoelectronic sequence perturbed by rare gases are listed in Table 6 and shown in Fig. 5. A systematic trend in the data is clear and is similar to that shown in Fig. 1.

3.5. *Validity of the Van der Waals formula*

In Figs. 1–5, the scatter of the data about the average value of w(experiment)/w(theory) is less for the larger values of $f(C_6, \mu, T)$. This is because the heavier perturbers have much larger polarisabilities and hence the longer-range part of the radiator-perturber interaction becomes the dominant factor determining the line width. Our results also show that better agreement between theory and experiment is obtained if the Van der Waals formula is multiplied by a factor of about 1.25–1.5. This can be explained by studying Fig. 6 where accurate potentials for Na–Ne are plotted as a ratio to their asymptotic value. It is seen that true convergence to the Van der Waals limit only occurs for $R > 50$ a.u. a much larger value of R than is often assumed, but that the curves have a maximum at much lower

© European Southern Observatory • Provided by the NASA Astrophysics Data System

1990A&A...236..261D

Table 6. Half-half widths for resonance lines of atoms in the potassium isoelectronic sequence perturbed by He, Ne, Ar, Kr and Xe. The quantity tabulated is $w/(10^{-9}\,\mathrm{rad\,s^{-1}}\,N\,\mathrm{cm}^3)$

Transition	λ(Å)	T(K)	He	Ne	Ar	Kr	Xe	Reference
K I $4s^2S_{1/2}-4p^2P_{1/2}$	7699.0	410	1.55	0.85	2.45	2.31	2.75	a
K I $4s^2S_{1/2}-4p^2P_{3/2}$	7664.9	410	2.06	1.16	1.98	2.31	2.75	a
Ca II $4s^2S_{1/2}-4p^2P_{1/2}$	3968.5	655	1.05					b
		765			1.48			b
		7466	2.6					c
Ca II $4s^2S_{1/2}-4p^2P_{3/2}$	3933.7	655	1.46					b
		765			1.53			b

References: (a) Lwin et al. (1977). (b) Bowman and Lewis (1978). (c) Baur and Cooper (1977)

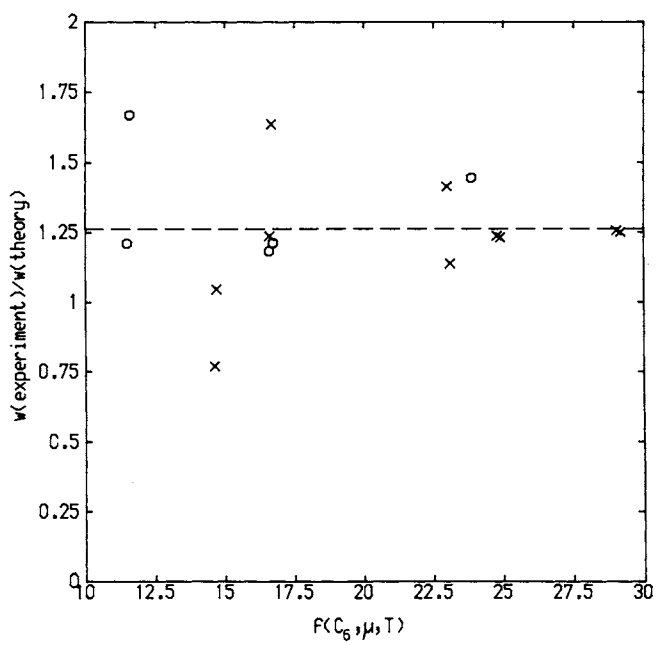

Fig. 5. The ratio w(experiment)/w(theory) as a function of $f(C_6, \mu, T)$ for resonance lines of atoms in the potassium isoelectronic sequence; the experimental data are listed in Table 6. The lines of K and Ca^+, are denoted by × and ○ respectively. The average value of the ratio is 1.262

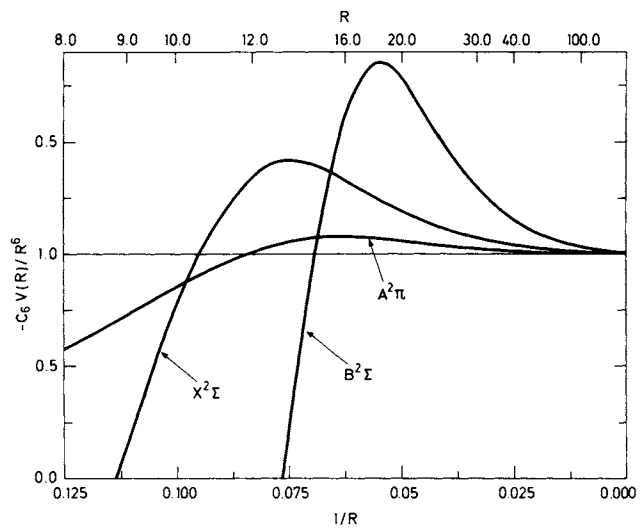

Fig. 6. The adiabatic potentials for the $X^2\Sigma$, $B^2\Sigma$ and $A^2\Pi$ states for the system Na–Ne plotted as a ratio to their asymptotic form, $-C_6/R^6$

values of R. This behaviour is typical of all the alkali-rare gas interactions.

4. Conclusions

Regularities and similarities in spectra have been clearly identified and have been examined in terms of departures from the Van der Waals formula. This approach provides a method by which discrepancies in experimental data can be identified and which can be used under certain circumstances to estimate new line width data.

Acknowledgements. This work is part of the ALIS link programme no: 198: 'Theory of atomic collisions' and is supported by the British Council. The work is also supported by RZN of Serbia and by SKNTI through the project 'Atomic and Plasma Spectroscopy'.

References

Allard, N., Kielkopf, J.F.: 1982, *Rev. Mod. Phys.* **54**, 1103
Allen, C.W.: 1973, Astrophysical Quantities, 3rd edn., Athlone, London
Al-Saqabi, B.N.I., Peach, G.: 1987, *J. Phys. B: At. Mol. Phys.* **20**, 1175
Baur, J.F., Cooper, J.: 1977, *J. Quant. Spectrosc. Radiat. Transfer* **17**, 311
Bernabeu, E., Alvarez, J.M.: 1980, *Phys. Rev. A* **22**, 2690
Bowman, N.J., Lewis, E.L.: 1978, *J. Phys. B: At. Mol.Phys.* **11**, 1703
Chatham, R.H., Gallagher, A., Lewis, E.L.: 1980, *J. Phys. B: At. Mol. Phys.* **13**, L7
Dalgarno, A., Kingston, A.E.: 1960, *Proc. R. Soc. A* **259**, 424
Deleage, J.P., Kunth, D., Testor, G., Rostas, F., Roueff, E.: 1973, *J. Phys. B: At. Mol. Phys.* **6**, 1892
Dimitrijević, M.S.: 1982, *Astron. Astrophys.* **112**, 251
Edlén, B., Risberg, P.: 1956, *Ark. Fys.* **10**, 553
Evans, J.M., Cooper, J.: 1972, *J. Quant. Spectrosc. Radiat. Transfer* **12**, 259
Evdokimov, Yu.V.: 1968, *Opt. Spectrosc.* **24**, 448
Gallagher, A.: 1975, *Phys. Rev. A* **12**, 133

© European Southern Observatory • Provided by the NASA Astrophysics Data System

1990A&A...236..261D

Johansson, I.: 1959, *Ark. Fys.* **15**, 169
Johansson, I.: 1961, *Ark. Fys.* **20**, 135
Kielkopf, J.F.: 1980, *J. Phys. B: At. Mol. Phys.* **13**, 3813
Kielkopf, J.F., Allard, N.F.: 1980, *J. Phys. B: At. Mol. Phys.* **13**, 709
Kleiman, H.: 1962, *J. Opt. Soc. Am.* **52**, 441
Konjević, N., Dimitrijević, M.S.: 1981, Spectral Line Shapes, ed. B. Wende, Walter de Gruyter, Berlin, p. 241
Lwin, N., McCartan, D.G., Lewis, E.L.: 1977, *Astrophys. J.* **213**, 599
McCartan, D.G., Farr, J.M.: 1976, *J. Phys. B: At. Mol. Phys.* **9**, 985
O'Neill, J.A., Smith, G.: 1980, *Astron. Astrophys.* **81**, 100
Ottinger, Ch., Scheps, R., York, G.W., Gallagher, A.: 1975, *Phys. Rev. A* **11**, 1815
Peach, G.: 1981, *Adv. Phys.* **30**, 367
Risberg, G.: 1968, *Ark. Fys.* **37**, 231
Risberg, P.: 1956, *Ark. Fys.* **10**, 583
Rostas, F., Lemaire, J.L.: 1971, *J. Phys. B: At. Mol. Phys.* **4**, 555
Saxon, R.P.: 1973, *J. Chem. Phys.* **59**, 1539
Smith, G.: 1972, *J. Phys. B: At. Mol. Phys.* **5**, 2310
Smith, G.: 1975, *J. Phys. B: At. Mol. Phys.* **8**, 2273
Smith, G., Collins, B.S.: 1976, *J. Phys. B: At. Mol. Phys.* **9**, L117
Smith, G., Raggett, D. St. J.: 1981, *J. Phys. B: At. Mol. Phys.* **14**, 4015
Thomas, M.A., Humberston, J.W.: 1972, *J. Phys. B: At. Mol. Phys.* **5**, L229
Wiese, W.L., Konjević, N.: 1982, *J. Quant. Spectrosc. Radiat. Transfer* **28**, 185

© European Southern Observatory • Provided by the NASA Astrophysics Data System

1992A&A...256..305M

Astron. Astrophys. 256, 305–308 (1992)

ASTRONOMY AND ASTROPHYSICS

Influence of ion–atom collisions on the absorption of radiation in white dwarfs

A.A. Mihajlov[1,2] **and M.S. Dimitrijević**[2,1]

[1] Institute of Physics, P.O. Box 57, 11001 Beograd, Yugoslavia
[2] Astronomical Observatory, Volgina 7, 11050 Beograd, Yugoslavia

Received March 28, accepted September 10, 1991

Abstract. In order to provide the relevant absorption coefficients for the interpretation of the continuum absorption spectra in a number of white dwarfs with helium dominated atmospheres, the processes $He_2^+ + \hbar\omega \rightarrow He + He^+$ and $He + He^+ + \hbar\omega \rightarrow He + He^+$ have been considered together. We present also the absorption coefficients for the conditions of DA white dwarf atmospheres calculated by taking into account together the processes $H_2^+ + \hbar\omega \rightarrow H + H^+$ and $H + H^+ + \hbar\omega \rightarrow H + H^+$.

Key words: radiation absorption – continuous spectrum – stellar spectrum – white dwarfs

1. Introduction

The significance of the combined study of the processes of the photodissociation

$$H_2^+ + \hbar\omega \rightarrow H + H^+ \tag{1a}$$

and the absorption of electromagnetic radiation by collisional ion–atom complexes

$$H + H^+ + \hbar\omega \rightarrow \begin{cases} H + H^+ \\ H^+ + H \end{cases} \tag{1b}$$

has been demonstrated recently by Mihajlov & Dimitrijević (1986), for the conditions characteristic for a stellar plasma ($T \lesssim 10\,000$ K). Here, H is a hydrogen atom in the ground (1s) state and ω the circular frequency of the absorbed photon. The simple method for the determination of absorption coefficients in the infrared and visible spectral range, proposed in the article, mentioned above is applicable not only in the case of processes (1a) and (1b), but for a more numerous class of atomic systems. For the application of this method, the potentials (as a function of the internuclear distance R) for low lying energy states of molecular ions and the corresponding dipole matrix elements are needed.

An interesting case where the developed method can be applied directly, is the process

$$He_2^+ + \hbar\omega \rightarrow He + He^+ \tag{2a}$$

$$He + He^+ + \hbar\omega \rightarrow \begin{cases} He + He^+ \\ He^+ + He, \end{cases} \tag{2b}$$

where He is in the ground state.

Recent calculations by Gaur et al. (1988) indicate that in helium-rich non-DA white dwarfs, He_2^+ is the most abundant molecule in the atmospheres. Since non-DA white dwarfs comprise 20 to 25% of all white dwarfs (Sion 1986), and the gas pressures typical for helium-rich white dwarf atmospheres are 10^7–10^{10} dyn cm^{-2} (Koester 1980), it is of interest to investigate the processes (1b) and (2b) and provide the corresponding absorption coefficients.

Calculations of Gaur et al. (1988) show also that H_2 and H_2^+ are the most abundant molecules in DA white dwarf atmospheres. In Mihajlov & Dimitrijević (1986), the H_2^+ case is presented as an example for the application of the method and approximate expressions for H_2^+ molecular potentials were used. The accuracy of our proposed method is equivalent to the accuracy of the method for the calculation of the spontaneous emission during ion–atom collisions [as demonstrated in Mihajlov & Dimitrijević (1986)]. Since it has been demonstrated recently (Ermolaev et al. 1989; Ermolaev & Mihajlov 1991), that the accuracy of those calculations is better than assumed previously, and consequently the accuracy of the proposed method, we will also provide here a table of improved data for the H_2^+ case using the accurate molecular potentials for H_2^+ instead of the simple asymptotic expansion used before (Mihajlov & Dimitrijević 1987).

2. Results and discussion

Let us consider the processes

$$A_2^+ + \hbar\omega \rightarrow A + A^+ \tag{3a}$$

$$A + A^+ + \hbar\omega \rightarrow \begin{cases} A + A^+ \\ A^+ + A, \end{cases} \tag{3b}$$

where A is H or He. The total absorption coefficient for processes (3a) and (3b) together, normalized to the density $N(A) = N(A^+) = 1$, is given by the expression (Mihajlov & Dimitrijević 1986)

$$K_\omega^{(ab)}(T) = 0.62\,10^{-42}\gamma^{-1}R_\omega^4 \exp(|U_1(R_\omega)|/kT) \quad (\mathrm{cm}^5). \tag{4}$$

Send offprint requests to: M.S. Dimitrijević

© European Southern Observatory • Provided by the NASA Astrophysics Data System

1992A&A...256..305M

In Eq. (4) R_ω (in a.u.) is determined from (Mihajlov & Popović 1981):

$$\varepsilon(R)=\hbar\omega=U_2(R_\omega)-U_1(R_\omega), \tag{5}$$

assuming that the photon absorption occurs in the direct vicinity of the resonant internuclear distance R_ω. Here, $U_1(R_\omega)$ and $U_2(R_\omega)$ are the corresponding energies of the molecular states. In the case of H_2^+, U_1 and U_2 correspond to the Σ_g^+ and Σ_u^+ electron states and were taken from Bates et al. (1953). In the case of He_2^+, U_1 and U_2 correspond to the Σ_u^+ and Σ_g^+ electron states and were taken from Gupta & Matsen (1967). The γ in Eq. (4) is defined as

$$|d\varepsilon/dR|=\gamma\varepsilon|_{R=R_\omega}. \tag{6}$$

Equation (6) may be successfully approximated for R_ω larger than some limiting value $R_1(R_1\approx 0$ for H and ≈ 1.5 for He) as $\gamma\approx\gamma_A[1-\mathcal{O}(\delta/\gamma_A R)]$; $\gamma_A^2/2=I_A$ (a.u.); $\delta=(2/\gamma_A)-1$; where I_A is the ionization potential of A. Fop $R_\omega>R_{min}$ (R_{min} corresponds to the minimum of the molecular potential), $\gamma\approx\gamma_A=$const ($\gamma=1$ for H and 1.345 for He). In Eq. (4) the square of the corresponding dipole matrix element is approximated as $\sim e^2R_\omega^4/4$ (for details see Appendix A in Mihajlov & Popović 1981, and the discussion in Ermolaev & Mihajlov 1991). In the case of hydrogen and helium, this approximation is valid for R_ω larger than the equilibrium distance for the state 1. This value is near 2 a.u. for hydrogen and helium and corresponding R_ω for He as a function of λ (Å) are presented in Table 1. This table may be used for the examination of the validity of the method (how far is R_ω from the equilibrium distance) and also to see the influence of differences in molecular potential calculations. We might use the proposed method up to 1000 Å as a reasonable extrapolation since for He $R_\omega\approx 2$ for 1000 Å. However in this region we need more precise matrix elements and γ. Moreover, in the He case, around $R=1.5$, $d\varepsilon/dR=0$, according to the data of Gupta & Matsen (1967). Consequently, the quasistatic model used in our method is not more correct ($K_\omega\to\infty$).

Table 1. The R_ω (a.u.) for H_2^+ and He_2^+ as a function of λ (Å)

λ (Å)	He_2^+ R_ω (a.u.)
3000.	2.895
4000.	3.078
5000.	3.252
6000.	3.399
7000.	3.517
8000.	3.617
9000.	3.710
10000.	3.804
11000.	3.886
12000.	3.957
13000.	4.010
14000.	4.047
15000.	4.082
16000.	4.124
17000.	4.168
18000.	4.211
19000.	4.251
20000.	4.289

The total absorption coefficient may be presented as the sum of the absorption coefficients for the processes a and b,

$$K_\omega^{(ab)}(T)=K_\omega^{(a)}(T)+K_\omega^{(b)}(T) \tag{7}$$

$$K_\omega^{(a)}(T)=K_\omega^{(ab)}(T)X^{(a)}(\omega, T) \tag{8}$$

$$K_\omega^{(b)}(T)=K_\omega^{(ab)}(T)X^{(b)}(\omega, T) \tag{9}$$

$$X^{(a)}(\omega, T)=\Phi(Z^{1/2})-2\pi^{1/2}Z\exp(-Z) \tag{10}$$

$$X^{(b)}(\omega, T)=1-X^{(a)}(\omega, T) \tag{11}$$

$$Z=|U_1(R_\omega)|/kT, \tag{12}$$

where Φ is the error function (Abramowitz & Stegun 1972).

The corresponding $Z^{1/2}$ and $X^{(b)}(\omega, T)=K_\omega^{(b)}(T)/K_\omega^{(ab)}(T)$ as a function of $Z^{1/2}$ are presented in Tables 2 and 3 for the He_2^+ case, as a function of λ and T, for conditions of interest for white dwarfs. Using Tables 2 and 3 it is very easy to see the influence of the processes a or b on the total absorption coefficient in white dwarfs. Moreover, these tables enable the determination of the corresponding spectral coefficients for the stimulated emission (negative absorption) denoted here as $Z_\omega^{(i)}(T)$. In the case of thermodynamic equilibrium:

$$Z_\omega^{(i)}(T)=Z_\omega^{(ab)}(T)X^{(i)}(\omega, T), \quad i=a, b \tag{13}$$

$$Z_\omega^{(ab)}(T)=K_\omega^{(ab)}(T)\exp(-\hbar\omega/kT). \tag{14}$$

Finally, we could determine the absolute coefficients of absorption, marked here by an asterisk:

$$K_\omega^{*(i)}(T)=K_\omega^{(i)}(T)-Z_\omega^{(i)}(T), \quad i=\text{a, b, ab}$$
$$=K_\omega^{(i)}(T)[1-\exp(-\hbar\omega/kT)]. \tag{15}$$

Table 2. The $X^{(b)}=K_\omega^{(b)}(T)/K_\omega^{(ab)}(T)$ as a function of $Z^{1/2}=(-U_1(R_\omega)/kT)^{1/2}$

$\sqrt{Z}$	$X^{(b)}$
0.3	0.7642
0.4	0.7255
0.5	0.6992
0.6	0.6795
0.7	0.6609
0.8	0.6390
0.9	0.6097
1.0	0.5724
1.1	0.5269
1.2	0.4747
1.3	0.4179
1.4	0.3592
1.5	0.3015
1.6	0.2470
1.7	0.1974
1.8	0.1541
1.9	0.1174
2.0	0.0874
2.2	0.0450
2.4	0.0212
2.6	0.0091
2.8	0.0036
3.0	0.0013

© European Southern Observatory • Provided by the NASA Astrophysics Data System

1992A&A...256..305M

Table 3. The $Z^{1/2}=(-U_1(R_\omega)/kT)^{1/2}$ as a function of T (K) and λ (Å). The case of He_2^+

λ [Å] \ T [K]	4000.	6000.	8000.	10000.	15000.	20000.	25000.	30000.
3000.	2.199	1.795	1.555	1.391	1.135	0.983	0.879	0.803
4000.	2.001	1.634	1.415	1.266	1.033	0.895	0.800	0.731
5000.	1.847	1.508	1.306	1.168	0.954	0.826	0.739	0.675
6000.	1.712	1.398	1.211	1.083	0.884	0.766	0.685	0.625
7000.	1.606	1.312	1.136	1.016	0.829	0.718	0.643	0.587
8000.	1.518	1.239	1.073	0.960	0.784	0.679	0.607	0.554
9000.	1.441	1.177	1.019	0.911	0.744	0.644	0.576	0.526
10000.	1.376	1.124	0.973	0.870	0.711	0.615	0.551	0.503
11000.	1.318	1.076	0.932	0.833	0.680	0.589	0.527	0.481
12000.	1.264	1.032	0.894	0.800	0.653	0.565	0.506	0.462
13000.	1.217	0.994	0.861	0.770	0.629	0.544	0.487	0.444
14000.	1.175	0.960	0.831	0.743	0.607	0.526	0.470	0.429
15000.	1.139	0.930	0.805	0.720	0.588	0.509	0.456	0.416
16000.	1.108	0.904	0.783	0.701	0.572	0.495	0.443	0.404
17000.	1.081	0.882	0.764	0.683	0.558	0.483	0.432	0.395
18000.	1.057	0.863	0.748	0.669	0.546	0.473	0.423	0.386
19000.	1.036	0.846	0.732	0.655	0.535	0.463	0.414	0.378
20000.	1.016	0.830	0.719	0.643	0.525	0.454	0.407	0.371

Table 4. The absorption coefficient $\times 10^{39}$ (cm^{-1}) as a function of T (K) and λ (Å). The case of H_2^+

λ [Å] \ T [K]	4000.	5000.	6000.	7000.	8000.	9000.	10000.	11000.
3000.	9.171	3.403	1.758	1.096	0.769	0.584	0.469	0.391
4000.	5.479	2.457	1.439	0.982	0.738	0.590	0.494	0.427
5000.	3.884	1.982	1.266	0.919	0.722	0.599	0.516	0.457
6000.	3.066	1.717	1.167	0.885	0.720	0.613	0.538	0.485
7000.	2.584	1.554	1.107	0.869	0.724	0.629	0.562	0.512
8000.	2.286	1.451	1.072	0.863	0.734	0.647	0.584	0.538
9000.	2.079	1.379	1.049	0.862	0.745	0.664	0.607	0.563
10000.	1.942	1.336	1.041	0.871	0.762	0.687	0.632	0.591
11000.	1.842	1.307	1.039	0.882	0.780	0.709	0.657	0.617
12000.	1.763	1.283	1.038	0.892	0.796	0.729	0.679	0.641
13000.	1.702	1.266	1.039	0.902	0.812	0.748	0.700	0.663
14000.	1.656	1.255	1.043	0.914	0.828	0.766	0.720	0.685
15000.	1.621	1.249	1.050	0.927	0.845	0.786	0.741	0.707
16000.	1.595	1.247	1.058	0.941	0.862	0.805	0.762	0.729
17000.	1.575	1.248	1.069	0.957	0.880	0.825	0.784	0.751
18000.	1.561	1.252	1.080	0.972	0.898	0.845	0.804	0.773
19000.	1.550	1.256	1.092	0.988	0.916	0.864	0.825	0.794
20000.	1.542	1.263	1.105	1.005	0.935	0.885	0.846	0.816

The absorption coefficients $K_\omega^{(ab)}$ for the H_2^+ and He_2^+ case as a function of λ and T and conditions in white dwarf atmospheres are presented in Tables 4 and 5. From Tables 2 and 3 one can see that the processes 1a and 1b as well as 2a and 2b must be treated together when the process 1a or 2a are taken into account since their contributions are comparable. Moreover, the process 1b (2b) becomes more significant towards the infrared part of the spectrum. The total absorption coefficient shows a weak dependence

© European Southern Observatory • Provided by the NASA Astrophysics Data System

1992A&A...256..305M

Table 5. The absorption coefficient $\times 10^{39}$ (cm^{-1}) as a function of T (K) and λ (Å). The case of He_2^+

λ[Å] \ T[K]	4000.	6000.	8000.	10000.	15000.	20000.	25000.	30000.
3000.	4.070	0.812	0.363	0.224	0.118	0.085	0.070	0.062
4000.	2.269	0.597	0.306	0.205	0.120	0.092	0.079	0.071
5000.	1.565	0.502	0.284	0.202	0.128	0.102	0.089	0.081
6000.	1.154	0.434	0.266	0.199	0.134	0.111	0.098	0.091
7000.	0.931	0.394	0.256	0.198	0.140	0.118	0.107	0.099
8000.	0.790	0.366	0.250	0.198	0.146	0.125	0.114	0.107
9000.	0.697	0.349	0.247	0.200	0.152	0.132	0.122	0.115
10000.	0.642	0.341	0.249	0.206	0.160	0.141	0.131	0.124
11000.	0.597	0.335	0.250	0.211	0.167	0.149	0.139	0.133
12000.	0.559	0.328	0.251	0.214	0.173	0.156	0.146	0.140
13000.	0.524	0.320	0.250	0.216	0.177	0.160	0.151	0.145
14000.	0.492	0.311	0.247	0.215	0.179	0.163	0.154	0.149
15000.	0.468	0.304	0.245	0.215	0.181	0.166	0.158	0.152
16000.	0.455	0.302	0.246	0.218	0.185	0.170	0.162	0.157
17000.	0.447	0.303	0.249	0.222	0.190	0.176	0.168	0.163
18000.	0.443	0.305	0.253	0.227	0.195	0.181	0.173	0.168
19000.	0.440	0.308	0.257	0.231	0.200	0.187	0.179	0.174
20000.	0.438	0.311	0.261	0.236	0.205	0.192	0.184	0.179

on λ and T except in the region of low temperatures and towards the UV part of the spectrum, where a significant increase of $K_{\omega}^{(ab)}$ exists.

Acknowledgement. The authors are indebted to Vladimir Kršljanin for useful discussions.

References

Abramowitz M., Stegun I., 1972, Handbook of Mathematical Functions. Dover, New York
Bates D.R., Ledsham K., Stewart A.L., 1953, Phil. Trans. R. Soc. London Ser. A 246, 215
Ermolaev A.M., Mihajlov A.A., 1991, J. Phys. B 24, 155
Ermolaev A.M., Mihajlov A.A., Popović M.M., 1989, in: Labat J.M. (ed.) Proc. XIX Int. Conf. Phen. Ioniz. Gases, Beograd. University of Belgrade Press, Belgrade, p. 656
Gaur V.P., Tripathi B.M., Joshi G.C., Pande M.C., 1988, Ap&SS 147, 107
Gupta B.K., Matsen F.A., 1967, J. Chem. Phys. 47, 4860
Koester D., 1980, Proc. Second European IUE Conf., Tübingen, ESA SP-157, p. 333
Mihajlov A.A., Dimitrijević M.S., 1986, A&A 155, 319
Mihajlov A.A., Popović M.M., 1981, Phys. Rev. A 23, 1679
Mihalas D., 1978, Stellar Atmospheres (Chap. 4.4). W.H. Freeman, San Francisco
Sion E.M., 1986, PASP 98, 821

© European Southern Observatory • Provided by the NASA Astrophysics Data System

1993A&A...276..187M

Astron. Astrophys. 276, 187–192 (1993)

ASTRONOMY AND ASTROPHYSICS

The contribution of ion–atom radiative collisions to the opacity of the solar atmosphere

A.A. Mihajlov[1,2], M.S. Dimitrijević[2], and Lj.M. Ignjatović[1]

[1] Institute of Physics, P.O. Box 57, 11001 Beograd, Yugoslavia
[2] Astronomical Observatory, Volgina 7, 11050 Beograd, Yugoslavia

Received June 16, 1992; accepted February 3, 1993

Abstract. We investigate the contribution to the opacity of the solar atmosphere of some processes other than formation and photodissociation of the H^- ion. We show that positive-ion–atom radiative collision processes are not negligible at certain layers of the photosphere and of the chromosphere, although they make only a negligible contribution to the solar continuous optical emission emergent intensity.

Key words: atomic processes–molecular processes–Sun: photosphere–Sun: chromosphere

1. Introduction

The continuum opacity of the solar atmosphere in the visible range is dominated by radiation exchange in formation and dissociation of the H^- ion (see Mihalas 1978). However other processes involving atoms and positive ions may also play a role in the opacity. The purpose of the present paper is to evaluate the contribution of some ion–atom radiative collision processes to the opacity of the solar atmosphere. We will limit ourselves to the optical part of the electromagnetic spectrum (350–1250 nm) where the theory of the processes involved can be considered as correct.

Section 2 describes the processes involved; Sect. 3 contains a calculation of the corresponding emissivities, and Sect. 4 shows an appliction to the solar atmosphere. Sect. 5 is the conclusion.

2. Atomic and molecular radiative processes in the solar atmosphere

The following positive-ion–atom radiative collision processes will be treated here:

$$A^+ + A \leftrightarrow \varepsilon_\lambda + \begin{cases} A + A^+ & \text{(radiative charge exchange)}, \\ A_2^+ & \text{(ion–atom photoassociation and photodissociation of molecular ion)}, \end{cases} \quad (1)$$

where all atomic particles are in their electronic ground states and $\varepsilon_\lambda = 2\pi\hbar c/\lambda$ is the energy of the photon with the wavelength λ.

The contribution of processes (1) to the opacity of the solar atmosphere will be compared here with the contribution of the following known radiative processes:

(i) free–free and free–bound process involving a positive ion:

$$A^+ + e \leftrightarrow \varepsilon_\lambda + \begin{cases} A^+ + e \\ A^*, \end{cases} \quad (2)$$

where A* is an atom in an excited state;

(ii) free–free processes in the field of an atom:

$$A + e \leftrightarrow \varepsilon_\lambda + A + e; \quad (3)$$

(iii) free–bound processes in the field of an atom (first of all formation and dissociation of H^-):

$$A + e \leftrightarrow \varepsilon_\lambda + A^-. \quad (4)$$

The theory of processes (1) has been given by Drukarev & Mihajlov (1974), Mihajlov & Popović (1981), Mihajlov & Dimitrijević (1986). The molecular ion (H_2^*) photodissociation have been described by e.g. Mihalas (1978). Process (2) has been treated by e.g. Menzel (1962) and Sobelman (1979). Process (3) has been studied by e.g. Firsov & Chibisov (1960) and Stilley & Callaway (1970), while process (4) has been investigated by e.g. Armstrong (1963), Weisner & Armstrong (1964), and Wishart (1979). Processes (3) and (4) have been described as well e.g. in Mihalas (1978).

The spectral emissivity corresponding to process (1) is:

$$\varepsilon_{ia}(\lambda) = \sum S_{ia}^{A}(\lambda)\, N(A^+)\, N(A), \quad (5a)$$

where $N(A^+)$ and $N(A)$ are the number density of the ion A^+ and the atom A respectively, the sum is over the different kinds of ions and atoms and $S_{ia}^{A}(\lambda)$ is the emission spectral coefficient characterizing the total contribution of both photoemissive channels. It is given in analytical form by Mihajlov & Popović (1981).

Similarly we have for process (2):

$$\varepsilon_{ei}(\lambda) = \sum S_{ei}^{A}(\lambda)\, N(A^+) N_e, \quad (5b)$$

Send offprint requests to : M.S. Dimitrijević

© European Southern Observatory • Provided by the NASA Astrophysics Data System

1993A&A...276..187M

where N_e is the electronic density and $S_{ei}^{A}(\lambda)$ is given analytically by Sobelman (1979).

For processes (3) and (4) we have respectively:

$$\varepsilon_{ea}^{ff}(\lambda)=\sum S_{ea}^{A,ff}(\lambda)\, N(A)N_e, \tag{5c}$$

$$\varepsilon_{ea}^{fb}(\lambda)=\sum S_{ea}^{A,fb}(\lambda)\, N(A)N_e. \tag{5d}$$

We also define the ratios of emissivities:

$$F_{ei}(\lambda)=\varepsilon_{ia}(\lambda)/\varepsilon_{ei}(\lambda), \tag{6a}$$

$$F_{ea}^{ff}(\lambda)=\varepsilon_{ia}(\lambda)/\varepsilon_{ea}^{ff}(\lambda), \tag{6b}$$

$$F_{ea}^{fb}(\lambda)=\varepsilon_{ia}(\lambda)/\varepsilon_{ea}^{fb}(\lambda), \tag{6c}$$

characterizing relative contribution of the process (1) in comparison with processes (2), (3) and (4) respectively.

In the case of local thermal equilibrium, these ratios are also the ratios of the corresponding absorption coefficients. We now proceed to calculating the quantities F.

3. Calculation of the emissivities

Hydrogen dominates the opacity in practice. Consequently we can write for process (1):

$$\varepsilon_{ia}(\lambda)=\xi_{ia}S_{ia}^{H}(\lambda)\, N(H^+)\, N(H), \tag{7a}$$

where $N(H^*)$ is the density of protons, $N(H)$ the density of hydrogen atoms in the 1s state. The coefficient ξ_{ia} takes into account the effect of real plasma composition differences from hydrogen case. Here $\xi_{ia}\cong 1$.

Other ions intervene in process (2) for which we can write:

$$\varepsilon_{ei}(\lambda)=\xi_{ei}S_{ei}^{H}(\lambda)\, N_e N_i, \tag{7b}$$

where $\xi_{ei}\approx 1$ is the Biberman–Norman factor and $N_i=\Sigma N(A^+)$ is the total density of single-charged positive ions.

Similarly we can write for processes (3) and (4):

$$\varepsilon_{ea}^{ff}(\lambda)=\xi_{ea}^{ff}S_{ea}^{H,ff}(\lambda)\, N_e\, N(H), \tag{7c}$$

$$\varepsilon_{ea}^{fb}(\lambda)=\xi_{ea}^{fb}S_{ea}^{H,fb}(\lambda)\, N_e\, N(H), \tag{7d}$$

where the coefficients $\xi_{ea}^{ff,fb}\cong 1$.

The expression of $S_{ia}^{H}(\lambda, T)$ is (Mihajlov & Popović 1981):

$$S_{ia}^{H}(\lambda, T)=4.7769\,10^{-34}\frac{C(R_\lambda)(R_\lambda/a_o)^4}{1-a_o/R_\lambda}\left(\frac{\varepsilon_\lambda}{2Ry}\right)^5 \times\exp\left[-\frac{U_2(R_\lambda)}{kT}\right],$$

$$C(R_\lambda)=\left[\frac{2D_{12}(R_\lambda)}{eR_\lambda}\right]^2\frac{1-a_o/R_\lambda}{\gamma(R_\lambda)}, \tag{8}$$

where R is the distance between protons (in the system $H^+ + H$),

$$\gamma(R_\lambda)=\left|\frac{d\ln[E_{12}(R)/2Ry]}{d(R/a_o)}\right|_{R=R_\lambda},$$

$$E_{12}(R)=U_2(R)-U_1(R), \tag{9}$$

$U_1(R)$ and $U_2(R)$–adiabatic terms of the ground ($1\Sigma_g$) and the first excited ($1\Sigma_u$) electronic states of ion H_2^+ and $D_{12}(R)$–modulus of dipole matrix element (between these states). Finally, R_λ is the root of the equation:

$$E_{12}(R)=\varepsilon_\lambda. \tag{10}$$

In Table 1 values of R_λ as well as of other parameters needed for the determination of $S_{ia}^{H}(\lambda, T)$ in 250 nm $\leq\lambda\leq$ 1500 nm range are presented in atomic units. These parameters have been determined using $U_1(R)$ and $U_2(R)$ values from Bates et al. (1953) and $D_{12}(R)$ values from Ramaker & Peek (1973).

The spectral coefficient $S_{ei}^{H}(\lambda, T, N_e)$ is evaluated in the quasi-classical approximation (Sobelman 1979) as:

$$S_{ei}^{H}(\lambda, T; N_e)=1.753\,10^{-33}\left(\frac{2Ry}{kT}\right)^{1/2}\left(\frac{\varepsilon_\lambda}{2Ry}\right)^2\exp\left[-\frac{\varepsilon_\lambda}{kT}\right] \times\left\{1+\frac{2Ry}{KT}\sum_{n>\sqrt{\lambda/\lambda_1}}^{n_{max}}\frac{1}{n^3}\exp\left[\frac{Ry}{n^2kT}\right]\right\}, \tag{11}$$

where

$$\lambda_1=\frac{2\pi c\hbar}{Ry},\qquad n_{max}=\left(\frac{e^2}{r_D Ry}\right)^{-1/2}, \tag{12}$$

n–principal quantum number of excited hydrogen state and $r_D=r_D(T; N_e)$–Debye radius.

With numerical coefficients given in Eqs. (8) and (11), corresponding spectral coefficients $S_{ia}^{H}(\lambda, T)$ and $S_{ei}^{H}(\lambda, T; N_e)$ are expressed in [$cm^3\,J\,s^{-1}\,nm^{-1}$] units.

For $\varepsilon_{ea}^{ff}(\lambda)$ we will use the tabulated data of Stilley & Callaway (1970), while the data for $\varepsilon_{ea}^{fb}(\lambda)$ are from tables of Wishart (1979).

4. Result for the solar atmosphere and discussion

We now apply the previous calculation to the solar atmosphere using the solar photospheric model of Maltby et al.

Table 1. Parameters of molecular ion H_2^+ in a.u., needed for the $S_{ia}^{H}(\lambda)$ calculation, by 250 nm $\leq\lambda\leq$ 1500 nm

λ (nm)	R_λ (a.u.)	$C(R_\lambda)$ (a.u.)	$E_{12}(R_\lambda)$ (a.u.)	$U_1(R_\lambda)$ (a.u.)	$U_2(R_\lambda)$ (a.u.)
250	3.17	0.875	0.1820	0.0684	0.1140
300	3.42	0.901	0.1520	0.0605	0.0913
350	3.63	0.922	0.1300	0.0544	0.0758
400	3.81	0.939	0.1140	0.0494	0.0645
450	3.98	0.954	0.1010	0.0453	0.0559
500	4.12	0.966	0.0911	0.0419	0.0492
600	4.37	0.987	0.0759	0.0364	0.0395
700	4.58	1.000	0.0651	0.0323	0.0328
800	4.77	1.020	0.0569	0.0291	0.0279
900	4.93	1.030	0.0506	0.0264	0.0242
1000	5.05	0.993	0.0456	0.0238	0.0217
1250	5.34	0.984	0.0364	0.0196	0.0169
1500	5.57	0.981	0.0304	0.0166	0.0137

© European Southern Observatory • Provided by the NASA Astrophysics Data System

1993A&A...276..187M

(1986) (their Table 11, photospheric reference model) for altitudes (h) lower than 605 km and chromospheric model of Vernazza et al. (1981) (their model C) for higher altitudes.

Taking into account Eqs. (5, 6, 7) we will represent quantities F as:

$$F_{ei}(\lambda)=f_{ei}\frac{S^{H}_{ia}(\lambda)}{S^{H}_{ei}(\lambda)}\eta_{ei},$$

$$F^{ff}_{ea}(\lambda)=f^{ff}_{ea}\frac{S^{H}_{ia}(\lambda)}{S^{H,ff}_{ea}(\lambda)}\eta_{ea},$$

$$F^{fb}_{ea}(\lambda)=f^{fb}_{ea}\frac{S^{H}_{ia}(\lambda)}{S^{H,fb}_{ea}(\lambda)}\eta_{ea},$$

$$\eta_{ei}=\frac{N(H^{+})N(H)}{N_e N_i},\qquad \eta_{ea}=\frac{N(H^{+})}{N_e},$$

where correction factors

$$f_{ei}=\frac{\xi_{ia}}{\xi_{ei}},\qquad f^{ff,fb}_{ea}=\frac{\xi_{ia}}{\xi^{ff,fb}_{ea}},$$

are close to unity since in our case quantities $\xi\cong 1$. The factor η_{ei} and η_{ea} values are presented in Table 2 together with basic parameters of the used solar models in the range $-100\ \mathrm{km}\leq h\leq 1605\ \mathrm{km}$.

The comparison of (1) and (2) processes contribution is presented in Figs. 1a, b where the behavior of $F_{ia}(\lambda)$ is shown. We can see two maxima, one in the photosphere and the other one in the chromosphere. This fact is explained by two corresponding strong maxima of the η_{ei} factor shown in Table 2. In consequence, although $S^{H}_{ia}/S^{H}_{ei}\ll 1$, $F_{ei}(\lambda)$ becomes larger than 1 at those locations, as illustrated in Figs. 1a and 1b.

Table 2. Values of η_{ei} and η_{ea} in the h-range considered. Up to $h=605$ km the model of photosphera (Maltby 1986) and for $h>605$ km the model of chromosphere (Vernazza et al. 1981) have been used

h (km)	T (k)	N_e (cm^{-3})	N_H (cm^{-3})	η_{ei}	η_{ea}
1605	6440	$0.601\,10^{11}$	$0.639\,10^{12}$	$0.963\,10^{1}$	$0.100\,10^{1}$
1515	6370	$0.646\,10^{11}$	$0.105\,10^{13}$	$0.152\,10^{2}$	$0.100\,10^{1}$
1380	6280	$0.760\,10^{11}$	$0.227\,10^{13}$	$0.289\,10^{2}$	$0.100\,10^{1}$
1280	6220	$0.749\,10^{11}$	$0.420\,10^{13}$	$0.551\,10^{2}$	$0.100\,10^{1}$
1180	6150	$0.811\,10^{11}$	$0.787\,10^{13}$	$0.960\,10^{2}$	$0.100\,10^{1}$
1065	6040	$0.935\,10^{11}$	$0.171\,10^{14}$	$0.182\,10^{3}$	$0.100\,10^{1}$
980	5925	$0.104\,10^{12}$	$0.315\,10^{14}$	$0.301\,10^{3}$	$0.100\,10^{1}$
855	5650	$0.106\,10^{12}$	$0.814\,10^{14}$	$0.764\,10^{3}$	$0.100\,10^{1}$
755	5280	$0.884\,10^{11}$	$0.186\,10^{15}$	$0.211\,10^{4}$	$0.100\,10^{1}$
705	5030	$0.766\,10^{11}$	$0.294\,10^{15}$	$0.383\,10^{4}$	$0.100\,10^{1}$
655	4730	$0.809\,10^{11}$	$0.479\,10^{15}$	$0.111\,10^{4}$	0.187
605	4420	$0.111\,10^{12}$	$0.812\,10^{15}$	$0.106\,10^{3}$	$0.145\,10^{-1}$
553	4410	$0.198\,10^{12}$	$0.164\,10^{16}$	$0.711\,10^{2}$	$0.856\,10^{-2}$
478	4410	$0.379\,10^{12}$	$0.337\,10^{16}$	$0.422\,10^{2}$	$0.476\,10^{-2}$
428	4510	$0.589\,10^{12}$	$0.527\,10^{16}$	$0.635\,10^{2}$	$0.708\,10^{-2}$
378	4610	$0.913\,10^{12}$	$0.817\,10^{16}$	$0.901\,10^{2}$	$0.101\,10^{-1}$
301	4770	$0.173\,10^{13}$	$0.156\,10^{17}$	$0.159\,10^{3}$	$0.177\,10^{-1}$
200	4990	$0.400\,10^{13}$	$0.350\,10^{17}$	$0.302\,10^{3}$	$0.344\,10^{-1}$
150	5150	$0.614\,10^{13}$	$0.509\,10^{17}$	$0.491\,10^{3}$	$0.593\,10^{-1}$
100	5410	$0.100\,10^{14}$	$0.714\,10^{17}$	$0.105\,10^{4}$	0.147
50	5790	$0.198\,10^{14}$	$0.960\,10^{17}$	$0.185\,10^{4}$	0.381
20	6180	$0.405\,10^{14}$	$0.110\,10^{18}$	$0.175\,10^{4}$	0.642
0	6520	$0.768\,10^{14}$	$0.119\,10^{18}$	$0.122\,10^{4}$	0.791
−20	6980	$0.173\,10^{15}$	$0.125\,10^{18}$	$0.652\,10^{3}$	0.901
−40	7590	$0.446\,10^{15}$	$0.129\,10^{18}$	$0.277\,10^{3}$	0.966
−60	8220	$0.105\,10^{16}$	$0.131\,10^{18}$	$0.124\,10^{3}$	0.994
−80	8860	$0.221\,10^{16}$	$0.133\,10^{18}$	$0.592\,10^{2}$	$0.100\,10^{1}$
−100	9400	$0.386\,10^{16}$	$0.136\,10^{18}$	$0342\,10^{2}$	$0.100\,10^{1}$

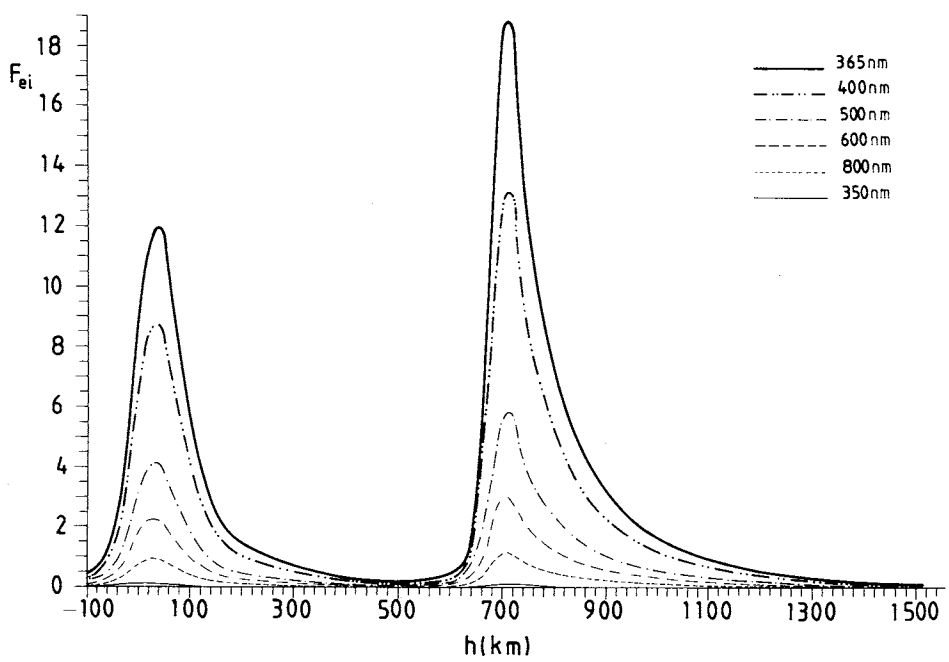

Fig. 1a. The parameter $F_{ei}(\lambda)$, for $f_{ei}=1$, in the $350\ \mathrm{nm}\leq\lambda\leq 800$ nm range ($350\ \mathrm{nm}<\lambda_2<365$ nm), as a function of h

© European Southern Observatory • Provided by the NASA Astrophysics Data System

1993A&A...276..187M

Figures 1a, b represent as well the behavior of $F_{ei}(\lambda)$ around $\lambda=\lambda_n$ for $n=2$ and 3. Here, $\lambda_n=n^2\lambda_1$ are continuum limits caused by free–bound electron transitions in n-states, and λ_1 is given by Eq. (12). The $\lambda=\lambda_n$ points are the discontinuity points of $S_{ei}^{H}(\lambda)$. In these points $S_{ei}^{H}(\lambda)$ has a jump caused by exclusion (when λ increases) or inclusion (when λ decreases) of the corresponding continuum. The described situation is well illustrated in Figs. 1a and 1b.

We can see that within the height range considered the contribution of processes (2) to the opacity may be neglected. However outside of this region its relative contribution to the processes (1) increases sharply.

The comparison of the contribution of processes (1) and (3) is presented in Fig. 2 where the behavior of $F_{ea}^{ff}(\lambda)$ is shown. One can see the photospheric and the chromospheric maximum of $F_{ea}^{ff}(\lambda)$ located in the same height range as for $F_{ei}(\lambda)$ in Figs. 1a, b. These maxima however are of smaller intensity.

In the considered photospheric and chromospheric regions, electron–atom processes are always dominant for wavelengths larger than 1250 nm, including the infrared part of the spectrum at 1650 nm, where the minimum in H^- absorption occurs. Our calculation however, show that for sophisticated investigations ion–atom processes

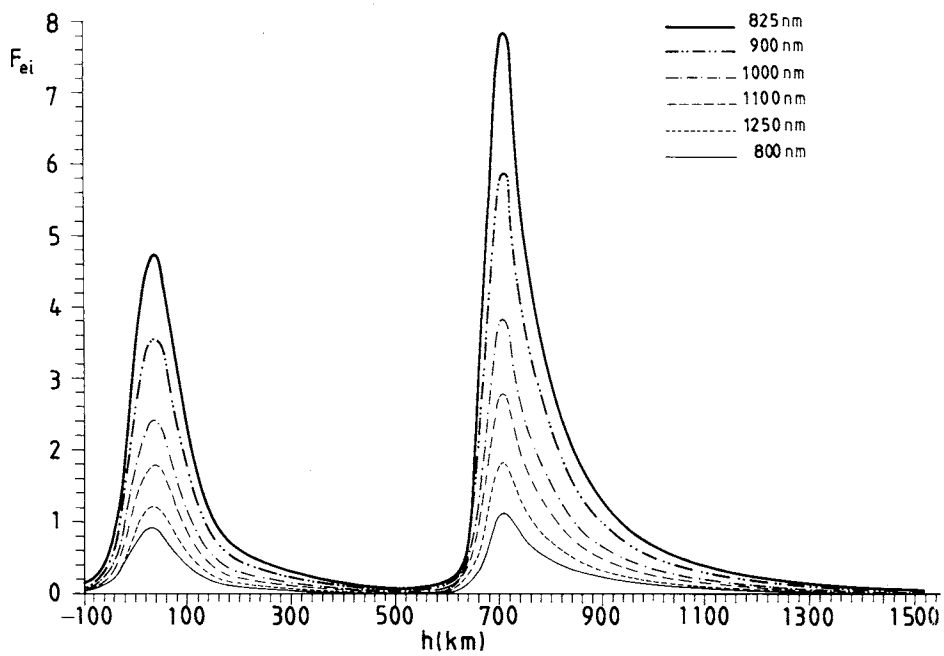

Fig. 1b. The parameter $F_{ei}(\lambda)$, for $f_{ei}=1$, in the 800 nm $\leq\lambda\leq$ 1250 nm range (800 nm $<\lambda_3<$ 850 nm), as a function of h

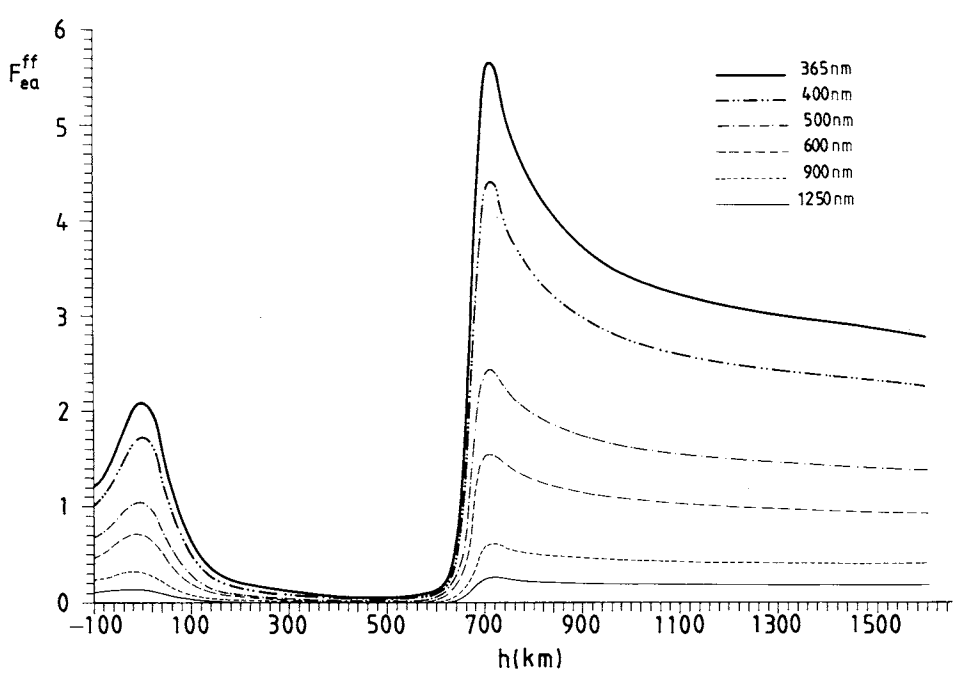

Fig. 2. The parameter $F_{ea}^{ff}(\lambda)$, for $f_{ea}^{ff}=1$, in the 350 nm $\leq\lambda\leq$ 1250 nm range, as a function of h

© European Southern Observatory • Provided by the NASA Astrophysics Data System

1993A&A...276..187M

must be taken into account around 1650 nm since in the layers considered, the contribution of these processes is 5–15% of that of electron–atom ones.

The comparison of the contributions of processes (1) and (4) is presented in Figs. 3a, b where the behavior of $F_{ea}^{fb}(\lambda)$ is shown. One can see in these figures that the behavior of $F_{ea}^{fb}(\lambda)$ is not a monotonous function of λ, which is the consequence of the behaviour of the electron radiative capture cross section or the ion H^- photodissociation cross section. These figures demonstrate that the values of $F_{ea}^{fb}(\lambda)$ parameter change from 0.15 up to 0.05 in the -100 km $\leq h \leq 50$ km, decrease slowly up to around 700 km and increases steeply up to 0.1. After 700 km they increase very slowly for all λ considered.

In Figs. (1)–(3) we can see that the processes (1), not taken into account up to now in photosphere and chromosphere research from the spectroscopical point of view are not negligible and that in particular layers it becomes in

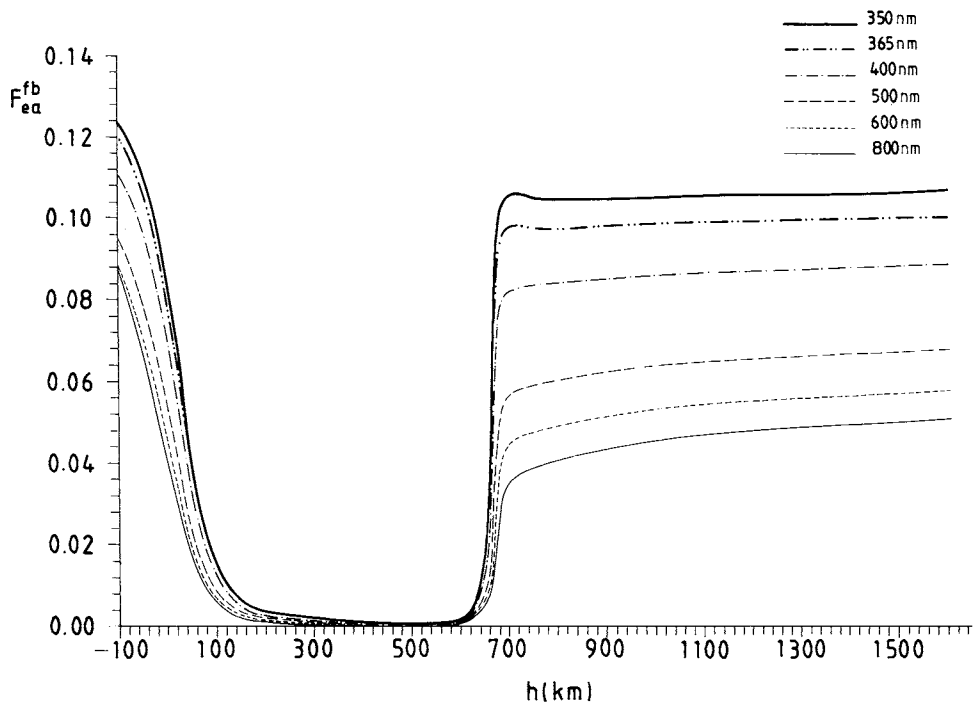

Fig. 3a. The parameter $F_{ea}^{fb}(\lambda)$, for $f_{ea}^{fb}=1$, in the 350 nm $\leq \lambda \leq$ 800 nm range, as a function of h

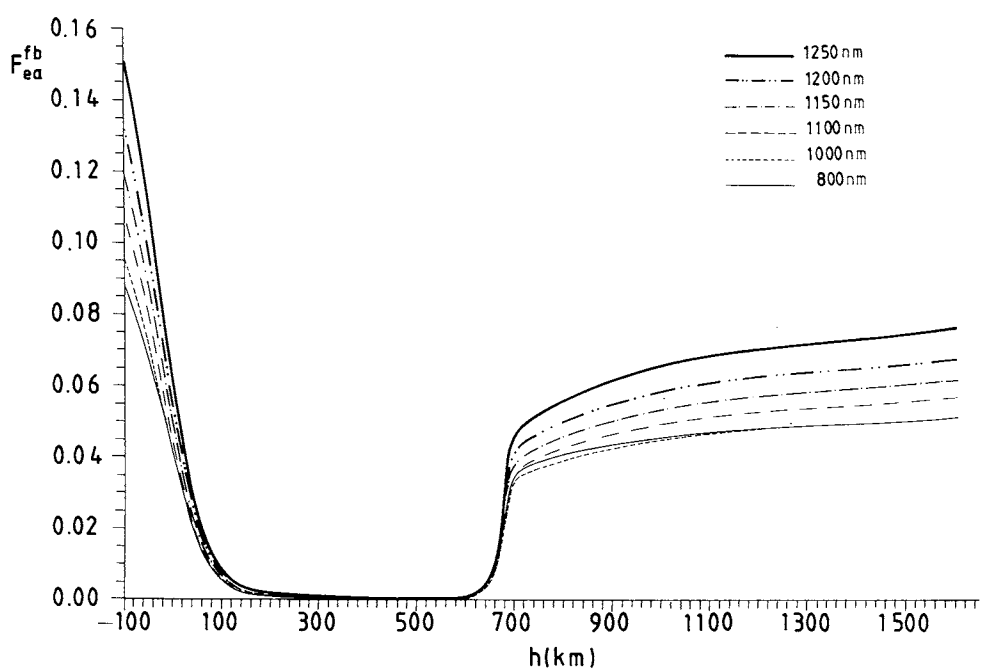

Fig. 3b. The parameter $F_{ea}^{fb}(\lambda)$, for $f_{ea}^{fb}=1$, in the 800 nm $\leq \lambda \leq$ 1250 nm range, as a function of h

© European Southern Observatory • Provided by the NASA Astrophysics Data System

1993A&A...276..187M

fact even comparable with processes (4), the most important for continuous emission (absorption) spectrum formation for the height range considered.

The importance of including H_2^+ in continuum opacity calculations is well known for A type star atmospheres (see e.g. Mihalas 1978), where hydrogen is approximately half ionized. In this case the H_2^+ photodissociation contribution to the total absorption is around 10%. We want to draw attention that on the basis of Fig. 3 one can see that the inclusion of radiative charge exchange processes together with H_2^+ photodissociation results in a combined contribution to the total absorption spectrum of around 10% for particular photospheric and chromospheric layers of the Sun, in spite of the fact that only 10^{-2}–10^{-4} of hydrogen is ionized.

Besides hydrogen, there is also helium but its density is below 10% of that of hyrogen in the regions considered (Vernazza et al. 1981). Consequently, taking into account the large ionization potential of helium, electron ion–radiative processes involving helium may be neglected in present case. We can neglect as well emission (absorption) due to electron scattering on He in comparison with emission (absorption) due to electron scattering on H. Our calculation on the basis of the paper by Bell et al. (1982) shows that the contribution of the e–He radiative process is always below 3% of that of e–H in the regions considered. Moreover, the He^- ion in the ground state is not stable and the He^- ion stable states are created from the excited helium atom and have thus a high creation threshold (around 20 eV, see e.g. Massey 1976). Consequently, radiative processes with He^- participation may be neglected in our case as well.

We have estimated (for hydrogen) the relative importance of processes (1) on the total optical depth of solar atmosphere in the range $0\ \mathrm{km} \leq h \leq 1065\ \mathrm{km}$, as well as on the emergent intensity (see e.g. Mihalas 1978). The calculations have been performed for radial rays. This shows that the contribution of processes (1) changes the optical depth of the atmospheric layer considered (photosphere and lower chromosphere) from 3.5 up to 1.5% when λ varies from 400 up to 800 nm.

Such an optical depth change is not negligible for sophisticated calculations. However it does not influence significantly the emergent intensity. Our calcultions show that for the photosphere ($0\ \mathrm{km} \leq h \leq 605\ \mathrm{km}$). the change of emergent intensity is between 0.28 to 0.14% for λ between 500 and 800 nm. In this layer for $\lambda \geq 500$ nm, the source function may be approximated by a Planck function, as used here.

5. Conclusions

The present results show that some atomic processes generally neglected can contribute appreciably to the opacity of some layers of the solar photosphere and chromosphere, and should not be neglected for local studies. So, the contribution of positive-ion–atom radiative collisions changes the optical depth of photosphere and lower chromosphere in the spectral range considered by 3.5–1.5%. However it changes only by about 0.2% of the emergent emission intensity from the solar photosphere in the 500–800 nm spectral range and can be neglected in this case. The processes we have studied may also be of importance in other stars where the temperature of the atmosphere is smaller than 10^4 K. Some other processes involving other elements than hydrogen or collisions between H^- and H might also be of interest.

Acknowledgements. We are indebted to Professor P. Maltby for very illuminating discussion. We are also grateful to Professor James Lequeux for his help to improve our article.

References

Armstrong B.H., 1963, Phys. Rev. 131, 1132
Bates D.R., Ledsham K., Stewart A.L., 1953, Phil. Trans. R. Soc. Lond., Ser. A 246, 215
Bell K.L., Berrington K.A., Croskery J.P., 1982, J. Phys. B 15, 977
Drukarev G.P., Mihajlov A.A., 1974, Opt. Spectrosk. 37, 384
Firsov O.B., Chibisov M.I., 1960, Zh. Ehksp. Teor. Fiz. 39, 1770
Maltby P., Avrett E.H., Carlsson M., Kjeldseth-Moe O., Kurucz R.L., Loeser R., 1986, ApJ 306, 284
Massey H.S.W., 1976, Negative Ions. Cambridge University Press, Cambridge
Menzel D.H., 1962, Selected Papers on Physical Processes in Ionized Plasmas. Dover Publications, New York
Mihalas D., 1978, Stellar Atmospheres, Chap. 7.7. W.H. Freeman, San Francisco
Mihajlov A.A., Popović M.M., 1981, Phys. Rev. A 23, 1679
Mihajlov A.A., Dimitrijević M.S., 1986, A&A 155, 319
Ramaker D.E., Peek J.M., 1973, Atomic Data 5, 167
Sobelman I.I., 1979, Atomic Spectra and Radiative Transitions, Chap. 9.5. Springer, Berlin
Stilley J.L., Callaway J., 1970, ApJ 160, 245
Vernazza J.E., Avrett E.H., Loeser R., 1981, ApJS 45, 635
Weisner J.D., Armstrong B.H., 1964, Proc. Phys. Soc. 83, 31
Wishart A.W., 1979, MNRAS 187, 59

© European Southern Observatory • Provided by the NASA Astrophysics Data System

1994A&A...287.1026M

Astron. Astrophys. 287, 1026–1028 (1994)

ASTRONOMY AND ASTROPHYSICS

Research Note

The influence of ion-atom radiative collisions on the continuous optical spectra in helium-rich DB white-dwarf atmospheres

A.A. Mihajlov[1,2], M.S. Dimitrijević[2], and Lj.M. Ignjatović[1]

[1] Institue of Physics, P.O. Box 57, 11001 Beograd, Yugoslavia
[2] Astronomical Observatory, Volgina 7, 11050 Beograd, Yugoslavia

Received 14 May 1993 / Accepted 17 December 1993

Abstract. We investigate the influence of radiative processes due to $He^+(1s)$-$He(1s^2)$ collisions on the continuous optical spectrum of the helium-rich DB white-dwarf atmospheres. We show that these ion-atom collision processes are important in certain layers of the studied white dwarf atmosphere, and that the corresponding contributions to the optical depth and continuous opacity are not negligible.

Key words: White dwarfs – radiation mechanisms: thermal – atomic processes – stars: atmospheres

1. Introduction

The influence of $H^+ + H(1s)$ radiative processes on the continuous spectra of low temperature solar-atmosphere layers where the $H(1s) + e$ radiative processes play the main role has been studied in Mihajlov et al. (1993, 1994). It was shown that $H^+ + H(1s)$ radiative processes are of importance for such layers, in spite of the fact that the main $H(1s) + e$ radiative processes include the very improtant process of H^- stable ion photo-creation and photo-dissociation. This suggests that radiative $He^+(1s) + He(1s^2)$ processes may be very important for low-temperature ($T \lesssim 20\,000$ K) atmospheric layers in helium-rich stars, where the influence of the competing $He^+(1s^2) + e$ radiative process is less significant since a stable negative atom ion does not exist for helium (Massey 1976).

We will consider the following ion-atom radiative processes

$$He^+(1s) + He^+(1s^2) \Leftrightarrow \epsilon_\lambda + He_2^+ , \tag{1a}$$

$$He^+(1s) + He^+(1s^2) \Leftrightarrow \epsilon_\lambda + \begin{cases} He^+(1s) + He^+(1s^2) \\ He^+(1s^2) + He^+(1s) \end{cases} \tag{1b}$$

where He_2^+ is the molecular ion in the electronic ground state ($1\sum_u^+$), and $\epsilon_\lambda = 2\pi\hbar c/\lambda$ – the energy of a photon with wavelength λ. In this paper we will show the importance of these processes for the DB white-dwarf atmosphere optical continuous spectra, on an example from Koester (1980). Consequently, we will investigate the contribution of processes (1) to the optical continuous spectra in comparison with the contribution of the following electron-atom and electron-ion radiative processes

$$He(1s^2) + e \Leftrightarrow \epsilon_\lambda + He(1s^2) + e ; \tag{2}$$

$$A^+ + e \Leftrightarrow \epsilon_\lambda + \begin{cases} A^+ + e \\ A^* \end{cases} \tag{3}$$

which are of importance for the DB white dwarf atmosphere plasma composition (Bues 1970). Here A^+ denotes helium, hydrogen or metallic atomic ion and A^* is the corresponding atom in an excited state.

2. Theory

The contributions of processes (1a), (1b), (2), (3) to the plasma absorption and emission continuous spectra is characterized by the spectral absorption coefficients $\kappa_{ia}^{(a)}$, $\kappa_{ia}^{(b)}$, κ_{ea}^{ff} κ_{ei} and the spectral emissivities $\varepsilon_{ia}^{(a)}$, $\varepsilon_{ia}^{(b)}$ ε_{ea}^{ff}, ε_{ei} where the index ff emphasizes that $e - He(1s^2)$ radiative processes are consequences of free-free electron transitions only. In the case of processes (1) we will use also quantities $\kappa_{ia}^{(ab)} = \kappa_{ia}^{(a)} + \kappa_{ia}^{(b)}$ and $\varepsilon_{ia}^{(ab)} = \varepsilon_{ia}^{(a)} + \varepsilon_{ia}^{(b)}$ which take into account the contribution of processes (1a) and (1b) together.

We will determine the relative contribution of the processes (1a,b) in comparison with electron-atom processes (2) and electron-ion processes (3) using the quantities

$$F_{ea}^{ff} = \frac{\varepsilon_{ia}^{(ab)}}{\varepsilon_{ea}^{ff}} = \frac{\kappa_{ia}^{(ab)}}{\kappa_{ea}^{ff}} , \quad F_{ei} = \frac{\varepsilon_{ia}^{(ab)}}{\varepsilon_{ei}} . \tag{4}$$

Send offprint requests to: M.S. Dimitrijević

© European Southern Observatory • Provided by the NASA Astrophysics Data System

1994A&A...287.1026M

In LTE, $\kappa_{\rm ia}^{\rm (ab)}/\kappa_{\rm ei} = \varepsilon_{\rm ia}^{\rm (ab)}/\varepsilon_{\rm ei}$. However, according to Koester (1980) the low-temperature layers of DB white dwarf atmosphere have relatively small optical depths. Consequently, considerable deviations of the excited atomic states (A^*) populations from LTE populations should exist. It means that the use of the ratio $\kappa_{\rm ia}^{\rm (ab)}/\kappa_{\rm ei}$ requires complete calculations of the excited atomic state population distribution function. For that reason we use here the ratio $\varepsilon_{\rm ia}^{\rm (ab)}/\varepsilon_{\rm ei}$ where $\varepsilon_{\rm ei}$ depends on the densities of only several atomic ions.

The spectral coefficients $\kappa_{\rm ia}^{\rm (ab)}$ and $\varepsilon_{\rm ia}^{\rm (ab)}$ take the form

$$\begin{aligned}\kappa_{\rm ia}^{\rm (ab)}(\lambda,T) &= K_{\rm ia}^{\rm (ab)}(\lambda,T)N({\rm He}^+)N({\rm He})\,,\\ \varepsilon_{\rm ia}^{\rm (ab)}(\lambda,T) &= S_{\rm ia}^{\rm (ab)}(\lambda,T)N({\rm He}^+)N({\rm He})\,,\end{aligned} \tag{5}$$

$$\begin{aligned}\frac{\kappa_{\rm ia}^{\rm (ab)}(\lambda,T)}{\varepsilon_{\rm ia}^{\rm (ab)}(\lambda,T)} &= \frac{K_{\rm ia}^{\rm (ab)}(\lambda,T)}{S_{\rm ia}^{\rm (ab)}(\lambda,T)}\\ &= \frac{2\pi^3\hbar^4c^3}{\epsilon_\lambda^5}\cdot\exp\left(\frac{\epsilon_\lambda}{kT}\right)\cdot\left[1-\exp\left(-\frac{\epsilon_\lambda}{kT}\right)\right],\end{aligned} \tag{6}$$

where $N({\rm He}^+)$ and $N({\rm He})$ are the ${\rm He}^+$ and He densities, and the factor $[1-\exp(-\epsilon_\lambda/kT)]$ describes the influence of the stimulated emission on the total absorption. The validity conditions of the Eqs. (4, 5) have been discussed in Mihajlov & Dimitrijević (1986) and (1992).

In our calculations we take $F_{\rm ea}^{\rm ff} = \kappa_{\rm ia}^{\rm (ab)}/\kappa_{\rm ea}^{\rm ff}$. Consequently, we will determine the quantities $F_{\rm ea}^{\rm ff}$ and $F_{\rm ei}$ from the spectral coefficients $\kappa_{\rm ea}^{\rm ff}$ and $\varepsilon_{\rm ei}$, where

$$\begin{aligned}\kappa_{\rm ea}^{\rm ff}(\lambda,T) &= K_{\rm ea}^{\rm ff}(\lambda,T)N({\rm He})N_{\rm e}\,,\\ \varepsilon_{\rm ei}(\lambda,T) &= \sum_A S_{\rm ei}^A(\lambda,T)N(A^+)N_{\rm e}\,.\end{aligned} \tag{7}$$

Here, $N_{\rm e}$ and $N(A^+)$ denote the free electron and A^+ ion densities, respectively.

In Eqs. (5) and (6) we use semiclassical values of $K_{\rm ia}^{\rm (ab)}(\lambda,T)$ from Mihajlov & Dimitrijević (1992), where these coefficients are given in analytical and tabular form. Values of $S_{\rm ia}^{\rm (ab)}(\lambda,T)$ were determined from Eq. (6).

In Eq. (7) we use tabulated values of $K_{\rm ea}^{\rm ff}(\lambda,T)$ from Bell et al. (1982). Values of $S_{\rm ei}^A(\lambda,T)$ were calculated with the help of a quasiclassical analytical expression from Menzel (1962) and Sobelman (1979).

3. Results and discussion

The calculations of quantities $F_{\rm ea}^{\rm ff}$ and $F_{\rm ei}$ from Eqs. (4–7), have been performed for DB white dwarf atmospheres in the case $\log g = 8$ and $T_{\rm eff} = 12\,000$ K. The plasma temperature (7942 K $\leq T \leq$ 21 039 K), Rosseland optical depth ($-5.60 \leq \log\tau \leq 2.75$) and other relevant data from Table 1 in Koester (1980) have been used. In the considered $\log\tau$ range the temperature T monotonically decreases from 8119 K up to 7942 K for $\log\tau \leq -3.60$ and after that monotonically increases up to 21 039 K for $\log\tau \leq 2.75$.

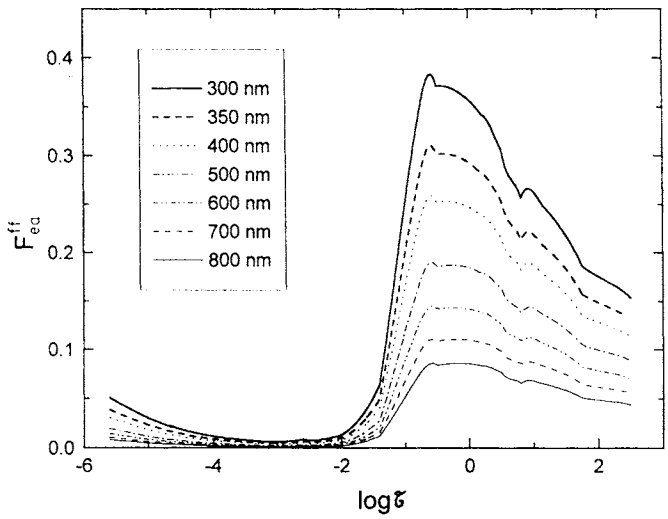

Fig. 1. The behavior of the parameter $F_{\rm ea}^{\rm ff}(\lambda,T)$ within the 300 nm $\leq \lambda \leq$ 800 nm range, as a function of Rosseland optical depth

The comparison of the contribution of processes (1) and (2) is presented in Fig. 1 where the behavior of the quantity $F_{\rm ea}^{\rm ff}(\lambda,T)$ for 300 nm$\leq \lambda \leq$ 800 nm is shown. We can see that $F_{\rm ea}^{\rm ff}(\lambda,T)$ increases fast for $-2.0 < \log\tau < -1.0$, reaches a maximum and after that decreases slowly with further increase of $\log\tau$. As a consequence there exists a relatively large region (with $-1.5 < \log\tau$) where the quantity $F_{\rm ea}^{\rm ff}(\lambda,T)$ is within the range 0.05–0.40, for the considered range of wavelengths.

The comparison of processes (1) and (3) is presented in Fig. 2 where the behavior of the quantity $F_{\rm ei}(\lambda,T)$, for the same λ range, is shown. We can see that for $-2.5 < \log\tau < 1.0$, $F_{\rm ei}(\lambda,T)$ has a maximum, which is more pronounced than the maximum of $F_{\rm ea}^{\rm ff}(\lambda,T)$. This maximum occurs around $\log\tau = -1.0$ where the quantity $F_{\rm ei}(\lambda,T)$ is within the range 5–40, i.e. two orders of magnitude larger than $F_{\rm ea}^{\rm ff}(\lambda,T)$. Outside the range, the quantity $F_{\rm ei}(\lambda,T)$ decreases more sharply than $F_{\rm ea}^{\rm ff}(\lambda,T)$. It shows that the electron-ion process (3) determines the border of the $\log\tau$ range where the processes (1) are of interest. Namely, Fig. 2 shows that this border is inside of the considered $\log\tau$ region for all the λ considered. Moreover, the behaviour of the quantities $F_{\rm ea}^{\rm ff}$ and $F_{\rm ei}$ as functions of $\log\tau$ is such that we can expect the electron-ion radiative processes to dominate in comparison with the electron-atom and ion-atom radiative processes outside of the considered $\log\tau \leq 2.75$ range.

Figure 1 shows the importance of the ion-atom radiative processes (1) and the necessity to take them into account when calculating the optical characteristics of DB white dwarf atmosphere. It is a direct consequence of the fact that a stable negative helium atomic ion does not exist. Conversely, we have seen that in the case of the solar atmosphere (see Mihajlov et al. 1993, 1994), where hydrogen negative stable atomic ion exist, the relative contribution of ion-atom radiative processes in compar-

© European Southern Observatory • Provided by the NASA Astrophysics Data System

1994A&A...287.1026M

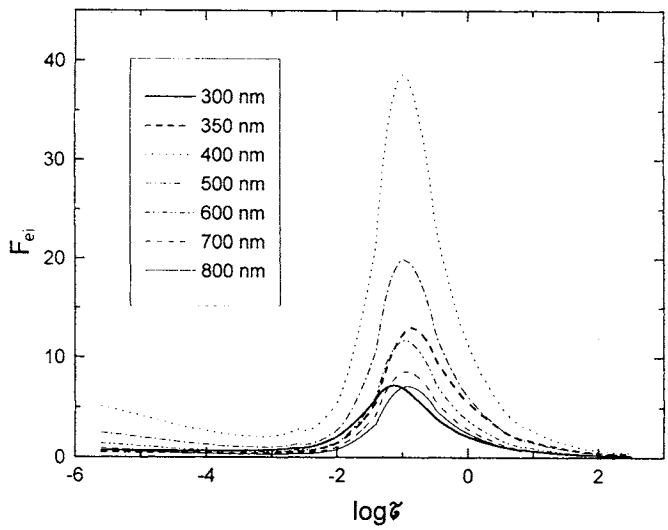

Fig. 2. The behavior of parameter $F_{ei}(\lambda, T)$, within the 300 nm $\leq \lambda \leq$ 800 nm range, as a function of Rosseland optical depth. The strong change between $F_{ei}(\lambda = 300\,\mathrm{nm})$ and $F_{ei}(\lambda = 350\,\mathrm{nm})$ is real, since between these λ are two thresholds of helium-photorecombination continuums with the principal quantum number 2

ison with electron-atom radiative processes is only within the 0.05–0.15 range.

We have estimated also the corresponding increase of the optical depth $\Delta\tau$ of the considered atmosphere layers and the change of the emergent intensity (see e.g. Mihalas 1978). The ratio $\Delta\tau/\tau$ for $\lambda = 500$ nm increases from about 0.0034 to about 0.1711 for $-2.00 \leq \log\tau \leq 0.30$ and after that decreases (to 0.0721 for $\log\tau \leq 2.75$). The calculations of the emergent intensity have been performed for radial rays. For the same λ we have that processes (1a,b) caused a decrease of the emergent intensity, for the considered $\log\tau \leq 2.75$ range by about 16 per cent.

In agreement with Mihajlov & Dimitrijević (1992), we have shown that in the considered case the radiative charge-exchange processes (1b) are more significant than the photoassociation/photodissociation processes (1a). Our calculations show that the decrease of the emergent intensity, for $\lambda = 500$ nm, is around 14 per cent when processes (1a) have not been taken into account.

4. Conclusion

It has been shown that the radiative ion-atom processes (1), not taken into account up to now in DB white dwarf research from the spectroscopical point of view, are of importance in the 300 nm $\leq \lambda \leq$ 800 nm range. In low temperature (8000 K $\lesssim T \lesssim$ 20 000 K) layers the contribution of processes (1) to the optical continuous spectra is more important than the contribution of electron-ion processes (3) and is comparable with the contribution of electron-atom processes (2). Consequently, the ion-atom processes (1) considered here should be taken into account for calculations of the characteristics for low-temperature ($T \lesssim$ 20 000 K) atmospheric layers in helium-rich stars

References

Bell K.L., Berrington K.A., Croskery J.P., 1982, J Phys B 15, 977
Buess I., 1970, A&A 7, 91
Koester D., 1980, A&AS 39, 401
Massey H.S.W., 1976, Negative ions, Cambridge University Press, Cambridge
Menzel D.H., 1962, Selected papers on physical processes in ionized plasmas, Dover Publications, New York
Mihajlov A.A., Dimitrijević M.S., 1986, A&A 155, 319
Mihajlov A.A., Dimitrijević M.S., 1992, A&A, 256, 305
Mihajlov A.A., Dimitrijević M.S., Ignjatović, Lj.M., 1993, A&A 276, 187
Mihajlov A.A., Dimitrijević M.S., Ignjatović, Lj.M., 1994, A&AS 103, 57
Sobelman I.I., 1979, Atomic spectra and radiative transitions (Chap. 9.5), Springer, Berlin

© European Southern Observatory • Provided by the NASA Astrophysics Data System

Astron. Astrophys. 324, 1206–1210 (1997)

ASTRONOMY AND ASTROPHYSICS

Processes of $H - H^+ - e$ and $H_2^+ - e$ recombination in the weakly-ionized layers of the solar atmosphere

A.A. Mihajlov[1,2], **Lj.M. Ignjatović**[1], **M.M. Vasilijević**[1], **and M.S. Dimitrijević**[2]

[1]Institute of Physics, P.O. Box 57, 11001 Belgrade, Serbia, Yugoslavia
[2]Astronomical Observatory, Volgina 7, 11050 Belgrade, Serbia, Yugoslavia

Received 26 August 1996 / Accepted 5 February 1997

Abstract. The influence of the $H - H^+ - e$ and $H_2^+ - e$ chemi - recombination processes on the highly excited hydrogen atom population in the photosphere and lower part of the chromosphere has been considered. It has been shown that these chemi - recombination processes have an important role in the large region around the temperature minimum in the Solar atmosphere, where they are comparable to the other relevant recombination processes, or even dominant and that they should be taken into account for the modelling of the weakly ionized layers in the Solar atmosphere.

Key words: molecular data – Sun: atmosphere

1. Introduction

In several previous papers (Mihajlov & Ljepojević, 1982 and Mihajlov et al. 1992, 1996), chemi-recombination processes during the free electron scattering on the quasi-molecular collisional complexes $H(1s) + H^+$ and molecular ions H_2^+ in the weakly bound rhovibrational states, have been introduced and investigated. It was assumed that these molecular ions are in the ground electronic state $X^2\Sigma_g^+(1s\sigma_g)$. The mentioned chemi-recombination processes are

$$H_2^+ + e \Rightarrow H^*(n) + H(1s), \qquad (1a)$$

$$H(1s) + H^+ + e \Rightarrow H^*(n) + H(1s), \qquad (1b)$$

where $H^*(n)$ denotes hydrogen atom in a highly excited (Rydberg) state with the principal quantum number $n \leq 4$. It has been shown that in partially ionized plasma the processes (1a) and (1b) may be significant for the $H^*(n)$ atom populations. This conclusion has been derived from the comparison of the (1a,b) processes with the electron - electron - ion recombination processes whose importance for hydrogen plasmas is well known (see e.g. Bates et al. 1962ab).

Send offprint requests to: M.S. Dimitrijević

In this paper we will consider the (1a,b) processes from the aspect of their influence on $H^*(n)$ atom populations of solar photosphere and lower part of chromosphere. We point out here that the taking into account of these processes may be particularly important when the conditions of LTE, concerning the excited atom population distribution function, are not satisfied. Such situation exist just for the above mentioned parts of the solar atmosphere (due to their small optical depth), which has been pointed out in Maltby et al. (1986) and Vernazza et al. (1981). The principal aim of this paper is to show that for particular layers of the solar atmosphere, the chemi - recombination processes (1a,b) could be comparable or sometimes even more important that the processes of the electron - electron - ion recombination as well as with the processes of electron - ion photorecombination, which have a particularly important role in the solar atmosphere. Consequently, we will show that the (1a,b) processes must be taken into account when modelling the solar atmosphere, together with other relevant recombination processes.

2. Theory

In accordance with Mihajlov & Ljepojević, 1982 and Mihajlov et al. 1992, 1996, recombination processes (1a,b) will be treated as the result of the energy exchange within the electronic component of the $H_2^+ + e$ or $H + H^+ + e$ system, which is caused by dipole interaction of the electron e with the ion - atomic subsystem H_2^+ or $H + H^+$. Here we have in mind that the energy exchange is connected with the transition of the just mentioned ion - atomic subsystems from the orbital $1s\sigma_g$ to the first excited orbital $2p\sigma_u$ and the simultaneous transition of the electron e from the free state to the highly excited bound state. It is assumed that the transition $1s\sigma_g \rightarrow 2p\sigma_u$ is performed without the energy exchange between electron and cores (protons). Also, it is assumed that the change of the electronic state of the $H_2^+ + e$ or $H + H^+ + e$ system, during the scattering of the free electron on the molecular ion or the quasi - molecular collisional complex, can happen only once. The difference between the (1a) and (1b) processes is that the ion - atomic subsystem H_2^+ is in the initial electronic state $X^2\Sigma_g^+(1s\sigma_g)$ with the proba-

bility equal to 1, and the subsystem $H + H^+$ with the probability equal to $1/2$. Consequently, the processes (1a) and (1b) may be treated as the corresponding channels of a more general chemi-recombination process (1) which is similar to the process of the direct disociative recombination.

Concerning the nuclei motion, it is treated classically for the (1b) processes where the ion - atomic subsystem is in the state of free motion, as well as for the (1a) processes, where within the input channel the ion - atomic subsystem is in a bound state. Here we take into account the assumption that these bound states are near the dissociation threshold, where the mentioned classical treatment is valid.

We will consider here the total influence of the (1a,b) chemi-recombination processes on the $H^*(n)$ atom populations in the considered Solar plasma. Consequently, as a quantitative characteristic of the above mentioned influence we will use the total chemi - recombination fluxes $I_r^{(ab)}(n) = I_r^{(a)}(n) + I_r^{(b)}(n)$, where $I_r^{(a)}(n)$ and $I_r^{(b)}(n)$ are the partial fluxes corresponding to the (1a) and (1b) chemi - recombination processes, respectively. It should be pointed out that the partial fluxes are denoted here as in our previous papers (Mihajlov et al. 1992, 1996). In Mihajlov et al. (1992, 1996) the recombination processes (1a,b) were treated for the more general non-equillibrium case for $T_e > T_a$, where T_e and T_a are the temperatures characterizing electron- and ion/atom - component. Here however, we take into account that in the standard models of solar photosphere (Maltby et al. 1986) and chromosphere (Vernazza et al. 1981), it has been taken that $T_a = T_e = T$. Consequently, we will assume that $I_r^{(a,b,ab)}(n) = I_r^{(a,b,ab)}(n;T)$.

According to Mihajlov et al. (1992, 1996), we will treat both partial chemi - recombination fluxes (for the case $T_a = T_e = T$) in the same form, i.e. as $I_r^{(a,b)}(n) = K_r^{(a,b)}(n;T)N(e)N(H^+)N(1)$, where $N(e)$ and $N(H^+)$ are the electron and proton densities and $N(1)$ is the density of $H(1s)$ atoms. Here $K_r^{(a)}(n;T)$ replaces the quantity $K_{dr}^{(a)}(n;T)N(H_2^+)[N(H^+)N(1)]^{-1}$, where $N(H_2^+)$ is the $H_2^+(1s\sigma)$ molecular ion density, and the $K_{dr}^{(a)}$ is the usuall dissociative recombination rate coefficient. This enables the total chemi-recombination flux $I_r^{(ab)}(n)$ to be presented in the form:

$$I_r^{(ab)}(n;T) = K_r^{(ab)}(n;T)N(e)N(H^+)N(1), \qquad (2)$$

where $K_r^{(ab)}(n;T) = K_r^{(a)}(n;T) + K_r^{(b)}(n;T)$. The advantage of such expression for the total chemi - recombination rate coefficient $K_r^{(ab)}(n;T)$ is, since the H_2^+ molecular ion density is absent in Eq. (2). This approach is constructive when the block of the weakly - bound rhovibrational states of the $H_2^+(1s\sigma)$ molecular ion, essential for the (1a) processes, is in the dissociative - associative equilibrium with the $H(1s)$ and H^+ components (with the same temperature T). Here, the assumption on existance of such dissociative - associative equilibrium is adopted on the basis of the above mentioned models of the solar atmosphere (Maltby et al. 1986, Vernazza et al. 1981). Namely, in these models the existance of LTE is assumed, when the radiation transfer out of the solar atmosphere is not taken into account. If such transfer is taken into account, some deviations from LTE are considered (in these models) which are not important for the discussed dissociative - associative equilibrium.

We will use here the total rate coefficient $K_r^{(ab)}(n;T)$ as in Mihajlov et al. (1996), i.e. as

$$K_r^{(ab)}(n;T) = \frac{(2\pi)^{5/2}}{3\sqrt{3}} \frac{(\hbar e a_0)^2}{(mkT)^{3/2}} \frac{\exp(I_n/kT)}{n^3} \int_0^{R_n} \exp\left[-\frac{U_2(R)}{kT}\right] \frac{R^4 dR}{a_0^5}, \qquad (3)$$

where the upper integration limit R_n is the root of the equation

$$U_2(R) - U_1(R) = I_n. \qquad (4)$$

Here, $I_n = R_y/n^2$ is the ionization potential of the $H^*(n)$ atom, while $U_1(R)$ and $U_2(R)$ are the adiabatic terms of the ground $(1\Sigma_g)$ and the first excited $(1\Sigma_u)$ electronic state of the molecular ion H_2^+, whose values are taken from Bates et al (1953).

According to the same paper, the lower integration limit instead of zero is taken as a_0 in Eq. (3) for the concrete calculations. The values of the R_n, for $n = 4-10$, are given in Mihajlov et al (1996) and here we will treat the processes (1a,b) just within this range of values for n.

The processes (1a,b) with $n = 2, 3$ are not treated here since our considerations are based on the previous papers (Mihajlov et al., 1992; Mihajlov et al., 1996), where only the region $n \geq 4$ was treated. This was imposed by the conditions of applicability of the used theory. For example, for $n = 3$ already the change of the electronic state of the $H_2^+ + e$ or $H + H^+ + e$ system (during the scattering of the free electron on the molecular ion or the quasi - molecular collisional complex) can happen more than once. Consequently, each of the processes (1a) and (1b) obtains the multi - channel character. That is why the inclusion of the processes (1a) and (1b) imposes a different approach. One of the possible solutions could be the adequate version of MQDT method, which was firstly developed for atoms (M. J. Seaton, 1966; see also U. Fano, 1970). In the case of a molecular system such methods have also been developing for a long time, and for the processes of dissociative recombination of the (1a) type some preliminary results already exist (see Giusti-Suzor, 1989; Hickman, 1989; and references therein).

The behaviour of the total rate coefficient $K_r^{(ab)}(n;T)$ as a function of the temperature T for $n = 4-10$, is shown in Table 1. This table covers the 4000 K$\leq T \leq$ 6500 K range, which is of interest for further consideration.

3. Results and discussions

The (1b) chemi - recombination processes may be significant only when the neutral atom component is dominant. Consequently, we will consider that part of the Solar atmosphere where the ionization degree is small enough. We will use here the Solar atmosphere plasma parameter data presented in Vernazza et al. (1981), similarly to Mihajlov et al. (1993, 1994), where the radiation processes during $H^+ + H(1s)$ collisions were considered.

Table 1. The values of the chemi-recombination rate coefficient $K_r^{(ab)}(n;T)$ in the case of the $T_a = T_e = T$, where T_a and T_e denote the temperatures of the atom/ion end electron components respectively, and n is the principal quantum number.

	$10^{28}K_r^{(ab)}(n;T)$ / $[cm^6s^{-1}]$						
T/[K]	n=4	n=5	n=6	n=7	n=8	n=9	n=10
4000	2.7824	1.6622	1.1602	.8884	.7201	.6038	.5203
4250	2.4277	1.4864	1.0512	.8105	.6593	.5537	.4774
4500	2.1421	1.3403	.9588	.7438	.6069	.5104	.4402
4750	1.9083	1.2172	.8796	.6860	.5612	.4726	.4077
5000	1.7143	1.1123	.8111	.6356	.5213	.4394	.3792
5250	1.5512	1.0221	.7514	.5907	.4859	.4100	.3539
5500	1.4126	.9438	.6988	.5515	.4546	.3839	.3314
5750	1.2938	.8752	.6524	.5166	.4265	.3604	.3112
6000	1.1909	.8148	.6110	.4854	.4013	.3394	.2930
6250	1.1011	.7613	.5739	.4572	.3786	.3203	.2766
6500	1.0223	.7135	.5406	.4318	.3580	.3030	.2617

Here we will use the chromospheric model C of Vernazza et al. (1981), since in this article temperatures, electron and ion densities are given, as well as the $H^*(n)$ atom densities as a function of the height h. The atomic densities calculations where performed there within the $1 \leq n \leq 8$ range. These atom densities are denoted here as $N(n)$.

We consider here the height range -75km $\leq h \leq$ 1605km with the plasma conditions illustrated in Table 2. In this table, first of all, temperatures T and $N(e)/N(H)$ ratios (where the $N(H)$ is the total hydrogen density) from Vernazza et al. (1981) are given. One can see that the temperature changes from 4170 K up to 6440 K for the presented h values . i.e. within the temperature range presented in Table 1. The $N(e)/N(H)$ ratio characterizes the plasma ionization degree, as long as its value remains much smaller than one. Table 2 shows that the $N(e)/N(H)$ ratio values remain smaller than 0.1 within the whole considered range and that for -75km$\leq h <$ 1180km these values decrease below 0.01. Also, Table 2 shows the values of

$$\eta(n) = \frac{N(n)}{N_{eq}(n)}, \tag{5}$$

as a function of h. Here, the $N_{eq}(n)$ denotes the equilibrium density of the $H^*(n)$ atoms which was determined by us, with the T, $N(e)$ and $N(H^+)$ taken from Vernazza et al. (1981) corresponding to the given h . From Table 2 one can see that the $\eta(n)$ parameter values vary between 0.6 and 1.2, which implies the difference of the $N(n)$ values from the equilibrium ones. These differences confirm that the chemi - recombination processes (1a,b), not taken into account in Vernazza et al. (1981) for $N(n)$ calculations, may be significant in comparison with the other recombination processes within the h range considered.

In order to estimate the importance of the (1a,b) chemi - recombination processes, we will compare them at first with the photorecombination processes

$$H^+ + e \Rightarrow H^*(n) + h\omega, \tag{6}$$

Table 2. Basic plasma parameters, for the solar chromospheric model of Vernazza et. al. (1981, model C), as a function of height h. The parameter $\eta(n) = N(H^*)(n)/N_{eq}(H^*)(n)$, where $N_{eq}(H^*)(n)$ is the equilibrium density of $H^*(n)$ atoms which corresponds to the electron density $N(e)$ and the proton density $N(H^+)$ from the same model.

			$\eta(n)$				
h/[km]	T/[K]	N(e)/N(H)	n=4	n=5	n=6	n=7	n=8
1605	6440	.9403E-01	.9860	.9381	.9316	.9014	.8996
1515	6370	.6160E-01	1.1407	1.0670	1.0503	1.0119	1.0088
1380	6280	.3344E-01	1.1496	1.0492	1.0248	.9848	.9820
1280	6220	.1782E-01	1.1271	1.0138	.9869	.9473	.9445
1180	6150	.1031E-01	1.1946	1.0618	1.0269	.9830	.9798
1065	6040	.5464E-02	1.2192	1.0721	1.0326	.9871	.9891
980	5925	.3308E-02	1.2286	1.0762	1.0348	.9882	.9853
905	5755	.1891E-02	1.1996	1.0563	1.0170	.9710	.9683
855	5650	.1308E-02	1.1747	1.0392	1.0015	.9560	.9537
755	5280	.4741E-03	1.0444	.9547	.9302	.8899	.8889
705	5030	.2611E-03	.9362	.8795	.8668	.8318	.8321
655	4730	.1686E-03	.8011	.7878	.8549	.7641	.7659
605	4420	.1370E-03	.6752	.7004	.7205	.6981	.7015
555	4230	.1254E-03	.6190	.6661	.6936	.6720	.6755
515	4170	.1190E-03	.6195	.6745	.7031	.6795	.6828
450	4220	.1132E-03	.6884	.7405	.7646	.7357	.7380
350	4465	.1112E-03	.8518	.8812	.8937	.8564	.8572
250	4780	.1155E-03	.9771	.9862	.9898	.9479	.9478
150	5180	.1317E-03	1.0323	1.0397	1.0397	.9973	.9967
100	5455	.1553E-03	1.0290	1.0438	1.0444	1.0042	1.0035
50	5840	.2306E-03	1.0273	1.0260	1.0416	1.0040	1.0035
0	6420	.5517E-03	1.0191	1.0359	1.0366	1.0029	1.0024
-25	6910	.1227E-02	1.0167	1.0326	1.0335	1.0022	1.0016
-50	7610	.3527E-02	1.0161	1.0303	1.0309	1.0024	1.0021
-75	8320	.8821E-02	1.0154	1.0285	1.0291	1.0031	1.0027

for the $n \geq 4$ range. As a quantitative characteristic of the relative influence of the (1a,b) chemi - recombination processes and the photorecombination processes (6) we will use the quantity

$$F_{phr}^{(ab)}(4;8) = \frac{\Sigma_4^8 I_r^{(ab)}(n;T)}{\Sigma_4^8 I_{phr}(n;T)}, \tag{7}$$

where $I_{phr}(n;T)$ denotes the photorecombination flux conditioning the process (6) for given n. In order to determine the $F_{phr}^{(ab)}(4;8)$ values, Eqs (2-4) have been used for $\Sigma_4^8 I_r^{(ab)}(n;T)$ calculations, while $\Sigma_4^8 I_{phr}(n;T)$ is estimated on the basis of data from Vernazza et al. (1981). Fig. 1 illustrates the behavior of the $F_{phr}^{(ab)}(4;8)$ quantity for 350 km $\leq h \leq$ 905 km. We show only this height range, since for $h >$905 km the values of quantity $F_{phr}^{(ab)}(4;8)$ decrease below 0.01, while for $h <$350 km these values continue to increase monotonically. One can see in Fig. 1 that above around 700 km the influence of the (1a,b) processes is much smaller in comparison with the photorecombination processes ($F_{phr}^{(ab)}(4;8) < 0.1$). For 650 km $< h <$ 700 km the influence of both processes is comparable and for $h <$ 650 km the (1a,b) chemi - recombination processes are dominant in comparison with the photorecombination processes (6) for $n \geq 4$.

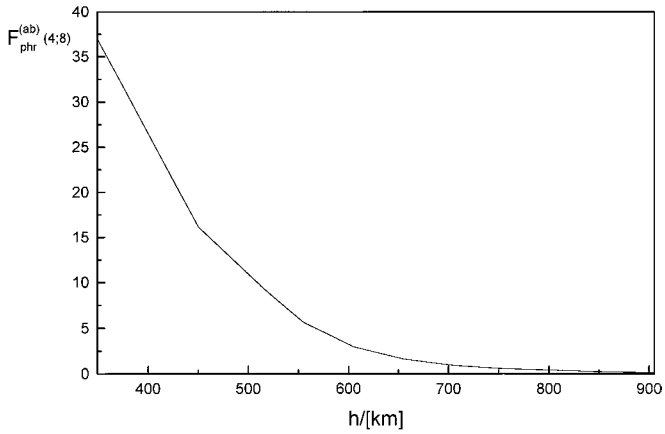

Fig. 1. The behaviour of the quantity $F^{(ab)}_{phr}(4;8)$, given by Eq. (7), as a function of height h.

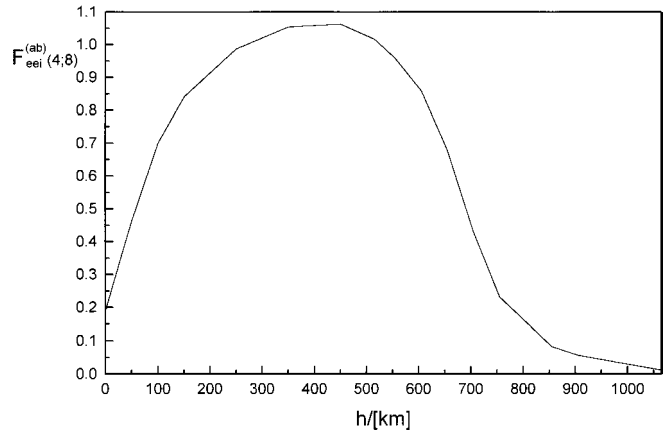

Fig. 2. The behaviour of the quantity $F^{(ab)}_{eei}(4;8)$, given by Eq. (9), as a function of height h.

This conclusion is not connected with our choice of the $n = 8$ as the upper limit of the considered n values region. Namely, our estimates performed in order to check this conclusion show that if we change even only $\Sigma_4^8 I_{phr}(n;T)$ with the sum for all $n \geq 4$, which have sense for given T and $N(e)$, the ratio values on Eq. (6) right side will be changed around 20 percent. It is clear that this change will be even smaller if $\Sigma_4^8 I_r^{(ab)}(n;T)$ in Eq. (7) will be changed in the adequate way. The performed estimates are possible with the help of results of the photorecombination fluxes calculations in Oesterbrock (1974) analyzed in Vernazza et al. (1981).

In the next step we will compare the (1a,b) chemi-recombination processes with the electron - electron - ion recombination processes

$$H^+ + e + e \Rightarrow H^*(n) + e, \tag{8}$$

for the same $n \geq 4$ range. As a quantitative characteristic of the relative influence of the (1a,b) chemi - recombination processes and the electron - electron - ion recombination processes (8) we will first of all use the quantity

$$F^{(ab)}_{eei}(4;8) = \frac{\Sigma_4^8 I_r^{(ab)}(n;T)}{\Sigma_4^8 I_r^{eei}(n;T)}, \tag{9}$$

where $I_r^{eei}(n;T)$ denotes the electron - electron - ion recombination flux conditioning the process (8) for given n, taken here in the form

$$I_r^{eei}(n) = \alpha_r^{eei}(T)[N(e)]^2 N(H^+). \tag{10}$$

For determination of the $F^{(ab)}_{eei}(4;8)$ values, the $\alpha_r^{eei}(T)$ rate coefficients have been calculated here by using the corresponding expressions in Vriens et al. (1980). The behavior of the $F^{(ab)}_{eei}(4;8)$ quantity for 0 km $\leq h \leq$ 1065 km illustrates Fig. 2. This Fig. shows that around 450 km, the (1a,b) chemi - recombination processes become even more influent than the electron - electron - ion recombination processes (8), while within 0 km $\leq h \leq$ 750 km range both processes are comparable ($F^{(ab)}_{eei}(4;8) > 0.2$). For $h <$ 0km and $h >$ 750km, the influence of the chemi - recombination processes becomes small in comparison with electron - electron - ion recombination processes ($F^{(ab)}_{eei}(4;8) < 0.1$ for $h < -25$km and $h >$ 850km).

Besides the $F^{(ab)}_{eei}(4;8)$ quantity, we will introduce also the quantities $f^{(ab)}_{eei}(n) = I_r^{(ab)}(n,T)/I_r^{eei}(n,T)$, characterizing the relative influence of the (1a,b) chemi - recombination processes in comparison with the electron - electron - ion recombination processes (8), on the $H^*(n)$ atom populations for the given n. From Eq. (2) and (10) we have that

$$f^{(ab)}_{eei}(n) = \frac{K_r^{(ab)}(n,T)}{\alpha_r^{eei}(T)} \frac{N(1)}{N(e)}. \tag{11}$$

Here, the ratio $N(1)/N(e)$ may be replaced with $[N(e)/N(H)]^{-1}$ from Table 2, for the $h \leq$ 750km range, practically without the decrease of accuraccy. The behavior of the $f^{(ab)}_{eei}(n)$ quantities as a function of height h for $n = 4 - 8$ is shown in Fig. 3. One can see in Fig. 3 that for n values considered, the chemi - recombination processes are comparable with the electron - electron - ion recombination processes (for $n = 6 - 8$) or dominant (for $n = 4, 5$) within a wide h range which lower limit changes for different n from -75 km up to 50 km and the upper one from 650 km up to 750km. For $n = 4$ and 5 the h range where the relative influence of the chemi - recombination processes remains comparable, is up to around 1200km.

The specific significance of the $f^{(ab)}_{eei}(n)$ quantities is in the fact that they are in the same time ratios of the total fluxes $I_{tot}^{(ab)}(n;T)$ and $I_{tot}^{eei}(n;T)$ characterizing the influence of the ionization processes inverse to the (1a,b) and the (8) recombination process. Namely, in the partially ionized plasma, the (1a,b) chemi - recombination processes occure together with the inverse chemi - ionization processes due to $H^*(n) + H(1s)$ collisions, while the electron - electron - ion processes (8) occure together with the impact ionization processes due to $H^*(n) + e$ collisions. The influence of these inverse processes on the $H^*(n)$ atom populations may be characterized by the

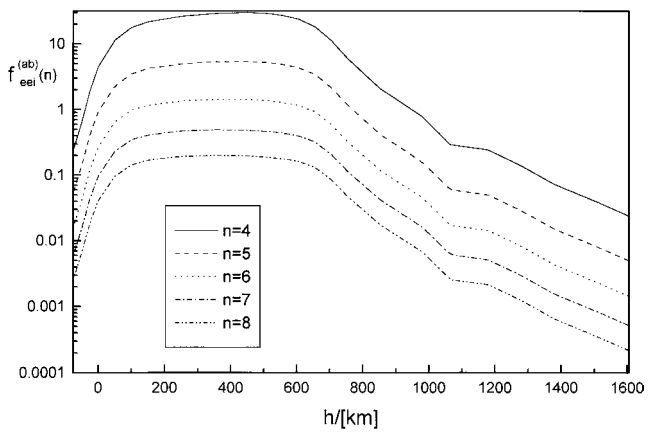

Fig. 3. The behaviour of the quantities $f_{eei}^{(ab)}(n)$, given by Eq. (11), as a function of height h for $n = 4 - 8$.

corresponding ionization fluxes $I_i^{(ab)}(n)$ and $I_i^{eei}(n)$. The total fluxes $I_{tot}^{(ab)}(n;T)$ and $I_{tot}^{eei}(n;T)$ are than being expressed as

$$I_{tot}^{(ab)}(n;T) = I_r^{(ab)}(n;T) - I_i^{(ab)}(n;T),$$

$$I_{tot}^{eei}(n;T) = I_r^{eei}(n;T) - I_i^{eei}(n;T).$$

On the basis of Mihajlov et al. (1996), when $T_e = T_a = T$, these total fluxes may be presented in the form

$$I_{tot}^{(ab)}(n;T) = I_r^{(ab)}(n;T)[1 - \eta(n)],$$

$$I_{tot}^{eei}(n;T) = I_r^{eei}(n;T)[1 - \eta(n)],$$

where, $\eta(n)$ is given by Eq. (5). From here follows that for the considered Solar plasma:

$$f_{eei}^{(ab)}(n) = \frac{I_{tot}^{(ab)}(n,T)}{I_{tot}^{eei}(n,T)}. \quad (12)$$

From the definition of $I_{tot}^{(ab)}(n,T)$ and $I_{tot}^{eei}(n,T)$ follows that their values may be also determined with the help of the parameter $\eta(n)$ values presented in Table 2. Moreover, the Table 2 makes it possible to find the limits of layers where the inverse ionization processes start to dominate in comparison with the recombination processes.

Obtained results show that the (1a,b) chemi - recombination processes evidently have an important role in the large region around the temperature minimum in the Solar atmosphere, where they are comparable or dominant in relation to the other recombination processes. Within this range they may be a quite significant factor contributing to the smaller decrease from LTE. Consequently, this shows the necessity of the inclusion of the (1a,b) processes in the modelling of the weakly ionized layers in the Solar atmosphere. For Solar and stellar atmosphere models where $T_e = T_a = T$, the expressions (2-4) for the (1a,b) chemi - recombination processes total rate coefficient $K_r^{(ab)}(n,T)$ may be used. However, for atmosphere models where the equality of T_e and T_a is not assumed, the corresponding tables and the general expressions for partially ionized nonequilibrium hydrogen plasma are given in Mihajlov et al. (1996).

References

Bates, D. R., Kingston, A. E. and McWhirter, R. W. P., 1962a, Proc. Roy. Soc. A267, 297

Bates, D. R., Kingston, A. E. and McWhirter, R. W. P., 1962b, Proc. Roy. Soc. A270, 155

Bates, D. R., Ledsham, K., Stewart, A. L., 1953, Phil. Trans. Roy. Soc. 246, 215

Fano, U., 1970, Phys. Rev. A. 2, 353

Giusti-Suzor, A., 1989, in Dissociative recombination: Theory, experiment and applications, eds. Mitchell, J. B. A., Guberman, S. L., World Scientific Publishing, Singapore, New Jersey, p. 14

Hickman, A. P., 1989, in Dissociative recombination: Theory, experiment and applications, eds. Mitchell, J. B. A., Guberman, S. L., World Scientific Publishing, Singapore, New Jersey, p. 35

Maltby, P., Avrett, E.H., Carlsson, M., Kjeldseth-Moe, O., Kurucz, R.L., Loeser, R., 1986, ApJ 306, 284

Mihajlov, A. A., Dimitrijević, M. S., Djurić, Z., 1996, Physica Scripta 53, 159

Mihajlov, A. A., Dimitrijević, M. S., Ignjatović, Lj. M., 1993, A&A 276, 187

Mihajlov, A. A., Dimitrijević, M. S., Ignjatović, Lj. M. and Djurić, Z., 1994, A&AS 103, 57

Mihajlov, A. A. & Ljepojević, N. N., 1982, Proc. Symp. on Physics of Ionized Gases (Dubrovnik, 1982), (Zagreb: Institute of Physics of the University of Zagreb), Contributed papers,

Mihajlov, A. A., Ljepojević, N. N., Dimitrijević, M. S., 1992, J. Phys. B: At. Mol. Opt. Phys. 25, 5121

Osterbrock, D.E., 1974, Astrophysics of Gaseous Nebulae, Freeman, San Francisco

Seaton, M.J., 1966, Proc. Phys. Soc., 88, 801

Vernazza, J. E., Avrett, E. H., Loeser, R., 1981, ApJS 45, 635

Vriens, L. & Smeets, A. H. M., 1980, Phys. Rev. A22, 940

This article was processed by the author using Springer-Verlag LaTeX A&A style file *L-AA* version 3.

Astron. Astrophys. 350, 719–724 (1999)

ASTRONOMY AND ASTROPHYSICS

The electron-impact broadening effect in CP stars: the case of La II, La III, Eu II, and Eu III lines

L.Č. Popović[1], M.S. Dimitrijević[1], and T. Ryabchikova[2,3]

[1] Astronomical Observatory, Volgina 7, 11160 Belgrade 74, Yugoslavia
[2] Institute of Astronomy of the Russian Academy of Sciences, Pyatnitskaya 48, 109017 Moscow, Russia (ryabchik@inasan.rssi.ru)
[3] Visiting scientist, Institute for Astronomy, Vienna University, Tuerkenschanzstrasse 17, 1180 Wien, Austria

Received 22 March 1999 / Accepted 26 August 1999

Abstract. The electron-impact widths and shifts for six Eu II lines and widths for three La II, and six La III multiplets have been calculated by using the modified semiempirical method. Estimation for Stark widths of 664.506 nm (Eu II) and 666.634 nm (Eu III) lines are given as well. The influence of the electron-impact mechanism on line shapes and equivalent widths in hot star atmospheres has been considered.

Key words: atomic data – plasmas – stars: chemically peculiar

1. Introduction

The lines of the ionized rare earth elements (REE) are present in the spectra of CP stars in a wide temperature domain (see e.g. Jaschek & Jaschek 1974, Bonsack & Wolf 1980, Magazzu & Cowley 1986, Ryabchikova & Ptitsyn 1986, Cowley & Greensberg 1988, Van't Veer et al. 1988, Sadakane 1993, Kupka et al. 1996, Gelbmann et al. 1997, Ryabchikova et al. 1997, 1999, etc), and many review articles on abundances of the REE exist (e.g. Jaschek & Jaschek 1974, Bonsack & Wolf 1980, Cowley 1984, Sadakane 1993). Cowley (1984) discussed the observed stellar lines of the REE and gave element by element summaries. Usually, REE abundance analysis is based on the lines of the first ions, which have experimentally determined oscillator strengths, but due to low ionization potentials the second ions of the REE are dominant in stellar atmospheres. The lack of atomic data for the lines of second ions of the REE did not allow to use them for abundance determinations, although line identifications were successfull. For example, Cowley (1984) identified Dy III lines in spectra of a few magnetic stars, Cowley & Greenberg (1988) surveyed lines of doubly ionized REE in UV spectra of five magnetic stars, Mathys & Cowley (1992) presented Pr III identification in optical spectra of a number of CP stars. The first calculations of the oscillator strengths for Ce III lines by Bord et al. (1997) made it possible to use the lines of the second ions of the REE for abundance determinations. Bord et al. (1997) analyzed Ce III lines in spectra of CP stars HD 200311, HD 192913, and HR 465, Cowley & Bord (1998) analyzed Nd III lines in CP stars γ Equ, and HD 168733, Ryabchikova et al. (1999) provided an identification and quantitative analysis of Eu III lines in the optical spectra of 10 CP stars.

The spectral lines of singly ionized lanthanum and europium are present in solar as well as in stellar spectra (see e.g. Grevesse & Blanquet 1969, Molnar 1972, Adelman 1987, Sadakane 1993, etc.). For example, Sadakane (1993) suggested overabundance of La in α CMa and o Peg, two hot Am-type stars, and Ryabchikova et al. (1999) revised abundance of Eu in 10 magnetic stars taking into account hyperfine structure and magnetic effects. The lines of Eu II in the optical spectra of CP stars are usually very strong and lie in the damping part of the curve-of-growth. Since in A-type stars mentioned here Stark broadening is the main pressure broadening mechanism (see e.g. Dimitrijević 1989) the corresponding data on Stark broadening of stellar spectral lines are needed for a number of astrophysical problems including the line formation and the abundance determinations.

Due to the poor knowledge on the energy levels as well as on the realiable transition probabilities for the rare earth emitters, the approximate methods are suitable for Stark broadening calculations. Here we have applied the modified semiempirical approach – MSE (Dimitrijević & Konjević 1980, Dimitrijević & Kršljanin 1986, Popović & Dimitrijević 1996a, 1997) whose applicability for complex spectra has been tested several times (see e.g. Popović & Dimitrijević 1996ab, 1997). This method is applicable only for the Stark broadening of ion lines while for neutral atom lines there exists e.g. the method of Dimitrijević & Konjević (1986).

In order to provide a complete set of Stark broadening data for astrophysical purposes, we started a project to calculate such data for a number of spectral lines of the ionized REE (see Popović & Dimitrijević 1998a). Here we present the Stark widths for three La II and six La III mulitplets, and Stark widths and shifts for six Eu II lines by using the MSE. Also, for Eu II λ 664.505 nm and for Eu III λ 666.635 nm lines estimates of the electron impact widths have been performed. Our data are the first Stark broadening calculations for spectral lines of ionized lanthanum and europium. For resonance lines of La II and Eu II

Send offprint requests to: L.Č. Popović (lpopovic@aob.bg.ac.yu)

Table 1. Stark full widths (FWHM) and shifts for Eu II lines, calculated within the modified semiempirical approach, as a function of temperature. The electron density is $10^{23}\mathrm{m}^{-3}$

Transition	T (K)	W (nm)	d (nm)
	5000.	0.293E-01	-0.432E-02
$6s\,^7S^0_3 - 6p\,^7P_2$	10000.	0.203E-01	-0.307E-02
	20000.	0.141E-01	-0.218E-02
$\lambda = 390.710\,\mathrm{nm}$	30000.	0.115E-01	-0.177E-02
	40000.	0.102E-01	-0.153E-02
	50000.	0.951E-02	-0.140E-02
	5000.	0.295E-01	-0.436E-02
$6s\,^7S^0_3 - 6p\,^7P_3$	10000.	0.205E-01	-0.309E-02
	20000.	0.142E-01	-0.220E-02
$\lambda = 393.048\,\mathrm{nm}$	30000.	0.116E-01	-0.179E-02
	40000.	0.103E-01	-0.155E-02
	50000.	0.959E-02	-0.142E-02
	5000.	0.300E-01	-0.436E-02
$6s\,^7S^0_3 - 6p\,^7P_4$	10000.	0.208E-01	-0.309E-02
	20000.	0.144E-01	-0.220E-02
$\lambda = 397.196\,\mathrm{nm}$	30000.	0.118E-01	-0.179E-02
	40000.	0.105E-01	-0.155E-02
	50000.	0.974E-02	-0.142E-02
	5000.	0.570E-01	-0.173E-01
$6s\,^9S^0_4 - 6p\,^9P_3$	10000.	0.397E-01	-0.125E-01
	20000.	0.276E-01	-0.916E-02
$\lambda = 420.505\,\mathrm{nm}$	30000.	0.226E-01	-0.776E-02
	40000.	0.200E-01	-0.705E-02
	50000.	0.185E-01	-0.671E-02
	5000.	0.557E-01	-0.169E-01
$6s\,^9S^0_4 - 6p\,^9P_4$	10000.	0.388E-01	-0.122E-01
	20000.	0.270E-01	-0.897E-02
$\lambda = 412.970\,\mathrm{nm}$	30000.	0.221E-01	-0.759E-02
	40000.	0.195E-01	-0.688E-02
	50000.	0.181E-01	-0.654E-02
	5000.	0.451E-01	-0.391E-02
$6s\,^9S^0_4 - 6p\,^9P_5$	10000.	0.314E-01	-0.278E-02
	20000.	0.219E-01	-0.198E-02
$\lambda = 381.967\,\mathrm{nm}$	30000.	0.179E-01	-0.161E-02
	40000.	0.158E-01	-0.142E-02
	50000.	0.146E-01	-0.132E-02

however, simple estimates of Stark widths and shifts, based on the regularities and systematic trends, exist (Lakićević 1983).

2. Method of calculations

In the case of three La II and six La III transitions, it was possible to use the MSE approach (Dimitrijević & Konjević 1980, Dimitrijević & Kršljanin 1986) in adequate way and calculate Stark widths (W - full width at half maximum) for the multiplet as a whole. For the simple spectrum Stark broadening parameters of different lines are nearly the same within a multiplet (Wiese & Konjević 1982, 1992). Consequently, one may take the averaged atomic data for a multiplet as a whole and calculate the corresponding Stark widths and shifts. If the wavelength of a particular line within the multiplet differs significantly from

Table 2. Stark full widths (FWHM) for La II and La III lines calculated within the modified semiempirical approach. The electron density is $10^{23}\mathrm{m}^{-3}$. The averaged wavelength of the multiplet is denoted as $\langle\lambda\rangle$.

Transition	T (K)	W (nm)
	5000.	0.336E-01
La II	10000.	0.232E-01
$a\,^3P - y\,^3D^0$	20000.	0.160E-01
	30000.	0.131E-01
$\langle\lambda\rangle = 463.20\,\mathrm{nm}$	40000.	0.116E-01
	50000.	0.109E-01
	5000.	0.493E-01
La II	10000.	0.348E-01
$a\,^3D - y\,^3D^0$	20000.	0.246E-01
	30000.	0.201E-01
$\langle\lambda\rangle = 403.58\,\mathrm{nm}$	40000.	0.174E-01
	50000.	0.148E-01
	5000.	0.219E-01
La II	10000.	0.152E-01
$a\,^3F - y\,^3D^0$	20000.	0.104E-01
	30000.	0.853E-02
$\langle\lambda\rangle = 379.44\,\mathrm{nm}$	40000.	0.756E-02
	50000.	0.707E-02
	5000.	0.260E-01
La III	10000.	0.182E-01
$6s\,^2S - 6p\,^2P^0$	20000.	0.126E-01
	30000.	0.103E-01
$\langle\lambda\rangle = 328.01\,\mathrm{nm}$	40000.	0.892E-02
	50000.	0.807E-02
	5000.	0.105E-01
La III	10000.	0.734E-02
$6s\,^2S - 7p\,^2P^0$	20000.	0.522E-02
	30000.	0.440E-02
$\langle\lambda\rangle = 124.28\,\mathrm{nm}$	40000.	0.400E-02
	50000.	0.376E-02
	5000.	0.747
La III	10000.	0.522
$7s\,^2S - 7p\,^2P^0$	20000.	0.374
	30000.	0.320
$\langle\lambda\rangle = 854.39\,\mathrm{nm}$	40000.	0.295
	50000.	0.281
	5000.	0.453E-01
La III	10000.	0.317E-01
$6p\,^2P^0 - 7s\,^2S$	20000.	0.226E-01
	30000.	0.191E-01
$\langle\lambda\rangle = 261.31\,\mathrm{nm}$	40000.	0.173E-01
	50000.	0.162E-01
	5000.	0.231E-01
La III	10000.	0.161E-01
$6p\,^2P^0 - 6d\,^2D$	20000.	0.115E-01
	30000.	0.978E-02
$\langle\lambda\rangle = 259.32\,\mathrm{nm}$	40000.	0.889E-02
	50000.	0.839E-02
	5000.	0.556
La III	10000.	0.388
$6d\,^2D - 7p\,^2P^0$	20000.	0.278
	30000.	0.238
$\langle\lambda\rangle = 876.37\,\mathrm{nm}$	40000.	0.220
	50000.	0.210

the averaged wavelength $\langle\lambda\rangle$ of the multiplet one may obtain more accurate values for each line by scaling multiplet values for widths and shifts:

$$W_{\rm line} = (\frac{\langle\lambda\rangle}{\lambda})^2 \cdot W, \quad (1)$$

In the above expression W and $\langle\lambda\rangle$ are values for the multiplet, and $W_{\rm line}$ and λ refer to a particular line of the multiplet.

It is not always possible to apply this approximation for complex spectra. If irregularities of atomic energy level structure, forbidden and intercombination transitions influence different lines of the multiplet in a different way, we have to calculate Stark broadening data for each line separately (Dimitrijević 1982, Popović & Dimitrijević 1997, Dimitrijević & Tankosić 1999). Such case is realized for Eu II and Eu III lines considered in our paper.

In the case of Eu II, taking into account very complex spectrum of this emitter and the absence of designation for higher levels, we were able to calculate the electron-impact broadening parameters only for six 6s-6p transitions using the MSE approach. Due to the complex spectrum we have applied here this method as it was described in Popović & Dimitrijević (1996a, 1997). We have estimated also the electron-impact width for Eu II ($5d\,^9D^0_6 - 6p\,^9P_5$) λ 664.506 nm line using the MSE approach with the estimate of the perturbation of the $5f$ levels (in accordance with Popović & Dimitrijević 1998b). We have also estimated Stark width for Eu III λ 666.635 nm line using the simplified MSE method (Dimitrijević & Konjević 1987) in LS coupling approximation.

Atomic energy levels needed for calculations have been taken from Sugar & Spector (1974) and from Martin et al. (1978). Matrix elements were calculated by the method of Bates & Damgaard (1949). The multiplet factors for calculations of La II and La III Stark broadening parameters were taken from Shore & Menzel (1968). Since for nonet terms the line factors are absent in the tables of Shore & Menzel (1968), the corresponding factors for Eu II lines were calculated according to formula:

$$\Re_{\rm line} = \sqrt{2J+1}\sqrt{2J'+1}\left\{\begin{array}{ccc} S & J & L \\ 1 & L' & J' \end{array}\right\} \quad (2)$$

where S is the total spin; J and J' are total angular momentum quantum numbers; while L and L' are total azimuthal quantum numbers. The quantum numbers of the perturbing level are denoted with the primes.

The details of the MSE and simplified MSE method have been given several times (Dimitrijević & Konjević 1980, Dimitrijević & Kršljanin 1986, Dimitrijević & Konjević 1987, Popović & Dimitrijević 1996a, 1997) and will not be repeated here again.

3. Results and discussion

Stark widths and shifts for six Eu II lines, and Stark widths for three La II and six La III multiplets are presented in Tables 1 and 2 for different temperatures, and for electron density of $10^{23}{\rm m}^{-3}$.

Table 3. Estimated Stark full widths (W) for Eu II 664.505 nm and Eu III 666.63 nm lines. The Eu II 664.505 nm line has been calculated within the modified semiempirical approach (MSE) with estimated perturbation of $5f$ levels. The Eu III 666.65 nm line has been calculated within the simplified MSE. The results are given for an electron density of $10^{23}{\rm m}^{-3}$ as a function of temperature.

Transition	T (K)	W (nm)
	5000.	0.930E-01
Eu II	10000.	0.644E-01
$5d\,^9D^0_6 - 6p\,^9P_5$	20000.	0.447E-01
	30000.	0.367E-01
$\lambda = 664.505$ nm	40000.	0.327E-01
	50000.	0.306E-01
	5000.	0.354E-01
Eu III	10000.	0.247E-01
$4f^7\,^6I^0_{17/2} - 4f^6 5d\,^6H_{15/2}$	20000.	0.171E-01
	30000.	0.137E-01
$\lambda = 666.63$ nm	40000.	0.117E-01
	50000.	0.104E-01

Stark widths for Eu II λ 664.505 nm line calculated by the MSE method with the estimated perturbation of unknown $5f$ levels, and Stark width for Eu III λ 666.63 nm line estimated with the simplified MSE method (Dimitrijević & Konjević 1987) are given in Table 3. In order to present our results in a more convenient form for synthetic spectrum calculations, all data from Tables 1–3 were fitted with the following expression:

$$W({\rm rad\,s^{-1}}) = A_0 \cdot T^{A_1}. \quad (3)$$

Here W is a full width at half maximum (FWHM) expressed in rad s^{-1} per electron, and constants A_0 and A_1 are determined numerically to obtain the best fit. The corresponding values of $\log A_0$ and A_1 are given in Table 4 together with the widths and shifts (in logarithmic form) per electron for T=10000 K. This temperature was chosen as the most representative for A-type stars where the Stark broadening becomes the dominant pressure broadening mechanism due to hydrogen ionization. This kind of presentation is similar to that used in the most complete set of atomic line parameters calculations by Kurucz (1993a) for Fe-peak elements.

There is no experimental data for the electron broadening parameters for La and Eu lines considered in the paper. The only estimates for the $5d^2\,^3F - 4f5d\,^3F^0$ (λ =580.82 nm) La II transition and the resonance Eu II line were made by Lakićević (1983) on the basis of regularities and systematic trends for the electron temperature of 20000 K and the electron density of $10^{23}{\rm m}^{-3}$. These estimates resulted in W=0.0338 nm; $|d|$=0.0149 nm for La II λ =580.82 nm, and in W=0.032 nm; $|d|$=0.014 nm for the resonance transition of Eu II. The energy level $4f\,^3F^0$ in Lakićević (1983) paper is obviously erroneous. We suppose that this is $5d\,^3F^0$ level in fact, but since we have not found the corresponding $5f$ levels in the literature the adequate MSE calculations cannot be performed. Concerning the results for Eu II, neither the transition nor the wavelength are specified in Lakićević (1983), making the comparison impossible.

Table 4. The Stark widths and shifts W (rad s^{-1}) and d (rad s^{-1}) per electron for T=10000 K, and constants $A_{0,1}$ as described in the text.

Ion λ (nm)	log[W(rad s^{-1})]	log A_0	A_1	log[d(rad s^{-1})]
Eu II 397.196	-5.6052	-0.36188E+01	-0.49620	-6.4333
Eu II 393.048	-5.6024	-0.36144E+01	-0.49674	-6.4242
Eu II 390.710	-5.6014	-0.36104E+01	-0.49733	-6.4218
Eu II 420.505	-5.3740	-0.33899E+01	-0.49574	-5.8759
Eu II 381.967	-5.3900	-0.34446E+01	-0.48596	-6.4458
Eu II 412.970	-5.3682	-0.33839E+01	-0.49580	-5.8707
Eu II 664.505	-5.5613	-0.35927E+01	-0.49160	
Eu III 666.635	-5.9803	-0.38493E+01	-0.53323	
La II $\langle 379.440\rangle$	-5.7017	-0.36967E+01	-0.50131	
La II $\langle 403.580\rangle$	-5.3955	-0.33450E+01	-0.51257	
La II $\langle 463.200\rangle$	-5.6913	-0.36932E+01	-0.49910	
La III $\langle 328.010\rangle$	-5.4969	-0.34520E+01	-0.51145	
La III $\langle 124.280\rangle$	-5.0483	-0.32345E+01	-0.45202	
La III $\langle 259.320\rangle$	-5.3461	-0.35580E+01	-0.44516	
La III $\langle 261.310\rangle$	-5.0585	-0.32468E+01	-0.45141	
La III $\langle 854.390\rangle$	-4.8709	-0.31376E+01	-0.43130	
La III $\langle 876.370\rangle$	-5.0218	-0.32939E+01	-0.42986	

In order to test the importance of the electron-impact broadening effect in stellar atmospheres, we have synthesized the line profiles of Eu II λ=420.505 nm and Eu III λ=666.63 nm lines using SYNTH code (Piskunov 1992) and the Kurucz's ATLAS9 code for stellar atmosphere models (Kurucz 1993b) in the temperature range of 6000 $\leq T_{\rm eff} \leq$ 16000 K, and 3.0$\leq \log g \leq$5.0. We have modified the SYNTH code, which uses $\log W$(rad s^{-1}) per electron for T=10000 K as an imput parameter replacing them by three imput parameters: A_0 and A_1 from Eq. 3 and Stark line shift (d).

For the spectrum synthezis it is more convenient to use the parameters A_0 and A_1 (from Table 4) than to take more accurate data from Tables 1–3. In Fig. 1 the comparison between calculated data (filled circles) and the fit with Eq. 3 (full line) for La III $\langle 876.37\rangle$ is shown. We present also the result of an approximate temperature scaling (dashed line) performed as

$$W_T = W_{T_m} \cdot (\frac{T}{T_m})^{-1/2}, \quad (4)$$

(T_m=10000 K) that may be used in astrophysics for ion lines.

As we can see from Fig. 1, if a particular accuracy is not necessary, Eqs. (3) and (4) provide a good approximation, especially for large scale calculations.

The synthesized line profiles for Eu II 420.505 nm line calculated for the model with $T_{\rm eff}$=9500 K, $\log g$=4.5 and the europium abundances A=log(Eu/H)=-5.9 and -7.5 are shown in Fig. 2. One can see that Stark effect leads to the growth of the line wings and hence to the increase of the line equivalent width (EW). In our cases enhancement factors are more than 2 for A=-5.9 and 1.6 for A=-7.5.

In Fig. 3(a,b) we show the ratio of the equivalent widths – $EW_{\rm St}/EW_0$ – as a function of the effective temperature. Here $EW_{\rm St}$ and EW_0 are the equivalent widths of the line calculated with and without Stark broadening effect. The calculations were performed for Eu II 420.505 nm (Fig. 3a) and for Eu III 666.63 nm (Fig. 3b) lines with the europium abundance log(Eu/H)= -6.9.

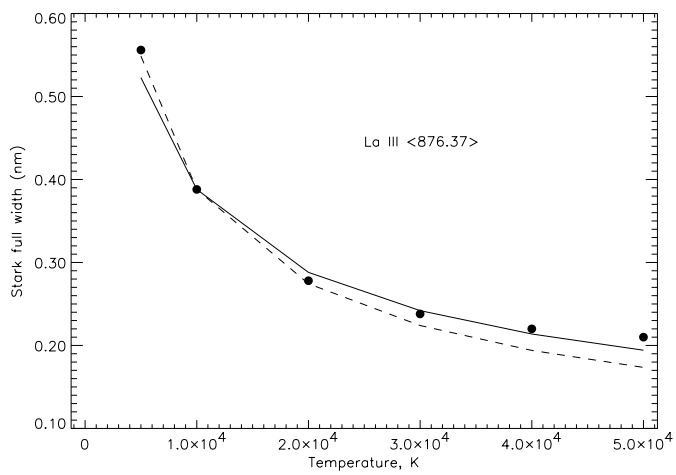

Fig. 1. Stark widths for La III $6d\,^2D - 7p\,^2P^0$ ($\langle\lambda\rangle$ =876.37 nm) line as a function of the electron temperature. Data from Table 2 are shown by filled circles, data obtained with the different approximations are shown by full line (Eq. 3) and by dashed line (Eq. 4), respectively

As one can see from Fig. 3(a,b) for Eu II 420.505 nm line the electron impact broadening has its maximum effect at $T_{\rm eff} \approx$ 8000–9000 K, while for Eu III 666.63 nm line this effect is important for $T_{\rm eff} >$ 8000 K and maximum is not present. Different trends in the dependence of the electron broadening effect on effective temperature for two lines may be explained by difference in the ionization potentials of Eu II and Eu III. The ionization potential of Eu II is 11.241 eV, and for higher effective temperatures this ion is practically absent in the layers where the electron impact broadening is important and where Eu III becomes to be a dominant ion. The small minimum around $T_{\rm eff}$=12000 K in Fig. 3b may be connected with the specific depth formation of the Eu III line. A decrease of the Stark broadening effect for Eu II

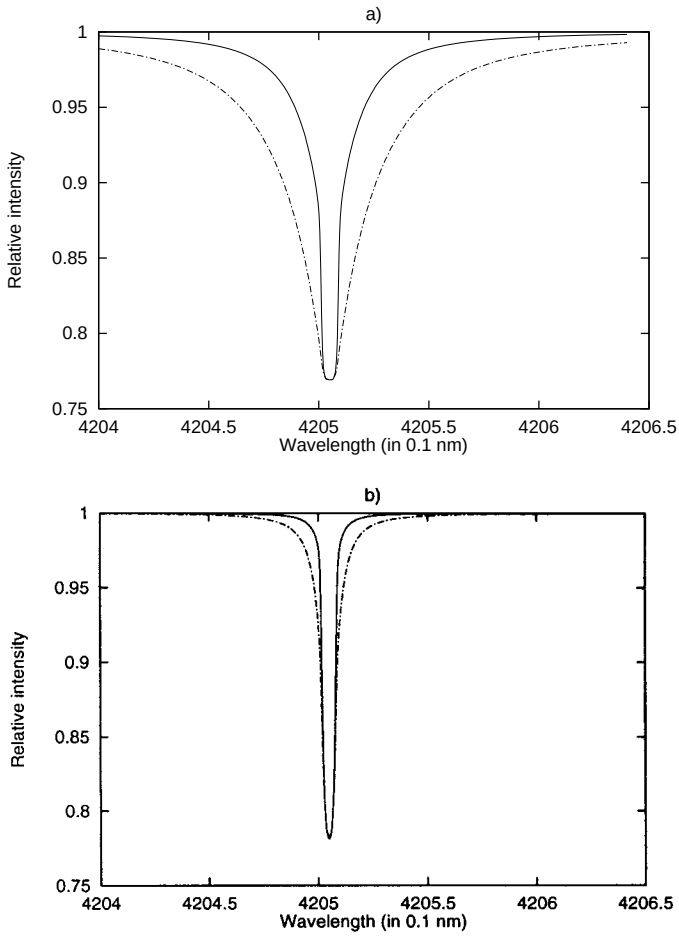

Fig. 2. The line profile of Eu II 420.505 nm line synthesized with Stark broadening mechanism taken into account (dashed line) and without it (full line). The calculations have been performed for the atmosphere model with $T_{\rm eff}$=9500 K and $\log g$=4.5. The abundances of europium are a) log(Eu/H)=-5.9 and b) log(Eu/H)=-7.5

line towards the lower temperatures when this ion becomes to be dominant occures due to rapid decrease of the electron density.

In Fig. 4 the influence of Stark broadening effect for different $\log g$ in the case of Eu III 666.63 nm line is shown. As one can see the importance of Stark broadening increases with $\log g$. This trend is expected, because the electron density, and hence the frequency of the electron-emitter collisions increases with $\log g$.

The influence of Stark broadening for Eu III 666.63 nm line as a function of europium abundance is shown in Fig. 5 for an A0 type star ($T_{\rm eff}$=10000 K, $\log\ g$=4.0).

It is interesting that the influence for the considered line has maximum about A=-5.

The Stark broadening influence as well as the equivalent width increase with abundance. For higher abundances of europium the contribution of the Van der Waals broadening effect starts to be more important too. Consequently, as one can see in Fig. 5. the ratio of the equivalent widths $EW_{\rm St}/EW_0$ decreases with abundance for A>-5.

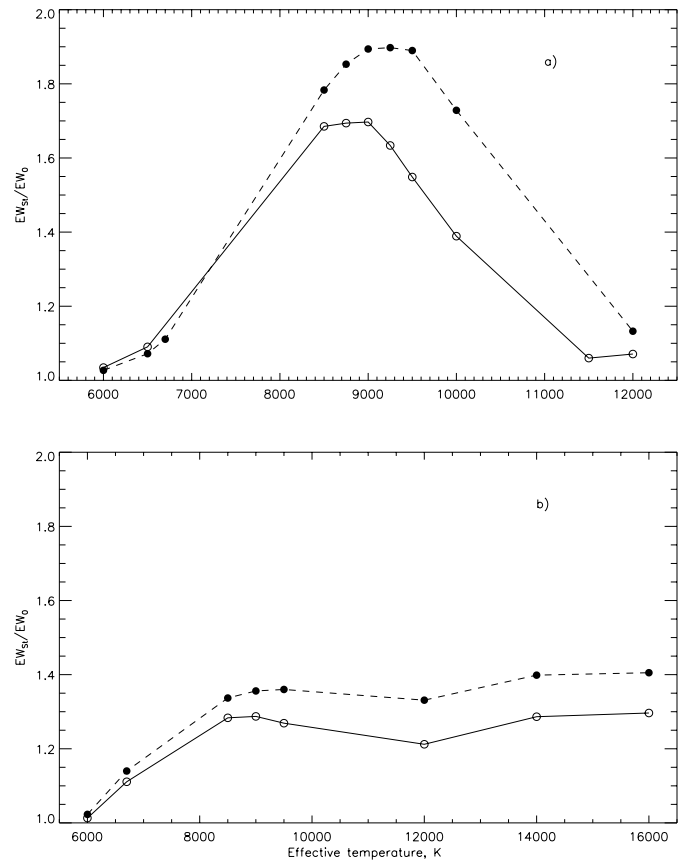

Fig. 3a and b. The ratio of equivalent widths for Eu II 420.505 nm line **a** and for Eu III 666.63 nm line **b** calculated with Stark broadening effect ($EW_{\rm St}$) and without it (EW_0) as a function of effective temperature. Results for $\log g$=4.0 and for $\log g$=4.5 are shown by the open circles and full circles respectively

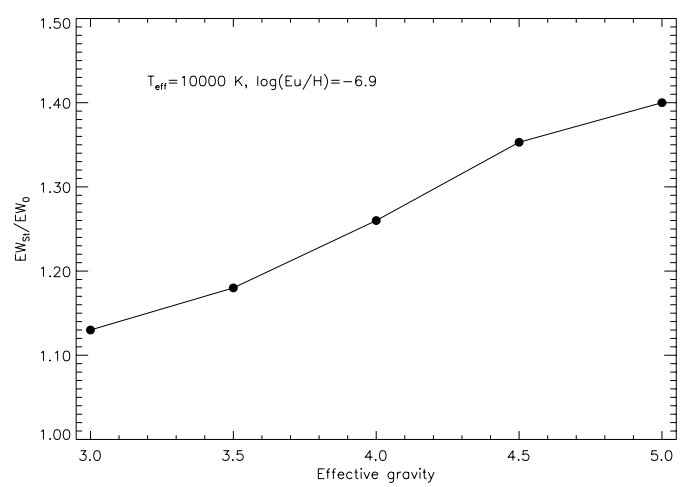

Fig. 4. The ratio of the equivalent widths $EW_{\rm St}/EW_0$ as a function of $\log g$ for Eu III 666.63 nm line

4. Conclusions

The Stark broadening widths and shifts for Eu II, Eu III, La II and La III lines calculated within the modified semiemprical approach are presented as the first reliable data on the Stark

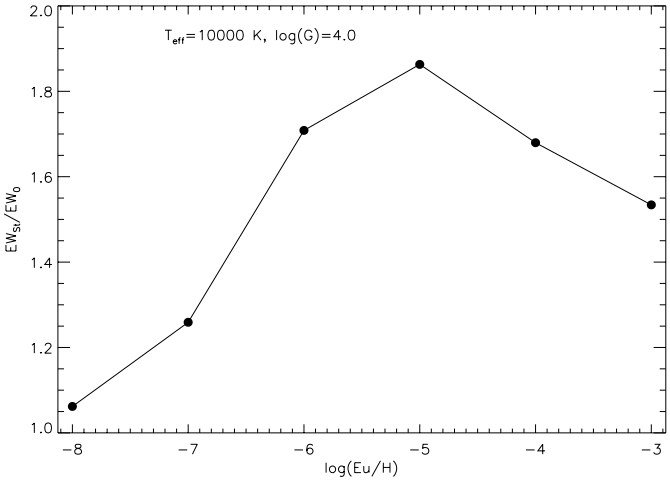

Fig. 5. The ratio of $EW_{\rm St}/EW_0$ for Eu III 666.63 nm line as a function of Eu abundance

broadening of the rare-earth elements, which is important in particular for the abundance analysis of CP stars.

The importance of the Stark broadening effect in stellar atmospheres under different conditions has been considered. Stark broadening becomes to be significant in hot stars, and it should be taken into account in the analysis of stellar spectral lines for the $T_{\rm eff}$>7000 K in particular if europium is overabundant.

Acknowledgements. This work has been supported by the Ministry of Science and Technology of Serbia through the project "Astrometrical, Astrodynamical and Astrophysical Researches" and Federal Ministry of Developement, Sciences and Environment Protection of Yugoslavia which supported Yugoslav-Russian scientific cooperation through the project "Investigation of the Impact Broadening Effect in Stellar Atmospheres". T.R. acknowledges support by the Austrian *Fonds zur Förderung der wissenschaftlichen Forschung, project S 7303-AST* during her stay in Austria.

References

Adelman S J., 1987, In: Adelman S.J., Lanz T. (eds.) Elemental Abundance Analyses. Proc. of the IAU working group on Ap stars Workshop, Institut d'Astronomie de l'Université de Lausanne, p. 58
Bates D.R., Damgaard A., 1949, Phil. Trans. R. Soc. London, Ser. A 242, 101
Bonsack W.K., Wolf S.C., 1980, ApJ 85, 599
Bord D.J., Cowley C.R., Norquist P.L., 1997, MNRAS 284, 869
Cowley C.R., 1984, Phys. Scr. T8, 28
Cowley C.R., Greensberg M., 1988, MNRAS 232, 763
Cowley C.R., Bord D.J., 1998, In: Brandt J.C., Ake T.B., Petersen C.C. (eds.) The Scientific Impact of the Goddard High Resolution Spectrograph. ASP Conf. Ser. 143, 346
Dimitrijević M. S., 1982, A&A 112, 251
Dimitrijević M. S., 1989, Bull. Obs. Astron. Belgrade 140, 111
Dimitrijević M.S., Konjević N., 1980, JQSRT 24, 451
Dimitrijević M.S., Kršljanin V., 1986, A&A 165, 269
Dimitrijević M.S., Konjević N., 1986, A&A 163, 297
Dimitrijević M.S., Konjević N., 1987, A&A 173, 345
Dimitrijević M. S., Tankosić D., 1999, Phys. Scr., submitted
Gelbmann M., Kupka F., Weiss W.W., Mathys G., 1997, A&A 319, 630
Grevesse N., Blanquet, G., 1969, Solar Phys. 8, 5
Jaschek M., Jaschek C., 1974, Vistas in Astron. 16, 131
Kupka F., Ryabchikova T.A., Weiss W.W., et al., 1996, A&A 308, 886
Kurucz R.L., 1993a, SAO, Cambridge, CDROM 20–22
Kurucz R.L., 1993b, Model atmosphere program ATLAS9 published on CDROM13
Lakićević I. S., 1983, A&A 127, 37
Magazzu A., Cowley C.R., 1986, ApJ 308, 254
Martin W.C, Zalubas R., Hagan L., 1978, Atomic Energy Levels. NSRDS-NBS 60, Washington D.C.
Mathys G., Cowley C.R., 1992, A&A 253, 199
Molnar H., 1972, A&A 20, 69
Piskunov N.E., 1992, In: Glagolevskij Yu.V., Romanyuk I.I. (eds.) Stellar magnetism. Nauka, St. Petersburg, p. 92
Popović L.Č., Dimitrijević M.S., 1996a, Phys. Scr. 53, 325
Popović L.Č., Dimitrijević M.S., 1996b, A&AS 116, 359
Popović L.Č., Dimitrijević M.S., 1997, In: Vujičić B., Djurović S., Purić J. (eds.) The Physics of Ionized Gas. Institute of Physics, Novi Sad, p. 477
Popović L.Č., Dimitrijević M.S., 1998a, In: North P., Schnel A., Žižňovský J. (eds.) Proc. of the 26th Meeting and Workshop of the European Working Group on CP Stars, Contributions of the Astron. Obs. Skalnaté Pleso 27, 353
Popović L.Č., Dimitrijević M.S., 1998b, Serb. Astron. J. 157, 109
Ryabchikova T.A., Landstreet J.D., Gelbmann M.J., et al., 1997, A&A 327, 1137
Ryabchikova T.A., Piskunov N., Savanov I., Kupka F., Malanushenko V., 1999, A&A 343, 229
Ryabchikova T.A., Ptitsyn D.A., 1986, In: Cowley C.R., et al. (eds.) Upper Main Sequence Stars with Anomalous Abundances. IAU Coll. 90, Reidel, Dordrecht, p. 319
Sadakane K., 1993, In: Peculiar Versus Normal Phenomena in A-type and Related Stars. ASP Conf. Ser. 44, 72
Shore B.W., Menzel D.H., 1965, ApJ 12, 187
Sugar J., Spector N., 1974, JOSA 64, 1484
Van't Veer C., Bukhart C., Coupry M.F., 1988, A&A 203, 123
Wiese W.L., Konjević N., 1982, JQSRT 28, 185
Wiese W.L., Konjević N., 1992, JQSRT 47, 185

A&A 365, 656–659 (2001)
DOI: 10.1051/0004-6361:20000013
© ESO 2001

Astronomy & Astrophysics

The electron-impact broadening effect in hot star atmospheres: The case of singly- and doubly-ionized zirconium*

L. Č. Popović, N. Milovanović, and M. S. Dimitrijević

Astronomical Observatory, Volgina 7, 11160 Belgrade 74, Serbia, Yugoslavia

Received 14 December 1999 / Accepted 31 August 2000

Abstract. The electron-impact widths for 30 Zr III lines were calculated using the modified semi-empirical (MSE) method. For two Zr II and four Zr III astrophysically important UV lines, only electron-impact widths are given, since for their calculation the experimental oscillator strengths were used and consequently the accuracy of the parameters is lower than in the case of other lines. The influence of the electron-impact mechanism on line shapes and equivalent widths in hot star atmospheres was also considered. The impact of the electron-impact broadening effect on abundance determination, particularly its effect on "zirconium conflict" is discussed as well.

Key words. atomic data – plasma – stars: atmospheres

1. Introduction

Electron-impact broadening is the main broadening mechanism in A and B type star atmospheres (see e.g. Popović et al. 1999). Electron-impact broadening data are needed to solve various problems in astrophysics and physics, for example, diagnosis and modeling of laboratory and stellar plasma, investigation of its physical properties and for abundance determination. These investigations provide information useful for the modeling of stellar evolution, e.g. abundance studies in stellar atmospheres provide evidence of the chemical composition of the stellar primordial cloud, of processes occurring within the stellar interior, and the dynamic processes occuring in the stellar atmosphere.

Present abundance analyses for early-type stars show that 10%–20% of A and B stars have abundance anomalies, including anomalies in isotopic composition (Leckrone et al. 1993). The abundance anomalies in these stars, called CP stars, could be caused by diffusion occurring in the presence of selective radiative acceleration. The chemical species that absorb more of the outgoing photons are dragged by the photons to the stellar surface (see e.g. Michaud & Richter 1997). In order to investigate these processes, atomic data for multiple lines of numerous emitters are needed.

Here, we have considered electron-impact broadening parameters for Zr III spectral lines. Also, we present the electron-broadening widths for two astrophysically important UV Zr II lines. For six Zr II multiplets the electron-broadening widths and shifts were published in Popović & Dimitrijević (1996a). The zirconium lines are present in spectra of HgMn stars (Cowley & Aikman 1975; Heacox 1979; Leckrone et al. 1993; Sikström et al. 1999).

It is interesting that the zirconium abundance determination from weak Zr II optical lines and from strong Zr III lines (detected in UV) is quite different (see Leckrone et al. 1993; Sikström et al. 1999) in the HgMn star χ Lupi. This so-called "zirconium conflict" was supposed by Sikström et al. (1999) to be due to inadequate use of stellar models, e.g. if the influence of non-LTE effects or diffusion are not taken into account.

Zirconium, often overabundant in HgMn stars (see Heacox 1979), is one member of Sr-Y-Zr triad, which is vital for the study of *s*-process nucleosynthesis and has been suggested to represent a non-nuclear abundance pattern in HgMn stars. The most obvious interpretation of this anomaly involves diffusion theory or the inclusion of non-LTE effects.

Due to poor knowledge of the energy levels as well as the transition probabilities for singly- and doubly-ionized zirconium, the approximate methods are suitable for Stark broadening calculations.

Here, we present the results of electron-impact broadening parameter calculations of two astrophysically important Zr II and 34 Zr III lines. Also, we tested the influence of electron-impact broadening on the determination of equivalent widths and have discussed the possible

Send offprint requests to: L. Č. Popović,
e-mail: lpopovic@aob.bg.ac.yu

* Tables 1 and 2 are only available in electronic form at the CDS via anonymous ftp to cdsarc.u-strasbg.fr (130.79.128.5) or via
http://cdsweb.u-strasbg.fr/cgi-bin/qcat?J/A+A/365/656

influence of electron-impact broadening on zirconium abundance determination.

2. Method of calculation

We have applied the modified semiempirical approach – MSE (Dimitrijević & Konjević 1980; Dimitrijević & Kršljanin 1986), tested several times for complex spectra (see e.g. Popović & Dimitrijević 1996b,c, 1997). This method, applicable only for the Stark broadening of isolated, nonhydrogenic ion lines, has been described several times (Dimitrijević & Konjević 1980; Dimitrijević & Kršljanin 1986; Popović & Dimitrijević 1996b; Popović & Dimitrijević 1997)

Compared to the semiclassical perturbation approach, the modified semiempirical approach needs less atomic data. In fact, if there are no perturbing levels strongly violating the assumed approximation, we need only the energy levels with $\Delta n = 0$ and $\ell'_{\rm if} = \ell_{\rm if} \pm 1$, for e.g. the line width calculations, since all perturbing levels with $\Delta n \neq 0$, needed for a full semiclassical investigation, are lumped together and approximately estimated. E.g. for transition $5s^1D - 5p^1D^0$, the atomic energy levels needed explicitly as perturbing levels within the MSE formalism for the final energy level $5s^1D$ are the atomic energy levels $5p^1D^0$ ($E = 53\,648.88$ cm^{-1}), $5p^1P^0$ ($E = 62\,117.41$ cm^{-1}) and $5p^1F^0$ ($E = 62\,590.70$ cm^{-1}), while for the initial energy level $5p^1D^0$ we need the energy values for atomic energy levels $5s^1D$ ($E = 25\,068.35$ cm^{-1}), $5d^1F$ ($E = 103\,585.01$ cm^{-1}), $5d^1P$ ($E = 105\,554.66$ cm^{-1}) and $5d^1D$ ($E = 109\,272.70$ cm^{-1}). The perturbations by the other levels (with $\Delta n \neq 0$) are lumped together and estimated.

In the case of 30 Zr III transitions, it was possible to adequately use the MSE approach (Dimitrijević & Konjević 1980; Dimitrijević & Kršljanin 1986) and to calculate Stark widths (W – full width at half maximum) for the multiplet as a whole. For other transitions it was not possible to apply the MSE approach because of the lack of atomic data. In order to apply the MSE method (Dimitrijević & Konjević 1980), we must have reliable atomic energy data for the initial and final level of the transition forming the considered line. In addition, for each of the considered levels, we should have reliable data for the energy of levels with the same principal quantum number n and the orbital quantum numbers $\ell - 1$ and $\ell + 1$. Moreover, we should have good information concerning the levels with the principal quantum number different from that of the initial or final level, but which are close to the initial or final levels. These are required to check the validity of the assumed approximations and, if they are not satisfied, to take such levels into account separately. For the simple spectrum, the Stark broadening parameters of different lines are nearly the same within a multiplet (Wiese & Konjević 1982, 1992). Consequently, one may take the averaged atomic data for a multiplet as a whole and calculate the corresponding Stark widths. If the wavelength of a particular line within the multiplet differs significantly from the averaged wavelength $< \lambda >$ of the multiplet, one may obtain more accurate values for each line by scaling multiplet values for widths:

$$W_{\rm line} = \left(\frac{\lambda}{< \lambda >}\right)^2 \cdot W. \quad (1)$$

In the above expression, W and $< \lambda >$ are values for the multiplet, and $W_{\rm line}$ and λ refer to a particular line within the multiplet.

It is not always possible to apply this approximation to complex spectra. If irregularities of atomic energy level structure are present, forbidden and inter-combination transitions can influence different lines of the multiplet in different ways, and we have to calculate Stark broadening data for each line separately (Dimitrijević 1982; Popović & Dimitrijević 1997; Dimitrijević & Tankosić 2000). Such a situation occurred for two Zr II and four Zr III astrophysically important UV lines considered in our paper.

Atomic energy levels needed for the calculations have been taken from Reader & Acquista (1997) and oscillator strengths when available from Charro et al. (1999) and Sikström et al. (1999). In the paper of Reader & Acquista (1997) the spectrum of Zr III obtained with sliding spark discharges was observed from 630 Å to 4610 Å using the 10.7 m normal-incidence vacuum spectrograph. A total of 482 lines were classified as transitions between 139 energy levels. In their work, from the optimized energy level values, a system of Ritz-type wavelengths with uncertainties varying from about ±0.005 Å to ±0.003 Å was determined. From this paper, we obtained the determined energy level configurations and the values of the energy levels. In Charro et al. (1999) the oscillator strengths for the dipole-allowed transition in Zr III between the levels belonging to $4d^2$ and $4dn\ell$ configuration have been calculated using the relativistic quantum-defect orbital method. From this paper we obtained the oscillator strengths for matrix element calculations for $4d^2$–4d5p transitions. In Sikström et al. (1999), the lifetimes for the levels $v^2D_{3/2}$, $v^2F_{3/2}$ and $v^2F_{5/2}$ in the 4d5s5p configuration in Zr II have been measured, using the method of laser-induced fluorescence. Combined with branching fractions obtained with the Lund Ultraviolet Fourier Transform Spectrometer, experimental oscillator strengths also were derived. The estimated uncertainty in the obtained oscillator strengths is ±25% in lines with high observed intensities and no more than ±40% in the weakest line observed. From this paper we obtained the oscillator strengths for matrix element calculations for two Zr II lines considered. For other transitions, the matrix elements were calculated by the method of Bates & Damgaard (1949). The line and multiplet factors required were taken from Shore & Menzel (1968).

The accuracy of the MSE approximation is assumed to be about ±50% (Dimitrijević & Konjević 1980). In order to test the MSE method, Dimitrijević & Konjević (1980) selected experimental data for 36 multiplets (7 different ion species) of doubly-charged ions and 7 multiplets (4 different ion species) of triply-charged ions and compared

Table 3. The Stark widths (W) in rad s^{-1} per electron for $T = 10\,000$ K, and constants $A_{0,1}$ as described in the text

$<\lambda>$ (nm)	$\log A_0$	A_1	$\log W$
349.89	–3.4651	–0.5113	–5.5097
269.91	–3.3716	–0.5131	–5.4231
266.51	–3.4288	–0.5126	–5.4795
194.43	–3.3171	–0.4526	–5.1323
230.22	–3.2174	–0.4949	–5.1989
212.07	–3.2819	–0.4702	–5.1658
225.29	–3.2556	–0.4539	–5.0764
192.66	–3.2734	–0.4919	–5.2415
179.78	–3.3520	–0.4632	–5.2092
200.26	–3.2911	–0.4907	–5.2563
189.19	–3.3127	–0.4479	–5.1115
214.22	–3.3269	–0.4664	–5.1964
243.94	–3.2671	–0.4933	–5.2419
208.16	–3.3014	–0.4686	–5.1800
227.72	–3.2916	–0.4509	–5.1013
243.74	–3.4409	–0.5145	–5.4989
265.72	–3.4692	–0.5139	–5.5246
266.12	–3.4570	–0.5158	–5.5182
213.25	–3.2539	–0.4910	–5.2184
200.62	–3.3087	–0.4699	–5.1930
225.73	–3.2712	–0.5014	–5.2768
221.66	–3.2745	–0.4613	–5.1197
187.83	–3.3157	–0.4705	–5.2006
209.66	–3.2879	–0.5003	–5.2888
195.30	–3.3070	–0.4738	–5.2060
206.14	–3.2933	–0.4581	–5.1306
209.42	–3.2826	–0.5010	–5.2879
205.91	–3.2867	–0.4592	–5.1296
205.24	–3.2828	–0.4883	–5.2389
195.09	–3.2942	–0.4762	–5.2017

them with theoretical results. The averaged values of the ratios of measured to calculated widths are as follows: for doubly-charged ions 1.06±0.32 and for triply-charged ions 0.91±0.42. It was shown in Popović & Dimitrijević (1996c, 1998) that the MSE approach, even in the case of the emitters with very complex spectra (e.g. Xe II and Kr II), gives very good agreement with experimental measurements (in the interval ±30%). For example, for Xe II 6s−6p transitions, the averaged ratio between experimental and theoretical widths is 1.15±0.5 (Popović & Dimitrijević 1996c). In Kršljanin & Dimitrijević (1989) Stark shifts for 47 Ar II multiplets have been calculated within the framework of the MSE method and compared to selected (Konjević & Wiese 1976; Konjević et al. 1984) experimental data. Mean experimental-to-theoretical shift ratio of 1.26 ± 0.34 has been obtained. Generally, if the width and absolute shift values are comparable, the principal contributions to the shift will have the same sign and their accuracy will be similar. If the absolute shift values are considerably smaller (due to the mutual cancelations of important contributions with different signs), we assume that the error bars remain ±50% of the width value. The Stark shift data for Zr III are available upon request.

Table 4. Same as in the Table 3, but for two Zr II and four Zr III astrophysically important UV lines

	λ (nm)	$\log A_0$	A_1	$\log[W(\text{rad s}^{-1})]$
Zr II	193.85	–3.5886	–0.4223	–5.2864
Zr II	232.47	–4.0344	–0.4022	–5.6535
Zr III	193.725	–3.7247	–0.5198	–5.8025
Zr III	194.023	–3.7243	–0.5176	–5.7942
Zr III	194.105	–3.7055	–0.5189	–5.7799
Zr III	194.657	–3.7335	–0.5176	–5.8025

3. Results and discussion

The results of our calculations are presented in Tables 1 and 2 (accessible only in electronic form). In Table 1, the Stark widths calculated for a multiplet as a whole, and in Table 2 for particular lines within a multiplet, are given. The data are given for an electron density of 10^{23} m^{-3} and temperatures from 5 000 to 50 000 K. The electron-broadening data are a linear function of electron density. However, for higher densities, it is advisable to check whether the considered line is still isolated (Sahal-Bréchot 1969; Dimitrijević & Sahal-Bréchot 1984), as well as to verify the influence of Debye shielding (Griem 1974) and non-ideal plasma effects (Konjević & Uzelac 1990).

For the spectrum synthesis, it is convenient to use small numbers for the input parameters. We therefore have fitted each data set from Tables 1 and 2 with the expression (Popović et al. 1999):

$$\frac{W(\text{rad s}^{-1})}{N} = A_0 \cdot T^{A_1}, \tag{2}$$

where

$$W(\text{rad s}^{-1}) = \frac{W(\text{nm})}{\lambda(\text{nm})} \cdot \nu(\text{rad s}^{-1}),$$

and ν is the transition frequency. The parameters A_0 and A_1 as well as the Stark width $W(\text{rad s}^{-1})$ per electron for $T = 10\,000$ K are shown in Tables 3 and 4. In Eq. (2) W is a full width at half maximum (FWHM) expressed in rad s^{-1} per electron, and constants $A_{0,1}$ are determined numerically from the best fit. Equation (2) may be used to extrapolate toward higher temperatures. It is not advisable to extrapolate toward temperatures lower than those given in Tables 1 and 2 without checking the validity of the impact approximation. Moreover, at lower temperatures, the importance of quantum effects increases and the application of the MSE method (as well as the other semiclassical, classical or semiempirical methods which neglect quantum effects) becomes questionable.

We also have analyzed the influence of the electron-impact broadening mechanism on the equivalent width and consequently on the determination of zirconium abundance. We investigated the effect of the electron-impact broadening in the so-called "zirconium conflict" in the HgMn star χ Lupi. In order to test the importance of the electron-impact broadening effect in determinations of zirconium abundance, we synthesized the line profiles of Zr II (λ = 193.8 nm and λ = 232.5 nm) and Zr III

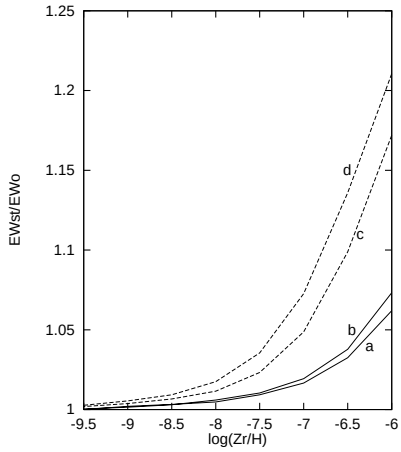

Fig. 1. The ratio of equivalent widths of: **a)** Zr II [232.5 nm], **b)** Zr II [193.85 nm], **c)** Zr III [194.1 nm] and **d)** Zr III [194.0 nm] lines calculated with Stark broadening effect ($EW_{\rm St}$) and without (EW) as a function of zirconium abundance

($\lambda = 194.02$ nm and $\lambda = 194.10$ nm) using SYNTH code (Piskunov 1992) where the LTE conditions are assumed and the Kurucz's ATLAS9 code for a model of stellar atmosphere (Kurucz 1993) ($T_{\rm eff} = 10\,000$ K and $\log g = 4.0$), i.e. with the stellar models with similar characteristics as those of χ Lupi ($T_{\rm eff} = 10\,650$ K and $\log g = 3.8$, see e.g. Leckrone et al. 1999). We have modified the SYNTH code, which uses $\log W(\,{\rm rad\,s^{-1}})$ per electron for $T = 10\,000$ K as an input parameter, replacing it with the two parameters: A_0 and A_1 from Eq. (2) (see Popović et al. 1999). We chose these lines because they have been commonly used for abundance determination, as they have a small wavelength displacement and are well resolved (Leckrone et al. 1993).

We have calculated the equivalent widths with and without the electron-impact broadening effect for different abundances of zirconium. The ratio of equivalent widths for the Zr II and Zr III lines considered here, calculated with and without the electron-impact broadening effect is presented in Fig. 1. As one can see from Fig. 1, the electron-broadening effect is more important in the case of higher abundances of zirconium. The equivalent width increases with abundances for both lines, but the equivalent widths for Zr III lines are more sensitive than Zr II lines. This may cause an error in abundance determination in cases where the electron-impact broadening effect is not taken into account. In any case, synthesizing of these two lines in order to measure the zirconium abundance without taking into account the electron-impact widths will result in Zr III lines suggesting an abundance of zirconium higher than that obtained with the Zr II lines. However, this effect is less than one order of magnitude of the abundance.

Although the "zirconium conflict" in the HgMn star χ Lupi cannot be explained only by this effect, one should be aware that the electron-impact broadening effect may cause errors in abundance determination.

In the case of Zr II and Zr III there are no measured Stark broadening data. Moreover, for Zr III there are no previously published theoretical electron-impact broadening parameters. We hope that the Stark broadening data presented here, as well as consideration of the influence of the electron-impact broadening mechanism on abundance determination will be of interest not only for consideration of "zirconium conflict" but also for different problems in astrophysical and physical plasma investigation and modeling.

Acknowledgements. This work was supported by the Ministry of Science and Technology of Serbia through the project "Astrometrical, Astrodynamical and Astrophysical Researches" and by the Federal Ministry of Development, Sciences and Environment Protection of Yugoslavia.

References

Bates, D. R., & Damgaard A. 1949, Phil. Trans. Roy. Soc. London, Ser. A, 242, 101
Charro, E., López-Ayuso, J. L., & Martin, I. 1999, J. Phys. B, 32, 4555
Cowley, C. R., & Aikman, G. C. L. 1975 ApJ, 196, 521
Dimitrijević, M. S. 1982, A&A, 112 251
Dimitrijević, M. S., & Konjević, N. 1980, JQSRT, 24, 451
Dimitrijević, M. S., & Kršljanin, V. 1986, A&A, 165, 269
Dimitrijević, M. S., & Sahal-Bréchot 1984, JQSRT, 31, 301
Dimitrijević, M. S., & Tankosić, D. 2000, Phys. Scr., 62, 177
Griem, H. R. 1974, Spectral Line Broadening by Plasmas (Academic Press, New York)
Heacox, W. D. 1979, ApJS, 41, 675
Konjević, N., Dimitrijević, M. S., & Wiese, W. L. 1984, J. Phys. Chem. Ref. Data, 13, 649
Konjević, N., & Uzelac, N. J. 1990, JQSRT, 44, 61
Konjević, N., & Wiese, W. L. 1976, J. Phys. Chem. Ref. Data, 5, 259
Kršljanin, V., & Dimitrijević, M. S. 1989, Z. Phys. D, 14, 273
Kurucz, R. L. 1993, Model atmosphere program ATLAS9 published on CDROM13
Leckrone, D. S., Proffitt, C. R., Wahlgren, G. M., Johansson, S. G., & Brage, T. 1999, AJ, 117, 1454L
Leckrone, D. S., Wahlgren, G. M., Johansson, S. G., & Adelman, S. J., 1993, in ASP Conf. Ser. 44, Peculiar Versus Normal Phenomena in A-Type and Related Stars, ed. M. M. Dworetsky, F. Castelli, & R. Faraggiana, 42
Michaud, G., & Richter, J. 1997, in Spectral Line Shapes, ed. M. Zoppi, & L. Ulivi, 9, 397
Piskunov, N. E. 1992, in Stellar magnetism, ed. Yu. V. Glagolevskij, & I. I. Romanyuk (Nauka, St. Petersburg), 92
Popović, L. Č., & Dimitrijević, M. S. 1996a, A&AS, 120, 373
Popović, L. Č., & Dimitrijević, M. S. 1996b, Phys. Scr., 53, 325
Popović, L. Č., & Dimitrijević, M. S. 1996c, A&AS, 116, 359
Popović, L. Č., & Dimitrijević, M. S. 1997, in The Physics of Ionized Gas, ed. B. Vujičić, S. Djurović, & J. Purić, Institute of Physics, Novi Sad, 477
Popović, L. Č., & Dimitrijević, M. S. 1998, A&AS, 127, 295
Popović, L. Č., Dimitrijević, M. S., & Ryabchikova, T. 1999, A&A, 350, 719.
Reader, J., & Acquista, N. 1997, Phys. Scr., 55, 310
Sahal-Bréchot, S. 1969, A&A, 1, 91
Sikström, C. M., Lundberg, H., Wahlgren, G. M., et al. 1999, A&A, 343, 297
Shore, B. W., & Menzel, D. H. 1968, ApJ, 12, 187
Wiese, W. L., & Konjević, N. 1982, JQSRT, 28, 185
Wiese, W. L., & Konjević, N. 1992, JQSRT, 47, 185

A&A 371, 354–359 (2001)
DOI: 10.1051/0004-6361:20010343
© ESO 2001

Astronomy & Astrophysics

Stark broadening in O III spectrum

A. Srećković[1], M. S. Dimitrijević[2], and S. Djeniže[1]

[1] Faculty of Physics[1], University of Belgrade, 11001 Belgrade, POBOX 368, Serbia, Yugoslavia
[2] Astronomical Observatory[2], 11001 Belgrade, Volgina 7, Serbia, Yugoslavia

Received 18 December 2000 / Accepted 20 February 2001

Abstract. The Stark widths and shifts of 7 doubly ionized oxygen (O III) spectral lines, in five multiplets, have been measured at electron densities between 1.66 10^{23} m^{-3} and 2.80 10^{23} m^{-3} and electron temperatures between 17 000 K and 54 000 K in a linear pulsed-arc discharge in N_2+ O_2 and CO_2 plasmas. The above mentioned species have been calculated using the semiclassical perturbation formalism. Our measured and calculated Stark width and shift values have been compared to the existing calculated and experimental data.

Key words. lines: profiles – atomic data

1. Introduction

Interest for the doubly ionized oxygen (O III) spectral lines is in recent years increasing in astrophysics because they are found in the spectra emitted by various kinds of cosmic light sources. In a recent publication by Nelson (2000) it was found that a relationship exists between nuclear black hole mass ($M_{\rm bh}$) and the O III spectral line widths for active galactic nuclei (AGNs). In their work, Cuesta & Phillips (2000) report on observations of the planetary nebula NGC 2440 in the transition O III (436.3 nm and 500.7 nm). Sako et al. (2000) present a preliminary analysis of the first high-resolution X-ray spectrum of a Seyfert 2 galaxy (Markarian 3) and notice that the soft X-ray emission is spatially extended along the O III ionization cone. Measurements of O III emission in Lyman-break galaxies (LBGs) have been presented by Teplitz et al. (2000) where the 500.7 nm line emission characteristics are used to estimate the star formation rate (SFR) of the LBGs. del Burgo et al. (2000) have discovered O III (495.9 nm and 500.7 nm) emission in the inner circumnuclear region of the M 31. Furthermore, the O III spectral line characteristics have been used in order to find nebular chemical abundances (Oey & Shields 2000; Dopita et al. 2000; Dopita & Sutherland 2000).

Therefore, the knowledge of the O III spectral line widths and shifts is of interest. If the Stark broadening is the principal pressure-broadening mechanism in plasmas, as e.g. for A and B type stars and white dwarfs, it is possible to obtain the other basic plasma parameters (Griem 1974, 1997) essential in the modelling of various plasma compositions and kinetic processes (Lesage 1994; Zeippen 1995) on the basis of the Stark width and shift values.

From the first experimental measurement of displacements of O III lines (Pretty 1931), Stark broadening parameters of O III lines have been measured several times (Platiša et al. 1975; Purić et al. 1988a,b; Blagojević et al. 2000). Theoretically, Stark broadening of O III lines has been investigated by Subrahmaniam (1968), Hey & Bryan (1977), Dimitrijević & Konjević (1980, 1981, 1987), Hey & Breger (1980, 1981) and Dimitrijević (1981, 1988a,b).

We have measured and calculated Stark $FWHM$ (full-width at half intensity maximum, W) and shift (d) of 7 O III spectral lines that belong to the wavelength range of interest for astrophysical observations. These belong to three transitions in 5 multiplets. Stark widths of 3 lines (334.07, 407.39 and 444.78 nm) have not been measured before (Lesage & Fuhr 1999). Stark shift values have been measured in only one experiment (Purić et al. 1988b). Thus, our five d data have not been measured before. We have calculated W and d values using the known semiclassical perturbation formalism (SCPF) (Sahal-Bréchot 1969a,b) updated several times (Sahal-Bréchot 1974; Fleurier et al. 1977; Dimitrijević & Sahal-Bréchot 1984; Dimitrijević et al. 1991; Dimitrijević & Sahal-Bréchot 1996b). It should be pointed out that for the O III lines Stark shifts no theoretical predictions exist (Lesage & Fuhr 1999 and references therein).

Send offprint requests to: S. Djeniže,
e-mail: steva@ff.bg.ac.yu

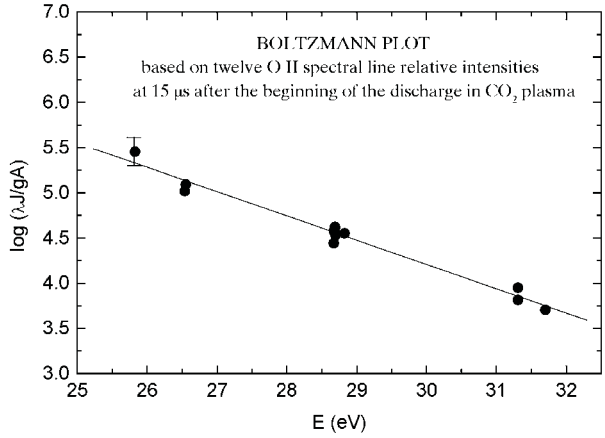

Fig. 1. Boltzmann plot in the CO_2 plasma

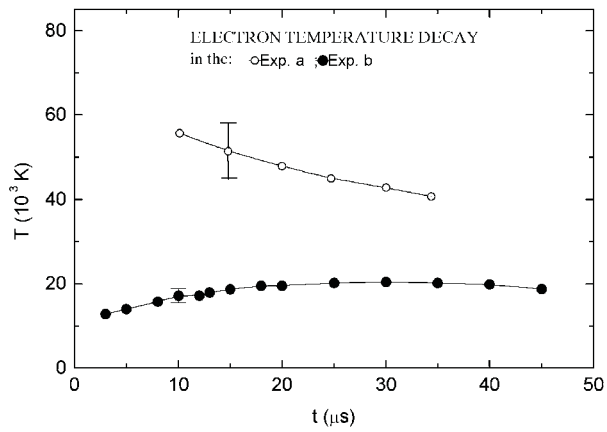

Fig. 2. Temporal evolution of the electron temperature (T) in the two different plasma compositions

Our measured and calculated W values have been compared with existing theoretical (Hey & Bryan 1977; Dimitrijević & Konjević 1981), experimental (Platiša et al. 1975; Purić et al. 1988a; Blagojević et al. 2000) and estimated values (Djeniže et al. 1990; Djeniže & Labat 1996; Djeniže 2000). Latest values are obtained on the basis of the regularities of the Stark widths found along the oxygen isonuclear sequences.

2. Experiment

A modified version of the linear-low pressure pulsed arc (Djeniže et al. 1992, 1998) has been used as a plasma source at two different discharge conditions. A pulsed discharge was driven in a quartz discharge tube of 5 mm inner diameter and effective plasma lengths of 5.8 cm and 6.3 cm (Fig. 1 in Djeniže et al. 1998). The tube has end-on quartz windows. On the opposite side of the electrodes the glass tube was expanded in order to reduce erosion of the glass wall and also sputtering of the electrode material onto the quartz windows. The working gas was a nitrogen-oxygen mixture (83% N_2 + 17% O_2) at 70 Pa filling pressure (Experiment a) and CO_2 at 133 Pa

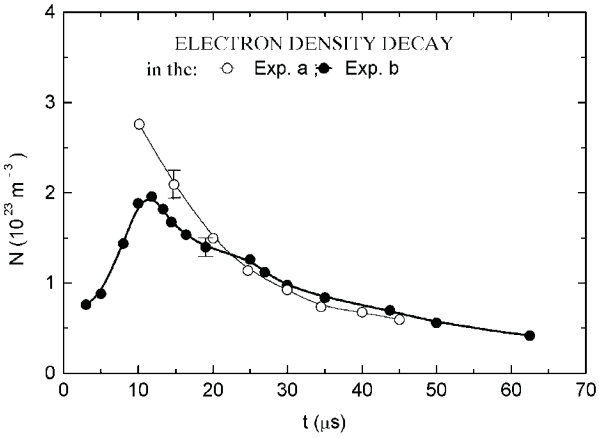

Fig. 3. Temporal evolution of the electron density (N) in the two different plasma compositions

filling pressure (Experiment b) with a constant flux flowing regime. The chosen flux and pressure provide minimal self-absorption of the investigated spectral lines. Spectroscopic observation of isolated spectral lines were made end-on along the axis of the discharge tube. A capacitor of 14 μF was charged up to 3.0 kV and 2.8 kV, in experiments a and b, respectively. The line profiles were recorded using a step-by-step technique with a photomultiplier (EMI 9789 QB) and a grating spectrograph (Zeiss PGS-2, reciprocal linear dispersion 0.73 nm/mm in the first order) system. The system was calibrated by using the EOA-101 standard lamp. The instrumental $FWHM$ of 0.008 nm was determined by narrow spectral lines emitted from the hollow cathode discharge. The spectrograph exit slit (10 μm) with the calibrated photomultiplier was micrometrically moved along the spectral plane in small wavelength steps (0.0073 nm). The photomultiplier signal was digitalized and averaged (five shots at each position) using an oscilloscope interfaced to a computer. Total line intensity (I) corresponds to the area under the line profile.

Plasma reproducibility was monitored by the O II and O III lines and, also, by the discharge current using the Rogowski coil signal (it was found that the signal is reproducible within ±3%).

The plasma parameters were determined using standard diagnostic methods (Rompe & Steenbeck 1967). Thus, in the case of the Exp. b, the electron temperature was determined from the Boltzmann plot of twelve O II lines (394.505; 395.437; 407.216; 407.587; 407.886; 408.512; 409.294; 408.716; 413.281; 432.577; 418.546; 418.979 nm) within an energy interval of 5.88 eV for corresponding upper-levels with an estimated error within ±5%, assuming the existence of LTE, according to criterion from Griem (1974). The Boltzmann plot, as an example, obtained at 15 μs after the beginning of the discharge is presented in Fig. 1. In the case of Exp. a, the electron temperature was determined from the ratios of the relative intensities of 348.49 nm N IV to 393.85 nm N III and the previous N III to the 399.50 nm N II spectral line,

assuming the existence of LTE, with an estimated error of ±12%. The necessary atomic data were taken from the available literature (Wiese et al. 1966; Lide 1994; NIST 2000; Kurucz 2000). Forms of the electron temperature decays are presented in Fig 2.

The electron density decay was measured using a well-established single laser interferometry technique (Ashby et al. 1965) for the 632.8 nm He-Ne laser wavelength with an estimated error of ±5%. The electron density decays are presented in Fig. 3.

3. Stark widths and shifts measurements

The measured profiles were of the Voigt type due to the convolutions of the Lorentzian Stark and Gaussian profiles caused by Doppler and instrumental broadening. For the electron density and temperature in our experiments, the Lorentzian fraction was dominant (over 87%). van der Waals (Griem 1974) and resonance (Griem 1974) broadening were estimated to be smaller by more than one order of magnitude in comparison to Stark, Doppler and instrumental broadening. The standard deconvolution procedure (Davies & Vaughan 1963) was computed using the least squares algorithm. The Stark widths were measured with ±12% error. Great care was taken to minimize the influence of self-absorption on Stark width determination. The opacity was checked by measuring relative line intensity ratios within the multiplet No. 2 during the plasma decay. The obtained values were compared with calculated ratios of the products of the spontaneous emission probabilities (A) and the corresponding statistical weights (g) of the upper levels of the lines. The necessary atomic data were taken from Wiese et al. (1966), Lide (1994) and NIST (2000). It turns out that the experimental relative line intensity ratios are constant during the whole plasma decay period, testifying to the absence of self-absorption and agree, within ±11% accuracy, with calculated relative intensity ratio values.

The Stark shifts were measured using the well-known method based on the line center position observations during the whole plasma decay period (Djeniže et al. 1998 and references therein). The Stark shift data were corrected for the electron temperature decay (Popović et al. 1992). Stark shift data are determined with a ±0.0008 nm error at a given N and T.

4. Method of calculation

The semiclassical perturbation formalism, as well as the corresponding computer code (Sahal-Bréchot 1969a,b), have been updated and optimized several times (Sahal-Bréchot 1974; Fleurier et al. 1977; Dimitrijević & Sahal-Bréchot 1984; Dimitrijević et al. 1991; Dimitrijević & Sahal-Bréchot 1996b). The calculation procedure, with the discussion of updatings and validity criteria, has been briefly reviewed e.g. in Dimitrijević & Sahal-Bréchot (1996a,b) so that only the basic details of calculations will be presented here. Stark full width (W) at the intensity half maximum ($FWHM$) and shift (d) of an isolated spectral line may be expressed as (Sahal-Bréchot 1996a,b; Fleurier et al. 1977):

$$W = N \int v f(v) \mathrm{d}v \Big(\sum_{i' \neq i} \sigma_{ii'}(v) + \sum_{f' \neq f} \sigma_{ff'}(v) + \sigma_{\mathrm{el}}\Big) + W_{\mathrm{R}}$$
$$d = N \int v f(v) \mathrm{d}v \int_{R_3}^{R_D} 2\pi\rho \mathrm{d}\rho \sin 2\phi_{\mathrm{p}} \quad (1)$$

where N is the electron density, $f(v)$ the Maxwellian velocity distribution function for electrons, ρ denotes the impact parameter of the incoming electron, i and f denote the initial and final atomic energy levels, and i', f' their corresponding perturber levels, while W_{R} gives the contribution of the Feshbach resonances (Fleurier et al. 1977). The inelastic cross section $\sigma_{j,j'}(v)$ can be expressed by an integral over the impact parameter of the transition probability $P_{jj'}(\rho, v)$ as

$$\sum_{j' \neq j} \sigma_{jj'}(v) = \frac{1}{2}\pi {R_1}^2 + \int_{R_1}^{R_{\mathrm{D}}} \sum_{j \neq j'} P_{jj'}(\rho, v), j = i, f \quad (2)$$

and the elastic cross section is given by

$$\sigma_{\mathrm{el}} = 2\pi R_2^2 + \int_{R_2}^{R_{\mathrm{D}}} 8\pi\rho \mathrm{d}\rho \sin^2 \delta$$
$$\delta = (\phi_{\mathrm{p}}^2 + \phi_{\mathrm{q}}^2)^{1/2}. \quad (3)$$

The phase shifts ϕ_{p} and ϕ_{q} due respectively to the polarization potential (r^{-4}) and to the quadrupolar potential (r^{-3}), are given in Sect. 3 of Chap. 2 in Sahal-Bréchot (1969a). R_{D} is the Debye radius. All the cut-offs R_1, R_2, R_3 are described in Sect. 1 of Chap. 3 in Sahal-Bréchot (1969b). For electrons, hyperbolic paths due to the attractive Coulomb force were used, while for perturbing ions the paths are different since the force is repulsive. The formulae for the ion-impact widths and shifts are analogous to Eqs. (1–3), without the resonance contribution to the width. The difference in calculation of the corresponding transition probabilities and phase shifts as functions of the impact parameter in Eqs. (2) and (3) is in the ion perturber trajectories which are influenced by the repulsive Coulomb force, instead of an attractive one as for electrons. Atomic energy levels have been taken from Moore (1985).

The contribution of ion impact widths and shifts to the total line widths and shifts can be neglected since our results for $T = 20\,000$ K are two order of magnitude smaller.

5. Results

Our measured Stark $FWHM$ (W_{m}) and shift (d_{m}) values at various electron temperatures (T) and densities (N) together with other authors data are given in Table 1.

Table 1. Measured Stark $FWHM$ (W_{m}) and shift (d_{m}) values for the O III spectral lines at observed electron temperatures (T) and densities (N). a, this work; b, Platiša et al. (1975); c, Purić et al. (1988a); d, Purić et al. (1988b) and e, Blagojević et al. (2000). $W_{\mathrm{m}}/W_{\mathrm{th}}$ represents the ratio between measured and our calculated (SCPF) values taken from Table 2

Transition	Multiplet	λ (nm)	T (10^4 K)	N (10^{23} m^{-3})	W_{m} (pm)	d_{m} (pm)	$W_{\mathrm{m}}/W_{\mathrm{th}}$	Ref.
2p3s − 2p (^{2}P^0) 3p	^{3}P^0−^{3}D (2)	375.47	5.40	2.80	38	0.0	0.85	a
			2.59	0.52	7.6		0.69	b
			1.83−1.99	0.33−0.47	7.5−9.1		0.87−0.78	e
		375.72	5.40	2.80	40	0.0	0.90	a
	^{3}P^0−^{3} S (3)	334.07	5.40	2.80	26	0.0	0.74	a
	^{1}P^0−^{1} D (6)	298.38	1.70	1.87	39.6		1.12	a
			1.78	1.96	39.4		1.10	a
			1.83	1.82	38.9		1.19	a
			1.90	1.66	38.0	0.9	1.33	a
			5.40	2.80	34.0	0.0	1.10	a
			4.25	2.18	27.4	0.0	1.07	c,d
2s2p^{2}3s′−2s2p^2(^{4}P)3p′	^{3}P−^{3}D^0 (23)	407.39	1.83	1.82	52.2		0.84	a
			1.90	1.66	51.2		0.84	a
		408.11	1.70	1.78	53.2		0.84	a
			1.78	1.96	57.1		0.84	a
			1.83	1.82	58.9		0.95	a
			1.90	1.66	59.7	−1.3	1.10	a
			4.25	2.18	59.0	0.0	1.17	c,d
2p^{2}3p′−2p^{2}3d′	^{3}S^0−^{3}P (33)	444.78	5.40	2.80	94.0	0.0	1.32	a

Our calculated W and d data at 10^{23} m^{-3} electron density are given in Table 2 for the mean wavelength $< \lambda >$ in the multiplet. The width and shift of each multiplet component can by easily evaluated if one takes into account that the W and d are proportional to λ^2.

6. Discussion

In order to compare measured and calculated Stark $FWHM$ and shift values, the theoretical Stark $FWHM$ and shift dependences on the electron temperature, together with the values of other authors and our experimental results, at an electron density of 10^{23} m^{-3} are presented graphically in Figs. 4 and 5.

The first O III W values were calculated on the basis of various approximations initiated by Griem (1974); Hey & Bryan (1977) and Dimitrijević & Konjević (1980). Thus, SE and SEM denote the results of semi-empirical (Griem 1968) and modified semi-empirical predictions using Eqs. (4), (5) and Eqs. (7)–(10), respectively from Dimitrijević & Konjević (1981). G and GM denote W values obtained on the basis of the simplified semiclassical method (Griem 1974). For the GM values the low temperature part is modified (Dimitrijević & Konjević 1980). The estimated W values, based on the obtained regularities of the Stark $FWHM$ along an oxygen isonuclear sequences (INS), have been taken from Djeniže (1990, 1996, 2000).

On the basis of the Tables 1, 2, and Fig. 4 one can conclude that our measured (W_{m}) and calculated (SCPF) Stark $FWHM$ values are in satisfactory mutual agreement (within ±13% in average). We notice, also, fair agreement between W_{m} and W_{G} and W_{INS} values. Values W measured earlier (Purić et al. 1988a; Blagojević et al. 2000) agree, also, with W_{SCPF}, W_{G} and W_{INS} calculated values within the accuracy of experiments (up to ±15%) and uncertainties of the approximations (up to ±30%).

Our calculated Stark shift values are small and have a negative sign. The measured d_{m} values are, in most of the cases (see Table 2), equal to zero. The only exception is the 408.11 nm O III line which we have measured and, also, it has a calculated shift different from zero. It turns out that the calculated d values of the particular wavelengths are approximately constant over a wide range of the electron temperatures from 20 000 K up to 500 000 K.

7. Conclusion

We have found very good agreement (within ±10%) between measured, calculated and estimated Stark $FWHM$ values in the cases of the O III wavelengths that belong to the multiplets Nos. 2, 6 and 23. These facts allow us to

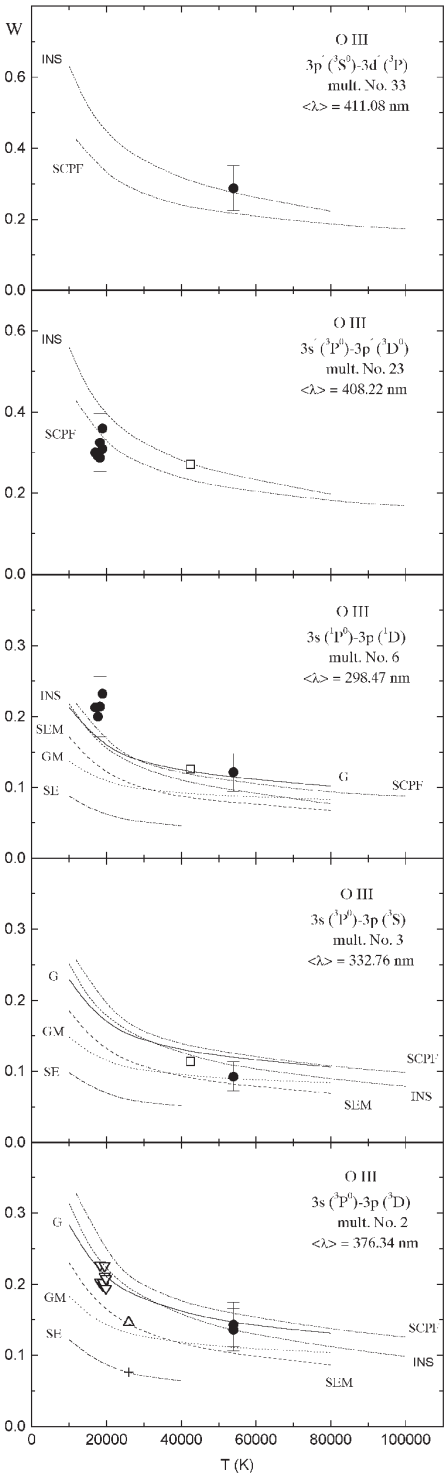

Fig. 4. Stark $FWHM$ (W in 0.1 nm) dependence on the electron temperature (T) for the most investigated O III spectral lines belonging to various transitions at 10^{23} m^{-3} electron density. SCPF, our calculations by using the semiclassical perturbation formalism. •, our experimental results and those of other authors: △, Platiša et al. (1975); □, Purić et al. (1988a); ▽, Blagojević et al. (2000). SE, SEM, G and GM denote theoretical W values (see text). +, calculations by Hey & Bryan (1977). INS denote estimated W values (Djeniže et al. 1990; Djeniže & Labat 1996; Djeniže 2000). The error bars include the uncertanties of the width and electron density measurements. $< \lambda >$ is the mean wavelength in the multiplet

Table 2. Electron Stark $FWHM$ (W in pm) and shift (d in pm) calculated by using the semiclassical perturbation formalism (SCPF) (Eqs. (1)–(3)) at 10^{23} m^{-3} electron density and various electron temperatures (T in 10^4 K). $< \lambda >$ is the mean wavelength (in nm) in the multiplet. Negative shift is toward the blue

Transition	Multiplet	$< \lambda >$	T	W	d
2p3s−	^{3}P^0−^{3}D	376.34	1	34.6	−0.280
2p(^{2}P^0)3p	(2)		2	24.6	−0.572
			5	16.2	−0.502
			10	12.6	−0.639
			20	10.2	−0.572
			30	9.18	−0.554
			50	8.12	−0.532
	^{3}P^0−^{3}S	332.76	1	27.1	−0.192
	(3)		2	19.3	−0.396
			5	12.8	−0.345
			10	9.90	−0.436
			20	8.06	−0.394
			30	7.26	−0.383
			50	6.44	−0.369
	^{1}P^0−^{1}D	298.47	1	23.1	−0.127
	(6)		2	16.6	−0.141
			5	11.2	−0.198
			10	8.81	−0.229
			20	7.25	−0.229
			30	6.56	−0.228
			50	5.83	−0.214
2s2p^{2}3s′−	^{3}P−^{3}D^0	408.22	1	45.2	−0.778
2s2p^2(^{4}P)3p′	(23)		2	32.1	−0.906
			5	21.5	−0.873
			10	16.9	−0.982
			20	13.8	−0.924
			30	12.4	−0.891
			50	11.0	−0.840
2p^{2}3p′−	^{3}S^0−^{3}P	411.08	1	44.9	0.072
2p^{2}3d′	(33)		2	32.5	−0.608
			5	22.0	−0.464
			10	17.3	−0.684
			20	14.2	−0.511
			30	12.9	−0.492
			50	11.6	−0.470

recommend these lines (375.47 nm, 375.72 nm, 298.38 nm; 407.39 nm and 408.11 nm) for plasma diagnostics as lines with convenient Stark $FWHM$ data. Because the found Stark shift values are very small, and show negligible dependence on the electron temperature, these can be used, also, for diagnostic purposes as data independent of the self-absorption in the optically thick astrophysical plasmas.

Acknowledgements. This work is a part of the project "Astrometrical, Astrodynamical and Astrophysical Investigations", supported by the Ministry of Science and Technology of the Republic of Serbia.

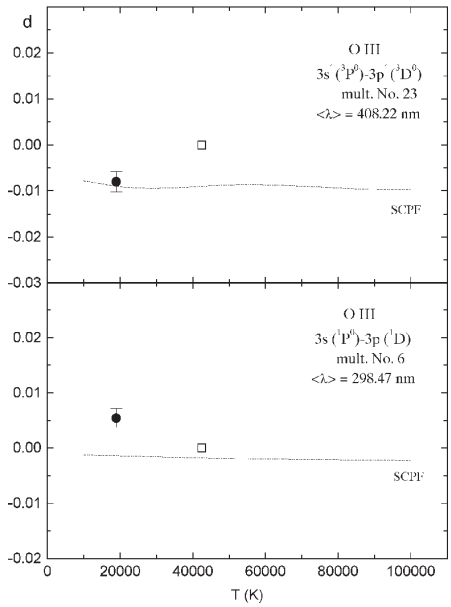

Fig. 5. Stark shift (d in 0.1 nm) dependence on the electron temperature (T) for the O III spectral lines belonging to various transitions at 10^{23} m^{-3} electron density. SCPF, our calculations by using the semiclassical perturbation formalism. •, our experimental results and those of other authors: □, Purić et al. (1988b). The error bars include the uncertanties of the shift and electron density measurements. $< \lambda >$ is the mean wavelength in the multiplet

References

Ashby, D. E. T. F., Jephcott, D. F., Malein, A., & Raynor, F. A. 1965, Appl. Phys., 36, 29

Blagojević, B., Popović, M. V., & Konjević, N. 2000, JQSRT, 67, 9

Cuesta, L., & Phillips, J. P. 2000, ApJ, 543, 754

Davies, J. I., & Vaughan, J. M. 1963, ApJ, 137, 1302

del Burgo, C., Mediavilla, E., & Arribas, S. 2000, ApJ, 540, 741

Dimitrijević, M .S., & Konjević, N. 1980, JQSRT, 24, 451

Dimitrijević, M. S. 1981, Publ. Astron. Obs. Sarajevo, 1, 215

Dimitrijević, M. S., & Konjević, N. 1981, in Spectral Line Shapes, vol. 1, ed. B. Wende (Walter de Gruyter, & Co., New York), 211

Dimitrijević, M. S., & Sahal-Bréchot, S. 1984, JQSRT, 31, 301

Dimitrijević, M. S., & Konjević, N. 1987, A&A, 172, 345

Dimitrijević, M. S. 1988a, A&AS, 76, 53

Dimitrijević, M. S. 1988b, Bull. Astron. Belgrade, 139, 31

Dimitrijević, M. S., Sahal-Bréchot, S., & Bommier, V. 1991, A&AS, 89, 581

Dimitrijević, M. S., & Sahal-Bréchot, S. 1996a, A&AS, 119, 369

Dimitrijević, M. S., & Sahal-Bréchot, S. 1996b, Phys. Scr., 54, 50

Djeniže, S., Labat, J., Platiša, M., Srećković, A., & Purić, J. 1990, A&A, 227, 291

Djeniže, S., Srećković, A., & Labat, J. 1992, A&A, 253, 632

Djeniže, S., & Labat, J. 1996, Bull. Astron. Belgrade, 153, 35

Djeniže, S., Milosavljević, V., & Srećković, A. 1998, JQSRT, 59, 71

Djeniže, S. 2000, Phys. Scr., 61, 412

Dopita, M. A., & Sutherland, R. S. 2000, ApJ, 539, 742

Dopita, M. A., Kewley, L. J., Heisler, C. A., & Sutherland, R. S. 2000, ApJ, 542, 224

Fleurier, C., Sahal-Bréchot, S., & Chapelle, J. 1977, JQSRT, 17, 595

Griem, H. R. 1968, Phys. Rev., 165, 258

Griem, H. R. 1974, Spectral Line Broadening by Plasmas (Academic Press, New York)

Griem, H. R. 1997 Principles of Plasma Spectroscopy (Cambridge University Press, Cambridge)

Hey, J. D., & Bryan, R. J. 1977, JQSRT, 17, 221

Hey, J. D., & Breger, P. 1980, JQSRT, 24, 349

Hey, J. D., & Breger, P. 1981, in Spectral Line Shapes, vol. 1, ed. B. Wende (Walter de Gruyter, & Co., New York), 201.

Kurucz, R. L. 2000, Harward-Smitshonian Center for Astrophysics, CDRom-23

Lesage, A. 1994, Proc. of the XXIInd General Assembly of the International Astronomical Union la Haie

Lesage, A., & Fuhr, J. R. 1999, Bibliography of Atomic Line Shapes and Shifts (April 1992 through June 1999), Observatoire de Paris

Lide, D. R. 1994 (Editor-in-Chief), CRC Handbook of Chemistry and Physics, 74th edition (CRC Press, Boca Raton, USA)

Moore, C. E. 1985, Selected Tables of Atomic Spectra, A.Atomic Energy Levels-II.nd ed.; B. Multiplet Table; O III, U.S. Department of Commerce, NBS

Nelson, Ch. H. 2000, ApJ, 544, L91

NIST-Atomic Spectra Database Lines Data, 2000, (Wavelengths ordered), `http://nist.search.html`

Oey, M. S., & Shields J. C. 2000, ApJ, 539, 687

Platiša, M., Popović, M. V., & Konjević, N. 1975, A&A, 45, 325

Popović, L. Č., Srećković, A., & Djeniže, S. 1992, Proc. of the 11th ICSLS, A25, Carry le Rouet, France

Pretty, W. E. 1931, Proc. Phys. Soc. London, 43, 279

Purić, J., Djeniže, S., Srećković, A., Platiša, M., & Labat, J. 1988a, Phys. Rev. A, 37, 498

Purić, J., Djeniže, S., Srećković, A., et al. 1988b, Proc. of the 14th SPIG, ed. N. Konjević, L. Tanović, & N. Tanović, Sarajevo, Yugoslavia, 345

Rompe, R., & Steenbeck, M. 1967, Ergebnisse der Plasmaphysik und der Gaselektronik, Band 1 (Berlin: Akademie Verlag)

Sahal-Bréchot, S. 1969a, A&A, 1, 91

Sahal-Bréchot, S. 1969b, A&A, 2, 322

Sahal-Bréchot, S. 1974, A&A, 35, 321

Sako, M., Kahn, S. M., Paerels, F., & Liedahl, D. A. 2000, ApJ, 543, L115

Subrahmaniam, P. 1968, MNRAS, 140, 1

Teplitz, H. I., et al. 2000, ApJ, 542, 18

Wiese, W. L, Smith, M. W., & Glennon, B. M. 1966, Atomic Transition Probabilities, NSRDS NBS 4, vol. 1 (Washington DC: US Govt. Printing Office)

Zeippen, C. J. 1995, Phys. Scr., 58, 43

A&A 382, 359–367 (2002)
DOI: 10.1051/0004-6361:20011549
© ESO 2002

Astronomy & Astrophysics

Stark shifts and transition probabilities in the Ne II spectrum

S. Djeniže[1,3], V. Milosavljević[1], and M. S. Dimitrijević[2]

[1] Faculty of Physics, University of Belgrade, PO Box 368, Belgrade, Serbia, Yugoslavia
[2] Astronomical Observatory, Belgrade, Volgina 7, Serbia, Yugoslavia
[3] Hungarian Academy of Science, Budapest, Hungary

Received 13 June 2001 / Accepted 2 November 2001

Abstract. Stark shifts (d) and transition probabilities of the spontaneous emission (Einstein's A values) of forty two singly charged neon (Ne II) ion spectral lines have been measured in a linear, low pressure, pulsed arc at 35 300 K electron temperature and 1.83×10^{23} m^{-3} electron density. Transition probabilities have been obtained using the relative line intensity ratio (RLIR) method. Stark shift values have also been calculated, using the semiclassical perturbation formalism (SCPF). The measured and calculated shift values and the measured A values have been compared to the existing data taken from available data sources.

Key words. atomic data – radiation mechanisms: general – methods: laboratory

1. Introduction

Atomic data such as Stark widths (W) and shifts (d) and transition probabilities (A) play an important role in the diagnostics and modelling of various cosmic and laboratory plasmas (Griem 1964; Wiese 1968; Rompe & Steenbeck 1967; Griem 1974; Wiese et al. 1966; Griem 1997). The basic plasma parameters such as electron temperature (T) and density (N) may be obtained on the basis of the known d and W values. However, various optical depths of the emitting plasma may result in self-absorption influencing the line width value (screening the Stark contribution). Thus, Stark shifts independent of self-absorption are more reliable and consequently more interesting for diagnostic purposes. On the other hand, various kinetic processes appearing in plasma modelling require reliable knowledge of the A values (Griem 1997; Lesage & Fuhr 1999; Zeippen 1995). Furthermore, knowledge of the A values gives the possibility to determine the (B) coefficients which characterize the absorption and stimulated emission. These processes are also important in the laser physics and astrophysics.

Neon is the most abundant element in the Universe after H, He, O and C and it is one of products of hydrogen and helium burning in orderly evolution of stellar interiors (Trimble 1991). After the hydrogen, helium and carbon-burning periods, in massive stars neon burning starts. Neon also occurs in supernovae ejecta (Thieleman et al. 1986). After the earlier investigation of Ne II Stark shifts (Pretty 1931; Maissel 1959; Mandel'shtam 1962; Mandel'shtam et al. 1963; Mazing & Vrublevskaya 1962) the first measurements of d values at convenient plasma parameters (T and N) were performed in only one experiment (Purić et al. 1987). In this experiment (Purić et al. 1987) d values of 18 Ne II spectral lines from 13 multiplets were measured at 35 000 K electron temperature and 1.42×10^{23} m^{-3} electron density.

Unique theoretical calculations, made on the basis of the semiclassical (G) approximation (Griem 1974), are performed up to $T = 40\,000$ K only for seven Ne II multiplets (^{4}P–^{4}P^0, ^{4}P–^{4}D^0 and ^{2}P–^{2}D^0 in transition 3s–3p; ^{4}P^0–^{4}D, ^{2}D^0–^{2}F, ^{2}S^0–^{2}P and ^{4}S^0–^{4}P in transition 3p–3d).

We have measured Stark shift values of 42 Ne II spectral lines that belong to 23 multiplets and calculated Stark shift values for 22 multiplets. Shift values of 30 lines were not known before. Measurements were realized at plasma parameters of $T = 35\,300$ K and $N = 1.83 \times 10^{23}$ m^{-3}. Our N value is about 30% higher than those in the experiment of Purić et al. (1987) giving a higher accuracy of the determined d values. The known semiclassical perturbation formalism (SCPF), updated several times, has been used for the calculations of d values.

Existing measured and calculated Ne II A values are collected in a number of articles (Wiese et al. 1966; NIST 2001; Kurucz 2001; Burshtein & Vujnović 1991; Blackford & Hibbert 1994; Griesmann et al. 1997; Fischer & He 1999; Zeippen 1995). Existing transition probability values

Send offprint requests to: V. Milosavljević,
e-mail: vladimir@ff.bg.ac.yu

of the spontaneous emission (Einstein's A values) corresponding to the Ne II transitions investigated have also been checked using the known relative line intensity ratio (RLIR) method described in Djeniže & Bukvić (2001). It was found that 32 A values of the investigated 41 transitions need a correction.

2. Experiment

A modified version of the linear low-pressure pulsed arc (Djeniže et al. 1991; Djeniže et al. 1992; Djeniže et al. 1998; Milosavljević et al. 2000) has been used as an optically thin plasma source. A pulsed discharge was driven in a quartz discharge tube of 5 mm inner diameter and effective plasma length of 7.2 cm (Fig. 1 in Djeniže et al. 1991; Djeniže et al. 1998). The tube has end-on quartz windows on the side of the spectrograph. On the opposite side of the electrodes the glass tube was expanded in order to reduce erosion of the glass wall and also sputtering of the electrode material onto the quartz windows. The working gas was pure neon at 133 Pa filling pressure in the flowing regime. Spectroscopic observations of isolated spectral lines were made along the axis of the discharge tube. A capacitor of 14 μF was charged up to 2.5 kV. The line profiles were recorded using a step-by-step technique with a photomultiplier (EMI 9789 QB) and a grating spectrograph (Zeiss PGS–2, reciprocal linear dispersion 0.73 nm/mm in the first order) system. The system was calibrated by using an EOA–101 standard lamp located at 40 cm distance from the spectrograph input slit. The instrumental $FWHM$ of 0.008 nm was determined by using the narrow spectral lines emitted by the hollow cathode discharge. The recorded profiles of these lines are Gaussian in shape to within 8% accuracy within the wavelength range of the investigated spectral lines. The spectrograph exit slit (10 μm) with the calibrated photomultiplier was micrometrically moved along the spectral plane in small wavelength steps (0.0073 nm). The averaged photomultiplier signal (five shots at the same spectral range) was digitalized using an oscilloscope, interfaced to a computer. All spectral line profiles were recorded at the same detection conditions. A sample output, as example, is shown in Fig. 1.

Plasma reproducibility was monitored by the Ne II line radiation and by the discharge current (it was found to be within ±3%). The discharge characteristics were determined by analyzing the Rogowski coil signal. The values found were: discharge current = 2.95 kA, discharge period = 70 μs, thermal resistance = 0.44 Ω, and decrement = 2.6.

The measured profiles were of the Voigt type due to the convolution of the Lorentz, Stark, and Gaussian profiles with Doppler and instrumental broadening. For the electron density and temperature of our experiments the Lorentz fraction in the Voigt profile was dominant (over 88%). Van der Waals and resonance broadening were estimated to be smaller by more than one order of magnitude

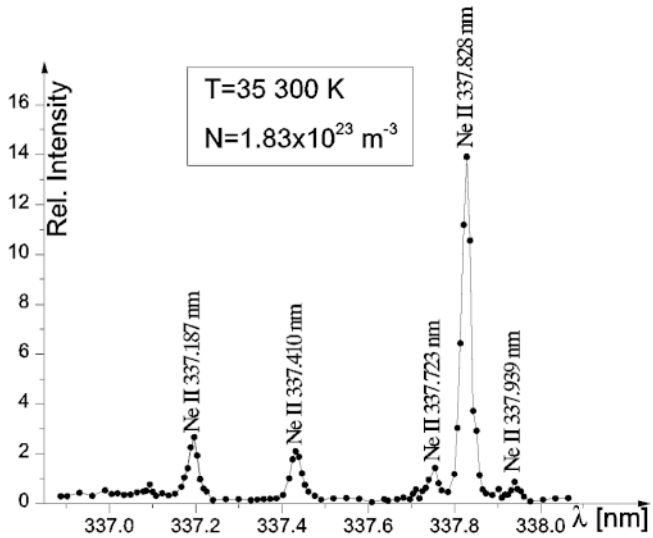

Fig. 1. Recorded spectrum with several investigated Ne II lines.

in comparison to Stark, Doppler and instrumental broadening. The standard deconvolution procedure (Davies & Vaughan 1963; Milosavljević & Poparić 2001) was computerized using a least squares algorithm. Total line intensity (I) corresponds to the area under the line profile. One can notice, see Fig. 1, that the investigated spectral lines are well isolated while the continuum is close to the zero value within the same range of wavelengths. These facts are important for accurate determination of the total line intensities and the values are very convenient as they increase the reliability of the results. Great care was taken to minimize the influence of self-absorption on the total line intensity determination. The opacity was checked by measuring relative line intensity (I) ratios within the low lying multiplets (Nos. 1, 2 and 7) in the Ne II spectrum during the decaying plasma. Absence of the self-absorption would cause constant relative line intensity ratio (Djeniže & Bukvić 2001). This is fullfilled in the case of the low lying multiplets within ±5% (see Fig. 4). Therefore, the influence of the self-absorption on the total line intensity values for Ne II lines can be neglected.

Basic investigations were made of the electrical and optical characteristics of the part of the discharge channel connecting the narrow linear tube and the electrodes. We have inspected the shape of the discharge using a low current DC discharge. We found that the diameter of the discharge channel outside the narrow tube is about three times wider than in the tube and the discharge channel is bent toward the electrodes. Therefore, the current density is approximately 10 times lower than in the tube. We also found that the brightness of the narrow tube is nearly 10 times higher than outside the tube. In the pulsed regime the shape of the discharge was checked photographically and we found that the shape does not change with respect to that of the DC discharge. Taking into account these measurements we estimated that the density of the radiation coming from outside the narrow tube is on average at

least 5 to 10 times lower than the radiation density coming from the tube. We also estimated that the length of the discharge outside the tube, contributing to the light captured by the spectrograph, does not exceed 10 mm i.e. it is 7 times shorter than the tube. Therefore, the overall contribution of the light coming from the discharge outside the narrow tube is 1.5%–3% of the total intensity. Thus, the line profile is "spoiled" by the same amount by an unknown profile coming from the part which connects the linear tube to the electrodes. Fluctuations of the light intensity in the shot-by-shot technique that we have applied are of the order of 3%–5% if the lines under consideration originate from buffer gas, or up to 20% if the spectral lines originate from sputtered material. So it can be concluded that the contribution of the "cold" plasma is masked by the uncertainty caused by fluctuations of the plasma source. The "effective length" is related to the interferometric measurements. It is a few percent longer than the geometrical length of the tube due to the fact that plasma is not restricted just to the area inside the narrow tube. The value of the "effective length" is estimated on an empirical basis. The effective plasma length used can be treated as optically thin for the Ne II lines under investigation.

The plasma parameters were determined using standard diagnostic methods (Griem 1964; Wiese 1968; Rompe & Steenbeck 1967). Thus, the electron temperature (T) was determined from the Boltzmann plot of the relative intensities of Ne II spectral lines. First, this was done for 14 Ne II lines (331.98 nm, 336.06 nm, 337.18 nm, 341.48 nm, 341.69 nm, 341.77 nm, 350.36 nm, 356.83 nm, 366.41 nm, 369.42 nm, 429.04 nm, 439.19 nm, 440.93 nm and 441.32 nm) within an energy interval of 7.13 eV for corresponding upper-levels, assuming the existence of local thermodynamic equilibrium (LTE), according to the criterion in Griem (1964). All necessary atomic data were taken from Wiese et al. (1966) and Striganov & Sventickij (1966). The electron temperature obtained at 17 μs after the beginning of the discharge was 34 500 K ± 6%. Second, it was done for all investigated (41 Ne II) lines, within an energy interval of 7.45 eV, using our new A values. At 17 μs after the beginning of the discharge we found an electron temperature of 35 300 K ± 3%. It turns out that the fitting correlation factor was excellent (0.997).

As an example, the Boltzmann plot obtained at 17μs after the beginning of the discharge is presented in Fig. 2. The electron temperature decay is presented in Fig. 3, together with the electron density (N) decay. The latter was measured using the well-known single laser interferometry technique (Ashby et al. 1965) for the 632.8 nm He-Ne laser wavelength with an estimated error of ±4% (this corresponds to 1/4 fringe uncertainty on a total of 7 fringes). The electron density decay is presented, also, in Fig. 3. Taking into account the temporal dependence of T and N and the criteria for the existence of LTE (Griem 1964; Hey 1976), we can conclude that relevant Ne II ion level populations remain in LTE up to 50 μs after the beginning of the discharge.

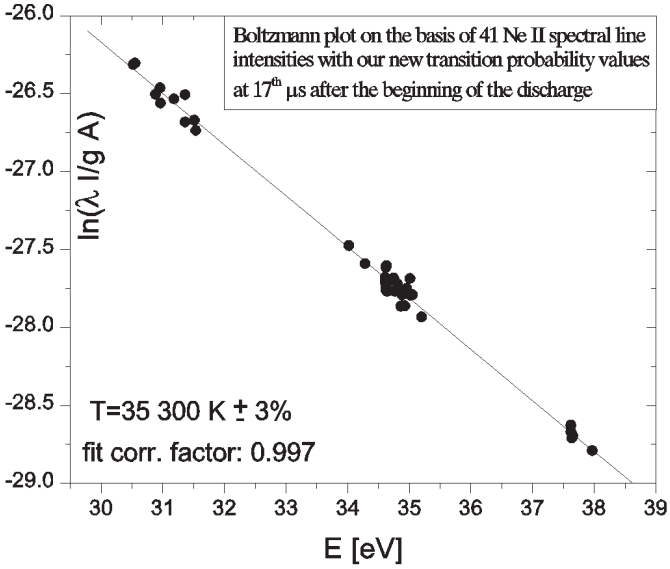

Fig. 2. Boltzmann plot.

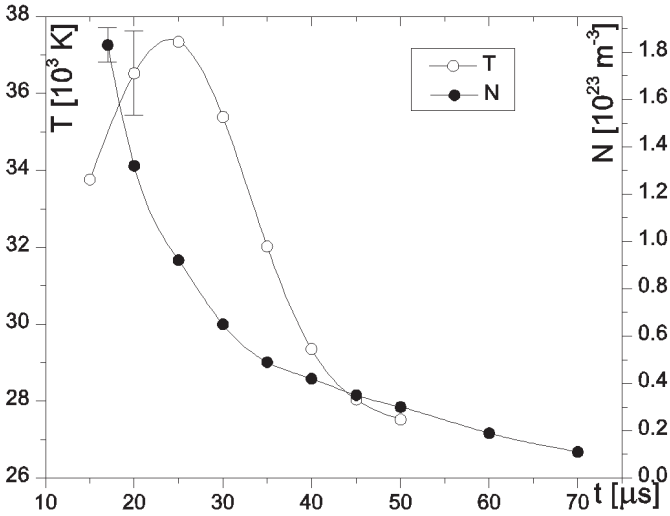

Fig. 3. Temporal evolution of the electron temperature (T) and electron density (N) during plasma decay.

At 17 μs after the beginning of the discharge, when the shifted Ne II spectral line profile center positions were monitored, the electron temperature found was 35 300 K and the electron density 1.83×10^{23} m^{-3}.

2.1. Stark shift measurements

The Stark shifts were measured relative to the unshifted spectral lines emitted by the same plasma (Milosavljević et al. 2000 and references therein). The Stark shift of A spectral line can be measured experimentally by evaluating the position of the spectral line center (X_c) recorded at two different electron density values during plasma decay. In principle, the method requires recording the spectral line profile at the high electron density (N_1) that causes an appreciable shift and then later when the electron concentration has dropped to a value (N_2) lower by at least

an order of magnitude. The difference of the line center positions in these two cases is Δd, so that the shift d_1 at the higher electron density N_1 is:

$$d_1 = N_1 \cdot \Delta d/(N_1 - N_2). \quad (1)$$

The Stark shift data were corrected for the electron temperature decay (Popović et al. 1992). Stark shift data are determined with ± 0.0008 nm error at a given N and T.

2.2. Transition probability measurements

Transition probabilities of spontaneous emission of 41 transitions in the Ne II spectrum have been obtained using the RLIR method (Djeniže & Bukvić 2001). The total line intensities (I) have been measured with high accuracy (3%–5%) using the step-by-step technique (described above) for the line profiles recording. In the case when plasma remains at LTE the well-known formula (Griem 1974):

$$(I_1/I_2)_{\rm EXP} = (A_1 g_1 \lambda_2 / A_2 g_2 \lambda_1) \exp(\Delta E_{21}/kT), \quad (2)$$

can be used for a comparison between measured relative line intensity ratios and corresponding calculated values, taking into account the validity of the Boltzmann distribution for the population of the excited levels in emitters. In this expression I denotes the measured relative intensity, λ the wavelength of the transition, A the transition probability of the spontaneous emission, E the excitation energy from the ground energy level, and g the corresponding statistical weight. T is the electron temperature of the plasma in LTE and k is the Boltzmann constant. In the case where the spectral lines to be compared belong to the same multiplet, Eq. (2) can be re-written in the form:

$$(I_1/I_2)_{\rm EXP} = A_1 g_1 / A_2 g_2, \quad (3)$$

due to the very small difference between excitation energies and wavelengths related to the compared lines. Eq. (3) provides a possibility for checking the existing A values associated with the transitions within a multiplet.

We found that the experimental ratios are constant (within $\approx\pm 5\%$) within the same multiplet during the plasma decay. This offers the possibility to use the comparison between measured and calculated relative line intensity ratios as a method (Djeniže & Bukvić 2001) for estimating the transition probabilities relative to the A value selected as reference.

The choice of the A reference value is important, but it is not crucial. In fact, the information contained in the ratios of relative line intensities is essential. In this paper we have taken the transition probabilities of the most intensive lines (333.487 nm and 303.448 nm) as the reference values. There are two practical reasons for such a choice. First, the transition probability values for these lines have remained unchanged for many years in NIST (NBS) (NIST 2001) and in the tables in Wiese et al. (1966). Second, due to their high intensity, measurements related to these lines are most reliable. Using the Eqs. (2) and (3) we found that 32 of the existing A values (NIST) in the investigated Ne II transitions need corrections which are, in most of the cases, within the given uncertainties (NIST) of these lines.

3. Method of calculation

The semiclassical perturbation formalism, as well as the corresponding computer code (Dimitrijević & Sahal–Bréchot 1996a,b), have been updated and optimized several times (Sahal–Bréchot 1974; Fleurier et al. 1977; Dimitrijević & Sahal–Bréchot 1984; Dimitrijević et al. 1991; Dimitrijević & Sahal–Bréchot 1996b). The calculation procedure, with a discussion of updating and validity criteria, has been briefly reviewed (e.g. in Dimitrijević & Sahal–Bréchot 1996a,b), so that only the basic details of the calculations will be presented here. The Stark full width (W) at the intensity half maximum (FWHM) and the shift (d) of an isolated spectral line may be expressed as (Dimitrijević & Sahal–Bréchot 1996a,b; Fleurier et al. 1977)

$$W = N \int v f(v) {\rm d}v \left(\sum_{i' \neq i} \sigma_{ii'}(v) + \sum_{f' \neq f} \sigma_{ff'}(v) + \sigma_{\rm el} \right) + W_{\rm R}$$

$$d = N \int v f(v) {\rm d}v \int_{R_3}^{R_{\rm D}} 2\pi\rho {\rm d}\rho \sin 2\phi_p, \quad (4)$$

where N is the electron density, $f(v)$ is the Maxwellian velocity distribution function for electrons, ρ denotes the impact parameter of the incoming electron, i and f denote the initial and final atomic energy levels, and i', f' their corresponding perturbing levels, while $W_{\rm R}$ gives the contribution of the Feshbach resonances (Fleurier et al. 1977). The inelastic cross section $\sigma_{j,j'}(v)$, $j = i, f$ can be expressed by an integral over the impact parameter of the transition probability $P_{jj'}(\rho, v)$ as

$$\sum_{j' \neq j} \sigma_{jj'}(v) = \frac{1}{2}\pi {R_1}^2 + \int_{R_1}^{R_{\rm D}} \sum_{j \neq j'} P_{jj'}(\rho, v), j = i, f \quad (5)$$

and the elastic cross section is given by

$$\sigma_{\rm el} = 2\pi R_2^2 + \int_{R_2}^{R_{\rm D}} 8\pi\rho {\rm d}\rho \sin^2 \delta$$

$$\delta = (\phi_{\rm p}^2 + \phi_{\rm q}^2)^{1/2}. \quad (6)$$

The phase shifts $\phi_{\rm p}$ and $\phi_{\rm q}$ due respectively to the polarization potential (r^{-4}) and to the quadripolar potential (r^{-3}), are given in Sect. 3 of Chapter 2 in Sahal–Bréchot (1969a). $R_{\rm D}$ is the Debye radius. All the cut-offs R_1, R_2,

R_3 are described in Sect. 1 of Chapter 3 in Sahal–Bréchot (1969b). For electrons hyperbolic paths due to the attractive Coulomb force were used, while for perturbing ions the paths are different since the force is repulsive. The formulae for the ion-impact widths and shifts are analogous to Eqs. (4)–(6) , without the resonance contribution to the width. The difference in calculation of the corresponding transition probabilities and phase shifts as functions of the impact parameter in Eqs. (5)–(6) is in the ion perturber trajectories which are influenced by the repulsive Coulomb force instead of an attractive one as for electrons.

Atomic energy levels not existing (or revised) in (Moore 1971; Bashkin & Stoner 1978) have been taken in (Quinet et al. 1994). It should be mentioned that the Ne II spectrum is not well determined experimentally so that the set of experimental perturbing atomic energy levels needed for a semiclassical perturbation method calculation with the usual average accuracy of ±30%, is not complete.

4. Results

4.1. Stark shift

The results of the measured Stark shift (d_{m}) values at electron temperature $T = 35\,300$ K and electron density 1.83×10^{23} m^{-3} are shown in Table 1.

Our calculated Stark shift values are presented in Table 2.

4.2. Transition probabilities

We have monitored the ratios $(I_1/I_2)_{\mathrm{EXP}}$ for spectral lines that belong to the same multiplet in a wide range of the decaying plasma up to the moment when the line intensity maximum dropped down to 8% of its maximal value. We have found that these experimental ratios are constant to within ±5% during the plasma decay. This suggests that the comparison between the measured and calculated relative line intensity ratios can be used as a method for estimating the transition probabilities relative to the selected reference A values. We suppose that there is at least one pair of lines, belonging to the same multiplet, for which measured and calculated relative line intensity ratios are in agreement (to within the accuracy of the measurements) during the whole plasma decay period. If such agreement really exist one can accept these lines, with the corresponding transition probabilities, as the reference lines. Among the lines that we have investigated such behavior is found for the 333.487 nm and 332.716 nm lines in multiplet No. 2 and for the 303.448 nm and 303.773 nm lines in multiplet No. 8. These facts allow us to conclude that the existing transition probability values of the strong 333.487 nm and 303.448 nm Ne II lines can be used as reference A values.

As an example, relative line intensity ratios measured for the lines within the same multiplet, as an example, are presented in the Fig. 4.

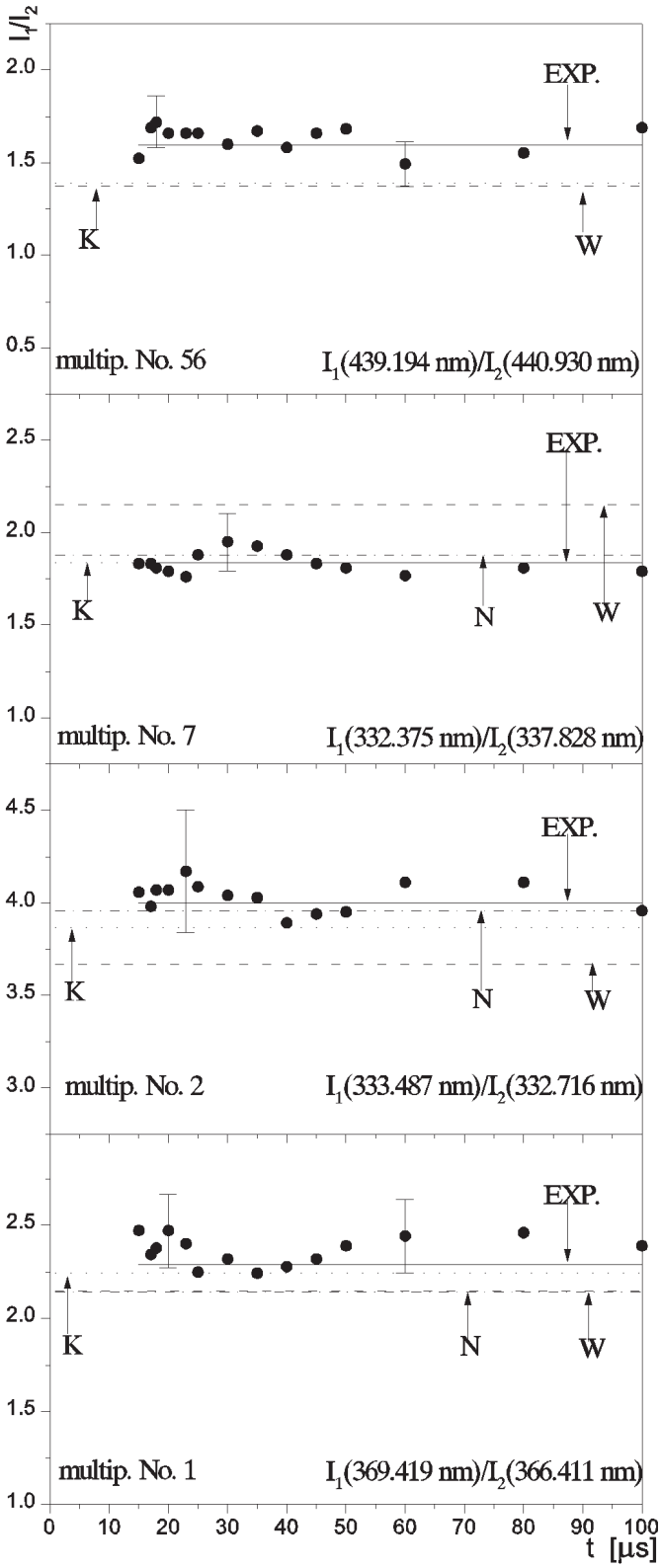

Fig. 4. Relative line intensity ratios (I_1/I_2) within the multiplets. • our experimental values during the plasma decay. Theoretical values (Eq. (3)): (- - -) W, from Wiese et al. (1966); (- · -) N, from NIST (2001); (· · ·) K, from Kurucz (2001) and (—) EXP, calculated with our experimentally obtained A values from Table 1. The error bars represent ±8% uncertainties.

Table 1. Our measured Stark shift (d_m) values for the Ne II spectral lines at 35 300 K electron temperature and 1.83×10^{23} m^{-3} electron density. Positive shift is toward the red. A_{exp} (in 10^8 s^{-1}) represent our measured transition probability values. A_W, A_N, A_K, A_{GMW} and A_{BV} denote values taken from Wiese et al. (1966), NIST (2001), Kurucz (2001), Griesmann et al. (1997) and Burshtein & Vujnović (1991), respectively (also in 10^8 s^{-1}).

Transition	Multiplet	λ (nm)	E (eV)	g	d_m (pm)	A_{exp}	A_W	A_N	A_K	A_{GMW}	A_{BV}
3s–3p	^4P–$^4P^0$	369.419	30.52	6	−0.7	1.13 ± 10%	0.96	1.0	1.002	0.947	0.870
	(1)	366.411	30.55	4	−0.2	0.74 ± 10%	0.67	0.70	0.6822	0.553	0.560
	^4P–$^4D^0$	333.487	30.88	8	−0.6	1.80 ± 10%	1.8	1.8	1.839		
	(2)	336.063	30.96	4	0.0	0.90 ± 10%	0.73	0.82	0.8298		
		332.716	30.95	4	−0.8	0.90 ± 10%	0.98	0.91	0.9499		
	^4P–$^4S^0$	300.166	31.36	4	−0.8	0.80 ± 16%	0.78	0.87	0.8853	0.763	0.690
	(4)	302.886	31.36	4	0.0	0.61 ± 16%	0.57	0.47	0.4669	0.420	0.420
	^2P–$^2D^0$	372.708	31.18	4	−2.5	1.26 ± 16%	1.0	0.98	1.146	0.870	0.800
	(5)										
	^2P–$^2P^0$	332.375	31.51	4	0.0	1.45 ± 10%	1.4	1.6	1.408	1.350	1.280
	(7)	337.828	31.53	2	0.0	1.58 ± 10%	1.3	1.7	1.533	1.620	1.350
3s′–3p′	^2D–$^2F^0$	356.853	34.02	8	−0.6	2.36 ± 16%	1.3	1.4	1.534		
	(9)										
	^2D–$^2P^0$	331.975	34.28	2	−1.0	2.10 ± 16%	1.7	1.6	1.701		
	(10)										
3p–3d	$^4P^0$–^4D	303.448	34.61	8	0.0	3.10 ± 10%	3.1	3.1	2.797	2.700	
	(8)	302.704	34.62	6	0.4	1.44 ± 10%	1.51	1.4	1.33		
		303.773	34.63	4	0.2	2.10 ± 10%	2.0	2.1	1.848		
	$^4D^0$–^4D	332.920	34.61	8	0.8	1.00 ± 16%	0.87	0.88	0.9039	0.858	
	(12)	335.790	34.62	6	1.4	0.66 ± 16%	0.55	0.50	0.5541		
		332.029	34.62	6	–	0.40 ± 16%	0.13	0.21	0.2106		
		337.410	34.63	4	3.1	0.38 ± 18%	0.38	0.30	0.3432		
		336.289	34.64	2	0.9	–					
		337.939	34.64	2	2.5	0.31 ± 20%	0.35	0.30	0.3127		
	$^2D^0$–^2F	341.771	34.75	8	2.4	1.65 ± 16%	2.0	1.6	1.457		
	(20)	341.482	34.81	6	3.1	0.70 ± 16%	0.41	0.018	0.3972		
	$^2D^0$–^2D	341.682	34.75	6	4.2	0.85 ± 16%	0.67	0.64	0.3877		
	(21)										
	$^2D^0$–^4P	337.187	34.86	6	0.7	0.35 ± 18%	0.12	0.22	0.7586		
	(22)										
	$^2S^0$–^2P	350.361	34.88	2	0.0	2.55 ± 16%	1.9	2.0	2.207		
	(28)										
	$^2P^0$–^2P	369.709	34.88	2	–	0.29 ± 18%	0.34	0.28	0.2495		
	(41)	362.806	34.93	4	3.5	0.40 ± 18%	0.57	0.60	0.5158		
	$^4S^0$–^2D	365.993	34.75	6	4.0	0.14 ± 18%	0.11	0.067	0.0629		
	(33)	363.275	34.77	4	6.9	0.23 ± 18%	0.09	0.13	0.3903		
	$^4S^0$–^4F	357.126	34.83	6	2.9	0.84 ± 16%	0.43	0.63	0.9687		
	(31)										
	$^4S^0$–^4P	356.584	34.84	4	2.2	0.84 ± 16%	0.82	0.62	0.1895		
	(34)										
3p′–3d′	$^2P^0$–^2D	333.612	37.97	4	1.3	1.20 ± 16%	–	1.10	0.9316		
3p–4s	$^2P^0$–^2P	337.728	35.20	2	5.4	0.64 ± 20%	–	–	0.6851		
	$^4D^0$–^4P	303.965	34.96	6	6.4	0.93 ± 16%	–	–	1.319	0.609	
		303.598	35.01	4	2.0	1.29 ± 16%	–	–	1.04		
		303.079	35.05	2	–	1.45 ± 16%	–	–	0.8506		
	$^4P^0$–^4P	278.002	35.01	4	–	0.14 ± 20%	–	–	0.1299		
3d–4f	^4F–$^4F^0$	439.194	37.62	10	−7.2	2.68 ± 10%	2.2	0.24	2.395		
	(56)	440.930	37.65	8	−5.5	2.10 ± 10%	2.0	–	2.163		
	^4F–$^4G^0$	429.040	37.62	12	−3.3	2.56 ± 10%	2.5	2.5	2.448		
	(57)	441.320	37.64	6	−14.9	2.25 ± 10%	2.0	2.0	1.477		

Our measured transition probability values (A_{exp}) are presented in Table 1 together with A values taken from various theoretical (Wiese et al. 1966; NIST 2001; Kurucz 2001) and experimental data sources (Burshtein & Vujnović 1991; Griesmann et al. 1997).

5. Discussion

5.1. Stark shift

In order to make easier the comparison between measured and calculated Stark shift values, the theoretical Stark

Table 2. Electron Stark shift (d in pm) calculated by using the semiclassical perturbation formalism (SCPF) [Eqs. (4)–(6)] for the Ne II spectral lines at 10^{23} m^{-3} electron density and for electron temperatures from 5000 K up to 100 000 K. $\bar{\lambda}$ is the mean wavelength in the multiplet. Positive shift is toward the red.

Transition	$\bar{\lambda}$ (nm)	T (10^4 K):	0.5	1	2	3	5	10
3s ^{4}P–3p ^{4}P^0	372.51		0.003	−0.365	−0.480	−0.432	−0.543	−0.455
3s ^{4}P–3p ^{4}D^0	334.33		−0.035	−0.136	−0.187	−0.178	−0.216	−0.189
3s ^{4}P–3p ^{4}S^0	298.83		−0.039	0.021	0.052	0.049	0.065	0.037
3s ^{2}P–3p ^{2}D^0	371.41		−0.113	−0.287	−0.394	−0.379	−0.455	−0.381
3s ^{2}P–3p ^{2}P^0	334.27		−0.107	−0.058	−0.047	−0.032	−0.036	−0.060
3s′ ^{2}D–3p′ ^{2}F^0	357.21		−0.128	−0.246	−0.332	−0.308	−0.377	−0.321
3s′ ^{2}D–3p′ ^{2}P^0	333.78		−0.056	−0.113	−0.141	−0.131	−0.158	−0.150
3p ^{4}P^0–3d ^{4}D	304.01		1.66	0.987	0.937	0.968	1.04	0.869
3p ^{4}D^0–3d ^{4}D	335.26		0.820	0.879	0.860	0.964	1.01	0.864
3p ^{2}D^0–3d ^{4}F	342.15		2.51	1.45	1.34	1.43	1.49	1.27
3p ^{2}D^0–3d ^{2}F	337.56		2.45	1.42	1.30	1.38	1.45	1.24
3p ^{2}D^0–3d ^{2}D	343.23		0.760	0.797	0.782	0.892	0.975	0.828
3p ^{2}D^0–3d ^{4}P	335.26		2.81	1.70	1.53	1.57	1.63	1.40
3p ^{2}S^0–3d ^{2}P	347.31		1.47	1.36	1.22	1.36	1.42	1.26
3p ^{2}P^0–3d ^{2}P	365.18		1.30	1.24	1.12	1.30	1.35	1.23
3p ^{4}S^0–3d ^{2}D	365.00		0.526	0.573	0.507	0.674	0.709	0.644
3p ^{4}S^0–3d ^{4}F	363.78		1.12	1.13	1.05	1.23	1.25	1.13
3p ^{4}S^0–3d ^{4}P	356.00		6.79	4.40	2.46	2.61	2.17	1.58
3p′ ^{2}P^0–3d′ ^{2}P	342.27		0.871	0.883	0.826	0.966	1.01	0.850
3p ^{2}P^0–4s ^{2}P	341.23		27.3	21.0	15.7	14.4	11.9	9.32
3p ^{4}D^0–4s ^{4}P	304.53		22.2	17.1	12.9	11.7	9.68	7.61
3p ^{4}P^0–4s ^{4}P	278.52		19.0	14.7	11.3	10.1	8.46	6.58

shift dependence on the electron temperature together with the values of the other authors and our experimental results at an electron density of 10^{23} m^{-3} are presented graphically in Fig. 5.

Generally, we have obtained very small shift values. Both, experimental and measured d values, are below of one pm, within our experimental accuracy (±0.8 pm). Our measured and calculated d values have the same sign (see Fig. 5, Tables 1 and 2).

Stark shifts corresponding to the 3p–3d and 3p–4s transition arrays have finite and positive values. Measured shift values corresponding to the 3d-4f transition are negative and confirm the earlier obtained sign in Purić et al. (1987). Our calculated (SCPF) d values are smaller than those from Griem (1974), by up to a factor 6. Moreover, our calculated d values have negative signs in the case of the lines that belong to the 3s–3p transition, contrary to the positive d values predicted in Griem (1974). These discrepancies in the sign of d and their magnitude can be explained taking into account the new atomic energy levels and differences in the theoretical methods.

Satisfactory agreement exists among our measured and calculated d values in the case of the lines that belong to the 3p–3d transition. Earlier measured 3p–3d shift values (Purić et al. 1987) also agree with our calculated values.

It should be pointed out that we have not performed calculations of d values belonging to lines in the 3d–4f transition because of the incompleteness of the set of the experimentally determined perturbing energy levels.

The large theoretical d values for 3p ^{2}P^0–4s ^{2}P, 3p ^{4}D^0–4s ^{4}P and 3p ^{4}P^0–4s ^{4}P multiplets are due to close 4p ^{2}P^0 and 4p ^{4}P^0 perturbing levels contributing positively to the shift. The reason for the strong disagreement with our measurements might indicate that 4p ^{2}P^0 and 4p ^{4}P^0 levels are in fact a combination of different contributions which results in decrease of their influence.

5.2. Transition probabilities

Generally, our measured A values are higher by about 19% on average than the data provided by NIST (NIST 2001).

In the case of the 3s–3p transition the measured A values (GMW – Griesmann et al. 1997 and BV – Burshtein & Vujnović 1991) show a tendency to increase in recent years (see Table 1).

We point out here that our four measured A data in the high-lying 3d–4f transition confirm the existing calculated values obtained by (Wiese et al. 1966; NIST 2001; Kurucz 2001), within 9%. It turns out that the recent theoretical calculations (Fischer & He 1999) give different A values which depend on the used approximations. This difference is, for example, in the case of the 3d ^{4}P$_{3/2}$–3p ^{4}S$^0_{3/2}$ transition, up to a factor 3 between the results obtained with the multiconfiguration Hartree-Fock (MCHF) method and the multiconfiguration Dirac-Fock (MCDF) method. Moreover, the calculated and measured A values presented in various data sources (Blackford & Hibbert 1994) and (Fischer & He 1999) show mutual discrepancies by up to a factor 100.

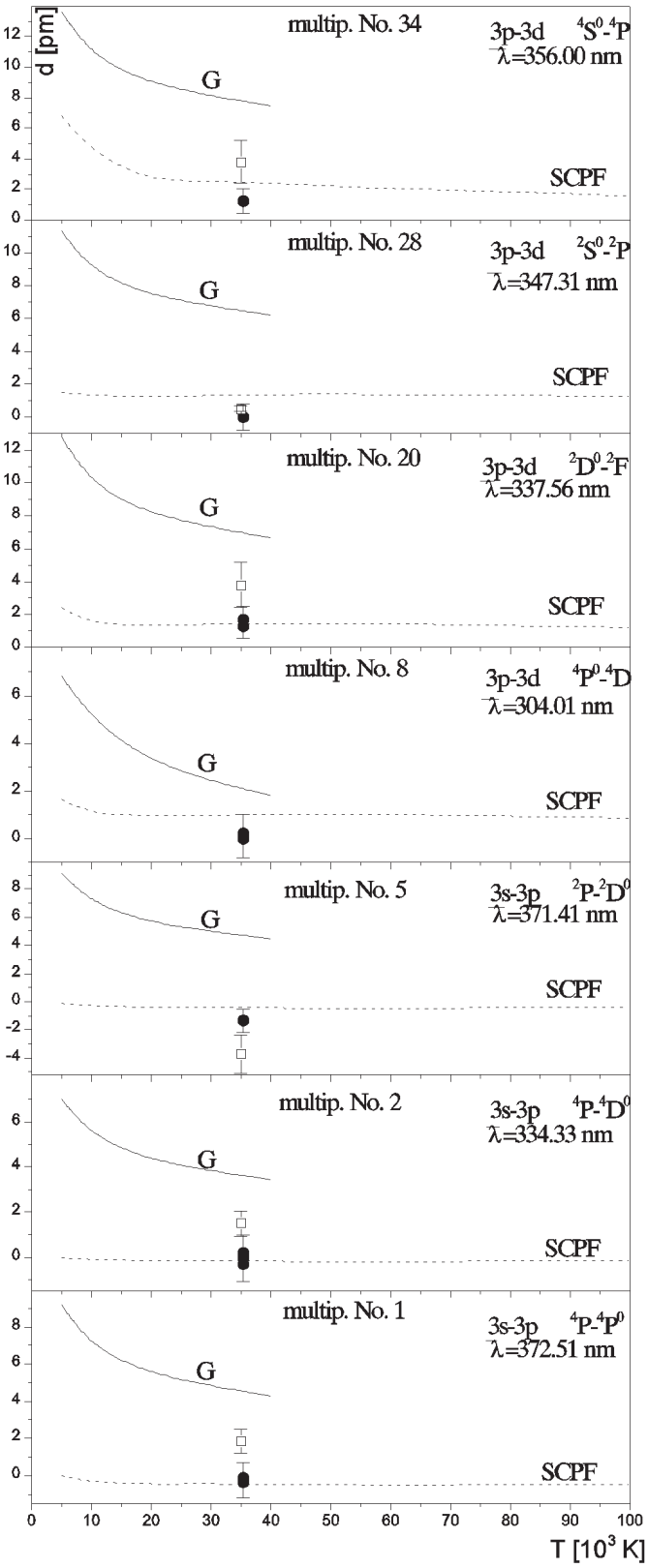

Fig. 5. Stark shift (d in pm) dependence on the electron temperature for various transitions at 10^{23} m^{-3} electron density. • our experimental data and □, from Purić et al. (1987). G, theoretical calculations taken form Griem (1974) and our calculated (SCPF) Stark shift values taken from Table 2. The error bars of ±0.0008 nm represent the uncertainties of the shift measurements. Positive shift is toward the red.

6. Conclusion

We have presented in this work experimental Stark shifts for 41 Ne II spectral lines at an electron temperature of 35 300 K and an electron density of 1.83×10^{23} m^{-3}, as well as calculated Stark shift values for 22 multiplets for an electron density of 10^{23} m^{-3} and for electron temperatures from 5000 K up to 100 000 K. The shift values found are, generally, small. In the case of the 3s–3p and 3s′–3p′ transitions they are practically equal to zero. The common characteristics of these d values is the weak dependence on the electron temperature up to 100 000 K. Thus, these can be used for diagnostics purposes as data independent of self-absorption in optically thick astrophysical plasmas.

Our measured A values, using the RLIR method, are generally higher than those published by NIST (NIST 2001). The difference is still within our experimental accuracy (±20%) and the known uncertainties for NIST values (±50%).

Acknowledgements. This work is a part of the projects "Determination of the atomic parameters on the basis of the spectral line profiles" and "Influence of collisional processes on astrophysical plasma lineshapes" supported by the Ministry of Science, Technologies and Development of the Republic of Serbia. S. Djeniže is grateful to the Foundation "Arany Janos Kozalapitvany" Budapest, Hungary

References

Ashby, D. E. T. F., Jephcott, D. F., Malein, A., & Raynor, F. A. 1965, Appl. Phys. B: Photophys. Laser Chem., 36, 29
Bashkin, S., & Stoner, J. O. Jr. 1978, Atomic Energy Levels and Grotrian Diagrams, vol. I (North Holland, Amsterdam)
Blackford, H. M. S., & Hibbert, A. 1994, At. Data Nucl. Data Tables, 58, 101
Burshtein, M. L., & Vujnović, V. 1991, A&A, 247, 252
Davies, J. T., & Vaughan, J. M. 1963, ApJ, 137, 1302
Dimitrijević, M. S., & Sahal–Bréchot, S. 1984, JQSRT, 31, 301
Dimitrijević, M. S., & Sahal–Bréchot, S. 1996a, Phys. Scr., 54, 50
Dimitrijević, M. S., & Sahal–Bréchot, S. 1996b, A&AS, 119, 369
Dimitrijević, M. S., Sahal–Bréchot, S., & Bommier, V. 1991, A&AS, 89, 581
Djeniže, S., Srećković, A., & Labat, J. 1992, A&A, 253, 632
Djeniže, S., Srećković, A., Labat, J., Konjević, R., & Popović, L. Č. 1991, Phys. Rev. A, 44, 410
Djeniže, S., Milosavljević, V., & Srećković, A. 1998, JQSRT, 59, 71
Djeniže, S., & Bukvić, S. 2001, A&A, 365, 252
Fischer, C. F., & He, X. 1999, Can. J. Phys., 77, 177
Fleurier, C., Sahal–Bréchot, S., & Chapelle, J. 1977, JQSRT, 17, 595
Griem, H. R. 1964, Plasma Spectroscopy (New York: McGraw-Hill Inc.)

Griem, H. R. 1974, Spectral Line Broadening by Plasmas (New York: Acad. Press)
Griem, H. R. 1997, Principles of Plasma Spectroscopy (Univ. Press Cambridge, Cambridge)
Griesmann, U., Musielok J., & Wiese, W. L. 1997, J. Opt. Soc. Am. B, 14, 2204
Hey, J. D. 1976, JQSRT, 16, 69
Kurucz, R. L. 2001, Harvard-Smithsonian Center for Astrophysics, CDROM 23
Lesage, A., & Fuhr, J. R. 1999, Bibliography on Atomic Line Shapes & Shifts (April 1992 through June 1999) Observatoire de Paris
Maissel, L. I. 1959, Proc. Phys. Soc. London, 74, 97
Mandel'shtam, S. L. 1962, in Optik und Spektroskopie Aller Wellenlängen (Akademie Verlag, Berlin), 372
Mandel'shtam, S. L., Mazing, M. A., Sobel'man I. I., & Vainshtein, L. A. 1963, Proc. VI Int. Conf. Phen. in Ioniz. Gases, ed. J. Taillet (S.E.R.M.A. Paris, 1963), vol. III, 331
Mazing, M. A., & Vrublevskaya, N. A. 1962, Opt. Spektrosk. (USSR), XIII, 308
Milosavljević, V., Djeniže, S., Dimitrijević, M. S., & Popović, L. Č. 2000, Phys. Rev. E, 62, 4137
Milosavljević, V., & Poparić, G. 2001, Phys. Rev. E, 63, 036404
Moore, C. E. 1971, Atomic Energy Levels, vol I, NS RDS-NBS 35 (US Department of Commerce, National Bureau of Standards, Washington D.C)
NIST – Atomic Spectra Data Base Lines (wavelength order) – `http://physics.nist.gov` (2001)
Popović, L. Č., Srećković, A., Djeniže, S. 1992, Proc. 11th ICSLS, A25, Carry le Rouet, France, ed. N. Feautrier et al. (Université de Provence en Marseille, Marseille, 1992)
Pretty, W. E. 1931, Proc. Phys. Soc. London, 43, 279
Purić, J., Djeniže, S., Srećković, A., Labat, J., & Ćirković, Lj. 1987, Phys. Rev. A, 35, 2111
Quinet, P., Palmeri, P., & Biémont, E. 1994, Phys. Scri., 49, 436
Rompe, R., & Steenbeck, M. 1967, Ergebnisse der Plasmaphysik und der Gaselektronik, Band 1 (Berlin: Akademie Verlag)
Sahal–Bréchot, S. 1969a, A&A, 1, 91
Sahal–Bréchot, S. 1969b, A&A, 2, 322
Sahal–Bréchot, S. 1974, A&A, 35, 321
Striganov, R. A., & Sventickij, N. S. 1966, Tablicy Spektral'nykh linij (Atomizdat, Moskva)
Thieleman, F. K., Nomoto, K., & Yokoi, K. 1986, A&A, 158, 17
Trimble, V. 1991, A&AR, 3, 1
Wiese, W. L., Smith, M. W., & Glennnon, B. M. 1966, Atomic Transition Probabilities, vol. I, Hydrogen through Neon, NSRDS-NBS4, US Department of Commerce, National Bureau of Standards, Washington D.C
Wiese, W. L. 1968, Methods of Experimental Physics, ed. B. Bederson, & W. L. Fite, vol. 7B (Academic Press, New York)
Zeippen, C. J. 1995, Phys. Scr., 58, 43

A&A 396, 331–336 (2002)
DOI: 10.1051/0004-6361:20021390
© ESO 2002

Astronomy & Astrophysics

Stark shifts and transition probabilities in Si III and Si IV spectra

S. Djeniže[1,2,3], M. S. Dimitrijević[2,4], A. Srećković[1,2], and S. Bukvić[1,2]

[1] Faculty of Physics, University of Belgrade 11001 Belgrade, PO Box 368, Serbia, Yugoslavia
[2] Isaac Newton Institute of Chile, Yugoslavia Branch, Belgrade, Yugoslavia
[3] Hungarian Academy of Sciences, Budapest, Hungary
[4] Astronomical Observatory, 11160 Belgrade, Volgina 7, Serbia, Yugoslavia

Received 24 May 2002 / Accepted 10 September 2002

Abstract. Stark shifts of nine doubly charged (Si III) and six triply charged (Si IV) silicon ion spectral lines have been measured in a linear, low-pressure, pulsed arc operated in O_2 and SF_6 discharges. Si III Stark shift values have been also calculated using the semiclassical perturbation formalism (SCPF) for electrons, protons and helium ions as perturbers. Transition probabilities of the spontaneous emission (Einstein's *A* values) of nine Si III transitions have been obtained using the relative line intensity ratio (RLIR) method, not applied before in Si III spectrum, and, also, calculated using the Coulomb approximation method. The measured Si IV shift and some calculated Si III shift values present the first published data in this field.

Key words. lines: profiles – atomic data

1. Introduction

Atomic data such as Stark shifts (*d*) and transition probabilities (*A*) play an important role in the diagnostics and modeling of various cosmic and laboratory plasmas (Griem 1964, 1974; Wiese 1968; Lesage 1995; Zeippen 1995). Silicon ions are among the most abundant emitters or absorbers in many kinds of cosmic plasmas. Thus, the knowledge of the doubly (Si III) and triply (Si IV) ionized silicon spectral lines' Stark parameters and transition probabilities is necessary in various astrophysical calculations. As an example, the silicon ionisation balance can be considered as a useful tool for temperature diagnosis in B-Stars. Thus, in a work by Becker & Butler (1990) spectral lines of Si II, Si III and Si IV emitted by non-LTE plasma have been used for temperature determination in B-Stars. In a recent publication (Monteverde et al. 2000) the ionization equilibria of Si II/Si III and Si III/Si IV have been used to observe the silicon abundance in M 33 early B Supergiants. Interstellar absorption by the young stars in the Magellanic Clouds was observed in the Si III and Si IV lines (Lehner et al. 2001). Presence of the Si III and Si IV spectral lines in the Quasar Q0122+0338 1 spectrum was observed using the Hubble Space Telescope (Papovich et al. 2000).

In the present work we will present the first Stark shifts measurements of six Si IV spectral lines and, also, the first measured Stark shift values of seven Si III spectral lines with their first calculated values, performed by us, on the basis of the semiclassical perturbation formalism (SCPF) (Sahal-Bréchot 1969a,b) for electrons, protons and helium ions as perturbers. Our work also contains the first experimental Si III transition probability values for nine Si III transitions obtained in emission spectra using the relative line intensity ratio (RLIR) method, already applied in the cases of the Ar III, Ar IV (Djeniže & Bukvić 2001), O II (Srećković et al. 2001a, 2002), Ne II (Djeniže et al. 2002a) and N III, N IV and N V (Djeniže et al. 2002b) spectra. We have also calculated the Si III transition probabilities using the Coulomb approximation method.

2. Experiment

The linear pulsed arc (Djeniže et al. 1992a,b, 2002a,b) was used as a plasma source. A pulsed discharge was driven in a Pyrex discharge tube of 5 mm inner diameter and plasma length of 7.7 cm. Spectroscopic observations of isolated spectral lines were made along the axis of the discharge tube. Atoms of silicon were obtained as impurities by sputtering from a Pyrex discharge tube. As a driving gas, oxygen and SF_6 have been used at filling pressures of 130 Pa and 70 Pa, respectively. Highly ionized oxygen, sulfur and fluorine ions facilitate erosion of the glass walls of the linear part of discharge tube. Furthermore, O_2 and SF_6, as working gases, left the observed lines of Si III and Si IV isolated. The Si III lines were investigated in the oxygen plasma, while lines of Si IV in O_2 and SF_6 plasmas. Discharge of the condenser of 8 μF capacity charged to 4 kV was selected for maximum efficiency in releasing silicon atoms.

Send offprint requests to: S. Djeniže,
e-mail: srdjan_bukvic@Softhome.net

The reproducibility of the investigated silicon spectral line radiation intensities was 90%, which can be taken as acceptable considering the method by which the impurity atoms were introduced.

The line profiles were recorded using a step-by-step technique described by Djeniže et al. (2002a). The Si III spectral line profiles were recorded at the same detection conditions. A sample of outputs are shown in Figs. 1 and 2.

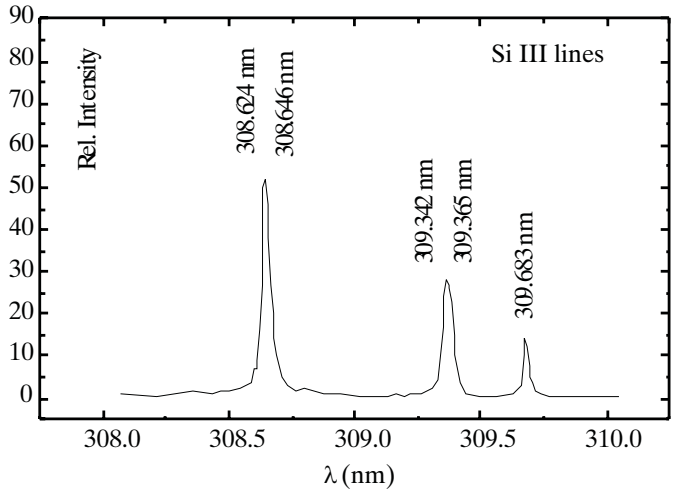

Fig. 1. Recorded spectrum with several investigated Si III lines at the 20th μs after the beginning of the discharge in oxygen plasma.

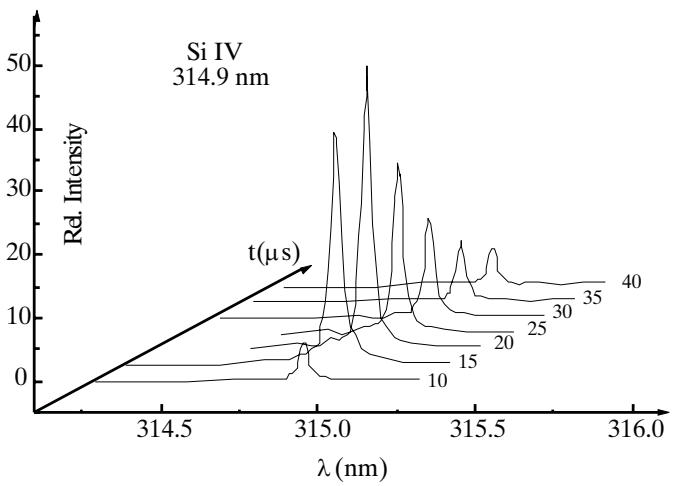

Fig. 2. Temporal evolution of the 314.9 nm Si IV spectral line profiles in oxygen plasma.

Total line intensity (I) corresponds to the area under the line profile (within 5%–7% accuracy). The Si III ion concentration is low because ions are produced as impurities originating from the Pyrex discharge tube. Therefore, the influence of the self-absorption on the total line intensity values for Si III lines can be neglected for the transition probability determination which is very important.

The plasma parameters were determined using standard diagnostic methods (Griem 1964). Thus, in the case of the oxygen plasma the electron temperature (T) was determined from

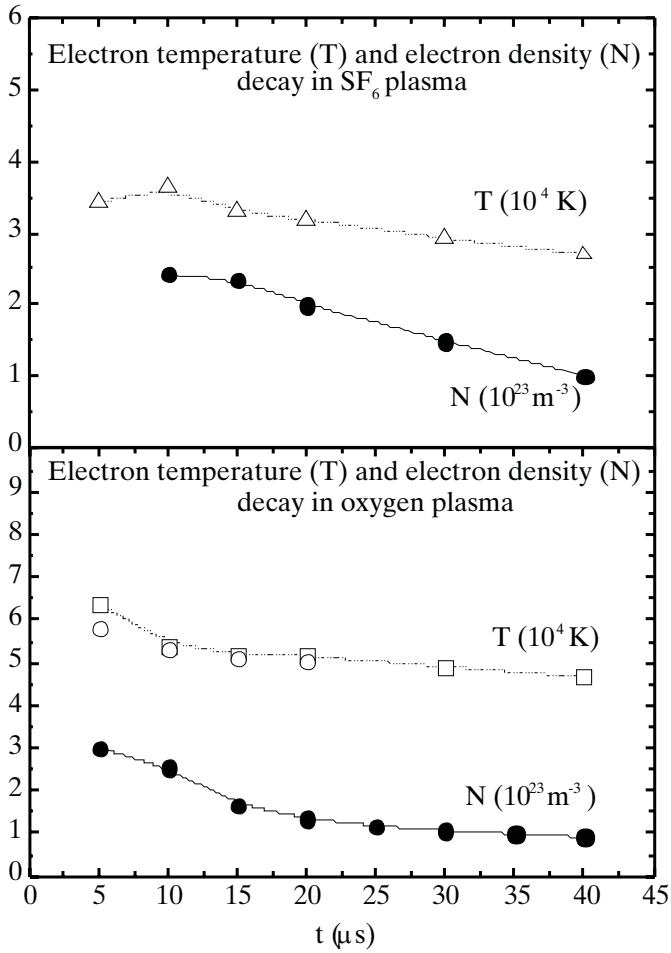

Fig. 3. Temporal evolution of the electron temperature (T) and electron density (N) during plasma decay. □, values obtained on the basis of 9 O III line relative intensities; ○, on the basis of the O IV/O III line intensity ratio and △, on the basis of the S III/S II line intensity ratio.

the Boltzmann plot of the relative intensities of nine O III spectral lines (375.9 nm, 326.1 nm, 326.5 nm, 326.7 nm, 371.5 nm, 396.1 nm, 369.5 nm, 369.9 nm and 409.1 nm) within an energy interval of 9.96 eV for corresponding upper levels, and, also, from the Saha equation applied to the 375.9 nm O III and 307.1 nm O IV spectral lines with an estimated error of ±13% assuming the existence of local thermodynamic equilibrium (LTE), according to the criteria from Griem (1974) and Hey (1976). Here we point out that the nine investigated Si III lines have been also included in the plasma diagnostics. The Boltzmann plot based on their relative line intensities gives T values (in the oxygen plasma) that agree well with the values presented in Fig. 3. The temperatures are: 51 700 K and 51 000 K in the 15th and 20th μs after the beginning of the discharge. These facts indicate that the relevant Si III energy level populations remain in the LTE needed for the A values calculation. In the case of the SF_6 plasma, the electron temperature was determined from the ratio of the relative intensities (Saha equation) of the 334.6 nm S III to the 481.6 nm S II spectral line, supposing the existence of LTE with an estimated

Table 1. Our measured (d_{exp} in pm) and calculated (d_{Th} in pm) electron Stark shift values at a given electron temperature (T in 10^4 K) and at 10^{23} m^{-3} electron density. Asteriks denote calculated values (electron shift) taken from Dimitrijević et al. (1991a). A^{rel}_{exp} and A^{rel}_{Th} denote our experimental and calculated relative transition probability (dimensionless) values. A_{Th}, A_N and A_K (all in 10^8 s^{-1}) represent our calculated transition probability values and those from NIST (2002) and Kurucz (2002), respectively. Atomic data (E_u in eV), λ and transitions are taken from NIST (2002) and Striganov & Sventickii (1966). Positive shift is toward the red.

Transition	λ (nm)	E_u	T	d_{exp}	d_{Th}	A^{rel}_{exp}	A^{rel}_{Th}	A_{Th}	A_N	A_K
Si III										
3p $^1P^o_1$–4p^2 $^1D_2$	254.181	15.15	5.3	−1.0 ± 0.8		0.087 ± 45%			0.32	0.158
3d $^3D_1$–4p $^3P^o_o$	309.683	21.73	5.3	−1.7 ± 0.8	0.45	0.696 ± 25%	0.917	1.65		1.403
3d $^3D_3$–4p $^3P^o_2$	308.624	21.74	5.3		0.45	0.609 ± 25%	0.777	1.40		1.178
4p $^3P^o_2$–4d $^3D_3$	380.653	24.99	5.3	6.3 ± 0.8	4.4		1.867	3.36	3.4	
4p $^3P^o_1$–5s $^3S_1$	323.395	25.56	5.3	11.6 ± 0.8	11.1	0.630 ± 12%	0.594	1.07	1.3	
4p $^3P^o_2$–5s $^3S_1$	324.163	25.56	5.3	6.8 ± 0.8	11.1	1.00 ± 6%	1.00	1.80	2.3	
4d $^1D_2$–5f $^1F^o_3$	471.665	27.96	5.3	1.5 ± 0.8	−2.8	0.870 ± 21%	1.444	2.60	2.8	
4f $^3F^o_2$–5g $^3G_3$	481.333	28.55	5.2	−12.8 ± 0.8	−42.1	0.913 ± 23%	1.244	2.24		2.910
4f $^3F^o_4$–5g $^3G_5$	482.895	28.55	5.2	−14.7 ± 0.8	−42.1	0.870 ± 23%	1.333	2.40		3.197
3d′ $^3D^o_3$–4p′ $^3P_2$	325.866	30.76	5.2	−2.5 ± 0.8		0.891 ± 28%	0.550	0.99		
Si IV										
4s $^2S_{1/2}$–4p $^2P^o_{3/2}$	408.886	27.08	3.3	−1.2 ± 0.8	−0.86*					
4p $^2P^o_{1/2}$–4d $^2D_{3/2}$	314.956	30.99	5.2	2.0 ± 0.8	1.15*					
4p $^2P^o_{3/2}$–4d $^2D_{5/2}$	316.569	30.99	3.1	1.7 ± 0.8	1.08*					
4d $^2D_{5/2}$–5p $^2P^o_{3/2}$	376.245	34.29	3.2	1.5 ± 0.8	−0.18*					
4d $^2D_{3/2}$–5p $^2P^o_{1/2}$	377.315	34.28	3.2	0.3 ± 0.8	−0.18*					
5p $^2P^0_{3/2}$–5d $^2D_{5/2}$	670.121	36.14	5.2	7.5 ± 0.8	22.3*					

error of ±11%. The electron temperature decay is presented in Fig. 3. Necessary atomic data were taken from NIST (2002).

Electron density (N), in the case of the oxygen plasma, was measured using the well-known single laser interferometry technique for the 632.8 nm He-Ne laser wavelength with an estimated error of ±6%. In the case of the SF_6 plasma, the electron density decay was observed by monitoring the Stark width values of the convenient 375.9 nm O III spectral line within an estimated error of ±8%. Oxygen ions produced as impurities in SF_6 discharge, due to their low concentration, give convenient Stark width values because of the absence of self-absorption. Corresponding N values, predicted by semi-classical theory (Griem 1974), were taken from Srećković et al. (2001b). The electron density decay is also presented in Fig. 3. Taking into account the temporal dependence of T and N and the criteria for the existence of LTE, one can conclude that relevant Si III ion level populations remain in LTE up to the 60th μs after the beginning of the discharge.

3. Stark shift measurements

The Stark shifts were measured relative to the unshifted spectral lines emitted by the same plasma (Djeniže et al. 2002a, and references therein). Stark shift data are determined with ±0.8 pm error at a given N and T. Our measured (d_{exp}) Stark shifts are presented in Table 1.

4. Transition probability measurements

In the case where plasma remains at LTE, the well-known formula (Griem 1964, 1974; Rompe & Steenbeck 1967; Wiese 1968)

$$(I_1/I_2)_{EXP} = (A_1 g_1 \lambda_2 / A_2 g_2 \lambda_1)\exp(\Delta E_{21}/kT) \quad (1)$$

can be used for a comparison between measured relative line intensity ratios and corresponding calculated values, taking into account the validity of the Boltzmann distribution for the population of the excited levels in emitters. In this expression, I denotes the measured relative intensity, λ the wavelength of the transition, A the transition probability of the spontaneous emission, E the excitation energy from the ground energy level, and g the corresponding statistical weight. T is the electron temperature of the plasma in LTE and k is the Boltzmann constant. On the basis of the measured relative line intensity ratio and determined electron temperature, Eq. (1) gives the possibility to obtain the ratio of the corresponding transition probabilities or the possibility of the determination of the particular transition probability value relative to the selected reference A values. As reference A value the transition probability corresponding to the Si III 324.163 nm transition was chosen. This line is the most intense and has the highest reproducibility among the investigated Si III spectral lines. Our experimental relative A values (A^{rel}_{exp}) are presented in Table 1 with estimated accuracies that contain the uncertainties of the line intensity and electron temperature determinations and the uncertainties

Table 2. Electron (a), proton (b) and helium ion (c) Stark shifts (in pm) calculated by using semiclassical perturbation formalism (SCPF) (Eqs. (4)–(6) in Djeniže et al. 2002a) for the Si III spectral lines at 10^{23} m^{-3} perturber density and electron temperatures from 10 000 K to 300 000 K. $< \lambda >$ is the mean wavelength in the multiplet. Positive shift is toward the red.

Transition	$< \lambda >$ (nm)	$T(10^4$ K):	1	2	5	10	15	30
3d ^{3}D–4p ^{3}P^o	309.07		a: 0.34	0.50	0.44	0.57	0.50	0.48
			b: 0.08	0.17	0.31	0.42	0.47	0.56
			c: 0.14	0.32	0.61	0.85	0.95	1.14
4p ^{3}P^o–4d ^{3}D	380.25		a: 4.17	3.74	4.38	3.76	3.71	3.37
			b: 1.33	2.14	3.20	3.85	4.28	4.97
			c: 2.32	4.00	6.31	7.82	8.61	10.0
4s ^{3}S–4p ^{3}P^o	456.14		a: −1.74	−2.31	−2.11	−2.34	−2.18	−2.02
			b: −0.46	−0.86	−1.46	−1.82	−2.04	−2.44
			c: −0.81	−1.63	−2.90	−3.69	−4.12	−4.92
4p ^{3}P^o–5s ^{3}S	323.88		a: 21.5	15.7	11.7	9.33	7.98	6.77
			b: 1.98	3.03	4.26	5.12	5.52	6.38
			c: 3.39	5.56	8.31	10.3	11.2	12.8
4d ^{1}D–5f ^{1}F^o	471.80		a: −7.4	−4.53	−2.85	−2.06	−1.44	−1.57
			b: −9.61	−14.1	−19.6	−23.1	−25.3	−28.3
			c:		−38.0	−46.7	−50.6	−56.8
4f ^{3}F^o–5g ^{3}G	482.35		a: −38.6	−42.4	−42.2	−36.6	−38.5	−34.1

of the calibration procedure. $A^{\rm rel}_{\rm exp}$ represent averaged values obtained during plasma decay in the time interval for which the criteria of the existence of the LTE is fulfilled. Our $A^{\rm rel}_{\rm exp}$ values provide the possibility for future comparison with absolute data as well as with data presented in relative form.

5. Method of calculation

5.1. Stark shifts

The semiclassical perturbation formalism, as well as the corresponding computer code (Dimitrijević & Sahal-Bréchot 1996a,b), has been updated and optimized several times (Dimitrijević & Sahal-Bréchot 1996b, 1984; Sahal-Bréchot 1974; Fleurier et al. 1977; Dimitrijević et al. 1991b). The calculation procedure, with the discussion of updates and validity criteria, has been briefly reviewed in Dimitrijević & Sahal-Bréchot (1996a,b) (see also Djeniže et al. 2002a). The formulae for the ion-impact widths and shifts are analogous to Eqs. (4)–(6) in Djeniže et al. (2002a), without the resonance contribution to the width. The difference in calculation of the corresponding transition probabilities and phase shifts as functions of the impact parameter in Eqs. (5), (6) is in the ion perturber trajectories which are influenced by the repulsive Coulomb force instead of an attractive one as for electrons. Atomic energy levels were taken from Martin & Zalubas (1983). Note that in the Si III spectrum many of the known terms are affected by configuration interactions and some needed here are not experimentally determined. Consequently, the obtained theoretical results might have errors larger than usual for the semiclassical perturbation method (±30%). Our calculated electron, proton and helium ion Stark shift values ($d_{\rm Th}$) are presented in Tables 1 and 2.

5.2. Transition probabilities

Due to its simplicity, the Coulomb approximation method of Bates & Damgaard (Bates & Damgaard 1949; Oertel & Shomo 1968) for the calculation of the Einstein A values (oscillator strengths) is often used in spite of the existence of more sophisticated methods. It is used particularly for complex calculations of e.g. line broadening parameters or stellar opacity. It is of interest therefore to compare oscillator strengths calculated with Coulomb approximation, with experimental values, as well as with theoretical ones obtained with sophisticated methods. This is particularly interesting for Si III, since many of the known terms in this spectrum are affected by configuration interactions. We took into account here that 3s4f^{3}F^o term has 23% of 3p3d^{3}F^o and that 3s5f^{1}F^o has a purity of 55%, while 31% are 3pnd ^{1}F^o and 14% is not determined. Consequently, the accuracy of the oscillator strength of the 471.67 nm line is lower than the others. Moreover, the composition of the 3s5g^{3}G term is not determined, so that oscillator strength of the 481.33 nm and 482.90 nm lines might be affected by the configuration interaction. The same discussion holds for the accuracy of the Stark shifts of these lines, which are more uncertain than other results. Our calculated A values ($A_{\rm Th}$) are presented in Table 1.

6. Results and discussion

The results of the measured Stark shift ($d_{\rm exp}$) and relative transition probability ($A^{\rm rel}_{\rm exp}$) as well as the calculated transition probability ($A_{\rm Th}$) values are shown in Table 1. $A^{\rm rel}_{\rm Th}$ represent our

calculated relative transition probability values. Our calculated Stark shift values (d_{Th}) are presented in Table 2.

On the basis of Tables 1 and 2 one can conclude that our measured (d_{exp}) and calculated (d_{Th}) Si III Stark shift values agree in the case of the lines that belong to the $4p^3P^o-4d^3D$ and $4p^3P^o-5s^3S$ transitions within the experimental accuracy and uncertainties of the calculations. In the case of the $4f^3F^o-5g^3G$ transition, the measured and calculated shifts have the same negative sign, but the calculated ones are about 3 times larger. This could be explained by the unknown composition of the $3s5g^3G$ term of these Si III lines and the unknown composition of ng^3G and nh^3H^o perturbing terms. Experimental d values for these lines obtained by González et al. (2000) also have a negative sign and lie below our calculated ones. Measured and calculated d values of the lines 309.683 nm and 471.665 in the $3d^3D-4p^3P^o$ and $4d^1D-5f^1F^o$ transitions, respectively, are small but have a different sign. This discrepancy can be considered as tolerable, taking into account the accuracy (±0.8 pm) of the experimental values and the uncertainties of the theoretical predictions related to the atomic data necessary for the Stark shift calculations. Incompleteness of the experimental perturbing energy levels in the case of the Si III 254.181 nm and 325.866 nm spectral lines is such that the semiclassical perturbation calculation results will be of very poor accuracy. On the basis of the calculated Si III Stark shift values (see Table 2), one can conclude that at electron temperatures below 30 000 K, the electron Stark shift is dominant. In the plasmas with electron temperatures higher than 50 000 K, proton and helium Stark shifts play an important role. The Stark shift generated by helium ions is about two times higher than the shift generated by protons. These results can be important in astrophysical plasmas where protons and helium ions represent the main plasma components.

In the case of the Si IV lines our measured Stark shifts and the calculated ones presented by Dimitrijević et al. (1991a) are very small and mutually agree very well within the experimental accuracy and uncertainties of the calculations. The only exception is the d value of the higher lying $5p^2P^o-5d^2D$ (670.121 nm) transition where the d_{Th} is higher than the measured ones by about 3 times. It should be pointed out that the d_{Th} values taken from Dimitrijević et al. (1991a) are also calculated on the basis of the semiclassical perturbation formalism (SCPF).

In the case of the transition probability values we can notice reasonable agreement between $A^{\mathrm{rel}}_{\mathrm{exp}}$ and $A^{\mathrm{rel}}_{\mathrm{Th}}$ values within the accuracies of the experiment (12–45%) and uncertainties of the calculations (<40%). The only exception is the 325.866 nm transition where the experimental A value is about 2 times higher than the calculated ones. It should be pointed out that our results for the mentioned transition are the first published data. Our calculated A values (A_{Th}) on the basis of the Coulomb approximation method agree with tabulated values in NIST (2002) and Kurucz (2002) predicted with about 50% uncertainties in NIST values (NIST 2002). Our smaller A_{Th} values in the case of the 481.333 nm and 482.895 nm transitions in comparison to the A_{K} values can be explained taking into account the cited (in Chap. 5.2) approximations used for our calculations. It should be pointed out that the ratio of the $A^{\mathrm{rel}}_{\mathrm{exp}}$, A_{Th} and A_{N} values related to the 323.395 nm and 324.163 nm transitions in the Si III $4p^3P^o-5s^3S$ multiplet are in very good mutual agreement (within 10%). They are: 0.630, 0.594 and 0.565, respectively. This fact confirm validity of our choice of the reference A value.

7. Conclusion

Generally, we have found satisfying agreement between measured and theoretical Stark shift values calculated on the basis of the semiclassical perturbation formalism (SCPF), especially in the case of the Si IV spectral lines. Difficulties about the knowledge of the perturbing energy levels increase the uncertainties of some calculated Si III Stark shift values, explaining the existing disagreement between some measured and calculated Stark shift values. Taking into account the agreement between measured and calculated finite d values, we recommend the 380.653, 323.395 and 324.163 nm Si III spectral lines as lines with convenient Stark shift values useful in astrophysical plasma diagnostics. Our experimental and calculated Si III transition probability values are in tolerable mutual agreement, within 40% on average.

Acknowledgements. This work is a part of the projects "Determination of the atomic parameters on the basis of the spectral line profiles" and "Influence of collision processes on astrophysical plasma lineshapes" supported by the Ministry of Science, Technologies and Development of the Republic of Serbia. S. Djeniže is grateful to the Foundation "Arany János Közalapitvány" Budapest, Hungary.

References

Bates, D. R., & Damgaard, A. 1949, Trans. Roy. Soc. London, Ser. A, 242, 101
Becker, S. R., & Butler, K. 1990, A&A, 235, 326
Dimitrijević, M. S., & Sahal-Bréchot, S. 1984, JQSRT, 31, 301
Dimitrijević, M. S., Sahal-Bréchot, S., & Bommier, V. 1991a, A&AS, 89, 591
Dimitrijević, M. S., Sahal-Bréchot, S., & Bommier, V. 1991b, A&AS, 89, 581
Dimitrijević, M. S., & Sahal-Bréchot, S. 1996a, Phys. Scr., 54, 50
Dimitrijević, M. S., & Sahal-Bréchot, S. 1996b, A&A, 119, 369
Djeniže, S., Srećković, A., & Labat, J. 1992a, A&A, 253, 632
Djeniže, S., Srećković, A., Labat, J., Purić, J., & Platiša, M. 1992b, J. Phys. B Atom. Molec. Optic., 25, 785
Djeniže, S., & Bukvić, S. 2001, A&A, 365, 252
Djeniže, S., Milosavljević, V., & Dimitrijević, M. S. 2002a, A&A, 382, 359
Djeniže, S., Srećković, A., & Bukvić, S. 2002b, Eur. Phys. J. D, 20, 11
Fleurier, C., Sahal-Bréchot, S., & Chapelle, J. 1977, JQSRT, 17, 595
González, V. R., Aparicio, J. A., del Val, J. A., & Mar, S. 2000, A&A, 363, 1177
Griem, H. R. 1964, Plasma Spectroscopy (McGraw-Hill Inc. New York)
Griem, H. R. 1974, Spectral Line Broadening by Plasmas (Acad. Press, New York)
Hey, J. D. 1976, JQSRT, 16, 69
Kurucz, R. L. 2002, Harvard-Smitshonian Center for Astrophysics, CD ROM 23

Lesage, A. 1995, ASP Conf. Ser. 78, ed. S. J. Adelman, & W. L. Wiese (Astronomical Society of the Pacific, San Francisco), 161
Lehner, N., Sembach, K. R., Dufton, P. L., Rolleston, W. R. J., & Keenan, F. P. 2001, ApJ, 551, 781
Martin, W. C., & Zalubas, R. 1983, J. Phys. Chem. Ref. Data, 12, 323
Monteverde, M. I., Herrero, A., & Lennon, D. J. 2000, ApJ, 545, 813
NIST 2002, Atomic Spectra Data Base Lines `http://physics.nist.gov`
Oertel, G. K., & Shomo, L. P. 1968, ApJS, 16, 175
Papovich, C., Norman, C. A., Bowen, D. V., et al. 2000, ApJ, 531, 654
Rompe, R., & Steenbeck, M. 1967, Ergebnisse der Plasmaphysik und der Gaselektronik, Band 1 (Akademie Verlag, Berlin)
Sahal-Bréchot, S. 1969a, A&A, 1, 91
Sahal-Bréchot, S. 1969b, A&A, 2, 322
Sahal-Bréchot, S. 1974, A&A, 35, 321
Srećković, A., Drinčić, V., Bukvić, S., & Djeniže, S. 2001a, Phys. Scr., 63, 306
Srećković, A., Dimitrijević, M. S., & Djeniže, S. 2001b, A&A, 371, 354
Srećković, A., Djeniže, S., & Bukvić, S. 2002, Phys. Scr., 65, 359
Striganov, R. A., & Sventickii, N. S. 1966, Tablicy Spektralnych Linij (Atomizdat, Moskva)
Wiese, W. L. 1968, Meth. Exper. Phys. 7B, ed. B. Bederson, & W. L. Fite (Academic Press, New York)
Zeippen, C. J. 1995, Phys. Scr., 58, 43

A&A 399, 795–797 (2003)
DOI: 10.1051/0004-6361:20021801
© ESO 2003

Astronomy & Astrophysics

The electron-impact broadening parameters for Co III spectral lines*

D. Tankosić[1,2], L. Č. Popović[1,2], and M. S. Dimitrijević[1,2]

[1] Astronomical Observatory, Volgina 7, 11160 Belgrade 74, Serbia, Yugoslavia
[2] Isaac Newton Institute of Chile, Yugosavia Branch

Received 11 October 2002 / Accepted 21 November 2002

Abstract. In hot star atmospheres, the Stark broadening mechanism is the main pressure broadening mechanism. An interesting application where such a mechanism is of interest is the modeling and investigation of hot star spectra, stellar atmospheres and subphotospheric layers. Consequently, for the investigation and modeling of the Hg-Mn star and other type of hot star atmospheres, the Stark broadening parameters for Co III spectral lines may be of interest.

Here we present Stark broadening data for 20 Co III spectral lines (from a^6D -z^6D^o and a^6D -z^6F^o Co III multiplets), as a function of temperature, calculated by using the modified semi-empirical approach. The importance of the electron-impact effect in the case of the Co III 194.98 nm line for several stellar atmosphere models has been tested.

Key words. atomic processes – line formation – stars: atmospheres – stars: early-type

1. Introduction

Spectral lines of doubly charged heavy element ions are present in hot star spectra, and they are of particular interest for modeling of CP star atmospheres. The spectral lines for singly ionized cobalt are present, e.g. in Hg-Mn star spectra (Bolcal & Didelon 1987). The investigation of cobalt abundance in Hg-Mn stars shows that most of the Hg-Mn stars are largely cobalt-deficient ([Co/H] ≤ -2 dex), except for the mildly cobalt-rich stars, ν Cnc and ϕ Her, and the cobalt-normal stars 87 Psc and 36 Lyn (Smith & Dworetsky 1993).

In hot star atmospheres the Stark broadening mechanism is the main pressure broadening mechanism (see e.g. Dimitrijević 1989; Popović et al. 1999, 2001). This broadening mechanism also may be important in the case of cooler stars, e.g. solar type stars, for transitions involving higher principal quantum numbers (Vince et al. 1985). An interesting application where such a mechanism is of interest is also the modeling and investigation of subphotospheric layers (Seaton 1987). Consequently, for the investigation and modeling of the Hg-Mn star and other types of hot star atmospheres, the Stark broadening parameters for Co III spectral lines are of interest. We underline that with instruments like the Goddard High Resolution Spectrograph on the Hubble Space Telescope, good resolution spectra with line profiles of trace elements become available. Here we present the Stark broadening data for 20 Co III spectral lines calculated using the modified semi-empirical approach (Dimitrijević & Konjević 1980; Dimitrijević & Kršljanin 1986; Popović & Dimitrijević 1996).

Send offprint requests to: D. Tankosić

* Table 1 is only available in electronic form at the CDS via anonymous ftp to `cdsarc.u-strasbg.fr` (`130.79.128.5`) or via `http://cdsweb.u-strasbg.fr/cgi-bin/qcat?J/A+A/399/795`

2. Theory

According to the modified semi-empirical (MSE) approach (Dimitrijević & Konjević 1980; Dimitrijević & Kršljanin 1986) the electron impact full width (*FHWM*) of an isolated ion line is given as

$$\begin{aligned} w_{MSE} = N\frac{4\pi}{3c}\frac{\hbar^2}{m^2}\left(\frac{2m}{\pi kT}\right)^{1/2}\frac{\lambda^2}{\sqrt{3}}\cdot\Bigg\{&\sum_{\ell_i\pm1}\sum_{L_{i'}J_{i'}}\mathfrak{R}^2_{\ell_i,\ell_i\pm1}\widetilde{g}(x_{\ell_i,\ell_i\pm1}) \\ &+\sum_{\ell_f\pm1}\sum_{L_{f'}J_{f'}}\mathfrak{R}^2_{\ell_f,\ell_f\pm1}\widetilde{g}(x_{\ell_f,\ell_f\pm1})+\left(\sum_{i'}\mathfrak{R}^2_{ii'}\right)_{\Delta n\neq0} \\ &\times g(x_{n_i,n_i+1})+\left(\sum_{f'}\mathfrak{R}^2_{ff'}\right)_{\Delta n\neq0} g(x_{n_f,n_f+1})\Bigg\}, \end{aligned} \tag{1}$$

and the corresponding Stark shift as

$$\begin{aligned} d = N\frac{2\pi}{3c}\frac{\hbar^2}{m^2}\left(\frac{2m}{\pi kT}\right)^{1/2}\frac{\lambda^2}{\sqrt{3}}\cdot\Bigg\{&\sum_{L_{i'}J_{i'}}\sigma_{J_iJ_{i'}}\mathfrak{R}^2_{\ell_i,\ell_i+1}\widetilde{g}_{\rm sh}(x_{\ell_i,\ell_i+1}) \\ &-\sum_{L_{i'}J_{i'}}\sigma_{J_iJ_{i'}}\mathfrak{R}^2_{\ell_i,\ell_i-1}\widetilde{g}_{\rm sh}(x_{\ell_i,\ell_i-1})\sum_{L_{f'}J_{f'}}\sigma_{J_fJ_{f'}}\mathfrak{R}^2_{\ell_f,\ell_f+1}\widetilde{g}_{\rm sh}(x_{\ell_f,\ell_f+1}) \\ &+\sum_{L_{f'}J_{f'}}\sigma_{J_fJ_{f'}}\mathfrak{R}^2_{\ell_f,\ell_f-1}\widetilde{g}_{\rm sh}(x_{\ell_f,\ell_f-1})+\left(\sum_{i'}\mathfrak{R}^2_{ii'}\right)_{\Delta n\neq0} g_{\rm sh}(x_{n_i,n_i+1}) \\ &-2\sum_{i'(\Delta E_{ii'}<0)}\sum_{L_{i'}J_{i'}}\mathfrak{R}^2_{\ell_i,\ell_{i'}}g_{\rm sh}(x_{\ell_i,\ell_{i'}})-\left(\sum_{f'}\mathfrak{R}^2_{ff'}\right)_{\Delta n\neq0} g_{\rm sh}(x_{n_f,n_f+1}) \\ &+2\sum_{f'(\Delta E_{ff'}<0)}\sum_{L_{f'}J_{f'}}\mathfrak{R}^2_{\ell_f,\ell_{f'}}g_{\rm sh}(x_{\ell_f,\ell_{f'}})+\sum_k\delta_k\Bigg\} \end{aligned} \tag{2}$$

where the initial level is denoted i, the final one with f, $\mathfrak{R}^2_{\ell_k,\ell_{k'}}$, $k = i, f$ is the square of the matrix element, and

$$\left(\sum_{k'} \mathfrak{R}^2_{kk'}\right)_{\Delta n \neq 0} = \left(\frac{3n^*_k}{2Z}\right)^2 \frac{1}{9}(n^{*2}_k + 3\ell^2_k + 3\ell_k + 11) \quad (3)$$

(in the Coulomb approximation).

In Eqs. (1) and (2)

$$x_{l_k,l_{k'}} = \frac{E}{\Delta E_{l_k,l_{k'}}}, k = i, f$$

where $E = \frac{3}{2}kT$ is the electron kinetic energy and $\Delta E_{l_k,l_{k'}} = |E_{l_k} - E_{l_{k'}}|$ is the energy difference between levels l_k and $l_k \pm 1$ (k = i, f),

$$x_{n_k,n_k+1} \approx \frac{E}{\Delta E_{n_k,n_k+1}},$$

where for $\Delta n \neq 0$ the energy difference between energy leves with n_k and $n_k + 1$, $\Delta E_{n_k,n_k+1}$, is estimated as $\Delta E_{n_k,n_k+1} \approx 2Z^2 E_{\rm H}/n^{*3}_k$. $n^*_k = [E_{\rm H}Z^2/(E_{\rm ion} - E_k)]^{1/2}$ is the effective principal quantum number, Z is the residual ionic charge, for example $Z = 1$ for neutral atoms and $E_{\rm ion}$ is appropriate spectral series limit.

In Eqs. (1)–(3) N and T are electron density and temperature, respectively, while with $g(x)$ (Griem 1968), $\widetilde{g}(x)$ (Dimitrijević & Konjević 1980) and $g_{\rm sh}(x)$ (Griem 1968), $\widetilde{g}_{\rm sh}(x)$ Dimitrijević & Kršljanin 1986) are the corresponding Gaunt factors for width and shift, respectively. The factor $\sigma_{kk'} = (E_{k'} - E_k)/|E_{k'} - E_k|$, where E_k and $E_{k'}$ are the energy of the considered and its pertubing level. The sum $\sum_k \delta_k$ is different from zero only if perturbing levels strongly violating the assumed approximations exist and may be evaluated as

$$\delta_i = \pm\mathfrak{R}^2_{ii'}\left[g_{\rm sh}\left(\frac{E}{\Delta E_{i,i'}}\right) \mp g_{\rm sh}(x_{n_i,n_i+1})\right], \quad (4)$$

for the upper level, and

$$\delta_f = \mp\mathfrak{R}^2_{ff'}\left[g_{\rm sh}\left(\frac{E}{\Delta E_{f,f'}}\right) \mp g_{\rm sh}(x_{n_f,n_f+1})\right], \quad (5)$$

for the lower level. In Eqs. (4) and (5) lower signs correspond to $\Delta E_{jj'} < 0$.

In comparison with the semiclasical perturbation approach (Sahal-Bréchot 1969a,b; Dimitrijević et al. 1991), the modified semi-empirical approach needs a considerably smaller amount of atomic data. In fact, if there are not perturbing levels strongly violating the assumed approximation, for e.g. the line width calculations, we need only the energy levels with $\Delta n = 0$ and $\ell_{if} = \ell_{if} \pm 1$, since all perturbing levels with $\Delta n \neq 0$, needed for a full semiclassical investigation are lumped together and approximately estimated. The modified semi-empirical method is used here, since we do not have a sufficiently complete set of published experimental Co III energy levels for an adequate semiclassical treatment.

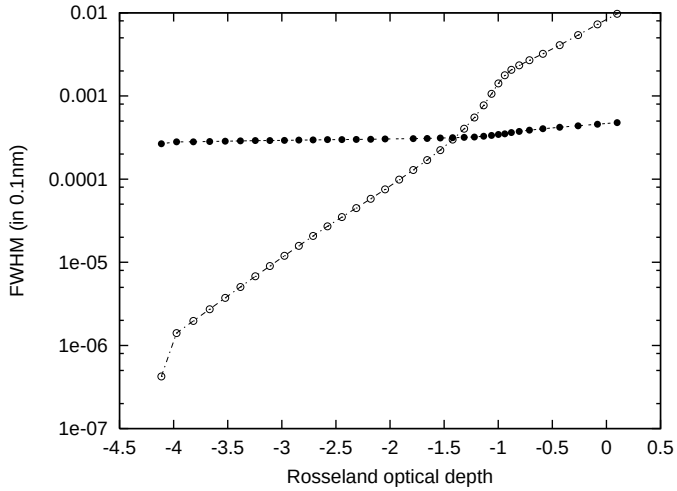

Fig. 1. Thermal Doppler (full circles) and Stark widths (open circles) for Co III (λ = 194.98 nm) spectral line as functions of optical depth for an A type star ($T_{\rm eff}$ = 10 000 K, log g = 4).

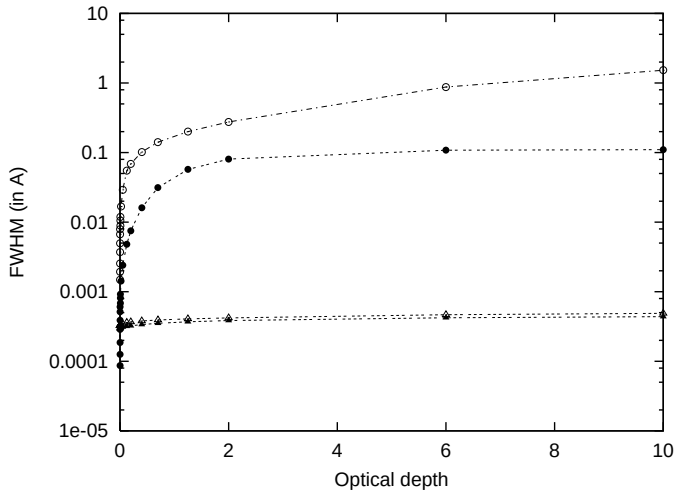

Fig. 2. Same as in Fig. 1 but for DA ($T_{\rm eff}$ = 10 000 K, log g = 6) and DB ($T_{\rm eff}$ = 15 000 K, log g = 7) white dwarfs with full circles is denoted Stark *FWHM* for DA and with open circles for DB white dwarfs. Full triangles denote thermal Doppler *FWHM* for DA and open triangles DA white dwarfs.

3. Results and discussion

The Stark broadening parameter calculations for 20 Co III spectral lines considered were performed using the modified semi-empirical approach (Dimitrijević & Konjević 1980; Dimitrijević & Kršljanin 1986; Popović & Dimitrijević 1996). Oscillator strengths have been calculated using the method of Bates & Damgaard (1949). The LS coupling approximation and the configuration mixing has been taken into account (see Popović & Dimitrijević 1996). The Co III energy levels needed for the Stark broadening parameter calculations as well as the purity of energy levels (configuration mixing) have been taken from Sugar & Corliss (1981). In Table 1, Stark widths and shifts for the 20 Co III spectral lines (from a^6D -z^6D^o and a^6D -z^6F^o multiplets), for an electron density of 10^{23} m^{-3} and temperature range 10 000–30 00 K, are shown. We have

calculated Stark broadening parameters for seven additional Co III lines, but the difference between lines from the same multiplet was too small and in Table 1 we only indicated that the results are practically the same. The average accuracy of the modified semi-empirical approach is ±50% (Dimitrijević & Konjević 1980).

In order to see the influence of Stark broadening mechanism for Co III spectral lines in stellar plasma conditions, we have calculated the Stark widths for the Co III 194.98 nm spectral line in different models of stellar atmospheres. In Figs. 1 and 2, the electron-impact and thermal Doppler widths as function of optical depth for a Kurucz's (1979) A type star ($T_{\rm eff}$ = 10 000 K, log g = 4) and models of DA ($T_{\rm eff}$ = 10 000 K, log g = 6) and DB ($T_{\rm eff}$ = 15 000 K, log g = 7) white dwarf atmospheres (Wickramasinghe 1972) are presented. From Fig. 1, in the case of an A type star, one can observe the existence of photospheric layers where Doppler and Stark widths are comparable and where the Stark width is dominant. In the case of white dwarf atmospheres (see Fig. 2) the Stark broadening mechanism is important in all considered layers of atmospheres and in deeper atmosphere layers the Stark width is three to four orders of magnitude larger than the termal Doppler width, so that in all considered cases the Stark broadening effect should be taken into account in abundance determination, spectra synthesis and modeling of stellar plasmas.

There are no experimental data or any other theoretical calculations for comparison, so an experimental determination of Co III Stark broadening parameters is of interest.

Acknowledgements. This work is a part of the projects "Influence of collisional processes on astrophysical plasma lineshapes" and "Astrophysical Spectroscopy of Extragalactic Objects", supported by the Ministry of Science, Technologies and Development of Serbia. The research was supported also by the Fonds zur Förderung der wissenschaftlichen Forschung (Project S7303-AST).

References

Bates, D. R., & Damgaard, A. 1949, Trans. Roy. Soc. London, Ser. A, 242, 101
Bolcal, C., & Didelon, P. 1987, Elemental Abundance Analyses, Institut d'Astronomie de l'Université de Lausanne, Chavannes-des-Bois, Switzerland, 152
Dimitrijević, M. S. 1989, Bull. Obs. Astron. Belgrade, 140, 111
Dimitrijević, M. S., & Konjević, N. 1980, J. Quant. Spectrosc. Radiat. Transfer, 24, 454
Dimitrijević, M. S., & Kršljanin, V. 1986, A&A, 165, 269
Dimitrijević, M. S., Sahal-Bréchot, S., Bommier, V. 1991, A&AS, 89, 581
Griem, H. R. 1968, Phys. Rev., 165, 258
Griem, H. R. 1974, Spectral Line Broadening by Plasmas (Academic Press, New York)
Kurucz, R. L. 1979, ApJS, 40, 1
Popović, L. Č., & Dimitrijević, M. S. 1996, Phys. Scr., 53, 325
Popović, L. Č., Dimitrijević, M. S., & Ryabchikova, T. 1999, A&A, 350, 719
Popović, L. Č., Simić, S., Milovanović, N., & Dimitrijević, M. S. 2001, ApJS, 135, 109
Sahal-Bréchot, S. 1969a, A&A, 1, 91
Sahal-Bréchot, S. 1969b, A&A, 2, 322
Seaton, M. J. 1987, J. Phys. B, 20, 6363
Smith, K. C., & Dworetsky, M. M. 1993, A&A, 274, 335
Sugar, J., & Corllis, C. 1981, J. Phys. Chem. Ref. Data, 10, 4
Vince, I., Dimitrijević, M. S., & Kršljanin, V. 1985, in Progress in Stellar Line Formation Theory, ed. J. Beckman, & L. Crivellari (Reidel, Dordrecht), 373
Wickramasinghe, D. T. 1972, Mem. R. Astron. Soc., 76, 129

A&A 400, 1155–1159 (2003)
DOI: 10.1051/0004-6361:20030064
© ESO 2003

Astronomy & Astrophysics

Stark broadening parameters in the S III spectrum

A. Srećković[1,2], M. S. Dimitrijević[2,3], S. Djeniže[1,2], and S. Bukvić[1,2]

[1] Faculty of Physics, University of Belgrade, 11001 Belgrade, POB 368, Serbia, Yugoslavia
[2] Isaac Newton Institute of Chile, Yugoslavia Branch, Belgrade, Yugoslavia
[3] Astronomical Observatory 11160 Belgrade, Volgina 7, Serbia, Yugoslavia
e-mail: steva@ff.bg.ac.yu

Received 2 December 2002 / Accepted 20 December 2002

Abstract. Stark widths and shifts of astrophysically important 10 doubly ionized sulfur (S III) spectral lines (within the 3d–4p and 4s–4p transitions) have been measured in a SF_6 plasma created in the linear, low-pressure, pulsed arc discharge at about 35 000 K electron temperature and about 2.8×10^{23} m^{-3} electron density. The widths and shifts have been calculated using the semiclassical perturbation formalism (SCPF) (taking into account the impurity of energy levels, i.e. that the atomic energy levels are expressed as a mix of different configurations due to the configuration interaction), modified semiempirical (SEM) approximation, simplified semiclassical theory (G) and its modification (GM) taking into account new energy level values. Calculations have been performed for electron temperatures between 10 000 K and 150 000 K for electrons, protons and helium ions as perturbers. The measured and calculated S III shifts present the first published data in this field.

Key words. plasmas – line: profiles – atomic data

1. Introduction

The ionized sulfur spectral lines play an important role in astrophysics. Recently, ultra-violet line emission from S III ions has been found in the spectra emitted from the diffuse interstellar medium (Shelton 2002). S III spectral lines have been obtained, also, in spectra of galaxies with Compact H II Regions (Vermeij & van der Hulst 2002; Martin-Hernández et al. 2002). Doubly ionized sulfur spectral lines have been used for the nebular chemical abundance diagnostics (Oey & Shields 2000). In the works: Kwitter & Henry (2001) and Castellanos et al. (2002) (and in many other works) presence of the S III ions was discovered in spectra of various cosmic light sources. Therefore, the S III spectral line characteristics are of interest in astrophysics. In hot stars with $T_{\rm eff}$ around or higher than 10 000 K, the hydrogen is mainly ionized and Stark broadening is the main pressure broadening mechanism. Thus, the knowledge of the Stark broadening parameters (the width and the shift) is important for the astrophysical and laboratory plasma diagnostics or modeling (Griem 1974, 1997; Zeippen 1995; Lesage & Fuhr 1999; Konjević et al. 2002).

In the present work we will present the first reliable Stark shift (d) measurements of S III spectral lines with their first calculated values, performed by us, on the basis of the semiclassical perturbation formalism (SCPF) (taking into account the impurity of energy levels, i.e. that the atomic energy levels are expressed as a mix of different configurations due to the configuration interaction), modified semiempirical (SEM) approximation (Dimitrijević & Konjević 1980) and the modification (GM) (Dimitrijević & Konjević 1980) of the simplified semiclassical theory (G) (Eq. (526) in Griem 1974) taking into account energy level values of Johansson et al. (1992) not available for earlier calculations (Dimitrijević & Konjević 1981; Dimitrijević 1988a,b). Calculation have been performed for electron temperatures between 10 000 K and 150 000 K for electrons, protons and helium ions as perturbers. Corresponding Stark *FWHM* (full-width at half intensity maximum, W) is also measured and calculated. Three of them are the first measured data. Our measured and calculated W and d values are compared to available experimental S III Stark parameters (Platiša et al. 1979; Djeniže et al. 1990).

2. Experiment

The linear pulsed arc that was used as plasma source was described in detail in our previous publications (Djeniže et al. 1992, 2002a,b; Srećković et al. 2001). Thus, only a few details will be given here. A pulsed discharge was occurred in a Pyrex discharge tube of 5 mm inner diameter and had plasma length of 6.3 cm. The tube had quartz windows. The working gas was SF_6 at 130 Pa filling pressure in a flowing regime (10 ml/min). The used experimental set-up system, recording procedure and applied diagnostics methods are presented in our earlier publication (Djeniže et al. 2002b, and references therein). The absence of the self-absorption was checked using the method described in Djeniže & Bukvić (2001). Obtained electron

Send offprint requests to: A. Srećković, e-mail: steva@ff.bg.ac.yu

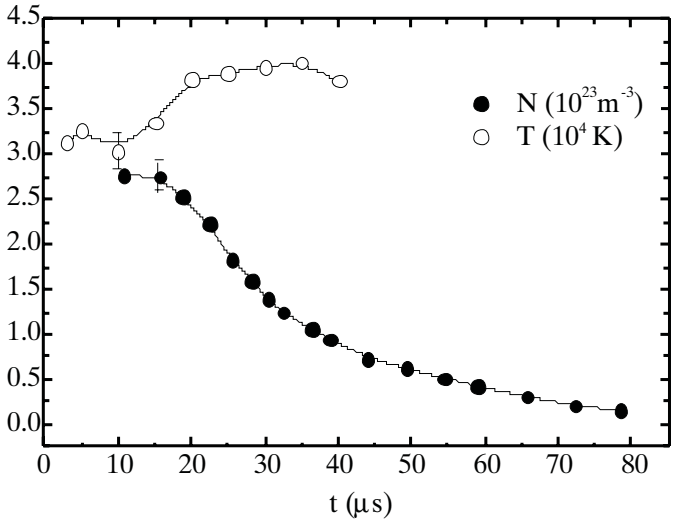

Fig. 1. Temporal evolutions of the electron temperature (T) and electron density (N). Error bars present ±7% and ±6%, respectively.

temperature (T) and electron density (N) decays are presented in Fig. 1.

2.1. Stark widths measurements

The measured profiles were of the Voigt type due to the convolutions of the Lorentzian Stark and Gaussian profiles caused by Doppler and instrumental broadening. For the electron density and temperature in our experiment the Lorentzian fraction was dominant. van der Waals (Griem 1974) and resonance (Griem 1974) broadening were estimated to be smaller by more than one order of magnitude in comparison to Stark, Doppler and instrumental broadening. The standard deconvolution procedure (Davies & Vaughan 1963) was applied using the least square algorithm. The Stark widths were measured with ±12% error at a given N and T. Our measured Stark *FWHM* (W_m) are presented in Table 1.

2.2. Stark shifts measurements

The Stark shifts were measured relative to the unshifted spectral lines emitted by the same plasma (Djeniže et al. 2002a, and references therein). Stark shift data are corrected to the electron temperature decay (Popović et al. 1992). Our measured Stark shifts (d_m) are presented in Table 1.

3. Theory

The S III Stark widths (W) and shift (d) values have been calculated using the semiclassical perturbation formalism (SCPF) (Sahal-Bréchot 1969a,b; 1974, 1991; Fleurier et al. 1974; Dimitrijević et al. 1991; Dimitrijević & Sahal-Bréchot 1996a,b) taking into account the impurity of energy levels, i.e. that the atomic energy levels are expressed as a mix of different configurations due to the configuration interaction, for electrons, protons and helium ions as perturbers. We have performed, also, calculations on the basis of the modified semiempirical theory (SEM) (Dimitrijević & Konjević 1980, 1981), and the modification (GM) (Dimitrijević & Konjević 1980) of the simplified semiclassical theory (G) (Eq. (526) in Griem 1974). Atomic energy levels needed for calculation have been taken in Johansson et al. (1992) for electrons as perturbers, only. Calculations have been performed for electron temperatures between 10 000 K and 150 000 K. Calculated W and d values are presented in Table 2.

Table 1. Measured S III Stark *FWHM* (W_m in pm) and shift (d_m in pm) at given T (in 10^3 K) and N (in 10^{23} m^{-3}). Transitions and wavelengths are taken from NIST (2002). Positive shift is toward the red.

Transition Multiplet	λ (nm)	T	N	W_m	d_m
3p3d–3p(^{2}P^0)4p ^{3}P^0–^{3}D (1)	370.9338	30.4	2.75	43.1	−1.1 ± 0.5
		31.2	2.84	36.1	
		33.6	2.80	36.0	
		38.3	2.43	37.9	
	371.0422	30.4	2.75	43.4	−1.4 ± 1.2
		31.2	2.84	44.0	
		33.6	2.80	45.6	
		38.3	2.43	32.9	
^{3}P^0–^{3}P (2)	337.0351	30.4	2.75	51.8	0.0 ± 0.6
		31.2	2.84	47.7	
		33.6	2.80	42.1	
		38.3	2.43	42.3	
	338.7092	30.4	2.75	61.5	0.0 ± 0.3
		31.2	2.84	47.0	
		33.6	2.80	46.2	
		38.3	2.43	47.8	
^{3}D^0–^{3}P (8)	392.8556	30.4	2.75	68.3	5.2 ± 0.9
		31.2	2.84	66.9	
		33.6	2.80	61.8	
		38.3	2.43	62.9	
	398.3723	30.4	2.75	72.5	7.6 ± 1.2
		31.2	2.84	69.5	
		33.6	2.80	74.3	
		38.3	2.43	72.4	
3p4s–3p(^{2}P^0)4p ^{3}P^0–^{3}P (4)	436.1468	30.4	2.75	80.2	0.3 ± 0.1
		31.2	2.84	66.5	
		33.6	2.80	62.6	
		38.3	2.43	63.0	
^{3}P^0–^{3}P (5)	389.9093	30.4	2.75	75.5	1.1 ± 0.5
		31.2	2.84	64.7	
		33.6	2.80	64.0	
		38.3	2.43	61.4	
^{3}P^0–^{3}S (6)	366.1942	30.4	2.75	78.5	3.7 ± 0.7
		31.2	2.84	79.4	
		33.6	2.80	78.1	
		38.3	2.43	77.0	
	371.7717	30.4	2.75	72.2	1.2 ± 0.6
		31.2	2.84	66.9	
		33.6	2.80	66.3	
		38.3	2.43	63.8	

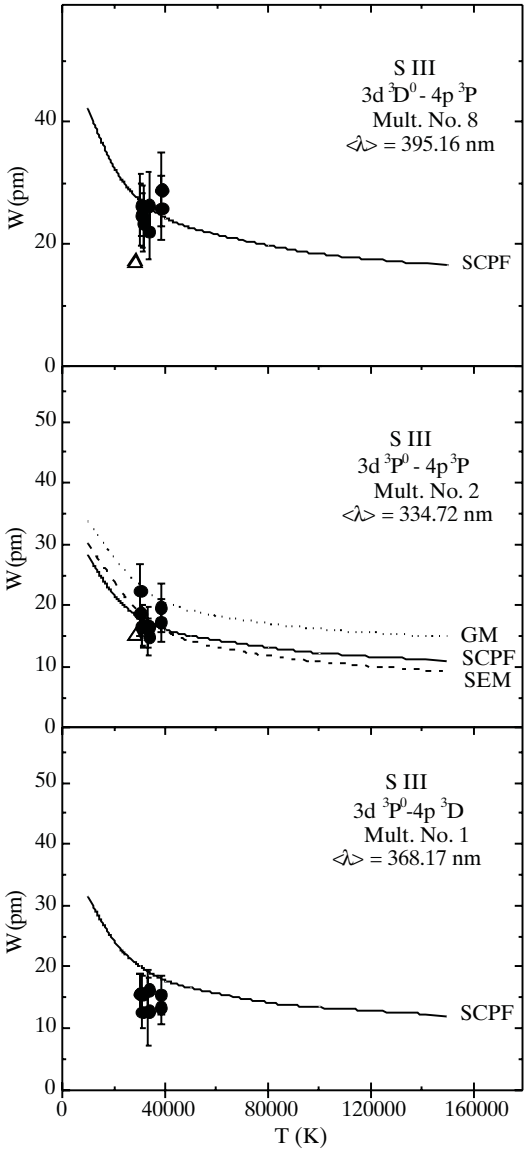

Fig. 2. Stark *FWHM* (*W* in pm) vs. electron temperature at 10^{23} m^{-3} electron density in the 3d–4p transition. SCPF, SEM and GM present our calculated *W* values using semiclassical perturbation formalism, modified semiempirical approaches and simplified semiclassical theory, respectively, for electrons as perturbers. •, our experimental data; △, Platiša et al. (1979); ◯, Djeniže et al. (1990). $< \lambda >$ is the mean wavelength in the multiplet. Error bars represent estimated uncertainties (±18%).

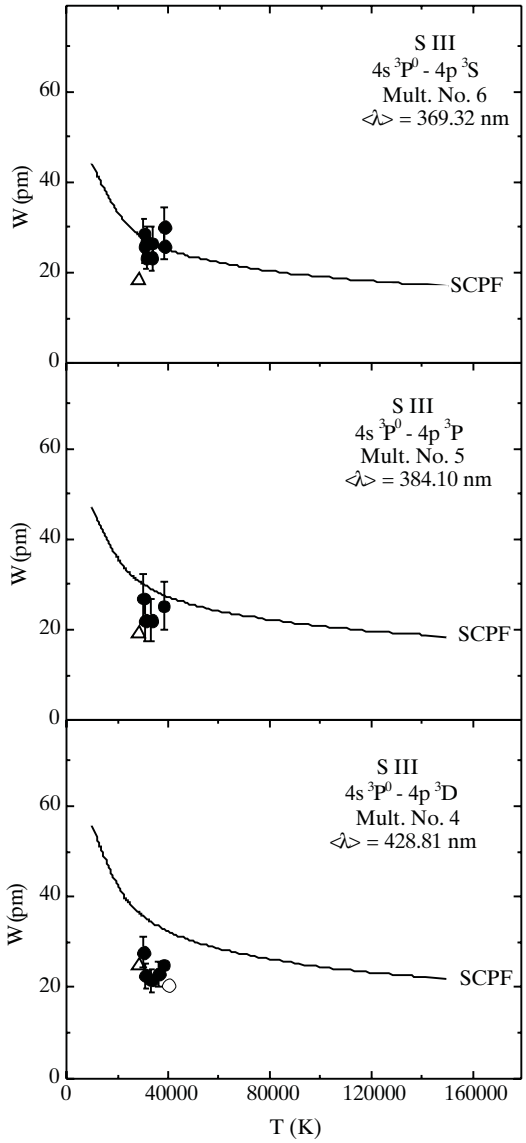

Fig. 3. Stark *FWHM* (*W* in pm) vs. electron temperature at 10^{23} m^{-3} electron density in the 4s–4p transition. The symbols are the same as in Fig. 2.

4. Results and discussion

Our measured (W_m and d_m) and calculated (W and d) values are presented in Tables 1 and 2, respectively. For each value given in Table 2, the collision volume multiplied by perturber density is much less than one and the impact approximation is valid (Sahal-Bréchot 1969a,b). When the impact approximation is not valid, the ion broadening contribution may be estimated by using quasistatic approach (Sahal-Bréchot 1991 or Griem 1974).

In order to compare the measured and calculated Stark *FWHM* values, we have presented in Figs. 2 and 3 existing experimental data set including our results, together with our theoretical predictions.

On the basis of the found *W* and *d* values one can conclude:

Very good agreement was found among our measured and calculated (SCPF) *W* values in the 3d–4p and 4s–4p transitions except in the multiplet No. 4 where SCPF values overvalue experimental data at about 35%. It turns out that SEM and GM *W* values also agree with our W_m data (see Fig. 2).

We have found that Stark width generated by electrons is dominant and the proton and helium ion contributions to the total Stark width can be neglected up to 150 000 K temperature.

Our calculated *d* values are very small. In the case of the 3d–4p transition they are practically equal to zero (within the uncertainties of the theory). In the case of the 4s–4p transition they are about 2 pm. Measured d_m values are also small. In the 4s–4p transition they show different sign in comparison to calculated ones. Evident finite d_m values are found in the case of

Table 2. Calculated S III Stark *FWHM* (*W* in pm) and shift (*d* in pm) for electrons (a), protons (b) and helium ions (c) as preturbers for various plasma temperatures (T in 10^4 K) and 10^{23} m^{-3} perturber density. A, B and C denote values obtained by semiclassical perturbation formalism (SCPF), modified semiempirical method (SEM) and modified simplified semiclassical theory (GM), respectively. Positive shift is toward the red. $< \lambda >$ is the mean wavelength in the multiplet. For each value given in Table 2, the collision volume multiplied by perturber density is much less than one and the impact approximation is valid (Sahal-Bréchot 1969a,b). When the impact approximation is not valid, the ion broadening contribution may be estimated by using quasistatic approach (Sahal-Bréchot 1991 or Griem 1974).

	Transition Multiplet	$< \lambda >$ (nm)		T (10^4 K)											
				1		2		3		5		10		15	
				W	*d*	*W*	*d*	*W*	*d*	*W*	*d*	*W*	*d*	*W*	*d*
A	$3d^3P^0$–$4p\ ^3D$	368.17	a	30.5	1.50	22.9	1.01	19.7	0.86	16.4	0.69	13.3	0.69	12.0	0.57
	(1)		b	0.82	0.09	1.42	0.02	1.75	0.03	2.14	0.05	2.43	0.08	2.60	0.10
			c	1.18	0.09	1.77	0.02	2.10	0.03	2.32	0.04	2.61	0.07	2.76	0.08
	$3d^3P^0$–$4p\ ^3P$	334.72	a	26.9	1.07	20.5	0.61	17.6	0.56	14.8	0.47	12.1	0.41	10.9	0.41
	(2)		b	0.73	0.01	1.25	0.03	1.54	0.04	1.87	0.06	2.12	0.10	2.26	0.12
			c	1.05	0.01	1.56	0.03	1.83	0.04	2.02	0.06	2.27	0.09	2.40	0.11
	$3d^3D^0$–$4p\ ^3P$	395.16	a	42.1	−0.64	31.5	−0.28	26.8	−0.18	22.4	−0.18	18.2	−0.20	16.5	−0.11
	(8)		b	1.04	−0.07	1.78	−0.14	2.19	−0.20	2.65	−0.29	3.00	−0.40	3.20	−0.47
			c	1.49	−0.07	2.21	−0.14	2.60	−0.19	2.86	−0.25	3.21	−0.35	3.38	−0.38
	$4s^3P^0$–$4p\ ^3D$	428.81	a	55.7	−1.97	41.3	−2.39	35.1	−2.26	29.3	−2.05	24.1	−2.31	21.9	−2.04
	(4)		b	0.98	−0.40	1.77	−0.75	2.20	−0.99	2.78	−1.28	3.23	−1.60	3.52	−1.79
			c	1.42	−0.39	2.17	−0.69	2.62	−0.86	2.94	−1.10	3.36	−1.32	3.59	−1.47
	$4s^3P^0$–$4p\ ^3P$	384.10	a	47.1	−1.34	34.8	−1.81	29.6	−1.70	24.7	−1.53	20.4	−1.75	18.5	−1.54
	(5)		b	0.85	−0.30	1.51	−0.57	1.87	−0.75	2.33	−0.97	2.70	−1.22	2.93	−1.36
			c	1.23	−0.29	1.87	−0.52	2.23	−0.65	2.48	−0.84	2.82	−1.01	3.00	−1.12
	$4s^3P^0$-$4p\ ^3S$	369.32	a	44.1	−1.01	32.2	−1.44	27.2	−1.35	22.7	−1.22	18.7	−1.42	17.0	−1.26
	(6)		b	0.81	−0.24	1.43	−0.46	1.76	−0.62	2.18	−0.80	2.51	−1.02	2.72	−1.14
			c	1.17	−0.24	1.76	−0.43	2.10	−0.53	2.33	−0.69	2.64	−0.84	2.80	−0.94
B	$3d^3P^0$–$4p\ ^3P$	334.72	a	30.1				17.4		13.5		10.5		9.32	
	(2)														
C	$3d^3P^0$–$4p\ ^3P$	334.72	a	33.7				21.8		18.6		15.9		14.9	
	(2)														

the multiplet No. 8 in the 3d–4p transition. It should be noted that within the semiclassical perturbation approach, dipole contributions to the width are positive while the corresponding contribution to the shift have different signs. Consequently, if the width and shift values are of the same order of magnitude, the accuracy is also the same. However, if due to mutual cancelations of contributions with different signs, shift values are smaller for an order of magnitude or even more, as is the case here, the accuracy of such shift values are smaller. A reasonable estimate is to take as the error bars for theoretical shifts ±30 percent of the corresponding width value, which indicates that in the present case uncertainties of theoretical shifts are such that different signs for small theoretical and experimental shifts are without meaning. Consequently, one can consider measured shift values more reliable for further applications.

5. Conclusion

We have found a dominant contribution of the electron impact in comparison with proton and ionized helium impact to the total Stark width of the S III lines belonging to the 3d–4p and 4s–4p transitions. Protons and helium ions generate small Stark widths which can be neglected for lines considered up to a temperature of 150 000 K.

On the basis of the found agreement among measured and calculated *W* and *d* values we recommend the 337.0351 nm and 338.7092 nm S III spectral lines as lines with convenient Stark broadening parameters in astrophysical plasma diagnostics.

Acknowledgements. This work is a part of the projects "Determination of the atomic parameters on the basis of the spectral line profiles" and "Influence of collision processes on astrophysical plasma lineshapes" supported in part by the Ministry of Science, Technologies and Development of the Republic of Serbia.

References

Castellanos, M., Diaz, A. I., & Tenorio-Tagle, G. 2002, ApJ, 565, L79
Davies, J. I., & Vaughan, J. M. 1963, ApJ, 137, 1302
Dimitrijević, M. S., & Konjević, N. 1980, JQSRT, 24, 451

Dimitrijević, M. S., & Konjević, N. 1981, in Spectral Line Shapes, vol. 1, ed. B. Wende (Walter de Gruyter & Co., New York), 211
Dimitrijević, M. S. 1988a, A&A, 76, 53
Dimitrijević, M. S. 1988b, Bul. Obs. Astron. Belgrade, 139, 31
Dimitrijević, M. S., Sahal-Bréchot, S., & Bommier, V. 1991, A&AS, 89, 581
Dimitrijević, M. S., & Sahal-Bréchot, S. 1996a, Phys. Scr., 54, 50
Dimitrijević, M. S., & Sahal-Bréchot, S. 1996b, A&A, 119, 369
Djeniže, S., Srećković, A., Platiša, M., et al. 1990, Phys. Rev. A, 42, 2379
Djeniže, S., Srećković, A., & Labat, J. 1992, A&A, 253, 632
Djeniže, S., & Bukvić, S. 2001, A&A, 365, 252
Djeniže, S., Milosavljević, V., & Dimitrijević, M. S. 2002a, A&A, 382, 359
Djeniže, S., Srećković, A., Jelisavčić, M., & Bukvić, S. 2002b, A&A, 389, 1086
Fleurier, C., Sahal-Bréchot, S., & Chapelle, J. 1977, JQSRT, 17, 595
Griem, H. R. 1974, Spectral Line Broadening by Plasmas (New York: Academic Press)
Griem, H. R. 1997, Principles of Plasma Spectroscopy (Cambridge: Univ. Press Cambridge)
Johansson, L., Magnusson, C. E., Joelsson, I., & Zetterberg, P. O. 1992, Phys. Scr., 46, 221
Konjević, N., Lesage, A., Fuhr, J. R., & Wiese, W. L. 2002, J. Phys. Chem. Ref. Data, 31, 3, 819
Kwitter, K. B., & Henry, R. B. C. 2001, ApJ, 562, 804
Lesage, A., & Fuhr, J. R. 1999, Bibliography of Atomic Line Shapes and Shifts (April 1992 through June 1999), Observatoire de Paris
Martin-Hernández, N. L., Peeters, E., Morisset, C., et al. 2002, A&A, 381, 606
NIST-Atomic Spectra Database Lines Data, 2002 (Wavelengths ordered)
Oey, M. S., & Shields, J. C. 2000, ApJ, 539, 687
Platiša, M., Popović, M., Dimitrijević, M. S., & Konjević, N. 1979, JQSRT, 22, 333
Popović, L. Č., Srećković, A., & Djeniže, S. 1992, Proc. of the 11th ICSLS, A25, Carry le Rouet, France
Sahal-Bréchot, S. 1969a, A&A, 1, 91
Sahal-Bréchot, S. 1969b, A&A, 2, 322
Sahal-Bréchot, S. 1974, A&A, 35, 321
Sahal-Bréchot, S. 1991, A&A, 245, 322
Shelton, R. L. 2002, ApJ, 569, 758
Srećković, A., Dimitrijević, M. S., & Djeniže, S. 2001, A&A, 371, 354
Vermeij, R., & van der Hulst, J. M. 2002, A&A, 391, 1081
Zeippen, C. J. 1995, Phys. Scr., 58, 43

A&A 400, 791–793 (2003)
DOI: 10.1051/0004-6361:20021904
© ESO 2003

Astronomy & Astrophysics

Stark broadening of spectral lines of multicharged ions of astrophysical interest. XXIII. Be III*

M. S. Dimitrijević[1,2], M. Dačić[1,2], Z. Cvetković[1,2], and S. Sahal–Bréchot[3]

[1] Astronomical Observatory, Volgina 7, 11160 Belgrade, Serbia, Yugoslavia
[2] Institute Isaac Newton of Chile, Yugoslavia Branch
[3] LERMA, UMR CNRS 8112, Observatoire de Paris–Meudon, 92195 Meudon, France

Received 6 November 2002 / Accepted 17 December 2002

Abstract. Using a semiclassical perturbation method, we have calculated electron–, proton–, and ionized helium–impact line widths and shifts for 52 Be III multiplets as a function of temperature and perturber density. Electron temperatures are 10 000 K; 20 000 K; 50 000 K; 100 000 K; 200 000 K and 300 000 K and perturber densities are from 10^{11} cm^{-3} up to 10^{21} cm^{-3}. The obtained results have been used for discussion of regularities and systematic trends along spectral series.

Key words. lines: profiles – atomic data – atomic processes – line: formation

1. Introduction

The astrophysical importance of light element ions line profile study is obvious, since such lines are present in stellar atmospheres. Such results are of interest e.g. for numerical modeling of stellar atmospheres or abundance determinations. The Be III Stark broadening parameters are additionally interesting for problems correlated with nucleogenesis, mixing between atmospheres and the interior, stellar structure and evolution (see e.g. Boesgaard 1988), and opacity calculations (Seaton 1988). Moreover, Stark broadening parameters of Be III lines are of interest for the investigation and diagnostic of laboratory and laser-produced plasma, as well as for the consideration of regularities and systematic trends. First experimental investigations of Be III plasma spectral line shapes, have been made by Fraenkel et al. (1968) who investigated high energy satellites in Be III spectrum and Malvezi et al. (1975) who investigated high-density laser-produced Be plasma. Rosznayi (1977) performed a theoretical study of Be III lines Stark broadening for a high density plasma with $kT = 21$ eV, and atom density 10^{19}–10^{21} cm^{-3}. In Dimitrijević & Konjević (1981) and Dimitrijević (1988a,b) Stark widths of Be III lines have been calculated within the semiempirical method (Griem 1968), the modified semiempirical method (Dimitrijević & Konjević 1980), the symplified semiclassical method (Griem 1974, Eq. (526)) and its modification (Dimitrijević & Konjević 1980). In Dimitrijević & Sahal-Bréchot (1996a,b) Stark broadening parameters of 12 Be III spectral lines have been obtained within the semiclassical perturbation approach (Sahal–Bréchot 1969a, b; see also Sahal–Bréchot 1974, 1991; Fleurier et al. 1977; Dimitrijević & Sahal–Bréchot 1984; Dimitrijević et al. 1991; Dimitrijević & Sahal–Bréchot 1995a,b). However, the recently published analysis of the spectrum and term system of Be III (Jupén et al. 2001) enables the calculation of Stark broadening parameters for 52 additional multiplets, with the standard accuracy. The aim of this work is to determine this additional parameters in order to extend the set of available Stark broadening data.

Obtained data are also of interest for investigations of regularities and systematic trends and have been used here for the investigations of such trends along spectral series. Results of such investigations are of interest for acquisition of new data by interpolation and for critical evaluation of existing experimental and theoretical data. Moreover, the obtained results are of interest for the investigation of regularities along the helium isoelectronic sequence since besides the results for Be III obtained here and in Dimitrijević & Sahal-Bréchot (1996a,b), the results for Li II (Dimitrijević & Sahal-Bréchot 1996c), C V (Dimitrijević & Sahal-Bréchot 1996d), O VII (Dimitrijević & Sahal–Bréchot 1998a), Na X (Dimitrijević & Sahal–Bréchot 1998b) and Si XIII (Dimitrijević & Sahal–Bréchot 1998c), have been published also.

This paper is the twenty third of a series devoted to the calculation of Stark broadening parameters of spectral lines of multicharged ions (see Dimitrijević & Sahal–Bréchot 1998b and references therein, Dimitrijević & Sahal–Bréchot 1988a,d; 1999), as the continuation of our previous research. A review of obtained results is given e.g. in Dimitrijević (1996).

Send offprint requests to: M. S. Dimitrijević,
e-mail: mdimitrijevic@aob.bg.ac.yu

* Table 1 is only available in electronic form at the CDS via anonymous ftp to cdsarc.u-strasbg.fr (130.79.128.5) or via http://cdsweb.u-strasbg.fr/cgi-bin/qcat?/A+A/400/791

2. Results and discussion

The semiclassical perturbation formalism used here, has been reviewed briefly e.g. in Dimitrijević & Sahal–Bréchot (1995a, 1996c). Energy levels for Be III have been taken in Jupén et al. (2001). Oscillator strengths have been calculated by using the method of Bates & Damgaard (1949) and the tables of Oertel & Shomo (1968). For higher levels, the method described by van Regemorter et al. (1979) has been used.

The results for 52 Be III multiplets, for Stark broadening due to electron−, proton−, and ionized helium−impacts are shown in Table 1 (accessible only in electronic form) for perturber densities 10^{11} cm^{-3}–10^{21} cm^{-3} and temperatures from 10 000 up to 300 000 K. Stark broadening parameters for densities lower than for tabulated values, are linear with perturber density. We also specify a parameter C (Dimitrijević & Sahal−Bréchot 1984), which gives an estimate for the maximum perturber density for which the line may be treated as isolated, when it is divided by the corresponding full width at half maximum. For each value given in Table 1 the collision volume (V) multiplied by the perturber density (N) is much less than one and the impact approximation is valid (Sahal−Bréchot 1969a,b). Values for $NV > 0.5$ are not given and values for $0.1 < NV \leq 0.5$ are denoted by an asterisk. When the impact approximation is not valid, the ion broadening contribution may be estimated by using quasistatic approach (Sahal−Bréchot 1991 or Griem 1974). In the region between where neither of these two approximations is valid, a unified type theory should be used. For example in Barnard et al. (1974), a simple analytical formula for such a case is given. The accuracy of the results obtained decreases when broadening by ion interactions becomes important.

In Figs. 1 and 2 the electron-impact full half widths and shifts for Be III $n_f s^1S$-$n_i p^1P^o$ lines as a function of n_i for different n_f, for $T = 50\,000$ K at $N_e = 10^{17}$ cm^{-3} is shown. Here, n_i is the principal quantum number of initial (upper), and n_f of the final (lower) level of the considered transition. We can see gradual change of Stark broadening parameters within particular $n_f s^1S$-$n_i p^1P^o$ spectral series, permitting the interpolation of new data or critical evaluation of mutual consistency of existing data as in our previous analyses (see e.g. Dimitrijević & Sahal−Bréchot 1996c). Exceptions of such behaviour have been analysed e.g. in Tankosić et al. (2001). As an addition to previous analyses (e.g. Dimitrijević & Sahal−Bréchot 1996c), where only one Li II $2s^3S$-np^3P^o series have been analysed in Figs. 1–2 are considered all calculated transitions belonging to different Be III $n_f s^1S$-$n_i p^1P^o$ series. One can be seen that differences between corresponding members with the same initial (upper) level of different spectral series are not large and increase gradually with the increase of the principal quantum number of the final (lower) level. Consequently, rough estimation of the mutual consistency of existing data or of an approximate value for a member of a different spectral series is possible in considered case on the basis of considered regularities if the upper (initial) level of the investigated transition is the same as for members of other spectral series with known Stark broadening parameters. Such regular behaviour of Stark broadening parameters within considered spectral series is the consequence of the gradual change of the energy separations between the initial (upper) level and the principal perturbing levels, shown in Fig. 3. It is of interest to determine experimentally Stark broadening parameters for several members of

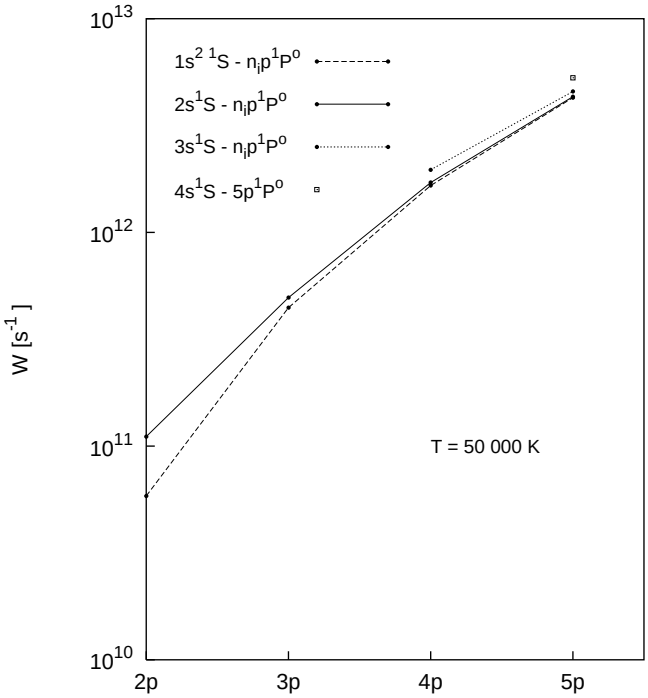

Fig. 1. Electron-impact full half widths (in angular frequency units) for Be III $n_f s^1S$-$n_i p^1P^o$ lines as a function of n_i for different n_f, for $T = 50\,000$ K at $N_e = 10^{17}$ cm^{-3}. Here, n_i is the principal quantum number of initial (upper), and n_f of the final (lower) level of the considered transition.

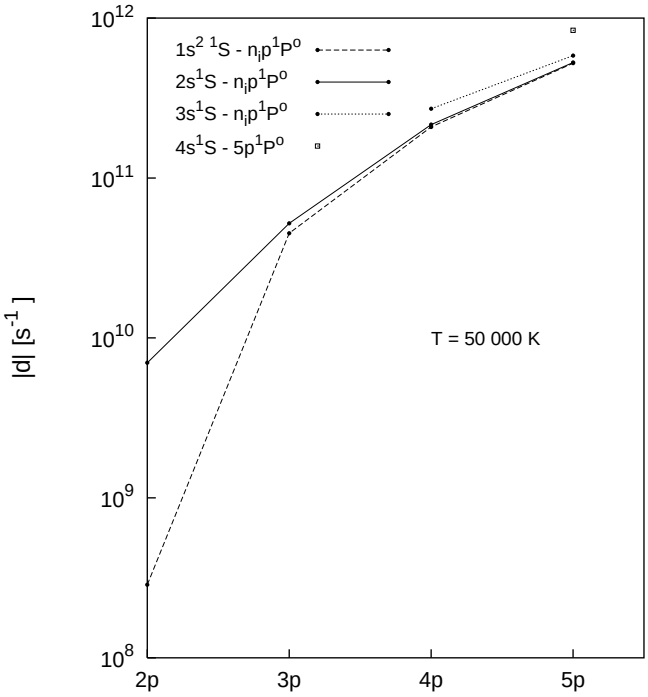

Fig. 2. As in Fig. 1 but for electron-impact shift.

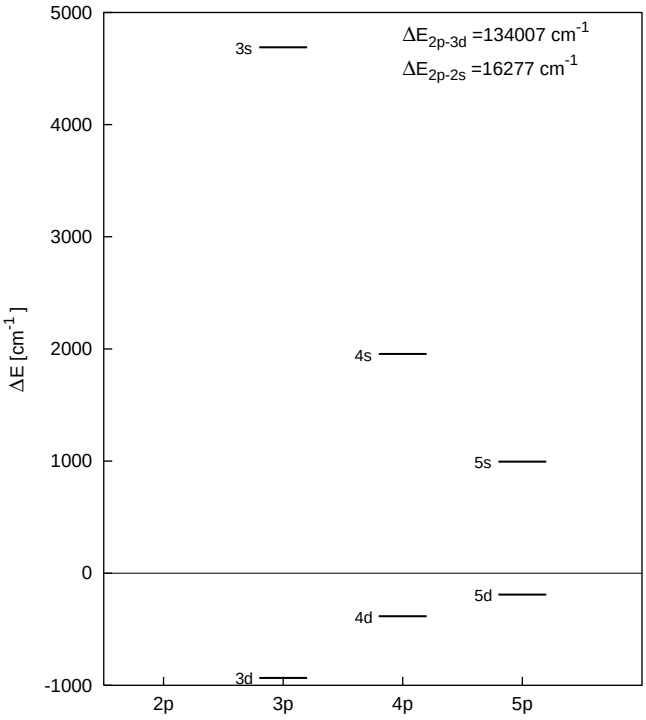

Fig. 3. Energy separations between the upper level $n_i p^1 P^o$ and the principal perturbing levels for Be III $n_f s^1 S$-$n_i p^1 P^o$ lines. Here, n_i is the principal quantum number of initial (upper), and n_f of the final (lower) level of the considered transition.

a Be III spectral series in order to test experimentally the possibilities of established regularities within spectral series for prediction of new data and checking the reliability and mutual consistency of existing ones.

Acknowledgements. This work is a part of the project "Influence of collisional processes on astrophysical plasma lineshapes", supported by Ministry of Science, Technologies and Development of Serbia. The research was supported also by the Fonds zur Förderung der wissenschaftlichen Forschung (Project S7303-AST).

References

Barnard, A. J., Cooper, J., & Smith, E. W. 1974, J. Quant. Spectrosc. Radiative Transfer, 14, 1025
Bates, D. R., & Damgaard, A. 1949, Trans. Roy. Soc. London, Ser. A, 242, 101
Boesgaard, A. M. 1988, Vistas Astron., 31, 167
Dimitrijević, M. S. 1996, Zh. Prikl. Spektrosk., 63, 810
Dimitrijević, M. S. 1988a, A&AS, 76, 53
Dimitrijević, M. S. 1988b, Bull. Obs. Astron. Belgrade, 139, 31
Dimitrijević, M. S., & Konjević, N. 1980, J. Quant. Spectrosc. Radiat. Transfer, 24, 451
Dimitrijević, M. S., & Konjević, N. 1981, in Spectral Line Shapes, ed. B. Wende, W. de Gryuter, & Co. Berlin, New York, 221
Dimitrijević, M. S., & Sahal−Bréchot, S. 1984, J. Quant. Spectrosc. Radiat. Transfer, 31, 301
Dimitrijević, M. S., & Sahal-Bréchot, S. 1995a, Phys. Scr., 52, 41
Dimitrijević, M. S., & Sahal−Bréchot, S. 1995b, A&AS, 109, 551
Dimitrijević, M. S., & Sahal−Bréchot, S. 1996a, A&AS, 119, 369
Dimitrijević, M. S., & Sahal−Bréchot, S. 1996b, Bull. Astron. Belgrade, 153, 101
Dimitrijević, M. S., & Sahal-Bréchot, S., 1996c, Phys. Scr., 54, 50
Dimitrijević, M. S., & Sahal−Bréchot, S. 1996d, A&AS, 115, 351
Dimitrijević, M. S., & Sahal−Bréchot, S. 1998a, A&AS, 131, 141
Dimitrijević, M. S., & Sahal−Bréchot, S. 1998b, A&AS, 130, 539
Dimitrijević, M. S., & Sahal−Bréchot, S. 1998c, A&AS, 129, 155
Dimitrijević, M. S., & Sahal−Bréchot, S. 1998d, A&AS, 131, 143
Dimitrijević, M. S., & Sahal−Bréchot, S. 1999, A&AS, 133, 227
Dimitrijević, M. S., Sahal-Bréchot, S., & Bommier, V. 1991, A&AS, 89, 581
Fleurier, C., Sahal-Bréchot, S., & Chapelle, J. 1977, J. Quant. Spectrosc. Radiat. Transfer, 17, 595
Fraenkel, B. S., Goldsmith, S., & Feldman, U. 1968, Phys. Lett. A, 27, 111
Griem, H. R. 1968, Phys. Rev., 165, 258
Griem, H. R. 1974, Spectral Line Broadening by Plasmas (Academic Press, New York)
Jupén, C., Meigs, A., von Hellermann, M., et al. 2001, Phys. Scr., 64, 566
Malvezi, A. M., Janitti, E., & Tondello, G. 1975, Opt. Commun., 13, 307
Oertel, G. K., & Shomo, L. P. 1968, ApJS, 16, 175
Rosznayi, B. F. 1977, J. Quant. Spectrosc. Radiat. Transfer, 17, 77
Sahal−Bréchot, S. 1969a, A&A, 1, 91
Sahal−Bréchot, S. 1969b, A&A, 2, 322
Sahal−Bréchot, S. 1974, A&A, 35, 321
Sahal−Bréchot, S. 1991, A&A, 245, 322
Seaton, M. J. 1988, J. Phys. B, 21, 3033
Tankosić, D., Popović, L. Č., & Dimitrijević, M. S. 2001, Phys. Scr., 63, 54
van Regemorter, H., Hoang Binh Dy, & Prud'homme, M. 1979, J. Phys. B, 12, 1073

A&A 403, 787–791 (2003)
DOI: 10.1051/0004-6361:20030463
© ESO 2003

Astronomy & Astrophysics

Influence of chemi-ionization and chemi-recombination processes on the population of hydrogen Rydberg states in atmospheres of late type dwarfs

A. A. Mihajlov[1,2], D. Jevremović[3,4], P. Hauschildt[5,6], M. S. Dimitrijević[2,4], Lj. M. Ignjatović[1,2], and F. Alard[7]

[1] Institute of Physics, PO Box 57, 11001 Belgrade, Serbia and Montenegro
[2] Institute Isaac Newton of Chile, Yugoslavia Branch, Belgrade, Serbia and Montenegro
[3] APS Division, Phys. Depart., Queen's University Belfast, BT7 1NN, Northern Ireland, UK
[4] Astronomical Observatory, Volgina 7, 11160 Belgrade, Serbia and Montenegro
[5] Depart. of Phys. and Astronomy and Center for Simulat. Physics, University of Georgia, Athens, GA 30602, USA
[6] Hamburger Sternwarte, Universitaet Hamburg, Gojenbergsweg 112, 21029 Hamburg, Germany
[7] CRAL/ENS, 46 Allée d'Italie, 69634 Lyon Cedex 07, France

Received 22 July 2002 / Accepted 4 February 2003

Abstract. We study the influence of a group of chemi-ionization and chemi-recombination processes on the populations of higher states of hydrogen in the layers of a stellar atmosphere. The group of processes includes ionization: $H^*(n) + H(1s) \Longrightarrow H_2^+ + e$, $H^*(n) + H(1s) \Longrightarrow H(1s) + H^+ + e$, and inverse recombination: $H_2^+ + e \Longrightarrow H^*(n) + H(1s)$, $H(1s) + H^+ + e \Longrightarrow H^*(n) + H(1s)$, where $H^*(n)$ is the hydrogen atom in a state with the principal quantum number $n \gg 1$, and H_2^+ is the hydrogen molecular ion in a weakly bound rho-vibrational state of the ground state. These processes have been treated within the framework of the semi-classical approximation, developed in several previous papers, and have been included in the general stellar atmosphere code PHOENIX. We present results for an M dwarf atmosphere with $T_{\rm eff} = 3800$ K and find that the inclusion of chemi-ionization and chemi-recombination processes is significant in the low temperature parts of the atmosphere.

Key words. atomic processes – molecular processes – stars: late type

1. Introduction

For several years we have studied the chemi-ionization atom-atom collisional processes and inverse chemi-recombination processes that may influence the populations of the hydrogen atom Rydberg states in the weakly ionized layers of stellar atmospheres (Mihajlov et al. 1996a, 1997). In the case of hydrogen, these processes are:

$$H^*(n) + H(1s) \Longrightarrow H_2^+ + e, \quad (1a)$$
$$H^*(n) + H(1s) \Longrightarrow H(1s) + H^+ + e, \quad (1b)$$

$$H_2^+ + e \Longrightarrow H^*(n) + H(1s), \quad (2a)$$
$$H(1s) + H^+ + e \Longrightarrow H^*(n) + H(1s), \quad (2b)$$

where $H^*(n)$ is a hydrogen atom in a state with the principal quantum number $n \gg 1$, and H_2^+ is a hydrogen molecular ion in a weakly bound rho-vibrational state of the ground electronic state. In the case of ionization (1a,b), the lower limit of the Rydberg state range that was considered was set to $n = 4$ (Mihajlov et al. 1996a, 1997). The block of rho-vibrational states with a dissociation energy less than 1 eV has an essential role in the case of formation of the molecular ion (processes (1a) and (2a)) and within the range of quantum numbers that was considered. In the case of cool stellar atmosphere layers (3000 K $\leq T \leq$ 5000 K), the block of such weakly bound rho-vibrational states can be considered to be in equilibrium with the collisional $H(1s) + H^+$ complexes, without the requirement that the lower rho-vibrational states of molecular ion are in equilibrium (Mihajlov & Ljepojević 1982; Mihajlov et al. 1992). This fact makes the description of recombination processes (2a) and (2b) easier, since it enables us to avoid the direct determination of the density of molecular ions in weakly ionized rho-vibrational states.

In our previous work (Mihajlov et al. 1997, 1998) we estimated the influence of the processes (1a,b; 2a,b) for the low temperature layers of the Solar atmosphere. We compared the ionization and recombination fluxes with and without inclusion of the above processes and found a significant difference in the population of the $H^*(n)$ atomic states with $4 < n < 8$.

Here we discuss the importance of these processes in stellar atmospheres of lower temperature. This paper is organized as follows: in Sect. 2 we summarize the theoretical framework and in Sect. 3 we describe the changes in the stellar atmosphere

Send offprint requests to: M. S. Dimitrijević,
e-mail: mdimitrijevic@aob.bg.ac.yu

code PHOENIX and parameters of the test model atmosphere. We present our results and discussion in Sect. 4 and draw our conclusions in Sect. 5.

2. Theoretical remarks

Let $I_{\rm i}^{(a,b)}(n)$ and $I_{\rm r}^{(a,b)}(n)$ denote ionization and recombination fluxes affecting population and depopulation of excited hydrogen atom atomic levels due to reactions. By definition, ionization fluxes $I_{\rm i}^{(a,b)}(n)$ determining the rate of depopulation of $H^*(n)$ states are given by

$$I_{\rm i}^{(a)}(n) = K_i^{(a)}(n) \cdot N({\rm H}) \cdot N({\rm H}^*(n)) \quad (3a)$$

$$I_{\rm i}^{(b)}(n) = K_i^{(b)}(n) \cdot N({\rm H}) \cdot N({\rm H}^*(n)) \quad (3b)$$

where N(H) and $N(H^*(n))$ are H(1s) and $H^*(n)$ atom densities, and $K_{\rm i}^{\rm a}(n)$ and $K_{\rm i}^{\rm b}(n)$ are rate coefficients of the reactions (1a) and (1b) respectively. The recombination flux $I_{\rm r}^{(a)}(n)$, determining the velocity of population of $H^*(n)$ states due to the reaction (2a), is given by definition as: $I_{\rm r}^{(a)} = K_{\rm dr} \cdot N(H_2^+) \cdot N({\rm e})$, where N(e) and $N(H_2^+)$ are the electron density and the density of molecular ion H_2^+ in the abovementioned weakly bound rho-vibrational states, and $K_{\rm dr}$ is the corresponding rate coefficient of the dissociative recombination reaction (2a). The expression for the recombination flux $I_{\rm r}^{(a)}$ may be written by:

$$I_{\rm r}^{(a)}(n) = K_{\rm r}^{(a)}(n) \cdot N({\rm H}) \cdot N({\rm H}^+) \cdot N({\rm e}) \quad (4a)$$

where $K_{\rm r}^{(a)} = K_{\rm dr}[N({\rm H}) \cdot N({\rm H}^+)/N(H_2^+)]^{-1}$. The advantage of expression (4a) for the recombination flux $I_{\rm r}^{(a)}(n)$ is the fact that it introduces a new effective rate coefficient of the reaction (2a). If the ionization rate coefficient $K_{\rm i}^{\rm a}(n)$ is known, the $K_{\rm r}^{(a)}(n)$ may be determined directly, under assumption of the equilibrium between H_2^+ weakly bound rho-vibrational states and the H + H^+ collisional complex (Mihajlov & Ljepojević 1982; Mihajlov et al. 1992). This makes the treatment of the problem easier and enables us to avoid the determination of the $K_{\rm dr}(n)$ rate coefficient. The recombination flux $I_{\rm r}^{(b)}(n)$, determining the rate of population of $H^*(n)$ states due to the reaction (2b), is given, by definition, by:

$$I_{\rm r}^{(b)}(n) = K_{\rm r}^{(b)}(n) \cdot N({\rm H}) \cdot N({\rm H}^+) \cdot N({\rm e}), \quad (4b)$$

where $K_{\rm r}^{(b)}(n)$ is the rate coefficient of the reaction (2b). The influence of the processes (1a,b) and (2a,b) on $H^*(n)$ atomic states populations may be estimated using only the N(H), $N(H^*(n))$, $N(H^+)$ and N(e) populations.

Rate coefficients for the processes (1, 2) have been determined within the semi-classical theory described in the previous papers (Janev & Mihajlov 1980; Mihajlov & Ljepojević 1982; Mihajlov et al. 1992). This theory takes into account atomic collisions, where the $H^*(n)$ + H system in the processes (1a,b) as well as the e + H^+ + H system in the processes (2b) go through the phase where they may be treated as a (H^+ + H) + e system. Here, (H^+ + H) denotes that the ion-atom subsystem may be treated as a quasi-molecular ion-atom complex under assumption that its electronic states may be described as superpositions of the ground and the first excited states of the H_2^+ molecular ion. Furthemore, this means that during the quasi-molecular phase the average electron distance from the center of mass of the H^+ + H subsystem is much larger than the internuclear distance between H^+ and H. Consequently, the dipole interaction between the (H^+ + H) and an electron (Smirnov & Mihajlov 1971) is the origin of the chemi-ionization/recombination processes (1a,b) and (2a,b). One can notice that within the frame of this approach, the processes (2a) and (2b) may be described practically in the same way. Expressions for the rate coefficients in the processes (1a,b) and (2a,b) which are used here as well as the method of determination of the rate coefficients are described in details in Mihajlov et al. (1996b).

3. Modeling

We included processess (1a,b) and (2a,b) into the general stellar atmosphere code PHOENIX described in Hauschildt et al. (1999), Short et al. (1999), Baron & Hauschildt (1998). PHOENIX solves simultaneously the equations of hydrostatic equilibrium, multi-level and multi-species statistical equilibrium and NLTE radiative transfer. The major advantage of PHOENIX is that it uses extensive atomic and molecular databases and can be used for modeling of very cool objects.

The main change in the code is in the addition of a new term in the statistical equilibrium equation which describes additional collisional processes. This change allows us to treat chemi-ionization/recombination processes consistently with all the other processes. Due to limits of the semi-classical approach, we include additional collisional term only for levels larger than $n = 4$.

We use for our calculation the plane-parallel, static option of PHOENIX which has been adopted for use in "chromospheric" type of problems. As a test atmosphere we use a "schematic" chromospheric structure with an effective temperature of 3800 K, logarithm gravity of 5.0, log $m_0 = -2.5$ being the column mass at temperature minimum, and log $m_{\rm TR}$ −4.8, $m_{\rm TR}$ standing for the column mass in the transition region. The choosen parameters represent a typical M0 dwarf of weak activity. The procedure of building this model is identical to that described in Jevremović et al. (2000) and its structure is shown in Fig. 1. As we are interested in behavior of hydrogen populations, we solve the NLTE problem for the 30 lowest levels. The standard collisional data for hydrogen are those from Vriens & Smeets (1980).

4. Results and discussion

In Figs. 2–4 we present the behavior of population ratios ζ without and with inclusion of chemi-ionization (1a,b) and chemi-recombination (2a,b) processes for the levels 3 to 20. The ratios are close to unity for $n = 3$, and start to differ for $n = 4$ and 5 (Fig. 2). For $n = 5$ the largest difference is around 10%. This is to be expected as we include the procesess for $n \geq 4$, which is based on the validity of the semi-classical approximation. The population of lower levels ($n = 2, 3$) is influenced by other processes included in the statistical equilibrium equation.

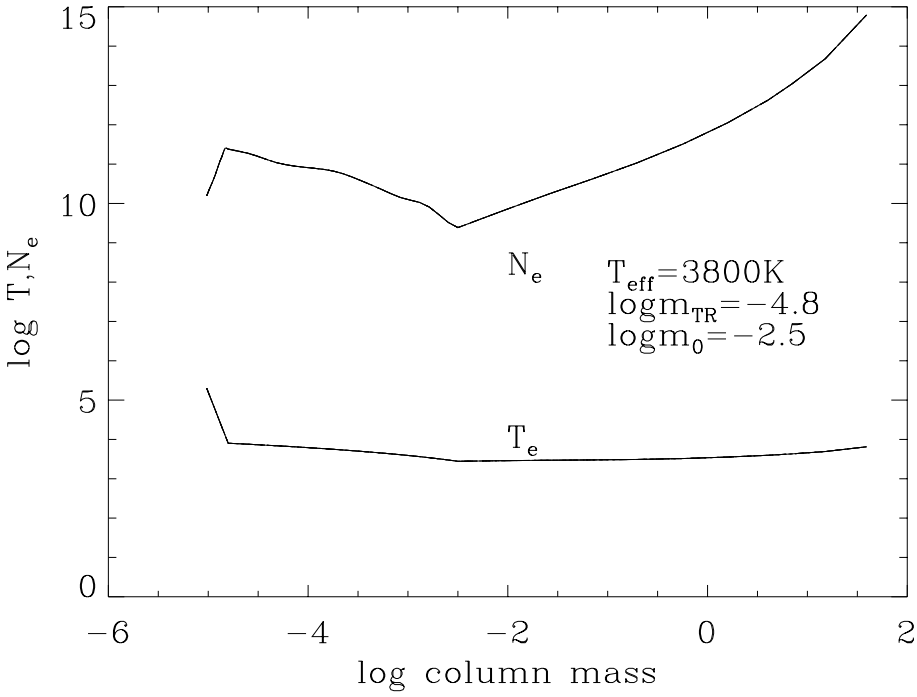

Fig. 1. Temperature and electron density structure for the model of test atmosphere.

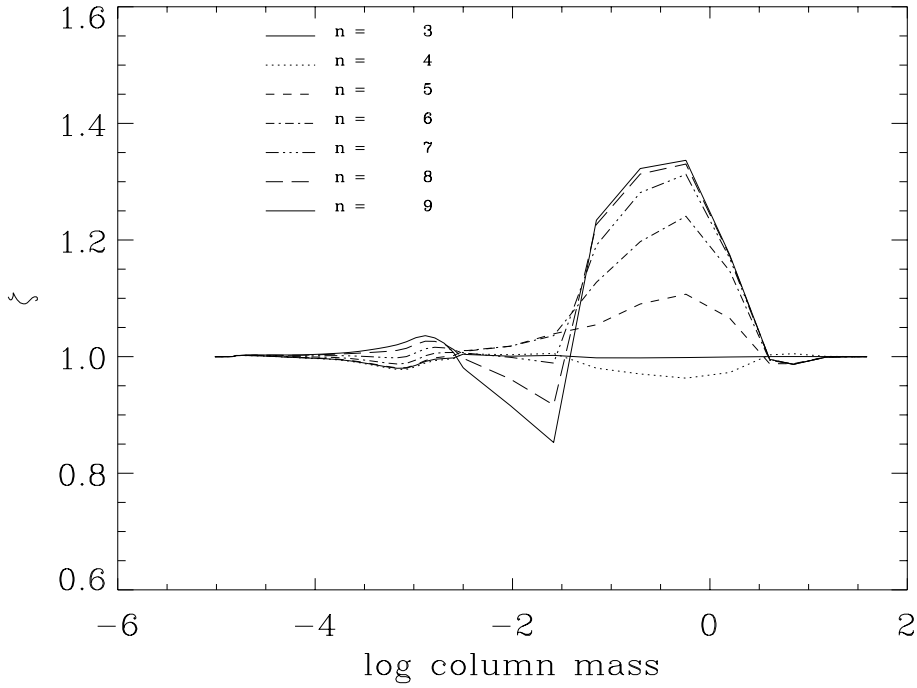

Fig. 2. The behaviour of the population ratio $\zeta(n)$ for $3 \leq n \leq 9$ as a function of the column mass.

As expected, the additional collisional term in statistical equilibrium brings the solution closer to local thermodynamical equilibrium (LTE). In terms of our population ratios, in the parts of atmosphere where populations, determined in our calculations using PHOENIX, are larger than LTE populations (departure coefficients $b_i > 1$), our parameter ζ is larger than one. This means that in such a case, chemi-ionization processes depopulate excited states and dominate in comparison with chemi-recombination processes. The result is that populations determined with processes (1, 2) included are smaller in comparison with populations calculated without them and consequently ζ is larger than one. In the reverse case ($b_i < 1$), parameter ζ is smaller than one, which means that in this case chemi-recombination processes dominate over chemi-ionization ones and increase the population of excited levels. As a result, in both cases, processes (1, 2) act as important factors closing the difference between the calculated and LTE populations.

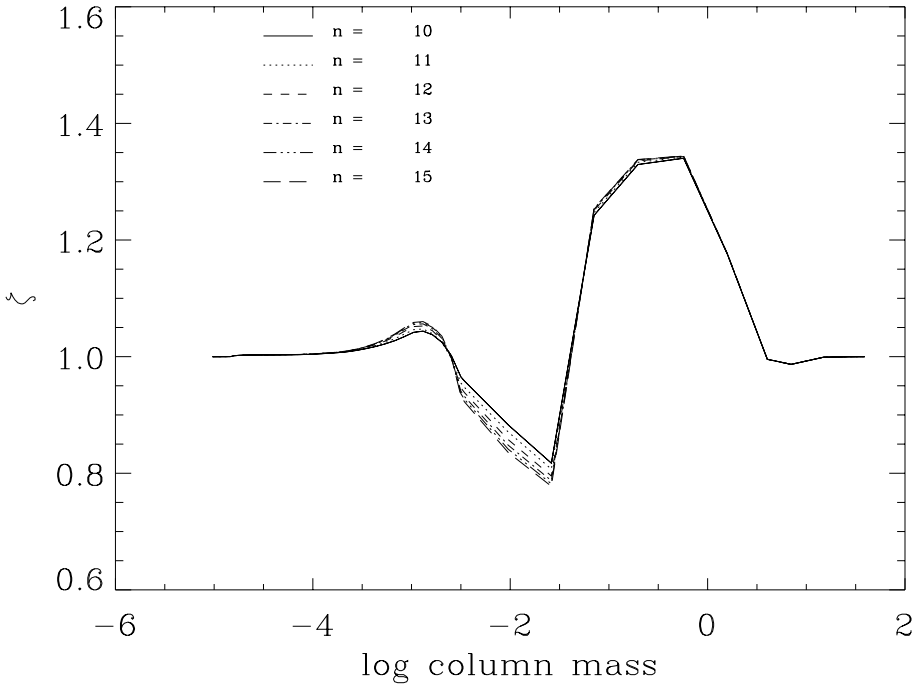

Fig. 3. The behaviour of the population ratio $\zeta(n)$ for $10 \leq n \leq 15$ as a function of the column mass.

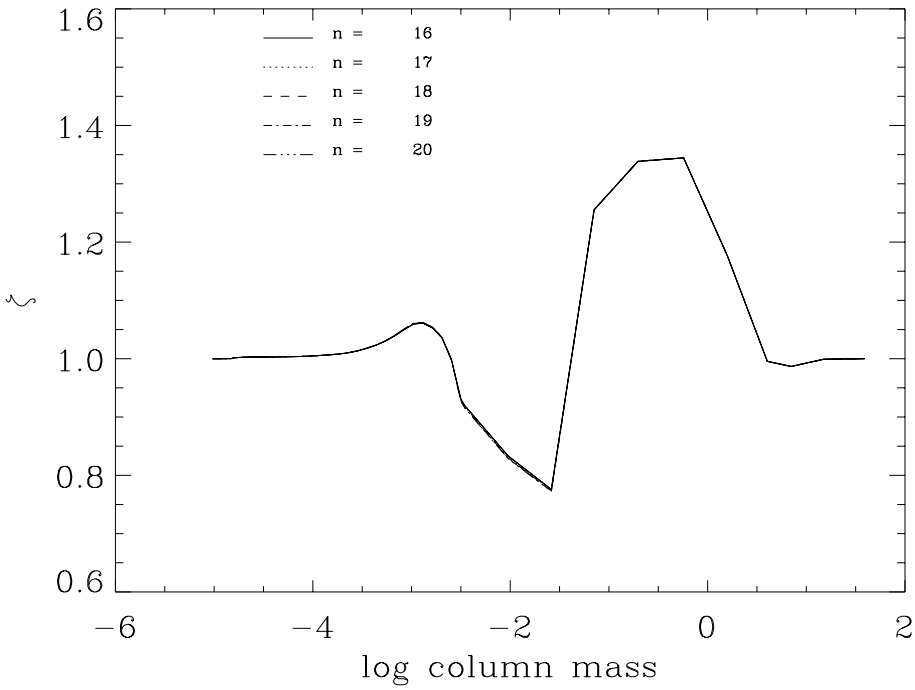

Fig. 4. The behaviour of the population ratio $\zeta(n)$ for $16 \leq n \leq 20$ as a function of the column mass.

As can be seen from Fig. 2, the behaviour of $\zeta(n)$ for $6 < n < 9$ shows a tendence to converge to a pattern, which may differ up to 40% from unity. For higher levels (Figs. 3 and 4) the convergence to a pattern is complete and it can be understood by assuming that highly excited hydrogen level populations have quasi-Boltzman distributions different from distributions for partial LTE. It is not suprising that the population ratios for the levels up to 30 and the proton density show the same behaviour as levels with $n > 15$. One also has to remember that in the layers with temperatures lower than 4500 K the main electron contributors are metals so, as expected, there is very little change in electron density.

5. Conclusion

We have demonstrated the importance of the inclusion of chemi-ionization (1a,b) and chemi-recombination (2a,b) processes in modeling of atmospheres of late type stars.

In previous work (Mihajlov et al. 1996a, 1997, 1998), it had been assumed that these processes were important up to $n = 10$. Here we have demonstrated that inclusion of processes (1a,b) and (2a,b) significantly changes the population of all Rydberg levels due to PLTE. However, in some atmospheric layers self-consistent modeling shows differences of up to 40% between calculations with and without inclusion of these processes.

We plan to continue these investigations for atmospheres with different effective temperatures, including stars with higher $T_{\rm eff}$, such as the Sun and Sun-like stars. Namely, on the basis of our previous results and those presented here, one could expect that for such stars, processes (1a,b) and (2a,b) should influence not only the population of higher levels of hydrogen, but also the electron density. Furthermore, we plan to include in PHOENIX the chemi-ionization/recombination processes similar to (1a,b) and (2a,b) in the He($1s^2$) atom which would be used in modeling of helium-rich stars.

Also, there is a need for a developement of a theory of processes similar to processes (1a,b) and (2a,b) for the lower levels of hydrogen, with the principal quantum numbers $n = 2$ and 3. This extension would enable more sophisticated modeling of stellar atmospheres as the population of lower levels may significantly alter the electron density and consequently the atmospheric structure.

Acknowledgements. This work is a part of the projects "Radiation and transport properties of the non-ideal laboratory and ionospheric plasma" (Project number 1466) and "Influence of collisional processes on astrophysical plasma lineshapes" (Project number GA 1195) and was supported by the *Ministry of Science, Technologies and Development of Serbia*. D.J. was supported at QUB through the PPARC grant PPA/G/S/1998/00034. Authors acknowledge the care of reviewer to improve this paper.

References

Baron, E., & Hauschildt, P. H. 1998, ApJ, 495, 370
Hauschildt, P. H., Allard, F., & Baron, E. 1999, ApJ, 512, 377
Janev, R. K., & Mihajlov, A. A. 1980, Phys. Rev., 21, 819
Jevremović, D., Doyle, J. G., & Short, C. I. 2000, A&A, 358, 575
Mihajlov, A. A., & Ljepojević, N. N. 1982, Proc. Symp. Phys. Ioniz. Gases, Dubrovnik, Contributed Papers, p. 385
Mihajlov, A. A., Ljepojević, N. N., & Dimitrijević, M. S. 1992, J. Phys. B: At. Mol. Phys., 25, 5127
Mihajlov, A. A., Dimitrijević, M. S., Ignjatović, Lj. M., & Vasilijević, M. M. 1996a, Int. Conf. in the memory of I. S. Shklovsky, S. A. Kaplan, S. B. Pikel'ner: Current problems in Astrophysics, Moscow, Russia, 23–28.09.1996
Mihajlov, A. A., Dimitrijević, M. S., & Djurić, Z. 1996b, Phys. Scr., 33, 159
Mihajlov, A. A., Ignjatović, Lj. M., Vasilijević, Lj. M., & Dimitrijević, M. S. 1997, A&A, 324, 1206
Mihajlov, A. A., Ignjatović, Lj. M., & Dimitrijević, M. S. 1998, Novyj cikl aktivnosty Solnca, Trudy, Sankt Peterburg, Pulkovo, p. 52
Short, C. I., Hauschildt, P. H., & Baron, E. 1999, ApJ, 525, 375
Smirnov, V. A., & Mihajlov, A. A. 1971, Opt. Spektrosk., 30, 984; Opt. Spectrosc., 30, 525
Vriens, L., & Smeets, A. H. M. 1980, Phys. Rev. A, 22, 940

A&A 404, 1099–1106 (2003)
DOI: 10.1051/0004-6361:20030561
© ESO 2003

Astronomy & Astrophysics

On the influence of Stark broadening on Si I lines in stellar atmospheres

M. S. Dimitrijević[1,2], T. Ryabchikova[3,4], L. Č. Popović[1,2], D. Shulyak[5], and V. Tsymbal[5]

[1] Astronomical Observatory, Volgina 7, 11160 Belgrade 74, Serbia
[2] Isaac Newton Institute of Chile, Yugoslavia Branch
[3] Institute of Astronomy, Russian Academy of Science, Pyatnitskaya 48, 119017 Moscow, Russia
[4] Institute for Astronomy, University of Vienna, Türkenschanzstrasse 17, 1180 Vienna, Austria
[5] Tavrian National University, Yaltinskaya 4, 330000 Simferopol, Crimea, Ukraine

Received 12 November 2002 / Accepted 27 March 2003

Abstract. We study the influence of Stark broadening and stratification effects on Si I lines in the rapidly oscillating (roAp) star 10 Aql, where the Si I 6142.48 Å and 6155.13 Å lines are asymmetrical and shifted. First we have calculated Stark broadening parameters using the semiclassical perturbation method for three Si I lines: 5950.2 Å, 6142.48 Å and 6155.13 Å. We revised the synthetic spectrum calculation code taking into account both Stark width and shift for these lines. From the comparison of our calculations with the observations we found that Stark broadening + the stratification effect can explain asymmetry of the Si I 6142.48 Å and 6155.13 Å lines in the atmospere of roAp star 10 Aql.

Key words. stars: chemically peculiar – line: profiles – atomic processes

1. Introduction

The Stark broadening is the most significant pressure broadening mechanism for A and B stars and one has to take into account this effect in investigation, analysis and modeling of their atmospheres. In one of our previous works (Popović et al. 2001) we have shown that the Stark effect may change the equivalent width of spectral lines by 10–45%, hence neglecting this mechanism, we may introduce a significant error in abundance determinations. On the other hand, high resolution spectra allow us to study different broadening effects using line profiles. In the course of the abundance analyses of peculiar (Ap) stars we noticed that some of the Si I lines are shifted relative to the laboratory wavelength. Moreover, few strong lines mainly from the multiplets $3p^3\ ^3D^0$–$5f^3D$ and $3p^3\ ^3D^0$–$5f^3G$ have asymmetrical line profiles, in particular the Si I 6155.13 Å line. We found that this line is slightly shifted and asymmetrical even in the solar spectrum, while in the hotter, e.g. Ap stars, the shift and asymmetry are more pronounced.

The aim of this paper is to explain the asymmetry of Si I lines within the framework of the Stark broadening effect. First we calculated the Stark broadening parameters for these lines, after that we calculated synthetic spectra and compared them with the observations, and finally, we discuss the effects causing shift and asymmetry in the line profile of the Si 6155.13 and 6142.48 Å lines.

2. Observations

For our analysis we used observations of one normal star HD 32115, two Ap stars HD 122970 and 10 Aql and Solar Flux Atlas by Kurucz et al. (1984). High resolution CCD spectra of 10 Aql and HD 122970 are described by Ryabchikova et al. (2000). High resolution CCD spectra ($R \approx 45\,000$) of HD 32115 in the wavelength region 4000–9500 Å were obtained with the coude-echell spectrometer mounted on the 2 m "Zeiss" telescope at Peak Terskol Observatory, Russia (see Bikmaev et al. 2002 for more details).

More Ap stars show peculiar line profiles of Si I lines but most stars have rather strong magnetic fields which distort line profiles through Zeeman splitting. Rather weak magnetic fields in Ap stars HD 122970 and 10 Aql allow us to ignore magnetic effects on line shape.

3. The Stark broadening parameter calculation

Calculations have been performed within the semiclassical perturbation formalism, developed and discussed in detail in Sahal-Bréchot (1969a,b). This formalism, as well as the corresponding computer code, have been optimized and updated

Send offprint requests to: M. S. Dimitrijević,
e-mail: mdimitrijevic@aob.bg.ac.yu

several times (see e.g. Sahal-Bréchot 1974; Dimitrijević & Sahal-Bréchot 1984a; Dimitrijević 1996).

Within this formalism, the full width of a neutral emitter isolated spectral line broadened by electron impacts can be expressed in terms of cross sections for elastic and inelastic processes as

$$W_{if} = \frac{2\lambda_{if}^2}{2\pi c} n_{\rm e} \int v f(v) {\rm d}v \left(\sum_{i' \neq i} \sigma_{ii'}(v) + \sum_{f' \neq f} \sigma_{ff'}(v) + \sigma_{\rm el} \right) \quad (1)$$

and the corresponding line shift as

$$d_{if} = \frac{\lambda_{if}^2}{2\pi c} n_{\rm e} \int v f(v) {\rm d}v \int_{R_3}^{R_D} 2\pi\rho {\rm d}\rho \sin 2\phi_{\rm p}. \quad (2)$$

Here, λ_{if} is the wavelength of the line originating from the transition with the initial atomic energy level i and the final level f, c is the velocity of light, $n_{\rm e}$ is the electron density, $f(v)$ is the Maxwellian velocity distribution function for electrons, m is the electron mass, k is the Boltzman constant, T is the temperature, and ρ denotes the impact parameter of the incoming electron. The inelastic cross section $\sigma_{jj'}(v)$ is determined according to Chap. 3 in Sahal-Bréchot (1969b), and elastic cross section $\sigma_{\rm el}$ according to Sahal-Bréchot (1969a). The cut-offs, included in order to maintain for the unitarity of the S-matrix, are described in Sect. 1 of Chap. 3 in Sahal-Bréchot (1969a).

The formulae for the ion-impact broadening parameters are analogous to the formulae for electron-impact broadening. We note that the fact that the colliding ions would impact in the far wings should be checked, even for stellar densities.

4. Line profile calculations

Model atmosphere calculations as well as calculations of the absorption coefficients were made with the local thermodynamical equilibrium (LTE) approximation. Model calculations were performed with the ATLAS9 code written by Kurucz (1993). The next step is the calculation of the outward flux at corresponding wavelengths points using the given model. For this we used the STARSP program written by Tsymbal (1996). In its current state this code includes the possibility of calculating a synthetic spectrum for an atmosphere with a vertical stratification of chemical elements.

The computational scheme is as follows. For each line we find the central opacity as

$$\alpha_\nu = \frac{\pi e^2}{mc} g f_{if} {\rm e}^{-\frac{\chi}{kT}} \frac{n}{\rho} \left(1 - {\rm e}^{-\frac{h\nu}{kT}}\right), \quad (3)$$

where α_ν is the mass absorption coefficient at frequency ν, e is the electron charge, g is the statistical weight, f_{if} is the oscillator strength for a given transition, χ is the excitation energy, n is the number density of a corresponding element in a given ionization stage multiplied by partition function, ρ is the density and h is the Planck constant. The last factor describes stimulated emission.

The Doppler width is

$$\Delta\nu_{\rm D} = \frac{\nu}{c} \sqrt{\frac{2kT}{m_{\rm A}} + \xi_{\rm t}^2}. \quad (4)$$

In this expression $m_{\rm A}$ is the mass of the absorber and $\xi_{\rm t}$ is the microturbulent velocity.

Next, we compute the total damping parameter

$$\gamma = \gamma_{\rm rad} + \gamma_{\rm Stark} + \gamma_{\rm neutral}. \quad (5)$$

Here $\gamma_{\rm rad}$, $\gamma_{\rm Stark}$ and $\gamma_{\rm neutral}$ are the radiative, Stark and damping parameters due to neutral atom collisions respectively. The values of $\gamma_{\rm rad}$, $\gamma_{\rm neutral}$, excitation energy χ and oscillator strength gf were taken from the Vienna Atomic Line Database (VALD) (Kupka et al. 1999). In the case of neutral atom broadening we assumed that perturbing particles are atoms of neutral hydrogen and helium only. This assumption is applicable to almost all types of stars due to high hydrogen and helium cosmic abundances. Usually this damping process is called Van der Waals broadening. The best theory for atomic hydrogen collisions which includes not only the Van der Waals potential is given in the papers by Anstee & O'Mara (1991) and Barklem & O'Mara (1998). Barklem et al. (2000) provided $\log \gamma_{\rm neutral}$ calculations for about 5000 lines of the neutral atoms and the first ions of many chemical elements. These damping parameters are included in VALD database per one perturbing particle and for a temperature of 10 000 K. Unfortunately, no calculations exist for Si I lines. We shall discuss the competition between the broadenings caused by the Stark effect and neutral hydrogen collisions in the atmospheres of our stars in Sect. 5.2.

In order to include Stark broadening effects we added the approximate formulas (see Eqs. (13) and (14) in Sect. 5.1) in the code. The Stark width and shift are

$$\gamma_{\rm Stark} = \gamma_{\rm Stark}^{\rm (e)} n_{\rm e} + \gamma_{\rm Stark}^{\rm (p)} n_{\rm p} + \gamma_{\rm Stark}^{\rm (HeII)} n_{\rm HeII}, \quad (6)$$

$$d_{\rm Stark} = d_{\rm Stark}^{\rm (e)} n_{\rm e} + d_{\rm Stark}^{\rm (p)} n_{\rm p} + d_{\rm Stark}^{\rm (HeII)} n_{\rm HeII}, \quad (7)$$

where $n_{\rm e}$, $n_{\rm p}$ and $n_{\rm HeII}$ are the corresponding densities of electrons, protons and He II ions respectively. The resulting opacity profile is given by the Voigt function (Doppler + pressure broadening).

Thus, at each point of a given spectral region (with resolution 0.01 Å for both lines) we computed line absorption coefficient ℓ_ν as follows

$$\ell_\nu = \alpha_\nu V(u, a), \quad (8)$$

where α_ν is given by Eq. (3) and $V(u, a)$ is a Voigt function with parameters

$$u = \frac{\nu - \nu_0 + d_{\rm Stark}}{\Delta\nu_{\rm D}}, \quad (9)$$

$$a = \frac{\gamma}{4\pi\Delta\nu_{\rm D}}. \quad (10)$$

The Stark shift $d_{\rm Stark}$ and the damping parameter γ have been found from (2) and (5), respectively.

The flux is given by the expression

$$H_\nu(\tau_\nu) = -\frac{1}{2} \int_0^{\tau_\nu} S_\nu E_2(\tau_\nu - t) {\rm d}t + \frac{1}{2} \int_{\tau_\nu}^{\infty} S_\nu E_2(t - \tau_\nu) {\rm d}t, \quad (11)$$

where τ_ν is the optical depth, S_ν is the source function and $E_n(x)$ is the exponential integral of the order n and argument x. The flux integral has been evaluated using matrix operators.

Table 1. Stark broadening parameters for Si I spectral lines. This table shows electron-, proton-, and ionized helium-impact broadening parameters for Si I for a perturber density of 10^{14} cm^{-3} and temperatures from 2500 up to 50 000 K. The quantity C (given in Å cm^{-3}), when divided by the corresponding full width at half maximum, gives an estimate for the maximum perturber density for which tabulated data may be used. The asterisk identifies cases for which the collision volume multiplied by the perturber density (the condition for validity of the impact approximation) lies beetwen 0.1 and 0.5. For higher densities, the isolated line approximation used in the calculations breaks down. *FWHM*(Å) denotes full line width at half maximum in Å, while *SHIFT*(Å) denotes line shift in Å.

Perturbers are:		Electrons		Protons		Helium ions	
Transition	T(K)	*FWHM*(Å)	*SHIFT*(Å)	*FWHM*(Å)	*SHIFT*(Å)	*FWHM*(Å)	*SHIFT*(Å)
SiI 4s−5p	2500	0.509E–02	0.333E–02	0.160E–02	0.701E–03		
^{1}P−^{1}D	5000	0.581E–02	0.409E–02	0.172E–02	0.898E–03		
5948.55 A	10 000	0.652E–02	0.381E–02	0.183E–02	0.109E–02	0.167E–02	0.851E–03
C = 0.36E+19	20 000	0.740E–02	0.328E–02	0.194E–02	0.127E–02	0.175E–02	0.101E–02
	30 000	0.811E–02	0.271E–02	0.202E–02	0.139E–02	0.181E–02	0.111E–02
	50 000	0.903E–02	0.212E–02	0.213E–02	0.153E–02	0.188E–02	0.123E–02
SiI 3p^3−5f	2500	0.967E–01	–0.576E–01	0.175E–01	–0.145E–01	*0.145E–01	–0.114E–01
^{3}D$_3$−^{3}D$_3$	5000	0.108	–0.624E–01	0.196E–01	–0.168E–01	0.160E–01	–0.134E–01
6142.48 Å	10 000	0.120	–0.609E–01	0.219E–01	–0.192E–01	0.178E–01	–0.154E–01
C = 0.52E+16	20 000	0.132	–0.472E–01	0.247E–01	–0.219E–01	0.198E–01	–0.176E–01
	30 000	0.140	–0.400E–01	0.266E–01	–0.235E–01	0.211E–01	–0.189E–01
	50 000	0.147	–0.326E–01	0.294E–01	–0.258E–01	0.228E–01	–0.208E–01
SiI 3p^3−5f	2500	0.905E–01	–0.622E–01	0.184E–01	–0.152E–01	*0.151E–01	–0.120E–01
^{3}D$_3$−^{3}G$_4$	5000	0.102	–0.707E–01	0.204E–01	–0.177E–01	0.168E–01	–0.141E–01
6155.13 Å	10 000	0.112	–0.706E–01	0.228E–01	–0.203E–01	0.187E–01	–0.162E–01
C = 0.20E+17	20 000	0.121	–0.571E–01	0.255E–01	–0.231E–01	0.208E–01	–0.185E–01
	30 000	0.129	–0.482E–01	0.273E–01	–0.248E–01	0.221E–01	–0.200E–01
	50 000	0.137	–0.392E–01	0.298E–01	–0.272E–01	0.240E–01	–0.219E–01

5. Results

5.1. Stark broadening data

The atomic energy levels needed for Stark broadening calculations were taken from Martin & Zalubas (1983) and Moore (1971), but LS determination of 5f^{3}D, 5f^{3}G, 6s^{1}P° and 7s^{1}P° terms have been adopted according to Moore (1971) and therfore, in order to obtain a consistent set of data, energy levels from Moore (1971) have been used as the principal source. Oscillator strengths have been calculated by using the method of Bates & Damgaard (1949) and tables of Oertel & Shomo (1968). For higher levels, the method described in van Regemorter et al. (1979) has been applied.

The spectrum of neutral silicon is complex and not known well enough for a good calculation of the considered lines. First of all upper and lower energy levels for 6142.48 Å and 6155.13 Å lines are not known reliably. According to Striganov & Sventickij (1966) they belong to the 3p^3 ^{3}D^0−5f^{3}D and 3p^3 ^{3}D^0−5f^{3}G multiplets respectively, while Moore et al. (1966) stated that the lower level of the corresponding transitions is 3d^{3}D°. It is also worth noting that in NIST (2002) the lower and upper levels of the corresponding transitions are not specified. Consequently, we adopted the identification of Striganov & Sventitskij (1966) as the only one enabling the corresponding calculations. Moreover, the 3s3p^3 ^{3}D$^\circ_3$ level is in fact a mixture of 39% of 3pnd^{3}D° and 56% of 3s3p^3 ^{3}D$^\circ_3$ states, and 5% is unknown. Also the 3pnd^{3}D° state is a mixture of states with $3 \leq n \leq 12$. In calculations, we assumed that we have 30% of 3p3d^{3}D° state, and our checks show that the difference in final results is negligible if we assume that this state is involved up to 20% only. An additional complication was that g levels, which might be very important for the perturbation of the considered 5f levels, are unknown. In accordance with the decrease of distance between 5s, 5p, 5d and 5f levels, we estimated that the distance from 5f^{3}D or 5f^{3}G term to the 5g levels should lie between 500 and 1500 cm^{-1}. We checked results without 5g levels and with a fictive 5g level at 500, 1000 and 1500 cm^{-1} from the corresponding 5f terms. In all cases, line widths differed by less than 1%, while the shift varies within the limits of 3.5% for 1000 or 1500 cm^{-1}. If the distance is 500 cm^{-1}, the shift value e.g. at 10 000 K for 6142.48 Å line differs by about 20%. If we include a fictive 6g level 500 cm^{-1} distant from 5g levels, the difference is negligible. Hence, in order to obtain the needed set of atomic energy levels, we adopted a fictive 5g level 1000 cm^{-1} distant from the 5f levels and a fictive 6g level 500 cm^{-1} distant from the 5g level. Since the average estimated error of the semiclassical method is ±30%, due to additional approximations and uncertainties, we estimate the error bars of our results to be ±50%.

Our results for electron-, proton-, and ionized helium-impact line widths and shifts for the three considered Si I spectral lines for a perturber density of 10^{14} cm^{-3} and temperatures

Table 2. The parameters A, B and C of the approximate formulae for Stark widths and shifts.

Line	5950.2 Å	6142.48 Å	6155.13 Å
		WIDTH	
		Electrons	
c_1	1E–16	1E–14	1E–14
A	–0.33801648	–0.87997007	–0.88824105
B	0.12759724	0.01704956	0.01525209
		Protons	
c_1	1E–16	1E–15	1E–15
A	–0.81663954	–0.77664655	–0.76856840
B	0.01728187	0.03913901	0.03758103
		He II	
c_1	1E–16	1E–15	1E–15
A	–0.83337682	–0.81987023	–0.81114334
B	0.01297813	0.02771659	0.02946282
		SHIFT	
		Electrons	
c_2	1E–16	1E–15	1E–15
A	0.38028502	–0.63997507	–0.69208568
B	1.33496618	0.88440353	1.18033516
C	–0.02047206	0.07950743	0.04721782
		Protons	
c_2	1E–16	1E–15	1E–15
A	–1.32564473	1.12387002	0.17032257
B	0.01917066	0.02838789	0.10512289
C	1.43394434	–1.31786299	–0.37318012
		He II	
c_2	1E–16	1E–15	1E–15
A	–1.67370868	0.14785217	0.14840180
B	0.01490401	0.10161093	0.10439166
C	1.75773489	–0.30183339	–0.31051296

$T = 2500–50\,000$ K, are shown in Table 1. For perturber densities lower than those tabulated here, Stark broadening parameters vary linearly with perturber density. The nonlinear behaviour of Stark broadening parameters at higher densities is the consequence of the influence of Debye shielding and has been analyzed in detail in Dimitrijević & Sahal-Bréchot (1984b).

In Table 1 the Stark widths and shifts for electron-, proton- and He II ion-impact broadening are presented as a function of temperature for a density of 10^{14} cm^{-3}. After testing the density dependence of Stark parameters, we have found that the width and shift are linear functions of density for perturber densities smaller than 10^{16} cm^{-3} and can be scaled by the simple formula:

$$(W, d)_N = (W, d)_0 \left(\frac{N}{10^{14}}\right), \tag{12}$$

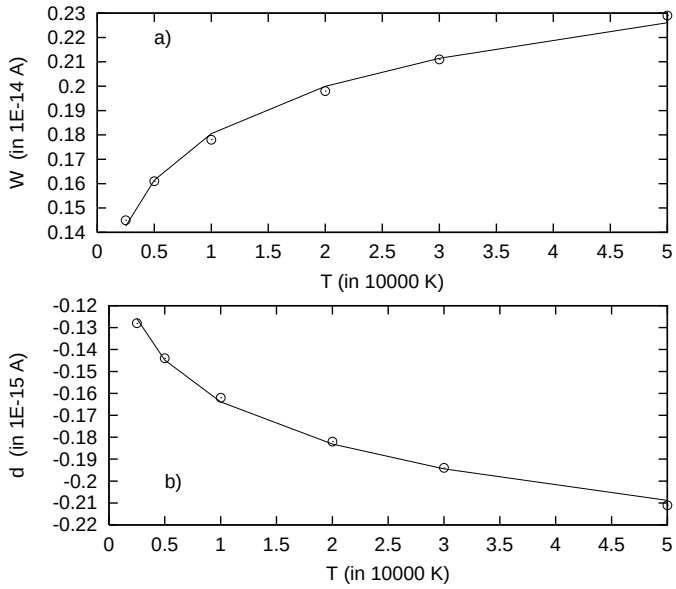

Fig. 1. The analytic fit of HeII-impact broadening data for Si I 6142 Å line: **a)** Stark width, and **b)** Stark shift. The shift and width are given for one perturber per cm^3.

where $(W, d)_N$ are the width and shift at a perturber density N (cm^{-3}), and $(W, d)_0$ are width and shift given in Table 1, respectively.

In order to simplify the use of Stark broadening data in the codes for stellar spectral synthesis, we have found an analytical expression for Stark widths and shifts

$$\frac{W}{n_e}[\text{Å}] = c_1 \left(A + T^B\right), \tag{13}$$

$$\frac{d}{n_e}[\text{Å}] = c_2 \left(A + CT^B\right). \tag{14}$$

The constants c_1, c_2, A, B and C are given in Table 2. We take T as $T/(10\,000$ K). The fits of our calculated data to the analytical functions given above are satisfactory (Fig. 1) and the differences are negligible in comparison with the expected error of our calculations (≈±50%).

5.2. The Stark broadening effect on the shape of Si I lines

The asymmetry and shift of Si I 6142.48 Å and (in particular) 6155.13 Å lines were observed, and it was obvious that the asymmetry is higher for the hotter stars. The most asymmetrical are λ 6142.48 Å and 6155.13 Å, the strongest lines of $3p^3\ ^3D^0–5f^3D$ and $3p^3\ ^3D^0–5f^3G$ multiplets, respectively. This line is slightly shifted and shows an asymmetry in the red wing even in a rather cool star like the Sun. It is not surprising if the Stark effect is responsible for the observed shifts and asymmetries. From Table 1 one can see that neither widths nor shifts have a strong temperature dependence, but they depend linearly on the perturber density. If a line is strong enough so that line core and line wings are formed at different atmospheric layers where electron density, differs significantly, then we should

Table 3. The atmospheric parameters and rotational velocities of the investigated stars.

Star name or HD	$T_{\rm eff}$	$\log g$	$\xi_{\rm t}$ km s^{-1}	$v \sin i$ km s^{-1}	$\log({\rm Si}/N_{\rm tot})$
Sun	5777	4.44	0.75	1.6	–4.49
HD 122970	6930	4.11	0.85	5.0	–4.45
HD 32115	7250	4.20	2.30	9.0	–4.65
10 Aql	7550	4.00	0.00	5.0	strat

observe line asymmetry due to different shifts at different atmospheric layers even with a homogeneous vertical distribution of the absorbing element in stellar atmosphere (the case of the observed asymmetries in normal stars). Vertical abundance stratification makes this effect more pronounced, and it is observed in cool Ap stars, where an element stratification takes place (Savanov et al. 2001; Ryabchikova et al. 2002; Wade et al. 2001).

Table 3 summarizes the model atmosphere parameters and rotational velocities for the stars of our sample. These data are taken from Ryabchikova et al. (2000) and Bikmaev et al. (2002). For the Sun corresponding parameters were taken from Valenti & Piskunov (1996) except $T_{\rm eff}$. Si abundances used in the present calculations are given in the last column.

In the Sun the most important broadening is due to collisions with neutral hydrogen and helium. In the hotter stars the importance of the Stark broadening increases. Barklem (priv. communic.) has provided us with the value of the broadening parameter due to collisions with atomic hydrogen for the Si I lines of our interest. This value per perturbing particle for a temperature 10 000 K, $\log \gamma_{\rm neutral} = -6.63$, is by 0.4 dex higher than the corresponding value obtained from the Unsöld (1955) approximation. According to Barklem his value may be overestimated by 0.1 dex which is proved by a comparison between the calculated and the observed blue wing of the solar Si I lines. The final value used in our calculations is $\log \gamma_{\rm neutral} = -6.75$. As for the shift due to collisions with the atomic hydrogen, a corresponding theory is not well developped, and the value of the shift is rather uncertain (Barklem, priv. communic.). The core and the wings of the strongest Si I λ 6155 line are formed in the layers with the temperatures 5000 and 5800 K respectively. In these layers the corresponding values for electron-, proton- and atomic hydrogen densities are 4.2×10^{12} cm^{-3}, 1.5×10^{11} cm^{-3}, 3.9×10^{16} cm^{-3} – line core, and 2.5×10^{13} cm^{-3}, 9.3×10^{12} cm^{-3}, 1.0×10^{17} cm^{-3} – line wings. The Stark width is 20 times smaller than $\gamma_{\rm neutral}$ at the depth of line core formation and 10 times smaller than $\gamma_{\rm neutral}$ at the depth of line wing formation. In the solar atmosphere, the Stark shift is 3 mÅ at the line core and about 20 mÅ for the line wings, which is not negligible. In the atmosphere of the hottest star of our sample, 10 Aql, the Stark width is of the order of $\gamma_{\rm neutral}$ at the depth of line core formation and exceeds $\gamma_{\rm neutral}$ by 5 times at the depth of line wing formation. Stark shifts are 10 and 100 mÅ, respectively. In 10 Aql the line core is formed at the layers with $T = 6500$ K, $N_{\rm e} = 1.4 \times 10^{13}$ cm^{-3}, $N_{\rm p} = 1.3 \times 10^{13}$ cm^{-3}, $N_{\rm HI} = 5.9\times10^{15}$ cm^{-3} while line wings are formed at the layers with $T = 7500$ K, $N_{\rm e} = 1.2\times10^{14}$ cm^{-3}, $N_{\rm p} = 1.2\times10^{13}$ cm^{-3}, $N_{\rm HI} = 1.1 \times 10^{16}$ cm^{-3}.

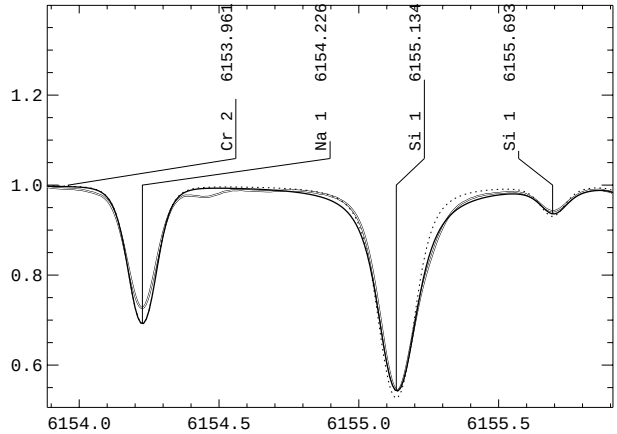

Fig. 2. A comparison between the observed Si I 6155 Å line profile in the solar spectrum and synthetic spectra calculated with Stark widths and shifts from Table 1 (solid line) and with Stark widths calculated by the approximate formulae and without Stark shift taken into account (dotted line). *X*- and *Y*-coordinates are wavelenghths and surface fluxes (normalized to unity).

5.3. The Sun

We first calculated Si I lines in the solar spectrum to check the Stark parameters. It was mentioned by Ryabchikova et al. (2002) that available theoretical oscillator strengths for the multiplets $3p^3\ ^3D^0$–$5f^3D$ and $3p^3\ ^3D^0$–$5f^3G$ are overestimated by about 0.5 dex compared to the multiplet $4s^1P^0$–$5p^1D$ (λ 5948.55 Å). The authors fitted the lines of $3p^3\ ^3D^0$–$5f^3D$ and $3p^3\ ^3D^0$–$5f^3G$ multiplets using the solar spectrum. Corrected oscillator strengths – $\log gf = -1.42$ (λ 6142.48 Å) and $\log gf = -0.77$ (λ 6155.13 Å) were published in Bikmaev et al. (2002). The latter value was reduced to $\log gf = -0.82$ to get a better fit for the solar Si I 6155 line. We also reduced the oscillator strength ($\log gf = -2.25$) of very weak Si line of the same multiplet, λ 6155.69 Å. We need to decrease both Stark widths and shifts for Si I 6142 and 6155 Å lines by 40% to get a reasonable fit of the synthetic line profiles to the solar ones. Due to relative weakness of the Si I 6142 Å line Stark effect is negligible but it is noticeable for the stronger line Si I 6155 Å. Figure 2 shows a comparison between the observed profile of the Si I 6155 Å line in the solar spectrum and synthetic profiles calculated with (solid line) and without (dashed

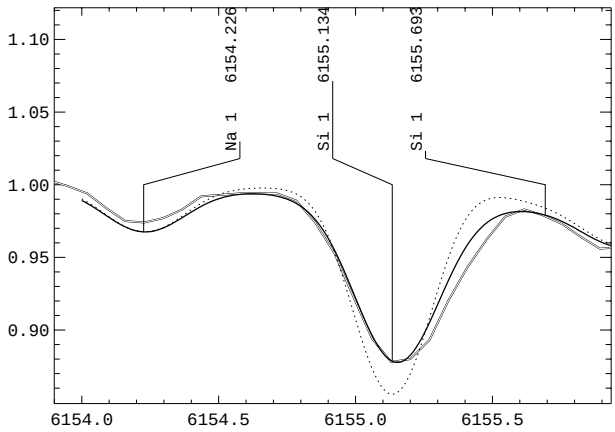

Fig. 3. The same as in Fig. 2 for normal star HD 32115.

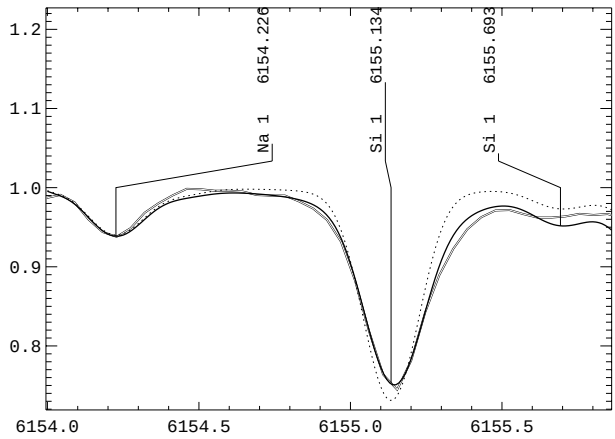

Fig. 4. The same as in Fig. 2 for Ap star HD 122970.

line) taking into account the Stark width and in particular, shift. The strongest Si I 5948.55 Å line in our study is fully symmetric as expected taking into account an order of magnitude smaller values for both the Stark width and shift (see Table 1).

With corrected Stark parameters we calculated Si I line profiles in spectra of other stars.

5.4. HD 32115

Spectra of this normal late A-type star have the smallest spectral resolution of our sample. As it may be seen from Fig. 3 the fit of the synthetic line profile of λ 6155.13 Å line to the observed one is much better when it was calculated with both Stark width and shift. As in the solar case, the Stark effect is negligible for the weaker Si I 6142.48 Å line. To get a better fit of the line profiles we decrease the Si abundance by 0.13 dex compared to the results published by Bikmaev et al. (2002) which were based mainly on the equivalent width measurements.

5.5. HD 122970

This is one of the coolest Ap stars and is expected to have a chemically stratified atmosphere. Results of the abundance determinations show that except for the rare-earth elements (REE) abundance stratification is marginal if it exists at all (Ryabchikova et al. 2000). Spectral synthesis of Si I lines seems to support this conclusion. We could reproduce the asymmetric and shifted line profile of Si I 6155.13 Å reasonably well, using the uniform distribution of Si and Stark broadening parameters presented here. Figure 4 shows a comparison between the observed and computed line profiles for two cases similar to Fig. 3. The best fit of Si I line profiles was obtained with the same Si abundance as was derived by Ryabchikova et al. (2000).

5.6. 10 Aql

10 Aql = HD 176232 is the hottest star in our sample. It has the most asymmetrical Si I 6155.13 Å line profile, which could not be reproduced by any combination of Stark parameters in a homogeneous atmosphere (Fig. 5). The even weaker line, Si I 6142.48 Å shows a noticeable line shift (Fig. 6). Ryabchikova et al. (2000) mentioned a possibility of Fe and the REE stratification in 10 Aql. Therefore we tried to find a simple distribution of Si in the atmosphere of 10 Aql by trial-and-error which would fit both Si I 6142.48 Å and 6155.13 Å lines. The simplest distribution shown in Fig. 7 gives a reasonable fit to the observed profiles of both Si I lines (Figs. 5 and 6). Moreover, the same Si distribution seems to fit much better the profiles of the strong Si II 6347, 6371 Å spectral lines compared to the calculations with the homogeneous Si abundance (−4.19) obtained by Ryabchikova et al. (2000). It is beyond the scope of the present paper to derive an exact Si abundance profile in the atmosphere of 10 Aql. We would like to stress here that with the present Stark parameters a sensitivity of 6155.13 Å line asymmetry to Si abundance changes in the stellar atmosphere can be successfully used in empirical studies of abundance stratification in the atmospheres of cool Ap stars.

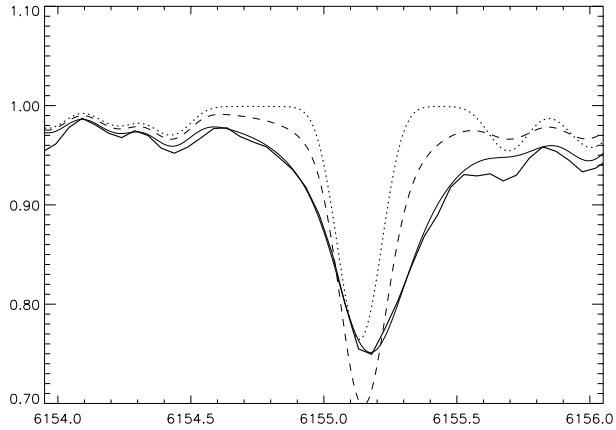

Fig. 5. A comparison between the observed Si I 6155 Å line profile in the spectrum of Ap star 10 Aql (thick line) and synthetic spectra calculated with Stark widths and shifts from Table 1 and Si abundance stratification (thin line), with the same Stark parameters but for homogeneous Si distribution (dashed line), and with Stark width calculated by approximate formulae for the same stratification (dotted line). X- and Y-coordinates are wavelenghths and surface fluxes (normalized to unity).

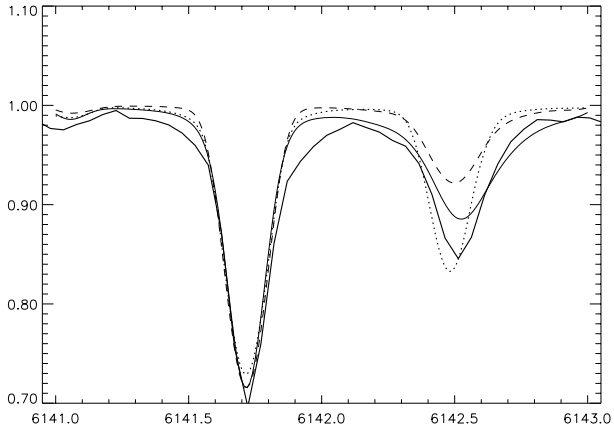

Fig. 6. The same as in Fig. 5 but for Si I 6142 Å line.

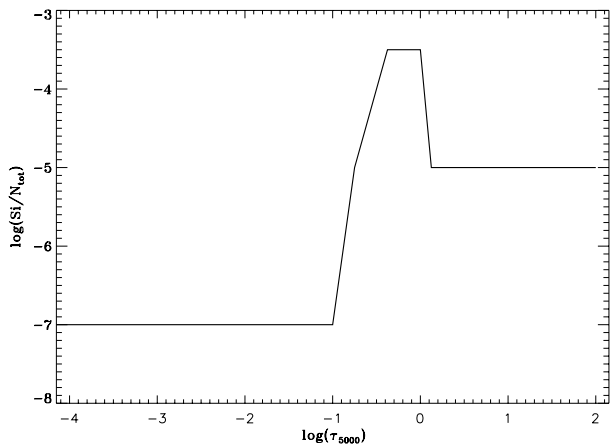

Fig. 7. Si abundance distribution in the atmosphere of Ap star 10 Aql.

6. Conclusions

In order to discuss the contribution of the Stark broadening effect to the asymmetry and the shift of Si I 6142.48 Å and 6155.13 Å lines we have calculated Stark broadening parameters for these lines by using the semiclasical perturbation method. The obtained results are the first calculated data for the considered lines. In order to include Stark broadening data we have changed the STARSP code and we have synthesized the considered lines. From our analyzis we can conclude that:

1) the Stark broadening effect is very important for these two lines. The contribution of electron impact is dominant but, impacts with protons and He II ions should be taken into accout as well;
2) the asymmetry as well as the shift of the Si I 6142.48 Å and 6155.13 Å lines in many stars including the Sun can be explained by the Stark broadening effect;
3) in hotter Ap stars, besides the Stark broadening effect, the stratification plays a very important role in producing line asymmetry. The sensitivity of the line asymmetry to changes in the number of Si atoms through the stellar atmosphere can be used in abundance distribution studies.

Acknowledgements. We are very grateful to Paul Barklem who provided us with the unpublished calculations of damping constants for Si I lines due to collisions with the atomic hydrogen. This work is a part of the projects "Influence of collisional processes on astrophysical plasma lineshapes" and "Astrophysical Spectroscopy of Extragalactic Objects" supported by the Ministry of Science, Technologies and Development of Serbia. The research was supported also by the Fonds zur Förderung der wissenschaftlichen Forschung *P14984* and Oštterreichische Nationalbank (Jubilaäumsfonds Nr. 7650). TR also thanks Russian Federal program "Astronomy" and the RFBR (grant 00-15-96722) for partial funding.

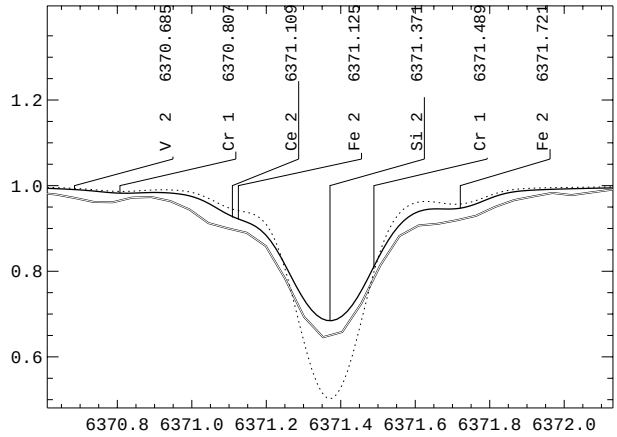

Fig. 8. A comparison between the observed Si II 6371 Å line profile in the spectrum of Ap star 10 Aql (double line) and the synthetic spectrum calculated with Si abundance distribution shown in Fig. 7 (solid line) and Si homogeneous abundance $\log(\mathrm{Si}/N_{\mathrm{tot}}) = -4.19$ (dotted line). X- and Y-coordinates are wavelenghths and surface fluxes (normalized to unity), respectively.

References

Anstee, S. D., & O'Mara, B. J. 1991, MNRAS, 253, 549
Barklem, P. S., & O'Mara, B. J. 1998, MNRAS, 300, 863
Barklem, P. S., Piskunov, N., & O'Mara, B. J. 2000, A&AS, 142, 467
Bates, D. R., & Damgaard, A. 1949, Trans. Roy. Soc. London, Ser. A, 242, 101
Bikmaev, I. F., Ryabchikova, T. A., Bruntt, H., et al. 2002, A&A, 389, 537
Dimitrijević, M. S. 1996, Zh. Priklad. Spektrosk., 63, 810
Dimitrijević, M. S., & Sahal-Bréchot, S. 1984a, JQSRT, 31, 301
Dimitrijević, M. S., & Sahal-Bréchot, S. 1984b, A&A, 136, 289
Griem, H. R. 1974, Spectral Line Broadening by Plasmas (New York: Academic Press)
Kupka, F., Piskunov, N. E., Ryabchikova, T. A., Stempels, H. C., & Weiss, W. W. 1999, A&AS, 138, 119
Kurucz, R. L. 1993, CDROM13, SAO, Cambridge
Kurucz, R. L., Furenlid, I., Brault, J., & Testerman, L. 1984, NSO Atlas No. 1: Solar Flux Atlas from 296 to 1300 nm, Sunspot, NSO
Martin, W. C., & Zalubas, R. 1983, J. Phys. Chem. Ref. Data, 12, 323
Moore, C. E. 1971, Atomic Energy Levels Vol. I, NSRDS-NBS 35 (Washington: U.S. Gov. Print. Office)
Moore, C. E., Minnaert, M. G. J., & Houtgast, J. 1966, The Solar Spectrum 2935 Å to 8770 Å, Second Revision of Rowland's Preliminary Table of Solar Spectrum Wavelengths, NBS Monograph 61 (Washington: U.S. Gov. Print. Office)
NIST 2002, Atomic Spectra Data Base, Lines, `http://physics.nist.gov`

Oertel, G. K., & Shomo, L. P. 1968, ApJS, 16, 175
Popović, L. Č., Simić, S., Milovanović, N., & Dimitrijević, M. S. 2001, ApJS, 135, 109
Ryabchikova, T., Piskunov, N., Kochukhov, O., et al. 2002, A&A, 384, 545
Ryabchikova, T. A., Savanov, I. S., Hatzes, A. P., Weiss, W. W., & Handler, G. 2000, A&A, 357, 981
Sahal–Bréchot, S. 1969a, A&A, 1, 91
Sahal–Bréchot, S. 1969b, A&A, 2, 322
Sahal–Bréchot, S. 1974, A&A, 35, 321
Savanov, I. S., Kochukhov, O. P., & Tsymbal, V. V. 2001, Ap, 44, 206
Striganov, A. R., & Sventickij, N. S. 1966, Tablicy Spektral'nykh Linij Nejtral'nykh i Ionizovannykh Atomov, Atomizdat, Moskva
Tsymbal, V. V. 1996, in Model Atmospheres and Spectral Synthesis, ed. S. J. Adelman, F. Kupka, & W. W. Weiss, ASP Conf. Ser., 108, 198
Unsöld, A. 1955, Physik der Stern Atmosphären, zweite Auflage (Springer-Verlag)
Valenti, J. A., & Piskunov, N. 1996, A&AS, 118, 595
van Regemorter, H., Hoang Binh Dy, & Prud'homme, M. 1979, J. Phys. B, 12, 1073
Wade, G. A., Ryabchikova, T. A., Bagnulo, S., & Piskunov, N. 2001, in Magnetic Fields Across the Hertzsprung-Russell Diagram, ed. G. Mathys, S. K. Solanki, & D. T. Wickramasinghe, ASP Conf. Ser., 248, 373

A&A 410, 735–739 (2003)
DOI: 10.1051/0004-6361:20031176
© ESO 2003

Astronomy & Astrophysics

Stark broadening of neutral germanium spectral lines

M. S. Dimitrijević[1,2], P. Jovanović[1,2], and Z. Simić[1,2]

[1] Astronomical Observatory, Volgina 7, 11160 Belgrade, Serbia and Montenegro
[2] Institute Isaac Newton of Chile, Yugoslavia Branch

Received 27 January 2003 / Accepted 7 July 2003

Abstract. Stark broadening of the 11 Ge I transitions, within the $4p^2$–4p5s transition array has been analyzed within the framework of the semiclassical perturbation method. Obtained results have been compared with available experimental and theoretical data. The importance of the electron-impact broadening in the case of the 4226.562 Å line for A star atmospheres has been tested

Key words. line: profiles – atomic data – molecular data – atomic processes – line: formation

1. Introduction

The interest in atomic data on larger numbers of emmiters/absorbers has increased considerably in the last years, since with space born spectrographs, one obtaines stellar spectra with such resolution that a large number of different spectral lines may be indentified. As an example, in the spectrum of Przybylski's star, Cowley et al. (2000) indentified lines belonging to 75 various atom/ion species. Consequently, data on the Stark broadening of neutral germanium spectral lines are of interest not only for laboratory but also for astrophysical plasma research as e.g. for germanium abundance determination and opacity calculations (Seaton 1988). Moreover, germanium is commonly associated with slow-neutron-capture nucleosynthesis in stellar interiors (see e.g. Leckrone et al. 1993). Also germanium lines are present in the Solar (see e.g. Moore et al. 1966; Grevesse 1984) spectrum and with the help of the Goddard High Resolution Spectrograph (GHRS) on the Hubble Space Telescope (HST), the presence of germanium is confirmed e.g. for the χ Lupi binary star (Leckrone et al. 1993). The primary component of this system has $T_{\rm eff} = 10\,650$ K and $\log g = 3.8$ and the secondary $T_{\rm eff} = 9200$ K and $\log g = 4.2$. Since around $T = 10\,000$ K hydrogen is mainly ionized, Stark broadening is the principal pressure broadening mechanism for such plasma conditions. It is interesting to note as well that beginning with germanium ($Z = 32$) and extending to heavier elements, there is a "dramatic increase in the magnitude of overabundances" (Leckrone et al. 1993) in chemically peculiar (CP) star spectra. An illustration of the increasing astrophysical interest for trace element spectra is also the work of Cardelli et al. (1991). With the GHRS they have for the first time detected in the interstellar medium the presence of trace elements like germanium and krypton, so that data on germanium spectral line shapes are obviously of interest for astrophysical plasma research. Moreover, Stark broadening parameters of germanium lines are of interest for the consideration of regularities and systematic trends (see e.g. Sarandaev et al. 2000) as well, and the corresponding results may be of interest in astrophysics for interpolation of new data and critical evaluation of existing data.

The first discussion on the Stark broadening of germanium lines was published in Minnhagen (1964), who considered correlation between observed wavelength shifts produced in electrodeless discharge tube and predicted Stark effect shifts in the spectrum of neutral germanium. Shifts in the wavelength of spectral lines in spark discharges have been investigated as well in the first experimental work on Ge I Stark broadening (Kondrat'eva 1970). After these pioneer works, reliable data on Ge I spectral line Stark broadening parameters have been obtained experimentally by Jones & Miller (1974) and Musiol et al. (1988). For the Ge I $4p^2\ {}^1S$–$5s^1S^0$ multiplet, Dimitrijević & Konjević (1983) performed a semiclassical calculation within the framework of the theory developed by Griem et al. (1962) (see also Griem 1974). Moreover, Lakićević (1983) estimated on the basis of regularities and systematic trends the Stark broadening parameters for the Ge I $4p^2\ {}^3P$–$5s^3P^0$ multiplet. The estimates based on regularities and systematic trends were performed also by Sarandaev et al. (2000) for the Ge I $4p^2\ {}^1S$–$5s^1P^0$ and $4p^2\ {}^1S$–$5s^3P^0$ multiplets. Here, we will calculate within the semiclassical perturbation approach the Stark broadening parameters of 11 Ge I transitions within the $4s^24p^2$–$4s^24p5s$ transition array, for conditions typical of astrophysical and laboratory plasmas. The obtained results will be compared with available experimental and theoretical values. Also, the importance of the electron-impact broadening for A type star atmospheres will be tested.

Send offprint requests to: M. S. Dimitrijević,
e-mail: mdimitrijevic@aob.bg.ac.yu

2. Results and discussion

For the determination of Stark broadening parameters (the full line width at half maximum – W and the line shift – d) of neutral germanium, the semiclassical perturbation formalism has been used. This formalism, as well as the corresponding computer code (Sahal-Bréchot 1969a,b), have been updated and optimized several times (Sahal-Bréchot 1974; Fleurier et al. 1977; Dimitrijević & Sahal-Bréchot 1984; Dimitrijević et al. 1991; Dimitrijević & Sahal-Bréchot 1996). The calculation procedure, with the discussion of updatings and validity criteria, has been briefly reviewed e.g. in Dimitrijević (1996). Atomic energy levels needed for calculations have been taken from Sugar & Musgrove (1993). The oscillator strengths have been calculated within the Coulomb approximation (Bates & Damgaard 1949; and the tables of Oertel & Shomo 1968). For higher levels, the method of van Regemorter et al. (1979) has been used.

In Table 1, electron-, proton-, and Ar II-impact broadening parameters for 11 Ge I transitions for a perturber density of 10^{16} cm^{-3} and temperatures from 2500 up to 50 000 K are shown. Moreover, we present in Table 1 a parameter C (Dimitrijević & Sahal-Bréchot 1984) which gives an estimate of the maximum perturber density for which the line may be treated as isolated, when it is divided by the corresponding full width at half maximum. After electrons, the most important charged perturbers in hot stellar atmospheres are protons, and Stark broadening parameters due to interaction of the emitter/absorber with them are included in Table 1. Due to its importance for laboratory and technological plasma investigations, Stark broadening parameters due to collisions with argon ions are included as well. The validity of the impact approximation has been estimated for data shown in Table 1, by checking if the collision volume (V) multiplied by the perturber density (N) is much less than one (Sahal-Bréchot 1969a,b), and in all considered cases the product NV is less than 0.1. When the impact approximation is not valid, the ion broadening contribution may be estimated by using the quasistatic approach (Sahal-Bréchot 1991 or Griem 1974). In the region between where neither of these two approximations is valid, a unified type theory should be used. For example in Barnard et al. (1974), a simple analytical formula for such a case is given. The accuracy of the results obtained decreases when broadening by ion interactions becomes important.

Jones & Miller (1974) determined experimentally Stark widths of Ge I $4p^2\ ^1S–5s^1P^0$ 4685.83 Å and $4p^2\ ^1S–5s^3P^0$ 4226.56 Å spectral lines by using a gas-driven spectroscopic shock tube with hydrogen as a driver gas, and runs were made with various filling pressures and different compositions of GeH_4, Ar and Ne. They used photographic techniques and Konjević & Wiese (1990) in his critical analysis of the experimental Stark broadening data stated that "self-absorption may have been an important factor for the 4226.56 Å line" in his experiment. In Konjević et al. (1984), the error bars of their results are critically estimated to be within ±50% (accuracy denoted as C in their notation).

Musiol et al. (1988) determined experimentally Stark widths of 9 lines from Ge I $4p^2$–4p5s and $4p^2$–4p4d transition arrays by using a wall-stabilized arc operated at atmospheric pressure with various mixtures of GeH_4 and Ar. In Konjević & Wiese (1990), the error bars of their results are critically estimated to be within ±50% (accuracy denoted as C in their notation), except for the 4226.56 Å line where the accuracy is denoted as D^+ (error bars larger than ±50%).

In Table 2, our results are compared with experimental results of Jones & Miller (1974) and Musiol et al. (1988). With W_m are denoted experimental full widths at half maximum in [Å], and with W_e and W_{GeII} our theoretical values for Stark widths due to electron- and Ge II-impacts, respectively. Since ionization potentials of H, Ar and Ge are 13.595 eV, 15.755 eV and 7.88 eV respectively, the most appropriate way to estimate the influence of ion-impact broadening for the considered experiments is to compare electron-impact widths with widths due to impacts with ions of heavy electron donors like germanium. One can see that the ion contribution is around 13−14 per cent which is well within the estimated error bars of the semiclassical perturbation approach of ±30 per cent (Griem 1974). Our results are in disagreement with experimental results of Jones & Miller (1974) for the 4226.56 Å line. This result is in disagreement with other theoretical (Dimitrijević & Konjević 1983; Sarandaev et al. 2000) and experimental (Musiol et al. 1988) results, and selfabsorption is indicated as a possible reason in Konjević & Wiese (1990). The ratio of the experimental Stark width of Jones & Miller (1974) for the 4685.83 Å line and our result is $W_m/W_e = 1.41$, that is within the estimated (Konjević et al. 1984) error bars of the experiment. The agreement of our values with experimental results of Musiol et al. (1988) is reasonable. The largest disagreement is for the 4226.56 Å line, where $W_m/W_e = 0.59$, that is however within the estimated (Konjević et al. 1984) error bars of ±50 per cent. The agreement for other lines is considerably better. However, if we analyse experimental and theoretical widths within the $4p^2\ ^3P–5s^3P^0$ multiplet, one can notice that the largest difference of experimental values is for 2754.59 Å $4p^2\ ^3P_2–5s^3P^0_1$ ($W_m = 0.0509$ Å) and 2651.57 Å $4p^2\ ^3P_0–5s^3P^0_1$ ($W_m = 0.0358$ Å) line. The corresponding theoretical values are $W_e = 0.0502$ Å and 0.0466 Å respectively. Since both lines have the same upper energy level and the lower level contribution is small, this is in contradiction with findings that if the perturbing energy level positions are regular, line widths within a multiplet should be approximately the same (Wiese & Konjević 1982). If we eliminate the influence of the wavelength differences multiplying values for the 2651.57 Å line by $(2754.59/2651.57)^2$, we will obtain for the theoretical width the value of 0.0503 Å which is practically equal to the calculated value for the 2754.59 Å line (0.0502 Å). Contrary, for experimental width the scaled value is 0.0386 Å, different to the experimental value of 0.0509 Å for the 2754.59 Å line. It is interesting to obtain new experimental results for these lines in order to see if the reason is configuration mixing.

For Ge I $4p^2\ ^1S–5s^1P^0$ multiplet, Dimitrijević & Konjević (1983) performed a semiclassical calculation within the framework of the theory developed by Griem et al. (1962) (see also Griem 1974). It should be noted that atomic data needed for calculations were not taken from Sugar & Musgrove (1993), not available at that time, but from Moore (1971) and

Table 1. This table shows electron-, proton- and Ar II-impact broadening parameters for Ge I for perturber density of 10^{16} cm^{-3} and temperatures from 2500 up to 50 000 K. Transitions and calculated (λ) and experimental (in the air – from NIST 2003 – λ_o) wavelengths (in Å) are also given in the table. By dividing C by the corresponding full width at half maximum (Dimitrijević et al. 1991), we obtain an estimate for the maximum perturber density for which the line may be treated as isolated and tabulated data may be used.

PERTURBER DENSITY IS 1.E+16 cm–3							
PERTURBERS ARE:		ELECTRONS		PROTONS		Ar II IONS	
TRANSITION	T (K)	WIDTH (10^{-1} Å)	SHIFT (10^{-1} Å)	WIDTH (10^{-1} Å)	SHIFT (10^{-1} Å)	WIDTH (10^{-1} Å)	SHIFT (10^{-1} Å)
	2500.	0.168	0.139	0.0439	0.0370	0.0271	0.0202
Ge I $4p^2\ ^1S_0$–$5s^1P^0_1$	5000.	0.201	0.162	0.0489	0.0429	0.0299	0.0241
	10 000.	0.235	0.190	0.0546	0.0491	0.0331	0.0279
λ = 4227.8 Å	20 000.	0.261	0.211	0.0611	0.0558	0.0367	0.0320
λ_o = 4226.562 Å	30 000.	0.272	0.213	0.0652	0.0600	0.0390	0.0345
C = 0.12E+20	50 000.	0.290	0.202	0.0709	0.0656	0.0423	0.0379
	2500.	0.172	0.145	0.0463	0.0389	0.0292	0.0214
Ge I $4p^2\ ^1S_0$–$5s^3P^0_1$	5000.	0.207	0.168	0.0515	0.0449	0.0320	0.0253
	10 000.	0.243	0.198	0.0574	0.0513	0.0352	0.0293
λ = 4687.1 Å	20 000.	0.273	0.223	0.0641	0.0583	0.0390	0.0335
λ_o = 4685.829 Å	30 000.	0.285	0.228	0.0684	0.0627	0.0414	0.0361
C = 0.18E+20	50 000.	0.306	0.217	0.0742	0.0685	0.0447	0.0396
	2500.	0.0843	0.0710	0.0221	0.0191	0.0132	0.0105
Ge I $4p^2\ ^1D_2$–$5s^3P^0_1$	5000.	0.101	0.0825	0.0247	0.0220	0.0147	0.0124
	10 000.	0.119	0.0969	0.0277	0.0252	0.0164	0.0144
λ = 3270.4 Å	20 000.	0.132	0.113	0.0310	0.0286	0.0183	0.0164
λ_o = 3269.489 Å	30 000.	0.136	0.112	0.0331	0.0307	0.0196	0.0177
C = 0.89E+19	50 000.	0.145	0.111	0.0360	0.0336	0.0212	0.0194
	2500.	0.0844	0.0721	0.0224	0.0193	0.0134	0.0106
Ge I $4p^2\ ^1D_2$–$5s^3P^0_2$	5000.	0.102	0.0838	0.0251	0.0224	0.0149	0.0126
	10 000.	0.120	0.0985	0.0281	0.0256	0.0166	0.0146
λ = 3125.7 Å	20 000.	0.135	0.111	0.0315	0.0291	0.0186	0.0167
λ_o = 3124.816 Å	30 000.	0.140	0.115	0.0337	0.0313	0.0198	0.0180
C = 0.67E+19	50 000.	0.148	0.109	0.0366	0.0342	0.0216	0.0198
	2500.	0.0873	0.0723	0.0223	0.0193	0.0133	0.0105
Ge I $4p^2\ ^1D$–$5s^1P^0$	5000.	0.104	0.0843	0.0250	0.0223	0.0148	0.0125
	10 000.	0.122	0.0986	0.0280	0.0255	0.0166	0.0145
λ = 3040.0 Å	20 000.	0.134	0.113	0.0314	0.0290	0.0185	0.0166
	30 000.	0.138	0.111	0.0336	0.0312	0.0198	0.0180
C = 0.62E+19	50 000.	0.147	0.109	0.0366	0.0341	0.0215	0.0197
	2500.	0.0557	0.0469	0.0145	0.0126	0.00855	0.00692
Ge I $4p^2\ ^3P_0$–$5s^3P^0_1$	5000.	0.0669	0.0545	0.0162	0.0146	0.00955	0.00819
	10 000.	0.0785	0.0640	0.0182	0.0166	0.0107	0.00948
λ = 2652.4 Å	20 000.	0.0869	0.0721	0.0204	0.0189	0.0120	0.0109
λ_o = 2651.568 Å	30 000.	0.0896	0.0742	0.0218	0.0203	0.0128	0.0117
C = 0.58E+19	50 000.	0.0948	0.0707	0.0237	0.0222	0.0139	0.0128
	2500.	0.0588	0.0494	0.0152	0.0133	0.00901	0.00729
Ge I $4p^2\ ^3P_1$–$5s^3P^0_0$	5000.	0.0707	0.0575	0.0171	0.0153	0.0101	0.00862
	10 000.	0.0827	0.0674	0.0191	0.0175	0.0113	0.00998
λ = 2710.4 Å	20 000.	0.0914	0.0758	0.0215	0.0199	0.0126	0.0114
λ_o = 2709.624 Å	30 000.	0.0940	0.0774	0.0230	0.0214	0.0135	0.0123
C = 0.63E+19	50 000.	0.0997	0.0767	0.0250	0.0234	0.0146	0.0135
	2500.	0.0573	0.0483	0.0149	0.0130	0.00881	0.00713
Ge I $4p^2\ ^3P_1$–$5s^3P^0_1$	5000.	0.0689	0.0561	0.0167	0.0150	0.00985	0.00843
	10 000.	0.0808	0.0659	0.0187	0.0171	0.0110	0.00977
λ = 2692.1 Å	20 000.	0.0895	0.0743	0.0210	0.0194	0.0123	0.0112
λ_o = 2691.341 Å	30 000.	0.0923	0.0764	0.0225	0.0209	0.0132	0.0121
C = 0.60E+19	50 000.	0.0977	0.0727	0.0244	0.0229	0.0143	0.0132

Table 1. continued.

PERTURBER DENSITY IS 1.E+16 cm–3							
PERTURBERS ARE:		ELECTRONS		PROTONS		Ar II IONS	
TRANSITION	T (K)	WIDTH (10^{-1} Å)	SHIFT (10^{-1} Å)	WIDTH (10^{-1} Å)	SHIFT (10^{-1} Å)	WIDTH (10^{-1} Å)	SHIFT (10^{-1} Å)
	2500.	0.0583	0.0498	0.0154	0.0134	0.00907	0.00731
Ge I $4p^2\ ^3P_1$–$5s^3P^0_2$	5000.	0.0701	0.0579	0.0172	0.0155	0.0101	0.00868
	10 000.	0.0831	0.0680	0.0193	0.0177	0.0114	0.0101
λ = 2593.3 Å	20 000.	0.0928	0.0769	0.0217	0.0201	0.0127	0.0115
λ_o = 2592.534 Å	30 000.	0.0962	0.0797	0.0232	0.0216	0.0136	0.0124
C = 0.46E+19	50 000.	0.101	0.0759	0.0253	0.0236	0.0148	0.0137
	2500.	0.0600	0.0505	0.0156	0.0136	0.00924	0.00746
Ge I $4p^2\ ^3P_2$–$5s^3P^0_1$	5000.	0.0721	0.0588	0.0175	0.0157	0.0103	0.00883
	10 000.	0.0846	0.0690	0.0196	0.0179	0.0115	0.0102
λ = 2755.4 Å	20 000.	0.0937	0.0777	0.0220	0.0204	0.0129	0.0117
λ_o = 2754.588 Å	30 000.	0.0965	0.0798	0.0235	0.0219	0.0138	0.0126
C = 0.63E+19	50 000.	0.102	0.0760	0.0256	0.0239	0.0150	0.0138
	2500.	0.0609	0.0521	0.0161	0.0140	0.00950	0.00764
Ge I $4p^2\ ^3P_2$–$5s^3P^0_2$	5000.	0.0733	0.0605	0.0180	0.0162	0.0106	0.00907
	10 000.	0.0868	0.0711	0.0202	0.0185	0.0119	0.0105
λ = 2652.0 Å	20 000.	0.0970	0.0804	0.0227	0.0210	0.0133	0.0121
λ_o = 2651.172 Å	30 000.	0.100	0.0832	0.0243	0.0226	0.0142	0.0130
C = 0.48E+19	50 000.	0.106	0.0793	0.0264	0.0247	0.0155	0.0143

Table 2. Comparison of our theoretical results for Stark broadening of Ge I lines with experimental results. With W_m are denoted experimental full widths at half maximum in [Å] and with W_e and W_{GeII} our theoretical values for Stark widths due to electron- and Ge II-impacts, respectively. Accuracy is denoted as in Konjević et al. (1984) and Konjević & Wiese (1990), C means that error bars are within ±50% and D^+ that they are larger than ±50%. Under Ref., 1 is for Musiol et al. (1988) and 2. for Jones & Miller (1974).

Transition	λ(Å)	T(K)	N_e 10^{17} cm^{-3}	W_m (Å)	W_e (Å)	W_{GeII} (Å)	Acc.	Ref.
$4p^2\ ^3P$–$5s^3P^0$	2754.59	12 450	0.57	0.0509	0.0502	0.00644	C	1
	2709.62	12 450	0.57	0.0434	0.0490	0.00628	C	1
	2651.57	12 450	0.57	0.0358	0.0466	0.00596	C	1
	2651.17	12 450	0.57	0.0427	0.0517	0.00662	C	1
	2592.53	12 450	0.57	0.0452	0.0494	0.00633	C	1
$4p^2\ ^1S$–$5s^3P^0$	4685.83	11 000	1	0.35	0.248	0.0339	C	2
$4p^2\ ^1D$–$5s^3P^0$	3124.82	12 450	0.57	0.0628	0.0715	0.00928	C	1
$4p^2\ ^1D$–$5s^1P^0$	3039.07	12 450	0.57	0.0622	0.0721	0.00924	C	1
$4p^2\ ^1S$–$5s^1P^0$	4226.56	11 000	1	3.18	0.239	0.0318	C	2
		12 450	0.57	0.0815	0.139	0.0185	D^+	1

Kaufman & Edlén (1974). The comparison of semiclassical method of Griem et al. (1962) (see also Griem 1974), used in Dimitrijević & Konjević (1983) and the semiclassical perturbation method (Sahal-Bréchot 1969a,b) used here, as well as an explanation of the differences, is given in Dimitrijević & Sahal-Bréchot (1996). The present results are considerably smaller. For example at T = 10 000 K and N_e = 10^{17} cm^{-3}, Dimitrijević & Konjević obtain a Stark width of 0.408 Å while the present results are 0.235 Å.

Lakićević (1983) estimated Stark broadening parameters for Ge I $4p^2\ ^3P$–$5s^3P^0$ multiplet on the basis of regularities and systematic trends, and he obtained that W is 0.1 Å and the absolute value of the shift is 0.055 Å for an electron density of 10^{17} cm^{-3} and T = 20 000 K. The distance between energy levels within the $5s^3P^0$ term is not negligible in comparison with the distance to the nearest perturbing levels. Consequently, the particular line widths within the corresponding multiplet differ. Our width values vary between 0.087 and 0.097 Å and shift values between 0.072 and 0.080 Å not taking into account the influence of wavelength differences. If one takes into account the simplicity of this method, the agreement is good for the width and within the error bars for the shift.

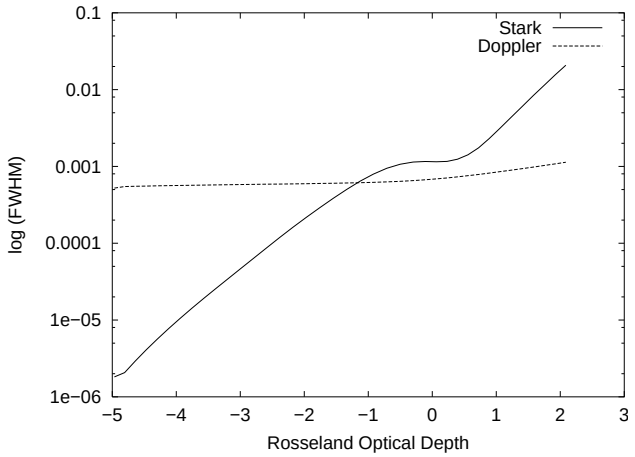

Fig. 1. Thermal Doppler (dotted line) and Stark widths (full line) for Ge I (λ = 4226.562 Å) spectral line as functions of Rosseland optical depth.

On the basis of examination of systematic trends (Purić et al. 1985, 1987, 1991, 1993; Purić 1996), dependencies enabling the estimation of the Stark widths of spectral lines due to s–p and p–s transitions of neutral atoms have been found by Sarandaev et al. (2000). These simple relations, based on the known ionization potential of the lower/upper level of the corresponding transitions and on the regularities and systematic trends, have been used to determine Stark widths for Ge I $4p^2\ {}^1S$–$5s^1P^0$ and $4p^2\ {}^1S$–$5s^3P^0$ transitions. For example at T = 20 000 K and $N_e = 10^{17}$ cm^{-3} they obtain for Ge I $4p^2\ {}^1S$–$5s^1P^0$ a Stark width of 0.33 Å while the present value is 0.261 Å.

In order to see the influence of the Stark broadening mechanism for Ge I spectral lines in stellar plasma conditions, we have calculated the Stark widths for the Ge I 4226.562 Å spectral line for a Kurucz's (1979) A type star atmosphere model with $T_{\rm eff}$ = 10 000 K and log g = 4. From Fig. 1 one can see the existence of atmospheric layers where Doppler and Stark widths are comparable and where the Stark width is dominant, and that the Stark broadening effect should be taken into account in abundance determination, spectra synthesis and modeling of stellar plasmas.

New experimental determination of Stark broadening of neutral germanium spectral lines will be obviously useful for comparison with experimental and theoretical data as well as for astrophysical plasma investigation and modeling.

Acknowledgements. This work is a part of the project GA-1195 "Influence of collisional processes on astrophysical plasma lineshapes", supported by the Ministry of Science, Technologies and Development of Serbia. The research was supported also by the Fonds zur Förderung der wissenschaftlichen Forschung (Project S7303-AST).

References

Barnard, A. J., Cooper, J., & Smith, E. W. 1974, J. Quant. Spectrosc. Radiat. Transfer, 14, 1025
Bates, D. R., & Damgaard, A. 1949, Trans. Roy. Soc. London, Ser. A, 242, 101
Cardelli, J. A., Savage, B. D., & Ebberts, D. C. 1991, ApJ, 383, L23
Cowley, C. R., Ryabchikova, T., Kupka, F., et al. 2000, MNRAS, 317, 299
Dimitrijević, M. S. 1996, Zh. Prikl. Spektrosk., 63, 810
Dimitrijević, M. S., & Konjević, N. 1983, J. Quant. Spectrosc. Radiat. Transfer, 30, 45
Dimitrijević, M. S., & Sahal-Bréchot, S. 1984, J. Quant. Spectrosc. Radiat. Transfer, 31, 301
Dimitrijević, M. S., & Sahal-Bréchot, S. 1996, Phys. Scr., 54, 50
Dimitrijević, M. S., Sahal-Bréchot, S., & Bommier, V. 1991, A&AS, 89, 581
Fleurier, C., Sahal-Bréchot, S., & Chapelle, J. 1977, J. Quant. Spectrosc. Radiative Transfer, 17, 595
Grevesse, N. 1984, Phys. Scr., T8, 49
Griem, H. R. 1974, Spectral Line Broadening by Plasmas (New York: Academic Press)
Griem, H. R., Baranger, M., Kolb, A. C., & Oertel, G. K. 1962, Phys. Rev., 125, 177
Jones, W. W., & Miller, M. H. 1974, Phys. Rev. A, 10, 1803
Kaufman, V., & Edlén, B. 1974, J. Phys. Chem. Ref. Data, 3, 825
Kondrat'eva, E. V. 1970, Opt. Spectrosc. (USSR) 29, 434
Konjević, N., Dimitrijević, M. S., & Wiese, W. L. 1984, J. Phys. Chem. Ref. Data, 13, 619
Konjević, N., & Wiese, W. L. 1990, J. Phys. Chem. Ref. Data, 19, 1307
Kurucz, R. L. 1979, ApJS, 40, 1
Lakićević, I. S. 1983, A&A, 127, 37
Leckrone, D. S., Wahlgren, G. M., Johansson, S. G., & Adelman, S. J. 1993, in Peculiar versus Normal Phenomena in A-Type and Related Stars, ed. M. M. Dworetsky, F. Castelli, & R. Faraggiana, ASP Conf. Ser., 44, 42
Minhagen, L. 1964, J. Opt. Soc. Am., 54, 320
Moore, C. E., Minnaert, M. G. J., & Houtgast, J. 1966, The Solar Spectrum 2935 Å to 8770 Å, NBS Monographs 61, US Department of Commerce, NBS, Washington DC
Moore, C. E. 1971, Atomic Energy Levels, Circular 467, vol. II, US Department of Commerce, NBS, Government Printing Office, Washington DC
Musiol, K., Labusz, S., & Pokrzywka, B. 1988, J. Quant. Spectrosc. Radiat. Transfer, 40, 143
NIST 2003, Atomic Spectra Data Base Lines, `http://physics.nist.org`
Oertel, G. K., & Shomo, L. P. 1968, ApJS, 16, 175
Purić, J. 1996, Zh. Prikl. Spektrosk., 63, 816
Purić, J., Ćuk, M., Dimitrijević, M. S., & Lesage, A. 1991, ApJ, 382, 353
Purić, J., Ćuk, M., & Lakićević, I. S. 1985, Phys. Rev. A, 32, 1106
Purić, J., Miller, M. H., & Lesage, A. 1993, ApJ, 416, 825
Purić, J., Srećković, A., Djeniže, S., & Platiša, M. 1987, Phys. Rev. A, 36, 3957
Sahal-Bréchot, S. 1969a, A&A, 1, 91
Sahal-Bréchot, S. 1969b, A&A, 2, 322
Sahal-Bréchot, S. 1974, A&A, 35, 321
Sahal-Bréchot, S. 1991, A&A, 245, 322
Sarandaev, E. V., Konovalova, O. A., & Salakhov, M. Kh. 2000, J. Quant. Spectrosc. Radiat. Transfer, 67, 105
Seaton, M. J. 1988, J. Phys. B, 21, 3033
Sugar, J., & Musgrove, A. 1993, J. Phys. Chem. Ref. Data, 22, 1213
van Regemorter, H., Hoang Binh Dy, & Prud'homme, M. 1979, J. Phys. B, 12, 1053
Wiese, W. L., & Konjević, N. 1982, J. Quant. Spectrosc. Radiat. Transfer, 28, 185

A&A 417, 375–380 (2004)
DOI: 10.1051/0004-6361:20034162
© ESO 2004

Astronomy & Astrophysics

Importance of collisions with charged particles for stellar UV line shapes: Cd III*

N. Milovanović[1,2], M. S. Dimitrijević[1,2], L. Č. Popović[1,2], and Z. Simić[1,2]

[1] Astronomical Observatory, Volgina 7, 11160 Belgrade, Serbia and Montenegro
[2] Isaac Newton Institute of Chile, Yugoslavia Branch

Received 6 August 2003 / Accepted 10 November 2003

Abstract. Stark broadening parameters, widths and shifts, for 84 spectral lines of doubly-ionized cadmium (Cd III) have been calculated using the modified semi-empirical approach (MSE). Calculated spectral lines belong to the transitions $4d^9 5s$–$4d^9 5p$ and $4d^9 5p$–$4d^9 5d$. Widths and shifts of the spectral lines are given for temperature range of 5000 K–60 000 K and an electron density of 10^{23} m^{-3}. The influence of collisions with charged particles on Cd III UV stellar lines along the HR diagram is discussed. Compared to the Doppler broadening, the influence of the Stark broadening mechanism is more important for deeper atmospheric layers and for larger values of $\log g$. Stark broadening does not depend on turbulent velocity for the considered stellar model of a standard main sequence hot star of A0 spectral type. The influence of the Stark widths for standard models of DA and DB white dwarfs is also discussed.

Key words. atomic processes – line: formation – stars: atmospheres – stars: early-type – stars: white dwarfs

1. Introduction

Spectral lines of multiply charged heavy elements are present in the UV spectra of early-type stars, especially in spectra of chemically peculiar (CP) ones. Investigation of these lines is important for example for spectral lines synthesis, diagnostics and modelling of laboratory and stellar plasma, abundance determination and opacity calculation.

Stark broadening of spectral lines is the dominant pressure broadening mechanism in hot, early-type, stars and white dwarf atmospheres. This type of broadening might also be important in interstellar molecular and ionized hydrogen clouds, as e.g. for radio recombination spectral lines in W51 emission nebulae (Lang & Wilson 1978), and in cooler stars such as solar type ones for transitions involving higher principal quantum numbers (Vince & Dimitrijević 1985).

Spectral lines of Cd I and Cd II are observed in stellar spectra of some CP stars, e.g. χ Lupi (Leckrone et al. 1999), so cadmium in various ionization stages is present in stellar atmospheres. With the development of space-born telescopes, spectral instruments like the Goddard High Resolution Spectrograph (GHRS) on the Hubble Space Telescope provide good resolution spectra of stellar objects so that the need for trace element data, like that for cadmium, increases.

Here, we present the computed electron-impact broadening parameters, widths and shifts, for 84 spectral lines (12 singlets and 72 triplets) of Cd III obtained using the modified semi-empirical method – MSE (Dimitrijević & Konjević 1980; Dimitrijević & Kršljanin 1986).

2. Method of calculation

Advanced calculation of the Stark broadening parameters using the strong-coupling quantum-mechanical method (Baranger 1958a, 1958b, 1958c; Kolb & Griem 1958; Griem 1974; Dimitrijević et al. 1981; Seaton 1988; Ralchenko et al. 1999; Zeng-xin et al. 1999) is so complicated that only a limited amount of data for spectral lines originating from low-lying transitions can be calculated adequately. On the other hand, the semi-classical method (Sahal-Bréchot 1969a, 1969b; Dimitrijević et al. 1991; see also a review of obtained results in Dimitrijević 1997) needs a large amount of atomic data, energy levels and oscillator strengths. This method is not applicable in an adequate way to the Stark broadening calculation of Cd III because there is insufficient number of reliable atomic data.

Here we use the modified semi-empirical approach (MSE, Dimitrijević & Konjević 1980; Dimitrijević & Kršljanin 1986) which includes explicitly only levels with $\Delta n = 0$ and $l'_{\rm if} = l_{\rm if} \pm 1$, where n is the principal quantum number, l is the orbital quantum number and i and f denote initial and final level, respectively. Levels with $\Delta n \neq 0$ are combined and approximately estimated, so that for Stark broadening parameter calculations we need less atomic data then in the semi-classical

Send offprint requests to: N. Milovanović,
e-mail: nmilovanovic@aob.bg.ac.yu

* Tables 1 and 2 are only available in electronic form at the CDS via anonymous ftp to cdsarc.u-strasbg.fr (130.79.128.5) or via http://cdsweb.u-strasbg.fr/cgi-bin/qcat?J/A+A/417/375

method. We note that the needed dipole matrix elements have been calculated using the Coulomb approximation method described in Bates & Damgaard (1949), Shore & Menzel (1965) and Oertel & Shomo (1967).

The modified semi-empirical method is applicable under the following conditions:

1. That the line is isolated, i.e. non-degenerate energy levels broadened by collisions do not overlap (Sahal-Bréchot 1969a; Dimitrijević & Sahal-Bréchot 1984).
2. That the minimal distance of the perturbing electron from an emitting particle is significantly smaller than distances between two perturbing electrons, i.e. that the probability that two or more electrons are close to an emitting particle is small (see e.g. Griem 1974).
3. That we can assume an impact approximation, which requires that the collision volume $V \sim \rho^3$ multiplied by electron density is much less than 1 (Sahal-Bréchot 1969a).
4. That the plasma is ideal. With the increase of the density the number of particles in the Debye sphere decreases and the plasma becomes non-ideal (Konjević & Uzelac 1990). The idealness of the plasma can be checked by calculating the number of perturbers in the Debye sphere which must be larger than 1 (Dimitrijević et al. 1991).

The accuracy of the MSE calculations for spectral line widths is around ±50% (Dimitrijević & Konjević 1980). The average ratio of calculated and experimental widths, determined in Dimitrijević & Konjević (1980) for 36 multiplets of 7 different doubly-charged ions is 1.06 ± 0.32 and for 7 multiplets for 4 triply-charged ions 0.91 ± 0.42. For 71 multiplets of 7 singly-charged ions with various couplings schemes Popović (1994) found that the overall average ratio of experimental to calculated widths is 1.4 ± 0.3. Even for relatively complex spectra of Xe II and Kr II with mixed jK and LS couplings, the accuracy found is about ±30% (Popović & Dimitrijević 1996). The accuracy of shifts usually gives higher errors compared to experimental values. This is a consequence of the cancellations of important contributions with different signs (see Dimitrijević & Kršljanin 1986). The error of obtained shifts with MSE calculations is within ±50% of the corresponding width value.

3. Results

Doubly-ionized cadmium (Cd III) belongs to the palladium isoelectronic sequence with the ground state electronic configuration $4d^{10}\ ^1S_0$ and ionization potential of 302 200 ± 50 cm^{-1}. Atomic data needed for our MSE calculation were taken from Van Kleef et al. (1980). They observed Cd III spectra in the UV spectral range from 50 to 210 nm with the 6.65 and 10.7 m normal-incidence vacuum spectrograph. Experimental values of energy levels were checked with the least-square level fitting of Hartee-Fock (HF) calculations of atomic parameters. They give a more complete analysis of energy level values compared to the first observed spectra of Cd III presented in the paper of Shenstone & Pittenger (1949). Van Kleef et al. (1980) estimated that the energy levels error for sharp lines is ±0.5 cm^{-3} and several cm^{-3} for strong and asymmetric lines.

Even if coupling schemes slowly go from LS to jj coupling as we go through the isoelectronic sequence from Pd I to Sn V, most of the energy levels, without losing accuracy, can be represented with LS coupling (van Kleef et al. 1980). Consequently an LS coupling scheme is adopted here.

The calculated Stark widths and shifts of Cd III spectral lines are given in Table 1 (available only in electronic form) as a function of temperature (from 5000 to 60 000 K) for an electron density of $N = 10^{23}$ m^{-3}. In Table 1 we present results for 84 spectral lines, where 22 belong to $4d^9\ 5s$–$4d^9\ 5p$ and 62 to $4d^9\ 5p$–$4d^9\ 5d$ transition.

For spectrum synthesis programs, as e.g. the frequently used SYNTH code (Piskunov 1992), it is more convenient to present the temperature dependence of Stark width by using parameters A_0, A_1 and Stark widths w[rad s^{-1}] per electron for temperature T = 10 000 K. These parameters can be derived numerically from the best fit of data given in Table 1 using equation (see Popović et al. 1999)

$$\frac{w[\mathrm{rad\ s^{-1}}]}{N} = A_0 \cdot T^{A_1}, \tag{1}$$

where

$$w[\mathrm{rad\ s^{-1}}] = w[\mathrm{nm}]\ \frac{2\pi c \times 10^{-8}}{\lambda^2[\mathrm{nm}]}.$$

The parameters $\log A_0$, A_1 and $\log w$[rad s^{-1}] for 84 spectral lines are given in Table 2 (available only in electronic form).

The Eq. (1) may be used for reasonable extrapolations toward higher temperatures. It is not advisable to extrapolate toward temperatures lower than given in Table 1 (T < 5000 K), without checking the validity of the impact approximation. Moreover, at lower temperatures, the importance of quantum effects increases and the application of MSE method as well as the other semi-classical, classical or semi-empirical ones neglecting quantum effects becomes questionable.

The extrapolation toward lower electron densities N is linear. For higher densities however, it is preferable to check the influence of Debye shielding, non-ideal plasma effect and that the spectral line is isolated.

4. Discussion

We used our results for Stark widths given in Tables 1 and 2 to examine the importance of electron-impact broadening in hot stars and white dwarf atmospheres for trace elements like Cd III. Behavior of Stark and Doppler spectral line widths in stellar atmospheres were calculated for Cd III $5p\ ^3F^0_3$–$5d\ ^3G_3$ (λ = 144.754 nm), a strong spectral line in various atmospheric models.

These calculations were performed for solar element abundance atmospheric models given in Kurucz (1979) and Kurucz's web site (`http://kurucz.harvard.edu/`). Each model is characterized by the effective temperature T_{eff}, logarithm of gravity $\log g$ and turbulent velocity v_{t} and each atmospheric layer within the model is characterized by electron density N and temperature T. Stark widths for λ = 144.754 nm spectral line for a particular model were calculated using Eq. (1). In this equation the Stark width is a function of N

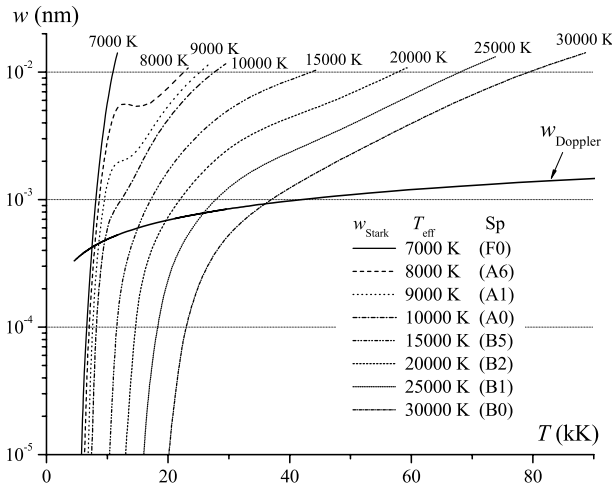

Fig. 1. Stark widths (FWHM) (thinner lines) and Doppler width (thicker line) for Cd III 5p $^3F^0_3$–5d $^3G_3$ (λ = 144.754 nm) spectral line as a function of atmospheric layer temperatures. Stark widths are shown for 8 atmospheric models with effective temperatures $T_{\rm eff}$ = 7000–30 000 K, corresponding to spectral classes (Sp) from F0 to B0, $\log g$ = 4.0 and turbulent velocity $v_{\rm t}$ = 0 km s^{-1}.

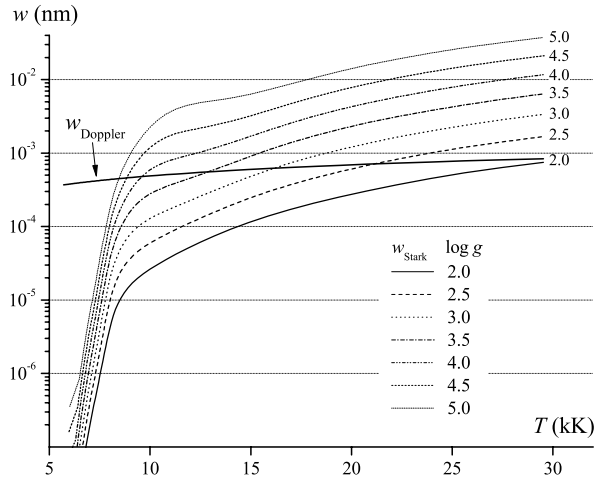

Fig. 2. Same as in Fig. 1 but Stark widths are shown for 7 values of model gravity $\log g$ = 2–5, $T_{\rm eff}$ = 10 000 K and $v_{\rm t}$ = 0 km s^{-1}.

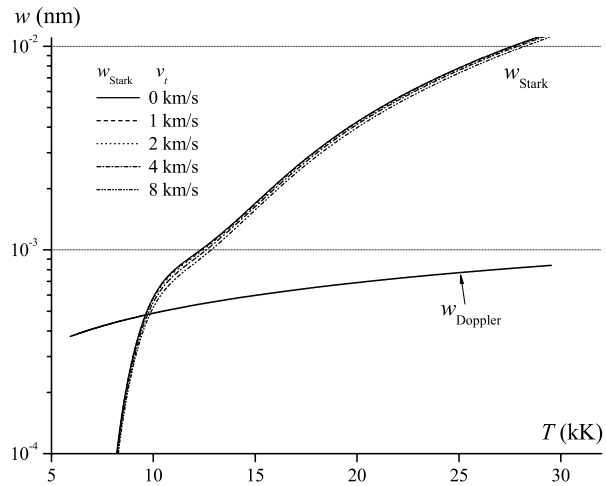

Fig. 3. Same as in Fig. 1 but Stark widths are shown for 5 values of turbulent velocity $v_{\rm t}$ = 0–8 km s^{-1}, $T_{\rm eff}$ = 10 000 K and $\log g$ = 4.0.

and T. For these line parameters $\log A_0$ is −3.64248 and A_1 = −0.50410.

In hot star atmospheres, besides electron-impact broadening (Stark broadening) the important broadening mechanism is a Doppler (thermal) one as well as the broadening due to the turbulence and stellar rotation. Other types of spectral line broadening, such as van der Waals, resonance and natural broadening, are usually negligible. For a Doppler-broadened spectral line the intensity distribution is not Lorentzian as for electron-impact broadening but Gaussian, whose full half width of the spectral line may be determined by the equation (see e.g. Konjević 1999)

$$w_{\rm D}[{\rm nm}] = 7.16 \times 10^{-7} \lambda[{\rm nm}] \sqrt{\frac{T[{\rm K}]}{M_{\rm Cd}}},$$

where atomic weight for cadmium is $M_{\rm Cd}$ = 112.411 a.u.

The importance of Stark broadening in hot star atmospheres is illustrated in Figs. 1–5. In Fig. 1 Stark (FWHM) and Doppler widths for Cd III 5p $^3F^0_3$–5d $^3G_3$ (λ = 144.754 nm) spectral line as a function of atmospheric layer temperatures are shown. Stark widths are shown for 8 atmospheric models with effective temperatures $T_{\rm eff}$ = 7000–30 000 K, corresponding to spectral classes (Sp) from F0 to B0, logarithm of surface gravity $\log g$ = 4.0 and turbulent velocity $v_{\rm t}$ = 0 km s^{-1}. In Fig. 1 one can see that Stark widths are lager than Doppler ones for stars with lower effective temperatures. For stars with higher effective temperatures, Stark broadening is more important than Doppler one for deeper atmospheric layers (larger layer temperature T). For example, for stars with effective temperature $T_{\rm eff}$ = 30 000 K (B0 stars), Stark and Doppler widths are equal for temperature layer $T \approx$ 35 000 K and for stars with $T_{\rm eff}$ = 7000 K (F0 stars), they are equal for $T \approx$ 5000 K.

The dependence of Stark and Doppler broadening on atmospheric layer temperature for 7 values of surface gravity is shown in Fig. 2. Models used here have $T_{\rm eff}$ = 10 000 K and $v_{\rm t}$ = 0 km s^{-1}. The Stark broadening in stellar atmospheres with higher values of surface gravity is significantly larger than Doppler broadening. For stars with surface gravity $\log g$ = 2, Stark broadening is comparable to Doppler widths only for deeper hot atmospheric layers. For upper parts of stellar atmospheres (T < 10 000 K) Stark widths rapidly decrease and for layer temperature $T \approx$ 6000–7000 K Stark widths are several magnitudes lower than Doppler ones for all shown values of surface gravity $\log g$.

Figure 3 represents the dependence of Stark and Doppler widths on atmosphere layer temperature for a solar abundance Kurucz model $T_{\rm eff}$ = 10 000 K, $\log g$ = 4 and 5, and values of the turbulent velocity $v_{\rm t}$ = 0–8 km s^{-1}. As one can see in Fig. 3, Stark widths do not show any significant dependence as a function of turbulent velocity.

The ratio of Stark and Doppler widths along the Hertzsprung-Russell diagram, from K0 to O5 spectral class, and within the range of the column mass at temperature minimum $\log m$ from −3 up to 0 are shown in Fig. 4. In deeper parts of atmospheres, e.g. $\log m$ = 0, Stark broadening is larger than

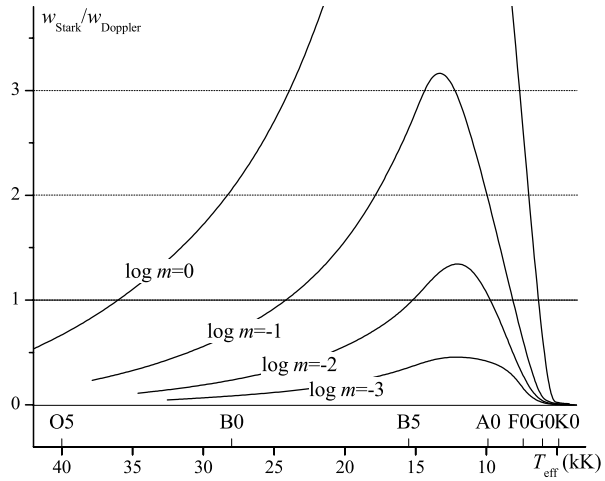

Fig. 4. Ratio of Stark and Doppler widths $w_{\rm Stark}/w_{\rm Doppler}$ as a function of the model effective temperature $T_{\rm eff}$ (upper part of x-axis is spectral class). Dependance is shown for 4 values of logarithm of the column mass at temperature minimum $\log m$ from 0 to −3, $\log g = 4.0$ and velocity $v_{\rm t} = 0$ km s^{-1}.

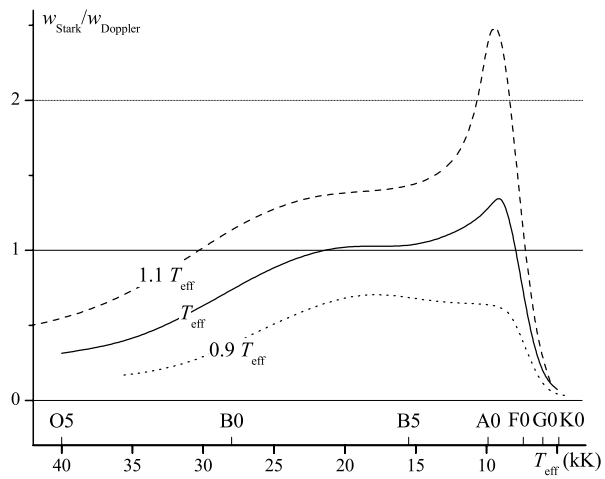

Fig. 5. Same as in Fig. 4 but the ratio is shown for 3 values of layer temperature $T = 0.9\ T_{\rm eff}$, $T_{\rm eff}$ and $1.1\ T_{\rm eff}$, $\log g = 4.0$ and velocity $v_{\rm t} = 0$ km s^{-1}.

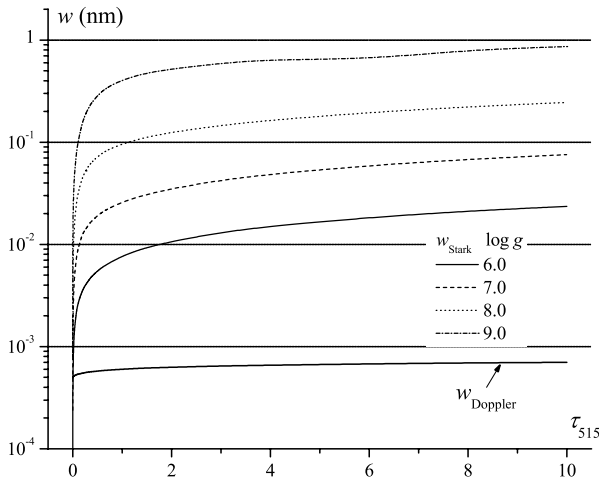

Fig. 6. Stark and Doppler widths for Cd III $\lambda = 144.754$ nm spectral line as a function of optical depth for standard wavelength $\lambda_{\rm st} = 515$ nm for DA white dwarfs. Widths are given for 4 values of logarithm of surface gravity $\log g = 6.0$–9.0. Effective model temperature is $T_{\rm eff} = 15\,000$ K.

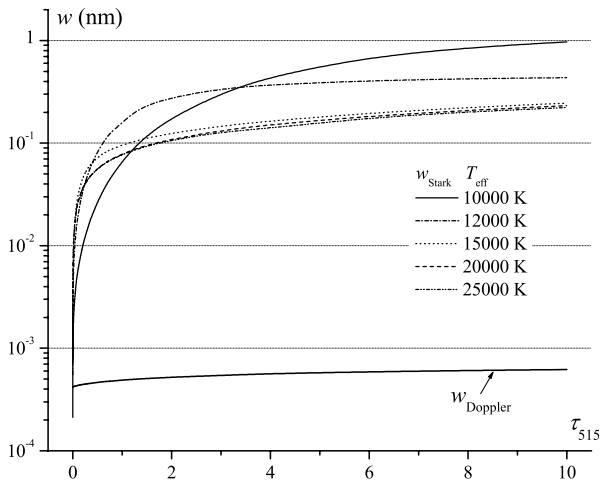

Fig. 7. Same as in Fig. 6 but widths are given for 5 values of effective temperature $T_{\rm eff} = 10\,000$–$25\,000$ and $\log g = 8$.

the Doppler one for stars of G, F, A and B spectral type. For $\log m = -3$ (upper atmospheric parts) Doppler widths are comparable (approximately one-half) with Stark widths for spectral classes A0 to B5.

In Fig. 5 are shown ratios of Stark and Doppler widths as a function of star effective temperature (spectral class) for a Kurucz atmospheric model $\log g = 4$ and $v_{\rm t} = 0$ km s^{-1}. Stark and Doppler width ratio is given for 3 values of layer temperature $T = 0.9\ T_{\rm eff}$, $T_{\rm eff}$ and $1.1\ T_{\rm eff}$. In this figure one can see that Stark broadening is the dominant broadening mechanism for deeper atmospheric layers ($T = 1.1\ T_{\rm eff}$) for stars of G, F, A and B spectral class. For upper layers ($T = 0.9\ T_{\rm eff}$) Stark broadening is comparable to the Doppler one and should be taken into account for stars of A and B spectral class, since differences of Lorentz (for Stark) and Gauss (for Doppler) distributions may be important in the line wings.

To compare Stark and Doppler broadening we have calculated spectral line widths for Cd III $\lambda = 144.754$ nm for DA and DB white dwarf atmospheres. Models were taken from Wickramasinghe (1972). DA dwarfs are helium and metal underabundant and DB white dwarfs are helium and metal overabundant compared to hydrogen.

As one can see in Figs. 6–9 Stark broadening is by one or two order of magnitudes higher than Doppler one. Consequently, with the increases in pressure, electron density or effective temperature in DA and DB white dwarf models, the importance of Stark broadening increases as well.

The comparison of Stark and thermal Doppler contributions to the line widths is calculated for one line of Cd III ($\lambda = 144.754$ nm), and we can expect a similar contribution of the Stark broadening for all UV Cd III lines. The contribution of the Stark effect to line widths increases with the principal quantum number (Vince & Dimitrijević 1985) and also one should take into account that in some cases, due to close perturbing

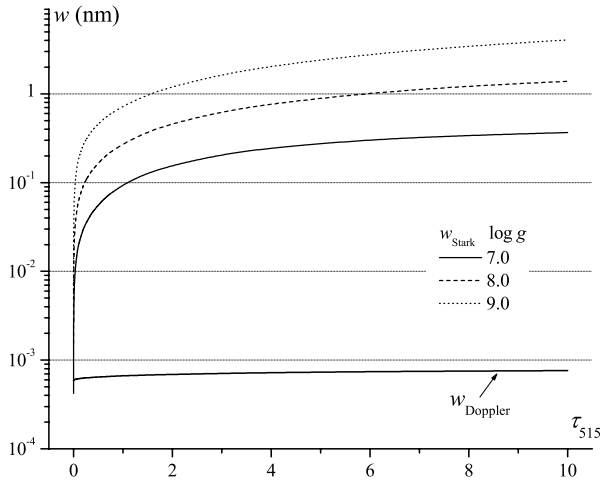

Fig. 8. Same as in Fig. 6 but for DB white dwarfs. Effective model temperature is $T_{\rm eff}$ = 20 000 K.

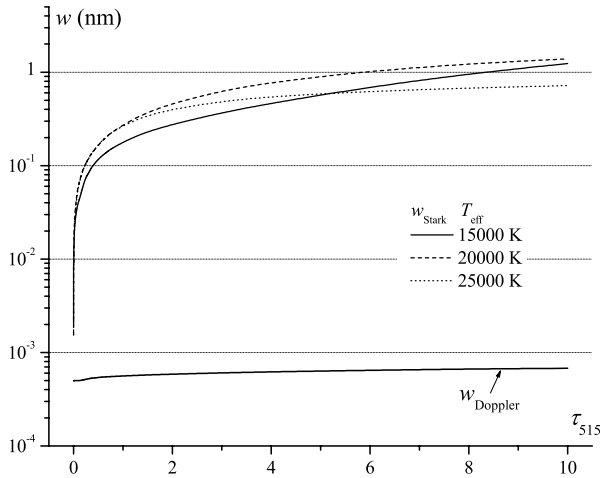

Fig. 9. Same as in Fig. 8 but widths are given for $T_{\rm eff}$ = 10 000 K, 20 000 K and 25 000 K and $\log g$ = 8.

levels, Stark widths might also be large. In some cases the Stark broadening may significantly contribute to the line widths as well as to the line shapes (see e.g. Dimitrijević et al. 2003, as well as results of our similar investigations for Zr II and Zr III in Popović et al. 2001a and Nd II in Popović et al. 2001b).

5. Conclusion

We have calculated Stark broadening parameters, widths and shifts, for 84 UV spectral lines of Cd III by using the MSE method. We estimate that the errors bars of obtained data are ±50%. There is no possibility for the moment to calculate them in an adequate way by more sophisticated semi-classical methods since a sufficiently complete set of reliable experimental Cd III atomic energy levels is not available. When results of reliable Stark broadening calculations are not available (for example for Cd III lines not included here) more approximate methods are often used for stellar atmosphere analysis, e.g. data obtained by using methods based on regularities and systematic trends (see e.g. Lakićević 1983; Purić et al. 1991), on classical approaches, other approaches (see e.g. Griem 1974 and references therein) or even sometimes the value of 1 to 10 times the classical damping (see e.g. Lanz et al. 1988).

There are no measured or even theoretically calculated electron-impact broadening parameters for Cd III. Our analysis of the influence of Stark broadening on the Cd III 144.754 nm spectral line demonstrates the importance of this broadening mechanism for hot star atmosphere analysis. However, for very hot stars, of the spectral class O, the influence of Stark broadening is reduced due to lower pressure in lower atmospheric layers. The effect of electron-impact broadening for DA and DB white dwarfs is even more significant.

Since with the development of space-born techniques, more good quality data on trace elements spectra will become available, we hope that the presented set of Cd III electron-impact broadening parameters will be of interest for future investigations of astrophysical and laboratory plasma, modelling of stellar atmospheres and stellar spectra synthesis and analysis. An example of the interest for as possible a large set of atomic data is the PHOENIX (see e.g. Hauschildt & Baron 1999) computer code for stellar modelling which includes a database containing 4.2×10^7 atomic, ionic and molecular spectral lines. Moreover, data on Stark broadening of Cd III spectral lines might be of interest not only for modelling and interpretation of stellar spectra but also for abundance determination and investigation of stratification of chemical elements (see e.g. Dimitrijević et al. 2003).

Acknowledgements. This work is a part of the projects "Influence of collisional processes on astrophysical plasma lineshapes" (GA 1195) and "Astrophysical Spectroscopy of Extragalactic Objects" (GA 1196) supported by the Ministry of Science, Technologies and Development of Serbia.

References

Baranger, M. 1958a, Phys. Rev., 111, 481
Baranger, M. 1958b, Phys. Rev., 111, 494
Baranger, M. 1958c, Phys. Rev., 112, 855
Bates, D. R., & Damgaard, A. 1949, Phil. Trans. Roy. Soc., A242, 101
Dimitrijević, M. S. 1997, Ap&SS, 252, 415
Dimitrijević, M. S., & Konjević, N. 1980, JQSRT, 24, 451
Dimitrijević, M. S., & Kršljanin, V. 1986, A&A, 165, 269
Dimitrijević, M. S., & Sahal-Bréchot, S. 1984, JQSRT, 31, 301
Dimitrijević, M. S., Feautrier, N., & Sahal-Bréchot, S. 1981, J. Phys., B14, 2559
Dimitrijević, M. S., Sahal-Bréchot, S., & Bomier, V. 1991, A&AS, 89, 581
Dimitrijević, M. S., Ryabchikova, T., Popović, L. Č., Shulyak, D., & Tsymbal, V. 2003, A&A, 404, 1099
Griem, H. R. 1974, Spectral Line Broadening by Plasmas (New York and London: Academic Press)
Hauschildt, P. H., & Baron, E. 1999, J. Comput. Appl. Math, 109, 41
Kolb, A. C., & Griem, H. R. 1958, Phys. Rev., 111, 514
Konjević, N. 1999, Phys. Rep., 316, 351
Konjević, N., & Uzelac, N. J. 1990, JQSRT, 44, 61
Kurucz, R. L. 1979, A&AS, 40, 1
Lakićević, I. S. 1983, A&A, 127, 37
Lang, K. R., & Wilson, R. F. 1978, MNRAS, 183, 5
Lanz, T., Dimitrijević, M. S., & Artru, M.-C. 1988, A&A, 192, 254

Leckrone, D. S., Proffitt, C. R., Wahlgren, G. M., Johansson, S. G., & Brage, T. 1999, AJ, 117, 1454
Oertel, G. K., & Shomo, L. P. 1967, ApJS, 16, 175
Piskunov, N. E. 1992, in Stellar Magnetism, ed. Yu. V. Glagolevskij, & I. I. Romanyuk (St. Petersburg: Nauka), 92
Popović, L. Č. 1994, Publ. Astron. Obs. Belgrade, 46, 1
Popović, L. Č., & Dimitrijević, M. S. 1996, A&AS, 120, 373
Popović, L. Č., Dimitrijević, M. S., & Ryabchikova, T. 1999, A&A, 127, 295
Popović, L. Č., Milovanović, N., & Dimitrijević, M. S. 2001a, A&A, 365, 656
Popović, L. Č., Simić, S., Milovanović, N., & Dimitrijević, M. S. 2001b, ApJS, 135, 109
Purić, J., Ćuk, M., Dimitrijević, M. S., & Lesage, A. 1991, ApJ, 382, 353
Ralchenko, Yu. V., Griem, H. R., Bray, I., & Fursa, D. V. 1999, Phys. Rev. A, 59, 1890
Sahal-Bréchot, S. 1969a, A&A, 1, 91
Sahal-Bréchot, S. 1969b, A&A, 2, 322
Seaton, M. J. 1988, J. Phys. B, 21, 3033
Shenstone, A. G., & Pittenger, J. T. 1949, J. Opt. Soc. Am., 39, 219
Shore, B. W., & Menzel, D. H. 1965, ApJS, 12, 187
Van Kleef, Th. A. M., Joshi, Y. N., & Uijlings, P. 1980, Phys. Scr, 22, 353
Vince, I., & Dimitrijević, M. S. 1985, Publ. Obs. Astron. de Belgrade, 33, 15
Wickramasinghe, D. T. 1972, Mem. R. Astron. Soc., 76, 129
Zeng-xin, Z., Jian-min, Y., & Yong-sheng, S. 1999, Chin. Phys. Lett., 16, 885

A&A 420, 769–774 (2004)
DOI: 10.1051/0004-6361:20035728
© ESO 2004

Astronomy & Astrophysics

Stark broadening parameters in singly and doubly ionized fluorine spectra

A. Srećković[1,2], S. Bukvić[1,2], S. Djeniže[1,2], and M. S. Dimitrijević[2,3]

[1] Faculty of Physics, University of Belgrade, 11001 Belgrade, PO Box 368, Serbia
[2] Isaac Newton Institute of Chile, Yugoslavia Branch, Belgrade, Serbia
[3] Astronomical Observatory, 11160 Belgrade, Volgina 7, Serbia
e-mail: steva@ff.bg.ac.yu

Received 22 November 2003 / Accepted 1 March 2004

Abstract. Stark widths (W) and shifts (d) of 5 singly ionized fluorine (F II) spectral lines within the 3s−3p, 3s′−3p′ and 3d−4f transitions and 5 doubly ionized fluorine (F III) spectral lines within the 3s−3p transition have been measured in a linear, low-pressure, pulsed arc discharge created in SF_6 plasma at 30 400−33 600 K electron temperatures and at $(2.75–2.80) \times 10^{23}$ m^{-3} electron densities. For Stark parameters of two F II and five F III lines there are no other experimental data. The widths and shifts have also been calculated using the semiclassical perturbation formalism (SCPF) (taking into account the impurity of energy levels, i.e. that the atomic energy levels are expressed as a mix of different configurations due to the configuration interaction). Calculations have been performed for temperatures between 5000 K and 100 000 K for the F II spectral lines and between 10 000 K and 300 000 K for the F III spectral lines for electrons, protons and helium ions as perturbers. Our measured and theoretical Stark parameters are compared with existing experimental and theoretical data. Tolerable agreement was found among them.

Key words. lines: profiles – atomic data

1. Introduction

Atomic data, such a Stark widths (W) and shifts (d) are useful for plasma diagnostic purposes in a wide range of electron temperatures (T) for astrophysical and laboratory plasmas. In the last five years fluorine spectral lines have become important for abundance investigations in various astrophysical plasmas (Lodders 2003; Zhu et al. 2002; Highberger et al. 2001). Only four experiments (Platiša et al. 1977; Purić et al. 1988; Djeniže et al. 1991; Blagojević et al. 1999; see also Lesage & Fuhr 1999; Konjević et al. 2002, and references therein), deal with investigations of Stark broadening parameters (W, d) of singly ionized fluorine spectral lines. A number of calculations of the Stark parameters, related to the F II, F III spectral lines, on the basis of different theoretical approaches is presented in the literature (Griem 1974; Hey 1976; Hey & Breger 1981; Dimitrijević & Konjević 1981; Dimitrijević 1988a,b). Furthermore, in Djeniže (2000), on the basis of regularities within an isonuclear sequence, Stark widths of F II 402.50 nm spectral lines (3s−3p transition) are predicted. In Djeniže et al. (1999) regularities of Stark widths of several F II spectral lines within the same transition (3s′−3p′) are presented.

The aim of this work is to present measured Stark *FWHM* (full-width at half intensity maximum, W) and shift (d) values at (30 400–33 600) K electron temperatures and at $(2.75–2.80) \times 10^{23}$ m^{-3} electron densities for 5 F II spectral lines belonging to the 3s−3p, 3s′−3p′, and 3d−4f transitions and 5 doubly ionized fluorine (F III) spectral lines within the 3s ^{4}P−3p ^{4}D° transition together with their calculated values using the semiclassical perturbation formalism (SCPF) updated several times (Sahal-Bréchot 1969a,b, 1974, 1991; Fleurier et al. 1977; Dimitrijević & Sahal-Bréchot 1984, 1996b, see also a review in Dimitrijević 1996). A unique exception is the transition 3p−3d from the F II spectrum (multiplet No. 3) for which only calculated values are presented. Our measured and calculated Stark parameters are compared with the existing experimental and theoretical data (Griem 1974; Platiša et al. 1977; Dimitrijević & Konjević 1981; Purić et al. 1988; Djeniže et al. 1991).

2. The experiment

A linear pulsed arc, used as plasma source, was described in detail in our previous publications (Djeniže et al. 1992, 2002a; Srećković et al. 2001, 2003). The working gas was SF_6 at 130 Pa filling pressure in a flowing regime (10 ml/min).

Send offprint requests to: M. S. Dimitrijević,
e-mail: mdimitrijevic@aob.bg.ac.yu

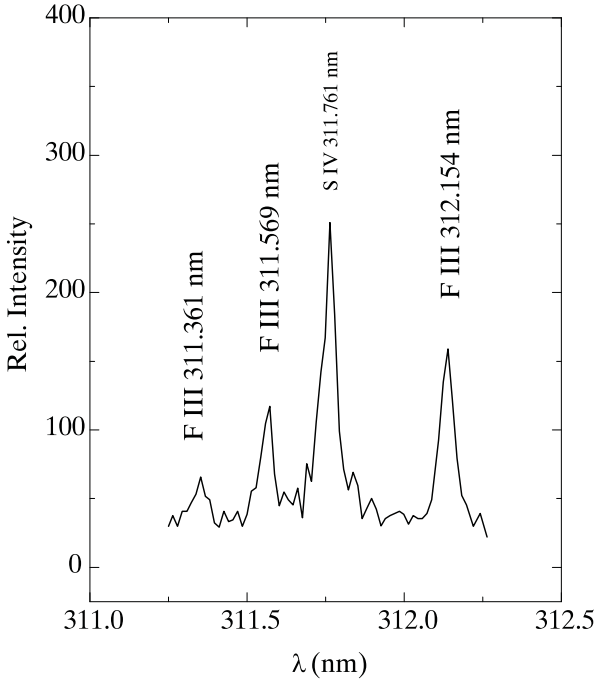

Fig. 1. Recorded spectrum with several investigated F III spectral line profiles.

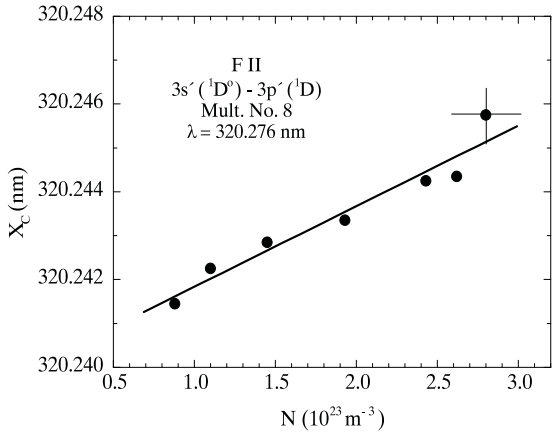

Fig. 2. The dependence of the position of the observed line center (X_C) as a function of the electron density (N) during the plasma decay.

The complete experimental procedure, plasma diagnostic techniques and set-up of the system used are described in Djeniže et al. (2002a). The absence of self-absorption was checked using the method described in Djeniže & Bukvić (2001). Part of the recorded F III spectrum, is presented, as an example, in Fig. 1.

The obtained electron temperature (T) and the electron density (N) decays are presented in Fig. 1 of Djeniže et al. (2002b).

3. Stark width measurements

The measured profiles were of the Voigt type due to the convolutions of the Lorentzian Stark and Gaussian profiles caused by Doppler and instrumental broadening. For the electron density and temperature presented in our experiment, the Lorentzian fraction was dominant. Van der Waals (Griem 1974) and resonance (Griem 1974) broadening were estimated to be smaller by more than one order of magnitude in comparison to Stark, Doppler and instrumental broadening. The standard deconvolution procedure (Davies & Vaughan 1963) has been applied using the least squares algorithm. The Stark widths were measured with ±12% error at a given N and T. Our measured Stark *FWHM* (W_m) values are presented in Table 1.

3.1. Stark shift measurements

The Stark shifts were measured relative to the unshifted spectral lines emitted by the same plasma using a method established and applied first by Purić & Konjević (1972). According to this method the Stark shift of a spectral line can be measured experimentally by evaluating the position of the spectral line center (X_C) recorded at different electron density values during plasma decay (Srećković et al. 2000). In principle, the method requires recording the spectral line profile at a higher electron density (N_1) resulting in an appreciable shift and then, later, when the electron concentration has dropped to a value (N_2) lower by at least an order of magnitude. The difference of the line center position in these two cases is ΔX_C, so that the shift d_1 at the higher electron density N_1 is

$$d_1 = N_1 \Delta X_C/(N_2 - N_1).$$

Our Stark shift values have been obtained for line center positions corresponding to the 15th μs and 45th μs after the beginning of the discharge. The dependence of the position of the observed line center (X_C) on the electron density (N) during the plasma decay of the investigated 320.650 nm F II spectral line is presented in Fig. 2, as an example.

The Stark shift data are corrected for the electron temperature decay (Popović et al. 1992). Stark shift data are determined with ±0.8 pm error at a given N and T. Measured (d_m) Stark shifts are presented in Table 1.

4. Method of calculation

The semiclassical perturbation formalism, as well as the corresponding computer code (Sahal-Bréchot 1969a,b), has been updated and optimized several times (Sahal-Bréchot 1974; Fleurier et al. 1977; Dimitrijević & Sahal-Bréchot 1984, 1996b; Dimitrijević et al. 1991). The calculation procedure, with a discussion of updates and validity criteria, has been briefly reviewed e.g. in Dimitrijević & Sahal-Bréchot (1996a,b) and in Dimitrijević (1996) so that only the basic details of calculations will be presented here. Stark full width (W) at intensity half maximum (*FWHM*) and shift (d) of an isolated spectral line, may be expressed as (Sahal-Bréchot 1969a,b; Fleurier et al. 1977):

$$W = N \int v f(v) \mathrm{d}v \left(\sum_{i' \neq i} \sigma_{ii'}(v) + \sum_{f' \neq f} \sigma_{ff'}(v) + \sigma_{\mathrm{el}} \right) + W_{\mathrm{R}}$$

$$d = N \int v f(v) \mathrm{d}v \int_{R_3}^{R_{\mathrm{D}}} 2\pi\rho \mathrm{d}\rho \sin 2\phi_{\mathrm{p}} \qquad (1)$$

Table 1. Measured F II and F III Stark *FWHM* (W_m in pm) and shift (d_m in pm) at a given T (in 10^4 K) and N (in 10^{23} m^{-3}). Transitions and wavelengths (λ in nm) are taken from NIST (2003). Negative shift is toward the blue.

Ion	Transition multiplet	λ	T	N	W_m	d_m
F II	$2p^33s-2p^3$ ($^4S^o$)3p	385.167	3.36	2.80	64.8	–3.4
	$^5S^o-^5P$					
	(1)					
	$2p^33s'-2p^3$ ($^2D^o$)3p′	410.916	3.04	2.75	61.0	−1.8
	$^3D^o-^3D$		3.36	2.80	54.8	
	(5)					
	$^1D^o-^1F$	429.916	3.04	2.75	74.4	
	(7)		3.36	2.80	71.8	−0.6
	$^1D^o-^1D$	320.276	3.04	2.75	61.0	
	(8)		3.36	2.80	57.8	−5.0
	$2p^33d-2p^3$ ($^4S^o$)4f	424.666	3.04	2.75	381	−1.8
	$^5D^o-^5F$		3.36	2.80	355	4
	(9)					
F III	$2p^23s-2p^2$ (^3P)3p	311.361	3.04	2.75	35.9	−2.8
	$^4P-^4D^o$	311.569	3.04	2.75	32.7	1.4
	(1)		3.36	2.80	31.1	
		312.154	3.04	2.75	39.7	−1.9
			3.36	2.80	37.7	
		312.478	3.04	2.75	38.7	0.3
			3.36	2.80	39.6	
		313.422	3.04	2.75	40.6	−2.8
			3.36	2.80	39.6	

where N is the electron density, $f(v)$ the Maxwellian velocity distribution function for electrons, ρ denotes the impact parameter of the incoming electron, i and f denote the initial and final atomic energy levels, and i', f' their corresponding perturbing levels, while W_R gives the contribution of the Feshbach resonances (Fleurier et al. 1977). The inelastic cross section $\sigma_{j,j'}(v)$ can be expressed by an integral over the impact parameter of the transition probability $P_{jj'}(\rho, v)$ as

$$\sum_{i'\neq i} \sigma_{jj'}(v) = \frac{1}{2}\pi {R_1}^2 + \int_{R_1}^{R_D} \sum_{j\neq j'} P_{jj'}(\rho, v),\ j = i, f \tag{2}$$

and the elastic cross section is given by

$$\sigma_{el} = 2\pi R_2^2 + \int_{R_2}^{R_D} 8\pi\rho \mathrm{d}\rho \sin^2\delta \tag{3}$$

$$\delta = (\phi_p^2 + \phi_q^2)^{1/2}. \tag{4}$$

The phase shifts ϕ_p and ϕ_q due respectively to the polarization potential (r^{-4}) and to the quadrupolar potential (r^{-3}), are given in Sect. 3 of Chapter 2 in Sahal-Bréchot (1969a). R_D is the Debye radius. All the cut-offs R_1, R_2, R_3 are described in Sect. 1 of Chapter 3 in Sahal-Bréchot (1969b). The formulae for the ion-impact widths and shifts are analogous to Eqs. (1)–(3), without the resonance contribution to the width. The difference in calculation of the corresponding transition probabilities and phase shifts as functions of the impact parameter in Eqs. (2) and (3) is in the ion perturbing trajectories which are influenced by a repulsive Coulomb force instead of an attractive one as for electrons.

Atomic energy levels needed for the calculation have been taken from Bashkin & Stoner (1975). The calculations have been performed for electron temperatures between 5000 K and 100 000 K for F II spectral lines and 10 000 K and 300 000 K for F III spectral lines for electrons, protons and helium ions as perturbers. Calculated W and d values are presented in Tables 2 and 3.

5. Results and discussion

Our measured (W_m and d_m) and calculated (W and d) values at a given electron temperature (T) and density (N) are given in Tables 1 and 2, respectively. For each value given in Table 2, the collision volume multiplied by the perturber density is much less than one and the impact approximation is valid (Sahal-Bréchot 1969a,b). When the impact approximation is not valid, the ion broadening contribution may be estimated by using the quasistatic approach (Sahal-Bréchot 1991; or Griem 1974).

To compare the measured and calculated Stark *FWHM* values, we have presented in Figs. 3–8 an existing experimental data set including our results, together with our (SCPF) theoretical results and those from Griem (1974) (G). In the case of F III lines the previous calculations made by Dimitrijević & Konjević (1981) have also been included for comparison.

The F II W values generated by protons and helium ions are up to 5–10 times smaller than the widths generated by electrons and show weak dependence on the temperature (see Table 2). The F II d values generated by electrons, protons and helium

Table 2. Calculated F II Stark *FWHM* (W in pm) and shift (d in pm) values for electrons (a), protons (b) and helium ions (c) as perturbers for various plasma temperatures (T in 10^3 K) and 10^{23} m^{-3} perturber density. $\langle\lambda\rangle$ is the mean wavelength in the multiplet. The negative shift is toward the blue.

Transition multiplet	$\langle\lambda\rangle$ (nm)		T (10^3 K)											
			5		10		20		30		50		100	
			W	d	W	d	W	d	W	d	W	d	W	d
3s ^{5}S^o–3p ^{5}P	385.01	a	38.5	−0.17	27.9	−0.34	20.4	−0.44	17.6	−0.43	15.3	−0.52	13.7	−0.46
(1)		b	0.64	−0.08	1.12	−0.16	1.58	−0.28	1.75	−0.34	1.92	−0.43	2.15	−0.52
		c	0.91	−0.08	1.14	−0.15	1.75	−0.24	1.89	−0.30	2.05	−0.36	2.22	−0.43
3s′ ^{3}D^o–3p′ ^{3}D	411.48	a	44.7	0.08	32.3	−0.45	23.5	−0.62	20.2	−0.61	17.6	−0.74	15.7	−0.64
(5)		b	0.72	−0.11	1.27	−0.24	1.79	−0.39	1.99	−0.48	2.19	−0.60	2.45	−0.71
		c	1.02	−0.11	1.55	−0.22	1.98	−0.34	2.14	−0.42	2.32	−0.49	2.53	−0.59
3s′ ^{3}D^o–3p′ ^{3}P	354.08	a	34.0	0.40	24.6	−0.07	18.0	−0.14	15.6	−0.13	13.7	−0.16	12.3	−0.16
(6)		b	0.64	−0.02	1.08	−0.05	1.51	−0.09	1.65	−0.12	1.81	−0.16	2.01	−0.20
		c	0.90	−0.02	1.33	−0.05	1.65	−0.08	1.78	−0.11	1.93	−0.14	2.08	−0.17
3s′ ^{1}D^o–3p′ ^{1}F	430.54	a	49.5	−0.06	35.8	−0.56	26.3	−0.61	22.8	−0.66	20.2	−0.78	18.2	−0.73
(7)		b	0.87	−0.13	1.50	−0.26	2.10	−0.44	2.32	−0.53	2.55	−0.66	2.86	−0.79
		c	1.23	−0.12	1.84	−0.24	2.31	−0.38	2.50	−0.47	2.72	−0.54	2.94	−0.66
3s′ ^{1}D^o–3p′ ^{1}D	320.65	a	29.8	0.62	21.6	0.43	16.1	0.25	14.1	0.35	12.7	0.40	11.7	0.32
(8)		b	0.70	0.08	1.14	0.17	1.55	0.27	1.68	0.33	1.84	0.41	2.04	0.49
		c	0.96	0.08	1.40	0.15	1.67	0.24	1.80	0.29	1.95	0.34	2.08	0.41
3p ^{5}P–3d ^{5}D^o	350.54	a	41.4	0.96	30.9	1.00	23.4	0.96	20.6	1.07	18.4	1.14	16.8	1.01
(3)		b	1.50	0.22	2.26	0.42	2.84	0.64	3.07	0.76	3.34	0.88	3.63	1.06
		c	1.90	0.21	2.65	0.38	3.05	0.55	3.27	0.63	3.52	0.73	3.69	0.87
3d ^{5}D^o–4f ^{5}F	424.70	a	990	−2.01	158	−3.88	129	−3.1	120	−2.75	110	−3.28	99.9	−3.02
(9)		b	11.5	−7.37	15.7	−10.7	19.6	−14.8	21.9	−16.5	24.8	−19.0	28.2	−21.5
		c	11.9	−5.98	15.0	−8.59	18.0	−12.2	19.4	−13.3	21.5	−15.4	23.3	−17.7

Table 3. Calculated F III Stark *FWHM* (W in pm) and shift (d in pm) values for electrons (a), protons (b) and helium ions (c) as perturbers for various plasma temperatures (T in 10^3 K) and 10^{23} m^{-3} perturber density. $\langle\lambda\rangle$ represents the mean wavelength in the multiplet. Negative shift is toward the blue.

Transition multiplet	$\langle\lambda\rangle$ (nm)		T (10^3 K)											
			10		20		50		100		150		300	
			W	d	W	d	W	d	W	d	W	d	W	d
3s ^{4}P–3p ^{4}D^o	312.52	a	21.5	−0.40	15.3	−0.61	10.4	−0.60	8.41	−0.70	7.59	0.68	6.51	−0.62
(1)		b	0.14	−0.10	0.30	−0.20	0.59	−0.37	0.78	−0.50	0.87	−0.55	1.02	−0.66
		c	0.22	−0.10	0.42	−0.19	0.68	−0.33	0.80	0.41	0.87	−0.46	0.99	−0.55

ions are very small, except for the multiplet No. 9, and are of the same magnitude. Similar conclusions can be obtained for the F III W and d values in the multiplet No. 1 (see Table 3).

Very good agreement has been found among our measured and calculated F II W and d values. Existing experimental W values (Djeniže et al. 1991; Platiša et al. 1977) also agree with our calculated values (see Figs. 3 and 4). Griem's (1974) W values lie below ours. In the case of the F II d values our SCPF calculations provide smaller values than those predicted by Griem (1974) (see Fig. 6).

Our measured and calculated F III W values agree mutually (within 5%) and both lie above previously calculated (Dimitrijević & Konjević 1981) and measured (Purić et al. 1988) values. Measured F III d values show evident scatter and within the experimental accuracy are practically equal to zero. Our calculation provides a very small negative shift which is practically independent on the electron temperature.

On the basis of the obtained W and d values we can conclude that a good agreement is found between our measured and calculated (SCPF) W values (within the experimental accuracy and uncertainties of the calculations) in the case of the F II lines that belong to the 3s–3p, 3d–4f and 3s′–3p′ transition.

We found that the Stark width generated by electrons is dominant and that the proton and helium ion contributions to the total Stark width can be neglected up to 150 000 K.

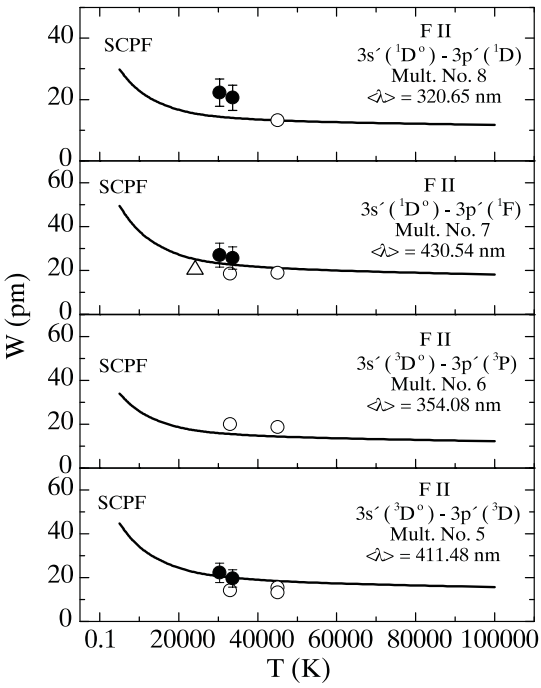

Fig. 3. F II Stark widths (W in pm) as a function of the electron temperature (T) in the 3s−3p transition at 10^{23} m^{-3} electron density. •, our experimental results, △, Platiša et al. (1977) and ○, Djeniže et al. (1991). SCPF (full line) represents our calculations using the semiclassical perturbation formalism. Error bars include the uncertainties of the width and electron density measurements (±20%).

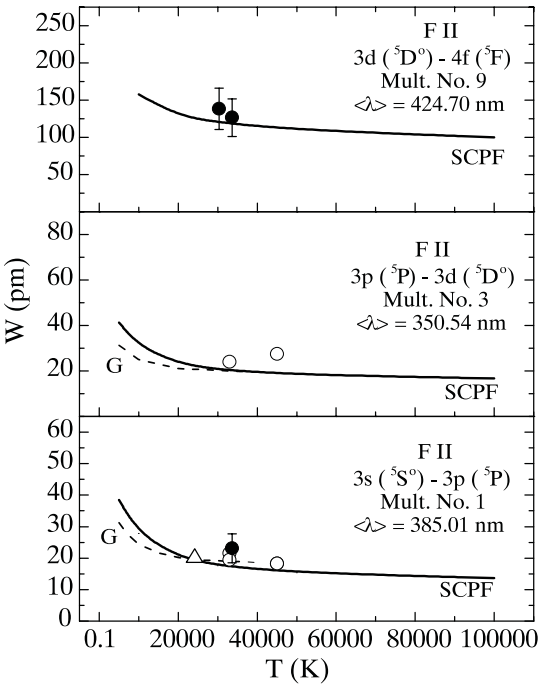

Fig. 4. F II Stark widths (W in pm) as a function of the electron temperature (T) in the 3s−3p, 3p−3d and 3d−4f transitions at 10^{23} m^{-3} electron density. •, our experimental results; △, Platiša et al. (1977) and ○, Djeniže et al. (1991). SCPF (full line) represents our calculations using the semiclassical perturbation formalism. G (dashed lines), denotes values calculated by Griem (1974). Error bars include the uncertainties of the width and electron density measurements (±20%). $\langle\lambda\rangle$ is the mean wavelength in the multiplet.

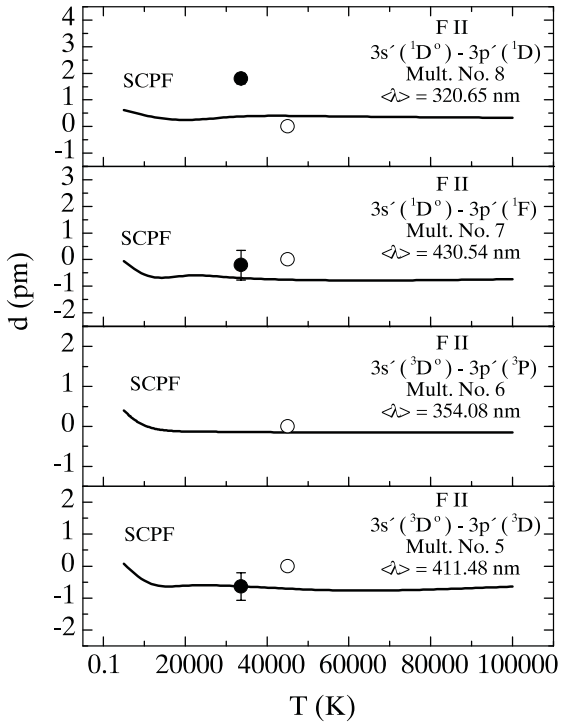

Fig. 5. F II Stark shifts (d in pm) as a function of the electron temperature (T) at 10^{23} m^{-3} electron density. •, our experimental results and ○, results from Djeniže et al. (1991). SCPF (full line) represents our calculations using the semiclassical perturbation formalism. $\langle\lambda\rangle$ is the mean wavelength of the multiplet.

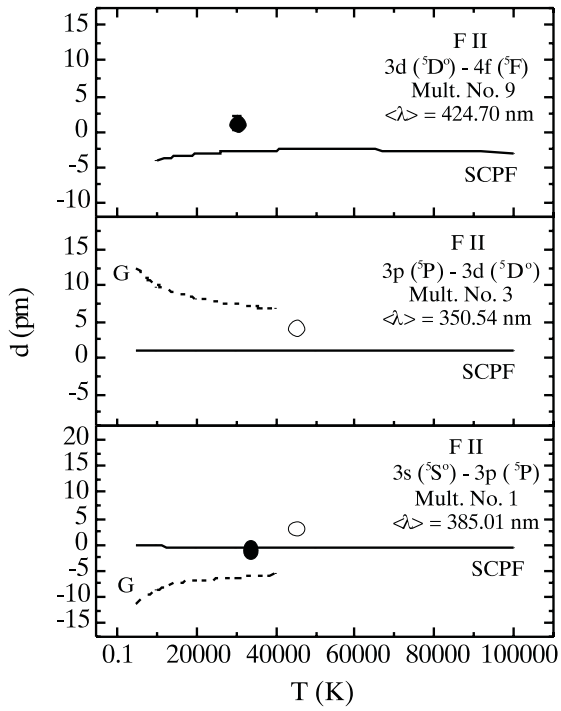

Fig. 6. F II electron Stark shifts (d in pm) as a function of the electron temperature (T) in the 3s−3p, 3p−3d and 3d−4f transitions at 10^{23} m^{-3} electron density. •, our experimental results and ○, from Djeniže et al. (1991). SCPF (full line) represents our calculations using the semiclassical perturbation formalism. G (dashed line), denotes calculations of Griem (1974). $\langle\lambda\rangle$ is the mean wavelength of the multiplet.

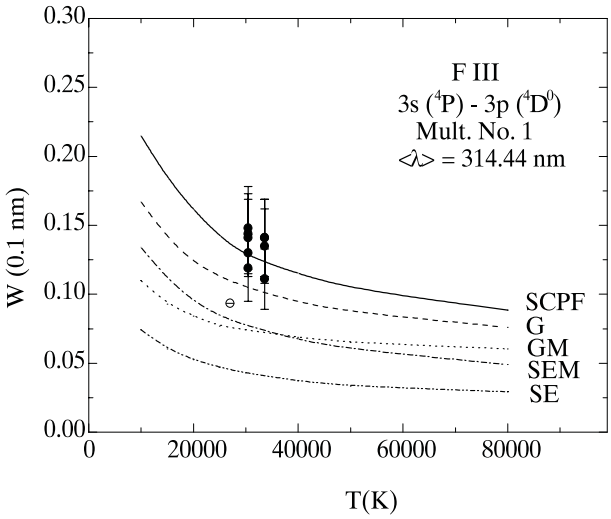

Fig. 7. F III electron Stark *FWHM* vs. electron temperature at 10^{23} m^{-3} electron density. G represents (dashed line) results from Dimitrijević & Konjević (1981) based on Griem's semiclassical method (see Griem 1974, Eq. (526)). GM denotes its modification by Dimitrijević & Konjević (1980). SEM denotes the modified semiempirical method (Dimitrijević & Konjević 1980). SE denotes the result from Griem's semiempirical calculation (Griem 1968). SCPF denotes our electron Stark width values calculated on the basis of the semiclassical perturbation formalism. • denotes our new experimental data and ⊘ denotes results from Purić et al. (1988).

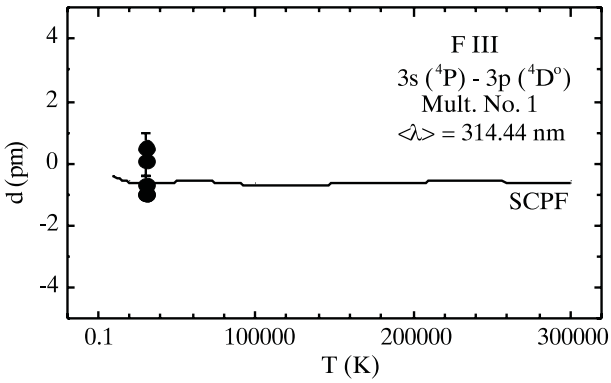

Fig. 8. F III electron Stark shift (*d*) vs. electron temperature at 10^{23} m^{-3} electron density. • denotes our experimental data. SCPF (full line) represents our electron Stark shift values calculated on the basis of the semiclassical perturbation formalism.

Our calculated Stark shift *d* values are generally very small (<1 pm) with negative sign in the case of the F II lines belonging to the 3s−3p and 3s′−3p′ transitions except for the muliplet No. 8 where the calculated *d* values have a positive sign. Small *d* values with positive sign are found for the 3p−3d transition. In the case of the 3d−4f transition the calculated *d* values are less than 4 pm with a negative sign.

We hope that the results presented in this paper, for Stark broadening parameters of the F II and F III spectral lines, will be of interest for a number of problems in plasma physics and astrophysics.

Acknowledgements. This work is a part of the projects "Determination of the atomic parameters on the basis of the spectral line profiles" (OI 1228) and "Influence of collision processes on astrophysical plasma line shapes" (GA 1195) supported by the Ministry of Science, Technologies and Development of the Republic of Serbia.

References

Bashkin, S., & Stoner, J. J. Jr. 1975, Atomic Energy Levels and Grotrian Diagrams (Amsterdam: North-Holland), 1
Blagojević, B., Popović, M. V., & Konjević, N. 1999, Phys. Scr., 59, 374
Davies, J. I., & Vaughan, J. M. 1963, ApJ, 137, 1302
Dimitrijević, M. S. 1988a, A&AS, 76, 53
Dimitrijević, M. S. 1988b, Bull. Astron. Belgrade, 139, 31
Dimitrijević, M. S. 1996, Zh. Prikl. Spectrosk., 63, 810
Dimitrijević, M. S., & Konjević, N. 1980, JQSRT, 24, 541
Dimitrijević, M. S., & Konjević, N. 1981, in Spectral Line Shapes, ed. B. Wende (New York: Walter de Gruyter, & Co.), 1, 211
Dimitrijević, M. S., & Sahal-Bréchot, S. 1984, JQSRT, 31, 301
Dimitrijević, M. S., & Sahal-Bréchot, S. 1996a, A&AS, 119, 369
Dimitrijević, M. S., & Sahal-Bréchot, S. 1996b, Phys. Scr., 54, 50
Djeniže, S. 2000, Serb. Astron. J., 161, 15
Djeniže, S., & Bukvić, S. 2001, A&A, 365, 252
Djeniže, S., Labat, J., Srećković, A., et al. 1991, Phys. Scr., 44, 148
Djeniže, S., Srećković, A., & Labat, J. 1992, A&A, 253, 632
Djeniže, S., Srećković, A., Labat, J., & Platiša, M. 1999, Phys. Scr., 53, 98
Djeniže, S., Srećković, A., Jelisavčić, M., & Bukvić, S. 2002a, A&A, 389, 1086
Djeniže, S., Dimitrijević, M. S., Srećković, A., & Bukvić, S. 2002b, A&A, 396, 331
Fleurier, C., Sahal-Bréchot, S., & Chapelle, J. 1977, JQSRT, 17, 595
Griem, H. R. 1968, Phys. Rev., 165, 258
Griem, H. R. 1974, Spectral Line Broadening by Plasmas (New York: Academic Press)
Hey, J. D. 1976, JQSRT, 16, 69
Hey, J. D., & Breger, P. 1981, in Spectral Line Shapes, ed. B. Wende (New York: Walter de Gruyter & Co.), 1, 201
Highberger, J. L., Savage, C., Bieging, J. H., & Ziurys, L. M. 2001, ApJ, 562, 790
NIST 2003, Atomic Spectra Data Base Lines (Wavelengths ordered), `http://www.physics.nist.gov`
Konjević, N., Lesage, A., Fuhr, J.R., & Wiese, W. L. 2002, J. Phys. Chem. Ref. Data, 31, 3, 819
Lesage, A., & Fuhr, J. R. 1999, Bibliography of Atomic Line Shapes and Shifts (April 1992 though June 1999), Observatoire de Paris
Lodders, K. 2003, ApJ, 591, 1220
Platiša, M., Dimitrijević, M. S., Popović, M. V., & Konjević, N. 1977, A&A, 54, 837
Popović, L. Č., Srećković, A., & Djeniže, S. 1992, Proc. 11th ICSLS, A25, Carry de Rouet, France
Purić, J., & Konjević, N. 1972, Z. Phys., 249, 440
Purić, J., Srećković, A., Djeniže, S., & Platiša, M. 1988, Phys. Rev. A, 37, 11, 4380
Sahal-Bréchot, S. 1969a, A&A, 1, 91
Sahal-Bréchot, S. 1969b, A&A, 2, 322
Sahal-Bréchot, S. 1974, A&A, 35, 321
Sahal-Bréchot, S. 1991, A&A, 245, 322
Srećković, A., Drinčić, V., Bukvić, S., & Djeniže, S. 2000, J. Phys. B, 33, 4873
Srećković, A., Dimitrijević, M. S., & Djeniže, S. 2001, A&A, 371, 354
Srećković, A., Dimitrijević, M. S., Djeniže, S., & Bukvić, S. 2003, A&A, 400, 1155
Zhu, C., Krems, R., Dolgano, A., & Balakrishnan, N. 2002, ApJ, 577, 795

A&A 423, 397–400 (2004)
DOI: 10.1051/0004-6361:20047100
© ESO 2004

Astronomy & Astrophysics

Stark broadening of the four times ionized silicon spectral lines*

N. Ben Nessib[1], M. S. Dimitrijević[2,3], and S. Sahal-Bréchot[4]

[1] Groupe de Recherche en Physique Atomique et Astrophysique, Faculté des Sciences de Bizerte, 7021 Zarzouna, Tunisia
[2] Astronomical Observatory, Volgina 7, 11160 Belgrade, Serbia
e-mail: mdimitrijevic@aob.bg.ac.yu
[3] Institute Isaac Newton of Chile, Yugoslavia Branch, Yugoslavia
[4] Laboratoire d'étude du Rayonnement et de la Matière en Astrophysique, UMR CNRS 8112, Observatoire de Paris-Meudon, 92195 Meudon, France

Received 19 January 2004 / Accepted 3 May 2004

Abstract. Using a semiclassical perturbation approach, we have obtained Stark broadening parameters for 16 Si V multiplets using atomic data calculated ab initio with the SUPERSTRUCTURE code. In order to complete Stark broadening data for the most important charged perturbers in stellar atmospheres, Stark broadening parameters for proton-, He II-, and Si II-impact line widths and shifts are also presented. Results have been obtained for an electron density of 10^{17} cm^{-3} as a function of temperature. Moreover, we have performed the same calculations with oscillator strengths calculated within the Coulomb approximation. The differences, which are within the error bars of the semiclassical perturbation approach (±20−30%) confirm that the Bates & Damgaard approximation may be used to complete the atomic data set needed for the Stark broadening calculations for multicharged ions like Si V, where more reliable oscillator strength values are not available.

Key words. atomic processes – line: profiles – atomic data

1. Introduction

The semiclassical perturbation formalism (Sahal-Bréchot 1969a,b) has been used in a series of papers for large scale calculations of Stark broadening parameters for a number of spectral lines of various emitters from neutral atoms up to twelve times ionized atoms (see e.g., Dimitrijević 1997, and references therein). The results of such calculations are of interest for a number of different problems in physics, astrophysics and plasma technology. In astrophysics, such atomic data are of interest e.g. for numerical modelling of stellar atmospheres or abundance determinations, problems correlated with nucleogenesis, mixing between atmosphere and interior, stellar structure and evolution (see e.g., Boesgaard 1988), and opacity calculations (Seaton 1988). Moreover, Stark broadening parameters are of interest for the investigation and diagnostics of laboratory and laser-produced plasmas, as well as for the theoretical studies of regularities and systematic trends.

In the case of four-times ionized atoms there exists a sufficiently complete set of the needed atomic data required for sophisticated semiclassical calculations for a number of astrophysically interesting lines. Therefore, large scale calculations have been performed with the semiclassical perturbation formalism (Sahal-Bréchot 1969a,b) for C V (Dimitrijević & Sahal-Bréchot 1995a, 1996a), N V (Dimitrijević & Sahal-Bréchot 1992), O V (Dimitrijević & Sahal-Bréchot 1995b,c), P V (Dimitrijević & Sahal-Bréchot 1995a, 1996a), S V (Dimitrijević & Sahal-Bréchot 1997, 1998a) and V V (Dimitrijević & Sahal-Bréchot 1998b) spectral lines. When we did not have a sufficiently complete set of reliable atomic data, the full semiclassical method could not be applied adequately, and simpler methods (Dimitrijević & Konjević 1980; Griem 1974, Eq. (526)) were used for the calculation of C V, O V, F V, Ne V and Al V Stark broadening parameters, including 6 multiplets of Si V (Dimitrijević 1993a,b). Such data are of interest for the consideration of radiative transfer through subphotospheric layers (Seaton 1988), for modelling of some hot star atmospheres such as PG 1159 pre-white dwarfs with an effective temperature between 100 000 and 140 000 K (Werner & Heber 1991), as well as for fusion plasmas and laser-produced plasmas. The development of soft X-ray lasers, where Stark broadening data are needed to calculate gain values, to model radiation trapping and to consider photoresonant pumping schemes (see e.g., Fill & Schöning 1994; Griem & Moreno 1980), provided an additional interest in such results.

With the development of space-borne spectroscopy, together with the possibility of obtaining high resolution spectra for a wide wavelength range including X-rays not detectable from the Earth's surface, the interest in such results is

* Tables 1 and 2 are only available in electronic form at the CDS via anonymous ftp to cdsarc.u-strasbg.fr (130.79.128.5) or via http://cdsweb.u-strasbg.fr/cgi-bin/qcat?J/A+A/423/397

increasing. For example the Low Energy Transmission Grating (LETG) on board the X-ray space observatory CHANDRA provides high quality spectra in the wavelength region between 5 and 140 Å, and contains a series of lines which can provide density and temperature diagnostics for relatively hot and dense stellar plasmas. An analysis of the X-ray high resolution spectrum of some stars shows spectra which may be rich in emission lines in the soft X-ray region, including Si V lines.

The aim of this paper is twofold. First we will compute Si V Stark broadening parameters within the semiclassical formalism by using oscillator strengths from the SUPERSTRUCTURE code to provide new Stark broadening data of astrophysical interest. Additionally, we perform the same calculations using the Coulomb approximation (Bates & Damgaard 1949; Oertel & Shomo 1968), in order to estimate the error introduced in the Stark broadening parameters due to uncertainties in the oscillator strengths obtained from the Coulomb approximation.

2. Theory

The energy levels of SiV are calculated using the general atomic structure code SUPERSTRUCTURE developed at the University College, London and described by Eissner et al. (1974). SUPERSTRUCTURE can calculate electric dipole (E1), electric quadrupole (E2), magnetic dipole (M1) and magnetic quadrupole (M2) transition probabilities. The wave functions are determined by diagonalization of the non-relativistic Hamiltonian using orbitals calculated in a scaled Thomas-Fermi-Dirac-Amaldi (TFDA) potential. The scaling parameters have been obtained by a self-consistent energy minimization procedure on all term energies of the eleven configurations $(1s^2)2s^22p^6$, $2s^22p^53l$, $2s2p^63l$ and $2s^22p^54l$ ($l \leq n-1$). The relativistic corrections: spin-orbit, mass, Darwin and one-body, are introduced according to the Breit-Pauli approach of Bethe & Salpeter (1957) in intermediate coupling LSJ. The main input data of this code are the charge of the ion and the configurations to be used in the model.

Stark broadening parameter calculations have been performed within the semiclassical perturbation method (Sahal-Bréchot 1969a,b). A detailed description of this formalism with all the innovations and optimizations is given in Sahal-Bréchot (1969a,b, 1974, 1991), Fleurier et al. (1977), Dimitrijević et al. (1991), Dimitrijević & Sahal-Bréchot (1996b), and only the basic details of calculations will be presented here. The Stark full width (W) at the intensity half maximum (FWHM) and shift (d) of an isolated spectral line, may be expressed as (Sahal-Bréchot 1969a,b)

$$W = N \int v f(v) \mathrm{d}v \left(\sum_{i' \neq i} \sigma_{ii'}(v) + \sum_{f' \neq f} \sigma_{ff'}(v) + \sigma_{\mathrm{el}} \right) + W_{\mathrm{R}}$$

$$d = N \int v f(v) \mathrm{d}v \int_{R_3}^{R_{\mathrm{D}}} 2\pi\rho \mathrm{d}\rho \sin 2\phi_{\mathrm{p}} \qquad (1)$$

where N is the electron density, $f(v)$ the Maxwellian velocity distribution function for electrons, ρ denotes the impact parameter of the incoming electron and v is the velocity, i and f denote the initial and final atomic energy levels, and i', f' their corresponding perturber levels, while W_{R} gives the contribution of the Feshbach resonances (Fleurier et al. 1977). The inelastic cross section $\sigma_{j,j'}(v)$ can be expressed by an integral over the impact parameter of the transition probability $P_{jj'}(\rho, v)$ as

$$\sum_{i' \neq i} \sigma_{jj'}(v) = \frac{1}{2}\pi {R_1}^2 + \int_{R_1}^{R_{\mathrm{D}}} \sum_{j \neq j'} P_{jj'}(\rho, v),\ j = i, f \qquad (2)$$

and the elastic cross section is given by

$$\sigma_{\mathrm{el}} = 2\pi R_2^2 + \int_{R_2}^{R_{\mathrm{D}}} 8\pi\rho \mathrm{d}\rho \sin^2 \delta$$

$$\delta = \left(\phi_{\mathrm{p}}^2 + \phi_{\mathrm{q}}^2\right)^{1/2}. \qquad (3)$$

The phase shifts ϕ_{p} and ϕ_{q} due respectively to the polarisation potential (r^{-4}) and to the quadrupolar potential (r^{-3}), are given in Sect. 3 of Chapter 2 in Sahal-Bréchot (1969a). R_{D} is the Debye radius. All the cut-offs R_1, R_2, R_3 are described in Sect. 1 of Chapter 3 in Sahal-Bréchot (1969b).

For electrons hyperbolic paths due to the attractive Coulomb force were used, while for perturbing ions the hyperbolic paths are different since the force is repulsive.

The formulae for the ion-impact widths and shifts are analogous to Eqs. (1)–(3), without the resonance contribution to the width. The results obtained within the semiclassical perturbation approach (Sahal-Bréchot 1969a,b) have been compared with critically selected experimental data for 13 He I multiplets (Dimitrijević & Sahal-Bréchot 1985) and it was found that the agreement between experimental data and semiclassical calculations is within ±20%, which is within the limits of predicted accuracy of the semiclassical method (Griem 1974). In addition, recent measurements of line widths for F V (Uzelac et al. 1993; Blagojević et al. 1996), N V (Glenzer et al. 1992; Blagojević et al. 1999) and O V (Blagojević et al. 1999) are in excellent agreement with the corresponding semiclassical perturbation calculations (Blagojević et al. (1996) for F V, Dimitrijević & Sahal-Bréchot (1992) for N V and Dimitrijević & Sahal-Bréchot (1995b,c) for O V).

3. Results and discussion

By combining the SUPERSTRUCTURE code for calculating energy levels and oscillator strengths and the code for the Stark broadening calculations we calculated Stark broadening parameters ab initio.

Using atomic energy levels obtained from the SUPERSTRUCTURE code, we have also calculated oscillator strengths using the Coulomb approximation. For higher levels, the method described by van Regemorter et al. (1979) has been used.

Electron-impact broadening widths (FWHM) and shifts for 16 Si V multiplets, have been calculated with atomic energy levels and oscillator strengths obtained using the SUPERSTRUCTURE Code. Results have also been obtained using the Bates & Damgaard method for the oscillator strengths. These data are shown in Table 1 (available only in

electronic form) for a perturber density of 10^{17} cm^{-3} and temperatures from 50 000 up to 500 000 K. Additionally, in order to provide Stark broadening data for the most important ionic perturbers in stellar atmospheres, proton-, ionized helium-, and Si II-impact broadening parameters are calculated for the same perturber densities and temperatures. Again, atomic energy levels and oscillator strengths are obtained using the SUPERSTRUCTURE code, and the results are shown in Table 2 (available only in electronic form). We found results similar to those obtained using the Bates & Damgaard approximation for the set of oscillator strengths for transitions to the perturbing levels. Such temperatures are of interest for the modelling and analysis of X-ray spectra, such as the spectra obtained by CHANDRA, modelling of some hot star atmospheres (e.g. PG 1195 type), subphotospheric layers, soft X-ray lasers and laser-produced plasmas. Higher temperatures are of interest for fusion plasmas as well as for stellar interiors. We also specify a parameter C (Dimitrijević & Sahal-Bréchot 1984), which gives an estimate for the maximum perturber density for which the line may be treated as isolated, when it is divided by the corresponding full width at half maximum. For each value given in Table 1 the collision volume (V) multiplied by the perturber density (N) is much less than one and the impact approximation is valid (Sahal-Bréchot 1969a,b). When the impact approximation is not valid, the ion broadening contribution may be estimated by using the quasistatic approach (Griem 1974; Sahal-Bréchot 1991). In the region where neither approximation is valid, a unified-type theory should be used. For example, in Barnard et al. (1974) a simple analytical formula for such a case is given. The accuracy of the results shown in Tables 1 and 2 decreases when broadening by ion interactions becomes important.

If we compare results for Stark widths obtained with oscillator strengths calculated with SUPERSTRUCTURE (W_S) and by using the Bates & Damgaard approximation (W_{BD}), the average ratio of W_{BD} and W_S is 1.09 for $T = 50\,000$ K and 1.10 for 500 000 K. Since in Stark broadening calculations we use a set of atomic data where a particular oscillator strength value is not always critical, the result obtained confirms that the Bates & Daamgard approximation may be useful for Stark broadening calculations in the case of ions such as Si V, when more reliable data are not available. For shifts the disagreements are larger, but the shifts obtained here are typically 2–3 orders of magnitude smaller than the widths. In fact, for the widths all the important contributions have a positive sign. For the present shifts important contributions have different signs, leading to mutual cancellations. Therefore, since the usual final accuracy for the shift is about 20–30 per cent of the width value, the accuracy of the shifts determined here is bad. If we compare our present results with Stark width results obtained in Dimitrijević (1993a) by using the modified semiempirical method (Dimitrijević & Konjević 1980) and with the results obtained in Dimitrijević (1993b) by using Griem's simplified semiclassical approach (Griem 1974, Eq. (526)) we can see that the average ratio of the present widths to the simplified semiclassical ones is 1.30, and to the modified semiempirical method 1.77. As to the difference between the present work and that of Dimitrijević (1993a,b), we have here a complete set of atomic energy levels needed for an adequate application of the semiclassical perturbation approach. One also has to take into account that these energy levels are calculated, while in Dimitrijević (1993a,b), experimental atomic energy levels were used.

In conclusion, we see that using the SUPERSTRUCTURE code one obtains a set of energy levels and oscillators strengths, enabling an ab initio calculation of Stark broadening parameters. This is suitable especially for multicharged ions when other theoretical and experimental atomic data are scarce. This work also suggests that the set of oscillator strength values obtained with the Bates & Damgaard approximation may be useful for Stark broadening calculations when more reliable data are not available.

Acknowledgements. This work is a part of the project "Influence of collisional processes on astrophysical plasma line shapes" (GA 1195), supported by the Ministry of Science and Environment Protection of Serbia.

References

Barnard, A. J., Cooper, J., & Smith, E. W. 1974, J. Quant. Spectrosc. Radiat. Transfer, 14, 1025
Bates, D. R., & Damgaard, A. 1949, Phil. Trans. Roy. Soc. London A, 242, 101
Bethe, H., & Salpeter, E. 1957, Quantum mechanics of one- and two-electron atoms (Berlin, Göttingen: Springer)
Blagojević, B., Popović, M. V., Konjević, N., & Dimitrijević, M. S. 1996, Phys. Rev. E, 54, 743
Blagojević, B., Popović, M. V., Konjević, N., & Dimitrijević, M. S. 1999, J. Quant. Spectrosc. Radiat. Transfer, 61, 361
Boesgaard, A. M. 1988, Vist. Astron., 31, 167
Dimitrijević, M. S. 1984, A&A, 131, 327
Dimitrijević, M. S. 1993a, A&AS, 100, 237
Dimitrijević, M. S. 1993b, Astrophys. Lett. Commun., 28, 385
Dimitrijević, M. S. 1997, Astrophys. Space Sci., 252, 415
Dimitrijević, M. S., & Konjević, N. 1980, J. Quant. Spectrosc. Radiat. Transfer, 24, 451
Dimitrijević, M. S., & Sahal-Bréchot, S. 1984, J. Quant. Spectrosc. Radiat. Transfer, 31, 301
Dimitrijević, M. S., & Sahal-Bréchot, S. 1985, Phys. Rev. A, 31, 316
Dimitrijević, M. S., & Sahal-Bréchot, S. 1992, A&AS, 95, 109
Dimitrijević, M. S., & Sahal-Bréchot, S. 1995a, Bull. Astron. Belgrade, 152, 99
Dimitrijević, M. S., & Sahal-Bréchot, S. 1995b, A&AS, 109, 551
Dimitrijević, M. S., & Sahal-Bréchot, S. 1995c, Bull. Astron. Belgrade, 150, 95
Dimitrijević, M. S., & Sahal-Bréchot, S. 1996a, A&AS, 115, 351
Dimitrijević, M. S., & Sahal-Bréchot, S. 1996b, Phys. Scr., 54, 50
Dimitrijević, M. S., & Sahal-Bréchot, S. 1997, Bull. Astron. Belgrade, 155, 131
Dimitrijević, M. S., & Sahal-Bréchot, S. 1998a, A&AS, 127, 543
Dimitrijević, M. S., & Sahal-Bréchot, S. 1998b, Atomic Data and Nuclear Data Tables, 68, 241
Dimitrijević, M. S., Sahal-Bréchot, S., & Bommier, V. 1991, A&AS, 89, 581
Eissner, W., Jones, M., & Nussbaumer, H. 1974, Computer Phys. Commun., 8, 270

Fill, E. E., & Schöning, T. 1994, J. Appl. Phys., 76, 1423
Fleurier, C., Sahal-Bréchot, S., & Chapelle, J. 1977, J. Quant. Spectrosc. Radiat. Transfer, 17, 595
Glenzer, S., Uzelac, N. I., & Kunze, H. J. 1992, Phys. Rev. A, 49, 8795
Griem, H. R. 1974, Spectral line broadening by plasmas (New York: McGraw-Hill)
Griem, H. R., & Moreno, J. C. 1980, in X-ray lasers, ed. G. Tallents (Bristol: Institute of Physics), 301
Oertel, G. K., & Shomo, L. P. 1968, ApJ, 136, 906
Sahal-Bréchot, S. 1969a, A&A, 1, 91
Sahal-Bréchot, S. 1969b, A&A, 2, 322
Sahal-Bréchot, S. 1974, A&A, 35, 321
Sahal-Bréchot, S. 1991, A&A, 245, 322
Seaton, M. J. 1988, J. Phys. B., 21, 3033
Uzelac, N. I., Glenzer, S., Konjević, N., Hey, J. D., & Kunze, H. J. 1993, Phys. Rev. E, 47, 3623
Van Regemorter, H., Hoang Binh Dy, & Prud'homme, M. 1979, J. Phys. B, 12, 1073
Werner, K., & Heber, U. 1991, A&A, 247, 476

A&A 425, 1147–1152 (2004)
DOI: 10.1051/0004-6361:20047066
© ESO 2004

Astronomy & Astrophysics

Stark broadening of Ga I spectral lines*

M. S. Dimitrijević[1,2], M. Dačić[1,2], Z. Cvetković[1,2], and Z. Simić[1,2]

[1] Astronomical Observatory, Volgina 7, 11160 Belgrade, Serbia and Montenegro
e-mail: mdimitrijevic@aob.bg.ac.yu
[2] Institute Isaac Newton of Chile, Yugoslavia Branch

Received 13 January 2004 / Accepted 10 May 2004

Abstract. Stark broadening of the 18 Ga I transitions has been analyzed within the framework of the semiclassical perturbation method. Results obtained have been compared with available experimental and theoretical data and used for the consideration of the influence of the Stark broadening effect in stellar atmospheres

Key words. line: profiles – atomic data – atomic processes – line: formation – stars: atmospheres

1. Introduction

Data on the Stark broadening of neutral gallium spectral lines are of interest not only for the laboratory but also for astrophysical plasma research as e.g. for stellar spectra analysis and synthesis, for gallium abundance determination (Smith 1996) and opacity calculations (Seaton 1988). Spectral lines of this element are present in the Solar spectrum (see e.g., Moore et al. 1966; Grevesse 1984). Moreover Jaschek & Jaschek (1987) have found gallium lines not only in the spectra of HgMn, Si-4200 and He-weak chemically peculiar stars but also in the spectra of a few stars otherwise classified as normal. Dworetsky (1993) reports on neutral gallium lines in A-type star spectra, and Ryabchikova & Smirnov (1994) in the spectrum of HgMn star Kappa Cancri. Smith (1995) investigated anomalous gallium line profiles in HgMn stars and found evidence for chemical stratification in their atmospheres. The fact that this element is often overabundant in chemically peculiar stars contributes to the astrophysical importance of gallium spectral lines. The problem of gallium in HgMn chemically peculiar stars is discussed for example in Dworetsky et al. (1998).

Zverko & Zboril (1989) tried to derive the gallium abundance of 53 Tau from Ga I 4032.98 Å and 4172.06 Å spectral lines and Smith (1996) reports on elemental abundance of gallium in normal late-B and HgMn stars. Smith (1995, 1996) concluded that HgMn stars have enhanced gallium abundances, and Zboril & Berrington (1901) have published the Non-LTE gallium equivalent widths for the most prominent gallium transitions as identified in real spectra and in (hot) mercury-manganese stars.

Data on Stark broadening parameters are also significant for the calculation of opacity coefficients (Artru 1993) in stellar interiors and envelopes. For example Rogers & Iglesias (1992, see also comment in Artru 1993) developed the OPAL code for opacity calculations, where line broadening effects (including Stark broadening) are included, as well as gallium spectral lines.

Since around T = 10 000 K (a temperature of particular interest for chemically peculiar star atmospheres) hydrogen is mainly ionized, Stark broadening is the principal pressure broadening mechanism for such plasma conditions.

With the development of space-borne telescopes and instruments like the Goddard High Resolution Spectrograph on the Hubble Space Telescope and the Keck telescopes, the quality and quantity of spectroscopic data has increased so that for their interpretation data of line profiles are of increasing interest. Additionally, Stark broadening parameters of gallium lines are of interest for the consideration of regularities and systematic trends.

The first investigations of the influence of the Stark broadening mechanism on gallium lines have been performed by Kondrat'eva & Fomichenko (1970) in a spark discharge and by Venkatesan et al. (1981). Lakićević (1983) estimated, on the basis of regularities and systematic trends, Stark width and shift of the Ga I $4p^2P^0 - 5s^2S$ transition and N'Dollo & Fabry (1987) used the semiclassical method and experimentally determined Ga I Stark widths.

Here, we will use the semiclassical perturbation approach (Sahal-Bréchot 1969a,b) to determine Stark broadening parameters of 18 Ga I transitions for conditions typical of astrophysical and laboratory plasmas. The obtained results will be compared with available experimental and theoretical values, and used for the investigation of the influence of the Stark broadening mechanism on spectral line shapes in stellar atmospheres.

* Table 1 is also available in electronic form at the CDS via anonymous ftp to cdsarc.u-strasbg.fr (130.79.128.5) or via http://cdsweb.u-strasbg.fr/cgi-bin/qcat?J/A+A/425/1147

2. Results and discussion

Stark broadening parameters (the full line width at half maximum – W and the line shift – d) of neutral gallium spectral lines were determined by using the semiclassical perturbation formalism. This formalism, as well as the corresponding computer code (Sahal-Bréchot 1969a,b), has been updated and optimized several times (Sahal-Bréchot 1974, 1991; Fleurier et al. 1977; Dimitrijević & Sahal-Bréchot 1984; Dimitrijević et al. 1991; Dimitrijević & Sahal-Bréchot 1996). The calculation procedure, with the discussion of updating and validity criteria, has been briefly reviewed e.g. in Dimitrijević (1996). Atomic energy levels needed for calculations have been taken from Moore (1971). The oscillator strengths have been calculated within the Coulomb approximation (Bates & Damgaard 1949) and the tables of Oertel & Shomo (1968). For higher levels, the method of van Regemorter et al. (1979) has been used.

In Table 1 (available also in electronic form at the CDS), electron-, and proton-impact broadening parameters for 18 Ga I transitions for a perturber density of 10^{14} cm^{-3}, typical of stellar atmosphere conditions and temperatures from 2500 up to 50 000 K, are shown. Moreover, we present in Table 1 a parameter C (Dimitrijević & Sahal-Bréchot 1984), which gives an estimate of the maximum perturber density for which the line may be treated as isolated, when it is divided by the corresponding full width at half maximum. The validity of the impact approximation has been estimated for data shown in Table 1, by checking if the collision volume (V) multiplied by the perturber density (N) is much less than one (Sahal-Bréchot 1969a,b). When the impact approximation is not valid, the ion broadening contribution may be estimated by using the quasistatic approach (Sahal-Bréchot 1991; or Griem 1974). In the region between, where neither of these two approximations is valid, a unified type theory should be used. For example in Barnard et al. (1974), a simple analytical formula for such a case is given. The accuracy of the results obtained decreases when broadening by ion interactions becomes important.

N'Dollo & Fabry (1987) calculated Stark widths for four Ga I multiplets (Ga I $4p^2P^0$–$5s^2S$, $5s^2S$–$6p^2P^0$, $5s^2S$–$7p^2P^0$ and $5p^2P^0$–$10s^2S$) using the semiclassical theory of Griem et al. (1962) for the electron contribution and the quasistatic theory (Griem 1974) for ion contribution. They also obtained experimentally, observing spectroscopically a potassium-gallium arc, Stark widths for Ga I $4p^2P^0_{1/2}$–$5s^2S_{1/2}$ 4034.1 Å and $4p^2P^0_{3/2}$–$5s^2S_{1/2}$ 4173.2 Å spectral lines. A potassium-gallium mixture was used as the cathode, while the plasma was initiated in the presence of argon. In Figs. 1–3, our results are compared with experimental and theoretical results of N'Dollo & Fabry (1987). One can see that both calculations are in agreement with experimental data within the error bars. However, the temperature trend obtained by us diverges condiderably from the N'Dollo & Fabry (1987) result. In N'Dollo & Fabry (1987), the ion broadening contribution has been estimated within Griem's quasistatic approach (Griem 1974), and comparing calculated values in N'Dollo & Fabry (1987) with electron broadening and with electron + ion broadening. Within this approach the obtained contribution of ion broadening is negligible. However, if the impact approximation is valid, the result is different.

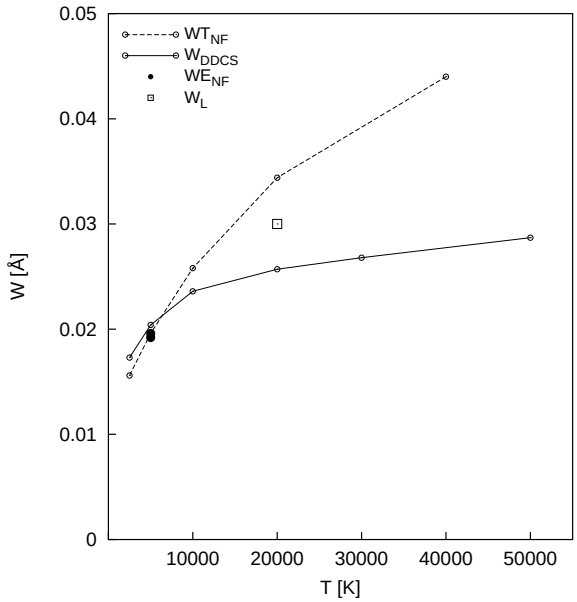

Fig. 1. Stark full widths at half maximum W[Å] for Ga I $4p^2P^0$–$5s^2S$ multiplet in function of T[K]. Theoretical calculations: W_{DDCS} – present work; WT_{NF} – N'Dollo & Fabry (1987); W_L – Lakićević (1983). Experimental data: WE_{NF} – N'Dollo & Fabry (1987).

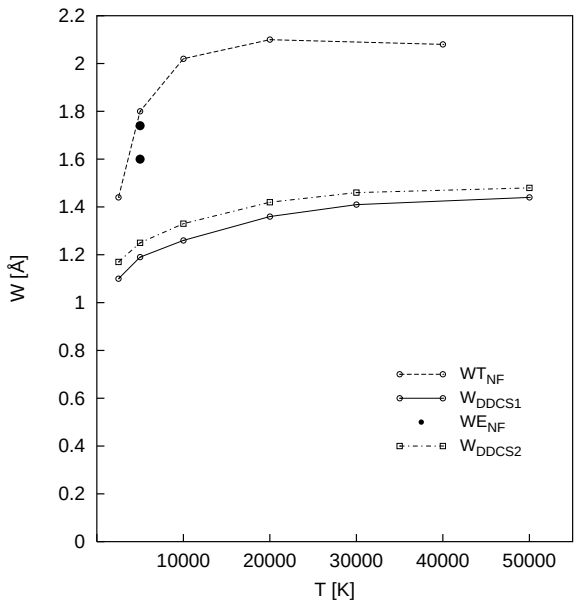

Fig. 2. Stark full widths at half maximum W[Å] for Ga I $5s^2S$–$6p^2P^0$ multiplet in function of T[K]. Theoretical calculations: W_{DDCS1} – present values for transition $S_{1/2}$–$P^0_{1/2}$; W_{DDCS2} – present values for transition $S_{1/2}$–$P^0_{3/2}$; WT_{NF} – N'Dollo & Fabry (1987). Experimental data: WE_{NF} – N'Dollo & Fabry (1987).

Since ionization potentials of Ga, K and Ar are 6.00 eV, 4.339 eV and 15.755 eV respectively, the most appropriate way to estimate the influence of ion-impact broadening for the considered experiment is to compare electron-impact widths with widths due to impacts with ions of the electron donors potassium and gallium. We obtained that the ion contribution is

Table 1. Electron-, proton- and He II-impact broadening parameters for Ga I for perturber density of 10^{14} cm^{-3} and temperatures from 2500 up to 50 000 K. Transitions and wavelengths (λ in Å) are also given in the table. By dividing C by the corresponding full width at half maximum (Dimitrijević et al. 1991), we obtain an estimate for the maximum perturber density for which the line may be treated as isolated and tabulated data may be used. The validity of the impact approximation has been estimated for data shown in this table, by checking if the collision volume (V) multiplied by the perturber density (N) is much less than one (Sahal-Bréchot 1969a,b).

Perturber density is 1.E+14 cm^{-3}					
Perturbers are:		Electrons		Protons	
Transition	T(K)	Width(Å)	Shift(Å)	Width(Å)	Shift(Å)
Ga I $4p^2P^0-5s^2S$	2500.	0.173E−03	0.142E−03	0.438E−04	0.400E−04
	5000.	0.204E−03	0.166E−03	0.488E−04	0.450E−04
4125.8 A	10 000.	0.236E−03	0.196E−03	0.546E−04	0.506E−04
C = 0.14E+18	20 000.	0.257E−03	0.223E−03	0.610E−04	0.569E−04
	30 000.	0.268E−03	0.209E−03	0.652E−04	0.608E−04
	50 000.	0.287E−03	0.204E−03	0.708E−04	0.662E−04
Ga I $4p^2P^0-4d^2D$	2500.	0.311E−03	−0.181E−03	0.757E−04	−0.452E−04
	5000.	0.311E−03	−0.176E−03	0.793E−04	−0.509E−04
2921.0 A	10 000.	0.315E−03	−0.163E−03	0.838E−04	−0.572E−04
C = 0.14E+17	20 000.	0.330E−03	−0.129E−03	0.894E−04	−0.644E−04
	30 000.	0.339E−03	−0.117E−03	0.933E−04	−0.689E−04
	50 000.	0.341E−03	−0.988E−04	0.990E−04	−0.751E−04
Ga I $4p^2P^0-5d^2D$	2500.	0.124E−02	−0.762E−03	0.297E−03	−0.221E−03
	5000.	0.128E−02	−0.678E−03	0.322E−03	−0.251E−03
2484.0 A	10 000.	0.135E−02	−0.496E−03	0.351E−03	−0.285E−03
C = 0.25E+16	20 000.	0.140E−02	−0.375E−03	0.386E−03	−0.321E−03
	30 000.	0.138E−02	−0.303E−03	0.410E−03	−0.343E−03
	50 000.	0.135E−02	−0.219E−03	0.445E−03	−0.375E−03
Ga I $5s^2S-5p^2P^0$	2500.	0.504E−02	0.368E−02	0.170E−02	0.954E−03
	5000.	0.581E−02	0.339E−02	0.177E−02	0.107E−02
12005.6 A	10 000.	0.696E−02	0.268E−02	0.186E−02	0.121E−02
C = 0.24E+18	20 000.	0.889E−02	0.155E−02	0.197E−02	0.136E−02
	30 000.	0.100E−01	0.105E−02	0.205E−02	0.146E−02
	50 000.	0.112E−01	0.508E−03	0.216E−02	0.159E−02
Ga I $5s^2S_{1/2}-6p^2P^0_{1/2}$	2500.	0.110E−01	0.808E−02	0.273E−02	0.210E−02
	5000.	0.119E−01	0.818E−02	0.297E−02	0.239E−02
6415.2 A	10 000.	0.126E−01	0.732E−02	0.326E−02	0.271E−02
C = 0.18E+17	20 000.	0.136E−01	0.555E−02	0.359E−02	0.305E−02
	30 000.	0.141E−01	0.464E−02	0.382E−02	0.327E−02
	50 000.	0.144E−01	0.363E−02	0.414E−02	0.357E−02
Ga I $5s^2S_{1/2}-6p^2P^0_{3/2}$	2500.	0.117E−01	0.855E−02	0.286E−02	0.223E−02
	5000.	0.125E−01	0.854E−02	0.313E−02	0.254E−02
6398.3 A	10 000.	0.133E−01	0.754E−02	0.344E−02	0.289E−02
C = 0.16E+17	20 000.	0.142E−01	0.573E−02	0.380E−02	0.326E−02
	30 000.	0.146E−01	0.476E−02	0.404E−02	0.349E−02
	50 000.	0.148E−01	0.369E−02	0.439E−02	0.381E−02
Ga I $5s^2S_{1/2}-7p^2P^0_{1/2}$	2500.	0.311E−01	0.216E−01	0.732E−02	0.591E−02
	5000.	0.324E−01	0.198E−01	0.811E−02	0.684E−02
5361.3 A	10 000.	0.338E−01	0.163E−01	0.903E−02	0.783E−02
C = 0.40E+16	20 000.	0.344E−01	0.124E−01	0.101E−01	0.890E−02
	30 000.	0.341E−01	0.994E−02	0.109E−01	0.957E−02
	50 000.	0.333E−01	0.694E−02	0.119E−01	0.105E−01

around 20 per cent. N'Dollo & Fabry (1987) obtained their result for electron densities between 10^{14} cm^{-3} and 2×10^{15} cm^{-3} and scaled and presented them on 10^{16} cm^{-3}, where the impact approximation is not valid. However, since for some experimental densities this approximation is valid, the ion broadening contribution is probably underestimated.

Table 1. continued.

Perturber density is 1.E+14 cm^{-3}					
Perturbers are:		Electrons		Protons	
Transition	T(K)	Width(Å)	Shift(Å)	Width(Å)	Shift(Å)
Ga I $5s^2S_{1/2}-7p^2P^0_{3/2}$	2500.	0.375E−01	0.248E−01	0.898E−02	0.735E−02
	5000.	0.390E−01	0.216E−01	0.100E−01	0.855E−02
5349.6 A	10 000.	0.399E−01	0.175E−01	0.112E−01	0.981E−02
C = 0.28E+16	20 000.	0.391E−01	0.129E−01	0.126E−01	0.112E−01
	30 000.	0.382E−01	0.102E−01	0.136E−01	0.120E−01
	50 000.	0.368E−01	0.693E−02	0.151E−01	0.132E−01
Ga I $5p^2P^0-5d^2D$	2500.	0.419E−01	−0.259E−01	0.914E−02	−0.688E−02
	5000.	0.450E−01	−0.263E−01	0.992E−02	−0.782E−02
13004.3 A	10 000.	0.479E−01	−0.241E−01	0.108E−01	−0.886E−02
C = 0.68E+17	20 000.	0.500E−01	−0.202E−01	0.119E−01	−0.999E−02
	30 000.	0.507E−01	−0.175E−01	0.127E−01	−0.107E−01
	50 000.	0.509E−01	−0.143E−01	0.138E−01	−0.117E−01
Ga I $4d^2D-5p^2P^0$	2500.	0.253	0.147	0.608E−01	0.389E−01
	5000.	0.284	0.168	0.642E−01	0.440E−01
59974.3 A	10 000.	0.308	0.175	0.685E−01	0.496E−01
C = 0.60E+19	20 000.	0.327	0.161	0.736E−01	0.558E−01
	30 000.	0.338	0.144	0.772E−01	0.597E−01
	50 000.	0.351	0.122	0.823E−01	0.651E−01
Ga I $4d^2D-6p^2P^0_{1/2}$	2500.	0.946E−01	0.649E−01	0.220E−01	0.168E−01
	5000.	0.103	0.681E−01	0.239E−01	0.192E−01
17885.8 A	10 000.	0.110	0.639E−01	0.262E−01	0.217E−01
C = 0.14E+18	20 000.	0.115	0.542E−01	0.289E−01	0.245E−01
	30 000.	0.117	0.467E−01	0.307E−01	0.263E−01
	50 000.	0.118	0.365E−01	0.333E−01	0.287E−01
Ga I $4d^2D-6p^2P^0_{3/2}$	2500.	0.990E−01	0.678E−01	0.228E−01	0.177E−01
	5000.	0.107	0.701E−01	0.249E−01	0.202E−01
17754.4 A	10 000.	0.114	0.647E−01	0.273E−01	0.229E−01
C = 0.12E+18	20 000.	0.119	0.544E−01	0.302E−01	0.258E−01
	30 000.	0.120	0.465E−01	0.321E−01	0.277E−01
	50 000.	0.121	0.360E−01	0.349E−01	0.302E−01
Ga I $4d^2D-7p^2P^0_{1/2}$	2500.	0.148	0.100	0.342E−01	0.275E−01
	5000.	0.154	0.908E−01	0.378E−01	0.319E−01
11553.5 A	10 000.	0.161	0.733E−01	0.421E−01	0.365E−01
C = 0.18E+17	20 000.	0.163	0.506E−01	0.472E−01	0.415E−01
	30 000.	0.162	0.364E−01	0.507E−01	0.446E−01
	50 000.	0.157	0.268E−01	0.557E−01	0.488E−01
Ga I $4d^2D-7p^2P^0_{3/2}$	2500.	0.177	0.114	0.416E−01	0.341E−01
	5000.	0.184	0.970E−01	0.464E−01	0.396E−01
11499.2 A	10 000.	0.188	0.766E−01	0.519E−01	0.454E−01
C = 0.13E+17	20 000.	0.184	0.511E−01	0.586E−01	0.517E−01
	30 000.	0.180	0.344E−01	0.632E−01	0.556E−01
	50 000.	0.173	0.257E−01	0.701E−01	0.610E−01
Ga I $5d^2D-6p^2P^0_{1/2}$	2500.	24.0	14.7	4.83	3.68
	5000.	26.0	14.6	5.26	4.20
231830.3 A	10 000.	27.3	13.2	5.77	4.77
C = 0.22E+20	20 000.	28.7	10.0	6.38	5.39
	30 000.	29.3	8.31	6.79	5.78
	50 000.	29.3	6.75	7.38	6.31

Table 1. continued.

Perturber density is 1.E+14 cm^{-3}					
Perturbers are:		Electrons		Protons	
Transition	T(K)	Width(Å)	Shift(Å)	Width(Å)	Shift(Å)
Ga I $5d^2D-6p^2P^0_{3/2}$	2500.	30.6	18.8	6.12	4.70
	5000.	33.0	18.5	6.68	5.37
256416.8 A	10 000.	34.6	16.5	7.33	6.10
C = 0.26E+20	20 000.	36.2	12.5	8.11	6.90
	30 000.	36.8	10.3	8.64	7.40
	50 000.	36.7	8.25	9.42	8.07
Ga I $5d^2D-7p^2P^0_{1/2}$	2500.	1.81	1.15	0.385	0.309
	5000.	1.91	1.08	0.427	0.358
37979.6 A	10 000.	1.99	0.890	0.475	0.410
C = 0.20E+18	20 000.	2.02	0.624	0.532	0.466
	30 000.	2.00	0.491	0.571	0.501
	50 000.	1.95	0.336	0.628	0.548
Ga I $5d^2D-7p^2P^0_{3/2}$	2500.	2.08	1.30	0.454	0.370
	5000.	2.18	1.14	0.506	0.430
37398.7 A	10 000.	2.23	0.917	0.566	0.494
C = 0.14E+18	20 000.	2.19	0.620	0.639	0.562
	30 000.	2.15	0.486	0.689	0.605
	50 000.	2.07	0.310	0.764	0.663

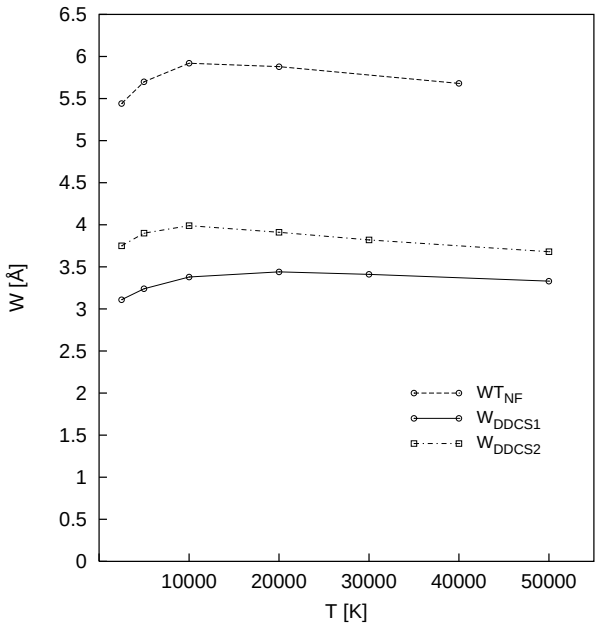

Fig. 3. Stark full widths at half maximum W[Å] for Ga I $5s^2S-7p^2P^0$ multiplet in function of T[K]. Theoretical calculations: W_{DDCS1} – present values for transition $S_{1/2}-P^0_{1/2}$; W_{DDCS2} – present values for transition $S_{1/2}-P^0_{3/2}$; WT_{NF} – N'Dollo & Fabry (1987).

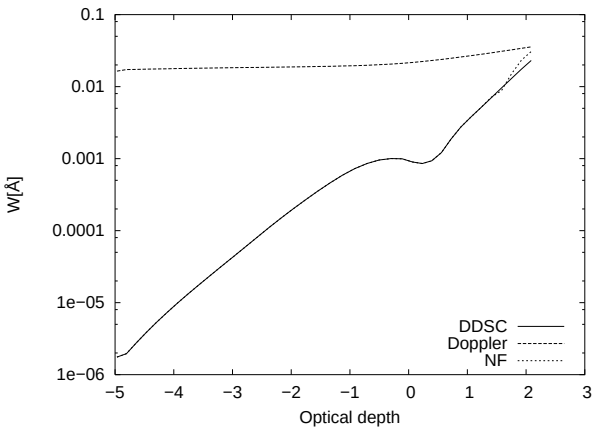

Fig. 4. Thermal Doppler and Stark widths for for Ga I $4p^2P^0-5s^2S$ multiplet as functions of optical depth for an A type star ($T_{\rm eff}$ = 10 000 K, log g = 4). Theoretical Stark line width calculations: DDCS – present work; NF – N'Dollo & Fabry (1987).

Lakićević (1983) estimated Stark broadening parameters for Ga I $4p^2P^0-5s^2S$ multiplet on the basis of regularities and systematic trends and he obtained that W is 0.30 Å and the absolute value of the shift 0.16 Å for an electron density of 10^{17} cm^{-3} and T = 20 000 K. Our width value is 0.257 Å and the shift value is 0.223 Å which is, taking into account the simplicity of the method, excellent for the width and within error bars for the shift.

To see the influence of the Stark broadening mechanism for Ga I spectral lines in stellar plasma conditions, we have calculated for our and N'Dollo & Fabry (1987) results included in Figs. 1–3 the Stark widths for a Kurucz's (1979). A type star ($T_{\rm eff}$ = 10 000 K, log g = 4) atmosphere model and compared them with Doppler ones. Results obtained as a function of the Rosseland optical depth are presented in Figs. 4–6. One can see that photospheric layers exist where Doppler and Stark widths are comparable and where the Stark width is dominant which is

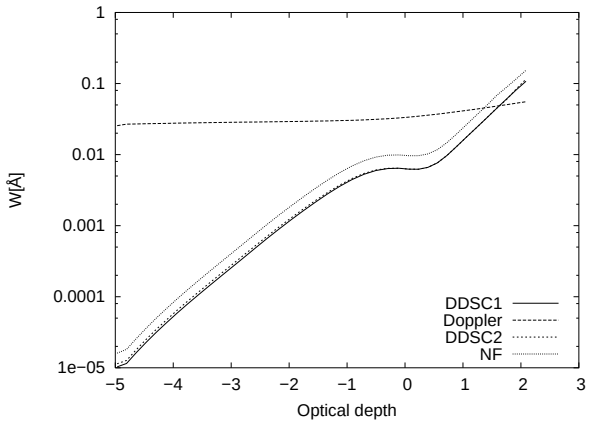

Fig. 5. Thermal Doppler and Stark widths for for Ga I $5s^2S$–$6p^2P^0$ multiplet as functions of optical depth for an A type star ($T_{\rm eff}$ = 10 000 K, log g = 4). Theoretical Stark line width calculations: DDCS1 – present values for transition $S_{1/2}$–$P^0_{1/2}$; DDCS2 – present values for transition $S_{1/2}$–$P^0_{3/2}$; NF – N'Dollo & Fabry (1987).

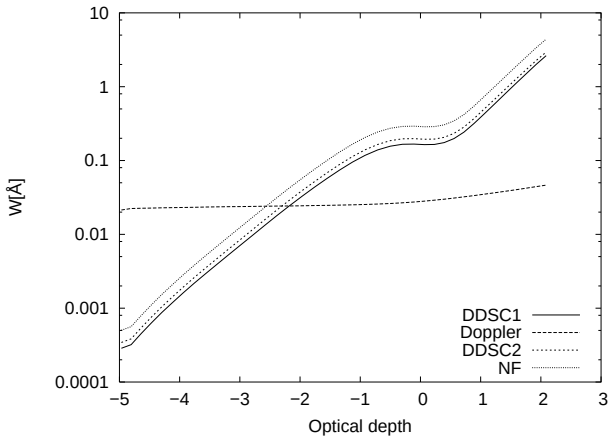

Fig. 6. Thermal Doppler and Stark widths for for Ga I $5s^2S$–$7p^2P^0$ multiplet as functions of optical depth for an A type star ($T_{\rm eff}$ = 10 000 K, log g = 4). Theoretical Stark line width calculations: DDCS1 – present values for transition $S_{1/2}$–$P^0_{1/2}$; DDCS2 – present values for transition $S_{1/2}$–$P^0_{3/2}$; NF – N'Dollo & Fabry (1987).

of interest when for example the stratification of gallium across the stellar photosphere is considered. Also, one can see that for transitions involving energy levels with higher principal quantum numbers, the importance of the Stark broadening mechanism increases. This increase is well illustrated in Figs. 5 and 6, where two members of the same spectral series, Ga I $5s^2S$–$6p^2P^0$ and $5s^2S$–$7p^2P^0$ are shown. This is due to the fact that with the increase of the principal quantum number of the upper level of the transition, the difference between this and the closest perturbing energy level decreases, resulting in the increase of the Stark broadening influence.

The new experimental evaluations of the Stark broadening parameters for Ga I spectral lines, especially at higher temperatures, will be of interest not only from the theoretical point of view but also for astrophysical and laboratory plasma diagnostics and modeling.

Acknowledgements. This work is a part of the project GA 1195 "Influence of collisional processes on astrophysical plasma lineshapes", supported by Ministry of Science and Environment Protection of Serbia. The research was supported also by the Fonds zur Förderung der wissenschaftlichen Forschung (Project S7303-AST).

References

Artru, M.-C. 1993, in Peculiar versus Normal Phenomena in A-Type and Related Stars, ed. M. M. Dworetsky, F. Castelli, R. Faraggiana, ASP Conf. Ser., 44, 113
Barnard, A. J., Cooper, J., & Smith, E. W. 1974, J. Quant. Spectrosc. Radiative Transfer, 14, 1025
Bates, D. R., & Damgaard, A. 1949, Phil. Trans. Roy. Soc. London, Ser. A, 242, 101
Dimitrijević, M. S. 1996, Zh. Prikl. Spektrosk., 63, 810
Dimitrijević, M. S., & Sahal-Bréchot, S. 1984, J. Quant. Spectrosc. Radiat. Transfer, 31, 301
Dimitrijević, M. S., & Sahal-Bréchot, S. 1996, Phys. Scr., 54, 50
Dimitrijević, M. S., Sahal-Bréchot, S., & Bommier, V. 1991, A&AS, 89, 581
Dworetsky, M. M. 1993, in Peculiar versus Normal Phenomena in A-Type and Related Stars, ed. M. M. Dworetsky, F. Castelli, & R. Faraggiana, ASP Conf. Ser., 44, 42
Dworetsky, M., Jomaron, C. M., & Smith, C. A. 1998, A&A, 333, 665
Fleurier, C., Sahal-Bréchot, S., & Chapelle, J. 1977, J. Quant. Spectrosc. Radiative Transfer, 17, 595
Grevesse, N. 1984, Phys. Scripta, T8, 49
Griem, H. R. 1974, Spectral Line Broadening by Plasmas (New York: Academic Press)
Griem, H. R., Baranger, M., Kolb, A. C., & Oertel, G. K. 1962, Phys. Rev., 125, 177
Jaschek, M., & Jaschek, C. 1987, A&A, 171, 380
Kondrat'eva, E. V., & Fomichenko, L. I. 1970, Opt. Spectrosc. (USSR), 29, 434
Kurucz, R. L. 1979, ApJS, 40, 1
Lakićević, I. S. 1983, A&A, 127, 37
Moore, C. E. 1971, Atomic Energy Levels, Circular 467, Vol. II, U. S. Department of Commerce, NBS (Washington DC: Government Printing Office)
Moore, C. E., Minnaert, M. G. J., & Houtgast, J. 1966, The Solar Spectrum 2935 Å to 8770 Å, NBS Monograph 61, U.S. Department of Commerce, NBS, Washington DC
N'Dollo, M., & Fabry, M. 1987, J. Phys. France, 48, 703
Oertel, G. K., & Shomo, L. P. 1968, ApJS, 16, 175
Rogers, F. J., & Iglesias, C. A. 1992, ApJS, 79, 507
Ryabchikova, T. A., & Smirnov, Ya. M. 1994, Astron. Zh., 71, 83
Sahal-Bréchot, S. 1969a, A&A, 1, 91
Sahal-Bréchot, S. 1969b, A&A, 2, 322
Sahal-Bréchot, S. 1974, A&A, 35, 321
Sahal-Bréchot, S. 1991, A&A, 245, 322
Seaton, M. J. 1988, J. Phys. B, 21, 3033
Smith, K. C. 1995, A&A, 297, 237
Smith, K. C. 1996, A&A, 305, 902
van Regemorter, H., Hoang Binh Dy, & Prud'homme, M. 1979, J. Phys. B, 12, 1073
Venkatesan, T., Wagner, A., Nach, D. L., Mungo, A. J., & Barr, D. 1981, Appl. Phys. Lett., 39, 9
Zboril, M., & Berrington, K. A. 2001, A&A, 373, 987
Zverko, J., & Zboril, M. 1989, Proc. 8th meeting of the subcomittee Magnetic stars, Potsdam, 176

A&A 434, 773–778 (2005)
DOI: 10.1051/0004-6361:20041574
© ESO 2005

Astronomy & Astrophysics

Modified semiempirical electron width calculations of singly-ionized oxygen spectral lines*

W. F. Mahmoudi[1], N. Ben Nessib[1], and M. S. Dimitrijević[2,3]

[1] Groupe de Recherche en Physique Atomique et Astrophysique, Faculté des Sciences de Bizerte, 7021 Zarzouna, Tunisia
[2] Astronomical Observatory, Volgina 7, 11160 Belgrade, Serbia
e-mail: mdimitrijevic@aob.bg.ac.yu
[3] Isaac Newton Institute of Chile, Yugoslavia Branch, Serbia

Received 2 July 2004 / Accepted 8 November 2004

Abstract. Using a modified semiempirical approach, we have calculated Stark broadening full widths at half maximum for 25 OII multiplets for temperatures from 5000 K up to 80 000 K using the needed oscillator strengths from the sophisticated atomic structure data base TOPbase. Then we compared our results with experimental data for 41 OII spectral lines and with the available semi-classical calculations to test the applied method and the accuracy of the results obtained.

Key words. line: profiles – atomic data

1. Introduction

Charged oxygen (OII) atoms, as emitters or absorbers, are especially important due to their presence in many kinds of cosmic sources of radiation. The abundance of oxygen and the large number of ionized oxygen spectral lines in stellar plasmas make these of great importance for diagnostic purposes. In astrophysics, Stark broadening data are required e.g. for the evaluation of the physical conditions in stellar atmospheres from the analysis of stellar spectra. Further, Stark broadening data are also required for determination of the abundances of elements and for evaluation of radiative transfer through the stellar interior.

For Stark linewidth determination, Griem (1968) suggested a simple semiempirical method based on Baranger's original formulation (Baranger 1958, see also 1962), together with the use of an effective Gaunt-factor approximation proposed by Seaton (1962) and Van Regemorter (1962). For singly ionized atoms, this semiempirical formula agrees on the average within ±50% with experiments (Griem 1974). This formula has been modified by Dimitrijević & Konjević (1980) to minimize the atomic data needed and to extend its validity to multiply charged ion lines. An effort has been made to obtain new Stark broadening data with this modified formula (see Dimitrijević & Popović 2001, and references therein), especially in the case when more sophisticated methods are not adequately applicable due to the lack of needed atomic data.

The aim of this paper is twofold: to provide new Stark broadening data for astrophysically important OII lines and to test the modified semiempirical approach (Dimitrijević & Konjević 1980). Also, we compared our results to available experimental and other theoretical results for OII.

2. Theory

Within the impact approximation, Baranger (1958) derived a quantum-mechanical expression for the width of an isolated line:

$$W = N\left(v\sum_{i'}\sigma_{i'i}(v) + \sum_{f'}\sigma_{f'f}(v)\right)_{\rm av} + W_{\rm el} \quad (1)$$

where W is $FWHM$ (Full Width at Half Maximum) in units of angular frequency and N is the electron concentration. The symbols $\sigma_{i'i}$, $\sigma_{f'f}$ represent the inelastic cross sections for collisional transitions to i', f' from the initial (i) and final (f) levels of the optical transition respectively. $W_{\rm el}$ is the line width induced by elastic collisions. The averaging in Eq. (1) has to be performed over the electron velocity v distribution.

Within the framework of the dipole approximation, one may use Bethe's relation (Bethe 1930)

$$\sigma_{j'j} = \frac{8\pi}{3}\bar{\lambda}^2\overline{R^2_{j'j}}\frac{\pi}{\sqrt{3}}g \quad (2)$$

to evaluate inelastic cross sections. In this expression $\bar{\lambda}$ is the reduced de Broglie wavelength of an electron and $\overline{R^2_{j'j}}$ (in units of the Bohr radius a_0) is the square of the coordinate operator

* Table 3 is only available in electronic form at the CDS via anonymous ftp to cdsarc.u-strasbg.fr (130.79.128.5) or via http://cdsweb.u-strasbg.fr/cgi-bin/qcat?/A+A/434/773

matrix element summed over all components of the operator, the magnetic substates of total angular momentum J', and averaged over the magnetic substates of J.

For higher electron temperatures, Griem (1968) assumed that the contribution of elastic collisions to the line width can be neglected (cf. Eq. (1)) and made an attempt to take elastic collisions into account in the low temperature limit by extrapolating the threshold value of the inelastic cross section below the threshold. The Stark line width can then be calculated from the well-know semiempirical formula (Griem 1968)

$$W = N\frac{8\pi}{3}\left(\frac{\hbar}{m}\right)^2\left(\frac{2m}{\pi kT}\right)^{\frac{1}{2}}\frac{\pi}{\sqrt{3}} \times\left[\sum_{i'} R^2_{i'i}g\left(\frac{E}{\Delta E_{ii'}}\right)+\sum_{f'} R^2_{f'f}g\left(\frac{E}{\Delta E_{ff'}}\right)\right]. \quad (3)$$

Here, $E = \frac{3kT}{2}$ is the energy of the perturbing electron and $\Delta E_{j'j} = \left[E_{j'} - E_j\right]$ is the energy difference between level j and j' (j and $j' = i, f, i', f'$ where i denotes initial and f final atomic energy level and i', f' are their corresponding perturbing levels), $g(x) = 0.20$ for $x \leq 2$ and $g(x) = 0.24$, 0.33, 0.56, 0.98, and 1.33 for $x = 3$, 5, 10, 30, and 100. Also

$$x = \frac{E}{\Delta E_{jj'}}, \quad (4)$$

$$R^2_{jj} = \sum_{j'} R^2_{j'j} \simeq \frac{1}{2}\left(\frac{n^*_j}{Z}\right)^2\left[5n^{*2}_j + 1 - 3l_j(l_j+1)\right], \quad (5)$$

n^*_j is the effective principal-, and l_j the orbital angular momentum-quantum numbers, while $(Z-1)$ is the ionic charge.

If one uses Eq. (3) to calculate Stark line widths, we need the same set of atomic data as for a more sophisticated semiclassical method, and a lack of atomic data causes the same difficulties for both methods in the evaluation of necessary matrix elements. These difficulties are especially serious for multiply-ionized atoms for which data on higher perturbing levels are sometimes completely missing in the literature. Moreover for multiply charged ions the Griem's semiempirical formula becomes inapplicable. To overcome these problems, Dimitrijević & Konjević (1980) have separated the transitions with $\Delta n = 0$ and with $\Delta n \neq 0$. In the first case, only two matrix elements are calculated for the initial state, one for the transition array $l \to l+1$ $\left(R^2_{l,l+1}\right)$ and the other for $l \to l-1$ $\left(R^2_{l,l-1}\right)$. Also, only two matrix elements are needed for the final state. The effective Gaunt factor $\widetilde{g}(x)$ for the transitions with the principal quantum number n unchanged is taken as

$$\widetilde{g}(x) = 0.7 - \frac{1.1}{Z} + g(x). \quad (6)$$

All perturbing levels with $\Delta n \neq 0$ are lumped together and the energy separation to the nearest perturbing level is estimated from

$$\Delta E_{n,n+1} = \frac{2Z^2E_H}{n^{*3}}. \quad (7)$$

At high temperatures (say $x \geq 50$), all Gaunt factors are calculated in accordance with the GBKO high temperature limit (Griem et al. 1962)

$$g_{j'j} = \frac{\sqrt{3}}{\pi}\left[\frac{1}{2} + \ln\left(\frac{2ZkT}{n^{*2}_j\Delta E_{j'j}}\right)\right]. \quad (8)$$

For $\Delta n = 0$

$$R^2_{ij} = f_{ij}\frac{\lambda_{ij}(\text{Å})}{303.7}, \quad (9)$$

where f_{ij} is the oscillator strength between levels i and j, and for $\Delta n \neq 0$

$$\sum_{i'}\left(R^2_{ii'}\right)_{\Delta n\neq 0} \simeq \left(\frac{3n^*_i}{2Z}\right)^2\frac{1}{9}\left(n^{*2}_i + 3l^2_i + 3l_i + 11\right), \quad (10)$$

where l_i is the orbital quantum number of the valence electron. In such a way Dimitrijević & Konjević (1980) extended the validity of the semiempirical method to multiply charged ions, and optimized the needed set of atomic data ensuring that the method is applicable when, due to the lack of atomic data, more sophisticated approaches are not adequately applicable.

When the wavelength of a particular line within the multiplet differs significantly from the average wavelength $\langle\lambda\rangle$ of the whole multiplet, we use the following scaling (Popović et al. 2001):

$$W_{\text{line}} = \left(\frac{\lambda}{\langle\lambda\rangle}\right)^2 W. \quad (11)$$

In the above expression, W and $\langle\lambda\rangle$ are values for the multiplet, and W_{line} and λ refer to a particular line within the multiplet.

3. Results and discussion

The atomic energy levels and oscillator strengths for OII have been taken from TOPbase (Cunto et al. 1993; Zeippen 1995). TOPbase does not provide mean square radii. Therefore we have calculated them by using the oscillator strengths (cf. Eq. (9)) and the effective quantum numbers n^*_i obtained from the TOPbase (cf. Eq. (10)). By using the modified semiempirical approach (Dimitrijević & Konjević 1980), we have calculated Stark broadening widths of forty one OII spectral lines. The obtained Stark *FWHM* values at various electron temperatures and electron densities and comparisons with other experimental and theoretical data are shown in Tables 1 and 2. With W_{m} are denoted the measured widths, W_{MBS} is the electron-impact width calculated by Mahmoudi et al. (2004) on the basis of the semi-classical approach of Sahal-Bréchot (1969a,b), W_{MSE} present calculations with the modified semiempirical approach of Dimitrijević and Konjević (1980) (corresponding to Eqs. (6)-(10)), and W_{eG} the semi-classical approach by Griem (1974).

Table 1. Experimental OII Stark widths W_m (*FWHM*), and different calculations: the semi-classical values calculated by Mahmoudi et al. (2004) W_{MBS}, our data obtained with the modified semiempirical approach (Dimitrijević & Konjević 1980) W_{MSE} and semi-classical values of Griem (1974) W_{eG}. References: a. Platiša et al. (1975); b. del Val et al. (1999); c. Djeniže et al. (1998); d. Blagojević et al. (1999); e. Djeniže et al. (1991), with e* is denoted the line where only the shift is reported by Djeniže et al. (1991) and f. Srećković et al. (2001). The data indicated by † are calculated here and not in the cited paper. The W_{eG} data for $T = 60000$ K denoted by ⊤ are extrapolated Griem (1974) values from Djeniže et al. (1991).

Multiplet	λ Å	T K	N_e 10^{17} cm^{-3}	W_m Å	W_{MBS} Å	W_{MSE} Å	W_{eG} Å	$\frac{\Delta S}{S}$	Ref.
3s ^{4}P–3p ^{4}D^0	4649.13	25 900	0.52	0.119		0.188	0.172	0.31	a
		40 000	1.0	0.209		0.290	0.314	0.31	b
	4641.81	40 000	1.0	0.223		0.289	0.313	0.31	b
		54 000	2.8	0.620		0.725		0.31	c
	4638.86	40 000	1.0	0.220		0.289	0.312	0.31	b
		54 000	2.8	0.640		0.724		0.31	c
	4650.84	25 900	0.52	0.123		0.188	0.171	0.31	a
		40 000	1.0	0.225		0.291	0.314	0.31	b
^{4}P–^{4}P^0	4349.43	40 000	1.0	0.253	0.249	0.263	0.219	0.32	b
	4336.86	40 000	1.0	0.202	0.248	0.261	0.218	0.32	b
	4366.89	25 900	0.52	0.115	0.147†	0.171	0.124	0.32	a
		40 000	1.0	0.248	0.251	0.265	0.221	0.32	b
	4345.56	40 000	1.0	0.258	0.249	0.262	0.218	0.32	b
	4319.63	40 000	1.0	0.261	0.246	0.259	0.216	0.32	b
	4317.14	25 900	0.52	0.114	0.144†	0.167	0.124	0.32	a
		40 000	1.0	0.256	0.246	0.259	0.216	0.32	b
^{4}P–^{4}S^0	3749.48	54 000	2.8	0.380	0.422	0.489		0.23	c
^{2}P–^{2}D^0	4414.90	18 800	0.31	0.087	0.106	0.128	0.094	0.26	d
		19 100	0.41	0.113	0.139	0.168	0.124	0.26	d
		19 500	0.46	0.133	0.155	0.187	0.138	0.26	d
		19 500	0.39	0.110	0.132	0.159	0.117	0.26	d
		19 800	0.44	0.125	0.147	0.178	0.132	0.26	d
		19 900	0.47	0.135	0.157	0.189	0.141	0.26	d
		25 900	0.52	0.139	0.158	0.184	0.149	0.26	a
	4416.97	18 800	0.31	0.086	0.106	0.128	0.093	0.26	d
		19 100	0.41	0.121	0.140	0.169	0.123	0.26	d
		19 500	0.46	0.130	0.155	0.187	0.138	0.26	d
		19 500	0.39	0.109	0.132	0.159	0.117	0.26	d
		19 800	0.44	0.124	0.147	0.178	0.132	0.26	d
		19 900	0.47	0.132	0.157	0.189	0.140	0.26	d
^{2}P–^{2}P^0	3954.36	25 900	0.52	0.118	0.127	0.157		0.28	a
		54 000	2.8	0.540	0.575	0.622		0.28	c
3p ^{4}D^0 – 3d ^{4}F	4075.86	25 900	0.52	0.122	0.156†	0.158	0.140	0.13	a
		40 000	1.0	0.197	0.270	0.244	0.258	0.13	b
	4072.15	25 900	0.52	0.118	0.156†	0.157	0.140	0.13	a
		40 000	1.0	0.239	0.269	0.244	0.258	0.13	b
	4092.93	25 900	0.52	0.122	0.158†	0.159	0.140	0.13	a
		40 000	1.0	0.213	0.272	0.246	0.260	0.13	b
^{2}D^0–^{4}D	4710.01	60 000	0.81	0.240		0.245		0.08	e
^{2}D^0–^{2}F	4705.35	18 800	0.31	0.115	0.145	0.165	0.126	0.10	d
		19 100	0.41	0.170	0.190	0.216	0.167	0.10	d
		19 500	0.46	0.195	0.212	0.240	0.186	0.10	d
		19 500	0.39	0.146	0.179	0.204	0.157	0.10	d
		19 800	0.44	0.174	0.202	0.228	0.178	0.10	d
		19 900	0.47	0.189	0.215	0.243	0.189	0.10	d
		60 000	0.7	0.240	0.253†	0.228	0.255	0.10	e
^{2}D^0–^{2}D	4395.93	60 000	0.81	0.254		0.238		0.07	e
^{4}S^0–^{4}P	4890.86	54 000	2.8	0.940	0.936	0.919		0.07	c
	4924.53	60 000	0.81	0.232	0.272	0.260	0.336$^\top$	0.07	e

Table 1. continued.

Multiplet	λ Å	T K	N_e 10^{17} cm^{-3}	W_m Å	W_{MBS} Å	W_{MSE} Å	W_{eG} Å	$\frac{\Delta S}{S}$	Ref.
$^2P^0-^2P$	5206.65	60 000	0.81	0.362		0.364	$0.326^{\top}$	0.10	e
$^2P^0-^2D$	4955.71	60 000	0.81	0.328	0.328	0.320	$0.331^{\top}$	0.09	e
3p′ $^2F^0$ – 3d′ ^2G	4185.46	15 700	1.45	0.448	0.595	0.633		0.11	f
		18 300	1.82	0.356	0.706	0.735		0.11	f
		20 500	0.98	0.232	0.364	0.374		0.11	f
		25 900	0.52	0.104	0.177	0.177		0.11	a
	4189.79	15 700	1.45	0.419	0.596	0.634		0.11	f
		18 300	1.82	0.358	0.707	0.737		0.11	f
		20 500	0.98	0.222	0.365	0.375		0.11	f
$^2F^0-^2F$	4448.19	40 000	1.0	0.343		0.308		0.15	b
$^2D^0-^2D$	4327.46	40 000	1.0	0.382		0.314		0.10	b
$^2P^{\circ}-^2D$	4860.97	60 000	0.81	0.284	0.285	0.336		0.13	e
	4871.52	60 000	0.81	0.284	0.287	0.338		0.13	e
$^2P^0-^2S$	4319.87	60 000	0.81	0.208		0.277		0.06	e
3s′ ^2D–3p′ $^2F^0$	4590.97	25 900	0.52	0.132	$0.186^{\dagger}$	0.196		0.30	a
		40 000	1.0	0.223	0.319	0.306		0.30	b
	4596.18	25 900	0.52	0.128	$0.187^{\dagger}$	0.196		0.30	a
		40 000	1.0	0.272	0.320	0.306		0.30	b
		54 000	2.8	0.420	0.843	0.776		0.30	c
	4595.96	54 000	2.8	0.380	0.843	0.776		0.30	c
3p $^2D^0$ – 4s ^2P	3470.67	54 000	2.8	1.00		1.481		0.10	c
$^4P^0-^4P$	3289.98	60 000	0.81	0.344		0.373	$0.355^{\top}$	0.18	e
$^4S^0-^4P$	3739.76	60 000	0.81	0.426		0.483	$0.473^{\top}$	0.14	e
$^2P^0-^2P$	3802.98	60 000	0.81	0.418		0.525	$0.492^{\top}$	0.11	e
3p′ $^2F^0$ – 4s′ ^2D	3270.86	60 000	0.81			0.348		0.09	e*
$^2P^0-^2D$	3729.22	60 000	0.81	0.132		0.499		0.11	e
3d ^4F–4p $^4D^0$	6895.10	60 000	0.81	0.976	1.480	1.777	$1.683^{\top}$	0.07	e

Table 2. Calculated OII widths for the transition array $2p^2(^3P)3s$ – $2p^2(^3P)3p$: semi-classical (Griem 1974) values W_D calculated by Dimitrijević (1982), semi-classical (Sahal-Bréchot 1969a,b) values W_{MBS} calculated by Mahmoudi, Ben Nessib and Sahal-Bréchot (2004) and our calculation with the modified semiempirical approach (Dimitrijević & Konjević 1980) W_{MSE}. λ_m is the average wavelength for the multiplet.

Multiplet	λ_m Å	T K	N_e 10^{17} cm^{-3}	W_D Å	W_{MBS} Å	W_{MSE} Å
$^4P-^4D^0$	4652	20 000	1.0	0.338		0.423
		30 000	1.0	0.314		0.345
		60 000	1.0	0.294		0.260
		80 000	1.0	0.288		0.244
$^4P-^4P^0$	4341	20 000	1.0	0.294	0.312	0.377
		30 000	1.0	0.274	0.272	0.308
		60 000	1.0	0.258	0.234	0.231
		80 000	1.0	0.254	0.225	0.217
$^4P-^4S^0$	3736	20 000	1.0	0.232	0.192	0.275
		30 000	1.0	0.218	0.169	0.224
		60 000	1.0	0.204	0.149	0.171
		80 000	1.0	0.200	0.145	0.161

Calculated $\frac{\Delta S}{S}$ ratios are also included in the Table 1. This ratio is a measure of the completeness of the set of perturbing levels with respect to the sums of dipole matrix elements and it is calculated from the following relation

$$\frac{\Delta S}{S} = \frac{\sum_{i'} R^2_{ii'} + \sum_{f'} R^2_{ff'} - R^2_{ii} - R^2_{ff}}{R^2_{ii} + R^2_{ff}}, \tag{12}$$

where in the summation enter terms for $\Delta n = 0$ defined by Eq. (9) and terms for $\Delta n \neq 0$ by Eq. (10). For a complete set of perturbing levels, $\frac{\Delta S}{S} = 0$. One can see in Table 1 that in all considered cases $\frac{\Delta S}{S}$ is greater than 0, i.e. the sum in Eq. (12) obtained with the help of Eqs. (9), (10) is larger than the sum (Eq. (5)) within the Coulomb approximation for up to 30%. This demonstrates that the introduction of a fictive common energy level for all perturbing energy levels with $\Delta n \neq 0$ (Eq. (7)) overestimates the theoretical sum rule Eq. (5) by up to 30%, but the agreement with experiments indicates that this is equilibrated by the underestimation of the contribution of elastic collisions.

Table 2 present a comparison of our calculations (W_{MSE}) with theoretical results of Dimitrijević (1982) (W_D) obtained using the semi-classical approach of Griem (1974) and theoretical data (W_{MBS}) calculated by Mahmoudi et al. (2004) using the semi-classical method of Sahal-Bréchot (1969a,b).

One can see from Tables 1 and 2 that the MSE results are in good agreement with experiments and more sophisticated

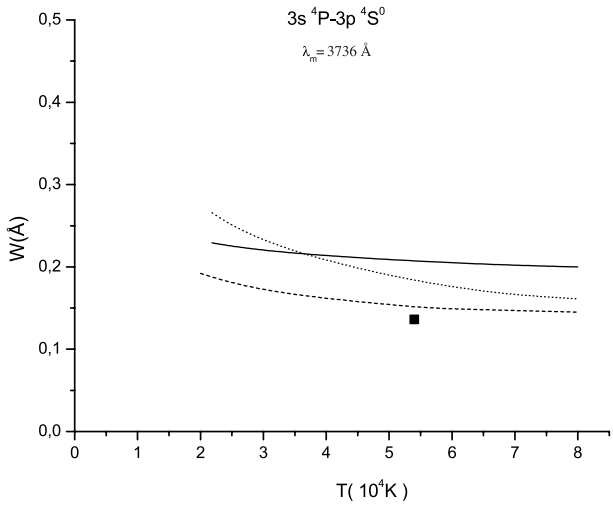

Fig. 1. Theoretical Stark width dependence on electron temperature for an electron density of 1×10^{17} cm^{-3}. ■, Djeniže et al. (1998); the solid line denotes results of Dimitrijević (1982) obtained by the semi-classical theory of Griem (1974); the dashed line denotes data calculated by Mahmoudi et al. (2004) and the doted line denotes our calculation with the modified semiempirical formalism (Dimitrijević & Konjević 1980). λ_m is the average wavelength for the multiplet.

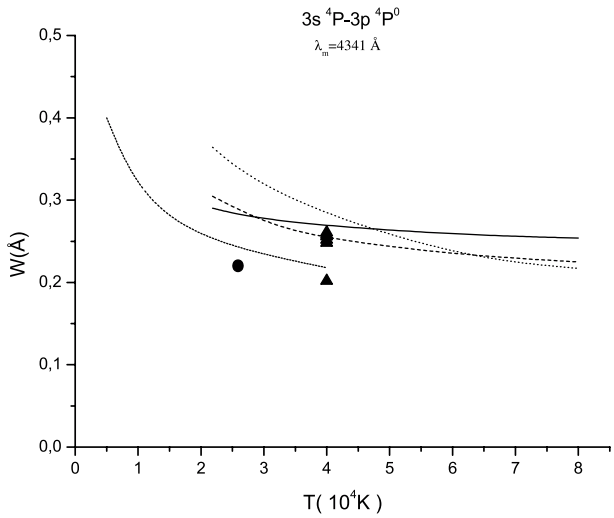

Fig. 2. Theoretical Stark width dependence on electron temperature for an electron density of 1×10^{17} cm^{-3}. •, Platiša et al. (1975); ▲, del Val et al. (1999); the solid line denotes results of Dimitrijević (1982) obtained by the semi-classical theory of Griem (1974); the dashed line denotes data calculated by Mahmoudi et al. (2004); the doted line denotes our calculation with the modified semiempirical formalism (Dimitrijević & Konjević 1980) and the short dashed one denotes the theoretical values of Griem (1974). λ_m is the average wavelength for the multiplet.

theoretical calculations (Mahmoudi et al. 2004; Griem 1974) for all considered experimental conditions (T and N_e). Indeed the ratio $\frac{W_m}{W_{MSE}}$ and $\frac{W_m}{W_{MBS}}$ shows on average an agreement within 20% and 16% respectively. This is well within the error bars of the semiempirical and the modified semiempirical methods estimated to be ±50% (Griem 1974; Dimitrijević & Konjević 1980) which is a very good agreement especially taking into account that the needed atomic data set is much smaller than for more sophisticated semi-classical calculations (Sahal-Bréchot 1969a,b; Griem 1974; Mahmoudi et al. 2004). The exceptions are in the multiplets $2p^2(^1D)3p\ ^2F^0 - 2p^2(^1D)3d\ ^2G$ at 18 300 K, $2p^2(^1D)3s\ ^2D - 2p^2(^1D)3p\ ^2F^0$ at 54 000 K, $2p^2(^3P)3d\ ^4F - 2p^2(^3P)4p\ ^4D^0$ and $2p^2(^1D)3p\ ^2P^0 - 2p^2(^1D)4s\ ^2D$ where the discrepancy between experiment and theoretical calculations is of the order of 50% which is also within the error bars of the semi-classical and the modified semiempirical method.

The results of Table 2 are compared in Figs. 1–3 with available experimental data but we note that the experimental results are for particular spectral lines within a multiplet while the theoretical data are calculated for the multiplet as a whole. One can see that our results obtained with the modified semiempirical method (Dimitrijević & Konjević 1980) are in agreement within the error bars with the experimental data and with more sophisticated semi-classical calculations of Dimitrijević (1982) and Mahmoudi et al. (2004) which demonstrates that this method can be used especially for large scale calculations and when due to lack of the needed atomic data more sophisticated methods are not adequately applicable.

In Table 3 (available only in electronic form at the CDS) our Stark width (*FWHM*) results for 25 OII multiplets calculated for an electron density of 10^{17} cm^{-3} and temperatures of 5000, 10 000, 20 000, 30 000, 60 000 and 80 000 K are given for the modelling, analysis and diagnostics of astrophysical

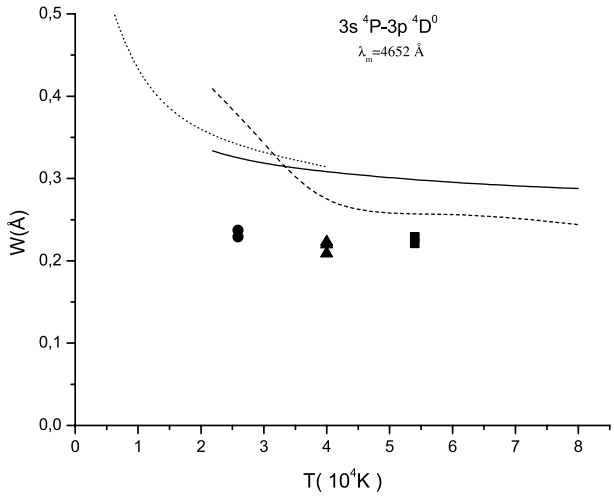

Fig. 3. Theoretical Stark width dependence on electron temperature for an electron density of 1×10^{17} cm^{-3}. •, Platiša et al. (1975); ▲, del Val et al. (1999); ■, Djeniže et al. (1998); the solid line denotes results of Dimitrijević (1982) calculated with the semi-classical theory of Griem (1974); the dashed line denotes our calculation with the modified semiempirical formalism (Dimitrijević & Konjević 1980) and the doted line denotes the theoretical value of Griem (1974). λ_m is the average wavelength for the multiplet.

plasmas. We note also that for lower densities a linear scaling is sufficient. For higher densities, linearity with the electron density may be assumed if the plasma is ideal. The idealness of the plasma can be checked by calculating the number of perturbers in the Debye sphere, i.e. $(4\pi/3)R_D^3 N > 1$ or $N < 1.9 \times 10^6 T^3$ cm^{-3} (Dimitrijević et al. 1991), where R_D is

the Debye radius. For non-ideal plasmas, the method used here is not suitable. Stark broadening in a strongly correlated plasma has been considered recently by Ben Chaouacha et al. (2004). The other criteria for the applicability of the modified semiempirical approach have been dicussed in detail in Milovanović et al. (2004).

4. Conclusion

We have calculated by using the modified semiemirical method (Dimitrijević & Konjević 1980) Stark widths (*FWHM*) for 25 OII multiplets for an electron density of 10^{17} cm^{-3} and temperatures from 5000 to 80 000 K. In order to test the applicability of the used method, we have compared the results obtained with experimental results for 41 OII spectral lines and with more sophisticated semi-classical calculations of Griem (1974), Dimitrijević (1982) and Mahmoudi et al. (2004). We found that the ratio of experimental and our theoretical values is on average in agreement within 20%, which is well within the estimated error bars of this method (±50%), with several exceptions of the order of 50%. The agreement found between experimental and semi-classical values demonstrates that the method can be used for OII Stark width calculations, especially when more sophisticated methods are not applicable in an adequate way. Consequently, one can expect that the accuracy of the obtained OII Stark width data presented in Table 3 is better on average than that estimated for this method of (±50%).

Acknowledgements. This work is a part of the project "Influence of collisional processes on astrophysical plasma line shapes" (GA 1195), supported by the Ministry of Science and Environment protection of Serbia. Part of this work has been supported by the Ministry of Higher Education, Scientific Research and Technology in Tunisia under the project LMA, FSB, 2001–2004.

References

Baranger, M. 1958, Phys. Rev. A, 112, 855
Baranger, M. 1962, in Atomic and Molecular Processes, ed. D. R., Bates (New York: Academic Press), Chap. 13
Ben Chaouacha, H., Ben Nessib, N., & Sahal-Bréchot, S. 2004, A&A, 419, 771
Bethe, H. A. 1930, Ann. Phys. (Leipzig), 5, 3251
Blagojević, B., Popović, M. V., & Konjević, N. 1999, Phys. Scr., 59, 374
Cunto, W., Mendoza, C., Ochsenbein, F., & Zeippen, C. J. 1993, A&A, 275, L5
del Val, J. A., Aparicio, J. A., Gonzales, V., & Mar, S. 1999, A&AS, 140, 171
Dimitrijević, M. S. 1982, A&A, 112, 251
Dimitrijević, M. S., & Konjević, N. 1980, JQSRT, 24, 451
Dimitrijević, M. S., & Popović, L. Č. 2001, J. Appl. Spectrosc., 68, 893
Dimitrijević, M. S., Sahal-Bréchot, S., & Bommier, V., 1991, A&AS, 89, 581
Djeniže, S., Milosavljević, V., & Srećković, A. 1998, JQSRT, 59, 71
Djeniže, S., Srećković, A., Labat, J., & Platiša, M. 1991, Z. Phys., D 21, 295
Griem, H. R. 1968, Phys. Rev., 165, 258
Griem, H. R. 1974, Spectral Line Broadening by Plasmas (New York (USA) and London (UK): Academic Press Inc.)
Griem, H. R., Baranger, M., Kolb, A. C., & Oertel, G. 1962, Phys. Rev., 125, 177
Mahmoudi, W. F., Ben Nessib, N., & Sahal-Bréchot, S. 2004, Phys. Scr., 70, 142
Milovanović, N., Dimitrijević, M. S., Popović, L. Č., & Simić, Z., 2004, A&A, 417, 365
Platiša, M., Popović, M., & Konjević, N. 1975, A&A, 45, 325
Popović, L. Č., Milovanović, N., & Dimitrijević, M. S. 2001, A&A, 365, 656
Sahal-Bréchot, S. 1969a, A&A, 1, 91
Sahal-Bréchot, S. 1969b, A&A, 2, 322
Seaton, M. J. 1962, in Atomic and Molecular Processes, ed. D. R. Bates (New York: Academic Press), Chap. 11
Srećković, A., Drinčić, V., Bukvić, S., & Djeniže, S. 2001, Phys. Scr., 36, 306
van Regemorter, H. 1962, ApJ, 136, 906
Zeippen, C. J. 1995, Phys. Scr., T58, 43

A&A 435, 1191–1198 (2005)
DOI: 10.1051/0004-6361:20042318
© ESO 2005

Astronomy & Astrophysics

On the influence of Stark broadening on Cr I lines in stellar atmospheres

M. S. Dimitrijević[1,2], T. Ryabchikova[3,4], L. Č. Popović[1,2,5], D. Shulyak[6], and S. Khan[6]

[1] Astronomical Observatory, Volgina 7, 11160 Belgrade 74, Serbia
[2] Isaac Newton Institute of Chile, Yugoslavia Branch, Yugoslavia
e-mail: mdimitrijevic@aob.bg.ac.yu
[3] Institute of Astronomy, Russian Academy of Science, Pyatnitskaya 48, 119017 Moscow, Russia
[4] Institute for Astronomy, University of Vienna, Türkenschanzstrasse 17, 1180 Vienna, Austria
[5] Astrophysikalisches Institut Potsdam, An der Sternwarte 16, 14482 Potsdam, Germany
[6] Tavrian National University, Yaltinskaya 4, 330000 Simferopol, Crimea, Ukraine

Received 5 November 2004 / Accepted 17 January 2005

Abstract. Using the semiclassical perturbation method, electron-, proton-, and ionized helium-impact line widths and shifts for the nine Cr I spectral lines from the $4p^7P^0-4d^7D$ multiplet were calculated for a perturber density of 10^{14} cm^{-3} and for temperatures $T = 2500-50\,000$ K. The results were used to investigate the influence of Stark broadening effect in the Cr-rich Ap star β CrB atmosphere on line shapes of these lines. It was found that the contribution of proton and He II collisions to the line width and shift is significant and comparable, and is sometimes even larger than electron-impact contribution depending of the electron temperature. Moreover, not only the Stark line width, but also the Stark shift may contribute to the blue as well as to the red asymmetry of the same line depending on the electron-, proton-, and He II density in stellar atmosphere. The results were used to investigate the influence of Stark broadening effect on Cr I line shapes in the atmosphere of the Cr-rich Ap star β CrB.

Key words. atomic processes – line: profiles – stars: chemically peculiar – stars: individual: β CrB

1. Introduction

Stark broadening is the most significant pressure broadening mechanism for A and B stars, such that this effect should be taken into account in investigation, analysis, and modelling of their atmospheres. In our previous works (Popović et al. 1999, 2001; Dimitrijević et al. 2003) we have shown that Stark broadening may change spectral line equivalent widths by 10–45%; hence neglecting this mechanism may introduce significant errors in abundance determinations. Stark data become extremely important after discovering abundance gradients in the atmospheres of magnetic, chemically peculiar (Ap) stars (Babel 1992; Ryabchikova et al. 2002; Wade et al. 2003). High resolution spectra allow us to perform stratification analysis using line profiles, and strong lines with developed wings provide us with the most accurate information about distribution of the element through the stellar atmosphere (see Dimitrijević et al. 2003 for Si).

Chromium is one of the most anomalous elements in Ap stars. It was shown to be concentrated in the deeper atmospheric layers in Ap stars β CrB (Wade et al. 2003) and in γ Equ (Ryabchikova et al. 2002), where electron density is high enough to favor the Stark effect. Most Cr I and Cr II lines in the optical spectral region have rather small Stark damping constants so no measurable Stark wings appeared. However, Cr I lines from 4p–4d transitions are known to have fairly large Stark damping constants according to calculations made by Kurucz (1993).

We present new calculations of Cr I line Stark widths and shifts based on the semiclassical perturbation approach (Sahal-Bréchot 1969a,b, 1974; Dimitrijević & Sahal-Bréchot 1984a). Calculation method is described in Sect. 2 and magnetic synthetic spectrum calculations are described in Sect. 3. Results of Stark broadening calculations are given in Sect. 4.1, while an application of new data to spectrum synthesis in magnetic Ap star β CrB is considered in Sect. 4.2.

2. The Stark broadening parameter calculation

Calculations have been performed within the semiclassical perturbation formalism, as developed and discussed in detail in Sahal-Bréchot (1969a,b). This formalism, as well as the corresponding computer code, have been optimized and updated several times (see e.g. Sahal-Bréchot 1974; Dimitrijević & Sahal-Bréchot 1984a; Dimitrijević 1996).

Within this formalism, the full width of a neutral emitter isolated spectral line broadened by electron impacts can be

Article published by EDP Sciences and available at http://www.edpsciences.org/aa or http://dx.doi.org/10.1051/0004-6361:20042318

expressed in terms of cross sections for elastic and inelastic processes as

$$W_{if} = \frac{2\lambda_{if}^2}{2\pi c} n_{\rm e} \int v f(v) {\rm d}v \left(\sum_{i' \neq i} \sigma_{ii'}(v) + \sum_{f' \neq f} \sigma_{ff'}(v) + \sigma_{\rm el} \right) \quad (1)$$

and the corresponding line shift as

$$d_{if} = \frac{\lambda_{if}^2}{2\pi c} n_{\rm e} \int v f(v) {\rm d}v \int_{R_3}^{R_D} 2\pi\rho {\rm d}\rho \sin 2\phi_{\rm p}. \quad (2)$$

Here, λ_{if} is the wavelength of the line originating from the transition with the initial atomic energy level i and the final level f; c is the velocity of light; $n_{\rm e}$ the electron density; $f(v)$ the Maxwellian velocity distribution function for electrons; m the electron mass; k the Boltzmann constant; T the temperature, and ρ denotes the impact parameter of the incoming electron. The inelastic cross section $\sigma_{jj'}(v)$ is determined according to Chap. 3 in Sahal-Bréchot (1969b) and elastic cross section $\sigma_{\rm el}$ according to Sahal-Bréchot (1969a). The cut-offs, included in order to maintain unitarity of the S-matrix, are described in Sect. 1 of Chap. 3 in Sahal-Bréchot (1969a).

The formulae for the ion-impact broadening parameters are analogous to the formulae for electron-impact broadening. For the colliding ions, the validity of the impact approximation has to be checked in the far wings.

3. Line profile calculations

Model atmosphere calculations, as well as calculations of the absorption coefficients, were made with the local thermodynamical equilibrium (LTE) approximation. Model calculations were performed with the ATLAS9 code (Kurucz 1993), modified by Piskunov & Kupka (2001) to include individual chemical composition of the star in line opacity calculations (see Kupka et al. 2004).

The next step is to calculate the outward flux at corresponding wavelength points using the given model. For this purpose we used SYNTHM code written by Khan (2004). This code allows synthetic spectra of early and intermediate type of stars to be calculated taking magnetic field effects into account along with stratification of chemical elements.

The computational scheme is as follows. For each line we find the central opacity as

$$\alpha_{\rm line} = \frac{\pi e^2}{mc} g f_{if} {\rm e}^{-\frac{\chi}{kT}} \frac{n}{\rho} \left(1 - {\rm e}^{-\frac{h\nu}{kT}}\right), \quad (3)$$

where α_ν is the mass absorption coefficient at frequency ν; e the electron charge; g the statistical weight; f_{if} the oscillator strength for a given transition; χ the excitation energy; n the number density of a corresponding element in a given ionization stage multiplied by partition function; ρ the density and h the Planck constant. The last factor describes stimulated emission.

Next, we compute the total damping parameter

$$\gamma = \gamma_{\rm rad} + \gamma_{\rm Stark} + \gamma_{\rm neutral}. \quad (4)$$

Here $\gamma_{\rm rad}$, $\gamma_{\rm Stark}$, and $\gamma_{\rm neutral}$ are the radiative broadening, Stark broadening, and damping parameters due to neutral atom collisions, respectively. The values of $\gamma_{\rm rad}$, $\gamma_{\rm neutral}$, excitation energy χ and oscillator strength gf were taken from the Vienna Atomic Line Database (VALD) (Kupka et al. 1999). In the case of neutral atom broadening we assumed that perturbing particles are only neutral hydrogen and helium atoms (Van der Waals broadening). This assumption is applicable to almost all types of stars due to high hydrogen and helium cosmic abundances. We shall discuss competition between the broadenings caused by the Stark effect and by neutral hydrogen collisions in the atmospheres of our template star β CrB in Sect. 4.2.

In order to take into account Stark broadening effects we added the approximate formulas Eqs. (20) and (21) (Sect. 4.1) to the code. The Stark width and shift are

$$\gamma_{\rm Stark} = \gamma_{\rm Stark}^{\rm (e)} n_{\rm e} + \gamma_{\rm Stark}^{\rm (p)} n_{\rm p} + \gamma_{\rm Stark}^{\rm (HeII)} n_{\rm HeII}, \quad (5)$$

$$d_{\rm Stark} = d_{\rm Stark}^{\rm (e)} n_{\rm e} + d_{\rm Stark}^{\rm (p)} n_{\rm p} + d_{\rm Stark}^{\rm (HeII)} n_{\rm HeII}, \quad (6)$$

where $n_{\rm e}$, $n_{\rm p}$ and $n_{\rm HeII}$ are the corresponding densities of electrons, protons, and He II ions respectively. The resulting opacity profile is given by the Voigt function (Doppler + pressure broadening).

The next step is to solve the transfer equation with new Stark damping parameters. In the presence of magnetic field, atomic level k determined by quantum numbers J_k, L_k, S_k splits into $2J_k + 1$ states with $M_k = -J_k, \ldots, +J_k$. The absolute value of splitting is defined by field modulus $|\boldsymbol{B}|$ and Landé factor g_k, which in the case of LS coupling is calculated as

$$g_k = \frac{3}{2} + \frac{S_k(S_k+1) - L_k(L_k+1)}{2J_k(J_k+1)}. \quad (7)$$

The possible transitions between split levels (u – upper and l – lower level) are allowed by selection rules

$$\Delta M = M_u - M_l = \begin{cases} +1 \equiv b, \\ 0 \equiv p, \\ -1 \equiv r. \end{cases} \quad (8)$$

For a normal Zeeman triplet the subscript p corresponds to the unshifted π component, whereas b and r correspond to the blue- and red-shifted σ components, respectively. In the general case of an anomalous splitting, indices p, b, r refer to the series of the π and σ components.

The wavelength shift of the component relative to the laboratory line centre λ_0 is defined by

$$\Delta\lambda = \frac{e\lambda_0^2 |\boldsymbol{B}|}{4\pi mc^2} \left(g_l M_l - g_u M_u\right). \quad (9)$$

The relative strengths of components $S_{p,r,b}$ in accordance with Sobelman (1977) are proportional to

$$\begin{pmatrix} J_u & 1 & J_l \\ -M_u & (M_u - M_l) & M_l \end{pmatrix}^2, \quad (10)$$

where the last structure is a $3j$-symbol. The normalization of components is done so that

$$\sum S_p = \sum S_b = \sum S_r = 1. \quad (11)$$

Article published by EDP Sciences and available at http://www.edpsciences.org/aa or http://dx.doi.org/10.1051/0004-6361:20042318

In a general case the polarized radiation can be described by means of Stokes $IQUV$ parameters. The transfer equation is

$$\frac{\mathrm{d}\boldsymbol{I}}{\mathrm{d}z} = -\boldsymbol{K}\boldsymbol{I} + \boldsymbol{J}. \tag{12}$$

Here $\boldsymbol{I} = (I, Q, U, V)^T$ is the Stokes vector, $\boldsymbol{K}$ the absorption matrix and $\boldsymbol{J}$ the emission vector,

$$\boldsymbol{K} = \alpha_{\mathrm{c}}\mathbf{1} + \sum_{\mathrm{lines}} \alpha_{\mathrm{line}}\boldsymbol{\Phi}_{\mathrm{line}}, \tag{13}$$

$$\boldsymbol{J}_\nu = \alpha_{\mathrm{c}} B_\nu(T)\boldsymbol{e_0} + B_\nu(T)\sum_{\mathrm{lines}} \alpha_{\mathrm{line}}\boldsymbol{\Phi}_{\mathrm{line}}\boldsymbol{e_0}, \tag{14}$$

where $\mathbf{1}$ is the 4×4 unit matrix, $\boldsymbol{e_0} = (1, 0, 0, 0)^T$, α_{c} the continuum absorption coefficient, α_{line} the line central opacity for zero damping and the zero magnetic field given by Eq. (3). Here we also assume LTE, so that the source function is equal to Planck function $B_\nu(T)$.

The line absorption matrix $\boldsymbol{\Phi}_{\mathrm{line}}$ is created with absorption profiles ϕ_j and anomalous dispersion profiles ψ_j of π and of $\sigma_\pm$ components in accordance with Rees et al. (1989). These profiles are calculated as (for $j = p, b, r$)

$$\phi_j = \sum_{i_j=1}^{N_j} S_{i_j} H\left(a, \upsilon - \frac{\Delta\lambda_{i_j}}{\Delta\lambda_{\mathrm{D}}}\right), \tag{15}$$

$$\psi_j = 2\sum_{i_j=1}^{N_j} S_{i_j} F\left(a, \upsilon - \frac{\Delta\lambda_{i_j}}{\Delta\lambda_{\mathrm{D}}}\right), \tag{16}$$

where $H(a, u)$ and $F(a, u)$ are the Voigt and Faraday-Voigt functions,

$$a = \frac{\gamma\,\lambda_0^2}{4\pi c\,\Delta\lambda_{\mathrm{D}}}, \tag{17}$$

$$\upsilon = \frac{\lambda - \lambda_0 + d_{\mathrm{Stark}}}{\Delta\lambda_{\mathrm{D}}}. \tag{18}$$

The Stark shift d_{Stark} and the damping parameter γ have been calculated from Eqs. (6) and (4), respectively. The Doppler width $\Delta\lambda_{\mathrm{D}}$ is

$$\Delta\lambda_{\mathrm{D}} = \frac{\lambda}{c}\sqrt{\frac{2kT}{m_{\mathrm{A}}} + \xi_{\mathrm{t}}^2}, \tag{19}$$

where m_{A} is the mass of the absorber atom and ξ_{t} the microturbulent velocity.

The transfer equation Eq. (12) is solved by the DELO method (Rees et al. 1989) with quadratic approximation for the source function, suggested by Socas-Navarro et al. (2000) and written in Fortran by Piskunov & Kochukhov (2000). Also, we used the fast Humlicek (1982) algorithm for approximations of the Voigt and Faraday-Voigt functions.

Convolution of the synthetic spectra due to stellar rotation was produced by IDL procedure of Valenti & Anderson implemented in the ROTATE IDL code by N. Piskunov.

4. Results

4.1. Stark broadening data

The atomic energy levels needed for Stark broadening calculations were taken from Wiese & Musgrove (1989). Oscillator strengths were calculated using the method of Bates & Damgaard (1949) and tables in Oertel & Shomo (1968). For higher levels, the method described in van Regemorter et al. (1979) was applied.

The neutral chromium spectrum is complex and not known well enough for a good calculation of the line being considered. The principal problem is the absence of reliable experimental data for f levels. However, by inspecting theoretically predicted Cr I levels in Moore (1971), one can see that the 4f level is missing. In accordance with the decrease in distance between existing s, p, and d levels, we estimated that the eventual 5f level should be around 52 000 cm^{-1} and not closer than 50 000 cm^{-1}. We checked results without 5f level and with a fictive 5f level at 52 000 and 50 000 cm^{-1}. In all cases, line widths differed by less than 1%, while the shift varies by several percents, so we performed calculations without the contribution of f energy levels. Since the average estimated error of the semiclassical method is ±30%, due to additional approximations and uncertainties, we estimate the error bars of our results to be ±50%.

Our results for electron-, proton-, and ionized helium-impact line widths and shifts for the nine Cr I spectral lines for a perturbed density of 10^{14} cm^{-3} and temperatures T = 2500–50 000 K are all shown in Table 1. For perturber densities lower than those tabulated here, Stark broadening parameters vary linearly with perturber density. The nonlinear behavior of Stark broadening parameters at higher densities is the consequence of the influence of Debye shielding, which has been analyzed in detail in Dimitrijević & Sahal-Bréchot (1984b).

After testing the density dependence of Stark parameters, we found that the width and shift are linear functions of density for perturber densities smaller than 10^{16} cm^{-3}. They can be scaled by the simple formula

$$(W, d)_N = (W, d)_0\left(\frac{N}{10^{14}}\right), \tag{20}$$

where $(W, d)_N$ are the width and shift at a perturber density N (cm^{-3}) and $(W, d)_0$ are width and shift given in Table 1, respectively.

In order to simplify the input of Stark broadening data in the codes for stellar spectral synthesis, we developed an analytical expression for Stark widths and shifts

$$\frac{W}{n_{\mathrm{e}}}\left[\text{Å}\right] = c_1 \cdot \left(A + T^B\right), \tag{21}$$

$$\frac{d}{n_{\mathrm{e}}}\left[\text{Å}\right] = c_2 \cdot \left(A + C \cdot T^B\right). \tag{22}$$

The constants c_1, c_2, A, B, and C are given in Table 2. We take T as $T/(10\,000\ \mathrm{K})$. As one can see from the analytical fit in Figs. 1 and 2, Eqs. (21) and (22) fit the calculated values in both Stark widths and shifts. In some lines here (as e.g. in Cr I λ = 5329.14 Å), the analytical fit in the case of proton

Article published by EDP Sciences and available at http://www.edpsciences.org/aa or http://dx.doi.org/10.1051/0004-6361:20042318

Table 1. Stark broadening parameters for Cr I 4p–4d spectral lines. This table shows electron-, proton-, and ionized helium-impact broadening parameters for Cr I for a perturber density of 10^{14} cm^{-3} and temperatures from 2500 up to 50 000 K. Quantity C is given in Å cm^{-3} and divided by the corresponding full width at half maximum (*FWHM*), gives an estimate for the maximum perturber density for which tabulated data may be used. The asterisk identifies cases for which the collision volume multiplied by the perturber density lies between 0.1 and 0.5. When it is larger than 0.5 results are omitted.

PERTURBERS ARE:		ELECTRONS		PROTONS		HELIUM IONS	
TRANSITION	T(K)	*FWHM*(A)	SHIFT(A)	*FWHM*(A)	SHIFT(A)	*FWHM*(A)	SHIFT(A)
Cr I $^7P^0_2$–$^7D_1$	2500.	0.890E–02	–0.205E–02	0.461E–02	–0.379E–02	0.344E–02	–0.299E–02
	5000.	0.772E–02	–0.146E–02	0.551E–02	–0.437E–02	0.388E–02	–0.346E–02
5276.07 A	10 000.	0.655E–02	–0.104E–02	0.678E–02	–0.505E–02	0.439E–02	–0.396E–02
C = 0.43E+15	20 000.	0.548E–02	–0.767E–03	0.832E–02	–0.592E–02	0.503E–02	–0.451E–02
	30 000.	0.493E–02	–0.660E–03	0.915E–02	–0.651E–02	0.547E–02	–0.488E–02
	50 000.	0.431E–02	–0.559E–03	0.993E–02	–0.719E–02	0.602E–02	–0.544E–02
Cr I $^7P^0_2$–$^7D_2$	2500.	0.193E–01	–0.216E–02				
	5000.	0.164E–01	–0.155E–02				
5275.75 A	10 000.	0.136E–01	–0.108E–02				
C = 0.11E+14	20 000.	0.111E–01	–0.790E–03	*0.717E–01	–0.298E–01		
	30 000.	0.983E–02	–0.675E–03	*0.702E–01	–0.273E–01		
	50 000.	0.841E–02	–0.569E–03	*0.664E–01	–0.239E–01	*0.135E–01	–0.346E–01
Cr I $^7P^0_2$–$^7D_3$	2500.	0.240E–01	–0.939E–03	*0.216E–01	–0.138E–01	*0.131E–01	–0.102E–01
	5000.	0.210E–01	–0.677E–03	*0.253E–01	–0.170E–01	*0.151E–01	–0.124E–01
5275.28 A	10 000.	0.178E–01	–0.473E–03	*0.274E–01	–0.193E–01	*0.169E–01	–0.150E–01
C = 0.60E+14	20 000.	0.147E–01	–0.401E–03	0.280E–01	–0.193E–01	*0.170E–01	–0.179E–01
	30 000.	0.131E–01	–0.393E–03	0.283E–01	–0.180E–01	*0.157E–01	–0.193E–01
	50 000.	0.112E–01	–0.393E–03	0.289E–01	–0.155E–01	*0.127E–01	–0.200E–01
Cr I $^7P^0_3$–$^7D_2$	2500.	0.195E–01	–0.219E–02				
	5000.	0.165E–01	–0.156E–02				
5298.49 A	10 000.	0.137E–01	–0.109E–02				
C = 0.12E+14	20 000.	0.112E–01	–0.801E–03	*0.723E–01	–0.301E–01		
	30 000.	0.992E–02	–0.685E–03	*0.708E–01	–0.276E–01		
	50 000.	0.849E–02	–0.578E–03	*0.670E–01	–0.242E–01	*0.136E–01	–0.349E–01
Cr I $^7P^0_3$–$^7D_3$	2500.	0.243E–01	–0.950E–03	*0.218E–01	–0.140E–01	*0.133E–01	–0.103E–01
	5000.	0.212E–01	–0.687E–03	*0.256E–01	–0.171E–01	*0.153E–01	–0.125E–01
5298.02 A	10 000.	0.179E–01	–0.481E–03	*0.276E–01	–0.195E–01	*0.171E–01	–0.151E–01
C = 0.60E+14	20 000.	0.148E–01	–0.408E–03	0.283E–01	–0.195E–01	*0.171E–01	–0.180E–01
	30 000.	0.132E–01	–0.400E–03	0.286E–01	–0.182E–01	*0.158E–01	–0.195E–01
	50 000.	0.113E–01	–0.400E–03	0.291E–01	–0.157E–01	*0.128E–01	–0.201E–01

and He II impact broadening parameters does not exactly fit the calculated values (see e.g. Fig. 2, with a fit for proton-impact shift), but the differences are smaller than the expected error of our calculations (≈±50%).

4.2. The Stark broadening effect on the shape of Cr I lines

In spite of the rather large Stark damping constants, the effect is not observable in stars with solar Cr abundance. In hot stars where electron and proton densities are high, the Cr I lines considered here are generally very weak, while in cooler stars (solar type) other broadening effects are more significant where these lines are strong enough. The only chance to look at Stark effect is in stratified atmosphere of a Cr-rich Ap star, such as the well known magnetic star β CrB.

Our spectral analysis was based on the β CrB spectrum obtained in February 1998 with the MuSiCoS spectropolarimeter mounted on the 2 m telescope at Pic du Midi observatory (R = 35 000). This spectrum was used by Wade et al. (2001, 2003) in stratification analysis. Starting Cr and Fe distributions were taken from this analysis and were slightly corrected using a set of spectral lines of Cr I Cr II Fe I Fe II with different lower level excitation energies. The adapted distributions are shown in Fig. 3. Fe stratification is necessary to correctly account for blends.

Synthetic spectrum calculation in our Cr I line regions was performed following the method described in Sect. 3. The surface magnetic field B_s = 5.4 kG was derived from the

Article published by EDP Sciences and available at http://www.edpsciences.org/aa or http://dx.doi.org/10.1051/0004-6361:20042318

Table 1. continued.

PERTURBERS ARE:		ELECTRONS		PROTONS		HELIUM IONS	
TRANSITION	T(K)	*FWHM*(A)	SHIFT(A)	*FWHM*(A)	SHIFT(A)	*FWHM*(A)	SHIFT(A)
Cr I $^7P^0_3$–$^7D_4$	2500.	0.182E–01	0.452E–03	0.109E–01	–0.737E–02	*0.683E–02	–0.564E–02
	5000.	0.156E–01	0.277E–03	0.130E–01	–0.902E–02	*0.788E–02	–0.664E–02
5297.38 A	10 000.	0.131E–01	0.129E–03	0.144E–01	–0.102E–01	0.909E–02	–0.787E–02
C = 0.12E+15	20 000.	0.108E–01	–0.434E–04	0.168E–01	–0.945E–02	0.956E–02	–0.934E–02
	30 000.	0.956E–02	–0.141E–03	0.172E–01	–0.830E–02	0.945E–02	–0.100E–01
	50 000.	0.822E–02	–0.240E–03	0.194E–01	–0.603E–02	0.793E–02	–0.100E–01
Cr I $^7P^0_4$–$^7D_3$	2500.	0.245E–01	–0.956E–03	*0.220E–01	–0.141E–01	*0.134E-01	–0.104E–01
	5000.	0.214E–01	–0.701E–03	*0.259E–01	–0.173E–01	*0.155E–01	–0.127E–01
5329.78 A	10 000.	0.181E–01	–0.492E–03	*0.280E–01	–0.197E–01	*0.173E–01	–0.153E–01
C = 0.61E+14	20 000.	0.150E–01	–0.419E–03	0.286E–01	–0.197E–01	*0.173E–01	–0.182E–01
	30 000.	0.134E–01	–0.411E–03	0.289E–01	–0.184E–01	*0.160E–01	–0.197E–01
	50 000.	0.115E–01	–0.410E–03	0.295E–01	–0.159E–01	*0.130E–01	–0.204E–01
Cr I $^7P^0_4$–$^7D_4$	2500.	0.184E–01	0.460E–03	0.110E–01	–0.746E–02	*0.692E–02	–0.570E–02
	5000.	0.158E–01	0.276E–03	0.132E–01	–0.911E–02	*0.798E–02	–0.672E–02
5329.14 A	10 000.	0.132E–01	0.127E–03	0.146E–01	–0.103E–01	0.920E–02	–0.796E–02
C = 0.12E+15	20 000.	0.109E–01	–0.484E–04	0.170E–01	–0.956E–02	0.967E–02	–0.946E–02
	30 000.	0.968E–02	–0.147E–03	0.174E–01	–0.840E–02	0.956E–02	–0.101E–01
	50 000.	0.832E–02	–0.248E–03	0.197E–01	–0.610E–02	0.802E–02	–0.101E–01
Cr I $^7P^0_4$–$^7D_5$	2500.	0.920E–02	0.162E–02	0.499E–02	0.407E–02	0.370E–02	0.321E–02
	5000.	0.800E–02	0.979E–03	0.599E–02	0.470E–02	0.417E–02	0.372E–02
5328.32 A	10 000.	0.678E–02	0.474E–03	0.739E–02	0.544E–02	0.473E–02	0.426E–02
C = 0.40E+15	20 000.	0.567E–02	0.103E–03	0.902E–02	0.641E–02	0.543E–02	0.485E–02
	30 000.	0.509E–02	–0.604E–04	0.987E–02	0.709E–02	0.590E–02	0.526E–02
	50 000.	0.445E–02	–0.208E–03	0.106E–01	0.784E–02	0.647E–02	0.589E–02

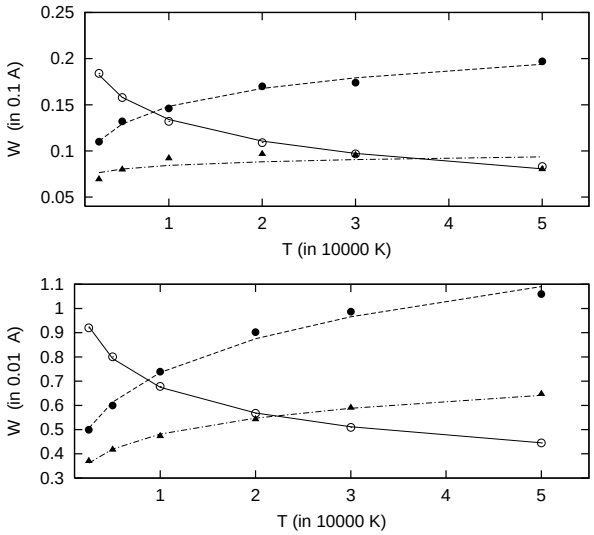

Fig. 1. The analytic fit of Cr I λ = 5329.14 Å (*upper figure*) and λ = 5328.32 Å (*down*) Stark widths due to impact with electrons (open circles), protons (full circles), and He II (full triangles).

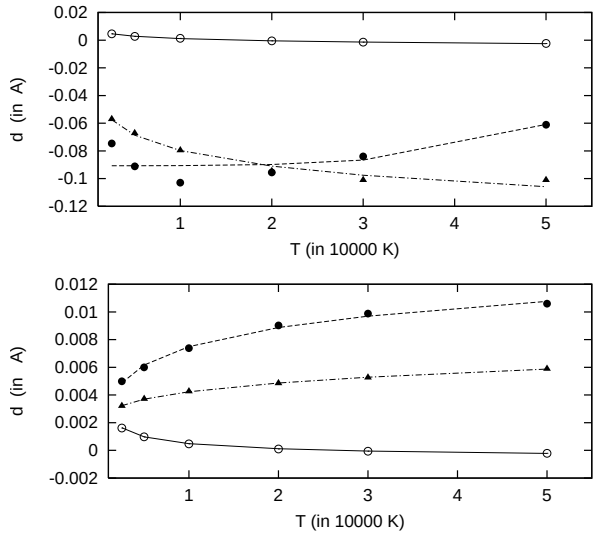

Fig. 2. The same as in Fig. 1, but for Stark shift.

magnetically split lines and used in all calculations. In the calculation process we found that Cr I lines have incorrect wavelengths with shifts up to 0.05 Å. We adjusted wavelengths by calculating the solar synthetic spectrum and comparing it with the Solar Flux Atlas (Kurucz et al. 1984). Improved wavelengths of Cr I lines derived this way agree within 0.005 Å and better with the precise measurements of J. E. Murray (1992), kindly provided to us by R. Kurucz[1]. We placed Murray's

[1] http://cfaku5.cfa.harvard.edu/atoms/2400/

Article published by EDP Sciences and available at http://www.edpsciences.org/aa or http://dx.doi.org/10.1051/0004-6361:20042318

Table 2. The parameters *A*, *B*, and *C* of the approximate formulas for Stark widths and shifts. * - fit with 3 values.

Line	5276.07 Å	5275.75 Å	5275.28 Å	5298.49 Å	5298.02 Å	5297.38 Å	5329.78 Å	5329.14 Å	5328.32 Å
					WIDTH				
					Electrons				
c_1	1E–16	1E–15	1E–15	1E–15	1E–15	1E–15	1E–15	1E–15	1E–16
A	–0.3474	–0.86156	–0.8218	–0.86039	–0.82019	–0.8674	–0.81818	–0.86596	–0.325497
B	–0.15596	–0.03684	–0.04346	–0.03716	–0.04412	–0.0337	–0.04412	–0.03410	–0.161576
					Protons				
c_1	1E–16	1E–15	1E–15	1E–15	1E–15	1E–15	1E–15	1E–15	1E–15
A	–0.3194	–0.23723*	–0.7393	–0.2312*	–0.7368	–0.85357	–0.7338	–0.85169	–0.924767
B	0.1789	–0.06276*	0.02231	–0.062768*	0.02238	0.02723	0.02281	0.027692	0.01959
					He II				
c_1	1E–16	–	1E–15	–	1E–15	1E–16	1E–15	1E–16	1E–16
A	–0.5525	–	–0.84377	–	–0.84219	–0.14236	–0.84037*	–0.13199	–0.51847
B	0.08565	–	0.01192	–	0.011451	0.11010	0.01177*	0.110894	0.092283
					SHIFT				
					Electrons				
c_2	1E–16	1E–16	1E–17	1E–16	1E–17	1E–17	1E–17	1E–17	1E–16
A	–3.4929	–6.7617	–81.5107	–2.5259	–9.0041	49.6736	–16.5511	40.5533	23.3420
B	0.01451	0.00793	0.00221	0.02206	0.02144	0.00526	0.01131	0.00586	0.00261
C	3.3728	6.6362	80.9250	2.3985	8.4079	–49.60704	15.9454	–40.4305	–23.2800
					Protons				
c_2	1E–16	1E–15	1E–15	1E–15	1E–15	1E–16	1E–15	1E–16	1E–16
A	–0.0170	0.25969*	3.0908	–3.3759*	0.5500	–2.4538	3.7646	18.8373	50.1882
B	0.22391	–0.122027*	0.00215	0.00846*	0.00990	0.02228	0.00188	–0.00173	–0.002557
C	–0.4916	–0.6076*	–3.2607	3.0621*	–0.7217	1.6060	–3.9381	–19.6934	–49.62339
					He II				
c_2	1E–16	–	1E–15	–	1E–15	1E–16	1E–15	1E–16	1E–16
A	–0.0174	–	1.7973	–	2.4949	37.4669	2.0440	36.5920	0.0405
B	0.20567	–	0.01778	–	0.01314	0.00418	0.01604	0.00431	0.22021
C	–0.3771	–	–1.9474	–	–2.6462	–38.2561	–2.1971	–37.3904	0.3832

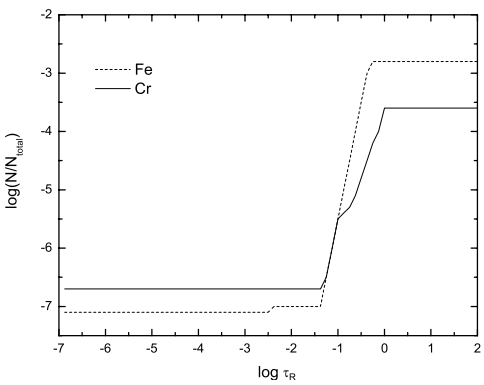

Fig. 3. Empirically derived Cr and Fe distributions in the atmosphere of magnetic Ap star β CrB.

wavelengths in Tables 1 and 2 and used them in spectral synthesis. We also estimated the contribution of Van der Waals broadening and found it to be one order of magnitude smaller than Stark broadening through the whole atmosphere above $\log(\tau_{5000}) = -0.2$ with rapid decrease below the photosphere.

We varied Stark broadening parameters given in Table 1 to achieve a best fit of the calculated Cr I line profiles to observations. Figure 4 shows a comparison between observations and calculations in the region of 3 groups of Cr I lines. For comparison we present synthetic calculations with homogeneous mean abundances $\log(\mathrm{Cr}/N_{\mathrm{tot}}) = -4.80$ and $\log(\mathrm{Fe}/N_{\mathrm{tot}}) = -4.15$, which were used in model atmosphere calculations (Kupka et al. 2004). To fit Cr I line wings we need to decrease current Stark widths by 60−70%. The same order of overestimation of Stark damping constants, was obtained for Si I lines (see Dimitrijević et al. 2003) calculated within the semiclassical perturbation formalism. Any change in Cr distribution, that may be responsible for line profiles, too, is critical for nearby Cr I λ 5296.691 Å, which is insensitive to the Stark broadening mechanism because of the small value of the Stark damping constant and because it is only sensitive to Cr distribution in stellar atmospheres. We also compare observations with a

Article published by EDP Sciences and available at http://www.edpsciences.org/aa or http://dx.doi.org/10.1051/0004-6361:20042318

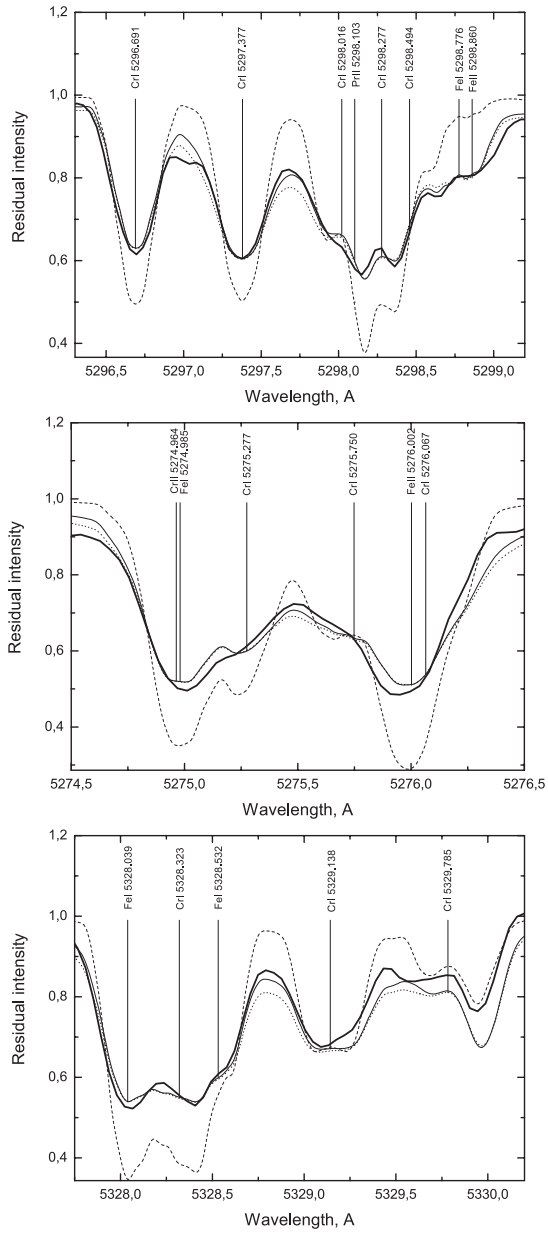

Fig. 4. A comparison between synthetic spectrum calculations and the observed spectrum (thick line) of magnetic Ap star β CrB in the regions of Cr I lines 5297 Å (*top panel*), 5276 Å (*middle panel*), and 5329 Å (*bottom panel*). Full thin line – calculations with stratification shown in Fig. 3 and Stark broadening data from Table 1 decreased by 70%; dashed line – the same Stark broadening data but homogeneous Cr and Fe abundances (see text); dotted line – stratified Cr and Fe abundances, but Stark broadening calculated with the approximation formula.

synthetic spectrum calculated using stratified Cr distribution and an approximation formula for Stark broadening (Cowley 1971). This formula is used in the cases where Stark broadening data, experimental or theoretical, are not available. Evidently, Stark broadening is overestimated when calculations are performed with this approximation formula.

For a more detailed investigation of the influence of Stark shifts on the observed line profile, we calculated theoretical spectra with and without shifts for two separate

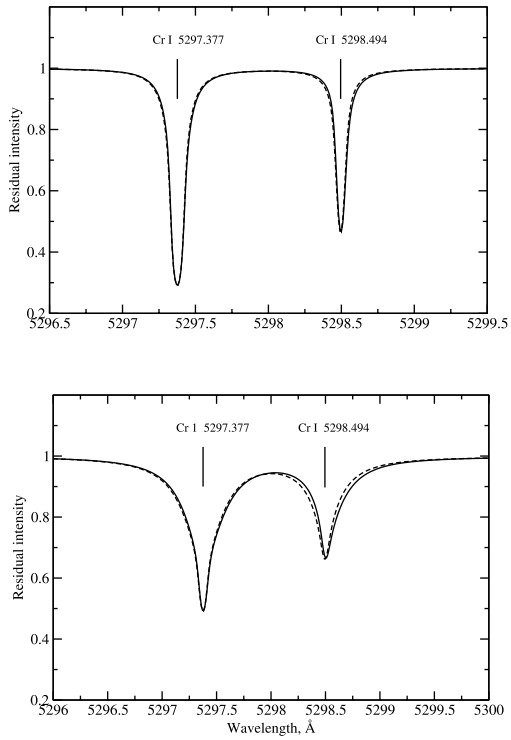

Fig. 5. Influence of Stark shift on Cr I line shapes in homogeneous (*upper panel*) and in stratified (*lower panel*) atmospheres. Calculations with both Stark widths and shifts are shown by solid lines, while those without Stark shifts are shown by a dashed line.

Cr I lines 5297.377 Å and 5298.494 Å in homogeneous and stratified atmospheres of the non-rotating star. These two lines have the smallest and largest shift values, therefore one can make a relative comparison. Figure 5 illustrates the influence of the Stark shift on line shape. The total shift in line position due to the Stark broadening effect is negligible for Cr I 5297.377 Å line both in homogeneous and stratified atmospheres. For the second line, Stark broadening leads to a theoretically measurable shift in the line position, in particular, in the case of Cr stratification resulting in a small line asymmetry. Unfortunately, in spectra of real stars, the effect is difficult to measure due to other broadening mechanisms (rotation, magnetic field) and mainly due to severe blending in the regions with Cr I lines from 4p−4d transitions.

5. Conclusions

Stark broadening parameters for Cr I spectral lines from the $4p^7P^0$–$4d^7D$ multiplet were calculated and the influence of Stark broadening effect was investigated in stellar atmospheres for these lines. From our investigation we can conclude:

(i) Although they belong to the same multiplet, the widths and shifts of the different lines can be quite different.

(ii) Contribution of the proton and He II collisions to the line width and shift is significant and is comparable and, depending of the electron temperature, even larger than electron-impact contribution.

(iii) Depending on the electron-, proton-, and He II density in stellar atmospheres, the Stark shift may contribute to the

Article published by EDP Sciences and available at http://www.edpsciences.org/aa or http://dx.doi.org/10.1051/0004-6361:20042318

blue, as well as to the red, asymmetry of the same line (see Fig. 2).

(iv) To fit Cr I line wings well we need to decrease the calculated Stark widths by 60−70%, which is the same order of overestimation as for Si I lines (Dimitrijević et al. 2003). Used in the cases where the adequate semiclassical calculation is not possible due to the lack of reliable atomic data, the approximation formula of Cowley (1971) also predicts the overestimated influence of Stark broadening in comparison with observations.

Acknowledgements. We are very thankful to G. Wade and R. Kurucz who provided us with the data necessary for our analysis. This work is a part of the projects GA-1195 "Influence of collisional processes on astrophysical plasma lineshapes" and GA-1196 "Astrophysical Spectroscopy of Extragalactic Objects" supported by the Ministry of Science and Environment protection of Serbia. The research was supported also by the Fonds zur Förderung der wissenschaftlichen Forschung *P14984*. T.R. thanks Leading Scientific School grant 162.2003.02 and the RFBR (grant 03-02-16342) for partial funding. L.Č.P. is supported by Alexander von Humboldt Foundation through the program for foreign scholars. D.S. acknowledges financial support from INTAS grant 03-55-652.

References

Babel, J. 1992, A&A, 258, 449
Bates, D. R., & Damgaard, A. 1949, Trans. Roy. Soc. London, Ser. A, 242, 101
Cowley, C. R. 1971, Obs., 91, 139
Dimitrijević, M. S. 1996, Zh. Priklad. Spektrosk., 63, 810
Dimitrijević, M. S., & Sahal-Bréchot, S. 1984a, JQSRT, 31, 301
Dimitrijević, M. S., & Sahal-Bréchot, S. 1984b, A&A, 136, 289
Dimitrijević, M. S., Ryabchikova, T., Popović, L. Č., Shulyak, D., & Tsymbal, V. 2003, A&A, 404, 1099
Humlicek, J. 1982, JQSRT, 27, 437
Khan, S. 2004, JQSRT, 88, 71
Kupka, F., Piskunov, N. E., Ryabchikova, T. A., Stempels, H. C., & Weiss, W. W. 1999, A&AS, 138, 119
Kupka, F., Paunzen, E., Iliev, I. Kh., & Maitzen, H. M. 2004, MNRAS, 352, 863
Kurucz, R. L. 1993, CDROM13, SAO, Cambridge
Kurucz, R. L., Furenlid, I., Brault, J., & Testerman, L. 1984, NSO Atlas No. 1: Solar Flux Atlas from 296 to 1300 nm, Sunspot, NSO
Moore, C. E. 1971, Atomic Energy Levels Vol. II, NSRDS-NBS 35 (Washington: US Gov. Print. Office)
Murray, J. E. 1992, Ph.D. Thesis, Imperial College, London
Oertel, G. K., & Shomo, L. P. 1968, ApJS, 16, 175
Piskunov, N., & Kupka, F. 2001, ApJ, 547, 1040
Piskunov, N., & Kochukhov, O. 2002, A&A, 381, 736
Popović, L. Č., Dimitrijević, M. S., & Ryabchikova, T. 1999, A&A, 350, 719
Popović, L. Č., Simić, S., Milovanović, N., & Dimitrijević, M. S. 2001, ApJS, 135, 109
Rees, D. E., Murphy, G. A., & Durrant, C. J. 1989, ApJ, 339, 1093
Ryabchikova, T., Piskunov, N., Kochukhov, O., et al. 2002, A&A, 384, 545
Ryabchikova, T., Wade, G., & LeBlanc, F. 2003, in Modelling of Stellar Atmospheres, ed. N. E. Piskunov, W. W. Weiss, & D. F. Gray, ASP, IAU Symp., 210, 301
Sahal-Bréchot, S. 1969a, A&A, 1, 91
Sahal-Bréchot, S. 1969b, A&A, 2, 322
Sahal-Bréchot, S. 1974, A&A, 35, 321
Sobelman, I. I. 1977, Introduction to the theory of atomic spectra (Moscow: Nauka)
Socas-Navarro, H., Trujillo Bueno, J., & Ruiz Cobo, B. 2000, ApJ, 530, 97
van Regemorter, H., Hoang Binh Dy, & Prud'homme, M. 1979, J. Phys. B, 12, 1073
Wade, G. A., Ryabchikova, T. A., Bagnulo, S., & Piskunov, N. 2001, in Magnetic Fields Across the Hertzsprung-Russell Diagram, ed. G. Mathys, S. K. Solanki, & D. T. Wickramasinghe, ASP Conf. Ser., 248, 341
Wade, G. A., LeBlanc, F., Ryabchikova, T. A., & Kudryavtsev, D. 2003, in Modelling of Stellar Atmospheres, ed. N. E. Piskunov, W. W. Weiss, & D. F. Gray, CD-D7, IAU Symp., 210
Wiese, W. L., & Musgrove, A. 1989, Atomic Data for Fusion Vol. 6, Spectroscopic Data for Titanium, Chromium and Nickel, Vol. 2. Chromium, Controled Fusion Atomic Data Center, Oak Ridge National Laboratory, Oak Ridge

Article published by EDP Sciences and available at http://www.edpsciences.org/aa or http://dx.doi.org/10.1051/0004-6361:20042318

A&A 437, 1023–1027 (2005)
DOI: 10.1051/0004-6361:20052694
© ESO 2005

Astronomy & Astrophysics

Processes of ($n - n'$)-mixing in collisions of Rydberg $H^*(n)$ atoms with H(1s) in the Solar atmosphere

A. A. Mihajlov[1,2], Lj. M. Ignjatović[1,2], and M. S. Dimitrijević[2,3]

[1] Institute of Physics, PO Box 57, 11001 Belgrade, Serbia and Montenegro
e-mail: mihajlov@phy.bg.ac.yu
[2] Institute Isaac Newton of Chile, Yugoslavia Branch, and Universidad Diego Portales, Chile
[3] Astronomical Observatory, Volgina 7, 11160 Belgrade 74, Serbia and Montenegro

Received 13 January 2005 / Accepted 17 March 2005

Abstract. The significance of ($n - n'$)-mixing processes in $H^*(n) + H(1s)$ collisions, for the principal quantum number $n \geq 4$, in the Solar photosphere and lower chromosphere has been investigated. These processes have been treated by the mechanism of resonant energy exchange within the electron component of the considered collision system. These processes must have significant influence in comparison with corresponding electron-atom collision processes on the populations of hydrogen Rydberg atoms in weakly ionized layers of the Solar atmosphere (ionization degree of the order of 10^{-4}). From the results obtained it follows that the examined ($n - n'$)-mixing processes have to be included in any modelling and investigation of Solar plasma, especially in the region of the temperature minimum in the Solar photosphere.

Key words. atomic processes – molecular processes – Sun: atmosphere

1. Introduction

Mihajlov et al. (1997, 1999, 2003) drew attention to the importance of inelastic processes in slow collisions of Rydberg state atoms with ground state H atoms in solar and stellar atmospheres. These papers were devoted to an investigation of the processes of chemi-ionization

$$\mathrm{H} + \mathrm{H}^*(n) \rightarrow \boldsymbol{e} + \begin{cases} \mathrm{H}^+ + \mathrm{H} \\ \mathrm{H} + \mathrm{H}^+, \end{cases} \tag{1}$$

and the inverse process of chemi-recombination

$$\boldsymbol{e} + \mathrm{H}^+ + \mathrm{H} \rightarrow \begin{cases} \mathrm{H} + \mathrm{H}^*(n), \\ \mathrm{H}^*(n) + \mathrm{H}, \end{cases} \tag{2}$$

where H designates a ground state H(1s) atom, $H^*(n)$ a Rydberg state hydrogen atom with principal quantum number $n \geq 4$ and $\boldsymbol{e}$ is a free electron. The processes (1) and (2) were treated using the resonant energy exchange mechanism (Smirnov & Mihajlov 1971; Janev & Mihajlov 1979) between the electrons of the $\mathrm{H} + \mathrm{H}^*(n)$ system, to which we subsequently refer to as the resonant mechanism. It was shown that the processes (1) and (2) can be of great importance in weakly ionized layers of many stellar atmospheres, in comparison with other possible ionization and recombination processes involving electrons or photons, namely direct ionization by electron impact

$$\boldsymbol{e} + \mathrm{H}^*(n) \rightarrow \mathrm{H}^+ + \boldsymbol{e} + \boldsymbol{e}, \tag{3}$$

the inverse 3-body electron recombination

$$\boldsymbol{e} + \boldsymbol{e} + \mathrm{H}^+ \rightarrow \boldsymbol{e} + \mathrm{H}^*(n), \tag{4}$$

and the radiative recombination

$$\boldsymbol{e} + \mathrm{H}^+ \rightarrow \mathrm{H}^*(n) + \epsilon_{\mathrm{ph}}, \tag{5}$$

where ϵ_{ph} is the energy of the emitted photon.

However, Mihajlov et al. (1997, 1999, 2003) adopted the usual assumption that the distribution of Rydberg states was determined by electron collisions

$$\boldsymbol{e} + \mathrm{H}^*(n) \rightarrow \boldsymbol{e} + \mathrm{H}^*(n'). \tag{6}$$

More recently, Mihajlov et al. (2004) showed that the Rydberg state distribution in a weakly ionized hydrogen plasma could also be strongly influenced by ($n - n'$)-mixing processes in $\mathrm{H}^*(n) + \mathrm{H}$ collisions. These conclusions were based on the results of an investigation of the excitation processes

$$\mathrm{H}^*(n) + \mathrm{H} \rightarrow \begin{cases} \mathrm{H}^*(n' = n + p) + \mathrm{H} \\ \mathrm{H} + \mathrm{H}^*(n' = n + p) \end{cases}, \qquad n \geq 4, \quad p \geq 1, \tag{7}$$

and the inverse de-excitation process

$$\mathrm{H}^*(n) + \mathrm{H} \rightarrow \begin{cases} \mathrm{H}^*(n' = n - p) + \mathrm{H} \\ \mathrm{H} + \mathrm{H}^*(n' = n - p) \end{cases}, \qquad n - p \geq 4, \tag{8}$$

which were caused by the same resonant mechanism as the processes of chemi-ionization and chemi-recombination. The results obtained impose the necessity of an investigation of

Article published by EDP Sciences and available at http://www.edpsciences.org/aa or http://dx.doi.org/10.1051/0004-6361:20052694

the processes (7) and (8) in weakly ionized layers of stellar atmospheres and particularly in the Solar atmosphere. The confirmation of the importance of these processes in the Solar photosphere would support the necessity of including of the whole group of non-elastic processes in $H^*(n)$ + H collisions, i.e. Eqs. (1), (2), (7) and (8), in models of weakly ionized layers of Solar and stellar atmospheres. That should be confirmed by one of the known and widely used non-LTE models of the Solar atmosphere.

For the reason mentioned we shall examine here in more detail the significance of $(n - n')$-mixing processes (7) and (8) in the Solar photosphere and lower chromosphere. For this purpose we shall calculate the rate coefficients of these processes for different n and p using a semiclassical method developed by Mihajlov et al. (2004). The rate coefficients obtained will be compared with the rate coefficients of electron-atom mixing processes (6) for electron and hydrogen atom densities and temperatures from the model C of the Solar photosphere and the lower chromosphere of Vernazza et al. (1981).

2. Theoretical comments

The resonant mechanism. Since the resonant mechanism for processes (1)–(8) has been discussed in several previous papers, and especially has been described in detail in Mihajlov et al. (2004), only the basic facts will be given here. On the basis of the resonant mechanism the $H^*(n)$ + H collision system is treated within the domain

$$R \ll r_n, \tag{9}$$

where R is the internuclear distance and $r_n \sim n^2$ is the average radius of the Rydberg atom $H^*(n)$. Within this domain the $H^*(n)$ + H system is treated in the form: e + (H^+ + H), where e is the outer electron of the $H^*(n)$ Rydberg atom. The electronic states of the subsystem (H^+ + H) are described using the adiabatic electronic ground state $|1s\sigma_g; R\rangle$, or of the first excited state $|2p\sigma_u; R\rangle$ of the molecular ion H_2^+. The relative internuclear motion is described in the approximation of two classical trajectories: the first one, which corresponds to the adiabatic $1s\sigma_g$-term, and the other, which corresponds to the $2p\sigma_u$-term. It is assumed that each of these trajectories is realized with the same probability $p_{\rm in}$ which is equal to 1/2.

The processes (7) and (8) of $(n - n')$-mixing, as well as the processes of chemi-ionization/recombination (1) and (2), are treated as a result of the resonant energy exchange between the outer electron e and the electronic component of the H^+ + H subsystem. This means that the transition of the outer electron from the initial energetic state to the upper ones occurs simultaneously with the transition of the H^+ + H subsystem from the electronic excited state $|2p\sigma_u; R\rangle$ to the ground state $|1s\sigma_g; R\rangle$, and the transition of the outer electron to the lower energetic state occurs simultaneously with the transition of the H^+ + H subsystem from the ground electronic state $|1s\sigma_g; R\rangle$ to the excited state $|2p\sigma_u; R\rangle$ as illustrated in Fig. 1. Within the considered mechanism one assumes that all mentioned transitions are caused by the interaction of the outer electron with the dipole momentum of the H^+ + H subsystem.

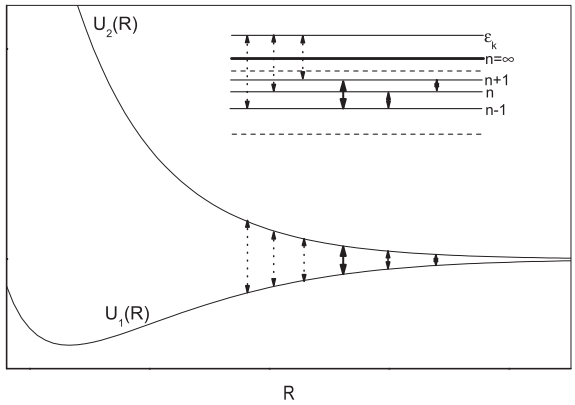

Fig. 1. The resonant mechanism in chemi-ionization/recombination channels (dashed arrows), and $(n - n')$-mixing channels (full arrows).

In Janev & Mihajlov (1979, 1980) the resonant mechanism described was applied in the range $n > 4$ where there are no crossings of the terms of $H^*(n)$ + H(1s) systems with the term of H^+ + H^- system. However, following our later papers, we will take $n = 4$ as a lower boundary of the considered principal quantum number region. In accordance with Sidis et al. (1983) the corresponding crossing point is placed at such a large internuclear distance that it does not influence the considered processes.

The resonant mechanism was also treated within the framework of theories related to a wider class of collision atomic systems $A^*(n) + B$, where in the general case A and B denote different atoms (Flannery 1980; Lebedev 1991b; Lebedev & Fabrikant 1996). However, in the symmetrical case these theories give the same results as the theory presented in Janev & Mihajlov (1979, 1980) and Mihajlov & Janev (1981). Besides, the processes of $(n - n')$-mixing in the $Li^*(n)$ + Li collisions were experimentally studied in Dubreuil (1983). The experimental results obtained were compared with the results from Janev & Mihajlov (1979). It was demonstrated that the agreement of these results is good enough to confirm the validity of the described resonant mechanism.

The processes (1)–(8), caused by the resonant mechanism, should not be confused with the processes in $H^*(n) + A$ collisions caused by the direct interaction of the electron of atom H^* with atom A whose electronic state does not change during the collision (Matsuzawa 1974; Gerstein 1976; Olson 1977; Percival 1978; Lebedev 1991a; Lebedev & Fabrikant 1996). The influence of such processes can be neglected in comparison with the influence of processes (7) and (8) at thermal collision energies ($\lesssim$1 eV), as was discussed in Janev & Mihajlov (1979).

The rate coefficients of processes (7) and (8) for fixed n and $n' = n \pm p$ have been determined semi-classically, describing the internuclear motion by using the trajectories determined in the potential corresponding to the excited electronic state $|2p\sigma_u; R\rangle$ of the H^+ + H subsystem. For the calculations of the considered rate coefficient an approximation was used where a block of Rydberg states with the principal quantum numbers from $n + p_1$ to $n + p_2$, where $p_2 \geq p_1 \geq 1$, is "smeared" to a continuum within the effective principal quantum number range

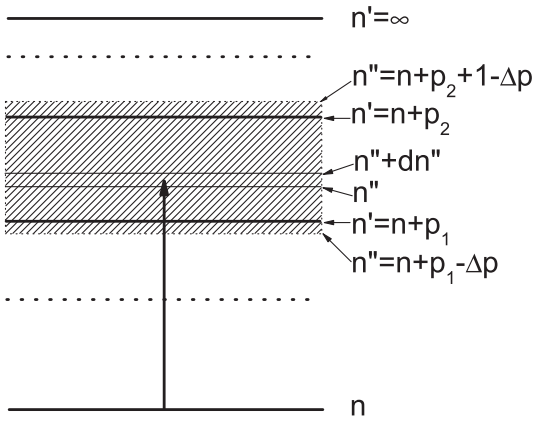

Fig. 2. The partial "smearing" of the discrete Coulomb spectrum to a continuum.

from $n + p_1 - \Delta p$ to $n + p_2 + 1 - \Delta p$, where $0 < \Delta p < 1$, as is shown in Fig. 2. Such "smearing" is performed under the conditions described in Mihajlov et al. (2004).

The described procedure for determination of the rate coefficients of the examined $(n - n')$-mixing processes means that the hydrogen (nl)-states with fixed n are populated according to their statistical weights. This assumption is based on the properties of the existing models of the photosphere and lower chromosphere of the Sun and similar stars, of some cooler stars (as for example M and K type stars), and of some other stars (like some of DB white dwarfs for example). It is well known that these models assume only limited deviations from the LTE. For example in Vernazza's model C of the Solar atmosphere used here it is assumed that the distribution of the total populations of the atomic shells with different principal quantum number n can deviate from the corresponding Boltzman distribution, but that there are no such deviations within particular shells. There are physical reasons for such an approach. Namely, it is well known that the processes of $(l - l')$-mixing for fixed n are practically resonant and are very effective over the distances proportional to an average Rydberg atom radius (Olson 1977; Percival 1978; Lebedev 1991a). Consequently such processes are much faster that the $(n - n')$-mixing processes, especially within the region where the $(n - n')$ transition energy is of the order of kT. A similar assumption for the population distribution of (nl) – states with fixed n was used and discussed in many previous articles, including Janev & Mihajlov (1979, 1980).

The procedure of "smearing" a discrete spectrum has already been used. For example in Sobel'man (1979) this has been used for description of the electron – ion recombination with transition of the free electron in a block of Rydberg states. In Duman & Shmatov (1980), "smearing" the discrete spectrum of the molecular ion A_2^+ has been used to describe the chemi – ionization processes in $A^*(n) + A$ collisions. In these cases it was used as physically acceptable approximation without special justifications.

In our case however, well-determined physical reasons exist for the approximation of "smearing". Concerning the "smearing" of the hydrogen Rydberg spectrum, some results from Janev & Mihajlov (1979) have been taken into account. These are the results related to the behavior of the $(n - n')$ transition probability due to $H^*(n) + H(1s)$ collisions as a function of collision parameters for fixed impact energies. On the basis of the results obtained one can consider that the $(n - n')$ transition occurs within some interval of internuclear distances whose center is a point of resonance (where the observed transition may be treated as a result of the strictly resonant energy exchange within the electronic component of the considered system) and that such intervals overlap significantly for n' and $n' \pm 1$. These results are related to the case when the atom – atom impact energy is at least several times greater than energies for the considered $(n - n')$ transitions, which justified the use of the straight line trajectory approximation in the mentioned article.

This allows the considered process to be treated as the continuous decay of the initial electronic state (of the total system), during the internuclear motion within the reaction zone (the internuclear distance range being less or close to the resonant distance for the transition $n \to n + 1$).

The rate coefficients. Since the procedure of obtaining the rate coefficients for the processes (7) and (8) is described in detail in Mihajlov et al. (2004), only the corresponding final expressions are presented here. The rate coefficients $K_{n;n+p}(T)$ for the excitation processes (7), for given n, p and the temperature T, are obtained in the form

$$K_{n;n+p}(T) = \frac{2\pi}{3\sqrt{3}} \frac{(ea_0)^2}{\hbar} \cdot n^{-5} \cdot g_{n;n+p} \times p_{\rm in} \cdot 2 \cdot \int\limits_{R_{\min}(n,n+p)}^{R_{\max}(n,n+p)} X(R) \cdot \exp\left[-\frac{U_2(R)}{kT}\right] \frac{R^4 \cdot {\rm d}R}{a_0^5}, \tag{10}$$

where e and a_0 are the electron charge and the atomic unit of length, $g_{n;n+p}$ is the Gaunt factor defined in Johnson (1972), $R_{\min}(n, n + p)$ and $R_{\max}(n, n + p)$ are roots of equations

$$\begin{aligned} \epsilon(R_{\min}) &= \epsilon_{n+p+1-\Delta p} - \epsilon_n, \\ \epsilon(R_{\max}) &= \epsilon_{n+p-\Delta p} - \epsilon_n, \end{aligned} \tag{11}$$

with $\epsilon(R) = U_2(R) - U_1(R)$ and $\Delta p = 0.380$. Here, $U_1(R)$ and $U_2(R)$ are adiabatic terms corresponding to the electronic states $|1s\sigma_g; R\rangle$ and $|2p\sigma_u; R\rangle$, respectively, and $\epsilon_n = -Ry/n^2$. $X(R)$ denotes the function

$$X(R) = \frac{\Gamma\left(3/2; \frac{|U_1(R)|}{kT}\right)}{\Gamma(3/2)}, \tag{12}$$

where $\Gamma(3/2; x)$ and $\Gamma(3/2)$ are the corresponding values of the incomplete and complete Gamma functions. The factor $p_{\rm in} = 1/2$ in Eq. (10) is the mentioned above probability for the realization of a trajectory which describes the internuclear motion in the potential $U_2(R)$, while the factor 2 reflects the fact that the system $H^*(n) + H$ crosses the transition zone twice: once on entry and once on leaving.

The rate coefficients $K_{n;n-p}(T)$ for de-excitation processes (8) are obtained from the thermodynamic balance principle in the form

$$K_{n;n-p}(T) = K_{n-p;n}(T) \cdot \frac{(n-p)^2}{n^2} \cdot \exp\left(\frac{\epsilon_{n-p;n}}{kT}\right), \tag{13}$$

where $\epsilon_{n-p;n} = \epsilon_n - \epsilon_{n-p}$.

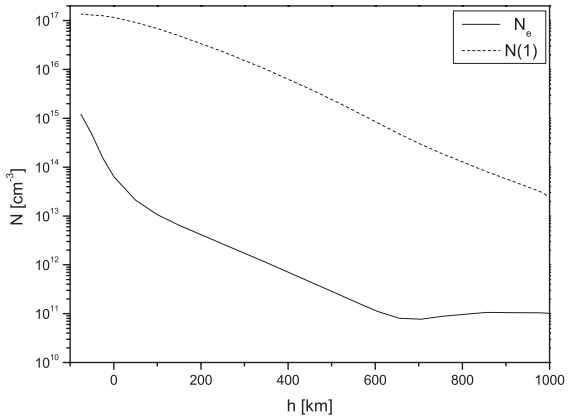

Fig. 3. The behavior of N_e and $N(1)$ in [cm^{-3}] as functions of height h within the considered part of the Solar atmosphere from model C of Vernazza et al. (1981)

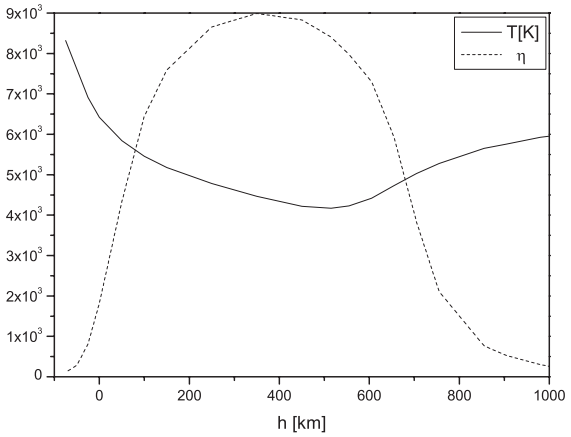

Fig. 4. The behavior of the temperature T and the parameter $\eta = N(1)/N_e$ as functions of height h within the considered part of the Solar atmosphere from model C of Vernazza et al. (1981)

3. Results and discussion

As in the previous article related to the chemi-ionization/recombination processes (1) and (2), we will treat the Solar photosphere and lower chromosphere using the standard C model of Vernazza et al. (1981). For our calculations we need to take from this model the electron density N_e, the density of hydrogen atoms in the ground state ($n = 1$), denoted here by $N(1)$, and the temperature T. The behavior of N_e and $N(1)$ in the Solar atmosphere as a function of height (h) is shown in Fig. 3, while Fig. 4 shows the behavior of T and the parameter η defined by the relation

$$\eta_{ea} = \frac{N(1)}{N_e}. \tag{14}$$

In our case the parameter η is close to the inverse value of the considered plasma's degree of ionization. Also, we will use the data about the hydrogen atom excited state population ($n \geq 2$) from Vernazza et al. (1981). In order to determine the relative influence of processes (7) and (8) in the considered parts of Solar atmosphere, we will compare them with electron-atom collision processes (6). Following the mentioned above papers related to chemi-ionization/recombination processes,

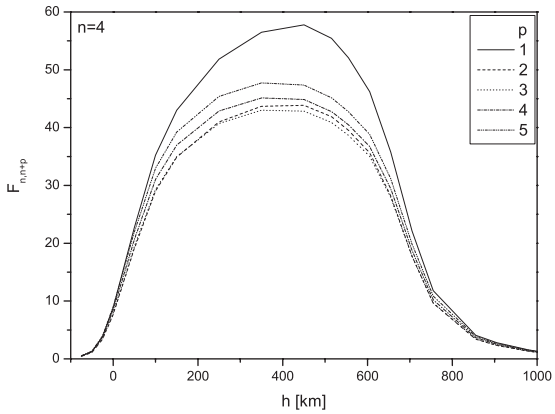

Fig. 5. The behavior of the parameter $F_{n,n+p} = (K_{n,n+p} \cdot \eta)/\alpha_{n,n+p}$, characterizing the relative efficiency of atom-atom and electron-atom $(n - n')$- mixing processes, as a function of height h for $n = 4$ and $p = 1$–5. The atom-atom rate coefficient $K_{n,n+p}$ is given by Eqs. (10)–(12) and the parameter η- by Eq. (14). The electron-atom rate coefficient $\alpha_{n,n+p}$ is taken from Vriens & Smeets (1980).

we compare the studied collision processes only with other relevant collision processes, omitting the radiative decay of hydrogen Rydberg states. The radiative decay, which causes the deviation from LTE in the considered part of the Solar atmosphere, is already included in Vernazza's model, so that the "optical part" of this model does not need to undergo any changes. We show that the "collision part" of Vernazza's model has to be changed by adding atomic collision processes (1)–(8).

The relative efficiency of processes (7) and (8) in comparison to process (6) is characterized by the parameter $F_{n;n\pm p}(T)$

$$F_{n;n\pm p}(T) = \frac{K_{n;n\pm p}(T)N(n)N(1)}{\alpha_{n;n\pm p}(T)N(n)N_e} = \frac{K_{n;n\pm p}(T)\eta_{ea}}{\alpha_{n;n\pm p}(T)}, \tag{15}$$

where $N(n)$ is the excited atom states population for given n, the parameter η_{ea} is defined by Eq. (14), and $\alpha_{n;n\pm p}(T_e)$ is the rate coefficient for the electron-atom process (6) taken from Vriens & Smeets (1980).

We have calculated the values of the parameter $F_{n;n\pm p}$ for $n \geq 4$ and $p \geq 1$, within the range of h corresponding to the Vernazza et al. (1981) model C of the Solar photosphere. Our results are illustrated in Figs. 5–7. In these figures the behavior of the parameter $F_{n;n+p}$ is shown, for $4 \leq n \leq 8$ and $1 \leq p \leq 5$, as a function of h within the range -50 km $\leq h \leq 1000$ km. In the largest part of the photosphere the $(n-n')$-mixing processes (7) and (8) are totally dominant in comparison to the electron-atom processes (6) for $n = 4$, 5, 6 and practically any $p \geq 1$, and have similar intensities for $n = 7$, 8. Comparing Figs. 5–7 with Fig. 4 one can see that the region of the maximal $F_{n;n\pm p}$ values corresponds to an h region near the temperature minimum, where the parameter η, defined by Eq. (14), is also maximal.

To demonstrate the significance of the obtained results we introduce the quantities $n = n^{(V)}_{\min}$ and $n = n^{(eq)}_{\min}$ dependent on h. The first value of n is defined by the condition:

$$N^{(V)}\left(n = n^{(V)}_{\min}\right) = \min_{n\geq 1} N^{(V)}(n), \tag{16}$$

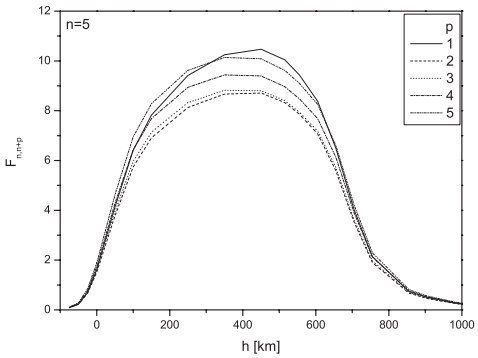

Fig. 6. The same as in Fig. 5, but for $n = 5$.

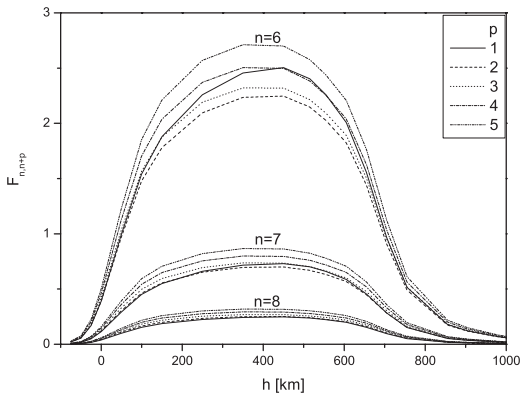

Fig. 7. The same as in Fig. 5, but for $n = 6, 7, 8$.

Table 1. The values of $n_{\min}^{(\mathrm{eq})}$ and $n_{\min}^{(V)}$ for h and T from Vernazza et al. (1981) model C.

	$h\,(km)$								
	–50	0	100	250	350	555	755	980	1065
$n_{\min}^{(\mathrm{eq})}$	4	4	5	5	5	6	5	5	5
$n_{\min}^{(V)}$	5	5	5	6	6	6	6	6	5

where $N^{(V)}(n)$ are excited atom populations from model C for a given h, and the second one is the value of n defined by the condition:

$$N^{(\mathrm{eq})}(n = n_{\min}^{(\mathrm{eq})}; T) = \min_{n\geq 1} N^{(\mathrm{eq})}(n; T) \tag{17}$$

where $N^{(\mathrm{eq})}(n; T)$ are equilibrium (Boltzmanian) excited atom populations for T from model C for the same h as in the previous case. It could be shown that in the considered temperature range, $n_{(\min)}^{(\mathrm{eq})}$ is close to the value of $(Ry/kT)^{(1/2)}$. In Table 1 the values of $n = n_{\min}^{(V)}$ and $n = n_{\min}^{(\mathrm{eq})}$ are presented for a series of h values in –50 km to 1065 km range. Within the considered domain of h the values of $n = n_{\min}^{(V)}$ and $n = n_{\min}^{(\mathrm{eq})}$ are 4, 5 and 6 for which domination of the processes (7) and (8) in comparison with the processes (6) is demonstrated.

For plasmas similar to the considered photospheric one, the exchange rate between both hydrogen basic components, atoms H(1s) and ions H^+, is limited by the group of excited atom states with n close to the $n_{\min}^{(V)}$ or $n_{\min}^{(\mathrm{eq})}$. However, one can see that the processes (7) and (8) play the dominant role in this group of excited states. This means that the exchange between the excited state atom populations within the lower part of the Rydberg region of n is determined by the processes (7) and (8). If we add to this the fact that the exchange between the mentioned group of Rydberg states and the continuum is determined by the chemi-ionization/recombination processes (1) and (2), one can conclude that the processes (1), (2), (7) and (8), closely connected by the resonant mechanism, completely dominate for the excited states with n close to $n_{\min}^{(V)}$ or $n_{\min}^{(\mathrm{eq})}$.

We gave here all relevant results demonstrating the significance of the processes (7) and (8) for a large part of the Solar photosphere and lower chromosphere, particularly in the neighborhood of the temperature minimum. On the basis of presented results we can conclude that the influence of the $(n - n')$-mixing processes (7) and (8), as well as the chemi-ionization/recombination processes (1) and (2), must be taken into account for any modelling of the Solar photosphere and lower chromosphere. Our findings are also related to similar stellar atmospheres as well as to stellar atmospheres with lower effective temperatures but where the atomic component is still dominant over the molecular one.

Acknowledgements. The authors wish to thank Prof. E. V. Kononovich for useful suggestions regarding the Solar atmosphere. This work is a part of the "Radiation and transport properties of the non-ideal laboratory and ionospheric plasma" project (Project number 1466), and "Influence of collision processes on the spectra of astrophysical plasmas" (Project number GA 1195) and was supported by the *Ministry of Science, Technology and Development of the Republic of Serbia*.

References

Dubreuil, B. 1983, Phys. Rev. A, 27, 2479
Duman, E. L., & Shmatov, I. P. 1980, JETP, 51, 1061
Gerstein, J. I. 1976, Phys. Rev. A, 14, 1354
Flannery, M. R. 1980, Phys. Rev. A, 22, 2408
Johnson, L. C. 1972, ApJ, 174, 227
Janev, R. K., & Mihajlov, A. A. 1979, Phys. Rev., 20, 1890
Janev, R. K., & Mihajlov, A. A. 1980, Phys. Rev., 21, 819
Lebedev, V. S. 1991a, J. Phys. B: At. Mol. Opt. Phys., 24, 1977
Lebedev, V. S. 1991b, J. Phys. B: At. Mol. Opt. Phys., 24, 1993
Lebedev, V. S., & Fabrikant, I. I. 1996, Phys. Rev. A, 54, 2888
Matsuzawa, M. 1974, J. Electron Spectrosc. Relat. Phen., 4, 1
Mihajlov, A. A., & Janev, R. K. 1981, J. Phys. B: At. Mol. Opt. Phys., 14, 1639
Mihajlov, A. A., Ignjatović Lj, M., Vasilijević, M. M., & Dimitrijević, M. S. 1997, A&A, 324, 1206
Mihajlov, A. A., Dimitrijević, M. S., Ignjatović, Lj. M., & Vasilijević, M. M. 1999, A&ATr, 18, 145
Mihajlov, A. A., Jevremović, D., Hauschildt, P., et al. 2003, A&A, 403, 787
Mihajlov, A. A., Ignjatović, Lj. M., Djurić, Z., & Ljepojević, N. N. 2004, J. Phys. B, 37, 4493
Olson, R. E. 1977, Phys. Rev. A, 15, 631
Percival, I. C. 1978, in Electronic and Atomic Collisions: Invited Papers, ed. G. Watel, North-Holland, 569
Sidis, V., Kubach, C., & Fussen, D. 1983, Phys. Rev. A, 27, 2431
Smirnov, V. A., & Mihajlov, A. A. 1971, Opt. Spektrosk., 30, 984 (Opt. Spectrosc., USSR 5, 525)
Sobel'man, I. I. 1979, it Atomic Spectra and Radiative Transitions (Berlin: Springer)
Vernazza, J. E., Avrett, E. H., & Loser, R. 1981, ApJS, 45, 635
Vriens, L., & Smeets, A. 1980, Phys. Rev. A, 22, 940

A&A 441, 391–393 (2005)
DOI: 10.1051/0004-6361:20052701
© ESO 2005

Astronomy & Astrophysics

Stark broadening of Cd I spectral lines*

Z. Simić[1,2], M. S. Dimitrijević[1,2], N. Milovanović[1,2], and S. Sahal-Bréchot[3]

[1] Astronomical Observatory, Volgina 7, 11160 Belgrade, Serbia and Montenegro
e-mail: [zsimic;mdimitrijevic]@aob.bg.ac.yu
[2] Institute Isaac Newton of Chile Yugoslavia Branch, and Universidad Diego Portales, Chile
[3] Observatoire de Paris-Meudon, 92195 Meudon, France

Received 14 January 2005 / Accepted 7 March 2005

Abstract. Stark broadening parameters, widths, and shifts for 33 Cd I singlets and 37 triplets were calculated using the semiclassical perturbation method. The results were compared with available experimental and theoretical data. Also, regularity in the spectral series $5s^2\ ^1S$–np $^1P^\circ$ was investigated. The influence of Stark broadening was analyzed in A-type stellar atmospheres.

Key words. line: profiles – atomic data – atomic processes – lines formation – stars: atmospheres

1. Introduction

Cadmium lines are interesting due to their presence in stellar atmospheres. They have been identified in A-type star spectra, as e.g. 68 Tauri (Adelman 1994a,b), χ Lupi (Leckrone et al. 1999), V816 Centauri (Cowley et al. 2000). As an example Adelman has shown for 68 Tau that the [Cd/H] value (-6.57 ± 0.15) is very large in comparison to the one for the Sun (-10.14). It is worth noting that for the atmosphere modelisation of this star with $T_{\rm eff} = 9025$ K and $\log g = 3.95$ (Adelman 1994a,b), Stark broadening data for C II, Mg II, Si II, and Ca II lines (Sahal-Bréchot 1969a,b; Chapelle & Sahal-Bréchot 1970; Lanz et al. 1988) have been used, which shows the usefulness of such data for A-type star spectra analysis.

The particularity of neutral cadmium is that the line 6438.4696 Å, $5p\ ^1P^\circ_1$–$5d\ ^1D_2$ is the fundamental wavelength on which other standards are based. Moreover, neutral cadmium is important in analytical spectrochemistry because of its significance in toxicological and environmental studies.

The first experimental investigations of the influence of the Stark broadening mechanism on cadmium lines were performed by Nagibina (1958) and by Gorodnichyute & Gorodnichyus (1961). Here, the experimental results obtained by Kusch & Oberschelp (1967) are of interest. Also, the first theoretical determination was by Grechikhin (1969), and in our case we will use the results obtained by Dimitrijević & Konjević (1983) for comparison.

Stark broadening of cadmium lines is also useful when considering of regularities and systematic trends, and the corresponding results may be of interest in astrophysics for interpolation of new data and critical evaluation of existing ones. We note here that the first investigation of regularity in spectral series was that of Wiese & Konjević (1982).

Here, we use the semiclassical perturbation approach (Sahal-Bréchot 1969a,b) to calculate the Stark broadening parameters of 33 Cd I singlets and 37 triplets as a function of electron density for temperatures between 2500 K and 50 000 K, which are particularly interesting for stellar investigation. The results obtained are then used for analysing of the influence of Stark broadening in A-type stellar atmospheres.

2. Results and discussion

For neutral cadmium lines Stark broadening parameters (the full line width at half maximum – W and the line shift – d) were calculated by using the semiclassical perturbation formalism (Sahal-Bréchot 1969a,b). This formalism, as well as the corresponding computer code, has been updated and optimized several times (Sahal-Bréchot 1974, 1991; Fleurier et al. 1977; Dimitrijević & Sahal-Bréchot 1984; Dimitrijević et al. 1991; Dimitrijević & Sahal-Bréchot 1996). A brief review of the calculation procedure, with discussion of updatings and validity criteria is given by Dimitrijević (1996). The atomic energy levels needed for the calculations were taken from Moore (1971). The oscillator strengths were calculated within the Coulomb approximation (Bates & Damgaard 1949; and the tables of Oertel & Shomo 1968). For higher levels, the method of van Regemorter et al. (1979) was used.

In Tables 1 and 2 (available only in the electronic form at the CDS), electron-, proton-, and He II-impact broadening parameters for 33 Cd I singlets (Table 1) and 37 Cd I triplets (Table 2) for perturber densities from 10^{13} cm^{-3} up to

* Tables 1 and 2 are only available in electronic form at the CDS via anonymous ftp to cdsarc.u-strasbg.fr (130.79.128.5) or via http://cdsweb.u-strasbg.fr/cgi-bin/qcat?J/A+A/441/391

Article published by EDP Sciences and available at http://www.edpsciences.org/aa or http://dx.doi.org/10.1051/0004-6361:20052701

Table 3. Experimental Stark widths – W_m, our theoretical results – W_{th}, theoretical results within GBKO approach – $W_{th'}$.

TRANSITION	λ (Å)	W_m(Å)	W_m/W_{th}	$W_m/W_{th'}$
CdI	5085.8	3.67	6.41	6.34
	4799.9	3.84	7.53	6.63
5p ^{3}P°–6s ^{3}S°	4678.2	1.74	3.59	3.00

10^{19} cm^{-3} along with temperatures from 2500 to 50 000 K, are shown. Parameter C (Dimitrijević & Sahal-Bréchot 1984) is also given as an estimate for the maximum perturber density for which the line may be treated as isolated, obtained when C is divided by the corresponding full width at half maximum. For perturber densities lower than the lowest tabulated value, the behavior of the corresponding Stark broadening parameters is linear. The validity of the impact approximation was estimated for data shown in Tables 1 and 2, by checking if the collision volume (V) multiplied by the perturber density (N) is much less than one (Sahal-Bréchot 1969a,b), and in all cases consider the product NV is less than 0.1. When the impact approximation is not valid, the ion broadening contribution may be estimated by using the quasistatic approach (Sahal-Bréchot 1991; or Griem 1974). In the region between, where neither of these two approximations is valid, a unified type theory should be used. For example in Barnard et al. (1974), a simple analytical formula for such a case is given. The accuracy of the results obtained decreases when broadening by ion interactions increases.

We compare our results (see Table 3) for Cd I 5p ^{3}P°–6s ^{3}S° multiplet with existing experimental data (Kusch & Oberschelp 1967). In this experiment Stark widths were determined by using spark discharge tube with $Cd(CH_3)_2$ and $Cd(C_2H_5)_2$ for perturber density normalized at value of 10^{17} cm^{-3} and for temperature of 11 100 K. Also, for the same multiplet there are theoretical results obtained within GBKO approach (Griem et al. 1962) by Dimitrijević & Konjević (1983). Both theoretical results disagree with experimental ones. Konjević et al. (1984a) indicate selfabsorption as a possible reason for this.

In cases where there are no reliable data for Stark broadening, investigation of regularities and systematic trends can quickly estimate missing values, especially if it is not necessary to have high accuracy for each particular line and good accuracy for a large number of lines is sufficient (see e.g. Purić et al. 1980, 1991; Dimitrijević 1982; Wiese & Konjević 1982, 1992; Tankosić et al. 2001).

The regular behavior of spectral line Stark widths in spectral series has been shown first by Wiese & Konjević (1982). This was also investigated by Dimitrijević & Sahal-Bréchot (1984, 1996), Tankosić et al. (2001), and Dimitrijević (2003, 2004). One of the goals is to investigate regularity within a spectral series of Cd I and then obtain an analytical expression that can be useful for estimating new data.

Sarandev et al. (2000) developed an approximate method for estimation of Stark spectral line widths and applied to the determination of spectral line widths for several heavy ions such as Cd I, Ge I, Hg I, Pb I, Rb I, Sn I, Zn I. Estimates were done for T = 20 000 K and N_e = 10^{17} cm^{-3}. For 5p ^{3}P°–6s ^{3}S transition of Cd I, they obtained full line width at half maximum W = 0.58 Å, which is very close to the semiclassical result of Dimitrijević & Konjević (1983), W = 0.62 Å, as well as to our result W = 0.47 Å.

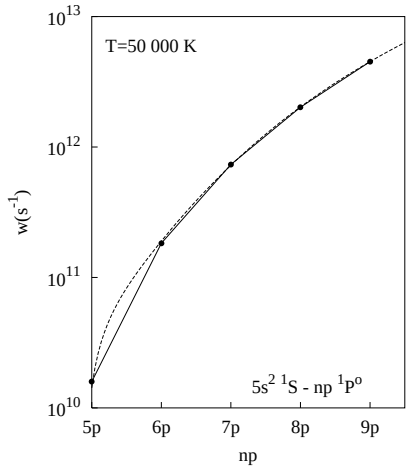

Fig. 1. Electron-impact widths for Cd I 5s^2 ^{1}S–np ^{1}P° spectral series in angular frequency units as a function of main quantum number n for the upper atomic energy level.

In Fig. 1 electron-impact full half widths W in angular frequency units, for Cd I 5s^2 ^{1}S–np ^{1}P° lines are shown as a function of quantum number n, for T = 50 000 K at N_e = 10^{16} cm^{-3}. We see a gradual changing in Stark widths within the 5s^2 ^{1}S–np ^{1}P° spectral series. Such regular behavior of Stark widths is the consequence of the gradual change in the energy separations between the initial (upper) level and the principal perturbing levels. This function $W(n)$ has been interpolated using the third power polynominal

$$W(n) = an^3 + bn^2 + cn + d.$$

Here W is a full width at half maximum ($FWHM$) expressed in rad/s per electron, and constants are $a = 6.83417 \times 10^{10}$, $b = -1.05083 \times 10^{12}$, $c = 5.15558 \times 10^{12}$, and $d = -9.83561 \times 10^{12}$. The polynomial function is represented by a dotted line in Fig. 1. Using the previous expression, it is estimated that the Stark width for the Cd I 5s^2 ^{1}S–10p ^{1}P° spectral line for which there is no enough atomic data is $W = 8.564 \times 10^{12}$ s^{-1} i.e. W = 0.911 Å.

One of our aims here is to use the results to investigate the influence of Stark broadening within a spectral series in A-type stellar atmospheres. Consequently, Stark widths within the 5s^2 ^{1}S–np ^{1}P° spectral series were compared in Fig. 2 with Doppler widths for a model (T_{eff} = 10 000 K, log g = 4) of an A-type stellar atmosphere (Kurucz 1979), close to the conditions for 68 Tauri (T_{eff} = 9025 K, log g = 3.95) where Stark broadening is of interest for the atmosphere modelisation (Adelman 1994a,b). We note also that one of the lines (2288.7 Å) within the first member of this series, the multiplet 5s^2 ^{1}S–5p ^{1}P°, has an intensity of 1500 according to the NIST Atomic Spectra Database. Our results are presented as a function of Rosseland optical depth – log τ. With an increasing the principal quantum number the importance of Stark broadening in comparison to the Doppler width increases as well. For lines

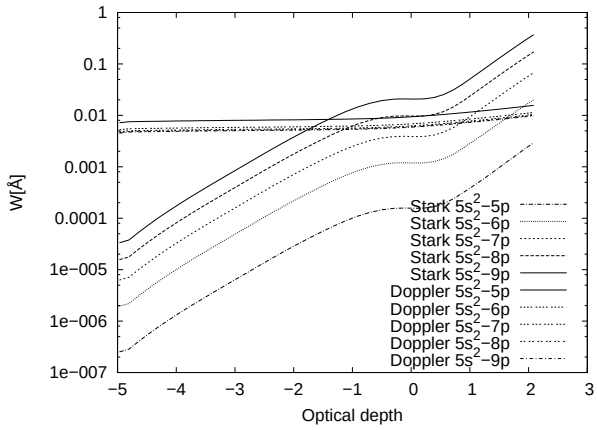

Fig. 2. Thermal Doppler and Stark widths for Cd I singlet spectral lines: $5s^2\ ^1S-5p\ ^1P^\circ$ (2288.7 Å), $5s^2\ ^1S-6p\ ^1P^\circ$ (1669.3 Å), $5s^2\ ^1S-7p\ ^1P^\circ$ (1526.9 Å), $5s^2\ ^1S-8p\ ^1P^\circ$ (1469.4 Å), $5s^2\ ^1S-9p\ ^1P^\circ$ (1440.2 Å) as a function of optical depth.

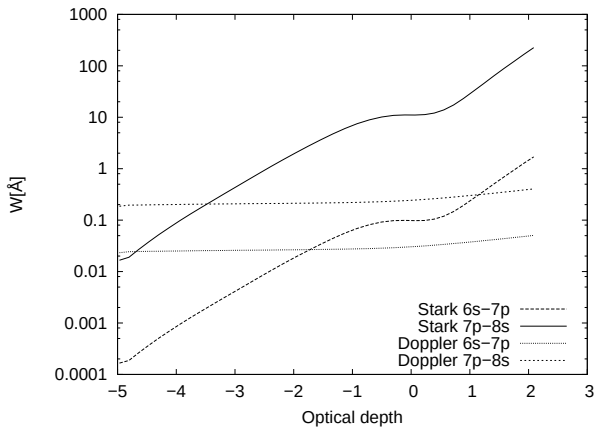

Fig. 3. Thermal Doppler and Stark widths for Cd I triplet spectral line: $6s\ ^3S^\circ$–$7p\ ^3P^\circ$ (7400.9 Å) and $7p\ ^3P^\circ$–$8s\ ^3S^\circ$ (59 346.5 Å) as a function of optical depth.

with higher initial quantum number, Stark broadening is more than one magnitude larger than the Doppler mechanism.

This model for the stellar atmosphere has been used for two other spectral lines, the first (7400.9 Å) in the optical range and the second (59 346.5 Å) in the IC range (see Fig. 3). It is interesting to see in Fig. 3, that the Stark broadening mechanism is absolutely dominant in comparison with the thermal Doppler mechanism throughout the considered stellar atmosphere layers ($\log \tau > -3.5$) for the 59 346.5 Å line. This is the consequence of the fact that infrared spectral lines originate from transitions with longer wavelengths than the lines in UV and optical ranges, and the corresponding Stark broadening, proportional to the square of the wavelength, is larger in comparison to the Doppler one, which is proportional to λ.

For the atmosphere model considering, the Stark broadening effect should be taken into account in abundance determinations and other investigations of stellar plasmas.

Acknowledgements. This work is part of the project GA 1195 "Influence of collisional processes on astrophysical plasma lineshapes", supported by the Ministry of Science and Environment Protection of Serbia. The research was also supported by the Fonds zur förderung der wissenschaftlichen Forschung (Project S7303-AST).

References

Adelman, S. J. 1994a, MNRAS, 266, 97
Adelman, S. J. 1994b, MNRAS, 271, 355
Barnard, A. J., Cooper, J., & Smith, E .W. 1974, J. Quant. Spectrosc. Radiative Transfer, 14, 1025
Bates, D. R., & Damgaard, A. 1949, Phil. Trans. Roy. Soc. London, Ser. A, 242, 101
Cowley, C. R., Ryabchikova, T., Kupka, F., et al. 2000, MNRAS, 317, 299
Chapelle, J., & Sahal-Bréchot, S. 1970, A&A, 6, 415
Dimitrijević, M. S. 1982, A&A, 112, 251
Dimitrijević, M. S. 1996, Zh. Prikl. Spektrosk., 63, 810
Dimitrijević, M. S., & Konjević, N. 1983, J. Quant. Spectrosc. Radiat. Transfer, 30, 45
Dimitrijević, M. S., & Sahal-Bréchot, S. 1984, J. Quant. Spectrosc. Radiat. Transfer, 31, 301
Dimitrijević, M. S., & Sahal-Bréchot, S. 1996, Phys. Scr., 54, 50
Dimitrijević, M. S., Sahal-Bréchot, S., & Bommier, V. 1991, A&AS, 89, 581
Dimitrijević, M. S., Dačić, M., Cvetković, Z., & Sahal-Bréchot, S. 2003, A&A, 400, 791
Dimitrijević, M. S., Dačić, M., Cvetković, Z., & Simić, Z. 2004, A&A, 425, 1147
Fleurier, C., Sahal-Bréchot, S., & Chapelle, J. 1977, J. Quant. Spectrosc. Radiative Transfer, 17, 595
Gorodnichyute, M. G., & Gorodnichyus, G. A. 1961, Litov. Fiz. Sb., 1, 163
Grechikhin, L. I. 1969, J. Appl. Spectrosc., 11, 870
Griem, H. R. 1974, Spectral Line Broadening by Plasmas (New York: Academic Press)
Griem, H. R., Baranger, M., Kolb, A. C., & Oertel, G. K. 1962, Phys. Rev., 125, 177
Konjević, N., Dimitrijević, M. S., & Wiese, W. L. 1984a, J. Phys. Chem. Ref. Data, 13, 619
Kurucz, R. L. 1979 ApJS, 40, 1
Kusch, H. J., & Oberschelp, E. 1967, Z. Astrophys., 67, 77
Lanz, T., Dimitrijević, M. S., & Artru, M.-C. 1988, A&A, 192, 249
Leckrone, D. S., Proffitt, C. R., Wahlgren, G. M., Johansson, S. G., & Brage, T. 1999, AJ, 117, 1454
Moore, C. E. 1971, Atomic Energy Levels, Circular 467, Vol. III (Washington D.C.: US Department of Commerce, NBS, Government Printing Office)
Nagibina. 1958, Opt. Spek., 4, 430
Oertel, G. K., & Shomo, L. P. 1968, ApJS, 16, 175
Purić, J., Lakićević, I., & Glavonjić, V. 1980, Phys. Lett. A, 76, 128
Purić, J., Ćuk, M., Dimitrijević, M. S., & Lesage, A. 1991, ApJ, 382, 353
Sahal-Bréchot, S. 1969a, A&A, 1, 91
Sahal-Bréchot, S. 1969b, A&A, 2, 322
Sahal-Bréchot, S. 1974, A&A, 35, 321
Sahal-Bréchot, S. 1991, A&A, 245, 322
Sarandev, E. V., Konovalova, C. A., & Salakhov, M. Kh. 2000, J. Quant. Spectrosc. Radiative Transfer, 67, 110
Tankosić, D., Popović, L.Č., & Dimitrijević, M. S. 2001, Phys. Scr., 63, 54
van Regemorter, H., Hoang Binh Dy, & Prud'homme, M. 1979, J. Phys. B, 12, 1073
Wiese, W. L., & Konjević N. 1982, J. Quant. Spectrosc. Radiat. Transfer, 28, 185
Wiese, W. L., & Konjević N. 1992, J. Quant. Spectrosc. Radiat. Transfer, 47, 185

1977A&A....54..837P

Astron. Astrophys. 54, 837—840 (1977)

ASTRONOMY AND ASTROPHYSICS

Stark Broadening of F II and Cl III Lines*

M. Platiša, M. Dimitrijević, M. Popović and N. Konjević
Institute of Physics, 11001 Beograd, P.O. Box 57, Yugoslavia

Received June 3, 1976

Summary. A pulsating low pressure arc was the plasma source used to measure, on a shot-by-shot basis, the profiles of 5 lines of singly ionized fluorine and 15 lines of doubly ionized chlorine. An electron density of $5.8\ 10^{16}\ \mathrm{cm}^{-3}$ was determined by laser interferometry while an electron temperature of 24200 K was deduced from a Boltzmann plot of relative intensities of Cl III lines. The experimental F II and Cl III Stark profile half-widths were compared with the values calculated by using various approximations of the semiclassical theoretical approach.

Key words: atomic physics — spectral line broadening

Introduction

The available data on experimental Stark broadening of singly and multiply ionized atom lines has been recently evaluated critically by Konjević and Wiese (1976) and earlier by Griem (1974). In both reviews one can notice that reliable experimental results for singly ionized atoms from some elements are missing completely, even in the two first periods of the periodic system of elements: alkaline metals, boron, fluorine and neon. The situation with multiply ionized atoms is even worse and one can only find experimental data for some lines of C III and C IV (Bogen, 1972), Si III (Purić et al., 1974), A III and A IV (Platiša et al., 1975a), N III (Popović et al., 1975), O III (Platiša et al., 1975b).

The intention of this work is to supply Stark broadening data for some prominent lines of F II and Cl III. The experimental results will be compared with available theoretical results (Griem, 1974) and calculated values obtained by various theoretical approximations.

Send offprint requests to: Dr. M. Platiša

* This work was partially performed under a grant from U.S. National Bureau of Standards

Calculations of the Line Widths

Most of the details and further references for the theoretical calculations can be found in our previous paper (Platiša et al., 1975a). For completeness we shall only state the semi-classical theoretical approaches that were employed: a) hyperbolic perturber-path approximation (Baranger, 1962), b) combination of hyperbolic and straight perturber path approximation with all the sophistications used by Cooper and Oertel (1967 and 1969) and c) Griem's (1968) semiempirical formula.

Data for atomic energy levels necessary for these computations were taken from Palenius (1968) for F II and from Edlen (1970) and Moore (1971) for Cl III.

Experimental Apparatus and Procedure

The experimental apparatus and procedure were described in more detail previously (Konjević et al., 1971; Platiša et al., 1975a). The plasma sources was a low pressure (0.1 Torr) pulsed arc 20 cm long with Pyrex discharge tube 24 mm i.d. The light from the pulsed arc was observed end-on and shot-by-shot with a 1 m-monochromator, McPherson, Model 2051 (inverse linear dispersion in the first order 4.15 Å/mm) equipped with photomultiplier tube EMI 6255 B. The instrumental half-width with 10 μ slits was 0.047 Å.

In order to obtain optically thin lines of F II and Cl III, freon 12 was diluted with argon. The ratio 1:11 was determined after a number of experiments in which freon 12 was gradually diluted while line shapes and line intensities within multiplets were carefully observed. Two criteria were used to determine when to stop further dilution: a) line intensities within multiplets should agree within 5% with the values derived from transition probability data given by Wiese et al. (1966 and 1969) and b) the line intensity should start to decrease while the line width remains constant for the strongest lines in the investigated spectrum. Here, it should be noted that with high dilution ratios (1:6 to 1:11) plasma parameters (electron density and tempera-

© European Southern Observatory • Provided by the NASA Astrophysics Data System

1977A&A....54..837P

ture), at constant pressure, do not change within the limits of statistical measurement errors.

The observed line shapes of F II and Cl III lines result from two broadening mechanisms in the plasma, Stark and Doppler effects combined with instrumental broadening. The influence of other types of broadening mechanisms (Van der Waals and resonance broadening) can be neglected in our pulsed arc operating at low pressure (see e.g. Griem, 1964).

Stark profiles were deduced from experimental ones using standard deconvolution procedures for gaussian and dispersion profiles (Davies and Vaughan, 1963). Since Doppler broadening was not negligible, in particular for fluorine lines, the gaussian part of the experimental profile consisted of two parts: the instrumental profile and the line width due to the motion of emitters in the plasma. Therefore, knowing the instrumental width, it was also possible to deduce the ion temperature in the plasma. Here, it should be mentioned that there is good agreement (within the limits of experimental error) between deduced temperature and that obtained from relative line intensities. This indicates that the ion and electron temperatures are the same, for the present experimental conditions, at the peak of the electron density in our pulsed discharge and at the same time justifies the LTE assumption used for electron temperature determination.

Finally it should be noted that the experimental results for F II and Cl III lines given in Tables 1 and 2 were obtained axially, end-on from the discharge vessel, which was filled up to 0.10 Torr with freon 12-argon mixture at a ratio 1:11.

Plasma Diagnostics

A helium-neon laser interferometer with a plane external mirror was used to determine the axial electron density. Interferometric fringes at 6328 Å were detected by a photomultiplier placed behind the monochromator to separate the signal from plasma radiation. The peak

Table 1. Experimental F II full half-widths in Å units compared with the theoretical values of Jones et al. (1971) (W_G) and calculated values obtained by using various theoretical approaches: Baranger (1962) (W_B), Cooper and Oertel (1967 and 1969) (W_{CO}) and Griem (1968) (W_{SE})

Transition array	Designation (mult. No.)	Wavelength (Å)	W_m (Å)	W_G (Å)	W_B (Å)	W_{CO} (Å)	W_{SE} (Å)	α	$\Delta S/S$
$2p^3 3s - 2p^3(^4S^0)3p$	$^5S^0 - ^5P$	3847.10	0.11_8	0.113	0.171	0.118	0.132	0.0110	−0.09
	(1)	3849.99	0.11_7	0.113	0.171	0.118	0.132	0.0110	−0.09
$2p^3 3s' - 2p^3(^2D^0)3p'$	$^3D^0 - ^3D$	4109.17	0.11_2	—	0.177	0.090	0.147	0.0148	+0.12
	(5)	4119.22	0.11_0	—	0.177	0.090	0.147	0.0148	+0.12
	$^1D^0 - ^1F$	4299.17	0.11_8	—	0.203	0.100	0.171	0.0131	+0.01
	(7)								

Experimental conditions $N_e = 5.8\ 10^{16}\ \mathrm{cm}^{-3}$, $T = 24\,200$ K

Table 2. Experimental Cl III full half-widths in Å units compared with calculated values obtained by using various theoretical approaches: Baranger (1962) (W_B), Cooper and Oertel (1967 and 1969) (W_{CO}) and Griem (1968) (W_{SE})

Transition array	Designation (mult. No.)	Wavelength (Å)	W_m (Å)	W_B (Å)	W_{CO} (Å)	W_{SE} (Å)	α	$\Delta S/S$
$3p^2 3d - 3p^2(^3P)4p$	$^4P - ^4P^0$	4018.50	0.11_1	0.098	0.070	0.130	0.0052	−0.26
	(7)	4059.07	0.10_9	0.098	0.070	0.130	0.0052	−0.26
		4106.83	0.11_5	0.098	0.070	0.130	0.0052	−0.26
$3p^2 4s - 3p^2(^3P)4p$	$^4P - ^4D^0$	3602.10	0.10_6	0.097	0.056	0.126	0.0108	−0.06
	(1)	3612.85	0.10_3	0.097	0.056	0.126	0.0108	−0.06
		3656.95	0.10_3	0.097	0.056	0.126	0.0108	−0.06
		3705.45	0.09_9	0.097	0.056	0.126	0.0108	−0.06
	$^4P - ^4P^0$	3283.41	0.09_7	0.085	0.049	0.109	0.0124	0.00
	(2)	3289.80	0.09_7	0.085	0.049	0.109	0.0124	0.00
		3340.42	0.10_0	0.085	0.049	0.109	0.0124	0.00
	$^4P - ^4S^0$	3191.45	0.09_6	0.070	0.039	0.100	0.0104	−0.06
	(3)							
	$^2P - ^2D^0$	3748.81	0.10_8	0.092	0.053	0.114	0.0146	−0.25
	(5)							
$3p^2 4s' - 3p^2(^1D)4p'$	$^2D - ^2F^0$	3530.03	0.10_5	0.089	0.053	0.109	0.0183	−0.23
	(10)							
	$^2D - ^2D^0$	3392.89	0.08_5	0.097	0.057	0.113	0.0120	+0.04
	(11)	3393.45	0.08_1	0.097	0.057	0.113	0.0120	+0.04

Experimental conditions $N_e = 5.8\ 10^{16}\ \mathrm{cm}^{-3}$, $T_e = 24\,200$ K

© European Southern Observatory • Provided by the NASA Astrophysics Data System

1977A&A....54..837P

electron density was $5.8\ 10^{16}\ \mathrm{cm}^{-3}$ with an estimated error not exceeding $\pm 7\%$.

The electron temperature of 24200 K $\pm 10\%$ was determined from the Boltzmann plot of the relative intensities of Cl III lines (3191.45, 3289.80, 3393.45, 3530.03, 3612.85, 3748.81 Å), assuming thermal equilibrium (Griem, 1964), the transition probabilities being those of Wiese et al. (1969). For these measurements the spectral response of the photomultiplier-monochromator system was calibrated against a standard tungsten coiled-coil quartz iodine lamp. The quoted electron density and temperature were taken at the peak of electron density.

Results and Discussion

Experimentally determined full halfwidths of F II and Cl III lines in Å units at an electron concentration of $5.8\ 10^{16}\ \mathrm{cm}^{-3}$ and electron temperature of 24200 K are given in Tables 1 and 2. The estimated errors of these line widths are typically $\pm 17\%$ for F II and $\pm 15\%$ for Cl III lines. These errors do not include uncertainties in electron density and temperature measurements.

For the same experimental conditions three sets of theoretical data were calculated and are also given in the tables. Semiclassical results for the line widths according to the theory of Baranger (1962) with hyperbolic perturber-path trajectories are introduced in the tables under W_B. The results obtained from the combination of Baranger's approach with the GBKO straight perturber path approximation for high perturber velocities (Cooper and Oertel, 1967 and 1969) are introduced in the tables under W_{CO} and the results evaluated from Griem's semiempirical formula are given under W_{SE}. For the first multiplet of F II in Table 1, under W_G, is also given the theoretical results obtained from semiclassical, hyperbolic perturber path calculations by Jones et al. (1971) published later and also in the Griem's book (1974).

An attempt is made to estimate the contribution of ion broadening to the total line width. Therefore, the ion broadening parameter α is calculated (Griem, 1964) and the results are given in the tables. It was found that the contribution of ion broadening to the total line width, in our experimental conditions, was of the order of 1%.

In order to illustrate the completeness of the sets of perturbing energy levels in regard to the dipole matrix elements, the parameter $\Delta S/S$ is introduced, for each particular line in the tables, as defined by Jones et al. (1971):

$$\frac{\Delta S}{S} = \left\{ \sum_{i'} |\langle i|\boldsymbol{R}|i'\rangle|^2 + \sum_{f'} |\langle f|\boldsymbol{R}|f'\rangle|^2 - R^2 \right\} R^{-2}$$

where $|\langle j|\boldsymbol{R}|j'\rangle|^2$ is the square of the matrix element of the electron position vector calculated by Coulomb approximation (Bates and Damgaard, 1949; Oertel and Shomo, 1968) and R^2 is obtained from the usual sum rule for a complete set of states:

$$R^2 = \frac{n_i^{*2}}{2Z^2}\left[5n_i^{*2} + 1 - 3l_i(l_i+1)\right] + \frac{n_f^{*2}}{2Z^2} \cdot \left[5n_f^{*2} + 1 - 3l_f(l_f+1)\right]$$

where $n_{i,f}^*$ and $l_{i,f}$ are effective principal and orbital quantum numbers for initial and final states respectively and Z is the ionization stage.

The agreement between experiment and the theoretical semiclassical calculations W_G and W_{CO} for singly ionized fluorine (Table 1) is well within the limits of experimental error, while the results based on Baranger's theoretical approach W_B are systematically higher. However, for Cl III (Table 2) experimental data agrees well with theoretical results W_B, obtained by using only hyperbolic perturber path trajectories, while W_{CO} are systematically lower. One can make a similar conclusion comparing theory and experiment for A III and A IV (Platiša et al., 1975a). This suggests that the approach of Baranger is much better for higher ionization stages than one can expect on the basis of comparison with the results for singly ionized atoms. This conclusion may be of some practical importance since Baranger's approach offers by far the simplest method to evaluate line widths.

On the basis of the comparison of W_{CO} with experimental results for Cl III, A III and A IV, one can suggest that for higher ionization stages Cooper and Oertel's way of dividing perturber trajectories into hyperbolic for $\varrho'_{\min} > \varrho_{\min}$ [$\varrho'_{\min} = ((Z-1)e^2/mv^2)$ is the Coulomb cutoff and $\varrho_{\min}$ is obtained from the straight line perturber path approximation] and straight $\varrho'_{\min} < \varrho_{\min}$ for higher perturber velocities is not adequate. Therefore, the suggestion that the contribution of the perturbers with small path deflections is overestimated in Baranger's approach (Cooper and Oertel, 1967) is not justified for higher ionization stages.

Finally, from both tables one can notice good agreement between experiment and the results obtained from Griem's semiempirical formula. It is, in particular, in encouragingly good agreement with Cl III experimental data. Similar agreement was also found in the case of C III (Bogen, 1971) and N III (Hey, 1976) which indicates that the applicability of the semiempirical formula may be successfully extended to the higher ionization stage.

Acknowledgement. The authors gratefully acknowledge the interest of Dr. W. L. Wiese for this work.

References

Baranger, M.: 1962, in Atomic and Molecular Processes, edited by D. R. Bates, Academic Press Inc., New York
Bates, D. R., Damgaard, A.: 1949, *Phil. Trans. Roy. Soc. London*, Ser. A **242**, 101
Bogen, P.: 1972, *Z. Naturforsch.* **27**a, 270
Cooper, J., Oertel, G. K.: 1967, *Phys. Rev. Letters* **18**, 985
Cooper, J., Oertel, G. K.: 1969, *Phys. Rev.* **180**, 286

© European Southern Observatory • Provided by the NASA Astrophysics Data System

1977A&A....54..837P

Davies, J.T., Vaughan, J.M.: 1963, *Astrophys. J.* **137**, 1302
Edlen, B.: 1970, Nuclear Instrum. Methods **90**, 1
Griem, H.R.: 1964, Plasma Spectroscopy, McGraw-Hill, New York
Griem, H.R.: 1968, *Phys. Rev.* **165**, 258
Griem, H.R.: 1974, Spectral Line Broadening by Plasmas, Academic Press Inc., New York
Hey, D.J.: 1976, *J. Quant. Spectroscop. Radiat. Transfer* **16**, 575
Jones, W.W., Benett, S., Griem, H.R.: 1971, University of Maryland Technical Report 71—128
Konjević, N., Platiša, M., Purić, J.: 1971, *J. Phys. B. Atom. Molec. Phys.* **4**, 1541
Konjević, N., Wiese, W.L.: 1976, J. Phys. Chem. Ref. Data (in press)
Moore, C.E.: 1971, Atomic Energy Levels National Bureau of Standards, NSRDS-NBS 35, Vol. 1
Oertel, G.K., Shomo, L.P.: 1968, *Astrophys. J. Suppl. Series* **16**, 175
Palenius, H.: 1968, *Arkiv för Fysik* **39**, 15
Platiša, M., Popović, M., Dimitrijević, M., Konjević, N.: 1975a, *Z. Naturforsch.* **30**a, 212
Platiša, M., Popović, M., Konjević, N.: 1975b, *Astron. Astrophys.* **45**, 325
Popović, M., Platiša, M., Konjević, N.: 1975, *Astron. Astrophys.* **41**, 463
Purić, J., Djeniže, S., Labat, J., Ćirković, Lj.: 1974, *Z. Phys.* **267**, 71
Wiese, W.L., Smith, M.W., Glennon, B.M.: 1966, Atomic Transition Probabilities, Vol. 1, Hydrogen Through Neon, U.S. Government Printing Office, NSRDS-NBS 4
Wiese, W.L., Smith, M.W., Miles, B.M.: 1969, Atomic Transition Probabilities, Vol. 2, Sodium Through Calcium, U.S. Government Printing Office, NSRDS-NBS 22

© European Southern Observatory • Provided by the NASA Astrophysics Data System

1978A&A....67..103P

Astron. Astrophys. 67, 103—105 (1978)

ASTRONOMY AND ASTROPHYSICS

Stark Broadening of Ne II Lines*

M. Platiša, M. S. Dimitrijević and N. Konjević

Institute of Physics, 11001 Beograd, P.O. Box 57, Yugoslavia

Received November 3, revised December 12, 1977

Summary. The half-widths of twelve Ne II lines have been measured in a pulsed arc plasma. The electron density of $5.1 \times 10^{16}\,\mathrm{cm}^{-3}$ was determined by laser interferometry while the electron temperature 28300 K was measured from a Boltzmann plot of relative intensities of Ne II lines. When compared with semiclassical and semiempirical theoretical values the experimental Ne II Stark profile half-widths agree within the uncertainty of the theory and the experiment.

Key words: atomic physics — spectral line broadening

Introduction

Reliable theory of the Stark broadening of spectral lines in plasmas is needed for evaluation of line broadening parameters which can be used with the confidence for stellar and laboratory plasma diagnostics and radiative transfer calculations. For the purpose of verification of the present theories numerous experimental attempts have been made to investigate Stark broadening of prominent spectral lines in laboratory plasmas (see e.g. Fuhr et al., 1972, 1974a,b). However, recently published critical review and the tables of selected data (Konjević and Wiese, 1976) indicate that there are no experimental results for Ne II which can be used for the comparison with the theory.

The aim of this work is to furnish Stark broadening data for some prominent Ne II lines and to compare them with the results obtained from semiclassical and semiempirical theoretical approaches.

Experimental Apparatus and Procedure

The experimental apparatus and the procedure are described in more details elsewhere (Konjević et al., 1971 and Platiša et al., 1977). The light source was a low pressure (0.2 mbar), pulsed arc with Pyrex discharge tube 24 mm internal diameter. The distance between electrodes was 20 cm and 1 mm diameter holes are located at the centre of both electrodes to allow axial laser interferometric measurements and end-on plasma observations to be made. During the experiment a continuous flow of nitrogen–neon mixture was maintained at a pressure of about 0.2 mbar.

The light from the pulsed arc was observed end-on and shot by shot with 1 m-monochromator (McPherson, Model 2051, inverse linear dispersion in the first order 4.15 Å/mm) equipped with photomultiplier tube. The instrumental half-width with 10 μm slits was 0.047 Å.

In order to obtain optically thin Ne II lines neon was diluted with nitrogen. The ratio $Ne:N_2 = 1:5$ was determined after a number of experiments in which Ne was diluted gradually. Two criteria were used when to stop further dilution: (a) line intensities within multiplet should agree within 5% with the values derived from transition probabilities (Wiese et al., 1966) and (b) the line intensity should start to decrease while the line width remains constant for the strongest lines in the spectrum investigated. It should be pointed out here that at high dilution ratios plasma parameters (electron density and temperature) at constant pressure and condenser bank energy do not change within the limits of the experimental scatter.

Plasma Diagnostics

A helium–neon laser interferometer with a plane external mirror was used to determine the axial electron density. Interferometric fringes at 6328 Å were detected by a photomultiplier placed behind the monochromator to separate the signal from the plasma radiation. The peak electron density was $5.1 \times 10^{16}\,\mathrm{cm}^{-3}$ with an estimated error not exceeding $\pm 8\%$.

The electron temperature of 28300 K $\pm$ 12% was determined from the Boltzmann plot of the relative intensities of the Ne II lines (3694.22, 3734.54, 3766.29,

Send offprint requests to: M. Platiša

* This work was partially performed under a grant from the U.S. National Bureau of Standards

© European Southern Observatory • Provided by the NASA Astrophysics Data System

1978A&A....67..103P

Table 1. Full-halfwidths in Å units caused by various broadening mechanisms

Multiplet	Natural broad.	Ion. broad.[a]	Doppler	Resonance[b]	Van der Waals[b]
$3s^4P$–$3p^4P^0$ (1)	0.0002	0.0018	0.0997	0.0	$1.42 \times 10^{-20} N_N$
$3s^4P$–$3p^4D^0$ (2)	0.0002	0.0017	0.0895	0.0	$1.16 \times 10^{-20} N_N$
$3s^2P$–$3p^2D^0$ (5)	0.0002	0.0020	0.0995		$1.43 \times 10^{-20} N_N$
$3p^4D^0$–$3d^4F$ (13)	0.0002	0.0036	0.0859	0.0	$1.18 \times 10^{-20} N_N$
$3p^4S^0$–$3d^4P$ (34)	0.0008	0.0042	0.0954	0.0	$1.18 \times 10^{-20} N_N$

Experimental conditions: $N_e = 5.1 \times 10^{16}$ cm^{-3}, $T_{\rm ion} = 28300$ K, $N_N < 1 \times 10^{16}$ cm^{-3}
Transition probabilities taken from Wiese et al., 1966
[a] Evaluated from Griem 1974, Equation 218b
[b] Resonance and van der Waals broadening are calculated from Griem (1964) Equations 4.104 and 4.113 respectively

3355.05, 3297.74, 3713.09, 3727.08) assuming thermal equilibrium (Griem, 1964); the transition probabilities were taken from Wiese et al. (1966).

Both quoted values, for the electron density and the temperature, were taken at the peak of electron density where all the measurements of the line profiles were performed.

Determination of Line Profiles

The experimental line profiles represent the result of the superposition of a Stark profile, an instrumental profile and the profiles induced by other broadening mechanisms. To assess the importance of different broadening processes apart from electron impact Stark broadening, Table 1 gives calculated line widths for various multiplets of Ne II.

From this table it is obvious that apart from electron impact broadening (typical full halfwidth under present experimental conditions is around 0.08 Å) Doppler broadening makes by far the largest contribution to the experimental line width. If one takes into account the initial pressure of nitrogen–neon mixture (0.2 mbar) resonance and van der Waals broadening are found to be negligible. The quadrupole impact broadening however are not completely negligible in comparison with the electron impact broadening.

Therefore, the experimental line profile consists of two parts: dispersion (caused mainly by electron impact and to the smaller extent by ion quadrupole broadening) and Gaussian (caused by Doppler and instrumental broadening). To obtain the Stark profile from measured it was first necessary to use deconvolution procedure for the dispersion and Gaussian profiles as described by Davies and Vaughan (1963). If the natural and the ion linewidth are known it is simple to deduce the electron impact Stark line width from the dispersion part of experimental profile. It should be pointed out here that the natural and the ion line width together did not exceed 5% of the dispersion profile line width.

Since we know intrumental width it was possible to deduce the ion temperature from the Gaussian part of the experimental line width. It was found that the ion temperature and measured electron temperature are the same (within the limits of experimental errors of both measurements) for the present experimental conditions at the peak of the electron density. If we also take into account the relatively high electron concentration ($\sim 5 \times 10^{+16}$ cm^{-3}) it is possible to justify the assumption of partial LTE used for determination of the electron temperature in our plasma (Griem, 1964).

Results and Conclusions

The experimentally determined electron impact full halfwidths of twelve Ne II lines in Å at an electron concentration of 5.1×10^{16} cm^{-3} and electron temperature of 28 300 K are given in Table 2. The estimated errors of these line widths are typically $\pm 17\%$. This estimate does not include uncertainty in the electron density and temperature measurements.

For the same experimental conditions two sets of theoretical data are also given in Table 2. Semiclassical results for the electron impact line width (Jones et al., 1971 and Griem, 1974) are introduced in Table 2 under $W_{\rm SC}$. The results obtained from Griem's (1968) semi-empirical approach are shown in the table under $W_{\rm SE}$.

© European Southern Observatory • Provided by the NASA Astrophysics Data System

1978A&A....67..103P

Table 2. Experimental Ne II electron impact full-halfwidths W_m in Å units compared with the theoretical values of Jones et al. (1971) (W_{SC}) and Griem (1968) (W_{SE})

Transition array	Designation (Mult. No.)	Wavelength	W_m (Å)	W_{SC} (Å)	W_{SE} (Å)
$2p^43s$–$2p^4(^3P)3p$	^4P–$^4P^0$ (1)	3694.22	0.07_2	0.068	0.044
		3734.94	0.07_2		
		3709.64	0.07_1		
		3766.29	0.06_8		
		3777.16	0.07_2		
	^4P–$^4D^0$ (2)	3334.87	0.08_1	0.060	0.037
		3355.05	0.08_3		
		3297.74	0.08_3		
	^2P–$^2D^0$ (5)	3713.09	0.08_2	0.076	0.050
		3727.08	0.08_0		
$2p^43p$–$2p^4(^3P)3d$	$^4D^0$–^4F (13)	3218.21	0.08_8	0.072	0.066
	$^4S^0$–^4P (34)	3542.90	0.09_5	0.097	0.090

Experimental conditions: $N_e = 5.1 \times 10^{16}$ cm^{-3}, $T_e = 28300$ K

Here it should be noted that using semiempirical approach perturbing electron energy levels were treated individually as recommended by Griem (1968) whenever Gaunt factors are away from the threshold value 0.2. All relevant atomic data for Ne II are taken from Persson (1971).

From the comparison between the experiment and semiclassical results (Jones et al., 1971) one can conclude that the agreement is excellent (within 7%) for multiplets 1, 5 and 34. The discrepancy is larger (within 19%) for multiplet 13 while in case of multiplet 2 the disagreement goes up to 28%. It is interesting to notice here that both theoretical approaches (semiclassical and semiempirical) predict in contradiction with the experiment, the Stark line widths for multiplet 2 smaller than for multiplet 1. We cannot find a sound explanation for this discrepancy between the theory and the experiment.

The agreement between semiempirical results and the experiment is worse (with exception of multiplet 34) but still well within 50% as predicted by Griem (1968).

Acknowledgement. The authors gratefully acknowledge the interest of Dr. W. L. Wiese for this work.

References

Davies, J. T., Vaughan, J. M.: 1963, *Astrophys. J.* **137**, 1302
Fuhr, J. R., Wiese, W. L., Roszman, J. L.: 1972, Bibliography on Atomic Line Shapes and Shifts, *Natl. Bur. Std. (U.S.) Spec. Publ.* **366**
Fuhr, J. R., Roszman, L. J., Wiese, W. L.: 1974a, *NBS Spec. Publ.* **366**, Suppl. 1
Fuhr, J. R., Martin, G. A., Specht, B. J.: 1974b, *NBS Spec. Publ.* **366**, Suppl. 2
Griem, H. R.: 1964, Plasma Spectroscopy, McGraw-Hill, New York
Griem, H. R.: 1968, *Phys. Rev.* **165**, 258
Griem, H. R.: 1974, Spectral Line Broadening by Plasmas, Academic Press Inc., New York
Jones, W. W., Benett, S., Griem, H. R.: 1971, University of Maryland Technical Report 71–128
Konjević, N., Platiša, M., Purić, J.: 1971, *J. Phys. B: Atom. Molec. Phys.* **4**, 1541
Konjević, N., Wiese, W. L.: 1976, *J. Phys. Chem. Ref. Data* **5**, 259
Persson, W.: 1971, *Physica Scripta* **3**, 133
Platiša, M., Dimitrijević, M., Popović, M., Konjević, N.: 1977, *J. Phys. B: Atom. Molec. Phys.* to be published
Wiese, W. L., Smith, M. W., Glennon, B. M.: 1966, Atomic Transition Probabilities, Vol. 1, Hydrogen Through Neon, U.S. Government Printing Office, NSRDS-NBS 4

© European Southern Observatory • Provided by the NASA Astrophysics Data System

Astronomical and Astrophysical Transactions (*AApTr*), 2012, Vol. 27, Issue 4, pp. 665–672,
ISSN 1055-6796, Photocopying permitted by license only, ©Cambridge Scientific Publishers

The era of Aries and Kriophoros statues

E. Theodossiou[1*], P. Mantarakis[2†], M.S. Dimitrijević[3‡]

[1] *Department of Astrophysics, Astronomy and Mechanics, Faculty of Physics, University of Athens, Zographou 157 84, Greece*
[2] *22127 Needles St, Chatsworth, California, USA*
[3] *Astronomical Observatory, Volgina 7, 11060 Belgrade, Serbia*

Received 20 November, 2012

We discuss the possibility that the great number of ancient Greek statues of Kriophoros (= 'ram-bearer') before 1 BC may have been the result of religious influence stemming from the knowledge that the constellation of Aries marked the point of vernal equinox rather than Pisces.

Keywords: Constellations; Zodiacal signs; Precession; Vernal equinox; Sculpture

1 Introduction

We will discuss here the possibility of the influence of astronomical knowledge on the commissioning of some Kriophoros ('ram-bearer') statues in Ancient Greece. Namely, in that period (approximately 2000–1 BC), due to the precession of the Earth's axis, the point of vernal equinox, marking the beginning of spring and new life, was in the constellation of Aries (ram), and not Pisces.

In the first part of the paper we will briefly review the Ancient Greek knowledge of constellations and the Earth's orbital precession, and then we will discuss the possibility of the influence of this knowledge on the number of Kriophoros statues.

2 The four seasons and the position of the zodiacal constellations

By the 1st millennium BC, the early Babylonian calendar had evolved from 12 lunar months to an ideal solar year of 12 months, each consisting of 30 days. They had also developed 12 zodiacal constellations (among many others) to mark each month. We know this from a cuneiform list written on a clay tablet (the *mul-Apin* series) that dates to around 700 BC. It was the ancient Greeks, however, who organised and codified the celestial knowledge and tied it to their mythology. The Greek astro-

*Email: etheodos@phys.uoa.gr
†Email: zanispetros@socal.rr.com
‡Email: mdimitrijevic@aob.bg.ac.rs

nomer Eudoxus (*ca.* 390–340 BC) first described the constellations in two works called *Enoptron* ('Mirror') and *Phaenomena* ('Appearances'), neither of which exist today. The Greek poet Aratus of Soli (*ca.* 315–245 BC) wrote a poem, also named *Phaenomena*, which does survive and gives us a complete guide to the constellations as they were known at that time. In his poem, Aratus identified 47 constellations and six individual stars along with a list of their risings and settings. It was the great astronomer Hipparchus (2nd Century BC), however, who created the first star catalogue around 129 BC. To his credit, he: 1) calculated the length of a year to within six and half minutes, 2) devised a coordinate system to plot each star's location, 3) developed a scale to rank star brightness that is still in use today, 4) corrected errors that Eudoxus and Aratus had made and precisely defined all the constellations for the first time, and 5) figured out that the Earth's axis wobbles as it spins, what is called precession.

It is fairly certain that the zodiacal zone was initially conceived in order to mark the annual apparent path of the Sun on the ecliptic. As an aside, Achilles Tatius (3rd century AD) gave the name 'ecliptic', which replaced the previous 'circle among the zodia (zodiacal signs)'. This significant astronomer, philosopher and priest justified the new name based on the fact that whenever the Moon happens to be at the center of the zodiacal zone during one of its synods, an eclipse happens. So the twelve zodiacal constellations were marking the apparent path of the Sun in the sky. And these constellations are twelve because of the fact that the Sun traces approximately 30 degrees per month on the celestial sphere during its apparent annual motion, thus making a complete circle. One should mention that their number was smaller in the beginning. Ovenden (1966) supposed that they were created between 2000 and 3000 BC by the people who lived near the 36° northern geographical latitude. Roy (1984) tried to identify the possible creators of zodiacal constellations, and concluded that the Phoenicians, Egyptians, Babylonians and Minoans were the most likely candidates.

Thanks to long-term and systematic observations, ancient sky watchers were able to associate a view of the starlit sky with the respective seasons of the solar-tropical year. Relating the position of the Sun when it has its maximum altitude with the respective duration of the day and night, or with the azimuth of its rising or setting, they determined four principal points of the apparent annual motion of the Sun on the ecliptic: the two equinoctial points (Υ and Υ') and the two solstices (E and E$'$). The discovery of these four basic positions of the Sun on the ecliptic was very important, since these positions signalled the start and the succession of the four seasons of the year.

Though the origin of some of the constellations (e.g. Gemini and Cancer) can be traced back to the Bronze Age (3300–1200 BC), the first record that we have of a star catalogue which listed numerous constellations dates to around 1000 BC by the Babylonians (Rogers, 1998, pp. 9–28). A 7th century BC copy of the text is preserved on two clay tablets (i.e., *mu-lapin),* that list the names of 66 stars and constellations as well as their rising, setting and culmination dates. Babylonian astronomers divided the ecliptic into twelve segments; each one identified by a different zodiacal sign and constellation. Their calendar began with the new moon following the vernal equinox, which at the time was in the constellation of Aries. The Babylonian constellations were grouped into two distinct sets: one set (called the "divine set") represented various gods and animals while the other represented daily activities,

tools and workers. Thus Aries the Ram was also known as "The Agrarian Worker" (Rogers). For unknown reasons, only the divine set was transmitted and integrated into Greek astronomy. Eudoxus of Cnidus (408–355 BC) described the constellations schematically and ascribed seasonal phases to each in his two works *Phenomena* and *Enoptron* (Treatise on astronomy, discussed by Aratus). Greek astronomers visualized Aries as a ram lying on its side with its head turned up and to the right. The stars Alpha, Beta and Gamma Arietis mark the ram's head and horns. The horns were a symbol of fertility and renewal; thus Aries carried special importance in that it ushered in the beginning of spring.

Prior to the Era of Aries, the vernal equinox occurred in the constellation of Taurus (the Bull). Though there are no records of the knowledge of constellations at this time, it is known that the bull cult of the Minoan Civilization (approximately 3000–1500 BC) coincided with the Era of Taurus. Also, Bronze Age Egyptians, Persians and Assyrians all represented their solar deities with bull-like characteristics.

Over a period of time, the precession of the terrestrial axis led to the constellations shifting position in the sky (known as 'precession of the equinoxes'). A slow but continuous westward shift of the points where the celestial equator intersects the ecliptic occurs such that the Υ, Υ', E and E$'$ shift by approximately 50 arc seconds per year, or 1° every 72 years. Therefore, approximately every 2140 years the zodiacal constellations, which define these four main positions of the solar motion, change, and every 25,800 years every constellation returns to its initial position after a complete cycle.

Table 1 The quartets of the basic zodia (signs) from 6000 BC to 4500 AD.

Era	Spring	Summer	Autumn	Winter
6000–4500 BC	Gemini	Virgo	Sagittarius	Pisces
4500–2000 BC	Taurus	Leo	Scorpius	Aquarius
2000–1 BC	Aries	Cancer	Libra	Capricornus
1–1950 AD	Pisces	Gemini	Virgo	Sagittarius
1950–4500 AD	Aquarius	Taurus	Leo	Scorpius

Table 1 presents the approximate periods when the various equal-length constellations were, are or will be at the equinox and solstice positions. But the earliest constellations were not of equal length, even within a quartet! This fact was supported by Geminus of Rhodes: *'But the signs made up of fixed stars are neither equal in size nor made up of an equal number of stars'* (2006, p. 126). This fact creates considerable scatter in the actual dates. It is also important that these dates are for the equinoctial (or solsticial) Sun appearing inside the limits of the constellations and this is an intrinsically un-observable event. All these led us to the conclusion that there must be more or less a systematic shift of about one epoch in Table 1.

Each constellation quartet assumes the name of the constellation being at the point of the vernal equinox (Υ) during the respective season. But since the ordering of the constellations took place in the first millennium BC, when the constellation of Aries was at the vernal equinox, we generally call (Υ) *the first point of Aries* even today and the symbol (Υ) is actually a depiction of the head and horns of Aries (the Ram).

In the era of Hipparchus, the constellation of Aries was in the first twelfth (0° to 30°) of the zodiacal circle (the sign and the constellation were identical), while

today it is in the last (330° to 360°). Aries was called *Princeps signorum coelestium* (Leader of the Celestial Signs), *Princeps zodiaci* (Leader of the Zodiacal) and *Ductor exercitus zodiaci* (Guide of the Zodiacal Army), while today Pisces has the title of the Leader of the Celestial Host (Allen, 1963, pp. 76, 337).

Middle eastern mythologies were profoundly influenced by this astronomical phenomenon; they assigned to it an intense astrological meaning, taking the entrance of the Sun into each new zodiacal sign as the start of a new solar / cosmic era for the universe. During each one of these periods they assigned to the Sun-god a form corresponding to the zodiacal constellation upon which it was projected. For example, when the vernal equinox was occurring in Aries, the solar deity, Apollo, was represented in the form of a golden-haired shepherd bearing a ram on his shoulders.

3 Kriophoros (Ram-Bearer) statues and the era of Aries

We pose the question: Does the fact that the vernal equinox occurred in the constellation of Aries have anything to do with the number of ancient Greek statues of Hermes Kriophoros? The knowledge of the natural philosophers and astronomers was also shared by the priesthood. Priests possessed the proper astronomical background and they knew well the time periods adopted from the Sun and the Moon, as well as the constellations. This was certainly true after approximately 400 BC (when Eudoxus of Cnidus recorded this knowledge), but it could have come from an earlier age as well. Many of the Greek Kriophoros statues were sculpted in the latter part of the era of Aries. It is possible that the priests who possessed this astronomical knowledge had an influence on the theme of public works and statues at the time.

Ancient Greek sculptors and craftsmen were considered lowly manual laborers. Plutarch (46–120 AD) wrote, in his *Life of Pericles II,* "We admire the work of art but despise the maker of it". This was a common view in the ancient world, and, consequently, artisans relied on commissions from benefactors to create major sculptures. Works could be commissioned by wealthy individuals or by the state, and used in public buildings, temples, or as grave markers (as is frequently shown by inscriptions on the base of the statues). We know, for example, that many of the great works of Phidias were commissioned by Pericles in 447 BC to commemorate Greece's victory against the Persians at the Battle of Marathon (490 BC), and to give thanks to Athena and Zeus for their protection. Regarding the Kriophoros statues, it is our hypothesis that priests, either directly or indirectly (by influencing aristocrats or state officials), commissioned these sculptures to honor both the god Hermes (the Greek equivalent of Mercury) and the Ram (Krios), symbolizing the astronomical beginning of the new spring. A number of Kriophoros statues exist, as for example:

1. The Giant Kriophoros in the Museum of the island Thassos (580 BC, H = 3.5 m)
2. The Archaic or archaizing bronze Hermes Kriophoros from Arcadia in the Boston Museum of Fine Arts, acc. no. 99.489 (520–510 BC, H = 16.7 cm 6 9/16 in)
3. Hermes Kriophoros from Sparta (500 BC). Boston Museum of Fine Arts
4. Hermes Krioforos of Kalamis, V 1010658.JPG. (First half of the 5th century BC) in the Museo Barracco–Roma

5. Hermes Krioforos from Thebes in Boeotia, ca 450 BC (Musée du Louvre)
6. Cleveland Museum of Art. Archaic painted terracotta warrior Kriophoros from Crete, Crete, 7th c. BC, Acc. no. 1998.172
7. Krioforos from Crete (620 BC). Old Museum–Berlin
8. Another one in Berlin: Abb.4. Archaische Hermes Berlin. Statuette. SMPK. INV. 30552.
9. Hermes Krioforos (No 54) and Goddess Relief (No 54), National Archaeological Museum of Athens (Part of a Throne)
10. Hermes Kriophoros (ram-bearer), bronze, Peloponnesian workshop, 550–525 BC. National Archaeological Museum of Athens
11. Archaic Hermes Krioforos in the new Acropolis Museum, Athens, ca 570 BCE, Acc. no. 624
12. Hermes Krioforos ca 450 BC (Museo di Palermo)
13. Hermes Krioforos. Attic black-figure olpe, 515–510 BC. H. 21.30 cm; D. 12.60 cm, Musée du Louvre F159)
14. The stone Krioforos from the Temple of Apollo in Curio Cyprus
15. Hermes Krioforos, from a terracotta relief, British Museum, terracotta room, case C, B 486. [Wilton House Stables, archaizing marble Hermes Kriophoros with a wedge-shaped beard. (Cornelius Vermeule and Dietrich von Bothmer, "Notes on a New Edition of Michaelis: Ancient Marbles in Great Britain Part Two". *American Journal of Archaeology* **60**.4 (October 1956:321–350) p. 347 and pl. 105, fig. 6)].

4 Hermes as protector of flocks

Hermes is mentioned in the *Iliad* as the god that protected the flocks of sheep-and-goats; Hermes had a son, Eudorus, with the Nymph Polymele (= the one with many sheep) and another son with Rhene (the deity of the sheep): Samon, the eponymous hero of Samothrace. Still other sons of Hermes were Polybous (= the one with many cattle, king of Corinth) and the pastoral gods Pan and Priapus.

Arcadians, as a stock-breeding people, prayed to Hermes to favor the proliferation of their flocks; and, since the main breeding animal is the ram, it occupied a vital place in the god's worship in Arcadia. Pausanias writes: *"on the road from Lechaeon to Corinth there is a statue of Hermes with a ram besides him. According to Homer Hermes is the protector god of flocks and their guard. They utter some secret phrase about Hermes and the ram during the initiations of the Mother goddess, but I can't tell it"* (Pausanias, 1935, *Description of Greece* 9.22.1–2).

Hermes is frequently depicted wearing head-dress and seated upon a male goat or holding a ram. According to a Homeric Hymn, he is considered as the patron not only of cattle, sheep, rams and goats, but also of horses, mules and dogs, even of the wild animals. With reference to this identity, the appellations and adjectives describe Hermes as: *Kriophoros, nomios, epimelios, melossoos, agroter, tereuter* and *courotrophos.*

However, despite the fact that Hermes is the protector of almost all domestic animals (cattle, rams, sheep, horses, mules and dogs), as well as of the wild animals, in his statues he is mainly depicted as *Hermes Kriophoros*. This fact is quite impressive given that this is the astronomical era of Aries (i.e. the beginning of spring and the renovation of life commenced when the point of vernal equinox was in the constellation of Aries). This is wholly compatible with our proposition, at least as a hypothesis for further study.

When the flock exits the sheep-cote, the ram goes in front and leads the other animals: the ram is the leading animal that through its fertilizing power conserves and multiplies the life of the flock. We could compare this with the position of constellation of Aries at that time, as *Ductor exercitus zodiaci* (Guide of the Zodiacal Army), which is the sign of the spring and the beginning of new cycle of life after winter.

5 Conclusion

We have proposed the hypothesis that one of the possible factors contributing to the number of statues of Hermes Kriophoros in ancient Greece is that the knowledge of the natural philosophers and astronomers was also shared by the priesthood and those who commissioned such statues. Priests possessed the proper astronomical background and they knew well the time periods adopted from the Sun and the Moon, as well as the constellations, and the fact that the constellation of Aries, with the point of vernal equinox, at that time was the sign of the beginning of the new cycle of life – the beginning of spring.

References

Allen, R.H. (1963) *Star Names: Their Lore and Meaning.* (1st edition 1899), Dover Publications, New York.

Geminos' *Introduction to the Phenomena*: *a translation and study of a Hellenistic survey of astronomy* (2006), transl. and commentary by James Evans and J. Lennart Berggren, Princeton University Press, Princeton.

Ovenden, M. (1966) The Origin of the Constellations, *Philosophical Journal*, vol. 3, 1–18.

On-line:
http://books.google.gr/books?id=HPBE3RbeceQC&pg=PA2&lpg=PA2&dq=Geminus,+Introduction+to+Phenomena &source

Pausanias, (1935), *Description of Greece*, Vol. IV: *Arcadia, Boeotia, Phocis and Ozolian Locri,* Books 8. 22–10, trans. by W.H.S. Jones. The Loeb Classical Library No. 297. Heinemann, London.

Rogers, J.H. (1998) "Origins of the ancient constellations", *Journal of British Astronomical Association*, vol. 108, 9–27.

Roy, P., (1984), "The Origin of the Constellations", *Vistas in Astronomy*, vol. 27, 171–197.

Vermeule Cornelius and von Bothmer Dietrich, "Notes on a New Edition of Michaelis: Ancient Marbles in Great Britain Part Two". *American Journal of Archaeology* **60**.4 (October 1956:321–350) p. 347 and pl. 105, fig. 6.

Astronomical and Astrophysical Transactions (*AApTr*), 2013, Vol. 28, Issue 1, pp. 73–78,
ISSN 1055-6796, Photocopying permitted by license only, ©Cambridge Scientific Publishers

The influence of the radiative non-symmetric ion–atom collisions on the stellar atmospheres in VUV region

V.A. Srećković[1*], A.A. Mihajlov[1], Lj.M. Ignjatović[1], M.S. Dimitrijević[2]

[1] *University of Belgrade, Institute of Physics, P.O. Box 57, 11001, Belgrade, Serbia*
[2] *Astronomical Observatory, Volgina 7, 11060 Belgrade Serbia*
and Observatoire de Paris, 92195 Meudon Cedex, France

Received 4 June, 2012

The aim of this work is to draw attention to the processes of radiative charge exchange in non-symmetric ion-atom collisions as a factor of influence on the opacity of stellar atmospheres in VUV region. For that purpose calculations of the spectral absorption coefficients for several ion–atom systems, namely He + H^+ and H + X^+, where X = Na and Li, have been performed. On chosen examples it has been established that the examined processes generate rather wide molecular absorption bands in the VUV region, which should be taken into account for the interpretation of data obtained from laboratory measurements or astrophysical observations. This paper discusses the potential significance of the considered radiative processes for DB white dwarfs and solar atmospheres, as well as for the atmospheres of the so-called lithium stars.

Keywords: Atomic processes — stellar atmospheres

1 Introduction

A series of previous papers studied the influence of the processes of radiative charge exchange in symmetric $H(1s) + H^+$ and $He(1s^2) + He^+(1s)$ collisions and corresponding photo-association/dissociation processes on the opacity of stellar atmospheres. In the hydrogen case, these processes were shown to be important for the atmospheres of the Sun and some DA white dwarfs (Stancil, 1994); in the helium case, for the atmospheres of some DB and DA white dwarfs (Mihajlov and Dimitrijević, 1992; Stancil, 1994). Thus, the mentioned papers made it clear that at least symmetric ion–atom radiative collisions play a significant role in stellar atmospheres. But the question whether some non-symmetric ion–atom radiative processes can also influence the optical characteristics of the considered stellar atmospheres is still open. A detailed study of such non-symmetric processes in connection with stellar atmospheres would require very extensive research, and remains a task for the future. The aim of this short article is to point out at least some objects where such processes could be of

*Email: vlada@ipb.ac.rs

interest, and to show the possible ways of describing their influence. For this purpose it was natural to start from the same DB white dwarfs' and the solar atmosphere (which were considered in previous papers, since adequate models exist for them). In the case of DB white dwarfs we mean models presented in Koester (1980), as well as in Bergeron et al. (1995). The necessary models of the solar atmosphere were described in Vernazza et al. (1981) and Maltby et al. (1986), and in Fontenla et al. (2006, 2009).

The composition of the mentioned models and the previous results for the ion–atom symmetric radiative process suggest that in the considered atmospheres the following non-symmetric absorption processes have to be taken into account

$$\varepsilon_\lambda + \mathrm{HeH}^+ \longrightarrow \mathrm{He}^+ + \mathrm{H}, \tag{1}$$

$$\varepsilon_\lambda + \mathrm{He} + \mathrm{H}^+ \longrightarrow \mathrm{He}^+ + \mathrm{H}, \tag{2}$$

$$\varepsilon_\lambda + \mathrm{H}X^+ \longrightarrow \mathrm{H}^+ + X, \tag{3}$$

$$\varepsilon_\lambda + \mathrm{H} + X^+ \longrightarrow \mathrm{H}^+ + X, \tag{4}$$

where $\mathrm{He}, \mathrm{He}^+, \mathrm{H} \equiv \mathrm{He}(1s^2)$, $\mathrm{He}^+(1s)$ and $\mathrm{H}(1s)$ respectively, HeH^+ and $\mathrm{H}X^+$ are the molecular ions in the corresponding electronic ground states, and X and X^+ are a metal atom and its ground-state ion. In the general case, apart from these absorption processes, the corresponding inverse emission processes should also be considered. However, it can be shown that, under the conditions of plasma taken from the models mentioned above, the significance of such emission processes can be neglected in comparison with other relevant emission processes. In this work we will consider the absorption processes (1) and (2) in connection with DB white dwarfs and solar atmospheres, and the processes (3) and (4) with $X = \mathrm{Na}$ and $X = \mathrm{Li}$ – in connection with the solar and so-called lithium stars' atmospheres.

2 Theoretical remark

The ground and first excited electronic state of the considered molecular ion (HeH^+ or $\mathrm{H}X^+$) will be denoted here by $|1>$ and $|2>$, and the corresponding adiabatic potential curves – by $U_1(R)$ and $U_2(R)$, where R is the internuclear distance. By $D_{12}(R)$ will be denoted the modulus of the dipole matrix element for the transition $|1> \rightarrow |2>$, i.e. $D_{12}(R) = |<1|\mathbf{D}(R)|2>|$, where $\mathbf{D}$ is the operator of dipole moment of AX^+. Keeping in mind the results of the previous papers, we will treat the non-symmetric radiative processes (1)–(4) within the dipole approximation where the data about $U_1(R)$, $U_2(R)$ and $D_{12}(R)$ are sufficient for all the necessary calculations. In accordance with Mihajlov et al. (2007) and Ignjatović et al. (2009) the quantum-mechanical treatment is applied here to the photo-dissociative processes (1) and (3), while the absorption charge exchange processes (2) and (4) are described within the semi-classical approximation.

The efficiencies of the photo-dissociative process (1) and (3) are characterized here by the partial spectral absorbtion coefficients $\kappa_{1,3}^{(a)}(\lambda) = \sigma_{1,3}^{\mathrm{phd}}(\lambda, T) \cdot N_{\mathrm{mi}}$, where $\sigma_{1,3}^{\mathrm{phd}}(\lambda, T)$ is the the photo-dissociation cross-section, and the absorption charge exchange processes (2) and (4) by the coefficients

$$\kappa_{2,4}^{(b)}(\lambda) \equiv \kappa_{2,4}^{(b)}(\lambda; T, N_{\mathrm{a}}, N_{\mathrm{i}}) = K_{2,4}^{(b)}(\lambda, T) N_{\mathrm{a}} N_{\mathrm{i}}, \tag{5}$$

where T, $N_{\rm a}$, $N_{\rm i}$ and $N_{\rm mi}$ denote the local plasma temperature and the densities of the atoms (He or H), ions (H^+ or X^+) and molecular ions (HeH^+ or HeX^+). Assuming the existence of LTE, we will take the photo-dissociation coefficient $\kappa_{1,3}^{(a)}(\lambda)$ in an equivalent form (suitable for further considerations), given by the relations

$$\kappa_{1,3}^{(a)}(\lambda) \equiv \kappa_{1,3}^{(a)}(\lambda; T, N_{\rm mi}) = K_{1,3}^{(a)}(\lambda, T) N_{\rm a} N_{\rm i}, \tag{6}$$

$$K_{1,3}^{(a)}(\lambda, T) = \sigma_{1,3}^{\rm phd}(\lambda, T) \cdot \chi_{1,3}^{-1}(T), \quad \chi_{1,3}(T) = (N_{\rm a} N_{\rm i})/N_{\rm mi}, \tag{7}$$

where the photo-dissociation cross-section and the quantity $\chi_{1,3}(T)$ are determined in a way similar to that in Ignjatović et al. (2009).

The efficiency of the processes (1) and (2), and (3) and (4) together is characterized by the total spectral absorbtion coefficients

$$\kappa_{12}(\lambda) = \kappa_1^{(a)}(\lambda) + \kappa_2^{(b)}(\lambda) = K_{12}(\lambda, T) N_{\rm a} N_{\rm i}, \quad K_{12}(\lambda, T) = K_1^{(a)}(\lambda, T) + K_2^{(b)}(\lambda, T), \tag{8}$$

$$\kappa_{34}(\lambda) = \kappa_3^{(a)}(\lambda) + \kappa_4^{(b)}(\lambda) = K_{34}(\lambda, T) N_{\rm a} N_{\rm i}, \quad K_{34}(\lambda, T) = K_3^{(a)}(\lambda, T) + K_4^{(b)}(\lambda, T), \tag{9}$$

where $K_{1,3}^{(a)}(\lambda, T)$ is given by Eqs. (7).

3 Results and discussion

The data needed for determination of $U_{1,2}(R)$ and $D_{12}^2(R)$ in the case HeH^+ are taken here from Green et al. (1974). For the molecular ions HNa^+ and HLi^+ the values of $U_{1,2}(R)$ and $D_{12}^2(R)$ are obtained here, using the method of calculation described in detail in Ignjatović and Mihajlov (2005).

As the main aim of this work is to draw attention to processes (1)–(4) as factors of influence on the opacity of the stellar atmospheres in UV and VUV region, the spectral absorption coefficients (for Na, Ni = 1) $K_{12}(\lambda, T)$ and $K_{34}(\lambda, T)$, which characterize the total efficiency of the processes (1) and (2), and (3) and (4) respectively, will be determined. The necessary calculations are performed here in accordance with (5)–(9) in the part of the VUV region, namely 70 nm $\leq \lambda \leq$ 170 nm, for several values of T which are relevant for the photospheres of the Sun and of the considered DB white dwarfs.

The behavior of the total spectral absorption coefficients $K_{12}(\lambda, T)$ for 70 nm $\leq \lambda \leq$115 nm and T = 5500 K and 12000 K is shown in Figs. 1 and 2. The first temperature is characteristic of a large part of the solar photosphere, and the second – of a part of the atmosphere of DB white dwarfs with $T_{\rm eff}$ = 12000 K.

The behavior of the total spectral absorption coefficients $K_{34}(\lambda, T)$, in the case of the processes (3) and (4) with X = Na, for 130 nm $\leq \lambda \leq$ 170 nm and T = 4000 K, is shown in Fig. 3. Let us note that the chosen temperature corresponds to a sunspot (see Maltby et al. (1986)).

Finally, taking into account the existence of the so-called lithium stars, intensively discussed in the literature (see North et al., 1998; Shavrina et al., 2003), Fig. 4 shows the behavior of the total spectral absorption coefficients $K_{34}(\lambda, T)$ in the case of processes (3) and (4) with X = Li for the same λ and T as in the case X = Na.

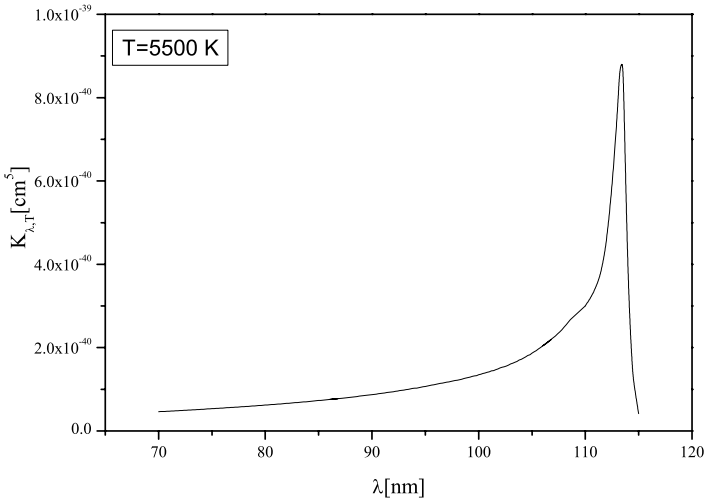

Figure 1 Rate coefficients $K_{\rm ia}(\lambda, T)$ (spectral absorption coefficients for Na, Ni = 1) at $T = 5500$ K, for HeH^+.

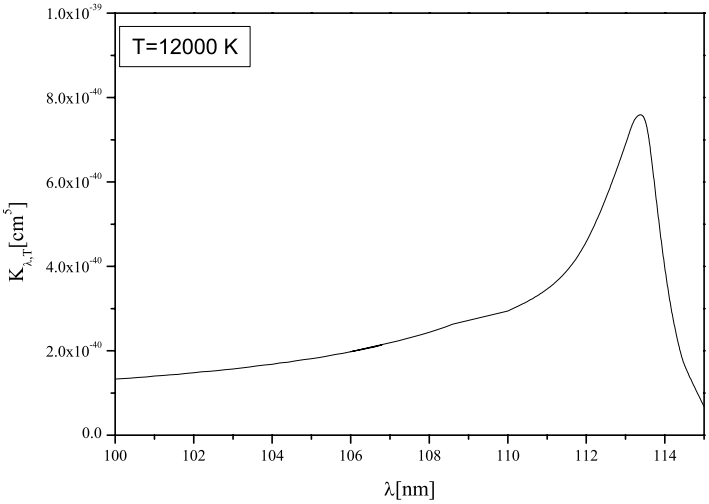

Figure 2 Rate coefficients $K_{\rm ia}(\lambda, T)$ at $T = 12000$ K, for HeH^+.

The presented figures illustrate the fact that the considered non-symmetric processes (1)–(4) generate rather wide molecular absorption bands in the VUV region. Moreover, the comparison of $K_{12}(\lambda, T)$ and $K_{34}(\lambda, T)$ with the corresponding characteristics of other relevant absorption processes (symmetric ion–atom absorption processes etc.), as well as the corresponding particle densities, suggest a conclusion that in the regions of λ which correspond to the most parts of the mentioned bands the efficiency of processes (1)–(4) is at least not negligible, and sometimes it is just these processes that determine the opacity of the considered stellar atmospheres.

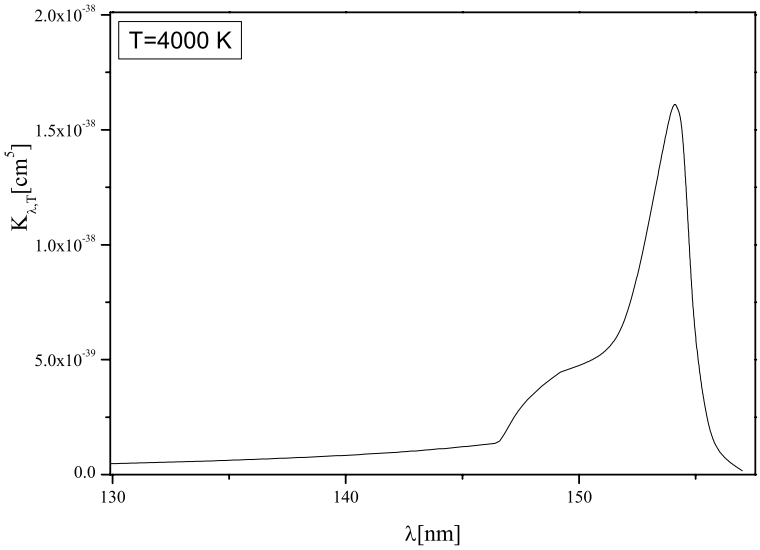

Figure 3 Rate coefficients $K_{\mathrm{ia}}(\lambda, T)$ at $T = 4000$ K, for HNa^+.

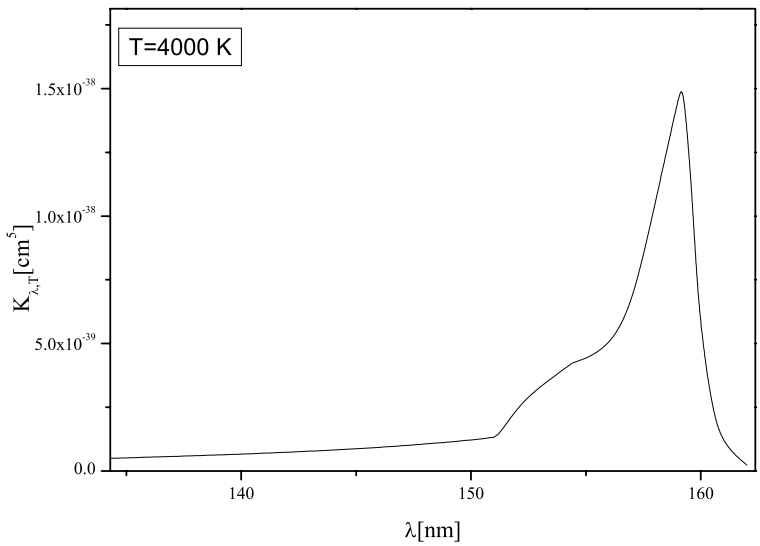

Figure 4 Rate coefficients $K_{\mathrm{ia}}(\lambda, T)$ at $T = 4000$ K, for HLi^+.

Acknowledgments This work was supported by the Ministry of Education, Science and Technological Development of the Republic of Serbia as a part of the projects 176002, III4402.

References

Bergeron, P., Wesemael, F., and Beauchamp, A. (1995). *PASP*, 107:1047–1054.

Fontenla, J. M., Avrett, E., Thuillier, G., and Harder, J. (2006). *ApJ*, 639:441–458.

Fontenla, J. M., Curdt, W., Haberreiter, M., Harder, J., and Tian, H. (2009). *ApJ*, 707:482–502.

Green, T. A., Michels, H. H., Browne, J. C., and Madsen, M. M. (1974). *J. Chem. Phys.*, 61(12):5186–5197.

Ignjatović, L. and Mihajlov, A. A. (2005). *Phys. Rev. A.*, 72:022715.

Ignjatović, L. M., Mihajlov, A. A., Sakan, N. M., Dimitrijević, M. S., and Metropoulos, A. (2009). *MNRAS*, 396:2201–2210.

Koester, D. (1980). *A&AS*, 39:401.

Maltby, P., Avertt, E. H., Carlsson, M., Kjeldseth-Moe, O., Kurucz, R. L., and Loeser, R. (1986). *ApJ*, 306:284.

Mihajlov, A. A. and Dimitrijević, M. S. (1992). *A&A*, 256:305.

Mihajlov, A. A., Ignjatović, L. M., Sakan, N. M., and Dimitrijević, M. S. (2007). *A&A*, 437.

North, P., Polosukhina, N., Malanushenko, V., and Hack, M. (1998). *A&A*, 333:644–646.

Shavrina, A. V., Polosukhina, N. S., Pavlenko, Y. V., Yushchenko, A. V., Quinet, P., Hack, M., North, P., Gopka, V. F., Zverko, J., Žhižnovský, J., and Veles, A. (2003). *A&A*, 409:707–713.

Stancil, P. C. (1994). *ApJ*, 430:360.

Vernazza, J., Avrett, E., and Loser, R. (1981). *ApJS*, 45:635.

ASTRONOMY & ASTROPHYSICS
SUPPLEMENT SERIES

SEPTEMBER **1993**, PAGE 593

Astron. Astrophys. Suppl. Ser. **100**, 593-594 (1993)

Stark-broadening parameters of spectral lines of astrophysical interest of neutral palladium

M.S. Dimitrijević

Astronomical Observatory, Volgina 7, 11050 Beograd, Yugoslavia

Received November 19, 1992; accepted January 4, 1993

Abstract. — Using a semiclassical approach, we have calculated electron-, proton-, and ionized-helium-impact line widths and shifts for 3 neutral palladium multiplets, observed in stellar and solar spectra.

Key words: lines: profiles-atomic and molecular data, Stark broadening

Neutral palladium lines are present in solar spectrum where fifteen lines of this element have been identified (Moore et al. 1966; Biémont et al. 1982). The development of satellite astronomy providing high resolution spectrograms, gives the possibility to determine palladium abundance in stellar atmospheres as well. Recently, Orlov & Shavrina (1991) have analyzed Pd I lines in stellar spectra and particularly 14 Pd I lines observed in the Procyon (α CMi) spectrum (Griffin & Griffin 1979). They have shown that the only line suitable for determining the palladium abundance in stellar atmospheres is the Pd I λ = 3242.70 Å line. Since α CMi is a rather hot star with $T_{\rm eff}$ = 6750 K and log g = 4.0, and since all sky surveys by satellites should provide high resolution spectra for other hot stars with a non negligible influence of electron impacts on spectral line shapes (e.g. hot white dwarfs), it is of interest to provide corresponding Stark broadening data enabling to perform better determination of palladium abundance.

In order to provide such data, we have calculated electron-, proton-, and ionized-helium-impact line widths and shifts for 3 Pd I multiplets by using the semiclassical-perturbation formalism (Sahal-Bréchot 1969ab). A summary of the method is given in Dimitrijević et al. (1991).

The energy levels for Pd I lines have been taken from Moore (1971), and the oscillator strengths have been calculated using the method of Bates & Damgaard (1949) and the tables of Oertel & Shomo (1968). For higher levels, the method described in Van Regemorter et al. (1979) has been applied. For the most critical transitions, the values for oscillator strengths obtained by Biémont et al. (1982) from lifetime measurements by using laser excitation which are combined with branching ratios taken from Corliss & Bozman (1962) have been used. Using available values, the partial average $\bar{f}$ value for 5s − 5p transition array has been formed as

$$\bar{f} = (2\ell + 1)^{-1} \sum (g^2 f / R^2_{\rm mult}\ R^2_{\rm line}) / \sum g,$$

where $R^2_{\rm mult}$ and $R^2_{\rm line}$ are the squares of the corresponding multiplet and line factors of Shore & Menzel (1985).

In addition to the electron-impact full halfwidths and shifts, Stark-broadening parameters due to proton and ionized-helium impacts have been calculated. Thus, we have provided Stark broadening data for the important charged perturbers in stellar atmospheres. Our results are shown in Table 1 for a perturber density of 10^{17} cm^{-3} and temperatures T from 3 000 to 100 000 K. For perturber densities lower than 10^{17} cm^{-3}, all of the corresponding data vary almost linearly with density, because the effect of Debye screening is negligible. We also specify the parameter c (Dimitrijević & Sahal-Bréchot 1984) which gives an estimate for the maximum perturber density for which the line may be treated as isolated, when it is divided by 2W.

For each value given in Table 1, the collision volume (V) multiplied by the perturber density (N) is much less than unity and the impact approximation is valid (Sahal-Bréchot 1969ab). When the impact approximation is not valid, the ion-broadening contribution may be estimated by using quasistatic estimations (Sahal-Bréchot 1991). One should note that the accuracy of the results obtained decreases when broadening by ion interactions becomes important.

We hope that the present results enable a better determination of palladium stellar abundances, especially in the case of white dwarfs and stars of A and B type.

© European Southern Observatory • Provided by the NASA Astrophysics Data System

Acknowledgements. I am indebted to Sylvie Sahal-Bréchot for providing me with the semiclassical computer code.

References

Bates D.R. & Damgaard A. 1949, Trans. Roy. Soc. London, Ser. A 242, 101
Biémont E., Grevesse N., Kwiatkowski N., Zimmerman P. 1982, A&A 108, 127
Corliss C.H. & Bozman W.R. 1962, NBS Monographs 53, Washington D.C.
Dimitrijević M.S. & Sahal-Bréchot S. 1984, JQSRT 31, 301
Dimitrijević M.S., Sahal-Bréchot S., Bommier V. 1991, A&AS 89, 581
Griffin R. & Griffin R. 1979, A Photometric Atlas of the Spectrum of Procyon $\lambda\lambda$ 3140 - 7470 Å, Cambridge, England
Griem H.R. 1974, Spectral Line Broadening by Plasmas (Academic Press, New York)
Moore C.E. 1971, Atomic Energy Levels III, NSRDS-NBS 35, Washington
Moore C.E., Minnaert M.G.J., Houtgast J. 1966, NBS Monograph 61, Washington D.C.
Oertel G.K. & Shomo L.P. 1968, ApJS 16, 175
Orlov M.Ya. & Shavrina A.V. 1991, Sov. Astron. Lett. 17, 227
Sahal-Bréchot S. 1969a, A&A 1, 91
Sahal-Bréchot S. 1969b, A&A 2, 322
Sahal-Bréchot S. 1991, A&A 245, 322
Shore B.W. & Menzel D.H. 1985, ApJS 12, 187
Van Regemorter H., Hoang Binh Dy, Prud'homme M. 1979, J. Phys. B 12, 1073

Table 1. This table shows electron, proton, and ionized-helium impact broadening parameters for neutral palladium multiplets, at a perturber density of 10^{17} cm^{-3} and temperatures from 3 000 to 100 000 K. Transitions and wavelengths (in Å) are also given. By using the parameter c [see Eq. (5) in Dimitrijević & Sahal-Bréchot 1984], we obtain an estimate for the maximum perturber density for which the line may be treated as isolated and tabulated data may be used. Data for densities N lower than 10^{17} cm^{-3} can be obtained by multiplying the results given at 10^{17} cm^{-3} by $N/10^{17}$

PERTURBER DENSITY= 0.1D(+17) cm(-3)

		ELECTRONS		PROTONS		IONIZED HELIUM	
TRANSITION	T(K)	WIDTH(A)	SHIFT(A)	WIDTH(A)	SHIFT(A)	WIDTH(A)	SHIFT(A)
5s3D - 5p3Po	3000.	0.426E-02	0.156E-02	0.251E-02	0.400E-03	0.251E-02	0.317E-03
3629.5 A	5000.	0.451E-02	0.168E-02	0.252E-02	0.439E-03	0.251E-02	0.349E-03
C= 0.19E+20	10000.	0.469E-02	0.167E-02	0.252E-02	0.497E-03	0.252E-02	0.395E-03
	20000.	0.542E-02	0.120E-02	0.253E-02	0.559E-03	0.252E-02	0.446E-03
	50000.	0.787E-02	0.675E-03	0.254E-02	0.654E-03	0.253E-02	0.521E-03
	100000.	0.102E-01	0.389E-03	0.256E-02	0.735E-03	0.253E-02	0.586E-03
5s3D - 5p3Do	3000.	0.443E-02	0.238E-02	0.259E-02	0.641E-03	0.257E-02	0.507E-03
3313.2 A	5000.	0.481E-02	0.270E-02	0.261E-02	0.705E-03	0.258E-02	0.559E-03
C= 0.13E+20	10000.	0.515E-02	0.305E-02	0.262E-02	0.800E-03	0.259E-02	0.636E-03
	20000.	0.589E-02	0.306E-02	0.265E-02	0.904E-03	0.261E-02	0.720E-03
	50000.	0.806E-02	0.212E-02	0.269E-02	0.106E-02	0.263E-02	0.842E-03
	100000.	0.103E-01	0.170E-02	0.274E-02	0.119E-02	0.266E-02	0.948E-03
5s3D - 5p3Fo	3000.	0.385E-02	0.114E-02	0.253E-02	0.308E-03	0.252E-02	0.245E-03
3473.6 A	5000.	0.409E-02	0.118E-02	0.253E-02	0.338E-03	0.252E-02	0.269E-03
C= 0.16E+20	10000.	0.434E-02	0.101E-02	0.253E-02	0.383E-03	0.253E-02	0.305E-03
	20000.	0.510E-02	0.528E-03	0.254E-02	0.431E-03	0.253E-02	0.343E-03
	50000.	0.737E-02	0.650E-04	0.254E-02	0.503E-03	0.253E-02	0.401E-03
	100000.	0.932E-02	-0.162E-03	0.255E-02	0.566E-03	0.254E-02	0.451E-03

© European Southern Observatory • Provided by the NASA Astrophysics Data System

1993A&AS..100..237D

ASTRONOMY & ASTROPHYSICS
SUPPLEMENT SERIES

AUGUST 1993, PAGE 237

Astron. Astrophys. Suppl. Ser. **100**, 237-241 (1993)

Electron-impact widths of four- and five-times charged ion lines of astrophysical importance

M.S. Dimitrijević

Astronomical Observatory, Volgina 7, 11050 Beograd, Yugoslavia

Received August 24; accepted November 20, 1992

Abstract. — Stark widths of astrophysically important spectral lines within 3 C V, 50 O V, 12 F V, 9 Ne V, 3 Al V, 6 Si V, 11 N VI, 28 F VI, 8 Ne VI, 7 Na VI, 15 Si VI, 6 P VI, and 1 Cl VI multiplets, have been calculated by using a modified semi-empirical approach.

Key words: line: profiles-atomic and molecular data — Stark broadening

1. Introduction

Important astrophysical applications of Stark broadening of multiply charged ion spectral lines are in the physics of stellar interiors (Seaton 1987). In subphotospheric layers, the modelling of energy transport requires radiative opacities and thus, certain atomic processes must be known with accuracy. At these high temperatures (10^5 K or more) and densities ($10^{17} - 10^{22}$cm^{-3}) Stark broadening of strong multicharged ionic lines plays a non-negligible role in the calculation of the opacities, especially in the UV. Moreover, with the development of spectroscopic investigations from space, UV and extreme UV spectral line research has been further stimulated.

In order to provide such data for four- and five-times charged ions, comprehensive studies of electron-, proton- and ionized helium-impact broadening parameters for 30 N V (Dimitrijević & Sahal-Bréchot 1992a) and 30 O VI (Dimitrijević & Sahal-Bréchot 1992b) multiplets have been made recently, by using the semiclassical perturbation approach (Sahal-Bréchot 1969ab). In the case of C V, O V, P V and S VI lines, there exist sufficient atomic data for sophisticated semiclassical calculations for some or all astrophysically interesting lines. But, for other four- and five-times charged ions, the atomic data set are not sufficiently complete.

Whenever the semiclassical method is not applicable, e.g., due to the lack of reliable atomic data and the high precision of every particular result is not so important, but a good average accuracy for a large number of lines is required, the modified semi-empirical method (Dimitrijević & Konjević 1980, 1981, 1987; Dimitrijević & Kršljanin 1986; Dimitrijević 1988a) is useful. In order to test the modified semi-empirical approach, selected experimental data for 36 multiplets (7 different ion species) of triply-charged ions were compared with theoretical linewidths. The averaged values of the ratios of measured to calculated widths are as follows (Dimitrijević & Konjević 1980): for doubly charged ions 1.06 ± 0.32 and for triply-charged ions 0.91 ± 0.42. Comparison is made also with the results of comprehensive width calculations for doubly and triply ionized atoms (Dimitrijević & Konjević 1981). The discrepancy did not exceed ±30% on the average (Dimitrijević & Konjević 1987). Moreover, the modified semi-empirical approach has been tested several times on numerous examples (Dimitrijević 1990 and references therein). The width data for the most intense lines for the following atom and ion species are available: Be III, B III, B IV, C III, C IV, N III, N IV, O III, O IV, F III, Ne III, Ne IV, Na III, Mg IV, Al III, Si III, Si IV, P III, P IV, S III, S IV, Cl III, Cl IV, Ar III, Ar IV (Dimitrijević & Konjević 1981; Dimitrijević 1988a). Moreover, width data are published for particular lines of Ti II, Mn II (Dimitrijević 1982), Fe II (Dimitrijević 1988b), Cu IV (Dimitrijević et al. 1989) and shift data for Ar II lines (Kršljanin & Dimitrijević 1989ab).

The aim of this paper is to provide Stark broadening data of astrophysical interest for four- and five-times charged ion lines. In such a way, our intention is to complete such data, together with the published studies for N V and O VI lines (Dimitrijević & Sahal-Bréchot 1992ab) and with studies of C V, O V, P V and S VI lines, which are in preparation. Consequently, in the case of C V and O V, data will be presented here only for such cases for which atomic data set is not sufficient for semiclassical perturbation calculations. Since theoretical errors for

© European Southern Observatory • Provided by the NASA Astrophysics Data System

1993A&AS..100..237D

shifts are considerably larger than for line widths, and since the astrophysical importance of multiply charged ion Stark widths is greater, only width calculations are presented in this article.

2. Results and discussion

Atomic energy levels have been taken from Moore (1980) for O V, Martin & Zalubas (1983) for Si V and Si VI, Martin et al. (1985) for P VI and from Bashkin & Stoner (1975) for other cases. Oscillator strengths have been calculated by using the method of Bates & Damgaard (1949) and the tables of Oertel & Shomo (1968). For higher levels, the method described by Van Regemorter et al. (1979) has been used. In the case of equivalent electrons, the corresponding coefficients of fractional parentage have been taken from Shore & Menzel (1965).

Table 3. Comparison of present results for Stark broadening full half width (WMSE) with values obtained by using the Eq. (526) in Griem (1974) (WG). The electron density is 10^{17} cm^{-3}

ELEMENT/TRANSITION LAMBDA(A)		T(K)	WMSE(A)	WG(A)
C V	3s1S - 3p1P	50000.	1.79	1.63
		100000.	1.57	1.36
	12202.6	200000.	1.46	1.18
	X=56.5	400000.	1.22	1.05
		800000.	1.21	0.949
N VI	2s1S - 2p1P	50000.	0.700E-02	0.812E-02
		100000.	0.516E-02	0.607E-02
	2833.7	200000.	0.420E-02	0.475E-02
	X=2.95	400000.	0.357E-02	0.395E-02
		800000.	0.305E-02	0.349E-02
O V	4p1P -4d1D	50000.	4.35	4.16
		100000.	3.79	3.43
	11913.1	200000.	3.30	2.96
	X=29.2	400000.	2.98	2.64
		800000.	2.81	2.41

Our results for 88 Stark line widths (FWHM) calculated using the modified semi-empirical approach (Dimitrijević & Konjević 1980) – (WMSE) are presented in Table 1 for multiplets with $\lambda > 1000$ Å. Results in the extreme ultraviolet, for 71 multiplets with $\lambda < 1000$ Å, are presented in Table 2. In both tables data are presented for an electron density of 10^{17} cm^{-3} and temperatures from 50,000 to 800,000 K. Data are linear with electron density, but at very high densities Debye screening should be considered (see e.g. Griem 1974). Moreover, for lines with very near perturbing levels broadening by inelastic proton collisions may be also important. The parameter X given in Tables is the maximal argument of all Gaunt factors $g(X)$ for $T = 100,000$ K and gives indications for the extrapolation outside the temperature range presented in Tables. For temperatures outside the Table limits

$$W_2 = (T_1/T_2)^{1/2}\ W_1 \quad \text{for} \quad (T_2/100,000)\,X \leq 2,$$

where T_2 is the actual temperature and T_1 the closest temperature given in Tables.

Comparison of the present values with values calculated by using Eq. (526) in Griem (1974) have been performed, and the obtained agreement is satisfactory. As an example, the comparison for C V $3s^1S - 3p^1P$, N VI $2s^1S - 2p^1P$ and O V $4p^1P - 4d^1D$ cases is presented in Table 3. In comparison with the experiment of Purić et al. (1988) for two O V lines, both approaches give about two times smaller values.

References

Bashkin S. & Stoner J.O. Jr. 1975, Atomic Energy Levels and Grotrian Diagrams, Vol. 1, North Holland, Amsterdam

Bates D.R. & Damgaard A. 1949, Trans. Roy. Soc. London, Ser. A 242, 101

Dimitrijević M.S. 1982, in Sun and Planetary System, eds. W. Fricke & Teleki, Astrophys. and Space Library 96, D. Reidel P.C., Dordrecht, Boston, London 101

Dimitrijević M.S. 1988a, A&AS 76, 53

Dimitrijević M.S. 1988b, in Physics of Formation of Fe II Lines Outside LTE, eds. R. Viotti, A. Vitone, M. Friedjung, D. Reidel P.C. 211

Dimitrijević M.S. 1990, in Accuracy of Element Abundances from Stellar Atmospheres (ed. R. Wehrse), Lecture Notes in Physics 356, (Springer: Berlin- Heidelberg), pp. 31-45

Dimitrijević M.S., Djurić Z. & Mihajlov A.A. 1989, J. Phys. Coll. C 1, Suppl. au No 1, 50 C1-623

Dimitrijević M.S. & Konjević N. 1980, JQSRT 24, 451

Dimitrijević M.S. & Konjević N. 1981, in Spectral Line Shapes, Ed. B. Wende, W. de Gruyter, Berlin, New York, p. 211

Dimitrijević M.S. & Konjević N. 1987, A&A 172, 345

Dimitrijević M.S. & Kršljanin V. 1986, A&A 165, 269

Dimitrijević M.S. & Sahal-Bréchot S. 1992a, A&AS 95, 109

Dimitrijević M.S. & Sahal-Bréchot S. 1992b, A&AS 93, 359

Griem H.R. 1974, Spectral Line Broadening by Plasmas (Academic Press, New York)

Kršljanin V. & Dimitrijević M.S. 1989a, Bull. Obs. Astron. Belgrade 140 (1989) 7

Kršljanin V. & Dimitrijević M.S. 1989b, Z. Phys. D 14, 273

Martin W.C. & Zalubas R. 1983, J. Phys. Chem. Ref. Data 12, 323

© European Southern Observatory • Provided by the NASA Astrophysics Data System

1993A&AS..100..237D

Martin W.C., Zalubas R. & Musgrove A. 1985, J. Phys. Chem. Ref. Data 14, 751
Moore C. 1980, Selected Tables of Atomic Spectra, O V, NSRDS-NBS 3, Section 9, U.S. Govt. Printing Office, Washington D.C
Oertel G.K. & Shomo L.P. 1968, ApJS 16, 175
Purić J., Djeniže S., Srećković A., Platiša M., Labat J. 1988, Phys. Rev. A 37, 498
Sahal-Bréchot S. 1969a, A&A 1, 91
Sahal-Bréchot S. 1969b, A&A 2, 322
Seaton M.J. 1987, J. Phys. B 20, 6363
Shore B.W. & Menzel D.H. 1965, ApJS 12, 187
Van Regemorter H., Hoang Binh Dy & Prud'homme M. 1979, J. Phys. B 12, 1073

© European Southern Observatory • Provided by the NASA Astrophysics Data System

1993A&AS..100..237D

Table 1. Electron impact full half widths (in Å units) of multicharged ion isolated lines with $\lambda > 1000$Å, at an electron density of 10^{17} cm^{-3}. Transitions and averaged wavelengths for the multiplet (in Å units) are also given. The value of X is the maximal argument of all Gaunt factors at $T = 100,000$ K

Transition	Lambda(A)	T(K)=50000	100000	200000	400000	800000	X
C V 3s1S - 3p1P	12202.6	1.79	1.57	1.46	1.22	1.21	56.5
N VI 2s1S - 2p1P	2833.7	0.700E-02	0.516E-02	0.420E-02	0.357E-02	0.305E-02	2.95
N VI 2s3S - 2p3P	1901.5	0.286E-02	0.202E-02	0.158E-02	0.131E-02	0.111E-02	1.98
N VI 3s3S - 3p3P	6596.3	0.282	0.240	0.207	0.180	0.168	14.3
N VI 3p3P - 3d3D	13698.6	0.882	0.744	0.634	0.550	0.551	14.3
O V 3s1S - 3p1P	5115.5	0.168	0.135	0.118	0.103	0.891E-01	5.33
O V 3p1P -3d1D	3145.6	0.472E-01	0.363E-01	0.305E-01	0.261E-01	0.234E-01	5.33
O V 4s1S - 4p1P	16102.3	8.82	7.74	6.72	6.01	5.76	16.8
O V 4p1P -4d1D	11913.1	4.35	3.79	3.30	2.98	2.81	29.2
O V 4p1P -5d1D	1419.0	0.162	0.139	0.118	0.999E-01	0.862E-01	185.
O V 4f1F -5d1D	1709.1	0.209	0.179	0.150	0.128	0.108	185.
O V 3s'1P -3p'1S	2317.5	0.448E-01	0.379E-01	0.327E-01	0.281E-01	0.296E-01	12.7
O V 3s'1P -3p'1P	12183.4	1.15	0.987	0.862	0.740	0.797	12.7
O V 3s'1P -3p'1D	3059.6	0.872E-01	0.736E-01	0.678E-01	0.590E-01	0.572E-01	41.3
O V 3p'1S -3d'1P	8591.5	0.441	0.361	0.305	0.259	0.250	8.96
O V 3p'1P -3d'1P	2146.8	0.248E-01	0.206E-01	0.177E-01	0.150E-01	0.150E-01	12.7
O V 3p'1P -3d'1D	4555.8	0.119	0.985E-01	0.895E-01	0.773E-01	0.713E-01	41.3
O V 3p'1D -3d'1P	4523.9	0.142	0.117	0.108	0.937E-01	0.816E-01	41.3
O V 3d'1D -3p'1D	39582.0	11.4	9.34	9.00	7.90	6.54	41.3
O V 4s3S -4p3P	7431.7	1.53	1.33	1.16	1.03	0.945	16.5
O V 4s3S -5p3P	1243.9	0.949E-01	0.828E-01	0.720E-01	0.640E-01	0.554E-01	29.1
O V 4p3P -5s3S	1662.9	0.152	0.133	0.117	0.102	0.935E-01	16.5
O V 4p3P -5d3D	1418.2	0.135	0.117	0.102	0.899E-01	0.775E-01	48.2
O V 5s3S -5p3P	14706.1	19.1	16.8	14.7	12.9	11.4	29.1
O V 5p3P -5d3D	27944.7	78.8	68.4	59.6	52.7	44.7	48.2
O V 3s'3P -3p'3S	3258.4	0.667E-01	0.530E-01	0.457E-01	0.398E-01	0.348E-01	4.32
O V 3s'3P -3p'3P	2750.4	0.495E-01	0.397E-01	0.342E-01	0.298E-01	0.263E-01	7.11
O V 3s'3P -3p'3D	4131.6	0.107	0.875E-01	0.758E-01	0.661E-01	0.578E-01	6.77
O V 3p'3S -3d'3P	4147.5	0.842E-01	0.663E-01	0.562E-01	0.481E-01	0.428E-01	5.65
O V 3p'3P -3d'3P	5422.1	0.151	0.121	0.102	0.878E-01	0.791E-01	7.11
O V 3p'3P -3d'3D	6817.3	0.240	0.193	0.163	0.139	0.127	7.11
O V 3p'3D -3d'3P	3268.3	0.525E-01	0.426E-01	0.364E-01	0.312E-01	0.277E-01	6.77
O V 3p'3D -3d'3D	3728.2	0.684E-01	0.561E-01	0.477E-01	0.408E-01	0.367E-01	7.11
O V 3p'3D -3d'3F	6489.3	0.201	0.165	0.140	0.120	0.107	6.77
F V 3s2S -3p2P0	2454.2	0.306E-01	0.223E-01	0.182E-01	0.160E-01	0.142E-01	2.82
F V 2p3s2P-2p3p2D	2702.7	0.435E-01	0.352E-01	0.304E-01	0.265E-01	0.230E-01	6.08
F V 3s'2P -3p'2S	2101.4	0.231E-01	0.170E-01	0.139E-01	0.122E-01	0.108E-01	3.16
F V 3s'2P -3p'2P	2450.6	0.308E-01	0.227E-01	0.186E-01	0.164E-01	0.145E-01	3.05
F V 3s'2P -3p'2D	2585.3	0.342E-01	0.252E-01	0.208E-01	0.183E-01	0.162E-01	3.24
F V 3s4P - 3p4S	2241.5	0.259E-01	0.190E-01	0.156E-01	0.137E-01	0.121E-01	2.84
F V 3s4P - 3p4D	2713.2	0.372E-01	0.273E-01	0.225E-01	0.198E-01	0.175E-01	2.83
F V 3s"4P - 3p"4S	2000.5	0.181E-01	0.139E-01	0.118E-01	0.102E-01	0.897E-02	4.05
F V 3s"4P - 3p"4P	2584.3	0.292E-01	0.219E-01	0.182E-01	0.158E-01	0.140E-01	3.25
F V 3s"4P - 3p"4D	3118.4	0.417E-01	0.310E-01	0.257E-01	0.223E-01	0.197E-01	3.25
F VI 3s1S -3p1P	4266.0	0.872E-01	0.682E-01	0.581E-01	0.506E-01	0.434E-01	4.45
F VI 3p1P -3d1D	2562.8	0.231E-01	0.172E-01	0.140E-01	0.120E-01	0.104E-01	4.45
F VI 4s1S -4p1P	9843.5	2.33	2.05	1.80	1.60	1.45	32.2
F VI 4p1P -4d1D	20128.8	8.69	7.60	6.48	5.93	5.43	21.0
F VI 4s'1P -4p'1D	7244.3	2.57	2.09	1.69	1.45	1.16	0.290E+04
F VI 4s'1P -4p'1P	27480.1	20.5	17.9	15.6	14.8	12.6	28.7
F VI 3s3S -3p3P	2320.1	0.244E-01	0.182E-01	0.149E-01	0.131E-01	0.113E-01	4.79
F VI 3s'3P -3p'3S	2665.2	0.336E-01	0.250E-01	0.207E-01	0.180E-01	0.157E-01	3.55
F VI 3s'3P -3p'3P	2281.8	0.252E-01	0.191E-01	0.159E-01	0.139E-01	0.120E-01	5.73
F VI 3s'3P -3p'3D	3420.2	0.545E-01	0.407E-01	0.338E-01	0.293E-01	0.256E-01	3.18
Ne V 3s1P -3p1S	1364.8	0.957E-02	0.733E-02	0.610E-02	0.526E-02	0.462E-02	4.36
Ne V 3s1P -3p1P	3314.7	0.499E-01	0.376E-01	0.314E-01	0.271E-01	0.237E-01	3.46
Ne V 3s1P -3p1D	1716.2	0.145E-01	0.111E-01	0.923E-02	0.797E-02	0.700E-02	3.83
Ne V 3s3P -3p3S	2007.5	0.181E-01	0.129E-01	0.103E-01	0.892E-02	0.787E-02	2.37
Ne V 3s3P -3p3P	1843.4	0.155E-01	0.111E-01	0.886E-02	0.769E-02	0.679E-02	2.37
Ne V 3s3P -3p3D	2269.7	0.229E-01	0.164E-01	0.132E-01	0.115E-01	0.101E-01	2.37
Ne VI 2s2p3s4P-2s2p3p4D	2172.6	0.188E-01	0.134E-01	0.107E-01	0.928E-02	0.808E-02	2.27
Ne VI 2s2p3s4P-2s2p3p4S	1866.8	0.141E-01	0.101E-01	0.801E-02	0.692E-02	0.602E-02	2.38
Ne VI 3s2S -3p2P	2046.4	0.167E-01	0.119E-01	0.948E-02	0.815E-02	0.708E-02	2.32
Ne VI 3s'2P -3p'2S	2270.0	0.153E-01	0.117E-01	0.977E-02	0.843E-02	0.719E-02	4.63
Ne VI 3s'2P -3p'2P	4445.0	0.573E-01	0.446E-01	0.380E-01	0.328E-01	0.279E-01	4.63
Ne VI 3s'2P -3p'2D	1999.3	0.121E-01	0.944E-02	0.806E-02	0.697E-02	0.591E-02	4.80
Na VI 3s1P -3p1D	1422.8	0.690E-02	0.511E-02	0.417E-02	0.357E-02	0.309E-02	3.18
Na VI 3s'1D -3p'1D	2245.6	0.192E-01	0.139E-01	0.110E-01	0.949E-02	0.825E-02	2.70
Na VI 3s3P -3p3P	1542.9	0.862E-02	0.609E-02	0.475E-02	0.401E-02	0.346E-02	1.98
Na VI 3s'3D -3p'3D	4175.5	0.607E-01	0.472E-01	0.392E-01	0.335E-01	0.286E-01	4.35
Al V 3s2P -3p2S	1440.5	0.695E-02	0.491E-02	0.361E-02	0.298E-02	0.261E-02	1.50
Al V 3s4P -3p4S	1187.8	0.455E-02	0.322E-02	0.233E-02	0.186E-02	0.166E-02	1.24
Si V 3s1P -3p1D	1319.6	0.527E-02	0.373E-02	0.271E-02	0.220E-02	0.192E-02	1.38
Si V 3s1P -3p1P	1291.4	0.505E-02	0.357E-02	0.260E-02	0.210E-02	0.184E-02	1.38
Si V 3s3P -3p3S	1496.6	0.641E-02	0.453E-02	0.335E-02	0.276E-02	0.239E-02	1.56
Si V 3s3P -3p3D	1259.1	0.471E-02	0.333E-02	0.245E-02	0.200E-02	0.174E-02	1.56
Si V 3s3P -3p3P	1132.0	0.391E-02	0.276E-02	0.203E-02	0.166E-02	0.145E-02	1.56
Si VI 3s2P -3p2D	1228.5	0.415E-02	0.294E-02	0.212E-02	0.169E-02	0.147E-02	1.28
Si VI 3s2P -3p2P	1165.2	0.375E-02	0.265E-02	0.191E-02	0.152E-02	0.132E-02	1.28
Si VI 3s'2D -3p'2F	1212.1	0.389E-02	0.275E-02	0.198E-02	0.158E-02	0.137E-02	1.26
Si VI 3s'2D -3p'2D	1076.4	0.312E-02	0.220E-02	0.158E-02	0.126E-02	0.109E-02	1.26
Si VI 3s4P -3p4P	1293.5	0.436E-02	0.309E-02	0.224E-02	0.180E-02	0.155E-02	1.35
Si VI 3s4P -3p4D	1133.2	0.343E-02	0.242E-02	0.175E-02	0.141E-02	0.122E-02	1.35
P VI 3s1P -3p1D	1108.8	0.309E-02	0.219E-02	0.156E-02	0.123E-02	0.105E-02	1.16

© European Southern Observatory • Provided by the NASA Astrophysics Data System

1993A&AS..100..237D

Table 2. The same as in Table 1 but for multiplets with $\lambda < 1000$ Å

Transition	Lambda(A)	T(K)=50000	100000	200000	400000	800000	X
C V 1s21S - 3p1P	35.0	0.100E-04	0.881E-05	0.846E-05	0.700E-05	0.660E-05	56.5
C V 2s1S - 3p1P	247.3	0.431E-03	0.372E-03	0.362E-03	0.298E-03	0.266E-03	56.5
N VI 1s21S - 2p1P	28.8	0.418E-06	0.307E-06	0.248E-06	0.208E-06	0.176E-06	2.95
N VI 2s3S - 3p3P	161.2	0.951E-04	0.792E-04	0.676E-04	0.588E-04	0.575E-04	14.3
N VI 2p3P - 3d3D	173.9	0.553E-04	0.447E-04	0.367E-04	0.311E-04	0.312E-04	14.3
N VI 2p3P - 4d3D	130.3	0.368E-03	0.295E-03	0.239E-03	0.199E-03	0.159E-03	0.130E+04
N VI 2p3P - 5d3D	116.8	0.846E-03	0.697E-03	0.577E-03	0.467E-03	0.374E-03	474.
N VI 3p3P - 4d3D	500.9	0.616E-02	0.499E-02	0.408E-02	0.342E-02	0.283E-02	0.130E+04
N VI 3p3P - 5d3D	346.7	0.780E-02	0.644E-02	0.534E-02	0.434E-02	0.352E-02	474.
O V 2s21S - 3p1P	172.2	0.148E-03	0.115E-03	0.978E-04	0.838E-04	0.723E-04	5.33
O V 2s21S - 4p1P	135.5	0.424E-03	0.370E-03	0.320E-03	0.284E-03	0.271E-03	16.8
O V 2p1P -5d1D	154.0	0.153E-02	0.131E-02	0.110E-02	0.921E-03	0.766E-03	185.
O V 3s1S - 4p1P	566.2	0.627E-02	0.543E-02	0.475E-02	0.419E-02	0.398E-02	16.8
O V 3p1P -4s1S	662.9	0.606E-02	0.510E-02	0.437E-02	0.394E-02	0.370E-02	16.8
O V 3p1P -4d1D	604.4	0.641E-02	0.546E-02	0.474E-02	0.433E-02	0.395E-02	29.2
O V 3p1P -5d1D	439.5	0.130E-01	0.111E-01	0.931E-02	0.782E-02	0.652E-02	185.
O V 3d1D - 4p1P	798.3	0.887E-02	0.756E-02	0.649E-02	0.579E-02	0.559E-02	16.8
O V 2p21S -3s'1P	265.6	0.324E-03	0.282E-03	0.246E-03	0.210E-03	0.237E-03	12.7
O V 2p21S -3d'1P	231.8	0.940E-04	0.757E-04	0.617E-04	0.502E-04	0.495E-04	8.96
O V 2p21D -3s'1P	231.1	0.246E-03	0.214E-03	0.187E-03	0.159E-03	0.179E-03	12.7
O V 2p21D -3d'1P	205.1	0.841E-04	0.685E-04	0.564E-04	0.463E-04	0.455E-04	8.96
O V 2p21D -3d'1D	216.0	0.107E-03	0.861E-04	0.808E-04	0.691E-04	0.574E-04	41.3
O V 2p21D -3d'1F	207.8	0.796E-04	0.633E-04	0.516E-04	0.427E-04	0.390E-04	6.60
O V 3s3S -4p3P	529.2	0.508E-02	0.432E-02	0.373E-02	0.333E-02	0.310E-02	16.5
O V 3s3S -5p3P	390.8	0.790E-02	0.686E-02	0.594E-02	0.529E-02	0.454E-02	29.1
O V 3p3P -5s3S	469.1	0.940E-02	0.820E-02	0.722E-02	0.626E-02	0.566E-02	15.3
O V 3p3P -5d3D	447.3	0.110E-01	0.944E-02	0.826E-02	0.724E-02	0.609E-02	48.2
O V 2p23P -3d'3D	203.9	0.110E-03	0.894E-04	0.744E-04	0.624E-04	0.569E-04	7.11
O V 2p23P -3d'3P	202.3	0.107E-03	0.853E-04	0.716E-04	0.603E-04	0.532E-04	5.65
O V 2p23P -3s'3P	227.5	0.177E-03	0.141E-03	0.122E-03	0.106E-03	0.910E-04	4.31
F V 2p3s2P-2p3p2S	154.2	0.734E-04	0.543E-04	0.447E-04	0.384E-04	0.342E-04	3.38
F V 2p3s2P-2p3p2P	162.0	0.710E-04	0.590E-04	0.509E-04	0.439E-04	0.376E-04	6.08
F VI 2s21S -2p1P	535.2	0.295E-03	0.209E-03	0.148E-03	0.105E-03	0.830E-04	0.558
F VI 2s21S -3p1P	126.9	0.606E-04	0.462E-04	0.381E-04	0.324E-04	0.276E-04	4.45
F VI 2s21S -4p1P	99.2	0.173E-03	0.150E-03	0.132E-03	0.119E-03	0.104E-03	32.2
F VI 2p1P -3s1S	173.1	0.841E-04	0.667E-04	0.570E-04	0.491E-04	0.417E-04	4.45
F VI 2p1P -4s1S	123.3	0.169E-03	0.149E-03	0.130E-03	0.111E-03	0.106E-03	10.3
F VI 2p1P -3d1D	121.2	0.232E-04	0.173E-04	0.148E-04	0.121E-04	0.102E-04	55.8
F VI 2p1P -4d1D	121.1	0.140E-03	0.121E-03	0.102E-03	0.931E-04	0.857E-04	21.0
F VI 3s1S -4p1P	410.7	0.266E-02	0.228E-02	0.201E-02	0.184E-02	0.158E-02	32.2
F VI 3p1P -4s1S	476.5	0.297E-02	0.257E-02	0.224E-02	0.191E-02	0.180E-02	10.3
F VI 2p21S -3s'1P	183.9	0.111E-03	0.961E-04	0.831E-04	0.699E-04	0.694E-04	9.48
F VI 2p21S -4s'1P	129.5	0.263E-03	0.228E-03	0.198E-03	0.195E-03	0.159E-03	28.7
F VI 3s'1P -3p'1S	117.6	0.374E-04	0.288E-04	0.242E-04	0.208E-04	0.178E-04	5.56
F VI 3s'1P -3p'1P	123.3	0.364E-04	0.300E-04	0.256E-04	0.217E-04	0.202E-04	9.48
F VI 3s'1P -3p'1D	118.9	0.471E-04	0.384E-04	0.330E-04	0.330E-04	0.270E-04	29.2
F VI 3s'1P -4p'1D	413.5	0.627E-02	0.496E-02	0.392E-02	0.309E-02	0.250E-02	0.290E+04
F VI 3s'1P -4p'1P	431.6	0.275E-02	0.241E-02	0.210E-02	0.188E-02	0.172E-02	10.2
F VI 2p3P -3s3S	153.8	0.566E-04	0.408E-04	0.326E-04	0.285E-04	0.248E-04	2.42
F VI 2p2'3P-3s'3P	161.3	0.685E-04	0.502E-04	0.409E-04	0.354E-04	0.307E-04	2.78
Ne V 2p21S -3s1P	184.7	0.895E-04	0.684E-04	0.575E-04	0.494E-04	0.428E-04	3.46
Ne V 2p21D -3s1P	173.9	0.790E-04	0.605E-04	0.509E-04	0.437E-04	0.379E-04	3.46
Ne V 2p23P -3s3P	167.7	0.686E-04	0.494E-04	0.393E-04	0.342E-04	0.298E-04	2.37
Ne VI 2p34S-2p23s4P	142.5	0.471E-04	0.344E-04	0.278E-04	0.241E-04	0.209E-04	2.69
Ne VI 2p2P -3s2S	138.6	0.404E-04	0.288E-04	0.229E-04	0.196E-04	0.169E-04	2.13
Na VI 2p21S -3s1P	134.5	0.356E-04	0.252E-04	0.186E-04	0.153E-04	0.131E-04	1.48
Na VI 2p21D -3s1P	127.8	0.321E-04	0.227E-04	0.168E-04	0.138E-04	0.118E-04	1.48
Na VI 2p23P -3s3P	123.9	0.301E-04	0.213E-04	0.168E-04	0.141E-04	0.121E-04	1.98
Al V 2p52P -3s2P	130.9	0.325E-04	0.229E-04	0.170E-04	0.139E-04	0.119E-04	1.50
Si V 3s1P -3p1S	873.8	0.258E-02	0.182E-02	0.133E-02	0.107E-02	0.943E-03	1.41
Si VI 2p52P - 3s2P	99.5	0.154E-04	0.109E-04	0.791E-05	0.628E-05	0.541E-05	1.28
Si VI 2p52P - 3d2P	83.2	0.194E-04	0.137E-04	0.969E-05	0.747E-05	0.631E-05	0.935
Si VI 2p52P - 3d2D	83.3	0.193E-04	0.137E-04	0.967E-05	0.748E-05	0.631E-05	0.947
Si VI 2p52P - 3s'2D	96.1	0.139E-04	0.984E-05	0.712E-05	0.564E-05	0.486E-05	1.26
Si VI 2p52P - 3d'2S	80.8	0.178E-04	0.126E-04	0.902E-05	0.710E-05	0.612E-05	1.15
Si VI 2p52P - 3d'2P	80.6	0.179E-04	0.126E-04	0.904E-05	0.710E-05	0.610E-05	1.13
Si VI 2p52P - 3d'2D	80.5	0.179E-04	0.127E-04	0.905E-05	0.711E-05	0.609E-05	1.10
Si VI 3s'2D -3p'2P	931.5	0.241E-02	0.171E-02	0.123E-02	0.976E-03	0.845E-03	1.26
Si VI 3s4P -3p4S	983.8	0.263E-02	0.186E-02	0.134E-02	0.107E-02	0.923E-03	1.35
P VI 3s1P -3p1S	717.0	0.142E-02	0.101E-02	0.719E-03	0.563E-03	0.483E-03	1.16
Cl VI 2s21S - 3p1P	671.4	0.142E-02	0.100E-02	0.711E-03	0.531E-03	0.440E-03	1.30

© European Southern Observatory • Provided by the NASA Astrophysics Data System

1993A&AS..100..593D

ASTRONOMY & ASTROPHYSICS
SUPPLEMENT SERIES

Astron. Astrophys. Suppl. Ser. **100,** 593-594 (1993)

Stark-broadening parameters of spectral lines of astrophysical interest of neutral palladium

M.S. Dimitrijević

Astronomical Observatory, Volgina 7, 11050 Beograd, Yugoslavia

Received November 19, 1992; accepted January 4, 1993

Abstract. — Using a semiclassical approach, we have calculated electron-, proton-, and ionized-helium-impact line widths and shifts for 3 neutral palladium multiplets, observed in stellar and solar spectra.

Key words: lines: profiles-atomic and molecular data, Stark broadening

Neutral palladium lines are present in solar spectrum where fifteen lines of this element have been identified (Moore et al. 1966; Biémont et al. 1982). The development of satellite astronomy providing high resolution spectrograms, gives the possibility to determine palladium abundance in stellar atmospheres as well. Recently, Orlov & Shavrina (1991) have analyzed Pd I lines in stellar spectra and particularly 14 Pd I lines observed in the Procyon (α CMi) spectrum (Griffin & Griffin 1979). They have shown that the only line suitable for determining the palladium abundance in stellar atmospheres is the Pd I λ = 3242.70 Å line. Since α CMi is a rather hot star with $T_{\rm eff}$ = 6750 K and log g = 4.0, and since all sky surveys by satellites should provide high resolution spectra for other hot stars with a non negligible influence of electron impacts on spectral line shapes (e.g. hot white dwarfs), it is of interest to provide corresponding Stark broadening data enabling to perform better determination of palladium abundance.

In order to provide such data, we have calculated electron-, proton-, and ionized-helium-impact line widths and shifts for 3 Pd I multiplets by using the semiclassical-perturbation formalism (Sahal-Bréchot 1969ab). A summary of the method is given in Dimitrijević et al. (1991).

The energy levels for Pd I lines have been taken from Moore (1971), and the oscillator strengths have been calculated using the method of Bates & Damgaard (1949) and the tables of Oertel & Shomo (1968). For higher levels, the method described in Van Regemorter et al. (1979) has been applied. For the most critical transitions, the values for oscillator strengths obtained by Biémont et al. (1982) from lifetime measurements by using laser excitation which are combined with branching ratios taken from Corliss & Bozman (1962) have been used. Using available values, the partial average $\bar{f}$ value for 5s − 5p transition array has been formed as

$$\bar{f} = (2\ell + 1)^{-1} \sum (g^2 f / R^2_{\rm mult}\ R^2_{\rm line}) / \sum g,$$

where $R^2_{\rm mult}$ and $R^2_{\rm line}$ are the squares of the corresponding multiplet and line factors of Shore & Menzel (1985).

In addition to the electron-impact full halfwidths and shifts, Stark-broadening parameters due to proton and ionized-helium impacts have been calculated. Thus, we have provided Stark broadening data for the important charged perturbers in stellar atmospheres. Our results are shown in Table 1 for a perturber density of 10^{17} cm^{-3} and temperatures T from 3 000 to 100 000 K. For perturber densities lower than 10^{17} cm^{-3}, all of the corresponding data vary almost linearly with density, because the effect of Debye screening is negligible. We also specify the parameter c (Dimitrijević & Sahal-Bréchot 1984) which gives an estimate for the maximum perturber density for which the line may be treated as isolated, when it is divided by 2W.

For each value given in Table 1, the collision volume (V) multiplied by the perturber density (N) is much less than unity and the impact approximation is valid (Sahal-Bréchot 1969ab). When the impact approximation is not valid, the ion-broadening contribution may be estimated by using quasistatic estimations (Sahal-Bréchot 1991). One should note that the accuracy of the results obtained decreases when broadening by ion interactions becomes important.

We hope that the present results enable a better determination of palladium stellar abundances, especially in the case of white dwarfs and stars of A and B type.

© European Southern Observatory • Provided by the NASA Astrophysics Data System

1993A&AS..100..593D

Acknowledgements. I am indebted to Sylvie Sahal-Bréchot for providing me with the semiclassical computer code.

References

Bates D.R. & Damgaard A. 1949, Trans. Roy. Soc. London, Ser. A 242, 101

Biémont E., Grevesse N., Kwiatkowski N., Zimmerman P. 1982, A&A 108, 127

Corliss C.H. & Bozman W.R. 1962, NBS Monographs 53, Washington D.C.

Dimitrijević M.S. & Sahal-Bréchot S. 1984, JQSRT 31, 301

Dimitrijević M.S., Sahal-Bréchot S., Bommier V. 1991, A&AS 89, 581

Griffin R. & Griffin R. 1979, A Photometric Atlas of the Spectrum of Procyon $\lambda\lambda$ 3140 - 7470 Å, Cambridge, England

Griem H.R. 1974, Spectral Line Broadening by Plasmas (Academic Press, New York)

Moore C.E. 1971, Atomic Energy Levels III, NSRDS-NBS 35, Washington

Moore C.E., Minnaert M.G.J., Houtgast J. 1966, NBS Monograph 61, Washington D.C.

Oertel G.K. & Shomo L.P. 1968, ApJS 16, 175

Orlov M.Ya. & Shavrina A.V. 1991, Sov. Astron. Lett. 17, 227

Sahal-Bréchot S. 1969a, A&A 1, 91

Sahal-Bréchot S. 1969b, A&A 2, 322

Sahal-Bréchot S. 1991, A&A 245, 322

Shore B.W. & Menzel D.H. 1985, ApJS 12, 187

Van Regemorter H., Hoang Binh Dy, Prud'homme M. 1979, J. Phys. B 12, 1073

Table 1. This table shows electron, proton, and ionized-helium impact broadening parameters for neutral palladium multiplets, at a perturber density of 10^{17} cm^{-3} and temperatures from 3 000 to 100 000 K. Transitions and wavelengths (in Å) are also given. By using the parameter c [see Eq. (5) in Dimitrijević & Sahal-Bréchot 1984], we obtain an estimate for the maximum perturber density for which the line may be treated as isolated and tabulated data may be used. Data for densities N lower than 10^{17} cm^{-3} can be obtained by multiplying the results given at 10^{17} cm^{-3} by $N/10^{17}$

PERTURBER DENSITY= 0.1D(+17) cm(-3)

		ELECTRONS		PROTONS		IONIZED HELIUM	
TRANSITION	T(K)	WIDTH(A)	SHIFT(A)	WIDTH(A)	SHIFT(A)	WIDTH(A)	SHIFT(A)
5s3D - 5p3Po	3000.	0.426E-02	0.156E-02	0.251E-02	0.400E-03	0.251E-02	0.317E-03
3629.5 A	5000.	0.451E-02	0.168E-02	0.252E-02	0.439E-03	0.251E-02	0.349E-03
C= 0.19E+20	10000.	0.469E-02	0.167E-02	0.252E-02	0.497E-03	0.252E-02	0.395E-03
	20000.	0.542E-02	0.120E-02	0.253E-02	0.559E-03	0.252E-02	0.446E-03
	50000.	0.787E-02	0.675E-03	0.254E-02	0.654E-03	0.253E-02	0.521E-03
	100000.	0.102E-01	0.389E-03	0.256E-02	0.735E-03	0.253E-02	0.586E-03
5s3D - 5p3Do	3000.	0.443E-02	0.238E-02	0.259E-02	0.641E-03	0.257E-02	0.507E-03
3313.2 A	5000.	0.481E-02	0.270E-02	0.261E-02	0.705E-03	0.258E-02	0.559E-03
C= 0.13E+20	10000.	0.515E-02	0.305E-02	0.262E-02	0.800E-03	0.259E-02	0.636E-03
	20000.	0.589E-02	0.306E-02	0.265E-02	0.904E-03	0.261E-02	0.720E-03
	50000.	0.806E-02	0.212E-02	0.269E-02	0.106E-02	0.263E-02	0.842E-03
	100000.	0.103E-01	0.170E-02	0.274E-02	0.119E-02	0.266E-02	0.948E-03
5s3D - 5p3Fo	3000.	0.385E-02	0.114E-02	0.253E-02	0.308E-03	0.252E-02	0.245E-03
3473.6 A	5000.	0.409E-02	0.118E-02	0.253E-02	0.338E-03	0.252E-02	0.269E-03
C= 0.16E+20	10000.	0.434E-02	0.101E-02	0.253E-02	0.383E-03	0.253E-02	0.305E-03
	20000.	0.510E-02	0.528E-03	0.254E-02	0.431E-03	0.253E-02	0.343E-03
	50000.	0.737E-02	0.650E-04	0.254E-02	0.503E-03	0.253E-02	0.401E-03
	100000.	0.932E-02	-0.162E-03	0.255E-02	0.566E-03	0.254E-02	0.451E-03

© European Southern Observatory • Provided by the NASA Astrophysics Data System

1993A&AS..100...91D

ASTRONOMY & ASTROPHYSICS
SUPPLEMENT SERIES

JULY 1993, PAGE 91

Astron. Astrophys. Suppl. Ser. **100**, 91-101 (1993)

Stark broadening of spectral lines of multicharged ions of astrophysical interest. VIII. S VI lines

M.S. Dimitrijević[1] and S. Sahal-Bréchot[2]

[1] Astronomical Observatory, Volgina 7, 11050 Beograd, Yugoslavia
[2] Laboratoire "Astrophysique, Atomes et Molécules", Département Atomes et Molécules en Astrophysique, Unité associée au C.N.R.S. N° 812, Observatoire de Paris-Meudon, 92190 Meudon, France

Received October 12; accepted October 26, 1992

Abstract. — Using a semiclassical approach, we have calculated electron-, proton-, and He III-impact line widths and shifts for 21 S VI multiplets, of interest for stellar opacities calculations.

Key words: lines: profile-atomic and molecular data

1. Introduction

This paper is the eighth in a series devoted to the calculation of Stark broadening parameters of spectral lines of multicharged ions, and is the continuation of our efforts to provide Stark broadening data of interest for stellar opacities and stellar plasma investigations (Dimitrijević & Sahal-Bréchot 1992 and references therein). By using the semiclassical-perturbation formalism (Sahal-Bréchot 1969ab), we have calculated electron-, proton-, and He III-impact line widths and shifts for 21 S VI multiplets. A summary of the formalism is given in Dimitrijević et al. (1991). Here, we present and discuss the results for S VI multiplets of interest for stellar plasma research. Moore (1950) e.g., gives a list of first five S VI multiplets in far UV to be of interest for astrophysics, and Seaton (1987) discuss the interest of Stark broadening data of spectral lines of multicharged ions for stellar opacities research.

2. Results and discussion

Energy levels for S VI lines have been taken from Joelsson et al. (1979). Oscillator strengths have been calculated by using the method of Bates & Damgaard (1949) and the tables of Oertel & Shomo (1968). For higher levels, the method described by Van Regemorter et al. (1979) has been used.

In addition to electron-impact full halfwidths and shifts, Stark-broadening parameters due to proton-, and He III-impacts have been calculated. Our results for Stark broadening parameters of S VI multiplets are shown in Table 1, for perturber densities $10^{17}-10^{21}$ cm^{-3} and temperatures $T = 100{,}000 - 1{,}000{,}000$ K. Data for other densities may be provided by authors upon request. We also specify a parameter c (Dimitrijević & Sahal-Bréchot 1984), which gives an estimate for the maximum perturber density for which the line may be treated as isolated when it is divided by the corresponding electron-impact full width at half maximum. For each value given in Table 1, the collision volume (V) multiplied by the perturber density (N) is much less than one and the impact approximation is valid (Sahal-Bréchot, 1969ab). Values for $NV > 0.5$ are not given and values for $0.1 < NV \leq 0.5$ are denoted by an asterisk. When the impact approximation is not valid, the ion broadening contribution may be estimated by using quasistatic estimations (Sahal-Bréchot 1991 or Griem 1974). The accuracy of the results obtained decreases when broadening by ion interactions becomes important.

Acknowledgements. This work is a part of French-Yugoslav collaboration through the project "L'élargissement Stark des raies spectrales des plasmas astrophysiques et de Laboratoire". It is also a part of the project "Physics and Dynamics of Celestial Bodies" supported by the Ministery of science and technology of Serbia.

References

Bates D.R. and Damgaard A. 1949, Trans. Roy. Soc. London, Ser. A 242, 101

Dimitrijević M.S. and Sahal-Bréchot S. 1984, JQSRT 31, 301

© European Southern Observatory • Provided by the NASA Astrophysics Data System

1993A&AS..100...91D

Dimitrijević M.S., Sahal-Bréchot S. and Bommier V. 1991, A&AS 89, 581
Dimitrijević M.S. and Sahal-Bréchot S. 1992, A&AS 95, 109 and 121
Griem H.R. 1974, Spectral Line Broadening by Plasmas, Academic Press, New York and London
Joelsson I., Zetterberg P.O. and Magnusson C.E. 1979, Physica Scripta 20, 145
Moore C.E. 1950, An Ultraviolet Multiplet Table, Circular of Nat. Bur. of Standards 488 Sect. 1, U.S. Dept. of Commerce, NBS, Washington D.C.
Oertel G.K. and Shomo L.P. 1968, ApJS 16, 175
Sahal-Bréchot S. 1969a, A&A 1, 91
Sahal-Bréchot S. 1969b, A&A 2, 322
Sahal-Bréchot S. 1991, A&A 245, 322
Seaton M.J. 1987, J. Phys. B 20, 6363
Van Regemorter H., Hoang Binh Dy and Prud'homme M. 1979, J. Phys. B 12, 1073

© European Southern Observatory • Provided by the NASA Astrophysics Data System

1993A&AS..100...91D

Table 1. This table shows electron-, proton-, and He III-impact broadening parameters for S VI, for perturber densities of $10^{17} - 10^{21}$ cm^{-3} and temperatures from 100,000 to 1,000,000 K. Transitions and averaged wavelengths for the multiplet (in Å) are also given. By using c (see Eq. (5) in Dimitrijević et al. 1991), we obtain an estimate for the maximum perturber density for which the line may be treated as isolated and tabulated data may be used. The asterisk identifies cases for which the collision volume multiplied by the perturber density (the condition for validity of the impact approximation) lies between 0.1 and 0.5

PERTURBER DENSITY = 0.1E+18 cm-3

PERTURBERS ARE:		ELECTRONS		PROTONS		He III	
TRANSITION	T(K)	WIDTH(A)	SHIFT(A)	WIDTH(A)	SHIFT(A)	WIDTH(A)	SHIFT(A)
S VI 3S-3P	100000.	0.276E-02	-0.431E-04	0.434E-04	-0.212E-04	0.839E-04	-0.421E-04
937.1 A	200000.	0.199E-02	-0.316E-04	0.868E-04	-0.391E-04	0.170E-03	-0.785E-04
C=0.94E+20	400000.	0.149E-02	-0.462E-04	0.134E-03	-0.615E-04	0.263E-03	-0.124E-03
	800000.	0.115E-02	-0.411E-04	0.176E-03	-0.845E-04	0.351E-03	-0.171E-03
S VI 3S-4P	100000.	0.506E-03	0.747E-05	0.299E-04	0.451E-05	0.588E-04	0.895E-05
249.1 A	200000.	0.379E-03	0.727E-05	0.428E-04	0.758E-05	0.846E-04	0.152E-04
C=0.24E+19	400000.	0.295E-03	0.761E-05	0.511E-04	0.107E-04	0.102E-03	0.216E-04
	800000.	0.239E-03	0.716E-05	0.578E-04	0.135E-04	0.115E-03	0.272E-04
S VI 3S-5P	100000.	0.662E-03	0.178E-04	0.704E-04	0.155E-04	0.139E-03	0.308E-04
191.5 A	200000.	0.523E-03	0.236E-04	0.844E-04	0.215E-04	0.168E-03	0.434E-04
C=0.66E+18	400000.	0.427E-03	0.208E-04	0.956E-04	0.268E-04	0.191E-03	0.543E-04
	800000.	0.358E-03	0.200E-04	0.104E-03	0.324E-04	0.210E-03	0.654E-04
S VI 4S-4P	100000.	0.707E-01	-0.152E-02	0.341E-02	-0.164E-02	0.670E-02	-0.327E-02
2598.4 A	200000.	0.539E-01	-0.218E-02	0.494E-02	-0.240E-02	0.979E-02	-0.482E-02
C=0.26E+21	400000.	0.427E-01	-0.196E-02	0.606E-02	-0.315E-02	0.121E-01	-0.639E-02
	800000.	0.349E-01	-0.188E-02	0.702E-02	-0.380E-02	0.141E-01	-0.767E-02
S VI 4S-5P	100000.	0.800E-02	0.526E-04	0.752E-03	0.636E-04	0.148E-02	0.127E-03
628.2 A	200000.	0.634E-02	0.794E-04	0.898E-03	0.967E-04	0.179E-02	0.195E-03
C=0.71E+19	400000.	0.520E-02	0.598E-04	0.101E-02	0.133E-03	0.202E-02	0.268E-03
	800000.	0.437E-02	0.596E-04	0.111E-02	0.159E-03	0.221E-02	0.322E-03
S VI 5S-5P	100000.	0.812	-0.355E-01	0.631E-01	-0.331E-01	0.125	-0.658E-01
5536.1 A	200000.	0.649	-0.334E-01	0.780E-01	-0.429E-01	0.155	-0.872E-01
C=0.55E+21	400000.	0.535	-0.328E-01	0.908E-01	-0.516E-01	0.182	-0.104
	800000.	0.451	-0.304E-01	0.103	-0.620E-01	0.203	-0.123
S VI 3P-4S	100000.	0.856E-03	0.613E-04	0.243E-04	0.483E-04	0.477E-04	0.960E-04
390.2 A	200000.	0.644E-03	0.731E-04	0.499E-04	0.688E-04	0.993E-04	0.139E-03
C=0.59E+19	400000.	0.503E-03	0.712E-04	0.823E-04	0.872E-04	0.165E-03	0.177E-03
	800000.	0.404E-03	0.672E-04	0.108E-03	0.106E-03	0.215E-03	0.215E-03
S VI 3P-5S	100000.	0.789E-03	0.111E-03	0.572E-04	0.854E-04	0.114E-03	0.170E-03
251.6 A	200000.	0.614E-03	0.114E-03	0.962E-04	0.107E-03	0.196E-03	0.217E-03
C=0.11E+19	400000.	0.492E-03	0.108E-03	0.128E-03	0.130E-03	0.262E-03	0.262E-03
	800000.	0.403E-03	0.101E-03	0.161E-03	0.153E-03	0.325E-03	0.309E-03
S VI 4P-5S	100000.	0.162E-01	0.147E-02	0.100E-02	0.124E-02	0.199E-02	0.246E-02
974.2 A	200000.	0.126E-01	0.155E-02	0.156E-02	0.156E-02	0.315E-02	0.317E-02
C=0.17E+20	400000.	0.102E-01	0.144E-02	0.203E-02	0.189E-02	0.410E-02	0.385E-02
	800000.	0.840E-02	0.135E-02	0.249E-02	0.222E-02	0.509E-02	0.447E-02
S VI 3P-3D	100000.	0.145E-02	-0.156E-05	0.208E-04	-0.295E-05	0.402E-04	-0.586E-05
710.6 A	200000.	0.105E-02	-0.506E-05	0.420E-04	-0.581E-05	0.821E-04	-0.116E-04
C=0.54E+20	400000.	0.783E-03	-0.690E-05	0.650E-04	-0.104E-04	0.128E-03	-0.209E-04
	800000.	0.610E-03	-0.428E-05	0.863E-04	-0.158E-04	0.172E-03	-0.318E-04

© European Southern Observatory • Provided by the NASA Astrophysics Data System

1993A&AS..100...91D

Table 1. continued

PERTURBER DENSITY = 0.1E+18 cm-3

PERTURBERS ARE:		ELECTRONS		PROTONS		He III	
TRANSITION	T(K)	WIDTH(A)	SHIFT(A)	WIDTH(A)	SHIFT(A)	WIDTH(A)	SHIFT(A)
S VI 3P-4D	100000.	0.770E-03	0.307E-04	0.447E-04	0.425E-04	0.884E-04	0.848E-04
289.8 A	200000.	0.586E-03	0.263E-04	0.692E-04	0.589E-04	0.138E-03	0.119E-03
C=0.91E+18	400000.	0.461E-03	0.262E-04	0.893E-04	0.720E-04	0.181E-03	0.146E-03
	800000.	0.373E-03	0.228E-04	0.109E-03	0.857E-04	0.221E-03	0.175E-03
S VI 3P-5D	100000.	0.119E-02	0.751E-04	0.132E-03	0.113E-03	0.262E-03	0.226E-03
227.6 A	200000.	0.949E-03	0.674E-04	0.169E-03	0.138E-03	0.340E-03	0.280E-03
C=0.30E+18	400000.	0.773E-03	0.655E-04	0.205E-03	0.166E-03	0.410E-03	0.335E-03
	800000.	0.641E-03	0.512E-04	0.251E-03	0.190E-03	0.506E-03	0.392E-03
S VI 4P-4D	100000.	0.453E-01	0.774E-03	0.202E-02	0.176E-02	0.400E-02	0.350E-02
1986.9 A	200000.	0.349E-01	0.633E-03	0.311E-02	0.245E-02	0.618E-02	0.493E-02
C=0.43E+20	400000.	0.278E-01	0.539E-03	0.398E-02	0.303E-02	0.799E-02	0.612E-02
	800000.	0.228E-01	0.434E-03	0.481E-02	0.361E-02	0.974E-02	0.738E-02
S VI 4P-5D	100000.	0.118E-01	0.612E-03	0.111E-02	0.103E-02	0.222E-02	0.205E-02
691.8 A	200000.	0.937E-02	0.549E-03	0.147E-02	0.126E-02	0.294E-02	0.254E-02
C=0.28E+19	400000.	0.765E-02	0.521E-03	0.179E-02	0.151E-02	0.356E-02	0.302E-02
	800000.	0.636E-02	0.395E-03	0.222E-02	0.175E-02	0.444E-02	0.358E-02
S VI 5P-5D	100000.	0.532	0.162E-01	0.407E-01	0.348E-01	0.812E-01	0.691E-01
4192.5 A	200000.	0.431	0.110E-01	0.526E-01	0.425E-01	0.107	0.863E-01
C=0.10E+21	400000.	0.357	0.114E-01	0.641E-01	0.507E-01	0.130	0.103
	800000.	0.300	0.696E-02	0.769E-01	0.603E-01	0.153	0.123
S VI 3D-4P	100000.	0.322E-02	0.732E-04	0.169E-03	0.419E-04	0.332E-03	0.832E-04
649.2 A	200000.	0.241E-02	0.691E-04	0.247E-03	0.678E-04	0.488E-03	0.137E-03
C=0.16E+20	400000.	0.188E-02	0.797E-04	0.304E-03	0.943E-04	0.604E-03	0.190E-03
	800000.	0.152E-02	0.720E-04	0.346E-03	0.117E-03	0.689E-03	0.235E-03
S VI 3D-5P	100000.	0.233E-02	0.721E-04	0.239E-03	0.584E-04	0.471E-03	0.116E-03
364.0 A	200000.	0.184E-02	0.919E-04	0.289E-03	0.812E-04	0.575E-03	0.164E-03
C=0.24E+19	400000.	0.150E-02	0.840E-04	0.328E-03	0.101E-03	0.654E-03	0.203E-03
	800000.	0.126E-02	0.796E-04	0.360E-03	0.120E-03	0.721E-03	0.245E-03
S VI 4D-5P	100000.	0.415E-01	0.339E-03	0.304E-02	-0.214E-03	0.599E-02	-0.426E-03
1420.9 A	200000.	0.330E-01	0.738E-03	0.376E-02	-0.344E-03	0.749E-02	-0.693E-03
C=0.22E+20	400000.	0.271E-01	0.619E-03	0.426E-02	-0.478E-03	0.848E-02	-0.963E-03
	800000.	0.227E-01	0.645E-03	0.469E-02	-0.588E-03	0.933E-02	-0.119E-02
S VI 3D-4F	100000.	0.145E-02	-0.316E-04	0.664E-04	-0.770E-04	0.131E-03	-0.153E-03
464.7 A	200000.	0.109E-02	-0.288E-04	0.110E-03	-0.108E-03	0.219E-03	-0.219E-03
C=0.23E+19	400000.	0.849E-03	-0.146E-04	0.155E-03	-0.136E-03	0.310E-03	-0.275E-03
	800000.	0.686E-03	-0.148E-04	0.195E-03	-0.164E-03	0.392E-03	-0.332E-03
S VI 4D-4F	100000.	0.885	-0.438E-01	0.456E-01	-0.636E-01	0.914E-01	-0.127
9213.0 A	200000.	0.684	-0.388E-01	0.785E-01	-0.867E-01	0.157	-0.175
C=0.92E+21	400000.	0.547	-0.334E-01	0.106	-0.104	0.213	-0.210
	800000.	0.448	-0.297E-01	0.134	-0.124	0.269	-0.251

© European Southern Observatory • Provided by the NASA Astrophysics Data System

1993A&AS..100...91D

Table 1. continued

PERTURBER DENSITY = 0.1E+18 cm-3							
PERTURBERS ARE:		ELECTRONS		PROTONS		He III	
TRANSITION	T(K)	WIDTH(A)	SHIFT(A)	WIDTH(A)	SHIFT(A)	WIDTH(A)	SHIFT(A)
S VI 4F-5D	100000.	0.350E-01	0.230E-02	0.346E-02	0.340E-02	0.688E-02	0.674E-02
1199.4 A	200000.	0.279E-01	0.208E-02	0.454E-02	0.409E-02	0.922E-02	0.827E-02
C=0.84E+19	400000.	0.227E-01	0.194E-02	0.572E-02	0.491E-02	0.116E-01	0.100E-01
	800000.	0.189E-01	0.153E-02	0.657E-02	0.559E-02	0.137E-01	0.112E-01
PERTURBER DENSITY = 0.1E+19 cm-3							
S VI 3S-3P	100000.	0.276E-01	-0.448E-03	0.434E-03	-0.207E-03	0.838E-03	-0.401E-03
937.1 A	200000.	0.199E-01	-0.324E-03	0.868E-03	-0.390E-03	0.170E-02	-0.776E-03
C=0.94E+21	400000.	0.149E-01	-0.467E-03	0.134E-02	-0.614E-03	0.263E-02	-0.124E-02
	800000.	0.115E-01	-0.411E-03	0.176E-02	-0.845E-03	0.351E-02	-0.171E-02
S VI 3S-4P	100000.	0.506E-02	0.724E-04	0.299E-03	0.440E-04	0.586E-03	0.850E-04
249.1 A	200000.	0.379E-02	0.715E-04	0.428E-03	0.757E-04	0.845E-03	0.150E-03
C=0.24E+20	400000.	0.295E-02	0.763E-04	0.511E-03	0.107E-03	0.102E-02	0.216E-03
	800000.	0.239E-02	0.716E-04	0.578E-03	0.135E-03	0.115E-02	0.271E-03
S VI 3S-5P	100000.	0.662E-02	0.170E-03	0.703E-03	0.150E-03	*0.138E-02	*0.289E-03
191.5 A	200000.	0.523E-02	0.237E-03	0.844E-03	0.215E-03	*0.168E-02	*0.426E-03
C=0.66E+19	400000.	0.427E-02	0.207E-03	0.956E-03	0.268E-03	0.191E-02	0.542E-03
	800000.	0.358E-02	0.200E-03	0.104E-02	0.324E-03	0.210E-02	0.653E-03
S VI 4S-4P	100000.	0.707	-0.148E-01	0.340E-01	-0.160E-01	0.668E-01	-0.308E-01
2598.4 A	200000.	0.539	-0.217E-01	0.494E-01	-0.239E-01	0.978E-01	-0.474E-01
C=0.26E+22	400000.	0.427	-0.195E-01	0.606E-01	-0.315E-01	0.121	-0.638E-01
	800000.	0.349	-0.188E-01	0.702E-01	-0.380E-01	0.141	-0.766E-01
S VI 4S-5P	100000.	0.800E-01	0.472E-03	0.751E-02	0.619E-03	*0.147E-01	*0.120E-02
628.2 A	200000.	0.634E-01	0.810E-03	0.898E-02	0.965E-03	*0.178E-01	*0.192E-02
C=0.71E+20	400000.	0.520E-01	0.595E-03	0.101E-01	0.132E-02	0.202E-01	0.268E-02
	800000.	0.437E-01	0.596E-03	0.111E-01	0.159E-02	0.221E-01	0.322E-02
S VI 5S-5P	100000.	8.11	-0.346	0.630	-0.318	*1.25	*-0.604
5536.1 A	200000.	6.49	-0.335	0.780	-0.428	*1.55	*-0.850
C=0.55E+22	400000.	5.35	-0.327	0.907	-0.515	*1.82	*-1.04
	800000.	4.51	-0.304	1.03	-0.620	2.03	-1.23
S VI 3P-4S	100000.	0.857E-02	0.601E-03	0.243E-03	0.469E-03	0.477E-03	0.903E-03
390.2 A	200000.	0.644E-02	0.728E-03	0.499E-03	0.687E-03	0.992E-03	0.136E-02
C=0.59E+20	400000.	0.503E-02	0.713E-03	0.823E-03	0.871E-03	0.165E-02	0.176E-02
	800000.	0.404E-02	0.672E-03	0.108E-02	0.106E-02	0.215E-02	0.215E-02
S VI 3P-5S	100000.	0.789E-02	0.108E-02	0.573E-03	0.817E-03	0.113E-02	0.155E-02
251.6 A	200000.	0.614E-02	0.115E-02	0.962E-03	0.107E-02	0.196E-02	0.211E-02
C=0.11E+20	400000.	0.492E-02	0.108E-02	0.128E-02	0.129E-02	0.262E-02	0.262E-02
	800000.	0.403E-02	0.101E-02	0.161E-02	0.153E-02	0.325E-02	0.308E-02
S VI 4P-5S	100000.	0.162	0.142E-01	0.100E-01	0.119E-01	0.199E-01	0.225E-01
974.2 A	200000.	0.126	0.155E-01	0.156E-01	0.156E-01	0.315E-01	0.308E-01
C=0.17E+21	400000.	0.102	0.144E-01	0.203E-01	0.188E-01	0.410E-01	0.384E-01
	800000.	0.840E-01	0.135E-01	0.249E-01	0.222E-01	0.509E-01	0.445E-01

© European Southern Observatory • Provided by the NASA Astrophysics Data System

1993A&AS..100...91D

Table 1. continued

PERTURBER DENSITY = 0.1E+19 cm-3

PERTURBERS ARE:		ELECTRONS		PROTONS		He III	
TRANSITION	T(K)	WIDTH(A)	SHIFT(A)	WIDTH(A)	SHIFT(A)	WIDTH(A)	SHIFT(A)
S VI 3P-3D	100000.	0.145E-01	-0.214E-05	0.208E-03	-0.288E-04	0.401E-03	-0.558E-04
710.6 A	200000.	0.105E-01	-0.455E-04	0.420E-03	-0.581E-04	0.821E-03	-0.115E-03
C=0.54E+21	400000.	0.783E-02	-0.708E-04	0.650E-03	-0.104E-03	0.128E-02	-0.209E-03
	800000.	0.610E-02	-0.428E-04	0.863E-03	-0.158E-03	0.172E-02	-0.318E-03
S VI 3P-4D	100000.	0.770E-02	0.298E-03	0.447E-03	0.412E-03	0.883E-03	0.792E-03
289.8 A	200000.	0.586E-02	0.264E-03	0.691E-03	0.588E-03	0.138E-02	0.117E-02
C=0.91E+19	400000.	0.461E-02	0.261E-03	0.893E-03	0.719E-03	0.181E-02	0.146E-02
	800000.	0.373E-02	0.228E-03	0.109E-02	0.857E-03	0.221E-02	0.175E-02
S VI 3P-5D	100000.	0.119E-01	0.698E-03	0.131E-02	0.108E-02	*0.262E-02	*0.204E-02
227.6 A	200000.	0.949E-02	0.670E-03	0.169E-02	0.138E-02	*0.340E-02	*0.271E-02
C=0.30E+19	400000.	0.773E-02	0.649E-03	0.205E-02	0.166E-02	*0.410E-02	*0.333E-02
	800000.	0.641E-02	0.512E-03	0.251E-02	0.190E-02	*0.506E-02	*0.391E-02
S VI 4P-4D	100000.	0.453	0.740E-02	0.202E-01	0.170E-01	0.399E-01	0.328E-01
1986.9 A	200000.	0.349	0.639E-02	0.311E-01	0.244E-01	0.617E-01	0.484E-01
C=0.43E+21	400000.	0.278	0.532E-02	0.398E-01	0.302E-01	0.799E-01	0.610E-01
	800000.	0.228	0.434E-02	0.481E-01	0.361E-01	0.974E-01	0.736E-01
S VI 4P-5D	100000.	0.118	0.564E-02	0.111E-01	0.980E-02	*0.220E-01	*0.185E-01
691.8 A	200000.	0.937E-01	0.546E-02	0.147E-01	0.125E-01	*0.294E-01	*0.246E-01
C=0.28E+20	400000.	0.765E-01	0.515E-02	0.179E-01	0.150E-01	*0.355E-01	*0.301E-01
	800000.	0.636E-01	0.395E-02	0.222E-01	0.175E-01	*0.444E-01	*0.357E-01
S VI 5P-5D	100000.	5.32	0.148	0.406	0.331	*0.805	*0.622
4192.5 A	200000.	4.31	0.108	0.526	0.424	*1.06	*0.835
C=0.10E+22	400000.	3.57	0.112	0.641	0.505	*1.30	*1.03
	800000.	3.00	0.696E-01	0.769	0.603	*1.53	*1.23
S VI 3D-4P	100000.	0.322E-01	0.714E-03	0.169E-02	0.408E-03	0.331E-02	0.789E-03
649.2 A	200000.	0.241E-01	0.682E-03	0.247E-02	0.677E-03	0.488E-02	0.135E-02
C=0.16E+21	400000.	0.188E-01	0.803E-03	0.304E-02	0.942E-03	0.604E-02	0.190E-02
	800000.	0.152E-01	0.720E-03	0.346E-02	0.117E-02	0.689E-02	0.235E-02
S VI 3D-5P	100000.	0.233E-01	0.690E-03	0.238E-02	0.565E-03	*0.468E-02	*0.109E-02
364.0 A	200000.	0.184E-01	0.920E-03	0.289E-02	0.811E-03	*0.574E-02	*0.161E-02
C=0.24E+20	400000.	0.150E-01	0.840E-03	0.328E-02	0.100E-02	0.654E-02	0.203E-02
	800000.	0.126E-01	0.796E-03	0.360E-02	0.120E-02	0.721E-02	0.245E-02
S VI 4D-5P	100000.	0.415	0.317E-02	0.304E-01	-0.209E-02	*0.595E-01	-0.403E-02
1420.9 A	200000.	0.330	0.742E-02	0.376E-01	-0.343E-02	0.749E-01	-0.683E-02
C=0.22E+21	400000.	0.271	0.619E-02	0.426E-01	-0.477E-02	0.848E-01	-0.962E-02
	800000.	0.227	0.645E-02	0.469E-01	-0.588E-02	0.933E-01	-0.119E-01
S VI 3D-4F	100000.	0.145E-01	-0.289E-03	0.664E-03	-0.747E-03	0.130E-02	-0.144E-02
464.7 A	200000.	0.109E-01	-0.294E-03	0.110E-02	-0.108E-02	0.219E-02	-0.215E-02
C=0.23E+20	400000.	0.849E-02	-0.141E-03	0.155E-02	-0.136E-02	0.310E-02	-0.275E-02
	800000.	0.686E-02	-0.148E-03	0.195E-02	-0.164E-02	0.392E-02	-0.332E-02

© European Southern Observatory • Provided by the NASA Astrophysics Data System

1993A&AS..100...91D

Table 1. continued

PERTURBER DENSITY = 0.1E+19 cm-3							
PERTURBERS ARE:		ELECTRONS		PROTONS		He III	
TRANSITION	T(K)	WIDTH(A)	SHIFT(A)	WIDTH(A)	SHIFT(A)	WIDTH(A)	SHIFT(A)
S VI 4D-4F	100000.	8.85	-0.416	0.456	-0.612	0.914	-1.17
9213.0 A	200000.	6.84	-0.390	0.785	-0.865	1.57	-1.72
C=0.92E+22	400000.	5.47	-0.332	1.06	-1.04	2.13	-2.10
	800000.	4.48	-0.297	1.34	-1.24	2.69	-2.51
S VI 4F-5D	100000.	0.350	0.213E-01	0.346E-01	0.323E-01	*0.688E-01	*0.605E-01
1199.4 A	200000.	0.279	0.207E-01	0.454E-01	0.408E-01	*0.921E-01	*0.799E-01
C=0.84E+20	400000.	0.227	0.192E-01	0.572E-01	0.489E-01	*0.116	*0.996E-01
	800000.	0.189	0.153E-01	0.657E-01	0.559E-01	*0.137	*0.111
PERTURBER DENSITY = 0.1E+20 cm-3							
S VI 3S-3P	100000.	0.276	-0.422E-02	0.432E-02	-0.192E-02	0.825E-02	-0.350E-02
937.1 A	200000.	0.199	-0.315E-02	0.867E-02	-0.379E-02	0.169E-01	-0.730E-02
C=0.94E+22	400000.	0.149	-0,458E-02	0.133E-01	-0.609E-02	0.263E-01	-0.122E-01
	800000.	0.115	-0.412E-02	0.176E-01	-0.844E-02	0.351E-01	-0.171E-01
S VI 3S-4P	100000.	0.506E-01	0.669E-03	0.296E-02	0.407E-03	*0.570E-02	*0.739E-03
249.1 A	200000.	0.379E-01	0.668E-03	0.427E-02	0.731E-03	*0.838E-02	*0.140E-02
C=0.24E+21	400000.	0.295E-01	0.755E-03	0.511E-02	0.106E-02	*0.101E-01	*0.211E-02
	800000.	0.239E-01	0.714E-03	0.578E-02	0.134E-02	*0.115E-01	*0.271E-02
S VI 3S-5P	100000.	0.662E-01	0.153E-02	*0.690E-02	*0.136E-02		
191.5 A	200000.	0.523E-01	0.226E-02	*0.840E-02	*0.204E-02		
C=0.66E+20	400000.	0.427E-01	0.203E-02	*0.955E-02	*0.263E-02		
	800000.	0.358E-01	0.198E-02	0.104E-01	0.323E-02		
S VI 4S-4P	100000.	7.07	-0.135	0.337	-0.146	*0.651	*-0.262
2598.4 A	200000.	5.39	-0.205	0.493	-0.229	*0.972	*-0.432
C=0.26E+23	400000.	4.27	-0.191	0.605	-0.310	*1.21	*-0.620
	800000.	3.49	-0.186	0.701	-0.379	*1.41	*-0.764
S VI 4S-5P	100000.	0.800	0.409E-02	*0.737E-01	*0.570E-02		
628.2 A	200000.	0.634	0.801E-02	*0.894E-01	*0.926E-02		
C=0.71E+21	400000.	0.520	0.574E-02	*0.101	*0.131E-01		
	800000.	0.437	0.591E-02	0.110	0.159E-01		
S VI 3P-4S	100000.	0.857E-01	0.554E-02	0.242E-02	0.428E-02	0.474E-02	0.763E-02
390.2 A	200000.	0.644E-01	0.687E-02	0.498E-02	0.655E-02	0.988E-02	0.123E-01
C=0.59E+21	400000.	0.503E-01	0.699E-02	0.823E-02	0.858E-02	0.165E-01	0.171E-01
	800000.	0.404E-01	0.668E-02	0.108E-01	0.105E-01	0.215E-01	0.214E-01
S VI 3P-5S	100000.	0.789E-01	0.963E-02	0.571E-02	0.716E-02		
251.6 A	200000.	0.614E-01	0.106E-01	0.959E-02	0.984E-02		
C=0.11E+21	400000.	0.492E-01	0.104E-01	0.128E-01	0.126E-01		
	800000.	0.403E-01	0.100E-01	0.161E-01	0.152E-01		
S VI 4P-5S	100000.	1.62	0.126	*0.993E-01	*0.104		
974.2 A	200000.	1.26	0.143	0.156	0.143		
C=0.17E+22	400000.	1.02	0.138	0.203	0.183		
	800000.	0.840	0.134	0.249	0.221		

© European Southern Observatory • Provided by the NASA Astrophysics Data System

1993A&AS..100...91D

Table 1. continued

PERTURBER DENSITY = 0.1E+20 cm-3

PERTURBERS ARE:		ELECTRONS		PROTONS		He III	
TRANSITION	T(K)	WIDTH(A)	SHIFT(A)	WIDTH(A)	SHIFT(A)	WIDTH(A)	SHIFT(A)
S VI 3P-3D	100000.	0.145	-0.741E-04	0.207E-02	-0.268E-03	0.395E-02	-0.489E-03
710.6 A	200000.	0.105	-0.484E-03	0.420E-02	-0.565E-03	0.818E-02	-0.109E-02
C=0.54E+22	400000.	0.783E-01	-0.720E-03	0.650E-02	-0.103E-02	0.128E-01	-0.206E-02
	800000.	0.610E-01	-0.430E-03	0.863E-02	-0.157E-02	0.172E-01	-0.318E-02
S VI 3P-4D	100000.	0.770E-01	0.253E-02	0.443E-02	0.372E-02	*0.864E-02	*0.657E-02
289.8 A	200000.	0.586E-01	0.233E-02	0.690E-02	0.556E-02	*0.137E-01	*0.104E-01
C=0.91E+20	400000.	0.461E-01	0.247E-02	0.892E-02	0.706E-02	*0.181E-01	*0.141E-01
	800000.	0.373E-01	0.226E-02	0.109E-01	0.855E-02	*0.221E-01	*0.174E-01
S VI 3P-5D	100000.	0.119	0.517E-02	*0.130E-01	*0.924E-02		
227.6 A	200000.	0.949E-01	0.531E-02	*0.168E-01	*0.125E-01		
C=0.30E+20	400000.	0.772E-01	0.600E-02	*0.204E-01	*0.159E-01		
	800000.	0.641E-01	0.501E-02	*0.251E-01	*0.189E-01		
S VI 4P-4D	100000.	4.53	0.573E-01	0.201	0.155	*0.390	*0.274
1986.9 A	200000.	3.49	0.529E-01	0.310	0.232	*0.613	*0.434
C=0.43E+22	400000.	2.78	0.474E-01	0.397	0.297	*0.798	*0.590
	800000.	2.28	0.425E-01	0.481	0.360	*0.974	*0.734
S VI 4P-5D	100000.	1.18	0.403E-01	*0.110	*0.841E-01		
691.8 A	200000.	0.936	0.422E-01	*0.145	*0.114		
C=0.28E+21	400000.	0.764	0.471E-01	*0.178	*0.145		
	800000.	0.636	0.385E-01	*0.222	*0.174		
S VI 3D-4P	100000.	0.322	0.669E-02	0.168E-01	0.377E-02	*0.322E-01	*0.684E-02
649.2 A	200000.	0.241	0.648E-02	0.247E-01	0.652E-02	*0.484E-01	*0.125E-01
C=0.16E+22	400000.	0.188	0.794E-02	0.303E-01	0.932E-02	*0.603E-01	*0.186E-01
	800000.	0.152	0.719E-02	0.346E-01	0.117E-01	0.689E-01	0.235E-01
S VI 3D-5P	100000.	0.233	0.629E-02	*0.234E-01	*0.513E-02		
364.0 A	200000.	0.184	0.882E-02	*0.288E-01	*0.770E-02		
C=0.24E+21	400000.	0.150	0.822E-02	*0.328E-01	*0.987E-02		
	800000.	0.126	0.791E-02	0.360E-01	0.120E-01		
S VI 4D-5P	100000.	4.15	0.331E-01	*0.299	*-0.193E-01		
1420.9 A	200000.	3.30	0.756E-01	*0.375	*-0.331E-01		
C=0.22E+22	400000.	2.71	0.626E-01	0.425	-0.472E-01		
	800000.	2.27	0.642E-01	0.469	-0.587E-01		
S VI 3D-4F	100000.	0.145	-0.219E-02	0.660E-02	-0.681E-02	*0.128E-01	-0.121E-01
464.7 A	200000.	0.109	-0.235E-02	0.110E-01	-0.103E-01	*0.218E-01	-0.194E-01
C=0.23E+21	400000.	0.849E-01	-0.117E-02	0.155E-01	-0.134E-01	*0.310E-01	-0.266E-01
	800000.	0.686E-01	-0.143E-02	0.195E-01	-0.163E-01	0.392E-01	-0.331E-01
S VI 4F-5D	100000.	3.49	0.159	*0.341	*0.274		
1199.4 A	200000.	2.78	0.165	*0.458	*0.370		
C=0.84E+21	400000.	2.27	0.176	*0.567	*0.473		
	800000.	1.89	0.150	*0.657	*0.556		

© European Southern Observatory • Provided by the NASA Astrophysics Data System

1993A&AS..100...91D

Table 1. continued

PERTURBER DENSITY = 0.1E+21 cm-3

PERTURBERS ARE:		ELECTRONS		PROTONS		He III	
TRANSITION	T(K)	WIDTH(A)	SHIFT(A)	WIDTH(A)	SHIFT(A)	WIDTH(A)	SHIFT(A)
S VI 3S-3P	100000.	2.76	-0.368E-01	0.416E-01	-0.156E-01	*0.682E-01	-0.219E-01
937.1 A	200000.	1.99	-0.275E-01	0.858E-01	-0.347E-01	*0.165	*-0.620E-01
C=0.94E+23	400000.	1.49	-0.433E-01	0.133	-0.587E-01	*0.261	*-0.112
	800000.	1.15	-0.399E-01	0.176	-0.833E-01	0.351	-0.166
S VI 3S-4P	100000.	0.506	0.557E-02	*0.277E-01	*0.326E-02		
249.1 A	200000.	0.379	0.598E-02	*0.417E-01	*0.660E-02		
C=0.24E+22	400000.	0.295	0.697E-02	*0.508E-01	*0.101E-01		
	800000.	0.239	0.693E-02	*0.577E-01	*0.132E-01		
S VI 3S-5P	100000.	0.661	0.106E-01				
191.5 A	200000.	0.522	0.190E-01				
C=0.66E+21	400000.	0.426	0.182E-01				
	800000.	0.358	0.189E-01				
S VI 4S-5P	100000.	8.00	0.244E-01				
628.2 A	200000.	6.34	0.638E-01				
C=0.71E+22	400000.	5.19	0.505E-01				
	800000.	4.37	0.558E-01				
S VI 3P-4S	100000.	0.857	0.413E-01	0.239E-01	0.326E-01		
390.2 A	200000.	0.644	0.592E-01	0.498E-01	0.565E-01		
C=0.59E+22	400000.	0.503	0.635E-01	*0.814E-01	*0.794E-01		
	800000.	0.404	0.640E-01	*0.108	*0.102		
S VI 3P-5S	100000.	0.787	0.592E-01				
251.6 A	200000.	0.613	0.797E-01				
C=0.11E+22	400000.	0.491	0.871E-01				
	800000.	0.402	0.924E-01				
S VI 4P-5S	100000.	16.1	0.724				
974.2 A	200000.	12.6	1.05				
C=0.17E+23	400000.	10.2	1.14				
	800000.	8.39	1.23				
S VI 3P-3D	100000.	1.45	-0.472E-03	0.200E-01	-0.218E-02	0.327E-01	-0.307E-02
710.6 A	200000.	1.05	-0.436E-02	0.416E-01	-0.521E-02	0.797E-01	-0.937E-02
C=0.54E+23	400000.	0.783	-0.656E-02	0.649E-01	-0.100E-01	0.127	-0.192E-01
	800000.	0.610	-0.394E-02	0.863E-01	-0.156E-01	0.171	-0.312E-01
S VI 3P-4D	100000.	0.766	0.105E-01	*0.422E-01	*0.273E-01		
289.8 A	200000.	0.584	0.128E-01	*0.682E-01	*0.470E-01		
C=0.91E+21	400000.	0.459	0.181E-01	*0.888E-01	*0.649E-01		
	800000.	0.372	0.195E-01	*0.109	*0.823E-01		
S VI 3P-5D	100000.	1.15	-0.487E-02				
227.6 A	200000.	0.923	0.135E-01				
C=0.30E+21	400000.	0.754	0.332E-01				
	800000.	0.628	0.371E-01				

© European Southern Observatory • Provided by the NASA Astrophysics Data System

1993A&AS..100...91D

Table 1. continued

PERTURBER DENSITY = 0.1E+21 cm-3

PERTURBERS ARE:		ELECTRONS		PROTONS		He III	
TRANSITION	T(K)	WIDTH(A)	SHIFT(A)	WIDTH(A)	SHIFT(A)	WIDTH(A)	SHIFT(A)
S VI 4P-5D	100000.	11.4	-0.108				
691.8 A	200000.	9.12	0.629E-01				
C=0.28E+22	400000.	7.48	0.230				
	800000.	6.24	0.267				
S VI 3D-4P	100000.	3.22	0.564E-01	*0.158	*0.300E-01		
649.2 A	200000.	2.41	0.577E-01	*0.242	*0.585E-01		
C=0.16E+23	400000.	1.88	0.738E-01	*0.302	*0.886E-01		
	800000.	1.52	0.696E-01	*0.345	*0.114		
S VI 3D-5P	100000.	2.32	0.450E-01				
364.0 A	200000.	1.84	0.743E-01				
C=0.24E+22	400000.	1.50	0.741E-01				
	800000.	1.26	0.755E-01				
S VI 3D-4F	100000.	1.44	0.286E-02	*0.636E-01	-0.514E-01		
464.7 A	200000.	1.09	-0.621E-02	*0.108	*-0.881E-01		
C=0.23E+22	400000.	0.847	-0.134E-02	*0.156	*-0.124		
	800000.	0.684	-0.961E-02	*0.194	*-0.158		
PERTURBER DENSITY = 0.1E+22 cm-3							
S VI 3S-4P	100000.	*5.02	*0.124E-01				
249.1 A	200000.	*3.78	*0.339E-01				
C=0.24E+23	400000.	2.95	0.512E-01				
	800000.	2.38	0.571E-01				
S VI 3S-5P	100000.						
191.5 A	200000.	*4.97	*0.669E-01				
C=0.66E+22	400000.	*4.11	*0.952E-01				
	800000.	3.48	0.135				
S VI 3P-4S	100000.	8.47	-0.160				
390.2 A	200000.	6.39	0.250				
C=0.59E+23	400000.	5.00	0.395				
	800000.	4.02	0.483				
S VI 3P-5S	100000.	*6.73	*-0.710				
251.6 A	200000.	5.56	-0.282E-01				
C=0.11E+23	400000.	4.56	0.292				
	800000.	3.78	0.537				
S VI 3P-3D	100000.	14.5	0.209E-01	*0.145	*-0.110E-01		
710.6 A	200000.	10.5	-0.290E-01	*0.390	*-0.409E-01		
C=0.54E+24	400000.	7.82	-0.540E-01	*0.636	*-0.905E-01		
	800000.	6.10	-0.336E-01	*0.859	*-0.149		
S VI 3P-4D	100000.	*6.99	*-0.236				
289.8 A	200000.	5.47	-0.112				
C=0.91E+22	400000.	4.36	0.489E-02				
	800000.	3.57	0.686E-01				

© European Southern Observatory • Provided by the NASA Astrophysics Data System

1993A&AS..100...91D

Table 1. continued

PERTURBER DENSITY = 0.1E+22 cm-3

PERTURBERS ARE:		ELECTRONS		PROTONS		He III	
TRANSITION	T(K)	WIDTH(A)	SHIFT(A)	WIDTH(A)	SHIFT(A)	WIDTH(A)	SHIFT(A)
S VI 3P-5D	100000.						
227.6 A	200000.	*7.55	*-0.285				
C=0.30E+22	400000.	*6.45	*-0.483E-01				
	800000.	5.54	0.548E-01				
S VI 3D-4F	100000.	*13.1	*0.584				
464.7 A	200000.	10.1	0.333				
C=0.23E+23	400000.	8.03	0.283				
	800000.	6.55	0.119				

© European Southern Observatory • Provided by the NASA Astrophysics Data System

1993A&AS..101..583D

ASTRONOMY & ASTROPHYSICS
SUPPLEMENT SERIES

Astron. Astrophys. Suppl. Ser. **101**, 583-586 (1993)

Stark broadening of Bi II lines of astrophysical interest

M.S. Dimitrijević and L.Č. Popović

Astronomical Observatory, Volgina 7, 11050 Beograd, Serbia, Yugoslavia

Received August 24, 1992; accepted February 18, 1993

Abstract. — We report here results of Bi II spectral line Stark broadening research within a modified semi-empirical approach. The strong absorption Bi II lines observed in Hg-Mn star atmospheres have been investigated, as well as other Bi II lines of importance for astrophysical and laboratory plasma. Stark width and shift data for 26 Bi II lines are presented as a function of temperature. The obtained results have been compared with experiments and with other estimations.

Key words: lines; profile — atomic and molecular data; Hg−Mn stars

1. Introduction

Stark broadening data are needed for a number of problems in astrophysical and laboratory plasma spectroscopy, as e.g. for evaluation and modelling of stellar atmosphere physical properties and abundance determinations (Grevesse 1967). The Stark broadening mechanism is particularly important in comparison with other pressure broadening mechanisms for white dwarfs and O, B and A type stars, to which belongs a class of chemically peculiar, Hg-Mn stars. Seven strong absorption lines of ionized bismuth have been found in the Hg-Mn star HR 7775 in high-resolution spectra obtained with IUE (Jacobs & Dworetsky 1982). The performed analysis shows the existence of an overabundance of Bi of 10^6 while Jacobs & Dworetsky (1982) have not detected Bi II in the spectra of several other Hg-Mn stars. Since plasma conditions in the HR 7775 star atmosphere are $T_{\rm eff} = 11000$ K, $\log g = 4.0$ (Jacobs & Dworetsky 1982) and the electron density $N_{\rm e}$ is $10^{14} - 10^{15}$ cm^{-3} in the layers where the Bi II lines are formed, it is of interest to provide the corresponding Stark broadening parameters which might be of significance for abundance investigation, determination of astrophysical gf values and other stellar plasma research. Besides its astrophysical importance, Stark broadening of Bi II lines is interesting for pumped laser developement (Keydan & Mikhalevskii 1968) as well as for laboratory plasma research and was investigated experimentally by Miller & Bengston (1980) and Purić et al. (1985).

2. Results and discussion

The term analysis of Bi II is due to Crawford & McLay (1934) and Murakawa & Suwa (1947) suggested the LS-designation for nearly all levels.

Table 1. Energy level mixing parameters K_1 and K_2

Config.	level	K_1 L_1	K_2 L_2
	$^1D_2$	0.535 $^1D_2$	0.465 $^3P_2$
np^2	$^3P_2$	0.535 $^3P^2$	0.465 $^1D_2$
	$^3P_0$	0.832 $^3P_0$	0.168 $^1S_0$
	$^1S_0$	0.832 $^1S_0$	0.168 $^3P_0$
npms	$^3P^0_1$	0.701 $^3P^0_1$	0.299 $^1P^0_1$
	$^1P^0_1$	0.701 $^1P^0_1$	0.299 $^3P^0_1$

The needed Bates & Damgaard (1949) factors have been calculated by using tables of Oertel & Shomo (1968). For $6p^2 - 6p7s$ transitions we have derived the needed Bates & Damgaard (1949) factors φ from oscillator strengths calculated by Gruzdev (1968). Moreover, Gruzdev demonstrated that departure from LS coupling of $6p^2$ and 6p7s terms may be taken into account by representing the corresponding term as a mixture of singlet and triplet states, and has provided corresponding partition coefficients. For example $6p^2$ $^3P_2$ may be represented as a mixture of K_1 $6p^2$ $^3P_2$ and K_2 $6p^2$ $^1D_2$ (the corresponding coefficients K_1 and K_2 used in this article are presented in Table 1.), where $K_1 + K_2 = 1$. We calculated the corresponding squares of the coordinate

© European Southern Observatory • Provided by the NASA Astrophysics Data System

1993A&AS..101..583D

operator matrix element in the form:

$$\vec{R}^2_{jj'} = K_\alpha \cdot \vec{R}^2_{\alpha\alpha'} + K_\beta \cdot \vec{R}^2_{\beta\beta'}$$

where α, α' denote the part with other multiplicity and the corresponding perturbing levels.

Our results for Stark full widths (FWHM) and shifts for 26 Bi II multiplets, calculated by using the modified semi-empirical approach (Dimitrijević & Konjević 1980), are presented in Table 2 for electron density of 10^{17} cm^{-3} and temperatures from 5,000 to 50,000 K. The multiplets are selected according to their astrophysical importance (see e.g. Moore 1962; Jacobs & Dworetsky 1982) as well as according to their interest for laboratory plasma (Miller & Bengston 1980; Purić et al. 1985), and ordered in Table as in Wiese et al. (1966).

The stellar absorption line equivalent widths are particularly influenced by Stark effect in two cases (Lanz et al. 1988). First, if the Stark width is larger than the Doppler width, it contributes to desaturate the core of the line. The other case is the case of very strong lines beyond the saturation plateau, when most of the absorbed energy lies in the wings dominated by Stark effect. For the considered Bi II lines, the Doppler width (FWHM) at 10000 K varies between 0.00061 nm for $\lambda = 124.11$ nm and 0.0028 nm for $\lambda = 571.9$ nm line. We see that for UV lines the Stark widths are much smaller than the corresponding Doppler widths for the electron densities of interest for Hg-Mn stars atmospheres. For optical lines, however, Stark broadening may be important in the wings.

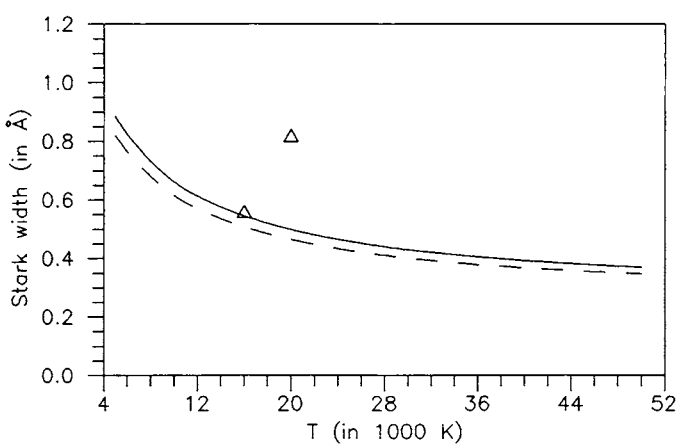

Fig. 1. Stark full width (FWHM) for Bi II 5209 Å $(7s^3P^0_1 - 7p^3D_2)$ spectral line as a function of temperature (T), at electron density $N = 10^{17}$ cm^{-3}. The used notation is: (—) - present results; (- - -) - pure LS coupling assumption; experimental data of (Δ) Purić et al. (1985), and (O) Miller & Bengston (1980)

If we consider fine or hyperfine components (data on hyperfine structure may be found in Bouazza & Bauche 1988), each particular component has the same line width in angular frequency units, since the energy differences between fine or hyperfine components are always much smaller than the inverse of colision time. For the hyperfine components e.g., Roueff & Spielfiedel (1983) and Omont (1973) demonstrated that Stark widths of particular hyperfine components are practically identical.

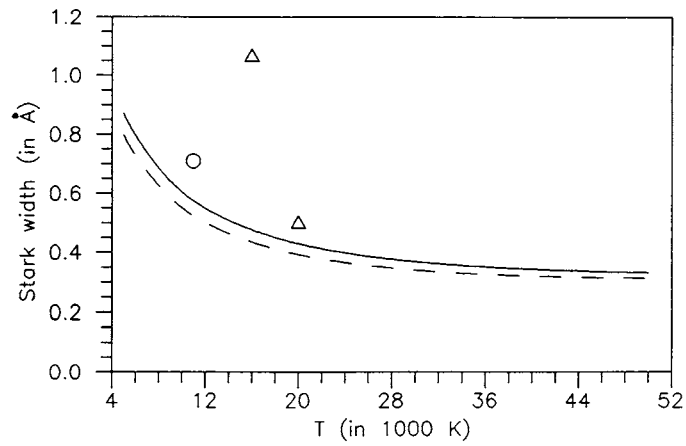

Fig. 2. Same as in Fig. 1. but for Bi II 5719 Å spectral line $(7s^3P_1 - 7p^3P_0)$

In Figs. 1 and 2 our results are compared with available experimental (Miller & Bengston 1980; Purić et al. 1985) data. The dashed line corresponds to calculations with pure LS coupling Taking into account that it is not easy to estimate the accuracy of the present results due to the complexity of the Bi II spectrum, these differences might give an impression of the influence of the breaking of LS coupling approximation on the accuracy of Bi II Stark width data. The agreement of the theoretical results with the experimental data of Miller & Bengston (1980) and Purić et al. (1985) is very encouraging. We hope that present results will be of help for determinations of the Bi stellar abundance and for investigations of astrophysical and laboratory plasmas.

References

Bates D.R. & Damgaard A. 1949, Phyl. Trans. Roy. Soc. London A242, 101
Bouazza S. & Bauche J. 1988, Z. Phys. D 10, 1
Crawford M.F. & McLay A.B. 1934, Proc. Roy. Soc. A 143, 540
Dimitrijević M.S. 1988, A&AS 76, 53-59
Dimitrijević M.S. & Konjević N. 1980, JQSRT 24, 451
Dimitrijević M.S. & Kršljanin V. 1986, A&A 165, 269
Grevesse N. 1967, ApJ 149, 37
Griem H.R. 1968, Phys. Rev. 165, 258
Gruzdev P.F. 1968, Opt. Spectrosc. 25, 3
Jacobs J.M. & Dworetsky M.M. 1982, Nature 299, 535
Keydan V.F. & Mikhalevskii V.S. 1968, Zh. Prikl. Spektrosk. 9, 713

© European Southern Observatory • Provided by the NASA Astrophysics Data System

1993A&AS..101..583D

Lanz T., Dimitrijević M.S. & Artru M.C. 1988, A&A 192, 249
Miller M.H. & Bengtson R.D. 1980, JQSRT 23, 411
Moore C.E. 1962, An Ultraviolet Multiplet Table, Circular of the NBS 488, Section 3, US Dept. of Commerce, NBS, Washington D.C.
Murakawa K. & Suwa S. 1947, Reports Inst. Sci. Tech., Tokyo Univ. 1, 121
Oertel G.K. & Shomo L.P. 1968, ApJS 16, 175
Omont A. 1973, J. Phys. 34, 179
Purić J., Ćuk M. & Lakićević I.S. 1985, Phys. Rev. A 32, 1106
Roueff E. & Spielfiedel A. 1983, J. Phys. B 16, 506
Wiese W.L., Smith M.W. & Glennon B.M. 1966, Atomic Transition Probabilities I, NSRDS-NBS 4, U.S. Dept. of Commerce, Washington D.C.

Table 2. Stark full widths (FWHM) and shifts of Bi II spectral lines of astrophysical interest. The electron density is 10^{17} cm^{-3}. The parameter $X = \frac{3kT}{2|\Delta E|}$, where ΔE is the energy difference between the closest perturbing level and the corresponding initial or final level, is calculated for $T = 10,000$ K

TRANSITION	T (K)	WIDTH [nm]	SHIFT [nm]	TRANSITION	WIDTH [nm]	SHIFT [nm]
	5000.	.386E-02	.101E-02		.546E-02	.426E-03
$6p^2\ ^3P_0 - 7s^3P^0_1$	10000.	.270E-02	.759E-03	$6p^2\ ^3P_1 - 7s^3P^0_0$	.380E-02	.321E-03
$\lambda = 143.68$ nm	20000.	.189E-02	.577E-03	$\lambda = 179.18$ nm	.266E-02	.258E-03
$X = 0.71$	30000.	.155E-02	.512E-03	$X = 0.68$	.222E-02	.244E-03
	40000.	.136E-02	.491E-03		.198E-02	.246E-03
	50000.	.125E-02	.485E-03		.184E-02	.251E-03
	5000.	.600E-02	.156E-02		.790E-02	.164E-02
$6p^2\ ^3P_1 - 7s^3P^0_1$	10000.	.418E-02	.114E-02	$6p^2\ ^3P_1 - 7s^3P^0_2$	.610E-02	.119E-02
$\lambda = 177.70$nm	20000.	.292E-02	.870E-03	$\lambda = 132.55$ nm	.470E-02	.904E-03
$X = 0.71$	30000.	.240E-02	.771E-03	$X = 517.70$	.408E-02	.801E-03
	40000.	.210E-02	.740E-03		.374E-02	.767E-03
	50000.	.183E-02	.731E-03		.350E-02	.781E-03
	5000.	.686E-02	.178E-02		.874E-02	.181E-02
$6p^2\ ^3P_2 - 7s^3P^0_1$	10000.	.480E-02	.131E-02	$6p^2\ ^3P_2 - 7s^3P^0_2$	.674E-02	.132E-02
$\lambda = 190.23$ nm	20000.	.334E-02	.993E-03	$\lambda = 139.39$ nm	.520E-02	.997E-03
$X = 0.71$	30000.	.274E-02	.879E-03	$X = 517.70$	.452E-02	.883E-03
	40000.	.242E-02	.845E-03		.139E-02	.540E-03
	50000.	.222E-02	.834E-03		.388E-02	.861E-03
	5000.	.236E-02	.627E-03		.342E-02	.885E-03
$6p^2\ ^3P_0 - 6d^3D^0_1$	10000.	.163E-02	.471E-03	$6p^2\ ^3P_1 - 6d^3D^0_2$	.236E-02	.665E-03
$\lambda = 124.11$ nm	20000.	.113E-02	.377E-03	$\lambda = 152.06$ nm	.164E-02	.531E-03
$X = 2.79$	30000.	.948E-03	.350E-03	$X = 1.99$	.136E-02	.492E-03
	40000.	.868E-03	.343E-03		.124E-02	.484E-03
	50000.	.834E-03	.353E-03		.119E-02	.494E-03
	5000.	.344E-02	.886E-03		.384E-02	.989E-03
$6p^2\ ^3P_1 - 6d^3D^0_1$	10000.	.236E-02	.665E-03	$6p^2\ ^3P_2 - 6d^3D^0_2$	.264E-02	.743E-03
$\lambda = 148.69$ nm	20000.	.165E-02	.532E-03	$\lambda = 161.14$ nm	.183E-02	.593E-03
$X = 2.79$	30000.	.138E-02	.494E-03	$X = 1.99$	.153E-02	.549E-03
	40000.	.126E-02	.484E-03		.134E-02	.552E-03
	50000.	.121E-02	.498E-03		.414E-02	.847E-03
	5000.	.384E-02	.987E-03		.394E-02	.832E-03
$6p^2\ ^3P_2 - 6d^3D^0_1$	10000.	.266E-02	.742E-03	$6p^2\ ^3P_1 - 6d^3F^0_2$	.272E-02	.623E-03
$\lambda = 157.37$ nm	20000.	.184E-02	.593E-03	$\lambda = 145.51$ nm	.190E-02	.493E-03
$X = 2.79$	30000.	.154E-02	.551E-03	$X = 4.63$	.157E-02	.451E-03
	40000.	.141E-02	.540E-03		.142E-02	.437E-03
	50000.	.135E-02	.556E-03		.134E-02	.441E-03
	5000.	.438E-02	.924E-03		.394E-02	.926E-03
$6p^2\ ^3P_2 - 6d^3F^0_2$	10000.	.304E-02	.692E-03	$6p^2\ ^3P_2 - 6d^3F^0_3$	.272E-02	.697E-03
$\lambda = 153.81$ nm	20000.	.212E-02	.548E-03	$\lambda = 153.32$ nm	.190E-02	.559E-03
$X = 4.63$	30000.	.176E-02	.502E-03	$X = 1.58$	.159E-02	.519E-03
	40000.	.159E-02	.486E-03		.145E-02	.508E-03
	50000.	.150E-02	.490E-03		.139E-02	.522E-03
	5000.	.756E-02	-.214E-02		.154E-01	.366E-02
$6p^2\ ^3P_2 - 7s^1P^0_1$	10000.	.680E-02	-.191E-02	$6p^2\ ^1D_2 - 7s^3P^0_1$	.107E-01	.268E-02
$\lambda = 137.26$ nm	20000.	.610E-02	-.155E-02	$\lambda = 280.41$ nm	.750E-02	.204E-02
$X = 9.46$	30000.	.584E-02	-.131E-02	$X = 0.71$	.614E-02	.181E-02
	40000.	.536E-02	-.112E-02		.540E-02	.174E-02
	50000.	.492E-02	-.939E-03		.496E-02	.172E-02

© European Southern Observatory • Provided by the NASA Astrophysics Data System

1993A&AS..101..583D

Table 2. continued

TRANSITION	T (K)	WIDTH [nm]	SHIFT [nm]	TRANSITION	WIDTH [nm]	SHIFT [nm]
	5000.	.756E-02	.174E-02		.742E-02	.171E-02
$6p^2\ ^1D_2 - 6d^3D^0_2$	10000.	.520E-02	.131E-02	$6p^2\ ^1D_2 - 6d^3D^0_1$	.512E-02	.129E-02
$\lambda = 221.47$ nm	20000.	.362E-02	.105E-02	$\lambda = 214.41$ nm	.356E-02	.103E-02
$X = 1.99$	30000.	.300E-02	.972E-03	$X = 2.79$	.298E-02	.960E-03
	40000.	.274E-02	.958E-03		.273E-02	.944E-03
	50000.	.262E-02	.982E-03		.260E-02	.975E-03
	5000.	.784E-02	.207E-02		.744E-02	.157E-02
$6p^2\ ^1D_2 - 6d^3D^0_3$	10000.	.632E-02	.168E-02	$6p^2\ ^1D_2 - 6d^3F_3$	.514E-02	.118E-02
$\lambda = 144.79$ nm	20000.	.590E-02	.159E-02	$\lambda = 206.96$ nm	.358E-02	.953E-03
$X = 4.98$	30000.	.580E-02	.187E-02	$X = 1.58$	.300E-02	.887E-03
	40000.	.568E-02	.186E-02		.274E-02	.871E-03
	50000.	.566E-02	.194E-02		.262E-02	.899E-03
	5000.	.151E-01	.300E-02		.130E-01	-.371E-02
$6p^2\ ^1D_2 - 7s^3P^0_2$	10000.	.116E-01	.219E-02	$6p^2\ ^1D_2 - 7s^1P^0_1$	.116E-01	-.330E-02
$\lambda = 182.37$ nm	20000.	.900E-02	.166E-02	$\lambda = 178.74$ nm	.104E-01	-.267E-02
$X = 517.70$	30000.	.780E-02	.147E-02	$X = 9.46$	.996E-02	-.227E-02
	40000.	.714E-02	.141E-02		.916E-02	-.194E-02
	50000.	.670E-02	.143E-02		.840E-02	-.163E-02
	5000.	.198E-01	-.628E-02		.220E-01	.583E-02
$6p^2\ ^1S_0 - 7s^1P^0_1$	10000.	.177E-01	-.547E-02	$6p^2\ ^1S_0 - 8s^3P^0_1$	.158E-01	.457E-02
$\lambda = 218.77$ nm	20000.	.157E-01	-.439E-02	$\lambda = 174.92$ nm	.124E-01	.422E-02
$X = 9.46$	30000.	.150E-01	-.372E-02	$X = 2.62$	.114E-01	.415E-02
	40000.	.133E-01	-.320E-02		.110E-01	.374E-02
	50000.	.127E-01	-.271E-02		.107E-02	.336E-02
	5000.	.177	-.194E-01		.174	-.266E-01
$7s^3P^0_1 - 7p^3D_2$	10000.	.132	-.136E-01	$7s^3P^0_1 - 7p^3P_0$	.121	-.189E-01
$\lambda = 520.9$ nm	20000.	.998E-01	-.955E-02	$\lambda = 571.9$ nm	.862E-01	-.135E-01
$X = 517.67$	30000.	.860	-.772E-02	$X = 0.71$	.740	-.112E-01
	40000.	.786E-01	-.646E-02		.688E-01	-.928E-02
	50000.	.740E-01	-.521E-02		.664E-01	-.853E-02

* In the table $X = \frac{3kT}{2|\Delta E|}$ for temperature T=10000 K

© European Southern Observatory • Provided by the NASA Astrophysics Data System

1993A&AS..101..587D

ASTRONOMY & ASTROPHYSICS
SUPPLEMENT SERIES

NOVEMBER I 1993, PAGE 587

Astron. Astrophys. Suppl. Ser. **101**, 587-597 (1993)

Stark broadening of spectral lines of multicharged ions of astrophysical interest. IX. F VII lines

M.S. Dimitrijević[1] and S. Sahal-Bréchot[2]

[1] Astronomical Observatory, Volgina 7, 11050 Beograd, Yugoslavia
[2] Laboratoire "Astrophysique, Atomes et Molécules", Département Atomes et Molécules en Astrophysique, Unité associée au C.N.R.S. N 812, Observatoire de Paris-Meudon, 92190 Meudon, France

Received January 19; accepted February 8, 1993

Abstract. — Using a semiclassical approach, we have calculated electron-, proton-, and He II-impact line widths and shifts for 20 F VII multiplets. The results obtained have been compared with available experimental and theoretical data.

Key words: lines: profile-atomic and molecular data

1. Introduction

This paper is the ninth of a series devoted to the calculation of Stark broadening parameters of spectral lines of multicharged ions (see Dimitrijević & Sahal-Bréchot 1993 and references therein). By using the semiclassical-perturbation formalism (Sahal-Bréchot 1969ab), we have calculated electron-, proton-, and He III- impact line widths and shifts for 20 F VII multiplets. A summary of the formalism is given in Dimitrijević et al. (1991). Here, we present and discuss the results obtained.

2. Results and discussion

Energy levels for F VII lines have been taken from Bashkin & Stoner (1975). The oscillator strengths have been calculated by using the method of Bates & Damgaard (1949) and the tables of Oertel & Shomo (1968). For higher levels, the method described by Van Regemorter et al. (1979) has been used.

In addition to electron-impact full halfwidths and shifts, Stark-broadening parameters due to proton-, and He III- impacts have been calculated. Our results for 20 F VII multiplets are shown in Table 1, for perturber densities $10^{17} - 10^{22}$ cm^{-3} and temperatures $T = 100,000 - 2,000,000$ K. We also specify a parameter c (Dimitrijević & Sahal-Bréchot 1984), which gives an estimate for the maximum perturber density for which the line may be treated as isolated when it is divided by the corresponding electron-impact full width at half maximum. For each value given in Table 1, the collision volume (V) multiplied by the perturber density (N) is much less than one and the impact aproximation is valid (Sahal-Bréchot 1969ab). Values for $NV > 0.5$ are not given and values for $0.1 < NV \leq 0.5$ are denoted by an asterisk. When the impact approximation is not valid, the ion broadening contribution may be estimated by using quasistatic estimations (Sahal-Bréchot 1991 and Griem 1974). The accuracy of the results obtained decreases when broadening by ion interactions becomes important.

The results obtained for the $3s^2S - 3p^2P^o$ multiplet have been compared in Table 2 with existing experimental data (Glenzer et al. 1992) and with other calculations (Glenzer et al. 1992) by using different approximate approaches (Griem 1974 Eq. 526; Dimitrijević & Konjević 1980; Hey & Breger 1982). We can see that there is good agreement between experimental data and semiclassical calculations and reasonable agreement between different approximate approaches and more sophisticated semiclassical calculations. For F VII $3s^2S - 3p^2P^o$ Stark width a simple estimate has been made by Purić et al. (1988), based on regularities investigations. For an electron density of 10^{17} cm^{-3} and a temperature of 60000 K, they give a full width of 0.070 Å while we obtain 0.079 Å, which is a very encouraging agreement.

Acknowledgements. This work has been supported by the French C.N.R.S. and is a part of French-Yugoslav collaboration through the project "L'élargissement Stark des raies spectrales des plasmas astrophysiques et de laboratoire". It is also a part of the project "Physics and

© European Southern Observatory • Provided by the NASA Astrophysics Data System

1993A&AS..101..587D

Dynamics of Celestial Bodies" supported by the Ministry of Science and Technology of Serbia.

References

Bashkin S. and Stoner J.O.Jr. 1975, Atomic Energy Levels and Grotrian Diagrams, Vol. 1, North Holland, Amsterdam

Bates D.R. and Damgaard A., 1949, Trans. Roy. Soc. London, Ser. A 242, 101

Dimitrijević M.S. and Sahal-Bréchot S. 1984, JQSRT 31, 301

Dimitrijević M.S., Sahal-Bréchot S. and Bommier V. 1991, A&AS 89, 581

Dimitrijević M.S. and Sahal-Bréchot S. 1993, A&AS in press

Glenzer S., Uzelac N.I., Kunze H.-J. 1992, 11th Int. Conf. on Spectral Line Shapes, Carry le Rouet, A-01

Griem H.R. 1974, Spectral Line Broadening by Plasmas, Academic Press, New York and London

Hey J.D., Breger P. 1982, S. Afr. J. Phys. 5, 111

Oertel G.K. and Shomo L.P. 1968, ApJS 16, 175

Purić J., Djeniže S., Labat J., Platiša M., Srećković A., Ćuk M. 1988, Z. Phys. D 10, 431

Sahal-Bréchot S. 1969a, A&A 1, 91

Sahal-Bréchot S. 1969b, A&A 2, 322

Sahal-Bréchot S. 1991, A&A 245, 322

Van Regemorter H., Hoang Binh Dy and Prud'homme M. 1979, J. Phys. B 12, 1073

© European Southern Observatory • Provided by the NASA Astrophysics Data System

1993A&AS..101..587D

Table 1. This table shows electron-, proton-, and He III- impact broadening parameters for F VII, for perturber densities of $10^{17} - 10^{22}$cm^{-3} and temperatures from 100,000 to 2,000,000 K. Transitions and averaged wavelengths for the multiplet (in Å) are also given. By using c [see Eq. (5) in Dimitrijević et al. 1991], we obtain an estimate for the maximum perturber density for which the line may be treated as isolated and tabulated data may be used. The asterisk identifies cases for which the collision volume multiplied by the perturber density (the condition for validity of the impact approximation) lies between 0.1 and 0.5

PERTURBER DENSITY = 0.1E+18 cm-3

PERTURBERS ARE:		ELECTRONS		PROTONS		He III	
TRANSITION	T(K)	WIDTH(A)	SHIFT(A)	WIDTH(A)	SHIFT(A)	WIDTH(A)	SHIFT(A)
FVII 2S-2P	100000.	0.893E-03	-0.165E-04	0.174E-05	-0.692E-05	0.324E-05	-0.138E-04
885.6 A	200000.	0.653E-03	-0.167E-04	0.557E-05	-0.137E-04	0.105E-04	-0.274E-04
C= 0.89E+20	500000.	0.428E-03	-0.186E-04	0.201E-04	-0.285E-04	0.389E-04	-0.575E-04
	1000000.	0.318E-03	-0.181E-04	0.368E-04	-0.411E-04	0.727E-04	-0.833E-04
FVII 2S-3P	100000.	0.562E-04	0.874E-06	0.114E-05	0.182E-05	0.218E-05	0.364E-05
113.0 A	200000.	0.418E-04	0.769E-06	0.254E-05	0.297E-05	0.498E-05	0.601E-05
C= 0.13E+18	500000.	0.292E-04	0.657E-06	0.480E-05	0.450E-05	0.958E-05	0.918E-05
	1000000.	0.227E-04	0.567E-06	0.620E-05	0.540E-05	0.125E-04	0.110E-04
FVII 2S-4P	100000.	0.967E-04	0.333E-05	0.678E-05	0.840E-05	0.136E-04	0.169E-04
86.7 A	200000.	0.744E-04	0.323E-05	0.113E-04	0.115E-04	0.227E-04	0.235E-04
C= 0.32E+17	500000.	0.541E-04	0.274E-05	0.157E-04	0.147E-04	0.322E-04	0.298E-04
	1000000.	0.432E-04	0.206E-05	0.202E-04	0.175E-04	0.402E-04	0.360E-04
FVII 2S-5P	100000.	0.189E-03	0.925E-05	0.243E-04	0.252E-04	0.487E-04	0.509E-04
78.4 A	200000.	0.149E-03	0.885E-05	0.321E-04	0.306E-04	0.656E-04	0.623E-04
C= 0.14E+17	500000.	0.111E-03	0.658E-05	0.432E-04	0.389E-04	0.861E-04	0.796E-04
	1000000.	0.895E-04	0.523E-05	0.511E-04	0.436E-04	0.108E-03	0.909E-04
FVII 3S-3P	100000.	0.629E-01	-0.821E-03	0.700E-03	0.134E-04	0.132E-02	0.266E-04
3257.4 A	200000.	0.472E-01	-0.132E-02	0.139E-02	0.268E-04	0.268E-02	0.537E-04
C= 0.11E+21	500000.	0.334E-01	-0.133E-02	0.239E-02	0.652E-04	0.468E-02	0.131E-03
	1000000.	0.264E-01	-0.133E-02	0.289E-02	0.113E-03	0.574E-02	0.227E-03
FVII 3S-4P	100000.	0.161E-02	0.334E-04	0.966E-04	0.117E-03	0.192E-03	0.236E-03
335.2 A	200000.	0.124E-02	0.275E-04	0.160E-03	0.161E-03	0.320E-03	0.328E-03
C= 0.48E+18	500000.	0.905E-03	0.211E-04	0.226E-03	0.205E-03	0.455E-03	0.416E-03
	1000000.	0.725E-03	0.117E-04	0.276E-03	0.246E-03	0.544E-03	0.498E-03
FVII 3S-5P	100000.	0.182E-02	0.766E-04	0.220E-03	0.229E-03	0.441E-03	0.461E-03
237.2 A	200000.	0.143E-02	0.707E-04	0.292E-03	0.277E-03	0.595E-03	0.565E-03
C= 0.12E+18	500000.	0.106E-02	0.503E-04	0.392E-03	0.354E-03	0.771E-03	0.720E-03
	1000000.	0.859E-03	0.383E-04	0.462E-03	0.394E-03	0.959E-03	0.827E-03
FVII 4S-4P	100000.	1.21	-0.279E-01	0.340E-01	0.227E-01	0.659E-01	0.454E-01
7961.1 A	200000.	0.935	-0.287E-01	0.520E-01	0.332E-01	0.102	0.671E-01
C= 0.27E+21	500000.	0.688	-0.296E-01	0.719E-01	0.463E-01	0.144	0.940E-01
	1000000.	0.554	-0.298E-01	0.842E-01	0.555E-01	0.168	0.112
FVII 4S-5P	100000.	0.201E-01	0.340E-03	0.194E-02	0.200E-02	0.388E-02	0.403E-02
736.5 A	200000.	0.158E-01	0.304E-03	0.261E-02	0.244E-02	0.522E-02	0.494E-02
C= 0.12E+19	500000.	0.118E-01	0.130E-03	0.339E-02	0.302E-02	0.699E-02	0.620E-02
	1000000.	0.952E-02	0.575E-04	0.403E-02	0.354E-02	0.809E-02	0.714E-02
FVII 5S-5P	100000.	11.8	-0.345	0.529	0.404	1.04	0.809
15703.5 A	200000.	9.34	-0.323	0.708	0.525	1.41	1.07
C= 0.54E+21	500000.	7.00	-0.360	0.912	0.666	1.85	1.38
	1000000.	5.67	-0.300	1.03	0.773	2.13	1.60

© European Southern Observatory • Provided by the NASA Astrophysics Data System

1993A&AS..101..587D

Table 1. continued

PERTURBER DENSITY = 0.1E+18 cm-3

PERTURBERS ARE:		ELECTRONS		PROTONS		He III	
TRANSITION	T(K)	WIDTH(A)	SHIFT(A)	WIDTH(A)	SHIFT(A)	WIDTH(A)	SHIFT(A)
FVII 2P-3S	100000.	0.486E-04	0.304E-05	0.690E-06	0.272E-05	0.133E-05	0.543E-05
134.8 A	200000.	0.365E-04	0.375E-05	0.227E-05	0.440E-05	0.449E-05	0.890E-05
C= 0.56E+18	500000.	0.257E-04	0.364E-05	0.533E-05	0.664E-05	0.107E-04	0.135E-04
	1000000.	0.202E-04	0.351E-05	0.754E-05	0.795E-05	0.154E-04	0.162E-04
FVII 2P-4S	100000.	0.702E-04	0.860E-05	0.499E-05	0.855E-05	0.995E-05	0.173E-04
97.3 A	200000.	0.545E-04	0.858E-05	0.900E-05	0.119E-04	0.180E-04	0.241E-04
C= 0.12E+18	500000.	0.401E-04	0.811E-05	0.145E-04	0.152E-04	0.296E-04	0.310E-04
	1000000.	0.323E-04	0.728E-05	0.184E-04	0.178E-04	0.384E-04	0.367E-04
FVII 2P-5S	100000.	0.139E-03	0.220E-04	0.177E-04	0.236E-04	0.355E-04	0.476E-04
86.4 A	200000.	0.109E-03	0.208E-04	0.272E-04	0.290E-04	0.550E-04	0.591E-04
C= 0.48E+17	500000.	0.819E-04	0.191E-04	0.374E-04	0.368E-04	0.755E-04	0.754E-04
	1000000.	0.662E-04	0.156E-04	0.461E-04	0.420E-04	0.944E-04	0.854E-04
FVII 2P-6S	100000.	0.272E-03	0.477E-04	0.480E-04	0.528E-04	0.976E-04	0.106E-03
81.5 A	200000.	0.216E-03	0.453E-04	0.622E-04	0.642E-04	0.129E-03	0.130E-03
C= 0.24E+17	500000.	0.163E-03	0.387E-04	0.830E-04	0.783E-04	*0.175E-03	*0.156E-03
	1000000.	0.131E-03	0.308E-04	0.949E-04	0.890E-04	*0.199E-03	*0.182E-03
FVII 3P-4S	100000.	0.163E-02	0.125E-03	0.743E-04	0.126E-03	0.147E-03	0.253E-03
392.0 A	200000.	0.125E-02	0.126E-03	0.134E-03	0.174E-03	0.268E-03	0.354E-03
C= 0.16E+19	500000.	0.915E-03	0.120E-03	0.219E-03	0.223E-03	0.445E-03	0.457E-03
	1000000.	0.734E-03	0.108E-03	0.277E-03	0.268E-03	0.558E-03	0.549E-03
FVII 3P-5S	100000.	0.147E-02	0.193E-03	0.157E-03	0.210E-03	0.315E-03	0.423E-03
260.1 A	200000.	0.115E-02	0.182E-03	0.242E-03	0.258E-03	0.489E-03	0.526E-03
C= 0.43E+18	500000.	0.857E-03	0.168E-03	0.336E-03	0.327E-03	0.667E-03	0.668E-03
	1000000.	0.692E-03	0.137E-03	0.405E-03	0.373E-03	0.841E-03	0.759E-03
FVII 3P-6S	100000.	0.213E-02	0.343E-03	0.349E-03	0.384E-03	0.710E-03	0.767E-03
220.3 A	200000.	0.169E-02	0.326E-03	0.452E-03	0.466E-03	0.940E-03	0.943E-03
C= 0.18E+18	500000.	0.127E-02	0.279E-03	0.600E-03	0.568E-03	*0.129E-02	*0.114E-02
	1000000.	0.102E-02	0.222E-03	0.690E-03	0.647E-03	*0.144E-02	*0.133E-02
FVII 4P-5S	100000.	0.220E-01	0.181E-02	0.138E-02	0.182E-02	0.276E-02	0.366E-02
855.8 A	200000.	0.173E-01	0.170E-02	0.215E-02	0.228E-02	0.438E-02	0.465E-02
C= 0.31E+19	500000.	0.129E-01	0.159E-02	0.294E-02	0.288E-02	0.610E-02	0.584E-02
	1000000.	0.104E-01	0.131E-02	0.358E-02	0.332E-02	0.729E-02	0.681E-02
FVII 4P-6S	100000.	0.150E-01	0.193E-02	0.198E-02	0.216E-02	0.402E-02	0.435E-02
536.9 A	200000.	0.119E-01	0.183E-02	0.262E-02	0.262E-02	0.535E-02	0.537E-02
C= 0.11E+19	500000.	0.894E-02	0.157E-02	0.358E-02	0.315E-02	0.746E-02	0.667E-02
	1000000.	0.721E-02	0.125E-02	0.401E-02	0.367E-02	*0.798E-02	*0.741E-02
FVII 5P-6S	100000.	0.176	0.141E-01	0.136E-01	0.141E-01	0.274E-01	0.285E-01
1586.7 A	200000.	0.140	0.134E-01	0.177E-01	0.171E-01	0.361E-01	0.352E-01
C= 0.56E+19	500000.	0.105	0.119E-01	0.233E-01	0.213E-01	0.491E-01	0.435E-01
	1000000.	0.851E-01	0.947E-02	0.278E-01	0.250E-01	0.560E-01	0.503E-01

© European Southern Observatory • Provided by the NASA Astrophysics Data System

1993A&AS..101..587D

Table 1. continued

PERTURBER DENSITY = 0.1E+19 cm-3

PERTURBERS ARE:		ELECTRONS		PROTONS		He III	
TRANSITION	T(K)	WIDTH(A)	SHIFT(A)	WIDTH(A)	SHIFT(A)	WIDTH(A)	SHIFT(A)
FVII 2S-2P	100000.	0.911E-02	-0.466E-04	0.173E-04	-0.675E-04	0.323E-04	-0.130E-03
885.6 A	200000.	0.651E-02	-0.168E-03	0.557E-04	-0.136E-03	0.105E-03	-0.270E-03
C= 0.89E+21	500000.	0.428E-02	-0.186E-03	0.201E-03	-0.285E-03	0.389E-03	-0.574E-03
	1000000.	0.318E-02	-0.181E-03	0.368E-03	-0.411E-03	0.727E-03	-0.833E-03
FVII 2S-3P	100000.	0.563E-03	0.656E-05	0.114E-04	0.178E-04	0.218E-04	0.341E-04
113.0 A	200000.	0.418E-03	0.740E-05	0.254E-04	0.294E-04	0.498E-04	0.591E-04
C= 0.13E+19	500000.	0.292E-03	0.667E-05	0.480E-04	0.450E-04	0.958E-04	0.917E-04
	1000000.	0.227E-03	0.567E-05	0.620E-04	0.540E-04	0.125E-03	0.110E-03
FVII 2S-4P	100000.	0.967E-03	0.282E-04	0.677E-04	0.808E-04	0.135E-03	0.154E-03
86.7 A	200000.	0.744E-03	0.307E-04	0.113E-03	0.114E-03	0.227E-03	0.229E-03
C= 0.32E+18	500000.	0.541E-03	0.271E-04	0.157E-03	0.147E-03	0.322E-03	0.297E-03
	1000000.	0.432E-03	0.206E-04	0.202E-03	0.175E-03	0.402E-03	0.359E-03
FVII 2S-5P	100000.	0.189E-02	0.743E-04	0.243E-03	0.239E-03	*0.483E-03	*0.444E-03
78.4 A	200000.	0.149E-02	0.820E-04	0.321E-03	0.299E-03	*0.656E-03	*0.595E-03
C= 0.14E+18	500000.	0.111E-02	0.648E-04	0.432E-03	0.388E-03	*0.861E-03	*0.791E-03
	1000000.	0.895E-03	0.523E-04	0.511E-03	0.436E-03	*0.108E-02	*0.906E-03
FVII 3S-3P	100000.	0.629	-0.814E-02	0.700E-02	0.130E-03	0.132E-01	0.250E-03
3257.4 A	200000.	0.472	-0.134E-01	0.139E-01	0.267E-03	0.268E-01	0.530E-03
C= 0.11E+22	500000.	0.334	-0.131E-01	0.239E-01	0.651E-03	0.468E-01	0.131E-02
	1000000.	0.264	-0.133E-01	0.289E-01	0.113E-02	0.574E-01	0.227E-02
FVII 3S-4P	100000.	0.161E-01	0.278E-03	0.964E-03	0.113E-02	0.192E-02	0.215E-02
335.2 A	200000.	0.124E-01	0.251E-03	0.160E-02	0.159E-02	0.319E-02	0.320E-02
C= 0.48E+19	500000.	0.905E-02	0.208E-03	0.226E-02	0.204E-02	0.455E-02	0.414E-02
	1000000.	0.725E-02	0.117E-03	0.276E-02	0.246E-02	0.544E-02	0.497E-02
FVII 3S-5P	100000.	0.182E-01	0.609E-03	0.220E-02	0.216E-02	*0.437E-02	*0.401E-02
237.2 A	200000.	0.143E-01	0.647E-03	0.292E-02	0.271E-02	*0.595E-02	*0.540E-02
C= 0.12E+19	500000.	0.106E-01	0.495E-03	0.392E-02	0.353E-02	*0.771E-02	*0.716E-02
	1000000.	0.859E-02	0.383E-03	0.462E-02	0.394E-02	*0.959E-02	*0.824E-02
FVII 4S-4P	100000.	12.1	-0.286	0.340	0.220	0.657	0.422
7961.1 A	200000.	9.35	-0.287	0.520	0.329	1.02	0.658
C= 0.27E+22	500000.	6.88	-0.297	0.719	0.462	1.44	0.938
	1000000.	5.54	-0.298	0.842	0.555	1.68	1.12
FVII 4S-5P	100000.	0.201	0.209E-02	0.194E-01	0.189E-01	*0.388E-01	*0.352E-01
736.5 A	200000.	0.158	0.257E-02	0.261E-01	0.238E-01	*0.521E-01	*0.474E-01
C= 0.12E+20	500000.	0.118	0.123E-02	0.339E-01	0.301E-01	*0.699E-01	*0.616E-01
	1000000.	0.952E-01	0.575E-03	0.403E-01	0.354E-01	*0.809E-01	*0.712E-01
FVII 2P-3S	100000.	0.490E-03	0.246E-04	0.691E-05	0.265E-04	0.133E-04	0.509E-04
134.8 A	200000.	0.364E-03	0.375E-04	0.227E-04	0.436E-04	0.449E-04	0.876E-04
C= 0.56E+19	500000.	0.257E-03	0.363E-04	0.533E-04	0.663E-04	0.107E-03	0.135E-03
	1000000.	0.202E-03	0.351E-04	0.754E-04	0.795E-04	0.154E-03	0.162E-03

© European Southern Observatory • Provided by the NASA Astrophysics Data System

1993A&AS..101..587D

Table 1. continued

PERTURBER DENSITY = 0.1E+19 cm-3

PERTURBERS ARE:		ELECTRONS		PROTONS		He III	
TRANSITION	T(K)	WIDTH(A)	SHIFT(A)	WIDTH(A)	SHIFT(A)	WIDTH(A)	SHIFT(A)
FVII 2P-4S	100000.	0.705E-03	0.795E-04	0.498E-04	0.824E-04	0.994E-04	0.158E-03
97.3 A	200000.	0.545E-03	0.838E-04	0.901E-04	0.117E-03	0.180E-03	0.235E-03
C= 0.12E+19	500000.	0.401E-03	0.809E-04	0.145E-03	0.151E-03	0.296E-03	0.309E-03
	1000000.	0.323E-03	0.728E-04	0.184E-03	0.178E-03	0.384E-03	0.366E-03
FVII 2P-5S	100000.	0.139E-02	0.203E-03	0.176E-03	0.224E-03	*0.353E-03	*0.418E-03
86.4 A	200000.	0.109E-02	0.201E-03	0.272E-03	0.284E-03	*0.550E-03	*0.568E-03
C= 0.48E+18	500000.	0.819E-03	0.190E-03	0.374E-03	0.367E-03	*0.755E-03	*0.749E-03
	1000000.	0.662E-03	0.156E-03	0.461E-03	0.420E-03	*0.945E-03	*0.851E-03
FVII 2P-6S	100000.	0.272E-02	0.428E-03	*0.478E-03	*0.486E-03		
81.5 A	200000.	0.216E-02	0.433E-03	*0.620E-03	*0.625E-03		
C= 0.24E+18	500000.	0.163E-02	0.384E-03	*0.830E-03	*0.780E-03		
	1000000.	0.131E-02	0.308E-03	*0.949E-03	*0.890E-03		
FVII 3P-4S	100000.	0.163E-01	0.120E-02	0.743E-03	0.121E-02	0.147E-02	0.232E-02
392.0 A	200000.	0.125E-01	0.124E-02	0.134E-02	0.172E-02	0.268E-02	0.345E-02
C= 0.16E+20	500000.	0.915E-02	0.119E-02	0.219E-02	0.222E-02	0.445E-02	0.456E-02
	1000000.	0.734E-02	0.108E-02	0.277E-02	0.268E-02	0.558E-02	0.548E-02
FVII 3P-5S	100000.	0.147E-01	0.180E-02	0.157E-02	0.199E-02	*0.314E-02	*0.372E-02
260.1 A	200000.	0.115E-01	0.176E-02	0.242E-02	0.253E-02	*0.490E-02	*0.506E-02
C= 0.43E+19	500000.	0.857E-02	0.167E-02	0.336E-02	0.326E-02	*0.667E-02	*0.665E-02
	1000000.	0.692E-02	0.137E-02	0.405E-02	0.373E-02	*0.841E-02	*0.757E-02
FVII 3P-6S	100000.	0.213E-01	0.309E-02	*0.348E-02	*0.353E-02		
220.3 A	200000.	0.169E-01	0.312E-02	*0.450E-02	*0.454E-02		
C= 0.18E+19	500000.	0.127E-01	0.277E-02	*0.600E-02	*0.565E-02		
	1000000.	0.102E-01	0.222E-02	*0.690E-02	*0.647E-02		
FVII 4P-5S	100000.	0.220	0.170E-01	0.138E-01	0.174E-01	*0.276E-01	*0.325E-01
855.8 A	200000.	0.173	0.165E-01	0.215E-01	0.224E-01	*0.438E-01	*0.448E-01
C= 0.31E+20	500000.	0.129	0.158E-01	0.294E-01	0.287E-01	*0.610E-01	*0.581E-01
	1000000.	0.104	0.131E-01	0.358E-01	0.332E-01	*0.729E-01	*0.679E-01
FVII 4P-6S	100000.	0.150	0.174E-01	*0.200E-01	*0.200E-01		
536.9 A	200000.	0.119	0.175E-01	*0.261E-01	*0.253E-01		
C= 0.11E+20	500000.	0.894E-01	0.155E-01	*0.358E-01	*0.314E-01		
	1000000.	0.721E-01	0.125E-01	*0.401E-01	*0.367E-01		
FVII 5P-6S	100000.	1.76	0.130	*0.136	*0.132		
1586.7 A	200000.	1.40	0.129	0.177	0.166		
C= 0.56E+20	500000.	1.05	0.118	0.233	0.213		
	1000000.	0.851	0.947E-01	0.278	0.250		

PERTURBER DENSITY = 0.1E+20 cm-3

FVII 2S-2P	100000.	0.914E-01	-0.838E-03	0.172E-03	-0.619E-03	0.318E-03	-0.110E-02
885.6 A	200000.	0.653E-01	-0.159E-02	0.557E-03	-0.132E-02	0.105E-02	-0.252E-02
C= 0.89E+22	500000.	0.428E-01	-0.186E-02	0.201E-02	-0.285E-02	0.389E-02	-0.568E-02
	1000000.	0.318E-01	-0.181E-02	0.368E-02	-0.411E-02	0.727E-02	-0.832E-02

© European Southern Observatory • Provided by the NASA Astrophysics Data System

1993A&AS..101..587D

Table 1. continued

PERTURBER DENSITY = 0.1E+20 cm-3

PERTURBERS ARE:		ELECTRONS		PROTONS		He III	
TRANSITION	T(K)	WIDTH(A)	SHIFT(A)	WIDTH(A)	SHIFT(A)	WIDTH(A)	SHIFT(A)
FVII 2S-3P	100000.	0.563E-02	0.538E-04	0.114E-03	0.162E-03	0.214E-03	0.288E-03
113.0 A	200000.	0.418E-02	0.614E-04	0.254E-03	0.283E-03	0.497E-03	0.542E-03
C= 0.13E+20	500000.	0.292E-02	0.645E-04	0.480E-03	0.449E-03	0.957E-03	0.898E-03
	1000000.	0.227E-02	0.559E-04	0.620E-03	0.539E-03	0.125E-02	0.110E-02
FVII 2S-4P	100000.	0.966E-02	0.161E-03	0.673E-03	0.703E-03		
86.7 A	200000.	0.743E-02	0.226E-03	0.113E-02	0.107E-02		
C= 0.32E+19	500000.	0.540E-02	0.265E-03	0.157E-02	0.146E-02		
	1000000.	0.432E-02	0.200E-03	0.202E-02	0.174E-02		
FVII 2S-5P	100000.	0.186E-01	0.197E-03				
78.4 A	200000.	0.147E-01	0.456E-03				
C= 0.14E+19	500000.	0.110E-01	0.619E-03	*0.432E-02	*0.385E-02		
	1000000.	0.886E-02	0.497E-03	*0.511E-02	*0.433E-02		
FVII 3S-3P	100000.	6.29	-0.843E-01	0.694E-01	0.120E-02	0.129	0.213E-02
3257.4 A	200000.	4.72	-0.134	0.139	0.260E-02	0.267	0.495E-02
C= 0.11E+23	500000.	3.34	-0.132	0.239	0.651E-02	0.467	0.129E-01
	1000000.	2.64	-0.133	0.289	0.113E-01	0.574	0.227E-01
FVII 3S-4P	100000.	0.161	0.103E-02	0.958E-02	0.984E-02		
335.2 A	200000.	0.124	0.142E-02	0.160E-01	0.149E-01		
C= 0.48E+20	500000.	0.904E-01	0.199E-02	0.226E-01	0.203E-01		
	1000000.	0.724E-01	0.108E-02	0.276E-01	0.245E-01		
FVII 3S-5P	100000.	0.179	0.112E-02				
237.2 A	200000.	0.141	0.319E-02				
C= 0.12E+20	500000.	0.105	0.468E-02	*0.392E-01	*0.351E-01		
	1000000.	0.851E-01	0.360E-02	*0.462E-01	*0.391E-01		
FVII 4S-5P	100000.	1.98	-0.213E-01				
736.5 A	200000.	1.56	-0.244E-02	*0.259	*0.213		
C= 0.12E+21	500000.	1.17	0.101E-01	*0.339	*0.299		
	1000000.	0.944	0.387E-02	*0.403	*0.352		
FVII 2P-3S	100000.	0.491E-02	0.242E-03	0.691E-04	0.241E-03	0.132E-03	0.428E-03
134.8 A	200000.	0.365E-02	0.354E-03	0.228E-03	0.420E-03	0.449E-03	0.801E-03
C= 0.56E+20	500000.	0.257E-02	0.362E-03	0.533E-03	0.662E-03	0.107E-02	0.132E-02
	1000000.	0.202E-02	0.349E-03	0.753E-03	0.793E-03	0.154E-02	0.162E-02
FVII 2P-4S	100000.	0.705E-02	0.693E-03	0.499E-03	0.724E-03	*0.994E-03	*0.124E-02
97.3 A	200000.	0.545E-02	0.768E-03	0.902E-03	0.110E-02	*0.180E-02	*0.202E-02
C= 0.12E+20	500000.	0.401E-02	0.802E-03	0.145E-02	0.151E-02	*0.296E-02	*0.297E-02
	1000000.	0.323E-02	0.721E-03	0.184E-02	0.178E-02	*0.384E-02	*0.364E-02
FVII 2P-5S	100000.	0.139E-01	0.159E-02	*0.177E-02	*0.186E-02		
86.4 A	200000.	0.109E-01	0.174E-02	*0.269E-02	*0.257E-02		
C= 0.48E+19	500000.	0.818E-02	0.188E-02	*0.374E-02	*0.364E-02		
	1000000.	0.662E-02	0.154E-02	*0.461E-02	*0.418E-02		

© European Southern Observatory • Provided by the NASA Astrophysics Data System

1993A&AS..101..587D

Table 1. continued

PERTURBER DENSITY = 0.1E+20 cm-3

PERTURBERS ARE:		ELECTRONS		PROTONS		He III	
TRANSITION	T(K)	WIDTH(A)	SHIFT(A)	WIDTH(A)	SHIFT(A)	WIDTH(A)	SHIFT(A)
FVII 2P-6S	100000.	0.270E-01	0.276E-02				
81.5 A	200000.	0.214E-01	0.336E-02				
C= 0.24E+19	500000.	0.162E-01	0.377E-02				
	1000000.	0.130E-01	0.300E-02				
FVII 3P-4S	100000.	0.163	0.104E-01	0.741E-02	0.107E-01	*0.146E-01	*0.184E-01
392.0 A	200000.	0.125	0.114E-01	0.133E-01	0.162E-01	*0.269E-01	*0.301E-01
C= 0.16E+21	500000.	0.915E-01	0.119E-01	0.219E-01	0.222E-01	*0.445E-01	*0.439E-01
	1000000.	0.734E-01	0.107E-01	0.277E-01	0.267E-01	*0.558E-01	*0.545E-01
FVII 3P-5S	100000.	0.147	0.140E-01	*0.157E-01	*0.165E-01		
260.1 A	200000.	0.115	0.152E-01	*0.240E-01	*0.228E-01		
C= 0.43E+20	500000.	0.857E-01	0.165E-01	*0.336E-01	*0.324E-01		
	1000000.	0.691E-01	0.134E-01	*0.405E-01	*0.371E-01		
FVII 3P-6S	100000.	0.212	0.199E-01				
220.3 A	200000.	0.168	0.242E-01				
C= 0.18E+20	500000.	0.126	0.271E-01				
	1000000.	0.102	0.216E-01				
FVII 4P-5S	100000.	2.20	0.138	*0.137	*0.146		
855.8 A	200000.	1.72	0.146	*0.215	*0.203		
C= 0.31E+21	500000.	1.28	0.156	*0.294	*0.285		
	1000000.	1.04	0.129	*0.358	*0.330		
FVII 4P-6S	100000.	1.49	0.113				
536.9 A	200000.	1.18	0.136				
C= 0.11E+21	500000.	0.889	0.152				
	1000000.	0.718	0.122				
FVII 5P-6S	100000.	17.4	0.951				
1586.7 A	200000.	13.8	1.08				
C= 0.56E+21	500000.	10.4	1.16				
	1000000.	8.45	0.927				
PERTURBER DENSITY = 0.1E+21 cm-3							
FVII 2S-2P	200000.	0.653	-0.144E-01	0.553E-02	-0.120E-01	0.103E-01	-0.210E-01
885.6 A	500000.	0.428	-0.176E-01	0.201E-01	-0.276E-01	0.389E-01	-0.532E-01
C=0.89E+23	1000000.	0.318	-0.181E-01	0.368E-01	-0.407E-01	0.726E-01	-0.817E-01
	2000000.	0.243	-0.163E-01	0.565E-01	-0.529E-01	0.114	-0.108
FVII 2S-3P	200000.	0.417E-01	0.182E-03	0.251E-02	0.249E-02	*0.484E-02	*0.422E-02
113.0 A	500000.	0.291E-01	0.362E-03	0.479E-02	0.424E-02	*0.958E-02	*0.797E-02
C=0.13E+21	1000000.	0.227E-01	0.538E-03	0.620E-02	0.528E-02	*0.125E-01	*0.106E-01
	2000000.	0.180E-01	0.369E-03	0.752E-02	0.646E-02	*0.152E-01	*0.130E-01
FVII 2S-4P	200000.	0.715E-01	-0.137E-03				
86.7 A	500000.	0.524E-01	0.897E-03				
C=0.32E+20	1000000.	0.420E-01	0.184E-02				
	2000000.	0.341E-01	0.155E-02	*0.230E-01	*0.194E-01		

© European Southern Observatory • Provided by the NASA Astrophysics Data System

1993A&AS..101..587D

Table 1. continued

PERTURBER DENSITY = 0.1E+21 cm-3

PERTURBERS ARE:		ELECTRONS		PROTONS		He III	
TRANSITION	T(K)	WIDTH(A)	SHIFT(A)	WIDTH(A)	SHIFT(A)	WIDTH(A)	SHIFT(A)
FVII 2S-5P	200000.	0.131	-0.125E-02				
78.4 A	500000.	0.997E-01	0.739E-03				
C=0.14E+20	1000000.	0.817E-01	0.426E-02				
	2000000.	0.673E-01	0.348E-02				
FVII 3S-4P	200000.	1.20	-0.182E-01				
335.2 A	500000.	0.879	-0.399E-02				
C=0.48E+21	1000000.	0.706	0.861E-02				
	2000000.	0.574	0.681E-02	*0.332	*0.273		
FVII 3S-5P	200000.	1.26	-0.196E-01				
237.2 A	500000.	0.962	-0.195E-02				
C=0.12E+21	1000000.	0.788	0.296E-01				
	2000000.	0.649	0.237E-01				
FVII 4S-5P	200000.	14.1	-0.386				
736.5 A	500000.	10.8	-0.282				
C=0.12E+22	1000000.	8.83	-0.169E-01				
	2000000.	7.26	-0.932E-02				
FVII 2P-3S	200000.	0.365E-01	0.296E-02	0.226E-02	0.369E-02	*0.447E-02	*0.623E-02
134.8 A	500000.	0.257E-01	0.322E-02	0.532E-02	0.624E-02	*0.107E-01	*0.117E-01
C=0.56E+21	1000000.	0.202E-01	0.347E-02	0.753E-02	0.778E-02	*0.154E-01	*0.156E-01
	2000000.	0.161E-01	0.302E-02	0.964E-02	0.946E-02	*0.192E-01	*0.193E-01
FVII 2P-4S	200000.	0.542E-01	0.502E-02	*0.901E-02	*0.881E-02		
97.3 A	500000.	0.399E-01	0.628E-02	*0.145E-01	*0.136E-01		
C=0.12E+21	1000000.	0.322E-01	0.710E-02	*0.182E-01	*0.170E-01		
	2000000.	0.259E-01	0.574E-02	*0.219E-01	*0.204E-01		
FVII 2P-5S	200000.	0.104	0.698E-02				
86.4 A	500000.	0.786E-01	0.118E-01				
C=0.48E+20	1000000.	0.640E-01	0.149E-01				
	2000000.	0.516E-01	0.119E-01				
FVII 2P-6S	200000.	0.185	0.571E-02				
81.5 A	500000.	0.144	0.171E-01				
C=0.24E+20	1000000.	0.118	0.281E-01				
	2000000.	0.955E-01	0.229E-01				
FVII 3P-4S	200000.	1.25	0.763E-01	*0.132	*0.131		
392.0 A	500000.	0.911	0.941E-01	*0.220	*0.197		
C=0.16E+22	1000000.	0.732	0.105	*0.277	*0.259		
	2000000.	0.590	0.854E-01	*0.339	*0.304		
FVII 3P-5S	200000.	1.10	0.608E-01				
260.1 A	500000.	0.828	0.103				
C=0.43E+21	1000000.	0.671	0.130				
	2000000.	0.542	0.104				

© European Southern Observatory • Provided by the NASA Astrophysics Data System

1993A&AS..101..587D

Table 1. continued

PERTURBER DENSITY = 0.1E+21 cm-3							
PERTURBERS ARE:		ELECTRONS		PROTONS		He III	
TRANSITION	T(K)	WIDTH(A)	SHIFT(A)	WIDTH(A)	SHIFT(A)	WIDTH(A)	SHIFT(A)
FVII 3P-6S	200000.	1.46	0.399E-01				
220.3 A	500000.	1.13	0.122				
C=0.18E+21	1000000.	0.927	0.202				
	2000000.	0.750	0.165				
FVII 4P-5S	200000.	16.4	0.679				
855.8 A	500000.	12.4	1.05				
C=0.31E+22	1000000.	10.0	1.26				
	2000000.	8.15	0.999				
FVII 4P-6S	200000.	10.4	0.244				
536.9 A	500000.	8.06	0.700				
C=0.11E+22	1000000.	6.60	1.14				
	2000000.	5.35	0.927				
PERTURBER DENSITY = 0.1E+22 cm-3							
FVII 2S-3P	200000.	0.396	-0.663E-02				
113.0 A	500000.	0.280	-0.214E-02				
C=0.13E+22	1000000.	0.219	0.151E-03	*0.624E-01	*0.481E-01		
	2000000.	0.175	0.115E-02	*0.745E-01	*0.620E-01		
FVII 2S-4P	200000.	*0.586	*-0.107E-01				
86.7 A	500000.	0.450	-0.304E-02				
C=0.32E+21	1000000.	0.370	0.448E-03				
	2000000.	0.306	0.608E-02				
FVII 2S-5P	200000.	*0.918	*-0.108E-01				
78.4 A	500000.	*0.763	*-0.387E-02				
C=0.14E+21	1000000.	0.655	0.454E-02				
	2000000.	0.560	0.156E-01				
FVII 2P-3S	200000.	0.360	0.872E-02	*0.223E-01	*0.237E-01		
134.8 A	500000.	0.254	0.196E-01	*0.530E-01	*0.518E-01		
C=0.56E+22	1000000.	0.200	0.253E-01	*0.756E-01	*0.704E-01		
	2000000.	0.160	0.264E-01	*0.948E-01	*0.912E-01		
FVII 2P-4S	200000.	0.461	-0.215E-01				
97.3 A	500000.	0.356	0.176E-01				
C=0.12E+22	1000000.	0.292	0.339E-01				
	2000000.	0.239	0.407E-01				
FVII 2P-5S	200000.	0.676	-0.789E-01				
86.4 A	500000.	0.583	0.882E-02				
C=0.48E+21	1000000.	0.501	0.410E-01				
	2000000.	0.420	0.671E-01				
FVII 2P-6S	200000.	0.896	-0.153				
81.5 A	500000.	0.880	-0.183E-01				
C=0.24E+21	1000000.	0.796	0.434E-01				
	2000000.	0.687	0.110				

© European Southern Observatory • Provided by the NASA Astrophysics Data System

1993A&AS..101..587D

Table 1. continued

PERTURBER DENSITY = 0.1E+23 cm-3

PERTURBERS ARE:		ELECTRONS		PROTONS		He III	
TRANSITION	T(K)	WIDTH(A)	SHIFT(A)	WIDTH(A)	SHIFT(A)	WIDTH(A)	SHIFT(A)
FVII 2S-3P	200000.	*3.26	*-0.121E-01				
113.0 A	500000.	*2.40	*-0.155E-01				
C=0.13E+23	1000000.	1.93	-0.815E-02				
	2000000.	1.57	-0.660E-02				
FVII 2S-4P	200000.						
86.7 A	500000.	*3.25	*-0.146E-02				
C=0.32E+22	1000000.	*2.82	*0.331E-02				
	2000000.	2.44	0.259E-01				
FVII 2S-5P	200000.						
78.4 A	500000.						
C=0.14E+22	1000000.	*4.44	*0.122E-01				
	2000000.	*4.10	*0.544E-01				
FVII 2P-3S	200000.	2.71	-0.355				
134.8 A	500000.	2.14	-0.826E-01				
C=0.56E+23	1000000.	1.75	0.440E-01				
	2000000.	1.43	0.115				
FVII 2P-4S	200000.	1.95	-0.657				
97.3 A	500000.	2.03	-0.229				
C=0.12E+23	1000000.	1.90	-0.342E-01				
	2000000.	1.69	0.922E-01				
FVII 2P-5S	200000.	*1.24	*-1.03				
86.4 A	500000.	2.17	-0.393				
C=0.48E+22	1000000.	2.44	-0.127				
	2000000.	2.40	0.113				

Table 2. Comparison between F VII $3s^2S - 3p^2P^o$ experimental Stark widths (FWHM) W_m – Glenzer et al. 1992, with calculated widths: W_{DSB} – present results; W_G – calculations from Glenzer et al. (1992) by using the simplified semiclassical approach (Griem 1974, Eq. 526); W_{DK} – calculations from Glenzer et al. (1992) by using the modified semiempirical approach (Dimitrijević & Konjević 1980); W_{HB} – calculations from Glenzer et al. (1992) by using the method of Hey & Breger (1992). N_e is the perturber density and T is temperature

Ne(10+18 cm-3)	kT(eV)	Wm(A)	Wm/WDSB	Wm/WG	Wm/WDK	Wm/WHB
2.92	18.5	1.49	1.08	1.51	1.69	1.35
2.10	16.6	1.11	1.07	1.48	1.71	1.34
1.57	14.4	0.87	1.07	1.51	1.75	1.36

© European Southern Observatory • Provided by the NASA Astrophysics Data System

1993A&AS..102...17P

ASTRONOMY & ASTROPHYSICS
SUPPLEMENT SERIES

Astron. Astrophys. Suppl. Ser. **102**, 17-23 (1993)

Stark broadening of Zn II and Cd II spectral lines of astrophysical interest

L.Č. Popović, I. Vince and M.S. Dimitrijević

Astronomical Observatory, Volgina 7, 11050 Belgrade, Yugoslavia

Received December 22, 1992; accepted March 23, 1993

Abstract. — Using a modified semi-empirical approach, Stark broadening parameters for 12 Zn II and 8 Cd II spectral lines have been calculated as a function of temperature. The results obtained have been compared with available experimental data. The influence of the oscillator strengths accuracy on Stark broadening parameter calculation has been investigated.

Key words: lines; profile — atomic and molecular data

1. Introduction

Stark broadening data for singly charged zinc and cadmium ion lines are of interest for analysis of hot star spectra. The Zn II spectaral lines have been observed in different stellar spectra as e.g. in the case of several Hg-Mn stars (Sadakane et al. 1988) and Be stars (Danezis & Theodossiou 1990; Danezis et al. 1991), where Stark broadening is the principal pressure broadening mechanism. Sadakane et al. (1988) observed two spectral lines of Zn II (λ =206.2 nm and 206.4 nm) in 23 Hg-Mn stars. When compared with spectra of reference (normal) stars, Zn II lines in several Hg-Mn stars are found to be stronger. Danezis & Theodossiou (1990) and Danezis et al. (1991) indentified several Zn II lines in spectra of Be stars. In spectra of AX Mon, Zn II resonance lines have been observed with radial velocities −58 km/s (λ =202.5 nm) and −230 km/s (λ =206.2 nm). Zinc is also important in astrophysics for nucleosynthesis research since it is likely produced by explosive Si – burning in SNe. Moreover, the observed Cu/Zn ratio as a function of metal abundance is not in accordance with current predictions (Sneden et al. 1991).

Besides the astrophysical importance, Stark broadening data of considered ions are significant for investigation of laboratory plasma as well. Measurements of Stark widths and shifts of singly ionized Zn and Cd spectral lines have been performed by Kusch & Oberschelp (1967ab), and Djeniže et al. (1991ab). In this paper we present calculated Stark width and shift data for 12 Zn II, and 8 Cd II spectral lines, for electron density $N_e = 10^{23}$ m^{-3}. Our results have been compared with available experimental data (Djeniže et al. 1991ab; Kusch & Oberschelp 1967ab). The influence of the oscillator strength accuracy on Stark broadening parameters has been investigated as well.

2. Theory

According to the modified semi-empirical approach (MSE), electron impact half width (HWHM) of an ion line is given by the expression (Dimitrijević & Konjević 1980; Dimitrijević & Kršljanin 1986; Dimitrijević 1988):

$$w + id = N\frac{h^2}{3m^2}\left(\frac{2m}{3\pi kT}\right)^{1/2} \cdot \left\{\sum_{j=\mathrm{i,f}} \mathbf{R}^2_{l_j,l_j+1}\left[\tilde{g}\left(x_{l_j,l_j+1}\right) + i\epsilon_j\tilde{g}_{\mathrm{sh}}\left(x_{l_j,l_j+1}\right)\right] + \sum_{j=\mathrm{i,f}} \mathbf{R}^2_{l_j,l_j-1}\left[\tilde{g}\left(x_{l_j,l_j-1}\right) - i\epsilon_j\tilde{g}_{\mathrm{sh}}\left(x_{l_j,l_j-1}\right)\right] + \sum_{j'}\left(\mathbf{R}^2_{jj'}\right)_{\Delta n\neq 0}\left[g\left(x_j\right) + i\epsilon_j\, g_{\mathrm{sh}}\left(x_j\right)\right] - 2i\epsilon_j \sum_{\Delta E_{jj'}<0}\left(\mathbf{R}^2_{jj'}\right)_{\Delta n\neq 0} g_{\mathrm{sh}}\left(x_j\right)\right\}, \quad (1)$$

where $\mathbf{R}^2_{jj'}(j = \mathrm{i,f})$ (in units of the Bohr radius a_0^2) is the square of the coordinate operator matrix element

$$\mathbf{R}^2_{l,l'} \approx \left(\frac{3n^*}{2Z}\right)^2 \frac{l_>}{2l+1}\left[n^{*2} - l_>^2\right]\varphi^2_{l,l'}, \quad (2)$$

Send offprint requests to: L.Č. Popović or M.S. Dimitrijević

© European Southern Observatory • Provided by the NASA Astrophysics Data System

1993A&AS..102...17P

$$\sum_{j'} \left(\mathbf{R}^2_{jj'}\right)_{\Delta n \neq 0} \approx \left(\frac{3n^*}{2Z}\right)^2 \frac{1}{9}\left(n_j^{*2} + 3l_j^2 + 3l_j + 11\right). \quad (3)$$

If we want to calculate separately Stark broadening parameters for a line within a particular multiplet, instead of $\mathbf{R}^2_{l,l'}$ we have $\sum_{J',L'} \mathbf{R}^2_{J,J'}$ where

$$\mathbf{R}^2_{J,J'} \approx \left(\frac{3n^*}{2Z}\right)^2 \frac{l_>}{2J+1}\left[n^{*2} - l_>^2\right] \mathcal{R}^2_{\rm line}\mathcal{R}^2_{\rm mult.}\varphi^2_{J,J'}, \quad (4)$$

or (if we know oscillator strengths, see e.g. Griem, 1974. Eq. (76))

$$\mathbf{R}^2_{J,J'} \approx 3\frac{E_{\rm H}}{E_{J'} - E_J}.f_{J'J} \quad \text{for} \quad (E_{J'} > E_J),$$

or

$$\mathbf{R}^2_{J,J'} \approx 3\frac{E_{\rm H}}{E_J - E_{J'}}\frac{2J'+1}{2J+1}\,.\,f_{JJ'} \quad \text{for} \quad (E_{J'} < E_J), \quad (5)$$

where the summation is performed over corresponding L' and J' quantum numbers (transitions $nlSLJ \rightarrow nl'SL'J'$); $\mathcal{R}_{\rm line}$, $\mathcal{R}_{\rm mult.}$, are the line and multiplet factors (Shore & Menzel 1965), and $f_{J'J}$ for $E_{J'} > E_J$ or $f_{JJ'}$ for $E_{J'} < E_j$ are the absorption oscillator strengths. If we want to use oscillator strength values (e.g. from literature) for particular $J \rightarrow J'$ transitions, but not to make a disctinction between particular lines within a multiplet, we must take into account that we will consider an averaged value for the multiplet as a whole, instead of a bulk of lines within this multiplet, characterized with different J-values. Consequently, we must introduce an averaging over different J-values within the multiplet considered, i.e. instead of $R_{l,l'}$ we have

$$\frac{\sum_{JJ'L'}(2J+1)\,\mathbf{R}^2_{JJ'}}{\sum_J(2J+1)} = \frac{\sum_{JJ'L'}(2J+1)\,\mathbf{R}^2_{JJ'}}{(2L+1)(2S+1)}. \quad (6)$$

In Eqs. (1-6) with i, f, i′, f′ are denoted initial and final level respectively and their corresponding perturbing levels, l_j is the angular momentum quatum number, $l_> = \max(l, l')$, and φ is the Bates-Damgaard factor (Bates & Damgaard 1949; Oertel & Shomo 1968), g, $g_{\rm sh}$ (Griem 1968) and $\tilde{g}$, $\tilde{g}_{\rm sh}$ (Dimitrijević & Konjević 1980; Dimitrijević & Kršljanin 1986) are the corresponding Gaunt factors; $x_{j,j'} = 3kT/2\,|\Delta E_{j,j'}|$ $(\Delta E_{jj'} = E_{j'} - E_j)$, T is the electron temperature, $x_{n_j} = 3kTn_j^{*3}/4Z^2E_{\rm H}$ ($E_{\rm H}$ is the hydrogen ionization energy, Z is the residual ionic charge ($Z = 1$ for neutrals, 2 for single charged ions, etc.), $n_j^* = \left[E_{\rm H}Z^2/\left(E_{\rm ion} - E_j\right)\right]^{1/2}$ is the effective principal quantum number ($E_{\rm ion}$ is appropriate spectral series limit), and N is the electron density.

In the cases when perturbing levels which strongly violate the assumed approximations exist, i.e. if there are levels with $|\Delta E_{jj'}| < \left(2Z^2E_{\rm H}\right)/n_j^{*3}$ for $x_{jj'} > 2$, the correction to Eq. (1) may be done by adding the following expression (Dimitrijević 1988):

$$w_c + id_c = N\frac{h^2}{3m^2}\left(\frac{2m}{3\pi kT}\right)^{1/2}.$$

$$\sum_{m'} \mathbf{R}^2_{jj'}\left\{g\left(x_{jj'}\right) - g\left(x_j\right) \pm i\epsilon_j\left[g_{\rm sh}\left(x_{jj'}\right) \pm g_{\rm sh}\left(x_j\right)\right]\right\}. \quad (7)$$

Here, m' is the number of such perturbing levels.

3. Results and discussion

Atomic energy levels needed for calculation have been taken from Moore (1971). Oscillator strengths from Wiese & Martin (1980) for Zn II and from Kunisz et al. (1975) for Cd II lines, have been used when available. Otherwise Coulomb approximation (Bates & Damgaard 1949) has been applied.

Stark line full widths (FWHM) and shifts for 12 Zn II and 8 Cd II spectral lines obtained by using the MSE method (Dimitrijević & Konjević 1980), are presented in Table 1 and Table 2, respectively. Stark widths and shifts are calculated for an electron density of 10^{23} m^{-3} and temperatures from 5,000 up to 50,000 K. The multiplets are selected according to their astrophysical importance (see e.g. Moore 1952, and 1962; Sadakane et al. 1988; etc.) and according to the available experimental data (Djeniže et al. 1991ab; Kusch & Oberschelp 1967ab).

In Figs. 1-6 and Table 3 our results for Zn II and Cd II Stark widths and shifts have been compared with available experimental data (Kusch & Oberschelp 1967ab; Djeniže et al. 1991ab) and with simple estimates (Lakićević 1983) based on regularities examination. One can see that in the case of more recent experimental values of Djeniže et al. (1991ab) the agreement between experimental and theoretical data for line width is slightly better in the case of the modified semi-empirical approach (Dimitrijević & Konjević 1980) than for Griem's (1968) semi-empirical method. All measured shifts are much smaller than corresponding widths. Taking into account the complexity of radiators and the fact that calculated shifts are of less accuracy than widths (see e.g. Dimitrijević et al. 1981) when they are much less than widths (Wiese & Konjević 1992) as in the present case, the presented ratios of experimental to theoretical shifts are of much less importance and are given here only for completeness. As a check of the influence of the oscillator strength uncertainty, our results are presented in Figs. 1-6 together with results obtained with oscillator strengths with Bates & Damgaard (1949) approximation only. Moreover, for Cd II lines results obtained by using oscillator strengths from Wiese & Martin (1980) have been added to previously mentioned results in Figs. 3-6. Different oscillator strengths for Cd II spectral lines are compared in the Table 4. We can see that the obtained differences in Stark broadening parameters are

© European Southern Observatory • Provided by the NASA Astrophysics Data System

1993A&AS..102...17P

within the error bars of the method, but in the case of the shift the accuracy of oscillator strengths may be very important. This is well illustrated in Fig. 6 where even the sign of shift is different for two different oscillator strength sets. We can conclude that shifts are more sensitive to the oscillator strength accuracy than widths as discussed e.g. in Sahal-Bréchot (1969). While oscillator strengths enter in the semi-empirical calculations directly, different short range effects enter implicitely in the semi-empirical Gaunt factor. Since this part is determined in order to be in accordance with experimental data, it is not surprising that, when quantum effects are important, semi-empirical values are sometimes in better accordance with experimental data than the semi-classical ones. The Stark broadening parameter differences with oscillator strength variation we have presented, might also give an impression of the errors of obtained results.

Table 4. Comparison between different oscillator strengths for CdII; $f_{\rm WM}$ – Wiese & Martin (1980), $f_{\rm KMR}$ – Kunisz et al. (1975), $f_{\rm C}$ – present calculations by using Bates & Damgard (1949) method (Coulomb approximation)

Transition	λ [nm]	f_{WM}	f_{KMR}	f_C
$5s^2S_{1/2} - 5p^2P^0_{1/2}$	226.50	0.23	0.321	0.291
$5s^2S_{1/2} - 5p^2P^0_{3/2}$	214.44	0.39	0.674	0.612
$5p^2P^0_{1/2} - 6s^2S_{1/2}$	257.29	0.17	0.148	0.119
$5p^2P^0_{3/2} - 6s^2S_{1/2}$	274.85	0.16	0.136	0.135
$5p^2P^0_{3/2} - 5s^2\ ^2D_{5/2}$	441.56	0.006	-	-

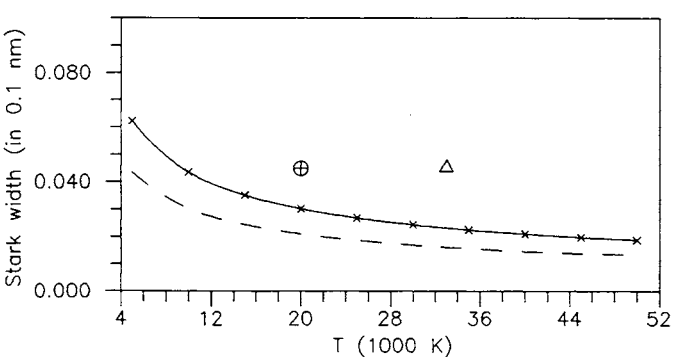

Fig. 1. Stark full width (FWHM) for the Zn II 206.20 nm $\left(4s^2S_{1/2} - 4p^2P^0_{1/2}\right)$ spectral line as a function of temperature (T), at electron density of $N = 10^{23}$ m^{-3}. The used notations are: (***) present results calculated by using the modified semi-empirical method (Dimitrijević & Konjević 1980) with oscillator strenghts by Wiese & Martin (1980) when available, (- - -) present results with Coulomb approximation only for oscillator strengths. Experimental data: (Δ)Djeniže et al. (1991a); (⊕) the estimate of Lakićević (1983)

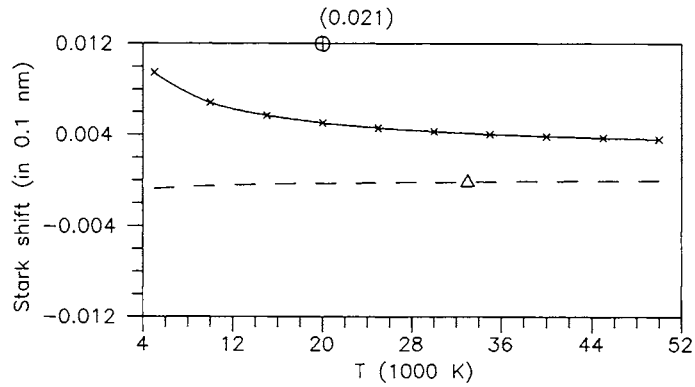

Fig. 2. Same as in Fig. 1 but for the shift

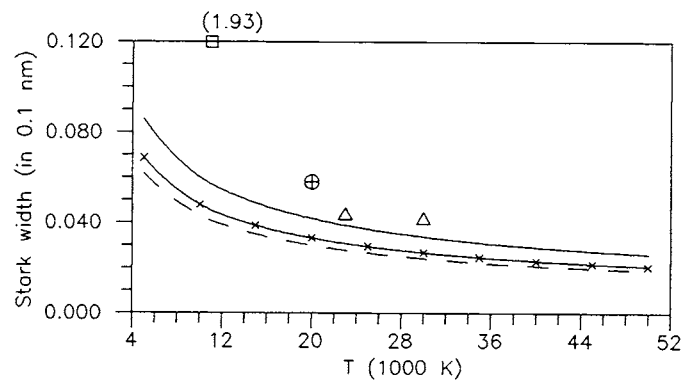

Fig. 3. Stark full width (FWHM) for the Cd II 226.50 nm $\left(5s^2S_{1/2} - 5p^2P^0_{1/2}\right)$ spectral line as a function of temperature (T), at electron density of $N = 10^{23}$ m^{-3}. The notations used are: (—) present results calculated by using the modified semi-empirical method (Dimitrijević & Konjević 1980) with oscillator strengths by Kunisz et al. (1975) when available, (**) present results with oscillator strengths by Wiese & Martin (1980) when available, (- - -) present results with Coulomb approximation only for oscillator strengths. Experimental data: (Δ)Djeniže et al. (1991ab); (□) Kusch & Oberschelp (1967b); ⊕ the estimate of Lakićević (1983)

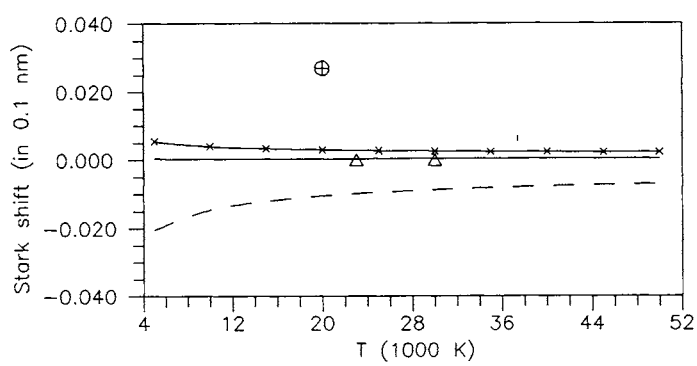

Fig. 4. Same as in Fig. 3 but for the shift

© European Southern Observatory • Provided by the NASA Astrophysics Data System

1993A&AS..102...17P

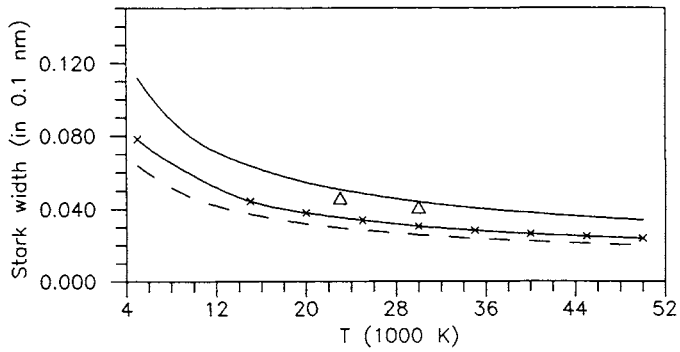

Fig. 5. Same as in Fig. 3. but for the Cd II 214.44 nm $\left(5s^2S_{1/2} - 5p^2P^0_{3/2}\right)$ spectral line

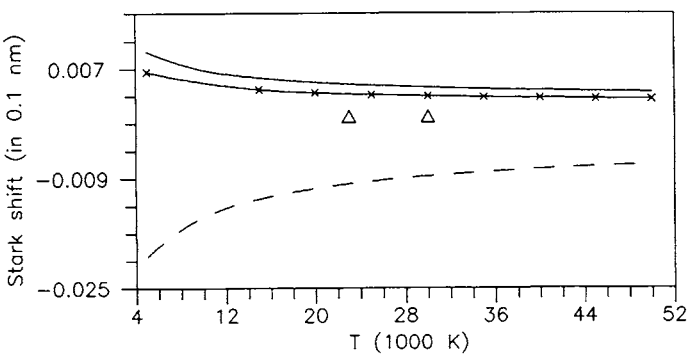

Fig. 6. Same as in Fig. 5 but for the shift

References

Bates D.R. & Damgaard A. 1949, Phyl. Trans. Roy. Soc. London A242, 101

Danezis E. & Theodossiou E. 1990, Ap&SS 174, 49

Danezis E., Theodossiou E. & Laskarides P.G. 1991, Ap&SS 179, 111

Dimitrijević M.S. 1988, A&AS 76, 451

Dimitrijević M.S., Feautrier N. & Sahal-Bréchot S. 1981, J. Phys. B14, 2559

Dimitrijević M.S. & Konjević N. 1980, JQSRT 24, 451

Dimitrijević M.S. & Kršljanin V. 1986, A&A 165, 269

Djeniže S., Srećković A., Labat J., Konjević R. & Popović L. 1991a, Phys. Rev. A 44, 410

Djeniže S., Srećković A., Labat J. & Nikolić B. 1991b, Proceedings of the XX ICPIG, Pisa, p. 1410

Griem H.R. 1968, Phys. Rev. 165, 258

Griem H.R. 1974, Spectral line Broadening by Plasmas, Academic Press, New York and London

Kunisz M.D., Migdalek J. & Rutkowski J. 1975, Acta Phys. Pol. A47, 227

Kusch H.J. & Oberschelp E. 1967a, Z. Astrophys. 67, 77

Kusch H.J. & Oberschelp E. 1967b, Z. Astrophys. 67, 85

Lakićević I.S. 1983, A&A 127, 37

Moore C.E. 1952, An Ultraviolet Multiplet table, Section 2, US Department of Commerce, Washington D.C.

Moore C.E. 1962, An Ultraviolet Multiplet table, Section 3, US Department of Commerce, Washington D.C.

Moore C.E. 1971, Atomic Energy Levels, Vols. II, III, NSRDS-NBS 35, US Department of Commerce, Washington D.C.

Oertel G.K. & Shomo L.P. 1968, ApJS 16, 175

Sadakane K., Jugaku J. & Takada-Hidai M. 1988, ApJ 325, 776

Sahal-Bréchot S. 1969, A&A 2, 322

Shore B.W. & Menzel D.H. 1965, ApJ 12, 187

Sneden C., Gratton R.G. & Crocker D.A. 1991, A&A 246, 354

Wiese W.L. & Konjević N. 1992, JQSRT 47, 185

Wiese W.L. & Martin G.A. 1980, Wavelengths and Transition Probabilities for Atoms and Atomic Ions, Part II, U.S. Department of commerce/National Bureau of Standard, Washington D.C.

© European Southern Observatory • Provided by the NASA Astrophysics Data System

1993A&AS..102...17P

Table 1. Stark full width (FWHM) and shift of Zn II spectral lines of astrophysical interest. The electron density is 10^{23} m^{-3}. The parameter $X = \frac{3kT}{2|\Delta E|}$, where ΔE is the energy difference between the closest perturbing level and the corresponding initial or final level, is calculated for $T = 10,000$ K. The averaged wavelength of the multiplet is denoted by $\bar{\lambda}$

TRANSITION	T (K)	WIDTH [nm]	SHIFT [nm]	TRANSITION	WIDTH [nm]	SHIFT [nm]
	5000.	.622E-02	.950E-03		.668E-02	.123E-02
$4s^2S_{1/2} - 4p^2P^0_{1/2}$	10000.	.434E-02	.685E-03	$4s^2S_{1/2} - 4p^2P^0_{3/2}$	.466E-02	.882E-03
$\lambda = 206.19$ nm	20000.	.302E-02	.504E-03	$\lambda = 202.55$ nm	.324E-02	.646E-03
$X = 0.258$	30000.	.244E-02	.428E-03	$X = 0.269$	.262E-02	.548E-03
Zn II	40000.	.210E-02	.386E-03	Zn II	.226E-02	.493E-03
	50000.	.187E-02	.360E-03		.202E-02	.457E-03
	5000.	.328E-02	.390E-03		.738E-01	.306E-01
$4s^2S - 5p^2P^0$	10000.	.228E-02	.298E-03	$4p^2P^0 - 4s^2\ ^2D$	.516E-01	.218E-01
$\bar{\lambda} = 98.49$ nm	20000.	.164E-02	.244E-03	$\bar{\lambda} = 678.13$ nm	.358E-01	.157E-01
$X = 2.256$	30000.	.144E-02	.232E-03	$X = 0.269$	.288E-01	.130E-01
Zn II	40000.	.135E-02	.258E-03	Zn II	.248E-01	.114E-01
	50000.	.122E-02	.291E-03		.222E-01	.104E-01
	5000.	.244E-01	.814E-02		.272E-01	.108E-01
$4p^2P^0 - 5s^2S$	10000.	.170E-01	.606E-02	$4p^2P^0 - 6s^2S$	.197E-01	.870E-02
$\bar{\lambda} = 253.98$nm	20000.	.120E-01	.476E-02	$\bar{\lambda} = 152.82$ nm	.156E-01	.819E-02
$X = 0.791$	30000.	.116E-01	.449E-02	$X = 1.904$	.147E-01	.776E-02
Zn II	40000.	.922E-02	.442E-02	Zn II	.144E-01	.704E-02
	50000.	.866E-02	.439E-02		.142E-01	.645E-02
	5000.	.928E-02	.112E-02		.137E-01	.180E-02
$4p^2P^0 - 4d^2D$	10000.	.642E-02	.899E-03	$4p^2P^0 - 5d^2D$	.964E-02	.153E-02
$\bar{\lambda} = 208.87$ nm	20000.	.452E-02	.814E-03	$\bar{\lambda} = 145.10$ nm	.726E-02	.150E-02
$X = 2.256$	30000.	.386E-02	.851E-03	$X = 14.374$	.656E-02	.156E-02
Zn II	40000.	.360E-02	.921E-03	Zn II	.632E-02	.173E-02
	50000.	.348E-02	.111E-02		.622E-02	.161E-02
	5000.	.278E-01	-.159E-02		.188E-01	.324E-02
$4s^2\ ^2D - 5p^2P^0$	10000.	.193E-01	-.997E-03	$4s^2\ ^2D - 4f^2F^0$	.133E-01	.304E-02
$\bar{\lambda} = 265.12$ nm	20000.	.139E-01	-.515E-03	$\bar{\lambda} = 187.08$ nm	.109E-01	.374E-02
$X = 2.256$	30000.	.120E-01	-.226E-03	$X = 14.374$	.106E-01	.450E-02
Zn II	40000.	.112E-01	.183E-03	Zn II	.105E-01	.486E-02
	50000.	.108E-01	.565E-03		.105E-01	.510E-02
	5000.	.324	-.469E-01		.128	.323E-01
$5s^2S - 5p^2P^0$	10000.	.224	-.346E-01	$4d^2D - 4f^2F^0$	.912E-01	.275E-01
$\bar{\lambda} = 763.82$ nm	20000.	.162	-.269E-01	$\bar{\lambda} = 492.03$ nm	.768E-01	.296E-01
$X = 2.256$	30000.	.142	-.255E-01	$X = 14.374$	.764E-01	.332E-01
Zn II	40000.	.134	-.235E-01	Zn II	.762E-01	.346E-01
	50000.	.132	-.214E-01		.760E-01	.346E-01

© European Southern Observatory • Provided by the NASA Astrophysics Data System

1993A&AS..102...17P

Table 2. Same as in Table 1, but for Cd II spectral lines

TRANSITION	T (K)	WIDTH [nm]	SHIFT [nm]	TRANSITION	WIDTH [nm]	SHIFT [nm]
	5000.	.874E-02	.391E-04		.112E-01	.154E-02
$5s^2S_{1/2} - 5p^2P^0_{1/2}$	10000.	.610E-02	.354E-04	$5s^2S_{1/2} - 5p^2P^0_{3/2}$	.786E-02	.111E-02
$\lambda = 226.50$nm	20000.	.424E-02	.365E-04	$\lambda = 214.44$nm	.546E-02	.817E-03
$X = 0.235$	30000.	.342E-02	.400E-04	$X = 0.285$	.440E-02	.693E-03
Cd II	40000.	.294E-02	.443E-04	Cd II	.380E-02	.625E-03
	50000.	.264E-02	.489E-04		.340E-02	.581E-03
	5000.	.322E-02	-.296E-02		.292E-01	.129E-01
$5s^2S - 6p^2P^0$	10000.	.226E-02	-.220E-03	$5p^2P^0 - 5s^2\ ^2D$	.204E-01	.921E-02
$\overline{\lambda} = 105.09$nm	20000.	.150E-02	-.181E-03	$\overline{\lambda} = 388.78$nm	.141E-01	.663E-02
$X = 1.928$	30000.	.139E-02	-.191E-03	$X = 0.278$	.114E-01	.551E-02
Cd II	40000.	.128E-02	-.226E-03	Cd II	.982E-02	.486E-02
	50000.	.122E-02	-.240E-03		.880E-02	.443E-02
	5000.	.302E-01	.907E-02		.186E-01	.106E-03
$5p^2P^0 - 6s^2S$	10000.	.210E-01	.678E-02	$5p^2P^0 - 5d^2D$	.131E-01	.580E-04
$\overline{\lambda} = 268.82$ nm	20000.	.150E-01	.541E-02	$\overline{\lambda} = 227.32$ nm	.914E-02	.842E-04
$X = 0.851$	30000.	.127E-01	.517E-02	$X = 1.928$	.744E-02	-.359E-03
Cd II	40000.	.166E-01	.511E-02	Cd II	.644E-02	-.849E-04
	50000.	.109E-01	.512E-02		.584E-02	-.180E-03
	5000.	.176	-.166		.428	.142E-01
$5d^2D - 4f^2F^0$	10000.	.125	-548E-02	$6p^2P^0 - 6d^2D$	.300	.135E-01
$\overline{\lambda} = 536.34$ nm	20000.	.998E-01	.939E-01	$\overline{\lambda} = 664.05$nm	.218	.141E-01
$X = 5.779$	30000.	.990E-01	.211E-01	$X = 5.779$	.194	.154E-01
Cd II	40000.	.984E-01	.283E-01	Cd II	.184	.167E-01
	50000.	.982E-01	.361E-01		.181	.131E-01

© European Southern Observatory • Provided by the NASA Astrophysics Data System

1993A&AS..102...17P

Table 3. Comparison of experimental and theoretical results: w_m – experimental data; a) Djeniže et al. (1991a), b) Kusch & Oberschelp (1967a), c) Kusch & Oberschelp (1967b) and d) Djeniže et al. (1991b). $w_{\rm MSE}$, $d_{\rm MSE}$ are Stark width and shift values calculated according to the modified semi-empirical approach (MSE) (Dimitrijević & Konjević 1980, Dimitrijević & Kršljanin 1986), and $w_{\rm SE}$ – calculated by Djeniže et al. (1991a) within semi-empirical approach (Griem 1968). The electron density is 10^{23} cm^{-3}

TRANSITION	λ	T [10^3 K]	$w_{\rm exp}/w_{MSE}$	$w_{\rm exp}/w_{SE}$	$d_{\rm exp}/d_{MSE}$	Ref.
Zn II						
$4s^2S - 4p^2P^0$	206.19	33.0	1.95	2.80	*	a
$4p^2P^0 - 4s^2\ ^2D$	589.44	33.0	1.69	1.43		a
	747.44	33.0	1.64	0.87	0.39	a
$4p^2P^0 - 5s^2S$	255.80	11.1	5.17	6.5		b
		33.0	0.94	0.85	0.45	a
	250.20	11.1	3.74			b
$5s^2S - 5p^2P^0$	758.85	33.0	0.32	0.16	-0.24	a
$4d^2D - 4f^2F$	491.17	11.1	2.68	1.33		b
		33.0	0.45	0.20	-0.20	a
	492.4	11.1	1.99			b
Cd II						
$5s^2S - 5p^2P^0$	214.41	23.0	0.92	1.65	*	a
		30.0	0.95	1.74	*	a
	226.50	11.1	31.63	43.4		c
		23.0	1.06	1.09	*	a
		30.0	1.16	1.50	*	a
$5p^2P^0 - 5s^2\ ^2D$	441.56	23.0	1.47	0.82	0.35	a
		30.0	1.21	0.63	0.36	a
	325.03	11.1	2.61			c
$5p^2P^0 - 6s^2S$	274.86	23.0	0.67	0.55	0.38	a
	257.29	11.1	2.31			c
$5p^2P^0 - 5d^2D$	231.28	11.1	4.03			c
	232.11	11.1	3.82	4.06		c
		23.0	1.02	0.81	*	a
	219.46	11.1	4.32			c
		23.0	1.02	0.92	*	a
$5d^2D - 4f^2F^0$	537.81	11.1	4.62			c
		23.0	0.20		0.85	d
		30.0	0.21		0.46	d
	533.75	11.1	3.52			c
		23.0	0.15		0.39	d
		30.0	0.19		0.26	d

* The measured Stark shifts are -0.002 nm $< d < +0.002$ nm and obtained theoretical results are within this erorr bar.

© European Southern Observatory • Provided by the NASA Astrophysics Data System

1994A&AS..103...57M

ASTRONOMY & ASTROPHYSICS
SUPPLEMENT SERIES

JANUARY 1994, PAGE 57

Astron. Astrophys. Suppl. Ser. **103**, 57-66 (1994)

Spectral coefficients of emission and absorption due to ion-atom radiation collisions in the solar atmosphere*

A.A. Mihajlov[1,2], M.S. Dimitrijević[2], Lj. Ignjatović[1] and Z. Djurić[1]

[1] Institute of Physics, P.O. Box 57, 11001 Beograd, Yugoslavia
[2] Astronomical Observatory, Volgina 7, 11050 Beograd, Yugoslavia

Received July 10, 1992; accepted May 28, 1993

Abstract. — Spectral coefficients of spontaneous emission and absorption (for 365 nm $\leq \lambda \leq$820 nm range) due to ion-atom radiation processes $H^+ + H(1s) \leftrightarrow H_2^+ (1\Sigma_g)$ and $H^+ + H(1s) \leftrightarrow H(1s) + H^+$ are presented. Calculations have been performed within semiclassical approach for standard solar photosphere and chromosphere models. The presented numerical results enable the inclusion of considered ion-atom radiative processes in the optical depth calculation for the layers mentioned. These results might be of interest as well for other astrophysical plasmas with dominant hydrogen component and temperatures around 6000 K.

Key words: sun: atmosphere — radiation mechanisms: thermal — atomic data — atomic processes

1. Introduction

We present here results of our calculations of the contribution of ion-atom radiative processes:

$$H^+ + H(1s) \leftrightarrow \varepsilon_\lambda + H_2^+ (1\Sigma_g)\,, \tag{1a}$$

$$H^+ + H(1s) \leftrightarrow \varepsilon_\lambda + H(1s) + H^+, \tag{1b}$$

to the solar photosphere and chromosphere continuous spectra in the optical range. Here ε_λ is the energy of photon with wavelength λ, where 365 nm $\leq \lambda \leq$ 820 nm. Our calculations have been made within semiclassical approach (Drukarev & Mihajlov 1974; Mihajlov & Popović 1981; Mihajlov & Dimitrijević 1986). It was demonstrated recently (Mihajlov et al. 1993) that the influence of processes (1a, b), neglected up to now, is significant in some photospheric and chromospheric layers.

In this paper, the calculations of the contribution of processes (1a,b) to the solar continuous spectra, for the commonly used photospheric (Maltby et al. 1986, their Table 11) and chromospheric (Vernazza et al. 1981, their model C) models are presented. We provide data for the whole height range for both models in order to avoid inconveniences due to artificial interruption near the fitting point. In the considered range we compare the contribution of processes (1a,b) with the contribution of electron-ion and electron-atom radiative processes, including the processes of creation and photodissociation of H^- ion (Mihalas 1978). The particular contribution of process (1a) and (1b) has been determined separately.

2. Basic relations

Spectral characteristics of the solar plasma, related to ion-atom processes (1a) and (1b), i.e. partial spectral emissivity $\varepsilon_{ia}^{(a,b)}(\lambda)$ and partial spectral absorption coefficient $\kappa_{ia}^{(a,b)}(\lambda)$ will be searched in the form

$$\begin{aligned} \varepsilon_{ia}^{(a,b)}(\lambda) &= S_{ia}^{(a,b)}(\lambda) N\left(H^+\right) N(H), \\ \kappa_{ia}^{(a,b)}(\lambda) &= K_{ia}^{(a,b)}(\lambda) N\left(H^+\right) N(H) \end{aligned} \tag{2}$$

where $N\left(H^+\right)$ and $N(H)$ are proton (H^+) and atom H(1s) densities. The total spectral emissivity and total spectral absorption coefficient, i.e.

$$\varepsilon_{ia}(\lambda) = \varepsilon_{ia}^{(a)}(\lambda) + \varepsilon_{ia}^{(b)}(\lambda) \quad \text{and} \quad \kappa_{ia}(\lambda) = \kappa_{ia}^{(a)}(\lambda) + \kappa_{ia}^{(b)}(\lambda),$$

will be presented here in the same form:

$$\begin{aligned} \varepsilon_{ia}(\lambda) &= S_{ia}(\lambda) N\left(H^+\right) N(H), \\ \kappa_{ia}(\lambda) &= K_{ia}(\lambda) N\left(H^+\right) N(H), \end{aligned} \tag{3}$$

Send offprint requests to: M.S. Dimitrijević

* Tables 1.1; 1.2; 2.1; 2.2; 3.1 and 3.2 are also available in electronic form: see the editorial in A&A 1992, Vol. 266, No. 2, page E1

© European Southern Observatory • Provided by the NASA Astrophysics Data System

1994A&AS..103...57M

where

$$S_{\rm ia}(\lambda) = S_{\rm ia}^{(a)}(\lambda) + S_{\rm ia}^{(b)}(\lambda),$$
$$K_{\rm ia}(\lambda) = K_{\rm ia}^{(a)}(\lambda) + K_{\rm ia}^{(b)}(\lambda); \quad (4)$$

The spontaneous emission spectral coefficient $S_{\rm ia}$ characterizes the total contribution of the photoassociation process (1a) and photoemission charge exchange process (1b). Similarly, the absorption spectral coefficient $K_{\rm ia}$ characterizes the total contribution of the photodissociation process (1a) and the photoabsorption charge exchange process (1b).

The coefficients $S_{\rm ia}$ and $K_{\rm ia}$ have been determined within the semiclassical approximation by Mihajlov & Popović (1981) and Mihajlov & Dimitrijević (1986) and may be expressed as

$$S_{\rm ia}(\lambda,T) = 4.7769\ 10^{-34} \frac{C\,(R_\lambda)\,(R_\lambda/a_0)^4}{1-a_0/R_\lambda} \left(\frac{\varepsilon_\lambda}{2R_y}\right)^5 \exp\left[-\frac{U_2\,(R_\lambda)}{kT}\right], \quad (5)$$

$$K_{\rm ia}(\lambda,T) = 0.620\ 10^{-42} \frac{C\,(R_\lambda)\,(R_\lambda/a_0)^4}{1-a_0/R_\lambda} \theta(\lambda,T) \exp\left[-\frac{U_1\,(R_\lambda)}{kT}\right], \quad (6)$$

where T is the plasma temperature and

$$C\,(R_\lambda) = \left[\frac{2D_{12}\,(R_\lambda)}{{\rm e}\,R_\lambda}\right]^2 \times \frac{1-a_0/R_\lambda}{\gamma\,(R_\lambda)},$$
$$\theta(\lambda,T) = 1-\exp\left(-\frac{\varepsilon_\lambda}{kT}\right),$$
$$\gamma\,(R_\lambda) = \left|\frac{{\rm dln}\,[E_{12}(R)/2R_y]}{{\rm d}\,(R/a_0)}\right|_{R=R_\lambda},$$
$$E_{12}(R) = U_2(R) - U_1(R). \quad (7)$$

Here, R is the distance between protons (in the system $H^+ + H$), $U_1(R)$ and $U_2(R)$ - adiabatic terms of the ground ($1\Sigma_g$) and the first excited ($1\Sigma_u$) electronic states of the ion H_2^+, and $D_{12}(R)$ - module of dipole matrix element (between these states). Finally, R_λ is the root of the equation:

$$E_{12}(R) = \varepsilon_\lambda, \quad (8)$$

where $\varepsilon_\lambda = 2\pi\hbar c/\lambda$. The adiabatic terms $U_{1,2}(R)$ and the matrix element $D_{12}(R)$ are tabulated (as functions of R) in Bates et al. (1953) and Ramaker & Peak (1973), respectively.

With given numerical coefficients in Eqs.(5) and (6) spectral coefficients $S_{\rm ia}(\lambda,T)$ and $K_{\rm ia}(\lambda,T)$ are expressed here in $[J\ {\rm cm}^3\ {\rm s}^{-1}\ {\rm nm}^{-1}]$ and $[{\rm cm}^{-1}]$ units, respectively.

We will take here the partial spectral coefficients $S_{\rm ia}^{(a,b)}$ and $K_{\rm ia}^{(a,b)}$ in the form:

$$S_{\rm ia}^{(a,b)} = S_{\rm ia} X^{(a,b)}, \quad K_{\rm ia}^{(a,b)} = K_{\rm ia}^{(a,b)} X^{(a,b)}, \quad (9)$$

where

$$X^{(a)} + X^{(b)} \equiv 1. \quad (10)$$

According to Mihajlov & Dimitrijević (1986), parameters $X^{(a,b)}$ may be expressed as

$$X^{(a)}(Z) = \frac{\gamma(3/2;Z)}{\Gamma(3/2)}, \quad X^{(b)}(Z) = \frac{\Gamma(3/2;Z)}{\Gamma(3/2)}, \quad (\text{for } Z \geq 0)$$
$$X^{(a)}(Z) = 0, \quad X^{(b)}(Z) = 1, \quad (\text{for } Z \leq 0) \quad (11)$$

where

$$Z = -\frac{U_1\,(R_\lambda)}{kT}, \quad (12)$$

and $\gamma(3/2;Z)$, $\Gamma(3/2;Z)$ are incomplete Gamma functions. In the considered λ range we have $U_1\,(R_\lambda) < 0$ and $Z = |U_1\,(R_\lambda)|\,/kT$.

Since according to Eq. (10) it is sufficient to determine only one of these parameters, we will use the parameter $X^{(b)}$ characterizing only radiative charge exchange, i.e. process (1b), in accordance with our previous article (Mihajlov & Dimitrijević 1986).

Parameters R_λ and $U_{1,2}\,(R_\lambda)$, needed for the calculation of $S_{\rm ia}$ and $K_{\rm ia}$ for 250 nm $\leq \lambda \leq$ 950 nm range, are tabulated in Mihajlov et al. (1983). In this λ range R_λ and $U_2\,(R_\lambda)$ may be fitted well with the following expressions:

$$R_\lambda = 1.37347\,{\rm ln}\lambda - 4.41481, \quad U_2\,(R_\lambda) = 90.5631\,\lambda^{-1.20962}, \quad (13)$$

where R_λ and $U_2\,(R_\lambda)$ are expressed in atomic units and λ in nm.

The function $X^{(b)}(Z)$ is tabulated in Mihajlov & Dimitrijević 1986, for $0.6 \leq \sqrt{Z} \leq 3.0$ range. As shown in this Ref., $X^{(b)}(Z)$ may be expressed in the form

$$X^{(b)}(Z) = 1 - \Phi\left(\sqrt{Z}\right) + \left(2/\sqrt{\pi}\right) \cdot \sqrt{Z}{\rm exp}(-Z), \quad (14)$$

where Φ is the error function (Abramowitz & Stegun 1972).

3. Results and discussion

Our calculations have been based on standard photospheric model of Maltby et al. (1986) and standard chromospheric model of Vernazza et al. (1981, model C). Plasma parameters T, $N_{\rm e}$, $N({\rm H})$ and $N\,({\rm H}^+)$ for the mentioned models are presented in tables 1.1 and 1.2 as functions of height (h). In these tables are presented as well parameters

$$\eta_{\rm ea} = \frac{N\,({\rm H}^+)}{N_{\rm e}} \quad \text{and} \quad \eta_{\rm ei} = \eta_{\rm ea} \cdot \frac{N({\rm H})}{N_{\rm i}}, \quad (15)$$

© European Southern Observatory • Provided by the NASA Astrophysics Data System

1994A&AS..103...57M

where N_i is the total density of positive atomic ions. They help to represent relative contributions of (1a,b) processes compared to electron-ion (η_{ei}) and electron-atom (η_{ea}) processes separately (see Mihajlov et al. 1993).

Spectral coefficients $S_{ia}(\lambda, T)$ and $K_{ia}(\lambda, T)$ as function of T for different λ are shown in Figs. 1 and 2 for $T \leq 10^4$K. The behavior of factor $X^b(Z)$ is illustrated in Fig. 3.

Emissivity $\varepsilon_{ia}(\lambda, T)$ and absorption coefficient $\kappa_{ia}(\lambda, T)$ are presented in Tables 2.1, 2.2 and 3.1, 3.2, respectively. Tables 2.1, 3.1 correspond to photospheric, and 2.2, 3.2 to chromospheric models. In these tables the temperature range is limited to $T < 10^4$K and the wavelength range is 365 nm $\leq \lambda \leq$ 820 nm. The presented tables enable direct inclusion of the influence of (1a,b) processes for calculations of spectral characteristics (first of all the optical depth) of the considered photospheric and chromospheric layers, within standard solar atmosphere models used here.

The relative contribution of (1a) and (1b) processes together, compared to the total electron-atom and electron-ion processes contribution is illustrated in Figs. 4.1 and 4.2. These figures show the change of

$$F = \frac{\varepsilon_{ia}}{\varepsilon_{ei} + \varepsilon_{ea}} \tag{16}$$

quantity as a function of height (h), where ε_{ei} and ε_{ea} are total contributions of free-free and free-bound transitions during electron-ion and electron-atom scattering respectively. If LTE exists, the quantity F represents the ratio of corresponding absorption coefficients as well. We assume here that

$$\varepsilon_{ei} = \xi_{ei} S_{ei} N_e^2, \quad \varepsilon_{ea} = \xi_{ea} S_{ea} N(\mathrm{H}) N_e, \tag{17}$$

where the corresponding spectral coefficients S_{ei} and S_{ea} have been determined for the purely hydrogenic plasma and the Biberman-Norman factor ξ_{ei} as well as the factor ξ_{ea} take into account the real composition of photospheric and chromospheric plasma, i.e. the presence of Na^+, Mg^+, Al^+, Ca^+ ions as well as the presence of helium atoms.

Figures 4.1 and 4.2 show that F, as a function of h, has a minimum in 100 km $< h <$ 600 km range which coincides with the temperature minimum (see Tables 1.1 and 1.2). The minimum of F appears because the relative hydrogen contribution to the free electron density in this range is very small (Vernazza et al. 1981).

The behavior of $X^{(b)}$ parameter, defined by Eqs. (9-14), as a function of h, is presented in Figs. 5.1 and 5.2. These figures show that $X^{(b)}$ has a minimum which coincides with the minimum of function F. This minimum is the result of $X^{(b)}(Z)$ dependency (see Eq. (11) and Fig. 3) where is $Z \sim 1/T$ (see Eq. (12)).

In Figs. 4.1 and 4.2 the ranges where processes (1a,b) are of influence (e.g. where the value of the quantity F is $0.04 - 0.12$) are shown. Moreover, in Figs. 5.1 and 5.2, is shown that outside the photospheric minimum surroundings, the influence of the radiation charge exchange processes (1b), due to H^+ and H(1s) collisions, is comparable and somewhere surpasses the influence of (1a), i.e. photoassociation H^+ and H(1s) and photodissociation of molecular ion H_2^+ $(1\Sigma_g)$.

Figures 4.1, 5.1 concern the photospheric and 4.2, 5.2 the chromospheric model. We can see that within both models, the results obtained are qualitatively similar but for particular layers quantitative differences exist as expected.

4. Conclusion

These results illustrate the influence of (1a,b) radiative processes involving H^+ and H(1s) on spectral characteristics for particular photospheric and chromospheric layers. The numerical results presented enable the inclusion of ion-atom radiative processes (1a,b) in the optical depth calculation for the mentioned layers. Our results might be of interest as well for other astrophysical plasmas with a dominant hydrogen component and temperatures around 6000 K.

References

Abramowitz M., Stegun I. 1972, Handbook of Mathematical Functions, Dover, New York

Bates D.R., Ledsham K., Stewart A.L. 1953, Phil. Trans. R. Soc., London Ser. A 246, 215

Biberman L.M., Norman G.E. 1963, J.Q.S.R.T., 3, 221

Boggess A. 1959, ApJ., 129, 432

Drukarev G.P. and Mihajlov A.A. 1974, Opt. Spectrosk., 37, 200

Maltby P., Avrett E.H., Carlsson M., Kjeldseth-Moe O., Kurucz R.L. and Loeser R. 1986, ApJ 306, 284

Mihalas D. 1978, Stellar Atmospheres (Chap. 7.7), W.H. Freeman, San Francisco

Mihajlov A.A., Popović M.M. 1981, Phys. Rev. A 23, 1679

Mihajlov A.A., Dimitrijević M.S. 1986, A&A 155, 319

Mihajlov A.A., Dimitrijević M.S. and Ignjatović Lj. 1993, A&A 276, 187

Ramaker D.E. and Peek J.M. 1973, Atomic Data 5, 167

Sobelman I.I. 1979, Atomic Spectra and Radiative Transitions (Chap. 9.5), Springer-Verlag, Berlin

Vernazza J.E., Avrett E.H. and Loeser R. 1981, ApJS 45, 635

© European Southern Observatory • Provided by the NASA Astrophysics Data System

1994A&AS..103...57M

Table 1.1. Basic plasma parameters (temperature T, electron density N_e, total hydrogen density $N(\mathrm{H})$) as well as parameter η_{ei} and η_{ea} defined by Eq. (15), for solar photospheric model of Maltby et al. (1986), as a function of height h

h[km]	T[K]	N_e [cm^{-3}]	N(H)[cm^{-3}]	η_{ei}	η_{ea}
2040	7360	.4745E +11	.1068E +12	.122E +01	.100E +01
1948	6940	.5303E +11	.1611E +12	.203E +01	.100E +01
1810	6630	.4475E +11	.3165E +12	.606E +01	.100E +01
1634	6440	.4768E +11	.7729E +12	.152E +02	.100E +01
1406	6280	.7199E +11	.2706E +13	.366E +02	.100E +01
1198	6150	.1118E +12	.9317E +13	.823E +02	.100E +01
1079	6040	.1414E +12	.2043E +14	.143E +03	.100E +01
912	5755	.1624E +12	.6686E +14	.411E +03	.100E +01
862	5650	.1649E +12	.9819E +14	.594E +03	.100E +01
761	5280	.1298E +12	.2246E +15	.173E +04	.100E +01
711	5030	.1078E +12	.3553E +15	.206E +04	.624E +00
655	4750	.1030E +12	.6014E +15	.975E +03	.167E +00
605	4550	.1321E +12	.9871E +15	.271E +03	.363E -01
553	4410	.1976E +12	.1642E +16	.711E +02	.856E -02
528	4400	.2445E +12	.2090E +16	.559E +02	.654E -02
503	4400	.3040E +12	.2654E +16	.469E +02	.537E -02
478	4410	.3793E +12	.3365E +16	.422E +02	.476E -02
453	4460	.4714E +12	.4218E +16	.525E +02	.587E -02
428	4510	.5886E +12	.5273E +16	.635E +02	.708E -02
403	4560	.7337E +12	.6579E +16	.761E +02	.849E -02
378	4610	.9128E +12	.8168E +16	.901E +02	.101E -01
352	4660	.1133E +13	.1016E +17	.107E +03	.119E -01
301	4770	.1733E +13	.1556E +17	.159E +03	.177E -01
250	4880	.2642E +13	.2350E +17	.223E +03	.251E -01
200	4990	.3997E +13	.3502E +17	.302E +03	.344E -01
175	5060	.4939E +13	.4236E +17	.370E +03	.431E -01
150	5150	.6142E +13	.5088E +17	.491E +03	.593E -01
125	5270	.7751E +13	.6052E +17	.720E +03	.922E -01
100	5410	.1001E +14	.7136E +17	.105E +04	.147E +00
75	5580	.1352E +14	.8328E +17	.148E +04	.240E +00
50	5790	.1977E +14	.9598E +17	.185E +04	.381E +00
35	5980	.2772E +14	.1031E +18	.193E +04	.520E +00
20	6180	.4052E +14	.1102E +18	.175E +04	.642E +00
10	6340	.5484E +14	.1146E +18	.151E +04	.721E +00
0	6520	.7676E +14	.1187E +18	.122E +04	.791E +00
-10	6720	.1104E +15	.1224E +18	.940E +03	.848E +00
-20	6980	.1725E +15	.1250E +18	.652E +03	.901E +00
-30	7280	.2798E +15	.1269E +18	.426E +03	.941E +00
-40	7590	.4463E +15	.1285E +18	.277E +03	.966E +00
-50	7900	.6897E +15	.1300E +18	.184E +03	.982E +00
-60	8220	.1046E +16	.1312E +18	.124E +03	.994E +00
-70	8540	.1540E +16	.1322E +18	.848E +02	.100E +01
-80	8860	.2207E +16	.1330E +18	.592E +02	.100E +01
-90	9140	.2970E +16	.1343E +18	.442E +02	.100E +01
-100	9400	.3856E +16	.1357E +18	.342E +02	.100E +01

Table 1.2. Same as in Table 1.1. but for the chromospheric model of Vernazza et al. (1981, model C)

h[km]	T[K]	N_e [cm^{-3}]	N(H)[cm^{-3}]	η_{ei}	η_{ea}
2016	7360	.3811E +11	.9075E +11	.135E +01	.100E +01
1990	7160	.3858E +11	.1033E +12	.166E +01	.100E +01
1925	6940	.4028E +11	.1380E +12	.241E +01	.100E +01
1785	6630	.4771E +11	.2601E +12	.444E +01	.100E +01
1605	6440	.6005E +11	.6386E +12	.963E +01	.100E +01
1515	6370	.6456E +11	.1048E +13	.152E +02	.100E +01
1380	6280	.7600E +11	.2273E +13	.289E +02	.100E +01
1280	6220	.7486E +11	.4200E +13	.551E +02	.100E +01
1180	6150	.8108E +11	.7865E +13	.960E +02	.100E +01
1065	6040	.9349E +11	.1711E +14	.182E +03	.100E +01
980	5925	.1041E +12	.3147E +14	.301E +03	.100E +01
905	5755	.1049E +12	.5546E +14	.528E +03	.100E +01
855	5650	.1064E +12	.8135E +14	.764E +03	.100E +01
755	5280	.8838E +11	.1864E +15	.211E +04	.100E +01
705	5030	.7664E +11	.2935E +15	.383E +04	.100E +01
655	4730	.8085E +11	.4794E +15	.111E +04	.187E +00
605	4420	.1112E +12	.8119E +15	.106E +03	.145E -01
555	4230	.1733E +12	.1382E +16	.153E +02	.192E -02
515	4170	.2495E +12	.2096E +16	.675E +01	.803E -03
450	4220	.4516E +12	.3989E +16	.657E +01	.744E -03
350	4465	.1110E +13	.9979E +16	.235E +02	.261E -02
250	4780	.2674E +13	.2315E +17	.103E +03	.119E -01
150	5180	.6476E +13	.4917E +17	.472E +03	.621E -01
100	5455	.1066E +14	.6866E +17	.104E +04	.161E +00
50	5840	.2122E +14	.9203E +17	.176E +04	.406E +00
0	6420	.6433E +14	.1166E +18	.134E +04	.741E +00
-25	6910	.1547E +15	.1261E +18	.721E +03	.885E +00
-50	7610	.4645E +15	.1317E +18	.274E +03	.969E +00
-75	8320	.1204E +16	.1365E +18	.112E +03	.100E +01

© European Southern Observatory • Provided by the NASA Astrophysics Data System

1994A&AS..103...57M

Table 2.1. Emissivity $\varepsilon_{ia}(\lambda)$ due to (1a) and (1b) reactions together as a function of λ and height h, for the photospheric model of Maltby et al. (1986)

h[km]	$\varepsilon_{ia}(\lambda)$; λ [nm], ε_{ia} [$cm^{-3}s^{-1}$* J/nm]					
	365	400	500	600	700	820
2040	.426E -15	.427E -15	.368E -15	.285E -15	.213E -15	.149E -15
1948	.731E -15	.747E -15	.669E -15	.532E -15	.405E -15	.287E -15
1810	.134E -14	.139E -14	.128E -14	.104E -14	.804E -15	.577E -15
1634	.344E -14	.360E -14	.341E -14	.280E -14	.218E -14	.158E -14
1406	.172E -13	.182E -13	.176E -13	.146E -13	.115E -13	.839E -14
1198	.866E -13	.924E -13	.905E -13	.762E -13	.603E -13	.443E -13
1079	.226E -12	.243E -12	.241E -12	.205E -12	.163E -12	.120E -12
912	.707E -12	.775E -12	.801E -12	.698E -12	.566E -12	.424E -12
862	.981E -12	.108E -11	.114E -11	.100E -11	.816E -12	.615E -12
761	.133E -11	.152E -11	.169E -11	.154E -11	.129E -11	.997E -12
711	.882E -12	.103E -11	.120E -11	.113E -11	.963E -12	.754E -12
655	.293E -12	.350E -12	.432E -12	.421E -12	.369E -12	.295E -12
605	.108E -12	.133E -12	.171E -12	.172E -12	.153E -12	.125E -12
553	.543E -13	.675E -13	.901E -13	.924E -13	.838E -13	.690E -13
528	.646E -13	.804E -13	.108E -12	.110E -12	.100E -12	.827E -13
503	.837E -13	.104E -12	.139E -12	.143E -12	.130E -12	.107E -12
478	.119E -12	.148E -12	.197E -12	.202E -12	.183E -12	.151E -12
453	.242E -12	.299E -12	.394E -12	.401E -12	.362E -12	.296E -12
428	.482E -12	.592E -12	.772E -12	.779E -12	.699E -12	.571E -12
403	.950E -12	.116E -11	.149E -11	.150E -11	.134E -11	.109E -11
378	.184E -11	.223E -11	.284E -11	.283E -11	.251E -11	.203E -11
352	.354E -11	.428E -11	.539E -11	.532E -11	.470E -11	.379E -11
301	.138E -10	.164E -10	.202E -10	.196E -10	.172E -10	.137E -10
250	.500E -10	.590E -10	.709E -10	.680E -10	.588E -10	.466E -10
200	.172E -09	.200E -09	.235E -09	.223E -09	.191E -09	.150E -09
175	.342E -09	.397E -09	.460E -09	.432E -09	.368E -09	.288E -09
150	.761E -09	.875E -09	.998E -09	.926E -09	.784E -09	.609E -09
125	.196E -08	.223E -08	.249E -08	.228E -08	.191E -08	.147E -08
100	.533E -08	.600E -08	.654E -08	.590E -08	.489E -08	.374E -08
75	.156E -07	.173E -07	.183E -07	.163E -07	.133E -07	.101E -07
50	.484E -07	.529E -07	.544E -07	.472E -07	.382E -07	.285E -07
35	.113E -06	.121E -06	.122E -06	.104E -06	.830E -07	.614E -07
20	.246E -06	.262E -06	.255E -06	.214E -06	.169E -06	.124E -06
10	.426E -06	.450E -06	.430E -06	.357E -06	.279E -06	.203E -06
0	.748E -06	.781E -06	.732E -06	.599E -06	.465E -06	.335E -06
-10	.132E -05	.136E -05	.125E -05	.101E -05	.774E -06	.554E -06
-20	.254E -05	.258E -05	.231E -05	.183E -05	.139E -05	.985E -06
-30	.498E -05	.500E -05	.434E -05	.338E -05	.254E -05	.178E -05
-40	.938E -05	.929E -05	.785E -05	.601E -05	.445E -05	.309E -05
-50	.167E -04	.164E -04	.135E -04	.102E -04	.745E -05	.512E -05
-60	.289E -04	.280E -04	.225E -04	.167E -04	.121E -04	.826E -05
-70	.477E -04	.456E -04	.359E -04	.263E -04	.189E -04	.128E -04
-80	.753E -04	.714E -04	.550E -04	.397E -04	.283E -04	.190E -04
-90	.110E -03	.103E -03	.784E -04	.560E -04	.396E -04	.264E -04
-100	.154E -03	.143E -03	.107E -03	.758E -04	.533E -04	.353E -04

Table 2.2. Same as in Table 2.1. but for the chromospheric model of Vernazza et al. (1981, model C)

h[km]	$\varepsilon_{ia}(\lambda)$; λ [nm], ε_{ia} [$cm^{-3}s^{-1}$* J/nm]					
	365	400	500	600	700	820
2016	.303E -15	.303E -15	.261E -15	.202E -15	.151E -15	.106E -15
1990	.350E -15	.353E -15	.310E -15	.243E -15	.183E -15	.129E -15
1925	.502E -15	.512E -15	.459E -15	.365E -15	.278E -15	.197E -15
1785	.111E -14	.115E -14	.107E -14	.867E -15	.670E -15	.481E -15
1605	.345E -14	.362E -14	.342E -14	.282E -14	.220E -14	.159E -14
1515	.607E -14	.639E -14	.609E -14	.504E -14	.394E -14	.286E -14
1380	.152E -13	.161E -13	.155E -13	.129E -13	.101E -13	.739E -14
1280	.271E -13	.288E -13	.279E -13	.234E -13	.184E -13	.135E -13
1180	.531E -13	.567E -13	.555E -13	.467E -13	.370E -13	.271E -13
1065	.125E -12	.134E -12	.134E -12	.114E -12	.904E -13	.667E -13
980	.239E -12	.259E -12	.261E -12	.224E -12	.180E -12	.133E -12
905	.379E -12	.415E -12	.430E -12	.374E -12	.303E -12	.227E -12
855	.524E -12	.579E -12	.608E -12	.535E -12	.437E -12	.329E -12
755	.753E -12	.857E -12	.955E -12	.873E -12	.732E -12	.563E -12
705	.831E -12	.966E -12	.113E -11	.106E -11	.906E -12	.710E -12
655	.200E -12	.240E -12	.298E -12	.291E -12	.256E -12	.205E -12
605	.260E -13	.322E -13	.429E -13	.439E -13	.398E -13	.328E -13
555	.722E -14	.918E -14	.128E -13	.136E -13	.126E -13	.105E -13
515	.611E -14	.783E -14	.111E -13	.119E -13	.111E -13	.934E -14
450	.208E -13	.265E -13	.371E -13	.393E -13	.364E -13	.305E -13
350	.603E -12	.744E -12	.980E -12	.996E -12	.898E -12	.736E -12
250	.214E -10	.256E -10	.313E -10	.304E -10	.266E -10	.212E -10
150	.833E -09	.955E -09	.108E -08	.100E -08	.846E -09	.656E -09
100	.618E -08	.693E -08	.750E -08	.673E -08	.557E -08	.424E -08
50	.548E -07	.597E -07	.610E -07	.527E -07	.425E -07	.317E -07
0	.547E -06	.574E -06	.544E -06	.448E -06	.350E -06	.253E -06
-25	.218E -05	.223E -05	.200E -05	.160E -05	.122E -05	.865E -06
-50	.101E -04	.100E -04	.844E -05	.645E -05	.478E -05	.332E -05
-75	.360E -04	.347E -04	.277E -04	.205E -04	.148E -04	.101E -04

© European Southern Observatory • Provided by the NASA Astrophysics Data System

1994A&AS..103...57M

Table 3.1. Spectral absorption coefficient $\kappa_{ia}(\lambda)$ due to (1a) and (1b) reactions together as a function of λ and height h for the photospheric model of Maltby et al. (1986)

h[km]	$\kappa_{1a}(\lambda)$; λ [nm], κ_{1a} [cm^{-1}]					
	365	400	500	600	700	820
2040	.386E -17	.381E -17	.372E -17	.367E -17	.364E -17	.360E -17
1948	.916E -17	.897E -17	.861E -17	.840E -17	.826E -17	.813E -17
1810	.218E -16	.212E -16	.201E -16	.194E -16	.190E -16	.186E -16
1634	.670E -16	.648E -16	.608E -16	.583E -16	.567E -16	.553E -16
1406	.393E -15	.379E -15	.352E -15	.336E -15	.325E -15	.316E -15
1198	.225E -14	.217E -14	.200E -14	.190E -14	.183E -14	.178E -14
1079	.660E -14	.633E -14	.580E -14	.548E -14	.527E -14	.510E -14
912	.286E -13	.272E -13	.244E -13	.228E -13	.218E -13	.209E -13
862	.450E -13	.427E -13	.381E -13	.354E -13	.336E -13	.322E -13
761	.999E -13	.934E -13	.811E -13	.739E -13	.692E -13	.655E -13
711	.958E -13	.887E -13	.753E -13	.676E -13	.627E -13	.587E -13
655	.505E -13	.461E -13	.381E -13	.336E -13	.307E -13	.284E -13
605	.269E -13	.244E -13	.197E -13	.171E -13	.155E -13	.142E -13
553	.177E -13	.160E -13	.127E -13	.109E -13	.977E -14	.889E -14
528	.215E -13	.193E -13	.154E -13	.132E -13	.118E -13	.107E -13
503	.279E -13	.251E -13	.200E -13	.171E -13	.153E -13	.139E -13
478	.388E -13	.349E -13	.278E -13	.238E -13	.214E -13	.195E -13
453	.715E -13	.644E -13	.516E -13	.444E -13	.400E -13	.365E -13
428	.129E -12	.117E -12	.941E -13	.813E -13	.734E -13	.672E -13
403	.231E -12	.210E -12	.170E -12	.147E -12	.133E -12	.122E -12
378	.407E -12	.370E -12	.301E -12	.263E -12	.238E -12	.219E -12
352	.717E -12	.653E -12	.535E -12	.468E -12	.426E -12	.392E -12
301	.229E -11	.210E -11	.174E -11	.153E -11	.140E -11	.130E -11
250	.691E -11	.635E -11	.532E -11	.473E -11	.435E -11	.405E -11
200	.198E -10	.183E -10	.155E -10	.139E -10	.129E -10	.120E -10
175	.355E -10	.329E -10	.280E -10	.252E -10	.234E -10	.219E -10
150	.688E -10	.640E -10	.550E -10	.497E -10	.463E -10	.436E -10
125	.149E -09	.139E -09	.121E -09	.110E -09	.103E -09	.975E -10
100	.334E -09	.314E -09	.275E -09	.252E -09	.238E -09	.226E -09
75	.781E -09	.738E -09	.655E -09	.607E -09	.575E -09	.549E -09
50	.188E -08	.178E -08	.161E -08	.150E -08	.144E -08	.138E -08
35	.352E -08	.336E -08	.307E -08	.289E -08	.278E -08	.268E -08
20	.619E -08	.596E -08	.551E -08	.523E -08	.506E -08	.491E -08
10	.915E -08	.884E -08	.824E -08	.788E -08	.765E -08	.745E -08
0	.135E -07	.131E -07	.123E -07	.119E -07	.116E -07	.113E -07
-10	.199E -07	.194E -07	.184E -07	.179E -07	.175E -07	.172E -07
-20	.307E -07	.301E -07	.290E -07	.283E -07	.278E -07	.274E -07
-30	.478E -07	.471E -07	.459E -07	.452E -07	.447E -07	.443E -07
-40	.720E -07	.714E -07	.703E -07	.698E -07	.694E -07	.690E -07
-50	.105E -06	.104E -06	.104E -06	.104E -06	.104E -06	.103E -06
-60	.149E -06	.149E -06	.150E -06	.150E -06	.151E -06	.151E -06
-70	.205E -06	.206E -06	.209E -06	.211E -06	.212E -06	.213E -06
-80	.273E -06	.276E -06	.282E -06	.286E -06	.289E -06	.291E -06
-90	.348E -06	.352E -06	.362E -06	.369E -06	.374E -06	.377E -06
-100	.430E -06	.437E -06	.451E -06	.462E -06	.469E -06	.474E -06

Table 3.2. Same as in Table 3.1. but for the chromospheric model of Vernazza et al. (1981, model C)

h[km]	$\kappa_{1a}(\lambda)$; λ [nm], κ_{1a} [cm^{-1}]					
	365	400	500	600	700	820
2016	.274E -17	.270E -17	.264E -17	.260E -17	.258E -17	.256E -17
1990	.367E -17	.361E -17	.350E -17	.344E -17	.339E -17	.335E -17
1925	.628E -17	.615E -17	.591E -17	.576E -17	.567E -17	.558E -17
1785	.182E -16	.177E -16	.167E -16	.162E -16	.158E -16	.155E -16
1605	.673E -16	.652E -16	.611E -16	.586E -16	.570E -16	.556E -16
1515	.127E -15	.122E -15	.114E -15	.109E -15	.106E -15	.103E -15
1380	.346E -15	.333E -15	.310E -15	.296E -15	.286E -15	.278E -15
1280	.656E -15	.632E -15	.585E -15	.557E -15	.539E -15	.523E -15
1180	.138E -14	.133E -14	.123E -14	.116E -14	.112E -14	.109E -14
1065	.366E -14	.351E -14	.321E -14	.304E -14	.292E -14	.283E -14
980	.793E -14	.758E -14	.689E -14	.648E -14	.622E -14	.599E -14
905	.153E -13	.146E -13	.131E -13	.122E -13	.117E -13	.112E -13
855	.241E -13	.228E -13	.204E -13	.189E -13	.180E -13	.172E -13
755	.564E -13	.528E -13	.458E -13	.417E -13	.391E -13	.370E -13
705	.902E -13	.835E -13	.709E -13	.637E -13	.590E -13	.553E -13
655	.358E -13	.327E -13	.270E -13	.237E -13	.217E -13	.200E -13
605	.832E -14	.748E -14	.596E -14	.512E -14	.459E -14	.418E -14
555	.345E -14	.307E -14	.239E -14	.202E -14	.179E -14	.161E -14
515	.334E -14	.296E -14	.228E -14	.192E -14	.169E -14	.152E -14
450	.102E -13	.903E -14	.702E -14	.592E -14	.524E -14	.472E -14
350	.176E -12	.159E -12	.127E -12	.110E -12	.988E -13	.902E -13
250	.351E -11	.321E -11	.266E -11	.235E -11	.215E -11	.200E -11
150	.721E -10	.671E -10	.578E -10	.523E -10	.489E -10	.460E -10
100	.364E -09	.343E -09	.302E -09	.278E -09	.262E -09	.249E -09
50	.201E -08	.191E -08	.173E -08	.162E -08	.155E -08	.149E -08
0	.109E -07	.105E -07	.984E -08	.944E -08	.918E -08	.895E -08
-25	.280E -07	.274E -07	.263E -07	.256E -07	.252E -07	.248E -07
-50	.766E -07	.760E -07	.749E -07	.743E -07	.740E -07	.736E -07
-75	.175E -06	.175E -06	.176E -06	.178E -06	.178E -06	.179E -06

© European Southern Observatory • Provided by the NASA Astrophysics Data System

1994A&AS..103...57M

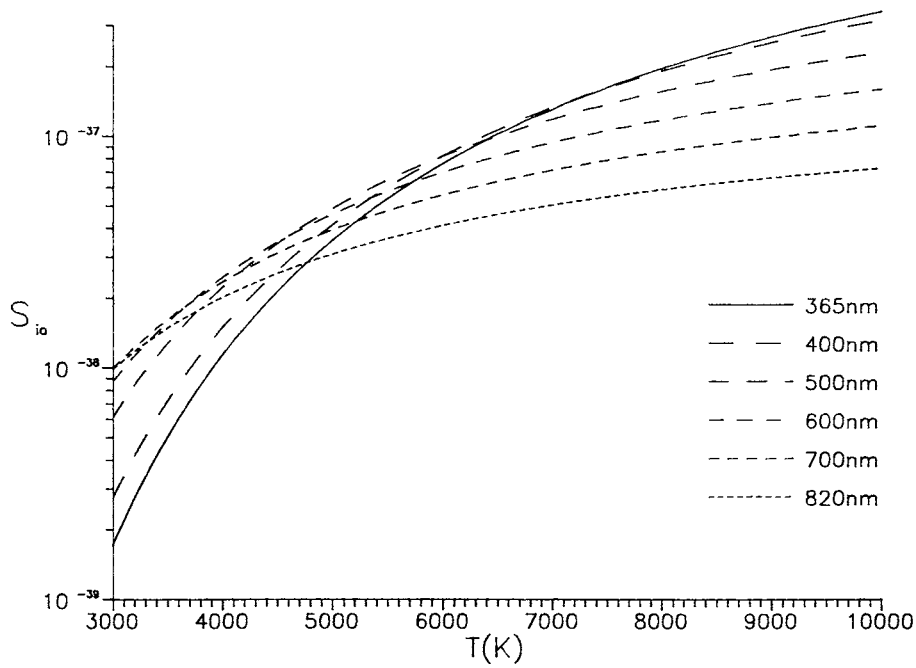

Fig. 1. Spectral coefficients $S_{\rm ia}(\lambda, T)$ for spontaneous emission due to (1a) and (1b) reactions together, are presented as a function of T for 365 nm $\leq \lambda \leq$ 820 nm

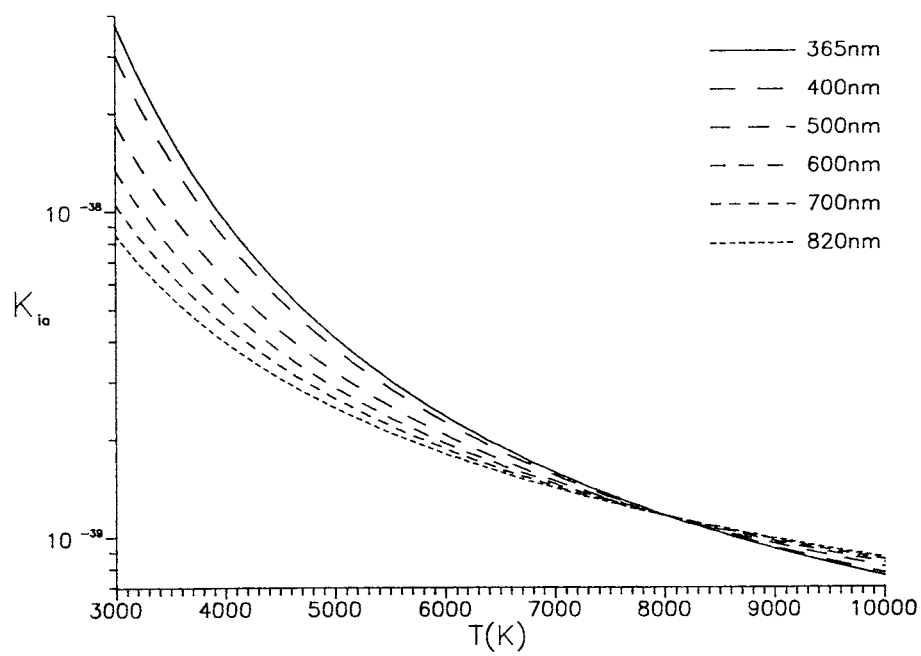

Fig. 2. Spectral coefficients $K_{\rm ia}(\lambda, T)$ for absorption due to (1a) and (1b) reactions together are presented as a function of T for 365 nm $\leq \lambda \leq$ 820 nm

© European Southern Observatory • Provided by the NASA Astrophysics Data System

1994A&AS..103...57M

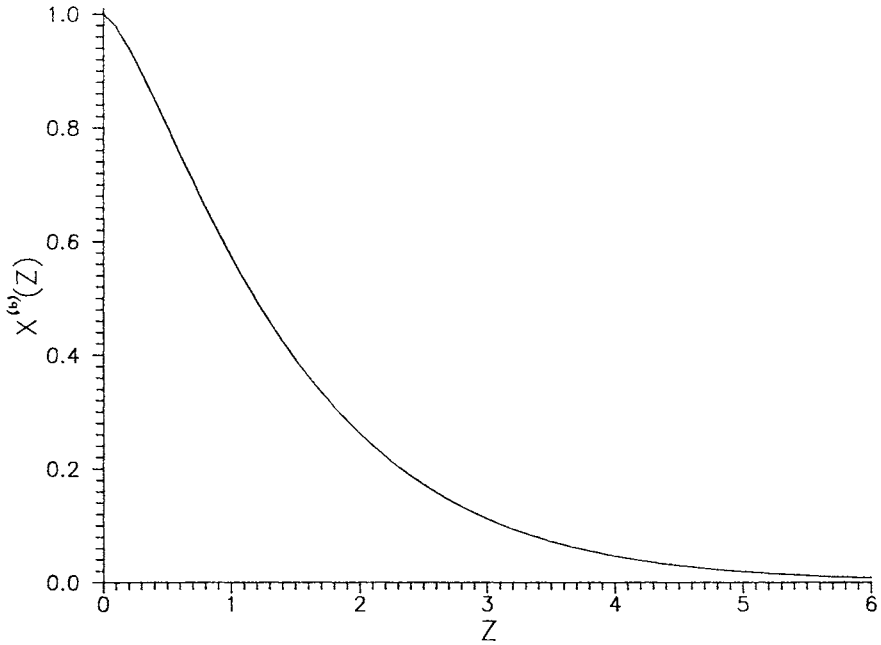

Fig. 3. Parameter $X^{(b)}(Z)$ defined by Eq. (11), for $Z \geq 0$

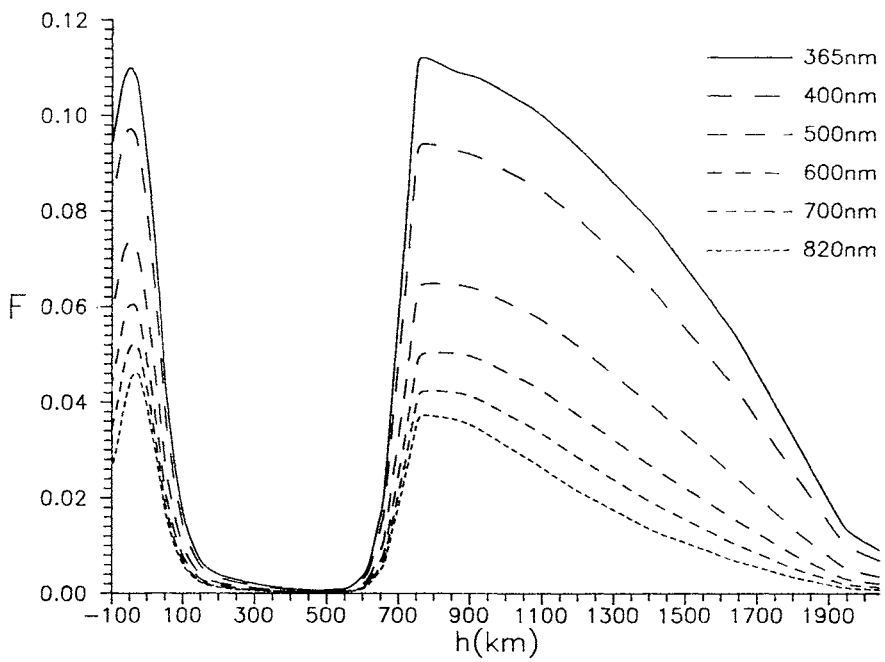

Fig. 4.1. Behavior of parameter $F(\lambda)$, defined by Eqs. (16) and (17), as a function of height h, for 365 nm $\leq \lambda \leq$ 820 nm for the photospheric model of Maltby et al. (1986)

© European Southern Observatory • Provided by the NASA Astrophysics Data System

1994A&AS..103...57M

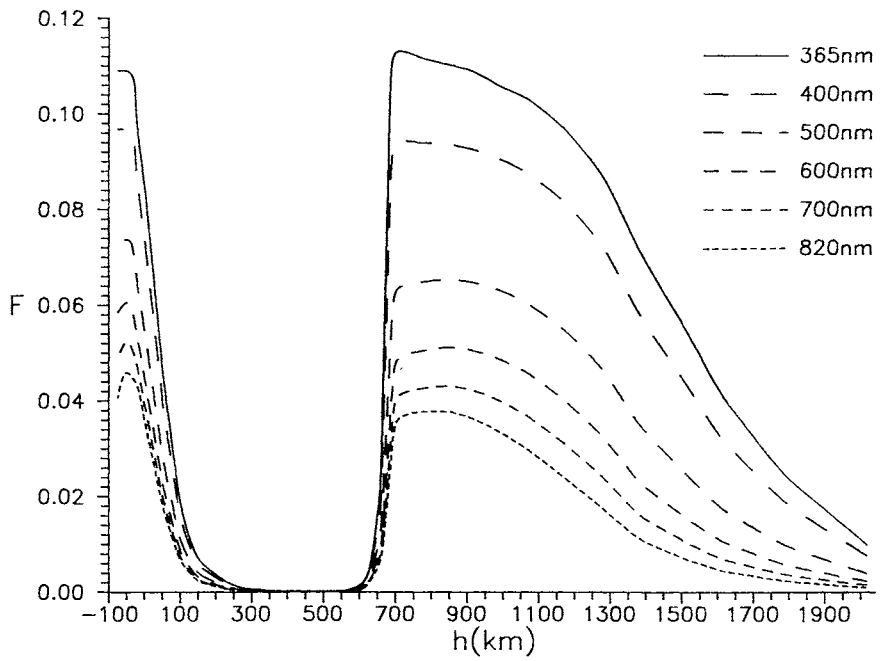

Fig. 4.2. Same as in Fig. 4.1. but for the chromospheric model of Vernazza et al. (1981, model C)

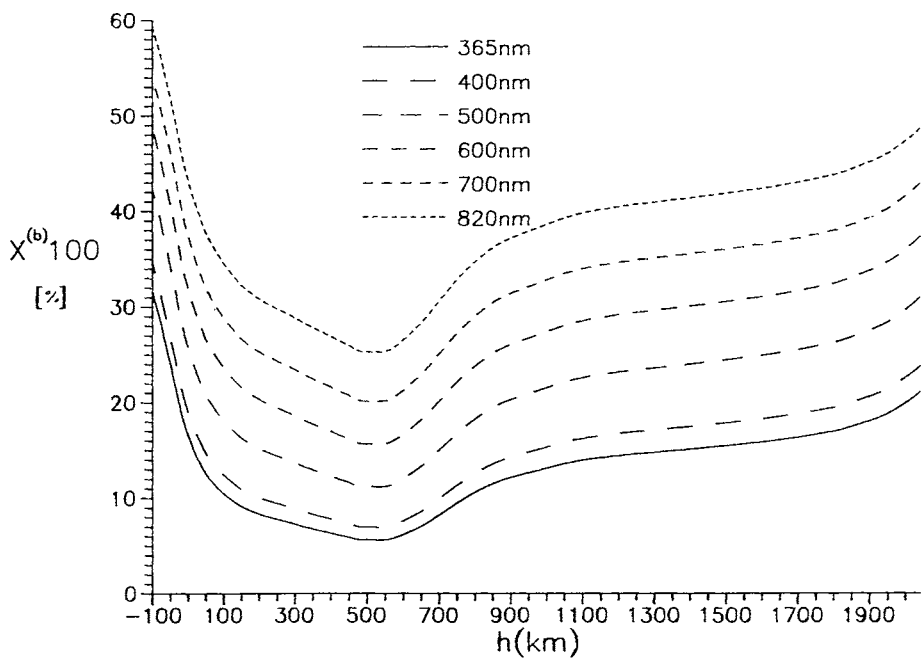

Fig. 5.1. Behavior of parameter $X^{(b)}(Z)$, where $Z = |U_1(R_\lambda)|/kT$, defined by Eqs. (9-14), as a function of height h, for 365 nm $\leq \lambda \leq$ 820 nm for the photospheric model of Maltby et al. (1986)

© European Southern Observatory • Provided by the NASA Astrophysics Data System

1994A&AS..103...57M

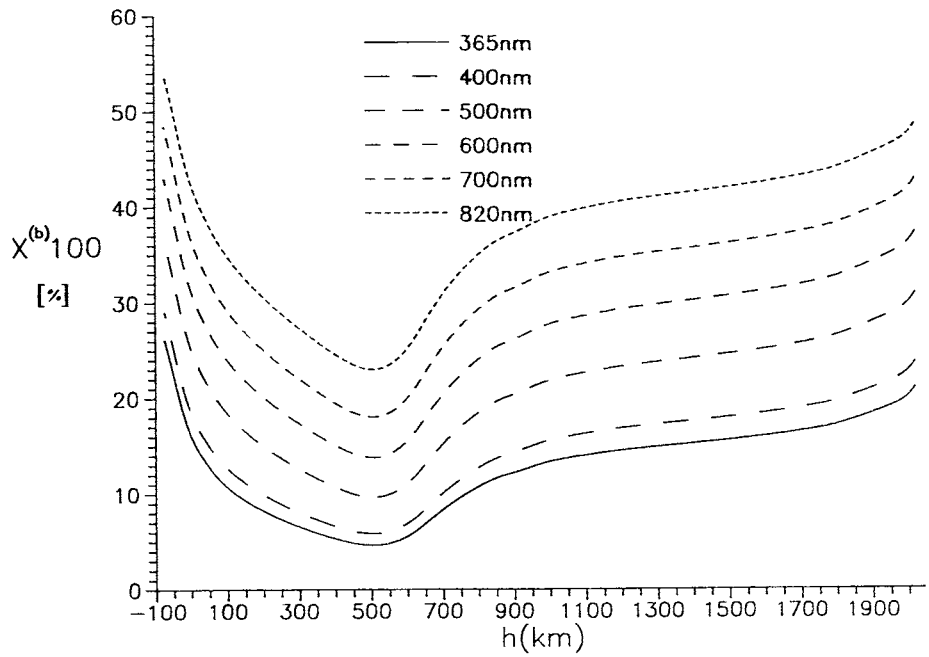

Fig. 5.2. Same as in Fig. 5.1. but for the chromospheric model of Vernazza et al. (1981, model C)

© European Southern Observatory • Provided by the NASA Astrophysics Data System

1994A&AS..105..243D

ASTRONOMY & ASTROPHYSICS
SUPPLEMENT SERIES

JUNE I **1994**, PAGE 243

Astron. Astrophys. Suppl. Ser. **105**, 243-244 (1994)

Stark broadening of Be I spectral lines*

M.S. Dimitrijević[1] and S. Sahal-Bréchot[2]

[1] Astronomical Observatory, Volgina 7, 11050 Beograd, Yugoslavia

[2] Laboratoire "Astrophysique, Atomes et Molécules", Unité associée au C.N.R.S. No 812, Département Atomes et Molécules en Astrophysique, Observatoire de Paris-Meudon, 92190 Meudon, France

Received May 17; accepted December 16, 1993

Abstract. — Using a semiclassical approach, we have calculated electron-, proton-, and ionized helium-impact line widths and shifts for 28 Be I multiplets. The resulting data have been compared with existing theoretical values.

Key words: lines: profile-atomic and molecular data

1. Introduction

As discussed in our previous article concerning Be II (Dimitrijević & Sahal-Bréchot 1992), beryllium Stark-broadening parameters are important to astrophysicists since the surface content (abundance) of light elements involves problems correlated with nucleogenesis, mixing between the atmosphere and the interior, and stellar structure and evolution (Boesgaard 1988). Moreover, due to the development of infrared astronomy from space, lines originating from higher energy levels have an increasing interest. For such lines the importance of Stark broadening contribution increases with the increase of the relevant principal quantum number, since the optical electron becomes less influenced by the core and more sensitive to weak external electric fields. Consequently, for such lines Stark broadening might be of interest even for cooler star plasmas.

By using the semiclassical-perturbation formalism (Sahal-Bréchot 1969a,b) we have calculated electron-, proton-, and ionized helium-impact line widths and shifts for 28 Be I multiplets. A summary of the formalism is given in Dimitrijević & Sahal-Bréchot (1984). Here, we present and discuss the results for Be I, along with a comparison with other semiclassical results (Benett & Griem 1971; Griem 1974).

* Table 1 is only available in electronic form: see the Editorial in A&AS 1994, Vol. 103, No. 1

2. Results and discussion

Energy levels for Be I lines have been taken from Bashkin & Stoner (1975). Oscillator strengths have been calculated by using the method of Bates & Damgaard (1949) and tables of Oertel & Shomo (1968). For higher levels, the method described in Van Regemorter et al. (1979) has been used.

Our results are shown in Table 1 (accessible in electronic form) for a perturber density of 10^{15} cm^{-3} and temperatures $T = 3,000 - 50,000$ K. For perturber densities lower than 10^{15} cm^{-3}, all of the data are practically linear functions of the density because the effect of Debye screening is negligible. We also specify a parameter c (Dimitrijević & Sahal-Bréchot 1984) which, when it is divided by the corresponding electron-impact full width at half maximum, gives an estimate for the maximum perturber density for which the line may be treated as isolated. For each value given in Table 1, the collision volume (V) multiplied by the perturber density (N) is much less than one and the impact approximation is valid (Sahal-Bréchot 1969a,b). Values for $0.1 < NV \leq 0.5$ are denoted by an asterisk. When the impact approximation is not valid, the ion-broadening contribution may be estimated by using quasistatic estimations (Griem 1974; Sahal-Bréchot 1991). The accuracy of the results obtained decreases when broadening by ion interactions becomes important.

In Table 2, the present results are compared with other semiclassical calculations (Benett & Griem 1971, given also in Griem 1974). We see that the agreement is within error limits of the semiclassical method except

© European Southern Observatory • Provided by the NASA Astrophysics Data System

1994A&AS..105..243D

Table 2. Comparison between the semiclassical calculation of Stark width (FWHM) W and shift d, at electron density of 10 cm and $T = 5000$ K and 20,000 K. DSB - present results; BG - Benett and Griem (1971) (Bennet & Griem 1971 and Griem 1974)

Transition	T(K)	WDSB(A)	WBG(A)	dDSB(A)	dBG(A)
Singlets 2s-2p	5000 20000	0.00184 0.00234	0.00142 0.00232	0.00103 0.000820	0.000933 0.000863
2s-3p	5000 20000	0.00859 0.0109	0.00928 0.0138	0.00549 0.00639	0.00523 0.00572
2p-3s	5000 20000	0.145 0.175	0.170 0.232	0.105 0.129	0.0997 0.115
2p-3d	5000 20000	0.0940 0.122	0.102 0.159	0.0594 0.0683	0.0536 0.0564
2p-4s	5000 20000	0.230 0.262	0.272 0.364	0.175 0.198	0.161 0.171
2p-4d	5000 20000	0.251 0.364	0.326 0.512	-0.0303 0.0121	-0.0542 -0.0133
Triplets 2p-3s	5000 20000	0.0163 0.0211	0.0218 0.0280	0.0133 0.0173	0.0129 0.0158

for transitions involving highly excited levels (2p-4s and 2p-4d) where our widths are smaller due to Debye screening effect not taken into account explicitly in Benett & Griem (1971, also in Griem 1974) (but the corresponding correction is suggested).

Acknowledgements. This work is a part of the project "Physics and Dynamics of Celestial Bodies", supported by Ministry of Science and Technology of Serbia.

References

Bashkin S., Stoner J.O. Jr. 1975, Atomic Energy Levels and Grotrian Diagrams, Vol. 1 (North Holland, Amsterdam)

Bates D.R., Damgaard A. 1949, Trans. Roy. Soc. London, Ser. A 242, 101

Benett S.M., Griem H.R. 1971, Calculated Stark Broadening Parameters for Isolated Spectral Lines from the Atom Helium through Calcium and Cesium, Univ. Maryland, Tech. Rep. No 71-097 (College Park, Maryland)

Boesgaard A.M. 1988, Vistas in Astronomy 31, 167

Dimitrijević M.S., Sahal-Bréchot S. 1984, JQSRT 31, 301

Dimitrijević M.S., Sahal-Bréchot S. 1992, JQSRT 48, 397

Griem H.R. 1974, Spectral Line Broadening by Plasmas (Academic Press, New York and London)

Oertel G.K., Shomo L.P. 1968, ApJS 16, 175

Sahal-Bréchot S. 1969a, A&A 1, 91

Sahal-Bréchot S. 1969b, A&A 2, 322

Sahal-Bréchot S. 1991, A&A 245, 322

Van Regemorter H., Hoang Binh Dy, Prud'homme M. 1979, J. Phys. B 12, 1073

© European Southern Observatory • Provided by the NASA Astrophysics Data System

1994A&AS..105..245D

ASTRONOMY & ASTROPHYSICS
SUPPLEMENT SERIES

JUNE I 1994, PAGE 245

Astron. Astrophys. Suppl. Ser. **105**, 245-246 (1994)

Stark broadening of spectral lines of multicharged ions of astrophysical interest. XI. Al XI and Si XII*

M.S. Dimitrijević[1] and S. Sahal-Bréchot[2]

[1] Astronomical Observatory, Volgina 7, 11050 Beograd, Yugoslavia

[2] Laboratoire "Astrophysique, Atomes et Molécules", Département Atomes et Molécules en Astrophysique, Unité associée au C.N.R.S. N 812, Observatoire de Paris-Meudon, 92190 Meudon, France

Received May 25; accepted December 16, 1993

Abstract. — Using a semiclassical approach, we have calculated electron-, proton-, and He III -impact line widths and shifts for 7 Al XI and 9 Si XII multiplets. The results obtained have been used for the study of the behavior of Stark broadening parameters within an isoelectronic sequence.

Key words: lines: profile-atomic and molecular data

1. Introduction

This paper is the eleventh of a series devoted to the calculation of Stark broadening parameters of spectral lines of multicharged ions (Dimitrijević et al. 1991a,b; Dimitrijević & Sahal-Bréchot 1992a-c; 1993a-d). In previous articles Stark broadening data for C IV (Dimitrijević et al. 1991a), NV (Dimitrijević & Sahal-Bréchot 1992b), O VI (Dimitrijević & Sahal-Bréchot 1992a), F VII (Dimitrijević & Sahal-Bréchot 1993c), Ne VIII and Na IX (Dimitrijević & Sahal-Bréchot 1993d) all belonging to the lithium isoelectronic sequence have been calculated.

Due to the simplicity (one optical electron), Stark broadening parameters for spectral lines for ions within this electronic sequence have particular importance for the investigation of regularities and systematic trends. Results of such investigations are of interest for acquisition of new data by interpolation and for critical evaluation of existing experimental and theoretical data, particularly in astrophysics. The astrophysical importance of multiply charged ion lines is increasing due to the development of UV astronomy from space and owing to the development of researches on the physics of stellar interiors (Seaton 1987).

In the case of Mg X, the reliable data on $4s^2S$ energy level are missing (Martin & Zalubas 1980), so that we could not complete atomic data set needed for reliable semiclassical calculations. In order to investigate the behavior of Stark broadening parameters along an isoelectronic sequence as far as possible without the significant influence of relativistic effects, we have calculated electron-, proton-, and He III-impact line widths and shifts for 7 Al XI and 9 Si XII multiplets, by using the semiclassical-perturbation formalism (Sahal-Bréchot 1969a,b). A summary of the formalism is given in Dimitrijević & Sahal-Bréchot (1991). Here, we present and discuss the results obtained as well as the Stark broadening parameter behaviour within the lithium isoelectronic sequence.

2. Results and discussion

Energy levels for Al XI and Si XII lines have been taken from Martin & Zalubas (1979, 1983) respectively. Oscillator strengths have been calculated by using the method of Bates & Damgaard (1949) and the tables of Oertel & Shomo (1968). For higher levels, the method described by Van Regemorter et al. (1979) has been used. In addition to electron-impact full halfwidths and shifts, Stark-broadening parameters due to proton-, and He III- impacts have been calculated.

Our results for 7 Al XI and 9 Si XII multiplets are shown in Table 1 (accessible only in electronic form),

* Table 1 is only available in electronic form: see the Editorial in A&AS 1994, Vol. 103, No. 1

© European Southern Observatory • Provided by the NASA Astrophysics Data System

1994A&AS..105..245D

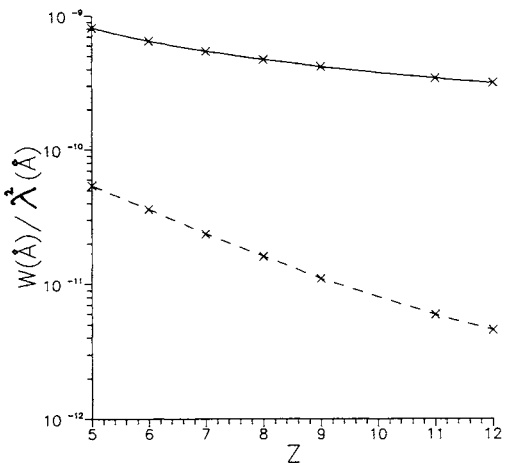

Fig. 1. The behavior of W(FWHM) [Å]/(λ[Å])^2 for (—) electron- and (- - - - -) proton-impact along the lithium isoelectronic sequence. With Z is denoted the residual charge as "seen" by the optical electron ($Z = 1$ for neutrals, 2 for singly charged ions etc). The considered transition is 2s-2p, electron density 10^{17}cm^{-3} and temperature 500,000 K

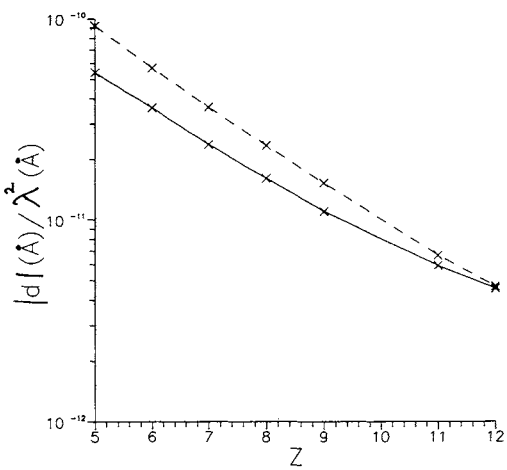

Fig. 2. Same as in Fig. 1 but for the shift

for perturber densities $10^{18} - 10^{23}$cm^{-3} and temperatures $T = 500,000 - 4,000,000$ K. We also specify a parameter c (Dimitrijević & Sahal-Bréchot 1984), which gives an estimate for the maximum perturber density for which the line may be treated as isolated when it is divided by the corresponding electron-impact full width at half maximum. For each value given in Table 1, the collision volume (V) multiplied by the perturber density (N) is much less than one and the impact approximation is valid (Sahal-Bréchot 1969a,b). Values for $NV > 0.5$ are not given and values for $0.1 < NV \leq 0.5$ are denoted by an asterisk. When the impact approximation is not valid, the ion broadening contribution may be estimated by using quasistatic estimations (Sahal-Bréchot 1991 and Griem 1974). The accuracy of the results obtained decreases when broadening by ion interactions becomes important.

In Figs. 1 and 2, the behavior of electron-, and proton-impact widths and shifts within the lithium isoelectronic sequence is shown. We can see that the behavior is regular. This fact might be of interest for the interpolation of new data and for critical selection of existing results.

Acknowledgements. This work is a part of the project "Physics and Dynamics of Celestial Bodies" supported by the Ministry for Science and Technology of Serbia.

References

Bates D.R. & Damgaard A. 1949, Trans. Roy. Soc. London, Ser. A 242, 101
Dimitrijević M.S. & Sahal-Bréchot S. 1984, JQSRT 31, 301
Dimitrijević M.S., Sahal-Bréchot S. & Bommier V. 1991a, A&AS 89, 581
Dimitrijević M.S., Sahal-Bréchot S. & Bommier V. 1991b, A&AS 89, 591
Dimitrijević M.S. & Sahal-Bréchot S. 1992a, A&AS 93, 359
Dimitrijević M.S. & Sahal-Bréchot S. 1992b, A&AS 95, 109
Dimitrijević M.S. & Sahal-Bréchot S. 1992c, A&AS 95, 121
Dimitrijević M.S. & Sahal-Bréchot S. 1993a, A&AS 99, 585
Dimitrijević M.S. & Sahal-Bréchot S. 1993b, A&AS 100, 91
Dimitrijević M.S. & Sahal-Bréchot S. 1993c, A&AS, in press
Dimitrijević M.S. & Sahal-Bréchot S. 1993d, A&AS, in press
Griem H.R. 1974, Spectral Line Broadening by Plasmas (Academic Press, New York and London)
Martin W.C. & Zalubas P. 1980, J. Phys. Chem. Ref. Data 9, 1
Martin W.C. & Zalubas P. 1983, J. Phys. Chem. Ref. Data 12, 323
Oertel G.K. & Shomo L.P. 1968, ApJS 16, 175
Sahal-Bréchot S. 1969a, A&A 1, 91
Sahal-Bréchot S. 1969b, A&A 2, 322
Sahal-Bréchot S. 1991, A&A 245, 322
Seaton M.J. 1987, J. Phys. B 20, 6363
Van Regemorter H., Hoang Binh Dy & Prud'homme M. 1979, J. Phys. B 12, 1073

© European Southern Observatory • Provided by the NASA Astrophysics Data System

1994A&AS..107..191D

ASTRONOMY & ASTROPHYSICS
SUPPLEMENT SERIES

Astron. Astrophys. Suppl. Ser. **107**, 191 (1994)

Erratum

Stark broadening of Bi II lines of astrophysical interest

M.S. Dimitrijević and L.Č. Popović

(*Astron. Astrophys. Suppl. Series* **101** (1993) 583-586)

In Fig. 1 caption instead of Stark full width (FWHM) must be Stark half width (HWHM).

In Table 2 for the Stark width of $7s^3P_1^0 - 7p^3D_2$ for $T = 30000$ K instead of .860 must be .860E-01. As well for $7s^3P_1^0 - 7p^3P_0$ for $T = 30000$ K instead of .740 must be .740E-01.

© European Southern Observatory • Provided by the NASA Astrophysics Data System

1994A&AS..107..191D

Commission paritaire N° 62.321

© Les Editions de Physique 1994

Directrice de la Publication : Jeanne BERGER

Saisie, composition MATHOR5-TEX
Impression JOUVE, 18, rue Saint-Denis, 75001 PARIS
N° 221028C Dépôt légal : Septembre 1994

© European Southern Observatory • Provided by the NASA Astrophysics Data System

1994A&AS..107..349D

ASTRONOMY & ASTROPHYSICS
SUPPLEMENT SERIES

OCTOBER II 1994, PAGE 349

Astron. Astrophys. Suppl. Ser. **107**, 349-351 (1994)

Stark broadening of spectral lines of multicharged ions of astrophysical interest. X. Ne VIII and Na IX*

M.S. Dimitrijević[1] and S. Sahal-Bréchot[2]

[1] Astronomical Observatory, Volgina 7, 11050 Beograd, Yugoslavia
[2] Laboratoire "Astrophysique, Unité associée au C.N.R.S. N° 812, Observatoire de Paris-Meudon, 92190 Meudon, France

Received January 26; accepted March 31, 1994

Abstract. — Using a semi classical approach, we have calculated electron-, proton-, and He III-impact line widths and shifts for 20 Ne VIII and 8 Na IX multiplets. Obtained results have been compared with available experimental and theoretical data. The influence of the perturber charge on the ion broadening contribution has been investigated and discussed.

Key words: lines: profile-atomic and molecular data

1. Introduction

The development of UV astronomy from space as well as the development of researches on the physics of stellar interiors (Seaton 1987), increases the significance of multiply charged ion lines in astrophysics. As the result of our attempt to provide the needed data for astrophysicist, this paper is the tenth of a series devoted to the calculation of Stark broadening parameters of spectral lines of multicharged ions (see Dimitrijević & Sahal-Bréchot 1992a and references therein as well as Dimitrijević & Sahal-Bréchot 1992b,c; 1993a-c).

By using the semi classical-perturbation formalism (Sahal-Bréchot 1969ab), we have calculated electron-, proton-, and ionized helium-impact line widths and shifts for 20 Ne VIII and 8 Na IX multiplets, in order to continue our research of multiply charged ion line Stark broadening parameters, with the special emphasis on the lithium isoelectronic sequence. A summary of the formalism is given in Dimitrijević et al. (1991). Here, we present and discuss the obtained results, and also the comparison with experimental data (Glenzer et al. 1992) and other theoretical calculations (Glenzer et al. 1992; Seaton 1988) and estimates (Purić et al 1988). Moreover, the influence of the perturber charge on the ion broadening contribution has been investigated and discussed.

2. Results and discussion

Energy levels for Ne VIII lines have been taken from Bashkin & Stoner (1975). For Na IX lines corresponding energy levels have been taken from Martin & Zalubas (1980). Oscillator strengths have been calculated by using the method of Bates & Damgaard (1949) and the tables of Oertel & Shomo (1968). For higher levels, the method described by Van Regemorter et al. (1979) has been used. In addition to electron-impacts full halfwidths and shifts, Stark- broadening parameters due to proton-, and He III-impacts have been calculated.

Our results for 20 Ne VIII and 8 Na IX multiplets are shown in Table 1 (accessible only in electronic from), for perturber densities $10^{16} - 10^{22}\mathrm{cm}^{-3}$ and temperatures $T = 200,000 - 2,000,000$ K. We also specify a parameter c (Dimitrijević & Sahal-Bréchot 1984), which gives an estimate for the maximum perturber density for which the line may be treated as isolated when it is divided by the corresponding electron-impact full width at half maximum. For each value given in Table 1, the collision volume (V) multiplied by the perturber density (N) is much less than one and the impact approximation is valid (Sahal-Bréchot 1969ab). Values for $NV > 0.5$ are not given and values for $0.1 < NV \leq 0.5$ are denoted

* Table 1 is only available in electronic form: see the Editorial in A&AS 1994, Vol. 103, No. 1

© European Southern Observatory • Provided by the NASA Astrophysics Data System

1994A&AS..107..349D

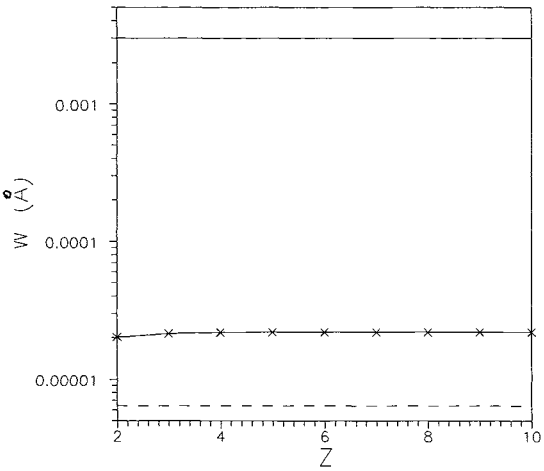

Fig. 1. The behavior of W(FWHM)[Å] for Na Z - Na IX impacts (-×-×-×-) ($Z = 1$ for neutrals, 2 for singly charged ions etc). Electron-impact (—) and proton-impact (- - - -) widths are shown as well. The considered transition is 2s−2p, electron density 10^{17}cm^{-3} and temperature 200,000 K

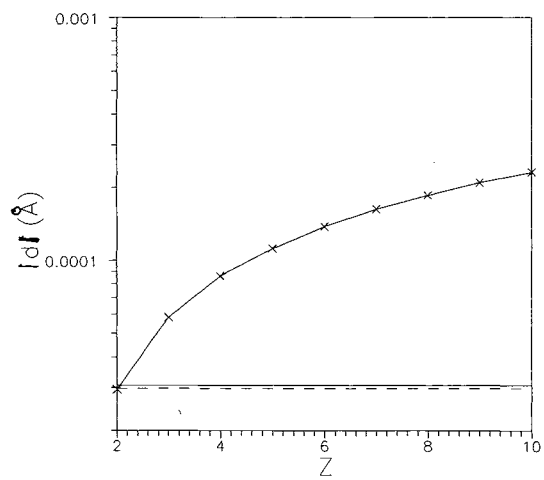

Fig. 2. Same as in Fig. 1 but for the shift

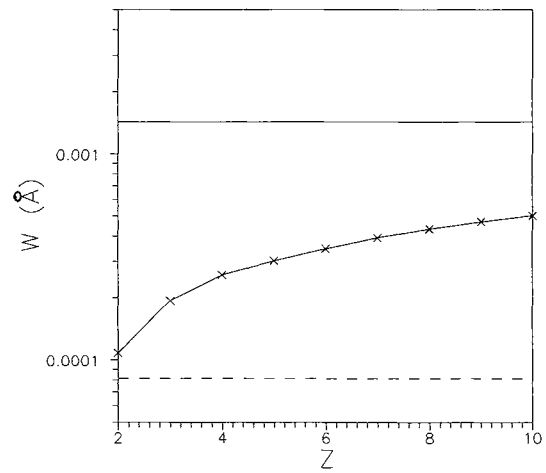

Fig. 3. Same as in Fig. 1 but for temperature of 1,000,000 K

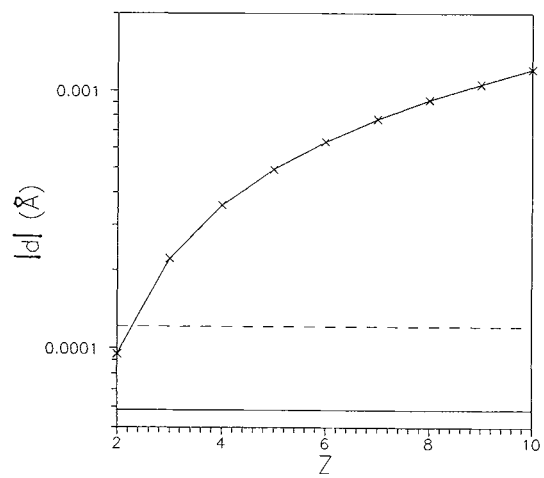

Fig. 4. Same as in Fig. 3 but for the shift

by an asterisk. When the impact approximation is not valid, the ion broadening contribution may be estimated by using quasistatic estimations (Sahal-Bréchot 1991 and Griem 1974). The accuracy of the results obtained decreases when broadening by ion interactions becomes important.

In Figs. 1-4, the influence of perturber charge on the ion broadening contribution is analyzed. Full half widths (W) and shifts (d) due to Na IX collisions with Na ions with the charge between 1 and 9 ($z = 2 - 10$) are compared with the electron- and proton-impact widths and shifts. When the perturber charge increases, we have that the repulsive force between the emitter and the perturber increases as well. On the other hand, a perturber with higher charge has the stronger influence on the emitter than a perturber with smaller charge at the same distance. For lower temperatures, i.e. smaller perturber velocities, the repulsive force is more effective since the collision duration is larger and highly charged perturber has smaller chance to come closer to the emitter. Consequently, for the lower temperatures (Figs. 1, 2) the Stark broadening parameters have smaller change with Z than for $T = 10^6$ K (Figs. 3, 4). One can see as well that shifts are more sensitive to the perturber charge increase than widths.

In Table 2, our results for Ne VIII $3s^2S-3p^2P^\circ$ 2820.7 Å line are compared with the available experimental data (Glenzer et al. 1992) and with calculations of Glenzer et al. (1992) by using different approximate methods (Eq. 526 in Griem 1974; Dimitrijević & Konjević 1980; Hey & Breger 1982). In our results the ion broadening contribution is included. However, the inelastic collisions have been neglected for ion-impact width. The best agreement of our results is with the results (Glenzer et al 1992) obtained by using the quasiclassical Gaunt factor approximation of Hey & Breger (1982), and the largest disagreement with the quantum mechanical results (Seaton 1988). All calculations give lower values than the experimental ones. For Ne VIII 3s−3p line, Purić et al.

© European Southern Observatory • Provided by the NASA Astrophysics Data System

1994A&AS..107..349D

Table 2. Experimental (Wm) Stark widths (FWHM) in Å for Ne VIII $3s^2S-3p^2P^\circ$, $\lambda = 2820.7$ Å line, compared with the theory. WDSB - the present semi-classical calculations; WS - Seaton (1988); WG - Glenzer et al (1992) by using Eq. (526) in Griem (1974); WDK - Glenzer et al (1992) by using the modified semiempirical approach (Dimitrijević & Konjević (1980); WH - calculated by Hey (cited as private communication in Glenzer et al 1992) by using the quasiclassical Gaunt factor approach (Hey & Breger 1982)

Transition	kT[eV]	Ne[10^{18}cm^{-3}]	Wm[Å]	Wm/WDSB	Wm/WS	Wm/WG	Wm/WDK	Wm/WH
Ne VIII	29.7	2.8	1.2	1.91	3.29	2.22	2.55	1.83
$3s^2S-3p^2P^\circ$								
2820.7 Å	42.5	3.2	1.2	1.67	3.47	2.07	2.45	1.77

(1988) estimated the Stark width (FWHM) at 80,000 K as 0.032 Å by using regularities and systematic trends. Our result is 0.045 Å which shows that simple approximate methods might be useful for quick estimates.

Acknowledgements. This work is a part of the project "Physics and Dynamics of Celestial Bodies" supported by the Ministry for Science and Technology of Serbia.

References

Bashkin S., Stoner J.O.Jr 1975, Atomic Energy Levels and Grotrian Diagrams, Vol. 1, North Holland, Amsterdam
Bates D.R., Damgaard A. 1949, Trans. Roy. Soc. London, Ser. A 242, 101
Dimitrijević M.S., Konjević N. 1980, JQSRT 24, 451
Dimitrijević M.S., Sahal-Bréchot S. 1984, JQSRT 31, 301
Dimitrijević M.S., Sahal-Bréchot S., Bommier V. 1991, A&AS 89, 581
Dimitrijević M.S., Sahal-Bréchot S. 1992a, A&AS 95, 109
Dimitrijević M.S., Sahal-Bréchot S. 1992b, A&AS 93, 359
Dimitrijević M.S., Sahal-Bréchot S. 1992c, A&AS 95, 121
Dimitrijević M.S., Sahal-Bréchot S. 1993a, A&AS 99, 585
Dimitrijević M.S., Sahal-Bréchot S. 1993b, A&AS 100, 91
Dimitrijević M.S., Sahal-Bréchot S. 1993c, A&AS 101, 587
Glenzer S., Uzelac N.I., Kunze H.-J. 1992, Phys. Rev. 45, 8795
Griem H.R. 1974, Spectral Line Broadening by Plasmas (Academic Press, New York and London)
Hey J.D., Breger P. 1982, S. Afr. J. Phys. 5, 111
Martin W.C., Zalubas P. 1980, J. Phys. Chem. Ref. Data 9, 1
Oertel G.K., Shomo L.P. 1968, ApJS 16, 175
Purić J., Djeniže S., Labat J., Platiša M., Srećković A., Ćuk M. 1988, Z. Phys. D 10, 431
Sahal-Bréchot S. 1969a, A&A 1, 91
Sahal-Bréchot S. 1969b, A&A 2, 322
Sahal-Bréchot S. 1991, A&A 245, 322
Seaton M.J. 1987, J. Phys. B 20, 6363
Seaton M.J. 1988, J. Phys. B 21, 3033
Van Regemorter H., Hoang Binh Dy, Prud'homme M. 1979, J. Phys. B 12, 1073

© European Southern Observatory • Provided by the NASA Astrophysics Data System

1994A&AS..107..349D

© European Southern Observatory • Provided by the NASA Astrophysics Data System

1995A&AS..109..551D

ASTRONOMY & ASTROPHYSICS
SUPPLEMENT SERIES

MARCH 1995, PAGE 551

Astron. Astrophys. Suppl. Ser. **109**, 551-552 (1995)

Stark broadening of spectral lines of multicharged ions of astrophysical interest. XII. O IV and O V*

M.S. Dimitrijević[1] and S. Sahal-Bréchot[2]

[1] Astronomical Observatory, Volgina 7, 11050 Beograd, Yugoslavia
[2] Laboratoire "Astrophysique, Atomes et Molécules" Département Atomes et Molécules en Astrophysique Unité associée au C.N.R.S. N 812, Observatoire de Paris-Meudon, 92190 Meudon, France

Received August 16; accepted October 14, 1994

Abstract. — Using a semiclassical approach, we have calculated electron-, proton-, and He III-impact line widths and shifts for 5 O IV and 19 O V multiplets.

Key words: lines: profile-atomic and molecular data

1. Introduction

The astrophysical interest of oxygen is obvious due to its high cosmical abundance and presence of its different ionization stages in stellar atmospheres. Stark broadening of O IV and O V spectral lines has been investigated several times theoretically (Dimitrijević & Konjević 1981; Dimitrijević 1988ab; 1993ab, Purić et al. 1988; Djeniže et al. 1990; Sahal-Bréchot 1991; Glenzer et al. 1994; Blagojević et al. 1994) and experimentally Purić et al. 1988; Glenzer et al. 1994; Blagojević et al. 1994). In previous theoretical evaluations various approximate approaches have been used or more sophisticated semiclassical calculations have been performed only for particular lines. This paper is the twelth of a series devoted to the calculation of Stark broadening parameters of spectral lines of multicharged ions (see Dimitrijević & Sahal-Bréchot 1992a and references therein as well as Dimitrijević & Sahal-Bréchot 1992b,c; 1993a-c, 1994).

By using the semiclassical-perturbation formalism (Sahal-Bréchot 1969a,b), we have calculated electron-, proton-, and ionized helium-impact line widths and shifts for 5 O IV and 19 O V multiplets, in order to continue our research of multiply charged ion line Stark broadening parameters. A summary of the formalism is given in Dimitrijević et al. (1991).

* Table 1 is only available in electronic form: see the Editorial in A&AS 1994, Vol. 103 No. 1.

2. Results and discussion

Energy levels for O IV and O V lines have been taken from Moore (1983, 1980). Oscillator strengths have been calculated by using the method of Bates & Damagaard (1949) and the tables of Oertel & Shomo (1968). For higher levels, the method described by Van Regemorter et al. (1979) has been used. In addition to electron-impact full halfwidths and shifts, Stark-broadening parameters due to proton-, and He III-impacts have been calculated.

Our results for 5 O IV and 19 O V multiplets are shown in Table 1 (accessible only in electronic form), for perturber densities $10^{17} - 10^{22}$ cm^{-3} and temperatures $T = 200,000 - 2,000,000$ K. We also specify a parameter c (Dimitrijević & Sahal-Bréchot 1984), which gives an estimate for the maximum perturber density for which the line may be treated as isolated when it is divided by the corresponding electron-impact full width at half maximum. For each value given in Table 1, the collision volume (V) multiplied by the perturber density (N) is much less than one and the impact approximation is valid (Sahal-Bréchot 1969a,b). Values for $NV > 0.5$ are not given and values for $0.1 < NV \leq 0.5$ are denoted by an asterisk. When the impact approximation is not valid, the ion broadening contribution may be estimated by using quasistatic estimations (Sahal-Bréchot 1991 and Griem 1974). The accuracy of the results obtained decreases when broadening by ion interactions becomes important.

© European Southern Observatory • Provided by the NASA Astrophysics Data System

1995A&AS..109..551D

Data for 3s-3p and 3p-3d multiplets of O IV for a perturber density of 10^{17} cm^{-3} have been tabulated in Blagojević et al. (1994) and have been compared with experimental results (Purić et al. 1988; Glenzer et al. 1994); Blagojević et al. 1994) as well as with simple theoretical estimates. This comparison shows good agreement between experimental and semiclassical values. In addition to the present data for 19 O V multiplets, Stark broadening data for 50 O V multiplets for which the set of atomic data needed for semiclassical calculation presently does not exist, have been calculated within the modified semiempirical approach (Dimitrijević & Konjević 1980) and published recently (Dimitrijević 1993a). For 29 of these 50 O V multiplets not included here, exist as well in Dimitrijević (1993b) data calculated within the approximate semiclassical approach (Eq. 526 in Griem 1974).

Acknowledgements. This work is a part of the project "Physics and Dynamics of Celestial Bodies" supported by the Ministry for Science and Technology of Serbia.

References

Bates D.R., Damgaard A. 1949, Trans. Roy. Soc. London, Ser. A 242, 101
Blagojević B., Popović M.V., Konjević N., Dimitrijević M.S. 1994, Phys. Rev. B 50, 2986
Dimitrijević M.S. 1988a, A&AS 76, 53
Dimitrijević M.S., 1988b, Bull. Obs. Astron. Belgrade 139, 31
Dimitrijević M.S. 1993a, A&AS 100, 237
Dimitrijević M.S. 1993b, Astro. Lett. Communications 28, 385
Dimitrijević M.S., Konjević N. 1980, JQSRT 24, 451
Dimitrijević M.S., Konjević N. 1981, in Spectral Line Shapes, eds. B. Wende, W. de Gruyter & Co., New York, 521
Dimitrijević M.S., Sahal-Bréchot S. 1984, JQSRT 31, 301
Dimitrijević M.S., Sahal-Bréchot S., Bommier V. 1991, A&AS 89, 581
Dimitrijević M.S., Sahal-Bréchot S. 1992a, A&AS 95, 109
Dimitrijević M.S., Sahal-Bréchot S. 1992b, A&AS 93, 359
Dimitrijević M.S., Sahal-Bréchot S. 1992c, A&AS 95, 121
Dimitrijević M.S., Sahal-Bréchot S. 1993a, A&AS 99, 585
Dimitrijević M.S., Sahal-Bréchot S. 1993b, A&AS 100, 91
Dimitrijević M.S., Sahal-Bréchot S. 1993c, A&AS 101, 587
Dimitrijević M.S., Sahal-Bréchot S. 1994, A&AS 107, 349
Djeniže S., Labat J., Platiša M., Srećković A., Purić J. 1990, A&AS 227, 291
Glenzer S., Hey J.D., Kunze H.J. 1994, J. Phys. B 27, 413
Griem H.R. 1974, Spectral Line Broadening by Plasmas (Academic Press, New York and London)
Moore C.E. 1980, Selected Tables of Atomic Spectra, Atomic Energy Levels and Multiplet Tables, O V, NSRDS-NBS 3, Section 9, U.S. Dept. of Commerce, Washington
Moore C.E. 1983, Selected Tables of Atomic Spectra, Atomic Energy Levels and Multiplet Tables, O IV, NSRDS-NBS 3, Section 10, U.S. Dept. of Commerce, Washington
Oertel G.K., Shomo L.P. 1968, ApJS 16, 175
Purić J., Djeniže S., Srećković A., Platiša M., Labat J. 1988, Phys Rev. A 37, 498
Sahal-Bréchot S. 1969a, A&A 1, 91
Sahal-Bréchot S. 1969b, A&A 2, 322
Sahal-Bréchot S. 1991, A&A 245, 322
Van Regemorter H., Hoang Binh Dy, Prud'homme M. 1979, J. Phys. B 12, 1073

© European Southern Observatory • Provided by the NASA Astrophysics Data System

1995A&AS..111..565D

ASTRONOMY & ASTROPHYSICS
SUPPLEMENT SERIES

JUNE II **1995**, PAGE 565

Astron. Astrophys. Suppl. Ser. **111**, 565-568 (1995)

Stark broadening of singly-ionized iron spectral lines

M.S. Dimitrijević

Astronomical Observatory, Volgina 7, 11050 Beograd, Yugoslavia

Received November 9 1994; accepted January 6 1995

Abstract. — Stark broadening parameters for singly-ionized iron $a^6D-z^6P^0$, $a^6D-z^6D^0$ and $a^6D-z^6F^0$ multiplets, have been calculated by using the semiclassical-perturbation approach. The obtained results have been compared with experimental data and simpler estimates.

Key words: lines: profile-atomic and molecular data

1. Introduction

The investigation of neutral and ionized iron is of great astrophysical importance due to its high abundance and its role in various processes in stellar plasma. Fe II lines are present in solar and stellar spectra and for their analysis or the calculations of synthetic spectra corresponding Stark broadening data are of importance. For example Yo-ici Takeda (1984) and Bolkal et al. (1992) have considered Fe II lines in the spectra of Am 15 Vul and Am 32 Aqr stars, while Adelman et al. (1992) have found such lines in several stars like e.g. Ao V type stars gamma Geminorum and 7 Sextantis. For all mentioned stars Stark broadening is the dominant pressure broadening mechanism in the line formation regions. In spite of its astrophysical meaning, we found only two published experimental investigations of Stark broadening parameters of Fe II lines. Manning et al. (1990) have investigated shifts of Fe II $a^4D - z^4F^0$ 2755.73 Å line and Purić et al. (1993) widths of 14 lines from $a^6D - z^6D^0$ and $a^6D - z^6F^0$ multiplets. Electron-impact widths for 3 solar multiplets ($a^4H-z^4F^0$, $a^6D - z^6D^0$ and $a^4F - z^4F^0$) and 3 multiplets observed in the spectrum of 15 Vulpeculae (Yo-ichi Takeda 1984) ($b^4P-z^4F^0$, $b^4F-z^4D^0$ and $b^4P-z^4D^0$), have been calculated by Dimitrijević (1988) within the modified semiempirical approach (Dimitrijević & Konjević 1980). Simple estimates based on the regularities and systematic trends, by Lakićević (1983) and Purić et al. (1993) exist as well.

The strongest Fe II lines correspond to 4s−4p and 3d−4p transitions in $3d^6nl$ and $3d^54snl$ configurations, covering some 1500 observed lines and accounting for the main part of the intensity of the Fe II spectrum (Johanson 1984). However, if one wishes to perform a more sophisticated calculation it is not easy to collect the sufficiently complete energy level set and to avoid the additional difficulties due to configuration interaction and violation of the LS selection rules. The best situation is just with 4s−4p sextets, measured by Purić et al. (1993), where the sufficiently complete energy level set exists and there is not pronounced configuration interactions or critical violations of the LS selection rules (Fawcet 1987), so that the semiclassical calculations may provide more reliable Stark broadening parameters.

By using the semiclassical-perturbation formalism (Sahal-Bréchot 1969ab), we have calculated Stark broadening parameters for singly-ionized iron $a^6D-z^6P^0$, $a^6D-z^6D^0$ and $a^6D-z^6F^0$ multiplets. Perturbers are electrons, protons and a singly charged perturber with the mass equal to 35 a.u. corresponding to the averaged mass of perturbing ions in Solar atmosphere. In the low chromosphere in the vicinity of the temperature minimum, hydrogen is mostly neutral. Consequently electrons are due to ionization of metals, positive ions are not protons and a mean ionic mass of 35 a.u. is relevant. On the other hand, in hotter stars hydrogen is partially (or mostly) ionized, thus positive ions are mainly protons. Moreover, data for the ionic mass of 35 a.u. may be of interest for the laboratory plasma as well since a group of possible perturbers (P II, S II, Cl II, Ar II, K II, Ca II) have the mass between 30 and 40 a.u. A summary of the formalism is given in Dimitrijević et al. (1991). The obtained results have been compared with experimental data and simpler evaluations.

2. Results and discussion

Energy levels for Fe II lines have been taken from Corlis & Sugar (1982). Oscillator strengths have been calculated by using the method of Bates & Damgaard (1949) and the tables of Oertel & Shomo (1968). For higher levels, the method described by Van Regemorter et al. (1979) has been used. In addition to electron-impact full halfwidths

© European Southern Observatory • Provided by the NASA Astrophysics Data System

1995A&AS..111..565D

Table 1. This table shows Stark broadening full half-widths (FWHM) and shifts for Fe II for a perturber density of 10^{17} cm^{-3} and temperatures from 5,000 up to 150,000 K. Perturbers are electrons, protons and a singly charged perturber with the mass equal to 35 a.u. corresponding to the averaged mass of perturbing ions in Solar atmosphera. By using c (see Eq. (5) in Dimitrijević et al. 1991), we obtain an estimate for the maximum perturber density for which the line may be treated as isolated and tabulated data may be used

PERTURBER DENSITY = 1xE+17cm-3

		ELECTRONS		PROTONS		IONS WITH M=35a.u.	
TRANSITION	T(K)	WIDTH(A)	SHIFT(A)	WIDTH(A)	SHIFT(A)	WIDTH(A)	SHIFT(A)
Fe II a6D-z6F	5000.	0.117	0.262E-03	0.169E-02	-0.546E-04	0.364E-02	-0.543E-04
2392.9 A	10000.	0.854E-01	-0.325E-03	0.313E-02	-0.121E-03	0.506E-02	-0.115E-03
C= 0.21E+21	30000.	0.519E-01	-0.304E-03	0.519E-02	-0.323E-03	0.620E-02	-0.244E-03
	50000.	0.432E-01	-0.411E-03	0.571E-02	-0.436E-03	0.664E-02	-0.313E-03
	100000.	0.362E-01	-0.398E-03	0.638E-02	-0.599E-03	0.694E-02	-0.380E-03
	150000.	0.336E-01	-0.391E-03	0.669E-02	-0.664E-03	0.708E-02	-0.422E-03
Fe II a6D-z6D	5000.	0.137	0.158E-03	0.173E-02	-0.196E-03	0.387E-02	-0.190E-03
2611.4 A	10000.	0.993E-01	-0.138E-02	0.329E-02	-0.422E-03	0.544E-02	-0.367E-03
C= 0.26E+21	30000.	0.600E-01	-0.113E-02	0.562E-02	-0.972E-03	0.671E-02	-0.698E-03
	50000.	0.496E-01	-0.153E-02	0.620E-02	-0.124E-02	0.722E-02	-0.814E-03
	100000.	0.411E-01	-0.146E-02	0.696E-02	-0.155E-02	0.759E-02	-0.980E-03
	150000.	0.380E-01	-0.145E-02	0.735E-02	-0.172E-02	0.769E-02	-0.109E-02
Fe II a6D-z6P	5000.	0.112	0.135E-03	0.168E-02	-0.362E-04	0.359E-02	-0.361E-04
2334.8 A	10000.	0.816E-01	-0.211E-03	0.310E-02	-0.806E-04	0.497E-02	-0.777E-04
C= 0.19E+21	30000.	0.498E-01	-0.222E-03	0.509E-02	-0.224E-03	0.608E-02	-0.176E-03
	50000.	0.414E-01	-0.278E-03	0.560E-02	-0.314E-03	0.651E-02	-0.226E-03
	100000.	0.347E-01	-0.285E-03	0.625E-02	-0.435E-03	0.681E-02	-0.281E-03
	150000.	0.323E-01	-0.274E-03	0.655E-02	-0.490E-03	0.691E-02	-0.313E-03

and shifts, Stark-broadening parameters due to proton-impacts, and to impacts with a singly charged perturber with the mass equal to 35 a.u. corresponding to the averaged mass of perturbing ions in Solar atmosphere, have been calculated.

Our results for $a^6D - z^6P^0$, $a^6D - z^6D^0$ and $a^6D - z^6F^0$ Fe II multiplets, covering 34 lines within 2328.11 – 2632.108 Å range, are shown in Table 1, for a perturber density of 10^{17}cm^{-3} and temperatures $T = 5,000 - 150,000$ K. We also specify a parameter c (Dimitrijević et al. 1991), which gives an estimate for the maximum perturber density for which the line may be treated as isolated when it is divided by the corresponding electron-impact full width at half maximum.

In Table 2 the present theoretical full half-widths have been compared with experimental results (Purić et al. 1993a) as well as with the calculations of Dimitrijević (1988) performed by using the modified semiempirical approach (1980) and with simple theoretical estimates of Purić et al. (1993b) based on regularities and systematic trends. For the experiment of Purić et al. (1993a) SF_6 has been used as a working gas. At $T = 30,000$ K and electron density of 10^{17}cm^{-3} full half width for F II-impact broadening of Fe II 2392.9 Å line is 0.00606 and for S II-impact broadening 0.00618. Since the difference is negligible in comparison with electron-impact broadening, and since the ionized sulphur has the lower ionization potential and the corresponding linewidth is larger, full half width due to S II-impacts has been presented in Table 2 as an upper limit of ion broadening contribution. We can see that semiclassical calculations with the ion broadening contribution included, give larger widths than experiment but within the error bars of theory and experiment. Taking into account the complexity of the Fe II spectrum, the results (Dimitrijević 1988) obtained by using the modified semiempirical method (Dimitrijević & Konjević 1980) are in satisfactory agreement with the experimental values. The agreement of simple estimates of Purić et al.

© European Southern Observatory • Provided by the NASA Astrophysics Data System

1995A&AS..111..565D

Table 2. Comparison of experimental and theoretical Stark widths (FWHM) at corresponding electron densities N, and temperatures T. W_M - experimental widths (FWHM) of Purić et al. 1993a; W_e - present semiclassical widths (FWHM) for electron-impact broadening; W_{SII} - present semiclassical widths (FWHM) for SII-impact broadening; W_{DK} - Dimitrijević (1988); W_P - Purić et al. 1993b

Transition	Wavelength [A]	T [10^4K]	N [10^{17}cm^{-3}]	W_M[A]	W_e[A]	W_{SII}[A]	W_{DK}[A]	W_P[A]
a^6D-z^6D^o	2598.37	3.00	1.95	0.070	0.117	0.0130	0.068	0.126
		2.90	1.64	0.058	0.100	0.0109	0.059	0.108
		2.80	1.06	0.044	0.066	0.0070	0.038	0.072
	2607.52	3.00	1.95	0.100	0.117	0.0130	0.068	0.126
		2.90	1.64	0.076	0.100	0.0109	0.059	0.108
		2.90	1.27	0.058	0.077	0.0084	0.045	0.084
	2611.87	3.00	1.95	0.096	0.117	0.0130	0.068	0.126
		2.90	1.64	0.090	0.100	0.0109	0.059	0.108
		2.80	1.06	0.072	0.066	0.0070	0.038	0.070
	2613.82	3.00	1.95	0.088	0.117	0.0130	0.068	0.126
		2.90	1.64	0.072	0.100	0.0109	0.059	0.108
		2.80	1.06	0.044	0.066	0.0070	0.038	0.070
	2617.62	3.00	1.95	0.084	0.117	0.0130	0.068	0.126
		2.90	1.64	0.072	0.100	0.0109	0.059	0.108
		2.80	1.06	0.050	0.066	0.0070	0.038	0.070
a^6D-z^6F^o	2373.74	2.80	1.06	0.062	0.057	0.0065	0.034	0.064
	2382.04	3.00	1.95	0.090	0.101	0.0121	0.060	0.114
		2.90	1.64	0.080	0.086	0.0101	0.051	0.098
		2.80	1.06	0.048	0.057	0.0065	0.034	0.064
	2388.63	3.00	1.95	0.076	0.101	0.0121	0.060	0.114
		2.80	1.06	0.044	0.057	0.0065	0.034	0.064
	2404.43	2.70	0.63	0.030	0.034	0.0038	0.020	0.038
	2404.89	3.00	1.95	0.086	0.101	0.0121	0.060	0.112
		2.90	1.64	0.066	0.086	0.0101	0.051	0.096
		2.80	1.06	0.042	0.057	0.0065	0.034	0.064
	2406.60	3.00	1.95	0.080	0.101	0.0121	0.060	0.112
		2.80	1.06	0.038	0.057	0.0065	0.034	0.064
	2410.52	2.80	1.06	0.042	0.057	0.0065	0.034	0.062
	2411.07	2.80	1.06	0.040	0.057	0.0065	0.034	0.062
	2413.31	3.00	1.95	0.094	0.101	0.0121	0.060	0.112
		2.90	1.64	0.068	0.086	0.0101	0.051	0.096

(1993b) with experimental and semiclassical values is encouraging as well. The simple estimate of Lakićević (1983) gives for $a^6D - z^0D^0$ Fe II multiplet for a perturber density of 10^{17} cm^{-3} and the temperature of 20,000 K, a full width = 0.068 Å which is in encouraging agreement with experimental and semiclassical results. On the other hand the shift of 0.032 Å has the different sign. New experimental data for Fe II Stark broadening parameters will be of interest for astrophysics as well as for theoretical investigations of Stark broadening for complex spectra.

Acknowledgements. This work is a part of the project "Physics and Dynamics of Celestial Bodies" supported by the Ministry for Science and Technology of Serbia.

References

Adelman S.J., Philip A.G.D., 1992, PASP 104, 316
Bates D.R., Damgaard A. 1949, Trans. Roy. Soc. London, Ser. A 242, 101
Bolkal C., Kocer D., Adelman S.J. 1992, MNRAS 258, 270
Corlis L., Sugar J. 1982, J. Phys. Chem. Ref. Data 11, 151
Dimitrijević M.S. 1988, in Physics of Formation of Fe II Lines Outside LTE, eds. R. Viotti, A. Vittone and M. Friedjung, Astrophysics and Space Science Library, Vol. 138 (D. Reidel P.C.) 211
Dimitrijević M.S., Konjević N. 1980, JQSRT 24, 451
Dimitrijević M.S., Sahal-Bréchot S., Bommier V. 1991, A&AS 89, 581
Fawcett B.C. 1987, Atomic and Nuclear Data Tables 37, 333

© European Southern Observatory • Provided by the NASA Astrophysics Data System

1995A&AS..111..565D

Johansson S. 1984, Phys. Scripta T8, 63
Lakićević I.S. 1983, A&A 127, 37
Manning J.T., Winefordner J.D., Palmer B.A., Hof D.E. 1990, Spectrochim. Acta 45B, 1031
Oertel G.K., Shomo L.P. 1968, ApJS 16, 175
Purić J., Djeniže S., Srećković A., Bukvić S., Pivalica S., Labat J., 1993a, A&AS 102, 607
Purić J., Miller M.H., Lesage A., 1993b, ApJ 416, 825
Sahal-Bréchot S. 1969a, A&A 1, 91
Sahal-Bréchot S. 1969b, A&A 2, 322
Van Regemorter H., Hoang Binh Dy, Prud'homme M. 1979, J. Phys. B 12, 1073
Yo-ichi Takeda 1984, Publ. Astron. Soc. Japan 36, 149

© European Southern Observatory • Provided by the NASA Astrophysics Data System

1995A&AS..114..171D

ASTRONOMY & ASTROPHYSICS
SUPPLEMENT SERIES

Astron. Astrophys. Suppl. Ser. **114**, 171-173 (1995)

Stark widths and shifts of Ni II spectral lines

M.S. Dimitrijević

Astronomical Observatory, Volgina 7, 11050 Beograd, Yugoslavia

Received February 1; accepted May 15, 1995

Abstract. — Stark widths and shifts for two spectral lines within the $a^4F - z^4G^\circ$ multiplet have been calculated using a semiclassical-perturbation approach. The obtained results have been compared with experimental data and simpler estimates.

Key words: lines: profile-atomic data

1. Introduction

Spectral lines of ionized nickel are present in stellar spectra. For example, such lines have been found in the spectra of Gamma Geminorum and 7 Sextantis (Adelman & Philip 1992), stars of A0 V type, where the main pressure broadening mechanism is the Stark effect. Consequently, the corresponding Stark broadening parameters are of astrophysical interest.

The first experimental determination of Ni II Stark widths and shifts has been performed recently (Djeniže et al. 1994). Obtained experimental widths have been compared with simple calculations (Djeniže et al. 1994) by using low temperature limits of the semiempirical (Griem 1968) and the modified semiempirical (Dimitrijević & Konjević 1980, 1987) approaches. As a result, a surprisingly large discrepancy between experimental and theoretical values has been reported. Since the sufficiently complete set of atomic data for the considered Ni II lines exists, it is of interest to perform a more elaborate theoretical analysis within the frame of the semiclassical approach. In spite of the fact that due to difficulties linked with Stark broadening calculations for heavy atoms (as e.g. configuration interaction, departure from LS coupling, less reliable and incomplete atomic data, limits of validity of various approximations included in the semiclassical - perturbation formalism), usual methods, such as the semiclassical perturbation one, reach their limits of validity, they are still only applied to emitters with complex spectra and results obtained by using close coupling collisional methods associated with sophysticated atomic structure calculations do no exist.

By using the semiclassical-perturbation formalism (Sahal-Bréchot 1969a, b), we have calculated Stark broadening parameters for two lines withins Ni II $a^4F - z^4G^\circ$ multiplet. Perturbers are electrons, protons and a singly charged perturber with the mass equal to 35 atomic mass units (a.u.). In the low chromosphere, in the vicinity of the temperature minimum, electrons are due to ionization of metals, positive ions are not protons and an average ionic mass of 35 a.u. is relevant, while in other regions of the solar atmosphere and in hotter stars, hydrogen is partly (or mostly) ionized and positive ions are protons. A summary of the formalism is given in Dimitrijević et al. (1991).

2. Results and discussion

Energy levels for Ni II lines have been taken from Corlis & Sugar (1981). Oscillator strengths have been calculated by using the Coulomb approximation method of Bates & Damgaard (1949) and the tables of Oertel & Shomo (1968). For higher levels, the method described by Van Regemorter et al. (1979) has been used. In order to test the applicability of the Coulomb approximation for the considered case, we compared presently calculated oscillator strengths with the experimental values of Bell et al. (1960), critically selected by Fuhr et al. (1981). For Ni II $a^4F - z^4G^\circ$, 2270.21 Å and 2264.46 Å lines Bell et al. (1960) obtained oscillator strengths equal to 0.24, while present result within the Coulomb approximation (Bates & Damgaard 1949) is 0.32, indicating that the Coulomb approximation is applicable for the considered transitions.

In addition to electron-impact full halfwidths and shifts, Stark-broadening parameters due to proton-impacts, and to impacts with a singly charged perturber with the mass equal to 35 a.u. corresponding to the averaged mass of perturbing ions in Solar atmosphera, have been calculated. Our results for two lines within the Ni II $a^4F - z^4G^\circ$ multiplet are shown in Table 1, for a perturber density of $10^{17}\mathrm{cm}^{-3}$ and temperatures $T = 5{,}000 - 150{,}000$ K. We also specify a parameter c (Dimitrijević et

© European Southern Observatory • Provided by the NASA Astrophysics Data System

1995A&AS..114..171D

Table 1. This table shows Stark broadening full half-widths (FWHM) and shifts in Å for Ni II for a perturber density of 10^{17} cm^{-3} and temperatures from 5,000 up to 150,000 K. Perturbers are electrons, protons and singly charged perturbers with the mass equal to 35 a.u. corresponding to the averaged mass of perturbing ions in Solar atmosphera. By using c (see Eq. (5) in Dimitrijević et al. 1991), we obtain an estimate for the maximum perturber density for which the line may be treated as isolated and tabulated data may be used

PERTURBERS ARE:		ELECTRONS		PROTONS		IONS WITH M=35a.u.	
TRANSITION	T(K)	WIDTH(A)	SHIFT(A)	WIDTH(A)	SHIFT(A)	WIDTH(A)	SHIFT(A)
Ni II 2264.5	5000.	0.984E-01	0.706E-03	0.128E-02	-0.751E-04	0.288E-02	-0.742E-04
2265.2 A	10000.	0.715E-01	-0.470E-03	0.243E-02	-0.166E-03	0.405E-02	-0.153E-03
C= 0.19E+21	30000.	0.432E-01	-0.493E-03	0.416E-02	-0.423E-03	0.499E-02	-0.310E-03
	50000.	0.355E-01	-0.552E-03	0.459E-02	-0.546E-03	0.537E-02	-0.383E-03
	100000.	0.291E-01	-0.617E-03	0.514E-02	-0.727E-03	0.563E-02	-0.459E-03
	150000.	0.269E-01	-0.562E-03	0.542E-02	-0.808E-03	0.575E-02	-0.511E-03
Ni II 2270.2	5000.	0.976E-01	0.518E-03	0.124E-02	-0.862E-04	0.281E-02	-0.850E-04
2270.9 A	10000.	0.710E-01	-0.557E-03	0.236E-02	-0.190E-03	0.396E-02	-0.173E-03
C= 0.20E+21	30000.	0.428E-01	-0.615E-03	0.408E-02	-0.476E-03	0.490E-02	-0.346E-03
	50000.	0.351E-01	-0.665E-03	0.450E-02	-0.613E-03	0.527E-02	-0.423E-03
	100000.	0.287E-01	-0.751E-03	0.505E-02	-0.800E-03	0.553E-02	-0.506E-03
	150000.	0.264E-01	-0.690E-03	0.533E-02	-0.890E-03	0.564E-02	-0.561E-03

Table 2. Comparison of experimental and theoretical Stark widths (FWHM) and shifts for Ni II lines within the $a^4F - z^4G^\circ$ multiplet at an electron density of 5.5 10^{17} cm^{-3} and temperature of 17000 K. WM, dM - experimental widths (FWHM) and shifts of Djeniže et al. 1994; W_{DSB}, d_{DSB} - present semiclassical electron - impact widths (FWHM) and shifts; $W_{Ar\ II}$, $d_{Ar\ II}$ - present semiclassical Ar II - impact widths and shifts; W_{MSE} - by using the method of Dimitrijević & Konjević (1980); W_{SMSE} - by using the method of Dimitrijević & Konjević (1987)

Wave-length (Å)	W_m (Å)	d_m (Å)	W_{DSB} (Å)	d_{DSB} (Å)	W_{ArII} (Å)	d_{ArII} (Å)	W_{MSE} (Å)	W_{SMSE} (Å)
2264.5	0.056	0.022	0.031	-0.00032	0.0025	-0.00013	0.018	0.015
2270.2	0.050	-	0.030	-0.00038	0.0025	-0.00014	0.018	0.014

al. 1991), which gives an estimate for the maximum perturber density for which the line may be treated as isolated when it is divided by the corresponding electron-impact full width at half maximum.

In Table 2 the present semiclassical full half-widths have been compared with experimental results (Djeniže et al. 1994) as well as with results of present calculations by using the modified semiempirical approach (MSE-Dimitrijević & Konjević 1980) and its simplified version (SMSE-Dimitrijević & Konjević 1987).

In Djeniže et al. (1994), the results of their calculations by using the SMSE method (Dimitrijević & Konjević 1987) have been presented and the ratios of measured and calculated Stark widths equal to 4.4 for 2264.5 Å line and 3.9 for 2270.2 Å line have been reported. However, the calculations of Djeniže et al. (1994) have been performed by using atomic energy levels from Moore (1958). Since the more recent and accurate atomic energy levels exist (Corlis & Sugar 1981) permitting the use of more sophysticated approaches as well, their calculations were repeated here. The ion broadening contribution has been neglected as well in Djeniže et al. (1994). As a working gas they used a mixture of 72% Ar and 28% He. Since there is more Ar and it has lower ionization potential than He, a reasonable assumption is that Ar II-impact broadening parameters may be used to estimate the ion broadening contribution. With more accurate atomic data and with the ion broadening contribution included, we obtain 3.2 and 3.0 as ratios of measured and calculated values for Ni II 2264.5 Å and 2270.2 Å lines instead of 4.4 and 3.9 obtained by Djeniže et al. (1994). With the use of the non simplified version of the MSE approach (Dimitrijević & Konjević 1980), the corresponding ratios are 2.7 and 2.4,

© European Southern Observatory • Provided by the NASA Astrophysics Data System

1995A&AS..114..171D

and for the ful semiclassical calculations 1.7 and 1.5, which is much better but still not satisfying.

The ratio of the semiclassical and the MSE values is also well too large, equal to 1.7 for both lines. If one performs an analysis of the contributions of different types of collisions, for Ni II 2264.5 Å line (T = 20000 K and the electron density 10^{17}cm^{-3}), the inelastic collision contribution is 0.875 10^{10}s^{-1} for the upper and 0.802 10^{10}s^{-1} for the lower level. The elastic collision contribution is 0.948 10^{10}s^{-1}. Moreover, the strong collision contribution to elastic and inelastic part is 0.597 10^{10}s^{-1}. The elastic collisions contribution consists of contributions due to strong collisions, the polarization and the quadrupole potentials. For the considered line the contribution due to the polarization potential is only 0.241 10^{9}s^{-1}. Consequently, for the considered line, elastic collisions, strong collisions and higher order interactions, taken as corrections implicitly in the modified semi-empirical approach or neglected, play an important role.

Our results for the shift have the different sign from experimental ones. Since the considered lines are an 4s−4p transition with a far 4d perturbing level with smaller influence, it is logical that the shift is around zero or negative. In spite of the fact that the agreement between the theory and experiment is better if one uses the more sophysticated semiclassical - perturbation approach, the differences are still such that a new experiment is of interest.

Acknowledgements. This work is a part of the project "Physics and Dynamics of Celestial Bodies" supported by the Ministry for Science and Technology of Serbia.

References

Adelman S.J., Philip A.G.D., 1992, PASP 104, 316
Bates D.R., Damgaard A., 1949, Trans. Roy. Soc. London, Ser. A 242, 101
Bell G.D., Paquet D.R., Wiese W.L., 1960, ApJ 143, 559
Corlis L., Sugar J., 1981, J. Phys. Chem. Ref. Data 10, 197
Dimitrijević M.S., Konjević N., 1980, JQSRT 24, 451
Dimitrijević M.S., Konjević N., 1987, A&A 172, 345
Dimitrijević M.S., Sahal-Bréchot S., Bommier V., 1991, A&AS 89, 581
Djeniže S., Skuljan Lj., Labat J., Bukvić S., Konjević R., 1994, A&AS 105, 115
Fuhr J.R., Martin G.A., Wiese W.L., Younger S.M., 1981, J. Phys. Chem. Ref. Data 10, 305
Griem H.R., 1968, Phys. Rev. 165, 258
Griem H.R., 1974, Spectral Line Broadening by Plasmas. Academic Press, New York
Moore C.E., 1958, Atomic Energy Levels, NSRDS-NBS 467, Vol.III, Washington
Oertel G.K., Shomo L.P., 1968, ApJS 16, 175
Sahal-Bréchot S., 1969a, A&A 1, 91
Sahal-Bréchot S., 1969b, A&A 2, 322
Van Regemorter H., Hoang Binh Dy, Prud'homme M., 1979, J. Phys. B 12, 1073

© European Southern Observatory • Provided by the NASA Astrophysics Data System

1996A&AS..115..351D

ASTRONOMY & ASTROPHYSICS
SUPPLEMENT SERIES

FEBRUARY 1996, PAGE 351

Astron. Astrophys. Suppl. Ser. **115**, 351-352 (1996)

Stark broadening of spectral lines of multicharged ions of astrophysical interest. XIII. C V and P V*

M.S. Dimitrijević[1] and S. Sahal-Bréchot[2]

[1] Astronomical Observatory, Volgina 7, 11050 Beograd, Yugoslavia
[2] Laboratoire "Astrophysique, Atomes et Molécules", Département Atomes et Molécules en Astrophysique, Unité Associée au CNRS No. 812, Observatoire de Paris Meudon, 92190 Meudon, France

Received June 6; accepted July 26, 1995

Abstract. — Using a semiclassical approach, we have calculated electron-, proton-, and He III-impact line widths and shifts for 25 C V and 51 P V multiplets.

Key words: lines: profile — atomic and molecular data

1. Introduction

Line profiles study of carbon ions in different ionization stages is of particular astrophysical interest, since such lines are present in stellar atmospheres. For studies as e.g. numerical modelling of stellar plasma or abundance determinations, data on C V lines are of importance. Stark broadening parameters are needed especially for hot and dense stars. A good example are the PG 1159 prewhite dwarfs with effective temperature 100,000−140,000 K where carbon and helium are the dominant constituents (C/He = 0.5, Werner et al. 1991). Other astrophysical applications have been pointed out in more detail in Dimitrijević & Sahal-Bréchot 1992). Stark broadening of C V lines is also of interest for the diagnostic of laser-produced plasma and for the research of regularities and systematic trends. For such a research P V lines are of interest as well. Recently, e.g., estimates of the Stark widths for P V 4s−4p and 4p−4d transitions have been performed within a study on Stark broadening regularities within successive ionization stages of phosphorus (Srećković et al. 1990).

Stark widths of two quasihydrogen - like C V lines (5-6 and 6-7 transitions) from plasma produced by laser irradiation of polyethylene foil in vacuum, have been measured by Irons (1973). Line profiles of C V, were measured in a carbon laser produced plasma by Iglesias & Griem (1988) and Wang et al. (1989). Stark widths of C V $3s^1S-3p^1P^0$, $1s^2\ ^1S-3p^1P^0$ and $2s^1S-3p^1P^0$, were determined within the modified semiempirical approach (Dimitrijević & Konjević 1980) in Dimitrijević (1993a). Stark widths for C V $3s^1S-3p^1P^0$ multiplet, obtained within the simplified semiclassical approach (Griem 1974), are given in Dimitrijević (1993b). Moreover, Stark broadening parameters for C V $2s^3S-2p^3P^0$ multiplet, were determined theoretically in McLean et al. (1984).

This paper is the 13th of a series devoted to the calculation of Stark broadening parameters of spectral lines of multicharged ions (see Dimitrijević & Sahal-Bréchot 1995 and references therein). By using the semiclassical-pertubation formalism (Sahal-Bréchot 1969a, b), we have calculated electron-, proton-, and ionized helium-impact line widths and shifts for 25 C V and 51 P V multiplets, in order to continue our research of multiply charged ion line Stark broadening parameters. A summary of the formalism is given in Dimitrijević et al. (1991).

2. Results and discussion

Energy levels for C V and P V lines have been taken from Bashkin & Stoner (1975). Oscillator strengths have been calculated by using the method of Bates & Damgaard (1949) and the tables of Oertel & Shomo (1968). For higher levels, the method described by Van Regemorter et al. (1979) has been used.

In addition to electron-impact full halfwidths and shifts, Stark-broadening parameters due to proton-, and He III- impacts have been calculated.

Our results for 25 C V and 51 P V multiplets are shown in Table 1 (accessible only in electronic form),

Send offprint requests to: M.S. Dimitrijević
*Table 1 is only available in electronic form at the CDS via anonymous ftp 130.79.128.5

© European Southern Observatory • Provided by the NASA Astrophysics Data System

1996A&AS..115..351D

for perturber densities $10^{17}-10^{22}$ cm^{-3} and temperatures T=50,000−1,000,000 K. We also specify a parameter c (Dimitrijević & Sahal-Bréchot 1984), which gives an estimate for the maximum perturber density for which the line may be treated as isolated when it is divided by the corresponding electron-impact full width at half maximum. For each value given in Tables 1, the collision volume (V) multiplied by the perturber density (N) is much less than one and the impact approximation is valid (Sahal-Bréchot 1969a, b). Values for $NV > 0.5$ are not given and values for $0.1 < NV \leq 0.5$ are denoted by an asterisk. When the impact approximation is not valid, the ion broadening contribution may be estimated by using quasistatic estimations (Sahal-Bréchot 1991; Griem 1974). The accuracy of the results obtained decreases when broadening by ion interactions becomes important.

In addition to the data presented here, Stark widths of C V $3s^1S-3p^1P^0$, $1s^2\,{}^1S-3p^1P^0$ and $2s^1S-3p^1P^0$ (where a sufficiently complete set of reliable energy levels needed for the adequate application of the semiclassical perturbation method does not exist), determined within the modified semiempirical approach (Dimitrijević & Konjević 1980) are given in Dimitrijević (1993a). Moreover, Stark widths for C V $3s^1S-3p^1P^0$ multiplet, obtained within the simplified semiclassical approach (Griem 1974), are given in Dimitrijević (1993b). Stark width for C V $2s^3S-2p^3P^0$ multiplet, was determined theoretically in McLean et al. (1984), but they obtain a considerably smaller value. Estimates of the Stark widths for P V 4s−4p transitions obtained by using regularities within successive ionization stages (Srećković et al. 1990), give for full width a value of 0.14 Å for T=40000 K and an electron density of 10^{17} cm^{-3}. We obtain a full width of 0.17 Å at T=50000 K, which is an excellent agreement encouraging the use of regularities and systematic trends for predictions and interpolations of Stark broadening parameters.

Acknowledgements. This work is a part of the project "Physics and Dynamics of Celestial Bodies" supported by the Ministry for Science and Technology of Serbia.

References

Bashkin S., Stoner J.O. Jr., 1975, Atomic Energy Levels and Grotrian Diagrams, Vol. 1, North Holland, Amsterdam
Bates D.R., Damgaard A., 1949, Trans. Roy. Soc. London Ser. A 242, 101
Dimitrijević M.S., 1993a, A&AS 100, 237
Dimitrijević M.S., 1993b, Astro. Lett. Comm. 28, 385
Dimitrijević M.S., Konjević N., 1980, JQSRT 24, 451
Dimitrijević M.S., Konjević N., 1981, in Spectral Line Shapes. In: Wende B., de Gruyter W. et al. (eds.), New York, 521
Dimitrijević M.S., Sahal-Bréchot S., 1984, JQSRT 31, 301
Dimitrijević M.S., Sahal-Bréchot S., Bommier V., 1991, A&AS 89, 581
Dimitrijević M.S., Sahal-Bréchot S., 1992, A&AS 96, 613
Dimitrijević M.S., Sahal-Bréchot S., 1995, A&AS 109, 551
Griem H.R., 1974, Spectral Line Broadening by Plasmas. Academic Press, New York and London
Iglesias E.J., Griem H.R., 1988, Phys. Rev. A 38, 301
Irons F.E., 1973, J. Phys. B 6, 1562
McLean A., Stamper J.A., Manka C.K., et al., 1984, Phys. Fluids 27, 1327
Oertel G.K., Shomo L.P., 1968, ApJS 16, 175
Sahal-Bréchot S., 1969a, A&A 1, 91
Sahal-Bréchot S., 1969b, A&A 2, 322
Sahal-Bréchot S., 1991, A&A 245, 322
Srećković A., Djeniže S., Labat J., Platiša M., Purić J., 1990, Fizika 22, 583
Van Regemorter H., Hoang Binh Dy, Prud'homme M., 1979, J. Phys. B 12, 1073
Wang J.S., Griem H.R., Iglesias E.J., 1989, Phys. Rev. A 40, 4115
Werner K., Heber U., Hunger K., 1991, A&A 244, 437

© European Southern Observatory • Provided by the NASA Astrophysics Data System

ASTRONOMY & ASTROPHYSICS
SUPPLEMENT SERIES

Astron. Astrophys. Suppl. Ser. **116,** 359-365 (1996)

Stark broadening of Xe II lines*

L.Č. Popović and M.S. Dimitrijević

Astronomical Observatory, Volgina 7, 11000 Belgrade, Yugoslavia

Received May 10; accepted September 13, 1995

Abstract. — We present here Stark widths and shifts for 20 Xe II multiplets which are of interest for laboratory plasma research as well as for the analysis of Hg – Mn stars spectra. For calculations the modified semiempirical approach was used. The obtained results are compared with the available experimental data.

Key words: atomic data — plasmas — stars: chemically peculiar

1. Introduction

Stark broadening data are of interest for diagnostic and modelling of laboratory and stellar plasma, investigation of its physical properties and abundance determination. Spectral lines of Xe II are present in spectra of hot (Hg – Mn) stars, (see, e.g., Whitford 1962; Aller 1970; Heacox 1979; Dobrichev et al. 1990), where Stark broadening is the main pressure broadening mechanism. On the basis of analysis of the Xe II spectral lines one can conclude that the abundance of Xe in Hg – Mn stars is about two times larger than in the Sun (Heacox 1979). Stark broadening of Xe II lines is important for laboratory plasma investigation (see e.g. Konjević & Uzelac 1990) as well.

A number of experimental and theoretical papers concerning Stark widths and shifts of Xe II lines have been published (e.g. Lesage et al. 1981; Miller et al. 1981; Richou et al. 1984; Nick & Helbig 1986; Pittman & Konjević 1986; Vitel & Skowronek 1987; Manola et al. 1988; Lesage et al. 1989; Di Rocco 1990a, b; Konjević & Uzelac 1990; Bertuccelli et al. 1991; Mar et al. 1992; Gigosos et al. 1994). We present here Stark broadening data for 20 Xe II multiplets. Due to the lack of reliable atomic data for Xe II lines, it is not possible to apply a semi-classical perturbation approach (Griem 1974; Sahal–Bréchot 1969a, b) in an adequate way, so the modified semiempirical approach (Dimitrijević & Konjević 1980; Dimitrijević & Kršljanin 1986) will be used here.

Our results are compared with numerous available experimental data (Lesage et al. 1981; Miller et al. 1981; Richou et al. 1984; Nick & Helbig 1986; Vitel & Skowronek 1987; Manola et al. 1988; Lesage et al. 1989; Di Rocco 1990b; Konjević & Uzelac 1990; Bertuccelli et al. 1991; Gigosos et al. 1994).

2. Results and discusion

Atomic energy levels for calculation have been taken from Hansen & Persson (1987), where it is indicated that the jK coupling scheme is the most appropriate for Xe II. Consequently the jK coupling scheme was used for matrix element calculation. An illustration of the influence of the applied coupling scheme on the Stark width calculation is shown in Figs. 1-4. In these figures, Stark widths for several Xe II lines (6s−6p transition), with jK and LS coupling scheme for the matrix element calculations are compared. As one can see from Figs. 1-4 the differences are relatively small in comparison with the accuracy of the method (±50%). Moreover, the calculations within jK coupling scheme are in slightly better agreement with experimental data.

Our results for Stark widths and shifts of Xe II spectral lines are presented in Table 1 (accessible only in electronic form). The values obtained for temperatures from 5000 K up to 50000 K and an electron density of 10^{23} m^{-3} are compared (in Table 2 and in Figs. 1-4) with the available experimental data (Lesage et al. 1981; Miller et al. 1981; Richou et al. 1984; Nick & Helbig 1986; Vitel & Skowronek 1987; Manola et al. 1988; Lesage et al. 1989; Di Rocco 1990b; Konjević & Uzelac 1990; Bertuccelli et al. 1991; Gigosos et al. 1994). Since we found that the ion broadening contribution is about several per cent, only the electron broadening contribution is given. As evident, the calculated Stark widths give satisfactory agreement with the experimental ones. From Table 2, it can be noticed that for the 6s−6p transition a large disagreement

Send offprint requests to: L.Č. Popović

*Table 1 is only available in electronic form and Table 2 is also available in electronic form via anonymous ftp 130.79.128.5 at the CDS in Strasbourg

Table 2. Comparison of measured (m) and theoretical (th) values for Stark widths (w) and shifts (d). Experimental results w_m, d_m are taken from: (1) – Nick & Helbig 1986, (2) – Di Rocco 1990b, (3) – Gigosos et al. 1994, (4) – Lesage et al. 1981, (5) – Lesage et al. 1989, (6) – Miller et al. 1981, (7) – Bertuccelli et al. 1991, (8) – Richou et al. 1984, (9) – Vitel & Skowronek 1987, (10) – Konjević & Uzelac 1990, (11) – Manola et al. 1988, the electron density is 10^{23} m^{-3}

Transition	λ (nm)	T (1000 K)	w_m (nm)	d_m (nm)	w_m/w_{th}	d_m/d_{th}	Ref.
$(^3P_2)6s[2]-(^3P_2)6p[1]$	460.3	10.0	0.0436	–	1.1		(1)
		10.0		0.00		–	(2)
		10.0	0.0683		1.7		(3)
		11.0	0.081		2.0		(4)
		11.0	0.065		1.6		(5)
		11.2	0.084		2.1		(6)
		14.5	0.0576		1.7		(7)
		15.0		>-0.001		–	(3)
	421.56	10.0		-0.00178		0.2	(2)
		14.5	0.0463		1.6		(7)
	537.24	8.0	0.067		1.0		(8)
		10.0	0.048		0.9		(1)
		10.0		-0.00866		0.5	(2)
		10.0	0.069		1.3		(3)
		11.0	0.088		1.7		(4)
		11.0	0.065		1.2		(5)
		11.2	0.093		1.8		(6)
		14.5	0.0588		1.3		(7)
		15.0		>-0.001		–	(3)
$(^3P_2)6s[2]-(^3P_2)6p[2]$	529.2	10.0	0.0427		0.8		(1)
		10.0		-0.031		1.6	(2)
		10.0	0.0805		1.6		(3)
		11.0	0.079		1.5		(5)
		11.0	0.088		1.7		(4)
		11.2	0.093		1.7		(6)
		12.6	0.0411	-0.00274	0.9	0.2	(9)
		13.0	0.0591		1.2		(10)
		13.9	0.039	-0.00488	0.9	0.3	(9)
		14.8	0.045	-0.00651	1.1	0.4	(9)
		15.0		-0.007		0.5	(3)
		15.8	0.041	-0.00508	1.0	0.3	(9)
	533.9	8.0	0.060		1.0		(8)
		10.0		-0.0199		1.0	(2)
		10.0	0.0679		1.3		(3)
		11.0	0.064		1.2		(5)
		13.0	0.0591		1.2		(10)

Table 2. continued

Transition	λ (nm)	T (1000 K)	w_m (nm)	d_m (nm)	w_m/w_{th}	d_m/d_{th}	Ref.
		13.4	0.0408	-0.00714	0.9	0.4	(9)
		14.3	0.0388	-0.00597	0.9	0.4	(9)
		14.8	0.0468	-0.00851	1.1	0.5	(9)
		15.0		-0.008		0.5	(3)
		15.8	0.0407	-0.00678	1.0	0.4	(9)
	597.6	10.0	0.0575		0.9		(1)
		10.0		-0.0214		0.9	(2)
		10.0	0.0791		1.2		(3)
		14.5	0.070		1.3		(7)
		15.0		-.009		0.5	(3)
$(^3P_2)6s[2]-(^3P_2)6p[3]$	484.4	10.0	0.0367		0.8		(1)
		10.0		.0258		1.8*	(2)
		10.0	0.0826		1.8		(3)
		11.0	0.072		1.5		(5)
		11.0	0.081		1.8		(4)
		11.2	0.086		1.9		(6)
		12.5	0.0556		1.2		(10)
		13.0	0.0536		1.1		(10)
		13.4	0.0370	0.00	1.0	-	(9)
		14.3	0.0358	-0.00312	1.0	0.3	(9)
		14.8	0.0383	0.00	1.0	–	(9)
		15.0		-0.003		0.3	(3)
		15.8	0.0390	0.00	1.1	–	(9)
	489.0	10.0		-0.0622		4.3	(2)
		10.0	0.0465		1.0		(3)
		14.5	0.0469		1.2		(7)
		15.0		-0.006		0.5	(3)
	541.9	8.0	0.090		1.3		(8)
		8.0	0.115		1.7		(11)
		9.0	0.096		1.5		(11)
		9.9	0.076		1.3		(11)
		10.0	0.0556		1.0		(1)
		10.0		-0.0029		0.2	(2)
		10.0	0.0897		1.5		(3)

* The measured and the calculated values of Stark shift have different sign.

Table 2. continued

Transition	λ (nm)	T (1000 K)	w_m (nm)	d_m (nm)	w_m/w_{th}	d_m/d_{th}	Ref.
		11.0	0.062		1.1		(11)
		11.0	0.081		1.4		(4)
		11.2	0.095		1.7		(6)
		12.1	0.065		1.2		(11)
		12.5	0.0667		1.2		(10)
		13.0	0.0682		1.3		(10)
		13.4	0.0459	-0.00102	1.0	0.1	(9)
		13.7	0.070		1.4		(11)
		14.3	0.0417	-0.00139	0.9	0.1	(9)
		14.5	0.062		1.3		(11)
		14.8	0.0553	-0.00213	1.2	0.1	(9)
		15.0		-0.006		0.3	(3)
		15.8	0.049	-0.0034	1.3	0.2	(9)
		16.2	0.0527		1.2		(11)
$(^3P_1)6s[1]-(^3P_1)6p[0]$	543.89	8.0	0.067		0.9		(8)
		10.0	0.0456		0.8		(1)
		10.0		-0.0148		0.7	(2)
		10.0	0.0608		1.0		(3)
		11.0	0.054		0.9		(5)
		14.5	0.0580		1.2		(7)
		15.0		-0.007		0.4	(3)
	465.2	10.0	0.0473		1.0		(1)
$(^3P_1)6s[1]-(^3P_1)6p[1]$	575.10	10.0		-0.0529		2.2	(2)
		14.5	0.0749		1.3		(7)
$(^3P_1)6s[1]-(^3P_1)6p[2]$	492.15	10.0		-0.0533		2.7	(2)
		10.0	0.0656		1.1		(3)
		11.0	0.056		1.0		(5)
		14.5	0.0557		1.3		(7)
		15.0		-0.004		0.3	(3)
	488.73	10.0		-0.0621		3.2	(2)
		10.0	0.0623		1.2		(3)
		14.5	0.0451		1.0		(7)
		15.0		<-0.001		–	(3)

Table 2. continued

Transition	λ (nm)	T (1000 K)	w_m (nm)	d_m (nm)	w_m/w_{th}	d_m/d_{th}	Ref.
$(^3P_0)6s[0]-(^3P_0)6p[1]$	488.35	10.0	0.0348		0.7		(1)
		10.0		-0.0143		0.7	(2)
		10.0	0.0542		1.0		(3)
		14.5	0.0486		1.2		(7)
		15.0		<-0.001		–	(3)
	519.14	10.0	0.0458		0.8		(1)
		10.0		-0.0135		0.6	(2)
		14.5	0.0529		1.1		(7)
$(^1D_2)6s[2]-(^1D_2)6p[2]$	526.2	10.0	0.0618		1.1		(1)
		10.0		-0.0277		1.7	(2)
		10.0	0.0583		1.0		(3)
		14.5	0.0554		1.3		(7)
		15.0		>-0.001		–	(3)
$(^3P_2)6p[2]-(^3P_2)6d[2]$	418.01	11.0	0.116		2.0		(5)
$(^3P_2)6p[2]-(^3P_2)6d[3]$	444.81	11.0	0.132		1.7		(5)
$(^3P_2)6p[3]-(^3P_2)6d[3]$	458.55	10.0	0.1455		1.7		(3)
		11.0	0.132		1.5		(5)
		15.0		0.082		3.2	(3)
$(^3P_2)6p[3]-(^3P_2)6d[4]$	433.05	10.0	0.1916		2.8		(3)
		11.0	0.132		1.9		(5)
		15.0		0.068		3.4	(3)

between our theoretical Stark widths and experimental data exists only with Lesage et al. (1981) and Miller et al (1981). Here, the ratio of measured and our calculated Stark widths is $w_{\rm exp}/w_{\rm th}$ =2.1 respectively for λ= 460.3 nm. Moreover, these experimental results are larger than our calculated results from 70% to 100%. Since more recent results exist from basically the same group (Richou et al. 1984; Manola et al. 1988; Lesage et al. 1989) we will exclude Lesage et al. (1981) and Miller et al. (1981) from further considerations. Excluding these measurements, we may conclude that our theoretical Stark width calculations are in good agreement with experimental data for 6s−6p transitions. It should be noticed that our results are in excellent agreement with experimental data of Nick & Helbig (1986) and Richou et al. (1984) which have the highest accuracy among critically selected experimental data for Xe II lines in Konjević & Wiese (1990). Our theoretical results are in excellent agreement as well with the experimental values of Vitel & Skowronek (1987) and Konjević & Uzelac (1990). The agreement with Manola et al. (1988), Lesage et al. (1989), Bertuccelli et al. (1991) and Gigosos et al. (1994) is also within the error bars of theory and experiment. For 6p−6d transitions there exist only experimental data by Lesage et al. (1989) and Gigosos et al. (1994). The ratio of measured and calculated data varies between 1.5 and 2.8. Since all data for 6p−6d transitions are obtained at temperatures of 10000 K and 11000 K, new measurements at different temperatures are of interest. Experimental data being within a narrower temperature range between 8000 K and

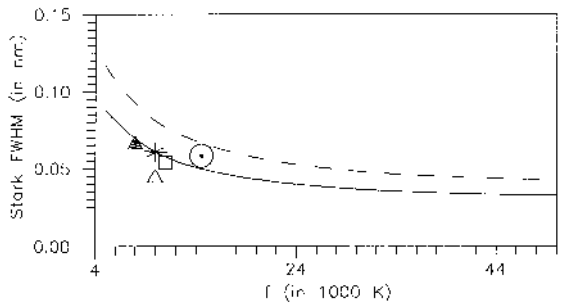

Fig. 1. Stark full width (FWHM) for Xe II $\lambda = 543.8$ nm spectral line as a function of temperature, at an electron density of $N = 10^{23}$ m^{-3}. The used notation is: (—) - present results calculated within the jK coupling approximation, (– – –) - present results within the LS coupling approximation. Experimental data: (+) – Lesage et al. 1981, (×) – Miller et al. 1981, (▲) – Richou et al. 1984, (Δ) – Nick & Helbig 1986, (◯) – Vitel & Skowronek 1987, (■) – Manola et al. 1988, (□) – Lesage et al. 1989, (⊕) – Konjević & Uzelac 1990, (⊙) – Bertuccelli et al. 1991, (*) – Gigosos et al. 1994

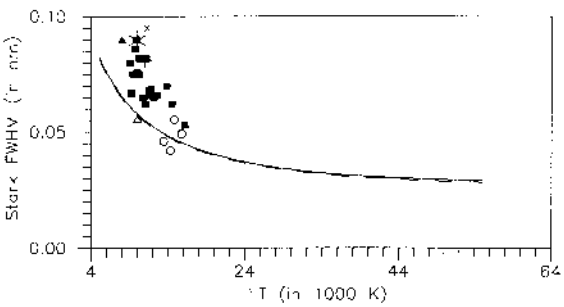

Fig. 2. Same as in Fig. 1, but for line $\lambda = 541.9$ nm

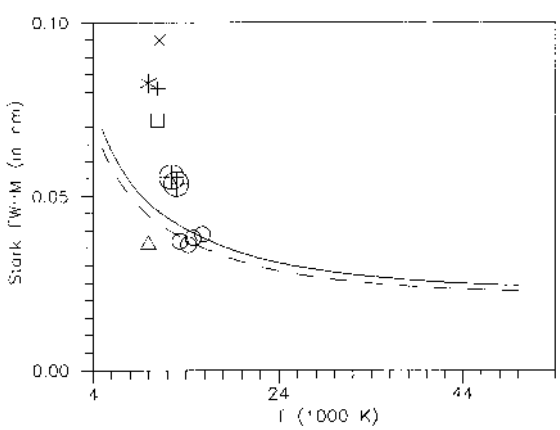

Fig. 3. Same as in Fig. 1, but for line $\lambda = 484.4$ nm

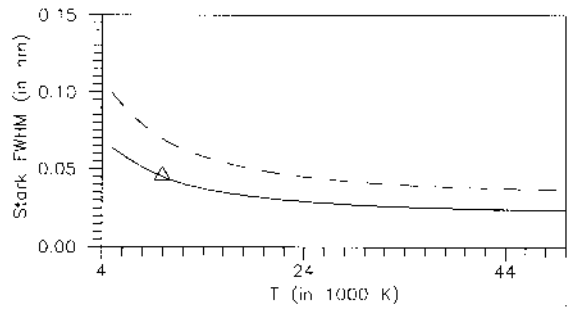

Fig. 4. Same as in Fig. 1, but for line $\lambda = 465.2$ nm

16200 K, where the Stark widths decrease quickly, it is important to provide experimental data for higher temperatures in order to check the dependence on temperature over a wider range. Without the data of Lesage et al. (1981) and Miller et al. (1981) the average value of the ratio of experimental and theoretical results is $w_{\rm exp}/w_{\rm th} = 1.29 \pm 0.07$ the indicated error represents an average quadratic error δ calculated from

$$\delta = \sqrt{\frac{\sum_{i=1}^{m} \Delta_i^2}{m(m-1)}}$$

where Δ_i is the difference between the $i^{\rm th}$ average ratio for a line and the average ratio for all lines. If there are several values at different temperature from the same reference for the same line, before making an average ratio for the line, these values have been averaged. For 6s−6p transitions alone the average ratio, excluding the above mentioned experiments, is 1.15±0.05.

For Xe II Stark shifts, we have only experimental data of Vitel & Skowronek (1987), estimated by Konjević & Wiese (1990) to be of low accuracy, data of Di Rocco (1990b) and data of Gigosos et al. (1994). The typical shifts are smaller by an order of magnitude than the widths or around zero and the difference between the two experiments is even one order of magnitude. The agreement with our shift calculations is very poor and new reliable shift measurements are of interest. One should notice also that the theoretical shifts are generally of lower accuracy than widths, since for the shift contributions from different perturbing terms have different signs. If shifts are much smaller than widths, i.e. if contributions with both signs are similar, the shift accuracy is much lower.

References

Aller M.F., 1970, A&A 6, 67
Bertuccelli D., Bertuccelli G., Di Rocco H.O., 1991, Phys. Scr. 43, 469
Dimitrijević M.S., Konjević N., 1980, JQSRT 24, 451
Dimitrijević M.S., Kršljanin V., 1986, A&A 165, 269
Di Rocco H.O., 1990a, Spectrosc. Lett. 23, 283
Di Rocco H.O., 1990b, Il Nuovo Cimento 12D, 1485

Dobrichev V.M., Ryabchikova T.A., Rajkova D.V., 1990, Nauchn. Inf. 68, 92
Gigosos M.A., Mar S., Pérez C., I. de la Rosa, 1994, Phys. Rev. E 49, 1575
Griem H.R., 1974, Spectral Line Broadening by Plasma. Academic Press, New York
Hansen J.E., Persson W., 1987, Phys. Scr. 36, 602
Heacox W.D., 1979, ApJS 41, 675
Konjević N., Uzelac N.I., 1990, JQSRT 44, 61
Konjević N., Wiese W.L., 1990, J. Phys. Chem. Ref. Data 19, 1307
Lesage A., Abadie D., Miller M.H., 1989, Phys. Rev. A 40, 1367
Lesage A., Miller M.H., Richou J., Bach T., 1981, in Spectral Line Shapes. In: Wende B., de Gruyter W. (eds.), Berlin, New York, p. 257
Manola S., Konjević N., Richou J., Lebrun J. L., Lesage A., 1988, Phys. Rev. A38, 5742
Mar S., Gigosos M.A., de la Rosa I., Pérez C., 1992, 11th ICSLS, A23, Carry le Rouet, France
Miller M.H., Lesage A., Abadie D., 1981, Phys. Rev. A 25, 2064
Nick K.P., Helbig V., 1986, Phys. Scr. 33, 55
Pittman T.L., Konjević N., 1986, JQSRT 35, 247
Richou J., Manola S., Lebrun J.L., Lesage A, 1984, Phys. Rev. A29, 3181
Sahal-Bréchot S., 1969a, A&A 1, 91
Sahal-Bréchot S., 1969b, A&A 2, 322
Vitel Y., Skowronek M., 1987, J. Phys. B 20, 6493
Whitford A.E., 1962, AJ 67, 640

ASTRONOMY & ASTROPHYSICS
SUPPLEMENT SERIES

Astron. Astrophys. Suppl. Ser. **117,** 127-129 (1996)

Stark broadening of solar Mg I lines*

M.S. Dimitrijević[1] and S. Sahal-Bréchot[2]

[1] Astronomical Observatory, Volgina 7, 11050 Beograd, Yugoslavia
[2] Laboratoire "Astrophysique, Atomes et Molécules", Département Atomes et Molécules en Astrophysique Unité associée au CNRS No. 812, observatoire de Paris-Meudon, 92190 Meudon, France

Received July 31; accepted September 27, 1995

Abstract. — Using a semiclassical approach, we have calculated electron-, proton-, Mg II-, Si II-, Fe II-, and Ar II- impact line widths and shifts for 267 Mg I multiplets, in order to provide the needed Stark broadening parameters for all important perturbers for investigation of Solar and laboratory plasma. An analysis of Solar Rydberg lines in the far infrared spectrum has been performed as well.

Key words: lines: profile-atomic and molecular data — Sun: photosphere — Sun: chromosphere

1. Introduction

Lines of neutral magnesium are present in the Solar spectrum and the corresponding Stark broadening parameters are of interest for their analysis as well as for the diagnostic of Solar plasma. Especially the infrared lines of Mg I have been observed in the Solar spectrum at Kitt Peak and during the Atmos experiment on Spacelab (Brault & Noyes 1983; Chang & Noyes 1983; Farmer & Norton 1989; Jefferies 1991). Other observations of such lines have been described by Deming et al. 1988, 1991; Glenar et al. 1988). Due to the suitability of these lines for the solar atmosphere investigations (see e.g. Van Regemorter & Hoang-Binh 1993) and to the fact that with the increase of the principal quantum number increases the importance of Stark broadening as well, the corresponding Stark widths and shifts are of importance for the structure of the Solar atmosphere research and solar plasma diagnostic (see e.g. Chang et al. 1991; Carlson et al. 1992). Stark broadening data for Mg I lines are also of interest for laboratory plasma research and have been investigated experimentally (Helbig & Kusch 1972; Kusch & Schweicker 1976; Goldbach et al. 1982) and theoretically (Benett & Griem 1971; Griem 1974; Brissaud et al. 1976; Dimitrijević & Konjević 1986; Marasinghe et al. 1986; Regemorter & Hoang Binh 1993; Dimitrijević & Sahal-Bréchot 1995).

By using the semiclassical-perturbation formalism (Sahal-Bréchot 1969a, b), electron-, proton-, and ionized argon-impact line widths and shifts for 99 Mg I multiplets have been published recently at an electron density of 10^{15} cm^{-3}, in order to provide Stark broadening data needed for laboratory plasma research and diagnostic (Dimitrijević & Sahal-Bréchot 1995). Using the same semiclassical approach, we have calculated here electron-, proton-, Mg II-, Si II-, Fe II-, and Ar II-impact line widths and shifts for 267 Mg I multiplets at an electron density of 10^{11} cm^{-3}, in order to provide the needed Stark broadening parameters for all important perturbers in the investigation and modelling of Solar plasma. A summary of the formalism is given in Dimitrijević et al. (1991).

2. Results and discussion

Energy levels for Mg I lines have been taken from Bashkin & Stoner (1975). For high n and ℓ, needed atomic energy levels not existing in Bashkin & Stoner, have been calculated by using the theoretical polarization formula of Waller (1926) (see e.g. Regemorter & Hoang Binh 1993 or Edlen 1964) valid for the angular momenta ℓ larger than 3. Oscillator strengths have been calculated by using the method of Bates & Damgaard (1949) and the tables of Oertel & Shomo (1968). For higher levels, the method described by Regemorter et al. (1979) has been used. In order to check the applicability of Bates & Damgaard's (1949) method for the calculation of oscillator strengths within the Coulomb approximation, line width calculations with line strengths from TOP base (the complete package of the opacity project (OP) data with the database management system is usually referred to as TOP base, see Butler et al. (1993) and Cunto et al. (1993)) have been performed at an electron density of 10^{12} cm^{-3} and T= 5000 K. For the $3s^2\ ^1S-3s3p\,^1P^0$ resonance line the

Send offprint requests to: M.S. Dimitrijević
*Tables 1-3 are only available in electronic form via anonymous ftp 130.79.128.5

full width with Bates & Damgaard line strengths is 0.63 10^{-6} Å and with TOP base line strengths 0.52 10^{-6} Å. For $6s^3S-6p^3P^0$ infrared line the full halfwidth is 0.162 Å in both cases. One can see that for transitions between low levels small differences exist. However, for lines that are of interest for solar infrared astrophysics, corresponding to transitions between high levels, the use of Bates & Damgaard oscillator strengths is sufficient for line widths. In addition to electron-impact full halfwidths and shifts, Stark-broadening parameters due to proton-, Mg II-, Si II- and Fe II- impacts have been calculated in order to provide an as much as possible complete set of Stark broadening data for Solar plasma research. Moreover, Stark-broadening parameters due to Ar II-impacts have been calculated as well, since argon is usually used as a carrier gas for experimental determination of Mg I Stark widths and shifts.

Our results for Stark broadening parameters due to e-, p-, and Ar II-impacts for 267 Mg I multiplets are shown in Table 1 (accessible only in electronic form), and due to Si II-, Fe II-, and Mg II-impacts in Table 2 (accessible only in electronic form) for perturber density of 10^{11} cm^{-3} and temperatures T= 2.500−50.000 K. Stark broadening parameters due to e-, p-, and Ar II-impacts for perturber densities 10^{15} cm^{-3}−10^{19} cm^{-3} are shown in Table 3 (accessible only in electronic form). We also specify a parameter c (Dimitrijević & Sahal-Bréchot 1984), which gives an estimate for the maximum perturber density for which the line may be treated as isolated when it is divided by the corresponding electron-impact full width at half maximum. For each value given in Table 1, the collision volume (V) multiplied by the perturber density (N) is much less than one and the impact approximation is valid (Sahal-Bréchot 1969a, b). Values for $NV > 0.5$ are not given and values for $0.1 < NV \leq 0.5$ are denoted by an asterisk. When the impact approximation is not valid, the ion broadening contribution may be estimated by using quasistatic estimations (Sahal-Bréchot 1991; Griem 1974). The accuracy of the results obtained decreases when broadening by ion interactions becomes important.

Regemorter & Hoang Binh (1993) have discussed recently the important simplification of theory for solar Rydberg lines corresponding to the transitions between nearly degenerate states, where the differences of energy $E(n\ell,\ n\ell+1)$ are of the order of a few cm^{-1}. These energy differences are much larger than the width so that the considered lines are isolated. They are however considerably smaller than the energy distances to the other perturbing levels $n'\ell'$ which may be neglected so that the Stark broadening problem corresponds to a simple three level close coupling system including $n\ell,\ n\ell+1$ atomic energy levels. In order to investigate such approximation, contributions (in angular frequency units) to the Mg I $5g^1G-6h^1H$ line widths, due to different types of collisions, have been calculated as a function of the number of perturbing levels at an electron density of 10^{12} cm^{-3} and temperature of 5000 K and shown in Table 4. One can see that the inelastic collision contribution practically does not vary with the addition of new perturbing levels and that the variation of strong collision contribution is as well of the order of several percents. The elastic collision contribution has however a non negligible dependence on the perturbing level number. Since for solar Rydberg lines the elastic contribution to the width is for an order of magnitude smaller in comparison with other considered contributions, we may conclude that the approximation of Regemorter & Hoang Binh (1993) is very good for Stark widths of the considered lines.

Table 4. Contribution of different types of collisions to the line widths (in angular frequency units) as a function of the number of perturbing levels of the initial level (i) for Mg I $5g^1G-6h^1H$ transition at an electron density of 10^{12} cm^{-3} for T=5000 K. Perturbing energy levels for the final level are 4f, 5f, 6f, 7f, 6h, 7h, 8h

Perturbing levels i'	6g	6g,7i	5g,6g,7i	5g,6g,7g,8g, 7i,8i,9i
coll. upper level	0.452(+9)	0.456(+9)	0.456(+9)	0.456(+9)
coll. lower level	0.109(+9)	0.109(+9)	0.109(+9)	0.109(+9)
strong coll.	0.119(+9)	0.135(+9)	0.128(+9)	0.129(+9)
elastic coll.	0.368(+8)	0.590(+8)	0.468(+8)	0.495(+8)

Since the elastic collisions have an important role for the Stark shift determination, for Stark shifts such approximation may become questionable.

In Table 5 our results (denoted as DSB) for Stark full widths for Mg I $5g^1G-6h^1H$ and $6g^1G-7h^1H$ transitions have been compared with results of Regemorter & Hoang Binh (1993) (denoted as RHB), with calculation within the Griem's (1968) semiempirical approach of Carlsson et al. (1992) (denoted as GCRS) and with calculations of Chang & Schoenfeld (1991) by using the Lindholm (1941) adiabatic theory (LCS). One can see that our calculations are in good agreement with the width calculations of Regemorter & Hoang Binh (1993) while for shifts the differences due to the omission of perturbing levels with the different principal quantum number (as discussed concerning Table 4) exist. The agreement with adiabatic theory of Lindholm (1941) used by Chang & Schoenfeld (1991), is apparently fortuitous for the width but shifts are largely overestimated, while the Griem's (1968) semiempirical approach, not appropriate for transitions between nearly degenerate states (GCRS), is in agreement with our results

Table 5. Comparison of electron-impact width (W-FWHM) and shift (d) values calculated according to various approaches, for Mg I $5g^1G-6h^1H$ and $6g^1G-7h^1H$ transitions at an electron density of 10^{12} cm^{-3} for T=5000 K. The notation is: DSB - present calculations; RHB - Regemorter & Hoang Binh (1993); GCRS - calculated by Carlson et al. (1992) by using the Griem's (1968) semiempirical formula with an effective Gaunt factor $g = 0.5$; LCS - calculated by Chang & Schoenfeld (1991) by using the Lindholm (1941) adiabatic theory

Transition	DSB	RHB	GCRS	LCS
5g - 6h				
W[Å]	0.18	0.16	0.21	0.25
d[Å]	0.0034	0.013	-	0.22
6g - 7h				
W[Å]	2.48	2.67	1.07	2.73
d[Å]	-0.0128	0.052	-	2.36

for Mg I $5g^1G-6h^1H$ transition but gives more than two times smaller result for $6g^1G-7h^1H$ transition.

We hope that the comprehensive set of Stark broadening parameters of Mg I lines will enable the better use of Mg I spectral lines for solar plasma research.

Acknowledgements. This work is a part of the project "Physics and Dynamics of Celestial Bodies" supported by the Ministry for Science and Technology of Serbia.

References

Bashkin S., Stoner J.O. Jr., 1975, Atomic Energy Levels and Grotrian Diagrams, Vol. 1, North Holland, Amsterdam
Bates D.R., Damgaard A., 1949, Trans. Roy. Soc. London, ser. A 242, 101
Benett S.M., Griem H.R., 1971, Calculated Stark Broadening Paramaters for Isolated Spectral Lines from the Atoms Helium through Calcium and Cesium, Techn. Rep. No. 71-097, Univ. Maryland
Brault J., Noyes R.W., 1983, ApJ 269, L61
Brissaud A., Goldbach C., Leorat J., Mazure A., Nollez G., 1976, J. Phys. B 9, 1147
Butler K., Mendoza G., Zeippen C.J., 1993, J. Phys. B 26, 4409
Carlsson M., Rutten R.J., Shchukina N.G., 1992, A&A 253, 567
Chang E.S., Avrett E.H., Manas P.J., Noyes R.W., Loeser R., 1991, ApJ 379, L79
Chang E.S., Noyes R.W., 1983, ApJ 275, L11
Chang E.S., Schoenfeld W.G., 1991, ApJ 383, 450
Cunto W., Mendoza C., Ochsenbein F., Zeippen C.J., 1993, A&A 275, L5
Deming D., Boyle R.J., Jennings D.E., Widemann G., 1988, ApJ 333, 978
Deming D., Jennings D.E., Jefferies J., Lindsey C., 1991, In: The Solar Atmosphere and Interior, Cox A.N., Livingston W., Matthews M. (eds.). Univ. of Arizona Press, Tucson
Dimitrijević M.S., Konjević N., 1986, A&A 163, 297
Dimitrijević M.S., Sahal-Bréchot S., 1984, JQSRT 31, 301
Dimitrijević M.S., Sahal-Bréchot S., Bommier V., 1991, A&AS 89, 581
Dimitrijević M.S., Sahal-Bréchot S., 1995, Phys. Scripta 52, 41
Edlen B., 1964, Handbuch der Physik 27. Springer, Berlin
Farmer C.B., Norton R.H., 1989, A High-Resolution Atlas of the Infrared Spectrum of the Sun and the Earth's Atmosphere from Space, NASA Ref. Publ. 1224, Vol. 1, Washington, Gov. Print. Office
Glenar D.A., Reuter D.C., Deming D., Chang E.S., 1988, ApJ 335, L35
Goldbach C., Nollez G., Plomdeur P., Zimmermann P., 1982, Phys. Rev. A 25, 2596
Griem H.R., 1968, Phys. Rev. 165, 258
Griem H.R., 1974, Spectral Line Broadening by Plasmas. Academic Press. New York and London
Helbig V., Kusch H.J., 1972, A&A 20, 299
Jefferies J.T., 1991, ApJ 377, 337
Kusch H.J., Schweiker H., 1976, A&A 53, 59
Lindholm E., 1941, Ark. Math. Astron. Fysik 28B, 3
Marasinghe P.A.B., Lovett R.J., 1986, Spectrochim. Acta B 41, 349
Oertel G.K., Shomo L.P., 1968, ApJS 16, 175
Regemorter van H., Hoang Binh Dy, 1993, A&A 277, 623
Sahal-Bréchot S., 1969a, A&A 1, 91
Sahal-Bréchot S., 1969b, A&A 2, 322
Sahal-Bréchot S., 1991, A&A 245, 322
Waller I., 1926, Z. Phys. 38, 635

ASTRONOMY & ASTROPHYSICS
SUPPLEMENT SERIES

Astron. Astrophys. Suppl. Ser. **119,** 369-371 (1996)

Stark broadening of spectral lines of multicharged ions of astrophysical interest. XIV. Be III and B III*

M.S. Dimitrijević[1] and S. Sahal-Bréchot[2]

[1] Astronomical Observatory, Volgina 7, 11050 Beograd, Yugoslavia
[2] Laboratoire "Astrophysique, Atomes et Molécules" Département Atomes et Molécules en Astrophysique Unité associée au C.N.R.S. No. 812, Observatoire de Paris-Meudon, 92190 Meudon, France

Received February 20; accepted March 15, 1996

Abstract. — Using a semiclassical approach, we have calculated electron-, proton-, and ionized helium-impact line widths and shifts for 12 Be III and 27 B III multiplets. The obtained results have been compared with available experimental and theoretical data.

Key words: lines: profiles-atomic and molecular data

1. Introduction

Line profiles study of light element ions in different ionization stages is of astrophysical interest, since such lines are present in stellar atmospheres. For studies as e.g. numerical modelling of stellar plasma or abundance determinations, data on Be III and B III lines may be of interest. The Be III Stark broadening parameters are additionally interesting, since the surface content (abundance) of Be, involves problems correlated with nucleogenesis, mixing between the atmospheres and the interior, and stellar structure and evolution (Boesgaard 1988). Line profiles of Be and B in various ionization stages, are of interest for opacity calculations as well (Seaton 1988). Moreover, Stark broadening of Be III and B III lines are of interest for the investigation and diagnostic of laboratory and laser-produced plasma, as well as for the research of regularities and systematic trends. For example Fraenkel et al. (1968) investigated high energy satellites in the vacuum UV Be III spectrum, while Malvezi et al. (1975) reported electron densities up to 10^{21} cm^{-3} in a laser produced Be plasma. Rosznayi (1977) studied theoretically, Stark broadening of Be III lines for a high density plasma with $kT = 21$ eV, and atom density $10^{19} - 10^{22}$ cm^{-3}. In this study, the inelastic contribution has been approximated by a formula for electron - impact ionization, and elastic contribution has been calculated first for $1s^2-2p$ transition, and subsequently has been generalized. In Dimitrijević & Konjević (1981) and Dimitrijević (1988ab) Stark widths of Be III and B III lines have been calculated within the semiempirical method (Griem 1968), the modified semiempirical method (Dimitrijević & Konjević 1980), the simplified semiclassical method (Griem 1974, Eq. (526)) and its modification (Dimitrijević & Konjević 1980). Moreover, Stark widths and shifts for B III 2s − 2p, 2s − 3p, 2p − 3s, 2p − 3d, 3s − 3p and 3p − 3d have been calculated by Seaton (1988) within the quantum mechanical strong coupling method. Stark broadening parameters of B III have been investigated experimentaly as well in two contributions. In Djeniže et al. (1992), the results concerning B III $4f^2F^\circ - 5g^2G$ 4497.6 Å line, measured in a pulsed linear arc plasma, have been reported. Srećković et al. (1993) measured in a linear, low - pressure pulsed arc operating in O_2, the Stark widths of two lines within the B III $2s^2S - 2p^2P^\circ$ multiplet.

The Be III and B III Stark broadening data are of interest and for studies of regularities and systematic trends within isoelectronic sequences. In previous articles Stark broadening data for Be II (Dimitrijević & Sahal-Bréchot 1992a), C IV (Dimitrijević et al. 1991), N V (Dimitrijević & Sahal-Bréchot 1992b), O VI (Dimitrijević & Sahal-Bréchot 1992c), F VII (Dimitrijević & Sahal-Bréchot 1993), Ne VIII and Na IX (Dimitrijević & Sahal-Bréchot 1994a) and Al XI and Si XII (Dimitrijević & Sahal-Bréchot 1994b) all belonging to the lithium isoelectronic sequence have been calculated. Consequently, the results for B III will complete this set of data. Moreover,

Send offprint requests to: M.S. Dimitrijević
*Table 1 is only available in electronic form at the CDS via anonymous ftp 130.79.128.5

Stark broadening data for Li II (Dimitrijević & Sahal-Bréchot 1996a) and C V (Dimitrijević & Sahal-Bréchot 1996b), belonging to the helium isoelectronic sequence as Be III, have been published also. Results of the investigations of regularities and systematic trends are of interest for acquisition of new data by interpolation and for critical evaluation of existing experimental and theoretical data.

This paper is the fourteenth of a series devoted to the calculation of Stark broadening parameters of spectral lines of multicharged ions (see Dimitrijević & Sahal-Bréchot 1995 and references therein and Dimitrijević & Sahal-Bréchot 1996b). By using the semiclassical-perturbation formalism (Sahal-Bréchot 1969ab), we have calculated electron-, proton-, and ionized helium-impact line widths and shifts for 12 Be III and 27 B III multiplets, in order to continue our research of multiply charged ion line Stark broadening parameters. A summary of the formalism is given in Dimitrijević et al. (1991) and Dimitrijević & Sahal-Bréchot (1996a).

2. Results and discussion

Energy levels for Be III and B III lines have been taken from Bashkin & Stoner (1975). Oscillator strengths have been calculated by using the method of Bates & Damgaard (1949) and the tables of Oertel & Shomo (1968). For higher levels, the method described by Van Regemorter et al. (1979) has been used. In addition to electron-impact full halfwidths and shifts, Stark-broadening parameters due to proton-, and ionized helium - impacts have been calculated.

Our results for 12 Be III and 27 B III multiplets are shown in Table 1 (accessible only in electronic form), for perturber densities $10^{17} - 10^{21}\mathrm{cm}^{-3}$ and temperatures $T = 10.000 - 300.000$ K. We also specify a parameter c (Dimitrijević & Sahal-Bréchot 1984), which gives an estimate for the maximum perturber density for which the line may be treated as isolated when it is divided by the corresponding electron-impact full width at half maximum. For each value given in Table 1, the collision volume (V) multiplied by the perturber density (N) is much less than one and the impact approximation is valid (Sahal-Bréchot 1969a,b). Values for $NV > 0.5$ are not given and values for $0.1 < N \leq 0.5$ are denoted by an asterisk. When the impact approximation is not valid, the ion broadening contribution may be estimated by using quasistatic estimations (Sahal-Bréchot 1991; Griem 1974). The accuracy of the results obtained decreases when broadening by ion interactions becomes important.

The unique experimental result convenient for comparison, are the Stark widths of two lines within the B III $2s^2S - 2p^2P^\circ$ multiplet, measured by Srećković et al. (1993) in a linear, low - pressure pulsed arc operating in O_2. They found a large disagreement between their Stark widths and results (Dimitrijević & Konjević 1981), obtained within the modified semiempirical approach (Dimitrijević & Konjević 1980). For B III 2065.77 Å line, they found that the ratio of measured to theoretical Stark width is 7.8 and for 2067.23 Å line 6.7 for the temperature of 48000 K at an electron density of 2.55 $10^{17}\mathrm{cm}^{-3}$. Corresponding ratios with our results with ionized oxygen-impact broadening included, are 3.9 and 3.5 respectively, which is better but not satisfying.

We may compare available theoretical results for B III $2s^2S - 2p^2P^\circ$ multiplet for the temperature of 160000 K at an electron density of 1 $10^{17}\mathrm{cm}^{-3}$. Our full width at half maximum $W = 0.0103$ Å, and the agreement is closest with calculations of Dimitrijević & Konjević (1981) by using the symplified semiclassical approach of Griem (1974, Eq. (526)), which obtained $W = 0.00892$ Å. Within the modified semiempirical approach (Dimitrijević & Konjević 1980), same authors obtained $W = 0.00449$ Å, which is two times smaller. Within the close coupling quantum mechanical approach Seaton (1988) obtained $W = 0.00602$ Å, which is also in disagreement with experiment and our calculations. In order to clarify the situation, particularly since B III $2s^2S - 2p^2P^\circ$ multiplet is important for the consideration of Stark broadening parameters within the lithium isoelectronic sequence, we recomend a new experimental determination of Stark broadening parameters particularly for this multiplet.[1]

Acknowledgements. This work is a part of the project "Physics and Dynamics of Celestial Bodies" supported by the Ministry for Science and Technology of Serbia.

References

Bashkin S., Stoner J.O.Jr., 1975, Atomic Energy Levels and Grotrian Diagrams, Vol. 1, North Holland, Amsterdam
Bates D.R., Damgaard A., 1949, Trans. Roy. Soc. London, Ser. A 242, 101
Boesgaard A.M., 1988, Vistas Astron. 31, 167
Dimitrijević M.S., 1988a, A&AS 76, 53
Dimitrijević M.S., 1988b, Bull. Obs. Astron. Belgrade 139, 31
Dimitrijević M.S., Konjević N., 1980, JQSRT 24, 451
Dimitrijević M.S., Konjević N., 1981, in Spectral Line Shapes. In: Wende B. (ed.). de Gruyter W. & Co., New York, p. 521
Dimitrijević M.S., Sahal-Bréchot S., 1984, JQSRT 31, 301
Dimitrijević M.S., Sahal-Bréchot S., Bommier V., 1991, A&AS 89, 581
Dimitrijević M.S., Sahal-Bréchot S., 1992a, JQSRT 48, 397
Dimitrijević M.S., Sahal-Bréchot S., 1992b, A&AS 95, 109
Dimitrijević M.S., Sahal-Bréchot S., 1992c, A&AS 93, 359
Dimitrijević M.S., Sahal-Bréchot S., 1993, A&AS 101, 587
Dimitrijević M.S., Sahal-Bréchot S., 1994a, A&AS 107, 351
Dimitrijević M.S., Sahal-Bréchot S., 1994b, A&AS 105, 245
Dimitrijević M.S., Sahal-Bréchot S., 1995, A&AS 109, 551
Dimitrijević M.S., Sahal-Bréchot S., 1996a, Phys. Scripta (in press)

[1]The very recent experimental results for this resonance multiplet (Glenzer S. & Kunze H.-J., 1996, Phys. Rev. A 53, 1225) agree with our semi-classical results within 10 percent.

Djeniže S., Srećković A., Labat J., Platiša M., 1992, Phys. Scripta 45, 320
Dimitrijević M.S., Sahal-Bréchot S., 1996b, A&AS 115, 351
Fraenkel B.S., Goldsmith S., Feldman U., 1968, Phys. Lett A 27, 111
Griem H.R., 1968, Phys. Rev. 165, 258
Griem H.R., 1974, Spectral Line Broadening by Plasmas. Academic Press, New York and London
Malvezi A.M., Janitti E., Tondello G., 1975, Opt. Commun. 13, 307
Rosznayi B.F., 1977, J. Quant. Spectrosc. Radiative Transfer 17, 77
Oertel G.K., Shomo L.P., 1968, ApJS 16, 175
Sahal-Bréchot S., 1969a, A&A 1, 91
Sahal-Bréchot S., 1969b, A&A 2, 322
Sahal-Bréchot S., 1991, A&A 245, 322
Seaton M.J., 1988, J. Phys. B 21, 3033
Srećković A., Djeniže S., Platiša M., 1993, XVI Int. Symp. Phys. Ioniz. Gases, Beograd, Contributed papers and Abstracts of Invited Lectures and Progress Reports. In: Milosavljević M. (ed.), Institute of Nuclear Sciences "Vinča", Beograd, 201
Van Regemorter H., Hoang Binh Dy, Prud'homme M., 1979, J. Phys. B 12, 1073

ASTRONOMY & ASTROPHYSICS
SUPPLEMENT SERIES

Astron. Astrophys. Suppl. Ser. **119,** 529-530 (1996)

Stark broadening of Sr I spectral lines*

M.S. Dimitrijević[1] and S. Sahal-Bréchot[2]

[1] Astronomical Observatory, Volgina 7, 11050 Belgrade, Yugoslavia
[2] Laboratoire "Astrophysique, Atomes et Molécules", Département Atomes et Molécules en Astrophysique, Unité associée au C.N.R.S. No. 812, Observatoire de Paris-Meudon, 92190 Meudon, France

Received March 13; accepted March 26, 1996

Abstract. — Using a semiclassical approach, we have calculated electron−, proton−, and ionized helium−impact line widths and shifts for 33 Sr I multiplets for perturber densities 10^{13} cm^{-3} (for stellar plasma research) and $10^{15}-10^{18}$ cm^{-3} (for laboratory plasma research) and temperatures $T = 2\ 500 - 50\ 000$ K.

Key words: lines: profile-atomic data

1. Introduction

Strontium lines are present in solar and stellar spectra. E.g. Komarov & Basak (1993) have found neutral strontium lines in the spectra of Sun and two Praesepe's stars. They are also of interest since Sr is one of thermonuclear s - processes product in stars and its overabundance is observed in CH and metal deficient barium stars (Šleivyté & Bartkevičius 1995). Neutral strontium lines are also of interest for the investigation of laboratory plasmas. Consequently, Kato et al. (1984) investigated wavelength shifts of Sr I lines emitted by an inductively coupled plasma and Karabut et al. (1980) dynamics of strontium line shapes during a pulsed discharge. Such lines have been considered theoretically as well by Davis (1972), for research of a laser - generated barium plasma. In order to continue our research of Stark broadening parameters needed for the investigation of astrophysical and laboratory plasmas and to provide the needed Stark broadening data, we have calculated within the semiclassical-perturbation formalism (Sahal−Bréchot 1969a,b) electron-, proton-, and ionized helium-impact line widths and shifts for 33 Sr I multiplets. A summary of the formalism is given in Dimitrijević & Sahal-Bréchot (1984).

2. Results and discussion

Energy levels for Sr I lines have been taken from Moore (1971). Oscillator strengths have been calculated by using the method of Bates & Damgaard (1949) and the tables of Oertel & Shomo (1968). For higher levels, the method described by Van Regemorter et al. (1979) has been used. We note that Gruzdev (1967) has found that the semiempirical and Hartree - Fock calculations of Sr I oscillator strengths agree fairly well with the f values calculated by the method of Coulomb approximation.

In addition to electron-impact full halfwidths and shifts, Stark-broadening parameters due to proton-, and He II- impacts have been calculated. Our results for 33 Sr I multiplets are shown in Table 1 (accesible only in electronic form), for perturber densities 10^{13} cm^{-3} (for stellar plasma research) and $10^{15}-10^{18}$ cm^{-3} (for laboratory plasma research) and temperatures $T = 2\ 500 - 50\ 000$ K. We also specify a parameter c (Dimitrijević & Sahal−Bréchot 1984), which gives an estimate for the maximum perturber density for which the line may be treated as isolated when it is divided by the corresponding full width at half maximum. For each value given in Table 1, the collision volume (V) multiplied by the perturber density (N) is much less than one and the impact approximation is valid (Sahal−Bréchot 1969a,b). Values for $NV > 0.5$ are not given and values for $0.1 < NV \leq 0.5$ are denoted by an asterisk. When the impact approximation is not valid, the ion broadening contribution may be estimated by using quasistatic approach (Sahal−Bréchot 1991; Griem 1974). In the region between where neither of these two approximations is valid, a unified type theory should be used. For example in Barnard et al. (1974), a simple analytical formulas for such a case are given. The accuracy of the results obtained decreases when broadening by ion interactions becomes important.

Send offprint requests to: M.S. Dimitrijević

*Table 1 is only available in electronic form: The material published electronically can be accessed: by ftp at cdsarc.u-strasbg.fr or 130.79.128.5 or on WWW at: http//cdsweb.u-strasbg.fr/abstract.html

Acknowledgements. This work is a part of the project "Physics and dynamics of celestial bodies", supported by Ministry of Science and Technology of Serbia.

References

Barnard A.J., Cooper J., Smith E.W., 1974, JQSRT 14, 1025
Bates D.R., Damgaard A., 1949, Trans. Roy. Soc. London Ser. A 242, 101
Davis J., 1972, JQSRT 12, 1351
Dimitrijević M.S., Sahal−Bréchot S., 1984, JQSRT 31, 301
Griem H.R., 1974, Spectral Line Broadening by Plasmas. Academic Press, New York
Gruzdev P.F., 1967, Opt. Spektrosk. 22, 169
Karabut E.K., Kravchenko V.F., Mikhalevskii V.S., 1980, Opt. Spectrosc. 48, 386
Kato K., Fukushima H., Nakajima T., 1984, Spectrochim. Acta B 39, 979
Komarov N.S., Basak N.Yu., 1993, Astron. Zh. 70, 111
Moore C.E., 1971, Atomic Energy Levels II, NSRDS-NBS 35, Washington
Oertel G.K., Shomo L.P., 1968, ApJS 16, 175
Sahal−Bréchot S., 1969a, A&A 1, 91
Sahal−Bréchot S., 1969b, A&A 2, 322
Sahal−Bréchot S., 1991, A&A 245, 322
Šleivyté J., Bartkevičius A., 1995, Vilniaus Astron. Obs. Biuletenis 85, 3
Van Regemorter H., Hoang Binh Dy, Prud'homme M., 1979, J. Phys. B 12, 1073

1996A&AS..120..373P

ASTRONOMY & ASTROPHYSICS
SUPPLEMENT SERIES

Astron. Astrophys. Suppl. Ser. **120**, 373-374 (1996)

Stark widths for astrophysically important ns−np transitions in Sc II, Y II and Zr II spectra*

L.Č. Popović and M.S. Dimitrijević

Astronomical Observatory, Volgina 7, 11000 Belgrade, Yugoslavia

Received April 16; accepted April 22, 1996

Abstract. — Here we present Stark widths for some astrophysically important ns−np transitions of Sc II, Y II and Zr II. Stark widths were calculated within the modified semiempirical approach. The obtained results were compared with simple estimates based on regularities and systematic trends.

Key words: atomic data — lines: profiles

1. Introduction

Spectral lines of Sc II, Y II and Zr II are present in spectra of hot stars, as e.g. in spectra of ϕ Her ($T_{\rm eff} \approx$ 11500 K, log$g$=3.5) and o And ($T_{\rm eff} \approx$ 9500 K, log$g$=3.5) (Adelman & Lanz 1987) as well as in other hot stars (see e.g. Adelman et al. 1979; Redfors & Cowley 1993; Kupka et al. 1994). Lines of these ions are also observed in the Solar spectrum (see e.g. Moore 1950, 1952; Krueger et al. 1968).

The electron impact broadening mechanism is the main pressure broadening mechanism in the hot star atmospheres ($T_{\rm eff} \gtrsim$ 10000 K), and it is of interest especially for A type stars and white dwarfs. Moreover, Stark broadening of lines orginating from energy levels with high principal quantum numbers may be important and for some lines in atmospheres of cooler stars (see e.g. Vince et al. 1985).

In this paper we present Stark widths for 18 transitions of Sc II, Y II and Zr II, which are needed for stellar atmospheres investigations (Lanz & Artru 1987).

2. Results and discussions

For the Stark broadening parameters calculation the modified semiempirical approach (Dimitrijević & Konjević 1980, for the case of complex heavy ions see also Popović & Dimitrijević 1996) was used. Calculations were carried out for ns−np transitions from 6 multiplets for each of considered ions. We have selected only such multiplets where it was possible to calculate Stark widths within the accuracy of the modified semiempirical approch. For these ions it is not possible to use more elaborate methods (as e.g. semiclassical one), because of the lack of atomic data.

The atomic data (energy levels) needed for calculations were taken from Moore (1971), Bashkin & Stoner (1978) and Andersen et al. (1978). Oscillator strengths have been calculated by using Bates & Damgaard (1949) method and the tables of Oertel & Shomo (1968). For some lines of considered ions, the oscillator strengths from the Sollar and the stellar spectra (as e.g. Boyarchuk & Boyarchuk 1960; Allen 1976), as well as determined theoretically and experimentally (see e.g. Andersen et al. 1978 and Malloy & Czyzak 1978) have been used.

In Tables 1–3 Stark full widths for Sc II, Y II and Zr II, respectively, are presented. The data are given for an electron density of 10^{23}m^{-3} and temperatures from 5000 to 50000 K.

In the case of these ions there is not measured or calculated Stark broadening parameters, only the simple estimates of Lakićević (1983) based on regularities and systematic trends for Sc II ($a^3D-z^3F^0$) and Zr II ($a^4F-z^4G^0$) were published. Comparison of our calculated Stark widths with the estimates given by Lakićević (1983) are shown in Table 4.

As one can see, our calculated Stark widths are in good agremeent with the simple estimates of Lakićević (1983).

In order to show how much is important to take into account the Stark broadening effect for the modelling and analyses of hot star atmospheres, we have compared termal Doppler and Stark widths for Kurucz's (1979) model of an A type star with log$g$=4.0 and $T_{\rm eff}$=10000 K. In Figs. 1 and 2 termal Doppler and Stark widths are

Send offprint requests to: L.Č. Popović

*Tables only in electronic form can be accessed by ftp at cdsarc.u-strasbg.fr or 130.79.128.5 or on www at http://cdsweb.u-strasbg.fr/abstract.html

© European Southern Observatory • Provided by the NASA Astrophysics Data System

1996A&AS..120..373P

Transition	$(FWHM)_1$	$(FWHM)_2$	$(FWHM)_1/(FWHM)_2$
	this paper	Lakićević (1983)	
Sc II ($a^3D-z^3F^0$)	0.0107 nm	0.0091 nm	1.17
Zr II ($a^4F-z^4G^0$)	0.00761 nm	0.0084 nm	0.91

presented as functions of temperature and optical depth, respectively, for an Y II line (λ=437.9 nm). One can see that exist conditions where Stark width is comparable and even up to one order of magnitude larger than the termal Doppler width. Consequently, one can see that exist conditions where Stark broadening may be principal broadening mechanism influencing line shape formation.

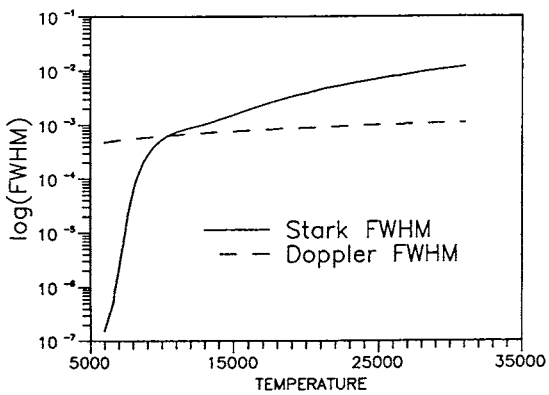

Fig. 1. Comparison of termal Doppler and Stark widths for 437.9 nm (Y II) line as a function of temperature for an A star ($T_{\rm eff}$=10000 K, log$g$=4.0). The abundance of ytrium is as in Solar atmosphere

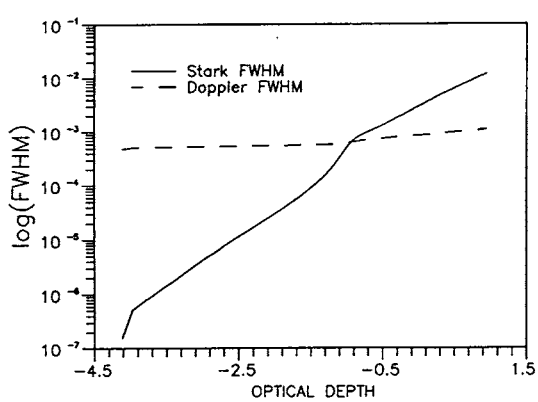

Fig. 2. Same as in Fig. 1, but the widths are presented as a function of optical depth

We hope that the presented results will be useful for astrophysical purposes.

References

Adelman S.J., Bidelman W.P., Pyper D.M., 1979, ApJS 40, 371

Adelman S.J., Lanz T., 1987, Elemental abundance analyses, the Institut d'Astronomie de l'Université de Lausanne

Allen M.S., 1976, PASP 88, 338

Andersen T., Ramanujam P.S., Bahr K., 1978, ApJ 223, 344

Bashkin S., Stoner J.O., 1987, Atomic energy levels & Grotrian diagrams 2. North-Holland Publishing Company, Amsterdam - Oxford - New York

Bates D.R., Damgaard A., 1949, Phyl. Roy. Soc. London A 242, 101

Boyarchuk M.E., Boyarchuk A.A., 1960, Izv. Krymskoy Astrophys. Obs. 22, 234

Dimitrijević M.S., Konjević N., 1980, JQSRT 24, 451

Krueger T.K., Aller L.H., Ross J., Czyzak S.J., 1968, ApJ 152, 765

Kupka F., Ryabchikova T., Bolgova G., et al., 1994, In: Chemically peculiar and magnetic stars on and close to upper main sequence, Tatranska Lomnica, pp. 130-136

Kurucz R.L., 1979, ApJS 40, 1

Lakićević I.S., 1983, A&A 127, 37

Lanz T., Artru M.-C., 1987, Elemental abundance analyses. In: Adelman S.J. and Lanz T. (eds.), the Institut d'Astronomie de l'Université de Lausanne, p. 156

Malloy P.J., Czyzak S.J., 1978, Astrophys. Space Sci. 58, 365

Moore C.E., 1950, An Ultraviolet Multplet Table, Circular of the NBS 488, Sect. 1, Washington D.C.

Moore C.E., 1952, An Ultraviolet Multplet Table, Circular of the NBS 488, Sect. 2, Washington D.C.

Moore C.E., 1971, Atomic energy levels, Nat. Stand. Ref. Data Ser., NBS, Vols. I, II, Washington D.C.

Oertel G.K., Shomo L.P., 1968, ApJS 16, 175

Popović L. Č., Dimitrijević M.S., 1996, Phys. Scr. 53, 325

Redfors A., Cowley C.R., 1993, A&A 271, 273

Vince I., Dimitrijević M.S., Kršljanin V., 1985, in Progres in Stellar Spectral Line Formation Theory. In: Beckman J., Crivellari L., Reidel D. (eds.). Dordrecht, p. 373

© European Southern Observatory • Provided by the NASA Astrophysics Data System

ASTRONOMY & ASTROPHYSICS
SUPPLEMENT SERIES

Astron. Astrophys. Suppl. Ser. **122,** 163-166 (1997)

Stark broadening of Ba I and Ba II spectral lines*

M.S. Dimitrijević[1] and S. Sahal-Bréchot[2]

[1] Astronomical Observatory, Volgina 7, 11050 Belgrade, Serbia, Yugoslavia
[2] Laboratoire "Astrophysique, Atomes et Molécules", Département Atomes et Molécules en Astrophysique, Unité associée au CNRS No. 812, Observatoire de Paris-Meudon, 92190 Meudon, France

Received June 11; accepted June 14, 1996

Abstract. Using a semiclassical approach, we have calculated electron-, proton-, and ionized helium-impact line widths and shifts for 14 Ba I and 64 Ba II multiplets for perturber densities $10^{15}-10^{18}$ cm^{-3} and temperatures $T = 2\,500 - 50\,000$ K for Ba I and $5\,000 - 100\,000$ K for Ba II. The results have been compared with available experimental and theoretical data.

Key words: line: profiles-atomic data

1. Introduction

Barium is one of thermonuclear s - processes product in stars and its overabundance is observed in CH subgiants, characterized by enhanced Sr and Ba lines, and in metal deficient barium stars, giants showing overabundance of s-processes elements (Šleivyté & Bartkevičius 1995). Barium lines are present in solar and stellar spectra. E.g. Komarov & Basak (1993) have found Ba I and Ba II lines in the spectra of the Sun and of two Praesepe's stars (for Solar barium lines see also Anders & Grevesse 1989).

Barium lines are also of interest for the investigation of laboratory plasmas. Since the research of Aulehla & Herman (1958) who have determined neutral barium Stark effect constants by investigating metallic lines broadened by an intermolecular field, Stark broadening of Ba I and Ba II lines has been considered experimentally and theoretically in a number of articles. Kato et al. (1984) investigated wavelength shifts of Ba I and Ba II lines emitted by an inductively coupled plasma. Manning et al. (1990) performed a study of the effect of pressure and electron density on wavenumber position for Ba II lines. Experimental Stark broadening parameters for ionized barium lines of Jaeger (1969), obtained with the help of a discharge sliding along the surface of a liquid jet, Purić & Konjević (1972), where the plasma source was a T-tube, Hadžiomerspahić et al. (1973, superseeding according to Konjević & Wiese 1976, the similar work of Platiša et al. 1971), with Z-pinch as the experimental apparatus, and of Fleurier et al. (1987), provided with a plasma jet, have been critically reviewed in Konjević & Wiese (1976) and Konjević et al. (1984b).

Stark widths of Ba II lines have been calculated by Cooper & Oertel (1967) within the semiclassical approach taking into account hyperbolic classical perturber paths and lower level broadening. For Ba II 1, 2, 3, and 4 multiplet they give full width at half maximum (FWHM) values of 0.42 Å, 0.84 Å, 1.02 Å and 1.20 Å respectively, but without the electron temperature specified. Theoretically, Ba I lines have been investigated by Grechikhin (1969), considering their applicability to plasma diagnostics. Ba I and Ba II lines have been considered theoretically as well by Davis (1972), for research of a laser - generated barium plasma and, Ba II lines by Sahal-Bréchot (1969b) within the semiclassical - perturbation formalism and by Fleurier et al. (1977) within the same formalism but with the effect of Feshbach resonances included. The semiclassical calculations by using the theoretical approach developed by Griem et al. (1962) and further improved and described in detail by Jones et al. (1971) and Griem (1974), were performed by Purić et al. (1978). For Ba II $6s^2S - 6p^2P^\circ$ multiplet, at an electron density of $N_e = 10^{17}$ cm^{-3} and electron temperature $T = 15000$ K, they obtain FWHM = 0.428 Å. In Konjević & Wiese (1976) and Konjević et al. (1984b) the theoretical comparison data have been calculated by W.W. Jones (private communication in Konjević & Wiese 1976), by using the same method. Stark broadening parameters of Ba II mult. 1 and 2, for $T = 16000$ K have been calculated also by Gorchakov & Demkin (1978) within the semiclassical approach of Vainshtein & Sobel'man (1959). Griem's (1968) semiempirical formula has been applied to Ba II lines in Hadžiomerspahić et al. (1973), Fleurier et al. (1977) and Dimitrijević & Konjević (1981). Moreover, Dimitrijević & Konjević (1981) performed for Ba II $6s^2S - 6p^2P^\circ$ multiplet 1, linewidth calculations within the modified

* Tables 1 and 2 are only available in electronic form: see the Editorial in A&AS 1994, Vol. 103, No. 1.

semiempirical method (Dimitrijević & Konjević 1980) and within the same approach but with the Gaunt factor derived from the work of Younger & Wiese (1979) for the perturbing transitions without the change of the principal quantum number, Lakićević (1983) estimated line widths and shifts for Ba I $6s^{21}S - 6p^{1}P^{\circ}$ and Ba II $6s^{2}S - 6p^{2}P^{\circ}$ multiplet for $T = 20000$ K, on the basis of the Stark broadening parameter dependence on the ionization potential from the lower level of the corresponding transition. By using Ba II 4899.9 Å and 4524.9 Å lines as example, Dimitrijević & Popović (1989) demonstrated a simple method (developed for neutrals by Vitel et al. 1988), suitable for critical evaluation of existing data and interpolation of new Stark widths along homologous sequences, by using a normalization factor for analogous transitions.

In order to continue our research of Stark broadening parameters needed for the investigation of astrophysical and laboratory plasmas and to provide the needed Stark broadening data, we have calculated within the semiclassical-perturbation formalism (Sahal-Bréchot 1969a,b) electron-, proton-, and ionized helium-impact line widths and shifts for 14 Ba I and 64 Ba II multiplets. A summary of the formalism for neutral emitters is given in Dimitrijević & Sahal-Bréchot (1984), and for ionized emitters in Dimitrijević et al. (1991) and Dimitrijević & Sahal-Bréchot (1996). We note here that the inelastic collision contribution is included in the ion-impact line widths.

2. Results and discussion

Energy levels for Ba I lines have been taken from Moore (1971). Roig & Tondello (1975) have been studied the spectrum of Ba II in absorption, by flash pyrolysis. They found a general agreement with previous results obtained in emission spectra (see the critical compilation of Moore 1971) but fifteen new levels have been established as well. For Ba II lines, energy levels were taken from Moore (1971), but values for $8 - 12p^{2}P^{\circ}$, $10f^{2}F^{\circ}$ and $11f^{2}F^{\circ}$, have been taken from Roig & Tondello (1975). Oscillator strengths have been calculated by using the method of Bates & Damgaard (1949) and the tables of Oertel & Shomo (1968). For higher levels, the method described by Van Regemorter et al. (1979) has been used.

In addition to electron-impact full halfwidths and shifts, Stark-broadening parameters due to proton-, and He II- impacts have been calculated. Our results for 14 Ba I multiplets and 64 Ba II multiplets are shown in Tables 1 and 2 (accessibles only in electronic form) respectively, for perturber densities $10^{15} - 10^{18}$ cm^{-3} and temperatures $T = 2\,500 - 50\,000$ K for Ba I and $T = 5\,000 - 100\,000$ K for Ba II. We also specify a parameter c (Dimitrijević & Sahal-Bréchot 1984), which gives an estimate for the maximum perturber density for which the line may be treated as isolated when it is divided by the corresponding full width at half maximum. For each value given in Table 1, the collision volume (V) multiplied by the perturber density (N) is much less than one and the impact approximation is valid (Sahal-Bréchot 1969a,b). Values for $NV > 0.5$ are not given and values for $0.1 < NV \leq 0.5$ are denoted by an asterisk. Tabulated Stark broadening parameters are linear with perturber density for perturber densities lower than 10^{15} cm^{-3}. When the impact approximation is not valid, the ion broadening contribution may be estimated by using the quasistatic approach (Sahal-Bréchot 1991; Griem 1974). In the region between, where neither of these two approximations is valid, a unified type theory should be used. For example in Barnard et al. (1974), a simple analytical formula for such a case is given. The accuracy of the results obtained decreases when broadening by ion interactions becomes important.

In Table 3 our results are compared with the experimental results (Jaeger 1969; Purić & Konjević 1972; Hadžiomerspahić et al. 1973; Fleurier et al. 1977) critically selected by Konjević & Roberts (1976); Konjević & Wiese (1976, 1990) and Konjević et al. (1984a,b). One can see that large differences between particular experiments and between theory and experiment exist. An agreement exists between widths of Fleurier et al. (1977), whose experiment was critically estimated by Konjević et al. (1984b) to have the highest accuracy among Ba II experimental data, and our results for $6s^{2}S - 6p^{2}P^{\circ}$ multiplet. For the shift, the best agreement is with the results of Purić & Konjević (1972) for the same multiplet.

Our results for Stark width are in agreement with the semiclassical calculations of Cooper & Oertel (1967) as well as with the semiclassical calculations by using the theoretical approach developed by Griem et al. (1962) and further improved and described in detail by Jones et al. (1971) and Griem (1974), performed by W.W. Jones (private communication in Konjević & Wiese 1976), and Purić et al. (1978). Our Stark width calculation are also in agreement within the error bars of the methods with various semiempirical calculations (Hadžiomerspahić et al. 1973; Fleurier et al. 1977; Dimitrijević & Konjević 1981) as well as with simple Stark width estimates of Lakićević (1983), on the basis of the Stark broadening parameter dependence on the ionization potential from the lower level of the corresponding transition. For Ba I $6s^{21}S - 6p^{1}P^{\circ}$ Lakićević (1983) obtained FWHM = 0.48 Å at an electron density of $N_{\rm e} = 10^{17}$ cm^{-3} and electron temperature $T = 20000$ K, and our result is 0.30 Å. For Ba II $6s^{2}S - 6p^{2}P^{\circ}$ multiplet for the same plasma conditions, Lakićević obtains FWHM = 0.50 Å and our result is 0.43 Å.

Our results for the shift are in agreement within the error of the method with the semiclassical calculations of W.W. Jones (private communication in Konjević & Wiese 1976), but in strong disagreement with calculations of Gorchakov & Demkin (1978), performed within the semiclassical approach of Vainshtein & Sobel'man (1959), with

Table 3. Experimental Stark full widths at half maximum (Wm) and shifts (dm) in Å compared with theory. The Wth and dth are present semi - classical calculations. Experimental values: (a) - Fleurier et al. (1977); (b) - Jaeger (1969); (c) - Purić & Konjević (1972); (d) - Hadžiomerspahić et al. (1973)

Transition (Mult.)	Wawelength	T(K)	Ne [10(+17) cm(-3)]	Wm [A]	Wth [A]	dm [A]	dth [A]	Ref.
5d−6p	6141.72	13000	1.13	0.50	0.91	-	-	a
(2)		13200	1	1.58	0.80	-	-	b
		16800	1	-	-	0.07	0.002	c
		27100	1	0.28	0.62	-	-	d
		31700	1	0.28	0.59	-	-	d
	6496.9	16800	1	-	-	0.07	0.002	c
		27100	1	0.28	0.62	0.05	0.002	d
		31700	1	0.28	0.59	-	-	d
	5853.7	13200	1	1.32	0.80	-	-	b
6s−6p	4554.03	13000	1.13	0.49	0.58	−0.050	−0.095	a
(1)		13200	1	0.80	0.51	-	-	b
		16800	1	-	-	−0.06	−0.076	c
		27100	1	0.26	0.39	-	-	d
	4934.09	13000	1.13	0.49	0.58	−0.050	−0.095	a
		13200	1	0.94	0.51	-	-	b
		16800	1	-	-	−0.07	−0.076	c
		27100	1	0.24	0.39	-	-	d
6p−6d	4130.6	13200	1	1.24	1.07	-	-	b
(4)								
	4166.0	13200	1	1.26	1.07	-	-	b
	3891.8	16800	1	-	-	0.26	0.49	d
		31700	1	0.28	0.93	0.33	0.40	d
6p−7s	4899.9	13200	1	1.48	1.10	-	-	b
(3)	4524.9	13200	1	1.28	1.10	-	-	b

the semi the empirical calculations of Purić & Konjević (1972) and with the simple estimates of Lakićević (1983). New high precision measurements of Stark broadening parameters for Ba I and Ba II lines will be of interest for the development of theoretical methods for heavy atoms and ions.

Acknowledgements. This work is a part of the project "Astrometrical, Astrodynamical and Astrophysical Investigations", supported by Ministry of Science and Technology of Serbia.

References

Anders E., Grevesse N., 1989, Geochim. Cosmochim. Acta 53, 197
Aulehla E., Herman L., 1958, C. R. H. Acad. Sci. 246, 1676
Barnard A.J., Cooper J., Smith E.W., 1974, JQSRT 14, 1025
Bates D.R., Damgaard A., 1949, Trans. Roy. Soc. London Ser. A 242, 101
Cooper J., Oertel G.K., 1967, Phys. Rev. Lett. 18, 985
Davis J., 1972, JQSRT 12, 1351
Dimitrijević M.S., Konjević N., 1980, JQSRT 24, 451
Dimitrijević M.S., Konjević N., 1981, A&A 102, 93
Dimitrijević M.S., Popović M.M., 1989, A&A 217, 203
Dimitrijević M.S., Sahal-Bréchot S., 1984, JQSRT 31, 301
Dimitrijević M.S., Sahal-Bréchot S., 1996, Phys. Scr. 54, 50
Dimitrijević M.S., Sahal-Bréchot S., Bommier V., 1991, A&AS 89, 581
Fleurier C., Sahal-Bréchot S., Chapelle J., 1977, JQSRT 17, 595
Gorchakov L.V., Demkin V.P., 1978, Izv.Vysshikh Uchebnykh Zavedenij, Fizika 4, 113
Grechikhin L.I., 1969, J. Appl. Spectrosc. (USSR) 10, 870
Griem H.R., 1968, Phys. Rev. 165, 258
Griem H.R., 1974, Spectral Line Broadening by Plasmas. Academic Press, New-York
Griem H.R., Baranger M., Kolb A.C., Oertel G.K., 1962, Phys. Rev. 125, 177
Hadžiomerspahić D., Platiša M., Konjević N., Popović M., 1973, Z. Physik 262, 169
Jaeger H., 1969, Z. Physik 223, 19
Jones W.W., Benett S.M., Griem H.R., 1971, Calculated Electron Impact Broadening Parameters for Isolated

Spectral Lines from the Singly Charged Ions: Lithium through Calcium, Techn. Report No. 71-128, University of Maryland, College Park, MD
Kato K., Fukushima H., Nakajima T., 1984, Spectrochim. Acta B 39, 979
Komarov N.S., Basak N. Yu., 1993, Astron. Zh. 70, 111
Konjević N., Roberts J.R., 1976, J. Phys. Chem. Ref. Data 5, 209
Konjević N., Wiese W.L., 1976, J. Phys. Chem. Ref. Data 5, 259
Konjević N., Wiese W.L., 1990, J. Phys. Chem. Ref. Data 19, 1307
Konjević N., Dimitrijević M.S., Wiese W.L., 1984a, J. Phys. Chem. Ref. Data 13, 619
Konjević N., Dimitrijević M.S., Wiese W.L., 1984b, J. Phys. Chem. Ref. Data 13, 649
Lakićević I.S., 1983, A&A 127, 37
Manning T.J., Winefordner J.D., Palmer B.A., Hof D.E., 1990, Spectrochim. Acta B 45, 1031
Moore C.E., 1971, Atomic Energy Levels II, NSRDS-NBS 35, Washington
Oertel G.K., Shomo L.P., 1968, ApJS 16, 175
Platiša M., Purić J., Konjević N., Labat J., 1971, A&A 15, 325
Purić J., Dimitrijević M.S., Lakićević I.S., 1978, Phys. Lett. A 67, 188
Purić J., Konjević N., 1972, Z. Physik. 249, 440
Roig R.A., Tondello G., 1975, J. Opt. Soc. 65, 829
Sahal-Bréchot S., 1969a, A&A 1, 91
Sahal-Bréchot S., 1969b, A&A 2, 322
Sahal-Bréchot S., 1991, A&A 245, 322
Šleivyté J., Bartkevičius A., 1995, Vilniaus Astron. Obs. Biul. 85, 3
Van Regemorter H., Hoang Binh Dy Prud'homme M., 1979, J. Phys. B 12, 1073
Vainshtein L.A., Sobel'man I.I., 1959, Opt. Spektrosk. 6, 440
Vitel Y., Skowronek M., Dimitrijević M.S., Popović M.M., 1988, A&A 200, 285
Younger S.M., Wiese W.L., 1979, JQSRT 22, 161

ASTRONOMY & ASTROPHYSICS
SUPPLEMENT SERIES

Astron. Astrophys. Suppl. Ser. **122,** 533-534 (1997)

Stark broadening of spectral lines of multicharged ions of astrophysical interest

XV. P IV spectral lines*

M.S. Dimitrijević[2] and S. Sahal-Bréchot[2]

[1] Astronomical Observatory, Volgina 7, 11050 Belgrade, Yugoslavia
[2] Laboratoire "Astrophysique, Atomes et Molécules", Département Atomes et Molécules en Astrophysique, Unité associée au C.N.R.S. No. 812, Observatoire de Paris-Meudon, 92190 Meudon, France

Received August 7; accepted August 19, 1996

Abstract. Using a semiclassical approach, we have calculated electron-, proton-, and He III-impact line widths and shifts for 114 P IV multiplets for perturber densities 10^{15}–10^{20} cm^{-3} and temperatures $T = 5000$–$1\,000\,000$ K. The obtained results have been compared with results obtained by using various simpler approaches.

Key words: lines: profile-atomic data

1. Introduction

The Stark broadening parameters of P IV lines are of interest not only for the plasma diagnostic but for the research of regularities and systematic trends and theoretical considerations as well. Consequently, Stark widths for P IV $4s^1S - 4p^1P^\circ$, $4s^3S - 4p^3P^\circ$ and $3p^3P^\circ - 3d^3D$ multiplets have been determined (Dimitrijević & Konjević 1981; Dimitrijević 1988a,b) within the modified semiempirical approach (Dimitrijević & Konjević 1980), Griem's semiempirical approach (Griem 1968), simplified semiclassical approach (Eq. (526) in Griem 1974) and its modification (Dimitrijević & Konjević 1980).

This paper is the fifteenth of a series devoted to the calculation of Stark broadening parameters of spectral lines of multicharged ions (see Dimitrijević & Sahal-Bréchot 1995 and references therein, as well as Dimitrijević & Sahal-Bréchot 1996a,b). In order to continue our research of Stark broadening parameters needed for the investigation of astrophysical and laboratory plasmas and to provide the needed Stark broadening data, we have calculated within the semiclassical-perturbation formalism (Sahal-Bréchot 1969a,b) electron-, proton-, and He III-impact line widths and shifts for 114 PIV multiplets. The original computer code (Sahal-Bréchot 1969a,b), has been updated and optimized several times (Sahal-Bréchot 1974; Fleurier et al. 1977; Dimitrijević et al. 1991; Dimitrijević & Sahal-Bréchot 1996c). A summary of the formalism is given in Dimitrijević & Sahal-Bréchot (1996c).

2. Results and discussion

The energy levels for P IV lines have been taken from Martin et al. (1985). Oscillator strengths have been calculated by using the method of Bates & Damgaard (1949) and the tables of Oertel & Shomo (1968). For higher levels, the method described by Van Regemorter et al. (1979) has been used.

In addition to electron-impact full halfwidths and shifts, Stark-broadening parameters due to proton-, and He III- impacts have been calculated. Our results for 114 P IV multiplets are shown in Table 1 (published only in electronic form), for perturber densities $10^{15} - 10^{20}$ cm^{-3} and temperatures $T = 5000 - 1\,000\,000$ K. We also specify a parameter c (Dimitrijević & Sahal–Bréchot 1984), which gives an estimate for the maximum perturber density for which the line may be treated as isolated when it is divided by the corresponding full width at half maximum. For each value given in Table 1, the collision volume (V) multiplied by the perturber density (N) is much less than unity and the impact approximation is valid (Sahal–Bréchot 1969a,b). Values for $NV > 0.5$ are not given and values for $0.1 < NV \leq 0.5$ are denoted by an asterisk. When the impact approximation is not valid, the ion broadening contribution may be estimated by using quasistatic approach (Sahal–Bréchot 1991 and Griem 1974). In the region between where neither of these two

Send offprint requests to: M.S. Dimitrijević

* Table 1 is only available in electronic form: The material published electronically can be accessed: by ftp at cdsarc.u-strasbg.fr or 130.79.128.5 or on WWW at: http//cdsweb.u-strasbg.fr/abstract.html

Table 2. Present semiclassical Stark full widths at half maximum (WDSB) in Å compared with the calculations of Dimitrijević (1988a,b) by using the modified semiempirical approach (Dimitrijević & Konjević 1980), Griem's semiempirical approach (Griem 1968), symplified semiclassical approach (Eq. (526) in Griem 1974) and its modification (Dimitrijević & Konjević 1980)

PERTURBER DENSITY = 1.E+17cm-3

TRANSITION	T(K)	WDSB(A)	WG(A)	WGM(A)	WSEM(A)	WSE(A)
P IV 4S 4P	10000.	0.714	0.653	0.363	0.565	0.264
4250.9 A	20000.	0.502	0.477	0.279	0.399	0.186
C= 0.43E+21	40000.	0.367	0.360	0.229	0.282	0.132
	80000.	0.280	0.285	0.202	0.215	---
	160000.	0.225	0.238	0.188	0.183	---
P IV 4S 4P	10000.	0.411	0.385	0.216	0.330	0.158
3356.9 A	20000.	0.291	0.281	0.165	0.233	0.112
C= 0.34E+21	40000.	0.210	0.211	0.134	0.165	0.790E-01
	80000.	0.159	0.166	0.117	0.121	0.648E-01
	160000.	0.127	0.138	0.108	0.100	---
P IV 3P 3D	10000.	0.743E-02	0.573E-02	0.477E-02	0.350E-02	0.260E-02
826.3 A	20000.	0.521E-02	0.417E-02	0.350E-02	0.248E-02	0.184E-02
C= 0.46E+20	40000.	0.375E-02	0.313E-02	0.267E-02	0.175E-02	0.130E-02
	80000.	0.271E-02	0.248E-02	0.216E-02	0.124E-02	0.920E-02
	160000.	0.200E-02	0.211E-02	0.190E-02	0.873E-03	0.690E-03

approximations is valid, a unified type theory should be used. For example in Barnard et al. (1974), a simple analytical formula for such a case is given. The accuracy of the results obtained decreases when broadening by ion interactions becomes important.

In Table 2, present semiclassical Stark full widths at half maximum (WDSB) in Å are compared with the calculations in Dimitrijević (1988a,b) by using the modified semiempirical approach (Dimitrijević & Konjević 1980), Griem's semiempirical approach (Griem 1968), simplified semiclassical approach (Eq. (526) in Griem 1974) and its modification (Dimitrijević & Konjević 1980). One can see that the best agreement is with the results obtained by using the simplified semiclassical approach.

For further development and refinement of the theory, the corresponding experimental data will be very useful.

Acknowledgements. This work is a part of the project "Astrometrical, Astrodynamical and Astrophysical Investigations", supported by Ministry of Science and Technology of Serbia.

References

Barnard A.J., Cooper J., Smith E.W., 1974, J. Quant. Spectrosc. Radiat. Trans. 14, 1025
Bates D.R., Damgaard A., 1949, Trans. Roy. Soc. London Ser. A 242, 101
Dimitrijević M.S., 1988a, Bul. Obs. Astron. Belgrade 139, 31
Dimitrijević M.S., 1988b, A&AS 76, 53
Dimitrijević M.S., Konjević N., 1980, J. Quant. Spectrosc. Radiat. Trans. 24, 451
Dimitrijević M.S., Konjević N., 1981, in Spectral Line Shapes, Wende B., de Gruyter W. (eds.) Berlin, New York, p. 211
Dimitrijević M.S., Sahal-Bréchot S., 1984, J. Quant. Spectrosc. Radiat. Trans. 31, 301
Dimitrijević M.S., Sahal-Bréchot S., Bommier V., 1991, A&AS 89, 581
Dimitrijević M.S., Sahal-Bréchot S., 1995, A&AS 109, 551
Dimitrijević M.S., Sahal-Bréchot S., 1996a, A&AS 115, 351
Dimitrijević M.S., Sahal-Bréchot S., 1996b, A&AS 119, 369
Dimitrijević M.S., Sahal-Bréchot S., 1996c, Phys. Scr. 54, 50
Fleurier C., Sahal-Bréchot S., Chapelle J., 1977, J. Quant. Spectrosc. Radiat. Trans. 17, 595
Griem H.R., 1968, Phys. Rev. 165, 258
Griem H.R., 1974, Spectral Line Broadening by Plasmas. Academic Press, New York.
Martin, W.C., Zalubas, R., Musgrove, A., 1985, J. Phys. Chem. Ref. Data 14, 751
Oertel G.K., Shomo L.P., 1968, ApJS 16, 175
Sahal-Bréchot S., 1969a, A&A 1, 91
Sahal-Bréchot S., 1969b, A&A 2, 322
Sahal-Bréchot S., 1974, A&A 35, 321
Sahal-Bréchot S., 1991, A&A 245, 322
Van Regemorter H., Hoang Binh Dy, Prud'homme M., 1979, J. Phys. B 12, 1073

ASTRONOMY & ASTROPHYSICS
SUPPLEMENT SERIES

Astron. Astrophys. Suppl. Ser. **127,** 295-297 (1998)

Stark broadening parameters for Kr II lines from 5s – 5p transitions*

L.Č. Popović and M.S. Dimitrijević

Astronomical Observatory, Volgina 7, 11050 Beograd, Serbia, Yugoslavia

Received November 28, 1996; accepted April 14, 1997

Abstract. With the development of space-borne spectroscopy, spectral line parameters for a large number of lines become of increasing interest for astrophysics. To provide Stark broadening data for ion lines from complex spectra, we present here calculated Stark widths for 37 Kr II lines from the 5s – 5p transition. The calculations were performed by using a modified semiempirical approach. The obtained Stark widths are on average in satisfactory agreement with available experimental data.

Key words: atomic data — lines, profiles

1. Introduction

Stark broadening data for many transitions of many atoms and ions are needed for diagnosis of laboratory and astrophysical plasmas. As an example, data for more than 10^6 transitions, including line-profile parameters, are needed for the calculation of stellar opacities (Seaton 1988). With the development of space-borne spectroscopy, interest increases even more for a large number of spectral line profile parameters. For example, Leckrone et al. (1993) stated that with the Goddard High Resolution Spectrograph (GHRS) on Hubble Space Telescope they "have doubled the number of heavy elements ($22 \leq Z \leq 80$) for which abundances in χ Lupi can be estimated, compared to ground-based data alone". Cardelli et al. (1991) have used the GHRS for investigation of spectra of the interstellar medium, which more accurately represents the pre-stellar material from which the Ap and Bp stars (where Stark broadening data are of interest) are formed (Leckrone et al. 1993). For the first time, they have begun to detect elements such as krypton and germanium.

Stark broadening for Kr II lines has additional theoretical interest for the investigation of regularities and systematic trends for singly-charged noble gas ions (e.g. Dimitrijević & Popović 1989; Di Rocco 1990; Purić et al. 1991; Bertuccelli & Di Rocco 1993). Stark broadening data for Xe II, which is homologous with Kr II, have been published recently (Popović & Dimitrijević 1996a). A consistent set of Stark broadening data for Kr II and Xe II enables the investigation and testing of regularities in the case of homologous atoms, as well as Stark width estimates for homologous sequences for noble gas ions.

Stark broadening of Kr II lines have been considered experimentally (see e.g. Brandt et al. 1981; Pittman & Konjević 1986; Vitel & Skowronek 1987; Uzelac & Konjević 1989; Lesage et al. 1989; Bertuccelli & Di Rocco 1991) and theoretically (see e.g. Bertuccelli & Di Rocco 1993). Bertuccelli & Di Rocco (1993) have calculated Kr II Stark widths for several lines by using analytical expressions for the cross sections and rate coefficients based on the Born approximation, with and without the empirical modification for the collision strength suggested by Robb and with the help of a semiempirical method (Griem 1968). Estimates also exist based on the dependence on atomic number and the upper level ionization potential, established from the consideration of regularities (Di Rocco 1990; Purić et al. 1991; Bertuccelli & Di Rocco 1991, 1993). Here we present Stark widths for 37 spectral lines from the 5s – 5p transition array of singly-charged krypton, calculated by using a modified semiempirical approach (Dimitrijević & Konjević 1980; Dimitrijević & Kršljanin 1986). Due to the complexity of the Kr II spectrum, calculations were performed as in Popović & Dimitrijević (1996b). Our results for Stark widths and shifts are compared with the available experimental and theoretical data.

2. Results and discusion

The atomic energy levels needed for the calculation were taken from Sugar & Musgrove (1991). Oscillator

Send offprint requests to: L.Č. Popović

* Tables 1-4 are only available in electronic form via anonymous ftp 130.79.128.5 at the CDS in Strasbourg or via http://cdsweb.u-strasbg.fr/Abstract.html

strengths have been calculated using the method of Bates & Damgaard (1949). Our investigation of the influence of the departure from the LS coupling scheme on the Xe II Stark broadening parameters (Popović & Dimitrijević 1996a) has demonstrated that the differences between results obtained by using the LS and jK coupling schemes are relatively small in comparison with the accuracy of the modified semiempirical method (±50% in average). The differences for the homologous Kr II radiator should not be larger, so that the use of the LS coupling approximation should not influence the accuracy significantly, especially for transitions between lower levels. In Table 1 (accessible only in electronic form), we present Stark widths for 37 Kr II lines obtained for temperatures from 5000 K up to 50000 K and at an electron density of 10^{23} m^{-3}. Since we have found that the ion broadening contribution to the line widths is several percent, only the electron broadening contribution is given.

Our results for Stark widths have been compared in Table 2 (accessible only in electronic form) and Figs. 1-3 with available experimental data (Brandt et al. 1981; Vitel & Skowronek 1987; Uzelac & Konjević 1989; Lesage et al. 1989; Bertuccelli & Di Rocco 1990). The ratio of measured and calculated data varies between 0.73 and 1.97 (or 1.60 if we exclude the results of Bertuccelli & Di Rocco 1991). This is similar agreement as for the homologous 5s − 5p Xe II transitions, where this ratio varies between 0.7 and 1.4 (Popović & Dimitrijević 1996a). One can see from Table 2 that the largest disagreement exists between our theoretical Stark widths and the experimental data given by Bertuccelli & Di Rocco (1990) ($w_{\rm m}/w_{\rm th}$ vary from 0.73 up to 1.97). One should notice however, that they have not determined the electron density directly. They estimated the electron density by comparing the experimental widths of five selected lines with those obtained in Lesage et al. (1989) and Vitel & Skowronek (1987). The measured and calculated width ratios in the case of Uzelac & Konjević (1989), Brandt et al. (1981) and Vitel & Skowronek (1987) are well within the error bars of the modified semiempirical method (±50). This is the case for Lesage et al. (1989) as well, with the exception of the 461.9 nm line. Since all experimental data are within a narrow temperature range between 11000 K and 17400 K, where the Stark widths decrease quicker than for higher temperatures, it is significant to provide new reliable experimental data for higher temperatures in order to check the theoretical temperature dependence.

In Table 1, data are presented for each particular line within a multiplet. One should notice that the atomic energy level differences within the considered multiplets are comparable to the distances to the nearest perturbing level. Consequently, the line widths within a multiplet differ (Dimitrijević 1982). For example, for the lines $\lambda = 429.29$ nm ($5s^4P_{3/2} - 5p^4D^0_{3/2}$) and $\lambda = 476.57$ nm ($5s^4P_{3/2} - 5p^4D^0_{5/2}$), the lower ($5s^4P_{3/2}$) level is the same.

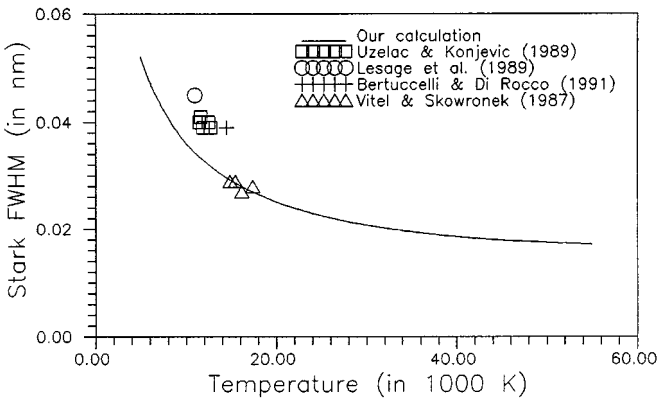

Fig. 1. Stark full-width (FWHM) for Kr II $\lambda = 465.9$ nm spectral line as a function of temperature, at an electron density of $N = 10^{23}$ m^{-3}

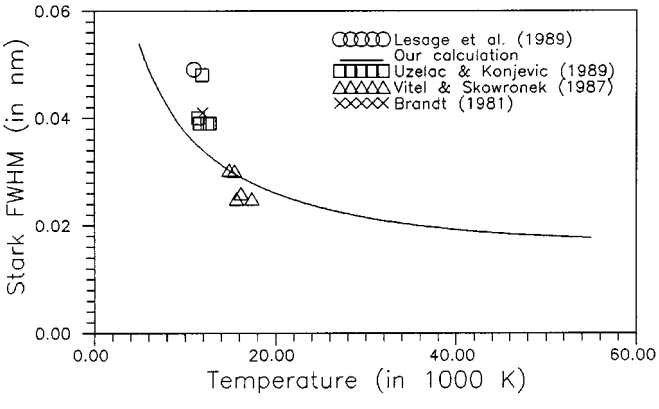

Fig. 2. Same as in Fig. 1, but for line $\lambda = 473.9$ nm

On the other hand, the upper level of the 476.57 line, i.e. $5p^4D^0_{5/2}$, is much closer to the 4d perturbing levels and especially to the $4d^4P_{5/2}$ and $4d^4P_{3/2}$ perturbing levels than the upper level ($5p^4D^0_{3/2}$) of the 429.29 nm line. Consequently, the 476.57 nm line width should be larger than the 429.29 nm line width. Indeed, the ratio of the corresponding widths is $w_{476.57}/w_{429.29} = 1.34$ from our calculations, $w_{476.57}/w_{429.29} = 1.7$ (Lesage et al. 1989) and $w_{476.57}/w_{429.29} = 1.16$ (Bertuccelli & Di Rocco 1991) from experiment.

The averaged value of the experimental and the theoretical data ratio is $w_{\rm exp}/w_{\rm th} = 1.25 \pm 0.05$, where the indicated error is an average quadratic error calculated in the same way as in Popović & Dimitrijević (1996a). If there are several values at different temperatures from the same reference for the same line, these values have been averaged before making an average ratio for the line. As one can see, the calculated Stark widths give a satisfactory agreement with experimental values on average.

The theoretical Stark widths for several lines are given in Bertuccelli & Di Rocco (1993). They have calculated Stark widths (only for $T = 10000$ and $N_{\rm e} = 10^{23}$ m^{-3}) by

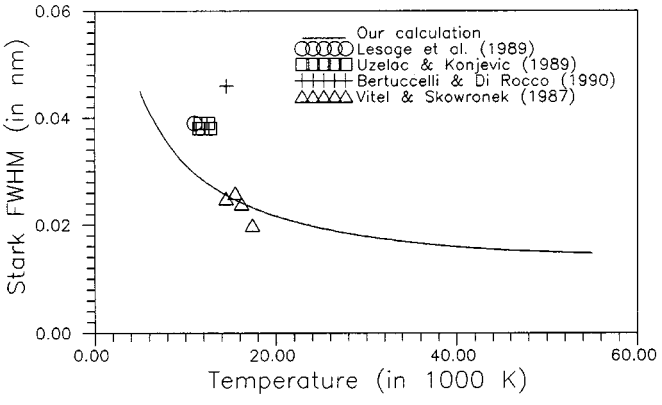

Fig. 3. Same as in Fig. 1, but for line $\lambda = 435.5$ nm

using Griem's semiempirical formula (Griem 1968) and by using the approach based on the Born approximation with and without the empirical modification for the collision strength suggested by Robb (see Bertuccelli & Di Rocco 1993). In Table 3 (accessible only in electronic form), we have compared our theoretical data with the theoretical data calculated by Bertucceli & Di Rocco (1993) and with the experimental data (Brandt et al. 1981; Vitel & Skowronek 1987; Uzelac & Konjević 1989; Lesage et al. 1989; Bertuccelli & Di Rocco 1991) for several lines. Data presented for a particular line are averaged if several values exist. As one can see, the ratios of calculations performed by Bertuccelli & Di Rocco (1993) and our calculations are 1.95, 1.76 and 1.56 for the calculations by using the approach based on the Born approximation with and without the empirical modification for the collision strength suggested by Robb and by using the Griem's semiempirical approach, respectively. Also, their calculations are significantly larger in comparison with experimental data.

There are Stark shift experimental data for three Kr II lines (Vitel & Skowronek 1987). The comparison between our calculations and experimental Stark shifts is shown in Table 4 (accessible only in electronic form). One should notice that the theoretical shifts are generally of lower accuracy than widths (see e.g. Dimitrijević et al. 1981; Popović et al. 1993). Namely, the contributions from different perturbing levels to the shift have different signs. If contributions with both signs are similar, shift accuracy is much lower. In view of these facts, the agreement between calculated and experimental shifts is satisfactory with the exception of the 435.55 nm line. The calculated data for Stark shifts can be obtained on request from the authors.

We hope that the presented data set on Kr II Stark widths will be of help for the analysis of the trace element spectral lines and abundances (especially by using spaceborne telescopes and instruments such as HST/GHRS), as well as for the investigation of regularities within homologous atom/ion sequences and their use for the interpolation of new data.

Acknowledgements. This work has been supported by the Ministry of Science and Technology of Serbia through the project "Astrometrical, Astrodynamical and Astrophysical Researches".

References

Bates D.R., Damgaard A., 1949, Trans. Roy. Soc. London, Ser A 242, 101
Bertuccelli D., Di Rocco H.O., 1991, Phys. Scr. 44, 138
Bertuccelli D., Di Rocco H.O., 1993, Phys. Scr. 47, 747
Brandt T., Helbig V., Nick K.P., 1981, Spectral line shapes, Wende B. (ed.). Berlin, W. de Gruyter
Cardelli J.A., Savage B.D., Ebbets D.C., 1991, ApJ 383, L23
Dimitrijević M.S., 1982, A&A 112, 251
Dimitrijević M.S., Feutrier N., Sahal-Bréchot S., 1981, J. Phys. B 14, 2559
Dimitrijević M.S., Konjević N., 1980, J. Quant. Spectrosc. Radiat. Transfer 24, 451
Dimitrijević M.S., Kršljanin V., 1986, A&A 165, 269
Dimitrijević M.S., Popović M.M., 1989, A&A 217, 201
Di Rocco H.O., 1990, J. Appl. Phys. 68, 3732
Griem R.H., 1968, Phys. Rev. 165, 258
Leckrone D.S., Wahlgren G.M., Johansson S.G., Adelman S.J., 1993, in Peculiar Versus Normal Phenomena in A-type and Related Stars, ASP Conf. Ser. 44, 42
Lesage A., Abadie D., Miller M.H., 1989, Phys. Rev. A 40, 1367
Pittman T.L., Konjević N., 1986, J. Quant. Spectrosc. Radiat. Transfer 35, 247
Popović L.Č., Dimitrijević M.S., 1996a, A&AS 116, 359
Popović L.Č., Dimitrijević M.S., 1996b, Phys. Scr. 53, 325
Popović L.Č., Vince I., Dimitrijević M.S., 1993, A&AS 102, 17
Purić J., Djeniže S., Labat J., Srećković A., Platiša M., 1991, Contrib. Plasma Phys. 31, 63
Seaton M.J., 1988, J. Phys. B: At. Mol. Opt. Phys. 21, 3033
Sugar J., Musgrove A., 1991, J. Phys. Chem. Ref. Data 20, 875
Uzelac N.I., Konjević N., 1989, J. Phys. B 22, 2517
Vitel Y., Skowronek, M. 1987, J. Phys. B 20, 6493

ASTRONOMY & ASTROPHYSICS
SUPPLEMENT SERIES

Astron. Astrophys. Suppl. Ser. **127,** 543-544 (1998)

Stark broadening of spectral lines of multicharged ions of astrophysical interest

XVI. S V spectral lines*

M.S. Dimitrijević[1] and S. Sahal-Bréchot[2]

[1] Astronomical Observatory, Volgina 7, 11050 Belgrade, Yugoslavia
[2] Laboratoire "Astrophysique, Atomes et Molécules", Département Atomes et Molécules en Astrophysique, Unité associée au CNRS No. 812, Observatoire de Paris-Meudon, 92190 Meudon, France

Received May 23; accepted May 27, 1997

Abstract. Using a semiclassical approach, we have calculated electron−, proton−, and He III−impact line widths and shifts for 34 S V multiplets for perturber densities $10^{17} - 10^{21}$ cm^{-3} and temperatures $T = 20\,000 - 1\,000\,000$ K. For lower perturber densities, the obtained results are linear with perturber density.

Key words: lines: profile — atomic data

1. Introduction

Stark widths and shifts of S V lines are of interest not only for the laboratory plasma research and for testing and developping of the Stark broadening theory for shapes of multicharged ion lines, but as well for the consideration of subphotosperic layers and atmospheres of hot stars. They are also of importance for the considerations of regularities and systematic trends particularly along isoelectronic sequences. Recently, S V spectral lines have been observed in spectra of some sdO stars (Rauch 1996). The relevant parameter range for the spectrum synthesis is for the electron density up to $N_e = 10^{17}$ cm^{-3} and the effective temperature $20\,000$ K $\leq T_{\rm eff} \leq 160\,000$ K. For such conditions, Stark broadening is the main pressure broadening mechanism, and toward the density of $N_e = 10^{17}$ cm^{-3} it becomes comparable with Doppler width or even dominant. Consequently, data on the shape of S V spectral lines are of interest for the modelling and interpretation of sdO star spectra, as well as for consideration and modelling of subphotospheric layers in other stars.

This paper is the sixteenth of a series devoted to the investigation of Stark broadening parameters of spectral lines of multicharged ions (see Dimitrijević & Sahal-Bréchot 1995 and references therein, as well as Dimitrijević & Sahal-Bréchot 1996a,b). In order to continue the attempt to provide to astrophysicists and plasma physicists Stark broadening parameters needed for the research of astrophysical and laboratory plasmas as well as plasmas in various plasma devices in technology, we have calculated within the semiclassical-perturbation formalism (Sahal-Bréchot 1969a,b), electron-, proton-, and He III-impact line widths and shifts for 34 S V multiplets.

2. Results and discussion

The original computer code (Sahal-Bréchot 1969a,b), has been modernized, updated and optimized several times (Sahal-Bréchot 1974; Fleurier et al. 1977; Dimitrijević & Sahal-Bréchot 1984; Dimitrijević et al. 1991; Dimitrijević & Sahal-Bréchot 1996b). A summary of the formalism is given in Dimitrijević & Sahal-Bréchot (1996b), and will not be repeated here. Atomic energy levels needed for calculations have been taken from Martin et al. (1990). Oscillator strengths have been calculated within the Coulomb approximation (Bates & Damgaard 1949, and the tables of Oertel & Shomo 1968). For higher levels, the method of Van Regemorter et al. (1979) has been used.

Our results for 34 S V multiplets are shown in Table 1 (accessible only in electronic form), for perturber densities $10^{17} - 10^{21}$ cm^{-3} and temperatures $T = 20\,000 - 1\,000\,000$ K. The complete set of data is given for the perturber density of 10^{18} cm^{-3}. For perturber density of 10^{17} cm^{-3}, only data for higher transitions, needed for better interpolation with perturber density are given. Stark broadening parameters for densities lover than tabulated, are linear with perturber density. We also specify a parameter c (Dimitrijević & Sahal-Bréchot 1984), which

* Table 1 is only available in electronic form: The material published electronically can be accessed: by ftp at cdsarc.u-strasbg.fr or 130.79.128.5 or on WWW at: http//cdsweb.u-strasbg.fr/abstract.html

gives an estimate for the maximum perturber density for which the line may be treated as isolated when it is divided by the corresponding full width at half maximum. For each value given in Table 1, the collision volume (V) multiplied by the perturber density (N) is much less than one and the impact approximation is valid (Sahal-Bréchot 1969a,b). Values for $NV > 0.5$ are not given and values for $0.1 < NV \leq 0.5$ are denoted by an asterisk. When the impact approximation is not valid, the ion broadening contribution may be estimated by using quasistatic approach (Sahal-Bréchot 1991 or Griem 1974). In the region between where neither of these two approximations is valid, a unified type theory should be used. For example in Barnard et al. (1974), a simple analytical formulas for such a case are given. The accuracy of the results obtained decreases when broadening by ion interactions becomes important.

We hope that presented results will be useful for the interpretation and modelling of sdO stars spectra as well as for subphotospheric layers research and for laboratory plasma considerations. For further development and rafinement of the Stark broadening theory for multicharged ion lineshapes, as well as for the investigation of regularities and systematic trends of Stark broadening parameters along isoelectronic sequences, the corresponding experimental data will be very useful.

Acknowledgements. This work is a part of the project "Astrometrical, Astrodynamical and Astrophysical Investigations", supported by Ministry of Science and Technology of Serbia.

References

Barnard A.J., Cooper J., Smith E.W., 1974, J. Quant. Spectrosc. Radiat. Transfer 14, 1025
Bates D.R., Damgaard A., 1949, Trans. Roy. Soc. London Ser. A 242, 101
Dimitrijević M.S., 1988a, Bul. Obs. Astron. Belgrade 139, 31
Dimitrijević M.S., 1988b, A&AS 76, 53
Dimitrijević M.S., Konjević N., 1980, J. Quant. Spectrosc. Radiat. Transfer 24, 451
Dimitrijević M.S., Konjević N., 1981, in Spectral Line Shapes, Wende B., de Gruyter W. (eds.). Berlin, New York, p. 211
Dimitrijević M.S., Sahal-Bréchot S., 1984, J. Quant. Spectrosc. Radiat. Transfer 31, 301
Dimitrijević M.S., Sahal-Bréchot S., Bommier V., 1991, A&AS 89, 581
Dimitrijević M.S., Sahal-Bréchot S., 1995, A&AS 109, 551
Dimitrijević M.S., Sahal-Bréchot S., 1996a, A&AS 115, 351
Dimitrijević M.S., Sahal-Bréchot S., 1996b, Phys. Scr. 54, 50
Fleurier C., Sahal-Bréchot S., Chapelle J., 1977, J. Quant. Spectrosc. Radiat. Transfer 17, 595
Griem H.R., 1968, Phys. Rev. 165, 258
Griem H.R., 1974, Spectral Line Broadening by Plasmas. Academic Press, New York
Martin W.C., Zalubas R., Musgrove A., 1990, J. Phys. Chem. Ref. Data 10, 821
Oertel G.K., Shomo L.P., 1968, ApJS 16, 175
Rauch T., 1996 (private communication)
Sahal-Bréchot S., 1969a, A&A 1, 91
Sahal-Bréchot S., 1969b, A&A 2, 322
Sahal-Bréchot S., 1974, A&A 35, 321
Sahal-Bréchot S., 1991, A&A 245, 322
Van Regemorter H., Hoang Binh Dy, Prud'homme M., 1979, J. Phys. B 12, 1073

ASTRONOMY & ASTROPHYSICS
SUPPLEMENT SERIES

Astron. Astrophys. Suppl. Ser. **128,** 203-205 (1997)

The electron impact broadening parameters in hot star atmospheres: Mn II, Mn III, Ga III, Ge III and Ge IV lines*

L.Č. Popović and M.S. Dimitrijević

Astronomical Observatory, Volgina 7, 11050 Beograd, Serbia, Yugoslavia

Received June 5; accepted June 6, 1997

Abstract. The electron - impact line widths and shifts for 16 Mn II, 3 Mn III, 10 Ga III, 8 Ge III and 14 Ge IV multiplets, have been considered within a modified semiempirical approach. Moreover, using a semiclassical approach, we have considered electron−, proton−, and He III-impact line widths and shifts for 3 Ge IV multiplets. The obtained results have been compared with other theoretical results.

Key words: lines: profile-atomic data — stars: chemically peculiar

1. Introduction

Lines of doubly- and triply-charged emitters are present in atmospheres of hot (A and B) stars ($T_{\rm eff} \gtrsim$10000 K) where Stark broadening mechanism is important. Moreover for such plasma conditions, it is the main pressure broadening mechanism. Also, as it was shown in Popović & Dimitrijević (1996a), in stellar atmospheres there exist conditions where Stark widths are comparable and even up to one order magnitude larger than the corresponding thermal Doppler widths. Consequently, Stark width data for a large number of transitions in many atomic and ionic spectra are needed for modeling of hot stellar plasma. Even in cooler stars, Stark broadening data for multicharged ion species may be of interest for the modeling of subphotospheric layers, for radiative transfer and opacity calculations, as well as for further developement of the physics of stellar interiors (Seaton 1987).

The increase of the number of spectral lines of astrophysical interest is additionally stimulated with the development of the space observations. Leckrone et al. (1993) investigating chemically peculiar stars with the Goddard High Resolution Spectrograph (GHRS) on the Hubble Space Telescope (HST) have found that "begining at $Z = 32$ (germanium) and extending to heavier elements, there is a dramatic increase in the magnitude of overabundance. All species between $Z = 32$ and $Z = 56$ analysed are overabundant relative to the Sun".

Here we present Stark broadening parameters for three ionized elements which lines are present in spectra of hot star atmospheres. Manganese is overabundant in atmospheres of Hg-Mn stars (Heacox 1979; Cowley 1980; Smith & Dworetsky 1993 etc.), and lines of singly and doubly charged manganese ions are observed in stellar atmospheres (Heacox 1979; Cowley 1980; Smith & Dworetsky 1993). Takada-Hidai et al. (1986) have analysed Ga II and Ga III lines in high resolved IUE spectra observed for 53 B and A stars and they have found an overabundance of gallium in the magnetic Si and Si Cr Eu stars, in the nonmagnetic Hg-Mn stars and in the He-weak PGa stars (for gallium overabundance analyses see also e.g. Heacox 1979 and Smith 1995). They have used for the spectrum synthesis models with $T_{\rm eff} = 11000$ K – 17000 K and $\log g = 3.5$, where the Stark broadening is the main pressure broadening mechanism and where the inclusion of this mechanism is of importance (Dimitrijević & Artru 1986). Moreover, Smith (1995) underlines the importance of gallium spectral lines for the detection of stratification effects in HgMn stars.

Spectral lines of germanium (Ge II, Ge III) are present in hot star spectra, as e.g. in β Ori (Selvelli et al. 1977) spectrum. They may be additionally of interest for stellar interior physics since germanium is commonly associated with slow-neutron capture nucleosynthesis (Leckrone et al. 1993).

In order to provide to astrophysicists the Stark broadening data needed for stellar spectra analysis and synthesis as well as for astrophysical and physical plasmas research and modelling, an effort has been made (see Dimitrijević 1996 and references therein) to obtain the

Send offprint requests to: L.Č. Popović

* Tables 1-4 are only available in electronic form via anonymous ftp 130.79.128.5 at the CDS in Strasbourg or via http://cdsweb.u-strasbg.fr/Abstract.html

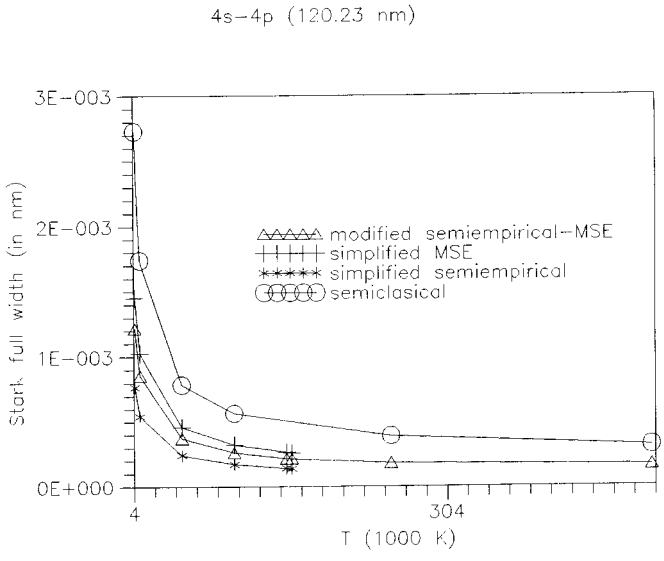

Fig. 1. Stark full widths for $4s^2S - 4p^2P^0$ transition of Ge IV calculated by using different approximations, as functions of temperature. The electron density is 10^{23} m^{-3}

needed data within the semiclassical perturbation approach, developed by Sahal-Bréchot (1969a,b) and improved and updated several times (Sahal-Bréchot 1974; Fleurier et al. 1977; Dimitrijević & Sahal-Bréchot 1984 1995; Dimitrijević et al. 1991). In the case where the semiclassical perturbation approach is not applicable with an appropriate accuracy due to the lack of reliable atomic energy levels data, the simpler, modified semiempirical approach (Dimitrijević & Konjević 1980) has been applied.

Table 5. Stark widths for Mn II $a^5D - z^5P^0$ multiplet obtained by using different approximations (Dimitrijević 1982). Used notation: $W_{\rm MSE}$ – calculation with the modified semiempirical approach (Dimitrijević & Konjević 1980), $W_{\rm SE}$ – semiempirical approach (Griem 1968), $W_{\rm SC}$ – semiclassical theory of Jones et al. (1971)

Transition	T (K)	$W_{\rm SEM}$(nm)	$W_{\rm SE}$(nm)	$W_{\rm SC}$(nm)
$a^5D - z^5P^0$	2500	.0246	.0166	.0266
Mn II	5000	.0174	.0117	.0190
$\overline{\lambda} = 346.4$ nm	10000	.0123	.0083	.0144
	20000	.00870	.00587	.0114

Here we have calculated within the semiclassical perturbation formalism (Sahal-Bréchot 1969a,b) electron-, proton-, and He III-impact line widths and shifts for 3 Ge IV lines. Moreover, Stark widths and shifts for 16 Mn II, 3 Mn III, 7 Ga III, 8 Ge III and 13 Ge IV lines for which there is not a set of reliable atomic energy level data sufficiently complete to achieve the appropriate accuracy of the semiclassical perturbation method, have been calculated within the modified semiempirical approach (Dimitrijević & Konjević 1980 and for ions with complex spectra see also Popović & Dimitrijević 1996b).

Table 6. Same as in Table 5, but for Ga III $4s^2S - 4p^2P^0$ multiplet (Dimitrijević & Artru 1986). $W_{\rm G}$ – aproximate semiclassical method (Griem 1974)

Transition	T (K)	$W_{\rm SEM}$(nm)	$W_{\rm SE}$(nm)	W_G(nm)
$4s^2S - 4p^2P^0$	2500	.00325	.00229	.00436
Ga III	5000	.00230	.00162	.00311
$\overline{\lambda} = 150.8$ nm	10000	.00163	.00114	.00223
	20000	.00115	.000808	.00163
	40000	.000814	.000571	.00123

2. Results and discussion

Summaries of the semiclassical perturbation formalism (Sahal-Bréchot 1969a,b) and of the modified semiempirical formalism (Dimitrijević & Konjević 1980) are given in Dimitrijević & Sahal-Bréchot (1995) and Popović & Dimitrijević (1996b) and will not be repeated here. The atomic energy levels needed for calculations were taken from Bashkin & Stoner (1987) for Mn II, Moore (1971) for Mn III, Ryabtsev & Wyart (1987) and Isberg & Litzén (1986) for Ga III, Sugar & Musgrove (1993) for Ge III, and in Ryabtsev & Wyart (1987) and Sugar & Musgrove (1993) for Ge IV. Oscillator strengths have been calculated by using the method of Bates & Damgaard (1949) and the tables of Oertel & Shomo (1968). For higher levels, the method described by Van Regemorter et al. (1979) has been used.

Results obtained within the modified semiempirical approach – MSE (Dimitrijević & Konjević 1980) for electron − impact line widths and shifts for 16 Mn II, 3 Mn III, 10 Ga III, 8 Ge III and 14 Ge IV multiplets as a function of temperature are presented in Tables 1 – 3 (accessibles only in electronic form). The calculations were performed for the perturber density of 10^{23} m^{-3}. Within the used approach, results for electron-impact broadening parameters are linear with electron density. For three lines of Ge IV it is possible to calculate Stark broadening parameters within the semiclassical perturbation approach (Sahal-Bréchot 1969a,b). For electron−, proton−, and He III-impact line widths and shifts for 3 Ge IV multiplets for the perturber densities of $10^{23} - 10^{26}$ m^{-3} and temperatures $T = 5000 - 500000$ K, are shown in Table 4 (accessible only in electronic form). For electron densities lower than tabulated, a linear interpolation with density is sufficient. We also specify a parameter C (Dimitrijević & Sahal-Bréchot 1984), which gives an estimate for the maximum perturber density for which the line may be treated as isolated when it is divided by the corresponding full width at half maximum. For each value given

in Table 1, the collision volume (V) multiplied by the perturber density (N) is much less than one and the impact approximation is valid (Sahal-Bréchot 1969a,b). Values for $NV > 0.5$ are not given and values for $0.1 < NV \leq 0.5$ are denoted by an asterisk. For higher densities, when the impact approximation is not valid, the ion broadening contribution may be estimated by using quasistatic approach (Sahal-Bréchot 1991 or Griem 1974). In the region between where neither of these two approximations is valid, a unified type theory should be used. For example in Barnard et al. (1974), simple analytical formulas for such a case are given. The accuracy of the results decreases when broadening by ion interactions becomes important. As an illustration, in Fig. 1. we have compared Stark widths calculated by using the semiclassical, MSE, simplified MSE and Griem's semiempirical appraoch.

In the case of these ions there is not measured Stark broadening parameters. For Mn II $a^5D - z^5P^0$ transition Dimitrijević (1982) performed calculations by using the MSE, Griem's semiempirical approach – SE (Griem 1968) and semiclassical approach of Griem (see Jones et al. 1971; Griem 1974). Since these data complete MSE results for Mn II they are shown here in Table 5, together with semiempirical and semiclassical results. The MSE results are in good agreement with more sophisticated semiclassical calculations. For Ga III $4s^2S - 4p^2P^0$ multiplet calculations by using the MSE and the SE approach as well as calculations by using approximate semiclassical method (Griem 1974) and the modification of this method (Dimitrijević & Konjević 1980) were performed by Dimitrijević & Artru (1986). For this multiplet calculations within the SE approach are given in Purić et al. (1978) as well. Results according to the approximate semiclassical method are slightly larger than MSE results and results obtained by the modification of approximate semiclassical method which are in good agreement.

Also, for Mn II $a^7S - z^7P^0$ multiplet, width and shift estimated on the basis of Stark broadening parameters dependence on ionized potential from the lower level of the corresponding transition exist as well (Lakićević 1983). For an electron density of 10^{23} m^{-3} and an electron temperature of 20000 K, Lakićević obtains $W_{\rm L} = 0.008$ nm and $|d|_{\rm L} = 0.0036$ nm, while our results are $W_{\rm MSE} = 0.0041$ nm and $|d|_{\rm MSE} = 0.00093$ nm.

We hope that Stark broadening data presented here will be of interest for space spectroscopy and for chemically peculiar star research as well as for laboratory plasma spectroscopy. Experimental data for considered ion lines will be of interest for the discussion and developement of Stark broadening theory for heavier emitters with more complex spectra.

Acknowledgements. This work is a part of the project "Astrometrical, Astrodynamical and Astrophysical Investigations", supported by Ministry of Science and Technology of Serbia.

References

Barnard A.J., Cooper J., Smith E.W., 1974, J. Quant. Spectrosc. Radiat. Transfer 14, 1025
Bashkin S., Stoner J.O., 1987, Atomic energy levels and Grotrian diagrams 2. North-Holland Publishing Company, Amsterdam, Oxford, New York
Bates D.R., Damgaard A., 1949, Phil. Trans. Roy. Soc. London, Ser. A 242, 101
Cowley C.R., 1980, PASP 92, 159
Dimitrijević M.S., 1982, in: Sun and Planetary System, Fricke W. and Teleki G. (eds.). D. Reidel Publishing Company, p. 101
Dimitrijević M.S., 1996, Zh. Prikl. Spektrosk. 63, 810
Dimitrijević M.S., Artru M.-C., 1986, The Physics of Ionized Gases, Contributed papers of SPIG'86, Šibenik, Kurepa M.V. (ed.), Dept. of Physics and Meteorology, University of Belgrade, p. 317
Dimitrijević M.S., Konjević N., 1980, J. Quant. Spectrosc. Radiat. Transfer 24, 451
Dimitrijević M.S., Sahal-Bréchot S., 1984, J. Quant. Spectrosc. Radiat. Transfer 31, 301
Dimitrijević M.S., Sahal-Bréchot, S., 1995, Phys. Scr. 52, 41
Dimitrijević M.S., Sahal-Bréchot S., Bommier V., 1991, A&AS 89, 581
Griem H.R., 1968, Phys. Rev. 165, 258
Griem H.R., 1974, Spectral Line Broadening by Plasmas. Academic Press, New York
Fleurier C., Sahal-Bréchot S., Chapelle J., 1977, J. Quant. Spectrosc. Radiat. Transfer 17, 595
Heacox W.D., 1979, ApJS 41, 675
Isberg B., Litzén U., 1986, Phys. Scr. 33, 420
Jones W.W., Benett S.M., Griem H.R., Univ. of Meryland Techn. Rep. No 1971-128, College Park, Maryland
Lakićevć I.S., 1983, A&A 127, 37
Leckrone D.S., Wahlgren G.M., Johansson S.G., Adelman S.J., 1993, in Peculiar versus Normal Phenomena in A-Type and Related Stars, Dworetsky M.M., Castelli F., Faraggiana R. (eds.), ASP Conf. Ser. 44, 42
Migdalek By.J., 1997, Acta Phys. Polonica A52, 465
Moore C.E., 1971, Atomic Energy Levels, NSRDS- NBS, Vol. 2, Washington D.C.
Oertel G.K., Shomo L.P., 1968, ApJS 16, 175
Popović L.Č., Dimitrijević M.S., 1996a, A&AS 120, 373
Popović L. Č., Dimitrijević M.S., 1996b, Phys. Scr. 53, 325
Purić J., Dimitrijević M.S., Lakićević I.S., 1978, Phys. Lett. 67A, 189
Ryabtsev A.N., Wyart J.-F., 1987, Phys. Scr. 36, 255
Sahal-Bréchot S., 1969a, A&A 1, 91
Sahal-Bréchot S., 1969b, A&A 2, 322
Sahal-Bréchot S., 1974, A&A 35, 321
Seaton M.J., 1987, J. Phys. B 20, 6363
Selvelli P.L., Crivellari L., Stalio R., 1977, A&AS 27, 1
Smith K.C., 1995, A&A 297, 237
Smith K.C., Dworetsky M.M., 1993, A&A 274, 335
Sugar J., Musgrove A., 1993, J. Phys. Chem. Ref. Data 22, 1238
Takada-Hidai M., Sadakane K., Jugaku J., 1986, ApJ 304, 425
Van Regemorter H., Hoang Binh Dy, Prud'homme M., 1979, J. Phys. B 12, 1073

ASTRONOMY & ASTROPHYSICS
SUPPLEMENT SERIES

Astron. Astrophys. Suppl. Ser. **128,** 359-360 (1998)

Stark broadening of spectral lines of multicharged ions of astrophysical interest

XVII. Ca IX and Ca X spectral lines*

M.S. Dimitrijević[1] and S. Sahal-Bréchot[2]

[1] Astronomical Observatory, Volgina 7, 11050 Belgrade, Yugoslavia
[2] Laboratoire "Astrophysique, Atomes et Molécules", Département Atomes et Molécules en Astrophysique, Unité associée au CNRS No. 812, Observatoire de Paris−Meudon, 92190 Meudon, France

Received July 2; accepted July 10, 1997

Abstract. Using a semiclassical approach, we have calculated electron−, proton−, and He III−impact line widths and shifts for 4 Ca IX multiplets for perturber densities $10^{18} - 10^{22}$ cm^{-3} and 48 Ca X multiplets for perturber densities $10^{17} - 10^{22}$ cm^{-3}. In both cases the temperature range is $T = 200000 - 5000000$ K. For lower perturber densities, obtained results are linear with perturber density.

Key words: lines: profile-atomic data — plasmas

1. Introduction

Stark widths and shifts of Ca IX and Ca X lines are obviously of interest for the laboratory plasmas, fusion plasmas and laser produced plasmas research as well as for testing and developing of the Stark-broadening theory for multicharged ion lines. Due to the abundance of calcium, such data are of interest for the consideration of solar and stellar plasma, particularly for subphotospheric layers, as well as for radiative transfer considerations. They are also of importance for the investigations of regularities and systematic trends particularly along isoelectronic sequences.

This paper is the seventeenth of a series devoted to the investigation of Stark broadening parameters of spectral lines of multicharged ions (see Dimitrijević & Sahal-Bréchot 1995 and references therein, as well as Dimitrijević & Sahal-Bréchot 1996a,b, 1997). As the continuation of our work with the objective to provide to astrophysicists and plasma physicists Stark broadening parameters needed for research on astrophysical and laboratory plasmas, we have calculated within the semiclassical-perturbation formalism (Sahal-Bréchot 1969a,b), electron-, proton-, and He III-impact line widths and shifts for 4 Ca IX and 48 Ca X multiplets.

2. Results and discussion

The semiclassical perturbation formalism and the relevant computer code (Sahal-Bréchot 1969a,b) used here, have been modernized, updated and optimized several times (Sahal-Bréchot 1974; Fleurier et al. 1977; Dimitrijević & Sahal-Bréchot 1984; Dimitrijević et al. 1991; Dimitrijević & Sahal-Bréchot 1996b). The used formalism has been reviewed e.g. in Dimitrijević & Sahal-Bréchot (1996c) and Dimitrijević (1996). The atomic energy levels of Ca IX and Ca X needed for calculations have been taken from Bashkin & Stoner (1975). The oscillator strengths have been calculated within the Coulomb approximation (Bates & Damgaard 1949, and the tables of Oertel & Shomo 1968). For higher levels, the method of Van Regemorter et al. (1979) has been used.

Our results for electron−, proton−, and He III−impact line widths and shifts for 4 Ca IX multiplets for perturber densities $10^{18} - 10^{22}$ cm^{-3} and 48 Ca X multiplets for perturber densities $10^{17} - 10^{22}$ cm^{-3}, for the electron temperatures $T = 200000 - 5000000$ K, are shown in Table 1 (accessible only in electronic form). The complete set of data is given for the perturber density of 10^{19} cm^{-3} for Ca IX and 10^{17} cm^{-3} for Ca X. For lower tabulated perturber densities, only data for higher transitions, needed for better interpolation are given. Stark broadening parameters for densities lower than tabulated, are linear with perturber density. We also specify a parameter c (Dimitrijević & Sahal-Bréchot 1984), which gives an estimate for the maximum perturber density for which the

Send offprint requests to: M.S. Dimitrijević

* Table 1 is only available in electronic form: The material published electronically can be accessed: by ftp at cdsarc.u-strasbg.fr or (130.79.128.5) or on WWW at: http://cdsweb.u-strasbg.fr/Abstract.html

line may be treated as isolated when it is divided by the corresponding full width at half maximum. For each value given in Table 1, the collision volume (V) multiplied by the perturber density (N) is much less than one and the impact approximation is valid (Sahal-Bréchot 1969a,b). Values for $NV > 0.5$ are not given and values for $0.1 < NV \leq 0.5$ are denoted by an asterisk. When the impact approximation is not valid, the ion broadening contribution may be estimated by using the quasistatic approach (Sahal-Bréchot 1991 or Griem 1974). In the region between where neither of these two approximations is valid, a unified type theory should be used. For example in Barnard et al. (1974), simple analytical formulas for such a case are given. The accuracy of the results obtained decreases when broadening by ion interactions becomes important.

We hope the presented results will be useful for the modelling and research of subphotospheric layers and that considerations of radiation transfer, as well as for laboratory plasma investigations. Besides the theoretical data, reliable experimental data will be of significance for further development and refinement of the Stark broadening theory for multicharged ion lineshapes, as well as for the investigation of regularities and systematic trends of Stark broadening parameters along isoelectronic sequences.

Acknowledgements. This work is a part of the project "Astrometrical, Astrodynamical and Astrophysical Investigations", supported by Ministry of Science and Technology of Serbia.

References

Barnard A.J., Cooper J., Smith E.W., 1974, J. Quant. Spectrosc. Radiat. Transfer 14, 1025
Bashkin S., Stoner J.O. Jr., 1975, Atomic Energy Levels and Grotrian Diagrams, Vol. 1, North Holland, Amsterdam
Bates D.R., Damgaard A., 1949, Trans. Roy. Soc. London, Ser. A 242, 101
Dimitrijević M.S., 1996, Zh. Prikl. Spektrosk. 63, 810
Dimitrijević M.S., Sahal-Bréchot S., 1984, J. Quant. Spectrosc. Radiat. Transfer 31, 301
Dimitrijević M.S., Sahal-Bréchot S., Bommier V., 1991, A&AS 89, 581
Dimitrijević M.S., Sahal-Bréchot S., 1995, A&AS 109, 551
Dimitrijević M.S., Sahal−Bréchot S., 1996a, A&AS 115, 351
Dimitrijević M.S., Sahal-Bréchot S., 1996b, A&AS 119, 369
Dimitrijević M.S., Sahal-Bréchot S., 1996c, Phys. Scripta 54, 50
Dimitrijević M.S., Sahal-Bréchot S., 1997, A&AS 122, 533
Fleurier C., Sahal-Bréchot S., Chapelle J., 1977, J. Quant. Spectrosc. Radiat. Transfer 17, 595
Griem H.R., 1974, Spectral Line Broadening by Plasmas. Academic Press, New York
Oertel G.K., Shomo L.P., 1968, ApJS 16, 175
Sahal-Bréchot S., 1969a, A&A 1, 91
Sahal-Bréchot S., 1969b, A&A 2, 322
Sahal-Bréchot S., 1974, A&A 35, 321
Sahal-Bréchot S., 1991, A&A 245, 322
Van Regemorter H., Hoang Binh Dy, Prud'homme M., 1979, J. Phys. B 12, 1073

ASTRONOMY & ASTROPHYSICS
SUPPLEMENT SERIES

Astron. Astrophys. Suppl. Ser. **129,** 155-156 (1998)

Stark broadening of spectral lines of multicharged ions of astrophysical interest

XVIII. Si XI and Si XIII spectral lines*

M.S. Dimitrijević[1] and S. Sahal-Bréchot[2]

[1] Astronomical Observatory, Volgina 7, 11050 Belgrade, Yugoslavia
[2] Laboratoire "Astrophysique, Atomes et Molécules", Département Atomes et Molécules en Astrophysique, Unité associée au CNRS 812, Observatoire de Paris-Meudon, 92190 Meudon, France

Received August 18; accepted September 3, 1997

Abstract. Using a semiclassical perturbation approach, we have calculated electron−, proton−, and He III−impact line widths and shifts for 4 Si XI multiplets for perturber densities 10^{18}− 10^{23} cm^{-3} and temperatures $T = 500\,000 - 4\,000\,000$ K, and for 61 Si XIII multiplets for perturber densities 10^{16}− 10^{23} cm^{-3} and temperatures $T = 500\,000 - 6\,000\,000$ K. For lower perturber densities, obtained results are linear with perturber density.

Key words: lines: profile — atomic data — plasmas

1. Introduction

Silicon is present in stellar atmospheres and important for the consideration of physical processes in stellar plasmas. Data on its spectral lines, as well as on spectral lines from its various ionization stages are consequently of particular astrophysical interest. Stark broadening parameters of Si XI and Si XIII spectral lines are important not only for astrophysics, as e.g. for the consideration of radiative transfer through subphotospheric layers, but also for the fusion plasmas and laser produced plasmas research. The development of soft X-ray lasers, where Stark broadening data are needed to calculate gain values, model radiation trapping and to consider photoresonant pumping schemes (see e.g. Griem & Moreno 1990; Fill & Schöning 1994), provided an additional interest for such results.

This paper is the eighteenth of a series devoted to the investigation of Stark broadening parameters of spectral lines of multicharged ions (see Dimitrijević & Sahal-Bréchot 1995 and references therein, as well as Dimitrijević & Sahal-Bréchot 1996a,b, 1997a,b). As a continuation of our programme (see e.g. Dimitrijević 1996) to obtain as large as possible set of reliable Stark broadening data needed for the consideration and modeling of astrophysical and laboratory plasmas as well as laser produced and fusion plasmas, and plasmas in various plasma devices in technology, we have calculated within the semiclassical-perturbation formalism (Sahal-Bréchot 1969a,b), electron-, proton-, and He III-impact line widths and shifts for 4 Si XI and 61 Si XIII multiplets. These data, together with Stark broadening data for Si IV (Dimitrijević et al. 1991b,c) and Si XII (Dimitrijević & Sahal-Bréchot 1993, 1994) will complete availlable results of large-scale Stark broadening calculations for multicharged silicon ion lines.

2. Results and discussion

The semiclassical perturbation formalism applied here as well as the corresponding computer code (Sahal-Bréchot 1969a,b), have been updated and improved several times (Sahal-Bréchot 1974; Fleurier et al. 1977; Dimitrijević & Sahal-Bréchot 1984; Dimitrijević et al. 1991a; Dimitrijević & Sahal-Bréchot 1996b). The semiclassical perturbation method used here, has been reviewed e.g. in Dimitrijević & Sahal-Bréchot (1996c) and Dimitrijević (1996). Atomic energy levels of Si XI and Si XIII needed for calculations, have been taken from Martin & Zalubas (1983). Oscillator strengths have been calculated within the Coulomb approximation (Bates & Damgaard 1949, and the tables of Oertel & Shomo 1968). For higher levels, the method of Van Regemorter et al. (1979) has been used.

Our results for electron−, proton−, and He III−impact line widths and shifts for 4 Si XI and 61 Si XIII multiplets are shown in Table 1 (accessible only in electronic form), for perturber densities $10^{18} - 10^{23}$ cm^{-3} and

Send offprint requests to: M.S. Dimitrijević

* Table 1 is only available in electronic form: The material published electronically can be accessed: by ftp at cdsarc.u-strasbg.fr or 130.79.128.5 or on WWW at: http//cdsweb.u-strasbg.fr/Abstract.html

$10^{16} - 10^{23}$ cm^{-3} respectively. The temperature range is $T = 500\,000 - 4\,000\,000$ K for Si XI and $500\,000 - 6\,000\,000$ K for Si XIII. For Si XIII, the complete set of data is given for the perturber density of 10^{19} cm^{-3}. For lower densities, only data needed for better interpolation are given. Stark broadening parameters for densities lover than tabulated, or for transitions not tabulated for perturber densities lower than 10^{19} cm^{-3} for Si XIII, are linear with perturber density. We present in the Table 1 as well, a parameter c (Dimitrijević & Sahal-Bréchot 1984), which gives an estimate for the maximum perturber density for which the line may be treated as isolated when it is divided by the corresponding full width at half maximum. For each value given in Table 1, the collision volume (V) multiplied by the perturber density (N) is much less than one and the impact approximation is valid (Sahal-Bréchot 1969a,b). Values for $NV > 0.5$ are not given and values for $0.1 < NV \leq 0.5$ are denoted by an asterisk. When the impact approximation is not valid, the ion broadening contribution may be estimated by using quasistatic approach (Sahal-Bréchot 1991 or Griem 1974). In the region between where neither of these two approximations is valid, a unified type theory should be used. For example in Barnard et al. (1974), a simple analytical formulas for such a case are given. The accuracy of the results obtained decreases when broadening by ion interactions becomes important.

Presented results may be of interest for the modelling and research of subphotospheric layers and the considerations of radiation transfer in stellar, fusion and laser produced plasmas, as well as for the investigation and modeling of soft X-ray lasers. They may be of significance as well for further development and rafinement of the Stark broadening theory for multicharged ion lineshapes, as well as for the investigation of regularities and systematic trends of Stark broadening parameters along isoelectronic sequences. The corresponding reliable experimental data will be certainly of particular interest.

Acknowledgements. This work is a part of the project "Astrometrical, Astrodynamical and Astrophysical Investigations", supported by Ministry of Science and Technology of Serbia.

References

Barnard A.J., Cooper J., Smith E.W., 1974, J. Quant. Spectrosc. Radiat. Transfer 14, 1025
Bates D.R., Damgaard A., 1949, Trans. Roy. Soc. London Ser. A 242, 101
Dimitrijević M.S., 1996, Zh. Prikl. Spektrosk. 63, 810
Dimitrijević M.S., Sahal-Bréchot S., 1984, J. Quant. Spectrosc. Radiat. Transfer 31, 301
Dimitrijević M.S., Sahal-Bréchot S., Bommier V., 1991a, A&AS 89, 581
Dimitrijević M.S., Sahal-Bréchot S., Bommier V., 1991b, A&AS 89, 591
Dimitrijević M.S., Sahal-Bréchot S., Bommier V., 1991c, Bull. Obs. Astron. Belgrade 144, 81
Dimitrijević M.S., Sahal-Bréchot S., 1995, A&AS 109, 551
Dimitrijević M.S., Sahal-Bréchot S., 1993, Bull. Astron. Belgrade 148, 21
Dimitrijević M.S., Sahal-Bréchot S., 1994, A&AS 105, 245
Dimitrijević M.S., Sahal-Bréchot S., 1996a, A&AS 115, 351
Dimitrijević M.S., Sahal-Bréchot S., 1996b, A&AS 119, 369
Dimitrijević M.S., Sahal-Bréchot S., 1996c, Phys. Scr. 54, 50
Dimitrijević M.S., Sahal-Bréchot S., 1997a, A&AS 122, 533
Dimitrijević M.S., Sahal-Bréchot S., 1997b, A&AS (in press)
Fill E.E., Schöning T., 1994, J. Appl. Phys. 76, 1423
Fleurier C., Sahal-Bréchot S., Chapelle J., 1977, J. Quant. Spectrosc. Radiat. Transfer 17, 595
Griem H.R., 1974, Spectral Line Broadening by Plasmas. Academic Press, New York
Griem H.R., Moreno J.C., 1990, in: X-ray Lasers, Tallents G. (ed.), Institute of Physics, Bristol, p. 301
Martin W.C., Zalubas R., 1983, J. Phys. Chem. Reference Data 12, 323
Oertel G.K., Shomo L.P., 1968, ApJS 16, 175
Sahal-Bréchot S., 1969a, A&A 1, 91
Sahal-Bréchot S., 1969b, A&A 2, 322
Sahal-Bréchot S., 1974, A&A 35, 321
Sahal-Bréchot S., 1991, A&A 245, 322
Van Regemorter H., Hoang Binh Dy, Prud'homme M., 1979, J. Phys. B 12, 1073

ASTRONOMY & ASTROPHYSICS
SUPPLEMENT SERIES

JUNE II **1998**, PAGE 539

Astron. Astrophys. Suppl. Ser. **130**, 539–540 (1998)

Stark broadening of spectral lines of multicharged ions of astrophysical interest

XIX. Na X spectral lines*

M.S. Dimitrijević[1] **and S. Sahal–Bréchot**[2]

[1] Astronomical Observatory, Volgina 7, 11050 Belgrade, Yugoslavia
[2] Laboratoire "Astrophysique, Atomes et Molécules", Département Atomes et Molécules en Astrophysique, Unité associée au CNRS 812, Observatoire de Paris–Meudon, 92190 Meudon, France

Received December 17; accepted December 18, 1997

Abstract. Using a semiclassical perturbation approach, we have calculated electron−, proton−, and He III−impact line widths and shifts for 57 Na X multiplets for perturber densities $10^{17}-10^{24}$ cm^{-3} and temperatures $T = 200\,000 - 5\,000\,000$ K. For lower perturber densities, the Stark broadening parameters are proportional to the perturber density.

Key words: lines: profile-atomic data

1. Introduction

Data on the sodium spectral lines, as well as on spectral lines from its various ionization stages are important not only for astrophysics, as e.g. for the consideration of radiative transfer through subphotospheric layers, but also for the fusion plasmas and laser-produced plasmas research. An additional interest for such results provides the development of soft X-ray lasers, where Stark broadening data are needed to calculate gain values, model radiation trapping and to consider photoresonant pumping schemes (see e.g. Griem & Moreno 1990; Fill & Schöning 1994), provided an additional interest for such results.

This paper is the nineteenth of a series devoted to the research of Stark broadening parameters of spectral lines of multicharged ions (see Dimitrijević & Sahal–Bréchot 1995 and references therein, as well as Dimitrijević & Sahal–Bréchot 1996a,b, 1997, 1998a-c). In accordance with our project (see e.g. Dimitrijević 1996) to obtain as large as possible set of reliable Stark broadening data needed for the consideration and modeling of astrophysical, laboratory, laser-produced, fusion plasmas, and plasmas in various devices, we have calculated within the semiclassical-perturbation formalism (Sahal–Bréchot 1969a,b), electron-, proton-, and He III-impact line widths and shifts for 57 Na X multiplets.

2. Results and discussion

Calculations have been performed within the frame of the semiclassical perturbation formalism, which, as well as the corresponding computer code (Sahal–Bréchot 1969a,b), have been updated and improved several times (Sahal–Bréchot 1974; Fleurier et al. 1977; Dimitrijević & Sahal–Bréchot 1984; Dimitrijević et al. 1991; Dimitrijević & Sahal–Bréchot 1996b). Short reviews of the semiclassical perturbation method used here, have been published several times as e.g. in Dimitrijević & Sahal–Bréchot (1996c) and Dimitrijević (1996). The atomic energy levels of Na X needed for calculations, have been taken from Martin & Zalubas (1981). The oscillator strengths have been calculated within the Coulomb approximation (Bates & Damgaard 1949, and the tables of Oertel & Shomo 1968). For higher levels, the method of Van Regemorter et al. (1979) has been used.

Our results for electron−, proton−, and He II−impact line widths and shifts for 57 Na X multiplets are shown in Table 1 (accessible only in electronic form), for perturber densities $10^{17} - 10^{24}$ cm^{-3} and temperatures $T = 200\,000 - 5\,000\,000$ K. The complete set of data is given for the perturber density of 10^{19} cm^{-3}, while for lower densities, only data needed for better interpolation are given. Stark broadening parameters for densities lower

Send offprint requests to: M.S. Dimitrijević

* Table 1 is only available in electronic form: The material published electronically can be accessed: by ftp at cdsarc.u-strasbg.fr or 130.79.128.5 or on WWW at: http//cdsweb.u-strasbg.fr/Abstract.html

than tabulated, or for transitions not tabulated for perturber densities lower than 10^{19} cm^{-3}, are proportional to the perturber density. We present in Table 1 as well, a parameter c (Dimitrijević & Sahal−Bréchot 1984), which gives an estimate for the maximum perturber density for which the line may be treated as isolated, when it is divided by the corresponding full width at half maximum. For each value given in Table 1, the collision volume (V) multiplied by the perturber density (N) is much less than one and the impact approximation is valid (Sahal–Bréchot 1969a,b). Values for $NV > 0.5$ are not given and values for $0.1 < NV \leq 0.5$ are denoted by an asterisk. When the impact approximation is not valid, the ion broadening contribution may be estimated by using the quasistatic approach (Sahal–Bréchot 1991 or Griem 1974). In the region between where neither of these two approximations is valid, a unified type theory should be used. For example in Barnard et al. (1974), a simple analytical formula for such a case is given. The accuracy of the results obtained decreases when broadening by ion interactions becomes important.

Acknowledgements. This work is a part of the project "Astrometrical, Astrodynamical and Astrophysical Investigations", supported by Ministry of Science and Technology of Serbia.

References

Barnard A.J., Cooper J., Smith E.W., 1974, J. Quant. Spectrosc. Radiat. Transfer 14, 1025
Bates D.R., Damgaard A., 1949, Trans. Roy. Soc. London, Ser. A 242, 101
Dimitrijević M.S., 1996, Zh. Prikl. Spektrosk. 63, 810
Dimitrijević M.S., Sahal–Bréchot S., 1984, J. Quant. Spectrosc. Radiat. Transfer 31, 301
Dimitrijević M.S., Sahal–Bréchot S., Bommier V., 1991, A&AS 89, 581
Dimitrijević M.S., Sahal–Bréchot S., 1995, A&AS 109, 551
Dimitrijević M.S., Sahal–Bréchot S., 1996a, A&AS 115, 351
Dimitrijević M.S., Sahal–Bréchot S., 1996b, A&AS 119, 369
Dimitrijević M.S., Sahal–Bréchot S., 1996c, Phys. Scri. 54, 50
Dimitrijević M.S., Sahal–Bréchot S., 1997, A&AS 122, 533
Dimitrijević M.S., Sahal–Bréchot S., 1998a, A&AS 127, 543
Dimitrijević M.S., Sahal–Bréchot S., 1998b, A&AS 128, 359
Dimitrijević M.S., Sahal–Bréchot S., 1998c, A&AS 129, 155
Fill E.E., Schöning T., 1994, J. Appl. Phys. 76, 1423
Fleurier C., Sahal–Bréchot S., Chapelle J., 1977, J. Quant. Spectrosc. Radiat. Transfer 17, 595
Griem H.R., 1974, Spectral Line Broadening by Plasmas. Academic Press, New York
Griem H.R., Moreno J.C., 1990, in: X-Ray Lasers, Tallents G. (ed.). Institute of Physics, Bristol, p. 301
Martin W.C., Zalubas R., 1981, J. Phys. Chem. Ref. Data 10, 153
Oertel G.K., Shomo L.P., 1968, ApJS 16, 175
Sahal–Bréchot S., 1969a, A&A 1, 91
Sahal–Bréchot S., 1969b, A&A 2, 322
Sahal–Bréchot S., 1974, A&A 35, 321
Sahal–Bréchot S., 1991, A&A 245, 322
Van Regemorter H., Hoang Binh Dy, Prud'homme M., 1979, J. Phys. B 12, 1073

ASTRONOMY & ASTROPHYSICS
SUPPLEMENT SERIES

JULY **1998**, PAGE 141

Astron. Astrophys. Suppl. Ser. **131**, 141–142 (1998)

Stark broadening of spectral lines of multicharged ions of astrophysical interest

XX. O VII and Mg XI spectral lines*

M.S. Dimitrijević[1] **and S. Sahal-Bréchot**[2]

[1] Astronomical Observatory, Volgina 7, 11050 Belgrade, Yugoslavia
[2] Laboratoire "Astrophysique, Atomes et Molécules", Département Atomes et Molécules en Astrophysique, Unité associée au CNRS 812, Observatoire de Paris-Meudon, 92190 Meudon, France

Received January 28; accepted January 29, 1998

Abstract. Using a semiclassical perturbation approach, we have calculated electron−, proton−, and He III−impact line widths and shifts for 14 O VII and 18 Mg XI multiplets. For O VII, perturber densities are 10^{17}−10^{23} cm^{-3} and temperatures $T = 100000 - 2000000$ K. For Mg XI, perturber densities are 10^{18}− 10^{24} cm^{-3} and temperatures $T = 500000 - 5000000$ K. For lower perturber densities, the Stark broadening parameters are proportional to the perturber density.

Key words: line: profiles-atomic data — plasmas

1. Introduction

The investigation of the influence of impacts with charged particles (Stark broadening) on spectral line shapes of oxygen and magnesium in various ionization stages is of importance for a number of problems in astrophysics, physics and technology. For example, Stark broadening parameters for such ions are needed for the modeling and theoretical considerations of subphotospheric layers (Seaton 1987), for stellar abundance determinations, opacity calculations, diagnostic of laser produced, fusion and laboratory plasmas. Data on O VII spectral lines are of interest for the interpretation and modelling of some hot star spectra as PG1159 type stars (Werner et al. 1991). The additional interest for such data is due to the development of soft X-ray lasers, where Stark broadening data are needed to calculate gain values, model radiation trapping and to consider photoresonant pumping schemes (see e.g. Griem & Moreno 1990; Fill & Schöning 1994).

This paper is the twentieth of a series devoted to the research of Stark broadening parameters of spectral lines of multicharged ions (see Dimitrijević & Sahal-Bréchot 1995 and references therein, as well as Dimitrijević & Sahal-Bréchot 1996a,b, 1997, 1998a-d). Within the frame of our project (see e.g. Dimitrijević 1996) to obtain as large as possible set of reliable semiclassical Stark broadening data needed for the investigation, diagnostics and modeling of various plasmas in stellar and solar physics, laboratory, laser physics, fusion research, and various devices, we have calculated within the semiclassical-perturbation formalism (Sahal-Bréchot 1969a,b), electron-, proton-, and He III-impact line widths and shifts for 14 O VII and 18 Mg XI multiplets.

2. Results and discussion

For the consideration of the influence of charged particle-impacts on spectral lines (Stark broadening), the semiclassical perturbation formalism has been used, which, as well as the corresponding computer code (Sahal-Bréchot 1969a,b), have been updated and improved several times (Sahal-Bréchot 1974; Fleurier et al. 1977, Dimitrijević & Sahal-Bréchot 1984; Dimitrijević et al. 1991; Dimitrijević & Sahal-Bréchot 1996b). Short reviews of the method of calculations, with the discussion of improvements and validity criteria, have been published several times as e.g. in Dimitrijević & Sahal-Bréchot (1996c) and Dimitrijević (1996). The atomic energy levels needed for calculations, have been taken from Isler et al. (1993) for O VII, and from Martin & Zalubas (1980) for Mg XI. The oscillator strengths have been calculated within the Coulomb approximation (Bates & Damgaard 1949, and the tables of

Send offprint requests to: M.S. Dimitrijević

* Tables 1 and 2 are only available in electronic form at the CDS via anonymous ftp (130.79.128.5) or via http://cdsweb.u-strasbg.fr/Abstract.html

Oertel & Shomo 1968). For higher levels, the method of Van Regemorter et al. (1979) has been used.

Our results for electron−, proton−, and He III−impact line widths and shifts for 14 O VII and 18 Mg XI multiplets are shown in Tables 1 and 2 (accessible only in electronic form), for perturber densities $10^{17} - 10^{23}$ cm^{-3} and temperatures $T = 100000 - 2000000$ K for O VII and for perturber densities $10^{18} - 10^{24}$ cm^{-3} and temperatures $T = 500000 - 5000000$ K for Mg XI. The complete set of data is given for the perturber density of 10^{19}cm^{-3} in both cases, while for lower densities, only data needed for better interpolation are given. Stark broadening parameters for densities lower than tabulated, or for transitions not tabulated for perturber densities lower than 10^{19} cm^{-3}, are proportional to the perturber density. Moreover, we present in Tables 1 and 2 as well, a parameter c (Dimitrijević & Sahal-Bréchot 1984), which gives an estimate for the maximum perturber density for which the line may be treated as isolated, when it is divided by the corresponding full width at half maximum. For each value given in Tables 1 and 2, the collision volume (V) multiplied by the perturber density (N) is much less than one and the impact approximation is valid (Sahal-Bréchot 1969a,b). Values for $NV > 0.5$ are not given and values for $0.1 < NV \leq 0.5$ are denoted by an asterisk. When the impact approximation is not valid, the ion broadening contribution may be estimated by using the quasistatic approach (Sahal-Bréchot 1991 or Griem 1974). In the region between where neither of these two approximations is valid, a unified type theory should be used. For example in Barnard et al. (1974), a simple analytical formula for such a case is given. The accuracy of the results obtained decreases when broadening by ion interactions becomes important.

One may conclude from Tables 1 and 2, that for multicharged ion lines like O VII and Mg XI lines, ion broadening is not always a small correction to the linewidth, as it is e.g. for singly- and doubly-charged ions, but it is often comparable or even dominant for temperatures of the order of 1000000 K or larger. One should note as well that shifts due to He III- and proton-impacts become dominant in comparison to electron - impact ones.

The presented results may be useful for a number of problems in stellar and laboratory plasma research, modeling and diagnostic. They are also of interest for investigation and modeling of fusion and laser-produced plasmas, as well as for the investigation and modeling of soft X-ray lasers. Such results also have an interest for further development and refinements of the Stark broadening theory for multicharged ion line shapes and different theoretical considerations, particularly for the investigation of systematic trends of Stark broadening parameters along isoelectronic sequences.

Acknowledgements. This work is a part of the project "Astrometrical, Astrodynamical and Astrophysical Investigations", supported by Ministry of Science and Technology of Serbia.

References

Barnard A.J., Cooper J., Smith E.W., 1974, J. Quant. Spectrosc. Radiat. Transfer 14, 1025
Bates D.R., Damgaard A., 1949, Trans. Roy. Soc. London, Ser. A 242, 101
Dimitrijević M.S., 1996, Zh. Prikl. Spektrosk. 63, 810
Dimitrijević M.S., Sahal-Bréchot S., 1984, J. Quant. Spectrosc. Radiat. Transfer 31, 301
Dimitrijević M.S., Sahal-Bréchot S., Bommier V., 1991, A&AS 89, 581
Dimitrijević M.S., Sahal-Bréchot S., 1995, A&AS 109, 551
Dimitrijević M.S., Sahal-Bréchot S., 1996a, A&AS 115, 351
Dimitrijević M.S., Sahal-Bréchot S., 1996b, A&AS 119, 369
Dimitrijević M.S., Sahal-Bréchot S., 1996c, Phys. Scr. 54, 50
Dimitrijević M.S., Sahal-Bréchot S., 1997, A&AS 122, 533
Dimitrijević M.S., Sahal-Bréchot S., 1998a, A&AS 127, 543
Dimitrijević M.S., Sahal-Bréchot S., 1998b, A&AS 128, 359
Dimitrijević M.S., Sahal-Bréchot S., 1998c, A&AS 129, 155
Dimitrijević M.S., Sahal-Bréchot S., 1998d, A&AS 130, 539
Fill E.E., Schöning T., 1994, J. Appl. Phys. 76, 1423
Fleurier C., Sahal-Bréchot S., Chapelle J., 1977, J. Quant. Spectrosc. Radiat. Transfer 17, 595
Griem H.R., 1974, Spectral Line Broadening by Plasmas. Academic Press, New York
Griem H.R., Moreno J.C., 1990, in: X-Ray Lasers, Tallents G. (ed.). Institute of Physics, Bristol, p. 301
Isler R.C., Jupen C., Martinson I., 1993, Phys. Scr. 47, 32
Martin W.C., Zalubas R., 1980, J. Phys. Chem. Ref. Data 9, 1
Oertel G.K., Shomo L.P., 1968, ApJS 16, 175
Sahal-Bréchot S., 1969a, A&A 1, 91
Sahal-Bréchot S., 1969b, A&A 2, 322
Sahal-Bréchot S., 1974, A&A 35, 321
Sahal-Bréchot S., 1991, A&A 245, 322
Seaton M.J., 1987, J. Phys. B 20, 6363
Werner K., Heber U., Hunger K., 1991, A&A 244, 437
Van Regemorter H., Hoang Binh Dy, Prud'homme M., 1979, J. Phys. B 12, 1073

ASTRONOMY & ASTROPHYSICS
SUPPLEMENT SERIES

JULY **1998**, PAGE 143

Astron. Astrophys. Suppl. Ser. **131**, 143–144 (1998)

Stark broadening of spectral lines of multicharged ions of astrophysical interest

XXI. Sc X, Sc XI, Ti XI and Ti XII spectral lines*

M.S. Dimitrijević[1] **and S. Sahal-Bréchot**[2]

[1] Astronomical Observatory, Volgina 7, 11050 Belgrade, Yugoslavia
[2] Laboratoire "Astrophysique, Atomes et Molécules", Département Atomes et Molécules en Astrophysique, Unité associée au CNRS 812, Observatoire de Paris−Meudon, 92190 Meudon, France

Received February 13; accepted February 16, 1998

Abstract. By using the semiclassical-perturbation formalism, we have calculated electron-, proton-, and He III-impact line widths and shifts for 4 Sc X, 10 Sc XI, 4 Ti XI and 27 Ti XII multiplets, significant for analysis, investigation and modeling of different plasmas in solar and stellar physics, physics and technology. The results are presented as a function of temperature and perturber density.

Key words: lines: profile — atomic data — plasmas

1. Introduction

A number of problems in solar and stellar physics, plasma physics and technology (see e.g. Griem 1974) depends on a comprehensive set of reliable data on the influence of impacts with charged particles on spectral line shapes, i.e. on the Stark broadening parameters. For example, Stark broadening parameters for multiply charged ions are needed for the modelling and theoretical considerations of subphotospheric layers (Seaton 1997), as well as for the examination of radiative transfer. Such data for multiply charged ion lines are of additional interest as well due to the development of soft X-ray lasers, where Stark broadening data are needed to calculate gain values, to model radiation trapping and to consider photoresonant pumping schemes (see e.g. Griem & Moreno 1990; Fill & Schöning 1994). Of course such data are also useful for the rafinement and checking of theory, as well as for the consideration of systematic trends along isoelectronic sequences. Scandium and titanium in various ionization stages are present in stellar plasma. For example Rogerson & Ewell (1985) have found 7 Ti IV lines in the τ Sco spectrum. One should mention as well that Stark broadening parameters for 10 scandium III and 10 Titanium IV multiplets, have been calculated recently within the semiclassical perturbation approach by Dimitrijević & Sahal-Bréchot (1992).

This paper is the twenty first of a series devoted to the research of Stark broadening parameters of spectral lines of multicharged ions (see Dimitrijević & Sahal-Bréchot 1995 and references therein, as well as Dimitrijević & Sahal-Bréchot 1996a,b, 1997, 1998a-e). As the continuation of our project (see e.g. Dimitrijević 1996) to make available to astrophysicists and physicists an as large as possible set of reliable semiclassical Stark broadening data needed for the investigation, diagnostics and modeling of various plasmas in stellar and solar physics, abundance determinations, opacity calculations, modeling and consideration of subphotospheric layers, diagnostics and investigation of laboratory plasma,as well as for laser physics, fusion research, and various devices as e.g. light sources, we have calculated within the semiclassical-perturbation formalism (Sahal-Bréchot 1969a,b), electron-, proton-, and He III-impact line widths and shifts for 4 Sc X, 10 Sc XI, 4 Ti XI and 27 Ti XII multiplets.

2. Results and discussion

In order to examinate Stark broadening of Sc X, Sc XI, Ti XI and Ti XII spectral lines and to determine the corresponding broadening parameters (the full line width at half maximum - W and the line shift - d), the semiclassical perturbation formalism has been used, which, as well as the corresponding computer code (Sahal-Bréchot 1969a,b), have been updated and optimized several times

Send offprint requests to: M.S. Dimitrijević

* Tables 1-4 are only available in electronic form at the CDS via anonymous ftp (130.79.128.5) or via http://cdsweb.u-strasbg.fr/Abstract.html

(Sahal-Bréchot 1974; Fleurier et al. 1977; Dimitrijević & Sahal-Bréchot 1984; Dimitrijević et al. 1991; Dimitrijević & Sahal-Bréchot 1996b). Also, we have published several times descriptions of the calculation procedure, with a discussion of updatings and validity criteria, as e.g. in Dimitrijević & Sahal-Bréchot (1996c) and Dimitrijević (1996). Atomic energy levels needed for calculations have been taken from Bashkin & Stoner (1978) for Sc X and Sc XI, and from Wiese & Musgrove (1989) for Ti XI and Ti XII. The oscillator strengths have been calculated within the Coulomb approximation (Bates & Damgaard 1949; and the tables of Oertel & Shomo 1968). For higher levels, the method of Van Regemorter et al. (1979) has been used.

Our results for electron−, proton−, and He III−impact line widths and shifts for 4 Sc X, 10 Sc XI, 4 Ti XI and 27 Ti XII multiplets are shown in Tables 1−4 (accessibles only in electronic form), for Sc X (Table 1) for temperatures from 200 000 K up to 5 000 000 K and perturber densities 10^{19} cm^{-3}−10^{22} cm^{-3}, for Sc XI (Table 2) for temperatures from 500 000 K up to 5 000 000 K and perturber densities 10^{18} cm^{-3}−10^{22} cm^{-3}, for Ti XI (Table 3) for temperatures from 500 000 K up to 5 000 000 K, and perturber densities 10^{18} cm^{-3}−10^{22} cm^{-3}, and for Ti XII (Table 4) for temperatures from 500 000 K up to 6 000 000 K, and perturber densities 10^{18} cm^{-3}−10^{23} cm^{-3}.

Stark broadening data for densities lower than for tabulated data, are proportional to the perturber density. Moreover, we present in Tables 1−4 as well, a parameter c (Dimitrijević & Sahal-Bréchot 1984), which gives an estimate for the maximum perturber density for which the line may be treated as isolated, when it is divided by the corresponding full width at half maximum. For each value given in Tables 1−4, the collision volume (V) multiplied by the perturber density (N) is much less than one and the impact approximation is valid (Sahal-Bréchot 1969a,b). Values for $NV > 0.5$ are not given and values for $0.1 < NV \leq 0.5$ are denoted by an asterisk. When the impact approximation is not valid, the ion broadening contribution may be estimated by using the quasistatic approach (Sahal-Bréchot 1991 or Griem 1974). In the region between where neither of these two approximations is valid, a unified type theory should be used. For example in Barnard et al. (1974), a simple analytical formula for such a case is given. The accuracy of the results obtained decreases when broadening by ion interactions becomes important.

The present results are the first Stark broadening data concerning scandium X and XI as well as titanium XI and XII spectral lines. We hope that the presented data will be of interest for some problems in stellar and laboratory plasma research, modeling and diagnostic, as well as for consideration of plasmas in various devices in physics and technology, as e.g. subphotospheric layers, radiative transfer, investigation and modeling of fusion and laser-produced plasmas, and of soft X-ray lasers. Such results also have an interest for the checking and development of the Stark broadening theory for multicharged ion line shapes as e.g. for investigations of systematic trends along isoelectronic sequences.

Acknowledgements. This work is a part of the project "Astrometrical, Astrodynamical and Astrophysical Investigations", supported by Ministry of Science and Technology of Serbia.

References

Barnard A.J., Cooper J., Smith E.W., 1974, J. Quant. Spectrosc. Radiat. Transfer 14, 1025
Bashkin S., Stoner J.O.Jr., 1978, Atomic Energy Levels and Grotrian Diagrams, Vol. 2, North Holland, Amsterdam
Bates D.R., Damgaard A., 1949, Trans. Roy. Soc. London, Ser. A 242, 101
Dimitrijević M.S., 1996, Zh. Prikl. Spektrosk. 63, 810
Dimitrijević M.S., Sahal-Bréchot S., 1984, J. Quant. Spectrosc. Radiat. Transfer 31, 301
Dimitrijević M.S., Sahal-Bréchot, 1992, A&AS, 95, 121
Dimitrijević M.S., Sahal-Bréchot S., 1995, A&AS 109, 551
Dimitrijević M.S., Sahal-Bréchot S., 1996a, A&AS 115, 351
Dimitrijević M.S., Sahal-Bréchot S., 1996b, A&AS 119, 369
Dimitrijević M.S., Sahal-Bréchot S., 1996c, Phys. Scr. 54, 50
Dimitrijević M.S., Sahal-Bréchot S., 1997, A&AS 122, 533
Dimitrijević M.S., Sahal-Bréchot S., 1998a, A&AS 127, 543
Dimitrijević M.S., Sahal-Bréchot S., 1998b, A&AS 128, 359
Dimitrijević M.S., Sahal-Bréchot S., 1998c, A&AS 129, 155
Dimitrijević M.S., Sahal-Bréchot S., 1998d, A&AS 130, 539
Dimitrijević M.S., Sahal-Bréchot S., 1998e, A&AS (in press)
Dimitrijević M.S., Sahal-Bréchot S., Bommier V., 1991, A&AS 89, 581
Fill E.E., Schöning T., 1994, J. Appl. Phys. 76, 1423
Fleurier C., Sahal-Bréchot S., Chapelle J., 1977, J. Quant. Spectrosc. Radiat. Transfer 17, 595
Griem H.R., 1974, Spectral Line Broadening by Plasmas. Academic Press, New York
Griem H.R., Moreno J.C., 1990, in: X-Ray Lasers, Tallents G., (ed.). Institute of Physics, Bristol, p. 301
Oertel G.K., Shomo L.P., 1968, ApJS 16, 175
Rogerson Jr.J.B., Ewell Jr.M.W., 1985, ApJS 58, 265
Sahal-Bréchot S., 1969a, A&A 1, 91
Sahal-Bréchot S., 1969b, A&A 2, 322
Sahal-Bréchot S., 1974, A&A 35, 321
Sahal-Bréchot S., 1991, A&A 245, 322
Seaton M.J., 1987, J. Phys. B 20, 6363
Van Regemorter H., Hoang Binh Dy, Prud'homme M., 1979, J. Phys. B 12, 1073
Wiese W.L., Musgrove A., 1989, Atomic Data for Fusion, Vol. VI: Spectroscopic Data for Titanium, Chromium and Nickel, Vol. 1. Titanium, ORNL-6551/V1, Controled Fusion Atomic Data Center, Oak Ridge National Laboratory, Oak Ridge

ASTRONOMY & ASTROPHYSICS
SUPPLEMENT SERIES

Astron. Astrophys. Suppl. Ser. **133**, 227–228 (1998)

Stark broadening of spectral lines of multicharged ions of astrophysical interest

XXII. K VIII and K IX spectral lines*

M.S. Dimitrijević[1] **and S. Sahal−Bréchot**[2]

[1] Astronomical Observatory, Volgina 7, 11050 Belgrade, Yugoslavia
[2] Laboratoire "Astrophysique, Atomes et Molécules", Département Atomes et Molécules en Astrophysique, Unité associée au CNRS 812, Observatoire de Paris−Meudon, 92190 Meudon, France

Received June 3; accepted June 4, 1998

Abstract. By using the semiclassical-perturbation formalism, we have calculated electron-, proton-, and He III-impact line widths and shifts for 4 K VIII and 30 K IX multiplets, of interest for analysis, investigation and modeling of different plasmas in solar and stellar subphotospheric layers research and plasma physics. The obtained results are presented as a function of temperature and perturber density. Results are compared with other theoretical estimates, based on regularities and systematic trends.

Key words: lines: profile-atomic data

1. Introduction

Potassium lines are present in Solar (Moore et al. 1966) and stellar spectra (Merrill 1956). For example potassium has been found in SN 1987 A ejecta (Trimble 1991). Potassium is a product of alpha processes - neutron capture on slow time scale, and the data on the spectral line broadening parameters of potassium in various ionization stages are of interest for modelling subphotospheric layers (Seaton 1987). Such data are as well of interest for the fusion plasmas and laser-produced plasmas research and for the investigation of soft X-ray lasers (see e.g. Griem & Moreno 1990; Fill & Schöning 1994).

This paper is the twenty second of a series devoted to the research of Stark broadening parameters of spectral lines of multicharged ions (see Dimitrijević & Sahal–Bréchot 1995 and references therein, as well as Dimitrijević & Sahal–Bréchot 1996a,b, 1997, 1998a-f). In accordance with our project (see e.g. Dimitrijević 1996) to make available to astrophysicists and physicists an as large as possible set of reliable semiclassical Stark broadening data needed for the investigation, diagnostics and modeling of various plasmas in astrophysics, physics and technology (see e.g. Dimitrijević & Sahal–Bréchot 1998f), we have calculated within the semiclassical-perturbation formalism (Sahal–Bréchot 1969a,b), electron-, proton-, and He III-impact line widths and shifts for 4 K VIII and 30 K IX multiplets.

2. Results and discussion

For the consideration of Stark broadening of K VIII and K IX spectral lines and the determination of the corresponding broadening parameters (the full line width at half maximum - W and the line shift - d), the semiclassical perturbation formalism has been used. This formalism, as well as the corresponding computer code (Sahal–Bréchot 1969a,b), have been updated and optimized several times (Sahal–Bréchot 1974; Fleurier et al. 1977; Dimitrijević & Sahal–Bréchot 1984; Dimitrijević et al. 1991; Dimitrijević & Sahal–Bréchot 1996b). The calculation procedure, with the discussion of updatings and validity criteria, has been briefly reviewed e.g. in Dimitrijević & Sahal–Bréchot (1996c) and Dimitrijević (1996). Atomic energy levels needed for calculations have been taken from Bashkin & Stoner (1978). The oscillator strengths have been calculated within the Coulomb approximation (Bates & Damgaard 1949, and the tables of Oertel & Shomo 1968). For higher levels, the method of Van Regemorter et al. (1979) has been used.

Our results for electron−, proton−, and He III−impact line widths and shifts for 4 K VIII and 30 K IX

Send offprint requests to: M.S. Dimitrijević

* Tables 1–2 are only available in electronic form at the CDS via anonymous ftp to cdsarc.u-strasbg.fr (130.79.128.5) or via http://cdsweb.u-strasbg.fr/Abstract.html

multiplets are shown in Tables 1 and 2 (accessibles only in electronic form), for K VIII (Table 1) for temperatures from 200 000 K up to 3 000 000 K and perturber densities 10^{18} cm^{-3} – 10^{22} cm^{-3}, and for K IX (Table 2) for temperatures from 200 000 K up to 5 000 000 K and perturber densities 10^{18} cm^{-3} – 10^{22} cm^{-3}.

Stark broadening data for densities lower than for tabulated data, are proportional to the perturber density. Moreover, we present in Tables 1–2 as well, a parameter c (Dimitrijević & Sahal–Bréchot 1984), which gives an estimate for the maximum perturber density for which the line may be treated as isolated, when it is divided by the corresponding full width at half maximum. For each value given in Tables 1–2, the collision volume (V) multiplied by the perturber density (N) is much less than one and the impact approximation is valid (Sahal–Bréchot 1969a,b). Values for $NV > 0.5$ are not given and values for $0.1 < NV \leq 0.5$ are denoted by an asterisk. When the impact approximation is not valid, the ion broadening contribution may be estimated by using the quasistatic approach (Sahal–Bréchot 1991 or Griem 1974). In the region between where neither of these two approximations is valid, a unified type theory should be used. For example in Barnard et al. (1974), a simple analytical formula for such a case is given. The accuracy of the results obtained decreases when broadening by ion interactions becomes important.

There is no experimental data concerning the Stark broadening of K VIII and K IX spectral lines. It exists however, a prediction for K IX $4s^2S-4p^2P^\circ$ Stark width (Djeniže & Labat 1996), obtained with the help of established regularities of the Stark widths along Na isoelectronic sequence. For $T = 500\,000$ K and an electron density of 10^{17} cm^{-3}, Djeniže & Labat (1996) obtained for the Stark full width (FWHM) the value of 0.0057 ± 25% Å, while the present result is 0.0099 Å. We hope that the presented data will be of interest for some problems in stellar and laboratory plasma research, especially for subphotospheric layers consideration, investigation and modeling of fusion and laser-produced plasmas, and of soft X-ray lasers, as well as for the checking and development of the Stark broadening theory for multicharged ion line shapes, as e.g. for investigations of systematic trends along isoelectronic sequences.

Acknowledgements. This work is a part of the project "Astrometrical, Astrodynamical and Astrophysical Investigations", supported by Ministry of Science and Technology of Serbia.

References

Barnard A.J., Cooper J., Smith E.W., 1974, J. Quant. Spectrosc. Radiat. Transfer 14, 1025
Bashkin S., Stoner J.O. Jr., 1978, Atomic Energy Levels and Grotrian Diagrams, Vol. 2, North Holland, Amsterdam
Bates D.R., Damgaard A., 1949, Trans. Roy. Soc. London Ser. A 242, 101
Dimitrijević M.S., 1996, Zh. Prikl. Spektrosk. 63, 810
Dimitrijević M.S., Sahal–Bréchot S., 1984, J. Quant. Spectrosc. Radiat. Transfer 31, 301
Dimitrijević M.S., Sahal–Bréchot S., 1992, A&AS 95, 121
Dimitrijević M.S., Sahal–Bréchot S., 1995, A&AS 109, 551
Dimitrijević M.S., Sahal–Bréchot S., 1996a, A&AS 115, 351
Dimitrijević M.S., Sahal–Bréchot S., 1996b, A&AS 119, 369
Dimitrijević M.S., Sahal–Bréchot S., 1996c, Phys. Scr. 54, 50
Dimitrijević M.S., Sahal–Bréchot S., 1997, A&AS 122, 533
Dimitrijević M.S., Sahal–Bréchot S., 1998a, A&AS 127, 543
Dimitrijević M.S., Sahal–Bréchot S., 1998b, A&AS 128, 359
Dimitrijević M.S., Sahal–Bréchot S., 1998c, A&AS 129, 155
Dimitrijević M.S., Sahal–Bréchot S., 1998d, A&AS 130, 539
Dimitrijević M.S., Sahal–Bréchot S., 1998e, A&AS 131, 141
Dimitrijević M.S., Sahal–Bréchot S., 1998f, A&AS 131, 143
Dimitrijević M.S., Sahal–Bréchot S., Bommier V., 1991, A&AS 89, 581
Djeniže S., Labat J., 1996, Bull. Astron. Belgrade 154, 17
Fill E.E., Schöning T., 1994, J. Appl. Phys. 76, 1423
Fleurier C., Sahal–Bréchot S., Chapelle J., 1977, J. Quant. Spectrosc. Radiat. Transfer 17, 595
Griem H.R., 1974, Spectral Line Broadening by Plasmas. Academic Press, New York
Griem H.R., Moreno J.C., 1990, in: X-Ray Lasers, Tallents G. (ed.). Institute of Physics, Bristol, p. 301
Merrill P.W., 1956, Lines of the Chemical Elements in Astronomical Spectra, Carnegie Inst. of Washington, Publication 610, Washington DC
Moore C.E., Minnaert M.G.J., Houtgast J., 1966, The Solar Spectrum 2935 Å to 8770 Å, NBS Monographs 61, U.S. Department of Commerce, NBS, Washington DC
Oertel G.K., Shomo L.P., 1968, ApJS 16, 175
Sahal–Bréchot S., 1969a, A&A 1, 91
Sahal–Bréchot S., 1969b, A&A 2, 322
Sahal–Bréchot S., 1974, A&A 35, 321
Sahal–Bréchot S., 1991, A&A 245, 322
Seaton M.J., 1987, J. Phys. B 20, 6363
Trimble V., 1991, The Origin and Abundance of the Chemical Elements Revisited, Astron. Astrophys. Rev. 3, 1
Van Regemorter H., Hoang Binh Dy, Prud'homme M., 1979, J. Phys. B 12, 1073

ASTRONOMY & ASTROPHYSICS
SUPPLEMENT SERIES

Astron. Astrophys. Suppl. Ser. **139**, 617–623 (1999)

The stark broadening effect in hot star atmospheres: Au I and Au II lines

L.Č. Popović, M.S. Dimitrijević, and D. Tankosić

Astronomical Observatory, Volgina 7, 11000 Belgrade, Yugoslavia

Received January 27; accepted June 16, 1999

Abstract. The Stark broadening parameters for six Au I lines and eight Au II transitions have been calculated. Two methods for calculation have been used: the semiclassical method (for Au I lines) and the modified semiempirical approach (for Au II transitions). In the case of Au II, the jj coupling approximation has been used for the matrix-element calculations. The importance of the electron-impact effect in the case of Au II $\lambda = 174.0476$ nm line for several stellar atmosphere models has been tested.

Key words: atomic processes — line formation — stars: atmospheres — stars: early-type

1. Introduction

Hg-Mn stars are nonmagnetic late B type stars that display unusually strong lines of many heavy ions (see e.g. Preston 1971; Heacox 1979; Dworetsky 1980; Dworetsky et al. 1984; Adelman 1987; Wahlgren et al. 1995). E.g. the mercury abundances in this type of stars are between 4000 and 40000 times larger than solar ones (see e.g. Aller & Ross 1967; Sargent 1964). In A and B type stars the electron-impact broadening is the main pressure broadening mechanism (e.g. Dimitrijević 1989). Considering that the resonant lines of ionized heavy elements ($z > 30$) are located in the ultraviolet spectral region, the abundance analysis of these elements has become possible due to satellite observations by high resolution spectrographs as e.g. International Ultraviolet Explorer (IUE) satellite ($R = 12000$) or Goddard High Resolution Spectrograph (GHSR) installed at Hubble Space Telescope. The number of heavy ion lines observations with the higher photometric quality and spectral resolution is growing up. Consequently, experimental and theoretical spectroscopic data for modelling of these lines are required.

In order to investigate the Hg-Mn star atmospheres as well as other types of hot stars, the Stark broadening parameters for heavy ion lines are needed. The most sophisticated theoretical method for the calculation of a Stark broadened line profile is of course the quantum mechanical close coupling approach. However, due to its complexity and numerical difficulties, only a small number of such calculations exist. In a lot of cases, such as e.g. the transitions between more excited energy levels, the more sophisticated quantum mechanical approach is very difficult or even practically impossible to use and the semiclassical approach (e.g. Sahal-Bréchot 1969a,b) remains the most efficient method for Stark broadening calculations. But for radiators with complex spectra, heavy elements or multiply charged ions, even the semiclassical method is often not applicable in an adequate way due to the lack of reliable data on atomic energy levels, or due to the complexity of the spectrum, problems of level mixing or problems with the adequate identification of atomic energy levels. Simpler approaches are as well of interest when line broadening data for a large number of lines are required (e.g. opacity calculations), and the high precision of every particular result is not so important, but only a good average accuracy is sufficient.

Here we present the electron-impact broadening parameters for six Au I lines and eight Au II transitions as a function of temperature, calculated by using the semiclassical (Sahal-Bréchot 1969a,b) and modified semiempirical approach (Dimitrijević & Konjević 1980; Dimitrijević & Kršljanin 1986; Popović & Dimitrijević 1996), respectively.

The Au II lines are observed in Hg-Mn and other CP stars (Wahlgren et al. 1995; Fuhrmann 1988; Adelman 1994). The investigation of gold in Hg-Mn stars shows that the abundances, obtained from the Au II λ174.0476 nm line, are between 4000 (for χ Lup) and 20000 (for k Cnc) times larger than solar ones (Wahlgren et al. 1995).

Send offprint requests to: L.Č. Popović,
e-mail: lpopovic@aob.bg.ac.yu

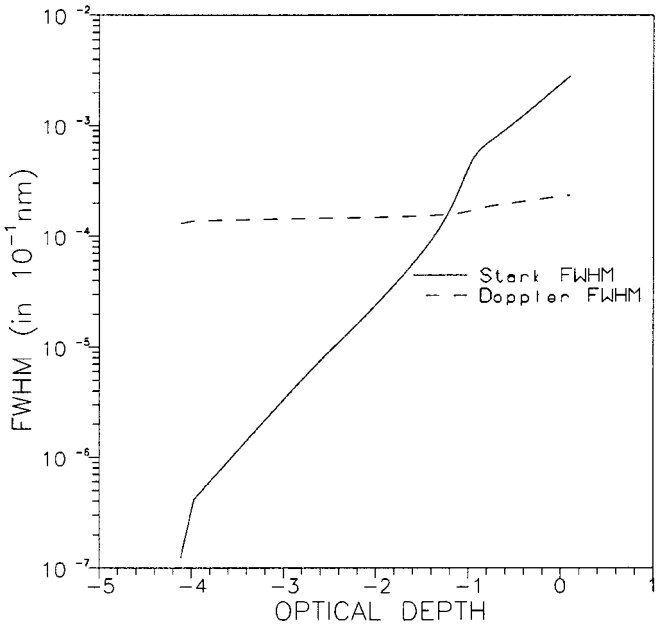

Fig. 1. Thermal Doppler and Stark widths for Au II (λ = 174.048 nm) line as functions of optical depth for an A type star ($T_{\rm eff}$ = 10000 K, $\log g = 4$)

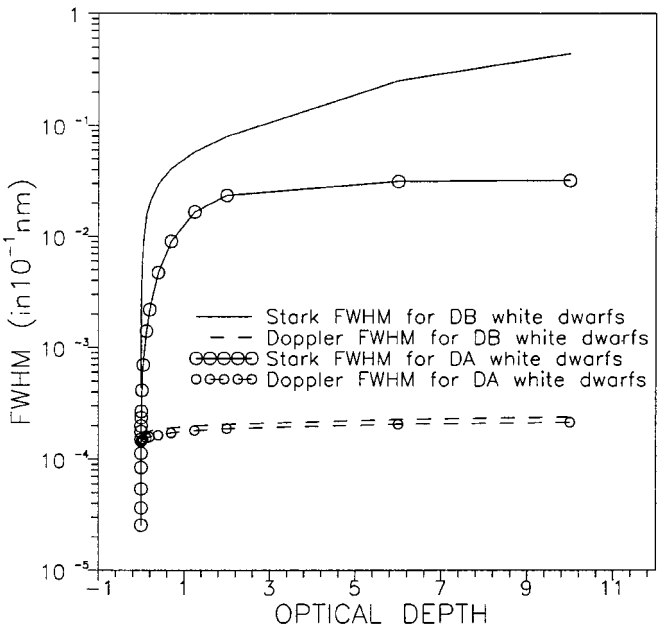

Fig. 2. Same as in Fig. 1, but for DA ($T_{\rm eff}$ = 10000 K, $\log g = 6$, curves with circles) and DB ($T_{\rm eff}$ = 15000 K, $\log g = 7$) white dwarfs

Since a sufficiently complete set of reliable atomic data needed for the application of the full semiclassical - perturbation approach (Sahal-Bréchot 1969a,b) in an adequate way does not exist, the modified semiempirical method (Dimitrijević & Konjević 1980; Dimitrijević & Kršljanin 1986; Popović & Dimitrijević 1996) has been used for Stark broadening calculation of Au II lines, whereas for Au I lines the more sophisticated semiclasical perturbation approach (Sahal-Bréchot 1969a,b) has been applied.

2. Results and discussion

For Au I spectral lines Stark broadening parameters, the full semiclassical perturbation formalism (Sahal-Bréchot 1969a,b), has been applied. A summary of the formalism for neutral emitters is given in Dimitrijević & Sahal-Bréchot (1984), and for ionized in Dimitrijević et al. (1991) and Dimitrijević & Sahal-Bréchot (1996). We note here that the inelastic collision contribution is included in the ion-impact line widths.

Energy levels for Au I lines have been taken from Moore (1971). Oscillator strengths have been calculated by using the method of Bates & Damgaard (1949) and the tables of Oertel & Shomo (1968). For higher levels, the method described by Van Regemorter et al. (1979) has been used. In addition to electron-impact full halfwidths and shifts, Stark-broadening parameters due to proton-, and He II- impacts have been calculated. Our results for six Au I lines are shown in Table 1, for perturber densities $10^{15} - 10^{19}$ cm^{-3} and temperatures $T = 2\,500 - 50\,000$ K. We also specify a parameter C (Dimitrijević & Sahal-Bréchot 1984), which gives an estimate for the maximum perturber density for which the line may be treated as isolated when it is divided by the corresponding full width at half maximum. For each value given in Table 1, the collision volume (V) multiplied by the perturber density (N) is much less than one and the impact approximation is valid (Sahal-Bréchot 1969a,b). Values for $NV > 0.5$ are not given and values for $0.1 < NV \leq 0.5$ are denoted by an asterisk. Tabulated Stark broadening parameters are linear with perturber density for perturber densities lower than 10^{15} cm^{-3}. The accuracy of the semiclasical method is $\pm$ 30% (Griem 1974). When the impact approximation is not valid, the ion broadening contribution may be estimated by using quasistatic approach (Sahal-Bréchot 1991 and Griem 1974). In the region between, where neither of these two approximations is valid, a unified type theory should be used. For example in Barnard et al. (1974), a simple analytical formulas for such a case are given. The accuracy of the results obtained decreases when broadening by ion interactions becomes important.

For Au II spectral lines, the electron-impact broadening calculation has been performed within the modified semiempirical approach. Considering the very complex spectrum of Au II, the jj coupling approximation for matrix-element calculation has been used. The needed atomic data for calculation have been taken from Rosberg & Wyart (1996). In Table 2, the electron-impact parameteres for eight Au II transitions as a function of temperature for an electron density of $N_{\rm e} = 10^{17}$ cm^3 are presented. The average accuracy of the MSE method is $\pm$ 50% (Dimitrijević & Konjević 1980).

In order to see the influence of Stark broadening mechanism for gold spectral lines in stellar plasma, we have

calculated the Stark widths for Au II $\lambda = 174.0476$ nm throught the different models of stellar atmospheres. In Figs. 1 and 2, the electron-impact and thermal Doppler widths as function of optical depth for Kurucz's (1979) A type star ($T_{\rm eff} = 10000$ K, $\log g = 4$) and models of DA ($T_{\rm eff} = 10000$ K, $\log g = 6$) and DB ($T_{\rm eff} = 15000$ K, $\log g = 7$) white dwarf atmospheres (Wickramasinghe 1972) are presented. As one can see from Fig. 1, for the case of hot A type star, in photospheric layers the line width due to Stark broadening is one order of magnitude larger than the width due to the thermal Doppler mechanism. In higher layers of the stellar atmosphere ($\tau \approx -4$) however, the thermal Doppler mechanism is more important. In the case of white dwarf atmospheres (see Fig. 2) the Stark broadening mechanism is important in all layers of atmospheres and in deeper atmosphere layers the Stark width is two or three order of magnitude larger than thermal Doppler width. For the three here considered atmosphere models Stark broadening effect should be taken into account in abundance determination and other investigations of stellar plasmas.

Acknowledgements. This work is a part of the project "Astrometrical, Astrodynamical and Astrophysical Investigations", supported by Ministry of Science and Technology of Serbia.

References

Adelman S.J., 1987, MNRAS 228, 573
Adelman S.J., 1994, MNRAS 266, 97
Aller L.H., Ross J.E., 1967, The Magnetic and Related Stars, Cameron R.C. (ed.). Baltimor, p. 339
Barnard A.J., Cooper J., Smith E.W., 1974, JQSRT 14, 1025
Bates D.R., Damgaard A., 1949, Trans. Roy. Soc. London, Ser. A 242, 101
Dimitrijević M.S., 1989, Bull. Obs. Astron. Belgrade 140, 111
Dimitrijević M.S., Konjević N., 1980, JQSRT 24, 454
Dimitrijević M.S., Kršljanin V., 1986, A&A 165, 269
Dimitrijević M.S., Sahal-Bréchot S., 1984, JQSRT 31, 301
Dimitrijević M.S., Sahal-Bréchot S., 1996, Phys. Scr. 54, 50
Dimitrijević M.S., Sahal-Bréchot S., Bommier V., 1991, A&AS 89, 581
Dworetsky M.M., 1980, A&A 84, 350
Dworetsky M.M., Storey P.J., Jacobs J.M., 1984, Phys. Scr. 8, 39
Griem H.R., 1974, Spectral Line Broadening by Plasmas. Academic Press, New York
Heacox W.D., 1979, ApJSS 41, 675
Fuhrmann K., 1988, ESA Spec. Publ 281, 1, 405
Kurucz R.L., 1979, ApJSS 40, 1
Moore C.E., 1971, Atomic Energy Levels Vol. III, NSRDS-NBS 35, Washington
Oertel G.K., Shomo L.P., 1968, ApJSS 16, 175
Preston G.W., 1971, PASP 83, 571
Popović L.Č., Dimitrijević M.S., 1996, Phys. Scr. 53, 325
Rosberg M., Wyart J.-F., 1996, Phys. Scr. 55, 690
Sahal-Bréchot S., 1969a, A&A 1, 91
Sahal-Bréchot S., 1969b, A&A 2, 322
Sahal-Bréchot S., 1991, A&A 245, 322
Sargent W.L., 1964, ARA&A 2, 297
Van Regemorter H., Hoang Binh Dy, Prud'homme M., 1979, J. Phys. B 12, 1073
Wahlgren G.M., Leckrone D.S., Johansson S.G., Rosberg M., Brage T., 1995, ApJ 444, 438
Wickramasinghe D.T., 1972, Mem. R. Astron. Soc. 76, 129

Table 1. This table shows electron-, proton-, and He II- impact broadening parameters for Au I, calculated within the full semiclassical perturbation approach (Sahal-Bréchot 1969a,b) for perturber densities of $10^{15} - 10^{19}$ cm^{-3} and temperatures from 2 500 up to 50 000 K. Transitions and averaged wavelengths for the multiplet (in nm) are also given. By dividing C by the corresponding full width at half maximum (Dimitrijević et al. 1991), we obtain an estimate for the maximum perturber density for which the line may be treated as isolated and tabulated data may be used. The asterisk identifies cases for which the collision volume multiplied by the perturber density (the condition for validity of the impact approximation) lies between 0.1 and 0.5. Stark broadening parameters for densities lower than tabulated, are linear with perturber density

PERTURBER DENSITY= 1.E+15cm-3							
PERTURBERS ARE:		ELECTRONS		PROTONS		IONIZED HELIUM	
TRANSITION	T(K)	W (0.1nm)	d (0.1nm)	W (0.1nm)	d (0.1nm)	W (0.1nm)	d (0.1nm)
6s2S-6p2Po1/2	2500.	0.144E-03	0.602E-04	0.957E-04	0.166E-04	0.955E-04	0.132E-04
Au I 267.67 nm	5000.	0.167E-03	0.690E-04	0.959E-04	0.186E-04	0.956E-04	0.148E-04
C=0.12E+19	10000.	0.175E-03	0.701E-04	0.961E-04	0.210E-04	0.957E-04	0.167E-04
	20000.	0.191E-03	0.627E-04	0.964E-04	0.236E-04	0.959E-04	0.188E-04
	30000.	0.213E-03	0.496E-04	0.966E-04	0.252E-04	0.960E-04	0.201E-04
	50000.	0.259E-03	0.360E-04	0.970E-04	0.275E-04	0.962E-04	0.219E-04
6s2S-6p2Po3/2	2500.	0.164E-03	0.101E-03	0.104E-03	0.278E-04	0.103E-03	0.221E-04
Au I 242.87 nm	5000.	0.192E-03	0.120E-03	0.105E-03	0.313E-04	0.104E-03	0.249E-04
C=0.79E+18	10000.	0.209E-03	0.132E-03	0.106E-03	0.352E-04	0.104E-03	0.280E-04
	20000.	0.230E-03	0.133E-03	0.107E-03	0.396E-04	0.105E-03	0.315E-04
	30000.	0.254E-03	0.134E-03	0.108E-03	0.424E-04	0.105E-03	0.338E-04
	50000.	0.295E-03	0.109E-03	0.109E-03	0.462E-04	0.106E-03	0.368E-04
6s2S-7p2Po1/2	2500.	0.117E-02	0.844E-03	0.381E-03	0.217E-03	0.356E-03	0.171E-03
Au I 166.58 nm	5000.	0.131E-02	0.965E-03	0.400E-03	0.248E-03	0.368E-03	0.196E-03
C=0.53E+17	10000.	0.145E-02	0.100E-02	0.422E-03	0.282E-03	0.382E-03	0.223E-03
	20000.	0.160E-02	0.917E-03	0.448E-03	0.319E-03	0.400E-03	0.253E-03
	30000.	0.171E-02	0.805E-03	0.466E-03	0.342E-03	0.413E-03	0.272E-03
	50000.	0.184E-02	0.672E-03	0.491E-03	0.373E-03	0.430E-03	0.297E-03
6s2S-7p2Po3/2	2500.	0.154E-02	0.114E-02	0.454E-03	0.290E-03	0.412E-03	0.228E-03
Au I 164.67 nm	5000.	0.172E-02	0.127E-02	0.483E-03	0.333E-03	0.432E-03	0.263E-03
C=0.33E+17	10000.	0.187E-02	0.127E-02	0.517E-03	0.379E-03	0.456E-03	0.300E-03
	20000.	0.202E-02	0.113E-02	0.558E-03	0.430E-03	0.484E-03	0.341E-03
	30000.	0.212E-02	0.990E-03	0.586E-03	0.461E-03	0.503E-03	0.366E-03
	50000.	0.222E-02	0.825E-03	0.626E-03	0.503E-03	0.530E-03	0.400E-03
6s2S-8p2Po1/2	2500.	0.403E-02	0.288E-02	0.119E-02	0.699E-03	*0.108E-02	*0.542E-03
Au I 150.14 nm	5000.	0.453E-02	0.326E-02	0.126E-02	0.817E-03	0.114E-02	0.640E-03
C=0.19E+17	10000.	0.501E-02	0.327E-02	0.134E-02	0.939E-03	0.119E-02	0.740E-03
	20000.	0.558E-02	0.279E-02	0.144E-02	0.107E-02	0.126E-02	0.847E-03
	30000.	0.600E-02	0.242E-02	0.150E-02	0.115E-02	0.131E-02	0.913E-03
	50000.	0.642E-02	0.201E-02	0.160E-02	0.126E-02	0.137E-02	0.100E-02
6s2S-8p2Po1/2	2500.	0.550E-02	0.396E-02	0.146E-02	0.949E-03	*0.129E-02	*0.731E-03
Au I 149.45 nm	5000.	0.605E-02	0.432E-02	0.157E-02	0.112E-02	*0.137E-02	*0.872E-03
C=0.12E+17	10000.	0.651E-02	0.419E-02	0.170E-02	0.129E-02	0.146E-02	0.102E-02
	20000.	0.705E-02	0.346E-02	0.185E-02	0.147E-02	0.157E-02	0.117E-02
	30000.	0.741E-02	0.297E-02	0.196E-02	0.159E-02	0.164E-02	0.126E-02
	50000.	0.770E-02	0.246E-02	0.210E-02	0.174E-02	0.175E-02	0.138E-02
PERTURBER DENSITY= 1.E+16cm-3							
6s2S-6p2Po1/2	2500.	0.144E-02	0.600E-03	0.956E-03	0.163E-03	0.952E-03	0.129E-03
Au I 267.67 nm	5000.	0.167E-02	0.688E-03	0.958E-03	0.185E-03	0.955E-03	0.146E-03
C=0.12E+20	10000.	0.175E-02	0.700E-03	0.961E-03	0.209E-03	0.957E-03	0.166E-03
	20000.	0.191E-02	0.627E-03	0.964E-03	0.235E-03	0.959E-03	0.187E-03
	30000.	0.213E-02	0.496E-03	0.966E-03	0.251E-03	0.960E-03	0.200E-03
	50000.	0.259E-02	0.360E-03	0.970E-03	0.274E-03	0.962E-03	0.218E-03
6s2S-6p2Po3/2	2500.	0.164E-02	0.101E-02	0.104E-02	0.271E-03	0.103E-02	0.214E-03
Au I 242.87 nm	5000.	0.192E-02	0.119E-02	0.105E-02	0.308E-03	0.104E-02	0.244E-03
C=0.79E+19	10000.	0.209E-02	0.132E-02	0.106E-02	0.349E-03	0.104E-02	0.277E-03
	20000.	0.230E-02	0.133E-02	0.107E-02	0.394E-03	0.105E-02	0.313E-03
	30000.	0.254E-02	0.134E-02	0.108E-02	0.422E-03	0.105E-02	0.336E-03
	50000.	0.295E-02	0.109E-02	0.109E-02	0.461E-03	0.106E-02	0.367E-03
6s2S-7p2Po1/2	2500.	0.117E-01	0.820E-02	0.377E-02	0.193E-02	*0.348E-02	*0.147E-02
Au I 166.58 nm	5000.	0.131E-01	0.949E-02	0.398E-02	0.231E-02	*0.365E-02	*0.179E-02
C=0.53E+18	10000.	0.145E-01	0.993E-02	0.421E-02	0.270E-02	0.381E-02	0.212E-02
	20000.	0.160E-01	0.916E-02	0.448E-02	0.310E-02	0.400E-02	0.245E-02
	30000.	0.171E-01	0.804E-02	0.466E-02	0.335E-02	0.412E-02	0.265E-02
	50000.	0.184E-01	0.671E-02	0.491E-02	0.368E-02	0.430E-02	0.292E-02

Table 1. continued

6s2S-7p2Po3/2	2500.	0.154E-01	0.111E-01	0.449E-02	0.253E-02	*0.403E-02	*0.190E-02
Au I 164.67 nm	5000.	0.172E-01	0.124E-01	0.481E-02	0.306E-02	*0.429E-02	*0.236E-02
C=0.33E+18	10000.	0.187E-01	0.126E-01	0.516E-02	0.360E-02	0.454E-02	0.281E-02
	20000.	0.202E-01	0.113E-01	0.558E-02	0.416E-02	0.483E-02	0.327E-02
	30000.	0.212E-01	0.989E-02	0.586E-02	0.450E-02	0.503E-02	0.355E-02
	50000.	0.222E-01	0.824E-02	0.626E-02	0.494E-02	0.530E-02	0.391E-02
6s2S-8p2Po1/2	2500.	0.403E-01	0.272E-01	*0.114E-01	*0.534E-02		
Au I 150.14 nm	5000.	0.453E-01	0.317E-01	*0.124E-01	*0.700E-02		
C=0.19E+18	10000.	0.501E-01	0.326E-01	*0.134E-01	*0.857E-02	*0.118E-01	*0.658E-02
	20000.	0.558E-01	0.277E-01	*0.144E-01	*0.101E-01	*0.126E-01	*0.789E-02
	30000.	0.600E-01	0.241E-01	*0.150E-01	*0.110E-01	*0.131E-01	*0.865E-02
	50000.	0.642E-01	0.200E-01	0.159E-01	0.122E-01	*0.137E-01	*0.964E-02
6s2S-8p2Po1/2	2500.	0.550E-01	0.369E-01				
Au I 149.45 nm	5000.	0.604E-01	0.414E-01	*0.155E-01	*0.926E-02		
C=0.12E+18	10000.	0.651E-01	0.418E-01	*0.169E-01	*0.116E-01		
	20000.	0.705E-01	0.345E-01	*0.185E-01	*0.138E-01	*0.157E-01	*0.107E-01
	30000.	0.741E-01	0.296E-01	*0.195E-01	*0.151E-01	*0.164E-01	*0.118E-01
	50000.	0.770E-01	0.246E-01	*0.210E-01	*0.168E-01	*0.174E-01	*0.132E-01
PERTURBER DENSITY= 1.E+17cm-3							
6s2S-6p2Po1/2	2500.	0.144E-01	0.590E-02	0.942E-02	0.153E-02	0.926E-02	0.119E-02
Au I 267.67 nm	5000.	0.167E-01	0.681E-02	0.953E-02	0.178E-02	0.946E-02	0.140E-02
C=0.12E+21	10000.	0.175E-01	0.696E-02	0.959E-02	0.204E-02	0.953E-02	0.161E-02
	20000.	0.191E-01	0.625E-02	0.963E-02	0.231E-02	0.957E-02	0.183E-02
	30000.	0.213E-01	0.495E-02	0.966E-02	0.249E-02	0.959E-02	0.197E-02
	50000.	0.259E-01	0.360E-02	0.970E-02	0.272E-02	0.961E-02	0.216E-02
6s2S-6p2Po3/2	2500.	0.164E-01	0.984E-02	0.102E-01	0.248E-02	0.993E-02	0.191E-02
Au I 242.87 nm	5000.	0.192E-01	0.118E-01	0.104E-01	0.292E-02	0.102E-01	0.228E-02
C=0.79E+20	10000.	0.209E-01	0.131E-01	0.105E-01	0.338E-02	0.104E-01	0.266E-02
	20000.	0.230E-01	0.132E-01	0.107E-01	0.386E-02	0.105E-01	0.305E-02
	30000.	0.254E-01	0.134E-01	0.108E-01	0.416E-02	0.105E-01	0.329E-02
	50000.	0.295E-01	0.109E-01	0.109E-01	0.456E-02	0.106E-01	0.362E-02
6s2S-7p2Po1/2	2500.	0.117	0.745E-01				
Au I 166.58 nm	5000.	0.131	0.896E-01	*0.383E-01	*0.178E-01		
C=0.53E+19	10000.	0.145	0.954E-01	*0.416E-01	*0.232E-01		
	20000.	0.160	0.895E-01	*0.446E-01	*0.284E-01	*0.396E-01	*0.218E-01
	30000.	0.171	0.794E-01	*0.465E-01	*0.313E-01	*0.411E-01	*0.243E-01
	50000.	0.184	0.669E-01	*0.491E-01	*0.351E-01	*0.429E-01	*0.275E-01
6s2S-7p2Po3/2	2500.	0.153	0.986E-01				
Au I 164.67 nm	5000.	0.172	0.116				
C=0.33E+19	10000.	0.187	0.120	*0.510E-01	*0.301E-01		
	20000.	0.202	0.109	*0.556E-01	*0.374E-01		
	30000.	0.212	0.973E-01	*0.585E-01	*0.415E-01	*0.500E-01	*0.321E-01
	50000.	0.222	0.821E-01	*0.625E-01	*0.468E-01	*0.529E-01	*0.365E-01
6s2S-8p2Po1/2	2500.	*0.401	*0.219				
Au I 150.14 nm	5000.	0.452	0.279				
C=0.19E+19	10000.	0.501	0.297				
	20000.	0.558	0.259				
	30000.	0.600	0.230				
	50000.	0.642	0.196				
6s2S-8p2Po1/2	2500.	*0.545	*0.279				
Au I 149.45 nm	5000.	*0.602	*0.350				
C=0.12E+19	10000.	0.649	0.369				
	20000.	0.704	0.315				
	30000.	0.740	0.278				
	50000.	0.769	0.239				

Table 1. continued

PERTURBER DENSITY= 1.E+18cm-3

6s2S-6p2Po1/2	2500.	0.144	0.561E-01	*0.810E-01	*0.124E-01	*0.676E-01	*0.903E-02
Au I 267.67 nm	5000.	0.167	0.661E-01	*0.906E-01	*0.157E-01	*0.852E-01	*0.119E-01
C=0.12E+22	10000.	0.175	0.681E-01	0.942E-01	0.189E-01	*0.920E-01	*0.146E-01
	20000.	0.191	0.614E-01	0.957E-01	0.221E-01	*0.946E-01	*0.173E-01
	30000.	0.213	0.487E-01	0.963E-01	0.240E-01	0.953E-01	0.189E-01
	50000.	0.259	0.356E-01	0.968E-01	0.266E-01	0.958E-01	0.210E-01
6s2S-6p2Po3/2	2500.	0.163	0.913E-01	*0.835E-01	*0.178E-01	*0.657E-01	*0.121E-01
Au I 242.87 nm	5000.	0.192	0.113	*0.974E-01	*0.243E-01	*0.892E-01	*0.179E-01
C=0.79E+21	10000.	0.209	0.128	*0.103	*0.303E-01	*0.990E-01	*0.231E-01
	20000.	0.230	0.130	0.106	0.361E-01	*0.103	*0.280E-01
	30000.	0.254	0.132	0.107	0.395E-01	*0.104	*0.309E-01
	50000.	0.295	0.108	0.109	0.440E-01	0.106	0.346E-01
6s2S-7p2Po1/2	2500.	* 1.14	*0.497				
Au I 166.58 nm	5000.	1.30	0.721				
C=0.53E+20	10000.	1.44	0.830				
	20000.	1.59	0.807				
	30000.	1.70	0.729				
	50000.	1.84	0.616				
6s2S-7p2Po3/2	2500.	* 1.47	*0.581				
Au I 164.67 nm	5000.	* 1.69	*0.872				
C=0.33E+20	10000.	1.85	0.994				
	20000.	2.01	0.949				
	30000.	2.11	0.847				
	50000.	2.21	0.734				
6s2S-8p2Po1/2	2500.						
Au I 150.14 nm	5000.						
C=0.19E+20	10000.	* 4.69	* 2.05				
	20000.	* 5.37	* 1.94				
	30000.	* 5.82	* 1.76				
	50000.	* 6.29	* 1.59				
6s2S-8p2Po1/2	2500.						
Au I 149.45 nm	5000.						
C=0.12E+20	10000.						
	20000.	* 6.45	* 2.12				
	30000.	* 6.92	* 1.93				
	50000.	* 7.32	* 1.80				

PERTURBER DENSITY= 1.E+19cm-3

6s2S-6p2Po1/2	2500.	1.40	0.468		
Au I 267.67 nm	5000.	1.66	0.595		
C=0.12E+23	10000.	1.75	0.634		
	20000.	1.91	0.581	*0.898	*0.188
	30000.	2.13	0.459	*0.930	*0.214
	50000.	2.59	0.336	*0.953	*0.245
6s2S-6p2Po3/2	2500.	1.59	0.688		
Au I 242.87 nm	5000.	1.90	0.966		
C=0.79E+22	10000.	2.09	1.16		
	20000.	2.30	1.22		
	30000.	2.54	1.25	* 1.03	*0.331
	50000.	2.95	1.03	* 1.07	*0.390
6s2S-7p2Po1/2	2500.				
Au I 166.58 nm	5000.				
C=0.53E+21	10000.	* 12.1	* 4.30		
	20000.	* 14.4	* 5.20		
	30000.	* 15.8	* 4.90		
	50000.	* 17.4	* 4.60		

Table 2. This table shows electron-impact broadening parameters for Au II, calculated within the modified semiempirical approach (Dimitrijević & Konjević 1980; Dimitrijević & Kršljanin 1986; Popović & Dimitrijević 1996) for a perturber density of 10^{17} cm^{-3} and temperatures from 5 000 up to 50 000 K. Transitions and averaged wavelengths for the multiplet ($\bar{\lambda}$ in nm) are also given. Stark broadening parameters for other pertuber densities may be obtained by linear scaling, taking into account that for sufficiently higher densities a correction for Debye shielding effect (Griem 1974) should be applied

Transition	T (K)	W (nm)	d (nm)
$6s(3/2,1/2)-6p(3/2,1/2)$	5000.	0.410E-02	−0.912E-03
$\overline{\lambda}=201.58$ nm	10000.	0.285E-02	−0.643E-03
	20000.	0.197E-02	−0.452E-03
	30000.	0.159E-02	−0.365E-03
	40000.	0.137E-02	−0.313E-03
	50000.	0.123E-02	−0.276E-03
$6s(3/2,1/2)-6p(3/2,3/2)$	5000.	0.330E-02	−0.623E-03
$\overline{\lambda}=175.89$ nm	10000.	0.229E-02	−0.435E-03
	20000.	0.159E-02	−0.300E-03
	30000.	0.128E-02	−0.237E-03
	40000.	0.111E-02	−0.198E-03
	50000.	0.100E-02	−0.169E-03
$6s(5/2,1/2)-6p(5/2,1/2)$	5000.	0.404E-02	−0.106E-02
$\overline{\lambda}=208.04$ nm	10000.	0.282E-02	−0.754E-03
	20000.	0.195E-02	−0.536E-03
	30000.	0.157E-02	−0.441E-03
	40000.	0.135E-02	−0.385E-03
	50000.	0.121E-02	−0.346E-03
$6s(5/2,1/2)-6p(5/2,3/2)$	5000.	0.308E-02	−0.658E-03
$\overline{\lambda}=174.53$ nm	10000.	0.215E-02	−0.464E-03
	20000.	0.149E-02	−0.326E-03
	30000.	0.120E-02	−0.264E-03
	40000.	0.103E-02	−0.226E-03
	50000.	0.927E-03	−0.199E-03
$6p(3/2,1/2)-7s(3/2,1/2)$	5000.	0.191E-01	0.816E-02
$\overline{\lambda}=235.45$ nm	10000.	0.133E-01	0.607E-02
	20000.	0.939E-02	0.478E-02
	30000.	0.792E-02	0.449E-02
	40000.	0.720E-02	0.451E-02
	50000.	0.679E-02	0.452E-02
$6p(3/2,3/2)-7s(3/2,1/2)$	5000.	0.282E-01	0.116E-01
$\overline{\lambda}=283.87$ nm	10000.	0.196E-01	0.860E-02
	20000.	0.139E-01	0.677E-02
	30000.	0.117E-01	0.638E-02
	40000.	0.106E-01	0.642E-02
	50000.	0.100E-01	0.642E-02
$6p(5/2,1/2)-7s(5/2,1/2)$	5000.	0.147E-01	0.387E-02
$\overline{\lambda}=226.38$ nm	10000.	0.103E-01	0.284E-02
	20000.	0.719E-02	0.218E-02
	30000.	0.594E-02	0.200E-02
	40000.	0.528E-02	0.197E-02
	50000.	0.487E-02	0.194E-02
$6p(5/2,3/2)-7s(5/2,1/2)$	5000.	0.241E-01	0.585E-02
$\overline{\lambda}=286.18$ nm	10000.	0.168E-01	0.430E-02
	20000.	0.118E-01	0.330E-02
	30000.	0.974E-02	0.304E-02
	40000.	0.865E-02	0.299E-02
	50000.	0.798E-02	0.295E-02

ASTRONOMY & ASTROPHYSICS
SUPPLEMENT SERIES

Astron. Astrophys. Suppl. Ser. **140**, 191–192 (1999)

Stark broadening of neutral calcium spectral lines

M.S. Dimitrijević[1] **and S. Sahal−Bréchot**[2]

[1] Astronomical Observatory, Volgina 7, 11000 Belgrade, Serbia, Yugoslavia
[2] Laboratoire "Astrophysique, Atomes et Molécules", Département Atomes et Molécules en Astrophysique, Unité associée au CNRS 812, Observatoire de Paris−Meudon, 92190 Meudon, France

Received June 24; accepted September 6, 1999

Abstract. Using the semiclassical perturbation approach, we have calculated electron−, proton−, He II−, Mg II-, Si II- and Fe II-impact line widths and shifts for 189 Ca I multiplets as a function of temperature and perturber density. Perturbers selected here are the main perturbers in solar atmospheres. Obtained results have been compared with the existing theoretical and experimental data.

Key words: atomic data — line: profiles

1. Introduction

Calcium lines are present in solar (see e.g. Moore et al. 1966; Holweger 1972; Grevesse 1984) and stellar spectra (see e.g. Merrill 1956; Adelman & Davis Philip 1992). Adelman & Davis Philip (1992) have found, for example, neutral calcium lines in the Gamma Geminorum spectrum and Trimble (1991) reports the presence of this product of alpha processes in SN 1987 A ejecta. Consequently, Stark broadening data of neutral calcium spectral lines are of interest for stellar plasma as well as for laboratory plasma research and modeling. Neutral calcium spectral lines broadened by Stark effect have been investigated experimentally (Kusch & Pritschow 1970; Hühn & Kusch 1973) and theoretically (Griem 1974; Marassinghe & Lovett 1986). Stark-effect interaction constants for seven solar calcium lines, whose abundances are sensitive to Stark broadening, have been estimated by Holweger (1972).

In accordance with our project (see e.g. Dimitrijević 1996a) to make available to astrophysicists and physicists an as large as possible set of reliable semiclassical Stark broadening data needed for the investigation, diagnostics and modeling of various plasmas in astrophysics, physics and technology, we have calculated within the semiclassical-perturbation formalism (Sahal−Bréchot 1969a,b see also Sahal−Bréchot 1974; Dimitrijević & Sahal−Bréchot 1984) electron-, proton-, ionized helium-, ionized magnesium-, ionized silicon-, and ionized iron-impact line widths and shifts for 189 neutral calcium multiplets. Consequently, the relevant data for all principal perturbers in the solar plasma are provided.

2. Results and discussion

For the determination of Stark broadening parameters (the full line width at half maximum - W and the line shift - d) of neutral calcium, the semiclassical perturbation formalism has been used. This formalism, as well as the corresponding computer code (Sahal−Bréchot 1969a,b), have been updated and optimized several times (Sahal−Bréchot 1974; Fleurier et al. 1977; Dimitrijević & Sahal−Bréchot 1984; Dimitrijević et al. 1991; Dimitrijević & Sahal−Bréchot 1996). The calculation procedure, with the discussion of updatings and validity criteria, has been briefly reviewed in Dimitrijević (1996, 1997). Atomic energy levels needed for calculations have been taken from Sugar & Corliss (1979). The oscillator strengths have been calculated within the Coulomb approximation (Bates & Damgaard 1949, and the tables of Oertel & Shomo 1968). For higher levels, the method of Van Regemorter et al. (1979) has been used.

All results are for temperatures from 2 500 up to 50 000 K. In Table 1 (accessible only in electronic form), electron-, proton-, and He II-impact broadening parameters for 189 Ca I multiplets for perturber density of 10^{11} cm^{-3} are shown. Data for electron-, proton-, and He II-impact broadening parameters for Ca I for perturber densities of 10^{12} cm^{-3} – 10^{19} cm^{-3} are shown in Table 2 (accessible only in electronic form). Table 3 (accessible only in electronic form) shows Mg II-, Si II-, and

Send offprint requests to: M.S. Dimitrijević
e-mail: mdimitrijevic@aob.bg.ac.yu

*Tables 1-3 are only available in electronic form: The material published electronically can be accessed: by ftp at cdsarc.u-strasbg.fr (130.79.128.5) or via http://cdsweb.u-strasbg.fr/Abstract.html

Fe II-impact broadening parameters for 189 Ca I multiplets, for perturber density of 10^{11} cm^{-3}.

Stark broadening data for densities lower than for tabulated data, are proportional to the perturber density. Moreover, we present in Tables 1-3 as well, a parameter C (Dimitrijević & Sahal−Bréchot 1984), which gives an estimate for the maximum perturber density for which the line may be treated as isolated, when it is divided by the corresponding full width at half maximum. The validity of the impact approximation has been estimated for data shown in Tables 1-3, by checking if the collision volume (V) multiplied by the perturber density (N) is much less than one (Sahal−Bréchot 1969a,b). Values for $NV > 0.5$ are not given and values for $0.1 < NV \leq 0.5$ are denoted by an asterisk. When the impact approximation is not valid, the ion broadening contribution may be estimated by using the quasistatic approach (Sahal−Bréchot 1991 or Griem 1974). In the region between where neither of these two approximations is valid, a unified type theory should be used. For example in Barnard et al. (1974), a simple analytical formula for such a case is given. The accuracy of the results obtained decreases when broadening by ion interactions becomes important.

There are two experimental studies reporting results of measurements of neutral calcium line Stark broadening parameters (Kusch & Pritschow 1970; Hühn & Kusch 1973). Kusch & Pritschow (1970) have investigated experimentaly Stark widths and shifts of four neutral calcium lines from plasma produced in a pulsed capillary discharge, and reported results for an electron density of 10^{18} cm^{-3}. Only for one line (the 5188.8 Å line from the $4p^1P^\circ - 5d^1D$ multiplet) exist a sufficiently complete set of atomic data needed for an adequate application of our approach. For this line, however, the impact approximation condition is not satisfied for the reported electron density. Hühn & Kusch (1973) published experimental Stark widths for the 4318.6 Å and 4425.4 Å lines from the $4s4p^3P^\circ - 4p^2\ ^3P$ and $4s4p^3P^\circ - 4s4d^3D$ multiplets, from plasma produced in a high pressure arc. Only the 4425.4 Å line may be compared with our results. For an electron density of 10^{17}cm^{-3} and the temperature 10 000 K, Hühn & Kusch (1973) obtain for the full width at half maximum the value of 0.29 Å, while our result is 1.26 Å. The semiclassical result of Griem (1974) is 1.51 Å. As one can see, the agreement between the experimental result and both theories is very poor. The differences between the calculation methods used by us and those of Griem (1974), have been discussed in detail in Dimitrijević & Sahal−Bréchot (1996). The reasons for such large difference between experiment and theory have been discussed in detail in Konjević & Roberts (1976), and the principal point of their remarks on the experiment is the lack of an independent measurement of electron density.

It is surprising that in spite of the importance of neutral calcium lines, there are not more experimental data. Reliable experimental data for Stark broadening of Ca I lines will be important for the check of theory, as well as for abundance determinations and other problems in astrophysics and plasma physics.

Acknowledgements. This work has been supported by the Ministry of Science and Technology of Serbia through the project "Astrometrical, Astrodynamical and Astrophysical Researches".

References

Adelman S.J., Davis Philip A.G., 1992, PASP 104, 316
Barnard A.J., Cooper J., Smith E.W., 1974, J. Quant. Spectrosc. Radiat. Transfer 14, 1025
Bates D.R., Damgaard A., 1949, Trans. Roy. Soc. London, Ser. A 242, 101
Dimitrijević M.S., 1996, Zh. Prikl. Spektrosk. 63, 810
Dimitrijević M.S., 1997, Astrophys. Space Sci. 252, 415
Dimitrijević M.S., Sahal−Bréchot S., 1984, J. Quant. Spectrosc. Radiat. Transfer 31, 301
Dimitrijević M.S., Sahal−Bréchot S., 1996, Phys. Scr. 54, 50
Dimitrijević M.S., Sahal−Bréchot S., Bommier V., 1991, A&AS 89, 581
Fleurier C., Sahal−Bréchot S., Chapelle J., 1977, J. Quant. Spectrosc. Radiat. Transfer 17, 595
Grevesse N., 1984, Phys. Scr. T8, 49
Griem H.R., 1974, Spectral Line Broadening by Plasmas. Academic Press, New York
Holweger H., 1972, Solar Phys. 25, 14
Hühn R., Kusch H.J., 1973, A&A 28, 159
Konjević N., Roberts J.R., 1976, J. Phys. Chem. Ref. Data 5, 209
Kusch H.J., Pritschow H.P., 1970, A&A 4, 31
Merrill P.W., 1956, Lines of the Chemical Elements in Astronomical Spectra, Carnegie Inst. of Washington. Publication 610, Washington DC
Moore C.E., Minnaert M.G.J., Houtgast J., 1966, The Solar Spectrum 2935 Å to 8770 Å, NBS Monographs 61, U.S. Department of Commerce, NBS, Washington DC
Oertel G.K., Shomo L.P., 1968, ApJS 16, 175
Sahal−Bréchot S., 1969a, A&A 1, 91
Sahal−Bréchot S., 1969b, A&A 2, 322
Sahal−Bréchot S., 1974, A&A 35, 321
Sahal−Bréchot S., 1991, A&A 245, 322
Sugar J., Corlis C., 1979, J. Phys. Chem. Ref. Data 8, 865
Trimble V., 1991, The Origin and Abundance of the Chemical Elements Revisited, Astron. Astrophys. Review, No. 3, 1
Van Regemorter H., Hoang Binh Dy, Prud'homme M., 1979, J. Phys. B 12, 1073

ASTRONOMY & ASTROPHYSICS
SUPPLEMENT SERIES

Astron. Astrophys. Suppl. Ser. **140**, 193–196 (1999)

Stark broadening of neutral zinc spectral lines

M.S. Dimitrijević[1] **and S. Sahal–Bréchot**[2]

[1] Astronomical Observatory, Volgina 7, 11000 Belgrade, Serbia, Yugoslavia
[2] Laboratoire "Astrophysique, Atomes et Molécules", Département Atomes et Molécules en Astrophysique, Unité associée au CNRS 812, Observatoire de Paris−Meudon, 92190 Meudon, France

Received June 24; accepted September 6, 1999

Abstract. Using the semiclassical perturbation approach, we have calculated electron−, proton− and He II−impact line widths and shifts for 32 Zn I multiplets as a function of temperature and perturber density. Obtained results have been compared with the existing theoretical and experimental data.

Key words: atomic data — line: profiles

1. Introduction

Neutral zinc spectral lines are present in stellar (see e.g. Sneden et al. 1991) and solar (see e.g. Biémont & Godefroid 1980; Grevesse 1984) spectra. Consequently, Stark broadening parameters of Zn I lines are of interest for a number of astrophysical problems, e.g. for abundance determinations, as well as for stellar plasma analysis, modeling and diagnostics. Such data are also of interest for laboratory plasma diagnostics, modeling and investigation (see Grechikhin 1969; Kusch & Oberschelp 1967; Salakhov 1975; Fishman et al. 1979; Dimitrijević & Konjević 1983; Lakićević 1983; Rathore et al. 1985; Rao et al. 1989).

Within the semiclassical-perturbation formalism (Sahal–Bréchot 1969a,b; see also Sahal–Bréchot 1974; Dimitrijević & Sahal–Bréchot 1984), we have calculated electron-, proton-, and ionized helium-impact line widths and shifts for 32 neutral zinc multiplets, as the continuation of our project to create a large Stark broadening data set for astrophysical and laboratory plasma research purposes.

Send offprint requests to: M.S. Dimitrijević
e-mail: mdimitrijevic@aob.bg.ac.yu

*Table 1 is only available in electronic form: The material published electronically can be accessed: by ftp at cdsarc.u-strasbg.fr (130.79.128.5) or via http://cdsweb.u-strasbg.fr/Abstract.html

2. Results and discussion

In order to determine the full line width at half maximum - W and the line shift - d of neutral calcium lines influenced by the Stark broadening mechanism, the semiclassical perturbation formalism has been used. This formalism, as well as the corresponding computer code (Sahal–Bréchot 1969a,b), have been updated and optimized several times (Sahal–Bréchot 1974; Fleurier et al. 1977; Dimitrijević & Sahal–Bréchot 1984; Dimitrijević et al. 1991; Dimitrijević & Sahal–Bréchot 1996). A review of the calculation procedure, with the discussion of updatings and validity criteria, is published, e.g., in Dimitrijević (1996, 1997).

Atomic energy levels needed for calculations have been taken from Sugar & Musgrove (1995). The oscillator strengths have been calculated within the Coulomb approximation (Bates & Damgaard 1949, and the tables of Oertel & Shomo 1968). For higher levels, the method of Van Regemorter et al. (1979) has been used.

Electron-, proton-, and He II-impact broadening parameters for Zn I for perturber densities of 10^{13} cm^{-3} – 10^{19} cm^{-3} and temperatures from 2 500 up to 50 000 K, are presented in Table 1 (accessible only in electronic form). For perturber density of 10^{13} cm^{-3}, only data for three multiplets are shown, since other data are linear with density for densities lower than 10^{14} cm^{-3}. For perturber densities lower than 10^{13} cm^{-3}, Stark broadening parameters for all tabulated multiplets are linear with perturber density. We also specify a parameter C (Dimitrijević & Sahal–Bréchot 1984), which gives an estimate for the maximum perturber density for which the line may be treated as isolated when it is divided by the corresponding full width at half maximum. For each value given in Table 1, the collision volume (V) multiplied by the perturber density (N) is much less than one and the impact approximation is valid (Sahal–Bréchot 1969a,b). Values for $NV > 0.5$ are not given and values for $0.1 < NV \leq 0.5$ are denoted by an asterisk. Stark broadening parameters for densities lower than tabulated are linear with perturber density.

Table 2. Comparison between experimental and theoretical Stark full widths at half maximum. Experimental data: a-Kusch & Oberschelp (1967); b-Fishman et al. (1979) c-Rathore et al. (1985). Theoretical data: WDSB - present results; WDK - Dimitrijević & Konjević (1983)

Transition	Wavelength (A)	T(K)	N/10(+17) (cm-3)	Wm (A)	Wm/WDSB	Wm/WDK	Ref.
Zn I 4p-5s (triplets)	4810.53	11000	1.0	1.65	3.56	3.25	a
		11000	4.5	0.92	0.43	0.40	b
		13700	1.0	1.00	2.24	2.02	c
		14800	1.0	0.90	1.99	1.79	c
		16300	1.0	0.52	1.13	1.01	c
		18100	1.0	0.40	0.86	0.76	c
	4722.16	11000	1.0	1.57	3.39	3.09	a
		11000	4.5	1.20	0.58	0.52	b
		13700	1.0	1.00	2.24	2.02	c
		14800	1.0	0.64	1.42	1.27	c
		16300	1.0	0.42	0.92	0.82	c
		18100	1.0	0.36	0.77	0.69	c
	4680.14	11000	1.0	0.84	1.81	1.66	a
		11000	4.5	1.29	0.62	0.56	b
4p-6s (triplets)	3072.06	11000	1.0	0.70	0.76	0.65	a
	3035.78	11000	1.0	0.61	0.66	0.57	a
	3018.36	11000	1.0	0.56	0.61	0.52	a
4p-4d (triplets)	3345.02	11000	1.0	1.74	2.87	2.66	a
	3302.58	11000	1.0	1.40	2.31	2.14	a
	3282.33	11000	1.0	0.91	1.50	1.39	a
4p-5d (triplets)	2800.9	11000	1.0	1.96	0.53	0.39	a
	2770.9	11000	1.0	2.49	0.67	0.50	a
	2756.45	11000	1.0	1.27	0.34	0.25	a

When the impact approximation is not valid, the ion broadening contribution may be estimated by using the quasistatic approach (Sahal–Bréchot 1991 or Griem 1974). In the region between where neither of these two approximations is valid, a unified type theory should be used. For example in Barnard et al. (1974), simple analytical formulas for such a case are given. The accuracy of the results obtained decreases when broadening by ion interactions becomes important.

There are three experimental studies with data of Stark widths and shifts of neutral zinc lines (Kusch & Oberschelp 1987; Fishman et al. 1979; Rathore et al. 1985). Theoretical data suitable for comparison with our results are published in Dimitrijević & Konjević (1983), Lakićević (1983), and Rathore et al. (1985).

In Tables 2 and 3, experimental (Kusch & Oberschelp 1987; Fishman et al. 1979; Rathore et al. 1985) Stark widths (Table 2) and shifts (Table 3) are compared with present results and with semiclassical Stark broadening parameters from Dimitrijević & Konjević (1983). In the experiments of Kusch & Oberschelp (1987) and Fishman et al. (1979), ion perturbers are protons, while in the experiment of Rathore et al. (1985) the carrier gas was neon. In order to make the adequate comparison, Stark broadening of neutral zinc by impacts with neon ions has been calculated and included in WDSB and dDSB (present

Table 3. Comparison between experimental and theoretical Stark shifts. Experimental data: c-Rathore et al. (1985). Theoretical data: dDSB - present results; dDK - Dimitrijević & Konjević (1983)

Transition	Wavelength (A)	T(K)	N/10(+17) (cm-3)	dm (A)	dm/dDSB	dm/dDK	Ref.
Zn I 4p-5s (triplets)	4810.53	13700	1.0	0.44	1.24	1.58	c
		14800	1.0	0.35	0.97	1.24	c
		16300	1.0	0.25	0.66	0.87	c
		18100	1.0	0.21	0.55	0.72	c
	4722.16	11000	4.5	0.78	0.49	0.69	b
		13700	1.0	0.44	1.24	1.58	c
		14800	1.0	0.35	0.97	1.24	c
		16300	1.0	0.256	0.67	0.89	c
		18100	1.0	0.175	0.46	0.60	c

calculation of Stark widths - WDSB and shifts - dDSB) values in Tables 2 and 3. For the $4p^3P^\circ - 5d^3D$ multiplet, the impact approximation is not valid for proton perturbers and the quasistatic ion broadening contribution is calculated according to Griem (1974). One can see in Table 2 that the agreement of all experiments with both calculations is very poor. The ratio of experimental widths of Kusch & Oberschelp (1967) and the theoretical ones vary from 0.25 up to 3.56. The experimental widths of Fishman et al. (1979) are two times larger than theoretical values from both approaches. The temperature trend of the experimental widths of Rathore et al. (1985) is in such disagreement with both theoretical approaches that the ratios of measured and calculated Stark widths vary e.g. for the 4722.16 Å line from 2.24 for $T = 13\,700$ K up to 0.77 for $T = 18\,100$ K for the present results, and from 2.02 up to 0.69 for the theoretical values of Dimitrijević & Konjević (1983). For the shift, ratios of experimental values of Rathore et al. (1985) and results of the present calculations vary from 1.24 to 0.46 for the same spectral line.

The experimental results of Fishman et al. (1979) and Rathore et al. (1985) were not selected for critical compilations of reliable Stark broadening experimental data (Konjević & Roberts 1976; Konjević et al. 1984; Konjević & Wiese 1990), while the results of Kusch & Oberschelp (1967) were selected with the attribution of the lowest accuracy (Konjević & Roberts 1976). In the analysis of the Kusch & Oberschelp (1967) experiment, Konjević & Roberts (1976) have found large variations of Stark widths within multiplets, and supposed that this may be caused by improper treatment of self-absorption. Moreover, Dimitrijević & Konjević (1983) have shown on the basis of the analysis of Stark width systematic trends within spectral series, that the experimental results of Kusch & Oberschelp (1967) are in disagreement with such trends.

Lakićević (1983) estimated on the basis of regularities and systematic trends Stark width and shift for the

Zn I $4s^2\ ^1S - 4p^1P^\circ$ transition for an electron temperature (T) of 20 000 K and an electron density of 10^{17} cm^{-3}. He obtained the value of 0.066 Å for the full width at half maximum, and 0.035 Å for the shift. We obtain the value of 0.039 Å for the width and 0.029 Å for the shift. On the basis of regularities and systematic trends as well, Stark widths and shifts for the Zn I $4p^3P^\circ - 5s^3S$ transition for electron temperatures of 10 000 and 20 000 K and an electron density of 10^{17} cm^{-3} have been estimated by Rathore et al. (1985). They obtained the value of 0.60 Å for the full width at half maximum, and 0.36 Å for the shift, for $T = 10\,000$ K, and our results are 0.371 Å for the width and 0.295 Å for the shift. For $T = 20\,000$ K, they obtained 0.61 Å for the width and 0.30 Å for the shift, and we 0.408 Å for the width and 0.336 Å for the shift. Particularly for the shift, this is in both cases an encouraging agreement of simple estimates with our semiclassical perturbation results.

The comparison between our semiclassical perturbation results and semiclassical results of Dimitrijević & Konjević (1983) is shown in Table 4. Differences between the present calculations and the semiclassical method described in Griem (1974) and used by Dimitrijević & Konjević (1983), have been discussed in detail in Dimitrijević & Sahal–Bréchot (1995) and may be attributed to the theoretical differences and the differences in input data.

First of all, the lower cut-offs are different in both methods. In Dimitrijević & Konjević (1983), the same cut-off for widths and shifts as well as for both elastic and inelastic collisions has been used. The effect of the change of the set of values for the cut-offs R_1, R_2, and R_3 has been studied and discussed in detail in Sahal–Bréchot (1969b): the final choice of the cut-offs was adopted for physical reasons (it allows for the unitarity of the S-matrix) and followed Seaton (1962).

Moreover, in the present method, with the help of the symmetrization procedure one takes into account the impact electron velocity change during an inelastic collision, which is not taken into account in Dimitrijević & Konjević (1983). The importance of the symmetrisation has been shown in Sahal–Bréchot (1969b). It has been demonstrated there that the symmetrisation improves considerably (factor two) semiclassical cross sections for small energies (close to the threshold), which are overestimated without symmetrisation. Also, for the difference of the semiclassical method (Griem 1974) used by Dimitrijević & Konjević (1983) we take into account explicitely the elastic collision contribution.

Another difference between methods used here and in Dimitrijević & Konjević (1983), is the Debye shielding effect. Griem (1974) gives the equation for the Debye shielding correction, which may be included when necessary, and here, the Debye cut-off is included in the calculations. Also, while in Dimitrijević & Konjević (1983) the ion-broadening contribution is only a correction within the quasistatic theory, the complete semiclassical perturbation calculation has been performed here for the ion-impact broadening, when the impact approximation is valid. The differences in the imput data are the more recent atomic energy level data (Sugar & Musgrove 1995).

Table 4. Comparison between present Stark full widths at half maximum (WDSB) and shifts (dDSB) and the corresponding results (WDK, dDK) of Dimitrijević & Konjević (1983)

Transition	Wavelength (A)	T(K)	WDSB (A)	dDSB (A)	WDK (A)	dDK (A)
Zn I 4p-5s (triplets)	4767.4	5000	0.320	0.243	0.408	0.195
		10000	0.371	0.295	0.432	0.226
		20000	0.408	0.336	0.502	0.251
		40000	0.443	0.337	0.596	0.253
4p-6s (triplets)	3054.7	5000	0.676	0.449	0.812	0.367
		10000	0.752	0.565	0.920	0.404
		20000	0.809	0.562	1.122	0.420
		40000	0.889	0.521	1.338	0.396
4p-4d (triplets)	3324.8	5000	0.423	-0.107	0.520	-0.137
		10000	0.488	-0.0469	0.582	-0.0999
		20000	0.543	0.714E-04	0.662	-0.0548
		40000	0.583	0.0367	0.726	-0.0163
4p-5d (triplets)	2786.7	5000	2.33	0.481	3.96	0.364
		10000	2.77	0.509	4.04	0.288
		20000	3.08	0.458	4.08	0.230
		40000	3.21	0.410	3.96	0.191

Both methods have been compared with critically selected experimental data for 13 He I multiplets (Dimitrijević & Sahal–Bréchot 1985) and it was found that the agreement between experimental data and both semiclassical methods is within the limits of 20 percent, which is the predicted accuracy of the semiclassical method (Griem 1974). One can see from Table 4 that for zinc differences are larger and increase with temperature, particularly for the shift. One must take into account that more recent and more complete energy levels have been used in our calculations.

The obtained Stark broadening data are of interest for a number of problems in astrophysics and plasma physics as e.g. abundance determinations, stellar spectra analysis and laboratory plasma diagnostics. Reliable experimental determinations of neutral zinc Stark broadening parameters will be of interest for checking and development of Stark broadening theory.

Acknowledgements. This work has been supported by the Ministry of Science and Technology of Serbia through the project "Astrometrical, Astrodynamical and Astrophysical Researches".

References

Barnard A.J., Cooper J., Smith E.W., 1974, J. Quant. Spectrosc. Radiat. Transfer 14, 1025

Bates D.R., Damgaard A., 1949, Trans. Roy. Soc. London, Ser. A 242, 101
Biémont E., Godefroid M., 1980, A&A 84, 361
Dimitrijević M.S., 1996, Zh. Prikl. Spektrosk. 63, 810
Dimitrijević M.S., 1997, Astrophys. Space Sci. 252, 415, Spektrosk. 63, 810
Dimitrijević M.S., Konjević N., 1983, J. Quant. Spectrosc. Radiat. Transfer 30, 45
Dimitrijević M.S., Sahal–Bréchot S., 1984, J. Quant. Spectrosc. Radiat. Transfer 31, 301
Dimitrijević M.S., Sahal–Bréchot S., 1985, Phys. Rev. A 31, 316
Dimitrijević M.S., Sahal–Bréchot S., 1995, Phys. Scr. 52, 42
Dimitrijević M.S., Sahal–Bréchot S., 1996, Phys. Scr. 54, 50
Dimitrijević M.S., Sahal–Bréchot S., Bommier V., 1991, A&AS 89, 581
Fishman I.S., Semin P.S., Desyatnik G.A., 1979, Opt. Spectrosc. 47, 245
Fleurier C., Sahal–Bréchot S., Chapelle J., 1977, J. Quant. Spectrosc. Radiat. Transfer 17, 595
Grechikhin L.I., 1969, J. Appl. Spectrosc. (USSR) 11, 870
Grevesse N., 1984, Phys. Scr. T8, 49
Griem H.R., 1974, Spectral Line Broadening by Plasmas. Academic Press, New York
Konjević N., Dimitrijević M.S., Wiese W.L., 1984, J. Phys. Chem. Ref. Data 13, 619
Konjević N., Roberts J.R., 1976, J. Phys. Chem. Ref. Data 5, 209
Konjević N., Wiese W.L., 1990 J. Phys. Chem. Ref. Data 19, 1307
Kusch H.J., Oberschelp E., 1967, Z. Astrophys. 67, 77
Lakićević I.S., 1983, A&A 127, 37
Oertel G.K., Shomo L.P., 1968, ApJS 16, 175
Rao P.M.R., Saraswathy P., Krishnamarty G., et al., 1989, Pramana 32, 627
Rathore B.A., Purić J., Ćuk M., Lakićević I.S., 1985, Sing. J. Phys. 2, 105
Sahal–Bréchot S., 1969a, A&A 1, 91
Sahal–Bréchot S., 1969b, A&A 2, 322
Sahal–Bréchot S., 1974, A&A 35, 321
Sahal–Bréchot S., 1991, A&A 245, 322
Salakhov M.H., 1975, Dep. VINITI 2070-75
Seaton M.J., 1962, Proc. Phys. Soc. 79, 1105
Sneden C., Gratton R.G., Crocker D.A., 1991, A&A 246, 354
Sugar J., Musgrove A., 1995, J. Phys. Chem. Ref. Data 24, 1803
Van Regemorter H., Hoang Binh Dy, Prud'homme M., 1979, J. Phys. B 12, 1073

1986A&AS...64..591D

ASTRONOMY & ASTROPHYSICS
SUPPLEMENT SERIES

JUNE 1986, PAGE 591

Astron. Astrophys. Suppl. Ser. **64**, 591-594 (1986)

On the stark broadening within a F I transition array

M. S. Dimitrijević

Astronomical Observatory, Volgina 7, 11050 Beograd, Yugoslavia

Received August 14, accepted September 26, 1985

Summary. — Using a semiclassical formalism, electron impact widths and shifts within 3s - 3p transition array of F I have been computed. A detailed analysis of Stark broadening parameters as functions of the impact electron angular momentum quantum number and the temperature is carried out. On the basis of the results obtained, the differences between the contribution of elastic, inelastic and strong collisions to the line widths within a transition array are discussed, as well as the Stark shift and width behaviour of the various components.

Key words : lines profile.

1. Introduction.

The Stark broadening of spectral lines of neutral fluorine has been investigated experimentally by several authors (Konjević *et al.*, 1972; Vujnović *et al.*, 1983; see also Konjević and Roberts, 1976; Konjević *et al.*, 1984). Theoretically, it has been treated by Benett and Griem (1971) and the results were published in Griem's book (1974). Recently, a semiclassical calculation of F I neutral lines has been performed at $T = 14000$ K by Vujnović *et al.* (1983), using a more complete set of energy levels (Bashkin and Stoner, 1975; Hansen and Persson, 1973), not available at the time of Benett and Griem's (1971) work. Numerical results have been compared with experimental ones and the good agreement was found.

In this article semiclassical calculations of Stark broadening parameters for F I 3s - 3p transition array are presented for various temperatures. We have performed also an analysis of the contribution of different angular momenta of the colliding electron to the linewidth and shift. The results obtained have also been used for the investigation of the behaviour of Stark broadening parameters within a given spectrum. In order to analyse similarities within a transition array, we have also computed contributions of various collisional processes to the impact Stark broadening of F I 3s - 3p lines for different angular momenta of the incoming perturbing electron.

2. Theory.

Within the frame of the semiclassical perturbation formalism (Sahal-Bréchot, 1969a, b), the half halfwidth and shift of an electron impact broadened line can be expressed in terms of cross sections for elastic and inelastic processes (Baranger, 1958)

$$w = N \int v f(v)\, \mathrm{d}v \left(\sum_{i' \neq i} \sigma_{ii'}(v) + \sum_{f' \neq f} \sigma_{ff'}(v) + \sigma_{\mathrm{el}} \right) \quad (1)$$

$$d = N \int v f(v)\, \mathrm{d}v \int 2\, \pi \rho\, \mathrm{d}\rho \sin 2\, \phi_{\mathrm{p}} \,. \quad (2)$$

Here, N is the electron density, $f(v)$ is the Maxwellian velocity distribution function for electrons, ρ denotes the impact parameter of the incoming electron, i and f denote the initial and final atomic energy level and i', f', their perturbing levels. The inelastic cross section $\sigma_{ii'}(v)$ can be expressed by an integration over the impact parameter of the transition probability $P_{ii'}(\rho, v)$

$$\sum_{i' \neq i} \sigma_{ii'}(v) = \frac{1}{2} \pi R_1^2 + \int_{R_1}^{R_{\mathrm{d}}} 2\, \pi \rho\, \mathrm{d}\rho \sum_{i' \neq i} P_{ii'}(\rho, v) \,, \quad (3)$$

and the elastic cross section is given by

$$\sigma_{\mathrm{el}} = 2\, \pi R_2^2 + \int_{R_1}^{R_{\mathrm{d}}} 8\, \pi \rho\, \mathrm{d}\rho \sin^2 \delta \quad (4)$$

$$\delta = (\phi_{\mathrm{p}}^2 + \phi_{\mathrm{q}}^2)^{1/2} \,. \quad (5)$$

The phase shifts ϕ_{p} and ϕ_{q}, the cut-offs R_1, R_2, R_{d}, and the symmetrization procedures in the inelastic cross sections are described by Sahal-Bréchot (1969a, b).

In order to exhibit the contribution of the collisions with a particular angular momentum l to the linewidth and shift, we have introduced the semiclassical Stark broadening parameters w_l and d_l corresponding to the collisions with perturbers with a particular l (Dimitrijević *et al.*, 1981, 1983). We replace the integration over the impact parameter ρ of the perturbing classical particle by the integration over l using the relation $l \sim \rho k$ with $k = mv$. The corresponding values for w_l and d_l are obtained using l/k

© European Southern Observatory • Provided by the NASA Astrophysics Data System

1986A&AS...64..591D

and $(l + 1)/k$ as the lower and the upper cut-offs in equations (1) to (5).

3. Results and discussion.

The data for atomic energy levels used in this calculation were taken from Bashkin and Stoner (1975). The required oscillator strengths were calculated in the Coulomb approximation using the method of Bates and Damgaard (1949) and tables of Oertel and Shomo (1968). The contribution of the $3s^4P$ - $3p^2D^0$ transition to the broadening of $3p^2D^0$ and $3s^4P$ levels is neglected, since the corresponding oscillator strength is small in comparison with oscillator strengths for allowed perturbing transitions (Lokner *et al.*, 1983). We recall here also that we did not use the one electron approximation (Benett and Griem, 1971), taking into account every particular transition within a supermultiplet properly (see Dimitrijević, 1982).

The results of calculations of electron impact linewidths and shifts are presented in table I. The results for P-D transitions are for several percents different from Vujnović *et al.* (1983), due to the improved oscillator strength values. It was shown earlier (Wiese and Konjević, 1982) that, the Stark linewidths (in angular frequency units) within a supermultiplet, differ within the limit of $\pm$ 30 %, while within a transition array the difference is within $\pm$ 40 %. In our case, the differences of linewidths (in angular frequency units) are consistent with the findings of Wiese and Konjević (1982). The results for the shift however, differ for more than three times within the transition array considered.

For $3s^4P$ - $3p^4P^0$ multiplet, we have evaluated the contributions w_l and d_l of the various angular momenta l to the half halfwidth w and shift d. Results for 5000, 20000 and 30000 K are presented in figure 1 and 2. If we compare obtained results with the similar ones for Li I $2s^2S$ - $2p^2P^0$ resonance line (Dimitrijević *et al.*, 1981), we can see that higher l values are more important for the F I lines, especially for the shift.

Figures 3 and 4 show the convergence of the sums $\sum_{i=0}^{l} w_i/w$ and $\sum_{i=0}^{l} d_i/d$ for F I $3s^4P$ - $3p^4P^0$ multiplet at various temperatures. We can see that 80 % of the width is given by $l \leqslant 2$ at 5000 K and $l \leqslant 7$ at 30000 K. For the shift the convergence is slower. For $T = 5000$ K a summation up to $l = 5$ is necessary to obtain 80 % of the final result while for $T = 30000$ K, only 50 % is obtained with $l \leqslant 12$.

In figures 5-7 are presented the halfwidths (in angular frequency units) due to strong, elastic and inelastic (only for lower level) collisions, of all the members considered of the 3s - 3p transition array. We can see that the largest differences within the transition array considered, exist for elastic contribution. It is clear now, why the line shift, produced mainly by elastic collisions, is more sensitive to the atomic parameters variations than the linewidth. It is confirmed by figure 8, where contributions d_l for the various angular momenta l of the colliding electron are presented. In this particular case the differences within the transition array considered are so large that differences due to the use of wavelength units are not so important. By the help of figure 8 we can conclude that large differences between shift values within F I 3s - 3p transition array are produced mainly due to elastic collisions with perturbers with $1 < l < 5$ and that the differences will be smaller towards the high temperature limit.

References

Baranger, M. : 1958, *Phys. Rev.* **112,** 855.
Bashkin, S. and Stoner, J. O. : 1975, *Atomic Energy Levels and Grotrian Diagrams,* Vol. **I** (North-Holland and Elsevier P. C., Amsterdam, New York, Oxford).
Bates, D. R. and Damgaard, A. : 1949, *Philos. Trans. R. Soc. London, Ser. A* **242,** 102.
Benett, S. M. and Griem, H. R. : 1971, « Calculated Stark Broadening Parameters for Isolated Spectral Lines from the Atoms Helium throughout Calcium and Cesium », *Tech. Rep.* No. 71-097 (Univ. Maryland).
Dimitrijević, M. S. : 1982, *Astron. Astrophys.* **112,** 251.
Dimitrijević, M. S., Feautrier, N. and Sahal-Brechot, S. : 1981, *J. Phys. B* **14,** 2559.
Dimitrijević, M. S., Feautrier, N. and Sahal-Brechot, S. : 1983, *Fizika* **15,** 205.
Griem, H. R. : 1974, *Spectral Line Broadening by Plasmas* (Academic Press, New York).
Hansen, J. E. and Persson, W. : 1973, *Phys. Scri.* **8,** 197.
Konjević, N., Dimitrijević, M. S. and Wiese, W. L. : 1984, *J. Phys. Chem. Ref. Data* **13,** 619.
Konjević, N., Platiša, M. and Popović, M. : 1972, *Z. Phys.* **257,** 235.
Konjević, N. and Roberts, J. R. : 1976, *J. Phys. Chem. Ref. Data* **5,** 209.
Lokner, V., Vadla, Č. and Vujnović, V. : 1983, *J. Quant. Spectrosc. Radiat. Transfer* **30,** 187.
Oertel, G. K. and Shomo, L. P. : 1968, *Astrophys. J. Suppl. Series* **16,** 175.
Purić, J., Lakićević, I., Labat, J., Djeniže, S. and Ćirković, Lj. : 1977, *Phys. Lett. A* **63,** 243.
Sahal-Bréchot, S. : 1969a, *Astron. Astrophys.* **1,** 91.
Sahal-Bréchot, S. : 1969b, *Astron. Astrophys.* **2,** 322.
Schulz-Gulde, E. and Wenzel, A. : 1980, *J. Phys. B* **13,** 3733.
Vujnović, V. Vadla, Č., Lokner, V. and Dimitrijević, M. S. : 1983, *Astron. Astrophys.* **123,** 249.
Wiese, W. L. and Konjević, N. : 1982, *J. Quant. Spectrosc. Radiat. Transfer* **28,** 185.

© European Southern Observatory • Provided by the NASA Astrophysics Data System

1986A&AS...64..591D

TABLE I. — *This table lists Stark broadening parameters for F I 3s-3p lines at an electron density of 10^{22} m^{-3} and for various temperatures. Transitions and averaged wavelengths for the multiplet (in nm) are also given. Under w are given electron impact half halfwidths while d denote corresponding shifts.*

Transition	Temperature (K)	w(nm)	d(nm)
$3s^4P-3p^4P^o$	5000	0.178	0.0862
λ=749.03nm	14000	0.235	0.0629
Mult.1	20000	0.277	0.0533
ΔS/S=-0.03	30000	0.340	0.0414
$3s^4P-3p^4D^o$	5000	0.176	0.162
λ=685.92nm	14000	0.226	0.164
Mult.2	20000	0.263	0.142
ΔS/S=-0.04	30000	0.317	0.118
$3s^4P-3p^4S^o$	5000	0.201	0.247
λ=630.42nm	14000	0.252	0.284
Mult.3	20000	0.286	0.300
ΔS/S=+0.06	30000	0.332	0.274
$3s^2P-3p^2D^o$	5000	0.242	0.212
λ=775.94nm	14000	0.316	0.200
Mult.4	20000	0.370	0.172
ΔS/S=+0.01	30000	0.449	0.144
$3s^2P-3p^2S^o$	5000	0.264	0.293
λ=736.93nm	14000	0.336	0.339
Mult.5	20000	0.385	0.332
ΔS/S=+0.11	30000	0.455	0.325
$3s^2P-3p^2P^o$	5000	0.255	0.288
λ=706.70	14000	0.325	0.305
Mult.6	20000	0.372	0.307
ΔS/S=+0.01	30000	0.439	0.261
$3s^4P-3p^2D^o$	5000	0.185	0.187
λ=659.94	14000	0.233	0.196
	20000	0.268	0.178
ΔS/S=+0.02	30000	0.320	0.151

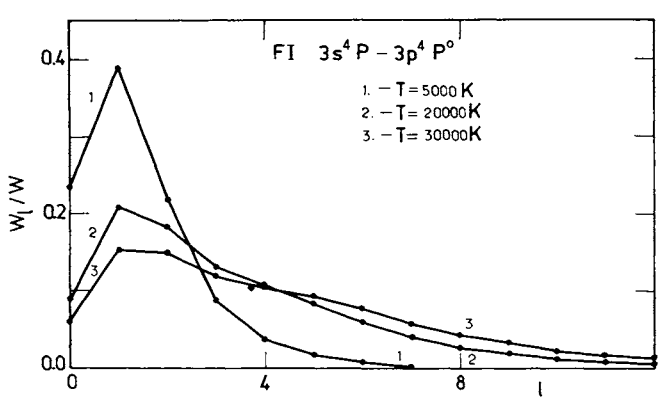

FIGURE 1. — Relative contributions, w_l/w, for the various angular momenta l of the colliding electron for the semiclassical half halfwidths at different temperatures.

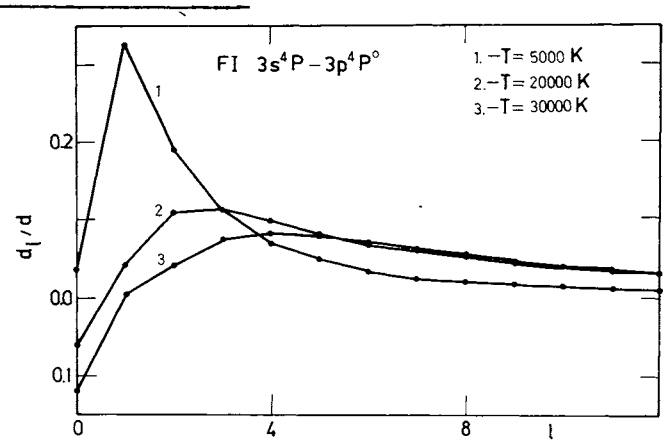

FIGURE 2. — Relative contributions, d_l/d, for the various angular momenta l of the colliding electron for the semiclassical shift at different temperatures.

© European Southern Observatory • Provided by the NASA Astrophysics Data System

1986A&AS...64..591D

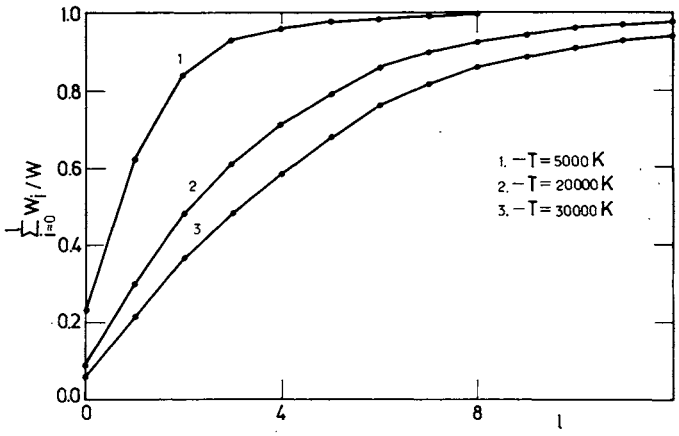

FIGURE 3. — Convergence of the sum $\sum_{i=0}^{l} w_i/w$ as a function of l for F I $3s^4P$ - $3p^4P^0$ multiplet.

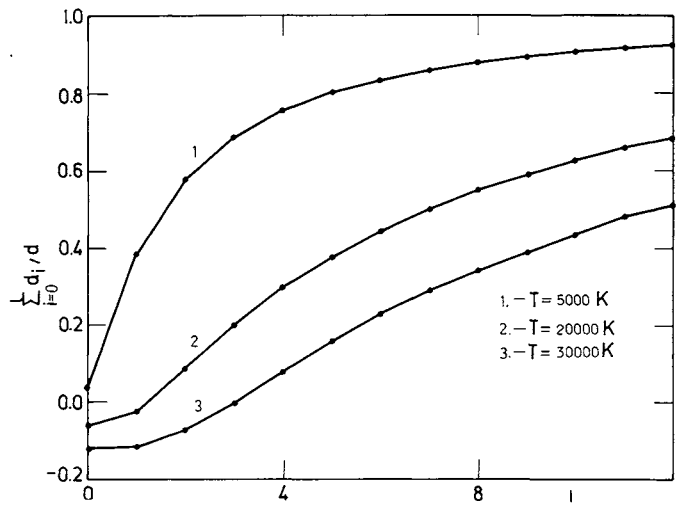

FIGURE 4. — Convergence of the sum $\sum_{i=0}^{l} d_i/d$ as a function of l for F I $3s^4P$ - $3p^4P^0$ multiplet

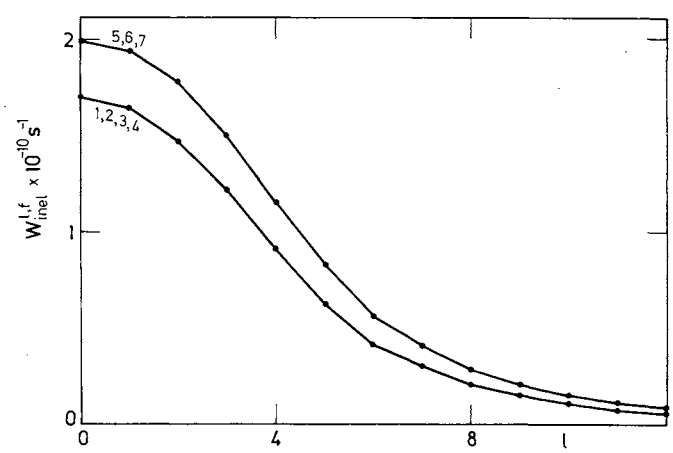

FIGURE 5. — The lower level inelastic contribution to the halfwidth as a function of l at T = 20000 K, for : 1) $3s^4P$ - $3p^4P^0$; 2) $3s^4P$ - $3p^4D^0$; 3) $3s^4P$ - $3p^4S^0$; 4) $3s^4P$ - $3p^2D^0$; 5) $3s^2P$ - $3p^2S^0$; 6) $3s^2P$ - $3p^2D^0$; 7) $3s^2P$ - $3p^2P^0$.

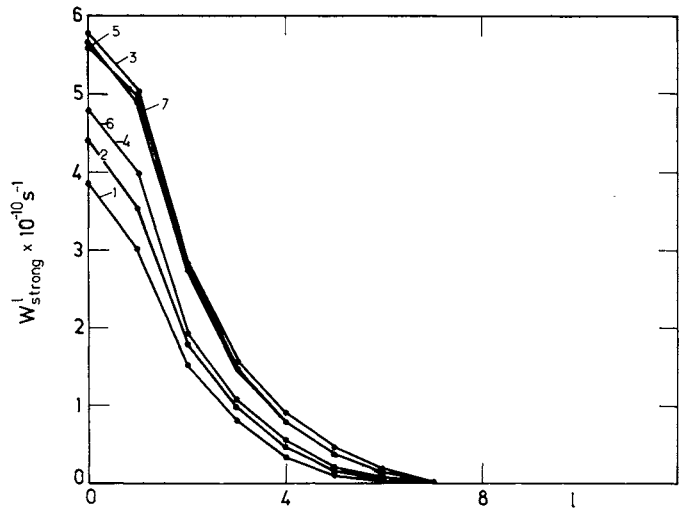

FIGURE 6. — Same as in figure 5 but for strong collision's contribution.

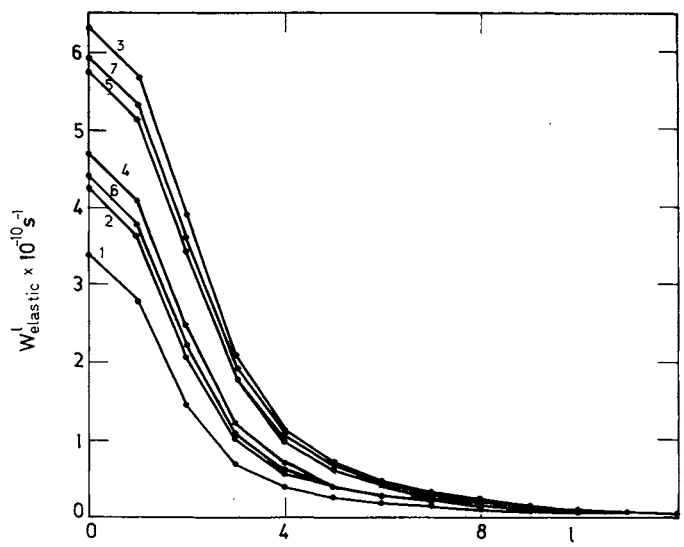

FIGURE 7. — Same as in figure 5 but for elastic collision's contribution.

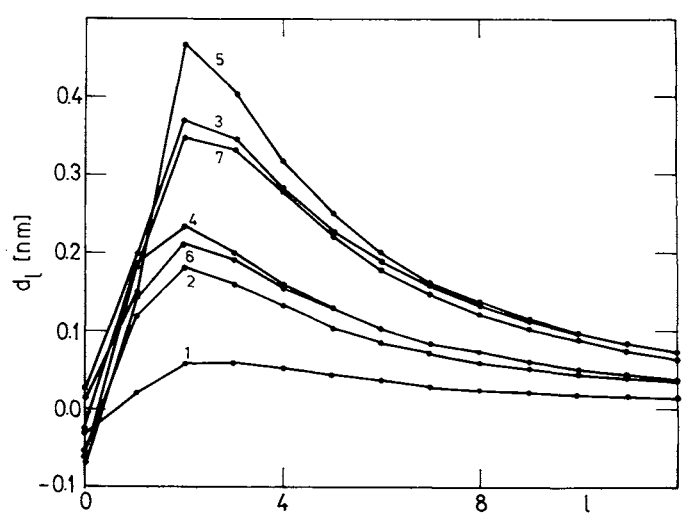

FIGURE 8. — Contributions d_l for the various angular momenta l of the colliding electron for the semiclassical shift at T = 20000 K. The notation is same as in figure 5.

© European Southern Observatory • Provided by the NASA Astrophysics Data System

1987A&AS...70...57D

ASTRONOMY & ASTROPHYSICS
SUPPLEMENT SERIES

Astron. Astrophys. Suppl. Ser. **70**, 57-61 (1987)

Stark broadening trends along homologous sequences

M. S. Dimitrijević ([1,2]), A. A. Mihajlov ([2,1]) and M. M. Popović ([2])

([1]) Astronomical Observatory, Volgina 7, 11050 Beograd, Yugoslavia
([2]) Institute of Physics, 11001 Beograd, P.O. Box 57, Yugoslavia

Received July 31, 1986; accepted February 11, 1987

Summary. — Using a semiclassical formalism, a detailed analysis of Stark broadening parameters as a function of the impact electron angular momentum quantum number and the temperature is carried out for resonance lines of the alkalis. On the basis of the results obtained, the differences between the contribution of elastic, inelastic and strong collisions to the line widths for analogous transitions in homologous atoms are discussed.

Key words: Stark broadening — line shapes.

1. Introduction.

Radiators with the same electronic charge and the same number of valence electrons, i.e. homologous atoms and ions often exhibit similar atomic structures. As a consequence a systematic behaviour of Stark broadening parameters such as gradual variations are expected in such cases. Purić and Ćirković (1973), and Purić *et al.* (1977, 1978) have studied in detail systematic trends of Stark widths of alkalis and alkali-like ions by appeal to the dependence of Stark widths on atomic oscillator strengths and their regularities. Mazure and Nollez (1978) also discussed regularities of Stark widths and shifts for alkali metal resonance lines at $T = 20000$ K, using the modified microfield approach. Miller *et al.* (1980), Lakićević and Purić (1983) and Purić *et al.* (1985) extended similar studies to the CII, SiII, GeII, PbII and NII, PII, AsII, SbII, BiIII sequence of homologous ions. More recently Miller *et al.* (1982) and Pittman and Konjević (1986) performed an analysis of Stark broadening along homologous sequence of singly ionized noble gases. In the case when a clear systematic trend for broadening is discernible for lines with the same upper level, accurate interpolations and critical evaluations of experimental data become feasible.

Since regularities apply especially to simple atomic systems with one or two electrons outside closed shells, the resonance lines of alkalis are very convenient for the study of the influence of various collisional processes on the regular or irregular behaviour of Stark broadening parameters for analogous transitions in homologous atoms.

In precedent studies of Stark broadening parameter regularities within a homologous sequence of neutral as well as charged emitters, the main attention has been paid to a very small temperature region where the coherent experimental data set for all homologous sequence exist. The analysis of the influence of different collisional processes on the Stark broadening within an FI transition array (Dimitrijević, 1986) shows that the largest differences within the transition array considered exist for elastic contribution. Consequently, one can conclude that in the case considered, the differences of Stark broadening parameters within a transition array will be smaller towards the high temperature limit, since the elastic collisions contribution decreases. It is of interest to perform a similar analysis in the case of homologous atoms in order to see if the regularities found in the small temperature region may be expected for other plasma conditions also.

For the analysis of the influence of different collisional processes on the Stark broadening similarities within a homologous sequence, it is interesting also to perform an analysis of the contribution of different angular momenta of the colliding electron to the line width and shift. In order to analyse similarities within a homologous sequence, we have computed contributions of various collisional processes to the impact Stark broadening of LiI, NaI, KI, RbI and CsI resonance lines for different angular momenta of the incoming perturbing electron. We have performed also an analysis of the contribution of different angular momenta of the colliding electron to

Send offprint requests to: M. S. Dimitrijević.

© European Southern Observatory • Provided by the NASA Astrophysics Data System

1987A&AS...70...57D

the line width and shift of resonance lines for the homologous sequence of alkalis.

2. Theory.

Using the semiclassical perturbation formalism (Sahal-Bréchot, 1969a, b) we can express the half halfwidth (w) and the shift (d) of an electron-impact broadened line as :

$$w = N \int v f(v)\, \mathrm{d}v \left(\sum_{i' \neq i} \sigma_{ii'}(v) + \sum_{f' \neq f} \sigma_{ff'}(v) + \sigma_{\mathrm{el}} \right) \quad (1)$$

$$d = N \int v f(v)\, \mathrm{d}v \int 2\, \pi \rho\, \mathrm{d}\rho\, \sin 2\, \phi_p\, . \quad (2)$$

Here, N is the electron density, $f(v)$ is the Maxwellian velocity distribution function for electrons, ρ denotes the impact parameter of the incoming electron, i and f denote the initial and final atomic energy level and i', f' their perturbing levels. The inelastic cross section $\sigma_{ii'}(v)$ can be expressed by an integration over the impact parameter of the transition probability $P_{ii'}(\rho, v)$:

$$\sum_{i' \neq i} \sigma_{ii'}(v) = \frac{1}{2}\, \pi R_1^2 + \int_{R_1}^{R_d} 2\, \pi \rho\, \mathrm{d}\rho \sum_{i' \neq i} P_{ii'}(\rho, v)\, , \quad (3)$$

and the elastic cross section is given by :

$$\sigma_{\mathrm{el}} = 2\, \pi R_2^2 + \int_{R_2}^{R_d} 8\, \pi \rho\, \mathrm{d}\rho\, \sin^2 \delta \quad (4)$$

$$\delta = (\phi_p^2 + \phi_q^2)^{1/2}\, . \quad (5)$$

The phase shifts ϕ_p and ϕ_q, the cut-offs R_1, R_2, R_3, R_d, and the symmetrization procedures in the inelastic cross sections are described by Sahal-Bréchot (1969a, b). More details on the calculation procedure are given also by Dimitrijević *et al.* (1981) or Dimitrijević and Truong Bach (1986).

In order to exhibit the contribution of the collisions with a particular angular momentum to the line width and shift, we have introduced the semiclassical Stark broadening parameters w_l and d_l corresponding to the collisions with perturbers with a particular l (Dimitrijević *et al.*, 1981, 1983, Dimitrijević, 1986). We replace the integration over the impact parameter ρ of the perturbing classical particle by the integration over l using the relation $l \sim \rho k$ with $k = mv$. The corresponding values for w_l and d_l are obtained using l/k and $(l+1)/k$ as the lower and upper cut-offs in equations (1) to (5).

3. Results and discussion.

The data for atomic energy levels used in this calculations were taken from Bashkin and Stoner (1975). The required oscillator strengths were calculated in the Coulomb approximation using the method of Bates and Damgaard (1949) and tables of Oertel and Shomo (1968).

For resonance lines of LiI, NaI, KI, RbI and CsI homologous sequencé we have evaluated relative contribution w_l/w and d_l/d of the various angular momenta l to the half halfwidth w and shift d. Results for $T = 2500$ K and 20000 K at the electron density $N_e = 10^{16}\ \mathrm{cm}^{-3}$ are presented in figures 1-4. We can see that the importance of higher l values increase along the homologous sequence, especially in the case of the shift. We can notice also that for higher temperatures the importance of higher l values increase as well as the difference between values for particular emitters. In the case of the shift, the smallest l values are equal to zero in some cases for higher temperatures, since $\rho = l/k < R_3$ and the strong collision contribution is neglected in the case of the shift.

If we look at the corresponding Grotrian diagrams (Bashkin and Stoner, 1975), we can notice that in the case of resonance lines, the important perturbing level nd is gradually moving closer to the upper level of the transition. Such situation is similar to the increase of the temperature. If the energy levels are closer, higher l values become important at lower temperatures.

The relative half-halfwidths due to the inelastic, elastic and strong collisions at $T = 2500$ K and 20000 K and $N_e = 10^{16}\ \mathrm{cm}^{-3}$ as function of l are shown in figures 5-10. It must be pointed out that strong and weak contributions are contained in the elastic and inelastic halfwidth while the strong halfwidth contains strong inelastic and strong elastic contribution. We can notice the importance of very low l values for all investigated contributions as well as the increase of the importance of electrons with higher l values with the temperature and along the homologous sequence, especially for the inelastic contribution.

The importance of low l values is pointed out by Bely *et al.* (1963). They concluded that for neutrals, typical l values for the incident electron are between 1 and 5. Dimitrijević *et al.* (1981) performed a quantum mechanical close coupling calculations for the Stark broadening of the LiI 2s-2p line including the polarisation of ^{2}S and ^{2}P terms by means of coupled polarised orbitals. The difference between the quantum mechanical and semiclassical calculations is most prominent for the lowest l values. With the increase of l the result converge together at around $l = 3$ for the widths and $l = 4$ for the shift. For other members of the homologous group analysed, the influence of the higher l values is larger and the semiclassical method is better. Moreover, homologous atoms have a similar structure and we expect that the roughness of the method in the case of the lowest l values is less meaningful, since we analyse only the relative relations between various members of the same homologous group.

The relative importance of elastic, inelastic and strong contributions for different alkalis and for $T = 2500$ K and 20000 K are compared in figures 11 and 12. We can

© European Southern Observatory • Provided by the NASA Astrophysics Data System

1987A&AS...70...57D

see that the elastic contribution is dominant at $T = 2500$ K while at $T = 20000$ K the dominant contribution is inelastic. We can notice also that for none of the collisional processes examined, relative differences along the homologous sequence are particularly larger in comparison with others. Consequently, the regular behaviour of Stark widths and shifts (Purić *et al.*, 1977, Mazure and Nollez, 1978) is not dominated by only one collisional process as in the case of a FI transition array examinated previously (Dimitrijević, 1986). We can conclude that the difference between particular linewidths along the homologous sequence has not a systematic temperature dependence in the range $2500\ \mathrm{K} \leqslant T \leqslant 20000\ \mathrm{K}$, since we have not a clear variation of contributions due to different collisional processes. E.g. $w_{\mathrm{Na}}/w_{\mathrm{Cs}} = 4.4$ at $T = 2500$ K and 5.1 at $T = 20000$ K. In the case of the shift, differences between various members of the homologous sequence decrease toward the higher temperatures, since the contribution of the lowest l values strongly contributing to the differences becomes zero (see Figs. 3 and 4). E.g. $d_{\mathrm{Na}}/d_{\mathrm{Cs}} = 4.8$ at 2500 K and 1.3 at $T = 20000$ K.

4. Conclusion.

We can conclude that the regular behaviour of Stark widths and shifts is not clearly dominated by a particular collisional process. Consequently, the relative differences between particular linewidths have not a systematic temperature dependence along the homologous sequence examined (for $2500\ \mathrm{K} \leqslant T \leqslant 20000\ \mathrm{K}$). In the case of the shift, relative differences between various members of the homologous sequence decrease towards the higher temperatures since the contribution of the lowest l values becomes zero.

Other conclusions are that the importance of higher l values increase with the temperature and along the homologous sequence, especially in the case of the shift. Consequently, the semiclassical method becomes better.

References

BASHKIN, S., STONER, J. O. : 1975, *Atomic Energy Levels and Grotrian Diagrams,* Vol. I (North-Holland and Elsevier P. C., Amsterdam, New York, Oxford).

BATES, D. R., DAMGAARD, A. : 1949, *Phil. Trans. R. Soc. London Ser. A* **242,** 102.

BELY, O., TULLY, J., REGEMORTER, VAN H. : 1963, *Ann. Phys. Fr.* **8,** 303.

DIMITRIJEVIĆ, M. S. : 1986, *Astron. Astrophys. Suppl. Ser.* **64,** 591.

DIMITRIJEVIĆ, M. S., FEAUTRIER, N., SAHAL-BRÉCHOT, S. : 1981, *J. Phys. B* **14,** 2559.

DIMITRIJEVIĆ, M. S., FEAUTRIER, N., SAHAL-BRÉCHOT, S. : 1983, *Fizika* **15,** 205.

DIMITRIJEVIĆ, M. S., TRUONG BACH : 1986, *Z. Naturforsch.* **41a,** 772.

LAKIĆEVIĆ, I. S., PURIĆ, J. : 1983, *J. Phys. B* **16,** 1525.

MAZURE, A., NOLLEZ, G. : 1978, *Z. Naturforsch.* **33a,** 1575.

MILLER, M. H., LESAGE, A., ABADIE, D. : 1982, *Phys. Rev. A* **25,** 2064.

MILLER, M. H., LESAGE, A., PURIĆ, J. : 1980, *Astrophys. J.* **239,** 410.

OERTEL, G. K., SHOMO, L. P. : 1968, *Astrophys. J. Suppl. Ser.* **16,** 175.

PITTMAN, T. L., KONJEVIĆ, N. : 1986, *J. Quant. Spectrosc. Radiat. Transfer.* **35,** 247.

PURIĆ, J., ĆIRKOVIĆ, Lj. : 1973, *Proc. 11th Int. Conf. Phen. Ioniz. Gases* (Prague) 398.

PURIĆ, J., ĆUK, M., LAKIĆEVIĆ, I. S. : 1985, *Phys. Rev. A* **32,** 1106.

PURIĆ, J., DIMITRIJEVIĆ, M. S., LAKIĆEVIĆ, I. S. : 1978, *Phys. Lett.* **67A,** 189.

PURIĆ, J., LABAT, J., ĆIRKOVIĆ, Lj., DJENIŽE, S. : 1977, *J. Phys. B* **10,** 2375.

SAHAL-BRÉCHOT, S. : 1969a, *Astron. Astrophys.* **1,** 91.

SAHAL-BRÉCHOT, S. : 1969b, *Astron. Astrophys.* **2,** 322.

© European Southern Observatory • Provided by the NASA Astrophysics Data System

1987A&AS...70...57D

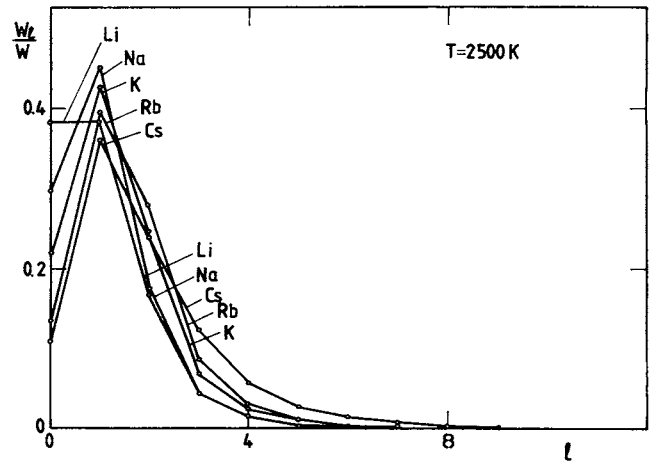

FIGURE 1. — Relative contributions, w_l/w for the various angular momenta l of the colliding electron for the semiclassical half halfwidths of the resonance lines of alkalis. $T = 2500$ K and $N_e = 10^{16}$ cm^{-3}.

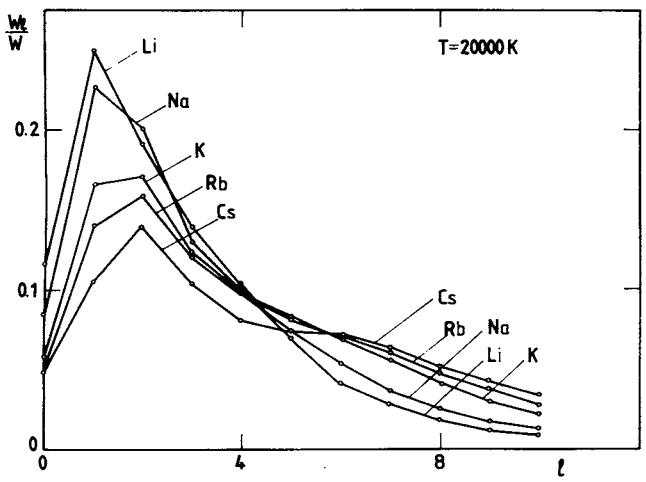

FIGURE 2. — Same as in figure 1, but for $T = 20000$ K.

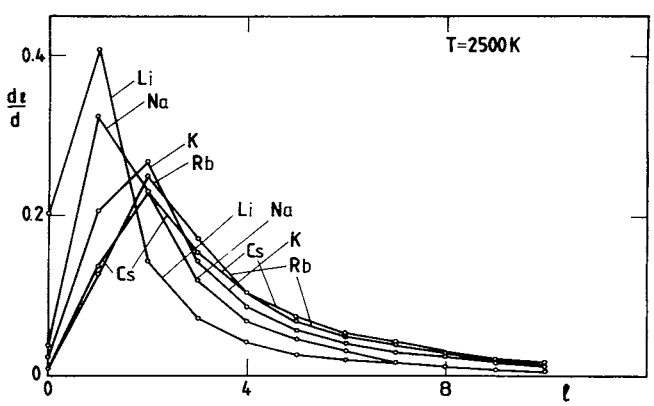

FIGURE 3. — Relative contributions, d_l/d for the various angular momenta l of the colliding electron for the semiclassical shift of the resonance lines of alkalis. $T = 2500$ K and $N_e = 10^{16}$ cm^{-3}.

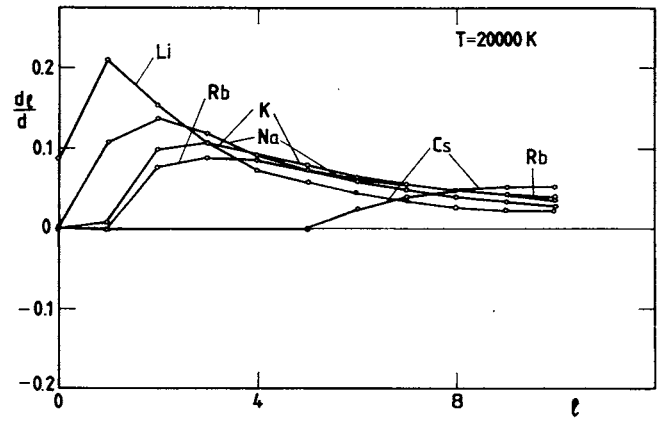

FIGURE 4. — Same as in figure 1 but for $T = 20000$ K.

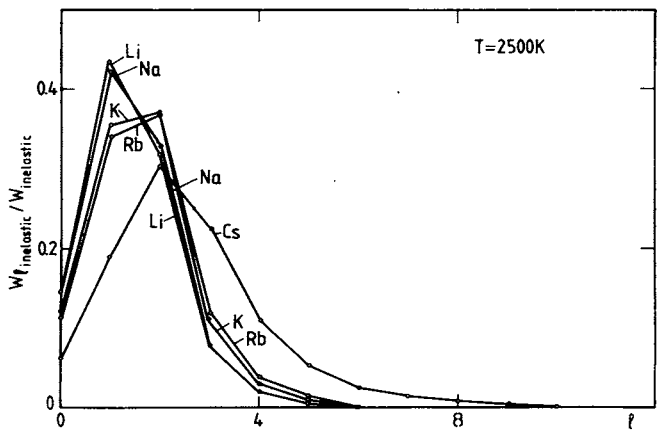

FIGURE 5. — Relative half halfwidths due to inelastic collisions as functions of l. $T = 2500$ K, $N_e = 10^{16}$ cm^{-3}.

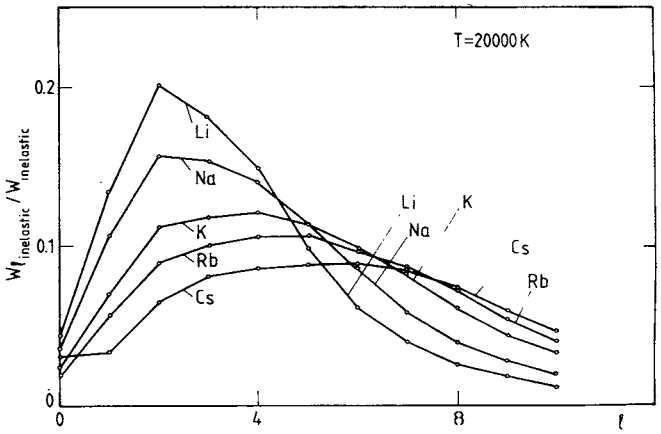

FIGURE 6. — Same as in figure 5 but for $T = 20000$ K.

© European Southern Observatory • Provided by the NASA Astrophysics Data System

1987A&AS...70...57D

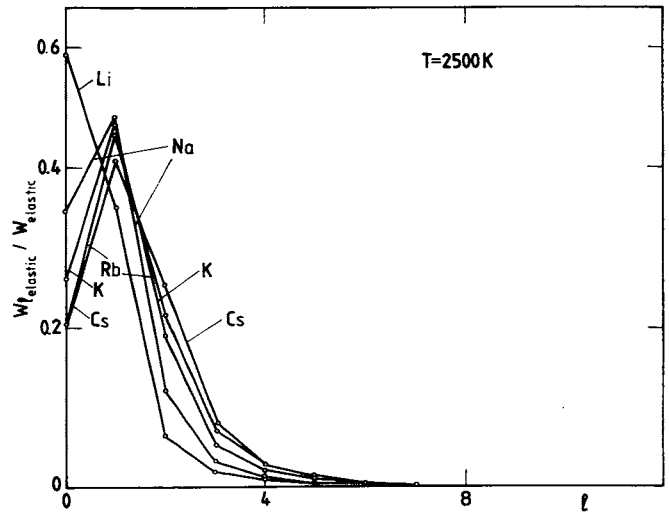

FIGURE 7. — Relative half halfwidths due to elastic collisions as functions of l. $T = 2500$ K, $N_e = 10^{16}$ cm^{-3}.

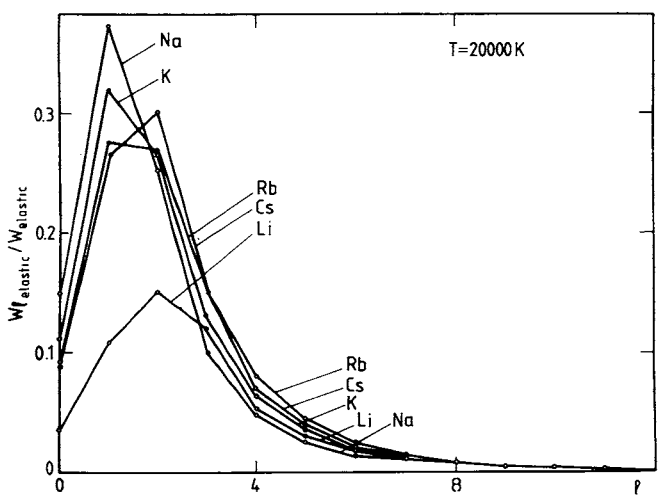

FIGURE 8. — Same as in figure 7 but for $T = 20000$ K.

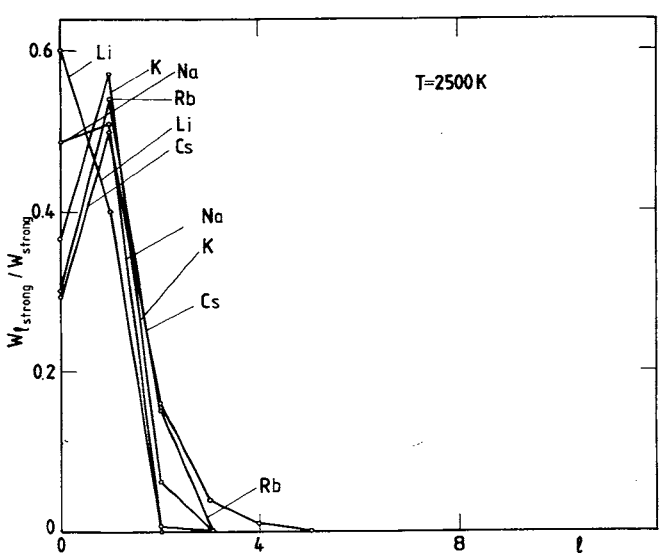

FIGURE 9. — Relative half halfwidths due to strong collisions as functions of l. $T = 2500$ K, $N_e = 10^{16}$ cm^{-3}.

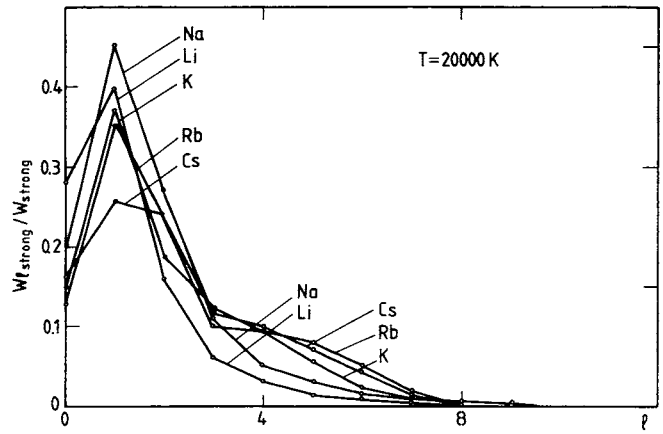

FIGURE 10. — Same as in figure 9 but for $T = 20000$ K.

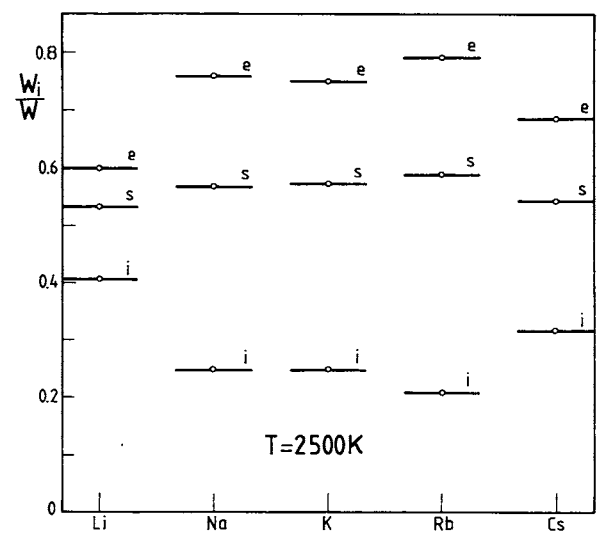

FIGURE 11. — Relative contributions of elastic (j = e), inelastic (j = i) and strong (j = s) collisions to the halfwidth for $T = 2500$ K, $N_e = 10^{16}$ cm^{-3}.

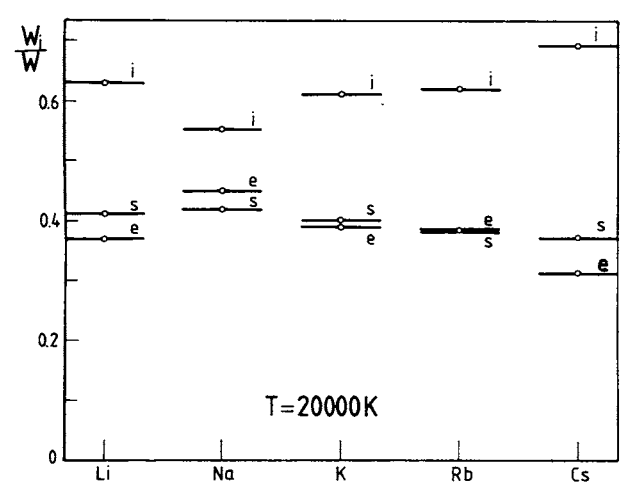

FIGURE 12. — Same as in figure 11 but for $T = 20000$ K.

© European Southern Observatory • Provided by the NASA Astrophysics Data System

1988A&AS...76...53D

ASTRONOMY & ASTROPHYSICS
SUPPLEMENT SERIES

NOVEMBER 1988, PAGE 53

Astron. Astrophys. Suppl. Ser. **76**, 53-59 (1988)

Electron-impact widths of doubly and triply charged ion lines of astrophysical importance

M. S. Dimitrijević

Astronomical Observatory, Volgina 7, 11050 Beograd, Yugoslavia

Received March 22, accepted June 8, 1988

Summary. — A recently developed modified semiempirical approach (Dimitrijević and Konjević, 1980, 1987 ; Dimitrijević and Kršljanin, 1986) is applied to the Stark broadening of spectral lines from 127 astrophysically important multiplets of doubly and triply charged ions.

Key words : lines : profiles — atomic and molecular data, Stark broadening.

1. Introduction.

In the spectra of O, B and A type stars, and white dwarfs, a large number of singly and multiply charged ion lines has been observed (see e.g. Peytremann, 1972, or Lanz *et al.*, 1982). In atmospheres of such stars, Stark broadening is the dominant pressure broadening mechanism and the knowledge of the Stark broadening parameters for a large number of elements in several ionization stages is very important for a number of astrophysical problems. Even in atmospheres of relatively cool stars as the Sun, where line broadening caused by collisions with neutral perturbers is dominant, Stark broadening may compete with other broadening mechanisms in line wings or for higher spectral series members (Vince *et al.*, 1985a). Moreover, Stark effect is also one of the causes of the stellar spectral line asymmetries (Vince *et al.*, 1985b) and its knowledge is important for more precise determination of other sources of asymmetry.

In many astrophysical problems, Stark broadening data for a large number of transitions in many atoms are needed. Quantum mechanical or semiclassical theories requiring the knowledge of numerous atomic data and time consuming computer codes, are often not suitable for large scale calculations when high accuracy of every particular line is not so important and only a reasonable average accuracy for a number of lines is required. Consequently an effort has been made to provide necessary simple approximate formulae with good average accuracy (see e.g. Griem, 1968 ; Hey and Bryan, 1977 ; Seaton, 1987).

A convenient method for Stark broadening calculations when more sophisticated theories are not needed or not applicable (e.g. large scale calculations, lack of atomic data, complex spectra or rough estimates) may be the modified semiempirical approach (Dimitrijević and Konjević, 1980, 1981a, 1987 ; Dimitrijević and Kršljanin, 1986) for Stark broadening parameters of ion lines and a simple method for Stark widths and shifts in the case of neutral atom lines (Dimitrijević and Konjević, 1986).

The modified semiempirical approach was tested several times (Dimitrijević and Konjević, 1981a, b, c ; Dimitrijević, 1982a, c, 1983, 1988 ; Konjević *et al.*, 1984 ; Lanz *et al.*, 1988 ; El-Farra and Hughes, 1983 ; Ackermann *et al.*, 1985) and on the average gives a satisfactory agreement with experiments.

In this paper, the modified semiempirical approach is applied to the Stark broadening of spectral lines from 127 astrophysically important multiplets of doubly and triply charged ions, in order to provide new Stark broadening data needed in astrophysics.

2. Modified semiempirical approach.

According to the modified semiempirical approach (Dimitrijević and Konjević, 1980, 1987 ; Dimitrijević and Kršljanin, 1986), the half-halfwidth w and the shift d of

Send offprint requests to : M. S. Dimitrijević.

© European Southern Observatory • Provided by the NASA Astrophysics Data System

1988A&AS...76...53D

an ion spectral line broadened by Stark effect are given by the following expression

$$w + i d = N \frac{4\pi}{3} \frac{\hbar^2}{m^2} \left(\frac{2m}{\pi k T} \right)^{1/2} \frac{\pi}{\sqrt{3}} \sum_{j=i,f} \{ \mathbf{R}^2_{k,k+1} [\mathbf{g}(x_{k,k+1}) + i \varepsilon_j \mathbf{g}_{sh}(x_{k,k+1})] + \mathbf{R}^2_{k,k-1} [\mathbf{g}(x_{k,k-1}) - i \varepsilon_j \mathbf{g}_{sh}(x_{k,k-1})] \} + \sum_{j'} (\mathbf{R}^2_{jj'})_{\Delta n \neq 0} [g(x_j) + i \varepsilon_j g_{sh}(x_j)] - 2 i \varepsilon_j \left[\sum_{\Delta E_{jj'} < 0} (\mathbf{R}^2_{jj'})_{\Delta n \neq 0} g_{sh}(x_{jj'}) \right] . \quad (1)$$

In this expression $\mathbf{R}^2_{j',j}$ (in units of the Bohr radius a_0^2) is the square of the coordinate operator matrix element summed over all components of the operator and the magnetic substates of total angular momentum J', and averaged over the magnetic substates of J.

$$\sum_{j'} (\mathbf{R}^2_{jj'})_{\Delta n \neq 0} = \left(\frac{3 n_j^*}{2 Z} \right)^2 \frac{1}{9} (n_j^{*2} + 3 \ell_j^2 + 3 \ell_j + 11)$$

$$\mathbf{R}^2_{jj'} = \left(\frac{3 n_j^{*2}}{2 Z} \right) \frac{\ell_>}{2 \ell + 1} (n_\ell^{*2} - \ell_>^2) \phi^2 (n_{\ell-1}^*, n_\ell^*, \ell) . \quad (2)$$

The cases where the one-electron model (i.e. only one energy level for each $n\ell$ electron) assumed in equation (2) is not satisfied, are analysed in detail by Dimitrijević (1982b). e.g. for a multiplet as a whole, $\mathbf{R}^2_{j'j}$ should be multiplied by $R^2_{\text{mult}}(2\ell+1)/(2L+1)$. The multiplet factor R^2_{mult} can be found in tables of Shore and Menzel (1965). The parameter $\varepsilon_j = +1$ if $j = i$, and -1 if $j = f$, $k = \ell_j$ (the orbital quantum number of the valence electron, i and f denote the initial and final energy states, $x_{jj'} = 3\,kT/2|\Delta E_{jj'}|$ $x_j = 3\,kTn_j^{*3}/4\,Z^2 E_{\text{H}}$, E_{H} is the hydrogen ionization energy, E_{ion} is the appropriate spectral series limit (In case that the term in question belongs to a series converging on an excited state of the resulting ion, the excitation energy of this state is added to the usual ionization energy). The residual ionic charge is denoted as Z, $\Delta E_{j'j} = E_{j'} - E_{j'}$ $\ell = \max(\ell_{j'}, \ell_j)$, N is electron density, $n_j^* = [E_{\text{H}} Z^2/(E_{\text{ion}} - E_j)]^{1/2}$ the effective principal quantum number, and ϕ^2 is the Bates-Damgaard (1949) factor, tabulated e.g. in Oertel and Shomo's (1968) paper.

All Gaunt factors g, $\mathbf{g}$, g_{sh} and $\mathbf{g}_{sh}$ are given in Dimitrijević and Kršljanin (1986). At high temperatures, say $3\,kT/2\,\Delta E > 50$, all Gaunt factors in equation (1) may be calculated in accordance with the GBKO high temperature limit (Griem *et al.*, 1962), viz.

$$\mathbf{g}_{j'j} = g_{j'j} = \frac{\sqrt{3}}{\pi} \left[\frac{1}{2} + ln \left(\frac{2\,ZkT}{n_j^{*2}\,\Delta E_{j'j}} \right) \right]$$

$$\mathbf{g}_{sh} = g_{sh} = \sqrt{3}/2 .$$

Equation (1) is obtained assuming the LS coupling approximation, separating the transitions with $\Delta n = 0$ and $\Delta n \neq 0$ and supposing that the nearest perturbing level in the $\Delta n \neq 0$ group may be obtained in the hydrogenic approximation as :

$$|\Delta E_{n,n+1}| \approx 2\,Z^2 E_{\text{H}}/n^{*3} .$$

In the cases when perturbing levels exist which strongly violate the assumed approximations, i.e. if there are levels with $|\Delta E_{j'j}| \ll |\Delta E_{n,n+1}|$, a correction of equation (1) may be done by summing equation (3) and equation (1). Here, m' is the number of such perturbing levels and $\varepsilon_k = +1$ if $k = i$ and -1 if $k = f$.

$$w_c + i d_c = N \frac{4\pi}{3} \frac{\hbar^2}{m^2} \left(\frac{2m}{\pi k T} \right)^{1/2} \frac{\pi}{\sqrt{3}} \times \sum_{m'} \mathbf{R}^2_{j'j} [g(x_{j'j}) - g(x_{n_i,n_{i+1}}) \pm i \varepsilon_k (g_{sh}(x_{j'j}) \mp g_{sh}(x_{n_i,n_{i+1}}))] . \quad (3)$$

For all cases when $3\,kT/2|\Delta E_{j'j}| \lesssim 2$ one can use the values $g = g_{sh} = 0.2$ and $\mathbf{g} = \mathbf{g}_{\text{sh}} = 0.9\text{-}1.1/Z$.

Furthermore, one can put in equations (1) and (2), $\phi^2 = 1$ (Dimitrijević and Konjević, 1987) what is a reasonable assumption for $\Delta n = 0$ since the exact values of ϕ^2 usually range between 0.8 and 1 (see Griem, 1974, p. 31). If one performs summation in equation (1) it is easy to obtain (Dimitrijević and Konjević, 1987)

$$w(\text{Å}) = 0.4430 \times 10^{-8} \frac{\lambda^2(\text{cm})\,N(\text{cm}^{-3})}{T^{1/2}(\text{K})} \times \sum_{j=i,f} \left[\mathbf{R}_j^2 + \frac{\mathbf{g}_{th} - g_{th}}{g_{th}} \left(\frac{3 n_j^*}{2 Z} \right)^2 (n_j^{*2} - \ell_j^2 - \ell_j - 1) \right]$$

$$\mathbf{R}_j^2 = \sum_{j'} \mathbf{R}^2_{jj'} . \quad (4)$$

Since the contribution to the total line width of transitions with $\Delta n \neq 0$ does not exceed 25 %, and it is compensated by assuming $\phi^2 = 1$, we can neglect them and finally obtain :

$$w(\text{Å}) = 2.2151 \times 10^{-8} \frac{\lambda^2(\text{cm})\,N(\text{cm}^{-3})}{T^{1/2}(\text{K})} \times \left(0.9 - \frac{1.1}{Z} \right) \sum_{j=i,f} \left(\frac{3 n_j^*}{2 Z} \right)^2 (n^{*2} - \ell_j^2 - \ell_j - 1) . \quad (5)$$

© European Southern Observatory • Provided by the NASA Astrophysics Data System

1988A&AS...76...53D

In order to test the modified semiempirical approach, selected experimental data for 36 multiplets (7 different ion species) of doubly ; and 7 multiplets (4 different ion species) of triply-charged ions, were compared with theoretical linewidths. The averaged values of the ratios of measured to calculated widths are as follows : for doubly-, 1.06 ± 0.32 and for triply-charged ions 0.91 ± 0.42 (Dimitrijević and Konjević, 1980). Furthermore, in order to test the equations obtained for low temperature limit of modified semiempirical formula, comparison is made between the linewidth results from equations (1) and (5) and previously mentioned selected experimental results (Dimitrijević and Konjević, 1980), in the case when equation (5) may be applied (32 multiplets). The average ratio of experimental and calculated values from equations (1) and (5) are 1.01 and 1.04 respectively (Dimitrijević and Konjević, 1987). Comparison is made also with the results of comprehensive width calculations for doubly and triply ionized atoms (Dimitrijević and Konjević, 1981a). The discrepancy did not exceed $\pm$ 30 on the average (Dimitrijević and Konjević, 1987).

Recently, the modified semiempirical theory is applied to the most intensive lines of Ti II and Mn II observed in the Solar spectrum (Dimitrijević, 1982a) as well as to the selected Fe II lines from the Solar spectrum and the spectrum of Am 15 Vulpeculae (Dimitrijević, 1988), in order to test the applicability of the approach to the case of more complex transitions and heavier elements. The obtained agreement between this approach and more sophisticated semiclassical calculations indicates that this method can be used for estimation of electron widths for heavier elements also.

3. Results.

Generally, the possibilities of the theory in the case of shifts are considerably smaller than for line widths (Dimitrijević *et al.*, 1981, Griem, 1974). Consequently in this article only width calculations are presented. The results of electron-impact line width calculations (FWHM) for the prominent isolated lines of Be III through Ar III and B IV through Ar IV are given in table I.

It is not necessary to discuss here uncertainties in all of the approximations involved in our calculations, since the criteria for their application are described in detail elsewhere (Griem, 1964, 1968, 1974 : Griem *et al.*, 1962). The use of a common Gaunt factor threshold value for all elements is a very crude approximation (see e.g. Dimitrijević and Konjević, 1978) which, however, introduces great simplification whenever it is necessary to calculate, with a reasonable accuracy, large number of line widths.

For evaluation of the radial integrals, the Coulomb approximation (Bates and Damgaard, 1949 ; Oertel and Shomo, 1968) has been used. Cases with an initial atomic state with equivalent electrons were avoided, when possible. If not, the corresponding coefficients of fractional parentage (Shore and Mensel, 1965) are included.

The principal deficiency in the comparison of theoretical results for doubly and triply charged ion lines with experiments comes from the lack of experimental linewidths at higher temperatures. However, on the basis on existing numerous comparisons for temperatures of the greatest importance for astrophysics (see e.g. Konjević *et al.*, 1984 ; Dimitrijević and Konjević, 1980) we hope that the present results will be useful for a number of astrophysical purposes.

Acknowledgements.

I am indebted to Dr Nicole Feautrier and Dr Françoise Praderie for encouraging me to perform the calculations presented in this article.

References

ACKERMANN, U., FINKEN, K. H. and MUSIELOK, J. : 1985, *Phys. Rev. A* **31,** 2597.
BATES, D. R. and DAMGAARD, A. : 1949, *Philos. Trans. R. Soc. London, Ser. A* **242,** 101.
DIMITRIJEVIĆ, M. S. : 1982a, Sun and Planetary System, Eds. W. Fricke, G. Teleki (D. Reidel P. C.) Dordrecht, p. 101.
DIMITRIJEVIĆ, M. S. : 1982b, *Astron. Astrophys.* **112,** 251.
DIMITRIJEVIĆ, M. S. : 1982c, The Physics of Ionized Gases (Inv. Lectures of SPIG-82), Ed. G. Pichler, Inst. Phys. University Zagreb, p. 397.
DIMITRIJEVIĆ, M. S. : 1983, *Astron. Astrophys.* **127,** 68.
DIMITRIJEVIĆ, M. S. : 1988, Physics of Formation of Fe II Lines Outside LTE, Ed. R. Viotti, A. Vittone, M. Friedjung (D. Reidel P. C.) Dordrecht, p. 211.
DIMITRIJEVIĆ, M. S. and KONJEVIĆ, N. : 1978, *J. Quant. Spectrosc. Radiat. Transfer* **20,** 223.
DIMITRIJEVIĆ, M. S. and KONJEVIĆ, N. : 1980, *J. Quant. Spestrosc. Radiat. Transfer* **24,** 451.
DIMITRIJEVIĆ, M. S. and KONJEVIĆ, N. : 1981a, Spectral Line Shapes, Ed. B. Wende (W. de Gruyter) Berlin, New York, p. 211.
DIMITRIJEVIĆ, M. S. and KONJEVIĆ, N. : 1981b, *Astron. Astrophys.* **102,** 93.
DIMITRIJEVIĆ, M. S. and KONJEVIĆ, N. : 1981c, *J. Quant. Spectrosc. Radiat. Transfer* **25,** 387.
DIMITRIJEVIĆ, M. S., FEAUTRIER, N., SAHAL-BRECHOT, S. : 1981, *J. Phys. B* **14,** 2559.
DIMITRIJEVIĆ, M. S. and KRŠLJANIN, V. : 1986, *Astron. Astrophys.* **165,** 269.
DIMITRIJEVIĆ, M. S. and KONJEVIĆ, N. : 1986, *Astron. Astrophys.* **163,** 297.
DIMITRIJEVIĆ, M. S. and KONJEVIĆ, N. : 1987, *Astron. Astrophys.* **172,** 345.
EL-FARRA, M. A., HUGHES, T. P. : 1983, *J. Quant. Spectrosc. Radiat. Transfer* **30,** 335.

© European Southern Observatory • Provided by the NASA Astrophysics Data System

1988A&AS...76...53D

GRIEM, H. R. : 1964, Plasma Spectroscopy, Chap. 4 (McGraw-Hill) New York.
GRIEM, H. R. : 1968, *Phys. Rev.* **165,** 258.
GRIEM, H. R. : 1974, Spectral Line Broadening by Plasmas (Academic Press) New York.
GRIEM, H. R., BARANGER, M., KOLB, A. C., OERTEL, G. K. : 1962, *Phys. Rev.* **125,** 177.
HEY, J. D. and BRYAN, R. J. : 1977, *J. Quant. Spectrosc. Radiat. Transfer* **17,** 221.
KONJEVIĆ, N., DIMITRIJEVIĆ, M. S. and WIESE, W. L. : 1984, *J. Phys. Chem. Ref. Data* **13,** 649.
LANZ, T., DIMITRIJEVIĆ, M. S. and ARTRU, M. C. : 1988, *Astron. Astrophys.* **192,** 249.
OERTEL, G. K. and SHOMO, L. P. : 1968, *Astrophys. J. Suppl. Ser.* **16,** 175.
PEYTREMANN, E. : 1972, *Astron. Astrophys.* **17,** 76.
SEATON, M. J. : 1987, *J. Phys. B* **20,** 6431.
SHORE, B. W. and MENZEL, D. H. : 1965, *Astrophys. J. Suppl. Ser.* **12,** 187.
VINCE, I., DIMITRIJEVIĆ, M. S. and KRŠLJANIN, V. : 1985a, Spectral Line Shapes III, Ed. F. Rostas (W. de Gruyter) Berlin, New York, 649.
VINCE, I., DIMITRIJEVIĆ, M. S. and KRŠLJANIN, V. : 1985b, Progress in Stellar Spectral Line Formation Theory, Eds. J. E. Beckman ; L. Crivellari (D. Reidel) Dordrecht, Boston, Lancaster, 373.

© European Southern Observatory • Provided by the NASA Astrophysics Data System

1988A&AS...76...53D

TABLE I. — *This table lists electron impact full half-widths of isolated lines from beryllium through argon at an electron density of* 1×10^{17} cm^{-3} *and electron temperatures from 10000 to 160000 K. Transition and averaged wavelength for the multiplet (in Angström units) are also given.*

Element/Transition	λ (Å)	W_{MSE} (Å) (FWHM)				
		T(K)=10000	20000	40000	80000	160000
BE III $2s^1S-2p^1P^o$	6141.0	0.227	0.160	0.117	0.947-1	0.843-1
BE III $2s^3S-2p^3P^o$	3721.8	0.701-1	0.496-1	0.351-1	0.263-1	0.221-1
BE III $2p^1P^o-3d^1D$	746.2	0.883-2	0.732-2	0.599-2	0.591-2	0.481-2
BE III $2p^3P^o-3d^3D$	675.6	0.559-2	0.449-2	0.370-2	0.309-2	0.312-2
B III $2s^2S-2p^2P^o$	2066.3	0.191-1	0.135-1	0.953-2	0.674-2	0.516-2
B III $2p^2P^o-3d^2D$	677.1	0.558-2	0.449-2	0.370-2	0.308-2	0.310-2
B III $4p^2P^o-5d^2D$	4243.6	10.1	8.46	6.92	5.84	4.83
B III $4d^2D-5f^2F^o$	4487.5	12.9	10.0	8.01	6.46	5.20
B IV $2s^3S-2p^3P^o$	2823.4	0.269-1	0.190-1	0.134-1	0.966-2	0.767-2
B IV $2s^3S-3p^3P^o$	344.2	0.665-3	0.496-3	0.403-3	0.343-3	0.295-3
C III $2p^3P^o-3s^3S$	538.2	0.344-2	0.243-2	0.172-2	0.139-2	0.121-2
C III $2p^2P^o-3d^3D$	459.6	0.199-2	0.141-2	0.109-2	0.891-3	0.748-3
C III $3s^3S-3p^3P^o$	4648.8	0.523	0.370	0.274	0.229	0.203
C III $3s^1P^o-3p^1D$	4326.0	0.486	0.346	0.280	0.249	0.223
C III $3p^1P^o-3d^1D$	5696.0	0.736	0.521	0.384	0.315	0.279
C III $3p^1P^o-4d^1D$	1531.8	0.185	0.160	0.139	0.125	0.115
C III $3d^1D-4f^1F^o$	2162.9	0.184	0.147	0.120	0.106	0.964-1
C III $4p^3P^o-5d^3D$	3609.3	3.33	2.95	2.64	2.26	2.04
C III $4f^1F^o-5g^1G$	4187.0	1.53	1.26	1.07	1.02	0.981
C IV $2s^2S-2p^2P^o$	1549.1	0.728-2	0.515-2	0.364-2	0.258-2	0.187-2
C IV $2s^2S-4p^2P^o$	244.9	0.295-2	0.250-2	0.218-2	0.188-2	0.176-2
C IV $2p^2P^o-3s^2S$	419.6	0.227-2	0.161-2	0.116-2	0.936-3	0.829-3
C IV $2p^2P^o-3d^2D$	384.1	0.106-2	0.811-3	0.656-3	0.538-3	0.440-3
C IV $2p^2P^o-4d^2D$	289.2	0.598-2	0.503-2	0.416-2	0.338-2	0.286-2
C IV $3s^2S-3p^2P^o$	5804.9	0.776	0.571	0.440	0.368	0.325

Element/Transition	λ (Å)	W_{MSE} (Å) (FWHM)				
		T(K)=10000	20000	40000	80000	160000
C IV $4d^2D-5f^2F^o$	2524.4	2.16	1.75	1.40	1.11	0.889
N III $2p^2P^o-3s^2S$	452.1	0.202-2	0.143-2	0.101-2	0.783-3	0.681-3
N III $2p^2P^o-3d^2D$	374.4	0.130-2	0.922-3	0.652-3	0.501-3	0.413-3
N III $3s^4P^o-3p^4D$	4517.3	1.30	1.09	0.967	0.968	0.946
N III $3s^4P^o-3p^4P$	3367.3	0.399	0.167	0.121	0.984-1	0.863-1
N III $3p^2P^o-3d^2D$	4640.6	0.415	0.294	0.208	0.163	0.139
N III $3p^4D-3d^4F^o$	4864.9	0.435	0.307	0.218	0.173	0.147
N III $3d^4P^o-4f^4D$	2063.8	0.171	0.141	0.116	0.976-1	0.944-1
N IV $2p^1P^o-3d^1D$	335.0	0.780-3	0.552-3	0.390-3	0.290-3	0.232-3
N IV $2p^3P^o-3d^3D$	283.5	0.471-3	0.333-3	0.244-3	0.194-3	0.160-3
N IV $3s^3S-3p^3P^o$	3480.8	0.213	0.151	0.108	0.837-1	0.715-1
N IV $3p^3P^o-3d^3D$	7117.0	0.735	0.520	0.379	0.304	0.259
O III $3s^3P^o-3p^3D$	3762.3	0.230	0.163	0.115	0.866-1	0.742-1
O III $3s^3P^o-3p^3S$	3326.6	0.185	0.131	0.925-1	0.697-1	0.598-1
O III $3s^3P^o-3p^3P$	3041.5	0.158	0.112	0.792-1	0.600-1	0.515-1
O III $3s^5P-3p^5D^o$	3706.1	0.223	0.158	0.112	0.841-1	0.722-1
O III $3s^5P-3p^5S^o$	2678.2	0.126	0.891-1	0.630-1	0.479-1	0.410-1
O III $3p^3S-3d^3P^o$	3127.3	0.171	0.121	0.854-1	0.626-1	0.515-1
O III $3p^3P-3d^3D^o$	3712.5	0.245	0.173	0.122	0.907-1	0.753-1
O III $3p^3D-3d^3F^o$	3265.9	0.178	0.126	0.891-1	0.668-1	0.556-1
O III $3p^5D^o-3d^5F$	3453.0	0.196	0.139	0.982-1	0.727-1	0.601-1
O III $3d^3P^o-4p^3S$	2601.6	0.321	0.227	0.175	0.150	0.137
O III $3d^1F^o-4p^1D$	2558.1	0.356	0.262	0.215	0.189	0.173
O IV $2p^2P^o-3s^2S$	279.8	0.596-3	0.421-3	0.298-3	0.217-3	0.176-3

© European Southern Observatory • Provided by the NASA Astrophysics Data System

1988A&AS...76...53D

TABLE I *(continued)*.

Element/Transition	λ(Å)	W_{MSE}(Å) (FWHM) T(K)=10000	20000	40000	80000	160000
O IV $2p^2P^o-3d^2D$	238.5	0.330-3	0.233-3	0.165-3	0.120-3	0.948-4
O IV $3s^4P^o-3p^4D$	3374.3	0.168	0.119	0.838-1	0.622-1	0.520-1
O IV $3p^4P-3d^4D^o$	4792.5	0.310	0.219	0.155	0.119	0.983-1
O IV $3p^2D-3d^2D^o$	5339.5	0.400	0.283	0.202	0.156	0.132
F III $3s^4P_6-3p^4P^o_6$	2916.3	0.119	0.839-1	0.593-1	0.431-1	0.355-1
F III $3s^4P-3p^4D^o$	3124.4	0.134	0.949-1	0.671-1	0.489-1	0.403-1
F III $3s^2P_4-3p^2P^o_4$	2811.4	0.130	0.918-1	0.652-1	0.505-1	0.436-1
F III $3s^2P-3p^2D^o$	3176.9	0.160	0.113	0.803-1	0.622-1	0.534-1
F III $3p'^2D^o-3d'^2D$	2788.1	0.128	0.903-1	0.638-1	0.463-1	0.373-1
NE III $3s^3S^o-3p^3P$	2678.2	0.965-1	0.683-1	0.483-1	0.348-1	0.285-1
NE III $3s^5S^o-3p^5P$	2592.3	0.820-1	0.580-1	0.410-1	0.292-1	0.235-1
NE III $3s'^3D^o-3p'^3F$	2612.4	0.832-1	0.588-1	0.416-1	0.298-1	0.241-1
NE III $3p^3P-3d^3D^o$	2413.0	0.540-1	0.382-1	0.270-1	0.192-1	0.150-1
NE III $3p'^3D-3d'^3D^o$	2091.7	0.625-1	0.442-1	0.312-1	0.223-1	0.175-1
NE III $3p^5P_7-3d^5D^o_9$	2163.8	0.685-1	0.484-1	0.342-1	0.243-1	0.189-1
NE IV $3s^4P-3p^4D^o$	2361.5	0.608-1	0.430-1	0.304-1	0.215-1	0.169-1
NE IV $3s'^2D-3p'^2F^o$	2289.1	0.588-1	0.416-1	0.294-1	0.208-1	0.163-1
NA III $3s^4P-3p^4P^o$	2515.6	0.667-1	0.472-1	0.333-1	0.237-1	0.189-1
NA III $3s^4P-3p^4D^o$	2232.5	0.545-1	0.385-1	0.272-1	0.193-1	0.154-1
NA III $3s^4P-3p^4S^o$	1971.5	0.441-1	0.311-1	0.220-1	0.156-1	0.124-1
NA III $3s^2P-3p^2D^o$	2458.9	0.689-1	0.487-1	0.345-1	0.244-1	0.195-1
NA III $3s^2P-3p^2P^o$	2247.4	0.593-1	0.419-1	0.296-1	0.210-1	0.168-1
NA III $3p^2D^o-3p^2F$	1995.9	0.558-1	0.394-1	0.279-1	0.197-1	0.152-1
NA III $3p^4P^o-3d^4D$	1852.0	0.447-1	0.316-1	0.223-1	0.158-1	0.121-1

Element/Transition	λ(Å)	W_{MSE}(Å) (FWHM) T(K)=10000	20000	40000	80000	160000
NA III $3p^4D^o-3d^4F$	1947.1	0.514-1	0.363-1	0.257-1	0.182-1	0.139-1
MG IV $3s^4P-3p^4S^o$	1477.8	0.199-1	0.140-1	0.993-2	0.702-2	0.520-2
MG IV $3s^4P-3p^4P^o$	1911.5	0.314-1	0.222-1	0.157-1	0.111-1	0.828-2
MG IV $3s^4P_6-3p^4D^o_8$	1683.0	0.249-1	0.176-1	0.125-1	0.882-2	0.654-2
MG IV $3p^4S^o_4-4d^4P_6$	1548.1	0.238-1	0.169-1	0.119-1	0.843-2	0.611-2
AL III $3s^2S-3p^2P^o$	1857.4	0.303-1	0.214-1	0.151-1	0.107-1	0.801-2
AL III $3s^2S-4p^2P^o$	696.0	0.136-1	0.964-2	0.688-2	0.549-2	0.494-2
AL III $3s^2S-5p^2P^o$	560.4	0.238-1	0.172-1	0.142-1	0.130-1	0.122-1
AL III $3p^2P^o-3d^2D$	1609.9	0.316-1	0.224-1	0.158-1	0.112-1	0.825-2
AL III $3d^2D-4f^2F^o$	1935.9	0.148	0.121	0.998-1	0.833-1	0.798-1
AL III $4s^2S-4p^2P^o$	5705.9	1.48	1.04	0.751	0.616	0.569
AL III $4p^2P^o-4d^2D$	4523.2	1.45	1.14	0.909	0.764	0.727
AL III $4d^2D-6f^2F^o$	2762.8	6.51	5.48	4.35	3.69	3.09
AL III $4f^2F^o-5d^2D$	4701.6	4.42	3.77	3.23	2.80	2.56
AL III $4f^2F^o-6g^2G$	2907.0	4.04	3.32	2.77	2.34	1.97
SI III $3p^3P^o-3d^3D$	1111.6	0.894-2	0.632-2	0.447-2	0.316-2	0.223-2
SI III $3p^3P^o-4s^3S$	996.1	0.175-1	0.124-1	0.876-2	0.702-2	0.613-2
SI III $4s^3S-4p^3P^o$	4560.1	0.728	0.514	0.364	0.289	0.257
SI III $4p^3P^o-4d^3D$	3801.4	0.762	0.546	0.411	0.342	0.316
SI III $4p^3P^o-5s^3S$	3237.8	0.793	0.571	0.458	0.411	0.379
SI IV $3s^2S-3p^2P^o$	1396.7	0.141-1	0.995-2	0.703-2	0.497-2	0.356-2
SI IV $3p^2P^o-3d^2D$	1126.4	0.109-1	0.768-2	0.543-2	0.384-2	0.273-2
SI IV $4s^2S-4p^2P^o$	4097.9	0.605	0.428	0.302	0.230	0.196
SI IV $4p^2P^o-4d^2D$	3160.3	0.467	0.346	0.267	0.213	0.180

© European Southern Observatory • Provided by the NASA Astrophysics Data System

1988A&AS...76...53D

TABLE I *(continued)*.

Element/Transition	λ(Å)	W_{MSE}(Å) (FWHM)				
		T(K)=10000	20000	40000	80000	160000
SI IV $4d^2D-5p^2P^o$	3766.0	1.19	0.866	0.675	0.568	0.507
SI IV $5p^2P^o-6s^2S$	4323.5	3.37	2.55	2.14	1.89	1.71
SI IV $5d^2D-6f^2F^o$	4212.4	8.51	7.23	6.08	4.92	4.20
P III $3d^2D-4p^2P^o$	4066.2	0.343	0.242	0.171	0.128	0.106
P III $4s^2S-4p^2P^o$	4230.4	0.531	0.375	0.265	0.206	0.180
P III $4s^4P^o-4p^4P$	3943.5	0.462	0.327	0.231	0.176	0.154
P III $3p^3P^o-3d^3D$	826.3	0.350-2	0.248-2	0.175-2	0.124-2	0.876-3
P IV $4s^3S-4p^3P^o$	3355.9	0.330	0.233	0.165	0.121	0.100
P IV $4s^1S-4p^1P^o$	4249.6	0.565	0.399	0.282	0.215	0.183
S III $3d^3P_o-4p^3P$	3346.2	0.202	0.143	0.101	0.745-1	0.609-1
S III $3d^3P^o-4p^3S$	3233.4	0.193	0.136	0.963-1	0.708-1	0.580-1
S III $3d^3D^o-4p^3P$	3950.5	0.284	0.201	0.142	0.104	0.853-1
S III $4s^3P^o-4p^3D$	4287.1	0.472	0.334	0.236	0.183	0.159
S III $4s^3P^o-4p^3S$	3692.3	0.364	0.258	0.182	0.140	0.121
S III $4s^3P^o-4p^3P$	3840.0	0.389	0.275	0.194	0.150	0.130
S III $4p^3P-4d^3D^o$	2961.0	0.248	0.175	0.124	0.909-1	0.814-1
S III $4p^3D-4d^3P^o$	2740.6	0.207	0.147	0.104	0.765-1	0.686-1
S III $4p^3D-4d^3F^o$	2865.7	0.222	0.157	0.111	0.819-1	0.729-1
S III $4p^3P-5s^3P^o$	2677.0	0.129	0.914-1	0.646-1	0.479-1	0.431-1
S III $4p^3D-5s^3P^o$	2495.6	0.107	0.756-1	0.534-1	0.400-1	0.360-1
S IV $3p^2P^o-4s^2S$	553.1	0.396-2	0.280-2	0.198-2	0.144-2	0.118-2
S IV $4s^2S-4p^2P^o$	3104.1	0.245	0.173	0.122	0.886-1	0.723-1
CL III $3d^4P-4p^4P^o$	4045.8	0.257	0.182	0.129	0.931-1	0.744-1
CL III $3d^4F-4p^4D^o$	1825.7	0.452-1	0.320-1	0.226-1	0.165-1	0.134-1
CL III $4s^4P-4p^4D^o$	3629.0	0.284	0.201	0.142	0.106	0.898-1
CL III $4s^4P-4p^4P^o$	3330.9	0.246	0.174	0.123	0.912-1	0.773-1

Element/Transition	λ(Å)	W_{MSE}(Å) (FWHM)				
		T(K)=10000	20000	40000	80000	160000
CL III $4s^4P-4p^4S^o$	3160.1	0.226	0.160	0.113	0.836-1	0.707-1
CL III $4s^2P-4p^2D^o$	3739.4	0.314	0.222	0.157	0.118	0.101
CL III $4s^2P-4p^2P^o$	3300.9	0.243	0.172	0.121	0.903-1	0.768-1
CL III $4s'^2D-4p'^2F^o$	3543.8	0.271	0.192	0.136	0.100	0.852-1
CL III $4s'^2D-4p'^2D^o$	3394.2	0.252	0.178	0.126	0.933-1	0.790-1
CL III $4s'^2D-4p'^2P^o$	2975.4	0.204	0.144	0.102	0.752-1	0.634-1
CL III $4p^2D^o-4d^2F$	2581.6	0.164	0.116	0.820-1	0.593-1	0.527-1
CL III $4p^2D^o-4d^2D$	2324.3	0.135	0.952-1	0.673-1	0.489-1	0.441-1
CL III $4p^4P^o-4d^4D$	2668.2	0.174	0.123	0.872-1	0.628-1	0.548-1
CL III $4p^4S^o-4d^4P$	2700.2	0.182	0.129	0.909-1	0.654-1	0.572-1
CL III $4p^4P^o-5s^4P$	2416.9	0.888-1	0.628-1	0.444-1	0.321-1	0.283-1
CL III $4p^4D^o-5s^4P$	2281.0	0.779-1	0.551-1	0.390-1	0.283-1	0.251-1
CL IV $4s^3P^o-4p^3D$	3082.2	0.162	0.114	0.808-1	0.589-1	0.479-1
CL IV $4s^3P^o-4p^3P$	2767.6	0.131	0.924-1	0.653-1	0.474-1	0.384-1
A III $3d^5D^o_9-4p^5P_7$	1669.7	0.342-1	0.242-1	0.171-1	0.123-1	0.986-2
A III $3d'^3D^o-4p'^3D$	2690.3	0.911-1	0.644-1	0.456-1	0.330-1	0.265-1
A III $3d''^3P^o-4p''^3P$	3432.6	0.164	0.116	0.822-1	0.587-1	0.461-1
A III $4s^5S^o-4p^5P$	3296.6	0.208	0.147	0.104	0.763-1	0.637-1
A III $4s'^3D^o-4p'^3D$	3492.1	0.238	0.168	0.119	0.877-1	0.741-1
A III $4s'^3D^o-4p'^3F$	3344.8	0.221	0.156	0.110	0.814-1	0.685-1
A IV $4s^4P-4p^4D^o$	2810.9	0.117	0.829-1	0.586-1	0.422-1	0.340-1
A IV $4s^4P-4p^4P^o$	2617.5	0.102	0.721-1	0.510-1	0.366-1	0.294-1
A IV $4s^2P-4p^2D^o$	2925.4	0.133	0.943-1	0.667-1	0.482-1	0.389-1
A IV $4s'^2D-4p'^2F^o$	2769.2	0.114	0.806-1	0.570-1	0.410-1	0.330-1

© European Southern Observatory • Provided by the NASA Astrophysics Data System

1990A&AS...82..519D

ASTRONOMY & ASTROPHYSICS
SUPPLEMENT SERIES

Astron. Astrophys. Suppl. Ser. **82**, 519-529 (1990)

Stark broadening of He I lines

M. S. Dimitrijević ([1]) and S. Sahal-Bréchot ([2])

([1]) Astronomical Observatory, Volgina 7, 11050 Beograd, Yugoslavia
([2]) Département "Atomes et Molécules en Astrophysique", Unité Associée au C.N.R.S. N° 812, Observatoire de Paris-Meudon, France

Received May 22, accepted October 16, 1989

Abstract. — Using a semiclassical approach for the Stark broadening of atomic lines, we have calculated electron-, proton- and ionized helium-impact line widths and shifts for 77 neutral helium multiplets in the ultraviolet, visible and infrared regions of the spectrum.

Key words : lines : profile-atomic and molecular data.

1. Introduction.

Stark broadening of neutral helium lines is of particular interest for a large number of problems which concern plasma laboratory spectroscopy and astrophysics as well. Moreover many experimental data are available (Konjević *et al.*, 1984) and He is a simple atomic system : these data provide an opportunity to test the various theoretical approximations. We have calculated in the present paper electron-, proton- and ionized helium-impact line widths and shifts for 77 neutral helium multiplets in the ultraviolet, visible and infrared regions of the spectrum. For that we have used the semiclassical perturbation formalism (Sahal-Bréchot, 1969 a,b) and the Stark broadening and shift computer code derived from that method. The present data extend and complete those of Dimitrijević and Sahal-Bréchot (1984 a,b ; 1985). They also correct a number of the previous data of Dimitrijević and Sahal-Bréchot (1984 a,b) which are erroneous for high quantum numbers ($n \geq 7$) : as a matter of fact the Stark broadening computer code of Sahal-Bréchot needs energies of the upper, lower and perturbing levels, associated mean radius and oscillator strengths. For the oscillator strengths we had used the computer code of Hoang Binh Dy based on the work of Van Regemorter *et al.* (1979) and in 1984, that code provided erroneous data for high values of n.

We have used now an improved code and the new oscillator strengths have modified some of our previous Stark broadening and shift data. We have also improved the integration procedure on the impact parameter in the Stark broadening and shift code in order to obtain shifts as reliable as possible at high temperatures, which yet remain rather uncertain, owing to the groving of the importance of the Debye cutoff. The Debye cutoff which has a physical sense but remains "ad hoc", leads also to a departure from the linear density law ; this is expected but it is another source of uncertainty. For most astrophysical cases, this departure is small and well within the expected accuracy of the method. However, when one wants to investigate regularities within spectral series, or when one wants to make precise comparisons with measurements which are made at different densities, computed data (especially for the shift) at a number of different densities are needed. We have thus calculated an extensive, self consistent set of data (perturber density = 10^{13} - 10^{19} cm^{-3}) as a basis for such investigations.

The present paper concerns the data at a perturber density 10^{13} cm^{-3} only. The data for higher densities will be published elsewhere (Dimitrijević and Sahal-Bréchot, 1990).

2. Theory.

The calculation procedure is well described elsewhere (Sahal-Bréchot, 1969 a,b ; see e.g. also Dimitrijević and Truong Bach, 1985) and only a few details will be given here. Within the framework of semiclassical-perturbational formalism (Sahal-Bréchot, 1969 a,b) used here, the full halfwidth ($2W$) and shift (D) of an electron-

Send offprint requests to : M. S. Dimitrijević.

© European Southern Observatory • Provided by the NASA Astrophysics Data System

1990A&AS...82..519D

impact broadened line can be expressed as :

$$2W = N_e \int_0^\infty v f(v) \mathrm{d}v \left[\sum_{i' \neq i} \sigma_{ii'}(v) + \sum_{f' \neq f} \sigma_{ff'}(v) + \sigma_{\mathrm{el}}(v) \right],$$
$$D = N_e \int_0^\infty v f(v) \mathrm{d}v \int_{R_3}^{R_D} 2\pi \varrho \, \mathrm{d}\varrho \sin 2\, \varphi_{\mathrm{p}}. \quad (1)$$

Here, N_e is the electron density, $f\ (v)$ the Maxwellian velocity distribution function for electrons, ρ denotes the impact parameter of the incoming electron, i, and f denote the initial and final atomic energy level and i', f' their perturbing levels. The inelastic cross section $\sigma_{ii'}(v)$ can be expressed by an integration over the impact parameter of the transition probability $P_{ii'}(\rho, v)$

$$\sum_{i' \neq i} \sigma_{ii'}(v) = \frac{1}{2} \pi R_1^2 + \int_{R_1}^{R_D} 2\pi \varrho \, \mathrm{d}\varrho \sum_{i' \neq i} P_{ii'}(\varrho, v), \quad (2)$$

and the elastic cross section is given by

$$\sigma_{\mathrm{el}} = 2\pi\, R_2^2 + \int_{R_2}^{R_D} 8\pi \varrho \, \mathrm{d}\varrho \sin^2 \delta,$$
$$\delta = \left[\varphi_{\mathrm{p}}^2 + \varphi_{\mathrm{q}}^2\right]^{1/2}. \quad (3)$$

The phase shifts ϕ_{p} and ϕ_{q} due respectively to the polarization potential (r^{-4}) and to the quadrupolar potential (r^{-3}) part, are given in paragraph 3 of section 2 in the paper of Sahal-Bréchot (1969a). All the cutoffs R_1, R_2, R_3, R_D are described in paragraph 1 of section 3 of Sahal-Bréchot (1969b).

If we want to make certain that a line is isolated, we can use the parameter c defined by Dimitrijević and Sahal-Bréchot (1984a) and given in tables I-III. For an electron concentration lower than

$$N_{\mathrm{I}}\,(\mathrm{cm}^{-3}) = c/2W\ (\text{Å}), \quad (4)$$

the line can be treated as isolated in the core, even if weak forbidden components due to the failure of this approximation still appear in the wing.

The formulae for the proton impact (or He^+- impact width and shift) are analogous, but inelastic collisions are negligible.

3. Results.

The calculated values are divided in three parts. Our results for electron-, proton- and ionized helium-impact full halfwidths $(2W)$ and shifts (D), respectively for He (I) resonance lines (which lie in the far ultraviolet are shown in table I for perturber density $NE = 10^{13}$ cm^{-3} and $T =$ 10 000 ; 20 000 ; 40 000 ; 100 000 ; 150 000 and 200 000 K. the results for lines between 2 500 and 7 000 Å are shown in table II for a number of temperatures (5 000 ; 10 000 ; 20 000 ; 30 000 ; 40 000 and 80 000 K) and $NE = 10^{13}$ cm^{-3}. The results for lines with $\lambda >$7 000 Å are presented in table III for $T =$ 2 500 ; 5 000 ; 10 000 ; 20 000 ; 40 000 and 80 000 K and $NE = 10^{13}$ cm^{-3}. In tables I-III, we also give a parameter denoted by c (see Eq. (4) which divided by $2W$, gives an estimate for the maximum perturber density for which the line may be treated as isolated.

We checked that for each value given in the tables the collision volume (V) multiplied by the perturber density NE is much less than one. In such a case the impact approximation is valid (Sahal-Bréchot, 1969). The values for which $NE \cdot V > 0.5$ are not given in the tables, while values where $0.1 < NE \cdot V \leq 0.5$ are denoted with an asterisk and are given in order to enable rough estimation. In the cases when the impact approximation is not valid, the ion broadening contribution may be estimated by the quasi-static ion-broadening parameter (Griem, 1974) introduced by Griem *et al.* (1962).

Data for needed energy levels were taken from Martin (1973). Mean atomic radius and mean squared radius are calculated in the hydrogenic approximation.

Acknowledgements.

Calculations have been made on the VAX 8600 of the Observatory of Paris-Meudon and on the IBM computers of the CIRCE (Orsay) during the stays of M.D. as associated astronomer of the Paris Observatory in 1988 and 1989. This work, supported by CNRS, is a part of French-Yugoslav collaboration through the project "L'Elargissement Stark des raies spectrales des plasmas astrophysiques et de laboratoire". Also this is a part of the project "Atomic, Molecular and Plasma Spectroscopy" supported by SKNTI and RZN of Serbia.

References

DIMITRIJEVIĆ M. S. and SAHAL-BRÉCHOT S. : 1984a, *J. Quant. Spectrosc. Radiat. Transfer* **31**, 301.
DIMITRIJEVIĆ M. S. and SAHAL-BRÉCHOT S. : 1984b, *Astron. Astrophys.* **136**, 289.
DIMITRIJEVIĆ M. S. and SAHAL-BRÉCHOT S. : 1985, *Phys. Rev. A* **31**, 316.

© European Southern Observatory • Provided by the NASA Astrophysics Data System

1990A&AS...82..519D

DIMITRIJEVIĆ M. S. and SAHAL-BRÉCHOT S. : 1990, *Bull. Obs. Astron. Belgrade,* in press.
DIMITRIJEVIĆ M. S. and TRUONG BACH : 1986, *Z. Naturforsch.* **41a,** 772.
GRIEM H. R., BARANGER M., KOLB A. C. and OERTEL G. : 1962, *Phys. Rev.* **125,** 177.
GRIEM H. R. : 1974, Spectral Line Broadening by Plasmas (Academic Press, New York).
KONJEVIĆ N., DIMITRIJEVIĆ M. S. and WIESE W. L. : 1984, *J. Phys. Chem. Ref. Data* **13,** 619.
KONJEVIĆ N. and ROBERTS J. R. : 1976, *J. Phys. Chem. Ref. Data* **5,** 209.
MARTIN W. C. : 1973, *J. Phys. Chem. Ref. Data* **2,** 257.
SAHAL-BRÉCHOT S. : 1969a, *Astron. Astrophys.* **1,** 91.
SAHAL-BRÉCHOT S. : 1969b, *Astron. Astrophys.* **2,** 322.
VAN REGEMORTER H., HOANG BINH DY and PRUD'HOMME M. : 1979, *J. Phys. B* **12,** 1073.

TABLE I. — *This table lists electron-, proton- and ionized helium-impact broadening parameters for* He I *resonance lines for perturber density* $NE = 10^{13}$ cm^{-3} *and temperatures from* 10 000 K *to* 200 000 K. *Transitions and averaged wavelengths for the multiplet (in* Å*) are also given. Under* $2W$ *are given full halfwidths (in* Å*) while* D *denote corresponding shifts. If we divide* c *by* $2W_e$, *we obtain an estimate for the maximum electron density for which the line may be treated as isolated and the tabulated values may be used. Asterisk denotes cases when the collision volume multiplied by the electron density (condition for the validity of the impact approximation) lies between* 0.1 *and* 0.5.

NE= 0.1E+14

TRANSITION	T(K)	ELECTRONS 2WE(A)	DE(A)	PROTONS 2WI(A)	DI(A)	IONIZED HELIUM 2WI(A)	DI(A)
1S - 5P	10000.	0.765E-04	-0.215E-04	0.299E-04	-0.274E-04	0.256E-04	-0.235E-04
516.6A	20000.	0.704E-04	-0.126E-04	0.338E-04	-0.310E-04	0.287E-04	-0.266E-04
c= 0.66E+15	40000.	0.630E-04	-0.505E-05	0.388E-04	-0.350E-04	0.325E-04	-0.299E-04
(5UV)	100000.	0.529E-04	-0.210E-05	0.458E-04	-0.422E-04	0.389E-04	-0.352E-04
	150000.	0.484E-04	-0.108E-05	0.475E-04	-0.462E-04	0.421E-04	-0.380E-04
	200000.	0.452E-04	0.220E-06	0.476E-04	-0.492E-04	0.443E-04	-0.403E-04
1S - 6P	10000.	0.174E-03	-0.387E-04	0.717E-04	-0.651E-04	0.613E-04	-0.557E-04
512.1A	20000.	0.159E-03	-0.251E-04	0.816E-04	-0.739E-04	0.691E-04	-0.633E-04
c= 0.37E+15	40000.	0.141E-03	-0.938E-05	0.937E-04	-0.843E-04	0.782E-04	-0.718E-04
(6UV)	100000.	0.117E-03	-0.370E-05	0.109E-03	-0.102E-03	0.938E-04	-0.846E-04
	150000.	0.107E-03	0.261E-06	0.112E-03	-0.112E-03	0.101E-03	-0.917E-04
	200000.	0.993E-04	0.580E-06	0.110E-03	-0.119E-03	0.106E-03	-0.976E-04
1S - 7P	10000.	0.349E-03	-0.711E-04	0.151E-03*	-0.135E-03*	0.129E-03*	-0.115E-03*
510.0A	20000.	0.316E-03	-0.264E-04	0.172E-03*	-0.154E-03*	0.145E-03*	-0.132E-03*
c= 0.23E+15	40000.	0.278E-03	-0.158E-04	0.198E-03	-0.177E-03	0.165E-03*	-0.150E-03*
(7UV)	100000.	0.229E-03	0.281E-06	0.227E-03	-0.216E-03	0.198E-03	-0.178E-03
	150000.	0.207E-03	0.796E-06	0.228E-03	-0.236E-03	0.213E-03	-0.194E-03
	200000.	0.193E-03	0.932E-06	0.221E-03	-0.249E-03	0.222E-03	-0.206E-03
1S - 8P	10000.	0.616E-03	-0.119E-03	0.268E-03*	-0.236E-03*		
508.6A	20000.	0.555E-03	-0.685E-04	0.305E-03*	-0.271E-03*	0.257E-03*	-0.231E-03*
c= 0.17E+15	40000.	0.489E-03	-0.243E-04	0.351E-03*	-0.311E-03*	0.293E-03*	-0.264E-03*
(8UV)	100000.	0.400E-03	-0.855E-05	0.401E-03*	-0.383E-03*	0.351E-03*	-0.315E-03*
	150000.	0.362E-03	0.231E-05	0.401E-03*	-0.418E-03*	0.378E-03*	-0.343E-03*
	200000.	0.336E-03	0.202E-05	0.390E-03	-0.441E-03	0.393E-03*	-0.366E-03*
1S - 9P	10000.	0.104E-02	-0.191E-03				
507.7A	20000.	0.930E-03	-0.972E-04				
c= 0.12E+15	40000.	0.815E-03	-0.378E-04				
(9UV)	100000.	0.663E-03	-0.105E-04	0.694E-03*	-0.675E-03*		
	150000.	0.599E-03	0.353E-05	0.685E-03*	-0.736E-03*	0.663E-03*	-0.604E-03*
	200000.	0.554E-03	0.282E-05	0.657E-03*	-0.772E-03*	0.686E-03*	-0.647E-03*
1S -10P	10000.	0.169E-02	-0.282E-03				
507.1A	20000.	0.150E-02	-0.125E-03				
c= 0.75E+14	40000.	0.131E-02	-0.565E-04				
(10UV)	100000.	0.105E-02	-0.106E-04				
	150000.	0.947E-03	0.474E-05				
	200000.	0.874E-03	0.362E-05	0.106E-02*	-0.134E-02*		

© European Southern Observatory • Provided by the NASA Astrophysics Data System

1990A&AS...82..519D

TABLE II. — *Same as in table I but for the* He I *lines in the range* 2 500 > λ (Å) ≤ 7 000, *for temperatures from* 5 000 *to* 80 000 K.

NE= 0.1E+14

TRANSITION	T(K)	ELECTRONS 2WE(A)	DE(A)	PROTONS 2WI(A)	DI(A)	IONIZED HELIUM 2WI(A)	DI(A)
2S - 3P	5000.	0.634E-03	-0.272E-03	0.187E-03	-0.172E-03	0.162E-03	-0.148E-03
5015.7A	10000.	0.601E-03	-0.196E-03	0.210E-03	-0.194E-03	0.181E-03	-0.166E-03
c= 0.26E+18	20000.	0.572E-03	-0.126E-03	0.237E-03	-0.218E-03	0.203E-03	-0.187E-03
(4)	30000.	0.552E-03	-0.861E-04	0.256E-03	-0.233E-03	0.217E-03	-0.200E-03
	40000.	0.536E-03	-0.722E-04	0.270E-03	-0.245E-03	0.228E-03	-0.210E-03
	80000.	0.494E-03	-0.465E-04	0.310E-03	-0.279E-03	0.259E-03	-0.236E-03
2S - 4P	5000.	0.168E-02	-0.669E-03	0.524E-03	-0.482E-03	0.451E-03	-0.412E-03
3964.7A	10000.	0.158E-02	-0.345E-03	0.589E-03	-0.544E-03	0.505E-03	-0.467E-03
c= 0.73E+17	20000.	0.148E-02	-0.221E-03	0.666E-03	-0.613E-03	0.567E-03	-0.526E-03
(5)	30000.	0.140E-02	-0.169E-03	0.720E-03	-0.657E-03	0.608E-03	-0.564E-03
	40000.	0.134E-02	-0.136E-03	0.762E-03	-0.691E-03	0.640E-03	-0.592E-03
	80000.	0.120E-02	-0.777E-04	0.873E-03	-0.790E-03	0.730E-03	-0.666E-03
2S - 5P	5000.	0.400E-02	-0.133E-02	0.130E-02	-0.118E-02	0.112E-02	-0.101E-02
3613.6A	10000.	0.375E-02	-0.933E-03	0.146E-02	-0.134E-02	0.125E-02	-0.115E-02
c= 0.32E+17	20000.	0.346E-02	-0.445E-03	0.165E-02	-0.152E-02	0.141E-02	-0.130E-02
(6)	30000.	0.325E-02	-0.316E-03	0.179E-02	-0.163E-02	0.151E-02	-0.140E-02
	40000.	0.309E-02	-0.250E-03	0.190E-02	-0.171E-02	0.159E-02	-0.146E-02
	80000.	0.273E-02	-0.496E-04	0.217E-02	-0.197E-02	0.182E-02	-0.165E-02
2S - 6P	5000.	0.848E-02	-0.304E-02	0.288E-02	-0.258E-02	0.248E-02*	-0.220E-02*
3447.6A	10000.	0.791E-02	-0.182E-02	0.325E-02	-0.295E-02	0.278E-02	-0.252E-02
c= 0.17E+17	20000.	0.722E-02	-0.806E-03	0.370E-02	-0.335E-02	0.313E-02	-0.287E-02
(7)	30000.	0.674E-02	-0.552E-03	0.401E-02	-0.361E-02	0.336E-02	-0.309E-02
	40000.	0.641E-02	-0.439E-03	0.425E-02	-0.382E-02	0.354E-02	-0.325E-02
	80000.	0.559E-02	-0.342E-04	0.481E-02	-0.441E-02	0.407E-02	-0.367E-02
2S - 7P	5000.	0.163E-01	-0.463E-02	0.579E-02*	-0.508E-02*	0.496E-02*	-0.431E-02*
3354.6A	10000.	0.151E-01	-0.324E-02	0.653E-02*	-0.584E-02*	0.558E-02*	-0.499E-02*
c= 0.99E+16	20000.	0.137E-01	-0.749E-03	0.745E-02*	-0.667E-02*	0.628E-02*	-0.570E-02*
(8)	30000.	0.127E-01	-0.930E-03	0.809E-02*	-0.722E-02*	0.677E-02*	-0.615E-02*
	40000.	0.120E-01	-0.744E-03	0.857E-02	-0.765E-02	0.714E-02*	-0.648E-02*
	80000.	0.104E-01	-0.306E-04	0.960E-02	-0.889E-02	0.821E-02*	-0.738E-02*
2S - 8P	5000.	0.278E-01	-0.760E-02				
3296.8A	10000.	0.259E-01	-0.336E-02	0.112E-01*	-0.991E-02*		
c= 0.70E+16	20000.	0.233E-01	-0.214E-02	0.128E-01*	-0.114E-01*	0.108E-01*	-0.971E-02*
(9)	30000.	0.217E-01	-0.151E-02	0.139E-01*	-0.123E-01*	0.116E-01*	-0.105E-01*
	40000.	0.205E-01	-0.120E-02	0.147E-01*	-0.131E-01*	0.123E-01*	-0.111E-01*
	80000.	0.177E-01	-0.566E-04	0.165E-01*	-0.153E-01*	0.141E-01*	-0.126E-01*
2S - 9P	5000.	0.462E-01	-0.140E-01				
3258.3A	10000.	0.428E-01	-0.835E-02				
c= 0.48E+16	20000.	0.383E-01	-0.320E-02				
	30000.	0.356E-01	-0.231E-02				
	40000.	0.336E-01	-0.515E-03				
	80000.	0.288E-01	-0.985E-04	0.282E-01	-0.264E-01		
2S -10P	5000.	0.747E-01	-0.102E-01				
3231.3A	10000.	0.686E-01	-0.121E-01				
c= 0.31E+16	20000.	0.609E-01	-0.453E-02				
	30000.	0.563E-01	-0.948E-03				
	40000.	0.530E-01	-0.256E-02				
	80000.	0.452E-01	-0.140E-03				
2P - 4S	5000.	0.104E-02	0.780E-03	0.231E-03	0.216E-03	0.198E-03	0.186E-03
5047.7A	10000.	0.107E-02	0.765E-03	0.259E-03	0.244E-03	0.222E-03	0.209E-03
c= 0.14E+19	20000.	0.110E-02	0.659E-03	0.291E-03	0.274E-03	0.250E-03	0.235E-03
(47)	30000.	0.112E-02	0.563E-03	0.311E-03	0.293E-03	0.267E-03	0.252E-03
	40000.	0.114E-02	0.504E-03	0.326E-03	0.308E-03	0.280E-03	0.264E-03
	80000.	0.112E-02	0.365E-03	0.367E-03	0.346E-03	0.315E-03	0.297E-03

© European Southern Observatory • Provided by the NASA Astrophysics Data System

1990A&AS...82..519D

TABLE II *(continued)*

NE= 0.1E+14

TRANSITION	T(K)	ELECTRONS 2WE(A)	DE(A)	PROTONS 2WI(A)	DI(A)	IONIZED HELIUM 2WI(A)	DI(A)
2P - 5S	5000.	0.228E-02	0.170E-02	0.516E-03	0.482E-03	0.443E-03	0.413E-03
4437.6A	10000.	0.232E-02	0.161E-02	0.579E-03	0.543E-03	0.497E-03	0.466E-03
c= 0.55E+18	20000.	0.236E-02	0.127E-02	0.650E-03	0.612E-03	0.558E-03	0.525E-03
(50)	30000.	0.242E-02	0.104E-02	0.696E-03	0.655E-03	0.597E-03	0.563E-03
	40000.	0.243E-02	0.907E-03	0.730E-03	0.688E-03	0.627E-03	0.591E-03
	80000.	0.233E-02	0.595E-03	0.822E-03	0.773E-03	0.704E-03	0.664E-03
2P - 6S	5000.	0.483E-02	0.341E-02	0.108E-02	0.100E-02	0.929E-03	0.857E-03
4169.0A	10000.	0.472E-02	0.306E-02	0.121E-02	0.113E-02	0.104E-02	0.972E-03
c= 0.28E+18	20000.	0.484E-02	0.227E-02	0.136E-02	0.128E-02	0.117E-02	0.110E-02
(52)	30000.	0.502E-02	0.184E-02	0.146E-02	0.137E-02	0.125E-02	0.118E-02
	40000.	0.497E-02	0.155E-02	0.153E-02	0.144E-02	0.132E-02	0.124E-02
	80000.	0.462E-02	0.912E-03	0.172E-02	0.162E-02	0.148E-02	0.139E-02
2P - 7S	5000.	0.924E-02	0.625E-02	0.209E-02	0.191E-02	0.179E-02	0.163E-02
4024.0A	10000.	0.880E-02	0.530E-02	0.234E-02	0.217E-02	0.201E-02	0.186E-02
c= 0.16E+18	20000.	0.918E-02	0.377E-02	0.263E-02	0.246E-02	0.226E-02	0.211E-02
(54)	30000.	0.942E-02	0.302E-02	0.282E-02	0.264E-02	0.242E-02	0.227E-02
	40000.	0.919E-02	0.232E-02	0.296E-02	0.277E-02	0.254E-02	0.238E-02
	80000.	0.854E-02	0.127E-02	0.333E-02	0.312E-02	0.285E-02	0.268E-02
2P - 8S	5000.	0.162E-01	0.109E-01	0.376E-02	0.340E-02	0.323E-02*	0.290E-02*
3935.9A	10000.	0.158E-01	0.860E-02	0.422E-02	0.388E-02	0.362E-02	0.332E-02
c= 0.10E+18	20000.	0.163E-01	0.585E-02	0.474E-02	0.441E-02	0.407E-02	0.377E-02
(57)	30000.	0.164E-01	0.461E-02	0.508E-02	0.474E-02	0.436E-02	0.406E-02
	40000.	0.159E-01	0.360E-02	0.533E-02	0.498E-02	0.457E-02	0.428E-02
	80000.	0.148E-01	0.173E-02	0.601E-02	0.561E-02	0.514E-02	0.482E-02
2P - 3D	5000.	0.746E-03	0.296E-03	0.232E-03	0.216E-03	0.200E-03	0.185E-03
6678.1A	10000.	0.697E-03	0.248E-03	0.261E-03	0.243E-03	0.224E-03	0.208E-03
c= 0.47E+18	20000.	0.632E-03	0.194E-03	0.296E-03	0.273E-03	0.252E-03	0.234E-03
(46)	30000.	0.594E-03	0.164E-03	0.321E-03	0.292E-03	0.270E-03	0.251E-03
	40000.	0.567E-03	0.141E-03	0.340E-03	0.308E-03	0.285E-03	0.263E-03
	80000.	0.515E-03	0.923E-04	0.387E-03	0.353E-03	0.325E-03	0.296E-03
2P - 4D	5000.	0.398E-02	0.983E-03	0.255E-02	0.226E-02	0.213E-02	0.191E-02
4921.9A	10000.	0.346E-02	0.642E-03	0.287E-02	0.263E-02	0.244E-02	0.218E-02
c= 0.12E+17	20000.	0.294E-02	0.370E-03	0.298E-02	0.306E-02	0.278E-02	0.252E-02
(48)	30000.	0.265E-02	0.292E-03	0.288E-02	0.328E-02	0.292E-02	0.276E-02
	40000.	0.246E-02	0.241E-03	0.274E-02	0.340E-02	0.298E-02	0.294E-02
	80000.	0.205E-02	0.151E-03	0.229E-02	0.349E-02	0.285E-02	0.332E-02
2P - 5D	5000.	0.100E-01	0.225E-02	0.630E-02*	0.546E-02*	0.527E-02*	0.462E-02*
4387.9A	10000.	0.870E-02	0.136E-02	0.716E-02	0.639E-02	0.604E-02*	0.532E-02*
c= 0.61E+16	20000.	0.736E-02	0.686E-03	0.763E-02	0.751E-02	0.690E-02	0.616E-02
(51)	30000.	0.662E-02	0.529E-03	0.752E-02	0.814E-02	0.735E-02	0.675E-02
	40000.	0.612E-02	0.434E-03	0.725E-02	0.851E-02	0.756E-02	0.721E-02
	80000.	0.503E-02	0.180E-03	0.613E-02	0.895E-02	0.747E-02	0.828E-02
2P - 6D	5000.	0.221E-01	0.363E-02				
4143.8A	10000.	0.190E-01	0.237E-02	0.185E-01*	0.167E-01*		
c= 0.26E+16	20000.	0.159E-01	0.112E-02	0.187E-01*	0.196E-01*		
(53)	30000.	0.142E-01	0.837E-03	0.176E-01*	0.210E-01*	0.188E-01*	0.178E-01*
	40000.	0.131E-01	0.675E-03	0.165E-01*	0.216E-01*	0.189E-01*	0.190E-01*
	80000.	0.107E-01	0.234E-03	0.130E-01	0.218E-01	0.174E-01*	0.213E-01*
2P - 7D	5000.	0.396E-01	0.623E-02				
4009.3A	10000.	0.342E-01	0.278E-02				
c= 0.21E+16	20000.	0.288E-01	0.185E-02				
(55)	30000.	0.259E-01	0.137E-02	0.320E-01*	0.352E-01*		
	40000.	0.238E-01	0.107E-02	0.305E-01*	0.367E-01*		
	80000.	0.195E-01	0.507E-03	0.250E-01*	0.383E-01*	0.317E-01*	0.361E-01*

© European Southern Observatory • Provided by the NASA Astrophysics Data System

1990A&AS...82..519D

TABLE II *(continued)*

NE= 0.1E+14

TRANSITION	T(K)	ELECTRONS 2WE(A)	DE(A)	PROTONS 2WI(A)	DI(A)	IONIZED HELIUM 2WI(A)	DI(A)
2P - 8D	5000.	0.707E-01	0.713E-02				
3926.5A	10000.	0.607E-01	0.427E-02				
c= 0.26E+15	20000.	0.509E-01	0.196E-02				
(58)	30000.	0.455E-01	0.147E-02				
	40000.	0.419E-01	0.560E-03				
	80000.	0.340E-01	0.336E-03	0.333E-01*	0.935E-01*		
2P - 9D	5000.	0.109	0.851E-02				
3871.8A	10000.	0.944E-01	0.534E-02				
c= 0.60E+14	20000.	0.795E-01	0.256E-02				
(60)	30000.	0.712E-01	0.196E-02				
	40000.	0.657E-01	0.156E-02				
	80000.	0.535E-01	0.380E-03	0.352E-01*	0.122*		
2S - 3P	5000.	0.143E-03	0.773E-04	0.398E-04	0.322E-04	0.358E-04	0.277E-04
3888.7A	10000.	0.166E-03	0.628E-04	0.434E-04	0.363E-04	0.387E-04	0.311E-04
c= 0.81E+18	20000.	0.182E-03	0.494E-04	0.477E-04	0.407E-04	0.422E-04	0.350E-04
(2)	30000.	0.188E-03	0.406E-04	0.505E-04	0.436E-04	0.445E-04	0.374E-04
	40000.	0.191E-03	0.340E-04	0.526E-04	0.457E-04	0.463E-04	0.393E-04
	80000.	0.193E-03	0.224E-04	0.585E-04	0.513E-04	0.510E-04	0.441E-04
2S - 4P	5000.	0.439E-03	0.232E-03	0.116E-03	0.100E-03	0.103E-03	0.860E-04
3187.7A	10000.	0.500E-03	0.179E-03	0.129E-03	0.113E-03	0.113E-03	0.968E-04
c= 0.23E+18	20000.	0.527E-03	0.131E-03	0.142E-03	0.127E-03	0.125E-03	0.109E-03
(3)	30000.	0.533E-03	0.926E-04	0.152E-03	0.136E-03	0.132E-03	0.117E-03
	40000.	0.534E-03	0.742E-04	0.159E-03	0.143E-03	0.138E-03	0.122E-03
	80000.	0.521E-03	0.352E-04	0.178E-03	0.160E-03	0.153E-03	0.138E-03
2S - 5P	5000.	0.114E-02	0.522E-03	0.296E-03	0.259E-03	0.259E-03	0.222E-03
2945.1A	10000.	0.128E-02	0.422E-03	0.328E-03	0.293E-03	0.286E-03	0.251E-03
c= 0.10E+18	20000.	0.131E-02	0.267E-03	0.365E-03	0.330E-03	0.318E-03	0.283E-03
(11UV)	30000.	0.132E-02	0.182E-03	0.390E-03	0.353E-03	0.338E-03	0.303E-03
	40000.	0.131E-02	0.148E-03	0.409E-03	0.371E-03	0.353E-03	0.319E-03
	80000.	0.125E-02	0.602E-04	0.461E-03	0.419E-03	0.394E-03	0.358E-03
2S - 6P	5000.	0.256E-02	0.103E-02	0.653E-03	0.575E-03	0.570E-03	0.492E-03
2829.1A	10000.	0.280E-02	0.813E-03	0.727E-03	0.652E-03	0.632E-03	0.558E-03
c= 0.54E+17	20000.	0.285E-02	0.434E-03	0.811E-03	0.737E-03	0.703E-03	0.632E-03
(12UV)	30000.	0.284E-02	0.326E-03	0.867E-03	0.789E-03	0.749E-03	0.677E-03
	40000.	0.281E-02	0.259E-03	0.909E-03	0.829E-03	0.784E-03	0.711E-03
	80000.	0.264E-02	0.113E-03	0.103E-02	0.935E-03	0.877E-03	0.801E-03
2P - 4S	5000.	0.585E-03	0.449E-03	0.128E-03	0.120E-03	0.110E-03	0.103E-03
4713.2A	10000.	0.616E-03	0.468E-03	0.143E-03	0.135E-03	0.123E-03	0.116E-03
c= 0.20E+19	20000.	0.638E-03	0.440E-03	0.161E-03	0.152E-03	0.138E-03	0.130E-03
(12)	30000.	0.642E-03	0.390E-03	0.172E-03	0.162E-03	0.148E-03	0.140E-03
	40000.	0.658E-03	0.347E-03	0.181E-03	0.170E-03	0.155E-03	0.146E-03
	80000.	0.684E-03	0.278E-03	0.203E-03	0.191E-03	0.174E-03	0.164E-03
2P - 5S	5000.	0.136E-02	0.103E-02	0.290E-03	0.272E-03	0.249E-03	0.233E-03
4120.8A	10000.	0.135E-02	0.987E-03	0.325E-03	0.306E-03	0.280E-03	0.262E-03
c= 0.77E+18	20000.	0.137E-02	0.864E-03	0.365E-03	0.344E-03	0.314E-03	0.295E-03
(16)	30000.	0.142E-02	0.731E-03	0.391E-03	0.369E-03	0.336E-03	0.317E-03
	40000.	0.146E-02	0.639E-03	0.410E-03	0.387E-03	0.352E-03	0.332E-03
	80000.	0.148E-02	0.460E-03	0.461E-03	0.435E-03	0.396E-03	0.373E-03
2P - 6S	5000.	0.274E-02	0.209E-02	0.615E-03	0.572E-03	0.529E-03	0.490E-03
3867.5A	10000.	0.291E-02	0.202E-02	0.691E-03	0.648E-03	0.593E-03	0.555E-03
c= 0.38E+18	20000.	0.285E-02	0.158E-02	0.775E-03	0.729E-03	0.666E-03	0.625E-03
(20)	30000.	0.302E-02	0.130E-02	0.830E-03	0.781E-03	0.713E-03	0.670E-03
	40000.	0.310E-02	0.110E-02	0.871E-03	0.820E-03	0.748E-03	0.704E-03
	80000.	0.298E-02	0.717E-03	0.979E-03	0.922E-03	0.840E-03	0.792E-03

© European Southern Observatory • Provided by the NASA Astrophysics Data System

1990A&AS...82..519D

NE= 0.1E+14

TRANSITION	T(K)	ELECTRONS 2WE(A)	ELECTRONS DE(A)	PROTONS 2WI(A)	PROTONS DI(A)	IONIZED HELIUM 2WI(A)	IONIZED HELIUM DI(A)
2P - 8S	5000.	0.918E-02	0.672E-02	0.216E-02	0.197E-02	0.186E-02	0.168E-02
3652.0A	10000.	0.935E-02	0.602E-02	0.243E-02	0.224E-02	0.208E-02	0.192E-02
c= 0.14E+18	20000.	0.988E-02	0.418E-02	0.273E-02	0.255E-02	0.234E-02	0.218E-02
(27)	30000.	0.105E-01	0.330E-02	0.292E-02	0.273E-02	0.251E-02	0.235E-02
	40000.	0.104E-01	0.258E-02	0.306E-02	0.287E-02	0.263E-02	0.246E-02
	80000.	0.983E-02	0.139E-02	0.345E-02	0.323E-02	0.295E-02	0.277E-02
2P -10S	5000.	0.260E-01	0.178E-01	0.595E-02*	0.528E-02*	0.511E-02*	0.448E-02*
3562.9A	10000.	0.249E-01	0.134E-01	0.668E-02*	0.607E-02*	0.573E-02*	0.518E-02*
c= 0.68E+17	20000.	0.269E-01	0.854E-02	0.750E-02*	0.692E-02*	0.644E-02*	0.592E-02*
(33)	30000.	0.276E-01	0.651E-02	0.803E-02	0.745E-02	0.689E-02*	0.638E-02*
	40000.	0.270E-01	0.495E-02	0.843E-02	0.785E-02	0.723E-02*	0.672E-02*
	80000.	0.257E-01	0.236E-02	0.949E-02	0.886E-02	0.812E-02	0.761E-02
2P - 3D	5000.	0.280E-03	-0.770E-04	0.591E-04	-0.499E-04	0.526E-04	-0.429E-04
5875.7A	10000.	0.302E-03	-0.425E-04	0.650E-04	-0.561E-04	0.574E-04	-0.482E-04
c= 0.19E+19	20000.	0.301E-03	-0.115E-04	0.718E-04	-0.630E-04	0.631E-04	-0.541E-04
(11)	30000.	0.300E-03	0.390E-05	0.763E-04	-0.674E-04	0.667E-04	-0.579E-04
	40000.	0.299E-03	0.832E-05	0.798E-04	-0.708E-04	0.696E-04	-0.608E-04
	80000.	0.296E-03	0.124E-04	0.896E-04	-0.794E-04	0.771E-04	-0.682E-04
2P - 4D	5000.	0.247E-02	0.618E-04	0.152E-02	0.135E-02	0.127E-02	0.115E-02
4471.5A	10000.	0.220E-02	-0.642E-04	0.173E-02	0.156E-02	0.145E-02	0.130E-02
c= 0.14E+17	20000.	0.191E-02	-0.146E-04	0.183E-02	0.184E-02	0.167E-02	0.152E-02
(14)	30000.	0.175E-02	-0.156E-04	0.174E-02	0.200E-02	0.178E-02	0.164E-02
	40000.	0.165E-02	-0.620E-05	0.163E-02	0.211E-02	0.183E-02	0.179E-02
	80000.	0.141E-02	0.120E-04	0.117E-02	0.204E-02	0.172E-02	0.202E-02
2P - 5D	5000.	0.671E-02	0.230E-03	0.404E-02	0.351E-02	0.337E-02*	0.298E-02*
4026.2A	10000.	0.591E-02	0.286E-04	0.462E-02	0.409E-02	0.386E-02	0.342E-02
c= 0.68E+16	20000.	0.508E-02	-0.851E-04	0.499E-02	0.483E-02	0.444E-02	0.395E-02
(18)	30000.	0.463E-02	-0.387E-04	0.487E-02	0.533E-02	0.477E-02	0.438E-02
	40000.	0.433E-02	-0.162E-04	0.459E-02	0.554E-02	0.494E-02	0.462E-02
	80000.	0.365E-02	0.201E-04	0.338E-02	0.566E-02	0.480E-02	0.540E-02
2P - 6D	5000.	0.147E-01	-0.204E-03	0.931E-02*	0.787E-02*		
3819.6A	10000.	0.129E-01	-0.441E-04	0.106E-01*	0.931E-02*	0.890E-02*	0.772E-02*
c= 0.36E+16	20000.	0.110E-01	-0.137E-03	0.117E-01*	0.113E-01*	0.102E-01*	0.899E-02*
(22)	30000.	0.100E-01	-0.618E-04	0.109E-01	0.121E-01	0.110E-01*	0.992E-02*
	40000.	0.933E-02	-0.231E-04	0.108E-01	0.132E-01	0.113E-01*	0.106E-01*
	80000.	0.779E-02	-0.172E-04	0.871E-02	0.132E-01	0.119E-01*	0.128E-01*
2P - 7D	5000.	0.288E-01	0.606E-04				
3705.0A	10000.	0.250E-01	-0.331E-03				
c= 0.17E+16	20000.	0.213E-01	-0.226E-03	0.250E-01*	0.263E-01*		
(25)	30000.	0.193E-01	-0.129E-03	0.229E-01*	0.288E-01*		
	40000.	0.179E-01	-0.827E-04	0.203E-01	0.293E-01	0.254E-01*	0.252E-01*
	80000.	0.149E-01	-0.194E-04	0.148E-01	0.288E-01	0.231E-01	0.297E-01
2P - 8D	5000.	0.475E-01	0.965E-04				
3634.2A	10000.	0.417E-01	-0.385E-03				
c= 0.15E+16	20000.	0.357E-01	-0.119E-03				
(28)	30000.	0.324E-01	-0.434E-04				
	40000.	0.302E-01	-0.406E-04				
	80000.	0.251E-01	-0.159E-05	0.278E-01*	0.452E-01*		
2P - 9D	5000.	0.738E-01	-0.277E-04				
3587.3A	10000.	0.652E-01	-0.529E-03				
c= 0.13E+16	20000.	0.562E-01	0.464E-04				
(31)	30000.	0.512E-01	0.398E-04				
	40000.	0.476E-01	-0.582E-04				
	80000.	0.396E-01	0.403E-05	0.391E-01*	0.649E-01*		
2P -10D	5000.	0.115	-0.423E-02				
3554.4A	10000.	0.101	-0.376E-02				
c= 0.55E+15	20000.	0.871E-01	-0.843E-03				
(34)	30000.	0.791E-01	-0.597E-03				
	40000.	0.736E-01	-0.801E-03				
	80000.	0.611E-01	-0.288E-04				

© European Southern Observatory • Provided by the NASA Astrophysics Data System

1990A&AS...82..519D

TABLE III. — *The same as in table I but for infrared* He I *lines with* $\lambda > 7\,000$ Å, *for temperatures from* 2 500 *to* 80 000 K.

NE= 0.1E+14

TRANSITION	T(K)	ELECTRONS 2WE(A)	DE(A)	PROTONS 2WI(A)	DI(A)	IONIZED HELIUM 2WI(A)	DI(A)
2S - 2P	2500.	0.717E-03	-0.399E-03	0.159E-03	-0.110E-03	0.148E-03	-0.944E-04
20581.3A	5000.	0.750E-03	-0.475E-03	0.169E-03	-0.123E-03	0.156E-03	-0.106E-03
c= 0.21E+21	10000.	0.798E-03	-0.457E-03	0.182E-03	-0.139E-03	0.166E-03	-0.119E-03
	20000.	0.876E-03	-0.427E-03	0.196E-03	-0.155E-03	0.177E-03	-0.134E-03
	40000.	0.100E-02	-0.313E-03	0.213E-03	-0.175E-03	0.191E-03	-0.150E-03
	80000.	0.113E-02	-0.251E-03	0.233E-03	-0.196E-03	0.208E-03	-0.168E-03
2P - 3S	2500.	0.491E-03	0.362E-03	0.107E-03	0.100E-03	0.924E-04	0.859E-04
7281.4A	5000.	0.556E-03	0.413E-03	0.120E-03	0.113E-03	0.103E-03	0.967E-04
c= 0.71E+19	10000.	0.589E-03	0.430E-03	0.135E-03	0.127E-03	0.116E-03	0.109E-03
(45)	20000.	0.617E-03	0.398E-03	0.151E-03	0.142E-03	0.130E-03	0.122E-03
	40000.	0.640E-03	0.314E-03	0.170E-03	0.160E-03	0.146E-03	0.137E-03
	80000.	0.660E-03	0.258E-03	0.190E-03	0.179E-03	0.164E-03	0.154E-03
3S - 3P	2500.	0.182	-0.966E-01	0.406E-01	-0.372E-01	0.351E-01	-0.318E-01
74351.0A	5000.	0.187	-0.932E-01	0.454E-01	-0.419E-01	0.392E-01	-0.359E-01
c= 0.58E+20	10000.	0.183	-0.804E-01	0.509E-01	-0.471E-01	0.438E-01	-0.404E-01
	20000.	0.176	-0.651E-01	0.573E-01	-0.530E-01	0.491E-01	-0.455E-01
	40000.	0.171	-0.480E-01	0.652E-01	-0.596E-01	0.552E-01	-0.511E-01
	80000.	0.163	-0.360E-01	0.746E-01	-0.676E-01	0.625E-01	-0.574E-01
3S - 4P	2500.	0.265E-01	-0.132E-01	0.684E-02	-0.621E-02	0.590E-02	-0.531E-02
15083.7A	5000.	0.260E-01	-0.108E-01	0.767E-02	-0.705E-02	0.660E-02	-0.604E-02
c= 0.11E+19	10000.	0.247E-01	-0.819E-02	0.862E-02	-0.797E-02	0.739E-02	-0.684E-02
	20000.	0.232E-01	-0.539E-02	0.975E-02	-0.897E-02	0.830E-02	-0.770E-02
	40000.	0.215E-01	-0.325E-02	0.111E-01	-0.101E-01	0.937E-02	-0.866E-02
	80000.	0.195E-01	-0.215E-02	0.128E-01	-0.116E-01	0.107E-01	-0.975E-02
3S - 5P	2500.	0.393E-01	-0.186E-01	0.108E-01	-0.962E-02	0.927E-02	-0.820E-02
11013.1A	5000.	0.378E-01	-0.139E-01	0.121E-01	-0.110E-01	0.104E-01	-0.940E-02
c= 0.30E+18	10000.	0.355E-01	-0.877E-02	0.136E-01	-0.125E-01	0.116E-01	-0.107E-01
(70)	20000.	0.330E-01	-0.431E-02	0.154E-01	-0.141E-01	0.131E-01	-0.121E-01
	40000.	0.298E-01	-0.270E-02	0.177E-01	-0.160E-01	0.148E-01	-0.136E-01
	80000.	0.264E-01	-0.112E-02	0.202E-01	-0.183E-01	0.169E-01	-0.154E-01
3S - 6P	2500.	0.698E-01	-0.264E-01	0.199E-01*	-0.174E-01*	0.171E-01*	-0.147E-01*
9603.4A	5000.	0.662E-01	-0.200E-01	0.224E-01	-0.201E-01	0.192E-01*	-0.171E-01*
c= 0.13E+18	10000.	0.619E-01	-0.910E-02	0.252E-01	-0.229E-01	0.216E-01	-0.196E-01
(71)	20000.	0.567E-01	-0.585E-02	0.287E-01	-0.260E-01	0.243E-01	-0.223E-01
	40000.	0.505E-01	-0.161E-02	0.330E-01	-0.297E-01	0.275E-01	-0.253E-01
	80000.	0.442E-01	-0.584E-03	0.374E-01	-0.342E-01	0.316E-01	-0.285E-01
3P - 4S	2500.	0.272E-01	0.162E-01	0.520E-02	0.481E-02	0.448E-02	0.412E-02
21132.0A	5000.	0.288E-01	0.173E-01	0.583E-02	0.543E-02	0.502E-02	0.466E-02
c= 0.47E+19	10000.	0.289E-01	0.163E-01	0.654E-02	0.612E-02	0.563E-02	0.525E-02
	20000.	0.285E-01	0.135E-01	0.735E-02	0.688E-02	0.631E-02	0.591E-02
	40000.	0.284E-01	0.100E-01	0.829E-02	0.774E-02	0.709E-02	0.664E-02
	80000.	0.273E-01	0.734E-02	0.940E-02	0.871E-02	0.798E-02	0.746E-02
3P - 5S	2500.	0.239E-01	0.159E-01	0.461E-02	0.425E-02	0.397E-02	0.364E-02
13411.8A	5000.	0.251E-01	0.168E-01	0.518E-02	0.482E-02	0.445E-02	0.413E-02
c= 0.19E+19	10000.	0.254E-01	0.154E-01	0.581E-02	0.544E-02	0.499E-02	0.467E-02
	20000.	0.254E-01	0.121E-01	0.653E-02	0.613E-02	0.560E-02	0.526E-02
	40000.	0.257E-01	0.831E-02	0.733E-02	0.690E-02	0.629E-02	0.592E-02
	80000.	0.245E-01	0.501E-02	0.826E-02	0.775E-02	0.707E-02	0.666E-02
3P - 6S	2500.	0.354E-01	0.246E-01	0.717E-02	0.654E-02	0.616E-02	0.558E-02
11225.9A	5000.	0.366E-01	0.254E-01	0.805E-02	0.745E-02	0.692E-02	0.637E-02
c= 0.13E+19	10000.	0.374E-01	0.230E-01	0.904E-02	0.844E-02	0.777E-02	0.723E-02
(87)	20000.	0.378E-01	0.167E-01	0.102E-01	0.952E-02	0.872E-02	0.817E-02
	40000.	0.381E-01	0.108E-01	0.114E-01	0.107E-01	0.979E-02	0.920E-02
	80000.	0.357E-01	0.515E-02	0.128E-01	0.121E-01	0.110E-01	0.104E-01

© European Southern Observatory • Provided by the NASA Astrophysics Data System

1990A&AS...82..519D

TABLE III *(continued)*

NE= 0.1E+14

TRANSITION	T(K)	ELECTRONS 2WE(A)	DE(A)	PROTONS 2WI(A)	DI(A)	IONIZED HELIUM 2WI(A)	DI(A)
3P - 4D	2500.	0.756E-01	0.242E-01	0.338E-01	0.298E-01	0.285E-01	0.254E-01
19089.4A	5000.	0.684E-01	0.180E-01	0.388E-01	0.343E-01	0.324E-01	0.291E-01
c= 0.18E+18	10000.	0.598E-01	0.105E-01	0.436E-01	0.400E-01	0.372E-01	0.333E-01
	20000.	0.512E-01	0.711E-02	0.455E-01	0.465E-01	0.423E-01	0.384E-01
	40000.	0.432E-01	0.371E-02	0.423E-01	0.518E-01	0.454E-01	0.447E-01
	80000.	0.363E-01	0.232E-02	0.360E-01	0.534E-01	0.438E-01	0.506E-01
3P - 5D	2500.	0.103	0.297E-01	0.481E-01*	0.410E-01*	0.407E-01*	0.347E-01*
12968.4A	5000.	0.917E-01	0.195E-01	0.552E-01*	0.478E-01*	0.461E-01*	0.404E-01*
c= 0.54E+17	10000.	0.796E-01	0.132E-01	0.627E-01	0.560E-01	0.528E-01*	0.466E-01*
	20000.	0.675E-01	0.695E-02	0.668E-01	0.657E-01	0.604E-01	0.539E-01
	40000.	0.563E-01	0.418E-02	0.636E-01	0.745E-01	0.662E-01	0.631E-01
	80000.	0.465E-01	0.191E-02	0.540E-01	0.784E-01	0.655E-01	0.725E-01
3P - 6D	2500.	0.181	0.412E-01				
11045.0A	5000.	0.160	0.275E-01				
c= 0.18E+17	10000.	0.137	0.141E-01	0.132*	0.118*		
(88)	20000.	0.115	0.888E-02	0.133*	0.139*		
	40000.	0.954E-01	0.513E-02	0.117*	0.153*	0.134*	0.135*
	80000.	0.779E-01	0.206E-02	0.922E-01*	0.155*	0.124*	0.152*
3D - 4P	2500.	0.124	-0.999E-02				
18555.6A	5000.	0.102	-0.738E-02	0.167*	-0.228*		
c= 0.15E+17	10000.	0.828E-01	-0.512E-02	0.110	-0.226	0.182*	-0.229*
	20000.	0.675E-01	-0.323E-02	0.599E-01	-0.196	0.128*	-0.235*
	40000.	0.549E-01	-0.211E-02	0.362E-01	-0.156	0.730E-01	-0.212
	80000.	0.448E-01	-0.123E-02	0.186E-01	-0.121	0.420E-01	-0.169
3D - 5P	2500.	0.545E-01	-0.252E-01	0.145E-01*	-0.130E-01*	0.125E-01*	-0.111E-01*
12755.7A	5000.	0.522E-01	-0.190E-01	0.163E-01*	-0.148E-01*	0.140E-01*	-0.127E-01*
c= 0.40E+18	10000.	0.487E-01	-0.117E-01	0.183E-01	-0.168E-01	0.157E-01*	-0.144E-01*
	20000.	0.448E-01	-0.706E-02	0.208E-01	-0.191E-01	0.176E-01	-0.163E-01
	40000.	0.400E-01	-0.356E-02	0.238E-01	-0.215E-01	0.200E-01	-0.184E-01
	80000.	0.352E-01	-0.139E-02	0.272E-01	-0.247E-01	0.228E-01	-0.207E-01
3D - 4F	2500.	0.405E-01	-0.676E-02	0.227E-01	-0.201E-01	0.191E-01	-0.171E-01
18696.9A	5000.	0.350E-01	-0.321E-02	0.262E-01	-0.232E-01	0.218E-01	-0.195E-01
c= 0.19E+18	10000.	0.295E-01	-0.142E-02	0.290E-01	-0.272E-01	0.250E-01	-0.224E-01
	20000.	0.247E-01	0.219E-03	0.287E-01	-0.317E-01	0.283E-01	-0.260E-01
	40000.	0.208E-01	0.459E-03	0.238E-01	-0.344E-01	0.293E-01	-0.304E-01
	80000.	0.178E-01	0.869E-03	0.167E-01	-0.335E-01	0.258E-01	-0.339E-01
3D - 5F	2500.	0.106	-0.518E-02	0.516E-01	0.528E-01	0.512E-01	0.415E-01
12790.3A	5000.	0.896E-01	-0.258E-02	0.466E-01	0.491E-01	0.533E-01	0.496E-01
c= 0.12E+17	10000.	0.737E-01	0.110E-03	0.368E-01	0.392E-01	0.467E-01	0.518E-01
	20000.	0.598E-01	0.442E-03	0.359E-01	0.199E-01	0.386E-01	0.461E-01
	40000.	0.483E-01	0.965E-03	0.276E-01	0.637E-02	0.362E-01	0.263E-01
	80000.	0.389E-01	0.950E-03	0.165E-01	-0.523E-02	0.320E-01	0.107E-01
2S - 2P	2500.	0.106E-03	-0.502E-04	0.301E-04	-0.142E-04	0.294E-04	-0.122E-04
10830.0A	5000.	0.107E-03	-0.605E-04	0.309E-04	-0.159E-04	0.299E-04	-0.137E-04
c= 0.11E+21	10000.	0.114E-03	-0.632E-04	0.320E-04	-0.179E-04	0.307E-04	-0.154E-04
(1)	20000.	0.131E-03	-0.622E-04	0.333E-04	-0.201E-04	0.316E-04	-0.172E-04
	40000.	0.156E-03	-0.475E-04	0.349E-04	-0.225E-04	0.328E-04	-0.194E-04
	80000.	0.188E-03	-0.383E-04	0.368E-04	-0.253E-04	0.343E-04	-0.217E-04
2P - 3S	2500.	0.266E-03	0.199E-03	0.610E-04	0.566E-04	0.527E-04	0.486E-04
7065.3A	5000.	0.312E-03	0.235E-03	0.683E-04	0.637E-04	0.589E-04	0.547E-04
c= 0.12E+20	10000.	0.342E-03	0.264E-03	0.765E-04	0.716E-04	0.659E-04	0.615E-04
(10)	20000.	0.360E-03	0.249E-03	0.857E-04	0.804E-04	0.738E-04	0.690E-04
	40000.	0.375E-03	0.216E-03	0.961E-04	0.902E-04	0.827E-04	0.775E-04
	80000.	0.404E-03	0.173E-03	0.108E-03	0.101E-03	0.927E-04	0.870E-04

© European Southern Observatory • Provided by the NASA Astrophysics Data System

1990A&AS...82..519D

TABLE III *(continued)*

NE= 0.1E+14

TRANSITION	T(K)	ELECTRONS 2WE(A)	DE(A)	PROTONS 2WI(A)	DI(A)	IONIZED HELIUM 2WI(A)	DI(A)
3S - 4P	2500.	0.622E-02	0.386E-02	0.159E-02	0.133E-02	0.142E-02	0.114E-02
12528.0A	5000.	0.704E-02	0.267E-02	0.175E-02	0.150E-02	0.155E-02	0.129E-02
c= 0.36E+19	10000.	0.819E-02	0.184E-02	0.193E-02	0.169E-02	0.170E-02	0.145E-02
	20000.	0.875E-02	0.103E-02	0.214E-02	0.190E-02	0.187E-02	0.163E-02
	40000.	0.908E-02	0.368E-03	0.238E-02	0.214E-02	0.207E-02	0.183E-02
	80000.	0.899E-02	-0.314E-04	0.267E-02	0.240E-02	0.230E-02	0.206E-02
3S - 5P	2500.	0.106E-01	0.654E-02	0.275E-02	0.235E-02	0.242E-02	0.201E-02
9463.6A	5000.	0.119E-01	0.439E-02	0.304E-02	0.266E-02	0.266E-02	0.228E-02
c= 0.10E+19	10000.	0.134E-01	0.326E-02	0.337E-02	0.301E-02	0.294E-02	0.258E-02
(67)	20000.	0.139E-01	0.140E-02	0.375E-02	0.338E-02	0.326E-02	0.290E-02
	40000.	0.140E-01	0.563E-03	0.420E-02	0.381E-02	0.363E-02	0.327E-02
	80000.	0.135E-01	0.127E-03	0.473E-02	0.428E-02	0.405E-02	0.368E-02
3S - 6P	2500.	0.198E-01	0.120E-01	0.513E-02	0.439E-02	0.449E-02	0.375E-02
8361.8A	5000.	0.224E-01	0.890E-02	0.569E-02	0.501E-02	0.497E-02	0.428E-02
c= 0.47E+18	10000.	0.246E-01	0.539E-02	0.634E-02	0.568E-02	0.551E-02	0.487E-02
(68)	20000.	0.251E-01	0.357E-02	0.707E-02	0.642E-02	0.613E-02	0.551E-02
	40000.	0.249E-01	0.113E-02	0.793E-02	0.722E-02	0.683E-02	0.620E-02
	80000.	0.235E-01	0.811E-03	0.897E-02	0.813E-02	0.765E-02	0.698E-02
3P - 4S	2500.	0.111E-01	0.634E-02	0.197E-02	0.177E-02	0.172E-02	0.152E-02
21120.0A	5000.	0.137E-01	0.744E-02	0.219E-02	0.199E-02	0.191E-02	0.171E-02
c= 0.24E+20	10000.	0.155E-01	0.796E-02	0.244E-02	0.224E-02	0.212E-02	0.192E-02
	20000.	0.170E-01	0.769E-02	0.273E-02	0.251E-02	0.236E-02	0.216E-02
	40000.	0.179E-01	0.625E-02	0.305E-02	0.282E-02	0.263E-02	0.242E-02
	80000.	0.186E-01	0.509E-02	0.341E-02	0.317E-02	0.294E-02	0.272E-02
3P - 5S	2500.	0.120E-01	0.840E-02	0.244E-02	0.226E-02	0.210E-02	0.193E-02
12846.0A	5000.	0.135E-01	0.957E-02	0.273E-02	0.255E-02	0.235E-02	0.219E-02
c= 0.75E+19	10000.	0.143E-01	0.943E-02	0.307E-02	0.287E-02	0.264E-02	0.247E-02
	20000.	0.149E-01	0.796E-02	0.344E-02	0.323E-02	0.296E-02	0.278E-02
	40000.	0.159E-01	0.585E-02	0.386E-02	0.364E-02	0.332E-02	0.312E-02
	80000.	0.161E-01	0.423E-02	0.434E-02	0.409E-02	0.372E-02	0.351E-02
3P - 6S	2500.	0.198E-01	0.143E-01	0.414E-02	0.380E-02	0.355E-02	0.325E-02
10667.6A	5000.	0.213E-01	0.157E-01	0.464E-02	0.431E-02	0.399E-02	0.369E-02
c= 0.29E+19	10000.	0.228E-01	0.152E-01	0.521E-02	0.488E-02	0.448E-02	0.419E-02
(73)	20000.	0.228E-01	0.116E-01	0.585E-02	0.549E-02	0.502E-02	0.472E-02
	40000.	0.243E-01	0.770E-02	0.657E-02	0.618E-02	0.564E-02	0.531E-02
	80000.	0.239E-01	0.447E-02	0.739E-02	0.695E-02	0.633E-02	0.597E-02
3P - 7S	2500.	0.362E-01	0.253E-01	0.720E-02	0.653E-02	0.619E-02	0.557E-02
9702.7A	5000.	0.354E-01	0.265E-01	0.809E-02	0.745E-02	0.695E-02	0.637E-02
c= 0.15E+19	10000.	0.368E-01	0.245E-01	0.908E-02	0.846E-02	0.780E-02	0.724E-02
(75)	20000.	0.382E-01	0.174E-01	0.102E-01	0.956E-02	0.876E-02	0.820E-02
	40000.	0.409E-01	0.114E-01	0.115E-01	0.108E-01	0.983E-02	0.924E-02
	80000.	0.389E-01	0.511E-02	0.129E-01	0.121E-01	0.110E-01	0.104E-01
3P - 4D	2500.	0.421E-01	0.115E-02	0.190E-01	0.169E-01	0.161E-01	0.144E-01
17002.0A	5000.	0.379E-01	-0.523E-03	0.219E-01	0.194E-01	0.182E-01	0.165E-01
c= 0.20E+18	10000.	0.343E-01	-0.983E-03	0.250E-01	0.225E-01	0.209E-01	0.188E-01
	20000.	0.304E-01	-0.139E-02	0.264E-01	0.265E-01	0.240E-01	0.216E-01
	40000.	0.266E-01	-0.108E-02	0.238E-01	0.308E-01	0.263E-01	0.253E-01
	80000.	0.231E-01	-0.159E-03	0.168E-01	0.293E-01	0.247E-01	0.290E-01
3P - 5D	2500.	0.673E-01	0.364E-02	0.310E-01*	0.268E-01*	0.263E-01*	0.227E-01*
11969.1A	5000.	0.602E-01	0.418E-03	0.356E-01	0.310E-01	0.298E-01*	0.264E-01*
c= 0.60E+17	10000.	0.534E-01	-0.203E-02	0.408E-01	0.361E-01	0.341E-01	0.302E-01
(72)	20000.	0.462E-01	-0.107E-02	0.441E-01	0.427E-01	0.393E-01	0.349E-01
	40000.	0.396E-01	-0.299E-03	0.405E-01	0.489E-01	0.436E-01	0.408E-01
	80000.	0.335E-01	-0.675E-05	0.298E-01	0.499E-01	0.424E-01	0.477E-01

© European Southern Observatory • Provided by the NASA Astrophysics Data System

1990A&AS...82..519D

TABLE III *(continued)*

NE= 0.1E+14

TRANSITION	T(K)	ELECTRONS 2WE(A)	DE(A)	PROTONS 2WI(A)	DI(A)	IONIZED HELIUM 2WI(A)	DI(A)
3P - 6D	2500.	0.121	-0.457E-03	0.590E-01*	0.486E-01*		
10311.0A	5000.	0.108	0.233E-02	0.679E-01*	0.573E-01*		
c= 0.26E+17	10000.	0.948E-01	-0.375E-02	0.782E-01*	0.678E-01*	0.649E-01*	0.562E-01*
(74)	20000.	0.813E-01	-0.128E-02	0.849E-01*	0.821E-01*	0.746E-01*	0.655E-01*
	40000.	0.690E-01	-0.122E-02	0.785E-01	0.959E-01	0.823E-01*	0.781E-01*
	80000.	0.578E-01	0.605E-04	0.634E-01	0.963E-01	0.866E-01*	0.930E-01*
3D - 4P	2500.	0.177E-01	0.110E-01	0.403E-02	0.346E-02	0.355E-02	0.296E-02
19543.0A	5000.	0.188E-01	0.940E-02	0.445E-02	0.390E-02	0.390E-02	0.335E-02
c= 0.87E+19	10000.	0.211E-01	0.698E-02	0.493E-02	0.440E-02	0.431E-02	0.377E-02
	20000.	0.222E-01	0.488E-02	0.548E-02	0.495E-02	0.477E-02	0.425E-02
	40000.	0.223E-01	0.255E-02	0.612E-02	0.556E-02	0.530E-02	0.477E-02
	80000.	0.218E-01	0.130E-02	0.688E-02	0.624E-02	0.591E-02	0.536E-02
3D - 5P	2500.	0.211E-01	0.138E-01	0.520E-02	0.447E-02	0.457E-02	0.382E-02
12985.0A	5000.	0.232E-01	0.106E-01	0.576E-02	0.507E-02	0.504E-02	0.434E-02
c= 0.20E+19	10000.	0.258E-01	0.850E-02	0.639E-02	0.573E-02	0.557E-02	0.492E-02
	20000.	0.266E-01	0.533E-02	0.712E-02	0.645E-02	0.618E-02	0.554E-02
	40000.	0.265E-01	0.310E-02	0.797E-02	0.726E-02	0.688E-02	0.623E-02
	80000.	0.253E-01	0.117E-02	0.899E-02	0.816E-02	0.769E-02	0.701E-02
3D - 6P	2500.	0.349E-01	0.215E-01	0.888E-02	0.762E-02	0.777E-02	0.650E-02
10996.6A	5000.	0.393E-01	0.160E-01	0.986E-02	0.869E-02	0.860E-02	0.743E-02
c= 0.81E+18	10000.	0.430E-01	0.128E-01	0.110E-01	0.986E-02	0.954E-02	0.844E-02
(78)	20000.	0.437E-01	0.781E-02	0.123E-01	0.111E-01	0.106E-01	0.956E-02
	40000.	0.431E-01	0.443E-02	0.137E-01	0.125E-01	0.118E-01	0.108E-01
	80000.	0.406E-01	0.176E-02	0.156E-01	0.141E-01	0.133E-01	0.121E-01
3D - 4F	2500.	0.359E-01	-0.364E-02	0.188E-01	-0.167E-01	0.158E-01	-0.143E-01
18686.0A	5000.	0.312E-01	-0.729E-03	0.216E-01	-0.192E-01	0.180E-01	-0.163E-01
c= 0.24E+18	10000.	0.264E-01	0.436E-03	0.244E-01	-0.223E-01	0.207E-01	-0.186E-01
	20000.	0.223E-01	0.156E-02	0.252E-01	-0.265E-01	0.236E-01	-0.214E-01
	40000.	0.190E-01	0.136E-02	0.225E-01	-0.300E-01	0.254E-01	-0.250E-01
	80000.	0.165E-01	0.142E-02	0.148E-01	-0.287E-01	0.232E-01	-0.286E-01
3D - 5F	2500.	0.168E-01	-0.171E-02	0.878E-02	-0.782E-02	0.741E-02	-0.668E-02
12785.0A	5000.	0.146E-01	-0.341E-03	0.101E-01	-0.897E-02	0.841E-02	-0.761E-02
c= 0.11E+18	10000.	0.124E-01	0.204E-03	0.114E-01	-0.104E-01	0.967E-02	-0.868E-02
	20000.	0.104E-01	0.730E-03	0.118E-01	-0.124E-01	0.111E-01	-0.100E-01
	40000.	0.888E-02	0.635E-03	0.105E-01	-0.140E-01	0.119E-01	-0.117E-01
	80000.	0.773E-02	0.664E-03	0.693E-02	-0.134E-01	0.108E-01	-0.134E-01

© European Southern Observatory • Provided by the NASA Astrophysics Data System

1991A&AS...89..581D

ASTRONOMY & ASTROPHYSICS
SUPPLEMENT SERIES

SEPTEMBER 1991, PAGE 581

Astron. Astrophys. Suppl. Ser. **89**, 581-590 (1991)

Stark broadening of spectral lines of multicharged ions of astrophysical interest. I. C IV lines

M.S. Dimitrijević[1], S. Sahal-Bréchot[2] and V. Bommier[2]

[1] Astronomical Observatory, Volgina 7, 11050 Beograd, Yugoslavia
[2] Laboratoire "Astrophysique, Atomes et Molécules", Département Atomes et Molécules en Astrophysique, Unité associée au C.N.R.S. N° 812, Observatoire de Paris-Meudon, France

Received November 19, 1990; accepted February 7, 1991

Abstract. — Using a semi-classical approach, we have calculated electron-, proton-, and ionized helium-impact line widths and shifts for 31 C IV multiplets. The obtained results have been compared with available experimental data. The comprehensive set of obtained data has also been used for the investigation of Stark broadening parameter regularities within the spectral series.

Key words: line profile — Stark broadening — atomic data.

1. Introduction.

This paper is the first one of a series devoted to the calculation of Stark broadening parameters of isolated spectral lines of multicharged ions: as a matter of fact, Stark broadening of spectral lines has been taking a new interest in astrophysics (Seaton 1987), owing to the recent development of researches on the physics of stellar interiors: in subphotospheric layers, the modeling of energy transport requires the knowledge of radiative opacities and thus, certain atomic processes must be known with accuracy. At these high temperatures (10^5 K or more) and densities ($10^{17} - 10^{22}$ cm^{-3}) the matter is mostly ionized: therefore Stark broadening of strong multicharged ionic lines plays a non-negligible role in the calculation of the opacities, especially in the UV. Stark broadening data for these lines are very scarce and many data are missing. The semi-classical-perturbation theory offers an interesting possibility for calculating numerous data, with an acceptable accuracy and without excessive computational time. Consequently, we have decided to undertake such calculations by using the computer code based on that theory (Sahal-Bréchot 1969ab).

The present paper concerns triply ionized carbon: beyond the interest for the modeling of stellar interiors, the knowledge of C IV Stark broadening parameters is of great importance for a number of problems in astrophysics and plasma physics, since carbon has a high cosmical abundance and is present as impurity in many laboratory plasma sources. For example the importance of reliable C IV Stark broadening parameters for the analysis of the extremely helium rich sdO type stars has been pointed out recently (Husfeld *et al.* 1989). In order to provide reliable data for C IV lines broadened by collisions with charged perturbers in stellar plasmas, we have calculated electron-, proton-, and ionized helium-impact line widths and shifts for 31 C IV multiplets, using the semi-classical-perturbation formalism (Sahal-Bréchot 1969ab). Our results are compared with available experimental data (Bogen 1972; El-Farra & Hughes 1983; Ackermann *et al.* 1985; Böttcher *et al.* 1987, 1988; and Djeniže *et al.* 1988). We have also compared calculated Stark widths with quantum mechanical results (Seaton 1988) and with results (Dimitrijević 1988; El-Farra & Hughes 1983) obtained using the modified semi-empirical approach (Dimitrijević & Konjević 1980).

The results obtained have also been used to continue our investigation of systematic trends for Stark broadening parameters within spectral series (Dimitrjević & Sahal-Bréchot 1984ab, 1985, 1987, 1990ab).

2. Theory.

The calculation procedure is well described elsewhere (Sahal-Bréchot 1969ab) and only few details will be given here. Within the framework of the semi-classical-perturbational formalism (Sahal-Bréchot 1969ab) used here, the full halfwidth (W) and shift (d) of an electron-impact broadened isolated spectral line can be expressed as:

© European Southern Observatory • Provided by the NASA Astrophysics Data System

1991A&AS...89..581D

$$W = N \int_0^\infty v\, f(v) \mathrm{d}v \left(\sum_{\mathrm{i}' \neq \mathrm{i}} \sigma_{\mathrm{ii}'}(v) + \sum_{\mathrm{f}' \neq \mathrm{f}} \sigma_{\mathrm{ff}'}(v) + \sigma_{\mathrm{el}} \right) + W_{\mathrm{R}}$$

$$d = N \int_0^\infty v\, f(v) \mathrm{d}v \int_{R_3}^{R_{\mathrm{D}}} 2\pi\rho\, \mathrm{d}\rho \sin\left(2\varphi_{\mathrm{p}}\right), \quad (1)$$

where N is the electron density, $f(v)$ the Maxwellian velocity distribution function for electrons, ρ denotes the impact parameters of the incoming electron, i and f denote the initial and final atomic energy levels, and i′, f′ their corresponding perturbing levels, while W_{R} gives the contribution of the Feshbach resonances (Fleurier *et al.* 1977). The inelastic cross section $\sigma_{jj'}(v)$ can be expressed by an integral over the impact parameter of the transition probability $P_{jj'}(\rho, v)$ as

$$\sum_{j \neq j'} \sigma_{jj'}(v) = \frac{1}{2}\pi R_1^2 + \int_{R_1}^{R_{\mathrm{D}}} 2\pi\rho\, \mathrm{d}\rho \sum_{j=j'}, P_{jj'}(\rho, v),\ j = \mathrm{i}, \mathrm{f} \quad (2)$$

and the elastic cross section is given by

$$\sigma_{\mathrm{el}} = 2\pi\, R_2^2 + \int_{R_2}^{R_{\mathrm{D}}} 8\pi\rho\, \mathrm{d}\rho \sin^2\delta,$$

$$\delta = \left(\varphi_{\mathrm{p}}^2 + \varphi_{\mathrm{q}}^2\right)^{\frac{1}{2}}. \quad (3)$$

The phase shifts φ_{p} and φ_{q} due respectively to the polarisation potential (r^{-4}) and to the quadrupolar potential (r^{-3}), are given in Section 3 of Chapter 2 in Sahal-Bréchot (1969a).

R_{D} is the Debye radius. All the cut-offs R_1, R_2, R_3 are described in Section 1 of Chapter 3 in Sahal-Bréchot (1969b). For multiply charged ions ($Z > 2$) the cut-off R_1 can become smaller than the mean atomic radii $\langle r_j \rangle$, $\langle r_{j'} \rangle$. In that case we have used the cutt-off of Seaton (1962), used also by Burgess (1964) for excitation of ions by electron impact and adpated by Feautrier (1968) for Stark broadening purposes:

$$\sum_{j \neq j} \sigma_{jj'} = \sum_{j' \neq j} \int_{\mathrm{Max}(\langle r_j \rangle,\, \langle r_{j'} \rangle)}^{R_{\mathrm{D}}} 2\pi\rho\, \mathrm{d}\rho P_{jj'}(\rho, v) \quad (4)$$

when $R_1 < \mathrm{Max}\left(\langle r_j \rangle, \langle r_{j'} \rangle\right)$.

The formulae for the ion-impact widths are analogous, but inelastic collisions have been neglected. One must beware of the fact that the accuracy of the obtained results decreases when the broadening by ion-impact is important.

At high densities or for lines arising from high levels, the electron impact width becomes comparable to the separation $\Delta E(nl,\ nl \pm 1)$ between the perturbing energy levels and the initial or final levels: the corresponding levels become degenerate and the isolated line approximation is then invalid (Griem 1974). We can use the parameter c defined in Dimitrijević & Sahal-Bréchot (1984a) and given in Table 1, in order to check the validity of this approximation. For an electron concentration lower than

$$N_l\ (\mathrm{cm}^{-3}) = c/2W \quad (5)$$

with $2W$ expressed in Å and obtained at the density $N = 10^{17}\ \mathrm{cm}^{-3}$, the line may be treated as isolated in the core, even if a weak forbidden component due to failure of this approximation remains in the wing.

For investigations of dense plasmas in subphotospheric layers, one must also take into account that with the increase of the density the number of particles in the Debye sphere decreases and the plasma becomes non-ideal (Konjević & Uzelac 1990). The ideality of the plasma can be checked by calculating the number of perturbers in the Debye sphere which must be larger than 1. The condition of validity is given by

$$\frac{4\pi}{3} R_{\mathrm{D}}^3 N > 1, \quad \text{or} : N < 1.9 \times 10^6\ \mathrm{T}^3\ \mathrm{cm}^{-3}. \quad (6)$$

For $T = 200\,000$ K, the condition is fulfilled if $N < 1.5 \times 10^{22}\ \mathrm{cm}^{-3}$.

Furthermore, at high densities, the impact approximation becomes invalid for collisions with the ions of the plasma: there is then more than one perturber in the collision volume (Baranger 1958; Sahal-Bréchot 1969ab). The quasistatic approximation is then more adequate. For lines arising from moderately excited levels, the quadrupolar interaction potential is predominant and the current quasistatic formula based on the quadratic interaction potential is not valid: the quadrupolar quasistatic profile for ionic lines perturbed by positive ions is in fact Gaussian (Sahal-Bréchot 1991), the Gaussian width being given by the following simple expression

$$\Delta\omega_{\mathrm{quas}} = 1.6 \times 10^{-4} \times \times \frac{\left[\left(B_{\mathrm{i}} \langle r_{\mathrm{i}}^2 \rangle\right)^2 + \left(B_{\mathrm{f}} \langle r_{\mathrm{f}}^2 \rangle\right)^2 - B_{\mathrm{if}} \langle r_{\mathrm{i}}^2 \rangle \langle r_{\mathrm{f}}^2 \rangle\right]^{\frac{1}{2}}}{a_0^2} \left(\frac{NT^3}{Z^3 Z_{\mathrm{p}}}\right)^{\frac{1}{2}} \quad (7)$$

where B_{i}, B_{f}, B_{if} are given in Sahal-Bréchot (1974). The corresponding Gaussian profile is

$$I_{\mathrm{quas}}(\Delta\omega) = \exp\left\{ -\left(\frac{\Delta\omega}{\Delta\omega_{\mathrm{quas}}}\right)^2 \right\} \quad (8)$$

For lines arising from high levels the quadratic interaction becomes predominant and a possibility is to evaluate the ion broadening contribution by using the quasistatic ion broadening parameter (Griem 1974) introduced by Griem *et al.* (1962).

3. Results and discussion.

Energy levels for C IV lines have been taken from Bashkin & Stoner (1975). Oscillator strengths have been calculated using the method of Bates and Damgaard (1949) and tables

© European Southern Observatory • Provided by the NASA Astrophysics Data System

1991A&AS...89..581D

of Oertel & Shomo (1968). Fior higher levels, the method described by Van Regemorter *et al.* (1979) has been used.

In addition to the electron-impact full halfwidths and shifts, Stark broadening parameters due to proton-, and ionized helium-impact have been calculated. In such a way we provide Stark broadening data for all important charged perturbers in stellar atmospheres. Our results are shown in Table 1 for a perturber density 10^{17} cm^{-3} and temperatures of T = 20 000; 50 000; 80 000; 100 000; 150 000 and 200 000 K. We also specify a parameter c [see Eq. (5)], which gives an estimate for the maximum perturber density for which the line may be treated as isolated when it is divided by $2W$.

For each value given in Table 1, the collision volume (V) multiplied by the perturber density (N) is much less than one and the impact approximation is valid (Sahal-Bréchot 1969ab). Values for $N\,V > 0.5$ are not given in Table 1; values for $0.1 < N\,V \leq 0.5$ are denoted by an asterisk. When the impact approximation is not valid, the ion broadening contribution may be estimated by using quasistatic formulae (cf. Sect. 2), bearing in mind that the accuracy of the obtained results decrease when the broadening by ions is important.

For high densities or when a perturbing level is close to the initial or to the final levels, the influence of Debye screening may be important. In order to scale to other densities, we will provide data for $N = 10^{15}$, and $10^{18} - 10^{21}$ cm^{-3} elsewhere (Dimitrijević *et al.* 1991).

In Table 2 our results ($W_{\rm DSB}$) are compared with the existing experimental values (Bogen 1972; El-Farra & Hughes 1983, Ackermann *et al.* 1985; Böttcher *et al.* 1987, 1988; and, Djeniže *et al.* 1988) as well as with the results (Dimitrijević 1988; El-Farra & Hughes 1983) obtained using the modified semi-empirical method ($W_{\rm MSE}$) (Dimitrijević & Konjević 1980). In the paper of Böttcher *et al.* (1987) two experimental values are given, one assuming the impact, and the other assuming the quasistatic approximation. Both are presented in Table 2. Values in Table 2 have been calculated for the experimental conditions specified in the corresponding papers. The agreement with experimental data is not good for transitions arising from high levels. In such cases the ion broadening contribution is important and a more sophisticated method for the quasistatic ion broadening should be elaborated. For the shift, there is only one result for the 2s-2p multiplet (Djeniže *et al.* 1988) which has the opposite sign from our and Seaton's (1988) values.

We notice a good agreement between semi-classical-perturbation theory and much simpler modified semi-empirical results, especially for high transitions. This is promising for the use of the simpler, modified semi-empirical method in the cases where there are no semi-classical results, or in the case where a considerably higher effort is needed to use a more sophisticated method which does not promise a considerably higher accuracy (e.g. lack of reliable atomic data). However, in the cases of the 3s-3p and particularly the 2s-2p transition great differences exist. For such transitions the contribution of resonances below the threshold for inelastic excitation is important. Such a contribution is only indirectly included in the modified semi-empirical approach, where the empirical part is chosen to be in accordance (on the average) with existing experiments.

The present semi-classical calculations are in relatively good agreement with strong coupling quantum mechanical calculations of Seaton (1988). They are also in agreement in available cases with the calculations of Romanov *et al.* (1979) for the 2s-2p and 3s-3p multiplets and with the calculations for the same multiplets of Dimitrijević (1988), obtained using the approximate semi-classical method of Griem (1974). We can also compare values given in Table 2 for the 3s-3p multiplet, $N = 1.8 \times 10^{18}$ cm^{-3} and T = 145 000 K (the experimental data of Böttcher *et al.* 1988; W = 10.0 Å and our result = 7.4 Å) with the calculations (Böttcher *et al.* 1988) based on the theoretical approaches of Hey & Breger 1980ab (W = 5.45 Å); 1980, 1982c (W = 6.09 Å) and Baranger 1962 (W = 10.8 Å). This is also illustrated in Figures 1-3 where various theoretical and experimental data have been compared for C IV 2s ^{2}S – 2p ^{2}P^0, 3s ^{2}S – 3p ^{2}P^0 and 3d ^{2}D – 4f ^{2}F^0 multiplets.

In Figures 4 and 5 the electron and proton full halfwidths within the 2s ^{2}S – np ^{2}P^0 series are reported. We see the variation of the results for different plasma temperatures and different perturber type (electrons and protons). By inspecting the energy separation between the upper level and the principal perturbing levels (see the Grotrian diagrams in Bashkin & Stoner (1975), we find that this separation decreases gradually within a spectral series. This is the reason why we obtain a gradual change of the Stark widths. In Table 3 we can see the situation in the case of the shift. This conclusion might be used for the critical evaluation of existing results as well as for the interpolation of new data needed in astrophysics.

Acknowledgements.

One of us (M.D.) has been supported by the Observatory of Paris-Meudon. This work has also been supported by the C.N.R.S. and is a part of the French-Yugoslav collaboration through the project "L'élargissement Stark des raies spectrales des plasmas astrophysiques et de laboratoire". This study has also been supported in part by SKNTI under the project "Atomic, Molecular and Plasma Spectroscopy". The numerical calculations have been performed on the VAX 8600 of the Observatory of Paris-Meudon.

© European Southern Observatory • Provided by the NASA Astrophysics Data System

1991A&AS...89..581D

References

Ackermann U., Finken K.H. and Musielok J. 1985, Phys. Rev. A 31, 2597
Baranger M. 1958a, Phys. Rev. A 111, 481
Baranger M. 1958b, Phys. Rev. A 111, 494
Baranger M. 1958c, Phys. Rev. A 112, 855
Bashkin S. and Stoner J.O.Jr. 1975, Atomic Energy Levels and Grotrian Diagrams, Vol. 1 (North Holland, Amsterdam)
Bates D.R. and Damgaard A. 1949, Trans. Roy. Soc. London, Ser. A 242, 101
Bogen P. 1972, Z. Naturforsch. 27a, 210
Böttcher F., Musielok J. and Kunze H.-J. 1987, Phys. Rev. A 36, 2265
Böttcher F., Breger P., Hey J.D. and Kunze H.-J. 1988, Phys. Rev. A 38, 2690
Burgess D. 1964, Proceedings of the Symposium on Atomic collision processes in plasmas (Culham, England)
Dimitrijević M.S. 1988a, A&AS 76, 53
Dimitrijević M.S. 1988b, Bull. Obs. Astron. Belgrade, 139, 31
Dimitrijević M.S. 1988c, Bull. Obs. Astron. Belgrade, 139, 70
Dimitrijević M.S. Konjević 1980, JQSRT 24, 451
Dimitrijević M.S. and Sahal-Bréchot S. 1984a, JQSRT 31, 301
Dimitrijević M.S. and Sahal-Bréchot S. 1984b, A&A 136, 289
Dimitrijević M.S. and Sahal-Bréchot S. 1985, JQSRT 34, 149
Dimitrijević M.S. and Sahal-Bréchot S. 1987, JQSRT 38, 37
Dimitrijević M.S. and Sahal-Bréchot S. 1990, A&AS 82, 519
Dimitrijević M.S., Sahal-Bréchot S. and Bommier V. 1991, Bull. Obs. Astron. Belgrade, 144, in press
Djeniže S., Srecković A., Milosavjević M., Labat O., Platiša M., Purić J. 1988, Z. Phys. D 9, 129
Feautrier N. 1968, Ann. Astrophys. 31, 305
El-Farra M.A. and Hughes T.P. 1983, JQSRT 30, 335
Fleurier C., Sahal-Bréchot S. and Chapelle J. 1977, JQSRT 17, 595
Griem H.R. 1974, Spectral Line Broadening by Plasmas (Academic Press, New York)
Griem H.R., Baranger M., Kolb A.C. and Oertel G.K. Phys. Rev. 125, 177
Hey J.D. and Breger P. 1980a, JQSRT 24, 349
Hey J.D. and Breger P. 1980b, JQSRT 24, 427
Hey J.D. and Breger P. 1980c, JQSRT 23, 311
Hey J.D. and Breger P. 1982, S. Afr. J. Phys. 5, 111
Husfeld D., Butler K., Heber U., Drilling J.S. 1989, A&A 222, 150
Konjević N. and Uzelac N.I. 1990, JQSRT 44, 61
Oertel G.K. and Shomo L.P. 1968, ApJS 16, 175
Romanov G.S., Stepanov K.L. and Sirkin M.I. 1979, Opt. Spektrosk. 47, 860
Sahal-Bréchot S. 1969a, A&A 1, 91
Sahal-Bréchot S. 1969b, A&A 2, 322
Sahal-Bréchot S. 1974, A&A 35, 319
Sahal-Bréchot S. 1991, A&A in press
Sahal-Bréchot S. and Segre E.R. 1971, A&A 13, 161
Seaton M.J. 1962, Proc. Phys. Soc. 79, 1105
Seaton M.J. 1987, J. Phys. B 20, 6363
Seaton M.J. 1990, J. Phys. B 23, 3255
Van Regemorter H., Hoang Binh Dy and Prud'homme M. 1979, J. Phys. B 12, 1073

© European Southern Observatory • Provided by the NASA Astrophysics Data System

1991A&AS...89..581D

TABLE 1. *This table gives electron-, proton-, and ionized-helium- impact broadening parameters for C IV lines, for a perturber density of* 10^{17} cm^{-3} *and temperatures from 20 000 K to 200 000 K. Transitions and averaged wavelengths for the multiplet (in Å) are also given. By using c (see Eq. (5)), we obtain an estimate for the maximum perturber density for which the line may be treated as isolated and tabulated data may be used. The asterisk identifies cases for which the collision volume multiplied by the perturber density (the condition for validity of the impact approximation) lies between 0.1 and 0.5. For high densities or when a perturbing level is close to the initial or to the final levels, the influence of Debye screening may be important. In order to scale to other densities, we will provide data for* $N = 10^{15}$, *and* $10^{18} - 10^{21}$ cm^{-3} *elsewhere (Dimitrijević et al. 1991).*

PERTURBER DENSITY = 0.1D+18

TRANSITION	T(K)	ELECTRONS WIDTH(A)	ELECTRONS SHIFT(A)	PROTONS WIDTH(A)	PROTONS SHIFT(A)	IONIZED HELIUM WIDTH(A)	IONIZED HELIUM SHIFT(A)
CIV 2S-2P	20000.	0.115E-01	0.825E-03	0.157E-04	-0.372E-04	0.279E-04	-0.371E-04
1549.1 A	50000.	0.722E-02	-0.142E-03	0.642E-04	-0.959E-04	0.992E-04	-0.935E-04
C= 0.15D+21	80000.	0.576E-02	-0.204E-03	0.120E-03	-0.145E-03	0.161E-03	-0.135E-03
	100000.	0.519E-02	-0.173E-03	0.152E-03	-0.170E-03	0.199E-03	-0.159E-03
	150000.	0.432E-02	-0.195E-03	0.226E-03	-0.222E-03	0.254E-03	-0.195E-03
	200000.	0.382E-02	-0.216E-03	0.268E-03	-0.253E-03	0.304E-03	-0.226E-03
CIV 2S-3P	20000.	0.179E-02	0.184E-04	0.268E-04	0.378E-04	0.367E-04	0.354E-04
312.4 A	50000.	0.121E-02	0.385E-04	0.679E-04	0.715E-04	0.757E-04	0.635E-04
C= 0.47D+18	80000.	0.101E-02	0.343E-04	0.944E-04	0.907E-04	0.981E-04	0.783E-04
	100000.	0.929E-03	0.326E-04	0.108E-03	0.988E-04	0.105E-03	0.828E-04
	150000.	0.804E-03	0.317E-04	0.126E-03	0.110E-03	0.119E-03	0.926E-04
	200000.	0.730E-03	0.310E-04	0.138E-03	0.118E-03	0.128E-03	0.993E-04
CIV 2S-4P	20000.	0.331E-02	0.127E-03	0.155E-03	0.169E-03	0.168E-03	0.149E-03
244.9 A	50000.	0.240E-02	0.135E-03	0.280E-03	0.261E-03	0.265E-03	0.221E-03
C= 0.12D+18	80000.	0.205E-02	0.134E-03	0.332E-03	0.303E-03	0.300E-03	0.255E-03
	100000.	0.192E-02	0.133E-03	0.353E-03	0.319E-03	0.323E-03	0.269E-03
	150000.	0.169E-02	0.127E-03	0.401E-03	0.353E-03	0.349E-03	0.297E-03
	200000.	0.155E-02	0.116E-03	0.444E-03	0.387E-03	0.377E-03	0.320E-03
CIV 2S-5P	20000.	0.617E-02	0.365E-03	0.558E-03	0.495E-03*	0.526E-03*	0.401E-03
222.8 A	50000.	0.487E-02	0.366E-03	0.794E-03	0.702E-03*	0.708E-03*	0.581E-03
C= 0.51D+17	80000.	0.432E-02	0.380E-03	0.915E-03	0.816E-03*	0.819E-03*	0.688E-03
	100000.	0.407E-02	0.364E-03	0.973E-03	0.872E-03*	0.824E-03*	0.704E-03
	150000.	0.366E-02	0.313E-03	0.106E-02	0.928E-03*	0.924E-03*	0.778E-03
	200000.	0.338E-02	0.279E-03	0.117E-02	0.976E-03*	0.104E-02*	0.825E-03
CIV 2P-3S	20000.	0.239E-02	0.846E-04	0.123E-04	0.527E-04	0.169E-04	0.502E-04
419.6 A	50000.	0.153E-02	0.140E-03	0.605E-04	0.104E-03	0.584E-04	0.912E-04
C= 0.30D+19	80000.	0.125E-02	0.165E-03	0.902E-04	0.131E-03	0.880E-04	0.115E-03
	100000.	0.114E-02	0.170E-03	0.109E-03	0.145E-03	0.107E-03	0.123E-03
	150000.	0.980E-03	0.159E-03	0.146E-03	0.162E-03	0.129E-03	0.137E-03
	200000.	0.883E-03	0.159E-03	0.166E-03	0.176E-03	0.142E-03	0.148E-03
CIV 2P-4S	20000.	0.318E-02	0.459E-03	0.947E-04	0.167E-03	0.966E-04	0.144E-03
296.9 A	50000.	0.225E-02	0.401E-03	0.220E-03	0.267E-03	0.201E-03	0.222E-03
C= 0.61D+18	80000.	0.193E-02	0.383E-03	0.285E-03	0.307E-03	0.245E-03	0.259E-03
	100000.	0.180E-02	0.374E-03	0.308E-03	0.326E-03	0.266E-03	0.276E-03
	150000.	0.158E-02	0.358E-03	0.363E-03	0.362E-03	0.300E-03	0.304E-03
	200000.	0.144E-02	0.345E-03	0.395E-03	0.388E-03	0.351E-03	0.325E-03
CIV 2P-5S	20000.	0.568E-02	0.133E-02	0.354E-03	0.448E-03	0.350E-03	0.379E-03
262.6 A	50000.	0.433E-02	0.113E-02	0.631E-03	0.644E-03	0.543E-03	0.538E-03
C= 0.24D+18	80000.	0.381E-02	0.101E-02	0.745E-03	0.742E-03	0.638E-03	0.627E-03
	100000.	0.358E-02	0.959E-03	0.790E-03	0.795E-03	0.673E-03	0.666E-03
	150000.	0.321E-02	0.888E-03	0.935E-03	0.853E-03	0.750E-03	0.709E-03
	200000.	0.297E-02	0.846E-03	0.954E-03	0.923E-03	0.847E-03	0.751E-03
CIV 2P-3D	20000.	0.166E-02	-0.502E-04	0.165E-04	-0.393E-04	0.240E-04	-0.376E-04
384.1 A	50000.	0.109E-02	-0.304E-04	0.581E-04	-0.795E-04	0.610E-04	-0.692E-04
C= 0.71D+18	80000.	0.892E-03	-0.190E-04	0.831E-04	-0.100E-03	0.866E-04	-0.879E-04
	100000.	0.815E-03	-0.206E-04	0.985E-04	-0.111E-03	0.995E-04	-0.949E-04
	150000.	0.696E-03	-0.190E-04	0.125E-03	-0.125E-03	0.116E-03	-0.106E-03
	200000.	0.628E-03	-0.158E-04	0.140E-03	-0.135E-03	0.127E-03	-0.114E-03
CIV 2P-4D	20000.	0.468E-02	-0.752E-04*	0.154E-02*	0.143E-02*	0.138E-02*	0.115E-02
289.2 A	50000.	0.351E-02	0.480E-04*	0.218E-02*	0.209E-02*	0.188E-02*	0.175E-02
C= 0.80D+16	80000.	0.304E-02	0.954E-04*	0.258E-02*	0.242E-02*	0.228E-02*	0.197E-02
	100000.	0.284E-02	0.849E-04*	0.286E-02*	0.254E-02*	0.231E-02*	0.208E-02
	150000.	0.251E-02	0.701E-04*	0.297E-02*	0.271E-02*	0.265E-02*	0.215E-02
	200000.	0.230E-02	0.713E-04*	0.306E-02*	0.284E-02*	0.292E-02*	0.239E-02

© European Southern Observatory • Provided by the NASA Astrophysics Data System

1991A&AS...89..581D

TABLE 1 *(continued)*

PERTURBER DENSITY = 0.1D+18

TRANSITION	T(K)	ELECTRONS WIDTH(A)	ELECTRONS SHIFT(A)	PROTONS WIDTH(A)	PROTONS SHIFT(A)	IONIZED HELIUM WIDTH(A)	IONIZED HELIUM SHIFT(A)
CIV 2P-5D	20000.	0.106E-01	-0.307E-03				
259.5 A	50000.	0.831E-02	0.448E-04				
C= 0.34D+16	80000.	0.728E-02	0.268E-03				
	100000.	0.683E-02	0.236E-03				
	150000.	0.605E-02	0.156E-03				
	200000.	0.553E-02	0.191E-03				
CIV 3S-3P	20000.	0.896	-0.111E-01	0.723E-02	0.390E-02	0.108E-01	0.382E-02
5801.0 A	50000.	0.603	-0.994E-02	0.172E-01	0.869E-02	0.206E-01	0.803E-02
C= 0.16D+21	80000.	0.502	-0.159E-01	0.223E-01	0.115E-01	0.260E-01	0.101E-01
	100000.	0.463	-0.181E-01	0.251E-01	0.127E-01	0.277E-01	0.113E-01
	150000.	0.402	-0.162E-01	0.290E-01	0.154E-01	0.302E-01	0.130E-01
	200000.	0.366	-0.162E-01	0.309E-01	0.167E-01	0.319E-01	0.141E-01
CIV 3S-4P	20000.	0.569E-01	0.148E-02	0.224E-02	0.240E-02	0.245E-02	0.211E-02
948.1 A	50000.	0.407E-01	0.142E-02	0.404E-02	0.374E-02	0.381E-02	0.315E-02
C= 0.18D+19	80000.	0.348E-01	0.128E-02	0.479E-02	0.431E-02	0.438E-02	0.361E-02
	100000.	0.324E-01	0.122E-02	0.515E-02	0.458E-02	0.468E-02	0.382E-02
	150000.	0.286E-01	0.119E-02	0.587E-02	0.505E-02	0.516E-02	0.419E-02
	200000.	0.263E-01	0.103E-02	0.627E-02	0.551E-02	0.544E-02	0.447E-02
CIV 3S-5P	20000.	0.620E-01	0.319E-02	0.524E-02	0.465E-02*	0.495E-02*	0.376E-02
684.9 A	50000.	0.485E-01	0.313E-02	0.746E-02	0.659E-02*	0.668E-02*	0.545E-02
C= 0.48D+18	80000.	0.429E-01	0.320E-02	0.864E-02	0.768E-02*	0.770E-02*	0.646E-02
	100000.	0.404E-01	0.303E-02	0.907E-02	0.815E-02*	0.781E-02*	0.659E-02
	150000.	0.363E-01	0.258E-02	0.990E-02	0.866E-02*	0.862E-02*	0.729E-02
	200000.	0.335E-01	0.226E-02	0.110E-01	0.919E-02*	0.981E-02*	0.775E-02
CIV 3P-4S	20000.	0.715E-01	0.552E-02	0.147E-02	0.247E-02	0.160E-02	0.216E-02
1230.0 A	50000.	0.514E-01	0.599E-02	0.338E-02	0.403E-02	0.321E-02	0.336E-02
C= 0.73D+19	80000.	0.441E-01	0.578E-02	0.435E-02	0.463E-02	0.389E-02	0.389E-02
	100000.	0.411E-01	0.569E-02	0.481E-02	0.492E-02	0.419E-02	0.410E-02
	150000.	0.363E-01	0.546E-02	0.549E-02	0.541E-02	0.486E-02	0.458E-02
	200000.	0.333E-01	0.525E-02	0.601E-02	0.583E-02	0.505E-02	0.493E-02
CIV 3P-5S	20000.	0.584E-01	0.118E-01	0.320E-02	0.404E-02	0.317E-02	0.343E-02
798.1 A	50000.	0.446E-01	0.998E-02	0.569E-02	0.582E-02	0.486E-02	0.485E-02
C= 0.22D+19	80000.	0.393E-01	0.895E-02	0.681E-02	0.673E-02	0.567E-02	0.567E-02
	100000.	0.370E-01	0.851E-02	0.706E-02	0.711E-02	0.606E-02	0.601E-02
	150000.	0.332E-01	0.785E-02	0.836E-02	0.780E-02	0.680E-02	0.639E-02
	200000.	0.308E-01	0.736E-02	0.864E-02	0.823E-02	0.774E-02	0.692E-02
CIV 3P-3D	20000.	9.23	-0.137	0.135	-0.269	0.168	-0.250
20754.0 A	50000.	6.30	-0.296	0.367	-0.484	0.383	-0.426
C= 0.21D+22	80000.	5.27	-0.250	0.540	-0.600	0.512	-0.503
	100000.	4.86	-0.242	0.612	-0.633	0.556	-0.534
	150000.	4.23	-0.236	0.713	-0.707	0.641	-0.596
	200000.	3.85	-0.227	0.789	-0.763	0.712	-0.642
CIV 3P-4D	20000.	0.781E-01	-0.119E-02	0.224E-01	0.208E-01*	0.200E-01*	0.169E-01
1107.6 A	50000.	0.583E-01	0.100E-03	0.318E-01	0.305E-01*	0.272E-01*	0.254E-01
C= 0.12D+18	80000.	0.505E-01	0.836E-03	0.377E-01	0.353E-01*	0.333E-01*	0.289E-01
	100000.	0.471E-01	0.722E-03	0.415E-01	0.372E-01*	0.338E-01*	0.304E-01
	150000.	0.417E-01	0.511E-03	0.436E-01	0.394E-01*	0.393E-01*	0.315E-01
	200000.	0.382E-01	0.530E-03	0.448E-01	0.412E-01*	0.423E-01*	0.351E-01
CIV 3P-5D	20000.	0.982E-01	-0.280E-02				
770.3 A	50000.	0.765E-01	0.908E-04				
C= 0.30D+17	80000.	0.670E-01	0.208E-02				
	100000.	0.628E-01	0.182E-02				
	150000.	0.556E-01	0.112E-02				
	200000.	0.509E-01	0.143E-02				

© European Southern Observatory • Provided by the NASA Astrophysics Data System

1991A&AS...89..581D

TABLE 1 *(continued)*

PERTURBER DENSITY = 0.1D+18

TRANSITION	T(K)	ELECTRONS WIDTH(A)	ELECTRONS SHIFT(A)	PROTONS WIDTH(A)	PROTONS SHIFT(A)	IONIZED HELIUM WIDTH(A)	IONIZED HELIUM SHIFT(A)
CIV 3P-4F	20000.	0.482E-01	-0.202E-03*	0.184E-01	-0.175E-01*	0.159E-01	-0.142E-01
1106.5 A	50000.	0.354E-01	-0.119E-02*	0.267E-01	-0.253E-01*	0.220E-01	-0.212E-01
C= 0.12D+18	80000.	0.304E-01	-0.170E-02*	0.302E-01	-0.298E-01*	0.254E-01	-0.240E-01
	100000.	0.283E-01	-0.152E-02*	0.324E-01	-0.304E-01*	0.266E-01	-0.257E-01
	150000.	0.250E-01	-0.115E-02*	0.355E-01	-0.333E-01*	0.303E-01	-0.278E-01
	200000.	0.229E-01	-0.101E-02*	0.407E-01	-0.365E-01*	0.315E-01	-0.304E-01
CIV 3D-4P	20000.	0.835E-01	0.327E-02	0.365E-02	0.423E-02	0.388E-02	0.373E-02
1198.6 A	50000.	0.603E-01	0.366E-02	0.677E-02	0.655E-02	0.630E-02	0.551E-02
C= 0.29D+19	80000.	0.517E-01	0.354E-02	0.809E-02	0.763E-02	0.737E-02	0.640E-02
	100000.	0.482E-01	0.352E-02	0.872E-02	0.812E-02	0.781E-02	0.671E-02
	150000.	0.426E-01	0.337E-02	0.973E-02	0.895E-02	0.868E-02	0.751E-02
	200000.	0.391E-01	0.308E-02	0.112E-01	0.954E-02	0.954E-02	0.806E-02
CIV 3D-5P	20000.	0.827E-01	0.490E-02	0.726E-02	0.653E-02*	0.682E-02*	0.529E-02
806.6 A	50000.	0.651E-01	0.499E-02	0.104E-01	0.926E-02*	0.921E-02*	0.768E-02
C= 0.67D+18	80000.	0.577E-01	0.513E-02	0.120E-01	0.108E-01*	0.108E-01*	0.911E-02
	100000.	0.545E-01	0.492E-02	0.129E-01	0.116E-01*	0.108E-01*	0.937E-02
	150000.	0.489E-01	0.424E-02	0.138E-01	0.123E-01*	0.121E-01*	0.103E-01
	200000.	0.452E-01	0.379E-02	0.152E-01	0.129E-01*	0.138E-01*	0.109E-01
CIV 3D-4F	20000.	0.470E-01	-0.216E-04*	0.201E-01	-0.192E-01*	0.174E-01	-0.157E-01
1169.0 A	50000.	0.346E-01	-0.556E-03*	0.293E-01	-0.281E-01*	0.240E-01	-0.232E-01
C= 0.13D+18	80000.	0.297E-01	-0.123E-02*	0.333E-01	-0.328E-01*	0.281E-01	-0.265E-01
	100000.	0.276E-01	-0.104E-02*	0.364E-01	-0.335E-01*	0.293E-01	-0.281E-01
	150000.	0.244E-01	-0.610E-03	0.391E-01	-0.366E-01*	0.334E-01	-0.305E-01
	200000.	0.223E-01	-0.468E-03	0.440E-01	-0.400E-01*	0.339E-01	-0.334E-01
CIV 3D-5F	20000.	0.804E-01	0.667E-04				
799.7 A	50000.	0.663E-01	-0.489E-03				
C= 0.55D+16	80000.	0.588E-01	-0.809E-03				
	100000.	0.553E-01	-0.799E-03				
	150000.	0.492E-01	-0.821E-03				
	200000.	0.451E-01	-0.684E-03				
CIV 4S-4P	20000.	17.0	-0.274	0.373	0.293	0.432	0.259
14343.7 A	50000.	12.5	-0.401	0.649	0.482	0.650	0.408
C= 0.42D+21	80000.	10.8	-0.379	0.750	0.556	0.735	0.467
	100000.	10.1	-0.372	0.797	0.591	0.773	0.498
	150000.	8.97	-0.362	0.891	0.658	0.840	0.546
	200000.	8.26	-0.374	0.968	0.715	0.898	0.589
CIV 4S-5P	20000.	0.670	0.186E-01	0.464E-01	0.411E-01*	0.447E-01*	0.335E-01
2104.7 A	50000.	0.525	0.146E-01	0.665E-01	0.579E-01*	0.602E-01*	0.488E-01
C= 0.46D+19	80000.	0.465	0.162E-01	0.757E-01	0.667E-01*	0.659E-01*	0.561E-01
	100000.	0.439	0.149E-01	0.795E-01	0.700E-01*	0.712E-01*	0.585E-01
	150000.	0.394	0.109E-01	0.905E-01	0.745E-01	0.766E-01	0.628E-01
	200000.	0.365	0.839E-02	0.949E-01	0.827E-01	0.836E-01	0.690E-01
C IV 4P-5S	20000.	0.900	0.999E-01	0.293E-01	0.347E-01	0.302E-01	0.300E-01
2698.0 A	50000.	0.691	0.918E-01	0.522E-01	0.511E-01	0.469E-01	0.428E-01
C= 0.15D+20	80000.	0.612	0.847E-01	0.624E-01	0.591E-01	0.539E-01	0.490E-01
	100000.	0.577	0.785E-01	0.665E-01	0.624E-01	0.573E-01	0.525E-01
	150000.	0.520	0.740E-01	0.746E-01	0.699E-01	0.625E-01	0.565E-01
	200000.	0.482	0.714E-01	0.829E-01	0.739E-01	0.702E-01	0.599E-01
CIV 4P-5D	20000.	1.11	-0.388E-01				
2405.0 A	50000.	0.863	-0.999E-02				
C= 0.29D+18	80000.	0.756	0.934E-02				
	100000.	0.709	0.677E-02				
	150000.	0.629	0.461E-03				
	200000.	0.576	0.452E-02				

© European Southern Observatory • Provided by the NASA Astrophysics Data System

1991A&AS...89..581D

TABLE 1 *(continued)*

PERTURBER DENSITY = 0.1D+18

TRANSITION	T(K)	ELECTRONS WIDTH(A)	ELECTRONS SHIFT(A)	PROTONS WIDTH(A)	PROTONS SHIFT(A)	IONIZED HELIUM WIDTH(A)	IONIZED HELIUM SHIFT(A)
CIV 4D-5P	20000.	1.09	0.544E-01	*0.867E-01	-0.793E-01	*0.791E-01	-0.644E-01
2595.1 A	50000.	0.862	0.464E-01	*0.123	*-0.113	*0.106	*-0.940E-01
C= 0.64D+18	80000.	0.764	0.446E-01	0.145	-0.132	*0.125	*-0.109
	100000.	0.720	0.432E-01	0.154	-0.138	*0.138	*-0.114
	150000.	0.646	0.374E-01	0.174	-0.151	*0.142	*-0.122
	200000.	0.596	0.328E-01	0.180	-0.160	*0.146	*-0.129
CIV 4D-5P	20000.	1.09	0.544E-01	*0.867E-01	-0.793E-01	*0.791E-01	-0.644E-01
2595.1 A	50000.	0.862	0.464E-01	*0.123	*-0.113	*0.106	*-0.940E-01
C= 0.64D+18	80000.	0.764	0.446E-01	0.145	-0.132	*0.125	*-0.109
	100000.	0.720	0.432E-01	0.154	-0.138	*0.138	*-0.114
	150000.	0.646	0.374E-01	0.174	-0.151	*0.142	*-0.122
	200000.	0.596	0.328E-01	0.180	-0.160	*0.146	*-0.129
CIV 4D-5F	20000.	1.01	0.308E-02				
2524.4 A	50000.	0.830	-0.102E-01				
C= 0.55D+17	80000.	0.737	-0.163E-01				
	100000.	0.693	-0.155E-01				
	150000.	0.617	-0.144E-01				
	200000.	0.566	-0.130E-01				
CIV 4F-5D	20000.	1.11	-0.271E-01				
2534.5 A	50000.	0.873	0.836E-02				
C= 0.33D+18	80000.	0.768	0.323E-01				
	100000.	0.720	0.284E-01				
	150000.	0.639	0.186E-01				
	200000.	0.585	0.211E-01				

TABLE 2. *Experimental Stark widths (W_m) compared with the theory. The W_{DSB} are present semi-classical calculations; W_{MSE} are calculations (Dimitrijević 1988 and El-Farra & Hughes 1983) using the modified semi-empirical approach (Dimitrijević & Konjević 1980). Experimental data are: a) El-Farra, Hughes (1983); b) Bogen (1972); c) Djeniže et al. (1988); d) Böttcher et al. (1988); e) Ackermann et al. (1985); f) Böttcher et al. (1987): f1) collisional case; f2) static case.*

Transition	λ(Å)	T(K)	$N_e(10^{17}cm^{-3})$	W_m(Å) (Ref.)	W_{DSB}(Å)	W_{MSE}(Å)
$2s^2S-2p^2P^o$	1548.20	53.000	15	0.043(a)	0.11	0.044
		58.000	4	0.024(b)	0.027	0.012
	1550.77	53.000	15	0.063(a)	0.11	0.044
		58.000	4	0.024(b)	0.027	0.012
$3s^2S-3p^2P^o$	5801.33	38.000	1.64	0.98(c)	1.08	
		53.000	15	6.2(a)	8.84	6.5
		58.000	4	1.6(b)	2.27	1.6
		145.000	18	10.(d)	7.33	6.0
		116.000	5	2.8(e)	2.20	1.8
	5811.98	38.000	1.64	0.71(c)		
		53.000	15	6.0(a)	8.84	6.5
		58.000	4	1.6(b)	2.27	1.6
		116.000	5	2.8(e)	2.20	1.8
$3p^2P^o-4s^2S$	1230.	116.000	5	0.58(e)	0.20	0.2
$3s^2S-4p^2P^o$	948.1	116.000	5	0.4(e)	0.16	0.16
$3p^2P^o-4d^2D$	1107.6	113.700	4.7	0.10(f1)	0.20	
				0.12(f2)		
		116.000	5	0.53(e)	0.21	0.23
		124.000	7.7	0.18(f1)	0.32	
				0.23(f2)		
$3p^2P^o-4f^2F$	1106.5	116.000	5	0.35(e)	0.13	0.12
$4p^2P^o-5s^2S$	2698	116.000	5	5.4(e)	2.78	3.7
$3d^2D-4f^2F^o$	1169	53.000	15	0.62(a)	0.43	0.58
		113.700	4.7	0.060(f1)	0.12	
				0.070(f2)		
		116.000	5	0.4(e)	0.12	0.12
		124.000	7.7	0.12(f1)	0.18	
				0.15(f2)		
$4p^2P^o-5d^2D$	2405	116.000	5	10.0(e)	3.13	4.0
$4d^2D-5f^2F^o$	2524.4	116.000	5	8.4(e)	2.89	3.8
		124.000	7.7	1.0(f2)	4.19	

© European Southern Observatory • Provided by the NASA Astrophysics Data System

1991A&AS...89..581D

TABLE 3. *Electron-* (d_e), *and proton-impact* (d_p) *shifts for the C IV* $2s\,^2S - np\,^2P^0$ *spectral series for* $T = 200\,000$ K *and* $N = 10^{17}$ cm^{-3} *in angular frequency units.*

Transition	T = 200,000 K	
	d_e (s^{-1})	d_p (s^{-1})
2s - 2p	-1.70 10^9	-1.99 10^9
2s - 3p	5.99 10^9	2.29 10^{10}
2s - 4p	3.65 10^{10}	1.22 10^{11}
2s - 5p	1.06 10^{11}	3.71 10^{11}

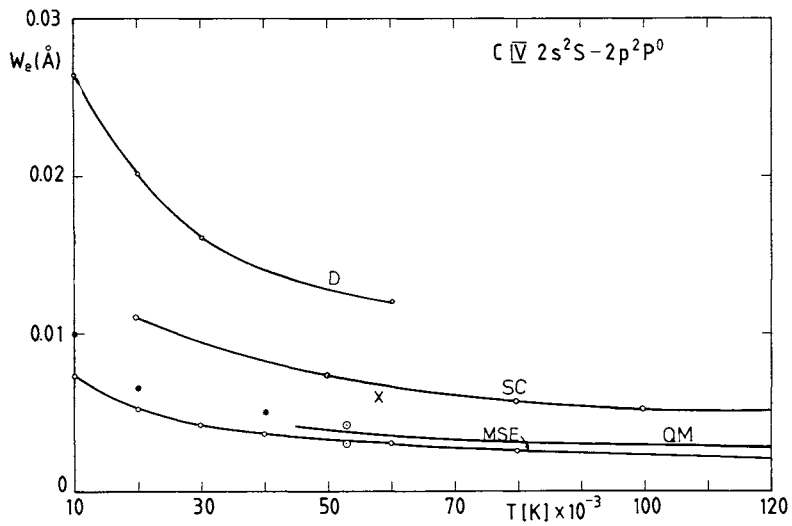

FIGURE 1. Full halfwidths for the C IV $2s\,^2S - 2p\,^2P^0$ multiplet ($\lambda = 1549.1$ Å) as a function of electron temperature for the density $N = 10^{17}$ cm^{-3}. Experimental points: (X) Bogen (1972); (⊙) El-Farra and Hughes (1983). Calculations: (SC) present semi-classical results; (QM) strong coupling quantum mechanical calculations by Seaton (1987); (D) Dimitrijević (1988b); (MSE) modified semi-empirical calculations (Dimitrijević 1988a). (*) Sahal-Bréchot and Segre (1971): semi-classical calculations anologous to present ones but without inclusion of the contribution of the Feshbach resonances.

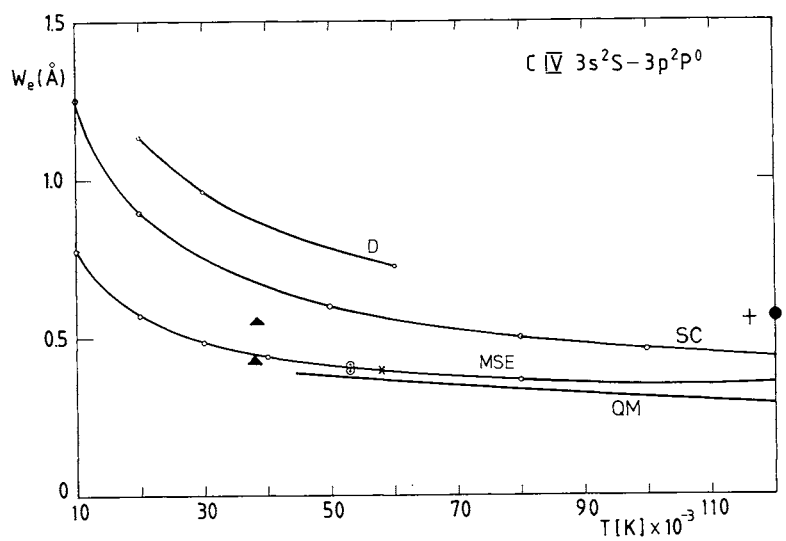

FIGURE 2. Full halfwidths for the C IV $3s\,^2S - 3p\,^2P^0$ multiplet ($\lambda = 5804.9$ Å) as a function of electron temperature for the density $N = 10^{17}$ cm^{-3}. Experimental points: (X) Bogen (1972); (⊙) El-Farra, Hughes (1983); (+) Ackermann *et al.* (1985); (Δ) Djeniže *et al.* (1988); (•) Böttcher *et al.* (1988), $T = 145000$ K. Calculations: (SC) present semi-classical results; (QM) strong coupling quantum mechanical calculations by Seaton (1987); (D) Dimitrijević (1988b); (MSE) modified semi-empirical calculations (Dimitrijević 1988a).

© European Southern Observatory • Provided by the NASA Astrophysics Data System

1991A&AS...89..581D

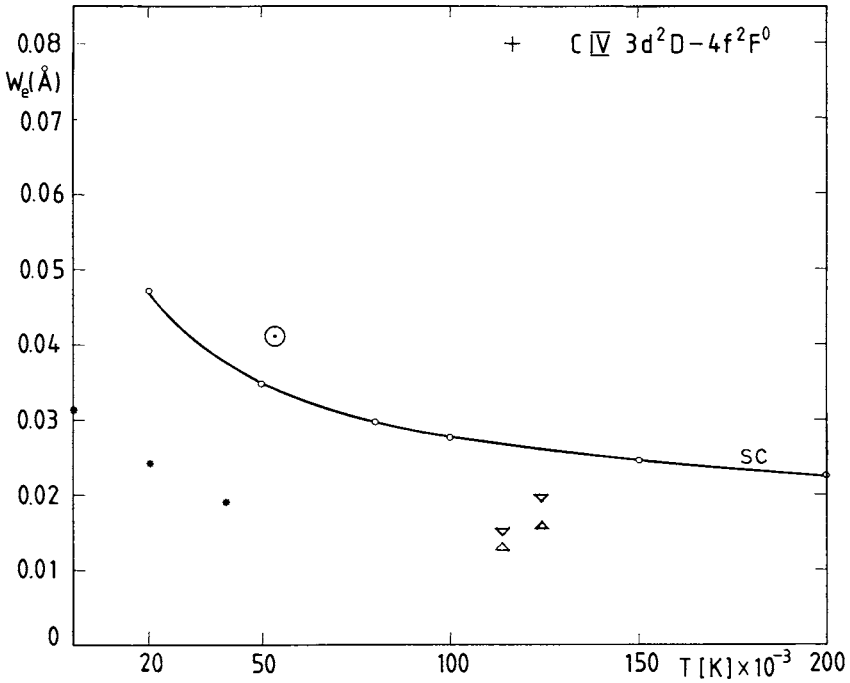

FIGURE 3. Full halfwidths for the C IV 3d ^{2}D – 4f ^{2}F^0 multiplet (λ = 1168.9 Å) as a function of electron temperature for the density $N = 10^{17}$ cm^{-3}. Experimental points: (⊙) El-Farra, Hughes (1983); (+) Ackermann *et al.* (1985); (Δ) Böttcher *et al.* (1987), collisional approximation, (∇) Böttcher *et al.* (1987), static approximation. Calculations: (SC) present semi-classical results. (*) Sahal-Bréchot and Segre (1971).

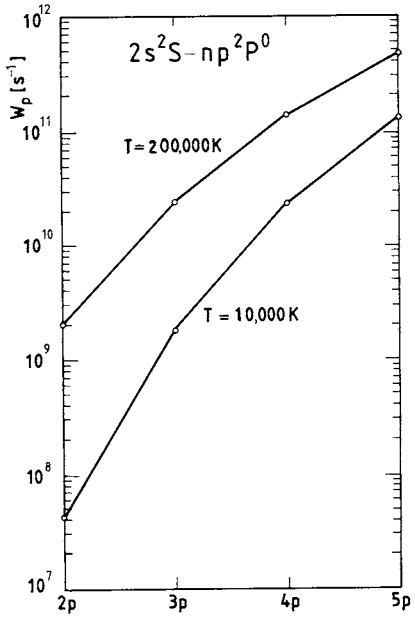

FIGURE 4. Electron-impact widths for C IV 2s ^{2}S – np ^{2}P^0 lines as function of n for T = 10 000 and 200 000 K, and $N = 10^{17}$ cm^{-3}.

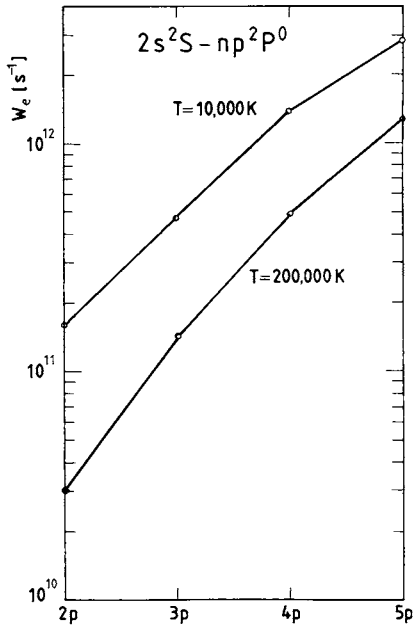

FIGURE 5. As in Figure 4 but for the proton-impact widths.

© European Southern Observatory • Provided by the NASA Astrophysics Data System

1991A&AS...89..581D

ASTRONOMY & ASTROPHYSICS
SUPPLEMENT SERIES

Astron. Astrophys. Suppl. Ser. **89**, 591-598 (1991)

Stark broadening of spectral lines of multicharged ions of astrophysical interest. II. Si IV lines

M.S. Dimitrijević[1], S. Sahal-Bréchot[2] and V. Bommier[2]

[1] Astronomical Observatory, Volgina 7, 11050 Beograd, Yugoslavia
[2] Laboratoire "Astrophysique, Atomes et Molécules", Unité associée au C.N.R.S. No 812, Département Atomes et Molécules en Astrophysique, Observatoire de Paris-Meudon, 92190 Meudon, France

Received November 19, 1990; accepted February 7, 1991

Abstract. — Using a semi-classical approach, we have calculated electron-, proton-, and ionized helium-impact line widths and shifts for 40 Si IV multiplets. The comprehensive set of obtained data has also been used for investigation of Stark broadening parameter regularities within spectral series.

Key words: line profile — atomic data — Stark broadening

1. Introduction.

This paper is the second one of a series devoted to the calculation of Stark broadening parameters of spectral lines of multicharged ions. The first has been concerned with C IV lines (Dimitrijević *et al.* 1991a, hereafter referred to as Paper I): as a matter of fact, Stark broadening of spectral lines has been taking a new interest in Astrophysics (Seaton 1987), owing to the recent development of researches on the physics of the stellar interiors.

For a number of astrophysical as well as physical applications, the knowledge of Si IV Stark broadening parameters is very important, due to its high cosmical abundance and its presence as an impurity in many laboratory plasma sources.

By using the semiclassical- perturbation formalism (Sahal- Bréchot 1969ab) we have calculated electron-, proton-, and ionized helium-impact line widths and shifts for 40 Si IV multiplets.

A summary of the formalism has been recalled in Paper I and will not be repeated here. In the present paper we will only discuss the results obtained by comparing with experiments and other calculations when they exist. They have also been used to continue our investigation of systematic trends for Stark broadening parameters within spectral series (Dimitrijević & Sahal- Bréchot 1984ab, 1985, 1987, 1990 and Paper 1).

2. Results and discussion

Energy levels for Si IV lines have been taken from Bashkin & Stoner (1975). Oscillator strengths have been calculated by using the method of Bates & Damgaard (1949) and the tables of Oertel & Shomo (1968). For higher levels, the method described by Van Regemorter *et al.* (1979) has been used.

In addition to the electron-impact full halfwidths and shifts, Stark broadening parameters due to proton-, and ionized helium- impact have been calculated. Thus we have provided Stark broadening data for all the important charged perturbers in stellar atmospheres. Our results are shown in Table 1 for a perturber density 10^{17} cm^{-3} and temperatures of T = 20 000; 50 000; 80 000; 100 000; 150 000 and 200 000 K. We also specify a parameter c (Dimitrijević & Sahal-Bréchot 1984a), which gives an estimate for the maximum perturber density for which the line may be treated as isolated when it is divided by 2W.

For each value given in Table 1, the collision volume (V) multiplied by the perturber density (N) is much less than one and the impact approximation is valid (Sahal-Bréchot 1969ab). Values for NV >0.5 are not given in Table 1; values for 0.1< NV ≤0.5 are denoted by an asterisk. When the impact approximation is not valid, the ion broadening contribution may be estimated by using quasistatic estimations (Sahal-Bréchot 1991, see also Paper I). One must be aware of the fact that the accuracy of the obtained results decreases when the broadening by ion interactions is important.

© European Southern Observatory • Provided by the NASA Astrophysics Data System

1991A&AS...89..581D

For high densities or when a perturbing level is close to the initial or to the final levels, the influence of Debye screening may be important. In order to scale to other densities, we will provide data for $N = 10^{15}$, and $10^{18} - 10^{21}$ cm^{-3} elsewhere (Dimitrijević *et al.* 1991b).

In Table 2 our results (W_{DSB}) are compared with the calculations of Dimitrijević (1988ab) using the modified semiempirical approach (Dimitrijević & Konjević, 1980) (W_{MSE}), the simplified semiclassical approach of Griem (1974) (W_G) and the modification of this approach (Dimitrijević & Konjević 1980) (W_{GM}). We can see that the simplified semiclassical approach agrees better with our calculations, in its original version for the low lying multiplets. For the higher transitions, the modified version is in better agreement with our values. The agreement with the simple modified semiempirical approach is also better for higher transitions. The experimental value (Platiša *et al.* 1977) for the 4s $^2S-4p\ ^2P^o$ multiplet at T =25600K and $N = 10^{17}$ cm^{-3} is $W = 0.22$ Å while our result is 0.44 Å. For the 4p $^2P^o-4d\ ^2D$ multiplet the experiment gives W =0.24 Å and our calculations 0.34 Å.

The obtained set of results has also been used for investigations of the behaviour of Stark widths and shifts parameters along spectral series.

In Figures 1 and 2 the electron and proton full halfwidths within the 3s $^2S-np\ ^2P^o$ series are illustrated. We see the variation of the results for different plasma temperatures and different perturber type (electrons and protons). By inspecting the energy separation between the upper level and the principal perturbing levels (see the Grotrian diagrams in Bashkin & Stoner (1975)), we find that this value decreases gradually within a spectral series. Thus we obtain a gradual change of the Stark widths as expected. In Table 3 we can see the same situation in the case of the shifts. Such a regular behaviour might be used for critical evaluation of existing results as well as for interpolation of new data needed in astrophysics.

Acknowledgements.

One of us (M.D.) has been supported by the Observatory of Paris-Meudon. This work has also been supported by the C.N.R.S. and is a part of the French-Yugoslav collaboration through the project "L'élargissement Stark des raies spectrales des plasmas astrophysiques et de laboratoire". This study has also been supported in part by SKNTI under the project "Atomic, Molecular and Plasma Spectroscopy". The numerical calculations have been performed on the VAX 8600 of the Observatory of Paris-Meudon.

References

Bashkin S. and Stoner J.O.Jr. 1975, Atomic Energy Levels and Grotrian Diagrams, Vol.1 (North Holand, Amsterdam)
Bates D.R. and Damgaard A. 1949, Trans. Roy. Soc. London, Ser. A 242, 101
Dimitrijević M.S. 1988a A&AS 76, 53
Dimitrijević M.S. 1988b, Bull. Obs. Astron. Belgrade 139, 31
Dimitrijević M.S. and Konjević N. 1980, JQSRT 24, 451
Dimitrijević M.S. and Sahal-Bréchot S. 1984a, JQSRT 31, 301
Dimitrijević M.S. and Sahal-Bréchot S. 1984b, A&A 136, 289
Dimitrijević M.S. and Sahal-Bréchot S. 1985, JQSRT 34, 149
Dimitrijević M.S. and Sahal-Bréchot S. 1987, JQRST 38, 37
Dimitrijević M.S. and Sahal-Bréchot S. 1990, A&AS 82, 519
Dimitrijević M.S., Sahal-Bréchot S. and Bommier V. 1991a, A&A in press (referred as Paper 1 in the text)
Dimitrijević M.S., Sahal-Bréchot S. and Bommier V. 1991b, Bull. Obs. Astron. Belgrade, 144, in press
Griem H.R. 1974, Spectral Line Broadening by Plasma (Academic Press, New York)
Oertel G.K. and Shomo L.P. 1968 ApJS 16, 175
Plastiša M., Dimitrijević M., Popović M. and Konjević N. 1977, J. Phys. B 10, 2997
Sahal-Bréchot S. 1969a A&A 1, 91
Sahal-Bréchot S. 1969b, A&A 2, 322
Sahal-Bréchot S. 1991, A&A in press
Sahal-Bréchot S. and Segre E.R. 1971 A&A 13, 161
Seaton M.J. 1987, J. Phys. B 20, 6363
Van Regemorter H., Hoang Binh Dy and Prud'homme M. 1979, J. Phys. B 12, 1073

© European Southern Observatory • Provided by the NASA Astrophysics Data System

1991A&AS...89..581D

TABLE 1. *This table shows electron-, proton-, and ionized-helium- impact broadening parameters for Si IV lines, for a perturber density of* 10^{17} cm^{-3} *and temperatures from 20 000 K to 200 000 K. Transitions and averaged wavelengths for the multiplet (in Å) are also given. By using c (see Eq. (5) of Paper 1), we obtain an estimate for the maximum perturber density for which the line may be treated as isolated and tabulated data may be used. The asterisk identifies cases for which the collision volume multiplied by the perturber density (the condition for validity of the impact approximation) lies between 0.1 and 0.5. For high densities or when a perturbing level is close to the initial or to the final levels, the influence of Debye screening may be important. In order to scale to other densities, we will provide data for* $N=10^{15}$, *and* $10^{18}-10^{21}$ cm^{-3} *elsewhere (Dimitrijević et al. 1991).*

PERTURBER DENSITY = 0.1D+18

TRANSITION	T(K)	ELECTRONS WIDTH(A)	ELECTRONS SHIFT(A)	PROTONS WIDTH(A)	PROTONS SHIFT(A)	IONIZED HELIUM WIDTH(A)	IONIZED HELIUM SHIFT(A)
SIIV3S-3P	20000.	0.176E-01	0.519E-04	0.907E-04	-0.304E-04	0.159E-03	-0.304E-04
1396.7 A	50000.	0.112E-01	-0.174E-03	0.272E-03	-0.784E-04	0.389E-03	-0.761E-04
C= 0.14D+21	80000.	0.899E-02	-0.166E-03	0.404E-03	-0.118E-03	0.507E-03	-0.110E-03
	100000.	0.812E-02	-0.119E-03	0.462E-03	-0.139E-03	0.571E-03	-0.129E-03
	150000.	0.684E-02	-0.162E-03	0.571E-03	-0.181E-03	0.670E-03	-0.157E-03
	200000.	0.612E-02	-0.187E-03	0.649E-03	-0.205E-03	0.707E-03	-0.181E-03
SIIV3S-4P	20000.	0.453E-02	0.352E-04	0.138E-03	0.175E-04	0.194E-03	0.172E-04
457.9 A	50000.	0.307E-02	0.701E-04	0.252E-03	0.402E-04	0.306E-03	0.373E-04
C= 0.51D+19	80000.	0.258E-02	0.544E-04	0.312E-03	0.548E-04	0.338E-03	0.473E-04
	100000.	0.240E-02	0.702E-04	0.328E-03	0.602E-04	0.354E-03	0.532E-04
	150000.	0.212E-02	0.826E-04	0.354E-03	0.736E-04	0.378E-03	0.627E-04
	200000.	0.195E-02	0.769E-04	0.371E-03	0.819E-04	0.396E-03	0.669E-04
SIIV3S-5P	20000.	0.558E-02	0.176E-03	0.405E-03	0.577E-04	0.501E-03	0.532E-04
361.6 A	50000.	0.429E-02	0.159E-03	0.588E-03	0.106E-03	0.634E-03	0.937E-04
C= 0.15D+19	80000.	0.384E-02	0.193E-03	0.642E-03	0.135E-03	0.686E-03	0.114E-03
	100000.	0.365E-02	0.211E-03	0.666E-03	0.146E-03	0.710E-03	0.119E-03
	150000.	0.335E-02	0.186E-03	0.710E-03	0.163E-03	0.746E-03	0.134E-03
	200000.	0.316E-02	0.186E-03	0.739E-03	0.175E-03	0.756E-03	0.144E-03
SIIV3S-6P	20000.	0.886E-02	0.464E-03	0.984E-03	0.132E-03*	0.109E-02*	0.117E-03
327.2 A	50000.	0.721E-02	0.412E-03	0.121E-02	0.220E-03*	0.129E-02*	0.185E-03
C= 0.64D+18	80000.	0.668E-02	0.416E-03	0.131E-02	0.255E-03*	0.138E-02*	0.212E-03
	100000.	0.646E-02	0.390E-03	0.135E-02	0.273E-03	0.140E-02	0.224E-03
	150000.	0.608E-02	0.378E-03	0.141E-02	0.301E-03	0.145E-02	0.250E-03
	200000.	0.583E-02	0.362E-03	0.144E-02	0.323E-03	0.147E-02	0.269E-03
SIIV3P-4S	20000.	0.128E-01	0.604E-03	0.769E-04	0.221E-03	0.109E-03	0.208E-03
817.1 A	50000.	0.805E-02	0.727E-03	0.291E-03	0.428E-03	0.290E-03	0.373E-03
C= 0.16D+20	80000.	0.655E-02	0.769E-03	0.415E-03	0.540E-03	0.425E-03	0.465E-03
	100000.	0.600E-02	0.823E-03	0.504E-03	0.595E-03	0.484E-03	0.492E-03
	150000.	0.517E-02	0.835E-03	0.630E-03	0.662E-03	0.561E-03	0.546E-03
	200000.	0.471E-02	0.794E-03	0.705E-03	0.717E-03	0.625E-03	0.590E-03
SIIV3P-5S	20000.	0.977E-02	0.204E-02	0.249E-03	0.449E-03	0.263E-03	0.384E-03
515.9 A	50000.	0.707E-02	0.166E-02	0.590E-03	0.727E-03	0.545E-03	0.595E-03
C= 0.30D+19	80000.	0.612E-02	0.147E-02	0.761E-03	0.838E-03	0.661E-03	0.691E-03
	100000.	0.579E-02	0.147E-02	0.846E-03	0.884E-03	0.712E-03	0.728E-03
	150000.	0.518E-02	0.130E-02	0.957E-03	0.984E-03	0.818E-03	0.805E-03
	200000.	0.478E-02	0.124E-02	0.106E-02	0.107E-02	0.914E-03	0.881E-03
SIIV3P-6S	20000.	0.136E-01	0.522E-02	0.748E-03	0.983E-03	0.716E-03	0.833E-03
438.4 A	50000.	0.108E-01	0.394E-02	0.139E-02	0.144E-02	0.117E-02	0.118E-02
C= 0.12D+19	80000.	0.983E-02	0.347E-02	0.165E-02	0.166E-02	0.140E-02	0.137E-02
	100000.	0.937E-02	0.321E-02	0.175E-02	0.177E-02	0.153E-02	0.144E-02
	150000.	0.853E-02	0.277E-02	0.207E-02	0.191E-02	0.173E-02	0.159E-02
	200000.	0.800E-02	0.255E-02	0.232E-02	0.204E-02	0.179E-02	0.165E-02
SIIV3P-3D	20000.	0.116E-01	0.340E-04	0.646E-04	0.836E-05	0.113E-03	0.836E-05
1126.4 A	50000.	0.751E-02	0.498E-04	0.190E-03	0.219E-04	0.271E-03	0.217E-04
C= 0.74D+20	80000.	0.604E-02	0.383E-04	0.279E-03	0.343E-04	0.350E-03	0.331E-04
	100000.	0.548E-02	0.342E-04	0.317E-03	0.416E-04	0.394E-03	0.391E-04
	150000.	0.465E-02	0.460E-04	0.390E-03	0.561E-04	0.457E-03	0.518E-04
	200000.	0.418E-02	0.472E-04	0.440E-03	0.681E-04	0.481E-03	0.594E-04
SIIV3P-4D	20000.	0.101E-01	0.339E-03	0.318E-03	0.359E-03	0.389E-03	0.319E-03
560.5 A	50000.	0.703E-02	0.496E-03	0.640E-03	0.604E-03	0.655E-03	0.510E-03
C= 0.13D+19	80000.	0.596E-02	0.484E-03	0.794E-03	0.703E-03	0.754E-03	0.585E-03
	100000.	0.554E-02	0.471E-03	0.869E-03	0.753E-03	0.805E-03	0.623E-03
	150000.	0.488E-02	0.462E-03	0.971E-03	0.831E-03	0.894E-03	0.685E-03
	200000.	0.450E-02	0.461E-03	0.107E-02	0.901E-03	0.960E-03	0.742E-03

© European Southern Observatory • Provided by the NASA Astrophysics Data System

1991A&AS...89..581D

TABLE 1. *(continued)*

PERTURBER DENSITY = 0.1D+18

TRANSITION	T(K)	ELECTRONS WIDTH(A)	ELECTRONS SHIFT(A)	PROTONS WIDTH(A)	PROTONS SHIFT(A)	IONIZED HELIUM WIDTH(A)	IONIZED HELIUM SHIFT(A)
SIIV3P-5D	20000.	0.154E-01	0.119E-02	0.110E-02	0.101E-02	0.118E-02	0.853E-03
454.7 A	50000.	0.120E-01	0.129E-02	0.172E-02	0.148E-02	0.159E-02	0.121E-02
C= 0.46D+18	80000.	0.107E-01	0.125E-02	0.199E-02	0.171E-02	0.182E-02	0.142E-02
	100000.	0.101E-01	0.122E-02	0.209E-02	0.180E-02	0.196E-02	0.150E-02
	150000.	0.911E-02	0.119E-02	0.243E-02	0.202E-02	0.213E-02	0.165E-02
	200000.	0.850E-02	0.110E-02	0.262E-02	0.214E-02	0.225E-02	0.172E-02
SIIV3P-6D	20000.	0.252E-01	0.290E-02*	0.284E-02*	0.222E-02*	0.266E-02*	0.176E-02
412.7 A	50000.	0.211E-01	0.279E-02*	0.379E-02*	0.321E-02*	0.339E-02*	0.258E-02
C= 0.22D+18	80000.	0.192E-01	0.282E-02*	0.431E-02*	0.366E-02*	0.387E-02*	0.300E-02
	100000.	0.184E-01	0.275E-02*	0.458E-02*	0.382E-02*	0.397E-02*	0.314F-02
	150000.	0.170E-01	0.246E-02*	0.510E-02*	0.413E-02*	0.442E-02*	0.346E-02
	200000.	0.160E-01	0.227E-02*	0.530E-02*	0.450E-02*	0.437E-02*	0.372E-02
SIIV3D-4P	20000.	0.636E-01	0.424E-03	0.154E-02	0.274E-03	0.221E-02	0.269E-03
1724.1 A	50000.	0.428E-01	0.116E-02	0.295E-02	0.622E-03	0.362E-02	0.576E-03
C= 0.73D+20	80000.	0.358E-01	0.947E-03	0.370E-02	0.842E-03	0.407E-02	0.727E-03
	100000.	0.332E-01	0.111E-02	0.395E-02	0.925E-03	0.426E-02	0.815E-03
	150000.	0.292E-01	0.132E-02	0.427E-02	0.113E-02	0.457E-02	0.956E-03
	200000.	0.270E-01	0.127E-02	0.450E-02	0.125E-02	0.478E-02	0.102E-02
SIIV3D-5P	20000.	0.310E-01	0.102E-02	0.213E-02	0.332E-03	0.263E-02	0.307E-03
860.7 A	50000.	0.239E-01	0.959E-03	0.313E-02	0.611E-03	0.338E-02	0.538E-03
C= 0.83D+19	80000.	0.214E-01	0.115E-02	0.342E-02	0.776E-03	0.365E-02	0.651E-03
	100000.	0.204E-01	0.123E-02	0.355E-02	0.838E-03	0.378E-02	0.686E-03
	150000.	0.187E-01	0.110E-02	0.379E-02	0.936E-03	0.397E-02	0.770E-03
	200000.	0.177E-01	0.110E-02	0.395E-02	0.100E-02	0.405E-02	0.829E-03
SIIV3D-6P	20000.	0.389E-01	0.211E-02	0.422E-02	0.588E-03*	0.468E-02*	0.518E-03
688.3 A	50000.	0.317E-01	0.187E-02	0.521E-02	0.980E-03*	0.557E-02*	0.821E-03
C= 0.28D+19	80000.	0.294E-01	0.189E-02	0.564E-02	0.113E-02*	0.594E-02*	0.943E-03
	100000.	0.284E-01	0.176E-02	0.582E-02	0.121E-02	0.604E-02	0.996E-03
	150000.	0.268E-01	0.171E-02	0.611E-02	0.134E-02	0.623E-02	0.111E-02
	200000.	0.257E-01	0.164E-02	0.621E-02	0.144E-02	0.632E-02	0.120E-02
SIIV3D-4F	20000.	0.288E-01	-0.821E-03	0.578E-03	-0.839E-03	0.766E-03	-0.774E-03
1066.6 A	50000.	0.195E-01	-0.599E-03	0.136E-02	-0.149E-02	0.145E-02	-0.128E-02
C= 0.47D+19	80000.	0.162E-01	-0.636E-03	0.187E-02	-0.181E-02	0.175E-02	-0.148E-02
	100000.	0.150E-01	-0.587E-03	0.203E-02	-0.190E-02	0.189E-02	-0.159E-02
	150000.	0.131E-01	-0.435E-03	0.234E-02	-0.213E-02	0.212E-02	-0.177E-02
	200000.	0.120E-01	-0.396E-03	0.260E-02	-0.230E-02	0.229E-02	-0.190E-02
SIIV3D-5F	20000.	0.581E-01	-0.352E-03*	0.145E-01*	0.125E-01		
749.9 A	50000.	0.438E-01	0.671E-03*	0.201E-01*	0.185E-01		
C= 0.67D+17	80000.	0.381E-01	0.121E-02*	0.237E-01*	0.218E-01		
	100000.	0.357E-01	0.115E-02*	0.252E-01*	0.226E-01*	0.199E-01*	0.182E-01
	150000.	0.317E-01	0.916E-03*	0.280E-01*	0.250E-01*	0.226E-01*	0.205E-01
	200000.	0.291E-01	0.904E-03*	0.299E-01*	0.264E-01*	0.230E-01*	0.208E-01
SIIV3D-6F	20000.	0.171E-01	-0.135E-03	0.352E-02	-0.971E-05*	0.395E-02	-0.969E-05
645.8 A	50000.	0.118E-01	-0.563E-04	0.437E-02	-0.246E-04*	0.468E-02	-0.237E-04
C= 0.89D+19	80000.	0.993E-02	-0.647E-04	0.472E-02	-0.361E-04*	0.499E-02	-0.335E-04
	100000.	0.924E-02	-0.644E-04	0.487E-02	-0.423E-04	0.508E-02	-0.383E-04
	150000.	0.822E-02	-0.655E-04	0.509E-02	-0.530E-04	0.521E-02	-0.464E-04
	200000.	0.764E-02	-0.678E-04	0.518E-02	-0.610E-04	0.530E-02	-0.532E-04
SIIV4S-4P	20000.	0.497	-0.720E-02	0.112E-01	-0.408E-02	0.157E-01	-0.390E-02
4097.9 A	50000.	0.336	-0.924E-02	0.209E-01	-0.834E-02	0.250E-01	-0.719E-02
C= 0.41D+21	80000.	0.284	-0.123E-01	0.260E-01	-0.105E-01	0.277E-01	-0.913E-02
	100000.	0.265	-0.131E-01	0.274E-01	-0.117E-01	0.290E-01	-0.987E-02
	150000.	0.235	-0.124E-01	0.299E-01	-0.132E-01	0.312E-01	-0.110E-01
	200000.	0.218	-0.117E-01	0.316E-01	-0.143E-01	0.328E-01	-0.118E-01

© European Southern Observatory • Provided by the NASA Astrophysics Data System

1991A&AS...89..581D

TABLE 1. *(continued)*

PERTURBER DENSITY = 0.1D+18

TRANSITION	T(K)	ELECTRONS WIDTH(A)	ELECTRONS SHIFT(A)	PROTONS WIDTH(A)	PROTONS SHIFT(A)	IONIZED HELIUM WIDTH(A)	IONIZED HELIUM SHIFT(A)
SIIV4S-5P	20000.	0.734E-01	0.784E-03	0.453E-02	0.208E-03	0.561E-02	0.201E-03
1211.0 A	50000.	0.556E-01	0.342E-03	0.656E-02	0.454E-03	0.710E-02	0.407E-03
C= 0.16D+20	80000.	0.495E-01	0.617E-03	0.715E-02	0.581E-03	0.767E-02	0.514E-03
	100000.	0.470E-01	0.678E-03	0.742E-02	0.655E-03	0.792E-02	0.567E-03
	150000.	0.431E-01	0.373E-03	0.790E-02	0.776E-03	0.832E-02	0.639E-03
	200000.	0.407E-01	0.487E-03	0.820E-02	0.833E-03	0.848E-02	0.694E-03
SIIV4S-6P	20000.	0.722E-01	0.225E-02	0.736E-02	0.800E-03*	0.814E-02*	0.721E-03
895.3 A	50000.	0.581E-01	0.205E-02	0.905E-02	0.137E-02*	0.968E-02*	0.117E-02
C= 0.48D+19	80000.	0.536E-01	0.213E-02	0.977E-02	0.161E-02*	0.103E-01*	0.135E-02
	100000.	0.517E-01	0.184E-02	0.101E-01	0.172E-02*	0.105E-01*	0.142E-02
	150000.	0.486E-01	0.182E-02	0.105E-01	0.191E-02	0.108E-01	0.158E-02
	200000.	0.465E-01	0.179E-02	0.107E-01	0.207E-02	0.109E-01	0.171E-02
SIIV4P-5S	20000.	0.205	0.227E-01	0.567E-02	0.735E-02	0.628E-02	0.631E-02
2125.0 A	50000.	0.150	0.205E-01	0.116E-01	0.119E-01	0.110E-01	0.982E-02
C= 0.50D+20	80000.	0.132	0.218E-01	0.142E-01	0.137E-01	0.130E-01	0.113E-01
	100000.	0.125	0.206E-01	0.156E-01	0.146E-01	0.139E-01	0.120E-01
	150000.	0.114	0.190E-01	0.175E-01	0.161E-01	0.157E-01	0.132E-01
	200000.	0.106	0.183E-01	0.189E-01	0.173E-01	0.169E-01	0.145E-01
SIIV4P-6S	20000.	0.120	0.384E-01	0.610E-02	0.769E-02	0.595E-02	0.650E-02
1230.0 A	50000.	0.943E-01	0.281E-01	0.111E-01	0.112E-01	0.948E-02	0.925E-02
C= 0.91D+19	80000.	0.857E-01	0.259E-01	0.131E-01	0.130E-01	0.113E-01	0.107E-01
	100000.	0.820E-01	0.230E-01	0.139E-01	0.138E-01	0.122E-01	0.112E-01
	150000.	0.752E-01	0.204E-01	0.167E-01	0.150E-01	0.137E-01	0.125E-01
	200000.	0.709E-01	0.189E-01	0.183E-01	0.161E-01	0.142E-01	0.129E-01
SIIV4P-4D	20000.	0.380	0.949E-02	0.922E-02	0.107E-01	0.115E-01	0.960E-02
3160.3 A	50000.	0.267	0.117E-01	0.189E-01	0.182E-01	0.196E-01	0.154E-01
C= 0.41D+20	80000.	0.228	0.121E-01	0.238E-01	0.213E-01	0.227E-01	0.177E-01
	100000.	0.214	0.112E-01	0.259E-01	0.228E-01	0.240E-01	0.188E-01
	150000.	0.190	0.101E-01	0.296E-01	0.253E-01	0.272E-01	0.209E-01
	200000.	0.177	0.102E-01	0.319E-01	0.271E-01	0.290E-01	0.224E-01
SIIV4P-5D	20000.	0.149	0.102E-01	0.928E-02	0.909E-02	0.981E-02	0.765E-02
1367.6 A	50000.	0.116	0.108E-01	0.149E-01	0.133E-01	0.136E-01	0.109E-01
C= 0.42D+19	80000.	0.102	0.106E-01	0.174E-01	0.153E-01	0.156E-01	0.127E-01
	100000.	0.967E-01	0.103E-01	0.181E-01	0.161E-01	0.168E-01	0.135E-01
	150000.	0.877E-01	0.987E-02	0.211E-01	0.182E-01	0.185E-01	0.149E-01
	200000.	0.819E-01	0.910E-02	0.229E-01	0.192E-01	0.195E-01	0.154E-01
SIIV4P-6D	20000.	0.168	0.181E-01*	0.179E-01*	0.143E-01*	0.166E-01*	0.113E-01
1046.7 A	50000.	0.139	0.174E-01*	0.239E-01*	0.206E-01*	0.214E-01*	0.166E-01
C= 0.14D+19	80000.	0.127	0.177E-01*	0.273E-01*	0.235E-01*	0.245E-01*	0.193E-01
	100000.	0.122	0.172E-01*	0.292E-01*	0.245E-01*	0.251E-01*	0.202E-01
	150000.	0.112	0.153E-01	0.325E-01	0.265E-01*	0.279E-01*	0.222E-01
	200000.	0.106	0.140E-01	0.339E-01	0.289E-01*	0.275E-01*	0.238E-01
SIIV4D-5P	20000.	0.787	0.200E-02	0.347E-01	-0.110E-01	0.426E-01	-0.101E-01
3766.0 A	50000.	0.604	-0.403E-02	0.529E-01	-0.194E-01	0.565E-01	-0.167E-01
C= 0.58D+20	80000.	0.539	0.497E-03	0.585E-01	-0.235E-01	0.614E-01	-0.193E-01
	100000.	0.512	0.285E-02	0.608E-01	-0.247E-01	0.640E-01	-0.205E-01
	150000.	0.469	0.101E-02	0.661E-01	-0.277E-01	0.675E-01	-0.230E-01
	200000.	0.442	0.133E-02	0.685E-01	-0.298E-01	0.694E-01	-0.248E-01
SIIV4D-6P	20000.	0.307	0.893E-02	0.261E-01	0.504E-03*	0.295E-01*	0.488E-03
1796.6 A	50000.	0.248	0.712E-02	0.326E-01	0.109E-02*	0.349E-01*	0.971E-03
C= 0.13D+20	80000.	0.229	0.769E-02	0.352E-01	0.139E-02	0.373E-01	0.122E-02
	100000.	0.221	0.697E-02	0.364E-01	0.156E-02	0.381E-01	0.135E-02
	150000.	0.207	0.690E-02	0.380E-01	0.184E-02	0.391E-01	0.151E-02
	200000.	0.198	0.657E-02	0.387E-01	0.196E-02	0.395E-01	0.164E-02

© European Southern Observatory • Provided by the NASA Astrophysics Data System

1991A&AS...89..581D

TABLE 1. *(continued)*

PERTURBER DENSITY = 0.1D+18

TRANSITION	T(K)	ELECTRONS WIDTH(A)	ELECTRONS SHIFT(A)	PROTONS WIDTH(A)	PROTONS SHIFT(A)	IONIZED HELIUM WIDTH(A)	IONIZED HELIUM SHIFT(A)
SIIV4D-4F	20000.	24.3	-1.08	0.641	-0.994	0.689	-0.850
24271.1 A	50000.	17.0	-1.23	1.41	-1.61	1.32	-1.32
C= 0.24D+22	80000.	14.5	-1.22	1.78	-1.86	1.58	-1.53
	100000.	13.5	-1.18	1.96	-1.96	1.68	-1.61
	150000.	12.0	-1.07	2.21	-2.18	1.92	-1.78
	200000.	11.1	-1.05	2.44	-2.36	2.14	-1.95
SIIV4D-5F	20000.	0.606	-0.113E-01	*0.132	*0.115		
2287.0 A	50000.	0.458	-0.365E-02	*0.185	*0.171		
C= 0.62D+18	80000.	0.400	0.173E-02	*0.214	*0.201	*0.179	*0.159
	100000.	0.375	0.134E-02	*0.229	*0.208	*0.181	*0.167
	150000.	0.334	-0.692E-03	*0.252	*0.229	*0.202	*0.189
	200000.	0.307	-0.800E-03	*0.274	*0.244	*0.212	*0.191
SIIV4D-6F	20000.	0.630	-0.166E-01				
1533.2 A	50000.	0.494	0.636E-03				
C= 0.18D+18	80000.	0.436	0.119E-01				
	100000.	0.410	0.101E-01				
	150000.	0.366	0.662E-02				
	200000.	0.337	0.688E-02				
SIIV4F-5D	20000.	0.607	0.457E-01	0.362E-01	0.372E-01	0.377E-01	0.315E-01
2675.2 A	50000.	0.467	0.475E-01	0.593E-01	0.544E-01	0.533E-01	0.448E-01
C= 0.16D+20	80000.	0.411	0.464E-01	0.694E-01	0.627E-01	0.618E-01	0.518E-01
	100000.	0.387	0.452E-01	0.740E-01	0.672E-01	0.653E-01	0.540E-01
	150000.	0.349	0.430E-01	0.841E-01	0.727E-01	0.741E-01	0.600E-01
	200000.	0.325	0.396E-01	0.921E-01	0.760E-01	0.748E-01	0.628E-01
SIIV4F-6D	20000.	0.443	0.494E-01	*0.460E-01	*0.370E-01	*0.426E-01	*0.294E-01
1672.6 A	50000.	0.366	0.472E-01	*0.623E-01	*0.539E-01	*0.550E-01	*0.435E-01
C= 0.37D+19	80000.	0.332	0.478E-01	*0.691E-01	*0.615E-01	*0.615E-01	*0.497E-01
	100000.	0.318	0.465E-01	*0.751E-01	*0.646E-01	*0.639E-01	*0.525E-01
	150000.	0.292	0.414E-01	0.817E-01	0.691E-01	*0.709E-01	*0.573E-01
	200000.	0.275	0.381E-01	0.884E-01	0.761E-01	*0.719E-01	*0.623E-01
SIIV5S-5P	20000.	4.92	-0.246	0.259	-0.112	0.316	-0.970E-01
8977.4 A	50000.	3.95	-0.266	0.385	-0.184	0.405	-0.153
C= 0.90D+21	80000.	3.60	-0.276	0.427	-0.212	0.443	-0.176
	100000.	3.46	-0.251	0.446	-0.225	0.459	-0.187
	150000.	3.21	-0.245	0.486	-0.251	0.491	-0.208
	200000.	3.04	-0.235	0.513	-0.273	0.495	-0.220
SIIV5S-6P	20000.	0.611	-0.318E-02	0.566E-01	-0.382E-02	*0.626E-01	-0.352E-02
2483.7 A	50000.	0.510	-0.553E-02	0.695E-01	-0.685E-02	*0.744E-01	-0.597E-02
C= 0.37D+20	80000.	0.476	-0.701E-02	0.751E-01	-0.848E-02	*0.795E-01	-0.697E-02
	100000.	0.462	-0.747E-02	0.775E-01	-0.896E-02	*0.808E-01	-0.748E-02
	150000.	0.436	-0.620E-02	0.808E-01	-0.100E-01	0.828E-01	-0.826E-02
	200000.	0.419	-0.616E-02	0.825E-01	-0.108E-01	0.839E-01	-0.888E-02
SIIV5P-6S	20000.	1.70	0.371	0.969E-01	0.924E-01	0.103	0.779E-01
4323.5 A	50000.	1.42	0.282	0.153	0.135	0.141	0.111
C= 0.11D+21	80000.	1.32	0.236	0.179	0.156	0.162	0.130
	100000.	1.28	0.243	0.187	0.165	0.174	0.136
	150000.	1.19	0.210	0.219	0.184	0.189	0.149
	200000.	1.13	0.199	0.235	0.195	0.200	0.155
SIIV5P-5D	20000.	3.97	0.204	0.217	0.210	0.233	0.178
6689.8 A	50000.	3.21	0.223	0.349	0.308	0.324	0.253
C= 0.99D+20	80000.	2.91	0.202	0.410	0.356	0.364	0.294
	100000.	2.77	0.191	0.436	0.376	0.395	0.312
	150000.	2.54	0.192	0.488	0.423	0.425	0.346
	200000.	2.39	0.172	0.529	0.445	0.449	0.354

© European Southern Observatory • Provided by the NASA Astrophysics Data System

1991A&AS...89..581D

TABLE 1. *(continued)*

PERTURBER DENSITY = 0.1D+18

TRANSITION	T(K)	ELECTRONS WIDTH(A)	ELECTRONS SHIFT(A)	PROTONS WIDTH(A)	PROTONS SHIFT(A)	IONIZED HELIUM WIDTH(A)	IONIZED HELIUM SHIFT(A)
SIIV5P-6D	20000.	1.16	0.111	*0.112	*0.927E-01	*0.104	*0.735E-01
2676.6 A	50000.	0.974	0.107	*0.151	*0.133	*0.135	*0.107
C= 0.94D+19	80000.	0.895	0.107	*0.175	*0.153	*0.155	*0.125
	100000.	0.858	0.103	*0.188	*0.159	*0.159	*0.131
	150000.	0.794	0.926E-01	0.211	0.174	*0.176	*0.145
	200000.	0.750	0.844E-01	0.218	0.188	*0.173	*0.154
SIIV5D-6P	20000.	6.13	-0.115	0.389	-0.211	*0.430	*-0.180
7055.2 A	50000.	5.11	-0.133	0.523	-0.314	*0.526	*-0.257
C= 0.11D+21	80000.	4.72	-0.113	0.577	-0.358	0.572	-0.297
	100000.	4.54	-0.120	0.610	-0.380	0.590	-0.314
	150000.	4.24	-0.113	0.645	-0.416	0.610	-0.342
	200000.	4.04	-0.963E-01	0.672	-0.444	0.650	-0.367
SIIV5D-6F	20000.	5.24	-0.210				
4212.4 A	50000.	4.16	-0.781E-01				
C= 0.13D+19	80000.	3.68	0.105E-01				
	100000.	3.47	-0.143E-02				
	150000.	3.11	-0.257E-01				
	200000.	2.87	-0.160E-01				
SIIV5F-6D	20000.	5.41	0.445	*0.433	*-0.373	*0.391	*-0.298
4950.1 A	50000.	4.42	0.381	*0.606	*-0.545	*0.522	*-0.444
C= 0.29D+19	80000.	3.98	0.360	*0.712	*-0.624	*0.611	*-0.518
	100000.	3.79	0.352	*0.749	*-0.675	*0.636	*-0.533
	150000.	3.45	0.321	*0.850	*-0.717	*0.728	*-0.584
	200000.	3.23	0.294	*0.923	*-0.725	*0.758	*-0.625

TABLE 2. *Comparison between different Stark width (W in Å) calculations for several Si IV lines at a density* $N=10^{17}$ cm^{-3}.

Transition	T(K)	W_{DSB} (Å)	W_{MSE} (Å)	W_{GM} (Å)	W_G (Å)	W_{SBS} (Å)
3s-3p	20000	0.176-1	0.995-2	0.764-2	0.122-1	0.103-1
	80000	0.899-2	0.497-2	0.484-2	0.691-2	
3p-3d	20000	0.116-1	0.768-2	0.856-2	0.114-1	0.100-1
	80000	0.604-2	0.384-2	0.233-2	0.670-2	
4s-4p	20000	0.497	0.428	0.298	0.512	
	80000	0.284	0.230	0.216	0.305	
4p-4d	20000	0.380	0.346	0.281	0.429	
	80000	0.228	0.213	0.211	0.270	
4d-5p	20000	0.787	0.866	0.692	1.09	
	80000	0.539	0.568	0.529	0.683	
5p-6s	20000	1.70	2.55	1.89	3.03	
	80000	1.32	1.89	1.51	1.93	
5d-6f	20000	5.24	7.23	5.39	6.34	
	80000	3.68	4.92	4.22	4.49	

W_{DSB} : present semi-classical calculations;
W_{MSE} : modified semi-empirical method (Dimitrijević 1988ab);
W_G : simplified semiclassical approach (Griem 1974);
W_{GM} : same approach, modified by Dimitrijević & Konjević (1980)
W_{SBS} :earlier semiclassical calculations (Sahal-Bréchot & Segre 1971) where Feshbach resonances were not included.

N.B. : The abbreviated notation 0.176-1 means 0.176×10^{-1} (and so on).

© European Southern Observatory • Provided by the NASA Astrophysics Data System

1991A&AS...89..581D

TABLE 3. *Electron- and proton-impact shifts along the 3s– np series in angular frequency units* (s^{-1}) *at* $N=10^{17}$ cm^{-3}.

Transition	T = 10,000 K		T = 200,000 K	
	$d_e(s^{-1})$	$d_p(s^{-1})$	$d_e(s^{-1})$	$d_p(s^{-1})$
3s - 3p	$3.98\ 10^{9}$	$-1.30\ 10^{8}$	$-1.80\ 10^{9}$	$-1.99\ 10^{9}$
3s - 4p	$-7.73\ 10^{9}$	$7.04\ 10^{9}$	$6.91\ 10^{9}$	$7.37\ 10^{9}$
3s - 5p	$8.84\ 10^{9}$	$4.00\ 10^{9}$	$2.68\ 10^{10}$	$2.53\ 10^{10}$
3s - 6p	$1.15\ 10^{11}$	$1.23\ 10^{10}$	$6.37\ 10^{10}$	$5.69\ 10^{10}$

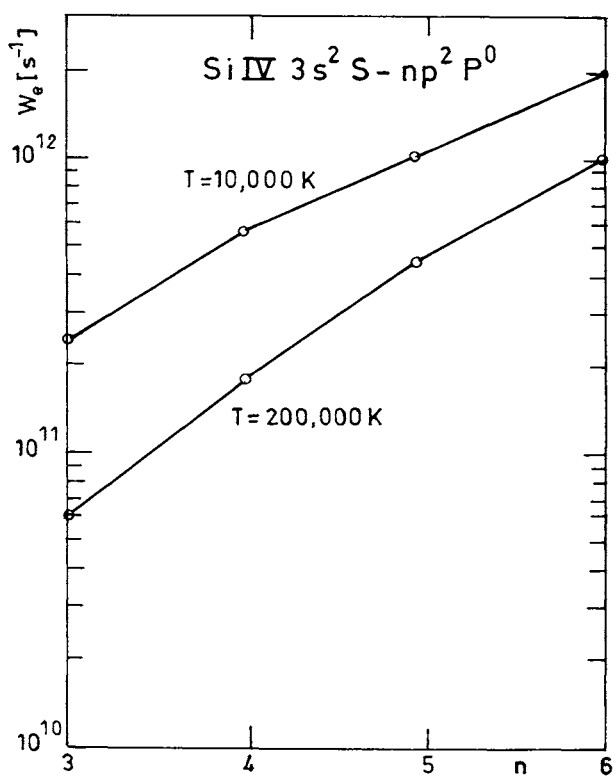

FIGURE 1. Electron-impact widths along the Si IV 3s ^2S–np $^2p^o$ series as a function of n for T =10 000 and 200 000 K, and N = 10^{17} cm^{-3} (angular frequency units).

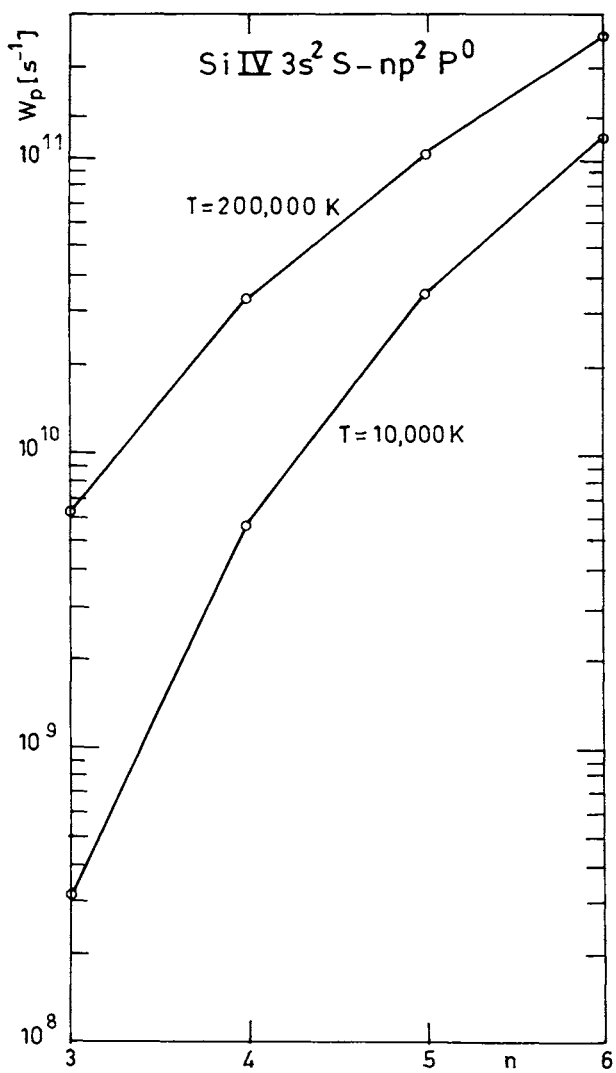

FIGURE 2. As in Figure 1 but for the proton-impact widths.

© European Southern Observatory • Provided by the NASA Astrophysics Data System

1991A&AS...89..591D

ASTRONOMY & ASTROPHYSICS
SUPPLEMENT SERIES

Astron. Astrophys. Suppl. Ser. **89**, 591-598 (1991)

Stark broadening of spectral lines of multicharged ions of astrophysical interest. II. Si IV lines

M.S. Dimitrijević[1], S. Sahal-Bréchot[2] and V. Bommier[2]

[1] Astronomical Observatory, Volgina 7, 11050 Beograd, Yugoslavia
[2] Laboratoire "Astrophysique, Atomes et Molécules", Unité associée au C.N.R.S. No 812, Département Atomes et Molécules en Astrophysique, Observatoire de Paris-Meudon, 92190 Meudon, France

Received November 19, 1990; accepted February 7, 1991

Abstract. — Using a semi-classical approach, we have calculated electron-, proton-, and ionized helium-impact line widths and shifts for 40 Si IV multiplets. The comprehensive set of obtained data has also been used for investigation of Stark broadening parameter regularities within spectral series.

Key words: line profile — atomic data — Stark broadening

1. Introduction.

This paper is the second one of a series devoted to the calculation of Stark broadening parameters of spectral lines of multicharged ions. The first has been concerned with C IV lines (Dimitrijević *et al.* 1991a, hereafter referred to as Paper I): as a matter of fact, Stark broadening of spectral lines has been taking a new interest in Astrophysics (Seaton 1987), owing to the recent development of researches on the physics of the stellar interiors.

For a number of astrophysical as well as physical applications, the knowledge of Si IV Stark broadening parameters is very important, due to its high cosmical abundance and its presence as an impurity in many laboratory plasma sources.

By using the semiclassical- perturbation formalism (Sahal- Bréchot 1969ab) we have calculated electron-, proton-, and ionized helium-impact line widths and shifts for 40 Si IV multiplets.

A summary of the formalism has been recalled in Paper I and will not be repeated here. In the present paper we will only discuss the results obtained by comparing with experiments and other calculations when they exist. They have also been used to continue our investigation of systematic trends for Stark broadening parameters within spectral series (Dimitrijević & Sahal- Bréchot 1984ab, 1985, 1987, 1990 and Paper 1).

2. Results and discussion

Energy levels for Si IV lines have been taken from Bashkin & Stoner (1975). Oscillator strengths have been calculated by using the method of Bates & Damgaard (1949) and the tables of Oertel & Shomo (1968). For higher levels, the method described by Van Regemorter *et al.* (1979) has been used.

In addition to the electron-impact full halfwidths and shifts, Stark broadening parameters due to proton-, and ionized helium- impact have been calculated. Thus we have provided Stark broadening data for all the important charged perturbers in stellar atmospheres. Our results are shown in Table 1 for a perturber density 10^{17} cm^{-3} and temperatures of T = 20 000; 50 000; 80 000; 100 000; 150 000 and 200 000 K. We also specify a parameter c (Dimitrijević & Sahal-Bréchot 1984a), which gives an estimate for the maximum perturber density for which the line may be treated as isolated when it is divided by 2W.

For each value given in Table 1, the collision volume (V) multiplied by the perturber density (N) is much less than one and the impact approximation is valid (Sahal-Bréchot 1969ab). Values for NV >0.5 are not given in Table 1; values for 0.1< NV ≤0.5 are denoted by an asterisk. When the impact approximation is not valid, the ion broadening contribution may be estimated by using quasistatic estimations (Sahal-Bréchot 1991, see also Paper I). One must be aware of the fact that the accuracy of the obtained results decreases when the broadening by ion interactions is important.

© European Southern Observatory • Provided by the NASA Astrophysics Data System

1991A&AS...89..591D

For high densities or when a perturbing level is close to the initial or to the final levels, the influence of Debye screening may be important. In order to scale to other densities, we will provide data for $N = 10^{15}$, and $10^{18} - 10^{21}$ cm^{-3} elsewhere (Dimitrijević *et al.* 1991b).

In Table 2 our results (W_{DSB}) are compared with the calculations of Dimitrijević (1988ab) using the modified semiempirical approach (Dimitrijević & Konjević, 1980) (W_{MSE}), the simplified semiclassical approach of Griem (1974) (W_G) and the modification of this approach (Dimitrijević & Konjević 1980) (W_{GM}). We can see that the simplified semiclassical approach agrees better with our calculations, in its original version for the low lying multiplets. For the higher transitions, the modified version is in better agreement with our values. The agreement with the simple modified semiempirical approach is also better for higher transitions. The experimental value (Platiša *et al.* 1977) for the 4s $^2S-4p\ ^2P^o$ multiplet at T =25600K and $N = 10^{17}$ cm^{-3} is $W = 0.22$ Å while our result is 0.44 Å. For the 4p $^2P^o-4d\ ^2D$ multiplet the experiment gives W =0.24 Å and our calculations 0.34 Å.

The obtained set of results has also been used for investigations of the behaviour of Stark widths and shifts parameters along spectral series.

In Figures 1 and 2 the electron and proton full halfwidths within the 3s $^2S-np\ ^2P^o$ series are illustrated. We see the variation of the results for different plasma temperatures and different perturber type (electrons and protons). By inspecting the energy separation between the upper level and the principal perturbing levels (see the Grotrian diagrams in Bashkin & Stoner (1975)), we find that this value decreases gradually within a spectral series. Thus we obtain a gradual change of the Stark widths as expected. In Table 3 we can see the same situation in the case of the shifts. Such a regular behaviour might be used for critical evaluation of existing results as well as for interpolation of new data needed in astrophysics.

Acknowledgements.

One of us (M.D.) has been supported by the Observatory of Paris-Meudon. This work has also been supported by the C.N.R.S. and is a part of the French-Yugoslav collaboration through the project "L'élargissement Stark des raies spectrales des plasmas astrophysiques et de laboratoire". This study has also been supported in part by SKNTI under the project "Atomic, Molecular and Plasma Spectroscopy". The numerical calculations have been performed on the VAX 8600 of the Observatory of Paris-Meudon.

References

Bashkin S. and Stoner J.O.Jr. 1975, Atomic Energy Levels and Grotrian Diagrams, Vol.1 (North Holand, Amsterdam)
Bates D.R. and Damgaard A. 1949, Trans. Roy. Soc. London, Ser. A 242, 101
Dimitrijević M.S. 1988a A&AS 76, 53
Dimitrijević M.S. 1988b, Bull. Obs. Astron. Belgrade 139, 31
Dimitrijević M.S. and Konjević N. 1980, JQSRT 24, 451
Dimitrijević M.S. and Sahal-Bréchot S. 1984a, JQSRT 31, 301
Dimitrijević M.S. and Sahal-Bréchot S. 1984b, A&A 136, 289
Dimitrijević M.S. and Sahal-Bréchot S. 1985, JQSRT 34, 149
Dimitrijević M.S. and Sahal-Bréchot S. 1987, JQRST 38, 37
Dimitrijević M.S. and Sahal-Bréchot S. 1990, A&AS 82, 519
Dimitrijević M.S., Sahal-Bréchot S. and Bommier V. 1991a, A&A in press (referred as Paper 1 in the text)
Dimitrijević M.S., Sahal-Bréchot S. and Bommier V. 1991b, Bull. Obs. Astron. Belgrade, 144, in press
Griem H.R. 1974, Spectral Line Broadening by Plasma (Academic Press, New York)
Oertel G.K. and Shomo L.P. 1968 ApJS 16, 175
Plastiša M., Dimitrijević M., Popović M. and Konjević N. 1977, J. Phys. B 10, 2997
Sahal-Bréchot S. 1969a A&A 1, 91
Sahal-Bréchot S. 1969b, A&A 2, 322
Sahal-Bréchot S. 1991, A&A in press
Sahal-Bréchot S. and Segre E.R. 1971 A&A 13, 161
Seaton M.J. 1987, J. Phys. B 20, 6363
Van Regemorter H., Hoang Binh Dy and Prud'homme M. 1979, J. Phys. B 12, 1073

© European Southern Observatory • Provided by the NASA Astrophysics Data System

1991A&AS...89..591D

TABLE 1. *This table shows electron-, proton-, and ionized-helium- impact broadening parameters for Si IV lines, for a perturber density of* 10^{17} cm^{-3} *and temperatures from 20 000 K to 200 000 K. Transitions and averaged wavelengths for the multiplet (in Å) are also given. By using c (see Eq. (5) of Paper 1), we obtain an estimate for the maximum perturber density for which the line may be treated as isolated and tabulated data may be used. The asterisk identifies cases for which the collision volume multiplied by the perturber density (the condition for validity of the impact approximation) lies between 0.1 and 0.5. For high densities or when a perturbing level is close to the initial or to the final levels, the influence of Debye screening may be important. In order to scale to other densities, we will provide data for* $N=10^{15}$, *and* $10^{18}-10^{21}$ cm^{-3} *elsewhere (Dimitrijević et al. 1991).*

PERTURBER DENSITY = 0.1D+18

TRANSITION	T(K)	ELECTRONS WIDTH(A)	ELECTRONS SHIFT(A)	PROTONS WIDTH(A)	PROTONS SHIFT(A)	IONIZED HELIUM WIDTH(A)	IONIZED HELIUM SHIFT(A)
SIIV3S-3P	20000.	0.176E-01	0.519E-04	0.907E-04	-0.304E-04	0.159E-03	-0.304E-04
1396.7 A	50000.	0.112E-01	-0.174E-03	0.272E-03	-0.784E-04	0.389E-03	-0.761E-04
C= 0.14D+21	80000.	0.899E-02	-0.166E-03	0.404E-03	-0.118E-03	0.507E-03	-0.110E-03
	100000.	0.812E-02	-0.119E-03	0.462E-03	-0.139E-03	0.571E-03	-0.129E-03
	150000.	0.684E-02	-0.162E-03	0.571E-03	-0.181E-03	0.670E-03	-0.157E-03
	200000.	0.612E-02	-0.187E-03	0.649E-03	-0.205E-03	0.707E-03	-0.181E-03
SIIV3S-4P	20000.	0.453E-02	0.352E-04	0.138E-03	0.175E-04	0.194E-03	0.172E-04
457.9 A	50000.	0.307E-02	0.701E-04	0.252E-03	0.402E-04	0.306E-03	0.373E-04
C= 0.51D+19	80000.	0.258E-02	0.544E-04	0.312E-03	0.548E-04	0.338E-03	0.473E-04
	100000.	0.240E-02	0.702E-04	0.328E-03	0.602E-04	0.354E-03	0.532E-04
	150000.	0.212E-02	0.826E-04	0.354E-03	0.736E-04	0.378E-03	0.627E-04
	200000.	0.195E-02	0.769E-04	0.371E-03	0.819E-04	0.396E-03	0.669E-04
SIIV3S-5P	20000.	0.558E-02	0.176E-03	0.405E-03	0.577E-04	0.501E-03	0.532E-04
361.6 A	50000.	0.429E-02	0.159E-03	0.588E-03	0.106E-03	0.634E-03	0.937E-04
C= 0.15D+19	80000.	0.384E-02	0.193E-03	0.642E-03	0.135E-03	0.686E-03	0.114E-03
	100000.	0.365E-02	0.211E-03	0.666E-03	0.146E-03	0.710E-03	0.119E-03
	150000.	0.335E-02	0.186E-03	0.710E-03	0.163E-03	0.746E-03	0.134E-03
	200000.	0.316E-02	0.186E-03	0.739E-03	0.175E-03	0.756E-03	0.144E-03
SIIV3S-6P	20000.	0.886E-02	0.464E-03	0.984E-03	0.132E-03*	0.109E-02*	0.117E-03
327.2 A	50000.	0.721E-02	0.412E-03	0.121E-02	0.220E-03*	0.129E-02*	0.185E-03
C= 0.64D+18	80000.	0.668E-02	0.416E-03	0.131E-02	0.255E-03*	0.138E-02*	0.212E-03
	100000.	0.646E-02	0.390E-03	0.135E-02	0.273E-03	0.140E-02	0.224E-03
	150000.	0.608E-02	0.378E-03	0.141E-02	0.301E-03	0.145E-02	0.250E-03
	200000.	0.583E-02	0.362E-03	0.144E-02	0.323E-03	0.147E-02	0.269E-03
SIIV3P-4S	20000.	0.128E-01	0.604E-03	0.769E-04	0.221E-03	0.109E-03	0.208E-03
817.1 A	50000.	0.805E-02	0.727E-03	0.291E-03	0.428E-03	0.290E-03	0.373E-03
C= 0.16D+20	80000.	0.655E-02	0.769E-03	0.415E-03	0.540E-03	0.425E-03	0.465E-03
	100000.	0.600E-02	0.823E-03	0.504E-03	0.595E-03	0.484E-03	0.492E-03
	150000.	0.517E-02	0.835E-03	0.630E-03	0.662E-03	0.561E-03	0.546E-03
	200000.	0.471E-02	0.794E-03	0.705E-03	0.717E-03	0.625E-03	0.590E-03
SIIV3P-5S	20000.	0.977E-02	0.204E-02	0.249E-03	0.449E-03	0.263E-03	0.384E-03
515.9 A	50000.	0.707E-02	0.166E-02	0.590E-03	0.727E-03	0.545E-03	0.595E-03
C= 0.30D+19	80000.	0.612E-02	0.147E-02	0.761E-03	0.838E-03	0.661E-03	0.691E-03
	100000.	0.579E-02	0.147E-02	0.846E-03	0.884E-03	0.712E-03	0.728E-03
	150000.	0.518E-02	0.130E-02	0.957E-03	0.984E-03	0.818E-03	0.805E-03
	200000.	0.478E-02	0.124E-02	0.106E-02	0.107E-02	0.914E-03	0.881E-03
SIIV3P-6S	20000.	0.136E-01	0.522E-02	0.748E-03	0.983E-03	0.716E-03	0.833E-03
438.4 A	50000.	0.108E-01	0.394E-02	0.139E-02	0.144E-02	0.117E-02	0.118E-02
C= 0.12D+19	80000.	0.983E-02	0.347E-02	0.165E-02	0.166E-02	0.140E-02	0.137E-02
	100000.	0.937E-02	0.321E-02	0.175E-02	0.177E-02	0.153E-02	0.144E-02
	150000.	0.853E-02	0.277E-02	0.207E-02	0.191E-02	0.173E-02	0.159E-02
	200000.	0.800E-02	0.255E-02	0.232E-02	0.204E-02	0.179E-02	0.165E-02
SIIV3P-3D	20000.	0.116E-01	0.340E-04	0.646E-04	0.836E-05	0.113E-03	0.836E-05
1126.4 A	50000.	0.751E-02	0.498E-04	0.190E-03	0.219E-04	0.271E-03	0.217E-04
C= 0.74D+20	80000.	0.604E-02	0.383E-04	0.279E-03	0.343E-04	0.350E-03	0.331E-04
	100000.	0.548E-02	0.342E-04	0.317E-03	0.416E-04	0.394E-03	0.391E-04
	150000.	0.465E-02	0.460E-04	0.390E-03	0.561E-04	0.457E-03	0.518E-04
	200000.	0.418E-02	0.472E-04	0.440E-03	0.681E-04	0.481E-03	0.594E-04
SIIV3P-4D	20000.	0.101E-01	0.339E-03	0.318E-03	0.359E-03	0.389E-03	0.319E-03
560.5 A	50000.	0.703E-02	0.496E-03	0.640E-03	0.604E-03	0.655E-03	0.510E-03
C= 0.13D+19	80000.	0.596E-02	0.484E-03	0.794E-03	0.703E-03	0.754E-03	0.585E-03
	100000.	0.554E-02	0.471E-03	0.869E-03	0.753E-03	0.805E-03	0.623E-03
	150000.	0.488E-02	0.462E-03	0.971E-03	0.831E-03	0.894E-03	0.685E-03
	200000.	0.450E-02	0.461E-03	0.107E-02	0.901E-03	0.960E-03	0.742E-03

© European Southern Observatory • Provided by the NASA Astrophysics Data System

1991A&AS...89..591D

TABLE 1. *(continued)*

PERTURBER DENSITY = 0.1D+18

TRANSITION	T(K)	ELECTRONS WIDTH(A)	ELECTRONS SHIFT(A)	PROTONS WIDTH(A)	PROTONS SHIFT(A)	IONIZED HELIUM WIDTH(A)	IONIZED HELIUM SHIFT(A)
SIIV3P-5D	20000.	0.154E-01	0.119E-02	0.110E-02	0.101E-02	0.118E-02	0.853E-03
454.7 A	50000.	0.120E-01	0.129E-02	0.172E-02	0.148E-02	0.159E-02	0.121E-02
C= 0.46D+18	80000.	0.107E-01	0.125E-02	0.199E-02	0.171E-02	0.182E-02	0.142E-02
	100000.	0.101E-01	0.122E-02	0.209E-02	0.180E-02	0.196E-02	0.150E-02
	150000.	0.911E-02	0.119E-02	0.243E-02	0.202E-02	0.213E-02	0.165E-02
	200000.	0.850E-02	0.110E-02	0.262E-02	0.214E-02	0.225E-02	0.172E-02
SIIV3P-6D	20000.	0.252E-01	0.290E-02*	0.284E-02*	0.222E-02*	0.266E-02*	0.176E-02
412.7 A	50000.	0.211E-01	0.279E-02*	0.379E-02*	0.321E-02*	0.339E-02*	0.258E-02
C= 0.22D+18	80000.	0.192E-01	0.282E-02*	0.431E-02*	0.366E-02*	0.387E-02*	0.300E-02
	100000.	0.184E-01	0.275E-02*	0.458E-02*	0.382E-02*	0.397E-02*	0.314F-02
	150000.	0.170E-01	0.246E-02*	0.510E-02*	0.413E-02*	0.442E-02*	0.346E-02
	200000.	0.160E-01	0.227E-02*	0.530E-02*	0.450E-02*	0.437E-02*	0.372E-02
SIIV3D-4P	20000.	0.636E-01	0.424E-03	0.154E-02	0.274E-03	0.221E-02	0.269E-03
1724.1 A	50000.	0.428E-01	0.116E-02	0.295E-02	0.622E-03	0.362E-02	0.576E-03
C= 0.73D+20	80000.	0.358E-01	0.947E-03	0.370E-02	0.842E-03	0.407E-02	0.727E-03
	100000.	0.332E-01	0.111E-02	0.395E-02	0.925E-03	0.426E-02	0.815E-03
	150000.	0.292E-01	0.132E-02	0.427E-02	0.113E-02	0.457E-02	0.956E-03
	200000.	0.270E-01	0.127E-02	0.450E-02	0.125E-02	0.478E-02	0.102E-02
SIIV3D-5P	20000.	0.310E-01	0.102E-02	0.213E-02	0.332E-03	0.263E-02	0.307E-03
860.7 A	50000.	0.239E-01	0.959E-03	0.313E-02	0.611E-03	0.338E-02	0.538E-03
C= 0.83D+19	80000.	0.214E-01	0.115E-02	0.342E-02	0.776E-03	0.365E-02	0.651E-03
	100000.	0.204E-01	0.123E-02	0.355E-02	0.838E-03	0.378E-02	0.686E-03
	150000.	0.187E-01	0.110E-02	0.379E-02	0.936E-03	0.397E-02	0.770E-03
	200000.	0.177E-01	0.110E-02	0.395E-02	0.100E-02	0.405E-02	0.829E-03
SIIV3D-6P	20000.	0.389E-01	0.211E-02	0.422E-02	0.588E-03*	0.468E-02*	0.518E-03
688.3 A	50000.	0.317E-01	0.187E-02	0.521E-02	0.980E-03*	0.557E-02*	0.821E-03
C= 0.28D+19	80000.	0.294E-01	0.189E-02	0.564E-02	0.113E-02*	0.594E-02*	0.943E-03
	100000.	0.284E-01	0.176E-02	0.582E-02	0.121E-02	0.604E-02	0.996E-03
	150000.	0.268E-01	0.171E-02	0.611E-02	0.134E-02	0.623E-02	0.111E-02
	200000.	0.257E-01	0.164E-02	0.621E-02	0.144E-02	0.632E-02	0.120E-02
SIIV3D-4F	20000.	0.288E-01	-0.821E-03	0.578E-03	-0.839E-03	0.766E-03	-0.774E-03
1066.6 A	50000.	0.195E-01	-0.599E-03	0.136E-02	-0.149E-02	0.145E-02	-0.128E-02
C= 0.47D+19	80000.	0.162E-01	-0.636E-03	0.187E-02	-0.181E-02	0.175E-02	-0.148E-02
	100000.	0.150E-01	-0.587E-03	0.203E-02	-0.190E-02	0.189E-02	-0.159E-02
	150000.	0.131E-01	-0.435E-03	0.234E-02	-0.213E-02	0.212E-02	-0.177E-02
	200000.	0.120E-01	-0.396E-03	0.260E-02	-0.230E-02	0.229E-02	-0.190E-02
SIIV3D-5F	20000.	0.581E-01	-0.352E-03*	0.145E-01*	0.125E-01		
749.9 A	50000.	0.438E-01	0.671E-03*	0.201E-01*	0.185E-01		
C= 0.67D+17	80000.	0.381E-01	0.121E-02*	0.237E-01*	0.218E-01		
	100000.	0.357E-01	0.115E-02*	0.252E-01*	0.226E-01*	0.199E-01*	0.182E-01
	150000.	0.317E-01	0.916E-03*	0.280E-01*	0.250E-01*	0.226E-01*	0.205E-01
	200000.	0.291E-01	0.904E-03*	0.299E-01*	0.264E-01*	0.230E-01*	0.208E-01
SIIV3D-6F	20000.	0.171E-01	-0.135E-03	0.352E-02	-0.971E-05*	0.395E-02	-0.969E-05
645.8 A	50000.	0.118E-01	-0.563E-04	0.437E-02	-0.246E-04*	0.468E-02	-0.237E-04
C= 0.89D+19	80000.	0.993E-02	-0.647E-04	0.472E-02	-0.361E-04*	0.499E-02	-0.335E-04
	100000.	0.924E-02	-0.644E-04	0.487E-02	-0.423E-04	0.508E-02	-0.383E-04
	150000.	0.822E-02	-0.655E-04	0.509E-02	-0.530E-04	0.521E-02	-0.464E-04
	200000.	0.764E-02	-0.678E-04	0.518E-02	-0.610E-04	0.530E-02	-0.532E-04
SIIV4S-4P	20000.	0.497	-0.720E-02	0.112E-01	-0.408E-02	0.157E-01	-0.390E-02
4097.9 A	50000.	0.336	-0.924E-02	0.209E-01	-0.834E-02	0.250E-01	-0.719E-02
C= 0.41D+21	80000.	0.284	-0.123E-01	0.260E-01	-0.105E-01	0.277E-01	-0.913E-02
	100000.	0.265	-0.131E-01	0.274E-01	-0.117E-01	0.290E-01	-0.987E-02
	150000.	0.235	-0.124E-01	0.299E-01	-0.132E-01	0.312E-01	-0.110E-01
	200000.	0.218	-0.117E-01	0.316E-01	-0.143E-01	0.328E-01	-0.118E-01

© European Southern Observatory • Provided by the NASA Astrophysics Data System

1991A&AS...89..591D

TABLE 1. *(continued)*

PERTURBER DENSITY = 0.1D+18

TRANSITION	T(K)	ELECTRONS WIDTH(A)	ELECTRONS SHIFT(A)	PROTONS WIDTH(A)	PROTONS SHIFT(A)	IONIZED HELIUM WIDTH(A)	IONIZED HELIUM SHIFT(A)
SIIV4S-5P	20000.	0.734E-01	0.784E-03	0.453E-02	0.208E-03	0.561E-02	0.201E-03
1211.0 A	50000.	0.556E-01	0.342E-03	0.656E-02	0.454E-03	0.710E-02	0.407E-03
C= 0.16D+20	80000.	0.495E-01	0.617E-03	0.715E-02	0.581E-03	0.767E-02	0.514E-03
	100000.	0.470E-01	0.678E-03	0.742E-02	0.655E-03	0.792E-02	0.567E-03
	150000.	0.431E-01	0.373E-03	0.790E-02	0.776E-03	0.832E-02	0.639E-03
	200000.	0.407E-01	0.487E-03	0.820E-02	0.833E-03	0.848E-02	0.694E-03
SIIV4S-6P	20000.	0.722E-01	0.225E-02	0.736E-02	0.800E-03*	0.814E-02*	0.721E-03
895.3 A	50000.	0.581E-01	0.205E-02	0.905E-02	0.137E-02*	0.968E-02*	0.117E-02
C= 0.48D+19	80000.	0.536E-01	0.213E-02	0.977E-02	0.161E-02*	0.103E-01*	0.135E-02
	100000.	0.517E-01	0.184E-02	0.101E-01	0.172E-02*	0.105E-01*	0.142E-02
	150000.	0.486E-01	0.182E-02	0.105E-01	0.191E-02	0.108E-01	0.158E-02
	200000.	0.465E-01	0.179E-02	0.107E-01	0.207E-02	0.109E-01	0.171E-02
SIIV4P-5S	20000.	0.205	0.227E-01	0.567E-02	0.735E-02	0.628E-02	0.631E-02
2125.0 A	50000.	0.150	0.205E-01	0.116E-01	0.119E-01	0.110E-01	0.982E-02
C= 0.50D+20	80000.	0.132	0.218E-01	0.142E-01	0.137E-01	0.130E-01	0.113E-01
	100000.	0.125	0.206E-01	0.156E-01	0.146E-01	0.139E-01	0.120E-01
	150000.	0.114	0.190E-01	0.175E-01	0.161E-01	0.157E-01	0.132E-01
	200000.	0.106	0.183E-01	0.189E-01	0.173E-01	0.169E-01	0.145E-01
SIIV4P-6S	20000.	0.120	0.384E-01	0.610E-02	0.769E-02	0.595E-02	0.650E-02
1230.0 A	50000.	0.943E-01	0.281E-01	0.111E-01	0.112E-01	0.948E-02	0.925E-02
C= 0.91D+19	80000.	0.857E-01	0.259E-01	0.131E-01	0.130E-01	0.113E-01	0.107E-01
	100000.	0.820E-01	0.230E-01	0.139E-01	0.138E-01	0.122E-01	0.112E-01
	150000.	0.752E-01	0.204E-01	0.167E-01	0.150E-01	0.137E-01	0.125E-01
	200000.	0.709E-01	0.189E-01	0.183E-01	0.161E-01	0.142E-01	0.129E-01
SIIV4P-4D	20000.	0.380	0.949E-02	0.922E-02	0.107E-01	0.115E-01	0.960E-02
3160.3 A	50000.	0.267	0.117E-01	0.189E-01	0.182E-01	0.196E-01	0.154E-01
C= 0.41D+20	80000.	0.228	0.121E-01	0.238E-01	0.213E-01	0.227E-01	0.177E-01
	100000.	0.214	0.112E-01	0.259E-01	0.228E-01	0.240E-01	0.188E-01
	150000.	0.190	0.101E-01	0.296E-01	0.253E-01	0.272E-01	0.209E-01
	200000.	0.177	0.102E-01	0.319E-01	0.271E-01	0.290E-01	0.224E-01
SIIV4P-5D	20000.	0.149	0.102E-01	0.928E-02	0.909E-02	0.981E-02	0.765E-02
1367.6 A	50000.	0.116	0.108E-01	0.149E-01	0.133E-01	0.136E-01	0.109E-01
C= 0.42D+19	80000.	0.102	0.106E-01	0.174E-01	0.153E-01	0.156E-01	0.127E-01
	100000.	0.967E-01	0.103E-01	0.181E-01	0.161E-01	0.168E-01	0.135E-01
	150000.	0.877E-01	0.987E-02	0.211E-01	0.182E-01	0.185E-01	0.149E-01
	200000.	0.819E-01	0.910E-02	0.229E-01	0.192E-01	0.195E-01	0.154E-01
SIIV4P-6D	20000.	0.168	0.181E-01*	0.179E-01*	0.143E-01*	0.166E-01*	0.113E-01
1046.7 A	50000.	0.139	0.174E-01*	0.239E-01*	0.206E-01*	0.214E-01*	0.166E-01
C= 0.14D+19	80000.	0.127	0.177E-01*	0.273E-01*	0.235E-01*	0.245E-01*	0.193E-01
	100000.	0.122	0.172E-01*	0.292E-01*	0.245E-01*	0.251E-01*	0.202E-01
	150000.	0.112	0.153E-01	0.325E-01	0.265E-01*	0.279E-01*	0.222E-01
	200000.	0.106	0.140E-01	0.339E-01	0.289E-01*	0.275E-01*	0.238E-01
SIIV4D-5P	20000.	0.787	0.200E-02	0.347E-01	-0.110E-01	0.426E-01	-0.101E-01
3766.0 A	50000.	0.604	-0.403E-02	0.529E-01	-0.194E-01	0.565E-01	-0.167E-01
C= 0.58D+20	80000.	0.539	0.497E-03	0.585E-01	-0.235E-01	0.614E-01	-0.193E-01
	100000.	0.512	0.285E-02	0.608E-01	-0.247E-01	0.640E-01	-0.205E-01
	150000.	0.469	0.101E-02	0.661E-01	-0.277E-01	0.675E-01	-0.230E-01
	200000.	0.442	0.133E-02	0.685E-01	-0.298E-01	0.694E-01	-0.248E-01
SIIV4D-6P	20000.	0.307	0.893E-02	0.261E-01	0.504E-03*	0.295E-01*	0.488E-03
1796.6 A	50000.	0.248	0.712E-02	0.326E-01	0.109E-02*	0.349E-01*	0.971E-03
C= 0.13D+20	80000.	0.229	0.769E-02	0.352E-01	0.139E-02	0.373E-01	0.122E-02
	100000.	0.221	0.697E-02	0.364E-01	0.156E-02	0.381E-01	0.135E-02
	150000.	0.207	0.690E-02	0.380E-01	0.184E-02	0.391E-01	0.151E-02
	200000.	0.198	0.657E-02	0.387E-01	0.196E-02	0.395E-01	0.164E-02

© European Southern Observatory • Provided by the NASA Astrophysics Data System

1991A&AS...89..591D

TABLE 1. *(continued)*

PERTURBER DENSITY = 0.1D+18

TRANSITION	T(K)	ELECTRONS WIDTH(A)	ELECTRONS SHIFT(A)	PROTONS WIDTH(A)	PROTONS SHIFT(A)	IONIZED HELIUM WIDTH(A)	IONIZED HELIUM SHIFT(A)
SIIV4D-4F	20000.	24.3	-1.08	0.641	-0.994	0.689	-0.850
24271.1 A	50000.	17.0	-1.23	1.41	-1.61	1.32	-1.32
C= 0.24D+22	80000.	14.5	-1.22	1.78	-1.86	1.58	-1.53
	100000.	13.5	-1.18	1.96	-1.96	1.68	-1.61
	150000.	12.0	-1.07	2.21	-2.18	1.92	-1.78
	200000.	11.1	-1.05	2.44	-2.36	2.14	-1.95
SIIV4D-5F	20000.	0.606	-0.113E-01	*0.132	*0.115		
2287.0 A	50000.	0.458	-0.365E-02	*0.185	*0.171		
C= 0.62D+18	80000.	0.400	0.173E-02	*0.214	*0.201	*0.179	*0.159
	100000.	0.375	0.134E-02	*0.229	*0.208	*0.181	*0.167
	150000.	0.334	-0.692E-03	*0.252	*0.229	*0.202	*0.189
	200000.	0.307	-0.800E-03	*0.274	*0.244	*0.212	*0.191
SIIV4D-6F	20000.	0.630	-0.166E-01				
1533.2 A	50000.	0.494	0.636E-03				
C= 0.18D+18	80000.	0.436	0.119E-01				
	100000.	0.410	0.101E-01				
	150000.	0.366	0.662E-02				
	200000.	0.337	0.688E-02				
SIIV4F-5D	20000.	0.607	0.457E-01	0.362E-01	0.372E-01	0.377E-01	0.315E-01
2675.2 A	50000.	0.467	0.475E-01	0.593E-01	0.544E-01	0.533E-01	0.448E-01
C= 0.16D+20	80000.	0.411	0.464E-01	0.694E-01	0.627E-01	0.618E-01	0.518E-01
	100000.	0.387	0.452E-01	0.740E-01	0.672E-01	0.653E-01	0.540E-01
	150000.	0.349	0.430E-01	0.841E-01	0.727E-01	0.741E-01	0.600E-01
	200000.	0.325	0.396E-01	0.921E-01	0.760E-01	0.748E-01	0.628E-01
SIIV4F-6D	20000.	0.443	0.494E-01	*0.460E-01	*0.370E-01	*0.426E-01	*0.294E-01
1672.6 A	50000.	0.366	0.472E-01	*0.623E-01	*0.539E-01	*0.550E-01	*0.435E-01
C= 0.37D+19	80000.	0.332	0.478E-01	*0.691E-01	*0.615E-01	*0.615E-01	*0.497E-01
	100000.	0.318	0.465E-01	*0.751E-01	*0.646E-01	*0.639E-01	*0.525E-01
	150000.	0.292	0.414E-01	0.817E-01	0.691E-01	*0.709E-01	*0.573E-01
	200000.	0.275	0.381E-01	0.884E-01	0.761E-01	*0.719E-01	*0.623E-01
SIIV5S-5P	20000.	4.92	-0.246	0.259	-0.112	0.316	-0.970E-01
8977.4 A	50000.	3.95	-0.266	0.385	-0.184	0.405	-0.153
C= 0.90D+21	80000.	3.60	-0.276	0.427	-0.212	0.443	-0.176
	100000.	3.46	-0.251	0.446	-0.225	0.459	-0.187
	150000.	3.21	-0.245	0.486	-0.251	0.491	-0.208
	200000.	3.04	-0.235	0.513	-0.273	0.495	-0.220
SIIV5S-6P	20000.	0.611	-0.318E-02	0.566E-01	-0.382E-02	*0.626E-01	-0.352E-02
2483.7 A	50000.	0.510	-0.553E-02	0.695E-01	-0.685E-02	*0.744E-01	-0.597E-02
C= 0.37D+20	80000.	0.476	-0.701E-02	0.751E-01	-0.848E-02	*0.795E-01	-0.697E-02
	100000.	0.462	-0.747E-02	0.775E-01	-0.896E-02	*0.808E-01	-0.748E-02
	150000.	0.436	-0.620E-02	0.808E-01	-0.100E-01	0.828E-01	-0.826E-02
	200000.	0.419	-0.616E-02	0.825E-01	-0.108E-01	0.839E-01	-0.888E-02
SIIV5P-6S	20000.	1.70	0.371	0.969E-01	0.924E-01	0.103	0.779E-01
4323.5 A	50000.	1.42	0.282	0.153	0.135	0.141	0.111
C= 0.11D+21	80000.	1.32	0.236	0.179	0.156	0.162	0.130
	100000.	1.28	0.243	0.187	0.165	0.174	0.136
	150000.	1.19	0.210	0.219	0.184	0.189	0.149
	200000.	1.13	0.199	0.235	0.195	0.200	0.155
SIIV5P-5D	20000.	3.97	0.204	0.217	0.210	0.233	0.178
6689.8 A	50000.	3.21	0.223	0.349	0.308	0.324	0.253
C= 0.99D+20	80000.	2.91	0.202	0.410	0.356	0.364	0.294
	100000.	2.77	0.191	0.436	0.376	0.395	0.312
	150000.	2.54	0.192	0.488	0.423	0.425	0.346
	200000.	2.39	0.172	0.529	0.445	0.449	0.354

© European Southern Observatory • Provided by the NASA Astrophysics Data System

1991A&AS...89..591D

TABLE 1. *(continued)*

PERTURBER DENSITY = 0.1D+18

TRANSITION	T(K)	ELECTRONS WIDTH(A)	ELECTRONS SHIFT(A)	PROTONS WIDTH(A)	PROTONS SHIFT(A)	IONIZED HELIUM WIDTH(A)	IONIZED HELIUM SHIFT(A)
SIIV5P-6D	20000.	1.16	0.111	*0.112	*0.927E-01	*0.104	*0.735E-01
2676.6 A	50000.	0.974	0.107	*0.151	*0.133	*0.135	*0.107
C= 0.94D+19	80000.	0.895	0.107	*0.175	*0.153	*0.155	*0.125
	100000.	0.858	0.103	*0.188	*0.159	*0.159	*0.131
	150000.	0.794	0.926E-01	0.211	0.174	*0.176	*0.145
	200000.	0.750	0.844E-01	0.218	0.188	*0.173	*0.154
SIIV5D-6P	20000.	6.13	-0.115	0.389	-0.211	*0.430	*-0.180
7055.2 A	50000.	5.11	-0.133	0.523	-0.314	*0.526	*-0.257
C= 0.11D+21	80000.	4.72	-0.113	0.577	-0.358	0.572	-0.297
	100000.	4.54	-0.120	0.610	-0.380	0.590	-0.314
	150000.	4.24	-0.113	0.645	-0.416	0.610	-0.342
	200000.	4.04	-0.963E-01	0.672	-0.444	0.650	-0.367
SIIV5D-6F	20000.	5.24	-0.210				
4212.4 A	50000.	4.16	-0.781E-01				
C= 0.13D+19	80000.	3.68	0.105E-01				
	100000.	3.47	-0.143E-02				
	150000.	3.11	-0.257E-01				
	200000.	2.87	-0.160E-01				
SIIV5F-6D	20000.	5.41	0.445	*0.433	*-0.373	*0.391	*-0.298
4950.1 A	50000.	4.42	0.381	*0.606	*-0.545	*0.522	*-0.444
C= 0.29D+19	80000.	3.98	0.360	*0.712	*-0.624	*0.611	*-0.518
	100000.	3.79	0.352	*0.749	*-0.675	*0.636	*-0.533
	150000.	3.45	0.321	*0.850	*-0.717	*0.728	*-0.584
	200000.	3.23	0.294	*0.923	*-0.725	*0.758	*-0.625

TABLE 2. *Comparison between different Stark width (W in Å) calculations for several Si IV lines at a density* $N=10^{17}$ cm^{-3}.

Transition	T(K)	W_{DSB} (Å)	W_{MSE} (Å)	W_{GM} (Å)	W_G (Å)	W_{SBS} (Å)
3s-3p	20000	0.176-1	0.995-2	0.764-2	0.122-1	0.103-1
	80000	0.899-2	0.497-2	0.484-2	0.691-2	
3p-3d	20000	0.116-1	0.768-2	0.856-2	0.114-1	0.100-1
	80000	0.604-2	0.384-2	0.233-2	0.670-2	
4s-4p	20000	0.497	0.428	0.298	0.512	
	80000	0.284	0.230	0.216	0.305	
4p-4d	20000	0.380	0.346	0.281	0.429	
	80000	0.228	0.213	0.211	0.270	
4d-5p	20000	0.787	0.866	0.692	1.09	
	80000	0.539	0.568	0.529	0.683	
5p-6s	20000	1.70	2.55	1.89	3.03	
	80000	1.32	1.89	1.51	1.93	
5d-6f	20000	5.24	7.23	5.39	6.34	
	80000	3.68	4.92	4.22	4.49	

W_{DSB} : present semi-classical calculations;
W_{MSE} : modified semi-empirical method (Dimitrijević 1988ab);
W_G : simplified semiclassical approach (Griem 1974);
W_{GM} : same approach, modified by Dimitrijević & Konjević (1980)
W_{SBS} :earlier semiclassical calculations (Sahal-Bréchot & Segre 1971) where Feshbach resonances were not included.

N.B. : The abbreviated notation 0.176-1 means 0.176×10^{-1} (and so on).

© European Southern Observatory • Provided by the NASA Astrophysics Data System

1991A&AS...89..591D

TABLE 3. *Electron- and proton-impact shifts along the 3s– np series in angular frequency units* (s^{-1}) *at* $N=10^{17}$ cm^{-3}.

Transition	T = 10,000 K		T = 200,000 K	
	$d_e(s^{-1})$	$d_p(s^{-1})$	$d_e(s^{-1})$	$d_p(s^{-1})$
3s - 3p	$3.98\ 10^{9}$	$-1.30\ 10^{8}$	$-1.80\ 10^{9}$	$-1.99\ 10^{9}$
3s - 4p	$-7.73\ 10^{9}$	$7.04\ 10^{9}$	$6.91\ 10^{9}$	$7.37\ 10^{9}$
3s - 5p	$8.84\ 10^{9}$	$4.00\ 10^{9}$	$2.68\ 10^{10}$	$2.53\ 10^{10}$
3s - 6p	$1.15\ 10^{11}$	$1.23\ 10^{10}$	$6.37\ 10^{10}$	$5.69\ 10^{10}$

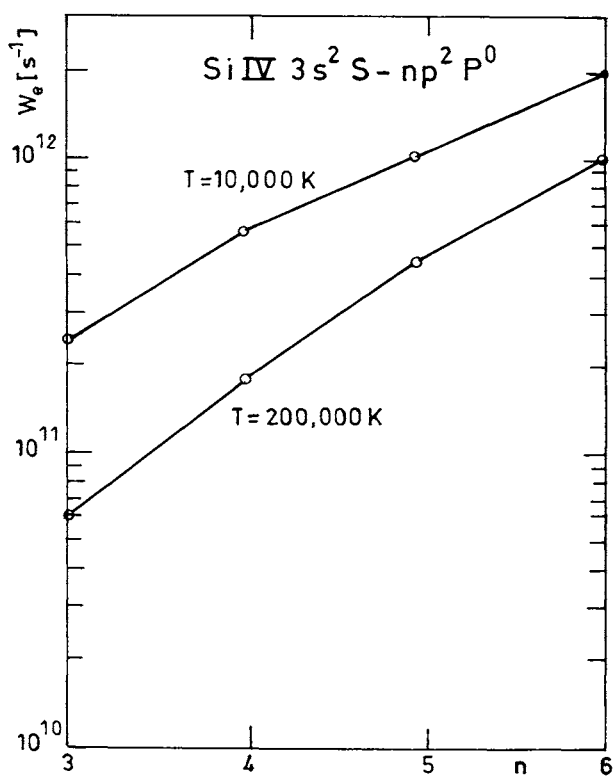

FIGURE 1. Electron-impact widths along the Si IV 3s ^2S–np $^2p^o$ series as a function of n for T =10 000 and 200 000 K, and N = 10^{17} cm^{-3} (angular frequency units).

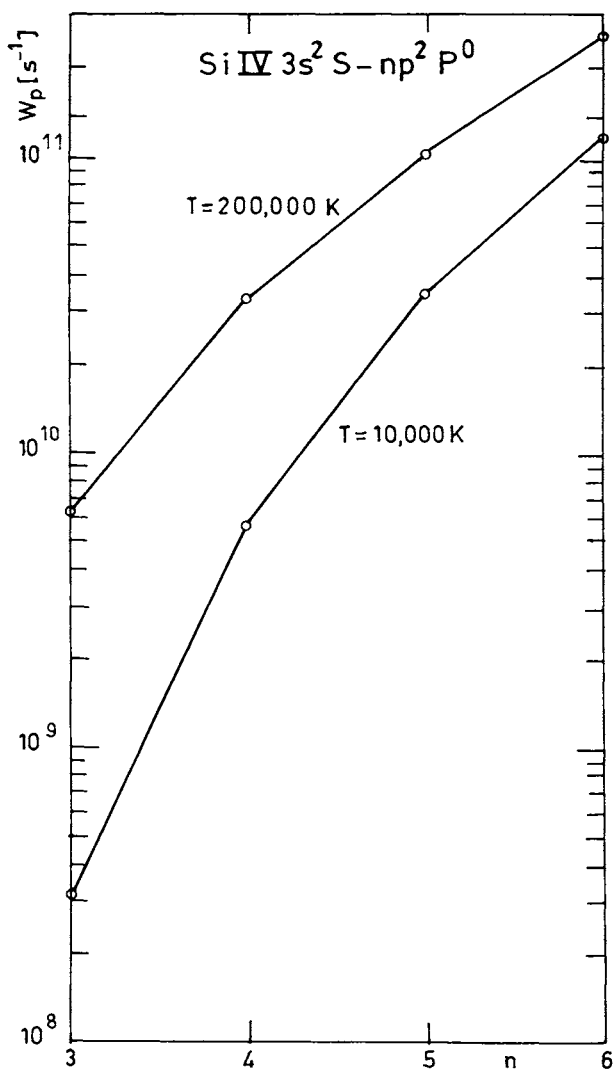

FIGURE 2. As in Figure 1 but for the proton-impact widths.

© European Southern Observatory • Provided by the NASA Astrophysics Data System

1992A&AS...93..359D

ASTRONOMY & ASTROPHYSICS
SUPPLEMENT SERIES

MAY 1992, PAGE 359

Astron. Astrophys. Suppl. Ser. **93**, 359-371 (1992)

Stark broadening of spectral lines of multicharged ions of astrophysical interest. III. O VI lines

M.S. Dimitrijević[1] and S. Sahal-Bréchot[2]

[1] Astronomical Observatory, Volgina 7, 11050 Beograd, Yugoslavia
[2] Laboratoire "Astrophysique, Atomes et Molécules", Unité associée au C.N.R.S. No 812, Département Atomes et Molécules en Astrophysique, Observatoire de Paris-Meudon, 92190 Meudon, France

Received May 15; accepted July 16, 1991

Abstract. — Using a semiclassical approach, we have calculated electron-, proton-, and ionized helium-impact line widths and shifts for 30 O VI multiplets. This comprehensive set of data has been used for the investigation of Stark broadening parameter regularities within spectral series.

Key words: line profile — atomic data — Stark broadening.

1. Introduction.

Stark broadening of multicharged ion spectral lines has been taking a new interest to Astrophysics (Seaton 1987), owing to the recent development of research on the physics of the stellar interiors. Knowledge of O VI Stark broadening parameters is useful also for the investigation of hot dense plasma in laboratory (see e.g. Böttcher *et al.* 1988), due to its presence as an impurity in many laboratory plasma sources.

This paper is the third of a series devoted to the calculation of Stark broadening parameters of spectral lines of multicharged ions. The first two were concerned with C IV and Si IV lines (Dimitrijević *et al.* 1991ab, hereafter referred as Papers I and II).

By using the semiclassical-perturbation formalism (Sahal-Bréchot 1969ab) we have calculated electron-, proton-, and ionized helium-impact line widths and shifts for 30 O VI multiplets. A summary of the formalism is given in Paper I. Here we present and discuss the results for O VI, along with a comparison with experimental data (Böttcher *et al.* 1988) and the results of other calculations (Seaton 1988, Böttcher *et al.* 1988). Our results have also been used to continue our investigation of systematic trends for Stark broadening parameters within spectral series (Dimitrijević & Sahal-Bréchot 1984ab, 1985, 1987, 1990 and Papers I and II).

Send offprint requests to: M.S. Dimitrijević.

2. Results and discussion.

Energy levels for O VI lines have been taken from Bashkin & Stoner (1975). Oscillator strengths have been calculated by using the method of Bates & Damgaard (1949) and the tables of Oertel & Shomo (1968). For higher levels, the method described by Van Regemorter *et al.* (1979) has been used.

In addition to the electron-impact full halfwidths and shifts, Stark broadening parameters due to proton-, and ionized helium-impacts have been calculated. Thus we have provided Stark broadening data for all the important charged perturbers in stellar atmospheres. Our results are shown in Table 1 for perturber densities $10^{17} - 10^{21}$ cm^{-3} and temperatures of $T = 100\,000 - 1\,500\,000$ K. For perturber densities lower than 10^{17} cm^{-3} all the corresponding data are practically linear with density, because the effect of Debye screening is negligible. In Table 2, data for 5s-5p and 6s-6p multiplets at perturber density 10^{15} cm^{-3} are presented. We also specify a parameter c (Dimitrijević & Sahal-Bréchot 1984a), which gives an estimate for the maximum perturber density for which the line may be treated as isolated when it is divided by 2W.

For each value given in Tables 1 and 2, the collision volume (V) multiplied by the perturber density (N) is much less than one and the impact approximation is valid (Sahal-Bréchot 1969ab). Values for $NV > 0.5$ are not given in Table 1; values for $0.1 < NV \leq 0.5$ are denoted by an asterisk. When the impact approximation is not valid, the ion broadening contribution may be estimated by using quasistatic estimations (Sahal-Bréchot 1991, see also

© European Southern Observatory • Provided by the NASA Astrophysics Data System

1992A&AS...93..359D

Paper I). One must be aware of the fact that the accuracy of the obtained results decreases when the broadening by ion interactions is important.

In Table 3 our results for the 3s-3p multiplets are compared with the experimental results and the calculations of Böttcher *et al.* (1988). The latter were performed using the simplified semiclassical method (Griem 1974), the modified semiempirical approach (Dimitrijević & Konjević 1980), the two variants of the quasiclassical Gaunt factor approximation of Hey & Breger (1980a,b,c; 1982), the approach of Baranger (1962) and the simple estimates based on regularities and systematic trends (Purić *et al.* 1987, 1988). The results are also compared in Table 3 with the strong coupling quantum mechanical calculations of Seaton (1988). The single experimental value seems to be out of line with all of the calculations. The additional experimental data for different plasma conditions will be important for the checking of different theoretical approaches. In Table 4 we compare our results with the thermally averaged collision strengths γ calculated by Seaton (1988), using strong coupling quantum mechanical method. The connection between Stark broadening parameters and γ is (Seaton 1988)

$$\gamma = 43.66\,(T/10^4)^{1/2}\,(10^4/\lambda)^2\,(10^{17}/N)\,(w + id)$$

with the temperature T in K, the electron density N in cm^{-3}, the wavelength λ, the half-width at half maximum w and the shift d in Å. We can see that a considerable difference exists between semiclassical and quantum mechanical (Seaton 1988) calculations, especially in the case of the shift. However, compared with widths, shifts are more difficult to calculate. Difficulties to obtain the Stark width and shift data of the same accuracy have been discussed in detail by Dimitrijević *et al.* (1981) and possibilities of the strong coupling quantum mechanical and semiclassical methods have been compared.

Our results have also been used for the investigation of the behaviour of Stark width and shift parameters along spectral series.

In Figures 1 and 2 the behaviour of the electron and proton full halfwidths within the $2s^2S - np^2p^0$ series are illustrated. We see the variation of the results for different plasma temperatures and different perturbers (electrons and protons). By inspecting the energy separation between the upper level and the principal perturbing levels (see the Grotrian diagrams in Bashkin & Stoner 1975), we find that this value decreases gradually within a spectral series. Thus we obtain a gradual change of the Stark widths as expected. In Figures 3 and 4 we can see the same situation in the case of the shifts. Such a regular behaviour might be used for critical evaluation of existing results as well as for interpolation of new data needed in astrophysics.

Since a systematic behaviour of linewidths is expected when the lower level quantum number increases, Figures 5-8 show that such trends exist also in the case of ns-np transitions and therefore they can be used for interpolation. In Table 5 it is shown that in the case of 3s-6p and 3d-6p transitions, electron impact widths are practically the same and that the electron impact shifts are similar. Consequently, if the principal quantum number of the upper level is quite larger than the corresponding one of the lower level, the change of the lower level angular momentum quantum number will produce only small changes in the electron impact broadening parameter values.

Acknowledgements.

One of us (M.D.) has been supported by the Observatory of Paris-Meudon. This work has also been supported by the French C.N.R.S. and is a part of French-Yugoslav collaboration through the project "L'elargissement Stark des raies spectrales des' plasmas astrophysiques et de laboratoire", it is also a part of the project "Physics and dynamics of celestial bodies", supported by RFN of Serbia.

References

Baranger M. 1962, in Atomic and Molecular Processes, D.R. Bates Ed. (Academic Press) New York

Bashkin S. and Stoner J.O.Jr. 1975, Atomic Energy Levels and Grotrian Diagrams, Vol. 1, North Holland, Amsterdam

Bates D.R. and Damgaard A. 1949, Trans. Roy. Soc. London, Ser. A 242, 101

Böttcher F., Breger P., Hey J.D., Kunze H.-J. 1988, Phys. Rev. 38, 2690

Dimitrijević M.S., Feautrier N. and Sahal-Bréchot S. 1981, J. Phys. B 14, 2559

Dimitrijević M.S., Konjević N. 1980, JQSRT 24, 451

Dimitrijević M.S. and Sahal-Bréchot S. 1984a, JQSRT 31, 301

Dimitrijević M.S. and Sahal-Bréchot S. 1984b, A&A 136, 289

Dimitrijević M.S. and Sahal-Bréchot S. 1985, JQSRT 34, 149

Dimitrijević M.S. and Sahal Bréchot S. 1987, JQSRT 38, 37

Dimitrijević M.S. and Sahal-Bréchot S. 1990, A&AS 82, 519

Dimitrijević M.S., Sahal-Bréchot S. and Bommier V. 1991a A&AS 89, **581** (referred as Paper I in the text)

Dimitrijević M.S., Sahal-Bréchot S. and Bommier V. 1991b, A&AS 89, **591** (referred as Paper II in the text)

Griem H.R. 1974, Spectral Line Broadening by Plasmas (Academic Press) New York

Hey J.D. and Breger P. 1980a, JQSRT 24, 349

© European Southern Observatory • Provided by the NASA Astrophysics Data System

1992A&AS...93..359D

Hey J.D. and Breger P. 1980b, JQSRT 24, 427
Hey J.D. and Breger P. 1980c, JQSRT 23, 311
Hey J.D. and Breger P. 1982, S. Afr. J. Phys. 5, 111
Oertel G.K. and Shomo L.P. 1968, ApJS 16, 175
Purić J., Djeniže S., Srećković A., Platiša M., Labat J. 1988, Phys. Rev. A 37, 498
Purić J., Srećković A., Djeniže S., Platiša M. 1987 Phys. Rev. A 36, 3957
Sahal-Bréchot S. 1969a, A&A 1, 91
Sahal-Bréchot S. 1969b, A&A 2, 322
Sahal-Bréchot S. 1991, A&A 245, 322
Seaton M.J. 1987, J. Phys. B 20, 6363
Seaton M.J. 1988, J. Phys. B 21, 3033
Van Regemorter H., Hoang Binh Dy and Prud'homme M. 1979, J. Phys. B 12, 1073

TABLE 1. *This table shows electron-, proton-, and ionized-helium- impact broadening parameters for O VI lines, for perturber densities of* $10^{17} - 10^{21}$ cm^{-3} *and temperatures from 100 000 K to 1 500 000 K. Transitions and averaged wavelengths for the multiplet (in Å) are also given. By using c (see Eq. 5 of Paper I), we obtain an estimate for the maximum perturber density for which the line may be treated as isolated and tabulated data may be used. The asterisk identifies cases for which the collision volume multiplied by the perturber density (the condition for validity of the impact approximation) lies between 0.1 and 0.5. Data for densities N lower than* 10^{17} cm^{-3} *can be obtained by multiplying the results given at* 10^{17} cm^{-3} *by* $N/10^{17}$.

PERTURBER DENSITY = 0.1D+18(cm-3)

TRANSITION	T(K)	ELECTRONS WIDTH(A)	ELECTRONS SHIFT(A)	PROTONS WIDTH(A)	PROTONS SHIFT(A)	IONIZED HELIUM WIDTH(A)	IONIZED HELIUM SHIFT(A)
OVI 2S-2P	100000.	0.146E-02	-0.329E-04	0.647E-05	-0.175E-04	0.111E-04	-0.174E-04
1033.8 A	200000.	0.105E-02	-0.310E-04	0.193E-04	-0.331E-04	0.274E-04	-0.314E-04
C= 0.10E+21	500000.	0.694E-03	-0.386E-04	0.536E-04	-0.609E-04	0.587E-04	-0.534E-04
	800000.	0.572E-03	-0.362E-04	0.739E-04	-0.760E-04	0.785E-04	-0.661E-04
OVI 2S-3P	100000.	0.121E-03	0.262E-05	0.456E-05	0.592E-05	0.577E-05	0.543E-05
150.1 A	200000.	0.910E-04	0.215E-05	0.818E-05	0.860E-05	0.902E-05	0.756E-05
C= 0.19E+18	500000.	0.647E-04	0.191E-05	0.135E-04	0.119E-04	0.127E-04	0.994E-05
	800000.	0.551E-04	0.166E-05	0.155E-04	0.134E-04	0.144E-04	0.112E-04
OVI 2S-4P	100000.	0.218E-03	0.905E-05	0.222E-04	0.244E-04	0.229E-04	0.210E-04
115.8 A	200000.	0.170E-03	0.872E-05	0.318E-04	0.303E-04	0.291E-04	0.251E-04
C= 0.47E+17	500000.	0.126E-03	0.696E-05	0.427E-04	0.385E-04	0.383E-04	0.321E-04
	800000.	0.108E-03	0.577E-05	0.472E-04	0.418E-04	0.429E-04	0.354E-04
OVI 2S-5P	100000.	0.441E-03	0.261E-04	0.700E-04	0.683E-04	0.640E-04	0.568E-04
104.8 A	200000.	0.351E-03	0.240E-04	0.898E-04	0.815E-04	0.794E-04	0.682E-04
C= 0.20E+17	500000.	0.264E-03	0.169E-04	0.111E-03	0.100E-03	0.999E-04	0.814E-04
	800000.	0.229E-03	0.147E-04	0.134E-03	0.112E-03	0.107E-03	0.939E-04
OVI 2S-6P	100000.	0.848E-03	0.596E-04	0.168E-03	0.156E-03*	0.147E-03*	0.128E-03
99.7 A	200000.	0.684E-03	0.492E-04	0.208E-03	0.181E-03	0.181E-03	0.152E-03
C= 0.10E+17	500000.	0.518E-03	0.354E-04	0.268E-03	0.209E-03	0.223E-03	0.183E-03
	800000.	0.450E-03	0.313E-04	0.277E-03	0.238E-03	0.217E-03	0.192E-03
OVI 2P-3S	100000.	0.115E-03	0.918E-05	0.333E-05	0.864E-05	0.400E-05	0.794E-05
184.1 A	200000.	0.869E-04	0.109E-04	0.785E-05	0.126E-04	0.773E-05	0.111E-04
C= 0.89E+18	500000.	0.621E-04	0.101E-04	0.158E-04	0.175E-04	0.139E-04	0.146E-04
	800000.	0.530E-04	0.985E-05	0.194E-04	0.197E-04	0.165E-04	0.166E-04
OVI 2P-4S	100000.	0.172E-03	0.253E-04	0.164E-04	0.246E-04	0.159E-04	0.214E-04
132.3 A	200000.	0.135E-03	0.237E-04	0.275E-04	0.310E-04	0.244E-04	0.260E-04
C= 0.19E+18	500000.	0.996E-04	0.225E-04	0.389E-04	0.396E-04	0.340E-04	0.330E-04
	800000.	0.862E-04	0.203E-04	0.464E-04	0.440E-04	0.406E-04	0.354E-04
OVI 2P-5S	100000.	0.348E-03	0.597E-04	0.561E-04	0.630E-04	0.489E-04	0.529E-04
117.4 A	200000.	0.275E-03	0.571E-04	0.746E-04	0.766E-04	0.635E-04	0.627E-04
C= 0.74E+17	500000.	0.206E-03	0.502E-04	0.100E-03	0.961E-04	0.857E-04	0.766E-04
	800000.	0.179E-03	0.435E-04	0.111E-03	0.102E-03	0.936E-04	0.800E-04
OVI 2P-6S	100000.	0.678E-03	0.134E-03	0.136E-03	0.141E-03	0.117E-03	0.118E-03
110.7 A	200000.	0.544E-03	0.126E-03	0.176E-03	0.170E-03	0.147E-03	0.140E-03
C= 0.37E+17	500000.	0.411E-03	0.101E-03	0.222E-03	0.203E-03	0.177E-03	0.165E-03
	800000.	0.356E-03	0.858E-04	0.264E-03	0.217E-03	0.201E-03	0.180E-03
OVI 2P-3D	100000.	0.949E-04	-0.210E-05	0.305E-05	-0.595E-05	0.389E-05	-0.554E-05
173.0 A	200000.	0.703E-04	-0.155E-05	0.657E-05	-0.882E-05	0.695E-05	-0.785E-05
C= 0.25E+18	500000.	0.490E-04	-0.123E-05	0.124E-04	-0.126E-04	0.113E-04	-0.106E-04
	800000.	0.414E-04	-0.695E-06	0.149E-04	-0.143E-04	0.132E-04	-0.119E-04

© European Southern Observatory • Provided by the NASA Astrophysics Data System

1992A&AS...93..359D

TABLE 1. *(continued)*

PERTURBER DENSITY = 0.1D+18(cm-3)

TRANSITION	T(K)	ELECTRONS WIDTH(A)	ELECTRONS SHIFT(A)	PROTONS WIDTH(A)	PROTONS SHIFT(A)	IONIZED HELIUM WIDTH(A)	IONIZED HELIUM SHIFT(A)
OVI 3S-3P	100000.	0.108	-0.179E-02	0.210E-02	0.392E-03	0.295E-02	0.385E-03
3820.0 A	200000.	0.818E-01	-0.285E-02	0.353E-02	0.715E-03	0.433E-02	0.665E-03
C= 0.12E+21	500000.	0.590E-01	-0.259E-02	0.522E-02	0.123E-02	0.561E-02	0.108E-02
	800000.	0.506E-01	-0.267E-02	0.572E-02	0.153E-02	0.607E-02	0.129E-02
OVI 3S-4P	100000.	0.366E-02	0.875E-04	0.313E-03	0.341E-03	0.328E-03	0.294E-03
447.8 A	200000.	0.285E-02	0.721E-04	0.452E-03	0.423E-03	0.419E-03	0.353E-03
C= 0.71E+18	500000.	0.211E-02	0.514E-04	0.602E-03	0.533E-03	0.528E-03	0.448E-03
	800000.	0.183E-02	0.348E-04	0.690E-03	0.595E-03	0.582E-03	0.487E-03
OVI 3S-5P	100000.	0.427E-02	0.217E-03	0.641E-03	0.622E-03	0.586E-03	0.518E-03
318.4 A	200000.	0.340E-02	0.192E-03	0.823E-03	0.747E-03	0.724E-03	0.625E-03
C= 0.18E+18	500000.	0.256E-02	0.129E-03	0.102E-02	0.908E-03	0.921E-03	0.745E-03
	800000.	0.222E-02	0.109E-03	0.120E-02	0.103E-02	0.970E-03	0.852E-03
OVI 3S-6P	100000.	0.662E-02	0.436E-03	0.128E-02	0.119E-02*	0.112E-02*	0.973E-03
275.4 A	200000.	0.534E-02	0.353E-03	0.159E-02	0.138E-02	0.137E-02	0.116E-02
C= 0.79E+17	500000.	0.404E-02	0.250E-03	0.205E-02	0.160E-02	0.170E-02	0.139E-02
	800000.	0.351E-02	0.220E-03	0.210E-02	0.181E-02	0.166E-02	0.145E-02
OVI 3P-4S	100000.	0.396E-02	0.373E-03	0.246E-03	0.362E-03	0.245E-03	0.316E-03
536.3 A	200000.	0.307E-02	0.353E-03	0.420E-03	0.461E-03	0.372E-03	0.387E-03
C= 0.24E+19	500000.	0.227E-02	0.335E-03	0.599E-03	0.589E-03	0.506E-03	0.486E-03
	800000.	0.196E-02	0.302E-03	0.724E-03	0.656E-03	0.598E-03	0.544E-03
OVI 3P-5S	100000.	0.364E-02	0.523E-03	0.501E-03	0.562E-03	0.440E-03	0.471E-03
354.0 A	200000.	0.287E-02	0.503E-03	0.654E-03	0.684E-03	0.566E-03	0.562E-03
C= 0.68E+18	500000.	0.215E-02	0.441E-03	0.880E-03	0.859E-03	0.769E-03	0.693E-03
	800000.	0.186E-02	0.382E-03	0.993E-03	0.904E-03	0.856E-03	0.714E-03
OVI 3P-6S	100000.	0.529E-02	0.963E-03	0.990E-03	0.103E-02	0.854E-03	0.857E-03
299.5 A	200000.	0.423E-02	0.909E-03	0.128E-02	0.124E-02	0.107E-02	0.102E-02
C= 0.27E+18	500000.	0.320E-02	0.730E-03	0.162E-02	0.148E-02	0.129E-02	0.120E-02
	800000.	0.277E-02	0.618E-03	0.194E-02	0.158E-02	0.147E-02	0.131E-02
OVI 3P-3D	100000.	0.824	-0.305E-01	0.373E-01	-0.606E-01	0.410E-01	-0.532E-01
11850.0 A	200000.	0.627	-0.248E-01	0.669E-01	-0.844E-01	0.689E-01	-0.730E-01
C= 0.12E+22	500000.	0.453	-0.228E-01	0.113	-0.112	0.989E-01	-0.924E-01
	800000.	0.388	-0.184E-01	0.132	-0.126	0.113	-0.105
OVI 3D-4P	100000.	0.469E-02	0.218E-03	0.469E-03	0.540E-03	0.477E-03	0.461E-03
529.9 A	200000.	0.367E-02	0.205E-03	0.684E-03	0.665E-03	0.611E-03	0.554E-03
C= 0.99E+18	500000.	0.272E-02	0.167E-03	0.923E-03	0.839E-03	0.832E-03	0.701E-03
	800000.	0.235E-02	0.137E-03	0.104E-02	0.948E-03	0.923E-03	0.766E-03
OVI 3D-5P	100000.	0.520E-02	0.317E-03	0.815E-03	0.804E-03	0.741E-03	0.668E-03
357.9 A	200000.	0.415E-02	0.290E-03	0.104E-02	0.956E-03	0.917E-03	0.800E-03
C= 0.23E+18	500000.	0.312E-02	0.207E-03	0.130E-02	0.118E-02	0.116E-02	0.953E-03
	800000.	0.271E-02	0.178E-03	0.158E-02	0.131E-02	0.128E-02	0.110E-02
OVI 3D-6P	100000.	0.796E-02	0.565E-03	0.157E-02	0.146E-02*	0.137E-02*	0.119E-02
304.4 A	200000.	0.642E-02	0.466E-03	0.194E-02	0.169E-02	0.168E-02	0.142E-02
C= 0.97E+17	500000.	0.486E-02	0.337E-03	0.248E-02	0.195E-02	0.208E-02	0.171E-02
	800000.	0.422E-02	0.297E-03	0.257E-02	0.222E-02	0.204E-02	0.180E-02
OVI 4S-4P	100000.	2.15	-0.640E-01	0.850E-01	0.592E-01	0.999E-01	0.522E-01
9362.9 A	200000.	1.69	-0.588E-01	0.121	0.814E-01	0.123	0.677E-0
C= 0.31E+21	500000.	1.26	-0.639E-01	0.154	0.103	0.151	0.869E-01
	800000.	1.09	-0.608E-01	0.169	0.116	0.163	0.979E-01
OVI 4S-5P	100000.	0.471E-01	0.946E-03	0.570E-02	0.547E-02	0.527E-02	0.458E-02
986.3 A	200000.	0.375E-01	0.843E-03	0.712E-02	0.656E-02	0.642E-02	0.541E-02
C= 0.17E+19	500000.	0.282E-01	0.282E-03	0.914E-02	0.799E-02	0.783E-02	0.666E-02
	800000.	0.245E-01	0.205E-03	0.103E-01	0.890E-02	0.829E-02	0.722E-02
OVI 4S-6P	100000.	0.413E-01	0.203E-02	0.716E-02	0.677E-02*	0.644E-02*	0.556E-02
664.7 A	200000.	0.333E-01	0.160E-02	0.926E-02	0.804E-02	0.791E-02	0.665E-02
C= 0.46E+18	500000.	0.252E-01	0.102E-02	0.120E-01	0.932E-02	0.971E-02	0.800E-02
	800000.	0.219E-01	0.897E-03	0.122E-01	0.104E-01	0.977E-02	0.839E-02

© European Southern Observatory • Provided by the NASA Astrophysics Data System

1992A&AS...93..359D

TABLE 1. *(continued)*

PERTURBER DENSITY = 0.1D+18(cm-3)

TRANSITION	T(K)	ELECTRONS WIDTH(A)	ELECTRONS SHIFT(A)	PROTONS WIDTH(A)	PROTONS SHIFT(A)	IONIZED HELIUM WIDTH(A)	IONIZED HELIUM SHIFT(A)
OVI 4P-5S	100000.	0.544E-01	0.493E-02	0.458E-02	0.501E-02	0.407E-02	0.417E-02
1172.1 A	200000.	0.431E-01	0.474E-02	0.602E-02	0.601E-02	0.517E-02	0.500E-02
C= 0.48E+19	500000.	0.324E-01	0.423E-02	0.818E-02	0.749E-02	0.671E-02	0.609E-02
	800000.	0.281E-01	0.370E-02	0.895E-02	0.814E-02	0.758E-02	0.677E-02
OVI 4P-6S	100000.	0.370E-01	0.542E-02	0.571E-02	0.587E-02	0.486E-02	0.489E-02
731.5 A	200000.	0.297E-01	0.512E-02	0.723E-02	0.705E-02	0.615E-02	0.578E-02
C= 0.16E+19	500000.	0.225E-01	0.412E-02	0.919E-02	0.840E-02	0.740E-02	0.667E-02
	800000.	0.195E-01	0.350E-02	0.107E-01	0.933E-02	0.867E-02	0.745E-02
OVI 5S-6P	100000.	0.365	0.595E-02	0.498E-01	0.457E-01	0.453E-01	0.382E-01
1836.9 A	200000.	0.295	0.292E-02	0.602E-01	0.551E-01	0.531E-01	0.443E-01
C= 0.35E+19	500000.	0.223	-0.107E-03	0.781E-01	0.669E-01	0.622E-01	0.552E-01
	800000.	0.194	0.114E-03	0.795E-01	0.703E-01	0.702E-01	0.574E-01
OVI 5P-6S	100000.	0.437	0.397E-01	0.381E-01	0.375E-01	0.337E-01	0.314E-01
2173.9 A	200000.	0.353	0.378E-01	0.485E-01	0.452E-01	0.419E-01	0.368E-01
C= 0.84E+19	500000.	0.268	0.315E-01	0.615E-01	0.535E-01	0.520E-01	0.457E-01
	800000.	0.233	0.266E-01	0.663E-01	0.589E-01	0.592E-01	0.480E-01

PERTURBER DENSITY = 0.1D+19(cm-3)

TRANSITION	T(K)	ELECTRONS WIDTH(A)	ELECTRONS SHIFT(A)	PROTONS WIDTH(A)	PROTONS SHIFT(A)	IONIZED HELIUM WIDTH(A)	IONIZED HELIUM SHIFT(A)
OVI 2S-2P	100000.	0.146E-01	-0.334E-03	0.647E-04	-0.171E-03	0.111E-03	-0.169E-03
1033.8 A	200000.	0.105E-01	-0.304E-03	0.193E-03	-0.331E-03	0.274E-03	-0.314E-03
C= 0.10E+22	500000.	0.694E-02	-0.384E-03	0.536E-03	-0.608E-03	0.587E-03	-0.534E-03
	1000000.	0.525E-02	-0.351E-03	0.869E-03	-0.838E-03	0.850E-03	-0.702E-03
OVI 2S-3P	100000.	0.121E-02	0.242E-04	0.456E-04	0.575E-04	0.577E-04	0.526E-04
150.1 A	200000.	0.910E-03	0.212E-04	0.818E-04	0.858E-04	0.902E-04	0.754E-04
C= 0.19E+19	500000.	0.647E-03	0.189E-04	0.135E-03	0.119E-03	0.127E-03	0.992E-04
	1000000.	0.512E-03	0.146E-04	0.168E-03	0.144E-03	0.149E-03	0.118E-03
OVI 2S-4P	100000.	0.218E-02	0.792E-04	0.222E-03	0.233E-03	0.229E-03	0.198E-03
115.8 A	200000.	0.170E-02	0.865E-04	0.318E-03	0.302E-03	0.291E-03	0.251E-0
C= 0.47E+18	500000.	0.126E-02	0.687E-04	0.427E-03	0.384E-03	0.383E-03	0.320E-03
	1000000.	0.101E-02	0.532E-04	0.498E-03	0.447E-03	0.442E-03	0.359E-03
OVI 2S-5P	100000.	0.440E-02	0.206E-03*	0.702E-03*	0.629E-03*	0.648E-03*	0.516E-03
104.8 A	200000.	0.351E-02	0.236E-03*	0.898E-03*	0.811E-03*	0.794E-03*	0.678E-03
C= 0.20E+18	500000.	0.264E-02	0.166E-03	0.111E-02	0.997E-03*	0.999E-03*	0.810E-03
	1000000.	0.214E-02	0.139E-03	0.127E-02	0.118E-02*	0.109E-02*	0.939E-03
OVI 2S-6P	100000.	0.844E-02	0.405E-03				
99.7 A	200000.	0.681E-02	0.478E-03*	0.208E-02*	0.180E-02		
C= 0.10E+18	500000.	0.516E-02	0.342E-03*	0.268E-02*	0.208E-02		
	1000000.	0.420E-02	0.287E-03*	0.274E-02*	0.244E-02*	0.264E-02*	0.203E-02
OVI 2P-3S	100000.	0.116E-02	0.886E-04	0.333E-04	0.839E-04	0.400E-04	0.769E-04
184.1 A	200000.	0.868E-03	0.109E-03	0.785E-04	0.125E-03	0.773E-04	0.110E-03
C= 0.89E+19	500000.	0.621E-03	0.101E-03	0.158E-03	0.174E-03	0.139E-03	0.146E-03
	1000000.	0.493E-03	0.960E-04	0.204E-03	0.210E-03	0.175E-03	0.173E-03
OVI 2P-4S	100000.	0.172E-02	0.243E-03	0.164E-03	0.235E-03	0.159E-03	0.203E-03
132.3 A	200000.	0.134E-02	0.237E-03	0.275E-03	0.309E-03	0.244E-03	0.259E-03
C= 0.19E+19	500000.	0.996E-03	0.223E-03	0.389E-03	0.396E-03	0.340E-03	0.330E-03
	1000000.	0.805E-03	0.190E-03	0.510E-03	0.463E-03	0.415E-03	0.377E-03
OVI 2P-5S	100000.	0.349E-02	0.556E-03	0.555E-03	0.591E-03*	0.490E-03*	0.490E-03
117.4 A	200000.	0.275E-02	0.569E-03	0.746E-03	0.763E-03*	0.635E-03*	0.624E-03
C= 0.74E+18	500000.	0.206E-02	0.498E-03	0.100E-02	0.958E-03	0.858E-03	0.763E-03
	1000000.	0.167E-02	0.403E-03	0.127E-02	0.103E-02	0.102E-02	0.893E-03

© European Southern Observatory • Provided by the NASA Astrophysics Data System

1992A&AS...93..359D

TABLE 1. *(continued)*

PERTURBER DENSITY = 0.1D+19(cm-3)

TRANSITION	T(K)	ELECTRONS WIDTH(A)	ELECTRONS SHIFT(A)	PROTONS WIDTH(A)	PROTONS SHIFT(A)	IONIZED HELIUM WIDTH(A)	IONIZED HELIUM SHIFT(A)
OVI 2P-6S	100000.	0.679E-02	0.120E-02	0.138E-02	0.128E-02		
110.7 A	200000.	0.544E-02	0.125E-02	0.176E-02	0.169E-02	0.147E-02	0.139E-02
C= 0.37E+18	500000.	0.411E-02	0.100E-02	0.222E-02	0.202E-02	0.177E-02	0.164E-02
	1000000.	0.332E-02	0.797E-03	0.257E-02	0.228E-02	0.201E-02	0.198E-02
OVI 2P-3D	100000.	0.950E-03	-0.195E-04	0.305E-04	-0.578E-04	0.389E-04	-0.538E-04
173.0 A	200000.	0.703E-03	-0.163E-04	0.657E-04	-0.880E-04	0.695E-04	-0.783E-04
C= 0.25E+19	500000.	0.490E-03	-0.126E-04	0.124E-03	-0.125E-03	0.113E-03	-0.106E-03
	1000000.	0.383E-03	-0.628E-05	0.162E-03	-0.152E-03	0.138E-03	-0.125E-03
OVI 3S-3P	100000.	1.08	-0.177E-01	0.210E-01	0.382E-02	0.295E-01	0.375E-02
3820.0 A	200000.	0.818	-0.288E-01	0.353E-01	0.715E-02	0.433E-01	0.664E-02
C= 0.12E+22	500000.	0.590	-0.258E-01	0.522E-01	0.123E-01	0.561E-01	0.108E-01
	1000000.	0.472	-0.271E-01	0.594E-01	0.163E-01	0.630E-01	0.136E-01
OVI 3S-4P	100000.	0.366E-01	0.726E-03	0.313E-02	0.325E-02	0.327E-02	0.279E-02
447.8 A	200000.	0.285E-01	0.710E-03	0.452E-02	0.422E-02	0.419E-02	0.352E-02
C= 0.71E+19	500000.	0.211E-01	0.504E-03	0.602E-02	0.532E-02	0.528E-02	0.447E-02
	1000000.	0.171E-01	0.293E-03	0.722E-02	0.621E-02	0.639E-02	0.517E-02
OVI 3S-5P	100000.	0.427E-01	0.167E-02*	0.645E-02*	0.574E-02*	0.595E-02*	0.473E-02
318.4 A	200000.	0.340E-01	0.188E-02*	0.823E-02*	0.743E-02*	0.724E-02*	0.621E-02
C= 0.18E+19	500000.	0.255E-01	0.126E-02	0.102E-01	0.905E-02*	0.922E-02*	0.742E-02
	1000000.	0.208E-01	0.102E-02	0.115E-01	0.107E-01*	0.988E-02*	0.851E-02
OVI 3S-6P	100000.	0.659E-01	0.291E-02				
275.4 A	200000.	0.531E-01	0.343E-02*	0.159E-01*	0.137E-01		
C= 0.79E+18	500000.	0.403E-01	0.241E-02*	0.205E-01*	0.159E-01		
	1000000.	0.328E-01	0.200E-02*	0.209E-01*	0.186E-01*	0.200E-01*	0.155E-01
OVI 3P-4S	100000.	0.396E-01	0.359E-02	0.246E-02	0.347E-02	0.246E-02	0.301E-02
536.3 A	200000.	0.307E-01	0.353E-02	0.420E-02	0.460E-02	0.372E-02	0.386E-02
C= 0.24E+20	500000.	0.227E-01	0.332E-02	0.599E-02	0.588E-02	0.506E-02	0.485E-02
	1000000.	0.183E-01	0.285E-02	0.736E-02	0.702E-02	0.641E-02	0.564E-02
OVI 3P-5S	100000.	0.364E-01	0.486E-02	0.493E-02	0.525E-02*	0.435E-02*	0.437E-02
354.0 A	200000.	0.287E-01	0.501E-02	0.654E-02	0.682E-02*	0.566E-02*	0.559E-02
C= 0.68E+19	500000.	0.215E-01	0.438E-02	0.880E-02	0.856E-02	0.769E-02	0.690E-02
	1000000.	0.174E-01	0.354E-02	0.116E-01	0.931E-02	0.910E-02	0.804E-02
OVI 3P-6S	100000.	0.529E-01	0.864E-02*	0.101E-01*	0.936E-02		
299.5 A	200000.	0.423E-01	0.903E-02*	0.128E-01*	0.123E-01*	0.107E-01*	0.101E-01
C= 0.27E+19	500000.	0.320E-01	0.722E-02*	0.162E-01*	0.148E-01*	0.129E-01*	0.120E-01
	1000000.	0.258E-01	0.575E-02*	0.189E-01*	0.165E-01*	0.144E-01*	0.144E-01
OVI 3P-3D	100000.	8.24	-0.287	0.373	-0.587	0.410	-0.513
11850.0 A	200000.	6.27	-0.249	0.669	-0.843	0.689	-0.729
C= 0.12E+23	500000.	4.53	-0.227	1.13	-1.11	0.989	-0.923
	1000000.	3.62	-0.166	1.40	-1.32	1.19	-1.11
OVI 3D-4P	100000.	0.469E-01	0.193E-02	0.470E-02	0.515E-02	0.477E-02	0.436E-02
529.9 A	200000.	0.367E-01	0.204E-02	0.684E-02	0.663E-02	0.611E-02	0.552E-02
C= 0.99E+19	500000.	0.272E-01	0.166E-02	0.923E-02	0.837E-02	0.832E-02	0.699E-02
	1000000.	0.219E-01	0.126E-02	0.114E-01	0.984E-02	0.932E-02	0.780E-02
OVI 3D-5P	100000.	0.520E-01	0.253E-02*	0.818E-02*	0.742E-02*	0.747E-02*	0.604E-02
357.9 A	200000.	0.415E-01	0.285E-02*	0.104E-01*	0.952E-02*	0.917E-02*	0.796E-02
C= 0.23E+19	500000.	0.312E-01	0.203E-02	0.130E-01	0.118E-01*	0.116E-01*	0.949E-02
	1000000.	0.253E-01	0.168E-02	0.150E-01	0.140E-01*	0.129E-01*	0.111E-01

© European Southern Observatory • Provided by the NASA Astrophysics Data System

1992A&AS...93..359D

TABLE 1. *(continued)*

PERTURBER DENSITY = 0.1D+19(cm-3)

TRANSITION	T(K)	ELECTRONS WIDTH(A)	ELECTRONS SHIFT(A)	PROTONS WIDTH(A)	PROTONS SHIFT(A)	IONIZED HELIUM WIDTH(A)	IONIZED HELIUM SHIFT(A)
OVI 3D-6P	100000.	0.792E-01	0.387E-02				
304.4 A	200000.	0.639E-01	0.454E-02	*0.194E-01	*0.168E-01		
C= 0.97E+18	500000.	0.484E-01	0.326E-02	*0.248E-01	*0.193E-01		
	1000000.	0.394E-01	0.272E-02	*0.255E-01	*0.229E-01	*0.246E-01	*0.190E-01
OVI 4S-4P	100000.	21.5	-0.664	0.849	0.571	0.998	0.501
9362.9 A	200000.	16.9	-0.591	1.21	0.812	1.23	0.675
C= 0.31E+22	500000.	12.6	-0.636	1.54	1.03	1.51	0.868
	1000000.	10.2	-0.576	1.74	1.21	1.66	1.01
OVI 4S-5P	100000.	0.470	0.518E-02	*0.567E-01	*0.510E-01	*0.525E-01	*0.420E-01
986.3 A	200000.	0.375	0.805E-02	0.712E-01	0.653E-01	*0.642E-01	*0.538E-01
C= 0.17E+20	500000.	0.282	0.262E-02	0.914E-01	0.797E-01	*0.783E-01	*0.663E-01
	1000000.	0.230	0.202E-02	0.102	0.908E-01	*0.931E-01	*0.728E-01
OVI 4S-6P	100000.	0.412	0.121E-01				
664.7 A	200000.	0.332	0.154E-01	*0.926E-01	*0.798E-01		
C= 0.46E+19	500000.	0.251	0.973E-02	*0.120	*0.926E-01		
	1000000.	0.205	0.809E-02	*0.123	*0.105	*0.113	*0.892E-01
OVI 4P-5S	100000.	0.544	0.464E-01	0.457E-01	0.469E-01	0.403E-01	0.389E-01
1172.1 A	200000.	0.431	0.473E-01	0.602E-01	0.598E-01	0.517E-01	0.498E-01
C= 0.48E+20	500000.	0.324	0.420E-01	0.818E-01	0.747E-01	0.671E-01	0.607E-01
	1000000.	0.263	0.342E-01	0.963E-01	0.868E-01	0.762E-01	0.693E-01
OVI 4P-6S	100000.	0.370	0.487E-01	*0.569E-01	*0.532E-01		
731.5 A	200000.	0.297	0.508E-01	*0.723E-01	*0.701E-01	*0.615E-01	*0.574E-01
C= 0.16E+20	500000.	0.225	0.407E-01	*0.919E-01	*0.836E-01	*0.740E-01	*0.662E-01
	1000000.	0.182	0.325E-01	*0.106	*0.965E-01	*0.807E-01	*0.788E-01
OVI 5S-6P	100000.	3.64	0.480E-02	*0.497	*0.410		
1836.9 A	200000.	2.94	0.250E-01	*0.602	*0.547		
C= 0.35E+20	500000.	2.23	-0.429E-02	*0.781	*0.665	*0.623	*0.549
	1000000.	1.81	-0.933E-04	*0.914	*0.738	*0.774	*0.625
OVI 5P-6S	100000.	4.37	0.368	*0.379	*0.340	*0.336	*0.281
2173.9 A	200000.	3.52	0.377	*0.485	*0.450	*0.419	*0.366
C= 0.84E+20	500000.	2.68	0.313	*0.615	*0.533	*0.520	*0.455
	1000000.	2.17	0.246	0.750	0.609	*0.585	*0.508

PERTURBER DENSITY = 0.1D+20(cm-3 = 0.1D+21(cm-3)

TRANSITION	T(K)	ELECTRONS WIDTH(A)	ELECTRONS SHIFT(A)	ELECTRONS WIDTH(A)	ELECTRONS SHIFT(A)
OVI 2S-2P	100000.	0.146	-0.303E-02	1.46	-0.243E-01
1033.8 A	200000.	0.105	-0.293E-02	1.05	-0.267E-01
C= 0.10E+23	500000.	0.694E-01	-0.385E-02	0.694	-0.372E-01
	1000000.	0.525E-01	-0.349E-02	0.525	-0.348E-01
OVI 2S-3P	100000.	0.121E-01	0.187E-03	0.120	-0.204E-04
150.1 A	200000.	0.910E-02	0.169E-03	0.905E-01	0.420E-03
C= 0.19E+20	500000.	0.647E-02	0.187E-03	0.644E-01	0.137E-02
	1000000.	0.512E-02	0.142E-03	0.509E-01	0.136E-02
OVI 2S-4P	100000.	0.217E-01	0.408E-03	0.203	-0.436E-02
115.8 A	200000.	0.170E-01	0.588E-03	0.160	-0.405E-03
C= 0.47E+19	500000.	0.125E-01	0.670E-03	0.120	0.355E-02
	1000000.	0.101E-01	0.512E-03	0.971E-01	0.467E-02
OVI 2S-5P	100000.	0.428E-01	0.441E-03	*0.353	*-0.962E-02
104.8 A	200000.	0.343E-01	0.111E-02	0.294	-0.242E-02
C= 0.20E+19	500000.	0.259E-01	0.155E-02	0.229	0.547E-02
	1000000.	0.211E-01	0.130E-02	0.190	0.111E-01

© European Southern Observatory • Provided by the NASA Astrophysics Data System

1992A&AS...93..359D

TABLE 1. *(continued)*

PERTURBER DENSITY = 0.1D+20(cm-3) = 0.1D+21(cm-3)

TRANSITION	T(K)	ELECTRONS WIDTH(A)	ELECTRONS SHIFT(A)	ELECTRONS WIDTH(A)	ELECTRONS SHIFT(A)
OVI 2S-6P	100000.	0.779E-01	0.148E-04	*0.563	*-0.130E-01
99.7 A	200000.	0.637E-01	0.122E-02	*0.492	*-0.527E-02
C= 0.10E+19	500000.	0.488E-01	0.310E-02	0.400	0.978E-02
	1000000.	0.401E-01	0.257E-02	0.338	0.214E-01
OVI 2P-3S	100000.	0.116E-01	0.797E-03	0.116	0.538E-02
184.1 A	200000.	0.869E-02	0.103E-02	0.869E-01	0.847E-02
C= 0.89E+20	500000.	0.621E-02	0.100E-02	0.621E-01	0.931E-02
	1000000.	0.493E-02	0.955E-03	0.493E-01	0.947E-02
OVI 2P-4S	100000.	0.173E-01	0.209E-02	0.170	0.984E-02
132.3 A	200000.	0.135E-01	0.212E-02	0.133	0.134E-01
C= 0.19E+20	500000.	0.996E-02	0.222E-02	0.987E-01	0.192E-01
	1000000.	0.805E-02	0.189E-02	0.799E-01	0.185E-01
OVI 2P-5S	100000.	0.348E-01	0.422E-02	0.318	0.101E-02
117.4 A	200000.	0.274E-01	0.468E-02	0.255	0.177E-01
C= 0.74E+19	500000.	0.206E-01	0.492E-02	0.195	0.370E-01
	1000000.	0.167E-01	0.395E-02	0.158	0.378E-01
OVI 2P-6S	100000.	0.668E-01	0.736E-02	0.518	-0.252E-01
110.7 A	200000.	0.536E-01	0.911E-02	0.441	0.164E-01
C= 0.37E+19	500000.	0.407E-01	0.979E-02	0.349	0.606E-01
	1000000.	0.328E-01	0.774E-02	0.288	0.718E-01
OVI 2P-3D	100000.	0.950E-02	-0.149E-03	0.943E-01	0.156E-03
173.0 A	200000.	0.703E-02	-0.127E-03	0.699E-01	0.442E-04
C= 0.25E+20	500000.	0.490E-02	-0.120E-03	0.487E-01	-0.724E-03
	1000000.	0.383E-02	-0.619E-04	0.382E-01	-0.541E-03
OVI 3S-3P	100000.	10.8	-0.179		
3820.0 A	200000.	8.18	-0.291		
C= 0.12E+23	500000.	5.90	-0.259		
	1000000.	4.72	-0.272		
OVI 3S-4P	100000.	0.365	0.198E-02	3.43	-0.920E-01
447.8 A	200000.	0.285	0.328E-02	2.71	-0.510E-01
C= 0.71E+20	500000.	0.211	0.479E-02	2.02	0.504E-02
	1000000.	0.170	0.266E-02	1.64	0.203E-01
OVI 3S-5P	100000.	0.416	0.198E-02	*3.46	*-0.103
318.4 A	200000.	0.332	0.742E-02	2.87	-0.451E-01
C= 0.18E+20	500000.	0.251	0.117E-01	2.23	0.262E-01
	1000000.	0.204	0.950E-02	1.85	0.772E-01
OVI 3S-6P	100000.	0.610	-0.147E-02	*4.45	*-0.110
275.4 A	200000.	0.498	0.722E-02	3.87	-0.574E-01
C= 0.79E+19	500000.	0.382	0.217E-01	3.14	0.564E-01
	1000000.	0.313	0.177E-01	2.66	0.144
OVI 3P-4S	100000.	0.396	0.311E-01	3.91	0.154
536.3 A	200000.	0.307	0.318E-01	3.04	0.207
C= 0.24E+21	500000.	0.227	0.331E-01	2.25	0.288
	1000000.	0.183	0.283E-01	1.82	0.277
OVI 3P-5S	100000.	0.364	0.369E-01	3.36	0.474E-02
354.0 A	200000.	0.286	0.412E-01	2.69	0.154
C= 0.68E+20	500000.	0.215	0.432E-01	2.04	0.325
	1000000.	0.174	0.347E-01	1.66	0.333

© European Southern Observatory • Provided by the NASA Astrophysics Data System

1992A&AS...93..359D

TABLE 1. *(continued)*

PERTURBER DENSITY = 0.1D+20(cm-3) = 0.1D+21(cm-3)

TRANSITION	T(K)	ELECTRONS WIDTH(A)	SHIFT(A)	ELECTRONS WIDTH(A)	SHIFT(A)
OVI 3P-6S	100000.	0.521	0.527E-01	4.11	-0.189
299.5 A	200000.	0.418	0.657E-01	3.48	0.115
C= 0.27E+20	500000.	0.317	0.706E-01	2.75	0.435
	1000000.	0.256	0.558E-01	2.27	0.518
OVI 3D-4P	100000.	0.468	0.107E-01	4.36	-0.862E-01
529.9 A	200000.	0.366	0.143E-01	3.45	-0.184E-02
C= 0.99E+20	500000.	0.271	0.162E-01	2.59	0.909E-01
	1000000.	0.219	0.122E-01	2.10	0.112
OVI 3D-5P	100000.	0.506	0.614E-02	*4.17	*-0.110
357.9 A	200000.	0.405	0.138E-01	3.48	-0.252E-01
C= 0.23E+20	500000.	0.306	0.191E-01	2.71	0.713E-01
	1000000.	0.249	0.159E-01	2.25	0.136
OVI 3D-6P	100000.	0.732	0.859E-03	*5.30	*-0.120
304.4 A	200000.	0.598	0.120E-01	*4.62	*-0.470E-01
C= 0.97E+19	500000.	0.459	0.296E-01	3.76	0.967E-01
	1000000.	0.376	0.244E-01	3.18	0.204
OVI 4S-5P	100000.	4.60	-0.732E-01		
986.3 A	200000.	3.67	-0.164E-01		
C= 0.17E+21	500000.	2.78	0.178E-01		
	1000000.	2.26	0.137E-01		
OVI 4S-6P	100000.	3.83	-0.504E-01		
664.7 A	200000.	3.12	0.233E-02		
C= 0.46E+20	500000.	2.39	0.834E-01		
	1000000.	1.96	0.679E-01		
OVI 4P-5S	100000.	5.43	0.371		
1172.1 A	200000.	4.30	0.401		
C= 0.48E+21	500000.	3.23	0.416		
	1000000.	2.62	0.336		
OVI 4P-6S	100000.	3.65	0.300		
731.5 A	200000.	2.94	0.372		
C= 0.16E+21	500000.	2.23	0.398		
	1000000.	1.81	0.316		

PERTURBER DENSITY = 0.1D+22(cm-3) = 0.1D+23(cm-3)

OVI 2S-2P	200000.	10.5	-0.171	*6.62	*-0.105E-01
1033.8 A	500000.	6.94	-0.309	*5.05	*-0.165E-01
C=0.10E+25	1000000.	5.25	-0.306	4.16	-0.146E-01
	1500000.	4.52	-0.307	3.73	-0.736E-02
OVI 2S-3P	200000.	0.842	-0.152E-01		
150.1 A	500000.	0.609	-0.385E-02	*6.83	*0.188E-02
C=0.19E+22	1000000.	0.485	-0.473E-03	*6.12	*0.102E-01
	1500000.	0.429	0.315E-02	*5.72	*0.709E-01
OVI 2S-4P	200000.	*1.26	*-0.212E-01		
115.8 A	500000.	0.996	-0.577E-02		
C=0.47E+21	1000000.	0.833	0.221E-02		
	1500000.	0.752	0.161E-01		
OVI 2S-5P	200000.	*1.95	*-0.158E-01		
104.8 A	500000.	*1.68	*-0.328E-02		
C=0.20E+21	1000000.	1.48	0.181E-01		
	1500000.	1.36	0.444E-01		

© European Southern Observatory • Provided by the NASA Astrophysics Data System

1992A&AS...93..359D

TABLE 1. *(continued)*

PERTURBER DENSITY = 0.1D+22(cm-3)				= 0.1D+23(cm-3)	
		ELECTRONS		ELECTRONS	
TRANSITION	T(K)	WIDTH(A)	SHIFT(A)	WIDTH(A)	SHIFT(A)
OVI 2S-6P	200000.			5.98	-0.859
99.7 A	500000.	*2.65	*0.442E-02	4.89	-0.192
C=0.10E+21	1000000.	*2.43	*0.371E-01	4.07	0.121
	1500000.	*2.29	*0.755E-01	3.65	0.257
OVI 2P-3S	200000.	0.848	0.252E-01	*3.99	*-1.53
184.1 A	500000.	0.609	0.526E-01	4.45	-0.484
C=0.89E+22	1000000.	0.485	0.670E-01	4.31	-0.725E-01
	1500000.	0.428	0.727E-01	4.09	0.180
OVI 2P-4S	200000.	1.08	-0.526E-01		
132.3 A	500000.	0.850	0.519E-01		
C=0.19E+22	1000000.	0.705	0.820E-01		
	1500000.	0.629	0.108		
OVI 2P-5S	200000.	1.54	-0.174		
117.4 A	500000.	1.37	0.229E-01		
C=0.74E+21	1000000.	1.19	0.930E-01		
	1500000.	1.08	0.172		
OVI 2P-6S	200000.	1.93	-0.325	*5.53	*0.188
110.7 A	500000.	1.99	-0.296E-01	4.00	0.161
C=0.37E+21	1000000.	1.84	0.108	3.22	0.149
	1500000.	1.71	0.283	2.87	0.127
OVI 2P-3D	200000.	0.651	0.233E-01		
173.0 A	500000.	0.461	0.118E-01		
C=0.25E+22	1000000.	0.364	0.924E-02		
	1500000.	0.320	0.482E-02		

TABLE 2. *The same as in Table 1 but for the perturber density* 10^{15} cm^{-3}.

PERTURBER DENSITY = 0.1D+16(cm-3)							
		ELECTRONS		PROTONS		IONIZED HELIUM	
TRANSITION	T(K)	WIDTH(A)	SHIFT(A)	WIDTH(A)	SHIFT(A)	WIDTH(A)	SHIFT(A)
OVI 5S-5P	100000.	0.218	-0.643E-02	0.131E-01	0.102E-01	0.130E-01	0.849E-02
18552.9 A	150000.	0.191	-0.647E-02	0.148E-01	0.114E-01	0.143E-01	0.948E-02
C= 0.61E+19	200000.	0.174	-0.657E-02	0.159E-01	0.123E-01	0.155E-01	0.103E-01
	500000.	0.132	-0.708E-02	0.207E-01	0.156E-01	0.186E-01	0.129E-01
OVI 6S-6P	100000.	1.48	-0.507E-01	0.102	0.799E-01	0.981E-01	0.661E-01
32786.9 A	150000.	1.30	-0.518E-01	0.114	0.889E-01	0.108	0.735E-01
C= 0.11E+20	200000.	1.20	-0.560E-01	0.122	0.953E-01	0.117	0.796E-01
	500000.	0.910	-0.498E-01	0.151	0.115	0.134	0.958E-01

TABLE 3. *Comparison between the experimental Stark full half width for* $3s^2S_{1/2} - 3p^2P_{1/2}$ *O VI line* (W_M*-Böttcher et al. 1988), with different Stark width (W in Å) calculations at the electron density* $N = 1.8 \times 10^{18} cm^{-3}$ *and* $T =$ *145 000 K.* W_{DSB} *: present semiclassical calculations;* W_S *: quantum mechanical calculations (Seaton 1988);* W_{DK} *: modified semiempirical method (Dimitrijević & Konjević 1980), calculated by Böttcher et al. (1988);* W_G *: simplified semiclassical approach (Griem 1974), calculated by Böttcher et al. (1988);* W_{HB1} *: quasiclassical Gaunt factor approach (Hey & Breger 1980a,b), calculated by Böttcher et al. (1988);* W_{HB2} *: quasiclassical Gaunt factor approach (Hey and Breger, 1980c, 1982), calculated by Böttcher et al. (1988);* W_B *: simplified approach of Baranger (1962), calculated by Böttcher et al. (1988);* W_P *: estimate based on regularities (Purić et al. 1987, 1988), calculated by Böttcher et al. (1988).*

O VI $3s^2S_{1/2}$-$3p^2P_{1/2}$, λ=3811.3 Å, T=145,000 K, N=1.8 $10^{18}cm^{-3}$								
W_M(Å)	W_{DSB}(Å)	W_S(Å)	W_{DK}(Å)	W_G(Å)	W_{HB1}(Å)	W_{HB2}(Å)	W_B(Å)	W_P(Å)
2.78	1.67	1.01	1.13	1.36	1.01	1.28	2.16	2.24

© European Southern Observatory • Provided by the NASA Astrophysics Data System

1992A&AS...93..359D

TABLE 4. *Comparison between Seaton's (1988) calculations of thermally averaged collision strengths for line profiles in O VI, and ours.*

PERTURBER DENSITY = 0.1D+18
THERMALLY AVERAGED COLLISION STRENGTH GAMMA FOR LINE PROFILES IN O VI

TRANSITION	T(K)	PRESENT RESULTS REAL	PRESENT RESULTS IMAGINARY	SEATON(1988) REAL	SEATON(1988) IMAGINARY
OVI 2S-2P	125000.	9.30	-0.487	5.9	-3.0
1033.8 A	250000.	9.65	-0.658	5.3	-2.3
C= 0.10D+21	500000.	10.0	-1.11	5.2	-2.0
	1000000.	10.7	-1.43	5.4	-2.0
OVI 2S-3P	125000.	37.7	1.54	25.	12.
150.1 A	250000.	40.4	2.08	24.	13.
C= 0.19D+18	500000.	44.3	2.62	24.	15.
	1000000.	49.6	2.82	24.	21.
OVI 2P-3S	125000.	23.8	4.46	20.	17.
184.1 A	250000.	25.7	6.84	23.	17.
C= 0.89D+18	500000.	28.3	9.22	24.	18.
	1000000.	31.8	12.4	25.	20.
OVI 2P-3D	125000.	22.1	-1.07	10.5	11.
173.0 A	250000.	23.4	-1.14	10.5	12.
C= 0.25D+18	500000.	25.2	-1.27	10.5	12.
	1000000.	28.0	-0.915	10.3	13.
OVI 3S-3P	125000.	52.0	-2.41	32.	-1.5
3820.0 A	250000.	56.3	-4.09	35.	-1.3
C= 0.12D+21	500000.	62.5	-5.48	37.	-1.1
	1000000.	70.6	-8.12	38.	-1.0
OVI 3P-3D	125000.	41.4	-3.10	24.	-4.4
11850.0 A	250000.	44.9	-3.88	25.	-4.8
C= 0.12D+22	500000.	49.8	-5.01	25.	-5.4
	1000000.	56.2	-5.17	25.	-6.1

TABLE 5. *Comparison between various contributions to the total width (FWHM) of the 3s-6p and 3d-6p O VI multiplets at $T = 100\ 000$ K and $N = 10^{15}$ cm^{-3}. The shift is also given for comparison. COLL.UPPER = contribution of inelastic collisions originating from the upper level. COLL.LOWER = idem, but from the lower level. STRONG.COLL = contribution of strong collisions. ELAST.COLL. = contribution of elastic collisions, upper + lower levels.*

	OVI 3S-6P	3D-6P
	T=100000 K	
COLLISIONS WITH ELECTRONS		
COL. UPPER :	0.123E+13	0.123E+13
COL. LOWER :	0.446E+11	0.232E+11
STRONG COL. :	0.238E+12	0.235E+12
ELAST. COL. :	0.371E+12	0.365E+12
TOTAL WIDTH :	0.165E+13	0.162E+13
SHIFT :	0.108E+12	0.115E+12
COLLISIONS WITH POSITIVE IONS		
TOTAL WIDTH :	0.318E+12	0.162E+13
SHIFT :	0.295E+12	0.115E+12

© European Southern Observatory • Provided by the NASA Astrophysics Data System

1992A&AS...93..359D

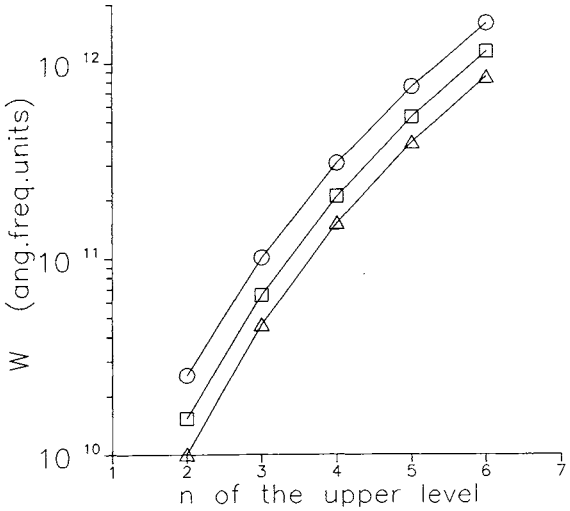

FIGURE 1. Electron-impact widths along the O VI $2s^2S$ - np^2P^0 series as a function of n for $T = 100\ 000$ K (o); 300 000 K (□), and 800 000 K (△) at $N = 10^{15}$ cm^{-3} (angular frequency units).

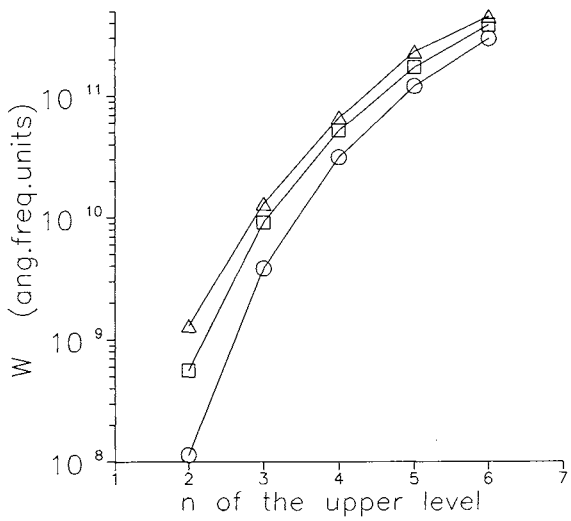

FIGURE 2. As in Figure 1 but for the proton-impact widths.

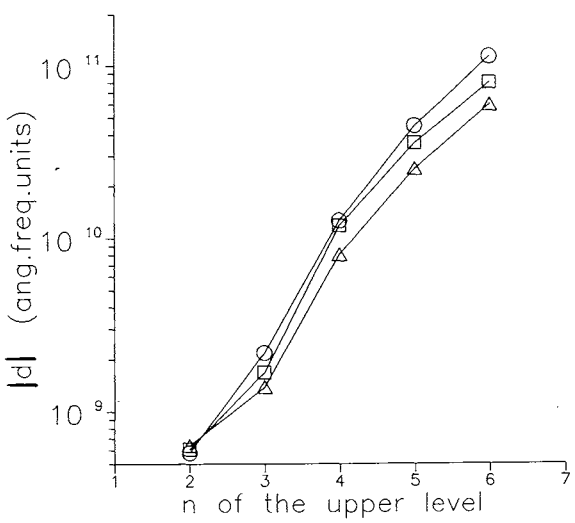

FIGURE 3. As in Figure 1 but for the electron-impact shifts.

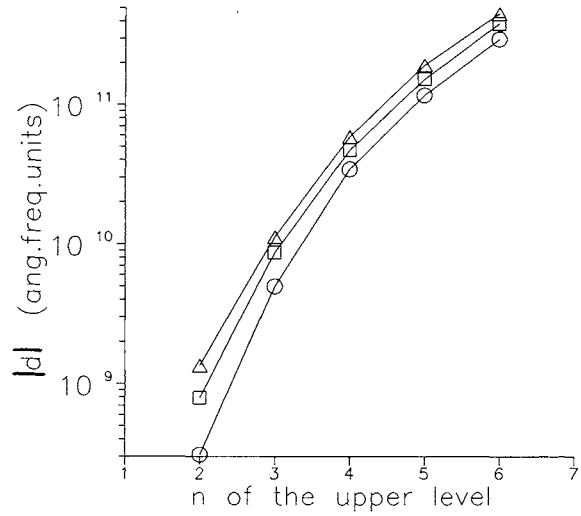

FIGURE 4. As in Figure 1 but for the proton-impact shifts.

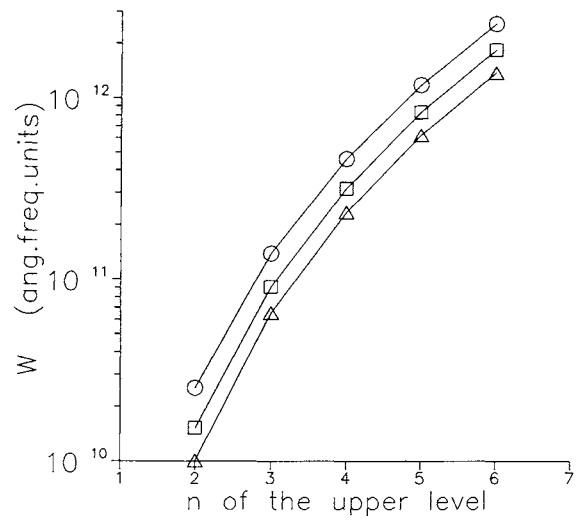

FIGURE 5. As in Figure 1 but for ns-np transitions.

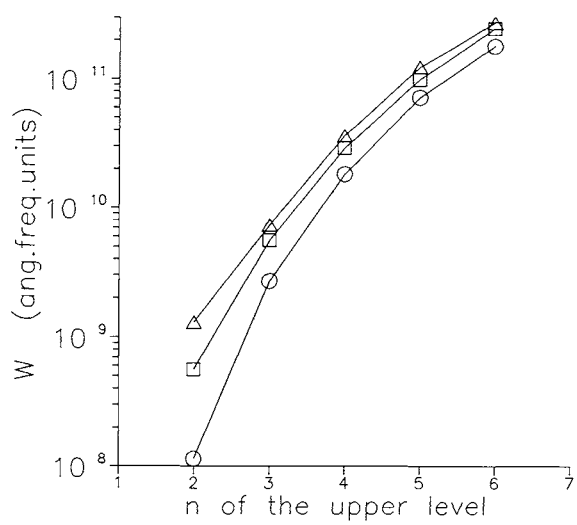

FIGURE 6. As in Figure 2 but for ns-np transitions.

© European Southern Observatory • Provided by the NASA Astrophysics Data System

1992A&AS...93..359D

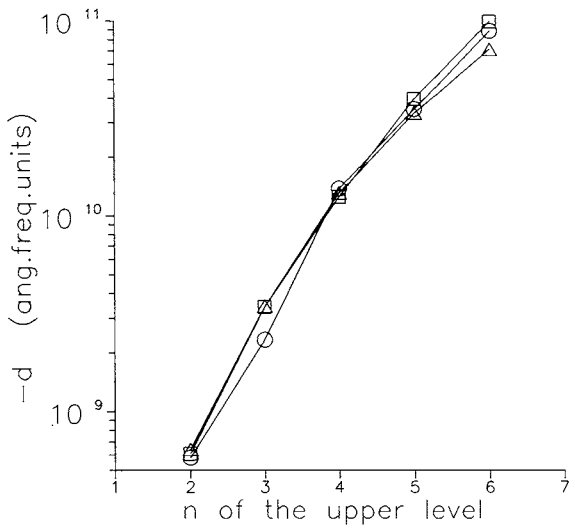

FIGURE 7. As in Figure 3 but for ns-np transitions.

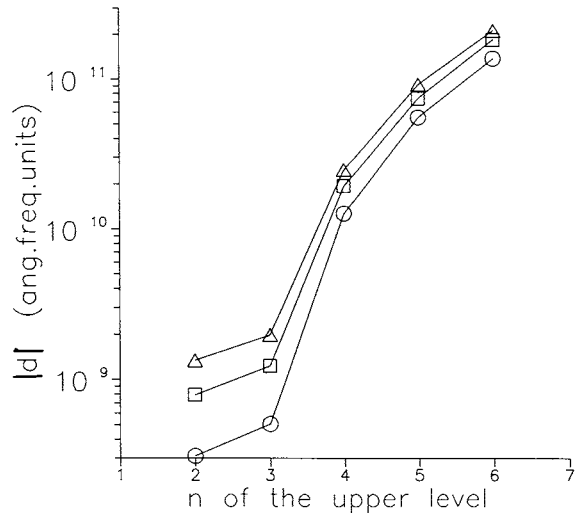

FIGURE 8. As in Figure 4 but for ns-np transitions.

© European Southern Observatory • Provided by the NASA Astrophysics Data System

1992A&AS...95..109D

ASTRONOMY & ASTROPHYSICS
SUPPLEMENT SERIES

Astron. Astrophys. Suppl. Ser. **95**, 109-120 (1992)

Stark broadening of spectral lines of multicharged ions of astrophysical interest. IV. N V lines

M.S. Dimitrijević[1] and S. Sahal-Bréchot[2]

[1] Astronomical Observatory, Volgina 7, 11050 Beograd
[2] Laboratoire"Astrophysique, Atomes et Molécules", Unité associée au C.N.R.S. N° 812, Département Atomes et Molécules en Astrophysique, Observatoire de Paris-Meudon, 92190 Meudon, France

Received September 17; accepted December 24, 1991

Abstract. — Using a semiclassical approach, we have calculated electron-, proton-, and ionized helium-impact line widths and shifts for 30 N V multiplets. The obtained data have been compared with the existing experimental values.

Key words: line profile; atomic data; Stark broadening.

1. Introduction.

Stark broadening of multicharged ion spectral lines has a new interest in Astrophysics owing to the recent development of research on the physics of the stellar interiors (Seaton 1987). Moreover, the knowledge of N V Stark broadening parameters is useful also for the spectroscopic diagnostic in atmospheres of hot stars and for the investigation of hot dense plasmas in the laboratory (see e.g. Böttcher *et al.* 1987, 1988; Purić *et al.* 1987), due to its presence as an impurity in many laboratory plasma sources.

This paper is the fourth of a series devoted to the calculation of Stark broadening parameters of spectral lines of multicharged ions. The first three were concerned with C IV, Si IV and O VI lines (Dimitrijević *et al.* 1991ab, Dimitrijević & Sahal-Bréchot 1992, hereafter referred as Papers I, II and III).

By using the semiclassical-perturbation formalism (Sahal-Bréchot 1969ab) we have calculated electron-, proton-, and ionized helium-impact line widths and shifts for 30 N V multiplets. A summary of the formalism is given in Paper I. In the present paper we present and discuss the results for N V, along with a comparison with experimental data (Böttcher *et al.* 1987, 1988; Purić *et al.* 1987).

2. Results and discussion.

Energy levels for N V lines have been taken from Bashkin & Stoner (1975). Oscillator strengths have been calculated by using the method of Bates & Damgaard (1949) and the tables of Oertel & Shomo (1968). For higher levels, the method described by Van Regemorter *et al.* (1979) has been used.

In addition to the electron-impact full halfwidths and shifts, the Stark broadening parameters due to proton and ionized helium He^+ impacts have been calculated. At high temperatures helium is ionized twice; yet the Stark broadening parameters due to the He^{++} have not been provided, because they are very small: the increase of the Coulomb repulsion entails a decrease of the line widths. Besides, owing to the neutrality plasma condition, the electron density is increased by the fact that helium is twice ionized and thus the relative contribution of the electron impact broadening is more important. Thus we have provided Stark broadening data for all the important charged perturbers in stellar atmospheres. Our results are shown in Table 1 for perturber densities $10^{17} - 10^{21}$ cm^{-3} and temperatures of T = 50,000 - 1,000,000 K. For perturber densities lower than 10^{17} cm^{-3} all the corresponding data are practically linear with density for the majority of the considered multiplets, because the effect of Debye screening is negligible for low excited levels. In Table 2, the exceptions are given together with the data for 4p-4d, 5s-5d multiplets at perturber densities 10^{15} cm^{-3} and 10^{16} cm^{-3}. We also specify a parameter (Dimitrijević & Sahal-Bréchot 1984), which gives an estimate for the maximum perturber density for which the line may be treated as isolated when it is divided by 2W.

For each value given in Tables 1 and 2, the collision volume (V) multiplied by the perturber density (N) is much less than one and the impact approximation is valid

© European Southern Observatory • Provided by the NASA Astrophysics Data System

1992A&AS...95..109D

(Sahal-Bréchot 1969ab). Values for $NV > 0.5$ are not given in the Table 1; values for $0.1 < NV \leq 0.5$ are denoted by an asterisk. When the impact approximation is not valid, the ion broadening contribution may be estimated by using quasistatic estimations (Sahal-Bréchot 1991, see also Paper I). One must be aware of the fact that the accuracy of the obtained results decreases when the broadening by ion interactions is important.

In Table 3 our results for the 3s-3p multiplets are compared with the experimental results and the calculations of Böttcher *et al.* (1988). The latter were performed using the simplified semiclassical method (Griem 1974), the modified semiempirical approach (Dimitrijević & Konjević 1980), the two variants of the quasiclassical Gaunt factor approximation of Hey & Breger (1980a, b, c; 1982), the approach of Baranger (1962) and the simple estimates based on regularities and systematic trends (Purić *et al.* 1987, 1988).

In Table 4 we compare our results with the experimental data of Purić *et al.* (1987) and Böttcher *et al.* (1987) as well as with the calculations (Böttcher *et al.* 1987) obtained by using the simplified semiclassical method (Griem 1974) and the simple estimates of Purić *et al.* (1987). Our results are in reasonable agreement with experimental data for the 3s-3p multiplet but disagree considerably with experimental values for the 3p-4d and 3d-4f lines. As a matter of fact, as shown in Table 1, the impact approximation for proton and He^+ collisions is neighbouring its limit of validity at the density of the experiment ($7.7 \times 10^{17} cm^{-3}$), but this cannot account for the discrepancy; actually the ion broadening cannot be due to collisions with multicharged ions in spite of the high temperature (124000 K): first, the carrier gas is hydrogen and nitrogen is only an impurity (1%); secondly, as aforesaid, the broadening by multicharged ions is very small, owing to the increase of the Coulomb repulsion. This is true in the frame of the impact approximation as well as in the frame of the quasistatic approximation (Sahal-Bréchot 1991). Thus the origin of the discrepancy is left unexplained.

In Figure 1 our results are compared with the experimental data (Böttcher *et al.* 1988) and with other calculations for the 3s-3p transition in the C IV, N V, O VI segment of the Li isoelectronic sequence. We can see that a regular behaviour exists but additional experimental and theoretical work for the investigated case is needed as well as the extension to the other members of the Li isoelectronic sequence.

Acknowledgements.

One of us (M.D.) has been supported by the Observatory of Paris-Meudon. This work has also been supported by the French C.N.R.S. and is a part of a French-Yugoslav collaboration through the project "L'élargissement Stark des raies spectrales des plasmas astrophysiques et de laboratoire"; it is also a part of the project "Physics and dynamics of celestial bodies", supported by RFN of Serbia.

References

Baranger M. 1962, in Atomic and Molecular Processes, Ed. D. R. Bates (Academic Press, New York)
Bashkin S. and Stoner J.O.Jr. 1975, Atomic Energy Levels and Grotrian Diagrams, Vol.1 (North Holland, Amsterdam)
Bates D.R. and Damgaard A. 1949, Trans. Roy. Soc. London Ser. A 242, 101
Böttcher F., Breger P., Hey J.D., Kunze H.-J. 1988, Phys. Rev. 38, 2690
Böttcher F., Musielok J., Kunze H.-J 1987, Phys. Rev. 36, 2265
Dimitrijević M.S., Konjević N. 1980, JQSRT 24, 451
Dimitrijević M.S. and Sahal-Bréchot S. 1984, JQSRT 31, 301
Dimitrijević M.S., Sahal-Bréchot S. and Bommier V. 1991a, A&AS 89, 581 (Paper I)
Dimitrijević M.S., Sahal-Bréchot S. and Bommier V. 1991b, A&AS 89, 591 (Paper II)
Dimitrijević M.S. and Sahal-Bréchot S. 1992, A&AS 93, 359 (Paper III)
Griem H.R. 1974, Spectral Line Broadening by Plasmas (Academic Press, New York)
Hey J.D. and Breger P. 1980a, JQSRT 24, 349
Hey J.D. and Breger P. 1980b, JQSRT 24, 427
Hey J.D. and Breger P. 1980c, JQSRT 23, 311
Hey J.D. and Breger P. 1982, S. Afr. J. Phys. 5, 111
Oertel G.K. and Shomo L.P. 1968, ApJS 16, 175
Purić J., Djeniže S., Srećković A., Platiša M., Labat J. 1988, Phys. Rev. A 37, 498
Purić J., Srećković A., Djeniže S., Platiša M. 1987 Phys. Rev. A 36, 3957
Sahal-Bréchot S. 1969a, A&A 1, 31
Sahal-Bréchot S. 1969b, A&A 2, 322
Sahal-Bréchot S. 1991, A&A 5, 322
Seaton M.J. 1987, J. Phys.B 20, 6363
Van Regemorter H., Hoang Binh Dy and Prud'homme M. 1979, J. Phys. B 12, 1073

© European Southern Observatory • Provided by the NASA Astrophysics Data System

1992A&AS...95..109D

TABLE 1. *This table shows electron-, proton-, and ionized- helium- impact broadening parameters for N V lines, for perturber densities of* $10^{17} - 10^{21} cm^{-3}$ *and temperatures from 50 000 K to 1 000 000 K. Transitions and averaged wavelengths for the multiplet (in Å) are also given. By using c (see Eq. (5) of Paper I), we obtain an estimate for the maximum perturber density for which the line may be treated as isolated and tabulated data may be used. The asterisk identifies cases for which the collision volume multiplied by the perturber density (the condition for validity of the impact approximation) lies between 0.1 and 0.5. Data for densities N lower than* $10^{17} cm^{-3}$ *can be obtained by multiplying the results given at* $10^{17} cm^{-3}$ *by* $N/10^{17}$.

PERTURBER DENSITY = 0.1D+18(cm-3)

PERTURBERS ARE		ELECTRONS		PROTONS		IONIZED HELIUM	
TRANSITION	T(K)	WIDTH(A)	SHIFT(A)	WIDTH(A)	SHIFT(A)	WIDTH(A)	SHIFT(A)
N V 2S-2P	50000.	0.358E-02	-0.371E-04	0.988E-05	-0.261E-04	0.173E-04	-0.260E-04
1240.2 A	100000.	0.253E-02	-0.804E-04	0.294E-04	-0.512E-04	0.448E-04	-0.495E-04
C= 0.12E+21	200000.	0.184E-02	-0.701E-04	0.705E-04	-0.880E-04	0.895E-04	-0.812E-04
	500000.	0.125E-02	-0.832E-04	0.146E-03	-0.142E-03	0.156E-03	-0.124E-03
N V 2S-3P	50000.	0.402E-03	0.735E-05	0.105E-04	0.142E-04	0.139E-04	0.132E-04
209.3 A	100000.	0.301E-03	0.783E-05	0.200E-04	0.215E-04	0.224E-04	0.192E-04
C= 0.29E+18	200000.	0.231E-03	0.699E-05	0.320E-04	0.293E-04	0.307E-04	0.244E-04
	500000.	0.168E-03	0.622E-05	0.429E-04	0.371E-04	0.403E-04	0.312E-04
N V 2S-4P	50000.	0.745E-03	0.325E-04	0.543E-04	0.609E-04	0.575E-04	0.531E-04
162.6 A	100000.	0.578E-03	0.307E-04	0.823E-04	0.785E-04	0.767E-04	0.661E-04
C= 0.73E+17	200000.	0.458E-03	0.292E-04	0.106E-03	0.951E-04	0.938E-04	0.783E-04
	500000.	0.344E-03	0.208E-04	0.138E-03	0.119E-03	0.119E-03	0.957E-04
N V 2S-5P	50000.	0.150E-02	0.849E-04	0.180E-03	0.172E-03	0.168E-03	0.144E-03
147.4 A	100000.	0.120E-02	0.857E-04	0.230E-03	0.215E-03	0.208E-03	0.177E-03
C= 0.31E+17	200000.	0.973E-03	0.735E-04	0.296E-03	0.254E-03	0.253E-03	0.212E-03
	500000.	0.741E-03	0.521E-04	0.381E-03	0.294E-03	0.309E-03	0.254E-03
N V 2P-3S	50000.	0.441E-03	0.290E-04	0.678E-05	0.204E-04	0.776E-05	0.190E-04
266.3 A	100000.	0.321E-03	0.343E-04	0.189E-04	0.314E-04	0.178E-04	0.278E-04
C= 0.15E+19	200000.	0.245E-03	0.353E-04	0.341E-04	0.431E-04	0.319E-04	0.360E-04
	500000.	0.178E-03	0.337E-04	0.537E-04	0.546E-04	0.462E-04	0.461E-04
N V 2P-4S	50000.	0.662E-03	0.770E-04	0.372E-04	0.597E-04	0.364E-04	0.528E-04
190.2 A	100000.	0.502E-03	0.846E-04	0.689E-04	0.810E-04	0.605E-04	0.674E-04
C= 0.32E+18	200000.	0.393E-03	0.793E-04	0.927E-04	0.973E-04	0.802E-04	0.806E-04
	500000.	0.294E-03	0.721E-04	0.127E-03	0.121E-03	0.110E-03	0.971E-04
N V 2P-5S	50000.	0.127E-02	0.219E-03	0.137E-03	0.162E-03	0.122E-03	0.133E-03
168.6 A	100000.	0.101E-02	0.204E-03	0.189E-03	0.198E-03	0.163E-03	0.165E-03
C= 0.13E+18	200000.	0.807E-03	0.189E-03	0.239E-03	0.238E-03	0.205E-03	0.195E-03
	500000.	0.612E-03	0.156E-03	0.305E-03	0.284E-03	0.250E-03	0.223E-03
N V 2P-3D	50000.	0.336E-03	-0.996E-05	0.695E-05	-0.146E-04	0.893E-05	-0.135E-04
247.7 A	100000.	0.247E-03	-0.571E-05	0.167E-04	-0.230E-04	0.172E-04	-0.201E-04
C= 0.40E+18	200000.	0.186E-03	-0.593E-05	0.281E-04	-0.317E-04	0.279E-04	-0.268E-04
	500000.	0.133E-03	-0.275E-05	0.425E-04	-0.406E-04	0.383E-04	-0.340E-04
N V 2P-4D	50000.	0.932E-03	0.215E-04	0.278E-03	0.300E-03	0.249E-03	0.252E-03
186.1 A	100000.	0.741E-03	0.221E-04	0.369E-03	0.372E-03	0.312E-03	0.311E-03
C= 0.88E+16	200000.	0.593E-03	0.144E-04	0.463E-03	0.440E-03	0.411E-03	0.363E-03
	500000.	0.443E-03	0.102E-04	0.567E-03	0.508E-03	0.521E-03	0.440E-03
N V 2P-5D	50000.	0.222E-02	0.317E-04				
166.9 A	100000.	0.182E-02	0.672E-04*	0.180E-02*	0.170E-02		
C= 0.21E+16	200000.	0.147E-02	0.444E-04*	0.206E-02*	0.194E-02		
	500000.	0.110E-02	0.251E-04*	0.256E-02*	0.214E-02*	0.187E-02*	0.201E-02
N V 3S-3P	50000.	0.274	-0.438E-02	0.379E-02	0.134E-02	0.543E-02	0.131E-02
4610.9 A	100000.	0.206	-0.528E-02	0.687E-02	0.241E-02	0.835E-02	0.224E-02
C= 0.14E+21	200000.	0.159	-0.616E-02	0.988E-02	0.362E-02	0.110E-01	0.322E-02
	500000.	0.117	-0.592E-02	0.125E-01	0.522E-02	0.131E-01	0.442E-02
N V 3S-4P	50000.	0.126E-01	0.340E-03	0.773E-03	0.855E-03	0.829E-03	0.749E-03
628.8 A	100000.	0.975E-02	0.291E-03	0.117E-02	0.111E-02	0.111E-02	0.937E-03
C= 0.11E+19	200000.	0.772E-02	0.259E-03	0.147E-02	0.134E-02	0.136E-02	0.112E-02
	500000.	0.581E-02	0.145E-03	0.185E-02	0.167E-02	0.172E-02	0.138E-02

© European Southern Observatory • Provided by the NASA Astrophysics Data System

1992A&AS...95..109D

TABLE 1. *(continued)*

PERTURBER DENSITY = 0.1D+18(cm-3)

PERTURBERS ARE		ELECTRONS		PROTONS		IONIZED HELIUM	
TRANSITION	T(K)	WIDTH(A)	SHIFT(A)	WIDTH(A)	SHIFT(A)	WIDTH(A)	SHIFT(A)
N V 3S-5P	50000.	0.148E-01	0.714E-03	0.167E-02	0.159E-02	0.156E-02	0.133E-02
450.1 A	100000.	0.118E-01	0.711E-03	0.211E-02	0.198E-02	0.193E-02	0.164E-02
C= 0.28E+18	200000.	0.952E-02	0.594E-03	0.271E-02	0.235E-02	0.232E-02	0.196E-02
	500000.	0.724E-02	0.400E-03	0.354E-02	0.276E-02	0.287E-02	0.236E-02
N V 3P-4S	50000.	0.149E-01	0.115E-02	0.580E-03	0.881E-03	0.575E-03	0.785E-03
778.0 A	100000.	0.114E-01	0.126E-02	0.104E-02	0.122E-02	0.947E-03	0.101E-02
C= 0.40E+19	200000.	0.896E-02	0.120E-02	0.144E-02	0.146E-02	0.125E-02	0.121E-02
	500000.	0.671E-02	0.109E-02	0.197E-02	0.180E-02	0.166E-02	0.152E-02
N V 3P-5S	50000.	0.131E-01	0.194E-02	0.122E-02	0.145E-02	0.111E-02	0.119E-02
510.0 A	100000.	0.104E-01	0.180E-02	0.172E-02	0.178E-02	0.148E-02	0.148E-02
C= 0.12E+19	200000.	0.837E-02	0.167E-02	0.213E-02	0.212E-02	0.184E-02	0.174E-02
	500000.	0.636E-02	0.138E-02	0.273E-02	0.252E-02	0.232E-02	0.199E-02
N V 3P-3D	50000.	2.36	-0.821E-01	0.663E-01	-0.122	0.813E-01	-0.111
15148.3 A	100000.	1.79	-0.746E-01	0.134	-0.177	0.139	-0.155
C= 0.15E+22	200000.	1.38	-0.694E-01	0.219	-0.226	0.200	-0.191
	500000.	1.02	-0.553E-01	0.303	-0.288	0.269	-0.241
N V 3P-4D	50000.	0.154E-01	0.214E-03	0.404E-02	0.436E-02	0.359E-02	0.367E-02
713.8 A	100000.	0.122E-01	0.205E-03	0.536E-02	0.540E-02	0.452E-02	0.453E-02
C= 0.13E+18	200000.	0.983E-02	0.107E-03	0.674E-02	0.638E-02	0.592E-02	0.530E-02
	500000.	0.736E-02	0.499E-04	0.819E-02	0.735E-02	0.740E-02	0.641E-02
N V 3P-5D	50000.	0.204E-01	0.229E-03				
495.3 A	100000.	0.166E-01	0.534E-03*	0.158E-01*	0.149E-01		
C= 0.19E+17	200000.	0.135E-01	0.340E-03*	0.182E-01*	0.171E-01		
	500000.	0.101E-01	0.173E-03*	0.226E-01*	0.188E-01*	0.165E-01*	0.177E-01
N V 3D-4P	50000.	0.171E-01	0.831E-03	0.120E-02	0.142E-02	0.125E-02	0.124E-02
764.9 A	100000.	0.133E-01	0.764E-03	0.183E-02	0.181E-02	0.170E-02	0.154E-02
C= 0.16E+19	200000.	0.105E-01	0.729E-03	0.237E-02	0.219E-02	0.208E-02	0.184E-02
	500000.	0.794E-02	0.518E-03	0.316E-02	0.275E-02	0.266E-02	0.221E-02
N V 3D-5P	50000.	0.200	0.868E-02	0.192E-01	0.188E-01	0.177E-01	0.158E-01
1583.6 A	100000.	0.160	0.889E-02	0.246E-01	0.231E-01	0.218E-01	0.193E-01
C= 0.35E+19	200000.	0.130	0.752E-02	0.307E-01	0.279E-01	0.254E-01	0.227E-01
	500000.	0.987E-01	0.539E-02	0.403E-01	0.333E-01	0.325E-01	0.283E-01
N V 3D-4F	50000.	0.927E-02	-0.379E-03	0.370E-02	-0.410E-02	0.321E-02	-0.343E-02
747.6 A	100000.	0.729E-02	-0.337E-03	0.493E-02	-0.505E-02	0.422E-02	-0.419E-02
C= 0.14E+18	200000.	0.581E-02	-0.209E-03	0.615E-02	-0.606E-02	0.513E-02	-0.489E-02
	500000.	0.437E-02	-0.875E-04	0.813E-02	-0.737E-02	0.638E-02	-0.613E-02
N V 3D-5F	50000.	0.177E-01	-0.191E-03				
511.8 A	100000.	0.147E-01	-0.269E-03				
C= 0.20E+16	200000.	0.120E-01	-0.306E-03				
	500000.	0.896E-02	-0.121E-03				
N V 4S-4P	50000.	5.56	-0.102	0.169	0.127	0.198	0.110
11345.1 A	100000.	4.32	-0.140	0.251	0.177	0.255	0.151
C= 0.36E+21	200000.	3.44	-0.132	0.306	0.216	0.301	0.180
	500000.	2.61	-0.147	0.389	0.275	0.362	0.225
N V 4S-5P	50000.	0.162	0.369E-02	0.149E-01	0.140E-01	0.139E-01	0.117E-01
1389.6 A	100000.	0.129	0.330E-02	0.190E-01	0.173E-01	0.171E-01	0.143E-01
C= 0.27E+19	200000.	0.105	0.244E-02	0.232E-01	0.208E-01	0.201E-01	0.168E-01
	500000.	0.797E-01	0.902E-03	0.295E-01	0.252E-01	0.240E-01	0.210E-01

© European Southern Observatory • Provided by the NASA Astrophysics Data System

1992A&AS...95..109D

TABLE 1. *(continued)*

PERTURBER DENSITY = 0.1D+18(cm-3)

PERTURBERS ARE		ELECTRONS		PROTONS		IONIZED HELIUM	
TRANSITION	T(K)	WIDTH(A)	SHIFT(A)	WIDTH(A)	SHIFT(A)	WIDTH(A)	SHIFT(A)
N V 4P-5S	50000.	0.198	0.182E-01	0.109E-01	0.127E-01	0.106E-01	0.107E-01
1702.9 A	100000.	0.158	0.170E-01	0.154E-01	0.156E-01	0.138E-01	0.132E-01
C= 0.80E+19	200000.	0.128	0.158E-01	0.199E-01	0.186E-01	0.169E-01	0.154E-01
	500000.	0.973E-01	0.134E-01	0.247E-01	0.226E-01	0.212E-01	0.188E-01
N V 4P-5D	50000.	0.230	-0.317E-03				
1549.1 A	100000.	0.187	0.286E-02	*0.154	*0.145		
C= 0.18E+18	200000.	0.152	0.106E-02	*0.175	*0.167		
	500000.	0.114	0.143E-03	*0.226	*0.182	*0.156	*0.171
N V 4D-5P	50000.	0.235	0.908E-02	0.956E-02	-0.507E-02	0.106E-01	-0.446E-02
1655.9 A	100000.	0.190	0.920E-02	0.119E-01	-0.676E-02	0.123E-01	-0.566E-02
C= 0.69E+18	200000.	0.154	0.826E-02	0.140E-01	-0.813E-02	0.140E-01	-0.686E-02
	500000.	0.117	0.592E-02	0.161E-01	-0.993E-02	0.155E-01	-0.831E-02
N V 4D-5F	50000.	0.215	-0.397E-02				
1616.3 A	100000.	0.179	-0.461E-02				
C= 0.20E+17	200000.	0.146	-0.440E-02				
	500000.	0.109	-0.210E-02				

PERTURBER DENSITY = 0.1D+19(cm-3)

N V 2S-2P	50000.	0.357E-01	-0.104E-03	0.987E-04	-0.247E-03	0.173E-03	-0.246E-03
1240.2 A	100000.	0.255E-01	-0.776E-03	0.294E-03	-0.506E-03	0.448E-03	-0.489E-03
C= 0.12D+22	200000.	0.184E-01	-0.736E-03	0.705E-03	-0.879E-03	0.895E-03	-0.811E-03
	500000.	0.125E-01	-0.832E-03	0.146E-02	-0.142E-02	0.156E-02	-0.124E-02
N V 2S-3P	50000.	0.402E-02	0.608E-04	0.105E-03	0.133E-03	0.139E-03	0.123E-03
209.3 A	100000.	0.301E-02	0.747E-04	0.200E-03	0.211E-03	0.224E-03	0.188E-03
C= 0.29D+19	200000.	0.231E-02	0.701E-04	0.320E-03	0.293E-03	0.307E-03	0.243E-03
	500000.	0.168E-02	0.622E-04	0.429E-03	0.370E-03	0.403E-03	0.312E-03
N V 2S-4P	50000.	0.745E-02	0.258E-03	0.539E-03	0.550E-03	*0.574E-03	*0.473E-03
162.6 A	100000.	0.578E-02	0.279E-03	0.823E-03	0.760E-03	0.766E-03	0.637E-03
C= 0.73D+18	200000.	0.458E-02	0.289E-03	0.106E-02	0.948E-03	0.938E-03	0.780E-03
	500000.	0.344E-02	0.208E-03	0.138E-02	0.119E-02	0.119E-02	0.954E-03
N V 2S-5P	50000.	0.150E-01	0.551E-03	*0.181E-02	*0.146E-02		
147.4 A	100000.	0.120E-01	0.743E-03	*0.230E-02	*0.204E-02		
C= 0.31D+18	200000.	0.972E-02	0.721E-03	*0.296E-02	*0.253E-02	*0.253E-02	*0.211E-02
	500000.	0.740E-02	0.521E-03	*0.381E-02	*0.292E-02	*0.309E-02	*0.252E-02
N V 2P-3S	50000.	0.438E-02	0.255E-03	0.678E-04	0.191E-03	0.777E-04	0.177E-03
266.3 A	100000.	0.322E-02	0.340E-03	0.189E-03	0.309E-03	0.178E-03	0.273E-03
C= 0.15D+20	200000.	0.245E-02	0.355E-03	0.341E-03	0.430E-03	0.319E-03	0.359E-03
	500000.	0.178E-02	0.337E-03	0.537E-03	0.545E-03	0.462E-03	0.460E-03
N V 2P-4S	50000.	0.659E-02	0.705E-03	0.371E-03	0.544E-03	0.361E-03	0.474E-03
190.2 A	100000.	0.502E-02	0.821E-03	0.689E-03	0.788E-03	0.605E-03	0.651E-03
C= 0.32D+19	200000.	0.393E-02	0.791E-03	0.927E-03	0.970E-03	0.802E-03	0.803E-03
	500000.	0.294E-02	0.721E-03	0.127E-02	0.121E-02	0.110E-02	0.968E-03
N V 2P-5S	50000.	0.126E-01	0.196E-02	*0.137E-02	*0.141E-02	*0.122E-02	*0.112E-02
168.6 A	100000.	0.101E-01	0.195E-02	*0.189E-02	*0.189E-02	*0.163E-02	*0.156E-02
C= 0.13D+19	200000.	0.807E-02	0.189E-02	*0.239E-02	*0.236E-02	*0.205E-02	*0.193E-02
	500000.	0.612E-02	0.156E-02	0.305E-02	0.283E-02	*0.250E-02	*0.222E-02
N V 2P-3D	50000.	0.336E-02	-0.108E-03	0.695E-04	-0.137E-03	0.891E-04	-0.127E-03
247.7 A	100000.	0.247E-02	-0.528E-04	0.167E-03	-0.227E-03	0.172E-03	-0.197E-03
C= 0.40D+19	200000.	0.186E-02	-0.564E-04	0.281E-03	-0.316E-03	0.279E-03	-0.268E-03
	500000.	0.133E-02	-0.275E-04	0.425E-03	-0.405E-03	0.383E-03	-0.339E-03

© European Southern Observatory • Provided by the NASA Astrophysics Data System

1992A&AS...95..109D

TABLE 1. *(continued)*

PERTURBER DENSITY = 0.1D+19(cm-3)

PERTURBERS ARE		ELECTRONS		PROTONS		IONIZED HELIUM	
TRANSITION	T(K)	WIDTH(A)	SHIFT(A)	WIDTH(A)	SHIFT(A)	WIDTH(A)	SHIFT(A)
N V 2P-4D	50000.	0.878E-02	-0.160E-03	*0.279E-02	*0.253E-02		
186.1 A	100000.	0.704E-02	0.288E-04	*0.369E-02	*0.352E-02		
C= 0.88D+17	200000.	0.568E-02	0.115E-03	*0.463E-02	*0.437E-02	*0.411E-02	*0.360E-02
	500000.	0.427E-02	0.102E-03	*0.567E-02	*0.505E-02	*0.519E-02	*0.437E-02
N V 2P-5D	50000.	0.189E-01	-0.661E-03				
166.9 A	100000.	0.158E-01	-0.131E-03				
C= 0.21D+17	200000.	0.131E-01	0.302E-03				
	500000.	0.995E-02	0.251E-03				
N V 3S-3P	50000.	2.74	-0.426E-01	0.378E-01	0.126E-01	0.541E-01	0.123E-01
4610.9 A	100000.	2.06	-0.541E-01	0.686E-01	0.238E-01	0.834E-01	0.221E-01
C= 0.14D+22	200000.	1.59	-0.616E-01	0.988E-01	0.362E-01	0.110	0.322E-01
	500000.	1.17	-0.592E-01	0.125	0.521E-01	0.131	0.441E-01
N V 3S-4P	50000.	0.126	0.253E-02	0.770E-02	0.773E-02	0.827E-02	0.669E-02
628.8 A	100000.	0.975E-01	0.250E-02	0.117E-01	0.108E-01	0.111E-01	0.903E-02
C= 0.11D+20	200000.	0.772E-01	0.255E-02	0.147E-01	0.133E-01	0.136E-01	0.112E-01
	500000.	0.581E-01	0.145E-02	0.185E-01	0.166E-01	0.172E-01	0.137E-01
N V 3S-5P	50000.	0.147	0.443E-02	*0.167E-01	*0.135E-01		
450.1 A	100000.	0.118	0.606E-02	*0.211E-01	*0.188E-01		
C= 0.28D+19	200000.	0.950E-01	0.580E-02	*0.271E-01	*0.234E-01	*0.232E-01	*0.195E-01
	500000.	0.723E-01	0.400E-02	*0.354E-01	*0.275E-01	*0.288E-01	*0.235E-01
N V 3P-4S	50000.	0.149	0.106E-01	0.578E-02	0.805E-02	0.574E-02	0.710E-02
778.0 A	100000.	0.114	0.123E-01	0.104E-01	0.118E-01	0.947E-02	0.975E-02
C= 0.40D+20	200000.	0.896E-01	0.119E-01	0.144E-01	0.146E-01	0.125E-01	0.121E-01
	500000.	0.671E-01	0.109E-01	0.197E-01	0.180E-01	0.166E-01	0.151E-01
N V 3P-5S	50000.	0.131	0.173E-01	*0.123E-01	*0.126E-01	*0.111E-01	*0.101E-01
510.0 A	100000.	0.104	0.171E-01	*0.172E-01	*0.170E-01	*0.148E-01	*0.140E-01
C= 0.12D+20	200000.	0.837E-01	0.167E-01	*0.213E-01	*0.211E-01	*0.184E-01	*0.173E-01
	500000.	0.636E-01	0.138E-01	0.273E-01	0.251E-01	*0.232E-01	*0.198E-01
N V 3P-3D	50000.	23.6	-0.748	0.664	-1.14	0.812	-1.02
15148.3 A	100000.	17.9	-0.707	1.34	-1.74	1.39	-1.52
C= 0.15D+23	200000.	13.8	-0.690	2.19	-2.26	2.00	-1.91
	500000.	10.2	-0.553	3.03	-2.88	2.69	-2.41
N V 3P-4D	50000.	0.146	-0.315E-02	*0.404E-01	*0.367E-01		
713.8 A	100000.	0.117	-0.719E-03	*0.536E-01	*0.512E-01		
C= 0.13D+19	200000.	0.945E-01	0.618E-03	*0.674E-01	*0.634E-01	*0.592E-01	*0.527E-01
	500000.	0.713E-01	0.499E-03	*0.819E-01	*0.732E-01	*0.738E-01	*0.637E-01
N V 3P-5D	50000.	0.175	-0.622E-02				
495.3 A	100000.	0.146	-0.171E-02				
C= 0.19D+18	200000.	0.120	0.214E-02				
	500000.	0.915E-01	0.173E-02				
N V 3D-4P	50000.	0.171	0.680E-02	0.120E-01	0.128E-01	*0.124E-01	*0.109E-01
764.9 A	100000.	0.133	0.697E-02	0.183E-01	0.176E-01	0.170E-01	0.148E-01
C= 0.16D+20	200000.	0.105	0.722E-02	0.237E-01	0.218E-01	0.208E-01	0.183E-01
	500000.	0.794E-01	0.518E-02	0.316E-01	0.274E-01	0.266E-01	0.220E-01
N V 3D-5P	50000.	2.00	0.555E-01	*0.189	*0.160		
1583.6 A	100000.	1.60	0.771E-01	*0.246	*0.219	*0.217	*0.181
C= 0.35D+20	200000.	1.30	0.736E-01	*0.307	*0.278	*0.254	*0.225
	500000.	0.986	0.539E-01	*0.403	*0.332	*0.325	*0.282

© European Southern Observatory • Provided by the NASA Astrophysics Data System

1992A&AS...95..109D

TABLE 1. *(continued)*

PERTURBER DENSITY = 0.1D+19(cm-3)

PERTURBERS ARE		ELECTRONS		PROTONS		IONIZED HELIUM	
TRANSITION	T(K)	WIDTH(A)	SHIFT(A)	WIDTH(A)	SHIFT(A)	WIDTH(A)	SHIFT(A)
N V 3D-4F	50000.	0.865E-01	0.939E-03	*0.369E-01	-0.348E-01	*0.321E-01	-0.285E-01
747.6 A	100000.	0.686E-01	-0.102E-02	*0.493E-01	-0.480E-01	*0.422E-01	-0.394E-01
C= 0.14D+19	200000.	0.551E-01	-0.168E-02	*0.615E-01	-0.602E-01	*0.513E-01	-0.485E-01
	500000.	0.418E-01	-0.875E-03	*0.813E-01	-0.734E-01	*0.636E-01	-0.610E-01
N V 3D-5F	50000.	0.137	0.228E-02				
511.8 A	100000.	0.118	-0.104E-02				
C= 0.20D+17	200000.	0.996E-01	-0.214E-02				
	500000.	0.767E-01	-0.121E-02				
N V 4S-5P	50000.	1.62	0.137E-01	*0.148	*0.119		
1389.6 A	100000.	1.29	0.242E-01	*0.190	*0.164		
C= 0.27D+20	200000.	1.04	0.232E-01	*0.232	*0.207	*0.201	*0.166
	500000.	0.796	0.902E-02	*0.295	*0.251	*0.240	*0.209
N V 4P-5S	50000.	1.98	0.165	0.110	0.113	*0.106	*0.917E-01
1702.9 A	100000.	1.58	0.164	0.154	0.150	*0.138	*0.125
C= 0.80D+20	200000.	1.28	0.158	0.199	0.186	*0.169	*0.153
	500000.	0.973	0.134	0.247	0.225	*0.212	*0.187
N V 4P-5D	50000.	2.01	-0.810E-01				
1549.1 A	100000.	1.67	-0.379E-01				
C= 0.18D+19	200000.	1.38	-0.148E-02				
	500000.	1.05	0.143E-02				
N V 4D-5P	50000.	2.31	0.824E-01	0.950E-01	-0.461E-01	*0.105	*-0.400E-01
1655.9 A	100000.	1.87	0.928E-01	0.119	-0.657E-01	*0.122	*-0.547E-01
C= 0.69D+19	200000.	1.52	0.832E-01	0.140	-0.811E-01	*0.140	*-0.683E-01
	500000.	1.16	0.592E-01	0.161	-0.991E-01	0.155	-0.829E-01
N V 4D-5F	50000.	1.70	0.301E-01				
1616.3 A	100000.	1.47	-0.150E-01				
C= 0.20D+18	200000.	1.24	-0.325E-01				
	500000.	0.952	-0.210E-01				
PERTURBER DENSITY = 0.1D+20(cm-3)							
N V 2S-2P	50000.	0.358	-0.165E-02	0.971E-03	-0.213E-02	0.170E-02	-0.212E-02
1240.2 A	100000.	0.255	-0.741E-02	0.293E-02	-0.473E-02	0.447E-02	-0.457E-02
C= 0.12D+23	200000.	0.184	-0.708E-02	0.704E-02	-0.866E-02	0.895E-02	-0.797E-02
	500000.	0.125	-0.830E-02	0.146E-01	-0.142E-01	0.156E-01	-0.124E-01
N V 2S-3P	50000.	0.402E-01	0.341E-03	0.103E-02	0.112E-02	0.135E-02	0.102E-02
209.3 A	100000.	0.301E-01	0.524E-03	0.200E-02	0.191E-02	0.224E-02	0.168E-02
C= 0.29D+20	200000.	0.231E-01	0.609E-03	0.320E-02	0.284E-02	0.307E-02	0.235E-02
	500000.	0.168E-01	0.607E-03	0.429E-02	0.369E-02	0.403E-02	0.311E-02
N V 2S-4P	50000.	0.738E-01	0.605E-03	*0.528E-02	*0.410E-02		
162.6 A	100000.	0.573E-01	0.125E-02	*0.812E-02	*0.631E-02		
C= 0.73D+19	200000.	0.455E-01	0.230E-02	*0.106E-01	*0.893E-02		
	500000.	0.342E-01	0.198E-02	*0.138E-01	*0.119E-01		
N V 2S-5P	50000.	0.142	-0.185E-02				
147.4 A	100000.	0.115	0.142E-02				
C= 0.31D+19	200000.	0.934E-01	0.449E-02				
	500000.	0.716E-01	0.475E-02				
N V 2P-3S	50000.	0.439E-01	0.225E-02	0.677E-03	0.161E-02	0.775E-03	0.147E-02
266.3 A	100000.	0.322E-01	0.308E-02	0.190E-02	0.281E-02	0.177E-02	0.244E-02
C= 0.15D+21	200000.	0.245E-01	0.341E-02	0.341E-02	0.419E-02	0.319E-02	0.347E-02
	500000.	0.178E-01	0.336E-02	0.537E-02	0.544E-02	0.462E-02	0.459E-02

© European Southern Observatory • Provided by the NASA Astrophysics Data System

1992A&AS...95..109D

TABLE 1. *(continued)*

PERTURBER DENSITY = 0.1D+20(cm-3)

PERTURBERS ARE		ELECTRONS		PROTONS		IONIZED HELIUM	
TRANSITION	T(K)	WIDTH(A)	SHIFT(A)	WIDTH(A)	SHIFT(A)	WIDTH(A)	SHIFT(A)
N V 2P-4S	50000.	0.660E-01	0.547E-02*	0.371E-02*	0.417E-02*	0.362E-02*	0.348E-02
190.2 A	100000.	0.502E-01	0.693E-02*	0.686E-02*	0.667E-02*	0.603E-02*	0.536E-02
C= 0.32D+20	200000.	0.393E-01	0.736E-02*	0.927E-02*	0.921E-02*	0.802E-02*	0.753E-02
	500000.	0.294E-01	0.713E-02*	0.127E-01*	0.120E-01*	0.110E-01*	0.962E-02
N V 2P-5S	50000.	0.126	0.129E-01				
168.6 A	100000.	0.100	0.142E-01				
C= 0.13D+20	200000.	0.804E-01	0.168E-01				
	500000.	0.610E-01	0.153E-01				
N V 2P-3D	50000.	0.336E-01	-0.725E-03	0.687E-03	-0.116E-02	0.878E-03	-0.106E-02
247.7 A	100000.	0.247E-01	-0.326E-03	0.167E-02	-0.207E-02	0.171E-02	-0.177E-02
C= 0.40D+20	200000.	0.186E-01	-0.481E-03	0.281E-02	-0.308E-02	0.279E-02	-0.259E-02
	500000.	0.133E-01	-0.260E-03	0.425E-02	-0.404E-02	0.383E-02	-0.338E-02
N V 2P-4D	50000.	0.755E-01	-0.195E-02				
186.1 A	100000.	0.619E-01	-0.139E-02				
C= 0.88D+18	200000.	0.509E-01	-0.535E-03				
	500000.	0.390E-01	0.465E-03				
N V 2P-5D	50000.	0.146	-0.124E-02				
166.9 A	100000.	0.128	-0.245E-02				
C= 0.21D+18	200000.	0.109	-0.261E-03				
	500000.	0.856E-01	0.491E-03				
N V 3S-3P	50000.	27.4	-0.460	0.370	0.109	0.526	0.105
4610.9 A	100000.	20.6	-0.557	0.682	0.220	0.827	0.205
C= 0.14D+23	200000.	15.9	-0.623	0.987	0.355	1.10	0.315
	500000.	11.7	-0.595	1.25	0.520	1.31	0.440
N V 3S-4P	50000.	1.25	-0.245E-02*	0.752E-01*	0.582E-01		
628.8 A	100000.	0.967	0.370E-02*	0.116	*0.896E-01		
C= 0.11D+21	200000.	0.767	0.173E-01*	0.147	*0.126		
	500000.	0.578	0.131E-01*	0.185	*0.165		
N V 3S-5P	50000.	1.39	-0.233E-01				
450.1 A	100000.	1.12	0.548E-02				
C= 0.28D+20	200000.	0.915	0.331E-01				
	500000.	0.701	0.358E-01				
N V 3P-4S	50000.	1.49	0.834E-01*	0.575E-01*	0.623E-01*	0.568E-01*	0.527E-01
778.0 A	100000.	1.14	0.105	*0.103	*0.101	*0.946E-01*	0.810E-01
C= 0.40D+21	200000.	0.896	0.111	*0.144	*0.139	*0.125	*0.114
	500000.	0.671	0.107	*0.197	*0.179	*0.166	*0.151
N V 3P-5S	50000.	1.30	0.113				
510.0 A	100000.	1.04	0.125				
C= 0.12D+21	200000.	0.835	0.149				
	500000.	0.635	0.135				
N V 3P-4D	50000.	1.28	-0.336E-01				
713.8 A	100000.	1.05	-0.291E-01				
C= 0.13D+20	200000.	0.858	-0.174E-01				
	500000.	0.658	-0.301E-02				
N V 3P-5D	50000.	1.37	-0.135E-01				
495.3 A	100000.	1.19	-0.258E-01				
C= 0.19D+19	200000.	1.01	-0.690E-02				
	500000.	0.793	-0.433E-03				

© European Southern Observatory • Provided by the NASA Astrophysics Data System

1992A&AS...95..109D

TABLE 1. *(continued)*

PERTURBER DENSITY = 0.1D+20(cm-3)

PERTURBERS ARE		ELECTRONS		PROTONS		IONIZED HELIUM	
TRANSITION	T(K)	WIDTH(A)	SHIFT(A)	WIDTH(A)	SHIFT(A)	WIDTH(A)	SHIFT(A)
N V 3D-4P	50000.	1.69	0.211E-01	*0.117	*0.949E-01		
764.9 A	100000.	1.32	0.337E-01	*0.184	*0.145		
C= 0.16D+21	200000.	1.05	0.581E-01	*0.236	*0.205		
	500000.	0.790	0.495E-01	*0.316	*0.272		
N V 3D-5P	50000.	19.0	-0.210				
1583.6 A	100000.	15.3	0.143				
C= 0.35D+21	200000.	12.5	0.448				
	500000.	9.58	0.490				
N V 3D-4F	50000.	0.729	0.310E-01				
747.6 A	100000.	0.593	0.228E-01				
C= 0.14D+20	200000.	0.486	0.754E-02				
	500000.	0.377	-0.156E-02				
N V 3D-5F	50000.	0.972	0.298E-01				
511.8 A	100000.	0.884	0.199E-01				
C= 0.20D+18	200000.	0.776	-0.304E-02				
	500000.	0.626	-0.108E-01				
N V 4S-5P	50000.	15.5	-0.432				
1389.6 A	100000.	12.4	-0.224				
C= 0.27D+21	200000.	10.1	0.208E-01				
	500000.	7.75	0.534E-01				
N V 4P-5S	50000.	19.6	1.19				
1702.9 A	100000.	15.7	1.27				
C= 0.80D+21	200000.	12.7	1.44				
	500000.	9.69	1.32				
N V 4P-5D	50000.	16.4	-0.169				
1549.1 A	100000.	14.0	-0.338				
C= 0.18D+20	200000.	11.9	-0.243				
	500000.	9.27	-0.151				
N V 4D-5P	50000.	21.0	-0.762E-01				
1655.9 A	100000.	17.3	0.302				
C= 0.69D+20	200000.	14.3	0.622				
	500000.	11.0	0.577	*1.61	*-0.985		

PERTURBER DENSITY = 0.1D+21(cm-3) = 0.1D+22(cm-3)

PERTURBERS ARE		ELECTRONS		ELECTRONS	
N V 2S-2P	100000.	2.55	-0.643E-01	25.5	-0.281
1240.2 A	200000.	1.84	-0.635E-01	18.4	-0.411
C= 0.12E+24	500000.	1.25	-0.803E-01	12.5	-0.650
	1000000.	0.963	-0.748E-01	9.63	-0.682
N V 2S-3P	100000.	0.296	-0.137E-02	*2.59	*-0.696E-01
209.3 A	200000.	0.228	0.883E-03	2.05	-0.393E-01
C= 0.29E+21	500000.	0.166	0.418E-02	1.53	-0.968E-02
	1000000.	0.134	0.392E-02	1.25	0.808E-02
N V 2S-4P	100000.	0.516	-0.114E-01		
162.6 A	200000.	0.418	0.129E-03	*3.10	*-0.367E-01
C= 0.73E+20	500000.	0.319	0.914E-02	2.55	-0.123E-01
	1000000.	0.263	0.144E-01	2.19	0.505E-01

© European Southern Observatory • Provided by the NASA Astrophysics Data System

1992A&AS...95..109D

TABLE 1. *(continued)*

PERTURBER DENSITY = 0.1D+21(cm-3)				= 0.1D+22(cm-3)	
PERTURBERS ARE		ELECTRONS		ELECTRONS	
TRANSITION	T(K)	WIDTH(A)	SHIFT(A)	WIDTH(A)	SHIFT(A)
N V 2S-5P	100000.	*0.895	*-0.224E-01		
147.4 A	200000.	0.767	-0.548E-02		
C= 0.31E+20	500000.	0.614	0.163E-01	*4.32	*0.523E-02
	1000000.	0.516	0.335E-01	3.88	0.161
N V 2P-3S	100000.	0.322	0.219E-01	3.03	-0.111
266.3 A	200000.	0.245	0.272E-01	2.35	0.617E-01
C= 0.15E+22	500000.	0.178	0.311E-01	1.72	0.166
	1000000.	0.143	0.300E-01	1.39	0.241
N V 2P-4S	100000.	0.490	0.292E-01	3.31	-0.509
190.2 A	200000.	0.386	0.431E-01	2.94	-0.137
C= 0.32E+21	500000.	0.289	0.604E-01	2.37	0.152
	1000000.	0.234	0.566E-01	1.99	0.343
N V 2P-5S	100000.	0.877	0.676E-02	*3.83	*-1.12
168.6 A	200000.	0.723	0.590E-01	3.93	-0.433
C= 0.13E+21	500000.	0.560	0.110	3.67	0.680E-01
	1000000.	0.459	0.115	3.25	0.521
N V 2P-3D	100000.	0.243	0.327E-02	2.14	0.115
247.7 A	200000.	0.184	0.246E-03	1.66	0.660E-01
C= 0.40E+21	500000.	0.132	-0.768E-03	1.22	0.507E-01
	1000000.	0.106	-0.125E-02	0.990	0.198E-01
N V 2P-4D	100000.	0.486	0.726E-02	*3.26	*0.161
186.1 A	200000.	0.415	0.970E-03	*2.91	*0.108
C= 0.88E+19	500000.	0.331	0.211E-02	2.50	0.744E-01
	1000000.	0.276	0.213E-02	2.18	0.298E-01
N V 2P-5D	100000.	*0.873	*0.246E-01		
166.9 A	200000.	0.795	0.127E-01	*4.90	*0.188
C= 0.21E+19	500000.	0.667	-0.295E-02	*4.55	*0.123
	1000000.	0.570	-0.102E-01	4.15	-0.239E-01
N V 3S-4P	100000.	8.81	-0.274		
628.8 A	200000.	7.12	-0.132		
C= 0.11E+22	500000.	5.44	-0.153E-01		
	1000000.	4.48	0.681E-01		
N V 3S-5P	100000.	*8.91	*-0.262		
450.1 A	200000.	7.59	-0.120		
C= 0.28E+21	500000.	6.06	0.741E-01		
	1000000.	5.09	0.237		
N V 3P-4S	100000.	11.1	0.471		
778.0 A	200000.	8.79	0.678		
C= 0.40E+22	500000.	6.61	0.919		
	1000000.	5.38	0.862		
N V 3P-5S	100000.	9.21	0.488E-01		
510.0 A	200000.	7.58	0.519		
C= 0.12E+22	500000.	5.88	0.966		
	1000000.	4.82	1.01		
N V 3P-4D	100000.	8.45	0.998E-01		
713.8 A	200000.	7.17	-0.180E-01		
C= 0.13E+21	500000.	5.69	-0.447E-01		
	1000000.	4.73	-0.392E-01		

© European Southern Observatory • Provided by the NASA Astrophysics Data System

1992A&AS...95..109D

TABLE 1. *(continued)*

PERTURBER DENSITY = 0.1D+21(cm-3)				= 0.1D+22(cm-3)	
PERTURBERS ARE		ELECTRONS		ELECTRONS	
TRANSITION	T(K)	WIDTH(A)	SHIFT(A)	WIDTH(A)	SHIFT(A)
N V 3P-5D	100000.	8.31	0.213		
495.3 A	200000.	7.51	0.959E-01		
C= 0.19E+20	500000.	6.26	-0.624E-01		
	1000000.	5.32	-0.124		
N V 3D-4P	100000.	11.9	-0.259		
764.9 A	200000.	9.63	0.250E-01		
C= 0.16E+22	500000.	7.38	0.240		
	1000000.	6.07	0.360		
N V 3D-4F	100000.	4.87	0.181		
747.6 A	200000.	4.08	0.195		
C= 0.14E+21	500000.	3.27	0.105		
	1000000.	2.77	0.603E-01		
N V 3D-5F	100000.	6.17	0.140		
511.8 A	200000.	5.68	0.175		
C= 0.20E+19	500000.	4.87	0.114		
	1000000.	4.21	0.655E-01		

TABLE 2. *The same as in Table 1 but for the perturber densities* 10^{15} cm^{-3} *and* 10^{16} cm^{-3}.

PERTURBER DENSITY = 0.1D+16(cm-3)							
PERTURBERS ARE		ELECTRONS		PROTONS		IONIZED HELIUM	
TRANSITION	T(K)	WIDTH(A)	SHIFT(A)	WIDTH(A)	SHIFT(A)	WIDTH(A)	SHIFT(A)
N V 3P-5D	50000.	0.219E-03	0.105E-04	0.132E-03	0.129E-03	0.109E-03	0.107E-03
495.3 A	100000.	0.177E-03	0.707E-05	0.158E-03	0.151E-03	0.134E-03	0.126E-03
C= 0.19D+15	200000.	0.142E-03	0.459E-05	0.182E-03	0.172E-03	0.153E-03	0.136E-03
	500000.	0.105E-03	0.173E-05	0.226E-03	0.188E-03	0.165E-03	0.177E-03
N V 3D-5F	50000.	0.225E-03	0.188E-06	0.459E-03	0.401E-03	0.369E-03	0.327E-03
511.8 A	100000.	0.181E-03	-0.133E-05	0.487E-03	0.457E-03	0.449E-03	0.372E-03
C= 0.20D+14	200000.	0.144E-03	-0.214E-05	0.548E-03	0.542E-03	0.520E-03	0.405E-03
	500000.	0.105E-03	-0.121E-05	0.674E-03	0.567E-03	0.521E-03	0.539E-03
N V 4P-4D	50000.	0.600	-0.494E-02	0.936E-01	0.104	0.827E-01	0.878E-01
36239.8 A	100000.	0.478	-0.706E-02	0.121	0.125	0.106	0.105
C= 0.33D+19	200000.	0.385	-0.924E-02	0.157	0.150	0.130	0.125
	500000.	0.290	-0.719E-02	0.209	0.178	0.166	0.149
N V 4D-5F	50000.	0.262E-02	-0.269E-04	0.450E-02	0.400E-02	0.367E-02	0.327E-02
1616.3 A	100000.	0.212E-02	-0.337E-04	0.481E-02	0.449E-02	0.449E-02	0.367E-02
C= 0.20D+15	200000.	0.170E-02	-0.358E-04	0.531E-02	0.532E-02	0.517E-02	0.405E-02
	500000.	0.124E-02	-0.210E-04	0.658E-02	0.553E-02	0.514E-02	0.517E-02
N V 5S-5P	50000.	0.554	-0.173E-01	0.266E-01	0.212E-01	0.266E-01	0.180E-01
22592.2 A	100000.	0.447	-0.154E-01	0.332E-01	0.257E-01	0.318E-01	0.216E-01
C= 0.72D+19	200000.	0.363	-0.163E-01	0.405E-01	0.310E-01	0.376E-01	0.255E-01
	500000.	0.278	-0.155E-01	0.491E-01	0.370E-01	0.428E-01	0.310E-01
N V 5P-5D	50000.	6.96	0.159E-01	2.61	2.56	2.20	2.11
71174.4 A	100000.	5.65	-0.470E-01	3.11	2.94	2.62	2.45
C= 0.39D+19	200000.	4.58	-0.696E-01	3.61	3.35	3.18	2.69
	500000.	3.42	-0.785E-01	4.68	3.81	3.27	3.32
PERTURBER DENSITY = 0.1D+17(cm-3)							
N V 3D-5F	50000.	0.207E-02	-0.219E-04	*0.459E-02	*0.399E-02		
511.8 A	100000.	0.168E-02	-0.313E-04	*0.487E-02	*0.455E-02	*0.450E-02	*0.369E-02
C= 0.20D+15	200000.	0.135E-02	-0.214E-04	*0.548E-02	*0.542E-02	*0.520E-02	*0.405E-02
	500000.	0.990E-03	-0.121E-04	0.674E-02	0.567E-02	*0.521E-02	*0.539E-02
N V 4D-5F	50000.	0.245E-01	-0.496E-03	*0.450E-01	*0.398E-01		
1616.3 A	100000.	0.200E-01	-0.511E-03	*0.481E-01	*0.446E-01	*0.450E-01	*0.365E-01
C= 0.20D+16	200000.	0.161E-01	-0.358E-03	*0.531E-01	*0.532E-01	*0.517E-01	*0.405E-01
	500000.	0.119E-01	-0.210E-03	0.658E-01	0.553E-01	*0.514E-01	*0.517E-01

© European Southern Observatory • Provided by the NASA Astrophysics Data System

1992A&AS...95..109D

TABLE 3. *Comparison between the experimental Stark full half-width for the* $3s^2S_{1/2} - 3p^2P_{1/2}$ *N V line* (W_M-*Böttcher et al. 1988), with different Stark width (W in Å) calculations at the electron density* $N = 1.8\text{x}10^{18}$ cm^{-3} *and* $T = 145\ 000$ *K.*
W_{DSB}*: present semiclassical calculations;*
W_{DK}*: modified semiempirical method (Dimitrijević & Konjević 1980), calculated by Böttcher et al. (1988);*
W_G*: simplified semiclassical approach (Griem 1974), calculated by Böttcher et al. (1988);*
W_{HB1}*: quasiclassical Gaunt factor approach (Hey & Breger 1980a,b), calculated by Böttcher et al. (1988)*
W_{HB2}*: quasiclassical Gaunt factor approach (Hey & Breger 1980c, 1982), calculated by Böttcher et al. (1988)*
W_B*: simplified approach of Baranger (1962) calculated by Böttcher et al. (1988)*
W_p*: estimate based on regularities (Purić et al. 1987, 1988), calculated by Böttcher et al. (1988).*

N V $3s^2S_{1/2}-3p^2P_{1/2}$, λ=4603.7 Å, T=145,000 K, N=1.8 10^{18} cm^{-3}							
W_M(Å)	W_{DSB}(Å)	W_{DK}(Å)	W_G(Å)	W_{HB1}(Å)	W_{HB2}(Å)	W_B(Å)	W_P(Å)
4.92	3.71	2.41	3.03	2.12	2.51	4.39	1.99

TABLE 4. *Comparison between the experimental Stark full halfwidths of N V lines* (W_m)*with our results* (W_{DSB})*, calculations (Böttcher et al. 1987) using a simplified semiclassical method (Griem 1974)* (W_G) *and estimates based on regularities (Purić et al. 1987)* (W_P)*. Experimental data are obtained by: (a) Purić et al. (1987), (b) Böttcher et al. (1987).*

Transition	λ(Å)	N(10^{17} cm^{-3})	T(K)	W_M(Å)	W_{DSB}(Å)	W_P(Å)	W_G(Å)	Ref.
NV $3s^2S-3p^2P^o$	4603.8	1.78	50000	0.338	0.488	0.340		(a)
	4619.9	1.78	50000	0.338	0.488	0.340		(a)
NV $3p^2P^o-4d^2D$	713.8	7.7	124100	0.42	0.085		0.11	(b)
NV $3d^2D-4f^2F^o$	747.6	7.7	124100	0.30	0.050		0.071	(b)

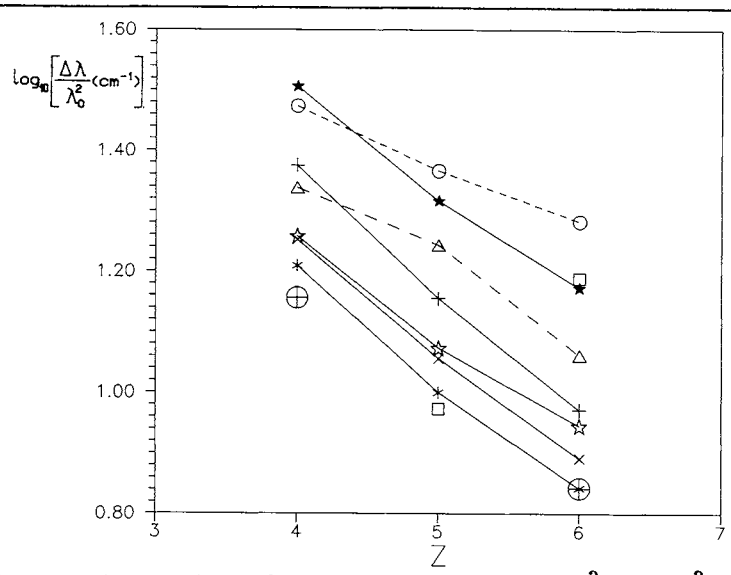

FIGURE 1. Comparison between the experimental Stark full half-widths for $3s^2S_{1/2}-3p^2P_{1/2}$ C IV, N V, and O IV lines (O) (Böttcher *et al.* 1988) with different Stark width (*W* in Å) calculations at the electron density $N = 1.8 \times 10^{18}$ cm^{-3} and $T = 145\ 000$ K. (△) present semi-classical calculations; (⊕) quantum mechanical strong coupling calculations (Seaton 1987); (X) modified semi-empirical method (Dimitrijević & Konjević 1980), calculated by Böttcher *et al.* (1988); (+) simplified semi-classical approach (Griem 1974), calculated by Böttcher *et al.* (1989); (*) quasiclassical Gaunt factor approach (Hey & Breger 1980a, b), calculated by Böttcher *et al.* (1988); (✱) quasiclassical Gaunt factor approach (Hey & Breger 1980c, 1982), calculated by Böttcher *et al.* (1988); (*) simplified approach of Baranger (1962) calculated by Böttcher *et al.* (1988); (□) estimate based on regularities (Purić *et al.* 1987, 1988), caculated by Böttcher *et al.* (1988).

© European Southern Observatory • Provided by the NASA Astrophysics Data System

1992A&AS...95..121D

ASTRONOMY & ASTROPHYSICS
SUPPLEMENT SERIES

Astron. Astrophys. Suppl. Ser. **95**, 121-128 (1992)

Stark broadening of spectral lines of multicharged ions of astrophysical interest. V. Sc III and Ti IV lines

M.S. Dimitrijević[1] and S. Sahal-Bréchot[2]

[1] Astronomical Observatory, Volgina 7, 11050 Beograd, Yugoslavia
[2] Laboratoire "Astrophysique, Atomes et Molécules" Département Atomes et Molécules en Astrophysique, Unité associée au C.N.R.S. N° 812, Observatoire de Paris-Meudon, 92190 Meudon, France

Received September 17; accepted December 24, 1991

Abstract. — Using a semiclassical approach, we have calculated electron-, proton-, and ionized helium-impact line widths and shifts for 10 Sc III and 10 Ti IV multiplets. This comprehensive set of data has been used for the investigation of Stark broadening parameter regularities within isoelectronic sequences.

Key words: line profile; atomic and molecular data.

1. Introduction.

The knowledge of multicharged ion Stark broadening parameters is of interest in astrophysics owing to the recent development of research on the physics of the stellar interiors (Seaton 1987), as well as for the investigation of hot star atmospheres. E.G. Rogerson & Ewell (1985) have found 7 Ti IV lines in the τ Sco spectrum.

This paper is the fifth of a series devoted to the calculation of Stark broadening parameters of spectral lines of multicharged ions. The first four were concerned with C IV, Si IV, O VI and N V lines (Dimitrijević *et al.* 1991ab, Dimitrijević & Sahal-Bréchot 1992ab, hereafter referred as Papers I-IV).

By using the semiclassical-perturbation formalism (Sahal-Bréchot 1969ab) we have calculated electron-, proton-, and ionized helium-impact line widths and shifts for 10 Sc III and 10 Ti IV multiplets. A summary of the formalism is given in Paper I. Here we present and discuss the results for Sc III and Ti IV, along with a discussion of the Stark broadening parameter regularities within an isoelectronic sequence.

2. Results and discussion.

Energy levels for Sc III and Ti IV lines have been taken from Bashkin & Stoner (1975). Oscillator strengths have been calculated by using the method of Bates & Damgaard (1949) and the tables of Oertel & Shomo (1968). For higher levels, the method described by Van Regemorter *et al.* (1979) has been used.

In addition to the electron-impact full halfwidths and shifts, Stark broadening parameters due to proton-, and ionized helium- impacts have been calculated. At high temperatures Helium is ionized twice; yet the Stark broadening parameters due to He^{++} have not been provided, because they are very small: the increase of the Coulomb repulsion entails a decrease of the line width. Besides, owing to the neutrality plasma condition, the electron density is increased by the fact that helium is twice ionized and thus the relative contribution of the electron impact broadening is more important. Thus we have provided Stark broadening data for all the important charged perturbers in stellar atmospheres and subphotospheric layers. Our results are shown in Table 1 for Sc III and in Table 2 for Ti IV lines, for perturber densities $10^{17} - 10^{20}$ cm^{-3} and temperatures of $T = 20\,000$ - $800\,000$ K. For perturber densities lower than 10^{17} cm^{-3} all the corresponding data are practically linear with density for the majority of the considered multiplets, because the effect of Debye screening is negligible. We also specify a parameter c (Dimitrijević & Sahaal-Bréchot 1984), which gives an estimate for the maximum perturber density for which the line may be treated as isolated when it is divided by width.

For each value given in Tables 1 and 2, the collision volume (V) multiplied by the perturber density (N) is much less than one and the impact approximation is valid (Sahal-Bréchot 1969ab). Values for $NV > 0.5$ are not given and values for $0.1 < NV \leq 0.5$ are denoted by an asterisk. When the impact approximation is not valid,

© European Southern Observatory • Provided by the NASA Astrophysics Data System

1992A&AS...95..121D

the ion broadening contribution may be estimated by using quasistatic estimations (Sahal-Bréchot 1991, see also Paper I). One must be aware of the fact that the accuracy of the obtained results decreases when the broadening by ion interactions is important.

In Figures 1 and 2 the line widths and shifts for the 3d - 4f multiplets of Sc III and Ti IV in angular frequency units are presented. We can see that the mutual relation of the corresponding isoelectronic Stark broadening parameters strongly depends on temperature. For the investigation of regularities in this isoelectronic sequence, calculations for other sequence members as well as experimental data are needed.

Acknowledgements.

One of us (M.D.) has been supported by the Observatory of Paris-Meudon. This work has also been supported by the French C.N.R.S. and is a part of a French-Yugoslav collaboration through the project "L'élargissement Stark des raies spectrales des plasmas astrophysiques et de laboratoire", it is also a part of the project "Physics and dynamics of celestial bodies", supported by RFN of Serbia.

References

Bashkin S. and Stoner J.O.Jr. 1975, Atomic Energy Levels and Grotrian Diagrams, Vol.1 (North Holland, Amsterdam)

Bates D.R. and Damgaard A. 1949, Trans.Roy.Soc. London, Ser. A 242, 101

Dimitrijević M.S. and Sahal-Bréchot S. 1984, JQSRT 31, 301

Dimitrijević M.S., Sahal-Bréchot S. and Bommier V 1991a, A&AS 89, 581 (referred as Paper I in the text)

Dimitrijević M.S., Sahal-Bréchot S. and Bommier V. 1991b, A&AS 89, 591 Paper II

Dimitrijević M.S. and Sahal-Bréchot S. 1992, A&AS 93, 359 Paper III

Dimitrijević M.S. and Sahal-Bréchot S. 1992, A&AS in press Paper IV

Oertel G.K. and Shomo L.P. 1968, ApJS 16, 175

Rogerson Jr. J.B. and Ewell Jr. M.W. 1985, ApJS 58, 265

Sahal-Bréchot S. 1969a, A&A 1, 91

Sahal-Bréchot S. 1969b, A&A 2, 322

Seaton M.J. 1987, J.Phys.B 20, 6363

Van Regemorter H., Hoang Binh Dy and Prud'homme M.: 1979, J.Phys.B 12, 1073

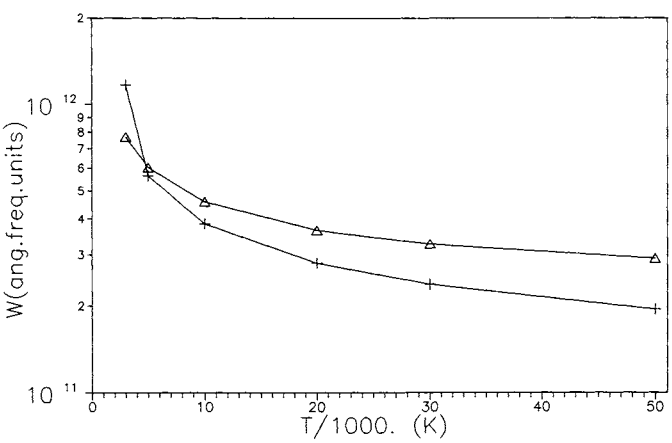

FIGURE 1. Electron impact widths in angular frequency units for the 3d – 4f Sc III and Ti IV multiplets as a function of temperature. The electron density is 10^{17} cm^{-3}.

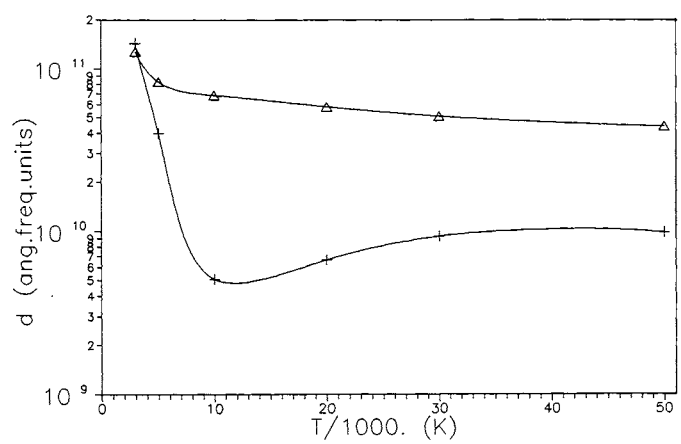

FIGURE 2. Same as in Figure 1 but for the shift.

© European Southern Observatory • Provided by the NASA Astrophysics Data System

1992A&AS...95..121D

TABLE 1. *This table shows electron-, proton-, and ionized- helium- impact broadening parameters for Sc III and Ti IV lines, for perturber densities of* $10^{17}-10^{20}$cm^{-3} *and temperatures from 20 000 K to 300 000 K. Transitions and average wavelengths for the multiplet (in Å) are also given. By using c (see Eq. (5) of Paper I), we obtain an estimate for the maximum perturber density for which the line may be treated as isolated and tabulated data may be used. The asterisk identifies cases for which the collision volume multiplied by the perturber density (the condition for validity of the impact approximation) lies betwen 0.1 and 0.5. Data for densities N lower than* 10^{17} cm^{-3} *can be obtained by multiplying the results given at* 10^{17} cm^{-3} *by* N/10^{17}.

PERTURBER DENSITY = 0.1D+18 (cm-3)

PERTURBERS ARE		ELECTRONS		PROTONS		IONIZED HELIUM	
TRANSITION	T(K)	WIDTH(A)	SHIFT(A)	WIDTH(A)	SHIFT(A)	WIDTH(A)	SHIFT(A)
SCIII 3D-4P	20000.	0.278E-01	0.836E-03	0.105E-02	0.153E-03	0.144E-02	0.149E-03
1605.1 A	50000.	0.183E-01	0.894E-03	0.184E-02	0.331E-03	0.216E-02	0.299E-03
C= 0.95E+20	100000.	0.140E-01	0.785E-03	0.227E-02	0.477E-03	0.245E-02	0.414E-03
	200000.	0.113E-01	0.869E-03	0.257E-02	0.613E-03	0.273E-02	0.507E-03
SCIII 3D-5P	20000.	0.177E-01	0.387E-03	0.186E-02	-0.393E-04	0.216E-02	-0.381E-04
780.6 A	50000.	0.138E-01	0.242E-03	0.237E-02	-0.844E-04	0.254E-02	-0.755E-04
C= 0.81E+19	100000.	0.121E-01	0.400E-03	0.265E-02	-0.121E-03	0.279E-02	-0.104E-03
	200000.	0.108E-01	0.326E-03	0.283E-02	-0.154E-03	0.290E-02	-0.127E-03
SCIII 3D-4F	20000.	0.103E-01	0.164E-02	0.878E-03	0.336E-03	0.108E-02	0.293E-03
731.2 A	50000.	0.825E-02	0.124E-02	0.126E-02	0.541E-03	0.134E-02	0.450E-03
C= 0.60E+19	100000.	0.725E-02	0.110E-02	0.145E-02	0.656E-03	0.151E-02	0.541E-03
	200000.	0.646E-02	0.941E-03	0.164E-02	0.792E-03	0.162E-02	0.637E-03
SCIII 4S-4P	20000.	0.117	-0.210E-02	0.344E-02	-0.974E-03	0.460E-02	-0.922E-03
2711.4 A	50000.	0.769E-01	-0.214E-02	0.596E-02	-0.190E-02	0.681E-02	-0.164E-02
C= 0.27E+21	100000.	0.592E-01	-0.314E-02	0.724E-02	-0.261E-02	0.774E-02	-0.217E-02
	200000.	0.484E-01	-0.265E-02	0.830E-02	-0.317E-02	0.862E-02	-0.261E-02
SCIII 4S-5P	20000.	0.319E-01	-0.177E-03	0.299E-02	-0.227E-03	0.344E-02	-0.209E-03
973.9 A	50000.	0.244E-01	-0.349E-03	0.378E-02	-0.403E-03	0.405E-02	-0.352E-03
C= 0.13E+20	100000.	0.211E-01	-0.115E-03	0.423E-02	-0.537E-03	0.444E-02	-0.441E-03
	200000.	0.188E-01	-0.190E-03	0.452E-02	-0.644E-03	0.459E-02	-0.531E-03
SCIII 4P-5S	20000.	0.106	0.307E-01	0.392E-02	0.501E-02	0.414E-02	0.438E-02
1906.9 A	50000.	0.766E-01	0.203E-01	0.745E-02	0.753E-02	0.675E-02	0.625E-02
C= 0.49E+20	100000.	0.644E-01	0.180E-01	0.972E-02	0.912E-02	0.829E-02	0.748E-02
	200000.	0.553E-01	0.139E-01	0.119E-01	0.107E-01	0.105E-01	0.874E-02
SCIII 4P-4D	20000.	0.881E-01	0.644E-02	0.333E-02	0.224E-02	0.401E-02	0.198E-02
2005.4 A	50000.	0.614E-01	0.543E-02	0.556E-02	0.366E-02	0.571E-02	0.307E-02
C= 0.64E+20	100000.	0.501E-01	0.633E-02	0.671E-02	0.448E-02	0.668E-02	0.366E-02
	200000.	0.428E-01	0.539E-02	0.787E-02	0.531E-02	0.772E-02	0.440E-02
SCIII 4D-5P	20000.	1.39	-0.499E-01	0.968E-01	-0.252E-01	0.115	-0.219E-01
6273.7 A	50000.	1.09	-0.518E-01	0.129	-0.406E-01	0.137	-0.336E-01
C= 0.53E+21	100000.	0.967	-0.482E-01	0.146	-0.490E-01	0.153	-0.407E-01
	200000.	0.871	-0.453E-01	0.159	-0.592E-01	0.161	-0.476E-01
SCIII 4D-4F	20000.	0.394	-0.185E-02	0.135E-01	0.741E-03	0.170E-01	0.726E-03
4066.8 A	50000.	0.322	0.331E-03	0.212E-01	0.164E-02	0.231E-01	0.151E-02
C= 0.19E+21	100000.	0.289	-0.194E-02	0.243E-01	0.241E-02	0.261E-01	0.211E-02
	200000.	0.263	-0.953E-03	0.272E-01	0.322E-02	0.285E-01	0.264E-02
SCIII 5S-5P	20000.	2.45	-0.316	0.187	-0.806E-01	0.209	-0.703E-01
7483.9 A	50000.	1.95	-0.268	0.243	-0.120	0.252	-0.997E-01
C= 0.75E+21	100000.	1.74	-0.215	0.281	-0.145	0.280	-0.120
	200000.	1.57	-0.186	0.312	-0.172	0.292	-0.136
PERTURBER DENSITY = 0.1D+19(cm-3)							
SCIII 3D-4P	20000.	0.278	0.862E-02	0.104E-01	0.139E-02	0.141E-01	0.134E-02
1605.1 A	50000.	0.183	0.897E-02	0.184E-01	0.320E-02	0.215E-01	0.287E-02
C= 0.95E+21	100000.	0.140	0.790E-02	0.226E-01	0.473E-02	0.245E-01	0.409E-02
	200000.	0.113	0.869E-02	0.257E-01	0.612E-02	0.273E-01	0.506E-02
SCIII 3D-5P	20000.	0.177	0.387E-02	0.181E-01	-0.355E-03	0.204E-01	-0.343E-03
780.6 A	50000.	0.138	0.250E-02*	0.235E-01	-0.815E-03*	0.251E-01	-0.726E-03
C= 0.81E+20	100000.	0.121	0.396E-02	0.265E-01	-0.119E-02*	0.277E-01	-0.103E-02
	200000.	0.108	0.330E-02	0.283E-01	-0.153E-02*	0.290E-01	-0.127E-02

© European Southern Observatory • Provided by the NASA Astrophysics Data System

1992A&AS...95..121D

TABLE 1. *(continued)*

PERTURBER DENSITY = 0.1D+19(cm-3)

PERTURBERS ARE TRANSITION	T(K)	ELECTRONS WIDTH(A)	ELECTRONS SHIFT(A)	PROTONS WIDTH(A)	PROTONS SHIFT(A)	IONIZED HELIUM WIDTH(A)	IONIZED HELIUM SHIFT(A)
SCIII 3D-4F	20000.	0.103	0.159E-01	0.858E-02	0.294E-02*	0.104E-01*	0.251E-02
731.2 A	50000.	0.825E-01	0.120E-01	0.126E-01	0.511E-02*	0.132E-01*	0.420E-02
C= 0.60E+20	100000.	0.725E-01	0.109E-01	0.145E-01	0.643E-02*	0.150E-01*	0.528E-02
	200000.	0.646E-01	0.939E-02	0.164E-01	0.790E-02	0.162E-01	0.634E-02
SCIII 4S-4P	20000.	1.17	-0.189E-01	0.339E-01	-0.876E-02	0.451E-01	-0.824E-02
2711.4 A	50000.	0.769	-0.201E-01	0.595E-01	-0.182E-01	0.679E-01	-0.156E-01
C= 0.27E+22	100000.	0.592	-0.310E-01	0.724E-01	-0.258E-01	0.774E-01	-0.214E-01
	200000.	0.484	-0.265E-01	0.830E-01	-0.316E-01	0.862E-01	-0.260E-01
SCIII 4S-5P	20000.	0.319	-0.162E-02*	0.289E-01	-0.203E-02*	0.326E-01	-0.185E-02
973.9 A	50000.	0.244	-0.321E-02*	0.376E-01	-0.386E-02*	0.400E-01	-0.334E-02
C= 0.13E+21	100000.	0.211	-0.118E-02	0.422E-01	-0.530E-02*	0.443E-01	-0.434E-02
	200000.	0.188	-0.184E-02	0.452E-01	-0.642E-02*	0.459E-01	-0.530E-02
SCIII 4P-5S	20000.	1.06	0.297	0.389E-01	0.424E-01	0.409E-01	0.361E-01
1906.9 A	50000.	0.766	0.198	0.748E-01	0.693E-01	0.665E-01	0.567E-01
C= 0.49E+21	100000.	0.644	0.177	0.970E-01	0.888E-01	0.830E-01	0.721E-01
	200000.	0.553	0.139	0.119	0.106	0.105	0.870E-01
SCIII 4P-4D	20000.	0.881	0.596E-01	0.329E-01	0.197E-01	0.392E-01	0.171E-01
2005.4 A	50000.	0.614	0.516E-01	0.556E-01	0.346E-01	0.571E-01	0.287E-01
C= 0.64E+21	100000.	0.501	0.621E-01	0.671E-01	0.440E-01	0.667E-01	0.358E-01
	200000.	0.428	0.538E-01	0.787E-01	0.530E-01	0.772E-01	0.438E-01
SCIII 4D-5P	20000.	13.9	-0.454	*0.941	*-0.221	*1.10	*-0.188
6273.7 A	50000.	10.9	-0.486	1.28	-0.384	*1.36	*-0.314
C= 0.53E+22	100000.	9.67	-0.475	1.46	-0.481	*1.52	*-0.397
	200000.	8.71	-0.449	1.59	-0.590	*1.61	*-0.474
SCIII 4D-4F	20000.	3.94	-0.148E-01	0.133	0.670E-02	0.166	0.655E-02
4066.8 A	50000.	3.22	0.291E-02	0.211	0.159E-01	0.230	0.146E-01
C= 0.19E+22	100000.	2.89	-0.198E-01	0.243	0.239E-01	0.261	0.209E-01
	200000.	2.63	-0.981E-02	0.272	0.321E-01	0.285	0.264E-01
SCIII 5S-5P	20000.	24.5	-3.01	*1.81	*-0.681	*1.98	*-0.577
7483.9 A	50000.	19.5	-2.57	*2.43	*-1.10	*2.47	*-0.913
C= 0.75E+22	100000.	17.4	-2.10	2.81	-1.42	*2.78	*-1.16
	200000.	15.7	-1.85	3.12	-1.71	*2.92	*-1.35

PERTURBER DENSITY = 0.1D+20(cm-3) = 0.1D+21(cm-3)

PERTURBERS ARE		ELECTRONS		ELECTRONS	
SCIII 3D-4P	50000.	1.83	0.875E-01	14.0	0.690
1605.1 A	100000.	1.40	0.762E-01	11.3	0.814
C= 0.95E+22	200000.	1.13	0.849E-01	10.2	0.788
	300000.	1.02	0.814E-01	8.41	0.739
SCIII 3D-5P	50000.	1.38	0.257E-01	12.0	0.428
780.6 A	100000.	1.21	0.394E-01	10.8	0.353
C= 0.81E+21	200000.	1.08	0.328E-01	10.1	0.300
	300000.	1.01	0.294E-01	8.72	0.303
SCIII 3D-4F	50000.	0.825	0.111	7.22	0.804
731.2 A	100000.	0.725	0.102	6.45	0.768
C= 0.60E+21	200000.	0.646	0.910E-01	6.06	0.787
	300000.	0.608	0.865E-01	5.23	0.664
SCIII 4S-4P	50000.	7.69	-0.181		
2711.4 A	100000.	5.92	-0.293		
C= 0.27E+23	200000.	4.84	-0.257		
	300000.	4.39	-0.265		

© European Southern Observatory • Provided by the NASA Astrophysics Data System

1992A&AS...95..121D

TABLE 1. *(continued)*

PERTURBER DENSITY = 0.1D+20(cm-3)				= 0.1D+21(cm-3)	
PERTURBERS ARE		ELECTRONS		ELECTRONS	
TRANSITION	T(K)	WIDTH(A)	SHIFT(A)	WIDTH(A)	SHIFT(A)
SCIII 4S-5P	50000.	2.44	-0.275E-01	21.0	0.560E-01
973.9 A	100000.	2.11	-0.901E-02	18.7	-0.753E-0
C= 0.13E+22	200000.	1.88	-0.170E-01	17.6	-0.158
	300000.	1.76	-0.205E-01	15.1	-0.107
SCIII 4P-5S	50000.	7.66	1.80		
1906.9 A	100000.	6.44	1.66		
C= 0.49E+22	200000.	5.53	1.33		
	300000.	5.09	1.23		
SCIII 4P-4D	50000.	6.14	0.457		
2005.4 A	100000.	5.01	0.577		
C= 0.64E+22	200000.	4.28	0.519		
	300000.	3.94	0.510		

© European Southern Observatory • Provided by the NASA Astrophysics Data System

1992A&AS...95..121D

TABLE 2. *The same as in Table 1 but for Ti IV lines.*

PERTURBER DENSITY = 0.1D+18(cm-3)

PERTURBERS ARE		ELECTRONS		PROTONS		IONIZED HELIUM	
TRANSITION	T(K)	WIDTH(A)	SHIFT(A)	WIDTH(A)	SHIFT(A)	WIDTH(A)	SHIFT(A)
TIIV 3D-4P	20000.	0.596E-02	0.758E-04	0.787E-04	0.128E-04	0.130E-03	0.128E-04
777.8 A	50000.	0.384E-02	0.913E-04	0.198E-03	0.326E-04	0.259E-03	0.314E-04
C= 0.29E+20	100000.	0.281E-02	0.912E-04	0.295E-03	0.563E-04	0.353E-03	0.511E-04
	200000.	0.215E-02	0.109E-03	0.373E-03	0.816E-04	0.403E-03	0.711E-04
TIIV 3D-5P	20000.	0.473E-02	0.553E-04	0.236E-03	0.127E-04	0.310E-03	0.125E-04
433.7 A	50000.	0.335E-02	0.891E-04	0.394E-03	0.298E-04	0.446E-03	0.275E-04
C= 0.35E+19	100000.	0.270E-02	0.891E-04	0.467E-03	0.457E-04	0.504E-03	0.400E-04
	200000.	0.227E-02	0.984E-04	0.525E-03	0.627E-04	0.558E-03	0.514E-04
TIIV 3D-4F	20000.	0.268E-02	0.634E-04	0.786E-04	0.212E-04	0.115E-03	0.207E-04
423.9 A	50000.	0.185E-02	0.926E-04	0.156E-03	0.471E-04	0.193E-03	0.427E-04
C= 0.41E+19	100000.	0.146E-02	0.965E-04	0.214E-03	0.688E-04	0.230E-03	0.599E-04
	200000.	0.121E-02	0.104E-03	0.246E-03	0.894E-04	0.261E-03	0.742E-04
TIIV 4S-4P	20000.	0.608E-01	-0.326E-03	0.637E-03	-0.232E-03	0.104E-02	-0.230E-03
2065.6 A	50000.	0.391E-01	-0.884E-03	0.158E-02	-0.558E-03	0.202E-02	-0.516E-03
C= 0.21E+21	100000.	0.288E-01	-0.927E-03	0.235E-02	-0.880E-03	0.274E-02	-0.759E-03
	200000.	0.223E-01	-0.112E-02	0.295E-02	-0.121E-02	0.313E-02	-0.101E-02
TIIV 4S-5P	20000.	0.129E-01	-0.108E-04	0.572E-03	-0.356E-05	0.747E-03	-0.356E-05
664.8 A	50000.	0.904E-02	0.248E-04	0.948E-03	-0.933E-05	0.107E-02	-0.919E-05
C= 0.81E+19	100000.	0.724E-02	0.315E-04	0.112E-02	-0.175E-04	0.121E-02	-0.162E-04
	200000.	0.604E-02	0.264E-04	0.126E-02	-0.279E-04	0.134E-02	-0.240E-04
TIIV 4P-5S	20000.	0.386E-01	0.310E-02	0.461E-03	0.901E-03	0.595E-03	0.830E-03
1196.1 A	50000.	0.255E-01	0.280E-02	0.124E-02	0.162E-02	0.131E-02	0.140E-02
C= 0.26E+20	100000.	0.195E-01	0.319E-02	0.205E-02	0.211E-02	0.186E-02	0.174E-02
	200000.	0.158E-01	0.287E-02	0.266E-02	0.254E-02	0.232E-02	0.209E-02
TIIV 4P-4D	20000.	0.377E-01	0.429E-03	0.433E-03	0.260E-03	0.679E-03	0.253E-03
1469.4 A	50000.	0.244E-01	0.893E-03	0.105E-02	0.575E-03	0.128E-02	0.521E-03
C= 0.73E+20	100000.	0.183E-01	0.935E-03	0.153E-02	0.840E-03	0.170E-02	0.731E-03
	200000.	0.145E-01	0.102E-02	0.191E-02	0.109E-02	0.196E-02	0.905E-03
TIIV 4D-5P	20000.	0.257	-0.965E-03	0.847E-02	-0.653E-03	0.115E-01	-0.643E-03
2944.3 A	50000.	0.181	-0.123E-02	0.147E-01	-0.151E-02	0.171E-01	-0.140E-02
C= 0.16E+21	100000.	0.146	-0.123E-02	0.179E-01	-0.230E-02	0.194E-01	-0.202E-02
	200000.	0.123	-0.128E-02	0.202E-01	-0.314E-02	0.216E-01	-0.256E-02
TIIV 4D-4F	20000.	0.119	-0.336E-03	0.116E-02	-0.152E-03	0.186E-02	-0.151E-03
2545.6 A	50000.	0.818E-01	-0.661E-03	0.276E-02	-0.384E-03	0.350E-02	-0.369E-03
C= 0.15E+21	100000.	0.652E-01	-0.513E-03	0.401E-02	-0.660E-03	0.464E-02	-0.595E-03
	200000.	0.547E-01	-0.574E-03	0.486E-02	-0.951E-03	0.525E-02	-0.824E-03
TIIV 5S-5P	20000.	1.17	-0.477E-01	0.398E-01	-0.175E-01	0.509E-01	-0.161E-01
5431.3 A	50000.	0.824	-0.439E-01	0.673E-01	-0.315E-01	0.738E-01	-0.274E-01
C= 0.54E+21	100000.	0.670	-0.546E-01	0.818E-01	-0.414E-01	0.847E-01	-0.343E-01
	200000.	0.565	-0.482E-01	0.943E-01	-0.496E-01	0.957E-01	-0.408E-01
PERTURBER DENSITY = 0.1D+19(cm-3)							
TIIV 4D-5P	50000.	1.81	-0.110E-01	0.146	-0.145E-01*	0.170	*-0.134E-01
2944.3 A	100000.	1.46	-0.123E-01	0.179	-0.226E-01	0.193	-0.199E-01
C= 0.16E+22	200000.	1.23	-0.127E-01	0.202	-0.313E-01	0.216	-0.256E-01
	300000.	1.12	-0.889E-02	0.215	-0.348E-01	0.223	-0.285E-01
TIIV 3D-4F	50000.	0.185E-01	0.933E-03	0.156E-02	0.451E-03	0.192E-02	0.407E-03
423.9 A	100000.	0.146E-01	0.948E-03	0.214E-02	0.678E-03	0.230E-02	0.589E-03
C= 0.41E+20	200000.	0.121E-01	0.104E-02	0.246E-02	0.892E-03	0.261E-02	0.740E-03
	300000.	0.110E-01	0.996E-03	0.266E-02	0.994E-03	0.277E-02	0.821E-03

© European Southern Observatory • Provided by the NASA Astrophysics Data System

1992A&AS...95..121D

TABLE 2. *(continued)*

PERTURBER DENSITY = 0.1D+19(cm-3)

PERTURBERS ARE		ELECTRONS		PROTONS		IONIZED HELIUM	
TRANSITION	T(K)	WIDTH(A)	SHIFT(A)	WIDTH(A)	SHIFT(A)	WIDTH(A)	SHIFT(A)
TIIV 4D-4F	50000.	0.818	-0.688E-02	0.276E-01	-0.370E-02	0.349E-01	-0.355E-02
2545.6 A	100000.	0.652	-0.443E-02	0.400E-01	-0.653E-02	0.463E-01	-0.587E-02
C= 0.15E+22	200000.	0.547	-0.564E-02	0.486E-01	-0.950E-02	0.525E-01	-0.823E-02
	300000.	0.502	-0.399E-02	0.524E-01	-0.113E-01	0.560E-01	-0.930E-02
TIIV 4P-5S	50000.	0.255	0.273E-01	0.123E-01	0.152E-01	0.130E-01	0.130E-01
1196.1 A	100000.	0.195	0.312E-01	0.205E-01	0.206E-01	0.186E-01	0.170E-01
C= 0.26E+21	200000.	0.158	0.286E-01	0.266E-01	0.253E-01	0.232E-01	0.208E-01
	300000.	0.141	0.269E-01	0.303E-01	0.278E-01	0.254E-01	0.231E-01
TIIV 4P-4D	50000.	0.244	0.905E-02	0.104E-01	0.551E-02	0.127E-01	0.497E-02
1469.4 A	100000.	0.183	0.880E-02	0.153E-01	0.828E-02	0.170E-01	0.719E-02
C= 0.73E+21	200000.	0.145	0.101E-01	0.191E-01	0.109E-01	0.196E-01	0.903E-02
	300000.	0.130	0.874E-02	0.210E-01	0.121E-01	0.212E-01	0.996E-02
TIIV 3D-4P	50000.	0.384E-01	0.935E-03	0.198E-02	0.314E-03	0.258E-02	0.302E-03
777.8 A	100000.	0.281E-01	0.944E-03	0.295E-02	0.556E-03	0.353E-02	0.505E-03
C= 0.29E+21	200000.	0.215E-01	0.109E-02	0.373E-02	0.815E-03	0.403E-02	0.709E-03
	300000.	0.189E-01	0.120E-02	0.403E-02	0.980E-03	0.431E-02	0.811E-03
TIIV 3D-5P	50000.	0.335E-01	0.934E-03	0.392E-02	0.286E-03*	0.442E-02*	0.263E-03
433.7 A	100000.	0.271E-01	0.855E-03	0.466E-02	0.451E-03	0.503E-02	0.394E-03
C= 0.35E+20	200000.	0.227E-01	0.979E-03	0.525E-02	0.626E-03	0.557E-02	0.513E-03
	300000.	0.207E-01	0.965E-03	0.556E-02	0.695E-03	0.574E-02	0.575E-03
TIIV 4S-4P	50000.	0.391	-0.893E-02	0.158E-01	-0.536E-02	0.202E-01	-0.494E-02
2065.6 A	100000.	0.288	-0.871E-02	0.235E-01	-0.869E-02	0.274E-01	-0.748E-02
C= 0.21E+22	200000.	0.223	-0.112E-01	0.295E-01	-0.121E-01	0.313E-01	-0.101E-01
	300000.	0.197	-0.928E-02	0.321E-01	-0.135E-01	0.337E-01	-0.112E-01
TIIV 4S-5P	50000.	0.904E-01	0.333E-03	0.944E-02	-0.899E-04*	0.106E-01	-0.885E-04
664.8 A	100000.	0.724E-01	0.260E-03	0.112E-01	-0.173E-03*	0.121E-01	-0.161E-03
C= 0.81E+20	200000.	0.604E-01	0.258E-03	0.126E-01	-0.279E-03*	0.134E-01	-0.240E-03
	300000.	0.552E-01	0.370E-03	0.133E-01	-0.338E-03*	0.138E-01	-0.294E-03
TIIV 5S-5P	50000.	8.24	-0.417	0.670	-0.297	*0.732	*-0.255
5431.3 A	100000.	6.70	-0.540	0.817	-0.405	*0.846	*-0.334
C= 0.54E+22	200000.	5.65	-0.480	0.943	-0.494	0.957	-0.406
	300000.	5.17	-0.456	1.02	-0.552	0.993	-0.445

PERTURBER DENSITY = 0.1D+20(cm-3) = 0.1D+21(cm-3)

PERTURBERS ARE		ELECTRONS		ELECTRONS	
TIIV 3D-4P	100000.	0.281	0.922E-02	2.81	0.827E-01
777.8 A	200000.	0.215	0.108E-01	2.15	0.100
C= 0.29E+22	300000.	0.189	0.120E-01	1.89	0.115
	800000.	0.145	0.106E-01	1.45	0.106
TIIV 3D-5P	100000.	0.270	0.852E-02	2.70	0.756E-01
433.7 A	200000.	0.227	0.966E-02	2.27	0.905E-01
C= 0.35E+21	300000.	0.207	0.961E-02	2.07	0.911E-01
	800000.	0.172	0.923E-02	1.72	0.916E-01
TIIV 3D-4F	100000.	0.146	0.900E-02	1.46	0.742E-01
423.9 A	200000.	0.121	0.101E-01	1.21	0.896E-01
C= 0.41E+21	300000.	0.110	0.995E-02	1.10	0.897E-01
	800000.	0.907E-01	0.898E-02	0.907	0.892E-01
TIIV 4S-4P	100000.	2.88	-0.814E-01	28.8	-0.645
2065.6 A	200000.	2.23	-0.108	22.3	-0.973
C= 0.21E+23	300000.	1.97	-0.931E-01	19.7	-0.818
	800000.	1.53	-0.906E-01	15.3	-0.901

© European Southern Observatory • Provided by the NASA Astrophysics Data System

1992A&AS...95..121D

TABLE 2. *(continued)*

PERTURBER DENSITY = 0.1D+20(cm-3)				= 0.1D+21(cm-3)	
PERTURBERS ARE		ELECTRONS		ELECTRONS	
TRANSITION	T(K)	WIDTH(A)	SHIFT(A)	WIDTH(A)	SHIFT(A)
TIIV 4S-5P	100000.	0.724	0.331E-02	7.24	0.350E-01
664.8 A	200000.	0.604	0.268E-02	6.04	0.301E-01
C= 0.81E+21	300000.	0.552	0.360E-02	5.51	0.398E-01
	800000.	0.456	0.441E-02	4.56	0.432E-01
TIIV 4P-5S	100000.	1.95	0.286	19.5	2.08
1196.1 A	200000.	1.58	0.275	15.8	2.14
C= 0.26E+22	300000.	1.41	0.268	14.1	2.19
	800000.	1.11	0.229	11.1	2.26
TIIV4P2P-4D	100000.	1.83	0.821E-01		
1469.4 A	200000.	1.45	0.977E-01		
C= 0.73E+22	300000.	1.30	0.874E-01		
	800000.	1.04	0.841E-01		
TIIV 4D-5P	100000.	14.6	-0.965E-01		
2944.3 A	200000.	12.3	-0.118		
C= 0.16E+23	300000.	11.2	-0.899E-01		
	800000.	9.35	-0.670E-01		
TIIV 4D-4F	100000.	6.52	-0.412E-01		
2545.6 A	200000.	5.47	-0.546E-01		
C= 0.15E+23	300000.	5.02	-0.396E-01		
	800000.	4.19	-0.450E-01		

© European Southern Observatory • Provided by the NASA Astrophysics Data System

1992A&AS...96..613D

ASTRONOMY & ASTROPHYSICS
SUPPLEMENT SERIES

DECEMBER II 1992, PAGE 613

Astron. Astrophys. Suppl. Ser. **96**, 613-624 (1992)

Stark broadening of spectral lines of multicharged ions of astrophysical interest. VI. C IV lines of large principal quantum number

M.S. Dimitrijević[1] and S. Sahal-Bréchot[2]

[1] Astronomical Observatory, Volgina 7, 11050 Beograd, Yugoslavia
[2] Laboratoire "Astrophysique, Atomes et Molécules", Département Atomes et Molécules en Astrophysique, Unité associée au C.N.R.S. N°812, Observatoire de Paris-Meudon, 92190 Meudon, France

Received March 10; accepted April 22, 1992

Abstract. — Using a semiclassical approach, we have calculated electron-, proton-, and ionized helium-impact line widths and shifts for 69 C IV multiplets of large principal quantum number. This comprehensive set of data has been used for the investigation of Stark broadening parameter regularities within spectral series.

Key words: lines: profile — atomic and molecular data.

1. Introduction.

We have recently calculated Stark broadening data for 39 C IV multiplets (Dimitrijević & Sahal-Bréchot 1991ab), persuaded that we had provided data for practically all C IV lines important for stellar research. Our tables however are not sufficiently complete for the investigation of PG 1159 stars (Werner *et al.* 1991; Werner & Heber 1991). The PG 1159 stars are not hydrogen deficient pre-white dwarfs with effective temperature 100,000 - 140,000 K and peculiar chemical composition. Carbon and helium are the dominant constituents (C/He = 0.5) (Werner *et al.* 1991). Due to the high surface gravity (log g = 7) Stark broadening is an important line broadening mechanism and Stark broadening data are needed for NLTE model atmosphere analysis (Werner *et al.* 1991) and other stellar plasma investigations (see e.g. Dimitrijević 1989 or Kršljanin & Dimitrijević 1992). In this class of stars a number of large principal quantum number C IV lines not included in our previous analysis were observed recently (Werner *et al.* 1991; Werner & Heber 1991). Moreover, Stark broadening data in the far and extreme ultraviolet, for lines originating from transitions between energy levels with large principal quantum number and low lying levels will become important for astrophysics in the near future. The Extreme Ultraviolet Explorer (EUVE) mission will provide the all sky survey in the $\lambda = 70 - 700$ Å range by four EUV telescopes in Earth orbit (Bowyer & Malina 1990). Moreover, the primary goal of the Far Ultraviolet Spectroscopy Explorer (FUSE) mission which is being developed by NASA is to obtain high resolution spectra with unprecedented sensitivity in the wavelength range 912 - 1250 Å (Soneborn 1991). Consequently, one of the principal aims of this paper is to complement available C IV Stark broadening data with the lines of large principal quantum number.

This paper is the sixth of a series devoted to the calculation of Stark broadening parameters of spectral lines of multicharged ions. The first five were concerned with C IV, Si IV, O VI, N V Sc III and Ti IV lines (Dimitrijević *et al.* 1991a-d, Dimitrijević & Sahal-Brechot 1992a-c). By using the semiclassical-perturbation formalism (Sahal-Bréchot 1969ab), we have calculated electron-, proton-, and ionized helium-impact line widths and shifts for 69 C IV multiplets of large principal quantum number. A summary of the formalism is given in Dimitrijević & Sahal-Bréchot (1991a). Here, we present and discuss the results for C IV multiplets of large principal quantum number, along with a discussion of the Stark broadening parameter regularities within spectral series.

2. Results and discussion.

Energy levels for C IV lines have been taken from Bashkin & Stoner (1975). Oscillator strengths have been calculated by using the method of Bates & Damgaard (1949) and the tables of Oertel & Shomo (1968). For higher levels, the method described by Van Regemorter *et al.* (1979) has been used.

In addition to electron-impact full halfwidths and shifts, Stark-broadening parameters due to proton-, and

© European Southern Observatory • Provided by the NASA Astrophysics Data System

1992A&AS...96..613D

ionized helium- impacts have been calculated. At high temperatures helium is ionized twice; yet the Stark broadening parameters due to doubly charged helium have not been provided, because they are smaller than previous one: the increase of the Coulomb repulsion entails a decrease of the line width. Besides, owing to the neutrality plasma condition, the electron density is twice larger than the corresponding doubly charged helium density due to the fact that helium is twice ionized and thus the relative contribution of the electron impact broadening is more important. Consequently, the influence of other multiply charged ions on the line broadening parameters is much smaller.

Our results for C IV multiplets of large principal quantum number are shown in Table 1, for perturber densities $10^{13} - 10^{18}$ cm^{-3} and temperatures $T = 20{,}000 - 200{,}000$ K. In table 2 Stark broadening parameters are presented for far UV C IV multiplets for temperatures $T = 20{,}000 - 200{,}000$ K and only for a perturber density of 10^{15}cm^{-3}, since these lines are not so important for model atmosphere analysis in comparison with previous ones. However, data for other densities may be provided by authors upon request. We also specify a parameter c (Dimitrijević & Sahal-Bréchot 1984), which gives an estimate for the maximum perturber density for which the line may be treated as isolated when it is divided by the corresponding electron-impact full width at half maximum. For each value given in Tables 1 and 2, the collision volume (V) multiplied by the perturber density (N) is much less than one and the impact approximation is valid (Sahal-Bréchot 1969ab). Values for $NV > 0.5$ are not given and values for $0.1 < NV < 0.5$ are denoted by an asterisk. When the impact approximation is not valid, the ion broadening contribution may be estimated by using quasistatic estimations (Sahal-Bréchot 1991 and Griem 1974). The accuracy of the results obtained decreases when broadening by ion interactions becomes important.

In Figures 1-4, the electron and proton full halfwidths and shifts within the $2p^2P^o - ns^2S$ series are reported. By inspecting the energy separation between the upper level and the principal perturbing levels (see the Grotrian diagrams in Bashkin & Stoner 1975), we find that this separation decreases gradually within a spectral series. We obtain therefore, a gradual change of the Stark widths as in the case analysed in Dimitrijević *et al.* (1991a) when the upper level was a p level. In Figures 5 and 6 the case of C IV $np^2P^o - 9s^2S$ transitions, i.e. the case when the upper level does not change is presented. We can see that particularly for shifts the changes of Stark broadening parameters are relatively small, permitting the interpolation of new data or critical evaluation of mutual consistency of existing data.

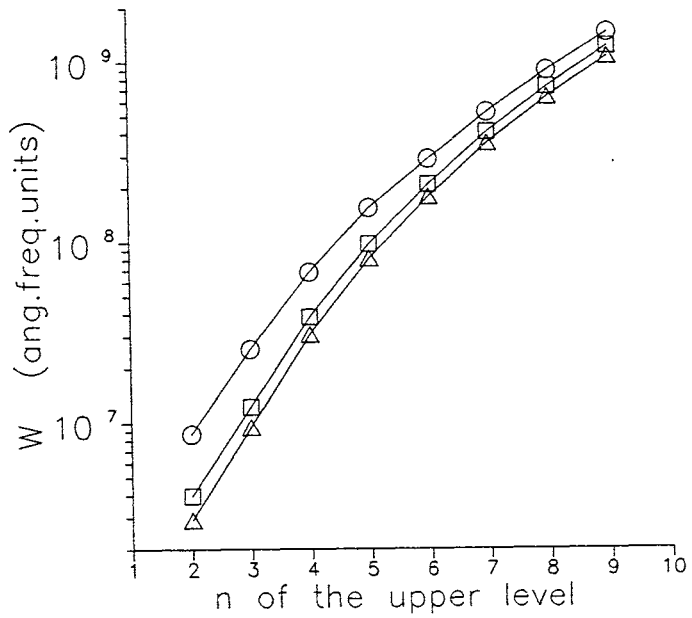

FIGURE 1. Electron-impact full half-widths (in angular frequency units) for the C IV $2p^2P^o - ns^2S$ lines as a function of n for $T = 20{,}000$ K (O); 100,000 K () and 200,000 K (Δ) at $N_e = 10^{13}$ cm^{-3}.

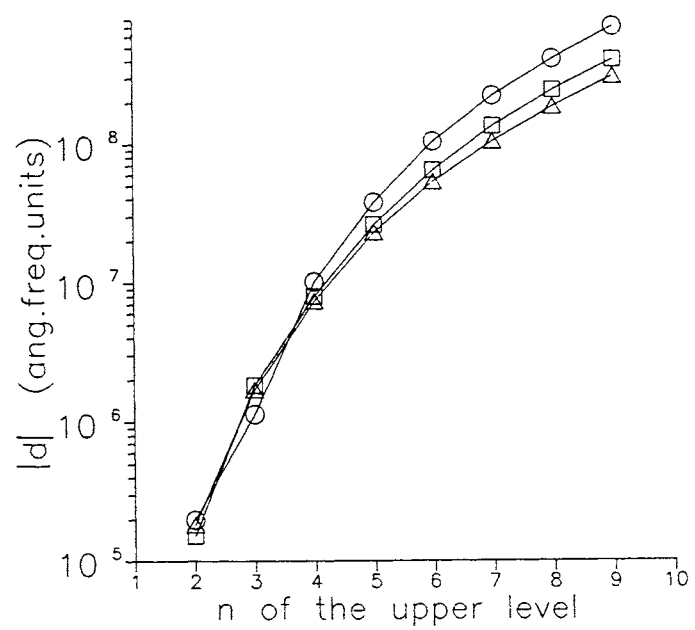

FIGURE 2. As in Fig. 1 but for the electron - impact shift.

© European Southern Observatory • Provided by the NASA Astrophysics Data System

1992A&AS...96..613D

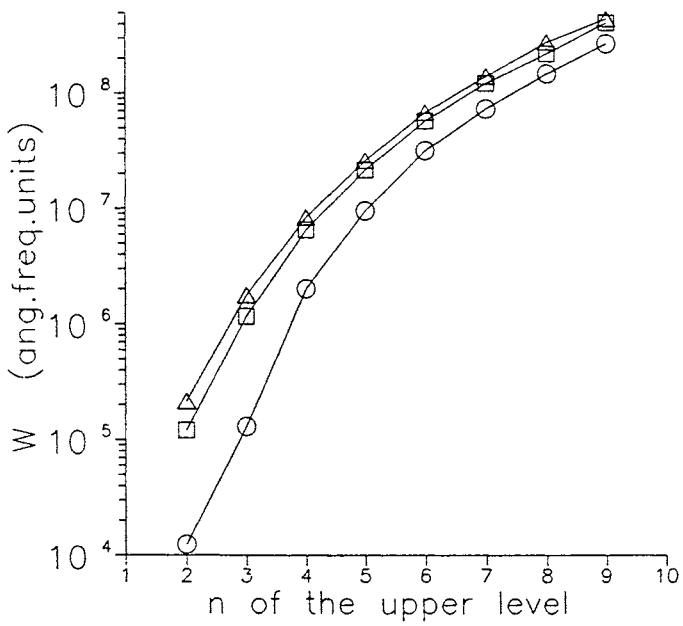

FIGURE 3. As in Fig. 1 but for the proton - impact full halfwidth.

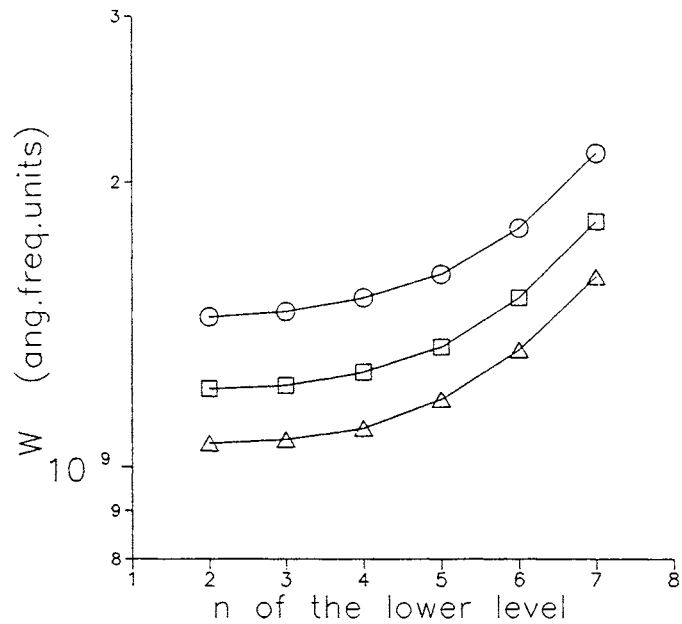

FIGURE 5. As in Fig. 1 but for the C IV $np^2P^o - 9s^2S$ electron - impact width.

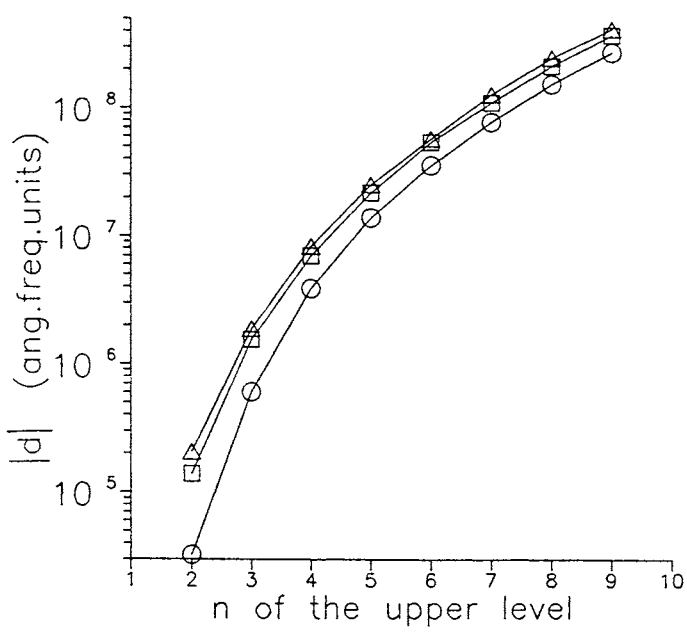

FIGURE 4. As in Fig. 1 but for the proton - impact shift.

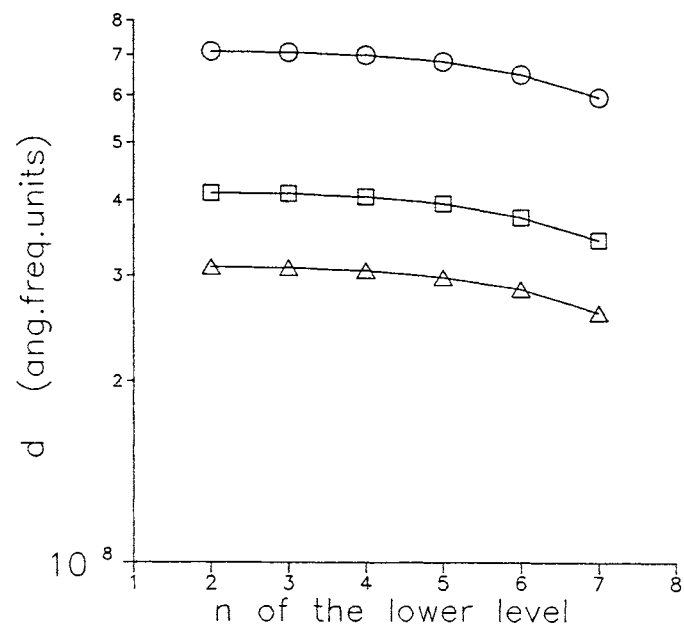

FIGURE 6. As in Fig. 1 but for the C IV $np^2P^o - 9s^2S$ electron - impact shift.

© European Southern Observatory • Provided by the NASA Astrophysics Data System

1992A&AS...96..613D

Acknowledgements.

This work has been supported by the French C.N.R.S. and is a part of French-Yugoslav collaboration through the project "L'élargissement Stark des raies spectrales des plasmas astrophysiques et de laboratoire". It is also a part of the project "Physics and Dynamics of Celestial Bodies" supported by RFN of Serbia.

References

Bashkin S., Stoner J.O. Jr. 1975, Atomic Energy Levels and Grotrian Diagrams, Vol.1, North Holland, Amsterdam

Bates D.R., Damgaard A. 1949, Trans.Roy.Soc. London, Ser. A 242, 101

Bowyer S., Malina R.F. 1991, Proc.Int.Symp. "Evolution in Astrophysics", Toulouse 1990, ESA SP-310, 189

Dimitrijević M.S. 1989, Bull. Obs. Astron. Belgrade 140, 111

Dimitrijević M.S., Sahal-Bréchot S. 1984, JQSRT 31, 301

Dimitrijević M.S., Sahal-Bréchot S., Bommier V. 1991a, A&AS 89, 581

Dimitrijević M.S., Sahal-Bréchot S., Bommier V. 1991b, Bull. Obs.Astron.Belgrade 144, 65

Dimitrijević M.S., Sahal-Bréchot S., Bommier V. 1991c, A&AS 89, 591

Dimitrijević M.S., Sahal-Bréchot S., Bommier V. 1991d, Bull. Obs. Astron. Belgrade 144, 81

Dimitrijević M.S., Sahal-Bréchot S. 1992a, A&AS 93, 359

Dimitrijević M.S., Sahal-Bréchot S. 1992b, A&AS in press

Dimitrijević M.S., Sahal-Bréchot S. 1992c, A&AS in press

Griem H.R. 1974, Spectral Line Broadening by Plasmas, Academic Press, New York and London

Kršljanin V., Dimitrijević M.S. 1992, in Atmospheres of Early-Type Stars, eds. S. Jeffery and U. Heber, Lect.Notes in Physics, in press

Oertel G.K., Shomo L.P. 1968, ApJS 16, 175

Sahal-Bréchot S. 1969a, A&A 1, 91

Sahal-Bréchot S. 1969b, A&A 2, 322

Sahal-Bréchot S. 1991, A&A 245, 322

Seaton M.J. 1987, J.Phys.B 20, 6363

Soneborn G., Malina R.F. 1991, Proc.Int.Symp. "Evolution in Astrophysics", Toulouse 1990, ESA SP-310, 189

Van Regemorter H., Hoang Binh Dy, Prud'homme M. 1979, J.Phys.B 12, 1073

Werner K., Heber U. 1991, A&A 247, 476

Werner K., Heber U., Hunger K. 1991, A&A 244, 437

TABLE 1. *This table shows electron-, proton-, and ionized- helium- impact broadening parameters for C IV lines of large principal quantum number, for perturber densities of* $10^{13} - 10^{18}$ cm^{-3} *and temperatures from 20,000 to 200,000 K. Transitions and averaged wavelengths for the multiplet (in Å) are also given. By using c [see Eq. (5) in Dimitrijevic et al., 1991a], we obtain an estimate for the maximum perturber density for which the line may be treated as isolated and tabulated data may be used. The asterisk identifies cases for which the collision volume multiplied by the perturber density (the condition for validity of the impact approximation) lies between 0.1 and 0.5.*

PERTURBER DENSITY = 0.1D+14(cm-3)

PERTURBERS ARE		ELECTRONS		PROTONS		IONIZED HELIUM	
TRANSITION	T(K)	WIDTH(A)	SHIFT(A)	WIDTH(A)	SHIFT(A)	WIDTH(A)	SHIFT(A)
CIV 4D-6F	20000.	0.154E-03	0.153E-05	0.223E-03	0.209E-03	0.185E-03	0.170E-03
1637.6 A	50000.	0.116E-03	-0.421E-06	0.256E-03	0.255E-03	0.244E-03	0.190E-03
C= 0.79E+12	100000.	0.922E-04	-0.154E-05	0.356E-03	0.275E-03	0.240E-03	0.209E-03
	200000.	0.720E-04	-0.118E-05	0.356E-03	0.324E-03	0.307E-03	0.232E-03
CIV 4D-7F	20000.	0.215E-03	0.348E-05	0.385E-03	0.323E-03	0.320E-03	0.280E-03
1351.3 A	50000.	0.160E-03	-0.616E-06	0.386E-03	0.406E-03	0.424E-03	0.319E-03
C= 0.35E+12	100000.	0.126E-03	-0.238E-05	0.516E-03	0.450E-03	0.462E-03	0.389E-03
	200000.	0.984E-04	-0.162E-05	0.521E-03	0.530E-03	0.489E-03	0.442E-03
CIV 4F-5G	20000.	0.697E-04	-0.310E-05	0.973E-04	-0.966E-04	0.832E-04	-0.795E-04
2530.7 A	50000.	0.523E-04	-0.155E-05	0.124E-03	-0.115E-03	0.102E-03	-0.908E-04
C= 0.55E+13	100000.	0.419E-04	-0.323E-06	0.144E-03	-0.130E-03	0.112E-03	-0.106E-03
	200000.	0.335E-04	0.453E-06	0.155E-03	-0.145E-03	0.158E-03	-0.128E-03
CIV 4F-6G	20000.	0.128E-03	-0.168E-05	0.341E-03	0.315E-03	0.306E-03	0.257E-03
1640.1 A	50000.	0.950E-04	-0.160E-05	0.436E-03	0.357E-03	0.313E-03	0.312E-03
C= 0.17E+12	100000.	0.744E-04	0.124E-06	0.445E-03	0.398E-03	0.414E-03	0.370E-03
	200000.	0.576E-04	0.189E-06	0.574E-03	0.431E-03	0.405E-03	0.397E-03
CIV 4F-7G	20000.	0.213E-03	-0.201E-05	0.647E-03	0.605E-03	*0.620E-03	*0.497E-03
1353.0 A	50000.	0.156E-03	-0.155E-05	0.853E-03	0.664E-03	0.635E-03	0.619E-03
C= 0.81E+11	100000.	0.121E-03	0.147E-06	0.117E-02	0.778E-03	0.663E-03	0.637E-03
	200000.	0.931E-04	-0.146E-06	0.956E-03	0.103E-02	0.107E-02	0.625E-03
CIV 5D-6F	20000.	0.147E-02	-0.696E-05	0.177E-02	0.163E-02	0.143E-02	0.134E-02
4647.0 A	50000.	0.111E-02	-0.158E-04	0.198E-02	0.198E-02	0.196E-02	0.154E-02
C= 0.64E+13	100000.	0.885E-03	-0.216E-04	0.282E-02	0.219E-02	0.196E-02	0.165E-02
	200000.	0.693E-03	-0.147E-04	0.286E-02	0.251E-02	0.252E-02	0.175E-02
CIV 5D-7F	20000.	0.108E-02	0.883E-05	0.177E-02	0.149E-02	0.145E-02	0.129E-02
2902.4 A	50000.	0.807E-03	-0.739E-05	0.177E-02	0.185E-02	0.194E-02	0.147E-02
C= 0.16E+13	100000.	0.638E-03	-0.142E-04	0.241E-02	0.209E-02	0.210E-02	0.180E-02
	200000.	0.498E-03	-0.914E-05	0.230E-02	0.241E-02	0.218E-02	0.203E-02
CIV 5F-6G	20000.	0.131E-02	-0.200E-04	0.267E-02	0.248E-02	0.239E-02	0.200E-02
4658.5 A	50000.	0.983E-03	-0.152E-04	0.358E-02	0.277E-02	0.242E-02	0.240E-02
C= 0.14E+13	100000.	0.774E-03	0.219E-06	0.350E-02	0.304E-02	0.290E-02	0.292E-02
	200000.	0.601E-03	0.274E-05	0.441E-02	0.331E-02	0.288E-02	0.312E-02
CIV 5F-7G	20000.	0.109E-02	-0.119E-04	0.297E-02	0.275E-02	*0.287E-02	*0.228E-02
2906.5 A	50000.	0.802E-03	-0.812E-05	0.392E-02	0.304E-02	0.290E-02	0.284E-02
C= 0.37E+12	100000.	0.626E-03	0.335E-06	0.538E-02	0.361E-02	0.296E-02	0.287E-02
	200000.	0.483E-03	-0.212E-06	0.429E-02	0.464E-02	0.497E-02	0.288E-02
CIV 5G-6F	20000.	0.130E-02	0.337E-04	0.196E-02	0.180E-02	0.155E-02	0.147E-02
4661.0 A	50000.	0.979E-03	0.861E-05	0.242E-02	0.219E-02	0.203E-02	0.165E-02
C= 0.64E+13	100000.	0.775E-03	-0.692E-05	0.310E-02	0.241E-02	0.202E-02	0.183E-02
	200000.	0.604E-03	-0.885E-05	0.320E-02	0.281E-02	0.269E-02	0.197E-02

© European Southern Observatory • Provided by the NASA Astrophysics Data System

1992A&AS...96..613D

TABLE 1. *(continued)*

PERTURBER DENSITY = 0.1D+14(cm-3)

PERTURBERS ARE		ELECTRONS		PROTONS		IONIZED HELIUM	
TRANSITION	T(K)	WIDTH(A)	SHIFT(A)	WIDTH(A)	SHIFT(A)	WIDTH(A)	SHIFT(A)
CIV 5G-7F	20000.	0.101E-02	0.245E-04	0.174E-02	0.151E-02	0.151E-02	0.132E-02
2907.4 A	50000.	0.755E-03	0.204E-05	0.181E-02	0.197E-02	0.198E-02	0.147E-02
C= 0.16E+13	100000.	0.596E-03	-0.853E-05	0.233E-02	0.215E-02	0.221E-02	0.179E-02
	200000.	0.464E-03	-0.688E-05	0.259E-02	0.249E-02	0.233E-02	0.205E-02
CIV 5G-6H	20000.	0.561E-03	-0.670E-05	0.290E-02	-0.287E-02	0.246E-02	-0.228E-02
4660.2 A	50000.	0.418E-03	0.606E-05	0.349E-02	-0.313E-02	0.285E-02	-0.296E-02
C= 0.14E+13	100000.	0.332E-03	0.620E-05	0.377E-02	-0.365E-02	0.338E-02	-0.323E-02
	200000.	0.262E-03	0.583E-05	0.458E-02	-0.369E-02	0.393E-02	-0.349E-02
CIV 6D-7F	20000.	0.886E-02	-0.401E-04	0.122E-01	0.103E-01	0.983E-02	0.892E-02
7708.6 A	50000.	0.668E-02	-0.116E-03	0.125E-01	0.127E-01	0.134E-01	0.103E-01
C= 0.11E+14	100000.	0.530E-02	-0.138E-03	0.166E-01	0.147E-01	0.137E-01	0.122E-01
	200000.	0.414E-02	-0.855E-04	0.159E-01	0.164E-01	0.148E-01	0.138E-01
CIV 6F-7D	20000.	0.762E-02	0.274E-03	0.422E-02	-0.369E-02	0.360E-02	-0.313E-02
7746.1 A	50000.	0.588E-02	0.207E-03	0.498E-02	-0.431E-02	0.432E-02	-0.371E-02
C= 0.18E+14	100000.	0.474E-02	0.161E-03	0.536E-02	-0.535E-02	0.519E-02	-0.386E-02
	200000.	0.376E-02	0.947E-04	0.655E-02	-0.584E-02	0.589E-02	-0.472E-02
CIV 6F-7G	20000.	0.965E-02	-0.132E-03	0.207E-01	0.178E-01	*0.183E-01	*0.154E-01
7726.7 A	50000.	0.713E-02	-0.609E-04	0.261E-01	0.201E-01	0.166E-01	0.183E-01
C= 0.26E+13	100000.	0.557E-02	0.262E-04	0.315E-01	0.255E-01	0.211E-01	0.191E-01
	200000.	0.428E-02	0.151E-04	0.296E-01	0.281E-01	0.321E-01	0.212E-01
CIV 6G-7F	20000.	0.919E-02	0.182E-03	0.713E-02	0.665E-02	0.653E-02	0.543E-02
7729.6 A	50000.	0.684E-02	0.359E-04	0.974E-02	0.767E-02	0.665E-02	0.638E-02
C= 0.38E+13	100000.	0.537E-02	-0.660E-04	0.977E-02	0.820E-02	0.750E-02	0.781E-02
	200000.	0.416E-02	-0.485E-04	0.127E-01	0.872E-02	0.757E-02	0.816E-02

PERTURBER DENSITY = 0.1D+15(cm-3)

PERTURBERS ARE		ELECTRONS		PROTONS		IONIZED HELIUM	
TRANSITION	T(K)	WIDTH(A)	SHIFT(A)	WIDTH(A)	SHIFT(A)	WIDTH(A)	SHIFT(A)
CIV 4D-5G	20000.	0.825E-03	-0.646E-04	0.106E-02	-0.102E-02	0.890E-03	-0.846E-03
2524.6 A	50000.	0.621E-03	-0.376E-04	0.132E-02	-0.122E-02	0.107E-02	-0.998E-03
C= 0.55E+14	100000.	0.500E-03	-0.190E-04	0.154E-02	-0.137E-02	0.119E-02	-0.119E-02
	200000.	0.400E-03	-0.470E-05	0.160E-02	-0.153E-02	0.166E-02	-0.128E-02
CIV 4F-5G	20000.	0.690E-03	-0.310E-04	0.973E-03	-0.966E-03	0.832E-03	-0.795E-03
2530.7 A	50000.	0.518E-03	-0.155E-04	0.124E-02	-0.115E-02	0.102E-02	-0.908E-03
C= 0.55E+14	100000.	0.416E-03	-0.323E-05	0.144E-02	-0.130E-02	0.112E-02	-0.106E-02
	200000.	0.332E-03	0.453E-05	0.155E-02	-0.145E-02	0.158E-02	-0.128E-02
CIV 4F-6G	20000.	0.117E-02	-0.168E-04	*0.341E-02	*0.315E-02	*0.306E-02	*0.257E-02
1640.1 A	50000.	0.877E-03	-0.160E-04	0.436E-02	0.357E-02	*0.313E-02	*0.312E-02
C= 0.17E+13	100000.	0.692E-03	0.124E-05	0.445E-02	0.398E-02	*0.414E-02	*0.370E-02
	200000.	0.539E-03	0.189E-05	0.574E-02	0.431E-02	0.405E-02	0.397E-02
CIV 4F-7G	20000.	0.187E-02	-0.201E-04				
1353.0 A	50000.	0.139E-02	-0.155E-04	*0.853E-02	*0.664E-02		
C= 0.81E+12	100000.	0.109E-02	0.147E-05	*0.117E-01	*0.778E-02	*0.663E-02	*0.637E-02
	200000.	0.849E-03	-0.146E-05	*0.956E-02	*0.103E-01	*0.107E-01	*0.625E-02
CIV 5D-6P	20000.	0.905E-02	0.257E-03	0.152E-02	-0.150E-02	0.128E-02	-0.125E-02
4786.8 A	50000.	0.734E-02	0.312E-03	0.203E-02	-0.187E-02	0.171E-02	-0.153E-02
C= 0.12E+16	100000.	0.620E-02	0.277E-03	0.239E-02	-0.201E-02	0.205E-02	-0.178E-02
	200000.	0.513E-02	0.233E-03	0.261E-02	-0.235E-02	0.247E-02	-0.196E-02
CIV 5D-7P	20000.	0.516E-02	0.319E-03	0.310E-03	-0.247E-03	0.299E-03	-0.208E-03
2935.9 A	50000.	0.434E-02	0.316E-03	0.394E-03	-0.310E-03	0.368E-03	-0.256E-03
C= 0.44E+15	100000.	0.374E-02	0.242E-03	0.470E-03	-0.358E-03	0.403E-03	-0.294E-03
	200000.	0.314E-02	0.202E-03	0.542E-03	-0.416E-03	0.449E-03	-0.335E-03

PERTURBER DENSITY = 0.1D+15(cm-3)

CIV 4P-6D	20000.	0.116E-02	0.640E-04	0.537E-03	0.517E-03	0.436E-03	0.431E-03
1586.0 A	50000.	0.885E-03	0.386E-04	0.720E-03	0.612E-03	0.573E-03	0.516E-03
C= 0.81E+14	100000.	0.718E-03	0.230E-04	0.780E-03	0.673E-03	0.683E-03	0.574E-03
	200000.	0.574E-03	0.110E-04	0.903E-03	0.849E-03	0.757E-03	0.589E-03
CIV 4P-7D	20000.	0.144E-02	0.875E-04	0.638E-03	0.582E-03	0.516E-03	0.475E-03
1315.9 A	50000.	0.112E-02	0.548E-04	0.793E-03	0.694E-03	0.642E-03	0.573E-03
C= 0.53E+14	100000.	0.913E-03	0.337E-04	0.959E-03	0.762E-03	0.693E-03	0.628E-03
	200000.	0.734E-03	0.169E-04	0.999E-03	0.799E-03	0.789E-03	0.747E-03
CIV 4D-6F	20000.	0.149E-02	0.153E-04	0.223E-02	0.209E-02	*0.185E-02	*0.170E-02
1637.6 A	50000.	0.113E-02	-0.421E-05	0.256E-02	0.255E-02	0.244E-02	0.190E-02
C= 0.79E+13	100000.	0.900E-03	-0.154E-04	0.356E-02	0.275E-02	0.240E-02	0.209E-02
	200000.	0.705E-03	-0.118E-04	0.356E-02	0.324E-02	0.307E-02	0.232E-02
CIV 4D-7F	20000.	0.203E-02	0.348E-04	*0.385E-02	*0.323E-02	*0.320E-02	*0.280E-02
1351.3 A	50000.	0.152E-02	-0.616E-05	*0.386E-02	*0.406E-02	*0.424E-02	*0.319E-02
C= 0.35E+13	100000.	0.121E-02	-0.238E-04	*0.516E-02	*0.450E-02	*0.462E-02	*0.389E-02
	200000.	0.946E-03	-0.162E-04	0.521E-02	0.530E-02	*0.489E-02	*0.442E-02
CIV 5D-6F	20000.	0.143E-01	-0.696E-04	0.177E-01	0.163E-01	*0.143E-01	*0.134E-01
4647.0 A	50000.	0.109E-01	-0.158E-03	0.198E-01	0.198E-01	0.196E-01	0.154E-01
C= 0.64E+14	100000.	0.867E-02	-0.216E-03	0.282E-01	0.219E-01	0.196E-01	0.165E-01
	200000.	0.680E-02	-0.147E-03	0.286E-01	0.251E-01	0.252E-01	0.175E-01
CIV 5D-7F	20000.	0.102E-01	0.883E-04	*0.177E-01	*0.149E-01	*0.145E-01	*0.129E-01
2902.4 A	50000.	0.772E-02	-0.739E-04	*0.177E-01	*0.185E-01	*0.194E-01	*0.147E-01
C= 0.16E+14	100000.	0.613E-02	-0.142E-03	*0.241E-01	*0.209E-01	*0.210E-01	*0.180E-01
	200000.	0.480E-02	-0.914E-04	0.230E-01	0.241E-01	*0.218E-01	*0.203E-01
CIV 5F-6D	20000.	0.124E-01	0.615E-03	0.207E-02	0.205E-02	0.175E-02	0.172E-02
4665.0 A	50000.	0.959E-02	0.404E-03	0.278E-02	0.254E-02	0.225E-02	0.205E-02
C= 0.19E+15	100000.	0.776E-02	0.268E-03	0.331E-02	0.293E-02	0.265E-02	0.235E-02
	200000.	0.618E-02	0.164E-03	0.390E-02	0.328E-02	0.282E-02	0.258E-02
CIV 5F-7D	20000.	0.798E-02	0.453E-03	0.235E-02	0.216E-02	0.190E-02	0.178E-02
2909.3 A	50000.	0.622E-02	0.296E-03	0.273E-02	0.256E-02	0.244E-02	0.206E-02
C= 0.73E+14	100000.	0.507E-02	0.193E-03	0.338E-02	0.303E-02	0.283E-02	0.228E-02
	200000.	0.406E-02	0.110E-03	0.430E-02	0.331E-02	0.275E-02	0.256E-02

© European Southern Observatory • Provided by the NASA Astrophysics Data System

1992A&AS...96..613D

TABLE 1. *(continued)*

PERTURBER DENSITY = 0.1D+15(cm-3)

PERTURBERS ARE		ELECTRONS		PROTONS		IONIZED HELIUM	
TRANSITION	T(K)	WIDTH(A)	SHIFT(A)	WIDTH(A)	SHIFT(A)	WIDTH(A)	SHIFT(A)
CIV 5F-6G	20000.	0.122E-01	-0.200E-03	*0.267E-01	*0.248E-01	*0.239E-01	*0.200E-01
4658.5 A	50000.	0.925E-02	-0.152E-03	0.358E-01	0.277E-01	*0.242E-01	*0.240E-01
C= 0.14E+14	100000.	0.733E-02	0.219E-05	0.350E-01	0.304E-01	0.290E-01	0.292E-01
	200000.	0.572E-02	0.274E-04	0.441E-01	0.331E-01	0.288E-01	0.312E-01
CIV 5F-7G	20000.	0.971E-02	-0.119E-03				
2906.5 A	50000.	0.728E-02	-0.812E-04	*0.392E-01	*0.304E-01		
C= 0.37E+13	100000.	0.573E-02	0.335E-05	*0.538E-01	*0.361E-01		
	200000.	0.445E-02	-0.212E-05	*0.429E-01	*0.464E-01		
CIV 5G-6F	20000.	0.126E-01	0.337E-03	0.196E-01	0.180E-01	*0.155E-01	*0.147E-01
4661.0 A	50000.	0.953E-02	0.861E-04	0.242E-01	0.219E-01	0.203E-01	0.165E-01
C= 0.64E+14	100000.	0.756E-02	-0.692E-04	0.310E-01	0.241E-01	0.202E-01	0.183E-01
	200000.	0.591E-02	-0.885E-04	0.320E-01	0.281E-01	0.269E-01	0.197E-01
CIV 5G-7F	20000.	0.956E-02	0.245E-03	*0.174E-01	*0.151E-01	*0.151E-01	*0.132E-01
2907.4 A	50000.	0.720E-02	0.204E-04	*0.181E-01	*0.197E-01	*0.198E-01	*0.147E-01
C= 0.16E+14	100000.	0.571E-02	-0.853E-04	*0.233E-01	*0.215E-01	*0.221E-01	*0.179E-01
	200000.	0.446E-02	-0.688E-04	0.259E-01	0.249E-01	*0.233E-01	*0.205E-01
CIV 5G-6H	20000.	0.511E-02	-0.670E-04	*0.290E-01	-0.287E-01	*0.246E-01	-0.228E-01
4660.2 A	50000.	0.386E-02	0.606E-04	0.349E-01	-0.313E-01	*0.285E-01	-0.296E-01
C= 0.14E+14	100000.	0.309E-02	0.620E-04	0.377E-01	-0.365E-01	*0.338E-01	-0.323E-01
	200000.	0.246E-02	0.583E-04	0.458E-01	-0.369E-01	0.393E-01	-0.349E-01
CIV 6D-7F	20000.	0.847E-01	-0.401E-03	*0.122	*0.103	*0.983E-01	*0.892E-01
7708.6 A	50000.	0.643E-01	-0.116E-02	*0.125	*0.127	*0.134	*0.103
C= 0.11E+15	100000.	0.513E-01	-0.138E-02	*0.166	*0.147	*0.137	*0.122
	200000.	0.402E-01	-0.855E-03	0.159	0.164	*0.148	*0.138
CIV 6F-7D	20000.	0.751E-01	0.274E-02	0.422E-01	-0.369E-01	0.360E-01	-0.313E-01
7746.1 A	50000.	0.581E-01	0.207E-02	0.498E-01	-0.431E-01	0.432E-01	-0.371E-01
C= 0.18E+15	100000.	0.469E-01	0.161E-02	0.536E-01	-0.535E-01	0.519E-01	-0.386E-01
	200000.	0.372E-01	0.947E-03	0.655E-01	-0.584E-01	0.589E-01	-0.472E-01
CIV 6F-7G	20000.	0.871E-01	-0.132E-02				
7726.7 A	50000.	0.654E-01	-0.609E-03	*0.261	*0.201	*0.166	*0.183
C= 0.26E+14	100000.	0.515E-01	0.262E-03	*0.315	*0.255	*0.211	*0.191
	200000.	0.399E-01	0.151E-03	*0.296	*0.281	*0.321	*0.212
CIV 6G-7F	20000.	0.854E-01	0.182E-02	*0.713E-01	*0.665E-01	*0.653E-01	*0.543E-01
7729.6 A	50000.	0.643E-01	0.359E-03	0.974E-01	0.767E-01	*0.665E-01	*0.638E-01
C= 0.38E+14	100000.	0.508E-01	-0.660E-03	0.977E-01	0.820E-01	0.750E-01	0.781E-01
	200000.	0.396E-01	-0.485E-03	0.127	0.872E-01	0.757E-01	0.816E-01

PERTURBER DENSITY = 0.1D+16(cm-3)

PERTURBERS ARE		ELECTRONS		PROTONS		IONIZED HELIUM	
TRANSITION	T(K)	WIDTH(A)	SHIFT(A)	WIDTH(A)	SHIFT(A)	WIDTH(A)	SHIFT(A)
CIV 4S-7P	20000.	0.702E-02	0.651E-03	0.104E-02	0.961E-03	0.902E-03	0.799E-03
1210.6 A	50000.	0.599E-02	0.583E-03	0.137E-02	0.121E-02	0.118E-02	0.981E-03
C= 0.53E+16	100000.	0.524E-02	0.429E-03	0.157E-02	0.129E-02	0.140E-02	0.114E-02
	200000.	0.445E-02	0.331E-03	0.168E-02	0.151E-02	0.165E-02	0.125E-02
C IV 4P-6S	20000.	0.519E-02	0.141E-02	0.433E-03	0.482E-03	0.383E-03	0.410E-03
1653.9 A	50000.	0.433E-02	0.106E-02	0.614E-03	0.615E-03	0.531E-03	0.518E-03
C= 0.55E+17	100000.	0.376E-02	0.869E-03	0.738E-03	0.721E-03	0.656E-03	0.608E-03
	200000.	0.322E-02	0.721E-03	0.970E-03	0.828E-03	0.782E-03	0.704E-03
C IV 4P-7S	20000.	0.565E-02	0.207E-02	0.691E-03	0.729E-03	0.586E-03	0.612E-03
1344.3 A	50000.	0.488E-02	0.152E-02	0.957E-03	0.929E-03	0.774E-03	0.769E-03
C= 0.22E+17	100000.	0.436E-02	0.125E-02	0.115E-02	0.104E-02	0.104E-02	0.865E-03
	200000.	0.378E-02	0.971E-03	0.131E-02	0.119E-02	0.110E-02	0.946E-03
C IV 4P-8S	20000.	0.730E-02	0.310E-02	0.112E-02	0.115E-02	0.965E-03	0.949E-03
1200.0 A	50000.	0.650E-02	0.228E-02	0.148E-02	0.140E-02	0.125E-02	0.118E-02
C= 0.12E+17	100000.	0.589E-02	0.184E-02	0.168E-02	0.161E-02	0.150E-02	0.126E-02
	200000.	0.515E-02	0.139E-02	0.211E-02	0.187E-02	0.164E-02	0.139E-02
C IV 4P-9S	20000.	0.100E-01	0.464E-02	0.179E-02	0.178E-02	0.157E-02	0.147E-02
1118.4 A	50000.	0.910E-02	0.347E-02	0.233E-02	0.214E-02	0.203E-02	0.170E-02
C= 0.72E+16	100000.	0.834E-02	0.270E-02	0.275E-02	0.244E-02	0.219E-02	0.200E-02
	200000.	0.733E-02	0.203E-02	0.296E-02	0.269E-02	0.289E-02	0.244E-02
CIV 4P-6D	20000.	0.115E-01	0.606E-03	0.537E-02	0.514E-02	*0.436E-02	*0.428E-02
1586.0 A	50000.	0.882E-02	0.386E-03	0.720E-02	0.612E-02	*0.573E-02	*0.516E-02
C= 0.81E+15	100000.	0.716E-02	0.230E-03	0.780E-02	0.673E-02	0.683E-02	0.574E-02
	200000.	0.573E-02	0.110E-03	0.903E-02	0.849E-02	0.757E-02	0.589E-02
CIV 4P-7D	20000.	0.143E-01	0.828E-03	*0.639E-02	*0.577E-02	*0.516E-02	*0.470E-02
1315.9 A	50000.	0.111E-01	0.548E-03	*0.793E-02	*0.694E-02	*0.642E-02	*0.573E-02
C= 0.53E+15	100000.	0.910E-02	0.337E-03	*0.959E-02	*0.762E-02	*0.693E-02	*0.628E-02
	200000.	0.732E-02	0.169E-03	0.999E-02	0.799E-02	*0.789E-02	*0.747E-02
CIV 4D-6P	20000.	0.785E-02	0.536E-03	0.510E-03	0.429E-03	0.496E-03	0.361E-03
1654.5 A	50000.	0.648E-02	0.519E-03	0.665E-03	0.548E-03	0.621E-03	0.453E-03
C= 0.26E+16	100000.	0.555E-02	0.434E-03	0.790E-03	0.630E-03	0.702E-03	0.528E-03
	200000.	0.466E-02	0.332E-03	0.909E-03	0.736E-03	0.760E-03	0.603E-03
CIV 4D-7P	20000.	0.908E-02	0.837E-03	0.114E-02	0.105E-02	0.103E-02	0.877E-03
1358.5 A	50000.	0.776E-02	0.775E-03	0.148E-02	0.129E-02	0.126E-02	0.109E-02
C= 0.18E+16	100000.	0.676E-02	0.589E-03	0.179E-02	0.153E-02	0.144E-02	0.128E-02
	200000.	0.574E-02	0.469E-03	0.200E-02	0.166E-02	0.176E-02	0.143E-02

PERTURBER DENSITY = 0.1D+16(cm-3)

CIV 4S-6P	20000.	0.568E-02	0.389E-03	0.635E-03	0.605E-03	0.577E-03	0.508E-03
1440.3 A	50000.	0.467E-02	0.345E-03	0.841E-03	0.767E-03	0.750E-03	0.633E-03
C= 0.12E+17	100000.	0.402E-02	0.271E-03	0.102E-02	0.873E-03	0.859E-03	0.727E-03
	200000.	0.339E-02	0.190E-03	0.122E-02	0.102E-02	0.983E-03	0.825E-03
CIV 4D-6F	20000.	0.137E-01	-0.423E-04				
1637.6 A	50000.	0.105E-01	-0.421E-04	*0.256E-01	*0.255E-01		
C= 0.79E+14	100000.	0.843E-02	-0.154E-03	*0.356E-01	*0.275E-01		
	200000.	0.665E-02	-0.118E-03	*0.356E-01	*0.324E-01	*0.307E-01	*0.232E-01

© European Southern Observatory • Provided by the NASA Astrophysics Data System

1992A&AS...96..613D

TABLE 1. *(continued)*

PERTURBER DENSITY = 0.1D+16(cm-3)

PERTURBERS ARE		ELECTRONS		PROTONS		IONIZED HELIUM	
TRANSITION	T(K)	WIDTH(A)	SHIFT(A)	WIDTH(A)	SHIFT(A)	WIDTH(A)	SHIFT(A)
CIV 4D-7F	20000.	0.181E-01	-0.128E-04				
1351.3 A	50000.	0.139E-01	-0.616E-04				
C= 0.35E+14	100000.	0.111E-01	-0.238E-03				
	200000.	0.877E-02	-0.162E-03				
CIV 4D-5G	20000.	0.793E-02	-0.585E-03	0.106E-01	-0.102E-01	*0.890E-02	-0.840E-02
2524.6 A	50000.	0.601E-02	-0.376E-03	0.132E-01	-0.122E-01	0.107E-01	-0.998E-02
C= 0.55E+15	100000.	0.486E-02	-0.190E-03	0.154E-01	-0.137E-01	0.119E-01	-0.119E-01
	200000.	0.390E-02	-0.470E-04	0.160E-01	-0.153E-01	0.166E-01	-0.128E-01
CIV 4F-6D	20000.	0.119E-01	0.794E-03	0.596E-02	0.560E-02	*0.492E-02	*0.468E-02
1641.0 A	50000.	0.914E-02	0.521E-03	0.806E-02	0.656E-02	*0.632E-02	*0.568E-02
C= 0.87E+15	100000.	0.742E-02	0.337E-03	0.830E-02	0.731E-02	0.745E-02	0.629E-02
	200000.	0.594E-02	0.183E-03	0.100E-01	0.928E-02	0.828E-02	0.668E-02
CIV 4F-7D	20000.	0.149E-01	0.977E-03	*0.684E-02	*0.616E-02	*0.557E-02	*0.505E-02
1353.6 A	50000.	0.116E-01	0.655E-03	*0.849E-02	*0.745E-02	*0.692E-02	*0.606E-02
C= 0.56E+15	100000.	0.947E-02	0.420E-03	*0.102E-01	*0.813E-02	*0.749E-02	*0.663E-02
	200000.	0.762E-02	0.225E-03	0.106E-01	0.851E-02	*0.833E-02	*0.792E-02
CIV 4F-5G	20000.	0.658E-02	-0.255E-03	0.972E-02	-0.961E-02	0.832E-02	-0.790E-02
2530.7 A	50000.	0.498E-02	-0.155E-03	0.124E-01	-0.115E-01	0.102E-01	-0.908E-02
C= 0.55E+15	100000.	0.401E-02	-0.323E-04	0.144E-01	-0.130E-01	0.112E-01	-0.106E-01
	200000.	0.322E-02	0.453E-04	0.155E-01	-0.145E-01	0.158E-01	-0.128E-01
CIV 4F-6G	20000.	0.989E-02	-0.166E-03				
1640.1 A	50000.	0.764E-02	-0.160E-03				
C= 0.17E+14	100000.	0.612E-02	0.124E-04				
	200000.	0.483E-02	0.189E-04	*0.574E-01	*0.431E-01		
CIV 4F-7G	20000.	0.153E-01	-0.240E-03				
1353.0 A	50000.	0.118E-01	-0.155E-03				
C= 0.81E+13	100000.	0.943E-02	0.147E-04				
	200000.	0.742E-02	-0.146E-04				
CIV 5S-6P	20000.	0.484E-01	0.139E-02	0.439E-02	0.414E-02	0.400E-02	0.345E-02
3935.8 A	50000.	0.400E-01	0.106E-02	0.585E-02	0.521E-02	0.526E-02	0.440E-02
C= 0.92E+17	100000.	0.345E-01	0.637E-03	0.705E-02	0.615E-02	0.606E-02	0.492E-02
	200000.	0.292E-01	0.159E-03	0.822E-02	0.716E-02	0.676E-02	0.563E-02
CIV 5S-7P	20000.	0.348E-01	0.241E-02	0.469E-02	0.432E-02	0.415E-02	0.358E-02
2592.0 A	50000.	0.297E-01	0.206E-02	0.618E-02	0.544E-02	0.535E-02	0.439E-02
C= 0.24E+17	100000.	0.260E-01	0.139E-02	0.725E-02	0.576E-02	0.622E-02	0.509E-02
	200000.	0.221E-01	0.983E-03	0.769E-02	0.683E-02	0.735E-02	0.569E-02
CIV 5P-6S	20000.	0.633E-01	0.109E-01	0.288E-02	0.296E-02	0.272E-02	0.247E-02
5022.2 A	50000.	0.536E-01	0.816E-02	0.406E-02	0.375E-02	0.364E-02	0.315E-02
C= 0.26E+18	100000.	0.468E-01	0.653E-02	0.508E-02	0.452E-02	0.423E-02	0.370E-02
	200000.	0.401E-01	0.567E-02	0.597E-02	0.506E-02	0.543E-02	0.425E-02

PERTURBER DENSITY = 0.1D+16(cm-3)

PERTURBERS ARE		ELECTRONS		PROTONS		IONIZED HELIUM	
TRANSITION	T(K)	WIDTH(A)	SHIFT(A)	WIDTH(A)	SHIFT(A)	WIDTH(A)	SHIFT(A)
C IV 5P-7S	20000.	0.322E-01	0.929E-02	0.306E-02	0.317E-02	0.265E-02	0.264E-02
2954.6 A	50000.	0.282E-01	0.679E-02	0.405E-02	0.394E-02	0.353E-02	0.330E-02
C= 0.90E+17	100000.	0.252E-01	0.554E-02	0.497E-02	0.464E-02	0.424E-02	0.387E-02
	200000.	0.218E-01	0.435E-02	0.564E-02	0.499E-02	0.504E-02	0.431E-02
C IV 5P-8S	20000.	0.305E-01	0.113E-01	0.407E-02	0.417E-02	0.361E-02	0.348E-02
2337.0 A	50000.	0.274E-01	0.828E-02	0.540E-02	0.508E-02	0.453E-02	0.425E-02
C= 0.45E+17	100000.	0.249E-01	0.669E-02	0.622E-02	0.578E-02	0.560E-02	0.468E-02
	200000.	0.218E-01	0.507E-02	0.763E-02	0.688E-02	0.639E-02	0.518E-02
C IV 5P-9S	20000.	0.356E-01	0.151E-01	0.600E-02	0.586E-02	0.526E-02	0.484E-02
2046.0 A	50000.	0.325E-01	0.113E-01	0.772E-02	0.702E-02	0.696E-02	0.562E-02
C= 0.24E+17	100000.	0.298E-01	0.879E-02	0.913E-02	0.808E-02	0.712E-02	0.654E-02
	200000.	0.262E-01	0.663E-02	0.992E-02	0.878E-02	0.927E-02	0.816E-02
CIV 5P-6D	20000.	0.101	0.347E-02	0.414E-01	0.399E-01	*0.335E-01	*0.331E-01
4441.8 A	50000.	0.783E-01	0.191E-02	0.557E-01	0.476E-01	*0.444E-01	*0.406E-01
C= 0.64E+16	100000.	0.641E-01	0.759E-03	0.603E-01	0.525E-01	0.532E-01	0.447E-01
	200000.	0.517E-01	0.122E-03	0.691E-01	0.659E-01	0.600E-01	0.460E-01
CIV 5P-7D	20000.	0.700E-01	0.328E-02	*0.291E-01	*0.264E-01	*0.237E-01	*0.214E-01
2820.7 A	50000.	0.548E-01	0.207E-02	*0.365E-01	*0.317E-01	*0.290E-01	*0.261E-01
C= 0.24E+16	100000.	0.450E-01	0.113E-02	0.436E-01	0.349E-01	*0.317E-01	*0.289E-01
	200000.	0.363E-01	0.483E-03	0.459E-01	0.366E-01	*0.360E-01	*0.343E-01
CIV 5D-6P	20000.	0.904E-01	0.262E-02	0.152E-01	-0.150E-01	0.128E-01	-0.124E-01
4786.8 A	50000.	0.734E-01	0.312E-02	0.203E-01	-0.187E-01	0.171E-01	-0.153E-01
C= 0.12E+17	100000.	0.620E-01	0.277E-02	0.239E-01	-0.201E-01	0.205E-01	-0.178E-01
	200000.	0.513E-01	0.233E-02	0.261E-01	-0.235E-01	0.247E-01	-0.196E-01
CIV 5D-7P	20000.	0.516E-01	0.320E-02	0.310E-02	-0.246E-02	0.299E-02	-0.207E-02
2935.9 A	50000.	0.434E-01	0.316E-02	0.394E-02	-0.310E-02	0.368E-02	-0.256E-02
C= 0.44E+16	100000.	0.374E-01	0.242E-02	0.470E-02	-0.358E-02	0.403E-02	-0.294E-02
	200000.	0.314E-01	0.202E-02	0.542E-02	-0.416E-02	0.449E-02	-0.335E-02
CIV 5D-6F	20000.	0.133	-0.221E-02				
4647.0 A	50000.	0.102	-0.158E-02	*0.198	*0.198		
C= 0.64E+15	100000.	0.821E-01	-0.216E-02	*0.282	*0.219		
	200000.	0.648E-01	-0.147E-02	*0.286	*0.251	*0.252	*0.175
CIV 5D-7F	20000.	0.920E-01	-0.759E-03				
2902.4 A	50000.	0.708E-01	-0.739E-03				
C= 0.16E+15	100000.	0.568E-01	-0.142E-02				
	200000.	0.448E-01	-0.914E-03				
CIV 5F-6D	20000.	0.122	0.608E-02	0.207E-01	0.205E-01	0.175E-01	0.171E-01
4665.0 A	50000.	0.947E-01	0.404E-02	0.278E-01	0.254E-01	0.225E-01	0.205E-01
C= 0.19E+16	100000.	0.768E-01	0.268E-02	0.331E-01	0.293E-01	0.265E-01	0.235E-01
	200000.	0.612E-01	0.164E-02	0.390E-01	0.328E-01	0.282E-01	0.258E-01

© European Southern Observatory • Provided by the NASA Astrophysics Data System

1992A&AS...96..613D

TABLE 1. *(continued)*

PERTURBER DENSITY = 0.1D+16(cm-3)

PERTURBERS ARE		ELECTRONS		PROTONS		IONIZED HELIUM	
TRANSITION	T(K)	WIDTH(A)	SHIFT(A)	WIDTH(A)	SHIFT(A)	WIDTH(A)	SHIFT(A)
CIV 5F-7D	20000.	0.789E-01	0.438E-02	*0.235E-01	*0.215E-01	*0.190E-01	*0.176E-01
2909.3 A	50000.	0.616E-01	0.296E-02	0.273E-01	0.256E-01	*0.244E-01	*0.206E-01
C= 0.73E+15	100000.	0.503E-01	0.193E-02	0.338E-01	0.303E-01	*0.283E-01	*0.228E-01
	200000.	0.403E-01	0.110E-02	0.430E-01	0.331E-01	0.275E-01	0.256E-01
CIV 5F-6G	20000.	0.106	-0.177E-02				
4658.5 A	50000.	0.825E-01	-0.152E-02				
C= 0.14E+15	100000.	0.662E-01	0.219E-04				
	200000.	0.522E-01	0.274E-03	*0.441	*0.331		
CIV 5F-7G	20000.	0.810E-01	-0.130E-02				
2906.5 A	50000.	0.626E-01	-0.812E-03				
C= 0.37E+14	100000.	0.501E-01	0.335E-04				
	200000.	0.394E-01	-0.212E-04				
CIV 5G-6F	20000.	0.114	0.157E-02				
4661.0 A	50000.	0.881E-01	0.861E-03	*0.242	*0.219		
C= 0.64E+15	100000.	0.706E-01	-0.692E-03	*0.310	*0.241		
	200000.	0.556E-01	-0.885E-03	*0.320	*0.281	*0.269	*0.197
CIV 5G-7F	20000.	0.850E-01	0.691E-03				
2907.4 A	50000.	0.653E-01	0.204E-03				
C= 0.16E+15	100000.	0.524E-01	-0.853E-03				
	200000.	0.413E-01	-0.688E-03				
CIV 5G-6H	20000.	0.444E-01	0.268E-03				
4660.2 A	50000.	0.344E-01	0.606E-03				
C= 0.14E+15	100000.	0.280E-01	0.620E-03				
	200000.	0.225E-01	0.583E-03	*0.458	*-0.369		
CIV 6S-7P	20000.	0.251	0.208E-02	0.275E-01	0.252E-01	0.247E-01	0.211E-01
6593.7 A	50000.	0.218	0.308E-02	0.352E-01	0.311E-01	0.307E-01	0.264E-01
C= 0.16E+18	100000.	0.193	0.690E-03	0.446E-01	0.366E-01	0.353E-01	0.307E-01
	200000.	0.165	-0.576E-03	0.480E-01	0.401E-01	0.426E-01	0.343E-01
C IV 6P-7S	20000.	0.340	0.638E-01	0.160E-01	0.143E-01	0.153E-01	0.121E-01
8385.0 A	50000.	0.299	0.454E-01	0.213E-01	0.183E-01	0.198E-01	0.153E-01
C= 0.42E+18	100000.	0.268	0.371E-01	0.267E-01	0.214E-01	0.228E-01	0.176E-01
	200000.	0.232	0.298E-01	0.281E-01	0.235E-01	0.272E-01	0.201E-01
C IV 6P-8S	20000.	0.153	0.438E-01	0.154E-01	0.151E-01	0.129E-01	0.126E-01
4791.4 A	50000.	0.138	0.318E-01	0.207E-01	0.190E-01	0.175E-01	0.154E-01
C= 0.14E+18	100000.	0.126	0.257E-01	0.239E-01	0.203E-01	0.211E-01	0.179E-01
	200000.	0.110	0.196E-01	0.257E-01	0.238E-01	0.249E-01	0.196E-01
C IV 6P-9S	20000.	0.131	0.474E-01	0.187E-01	0.183E-01	0.162E-01	0.154E-01
3709.7 A	50000.	0.120	0.354E-01	0.244E-01	0.219E-01	0.217E-01	0.184E-01
C= 0.80E+17	100000.	0.111	0.274E-01	0.280E-01	0.253E-01	0.234E-01	0.203E-01
	200000.	0.971E-01	0.208E-01	0.314E-01	0.278E-01	0.269E-01	0.255E-01

PERTURBER DENSITY = 0.1D+16(cm-3)

PERTURBERS ARE		ELECTRONS		PROTONS		IONIZED HELIUM	
TRANSITION	T(K)	WIDTH(A)	SHIFT(A)	WIDTH(A)	SHIFT(A)	WIDTH(A)	SHIFT(A)
CIV 6P-7D	20000.	0.535	0.154E-01	*0.194	*0.179	*0.161	*0.145
7389.4 A	50000.	0.425	0.728E-02	*0.245	*0.216	*0.193	*0.174
C= 0.17E+17	100000.	0.352	0.254E-02	0.297	0.238	*0.208	*0.194
	200000.	0.286	-0.658E-03	0.318	0.246	*0.240	*0.233
CIV 6D-7P	20000.	0.517	0.133E-01	0.114	-0.108	*0.984E-01	-0.890E-01
7949.8 A	50000.	0.425	0.165E-01	0.145	-0.132	0.114	-0.108
C= 0.20E+17	100000.	0.361	0.138E-01	0.166	-0.151	0.142	-0.127
	200000.	0.299	0.126E-01	0.168	-0.171	0.182	-0.138
CIV 6D-7F	20000.	0.775	-0.150E-01				
7708.6 A	50000.	0.597	-0.116E-01				
C= 0.11E+16	100000.	0.480	-0.138E-01				
	200000.	0.379	-0.855E-02				
CIV 6F-7D	20000.	0.721	0.302E-01	*0.422	*-0.365		
7746.1 A	50000.	0.561	0.207E-01	*0.498	*-0.431		
C= 0.18E+16	100000.	0.455	0.161E-01	*0.536	*-0.535	*0.519	*-0.386
	200000.	0.362	0.947E-02	*0.655	*-0.584	*0.589	*-0.472
CIV 6F-7G	20000.	0.733	-0.101E-01				
7726.7 A	50000.	0.566	-0.609E-02				
C= 0.26E+15	100000.	0.453	0.262E-02				
	200000.	0.355	0.151E-02				
CIV 6G-7F	20000.	0.742	0.630E-02				
7729.6 A	50000.	0.573	0.359E-02				
C= 0.38E+15	100000.	0.459	-0.660E-02				
	200000.	0.360	-0.485E-02	*1.27	*0.872		
C IV 7P-8S	20000.	1.46	0.273	0.652E-01	0.496E-01	0.637E-01	0.417E-01
12985.7 A	50000.	1.32	0.193	0.833E-01	0.631E-01	0.765E-01	0.520E-01
C= 0.61E+18	100000.	1.20	0.160	0.960E-01	0.719E-01	0.846E-01	0.597E-01
	200000.	1.04	0.121	0.112	0.837E-01	0.935E-01	0.679E-01
C IV 7P-9S	20000.	0.599	0.166	0.603E-01	0.576E-01	0.529E-01	0.474E-01
7253.4 A	50000.	0.553	0.123	0.781E-01	0.682E-01	0.643E-01	0.580E-01
C= 0.19E+18	100000.	0.507	0.959E-01	0.941E-01	0.775E-01	0.743E-01	0.648E-01
	200000.	0.444	0.724E-01	0.108	0.841E-01	0.747E-01	0.734E-01
PERTURBER DENSITY = 0.1D+17(cm-3)							
CIV 4S-6P	20000.	0.567E-01	0.370E-02	0.635E-02	0.586E-02	0.577E-02	0.489E-02
1440.3 A	50000.	0.467E-01	0.340E-02	0.841E-02	0.764E-02	0.750E-02	0.629E-02
C= 0.12E+18	100000.	0.402E-01	0.271E-02	0.102E-01	0.873E-02	0.859E-02	0.727E-02
	200000.	0.339E-01	0.190E-02	0.122E-01	0.102E-01	0.983E-02	0.825E-02
CIV 4S-7P	20000.	0.702E-01	0.608E-02	*0.104E-01	*0.919E-02	*0.906E-02	*0.760E-02
1210.6 A	50000.	0.599E-01	0.576E-02	*0.137E-01	*0.120E-01	*0.118E-01	*0.974E-02
C= 0.53E+17	100000.	0.524E-01	0.429E-02	0.157E-01	0.129E-01	*0.140E-01	*0.114E-01
	200000.	0.445E-01	0.331E-02	0.168E-01	0.151E-01	*0.165E-01	*0.125E-01

© European Southern Observatory • Provided by the NASA Astrophysics Data System

1992A&AS...96..613D

TABLE 1. *(continued)*

PERTURBER DENSITY = 0.1D+17(cm-3)

PERTURBERS ARE		ELECTRONS		PROTONS		IONIZED HELIUM	
TRANSITION	T(K)	WIDTH(A)	SHIFT(A)	WIDTH(A)	SHIFT(A)	WIDTH(A)	SHIFT(A)
C IV 4P-6S	20000.	0.519E-01	0.140E-01	0.434E-02	0.470E-02	0.383E-02	0.397E-02
1653.9 A	50000.	0.433E-01	0.106E-01	0.614E-02	0.612E-02	0.532E-02	0.516E-02
C= 0.55E+18	100000.	0.376E-01	0.869E-02	0.738E-02	0.721E-02	0.656E-02	0.608E-02
	200000.	0.322E-01	0.721E-02	0.970E-02	0.828E-02	0.782E-02	0.704E-02
C IV 4P-7S	20000.	0.565E-01	0.204E-01	0.690E-02	0.703E-02	*0.586E-02	*0.586E-02
1344.3 A	50000.	0.488E-01	0.151E-01	0.957E-02	0.925E-02	0.773E-02	0.764E-02
C= 0.22E+18	100000.	0.436E-01	0.125E-01	0.115E-01	0.104E-01	0.104E-01	0.865E-02
	200000.	0.378E-01	0.971E-02	0.131E-01	0.119E-01	0.110E-01	0.946E-02
C IV 4P-8S	20000.	0.730E-01	0.301E-01	*0.112E-01	*0.110E-01	*0.973E-02	*0.894E-02
1200.0 A	50000.	0.650E-01	0.227E-01	*0.148E-01	*0.139E-01	*0.125E-01	*0.117E-01
C= 0.12E+18	100000.	0.589E-01	0.184E-01	0.168E-01	0.161E-01	*0.150E-01	*0.126E-01
	200000.	0.515E-01	0.139E-01	0.211E-01	0.187E-01	*0.164E-01	*0.139E-01
C IV 4P-9S	20000.	0.100	0.445E-01	*0.181E-01	*0.167E-01		
1118.4 A	50000.	0.911E-01	0.345E-01	*0.234E-01	*0.212E-01		
C= 0.72E+17	100000.	0.834E-01	0.268E-01	*0.275E-01	*0.244E-01	*0.219E-01	*0.200E-01
	200000.	0.733E-01	0.203E-01	*0.296E-01	*0.269E-01	*0.289E-01	*0.244E-01
CIV 4P-6D	20000.	0.109	0.229E-02				
1586.0 A	50000.	0.845E-01	0.318E-02				
C= 0.81E+16	100000.	0.689E-01	0.230E-02	*0.780E-01	*0.673E-01		
	200000.	0.555E-01	0.110E-02	*0.903E-01	*0.849E-01		
CIV 4D-6P	20000.	0.784E-01	0.527E-02	0.510E-02	0.419E-02	0.496E-02	0.350E-02
1654.5 A	50000.	0.647E-01	0.516E-02	0.665E-02	0.546E-02	0.621E-02	0.451E-02
C= 0.26E+17	100000.	0.555E-01	0.434E-02	0.790E-02	0.630E-02	0.702E-02	0.528E-02
	200000.	0.466E-01	0.332E-02	0.909E-02	0.736E-02	0.760E-02	0.603E-02
CIV 4D-7P	20000.	0.908E-01	0.793E-02	*0.114E-01	*0.101E-01	*0.102E-01	*0.834E-02
1358.5 A	50000.	0.775E-01	0.769E-02	0.148E-01	0.128E-01	*0.126E-01	*0.108E-01
C= 0.18E+17	100000.	0.676E-01	0.589E-02	0.179E-01	0.153E-01	*0.144E-01	*0.128E-01
	200000.	0.573E-01	0.469E-02	0.200E-01	0.166E-01	*0.176E-01	*0.143E-01
CIV 4D-5G	20000.	0.717E-01	-0.240E-02				
2524.6 A	50000.	0.554E-01	-0.283E-02	*0.132	*-0.121		
C= 0.55E+16	100000.	0.452E-01	-0.190E-02	*0.154	*-0.137	*0.119	*-0.119
	200000.	0.367E-01	-0.470E-03	*0.160	*-0.153	*0.166	*-0.128
CIV 4F-6D	20000.	0.112	0.374E-02				
1641.0 A	50000.	0.874E-01	0.446E-02				
C= 0.87E+16	100000.	0.714E-01	0.337E-02	*0.830E-01	*0.731E-01		
	200000.	0.574E-01	0.183E-02	*0.100	*0.928E-01		
CIV 4F-7D	20000.	0.139	0.402E-02				
1353.6 A	50000.	0.110	0.548E-02				
C= 0.56E+16	100000.	0.906E-01	0.420E-02				
	200000.	0.732E-01	0.225E-02				

PERTURBER DENSITY = 0.1D+17(cm-3)

PERTURBERS ARE		ELECTRONS		PROTONS		IONIZED HELIUM	
TRANSITION	T(K)	WIDTH(A)	SHIFT(A)	WIDTH(A)	SHIFT(A)	WIDTH(A)	SHIFT(A)
CIV 4F-5G	20000.	0.583E-01	0.244E-03	*0.963E-01	-0.898E-01		
2530.7 A	50000.	0.451E-01	-0.734E-03	*0.124	*-0.114		
C= 0.55E+16	100000.	0.368E-01	-0.323E-03	*0.144	*-0.130	*0.112	*-0.106
	200000.	0.299E-01	0.453E-03	*0.155	*-0.145	*0.158	*-0.128
CIV 5S-6P	20000.	0.484	0.126E-01	0.439E-01	0.401E-01	0.400E-01	0.333E-01
3935.6 A	50000.	0.400	0.103E-01	0.585E-01	0.519E-01	0.526E-01	0.438E-01
C= 0.92E+18	100000.	0.345	0.637E-02	0.705E-01	0.615E-01	0.606E-01	0.492E-01
	200000.	0.292	0.159E-02	0.822E-01	0.716E-01	0.676E-01	0.563E-01
CIV 5S-7P	20000.	0.348	0.222E-01	*0.469E-01	*0.414E-01	*0.413E-01	*0.340E-01
2591.9 A	50000.	0.297	0.202E-01	*0.617E-01	*0.540E-01	*0.535E-01	*0.436E-01
C= 0.24E+18	100000.	0.260	0.139E-01	0.725E-01	0.576E-01	*0.622E-01	*0.509E-01
	200000.	0.221	0.983E-02	0.769E-01	0.683E-01	*0.735E-01	*0.569E-01
CIV 5P-6S	20000.	0.634	0.108	0.288E-01	0.290E-01	0.272E-01	0.241E-01
5022.2 A	50000.	0.536	0.815E-01	0.406E-01	0.374E-01	0.364E-01	0.314E-01
C= 0.26E+19	100000.	0.468	0.653E-01	0.508E-01	0.452E-01	0.423E-01	0.370E-01
	200000.	0.401	0.567E-01	0.597E-01	0.506E-01	0.543E-01	0.425E-01
C IV 5P-7S	20000.	0.322	0.918E-01	0.305E-01	0.306E-01	*0.265E-01	*0.253E-01
2954.6 A	50000.	0.282	0.677E-01	0.405E-01	0.392E-01	*0.353E-01	*0.329E-01
C= 0.90E+18	100000.	0.252	0.553E-01	0.497E-01	0.464E-01	0.424E-01	0.387E-01
	200000.	0.218	0.435E-01	0.564E-01	0.499E-01	0.504E-01	0.431E-01
C IV 5P-8S	20000.	0.305	0.110	*0.407E-01	*0.397E-01	*0.362E-01	*0.330E-01
2337.0 A	50000.	0.274	0.824E-01	*0.540E-01	*0.505E-01	*0.453E-01	*0.421E-01
C= 0.45E+18	100000.	0.249	0.667E-01	0.622E-01	0.578E-01	*0.560E-01	*0.468E-01
	200000.	0.218	0.507E-01	0.763E-01	0.688E-01	*0.639E-01	*0.518E-01
C IV 5P-9S	20000.	0.356	0.145	*0.604E-01	*0.550E-01		
2046.0 A	50000.	0.325	0.113	*0.772E-01	*0.695E-01		
C= 0.24E+18	100000.	0.298	0.874E-01	*0.913E-01	*0.808E-01	*0.712E-01	*0.654E-01
	200000.	0.262	0.663E-01	*0.992E-01	*0.878E-01	*0.927E-01	*0.816E-01
CIV 5P-6D	20000.	0.961	0.541E-02				
4442.4 A	50000.	0.754	0.139E-01				
C= 0.64E+17	100000.	0.621	0.759E-02	*0.603	*0.525		
	200000.	0.502	0.122E-02	*0.691	*0.659		
CIV 5P-7D	20000.	0.659	0.840E-02				
2820.7 A	50000.	0.522	0.162E-01				
C= 0.24E+17	100000.	0.432	0.113E-01				
	200000.	0.350	0.483E-02				
CIV 5D-6P	20000.	0.894	0.336E-01	*0.152	*-0.143	*0.128	*-0.118
4786.8 A	50000.	0.727	0.323E-01	*0.203	*-0.186	*0.171	*-0.151
C= 0.12E+18	100000.	0.616	0.277E-01	0.239	-0.201	*0.205	*-0.178
	200000.	0.510	0.233E-01	0.261	-0.235	*0.247	*-0.196

© European Southern Observatory • Provided by the NASA Astrophysics Data System

1992A&AS...96..613D

TABLE 1. *(continued)*

PERTURBER DENSITY = 0.1D+17(cm-3)

TRANSITION	T(K)	ELECTRONS WIDTH(A)	ELECTRONS SHIFT(A)	PROTONS WIDTH(A)	PROTONS SHIFT(A)	IONIZED HELIUM WIDTH(A)	IONIZED HELIUM SHIFT(A)
	PERTURBERS ARE						
CIV 5D-7P	20000.	0.512	0.330E-01	0.310E-01	-0.239E-01	*0.298E-01	-0.199E-01
2935.9 A	50000.	0.431	0.318E-01	0.394E-01	-0.308E-01	*0.368E-01	-0.255E-01
C= 0.44E+17	100000.	0.372	0.242E-01	0.470E-01	-0.358E-01	0.403E-01	-0.294E-01
	200000.	0.313	0.202E-01	0.542E-01	-0.416E-01	0.449E-01	-0.335E-01
CIV 5D-6F	20000.	1.16	-0.269E-01				
4647.0 A	50000.	0.916	-0.256E-01				
C= 0.64E+16	100000.	0.746	-0.216E-01				
	200000.	0.594	-0.147E-01				
CIV 5F-6D	20000.	1.13	0.343E-01	0.206	0.193	0.176	0.160
4665.0 A	50000.	0.890	0.370E-01	0.278	0.252	0.225	0.203
C= 0.19E+17	100000.	0.728	0.268E-01	0.331	0.293	0.265	0.235
	200000.	0.584	0.164E-01	0.390	0.328	0.282	0.258
CIV 5F-7D	20000.	0.730	0.201E-01				
2909.3 A	50000.	0.579	0.257E-01				
C= 0.73E+16	100000.	0.477	0.193E-01				
	200000.	0.385	0.110E-01				
CIV 6S-7P	20000.	2.51	0.992E-02	*0.275	*0.241	*0.248	*0.201
6593.7 A	50000.	2.18	0.288E-01	0.351	0.309	*0.307	*0.262
C= 0.16E+19	100000.	1.93	0.690E-02	0.446	0.366	*0.353	*0.307
	200000.	1.65	-0.576E-02	0.480	0.401	*0.426	*0.343
C IV 6P-7S	20000.	3.40	0.635	0.160	0.139	0.153	0.117
8385.0 A	50000.	2.99	0.453	0.213	0.183	0.198	0.153
C= 0.42E+19	100000.	2.68	0.371	0.267	0.214	0.228	0.176
	200000.	2.32	0.298	0.281	0.235	0.272	0.201
C IV 6P-8S	20000.	1.53	0.427	*0.154	*0.144	*0.130	*0.120
4791.4 A	50000.	1.38	0.316	*0.207	*0.188	*0.175	*0.153
C= 0.14E+19	100000.	1.26	0.257	0.239	0.203	*0.211	*0.179
	200000.	1.10	0.196	0.257	0.238	*0.249	*0.196
C IV 6P-9S	20000.	1.30	0.455	*0.186	*0.173		
3709.7 A	50000.	1.20	0.352	*0.244	*0.217		
C= 0.80E+18	100000.	1.11	0.273	*0.280	*0.253	*0.234	*0.203
	200000.	0.971	0.208	*0.314	*0.278	*0.269	*0.255
CIV 6P-7D	20000.	5.07	-0.100E-01				
7389.4 A	50000.	4.07	0.424E-01				
C= 0.17E+18	100000.	3.40	0.254E-01				
	200000.	2.77	-0.658E-02				
CIV 6D-7P	20000.	5.02	0.210				
7949.8 A	50000.	4.16	0.179	*1.45	*-1.31		
C= 0.20E+18	100000.	3.54	0.138	*1.66	*-1.51		
	200000.	2.94	0.126	*1.68	*-1.71		

PERTURBER DENSITY = 0.1D+17(cm-3)

TRANSITION	T(K)	ELECTRONS WIDTH(A)	ELECTRONS SHIFT(A)	PROTONS WIDTH(A)	PROTONS SHIFT(A)	IONIZED HELIUM WIDTH(A)	IONIZED HELIUM SHIFT(A)
	PERTURBERS ARE						
CIV 6D-7F	20000.	6.61	-0.152				
7708.6 A	50000.	5.26	-0.174				
C= 0.11E+17	100000.	4.30	-0.138				
	200000.	3.43	-0.855E-01				
CIV 6F-7D	20000.	6.46	0.155				
7746.1 A	50000.	5.14	0.203				
C= 0.18E+17	100000.	4.22	0.161				
	200000.	3.39	0.947E-01				
C IV 7P-8S	20000.	14.6	2.72	0.651	0.481	*0.635	*0.401
12985.7 A	50000.	13.2	1.92	0.833	0.628	*0.764	*0.517
C= 0.61E+19	100000.	12.0	1.60	0.960	0.719	0.846	0.597
	200000.	10.4	1.21	1.12	0.837	0.935	0.679
C IV 7P-9S	20000.	5.99	1.60	*0.599	*0.543		
7253.4 A	50000.	5.53	1.22	*0.781	*0.676	*0.642	*0.575
C= 0.19E+19	100000.	5.07	0.955	*0.941	*0.775	*0.743	*0.648
	200000.	4.44	0.724	*1.08	*0.841	*0.747	*0.734
PERTURBE	R DENSI	TY = 0.1D+	18(cm-3)				
CIV 4S-6P	20000.	0.567	0.260E-01	*0.629E-01	*0.485E-01		
1440.3 A	50000.	0.467	0.302E-01	*0.847E-01	*0.724E-01		
C= 0.12E+19	100000.	0.401	0.264E-01	*0.102	*0.866E-01		
	200000.	0.339	0.190E-01	*0.122	*0.102	*0.983E-01	*0.825E-01
CIV 4S-7P	20000.	0.698	0.342E-01				
1210.6 A	50000.	0.596	0.487E-01				
C= 0.53E+18	100000.	0.522	0.414E-01				
	200000.	0.444	0.331E-01				
C IV 4P-6S	20000.	0.519	0.133	*0.433E-01	*0.402E-01	*0.382E-01	*0.330E-01
1653.9 A	50000.	0.433	0.104	*0.615E-01	*0.585E-01	*0.529E-01	*0.494E-01
C= 0.55E+19	100000.	0.376	0.864E-01	*0.738E-01	*0.716E-01	*0.656E-01	*0.603E-01
	200000.	0.322	0.717E-01	0.970E-01	0.828E-01	*0.782E-01	*0.704E-01
C IV 4P-7S	20000.	0.565	0.190				
1344.3 A	50000.	0.488	0.147				
C= 0.22E+19	100000.	0.436	0.124	*0.115	*0.103		
	200000.	0.378	0.964E-01	*0.131	*0.119		
C IV 4P-8S	20000.	0.730	0.274				
1200.0 A	50000.	0.650	0.216				
C= 0.12E+19	100000.	0.589	0.182				
	200000.	0.515	0.138				
C IV 4P-9S	20000.	0.998	0.388				
1118.4 A	50000.	0.909	0.322				
C= 0.72E+18	100000.	0.833	0.265				
	200000.	0.732	0.200				

© European Southern Observatory • Provided by the NASA Astrophysics Data System

1992A&AS...96..613D

TABLE 1. *(continued)*

PERTURBER DENSITY = 0.1D+18(cm-3)

PERTURBERS ARE		ELECTRONS		PROTONS		IONIZED HELIUM	
TRANSITION	T(K)	WIDTH(A)	SHIFT(A)	WIDTH(A)	SHIFT(A)	WIDTH(A)	SHIFT(A)
CIV 5S-6P	20000.	4.84	0.538E-01	*0.437	*0.334		
3935.6 A	50000.	4.00	0.771E-01	*0.581	*0.496		
C= 0.92E+19	100000.	3.45	0.585E-01	*0.705	*0.610	*0.606	*0.488
	200000.	2.92	0.159E-01	*0.822	*0.716	*0.676	*0.563
CIV 5S-7P	20000.	3.46	0.104				
2591.9 A	50000.	2.96	0.163				
C= 0.24E+19	100000.	2.59	0.132				
	200000.	2.21	0.983E-01				
CIV 5P-6S	20000.	6.33	1.05	0.286	0.255	*0.268	*0.206
5022.2 A	50000.	5.36	0.805	0.407	0.361	*0.361	*0.300
C= 0.26E+20	100000.	4.68	0.650	0.508	0.449	*0.423	*0.367
	200000.	4.01	0.565	0.597	0.506	*0.543	*0.425
C IV 5P-7S	20000.	3.22	0.857				
2954.6 A	50000.	2.82	0.657	*0.403	*0.368		
C= 0.90E+19	100000.	2.52	0.550	*0.497	*0.460		
	200000.	2.18	0.432	*0.564	*0.499	*0.504	*0.431
C IV 5P-8S	20000.	3.05	0.998				
2337.0 A	50000.	2.74	0.785				
C= 0.45E+19	100000.	2.49	0.661				
	200000.	2.18	0.502				
C IV 5P-9S	20000.	3.55	1.26				
2046.0 A	50000.	3.25	1.05				
C= 0.24E+19	100000.	2.98	0.865				
	200000.	2.62	0.653				
CIV 5P-6D	20000.	8.34	-0.402				
4442.4 A	50000.	6.75	-0.161				
C= 0.64E+18	100000.	5.65	-0.179E-01				
	200000.	4.63	0.122E-01				
CIV 5D-6P	20000.	8.47	0.460				
4786.8 A	50000.	6.98	0.413				
C= 0.12E+19	100000.	5.95	0.304				
	200000.	4.96	0.233				
CIV 5D-7P	20000.	4.92	0.266				
2935.9 A	50000.	4.19	0.316	*0.396	*-0.294		
C= 0.44E+18	100000.	3.64	0.247	*0.469	*-0.355		
	200000.	3.06	0.202	*0.542	*-0.416	*0.449	*-0.335
CIV 5D-6F	20000.	8.90	0.129				
4647.0 A	50000.	7.47	-0.122				
C= 0.64E+17	100000.	6.27	-0.218				
	200000.	5.10	-0.147				

PERTURBER DENSITY = 0.1D+18(cm-3)

PERTURBERS ARE		ELECTRONS		PROTONS		IONIZED HELIUM	
TRANSITION	T(K)	WIDTH(A)	SHIFT(A)	WIDTH(A)	SHIFT(A)	WIDTH(A)	SHIFT(A)
CIV 5G-6F	20000.	7.05	0.172E-02				
4661.0 A	50000.	6.03	-0.106				
C= 0.64E+17	100000.	5.09	-0.132				
	200000.	4.16	-0.885E-01				
C IV 6P-9S	20000.	13.0	3.99				
3709.7 A	50000.	12.0	3.29				
C= 0.80E+19	100000.	11.0	2.70				
	200000.	9.70	2.05				
PERTURBER DENSITY = 0.1D+19(cm-3)							
CIV 4S-6P	20000.	5.43	-0.573E-01				
1440.3 A	50000.	4.53	0.109				
C= 0.12E+20	100000.	3.92	0.170				
	200000.	3.32	0.173				
CIV 4S-7P	20000.	6.15	-0.209				
1210.6 A	50000.	5.48	0.109				
C= 0.53E+19	100000.	4.89	0.209				
	200000.	4.21	0.290				
C IV 4P-6S	20000.	5.18	1.12				
1653.9 A	50000.	4.32	0.913				
C= 0.55E+20	100000.	3.76	0.807				
	200000.	3.21	0.711				
C IV 4P-7S	20000.	5.59	1.43				
1344.3 A	50000.	4.85	1.19				
C= 0.22E+20	100000.	4.33	1.12				
	200000.	3.76	0.948				
C IV 4P-8S	20000.	*6.95	*1.77				
1200.0 A	50000.	6.30	1.60				
C= 0.12E+20	100000.	5.75	1.56				
	200000.	5.05	1.34				
C IV 4P-9S	20000.	*8.73	*2.03				
1118.4 A	50000.	8.39	2.10				
C= 0.72E+19	100000.	7.85	2.11				
	200000.	6.98	1.93				
CIV 4D-6P	20000.	7.22	0.516E-01				
1654.5 A	50000.	6.10	0.274				
C= 0.26E+19	100000.	5.29	0.338				
	200000.	4.48	0.320				
CIV 4D-7P	20000.	7.78					
1358.5 A	50000.	6.99	0.224				
C= 0.18E+19	100000.	6.23	0.337				
	200000.	5.36	0.425				

© European Southern Observatory • Provided by the NASA Astrophysics Data System

1992A&AS...96..613D

TABLE 2. *This table shows electron-, proton-, and ionized- helium- impact broadening parameters for far UV C IV lines of large principal quantum number of the upper level, for a perturber density of* 10^{15} cm^{-3} *and temperatures from 20,000 to 200,000 K. The other notation is the same as in Table 1. Data for other densities may be provided by author uppon request.*

PERTURBER DENSITY = 0.1D+16(cm-3)

PERTURBERS ARE		ELECTRONS		PROTONS		IONIZED HELIUM	
TRANSITION	T(K)	WIDTH(A)	SHIFT(A)	WIDTH(A)	SHIFT(A)	WIDTH(A)	SHIFT(A)
CIV 2S-6P	20000.	0.111E-03	0.998E-05	0.140E-04	0.133E-04	0.128E-04	0.112E-04
212.4 A	50000.	0.923E-04	0.933E-05	0.186E-04	0.170E-04	0.166E-04	0.140E-04
C= 0.27E+15	100000.	0.796E-04	0.768E-05	0.227E-04	0.193E-04	0.189E-04	0.160E-04
	200000.	0.672E-04	0.581E-05	0.270E-04	0.224E-04	0.218E-04	0.184E-04
CIV 2S-7P	20000.	0.193E-03	0.205E-04	0.304E-04	0.282E-04	0.264E-04	0.235E-04
206.6 A	50000.	0.166E-03	0.187E-04	0.403E-04	0.354E-04	0.344E-04	0.287E-04
C= 0.15E+15	100000.	0.145E-03	0.141E-04	0.453E-04	0.378E-04	0.408E-04	0.333E-04
	200000.	0.124E-03	0.112E-04	0.494E-04	0.445E-04	0.479E-04	0.366E-04
C IV 2P-6S	20000.	0.938E-04	0.340E-04	0.103E-04	0.116E-04	0.905E-05	0.978E-05
247.4 A	50000.	0.787E-04	0.258E-04	0.148E-04	0.147E-04	0.123E-04	0.123E-04
C= 0.12E+16	100000.	0.682E-04	0.212E-04	0.188E-04	0.175E-04	0.158E-04	0.142E-04
	200000.	0.582E-04	0.175E-04	0.223E-04	0.187E-04	0.188E-04	0.165E-04
C IV 2P-7S	20000.	0.159E-03	0.683E-04	0.223E-04	0.236E-04	0.192E-04	0.200E-04
239.1 A	50000.	0.138E-03	0.503E-04	0.313E-04	0.300E-04	0.258E-04	0.250E-04
C= 0.71E+15	100000.	0.123E-03	0.411E-04	0.372E-04	0.334E-04	0.336E-04	0.271E-04
	200000.	0.107E-03	0.320E-04	0.428E-04	0.386E-04	0.347E-04	0.307E-04
C IV 2P-8S	20000.	0.259E-03	0.121E-03	0.431E-04	0.444E-04	0.369E-04	0.365E-04
234.1 A	50000.	0.232E-03	0.887E-04	0.565E-04	0.538E-04	0.478E-04	0.451E-04
C= 0.45E+15	100000.	0.210E-03	0.717E-04	0.649E-04	0.616E-04	0.564E-04	0.483E-04
	200000.	0.184E-03	0.543E-04	0.816E-04	0.713E-04	0.623E-04	0.537E-04
C IV 2P-9S	20000.	0.408E-03	0.200E-03	0.766E-04	0.765E-04	0.670E-04	0.631E-04
230.9 A	50000.	0.373E-03	0.150E-03	0.996E-04	0.915E-04	0.863E-04	0.724E-04
C= 0.31E+15	100000.	0.342E-03	0.116E-03	0.117E-03	0.104E-03	0.935E-04	0.854E-04
	200000.	0.300E-03	0.878E-04	0.126E-03	0.116E-03	0.123E-03	0.104E-03
CIV 2P-6D	20000.	0.256E-03	0.163E-04	0.130E-03	0.124E-03	*0.106E-03	*0.103E-03
245.8 A	50000.	0.196E-03	0.108E-04	0.174E-03	0.147E-03	*0.138E-03	*0.124E-03
C= 0.19E+14	100000.	0.159E-03	0.695E-05	0.188E-03	0.162E-03	0.164E-03	0.138E-03
	200000.	0.127E-03	0.390E-05	0.218E-03	0.205E-03	0.181E-03	0.143E-03
CIV 2P-7D	20000.	0.450E-03	0.288E-04	*0.210E-03	*0.189E-03	*0.169E-03	*0.154E-03
238.2 A	50000.	0.350E-03	0.194E-04	*0.261E-03	*0.228E-03	*0.211E-03	*0.188E-03
C= 0.17E+14	100000.	0.286E-03	0.124E-04	*0.314E-03	*0.249E-03	*0.228E-03	*0.206E-03
	200000.	0.230E-03	0.671E-05	0.328E-03	0.262E-03	*0.260E-03	*0.245E-03
CIV 3S-6P	20000.	0.900E-03	0.756E-04	0.110E-03	0.105E-03	0.100E-03	0.879E-04
595.5 A	50000.	0.744E-03	0.707E-04	0.146E-03	0.133E-03	0.130E-03	0.110E-03
C= 0.21E+16	100000.	0.640E-03	0.572E-04	0.178E-03	0.151E-03	0.149E-03	0.125E-03
	200000.	0.540E-03	0.428E-04	0.213E-03	0.176E-03	0.170E-03	0.144E-03
CIV 3S-7P	20000.	0.140E-02	0.143E-03	0.217E-03	0.201E-03	0.189E-03	0.168E-03
552.2 A	50000.	0.120E-02	0.131E-03	0.288E-03	0.252E-03	0.246E-03	0.205E-03
C= 0.11E+16	100000.	0.105E-02	0.981E-04	0.325E-03	0.269E-03	0.291E-03	0.237E-03
	200000.	0.893E-03	0.773E-04	0.353E-03	0.318E-03	0.342E-03	0.261E-03

PERTURBER DENSITY = 0.1D+16(cm-3)

PERTURBERS ARE		ELECTRONS		PROTONS		IONIZED HELIUM	
TRANSITION	T(K)	WIDTH(A)	SHIFT(A)	WIDTH(A)	SHIFT(A)	WIDTH(A)	SHIFT(A)
C IV 3P-6S	20000.	0.730E-03	0.247E-03	0.759E-04	0.849E-04	0.665E-04	0.718E-04
672.4 A	50000.	0.611E-03	0.187E-03	0.109E-03	0.108E-03	0.912E-04	0.903E-04
C= 0.90E+16	100000.	0.530E-03	0.154E-03	0.137E-03	0.129E-03	0.117E-03	0.104E-03
	200000.	0.453E-03	0.127E-03	0.167E-03	0.137E-03	0.138E-03	0.121E-03
C IV 3P-7S	20000.	0.108E-02	0.447E-03	0.147E-03	0.155E-03	0.126E-03	0.132E-03
614.9 A	50000.	0.939E-03	0.329E-03	0.206E-03	0.198E-03	0.170E-03	0.165E-03
C= 0.47E+16	100000.	0.837E-03	0.269E-03	0.245E-03	0.221E-03	0.222E-03	0.179E-03
	200000.	0.725E-03	0.210E-03	0.282E-03	0.255E-03	0.230E-03	0.203E-03
C IV 3P-8S	20000.	0.164E-02	0.746E-03	0.267E-03	0.275E-03	0.228E-03	0.226E-03
582.8 A	50000.	0.146E-02	0.547E-03	0.350E-03	0.333E-03	0.296E-03	0.279E-03
C= 0.28E+16	100000.	0.132E-02	0.442E-03	0.401E-03	0.382E-03	0.350E-03	0.299E-03
	200000.	0.116E-02	0.335E-03	0.506E-03	0.442E-03	0.385E-03	0.333E-03
C IV 3P-9S	20000.	0.245E-02	0.119E-02	0.455E-03	0.454E-03	0.398E-03	0.375E-03
562.9 A	50000.	0.224E-02	0.888E-03	0.592E-03	0.544E-03	0.513E-03	0.431E-03
C= 0.18E+16	100000.	0.205E-02	0.690E-03	0.698E-03	0.619E-03	0.555E-03	0.507E-03
	200000.	0.180E-02	0.520E-03	0.745E-03	0.687E-03	0.730E-03	0.617E-03
CIV 3P-6D	20000.	0.188E-02	0.116E-03	0.937E-03	0.893E-03	*0.763E-03	*0.746E-03
660.9 A	50000.	0.144E-02	0.759E-04	0.126E-02	0.107E-02	*0.995E-03	*0.897E-03
C= 0.14E+15	100000.	0.117E-02	0.483E-04	0.136E-02	0.117E-02	0.118E-02	0.998E-03
	200000.	0.937E-03	0.263E-04	0.157E-02	0.148E-02	0.131E-02	0.103E-02
CIV 3P-7D	20000.	0.297E-02	0.186E-03	*0.137E-02	*0.124E-02	*0.111E-02	*0.101E-02
608.9 A	50000.	0.231E-02	0.125E-03	*0.170E-02	*0.149E-02	*0.138E-02	*0.123E-02
C= 0.11E+15	100000.	0.189E-02	0.794E-04	*0.205E-02	*0.163E-02	*0.149E-02	*0.135E-02
	200000.	0.152E-02	0.422E-04	0.214E-02	0.171E-02	*0.170E-02	*0.160E-02
CIV 3D-6P	20000.	0.117E-02	0.105E-03	0.145E-03	0.139E-03	0.132E-03	0.117E-03
685.4 A	50000.	0.971E-03	0.985E-04	0.194E-03	0.178E-03	0.172E-03	0.146E-03
C= 0.28E+16	100000.	0.837E-03	0.810E-04	0.235E-03	0.201E-03	0.196E-03	0.166E-03
	200000.	0.706E-03	0.615E-04	0.281E-03	0.234E-03	0.227E-03	0.192E-03
CIV 3D-7P	20000.	0.180E-02	0.191E-03	0.282E-03	0.261E-03	0.244E-03	0.218E-03
628.7 A	50000.	0.154E-02	0.174E-03	0.373E-03	0.328E-03	0.318E-03	0.266E-03
C= 0.14E+16	100000.	0.135E-02	0.132E-03	0.418E-03	0.350E-03	0.378E-03	0.309E-03
	200000.	0.115E-02	0.104E-03	0.456E-03	0.412E-03	0.443E-03	0.339E-03
CIV 3D-6F	20000.	0.221E-02	0.655E-05				
682.5 A	50000.	0.169E-02	0.267E-05	*0.448E-02	*0.447E-02		
C= 0.14E+14	100000.	0.135E-02	-0.201E-04	*0.616E-02	*0.475E-02	*0.414E-02	*0.367E-02
	200000.	0.107E-02	-0.160E-04	*0.620E-02	*0.564E-02	*0.538E-02	*0.406E-02
CIV 3D-7F	20000.	0.375E-02	0.897E-05				
627.1 A	50000.	0.287E-02	-0.486E-05				
C= 0.76E+13	100000.	0.230E-02	-0.454E-04				
	200000.	0.181E-02	-0.310E-04				

© European Southern Observatory • Provided by the NASA Astrophysics Data System

1993A&AS...99..585D

ASTRONOMY & ASTROPHYSICS
SUPPLEMENT SERIES

JUNE II 1993, PAGE 585

Astron. Astrophys. Suppl. Ser. **99**, 585-589 (1993)

Stark broadening of spectral lines of multicharged ions of astrophysical interest. VII: Al III lines

M.S. Dimitrijević[1] and S. Sahal-Bréchot[2]

[1] Astronomical Observatory, Volgina 7, 11050 Beograd, Yugoslavia
[2] Laboratoire "Astrophysique, Atomes et Molécules", Département Atomes et Molécules en Astrophysique, Unité associée au C.N.R.S. N 812, Observatoire de Paris-Meudon, 92190 Meudon, France

Received September 11; accepted October 12, 1992

Abstract. — Using a semiclassical approach, we have calculated electron-, proton-, and ionized helium-impact line widths and shifts for 23 Al III multiplets of astrophysical interest.

Key words: lines: profile — atomic and molecular data

1. Introduction

This paper is the seventh in a series devoted to the calculation of Stark broadening parameters of spectral lines of multicharged ions. The first six were concerned with C IV, Si IV, O VI, N V Sc III and Ti IV lines (Dimitrijević et al. 1991a-d; Dimitrijević & Sahal-Bréchot 1992a-c). By using the semiclassical-perturbation formalism (Sahal-Bréchot 1969a,b), we have calculated electron-, proton-, and ionized helium-impact line widths and shifts for 23 Al multiplets. A summary of the formalism is given in Dimitrijević & Sahal-Bréchot (1991a). Here, we present and discuss the results for Al III multiplets, which are of interest for the interpretation and analysis of stellar spectra. Namely, Al III absorption lines are very strong in hot star atmospheres (see e.g. Struve 1930), where Stark broadening is the principal pressure broadening mechanism. Moreover, results presented may be used for the diagnostic and modelling of an electrodynamic macro-particle accelerator arc plasma created by the evaporation of an Al-foil (see e.g. Rasheigh & Marshall 1978; or Rolader & Batteh 1989) and for spectroscopy of laboratory plasma (Davis & Morin 1971).

2. Results and discussion

Energy levels for Al III lines have been taken from Bashkin & Stoner (1975). Oscillator strengths have been calculated by using the method of Bates & Damgaard (1949) and the tables of Oertel & Shomo (1968). For higher levels, the method described by Van Regemorter et al. (1979) has been used.

In addition to electron-impact full halfwidths and shifts, Stark-broadening parameters due to proton-, and ionized helium- impacts have been calculated. Our results for Stark broadening parameters of Al III multiplets are shown in Table 1, for a perturber density of 10^{15} cm^{-3} and temperatures $T = 10,000 - 500,000$ K. Data for the 9 most important multiplets, for perturber densities $10^{17} - 10^{20}$ cm^{-3}, may be found in an article of Dimitrijević et al. (1993) concerned with the diagnostic of electrodynamical macroparticle accelerator arc plasma. Data for other densities may be provided by authors upon request or obtained from data in Table 1 taking into account that the linearity with density is not valid when the Debye screening effect becomes important. In such a case, the Debye shielding correction (see p. 321, in Griem 1974), divided by Z^2 must be used. Here, $Z = 1$, for neutrals, 2 for singly charged ions etc. We also specify a parameter c (Dimitrijević & Sahal-Bréchot 1984) which gives an estimate for the maximum perturber density for which the line may be treated as isolated when it is divided by the corresponding electron-impact full width at half maximum. For each value given in Tables 1 and 2, the collision volume (V) multiplied by the perturber density (N) is much less than one and the impact approximation is valid (Sahal-Bréchot 1969ab). When the impact approximation is not valid, the ion broadening contribution may be estimated by using quasistatic estimations (Sahal-Bréchot 1991 or Griem 1974). The accuracy of the results obtained decreases when broadening by ion interactions becomes important.

© European Southern Observatory • Provided by the NASA Astrophysics Data System

1993A&AS...99..585D

Acknowledgements. This work is a part of French-Yugoslav collaboration through the project "L'élargissement Stark des raies spectrales des plasmas astrophysiques et de laboratoire". It is also a part of the project "Physics and Dynamics of Celestial Bodies" supported by Ministery of science and technology of Serbia.

References

Bashkin S. and Stoner J.O. Jr. 1975, Atomic Energy Levels and Grotrian Diagrams, Vol. 1, North Holland, Amsterdam
Bates D.R. and Damgaard A. 1949, Trans. Roy. Soc. London, Ser. A 242, 101
Davis J. and Morin S. 1971, JQSRT 11, 495
Dimitrijević M.S., Djurić Z. and Mihajlov A. 1993, to be published
Dimitrijević M.S. and Sahal-Bréchot S. 1984, JQSRT 31, 301
Dimitrijević M.S., Sahal-Bréchot S. and Bommier V. 1991a, A&AS 89, 581
Dimitrijević M.S., Sahal-Bréchot S. and Bommier V. 1991b, Bull. Obs. Astron. Belgrade 144, 65
Dimitrijević M.S., Sahal-Bréchot S. and Bommier V. 1991c, A&AS 89, 591
Dimitrijević M.S., Sahal-Bréchot S. and Bommier V. 1991d, Bull. Obs. Astron. Belgrade 144, 81
Dimitrijević M.S. and Sahal-Bréchot S. 1992a, A&AS 93, 359
Dimitrijević M.S. and Sahal-Bréchot S. 1992b, A&AS 95, 109
Dimitrijević M.S. and Sahal-Bréchot S. 1992c, A&AS 95, 121
Dimitrijević M.S. and Sahal-Bréchot S. 1992d, A&AS 96, 613
Dimitrijević M.S. and Sahal-Bréchot S. 1992e, Bull. Astron. Belgrade 146, 105
Griem H.R. 1974, Spectral Line Broadening by Plasmas, Academic Press, New York and London
Oertel G.K. and Shomo L.P. 1968, ApJS 16, 175
Rasheigh S.C. and Marshall R.A. 1978, J. Appl. Phys. 49, 2540
Rolader G.E. and Batteh J.H. 1989, IEEE Transactions on Plasma Sci. 17439
Sahal-Bréchot S. 1969a, A&A 1, 91
Sahal-Bréchot S. 1969b, A&A 2, 322
Sahal-Bréchot S. 1991, A&A 245, 322
Struve O. 1930, ApJ 71, 671
Van Regemorter H., Hoang Binh Dy and Prud'homme M. 1979, J. Phys. B 12, 1073

Table 1. This table shows electron-, proton-, and ionized- helium- impact broadening parameters for Al III, for a perturber density of 10^{15} cm^{-3} and temperatures from 10,000 to 500,000 K. Transitions and averaged wavelengths for the multiplet (in Å) are also given. By using c (see Eq. (5) in Dimitrijević et al. 1991a), we obtain an estimate for the maximum perturber density for which the line may be treated as isolated and tabulated data may be used

PERTURBER DENSITY = 0.1E+16 cm-3

PERTURBERS ARE:		ELECTRONS		PROTONS		IONIZED HELIUM	
TRANSITION	T(K)	WIDTH(A)	SHIFT(A)	WIDTH(A)	SHIFT(A)	WIDTH(A)	SHIFT(A)
ALIII 3S-3P	10000.	0.518E-03	-0.140E-05	0.296E-05	-0.599E-06	0.506E-05	-0.599E-06
1857.4 A	20000.	0.371E-03	-0.388E-05	0.676E-05	-0.120E-05	0.983E-05	-0.118E-05
C= 0.19E+19	50000.	0.240E-03	-0.370E-05	0.133E-04	-0.264E-05	0.165E-04	-0.245E-05
	100000.	0.179E-03	-0.397E-05	0.182E-04	-0.399E-05	0.196E-04	-0.352E-05
	200000.	0.142E-03	-0.375E-05	0.208E-04	-0.545E-05	0.221E-04	-0.448E-05
	500000.	0.113E-03	-0.358E-05	0.240E-04	-0.692E-05	0.243E-04	-0.571E-05
ALIII 3S-4P	10000.	0.164E-03	0.145E-05	0.594E-05	0.672E-06	0.803E-05	0.658E-06
696.0 A	20000.	0.122E-03	0.295E-05	0.916E-05	0.123E-05	0.112E-04	0.114E-05
C= 0.85E+17	50000.	0.898E-04	0.258E-05	0.126E-04	0.210E-05	0.136E-04	0.184E-05
	100000.	0.757E-04	0.364E-05	0.142E-04	0.279E-05	0.151E-04	0.231E-05
	200000.	0.660E-04	0.303E-05	0.156E-04	0.334E-05	0.160E-04	0.276E-05
	500000.	0.564E-04	0.286E-05	0.167E-04	0.416E-05	0.167E-04	0.336E-05
ALIII 3S-5P	10000.	0.208E-03	0.136E-04	0.176E-04	0.175E-05	0.215E-04	0.163E-05
560.4 A	20000.	0.166E-03	0.843E-05	0.231E-04	0.281E-05	0.250E-04	0.243E-05
C= 0.25E+17	50000.	0.139E-03	0.794E-05	0.271E-04	0.422E-05	0.289E-04	0.346E-05
	100000.	0.128E-03	0.753E-05	0.298E-04	0.506E-05	0.304E-04	0.418E-05
	200000.	0.119E-03	0.651E-05	0.310E-04	0.601E-05	0.312E-04	0.489E-05
	500000.	0.106E-03	0.575E-05	0.317E-04	0.714E-05	0.318E-04	0.558E-05

© European Southern Observatory • Provided by the NASA Astrophysics Data System

1993A&AS...99..585D

Table 1. continued

PERTURBER DENSITY = 0.1E+16 cm-3

PERTURBERS ARE:		ELECTRONS		PROTONS		IONIZED HELIUM	
TRANSITION	T(K)	WIDTH(A)	SHIFT(A)	WIDTH(A)	SHIFT(A)	WIDTH(A)	SHIFT(A)
ALIII 3P-4S	10000.	0.580E-03	0.116E-03	0.390E-05	0.104E-04	0.526E-05	0.968E-05
1382.6 A	20000.	0.416E-03	0.767E-04	0.106E-04	0.167E-04	0.111E-04	0.145E-04
C= 0.33E+18	50000.	0.286E-03	0.575E-04	0.224E-04	0.252E-04	0.208E-04	0.207E-04
	100000.	0.232E-03	0.491E-04	0.304E-04	0.302E-04	0.270E-04	0.251E-04
	200000.	0.194E-03	0.426E-04	0.385E-04	0.359E-04	0.334E-04	0.291E-04
	500000.	0.158E-03	0.367E-04	0.489E-04	0.429E-04	0.429E-04	0.334E-04
ALIII 3P-5S	10000.	0.412E-03	0.204E-03	0.119E-04	0.208E-04	0.114E-04	0.180E-04
856.2 A	20000.	0.316E-03	0.151E-03	0.216E-04	0.288E-04	0.208E-04	0.242E-04
C= 0.57E+17	50000.	0.259E-03	0.113E-03	0.360E-04	0.370E-04	0.306E-04	0.306E-04
	100000.	0.230E-03	0.874E-04	0.455E-04	0.443E-04	0.382E-04	0.361E-04
	200000.	0.202E-03	0.696E-04	0.559E-04	0.508E-04	0.447E-04	0.417E-04
	500000.	0.169E-03	0.511E-04	0.690E-04	0.602E-04	0.515E-04	0.510E-04
ALIII 3P-3D	10000.	0.451E-03	0.326E-05	0.323E-05	0.122E-05	0.536E-05	0.121E-05
1609.8 A	20000.	0.328E-03	0.628E-05	0.706E-05	0.238E-05	0.996E-05	0.229E-05
C= 0.72E+18	50000.	0.216E-03	0.562E-05	0.132E-04	0.475E-05	0.159E-04	0.415E-05
	100000.	0.165E-03	0.695E-05	0.175E-04	0.661E-05	0.187E-04	0.570E-05
	200000.	0.135E-03	0.596E-05	0.201E-04	0.828E-05	0.210E-04	0.685E-05
	500000.	0.112E-03	0.572E-05	0.233E-04	0.104E-04	0.234E-04	0.849E-05
ALIII 3P-4D	10000.	0.491E-03	0.389E-04	0.218E-04	0.259E-04	0.236E-04	0.226E-04
893.3 A	20000.	0.386E-03	0.427E-04	0.358E-04	0.359E-04	0.345E-04	0.296E-04
C= 0.15E+17	50000.	0.297E-03	0.389E-04	0.512E-04	0.460E-04	0.462E-04	0.381E-04
	100000.	0.251E-03	0.364E-04	0.620E-04	0.537E-04	0.545E-04	0.442E-04
	200000.	0.214E-03	0.303E-04	0.716E-04	0.624E-04	0.640E-04	0.517E-04
	500000.	0.173E-03	0.230E-04	0.874E-04	0.749E-04	0.747E-04	0.607E-04
ALIII 3P-5D	10000.	0.770E-03	0.155E-03	0.745E-04	0.744E-04	0.708E-04	0.611E-04
740.5 A	20000.	0.661E-03	0.134E-03	0.987E-04	0.902E-04	0.878E-04	0.742E-04
C= 0.55E+16	50000.	0.560E-03	0.109E-03	0.128E-03	0.115E-03	0.109E-03	0.918E-04
	100000.	0.498E-03	0.934E-04	0.157E-03	0.132E-03	0.138E-03	0.107E-03
	200000.	0.436E-03	0.728E-04	0.168E-03	0.147E-03	0.146E-03	0.117E-03
	500000.	0.356E-03	0.532E-04	0.198E-03	0.187E-03	0.185E-03	0.131E-03
ALIII 3D-4P	10000.	0.434E-02	0.235E-04	0.124E-03	0.143E-04	0.172E-03	0.141E-04
3606.2 A	20000.	0.327E-02	0.591E-04	0.198E-03	0.267E-04	0.245E-03	0.248E-04
C= 0.23E+19	50000.	0.242E-02	0.533E-04	0.282E-03	0.466E-04	0.305E-03	0.412E-04
	100000.	0.205E-02	0.773E-04	0.320E-03	0.634E-04	0.340E-03	0.519E-04
	200000.	0.180E-02	0.653E-04	0.352E-03	0.763E-04	0.363E-03	0.625E-04
	500000.	0.155E-02	0.614E-04	0.372E-03	0.950E-04	0.379E-03	0.781E-04
ALIII 3D-5P	10000.	0.169E-02	0.742E-04	0.132E-03	0.136E-04	0.162E-03	0.127E-04
1600.0 A	20000.	0.135E-02	0.614E-04	0.176E-03	0.220E-04	0.190E-03	0.190E-04
C= 0.20E+18	50000.	0.113E-02	0.597E-04	0.206E-03	0.332E-04	0.220E-03	0.273E-04
	100000.	0.105E-02	0.565E-04	0.226E-03	0.397E-04	0.232E-03	0.332E-04
	200000.	0.978E-03	0.495E-04	0.239E-03	0.475E-04	0.239E-03	0.389E-04
	500000.	0.871E-03	0.438E-04	0.249E-03	0.565E-04	0.244E-03	0.447E-04

© European Southern Observatory • Provided by the NASA Astrophysics Data System

1993A&AS...99..585D

Table 1. continued

PERTURBER DENSITY = 0.1E+16 cm-3

PERTURBERS ARE:		ELECTRONS		PROTONS		IONIZED HELIUM	
TRANSITION	T(K)	WIDTH(A)	SHIFT(A)	WIDTH(A)	SHIFT(A)	WIDTH(A)	SHIFT(A)
ALIII 3D-4F	10000.	0.192E-02	-0.648E-04	0.561E-04	-0.815E-04	0.622E-04	-0.709E-04
1935.9 A	20000.	0.147E-02	-0.658E-04	0.975E-04	-0.114E-03	0.101E-03	-0.977E-04
C= 0.68E+17	50000.	0.108E-02	-0.594E-04	0.158E-03	-0.150E-03	0.141E-03	-0.124E-03
	100000.	0.890E-03	-0.419E-04	0.194E-03	-0.178E-03	0.171E-03	-0.149E-03
	200000.	0.751E-03	-0.315E-04	0.234E-03	-0.207E-03	0.206E-03	-0.167E-03
	500000.	0.609E-03	-0.145E-04	0.276E-03	-0.237E-03	0.239E-03	-0.195E-03
ALIII 3D-5F	10000.	0.452E-02	0.182E-03	0.115E-02	0.115E-02	0.989E-03	0.952E-03
1352.8 A	20000.	0.368E-02	0.145E-03	0.143E-02	0.138E-02	0.121E-02	0.114E-02
C= 0.96E+15	50000.	0.285E-02	0.900E-04	0.183E-02	0.169E-02	0.141E-02	0.137E-02
	100000.	0.236E-02	0.518E-04	0.213E-02	0.193E-02	0.176E-02	0.156E-02
	200000.	0.193E-02	0.276E-04	0.209E-02	0.220E-02	0.218E-02	0.166E-02
	500000.	0.146E-02	-0.123E-04	0.297E-02	0.264E-02	0.225E-02	0.176E-02
ALIII 4S-4P	10000.	0.143E-01	-0.613E-03	0.405E-03	-0.132E-03	0.544E-03	-0.125E-03
5706.9 A	20000.	0.107E-01	-0.518E-03	0.628E-03	-0.221E-03	0.762E-03	-0.194E-03
C= 0.57E+19	50000.	0.814E-02	-0.500E-03	0.873E-03	-0.341E-03	0.929E-03	-0.284E-03
	100000.	0.707E-02	-0.480E-03	0.100E-02	-0.410E-03	0.104E-02	-0.341E-03
	200000.	0.627E-02	-0.447E-03	0.111E-02	-0.494E-03	0.112E-02	-0.400E-03
	500000.	0.538E-02	-0.390E-03	0.120E-02	-0.583E-03	0.121E-02	-0.487E-03
ALIII 4S-5P	10000.	0.271E-02	0.108E-04	0.205E-03	0.125E-05	0.250E-03	0.124E-05
1912.3 A	20000.	0.216E-02	0.194E-06	0.269E-03	0.246E-05	0.291E-03	0.239E-05
C= 0.29E+18	50000.	0.183E-02	0.742E-05	0.315E-03	0.509E-05	0.335E-03	0.457E-05
	100000.	0.171E-02	0.203E-05	0.344E-03	0.727E-05	0.355E-03	0.631E-05
	200000.	0.159E-02	0.117E-05	0.356E-03	0.924E-05	0.363E-03	0.770E-05
	500000.	0.141E-02	0.938E-06	0.369E-03	0.118E-04	0.372E-03	0.974E-05
ALIII 4P-5S	10000.	0.908E-02	0.342E-02	0.302E-03	0.379E-03	0.322E-03	0.327E-03
3710.5 A	20000.	0.710E-02	0.247E-02	0.498E-03	0.525E-03	0.500E-03	0.442E-03
C= 0.11E+19	50000.	0.599E-02	0.185E-02	0.745E-03	0.679E-03	0.672E-03	0.560E-03
	100000.	0.549E-02	0.144E-02	0.926E-03	0.814E-03	0.807E-03	0.658E-03
	200000.	0.498E-02	0.113E-02	0.110E-02	0.921E-03	0.912E-03	0.752E-03
	500000.	0.428E-02	0.848E-03	0.129E-02	0.111E-02	0.100E-02	0.910E-03
ALIII 4P-4D	10000.	0.141E-01	0.846E-03	0.519E-03	0.647E-03	0.554E-03	0.565E-03
4524.9 A	20000.	0.112E-01	0.908E-03	0.862E-03	0.898E-03	0.838E-03	0.745E-03
C= 0.37E+18	50000.	0.879E-02	0.847E-03	0.124E-02	0.115E-02	0.111E-02	0.955E-03
	100000.	0.761E-02	0.747E-03	0.154E-02	0.135E-02	0.132E-02	0.110E-02
	200000.	0.662E-02	0.623E-03	0.178E-02	0.156E-02	0.154E-02	0.129E-02
	500000.	0.547E-02	0.447E-03	0.212E-02	0.186E-02	0.189E-02	0.154E-02
ALIII 4P-5D	10000.	0.720E-02	0.108E-02	0.638E-03	0.662E-03	0.605E-03	0.543E-03
2212.8 A	20000.	0.617E-02	0.984E-03	0.855E-03	0.803E-03	0.756E-03	0.660E-03
C= 0.49E+17	50000.	0.524E-02	0.890E-03	0.111E-02	0.102E-02	0.944E-03	0.815E-03
	100000.	0.468E-02	0.759E-03	0.138E-02	0.117E-02	0.119E-02	0.948E-03
	200000.	0.412E-02	0.609E-03	0.148E-02	0.131E-02	0.129E-02	0.104E-02
	500000.	0.338E-02	0.440E-03	0.173E-02	0.167E-02	0.165E-02	0.117E-02

© European Southern Observatory • Provided by the NASA Astrophysics Data System

1993A&AS...99..585D

Table 1. continued

PERTURBER DENSITY = 0.1E+16 cm-3

PERTURBERS ARE:		ELECTRONS		PROTONS		IONIZED HELIUM	
TRANSITION	T(K)	WIDTH(A)	SHIFT(A)	WIDTH(A)	SHIFT(A)	WIDTH(A)	SHIFT(A)
ALIII 4D-5P	10000.	0.592E-01	-0.139E-02	0.293E-02	-0.182E-02	0.351E-02	-0.157E-02
7891.9 A	20000.	0.482E-01	-0.185E-02	0.415E-02	-0.252E-02	0.428E-02	-0.211E-02
C= 0.11E+19	50000.	0.406E-01	-0.153E-02	0.517E-02	-0.323E-02	0.512E-02	-0.265E-02
	100000.	0.372E-01	-0.134E-02	0.608E-02	-0.386E-02	0.566E-02	-0.315E-02
	200000.	0.338E-01	-0.103E-02	0.662E-02	-0.439E-02	0.618E-02	-0.366E-02
	500000.	0.291E-01	-0.598E-03	0.735E-02	-0.516E-02	0.692E-02	-0.445E-02
ALIII 4D-4F	10000.	2.58	-0.190	0.940E-01	-0.140	0.955E-01	-0.122
54755.5 A	20000.	2.03	-0.204	0.168	-0.188	0.148	-0.155
C= 0.55E+20	50000.	1.56	-0.186	0.243	-0.237	0.209	-0.197
	100000.	1.33	-0.162	0.302	-0.280	0.247	-0.225
	200000.	1.13	-0.132	0.351	-0.324	0.283	-0.257
	500000.	0.908	-0.912E-01	0.403	-0.396	0.366	-0.292
ALIII 4D-5F	10000.	0.473E-01	0.834E-03	0.106E-01	0.107E-01	0.907E-02	0.891E-02
4151.2 A	20000.	0.387E-01	0.472E-03	0.134E-01	0.128E-01	0.111E-01	0.105E-01
C= 0.90E+16	50000.	0.302E-01	0.396E-04	0.171E-01	0.156E-01	0.132E-01	0.126E-01
	100000.	0.252E-01	-0.259E-03	0.196E-01	0.179E-01	0.166E-01	0.146E-01
	200000.	0.207E-01	-0.356E-03	0.200E-01	0.202E-01	0.207E-01	0.154E-01
	500000.	0.158E-01	-0.576E-03	0.279E-01	0.244E-01	0.217E-01	0.164E-01
ALIII 4F-5D	10000.	0.369E-01	0.625E-02	0.300E-02	0.320E-02	0.279E-02	0.262E-02
4702.6 A	20000.	0.311E-01	0.504E-02	0.401E-02	0.388E-02	0.359E-02	0.323E-02
C= 0.22E+18	50000.	0.259E-01	0.449E-02	0.543E-02	0.495E-02	0.465E-02	0.406E-02
	100000.	0.229E-01	0.382E-02	0.640E-02	0.552E-02	0.565E-02	0.434E-02
	200000.	0.199E-01	0.305E-02	0.722E-02	0.633E-02	0.573E-02	0.503E-02
	500000.	0.161E-01	0.218E-02	0.873E-02	0.812E-02	0.745E-02	0.573E-02
ALIII 5S-5P	10000.	0.144	-0.265E-01	0.954E-02	-0.406E-02	0.115E-01	-0.350E-02
12786.7 A	20000.	0.119	-0.187E-01	0.127E-01	-0.567E-02	0.134E-01	-0.480E-02
C= 0.13E+20	50000.	0.108	-0.141E-01	0.153E-01	-0.737E-02	0.158E-01	-0.611E-02
	100000.	0.104	-0.122E-01	0.171E-01	-0.875E-02	0.170E-01	-0.711E-02
	200000.	0.980E-01	-0.103E-01	0.187E-01	-0.102E-01	0.177E-01	-0.816E-02
	500000.	0.867E-01	-0.765E-02	0.202E-01	-0.121E-01	0.181E-01	-0.962E-02
ALIII 5P-5D	10000.	0.150	0.175E-01	0.118E-01	0.123E-01	0.112E-01	0.101E-01
9597.1 A	20000.	0.129	0.165E-01	0.158E-01	0.149E-01	0.141E-01	0.123E-01
C= 0.92E+18	50000.	0.113	0.150E-01	0.203E-01	0.189E-01	0.177E-01	0.152E-01
	100000.	0.103	0.128E-01	0.252E-01	0.218E-01	0.223E-01	0.177E-01
	200000.	0.929E-01	0.101E-01	0.272E-01	0.241E-01	0.241E-01	0.196E-01
	500000.	0.776E-01	0.715E-02	0.315E-01	0.312E-01	0.304E-01	0.220E-01

© European Southern Observatory • Provided by the NASA Astrophysics Data System

Available online at www.sciencedirect.com
SCIENCE DIRECT®
Atomic Data and Nuclear Data Tables 85 (2003) 269–290
Atomic Data AND Nuclear Data Tables
www.elsevier.com/locate/adt

Stark broadening of AgI spectral lines☆

M.S. Dimitrijević[a,*] and S. Sahal-Bréchot[b]

[a]*Astronomical Observatory, Volgina 7, 11160 Belgrade, Serbia and Montenegro*
[b]*LERMA, Unité de recherche du CNRS 8112, Observatoire de Paris-Meudon, 92190 Meudon, France*

Abstract

Using a semiclassical approach, we have calculated electron-, proton-, and ionized helium-impact line widths and shifts for 48 Ag I lines, for perturber densities 10^{13}–10^{19} cm^{-3} and temperatures $T = 2500$–$50{,}000$ K.
© 2003 Elsevier Inc. All rights reserved.

☆ Supplementary data associated with this article can be found at doi:10.1016/S0092-640X(03)00058-5.

* Corresponding author.
E-mail address: mdimitrijevic@aob.bg.ac.yu (M.S. Dimitrijević).

0092-640X/$ - see front matter © 2003 Elsevier Inc. All rights reserved.
doi:10.1016/S0092-640X(03)00058-5

Contents

1. Introduction 270

Explanation of Table 273

Table
1. Stark broadening parameters for Ag I spectral lines 274

1. Introduction

Stark broadening of neutral silver spectral lines has been considered experimentally [1,2] and theoretically [2,3]. In [3] quadratic Stark constants of neutral silver spectral lines in the Coulomb approximation have been determined. The objective of the present work is to continue our efforts to provide to plasma physicists and astrophysicists Stark broadening parameters needed for investigation and modeling of various plasmas (see [4,5], and references therein). We present here results of our calculations of electron-, proton-, and ionized helium-impact line widths and shifts for 48 Ag I spectral lines.

Calculations have been performed within the semiclassical perturbation formalism, developed and discussed in detail in [6,7]. This formalism, as well as the corresponding computer code, has been optimized and updated [4,8]. In [5] is presented a project to provide within this formalism Stark broadening data needed for the investigation of astrophysical and laboratory plasmas. Within this formalism, the full width of a neutral emitter isolated spectral line broadened by electron impacts can be expressed in terms of cross-sections for elastic and inelastic processes as

$$W_{if} = \frac{\lambda_{if}^2}{2\pi c} N \int v f(v)\, \mathrm{d}v \left(\sum_{i' \neq i} \sigma_{ii'}(v) + \sum_{f' \neq f} \sigma_{ff'}(v) + \sigma_{el} \right) \tag{1}$$

and the corresponding line shift as

$$d_{if} = \frac{\lambda_{if}^2}{2\pi c} N \int v f(v)\, \mathrm{d}v \int_{R_3}^{R_\mathrm{D}} 2\pi\rho\, \mathrm{d}\rho \sin 2\phi_p. \tag{2}$$

Here, λ_{if} is the wavelength of the line originating from the transition with the initial atomic energy level i and the final level f, c is the velocity of light, N is the electron density, and $f(v)$ is the Maxwellian velocity distribution function for electrons given by

$$f(v) = 4\pi \left(\frac{m}{2\pi kT} \right)^{3/2} v^2 \exp\left(-\frac{mv^2}{2kT} \right), \tag{3}$$

where m is the electron mass, k is Boltzmann's constant and ρ denotes the impact parameter of the incoming electron. The inelastic cross-section $\sigma_{jj'}(v)$ can be expressed as an integration of the transition probability $P_{jj'}(\rho, v)$ over the impact parameter:

$$\sum_{i' \neq i} \sigma_{jj'}(v) = \frac{1}{2}\pi R_1^2 + \int_{R_1}^{R_\mathrm{D}} 2\pi\rho d\rho \sum_{j \neq j'} P_{jj'}(\rho, v), \quad j = i, f. \tag{4}$$

For the evaluation of the elastic contribution, in [6] the transition matrices (T) are expanded to the first order for the quadrupolar contribution, with spin exchange included. For the dipolar contribution, only the imaginary part of the second-order terms of the T expansion have been retained. Consequently, according to Chapter 3 in [7] and Chapter 2 in [6], after averaging over angles and following the cut-off procedure and trajectory parameterization, the elastic contribution has been evaluated according to

$$\sigma_{el} = 2\pi R_2^2 + \int_{R_2}^{R_\mathrm{D}} 8\pi\rho\, \mathrm{d}\rho \sin^2 \times \left[\phi_q^2 + \left(\sum_{i \neq i'} \phi_{ii'} - \sum_{f \neq f'} \phi_{ff'} \right)^2 \right]^{1/2}, \tag{5}$$

where

$$\phi_p = \left(\sum_{i \neq i'} \phi_{ii'} - \sum_{f \neq f'} \phi_{ff'} \right)^2. \tag{6}$$

The phase shifts ϕ_p and ϕ_q due, respectively, to the polarization potential (r^{-4}) and to the quadrupole potential (r^{-3}) are given in Section 3 of Chapter 2 in [6]. R_D is the Debye radius, included in order to take into account the Debye shielding. All the cut-offs (R_1, R_2, R_3) are described in Section 1 of Chapter 3 in [6]. They are included in order to maintain the unitarity of the S-matrix.

The formulas for the ion-impact broadening parameters are analogous to the formulas for electron-impact broadening.

The atomic energy levels needed for calculations were taken from [9]. Oscillator strengths have been calculated by using the method of Bates and Damgaard [10,11].

For higher levels, the method described in [12] has been used. Our results for electron-, proton-, and ionized helium-impact line widths and shifts for 48 Ag I spectral lines, for perturber densities 10^{13}–$10^{19}\,\mathrm{cm}^{-3}$ and temperatures $T = 2500$–$50{,}000\,\mathrm{K}$, are shown in Table 1. Temperature and perturber density ranges in the table are determined taking into account not only physical conditions where the Stark broadening mechanism is the most important, but also for higher temperatures we took into account the fact that the ionization potential of Ag I is $61106.50\,\mathrm{cm}^{-1}$. (We note that for Na I and Rb I with ionization potentials of 41449.65 and $33690.81\,\mathrm{cm}^{-1}$, respectively, experimental measurements in T-tubes exist up to 26,000 K [13,14] and theoretical results, e.g. for Na I in [15], are given up to 40,000 K.)

For perturber densities lower than those tabulated here, Stark broadening parameters vary linearly with perturber density. By inspecting Eqs. (1) and (2) for Stark widths and shifts one can see that the nonlinear variation of those quantities is due to the Debye screening effect, through the upper cut-off parameter R_D, which depends on the perturber density N. This has been analyzed in detail in [16], where it has been demonstrated that the important quantities for an estimate of the influence of the Debye shielding on Stark broadening parameter values are the differences between R_D and R_1, R_2, and R_3. If these differences are small, Stark broadening parameters are not linear with the electron density (N_e) even if the photon energy is large in comparison with the plasmon energy. On the other hand if the electron density increases, R_D decreases and $R_\mathrm{D} - R_1$, $R_\mathrm{D} - R_2$, $R_\mathrm{D} - R_3$ differences decrease so that the behavior of Stark broadening parameters also becomes nonlinear. Moreover, in [16] it has been shown (see e.g. Fig. 9 in [16]) that within a spectral series, the density range of linear behavior of Stark broadening parameters decreases with the increase of the principal quantum number of the upper level, so that this range is maximal for the lowest member of a spectral series, as e.g. here for Ag I 5s–5p transition. This is a consequence of the fact that the energy gap between the initial energy level and the most important perturbing levels decreases with the increase of the principal quantum number (see e.g. Figs. 1 and 2 in [16]).

We also specify a quantity C (see [4]) with dimensions $\mathrm{Å\,cm}^{-3}$, which gives an estimate for the maximum perturber density for which the line may be treated as isolated when it is divided by the corresponding full width at half maximum. For perturber densities lower than $N_\ell\,(\mathrm{cm}^{-3}) = C\,(\mathrm{Å\,cm}^{-3})/W_{if}\,(\mathrm{Å})$, the line may be treated as isolated in the core, even if a weak forbidden component due to the failure of this approximation remains in the wing. At higher densities the impact width is comparable to the separation between the perturbing energy levels and the initial or final level of the transition: the corresponding energy levels become degenerate and the isolated line approximation is then invalid [15]. For each value given in Table 1, the collision volume (V) multiplied by the perturber density (N) is much less than one and the impact approximation is valid [6,7]. The collision volume is proportional to the cube of the typical emitter-perturber distance ρ^3_typ, and ρ^3_typ may be estimated from the width, representing the width as proportional to the perturber density N, the average velocity v, and the average total cross-section $\sigma_\mathrm{typ} = \pi\rho^2_\mathrm{typ}$. Values for $NV > 0.5$ are not given and values for $0.1 < NV \leqslant 0.5$ are denoted by an asterisk. When the impact approximation is not valid, the ion broadening contribution may be estimated by using the quasistatic approach [15,17]. In the region where neither of these two approximations is valid, a unified type theory should be used [18].

The sparse existing experimental data [1,2] were not included in the review of critically selected experimental Stark broadening data [19]. In order to make a comparison of theory with reliable experimental data, the results of corresponding experiments to determine the Stark broadening of Ag I lines will be of interest for future development and refinement of the theory.

A computer-readable file of Table 1 may be obtained from the authors by request (e-mail: mdimitrijevic@aob.bg.ac.yu) or through the journal's website.

Acknowledgments

This work is a part of the project GA 1195, "Influence of collisional processes on astrophysical plasma lineshapes," supported by the Ministry of Science, Technologies and Development of Serbia.

References

[1] J. Holtsmark, B. Trumpy, Z. Phys. 31 (1925) 803.
[2] V.F. Kitaeva, Tr. Fiz. Inst. Acad. Nauk SSSR 11 (1956) 3.
[3] G. Pichler, Fizika 4 (1972) 235.
[4] M.S. Dimitrijević, S. Sahal-Bréchot, J. Quant. Spectrosc. Radiat. Transfer 31 (1984) 301.
[5] M.S. Dimitrijević, Zh. Priklad. Spektrosk. 63 (1996) 810.
[6] S. Sahal-Bréchot, Astron. Astrophys. 1 (1969) 91.
[7] S. Sahal-Bréchot, Astron. Astrophys. 2 (1969) 322.
[8] S. Sahal-Bréchot, Astron. Astrophys. 35 (1974) 319.
[9] C.E. Moore, Atomic Energy Levels III, NSRDS-NBS 35, Washington, 1971.
[10] D.R. Bates, A. Damgaard, Trans. R. Soc. Lond. A 242 (1949) 101.
[11] G.K. Oertel, L.P. Shomo, Astrophys. J. Suppl. Series 16 (1968) 175.
[12] H. Van Regemorter, Hoang Binh Dy, M. Prud'homme, J. Phys. B 12 (1979) 1053.
[13] J. Purić, J. Labat, S. Djeniže, Lj. Ćirković, I. Lakićević, Phys. Lett. A 56 (1976) 83.

[14] J. Purić, J. Labat, L.j. Ćirković, S. Djeniže, J. Phys. B 10 (1977) 2375.
[15] S. Sahal-Bréchot, Astron. Astrophys. 245 (1991) 322.
[16] M.S. Dimitrijević, S. Sahal-Bréchot, Astron. Astrophys. 136 (1984) 289.
[17] H.R. Griem, Spectral Line Broadening by Plasmas, Academic Press, New York, 1974.
[18] A.J. Barnard, J. Cooper,, E.W. Smith, J. Quant. Spectrosc. Radiat. Transfer 14 (1974) 1025.
[19] N. Konjević, J.R. Roberts, J. Phys. Chem. Ref. Data 5 (1976) 209.

Explanation of Table

Table 1. Stark broadening parameters for Ag I spectral lines

This table shows electron-, proton-, and ionized helium-impact broadening parameters for Ag I for perturber densities from 10^{13} cm^{-3} up to 10^{19} cm^{-3} and temperatures from 2500 up to 50,000 K. For perturber (electron, proton, and ionized helium) densities lower than those tabulated, Stark broadening parameters vary linearly with perturber density. Consequently, the first appearance of a transition in the table is for the highest perturber density for which linear extrapolation to lower perturber density from the listed Stark broadening parameters is approximately correct. For perturber density lower than 10^{13} cm^{-3}, Stark broadening parameters do not vary linearly with N only for several transitions with larger n, and so only for such transitions are data given. Calculations have been performed for all transitions for which reliable data exist for all energy levels with $\Delta n = 0, \pm 1, \pm 2$, perturbing the initial and final energy levels of the considered transition. Transitions for a particular density are listed starting with the lowest n, ℓ, and j, first for the spectral series $n_f\ell - n_i(\ell+1)$, where n_i ($n_i \geqslant n_f$) increases through the full range of values before n_f is increased, then for the spectral series $n_f\ell - n_i(\ell-1)$. Within a multiplet $n_f\ell_f^2 L_f - n_i\ell_i^2 L_i$, particular lines are listed starting from the lowest j_f and j_i. First j_i increases and then j_f. Then, the same ordering is used for the next ℓ. For each value given in the table, the collision volume (V) multiplied by the perturber density (N) is much less than one and the impact approximation is valid [8]. Values for $NV > 0.5$ are not given and values for $0.1 < NV \leqslant 0.5$ are denoted by an asterisk.

Transition: Identification of the transition by the principal quantum numbers n and the angular momentum quantum numbers ℓ in the first row and by the total angular momentum quantum numbers j in the second row, for the electron making the transition. For example 5S 9P in the first row and 1.5 .5 in the second row means the silver atom spectral line originating from the transition between atomic energy levels $1s^22s^22p^63s^23p^63d^{10}4s^24p^64d^{10}5s^2S_{3/2}$ and $1s^22s^22p^63s^23p^63d^{10}4s^24p^64d^{10}9p^2P^0_{1/2}$.

WL (Å)	Transition wavelength in Å
T (K)	Temperature in kelvin
Density (cm^{-3})	Perturber density in cm^{-3}
C	The quantity C (given in Å cm^{-3}), when divided by the corresponding full width at half maximum, gives an estimate for the maximum perturber density for which tabulated data may be used. For higher densities, the isolated line approximation used in calculations breaks down.
Width (Å)	Full line width at half maximum in Å
Shift	Line shift in Å. A positive shift is towards the red

Table 1
Stark broadening parameters for Ag I spectral lines. See page 273 for Explanation of Table

Transition		*WL* (Å)	*T* (K)	Perturber density (cm^{-3})	*C*	Electrons		Protons		Ionized helium	
						Width (Å)	Shift (Å)	Width (Å)	Shift (Å)	Width (Å)	Shift (Å)
5S	9P	1723.3	2500	1.E + 13	.68E + 13	.157E − 2	.820E − 3	.410E − 3	.357E − 3	*.329E − 3	*.281E − 3
1.5	.5		5000			.158E − 2	.637E − 3	.462E − 3	.410E − 3	.367E − 3	.324E − 3
			10,000			.150E − 2	.427E − 3	.524E − 3	.467E − 3	.410E − 3	.371E − 3
			20,000			.140E − 2	.226E − 3	.603E − 3	.530E − 3	.460E − 3	.421E − 3
			30,000			.133E − 2	.171E − 3	.661E − 3	.569E − 3	.491E − 3	.453E − 3
			50,000			.123E − 2	.117E − 3	.752E − 3	.621E − 3	.535E − 3	.495E − 3
5S	10P	1699.7	2500	1.E + 13	.81E + 13	.234E − 2	.134E − 2	*.586E − 3	*.500E − 3	*.473E − 3	*.391E − 3
.5	.5		5000			.242E − 2	.969E − 3	.657E − 3	.577E − 3	*.527E − 3	*.455E − 3
			10,000			.241E − 2	.598E − 3	.741E − 3	.659E − 3	*.587E − 3	*.522E − 3
			20,000			.230E − 2	.398E − 3	.844E − 3	.748E − 3	.656E − 3	.594E − 3
			30,000			.222E − 2	.296E − 3	.917E − 3	.805E − 3	.701E − 3	.640E − 3
			50,000			.209E − 2	.195E − 3	.103E − 2	.878E − 3	.762E − 3	.701E − 3
5S	10P	1699.2	2500	1.E + 13	.36E + 13	.332E − 2	.149E − 2	*.900E − 3	*.761E − 3	*.717E − 3	*.592E − 3
1.5	.5		5000			.326E − 2	.102E − 2	*.102E − 2	*.885E − 3	*.802E − 3	*.696E − 3
			10,000			.306E − 2	.733E − 3	*.116E − 2	*.102E − 2	*.899E − 3	*.803E − 3
			20,000			.281E − 2	.346E − 3	.134E − 2	.116E − 2	*.101E − 2	*.917E − 3
			30,000			.265E − 2	.264E − 3	.148E − 2	.124E − 2	*.108E − 2	*.988E − 3
			50,000			.244E − 2	.181E − 3	.170E − 2	.137E − 2	*.118E − 2	*.108E − 2
6S	9P	6472.9	2500	1.E + 13	.19E + 15	.165E − 1	.103E − 1	.408E − 2	.354E − 2	.331E − 2	.279E − 2
.5	.5		5000			.171E − 1	.828E − 2	.457E − 2	.405E − 2	.367E − 2	.321E − 2
			10,000			.172E − 1	.617E − 2	.514E − 2	.460E − 2	.409E − 2	.366E − 2
			20,000			.166E − 1	.405E − 2	.583E − 2	.521E − 2	.456E − 2	.415E − 2
			30,000			.161E − 1	.289E − 2	.632E − 2	.559E − 2	.487E − 2	.446E − 2
			50,000			.153E − 1	.177E − 2	.707E − 2	.610E − 2	.529E − 2	.486E − 2
6S	9P	6463.7	2500	1.E + 13	.96E + 14	.221E − 1	.115E − 1	.577E − 2	.502E − 2	*.462E − 2	*.395E − 2
1.5	.5		5000			.222E − 1	.898E − 2	.650E − 2	.577E − 2	.516E − 2	.456E − 2
			10,000			.212E − 1	.623E − 2	.738E − 2	.657E − 2	.577E − 2	.521E − 2
			20,000			.197E − 1	.368E − 2	.848E − 2	.745E − 2	.646E − 2	.592E − 2
			30,000			.187E − 1	.272E − 2	.929E − 2	.801E − 2	.691E − 2	.637E − 2
			50,000			.174E − 1	.155E − 2	.106E − 1	.874E − 2	.753E − 2	.697E − 2
6S	10P	6143.2	2500	1.E + 13	.11E + 15	.305E − 1	.180E − 1	*.766E − 2	*.653E − 2	*.618E − 2	*.511E − 2
.5	.5		5000			.316E − 1	.141E − 1	.859E − 2	.754E − 2	*.688E − 2	*.594E − 2
			10,000			.315E − 1	.101E − 1	.968E − 2	.861E − 2	*.767E − 2	*.682E − 2
			20,000			.301E − 1	.638E − 2	.110E − 1	.977E − 2	.857E − 2	.776E − 2
			30,000			.290E − 1	.448E − 2	.120E − 1	.105E − 1	.915E − 2	.835E − 2
			50,000			.274E − 1	.254E − 2	.134E − 1	.115E − 1	.995E − 2	.915E − 2
6S	10P	6137.3	2500	1.E + 13	.48E + 14	.433E − 1	.201E − 1	*.117E − 1	*.992E − 2	*.936E − 2	*.772E − 2
1.5	.5		5000			.426E − 1	.152E − 1	*.133E − 1	*.115E − 1	*.105E − 1	*.908E − 2
			10,000			.399E − 1	.955E − 2	*.151E − 1	*.132E − 1	*.117E − 1	*.105E − 1
			20,000			.367E − 1	.569E − 2	.175E − 1	.151E − 1	*.131E − 1	*.120E − 1
			30,000			.347E − 1	.399E − 2	.193E − 1	.162E − 1	*.141E − 1	*.129E − 1
			50,000			.320E − 1	.209E − 2	.222E − 1	.178E − 1	*.153E − 1	*.141E − 1

7S	9P	16286.3	2500	1.E + 13	.61E + 15	.140	.722E − 1	.366E − 1	.319E − 1	*.293E − 1	*.250E − 1
1.5	.5		5000			.141	.559E − 1	.412E − 1	.366E − 1	.327E − 1	.289E − 1
			10,000			.135	.378E − 1	.468E − 1	.417E − 1	.366E − 1	.331E − 1
			20,000			.127	.217E − 1	.538E − 1	.473E − 1	.410E − 1	.376E − 1
			30,000			.121	.137E − 1	.590E − 1	.508E − 1	.438E − 1	.404E − 1
			50,000			.113	.698E − 2	.671E − 1	.555E − 1	.478E − 1	.442E − 1
7S	10P	14394.1	2500	1.E + 13	.58E + 15	.168	.985E − 1	*.420E − 1	*.358E − 1	*.339E − 1	*.280E − 1
.5	.5		5000			.174	.770E − 1	.471E − 1	.414E − 1	*.377E − 1	*.326E − 1
			10,000			.173	.546E − 1	.531E − 1	.472E − 1	*.421E − 1	*.374E − 1
			20,000			.166	.316E − 1	.605E − 1	.536E − 1	.470E − 1	.426E − 1
			30,000			.161	.215E − 1	.657E − 1	.577E − 1	.502E − 1	.458E − 1
			50,000			.152	.969E − 2	.738E − 1	.630E − 1	.546E − 1	.502E − 1
7S	10P	14361.9	2500	1.E + 13	.26E + 15	.237	.110	*.643E − 1	*.543E − 1	*.512E − 1	*.423E − 1
1.5	.5		5000			.233	.829E − 1	*.726E − 1	*.632E − 1	*.573E − 1	*.497E − 1
			10,000			.219	.528E − 1	*.828E − 1	*.725E − 1	*.642E − 1	*.574E − 1
			20,000			.202	.300E − 1	.959E − 1	.825E − 1	*.719E − 1	*.655E − 1
			30,000			.191	.182E − 1	.106	.888E − 1	*.770E − 1	*.706E − 1
			50,000			.177	.968E − 2	.122	.977E − 1	*.840E − 1	*.774E − 1
8S	9P	40886.3	2500	1.E + 13	.38E + 16	.880	.437	.230	.200	*.184	*.157
1.5	.5		5000			.898	.319	.259	.230	.206	.182
			10,000			.870	.182	.294	.262	.230	.208
			20,000			.827	.573E − 1	.338	.297	.258	.236
			30,000			.797	.427E − 1	.370	.319	.275	.254
			50,000			.755	.287E − 1	.422	.348	.300	.278
8S	10P	30741.2	2500	1.E + 13	.27E + 16	.764	.444	*.191	*.163	*.154	*.128
.5	.5		5000			.798	.322	.214	.188	*.172	*.148
			10,000			.801	.193	.242	.215	*.192	*.170
			20,000			.774	.119	.275	.244	.214	.194
			30,000			.753	.508E − 1	.299	.263	.229	.209
			50,000			.720	.359E − 1	.336	.287	.249	.229
8S	10P	30594.7	2500	1.E + 13	.12E + 16	1.08	.495	*.291	*.246	*.232	*.192
1.5	.5		5000			1.06	.358	*.329	*.287	*.260	*.225
			10,000			1.00	.204	*.375	*.329	*.291	*.260
			20,000			.934	.969E − 1	.435	.374	*.326	*.297
			30,000			.889	.523E − 1	.480	.403	*.349	*.320
			50,000			.826	.367E − 1	.551	.443	*.381	*.351
5S	8P	1766.1	2500	1.E + 14	.25E + 15	.512E − 2	.330E − 2	*.125E − 2	*.101E − 2	*.102E − 2	*.787E − 3
.5	.5		5000			.533E − 2	.277E − 2	.139E − 2	.119E − 2	*.113E − 2	*.931E − 3
			10,000			.543E − 2	.213E − 2	.156E − 2	.136E − 2	*.125E − 2	*.108E − 2
			20,000			.527E − 2	.145E − 2	.177E − 2	.156E − 2	.139E − 2	.123E − 2
			30,000			.512E − 2	.107E − 2	.191E − 2	.167E − 2	.149E − 2	.133E − 2
			50,000			.490E − 2	.769E − 3	.212E − 2	.184E − 2	.161E − 2	.146E − 2
5S	8P	1764.9	2500	1.E + 14	.12E + 15	.697E − 2	.354E − 2	*.179E − 2	*.145E − 2	*.144E − 2	*.112E − 2
1.5	.5		5000			.711E − 2	.304E − 2	*.202E − 2	*.171E − 2	*.161E − 2	*.134E − 2
			10,000			.683E − 2	.221E − 2	.228E − 2	.198E − 2	*.180E − 2	*.156E − 2
			20,000			.638E − 2	.132E − 2	.261E − 2	.227E − 2	*.201E − 2	*.180E − 2

Table 1 (*continued*)

Transition		*WL* (Å)	*T* (K)	Perturber density (cm^{-3})	*C*	Electrons		Protons		Ionized helium	
						Width (Å)	Shift (Å)	Width (Å)	Shift (Å)	Width (Å)	Shift (Å)
			30,000			.608E − 2	.101E − 2	.285E − 2	.244E − 2	*.215E − 2	*.194E − 2
			50,000			.568E − 2	.694E − 3	.324E − 2	.268E − 2	.234E − 2	.213E − 2
5S	9P	1724.0	2500	1.E + 14	.13E + 15	.117E − 1	.704E − 2	*.289E − 2	*.223E − 2		
.5	.5		5000			.122E − 1	.536E − 2	*.324E − 2	*.267E − 2		
			10,000			.122E − 1	.419E − 2	*.365E − 2	*.312E − 2	*.290E − 2	*.245E − 2
			20,000			.117E − 1	.254E − 2	*.414E − 2	*.359E − 2	*.324E − 2	*.284E − 2
			30,000			.114E − 1	.192E − 2	*.448E − 2	*.388E − 2	*.345E − 2	*.307E − 2
			50,000			.108E − 1	.128E − 2	.501E − 2	.426E − 2	*.375E − 2	*.338E − 2
5S	9P	1723.3	2500	1.E + 14	.68E + 14	.157E − 1	.773E − 2				
1.5	.5		5000			.158E − 1	.617E − 2	*.462E − 2	*.376E − 2		
			10,000			.150E − 1	.422E − 2	*.524E − 2	*.443E − 2		
			20,000			.140E − 1	.224E − 2	*.603E − 2	*.512E − 2	*.459E − 2	*.403E − 2
			30,000			.133E − 1	.171E − 2	*.660E − 2	*.554E − 2	*.491E − 2	*.438E − 2
			50,000			.123E − 1	.117E − 2	*.752E − 2	*.610E − 2	*.535E − 2	*.484E − 2
5S	10P	1699.7	2500	1.E + 14	.81E + 14	.234E − 1	.127E − 1				
.5	.5		5000			.242E − 1	.939E − 2				
			10,000			.241E − 1	.593E − 2				
			20,000			.230E − 1	.395E − 2	*.843E − 2	*.718E − 2		
			30,000			.222E − 1	.295E − 2	*.916E − 2	*.779E − 2		
			50,000			.209E − 1	.195E − 2	*.103E − 1	*.859E − 2		
5S	10P	1699.2	2500	1.E + 14	.36E + 14	.331E − 1	.135E − 1				
1.5	.5		5000			.325E − 1	.963E − 2				
			10,000			.305E − 1	.718E − 2				
			20,000			.281E − 1	.339E − 2				
			30,000			.265E − 1	.262E − 2				
			50,000			.244E − 1	.181E − 2				
6S	8P	7110.1	2500	1.E + 14	.40E + 16	.830E − 1	.534E − 1	*.202E − 1	*.164E − 1	*.165E − 1	*.127E − 1
.5	.5		5000			.864E − 1	.448E − 1	.226E − 1	.192E − 1	*.183E − 1	*.151E − 1
			10,000			.882E − 1	.348E − 1	.253E − 1	.221E − 1	*.203E − 1	*.175E − 1
			20,000			.859E − 1	.238E − 1	.286E − 1	.252E − 1	.226E − 1	.200E − 1
			30,000			.837E − 1	.173E − 1	.309E − 1	.271E − 1	.241E − 1	.215E − 1
			50,000			.803E − 1	.115E − 1	.344E − 1	.297E − 1	.261E − 1	.236E − 1
6S	8P	7090.0	2500	1.E + 14	.20E + 16	.112	.606E − 1	*.289E − 1	*.234E − 1	*.232E − 1	*.181E − 1
1.5	.5		5000			.115	.491E − 1	*.325E − 1	*.277E − 1	*.259E − 1	*.216E − 1
			10,000			.110	.365E − 1	.368E − 1	.320E − 1	*.290E − 1	*.252E − 1
			20,000			.103	.233E − 1	.422E − 1	.366E − 1	*.324E − 1	*.290E − 1
			30,000			.988E − 1	.168E − 1	.461E − 1	.394E − 1	*.346E − 1	*.313E − 1
			50,000			.925E − 1	.103E − 1	.522E − 1	.433E − 1	.377E − 1	.344E − 1
6S	9P	6472.9	2500	1.E + 14	.19E + 16	.165	.994E − 1	*.408E − 1	*.314E − 1		
.5	.5		5000			.171	.814E − 1	*.457E − 1	*.377E − 1		
			10,000			.172	.615E − 1	*.514E − 1	*.440E − 1	*.409E − 1	*.345E − 1
			20,000			.166	.404E − 1	*.583E − 1	*.506E − 1	*.456E − 1	*.400E − 1

			30,000			.161	.289E − 1	*.632E − 1	*.547E − 1	*.487E − 1	*.433E − 1
			50,000			.153	.177E − 1	.707E − 1	.601E − 1	*.529E − 1	*.477E − 1
6S	9P	6463.7	2500	1.E + 14	.96E + 15	.220	.109				
1.5	.5		5000			.222	.873E − 1	*.650E − 1	*.528E − 1		
			10,000			.212	.618E − 1	*.737E − 1	*.623E − 1		
			20,000			.197	.368E − 1	*.848E − 1	*.720E − 1	*.646E − 1	*.568E − 1
			30,000			.187	.272E − 1	*.929E − 1	*.779E − 1	*.691E − 1	*.616E − 1
			50,000			.174	.155E − 1	*.106	*.858E − 1	*.753E − 1	*.680E − 1
6S	10P	6143.2	2500	1.E + 14	.11E + 16	.305	.171				
.5	.5		5000			.316	.137				
			10,000			.314	.101				
			20,000			.301	.634E − 1	*.110	*.938E − 1		
			30,000			.290	.447E − 1	*.120	*.102		
			50,000			.274	.254E − 1	*.134	*.112		
6S	10P	6137.3	2500	1.E + 14	.48E + 15	.431	.182				
1.5	.5		5000			.424	.144				
			10,000			.398	.941E − 1				
			20,000			.367	.561E − 1				
			30,000			.346	.396E − 1				
			50,000			.319	.209E − 1				
7S	8P	21124.9	2500	1.E + 14	.35E + 17	.728	.456	*.177	*.144	*.145	*.112
.5	.5		5000			.764	.370	.198	.169	*.160	*.132
			10,000			.791	.267	.222	.194	*.178	*.153
			20,000			.783	.163	.251	.221	.198	.175
			30,000			.770	.110	.272	.238	.211	.189
			50,000			.748	.529E − 1	.302	.261	.229	.207
7S	8P	20948.6	2500	1.E + 14	.17E + 17	.977	.514	*.252	*.204	*.202	*.157
1.5	.5		5000			1.00	.405	*.283	*.241	*.226	*.188
			10,000			.975	.281	.320	.279	*.252	*.219
			20,000			.926	.161	.367	.318	*.282	*.252
			30,000			.893	.879E − 1	.401	.343	*.301	*.272
			50,000			.846	.507E − 1	.454	.377	.328	.299
7S	9P	16344.6	2500	1.E + 14	.12E + 17	1.05	.626	*.260	*.200		
.5	.5		5000			1.10	.508	*.291	*.240		
			10,000			1.11	.368	*.327	*.280	*.260	*.220
			20,000			1.07	.218	*.371	*.322	*.290	*.255
			30,000			1.04	.154	*.402	*.348	*.310	*.276
			50,000			.998	.689E − 1	.450	.382	*.337	*.304
7S	9P	16286.3	2500	1.E + 14	.61E + 16	1.40	.686				
1.5	.5		5000			1.41	.550	*.412	*.335		
			10,000			1.35	.378	*.468	*.395		
			20,000			1.27	.215	*.538	*.457	*.410	*.360
			30,000			1.21	.137	*.589	*.494	*.438	*.391
			50,000			1.13	.698E − 1	*.671	*.544	*.477	*.431

Table 1 (*continued*)

Transition		*WL* (Å)	*T* (K)	Perturber density (cm^{-3})	*C*	Electrons		Protons		Ionized helium	
						Width (Å)	Shift (Å)	Width (Å)	Shift (Å)	Width (Å)	Shift (Å)
7S	10P	14394.1	2500	1.E + 14	.58E + 16	1.68	.934				
.5	.5		5000			1.74	.755				
			10,000			1.73	.542				
			20,000			1.66	.314	*.605	*.515		
			30,000			1.61	.215	*.657	*.558		
			50,000			1.52	.969E − 1	*.738	*.616		
7S	10P	14361.9	2500	1.E + 14	.26E + 16	2.36	.996				
1.5	.5		5000			2.33	.801				
			10,000			2.19	.528				
			20,000			2.02	.296				
			30,000			1.91	.182				
			50,000			1.77	.968E − 1				
8S	8P	96206.6	2500	1.E + 14	.73E + 18	14.9	8.05	*3.60	*2.93	*2.94	*2.27
.5	.5		5000			16.4	4.90	4.02	3.42	*3.25	*2.68
			10,000			17.6	2.46	4.51	3.93	3.61	3.10
			20,000			17.9	.987	5.10	4.48	4.02	3.55
			30,000			18.0	.568	5.51	4.82	4.28	3.83
			50,000			18.0	−.133	6.13	5.29	4.64	4.20
8S	8P	92654.4	2500	1.E + 14	.34E + 18	19.1	7.06	*4.86	*3.94	*3.91	*3.04
1.5	.5		5000			20.3	4.93	*5.47	*4.65	*4.36	*3.63
			10,000			20.1	1.89	6.19	5.38	*4.87	*4.24
			20,000			19.7	.700	7.09	6.15	*5.44	*4.87
			30,000			19.4	.427	7.75	6.63	*5.82	*5.26
			50,000			18.8	−.335	8.79	7.27	6.33	5.78
8S	9P	41255.7	2500	1.E + 14	.76E + 17	6.68	3.84	*1.64	*1.27		
.5	.5		5000			7.04	2.83	*1.84	*1.52		
			10,000			7.25	1.69	*2.07	*1.77	*1.65	*1.39
			20,000			7.13	.585	*2.35	*2.04	*1.84	*1.61
			30,000			7.01	.426	*2.55	*2.20	*1.96	*1.75
			50,000			6.80	.280	2.85	2.42	*2.13	*1.92
8S	9P	40886.3	2500	1.E + 14	.38E + 17	8.80	4.10				
1.5	.5		5000			8.98	3.08	*2.59	*2.11		
			10,000			8.69	1.79	*2.94	*2.48		
			20,000			8.27	.569	*3.38	*2.87	*2.57	*2.26
			30,000			7.97	.427	*3.70	*3.10	*2.75	*2.46
			50,000			7.55	.287	*4.22	*3.42	*3.00	*2.71
8S	10P	30741.2	2500	1.E + 14	.27E + 17	7.64	4.17				
.5	.5		5000			7.98	3.09				
			10,000			8.01	1.89				
			20,000			7.74	1.19	*2.75	*2.34		
			30,000			7.53	.508	*2.99	*2.54		
			50,000			7.20	.359	*3.36	*2.80		

8S	10P	30594.7	2500	1.E + 14	.12E + 17	10.7	4.42					
1.5	.5		5000			10.6	3.34					
			10,000			10.0	1.97					
			20,000			9.33	.964					
			30,000			8.87	.523					
			50,000			8.25	.367					
7P	8S	64922.4	2500	1.E + 14	.68E + 18	2.31	−.741	.466	−.379	.389	−.299	
.5	.5		5000			2.84	−.354	.515	−.435	.425	−.344	
			10,000			3.21	−.591E − 1	.573	−.494	.467	−.392	
			20,000			3.52	.163	.643	−.560	.515	−.445	
			30,000			3.70	.209	.693	−.600	.546	−.478	
			50,000			3.89	.294	.768	−.654	.589	−.522	
7P	8S	68487.1	2500	1.E + 14	.38E + 18	3.69	−1.01	.786	−.665	.639	−.522	
.5	1.5		5000			4.18	−.598	.880	−.766	.708	−.605	
			10,000			4.38	−.771E − 1	.992	−.874	.787	−.693	
			20,000			4.56	.208	1.13	−.991	.877	−.787	
			30,000			4.66	.286	1.23	−1.07	.936	−.847	
			50,000			4.76	.376	1.39	−1.16	1.02	−.927	
5S	7P	1850.4	2500	1.E + 15	.56E + 16	.184E − 1	.121E − 1	*.444E − 2	*.323E − 2	*.365E − 2	*.244E − 2	
.5	.5		5000			.192E − 1	.108E − 1	*.494E − 2	*.392E − 2	*.404E − 2	*.303E − 2	
			10,000			.199E − 1	.885E − 2	.552E − 2	.461E − 2	*.447E − 2	*.361E − 2	
			20,000			.196E − 1	.670E − 2	.621E − 2	.532E − 2	*.495E − 2	*.420E − 2	
			30,000			.192E − 1	.542E − 2	.668E − 2	.576E − 2	*.527E − 2	*.456E − 2	
			50,000			.185E − 1	.393E − 2	.739E − 2	.633E − 2	.570E − 2	.502E − 2	
5S	7P	1847.7	2500	1.E + 15	.28E + 16	.249E − 1	.140E − 1	*.628E − 2	*.449E − 2			
1.5	.5		5000			.258E − 1	.118E − 1	*.704E − 2	*.556E − 2	*.565E − 2	*.426E − 2	
			10,000			.253E − 1	.943E − 2	*.794E − 2	*.661E − 2	*.630E − 2	*.515E − 2	
			20,000			.239E − 1	.658E − 2	*.903E − 2	*.767E − 2	*.703E − 2	*.604E − 2	
			30,000			.229E − 1	.517E − 2	.982E − 2	.832E − 2	*.750E − 2	*.657E − 2	
			50,000			.216E − 1	.366E − 2	.110E − 1	.917E − 2	*.815E − 2	*.727E − 2	
5S	8P	1766.1	2500	1.E + 15	.25E + 16	.512E − 1	.305E − 1					
.5	.5		5000			.533E − 1	.262E − 1					
			10,000			.543E − 1	.207E − 1					
			20,000			.527E − 1	.144E − 1	*.177E − 1	*.147E − 1			
			30,000			.512E − 1	.107E − 1	*.191E − 1	*.160E − 1			
			50,000			.490E − 1	.766E − 2	*.212E − 1	*.178E − 1	*.161E − 1	*.140E − 1	
5S	8P	1764.9	2500	1.E + 15	.12E + 16	.693E − 1	.324E − 1					
1.5	.5		5000			.708E − 1	.276E − 1					
			10,000			.681E − 1	.209E − 1					
			20,000			.636E − 1	.130E − 1					
			30,000			.607E − 1	.993E − 2					
			50,000			.567E − 1	.687E − 2	*.323E − 1	*.258E − 1			
5S	9P	1724.0	2500	1.E + 15	.13E + 16	*.116	*.609E − 1					
.5	.5		5000			.121	.502E − 1					
			10,000			.122	.395E − 1					
			20,000			.117	.250E − 1					

Table 1 (*continued*)

Transition		*WL* (Å)	*T* (K)	Perturber density (cm^{-3})	*C*	Electrons		Protons		Ionized helium	
						Width (Å)	Shift (Å)	Width (Å)	Shift (Å)	Width (Å)	Shift (Å)
			30,000			.113	.188E – 1				
			50,000			.108	.126E – 1				
5S	9P	1723.3	2500	1.E + 15	.68E + 15*	.151	*.605E – 1				
1.5	.5		5000			*.154	*.513E – 1				
			10,000			.147	.378E – 1				
			20,000			.138	.217E – 1				
			30,000			.131	.165E – 1				
			50,000			.122	.114E – 1				
5S	10P	1699.7	2500	1.E + 15	.81E + 15*	.225	*.102				
.5	.5		5000			*.236	*.833E – 1				
			10,000			*.236	*.575E – 1				
			20,000			.227	.382E – 1				
			30,000			.219	.285E – 1				
			50,000			.208	.191E – 1				
5S	10P	1699.2	2500	1.E + 15	.36E + 15	*.288	*.894E – 1				
1.5	.5		5000			*.295	*.754E – 1				
			10,000			*.284	*.570E – 1				
			20,000			.266	.314E – 1				
			30,000			.253	.241E – 1				
			50,000			.235	.170E – 1				
6S	6P	16821.9	2500	1.E + 15	.69E + 18	.390	.240	.100	.793E – 1	.831E – 1	.616E – 1
1.5	.5		5000			.421	.188	.111	.924E – 1	.912E – 1	.726E – 1
			10,000			.444	.139	.124	.106	.100	.838E – 1
			20,000			.449	.908E – 1	.140	.121	.111	.958E – 1
			30,000			.450	.646E – 1	.151	.130	.118	.103
			50,000			.450	.388E – 1	.167	.142	.128	.113
6S	7P	8707.1	2500	1.E + 15	.12E + 18	.405	.265	*.980E – 1	*.713E – 1	*.806E – 1	*.538E – 1
.5	.5		5000			.425	.231	*.109	*.865E – 1	*.891E – 1	*.668E – 1
			10,000			.442	.185	.122	.102	*.985E – 1	*.796E – 1
			20,000			.441	.134	.137	.117	*.109	*.926E – 1
			30,000			.435	.995E – 1	.147	.127	*.116	*.100
			50,000			.424	.701E – 1	.163	.140	.126	.111
6S	7P	8646.8	2500	1.E + 15	.61E + 17	.544	.304	*.137	*.982E – 1		
1.5	.5		5000			.565	.253	*.154	*.122	*.123	*.931E – 1
			10,000			.556	.201	*.173	*.144	*.138	*.113
			20,000			.529	.133	*.197	*.168	*.154	*.132
			30,000			.511	.966E – 1	.215	.182	*.164	*.144
			50,000			.487	.645E – 1	.241	.200	*.178	*.159
6S	8P	7110.1	2500	1.E + 15	.40E + 17	.830	.493				
.5	.5		5000			.864	.423				
			10,000			.882	.340				
			20,000			.859	.238	*.286	*.238		

			30,000			.837	.172	*.309	*.260		
			50,000			.803	.115	*.344	*.288	*.261	*.227
6S	8P	7090.0	2500	1.E + 15	.20E + 17	1.12	.531				
1.5	.5		5000			1.14	.446				
			10,000			1.10	.351				
			20,000			1.03	.229				
			30,000			.986	.165				
			50,000			.924	.103	*.522	*.417		
6S	9P	6472.9	2500	1.E + 15	.19E + 17	*1.64	*.857				
.5	.5		5000			1.71	.730				
			10,000			1.72	.585				
			20,000			1.65	.398				
			30,000			1.60	.284				
			50,000			1.53	.177				
6S	9P	6463.7	2500	1.E + 15	.96E + 16	*2.12	*.850				
1.5	.5		5000			*2.16	*.726				
			10,000			2.07	.569				
			20,000			1.94	.368				
			30,000			1.85	.263				
			50,000			1.72	.155				
6S	10P	6143.2	2500	1.E + 15	.11E + 17	*2.94	*1.32				
.5	.5		5000			*3.09	*1.13				
			10,000			*3.09	*.915				
			20,000			2.97	.618				
			30,000			2.87	.434				
			50,000			2.72	.254				
6S	10P	6137.3	2500	1.E + 15	.48E + 16	*3.75	*1.16				
1.5	.5		5000			*3.85	*1.03				
			10,000			*3.70	*.795				
			20,000			3.47	.528				
			30,000			3.30	.369				
			50,000			3.07	.209				
7S	7P	46425.0	2500	1.E + 15	.35E + 19	11.3	6.82	*2.71	*1.97	*2.23	*1.49
.5	.5		5000			12.1	5.00	*3.01	*2.39	*2.46	*1.84
			10,000			13.3	3.28	3.36	2.80	*2.72	*2.19
			20,000			13.7	1.73	3.78	3.23	*3.02	*2.55
			30,000			13.9	1.12	4.07	3.49	*3.20	*2.77
			50,000			14.0	.601	4.50	3.84	3.47	3.05
7S	7P	44759.2	2500	1.E + 15	.16E + 19	14.3	7.07	*3.61	*2.59		
1.5	.5		5000			15.3	5.12	*4.05	*3.20	*3.25	*2.45
			10,000			15.6	3.18	*4.57	*3.80	*3.62	*2.96
			20,000			15.3	1.11	*5.20	*4.41	*4.04	*3.47
			30,000			15.2	.704	5.65	4.79	*4.31	*3.78
			50,000			14.8	.379	6.36	5.27	*4.69	*4.18
7S	8P	21124.9	2500	1.E + 15	.35E + 18	7.28	4.20				
.5	.5		5000			7.63	3.47				

Table 1 (*continued*)

Transition		*WL* (Å)	*T* (K)	Perturber density (cm^{-3})	*C*	Electrons		Protons		Ionized helium	
						Width (Å)	Shift (Å)	Width (Å)	Shift (Å)	Width (Å)	Shift (Å)
			10,000			7.91	2.58				
			20,000			7.82	1.60	*2.51	*2.09		
			30,000			7.70	1.09	*2.71	*2.28		
			50,000			7.48	.526	*3.02	*2.53	*2.29	*2.00
7S	8P	20948.6	2500	1.E + 15	.17E + 18	9.71	4.48				
1.5	.5		5000			9.99	3.63				
			10,000			9.72	2.66				
			20,000			9.24	1.59				
			30,000			8.91	.865				
			50,000			8.45	.501	*4.54	*3.63		
7S	9P	16344.6	2500	1.E + 15	.12E + 18	*10.4	*5.39				
.5	.5		5000			10.9	4.50				
			10,000			11.0	3.41				
			20,000			10.7	2.11				
			30,000			10.4	1.52				
			50,000			9.96	.681				
7S	9P	16286.3	2500	1.E + 15	.61E + 17	*13.5	*5.32				
1.5	.5		5000			*13.8	*4.48				
			10,000			13.2	3.36				
			20,000			12.5	2.02				
			30,000			11.9	1.34				
			50,000			11.2	.686				
7S	10P	14394.1	2500	1.E + 15	.58E + 17	*16.1	*7.22				
.5	.5		5000			*17.0	*6.12				
			10,000			*17.0	*4.72				
			20,000			16.4	2.92				
			30,000			15.9	2.11				
			50,000			15.1	.947				
7S	10P	14361.9	2500	1.E + 15	.26E + 17	*20.6	*6.33				
1.5	.5		5000			*21.1	*5.55				
			10,000			*20.3	*4.14				
			20,000			19.1	2.57				
			30,000			18.2	1.74				
			50,000			17.0	.929				
5P	8S	3982.7	2500	1.E + 15	.16E + 18	.372E − 1	.261E − 1	.767E − 2	.644E − 2	.612E − 2	.497E − 2
.5	1.5		5000			.428E − 1	.314E − 1	.861E − 2	.757E − 2	.687E − 2	.592E − 2
			10,000			.470E − 1	.326E − 1	.966E − 2	.873E − 2	.771E − 2	.689E − 2
			20,000			.531E − 1	.309E − 1	.108E − 1	.997E − 2	.865E − 2	.790E − 2
			30,000			.573E − 1	.271E − 1	.116E − 1	.107E − 1	.926E − 2	.853E − 2
			50,000			.649E − 1	.231E − 1	.126E − 1	.118E − 1	.101E − 1	.936E − 2
6P	8S	13728.9	2500	1.E + 15	.84E + 18	.484	.243	.731E − 1	.587E − 1	.601E − 1	.456E − 1
.5	.5		5000			.597	.301	.812E − 1	.685E − 1	.664E − 1	.538E − 1

			10,000			.692	.315	.904E − 1	.788E − 1	.734E − 1	.623E − 1
			20,000			.795	.294	.101	.898E − 1	.814E − 1	.712E − 1
			30,000			.867	.265	.108	.967E − 1	.866E − 1	.768E − 1
			50,000			.968	.221	.118	.106	.938E − 1	.843E − 1
5S	6P	2070.5	2500	1.E + 16	.19E + 18	.459E − 1	.312E − 1	*.116E − 1	*.723E − 2	*.970E − 2	*.528E − 2
.5	.5		5000			.493E − 1	.303E − 1	*.128E − 1	*.912E − 2	*.107E − 1	*.693E − 2
			10,000			.521E − 1	.268E − 1	.141E − 1	.110E − 1	*.117E − 1	*.850E − 2
			20,000			.529E − 1	.221E − 1	.157E − 1	.128E − 1	*.128E − 1	*.100E − 1
			30,000			.525E − 1	.190E − 1	.168E − 1	.139E − 1	*.135E − 1	*.110E − 1
			50,000			.518E − 1	.149E − 1	.183E − 1	.154E − 1	.146E − 1	.122E − 1
5S	6P	2061.8	2500	1.E + 16	.10E + 18	.612E − 1	.370E − 1	*.153E − 1	*.949E − 2		
1.5	.5		5000			.649E − 1	.338E − 1	*.171E − 1	*.123E − 1	*.140E − 1	*.927E − 2
			10,000			.661E − 1	.293E − 1	*.191E − 1	*.150E − 1	*.155E − 1	*.116E − 1
			20,000			.638E − 1	.233E − 1	.215E − 1	.177E − 1	*.171E − 1	*.138E − 1
			30,000			.621E − 1	.196E − 1	.232E − 1	.193E − 1	*.182E − 1	*.152E − 1
			50,000			.598E − 1	.148E − 1	.258E − 1	.214E − 1	*.197E − 1	*.169E − 1
5S	7P	1850.4	2500	1.E + 16	.56E + 17	.183	.104				
.5	.5		5000			.192	.966E − 1				
			10,000			.199	.830E − 1				
			20,000			.196	.663E − 1				
			30,000			.192	.536E − 1				
			50,000			.185	.389E − 1	*.738E − 1	*.599E − 1		
5S	7P	1847.7	2500	1.E + 16	.28E + 17	.241	.110				
1.5	.5		5000			.253	.979E − 1				
			10,000			.249	.843E − 1				
			20,000			.236	.646E − 1				
			30,000			.227	.506E − 1				
			50,000			.214	.358E − 1				
5S	8P	1766.1	2500	1.E + 16	.25E + 17	*.481	*.219				
.5	.5		5000			*.511	*.203				
			10,000			*.527	*.174				
			20,000			.516	.140				
			30,000			.503	.107				
			50,000			.483	.743E − 1				
5S	8P	1764.9	2500	1.E + 16	.12E + 17	*.574	*.196				
1.5	.5		5000			*.625	*.184				
			10,000			*.622	*.158				
			20,000			.595	.123				
			30,000			.573	.937E − 1				
			50,000			.540	.644E − 1				
5S	9P	1724.0	2500	1.E + 16	.13E + 17						
.5	.5		5000								
			10,000			*1.10	*.286				
			20,000			*1.09	*.236				
			30,000			*1.06	*.177				
			50,000			1.02	.117				

Table 1 (*continued*)

Transition		*WL* (Å)	*T* (K)	Perturber density (cm^{-3})	*C*	Electrons		Protons		Ionized helium	
						Width (Å)	Shift (Å)	Width (Å)	Shift (Å)	Width (Å)	Shift (Å)
5S	9P	1723.3	2500	1.E + 16	.68E + 16						
1.5	.5		5000								
			10,000			*1.20	*.240				
			20,000			*1.18	*.191				
			30,000			*1.15	*.144				
			50,000			*1.10	*.979E − 1				
5S	10P	1699.7	2500	1.E + 16	.81E + 16						
.5	.5		5000								
			10,000								
			20,000								
			30,000			*1.93	*.249				
			50,000			*1.87	*.163				
5S	10P	1699.2	2500	1.E + 16	.36E + 16						
1.5	.5		5000								
			10,000								
			20,000								
			30,000			*2.04	*.180				
			50,000			*1.97	*.123				
6S	6P	17417.9	2500	1.E + 16	.14E + 20	3.07	1.94	*.787	*.490	*.663	*.359
.5	.5		5000			3.34	1.67	*.867	*.616	*.729	*.469
			10,000			3.73	1.23	.957	.738	*.796	*.573
			20,000			4.02	.900	1.06	.861	*.871	*.676
			30,000			4.12	.690	1.13	.936	.919	.738
			50,000			4.23	.453	1.24	1.03	.986	.818
6S	6P	16821.9	2500	1.E + 16	.69E + 19	3.90	2.22	*.992	*.617		
1.5	.5		5000			4.21	1.75	*1.11	*.799	*.906	*.601
			10,000			4.44	1.32	*1.24	*.973	*1.00	*.750
			20,000			4.49	.877	1.40	1.15	*1.11	*.896
			30,000			4.50	.630	1.50	1.25	*1.18	*.981
			50,000			4.50	.384	1.67	1.38	*1.27	*1.09
6S	7P	8707.1	2500	1.E + 16	.12E + 19	4.03	2.29				
.5	.5		5000			4.23	2.06				
			10,000			4.41	1.69				
			20,000			4.40	1.28				
			30,000			4.35	.957				
			50,000			4.24	.694	*1.63	*1.32		
6S	7P	8646.8	2500	1.E + 16	.61E + 18	5.26	2.39				
1.5	.5		5000			5.52	2.07				
			10,000			5.47	1.70				
			20,000			5.23	1.23				
			30,000			5.06	.897				
			50,000			4.83	.633				

6S	8P	7110.1	2500	1.E + 16	.40E + 18	*7.79	*3.54				
.5	.5		5000			*8.29	*3.25				
			10,000			*8.57	*2.75				
			20,000			8.41	2.14				
			30,000			8.23	1.55				
			50,000			7.92	1.13				
6S	8P	7090.0	2500	1.E + 16	.20E + 18	*9.26	*3.14				
1.5	.5		5000			*10.1	*2.93				
			10,000			*10.1	*2.49				
			20,000			9.65	1.86				
			30,000			9.32	1.37				
			50,000			8.81	.986				
6S	9P	6472.9	2500	1.E + 16	.19E + 18						
.5	.5		5000								
			10,000			*15.5	*3.97				
			20,000			*15.3	*3.02				
			30,000			*15.1	*2.29				
			50,000			*14.5	*1.67				
6S	9P	6463.7	2500	1.E + 16	.96E + 17						
1.5	.5		5000								
			10,000			*16.9	*3.32				
			20,000			*16.7	*2.46				
			30,000			*16.3	*1.88				
			50,000			*15.5	*1.38				
5P	6S	7689.9	2500	1.E + 16	.34E + 20	.113	.796E − 1	.265E − 1	.207E − 1	.220E − 1	.160E − 1
.5	.5		5000			.132	.954E − 1	.292E − 1	.242E − 1	.242E − 1	.190E − 1
			10,000			.148	.115	.324E − 1	.279E − 1	.266E − 1	.220E − 1
			20,000			.159	.120	.360E − 1	.318E − 1	.294E − 1	.252E − 1
			30,000			.170	.121	.383E − 1	.343E − 1	.312E − 1	.272E − 1
			50,000			.181	.106	.415E − 1	.376E − 1	.337E − 1	.298E − 1
5P	6S	8275.8	2500	1.E + 16	.39E + 20	.129	.914E − 1	.308E − 1	.237E − 1	.258E − 1	.184E − 1
.5	1.5		5000			.151	.112	.339E − 1	.278E − 1	.282E − 1	.218E − 1
			10,000			.169	.132	.375E − 1	.320E − 1	.309E − 1	.253E − 1
			20,000			.183	.137	.416E − 1	.365E − 1	.341E − 1	.289E − 1
			30,000			.197	.138	.443E − 1	.393E − 1	.362E − 1	.312E − 1
			50,000			.211	.119	.479E − 1	.431E − 1	.390E − 1	.343E − 1
5P	7S	4477.3	2500	1.E + 16	.43E + 19	.163	.113	.348E − 1	.258E − 1	*.278E − 1	*.192E − 1
.5	.5		5000			.190	.137	.391E − 1	.319E − 1	*.313E − 1	*.245E − 1
			10,000			.209	.162	.439E − 1	.379E − 1	.351E − 1	.295E − 1
			20,000			.226	.152	.492E − 1	.440E − 1	.393E − 1	.346E − 1
			30,000			.239	.147	.526E − 1	.477E − 1	.421E − 1	.377E − 1
			50,000			.262	.125	.573E − 1	.526E − 1	.458E − 1	.417E − 1
5P	7S	4669.8	2500	1.E + 16	.47E + 19	.177	.121	.379E − 1	.281E − 1	*.303E − 1	*.209E − 1
.5	1.5		5000			.206	.148	.425E − 1	.347E − 1	*.340E − 1	*.266E − 1
			10,000			.230	.172	.477E − 1	.412E − 1	.381E − 1	.321E − 1
			20,000			.246	.164	.535E − 1	.478E − 1	.428E − 1	.376E − 1

Table 1 (*continued*)

Transition		*WL* (Å)	*T* (K)	Perturber density (cm^{-3})	*C*	Electrons		Protons		Ionized helium	
						Width (Å)	Shift (Å)	Width (Å)	Shift (Å)	Width (Å)	Shift (Å)
			30,000			.260	.159	.572E − 1	.518E − 1	.457E − 1	.409E − 1
			50,000			.285	.134	.623E − 1	.571E − 1	.498E − 1	.453E − 1
5P	8S	3841.8	2500	1.E + 16	.15E + 19	.346	.226	*.709E − 1	*.434E − 1		
.5	.5		5000			.398	.274	*.800E − 1	*.587E − 1		
			10,000			.438	.298	*.899E − 1	*.730E − 1	*.717E − 1	*.558E − 1
			20,000			.497	.287	*.101	*.870E − 1	*.805E − 1	*.677E − 1
			30,000			.533	.252	*.108	*.952E − 1	*.862E − 1	*.746E − 1
			50,000			.603	.215	.118	.106	*.938E − 1	*.834E − 1
5P	8S	3982.7	2500	1.E + 16	.16E + 19	.372	.243	*.762E − 1	*.466E − 1		
.5	1.5		5000			.428	.302	*.860E − 1	*.631E − 1		
			10,000			.470	.319	*.966E − 1	*.784E − 1	*.771E − 1	*.600E − 1
			20,000			.531	.308	*.108	*.934E − 1	*.865E − 1	*.727E − 1
			30,000			.573	.270	*.116	*.102	*.926E − 1	*.802E − 1
			50,000			.649	.231	.126	.114	*.101	*.896E − 1
6P	7S	27858.3	2500	1.E + 16	.35E + 20	8.95	−.462	*1.41	*−.745	*1.28	*−.562
.5	.5		5000			11.8	.868	1.50	−.905	*1.35	*−.699
			10,000			14.0	2.09	1.61	−1.06	*1.43	*−.833
			20,000			16.0	2.84	1.75	−1.23	1.51	−.970
			30,000			17.0	2.68	1.86	−1.33	1.56	−1.05
			50,000			18.3	2.39	2.02	−1.46	1.64	−1.16
6P	7S	29531.5	2500	1.E + 16	.21E + 20	14.2	−1.73	*2.44	*−1.52	*2.04	*−1.11
.5	1.5		5000			17.1	.652E − 1	*2.71	*−1.92	*2.25	*−1.46
			10,000			19.0	1.96	3.01	−2.31	*2.47	*−1.79
			20,000			20.5	3.08	3.38	−2.70	*2.71	*−2.12
			30,000			21.3	3.00	3.65	−2.93	*2.86	*−2.31
			50,000			22.4	2.92	4.08	−3.24	3.08	−2.56
6P	8S	13728.9	2500	1.E + 16	.84E + 19	4.84	2.29	*.724	*.448		
.5	.5		5000			5.97	2.92	*.810	*.587	*.660	*.440
			10,000			6.92	3.11	*.904	*.719	*.733	*.553
			20,000			7.95	2.93	*1.01	*.849	*.814	*.663
			30,000			8.67	2.64	1.08	.927	*.866	*.728
			50,000			9.68	2.21	1.18	1.03	*.937	*.811
6P	8S	14123.3	2500	1.E + 16	.49E + 19	5.83	2.02	.601	*.375	*.499	*.272
.5	1.5		5000			7.11	2.68	.667	*.478	*.552	*.362
			10,000			8.06	3.14	.742	*.577	*.607	*.447
			20,000			9.01	3.02	.830	.676	*.668	*.530
			30,000			9.68	2.77	.890	.736	*.707	*.579
			50,000			10.7	2.34	.977	.815	.760	.643
5S	5P	3383.9	2500	1.E + 17	.15E + 21	.375E − 1	.174E − 1	.222E − 1	.444E − 2	.217E − 1	.343E − 2
.5	.5		5000			.422E − 1	.205E − 1	.227E − 1	.522E − 2	.224E − 1	.408E − 2
			10,000			.443E − 1	.223E − 1	.229E − 1	.602E − 2	.226E − 1	.475E − 2
			20,000			.500E − 1	.217E − 1	.231E − 1	.687E − 2	.228E − 1	.544E − 2

			30,000			.567E − 1	.182E − 1	.232E − 1	.740E − 2	.229E − 1	.587E − 2
			50,000			.691E − 1	.142E − 1	.234E − 1	.812E − 2	.230E − 1	.645E − 2
5S	5P	3281.6	2500	1.E + 17	.13E + 21	.384E − 1	.194E − 1	.225E − 1	.506E − 2	*.218E − 1	*.390E − 2
1.5	.5		5000			.437E − 1	.239E − 1	.230E − 1	.598E − 2	.226E − 1	.467E − 2
			10,000			.465E − 1	.272E − 1	.233E − 1	.692E − 2	.229E − 1	.545E − 2
			20,000			.523E − 1	.274E − 1	.235E − 1	.791E − 2	.231E − 1	.627E − 2
			30,000			.589E − 1	.240E − 1	.237E − 1	.853E − 2	.232E − 1	.677E − 2
			50,000			.707E − 1	.191E − 1	.239E − 1	.936E − 2	.234E − 1	.743E − 2
5S	6P	2070.5	2500	1.E + 17	.19E + 19	.455	.256				
.5	.5		5000			.490	.263				
			10,000			.518	.238				
			20,000			.527	.204				
			30,000			.524	.179	*.167	*.124		
			50,000			.517	.144	*.183	*.142		
5S	6P	2061.8	2500	1.E + 17	.10E + 19	.583	.274				
1.5	.5		5000			.628	.266				
			10,000			.645	.242				
			20,000			.627	.205				
			30,000			.612	.176				
			50,000			.591	.140				
5S	7P	1850.4	2500	1.E + 17	.56E + 18	*1.46	*.549				
.5	.5		5000			*1.67	*.615				
			10,000			*1.81	*.576				
			20,000			*1.83	*.493				
			30,000			1.82	.425				
			50,000			1.77	.338				
5S	7P	1847.7	2500	1.E + 17	.28E + 18	*1.48	*.453				
1.5	.5		5000			*1.88	*.517				
			10,000			*2.04	*.508				
			20,000			*2.04	*.422				
			30,000			2.01	.360				
			50,000			1.94	.287				
5S	8P	1766.1	2500	1.E + 17	.25E + 18						
.5	.5		5000								
			10,000								
			20,000			*4.20	*.791				
			30,000			*4.25	*.686				
			50,000			*4.22	*.544				
5P	6S	7689.9	2500	1.E + 17	.34E + 21	1.13	.744	*.261	*.155	*.213	*.108
.5	.5		5000			1.32	.916	.291	.205	*.240	*.153
			10,000			1.47	1.13	.324	.253	*.265	*.194
			20,000			1.59	1.19	.360	.300	.294	.234
			30,000			1.70	1.21	.383	.327	.312	.257
			50,000			1.81	1.06	.415	.363	.337	.287

Table 1 (*continued*)

Transition		*WL* (Å)	*T* (K)	Perturber density (cm^{-3})	*C*	Electrons		Protons		Ionized helium	
						Width (Å)	Shift (Å)	Width (Å)	Shift (Å)	Width (Å)	Shift (Å)
5P	6S	8275.8	2500	1.E + 17	.39E + 21	1.29	.854	*.303	*.178	*.249	*.124
.5	1.5		5000			1.51	1.08	.338	.236	*.279	*.176
			10,000			1.69	1.30	.375	.290	*.309	*.223
			20,000			1.83	1.36	.416	.344	.341	.268
			30,000			1.97	1.38	.442	.376	.361	.295
			50,000			2.11	1.19	.479	.417	.390	.329
5P	7S	4477.3	2500	1.E + 17	.43E + 20	1.63	.981				
.5	.5		5000			1.90	1.26				
			10,000			2.09	1.54	*.438	*.303		
			20,000			2.26	1.47	*.492	*.386		
			30,000			2.39	1.45	*.526	*.433		
			50,000			2.62	1.25	*.573	*.492	*.458	*.382
5P	7S	4669.8	2500	1.E + 17	.47E + 20	1.77	1.05				
.5	1.5		5000			2.06	1.37				
			10,000			2.30	1.63	*.476	*.329		
			20,000			2.46	1.60	*.535	*.420		
			30,000			2.60	1.56	*.572	*.471		
			50,000			2.85	1.33	*.623	*.534	*.498	*.416
5P	8S	3841.8	2500	1.E + 17	.15E + 20	*3.45	*1.73				
.5	.5		5000			*3.98	*2.36				
			10,000			4.38	2.71				
			20,000			4.97	2.71				
			30,000			5.33	2.44				
			50,000			6.03	2.10				
5P	8S	3982.7	2500	1.E + 17	.16E + 20	*3.71	*1.86				
.5	1.5		5000			*4.28	*2.62				
			10,000			4.70	2.91				
			20,000			5.31	2.90				
			30,000			5.73	2.62				
			50,000			6.49	2.25				
5S	5P	3383.9	2500	1.E + 18	.15E + 22	.374	.163	*.177	*.325E − 1	*.136	*.224E − 1
.5	.5		5000			.422	.197	*.210	*.437E − 1	*.191	*.324E − 1
			10,000			.443	.217	*.223	*.542E − 1	*.215	*.415E − 1
			20,000			.500	.213	.229	.645E − 1	*.224	*.502E − 1
			30,000			.567	.179	.231	.705E − 1	*.227	*.553E − 1
			50,000			.691	.140	.233	.784E − 1	*.229	*.618E − 1
5S	5P	3281.6	2500	1.E + 18	.13E + 22	.383	.198	*.175	*.353E − 1		
1.5	.5		5000			.437	.229	*.212	*.490E − 1		
			10,000			.465	.264	*.226	*.615E − 1	*.217	*.469E − 1
			20,000			.523	.269	.233	.737E − 1	*.227	*.572E − 1
			30,000			.589	.236	.236	.809E − 1	*.230	*.633E − 1
			50,000			.707	.189	.239	.901E − 1	*.233	*.709E − 1

5S	6P	2070.5	2500	1.E + 18	.19E + 20	*3.12	*.966		
.5	.5		5000			*3.98	*1.48		
			10,000			*4.54	*1.57		
			20,000			*4.81	*1.46		
			30,000			4.86	1.37		
			50,000			4.87	1.10		
5S	6P	2061.8	2500	1.E + 18	.10E + 20	*3.06	*.888		
1.5	.5		5000			*4.21	*1.25		
			10,000			*5.00	*1.43		
			20,000			*5.24	*1.31		
			30,000			*5.27	*1.23		
			50,000			5.25	.979		
5P	6S	7689.9	2500	1.E + 18	.34E + 22	11.2	5.78		
.5	.5		5000			13.2	7.99		
			10,000			14.7	10.4		
			20,000			15.9	11.3	*3.58	*2.41
			30,000			17.0	11.8	*3.82	*2.80
			50,000			18.1	10.5	*4.14	*3.26
5P	6S	8275.8	2500	1.E + 18	.39E + 22	12.9	6.65		
.5	1.5		5000			15.1	9.42		
			10,000			16.9	12.0		
			20,000			18.3	12.9	*4.14	*2.77
			30,000			19.7	13.5	*4.41	*3.21
			50,000			21.1	11.9	*4.78	*3.75
5P	7S	4477.3	2500	1.E + 18	.43E + 21	*15.6	*4.82		
.5	.5		5000			*18.8	*9.02		
			10,000			*20.9	*12.9		
			20,000			*22.6	*13.3		
			30,000			23.9	13.2		
			50,000			26.1	11.8		
5P	7S	4669.8	2500	1.E + 18	.47E + 21	*16.9	*5.07		
.5	1.5		5000			*20.4	*9.81		
			10,000			*22.9	*13.6		
			20,000			*24.6	*14.4		
			30,000			25.9	14.2		
			50,000			28.5	12.6		
5S	5P	3383.9	2500	1.E + 19	.15E + 23	*3.61	*1.24		
.5	.5		5000			*4.18	*1.70		
			10,000			4.42	1.98		
			20,000			5.00	2.00		
			30,000			5.66	1.68		
			50,000			6.90	1.32	*2.28	*.699
5S	5P	3281.6	2500	1.E + 19	.13E + 23	*3.69	*1.38		
1.5	.5		5000			*4.32	*1.94		

Table 1 (*continued*)

Transition	*WL* (Å)	*T* (K)	Perturber density (cm^{-3})	*C*	Electrons		Protons		Ionized helium	
					Width (Å)	Shift (Å)	Width (Å)	Shift (Å)	Width (Å)	Shift (Å)
		10,000			4.63	2.40				
		20,000			5.23	2.52				
		30,000			5.89	2.21				
		50,000			7.07	1.79	*2.33	*.793		

1991ApJ...382..353P

THE ASTROPHYSICAL JOURNAL, 382:353–357, 1991 November 20
© 1991. The American Astronomical Society. All rights reserved. Printed in U.S.A.

REGULARITIES OF STARK PARAMETERS ALONG THE PERIODIC TABLE

J. PURIĆ,[1] M. ĆUK,[1] M. S. DIMITRIJEVIĆ,[2] AND A. LESAGE[3]
Received 1991 February 20; accepted 1991 May 31

ABSTRACT

Stark width and shift dependence on the upper-level ionization potential of the corresponding transitions have been investigated on the basis of the semiclassical and semiempirical data. The simple formulas obtained from that dependence can be used to predict the Stark broadening and shift parameters of resonance $n_0 s - n_0 p$ and $n_0 s - (n_0 + 1)p$ (n_0 for ground level) and off-resonance [$(n_0 + 1)s - (n_0 + 1)p$ lines of neutral atoms and ions (up to several stages of the ionization).

The predicted data are compared with the known experimental and theoretical values. The agreement is found to be within the quoted experimental and theoretical uncertainties. All data are given at the electron density $N = 10^{17}$ cm^{-3} and different electron temperatures T (for neutral atoms and singly charged ions T = 10,000, 20,000, 40,000, and 80,000 K; for doubly and multiply charged ions T = 20,000, 40,000, 80,000, and 160,000 K).

Subject headings: atomic processes — laboratory spectra — line profiles

1. INTRODUCTION

Some recent reviews (Lanz & Artru 1987; Smith 1989) show that the experimental determination of Stark widths, as well as the existing theoretical data, cannot satisfy the need for all observed stellar lines, although it is an active field of research. Therefore, it is of interest to exploit any possible theoretical approach which might provide simple relations, for example, from the systematic trends found in the Stark broadening data (see e.g., Purić, Lakićević, & Glavonjić 1980). Several simple empirical formulas have been used in stellar studies, which take into account the variation of the Stark width with the electronic density, and its dependence on the excitation energy of the transition. For example, Cowley (1971) applied the semiempirical approach of Griem (1968), giving the width proportional to n^{*4}, n^* being the effective quantum number of the upper level. A simple formula giving the Stark broadening parameter dependence on n^* (leading term proportional to n^{*4}) and the angular momentum quantum number ℓ, is given by Dimitrijević & Konjević (1987). In the extensive work of Kurucz (1979), a simple empirical formula giving a width proportional to n^{*5} has been used. A different approach, based on the systematic trends found in Stark broadening parameters, has been developed in a series of articles (Purić et al. 1980; Purić 1981; Lakićević & Purić 1983; Purić, Ćuk, & Lakićević 1985a, b), in the case of neutral atoms and singly charged ion resonances and off-resonances ($ns - np$ transitions: $\Delta n = 0$ or 1 for resonances and $n = n_0 + 1$ for off-resonances; n_0 is the main quantum number of the ground energy level of a corresponding emitter). Similar regularities were found for the isoelectronic sequences (Purić et al. 1988a, b); for the isonuclear sequences (the same type of transition within several stages of ionization of a particular emitter; Purić et al. 1987b, 1988a, b, c); and for the same type of transition within homologous groups of atoms or ions (Purić et al 1987a, 1988b). In the present work we apply this approach to doubly and triply charged ion resonant and off-resonant spectral lines.

The proposed method is based on the fact, demonstrated first by Purić et al. (1980), that the Stark widths and shifts (in Å (see Dimitrijević & Konjević 1984) or angular frequency units) exhibit a systematic dependence on the ionization potential, upper or lower energy level of the corresponding transition when measured from the ionization limit and not from the ground level (in order to avoid misunderstanding we will call the positive value of such quantity (χ) the "upper" or "lower level ionization potential," respectively). For the case of $np^{k-1}(n+1)s - np^k$ resonance transitions of singly ionized emitters, Dimitrijević (1985) derived theoretically expressions similar to those derived empirically by Purić et al. (1980). Moreover, a systematic dependence has been found also on the net core charge (z) of the emitter as seen by the electron undergoing transition. Since the simple relations based on such trends may be useful in astrophysics, when Stark broadening data for many lines are needed, we have tried here to obtain and analyze such relations. Therefore, the Stark parameter dependences on χ and z are deduced here from the large-scale semi-classical (Griem 1974) or semiempirical (Griem 1968) and modified semiempirical (Dimitrijević & Konjević 1980; Dimitrijević 1988) calculations. The relations we obtained were checked using the existing experimental and theoretical data (Griem 1974; Konjević & Roberts 1976; Konjević & Wiese 1976; Konjević, Dimitrijević & Wiese, 1984a, b; Dimitrijević 1988; Konjević & Wiese 1990).

Although the majority of existing data are for the lighter atoms and ions, we will try here to discuss the extension of the regularities to heavier elements, since this is of particular interest for astrophysical purposes.

2. THEORY

The relations for line width (W) and shift (d) are, as shown in previous articles (Purić et al. 1980; Lakićević 1983, 1985; Purić et al. 1985a, b; Ćuk 1989),

$$W = N_e f(T) a_1 z^{c_1} \chi^{-b_1} , \quad (1)$$

$$d = N_e f(T) a_2 z^{c_2} \chi^{-b_2} , \quad (2)$$

[1] Faculty of Physics, University of Belgrade, P.O. Box 550, 11001 Belgrade, Yugoslavia.
[2] Astronomical Observatory, Volgina 7, 11050 Belgrade, Yugoslavia.
[3] Département d'Astrophysique Stelaire et Galactique, Observatoire de Paris, 92195 Meudon Cedex, France.

© American Astronomical Society • Provided by the NASA Astrophysics Data System

1991ApJ...382..353P

where a_1 and a_2 are coefficients independent of the temperature, ionization potential, and the electron density for a particular transition.

For lower temperatures of astrophysical interest, $f(T)$ tends to be $f(T) = T^{-1/2}$ in the case of ionized emitters (see, e.g., Griem 1974). Here z is the net core charge of the emitter, as seen by the electron undergoing the transition. Equations (1) and (2) can be used (1) in the case of the lines originating from the same type of transition (e.g., resonances or off-resonances) within one stage of ionization (2) within particular isoelectronic sequences, and (3) within a given isonuclear sequence.

In the case of a particular transition within a given homologous group of atoms or ions, it is more convenient to use the slightly different relations in the function of the nuclear charge number of the emitter Z ($Z = z + 1$) (Purić et al. 1987b; Purić et al. 1988a):

$$W = N_e f(T) a_1 Z^{-1} \chi^{-b_1} , \quad (3)$$

$$d = N_e f(T) a_2 Z^{-1} \chi^{-b_2} . \quad (4)$$

For the same plasma conditions and for the exactly analogous transitions within the different atomic spectra, the corresponding a and b constants are similar. Consequently, we can determine empirically, from experiments or more sophisticated calculations, averaged empirical values for $A = aN_e f(T)$ and b.

For the ionized emitters, in the case of a low-temperature limit, we can scale the obtained empirical values to other temperatures by using $T^{-1/2}$ dependence (for validity conditions see, e.g., Griem 1974). In the case of higher temperatures the dependence on temperature is weaker. In some cases, when only an estimate is needed and temperature does not vary too much, we can use an averaged empirical value for a temperature range taking into account that the accuracy is lower.

In the semiclassical (Griem 1974) or the modified semiempirical (Dimitrijević & Konjević 1980) formulas, ionization potentials are included through the expression for effective quantum number, Stark broadening functions (see Griem 1974), and the wavelength; therefore one can always find an appropriate, more or less approximate expression for W and d satisfying mathematical conditions for a series expansion

$$f(x) = \sum k_n x^n \quad (5)$$

in terms of the ionization potential, where $f(x)$ stands for w or d and x for the ionization potential. Moreover, we can always try to fit w or d with an $f(x) = \alpha x^\beta$ expression. In astrophysics w is sometimes successfully represented as $w = \alpha T^\beta$ in order to make easier the use of data for the whole temperature range within a model of the stellar atmosphere. Here we propose that the expressions (eqs. [1]–[4]), all of the same type,

$$w, d = A\chi^{-b} , \quad (6)$$

are suitable for the calculations of new data by an interpolation if we determine the necessary coefficients from the known Stark parameter values within the particular stage of ionization.

One can try to obtain the corresponding coefficients A, b (see eq. [6]) or k_n, n (see eq. [5]) analytically (Purić 1981; Dimitrijević 1985) and investigate if the series expansion is convergent or how good the $f(x) = \alpha x^\beta$ fit is. For instance, Dimitrijević (1985) obtained analytical expressions for the corresponding coefficients of the series expansion over the ionization potential, for w- and d-values for a special case, starting from Griem's (1968) semiempirical formula. Such a procedure may provide usable analytical expressions only with additional approximations and for special cases. The other way, used here, is to try to obtain the proposed simple relations from the large set of results of more sophisticated calculations, in order to prove that Stark broadening parameters may be fitted with the proposed relations and to obtain the corresponding α- and β-coefficients on the basis of existing semiclassical and modified semiempirical calculations. Also, one attempt has been undertaken to find a generalized relation which appropriately fits the existing theoretical and experimental data within several ionization stages.

3. RESULTS AND DISCUSSION

Equations (1) and (2) have been verified using the existing theoretical and experimental results and the procedure described by Purić et al. (1985a), that is, plotting the W versus χ-data on a log-log graph, for a specific temperature and $N_e = 10^{17}$ cm^{-3}, and a linear regression is used in order to get the $A = aNf(T)$, b- and c-coefficients of equations (1) and (2). The data we have used are the Stark parameter values calculated by Griem (1974) in the case of the neutral atoms for the resonance transitions, as in the case of the singly ionized atoms for resonance and off-resonance [$(n_0 + 1)s - (n_0 + 1)p$ transitions, where n_0 is the principal quantum number of the ground state of the emitter]. In the case of doubly and triply charged ions, the data obtained by Dimitrijević (1988), who used the modified semiempirical formula of Dimitrijević & Konjević (1980), have been used. All Stark broadening parameters are full widths at half-maximum (FWHM) in angular frequency units normalized to the electron density 10^{17} cm^{-3}.

Our analysis of the semiclassical (Griem 1974) or modified semiempirical (Dimitrijević & Konjević 1980) results, shows

TABLE 1

	W		d	
T[10^4 K]	$A \times 10^{-19}$	b	$A \times 10^{-19}$	b
Neutral Atom Resonances: $\Delta n = 0$				
1.....	1.100	3.67	0.440	3.76
2.....	0.714	3.00	0.356	3.64
Neutral Atom Resonances: $\Delta n = 1$				
1.....	0.292	1.95	1.93	2.03
2.....	0.358	2.00	1.94	1.97
Singly Charged Ion Resonances: $\Delta n = 0$ and 1				
1.....	1.64	1.67	1.36	1.93
2.....	1.70	1.78	1.46	2.06
Singly Charged Ion Off-resonances: $(n_0 + 1)s - (n_0 + 1)p$				
1.....	1.36	1.58	0.716	1.75
2.....	1.56	1.73	0.884	2.01
4.....	2.60	2.06	...	...
Doubly Charged Ion Off-resonances: $(n_0 + 1)s - (n_0 + 1)p$				
4.....	6.35	2.06	...	...
Triply Charged Ion Off-resonances: $(n_0 + 1)s - (n_0 + 1)p$				
4.....	11.96	2.06	...	...

NOTES.—Coefficients A and b (eq. [6]) for several types of transition at different temperatures and $N = 10^{17}$ cm^{-3}.

© American Astronomical Society • Provided by the NASA Astrophysics Data System

1991ApJ...382..353P

that for $T = 10{,}000$ K and $N = 10^{17}$ cm^{-3}, $b = 3.67 \pm 17\%$ and $A = 1.1 \times 10^{13}$ (if χ is expressed in eV and w in angular frequency units) for the neutral atom resonances. In the case of neutrals, equations (1) and (6) are identical. However, we can use equation (6) for the ion lines also. The corresponding A- and b-coefficients for other considered cases (neutrals, singly, doubly, and triply charged ion lines) are given in Table 1. By using the coefficients from Table 1 and equation (6) we can obtain new data for other lines belonging to the same type of transition only knowing the corresponding χ-value and plasma conditions (N, T).

The analysis of the simultaneous Stark broadening parameter dependence on the z- and χ-factors for off-resonance transitions of ions from Li to Ar in the three successive stages of ionization (II, III, and IV) has been made, and the equation (1) with empirically determined coefficients becomes

$$w(\text{rad s}^{-1}) = 0.01133[T\ (\text{K})]^{-1/2} N_e(\text{cm}^{-3}) z^{2.2} [\chi\ (\text{eV})]^{-2.06} \quad (7)$$

as demonstrated in Figure 1, where theoretical data from Griem (1974) and Dimitrijević (1988) have been used. The theoretical data fit the linear regression formula given by equation (7) with a correlation factor of 0.98. Since all available data fit this relation so closely, we hope that such an equation will be useful for the prediction of Stark width parameters for spectral lines belonging to the same type of transitions, especially for astrophysical purposes.

Figure 2 presents a comparison of the results obtained by using equation (5) with the experimental data published in the

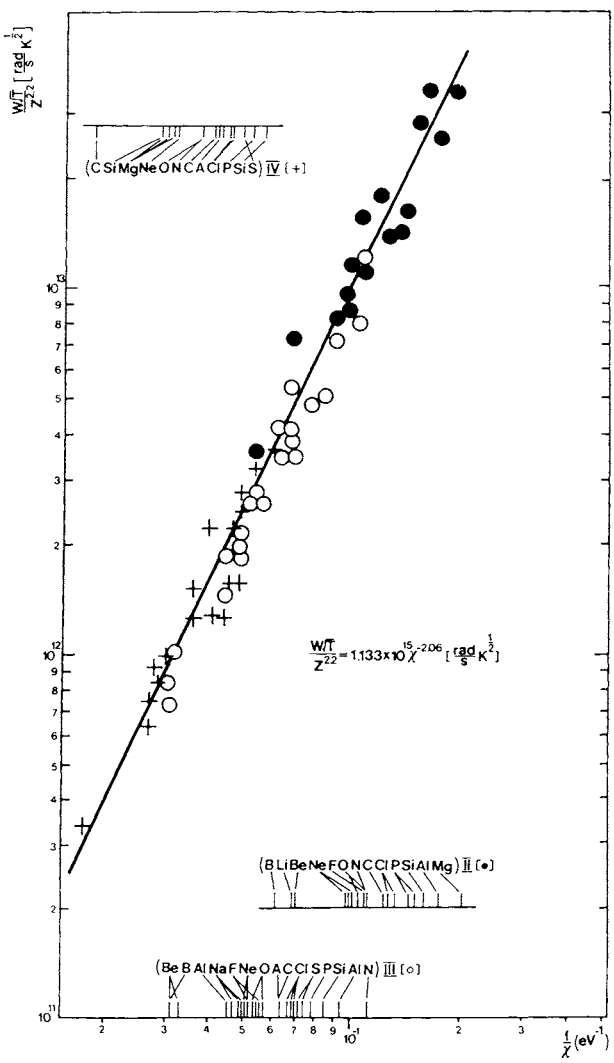

FIG. 1.—Theoretical reduced Stark width ($wT^{1/2}z^{-2.2}$) vs. inverse value of the upper level ionization potential (χ) for singly (*filled circles*) (Griem 1974), doubly (*open circles*), and triply (*crosses*) (Dimitrijević 1988) charged ion off-resonances; solid line is the best fit of the theoretical data (eq. [7]). All data are normalized at an electron density $N = 10^{17}$ cm^{-3}.

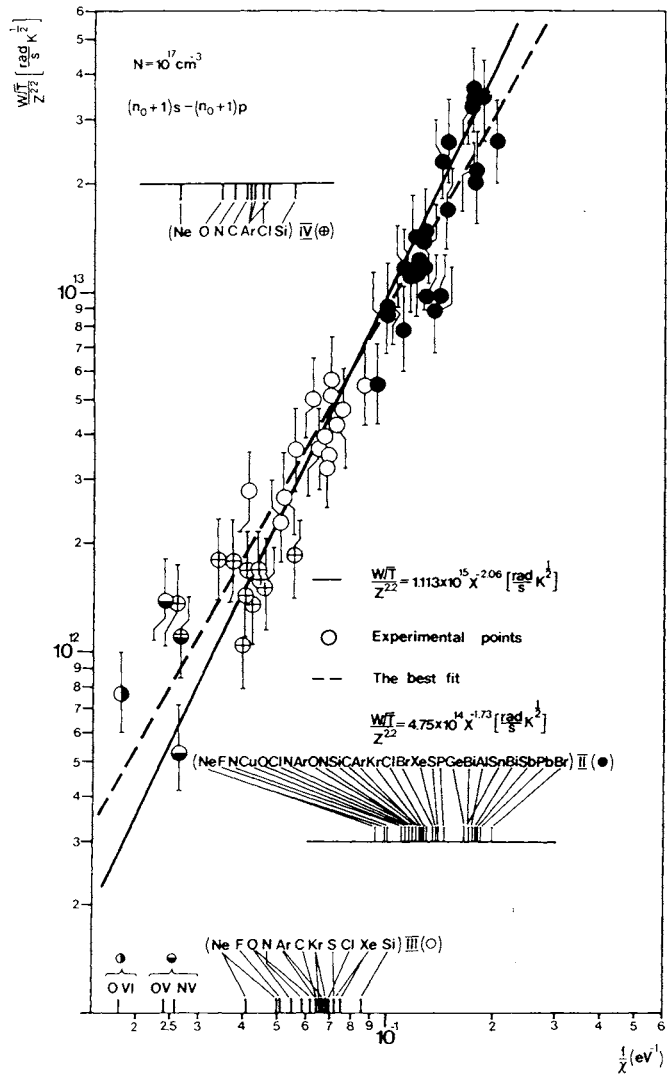

FIG. 2.—Experimental reduced Stark width ($wT^{1/2}z^{-2.2}$) vs. inverse value of the upper level ionization potential (χ) for singly, (*filled circles*), doubly (*open circles*), triply (*circles with cross*), quadruply, (*half-filled circles*), and quintuply (*vertically split circles*) charged ion off-resonances obtained by different authors. Al II, Bi II, Pb II, Sb II (Purić et al. 1985a); Ar II (Abbas, Basha, & Abdel-Aal 1988; Nick & Helbig 1986); Br II (Djeniže et al. 1988a; Jones & Miller 1974); C II (Djeniže, et al. 1988b); Cl II (Purić et al. 1988e); Cu II (Fleurier 1987); F II (Platiša et al. 1977a, b); Kr II (Richou et al. 1983; Brandt, Helbig, & Nick 1981); Ne II (Pittman & Konjević 1986; Purić et al. 1987a); N II (Purcell & Barnard 1984; Purić et al. 1987b); O II (Purić et al. 1988c); P II (Miller, Abadie, & Lesage 1985; Purić et al. 1985a); Si II (Lesage et al. 1983); S II (Miller et al. 1985; Djeniže et al. 1990a, b); Sn II (Djeniže et al. 1990a, b); Xe II (Miller, Roig, & Bengston 1979); Ar III, Ne III, Kr III, and Xe III (Konjević & Pittman 1987); Ar IV and Ne IV (Purić et al. 1988c); C III and C IV (Bogen 1972); C IV (Djeniže et al. 1988b); Cl III, Cl IV, and F III (Purić et al. 1988e); N III, N IV, and N V (Purić et al. 1987b; Böttcher et al. 1988); O III, O IV, and O V (Purić et al. 1988d); Si III (Kusch & Schröder 1982); S III (Platiša et al. 1979; Djeniže et al. 1990); *dashed line*—best fit of the experimental data (eq. [8]); *solid line*—the best fit of the theoretical data presented in Fig. 1 (eq. [7]). All data are normalized at an electron density $N = 10^{17}$ cm^{-3}.

© American Astronomical Society • Provided by the NASA Astrophysics Data System

1991ApJ...382..353P

critical reviews of Konjević & Roberts (1976), Konjević & Wiese (1976), Konjević et al. (1984a, b) and Konjević & Wiese (1990). Line widths from 18 elements including heavy ones such as Br, Kr, Sn, Sb, Xe, Pb, Bi, and five stages of ionization (II–VI) are plotted on the same log-log graph as in Figure 1. The linear regression line calculated with a 0.97% correlation factor

$$w(\text{rad s}^{-1}) = 0.00475[T(\text{K})]^{1/2} z^{2.2} N_e(\text{cm}^{-3})[\chi(\text{ev})]^{-1.73} \quad (8)$$

differs slightly from the line representing equation (7).

The agreement is within a $\pm 40\%$ error bar for the majority of cases. However, one can see that for large χ (small $1/\chi$) the dispersion of results is within a factor of 3. This is for the case of higher order ionization stages (e.g., fourth and fifth). In such a case we have only a few experimental results, corresponding to the much higher temperatures scaled with $T^{-1/2}$, for lower temperatures, which is an additional source of uncertainty. Moreover, the theory becomes more uncertain for higher ionization stages since at low temperatures small range effects may be of importance.

In the case of the doubly charged ion spectral lines the agreement of the calculated values with existing experimental values is better than $\pm 30\%$ except for N III 2677.90 Å and O III 2454.99 Å lines, where the ratios of measured to calculated values is 1.79 and 1.37, respectively. In the case of the triply charged ion spectral lines, the agreement is better than $\pm 25\%$, except for Ne IV 2357.96 and 2352.52 Å, N IV 3478.71 Å, and O IV 3063.43 Å, where the ratios are 1.67, 2.21, 1.39, and 1.67, respectively. Unfortunately there is a lack of experimental results in the case of quadruply and quintuply charged ion off-resonances. One can see in Figure 3 that the ratios of experimental results, when they exist (O V, 5114 Å; O VI 3811 Å; and N V 4603 and 6619 Å), to our predictions obtained by equation (7) are 2.68, 2.70, 1.77, and 0.86, respectively. Therefore, equation (7) might be used for the predictions of missing Stark broadening data in the case of singly, doubly, and triply charged ions. For astrophysical purposes, where sometimes the missing widths are estimated as 10 times the classical width (see, e.g., Lanz, Dimitrijević, & Artru 1988) equation (7) might be used for rough predictions even for higher ionization stages, for the lines of the $(n_0 + 1)s - (n_0 + 1)p$ type.

A comparison between the values calculated using equation (7) and experimental values is shown in Figure 3 where the ratio of experimental to theoretical values is plotted as a function of $1/\chi$.

Present results and comparisons show that the described method may be useful in astrophysics for the estimation of unknown Stark width values in the case of lines where the same type of transitions is involved.

4. CONCLUSION

It has been found that the relations given by equations (1) and (2) are very convenient for the prediction of new Stark broadening data, avoiding much more complicated procedures, or in the cases when accurate atomic data are missing. Moreover, the described method gives good possibilities for the quick estimation of the reliability of the experimental or theoretical Stark parameters (Purić 1981). In the case of large discrepancies one should reconsider both the possible influence of the close perturbing levels used in the theoretical calculations (see, e.g., Freudenstein & Cooper 1978; Dimitrijević 1982) and the accuracy of the experimental data included in the graphs. None of the points on our graphs were chosen to avoid closely interacting levels. In complex atoms the distance from the ionization limit depends on whether the parent term is from an excited level of the next ionization stage. In that case the parent's excitation has to be added to the ionization energy.

Finally, we conclude that the described approach might be used for the predictions of missing Stark broadening data in the case of singly, doubly, and triply charged ions. For doubly and triply charged ions, the described approach can be used with caution in order to predict missing Stark broadening

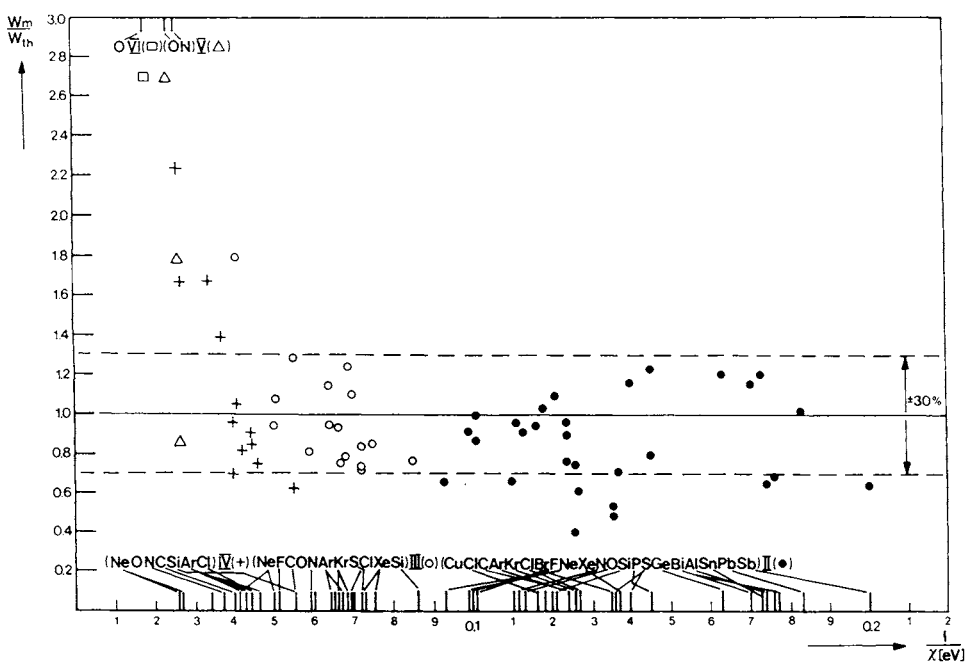

FIG. 3.—Ratio W_m/W_{th} (of the experimental data presented in Fig. 2 to the theoretical predictions calculated using eq. [7]) vs. inverse value of the upper level ionization potential χ.

© American Astronomical Society • Provided by the NASA Astrophysics Data System

1991ApJ...382..353P

data. For higher ionization stages, or heavier elements, the present method can provide a better estimate than the crude approximation frequently used in astrophysics, when missing widths are supposed to be 10 times the classical width (see, e.g., Lanz et al. 1988). For opacity calculations and investigation of stellar atmospheres, when a large number of line-broadening parameters is required, present investigations are useful in enlarging the number of existing data. This field of research remains largely open to the other demonstrations of regularities and similarities, even for heavier atoms and higher ionization stages, as long as one can compare the same kind of spectroscopic transition.

REFERENCES

Abbas, A., Basha, T. S., & Abdel-Aal, Z. A. 1988, Japanese J. Appl. Phys., 27, 804
Bogen, P. 1972, Zs. Naturforschung, 27a, 210
Böttcher, F., Breger, P., Hey, J. D., & Kunze, H.-J. 1988, Phys. Rev. A, 38, 2690
Böttcher, F., Musielok, J., & Kunze, H.-J. 1987, Phys. Rev. A, 36, 2265
Brandt, T., Helbig, V., & Nick, K. P. 1981, in Spectral Line Shapes, ed. B. Wende (Berlin: de Gruyter), 265
Cowley, C. R. 1971, Observatory, 91, 139
Ćuk, M. 1989, Ph.D. thesis, Beograd, Physical Faculty
Dimitrijević, M. S. 1982, A&A, 112, 251
———. 1985, A&A, 145, 439
———. 1988, A&AS, 76, 53
Dimitrijević, M. S., & Konjević, N. 1980, J. Quant. Spectrosc. Rad. Transf., 24, 451
———. 1984, Zs. Naturforschung, 39a, 553
———. 1987, A&A, 172, 345
Djeniže, S., Labat, O., Srećković, A., & Purić, J. 1988a, in Spectral Line Shapes, ed. J. Szudy (Warsaw: Ossolineum), A16
Djeniže, S., Srećković, A., & Labat, J. 1990a, Zs. Phys. D, 19, 85
Djeniže, S., Srećković, A., Milosavljević, M., Labat, J., Platiša, M., & Purić, J. 1988b, Zs. Phys. D, 9, 129
Djeniže, S., Srećković, A., Platiša, M., Konjević, R., Labat, J., & Purić, J. 1990b, Phys. Rev. A, 42, 2379
Fleurier, C. 1987, in Spectral Line Shapes III, ed. R. J. Exton (Hampton, VA: A. Deepak), 67
Freudenstein, S. A., & Cooper, J. 1978, ApJ, 224, 1079
Griem, H. R. 1968, Phys. Rev., 165, 258
———. 1974, Spectral Line Broadening by Plasmas (New York: Academic)
Jones, W. W., & Miller, M. H. 1974, Phys. Rev. A, 10, 1803
Konjević, N., Dimitrijević, M. S., & Wiese, W. L. 1984a, J. Phys. Chem. Ref. Data, 13, 619
———. 1984b, J. Phys. Chem. Ref. Data, 13, 649
Konjević, N., & Pittman, T. L. 1987, J. Quant. Spectrosc. Rad. Transf., 37, 311
Konjević, N., & Roberts, D. E. 1976, J. Phys. Chem. Ref. Data, 5, 209
Konjević, N., & Wiese, W. L. 1976, J. Phys. Chem. Ref. Data, 5, 259
———. 1990, J. Phys. Chem. Ref. Data, 19, 1308
Kurucz, R. L. 1979, ApJS, 40, 1
Kusch, H. J., & Schröder, K. 1982, A&A, 116, 255
Lakićević, I. S. 1983, A&A, 127, 37
———. 1985, A&A, 151, 457
Lakićević, I. S., & Purić, J. 1983, in Spectral Line Shapes II, ed. K. Burnett (Berlin: de Gruyter), 147
Lanz, T., & Artru, M.-C. 1987, Phys. Scripta, 32, 115
Lanz, T., Dimitrijević, M. S., & Artru, M.-C. 1988, A&A, 192, 249
Lesage, A., Rathore, B. A., Lakićević, I. S., & Purić, J. 1983, Phys. Rev. A, 28, 2264
Miller, M. H., Abadie, D., & Lesage, A. 1985, ApJ, 291, 219
Miller, M. H., Roig, R. A., & Bengston, R. D. 1979, Phys. Rev. A, 20, 499
Nick, K. P., & Helbig, V. 1986, Phys. Scripta, 33, 55
Pittman, T. L., & Konjević, N. 1986, J. Quant. Spectrosc. Rad. Transf., 35, 247
Platiša, M., Dimitrijević, M. S., Popović, M., & Konjević, N. 1977a, A&A, 54, 837
———. 1977b, J. Phys. B, 10, 2997
Platiša, M., Popović, M., Dimitrijević, M. S., & Konjević, N. 1979, J. Quant. Spectrosc. Rad. Transf., 22, 333
Purcell, S. T., & Barnard, J. 1984, J. Quant. Spectrosc. Rad. Transf., 32, 205
Purić, J. 1981, 16th ICPIG, Invited Papers, (Minsk: PIK Viniti) 311
Purić J., Ćuk, M., & Lakićević, I. 1985a, Phys. Rev. A, 32, 1106
———. 1985b, in Spectral Line Shapes III, ed. F. Rostas (Berlin: de Gruyter) 41
Purić, J., Djeniže, S., Labat, J., Platiša, M., Srećković, A., & Ćuk, M. 1988a, Z. Phys. D, 10, 431
Purić, J., Djeniže, S., Srećković, A., & Ćuk, M. 1988b, Fizika, 20, 485
Purić, J., Djeniže, S., Srećković, A., Ćuk, M., Labat, J., & Platiša, M. 1988c, Z. Phys. D, 8, 343
Purić, J., Djeniže, S., Srećković, A., Labat, J., & Ćirković, L., 1987a, Phys. Rev. A, 35, 2111
Purić, J., Djeniže, S., Srećković, A., Platiša, M. & Labat, J. 1988d, Phys. Rev. A, 37, 498
Purić, J., Lakićević, I., & Glavonjić, V. 1980, Phys. Letters, 76a, 128
Purić, J., Srećković, A., Djeniže, S., & Platiša, M. 1987b, Phys. Rev. A, 36, 3957
———. 1988e, Phys. Rev. A, 37, 4380
Richou, J., Manola, S., Lesage, A., Abadie, D., & Miller, M. H. 1983, Proc. 17th Internat. Conf. Phen. Ioniz. Gases, Vol. 4, ed. W. Böttcher, H. Wenk, & E. Schulz-Gulde (Düsseldorf: Institute of Theoretical Physics), 632
Smith, P. L. 1989, in Atomic and Molecular Data Required for Ultraviolet and Optical Astrophysics (Harvard College Observatory: Report of the Atomic and Molecular Astrophysics Laboratory)
Wiese, W. L., & Konjević, N. 1982, J. Quant. Spectrosc. Rad. Transf., 28, 185

© American Astronomical Society • Provided by the NASA Astrophysics Data System

1995ApJ...454..420M

THE ASTROPHYSICAL JOURNAL, 454:420–428, 1995 November 20
© 1995. The American Astronomical Society. All rights reserved. Printed in U.S.A.

RADIATIVE $He^+(1s) + He(1s^2)$ PROCESSES AS THE SOURCE OF THE DB WHITE DWARF ATMOSPHERE ELECTROMAGNETIC CONTINUOUS SPECTRA

A. A. MIHAJLOV,[1,2] M. S. DIMITRIJEVIĆ,[2] LJ. M. IGNJATOVIĆ,[1] AND Z. DJURIĆ[1]
Received 1994 August 12; accepted 1995 May 1

ABSTRACT

The influence of the processes of radiative charge transfer and photoassociation during $He^+ + He$ collisional processes, as well as the process of the photodissociation of the He_2^+ molecular ion, on the formation of the continuous spectrum of the DB white dwarf atmospheres with $T_{eff} = 12{,}000$–$30{,}000$ K, for log g (gravity) = 7 and 8, is studied within the wavelength range $\lambda = 200$–800 nm. It is shown that the contribution of these processes relative to other relevant radiative processes is particularly important for $T_{eff} \leq 16{,}000$ K and increases with the decrease of T_{eff}. Moreover, it is found that the influence of the considered $He^+ + He$ radiative processes is particularly pronounced in the UV range.

Subject headings: atomic processes — radiative transfer — stars: atmospheres — white dwarfs

1. INTRODUCTION

Radiative $He^+(1s) + He(1s^2)$ processes may be of importance for the formation of continuous spectra in helium-rich star low-temperature atmospheric layers (see, e.g., Mihajlov & Dimitrijević 1992; Stancil 1994). In this work, such radiative processes within DB white dwarf atmospheres are investigated in detail. Special attention is paid to their contribution to the formation of continuous optical spectra, as a function of the effective temperature T_{eff} and log g (gravity), in comparison with the contribution of other relevant radiative processes. Here we will consider the ion-atom processes of photoassociation and photodissociation

$$He^+(1s) + He(1s^2) \Leftrightarrow \epsilon_\lambda + He_2^+ , \tag{1a}$$

as well as the processes of the photoemission and photoabsorption charge exchange

$$He^+(1s) + He(1s^2) \Leftrightarrow \epsilon_\lambda + \begin{cases} He^+(1s) + He(1s^2) \\ He(1s^2) + He^+(1s) \end{cases} , \tag{1b}$$

where $He_2^+ = He_2^+(1\Sigma_u^+)$ and ϵ_λ is the energy of the photon with the wavelength λ. These processes will be considered here within the semiclassical approach (Mihajlov & Popović 1981; Mihajlov & Dimitrijević 1986, 1992). We will compare the influence of the ion-atom processes in equations (1a)–(1b) on the optical characteristics of the DB white dwarf atmospheres with the influence of other radiative processes which are also significant for these atmospheres. These include the processes of emission and absorption connected with the free-free transitions of an electron in the filed of atoms and atomic ions, as well as the processes of electron-ion photorecombination and photoionization of excited atoms. We take into account atoms and ions relevant for the assumed DB white dwarf atmosphere plasma composition (Bues 1970; Koester 1980). The contribution of the electron-atom processes will be estimated here in the manner of Bell, Berrington, & Croskery (1982), and the contribution of the electron-ion processes using the results of Sobelman (1979) and Menzel (1962).

The radiative processes investigated are considered within the optical range 200 nm $< \lambda <$ 800 nm. The needed calculations are performed for 12,000 K $\leq T_{eff} \leq$ 30,000 K and log g = 7 and 8. In such a way, the entire range of T_{eff} and log g parameters, considered in Koester (1980) concerning the white dwarf atmosphere modeling, is covered.

Our objective here is to estimate the importance of the ion-atom processes of photoassociation and photodissociation in equation (1a) and photoemission and photoabsorption charge exchange in equation (1b) in comparison with the relevant electron-atom and electron-ion processes in order to clarify the nature of the DB white dwarf photosphere continuous spectrum for different λ and T ranges. Therefore, we will study the influence of these processes on particular photospheric layers as well as their global characteristics. Such results may be of significance for DB white dwarf photosphere modeling.

The absorption channels (right to left implications) for the ion-atom reactions in equations (1a) and (1b) have been considered previously in Mihajlov & Dimitrijević (1992) and Stancil (1994). The contribution of emission channels (left to right implications) has been considered in Mihajlov, Ermolaev, & Dimitrijević (1993) for laboratory plasma and in Mihajlov, Dimitrijević, & Ignjatović (1994a) for a special case of DB white dwarf atmospheres.

2. THEORY

2.1. *Radiative Process Characteristics*

The contribution to the continuous spectra of the emission and absorption channels for ion-atom reactions in equations (1a) and (1b) can be characterized with the help of the corresponding partial spectral emissivities $\epsilon^{(a)}$ and $\epsilon^{(b)}$, the total emissivities $\epsilon^{(ab)} = \epsilon^{(a)} + \epsilon^{(b)}$, and the spectral absorption coefficients $\kappa^{(a)}$, $\kappa^{(b)}$, and $\kappa^{(ab)} = \kappa^{(a)} + \kappa^{(b)}$, respectively, where superscripts a and b denote the corresponding reactions. We will also use here the emissivity ϵ_{ea} and the absorption coefficient κ_{ea}, characterizing electron-atom radiative processes, and similarly ϵ_{ei} and κ_{ei}, characterizing electron-ion processes, as the source of the background opacity. All quantitities should be treated as functions of the wavelength (λ), temperature (T), and corresponding particle densities.

As a measure of the influence of the ion-atomic processes in equations (1a)–(1b) on the continuous spectra of white dwarf

[1] Institute of Physics, P.O. Box 57, 11001 Beograd, Yugoslavia.
[2] Astronomical Observatory, Volgina 7, 11050 Beograd, Yugoslavia.

© American Astronomical Society • Provided by the NASA Astrophysics Data System

1995ApJ...454..420M

atmospheres, we will use the quantity

$$F = \frac{\epsilon^{(ab)}}{\epsilon}, \quad (2)$$

where $\epsilon = \epsilon_{ea} + \epsilon_{ei}$. Besides this quantity, the ratio $\kappa^{(ab)}/\kappa$, with $\kappa = \kappa_{ea} + \kappa_{ei}$, may be used in principle as well. When LTE exists, then $\epsilon^{(ab)}/\epsilon = \kappa^{(ab)}/\kappa$. Outside LTE, however, these ratios are not equal, and one of them must be chosen. We consider here mainly outer atmospheric layers where the optical depth is less than or equal to unity. The radiation from such layers goes out, resulting in a departure from LTE by the excited atom population. For outer solar atmospheric layers, e.g., where a similar situation exists, this is confirmed by the direct plasma composition calculations (Vernazza, Avrett, & Loeser 1981). For DB white dwarfs, one may expect a similar situation. In the case of departure from LTE, the calculation of the absorption coefficient, κ, requires more information about excited atom populations. Consequently, we will take here the quantity F just given in equation (2) as in our previous work (see, e.g., Mihajlov et al. 1994a, b).

We will express $\epsilon^{(ab)}$ and $\kappa^{(ab)}$ in the form

$$\epsilon^{(ab)} = S^{(ab)} N(He^+) N(He), \quad \kappa^{(ab)} = K^{(ab)} N(He^+) N(He), \quad (3)$$

where $N(He^+)$ and $N(He)$ are densities of the helium ion and atom and $S^{(ab)}$ and $K^{(ab)}$ are the corresponding spectral coefficients for spontaneous emission and absorption, describing the ion-atom radiative processes in equations (1a) and (1b) together.

2.2. *Spectral Coefficients of Spontaneous Emission and Absorption*

Spectral coefficients $S^{(ab)}$ and $K^{(ab)}$ may be determined within the semiclassical approximation (Mihajlov & Popović 1981; Mihajlov & Dimitrijević 1992) and can be represented as functions of λ and temperature T in the form

$$S^{(ab)}(\lambda, T) = 4.777 \times 10^{-34} \frac{C(R_\lambda)}{1.345[1 - 0.362(a_0/R_\lambda)]} \times \left(\frac{R_\lambda}{a_0}\right)^4 \left(\frac{\epsilon_\lambda}{2Ry}\right)^5 \exp\left[\frac{-U_2(R_\lambda)}{kT}\right], \quad (4)$$

$$K^{(ab)}(\lambda, T) = 0.620 \times 10^{-42} \frac{C(R_\lambda)}{1.345[1 - 0.362(a_0/R_\lambda)]} \times \left(\frac{R_\lambda}{a_0}\right)^4 \theta(\lambda, T) \exp\left[\frac{-U_1(R_\lambda)}{kT}\right], \quad (5)$$

where the coefficient $C(R_\lambda)$ is given by

$$C(R_\lambda) = \left[\frac{2D_{12}(R_\lambda)}{eR_\lambda}\right]^2 \frac{1.345[1 - 0.362(a_0/R_\lambda)]}{\gamma(R_\lambda)},$$

$$\gamma(R_\lambda) = \left| \frac{d \ln \{[U_2(R) - U_1(R)]/2Ry\}}{d(R/a_0)} \right|_{R=R_\lambda}. \quad (6)$$

Here R denotes the internuclear distance in the $He^+ + He$ system; $U_1(R)$ and $U_2(R)$ are adiabatic terms of the ground ($1\,\Sigma_u$) and the first excited electronic states ($1\,\Sigma_g$) of the He_2^+ ion, which are given in Gupta & Madsen (1967); and R_λ denotes the R value such that

$$U_2(R_\lambda) - U_1(R_\lambda) = \epsilon_\lambda, \quad (7)$$

where $\epsilon_\lambda = 2\pi\hbar c/\lambda$, and $D_{12}(R)$ is the module of the dipole matrix element taken between these two states. In our previous work, the approximation $D_{12}(R) = eR/2$ was used. Here we use the following expression (Ermolaev & Mihajlov 1991), more accurate in the visible spectral range:

$$D_{12}(R) = \frac{eR}{2} \frac{1 - 0.695(a_0/R)}{(1 - s^2)^{1/2}},$$

$$s = \left[1 + 1.345\frac{R}{a_0} + \frac{1}{3}\left(1.345\frac{R}{a_0}\right)^2\right] \exp\left(-1.345\frac{R}{a_0}\right), \quad (8)$$

where s denotes the integral of the He $1s$ orbital overlapping for a given R. Finally, the coefficient $\theta(\lambda, T)$, which describes the decrease of the absorption coefficient resulting from stimulated emission, is given by the expression

$$\theta(\lambda, T) = 1 - \exp\left(-\frac{\epsilon_\lambda}{kT}\right). \quad (9)$$

From equations (4), (5), (7), and (9), it follows that the ratio $S^{(ab)}/K^{(ab)}$ represents the universal function of λ and T (see, e.g., Sobelman 1979), proportional to the Planck distribution function. One must take into account that numerical coefficients in equations (4) and (5) are chosen in such a manner that $S^{(ab)}$ is expressed in J cm^{-3} s^{-1} nm^{-1} and $K^{(ab)}$ is expressed in cm^5. All parameters needed for the calculation of spectral coefficients $S^{(ab)}$ and $K^{(ab)}$ in the 150 nm $\leq \lambda \leq$ 850 nm range are given in Table 1. The behavior of these coefficients as a function of T is presented in Figures 1 and 2.

Stancil (1992, his Figs. 4–5) compares his results for the absorption coefficient with the corresponding semiclassical results for H (Mihajlov & Dimitrijević 1986) and He (Mijajlov & Dimitrijević 1992). He found good agreement between quantum-mechanical and semiclassical results for He, better than for H. This is the consequence of the fact that in Mihajlov & Dimitrijević (1986), the approximate expressions for molecular terms and $\gamma(R_\lambda)$ factor (not used in Mihajlov & Dimitrijević 1992 for helium) have been used. Moreover, in comparison with Mihajlov & Dimitrijević (1992), the expressions given here are more accurate for the dipole matrix elements. In Stancil (1994), the photodissociation channel contribution has been considered using the quantum-mechanical approach, while the

TABLE 1

PARAMETERS NEEDED FOR CALCULATION OF SPECTRAL COEFFICIENTS[a]

λ (nm)	R_λ (a.u.)	ϵ_λ (a.u.)	$\lvert U_1(R_\lambda)\rvert$ (a.u.)	$U_2(R_\lambda)$ (a.u.)	$C(R_\lambda)$
150.....	2.20	0.3037	0.0832	0.2205	1.052
200.....	2.43	0.2278	0.0755	0.1523	1.037
250.....	2.62	0.1822	0.0672	0.1150	1.029
300.....	2.77	0.1519	0.0600	0.0918	1.025
350.....	2.90	0.1302	0.0540	0.0761	1.022
400.....	3.01	0.1139	0.0490	0.0649	1.020
450.....	3.11	0.1012	0.0448	0.0564	1.019
500.....	3.19	0.0911	0.0412	0.0499	1.018
550.....	3.27	0.0828	0.0382	0.0446	1.017
600.....	3.35	0.0759	0.0356	0.0404	1.017
650.....	3.41	0.0701	0.0333	0.0368	1.016
700.....	3.47	0.0651	0.0313	0.0338	1.016
750.....	3.53	0.0607	0.0295	0.0313	1.016
800.....	3.58	0.0569	0.0279	0.0291	1.016
850.....	3.64	0.0536	0.0264	0.0272	1.015

[a] Parameters of molecular ion He_2^+ needed for the $S^{(ab)}(\lambda)$ and $K^{(ab)}(\lambda)$ calculations, within the 150 nm $\leq \lambda \leq$ 850 nm range.

© American Astronomical Society • Provided by the NASA Astrophysics Data System

1995ApJ...454..420M

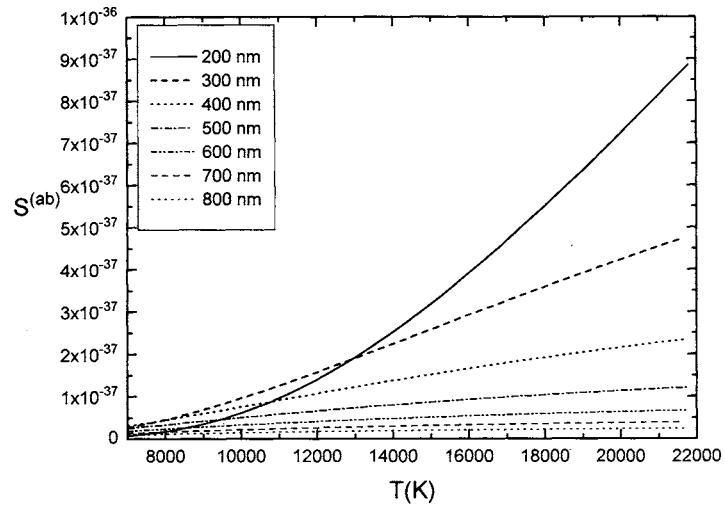

FIG. 1.—Spectral coefficients $S^{(ab)}(\lambda, T)$ for spontaneous emission resulting from ion-atom radiative processes in eqs. (1a)–(1b) together, as a function of T, for 200 nm $\leq \lambda \leq$ 800 nm.

second channel (the absorption during free-free ion-atom transitions) has been treated in a similar semiclassical way. One must recognize that both channels are, in fact, of equal importance. Moreover, for transitions in the photodissociation channel with initial rotational-vibrational states near the dissociation limit and wider (within the domain of the pronounced aharmonism), the semiclassical approach is applicable. Such a situation applies to the infrared and visible range as well. One advantage of the semiclassical approach is the simplicity of the corresponding expressions which may be easily implemented in computer codes for stellar atmosphere modeling. Moreover, eventual molecular term corrections within the presented semiclassical method need only a correction of input data given in Table 1, while in order to recalculate the quantum-mechanical results, first of all one must determine from the beginning the vibrational-rotational spectrum.

2.3. *Relative Intensities of Ion-Atom Radiative Processes*

Particular relative contributions of the ion-atom radiative processes in equations (1a) and (1b) can be characterized with the help of coefficients $X^{(a)}$ and $X^{(b)}$:

$$X^{(a,b)} = \frac{\epsilon^{(a,b)}}{\epsilon^{(ab)}} = \frac{\kappa^{(a,b)}}{\kappa^{(ab)}} . \tag{10}$$

According to Mihajlov & Dimitrijević (1992), we have that $X^{(a)} = 1 - X^{(b)}$ and

$$X^{(b)}(Z) = \begin{cases} 1 & \text{for } Z \leq 0 , \\ \Gamma(3/2;\, Z)/\Gamma(3/2) & \text{for } Z \geq 0 , \end{cases} \tag{11}$$

where $\Gamma(3/2;\, Z)$ is an incomplete gamma-function (Abramowitz & Stegun 1972) and $Z = -U_1(R_\lambda)/kT$. In considered wavelength range, we find that $U_1(R_\lambda) < 0$ and $Z = |U_1(R_\lambda)|/kT$. Here we use just the coefficient $X^{(b)}$. The behavior of this coefficient as a function of Z was shown in Mihajlov et al. (1994b).

3. RESULTS AND DISCUSSION

Our results are presented here in order to emphasize the role of the ion-atom radiative processes in equations (1a)–(1b) a

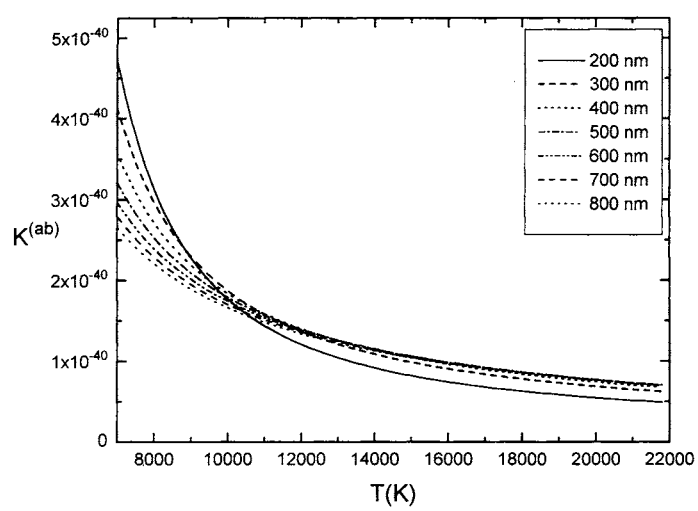

FIG. 2.—Spectral coefficients $K^{(ab)}(\lambda, T)$ for absorbtion resulting from ion-atom radiative processes in eqs. (1a)–(1b) together, as a function of T, for 200 nm $\leq \lambda \leq$ 800 nm.

© American Astronomical Society • Provided by the NASA Astrophysics Data System

1995ApJ...454..420M

source of the continuous spectrum of the DB white dwarf photospheres. The contribution of the ion-atom radiative processes in equations (1a)–(1b) is compared with the contribution of the electron-atom and electron-ion radiative processes. However, we do not consider here molecular bands generated by helium molecules in excited electronic states, or continuous spectra originating from blended lines. Present calculations for F given by equations (2) and (3) (performed by using the DB white dwarf atmospheric structures of Koester 1980) are presented in Figures 3*a*–3*e* for $\log g = 8$ and $\lambda = 200$, 300, 400, 600, and 800 nm, and in Figure 4 for $\log g = 7$ and $\lambda = 400$ nm (we note here that the figures are not on the same scale). These figures show the behavior of F as a function of the Rosseland optical depth τ (taken from Koester 1980) for $\tau \leq 2.75$. The curves in these figures correspond to the effective temperatures from 12,000 K $\leq T_{\rm eff} \leq$ 30,000 K.

In equation (2) the emissivity $\epsilon = \epsilon_{ea} + \epsilon_{ei}$. The term ϵ_{ea} is the emissivity which is due to free-free radiative transition at e-He scattering only. We take into account here the considered-atmosphere composition, in which the He component is 5 orders of magnitude larger than other components (Bues 1970; Koester 1980). We also consider the fact that the ion-atom radiative processes in equations (1a)–(1b) are significant for helium plasma with ionization degree less than or on the order of 10^{-3} (Mihajlov et al. 1993, 1994a), which also follows from our results. As a result it is quite sufficiently to take into account only e-He, among all electron-atom radiative processes. The nonexistence of the stable negative helium atomic ion, and consequently the absence of the electron photocapture during the e-He scattering, are also taken into account. The term ϵ_{ei} is the emissivity which is due to free-free (bremsstrahlung) and free-bound (photorecombination) radiative transition at e-A^+ scattering. Here A^+ denotes He^+ as well as H^+ and metal ions. We consider H^+ and metal ions have, since in a number of cases they are the significant part of the ionic component within the particular atmospheric layers; this confirms our results, which are based on Koester's (1980) data.

The term ϵ_{ea} is proportional to $N(e)$, and the term ϵ_{ei} is proportional to $N(e)^2$, where $N(e)$ is the free electron density. Consequently, the relative importance of ϵ_{ei} increases rapidly with the ionization degree; i.e., the temperature increases. Therefore, from the quick increase of just the term ϵ_{ei} follows the quick decrease of $F(\log \tau)$ in Figures 3*a*–3*e* and 4 as $T_{\rm eff}$ increases within the $T_{\rm eff} \geq 18{,}000$ K range for the UV part of the spectrum and within the $T_{\rm eff} \geq 20{,}000$ K range for the visible part of the spectrum. For 16,000 K for the UV range and 18,000 K for the visible range, electron-ion and electron-atom process contributions become comparable. The electron-ion term ϵ_{ei} is also responsible for the decrease of all $F(\log \tau)$ curves in these figures, for τ larger than or on the order of magnitude 1, where the temperature and the ionization degree increase quickly with the increase in τ.

When τ is less than or close to 1 and $T_{\rm eff}$ is less than or close to 16,000 K, the term ϵ_{ea} dominates in comparison to ϵ_{ei}. Consequently, within this region we find that $F(\log \tau) \approx \epsilon^{(\rm ab)}/\epsilon_{ea}$, where ϵ_{ea} may be taken as $\epsilon_{ea} = S^{\rm ff}_{ea}\, N(e)N({\rm He})$, and "ff" indicates that only the free-free electron-atom radiative processes are considered. The corresponding spectral coefficient $S^{\rm ff}_{ea}$ is taken here (as a function of λ and T) from Bell et al. (1982). It follows that

$$F(\log \tau) \approx \frac{\epsilon^{(\rm ab)}}{\epsilon_{(ea)}} = \frac{S^{(\rm ab)}}{S^{\rm ff}_{ea}} \frac{N({\rm He}^+)}{N(e)} .$$

The first multiplicator $S^{(\rm ab)}/S^{\rm ff}_{ea}$ in the above expression changes slowly (is practically constant) within the $\log \tau \leq -1$ range, but its decrease within the $\log \tau > -1$ range produces the beginning of the decrease of all $F(\log \tau)$ curves, around $\log \tau = 0$.

Figures 3*a*–3*e* illustrate the very significant influence of $T_{\rm eff}$ on the $F(\log \tau)$ curve shapes within the $\log \tau < -1$ range and for $T_{\rm eff} < 18{,}000$ K. This influence is particularly pronounced for the transition from the range of $T_{\rm eff} \geq 14{,}000$ K to $T_{\rm eff} =$ 12,000 K. This fact is the consequence of the behavior of the second multiplicator $N({\rm He}^+)/N(e)$ as a function of $\log \tau$ for different values of $T_{\rm eff}$. The ratio $N({\rm He}^+)/N(e)$ represents one significant characteristic of the considered plasma, namely, the relative contribution of the He atom component to the total free electron density. The behavior of this ratio as a $\log \tau$ function for $T_{\rm eff} =$ 12,000, 14,000, 16,000, and 18,000 K is shown in Figure 5*a*. One can see that within the small τ range, the He component contribution is dominant for $T_{\rm eff} \geq 16{,}000$ K, is still significant for 14,000 K, and decreases sharply for $T_{\rm eff} = 12{,}000$ K. Namely, at the transition between $T_{\rm eff} =$ 14,000 K and 12,000 K, the $N({\rm He}^+)/N(e)$ ratio decreases quickly for $\log \tau \leq -1$, and for $\log \tau < -1.5$, this ratio decreases for several orders of magnitude, starting from values close to 0.5 up to values close to zero (with the minimum of this ratio around $\log \tau = -3$). This follows from the Saha equation with T, $N(e)$, and $N({\rm He})$ from Koester (1980). One must take into account for the interpretation in Figure 5*a* that, for $T_{\rm eff} =$ 12,000 K and 14,000 K and $\log \tau < -1.5$, the ionization degree of the considered atmospheric layers is of the order of magnitude of 10^{-5}, and the relative contribution of the H and metals in comparison with He is 2.5×10^{-5} (Bues 1970; Koester 1980), i.e., of the same order of magnitude as the ionization degree. Accordingly, the lower curve in Figure 5*a* shows that within the $\log \tau \leq 1.5$ region, we see that an ionic component completely dominates H and metal ions for $T_{\rm eff} = 12{,}000$ K, and for $T_{\rm eff} = 14{,}000$ K, the contribution of the He ions becomes equal to the H and metal ion contribution. Two upper curves in Figure 5*a* illustrate the $N({\rm He}^+)/N(e)$ ratio for a further increase in $T_{\rm eff}$ from 18,000 to 20,000 K. One can see that the curve corresponding to $T_{\rm eff} = 18{,}000$ K has parts in which the calculated values of this ratio are equal to 1. These parts correspond to the τ ranges for which one obtains from Koester's (1980) data that $N({\rm He}^+)/N(e) > 1$. We assumed here that $N(e) = N({\rm He}^+) + N({\rm H}^+) + N({\rm metal\ ions})$, where the second and third terms are the densities of H^+ and metal ions. In such cases, we assumed that $N({\rm He}^+)/N(e) = 1$ and consequently, $N({\rm H}^+) + N({\rm metal\ ions}) = 0$.

Within the visible part of the spectrum, the increase in the $N({\rm He}^+)/N(e)$ ratio for the transition from 14,000 to 16,000 K produces the increase in the $F(\log \tau)$ value in Figures 3*c*–3*e*. Within the UV part of the spectrum, there is no such correlation resulting from the contribution of the electron-ion radiative processes. Moreover, the contribution of these processes stops the further $F(\log \tau)$ increase with the $T_{\rm eff}$ increase over 16,000 K, within the considered spectral range.

The $F(\log \tau)$ curve oscillations in Figures 3*a*–3*e* and 4 are produced by the nonmonotonical behavior of the temperature and the electron, atom, and ion densities (as well as some of their combinations) as functions of $\log \tau$ in (or calculated from) the Koester (1980) models, which are not easy to notice at first sight. Therefore, Figure 5*b* shows the origin of such oscillations for the example of a well-pronounced oscillation within the $-5.2 \leq \log \tau \leq -4.4$ range, for $\log g = 8$ and $T_{\rm eff} = 14{,}000$ K. It is taken into account that these oscillations are the most

© American Astronomical Society • Provided by the NASA Astrophysics Data System

1995ApJ...454..420M

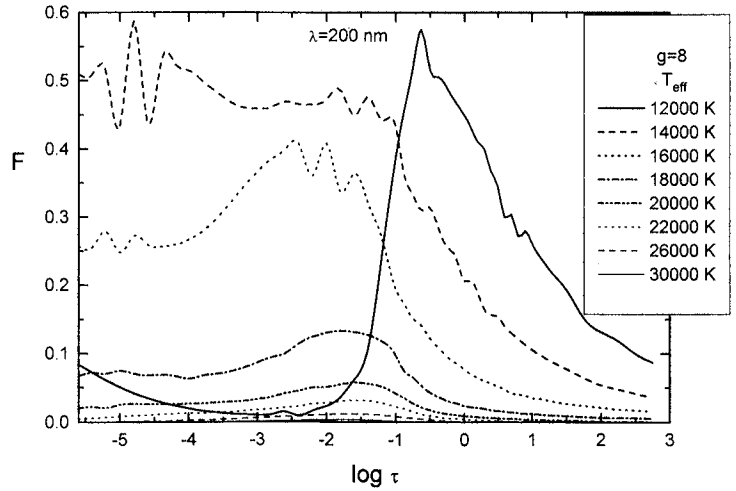

FIG. 3*a*

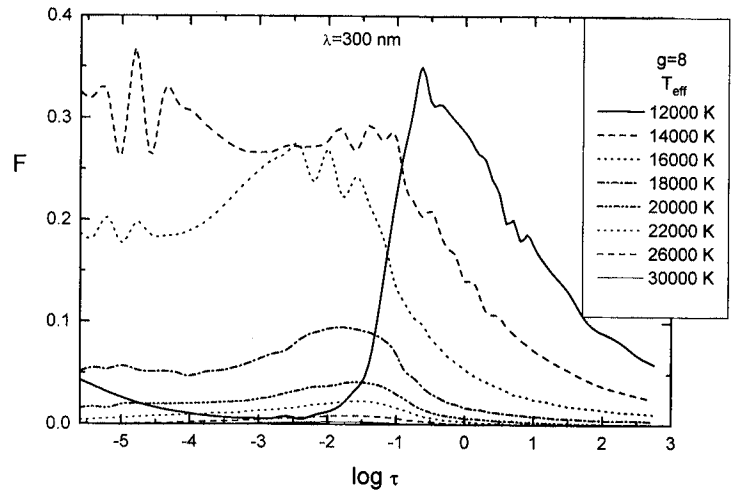

FIG. 3*b*

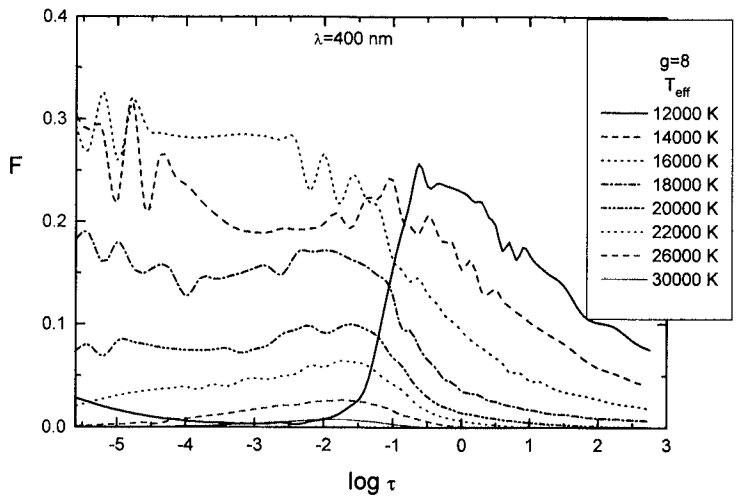

FIG. 3*c*

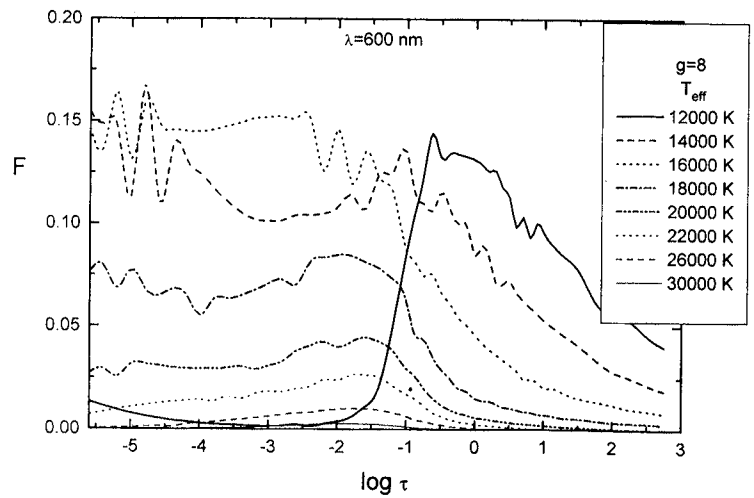

FIG. 3*d*

FIG. 3.—(*a*) Behavior of the parameter $F(\lambda, T)$, defined by eq. (2), as a function of Rosseland optical depth logarithm for $\lambda = 200$ nm and 12,000 K $\leq T_{eff} \leq$ 30,000 K, in the case of $\log g = 8$. (*b*) Same as (*a*), but for $\lambda = 300$ nm. (*c*) Same as (*a*), but for $\lambda = 400$ nm. (*d*) Same as (*a*), but for $\lambda = 600$ nm. (*e*) Same as (*a*), but for $\lambda = 800$ nm.

© American Astronomical Society • Provided by the NASA Astrophysics Data System

1995ApJ...454..420M

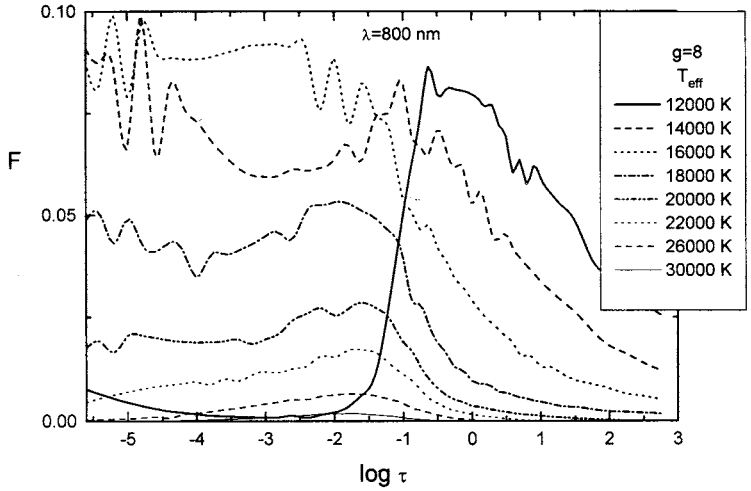

FIG. 3*e*

pronounced for $T_{\rm eff} = 14{,}000$ K. For such well-pronounced oscillations, it is found that they are very well correlated with the corresponding oscillations of the $N(\mathrm{He}^+)/N(e)$ ratio, which follows from the comparison of Figures 3*a*–3*e* with Figure 5*a*. In order to show the origin of oscillations, we will assume that

$$\frac{N(\mathrm{He}^+)}{N(e)} = f_{S;\mathrm{He}}(T)N(e)^{-2}N(\mathrm{He})\ ,$$

where $f_{S;\mathrm{He}}(T)$ is the Saha function of the helium component. Figure 5*b* shows the behavior of $f_{S;\mathrm{He}}(T)$, $f_{S;\mathrm{He}}(T)N(e)^{-2}$, and the $N(\mathrm{He}^+)/N(e)$ ratio around the considered oscillation. In the same figure, the behavior of temperature within the considered range is shown as well. In order to present all curves in the same figure, the corresponding quantities are normalized on their values at the point $\log\tau = -4.4$. The temperature curve in Figure 5*b* illustrates that the relative temperature changes around the oscillation are very small and it is difficult to notice them. So we will show here, on the basis of Koester's (1980) data, that for $\log\tau = -5.4$, -5.2, -5.0, -4.8, -4.6, and -4.4, the temperature has the values $T = 9540$, 9612, 9601, 9740, 9703, and 9806 K, respectively. These small temperature variations, however, produce the considerable changes of the Saha function $f_{S;\mathrm{He}}(T)$ initializating the oscillation, as shown by the lowest curve in Figure 5*b*. Such changes are the direct consequence of the large ionization potential of the He atom, but these changes are not the only reason for oscillations. The upper curve in Figure 5*b*, which shows the behavior of the product $f_{S;\mathrm{He}}(T)N(e)^{-2}$, illustrates the large influence of the electron density variations. Finally, one can see that only when the helium atom density variations are taken into account does one obtain the real oscillation shape on the $N(\mathrm{He}^+)/N(e)$ ratio curve. Such oscillations are not important here, however, since they are variations of several percent in relation to the general trend, which we report on here.

The change in $\log g$ from 8 to 7, however, has a considerably weaker influence on the change in the $F(\log\tau)$ curves. This may be seen by comparing Figures 3*c* and 4 for $\lambda = 400$ nm. Figures 3*a*–3*e* also show that in comparison with the electron-atom and electron-ion radiative processes, the relative influence of ion-atom radiative processes increases quickly with the λ decrease and becomes particularly significant in the UV spectral range.

In Figure 6, the relative contribution of the purely collisional

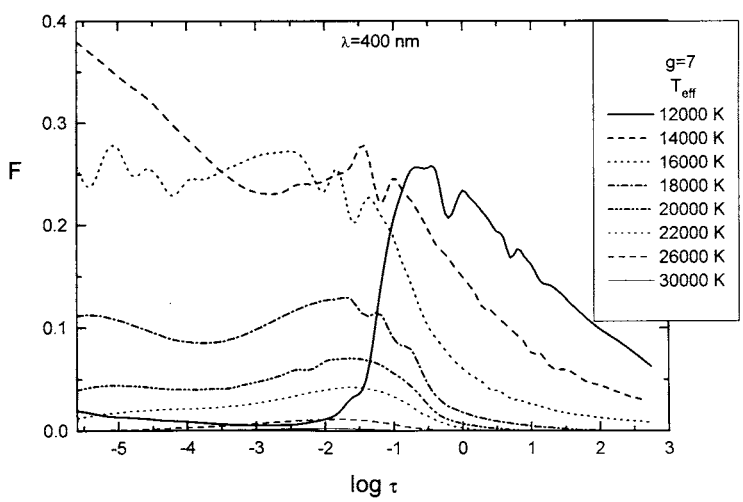

FIG. 4.—Same as Fig. 3*c*, but in the case of $\log g = 7$

© American Astronomical Society • Provided by the NASA Astrophysics Data System

1995ApJ...454..420M

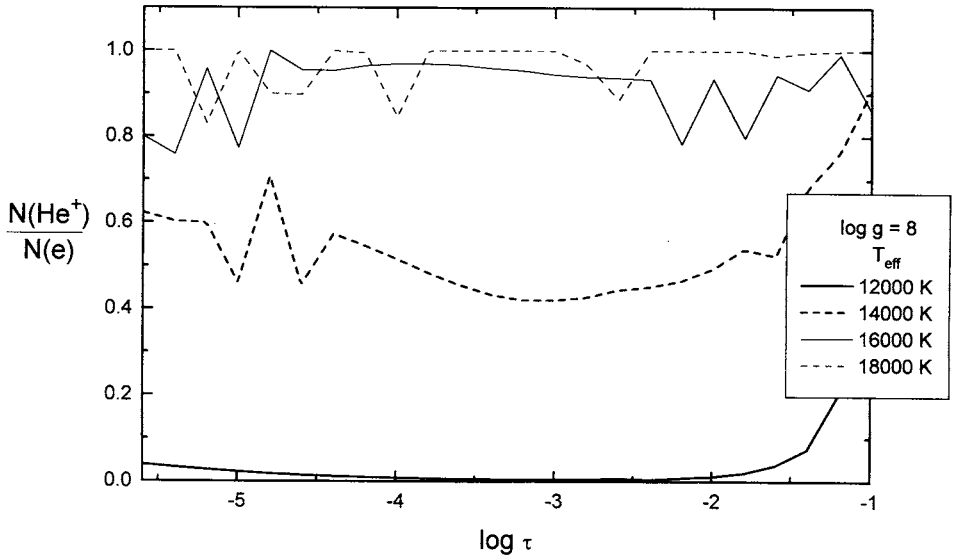

FIG. 5*a*

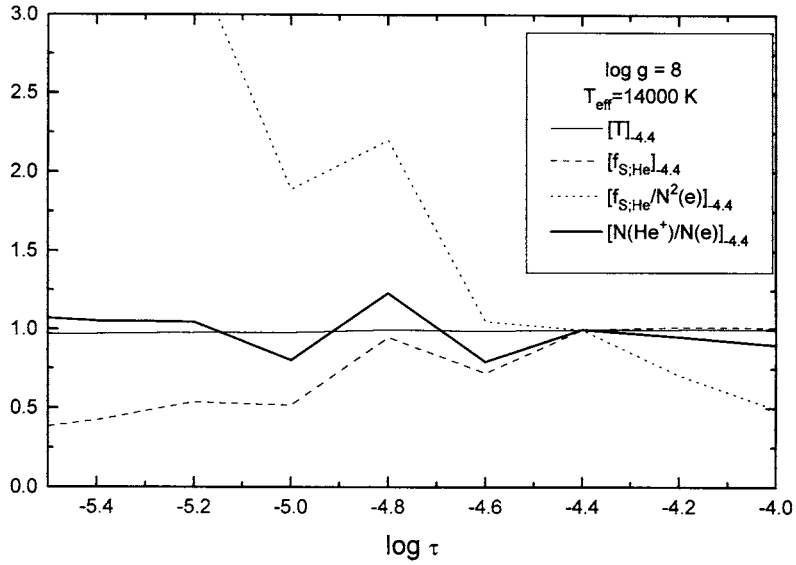

FIG. 5*b*

FIG. 5.—(*a*) Behavior of the $N(\mathrm{He}^+)/N(e)$ ratio as functions of Rosseland optical depths logarithm, based on DB white dwarf models from Koester (1980). Dependence on T_{eff} for 12,000 K $\leq T_{\mathrm{eff}} \leq$ 18,000 K and $\log g = 8$. (*b*) Behavior of the $N(\mathrm{He}^+)/N(e)$ ratio as functions of Rosseland optical depth logarithm, based on DB white dwarf models from Koester (1980). The origin of the oscillation of this ratio for $T_{\mathrm{eff}} = 14{,}000$ K and $\log g = 8$. Subscript "-4.4" denotes that the corresponding quantity is normalized with its value for $\log \tau = -4.4$; $f_{S;\mathrm{He}}$ the Saha function for the He component.

radiative charge exchange processes (eq. [16]), compared to the total contribution of the ion-atom radiative processes (eqs. [1a]–[1b]), is shown. This figure is for $\lambda = 400$ nm, and one can see that the coefficient $X^{(b)}$ is weakly dependent on $\log g$. The dependence on T_{eff} is pronounced in this case as well, but the shape of the $X^{(b)}$ variation with T_{eff} remains more or less the same in the T_{eff} range considered. One can see that $X^{(b)}$ increases quickly and becomes larger than 50% around $\log \tau = 0$, so that for $\log \tau \geq 0$ the purely collisional radiative exchange processes in equation (1b) become dominant.

The influence of the ion-atom radiative processes in equations (1a)–(1b) on the optical characteristics of the considered atmospheric layers will be illustrated here with the relative changes of the optical depth and the emergent radiation intensity calculated for radial rays (see, e.g., Mihalas 1978), i.e., the ratios $\Delta\Phi(\lambda, \log \tau)/\Phi(\lambda, \log \tau)$, $\Delta\tau(\lambda, \log \tau)/\tau$, where $\Delta\Phi(\lambda, \log \tau) = [\Phi'(\lambda, \log \tau) - \Phi(\lambda, \log \tau)]$, and $\Delta\tau(\lambda, \log \tau) = [\tau'(\lambda, \log \tau) - \tau]$. Here $\Phi'(\lambda, \log \tau)$ and $\Phi(\lambda, \log \tau)$ are emergent radiation intensities determined with and without ion-atom radiative processes (eqs. [1a]–[1b]), and $\tau'(\lambda, \log \tau)$ is the optical depth determined with the ion-atom radiative processes included. In Figures 7–8 the behavior of the ratios $\Delta\tau(\lambda, \log \tau)/\tau$ and $\Delta\Phi(\lambda, \log \tau)/\Phi(\lambda, \log \tau)$ as a function of $\log \tau$, for $\lambda = 200$, 400, and 600 nm, is demonstrated. Curves in these figures are for $T_{\mathrm{eff}} = 12{,}000$ and 14,000 K and $\log g = 8$. These curves show qualitative changes of curve shapes similar to the corresponding changes in Figures 3–4, at the transition from $T_{\mathrm{eff}} = 12{,}000$ K to $T_{\mathrm{eff}} = 14{,}000$ K. Moreover, similarly to Figures

© American Astronomical Society • Provided by the NASA Astrophysics Data System

1995ApJ...454..420M

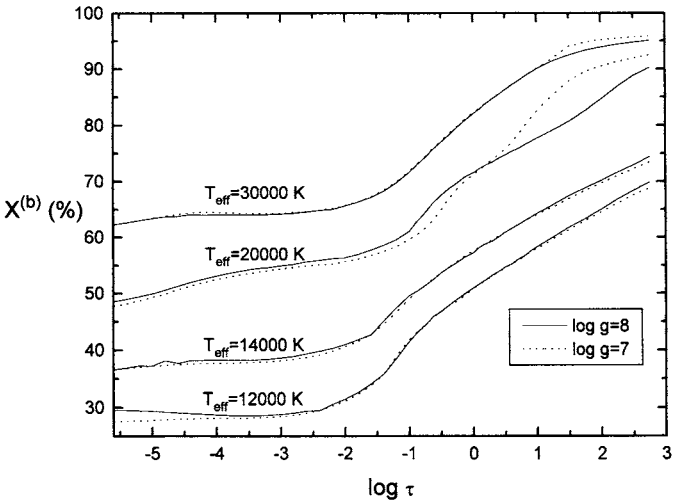

FIG. 6.—Behavior of the parameter $X^{(b)}(Z)$, where $Z = |U_1(R_\lambda)|/kT$, defined by eqs. (10)–(11), as a function of the Rosseland optical depth logarithm for $\lambda = 400$ nm, 12,000 $K \leq T_{eff} \leq 30{,}000$ K, and $\log g = 7$ and 8.

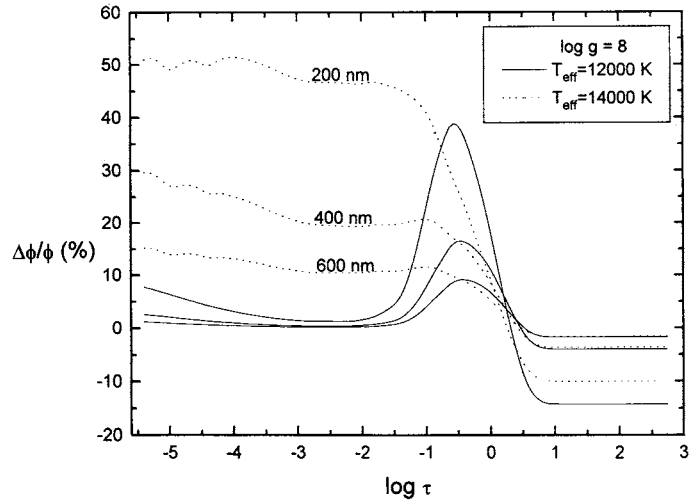

FIG. 8.—Behavior of the ratio $\Delta\Phi/\Phi$ as a function of the Rosseland optical depth logarithm for the same λ, T_{eff}, and $\log g$ as in Fig. 8.

3–4, they show the quick increase of the influence of the ion-atom processes with the λ decrease, especially at the transition from the visible to the UV spectral range. Our calculations also show that the transition from $\log g = 8$ to $\log g = 7$ is not connected with considerable changes of $\Delta\tau/\tau$ and $\Delta\Phi/\Phi$. It has been found that these changes are not larger than several percent in the largest part of the considered τ range (only for particular layers do these changes approach 20%).

The influence of the considered ion-atom radiative processes of equations (1a, b) on the optical characteristics of the atmosphere as a whole might be illustrated by the quantity $(\Delta\Phi/\Phi)_0$, i.e., by the ratio $\Delta\Phi/\Phi$, determined for $\log \tau = 0$, characterizing the whole outer layer with the optical depth $\tau = 1$. Namely, we found numerically that the further increase of the layer depth does not change the $\Delta\Phi/\Phi$ value, which is also in Figure 8. The behavior of the quantity $(\Delta\Phi/\Phi)_0$ is shown in Figure 9 as a function of λ within the 200 nm $\leq \lambda \leq$ 800 nm range, for 12,000 K $\leq T_{eff} \leq$ 20,000 K and $\log g = 8$. One can see that the relative intensity change is negative and decreases by up to 14%. We note that the final $(\Delta\Phi/\Phi)_0$ values characterize at the same time the influence of the absorption channel which decreases this value and the emission channel which leads to its increase. For the considered case, we find that in the contribution of the ion-atom radiative processes of equations (1a)–(1b) the influence of the absorption channels dominates. We found here that the final $(\Delta\Phi/\Phi)_0$ values are not negligible. Moreover, Figure 7 shows that changes in the optical depth $\Delta\tau$ represent a significant disturbance of the reference value τ for the tabular presentation of the white dwarf model, rather than a small perturbation. One can see in Figure 8 as well that $\Delta\Phi$ is a strong perturbation for energetic balance considerations of particular atmospheric layers. Consequently, the ion-atom radiative processes in equations (1a)–(1b) must be taken into account during the white dwarf atmosphere modeling and not added a posteriori as a correction to the result obtained by using the model when such processes have been neglected.

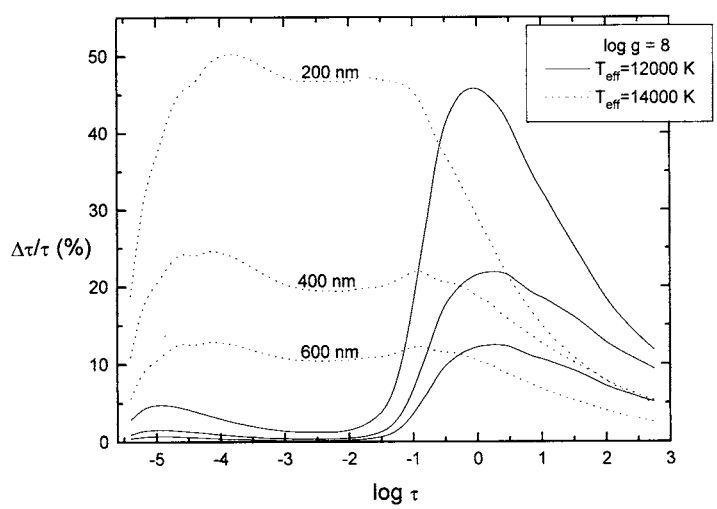

FIG. 7.—Behavior of the ratio $\Delta\tau/\tau$ as a function of the Rosseland optical depth logarithm for $\lambda = 200$, 400, and 600 nm and $T_{eff} = 12{,}000$ and 14,000 K, in the case of $\log g = 8$.

© American Astronomical Society • Provided by the NASA Astrophysics Data System

1995ApJ...454..420M

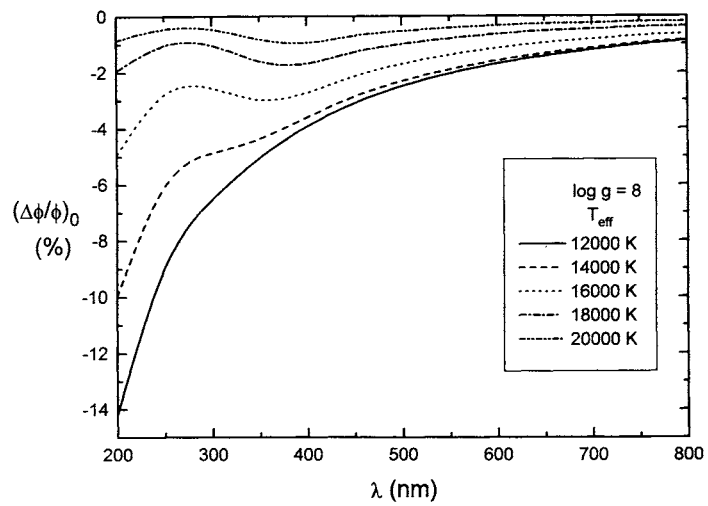

FIG. 9.—Behavior of the quantity $(\Delta\Phi/\Phi)_0$, i.e., the ratio of $\Delta\Phi/\Phi$ as a function of λ for T_{eff} and $\log g$ as in Fig. 6. Here $(\Delta\Phi/\Phi)_0$ denotes the ratio of $\Delta\Phi/\Phi$ for $\log\tau = 0$.

4. CONCLUSIONS

It is shown in this article that for $T_{eff} \leq 16{,}000$ K, DB white dwarf photosphere continuous spectra are formed under the important influence of the ion-atom radiative processes, while for larger T_{eff} values the electron-atom and electron-ion processes have a more basic role. This is the consequence of the fact that the influence of ion-atom radiative processes increases quickly when T_{eff} decreases around $T_{eff} = 16{,}000$ K. Moreover, a large increase in the H and metal relative contribution to the total electron density was found at the transition from $T_{eff} =$ 14,000 K to 12,000 K. This results with the very significant $He^+ + He$ relative emissivity curve shape change for $T_{eff} =$ 14,000 K and 12,000 K. It is also found that the influence of the radiative ion-atom processes increases quickly when λ decreases, especially at the transition from the visible to the UV spectral range.

From the results shown, it follows that for $T_{eff} \leq 16{,}000$ K and $\lambda \leq 400$ nm, ion-atom radiative processes may influence significantly the energetic balance and optical characteristics (opacity and optical depth) of white dwarf atmospheric layers where $\log(\tau) \leq 1$. Especially important is the influence on the optical depth values calculated with and without taking into account the ion-atom radiative processes. The facts presented suggest that it is necessary to include ion-atom radiative processes for the white dwarf atmosphere modeling from the beginning and not as an a posteriori correction, since they change the reference optical depths for the tabulated model parameters. All elements needed for the inclusion of the ion-atom radiative processes in the DB white dwarf atmosphere modeling are presented here.

REFERENCES

Abramowitz, M., & Stegun, I. 1972, Handbook of Mathematical Functions (New York: Dover)
Bell, K. L., Berrington, K. A., & Croskery, J. P. 1982, J. Phys. B, 15, 977
Bues, I. 1970, A&A, 7, 91
Ermolaev, A. M., & Mihajlov, A. A. 1991, J. Phys. B, 24, 155
Gupta, B. K., & Madsen, F. A. 1967, J. Chem. Phys., 47, 48
Koester, D. 1980, A&AS, 39, 401
Menzel, D. H. 1962, Selected Papers on Physical Processes in Ionized Plasmas (New York: Dover)
Mihajlov, A. A., & Dimitrijević, M. S. 1986, A&A, 155, 319
———. 1992, A&A, 256, 305
Mihajlov, A. A., Dimitrijević, M. S., & Ignjatović, Lj. 1994a, A&A, 287, 1026
Mihajlov, A. A., Dimitrijević, M. S., Ignjatović, Lj., & Djurić, Z. 1994b, A&AS, 103, 57
Mihajlov, A. A., Ermolaev, A. M., & Dimitrijević, M. S. 1993, J.Q.S.R.T., 50, 227
Mihajlov, A. A., & Popović, M. M. 1981, Phys. Rev. A, 23, 1679
Mihalas, D. 1978, Stellar Atmospheres (San Francisco: W. H. Freeman)
Sobelman, I. I. 1979, Atomic Spectra and Radiative Transitions (Berlin: Springer-Verlag)
Stancil, P. C. 1994, ApJ, 430, 360
Vernazza, J. E., Avrett, E. H., & Loeser, R. 1981, ApJS, 45, 635

© American Astronomical Society • Provided by the NASA Astrophysics Data System

The Astrophysical Journal Supplement Series, 170:243–250, 2007 May
© 2007. The American Astronomical Society. All rights reserved. Printed in U.S.A.

STARK BROADENING OF THE SPECTRAL LINES OF Ne v

R. Hamdi,[1] N. Ben Nessib,[1] M. S. Dimitrijević,[2,3] and S. Sahal-Bréchot[4]
Received 2006 October 6; accepted 2007 January 29

ABSTRACT

Using a semiclassical approach, we have calculated ab initio electron-, proton-, and ionized helium-impact line widths and shift for 26 Ne v multiplets. Energy levels and oscillator strengths have been calculated using SUPERSTRUCTURE code. Results have been presented for an electron density of 10^{17} cm^{-3} as a function of temperature, and are compared with experimental and other theoretical results.

Subject headings: atomic data — atomic processes — line: profiles

1. INTRODUCTION

Important astrophysical applications of Stark broadening of multiply charged ion spectral lines are in the physics of stellar interiors (Seaton 1987). In subphotospheric layers, the modeling of energy transport requires radiative opacities, so certain atomic processes should be known with sufficient accuracy. At these high temperatures (100,000 K and more) and densities (10^{17}–10^{22} cm^{-3}) Stark broadening of strong multiply charged ionic lines plays a nonnegligible role in the calculation of the opacities, especially in the UV. Moreover, with the development of spectroscopic investigations from space, UV and extreme-UV spectral line research has been further stimulated. The Stark broadening mechanism is also important for the investigation, analysis, and modeling of B-type, and particularly A-type, stellar atmospheres, as well as for white dwarf atmospheres. In Popović et al. (2001), the influence of Stark broadening on Nd ii lines in A-type stellar atmospheres was investigated. It was demonstrated that neglecting this mechanism introduces an error between 10% and 45% in the equivalent width determination and influences abundance determination.

Quadruply ionized neon (Ne v) is a unique probe of astrophysical plasma in the intermediate-temperature range [100,000–600,000 K], a temperature that bridges the low temperatures mapped in narrow band optical filters (5000–50,000 K) and the high-temperature regime imaged in X-rays ($T \geq 1{,}000{,}000$ K; Szentgyorgyi et al. 2000). Such temperatures are of interest not only for subphotospheric layers where Stark broadening is important (Seaton 1987). Temperatures of 100,000–150,000 K are typical for PG 1195-type stars (Werner & Heber 1991) and for DO white dwarfs, which have effective temperature from 50,000 to approximately 120,000 K at the hot end of the branch (Dreizler & Werner 1996).

For a number of quadruply ionized atoms there exist sufficient atomic data for sophisticated semiclassical calculations for astrophysically interesting lines. Thus, large-scale calculations have been performed with the semiclassical perturbation formalism (Sahal-Bréchot 1969a, 1969b) for C v (Dimitrijević & Sahal-Bréchot 1995, 1996a), N v (Dimitrijević & Sahal-Bréchot 1992), P v (Dimitrijević & Sahal-Bréchot 1995, 1996a), S v (Dimitrijević & Sahal-Bréchot 1997, 1998a), and V v (Dimitrijević & Sahal-Bréchot 1998b) spectral lines. But for other, as for Si v and Ne v, the needed atomic data set is not sufficiently complete. In a previous work, we calculate Stark broadening parameters of the quadruply ionized silicon (Ben Nessib et al. 2004).

Whenever the semiclassical method is not applicable, the modified semi-empirical method (Dimitrijević & Konjević 1980, 1981, 1987) is useful. This method was used for calculating the electron-impact widths of 88 multiplets of six ion species (C v, O v, F v, Ne v, Al v, and Si v) including nine multiplets of Ne v (Dimitrijević 1988).

Such data are of interest for the consideration of radiative transfer through subphotospheric layers (Seaton 1988), for modeling of some hot star atmospheres such as PG 1159 pre–white dwarfs with an effective temperature between 100,000 and 140,000 K (Werner & Heber 1991), as well as for fusion plasmas and laser-produced plasmas. The development of soft X-ray lasers, where Stark broadening data are needed to calculate gain values, to model radiation trapping, and to consider photoresonant pumping schemes (see, e.g., Fill & Schöning 1994; Griem & Moreno 1980), provided an additional interest in such results. The Low Energy Transmission Grating (LETG) on board the X-ray space observatory *Chandra* gives high-quality spectra in the wavelength region between 5 and 140 Å, and contains a series of lines that can provide density and temperature diagnostics for relatively hot and dense stellar plasmas objects. An analysis of X-ray spectrum of some stars with the high-resolution space observatory *Chandra* show spectra that can be rich in emission lines in the soft X-ray region.

The aim of this paper is to provide ab initio calculations of Stark broadening parameters due to electron, proton, and ionized helium impact of Ne v lines of astrophysical importance. Our results are compared with available experimental and theoretical data (Uzelac et al. 1993; Dimitrijević 1993). An outline of the theory is presented in § 2, and results are discussed in § 3.

2. THEORY

The energy levels and oscillator strengths were carried out with the general purpose atomic-structure program SUPERSTRUCTURE (Eissner et al. 1974), as modified by Nussbaumer & Storey (1978). The adopted atomic model for Ne v includes 17 configurations: $2s^22p^2$, $2s2p^3$, $2p^4$, $2s^22p3l$, $2s2p^23l$, $2s^22p4l$, $2s2p^24l$ ($l \leq n-1$). The wave functions are of configuration mixing type, and each configuration is expanded in terms of Slater states. The radial functions are calculated in scaled Thomas-Fermi

[1] Groupe de Recherche en Physique Atomique et Astrophysique, Institut National des Sciences Appliquées et de Technologie, Centre Urbain Nord B. P. No. 676, 1080 Tunis Cedex, Tunisia.
[2] Astronomical Observatory, Volgina 7, 11160 Belgrade 74, Serbia.
[3] Isaac Newton Institut of Chile, Yugoslavia Branch.
[4] Laboratoire d'Étude du Rayonnement et de la Matière en Astrophysique, UMR CNRS 8112, Observatoire de Paris-Meudon, 92195 Meudon, France.

TABLE 1

Electron Impact Broadening Parameters (FWHM-w and Shift-d) for Ne v Lines, for Perturber Density of 10^{17} cm^{-3}

Transition	T (K)	w_{SST} (Å)	d_{SST} (Å)	w_{BD} (Å)	d_{BD} (Å)
Ne v 2P–3S, 173.0 Å, C = 0.88E+18	50,000.0	0.992E−04	0.283E−05	0.935E−04	0.449E−05
	100,000.0	0.680E−04	0.559E−05	0.664E−04	0.610E−05
	150,000.0	0.570E−04	0.633E−05	0.557E−04	0.661E−05
	200,000.0	0.507E−04	0.678E−05	0.497E−04	0.709E−05
	300,000.0	0.435E−04	0.695E−05	0.427E−04	0.729E−05
	500,000.0	0.365E−04	0.667E−05	0.359E−04	0.701E−05
Ne v 2P–3D, 150.6 Å, C = 0.55E+18	50,000.0	0.874E−04	−0.283E−05	0.903E−04	−0.165E−05
	100,000.0	0.625E−04	−0.786E−06	0.653E−04	−0.101E−06
	150,000.0	0.521E−04	−0.459E−06	0.546E−04	0.133E−06
	200,000.0	0.460E−04	−0.708E−06	0.482E−04	−0.162E−06
	300,000.0	0.389E−04	−0.713E−06	0.409E−04	−0.103E−06
	500,000.0	0.320E−04	−0.414E−06	0.339E−04	0.325E−06
Ne v 2P-3D, 145.8 Å, C = 0.98E+18	50,000.0	0.974E−04	−0.272E−05	0.978E−04	−0.983E−06
	100,000.0	0.684E−04	−0.310E−06	0.701E−04	0.355E−06
	150,000.0	0.569E−04	0.369E−07	0.583E−04	0.478E−06
	200,000.0	0.503E−04	−0.312E−06	0.515E−04	0.943E−07
	300,000.0	0.426E−04	−0.174E−06	0.438E−04	0.319E−06
	500,000.0	0.353E−04	0.131E−06	0.364E−04	0.706E−06
Ne v 2P–3D, 145.7 Å, C = 0.67E+18	50,000.0	0.978E−04	−0.241E−05	0.968E−04	−0.940E−06
	100,000.0	0.692E−04	−0.271E−06	0.698E−04	0.289E−06
	150,000.0	0.578E−04	0.777E−07	0.582E−04	0.471E−06
	200,000.0	0.511E−04	−0.220E−06	0.515E−04	0.157E−06
	300,000.0	0.434E−04	−0.354E−07	0.438E−04	0.404E−06
	500,000.0	0.360E−04	0.265E−06	0.365E−04	0.760E−06
Ne v 2P–3S, 183.1 Å, C = 0.99E+18	50,000.0	0.116E−03	0.274E−05	0.105E−03	0.541E−05
	100,000.0	0.781E−04	0.609E−05	0.747E−04	0.693E−05
	150,000.0	0.654E−04	0.699E−05	0.627E−04	0.744E−05
	200,000.0	0.582E−04	0.750E−05	0.559E−04	0.798E−05
	300,000.0	0.499E−04	0.766E−05	0.481E−04	0.821E−05
	500,000.0	0.418E−04	0.735E−05	0.404E−04	0.790E−05
Ne v 2P–3D, 152.8 Å, C = 0.74E+18	50,000.0	0.110E−03	−0.298E−05	0.106E−03	−0.764E−06
	100,000.0	0.770E−04	−0.417E−06	0.765E−04	0.385E−06
	150,000.0	0.642E−04	0.201E−07	0.638E−04	0.541E−06
	200,000.0	0.567E−04	−0.309E−06	0.565E−04	0.200E−06
	300,000.0	0.482E−04	−0.124E−06	0.481E−04	0.475E−06
	500,000.0	0.399E−04	0.207E−06	0.400E−04	0.869E−06
Ne v 3S–3P, 3400.1 Å, C = 0.34E+21	50,000.0	0.806E−01	−0.169E−02	0.655E−01	−0.233E−03
	100,000.0	0.583E−01	−0.196E−02	0.473E−01	−0.269E−03
	150,000.0	0.491E−01	−0.219E−02	0.396E−01	−0.353E−03
	200,000.0	0.438E−01	−0.228E−02	0.352E−01	−0.319E−03
	300,000.0	0.376E−01	−0.224E−02	0.301E−01	−0.238E−03
	500,000.0	0.316E−01	−0.216E−02	0.252E−01	−0.212E−03
Ne v 3S–3P, 1620.9 Å, C = 0.64E+20	50,000.0	0.197E−01	−0.210E−03	0.162E−01	0.138E−03
	100,000.0	0.144E−01	−0.318E−03	0.118E−01	0.799E−04
	150,000.0	0.121E−01	−0.304E−03	0.990E−02	0.132E−03
	200,000.0	0.108E−01	−0.346E−03	0.882E−02	0.118E−03
	300,000.0	0.934E−02	−0.379E−03	0.758E−02	0.916E−04
	500,000.0	0.788E−02	−0.347E−03	0.636E−02	0.108E−03
Ne v 3P–3D, 1762.1 Å, C = 0.76E+20	50,000.0	0.204E−01	−0.182E−03	0.217E−01	−0.209E−03
	100,000.0	0.149E−01	−0.146E−03	0.158E−01	−0.103E−03
	150,000.0	0.125E−01	−0.123E−03	0.133E−01	−0.677E−04
	200,000.0	0.111E−01	−0.181E−03	0.119E−01	−0.139E−03
	300,000.0	0.950E−02	−0.212E−03	0.102E−01	−0.167E−03
	500,000.0	0.796E−02	−0.165E−03	0.854E−02	−0.100E−03
Ne v 3P–3D, 1264.5 Å, C = 0.47E+20	50,000.0	0.114E−01	−0.824E−04	0.119E−01	−0.636E−04
	100,000.0	0.831E−02	−0.412E−04	0.866E−02	−0.255E−04
	150,000.0	0.698E−02	−0.257E−04	0.728E−02	−0.955E−05
	200,000.0	0.621E−02	−0.603E−04	0.648E−02	−0.489E−04
	300,000.0	0.533E−02	−0.619E−04	0.557E−02	−0.486E−04
	500,000.0	0.448E−02	−0.362E−04	0.469E−02	−0.177E−04
Ne v 3P–3D, 2136.8 Å, C = 0.11E+21	50,000.0	0.347E−01	−0.538E−03	0.369E−01	−0.615E−03
	100,000.0	0.254E−01	−0.341E−03	0.271E−01	−0.464E−03
	150,000.0	0.214E−01	−0.412E−03	0.229E−01	−0.564E−03
	200,000.0	0.190E−01	−0.473E−03	0.204E−01	−0.576E−03
	300,000.0	0.164E−01	−0.405E−03	0.176E−01	−0.483E−03
	500,000.0	0.138E−01	−0.354E−03	0.148E−01	−0.427E−03

TABLE 1—*Continued*

Transition	T (K)	w_{SST} (Å)	d_{SST} (Å)	w_{BD} (Å)	d_{BD} (Å)
Ne v 3*P*–3*D*, 4087.1 Å, $C = 0.41E+21$	50,000.0	0.117	−0.209E−02	0.128	−0.271E−02
	100,000.0	0.861E−01	−0.160E−02	0.940E−01	−0.199E−02
	150,000.0	0.726E−01	−0.190E−02	0.794E−01	−0.233E−02
	200,000.0	0.647E−01	−0.207E−02	0.709E−01	−0.234E−02
	300,000.0	0.555E−01	−0.198E−02	0.610E−01	−0.216E−02
	500,000.0	0.467E−01	−0.181E−02	0.514E−01	−0.192E−02
Ne v 3*P*–3*D*, 2176.0 Å, $C = 0.12E+21$	50,000.0	0.357E−01	−0.633E−03	0.385E−01	−0.646E−03
	100,000.0	0.261E−01	−0.361E−03	0.281E−01	−0.467E−03
	150,000.0	0.220E−01	−0.435E−03	0.237E−01	−0.584E−03
	200,000.0	0.196E−01	−0.510E−03	0.211E−01	−0.611E−03
	300,000.0	0.168E−01	−0.450E−03	0.182E−01	−0.520E−03
	500,000.0	0.142E−01	−0.397E−03	0.154E−01	−0.455E−03
Ne v 3*P*–3*D*, 3158.2 Å, $C = 0.32E+21$	50,000.0	0.812E−01	−0.169E−02	0.961E−01	−0.255E−02
	100,000.0	0.595E−01	−0.130E−02	0.713E−01	−0.210E−02
	150,000.0	0.502E−01	−0.159E−02	0.604E−01	−0.244E−02
	200,000.0	0.448E−01	−0.172E−02	0.541E−01	−0.273E−02
	300,000.0	0.387E−01	−0.148E−02	0.468E−01	−0.248E−02
	500,000.0	0.327E−01	−0.138E−02	0.397E−01	−0.224E−02
Ne v 2*P*–3*S*, 166.2 Å, $C = 0.12E+19$	50,000.0	0.846E−04	0.227E−05	0.833E−04	0.448E−05
	100,000.0	0.581E−04	0.419E−05	0.595E−04	0.515E−05
	150,000.0	0.486E−04	0.510E−05	0.499E−04	0.584E−05
	200,000.0	0.433E−04	0.555E−05	0.444E−04	0.636E−05
	300,000.0	0.370E−04	0.560E−05	0.382E−04	0.645E−05
	500,000.0	0.309E−04	0.536E−05	0.320E−04	0.621E−05
Ne v 2*P*–3*D*, 141.9 Å, $C = 0.99E+18$	50,000.0	0.796E−04	−0.213E−05	0.833E−04	−0.633E−06
	100,000.0	0.564E−04	−0.271E−06	0.598E−04	0.369E−06
	150,000.0	0.468E−04	0.222E−07	0.497E−04	0.467E−06
	200,000.0	0.412E−04	−0.260E−06	0.439E−04	0.117E−06
	300,000.0	0.348E−04	−0.215E−06	0.372E−04	0.238E−06
	500,000.0	0.286E−04	0.460E−07	0.308E−04	0.619E−06
Ne v 2*P*–3*D*, 141.2 Å, $C = 0.11E+19$	50,000.0	0.873E−04	−0.283E−05	0.817E−04	−0.622E−06
	100,000.0	0.634E−04	−0.113E−05	0.591E−04	0.347E−06
	150,000.0	0.531E−04	−0.825E−06	0.493E−04	0.467E−06
	200,000.0	0.471E−04	−0.124E−05	0.435E−04	0.104E−06
	300,000.0	0.400E−04	−0.130E−05	0.369E−04	0.207E−06
	500,000.0	0.332E−04	−0.948E−06	0.306E−04	0.588E−06
Ne v 3*S*–3*P*, 2260.6 Å, $C = 0.23E+21$	50,000.0	0.353E−01	−0.594E−03	0.296E−01	−0.270E−04
	100,000.0	0.255E−01	−0.580E−03	0.214E−01	−0.269E−05
	150,000.0	0.215E−01	−0.656E−03	0.179E−01	−0.167E−04
	200,000.0	0.191E−01	−0.711E−03	0.159E−01	−0.854E−05
	300,000.0	0.164E−01	−0.706E−03	0.136E−01	0.165E−04
	500,000.0	0.138E−01	−0.673E−03	0.114E−01	0.261E−04
Ne v 3*S*–3*P*, 1947.6 Å, $C = 0.17E+21$	50,000.0	0.265E−01	−0.379E−03	0.222E−01	0.122E−04
	100,000.0	0.192E−01	−0.365E−03	0.160E−01	0.349E−04
	150,000.0	0.161E−01	−0.420E−03	0.134E−01	0.243E−04
	200,000.0	0.144E−01	−0.457E−03	0.119E−01	0.298E−04
	300,000.0	0.123E−01	−0.452E−03	0.102E−01	0.470E−04
	500,000.0	0.104E−01	−0.430E−03	0.852E−02	0.558E−04
Ne v 3*S*–3*P*, 1856.0 Å, $C = 0.15E+21$	50,000.0	0.233E−01	−0.421E−03	0.204E−01	0.355E−04
	100,000.0	0.169E−01	−0.419E−03	0.148E−01	0.429E−04
	150,000.0	0.142E−01	−0.457E−03	0.124E−01	0.549E−04
	200,000.0	0.126E−01	−0.510E−03	0.110E−01	0.528E−04
	300,000.0	0.108E−01	−0.523E−03	0.942E−02	0.561E−04
	500,000.0	0.907E−02	−0.487E−03	0.787E−02	0.700E−04
Ne v 3*P*–3*D*, 1941.0 Å, $C = 0.17E+21$	50,000.0	0.252E−01	−0.304E−03	0.268E−01	−0.225E−03
	100,000.0	0.182E−01	−0.278E−03	0.194E−01	−0.163E−03
	150,000.0	0.153E−01	−0.304E−03	0.162E−01	−0.181E−03
	200,000.0	0.135E−01	−0.375E−03	0.144E−01	−0.267E−03
	300,000.0	0.116E−01	−0.390E−03	0.123E−01	−0.270E−03
	500,000.0	0.968E−02	−0.340E−03	0.103E−01	−0.195E−03
Ne v 3*P*–3*D*, 1697.1 Å, $C = 0.13E+21$	50,000.0	0.193E−01	−0.175E−03	0.207E−01	−0.168E−03
	100,000.0	0.140E−01	−0.140E−03	0.150E−01	−0.112E−03
	150,000.0	0.117E−01	−0.154E−03	0.126E−01	−0.126E−03
	200,000.0	0.104E−01	−0.212E−03	0.112E−01	−0.197E−03
	300,000.0	0.892E−02	−0.214E−03	0.958E−02	−0.193E−03
	500,000.0	0.747E−02	−0.171E−03	0.805E−02	−0.136E−03

TABLE 1—*Continued*

Transition	T (K)	w_{SST} (Å)	d_{SST} (Å)	w_{BD} (Å)	d_{BD} (Å)
Ne v $3P$–$3D$, 1599.7 Å, $C = 0.11$E+21.....	50,000.0	0.183E−01	−0.244E−03	0.183E−01	−0.148E−03
	100,000.0	0.134E−01	−0.235E−03	0.133E−01	−0.101E−03
	150,000.0	0.113E−01	−0.246E−03	0.112E−01	−0.111E−03
	200,000.0	0.101E−01	−0.314E−03	0.993E−02	−0.176E−03
	300,000.0	0.863E−02	−0.329E−03	0.851E−02	−0.175E−03
	500,000.0	0.725E−02	−0.280E−03	0.715E−02	−0.124E−03
Ne v $3P$–$3D$, 1805.0 Å, $C = 0.17$E+21.....	50,000.0	0.235E−01	−0.364E−03	0.234E−01	−0.216E−03
	100,000.0	0.172E−01	−0.355E−03	0.170E−01	−0.160E−03
	150,000.0	0.145E−01	−0.371E−03	0.143E−01	−0.173E−03
	200,000.0	0.129E−01	−0.462E−03	0.127E−01	−0.255E−03
	300,000.0	0.111E−01	−0.481E−03	0.109E−01	−0.252E−03
	500,000.0	0.934E−02	−0.417E−03	0.916E−02	−0.189E−03
Ne v $3P$–$3D$, 2029.1 Å, $C = 0.20$E+21.....	50,000.0	0.269E−01	−0.228E−03	0.301E−01	−0.305E−03
	100,000.0	0.195E−01	−0.168E−03	0.218E−01	−0.213E−03
	150,000.0	0.163E−01	−0.204E−03	0.183E−01	−0.259E−03
	200,000.0	0.145E−01	−0.266E−03	0.163E−01	−0.352E−03
	300,000.0	0.124E−01	−0.251E−03	0.139E−01	−0.329E−03
	500,000.0	0.104E−01	−0.206E−03	0.117E−01	−0.257E−03
Ne v $3P$–$3D$, 1891.4 Å, $C = 0.18$E+21.....	50,000.0	0.249E−01	−0.321E−03	0.260E−01	−0.263E−03
	100,000.0	0.183E−01	−0.300E−03	0.189E−01	−0.188E−03
	150,000.0	0.154E−01	−0.329E−03	0.159E−01	−0.224E−03
	200,000.0	0.137E−01	−0.408E−03	0.141E−01	−0.307E−03
	300,000.0	0.118E−01	−0.412E−03	0.121E−01	−0.291E−03
	500,000.0	0.988E−02	−0.357E−03	0.102E−01	−0.228E−03

NOTES.—Transitions and averaged wavelength for the multiplet (in Å) are also given. We can consider line as isolated up to perturber density equal to C/w (Dimitrijević & Sahal-Bréchot 1984). SST denotes results obtained using SUPERSTRUCTURE, and BD denotes Bates and Damgaard oscillator strengths.

statistical model potential, which depends on parameters λ_{nl} determined variationally by optimizing the weighted sum of energy terms. Relativistic corrections are introduced by means of Breit-Pauli approximation in intermediate coupling. In particular spin-orbit, spin-spin, and spin-other-orbit interactions are included. The main input data of this code are the charge of the ion and the configurations to be used in the model. We have calculated mean radii and mean square radii within the hydrogenic approximation with a quantum defect, using the effective quantum numbers n_i^* obtained from the Ritz formula.

Stark broadening parameter calculations have been performed within the semiclassical perturbation method (Sahal-Bréchot 1969a, 1969b). A detailed description of this formalism with all the innovations is given in Sahal-Bréchot (1969a, 1969b, 1974, 1991), Fleurier et al. (1977), Dimitrijević et al. (1991), and Dimitrijević & Sahal-Bréchot (1996b). The full half-width (w) and shift (d) of an electron-impact broadened spectral line can be expressed as

$$W = N \int v f(v)\, dv \left[\sum_{i' \neq i} \sigma_{ii'}(v) + \sum_{f' \neq f} \sigma_{ff'}(v) + \sigma_{el} \right] + W_R,$$

$$d = N \int v f(v)\, dv \int_{R_3}^{R_D} 2\pi\rho\, d\rho \sin(2\varphi_p), \qquad (1)$$

where N is the electron density; $f(v)$ the Maxwellian velocity distribution function for electrons; ρ denotes the impact parameters of the incoming electron; i and f denote the initial and the final atomic energy levels, and i' and f' their corresponding perturbing levels; while W_R gives the contribution of the Feshbach resonances (Fleurier et al. 1977). The inelastic cross section $\sigma_{ii'}(v)$ can be expressed by an integral over the impact parameter of the transition probability $P_{jj'}(\rho, v)$ as

$$\sum_{j \neq j'} \sigma_{ii'}(v) = \frac{1}{2}\pi R_1^2 + \int_{R_1}^{R_D} 2\pi\rho\, d\rho \sum_{j=j'} P_{jj'}(\rho,\ v); \quad j = i,\ f, \qquad (2)$$

and the elastic cross section is given by

$$\sigma_{el} = 2\pi R_2^2 + \int_{R_2}^{R_D} 2\pi\rho\, d\rho \sin^2\delta,$$

$$\delta = \left(\varphi_p^2 + \varphi_q^2\right)^{1/2}. \qquad (3)$$

The phase shifts φ_p and φ_q due, respectively, to the polarization potential (r^{-4}) and to the quadrupolar potential (r^{-3}), are given in § 3 of chapter 2 in Sahal-Bréchot (1969a) and R_D is the Debye radius. All the cut-offs R_1, R_2, R_3 are described in § 1 of chapter 3 in Sahal-Bréchot (1969b).

For electrons, hyperbolic paths due to the attractive Coulomb force were used, while for perturbing ions the hyperbolic paths are different, since the force is repulsive. The formulae for the ion-impact widths and shifts are analogous to equations (1)–(3), without the resonance contribution to the width.

The results obtained within the semiclassical perturbation approach (Sahal-Bréchot 1969a, 1969b) have been compared with critically selected experimental data for 13 He I multiplets (Dimitrijević & Sahal-Bréchot 1985), and it was found that the agreement between experimental data and semiclassical

TABLE 2

Impact Broadening Parameters (FWHM-w and Shift-d) for Ne v Lines

Transition	T (K)	w_{H^+} (Å)	d_{H^+} (Å)	w_{He^+} (Å)	d_{He^+} (Å)	$w_{He^{++}}$ (Å)	$d_{He^{++}}$ (Å)
Ne v $2P$–$3S$, 173.0 Å, $C = 0.88$E+18	50,000.0	0.441E−06	0.270E−05	0.633E−06	0.261E−05	0.843E−06	0.527E−05
	100,000.0	0.179E−05	0.469E−05	0.215E−05	0.432E−05	0.354E−05	0.937E−05
	150,000.0	0.340E−05	0.601E−05	0.327E−05	0.521E−05	0.672E−05	0.122E−04
	200,000.0	0.426E−05	0.684E−05	0.419E−05	0.600E−05	0.859E−05	0.138E−04
	300,000.0	0.619E−05	0.826E−05	0.599E−05	0.696E−05	0.124E−04	0.168E−04
	500,000.0	0.867E−05	0.952E−05	0.752E−05	0.792E−05	0.174E−04	0.194E−04
Ne v $2P$–$3D$, 150.6 Å, $C = 0.55$E+18	50,000.0	0.119E−05	−0.481E−06	0.193E−05	−0.478E−06	0.225E−05	−0.937E−06
	100,000.0	0.255E−05	−0.931E−06	0.353E−05	−0.895E−06	0.490E−05	−0.186E−05
	150,000.0	0.355E−05	−0.129E−05	0.438E−05	−0.120E−05	0.689E−05	−0.260E−05
	200,000.0	0.417E−05	−0.158E−05	0.510E−05	−0.143E−05	0.817E−05	−0.318E−05
	300,000.0	0.518E−05	−0.196E−05	0.584E−05	−0.173E−05	0.101E−04	−0.397E−05
	500,000.0	0.614E−05	−0.250E−05	0.647E−05	−0.213E−05	0.121E−04	−0.508E−05
Ne v $2P$–$3D$, 145.8 Å, $C = 0.98$E+18	50,000.0	0.151E−05	−0.323E−06	0.240E−05	−0.322E−06	0.287E−05	−0.629E−06
	100,000.0	0.309E−05	−0.634E−06	0.418E−05	−0.615E−06	0.595E−05	−0.126E−05
	150,000.0	0.417E−05	−0.897E−06	0.513E−05	−0.834E−06	0.813E−05	−0.180E−05
	200,000.0	0.482E−05	−0.110E−05	0.588E−05	−0.102E−05	0.943E−05	−0.222E−05
	300,000.0	0.589E−05	−0.142E−05	0.655E−05	−0.123E−05	0.116E−04	−0.288E−05
	500,000.0	0.671E−05	−0.180E−05	0.720E−05	−0.156E−05	0.133E−04	−0.366E−05
Ne v $2P$–$3D$, 145.7 Å, $C = 0.67$E+18	50,000.0	0.153E−05	−0.395E−06	0.242E−05	−0.393E−06	0.290E−05	−0.770E−06
	100,000.0	0.312E−05	−0.769E−06	0.421E−05	−0.742E−06	0.602E−05	−0.153E−05
	150,000.0	0.421E−05	−0.107E−05	0.517E−05	−0.996E−06	0.822E−05	−0.216E−05
	200,000.0	0.487E−05	−0.132E−05	0.593E−05	−0.120E−05	0.953E−05	−0.265E−05
	300,000.0	0.596E−05	−0.166E−05	0.661E−05	−0.145E−05	0.117E−04	−0.337E−05
	500,000.0	0.681E−05	−0.211E−05	0.726E−05	−0.181E−05	0.135E−04	−0.427E−05
Ne v $2P$–$3S$, 183.1 Å, $C = 0.99$E+18	50,000.0	0.497E−06	0.301E−05	0.716E−06	0.291E−05	0.950E−06	0.588E−05
	100,000.0	0.201E−05	0.524E−05	0.242E−05	0.482E−05	0.397E−05	0.105E−04
	150,000.0	0.381E−05	0.671E−05	0.367E−05	0.582E−05	0.753E−05	0.136E−04
	200,000.0	0.477E−05	0.764E−05	0.470E−05	0.671E−05	0.962E−05	0.154E−04
	300,000.0	0.693E−05	0.923E−05	0.671E−05	0.778E−05	0.139E−04	0.188E−04
	500,000.0	0.971E−05	0.106E−04	0.843E−05	0.886E−05	0.195E−04	0.217E−04
Ne v $2P$–$3D$, 152.8 Å, $C = 0.74$E+18	50,000.0	0.169E−05	−0.441E−06	0.268E−05	−0.439E−06	0.321E−05	−0.860E−06
	100,000.0	0.345E−05	−0.860E−06	0.465E−05	−0.829E−06	0.665E−05	−0.171E−05
	150,000.0	0.465E−05	−0.120E−05	0.571E−05	−0.111E−05	0.908E−05	−0.241E−05
	200,000.0	0.537E−05	−0.147E−05	0.655E−05	−0.134E−05	0.105E−04	−0.296E−05
	300,000.0	0.658E−05	−0.184E−05	0.729E−05	−0.162E−05	0.129E−04	−0.375E−05
	500,000.0	0.752E−05	−0.235E−05	0.801E−05	−0.202E−05	0.149E−04	−0.476E−05
Ne v $3S$–$3P$, 3400.1 Å, $C = 0.34$E+21	50,000.0	0.976E−03	−0.109E−02	0.148E−02	−0.106E−02	0.186E−02	−0.214E−02
	100,000.0	0.210E−02	−0.190E−02	0.262E−02	−0.174E−02	0.406E−02	−0.379E−02
	150,000.0	0.284E−02	−0.241E−02	0.331E−02	−0.210E−02	0.562E−02	−0.490E−02
	200,000.0	0.342E−02	−0.275E−02	0.383E−02	−0.242E−02	0.671E−02	−0.557E−02
	300,000.0	0.431E−02	−0.332E−02	0.430E−02	−0.278E−02	0.854E−02	−0.673E−02
	500,000.0	0.513E−02	−0.383E−02	0.493E−02	−0.318E−02	0.102E−01	−0.778E−02
Ne v $3S$–$3P$, 1620.9 Å, $C = 0.64$E+20	50,000.0	0.281E−03	−0.127E−03	0.428E−03	−0.125E−03	0.535E−03	−0.248E−03
	100,000.0	0.550E−03	−0.234E−03	0.702E−03	−0.217E−03	0.106E−02	−0.469E−03
	150,000.0	0.712E−03	−0.312E−03	0.868E−03	−0.279E−03	0.140E−02	−0.630E−03
	200,000.0	0.831E−03	−0.364E−03	0.974E−03	−0.317E−03	0.163E−02	−0.739E−03
	300,000.0	0.100E−02	−0.442E−03	0.106E−02	−0.383E−03	0.198E−02	−0.897E−03
	500,000.0	0.114E−02	−0.535E−03	0.117E−02	−0.443E−03	0.224E−02	−0.109E−02
Ne v $3P$–$3D$, 1762.1 Å, $C = 0.76$E+20	50,000.0	0.407E−03	−0.509E−04	0.610E−03	−0.507E−04	0.774E−03	−0.992E−04
	100,000.0	0.762E−03	−0.997E−04	0.965E−03	−0.964E−04	0.147E−02	−0.198E−03
	150,000.0	0.961E−03	−0.140E−03	0.118E−02	−0.130E−03	0.188E−02	−0.282E−03
	200,000.0	0.112E−02	−0.172E−03	0.130E−02	−0.158E−03	0.218E−02	−0.346E−03
	300,000.0	0.131E−02	−0.220E−03	0.140E−02	−0.191E−03	0.258E−02	−0.446E−03
	500,000.0	0.145E−02	−0.279E−03	0.154E−02	−0.242E−03	0.285E−02	−0.567E−03
Ne v $3P$–$3D$, 1264.5 Å, $C = 0.47$E+20	50,000.0	0.241E−03	−0.220E−04	0.356E−03	−0.220E−04	0.458E−03	−0.429E−04
	100,000.0	0.442E−03	−0.434E−04	0.553E−03	−0.422E−04	0.856E−03	−0.864E−04
	150,000.0	0.550E−03	−0.617E−04	0.674E−03	−0.576E−04	0.108E−02	−0.124E−03
	200,000.0	0.639E−03	−0.759E−04	0.735E−03	−0.705E−04	0.125E−02	−0.153E−03
	300,000.0	0.735E−03	−0.987E−04	0.792E−03	−0.855E−04	0.145E−02	−0.200E−03
	500,000.0	0.815E−03	−0.126E−03	0.864E−03	−0.109E−03	0.160E−02	−0.255E−03
Ne v $3P$–$3D$, 2136.8 Å, $C = 0.11$E+21	50,000.0	0.831E−03	−0.281E−03	0.120E−02	−0.274E−03	0.159E−02	−0.548E−03
	100,000.0	0.150E−02	−0.505E−03	0.183E−02	−0.470E−03	0.291E−02	−0.101E−02
	150,000.0	0.185E−02	−0.666E−03	0.222E−02	−0.584E−03	0.361E−02	−0.135E−02
	200,000.0	0.215E−02	−0.762E−03	0.240E−02	−0.674E−03	0.422E−02	−0.155E−02
	300,000.0	0.244E−02	−0.927E−03	0.260E−02	−0.801E−03	0.485E−02	−0.188E−02
	500,000.0	0.272E−02	−0.110E−02	0.284E−02	−0.921E−03	0.539E−02	−0.224E−02

TABLE 2—*Continued*

Transition	T (K)	w_{H^+} (Å)	d_{H^+} (Å)	w_{He^+} (Å)	d_{He^+} (Å)	$w_{He^{++}}$ (Å)	$d_{He^{++}}$ (Å)
Ne v 3*P*–3*D*, 4087.1 Å, $C = 0.41$E+21	50,000.0	0.273E−02	−0.107E−02	0.398E−02	−0.104E−02	0.520E−02	−0.209E−02
	100,000.0	0.501E−02	−0.192E−02	0.616E−02	−0.178E−02	0.975E−02	−0.383E−02
	150,000.0	0.622E−02	−0.252E−02	0.751E−02	−0.220E−02	0.122E−01	−0.510E−02
	200,000.0	0.728E−02	−0.288E−02	0.818E−02	−0.255E−02	0.143E−01	−0.584E−02
	300,000.0	0.839E−02	−0.351E−02	0.887E−02	−0.302E−02	0.166E−01	−0.710E−02
	500,000.0	0.941E−02	−0.413E−02	0.972E−02	−0.346E−02	0.186E−01	−0.843E−02
Ne v 3*P*-3*D*, 2176.0 Å, $C = 0.12$E+21	50,000.0	0.856E−03	−0.276E−03	0.124E−02	−0.269E−03	0.164E−02	−0.538E−03
	100,000.0	0.154E−02	−0.499E−03	0.189E−02	−0.463E−03	0.300E−02	−0.997E−03
	150,000.0	0.190E−02	−0.660E−03	0.229E−02	−0.580E−03	0.373E−02	−0.133E−02
	200,000.0	0.221E−02	−0.757E−03	0.247E−02	−0.668E−03	0.435E−02	−0.154E−02
	300,000.0	0.252E−02	−0.920E−03	0.268E−02	−0.798E−03	0.500E−02	−0.187E−02
	500,000.0	0.280E−02	−0.109E−02	0.293E−02	−0.915E−03	0.555E−02	−0.224E−02
Ne v 3*P*–3*D*, 3158.2 Å, $C = 0.32$E+21	50,000.0	0.203E−02	−0.972E−03	0.290E−02	−0.938E−03	0.389E−02	−0.190E−02
	100,000.0	0.362E−02	−0.168E−02	0.439E−02	−0.154E−02	0.707E−02	−0.336E−02
	150,000.0	0.449E−02	−0.213E−02	0.530E−02	−0.186E−02	0.879E−02	−0.433E−02
	200,000.0	0.520E−02	−0.244E−02	0.568E−02	−0.214E−02	0.102E−01	−0.493E−02
	300,000.0	0.589E−02	−0.293E−02	0.618E−02	−0.245E−02	0.117E−01	−0.595E−02
	500,000.0	0.663E−02	−0.337E−02	0.678E−02	−0.281E−02	0.132E−01	−0.686E−02
Ne v 2*P*–3*S*, 166.2 Å, $C = 0.12$E+19	50,000.0	0.322E−06	0.217E−05	0.473E−06	0.211E−05	0.615E−06	0.424E−05
	100,000.0	0.141E−05	0.382E−05	0.166E−05	0.354E−05	0.278E−05	0.764E−05
	150,000.0	0.266E−05	0.496E−05	0.268E−05	0.429E−05	0.525E−05	0.100E−04
	200,000.0	0.348E−05	0.562E−05	0.342E−05	0.496E−05	0.704E−05	0.114E−04
	300,000.0	0.499E−05	0.686E−05	0.488E−05	0.582E−05	0.994E−05	0.139E−04
	500,000.0	0.713E−05	0.793E−05	0.629E−05	0.663E−05	0.145E−04	0.162E−04
Ne v 2*P*–3*D*, 141.9 Å, $C = 0.99$E+18	50,000.0	0.116E−05	−0.224E−06	0.188E−05	−0.223E−06	0.220E−05	−0.436E−06
	100,000.0	0.244E−05	−0.444E−06	0.337E−05	−0.433E−06	0.470E−05	−0.883E−06
	150,000.0	0.336E−05	−0.636E−06	0.416E−05	−0.600E−06	0.652E−05	−0.128E−05
	200,000.0	0.391E−05	−0.791E−06	0.482E−05	−0.735E−06	0.767E−05	−0.159E−05
	300,000.0	0.481E−05	−0.104E−05	0.546E−05	−0.913E−06	0.944E−05	−0.211E−05
	500,000.0	0.558E−05	−0.134E−05	0.601E−05	−0.117E−05	0.111E−04	−0.270E−05
Ne v 2*P*–3*D*, 141.2 Å, $C = 0.11$E+19	50,000.0	0.123E−05	−0.552E−06	0.196E−05	−0.547E−06	0.232E−05	−0.108E−05
	100,000.0	0.258E−05	−0.106E−05	0.352E−05	−0.100E−05	0.497E−05	−0.211E−05
	150,000.0	0.355E−05	−0.144E−05	0.434E−05	−0.133E−05	0.693E−05	−0.289E−05
	200,000.0	0.413E−05	−0.175E−05	0.503E−05	−0.154E−05	0.812E−05	−0.354E−05
	300,000.0	0.512E−05	−0.212E−05	0.569E−05	−0.188E−05	0.101E−04	−0.429E−05
	500,000.0	0.596E−05	−0.270E−05	0.629E−05	−0.226E−05	0.119E−04	−0.548E−05
Ne v 3*S*–3*P*, 2260.6 Å, $C = 0.23$E+21	50,000.0	0.426E−03	−0.307E−03	0.659E−03	−0.300E−03	0.809E−03	−0.599E−03
	100,000.0	0.875E−03	−0.554E−03	0.114E−02	−0.515E−03	0.169E−02	−0.111E−02
	150,000.0	0.118E−02	−0.731E−03	0.141E−02	−0.641E−03	0.232E−02	−0.148E−02
	200,000.0	0.138E−02	−0.837E−03	0.162E−02	−0.740E−03	0.270E−02	−0.170E−02
	300,000.0	0.172E−02	−0.102E−02	0.180E−02	−0.882E−03	0.340E−02	−0.206E−02
	500,000.0	0.198E−02	−0.121E−02	0.202E−02	−0.101E−02	0.394E−02	−0.247E−02
Ne v 3*S*–3*P*, 1947.6 Å, $C = 0.17$E+21	50,000.0	0.335E−03	−0.198E−03	0.517E−03	−0.194E−03	0.636E−03	−0.386E−03
	100,000.0	0.676E−03	−0.362E−03	0.879E−03	−0.335E−03	0.131E−02	−0.723E−03
	150,000.0	0.901E−03	−0.481E−03	0.109E−02	−0.426E−03	0.177E−02	−0.970E−03
	200,000.0	0.105E−02	−0.556E−03	0.124E−02	−0.487E−03	0.206E−02	−0.113E−02
	300,000.0	0.129E−02	−0.676E−03	0.137E−02	−0.586E−03	0.256E−02	−0.137E−02
	500,000.0	0.148E−02	−0.812E−03	0.153E−02	−0.676E−03	0.294E−02	−0.166E−02
Ne v 3*S*–3*P*, 1856.0 Å, $C = 0.15$E+21	50,000.0	0.315E−03	−0.207E−03	0.483E−03	−0.202E−03	0.598E−03	−0.403E−03
	100,000.0	0.636E−03	−0.373E−03	0.819E−03	−0.347E−03	0.123E−02	−0.746E−03
	150,000.0	0.847E−03	−0.492E−03	0.102E−02	−0.432E−03	0.166E−02	−0.996E−03
	200,000.0	0.990E−03	−0.564E−03	0.116E−02	−0.498E−03	0.194E−02	−0.114E−02
	300,000.0	0.122E−02	−0.686E−03	0.128E−02	−0.594E−03	0.242E−02	−0.139E−02
	500,000.0	0.140E−02	−0.814E−03	0.143E−02	−0.681E−03	0.278E−02	−0.166E−02
Ne v 3*P*–3*D*, 1941.0 Å, $C = 0.17$E+21	50,000.0	0.514E−03	−0.143E−03	0.766E−03	−0.141E−03	0.978E−03	−0.280E−03
	100,000.0	0.963E−03	−0.270E−03	0.121E−02	−0.251E−03	0.186E−02	−0.538E−03
	150,000.0	0.121E−02	−0.361E−03	0.148E−02	−0.328E−03	0.237E−02	−0.726E−03
	200,000.0	0.141E−02	−0.431E−03	0.163E−02	−0.373E−03	0.276E−02	−0.872E−03
	300,000.0	0.165E−02	−0.521E−03	0.176E−02	−0.457E−03	0.326E−02	−0.105E−02
	500,000.0	0.183E−02	−0.646E−03	0.193E−02	−0.532E−03	0.363E−02	−0.132E−02
Ne v 3*P*–3*D*, 1697.1 Å, $C = 0.13$E+21	50,000.0	0.408E−03	−0.878E−04	0.607E−03	−0.869E−04	0.777E−03	−0.171E−03
	100,000.0	0.758E−03	−0.167E−03	0.951E−03	−0.158E−03	0.147E−02	−0.333E−03
	150,000.0	0.950E−03	−0.226E−03	0.116E−02	−0.209E−03	0.186E−02	−0.455E−03
	200,000.0	0.111E−02	−0.274E−03	0.128E−02	−0.240E−03	0.216E−02	−0.555E−03
	300,000.0	0.128E−02	−0.331E−03	0.138E−02	−0.292E−03	0.254E−02	−0.670E−03
	500,000.0	0.142E−02	−0.420E−03	0.150E−02	−0.349E−03	0.281E−02	−0.853E−03

TABLE 2—*Continued*

Transition	T (K)	w_{H^+} (Å)	d_{H^+} (Å)	w_{He^+} (Å)	d_{He^+} (Å)	$w_{He^{++}}$ (Å)	$d_{He^{++}}$ (Å)
Ne v $3P$–$3D$, 1599.7 Å, C = 0.11E+21.....	50,000.0	0.373E−03	−0.120E−03	0.551E−03	−0.118E−03	0.710E−03	−0.234E−03
	100,000.0	0.694E−03	−0.221E−03	0.863E−03	−0.205E−03	0.134E−02	−0.442E−03
	150,000.0	0.867E−03	−0.295E−03	0.106E−02	−0.264E−03	0.170E−02	−0.595E−03
	200,000.0	0.101E−02	−0.345E−03	0.116E−02	−0.300E−03	0.199E−02	−0.701E−03
	300,000.0	0.117E−02	−0.419E−03	0.125E−02	−0.364E−03	0.233E−02	−0.850E−03
	500,000.0	0.131E−02	−0.509E−03	0.137E−02	−0.420E−03	0.260E−02	−0.104E−02
Ne v $3P$–$3D$, 1805.0 Å, C = 0.17E+21.....	50,000.0	0.496E−03	−0.179E−03	0.729E−03	−0.175E−03	0.945E−03	−0.349E−03
	100,000.0	0.919E−03	−0.325E−03	0.114E−02	−0.302E−03	0.178E−02	−0.650E−03
	150,000.0	0.115E−02	−0.432E−03	0.139E−02	−0.381E−03	0.225E−02	−0.872E−03
	200,000.0	0.134E−02	−0.497E−03	0.152E−02	−0.437E−03	0.263E−02	−0.101E−02
	300,000.0	0.155E−02	−0.604E−03	0.165E−02	−0.524E−03	0.307E−02	−0.123E−02
	500,000.0	0.172E−02	−0.724E−03	0.180E−02	−0.603E−03	0.344E−02	−0.148E−02
Ne v $3P$–$3D$, 2029.1 Å, C = 0.20E+21.....	50,000.0	0.617E−03	−0.126E−03	0.912E−03	−0.125E−03	0.118E−02	−0.246E−03
	100,000.0	0.114E−02	−0.240E−03	0.142E−02	−0.226E−03	0.220E−02	−0.478E−03
	150,000.0	0.142E−02	−0.324E−03	0.173E−02	−0.300E−03	0.278E−02	−0.652E−03
	200,000.0	0.165E−02	−0.393E−03	0.189E−02	−0.344E−03	0.323E−02	−0.795E−03
	300,000.0	0.190E−02	−0.474E−03	0.204E−02	−0.418E−03	0.377E−02	−0.960E−03
	500,000.0	0.210E−02	−0.601E−03	0.223E−02	−0.499E−03	0.417E−02	−0.122E−02
Ne v $3P$–$3D$, 1891.4 Å, C = 0.18E+21.....	50,000.0	0.550E−03	−0.168E−03	0.810E−03	−0.165E−03	0.105E−02	−0.327E−03
	100,000.0	0.101E−02	−0.310E−03	0.126E−02	−0.288E−03	0.197E−02	−0.620E−03
	150,000.0	0.126E−02	−0.414E−03	0.154E−02	−0.370E−03	0.248E−02	−0.833E−03
	200,000.0	0.147E−02	−0.483E−03	0.168E−02	−0.420E−03	0.289E−02	−0.982E−03
	300,000.0	0.170E−02	−0.587E−03	0.181E−02	−0.510E−03	0.337E−02	−0.119E−02
	500,000.0	0.189E−02	−0.712E−03	0.198E−02	−0.589E−03	0.375E−02	−0.145E−02

NOTES.—Proton- (H^+), singly and doubly charged helium- (He^+, He^{++}) impact broadening parameters (FWHM-w and shift-d) for Ne v lines calculated using SUPERSTRUCTURE oscillator strengths, for a perturber density of 10^{17} cm^{-3}. Transitions and averaged wavelength for the multiplet (in Å) are also given. We can consider line as isolated up to perturber density equal to C/w (Dimitrijević & Sahal-Bréchot 1984).

calculations is within ±20%, which is within the limits of predicted accuracy of the semiclassical method (Griem 1974).

3. RESULTS AND DISCUSSION

By combining the SUPERSTRUCTURE code for calculating energy levels and oscillator strengths and the code for the Stark broadening calculations, we calculated Stark broadening parameters ab initio. Calculated Stark broadening widths (FWHMs) and shifts for a perturber density of 10^{17} cm^{-3} and temperatures from 50,000 up to 500,000 K are shown in Table 1 for electron-impact broadening and in Table 2 for broadening by proton and singly and doubly charged helium ion collisions.

In order to check the error introduced by Bates & Damgaard (1949) method for oscillator strengths, often used when more reliable data are not available, we have also calculated oscillator strengths using the Coulomb approximation. Obtained results are used for Stark broadening parameter calculations. The obtained parameters are compared in Table 1 with present results for which oscillator strengths from SUPERSTRUCTURE code are used. We can see that the difference is tolerable.

We also specify a parameter C (Dimitrijević & Sahal-Bréchot 1984), which gives an estimate for the maximal perturber density for which the line may be treated as isolated, when it is divided by the corresponding FWHM. For each value given in Table 1 the collision volume V multiplied by the perturber density N is

TABLE 3

PRESENT RESULTS FOR STARK BROADENING FULL WIDTH AT HALF-INTENSITY MAXIMUM (W_{SC}) COMPARED WITH VALUES FROM UZELAC ET AL. (1993)

Transition	W_m (Å)	W_m/W_G	W_m/W_{DK}	W_m/W_{HB}	W_m/W_{SC}
$3s\,^3P^o - 3p\,^3D$, 2265.7 Å.....	0.64	1.28	1.71	1.32	1.16

NOTES.—W_m: experimental Stark width. W_G: Stark width calculated using approximate semiclassical method (Griem 1974, eq. [526]). W_{DK}: Stark width calculated using modified semiempirical formula (Dimitrijević & Konjević 1980). W_{HB}: Stark width calculated using classical-path approximation of Hey and Breger (Hey & Breger 1980). The electron density is 2.85×10^{18} cm^{-3}. The temperature is 298,000 K.

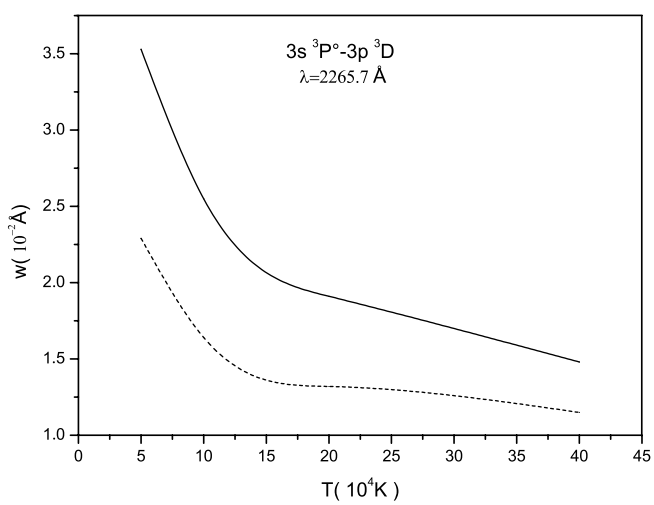

FIG. 1.—FWHM for the $3s^3P^o$–$3p\,^3D$ multiplet (λ = 2265.7 Å) as a function of electron temperature for the density $N = 10^{17}$ cm^{-3}. The solid line denotes our calculations with the semiclassical perturbation method (Sahal-Bréchot 1969a, 1969b); the dashed line denotes results of Dimitrijević (1993) obtained by the modified semiempirical approach (Dimitrijević & Konjević 1980).

much less than one, and the impact approximation is valid (Sahal-Bréchot 1969a, 1969b). When the impact approximation is not valid, the ion broadening contribution may be estimated by using the quasistatic approach (Griem 1974; Sahal-Bréchot 1991). In the region where neither approximation is valid, a unified-type theory should be used. For example, in Barnard et al. (1974) a simple analytical formula for such a case is given.

In Table 3 and Figure 1 is shown the comparison between our results and the experimental (Uzelac et al. 1993) and theoretical Stark widths (Uzelac et al. 1993; Dimitrijević 1993) for the $3s\ ^3P^o$–$3p\ ^3D$ multiplet. In Uzelac et al. (1993) Stark widths are calculated using the simplified semiclassical method (Griem 1974; eq. [526]; $W_{\rm G}$), the modified semiempirical formula (Dimitrijević & Konjević 1980, eqs. [7]–[9]; $W_{\rm DK}$), and a classical-path approximation of Hey and Breger (Hey & Breger 1980; $W_{\rm HB}$). The calculations of Dimitrijević (1993) are performed by using the modified semiempirical approach (Dimitrijević & Konjević 1980). The experimental value for this multiplet is $W_m = 0.64$ Å, and our result is $W_{\rm SC} = 0.55$ Å. The impact approximation for collisions with ions is valid ($C_{\rm imp} \simeq 10^{-8}$; Ben Nessib et al. 1996). $W_{\rm SC} = W_e + W_{\rm ion}$, where W_e is the electron impact Stark width and $W_{\rm ion}$ is the ionic-impact Stark width ($W_e = 0.495$ Å, $W_{\rm ion} = 0.059$ Å). Only collisions with protons are taken into account. Line broadening by other ion perturbers (Ne II, Ne III, and Ne IV) is neglected. The quadrupolar contribution coefficients B_i, B_f, and B_{if} of this multiplet have been evaluated following the expression of the quadrupole term for complex atoms with a two-electron configuration $l_1 l_2 LS$ (Sahal-Bréchot 1974).

We have reported results of Stark broadening parameters calculation for 26 spectral lines of Ne V. Obtained results are in relatively good agreement with experimental result of Uzelac et al. (1993). Such temperatures are of interest for the modeling and analysis of X-ray spectra, such as the spectra obtained by *Chandra*, modeling of some hot star atmospheres (e.g., PG 1195), subphotospheric layers, soft X-ray lasers, and laser-produced plasmas. Higher temperatures are of interest for fusion plasma as well as for stellar interiors.

We see that using the SUPERSTRUCTURE code one obtains a set of energy levels and oscillator strengths, enabling an ab initio calculation of Stark broadening parameters. This is suitable especially for multicharged ions when other theoretical and experimental atomic data scare. This work also suggest that the set of oscillator strength values obtained with the Bates and Damgaard approximation may be useful for Stark broadening calculations when more reliable data are not available.

This work is a part of the project 146001 "The influence of collisional processes on astrophysical plasmas line shapes," supported by the Ministry of Science and Environment Protection of Serbia.

REFERENCES

Barnard, A. J., Cooper, J., & Smith, E. W. 1974, J. Quant. Spectrosc. Radiat. Transfer, 14, 1025
Bates, D. R., & Damgaard, A. 1949, Philos. Trans. R. Soc. London A, 242, 101
Ben Nessib, N., Ben Lakhdar, Z., & Sahal-Bréchot, S. 1996, Phys. Scr., 54, 608
Ben Nessib, N., Dimitrijević, M. S., & Sahal-Bréchot, S. 2004, A&A, 423, 397
Dimitrijević, M. S. 1988, A&AS, 76, 53
———. 1993, A&AS, 100, 237
Dimitrijević, M. S., & Konjević, N. 1980, J. Quant. Spectrosc. Radiat. Transfer, 24, 451
———. 1981, A&A, 102, 93
———. 1987, A&A, 172, 345
Dimitrijević, M. S., & Sahal-Bréchot, S. 1984, J. Quant. Spectrosc. Radiat. Transfer, 31, 301
———. 1985, Phys. Rev. A, 31, 316
———. 1992, A&AS, 95, 109
———. 1995, Bull. Astron. Belgrade, 152, 99
———. 1996a, A&AS, 115, 351
———. 1996b, Phys. Scr., 54, 50
———. 1997, Bull. Astron. Belgrade, 155, 131
———. 1998a, A&AS, 127, 543
———. 1998b, Atomic Data and Nuclear Data Table, 68, 241
Dimitrijević, M. S., Sahal-Bréchot, S., & Bommier, V. 1991, A&AS, 89, 581
Dreizler, S., & Werner, K. 1996, A&A, 314, 217
Eissner, W., Jones, M., & Nussbaumer, H. 1974, Comput. Phys. Commun., 8, 270
Fill, E. E., & Schöning, T. 1994, J. Appl. Phys., 76, 1423
Fleurier, C., Sahal-Bréchot, S., & Chapelle, J. 1977, J. Quant. Spectrosc. Radiat. Transfer, 17, 595
Griem, H. R. 1974, Spectral line Broadening by Plasmas (New York: McGraw-Hill)
Griem, H. R., & Moreno, J. C. 1980, in X-Ray Lasers, ed. G. Tallents (Bristol: Institute of Physics), 301
Hey, J. D., & Breger, P. 1980, J. Quant. Spectrosc. Radiat. Transfer, 24, 349
Nussbaumer, H., & Storey, P. J. 1978, A&A, 64, 139
Popović, L. Č., Simić, S., Milovanović, N., & Dimitrijević, M. S. 2001, ApJS, 135, 109
Sahal-Bréchot, S. 1969a, A&A, 1, 91
———. 1969b, A&A, 2, 322
———. 1974, A&A, 35, 319
———. 1991, A&A, 245, 322
Seaton, M. J. 1987, J. Phys. B, 20, 6363
———. 1988, J. Phys. B, 21, 3033
Szentgyorgyi, A. H., Raymond, J. C., Hester, J. J., & Curiel, S. 2000, ApJ, 529, 279
Uzelac, N. I., Glenzer, S., Konjević, N., Hey, J. D., & Kunze, H. J. 1993, Phys. Rev. E, 47, 3623
Werner, K., & Heber, U. 1991, A&A, 247, 476

The Astrophysical Journal Supplement Series, 189:15–36, 2010 July doi:10.1088/0067-0049/189/1/15
© 2010. The American Astronomical Society. All rights reserved. Printed in the U.S.A.

ANALYSIS OF OPTICAL Fe II EMISSION IN A SAMPLE OF ACTIVE GALACTIC NUCLEUS SPECTRA

Jelena Kovačević[1,2], Luka Č. Popović[1,2], and Milan S. Dimitrijević[1,2,3]
[1] Astronomical Observatory, Volgina 7, 11060 Belgrade, Serbia; jkovacevic@aob.bg.ac.rs
[2] Isaac Newton Institute of Chile, Yugoslavia Branch, Belgrade, Serbia
[3] Laboratoire d'Étude du Rayonnement et de la Matière en Astrophysique, UMR CNRS 8112, Observatoire de Paris-Meudon, 92195 Meudon, France
Received 2009 November 12; accepted 2010 April 10; published 2010 June 15

ABSTRACT

We present a study of optical Fe II emission in 302 active galactic nuclei (AGNs) selected from the Sloan Digital Sky Survey. We group the strongest Fe II multiplets into three groups according to the lower term of the transition (b ^4F, a ^6S, and a ^4G terms). These approximately correspond to the blue, central, and red parts, respectively, of the "iron shelf" around Hβ. We calculate an Fe II template that takes into account transitions into these three terms and an additional group of lines, based on a reconstruction of the spectrum of I Zw 1. This Fe II template gives a more precise fit of the Fe II lines in broad-line AGNs than other templates. We extract Fe II, Hα, Hβ, [O III], and [N II] emission parameters and investigate correlations between them. We find that Fe II lines probably originate in an intermediate line region. We note that the blue, red, and central parts of the iron shelf have different relative intensities in different objects. Their ratios depend on continuum luminosity, FWHM Hβ, the velocity shift of Fe II, and the Hα/Hβ flux ratio. We examine the dependence of the well-known anti-correlation between the equivalent widths of Fe II and [O III] on continuum luminosity. We find that there is a Baldwin effect for [O III] but an inverse Baldwin effect for the Fe II emission. The [O III]/Fe II ratio thus decreases with $L_{\lambda 5100}$. Since the ratio is a major component of the Boroson & Green Eigenvector 1 (EV1), this implies a connection between the Baldwin effect and EV1 and could be connected with AGN evolution. We find that spectra are different for Hβ FWHMs greater and less than $\sim$3000 km s^{-1}, and that there are different correlation coefficients between the parameters.

Key words: atomic processes – galaxies: active – quasars: emission lines

Online-only material: machine-readable table

1. INTRODUCTION

Optical Fe II ($\lambda\lambda$4400–5400) emission is one of the most interesting features in active galactic nucleus (AGN) spectra. The emission arises from numerous transitions of the complex Fe II ion. Fe II emission is seen in almost all type-1 AGN spectra and it is especially strong in narrow-line Seyfert 1s (NLS1s). It can also appear in the polarized flux of type-2 AGNs when a hidden broad-line region (BLR) can be seen. Origin of the optical Fe II lines, the mechanisms of their excitation, and location of the Fe II emission region in AGN are still open questions. There are also many correlations between Fe II emission and other AGN properties which need a physical explanation.

Some of the problems connected with Fe II emission are as follows.

1. There have been suggestions that Fe II emission cannot be explained with standard photoionization models (see Collin & Joly 2000; Collin-Souffrin et al. 1980, and references therein). To explain the Fe II emission, additional mechanisms of excitation have been proposed: (a) continuum fluorescence (Phillips 1978a, 1979), (b) collisional excitation (Joly 1981, 1987, 1991; Veron et al. 2006), (c) self-fluorescence among Fe II transitions (Netzer & Wills 1983), and (d) fluorescent excitation by the Lyα and Lyβ lines (Penston 1988; Verner et al. 1999).
2. There are uncertainties about where the Fe II emission-line region is located in an AGN. A few proposed solutions are that the Fe II lines arise: (a) in the same emission region as the broad Hβ line (Boroson & Green 1992), (b) in the accretion disk near the central black hole, which produces the double-peaked broad Balmer emission lines (Collin-Souffrin et al. 1980; Zhang et al. 2006), (c) in a region that can be heated by shocks or from an inflow, located between BLR and narrow-line region (NLR)—the so-called the intermediate line region (ILR; Marziani & Sulentic 1993; Popović et al. 2004, 2007, 2009; Hu et al. 2008b; Kuehn et al. 2008), and (d) and in the shielded, neutral, outer region of a flattened BLR (Gaskell et al. 2007; Gaskell 2009).
3. It has long been established that the Fe II emission is correlated with the radio, X-ray, and IR continua. Fe II lines are stronger in spectra of radio-quiet (RQ) AGNs than in radio-loud (RL) objects (Osterbrock 1977; Bergeron & Kunth 1984). But, if we consider RL AGNs, Fe II emission is stronger in core dominant (CD) AGNs than in lobe dominant (LD) AGNs (Setti & Woltjer 1977; Joly 1991). The relative strength of the Fe II lines correlates with the soft X-ray slope, but anti-correlates with X-ray luminosity (Wilkes et al. 1987; Boller et al. 1996; Lawrence et al. 1997). Strong optical Fe II emission is usually associated with strong IR luminosity (Low et al. 1989; Lipari et al. 1993), but it is anti-correlated with IR color index α(60,25) (Wang et al. 2006).
4. Many correlations have been observed between Fe II and other emission lines. Boroson & Green (1992) give a number of correlations between the equivalent width (EW) of Fe II and properties of the [O III] and Hβ lines. The most interesting are the anti-correlations of EW Fe II versus EW [O III]/EW Hβ, EW Fe II versus peak [O III], EW Fe II/EW Hβ versus peak [O III], and the correlation of EW Fe II/EW Hβ versus Hβ asymmetry. An anti-correlation between EW Fe II and FWHM of Hβ has also been found (Gaskell 1985; Zheng & Keel 1991; Boroson & Green

1992). These correlations dominate the first eigenvector of the principal component analysis of Boroson & Green (1992; hereinafter EV1). Correlations between EV1 and some properties of C IV λ1549 lines have also been pointed out (Baskin & Laor 2004). With increasing continuum luminosity, the EW of the C IV lines decreases (the so-called Baldwin effect, Baldwin 1977; Wang et al. 1995), while the blueshift of the C IV line and the EW of Fe II increase. Recently, Dong et al. (2009) have found the Baldwin effect to be related to EV1. Fe II lines are usually strong in AGN spectra with low-ionization broad absorption lines (BALs; Harting & Baldwin 1986; Boroson & Meyers 1992).

Searching for a physical cause of these correlations may help in understanding of the origin of Fe II emission. Some of physical properties which may influence these correlations are the Eddington ratio ($L/L_{\rm Edd}$; Boroson & Green 1992; Baskin & Laor 2004), black hole mass ($M_{\rm BH}$), and inclination angle (Miley & Miller 1979; Wills & Browne 1986; Marziani et al. 2001).

In addition to these properties, Fe II emission strength may vary with evolution of AGNs. For example, Lipari & Terlevich (2006) have explained some properties of AGN (as BALs, Fe II strength, radio properties, emission line width, luminosity of narrow lines, etc.) by an "evolutive unification model." In this model, accretion arises from the interaction between nuclear starbursts and the supermassive black hole. This would mean that not only the orientation, but also the evolutionary state of an AGN influence its spectral properties. Thus, young AGNs have strong Fe II, BALs, and weak radio emission, also the NLR is compact and faint, and broad lines are relatively narrow. In contrast with this, old AGNs have weak Fe II, no BALs, strong radio emission with extended radio lobes, the NLR is extended and bright, and the broad lines have greater velocity widths.

In this paper, we investigate the Fe II emitting region by analyzing the correlations between the optical Fe II lines and the other emission lines in a sample of 302 AGNs from the Sloan Digital Sky Survey (SDSS). To do this we construct an Fe II template. The strongest Fe II multiplets within the 4400–5500 Å range are sorted into three groups, according to the lower terms of the transitions: $3d^6(^3F2)4s\ ^4F$, $3d^54s^2\ ^6S$, and $3d^6(^3G)4s\ ^4G$ (which we will hereinafter refer to as the F, S, and G groups of lines). The F group mainly contains the lines from the Fe II multiplets 37 and 38 and describes the blue part of the Fe II shelf relative to Hβ. The S group of lines describes the part of Fe II emission under Hβ and [O III] and contains lines from multiples 41, 42, and 43 Fe II. Finally, the G group contains lines from multiplets 48 and 49, and describes the red part of the Fe II shelf. A simplified Grotrian diagram of these transitions is shown in Figure 1. We separately analyze their relationships with other lines in AGN spectra (Hβ, [O III], Hα, [N II]). In this way, we try to connect details of the Fe II emission with physical properties of the AGN emission regions in which these lines arise. Each of the Fe II multiplet groups has specific characteristics, which may be reflected in a different percent of correlations with other lines, and gives us more information about the complex Fe II emission region.

The paper is organized as follows: in Section 2, we describe the procedure of sample selection and details of analysis; our results are presented in Section 3; in Section 4 we give discussion of obtained results, and finally in Section 5 we outline our conclusions.

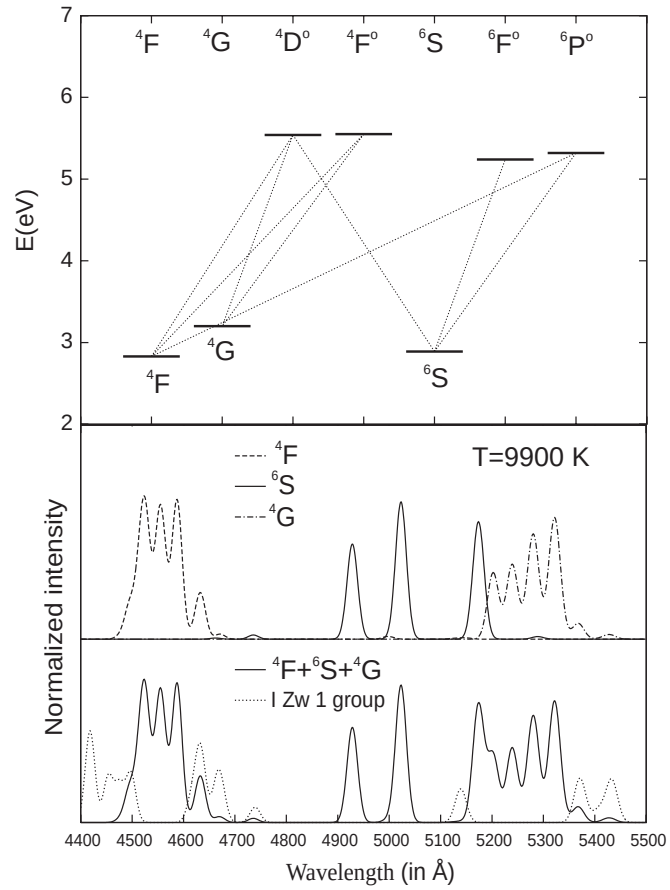

Figure 1. Top: Grotrian diagram showing the strongest Fe II transitions in the 4400–5500 Å region. Middle: Lines are separated into three groups according to the lower level of transition: F (dashed line), S (solid line), and G (dash-dotted line). Bottom: the lines from the three line groups (solid line) and lines measured from I Zw 1 (represented with dots).

2. THE SAMPLE AND ANALYSIS

2.1. The AGN Sample

Spectra for our data sample are taken from the seventh data release (Abazajian et al. 2009) of the SDSS. For the purposes of the work, we chose AGNs with the following characteristics.

1. High signal-to-noise ratio (S/N > 20).
2. Good pixel quality (profiles are not affected by distortions due to bad pixels on the sensors, the presence of strong foreground or background sources).
3. High-redshift confidence (zConf > 0.95) and with $z \leqslant 0.7$ in order to cover the optical Fe II lines around Hβ and [O III] lines.
4. Negligible contribution from the stellar component. We controlled for this by having the EWs of typical absorption lines be less than 1 Å (EW CaK 3934 Å, Mg 5177 Å, and Hδ 4102 Å > −1).[4] Because of this it was not necessary to remove a host galaxy starlight contribution.
5. Presence of the narrow [O III] and the broad Hβ component (FWHM Hβ > 1000 km s^{-1}).

We found 497 AGNs using the mentioned criteria. However, on inspection of the spectra we found that in some of them

[4] For some objects we were able to find estimates of the stellar component in the literature and to confirm that the host galaxy fraction is indeed small in our sample (see Appendix A).

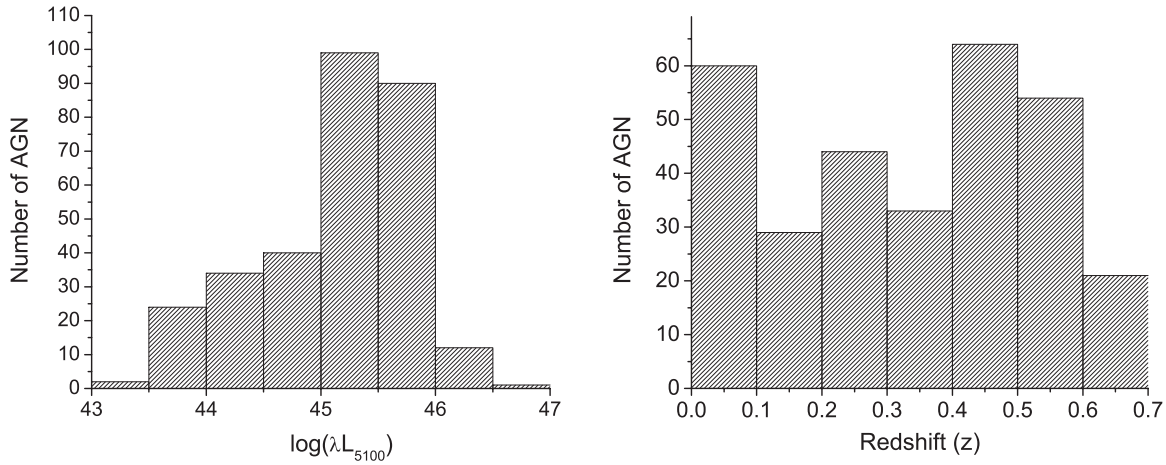

Figure 2. Distribution of continuum luminosity (left) and cosmological redshift (right) in the AGN sample.

the Fe II line emission is within the level of noise and could not be properly fitted, so we excluded these objects from further analysis (see Appendix A). As a result, our final sample contains 302 spectra, from which 137 have all Balmer lines, and the rest are without the Hα line (due to cosmological redshifts). The sample distribution by continuum luminosity (λ5100) and by cosmological redshift is given in Figure 2. Corrections for Galactic extinction were made using an empirical selective extinction function computed for each spectrum on the basis of Galactic extinction coefficients given by Schlegel (1998) and available from the NASA/IPAC Extragalactic Database.[5] Finally, all spectra were de-redshifted.

To subtract the continuum, we used the DIPSO software, finding the continuum level by using continuum windows given in the paper of Kuraszkiewicz et al. (2002; see Figure 3). The used continuum windows are 3010–3040 Å, 3240–3270 Å, 3790–3810 Å, 4210–4230 Å, 5080–5100 Å, 5600–5630 Å, and 5970–6000 Å. We used the same procedure to subtract the continuum in all objects. Continuum subtraction may cause systemic errors in the estimation of line parameters and continuum luminosity. We estimated that the error bars are smaller than 5%, especially within the Hα+[N II] region and in the red part of the "iron shelf."

We considered two spectral ranges: 4400–5500 Å and 6400–6800 Å. In the first range, dominant lines are the numerous Fe II lines, [O III] $\lambda\lambda$4959, 5007, Hβ and He II λ4686, and in the second range, Hα and [N II] $\lambda\lambda$6548, 6583.

To investigate correlations between the Fe II multiplets and other lines in spectra, we fit all considered lines with Gaussians. The optical Fe II lines were fitted with a template calculated as described in the next section.

2.2. The Fe II ($\lambda\lambda$4400–5500) Template

A number of authors have created an Fe II template in the UV and optical range (see Vestergaard & Wilkes 2001, and references therein). Boroson & Green (1992) applied an empirical template by removing all lines which are not Fe II, from the spectrum of I Zw 1. Similarly, Veron-Cetty et al. (2004) constructed an Fe II template by identifying systems of broad and of narrow Fe II lines in the I Zw 1 spectrum, and measuring their relative intensities. Dong et al. (2008) improve on that template by using two parameters of intensity—one for the broad and the other for the narrow Fe II lines. All these empirical templates are defined by the line width and the line strength, implying that relative strengths of the lines in the Fe II multiplets are the same in all objects.

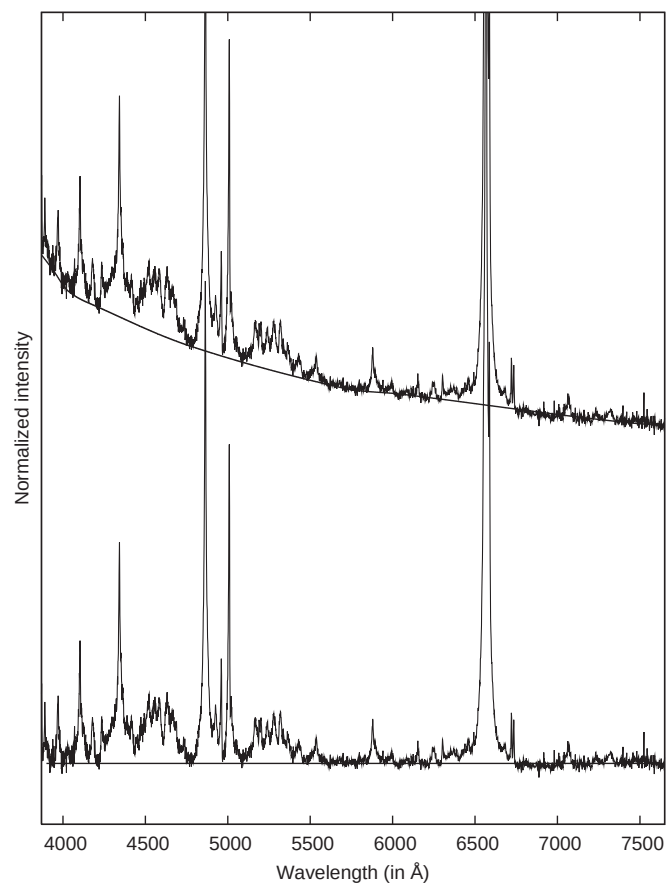

Figure 3. Example of removing the continuum from the spectrum of SDSS J075101.42 + 29174000.00; the level of the continuum is determined by interpolating between the chosen points at wavelengths without emission lines (top). The spectrum without continuum emission is shown at the bottom.

In theoretical modeling, significant effort has been made to calculate the iron emission by including a large number of Fe II atomic levels, going to high energy (Verner et al. 1999; Sigut & Pradhan 2003; Collin-Souffrin et al. 1980; Bruhweiler & Verner 2008). Bruhweiler & Verner (2008) calculated Fe II emission

[5] http://nedwww.ipac.caltech.edu/

using the CLOUDY code and the 830 level Fe II model. In this model, energies go up to 14.6 eV, producing 344,035 atomic transitions. For their calculations they used solar abundances for a range of physical conditions such as the flux of ionizing photons [Φ_H], hydrogen density [n_H], and microturbulence [ξ].

Using existing Fe II templates, we found that empirical and theoretical models can generally fit NLSy1 Fe II lines well, but that in some cases of spectra with broader Hβ lines, the existing models did not provide as good fit.

One of the problems in the analysis of Fe II emission is that it consists of numerous overlapping lines. This makes the identification and determination of relative intensities very difficult. Therefore, the list of Fe II lines used for the fit of the Fe II emission, as well as their relative intensities, is different in different models (Veron-Cetty et al. 2004; Bruhweiler & Verner 2008). Also, there is significant disagreement in values of oscillator strengths in different atomic data sources (Fuhr et al. 1981; Giridhar & Ferro 1995; Kurucz 1990).

To investigate the Fe II emission, we made an Fe II template taking into account the following: (1) the majority of multiplets dominant in the optical part ($\lambda\lambda$4400–5500), whose lines can be clearly identified in AGN spectra, have one of the three specific lower terms of their transitions: *F*, *S*, or *G*; and (2) beside these lines there are also lines whose origin is not well known but which presumably originate from higher levels.

We constructed an Fe II template consisting of 50 Fe II emission lines, identified as the strongest within the 4400–5500 Å range. Thirty-five of them are sorted into three line groups according to the lower term of their transition (*F*, *S*, and *G*). The *F* group consists of 19 lines (mainly multiplets 37 and 38) and dominates in the blue shelf of the iron template (4400–4700 Å). The *S* group consists of five lines (multiplets 41, 42, and 43) and describes the Fe II emission covering the [O III] and Hβ region of the spectrum and some of emission from the red Fe II bump (5150–5400 Å), and the *G* lines (11 lines from multiplets 48 and 49) dominate in the red bump (5150–5400 Å; see Figure 1).

We assume that the profiles of each of lines can be represented by a Gaussian, described by width (*W*), shift (*d*),[6] and intensity (*I*). Since all Fe II lines from the template probably originate in the same region, with the same kinematical properties, values of *d* and *W* are assumed to be the same for all Fe II lines in the case of one AGN.

Since the population of the lower term is influenced by transition probabilities and excitation temperature, we assumed that the relative intensities between lines within a line group (*F*, *S*, or *G*) can be obtained approximately from

$$\frac{I_1}{I_2} = \left(\frac{\lambda_2}{\lambda_1}\right)^3 \frac{f_1}{f_2} \cdot \frac{g_1}{g_2} \cdot e^{-(E_1-E_2)/kT}, \qquad (1)$$

where I_1 and I_2 are the intensities of lines with the same lower term, λ_1 and λ_2 are the wavelengths of the transition, g_1 and g_2 are the statistical weights for the upper energy levels, f_1 and f_2 are the oscillator strengths, E_1 and E_2 are the energies of the upper levels of transitions, *k* is the Boltzmann constant, and *T* is the excitation temperature. Details can be found in Appendix C. The excitation temperature is the same for all transitions in the case of partial local thermodynamic equilibrium (LTE) (see Griem 1997), but as it is shown in Appendix C, Equation (1) may also be used in some non-LTE cases.

[6] Here we used $W = \frac{W_D}{\lambda_0}$, $d = \frac{\Delta\lambda}{\lambda_0}$, where $W_D = \sigma\sqrt{2}$ is the Doppler width, $\Delta\lambda$ is the shift, and σ is the velocity dispersion.

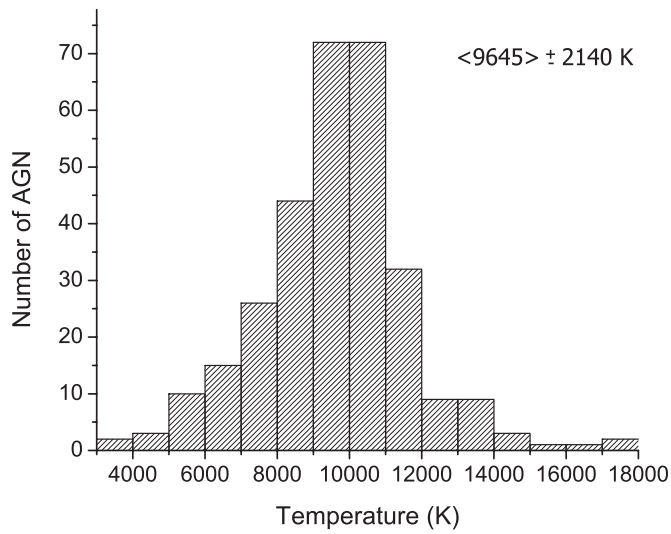

Figure 4. Distribution of the excitation temperatures for the sample of 302 AGNs. Temperatures are obtained by fits using Equation (1). The mean value and dispersion are shown in the figure.

Lines from the three above mentioned groups explain about 75% of the Fe II emission in the observed range (4400–5500 Å), but about 25% of Fe II emission cannot be explained with permitted lines for which the excitation energies are close to the lines of the three groups. The missing Fe II emission is around ∼4450 Å, ∼4630 Å, ∼5130 Å, and ∼5370 Å.

There are some indications that fluorescence processes may have a role in producing some Fe II lines (Verner et al. 1999; Hartman & Johansson 2000). Processes like self-fluorescence, continuum fluorescence, or Lyα and Lyβ pumping could supply enough energy to excite the Fe II lines with a high energy of excitation, which could provide one of the explanations for emission within these wavelength regions. To complete the template for approximately 25% of missing Fe II flux, we selected 15 lines from the Kurutz database[7] with wavelengths close to those of the extra emission, upper level excitation energies of up to ∼13 eV, and strong oscillator strengths. We measured their relative intensities in I Zw 1 which has a well-studied spectrum (Veron-Cetty et al. 2004), with strong and narrow Fe II lines. Relative intensities of these 15 lines were obtained by making the best fit of the I Zw 1 spectrum with the Fe II lines from the *F*, *S*, and *G* line groups. The extra lines are represented in Figure 1 (bottom), with a dotted line.

Our template of Fe II is described by seven free fitting parameters; the first six being width, shift, and four parameters of intensity (for the *F*, *S*, and *G* line groups and for the lines with relative intensities obtained from I Zw 1). The seventh parameter is the excitation temperature included in the calculation of relative intensities within *F*, *S*, and *G* line groups.

We found that for the majority of objects, the excitation temperature obtained from our fit is within the range of 9000 K–11,000 K (see Figure 4), which agrees well with theoretical predictions (Collin & Joly 2000). However, as it can be seen in Equation (1), our fit is not very sensitive to the temperature, especially for $T > 8000$ K. Equation (1) is also very approximate, so estimated temperatures should be treated with caution.

To estimate the error in the excitation temperature, we found our best fit for a number of objects. We then changed only the

[7] http://www.pmp.uni-hannover.de/cgi-bin/ssi/test/kurucz/sekur.html

Table 1
A List of the 35 Strongest Fe II Lines within the 4400–5500 Å Region Used to Calculate the Fe II Template

Wavelength	Multiplet	Transition	gf	Ref.	Relative Intensity		
					$T = 5000$ K	$T = 10{,}000$ K	$T = 15{,}000$ K
4472.929	37	b $^4F_{5/2}$–z $^4F^o_{3/2}$	4.02E-04	1	0.033	0.036	0.037
4489.183	37	b $^4F_{7/2}$–z $^4F^o_{5/2}$	1.20E-03	1	0.105	0.110	0.111
4491.405	37	b $^4F_{3/2}$–z $^4F^o_{3/2}$	2.76E-03	1	0.226	0.243	0.249
4508.288	38	b $^4F_{3/2}$–z $^4D^o_{1/2}$	4.16E-03	2	0.345	0.367	0.375
4515.339	37	b $^4F_{5/2}$–z $^4F^o_{5/2}$	3.89E-03	2	0.333	0.348	0.353
4520.224	37	b $^4F_{9/2}$–z $^4F^o_{7/2}$	2.50E-03	3	0.235	0.233	0.233
4522.634	38	b $^4F_{5/2}$–z $^4D^o_{3/2}$	9.60E-03	3	0.827	0.859	0.870
4534.168	37	b $^4F_{3/2}$–z $^4F^o_{5/2}$	3.32E-04	3	0.028	0.029	0.030
4541.524	38	b $^4F_{3/2}$–z $^4D^o_{3/2}$	8.80E-04	3	0.075	0.078	0.079
4549.474	38	b $^4F_{7/2}$–z $^4D^o_{5/2}$	1.10E-02	4	1.000	1.000	1.000
4555.893	37	b $^4F_{7/2}$–z $^4F^o_{7/2}$	5.20E-03	3	0.477	0.474	0.474
4576.340	38	b $^4F_{5/2}$–z $^4D^o_{5/2}$	1.51E-03	4	0.136	0.136	0.136
4582.835	37	b $^4F_{5/2}$–z $^4F^o_{7/2}$	7.80E-04	3	0.070	0.070	0.070
4583.837	38	b $^4F_{9/2}$–z $^4D^o_{7/2}$	1.44E-02	2	1.420	1.353	1.331
4620.521	38	b $^4F_{7/2}$–z $^4D^o_{7/2}$	8.32E-04	4	0.080	0.076	0.075
4629.339	37	b $^4F_{9/2}$–z $^4F^o_{9/2}$	4.90E-03	4	0.497	0.459	0.447
4666.758	37	b $^4F_{7/2}$–z $^4F^o_{9/2}$	6.02E-04	4	0.060	0.055	0.054
4993.358	36	b $^4F_{9/2}$–z $^6P^o_{7/2}$	3.26E-04	4	0.041	0.030	0.027
5146.127	35	b $^4F_{7/2}$–z $^6F^o_{7/2}$	1.22E-04	5	0.016	0.011	0.010
4731.453	43	a $^6S_{5/2}$–z $^4D^o_{7/2}$	1.20E-03	2	0.025	0.030	0.032
4923.927	42	a $^6S_{5/2}$–z $^6P^o_{3/2}$	2.75E-02	4	0.656	0.693	0.706
5018.440	42	a $^6S_{5/2}$–z $^6P^o_{5/2}$	3.98E-02	4	1.000	1.000	1.000
5169.033	42	a $^6S_{5/2}$–z $^6P^o_{7/2}$	3.42E-02	1	0.929	0.854	0.831
5284.109	41	a $^6S_{5/2}$–z $^6F^o_{7/2}$	7.56E-04	2	0.022	0.019	0.018
5197.577	49	a $^4G_{5/2}$–z $^4F^o_{3/2}$	7.92E-03	5	0.532	0.620	0.652
5234.625	49	a $^4G_{7/2}$–z $^4F^o_{5/2}$	8.80E-03	3	0.615	0.695	0.723
5264.812	48	a $^4G_{5/2}$–z $^4D^o_{3/2}$	1.08E-03	1	0.075	0.084	0.087
5276.002	49	a $^4G_{9/2}$–z $^4F^o_{7/2}$	1.148e-02	2	0.861	0.928	0.951
5316.615	49	a $^4G_{11/2}$–z $^4F^o_{9/2}$	1.17E-02	4	1.000	1.000	1.000
5316.784	48	a $^4G_{7/2}$–z $^4D^o_{5/2}$	1.23E-03	5	0.089	0.097	0.099
5325.553	49	a $^4G_{7/2}$–z $^4F^o_{7/2}$	6.02E-04	4	0.044	0.047	0.048
5337.732	48	a $^4G_{5/2}$–z $^4D^o_{5/2}$	1.28E-04	5	0.009	0.010	0.010
5362.869	48	a $^4G_{9/2}$–z $^4D^o_{7/2}$	1.82E-03	5	0.142	0.146	0.148
5414.073	48	a $^4G_{7/2}$–z $^4D^o_{7/2}$	1.60E-04	5	0.012	0.012	0.013
5425.257	49	a $^4G_{9/2}$–z $^4F^o_{9/2}$	4.36E-04	5	0.035	0.035	0.035

Notes. In the first column are wavelengths (in air), in the second multiplet numbers (Giridhar & Ferro 1995), in the third are terms of transitions, in the fourth are gf values used for the template calculation, in the fifth are the references for the source of oscillator strengths, and in the 6th–8th columns are relative intensities, calculated for $T = 5000$ K, 10,000 K, and 15,000 K. Intensities of lines from the F, S, and G groups are normalized to intensities of the λ4549.474, λ5018.44, and λ5316.6 lines (respectively).

References. (1) Fuhr et al. 1981; (2) Giridhar & Ferro 1995; (3) NIST Atomic Spectra Database (http://physics.nist.gov/PhysRefData/ASD/); (4) Kurucz 1990; (5) http://www.pmp.uni-hannover.de/cgi-bin/ssi/test/kurucz/sekur.html.

excitation temperature while keeping the other fit parameters fixed. We thus found $\chi^2_{\max}$ for which the fit is still reasonable. After that, we constructed χ^2 versus T and measured the dispersion in temperature at $0.1(\chi^2_{\max} - \chi^2_{\min})$. We obtained error bars that were mostly within the range ±25%, with the tendency for higher temperature to have a greater uncertainty. Therefore, in further analysis, we will not consider the temperatures obtained from the fit.

The wavelengths of the 50 template lines are presented in Tables 1 and 2. For the 35 lines from the three line groups we give multiplet names, configurations of the transitions generating those lines, oscillator strengths, and the relative intensities. The intensities have been calculated using the Equation (1) for excitation temperatures $T = 5000$, 10,000, and 15,000 K (Table 1). For the 15 lines for which relative intensities were measured in I Zw 1, we give wavelengths, configurations, and oscillator strengths taken from Kurucz database, as well as their measured relative intensities (Table 2).

The purpose of dividing the Fe II emission into four groups is to investigate the correlations between the iron lines that arise from different multiplets and some spectral properties, and to compare them with results obtained for the total Fe II within the observed range. Also, a template that has more parameters may give a better fit, since relative intensities among Fe II lines can be different even in the similar AGN spectra, as is, for example, the case for spectra of I Zw 1 and Mrk 42 (as, e.g., Phillips 1978b).

We applied this template to our sample of 302 AGNs from SDSS database, and we compare it with other theoretical and empirical models (see Appendix B). We found that the template

fits Fe II emission very well (Figure 23 and Figure 24). In the cases when the Fe II emission of an object has different properties from I Zw 1, small disagreements are noticed in the lines for which the relative intensity was obtained from I Zw 1. However, the Fe II emission in these objects shows larger disagreement with the empirical and theoretical models considered in Appendix B (see Figure 25). Although our Fe II template has more free parameters than other templates used for fitting the Fe II emission, it enables more precise fits of Fe II lines in some AGNs (especially with very broad Hβ line) than the other Fe II templates we considered.

2.3. Emission-line Decomposition and Fitting Procedure

We assume that broad emission lines (BELs) arise in two or more emission regions (Brotherton et al. 1994; Popović et al. 2004; Bon et al. 2006, 2009; Ilić et al. 2006), so that their profiles are sums of Gaussians with different shifts, widths, and intensities, which reflect the physical conditions of the emitting regions where the components arise.

For this reason, we fit the emission lines we considered ([O III] $\lambda\lambda$4959, 5007, Hβ, He II λ4686, Hα and [N II] $\lambda\lambda$6548, 6583) with a sum of Gaussians, describing one Gaussian with three parameters (width, intensity, and shift from the transition wavelength).

Both lines of the [O III] $\lambda\lambda$4959, 5007 doublet originate from the same lower energy level and both have a negligible optical depth since the transitions are strongly forbidden. Taking this into account, we assumed that the [O III] λ4959 and [O III] λ5007 lines have the same emission-line profile. We fit each line of the doublet with either a single Gaussian, or, in the case of a significant asymmetry, with two Gaussians. The Gaussian that describes the [O III] λ4959 has the same width and shift as the one which describes the [O III] λ5007 line, and we took their intensity ratio to be 2.99 (Dimitrijević et al. 2007). [N II] $\lambda\lambda$6548, 6583 were fitted using the same procedure, with an intensity ratio of the doublet components of $\approx$3. The He II λ4686 line was fitted with one broad Gaussian.

To fit the Balmer lines, a number of Gaussian functions were used for each line. It is usually assumed that there are two components for Hα and Hβ: a narrow component representing the NLR, and a broad one representing the BLR. However, the broad emission lines (BELs) are very complex and cannot be properly explained by single Gaussian (which would indicate an isotropic spherical region). Moreover, there are some papers (Brotherton et al. 1994; Corbin & Boroson 1996; Popović et al. 2004; Ilić et al. 2006; Bon et al. 2006, 2009; Hu et al. 2008a) where the broad lines are assumed to be emitted from two kinematically different regions: a "Very Broad Line Region" (VBLR) and an ILR. We therefore tested fitting the broad lines with one and two Gaussians. We found that in most AGNs in our sample, the fit with two Gaussians was significantly better than the fit with one Gaussian.

To apply a uniform model of the line-fitting procedure, we assumed that Balmer lines have three components from the NLR, ILR, and VBLR. We exclude four spectra from the sample in which the Hα line could not be decomposed in this way, so finally our sample contains 133 spectra (from 137) with all Balmer lines that could be analyzed within the 6400–6800 Å range. To check this assumption on the rest of the spectra, we examined the corresponding correlations and found that the luminosities and widths of the NLR, ILR, and VBLR components of Hα are highly correlated with the same parameters of the NLR, ILR, and VBLR components of Hβ.

Table 2
List of the Lines Taken from Kurucz Database[a]

Wavelength	Transitions	*gf*	Relative Intensity
4418.957	y $^4G_{5/2}$–e $^4F_{3/2}$	1.45E-02	3.00
4449.616	y $^4G_{9/2}$–e $^4F_{7/2}$	2.58E-02	1.50
4471.273	y $^4D_{5/2}$–f $^4D_{3/2}$	6.40E-03	1.20
4493.529	y $^4G_{10/2}$–e $^4F_{9/2}$	3.74E-02	1.60
4614.551	y $^6P_{5/2}$– $^6D_{7/2}$	2.69E-03	0.70
4625.481	x $^4D_{1/2}$–f $^4D_{1/2}$	8.51E-03	0.70
4628.786	x $^4D_{5/2}$–f $^4D_{5/2}$	1.83E-02	1.20
4631.873	x $^4D_{3/2}$–f $^4D_{3/2}$	1.34E-02	0.60
4660.593	$d^54s^2\ ^2G_{7/2}$–$(4G)sp\ ^2G_{7/2}$	1.15E-03	1.00
4668.923	x $^4D_{5/2}$–f $^4D_{7/2}$	3.13E-03	0.90
4740.828	y $^6P_{5/2}$–e $^6F_{7/2}$	1.98E-03	0.50
5131.210	y $^4P_{5/2}$–e $^4D_{5/2}$	2.13E-03	1.1
5369.190	e $^4D_{5/2}$– $^4D_{5/2}$	1.23E-03	1.45
5396.232	x $^4F_{5/2}$–f $^4D_{3/2}$	2.80E-03	0.40
5427.826	b $^4G_{11/2}$–w $^4F_{9/2}$	2.17E-02	1.40

Notes. In the first column are wavelengths (in air), in the second oscillator strengths, and in the third relative intensities measured in I Zw 1.
[a] http://www.pmp.uni-hannover.de/cgi-bin/ssi/test/kurucz/sekur.html.

This is in favor of our three-component decomposition (Table 3). For the 133 objects, which have both Hβ and Hα lines, it can be noticed that 16 spectra have large redshifts of the VBLR Hβ component relative to VBLR of Hα, which causes disagreement and reduces the correlation between the VBLR shifts of the rest of objects. Without these 16 objects, Hβ and Hα VBLR components correlate in width and shift, with coefficient of correlation ~ 0.40, $P < 0.0001$. An example of shifts between the Hα and Hβ VBLR components is shown in Figure 5. The AGN SDSS J111603.13 + 020852.2 has its VBLR Hβ component redshifted by $\approx$4258 km s^{-1}, while shift of the Hα VBLR component is ≈ -1200 km s^{-1}.

We assume that all narrow lines (and narrow components of the broad lines) originate from the same NLR, and thus expect that these lines will have the same shifts and widths. We therefore took the Gaussian parameters of the shift and width of [O III], [N II], and the NLR components of Hβ and Hα to have the same values.

We separately fit lines from the 4400–5500 Å range (Fe II lines, [O III], He II, and Hβ) with 23 free parameters, and lines from the 6400–6800 Å range (Hα and [N II]) with eight free parameters. We applied a χ^2 minimization routine (Popović et al. 2004) to obtain the best fit. Examples of an AGN spectrum fit in both ranges are shown in Figures 6 and 7.

2.4. Line Parameters

We compared the shifts, widths, EWs, and luminosities of the lines. The shifts and widths were obtained directly from the fit (parameters of width and shift). Luminosities were calculated using the formulae given in Peebles (1993), with adopted cosmological parameters $\Omega_M = 0.27$, $\Omega_\Lambda = 0.73$, and $\Omega_k = 0$. We adopt a Hubble constant, $H_o = 71$ km s^{-1}Mpc^{-1}. The continuum luminosity was obtained from the average value of the continuum flux measured between 5100 Å ($\lambda\lambda$5095–5100 and $\lambda\lambda$5100–5105). EWs were measured with respect to the continuum below the lines. The continuum was estimated by subtracting all fitted lines from the observed spectra. Then, the line of interest (or the Fe II template), which is fitted separately, is added to the continuum. EWs are obtained by normalizing the lines on continuum level, and by measuring their fluxes (see Figure 8). To determine the full width at half-maximum

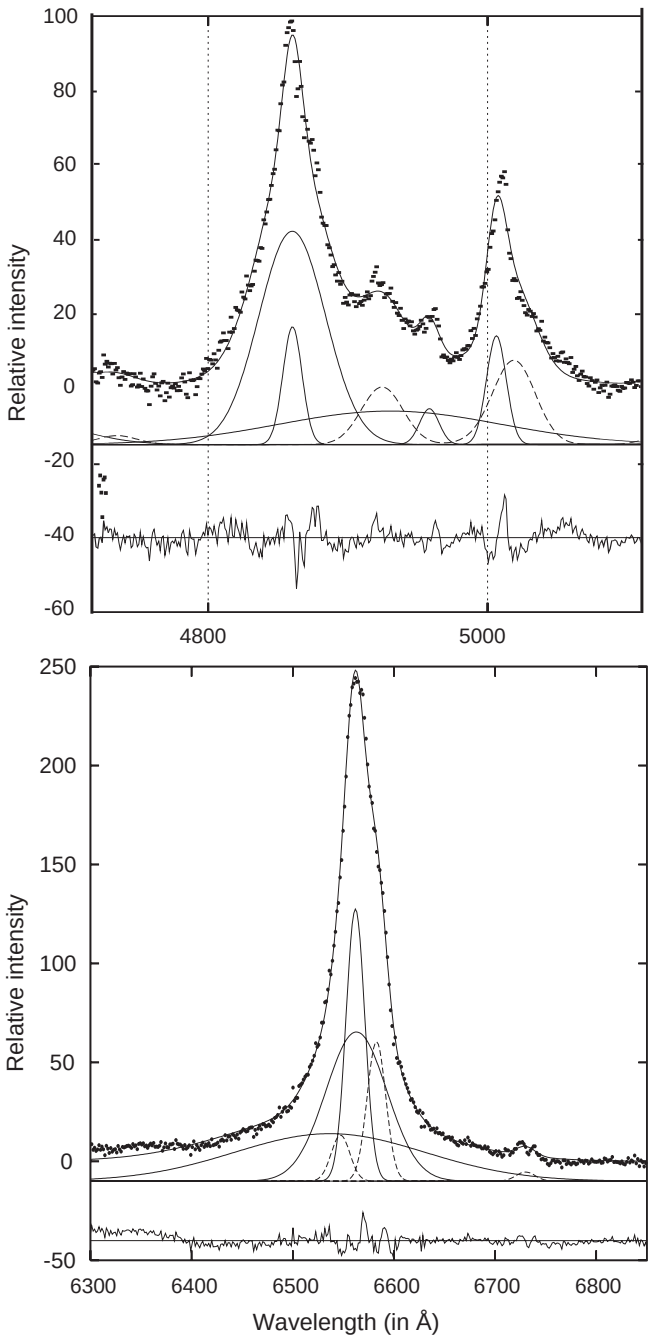

Figure 5. Balmer lines in the SDSS J111603.13 + 020852.2 spectrum. Top: Hβ with a highly redshifted Hβ VBLR component; bottom: Hα where the VBLR component is not redshifted.

(FWHM) of the broad component of the Balmer lines, the VBLR and ILR components from the fit are considered as it is shown in Figure 9. The broad Balmer line (VBLR+ILR) is then normalized on unity, and the FWHM is measured at half of the maximum intensity.

3. RESULTS

3.1. The Ratios of Fe II Line Groups versus Other Spectral Properties

Some objects have relative intensities of Fe II lines similar to I Zw 1, while others show significant disagreement, which usually shows up as stronger iron emission in the blue bump (mainly F lines) than one in the red bump (mainly G lines), comparing to I Zw 1. That objects could be fitted well with the template model which assumes that relative intensities between the Fe II lines from different line groups (F, S, and G) are different for different objects.

Difference between the relative intensities of the Fe II lines from different parts of iron shelf (blue, red, and central) can be illustrated well with histograms of distribution of the Fe II group ratio (F/G, F/S, and G/S) for the sample (Figure 10). The average value of the F/G luminosity ratio is 1.44 ± 0.55, of the F/S ratio 1.97 ± 1.05, and of the G/S ratio 1.39 ± 0.46.[8] We found that the majority of objects have Fe II group ratios close to the average values, but still a significant number of objects are showing a difference since the intensity ratios of Fe II line groups vary in different objects (see Figure 10). The ratios of the Fe II line groups in I Zw 1 are indicated by the vertical dashed lines ($F/G = 1.10$, $F/S = 1.56$, and $G/S = 1.41$).

We analyzed the flux ratios of the Fe II multiplet groups and the total Fe II flux (see histograms in Figure 11), and we found that lines from multiplets 37 and 38 (group F) generally have the largest contribution to the total Fe II emission within the 4400–5500 Å range (about 32%), while group S contributes about 18% and G about 23%. As expected, there are very strong correlations between the EWs of Fe II line groups (Table 4).

Since line intensities and their ratios are indicators of physical properties of the plasma where those lines arise, we have investigated relations among the ratios of Fe II line groups with various spectral properties. A correlation between the FWHM Hβ and the EW Fe II emission has previously been found (Gaskell 1985; Boroson & Green 1992; Sulentic et al. 2009). Consequently, one can expect that FWHM Hβ may be connected with the Fe II line group ratios. We therefore investigated correlations between the ratios of the Fe II groups (F/G, F/S, and G/S) and Hβ FWHM. We excluded the three outliers, which have negligible flux for the S group. As it can be seen in Figure 12 (first panel) there are different trends for spectra with FWHM Hβ less than and greater than $\sim$3000 km s^{-1}. Therefore, we divided the sample into two sub-samples: 158 objects with FWHM Hβ $<$ 3000 km s^{-1} and 141 objects with FWHM Hβ $>$ 3000 km s^{-1} (see Figure 12 and Table 5). A similar subdivision of AGN samples was performed by Sulentic et al. (2002, 2009) and Zamfir et al. (2010), but for FWHM Hβ $\approx$ 4000 km s^{-1} as the limiting FWHM of the subdivision. We found that FWHM Hβ $\approx$ 3000 km s^{-1} is a more appropriate place to divide the objects into two groups, since all objects with strongly redshifted VBLR Hβ component (see Figure 5) belong to the FWHM Hβ $>$ 3000 km s^{-1} sub-sample. Sulentic et al. (2002) also noticed that AGNs with FWHM Hβ $>$4000 km s^{-1} have a larger redshifted VBLR Hβ ($\sim$5000 km s^{-1}).

In Table 5, we present the correlations between the luminosity ratios of the Fe II line groups and other spectral properties such as FWHM Hβ, Doppler width of Hβ broad components, width and shift of iron lines, and continuum luminosity ($L_{\lambda 5100}$). They are examined for the total sample and for two sub-samples, divided according to FWHM Hβ, and denoted in Table 5 as (1) for FWHM Hβ $<$ 3000 km s^{-1} and (2) for Hβ FWHM $>$ 3000 km s^{-1}.

We found a difference in the correlations for those two sub-samples. For the Hβ FWHM $>$ 3000 km s^{-1} sub-sample (2), all three ratios (F/G, F/S, and G/S) increase as Hβ width increases. On the other hand, for the Hβ FWHM $<$

[8] Here we give the averaged ratio value and dispersion.

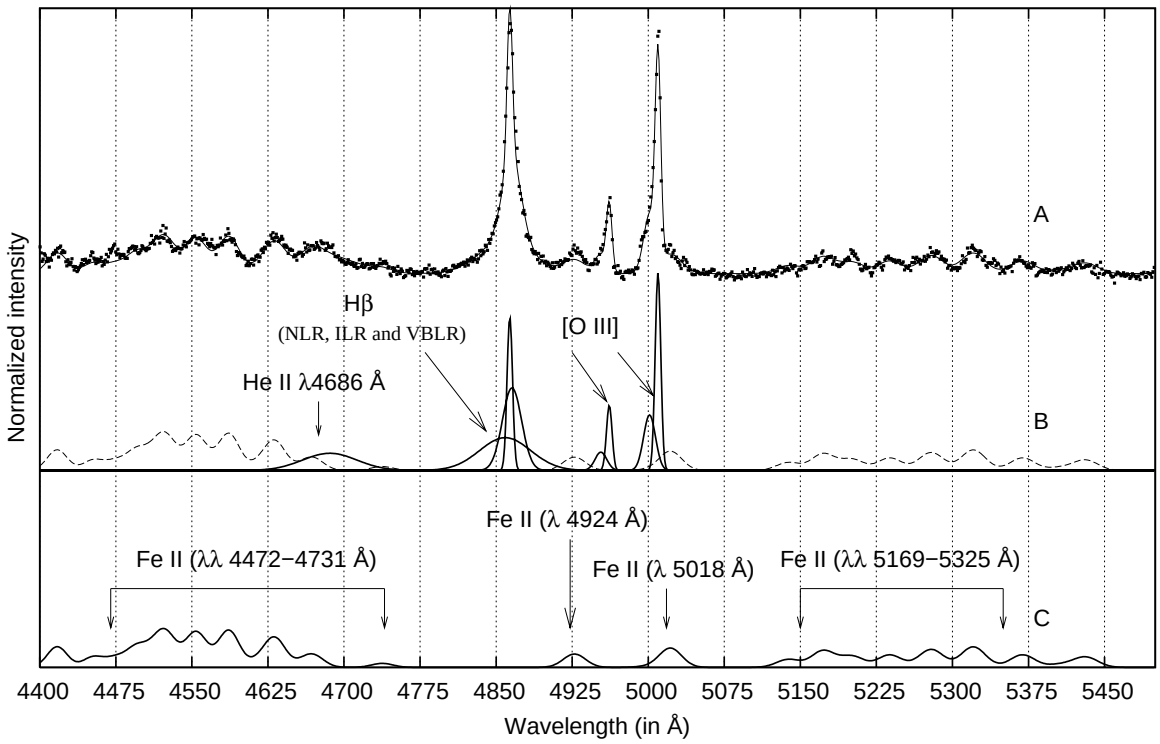

Figure 6. Spectrum of SDSS J141755.54 + 431155.8 in the 4400–5500 Å region: (A) the observed spectra (dots) and the best fit (solid line). (B) Hβ fit with the sum of three Gaussians representing emission from the NLR, ILR, and VBLR. The [O III] $\lambda\lambda$4959, 5007 lines are fitted with two Gaussians for each line of the doublet and He II λ4686 is fitted with one broad Gaussian. The Fe II template is denoted with a dashed line, and also represented separately in panel C (bottom).

Table 3
Correlations between Widths, Shifts, and Luminosities of the NLR, ILR, and VBLR Components of the Hα and Hβ Lines

Correlation (Hα and Hβ)	r	P	A	B
Hα NLR width vs. Hβ NLR width	0.99	<0.0001	6.19 ± 2.81	0.97 ± 0.01
Hα ILR width vs. Hβ ILR width	0.91	<0.0001	165.37 ± 43.29	0.74 ± 0.03
Hα VBLR width vs. Hβ VBLR width	0.50 (0.42)	<0.0001	1863.15 ± 352.50	0.54 ± 0.08
Hα NLR shift vs. Hβ NLR shift	0.97	<0.0001	16.40 ± 3.58	0.91 ± 0.02
Hα ILR shift vs. Hβ ILR shift	0.90	<0.0001	−1.86 ± 16.97	1.09 ± 0.05
Hα VBLR shift vs. Hβ VBLR shift	0.18 (0.41)	0.041 (<0.0001)	−93.64 ± 45.30	0.06 ± 0.03
L Hα NLR vs. L Hβ NLR	0.93	<0.0001	3.40 ± 1.29	0.93 ± 0.03
L Hα ILR vs. L Hβ ILR	0.96	<0.0001	1.93 ± 1.08	0.97 ± 0.03
L Hα VBLR vs. L Hβ VBLR	0.96	<0.0001	0.70 ± 1.03	0.99 ± 0.02

Notes. The values in brackets are for the sample without the 16 objects with highly redshifted Hβ VBLR components (>4000 km s^{-1}). The coefficient of correlation (r) is in the second column, the P-value which is a measure of significance of the correlation is given in the third column, and in the next columns are the coefficients A and B from the fit with a linear function: $H\beta = A + B \cdot H\alpha$. The slopes are from regressions where X is taken as the independent variable.

3000 km s^{-1} sub-sample (1) no correlation is observed between these properties.

The observed correlation between the G/S group ratio and Hβ FWHM may be caused by intrinsic reddening since reddening increases as objects get more edge-on (Gaskell et al. 2004) and the Hβ FWHM also increases (Wills & Browne 1986). However, this cannot explain the F/G and F/S correlation with Hβ FWHM, and also, a strong influence of reddening on the G/S ratio is not expected because of the close wavelengths of lines from those groups.

We also studied correlations between continuum luminosity ($L_{\lambda 5100}$) and Fe II group ratios, since these may indicate excitation processes in the emitting region. We found that the F/G and F/S ratios decrease in objects where the continuum level is higher. Observed correlations are stronger for the Hβ FWHM < 3000 km s^{-1} sub-sample (F/G versus $L_{\lambda 5100}$: $r = -0.51$, $P < 0.0001$ and F/S versus $L_{\lambda 5100}$: $r = -0.41$, $P < 0.0001$). The ratio of G/S seems not to be dependent on continuum luminosity.

These correlations are the opposite of what would be expected from reddening, since reddening decreases with luminosity (Gaskell et al. 2004). There are a few effects that could destroy the expected reddening effect: (1) incorrect continuum subtraction; (2) host galaxy fraction which depends on the Eddington ratio; and (3) a different contribution of starlight in SDSS fiber which depends on the luminosity of the host galaxy and the redshift (see Gaskell & Kormendy 2009). There is a small possibility that these effects are important. As we already noted, the error bar in the continuum subtraction is smaller than 5%. Also, we examined whether the host galaxy contributions

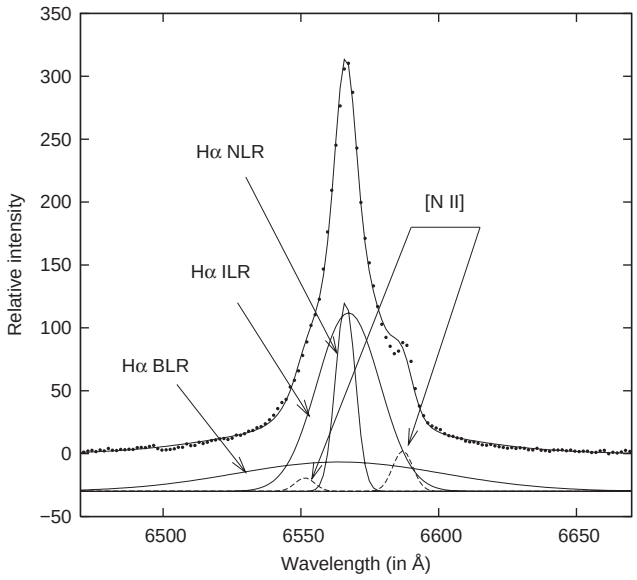

Figure 7. Fits of SDSS J141755.54 + 431155.8 in the 6400–6800 Å region: Hα is fitted with the sum of three Gaussians which represent emission from NLR, ILR, and VBLR and [N II] λλ6548, 6583 lines are fitted with one Gaussian for each line of doublet. Narrow [N II] lines are denoted with dashed lines.

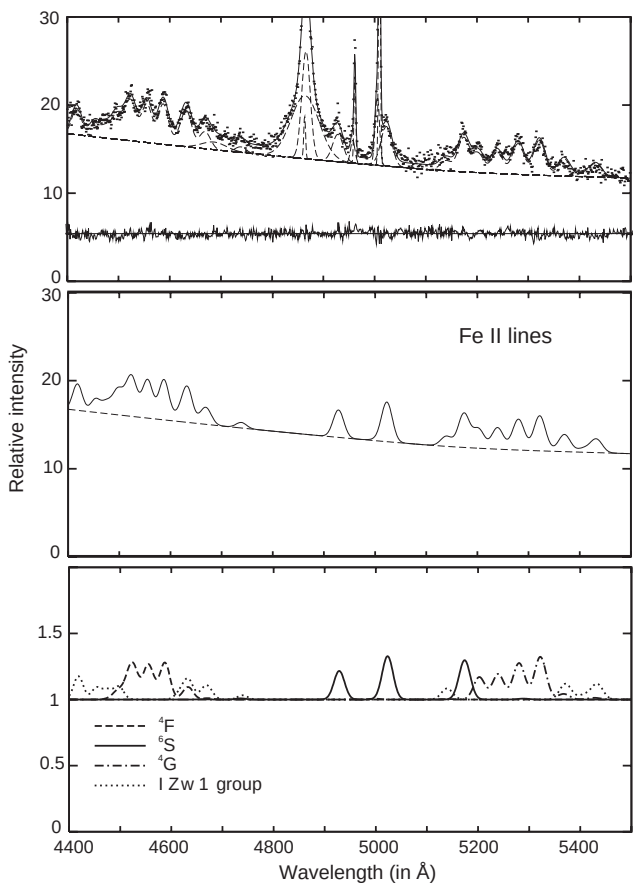

Figure 8. Example of measuring EWs of the Fe II group of lines. Top: fit spectrum (SDSS J020039.15−084554.9); middle: Fe II lines and continuum; bottom: Fe II lines normalized on the continuum level.

have influence on considered correlations. We found no correlations between the host galaxy fraction (determined in λ5100 Å) and Fe II group ratios.[9] The correlations appear instead to be

[9] The amount of stellar continuum is taken from Vanden Berk et al. (2006) for 106 common objects (see Appendix A).

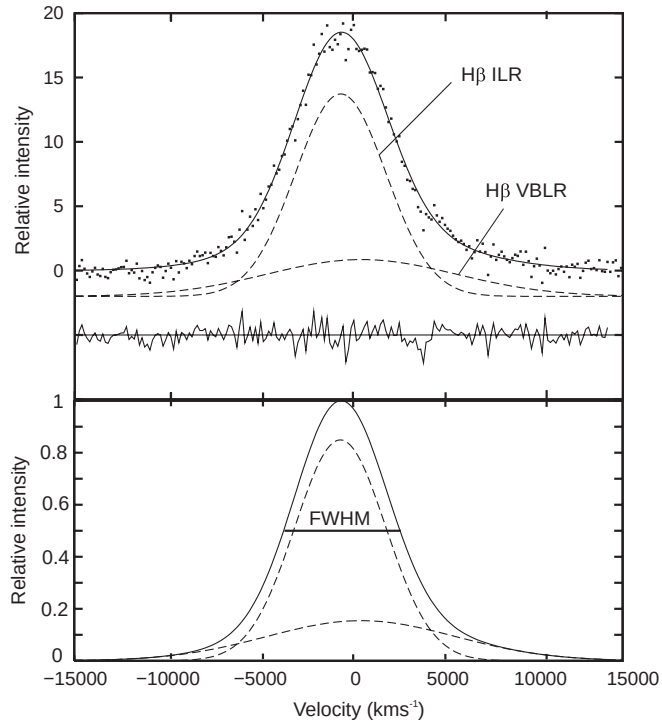

Figure 9. Example of measuring FWHM. Top: fitted broad Hβ (ILR+VBLR); bottom: FWHM is obtained as width on half maximum of the sum of ILR and VBLR Gaussians.

Table 4
Correlations Between Equivalent Widths (EWs) of the Fe II *F*, *S*, and *G* Multiplet Groups

X	*Y*	*r*	*P*	*A*	*B*
EW Fe II *F*	EW Fe II ^6S	0.76	<0.0001	0.21 ± 1.00	0.66 ± 0.03
EW Fe II *F*	EW Fe II ^4G	0.80	<0.0001	−0.17 ± 1.29	0.96 ± 0.04
EW Fe II ^6S	EW Fe II ^4G	0.83	<0.0001	5.39 ± 0.95	0.14 ± 0.04

Notes. Relationships are fitted with function $Y = A + B \cdot X$. The coefficient of correlations, *r*, the corresponding measure of the significance of correlations, *P*, as well as the *A* and *B* coefficients, are shown in the table.

connected with a weaker Baldwin effect for the *F* group (see Table 7).

We also investigated the correlation of the log(L Hα/L Hβ) with ratios of Fe II groups. We found correlations with F/G ($r = -0.36$, $P < 0.0001$) and with F/S ratio ($r = -0.34$, $P < 0.0001$), but there is no correlation with G/S (Figure 13, Table 6), i.e., between the ratio of red and central parts. There is a possibility that these correlations are caused by intrinsic reddening.

3.2. Connection between Kinematical Properties of Fe II Lines and Balmer Lines (Hα and Hβ)

We assume that the broadening of the lines arises by the Doppler effect caused by random velocities of emission clouds, and that the shifts of lines are a consequence of systemic motions of the emitting gas. We therefore studied the kinematical connection among emission regions by analyzing relationships between their widths and shifts obtained from our best fits.

The Doppler widths of Fe II and Balmer lines (Hβ and Hα) are compared in Figure 14. On the *X*-axis we present Fe II width and on the *Y*-axis the widths of the Hβ (first panel) and Hα (second panel) components. The widths of the NLR

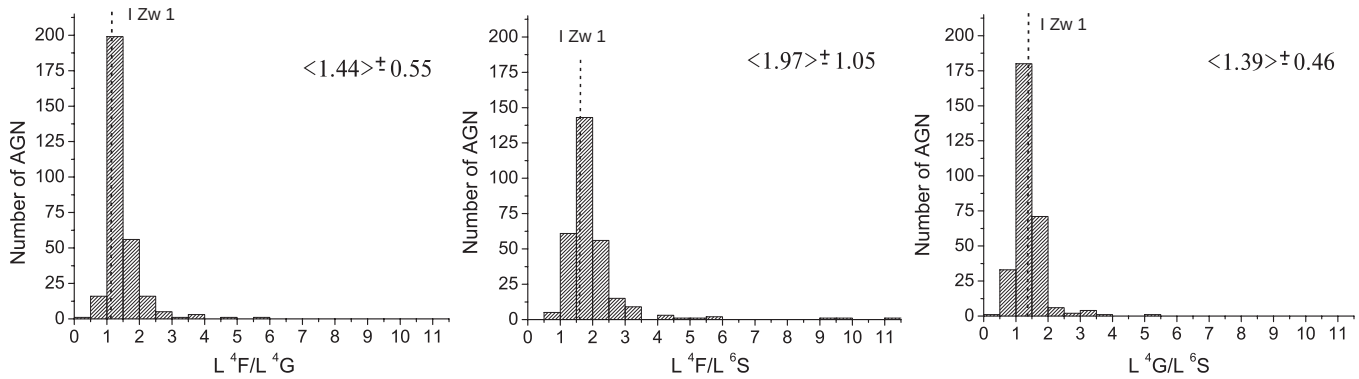

Figure 10. Distribution of the ratios of luminosities of the three Fe II groups (*F*, *S*, and *G*). The mean value and the dispersion of the distribution are given in the plots. We indicate with a dashed vertical line the ratio of Fe II groups we obtained in the I Zw 1 spectrum.

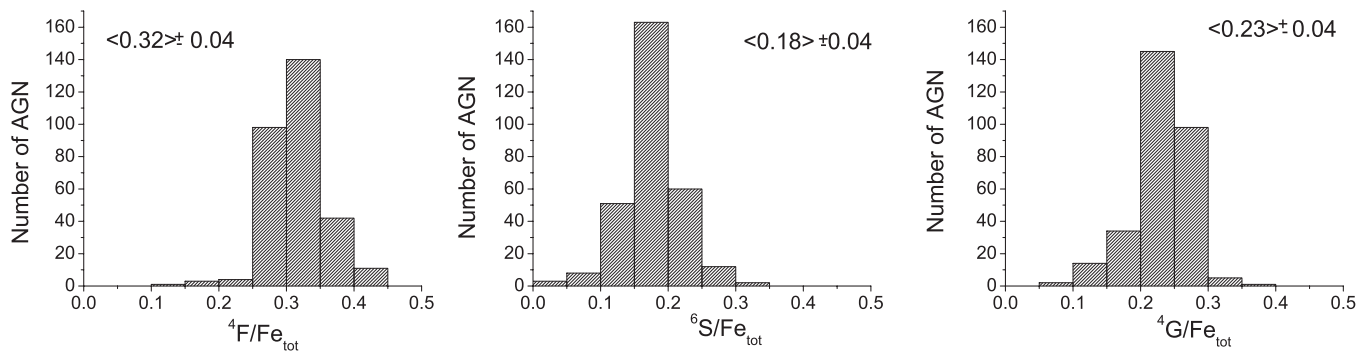

Figure 11. Distribution of the ratios of total Fe II (4400–5500 Å) and Fe II groups (*F*, *S*, and *G*). The mean value and the dispersion of the distribution are shown.

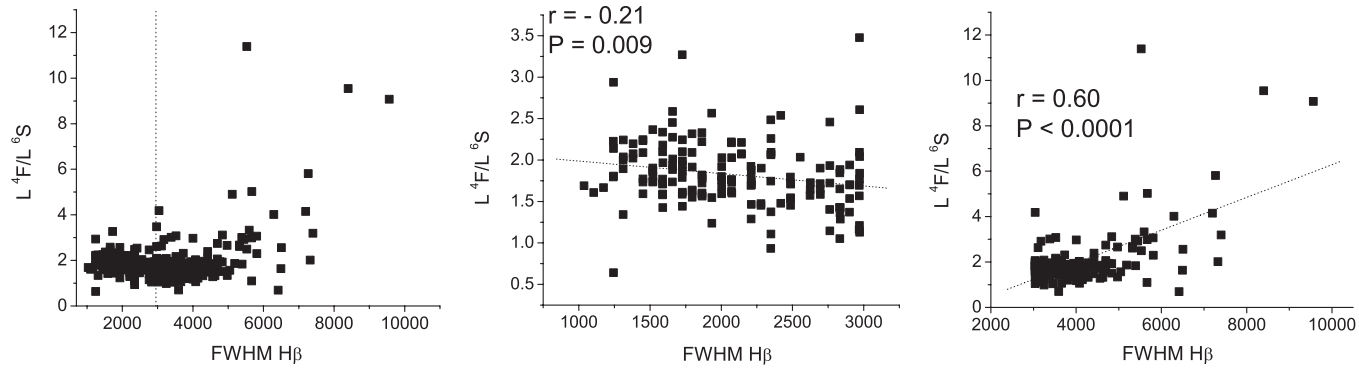

Figure 12. Relationship between F/S and Hβ FWHM, for total sample (left), sub-sample of Hβ FWHM < 3000 km s^{-1} (middle), and the sub-sample of Hβ FWHM > 3000 km s^{-1} (right).

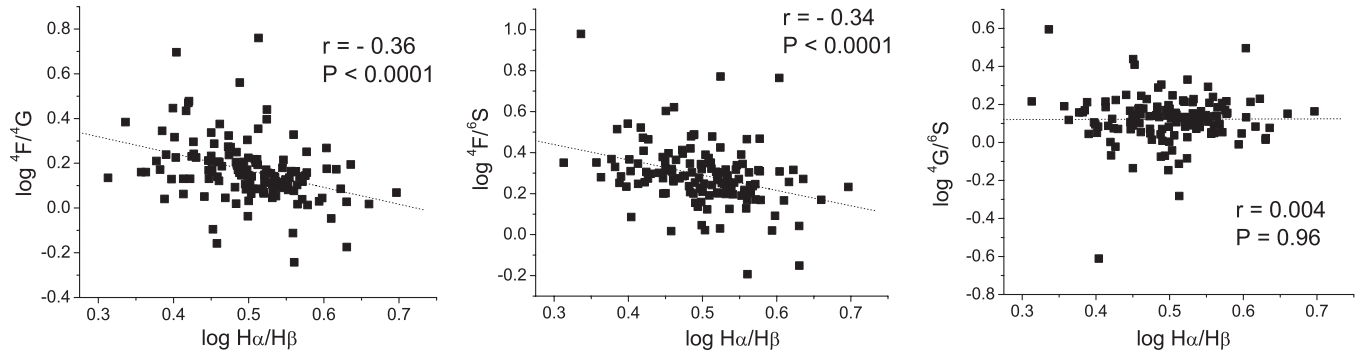

Figure 13. Relationship between Fe II group ratios and the Balmer decrement.

components are denoted by triangles, the ILR components with circles, and the VBLR components with squares. Dotted lines show the average values of the widths: vertical lines for Fe II components and horizontal lines for Hβ (or Hα). For the sample of 302 AGNs (first panel), the average value of Fe II width and dispersion of the sample is 1430 ± 440 km s^{-1}, while the average

Table 5
Correlations Between the Ratio of Fe II Line Groups and Spectral Properties

		Hβ FWHM	w Hβ ILR	w Hβ VBLR	w Fe II	sh Fe II	log λL_{5100}
F/G	r	**0.28**	**0.24**	**0.29**	0.18	**−0.27**	**−0.32**
	P	**7.13E-7**	**2.49E-5**	**2.37E-7**	0.002	**2.75E-6**	**1.82E-8**
(1) F/G	r	−0.10	−0.02	0.16	0.001	−0.10	**−0.51**
	P	0.20	0.831	0.046	0.987	0.189	**5.72E-12**
(2) F/G	r	**0.36**	0.27	0.31	0.17	−0.30	**−0.36**
	P	**1.22E-5**	0.001	1.82E-4	0.043	3.31E-4	**8.98E-6**
F/S	r	**0.41**	**0.26**	0.16	0.20	**−0.27**	−0.15
	P	**1.95E-13**	**4.05E-6**	0.004	5.47E-4	**2.44E-6**	0.011
(1) F/S	r	−0.21	−0.18	0.07	−0.23	−0.11	**−0.41**
	P	0.009	0.027	0.407	0.004	0.182	**7.90E-8**
(2) F/S	r	**0.59**	**0.33**	0.12	0.25	−0.29	−0.18
	P	**1.35E-14**	**5.08E-5**	0.157	0.002	5.29E-4	0.035
G/S	r	**0.26**	0.16	0.03	0.07	−0.11	0.06
	P	**3.92E-6**	0.004	0.646	0.213	0.048	0.312
(1) G/S	r	−0.09	−0.17	−0.09	−0.26	0.003	0.14
	P	0.243	0.036	0.277	0.001	0.965	0.076
(2) G/S	r	**0.44**	0.28	0.01	0.15	−0.13	0.006
	P	**6.15E-8**	8.26E-4	0.867	0.07	0.113	0.935

Notes. In the third column is FWHM of broad Hβ (ILR+VBLR), in the fourth and fifth columns are the Doppler widths of ILR and VBLR Hβ components, in the sixth and seventh the Doppler width and shift of Fe II lines, and in the eighth column is the continuum luminosity at 5100 Å. Correlation coefficients are calculated for the total sample, for objects with Hβ FWHM $< 3000\,\mathrm{km\,s^{-1}}$ (1) and with Hβ FWHM $> 3000\,\mathrm{km\,s^{-1}}$ (2). The correlations with $P < 0.0001$ are printed in boldface.

Table 6
The Relationship Between log(L Hα/L Hβ) and the Ratios of the Fe II Groups

		log(L Hα/L Hβ)
log(F/G)	r	−0.36
	P	<0.0001
log(F/S)	r	−0.34
	P	<0.0001
log(G/S)	r	0.004
	P	0.962

values for Hβ components are $300 \pm 150\,\mathrm{km\,s^{-1}}$ (NLR), $1570 \pm 700\,\mathrm{km\,s^{-1}}$ (ILR), and $4360 \pm 1440\,\mathrm{km\,s^{-1}}$ (VBLR). For the selected sample of 133 AGNs that have the Hα line in the spectra (second panel), the averaged value of the Fe II width is $1310 \pm 410\,\mathrm{km\,s^{-1}}$ and for the Hα components: $240 \pm 90\,\mathrm{km\,s^{-1}}$ (NLR), $1160 \pm 560\,\mathrm{km\,s^{-1}}$ (ILR), and $4060 \pm 1650\,\mathrm{km\,s^{-1}}$ (VBLR). It is obvious that the averaged Fe II width ($\sim$1400 km s^{-1}) is very close to the average widths of the ILR Hβ and Hα components (1568 km s^{-1} and 1156 km s^{-1}, respectively), while the averaged widths of NLR and VBLR components are significantly different from the Fe II width.

Relationships among the widths of the Fe II and ILR components are also presented in Figure 15 (Table 7). The correlation between the Fe II width and the width of Hα ILR is $r = 0.77$, $P < 0.0001$, and between the Fe II width and the Hβ ILR width it is $r = 0.73$, $P < 0.0001$. We also found a correlation between the widths of Fe II and the VBLR ($r = 0.66$, $P < 0.0001$ for the Hα VBLR, and $r = 0.45$, $P < 0.0001$ for Hβ VBLR).

Relationships between the shifts of Fe II and Hα and Hβ components were also considered (Table 7). We found correlations with the shifts of the Hα ILR ($r = 0.30$, $P = 0.0004$) and the Hβ ILR component ($r = 0.39$, $P < 0.0001$), but no correlation between the shift of Fe II and the shifts of other Hα and Hβ components.

We found that Fe II lines tend to have an averaged redshift of $270 \pm 180\,\mathrm{km\,s^{-1}}$ with respect to the transition wavelength, and with respect to narrow lines $100 \pm 240\,\mathrm{km\,s^{-1}}$ (see Figure 16).

3.3. Correlations between the Fe II Line Groups and Other Emission Lines

Correlations between the luminosity of the Fe II multiplet groups, total Fe II, and luminosities of the [N II] and [O III] lines are presented in Table 8. In the L [N II] versus L Fe II plot, seven outliers are observed with negligible [N II]. They are probably caused by an underestimate in the fit of the [N II] lines due to the blending with the Hα line. Without these outliers, the correlation is $\sim$0.70, $P < 0.0001$. There is no correlation between L [N II]/L [O III] and L Fe II.

We analyzed relationships among the luminosities of the Fe II line groups and the NLR, ILR, and VBLR Hα components (Table 8). All three Hα components are correlated with the Fe II line groups. Correlations are stronger with the ILR and VBLR components than with the NLR components. The same analysis was carried out for the luminosities of Fe II line groups and the NLR, ILR, and VBLR components of Hβ (Table 8). The NLR component of Hβ also has a weaker correlation with Fe II lines ($r \sim 0.60$, $P < 0.0001$) than broad Hβ components ($r \sim 0.90$, $P < 0.0001$).

We also investigated the anti-correlations between EW Fe II and EW [O III], and between EW Fe II and EW [O III]/EW Hβ (Boroson & Green 1992). We confirmed the existence of these relationships in our sample, with Fe II lines separated into F, S, and G line groups (Figure 17, Table 9). A difference from Boroson & Green (1992), who measured the EWs of all lines referring to the continuum level at the λ4861, is that we calculated the EWs by estimating the continuum below all the Fe II lines considered (see Figure 8). Note also that Boroson

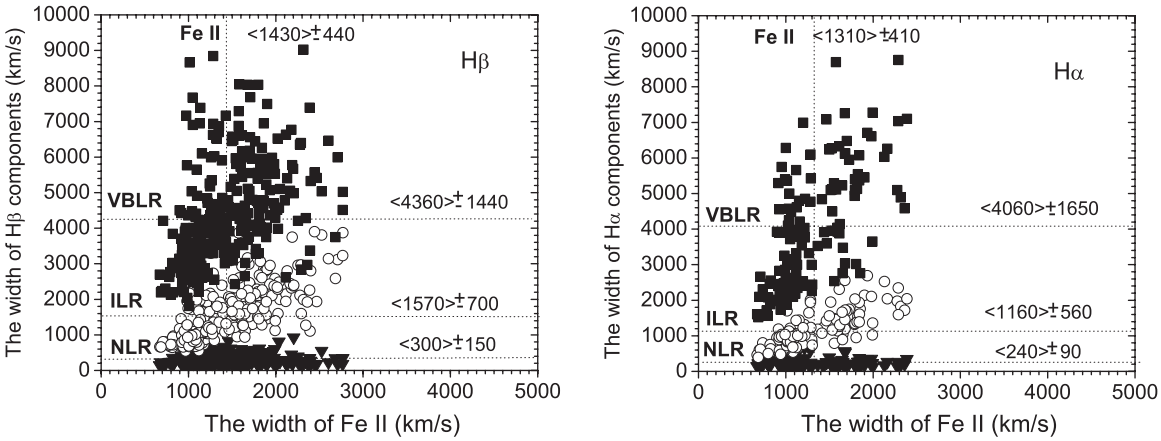

Figure 14. Widths of the Fe II lines compared with the widths of the Hβ (left) and Hα (right) components. On the *X*-axis are the widths of Fe II, and on *Y*-axis are the widths of the NLR (triangles), ILR (circles), and VBLR (squares) components of Hβ (Hα). The dotted vertical line shows the average value of Fe II widths, while the dotted horizontal lines show the average values of the Hβ (Hα) components. The average value of the Fe II lines is the same as or very close to the average width value of the ILR components of Hβ and Hα.

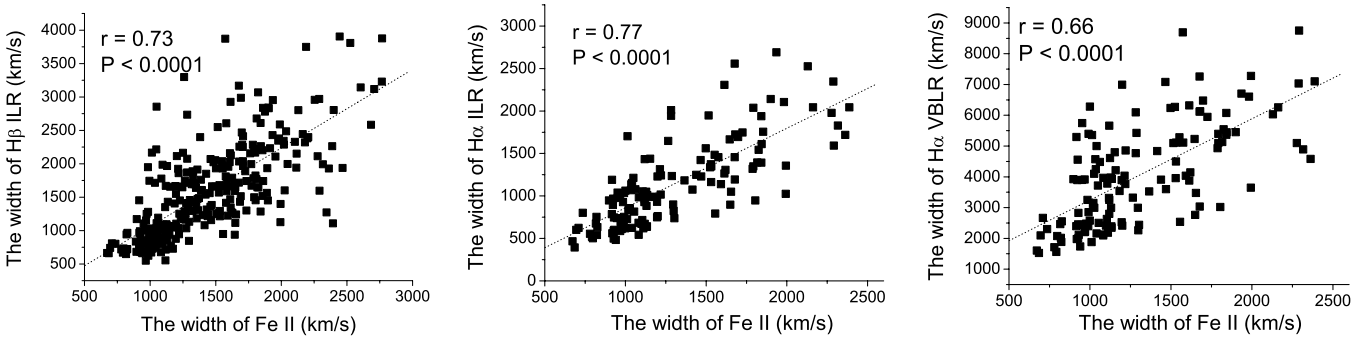

Figure 15. Correlation between the widths of Fe II and the Hβ ILR (left), Hα ILR (middle), and Hα VBLR components (right). In all cases, correlations are observed ($r = 0.67, 0.72, 0.62$), indicating kinematical connection between these emission regions.

Table 7

Relationships Between the Fe II Width and the Widths of the NLR, ILR, and VBLR Components of the Hα and Hβ (Left), and the Same but for the Shifts (Right)

		width Fe II	Corr.			shift Fe II	Corr.
w Hα NLR	*r*	0.01	No	sh Hα NLR	*r*	0.02	No
	P	0.871			*P*	0.84	
	A	232.71 ± 27.12			*A*	149.78 ± 8.88	
	B	0.00 ± 0.02			*B*	0.00 ± 0.02	
w Hα ILR	*r*	0.77	Yes	sh Hα ILR	*r*	0.30	Yes, weak
	P	<0.0001			*P*	0.0004	
	A	−94.35 ± 111.64			*A*	66.10 ± 26.11	
	B	0.96 ± 0.08			*B*	0.26 ± 0.07	
w Hα VBLR	*r*	0.66	Yes	sh Hα VBLR	*r*	0.01	No
	P	<0.0001			*P*	0.930	
	A	609.84 ± 356.76			*A*	−49.14 ± 44.47	
	B	2.63 ± 0.26			*B*	0.01 ± 0.12	
w Hβ NLR	*r*	0.05	No	sh Hβ NLR	*r*	0.00	No
	P	0.401			*P*	0.928	
	A	275.84 ± 30.17			*A*	165.22 ± 9.63	
	B	0.02 ± 0.02			*B*	0.00 ± 0.03	
w Hβ ILR	*r*	0.73	Yes	sh Hβ ILR	*r*	0.39	Yes
	P	< 0.0001			*P*	<0.0001	
	A	−114.23 ± 94.28			*A*	55.32 ± 14.80	
	B	1.17 ± 0.06			*B*	0.32 ± 0.04	
w Hβ VBLR	*r*	0.45	Yes	sh Hβ VBLR	*r*	−0.17	No
	P	<0.0001			*P*	0.003	
	A	2241.03 ± 251.81			*A*	1301.87 ± 96.29	
	B	1.48 ± 0.17			*B*	−0.83 ± 0.28	

Notes. Relationships are fitted with function $Y = A + B \cdot X$. The coefficient of correlations, *r*, the corresponding measure of the significance of correlations, *P*, as well as the *A* and *B* coefficients, are shown in the table.

Table 8
Correlations Between Luminosities (L) of the Fe II Lines (Total Fe II, F, S, and G Line Groups) and Luminosities of [N II], [O III], and Hα and Hβ Components

		log(L Fe II total)	log(LF)	log(LS)	log(LG)	log(L I Zw 1 Group)
log(L [N II])	r	0.73	0.72	0.67	0.73	0.72
	P	<0.0001	<0.0001	<0.0001	<0.0001	<0.0001
log(L [N II]/L [O III])	r	0.06	0.08	0.08	0.10	0.02
	P	0.51	0.38	0.35	0.25	0.84
log(L Hα NLR)	r	0.76	0.74	0.71	0.75	0.77
	P	<0.0001	<0.0001	<0.0001	<0.0001	<0.0001
log(L Hα ILR)	r	0.91	0.90	0.84	0.89	0.90
	P	<0.0001	<0.0001	<0.0001	<0.0001	<0.0001
log(L Hα VBLR)	r	0.90	0.89	0.82	0.87	0.90
	P	<0.0001	<0.0001	<0.0001	<0.0001	<0.0001
log(L Hβ NLR)	r	0.64	0.63	0.61	0.63	0.64
	P	<0.0001	<0.0001	<0.0001	<0.0001	<0.0001
log(L Hβ ILR)	r	0.93	0.93	0.88	0.92	0.92
	P	<0.0001	<0.0001	<0.0001	<0.0001	<0.0001
log(L Hβ VBLR)	r	0.95	0.95	0.90	0.93	0.95
	P	<0.0001	<0.0001	<0.0001	<0.0001	<0.0001

Notes. Relationships are fitted with the function $Y = A + B \cdot X$. The coefficient of correlations, r, and the corresponding measure of the significance of correlations, P, are shown in the table.

Table 9
The Same as in Table 8, but for EWs

		EW Fe II Total	EW F	EW S	EW G	EW I Zw 1 Group
EW [N II]	r	−0.27	−0.20	−0.22	−0.27	−0.25
	P	0.002	0.02	0.01	0.001	0.004
EW [O III]	r	−0.39	−0.40	−0.37	−0.42	−0.20
	P	<0.0001	<0.0001	<0.0001	<0.0001	0.0006
EW [O III]/EW Hβ	r	−0.46	−0.47	−0.43	−0.45	−0.28
	P	<0.0001	<0.0001	<0.0001	<0.0001	<0.0001
EW Hα NLR	r	−0.18	−0.18	−0.18	0.19	−0.06
	P	0.04	0.04	0.04	0.02	0.49
EW Hα ILR	r	−0.23	−0.17	−0.18	−0.29	−0.16
	P	0.007	0.04	0.04	7E-4	0.06
EW Hα VBLR	r	−0.28	−0.23	−0.28	−0.34	−0.12
	P	0.001	0.007	1E-4	<0.0001	0.18
EW Hβ NLR	r	0.01	0.01	−0.09	−0.04	0.15
	P	0.90	0.91	0.11	0.46	0.01
EW Hβ ILR	r	−0.02	0.02	0.07	−0.07	−0.08
	P	0.70	0.69	0.25	0.24	0.18
EW Hβ VBLR	r	0.12	0.11	0.11	0.04	0.21
	P	0.03	0.07	0.07	0.52	0.0003

& Green (1992) used mainly measurements from lines from multiplets 37 and 38.

We found a correlation between total EW Fe II and EW [O III]: $r = -0.39$, $P < 0.0001$. The correlation coefficient was significantly lower for the lines obtained from I Zw 1 ($r = -0.20$, $P = 0.0006$) than for the other three groups (see Table 9). We also analyzed relationships between EW Fe II line groups and EW [O III]/EW Hβ. For total EW Fe II, we found $r = -0.46$, $P < 0.0001$ (Figure 17, right), but for lines from I Zw 1 group we found $r = -0.28$, $P < 0.0001$.

No significant correlations were found between EW Fe II and EW [N II] lines (Table 9).

We also investigated whether there were any trends between EWs of Fe II F, S, G line groups and EWs of NLR, ILR, and VBLR Hα and Hβ components (Table 9). We found no significant correlations, besides a small correlation detected for EW Hα VBLR versus EW Fe II G.

The correlations between EW Fe II and the Doppler widths of Hβ components are also considered (Table 10). As was expected, an inverse correlation was found between EW Fe II and the widths of the broad Hβ components (ILR and VBLR, as well as for the Hβ FWHM, $r \sim -0.30$, $P < 0.0001$). These correlations are part of EV1. But, contrary to this, we found a positive correlation ($r = 0.30$, $P < 0.0001$) between the EW Fe II and the width of NLR component.

3.4. Relations Among Emission-line Strength and Continuum Luminosity

In Section 3.3. we have confirmed the anti-correlation EW Fe II versus EW [O III] (also EW Fe II versus EW [O III]/EW Hβ). To try to understand the underlying physics which governs this anti-correlation, we examined its dependence of the continuum luminosity and redshift.

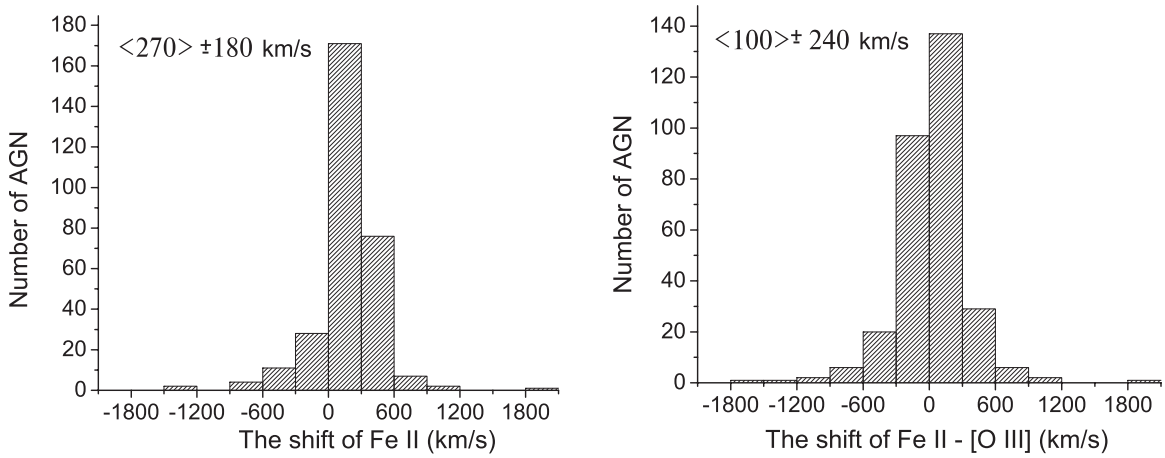

Figure 16. Distribution of the Fe II shift with respect to the transition wavelength (left) and distribution of the Fe II shift with respect to the [O III] lines (right).

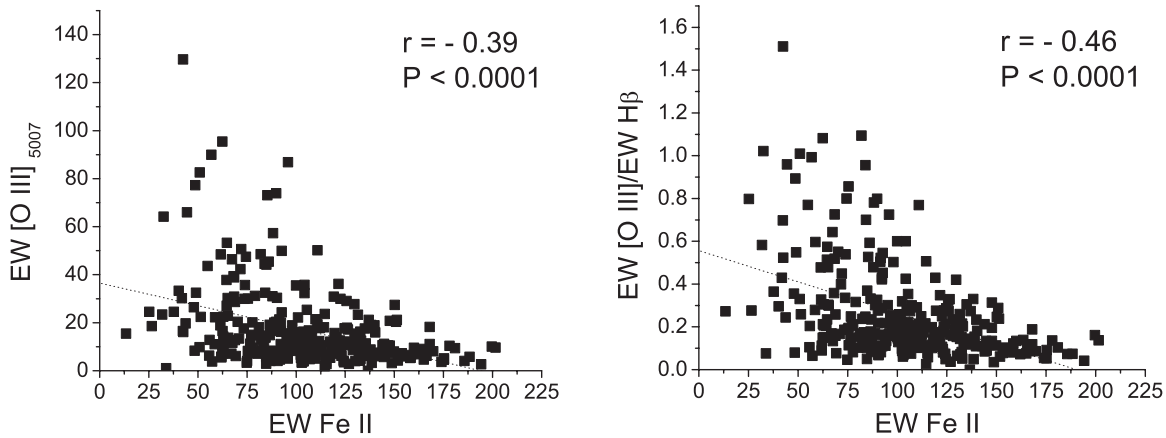

Figure 17. Relationship between the EW [O III] λ5007 vs. EW Fe II (left) and EW [O III]/EW Hβ vs. EW Fe II (right).

Table 10
The Equivalent Width of Fe II versus the Widths of the Hβ Components

		EW Fe II
Width Hβ NLR	r	0.30
	P	<0.0001
Width Hβ ILR	r	−0.31
	P	<0.0001
Width Hβ VBLR	r	−0.34
	P	<0.0001
Hβ FWHM	r	−0.30
	P	<0.0001

Because of selection effects, cosmological redshift, z, and continuum luminosity are highly correlated in our sample, so it is difficult to clearly distinguish which influence dominates in some correlations. Since our sample has a more uniform redshift distribution than continuum luminosity distribution (see Figure 2), we binned EWs of the [O III] and Fe II lines within the $z = 0$–0.7 range, using a $\Delta z = 0.1$ bin size. The binned data are presented in Figure 18. It can be seen that as redshift increases in the $z < 0.4$ range, EW Fe II also increases, but EW [O III] decreases (Figure 18). For $z > 0.4$, the trend is not so obvious, probably due to the larger scatter of the data at higher redshifts.

We derived correlation coefficients for the ratios of the [O III], Fe II, and Hβ lines and $L_{\lambda 5100}$ (also with redshift, see Figure 19, Table 11). A significant anti-correlation was found for the ratio of EW [O III]/EW Fe II versus $L_{\lambda 5100}$ and for EW [O III]/EW

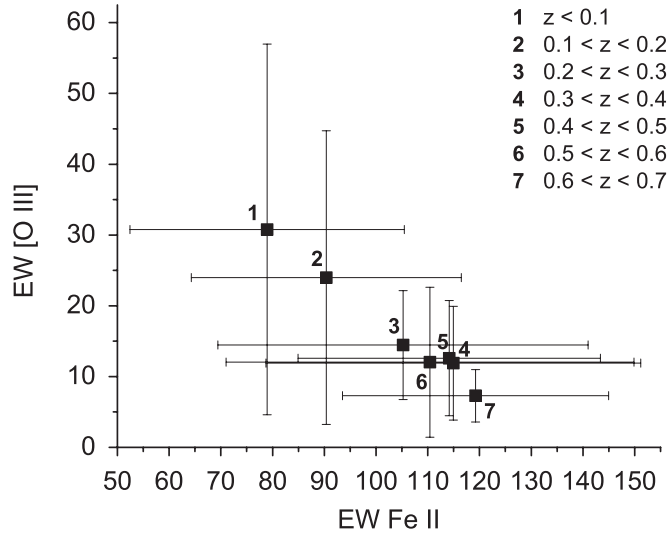

Figure 18. Relationship between the EWs, EW [O III]λ5007, and EW Fe II, binned for cosmological redshift. The error bars are the dispersions in each sub-sample within different redshift bins.

Fe II versus z ($r = -0.46$, $P = 0$ and $r = -0.48$, $P = 0$, respectively). We found that the ratios of EW [O III]/EW Hβ and EW Hβ NLR/EW Fe II also decrease as $L_{\lambda 5100}$ (redshift) increases. As in the previous case, the difference between the P-values for correlation with $L_{\lambda 5100}$ and with z is very small, so we cannot tell which effect dominates. In contrast to this, for EW H$\beta_{\rm total}$/EW Fe II versus $L_{\lambda 5100}$, no significant trend is

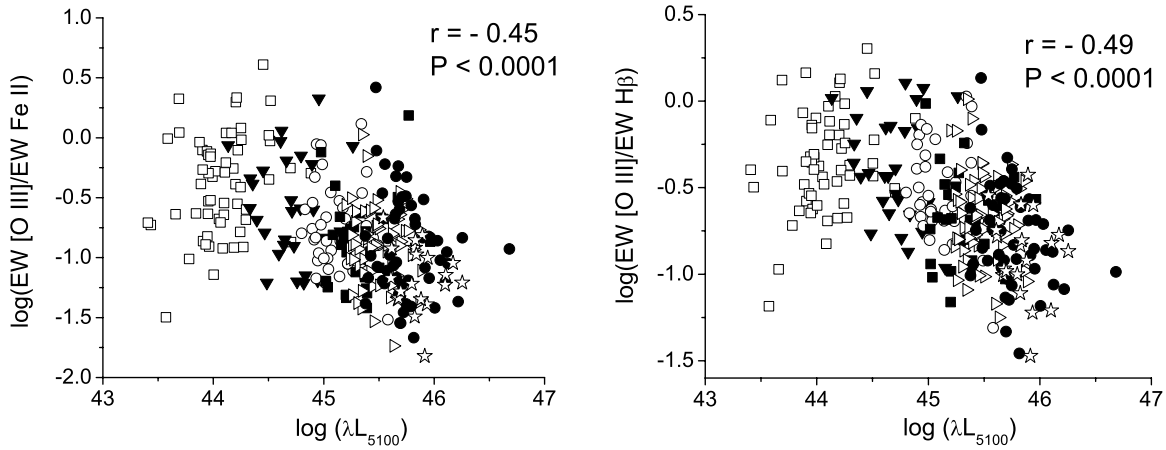

Figure 19. First panel: EW [O III]/EW Fe II ratio vs. continuum luminosity (λL_{5100}); second panel: the same for EW [O III]/EW Hβ ratio. Objects with redshift within range $z < 0.1$ are denoted with open squares, $0.1 < z < 0.2$ with filled triangles, $0.2 < z < 0.3$ with open circles, $0.3 < z < 0.4$ with filled squares, $0.4 < z < 0.5$ with open triangles, $0.5 < z < 0.6$ with filled circles, and $0.6 < z < 0.7$ with stars. [O III] includes only the λ5007 component.

Table 11

Correlations for the Total Sample (First and Second Columns), the Sub-sample with FWHM $H\beta < 3000$ km s^{-1} (1), and Sub-sample with FWHM $H\beta > 3000$ km s^{-1} (2)

		log λL_{5100}	log z	(1) log λL_{5100}	(1) log z	(2) log λL_{5100}	(2) log z
log (EW [O III]/EW Fe II)	r	**−0.46**	**−0.48**	**−0.44**	**−0.45**	**−0.55**	**−0.56**
	P	**0**	**0**	**5.67E-9**	**1.89E-9**	**1.69E-12**	**6.40E-13**
log(EW[O III]/EW Hβ)	r	**−0.49**	**−0.48**	**−0.43**	**−0.43**	**−0.50**	**−0.49**
	P	**0**	**0**	**1.66E-8**	**2.00E-8**	**2.14E-10**	**5.85E-10**
log(EWH$\beta_{\rm total}$/EW Fe II)	r	−0.19	**−0.28**	−0.28	**−0.31**	**−0.45**	**−0.49**
	P	0.001	**1.30E-6**	4.00E-4	**5.47E-5**	**2.40E-8**	**9.53E-10**
log(EWHβ NLR/EW Fe II)	r	**−0.42**	**−0.42**	**−0.52**	**−0.51**	−0.31	−0.31
	P	**2.35E-14**	**4.75E-14**	**2.42E-12**	**7.17E-12**	2.22E-4	1.97E-4
log(EW[O III])	r	**−0.43**	**−0.42**	**−0.33**	**−0.32**	**−0.54**	**−0.53**
	P	**4.00E-15**	**1.60E-14**	**1.89E-5**	**4.16E-5**	**3.35E-12**	**1.37E-11**
log(EW Fe II$_{\rm total}$)	r	**0.30**	**0.39**	**0.47**	**0.53**	**0.36**	**0.41**
	P	**1.89E-7**	**3.82E-12**	**7.05E-10**	**6.09E-13**	**1.06E-5**	**4.16E-7**
log(EW Fe II F)	r	0.16	**0.26**	0.23	0.28	0.27	**0.35**
	P	0.004	**5.99E-6**	0.003	2.81E-4	0.001	**2.36E-5**
log(EW Fe II S)	r	**0.33**	**0.40**	**0.52**	**0.58**	**0.37**	**0.39**
	P	**3.87E-9**	**1.04E-12**	**1.87E-12**	**8.88E-16**	**4.57E-6**	**1.37E-6**
log(EW Fe II G)	r	**0.44**	**0.50**	**0.61**	**0.65**	**0.50**	**0.51**
	P	**1.78E-15**	**0**	**0**	**0**	**2.52E-10**	**9.89E-11**
log(EW Fe II I Zw 1 group)	r	**0.32**	**0.23**	**0.31**	**0.39**	0.13	0.18
	P	**1.77E-8**	**4.58E-5**	**8.33E-5**	**4.29E-7**	0.120	0.031
log(EW Hβ NLR)	r	**−0.36**	**−0.33**	**−0.44**	**−0.41**	−0.21	−0.20
	P	**2.05E-10**	**6.78E-9**	**8.87E-9**	**8.79E-8**	0.010	0.015
log(EW Hβ ILR)	r	0.08	0.03	−0.04	−0.04	−0.11	−0.08
	P	0.161	0.545	0.611	0.603	0.21	0.315
log(EW Hβ VBLR)	r	0.16	0.17	**0.41**	**0.44**	−0.09	−0.09
	P	0.006	0.002	**6.98E-8**	**9.53E-9**	0.292	0.271

Note. The correlations with $P < 0.0001$ are given in bold print.

observed, but for EW H$\beta_{\rm total}$/EW Fe II versus z, there is a weak correlation ($r = 0.28$, $P = 1.3$E-6).

Because of discrepancies in the properties observed between sub-samples within different Hβ FWHM ranges (see Section 3.1), we analyzed the relationships separately for the sub-samples with FWHM H$\beta < 3000$ km s^{-1} and FWHM H$\beta > 3000$ km s^{-1}. It will be noticed that, in general, all the correlations considered are stronger for the FWHM H$\beta > 3000$ km s^{-1} sub-sample than for spectra with narrower Hβ lines (see Table 11). The only exception is the correlation of EW Hβ NLR/EW Fe II versus $L_{\lambda 5100}$, which is more significant for the FWHM H$\beta < 3000$ km s^{-1} sub-sample.

It is interesting to connect these anti-correlations (EW Fe II versus EW [O III] and considered ratios versus $L_{\lambda 5100}$) with the Baldwin effect. Baskin & Laor (2004) confirmed a correlation between the Baldwin effect and some of the emission parameters which define EV1 correlations (which are related to EW [O III]–EW Fe II anti-correlation). Also, it has been found that the [O III] lines show a strong Baldwin effect (Dietrich et al. 2002). On the other hand, no Baldwin effect has been noticed

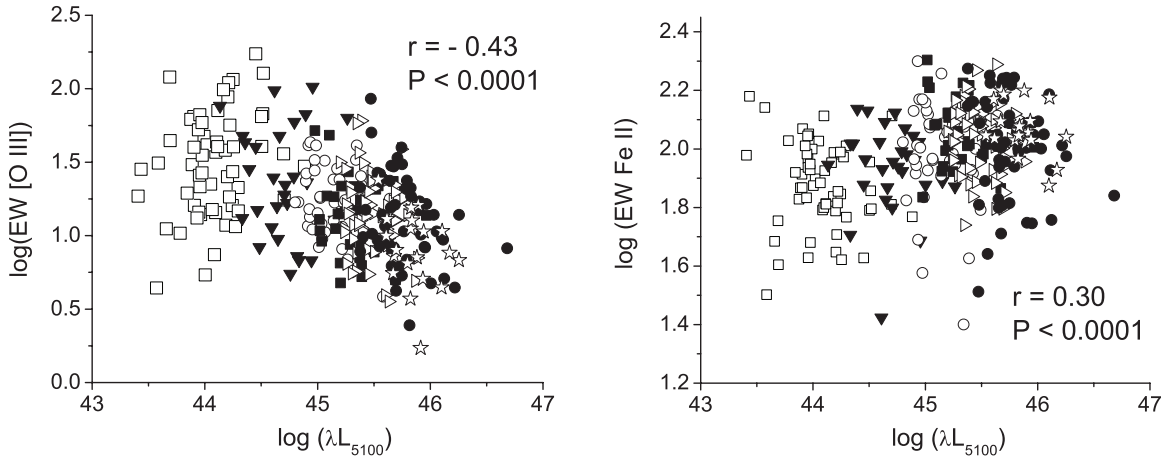

Figure 20. Baldwin effect is significant for the [O III] lines (first panel), while an inverse Baldwin effect is detected for the optical Fe II lines (second panel). Symbols have the same meaning as in Figure 19.

for the optical Fe II and Hβ lines (Dietrich et al. 2002), or even an inverse Baldwin Effect has been reported: Croom et al. (2002) found an inverse Baldwin effect in Hβ and Netzer & Trakhtenbrot (2007) found one for both Hβ and optical Fe II lines.

Because of this, we examined the dependence of the EWs of Fe II, Hβ and [O III] lines versus $L_{\lambda 5100}$ and z in our sample. Since Hβ is decomposed in NLR, ILR, and VBLR and the iron lines are separated in the groups, they can be considered in more detail. Also, we performed separate analyses for the sub-samples with different Hβ FWHM ranges (Table 11).

Analyzing the total sample (i.e., the whole Hβ FWHM range), it is obvious that Fe II lines show an inverse Baldwin effect, which is especially strong for the central ($r = 0.33$, $P < 0.0001$) and red part ($r = 0.44$, $P < 0.0001$) of the Fe II shelf (S and G groups), as well as for the group of lines from I Zw 1 ($r = 0.32$, $P < 0.0001$). The correlation of total Fe II versus $L_{\lambda 5100}$ is presented in Figure 20. What is interesting is that a strong inverse Baldwin effect is not observed for the F lines (blue part; $r = 0.16$, $P = 0.004$). In the relationship between Hβ components and continuum luminosity for the total sample, no trend is observed for broad Hβ (ILR and VBLR), but it can be noticed that the narrow Hβ component anti-correlates with continuum luminosity ($r = -0.36$, $P < 0.0001$),—i.e., they show a Baldwin effect—as well as the [O III] lines, for which the previously found trend is confirmed ($r = -0.43$, $P < 0.0001$—see Figure 20).

If we compare these correlations with the corresponding correlations with redshift, it is obvious that the iron lines (total Fe II and the multiplet groups) correlate more strongly with redshift than with luminosity. In the case of other lines we consider, the difference between the correlations with $L_{\lambda 5100}$ and z, is not so significant. Generally, it seems that the lines which show an inverse Baldwin effect (Fe II and Hβ VBLR) correlate more significantly with redshift than with luminosity, while the lines which show a (normal) Baldwin effect ([O III] and Hβ NLR) have more significant correlations with continuum luminosity.

We find that the coefficients of correlations between the EWs of lines and the continuum luminosity (and z) depend on the Hβ FWHM range of the sub-sample. It seems that continuum luminosity affects iron lines and Hβ more for the sub-sample with narrower Hβ line (FWHM Hβ < 3000 km s^{-1}). In that sub-sample, all Fe II groups show a stronger inverse Baldwin effect, Hβ NLR decreases more strongly with an increase in continuum luminosity, and an inverse Baldwin effect is also observed for Hβ VBLR ($r = 0.41$, $P < 0.0001$). This is not seen in the FWHM Hβ > 3000 km s^{-1} sub-sample. In contrast with this the Baldwin effect is stronger in the [O III] lines for the FWHM Hβ > 3000 km s^{-1} sub-sample.

4. DISCUSSION

From our analysis of optical Fe II lines ($\lambda\lambda$4400–5400), we can try to investigate physical and kinematical characteristics of the Fe II emitting region in AGN as well as the connection between the Fe II and other emission regions. We have investigated above correlations between the Fe II emission properties and some spectral features. Correlations of the Fe II lines were considered separately for different multiplet groups, which enable more detailed analysis. Here we give some discussion of the results we have obtained.

4.1. The Fe II Line Group Ratios—Possible Physical Conditions in the Fe II Emitting Region

Although we used very simple approximations to calculate the intensities of the observed Fe II lines, we found that the calculated intensities can satisfactorily fit the Fe II shelf within the 4400–5500 Å range. This approach is very simplified, but in some cases, it enables a better fit than much more complicated theoretical models (see Appendix B). We included excitation temperature in our calculation and found that it is in the most cases around 10,000 K (9646 ± 2143 K); see Figure 4. Roughly the estimated temperature of the Fe II emitting region from our fitting (assumed template) is in a good agreement with the prediction given earlier in literature (∼7000 K; Joly 1987).

We found that the most intensive emission in the optical part arises in transitions with the lower term b ^4F (multiplets 37 and 38). We also considered the ratios of multiplet groups. The line ratios may indicate some physical properties. For example, it has been shown that the Balmer line ratios are velocity dependent in AGNs (see, e.g., Shuder 1982, 1984; Crenshaw 1986; Stirpe 1990, 1991; Snedden & Gaskell 2007) and this is probably related to a range of physical conditions (electron temperature and density) and to the radiative transfer effects (see, e.g., Popović 2003, 2006). In general, the ratios between the F, G, and S groups indicate the ratio between the blue, red, and central parts of the Fe II shelf around Hβ lines. As can be seen in Table 5, there is correlation between the F/G, F/S, and G/S ratios versus FWHM of Hβ line. It is interesting that this correlation

is not present when we consider the cases where FWHM(Hβ) < 3000 km s^{-1}. We should note here that for the case FWHM(Hβ) < 3000 km s^{-1} we had only ΔFWHM(Hβ) $\approx$ 2000 km s^{-1} and this may affect the obtained results. As we mentioned above, the separation of the sample into two sub-samples according to the Hβ FWHM is similar as given in Sulentic et al. (2009, and reference therein). It seems that the characteristics of the Pop A (FWHM Hβ < 4000 km s^{-1}) and B (FWHM Hβ > 4000 km s^{-1}) of AGNs (as proposed by the above-mentioned authors) can be recognized in the Fe II line ratios: namely, the correlations and trends observed in Table 5 indicate that the ratios of blue and red (as well as blue and central) parts of Fe II shelf anti-correlate with continuum luminosity more strongly in Pop A than in Pop B. Also, for Pop B, all considered flux ratios (F/G, F/S, and G/S) increase with increasing Hβ width and with decreasing Fe II shift, while that trend is not observed in Pop A.

The observed anti-correlations of the F/G and F/S ratios versus $L_{\lambda 5100}$ could be affected by the differing degrees of the inverse Baldwin effect observed for the Fe II lines from the three line groups since the EWs of the S and G groups increase more significantly with $L_{\lambda 5100}$ ($r = 0.33$ and $r = 0.43$, $P < 0.0001$, respectively) than those of the F group ($r = 0.16$, $P = 0.04$, see Table 11). Note here that the ratio of G/S does not correlate with the continuum. Also, since the inverse Baldwin effect for the S and G groups is stronger for the FWHM Hβ <3000 km s^{-1} sub-sample, the correlations of F/G and F/S versus $L_{\lambda 5100}$ are stronger for FWHM Hβ < 3000 km s^{-1} (Table 5).

From the above-mentioned correlations, we can ask some intriguing questions about the physical conditions and processes in the Fe II emitting region: (1) Which processes cause the increase of Fe II EW with increasing $L_{\lambda 5100}$? Note that the EWs of the majority of the other emission lines in AGN spectra decrease with increasing $L_{\lambda 5100}$ (see Dietrich et al. 2002); (2) Why is the inverse Baldwin effect correlation lower for the F group compared with the S and G groups?; and (3) What causes that inverse Baldwin effect for Fe II (in S and G) to be more significant in the sub-sample with FWHM Hβ < 3000 km s^{-1} than in one with a broader Hβ line? Answering some of these questions may lead to a better understanding of the complex Fe II emitting region.

4.2. Location of the Fe II Emitting Region

Marziani & Sulentic (1993) and Popović et al. (2004) noted earlier that Fe II lines may originate in the ILR, which may be the transition from the torus to the BLR. Recently, other authors also found that the optical Fe II emission may arise from a region in the outer parts of the BLR or several times larger than the Hβ one (Hu et al. 2008b; Kuehn et al. 2008; Popović et al. 2004, 2007, 2009; Gaskell et al. 2007).

To explore the kinematics of the Fe II emitting region, which may indicate the location of the Fe II emission, we compared the derived widths and shifts of the Fe II and the Hβ and Hα components. As can be seen in Figures 14 and 15, there is an indication that Fe II emitting region is located as the IL-emitting region. Moreover, the correlation between the Doppler widths of the Fe II and IL regions is significantly higher than for the VBLR and NLR. There is no significant correlation between the Doppler widths of the Fe II and NL regions ($r = 0.01$, $P = 0.87$ for Hα, $r = 0.05$, $P = 0.40$ for Hβ), but there is a correlation between the Fe II and VBLR regions ($r = 0.66$, $P < 0.0001$ for Hα, $r = 0.45$, $P < 0.0001$ for Hβ). This may indicate that one more component of the Fe II lines is arising from the VBLR. Note here that, due to the complex Fe II template, we assumed only one component for each Fe II line (see Section 2.2). The reasonable fits of the Fe II shelf indicate that the VBLR component of Fe II should be significantly weaker than the ILR one.

These indications are also supported by the correlation between the shift of the Fe II lines and the ILR components of Hα and Hβ. The distribution of the Fe II line shifts is shown in Figure 16. The shift is obtained with respect to the transition wavelength (Figure 16, left) and with respect to the narrow lines (Figure 16, right). We found that Fe II lines are slightly redshifted, which is in agreement with the results of Hu et al. (2008b). But in this case, the average value of the Fe II shift relative to the transition wavelength is 270 ± 180 km s^{-1}, while the average value of the Fe II shift with respect to the narrow lines is 100 ± 240 km s^{-1}. This implies a significantly smaller redshift than that found in Hu et al. (2008b). A slightly redshifted Fe II emission may indicate that Fe II lines arise in an inflowing region (see Gaskell 2009).

4.3. EW Fe II versus EW [O III] Anti-correlation

One of the problems mentioned in Section 1 is the anti-correlation between the EWs of the [O III] and Fe II lines which is related to EV1 in the analysis of Boroson & Green (1992). Some physical causes proposed to explain EV1 correlations are (1) Eddington ratio $L/L_{\rm Edd}$ (Boroson & Green 1992; Baskin & Laor 2004), (2) black hole mass $M_{\rm BH}$, and (3) inclination angle (Miley & Miller 1979; Wills & Browne 1986; Marziani et al. 2001). Wang et al. (2006) also suggested that EV1 may be related to AGN evolution.

To try to understand the EW Fe II versus EW [O III] anti-correlation, we examined its relationship to continuum luminosity and redshift (see Section 3.4, Table 11). We found an anti-correlation between the EW [O III]/EW Fe II ratio and $L_{\lambda 5100}$. Also, we examined the relations of EWs of Fe II and [O III] lines versus $L_{\lambda 5100}$. We confirmed a strong Baldwin effect for [O III] lines, and an inverse Baldwin effect for EW Fe II lines, i.e., we found that as continuum luminosity increases, EW Fe II also increases, but EW [O III] decreases. This implies that the EW Fe II–EW [O III] anti-correlation may be influenced by a Baldwin effect for [O III] and an inverse Baldwin effect for Fe II lines. Also, in our analysis we found that the strength of the Baldwin effect depends on the Hβ FWHM of the sample (see Table 11). Note that Hβ FWHM is one of the parameters in EV1. As it is mentioned in Section 1, some indications of the connection between the Baldwin effect and EV1 have been given in Baskin & Laor (2004) and Dong et al. (2009). Ludwig et al. (2009) found that the significance of the EV1 relationships is a strong function of continuum luminosity, i.e., the relationships between EW Fe II, EW [O III], and Hβ FWHM can be detected only in a high-luminosity sample of AGNs ($\log\lambda L_{5100} > 44.7$), as well as a Baldwin effect for [O III] lines.[10]

The origin of the Baldwin effect is still not understood and is a matter of debate. The increase of the continuum luminosity may cause a decrease of the covering factor, or changes in the spectral energy distribution (softening of the ionizing continuum) which may result in the decrease of EWs. The inclination angle may also be related to Baldwin effect (for review see Green et al. 2001). The physical properties which are usually considered to be a primary cause of the Baldwin effect are $M_{\rm BH}$ (Warner et al.

[10] The majority of objects in our sample have continuum luminosities in the range $44.5 < \log\lambda L_{5100} < 46$ range (see Figure 2).

2003; Xu et al. 2008), $L/L_{\odot}$ (Boroson & Green 1992; Baskin & Laor 2004), and changes in gas metallicity (Dietrich et al. 2002). Also, a connection between the Baldwin effect and AGN evolution is possible (see Green et al. 2001).

We investigated whether the correlations observed between $L_{\lambda 5100}$ and the EWs of the lines (as well as EW [O III] versus EW Fe II) are primarily caused by evolution. Since continuum luminosity is strongly correlated with cosmological redshift in our sample, it is difficult to separate luminosity from evolutionary effects. The exceptions are correlations of EW Fe II versus z, as well as the ratio EW H$\beta_{\rm total}$/EW Fe II versus z, which are significantly stronger than correlations of the same quantities with $L_{\lambda 5100}$. This implies that the inverse Baldwin effect of Fe II may be governed first of all by an evolutionary effect. This result is in agreement with results of Green et al. (2001).

5. CONCLUSIONS

In this paper, we have investigated the characteristic of the Fe II emission region, using the sample of 302 AGNs from SDSS. To analyze the Fe II emission, an Fe II template was constructed by grouping the strongest Fe II multiplets into three groups, according to the atomic properties of transitions.

We have investigated the correlations of these Fe II groups and their ratios with other lines in spectra. In this way, we tried to find some physical connection between the Fe II and other emitting regions, as well as to connect Fe II atomic structure with the physical properties of the emitting plasma.

We also investigated the kinematical connection between Fe II and the Balmer emission region. In particular, the anti-correlation of EW Fe II–EW [O III] and its possible connection with AGN luminosity and evolution were analyzed. From our investigation we can outline the following conclusions.

1. We have proposed here an optical Fe II template for the 4400–5500 Å range, which consists of three groups of Fe II multiplets, grouped according to the lower terms of transitions (F, S, and G), and an additional group of lines reconstructed from the I Zw 1 spectrum. We found that the template can satisfactorily fit the Fe II lines. In spectra in which Fe II emission lines have different relative intensities than in I Zw 1, this template fits better than empirical and theoretical templates based on the I Zw 1 spectrum (see more in Appendix B). Using this template, we are able to consider different groups of transitions which contribute to the blue, central, and red parts of Fe II shelf around the Hβ+[O III] lines.
2. We find that the ratios of different parts of the iron shelf (F/G, F/S, and G/S) depend on some spectral properties such as continuum luminosity, Hβ FWHM, the shift of Fe II, and the Hα/Hβ flux ratio. Also, it is noticed that spectra with Hβ FWHM greater and less than $\sim$3000 km s^{-1} have different properties, which is reflected in significantly different coefficients of correlation between the parameters.
3. We found that the Fe II emission is mainly characterized with a random velocity of $\sim$1400 km s^{-1} that corresponds to the ILR origin, which is also supported by the significant correlation between the width of Fe II and Hα, Hβ ILR widths. This is in agreement with the previous investigations (Popović et al. 2004; Hu et al. 2008b; Kuehn et al. 2008), but unlike the earlier investigations, we found a slight correlation with the width of VBLR. Therefore, it is possible that Fe II is partly produced in the VBLR and cannot be resolved from continuum luminosity. Also, we found that the Fe II lines are slightly redshifted relative to the narrow lines ($\sim$100 km s^{-1}; see Figure 16).
4. The Balmer lines were decomposed into NLR, ILR, and VBLR components and relationships among Hβ components and some spectral properties were investigated. We found a positive correlation between the width of narrow lines and EW Fe II ($r = 0.30$, $P < 0.0001$), while the width of the broad Hβ components anti-correlates with EW Fe II. Also, we found a Baldwin effect in the case of the Hβ NLR component, while the ILR component showed no correlation with continuum luminosity, and the VBLR component shows an inverse Baldwin effect for the FWHM $<$ 3000 km s^{-1} sub-sample.
5. We confirm in our sample the anti-correlation between EW Fe II and EW [O III], which is related to EV1 in Boroson & Green (1992), and we examined its dependence on the continuum luminosity and redshift. We found an inverse Baldwin effect for Fe II lines from the central and red parts of the Fe II shelf (S and G), but for Fe II lines from blue part (F), no correlation was observed. A Baldwin effect was confirmed for the [O III] lines. Since EW Fe II increases, and EW [O III] decreases with increases of continuum luminosity (and also the trend of decreasing of the EW [O III]/EW Fe II ratio with luminosity is obvious), the observed EW Fe II versus EW [O III] anti-correlation is probably due to the same physical reason that causes the Baldwin effect. Moreover, it is observed that the coefficients of correlation due to Baldwin effect depend on the Hβ FWHM range of a sub-sample, which also implies the connection between the Baldwin effect and EV1. A decreasing trend is observed for EW [O III]/EW Hβ versus continuum luminosity.
6. We found that the EW of the Fe II lines and the EW H$\beta_{\rm total}$/EW Fe II ratio have a stronger correlation with redshift than with continuum luminosity. This implies that the inverse Baldwin effect of Fe II may be primarily caused by evolution.

This work is a part of the projects (146002): "Astrophysical Spectroscopy of Extragalactic Objects" and (146001): "Influence of Collisions with Charged Particles on Astrophysical Spectra," supported by Serbian Ministry of Science and Technological Development. Data for the present study have been entirely collected at the SDSS database. Funding for the SDSS and SDSS-II has been provided by the Alfred P. Sloan Foundation, the Participating Institutions, the National Science Foundation, the U.S. Department of Energy, the National Aeronautics and Space Administration, the Japanese Monbukagakusho, the Max Planck Society, and the Higher Education Funding Council for England. The SDSS Web Site is http://www.sdss.org/. The SDSS is managed by the Astrophysical Research Consortium for the Participating Institutions. The Participating Institutions are the American Museum of Natural History, Astrophysical Institute Potsdam, University of Basel, University of Cambridge, Case Western Reserve University, University of Chicago, Drexel University, Fermilab, the Institute for Advanced Study, the Japan Participation Group, John Hopkins University, the Joint Institute for Nuclear Astrophysics, the Kavli Institute for Particle Astrophysics and Cosmology, the Korean Scientist Group, the Chinese Academy of Sciences (LAMOST), Los Alamos National Laboratory, the Max-Planck-Institute for Astronomy (MPIA), the Max-Planck-Institute for Astrophysics (MPA), New Mexico State University, Ohio State University,

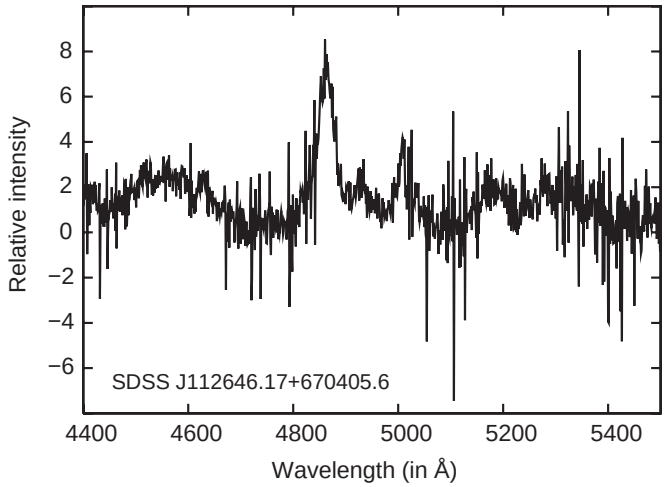

Figure 21. Example of a spectrum rejected because of strong noise which inhibited a precise fit to the iron lines.

University of Pittsburgh, University of Portsmouth, Princeton University, the United States Naval Observatory, and the University of Washington. This research has made use of NASA's Astrophysics Data System.

We thank M. Gaskell for very useful comments and suggestions.

Facilities: Nickel, HST (STIS), CXO (ASIS)

APPENDIX A

THE SAMPLE SELECTION

Using an SQL search with the requirements mentioned in Section 2.1, we obtained 497 AGN spectra with broad emission lines. From that number, 188 spectra were rejected because of noise in the iron emission line region. An example of the rejected spectrum is shown in Figure 21. Also, three spectra were rejected because of bad pixels, and one because of very strong double-peak emission in Hβ (SDSS J154213.91+183500.0).

Three more spectra with broad Hβ and practically without the Fe II emission were rejected since it was not possible to fit the Fe II lines (SDSS J132756.15+111443.6, SDSS J104326.47+110524.2, and SDSS J083343.47+074654.5). These three spectra are shown in Figure 22. There is also a possibility that in these three objects the Fe II lines are very broad and weak so that they cannot be distinguished from the continuum emission.

The sample contains 302 AGN spectra (tables with the SDSS identification and obtained parameters from the best fit are available electronically only in Table 12). To test the host galaxy contribution in the selected sample of 302 AGNs, we have compared our sample with the set of AGNs for which the host galaxy fraction is determined in Vanden Berk et al. (2006). We found 106 common objects. In the case of 48 AGNs (45% of the sample), there is practically no host galaxy contribution (0%), and in the rest of the objects, the contribution of the host galaxy is mainly smaller than 20%.

APPENDIX B

COMPARISON WITH OTHER Fe II TEMPLATES

We compared two Fe II templates (one empirical and one theoretical) with our template. The empirical Fe II template was taken from Dong et al. (2008) using 46 broad and 95 narrow lines

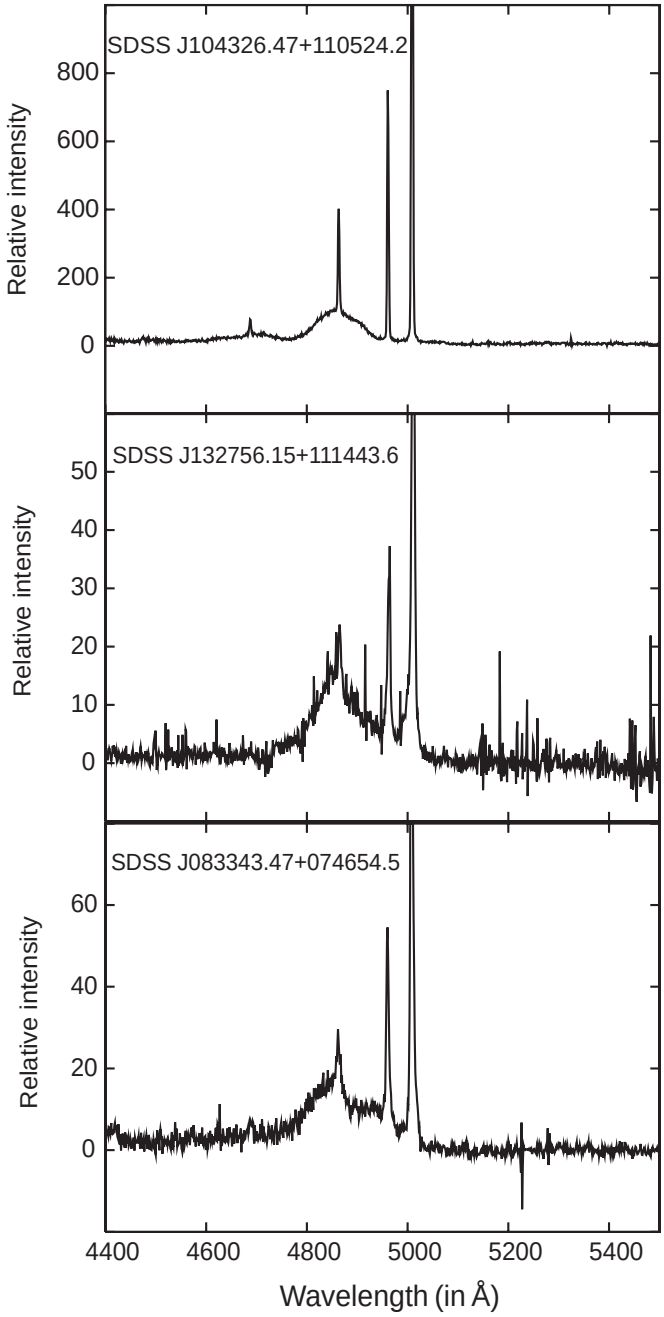

Figure 22. Three spectra with broad Hβ line and without Fe II emission.

identified by Veron-Cetty et al. (2004) in the I Zw 1 spectrum within a 4400–5500 Å range. The Fe II lines were fitted with six free parameters (the width, shift, and intensity for narrow lines and the width, shift and intensity for broad lines). We also considered the theoretical model from Bruhweiler & Verner (2008) calculated for $\log[n_{\rm H}/({\rm cm}^{-3})] = 11$, $[\xi]/(1\ {\rm km\ s}^{-1}) = 20$, and $\log[\Phi_{\rm H}/({\rm cm}^{-2}\ {\rm s}^{-1})] = 21$, since we found that this gave the best fit for those values of physical parameters. With this model, Fe II lines were fitted with three free parameters (width, shift, and intensity).

Figure 23 shows the spectrum of SDSS J020039.15−084554.9, an object in which the iron lines have relative intensities similar to I Zw 1. We fit that spectrum with our template (a), with a template based on line intensities from I Zw 1 (Dong et al. 2008) (b), and with a template calculated by the CLOUDY

Table 12
Parameters Used in Analyses of 302 AGN Samples

Name (SDSS J)	z	log (λL_{5100})	L H$\beta_{\rm total}$ (10^{40}erg s^{-1})	FWHM Hβ[a] (km s^{-1})	w Hβ NLR[b] (km s^{-1})	Shift Hβ NLR[c] (km s^{-1})	Hβ NLR/H$\beta_{\rm total}$	w Hβ ILR (km s^{-1})	shift Hβ ILR (km s^{-1})	Hβ ILR/H$\beta_{\rm total}$
000011.96+000225.29	0.478863	45.3826	856.7333	2835.2357	498.5579	−105.7368	0.0076	1245.3918	529.8802	0.3365
001224.03−102226.29	0.228075	45.1422	591.3836	2954.4480	377.8284	223.7951	0.0261	1285.4801	−1606.9775	0.2439
001335.38−095120.92	0.061570	44.0851	29.5634	3523.3501	172.2847	174.0595	0.0095	1975.1616	205.5797	0.6776
003618.41−105503.04	0.408479	45.4659	1106.6096	3246.2611	245.4581	217.2596	0.0096	1672.2153	132.8410	0.5109
004222.29−103743.70	0.423970	45.7358	2176.6337	2900.9095	313.0313	292.0068	0.0138	1431.1402	55.9203	0.4321
005812.85+160201.37	0.210642	45.2320	707.2841	3936.3637	278.4203	156.4947	0.0096	2262.8155	39.5246	0.7531
012159.82−010224.35	0.054234	44.2039	58.2980	4217.2466	226.8500	106.1595	0.1208	2469.0427	380.6375	0.6997
013418.19+001536.76	0.399966	45.6719	2193.5488	4562.5384	376.7642	409.5435	0.0204	1740.6250	−87.2726	0.2812
014631.99+133506.34	0.688737	45.9144	2420.6242	3593.5713	113.2796	45.6614	0.0087	1913.9080	325.8444	0.5801
014723.28+144320.92	0.432697	45.1977	365.7338	1657.0512	217.5084	269.9151	0.1000	671.3043	47.7360	0.2271
014942.51+001501.73	0.552141	46.0557	4681.0997	3940.7601	494.1209	96.5871	0.0348	2157.2436	364.4667	0.6578
015950.24+002340.91	0.162741	45.2646	677.2004	2970.4073	294.6930	196.7538	0.0655	1716.0900	207.0487	0.6449
020039.16−084555.01	0.431919	45.2859	512.0838	1589.0594	188.2487	133.3627	0.0603	967.1185	349.9747	0.4435
020435.19−093155.02	0.623804	45.6721	1345.1493	2072.8652	116.4124	335.5667	0.0145	1094.7521	306.1241	0.4650
021707.88−084743.41	0.291441	45.2660	335.3650	2347.9672	187.1275	111.6547	0.0149	1183.1579	146.4486	0.4298

Notes.
[a] Only broad Hβ components included.
[b] Doppler width of Hβ NLR and central [O III] components.
[c] Shift of Hβ NLR and central [O III] components.

(This table is available in its entirety in a machine-readable form in the online journal. A portion is shown here for guidance regarding its form and content.)

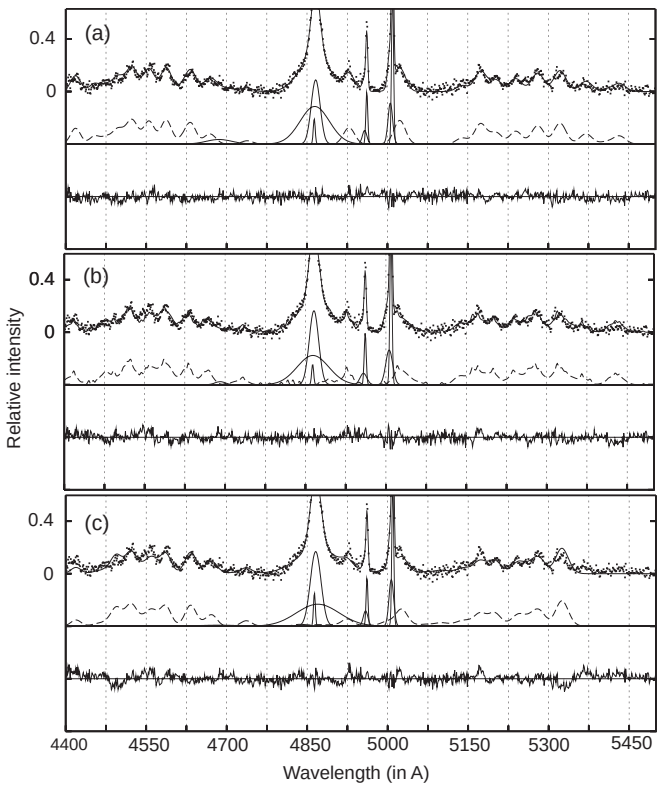

Figure 23. Examples of fits to SDSS J020039.15−084554.9: (a) with our template, (b) with the empirical template of Dong et al. (2008), and (c) with the theoretical template of Bruhweiler & Verner (2008). Since this AGN has iron emission equally strong in blue and red iron bumps (as I Zw 1), all three models fit the observed lines well.

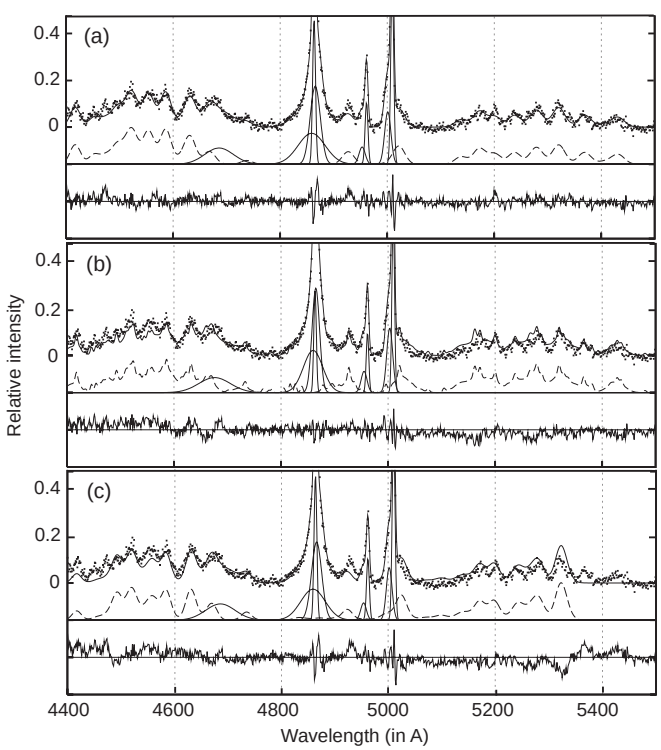

Figure 24. Examples of fits to SDSS J141755.54 + 431155.8: (a) with our template, (b) with the empirical template of Dong et al. (2008), and (c) with the theoretical template of Bruhweiler & Verner (2008). Iron emission is a bit stronger in the blue bump than in red. Our model fits this spectrum slightly better than the other two.

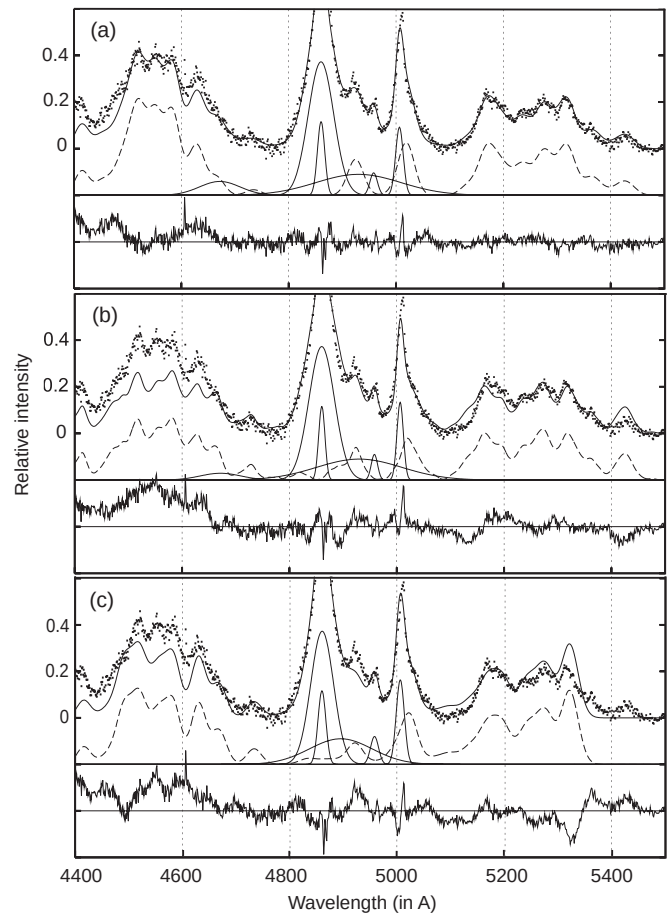

Figure 25. Examples of fits to SDSS J111603.13 + 020852.2: (a) with our template, (b) with the empirical template of Dong et al. (2008), and (c) with the theoretical template of Bruhweiler & Verner (2008). In this object, iron emission is much stronger in blue than in red bump. Our template shows disagreement for lines whose relative intensity is taken from I Zw 1, but the other three wavelength regions based on our three line groups fit the observed Fe II well. The other two models cannot fit this kind of Fe II emission well.

code (Bruhweiler & Verner 2008) (c). We found that for this object all three templates fit the iron lines well.

In the case of SDSS J141755.54 + 431155.8, however (Figure 24), the iron lines in the blue bump are slightly stronger compared with those in the red, and our model fits the iron emission slightly better than the other two templates. The discrepancy between the blue and red Fe II bumps is especially emphasized in the spectrum of the object SDSS J111603.13 + 020852.2 (Figure 25), which makes a significant difference for comparison with the Fe II properties of the I Zw 1 object. In this case, our template shows a small disagreement for the lines whose relative intensity is taken from I Zw 1, but other two models, cannot fit well this type of the Fe II emission. Disagreement is particularly strong in the blue bump (i.e., in the multiplets 37 and 38 of the *F* group).

APPENDIX C

THE RELATIVE INTENSITIES OF Fe II LINES

To estimate the relative intensities of Fe II lines within the three groups, we stated that the intensity of a line ($m \rightarrow n$) should be proportional to the number of emitters (N_m) (Osterbrock 1989; Griem 1997), i.e., for optically thin plasma (for Fe II lines) one can write: $I_{mn} = \text{const} \cdot \frac{A_{mn}}{\lambda_{mn}} \int_0^{\ell} N_m dx$, where

A_{mn} is the probability of the transition, λ_{mn} is the transition wavelength, and ℓ is the depth of the emitting region.

Of course, the density of emitters can be non-uniform across the region, but we can approximate here that it is uniform, and in the case of non-thermodynamical equilibrium it could be written (Osterbrock 1989) as

$$N_m \sim b(T, N_e) g_m \exp(-E_{mn}/kT),$$

where $b(T, N_e)$ represents deviation from thermodynamical equilibrium. In the case of lines which have the same lower level, one may approximate the ratio as (Griem 1997)

$$\frac{I_1}{I_2} = \frac{b_1(T, N_e)}{b_2(T, N_e)} \left(\frac{\lambda_2}{\lambda_1}\right)^3 \frac{f_1}{f_2} \cdot \frac{g_1}{g_2} \cdot e^{-(E1-E2)/kT}. \quad \text{(C1)}$$

Assuming that $\frac{b_1(T,N_e)}{b_2(T,N_e)} \approx 1$ we obtained Equation (1) for estimation of line ratios within one group.

REFERENCES

Abazajian, K. N., et al. 2009, ApJS, 182, 543A
Baldwin, J. A. 1977, ApJ, 214, 679
Baldwin, J. A., Ferland, G. J., Korista, K. T., Hamann, F., & LaCluyzé, A. 2004, ApJ, 615, 610B
Baskin, A., & Laor, A. 2004, MNRAS, 350, L31
Bergeron, J., & Kunth, D. 1984, MNRAS, 207, 263
Boller, T., Brandt, W. N., & Fink, H. 1996, A&A, 305, 53
Bon, E., Popović, L. Č., Ilić, D., & Mediavilla, E. G. 2006, New Astron. Rev., 50, 716
Bon, E., Popović, L. Č., Gavrilović, N., La Mura, G., & Mediavilla, E. G. 2009, MNRAS, 400, 924
Boroson, T. A., & Green, R. F. 1992, ApJS, 80, 109
Boroson, T. A., & Meyers, K. A. 1992, ApJ, 397, 442
Brotherton, M. S., Wills, B. J., Francis, P. J., & Steidel, C. C. 1994, ApJ, 430, 495
Bruhweiler, F., & Verner, E. 2008, ApJ, 675, 83
Crenshaw, D. M. 1986, ApJS, 62, 821
Collin, S., & Joly, M. 2000, New Astron. Rev., 44, 531
Collin-Souffrin, S., Joly, M., Dumont, S., & Heidmann, N. 1980, A&A, 83, 190
Corbin, M. R., & Boroson, T. A. 1996, ApJS, 107, 69
Croom, S. M., et al. 2002, MNRAS, 337, 275
Dietrich, M., Hamann, F., Shields, J. C., Constantin, A., Vestergaard, M., Chaffee, F., Foltz, C. B., & Junkkarinen, V. T. 2002, ApJ, 581, 912
Dimitrijević, M. S., Popović, L. Č., Kovačević, J., Dačić, M., & Ilić, D. 2007, MNRAS, 374, 1181
Dong, X., Wang, J., Wang, T., Wang, H., Fan, X., Zhou, H., & Yuan, W. 2009, arXiv:0903.5020D
Dong, X., Wang, T., Wang, J., Yuan, W., Zhou, H., Dai, H., & Zhang, K. 2008, MNRAS, 383, 581
Fuhr, J. R., Martin, G. A., Wiese, W. L., & Younger, S. M. 1981, J. Phys. Chem. Ref. Data, 10, 305
Gaskell, C. M. 1985, ApJ, 291, 112
Gaskell, C. M. 2009, New Astron. Rev., 53, 133
Gaskell, C. M., Goosmann, R. W., Antonucci, R. R. J., & Whysong, D. H. 2004, ApJ, 616, 147G
Gaskell, C. M., Klimek, E. S., & Nazarova, L. S. 2007, BAAS, 39, 947
Gaskell, C. M., & Kormendy, J. 2009, arXiv:0907.1652v1
Giridhar, S., & Ferro, A. A. 1995, RevMexAA, 31, 23
Green, P. J., Forster, K., & Kuraszkiewicz, J. 2001, ApJ, 556, 727
Griem, H. R. 1997, Principles of Plasma Spectroscopy (Cambridge: Cambridge Univ. Press)
Harting, G. F., & Baldwin, J. A. 1986, ApJ, 302, 64
Hartman, H., & Johansson, S. 2000, A&A, 359, 627
Hu, C., Wang, J.-M., Chen, Y.-M., Bian, W. H., & Xue, S. J. 2008a, ApJ, 683, 115
Hu, C., Wang, J.-M., Ho, L. C., Chen, Y.-M., Zhang, H.-T., Bian, W.-H., & Xue, S.-J. 2008b, ApJ, 687, 78
Ilić, D., Popović, L. Č., Bon, E., Mediavilla, E. G., & Chavushyan, V. H. 2006, MNRAS, 371, 1610
Joly, M. 1981, A&A, 102, 321
Joly, M. 1987, A&A, 184, 33
Joly, M. 1991, A&A, 242, 49
Kuehn, C. A., Baldwin, J. A., Peterson, B. M., & Korista, K. T. 2008, ApJ, 673, 69
Kuraszkiewicz, J. K., Green, P. J., Forster, K., Aldcroft, T. L., Evans, I. N., & Koratkar, A. 2002, ApJS, 143, 257
Kurucz, R. L. 1990, in Trans. IAU XXB, Proc. 20th General Assembly, ed. M. McNally (Dordrecht: Kluwer), 168
Lawrence, A., Elvis, M., Wilkes, B. J., McHardy, I., & Brandt, N. 1997, MNRAS, 285, 879
Lipari, S. L., & Terlevich, R. J. 2006, MNRAS, 368, 1001
Lipari, S., Terlevich, R., & Macchetto, F. 1993, ApJ, 406, 451
Low, F., Cutri, R., Kleinmann, S., & Huchra, J. 1989, ApJ, 340, L1
Ludwig, R. R., Wills, B., Greene, J. E., & Robinson, E. L. 2009, ApJ, 706, 995L
Marziani, P., & Sulentic, J. W. 1993, ApJ, 558, 553
Marziani, P., Sulentic, J. W., Zwitter, T., Dultzin-Hacyan, D., & Calvani, M. 2001, ApJ, 558, 553
Miley, G. K., & Miller, J. S. 1979, ApJ, 288, L55
Netzer, H., & Trakhtenbrot, B. 2007, ApJ, 654, 754
Netzer, H., & Wills, B. J. 1983, ApJ, 275, 445
Osterbrock, D. E. 1977, ApJ, 325, 733
Osterbrock, D. E. 1989, Astrophysics of Gaseous Nebulae and Active Galactic Nuclei (Sausalito, CA: Univ. Science Books)
Peebles, P. J. E. 1993, Principles of Physical Cosmology (Princeton, NJ: Princeton Univ. Press)
Penston, M. V. 1988, MNRAS, 233, 601
Phillips, M. M. 1978a, ApJ, 226, 736
Phillips, M. M. 1978b, ApJS, 38, 187
Phillips, M. M. 1979, ApJ, 39, 377
Popović, L. Č. 2003, ApJ, 599, 140
Popović, L. Č. 2006, Serb. Astron. J., 173, 1
Popović, L. Č., Mediavilla, E., Bon, E., & Ilić, D. 2004, A&A, 423, 909
Popović, L. Č., Smirnova, A., Ilić, D., Moiseev, A., Kovačević, J., & Afanasiev, V. 2007, in ASP Conf. Ser. 373, The Central Engine of Active Galactic Nuclei, ed. L. C. Ho & J.-M. Wang (San Francisco, CA: ASP), 552
Popović, L. Č., Smirnova, A., Kovačević, J., Moiseev, A., & Afanasiev, V. 2009, AJ, 137, 3548
Schlegel, M. 1998, ApJ, 500, 525
Setti, G., & Woltjer, L. 1977, ApJ, 218, L33
Shuder, J. M. 1982, ApJ, 259, 48
Shuder, J. M. 1984, ApJ, 280, 491
Sigut, T. A. A., & Pradhan, A. K. 2003, ApJS, 145, 15
Snedden, S. A., & Gaskell, C. M. 2007, ApJ, 669, 126
Stirpe, G. M. 1990, A&AS, 85, 1049
Stirpe, G. M. 1991, A&A, 247, 3
Sulentic, J. W., Marziani, P., Zamanov, R., Bachev, R., Calvani, M., & Dultzin-Hacyan, D. 2002, ApJ, 566, L71
Sulentic, J. W., Marziani, P., & Zamfir, S. 2009, New Astron. Rev., 53, 198
Vanden Berk, D. E., et al. 2006, AJ, 131, 84
Veron, M., Joly, M., Veron, P., Boroson, T., Lipari, S., & Ogle, X. 2006, A&A, 451, 851
Veron-Cetty, M.-P., Joly, M., & Veron, P. 2004, A&A, 417, 515
Verner, E. M., Verner, D. A., Korista, K. T., Ferguson, J. W., Hamann, F., & Ferland, G. J. 1999, ApJS, 120, 101
Vestergaard, M., & Wilkes, B. J. 2001, ApJS, 134, 1
Wang, J., Wei, J. Y., & He, X. T. 2006, ApJ, 638, 106
Wang, T. G., Zhou, Y. Y., & Gao, A. S. 1995, ApJ, 457, 111
Warner, C., Hamann, F., & Dietrich, M. 2003, ApJ, 596, 72
Wilkes, B. J., Elvis, M., & McHardy, I. 1987, ApJ, 321, L23
Wills, B. J., & Browne, I. W. A. 1986, ApJ, 302, 56
Xu, Y., Bian, W.-H., Yuan, Q.-R., & Huang, K.-L. 2008, MNRAS, 389, 1703
Zamfir, S., Sulentic, J. W., Marziani, P., & Dultzin, D. 2010, MNRAS, 403, 1759
Zhang, X-G, Dultzin-Hacyan, D., & Wang, T.-G. 2006, MNRAS, 372, L5
Zheng, W., & Keel, W. C. 1991, ApJ, 382, 121

The Astrophysical Journal Supplement Series, 193:2 (7pp), 2011 March doi:10.1088/0067-0049/193/1/2
© 2011. The American Astronomical Society. All rights reserved. Printed in the U.S.A.

CHEMI-IONIZATION IN SOLAR PHOTOSPHERE: INFLUENCE ON THE HYDROGEN ATOM EXCITED STATES POPULATION

Anatolij A. Mihajlov[1,2], Ljubinko M. Ignjatović[1,2], Vladimir A. Srećković[1], and Milan S. Dimitrijević[2,3,4]
[1] Institute of Physics, University of Belgrade, P.O. Box 57, 11001 Belgrade, Serbia; ljuba@ipb.ac.rs, mihajlov@ipb.ac.rs
[2] Isaac Newton Institute of Chile, Yugoslavia Branch, Volgina 7, 11060 Belgrade, Serbia
[3] Astronomical Observatory, Volgina 7, 11060 Belgrade, Serbia
[4] Observatoire de Paris, 92195 Meudon Cedex, France
Received 2010 May 30; accepted 2010 December 5; published 2011 January 18

ABSTRACT

In this paper, the influence of chemi-ionization processes in $H^*(n \geqslant 2) + H(1s)$ collisions, as well as the influence of inverse chemi-recombination processes on hydrogen atom excited-state populations in solar photosphere, are compared with the influence of concurrent electron–atom and electron–ion ionization and recombination processes. It has been found that the considered chemi-ionization/recombination processes dominate over the relevant concurrent processes in almost the whole solar photosphere. Thus, it is shown that these processes and their importance for the non-local thermodynamic equilibrium modeling of the solar atmosphere should be investigated further.

Key words: atomic processes – Sun: atmosphere

1. INTRODUCTION

In order to improve the modeling of the solar photosphere, as well as to model atmospheres of other similar and cooler stars where the main constituent is also hydrogen, it is necessary to take into account the influence of all the relevant collisional processes on the excited-atom populations in weakly ionized hydrogen plasmas. This is important for modeling since a strong connection between the changes in atom excited-state populations and the electron density exists in weakly ionized plasmas. For example, with an increase of the electron density, caused by a growth of the excited hydrogen atom population, the rate of thermalization by electron–atom collisions in the stellar atmosphere will become higher. A consequence will be that the radiative source function of the line center will be more closely coupled to the Planck function, making the synthesized spectral lines stronger for a given model structure, affecting the accuracy of plasma diagnostics and determination of the atmospheric pressure.

Therefore, in previous papers (Mihajlov et al. 1997, 2003a, 2003b, 2007b), just a group of chemi-ionization and chemi-recombination atom collisional processes in weakly ionized layers of stellar atmospheres (ionization degree less than 10^{-3}) was studied. In order to demonstrate the significance of these processes it was necessary to compare their efficiency, from the aspect of their influence on the free electron and excited atom populations, with the efficiency of the known concurrent processes of electron–atom impact ionization, electron–electron–ion recombination, and electron–ion photo-recombination. In the helium case, considered in Mihajlov et al. (2003b), it was established that the efficiency of chemi-ionization and chemi-recombination processes in weakly ionized layers of the examined DB white dwarf atmospheres was significantly greater than the efficiency of the relevant electron–atom and electron–ion processes or at least comparable to them. In the hydrogen case, considered in Mihajlov et al. (1997, 2003a, 2007b) in connection with solar and M red dwarf atmospheres, the relevant chemi-ionization processes are

$$H^*(n) + H(1s) \Rightarrow H_2^+ + e, \tag{1}$$

$$H^*(n) + H(1s) \Rightarrow H(1s) + H^+ + e, \tag{2}$$

and the corresponding inverse recombination processes are

$$H_2^+ + e \Rightarrow H^*(n) + H(1s), \tag{3}$$

$$H(1s) + H^+ + e \Rightarrow H^*(n) + H(1s), \tag{4}$$

where $H^*(n)$ is hydrogen in one of the excited states with the principal quantum number $n \geqslant 2$, H_2^+ is the hydrogen molecular ion in the ground electronic state ($1\Sigma_g^+$), and e is a free electron. Consequently, in this case the efficiency of the chemi-ionization and chemi-recombination processes has to be compared with the efficiency of the processes

$$H^*(n) + e \Rightarrow H^+ + 2e, \tag{5}$$

$$H^+ + 2e \Rightarrow H^*(n) + e, \tag{6}$$

$$H^+ + e \Rightarrow H^*(n) + \varepsilon_\lambda, \tag{7}$$

where ε_λ is the energy of a photon with wavelength λ.

Let us emphasize the fact that in this paper we focus only on the hydrogen case, since our main aim is to draw attention of astronomers to the processes (1)–(4), and to show that the importance of these processes for non-local thermodynamic equilibrium (LTE) modeling of solar atmosphere should be investigated. For this purpose, it should be demonstrated that in the solar photosphere the efficiency of these processes is greater than, or at least comparable to, the efficiency of processes (5)–(7) within those ranges of values of $n \geqslant 2$ and temperature T which are relevant to the chosen solar atmosphere model. However, by now only for chemi-recombination processes (3) and (4) it was qualitatively shown that for $4 \leqslant n \leqslant 8$ their efficiency is comparable with the efficiency of the concurrent processes (6) and (7) in a part of the solar photosphere (see Mihajlov et al. 1997).

Therefore, the results of new complete calculations are presented here, which are necessary for achieving the aim of this work. All the calculations are performed on the basis of the well-known model C of the solar atmosphere from Vernazza

et al. (1981), since it is only for this model that all the data needed for various calculations are provided in tabular form. Certainly, we keep in mind also that in Stix (2002) this model is cited as practically the single adequate non-LTE model of the solar atmosphere.

Besides all that is mentioned above, the fact that the processes (1)–(4) are very important for the solar photosphere is supported by the results obtained in Mihajlov et al. (2003a, 2007b), where these processes were included ab initio in a non-LTE modeling of an M red dwarf atmosphere with the effective temperature $T_{\rm eff} = 3800$ K, using PHOENIX code (see Baron & Hauschildt 1998; Hauschildt et al. 1999; Short et al. 1999). A fact was established that including even the chemi-ionization/recombination only for $4 \leqslant n \leqslant 8$ generates significant changes (by up to 50%), at least in the populations of hydrogen-atom excited states with $2 \leqslant n \leqslant 20$, and if all these processes (with $n \geqslant 2$) are included, a significant change (somewhere up to 2–3 times) is also generated of the free electron density N_e, and, as one of further consequences, significant changes in hydrogen line profiles. Keeping in mind that the compositions of the solar and the considered M red dwarf's photospheres are practically the same and the values of hydrogen-atom density, N_e, and T in these photospheres change within similar regions (Vernazza et al. 1981; Mihajlov et al. 2007b), one can expect that the influence of processes (1)–(4) on the hydrogen-atom excited states and free-electron populations in the solar atmosphere will be at least close to their influence in that of the M red dwarf, and that these processes will be very important for weakly ionized layers of the solar atmosphere.

Finally, let us note the fact concerning a group of collision ion–atom radiative processes. Namely, in several papers (Mihajlov & Dimitrijević 1986, 1992; Mihajlov et al. 1993, 1994a, 1994b, 2007a; Ermolaev et al. 1995; Ignjatović et al. 2009) it was suggested that these processes should be included in the stellar atmosphere models, and recently it was actually realized in Fontenla et al. (2009) and D. Koester (2010, private communication). Due to a principal similarity between the mechanisms of processes (1)–(4) and these radiative processes, one can hope that the chemi-ionization/recombination processes will be also included in the stellar atmosphere models.

In this paper all the needed theoretical data, about the chemi-ionization and chemi-recombination processes (1)–(4), are given in Section 2, while in Section 3 the obtained results are presented (in figures) demonstrating the significance of the considered processes. Apart from that, all the data used for the calculation of the rate coefficients of processes (1)–(4) are given here in three tables.

2. THEORY

2.1. The Chemi-ionization Processes: $n \geqslant 5$

Here we will consider processes (1)–(4) within the regions $n \geqslant 5$ and $2 \leqslant n \leqslant 4$ separately. Within the first region we will determine the rate coefficients for the chemi-ionization processes (1) and (2) directly, using the principle of thermodynamical balance for determination of the rate coefficients for the inverse chemi-recombination processes (3) and (4).

The parameters that are needed in further considerations are the following: $r_n \sim n^2$—the characteristic radius of Rydberg atom $H^*(n)$; R—the inter-nuclear distance in the collision system $H^*(n)+H(1s)$; and $U_1(R)$ and $U_2(R)$—the adiabatic potential energies of the ground and the first exited electronic states of molecular ion H_2^+.

In accordance with the previous papers (Mihajlov et al. 1997, 2003a, 2003b, 2007b) we will treat processes (1) and (2) with $n \geqslant 5$ on the basis of dipole resonant mechanism, which was introduced in the considerations of Smirnov & Mihajlov (1971) for inelastic processes in thermal $[H^*(n) + H(1s)]$ collisions. This means that such processes are considered as a result of resonant energy conversion within the electronic component of the collisional system $H^*(n) + H(1s)$, which is realized inside the region

$$R \ll r_n, \tag{8}$$

where the system $H^*(n) + H(1s)$ can be presented as $[H^+ + H(1s)] + e_n$, and which is caused by the dipole part of the interaction of the outer electron e_n with the subsystem $[H^+ + H(1s)]$. Already in Devdariani et al. (1978) just chemi-ionization processes in atom–Rydberg-atom collisions (the case of alkali metal atoms) were described on the basis of the same mechanism. After that, the methods based on the dipole resonant mechanism have been used in practice for investigation of chemi-ionization processes until now (see, for example, Beterov et al. 2005 and Ignjatović & Mihajlov 2005). Application of this mechanism is particularly successful within the so-called decay approximation, which was examined in Janev & Mihajlov (1980) and immediately demonstrated to be suitable for any inelastic processes in slow $[H^*(n)+H(1s)]$ collisions. Let us note that in the previous papers (Mihajlov et al. 2003a, 2003b, 2007b) a method from Mihajlov & Dimitrijević (1992) and Mihajlov et al. (1996) was used, which is based on this approximation.

Only the decay approximation will be used here for processes (1) and (2) with $n \geqslant 5$. First, it is assumed that in the region, Equation (8), the electronic state of the subsystem $[H^+ + H(1s)]$ can be approximated well by one of the two adiabatic electronic states of the molecular ion H_2^+: the ground one $|1\Sigma_g^+\vec{r}_{\rm mi}, R>$ and the first excited $|1\Sigma_u^+\vec{r}_{\rm mi}, R>$, and the state of the outer electron e_n—by one of the hydrogen Rydberg states $|n, l, m, \vec{r}>$. Then, it is assumed that, in the case of chemi-ionization processes (1) and (2), we can consider that the subsystem $[H^+ + H(1s)]$ is in the first excited electronic state $|1\Sigma_u^+\vec{r}_{\rm mi}, R>$ with a probability of 1/2, which means that we can describe the relative inter-nuclear motion as going on in the reflective potential $U_2(R)$. Finally, it means that we can expect (as a result of the mentioned electron–dipole interaction) a decay of the initial electronic state $|n, l, m, \vec{r}; 1\Sigma_u^+\vec{r}_{\rm mi}, R>= |n, l, m, \vec{r}> |1\Sigma_u^+\vec{r}_{\rm mi}, R>$ of the system $[H^+ + H(1s)] + e_n$, with a transition to the final state $|\epsilon, l', m', \vec{r}; 1\Sigma_g^+\vec{r}_{\rm mi}, R>= |\epsilon, l', m', \vec{r}> |1\Sigma_g^+\vec{r}_{\rm mi}, R>$ in a narrow neighborhood of the resonant point $R = R_{n;\epsilon}$, which is the root of the equation

$$U_{12}(R) \equiv U_2(R) - U_1(R) = \epsilon - \epsilon_n. \tag{9}$$

Here, $\epsilon_n \cong -I/n^2$ and ϵ are the energies of the initial (bound) and final (free) states of the outer electron and I is the ionization potential of the ground-state hydrogen atom. Here it is important that we have almost resonant simultaneous transitions: of the subsystem $[H^+ + H(1s)]$ to the ground electronic state $|1\Sigma_g^+\vec{r}_{\rm mi}, R>$, and of the outer electron to one of the free states $|\epsilon, l', m', \vec{r}>$.

In accordance with Janev & Mihajlov (1980), Mihajlov & Dimitrijević (1992), and Mihajlov et al. (1996), we will characterize processes (1) and (2) by quantities $W_n(R)$, $P_{\rm ci}^{(a)}(n; \rho, E)$, and $P_{\rm ci}^{(b)}(n; \rho, E)$. The first quantity has the meaning of mean decay velocity of the considered system's initial state and is

given by relations

$$W_n(R) = \frac{1}{n^2} \cdot \sum_{l,m} \frac{2\pi}{\hbar} \cdot | < 1u; n, l, m, \left| e^2 \cdot \frac{\vec{r} \cdot \vec{r}_{\rm mi}}{r^3} \right| \epsilon_k, l', m'; 1g^+ > |^2 \cdot g(\epsilon), \quad (10)$$

where e is the electron charge, $|1g, \epsilon, l', m' >= |\epsilon, l', m', \vec{r} > |1\Sigma_g^+ \vec{r}_{\rm mi}, R >$, $|1u, n, l, m >= |n, l, m, \vec{r} > |1\Sigma_u^+ \vec{r}_{\rm mi}, R >$, and $g(\epsilon)$ is the density of the free single-electron states in the energy space. Following Janev & Mihajlov (1980) and Ignjatović & Mihajlov (2005), we will transform Equation (10) to the simple form

$$W_n(R) = \frac{4}{3\sqrt{3}n^5} D_{12}^2(R) G_{nk},$$
$$D_{12}(R) = | < 1\Sigma_u^+ \vec{r}_{\rm mi}, R | r_{\rm mi;R} | 1\Sigma_g^+ \vec{r}_{\rm mi}, R > |, \quad (11)$$

where $r_{\rm mi;R}$ is the projection of $\vec{r}_{\rm mi}$ on the inter-nuclear axis, $G_{nk} \equiv \sigma_{\rm ph}(n,k)/\sigma_{\rm ph}^{\rm Kr}(n,k)$ is the generalized Gaunt factor, defined in Johnson (1972), $\sigma_{\rm ph}(n,k)$ is the mean photo-ionization cross section of the atom $H^*(n)$ for the given ϵ, and $\sigma_{\rm ph}^{\rm Kr}(n,k)$ is the same photo-ionization cross section, but in Kramers's approximation (Kramers 1923; Sobel'man 1979).

The quantities $P_{\rm ci}^{(a)}(n;\rho,E)$ and $P_{\rm ci}^{(b)}(n;\rho,E)$ are the probabilities of the realization of the chemi-ionization processes (1) and (2), respectively, for given ρ and E. In the previous papers (Mihajlov & Dimitrijević 1992; Mihajlov et al. 1996, 2003a, 2003b, 2007b), the influence of the initial state's decay (during the collision) on its amplitude was neglected in order to simplify the procedure that was used. However, it generates errors that are larger than 10% for $n \leqslant 8$. Consequently, in this work the said influence is taken into account and a procedure similar to the ones from Janev & Mihajlov (1980) and Ignjatović & Mihajlov (2005) is used. Therefore, we will present here only the final expressions for the ionization probabilities $P_{\rm ci}^{(a,b)}(n;\rho,E)$, the partial cross sections $\sigma_{\rm ci}^{(a,b)}(n;E)$, and the corresponding partial rate coefficients $K_{\rm ci}^{(a,b)}(n;T)$, where T is the temperature of the considered plasma, using additional parameters R_n, R_0, and R_E, which are the roots of equations

$$U_{12}(R) = |\epsilon_n|, \quad U_2(R) = E, \quad U_{12}(R) = E, \quad (12)$$

respectively.

In the case when only one of the processes (1) and 2) is realized, the ionization probabilities are obtained in the form

$$P_{\rm ci}^{(a,b)}(n,\rho,E) = \frac{1}{2}\left(1 - e^{-2\int_{R_0}^{R_n} \frac{W_n(R)dR}{v_{\rm rad}}}\right), \quad (13)$$

and in the case of realization of both processes we have it that

$$P_{\rm ci}^{(a)}(n,\rho,E) = \frac{1}{2}\left(1 - e^{-2\int_{R_0}^{R_E} \frac{W_n(R)dR}{v_{\rm rad}}}\right) e^{-\int_{R_E}^{R_n} \frac{W_n(R)dR}{v_{\rm rad}}}, \quad (14)$$

$$P_{\rm ci}^{(b)}(n,\rho,E) = \frac{1}{2}\left(1 - e^{-\int_{R_E}^{R_n} \frac{W_n(R)dR}{v_{\rm rad}}}\right)\left(1 + e^{-2\int_{R_0}^{R_n} \frac{W_n(R)dR}{v_{\rm rad}}}\right), \quad (15)$$

where ρ and $E = m_{\rm red}v^2/2$ are the impact parameter and the atom–Rydberg-atom impact energy, respectively ($m_{\rm red}$ being the reduced mass of the collision system).

$v_{\rm rad} = v_{\rm rad}(\rho, E; R)$ is the radial inter-nuclear velocity, which is given by

$$v_{\rm rad}(\rho, E; R) = \sqrt{\frac{2}{m_{\rm red}}\left[E - U_2(R) - \frac{E\rho^2}{R^2}\right]}. \quad (16)$$

Then, from Equations (13)–(16) the partial cross sections $\sigma_{\rm ci}^{(a,b)}(n;E)$ are determined, namely,

$$\sigma_{\rm ci}^{(a,b)}(n,E) = 2\pi \int_0^{\rho_{\rm max}^{(a,b)}(E)} P_{\rm ci}^{(a,b)}(n,\rho,E)\rho d\rho, \quad (17)$$

where $\rho_{(1a,b)}^{\rm max}(E)$ is the upper limit of values ρ, at which the corresponding region R is reached for a given E.

After that, the partial rate coefficients for the chemi-ionization processes (1) and (2) with $n \geqslant 5$ are determined by expressions

$$K_{\rm ci}^{(a,b)}(n,T) = \int_{E_{\rm min}^{(a,b)}(n)}^{E_{\rm max}} v\sigma_{\rm ci}^{(a,b)}(n,E) f(v;T) dv, \quad (18)$$

where $\sigma_{\rm ci}^{(a,b)}(n,E)$ is defined by Equation (17), v is the atom–Rydberg-atom impact velocity, $f(v;T)$ is the velocity distribution function for the given temperature T, and $E_{\rm min}^{(a,b)}(n) = 0$ if $U_2(R_n) \leqslant 0$; $E_{\rm min}^{(a,b)} = U_2(R_n)$ if $U_2(R_n) > 0$; $E_{\rm max}^{(a)} = U_2(R_{0;1}) = U_2(R_{0;1})$, where $R_{0;1}$ is such a point that $U_1(R_{0;1}) = 0$; $E_{\rm max}^{(b)} = \infty$.

Finally, using partial rate coefficients $K_{\rm ci}^{(a,b)}(n,T)$, we will determine the total one, namely,

$$K_{\rm ci}(n,T) = K_{\rm ci}^{(a)}(n,T) + K_{\rm ci}^{(b)}(n,T), \quad (19)$$

which characterizes the efficiency of the chemi-ionization processes (1) and (2) together.

2.2. The Chemi-recombination Processes: $n \geqslant 5$

Under the conditions which exist in the solar atmosphere, we can determine the chemi-recombination rate coefficients (as functions of T) from the principle of thermodynamical balance for processes (1, 2) and (3, 4), namely,

$$K_{\rm ci}^{(a)}(n,T) \cdot N_n N_1 = K_{\rm dr}(n,T) \cdot N_{\rm mi}^{\rm (eq)} N_e \equiv K_{\rm cr}^{(a)}(n,T) \cdot N_1 N_{ai} N_e \quad (20)$$

$$K_{\rm ci}^{(b)} \cdot N_n N_1 = K_{\rm cr}^{(b)}(n,T) \cdot N_1 N_{ai} N_e, \quad (21)$$

where the chemi-ionization rate coefficient $K_{\rm cr}^{(a)}(n,T)$ is expressed through the dissociative recombination rate coefficient $K_{\rm dr}(n,T)$ by relation

$$K_{\rm cr}^{(a)}(n,T) \equiv K_{\rm dr}(n,T) \cdot \chi^{-1}(T), \qquad \chi(T) = \left(\frac{N_{ai}N_1}{N_{\rm mi}^{\rm (eq)}}\right), \quad (22)$$

where N_1 and N_n denote the densities of ground- and excited-state hydrogen atoms, respectively, while N_{ai} and $N_{\rm mi}^{\rm (eq)}$ are the densities of atomic ions H^+ and molecular ions H_2^+, respectively. The index "eq" denotes that molecular ion density corresponds to thermodynamical equilibrium condition for given T. Factor $\chi(T)$ can be determined as in Mihajlov et al. (2007a) in connection with the contribution of $H^+ + H(1s)$ radiative collision processes to the solar atmosphere's opacity in UV and VUV region.

Taking quantity $K_{\rm cr}^{(a)}(n,T)$ as the rate coefficient for process (3), we can characterize both chemi-recombination processes (3) and (4) in a similar way. Namely, in accordance with Equations (20) and (21), rate coefficients $K_{\rm cr}^{(a)}(n,T)$ and $K_{\rm cr}^{(b)}(n,T)$ are given by relations

$$K_{\rm cr}^{(a,b)}(n,T) = K_{\rm ci}^{(a,b)}(n,T) \cdot S_n^{-1}(T),$$
$$S_n(T) \equiv \frac{N_i N_e}{N_n} = \frac{1}{n^2} \cdot \frac{mk_BT}{2\pi\hbar^2} \cdot \exp\left(-\frac{I_n}{k_BT}\right), \quad (23)$$

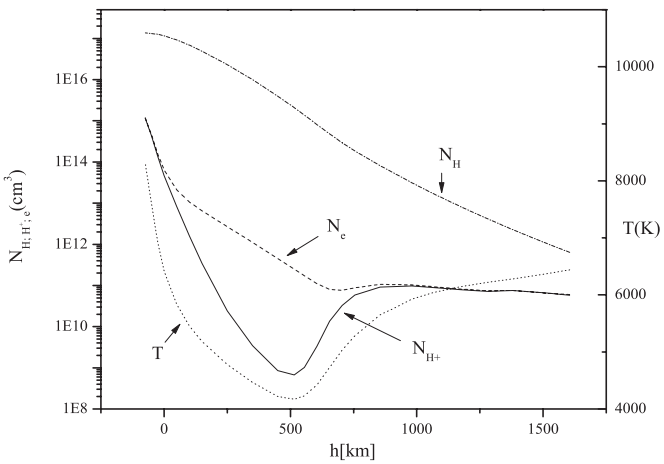

Figure 1. Basic plasma parameters, for the solar model of Vernazza et al. (1981), as a function of height *h*.

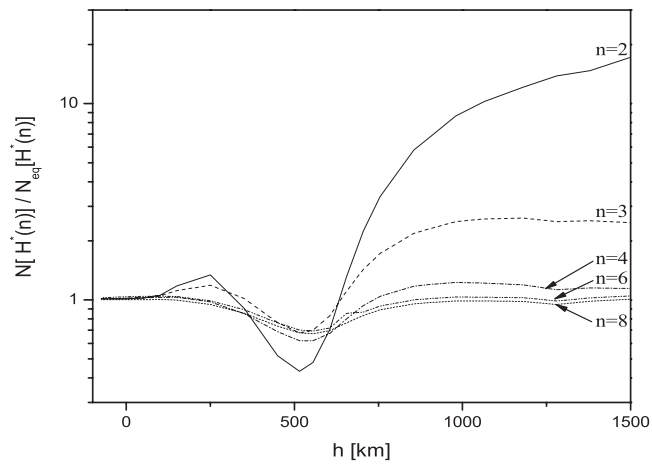

Figure 2. Parameter $\eta(n) = N(H^*)(n)/N^{(\mathrm{eq})}(H^*)(n)$, as a function of height *h*. The index "eq" denotes that excited atom densities correspond to thermodynamical equilibrium conditions for given *T*.

where *m* is the electron mass and k_B is the Boltzmann constant. Consequently, using such partial rate coefficients, we can introduce here the total one, i.e.,

$$K_{\mathrm{cr}}(n, T) = K_{\mathrm{cr}}^{(a)}(n, T) + K_{\mathrm{cr}}^{(b)}(n, T), \tag{24}$$

which characterizes the efficiency of processes (3) and (4) together for $n \geqslant 5$.

2.3. The Chemi-ionization/Recombination Processes: $2 \leqslant n \leqslant 4$

The reason why the regions $n \geqslant 5$ and $2 \leqslant n \leqslant 4$ are being considered separately is the behavior of the adiabatic potential curves of atom–atom systems $H^*(n) + H(1s)$. Namely, in the first region the atom–atom curves lie above the adiabatic curve of the ion–ion system $H^+ + H^-(1s^2)$ for any *R*, and the dipole resonant mechanism can be applied for $n \geqslant 5$ without any exceptions, while in the other region there are points where the atom–atom curves cross the ion–ion one and application of this mechanism generates some errors (see Janev & Mihajlov 1979). Since the corresponding cross points for $n \leqslant 4$ are so far from the point $R = 0$ that their existence could be neglected for $n = 4$ and 3, and with some caution even for $n = 2$, the dipole resonant mechanism was applicable, for example, in Mihajlov & Dimitrijević (1992) and Mihajlov et al. (1996) for $n = 4$ and in Zhdanov & Chibisov (1976) for $n = 3$. However, now we can determine the values of rate coefficients $K_{\mathrm{cr}}^{(a)}(n, T)$ of dissociative recombination process (3) for $n = 2$, 3, and 4 using the results deduced from the experimental data of Jones (1977), presented in Janev et al. (1987).

Due to this fact and the mentioned errors, we use here semi-empirical rate coefficients $K_{\mathrm{cr}}^{(a)}(n = 3, T)$ and $K_{\mathrm{cr}}^{(a)}(n = 4, T)$, which are obtained from Janev et al. (1987), for the dominant processes of the dissociative recombination, i.e., for process (3) with $n = 3$ and 4. The corresponding chemi-ionization rate coefficients $K_{\mathrm{ci}}^{(a)}(n = 3, T)$ and $K_{\mathrm{ci}}^{(a)}(n = 4, T)$ are then obtained from the principle of thermodynamical balance, as it has been described above. For relatively minor chemi-ionization/recombination processes, i.e., for processes (1) and (3) with $n = 2$, we use here rate coefficients $K_{\mathrm{ci}}^{(a)}(n = 2, T)$ and $K_{\mathrm{cr}}^{(a)}(n = 2, T)$, which are 10%–30% greater than the corresponding coefficients obtained using the data from Janev et al. (1987), in accordance with the calculated results from Urbain et al. (1991) and Rawlings et al. (1993). It gives a possibility to compensate the decrease of rate coefficients $K_{\mathrm{ci}}^{(a)}(n \geqslant 5, T)$ and $K_{\mathrm{cr}}^{(a)}(n \geqslant 5, T)$ in comparison with the corresponding ones obtained using Janev et al. (1987), due to the fact that here, unlike Janev et al. (1987), the decay of the considered system's initial electronic state has been taken into account. For other chemi-ionization and recombination processes (2) and (4) with $2 \leqslant n \leqslant 4$, whose contribution could really be neglected, the corresponding rate coefficients will be determined (in accordance with what was said above) by extrapolation of those from the region $n \geqslant 5$. Finally, let us note that in further considerations for chemi-ionization and recombination processes (1)–(4) with $n < 5$ we will use also total rate coefficients, which are given by the same expressions (19) and (24), but for $2 \leqslant n \leqslant 4$.

3. RESULTS AND DISCUSSION

3.1. The Considered Model of the Solar Photosphere

In accordance with the aim of this work, we consider here model C of solar atmosphere from Vernazza et al. (1981). Namely, this is a non-LTE model which is still actual (see Stix 2002), and it is only for this model that all the quantities necessary for our calculations are available in tabular form as functions of height (*h*) in solar photosphere. In Figure 1, basic plasma parameters for this model are shown. In Figure 2, deviations of non-LTE populations of excited hydrogen atom states with $2 \leqslant n \leqslant 8$ in solar photosphere within the C model of Vernazza et al. (1981) are illustrated. One can see that these deviations are particularly pronounced for $n = 2$. Around $h = 500$ km $N(H^*(n = 2))$ is one-half of the corresponding equilibrium density, and for *h* larger than 1000 km it is around 10 times greater. These deviations rapidly decrease with an increase of *n*. However, even for $n = 8$ this deviation is around 40% around $h = 500$ km, illustrating the importance of taking into account the considered processes ab initio in the modeling of solar atmosphere.

3.2. The Calculated Chemi-ionization/Recombination Rate Coefficients

The values of the total chemi-ionization and recombination rate coefficients $K_{\mathrm{ci}}(n, T)$ and $K_{\mathrm{cr}}(n, T)$, obtained in the described way, are presented in Tables 1 and 2, respectively. These tables cover the regions $2 \leqslant n \leqslant 8$ and $4000\,\mathrm{K} \leqslant \mathrm{T} \leqslant 10000\,\mathrm{K}$

Table 1
Calculated Values of Coefficient K_{ci} ($cm^3\ s^{-1}$) as a Function of n and T

T (K)	n						
	2	3	4	5	6	7	8
4000	0.150E−11	0.619E−09	0.126E−08	0.576E−09	0.554E−09	0.463E−09	0.366E−09
4250	0.202E−11	0.549E−09	0.106E−08	0.617E−09	0.583E−09	0.482E−09	0.378E−09
4500	0.260E−11	0.501E−09	0.900E−09	0.656E−09	0.611E−09	0.500E−09	0.389E−09
4750	0.324E−11	0.488E−09	0.833E−09	0.694E−09	0.637E−09	0.517E−09	0.400E−09
5000	0.403E−11	0.495E−09	0.815E−09	0.730E−09	0.662E−09	0.533E−09	0.410E−09
5250	0.504E−11	0.501E−09	0.800E−09	0.765E−09	0.686E−09	0.548E−09	0.420E−09
5500	0.623E−11	0.500E−09	0.782E−09	0.799E−09	0.709E−09	0.563E−09	0.428E−09
5750	0.756E−11	0.493E−09	0.764E−09	0.832E−09	0.731E−09	0.576E−09	0.437E−09
6000	0.909E−11	0.490E−09	0.757E−09	0.864E−09	0.752E−09	0.589E−09	0.445E−09
6250	0.108E−10	0.502E−09	0.766E−09	0.895E−09	0.772E−09	0.602E−09	0.453E−09
6500	0.128E−10	0.519E−09	0.783E−09	0.924E−09	0.791E−09	0.613E−09	0.460E−09
7000	0.175E−10	0.540E−09	0.808E−09	0.981E−09	0.827E−09	0.635E−09	0.473E−09
7500	0.232E−10	0.574E−09	0.848E−09	0.103E−08	0.860E−09	0.655E−09	0.485E−09
8000	0.300E−10	0.609E−09	0.891E−09	0.108E−08	0.892E−09	0.674E−09	0.497E−09
8500	0.380E−10	0.650E−09	0.939E−09	0.113E−08	0.920E−09	0.691E−09	0.507E−09
9000	0.470E−10	0.688E−09	0.986E−09	0.118E−08	0.948E−09	0.707E−09	0.516E−09
9500	0.574E−10	0.733E−09	0.104E−08	0.122E−08	0.973E−09	0.722E−09	0.525E−09
10000	0.689E−10	0.787E−09	0.109E−08	0.126E−08	0.997E−09	0.736E−09	0.533E−09

Table 2
Calculated Values of Recombination Coefficient K_{cr} ($cm^6\ s^{-1}$) as a Function of n and T

T (K)	n						
	2	3	4	5	6	7	8
4000	0.190E−27	0.732E−27	0.390E−27	0.114E−27	0.977E−28	0.831E−28	0.709E−28
4250	0.130E−27	0.458E−27	0.257E−27	0.102E−27	0.880E−28	0.753E−28	0.645E−28
4500	0.918E−28	0.305E−27	0.177E−27	0.914E−28	0.799E−28	0.688E−28	0.591E−28
4750	0.666E−28	0.223E−27	0.135E−27	0.828E−28	0.730E−28	0.631E−28	0.544E−28
5000	0.506E−28	0.174E−27	0.110E−27	0.755E−28	0.671E−28	0.582E−28	0.503E−28
5250	0.403E−28	0.138E−27	0.912E−28	0.693E−28	0.619E−28	0.540E−28	0.467E−28
5500	0.331E−28	0.111E−27	0.763E−28	0.639E−28	0.575E−28	0.502E−28	0.436E−28
5750	0.275E−28	0.889E−28	0.645E−28	0.592E−28	0.535E−28	0.469E−28	0.407E−28
6000	0.233E−28	0.731E−28	0.558E−28	0.551E−28	0.500E−28	0.440E−28	0.382E−28
6250	0.201E−28	0.627E−28	0.498E−28	0.514E−28	0.469E−28	0.413E−28	0.360E−28
6500	0.176E−28	0.548E−28	0.451E−28	0.482E−28	0.441E−28	0.389E−28	0.339E−28
7000	0.139E−28	0.421E−28	0.374E−28	0.427E−28	0.393E−28	0.348E−28	0.304E−28
7500	0.114E−28	0.341E−28	0.322E−28	0.382E−28	0.354E−28	0.314E−28	0.275E−28
8000	0.964E−29	0.284E−28	0.283E−28	0.345E−28	0.321E−28	0.286E−28	0.250E−28
8500	0.834E−29	0.243E−28	0.253E−28	0.314E−28	0.293E−28	0.261E−28	0.229E−28
9000	0.731E−29	0.211E−28	0.229E−28	0.287E−28	0.269E−28	0.240E−28	0.211E−28
9500	0.654E−29	0.187E−28	0.209E−28	0.264E−28	0.248E−28	0.222E−28	0.195E−28
10000	0.590E−29	0.169E−28	0.194E−28	0.245E−28	0.230E−28	0.206E−28	0.181E−28

which are relevant for solar photosphere considered on the basis of C model from Vernazza et al. (1981).

Relative contribution of partial chemi-ionization and recombination processes for given n and T characterizes corresponding branch coefficients $X_{ci}^{(a,b)}(n,T)$, namely,

$$X_{ci}^{(a,b)}(n,T) = \frac{K_{ci}^{(a,b)}(n,T)}{K_{ci}(n,T)}, \quad X_{cr}^{(a,b)}(n,T) = \frac{K_{cr}^{(a,b)}(n,T)}{K_{cr}(n,T)}. \tag{25}$$

Since $X_{ci,cr}^{(b)}(n,T) = 1 - X_{ci,cr}^{(a)}(n,T)$ and $X_{ci}^{(a,b)}(n,T) = X_{cr}^{(a,b)}(n,T) \equiv X^{(a,b)}(n,T)$, it is enough to present only the values of one of the coefficients $X^{(a,b)}(n,T)$. Here, the values of the coefficient $X^{(a)}(n,T)$, which directly describe relative contributions of the associative ionization and dissociative recombination processes (1) and (3), are presented in Table 3.

3.3. Comparison of Fluxes of the Considered Processes

Let $I_{ci}(n,T)$ and $I_{cr}(n,T)$ be the total chemi-ionization and chemi-recombination fluxes caused by the processes (1, 2) and (3, 4), i.e.,

$$\begin{aligned} I_{ci}(n,T) &= K_{ci}(n,T) \cdot N_n N_1, \\ I_{cr}(n,T) &= K_{cr}(n,T) \cdot N_1 N_i N_e, \end{aligned} \tag{26}$$

and $I_{i;ea}(n,T)$, $I_{r;eei}(n,T)$, and $I_{r;ph}(n,T)$ be the fluxes caused by ionization and recombination processes (5), (6), and (7), i.e.,

$$\begin{aligned} I_{i;ea}(n,T) &= K_{ea}(n,T) \cdot N_n N_e, \\ I_{r;eei}(n,T) &= K_{eei}(n,T) \cdot N_i N_e N_e, \\ I_{r;ph}(n,T) &= K_{ph}(n,T) \cdot N_i N_e, \end{aligned} \tag{27}$$

where N_1, N_n, N_i, and N_e are, respectively, the densities of the ground and excited states of a hydrogen atom, of ion H^+, and of free electron in the considered plasma with given T.

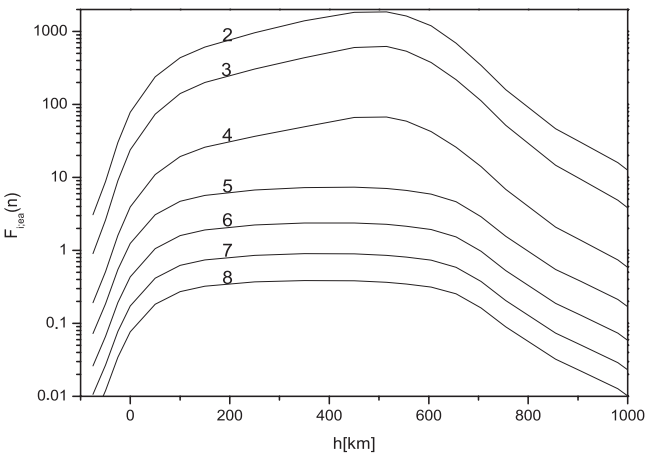

Figure 3. Behavior of the quantity $F_{i;\mathrm{ea}}^{(\mathrm{ab})}(n)$ given by Equation (5), as a function of height h.

Table 3
Calculated Values of Coefficient $X^{(a)} \equiv K_{\mathrm{ci}}^{(a)}/K_{\mathrm{ci}} = K_{\mathrm{cr}}^{(a)}/K_{\mathrm{cr}}$ as a Function of n and T

T (K)	n						
	2	3	4	5	6	7	8
4000	0.998	0.955	0.877	0.507	0.408	0.335	0.281
4250	0.969	0.934	0.827	0.484	0.388	0.318	0.266
4500	0.924	0.907	0.765	0.463	0.371	0.303	0.254
4750	0.872	0.881	0.709	0.443	0.354	0.289	0.242
5000	0.819	0.857	0.664	0.425	0.339	0.277	0.231
5250	0.769	0.831	0.619	0.408	0.325	0.265	0.221
5500	0.721	0.800	0.568	0.393	0.312	0.254	0.212
5750	0.673	0.764	0.515	0.378	0.300	0.244	0.203
6000	0.627	0.728	0.466	0.364	0.288	0.235	0.196
6250	0.585	0.699	0.430	0.351	0.278	0.226	0.188
6500	0.546	0.672	0.399	0.339	0.268	0.218	0.182
7000	0.474	0.610	0.336	0.317	0.250	0.204	0.169
7500	0.414	0.558	0.289	0.297	0.235	0.190	0.158
8000	0.363	0.510	0.250	0.280	0.221	0.179	0.149
8500	0.321	0.469	0.220	0.264	0.208	0.169	0.141
9000	0.287	0.429	0.193	0.250	0.197	0.160	0.133
9500	0.258	0.398	0.174	0.237	0.187	0.151	0.126
10000	0.234	0.376	0.160	0.225	0.177	0.144	0.120

Using these expressions, we will first calculate quantities $F_i(n, T)$ given by

$$F_i(n, T) = \frac{I_{\mathrm{ci}}(n, T)}{I_{i;\mathrm{ea}}(n, T)} = \frac{K_{\mathrm{ci}}(n, T)}{K_{\mathrm{ea}}(n, T)} \cdot N_1 N_e, \qquad (28)$$

which characterize the relative efficiency of partial chemi-ionization processes (1, 2) together and the impact electron–atom ionization (5) in the considered plasma. The total chemi-ionization and recombination rate coefficients $K_{\mathrm{ci}}(n, T)$ are determined here by the method described in the previous section, and impact ionization rate coefficients $K_{\mathrm{ea}}(n, T)$ are taken from Vriens & Smeets (1980). In Figure 3, the behavior of the quantities $F_{i,\mathrm{ea}}(n, T)$ for $2 \leqslant n \leqslant 8$ as functions of height h is shown, according to the data (N_1, N_e, and T) from Vernazza et al. (1981) for solar photosphere. One can see that the efficiency of the considered chemi-ionization processes in comparison with the electron–atom impact ionization is dominant for $2 \leqslant n \leqslant 6$ and becomes comparable for $n = 7$ and 8.

However, in order to compare the relative influence of the chemi-ionization processes (1) and (2) together to that of the impact electron–atom ionization process (5) on the whole block of the excited hydrogen atom states with $2 \leqslant n \leqslant 8$, we will calculate quantity $F_{i,\mathrm{ea};2-8}(T)$, given by

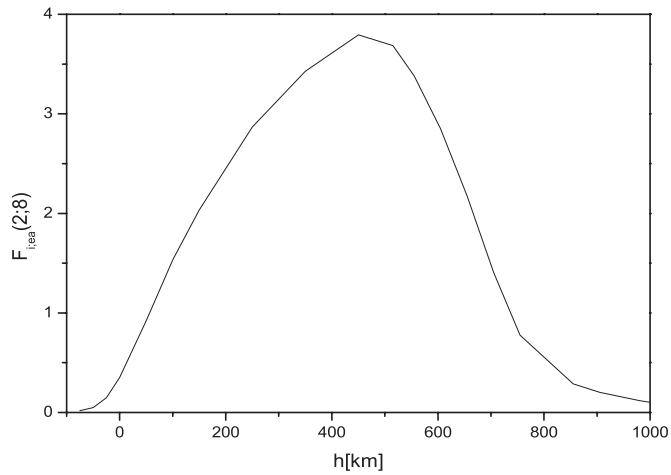

Figure 4. Behavior of the quantity $F_{i;\mathrm{ea}}(2; 8)$ given by Equation (29), as a function of height h.

$$F_{i,\mathrm{ea};2-8}(T) = \frac{\sum_{n=2}^{8} I_{\mathrm{ci}}(n, T)}{\sum_{n=2}^{8} I_{i;\mathrm{ea}}(n, T)} = \frac{\sum_{n=2}^{8} K_{\mathrm{ci}}(n, T) \cdot N_n}{\sum_{n=2}^{8} K_{\mathrm{ea}}(n, T) \cdot N_n} \cdot N_1 N_e, \qquad (29)$$

which can reflect the influence of the existing populations of excited hydrogen atom states within a non-LTE model of the solar atmosphere. In Figure 4, the behavior of the quantity $F_{i,\mathrm{ea};2-8}(T)$ as functions of height h is shown according to the same data from Vernazza et al. (1981). As one can see, the real influence of the chemi-ionization processes on the total populations of states with $2 \leqslant n \leqslant 8$ remains dominant with respect to the concurrent electron–atom impact ionization processes almost in the whole photosphere (50 km $\lesssim h \lesssim$ 750 km). This means that the chemi-ionization processes influence the radiative properties of the whole solar atmosphere in the optical region considerably.

Then, in order to compare the relative influence of chemi-recombination processes (3) and (4) together and electron–electron–H^+ ion recombination process (6) on the same block of excited hydrogen atom states with $2 \leqslant n \leqslant 8$, we calculated quantity $F_{r,\mathrm{eei};2-8}(T)$, given by

$$F_{r,\mathrm{eei};2-8}(T) = \frac{\sum_{n=2}^{8} I_{\mathrm{cr}}(n, T)}{\sum_{n=2}^{8} I_{r;\mathrm{eei}}(n, T)} = \frac{\sum_{n=2}^{8} K_{\mathrm{cr}}(n, T)}{\sum_{n=2}^{8} K_{\mathrm{eei}}(n, T)} \cdot \frac{N_1}{N_e}, \qquad (30)$$

taking rate coefficients $K_{\mathrm{eei}}(n, T)$ also from Vriens & Smeets (1980). In Figure 5, the behavior of this quantity as a function of height h is shown. One can see that the considered chemi-recombination processes dominate with respect to the concurrent electron–electron–ion recombination processes within the region 100 km $\lesssim h \lesssim$ 650 km. Consequently, the considered chemi-recombination processes are also very significant for the optical properties of the solar photosphere.

Finally, we compared the relative influence of chemi-recombination processes (3) and (4) together and photo-

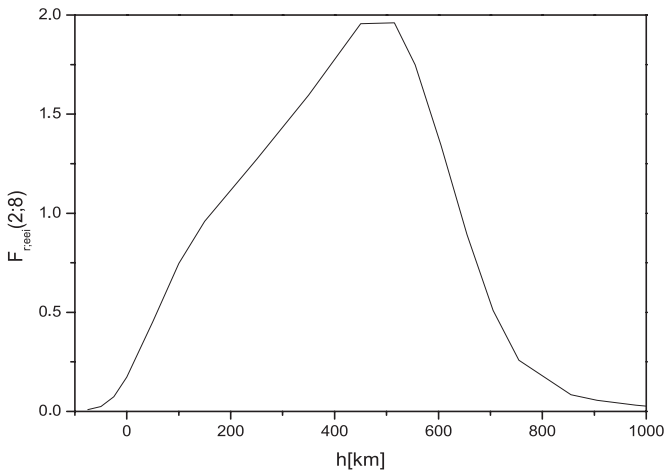

Figure 5. Behavior of the quantity $F_{r;\mathrm{eei}}(2;8)$ given by Equation (30), as a function of height h.

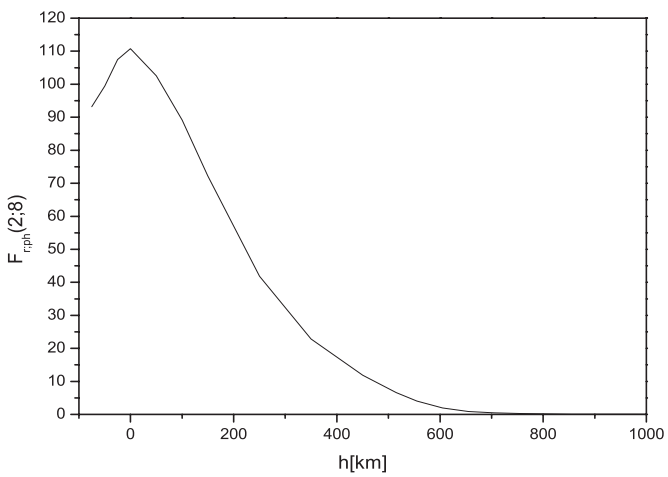

Figure 6. Behavior of the quantity $F_{r;\mathrm{ph}}(2;8)$ given by Equation (31), as a function of height h.

recombination electron–H^+ ion process (7), also within the block of the excited hydrogen atom states with $2 \leqslant n \leqslant 8$. For that sake we calculated quantity $F_{r,\mathrm{ph};2-8}(T)$, given by

$$F_{r,\mathrm{ph};2-8}(T) = \frac{\sum_{n=2}^{8} I_{\mathrm{cr}}(n,T)}{\sum_{n=2}^{8} I_{r;\mathrm{ph}}(n,T)} = \frac{\sum_{n=2}^{8} K_{\mathrm{cr}}(n,T)}{\sum_{n=2}^{8} K_{\mathrm{ph}}(n,T)} \cdot N_1, \tag{31}$$

taking rate coefficients $K_{\mathrm{ph}}(n,T)$ from Sobel'man (1979). This is necessary since in Mihajlov et al. (1997) only the states $4 \leqslant n \leqslant 8$ were considered. Still, it was a natural expectation that the inclusion of states with $n = 2$ and 3 will increase the influence of photo-recombination electron–ion processes. The behavior of quantity $F_{r,\mathrm{ph};2-8}(T)$ as a function of h is shown in Figure 6. One can see that here a domination of the chemi-recombination processes with $2 \leqslant n \leqslant 8$ over the electron–ion photo-recombination processes is confirmed (although to a slightly lesser extent) in a significant part of the photosphere (-50 km $\lesssim h \lesssim 600$ km).

4. CONCLUSION

The obtained results demonstrate the fact that the considered chemi-ionization/recombination processes must have a very significant influence on the optical properties of the solar photosphere in comparison with the concurrent electron–atom impact ionization and electron–ion recombination processes. Thus, it is shown that the importance of these processes for non-LTE modeling of solar atmosphere should be necessarily investigated.

This work was supported by the Ministry of Science and Technological Development of Serbia as a part of the project "Influence of collisional processes on astrophysical plasma line shapes" (Project number 176002).

REFERENCES

Baron, E., & Hauschildt, P. H. 1998, ApJ, 495, 370
Beterov, I. I., Tretyakov, D. B., Ryabtsev, I. I., Bezuglov, N. N., Miculis, K., Ekers, A., & Klucharev, A. N. 2005, J. Phys. B, 38, 4349
Devdariani, A. Z., Klyucharev, A. N., Lazarenko, A. B., & Sheverev, V. A. 1978, Pis'ma Zh. Tekh. Fiz., 4, 1013
Ermolaev, A. M., Mihajlov, A. A., Ignjatović, L. M., & Dimitrijević, M. S. 1995, J. Phys. D, 28, 1047
Fontenla, J. M., Curdt, W., Haberreiter, M., Harder, J., & Tian, H. 2009, ApJ, 707, 482
Hauschildt, P. H., Allard, F., & Baron, E. 1999, ApJ, 512, 377
Ignjatović, L. M., & Mihajlov, A. A. 2005, Phys. Rev. A, 72, 022715
Ignjatović, L. M., Mihajlov, A. A., Sakan, N. M., Dimitrijević, M. S., & Metropoulos, A. 2009, MNRAS, 396, 2201
Janev, R. K., Langer, W. D., Evans, K., Jr., & Post, D. E., Jr. 1987, Elementary Processes in Hydrogen–Helium Plasmas (Berlin: Springer)
Janev, R. K., & Mihajlov, A. A. 1979, Phys. Rev. A, 20, 1890
Janev, R. K., & Mihajlov, A. A. 1980, Phys. Rev. A, 21, 819
Johnson, L. C. 1972, ApJ, 174, 227
Jones, E. 1977, Report 175, Culham Laboratory, Abingdon, Oxon, London
Kramers, H. A. 1923, Phil. Mag., 46, 836
Mihajlov, A. A., & Dimitrijević, M. S. 1986, A&A, 155, 319
Mihajlov, A. A., & Dimitrijević, M. S. 1992, A&A, 256, 305
Mihajlov, A. A., Dimitrijević, M. S., & Djurić, Z. 1996, Phys. Scr., 53, 159
Mihajlov, A. A., Dimitrijević, M. S., & Ignjatović, L. M. 1993, A&A, 276, 187
Mihajlov, A. A., Dimitrijević, M. S., & Ignjatović, L. M. 1994a, A&A, 287, 1026
Mihajlov, A. A., Dimitrijević, M. S., Ignjatović, L. M., & Djurić, Z. 1994b, A&AS, 103, 57
Mihajlov, A. A., Ignjatović, L. M., Dimitrijević, M. S., & Djurić, Z. 2003a, ApJS, 147, 369
Mihajlov, A. A., Ignjatović, L. M., Sakan, N. M., & Dimitrijević, M. S. 2007a, A&A, 469, 749
Mihajlov, A. A., Ignjatovic, L. M., Vasilijević, M. M., & Dimitrijević, M. S. 1997, A&A, 324, 1206
Mihajlov, A. A., et al. 2003b, A&A, 403, 787
Mihajlov, A. A., et al. 2007b, A&A, 471, 671
Rawlings, J., Drew, J., & Barlow, M. 1993, MNRAS, 265, 968
Short, C. I., Hauschildt, P. H., & Baron, E. 1999, ApJ, 525, 375
Smirnov, V. M., & Mihajlov, A. A. 1971, Opt. Spektrosk., 30, 984
Sobel'man, I. I. 1979, Atomic Spectra and Radiative Transitions (Berlin: Springer)
Stix, M. 2002, The Sun (Section 4.3 Atmospheric Models) (2nd ed.; Berlin: Springer)
Urbain, X., Cornet, A., Brouillard, F., & Giusti-Suzor, A. 1991, Phys. Rev. Lett., 66, 1685
Vernazza, J., Avrett, E., & Loser, R. 1981, ApJS, 45, 635
Vriens, L., & Smeets, A. H. M. 1980, Phys. Rev. A, 22, 940
Zhdanov, V. P., & Chibisov, M. I. 1976, Sov. Phys. JETP, 43, 1089

THE ASTROPHYSICAL JOURNAL SUPPLEMENT SERIES, 135:109–114, 2001 July
© 2001. The American Astronomical Society. All rights reserved. Printed in U.S.A.

STARK BROADENING EFFECT IN STELLAR ATMOSPHERES: Nd II LINES

L. Č. POPOVIĆ,[1] S. SIMIĆ,[2] N. MILOVANOVIĆ,[1] AND M. S. DIMITRIJEVIĆ[1]
Received 2000 November 8; accepted 2001 January 31

ABSTRACT

The influence of the Stark broadening mechanism on line shapes and equivalent widths in stellar atmospheres was considered. The test of this influence was done for 38 astrophysically important Nd II lines for different types of stellar atmospheres. Moreover, the electron-impact widths for 284 Nd II lines are given. For calculation of the electron-impact widths we use the modified semiempirical method.

Subject headings: atomic data — plasmas — stars: chemically peculiar

1. INTRODUCTION

The atomic data are needed for various problems in astrophysics. For example, the reliability of the element abundance determinations in stellar atmospheres depends on a number of factors, where atomic data (transition probabilities, collisional widths, etc.) are among the most important. One of the needed set of atomic data for line synthesis are the electron-impact widths. They are needed in order to solve various problems in astrophysics and physics, for example, diagnostics and modeling of laboratory and stellar plasma, investigation of its physical properties and for abundance determination. These investigations provide information useful for the modeling of stellar evolution, e.g., abundance studies in stellar atmospheres provide evidence of the chemical composition of the stellar primordial cloud, of processes occurring within the stellar interior, and the dynamic processes occurring in the stellar atmospheres.

Spectroscopic data for rare earth elements (REE) are of interest for astrophysics since the lines of the ionized REE are present in stellar spectra. Moreover, the REE are overabundant in CP stars in a wide temperature domain (see, e.g., Jaschek & Jaschek 1974; Bonsack & Wolff 1980; Magazzu & Cowley 1986; Ryabchikova & Ptitsyn 1986; Cowley & Greenberg 1988; Van't Veer et al. 1988; Sadakane 1993; Kupka et al. 1996; Gelbmann et al. 1997; Ryabchikova et al. 1997, 1999; Cowley et al. 2000), and the atomic data for REE are needed in order to solve the astrophysical problems such as the relative abundance of *r*- and *s*-process elements in metal poor Halo stars and the evolution of CP stars (Cowley 1984; Sneden et al. 1996). Usually, REE abundance analysis is based on the lines for the first ionization stages, which have experimentally determined oscillator strengths. In some CP stars, e.g., HD 101065 (Cowley et al. 2000), very large excesses of REE are presented.

The lines of Nd II are observed in spectra of CP stars as well as in spectra of other stars (see e.g., Guthrie 1985; Adelman 1987, 1994; Sadakane 1993; Cowley et al. 2000). Due to conditions in stellar atmospheres, the Nd II lines are dominant in comparison with Nd I and Nd III lines, e.g., in spectra of HD 101065, a roAp star, Cowley et al. (2000) found 71 lines of Nd II and only six and seven lines of Nd I and Nd III, respectively. It is the reason why for determination of neodymium abundance in spectra of CP and other stars the Nd II lines are usually used. On the other side, due to complexity of Nd II spectrum, it is very difficult to obtain atomic data (oscillator strengths, Stark widths, etc.) needed for astrophysical purposes. In order to provide a complete set of Stark broadening data of astrophysical interest, we started a project to calculate such data for a number of spectral lines of REE (see Popović & Dimitirjević 1998a; Popović et al. 1999). Here we present Stark widths for 284 Nd II lines. Also, in order to stress the Stark broadening mechanism importance for different types of stars, we have analyzed the electron-impact effect influence on spectral line shapes and equivalent widths in the case of 38 Nd II lines which are observed in stellar spectra.

2. METHOD OF CALCULATION

When there is no enough atomic data for more sophisticated calculations, one may use the modified semiempirical approach (MSE, Dimitrijević & Konjević 1980, 1987; Dimitrijević & Kršljanin 1986), tested several times for complex spectra (see, e.g., Popović & Dimitrijević 1996a, 1996b, 1997). This method, applicable only for the Stark broadening of isolated, nonhydrogenic ion lines, has been described several times (Dimitrijević & Konjević 1980; Dimitrijević & Kršljanin 1986; Popović & Dimitrijević 1996b, 1997, 2000) and here will not be repeated.

Compared with the semiclassical perturbation approach, the modified semiempirical approach needs less atomic data. In fact, if there are no perturbing levels strongly violating the assumed approximation, we need only the energy levels with $\Delta n = 0$ and $\ell'_{if} = \ell_{if} \pm 1$, for, e.g., the line width calculations, since all perturbing levels with $\Delta n \neq 0$, needed for a full semiclassical investigation, are lumped together and approximately estimated.

The accuracy of the MSE approximation is assumed to be about $\pm 50\%$ (Dimitrijević & Konjević 1980). It was shown in Popović & Dimitrijević (1996b, 1998b) that the MSE approach, even in the case of the emitters with very complex spectra (e.g., Xe II and Kr II), gives a very good agreement with experimental measurements (in the interval $\pm 30\%$).

In the case of Nd II lines, due to a very complex spectrum, it was not possible to adequately use the MSE approach, so we use the simplified version of this approach given by Dimitrijević & Konjević (1987) and we calculated only the Stark widths. This formula is better than older approximate

[1] Astronomical Observatory Belgrade, Volgina 7, 11160 Belgrade, Serbia, Yugoslavia; lpopovic@aob.bg.ac.yu, nmilovanovic@aob.bg.ac.yu, mdimitrijevic@aob.bg.ac.yu.

[2] Faculty of Science, Institute of Physics, Radoja Domanovića 12, Yu-34000 Kragujevac, Serbia, Yugoslavia; simic@ptt.yu.

formula of Cowley (1971) often used for Stark width estimations when more sophisticated methods are not applicable.

Atomic energy levels needed for the calculations have been taken from Martin et al. (1978).

3. RESULTS AND DISCUSSION

The results of our calculations are presented in Table 1. In order to present our results in a more convenient form for synthetic spectrum calculations, all data calculated for different temperature were fitted with the following expression:

$$W\ (\mathrm{rad\ s^{-1}}) = A_0\, T^{-1/2}\ . \qquad (1)$$

Here W is a full width at half maximum (FWHM) expressed in rad s^{-1} per electron, and the constant A_0 is determined numerically in order to obtain the best fit. The corresponding values of log A_0 are given in Table 1 together with the widths (FWHM in logarithmic form) per electron for $T = 10{,}000$ K. Also, the electron-impact widths for $T = 10{,}000$ K and $N_e = 10^{23}$ m^{-3} are given in Table 1. This temperature ($T = 10{,}000$ K) was chosen as the most representative for A-type stars where the Stark broadening becomes the dominant pressure broadening mechanism due to hydrogen ionization. This kind of presentation is similar to that, used in the most complete set of atomic line parameters calculations by Kurucz (1993a) for Fe-peak elements.

In order to test the importance of the electron-impact broadening effect in stellar atmospheres, we have synthesized the line profiles of 38 Nd II lines using SYNTH code (Piskunov 1992) and the Kurucz ATLAS9 code for stellar atmosphere models (Kurucz 1993b) in the temperature range of $6000 \le T_{\mathrm{eff}} \le 16{,}000$ K, and $3.0 \le \log g \le 5.0$. The SYNTH code uses $\log W$ (rad s^{-1}) per electron for $T = 10{,}000$ K as an input parameter.

For the spectrum synthesis it is more convenient to use the parameters A_0 than to take Stark widths for each temperature, which we have calculated. In Figure 1 the comparison between calculated data (*filled circles*) and the fit with equation (1) (*solid line*) for Nd II $\lambda = 4013.3$ Å is shown. We present also the result of an approximate temperature

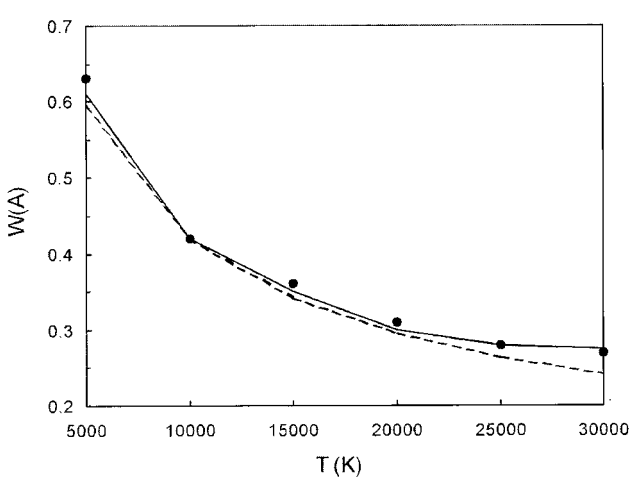

FIG. 1.—Stark widths for the Nd II 4013.3 Å line as a function of electron temperature. Calculated data are shown by filled circles. Data obtained with the different approximations are shown by the solid line (eq. [1]) and dashed line (eq. [2]), respectively.

TABLE 1

THE ELECTRON-IMPACT BROADENING PARAMETERS FOR Nd II LINES

Transition	λ (Å)	$\log(W)$[a]	$\log(A_0)$	w (Å)[b]
$6s\ ^6I_{13/2}-6p\ ^6H^0_{15/2}$	3555.9	−5.304	−3.304	0.332
$6s\ ^4I_{11/2}-6p\ ^4I^0_{13/2}$	3560.3	−5.296	−3.296	0.339
$6s\ ^6I_{11/2}-6p\ ^6H^0_{13/2}$	3576.0	−5.325	−3.325	0.320
$6s\ ^4I_{13/2}-6p\ ^4I^0_{15/2}$	3577.5	−5.273	−3.273	0.361
$6s\ ^4I_{9/2}-6p\ ^4I^0_{11/2}$	3592.6	−5.324	−3.324	0.324
$6s\ ^6I_{9/2}-6p\ ^6H^0_{11/2}$	3600.7	−5.344	−3.344	0.311
$6s\ ^6I_{7/2}-6p\ ^6H^0_{9/2}$	3646.3	−5.356	−3.356	0.310
$6s\ ^4I_{9/2}-6p\ ^4H^0_{9/2}$	3650.5	−5.329	−3.329	0.331
$6s\ ^6I_{9/2}-6p\ ^6H^0_{9/2}$	3715.8	−5.354	−3.354	0.323
$6s\ ^6I_{15/2}-6p\ ^6H^0_{15/2}$	3716.7	−5.299	−3.299	0.367
$6s\ ^6I_{13/2}-6p\ ^6H^0_{13/2}$	3724.5	−5.320	−3.320	0.351
$6s\ ^6I_{11/2}-6p\ ^6H^0_{11/2}$	3729.1	−5.339	−3.339	0.337
$6s\ ^4I_{13/2}-6p\ ^4I^0_{13/2}$	3753.5	−5.290	−3.290	0.382
$6s\ ^6I_{7/2}-6p\ ^6H^0_{7/2}$	3753.7	−5.366	−3.366	0.321
$6s\ ^4I_{9/2}-6p\ ^4H^0_{7/2}$	3764.5	−5.340	−3.340	0.343
$6s\ ^4I_{15/2}-6p\ ^4I^0_{15/2}$	3776.5	−5.267	−3.267	0.409
$6s\ ^6I_{15/2}-6p\ ^6I^0_{17/2}$	3781.4	−5.305	−3.305	0.375
$6s\ ^4I_{11/2}-6p\ ^4I^0_{11/2}$	3785.3	−5.318	−3.318	0.365
$6s\ ^6I_{11/2}-6p\ ^6I^0_{13/2}$	3806.0	−5.346	−3.346	0.346
$6s\ ^6I_{13/2}-6p\ ^6I^0_{15/2}$	3806.4	−5.328	−3.328	0.361
$6s\ ^4I_{9/2}-6p\ ^4I^0_{9/2}$	3806.4	−5.343	−3.343	0.348
$6s\ ^6I_{9/2}-6p\ ^6I^0_{11/2}$	3808.2	−5.362	−3.362	0.334
$6s\ ^6I_{7/2}-6p\ ^4I^0_{7/2}$	3815.8	−5.371	−3.371	0.328
$6s\ ^6I_{15/2}-6p\ ^4K^0_{15/2}$	3823.5	−5.309	−3.309	0.380
$6s\ ^6I_{9/2}-6p\ ^6H^0_{7/2}$	3827.4	−5.363	−3.363	0.336
$6s\ ^4I_{11/2}-6p\ ^4H^0_{9/2}$	3849.6	−5.323	−3.323	0.373
$6s\ ^6I_{13/2}-6p\ ^4H^0_{15/2}$	3852.7	−5.331	−3.331	0.366
$6s\ ^6I_{11/2}-6p\ ^6H^0_{9/2}$	3852.8	−5.350	−3.350	0.351
$6s\ ^6I_{7/2}-6p\ ^6I^0_{9/2}$	3864.4	−5.375	−3.375	0.334
$6s\ ^6I_{7/2}-6p\ ^6H^0_{5/2}$	3864.5	−5.375	−3.375	0.334
$6s\ ^6I_{11/2}-6p\ ^4K^0_{13/2}$	3870.1	−5.351	−3.351	0.353
$6s\ ^6I_{13/2}-6p\ ^4H^0_{13/2}$	3880.6	−5.334	−3.334	0.370
$6s\ ^6I_{11/2}-6p\ ^4K^0_{9/2}$	3881.4	−5.352	−3.352	0.355
$6s\ ^6I_{9/2}-6p\ ^4I^0_{11/2}$	3881.8	−5.368	−3.368	0.342
$6s\ ^6I_{13/2}-6p\ ^6H^0_{11/2}$	3891.0	−5.334	−3.334	0.371
$6s\ ^4I_{15/2}-6p\ ^4K^0_{17/2}$	3892.6	−5.277	−3.277	0.424
$6s\ ^6I_{15/2}-6p\ ^6H^0_{13/2}$	3901.3	−5.315	−3.315	0.390
$6s\ ^6I_{17/2}-6p\ ^6H^0_{15/2}$	3902.9	−5.293	−3.293	0.411
$5d\ ^6K_{13/2}-6p\ ^4H^0_{13/2}$	3905.2	−5.530	−3.530	0.238
$6s\ ^4I_{9/2}-6p\ ^4K^0_{11/2}$	3906.9	−5.351	−3.351	0.360
$6s\ ^4I_{13/2}-6p\ ^4K^0_{15/2}$	3908.9	−5.304	−3.304	0.402
$6s\ ^6I_{15/2}-6p\ ^4H^0_{15/2}$	3912.2	−5.316	−3.316	0.392
$6s\ ^4I_{11/2}-6p\ ^4K^0_{13/2}$	3922.0	−5.329	−3.329	0.382
$6s\ ^6I_{9/2}-6p\ ^6I^0_{9/2}$	3942.6	−5.372	−3.372	0.349
$6s\ ^6I_{11/2}-6p\ ^6I^0_{11/2}$	3952.2	−5.358	−3.358	0.363
$6s\ ^6I_{7/2}-6p\ ^6I^0_{7/2}$	3953.3	−5.381	−3.381	0.344
$6s\ ^4I_{15/2}-6p\ ^4I^0_{13/2}$	3973.2	−5.284	−3.284	0.435
$6s\ ^6I_{17/2}-6p\ ^6I^0_{17/2}$	3974.3	−5.299	−3.299	0.420
$6s\ ^6I_{13/2}-6p\ ^6I^0_{13/2}$	3974.7	−5.341	−3.341	0.382
$6s\ ^4I_{11/2}-6p\ ^4I^0_{9/2}$	3983.4	−5.334	−3.334	0.390
$6s\ ^6I_{15/2}-6p\ ^6I^0_{15/2}$	3991.2	−5.322	−3.322	0.402
$6s\ ^6I_{7/2}-6p\ ^6I^0_{7/2}$	3992.8	−5.384	−3.384	0.348
$6s\ ^6I_{13/2}-6p\ ^4K^0_{15/2}$	3995.8	−5.343	−3.343	0.384
$6s\ ^4I_{13/2}-6p\ ^4I^0_{11/2}$	4004.4	−5.311	−3.311	0.415
$6s\ ^6I_{17/2}-6p\ ^6K^0_{19/2}$	4013.3	−5.302	−3.302	0.426
$6s\ ^6I_{9/2}-6p\ ^6I^0_{9/2}$	4019.9	−5.378	−3.378	0.358
$6s\ ^6I_{13/2}-6p\ ^4K^0_{13/2}$	4021.9	−5.344	−3.344	0.388
$6s\ ^6I_{13/2}-6p\ ^4K^0_{15/2}$	4022.4	−5.344	−3.344	0.388
$6s\ ^4I_{11/2}-6p\ ^4I^0_{9/2}$	4023.3	−5.337	−3.337	0.395
$6s\ ^4I_{9/2}-6p\ ^4I^0_{9/2}$	4024.1	−5.360	−3.360	0.374
$6s\ ^4I_{15/2}-6p\ ^4H^0_{17/2}$	4032.9	−5.288	−3.288	0.444
$6s\ ^6I_{11/2}-6p\ ^4I^0_{13/2}$	4041.9	−5.364	−3.364	0.374
$6s\ ^6I_{15/2}-6p\ ^6K^0_{17/2}$	4062.2	−5.327	−3.327	0.411
$6s\ ^6I_{9/2}-6p\ ^6I^0_{11/2}$	4070.4	−5.381	−3.381	0.365

TABLE 1—*Continued*

Transition	λ (Å)	$\log(W)$[a]	$\log(A_0)$	w (Å)[b]
$6s\ ^6I_{9/2}-6p\ ^6I^0_{7/2}$	4076.4	−5.382	−3.382	0.365
$6s\ ^6I_{11/2}-6p\ ^6I^0_{9/2}$	4097.1	−5.368	−3.368	0.381
$6s\ ^6I_{13/2}-6p\ ^6K^0_{15/2}$	4110.6	−5.351	−3.351	0.399
$6s\ ^6I_{13/2}-6p\ ^6I^0_{11/2}$	4134.5	−5.352	−3.352	0.402
$6s\ ^4I_{11/2}-6p\ ^4K^0_{11/2}$	4135.8	−5.345	−3.345	0.410
$6s\ ^6I_{13/2}-6p\ ^4K^0_{11/2}$	4136.3	−5.352	−3.352	0.402
$6s\ ^4I_{15/2}-6p\ ^4K^0_{15/2}$	4147.7	−5.297	−3.297	0.460
$6s\ ^6I_{11/2}-6p\ ^6K^0_{13/2}$	4157.2	−5.372	−3.372	0.389
$6s\ ^4I_{13/2}-6p\ ^4K^0_{13/2}$	4157.8	−5.322	−3.322	0.436
$6s\ ^6I_{15/2}-6p\ ^6I^0_{13/2}$	4176.7	−5.335	−3.335	0.427
$6s\ ^6I_{9/2}-6p\ ^6K^0_{11/2}$	4178.4	−5.389	−3.389	0.378
$6s\ ^6I_{17/2}-6p\ ^6I^0_{15/2}$	4206.7	−5.316	−3.316	0.453
$6s\ ^6I_{9/2}-6p\ ^6K^0_{11/2}$	4233.5	−5.392	−3.392	0.385
$6s\ ^6I_{17/2}-6p\ ^6K^0_{17/2}$	4285.7	−5.321	−3.321	0.464
$6s\ ^6I_{7/2}-6p\ ^6K^0_{9/2}$	4304.7	−5.404	−3.404	0.387
$6s\ ^6I_{15/2}-6p\ ^6K^0_{15/2}$	4326.9	−5.345	−3.345	0.448
$6s\ ^6I_{11/2}-6p\ ^6K^0_{11/2}$	4352.5	−5.384	−3.384	0.415
$6s\ ^6I_{13/2}-6p\ ^6K^0_{13/2}$	4359.3	−5.367	−3.367	0.433
$6s\ ^4I_{13/2}-6p\ ^4K^0_{11/2}$	4398.8	−5.338	−3.338	0.471
$6s\ ^6I_{9/2}-6p\ ^6K^0_{9/2}$	4402.0	−5.402	−3.402	0.407
$6s\ ^4I_{15/2}-6p\ ^4K^0_{13/2}$	4429.1	−5.315	−3.315	0.503
$6s\ ^4I_{15/2}-6p\ ^6K^0_{17/2}$	4457.6	−5.317	−3.317	0.508
$6s\ ^4I_{13/2}-6p\ ^6K^0_{15/2}$	4464.2	−5.341	−3.341	0.481
$6s\ ^6I_{9/2}-6p\ ^4I^0_{11/2}$	4507.8	−5.407	−3.407	0.421
$5d\ ^6L_{17/2}-6p\ ^6K^0_{19/2}$	4518.0	−5.621	−3.621	0.258
$6s\ ^6I_{13/2}-6p\ ^6K^0_{11/2}$	4574.5	−5.378	−3.378	0.464
$6s\ ^6I_{17/2}-6p\ ^6K^0_{15/2}$	4581.4	−5.339	−3.339	0.510
$5d\ ^6L_{15/2}-6p\ ^6K^0_{17/2}$	4591.0	−5.668	−3.668	0.240
$6s\ ^6I_{11/2}-6p\ ^6K^0_{9/2}$	4595.6	−5.397	−3.397	0.448
$6s\ ^6I_{15/2}-6p\ ^6K^0_{13/2}$	4603.5	−5.360	−3.360	0.489
$5d\ ^6L_{13/2}-6p\ ^6K^0_{15/2}$	4667.4	−5.713	−3.713	0.223
$5d\ ^6K_{15/2}-6p\ ^6I^0_{17/2}$	4716.0	−5.610	−3.610	0.289
$5d\ ^6L_{11/2}-6p\ ^6K^0_{13/2}$	4742.2	−5.756	−3.756	0.209
$5d\ ^6K_{13/2}-6p\ ^6I^0_{15/2}$	4783.1	−5.651	−3.651	0.271
$5d\ ^6L_{19/2}-6p\ ^6K^0_{19/2}$	4799.3	−5.615	−3.615	0.296
$5d\ ^6K_{11/2}-6p\ ^6I^0_{13/2}$	4804.8	−5.684	−3.684	0.253
$5d\ ^6K_{9/2}-6p\ ^6I^0_{11/2}$	4815.3	−5.714	−3.714	0.237
$5d\ ^6L_{17/2}-6p\ ^6K^0_{17/2}$	4866.1	−5.662	−3.662	0.273
$5d\ ^6I_{13/2}-6p\ ^6H^0_{15/2}$	4909.1	−5.592	−3.592	0.326
$5d\ ^6L_{15/2}-6p\ ^6K^0_{15/2}$	4932.0	−5.708	−3.708	0.252
$5d\ ^6I_{11/2}-6p\ ^6H^0_{13/2}$	4980.9	−5.629	−3.629	0.309
$5d\ ^6K_{17/2}-6p\ ^6I^0_{17/2}$	4987.0	−5.604	−3.604	0.327
$5d\ ^6L_{13/2}-6p\ ^6K^0_{13/2}$	4990.8	−5.750	−3.750	0.234
$5d\ ^6L_{11/2}-6p\ ^6K^0_{11/2}$	4998.0	−5.785	−3.785	0.217
$5d\ ^6I_{7/2}-6p\ ^6H^0_{9/2}$	5025.0	−5.690	−3.690	0.273
$5d\ ^6K_{9/2}-6p\ ^6I^0_{9/2}$	5032.2	−5.738	−3.738	0.245
$5d\ ^6I_{9/2}-6p\ ^6H^0_{11/2}$	5033.9	−5.663	−3.663	0.292
$5d\ ^6K_{11/2}-6p\ ^6I^0_{11/2}$	5040.2	−5.710	−3.710	0.262
$5d\ ^6K_{15/2}-6p\ ^6I^0_{15/2}$	5046.8	−5.645	−3.645	0.305
$5d\ ^6K_{17/2}-6p\ ^6K^0_{19/2}$	5048.5	−5.611	−3.611	0.331
$5d\ ^6K_{13/2}-6p\ ^6I^0_{13/2}$	5052.0	−5.679	−3.679	0.283
$5d\ ^6L_{21/2}-6p\ ^6K^0_{19/2}$	5132.0	−5.609	−3.609	0.343
$5d\ ^6K_{15/2}-6p\ ^6K^0_{17/2}$	5160.9	−5.656	−3.656	0.311
$5d\ ^6I_{15/2}-6p\ ^6H^0_{15/2}$	5172.2	−5.587	−3.587	0.367
$5d\ ^6L_{19/2}-6p\ ^6K^0_{17/2}$	5194.0	−5.656	−3.656	0.316
$5d\ ^6I_{7/2}-6p\ ^6H^0_{7/2}$	5231.3	−5.710	−3.710	0.282
$5d\ ^6I_{13/2}-6p\ ^6H^0_{13/2}$	5236.3	−5.624	−3.624	0.345
$5d\ ^6L_{17/2}-6p\ ^6K^0_{15/2}$	5251.0	−5.701	−3.701	0.290
$5d\ ^6K_{9/2}-6p\ ^6I^0_{7/2}$	5252.2	−5.761	−3.761	0.253
$5d\ ^6I_{9/2}-6p\ ^6H^0_{9/2}$	5261.8	−5.685	−3.685	0.303
$5d\ ^6K_{13/2}-6p\ ^6K^0_{15/2}$	5273.5	−5.701	−3.701	0.293
$5d\ ^6L_{13/2}-6p\ ^6K^0_{11/2}$	5274.8	−5.780	−3.780	0.244
$5d\ ^6K_{11/2}-6p\ ^6I^0_{9/2}$	5278.3	−5.733	−3.733	0.272
$5d\ ^6I_{11/2}-6p\ ^6H^0_{11/2}$	5283.2	−5.658	−3.658	0.325
$5d\ ^6L_{15/2}-6p\ ^6K^0_{13/2}$	5294.6	−5.744	−3.744	0.267
$5d\ ^4K_{11/2}-6p\ ^4I^0_{13/2}$	5297.2	−5.572	−3.572	0.399

TABLE 1—*Continued*

Transition	λ (Å)	$\log(W)$[a]	$\log(A_0)$	w (Å)[b]
$5d\ ^6I_{15/2}-6p\ ^6I^0_{17/2}$	5298.4	−5.598	−3.598	0.375
$5d\ ^4K_{13/2}-6p\ ^4I^0_{15/2}$	5300.3	−5.533	−3.533	0.436
$5d\ ^6K_{19/2}-6p\ ^6I^0_{17/2}$	5303.7	−5.598	−3.598	0.376
$5d\ ^6K_{13/2}-6p\ ^6I^0_{11/2}$	5312.9	−5.704	−3.704	0.295
$5d\ ^6L_{11/2}-6p\ ^6K^0_{9/2}$	5321.2	−5.819	−3.819	0.227
$5d\ ^4L_{15/2}-6p\ ^4K^0_{17/2}$	5328.0	−5.556	−3.556	0.418
$5d\ ^6K_{15/2}-6p\ ^6I^0_{13/2}$	5347.1	−5.674	−3.674	0.321
$5d\ ^6K_{17/2}-6p\ ^6I^0_{15/2}$	5358.4	−5.639	−3.639	0.349
$5d\ ^6K_{19/2}-6p\ ^6K^0_{19/2}$	5373.4	−5.604	−3.604	0.380
$5d\ ^6K_{11/2}-6p\ ^6K^0_{13/2}$	5378.4	−5.743	−3.743	0.277
$5d\ ^6I_{13/2}-6p\ ^6I^0_{15/2}$	5399.6	−5.639	−3.639	0.355
$5d\ ^4L_{13/2}-6p\ ^4K^0_{15/2}$	5401.3	−5.601	−3.601	0.387
$5d\ ^6K_{9/2}-6p\ ^6K^0_{11/2}$	5422.9	−5.777	−3.777	0.260
$5d\ ^6I_{11/2}-6p\ ^6I^0_{13/2}$	5438.8	−5.672	−3.672	0.333
$5d\ ^6G_{13/2}-6p\ ^6H^0_{15/2}$	5442.7	−5.582	−3.582	0.411
$5d\ ^6I_{7/2}-6p\ ^6I^0_{9/2}$	5448.8	−5.730	−3.730	0.293
$5d\ ^6I_{7/2}-6p\ ^6H^0_{5/2}$	5449.0	−5.730	−3.730	0.293
$5d\ ^6I_{9/2}-6p\ ^6I^0_{11/2}$	5449.0	−5.702	−3.702	0.312
$5d\ ^6I_{17/2}-6p\ ^6H^0_{15/2}$	5480.2	−5.581	−3.581	0.417
$5d\ ^6G_{7/2}-6p\ ^6H^0_{9/2}$	5486.4	−5.681	−3.681	0.332
$5d\ ^6K_{17/2}-6p\ ^6K^0_{17/2}$	5487.2	−5.650	−3.650	0.357
$5d\ ^6I_{9/2}-6p\ ^6H^0_{7/2}$	5488.5	−5.705	−3.705	0.314
$5d\ ^6I_{11/2}-6p\ ^6H^0_{9/2}$	5534.9	−5.680	−3.680	0.339
$5d\ ^6I_{15/2}-6p\ ^6H^0_{13/2}$	5536.8	−5.619	−3.619	0.391
$5d\ ^6I_{13/2}-6p\ ^6H^0_{11/2}$	5571.4	−5.653	−3.653	0.366
$5d\ ^6K_{15/2}-6p\ ^6K^0_{15/2}$	5595.9	−5.695	−3.695	0.335
$5d\ ^6G_{5/2}-6p\ ^6H^0_{7/2}$	5604.2	−5.703	−3.703	0.329
$5d\ ^6I_{17/2}-6p\ ^6I^0_{17/2}$	5622.1	−5.593	−3.593	0.428
$5d\ ^6K_{13/2}-6p\ ^6K^0_{13/2}$	5690.0	−5.737	−3.737	0.314
$5d\ ^4K_{13/2}-6p\ ^4I^0_{13/2}$	5696.0	−5.565	−3.565	0.468
$5d\ ^6I_{17/2}-6p\ ^6K^0_{19/2}$	5700.4	−5.599	−3.599	0.434
$5d\ ^6I_{7/2}-6p\ ^6I^0_{7/2}$	5707.7	−5.752	−3.752	0.305
$5d\ ^6K_{11/2}-6p\ ^6K^0_{11/2}$	5709.8	−5.772	−3.772	0.292
$5d\ ^4K_{15/2}-6p\ ^4I^0_{15/2}$	5711.9	−5.526	−3.526	0.515
$5d\ ^6I_{15/2}-6p\ ^6I^0_{15/2}$	5719.7	−5.633	−3.633	0.403
$5d\ ^6I_{9/2}-6p\ ^6I^0_{9/2}$	5728.4	−5.725	−3.725	0.327
$5d\ ^6G_{7/2}-6p\ ^6H^0_{7/2}$	5733.3	−5.701	−3.701	0.347
$5d\ ^6I_{11/2}-6p\ ^6I^0_{11/2}$	5742.4	−5.697	−3.697	0.351
$5d\ ^6G_{11/2}-6p\ ^6H^0_{13/2}$	5742.8	−5.615	−3.615	0.424
$5d\ ^6H_{13/2}-6p\ ^6H^0_{15/2}$	5744.3	−5.577	−3.577	0.463
$5d\ ^6I_{13/2}-6p\ ^6I^0_{13/2}$	5744.7	−5.666	−3.666	0.377
$5d\ ^6G_{9/2}-6p\ ^6H^0_{11/2}$	5746.3	−5.650	−3.650	0.392
$5d\ ^4L_{17/2}-6p\ ^4K^0_{17/2}$	5755.8	−5.548	−3.548	0.497
$5d\ ^4G_{5/2}-6p\ ^4H^0_{7/2}$	5771.4	−5.652	−3.652	0.393
$5d\ ^6K_{9/2}-6p\ ^6K^0_{9/2}$	5805.6	−5.810	−3.810	0.276
$5d\ ^4K_{11/2}-6p\ ^4I^0_{11/2}$	5811.1	−5.612	−3.612	0.437
$5d\ ^4L_{15/2}-6p\ ^4K^0_{15/2}$	5817.9	−5.594	−3.594	0.457
$5d\ ^6G_{3/2}-6p\ ^6H^0_{5/2}$	5827.4	−5.723	−3.723	0.340
$5d\ ^6G_{13/2}-6p\ ^6H^0_{13/2}$	5847.9	−5.613	−3.613	0.441
$5d\ ^6G_{5/2}-6p\ ^6H^0_{5/2}$	5854.7	−5.723	−3.723	0.344
$5d\ ^6I_{15/2}-6p\ ^6K^0_{17/2}$	5866.6	−5.644	−3.644	0.414
$5d\ ^6K_{19/2}-6p\ ^6K^0_{17/2}$	5873.0	−5.644	−3.644	0.415
$5d\ ^4L_{13/2}-6p\ ^4K^0_{13/2}$	5888.3	−5.639	−3.639	0.422
$5d\ ^6H_{5/2}-6p\ ^6H^0_{7/2}$	5894.4	−5.698	−3.698	0.369
$5d\ ^4G_{7/2}-6p\ ^4H^0_{9/2}$	5944.8	−5.623	−3.623	0.445
$5d\ ^6H_{7/2}-6p\ ^6H^0_{9/2}$	5967.2	−5.673	−3.673	0.401
$5d\ ^6K_{17/2}-6p\ ^6K^0_{15/2}$	5981.5	−5.688	−3.688	0.388
$5d\ ^4K_{15/2}-6p\ ^4K^0_{17/2}$	5981.6	−5.545	−3.545	0.541
$5d\ ^6G_{7/2}-6p\ ^6H^0_{5/2}$	5995.8	−5.721	−3.721	0.362
$5d\ ^6I_{9/2}-6p\ ^6I^0_{7/2}$	6015.2	−5.747	−3.747	0.343
$5d\ ^6H_{9/2}-6p\ ^6H^0_{11/2}$	6032.8	−5.645	−3.645	0.436
$5d\ ^6I_{13/2}-6p\ ^6K^0_{15/2}$	6032.9	−5.687	−3.687	0.396
$5d\ ^6H_{11/2}-6p\ ^6H^0_{13/2}$	6043.3	−5.610	−3.610	0.475
$5d\ ^6G_{9/2}-6p\ ^6H^0_{9/2}$	6045.3	−5.671	−3.671	0.413
$5d\ ^4I_{13/2}-6p\ ^4I^0_{15/2}$	6045.4	−5.520	−3.520	0.584
$5d\ ^4I_{11/2}-6p\ ^4I^0_{13/2}$	6049.9	−5.559	−3.559	0.536

TABLE 1—*Continued*

Transition	λ (Å)	$\log(W)$[a]	$\log(A_0)$	w (Å)[b]
$5d\ ^6I_{11/2}-6p\ ^6I^0_{9/2}$	6053.5	−5.720	−3.720	0.370
$5d\ ^4K_{13/2}-6p\ ^4K^0_{15/2}$	6061.7	−5.590	−3.590	0.500
$5d\ ^6K_{13/2}-6p\ ^6K^0_{11/2}$	6062.3	−5.765	−3.765	0.334
$5d\ ^6K_{15/2}-6p\ ^6K^0_{13/2}$	6067.3	−5.731	−3.731	0.363
$5d\ ^6I_{13/2}-6p\ ^6I^0_{11/2}$	6084.5	−5.691	−3.691	0.399
$5d\ ^6I_{17/2}-6p\ ^6I^0_{15/2}$	6098.7	−5.627	−3.627	0.465
$5d\ ^6I_{15/2}-6p\ ^6I^0_{13/2}$	6108.4	−5.660	−3.660	0.432
$5d\ ^6K_{11/2}-6p\ ^6K^0_{9/2}$	6135.6	−5.804	−3.804	0.313
$5d\ ^4K_{11/2}-6p\ ^4K^0_{13/2}$	6139.7	−5.635	−3.635	0.463
$5d\ ^6G_{11/2}-6p\ ^6H^0_{11/2}$	6148.4	−5.643	−3.643	0.455
$5d\ ^4I_{9/2}-6p\ ^4I^0_{11/2}$	6158.2	−5.607	−3.607	0.497
$5d\ ^6H_{15/2}-6p\ ^6H^0_{15/2}$	6163.2	−5.570	−3.570	0.541
$5d\ ^6H_{5/2}-6p\ ^6H^0_{5/2}$	6172.1	−5.718	−3.718	0.387
$5d\ ^4K_{15/2}-6p\ ^4I^0_{13/2}$	6174.2	−5.557	−3.557	0.560
$5d\ ^6I_{11/2}-6p\ ^6K^0_{13/2}$	6185.6	−5.729	−3.729	0.379
$5d\ ^6H_{13/2}-6p\ ^6H^0_{13/2}$	6197.5	−5.608	−3.608	0.502
$5d\ ^6I_{9/2}-6p\ ^6K^0_{11/2}$	6240.2	−5.762	−3.762	0.356
$5d\ ^4G_{7/2}-6p\ ^4H^0_{7/2}$	6253.2	−5.644	−3.644	0.470
$5d\ ^6H_{7/2}-6p\ ^6H^0_{7/2}$	6260.4	−5.692	−3.692	0.422
$5d\ ^6I_{17/2}-6p\ ^6K^0_{17/2}$	6266.0	−5.637	−3.637	0.479
$5d\ ^6G_{13/2}-6p\ ^6H^0_{11/2}$	6269.0	−5.641	−3.641	0.475
$5d\ ^4L_{19/2}-6p\ ^4K^0_{17/2}$	6279.0	−5.540	−3.540	0.602
$5d\ ^4K_{13/2}-6p\ ^4I^0_{11/2}$	6294.5	−5.605	−3.605	0.522
$5d\ ^4K_{17/2}-6p\ ^4I^0_{15/2}$	6307.5	−5.516	−3.516	0.642
$5d\ ^4I_{9/2}-6p\ ^4H^0_{9/2}$	6330.2	−5.617	−3.617	0.512
$5d\ ^4L_{17/2}-6p\ ^4K^0_{15/2}$	6331.8	−5.586	−3.586	0.551
$5d\ ^6H_{15/2}-6p\ ^6I^0_{17/2}$	6343.2	−5.581	−3.581	0.559
$5d\ ^6G_{9/2}-6p\ ^6H^0_{7/2}$	6346.4	−5.691	−3.691	0.435
$5d\ ^6H_{9/2}-6p\ ^6H^0_{9/2}$	6363.1	−5.666	−3.666	0.462
$5d\ ^6I_{7/2}-6p\ ^6K^0_{9/2}$	6367.2	−5.800	−3.800	0.340
$5d\ ^4L_{13/2}-6p\ ^4K^0_{11/2}$	6383.8	−5.672	−3.672	0.460
$5d\ ^4L_{15/2}-6p\ ^4K^0_{13/2}$	6386.9	−5.631	−3.631	0.505
$5d\ ^4K_{11/2}-6p\ ^4I^0_{9/2}$	6391.7	−5.651	−3.651	0.484
$5d\ ^6H_{13/2}-6p\ ^6I^0_{15/2}$	6427.5	−5.622	−3.622	0.523
$5d\ ^6I_{15/2}-6p\ ^6K^0_{15/2}$	6435.2	−5.681	−3.681	0.457
$5d\ ^4I_{15/2}-6p\ ^4I^0_{15/2}$	6466.9	−5.514	−3.514	0.678
$5d\ ^6G_{11/2}-6p\ ^6H^0_{9/2}$	6491.9	−5.664	−3.664	0.484
$5d\ ^6H_{11/2}-6p\ ^6H^0_{11/2}$	6494.1	−5.638	−3.638	0.514
$5d\ ^6H_{5/2}-6p\ ^6I^0_{7/2}$	6506.2	−5.739	−3.739	0.409
$5d\ ^4G_{9/2}-6p\ ^4H^0_{9/2}$	6518.8	−5.615	−3.615	0.547
$5d\ ^4I_{13/2}-6p\ ^4I^0_{13/2}$	6565.7	−5.551	−3.551	0.642
$5d\ ^6H_{7/2}-6p\ ^6I^0_{9/2}$	6574.4	−5.711	−3.711	0.445
$5d\ ^6H_{7/2}-6p\ ^6H^0_{5/2}$	6574.7	−5.711	−3.711	0.445
$5d\ ^6I_{13/2}-6p\ ^6K^0_{13/2}$	6584.4	−5.722	−3.722	0.435
$5d\ ^4K_{15/2}-6p\ ^4K^0_{15/2}$	6606.2	−5.582	−3.582	0.605
$5d\ ^6I_{11/2}-6p\ ^6K^0_{11/2}$	6628.0	−5.756	−3.756	0.408
$5d\ ^4K_{17/2}-6p\ ^4K^0_{17/2}$	6638.0	−5.535	−3.535	0.681
$5d\ ^6H_{9/2}-6p\ ^6I^0_{11/2}$	6639.0	−5.682	−3.682	0.485
$5d\ ^6H_{13/2}-6p\ ^6H^0_{11/2}$	6672.5	−5.635	−3.635	0.546
$5d\ ^4K_{11/2}-6p\ ^4K^0_{11/2}$	6680.3	−5.667	−3.667	0.509
$5d\ ^4I_{9/2}-6p\ ^4H^0_{7/2}$	6681.0	−5.637	−3.637	0.545
$5d\ ^4K_{13/2}-6p\ ^4K^0_{13/2}$	6681.9	−5.627	−3.627	0.559
$5d\ ^6H_{15/2}-6p\ ^6H^0_{13/2}$	6687.9	−5.601	−3.601	0.595
$5d\ ^6H_{9/2}-6p\ ^6H^0_{7/2}$	6697.7	−5.686	−3.686	0.490
$5d\ ^4I_{11/2}-6p\ ^4I^0_{11/2}$	6729.5	−5.598	−3.598	0.605
$5d\ ^6H_{11/2}-6p\ ^6I^0_{13/2}$	6730.7	−5.651	−3.651	0.536
$5d\ ^6I_{9/2}-6p\ ^6K^0_{9/2}$	6752.3	−5.795	−3.795	0.388
$5d\ ^4I_{9/2}-6p\ ^4I^0_{9/2}$	6814.2	−5.645	−3.645	0.558
$5d\ ^4I_{15/2}-6p\ ^4K^0_{17/2}$	6814.8	−5.532	−3.532	0.722
$5d\ ^6H_{11/2}-6p\ ^6H^0_{9/2}$	6878.5	−5.659	−3.659	0.550
$5d\ ^4G_{9/2}-6p\ ^4H^0_{7/2}$	6891.5	−5.635	−3.635	0.584
$5d\ ^6I_{17/2}-6p\ ^6K^0_{15/2}$	6919.0	−5.674	−3.674	0.537
$5d\ ^6H_{13/2}-6p\ ^6I^0_{13/2}$	6922.6	−5.648	−3.648	0.570
$5d\ ^4I_{11/2}-6p\ ^4H^0_{9/2}$	6935.4	−5.609	−3.609	0.627
$5d\ ^6H_{7/2}-6p\ ^6I^0_{7/2}$	6955.1	−5.732	−3.732	0.475
$5d\ ^6H_{15/2}-6p\ ^6I^0_{15/2}$	6956.5	−5.614	−3.614	0.623

TABLE 1—*Continued*

Transition	λ (Å)	$\log(W)$[a]	$\log(A_0)$	w (Å)[b]
$5d\ ^4I_{13/2}-6p\ ^4K^0_{15/2}$	7056.3	−5.576	−3.576	0.701
$5d\ ^6H_{9/2}-6p\ ^6I^0_{9/2}$	7058.3	−5.705	−3.705	0.521
$5d\ ^4I_{15/2}-6p\ ^4I^0_{13/2}$	7065.9	−5.544	−3.544	0.755
$5d\ ^6I_{15/2}-6p\ ^6K^0_{13/2}$	7066.6	−5.716	−3.716	0.509
$5d\ ^6I_{13/2}-6p\ ^6K^0_{11/2}$	7088.0	−5.750	−3.750	0.473
$5d\ ^4I_{9/2}-6p\ ^4K^0_{11/2}$	7143.2	−5.661	−3.661	0.590
$5d\ ^4I_{11/2}-6p\ ^4K^0_{13/2}$	7174.2	−5.620	−3.620	0.654
$5d\ ^4G_{11/2}-6p\ ^4H^0_{9/2}$	7196.5	−5.605	−3.605	0.681
$5d\ ^6H_{11/2}-6p\ ^6I^0_{11/2}$	7202.0	−5.675	−3.675	0.581
$5d\ ^6I_{11/2}-6p\ ^6K^0_{9/2}$	7208.7	−5.788	−3.788	0.448
$5d\ ^4K_{13/2}-6p\ ^4K^0_{11/2}$	7327.2	−5.658	−3.658	0.625
$5d\ ^4K_{15/2}-6p\ ^4K^0_{13/2}$	7349.7	−5.618	−3.618	0.690
$5d\ ^4I_{13/2}-6p\ ^4I^0_{11/2}$	7373.9	−5.590	−3.590	0.741
$5d\ ^4K_{17/2}-6p\ ^4K^0_{15/2}$	7416.0	−5.571	−3.571	0.782
$5d\ ^6H_{13/2}-6p\ ^6I^0_{11/2}$	7422.1	−5.672	−3.672	0.621
$5d\ ^6H_{9/2}-6p\ ^6I^0_{7/2}$	7499.0	−5.725	−3.725	0.561
$5d\ ^4I_{11/2}-6p\ ^4I^0_{9/2}$	7520.7	−5.635	−3.635	0.694
$5d\ ^6H_{15/2}-6p\ ^6I^0_{13/2}$	7540.2	−5.641	−3.641	0.689
$5d\ ^4I_{15/2}-6p\ ^4K^0_{15/2}$	7637.4	−5.569	−3.569	0.834
$5d\ ^6H_{11/2}-6p\ ^6I^0_{9/2}$	7698.1	−5.696	−3.696	0.632
$5d\ ^4I_{13/2}-6p\ ^4K^0_{13/2}$	7911.2	−5.611	−3.611	0.811
$5d\ ^4I_{11/2}-6p\ ^4K^0_{11/2}$	7923.5	−5.651	−3.651	0.742
$5d\ ^4I_{15/2}-6p\ ^4K^0_{13/2}$	8649.0	−5.604	−3.604	0.987
$5d\ ^4I_{13/2}-6p\ ^4K^0_{11/2}$	8832.2	−5.642	−3.642	0.943

[a] Stark widths W(rad s^{-1}) per electron for $T = 10{,}000$ K.
[b] Stark widths W in Å for electron temperature of $T = 10{,}000$ K and electron density of $N_e = 10^{23}$ m^{-3}.

scaling performed as

$$W_T = W_{T_m}\left(\frac{T}{T_m}\right)^{-1/2} \tag{2}$$

($T_m = 10{,}000$ K) that may be used in astrophysics for ion lines (*dashed line*, Fig. 1).

As we can see from Figure 1, if a high accuracy is not necessary, equations (1) and (2) provide a good approximation, especially for large-scale calculations.

For 38 Nd II lines we have analyzed the influence of electron-impact broadening mechanism on equivalent widths. We have synthesized the line profiles with and without taking the electron-impact broadening mechanism for different type of stellar atmospheres. First, we have synthesized all considered line profiles for neodymium abundance of $A = \log(\mathrm{Nd/H}) = -7.0$, and two values of $\log g = 4.0$ and 4.5 for different effective temperatures ($T_{\mathrm{eff}} = 6000$–$16{,}000$). All considered lines have similar dependence on effective temperature; as an example in Figure 2, we show the ratio of the equivalent widths ($\mathrm{EW_{St}/EW_0}$) as a function of the effective temperature for Nd II 4013.3 Å line. As one can see from Figure 2 the maximum of the electron-impact broadening influence on equivalent widths is in the effective temperature range $T_{\mathrm{eff}} = 8000$–$10{,}000$ K. One should note here, that the Solar value for neodymium abundance is −10.55 which is three orders of magnitude lower than used in Figure 2, so that solar Nd II lines would be weak and relatively insensitive to the damping widths.

The dependence of electron-impact broadening influence on equivalent width vs. abundance of neodymium is investigated, and one example for Nd II $\lambda = 4062.2$ Å line is pre-

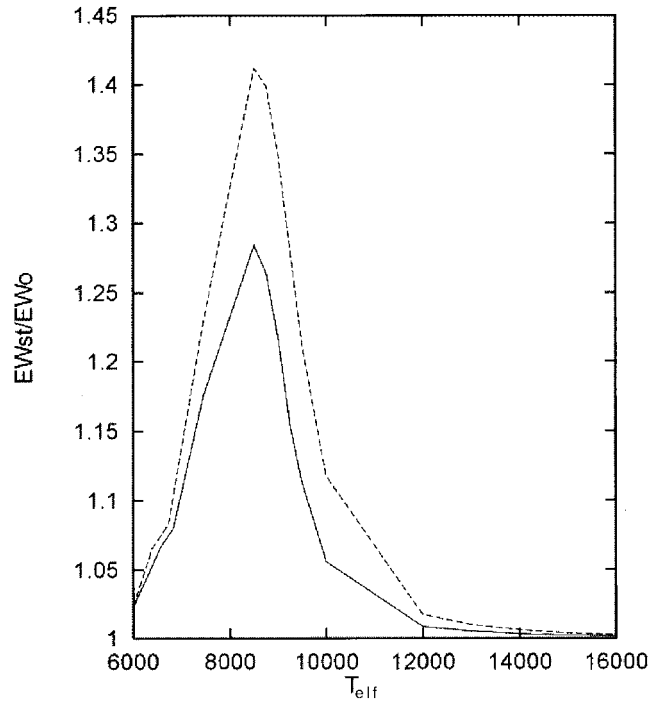

FIG. 2.—Ratio of equivalent widths for the Nd II 4013.3 Å line calculated with a Stark broadening effect (EW_{St}) and without it (EW_0) as a function of effective temperature. Results for $\log g = 4.0$ and for $\log g = 4.5$ are shown by the solid and dashed lines, respectively.

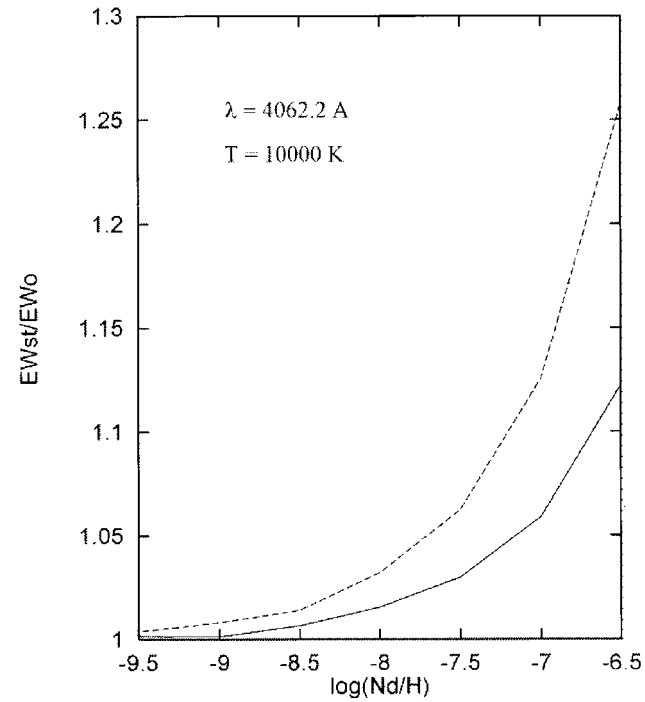

FIG. 4.—Ratio of the equivalent widths EW_{St}/EW_0 as a function of $\log g$ for the Nd II 4062.2 Å line. Results for $\log g = 4.0$ and 4.5 are shown by the solid and dashed lines, respectively.

sented in Figure 3. The influence is higher for higher abundance of neodymium, as expected. Similar results are obtained in the case of variation of effective surface gravity. One finds that this effect is more important in the case of the stars with higher values of surface gravity (Fig. 4).

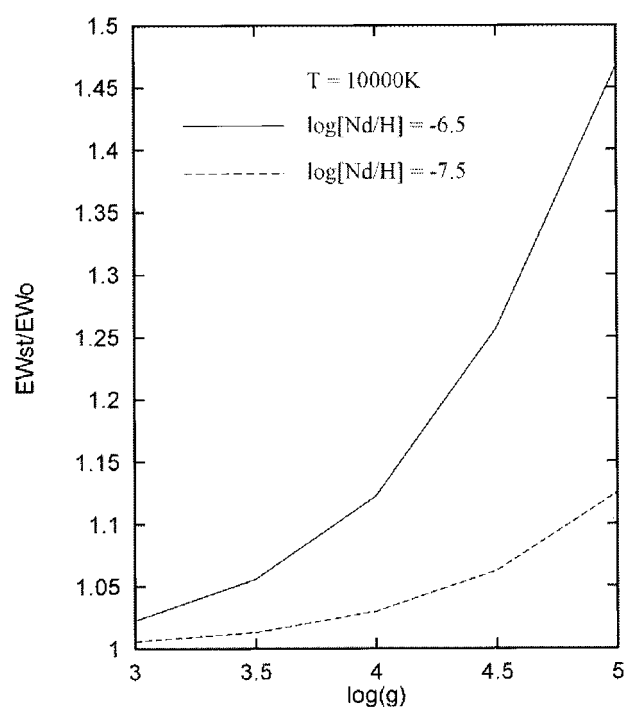

FIG. 3.—Ratio of EW_{St}/EW_0 for the Nd II 4062.2 Å line as a function of neodymium abundance. Results for $\log g = 4.0$ and 4.5 are shown by the solid and dashed lines, respectively.

In order to point out the type of stars where the electron-impact broadening effect is the most important, we summarized this influence in different types of stellar atmospheres, considering the minimum and maximum influence for all studied lines. The result is shown in Figure 5, where equivalent widths ratio vs. stellar spectral type is presented. As one can see from Figure 5, the most important influence of Stark broadening mechanism is in the A-type stellar atmospheres. Taking into account that Stark width depends on electron density (N) the effect is dominant in hot star atmospheres where electron density is higher (Fig. 6), since hydrogen becomes ionized. One can expect that the

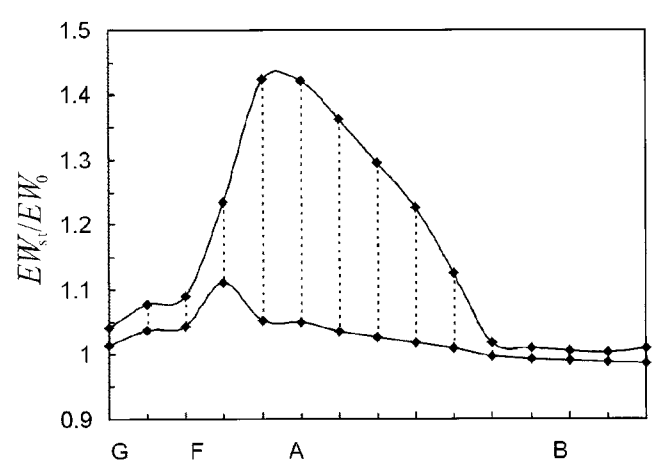

FIG. 5.—Maximum (*top line*) and minimum (*bottom line*) of the ratio of the equivalent widths EW_{St}/EW_0 for different types of stars. The maximum and minimum value for all 38 Nd II lines considered are summarized.

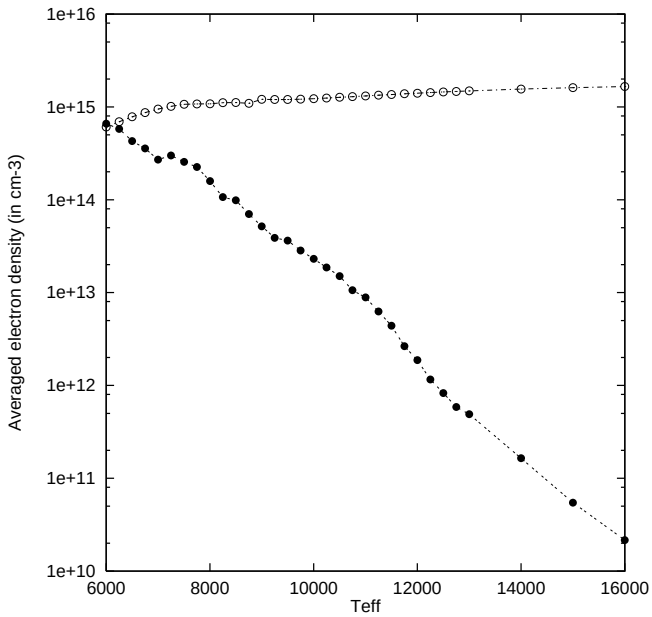

FIG. 6.—Average electron densities through the whole atmosphere (*open circles*) and for layers where the neodymium ion density is at maximum (T = 7000–9000 K, *filled circles*), as a function of the effective temperature corresponding to spectral types from G to B.

Stark broadening influence should be higher for hotter stars, but considering that Nd II ion is created in a part of stellar atmosphere with corresponding plasma parameters this is not the case. Starting from the fact that ionization potential of Nd II is 10.73 eV, consequently the layers where Nd II ion density is maximal have electron temperature between 7000 and 9000 K, we have calculated the averaged electron density in these layers of stellar atmosphere for different stellar types for $\log g = 4.0$, and as one can see from Figure 6, the averaged electron density decreases with effective temperature. This is the reason why the maximal influence of Stark broadening effect in the case of Nd II is in A-type stellar atmospheres.

4. CONCLUSION

In order to provide Stark broadening data for REE, we have calculated the Stark widths for 284 Nd II lines by using the MSE formalism. For a sample of 38 Nd II spectral lines, observed earlier in stellar atmospheres, we have analyzed the influence of Stark broadening mechanism on equivalent widths. The Stark broadening mechanism is very important for A and B type of stellar atmospheres as well as for white dwarfs atmospheres, and one has to take into account this effect for investigations, analysis and modeling of such stellar atmospheres. Also, we obtained that neglecting this mechanism, we introduce an error between 10% and 45% in the equivalent width determination, and corresponding errors in abundance determination.

We hope that the Stark broadening data and the qualitative analyze presented here, will be of interest for stellar spectroscopy, for CP star research and for laboratory plasma spectroscopy, too.

This work has been supported by the Ministry of Science and Technology of Serbia through the project Astrometrical, Astrodynamical, and Astrophysical Research and by the Federal Ministry of Development, Science, and Environment Protection.

REFERENCES

Adelman, S. J. 1987, in Elemental Abundance Analyses, ed. S. J. Adelman and T. Lanz (Lausanne: Inst. d'Astron.), 58
———. 1994, MNRAS, 266, 97
Bonsack, W. K., & Wolff, S. C. 1980, AJ, 85, 599
Cowley, C. R. 1971, Observatory, 91, 139
———. 1984, Phys. Scripta, T8, 28
Cowley, C. R., & Greenberg M. 1988, MNRAS, 232, 763
Cowley, C. R., Ryabchikova, T. A., Kupka, F., Bord, D.J., Mathys, G., & Bidelman, W.P. 2000, MNRAS, 317, 299
Dimitrijević, M. S., & Konjević N. 1980, J. Quant. Spectrosc. Radiat. Transfer, 24, 451
———. 1987, A&A, 173, 345
Dimitrijević, M. S., & Kršljanin, V. 1986, A&A, 165, 269
Gelbmann, M., Kupka, F., Weiss, W. W., & Mathys, G. 1997, A&A, 319, 630
Guthrie, B. N. G. 1985, MNRAS, 216, 15
Jaschek, M., & Jaschek, C. 1974, Vistas Astron., 16, 131
Kupka, F., Ryabchikova, T. A., Weiss, W. W., Kuschnig, R., Rogel, J., & Mathys, G. 1996, A&A, 308, 886
Kurucz, R. L. 1993a, CD-ROMs 20–22, Atomic Data (Cambridge: Smithsonian Astrophys. Obs.)
———. 1993b, CD-ROM 13, ATLAS9 Stellar Atmosphere Programs and 2 km/s Grid (Cambridge: Smithsonian Astrophys. Obs.)
Magazzu, A. & Cowley, C. R. 1986, ApJ, 308, 254
Martin, W. C., Zalubas, R., & Hagan, L. 1978, Atomic Energy Levels (NSRDS-NBS 60) (Washington: GPO)
Piskunov, N. E. 1992, in Stellar Magnetism, ed. Yu. V. Glagolevskij, I. I. Romanyuk (St. Petersburg: Nauka), 92
Popović, L. Č., & Dimitrijević, M. S. 1996a, Phys. Scr. 53, 325
———. 1996b, A&AS, 116, 359
———. 1997, in The Physics of Ionized Gas, ed. B. Vujičić, S. Djurović, & J. Purić (Novi Sad: Inst. Phys.), 477
———. 1998a, Proc. of the 26th Meeting and Workshop of the European Working Group on CP Stars, ed. P. North, A. Schnel, & J. Žižňovský (Tatranska Lomnica: Astron. Inst. Slovak Acad. Sci.), 27, 353
———. 1998b, A&AS, 127, 295
———. 2000, Phys. Scripta, 61, 192
Popović, L.Č., Dimitrijević, M. S., & Ryabchikova, T. 1999, A&A, 350, 719
Ryabchikova, T. A., Landstreet, J. D., Gelbmann, M. J., Bogova, G. T., Tsymbal, V. V., & Weiss, W. W. 1997, A&A, 327, 1137
Ryabchikova, T. A., Piskunov, N., Savanov, I., Kupka, F., & Malanushenko, V. 1999, A&A, 343, 229
Ryabchikova, T. A., Ptitsyn, D. A. 1986, in IAU Coll. 90, Upper Main Sequence Stars with Anomalous Abundances, ed. C. R. Cowley et al. (Dordrecht: Reidel), 319
Sadakane K. 1993, in ASP Conf. Ser. 44, Peculiar versus Normal Phenomena in A-Type and Related Stars, 72
Sneden, C., McWilliam, A., Preston, G. W., Cowan, J. J., Burris, D. L., & Armosky, B. J., 1996, ApJ, 467, 819
Van't Veer, C., Bukhart, C., & Coupry, M. F. 1988, A&A, 203, 123

THE ASTROPHYSICAL JOURNAL SUPPLEMENT SERIES, 135:115–124, 2001 July
© 2001. The American Astronomical Society. All rights reserved. Printed in U.S.A.

STARK WIDTHS OF THE Ne II, Ne III, AND Ne IV SPECTRAL LINES

V. MILOSAVLJEVIĆ[1]
Faculty of Physics, University of Belgrade, Studenski Trg 14-16, P.O. Box 368, 11000 Belgrade, Serbia, Yugoslavia
M. S. DIMITRIJEVIĆ[2]
Astronomical Observatory Belgrade, Volgina 7, 11160 Belgrade, Serbia, Yugoslavia
AND
S. DJENIŽE[3]
Faculty of Physics, University of Belgrade, Studenski Trg 14-16, P.O. Box 368, 11000 Belgrade, Serbia, Yugoslavia
Received 2000 October 10; accepted 2001 January 29

ABSTRACT

Stark widths of 42 single (Ne II), 10 double (Ne III), and five triple-charged (Ne IV) neon ion spectral lines, interesting for astrophysics, have been measured in a linear low-pressure pulsed arc at electron temperatures of 31,000 and 34,500 K and electron densities of 0.95×10^{23} and 1.83×10^{23} m^{-3}. The measured width values have been compared with the theoretical data calculated by us using semiclassical perturbation formalism. Our measured and calculated Stark width values have also been compared with existing experimental and theoretical data.

Subject headings: plasmas — methods: laboratory — line: profiles — atomic data

1. INTRODUCTION

The interest in Stark-broadening data of good quality for as large a number of spectral lines as possible of various emitters has been additionally stimulated in last 10 years by the development of space astronomy, with which an extensive amount of spectroscopic information over large spectral regions of all kinds of celestial objects has been and will be collected. There is a number of astrophysical problems for which Stark-broadening data are of interest. Such problems are, e.g., stellar spectra analysis and synthesis and stellar plasma investigations, diagnostics, and modeling. Stark broadening is the main broadening mechanism in O-, A-, and B-type star atmospheres, as well as in white dwarfs (see, e.g., Popović, Dimitrijević, & Ryabchikova 1999). The available abundance analyses for early-type stars show that about 10%–20% of A and B stars have abundance anomalies, including anomalies in isotopic compositions (Leckrone et al. 1993). The abundance anomalies in these stars, called CP stars, have been caused by different hydrodynamic processes in the outer stellar layers (aided and mitigated by magnetic fields, weak stellar winds, turbulence, rotation mixing, etc.). In order to investigate these processes, atomic data for numerous lines of various emitters, including Stark-broadening data, are needed, since the stellar chemical composition is not known a priori. Such investigations, in which Stark-broadening data are of interest, provide us with useful information for the modeling of stellar evolution. As an example, the abundance studies of stellar atmospheres provide evidence for the chemical composition of the stellar primordial cloud, the processes occurring within the stellar interior, and the dynamic processes in stellar atmospheres (see, e.g., Popović, Milovanović, & Dimitrijević 2001). Besides in white dwarfs and hot stars of B and A types, Stark broadening may be important in cooler star atmospheres as, e.g., a solar one. For example, the influence of Stark broadening within a spectral series increases with the increase of the principal quantum number of the upper level, and consequently the Stark-broadening contribution may become significant even in the spectrum of the Sun and cooler stars. Reliable Stark-broadening data are also needed for the determination of chemical abundances of elements from equivalent widths of absorption lines and for the estimation of the radiative transfer through the stellar plasmas, especially in subphotospheric layers, as well as for opacity calculations. Stark broadening is of interest as well for radiative acceleration considerations, nucleosynthesis research, and other astrophysical topics.

Neon is the most abundant element in the universe after H, He, O, and C, and it is one of the products of hydrogen and helium burning in the orderly evolution of stellar interiors, for example (Trimble 1991). After the hydrogen-, helium-, and carbon-burning periods end in massive stars, neon burning starts. Neon also occurs in supernovae ejecta (Thieleman, Nomoto, & Yokoi 1986; Woosley, Pinto, & Weaver 1988). We note as well that Ne III lines have been identified in the spectrum of a solar active region (Thomas & Neupert 1994). Moreover, Sigut (1999) recently provided non-LTE equivalent widths for Ne I, so that the astrophysical importance of Stark broadening of spectral lines of neon in various ionization stages is obvious.

The knowledge of the Stark width values of the single (Ne II), double (Ne III), and triple (Ne IV) charged neon spectral lines is of interest also for plasma diagnostic purposes. Namely, from the Stark width values, it is possible to obtain the basic plasma parameters, such as the electron temperature (T) and electron density (N), essential for the modeling of various cosmic plasmas. Moreover, neon is present in many laboratory light sources and lasers as the working gas.

From the first investigation of Ne II Stark shifts (Pretty 1931; Maissel 1959; Mandel'shtam 1962; Mandel'shtam et. al. 1963; Mazing & Vrublevskaya 1962), Stark widths of Ne II spectral lines have been investigated in several experiments (Mazing & Vrublevskaya 1962; Mandel'shtam 1962; Mandel'shtam et al. 1963; Platiša, Dimitrijević, & Konjević 1978; Pittman & Konjević 1986; Purić et al. 1987; Uzelac et al. 1993; Blagojević, Popović, & Konjević 1999;

[1] vladimir@ff.bg.ac.yu.
[2] mdimitrijevic@aob.bg.ac.yu.
[3] steva@ff.bg.ac.yu.

del Val, Aparicio, & Mar 2000) and in one (Griem 1974) theoretical publication. Moreover, Ne II Stark width estimates using regularities and systematic trends have been performed by Purić, Lakićević, & Glavonjić (1981), Bertucelli & Di Rocco (1993), and Djeniže et al. (1999). It should be pointed out that in a number of the mentioned experiments no significant results on the electron temperature and density have been reported, making the normalization of the Stark width values impossible. Thus, these results cannot be included in the comparison with our new Stark width data. In the case of the Ne III lines, four experiments deal with the Stark widths measurements (Konjević & Pittman 1987; Purić et al. 1988; Uzelac et. al. 1993; Blagojević, Popović, & Konjević 2000), and seven papers (Dimitrijević & Konjević 1981, 1987; Konjević & Pittman 1987; Dimitrijević 1988a, 1988b; Uzelac, et al. 1993; Blagojević et al. 2000) contain theoretical calculations of these values. Measured Stark width values of Ne IV spectral lines are presented in only two papers (Purić et al. 1988; Uzelac et al. 1993), and their calculated values are given in five publications (Dimitrijević & Konjević 1981, 1987; Dimitrijević 1988a, 1988b; Uzelac et al. 1993). Moreover, Purić et al. (1988) estimated Stark widths of Ne III and Ne IV lines by using regularities and systematic trends.

We have measured Stark FWHM (full width at half-maximum; W) of 42 Ne II spectral lines, at two discharge conditions, belonging to 24 multiplets, in six transitions. Stark widths in two multiplets ($3p\ ^4D^0$–$4s\ ^4P$, $3p\ ^4P^0$–$4s\ ^4P$) from them have not yet been investigated. Stark width values for 13 Ne II spectral lines are the first published data. Theoretical calculations for the W values investigated in this work exist only for the spectral lines from seven multiplets (Griem 1974). These calculations are based on the semiclassical theory. In the case of the Ne III and Ne IV spectral lines, we have measured Stark FWHM for 10 and five lines, respectively. The Ne III spectral lines investigated belong to five multiplets in three transitions, and two from these multiplets ($3p'\ ^3F$–$3d'\ ^3F^0$ and $3p'\ ^3D$–$3d'\ ^3D^0$) have not yet been investigated. The W values for four Ne III spectral lines are the first published data. The five Ne IV spectral lines investigated belong to two multiplets in one transition. One of them ($3s\ ^2P$–$3p\ ^2D^0$) was not investigated before, and the W values for three Ne IV lines are the first published data, according to atomic line shape bibliographies (Fuhr, Wiese, & Roszman 1972; Fuhr, Roszman, & Wiese 1974; Fuhr, Martin, & Spect 1975; Fuhr, Miller, & Martin 1978; Fuhr & Lesage 1993; Lesage & Fuhr 1999), covering the period 1889–1999. We have performed calculations of Ne II, Ne III, and Ne IV W values using the semiclassical perturbation formalism (SCPF; Sahal-Bréchot 1969a, 1969b) innovated several times (Sahal-Bréchot 1974; Fleurier, Sahal-Bréchot, & Chapelle 1977; Dimitrijević & Sahal-Bréchot 1984, 1996b; Dimitrijević, Sahal-Bréchot, & Bommier 1991).

Measurements were performed in optically thin neon plasma created in the linear, low-pressure, pulsed-arc discharge at two various plasma conditions.

2. EXPERIMENT

The modified version of the linear, low-pressure pulsed arc (Djeniže et al. 1991; Djeniže, Srećković, & Labat 1992; Djeniže, Milosavljević, & Srećković 1998; Milosavljević et al. 2000) has been used as a plasma source. A pulsed discharge was driven in a quartz discharge tube with an inner diameter of 5 mm and an effective plasma length of 7.2 cm (Fig. 1 in Djeniže et al. 1991; Djeniže et al. 1998). The tube had end-on quartz windows. On the opposite side of the electrodes, the glass tube was expanded in order to reduce the erosion of the glass wall and the sputtering of the electrode material onto the quartz windows. The working gas was pure neon at a filling pressure of 133 Pa in a flowing regime. Spectroscopic observations of isolated spectral lines were made end-on along the axis of the discharge tube. A capacitor of 14 μF was charged up to 1.5 and 2.5 kV, respectively. The line profiles were recorded using a step-by-step technique with a photomultiplier (EMI 9789 QB) and a grating spectrograph (Zeiss PGS-2, reciprocal linear dispersion of 0.73 nm mm^{-1} in first order) system. The instrumental FWHM of 0.008 nm was determined using the narrow spectral lines emitted by the hollow-cathode discharge. The recorded profiles of these lines are Gaussian in shape, with an 8% accuracy, within the range of the investigated spectral line wavelengths. The spectrograph exit slit (10 μm) with the calibrated photomultiplier was traversed along the spectral plane in micrometric wavelength steps (0.0073 nm). The averaged photomultiplier signal (five shots at the same spectral range) was digitized using an oscilloscope interfaced to a computer. A sample output is shown in Figure 1.

Plasma reproducibility was monitored by the Ne II line radiation and the discharge current (it was found to be within 3%). Discharge characteristics were determined by analyzing the Rogowski coil signal. The values found at an 1.5 and 2.5 kV bank voltage are as follows: the discharge current is 1.82 and 2.95 kA, the discharge period is 68 and 70 μs, the thermal resistance is 0.46 and 0.44 Ω, and the decrement is 2.8 and 2.6, respectively. A typical Rogowski coil signal is presented in Figure 2.

The measured profiles were of the Voigt type because of the convolutions of the Lorentzian, Stark, and Gaussian profiles from Doppler and instrumental broadening. For the electron density and temperature of our experiments, the Lorentzian fraction in the Voigt profile was dominant (over 88%). Van der Waals and resonance broadening were estimated to be smaller by more than an order of magnitude in comparison with Stark, Doppler, and instrumental

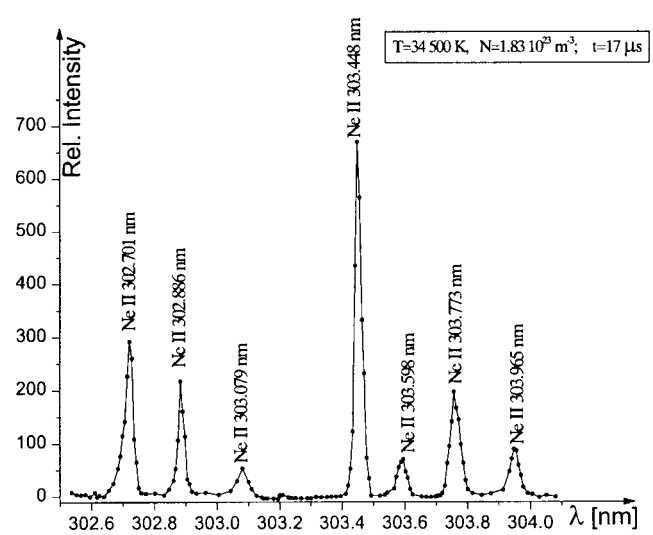

FIG. 1.—Recorded spectrum with several investigated Ne II lines at 17 μs after the beginning of the discharge, with a $U = 2.5$ kV bank voltage and a $p = 133$ Pa gas pressure.

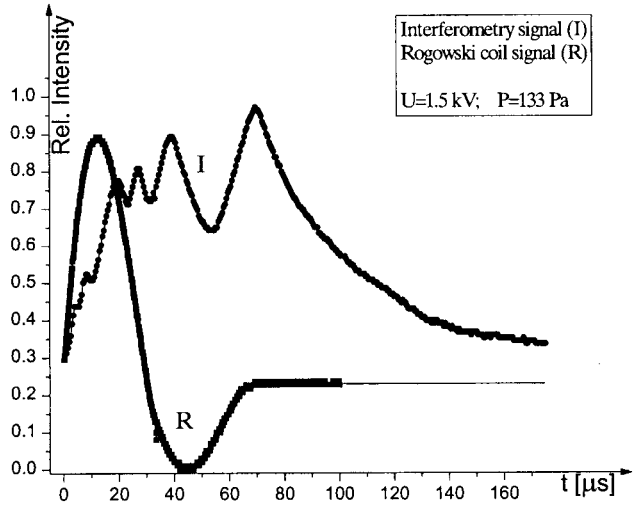

FIG. 2.—Temporal evolution of the Rogowski coil (R) and interferometry (I) signals.

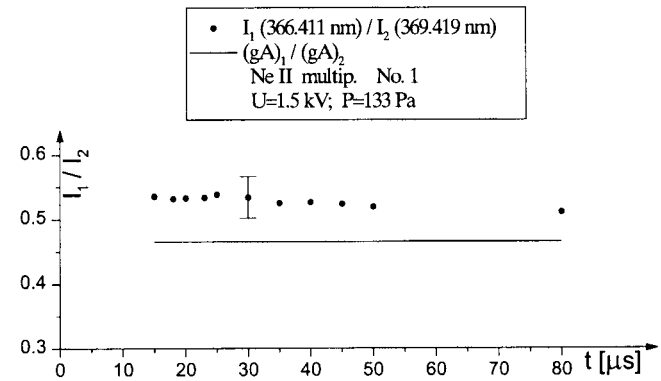

FIG. 3.—Intensity ratio (I_1/I_2) of two Ne II spectral lines belonging to the same multiplet, during the plasma decay. The solid line shows the theoretical prediction (Wiese et al. 1966); the filled circles show our measured values with a $\pm 6\%$ accuracy.

broadening. The standard deconvolution procedure (Davies & Vaughan 1963) was computerized using the least-square algorithm. The Stark widths were measured with $\pm 12\%$ estimated uncertainties for Ne II and $\pm 15\%$ estimated uncertainties for Ne III and Ne IV spectral lines at a given electron density and temperature. The estimated uncertainties come from the experimental technique and method used. Other uncertainties found, for example, in defining the length of the plasma (with possibly pronounced inhomogeneous end layers due to the expansion of the glass tube behind the electrodes), in the deconvolution procedure, and in the self-absorption tests are each 1 order of magnitude smaller. Consequently, the total error will not be significantly higher than the estimated one. Great care was taken to minimize the influence of self-absorption on Stark width determinations. The opacity was checked by measuring relative line intensity (I) ratios within the low-lying multiplet No. 1 in the Ne II spectrum during the decaying plasma (369.419 and 366.419 nm). The values obtained were compared with calculated ratios of the products of the spontaneous emission probabilities (A) and the corresponding statistical weights (g) of the upper levels of the lines. The necessary atomic data were taken from Wiese, Smith, & Glennon (1966), Lide (1994), and NIST (2001).[4] It turns out that these ratios differed by less than $\pm 14\%$ (in a wide part of the decaying plasma; see Fig. 3), testifying to the absence of self-absorption (Griem 1964; Wiese 1968).

In the 15th microsecond after the beginning of the discharge (when the Ne II profiles were analyzed at a lower electron density), the theoretical ratio I_1/I_2 is only 14% below the averaged experimental data. It should be pointed out that the experimental I_1/I_2 ratio is within a constant $\pm 3\%$ accuracy during the whole plasma-decay period. This fact also testifies to the absence of self-absorption. The constant difference among measured and calculated line intensity ratios can be explained (Djeniže & Bukvić 2001) by taking into account the high uncertainties ($\pm 50\%$) of the transition probabilities used. The same conclusions about self-absorption can also be obtained in the cases of the Ne III and Ne IV spectral lines. So, the effective plasma length used can be treated as optically thin for the Ne II, Ne III, and Ne IV spectral line radiation investigated.

The plasma parameters were determined using standard diagnostic methods (Rompe & Steenbeck 1967). Thus, the electron temperature (T) was determined from the Boltzmann plot of the relative intensities of 14 Ne II spectral lines (331.98, 336.06, 337.18, 341.48, 341.69, 341.77, 350.36, 356.83, 366.41, 369.42, 429.04, 439.19, 440.93, and 441.32 nm) within an energy interval of 7.1 eV for corresponding upper levels, with an estimated error of $\pm 6\%$, assuming the existence of LTE, according to the criterion from Griem (1964).

The Boltzmann plot obtained in the 15th microsecond after the beginning of the discharge is presented in the Figure 4 as an example. All necessary atomic data were taken from Wiese et. al. (1966), Lide (1994), NIST (2001), and Striganov & Sventickij (1966). The existing scatter between obtained values within the same multiplet can be explained by taking into account the high uncertainties of the existing A values. The electron temperature decay is presented in Figure 5. The electron density (N) decay was measured using a well-known single-laser interferometry technique (Ashby et al. 1965) for the 632.8 nm He-Ne laser wavelength, with an estimated error of $\pm 7\%$ (quarter-fringe uncertainties of four fringes for $U = 1.5$ kV bank energy

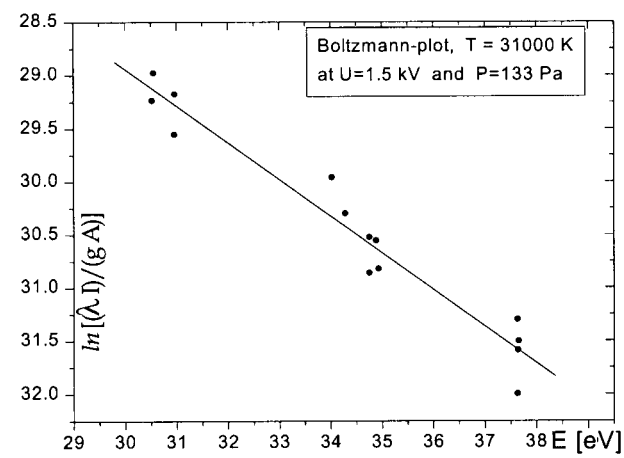

FIG. 4.—Boltzmann plot on the basis of 14 Ne II spectral lines at 15 μs after the beginning of the discharge, with a $U = 1.5$ kV bank voltage and a $p = 133$ Pa gas pressure.

[4] Available at http://physics.nist.gov.

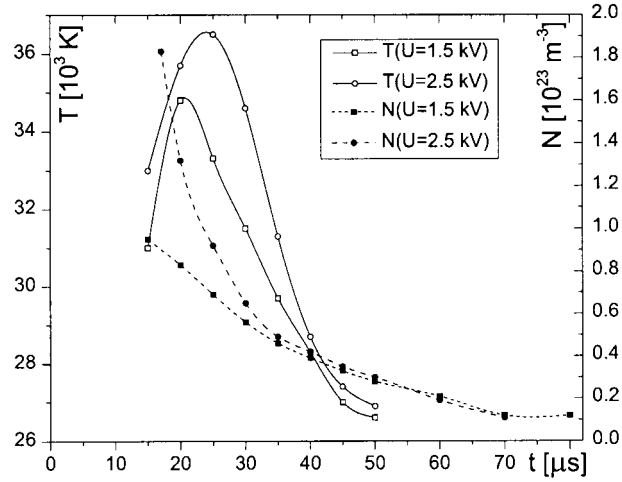

FIG. 5.—Temporal evolution of the electron temperatures (T) and electron densities (N) during the plasma decay at various discharge conditions.

and quarter-fringe uncertainties of seven fringes for $U = 2.5$ kV bank energy). Temporal evolution of the typical interferometry signal is presented in Figure 2. The electron density decay is presented in Figure 5.

At 15 and 17 μs after the beginning of the discharge, when the Ne II, Ne III, and Ne IV spectral line profiles were analyzed, the electron temperatures found were 31,000 and 34,500 K, and the electron densities were 0.95×10^{23} and 1.83×10^{23} m^{-3} for the 1.5 and 2.5 kV bank voltage, respectively.

3. METHOD OF CALCULATION

The semiclassical perturbation formalism, as well as the corresponding computer code (Sahal-Bréchot 1969a, 1969b), has been updated and optimized several times (Sahal-Bréchot 1974; Fleurier et al. 1977; Dimitrijević & Sahal-Bréchot 1984, 1996b; Dimitrijević et al. 1991). The calculation procedure, with the discussion of updatings and validity criteria, has been briefly reviewed, e.g., in Dimitrijević & Sahal-Bréchot (1996a, 1996b), so that only the basic details of calculations will be presented here. Stark full width (W) at half-maximum (FWHM) and shift (d) of an isolated spectral line, may be expressed as (Sahal-Bréchot 1969a, 1969b; Fleurier et al. 1977)

$$W = N \int v f(v) dv \left[\sum_{i' \neq i} \sigma_{ii'}(v) + \sum_{f' \neq f} \sigma_{ff'}(v) + \sigma_{\rm el} \right] + W_R ,$$

$$d = N \int v f(v) dv \int_{R_3}^{R_D} 2\pi\rho \, d\rho \, \sin 2\phi_p , \qquad (1)$$

where N is the electron density, $f(v)$ is the Maxwellian velocity distribution function for electrons, ρ denotes the impact parameter of the incoming electron, i and f denote the initial and final atomic energy levels, and i', f' denote their corresponding perturber levels, while W_R gives the contribution of the Feshbach resonances (Fleurier et al. 1977). The inelastic cross section $\sigma_{j,\,j'}(v)$ can be expressed by an integral over the impact parameter of the transition probability $P_{jj'}(\rho, v)$ as

$$\sum_{j' \neq j} \sigma_{jj'}(v) = \frac{1}{2} \pi R_1^2 + \int_{R_1}^{R_D} \sum_{j \neq j'} P_{jj'}(\rho, v), \; j = i, f , \qquad (2)$$

and the elastic cross section is given by

$$\sigma_{\rm el} = 2\pi R_2^2 + \int_{R_2}^{R_D} 8\pi\rho \, d\rho \, \sin^2 \delta ,$$

$$\delta = (\phi_p^2 + \phi_q^2)^{1/2} . \qquad (3)$$

The phase shifts ϕ_p and ϕ_q, due, respectively, to the polarization potential (r^{-4}) and the quadrupolar potential (r^{-3}), are given in § 3 of Sahal-Bréchot (1969a, p. 102). Here $R_{\rm D}$ is the Debye radius. All the cutoffs, R_1, R_2, and R_3, are described in § 1 of Sahal-Bréchot (1969b, p. 324). For the electrons, hyperbolic paths due to the attractive Coulomb force were used, while for perturbing ions, the paths were different, since the force is repulsive. The formulae for the ion impact widths and shifts are analogous to equations (1)–(3), without the resonance contribution to the width. The difference in calculation of the corresponding transition probabilities and phase shifts as functions of the impact parameter in equations (2) and (3) is in the ion perturber trajectories, which are influenced by the repulsive Coulomb force instead of an attractive one, as for electrons.

Atomic energy levels not found (or revised) in Moore (1971) and Bashkin & Stoner (1978) have been taken from Quinet, Palmeri, & Biémont (1994) for Ne II, from Persson, Wahlström, & Jönsson (1991) for Ne III, and from Kramida et al. (1999) for Ne IV. Corresponding ionization potentials for Ne III and Ne IV have been taken from Persson et al. (1991) and Kramida et al. (1999), and they differ from previously used values (Edlén 1964). One should mention that Ne II, Ne III, and Ne IV spectra are not well known, so the set of perturbing atomic energy levels needed for a semiclassical perturbation method calculation, with the usual average accuracy of $\pm 30\%$, is not complete.

4. RESULTS

The results of the measured Stark FWHM (W_m) values at obtained electron temperatures (T) and densities (N) are shown in Table 1 for the Ne II spectral lines and in Table 2 for the Ne III and Ne IV spectral lines. Ratios of $W_m/W_{\rm th}$ are also given, where $W_{\rm th}$ is the Stark FWHM calculated by us using the SCPF. Our calculated SCPF $W_{\rm th}$ values at an 10^{23} m^{-3} electron density are presented in Table 3 for Ne II lines and in Table 4 for the Ne III and Ne IV lines, respectively. Theoretical W values are given for the mean ($\langle\lambda\rangle$) wavelength in a multiplet. The width of each multiplet component can be easily evaluated if one takes into account that the line width is proportional to λ^2.

5. DISCUSSION

In order to make the comparison between measured and calculated Stark width values easier, the theoretical Stark FWHM dependence on the electron temperature, together with the values of the other authors and our experimental results at an electron density of 1×10^{23} m^{-3}, are presented graphically in Figures 6 and 7.

In the case of the most investigated Ne II spectral lines (Fig. 6), the existing calculated W values have been presented by Griem (1974; on the basis of the semiclassical [G] approach) and Uzelac et al. (1993; on the basis of the modified semiempirical [SEM] approximation). Moreover, theoretical Stark width values, calculated on the basis of the classical path (HB) approximation (Hey & Breger 1980a,

TABLE 1

MEASURED STARK FWHM (W_m) VALUES FOR THE Ne II SPECTRAL LINES

Transition	Multiplet	λ (nm)	T (10^4 K)	N (10^{23} m^{-3})	W_m (pm)	W_m/W_{th}	W_m/W_G
$3s$–$3p$	^4P–$^4P^0$ (1)	369.419	3.10	0.95	11.6	0.82	0.95
			3.45	1.83	20.5	0.78	0.90
		366.411	3.10	0.95	11.2	0.80	0.92
			3.45	1.83	19.6	0.76	0.86
	^4P–$^4D^0$ (2)	333.487	3.10	0.95	13.3	1.13	1.19
			3.45	1.83	20.7	0.94	0.98
		336.063	3.10	0.95	12.5	1.04	1.12
			3.45	1.83	21.8	0.97	1.03
		332.716	3.10	0.95	14.0	1.19	1.25
			3.45	1.83	22.0	1.00	1.04
	^4P–$^4S^0$ (4)	300.166	3.10	0.95	8.2	0.82	...
			3.45	1.83	14.6	0.79	...
		302.886	3.10	0.95	8.0	0.79	...
			3.45	1.83	15.0	0.80	...
	^2P–$^2D^0$ (5)	372.708	3.10	0.95	12.8	0.85	0.90
			3.45	1.83	22.5	0.80	0.84
	^2P–$^2P^0$ (7)	332.375	3.10	0.95	15.0	1.19	...
			3.45	1.83	23.8	1.02	...
		337.828	3.10	0.95	14.6	1.12	...
			3.45	1.83	24.2	1.00	...
$3s'$–$3p'$	^2D–$^2F^0$ (9)	356.853	3.10	0.95	13.2	1.00	...
			3.45	1.83	23.2	0.95	...
	^2D–$^2P^0$ (10)	331.975	3.10	0.95	12.0	1.03	...
			3.45	1.83	22.1	1.02	...
$3p$–$3d$	$^4P^0$–^4D (8)	303.448	3.10	0.95	10.1	0.73	0.93
			3.45	1.83	19.8	0.76	0.96
		302.704	3.10	0.95	11.1	0.80	1.03
			3.45	1.83	20.5	0.79	1.00
		303.773	3.10	0.95	11.2	0.81	1.04
			3.45	1.83	20.9	0.80	1.02
	$^4D^0$–^4D (12)	332.920	3.10	0.95	12.8	0.75	...
			3.45	1.83	24.3	0.77	...
		335.790	3.10	0.95	13.0	0.76	...
			3.45	1.83	24.7	0.77	...
		332.029	3.10	0.95	12.7	0.75	...
			3.45	1.83	24.5	0.77	...
		337.410	3.10	0.95	12.9	0.74	...
			3.45	1.83	24.5	0.75	...
		336.289	3.10	0.95	12.8	0.74	...
			3.45	1.83	24.5	0.76	...
		337.939	3.10	0.95	12.8	0.73	...
			3.45	1.83	24.3	0.74	...
	$^2D^0$–^4F (19)	333.078	3.10	0.95	16.1	0.90	...
			3.45	1.83	27.8	0.83	...
	$^2D^0$–^2F (20)	341.771	3.10	0.95	14.0	0.74	0.91
			3.45	1.83	25.1	0.70	0.86
		341.482	3.10	0.95	14.5	0.77	0.95
			3.45	1.83	26.2	0.73	0.90
	$^2D^0$–^2D (21)	341.682	3.10	0.95	15.6	0.85	...
			3.45	1.83	29.6	0.86	...
	$^2D^0$–^4P (22)	337.187	3.10	0.95	14.3	0.76	...
			3.45	1.83	26.5	0.73	...
	$^2S^0$–^2P (28)	350.361	3.10	0.95	16.5	0.81	0.98
			3.45	1.83	29.6	0.78	0.92
	$^2P^0$–^2P (41)	369.709	3.10	0.95	17.6	0.77	...
			3.45	1.83	32.0	0.74	...
		362.806	3.10	0.95	17.5	0.79	...
			3.45	1.83	32.0	0.77	...
	$^4S^0$–^2D (33)	365.993	3.10	0.95	17.6	0.84	...
			3.45	1.83	31.8	0.81	...
		363.275	3.10	0.95	17.5	0.85	...
			3.45	1.83	31.7	0.81	...
	$^4S^0$–^4F (31)	357.126	3.10	0.95	17.4	0.82	...
			3.45	1.83	31.8	0.79	...

TABLE 1—*Continued*

Transition	Multiplet	λ (nm)	T (10^4K)	N (10^{23}m^{-3})	W_m (pm)	W_m/W_{th}	W_m/W_G
	$^4S^0$–^4P (34)	356.584	3.10	0.95	17.7	0.73	0.97
			3.45	1.83	31.8	0.70	0.92
$3p'$–$3d'$	$^2P^0$–^2P	341.138	3.10	0.95	16.7	0.91	...
			3.45	1.83	30.9	0.90	...
$3p$–$4s$	$^2P^0$–^2P	337.728	3.10	0.95	16.0	0.55	...
			3.45	1.83	28.7	0.53	...
	^4D–^4P	303.965	3.10	0.95	15.9	0.68	...
			3.45	1.83	28.9	0.65	...
		303.598	3.10	0.95	16.4	0.70	...
			3.45	1.83	29.3	0.67	...
		303.079	3.10	0.95	16.2	0.69	...
			3.45	1.83	29.3	0.67	...
	$^4P^0$–^4P	278.002	3.45	1.83	20.7	0.56	...
$3d$–$4f$	^4F–$^4F^0$ (56)	439.194	3.45	1.83	107.8	...	...
		440.930	3.10	0.95	101.3	...	...
			3.45	1.83	185.4	...	...
	^4F–$^4G^0$ (57)	429.040	3.10	0.95	93.1	...	...
			3.45	1.83	170.2	...	...

NOTES.—Measured Stark FWHM (W_m) values for the Ne II spectral lines at an observed electron temperature (T) and electron density (N). Here W_m/W_{th} and W_m/W_G present the ratios between our measured (W_m) and our calculated (W_{th}) values (Table 3) and Griem's (1974) theoretical values (W_G), respectively.

TABLE 2

MEASURED STARK FWHM (W_m) VALUES FOR THE Ne III AND Ne IV SPECTRAL LINES

Emitter	Transition	Multiplet	λ (nm)	W_m (pm)	W_m/W_{th}
Ne III	$3s$–$3p$	$^5S^0$–^5P	259.004	13.5	1.05
		(11 UV)	259.360	12.1	0.94
			259.568	14.1	1.10
		$^3S^0$–^3P	267.864	14.1	0.95
		(12 UV)	267.790	15.0	1.00
	$3s'$–$3p'$	$^3D^0$–^3F	261.003	15.9	1.22
			261.341	14.1	1.08
			261.587	15.0	1.15
	$3p'$–$3d'$	^3F–$^3F^0$	226.491	12.1	1.10
		^3D–$^3D^0$	209.554	14.1	1.48
Ne IV	$3s$–$3p$	^4P–$^4D^0$	237.216	11.5	1.06
			235.252	12.1	1.12
			235.796	12.1	1.12
		^2P–$^2D^0$	236.549	15.0	1.21
			236.328	15.9	1.29

NOTES.—Measured Stark FWHM (W_m) values for the Ne III and Ne IV spectral lines at an observed electron temperature of 34,500 K and an electron density of 1.83×10^{23} m^{-3}. Here W_m/W_{th} presents the ratio between our measured (W_m) and calculated (W_{th}) values based on SCPF (Table 4).

1980b, 1982), are also presented in the work by Uzelac et al. (1993).

On the basis of Tables 1 and 3 and Figure 6, one can conclude that our measured W values agree, to within experimental accuracy, with existing experimental Stark width values in the case of the $3s$–$3p$ and $3p$–$3d$ transitions. Our calculated SCPF Stark width values, in general, lie above SEM and G values and agree, especially in the case of the multiplets Nos. 2, 5, 7, 9, and 10 (which belong to the $3s$–$3p$ and $3s'$–$3p'$ transitions), with our experimental W data and results from other experimental works (see Fig. 6). Generally, our W_m values lie, on average, up to 7% and 20% below our SCPF values in the case of the $3s$–$3p$ and $3p$–$3d$ transitions, respectively (see W_m/W_{th} values in Table 1). In the case of the higher lying multiplet in the $3p$–$4s$ transition, this discrepancy is higher. The averaged W_m/W_{th} ratios are 0.63. One of the reasons for the higher discrepancies in higher lying multiplets is the noncompleteness of the atomic energy levels needed for a reliable calculation, which are larger for higher lying multiplets. Because of this reason it was not possible to calculate Stark widths for Ne II $3d\,^4F$–$4f\,^4F^0$ and $3d\,^4F$–$4f\,^4G^0$ multiplets.

TABLE 3

ELECTRON STARK FWHM CALCULATED USING SCPF FOR THE Ne II SPECTRAL LINES

Transition	$\langle\lambda\rangle$ (nm)	T (10^4 K) 0.5	1	2	3	3.1	3.45	5	10
$3s\ ^4P$–$3p\ ^4P^0$	372.51	34.6	25.0	18.1	15.3	15.2	14.6	13.1	11.3
$3s\ ^4P$–$3p\ ^4D^0$	334.33	28.4	20.6	14.9	12.7	12.5	12.1	10.8	9.47
$3s\ ^4P$–$3p\ ^4S^0$	298.83	23.3	16.9	12.3	10.5	10.4	10.0	9.06	7.99
$3s\ ^2P$–$3p\ ^2D^0$	371.41	35.1	25.4	18.6	15.9	15.7	15.2	13.8	12.2
$3s\ ^2P$–$3p\ ^2P^0$	334.27	29.5	21.4	15.7	13.5	13.4	12.9	11.8	10.5
$3s'\ ^2D$–$3p'\ ^2F^0$	357.21	31.2	22.6	16.5	14.1	13.9	13.4	12.1	10.7
$3s'\ ^2D$–$3p'\ ^2P^0$	333.78	27.7	20.1	14.7	12.6	12.4	12.0	10.9	9.63
$3p\ ^4P^0$–$3d\ ^4D$	304.01	30.0	22.4	16.9	14.9	14.7	14.3	13.2	11.9
$3p\ ^4D^0$–$3d\ ^4D$	335.26	36.7	27.3	20.7	18.2	18.1	17.6	16.2	14.7
$3p\ ^2D^0$–$3d\ ^4F$	342.15	40.2	29.8	22.7	20.0	19.9	19.4	17.9	16.4
$3p\ ^2D^0$–$3d\ ^2F$	337.56	39.4	29.3	22.2	19.7	19.5	19.0	17.6	16.1
$3p\ ^2D^0$–$3d\ ^2D$	343.23	39.2	29.3	22.3	19.6	19.4	18.9	17.5	16.0
$3p\ ^2D^0$–$3d\ ^4P$	335.26	39.0	29.0	22.1	19.6	19.5	19.0	17.7	16.2
$3p\ ^2S^0$–$3d\ ^2P$	347.31	42.0	31.4	23.9	21.2	21.1	20.5	19.1	17.7
$3p\ ^2P^0$–$3d\ ^2P$	365.18	46.7	35.0	26.8	23.8	23.6	23.0	21.5	19.9
$3p\ ^4S^0$–$3d\ ^2D$	365.00	43.9	33.0	25.1	22.2	22.0	21.5	19.9	18.3
$3p\ ^4S^0$–$3d\ ^4F$	363.78	44.8	33.4	25.5	22.6	22.4	21.9	20.4	18.7
$3p\ ^4S^0$–$3d\ ^4P$	356.00	45.8	35.2	28.0	25.6	25.4	25.0	24.1	23.8
$3p'\ ^2P^0$–$3d'\ ^2P$	342.27	39.1	29.2	22.2	19.6	19.4	18.9	17.5	16.0
$3p\ ^2P^0$–$4s\ ^2P$	341.23	65.2	46.1	34.2	31.3	31.1	30.4	29.1	27.3
$3p\ ^4D^0$–$4s\ ^4P$	304.53	53.9	37.6	27.6	25.0	24.8	24.2	23.0	21.3
$3p\ ^4P^0$–$4s\ ^4P$	278.52	45.5	31.7	23.2	20.9	20.8	20.3	19.2	17.6

NOTES.—Electron Stark FWHM (W in pm) calculated using SCPF (eqs. [1]–[3]) for the Ne II spectral lines at a 10^{23} m^{-3} electron density and an electron temperature of up to T = 100,000 K. $\langle\lambda\rangle$ is the mean wavelength of the multiplet.

TABLE 4

ELECTRON STARK FWHM (W IN PM) CALCULATED USING SCPF FOR THE Ne III AND Ne IV SPECTRAL LINES

Emitter	Transition	$\langle\lambda\rangle$ (nm)	T (10^4 K) 2	3.45	5	10	20	30	50
Ne III.....	$3s\ ^5S$–$3p\ ^5P^0$	259.31	9.16	7.03	5.94	4.50	3.61	3.24	2.66
	$3s\ ^3S^0$–$3p\ ^3P$	267.90	10.6	8.13	6.88	5.25	4.24	3.82	3.39
	$3s'\ ^3D^0$–$3p'\ ^3F$	261.18	9.31	7.14	6.03	4.58	3.68	3.31	2.94
	$3p'\ ^3F$–$3d'\ ^3F^0$	226.51	7.71	6.03	5.13	3.98	3.25	2.96	2.67
	$3p'\ ^3D$–$3d'\ ^3D^0$	209.24	6.66	5.20	4.43	3.42	2.80	2.54	2.30
Ne IV.....	$3s\ ^4P$–$3p\ ^4D^0$	236.20	7.83	5.92	4.98	3.67	2.83	2.48	2.14
	$3s\ ^2P$–$3p\ ^2D^0$	237.67	8.95	6.75	5.69	4.20	3.25	2.86	2.47

NOTES.—Electron Stark FWHM (W in pm) calculated using SCPF (eqs. [1]–[3]) for the Ne III and Ne IV spectral lines at a 10^{23} m^{-3} electron density and an electron temperature of up to T = 500,000 K. $\langle\lambda\rangle$ is the mean wavelength of the multiplet.

The recently measured values presented by del Val et al. (2000; 48 Ne II lines) lie 25%, on average, above all other experimental and theoretical Stark FWHM values (see Fig. 6).

It should be pointed out that SCPF and G values show similar behavior at electron temperatures higher than 40,000–50,000 K and that both lie above SEM predictions (multiplets Nos. 2 and 7 in Fig. 6). Hey's predictions (HB) agree with our calculated (SCPF) values at temperatures higher than 30,000 K. Finally, we can conclude that the agreement between existing experimental and theoretical (G, HB, and SCPF) W values, to within the accuracy of the experiments and the uncertainties of the theories, is satisfactory. The only exceptions are the values from Uzelac et al. (1993) of electron temperatures obtained at 73,000 and 82,000 K. These lie below G, HB, and SCPF theoretical values but show agreement with SEM theoretical predictions.

In the case of the Ne III and Ne IV spectral lines, the W values were been calculated on the basis of various approximations initiated by Griem (1974) and Dimitrijević & Konjević (1981). Thus, SE and SEM denote the results of semiempirical predictions from Griem (1968) and modified semiempirical predictions using equations (4) and (5) and equations (7)–(10), respectively, from Dimitrijević & Konjević (1981). Here G and GM denote W values obtained on the basis of the simplified semiclassical approximations (Griem 1974). For the GM values, the Gaunt factor threshold value is modified (Dimitrijević & Konjević 1980). Theoretical W values from Uzelac et al. (1993), calculated by using the quasi-classical Gaunt factor method (Hey & Breger 1980a, 1980b, 1982), have also been taken into

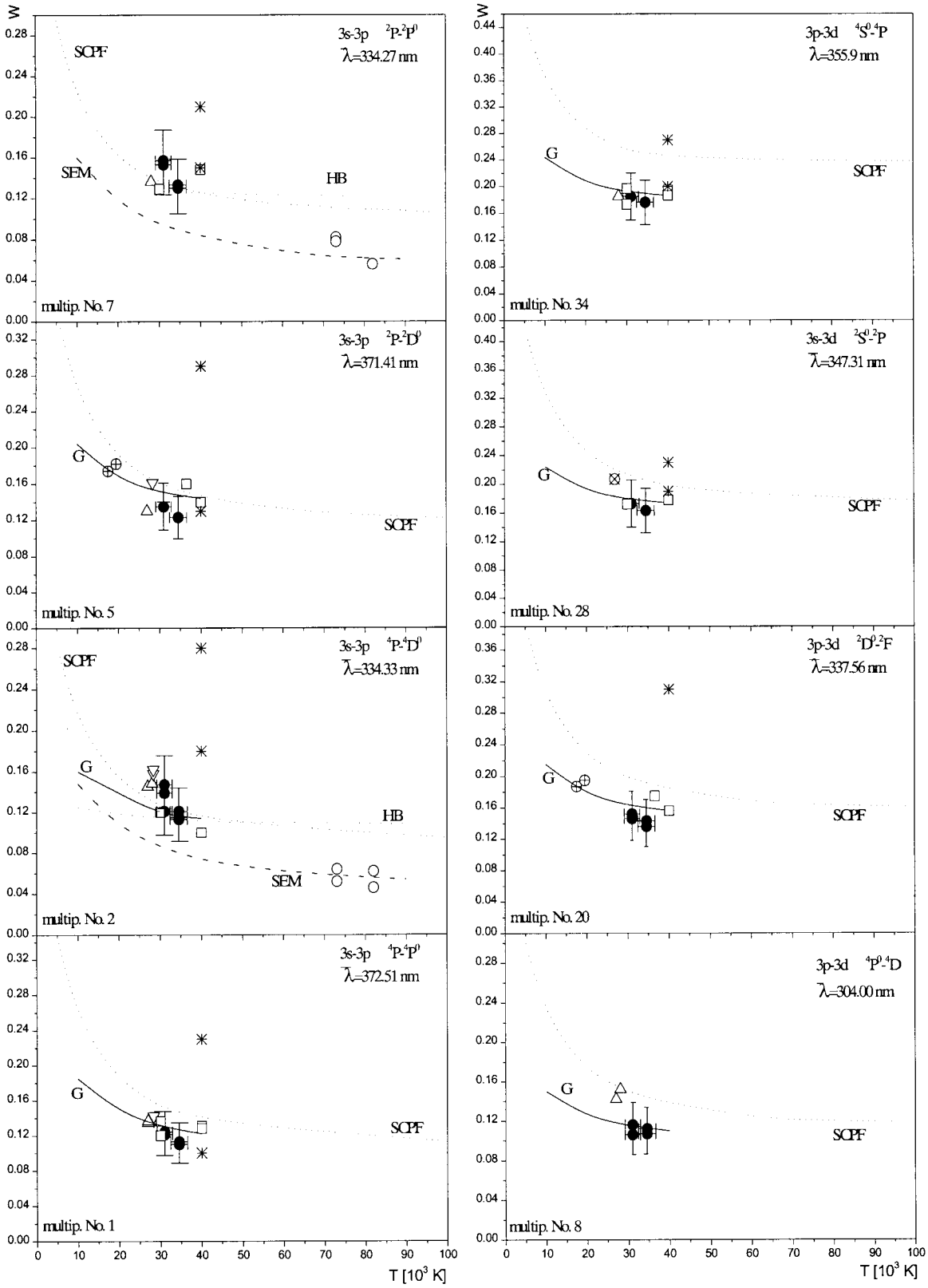

FIG. 6.—Stark FWHM (W in 0.1 nm) dependence on the electron temperature for the most investigated Ne II spectral lines belonging to various transitions at a 1×10^{23} m^{-3} electron density. The dotted lines show our calculations using SCPF. The filled circles show our experimental results. The results found by other authors are shown by the following symbols: inverted open triangles, Platiša et al. (1978); open triangles, Konjević & Pittman (1986); circled crosses, Pittman & Konjević (1986); open squares, Purić, et al. (1987); open circles, Uzelac et al. (1993); circled plus signs, Blagojević et al. (1999); and asterisks, del Val et al. (2000). Here G, SEM, and HB denote calculated W values on the basis of the semiclassical (Griem 1974), modified semiempirical (Dimitrijević & Konjević 1980; Uzelac et al. 1993), and quasi-classical Gaunt factor methods (Hey & Breger 1980a, 1980b, 1982), respectively. The error bars include the uncertainties of the width ($\pm 12\%$), electron density ($\pm 7\%$), and temperature measurements ($\pm 6\%$).

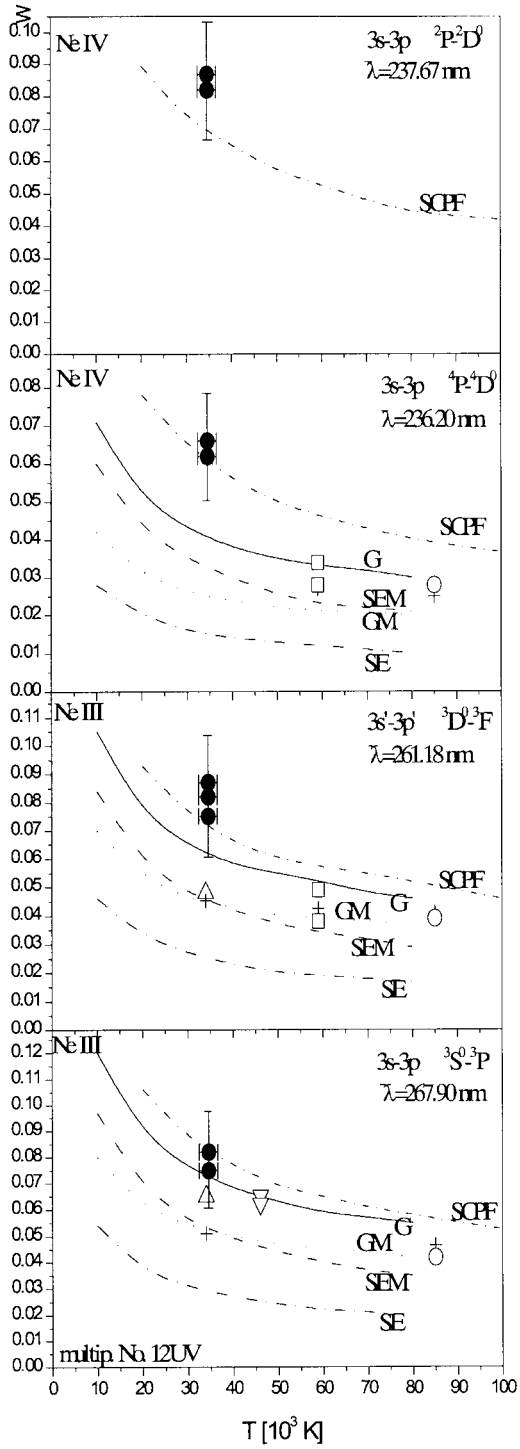

FIG. 7.—Stark FWHM (W in 0.1 nm) dependence on the electron temperature for the most investigated Ne III and Ne IV spectral lines belonging to the $3s$–$3p$ and $3s'$–$3p'$ transitions at a 1×10^{23} m^{-3} electron density. The dotted lines show our calculations using SCPF. The filled circles show our experimental results. The results found by other authors are shown by the following symbols: open triangles, Konjević & Pittman (1987); open squares, Purić et al. (1988); open circles, Uzelac et al. (1993), and inverted open triangles, Blagojević et al. (2000). Plus signs denote calculations using the quasi-classical Gaunt factor method (Hey & Breger 1980a, 1980b, 1982) performed only for the plasma parameters observed in the experiments in Uzelac et al. (1993), Konjević & Pittman (1987), and Purić et al. (1988). Here G, GM, SE, and SEM denote calculated W values on the basis of the semiclassical, simplified semiclassical, semiempirical, and modified semiempirical approaches, respectively, performed by Dimitrijević & Konjević (1981). The error bars include the uncertainties of the width ($\pm 15\%$), electron density ($\pm 7\%$), and temperature ($\pm 6\%$) measurements.

account. The latest values are presented only at electron temperatures observed in various experiments devoted to Ne III and Ne IV Stark width determination up to the year 1993.

On the basis of Tables 2 and 3 and Figure 7, one can conclude that our measured and calculated SCPF Ne III and Ne IV Stark FWHM values show satisfactory mutual agreement. It should be pointed out that our measured and calculated Stark FWHM values lie above all other experimental and theoretical data (see Fig. 7).

It should be pointed out that our SCPF values lie about 10% above theoretical predictions made by the simplified semiclassical (G) approximation in the case of the Ne III lines and much higher in the case of the Ne IV lines (see Fig. 7). Our W_m and W_{th} values are the first published data for the Ne IV $3s^2P$–$3p\ ^2D^0$ multiplet.

Such ratios of SCPF values and simplified semiclassical (G, GM) and semiempirical (SE, SEM) values are typical as for other emitters (see, e.g., Dimitrijević 1996, and references therein).

6. CONCLUSION

On the basis of the agreement found among experimental and theoretical Stark FWHM values, we can conclude that these represent convenient atomic data for the Ne II spectral lines, belonging to the multiplets Nos. 2, 5, 7, 9, and 10, needed in plasma spectroscopy.

In the case of the investigated Ne III and Ne IV spectral lines, our measured and calculated W values lie above all other Stark FWHM data, especially in the case of the Ne IV lines. New measurements at electron temperatures higher than 40,000 K can contribute to the clarification of this fact.

We hope as well that our semiclassical perturbation results for Ne II, Ne III, and Ne IV lines will be useful for astrophysical and laboratory plasma research, diagnostics, and modeling.

In order to underline the astrophysical interest of presented results, it is of interest to mention that the experimental temperatures (31,000 and 34,500 K) are the typical effective temperatures for late O-type stars. For example, for the O9 spectral type, in which Stark broadening is the principal pressure broadening mechanism (see, e.g., Griem 1974), the effective temperature is 32,600 K (Lang 1992). One should take into account, however, that within a stellar atmosphere model the temperature of interest varies, so that, e.g., for the Kurucz (1993) model of a typical B star, with an effective temperature of 16,000 K and a log of surface gravity equal to four, the temperature varies between 8600 and 47,000 K. For an A-type star with an effective temperature of 10,000 K and the same surface gravity, the temperature of interest is between 5800 and 29,000 K. Taking into account that scaling with electron density within the interval of interest is practically linear, our experimental and theoretical data cover plasma conditions of interest for A-, B-, and O-type stars, as well as white dwarfs, in which hydrogen is mainly ionized and Stark broadening is the principal pressure broadening mechanism.

This work is a part of the project "Astrometrical, Astrodynamical, and Astrophysical Investigations," supported by the Ministry of Science and Technology of the Republic of Serbia.

REFERENCES

Ashby, D. E. T. F., Jephcott, D. F., Malein, A., & Raynor, F. A. 1965, Appl. Phys., 36, 29
Bashkin, S., & Stoner, J. O., Jr. 1978, Atomic Energy Levels and Grotrian Diagrams, Vol. I (Amsterdam: North-Holland)
Bertucelli, D., & Di Rocco, H. O. 1993, Phys. Scr., 47, 747
Blagojević, B., Popović, M. V., & Konjević, N. 1999, Phys. Scr., 59, 374
———. 2000, J. Quant. Spectrosc. Radiat. Transfer, 67, 9
Davies, J. T., & Vaughan, J. M. 1963, ApJ, 137, 1302
del Val, J. A., Aparicio, J. A., & Mar, S. 2000, ApJ, 536, 998
Dimitrijević, M. S. 1988a, A&AS, 76, 53
———. 1988b, Bull. Obs. Astron. Belgrade, 139, 31
———. 1996, Zh. Prikl. Spektrosk., 63, 810
Dimitrijević, M. S., & Konjević, N. 1980, J. Quant. Spectrosc. Radiat. Transfer, 24, 451
———. 1981, in Spectral Line Shapes, ed. B. Wende (New York: de Gruyter), 211
———. 1987, A&A, 172, 345
Dimitrijević, M. S., & Sahal-Bréchot, S. 1984, J. Quant. Spectrosc. Radiat. Transfer, 31, 301
———. 1996a, A&AS, 119, 369
———. 1996b, Phys. Scr., 54, 50
Dimitrijević, M. S., Sahal-Bréchot, S., & Bommier, V. 1991, A&AS, 89, 581
Djeniže, S., & Bukvić, S. 2001, A&A, 365, 252
Djeniže, S., Milosavljević, V., & Srećković, A. 1998, J. Quant. Spectrosc. Radiat. Transfer, 5, 71
Djeniže, S., Srećković, A., & Labat, J. 1992, A&A, 253, 632
Djeniže, S., Srećković, A., Labat, J., Konjević, R., & Popović, L. Č. 1991, Phys. Rev. A, 44, 410
Djeniže, S., Srećković, A., Labat, J., & Platiša, M. 1999, Phys. Scr., 59, 98
Edlén, B. 1964, in Spectroscopy I, Handbuch der Physik, Vol. 27, ed. S. Flügge (Berlin: Springer), 198
Fleurier, C., Sahal-Bréchot, S., & Chapelle, J. 1977, J. Quant. Spectrosc. Radiat. Transfer, 17, 595
Fuhr, J. R., & Lesage, A. 1993, Bibliography on Atomic Line Shapes and Shifts (NBS Special Publ. 366, Suppl. 4) (Washington: NBS)
Fuhr, J. R., Martin, G. A., & Spect, B. J. 1975, Bibliography on Atomic Line Shapes and Shifts (NBS Special Publ. 366, Suppl. 2) (Washington: NBS)
Fuhr, J. R., Miller, B. J., & Martin, G. A. 1978, Bibliography on Atomic Line Shapes and Shifts (NBS Special Publ. 366, Suppl. 3) (Washington: NBS)
Fuhr, J. R., Roszman, L. J., & Wiese, W. L. 1974, Bibliography on Atomic Line Shapes and Shifts (NBS Special Publ. 366, Suppl. 1) (Washington: NBS)
Fuhr, J. R., Wiese, W. L., & Roszman, L. J. 1972, Bibliography on Atomic Line Shapes and Shifts (NBS Special Publ. 366) (Washington: NBS)
Griem, H. R. 1964, Plasma Spectroscopy (New York: McGraw-Hill)
———. 1968, Phys. Rev. A, 165, 258
———. 1974, Spectral Line Broadening by Plasmas (New York: Academic Press)
Hey, J. D., & Breger, P. 1980a, J. Quant. Spectrosc. Radiat. Transfer, 24, 349
———. 1980b, J. Quant. Spectrosc. Radiat. Transfer, 24, 427
———. 1982, S. Afr. J. Phys., 5, 111
Konjević, N., & Pittman, T. L. 1986, J. Quant. Spectrosc. Radiat. Transfer, 35, 473
———. 1987, J. Quant. Spectrosc. Radiat. Transfer, 37, 311
Kramida, A. E., Bastin, T., Biémont, E., Dumont, P.-D., & Garnir, H.-P. 1999, Eur. Phys. J. D., 7, 525
Kurucz, R. L. 1993, CD-ROM 13, ATLAS9 Stellar Atmosphere Programs and 2 km/s Grid (Cambridge: SAO)
Lang, K. R. 1992, Astrophysical Data I: Planets and Stars (New York: Springer)
Leckrone, D. S., Wahlgren, G. M., Johansson, S. G., & Adelman, S. J. 1993, in ASP Conf. Ser. 44, Peculiar Versus Normal Phenomena in A-Type and Related Stars, ed. M. M. Dworetsky, F. Castelli, & R. Faraggiana (IAU Colloq. 138) (San Francisco: ASP), 42
Lesage, A., & Fuhr, J. R. 1999, Bibliography on Atomic Line Shapes and Shifts (Paris: Observatoire de Paris)
Lide, D. R., ed. 1994, CRC Handbook of Chemistry and Physics (74th ed.; Boca Raton: CRC Press)
Maissel, L. I. 1959, Proc. Phys. Soc. London, 74, 97
Mandel'shtam, S. L. 1962, in Optik und Spektroskopie aller Wellenlängen (Berlin: Akademie Verlag), 372
Mandel'shtam, S. L., Mazing, M. A., Sobel'man, I. I., & Vainshtein, L. A. 1963, Proc. VI Int. Conf. Ioniz. Phen. in Gases, Vol. 3, (Paris: S.E.R.M.A.), 331
Mazing, M. A., & Vrublevskaya, N. A. 1962, Opt. Spectrosk., 13, 308
Milosavljević, V., Djeniže, S., Dimitrijević, M. S., & Popović, L. Č. 2000, Phys. Rev. E, 62, 4137
Moore, C. E. 1971, Atomic Energy Levels, Vol. I (Nat. Stand. Ref. Data Ser., 35) (Washington: NBS)
NIST. 2001, Atomic Spectra Database Lines (Washington: NIST)
Persson, W., Wahlström, C. G., & Jönsson, L. 1991, Phys. Rev. A, 43, 4791
Pittman, T. L., & Konjević, N. 1986, J. Quant. Spectrosc. Radiat. Transfer, 35, 247
Platiša, M., Dimitrijević, M. S., & Konjević, N. 1978, A&A, 67, 103
Popović L. Č., Dimitrijević, M. S., & Ryabchikova, T. 1999, A&A, 350, 719
Popović L. Č., Milovanović, N., & Dimitrijević, M. S. 2001, A&A, 365, 656
Pretty, W. E. 1931, Proc. Phys. Soc. London, 43, 279
Purić, J., Djeniže, S., Srećković, A., Ćuk, M., Labat, J., & Platiša, M. 1988, Z. Phys. D, 8, 343
Purić, J., Djeniže, S., Srećković, A., Labat, J., & Ćirković, Lj. 1987, Phys. Rev. A, 35, 2111
Purić, J., Lakićević, I. S., & Glavonjić, V. 1981, J. Quant. Spectrosc. Radiat. Transfer, 26, 65
Quinet, P., Palmeri, P., & Biémont, E. 1994, Phys. Scr., 49, 436
Rompe, R., & Steenbeck, M. 1967, Ergebnisse der Plasmaphysik und der Gaselektronik, Band 1 (Berlin: Akademie Verlag)
Sahal-Bréchot, S. 1969a, A&A, 1, 91
———. 1969b, A&A, 2, 322
———. 1974, A&A, 35, 319
Sigut, T. A. A. 1999, ApJ, 519, 303
Striganov, R. A., & Sventickij, N. S. 1966, Tablicy Spektralnych Linij Nejtalnych i Ionizovannych (Moskva: Atomizdat)
Trimble, V. 1991, A&A Rev., 3, 1
Thieleman, F. K., Nomoto, K., & Yokoi, K. 1986, A&A, 158, 17
Thomas, J. R., & Neupert, W. M. 1994, ApJS, 91, 461
Uzelac, N. I., Glenzer, S., Konjević, N., Hey, J. D., & Kunze, H. J. 1993, Phys. Rev. E, 47, 3623
Wiese W. L. 1968, Methods of Experimental Physics, Vol. 7B, ed. B. Bederson & W. L. Fite (New York: Academic Press)
Wiese, W. L., Smith, M. W., & Glennon, B. M. 1966, Atomic Transition Probabilities: Hydrogen through Neon (NSRDS-NBS 4) (Washington: NBS)
Woosley, S. E., Pinto, P. A., & Weaver, T. A. 1988, Proc. Astron. Soc. Australia, 7, 355

The Astrophysical Journal Supplement Series, 147:369–377, 2003 August
© 2003. The American Astronomical Society. All rights reserved. Printed in U.S.A.

SYMMETRICAL CHEMI-IONIZATION AND CHEMI-RECOMBINATION PROCESSES IN LOW-TEMPERATURE LAYERS OF HELIUM-RICH DB WHITE DWARF ATMOSPHERES

A. A. Mihajlov and Lj. M. Ignjatović
Institute of Physics, P. O. Box 57, 11001 Belgrade, Serbia, Yugoslavia;
and Institute Isaac Newton of Chile, Yugoslavia Branch, Belgrade, Serbia, Yugoslavia

M. S. Dimitrijević
Astronomical Observatory, Volgina 7, 11160 Belgrade, Serbia, Yugoslavia;
and Institute Isaac Newton of Chile, Yugoslavia Branch, Belgrade, Serbia, Yugoslavia

and

Z. Djurić
Department of Materials, University of Oxford, Parks Road, Oxford OX 3PH, UK
Received 2002 December 12; accepted 2003 March 28

ABSTRACT

The influence of symmetrical chemi-ionization and chemi-recombination processes on the helium atom Rydberg states' population in weakly ionized layers of helium-rich DB white dwarfs has been investigated. The ionization processes in $He^*(n) + He(1s^2)$ collisions and their inverse recombination processes $He_2^+ + e$ and $He(1s^2) + He^+ + e$ have been considered in domains of principal quantum numbers $n \geq 3$ and temperatures $12,000\ K \leq T_{eff} \leq 30,000\ K$. These processes have been treated within the frame of the semiclassical theory developed earlier. Their contributions to the Rydberg state populations have been compared with electron-electron-ion recombination, electron-excited atom ionization, and electron-ion photorecombination processes. Results showed that these processes can be dominant ionization/recombination mechanisms in helium-rich DB white dwarf atmosphere layers for $\log g = 7$ and 8 and $T_{eff} \leq 20,000$ K and have to be implemented in relevant models of weakly ionized helium plasmas.

Subject headings: atomic processes — stars: atmospheres — white dwarfs

1. INTRODUCTION

This work continues our investigations of the influence of ion-atom collisional processes on the properties of weakly ionized layers of helium-rich DB white dwarf atmospheres. It has been demonstrated in Mihajlov & Dimitrijević (1992), Mihajlov, Dimitrijević, & Ignjatović (1994a), and Mihajlov et al. (1995) that the processes of absorption and emission of electromagnetic radiation due to $He^+(1s)$ and $He(1s^2)$ collisions have a strong influence on the optical characteristics of DB white dwarf atmospheric layers. In plasma conditions, however, the ion-atom collisional complexes intensively interact not only with the EM field but also with charged particles, most importantly with free electrons. Consequently, it was necessary to consider processes based on $e + He^+(1s) + He(1s^2)$ collisions. Moreover, in a weakly ionized plasma the collisional complexes similar to the ion-atom one should be taken into account. These complexes consist of atoms in ground and highly excited (Rydberg) states and interact with an outer weakly bound electron of the Rydberg atom. Therefore, in helium plasmas the processes to be investigated are based on $He(1s^2) + He^*(n)$ collisions, with $He^*(n)$ representing the helium atom in a Rydberg state. The role of these complexes will be analyzed in a manner similar to the role of ion-atom complexes in a solar photosphere and lower chromosphere (Mihajlov et al. 1996, 1997b, 1999; Mihajlov, Ignjatović, & Dimitrijević 1998). We will consider the chemi-recombination processes resulting from free electron scattering on the collisional symmetrical ion-atom complexes and chemi-ionization processes during symmetrical atom–Rydberg atom collisions. The ionization/recombination processes with molecular ions in weakly bound rovibrational states will also be included. Therefore, for weakly ionized helium plasma of a DB white dwarf photosphere, the following chemi-ionization processes,

$$He^*(n) + He \Rightarrow He_2^+ + e\ , \tag{1a}$$

$$He^*(n) + He \Rightarrow He + H^+ + e\ , \tag{1b}$$

and the corresponding chemi-recombination processes,

$$He_2^+ + e \Rightarrow He^*(n) + He\ , \tag{2a}$$

$$He + He^+ + e \Rightarrow He^*(n) + He\ , \tag{2b}$$

are considered. He and He^+ are in their ground states $1s^2$ and $1s$, respectively, $He^*(n)$ is the helium atom in the highly excited (Rydberg) state with the principal quantum number $n \gg 1$, and He_2^+ is the molecular ion in the weakly bound rovibrational state belonging to its ground electronic state ($1\Sigma_u$). The main reasons for including (1a) and (2a) channels with molecular ions are the same as in the case of hydrogen plasmas, discussed in detail in Mihajlov & Ljepojević (1982) and Mihajlov, Ljepojević, & Dimitrijević (1992).

The chemi-ionization (eqs. [1a]–[1b]) and chemi-recombination (eqs. [2a]–[2b]) processes are investigated as mechanisms which may influence populations of helium atom Rydberg states. We will assume that the principal quantum number $n \geq 3$, as in Mihajlov et al. (1996, 1997a, 1999) and Djurić & Mihajlov (2001). The influence of examined processes is determined by comparison with other relevant ionization and recombination processes, namely,

electron-Rydberg atom impact ionization,

$$\mathrm{He}^*(n) + e \Rightarrow \mathrm{He}^+ + e + e \ , \tag{3}$$

electron-electron-ion recombination,

$$\mathrm{He}^+ + e + e \Rightarrow \mathrm{He}^*(n) + e \ , \tag{4}$$

and electron-ion photorecombination,

$$\mathrm{He}^+ + e \Rightarrow \mathrm{He}^*(n) + \epsilon_{\mathrm{phot}} \ , \tag{5}$$

where ϵ_{phot} denotes the emitted photon energy. The previous results for solar photosphere demonstrated that the influence of the chemi-ionization and chemi-recombination processes on Rydberg atom states populations is important, and in some layers even dominant in comparison with other ionization and recombination processes (Mihajlov et al. 1997b, 1998). It was found that the radiative ion-atom collisional processes are much more important for the helium-rich DB white dwarf than the solar photosphere (Mihajlov et al. 1994b, 1995). Taking into account these differences, we can expect that the importance of the chemi-ionization and chemi-recombination processes in the case of a helium-rich DB white dwarf atmosphere will be considerably greater than in the case of a solar photosphere.

2. THEORY

2.1. *Chemi-Ionization/Recombination Processes*

The importance of the chemi-recombination (eqs. [1a]–[1b]) and chemi-ionization (eqs. [2a]–[2b]) processes in a given plasma, relative to other recombination and ionization processes, is determined by comparing corresponding fluxes. This is performed under the standard assumption that in photosphere plasmas $T_e = T_a = T$, where T_e and T_a are the electron and atom temperatures and T is their common value. Under this assumption the deviation from LTE in a given plasma is manifested through the departure of the excited atom state populations from Boltzman's distribution. The possible cause of such deviations from LTE in the solar atmosphere is ongoing radiation (Vernazza, Avrett, & Loser 1981; Mihajlov et al. 1997b). Therefore, it is necessary to take into account all processes which can influence the excited atom state populations, particularly ionization/recombination processes (1) and (2).

Let $I_i^{(a,b)}(n;\ T)$ and $I_r^{(a,b)}(n;\ T)$ denote ionization and recombination fluxes conditioning population and depopulation of excited $\mathrm{He}^*(n)$ atomic states due to processes (1a)–(2b), respectively. By definition, we have

$$I_i^{(a)}(n;\ T) = K_i^{(a)}(n,T) \cdot N(\mathrm{He}) \cdot N(\mathrm{He}^*(n)) \ ,$$

$$I_i^{(b)}(n;\ T) = K_i^{(b)}(n,T) \cdot N(\mathrm{He}) \cdot N(\mathrm{He}^*(n)) \ , \tag{6}$$

where $N(\mathrm{He})$ and $N(\mathrm{He}^*(n))$ denote $\mathrm{He}(1s^2)$ atom and $\mathrm{He}^*(n)$ Rydberg atom ($n \geq 3$) densities, and $K_i^{(a)}(n;\ T)$ and $K_i^{(b)}(n;\ T)$ denote rate coefficients of processes (1a) and (1b). We also have

$$I_r^{(a)}(n;\ T) = K_{dr}^{(a)}(n,T) \cdot N(\mathrm{He}_2^+) \cdot N(e) \ ,$$

$$I_r^{(b)}(n;\ T) = K_r^{(b)}(n,T) \cdot N(\mathrm{He}) \cdot N(\mathrm{He}^+) \cdot N(e) \ , \tag{7}$$

where $N(\mathrm{He}^+)$, $N(e)$, and $N(\mathrm{He}_2^+)$ denote $\mathrm{He}^+(1s)$ ion, free electron, and He_2^+ molecular ion (in weakly bound rovibrational states) densities, and $K_{dr}^{(a)}(n,T)$ and $K_r^{(b)}(n,T)$ denote the rate coefficients of processes (2a) and (2b). The rate coefficient of process (2a) is denoted with $K_{dr}^{(a)}$ since this is a process of dissociative recombination. Following our method presented in Mihajlov et al. (1997a), flux $I_r^{(a)}(n;\ T)$ generated by chemi-recombination processes (eq. [2a]) is expressed as

$$I_r^{(a)}(n;\ T) = K_r^{(a)}(n,T) \cdot N(\mathrm{He}) \cdot N(\mathrm{He}^+) \cdot N(e) \ , \tag{8}$$

where $K_r^{(a)}(n,T)$ is given by the expression

$$K_r^{(a)}(n,T) = K_{dr}^{(a)}(n,T) \cdot \left[\frac{N(\mathrm{He})N(\mathrm{He}^+)}{N(\mathrm{He}_2^+)}\right]^{-1} \ . \tag{9}$$

We are interested in the total influence of processes (1a) and (1b) on the depopulation, and the total influence of processes (2a) and (2b) on the population of helium atom excited states. Consequently, we will consider the total chemi-ionization $I_i^{(ab)}(n;\ T)$ and chemi-recombination $I_r^{(ab)}(n;\ T)$ fluxes, where

$$I_i^{(ab)}(n;\ T) = I_i^{(a)}(n;\ T) + I_i^{(b)}(n;\ T) \ ,$$

$$I_r^{(ab)}(n;\ T) = I_r^{(a)}(n;\ T) + I_r^{(b)}(n;\ T) \ . \tag{10}$$

From equations (6)–(8) it follows that these fluxes can be expressed as

$$I_i^{(ab)}(n,T) = K_i^{(ab)}(n,T) \cdot N(\mathrm{He}) \cdot N(\mathrm{He}^*(n)) \ , \tag{11}$$

$$I_r^{(ab)}(n,T) = K_r^{(ab)}(n,T) \cdot N(\mathrm{He}) \cdot N(\mathrm{He}^+) \cdot N(e) \ , \tag{12}$$

where total chemi-ionization and chemi-recombination rate coefficients $K_i^{(ab)}(n;\ T)$ and $K_r^{(ab)}(n,T)$ are similarly defined as

$$K_i^{(ab)}(n;\ T) = K_i^{(a)}(n;\ T) + K_i^{(b)}(n;\ T) \ ,$$

$$K_r^{(ab)}(n,T) = K_r^{(a)}(n,T) + K_r^{(b)}(n,T) \ . \tag{13}$$

The rate coefficient $K_r^{(a)}(n,T)$ is given by equation (9).

The rate coefficients of the processes (1a)–(2b) have been determined by a method based on the semiclassical theory developed for hydrogen and alkalis in Mihajlov & Janev (1981), Mihajlov & Ljepojević (1982), and Mihajlov et al. (1992). This theory is based on the mechanism of resonant energy exchange within the electronic component of the symmetrical atom–Rydberg atom system collision, introduced in Smirnov & Mihajlov (1972), with more details to be found in Janev & Mihajlov (1979, 1980). The semiclassical theory has been adapted for helium in Mihajlov et al. (1996). The method used here is finalized and reviewed in detail in Mihajlov et al. (1997a).

Within the frame of the method used here, chemi-ionization rate coefficients $K_i^{(a)}(n,T)$, $K_i^{(b)}(n,T)$, and $K_i^{(ab)}(n,T)$ are determined directly, while chemi-recombination rate coefficients $K_r^{(a)}(n,T)$, $K_r^{(b)}(n,T)$, and $K_r^{(ab)}(n,T)$ are determined using the thermodynamical balance principle. For example, a simple way to find the partial rate coefficient $K_r^{(a)}(n,T)$ given by equation (9) is by using the thermodynamic balance principle and the partial chemi-ionization rate coefficient $K_i^{(a)}(n,T)$. The chemi-ionization and

chemi-recombination processes are additionally characterized by the parameters $X^{(ab)}_{ir;a,b}(n,T)$

$$X^{(ab)}_{ir;a,b}(n,T) = \frac{I^{(a,b)}_i(n,T)}{I^{(ab)}_i(n,T)} = \frac{I^{(a,b)}_r(n,T)}{I^{(ab)}_r(n,T)} \ , \qquad (14)$$

which describe the relative importance of the particular channel (" a " and " b ") of the considered processes. From equations (6)–(8), (11), (12), and (14), it follows that

$$X^{(ab)}_{ir;a}(n,T) = \frac{K^{(a)}_i(n,T)}{K^{(ab)}_i(n,T)} = \frac{K^{(a)}_r(n,T)}{K^{(ab)}_r(n,T)} \ . \qquad (15)$$

The procedure to obtain chemi-ionization and chemi-recombination rate coefficients $K^{(a,b)}_i(n,T)$, $K^{(ab)}_i(n,T)$, $K^{(a,b)}_r(n,T)$, and $K^{(ab)}_r(n,T)$ is described in detail in Mihajlov et al. (1997a), and the final expressions are

$$K^{(a,b)}_i(n,T) = \frac{2\pi}{3^{3/2}} n^{-5} a_0^2 v_0 \int_{R_{\min}}^{R_n} \exp\left[\frac{-U_2(R)}{kT}\right] \times X^{(a,b)}(R,T) \frac{R^4 dR}{a_0^5} \ , \qquad (16)$$

$$K^{(ab)}_i(n,T) = \frac{2\pi}{3^{3/2}} n^{-5} a_0^2 v_0 \int_{R_{\min}}^{R_n} \exp\left[\frac{-U_2(R)}{kT}\right] \frac{R^4 dR}{a_0^5} \ , \qquad (17)$$

$$K^{(a,b)}_r(n,T) = \frac{(2\pi)^{5/2}}{3^{3/2}} \frac{(\hbar e a_0)^2}{(mkT)^{3/2}} n^{-3} \exp\left(\frac{I_n}{kT}\right) \times \int_{R_{\min}}^{R_n} \exp\left[\frac{U_{12}(R)}{kT} - \frac{U_1(R)}{kT}\right] \times X^{(a,b)}(R,T) \frac{R^4 dR}{a_0^5} \ , \qquad (18)$$

$$K^{(ab)}_r(n,T) = \frac{(2\pi)^{5/2}}{3^{3/2}} \frac{(\hbar e a_0)^2}{(mkT)^{3/2}} n^{-3} \exp\left(\frac{I_n}{kT}\right) \times \int_{R_{\min}}^{R_n} \exp\left[\frac{U_{12}(R)}{kT} - \frac{U_1(R)}{kT}\right] \times X^{(ab)}(R,T) \frac{R^4 dR}{a_0^5} \ . \qquad (19)$$

The variable I_n denotes the ionization energy of $He^*(n)$ atoms, $U_{12}(R) = U_2(R) - U_1(R)$, R is the internuclear distance, and $U_1(R)$ and $U_2(R)$ are the ground and first excited electronic states of the molecular ion He_2^+ (see Gupta & Madsen 1967). The upper integration limit R_n is the largest root of the equation: $U_{12}(R) = I_n$, and its values for different n can be found in Mihajlov et al. (1997a). The lower integration limit, $R_{\min} = 1$, is determined empirically. The functions $X^{(a)}(R,T)$ and $X^{(b)}(R,T)$ are defined by relations $X^{(a)}(R,T) = \gamma(3/2;\ -U_1(R)/kT)/\Gamma(3/2)$ if $U_1(R) < 0$, where $\gamma(x;\ y)$ and $\Gamma(x)$ are incomplete and complete gamma functions, and $X^{(a)}(R,T) = 0$ if $U_1(R) \geq 0$, and $X^{(b)}(R,T) = 1 - X^{(a)}(R,T)$.

The total chemi-ionization and chemi-recombination rate coefficients, $K^{(ab)}_i(n,T)$ and $K^{(ab)}_r(n,T)$, in the temperature range $7000\ \mathrm{K} \leq T \leq 30,000\ \mathrm{K}$ and principal quantum numbers $n = 3$–10, are shown in Figures 1 and 2. The curves $K^{(ab)}_i(n=3,T)$ and $K^{(ab)}_i(n=4,T)$ in Figure 1 show an intersection close to the lower limit (7000 K) of the considered temperature range. The intersection occurs because processes (1a)–(1b) have an energy threshold which increases when n decreases. Because of this, when T decreases every rate coefficient $K^{(ab)}_i(n,T)$ decreases faster than any other rate coefficient $K^{(ab)}_i(n',T)$ with $n' > n$, and in domains of sufficiently low temperatures the intersection of the curves occurs.

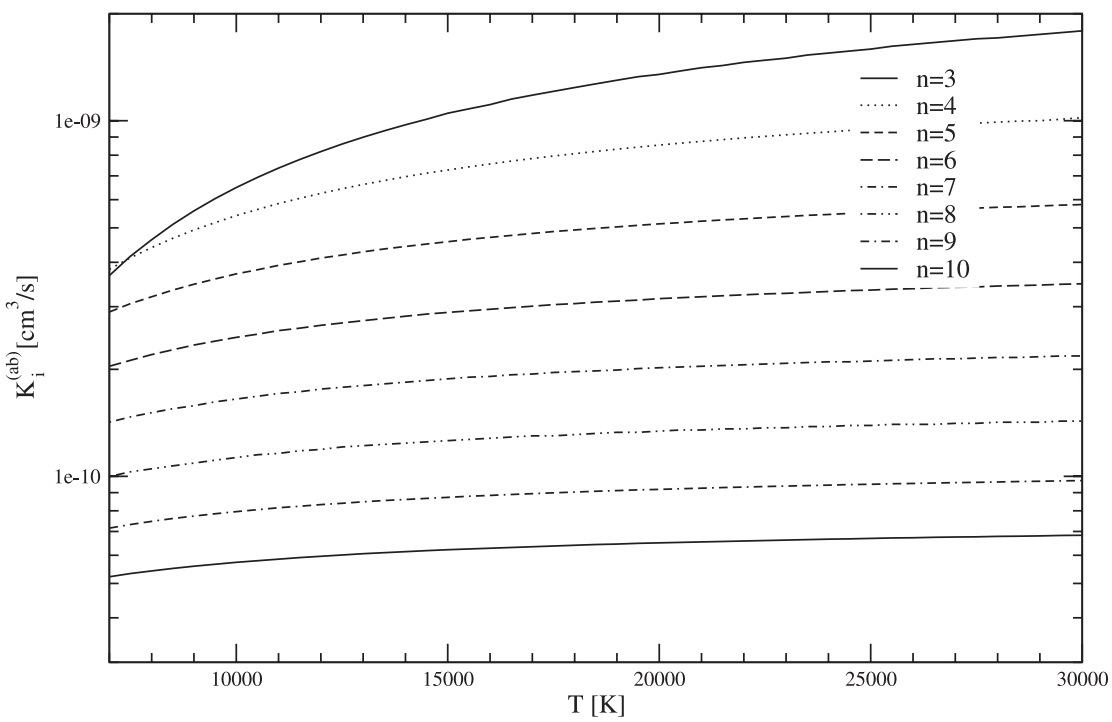

FIG. 1.—Total chemi-ionization rate coefficients, $K^{(ab)}_i(n,\ T)$, with $7000\ \mathrm{K} \leq T \leq 30,000\ \mathrm{K}$ and for principal quantum numbers $n = 3$–10

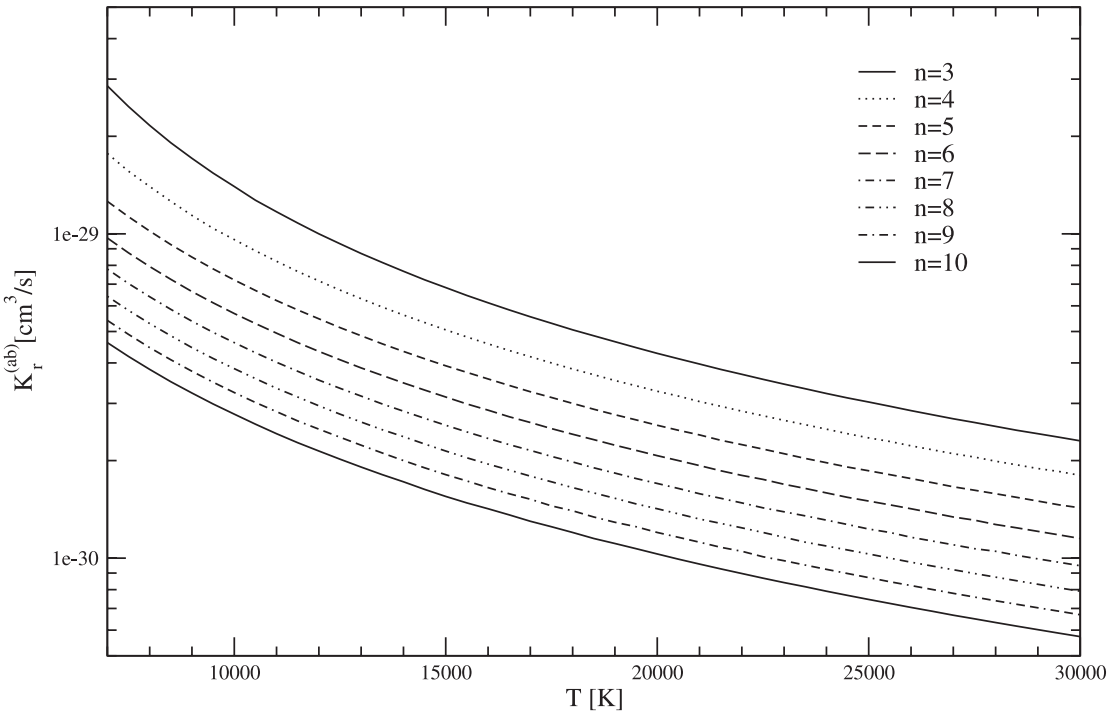

FIG. 2.—Same as in Fig. 1 but for the total chemi-recombination rate coefficients $K_r^{(ab)}(n,\ T)$

The function $X_{ir;a}^{(ab)}(n, T)$ is shown in Figure 3. From this figure and the definition of $X_{ir;b}^{(ab)}(n, T)$ it can be seen that the values of both parameters, in the temperature range 7000 K $\leq T \leq$ 30,000 K, are of the same order of magnitude. Consequently, in a given temperature domain the contributions of " a " and " b " channels of chemi-ionization (eqs. [1a]–[1b]) and chemi-recombination (eqs. [2a]–[2b]) processes in the population/depopulation of helium atom Rydberg states are comparable, which justifies the inclusion of both the " a " and " b " channels.

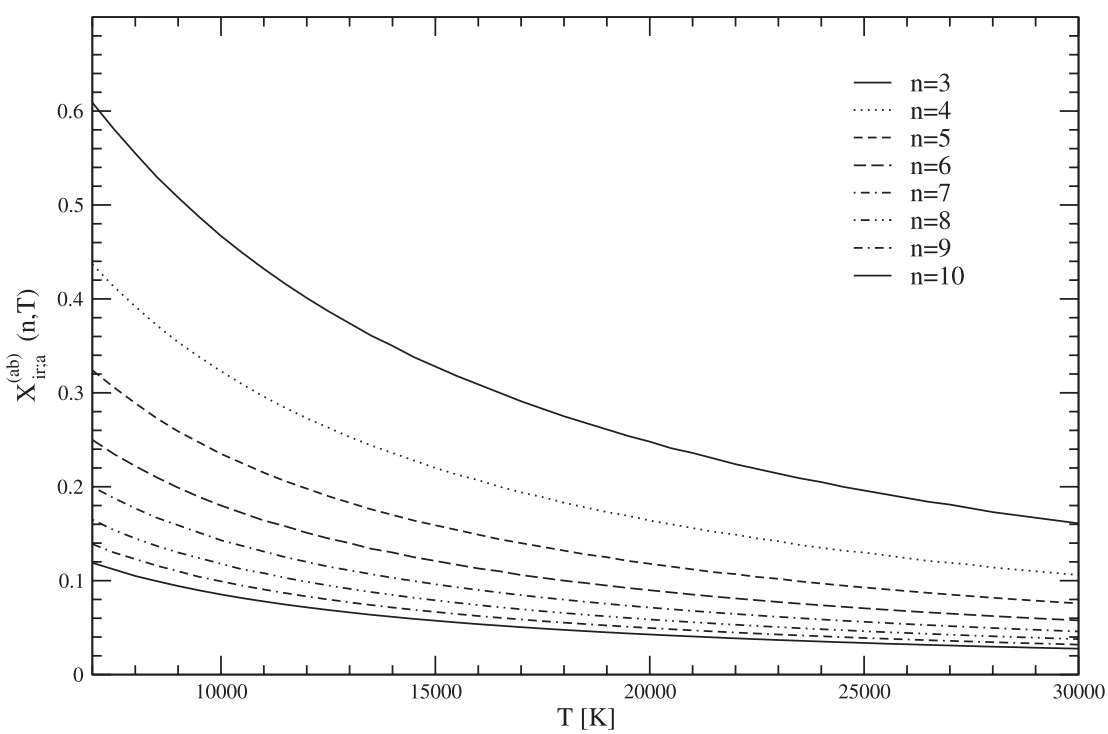

FIG. 3.—Same as in Fig. 1 but for the parameter $X_{ir;a}^{(ab)}(n,\ T)$, characterizing the relative importance of the particular channel (" a " and " b ") for the chemi-ionization and chemi-recombination processes.

2.2. *Other Ionization/Recombination Processes*

Fluxes generated in electron-excited atom impact ionization (eq. [3]) and electron-electron-ion recombination (eq. [4]) processes are given by expressions

$$I_i^{(ea)}(n,T) = \alpha_i^{(ea)}(n,T) \cdot N(\mathrm{He}^*(n)) \cdot N(e) \ , \qquad (20)$$

$$I_r^{(eei)}(n,T) = \alpha_r^{(eei)}(n,T) \cdot N(\mathrm{He}^+) \cdot N(e) \cdot N(e) \ , \qquad (21)$$

and the ionization and recombination rate coefficients $\alpha_i^{(ea)}(n,T)$ and $\alpha_r^{(eei)}(n,T)$ are determined by semiempirical expressions from Vriens & Smeets (1980).

Fluxes generated in electron-ion photorecombination (eq. [5]) processes are given by the expression

$$I_{\mathrm{phr}}^{(ei)}(n,T) = \alpha_{\mathrm{phr}}^{(ei)}(n,T) \cdot N(\mathrm{He}^+) \cdot N(e) \ , \qquad (22)$$

and the photorecombination rate coefficients $\alpha_{\mathrm{phr}}^{(ei)}(n,T)$ could be determined in accordance with Sobel'man (1979). However, these constants are determined here using relations found in our previous work on collisional ion-atom radiative processes (Mihajlov, Dimitrijević, & Ignjatović 1993; Mihajlov et al. 1995).

3. RESULTS AND DISCUSSION

The relative importance of chemi-ionization (eqs. [1a]–[1b]) and chemi-recombination (eqs. [2a]–[2b]) processes in comparison with electron-excited atom impact ionization (eq. [3]), electron-electron-ion recombination (eq. [4]) and electron-ion photorecombination (eq. [5]) processes is characterized by parameters $F_{ir}^{(ab)}(n,T)$ and $F_{\mathrm{phr}}^{(ab)}(n,T)$, defined as ratios of the corresponding fluxes:

$$F_{ir}^{(ab)}(n,T) = \frac{I_i^{(ab)}(n,T)}{I_i^{(ea)}(n,T)} = \frac{I_r^{(ab)}(n,T)}{I_r^{(eei)}(n,T)} \ ,$$

$$F_{\mathrm{phr}}^{(ab,ei)}(n,T) = \frac{I_r^{(ab)}(n,T)}{I_{\mathrm{phr}}^{(ei)}(n,T)} \ . \qquad (23)$$

From equations (11)–(12) and (20)–(23), it follows that these parameters can be shown in the form

$$F_{ir}^{(ab)}(n,T) = \frac{K_i^{(ab)}(n,T)}{\alpha_i^{(ea)}(n,T)} \cdot \eta_e^a = \frac{K_r^{(ab)}(n,T)}{\alpha_r^{(eei)}(n,T)} \cdot \eta_e^a \ , \qquad (24)$$

$$F_{\mathrm{phr}}^{(ab,ei)}(n,T) = \frac{K_r^{(ab)}(n,T) \cdot N(\mathrm{He})}{\alpha_{\mathrm{phr}}^{(ei)}(n,T)} \ , \qquad (25)$$

where η_e^a denotes He atom and free electron densities ratio

$$\eta_e^a = \frac{N(\mathrm{He})}{N(e)} \ . \qquad (26)$$

In the case of the DB white dwarf photosphere, all parameters have been determined for $12,000\ \mathrm{K} \leq T_{\mathrm{eff}} \leq 30,000\ \mathrm{K}$ and $\log g = 7$ and 8. The results presented are for the temperature range $12,000\ \mathrm{K} \leq T_{\mathrm{eff}} \leq 24,000\ \mathrm{K}$ and $\log g = 8$. The value of $\log g$ is chosen following Mihajlov et al. (1995), where the same DB white dwarf models have been analyzed with respect to radiative ion-atom collisional processes. The results for $\log g = 7$ are qualitatively the same. For temperatures $T_{\mathrm{eff}} > 24,000$ K, electron-excited atom impact ionization (eq. [3]) and electron-electron-ion recombination processes (eq. [4]) are dominant. The processes considered here are compared via parameters $F_{ir}^{(ab)}(n,T)$ and $F_{\mathrm{phr}}^{(ab)}(n,T)$, and the corresponding results are shown in Figures 4–7 and Figures 8–9, respectively. These parameters are shown as functions of $\log \tau$, where τ is the Rosseland optical depth. Temperatures and atom and electron densities needed to determine $F_{ir}^{(ab)}(n,T)$ and $F_{\mathrm{phr}}^{(ab)}(n,T)$ for given τ have been taken from Koester's (1980) DB white dwarf models for given T_{eff} and $\log g$ values. Figures 4, 5, 6, and 7 are related to $T_{\mathrm{eff}} = 12,000$, 14,000, 16,000, and 18,000 K, while Figures 8 and 9 are related to $T_{\mathrm{eff}} = 12,000$ and 24,000 K, respectively.

Our results show that for the lower temperatures the chemi-ionization (eqs. [1a]–[1b]) and chemi-recombination (eqs. [2a]–[2b]) processes are absolutely dominant over electron-excited atom ionization (eq. [3]) and electron-electron-atom recombination (eq. [4]) processes, for $n = 3$, 4, and 5 for almost all $\log \tau < 0$ values. For $n = 6$, 7, and 8 and in the same $\log \tau$ range, processes (1a)–(2b) are comparable with processes (3) and (4). This is illustrated in Figures 4 and 5, where $T_{\mathrm{eff}} = 12,000$ and 14,000 K. With the increase of temperature the influence of processes (1a)–(2b) decreases, which is manifested by the decrease of the $F_{ir}^{(ab)}(n,T)$ values. For example, $F_{ir}^{(ab)}(n,T)$ values for $n = 3$ and 4 decrease from $\sim 10^2$ for $T_{\mathrm{eff}} = 12,000$ K and ~ 10 for $T_{\mathrm{eff}} = 16,000$ K, down to ~ 0.1 for $T_{\mathrm{eff}} = 20,000$ K and ~ 0.01 for $T_{\mathrm{eff}} = 24,000$ K. This behavior indicates the effective temperature range where it is particularly important to take into account processes (1a)–(2b) for correct calculations of excited helium atom state populations.

It should be noted that the increase/decrease of populations with a principal quantum number n for considered plasma conditions causes the population increase/decrease of all states with a principal quantum number larger than n. Consequently, the increase/decrease of the populations with $3 \leq n \leq 8$ due to chemi-ionization (eqs. [1a]–[1b]) and chemi-recombination (eqs. [2a]–[2b]) processes causes an increase/decrease of all excited states' populations with $n > 8$, for the temperature and free electron density corresponding to the given $\log \tau$.

Regarding the relative importance of chemi-recombination (eqs. [2a]–[2b]) processes in comparison with photorecombination (eq. [5]), our results show that processes (2a)–(2b) are dominant within the whole effective temperature range $12,000\ \mathrm{K} \leq T_{\mathrm{eff}} \leq 30,000\ \mathrm{K}$ for $n > 4$ within the $\log \tau > -3$ range. For $n = 3$ and 4 the processes (1a)–(2b) are dominant within the $\log \tau > -4$ range. These results are illustrated in Figures 8 and 9, with $T_{\mathrm{eff}} = 12,000$ and 24,000 K.

Functions $F_{ir}^{(ab)}$ and $F_{\mathrm{phr}}^{(ab)}$ have several shallow local minimums/maximums, mainly in the range $\log(\tau) \in (-3, -2)$. This behavior was notified and analyzed in detail with respect to $\mathrm{He}^+ + \mathrm{He}$ radiative collisional processes in the same plasma (Mihajlov et al. 1995). The local oscillations of functions $F_{ir}^{(ab)}$ and $F_{\mathrm{phr}}^{(ab)}$ are caused by the temperature oscillations in helium-rich DB white dwarf plasma models, defined in Koester (1980) and used in this paper. Relatively small temperature fluctuations can produce the following effects: (*a*) pronounced oscillations in particles' densities because of the high ionization potential of helium atoms and (*b*) changes in rate coefficient values for all ionization/

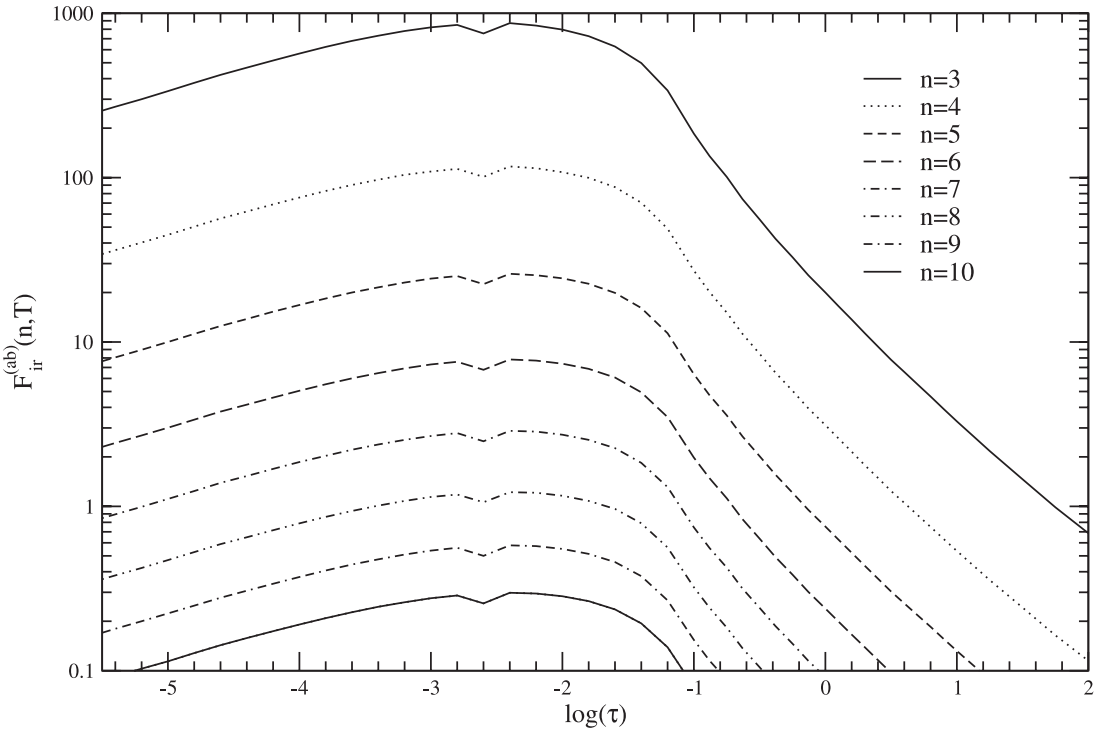

FIG. 4.—Parameter $F_{ir}^{(ab)}(n, T)$ as a function of the logarithm of Rosseland optical depth $\log \tau$, for principal quantum numbers $n = 3$–10, with $T_{\rm eff} = 12,000$ K and $\log g = 8$.

recombination processes considered. This is shown in Figures 4–9.

The presented results show a considerably greater influence of the chemi-ionization (eqs. [1a]–[1b]) and chemi-recombination (eqs. [2a]–[2b]) processes on populations of highly excited atomic states in the case of a helium-rich DB white dwarf atmosphere than in the case of the solar atmosphere (Mihajlov et al. 1997b). The reason for this is much

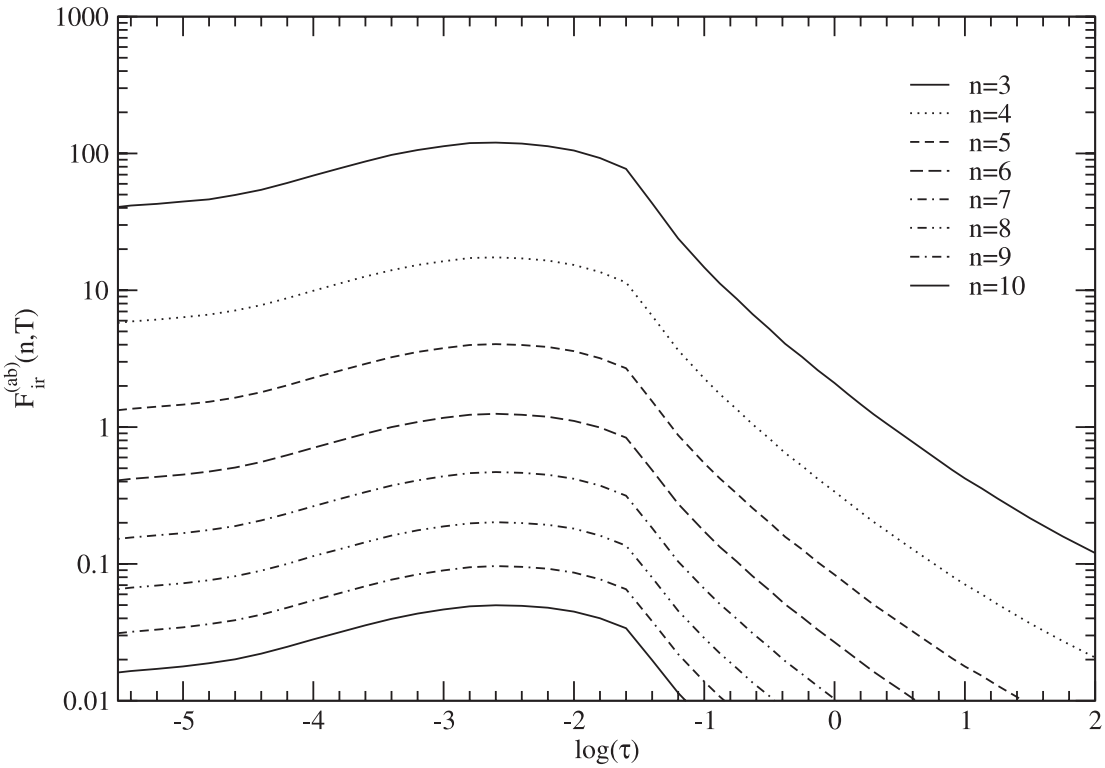

FIG. 5.—Same as in Fig. 4 but for $T_{\rm eff} = 14,000$ K

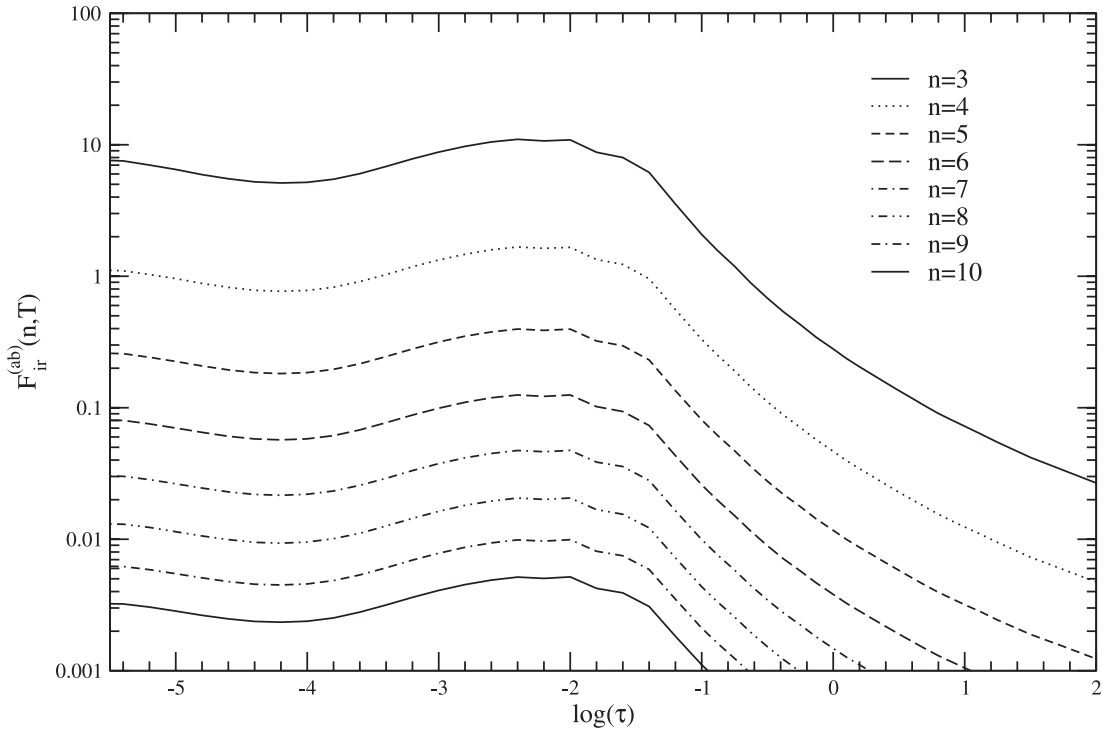

FIG. 6.—Same as in Fig. 4 but for $T_{\rm eff} = 16,000$ K

larger neutral atom densities in the DB white dwarf atmosphere than in the solar photosphere, which react with the same densities of free electrons. This is the consequence of a much higher (for almost 11 eV) ionization potential of helium atoms than of hydrogen. Therefore, for the same pressures and temperatures (~10,000 K) the ionization degree of the helium plasma is several orders of magnitude lower than that of the hydrogen plasma.

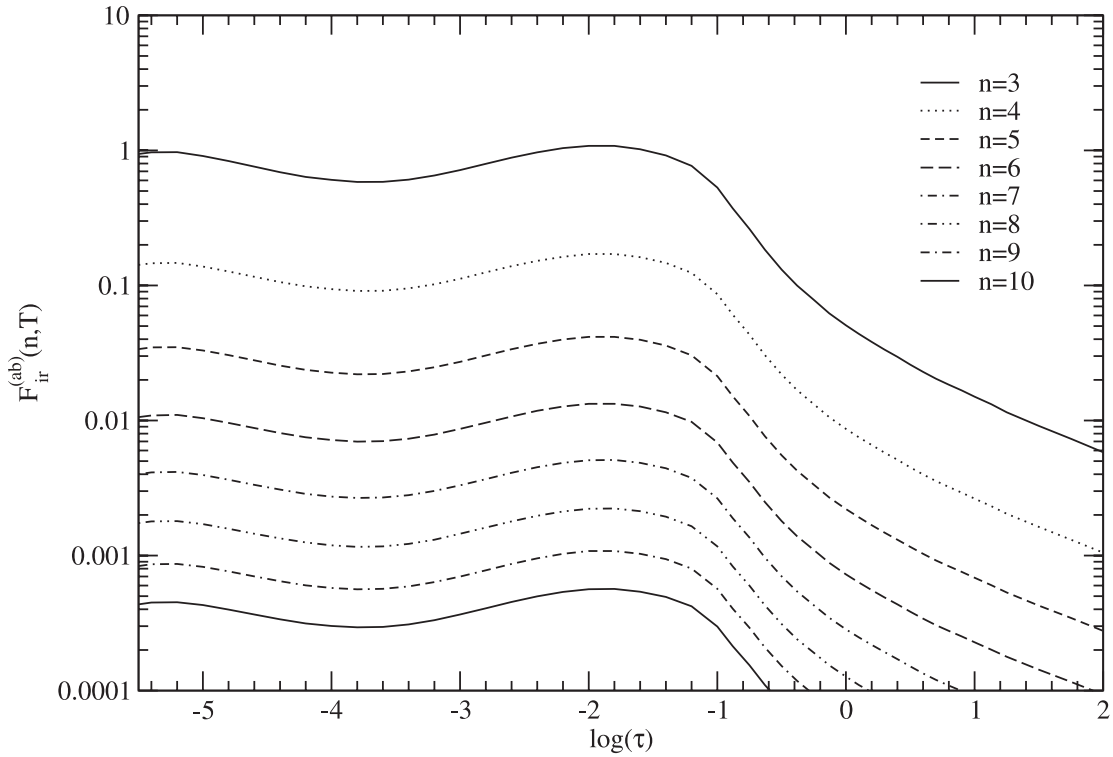

FIG. 7.—Same as in Fig. 4 but for $T_{\rm eff} = 18,000$ K

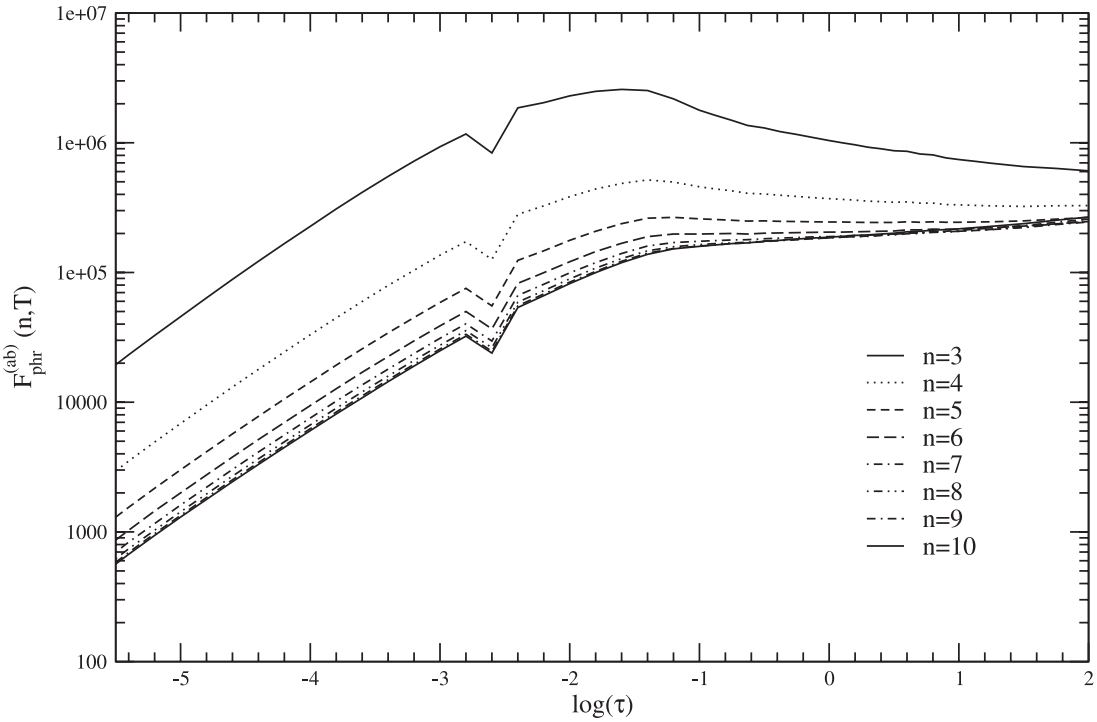

FIG. 8.—Parameter $F^{(ab)}_{\rm phr}(n,\ T)$ as a function of the logarithm of Rosseland optical depth $\log\tau$, for principal quantum numbers $n = 3$–10, with $T_{\rm eff} = 12,000$ K and $\log g = 8$.

4. CONCLUSION

The influence of the chemi-ionization (eqs. [1a]–[1b]) and chemi-recombination (eqs. [2a]–[2b]) processes shown in this paper must be taken into account for the ab initio modeling of helium-rich DB white dwarf atmospheres, for $\log g = 7$ and 8 and $T_{\rm eff} \leq 20,000$ K, since they would influence the basic structure of the atmosphere model. These results and similar ones for hydrogen solar plasma (Mihajlov et al. 1997b) clearly proved the importance of the symmetrical chemi-ionization and chemi-recombination processes in weakly ionized layers of stellar atmospheres.

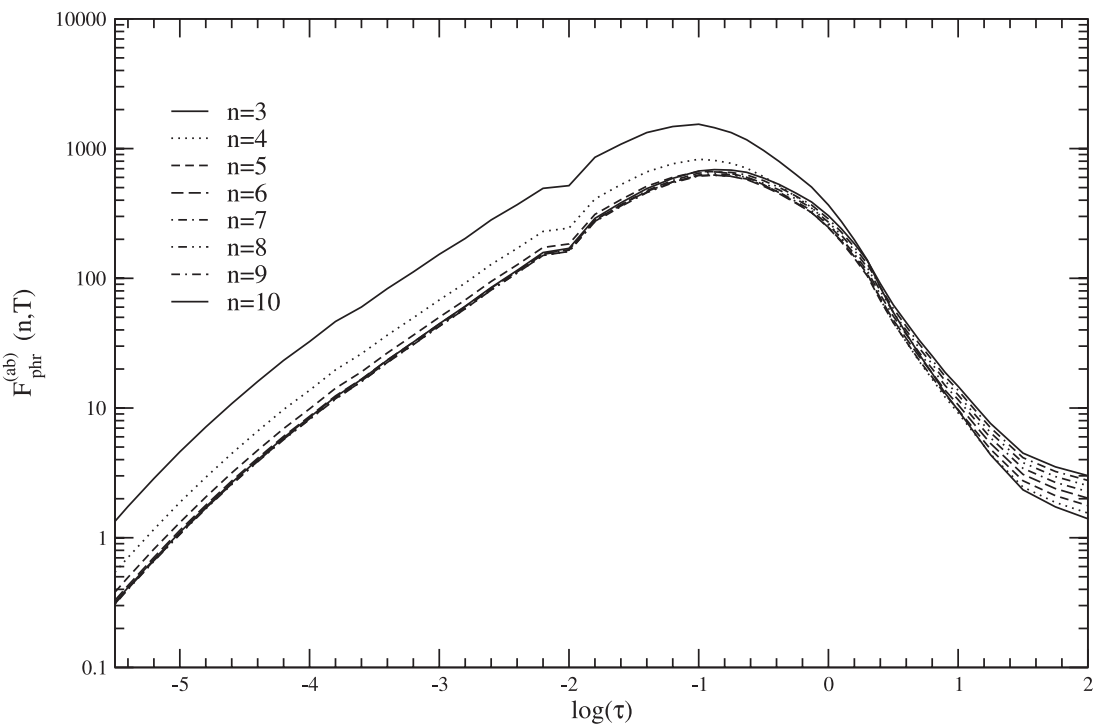

FIG. 9.—Same as in Fig. 8 but for $T_{\rm eff} = 24,000$ K

Further investigations of these processes should be performed by including them in sophisticated stellar atmosphere models and corresponding computing codes.

This work is part of the projects "Radiation and Transport Properties of the Non-ideal Laboratory and Ionospheric Plasma" (project no. 1466) and "Influence of Collisional Processes on Astrophysical Plasma Lineshapes" (project no. GA 1195) and was supported by the Ministry of Science, Technologies, and Development of Serbia.

REFERENCES

Djurić, Z., & Mihajlov, A. A. 2001, J. Quant. Spectrosc. Radiat. Transfer, 70, 285
Gupta, B. K., & Madsen, F. A. 1967, J. Chem. Phys., 47, 48
Janev, R. K., & Mihajlov, A. A. 1979, Phys. Rev., 20, 1890
———. 1980, Phys. Rev., 21, 819
Koester, D. 1980, A&AS, 39, 401
Mihajlov, A. A., & Dimitrijević, M. S. 1992, A&A, 256, 305
Mihajlov, A. A., Dimitrijević, M. S., & Ignjatović, Lj. 1993, A&AS, 276, 187
———. 1994a, A&A, 287, 1026
Mihajlov, A. A., Dimitrijević, M. S., Ignjatović, Lj., & Djurić, Z. 1994b, A&AS, 103, 57
———. 1995, ApJ, 454, 420
Mihajlov, A. A., Dimitrijević, M. S., Ignjatović, Lj. M., & Vasilijević, M. M. 1999, Astron. Astrophys. Trans., 18, 145
Mihajlov, A. A., Djurić, Z., & Dimitrijević, M. S. 1996, J. Quant. Spectrosc. Radiat. Transfer, 55, 141
Mihajlov, A. A., Djurić, Z., Dimitrijević, M. S., & Ljepojević, N. N. 1997a, Phys. Scr., 56, 631
Mihajlov, A. A., Ignjatović, Lj. M., & Dimitrijević, M. S. 1998, Novyj cikl aktivnosty Solnca, Trudy (Sankt Peterburg: Pulkovo), 52
Mihajlov, A. A., Ignjatović, Lj. M., Vasilijević, M. M., & Dimitrijević, M. S. 1997b, A&A, 324, 1206
Mihajlov, A. A., & Janev, R. K. 1981, J. Phys. B, 14, 1639
Mihajlov, A. A., & Ljepojević, N. N. 1982, Proc. Symp. Phys. Ionized Gases, Contributed Papers (Dubrovnik), 385
Mihajlov, A. A., Ljepojević, N. N., & Dimitrijević, M. S. 1992, J. Phys. B, 25, 5121
Smirnov, V. A., & Mihajlov, A. A. 1971, Opt. Spectrosc., 30, 525
Sobel'man, I. I. 1979, Atomic Spectra and Radiative Transitions (Berlin: Springer), chap. 11
Vernazza, J. E., Avrett, E. H., & Loser, R. 1981, ApJS, 45, 635
Vriens, L., & Smeets, A. 1980, Phys. Rev. A, 22, 940

Appl. Phys. B 78, 221–223 (2004)
DOI: 10.1007/s00340-003-1368-3

Applied Physics B
Lasers and Optics

L. CSILLAG[1,✉]
M.S. DIMITRIJEVIĆ[2]

On the Stark broadening of the 537.8 nm and 441.6 nm Cd^+ lines excited in a hollow cathode laser discharge

[1] Research Institute for Solid State Physics and Optics, Hungarian Academy of Science, 1525 Budapest, P.O. Box 49, Hungary
[2] Astronomical Observatory, Volgina 7, 11160 Belgrade, Serbia, Yugoslavia

Received: 20 March 2003/Revised version: 19 June 2003
Published online: 19 December 2003 • **© Springer-Verlag 2003**

ABSTRACT On the basis of available experimental and theoretical data the role of the Stark effect in the homogeneous line broadening of the green and blue laser lines in a hollow cathode He-Cd^+ laser discharge is discussed. It is found, that at typical laser discharge parameters, for the 538 nm line the Stark line-width amounts to $\Delta\nu_s(538\,\text{nm}) = 290$ MHz, which is comparable with the natural line-width broadened by collisions with neutral atoms $\Delta\nu_c(538\,\text{nm}) = 370$ MHz. For the 442 nm line, however, both are significantly smaller: $\Delta\nu_s(442\,\text{nm}) = 83$ MHz and $\Delta\nu_c(442\,\text{nm}) = 200$ MHz. The increased homogeneous line-width can result in single mode operation for the green line, while for the blue one it does not.

PACS 32.70.Jz; 32.60.+i

1 Introduction

It is well known that ionic lines can be effectively excited in a hollow cathode (HC) discharge due to the presence of high energy electrons. It was first used for laser purposes in 1970 for the excitation of the He-Cd^+ laser, where strong oscillation was observed at several red, green and blue Cd^+ transitions [1]. Since then a lot of metal vapor and noble gas HC laser transitions were found [2, 3].

An interesting feature of the HC lasers is that – in case of TEM_{00} transversal mode operation – they oscillate usually in a single axial mode without any optical selection. This property has been attributed to the large homogeneous line-width due to the collisional line broadening at the relatively large filling pressures or to the short lifetimes of the contributing levels. This assumption was proved for several HC systems [4]. It is curious, however, that while single mode operation in HC lasers was first found at the He-Cd^+ green laser transitions [5], recent studies have shown that the processes mentioned are not sufficient to explain single mode operation here [6].

The aim of this work is to show, that in HC laser discharges, the Stark broadening, in some cases, can be comparable with the broadening by collisions with neutral atoms and especially at the green Cd^+ transitions. This fact has to be taken into account in explaining the single mode operation. It is shown too, that, in contrast, the multi-mode operation of the blue He-Cd^+ laser can be attributed to the small natural, neutral atom collision-, and Stark-broadening. A short review of HC discharge properties and results of theoretical calculations of the Stark broadening of these transitions are given for typical HC discharge conditions.

2 The green and blue Cd^+ transitions

Due to the doublet level structure there are two green transitions: 533.75 nm and 537.80 nm ($5d\,^2D_{3/2,5/2} \leftarrow 4f^2F^0_{5/2,7/2}$) respectively. The excitation of the $4f^2F^0_{5/2,7/2}$ upper levels is assumed to be rather complex. A partial way of excitation is cascading from the $7g\,^2G_{9/2}$ level, but the main way is assumed to be a very effective de-excitation of highly excited Cd^+ ions by collisions with low energy electrons present in the HC discharge [7, 8].

Due to the large doublet splitting of the upper state ^2D there is a blue transition 441.56 nm ($5p\,^2P^0{}_{3/2} \leftarrow 5s^2\,^2D_{5/2}$) and an ultraviolet one 325.02 nm ($5p\,^2P^0{}_{1/2} \leftarrow 5s^2\,^2D_{3/2}$). The main excitation mechanism is accepted to be Penning ionisation of ground state Cd atoms by inelastic collisions with metastable He atoms [3].

3 The HC laser discharge

For laser purposes the discharge inside the cathode is used for excitation. Different HC geometries are applied; most frequently the "longitudinal" or "transversal" system. In the first case the discharge tube consists of a series of cylindrical cathodes and anodes. In the second one either a long cylindrical cathode is slotted and the anode is positioned outside the cathode but parallel with it, or there are a series of holes in the wall of a long cathode with anode rods inside the holes. The typical pressure in the tube is 10–25 hPa. It was found that the efficiency of the laser excitation depends on the HC geometry which can be attributed to the different electron energy distributions in them. The distributions have generally a nearly Maxwellian low energy part with a high energy tail [9–11]. The mean electron energy of the low energy part amounts to $E_e = 0.1$–1 eV, while the high energy tail can rise up to the cathode voltage which is commonly several hundred Volts.

✉ Fax: +36-1/392-2215, E-mail: csillag@szfki.hu

For laser purposes the high energy tail is of most importance, as this allows an effective population of high lying atomic or ionic levels, and therefore less attention was paid to the low energy electrons. But in several cases – like the Cd^+ green lines – they play an important role too. From the point of view of the Stark broadening, this low electron energy part is important: In a He-Zn^+ laser discharge, which is very similar to the He-Cd^+ one, it was found that in the middle of the cathode the electron density N_e, amounts to 5×10^{13}–10^{14} cm^{-3}, about two orders of magnitude larger, than that in the positive column of a glow discharge [12]. The electron density is proportional to the current density on the cathode surface, which is 50–100 mA cm^{-2} in a typical HC laser discharge. The actual values of the parameters E_e and N_e depend on the construction, the cathode voltage, the filling gas, and its pressure in the discharge tube. Different model calculations and measurements are available [13, 14]. Especially for the He-Cd gas mixture, in a transversal slotted hollow cathode discharge laser tube – studied by us earlier [6, 23], at 20–25 hPa filling pressure, and at ~ 100 mA cm^{-2} current density, $E_e \sim 0.2$ eV and $N_e \sim 10^{14}$ cm^{-3} can be assumed as a good estimation.

4 Stark broadening of the Cd^+ lines

Both experimental and theoretical results are available for the Stark broadening of the green and blue Cd^+ lines. Kusch and Oberschelp [15] have measured the half-widths of both and Djeniže et al. [16] has measured that of the blue line in a high temperature plasma of a pulsed discharge tube. The results of Kusch and Oberschelp [15] are considerably larger. In a critical analysis of existing experimental data, performed by Konjević et al. [17], it was stated that considering the high-density conditions and rather large dimensions of the employed pulse discharge, self absorption could be significant, but no check of it has been reported. Consequently, the accuracy, D, in their notation (uncertainties larger than 50 percent) is attributed to these results. In a critical analysis of Konjević et al. [18], the accuracy of results of Djeniže et al. [16], for blue line, is evaluated to be, B, (uncertainties within 30 percent) for $T = 23\,000$ K and C (uncertainties within 50 percent) for $T = 30\,000$ K. Theoretical calculations were performed by Djeniže et al. [16], and Popović et al. [19], using different approaches of the semiempirical theory [20–22].

4.0.1 The 538 nm Cd^+ *line.* In HC discharges, only broadening due to collisions with neutral atoms was studied experimentally for the 538 nm line [6], therefore the Stark broadening of this line is treated here. Due to large uncertainties of the line widths w_s (full widths at half maxima) measured by Kusch and Oberschelp [15], and discussed in [17] – the w_s value of Popović et al. [19], calculated within the modified semi-empirical approach [21], was used in extrapolating it to HC laser conditions: $T_e = 2300$ K electron temperature ($E_e \sim 0.2$ eV), and $N_e = 10^{14}$ cm^{-3} electron density respectively. At extrapolation it was assumed, that w_s is proportional to $T_e^{-1/2}$ and to N_e. This extrapolation resulted in:

$$w_{s,extr}(\lambda = 538\,\text{nm}, T_e = 2300\,\text{K}, N_e = 10^{14}\,\text{cm}^{-3}) = 2.75 \times 10^{-4}\,\text{nm}\,,$$

T_e (K)	Width (FWHM) (nm)	Width (FWHM) (MHz)	Shift (nm)	Shift (MHz)
1000	0.978×10^{-4}	150.4	0.862×10^{-5}	13.3
2000	0.566×10^{-4}	87.0	0.702×10^{-5}	10.8
5000	0.336×10^{-4}	51.7	0.598×10^{-5}	9.19
10 000	0.244×10^{-4}	37.5	0.466×10^{-5}	7.16
20 000	0.178×10^{-4}	27.4	0.346×10^{-5}	5.32
50 000	0.120×10^{-4}	18.4	0.240×10^{-5}	3.69

TABLE 1 Electron-impact broadening full half-widths (FWHM) and shifts for the Cd II 441.56 nm ($5p^2 P^0_{3/2} \leftarrow 5s^2\,{}^2D_{5/2}$) spectral line at a perturber density of 1.0×10^{14} cm^{-3} and temperatures from 1000 K up to 50 000 K

or in frequency units:

$$\Delta\nu_{s,extr}(\lambda = 538\,\text{nm}, T_e = 2300\,\text{K}, N_e = 10^{14}\,\text{cm}^{-3}) = 290\,\text{MHz}\,.$$

4.0.2 The 442 nm Cd^+ *line.* The Stark-width of the 441.6 nm Cd^+ line at $T_e = 23\,000$ K and $N_e = 10^{17}$ cm^{-3} was measured by Kusch and Oberschelp [15], and Djeniže et al. [16], and calculated by Djeniže et al. [16], and Popović et al. [19], using different approaches of the semiempirical theory [20–22]. Since there exists a complete set of atomic data needed for a full semiclassical perturbation approach [23–25], we performed such calculations and our semiclassical results for Stark full width at half maximum (FWHM) are shown in Table 1 for an electron density of 10^{14} cm^{-3} and temperatures $T = 1000$–$50\,000$ K.

For HC laser plasma conditions, i.e. for low electron densities and electron temperatures, the calculation yielded:

$$w_{s,calc}(\lambda = 442\,\text{nm}, T_e = 2300\,\text{K}, N_e = 10^{14}\,\text{cm}^{-3}) = 0.542 \times 10^{-4}\,\text{nm}\,,$$

or in frequency units:

$$\Delta\nu_{s,calc}(\lambda = 442\,\text{nm}, T_e = 2300\,\text{K}, N_e = 10^{14}\,\text{cm}^{-3}) = 83.3\,\text{MHz}\,.$$

This value is about 3.5 times smaller than that for the green line.

5 Single mode operation conditions

The mode structure of a laser is affected by many parameters like the resonator length L, the maximum of the gain coefficient g_0, the passive losses a, the saturation parameter p_s, and above all, the ratio of the homogeneous (Lorentzian) line-width to the inhomogeneous (Doppler) one in the frequency distribution of the gain curve $\Delta\nu_L/\Delta\nu_D$. The effect of these parameters on the mode structure of lasers was studied by Troicki' [26] on a He-Ne laser both experimentally and theoretically. He studied the laser mode pattern at different g_0/a and $\Delta\nu_L/\Delta\nu_D$ values by increasing the gas pressure in the gain tube. He derived critical values of $\Delta\nu_L/\Delta\nu_D$ depending on the ratio $X = g_0/a$, above which single mode operation takes place. His calculations agreed well with the experiments. As the main parameters L, g_0, a and p_s of a typical HC He-Cd^+ laser do not differ significantly from those

of a He-Ne laser, the results of Troicki' can be applied also for the green HC He-Cd^+ laser. At $g_0/a \sim 3$–4, at which such values are typical for this laser [27], the critical value for single mode operation of a HC He-Cd^+ laser can be estimated as: $\Delta\nu_L/\Delta\nu_D \sim 0.30$–0.32.

6 Results and discussion

We consider now the problem of single mode operation of the green He-Cd^+ laser. The broadening by collisions with neutral atoms was studied earlier in a HC He-Cd discharge tube at a moderate current density of about 10 mA cm^{-2} [6]. For the 538 nm line a broadening constant of 12 MHz/hPa was measured, and at 23 hPa – at the typical pressure for the green HC He-Cd^+ laser – 370 MHz was measured as the He-impact broadened line-width for this line. Due to the small current density, the Stark-broadening here is estimated to be only $\sim$ 30 MHz, which is less then the measuring error. (It has to be mentioned, however, that an increase of 26 MHz compared to the expected zero pressure line-width has been actually observed, but it was attributed to the uncertainty in the knowledge of the reflectivity of the Fabry Perot interferometer mirrors.)

In a HC laser discharge a current density of $\sim$ 100 mA cm^{-2} or more is applied. The Doppler line-width amounts to $\Delta\nu_D = 1200$–1300 MHz. As the natural line-width broadened by collisions with neutral atoms is only about 28%–31% of the Doppler line-width, this ratio is too small to explain the observed single mode operation. We have seen, however, that for the green line – at HC laser conditions – the Stark line-width (i.e. the broadening due to collisions of Cd^+ ions with slow electrons) amounts to 290 MHz which is already comparable to the broadening due to collisions of Cd^+ ions with neutral He atoms. These two broadenings are Lorentzian and therefore the half-widths can be added resulting in a homogeneous line-width of $\sim$ 660 MHz which is about 50% of the Doppler width. This ratio is already large enough to result in single mode operation of the green He-Cd^+ laser.

At the blue He-Cd^+ laser the situation differs from that of the green one. Here the natural line-width is only 47 MHz [28] and the broadening constant due to collisions with He atoms was found to be $\sim$ 6.5 MHz/hPa [29]. The resulting line-width at 23 hPa pressure amounts to $\sim$ 200 MHz. If we add to this the Stark half-width, it results only $\sim$ 283 MHz. So the homogeneous line-width is here only 18% of the inhomogeneous (Doppler) one which is estimated to be $\sim$ 1600 MHz using Cd monoisotope. Therefore the blue HC He-Cd^+ laser always operates in multi-mode.

As a conclusion it can be stated, that Stark broadening in HC laser discharges can give a significant contribution to the homogeneous line-width, but its actual role depend on the properties of the atomic or ionic levels involved.

ACKNOWLEDGEMENTS Thanks are due to Dr. M. Jánossy for his valuable suggestions.

This work is a part of the project "Influence of collisional processes on astrophysical plasma lineshapes", supported by Ministry of Science, Technologies and Development of Serbia.

REFERENCES

1 W.K. Schuebel: Appl. Phys. Lett. **16**, 470 (1970)
2 M. Jánossy, L. Csillag, Z. Donkó, K. Rózsa: Acta Phys. Hung. **93**, 311 (1993)
3 C.S. Willett: *Introduction to gas lasers: Population inversion mechanisms* (Pergamon Press 1974) pp. 202–206
4 L. Csillag, M. Jánossy: Appl. Phys. B **55**, 401 (1992)
5 T. Salamon, L. Csillag, M. Jánossy, K. Rózsa: Phys. Lett. A **46**, 17 (1973)
6 L. Csillag, M. Jánossy: Appl. Phys. B **73**, 55 (2001)
7 E.L. Latush, V.S. Michalevskij, M.F. Sem: Opt. Spektr. **34**, 214 (1973) (In Russian)
8 C. Boulmer-Leborgue, B. Dubreuil, J.C. Pellicer: J. Phys. D **22**, 512 (1989)
9 J. Mizeraczyk, W. Urbanik: J. Phys. D: Appl. Phys. **16**, 2119 (1983)
10 J. Mizeraczyk: Z. Naturforsch. **42a**, 587 (1986)
11 P. Gill, C.E. Webb: J. Phys. D: Appl. Phys. **10**, 299 (1977)
12 P. Gill, C.E. Webb: J. Phys. D: Appl. Phys. **11**, 245 (1978)
13 V. Derzhiev et al.: Appl. Phys. B **51**, 465 (1990)
14 K. Kutasi, Z. Donkó, P. Hartmann: Proc. WDS'01-10th Annual Meeting of Doctoral Students, Part II: Phys. of Plasmas and Ionized Media, Praga 2001, ed. by J.S. Šafrankova, Univ. Karlovyn, matfispress, pp. 366–371
15 H.J. Kusch, E. Oberschelp: Z. Astrophys. **67**, 85 (1967)
16 S. Djeniže, A. Srećković, J. Labat, R. Konjević, L. Popović: Phys. Rev. A **44**, 410 (1991)
17 N. Konjević, M.S. Dimitrijević, W.L. Wiese: J. Phys. Chem. Ref. Data **13**, 649 (1984)
18 N. Konjević, A. Lesage, J.R. Fuhr, W.L. Wiese: J. Phys. Chem. Ref. Data **31**, 819 (2002)
19 L.C. Popović, I. Vince, M.S. Dimitrijević: Astron. Astrophys. Suppl. **102**, 17 (1993)
20 H.R. Griem: Phys. Rev. **165**, 258 (1968)
21 M.S. Dimitrijević, N. Konjević: J. Quant. Spectrosc. Radiative Transfer **24**, 451 (1980)
22 M.S. Dimitrijević, N. Konjević: Astron. Astrophys. **172**, 345 (1987)
23 S. Sahal-Brechot: Astron. Astrophys. **1**, 91 (1969)
24 S. Sahal-Brechot: Astron. Astrophys. **2**, 322 (1969)
25 M.S. Dimitrijević, S. Sahal-Brechot, V. Bommier: Astron. Astrophys. Suppl. Ser. **89**, 581 (1991)
26 Yu.V. Troicki': Zh. Tehn. Fiz. **42**, 395 (1972) (In Russian)
27 M. Jánossy, K. Rózsa, L. Csillag, Le Trong Mu: Acta Phys. Hung. **56**, 147 (1984)
28 S.R. Baumann, H.W. Smith: J. Opt. Soc. Amer. **60**, 345 (1970)
29 S. Watanabe, K. Kuroda, I. Ogura: J. Appl. Phys. **47**, 4887 (1976)

Transactions IAU, Volume XXVIIIA
Reports on Astronomy 2009-2012
Ian Corbett, ed.
© 2012 International Astronomical Union
DOI: 00.0000/X000000000000000X

arXiv:1211.1481v1 [astro-ph.SR] 7 Nov 2012

DIVISION XII / COMMISSION 14 / WORKING GROUP COLLISION PROCESSES

CO-CHAIRS **Gillian Peach**
Milan S. Dimitrijevic

TRIENNIAL REPORT 2009-2012

1. Introduction

Research in atomic and molecular collision processes and spectral line broadening has been very active since our last report (Peach, Dimitrijević & Stancil 2009). Given the large volume of the published literature and the limited space available, we have attempted to identify work most relevant to astrophysics. Since our report can not be comprehensive, additional publications can be found in the databases at the web addresses listed in the final section. Elastic and inelastic collisions among electrons, atoms, ions, and molecules are included and charge transfer can be very important in collisions between heavy particles.

Numerous meetings on collision processes and line broadening have been held throughout the report period. Important international meetings that provide additional sources of data through their proceedings are: the 19th *International Conference on Spectral Line Shapes (ICSLS)* (Gigosos & González 2008), the 7th *Serbian Conference on Spectral Line Shapes in Astrophysics* (SCSLSA) (Popović & Dimitrijević 2009), the XXVI *International Conference on Photonic, Electronic, and Atomic Collisions* (ICPEAC) (Orel *et al.* 2009), the 20th *ICSLS* (Lewis & Predoi-Cross 2010), the 22nd *International Conference on Atomic Physics* (ICAP) (Bachor, Drummond & Hannaford 2011), and the 7th *International Conference on Atomic and Molecular Data and their Applications* (Bernotas, Karazija & Rudzikas 2011). The 8th SCSLSA and the XXVIIth ICPEAC took place in June and July 2011 and their proceedings will be published in *Baltic Astronomy* and *Journal of Physics: Conference Series*, respectively.

2. Electron collisions with atoms and molecules

Collisions of electrons with atoms, molecules and atomic and molecular ions are the major excitation mechanism for a wide range of astrophysical environments. In addition, electron collisions play an important role in ionization and recombination, contribute to cooling and heating of the gas, and may contribute to molecular fragmentation and formation. In the following sections we summarize recent work on collisions for astrophysically relevant species, including elastic scattering, excitation, ionization, dissociation, recombination and electron attachment and detachment.

A review has been published of the atomic data necessary for the non-LTE analysis of stellar spectra (Mashonkina 2009). Other references are listed below for scattering by the atoms and molecules specified.

2.1. *Electron scattering by neutral atoms*

Elastic scattering: H (screened Coulomb interactions) (Zhang *et al.* 2010), Mg (Zatsarinny *et al.* 2009), Ar (Gargioni & Grosswendt 2008), I (Zatsarinny *et al.* 2011), Mn, Cu, Zn, Ni, Ag, Cd (Felfli *et al.* 2011), Rb, Cs, Fr (Gangwar *et al.* 2010).

Excitation: H (screened Coulomb interactions) (Zhang *et al.* 2010, Zhang *et al.* 2011), He($2^{1,3}$S) (Wang *et al.* 2009, Wang *et al.* 2010), He, Ne (Kretinin *et al.* 2008), Mg (Zatsarinny *et al.* 2009), Ar (Gargioni & Grosswendt 2008).

Ionization: He (Bray *et al.* 2010, Ren *et al.* 2011), He(2^1S) (Wang *et al.* 2010), Ar (Gargioni & Grosswendt 2008).

Total cross section: Na (Jiao *et al.* 2010).

2.2. *Electron scattering by atomic ions*

Elastic scattering: Mg^+, Ca^+ (Mitroy & Zhang 2008).

Excitation: Hydrogen isoelectronic sequence Cr^{23+}–Ni^{27+} (Malespin et al. 2011), Lithium isoelectronic sequence Be^+–Kr^{33+} (Liang & Badnell 2011), Ne^{3+}, Ne^{6+} (Ludlow *et al.* 2011), Neon isoelectronic sequence Na^+–Kr^{26+} (Liang & Badnell 2010), Sodium isoelectronic sequence Mg^+–Kr^{25+} (Liang et al. 2009b), Mg^{4+} (Hudson *et al.* 2009), Mg^{8+} (Del Zanna *et al.* 2008), Si^{9+} (Liang et al. 2009a), S^{8+}–S^{11+} (Liang et al. 2011), K^+ (Tayal & Zatsarinny 2010), Fe^{10+} (Del Zanna *et al.* 2010), Fe^{12+} (Storey & Zeippen 2010), Fe^{18+} (Butler & Badnell 2008), Ni^{10+} (Aggarwal & Keenan 2008a), Ni^{18+} (Aggarwal & Keenan 2008c).

Recombination: H^+ (Chluba *et al.* 2010), N^+ (Fang *et al.* 2011), Aluminium isoelectronic sequence Si^+–Zn^{17+} (Abdel-Naby *et al.* 2011), Argon isoelectronic sequence K^+–Zn^{12+} (Nikolić *et al.* 2010), Fe^7+, Fe^{8+} (Schmidt *et al.* 2008), Selenium ions Se^{q+}, $q = 1 - 6$ (Sterling & Witthoeft 2011).

Energy levels, radiative and excitation rates: O^{3+} (Aggarwal & Keenan 2008b, Keenan *et al.* 2009), O^{6+} (Aggarwal & Keenan 2008d), Si^+ (Bautista *et al.* 2009), Ar^{17+} (Aggarwal *et al.* 2008), Selenium ions Se^{q+}, $q = 1 - 6$ (Sterling & Witthoeft 2011).

X-ray line emission: Na^{9+} (Phillips *et al.* 2010).
Radiative and Auger decay: Aluminium ions Al^{q+}, $q = 0 - 11$ (Palmeri *et al.* 2011).

2.3. *Electron scattering by molecules*

Elastic scattering: H_2O (Liu & Zhou 2010), $(H_2O)_2$ (Bouchiha *et al.* 2008), Li_2 (Tarana & Tennyson 2008), CO (Allan 2010), NH (Rajvanshi & Baluja 2010), NO_2 (Munjal *et al.* 2009), S_2 (Rajvanshi & Baluja 2011), SO_2 (Machado *et al.* 2011), SOS (Kaur *et al.* 2010), S_3 (Kaur *et al.* 2011).
Electron exchange: O_2, NO, NO_2 (Holtkötter & Hanne 2009).

Excitation: H_2 (Kretinin *et al.* 2008), Li_2 (Tarana & Tennyson 2008), CO (Allan 2010), N_2 (Kato *et al.* 2010, Johnson *et al.* 2010, Mavadat *et al.* 2011), NH (Rajvanshi & Baluja 2010), NO_2 (Munjal *et al.* 2009), S_2 (Rajvanshi & Baluja 2011), SOS (Kaur *et al.* 2010), S_3 (Kaur *et al.* 2011), C_2H_4 (da Costa *et al.* 2008).

Ionization: N_2 (Gochitashvili *et al.* 2010), NH (Rajvanshi & Baluja 2010), SiCl, $SiCl_2$, $SiCl_3$, $SiCl_4$ (Kothari *et al.* 2011), SO, SO_2 (Vinodkumar *et al.* 2008), SOS (Kaur *et al.* 2010), S_2 (Rajvanshi & Baluja 2011), S_3 (Kaur *et al.* 2011).

Total cross sections: SO, SO_2, SO_2Cl_2, SO_2ClF, SO_2F_2 (Joshipura & Gangopadhyay 2008), SO_2 (Machado *et al.* 2011), C_2H_4O (Szmytkowski *et al.* 2008), CH_3OH, CH_3NH_2 (Vinodkumar *et al.* 2008).

Dissociative processes: H_2 (Celiberto *et al.* 2009, Bellm *et al.* 2010, Celiberto *et al.* 2011), HCl (Fedor *et al.* 2010), HCl, DCl, HBr, DBr (Fedor *et al.* 2008), C_2H_2 (Chourou & Orel 2008).

Attachment: C_2H, C_2N (Harrison & Tennyson 2011).

2.4. *Electron scattering by molecular ions*

Detachment: C_2^- (Halmová *et al.* 2008).
Excitation: C_2^- (Halmová *et al.* 2008), CO^+ (Stäuber & Bruderer 2009).
Rotational cooling: HD^+ (Shafir *et al.* 2009).

Dissociative and recombination processes: HD^+ (Fifirig & Stroe 2008, Takagi *et al.* 2009, Stroe & Fifirig 2011), H_3^+ (Glosík *et al.* 2009), HF^+ (Roos *et al.* 2008, Roos *et al.* 2009), CH_3^+, CD_3^+ (Bahati *et al.* 2009), $CD_3OCD_2^+$, $(CD_3)_2OD^+$ (Hamberg *et al.* 2010a), CD_3CDOD^+, $CH_3CH_2OH_2^+$ (Hamberg *et al.* 2010b).

3. Collisions between heavy particles

A review entitled 'Energetic ion, atom and molecule reactions and excitation in H_2 discharges' has recently been published (Phelps 2009). Other references are listed below for the atomic and molecular processes specified.

3.1. *Collisions between neutral atoms and atomic ions*

Inelastic scattering: H + H (Barklem *et al.* 2011), Na + H (Barklem *et al.* 2010).
Excitation: H + H^+ (Winter 2009).

Charge transfer processes: H, D, T + He^{2+} (Stolterfoht *et al.* 2010), H^- + H^+, mutual neutralization (Stenrup *et al.* 2009), H + H^+ (Winter 2009), H + Li^{2+} (Mančev 2009), H + B^{5+}, C^{4+} (Barragán *et al.* 2010), H + C^{3+}, O^{3+}, Si^{3+} (Guevara *et al.* 2011), H^+ + Li^+, Be^{2+}, B^{3+}, C^{4+} (Samanta & Purkait 2011), He + H^+ (Guzmán *et al.* 2009, Harris *et al.* 2010, Fischer *et al.* 2010), He + H^+, He^{2+} (Zapukhlyak & Kirchner 2009), He + H^+, He^+, He^{2+} (Schöffler *et al.* 2009), He + $^3He^{2+}$ (Alessi *et al.* 2011), He + He^{2+}, Li^+, Li^{2+}, Li^{3+}, C^{6+}, O^{8+} (Samanta *et al.* 2011), He + C^{3+} (Wu *et al.* 2009b), He + N^{3+} (Liu *et al.* 2011b), He + O^{3+} (Kamber *et al.* 2008, Wu *et al.* 2009a), He, Ne, Ar, Kr, Xe + C^{3+} (Santos *et al.* 2010), He^+ + He^+ (Mančev 2009),
Li + H, H^+ (Cabrera-Trujillo *et al.* 2008), Li + H^+ (Liu *et al.* 2011a), Ne + C^{2+}, C^{3+}, O^{2+}, O^{3+} (Ding *et al.* 2008), Na + H ion-pair production (Barklem *et al.* 2010), Mg + H^+, He^{2+} (Kumari *et al.* 2011), Mg + Cs^+ (Sabido *et al.* 2008), Ar + H^+ (Cabrera-Trujillo *et al.* 2009), Ar + O^{3+} (Kamber *et al.* 2008).

Ionization: H + H^+ (Winter 2009), He + H^+ (Guzmán *et al.* 2009), He + He^{2+} (Ogurtsov *et al.* 2011), He, Ne, Ar, Kr, Xe + H^+ (Miraglia & Gravielle 2008), He, Ne, Ar, Kr, Xe + C^{3+} (Santos *et al.* 2010), Li^+, Na^+, K^+, Rb^+ + H^+ (Miraglia & Gravielle 2008).

Detachment: C^-, O^-, F^-, Na^-, Si^-, S^-, Cl^-, Ge^- + He, Ne, Ar (Jalbert *et al.* 2008), F^-, Cl^-, Br^-, I^- + H^+ (Miraglia & Gravielle 2008).

Energy loss and stopping cross sections: Li + H, H^+ (Cabrera-Trujillo *et al.* 2008), H, D, T + He^{2+} (Cabrera-Trujillo *et al.* 2011).

3.2. *Collisions between atoms and molecules*

Dissociative processes: H_2O + H^+ (Monce *et al.* 2009), H_2O + He^+ (Garcia *et al.* 2008).

Radiative association: H_2 + H^- (Ayouz *et al.* 2011).

Excitation and/or fragmentation: CN^- + H_2 (Agúndez *et al.* 2010), CO^+ + H (Andersson *et al.* 2008), CO_2^+ + He (González-Magaña *et al.* 2008), CO^+ + H, H_2 (Stäuber & Bruderer 2009).

Charge transfer processes: D_2, O_2, H_2O, CO_2 + O^{3+} (Kamber *et al.* 2008), H_2 + He^{2+}

(Khoma *et al.* 2009), CH_3 + H^+ (Nagao *et al.* 2008), CO_2 + He^+ (Lin & Mayer 2010), HCl + C^{2+} (Rozsályi *et al.* 2011).

Ionization and/or capture: H_2O + H^+, He^{2+}, C^{6+} (Illescas *et al.* 2011), C_2H_4 + H^+ (Getahun *et al.* 2010), N_2 + H^+ (Gochitashvili *et al.* 2010).

4. Stark broadening

Knowledge of Stark broadening parameters (line widths and shifts) for a large number of atomic transitions is very important for the analysis, interpretation and modelling of stellar spectra, circumstellar conditions and H II regions. For hot dense stars such as white dwarfs this is often the most important broadening mechanism.

4.1. *Developments in line broadening theory*

Rosato *et al.* (2009) have reexamined the Stark broadening of hydrogen lines in the presence of a magnetic field and developed an impact theory for ions, valid for low electron densities ($N_e \leqslant 10^{14}$ cm^{-3}), which takes into account the Zeeman splitting of the atomic energy levels. Rosato *et al.* (2010) have also studied numerically the role of time ordering in such plasmas, by using a simulation code that accounts for the evolution of the microscopic electric field generated by the charged particles moving close to the atom. Calisti *et al.* (2010) have developed a very fast method to account for the dynamical effects of charged particles on the spectral line shape emitted by plasmas, based on a formulation of the frequency fluctuation model.

Ab initio calculations of Stark broadening parameters, i.e. calculations where the required atomic energy levels and oscillator strengths are determined during the calculation and are not taken from other sources, have been considered and reviewed by Ben Nessib (2009). A book has recently been published (Gordon & Sorochenko 2009) that gives a detailed account of the surprising discovery in the 1960's of the radio recombination lines and their subsequent analysis. Even now some features have still not been satisfactorily explained.

4.2. *Isolated lines*

For isolated lines Stark broadening is dominated by collisions with plasma electrons. Broadening parameters have been determined theoretically for:

One line from the 3s-3p transition array for each of the spectra Si XI, Ti XI, Cr XIII, Cr XIV, Fe XV, Fe XVI, Ni XVIII and Fe XXIII and two lines from the array for K VIII, Ca IX, Sc X and Ti XI (Elabidi & Sahal-Bréchot 2011); two lines for 3s-3p transitions for ions C IV, N V, O VI, F VII, Na IX, Mg X, Al XI, Si XII and P XIII and one line for Ne VIII (Elabidi *et al.* 2009); the 2s-2p resonance doublets of C IV, N V, O VI, F VII and Ne VIII ions (Elabidi *et al.* 2011). These calculations all use a quantum mechanical approach.

For five lines of Cu I (Zmerli *et al.* 2010) and the lines Ne I 837.8 nm (Christova *et al.* 2010b) and Ar I 737.2 nm (Christova *et al.* 2010a), new Stark broadening parameters are obtained using a semiclassical perturbation approach. A semi-empirical approach, which uses a set of wave functions obtained from Hartree-Fock relativistic calculations and includes core polarization effects, has been applied to 58 lines of Pb IV (Alonso-Medina *et al.* 2010) and 171 lines of Sn III (Alonso-Medina & Colón 2011).

Broadening parameters have been obtained experimentally for the following numbers of lines:

34 Pb I (Alonso-Medina 2008), 25 Pb III (Alonso-Medina 2011), 34 Pb IV and 4

Pb V (Bukvić *et al.* 2011), 28 Cd III (Djeniže *et al.* 2009, Bukvić *et al.* 2009b), 13 Si I, 15 Si II, 28 Si III and 9 Si IV (Bukvić *et al.* 2009a), 29 (Bukvić *et al.* 2008) and 19 (Djurović *et al.* 2011) Ar III, 30 Kr III (Ćirišan *et al.* 2011), 12 Ne II, 8 Kr II and 5 Xe II (Peláez *et al.* 2010b), 38 Xe II (Peláez *et al.* 2009a, Peláez *et al.* 2009b), 10 Xe III (Peláez *et al.* 2009b), 5 Au I and 26 Au II (Djeniže 2009), 9 Sb III (Djeniže 2008), 15 Mn I and 10 Fe I (Zielinska *et al.* 2010), 21 Fe II (Aragón *et al.* 2011) and C I 833.5 nm (Bartecka *et al.* 2011).

The regularities and systematic trends of Stark broadening parameters and reasons for deviations have been investigated within the multiplets (Peláez *et al.* 2010b, Peláez *et al.* 2009a), along the homologous sequence of singly-ionized noble gases (Peláez *et al.* 2010a), within the spectral series (Christova *et al.* 2010a) and along isoelectronic sequences (Elabidi *et al.* 2009, Elabidi *et al.* 2011). Also the dependence of electron- and proton-impact Stark widths on the upper-level ionization potential within different series of spectral lines of neutral magnesium (Tapalaga *et al.* 2011) and as a function of charge on the atomic core (Elabidi & Sahal-Bréchot 2011) have been evaluated and discussed. This kind of trend and regularity analysis can be useful for the prediction of Stark broadening parameters and therefore for the spectroscopic diagnostic of astrophysical plasmas.

4.3. *Transitions in hydrogenic and helium-like systems*

Stark-broadened line profiles of the hydrogen Brackett series have been computed within the Model Microfield Method for the conditions of stellar atmospheres and circumstellar envelopes (Stéhle & Fouquet 2010), and Tremblay & Bergeron (2009) have performed improved calculations for the Stark broadening of hydrogen lines in dense plasmas typical of white-dwarf atmospheres. The central asymmetry of the Hβ line has been measured and analysed (Djurović *et al.* 2009) and new experimental results for Hα and Hγ have been published (Mijatović *et al.* 2010a, Mijatović *et al.* 2010b).

Omar (2010, 2011) published new calculations for the Stark broadening of the He I lines at 504.8 nm, 388.9 nm, 318.8 nm, 667.8 nm and 501.6 nm formed in a dense plasma. Tables of Stark broadening for the He I 447.1 nm line have been generated using computer simulations (Gigosos & González 2009). This line and its forbidden component have also been studied theoretically (González *et al.* 2011) and experimentally (Ivković *et al.* 2010, González *et al.* 2011). Gao *et al.* (2008) have carried out experiments for the He I 388.9 nm and 706.5 nm lines.

5. Broadening by neutral atoms and molecules

The analysis of experimental molecular spectra in order to extract line shape parameters is often very difficult. Line shapes can be affected by collisional narrowing and the dependence of collisional broadening and shifting on molecular speed. When these effects are sufficiently important, fitting Voigt profiles to experimental spectra produces systematic errors in the parameters retrieved. Here the experimental and theoretical results selected have been confined to the basic atomic and molecular data required for a description of the pressure broadening and shift of lines and molecular bands.

Since the last report an important book has been published (Hartman *et al.* 2008) that gives a comprehensive review of experimental and theoretical work on collisional effects in molecular spectra. In the following sections the items are labelled by 'E' and 'T' to indicate experimental work and theoretical analysis, respectively.

5.1. *Broadening and shift of atomic lines*

New research has been published in the period 2008-2011 and the transitions studied together with the perturbing atoms or molecules are listed below. The work is theoretical except where indicated by 'E'.

H: line wings of Lyα broadened by H and He (Allard *et al.* 2009a, Allard & Christova 2009); line wings of Lyγ by H^+ (Allard *et al.* 2009b) and Hα by H (Allard *et al.* 2008).
He: self broadening of line $3s^3S$–$2p^3P$ (Allard *et al.* 2009c, Allard *et al.* 2011).
Li: self broadening of resonance line (Reggami *et al.* 2009); resonance line broadened by He (Peach & Whittingham 2009, Peach 2010a, Peach 2010b); 2s-3d transition broadened by Ne and Ar (Rosenberry & Stewart 2011).
Na: resonance line broadened by H (Peach 2010b); lines 3s-3p and 3p-3d broadened by He (Peach & Whittingham 2009, Peach 2010a, Peach 2010b).
K: self broadening of resonance line (Reggami *et al.* 2009) and line wings (Talbi *et al.* 2008).
K, Rb and Cs: self broadening of principal series (E) (Vadla *et al.* 2009).
Rb: 5s-5p D2 line, broadening by He, CH_4, C_2H_6, C_3H_8, n-C_4H_{10} (E) (Zameroski *et al.* 2011).
Cs: 6s-6p D2 line, broadening by ^{3}He, H_2, HD, D_2, N_2, CH_4, C_2H_6, CF_4 (E) (Pitz *et al.* 2010).

5.2. *Broadening and shift of molecular lines*

Much new data have been published since the last report was prepared. The molecules are listed below with their perturbing atomic or molecular species and are labelled by 'E' and 'T' to indicate experimental work and theoretical analysis, respectively.

H_2-Ar: collision-induced absorption (T) (Tran *et al.* 2011b).
D_2-Kr: collision-induced absorption (E) (Abu-Kharma *et al.* 2010).
HI: lines broadened by N_2 (E) (Domanskaya *et al.* 2011).
HBr: self broadening (E) (Domanskaya *et al.* 2009).
HI and HBr: lines broadened by rare gases (E) (Domanskaya *et al.* 2009).
HDO: lines broadened by CO_2 (T) (Gamache *et al.* 2011).
HCl: lines broadened and shifted by N_2, He, Ar and Xe (E) (Hurtmans *et al.* 2009).
HCN: lines broadened by N_2, O_2 and air (E) (Yang *et al.* 2008).
H_2CO: lines broadened by H_2CO and N_2 (E+T) (Jacquemart *et al.* 2010).
HNO_3: lines broadened by N_2 (T) (Laraia *et al.* 2009).
HO_2: lines broadened by N_2 (E) (Miyano & Tonokura 2011).
H_2O_2: lines broadened by N_2, O_2 and air (E) (Sato *et al.* 2010).
H_2O: lines broadened by H_2 (E) (Krupnov 2010), (T) (Wiesenfeld & Faure 2010); by H_2 and He (E) (Dick *et al.* 2010); by N_2 (E) (Lavrentieva *et al.* 2010; by N_2 and O_2 (T) (Gamache & Laraia 2009); by O_2 (E) (Petrova *et al.* 2011; by H_2O (E) (Lisak *et al.* 2009, Ptashnik & Smith 2010); by H_2O, N_2, O_2 (E+T) (Cazzoli *et al.* 2008, Cazzoli *et al.* 2009, Koshelev 2011); by air (T) (Voronin *et al.* 2010); by CO_2 (T) (Sagawa *et al.* 2009); by H_2, He, N_2, O_2 and CO_2 (E) (Dick *et al.* 2009b); by rare gases (E+T) (Fiadzomor *et al.* 2008).
CH_4: lines broadened by N_2 (T) (Gabard & Boudon 2010); by N_2 and O_2 (E) (Lyulin *et al.* 2009); by CH_4 (E) (Smith *et al.* 2010, Lyulin *et al.* 2011); by CH_4 and N_2 (E) (McRaven *et al.* 2011); by O_2 and air (E) (Martin & Lepère 2009); by air (E) (Smith *et al.* 2009, Smith *et al.* 2011).
C_2H_2: broadened by H_2 (T) (Thibault *et al.* 2011a); by H_2 and D_2 (E+T) (Thibault *et al.* 2009); by N_2 (E) (Dhyne *et al.* 2009, Fissiaux *et al.* 2009, Dhyne *et al.* 2010); by C_2H_2 (E) (Li *et al.* 2010, Povey *et al.* 2011, Dhyne *et al.* 2011); by He and Ar (T) (Ivanov & Buzykin 2010); by Ne and Kr (E) (Nguyen *et al.* 2009a).
C_2H_4: lines broadened by C_2H_4 (E) (Flaud *et al.* 2011); by Ar (E+T) (Nguyen *et al.* 2009b).
C_2H_6: lines broadened by N_2 (E) (Blanquet *et al.* 2009); by C_2H_6 and N_2 (E) (Devi *et al.* 2010b,

Devi *et al.* 2010c); by O_2 and air (E) (Fissiaux *et al.* 2010).
CH_3Br: lines broadened by N_2 (T) (Boussetta *et al.* 2011); by CH_3Br, N_2 and O_2 (E) (Hoffman & Davies 2009); by CH_3Br (T) (Goméz *et al.* 2010).
CH_3F: lines broadened by CH_3F and He (E) (Koubek *et al.* 2011).
CO: lines broadened by CO, N_2 and O_2 (E) (Koshelev & Markov 2009); by H_2, N_2, O_2, CO, CO_2 and He (E) (Dick *et al.* 2009a).
CO_2: by O_2 (E) (Devi *et al.* 2010a); by CO_2 (E+T) (Predoi-Cross *et al.* 2010, Tran *et al.* 2011a); by CO_2, N_2 and O_2 (E) (Li *et al.* 2008); by air (T) (Hartmann 2009), (E) (Gulidova *et al.* 2010), (E+T) (Lamouroux *et al.* 2010); by He (E) (Deng *et al.* 2009); by air and Ar (E) (Farooq *et al.* 2010).
Cs_2: lines broadened by Cs_2 (E) (Misago *et al.* 2009).
N_2: lines broadened by H_2 (T) (Goméz *et al.* 2011); by N_2 (E+T) (Thibault *et al.* 2011b).
NH_3: lines broadened by H_2 and He (E) (Hanley *et al.* 2009); by He (T) (Dhib 2010; by NH_3 (E) (Aroui *et al.* 2009, Guinet *et al.* 2011); by NH_3 and O_2 (E+T) (Nouri *et al.* 2009).
O_2: lines broadened by O_2 (E) (Lisak *et al.* 2010, Wójtewicz *et al.* 2011); by O_2 and OO isotopologues (E) (Long *et al.* 2011); by O_2 and air (E) (Long *et al.* 2010).
O_2-CO_2: collision-induced absorption (E) (Vangvichith *et al.* 2009).
O_3: lines broadened by air (Drouin & Gamache 2008); by N_2 and air (E+T) (Tran *et al.* 2011c).
OH: lines broadened by N_2, H_2O and Ar (E) (Hwang *et al.* 2008).
OCS lines broadened by N_2, O_2 and OCS (E) (Koshelev & Tretyakov 2009); by N_2 and O_2 (E) (Galalou *et al.* 2011).
I_2: lines broadened by Ar (E) (Phillips & Perram 2008).

6. Databases

Some useful databases are:

Vienna Atomic Line Database (VALD) of atomic data for analysis of radiation from astrophysical objects, containing central wavelengths, energy levels, statistical weights, transition probabilities and line broadening parameters for all chemical elements of astronomical importance. It can be found at http://vald.astro.univie.ac.at/ (Kupka *et al.* 1999).

The database of Robert L. Kurucz comprises atomic line parameters, including line broadening. An update to this database is discussed by Kurucz 2011. (http://kurucz.harvard.edu)

CHIANTI database (Dere *et al.* 2009) contains a critically evaluated set of up-to-date atomic data for the analysis of optically thin collisionally ionized astrophysical plasmas. It lists experimental and calculated wavelengths, radiative data and rates for electron and proton collisions, see websites http://sohowww.nascom.nasa.gov/solarsoft and http://www.damtp.cam.ac.uk/user/astro/chianti/.

CDMS – Cologne Database for Molecular Spectroscopy, see website http://www.ph1.uni-koeln.de/vorhersagen/, provides recommendations for spectroscopic transition frequencies and intensities for atoms and molecules of astronomical interest in the frequency range 0-10 THz, i.e. 0-340 cm^{-1} (Müller *et al.* 2005).

BASECOL database (http://basecol.obspm.fr) contains excitation rate coefficients for ro-vibrational excitation of molecules by electrons, He and H_2 and it is mainly used for the study of interstellar, circumstellar and cometary atmospheres.

TIPTOPbase (http://cdsweb.u-strasbg.fr/topbase/home.html) contains:
(i) TOPbase, that lists atomic data computed in the Opacity Project; namely LS-coupling energy levels, gf-values and photoionization cross sections for light elements ($Z \leqslant 26$) of astrophysical interest and
(ii) TIPbase that lists intermediate-coupling energy levels, transition probabilities and

electron impact excitation cross sections and rates for astrophysical applications ($Z \leqslant 28$), computed by the IRON Project.

HITRAN – (HIgh-resolution TRANsmission molecular absorption database) is at http://www.cfa. harvard.edu/hitran/ (Rothman *et al.* 2009). It lists individual line parameters for molecules in the gas phase (microwave through to the UV), photoabsorption cross-sections for many molecules, and refractive indices of several atmospheric aerosols. A high temperature extension to HITRAN is HITEMP (To access the HITEMP data: ftp to cfa-ftp.harvard.edu; user = anonymous; password = e-mail address). It contains data for water, CO_2, CO, NO and OH (Rothman *et al.* 2010).

GEISA – (Gestion et Etude des Informations Spectroscopiques Atmosphériques) is a computer-accessible spectroscopic database, designed to facilitate accurate forward radiative transfer calculations using a line-by-line and layer-by-layer approach. It can be found at http://ether.ipsl.jussieu.fr/etherTypo/?id=950 (Jacquinet-Husson *et al.* 2008).

NIST – The National Institute of Standards and Technology hosts a number of useful databases for Atomic and Molecular Physics. A list can be found at http://www.nist.gov/srd/atomic.cfm. Among them are: An atomic spectra database and three bibliographic databases providing references on atomic energy levels and spectra, transition probabilities and spectral line shapes and line broadening.

STARK-B database (http://stark-b.obspm.fr) contains theoretical widths and shifts of isolated lines of atoms and ions due to collisions with charged perturbers, obtained using the impact approximation (Sahal-Bréchot 2010).

The European FP7 project will finish at the end of 2012. The virtual Atomic and Molecular Data Centre (VAMDC - http://www.vamdc.eu/) is being created with the aim of building an accessible and interoperable e-infrastructure for atomic and molecular data that will upgrade and integrate European (and other) A&M database services (Dubernet *et al.* 2011, Rixon *et al.* 2011).

References

Abdel-Naby, Sh. A., Nikolić, D., Gorczyca, T.W., *et al.* 2011, *A&A*, in press, DOI: http://dx.doi.org/10.1051/0004-6361/201117544

Abu-Kharma, M., Omari, H. Y., Shawaqfeh, N. & Stamp, C. 2010, *JMoSp*, 259, 111

Aggarwal, K. M., Hamada, K., Igarashi, A., *et al.* 2008, *A&A*, 487, 383

Aggarwal, K. M. & Keenan, F. P. 2008a, *EuPhJD*, 46, 205

Aggarwal, K. M. & Keenan, F. P. 2008b, *A&A*, 486, 1053

Aggarwal, K. M. & Keenan, F. P. 2008c, *A&A*, 488, 365

Aggarwal, K. M. & Keenan, F. P. 2008d, *A&A*, 489, 1377

Agúndez, M., Cernicharo, J., Guélin, M., *et al.* 2010, *A&A*, 517, L2

Alessi M., Otranto, S. & Focke, P. 2011, *PhRvA*, 83, 014701

Allan, M. 2010, *PhRvA*, 81, 042706

Allard, N. F., Kielkopf, J. F., Cayrel, R. & Van't Veer-memmerat, C. 2008, *A&A*, 480, 581

Allard, N. F. & Christova, M. 2009, *New Astron. Rev.*, 53, 252

Allard, N. F. & Kielkopf, J. F. 2009a, *A&A*, 493, 1155

Allard, N. F., Noselidze, I. & Kruk, J. W. 2009b, *A&A*, 506, 993

Allard, N. F., Deguilhem, B., Gadea, F. X., *et al.* 2009c, *EPL*, 88, 53002

Allard, N. F., Bonifaci, N. & Denat, A. 2011, *EuPhJD*, 61, 365

Alonso-Medina, A. 2008, *Spectrochim. Acta B*, 63, 598

Alonso-Medina, A., Colón, C., Montero, J. L., & Nation, L. 2010, *MNRAS*, 401, 1080

Alonso-Medina, A. 2011, *Spectrochim. Acta B*, 66, 439

Alonso-Medina, A. & Colón, C. 2011, *MNRAS*, 414, 713

Andersson, S., Barinovs, Ǵ. & Nyman, G. 2008, *ApJ*, 678, 1042

Aragón, C., Vega, P. & Aguilera, J. A. 2011, *JPhB: At. Mol. Opt. Phys.*, 44, 055002
Aroui, H., Laribi, H., Orphai, J. & Chelin, P. 2009, *JQSRT*, 110, 2037
Ayouz, M., Lopes, R., Raoult, M., *et al.* 2011, *PhRvA*, 83, 052712
Bachor, H., Drummond, P., & Hannaford, P., eds. 2011, Proc. 22nd *International Conference on Atomic Physics*, *JP-CS*, 264
Bahati, E. M., Fogle, M., Vane, C. R., *et al.* 2009, *PhRvA*, 79, 052703
Barklem, P. S., Belyaev, A. K., Dickinson, A. S. & Gadéa, F. X. 2010, *A&A*, 519, A20
Barklem, P. S., Belyaev, A. K., Guitou, M., *et al.* 2011, *A&A*, 530, A94
Barragán, P., Errea, L. F., Guzmán, F., *et al.* 2010, *PhRvA*, 81, 062712
Bartecka, A., Baclawski, A. & Musielok, J. 2011, *Cent. Eur. J. Phys.*, 9, 131
Bautista, M. A., Quinet, P., Palmeri, P., *et al.* 2009, *A&A*, 508, 1527
Bellm, S., Lower, J., Weigold, E. & Mueller, D. W. 2010, *PRL*, 104, 023202
Ben Nessib, N. 2009, *New Astron. Rev.*, 53, 255
Bernotas, A., Karazija, R. & Rudzikas, Z., eds. 2011, Proc. 7th *International Conference on Atomic and Molecular Data and their Applications*, *AIP-CP*, 1344
Blanquet, G., Auwera, J. V. & Lepère, M. 2009, *JMoSp*, 255, 72
Bouchiha, D., Caron, L. G., Gorfinkiel, J. D. & Sanche, L. 2008, *JPhB: At. Mol. Opt. Phys.*, 41, 045204
Boussetta, Z., Aroui, H., Jacquemart, D., *et al.* 2011, *JQSRT*, 112, 769
Bray, I., Fursa, D. V., Kadyrov, A. S. & Stelbovics, A. T. 2010, *PhRvA*, 81, 062704
Bukvić, S., Žigman, V., Srećković, A. & Djeniže, S. 2008, *JQSRT*, 109, 2869
Bukvić, S., Djeniže, S. & Srećković, A. 2009a, *A&A*, 508, 491
Bukvić, S., Djeniže, S., Srećković, A. & Nikolić, Z. 2009b, *Phys. Lett. A*, 373, 2750
Bukvić, S., Djeniže, S., Nikolić, Z. & Srećković, A. 2011, *A&A*, 529, A83
Butler, K. & Badnell, N. R. 2008, *A&A*, 489, 1369
Cabrera-Trujillo, R., Sabin, J. R., Deumens, E. & Öhrn, Y. 2008, *PhRvA*, 78, 012707
Cabrera-Trujillo, R., Amaya-Tapia, A. & Antillón, A. 2009, *PhRvA*, 79, 012712
Cabrera-Trujillo, R., Sabin, J. R., Öhrn, Y., *et al.* 2011, *PhRvA*, 83, 012715
Calisti, A., Mossé, C., Ferri, S., *et al.* 2010, *PhRvE*, 81, 016406
Cazzoli, G., Puzzarini, C., Buffa, G. & Tarrini, O. 2008, *JQSRT*, 109, 2820
Cazzoli, G., Puzzarini, C., Buffa, G. & Tarrini, O. 2009, *JQSRT*, 110, 609
Celiberto, R., Janev, R. K., Wadehra, J. M. & Laricchiuta, A. 2009, *PhRvA*, 80, 012712
Celiberto, R., Janev, R. K., Wadehra, J. M. & Laricchiuta, A. 2011, *PhRvA*, 84, 012707
Chluba, J., Vasil, G. M. & Dursi, L. J. 2010, *MNRAS*, 407, 599
Chourou, S. T. & Orel, A. E. 2008, *PhRvA*, 77, 042709
Christova, M., Dimitrijević, M. S. & Kovačević, A. 2010a, *JP-CS*, 207, 2024
Christova, M., Dimitrijević, M. S., Simić, S. & Sahal-Bréchot, S. 2010b, *JP-CS*, 207, 2025
Ćirišan, M., Peláez, R. J., Djurović, S., *et al.* 2011, *PhRvA*, 83, 012513
da Costa, R. F., Bettega, M. H. F. & Lima, M. A. P. 2008, *PhRvA*, 77, 042723
Del Zanna, G., Rozum, I. & Badnell, N. R. 2008 *A&A*, 487, 1203
Del Zanna, G., Storey, P. J. & Mason, H. E. 2010 *A&A*, 514, A40
Deng, W., Mondelain, D., Thibault, F., *et al.* 2009, *JMoSp*, 256, 102
Dere, K. P., Landi, E., Young, P. R., *et al.* 2009, *A&A*, 498, 915
Devi, V. M., Benner, D. C., Miller, C. E. & Predoi-Cross, A. 2010a, *JQSRT*, 111, 2355
Devi, V. M., Benner, D. C., Rinsland, C. P., *et al.* 2010b, *JQSRT*, 111, 2481
Devi, V. M., Rinsland, C. P., Benner, D. C., *et al.* 2010c, *JQSRT*, 111, 1234
Dhib, M. 2010, *JMoSp*, 259, 80
Dhyne, M., Fissiaux, L., Populaire, J.-C. & Lepère, M. 2009, *JQSRT*, 110, 358
Dhyne, M., Joubert, P., Populaire, J.-C. & Lepère, M. 2010, *JQSRT*, 111, 973
Dhyne, M., Joubert, P., Populaire, J.-C. & Lepère, M. 2011, *JQSRT*, 112, 969
Dick, M. J., Drouin, B. J., Crawford, T. J. & Pearson, J. C. 2009a, *JQSRT*, 110, 628
Dick, M. J., Drouin, B. J. & Pearson, J. C. 2009b, *JQSRT*, 110, 619
Dick, M. J., Drouin, B. J. & Pearson, J. C. 2010, *PhRvA*, 81, 022706
Ding, B. W., Chen, X. M., Yu, D. Y., *et al.* 2008, *PhRvA*, 78, 062718

Djeniže, S. 2008, *Phys. Lett. A*, 372, 6658
Djeniže, S. 2009, *Spectrochim. Acta B*, 64, 242
Djeniže, S., Srećković, A. & Bukvić, S. 2009, *EuPhJD*, 62, 185
Djurović, S., Ćirišan, M., Demura, A. V., *et al.* 2009, *PhRvE*, 79, 046402
Djurović, S., Mar, S., Peláez, R. J. & Aparicio, J. A. 2011, *MNRAS*, 414, 1389
Domanskaya, A. V., Bulanin, M. O., Kerl, K., & Maul, C. 2009, *JMoSp*, 253, 20
Domanskaya, A. V., Asfin, R. E., Maul, C., *et al.* 2011, *JMoSp*, 265, 69
Drouin, B. J. & Gamache, R. R. 2008, *JMoSp*, 251, 194
Dubernet, M. L., Boudon, V., Culhane, J. L., *et al.* 2011, *JQSRT*, 111, 2151
Elabidi, H. & Sahal-Bréchot, S. 2011, *EuPhJD*, 61, 285
Elabidi, H., Sahal-Bréchot, S. & Ben Nessib, N. 2009, *EuPhJD*, 54, 51
Elabidi, H., Sahal-Bréchot, S., Dimitrijević, M. S. & Ben Nessib, N. 2011, *MNRAS*, 417, 2624
Fang, X., Storey, P. J. & Liu, X.-W. 2011 *A&A*, 530, A18
Farooq, A., Jeffries, J. B. & Hanson, R. K. 2010, *JQSRT*, 111, 949
Fedor, J., May, O. & Allan, M. 2008, *PhRvA*, 78, 032701
Fedor, J., Winstead, C., McKoy, V., *et al.* 2010, *PhRvA*, 81, 042702
Felfi, Z., Msezane, A. Z. & Sokolovski, D. 2011, *PhRvA*, 83, 052705
Fiadzomor, P. A. Y., Keen, A. M., Grant, R. B. & Orr-Ewing, A. J. 2008, *Chem. Phys. Lett.*, 462, 188
Fifirig, M. & Stroe, M. 2008, *Phys. Scr.*, 78, 065302
Fischer, D., Gudmundsson, M., Berényi, Z., *et al.* 2010, *PhRvA*, 81, 012714
Fissiaux, L., Dhyne, M. & Lepère, M. 2009, *JMoSp*, 254, 10
Fissiaux, L., Blanquet, G. & Lepère, M. 2010, *JQSRT*, 111, 2037
Flaud, J.-M., Lafferty, W. J., Devi, V. M., *et al.* 2011, *JMoSp*, 267, 3
Gabard, T. & Boudon, V. 2010, *JQSRT*, 111, 1328
Galalou, S., Ben Mabrouk, K., Aroui, H., *et al.* 2011, *JQSRT*, 112, 2750
Gamache, R. R. & Laraia, A. L. 2009 *JMoSp*, 257, 116
Gamache, R. R., Laraia, A. L. & Lamouroux, J. 2011 *Icarus*, 213, 720
Gangwar, R. K., Tripathi, A.N., Sharma, L. & Srivastava, R. 2010, *JPhB: At. Mol. Opt. Phys.*, 43, 085205
Gao, H. M., Ma, S. I., Xu, C. M. & Vu, L. 2008, *EuPhJD*, 47, 191
Garcia, P. M. Y., Sigaud, G. M., Luna, H., *et al.* 2008, *PhRvA*, 77, 052708
Gargioni, E. & Grosswendt, B. 2008, *Rev. Mod. Phys.*, 80, 451
Getahun, H., Errea, L. F., Illescas, C., *et al.* 2010, *EuPhJD*, 60, 45
Gigosos, M. A. & González, M. Á. (eds.) 2008, Proc. 19th *International Conference on Spectral Line Shapes*, *AIP-CP*, 1058
Gigosos, M. A. & González, M. Á. 2009, *A&A*, 503, 293
Glosík, I., Plašil, R., Korolov, I., *et al.* 2009, *PhRvA*, 79, 052707
Gochitashvili, M. R., Kezerashvili, R. Ya. & Lomsadze, R. A. 2010, *PhRvA*, 82, 022702
Goméz, L., Jacquemart, D., Bouanich, J.-P., *et al.* 2010, *JQSRT*, 111, 1252
Goméz, L., Ivanov, S. V., Buzykin, O. G. & Thibault, F. 2011, *JQSRT*, 112, 1942
González-Magaña, O., Cabrera-Trujillo, R. & Hinojosa, G. 2008, *PhRvA*, 78, 052712
González, M. Á., Ivković, M., Gigosos, M. A., *et al.* 2011, *A&A*, 503, 293
Gordon, M. A. & Sorochenko, R. L. 2009, *Radio Recombination Lines* (New York:Springer Science+Business Media)
Guevara, N. L., Teixeira, E., Hall, B., *et al.* 2011, *PhRvA*, 83, 052709
Guinet, M., Jeseck, P., Mondelain, D., *et al.* 2011, *JQSRT*, 112, 1950
Gulidova, O. S., Asfin, R. E., Grigoriev, I. M. & Filippov, N. N. 2010, *JQSRT*, 111, 2315
Guzmán, F., Errea, L. F. & Pons, B. 2009, *PhRvA*, 80, 042708
Halmová, G., Gorfinkiel, J. D. & Tennyson, J. 2008, *JPhB: At. Mol. Opt. Phys.*, 41, 155201
Hamberg, M., Österdahl, F., Thomas, R. D., *et al.* 2010a, *A&A*, 514, A83
Hamberg, M., Zhaunerchyk, V., Vigren, E., *et al.* 2010b, *A&A*, 522, A90
Hanley, T. R., Steffes, P. G. & Karpowicz, B. M. 2009, *Icarus*, 202, 316
Harris, A. L., Peacher, J. L., Schulz, M. & Madison, D. H. 2010, *JP-CS*, 212, 012031

Harrison, S. & Tennyson, J. 2011, *JPhB: At. Mol. Opt. Phys.*, 44, 045206
Hartmann, J.-M. 2009, *JQSRT*, 110, 2019
Hartmann, J.-M., Boulet, C. & Robert, D. 2008, *Collisional Effects on Molecular Spectra* (Amsterdam:Elsevier)
Hoffman, K. J. & Davies, P. B. 2009, *JMoSp*, 254, 69
Holtkötter, I. & Hanne, G. F. 2009, *PhRvA*, 80, 022709
Hudson, C. E., Ramsbottom, C. A., Norrington, P. H. & Scott, M. P. 2009, *A&A*, 494, 729
Hurtmans, D., Henry, A., Valentin, A. & Boulet, C. 2009, *JMoSp*, 254, 126
Hwang, S. M., Kojima, J. N., Nguyen, Q.-V. & Rabinowitz, M. J. 2008, *JQSRT*, 109, 2715
Illescas, C., Errea, L. F., Méndez, L., *et al.* 2011, *PhRvA*, 83, 052704
Ivanov, S. V. & Buzykin, O. G. 2010, *JQSRT*, 111, 2341
Ivković, M., González, M. Á., Jovićević, S., *et al.* 2010, *Publ. Astron. Obs. Belgrade*, 89, 201
Jacquemart, D., Laraia, A. L., Tchana, F. K., *et al.* 2010, *JQSRT*, 111, 1209
Jacquinet-Husson, N., Scott, N. A., Chedin, A., *et al.* 2008, *JQSRT*, 109, 1043
Jalbert, G., Wolff, W., Magalhães, S. D. & de Castro Faria, N. V. 2008, *PhRvA*, 77, 012722
Jiao, L., Zhou, Y. & Wang, Y. 2010, *PhRvA*, 81, 042713
Johnson P. V., Young, J. A., Malone, C. P., *et al.* 2010, *JP-CS*, 204, 012003
Joshipura, K. N. & Gangopadhyay, S. 2008, *JPhB: At. Mol. Opt. Phys.*, 41, 215205
Kamber, E. Y., Abu-Haija, O. & Wardwell, J. A. 2008, *PhRvA*, 77, 012701
Kato, H., Suzuki, D., Ohkawa, M., *et al.* 2010, *PhRvA*, 81, 042717
Kaur, S. & Baluja, K. L. 2010, *PhRvA*, 82, 022717
Kaur, S., Bharadvaja, A. & Baluja, K. L. 2011, *PhRvA*, 83, 062707
Keenan, F. P. Crockett, P. J., Aggarwal, K. M., *et al.* 2009, *A&A*, 495, 359
Khoma, M. V., Lazur, V. Yu. & Janev, R. K. 2009, *PhRvA*, 80, 032706
Koshelev M. A. & Tretyakov, M. Yu. 2009, *JQSRT*, 110, 118
Koshelev M. A. & Markov, V. N. 2009, *JQSRT*, 110, 526
Koshelev M. A. 2011, *JQSRT* 112, 550
Kothari, H. N., Pandya, S. H. & Joshipura, K. N. 2011, *JPhB: At. Mol. Opt. Phys.*, 44, 125202
Koubek, J., Boulet, C., Perrin A., *et al.* 2011, *JMoSp*, 266, 12
Kretinin, I. Yu, Krisilov, A. V. & Zon, B. A. 2008 *JPhB: At. Mol. Opt. Phys.*, 41, 215206
Krupnov, A. F. 2010, *PhRvA*, 82, 036703
Kumari, S., Chatterjee, S. N., Jha, L. K. & Roy, B. N. 2011, *EuPhJD*, 61, 355
Kupka, F., Piskunov, N., Ryabchikova, T. A., *et al.* 1999, *A&AS*, 138, 119
Kurucz, R. L. 2011, *CanJPhys*, 89, 417
Lamouroux, J., Tran, H., Laraia, A. L., *et al.* 2010, *JQSRT*, 111, 2321
Laraia, A. L., Gamache, R. R., Hartmann, J.-M., *et al.* 2009, *JQSRT*, 110, 687
Lavrentieva, N. N., Petrova, T. M., Solodov, A. M. & Solodov, A. A. 2010, *JQSRT*, 111, 2291
Lewis, J. K. C. & Predoi-Cross, A. (eds.) 2010, Proc. 20th *International Conference on Spectral Line Shapes*, *AIP-CP*, 1290
Li, J. S., Liu, K., Zhang, W. J., *et al.* 2008, *JMoSp*, 252, 9
Li, J. S., Durry, G., Cousin, J., *et al.* 2010, *JQSRT*, 111, 2332
Liang, G. Y. Whiteford, A. D. & Badnell, N. R. 2009a, *A&A*, 499, 943
Liang, G. Y. Whiteford, A. D. & Badnell, N. R. 2009b, *A&A*, 500, 1263
Liang, G. Y. & Badnell, N. R. 2010, *A&A*, 518, A64
Liang, G. Y. & Badnell, N. R. 2011, *A&A*, 528, A69
Liang, G. Y., Badnell, N. R., Zhao, G., *et al.* 2011, *A&A*, 533, A87
Lin, Y. & Mayer, P. M. 2010, *Chem. Phys.*, 378, 103
Lisak, D., Havey, D. K. & Hodges, J. T. 2009, *PhRvA*, 79, 052507
Lisak, D., Masłowski, P., Cygan, A., *et al.* 2010, *PhRvA*, 81, 042504
Liu, J.-B. & Zhou, Ya.-J. 2010, *Chin. Phys. B*, 19, 093403
Liu, L., Liu, C. H., Wang, J. G. & Janev, R. K. 2011, *PhRvA*, 84, 032710
Liu, X. J., Wang, J. G., Qu, Y. Z. & Buenker, R. J. 2011, *PhRvA*, 84, 042706
Long, D. A., Havey, D. K., Okumura, M., *et al.* 2010, *JQSRT*, 111, 2021
Long, D. A., Havey, D. K., Yu, S. S., *et al.* 2011, *JQSRT*, 112, 2527

Ludlow, J. A., Lee, T. G., Ballance, C. P., *et al.* 2011, *PhRvA*, 84, 022701
Lyulin, O. M., Nikitin, A. V., Perevalov, V. I., *et al.* 2009, *JQSRT*, 110, 654
Lyulin, O. M., Perevalov, V. I., Morino, I., *et al.* 2011, *JQSRT*, 112, 531
Machado, L. E., Sugohara, R. T., dos Santos, A. S., *et al.* 2011, *PhRvA*, 84, 032709
McRaven, C. P., Cich, M. J., Lopez, G. V., *et al.* 2011, *JMoSp*, 266, 43
Malespin, C., Ballance, C. P., Pindzola, M. S., *et al.* 2011, *A&A*, 526, A115
Mančev, I. 2009, *EuPhJD*, 51, 213
Martin, B. & Lepère, M. 2009, *JMoSp*, 255, 6
Mashonkina, L. 2009, *Phys. Scr.*, T134, 014004
Mavadat, M., Ricard, A., Sarra-Bournet, C. & Laroche, G. 2011, *JPhD: Appl. Phys.*, 44, 155207
Mijatović, Z., Nikolić, D., Kobilarov, R. & Ivković, M. 2010a, *Publ. Astron. Obs. Belgrade*, 89, 217
Mijatović, Z., Nikolić, D., Kobilarov, R. & Ivković, M. 2010b, *JQSRT*, 111, 990
Miraglia, J. E. & Gravielle, M. S. 2008, *PhRvA*, 78, 052705
Misago, F., Lepèere, M., Bouanich, J.-P. & Blanquet, G. 2009, *JMoSp*, 254, 16
Mitroy, J. & Zhang, J. Y. 2008, *EuPhJD*, 46, 415
Miyano, S. & Tonokura, K. 2011, *JMoSp*, 265, 47
Monce, M. N., Pan, S., Radeva, N. L. & Pepper, J. L. 2009, *PhRvA*, 79, 012704
Müller, H. S. P., Schlöder, F., Stutzki, J. & Winnewisser, G. 2005, *JMoStr*, 742, 215
Munjal, H., Baluja, K. L. & Tennyson, J. 2009, *PhRvA*, 79, 032712
Nagao, M., Hida, K., Kimura, M., *et al.* 2008, *PhRvA*, 78, 012708
Nguyen, L., Blanquet, G., Dhyne, M. & Lepèere, M. 2009a, *JMoSp*, 254, 94
Nguyen, L., Blanquet, G., Populaire, J.-C. & Lepèere, M. 2009b, *JQSRT*, 110, 367
Nikolić, D., Gorczyca, T. W., Korista, K. T. & Badnell, N. R. 2010, *A&A*, 516, A97
Nouri, S., Ben Mabrouk, K., Chelin, P., *et al.* 2008, *JMoSp*, 258, 75
Ogurtsov, G. N., Ovchinnikov, S. Yu., Macek, J. H. & Mikoushkin, V. M. 2011, *PhRvA*, 84, 032706
Omar, B. 2010, *Int. J. Spectrosc.*, 506346
Omar, B. 2011, *J. At. Mol. Opt. Phys*, ID 850807
Orel, A. E., Starace, A. F., Nikolić, D., *et al.* (eds.) 2009, Proc. XXVI *International Conference on Photonic, Electronic & Atomic Collisions*, *JP-CS*, 194
Palmeri, P., Quinet, P., Mendoza, C., *et al.* 2011, *A&A*, 525, A59
Peach, G., Dimitrijević, M. S. & Stancil, P. C. 2009, in Karel A. van der Hucht (ed.), *Reports on Astronomy 2006-2009, IAU Transactions XXVIIA* (Cambridge: CUP), 385
Peach, G. & Whittingham, I. B. 2009, *New Astron. Rev.*, 53, 227
Peach, G. 2010a, in: *Mem. S.A.It. Suppl.*, 15, 68
Peach, G. 2010b, in: *Spectral Line Shapes*, Proc. 20th Intern. Conf., AIP-CP, 1290, 14
Peláez, R. J., Djurović, S., Ćirišan, M., *et al.* 2009a, *JPhB: At. Mol. Opt. Phys.*, 42, 125002
Peláez, R. J., Djurović, S., Ćirišan, M., *et al.* 2009b, *A&A*, 507, 1697
Peláez, R. J., Djurović, S., Ćirišan, M., *et al.* 2010a, *A&A*, 518, A60
Peláez, R. J., Djurović, S., Ćirišan, M., Aparicio, J. A. & Mar, S. 2010b, *JP-CS*, 257, 2021
Petrova, T. M., Solodov, A. M., Solodov, A. A., *et al.* 2011, *JQSRT*, 112, 2741
Phelps, A. V. 2009, *PhRvE*, 79, 066401
Phillips, G. T. & Perram, G. P. 2008, *JQSRT*, 109, 1875
Phillips, K. J. H., Aggarwal, K. M., Landi, E. & Keenan, F. P. 2010, *A&A*, 518, A41
Pitz, G. A., Fox, C. D. & Perram, G. P. 2010, *PhRvA*, 82, 042502
Popović, L. Č. and Dimitrijević, M. S. (eds.) 2009, Proc. 7th Serbian Conf. *Spectral Line Shapes in Astrophysics, New Astron. Rev.*, 53, 107
Povey, C., Predoi-Cross, A. & Hurtmans, D. R. 2011, *JMoSp*, 268, 177
Predoi-Cross, A., Liu, W., Murphy, R., *et al.* 2010, *JQSRT*, 111, 1065
Ptashnik, I. V. & Smith, K. M. 2010, *JQSRT*, 111, 1317
Rajvanshi, J. S. & Baluja, K. L. 2010, *PhRvA*, 82, 062710
Rajvanshi, J. S. & Baluja, K. L. 2011, *PhRvA*, 84, 042711
Reggami, L., Bouledroua, M., Allouche, A. R. & Aubert-Frécon, M. 2009, *JQSRT*, 110, 72

Ren, X., Bray, I., Fursa, D. V., *et al.* 2011, *PhRvA*, 83, 052711
Rixon, G., Dubernet, M. L., Piskunov, N., *et al.* 2011, *AIP-CP*, 1344, 107
Roos, J. B., Larson, Å. & Orel, A. E. 2008, *PhRvA*, 78, 022508
Roos, J. B., Orel, A. E., & Larson, Å. 2009, *PhRvA*, 79, 062510
Rosato, J., Marandet, Y., Capes, H., *et al.* 2009, *PhRvE*, 79, 046408
Rosato, J., Boland, D., Difallah, M., *et al.* 2010, *Int. J. Spectrosc.*, 374372
Rosenberry, M. A. & Stewart B. 2011, *JPhB: At. Mol. Opt. Phys.*, 44, 055207
Rothman, L. S., Gordon, I. E., Barbe, A., *et al.* 2009, *JQSRT*, 110, 533
Rothman, L. S., Gordon, I. E., Barbe, A., *et al.* 2010, *JQSRT*, 111, 2139
Rozsályi, E., Bene, E., Halász, G. J., *et al.* 2011, *PhRvA*, 83, 052713
Sabido, M, de Andrés, J., Sogas, J., *et al.* 2008, *EuPhJD*, 47, 63
Sagawa, H., Mendrok, J., Seta, T., *et al.* 2009, *JQSRT*, 110, 2027
Sahal-Bréchot, S. 2010, *JP-CS*, 257, 2037
Samanta, R. & Purkait, M. 2011, *EuPhJD*, 64, 311
Samanta, R., Purkait, M. & Mandal, C. R. 2011, *PhRvA*, 83, 032706
Santos, A. C. F., Sigaud, G. M., Melo, W. S., *et al.* 2010, *PhRvA*, 82, 012704
Sato, T. O., Mizoguchi, A., Mendrok, J., *et al.* 2010, *JQSRT*, 111, 821
Schmidt, E. W., Schippers, S., Bernhardt, D., *et al.* 2008, *A&A*, 492, 265
Schöffler, M. S., Titze, J., Schmidt, Ph. H., *et al.* 2009, *PhRvA*, 79, 064701
Shafir, D., Novotny, S., Buhr, H., *et al.* 2009, *PRL*, 102, 223202
Smith, M. A. H., Benner, D. C., Predoi-Cross, A. & Devi, V. M. 2009, *JQSRT*, 110, 639
Smith, M. A. H., Benner, D. C., Predoi-Cross, A. & Devi, V. M. 2010, *JQSRT*, 111, 1152
Smith, M. A. H., Benner, D. C., Predoi-Cross, A. & Devi, V. M. 2011, *JQSRT*, 112, 952
Stäuber, P. & Bruderer, S. 2009, *A&A*, 505, 195
Stéhle, C. & Fouquet, S. 2010, *Int. J. Spectrosc.*, 506346
Stenrup, M., Larson, Å. & Elander, N. 2009, *PhRvA*, 79, 012713
Sterling, N. C. & Witthoeft, M. C. 2011, *A&A*, 529, A147
Stolterfoht, N., Cabrera-Trujillo, R., Krstić, P. S., *et al.* 2010, *PhRvA*, 81, 052704
Storey, P. J. & Zeippen, C. J. 2010, *A&A*, 511, A78
Stroe, M. & Fifirig, M. 2011, *EuPhJD*, 61, 63
Szmytkowski, C., Domaracka, A. Możejko, P. & Ptasińska-Denga, E. 2008, *JPhB: At. Mol. Opt. Phys.*, 41, 065204
Takagi, H., Hara, S. & Sato, H. 2009, *PhRvA*, 79, 012715
Talbi, F., Bouledroua, M. & Alioua, K. 2008, *EuPhJD*, 50, 141
Tapalaga, I., Dojčinović, I. P. & Purić, J. 2011, *MNRAS*, 415, 503
Tarana, M. & Tennyson, J. 2008, *JPhB: At. Mol. Opt. Phys.*, 41, 205204
Tayal, S. S. & Zatsarinny, O. 2010, *A&A*, 510, A79
Thibault, F., Fuller, E. P., Grabow, K. A., *et al.* 2009, *JMoSp*, 256, 17
Thibault, F., Ivanov, S. V., Buzykin, O. G., *et al.* 2011a, *JQSRT*, 112, 1429
Thibault, F., Martinez, R. Z., Bermejo, D. & Goméz, L. 2011b, *JQSRT*, 112, 2542
Tran, H., Boulet, C., Stefani, S., *et al.* 2011a, *JQSRT*, 112, 925
Tran, H., Thibault, F. & Hartmann, J.-M. 2011b, *JQSRT*, 112, 1035
Tran, H., Picquet-Varrault, B., Boursier, C., *et al.* 2011c, *JQSRT*, 112, 2287
Tremblay, P.-E., & Bergeron, P. 2009, *ApJ*, 696, 1755
Vadla, C., Horvatic, V. & Niemax, K. 2009, *PhRvA*, 80, 052506
Vangvichith, M., Tran, H. & Hartmann, J.-M. 2009, *JQSRT*, 110, 2212
Vinodkumar, M., Limbachiya, C., Joshipura, K. N., *et al.* 2008, *JP-CS*, 115, 012013
Voronin, B. A., Lavrentieva, N. N., Mishina, T. P., *et al.* 2010, *JQSRT*, 111, 2308
Wang, Y. C., Zhou, Y., Cheng, Y. & Ma, J. 2009, *Chin. Phys. Lett.*, 26, 083401
Wang, Y. C., Zhou, Y., Cheng, Y., *et al.* 2010, *JPhB: At. Mol. Opt. Phys.*, 43, 045201
Wiesenfeld, L. & Faure, A. 2010, *PhRvA*, 82, 040702(R)
Winter, T. G. 2009, *PhRvA*, 80, 032701
Wójtewicz, S., Lisak, D., Cygan, A., it et al. 2011, *PhRvA*, 84, 032511
Wu, Y., Qi, Y. Y., Zou, S. Y., *et al.* 2009, *PhRvA*, 79, 062711

Wu, Y., Qi, Y. Y., Yan, J., *et al.* 2009, *PhRvA*, 80, 022715
Yang, C., Buldyreva, J., Gordon, I. E., *et al.* 2008 *JQSRT*, 109, 2857
Zameroski, N. D., Hager, G. D., Rudolph, W., *et al.* 2011, *JQSRT*, 112, 59
Zapukhlyak, M. & Kirchner, T. 2009, *PhRvA*, 80, 062705
Zatsarinny, O., Bartschat, K., Gedeon, S., *et al.* 2009, *PhRvA*, 79, 052709
Zatsarinny, O., Bartschat, K., Garcia, G., *et al.* 2011, *PhRvA*, 83, 042702
Zhang, S. B., Wang, J. G. & Janev, R. K. 2010, *PhRvA*, 81, 032707
Zhang, S. B., Wang, J. G., Janev, R. K. & Chen, X. J. 2011, *PhRvA*, 83, 032724
Zielinska, S., Pellerin, S., Dzierzega, K., *et al.* 2010, *JPhD: Appl. Phys.*, 43, 434005
Zmerli, B., Ben Nessib, N., Dimitrijević, M. S. & Sahal-Bréchot, S. 2010, *Phys. Scr.*, 82, 055301

Astronomy in Serbia

Milan S. Dimitrijević
Astronomical Observatory, Volgina 7,11050 Belgrade, Yugoslavia
mdimitrijevic@aob.bg.ac.yu

Abstract

A review of professional and amateur astronomy in Serbia is given.

1 Belgrade Astronomical Observatory

The principal astronomical institution in Serbia is the Belgrade Astronomical Observatory, one of the oldest scientific organizations and the only autonomous astronomical institute in Yugoslavia. Its past development forms an important part of the history of science and culture in these regions. The decree of its founding conjointly with the Meteorological Observatory was signed on 20 March (7 April) 1887 by the Minister of Education and Church Affaires of Kingdom of Serbia Milan Kujundžić on the initiative of Milan Nedeljković (Belgrade 27. Sept. 1857 - Belgrade 27 Dec. 1950), a professor of the Grand School (Belgrade University). Nedeljković was appointed first director of the newly founded Observatory.

On 1 May 1871 Nedeljković started his activity at the provisory Observatory in the rented Geizler family's house. Here the Observatory was operating until 1 May 1891, when it was moved into its own building constructed meanwhile - the one in which at present is Meteorological Observatory in the Karadjordje Park. In the minor museum section of this building there is, since the celebration of the Observatory's centenary in 1987, a room dedicated to the origins of astronomical science in Yugoslavia.

Nedeljković was at the head of the Observatory from 26 March (7 April) 1887 until 30 January 1924. A break took place only between 5 July 1899 and 31 October 1900, when he was sent into retirement for political reasons, in connection with the Ivanjdan attempt on King Milan, which was exploited by King Alexander for settling accounts with his political opponents. Nedeljković's place was filled during this period by Djordje Stanojević (Negotin, 7 April 1858 - Paris 24 Dec. 1921), the first Serbian astrophysicist, later on the rector of Belgrade University. Dj. Stanojević was a great popularizer of astronomy and science in general; he was the driving force in the introduction of electrical light in Belgrade, Užice, Čačak, Leskovac... He was the builder of the first hydroelectric power station in Serbia, a pioneer of industry of refrigerating appliances, the initiator of setting up a committee for cooling problems and of forming an international organization for cooling technique in Paris in 1903. He was also the pioneer of the color photography in Serbia.

Apart from its importance for astronomy and meteorology, the newly built Observatory, headed by Nedeljković, was a cradle of the seismic and geomagnetic researches in Serbia. Nedeljković borrowed the instruments for geomagnetic measurements from Tege Miklosh Konkoly, the founder of the Budapest Astronomical Observatory, and took care of building an earth-magnetism pavilion. Thanks to Konkoly, Nedeljković acquired in 1903 also a seismograph, installed next year in a special pavilion. The observations were carried out regularly and for these purposes the construction of what at present is the Seismological Institute was executed in 1906. This activity was taken over by Nedeljković's assistant Jelenko Mihailović (Vrbica, 11 Jan. 1869 - Belgrade 10 Oct. 1958) who worked at the Observatory since 1896.

During the Austro-Hungarian occupation of Serbia in World War I, the Observatory was administered by Victor Konrad from Vienna. During their flight from Serbia the Austrians took away or destroyed all the instruments. However, thanks to his extraordinary and professional skill Nedeljković contrived to acquire in Germany after the war, on account of war reparations, a number of instruments appertaining equipment for the new Observatory.

The instruments procured by Nedeljković constitute still practically the only observing basis of the Observatory, although some of them were taken away by the Germans during the World War II, two were ceded to each Ljubljana and Zagreb Universities (Djurković 1968), some of the smaller ones being left unmounted.

Currently mounted in appropriate pavilions are the following instruments procured by Nedeljković:

1. Large Refractor - ZEISS 650/10550mm equatorial;
2. Solar spectrograph (monochromatic) LITTROW, 9000 mm/100.000 developed by adapting to the ZEISS 200/3020 mm equatorial two astro cameras TESSAR and PETZVAL 160/800 mm;
3. Large Transit Instrument ASKANIA 190/2578 mm;
4. Large Vertical Circle ASKANIA 190/2578 mm;
5. Astrograph ZEISS 160/800 mm;
6. Photovisual Refractor ZEISS 135/1000 mm and 125/1000 mm;
7. Transit Instrument BAMBERG 100/1000 mm;
8. Zenith-telescope ASKANIA 110/1287 mm;

Large Meridian Circle ASKANIA 190/2578 mm burnt up on 11th of May 1999 during NATO air attack.

As Nedeljković was struggling for the new Observatory at which the acquired instruments were to be mounted and regular astronomical observations started, he suddenly was sent into retirement on 30 Jan. 1924. By ruling of the Faculty Council the Observatory was divided into two separate institutions: Astronomical Observatory and Meteorological Observatory of Belgrade University.

At the head of the Astronomical Observatory was appointed in 1925 Vojislav V. Mišković (Fužine 18 Jan. 1892 - Belgrade 25 Nov. 1976), at the time already

a well established astronomer engaged at Nice Observatory, France. He began his astronomical studies in Budapest and Göttingen before the World War I. On his demobilization at the end of 1918 from the Serbian Army, in which he served as a volunteer, he was sent to France to complete his studies. He graduated in 1919 and was appointed assistant at the Marseille Observatory. Since 1922 he was engaged as an astronomer at the Nice Observatory, receiving his doctor's degree in 1924 at the Montpellier University. In 1925 he won French Academy Prize for his studies in stellar statistics. In the period 1919-1925 he published a score of papers in the French scientific journals, treating the observation of the minor planets and comets and the determination of their orbits. He came to Belgrade in 1926 taking, in addition to the Astronomical Observatory, charge of the newly established Chair of Theoretical and Practical Astronomy at the Faculty of Philosophy, whereat he was elected associated professor. In 1929 he was elected corresponding member of the Serbian Royal Academy and in 1939 its full member. He directed the Observatory's activity to a considerable degree toward mathematical and numerical works, which yielded valuable results. Of importance are numerical works connected with the Mathematical Climatology of M. Milanković as well as with Mišković's own Precession Tables.

In 1929 Mišković succeeded in getting funds for the constructions of a new, modern, observatory, at 6 km distance southeast from the city's centre, occupying a 4.5 ha area at 253 m high hill Veliki Vračar, named since, along with the entire surrounding part of Belgrade, Zvezdara (=concerned with stars).

Exceptional and highly valued complex constituting the Astronomical Observatory was drawn up by Jan Dubovi, a member of GAMP (Group of Modern Outlook Architects) founded in 1928. It is thanks to this very achievement that Dubovi was conferred a doctor of science degree in Prague. The construction works were carried out in 1930 to 1932, the instruments being mounted during the following two years.

Mišković started also publishing the scientific periodical Mémoires de l'Obs. Astr. Belgrade (issued five volumes for: 1932, 1933, 1936, 1938 and 1949), Annuaire de l'Obs. Astr. Belgrade (six volumes for 1929 through 1934) containing sidereal time, short-period nutation terms, the mean and apparent places of 189 stars, newly discovered minor planets and directions for use. Nautički godišnjak (Nautical Almanac) for years 1934 through 1941) for navigation purposes in the Navy and Godišnjak Našeg Neba (Almanac of our Sky) an astronomical calendar in Serbian, issued in the years 1930 to 1941 and 1948 to 1952 (the 1948 issue was edited by F. Dominko and the issues for 1949, 1950 and 1951 by B. Popović.

In 1936 Mišković, assisted by Milorad Protić, organized the Minor Planets and Sun Observation Service. In the same year P. Djurković discovered at the Uccle Observatory, Belgium, a minor planet, subsequently named 1605 Milanković and M. Protić, at the Belgrade Observatory, discovered the minor planet 1564 Serbia, which marked the opening of a long series of 43 minor planets discovered by the Belgrade astronomers. Protić alone, in the period 1936-1956, made 33 discoveries. Of the 43 minor planets owing their discovery to Belgrade astronomers, 12 have obtained by the IAU permanent names, three of the discoveries having later been ascribed to other authors.

Besides Serbia, using his author's right, Protić gave the following names to the minor planets he discovered: 1507 Beograd, 1550 Tito, 1554 Yugoslavia, 1675 Simonida, 1724 Vladimir (after his grandson), 2244 Tesla and 2348 Mišković. P. Djurković discovered in the period 1936-1941, 5 minor planets, one of them - Zvezdara- named by him using his discover's prerogative. In 1980 Z. Knežević discovered on the photo-plates taken according to his instructions at Piszkesteto Observatory, Hungary, four minor planets, one of which having obtained the name 3276 Paolicchi, after one of his colleagues in Italy. In 1991, as a mark of honour, a minor planet was given the name 3900 Knežević - after our fellow. Another minor planet connected with the Belgrade Observatory is that named 1555 Dejan, after P. Djurković's son.

In 1936 Mišković started issuing Bulletin de l'Observatoire astronomique de Belgrade, a scientific periodical which from No. 145 for 1992 on appears under the name Bulletin astronomique de Belgrade, and from the number 157 for 1998 under the name Serbian astronomical Journal. This periodical's editors have been: V. V. Mišković (1936-1940, 1943 – 1948 and 1952-1956), M. Protić (1941-1942, 1955-1960 and 1971-1975), B. Popović (1950), V. Oskanjan (1964), P. Djurković (1964-1970), M. Mijatov (Nos. 127-131 in 1976-1981), D. Zulević (Nos. 132-133, in 1982-1983), Dj. Teleki (Nos. 134-136 in 1984-1986) and M. S. Dimitrijević (No. 137 in 1987 successively up to date).

Since July 1941 at the Observatory were quartered German military. The Wehrmacht brought along profs. Grotrian and Kippenheur from Potsdam, the two having inscribed the Observatory's instruments as German property, dispatching to Germany the spectroheliograph and the comet searcher. On the terraces of the Observaroty's edifice and on the water storage building pillboxes were erected for directing the flak, while the library was turned into officers mess. In the course of the liberation fightings in 1944 particularly heavy damages were inflicted on the main edifice, the water storage building and on "Large Refractor" pavilion. The Observatory's reconstruction was undertaken immediately after the war. Mišković remained its director until March 1946 when he submitted his resignation, accepted not before May 1948.

In 1945 P. Djurković started and edited the professional periodical Astonomska i Meteorološka Saopštenja (Astronomical and Meteorological Reports), published by the Observatory up to 1950 (seven issues in all). In 1947 Observatory started the series Publikacije Astronomske Opservatorije u Beogradu (Publications of Astronomical Observatory). Its editors in chief were: V. Oskanjan (No. 10), P. Djurković (Nos. 12-16), M. Protić (Nos. 17-19, 20-21) Dj. Teleki (Nos. 20, 26, 32, 34 and 35), M. Mijatov (Nos. 24, 25, 27-31), G. Popović (No. 33) and M. S. Dimitrijević (Nos. 36-69).

Up to 1 July the Observatory was, as it was before the war, under the Belgrade University. From that date on, up to 18 Dec. 1950. it is under the jurisdiction of the Serbian Academy of Sciences and thereafter, under the Committee for Scientific Institutions, University and Schools for Higher Education of SR Serbia. This status was kept until 27 March 1954, when the Observatory became institution with independent financing at the Executive Council of SR Serbia. On 9 Aug. 1985 the Observatory obtained the status of autonomous scientific research institute with the Executive Council of the Assembly of SR

Serbia as its founder, its name changed into Astronomical Observatory - Institute for Astronomical Researches. At the time it was financed by the Republic Community of Sciences of SR Serbia. After Community's dissolution it is being financed by the Republic Fund for Science of Serbia through the scientific project "Physics and Motion of Celestial Bodies and Artificial Earth's Satellites" (1985-1990). Leading the Project were: Dj. Teleki (1985-1987), A. Kubičela (1987-1989) and M. Dimitrijević (1990). In the period 1991-1995 the Project is named "Physics and Motion of Celestial Bodies" and was led by M. Dimitrijević (1991-1993) and Z. Knežević (1993-1996). For the period 1996-2000 the project is named "Astronomical, Astrodynamical and Astrophysical Researches", being led by Z. Knežević. The Time and Latitude Services are financed directly from the budget of SR Serbia. On 12 May 1992 the Observatory became a scientific institute financed through the mentioned scientific project at the Republic Ministry for Science and Technology, its founder being the Government of Republic Serbia. On 20 Dec. 1994 the Observatory was re-registrated as a scientific institute, resuming its old name.

When in May 1948 V. Mišković's resignation was accepted, to the post of Observatory's director was appointed academician Milutin Milanković (Dalj 28 May 1879 - Belgrade 12 Dec. 1958) who went down in history of science by his having explained the ice ages phenomenon through the slow changes in the Earth's insolation in consequence of the Earth's axis inclination and its motion around Sun, undergoing changes produced by various influences. Milanković elucidated also the history of the climate of Earth and other planets, being the originator of the mathematical theory of the Earth's poles motion. The Observatory's direction was entrusted to the Observatory's Council, at the head of which was the director and Council's president M. Milanković, with members Anton Bilimović, V. Mišković and Pavle Savić (Popović 1951). Milanković held this post till 26 June 1951.

In 1951 P. Djurković organized the Double Star Service. Within this Service, subsequently named Group, were discovered over 200 new double and multiple stars, the bulk of the which is due to Georgije Popović, working in this Group since 1960, being at its head since 1976.

In this same year the Variable Stars Service was organized by Vasilije Oskanjan. In this he was joined by Alexander Kubičela and Jelisaveta Arsenijević (at the Obsevatory since 1956) whereby an impetuous development of the astrophysical researches took place later directed toward stellar and solar physics and astronomical spectroscopy. Initially it was the photometry of eruptive stars which was pursued. Since 1959, after Oskanjan's return from his specialization in the Soviet Union, it was the work in the field of polarimetry of eruptive stars that was taken up. Formally, the Astrophysical Group was founded in 1960. In 1969 and 1970 working in the Group was Trajče Angelov. In 1972 the Group was joined by Ištvan Vince, in 1980 by Gojko Djurašević, in 1983 by Slobodan Jankov, in 1984 by Milan Dimitrijević, in 1985 - 1996 by Vladimir Kršljanin, in 1989-1996 by Olga Atanacković-Vukmanović (at the Observatory since 1982 first in the Absolute Declinations Group), in 1991 by Sanja Erkapić and Snežana Marković, in 1992 by Luka Popović, in 1994 by Darko Jevremović and in 1995 by Silvana Nikolic. Since 15 February 1997 the Group was joined

by Milan Ćirković, since 1st January of 1998 by Dragana Tankosić and Nataša Trajković (since 14 November 1998 Nataša Stanić), since 15 April 1998 up to 1 November 1999 by Desanka Šulić, since 1 January 1999 by Edi Bon, since 20 January 1999 by Nenad Milovanović and since 1 December 1999 by Oliver Vince.

From 26 June 1951 to March 1954 the Observatory's director is again V. Mišković. After he went into retirement the Observatory was headed by M. Protić in the capacity of deputy director and from 21 Nov. 1956 to 21 Nov. 1960 as a director.

After M. Protić at the head of the Observatory was Vasilije Oskanjan, first as acting director since 1960, then in 1964-1965 as the director. Following him, from July 1965 to 1970, the director was Pero Djurković. After him in the period 1971-1975 at the head of Observatory is again M. Protić. Since 1975, first as acting director and from 13 July 1977 to Sept 1981 as the director was M. Mijatov (Belgrade 3 July 1933 - Belgrade 19 Nov 1996). The director's post from 1982 to 1989 was held by Miodrag Mitrović, in 1990-1993 by Ištvan Vince and from 21 Nov 1994 on, by Milan Dimitrijević.

In 1986, on the part of the Assembly of SR Serbia and Republic Executive Council, the project was adopted and funds allocated for the building of an astrophysical observing station at Rgaj mountain near Prokuplje. Due to the investments in the Republic having meanwhile been suspended, the project has not been realized yet.

In 1987, in the presence of a number of statesmen and eminent guests from the country and abroad, the centenary of the Observatory's founding was solemnly celebrated in the hall of the Assembly of Serbia. On the occasion of this jubilee three international and one Yugoslav scientific conferences were held: IAU Colloquium 100 "Fundamental Astrometry" (8-11 Nov. - Chairman SOC H. Eichorn, Gainsville, USA), International Symposium on Astronomical Refraction in memory of Dj. Teleki, former President of IAU Working Group on Astronomical Refraction (3-4 Nov., Chairman SOC V. Milovanović), Second International Symposium on Catastrophic Collisions of the Small Sollar System Bodies (8-11 Nov., Chairman SOC V. Zappala, Italy) and Second Workshop "Astrophysics in Yugoslavia" (8-10 Nov Chairman SOC M. Dimitrijević). During these festivities a minor museum was opened in the old Observatory's building in Karadjordje Park, one of its rooms being dedicated to the development of the Astronomical Observatory.

In 1994 there took place a reorganization of the Observatory's inner structure, resulting in the establishment of : Department of Astrophysics, Department of Dynamical Astronomy and Department of Astrometry. Since 15 February 1997, Department of Astrometry was joined by Nataša Popović and since 20 May 1998 by Predrag Jovanović (working since 1 January 1996 in Time keeping and geographic coordinates determination service).

In 1995 the Observatory participated in the organization of the International Russian - Yugoslav Conference "Newcomb and Fundamental Astrometry" in St. Petersburg, of the First Hungarian-Yugoslav Conference in Baja and the First Romanian-Yugoslav Round Table on collaboration in astronomy in Temishoara; it organized the First Yugoslav Conference on Spectral Line Shapes in Krivaja.

In 1996 the Observatory organized the Second Yugoslav-Romanian Round Table on collaboration in astronomy in Belgrade and the Astrophysics Section at the 18th Summer School and International Symposium on the Physics and Ionized Gases in Kotor. The Observatory participated in the organization of the First Belaruss-Yugoslav Conference on Physics and Dynamics of Laboratory and Astrophysical Plasma in Minsk. The Observatory's fellows presented their results at 13 international and 6 national conferences. They published 129 bibliographic items of which 16 in the international leading journals. It published 4 volumes of Publ. Astron. Obs. Belgrade and 2 Nos. of its periodical Bull. Aston. Belgrade.

In 1997 the Observatory organized in the framework of celebration of its 110th anniversary the scientific conference "Development of Astronomy among Serbs". It took part also in the organization of the Third Romanian-Yugoslav Round Table on Cooperation in Astronomy in Kluj-Napoca, as well as in the Second Yugoslav Conference on Spectral Line Shapes in Bela Crkva. It fellows presented their results at 13 international and 4 national conferences. They published 152 bibliographic items, 11 of which in international journals of the highest standing.

During 1998, 154 bibliographic items have been published, with 19 among them in international scientific journals of the highest standing. Five invited lectures and progress reports have been given by fellows of Observatory at international conferences and one at national one. Four reviews and monographic texts in national publications have been published. Observatory's fellows have participated in works of 16 Scientific conferences abroad (28 participations by 19 fellows) and six conferences in Yugoslavia (61 participation by 28 fellows). Organized by the Observatory were IV Yugoslav - Romanian Astronomical Meeting, Belgrade, 5-8.05.1998; I Bulgarian - Serbian Astronomical Seminar, Belogradchik, 6-7.08 1998 and II Yugoslav - Belarussian Symposium on Physics and Diagnostics of Laboratory and Astrophysical Plasmas, Zlatibor, 5-6.09.1998. It issued four publications of the series Publ. Astron. Obs. Belgrade and two Nos. of its periodical Bull. Astron. Belgrade. As from 1998 Astronomical Observatory has an internet connection available from each personal computer on Observatory with Windows 95 installed.

During 1999, in spite of NATO air attacks on Yugoslavia and the destruction of the Big meridian circle, 112 bibliographic items have been published, 23 among them in international scientific journals of the highest standing. Six invited lectures have been given by Observatory's fellows at international conferences and five at national ones. Moreover, two Ph. D and one M. Sc Thesis have been published. Numbers 159 and 160 of the Observatory's publication Serbian Astronomical Journal, as well as Nos. 63, 64, 65 and 66 of the Publications of the Astronomical Observatory of Belgrade have been issued. These publications are regularly sent to 136 institutions and libraries in 45 countries and to 15 institutions and libraries within Yugoslavia. Observatory's fellows have participated in works of 8 scientific conferences abroad (9 participations by 6 fellows) and three conferences in Yugoslavia (35 participation by 22 fellows).

During 1999, Belgrade observatory organized or took part in the organi-

zation of the following conferences: III Yugoslav Conference on Spectral Line Shapes, Brankovac (Fruška gora), 4-6.10.1999; XII National Conference of Yugoslav Astronomers and International Workshop on the Development of Astronomical Databases, Belgrade, 19-21.11. 1999 and Symposium Milanković - juče, danas, sutra (Symposium Milanković - yesterday, today, tomorrow), Belgrade, 25-26.11. 1999.

Besides numerous newspaper articles and radio and TV emissions Observatory's fellows authored, explaining particularly the 11th August 1999 total Solar eclipse, they gave 48 lectures on astronomical subjects outside our institution contributing to the cultural life in our country. Moreover 4 lectures have been given at the Astronomical Observatory itself.

I note as well that Serbian Astronomical Journal is available on www through the Astrophysical Data System (ADS), thanks to the courtesy of the System's holders. The www address is: http://adswww.harvard.edu.BOBeo. During 1999, the web site of the Belgrade astronomical observatory has been made and the corresponding www address is: http://www.aob.bg.ac.yu. Moreover the database BELDATA has started to develop and it is available through internet with the address: http://www.aob.bg.ac.yu/BELDATA.

Currently there are 40 employees at the Observatory 32 of them are astronomers.

In the course of its history the Belgrade Astronomical Observatory grew to an institution of great importance in the history of science and culture of the Serbian people, not only in the field of astronomy but also in meteorology, seismology and geomagnetics. Linked to this institution are the names of the famous personalities in the history of science who contributed to the Observatory, and the scientific achievements of Serbian astronomers in general, having earned esteem in the international scientific community as well as to the young having a good perspective, in our country too, in engaging in this beautiful and challenging science, in an ambience enabling them to achieve results of the highest value.

2 University teaching of astronomy in Serbia after the Second world war

Beside Astronomical Observatory, there is in Belgrade also the Chair of Astronomy at the Faculty of Mathematics. As the Faculty of Sciences separated from the Philosophical Faculty in 1947, the Chair of Celestial Mechanics and Astronomy was formed, having shortly thereafter changed its name into Chair of Mechanics and Astronomy. The splitting up of this Chair into the Chair of Mechanics and the Chair of Astronomy began in 1960, being completed in 1962. The reorganization of the Faculty of Sciences in 1971 entailed the Chair of Astronomy becoming the Institute of Astronomy. In 1995 there took place the division of the Faculty of Sciences into several faculties. As the Faculty of Mathematics there remained the Chair of Astronomy which re-took, in the new organization, its old name.

In 1961 two study groups were formed - one for Astronomy, the other for

Astrophysics. Currently, there are at the Chair of Astronomy 12 full time astronomers and one engaged at one third-time basis, teaching fifteen subjects. The names of the Chair's fellows, the subjects they are lecturing on, as well as their electronic addresses are given in Appendix.

Beside Belgrade, Astronomy is taught at University in Novi Sad, Niš and Kragujevac. At the Faculty of Sciences of the Novi Sad University there is, since 1986, in 8th semester, the subject "Astrophysics and Astronomy", involving twice a week lectures and twice a week exercises. The subject is obligatory for students wishing to teach Physics in the secondary schools while being optional for students of Applied Physics.

At the Faculty of Philosophy of the Niš University in the study group for Physics, within the specialized training in General Physics, since the school year 1990/91 until 1993/94 there was taught twice a week in the 7th and 8th semesters, the subject Fundamentals of Astrophysics. The subject was thereafter dropped for two years from the curriculum, to be again taught within the 7th semester twice a week. In addition, there is in the study group for chemistry a Chair for Geo- and Cosmochemistry, occupying itself with the study of meteors and meteorites.

At the Faculty of Sciences of the Kragujevac University there has been introduced in the school year 1998/99 the subject Astrophysics and Astronomy in the 6th semester of the specialized training of the Group for Physics, with twice a week teaching and twice a week exercises.

3 Amateur astronomical societies

In addition to professional Astronomy, well developed in Serbia is also the amateur Astronomy. The largest and the oldest organization of amateur-astronomers is the Astronomical Society "Rudjer Bošković" in Belgrade (Kalemegdan, Gornji Grad 16, 11000 Belgrade), which in the course of 65 years of its existence was spreading astronomical knowledge in our country. The founding meeting was held on 22 April 1934. The first Society's President was Djordje Nikolić (1934-1936) and the second Vojin Djuričić (1936-1941), the governor of the State Mortgage Bank.

After the War, on 9 December 1951 was held the founding meeting of the Belgrade Astronomical Club "Rudjer Bošković" (as component part of the Association of students of the Natural-Mathematical Faculty (PMF)), Dr Radovan Danić being elect its President. Considering that already in 1952 there were in the Club 64 members, the majority of whom were not associated with the PMF, the Club Administrative Committee took decision on 23 March 1952, the Club to be re-registered into Astronomical Society "Rudjer Bošković". The founding meeting of the Society was held on 18 May 1952, Radovan Danić having been elected its President (1952-1966). Following him the Society' Presidents have been: Branislav Ševarlić (1966-1970), Pero Djurković (1970-1972), Nenad Janković (1972-1974), Božidar Popović (1974-1979), Zoran Knežević (1979-1982) and Milan S. Dimitrijević (1982-).

In 1953 the Society, jointly with the Aeronautical Association of Yugoslavia,

started publishing the periodical for astronomy and aeronautics (currently for astronomy) "Vasiona" (Universe). The periodical's editors in chief were: Nenad Dj. Janković (1953-1972), Pero Djurković (1973-1974), Jelena Milogradov-Turin (1975-1982), Branislav Ševarlić (1983-1984) and Milan S. Dimitrijević (1985-).

Thanks to the exertion of Pero Djurković and Radovan Danić with the authorities concerned, the Society obtained for itself the permises? in the Despot Tower at Kalemegdan where, on 20 December 1964 was solemnly opened the People's Observatory, whose regular activity started in June 1965. The Society managed also to procure a Zeiss planetarium, which was installed in an old spacious steam bath-house - Turkish Hamam - in the Kalemegdan Donji Grad. The Planetarium started operating in 1969, being formally opened on 17 February 1970.

The founding meeting of the Astronomical Society "Novi Sad", ADNOS (Jaroslav Francisti, Astronomska Opservatorija, Petrovaradinska tvrdjava, 21000 Novi Sad), took place on 4 March 1974. In 1976 the Society bought telescopes 20T Observatory 108/1600 mm and 10K 80/1200 mm and 14T 60/900 mm, of the American firm TASCO, and in 1991 purchased the reflector type telescopes Meade 200/1500 mm and 102/1000 mm. In 1989 the adaptation of the Astronomical Observatory at the Petrovaradin Fortress was completed while in 1996 the premises for the planetarium were secured and its adaptation is now finished. The Society's President in the period 1974-1980 was Živojin Ćulum, in the period 1980-1984 Božidar Jovanović, 1984-1998 Djura Paunić, from 1998 - up to 1 September 2000 Svetislav Krstić, and from 1 September 2000 the President is Dragoslav Petrović.

At Petnica near Valjevo the organization of the Young Researchers of Serbia is building the House of Young Researchers. This institution, initially of a recreative character, became the Research Station Petnica (Istraživačka stanica Petnica, Petnica, 14000 Valjevo). The first programmes were carried out in 1982, the first seminar in Astronomy in 1983 in preparation for going out for Rgaj Mountain, where astroclimatic explorations were conducted. In 1968 was obtained a Celestron telescope of Schmidt-Cassegrain type, objective diameter 20 cm. Later on were purchased Celestron, opening 102 cm, as well as a reflector of 33 cm opening, manufactured by Aljoša Jovanović. The heads of the seminar were Darko Jevremović, Silvana Nikolić, Samir Salim and Nikola Božinović, the duty being currently discharged by Oliver Vince.

In Valjevo, within the framework of the Society of researchers "Vladimir Mandić - Manda", founded on 16 February 1969, there is active also the Astronomical Group founded in 1972 (Nikola Božić, Birčaninova 68, p. fah 118, 14000 Valjevo).

In Kragujevac, on the roof of the Institute of Physics of the Faculty of Sciences, there is the Belerofont Observatory (Vukota Babović, Institut za fiziku PMF, Sestre Janjić 4, Kragujevac), opened on 20 February 1986. It disposes of a telescope Meniscus Cassegrain Spiegel 130/2250 mm.

In Niš, at the close of the sixties and the start of the seventies, there was operating a branch of the Astronomical Society "Rudjer Bošković, while at the Faculty of Philosophy there existed in the period 1876-1980 the "Astro-

Geophysical Society". In the year 1996 there was founded Astronomical Society "Alpha" (Dragan Ž. Gajić, Filozofski fakultet, Studijska grupa za Fiziku, p. fah 91, 18001 Niš). The first Society's President was Zoran Sekulić, while from March 1997 on, the President is Dragan Ž. Gajić.

In 1996 Zrenjanin too got an organization of amateur astronomers, Astronomical Society "Milutin Milanković" (Miša Bradić, Zrenjaninska gimnazija, Gimnazijska 2, 23000 Zrenjanin).

The amateur astronomers societies greatly contributed to the spreading of astronomical knowledge in our midst and to keeping step with the latest astronomical achievements and discoveries, the creating a more suitable climate for the development of Astronomy in Serbia.

References

[1] Babović Vukota: 1997, Multidisciplinarnost u razvoju Belerofonta, u Razvoj astronomije kod Srba, eds. M. S. Dimitrijević, J. Milogradov-Turin, L.Č. Popović, Publ. Astron. Obs. Belgrade, **56**, 95.

[2] Dimitrijević Milan S.: 1996, Beogradska Astronomska opservatorija u 1995, Belgrade Astronomical observatory in 1995, Publ. Obs. Astron. Belgrade, **52**.

[3] Dimitrijević Milan S.: 1997, 110 godina Astronomske opservatorije, u: Razvoj astronomije kod Srba, eds. M. S. Dimitrijević, J. Milogradov-Turin, L.Č. Popović, Publ. Astron. Obs. Belgrade, **56**, 9.

[4] Dimitrijević Milan S.: 1997, Beogradska Astronomska opservatorija u 1996, Belgrade Astronomical observatory in 1996, Publ. Astron. Obs. Belgrade, **55**.

[5] Dimitrijević Milan S.: 1998, Beogradska Astronomska opservatorija u 1997, Belgrade Astronomical observatory in 1997, Publ. Astron. Obs. Belgrade, **59**.

[6] Dimitrijević Milan S.: 1998, Belgrade Astronomical observatory, Proc. 4th Yugoslav-Romanian Astronomical Meeting, eds. M. S. Dimitrijević, L. Č. Popović, Publ. Astron. Obs. Belgrade, **60**, 162.

[7] Dimitrijević Milan S.: 1999, Beogradska Astronomska opservatorija u 1998, Belgrade Astronomical observatory in 1998, Publ. Astron. Obs. Belgrade, **63**.

[8] Dimitrijević Milan S.: 1998, Astronomija u Srbiji, Proc. I Bulgarian - Yugoslav Astronomical Meeting, eds. M. S. Dimitrijević, L. Č. Popović, M. Tsvetkov, Publ. Astron. Obs. Belgrade, **64**, 19.

[9] Djokić Milorad: 1989, Arhivska gradja o Opservatoriji Velike škole i Univerziteta u Beogradu u vremenu od 1887. do 1924. godine, u: Sto godina Astronomske opservatorije u Beogradu, Publ. Obs. Astron. Belgrade, **36**, 177.

[10] Djurković Pero: 1968, Sedamdeset pet godina rada Astronomske opservatorije u Beogradu, Publ. Obs. Astron. Belgrade, **12**, 15.

[11] Djurković P.: 1969, Rapport sur l'activité de l'Observatoire Astronomique de Belgrade de 1966 á 1969, Bull. Obs. Astron. Belgrade **XXII**, No 2, 143.

[12] Djurković P.: 1970, Rapport sur l'activité de l'Observatoire Astronomique de Belgrade en 1970, Bull. Obs. Astron. Belgrade **124**, 195.

[13] Francisti Jaroslav: 1997, Astronomsko društvo "Novi sad" - ADNOS, u Razvoj astronomije kod Srba, eds. M. S. Dimitrijević, J. Milogradov-Turin, L.Č. Popović, Publ. Astron. Obs. Belgrade, **56**, 91.

[14] Gajić Dragan Ž.: 1997, Astronomija i astrofizika na Univerzitetu u Nišu, u: Razvoj astronomije kod Srba, eds. M. S. Dimitrijević, J. Milogradov-Turin, L.Č. Popović, Publ. Astron. Obs. Belgrade, **56**, 109.

[15] Janković, Nenad Dj.: 1984, Zapisi i sećanja na Astronomsko društvo, Publ. Astron. Društva "Rudjer Bošković", No. 3.

[16] Janković Dj. Nenad: 1989, Milan Nedeljković, profesor Velike škole i osnivač njene Opservatorije, u: Sto godina Astronomske opservatorije u Beogradu, Publ. Obs. Astron. Belgrade, **36**, 107.

[17] Jeličić, Milan: 1984, Pedest godina Astronomskog društva "Rudjer Bošković", Vasiona, XXXII, No 1, 1.

[18] Michkovitch V.V.: 1930, Rapport annuel sur l'état et les travaux de l'Observatoire Astronomique de Belgrade pour l'année 1929, Annuaire pour l'an 1930, 125.

[19] Michkovitch V.V.: 1931, Rapport annuel sur l'état et les travaux de l'Observatoire Astronomique de Belgrade pour l'année 1930, Annuaire pour l'an 1931, 133.

[20] Michkovitch V.V.: 1932, Rapport annuel pour l'année 1931 sur l'état et les travaux de l'Observatoire Astronomique de l'Université de Belgrade, Mémoires I, 38.

[21] Michkovitch V.V.: 1941, Services et travaux d'observations en 1939 á l'Observatoire Astronomique de l'Université de Belgrade, Bull. Obs. Astron. Belgrade **V**, No 1-2, 1.

[22] Michkovitch V.V.: 1950, Services et travaux d'observations en 1940 á l'Observatoire Astronomique de l'Université de Belgrade, Bull. Obs. Astron. Belgrade **VI**, No 1-2, 1.

[23] Michkovitch V.V.: 1952, Rapport annuel présenté à l'Academie des sciences Serbe, sur l'état et l'activité de l'Observatoire en 1951, Bull. Obs. Astron. Belgrade **XVI**, No 1-4, 1.

[24] Milogradov - Turin J.: 1996, Astronomy education in FR Yugoslavia 1993 - 1996, Publ. Astron. Obs. Belgrade, **54**, 165.

[25] Milogradov - Turin J.: 1997, Jedan prilog istoriji Katedre za astronomiju Univerziteta u Beogradu, u Razvoj astronomije kod Srba, eds. M. S. Dimitrijević, J. Milogradov-Turin, L.Č. Popović, Publ. Astron. Obs. Belgrade, **56**, 65.

[26] Milogradov - Turin, J.: 1998, Chair of Astronomy of the University of Belgrade, Proc. 4th Yugoslav-Romanian Astronomical Meeting, eds. M. S. Dimitrijević, L. Č. Popović, Publ. Astron. Obs. Belgrade, **60**, 193.

[27] Milogradov - Turin, J.: 1999, Astronomy Education in FR Yugoslavia 1996 - 1999, Proc. XII Nat. Conf. Yug. Astronomers and Int. Workshop on the Development of Astronomical Databases, eds. L. Č. Popović, M. Dačić, Publ. Astron. Obs. Belgrade, **65**, 185.

[28] Naumovski Krste, Bradić Miša: 1997, Astronomsko društvo u Zrenjaninu, u: Razvoj astronomije kod Srba, eds. M. S. Dimitrijević, J. Milogradov-Turin, L.Č. Popović, Publ. Astron. Obs. Belgrade, **56**, 115.

[29] Nedeljković Milan: 1904, Izveštaj Opservatorije Velike škole i njenih meteoroloških stacija, 1899-1903, Državna štamparija, Beograd.

[30] Nedeljković Milan: 1905, Izveštaj Opservatorije i Meteoroloških stacija, 1904, Državna štamparija, Beograd.

[31] Nedeljković Milan: 1907, Izveštaj Opservatorije i Meteoroloških stacija, 1905-1906, Štamparija Davidović, Beograd.

[32] Nedeljković Milan: 1908, Izveštaj Opservatorije i Meteoroloških stacija, 1907, Državna štamparija, Beograd.

[33] Nedeljković Milan: 1909, Izveštaj Opservatorije i Meteoroloških stacija, 1908-1909, Državna štamparija, Beograd.

[34] Nedeljković Milan: 1910, Izveštaj Opservatorije i Meteoroloških stacija, 1910, Državna štamparija, Beograd.

[35] Nedeljković Milan: 1914, Izveštaj Opservatorije i Meteoroloških stacija, 1911-1912, Merkur, Beograd.

[36] Nedeljković Milan: 1923, Izveštaj Opservatorije, za 1919-1920, 1922 i 1923, Beogradska opservatorija, Beograd.

[37] Nedeljković Milan: 1925, Izveštaj Opservatorije, za 1924, Beogradska opservatorija, Beograd.

[38] Popović B.: 1950, Services et travaux d'observations en 1949 á l'Observatoire astronomique de l'Université de Belgrade, Bull. Obs. Astron. Belgrade **XIV- 1949**, VII.

[39] Popović B.: 1951, Rapport annuel sur l'état et l'activité de l'Observatoire astronomique de Belgrade en 1950, Bull. Obs. Astron. Belgrade **XV - 1950**, VII.

[40] Popović, L. Č.: 1997, Razvoj i aktivnosti Astronomskog društva "Rudjer Bošković", u Razvoj astronomije kod Srba, eds. M. S. Dimitrijević, J. Milogradov-Turin, L.Č. Popović, Publ. Astron. Obs. Belgrade, **56**, 77.

[41] Popović, Luka Č.: 1999, Amaterska astronomija u Jugoslaviji, Proc. I Bulgarian - Yugoslav Astronomical Meeting, eds. M. S. Dimitrijević, L. Č. Popović, M. Tsvetkov, Publ. Astron. Obs. Belgrade, **64**, 89.

[42] Protić, M.: 1975, Izveštaj o radu Astronomske opservatorije u Beogradu tokom 1973. godine, Publ. Obs. Astron. Belgrade, **20**, 231.

[43] Protitch M.: 1950, Services et travaux d'observations en 1941 á l'Observatoire astronomique de l'Université de Belgrade, Bull. Obs. Astron. Belgrade **VII - 1942**, 1.

[44] Protitch M.: 1956, Rapport annuel sur l'état et les travaux de l'Observatoire en 1955, Bull. Obs. Astron. Belgrade **XX**, No 3-4, 16.

[45] Protitch M.: 1960, Rapport annuel sur l'état et les travaux de l'Observatoire en 1959, Bull. Obs. Astron. Belgrade **XXIV**, No 3-4, 42.

[46] Salim Samir: 1997, Astronomija u Istraživačkoj stanici Petnica, u: Razvoj astronomije kod Srba, eds. M. S. Dimitrijević, J. Milogradov-Turin, L.Č. Popović, Publ. Astron. Obs. Belgrade, **56**, 101.

[47] Sekulić Miodrag: 1997, Astronomsko društvo "Alfa" - Niš, u: Razvoj astronomije kod Srba, eds. M. S. Dimitrijević, J. Milogradov-Turin, L.Č. Popović, Publ. Astron. Obs. Belgrade, **56**, 111.

[48] Simovljević Jovan: 1987, Astronomija, Četrdeset godina Prirodno - Matematičkog fakulteta u Beogradu, Beograd, 166.

[49] Stanojević M. Djordje: 1905b, Beogradska opservatorija i njen izveštaj za 1899 - 1903. god., str. 32, Beograd.

1993ApL&C..28..381D

Astro. Lett. and Communications, 1993, Vol. 28, pp. 381–383
Reprints available directly from the publisher
Photocopying by license only

© 1993 Gordon and Breach Science Publishers, S.A.
Printed in the United States of America

Stark Broadening of Pt II Lines in Chemically Peculiar Stars

MILAN S. DIMITRIJEVIĆ *Astronomical Observatory, Volgina 7, 11050 Beograd, Serbia, Yugoslavia*

(Received 10 August 1992; in final form 27 January 1993)

Stark widths of 1777.086 Å; 2245.518 Å; 1781.858 Å and 2144.244 Å Pt II lines observed in Hg Mn stars have been calculated by using the modified semiempirical approach.

1 INTRODUCTION

The need for a very extensive list of line broadening data has been particularly stimulated by spectroscopy from space. From instruments in orbit an extensive amount of spectroscopic information over large spectral regions of all kind of celestial objects has been and will be collected, stimulating the spectral-line-shape research.

Lines of Pt II have been discovered in the Hg Mn stars by Dworetsky (1969). An analysis of a few strong Pt II transitions which are also observed in IUE spectra of stars has shown (Dworetsky *et al.*, 1984) "that Pt is, like Hg, among the most overabundant elements in the atmospheres of Hg Mn stars, with enhancements of the order of 10^4 to 10^5 over the solar system abundances". Dworetsky *et al.* (1984) selected also the four Pt II lines which might be used for astrophysical applications. Moreover, they determined the corresponding theoretical gf values. The aim of this contribution is to investigate Stark broadening of these Pt II lines and to provide the corresponding Stark widths.

Whenever line broadening data for a large number of lines are required, and the high precision of every particular result is not so important, simple approximate formulae with good average accuracy may be very useful. Moreover, in the case of more complex atoms or multiply charged ions the lack of the accurate atomic data needed for more sophisticated calculations, decreases the reliability of the semiclassical results. In such cases approximate methods might be very interesting.

Good possibilities, in such cases, gave the modified semiempirical method (Dimitrijević and Konjević, 1980, 1981, 1987; Dimitrijević and Kršljanin, 1986; Dimitrijević, 1988). Such approximate methods might be useful particularly in the case of heavier elements. Atomic data for heavy element spectra are often insufficient for sophisticated semiclassical calculations. Moreover, the accuracy of usually applied

© Taylor & Francis • Provided by the NASA Astrophysics Data System

1993ApL&C..28..381D

approximations (e.g. Coulomb approximation) is lower for complex spectra. In such cases a reliable approximate method may be a useful tool for quick estimates of needed Stark widths.

2 RESULTS AND DISCUSSION

In this contribution we will present results of our calculations of Stark full width at half maximum using the modified semiempirical method (Dimitrijević and Konjević, 1980). Whenever possible, the corresponding Bates and Damgaard factors have been derived from known gf values (Dworetsky *et al.*, 1984). Our results for four Pt II lines selected by Dworetsky *et al.* (1984) as the most interesting ones from the astrophysical point of view, are presented in Table I. In order to see the influence of differences in oscillator strengths, results of calculations with gf values obtained using Coulomb approximation are presented as well. The differences might give an impression of the error bars of obtained results.

We can see also from Table I, that all lines belong to the same supermultiplet and that their width values are not very different. Using the analysis of Stark broadening

TABLE I

Full Stark widths in Å of astrophysically important Pt II lines as a function of temperature T in K. Electron density is 10^{17} cm^{-3}. Stark width W_1 has been calculated by using oscillator strengths of Dworetsky *et al.* (1984) and W_2 with oscillator strengths calculated within Coulomb approximation.

Transition	T(K)	W_1(Å)	W_2(Å)
$6s^4F_{9/2} - 6p^4G^0_{11/2}$	5000	0.0496	0.0353
	10000	0.0351	0.0249
$\lambda = 1777.1$ Å	20000	0.0248	0.0176
	40000	0.0176	0.0125
	80000	0.0124	0.00882
$6s^4F_{7/2} - 6p^4G^\circ_{9/2}$	5000	0.0529	0.0557
	10000	0.0374	0.0394
$\lambda = 2245.5$ Å	20000	0.0264	0.0279
	40000	0.0187	0.0197
	80000	0.0132	0.0139
$6s^4F_{9/2} - 6p^4F^\circ_{9/2}$	5000	0.0502	0.0358
	10000	0.0355	0.0253
$\lambda = 1781.9$ Å	20000	0.0251	0.0179
	40000	0.0177	0.0127
	80000	0.0125	0.00895
$6s^4F_{9/2} - 6p^4D^\circ_{7/2}$	5000	0.0692	0.0484
	10000	0.0489	0.0342
$\lambda = 2144.2$ Å	20000	0.0346	0.0242
	40000	0.0245	0.0171
	80000	0.0174	0.0122

© Taylor & Francis • Provided by the NASA Astrophysics Data System

1993ApL&C..28..381D

parameters within a supermultiplet (Dimitrijević, 1982) we can estimate Stark widths of other members within multiplets and supermultiplets as

$$W_\alpha = (\lambda_\alpha^2/\lambda_\beta^2)W_\beta, \tag{1}$$

taking as W_β the most appropriate value for the considered case (i.e. e.g. the closest available member of the same multiplet).

Optical Pt II lines selected by Dworetsky *et al.* (1984) are forbidden in LS coupling, two-electron transitions, or transitions to levels without well defined term assignation. If we use for them the term assignation used by Dworetsky and Vaughan (1973), in all considered cases dypole allowed perturbing terms of lower levels are not among terms with defined term assignation. Moreover, lower level configurations have series limits higher than the ionization limit and energy of corresponding terms in Pt III spectrum is not known. Since possible perturbing terms of lower levels are sufficiently far away, and since oscillator strengths for transition between upper and lower levels (Dworetsky *et al.*, 1984) are small, one can expect that the lower level broadening contribution is not higher than in the case of UV lines from Table I. For an order of magnitude estimate, we might use Eq. (1), taking as W_β data for transition with the same upper level (or the closest available member of the same multiplet). For optical Pt II lines given in Dworetsky *et al.* (1984) and Dworetsky and Vaughan (1973), we might scale by Eq. (1) $\lambda = 2245.5$ Å data for $\lambda = 4148.30$ Å, 4061.66 Å, 4034.17 Å, 4023.81 Å and 3447.78 Å lines; $\lambda = 1781.9$ Å data for 3806.91 Å line and $\lambda = 2144.2$ Å data for $\lambda =$ 4514.17 Å, 4288.40 Å, 4046.45 Å, 3766.40 Å and 3577.20 Å lines.

REFERENCES

Dimitrijević, M. S., 1982, *Astron. Astrophys.* **112,** 251.
Dimitrijević, M. S., 1988. *Astron. Astrophys. Suppl. Series* **76,** 53.
Dimitrijević, M. S. and Konjević, N., 1980. *JQSRT.* **24,** 451.
Dimitrijević, M. S. and Konjević, N., 1981, In Spectral Line Shapes, Ed. B. Wende, W. de Gruyter, Berlin, New York, p. 211.
Dimitrijević, M. S. and Konjević, N., 1987. *Astron. Astrophys.* **172,** 345.
Dimitrijević, M. S. and Kršljanin, V., 1986. *Astron. Astrophys.* **165,** 269.
Dworetsky, M. M., 1969. *Astrophys. J.* **156,** L101.
Dworetsky, M. M., Storey, P. J. and Jacobs, J. M., 1984. *Physica Scripta*, **T8,** 39.
Dworetsky, M. M. and Vaughan, Jr. H., 1973. *Astrophys. J.* **181,** 811.

© Taylor & Francis • Provided by the NASA Astrophysics Data System

ATMOP 3

5 - 8 APRIL 1993

ABSTRACT HANDBOOK

Daresbury Laboratory
Daresbury
Warrington WA4 4AD
UK

RECOMBINATION OF ELECTRONS ON BINARY ION-ATOM SYSTEMS

A A Mihajlov†, N N Ljepojevic‡ and M S Dimitrijevic§

†Institute of Physics, PO Box 57, 11001 Beograd, Yugoslavia; ‡School of Electrical, Electronic and Information Engineering, South Bank University, London SE1 0AA, England; §Astronomical Observatory, Volgina 7, 11050 Beograd, Yugoslavia

Collisions between atoms A and ions B^+ create quasi-molecular complexes, $\{A + B^+\}$, whose electronic state can be well described as a superposition of the lowest (ground) atractive and repulsive states of the molecular ion AB^+. Therefore, the process of dielectronic recombination of electrons has two channels

$$AB^+ + e \longrightarrow A + B^*(n) \tag{1a}$$

$$A + B^+ + e \longrightarrow A + B^*(n) \tag{1b}$$

where n denotes the principal quantum number of the excited state $B^*(n)$, and the ionisation potentials I_A and I_B must satisfy $I_A \geq I_B$. For the channel (1a) the initial state of the system is in the ground state with the probability 1, whereas for the channel (1b) the probability is given by the square modulus of the corresponding coefficient in the linear combination of the attractive and repulsive states.

The process (1a) is the well known process of dissociative recombination. The process (1b) was treated first in [1] and has largely been ignored in the literature. In a recent publication [2] an important symmetric case ($A = B$) of hydrogen was treated, where it was shown that the channel (1b) is not only comparable with the channel (1a), but is even dominant in a wide range of electron densities and temperatures. In the present work we treat the symmetric case of helium.

The rate coefficients for recombination are calculated for a plasma in the dissociation-recombination equilibrium [2]. For the calculation of the recombination coefficients, the differential rate coefficients for the inverse process of ionisation are required. The latter are obtained using the method developed in [3].

The rate cofficients for the recombination processes (1a) and (1b) are obtained as

$$K^{a,b}_{r,n}(T_a, T_e) = C_n(T_e) \int_{R_{min}}^{R_n} R^4 \exp\left[-\frac{U_1(R)}{kT_a} - \frac{\epsilon(r)}{kT_e}\right] X^{a,b}(R, T_a)\, dR \tag{2}$$

where R is the inter-nuclear distance, T_a and T_e the atom and electron temperatures, $X^a(R, T_a) = \gamma(3/2; |U_1(R)|/kT_a)/\Gamma(3/2)$, $X^b = 1 - X^a$, $U_1(R) < 0$ is the potential energy of the molecular ion He_2^+, $U_2(R)$ is the potential energy of the repulsive state of the ion-atom complex $\{He + He^+\}$, γ is the incomplete gamma function, $\epsilon(R) = U_2(R) - U_1(R)$, R_{min} and R_n are respectively distances of the closest approach and when $\epsilon(R_n)$ equals the ionisation energy ϵ_n of the state $He^*(n)$, and $C_n(T_e) = [8\pi^{5/2}/3(6^{1/2})n^3(kT_e)^{3/2}]\, exp[\epsilon_n/kT_e]$.

The total rate coefficient for the process (1) is $K_{r,n} = K^a_{r,n} + K^b_{r,n}$. The results obtained again show that none of the processes (1a) and (1b) must be neglected when calculating $K_{r,n}$.

References

[1] Mihajlov A A and Ljepojevic N N 1982 Proc. Symp. on Physics of Ionized Gases, Dubrovnik 1982, p 385

[2] Mihajlov A A, Ljepojevic N N and Dimitrijevic M S 1992, J Phys B **25**, 5121

[3] Mihajlov A A and Janev R K 1981, J Phys B **14**, 1639

INSTITUTE OF PHYSICS PUBLISHING JOURNAL OF PHYSICS B: ATOMIC, MOLECULAR AND OPTICAL PHYSICS

J. Phys. B: At. Mol. Opt. Phys. **37** (2004) 2713–2724 PII: S0953-4075(04)79539-5

Electron and ion contributions to the Ne I spectral line broadening

V Milosavljević[1], S Djeniže[1] and M S Dimitrijević[2]

[1] Faculty of Physics, University of Belgrade, PO Box 368, Belgrade, Serbia
[2] Astronomical Observatory, 11160 Belgrade, Volgina 7, Serbia

E-mail: vladimir@ff.bg.ac.yu

Received 3 April 2004
Published 11 June 2004
Online at stacks.iop.org/JPhysB/37/2713
doi:10.1088/0953-4075/37/13/009

Abstract
On the basis of the experimentally determined 26 prominent neutral neon (Ne I) line shapes (in the 3s–3p, 3s–3p′, 3s′–3p′, 3s′–3p and 3p–3d transitions) we have obtained electron (W_e) and ion (W_i) contributions to the total Stark width (W_t). Stark widths are also calculated using the semiclassical perturbation formalism for electrons and protons as perturbers up to 50 000 K electron temperatures. We made comparison of our measured and calculated W_e data and compared both of them with available experimental and theoretical W_e values.

1. Introduction

In thermal plasmas at local thermodynamic equilibrium (LTE), and for temperatures of about 1–2 eV (an electron density of about 1×10^{23} m^{-3}), the dominant pressure broadening mechanism is caused by collision processes with electrons and ions. Stark broadening in plasmas is important not only for theoretical understanding, but also for experimental methods, e.g. as a diagnostic tool. Plasma broadened and shifted spectral line profiles have been used for a number of years as a basis of an important non-interfering plasma diagnostic technique. Numerous theoretical and experimental efforts have been made to provide reliable data for such applications. This technique becomes, in some cases, the most sensitive and sometimes the only possible plasma diagnostic tool.

Classical emission laboratory plasmas spectroscopy has been mainly applied to optically thin plasma where absorption of the emitted radiation is negligible. Investigation of line profiles of atomic neon in medium dense plasmas, at about 1×10^{23} m^{-3}, is of particular interest for verifying predictions of theoretical approximations. Since neon is a constituent of laboratory plasmas the Ne I spectral line shapes represent important sources of information about the physical conditions in the place of birth of the radiation.

 © 2004 IOP Publishing Ltd Printed in the UK

Stark broadening of spectral lines is the dominant pressure broadening mechanism also in some astrophysical objects such as chemically peculiar A-type stars and white dwarf atmospheres. Moreover, even for cooler stars such as Solar-type ones, the Stark broadening data are needed also for the analysis and modelling of subphotospheric layers [1]. Consequently knowledge of the Stark broadening parameters of spectral lines is of interest for diagnostic, modelling and consideration of astrophysical, laboratory and technological plasmas. Particularly, from such data, it is possible to obtain the basic plasma parameters, such as the electron temperature and electron density.

In order to underline the astrophysical importance of neon data one should say that neon is the most abundant element in the universe after hydrogen, helium, oxygen and carbon, and it is for example [2] one of the products of hydrogen and helium burning in the orderly evolution of stellar interiors.

Stark broadening of neutral neon (Ne I) spectral lines has been studied experimentally several times [3–16]. The most complete existing calculation is in [17]. Also in [18] calculations have been performed for the Ne I 650.7 nm (3s–3p) spectral line using five different theoretical approaches. Results [18] are presented graphically and it is not easy to use them for detailed comparison. In [19] the quasistatic Stark broadening constant C_4 was calculated and some theoretical estimates exist also in [10].

Due to large uncertainties of the theoretically determined Stark broadening parameters (e.g. $\pm 30\%$ for the semiclassical method as estimated in [17]), the mutual agreement of experimental values independently obtained in various laboratories permits us to single out some lines as particularly reliable and suitable for diagnostic purposes.

Since the dependence of Stark broadening parameters on temperature is still not known with a large accuracy, it is of interest also to have experimental results in a wide temperature range.

Our experimental $W_{\mathrm{e}}^{\mathrm{exp}}$ and $W_{\mathrm{i}}^{\mathrm{exp}}$ values, presented here for 26 Ne I lines, are separated from the measured total Stark width using the line deconvolution procedure described in [20–22] which has already been applied for some He I [23–25], Ar I [26] and Kr I [27] lines. We note as well that in [28, 29] static (A) and dynamic (D) ion parameters, respectively, have been determined for a number of the Ne I lines considered here.

Using the semiclassical perturbation formalism (SCPF) (updated several times) [30–35], we have calculated $W_{\mathrm{e}}^{T_{\mathrm{w}}}$ values for 25 Ne I lines and also the $W_{\mathrm{i}}^{T_{\mathrm{w}}}$ values, generated by protons which are the main component in the astrophysical plasmas. Our values are compared with available experimental and theoretical data.

The basic plasma parameters, i.e. electron temperature (T^{D}) and electron density (N^{D}), have been obtained by using the line deconvolution procedure directly from the Ne I line profiles and also measured (T^{exp} and N^{exp}) using independent, well-known, experimental diagnostical techniques. Excellent agreement was found among the two sets of the obtained parameters (T^{D} and T^{exp}; and N^{D} and N^{exp}). Such a method is applicable for optically thin plasmas. For optically thick plasmas, the situation is more complicated due to weak asymmetry of the spectral line profile caused by self-absorption [17, 36].

2. Experiment and deconvolution procedure

A modified version of the linear low pressure pulsed arc [37–40] has been used as a plasma source. A pulsed discharge was driven in a pyrex tube of 5 mm inner diameter and effective plasma length of 7.2 cm (figure 1 in [38]). The working gas was neon (99.9% purity) at 133 Pa filling pressure in flowing regime. A capacitor of 14 μF was charged up to

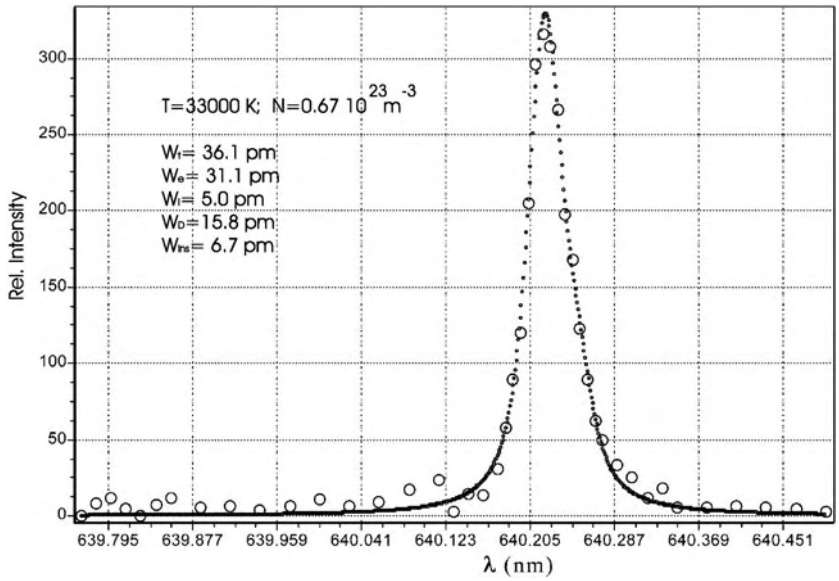

Figure 1. The recorded Ne I 640.225 nm line profile (o) with its fitting K function (dotted line) in the 25th μs after the beginning of the discharge at $U = 1.5$ kV bank voltage and $P = 133$ Pa gas pressure. This figure is an extension of figure 3.4.2 in [21]. W_t, W_e and W_i denote measured total, electron and ion Stark widths. W_D is the Doppler width determined at a measured T and N. W_{ins} is the instrumental width.

1.5 kV (experiment a) and 2.5 kV (experiment b), respectively. The complete experimental procedure with the set-up system used is described in [40]. Recorded Ne I spectral line profile with deconvolution fitting function, as an example, is shown in figure 1.

The absence of self-absorption was checked using the method described in [41]. The electron temperature (T^{exp}) was determined from the Boltzmann plot of the relative intensities of 14 Ne II spectral lines (331.98 nm, 336.06 nm, 337.18 nm, 341.48 nm, 341.69 nm, 341.77 nm, 350.36 nm, 356.83 nm, 366.41 nm, 369.42 nm, 429.04 nm, 439.19 nm, 440.93 nm and 441.32 nm) within energy interval of 7.1 eV for corresponding upper levels, with an estimated error of ±6%, assuming the existence of LTE, according to the criterion from [36]. All necessary atomic data were taken from [42–44]. The electron temperature decays are presented in figure 2. The electron density (N^{exp}) decay was measured using a well-known single laser interferometry technique [45] for the 632.8 nm He–Ne laser wavelength with an estimated error of ±7%. The electron density decays are presented also in figure 2. The T^D and N^D values obtained by deconvolution procedure [20] are also presented in figure 2. The experimental W_e^{exp}, W_i^{exp} and W_t^{exp} values are obtained using the deconvolution procedure.

The total line Stark FWHM (full-width at a half intensity maximum, W_t) is a function of W_e and W_i i.e.

$$W_t = f(W_e, W_i), \tag{1}$$

where W_e and W_i are the electron and ion contributions, respectively. For a non-hydrogenic, isolated neutral atom line the ion broadening is not negligible and the line profiles are described by an asymmetric K function (see equation (3) and [20, 26]). The

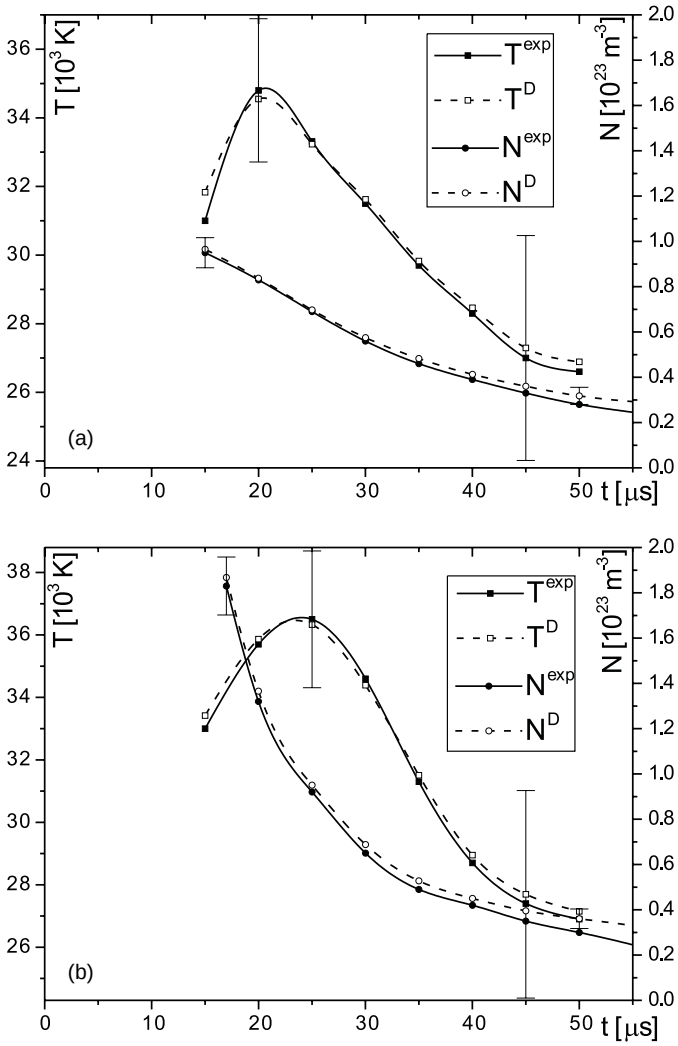

Figure 2. Electron temperature (T) and density (N) decays. Full lines represent measured data using independent experimental techniques. Dashed lines represent plasma parameters obtained using our line deconvolution procedure in different plasmas ((a) for 1.5 kV bank energy, (b) for 2.5 kV bank energy). Error bars represent estimated accuracies of the measurements (±6% and ±7% for T and N, respectively) and deconvolutions (±12%).

total Stark width with dynamic ion contribution $\left(W_{\mathrm{t}}^{\mathrm{dyn}}\right)$ and with static ion contribution ($W_{\mathrm{t}}^{\mathrm{st}}$; $W_{\mathrm{t}}^{\mathrm{st}} = W_{\mathrm{t}}^{\mathrm{dyn}}$ for $D = 1$) [17, 46, 47] may be calculated from the equation:

$$W_{\mathrm{t}}^{\mathrm{dyn}} \approx W_{\mathrm{e}}[1 + 1.75AD(1 - 0.75R)], \tag{2}$$

where R is the ratio of the mean ion separation to the Debye length. A is the quasi-static ion broadening parameter (see equation (224) in [17]) and D is a coefficient of the ion-dynamic contribution [26].

When $D = 1$ the influence of the ion-dynamical effect is negligible and the line shape is treated using the quasi-static ion approximation. From equations in [20, 26] it is possible to

obtain the plasma parameters (N and T) and the line broadening characteristics (W_t, W_e, W_i, A and D). One can see that the ion contribution, expressed in terms of the A and D parameters, directly determines the ion width (W_i) component in the total Stark width (equations (1) and (2)).

$$K(\lambda) = K_o + K_{max} \int_{-\infty}^{\infty} \exp(-t^2) \cdot \left[\int_0^{\infty} \frac{H_R(\beta)}{1 + \left(2\frac{\lambda-\lambda_o-\frac{W_G}{2\sqrt{\ln 2}}t}{W_e} - \alpha\beta^2\right)^2} \, d\beta \right] dt. \tag{3}$$

Here W_G is the Gaussian FWHM width given by (4) (i.e equation (2.3) in [20]).

$$W_G = 2\sqrt{\frac{2\ln 2kT}{m}}\frac{\lambda_o}{c}. \tag{4}$$

Where T is the emitter equivalent kinetic temperature, m is its mass, and k and c are the Boltzmann constant and velocity of light, respectively.

All other details about the asymmetric K function (3) and the complete numerical procedure for deconvolution of recorded spectral lines are described in earlier publications [20–22, 26, 29].

3. Method of calculation

A description of the semiclassical perturbation formalism used here is given in [30–35, 48]. For electrons hyperbolic paths due to the attractive Coulomb force were used, while for perturbing ions the paths are different since the force is repulsive. The expected accuracy of the semiclassical perturbation approach is ±30%.

Within the semiclassical perturbation formalism, we have calculated electron- and proton-impact line widths for 25 spectral lines of neutral neon. Energy levels have been taken from [49]. Oscillator strengths have been calculated by using the method of Bates and Damgaard [50, 51]. For higher levels, the method described in [52] has been used. The results obtained for Stark widths (FWHM) of 25 spectral lines of neutral neon are shown in table 2, for perturber density of 10^{22} m^{-3} and temperatures $T = 2500$–$50\,000$ K.

For each value given in table 2, the collision volume (V) multiplied by the perturber density (N) is much less than 1 and the impact approximation is valid [17, 30–35, 48]. When the impact approximation is not valid, the ion broadening contribution may be estimated by using the quasi-static approach ([17] or [53]).

In the region where neither of these two approximations is valid, a unified type theory should be used. For example, in [46], simple analytical formulae for such a case are given. The accuracy of the results obtained decreases when broadening by ion interactions becomes important.

4. Results and discussion

Our experimentally obtained W_t^{exp}, W_e^{exp} and W_i^{exp} data are shown in table 1 together with the ratios W_e^{exp}/W_e^{G} and $W_e^{exp}/W_e^{T_w}$ where G and T_w denote theoretical values from [17] and this work (see table 2), respectively.

Calculated Stark FWHM values (W^{T_w}) generated by electrons and protons for 25 Ne I lines in the 3s–3p, 3s–3p′, 3s′–3p′, 3s′–3p and 3p–4d transitions using semiclassical perturbation formalism are presented in table 2.

The measured N^{exp} and T^{exp} decays are presented in figure 2 together with the averaged (within 26 Ne I lines) N^D and T^D values obtained using the line profile deconvolution procedure

Table 1. Measured total Stark FWHM (W_t^{exp} in pm within ±12% accuracy), electron and ion (Ne^+, Ne^{2+}, ...) Stark widths (W_e^{exp} and W_i^{exp} in pm within ±12% accuracy) at measured electron temperatures T^{exp} (in 10^3 K) and electron densities N^{exp} (in 10^{22} m^{-3}). The indices G and T_w denote theoretical data taken from [17] and this work (see table 2), respectively at a given T^{exp} and N^{exp}.

Transition	Multiplet	λ (nm)	T^{exp}	N^{exp}	W_t^{exp}	W_e^{exp}	W_i^{exp}	W_e^{exp}/W_e^G	$W_e^{exp}/W_e^{T_w}$
3s–3p	$[3/2]_2^0$–$[1/2]_1$	703.241	3.30	6.7	44	39	5	0.86	1.10
			3.65	8.8	56	50	6	0.81	1.03
	$[3/2]_1^0$–$[1/2]_1$	724.517	3.30	6.7	46	43	3	0.87	1.14
			3.65	8.8	61	52	9	0.77	1.00
	$[3/2]_1^0$–$[1/2]_0$	607.434	3.30	6.7	34	31	3		0.88
			3.65	8.8	44	40	4		0.84
	$[3/2]_2^0$–$[3/2]_2$	614.306	3.30	6.7	37	32	5		0.97
			3.65	8.8	47	41	6		0.91
	$[3/2]_2^0$–$[3/2]_1$	621.728	3.30	6.7	43	39	4		1.16
			3.65	8.8	53	48	5		1.04
	$[3/2]_1^0$–$[3/2]_2$	630.479	3.30	6.7	37	32	5		0.92
			3.65	8.8	51	44	7		0.93
	$[3/2]_1^0$–$[3/2]_1$	638.299	3.30	6.7	30	27	3		0.76
			3.65	8.8	40	34	6		0.70
	$[3/2]_2^0$–$[5/2]_3$	640.225	3.30	6.7	36	31	5	0.72	0.92
			3.65	8.8	45	38	7	0.65	0.83
	$[3/2]_2^0$–$[5/2]_2$	633.443	3.30	6.7	35	30	5		0.91
			3.65	8.8	41	34	7		0.75
	$[3/2]_1^0$–$[5/2]_2$	650.653	3.30	6.7	36	33	3	0.74	0.95
			3.65	8.8	45	41	4	0.67	0.86
3s–3p′	$[3/2]_2^0$–$[1/2]_1$	588.190	3.30	6.7	29	25	4		0.83
			3.65	8.8	37	31	6		0.75
	$[3/2]_1^0$–$[1/2]_1$	603.000	3.30	6.7	37	32	5		1.01
			3.65	8.8	48	41	7		0.94
	$[3/2]_2^0$–$[3/2]_2$	594.483	3.30	6.7	32	27	5	0.72	0.90
			3.65	8.8	43	37	6	0.73	0.90
	$[3/2]_2^0$–$[3/2]_1^0$	597.553	3.30	6.7	40	36	4		1.18
			3.65	8.8	50	44	6		1.05
	$[3/2]_1^0$–$[3/2]_2$	609.616	3.30	6.7	30	28	2	0.70	0.88
			3.65	8.8	39	35	4	0.64	0.81
	$[3/2]_1^0$–$[3/2]_1$	612.846	3.30	6.7	26	22	4		0.69
			3.65	8.8	36	30	6		0.68
3s′–3p′	$[1/2]_1^0$–$[1/2]_1$	659.895	3.30	6.7	36	31	5		0.81
			3.65	8.8	50	43	7		0.82
	$[1/2]_1^0$–$[1/2]_0$	585.249	3.30	6.7	42	35	7		0.88
			3.65	8.8	54	45	9		0.84
	$[1/2]_0^0$–$[1/2]_1$	616.359	3.30	6.7	32	28	4		0.85
			3.65	8.8	44	38	6		0.84
	$[1/2]_1^0$–$[3/2]_2$	667.828	3.30	6.7	41	37	4	0.73	0.97
			3.65	8.8	55	50	5	0.73	0.96
	$[1/2]_1^0$–$[3/2]_1$	671.704	3.30	6.7	39	36	3		0.93
			3.65	8.8	50	46	4		0.87
	$[1/2]_0^0$–$[3/2]_1$	626.650	3.30	6.7	35	31	4	0.74	0.92
			3.65	8.8	46	41	5	0.72	0.89
	$[1/2]_0^0$–$[3/2]_1$	653.288	3.30	6.7	36	30	6	0.65	0.82
			3.65	8.8	44	37	7	0.59	0.74

Table 1. (Continued.)

Transition	Multiplet	λ (nm)	T^{exp}	N^{exp}	$W_{\mathrm{t}}^{\mathrm{exp}}$	$W_{\mathrm{e}}^{\mathrm{exp}}$	$W_{\mathrm{i}}^{\mathrm{exp}}$	$W_{\mathrm{e}}^{\mathrm{exp}}/W_{\mathrm{e}}^{\mathrm{G}}$	$W_{\mathrm{e}}^{\mathrm{exp}}/W_{\mathrm{e}}^{T_{\mathrm{w}}}$
3s′–3p	$[1/2]_1^0$–$[3/2]_2$	692.947	3.30	6.7	38	35	3	0.62	0.84
			3.65	8.8	50	45	5	0.59	0.79
	$[1/2]_1^0$–$[5/2]_1$	717.394	3.30	6.7	42	39	3		0.92
			3.65	8.8	53	49	4		0.85
3p–4d	$[3/2]_2$–$[5/2]_3^0$	597.463	3.30	6.7	42	36	6		
			3.65	8.8	53	45	8		

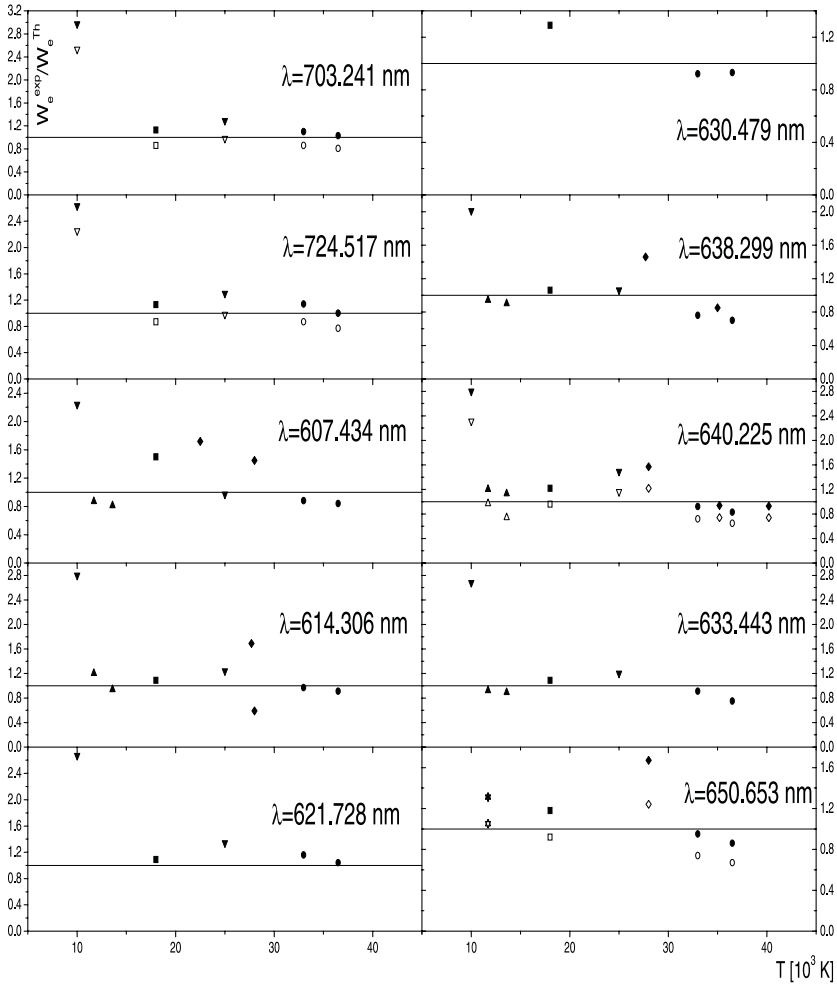

Figure 3. Ratios of the experimental $W_{\mathrm{e}}^{\mathrm{exp}}$ and theoretical $W_{\mathrm{e}}^{\mathrm{Th}}$ electron Stark widths versus electron temperature (T) for the Ne I lines in the 3s–3p transition (see also table 1). Empty and filled symbols are related to the Griem's (1974) (G) theoretical values and ones calculated by us (T_{w}) taken from table 2. ○, our experimental results and those of other authors: △, [6]; ✡, [7]; ▽, [11]; ◇, [12] and □, [16].

Table 2. Our calculated Ne I Stark FWHM (W^{T_w} in pm) for electrons (a) and protons (b) as perturbers for various temperatures (T) at 10^{22} m^{-3} perturber density.

		T ($\times 10^3$ K)					
λ (nm)		2.5	5.0	10.0	20.0	30.0	50.0
703.241	a	2.89	2.93	3.23	4.18	5.05	6.34
$3s[3/2]^0_2$–$3p[1/2]_1$	b	1.58	1.59	1.59	1.59	1.59	1.59
724.517	a	3.04	3.09	3.43	4.47	5.41	6.80
$3s[3/2]^0_1$–$3p[1/2]_1$	b	1.68	1.68	1.68	1.68	1.69	1.69
607.434	a	2.76	2.95	3.30	4.21	5.05	6.36
$3s[3/2]^0_1$–$3p[1/2]_0$	b	1.53	1.54	1.55	1.56	1.57	1.59
614.306	a	2.60	2.74	3.06	3.93	4.76	6.03
$3s[3/2]^0_2$–$3p[3/2]_2$	b	1.47	1.48	1.48	1.49	1.50	1.51
621.728	a	2.59	2.71	3.03	3.93	4.78	6.06
$3s[3/2]^0_2$–$3p[3/2]_1$	b	1.47	1.48	1.49	1.49	1.50	1.51
630.479	a	2.70	2.84	3.19	4.15	5.06	6.42
$3s[3/2]^0_1$–$3p[3/2]_2$	b	1.55	1.55	1.56	1.57	1.57	1.58
638.299	a	2.68	2.81	3.17	4.16	5.08	6.45
$3s[3/2]^0_1$–$3p[3/2]_1$	b	1.55	1.56	1.57	1.57	1.58	1.58
640.225	a	2.57	2.67	3.01	3.95	4.84	6.15
$3s[3/2]^0_2$–$3p[5/2]$	b	1.49	1.50	1.50	1.51	1.51	1.51
633.443	a	2.57	2.68	3.01	3.94	4.81	6.11
$3s[3/2]^0_2$–$3p[5/2]$	b	1.49	1.49	1.50	1.50	1.50	1.51
650.653	a	2.67	2.78	3.16	4.18	5.13	6.51
$3s[3/2]^0_1$–$3p[5/2]$	b	1.57	1.57	1.58	1.58	1.58	1.59
588.190	a	2.39	2.50	2.78	3.59	4.35	5.51
$3s[3/2]^0_2$–$3p'[1/2]_1$	b	1.34	1.34	1.35	1.36	1.36	1.37
603.000	a	2.47	2.58	2.91	3.78	4.61	5.85
$3s[3/2]^0_1$–$3p'[1/2]_1$	b	1.40	1.41	1.42	1.42	1.43	1.43
594.483	a	2.37	2.47	2.77	3.59	4.37	5.53
$3s[3/2]^0_2$–$3p'[3/2]_2$	b	1.34	1.35	1.35	1.36	1.36	1.37
597.553	a	2.37	2.46	2.76	3.59	4.37	5.55
$3s[3/2]^0_2$–$3p'[3/2]_1$	b	1.34	1.35	1.35	1.36	1.36	1.37
609.616	a	2.46	2.56	2.89	3.79	4.63	5.88
$3s[3/2]^0_1$–$3p'[3/2]_2$	b	1.41	1.42	1.42	1.42	1.43	1.43
612.846	a	2.46	2.55	2.88	3.79	4.64	5.89
$3s[3/2]^0_1$–$3p'[3/2]_1$	b	1.41	1.42	1.42	1.43	1.43	1.43
659.895	a	3.17	3.36	3.70	4.63	5.49	6.83
$3s'[1/2]^0_1$–$3p'[1/2]_1$	b	1.69	1.70	1.71	1.73	1.74	1.75
585.249	a	3.36	3.75	4.21	5.07	5.75	6.85
$3s'[1/2]^0_1$–$3p'[1/2]_0$	b	1.65	1.68	1.71	1.75	1.77	1.81
616.359	a	2.84	3.02	3.29	4.04	4.72	5.84
$3s'[1/2]^0_0$–$3p'[1/2]_1$	b	1.48	1.49	1.50	1.52	1.53	1.54
667.828	a	2.92	3.04	3.45	4.56	5.59	7.10
$3s'[1/2]^0_2$–$3p'[3/2]_2$	b	1.69	1.70	1.70	1.71	1.71	1.72
671.704	a	2.92	3.03	3.45	4.57	5.61	7.12
$3s'[1/2]^0_1$–$3p'[3/2]_1$	b	1.70	1.70	1.71	1.71	1.71	1.72
626.650	a	2.64	2.74	3.05	3.92	4.77	6.04
$3s'[1/2]^0_0$–$3p'[3/2]_1$	b	1.48	1.49	1.49	1.50	1.50	1.51
653.288	a	3.03	3.20	3.51	4.40	5.22	6.50
$3s'[1/2]^0_0$–$3p'[3/2]_1$	b	1.62	1.63	1.64	1.66	1.66	1.68
692.947	a	3.22	3.39	3.83	5.02	6.14	7.80

Table 2. (Continued.)

		T ($\times 10^3$ K)					
λ (nm)		2.5	5.0	10.0	20.0	30.0	50.0
$3s'[1/2]^0_1$–$3p[3/2]_2$	b	1.87	1.87	1.88	1.89	1.90	1.91
717.394	a	3.47	3.64	4.00	5.06	6.04	7.56
$3s'[1/2]^0_1$–$3p[5/2]_1$	b	1.89	1.90	1.91	1.92	1.94	1.95

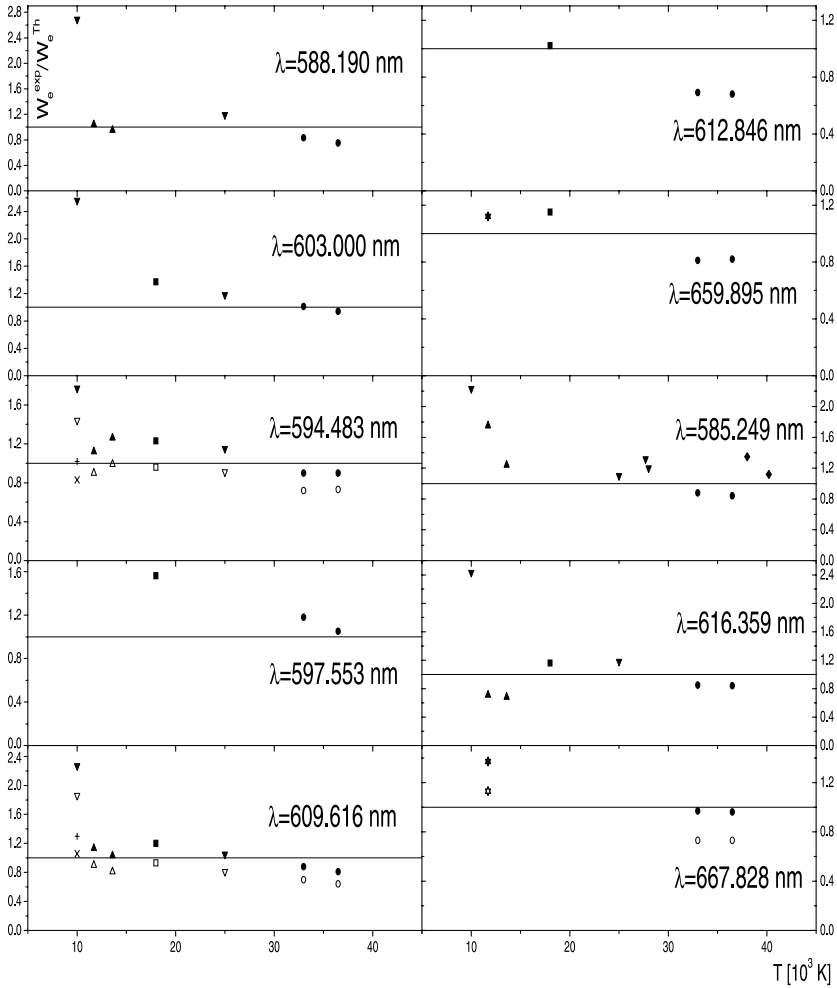

Figure 4. Same as in figure 3 but for the Ne I lines in the 3s–3p′ and 3s′–3p′ transitions. In addition: +, for the ratios of experimental data from [15] related to the Griem's (1974) (G) theoretical values; and ×, for their ratios related to our calculated (T_w) values.

for Ne I lines. One can conclude that the agreement between N^{exp} and N^D values is excellent (within 3% on average) in the two plasmas investigated. This fact confirms homogeneity of the investigated plasma in the linear part of our light source (see figure 1 in [38]). In the case of the electron temperature the situation is similar. The agreement between the two sets of the electron temperature decays (T^{exp} and T^D) is also excellent (within 2% on average).

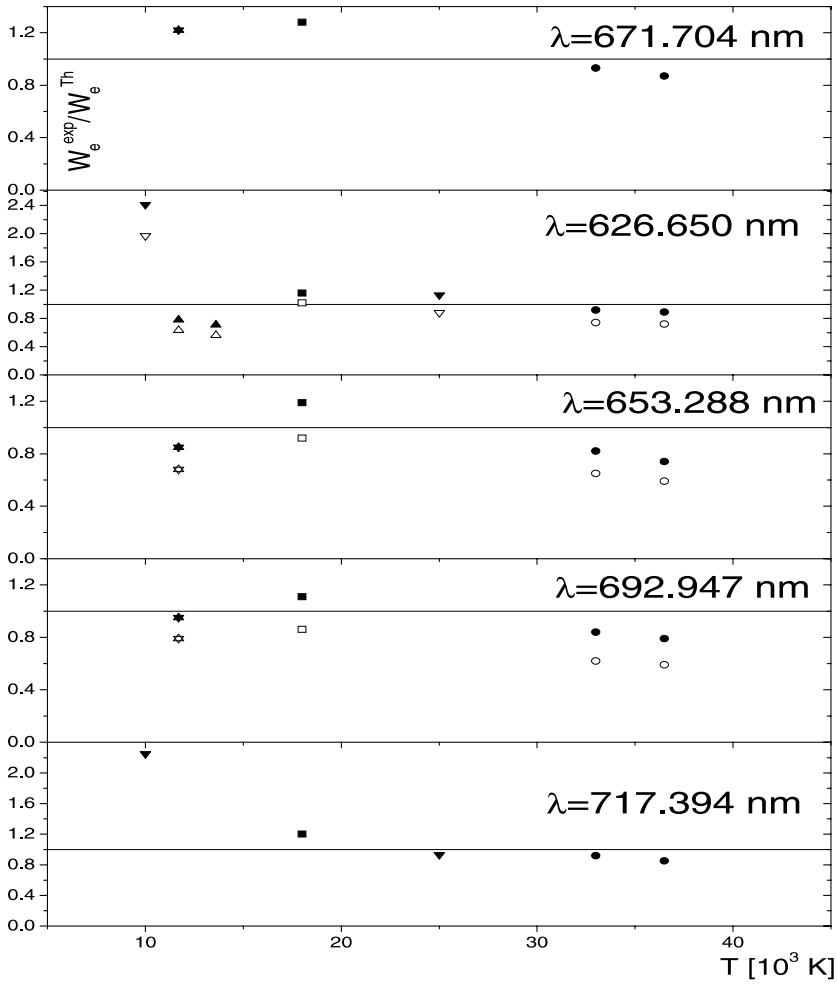

Figure 5. Same as in figure 3 but for the Ne I lines in the 3s′–3p′ and 3s′–3p transitions.

In order to make the comparison between the measured $\left(W_e^{exp}\right)$ and calculated $\left(W_e^{Th}\right)$ electron width values easier, the dependence of the ratio W_e^{exp}/W_e^{Th} on the electron temperature is presented graphically in figures 3–5. Experimental W_e^{exp} data are related to the Griem's (1974) (G) and our calculated (T_w) values taken from table 2.

We have found that the widths generated by protons show weak dependence on the electron temperature and are about three times smaller than the widths generated by electrons (see table 2) at $T = 30\,000$ K.

All our measured W_e^{exp} values lie below Griem's (1974) W_e^G values at about 29% (averaged through 10 lines). The greatest disagreement between them was found for the case of the 653.288 nm and 692.947 nm Ne I lines. Most of the W_e^{exp} values of the other authors lie also below Griem's data (see figures 3–5).

All calculated $W_e^{T_w}$ values (see table 2), generated by electrons, are smaller than W_e^G values at about 20%, but these are also higher than our measured ones. Within estimated experimental accuracy of ±12% our W_e^{exp} values agree with our calculated ones $\left(W_e^{T_w}\right)$ for the ten Ne I lines and all obtained ratios of our experimental and theoretical values are within

1.0 ± 0.3 interval which is less than combined experimental ($\pm$12%) and theoretical ($\pm$30%) error.

We have found that the electron contribution $\left(W_{\mathrm{e}}^{\mathrm{exp}}\right)$ to the total Stark widths is about 82%. At our plasma parameters the neon ions (Ne II, Ne III, ...) contribute about 18% (on average) to the total Stark widths.

The $W_{\mathrm{e}}^{\mathrm{exp}}$ values from [11] (∇ in figures 3–5) obtained at 10 000 K electron temperature are about 2.5 times higher from other experimental data. This is, probably, caused by unreliable measured electron density. We have excluded these values from all comparisons. Our $W_{\mathrm{e}}^{\mathrm{exp}}$ and $W_{\mathrm{e}}^{T_{\mathrm{w}}}$ values are within $\pm$20% on average in agreement with recently published [16] data for 19 Ne I lines.

Very good agreement was found among all existing $W_{\mathrm{e}}^{\mathrm{exp}}$ and $W_{\mathrm{e}}^{T_{\mathrm{w}}}$ values for the 626.650, 671.704, 717.394, 703.241, 724.517, 633.443, 588.190, 609.616 and 616.359 nm Ne I spectral lines in a wide range of electron temperatures.

5. Conclusion

It has been found that the electron contribution to the total Stark widths is about 82% and the neon ions contribute 18% (on average) to the total Stark widths. Generally, our measured and calculated electron Stark widths are smaller than those presented in [17] by about 20% on average.

In the electron temperature range between 10 000 K and 40 000 K very good agreement has been found among all existing $W_{\mathrm{e}}^{\mathrm{exp}}$ and our $W_{\mathrm{e}}^{T_{\mathrm{w}}}$ values for the 626.650, 671.704, 717.394, 703.241, 724.517, 633.443, 588.190, 609.616 and 616.359 nm Ne I spectral lines.

Acknowledgments

This work is a part of the projects OI1228 'Determination of the atomic parameters on the basis of the spectral line profiles' and GA1195 'Influence of collision processes on astrophysical plasma lineshapes' supported by the Ministry of Science, Technologies and Development of the Republic of Serbia.

References

[1] Seaton M J 1987 *J. Phys. B: At. Mol. Phys.* **20** 6363
[2] Trimble V 1991 *Astron. Astrophys. Rev.* **3** 1
[3] Mazing M A and Mandel'shtam S L 1957 *Opt. Spektrosk.* **2** 276
[4] Moo-Young G A, Greig J R and Griem H R 1970 *Phys. Rev.* A **2** 1617
[5] Miller M H and Bengston R D 1970 *Phys. Rev.* A **1** 983
[6] Nubbemeyer H, Stuck D and Wende B 1970 *Z. Phys.* **234** 29
[7] Miller M H, Roig R A and Moo-Young G A 1971 *Phys. Rev.* A **4** 971
[8] Im T D, Kazantsev A P, Routian S G, Saprykin E G and Shalagin A M 1974 *Sov. J. Quantum Electron.* **4** 234
[9] Im T D, Kochanov V P, Routian S G, Saprykin E G and Shalagin A M 1974 *Opt. Spectrosk. (USSR)* **36** 125
[10] Im T D, Kochanov V P, Routian S G, Saprykin E G and Shalagin A M 1976 *Sov. J. Quantum Electron.* **6** 283
[11] Purić J, Ćuk M and Rathore B H 1987 *Phys. Rev.* A **35** 1132
[12] Purić J, Srećković A, Djeniže S, Labat J and Ćirković Lj 1988 *Phys. Lett.* A **126** 280
[13] Deinezhenko A L and Protasevich E T 1988 *Opt. Spektrosk. (USSR)* **65** 303
[14] Windholz L and Neureiter C 1988 *Phys. Rev.* A **37** 1978
[15] Döhrn A and Helbig V 1996 *Phys. Rev.* E **53** 6581
[16] del Val J A, Aparicio J A and Mar S 1999 *Astrophys. J.* **513** 535
[17] Griem H R 1974 *Spectral Line Broadening by Plasmas* (New York: Academic)
[18] Syrkin M I 1981 *Opt. Spektrosk. (USSR)* **51** 431
[19] Krylova S I, Luizova L A, Solyanikova V A and Khakhaev A D 1971 *J. Appl. Spektrosk. (USSR)* **14** 676

[20] Milosavljević V and Poparić G 2001 *Phys. Rev.* E **63** 036404
[21] Milosavljević V 2001 *PhD Thesis* Faculty of Physics, University of Belgrade, Belgrade (unpublished)
[22] Milosavljević V 2002 *Monograph* (Belgrade: Zadužbina Andrejević)
[23] Milosavljević V and Djeniže S 2002 *Astron. Astrophys.* **393** 721
[24] Milosavljević V and Djeniže S 2002 *New Astron.* **7–8** 543
[25] Milosavljević V and Djeniže S 2003 *Eur. Phys. J.* D **23** 385
[26] Milosavljević V and Djeniže S 2003 *Astron. Astrophys.* **405** 397
[27] Milosavljević V, Djeniže S and Dimitrijević M S 2003 *Phys. Rev.* E **68** 016402
[28] Milosavljević V and Djeniže S 2002 *Phys. Lett.* A **305/1–2** 70
[29] Milosavljević V and Djeniže S 2003 *Astron. Astrophys.* **398** 1179
[30] Sahal-Bréchot S 1969 *Astron. Astrophys.* **1** 91
[31] Sahal-Bréchot S 1969 *Astron. Astrophys.* **2** 322
[32] Sahal-Bréchot S 1974 *Astron. Astrophys.* **35** 321
[33] Dimitrijević M S and Sahal-Bréchot S 1984 *J. Quant. Spectrosc. Radiat. Transfer* **31** 301
[34] Dimitrijević M S and Sahal-Bréchot S 1985 *Phys. Rev.* A **31** 316
[35] Dimitrijević M S, Sahal-Bréchot S and Bommier V 1991 *Astron. Astrophys. Suppl. Ser.* **89** 581
[36] Griem H R 1964 *Plasma Spectroscopy* (New York: McGraw-Hill)
[37] Djeniže S, Srećković A and Labat J 1992 *Astron. Astrophys.* **253** 632
[38] Djeniže S, Milosavljević V and Srećković A 1998 *J. Quant. Spectrosc. Radiat. Transfer* **59** 71
[39] Milosavljević V, Djeniže S, Dimitrijević M S and Popović L Č 2000 *Phys. Rev.* E **62** 4137
[40] Milosavljević V, Dimitrijević M S and Djeniže S 2001 *Astrophys. J. Suppl. Ser.* **135** 115
[41] Djeniže S and Bukvić S 2001 *Astron. Astrophys.* **365** 252
[42] NIST—Atomic Spectra Data Base Lines (wavelength order) 2003 Online at http://physics.nist.gov
[43] Wiese W L, Smith M W and Glennnon B M 1966 *Atomic Transition Probabilities, vol I Hydrogen Through Neon* (Washington, DC: US Department of Commerce, National Bureau of Standards) (NSRDS-NBS4)
[44] Striganov R A and Sventickij N S 1966 *Tablicy Spektral'nykh linij* (Moskva: Atomizdat)
[45] Ashby D E T F, Jephcott D F, Malein A and Raynor F A 1965 *Appl. Phys. B: Photophys. Laser Chem.* **36** 29
[46] Barnard A J, Cooper J and Smith E W 1974 *J. Quant. Spectrosc. Radiat. Transfer* **14** 1025
[47] Kelleher D E 1981 *J. Quant. Spectrosc. Radiat. Transfer* **25** 191
[48] Fleurier C, Sahal-Bréchot S and Chapelle J 1977 *J. Quant. Spectrosc. Radiat. Transfer* **17** 595
[49] Bashkin S and Stoner J J Jr 1975 *Atomic Energy Levels and Grotrian Diagrams* vol 1 (Amsterdam: North-Holland)
[50] Oertel G K and Shomo L P 1968 *Astrophys. J. Suppl. Ser.* **16** 175
[51] Bates D R and Damgaard A 1949 *Trans. R. Soc.* A **242** 101
[52] Van Regemorter H, Hoang Binh Dy and Prud'homme M 1979 *J. Phys. B: At. Mol. Phys.* **12** 1053
[53] Sahal-Bréchot S 1991 *Astron. Astrophys.* **245** 322

Bull. Astron. Belgrade № 145 (1992), 65 – 81.

UDC 52-355.3
Preliminary report

STARK BROADENING PARAMETER TABLES FOR Be II LINES OF ASTROPHYSICAL INTEREST

M. S. Dimitrijević[1], and S.Sahal–Bréchot[2]

[1] *Astronomical Observatory, Volgina 7, 11050 Beograd, Yugoslavia*
[2] *Laboratoire "Astrophysique, Atomes et Molécules" Département Atomes et Molécules en Astrophysique Unité associée au C.N.R.S. No 812 Observatoire de Paris–Meudon, 92190 Meudon, France*

(Received: November 4, 1991)

SUMMARY: Using a semiclassical approach, we have calculated electron–, proton–, and ionized helium–impact line widths and shifts for 30 Be II multiplets as a function of temperature for perturber densities 10^{13} and 10^{16}-10^{19}cm^{-3}.

1. INTRODUCTION

Stark broadening data for singly ionized beryllium lines are of interest in astrophysics since the surface content of Be provides informations on nucleogenesis, mixing between atmosphera and interior, the internal structure and evolution of a star (Boesgaard, 1988). Such data are of interest also for the analysis and diagnostics of stellar and laboratory plasmas. Moreover, the astrophysical importance of such data for the investigation of subphotospheric layers is discussed by Seaton (1987).

The present paper concerns singly ionized beryllium: In order to provide reliable data for Be II lines broadened by collisions with charged perturbers in stellar and laboratory plasmas, we have calculated electron–, proton–, and ionized helium–impact line widths and shifts for 30 Be II multiplets, using the semiclassical–perturbation formalism (Sahal – Bréchot, 1969ab). The obtained results for perturber density of 10^{15}cm^{-3}, together with discussion, analysis and comparison with existing experimental and theoretical data will be published in the principal article elsewhere (Dimitrijević, and Sahal–Bréchot, 1992). Since data are not linear with perturber density (N), due to the Debye screening effect, which is often important at high densities of interest for subphotospheric layers, we will present here the data for N = 10^{16} – 10^{19}cm^{-3}. Moreover, we will present also the data for N = 10^{13} cm^{-3} of special interest for stellar atmospheres.

2. RESULTS AND DISCUSSION

All details of the calculation procedure have been described in Dimitrijević, Sahal–Bréchot, Bommier (1991) and will not be repeated here. Energy levels for Be II lines have been taken from Bashkin and Stoner (1975). Oscillator strengths have been calculated using the method of Bates and Damgaard

(1949) and tables of Oertel and Shomo (1968). For the transitions including higher atomic energy levels, the method described by Van Regemorter et al. (1979) has been used.

In addition to the electron–impact full half-widths and shifts, Stark broadening parameters due to proton–, and ionized helium–impact have been calculated. In such a way we provide Stark broadening data for all important charged perturbers in stellar plasma. Our results are shown in Table 1 for perturber densities 10^{13} and 10^{16} – 10^{19}cm^{-3} and temperatures of T = 2,500; 5,000; 10,000; 20,000; 30,000 and 50,000 K. We also specify a parameter c (Dimitrijević and Sahal–Bréchot, 1984) which gives an estimate for the maximum perturber density for which the line may be treated as isolated when it is divided by the electron–impact full width at half maximum.

For each value given in Table 1, the collision volume (V) multiplied by the perturber density (N) is much less than one and the impact approximation is valid (Sahal–Bréchot, 1969ab). Values for NV > 0.5 are not given in Table 1; values for 0.1 < NV ≤ 0.5 are denoted by an asterisk. When the impact approximation is not valid, the ion broadening contribution may be estimated by using quasistatic formulae (cf. Sahal–Bréchot (1991) or Griem (1974)). The analysis of present results and comparison with available experimental and theoretical data is given in Dimitrijević and Sahal – Bréchot (1992).

Acknowledgments – This work is a part of French–Yugoslav collaboration through the project "L'élargissement Stark des raies spectrales des plasmas astrophysiques et de laboratoire". It is also a part of the project "Physics and dynamics of celestial bodies", supported by RFN of Serbia.

REFERENCES

Bashkin,S., and Stoner,J.O.Jr.: 1975, *Atomic Energy Levels and Grotrian Diagrams*, Vol.1, North Holland, Amsterdam.

Bates,D.R., and Damgaard,A.: 1949, *Trans. Roy. Soc. London, Ser. A* **242**, 101.

Boesgaard,A.M.: 1988, *Vistas in Astronomy*, **31**, 167.

Dimitrijević,M.S., and Sahal–Bréchot,S.: 1984, *JQSRT* **31**, 301.

Dimitrijević,M.S., and Sahal–Bréchot,S.: 1992, *JQSRT*, to be published.

Dimitrijević,M.S., Sahal–Bréchot,S., and Bommier, V.: 1991, *Astron. Astrophys. Suppl. Series.* **89**, 581.

Griem,H.R.: 1974, *Spectral Line Broadening by Plasmas*, Academic Press, New York.

Oertel,G.K., and Shomo,L.P.: 1968, *Astrophys. J. Suppl. Series* **16**, 175.

Sahal–Bréchot,S.: 1969a, *Astron.Astrophys.* **1**, 91.

Sahal–Bréchot,S.: 1969b, *Astron. Astrophys.* **2**, 322.

Sahal–Bréchot,S.: 1991, Astron.Astrophys. **245**, 322.

Seaton,M.J.: 1987, *J. Phys. B* **20**, 6363.

Van Regemorter,H., Hoang Binh Dy, and Prud'homme, M.: 1979, *J. Phys. B* **12**, 1073.

Table 1. This table gives electron–, proton–, and ionized–helium– impact broadening parameters for Be II lines, for perturber densities 10^{13} and 10^{16} – $10^{19} cm^{-3}$ and temperatures from 2,500 K to 50,000 K. Transitions and averaged wavelengths for the multiplet (in Å) are also given. By dividing c by the electron–impact full halfwidth, we obtain an estimate for the maximum perturber density for which the line may be treated as isolated and tabulated data may be used. The asterisk identifies cases for which the collision volume multiplied by the perturber density (the condition for validity of the impact approximation) lies between 0.1 and 0.5.

PERTURBER DENSITY = 0.1D+14(cm-3)

PERTURBERS ARE		ELECTRONS		PROTONS		IONIZED HELIUM	
TRANSITION	T(K)	WIDTH(A)	SHIFT(A)	WIDTH(A)	SHIFT(A)	WIDTH(A)	SHIFT(A)
Be II 2S-2P	2500.	0.126E-04	-0.110E-05	0.375E-07	-0.362E-07	0.638E-07	-0.362E-07
3131.5 A	5000.	0.801E-05	-0.102E-05	0.998E-07	-0.720E-07	0.154E-06	-0.712E-07
C= 0.31E+17	10000.	0.574E-05	-0.478E-06	0.219E-06	-0.134E-06	0.293E-06	-0.127E-06
	20000.	0.444E-05	-0.499E-06	0.366E-06	-0.216E-06	0.433E-06	-0.191E-06
	30000.	0.405E-05	-0.402E-06	0.460E-06	-0.261E-06	0.508E-06	-0.232E-06
	50000.	0.384E-05	-0.477E-06	0.552E-06	-0.326E-06	0.571E-06	-0.275E-06
Be II 2S-3P	2500.	0.652E-05	0.586E-06	0.164E-06	0.217E-06	0.212E-06	0.203E-06
1036.3 A	5000.	0.555E-05	0.368E-06	0.305E-06	0.322E-06	0.340E-06	0.290E-06
C= 0.17E+15	10000.	0.478E-05	0.476E-06	0.484E-06	0.437E-06	0.463E-06	0.367E-06
	20000.	0.420E-05	0.435E-06	0.611E-06	0.524E-06	0.574E-06	0.445E-06
	30000.	0.392E-05	0.399E-06	0.684E-06	0.577E-06	0.637E-06	0.493E-06
	50000.	0.362E-05	0.403E-06	0.795E-06	0.646E-06	0.719E-06	0.557E-06
Be II 2S-4P	2500.	0.126E-04	0.254E-05	0.873E-06	0.960E-06	0.925E-06	0.848E-06
842.0 A	5000.	0.111E-04	0.234E-05	0.130E-05	0.121E-05	0.122E-05	0.104E-05
C= 0.47E+14	10000.	0.101E-04	0.205E-05	0.166E-05	0.147E-05	0.151E-05	0.124E-05
	20000.	0.948E-05	0.170E-05	0.202E-05	0.172E-05	0.180E-05	0.146E-05
	30000.	0.915E-05	0.163E-05	0.221E-05	0.192E-05	0.195E-05	0.154E-05
	50000.	0.873E-05	0.139E-05	0.247E-05	0.196E-05	0.222E-05	0.175E-05
Be II 2S-5P	2500.	0.253E-04	0.822E-05	0.290E-05	0.279E-05	0.274E-05	0.238E-05
775.4 A	5000.	0.231E-04	0.704E-05	0.368E-05	0.340E-05	0.338E-05	0.285E-05
C= 0.20E+14	10000.	0.221E-04	0.542E-05	0.472E-05	0.401E-05	0.401E-05	0.340E-05
	20000.	0.214E-04	0.471E-05	0.526E-05	0.448E-05	0.493E-05	0.368E-05
	30000.	0.209E-04	0.416E-05	0.552E-05	0.507E-05	0.473E-05	0.404E-05
	50000.	0.202E-04	0.332E-05	0.618E-05	0.523E-05	0.577E-05	0.453E-05
Be II 2P-3S	2500.	0.184E-04	0.831E-05	0.683E-07	0.277E-06	0.929E-07	0.265E-06
1776.2 A	5000.	0.133E-04	0.631E-05	0.229E-06	0.459E-06	0.255E-06	0.410E-06
C= 0.26E+16	10000.	0.943E-05	0.488E-05	0.452E-06	0.640E-06	0.449E-06	0.564E-06
	20000.	0.722E-05	0.374E-05	0.730E-06	0.802E-06	0.651E-06	0.678E-06
	30000.	0.661E-05	0.334E-05	0.874E-06	0.888E-06	0.759E-06	0.755E-06
	50000.	0.605E-05	0.278E-05	0.105E-05	0.102E-05	0.903E-06	0.844E-06
Be II 2P-4S	2500.	0.223E-04	0.102E-04	0.451E-06	0.824E-06	0.443E-06	0.723E-06
1197.2 A	5000.	0.157E-04	0.924E-05	0.835E-06	0.113E-05	0.814E-06	0.977E-06
C= 0.47E+15	10000.	0.118E-04	0.750E-05	0.129E-05	0.138E-05	0.113E-05	0.117E-05
	20000.	0.100E-04	0.658E-05	0.162E-05	0.165E-05	0.143E-05	0.140E-05
	30000.	0.950E-05	0.585E-05	0.194E-05	0.183E-05	0.157E-05	0.155E-05
	50000.	0.900E-05	0.490E-05	0.220E-05	0.198E-05	0.181E-05	0.166E-05

PERTURBER DENSITY = 0.1D+14(cm-3)

PERTURBERS ARE		ELECTRONS		PROTONS		IONIZED HELIUM	
TRANSITION	T(K)	WIDTH(A)	SHIFT(A)	WIDTH(A)	SHIFT(A)	WIDTH(A)	SHIFT(A)
Be II 2P-5S	2500.	0.340E-04	0.180E-04	0.162E-05	0.227E-05	0.159E-05	0.196E-05
1048.2 A	5000.	0.272E-04	0.167E-04	0.257E-05	0.278E-05	0.222E-05	0.236E-05
C= 0.18E+15	10000.	0.220E-04	0.152E-04	0.332E-05	0.331E-05	0.285E-05	0.279E-05
	20000.	0.200E-04	0.129E-04	0.419E-05	0.395E-05	0.358E-05	0.325E-05
	30000.	0.190E-04	0.120E-04	0.471E-05	0.415E-05	0.396E-05	0.359E-05
	50000.	0.190E-04	0.102E-04	0.531E-05	0.471E-05	0.432E-05	0.384E-05
Be II 2P-3D	2500.	0.167E-04	0.837E-06	0.150E-06	-0.287E-06	0.195E-06	-0.269E-06
1512.4 A	5000.	0.124E-04	0.696E-06	0.349E-06	-0.454E-06	0.366E-06	-0.398E-06
C= 0.36E+15	10000.	0.927E-05	0.324E-06	0.580E-06	-0.626E-06	0.587E-06	-0.540E-06
	20000.	0.709E-05	0.154E-06	0.810E-06	-0.763E-06	0.742E-06	-0.646E-06
	30000.	0.612E-05	0.737E-07	0.909E-06	-0.844E-06	0.833E-06	-0.715E-06
	50000.	0.531E-05	0.272E-07	0.108E-05	-0.969E-06	0.962E-06	-0.801E-06
Be II 2P-4D	2500.	0.532E-04	0.344E-05	0.115E-04	0.121E-04	0.101E-04	0.102E-04
1143.0 A	5000.	0.438E-04	0.292E-05	0.145E-04	0.144E-04	0.121E-04	0.121E-04
C= 0.33E+13	10000.	0.363E-04	0.243E-05	0.178E-04	0.167E-04	0.152E-04	0.142E-04
	20000.	0.302E-04	0.196E-05	0.198E-04	0.195E-04	0.171E-04	0.154E-04
	30000.	0.272E-04	0.147E-05	0.227E-04	0.205E-04	0.191E-04	0.180E-04
	50000.	0.239E-04	0.101E-05	0.237E-04	0.213E-04	0.187E-04	0.201E-04
Be II 2P-5D	2500.	0.129E-03	0.999E-05	0.378E-04	0.369E-04	0.331E-04	0.315E-04
1026.9 A	5000.	0.108E-03	0.823E-05	0.471E-04	0.432E-04	0.393E-04	0.353E-04
C= 0.14E+13	10000.	0.914E-04	0.669E-05	0.562E-04	0.504E-04	0.452E-04	0.408E-04
	20000.	0.773E-04	0.477E-05	0.667E-04	0.561E-04	0.513E-04	0.446E-04
	30000.	0.700E-04	0.336E-05	0.637E-04	0.638E-04	0.625E-04	0.474E-04
	50000.	0.614E-04	0.234E-05	0.638E-04	0.670E-04	0.631E-04	0.550E-04
Be II 3S-3P	2500.	0.134E-02	-0.209E-03	0.192E-04	0.193E-04	0.255E-04	0.180E-04
12099.6 A	5000.	0.110E-02	-0.158E-03	0.353E-04	0.303E-04	0.402E-04	0.266E-04
C= 0.23E+17	10000.	0.881E-03	-0.107E-03	0.535E-04	0.417E-04	0.540E-04	0.359E-04
	20000.	0.756E-03	-0.749E-04	0.667E-04	0.507E-04	0.647E-04	0.428E-04
	30000.	0.715E-03	-0.700E-04	0.753E-04	0.569E-04	0.714E-04	0.477E-04
	50000.	0.671E-03	-0.541E-04	0.854E-04	0.640E-04	0.790E-04	0.535E-04
Be II 3S-4P	2500.	0.220E-03	0.308E-04	0.129E-04	0.141E-04	0.138E-04	0.125E-04
3275.6 A	5000.	0.190E-03	0.281E-04	0.192E-04	0.179E-04	0.183E-04	0.153E-04
C= 0.71E+15	10000.	0.169E-03	0.227E-04	0.246E-04	0.218E-04	0.224E-04	0.182E-04
	20000.	0.157E-03	0.173E-04	0.304E-04	0.253E-04	0.267E-04	0.218E-04
	30000.	0.151E-03	0.166E-04	0.318E-04	0.278E-04	0.298E-04	0.232E-04
	50000.	0.145E-03	0.139E-04	0.384E-04	0.293E-04	0.326E-04	0.261E-04
Be II 3S-5P	2500.	0.265E-03	0.734E-04	0.289E-04	0.278E-04	0.274E-04	0.238E-04
2454.6 A	5000.	0.241E-03	0.635E-04	0.366E-04	0.338E-04	0.337E-04	0.285E-04
C= 0.20E+15	10000.	0.228E-03	0.510E-04	0.469E-04	0.401E-04	0.399E-04	0.339E-04
	20000.	0.220E-03	0.416E-04	0.528E-04	0.446E-04	0.497E-04	0.371E-04
	30000.	0.216E-03	0.363E-04	0.552E-04	0.505E-04	0.473E-04	0.401E-04
	50000.	0.209E-03	0.289E-04	0.618E-04	0.521E-04	0.572E-04	0.451E-04

PERTURBER DENSITY = 0.1D+14(cm-3)

PERTURBERS ARE		ELECTRONS		PROTONS		IONIZED HELIUM	
TRANSITION	T(K)	WIDTH(A)	SHIFT(A)	WIDTH(A)	SHIFT(A)	WIDTH(A)	SHIFT(A)
Be II 3P-4S	2500.	0.470E-03	0.166E-03	0.752E-05	0.120E-04	0.836E-05	0.107E-04
5272.1 A	5000.	0.360E-03	0.155E-03	0.135E-04	0.167E-04	0.139E-04	0.147E-04
C= 0.43E+16	10000.	0.292E-03	0.125E-03	0.206E-04	0.209E-04	0.187E-04	0.177E-04
	20000.	0.268E-03	0.110E-03	0.261E-04	0.252E-04	0.235E-04	0.209E-04
	30000.	0.254E-03	0.979E-04	0.306E-04	0.275E-04	0.264E-04	0.231E-04
	50000.	0.244E-03	0.813E-04	0.336E-04	0.304E-04	0.289E-04	0.256E-04
Be II 3P-5S	2500.	0.336E-03	0.166E-03	0.149E-04	0.207E-04	0.147E-04	0.180E-04
3242.7 A	5000.	0.265E-03	0.163E-03	0.236E-04	0.256E-04	0.205E-04	0.216E-04
C= 0.16E+16	10000.	0.230E-03	0.140E-03	0.303E-04	0.305E-04	0.264E-04	0.258E-04
	20000.	0.214E-03	0.118E-03	0.366E-04	0.362E-04	0.326E-04	0.303E-04
	30000.	0.206E-03	0.109E-03	0.425E-04	0.391E-04	0.356E-04	0.328E-04
	50000.	0.206E-03	0.924E-04	0.484E-04	0.438E-04	0.391E-04	0.352E-04
Be II 3P-3D	2500.	0.422E-01	-0.502E-02	0.704E-03	-0.126E-02	0.857E-03	-0.115E-02
64174.1 A	5000.	0.336E-01	-0.285E-02	0.140E-02	-0.181E-02	0.145E-02	-0.160E-02
C= 0.64E+18	10000.	0.276E-01	-0.281E-02	0.227E-02	-0.231E-02	0.209E-02	-0.199E-02
	20000.	0.234E-01	-0.245E-02	0.288E-02	-0.278E-02	0.259E-02	-0.235E-02
	30000.	0.215E-01	-0.223E-02	0.330E-02	-0.306E-02	0.285E-02	-0.257E-02
	50000.	0.195E-01	-0.208E-02	0.370E-02	-0.345E-02	0.333E-02	-0.295E-02
Be II 3P-4D	2500.	0.820E-03	0.152E-04	0.167E-03	0.176E-03	0.146E-03	0.148E-03
4362.1 A	5000.	0.684E-03	0.200E-04	0.210E-03	0.209E-03	0.177E-03	0.175E-03
C= 0.48E+14	10000.	0.575E-03	0.175E-04	0.258E-03	0.242E-03	0.220E-03	0.206E-03
	20000.	0.484E-03	0.125E-04	0.286E-03	0.282E-03	0.249E-03	0.222E-03
	30000.	0.439E-03	0.910E-05	0.329E-03	0.298E-03	0.275E-03	0.261E-03
	50000.	0.389E-03	0.465E-05	0.346E-03	0.306E-03	0.268E-03	0.290E-03
Be II 3P-5D	2500.	0.115E-02	0.774E-04	0.333E-03	0.325E-03	0.291E-03	0.277E-03
3047.5 A	5000.	0.972E-03	0.621E-04	0.414E-03	0.380E-03	0.346E-03	0.311E-03
C= 0.13E+14	10000.	0.825E-03	0.491E-04	0.495E-03	0.444E-03	0.398E-03	0.360E-03
	20000.	0.701E-03	0.349E-04	0.586E-03	0.494E-03	0.453E-03	0.393E-03
	30000.	0.636E-03	0.251E-04	0.561E-03	0.561E-03	0.550E-03	0.417E-03
	50000.	0.560E-03	0.155E-04	0.561E-03	0.590E-03	0.555E-03	0.485E-03
Be II 3D-4P	2500.	0.487E-03	0.845E-04	0.283E-04	0.330E-04	0.296E-04	0.291E-04
4829.6 A	5000.	0.421E-03	0.780E-04	0.425E-04	0.416E-04	0.398E-04	0.355E-04
C= 0.15E+16	10000.	0.378E-03	0.708E-04	0.548E-04	0.501E-04	0.483E-04	0.422E-04
	20000.	0.348E-03	0.595E-04	0.673E-04	0.591E-04	0.608E-04	0.500E-04
	30000.	0.333E-03	0.560E-04	0.757E-04	0.645E-04	0.645E-04	0.528E-04
	50000.	0.316E-03	0.478E-04	0.795E-04	0.679E-04	0.737E-04	0.594E-04
Be II 3D-5P	2500.	0.467E-03	0.149E-03	0.502E-04	0.489E-04	0.473E-04	0.418E-04
3234.5 A	5000.	0.424E-03	0.127E-03	0.644E-04	0.597E-04	0.586E-04	0.500E-04
C= 0.35E+15	10000.	0.403E-03	0.970E-04	0.823E-04	0.700E-04	0.699E-04	0.596E-04
	20000.	0.387E-03	0.828E-04	0.917E-04	0.790E-04	0.848E-04	0.641E-04
	30000.	0.378E-03	0.733E-04	0.969E-04	0.894E-04	0.832E-04	0.710E-04
	50000.	0.364E-03	0.589E-04	0.106E-03	0.913E-04	0.995E-04	0.792E-04

PERTURBER DENSITY = 0.1D+14(cm-3)

PERTURBERS ARE		ELECTRONS		PROTONS		IONIZED HELIUM	
TRANSITION	T(K)	WIDTH(A)	SHIFT(A)	WIDTH(A)	SHIFT(A)	WIDTH(A)	SHIFT(A)
Be II 3D-4F	2500.	0.600E-03	-0.605E-06	0.153E-03	-0.164E-03	0.133E-03	-0.139E-03
4674.7 A	5000.	0.489E-03	-0.771E-05	0.192E-03	-0.195E-03	0.168E-03	-0.167E-03
C= 0.56E+14	10000.	0.398E-03	-0.734E-05	0.251E-03	-0.231E-03	0.210E-03	-0.189E-03
	20000.	0.324E-03	-0.852E-05	0.279E-03	-0.251E-03	0.254E-03	-0.220E-03
	30000.	0.290E-03	-0.551E-05	0.309E-03	-0.282E-03	0.265E-03	-0.228E-03
	50000.	0.253E-03	-0.166E-05	0.380E-03	-0.302E-03	0.272E-03	-0.249E-03
Be II 3D-5F	2500.	0.168E-02	0.375E-04	0.101E-02	0.905E-03	0.841E-03	0.763E-03
3198.1 A	5000.	0.136E-02	0.298E-04	0.115E-02	0.106E-02	0.104E-02	0.870E-03
C= 0.16E+13	10000.	0.110E-02	0.126E-04	0.135E-02	0.128E-02	0.119E-02	0.952E-03
	20000.	0.880E-03	-0.129E-05	0.165E-02	0.139E-02	0.119E-02	0.106E-02
	30000.	0.772E-03	-0.557E-05	0.159E-02	0.153E-02	0.143E-02	0.124E-02
	50000.	0.653E-03	-0.628E-05	0.197E-02	0.145E-02	0.125E-02	0.135E-02
Be II 4S-4P	2500.	0.240E-01	-0.332E-03	0.908E-03	0.892E-03	0.101E-02	0.798E-03
30339.8 A	5000.	0.207E-01	-0.675E-03	0.138E-02	0.119E-02	0.133E-02	0.100E-02
C= 0.61E+17	10000.	0.183E-01	-0.117E-02	0.172E-02	0.143E-02	0.161E-02	0.120E-02
	20000.	0.173E-01	-0.122E-02	0.212E-02	0.169E-02	0.189E-02	0.142E-02
	30000.	0.168E-01	-0.114E-02	0.233E-02	0.187E-02	0.205E-02	0.153E-02
	50000.	0.163E-01	-0.113E-02	0.247E-02	0.205E-02	0.215E-02	0.167E-02
Be II 4S-5P	2500.	0.264E-02	0.678E-03	0.256E-03	0.243E-03	0.241E-03	0.208E-03
7403.3 A	5000.	0.243E-02	0.479E-03	0.322E-03	0.292E-03	0.295E-03	0.247E-03
C= 0.19E+16	10000.	0.230E-02	0.303E-03	0.402E-03	0.351E-03	0.339E-03	0.287E-03
	20000.	0.222E-02	0.238E-03	0.470E-03	0.393E-03	0.430E-03	0.334E-03
	30000.	0.219E-02	0.200E-03	0.473E-03	0.430E-03	0.430E-03	0.339E-03
	50000.	0.213E-02	0.131E-03	0.562E-03	0.460E-03	0.503E-03	0.401E-03
Be II 4P-5S	2500.	0.517E-02	0.145E-02	0.139E-03	0.140E-03	0.154E-03	0.125E-03
11662.1 A	5000.	0.449E-02	0.144E-02	0.211E-03	0.185E-03	0.203E-03	0.157E-03
C= 0.90E+16	10000.	0.409E-02	0.140E-02	0.264E-03	0.223E-03	0.242E-03	0.187E-03
	20000.	0.392E-02	0.120E-02	0.319E-03	0.261E-03	0.293E-03	0.221E-03
	30000.	0.387E-02	0.109E-02	0.367E-03	0.286E-03	0.316E-03	0.239E-03
	50000.	0.385E-02	0.967E-03	0.388E-03	0.317E-03	0.325E-03	0.259E-03
Be II 4P-5D	2500.	0.120E-01	0.335E-03	0.320E-02	0.312E-02	0.279E-02	0.267E-02
9478.9 A	5000.	0.102E-01	0.327E-03	0.401E-02	0.365E-02	0.334E-02	0.299E-02
C= 0.12E+15	10000.	0.875E-02	0.224E-03	0.470E-02	0.428E-02	0.380E-02	0.346E-02
	20000.	0.750E-02	0.164E-03	0.558E-02	0.473E-02	0.435E-02	0.377E-02
	30000.	0.686E-02	0.632E-04	0.543E-02	0.539E-02	0.522E-02	0.404E-02
	50000.	0.610E-02	0.741E-05	0.532E-02	0.567E-02	0.537E-02	0.467E-02
Be II 4D-5P	2500.	0.828E-02	0.141E-02	0.710E-03	-0.735E-03	0.640E-03	-0.618E-03
10470.5 A	5000.	0.729E-02	0.114E-02	0.908E-03	-0.873E-03	0.806E-03	-0.742E-03
C= 0.28E+15	10000.	0.662E-02	0.871E-03	0.108E-02	-0.102E-02	0.955E-03	-0.873E-03
	20000.	0.608E-02	0.728E-03	0.141E-02	-0.118E-02	0.111E-02	-0.102E-02
	30000.	0.579E-02	0.661E-03	0.141E-02	-0.120E-02	0.125E-02	-0.106E-02
	50000.	0.541E-02	0.551E-03	0.168E-02	-0.141E-02	0.129E-02	-0.113E-02

PERTURBER DENSITY = 0.1D+14(cm-3)

PERTURBERS ARE		ELECTRONS		PROTONS		IONIZED HELIUM	
TRANSITION	T(K)	WIDTH(A)	SHIFT(A)	WIDTH(A)	SHIFT(A)	WIDTH(A)	SHIFT(A)
Be II 4D-5F	2500.	0.196E-01	0.105E-03	0.101E-01	0.888E-02	0.849E-02	0.753E-02
10098.4 A	5000.	0.160E-01	0.659E-04	0.111E-01	0.103E-01	0.104E-01	0.850E-02
C= 0.16E+14	10000.	0.130E-01	-0.798E-04	0.125E-01	0.124E-01	0.120E-01	0.937E-02
	20000.	0.106E-01	-0.168E-03	0.167E-01	0.131E-01	0.118E-01	0.101E-01
	30000.	0.934E-02	-0.185E-03	0.153E-01	0.150E-01	0.139E-01	0.121E-01
	50000.	0.796E-02	-0.145E-03	0.190E-01	0.135E-01	0.120E-01	0.125E-01
Be II 4F-5D	2500.	0.143E-01	0.141E-02	0.396E-02	0.392E-02	0.342E-02	0.324E-02
10138.4 A	5000.	0.120E-01	0.109E-02	0.491E-02	0.446E-02	0.403E-02	0.374E-02
C= 0.14E+15	10000.	0.102E-01	0.786E-03	0.591E-02	0.517E-02	0.469E-02	0.424E-02
	20000.	0.859E-02	0.557E-03	0.711E-02	0.569E-02	0.506E-02	0.472E-02
	30000.	0.777E-02	0.391E-03	0.727E-02	0.670E-02	0.622E-02	0.476E-02
	50000.	0.682E-02	0.248E-03	0.722E-02	0.710E-02	0.662E-02	0.581E-02
Be II 5S-5P	2500.	0.214	0.158E-01	0.148E-01	0.133E-01	0.141E-01	0.112E-01
61098.2 A	5000.	0.201	0.903E-03	0.184E-01	0.158E-01	0.173E-01	0.134E-01
C= 0.13E+18	10000.	0.194	-0.707E-02	0.231E-01	0.190E-01	0.205E-01	0.158E-01
	20000.	0.188	-0.106E-01	0.269E-01	0.215E-01	0.229E-01	0.181E-01
	30000.	0.187	-0.103E-01	0.286E-01	0.223E-01	0.260E-01	0.199E-01
	50000.	0.185	-0.110E-01	0.309E-01	0.254E-01	0.250E-01	0.218E-01

PERTURBER DENSITY = 0.1D+17(cm-3)

Be II 2S-2P	2500.	0.126E-01	-0.112E-02	0.370E-04	-0.311E-04	0.631E-04	-0.311E-04
3131.5 A	5000.	0.800E-02	-0.101E-02	0.997E-04	-0.682E-04	0.154E-03	-0.674E-04
C= 0.31E+20	10000.	0.574E-02	-0.485E-03	0.219E-03	-0.133E-03	0.293E-03	-0.125E-03
	20000.	0.445E-02	-0.513E-03	0.366E-03	-0.216E-03	0.433E-03	-0.190E-03
	30000.	0.405E-02	-0.401E-03	0.460E-03	-0.261E-03	0.508E-03	-0.232E-03
	50000.	0.384E-02	-0.477E-03	0.552E-03	-0.326E-03	0.571E-03	-0.275E-03
Be II 2S-3P	2500.	0.655E-02	0.514E-03	0.162E-03	0.181E-03	0.209E-03	0.167E-03
1036.3 A	5000.	0.555E-02	0.360E-03	0.304E-03	0.296E-03	0.339E-03	0.264E-03
C= 0.17E+18	10000.	0.478E-02	0.463E-03	0.484E-03	0.428E-03	0.463E-03	0.357E-03
	20000.	0.420E-02	0.433E-03	0.611E-03	0.522E-03	0.574E-03	0.443E-03
	30000.	0.392E-02	0.395E-03	0.684E-03	0.576E-03	0.637E-03	0.492E-03
	50000.	0.362E-02	0.403E-03	0.795E-03	0.646E-03	0.719E-03	0.557E-03
Be II 2S-4P	2500.	0.126E-01	0.222E-02	0.858E-03	0.722E-03	*0.900E-03	*0.610E-03
842.0 A	5000.	0.111E-01	0.216E-02	0.128E-02	0.104E-02	*0.120E-02	*0.861E-03
C= 0.47E+17	10000.	0.101E-01	0.198E-02	0.166E-02	0.140E-02	0.149E-02	0.117E-02
	20000.	0.948E-02	0.169E-02	0.202E-02	0.170E-02	0.180E-02	0.145E-02
	30000.	0.915E-02	0.162E-02	0.221E-02	0.191E-02	0.195E-02	0.153E-02
	50000.	0.873E-02	0.139E-02	0.247E-02	0.196E-02	0.222E-02	0.175E-02
Be II 2S-5P	2500.	0.253E-01	0.699E-02	*0.281E-02	*0.172E-02		
775.4 A	5000.	0.231E-01	0.622E-02	*0.371E-02	*0.257E-02		
C= 0.20E+17	10000.	0.221E-01	0.510E-02	*0.474E-02	*0.372E-02		
	20000.	0.214E-01	0.466E-02	*0.525E-02	*0.443E-02	*0.493E-02	*0.363E-02
	30000.	0.209E-01	0.411E-02	*0.552E-02	*0.503E-02	*0.473E-02	*0.400E-02
	50000.	0.202E-01	0.332E-02	*0.618E-02	*0.523E-02	*0.577E-02	*0.453E-02

PERTURBER DENSITY = 0.1D+17(cm-3)

PERTURBERS ARE		ELECTRONS		PROTONS		IONIZED HELIUM	
TRANSITION	T(K)	WIDTH(A)	SHIFT(A)	WIDTH(A)	SHIFT(A)	WIDTH(A)	SHIFT(A)
Be II 2P-3S	2500.	0.187E-01	0.827E-02	0.679E-04	0.236E-03	0.927E-04	0.223E-03
1776.2 A	5000.	0.133E-01	0.629E-02	0.229E-03	0.428E-03	0.255E-03	0.379E-03
C= 0.26E+19	10000.	0.943E-02	0.486E-02	0.451E-03	0.628E-03	0.448E-03	0.553E-03
	20000.	0.722E-02	0.374E-02	0.730E-03	0.800E-03	0.651E-03	0.676E-03
	30000.	0.661E-02	0.334E-02	0.874E-03	0.887E-03	0.759E-03	0.753E-03
	50000.	0.605E-02	0.278E-02	0.105E-02	0.102E-02	0.903E-03	0.844E-03
Be II 2P-4S	2500.	0.223E-01	0.998E-02	0.450E-03	0.661E-03	0.443E-03	0.560E-03
1197.2 A	5000.	0.156E-01	0.911E-02	0.841E-03	0.101E-02	0.824E-03	0.859E-03
C= 0.47E+18	10000.	0.117E-01	0.741E-02	0.129E-02	0.134E-02	0.113E-02	0.113E-02
	20000.	0.100E-01	0.658E-02	0.162E-02	0.165E-02	0.143E-02	0.139E-02
	30000.	0.950E-02	0.584E-02	0.194E-02	0.183E-02	0.157E-02	0.154E-02
	50000.	0.900E-02	0.490E-02	0.220E-02	0.198E-02	0.181E-02	0.166E-02
Be II 2P-5S	2500.	0.340E-01	0.172E-01	0.162E-02	0.163E-02	*0.158E-02	*0.133E-02
1048.2 A	5000.	0.272E-01	0.162E-01	0.255E-02	0.230E-02	*0.222E-02	*0.190E-02
C= 0.18E+18	10000.	0.220E-01	0.149E-01	0.333E-02	0.312E-02	*0.284E-02	*0.262E-02
	20000.	0.200E-01	0.128E-01	0.419E-02	0.392E-02	*0.358E-02	*0.322E-02
	30000.	0.190E-01	0.120E-01	0.471E-02	0.413E-02	0.396E-02	0.356E-02
	50000.	0.190E-01	0.101E-01	0.531E-02	0.471E-02	0.432E-02	0.384E-02
Be II 2P-3D	2500.	0.167E-01	0.931E-03	0.149E-03	-0.242E-03	0.193E-03	-0.224E-03
1512.4 A	5000.	0.124E-01	0.735E-03	0.348E-03	-0.422E-03	0.366E-03	-0.366E-03
C= 0.36E+18	10000.	0.926E-02	0.333E-03	0.580E-03	-0.614E-03	0.587E-03	-0.528E-03
	20000.	0.709E-02	0.154E-03	0.810E-03	-0.761E-03	0.742E-03	-0.643E-03
	30000.	0.612E-02	0.752E-04	0.909E-03	-0.842E-03	0.833E-03	-0.713E-03
	50000.	0.531E-02	0.272E-04	0.108E-02	-0.969E-03	0.962E-03	-0.801E-03
Be II 2P-4D	2500.	0.467E-01	-0.205E-02				
1143.0 A	5000.	0.394E-01	-0.864E-03				
C= 0.33E+16	10000.	0.333E-01	0.743E-03				
	20000.	0.281E-01	0.162E-02	*0.198E-01	*0.192E-01		
	30000.	0.255E-01	0.120E-02	*0.227E-01	*0.202E-01		
	50000.	0.225E-01	0.101E-02	*0.237E-01	*0.213E-01		
Be II 2P-5D	2500.	0.927E-01	-0.947E-02				
1026.9 A	5000.	0.838E-01	-0.553E-02				
C= 0.14E+16	10000.	0.744E-01	0.298E-04				
	20000.	0.654E-01	0.315E-02				
	30000.	0.602E-01	0.204E-02				
	50000.	0.539E-01	0.129E-02				
Be II 3S-3P	2500.	1.37	-0.211	0.189E-01	0.163E-01	0.251E-01	0.150E-01
12099.6 A	5000.	1.10	-0.161	0.352E-01	0.282E-01	0.400E-01	0.244E-01
C= 0.23E+20	10000.	0.880	-0.108	0.535E-01	0.409E-01	0.540E-01	0.351E-01
	20000.	0.756	-0.748E-01	0.667E-01	0.506E-01	0.646E-01	0.427E-01
	30000.	0.715	-0.703E-01	0.753E-01	0.568E-01	0.714E-01	0.476E-01
	50000.	0.671	-0.541E-01	0.854E-01	0.640E-01	0.790E-01	0.535E-01

PERTURBER DENSITY = 0.1D+17(cm-3)

PERTURBERS ARE		ELECTRONS		PROTONS		IONIZED HELIUM	
TRANSITION	T(K)	WIDTH(A)	SHIFT(A)	WIDTH(A)	SHIFT(A)	WIDTH(A)	SHIFT(A)
Be II 3S-4P	2500.	0.220	0.269E-01	0.127E-01	0.106E-01	*0.134E-01	*0.899E-02
3275.6 A	5000.	0.190	0.256E-01	0.190E-01	0.153E-01	*0.179E-01	*0.127E-01
C= 0.71E+18	10000.	0.169	0.217E-01	0.246E-01	0.208E-01	0.223E-01	0.172E-01
	20000.	0.157	0.172E-01	0.304E-01	0.251E-01	0.267E-01	0.216E-01
	30000.	0.151	0.165E-01	0.317E-01	0.277E-01	0.297E-01	0.230E-01
	50000.	0.145	0.139E-01	0.384E-01	0.293E-01	0.326E-01	0.261E-01
Be II 3S-5P	2500.	0.265	0.611E-01	*0.280E-01	*0.171E-01		
2454.6 A	5000.	0.241	0.564E-01	*0.370E-01	*0.257E-01		
C= 0.20E+18	10000.	0.228	0.477E-01	*0.472E-01	*0.372E-01		
	20000.	0.220	0.411E-01	*0.528E-01	*0.441E-01	*0.497E-01	*0.365E-01
	30000.	0.216	0.359E-01	*0.551E-01	*0.501E-01	*0.473E-01	*0.397E-01
	50000.	0.209	0.289E-01	*0.618E-01	*0.521E-01	*0.572E-01	*0.451E-01
Be II 3P-4S	2500.	0.470	0.164	0.749E-02	0.979E-02	0.827E-02	0.845E-02
5272.1 A	5000.	0.359	0.154	0.135E-01	0.151E-01	0.140E-01	0.131E-01
C= 0.43E+19	10000.	0.292	0.124	0.206E-01	0.202E-01	0.187E-01	0.171E-01
	20000.	0.268	0.110	0.261E-01	0.250E-01	0.235E-01	0.208E-01
	30000.	0.254	0.978E-01	0.306E-01	0.274E-01	0.264E-01	0.230E-01
	50000.	0.244	0.813E-01	0.336E-01	0.304E-01	0.289E-01	0.256E-01
Be II 3P-5S	2500.	0.336	0.160	0.149E-01	0.150E-01	*0.146E-01	*0.122E-01
3242.7 A	5000.	0.265	0.159	0.238E-01	0.213E-01	*0.207E-01	*0.173E-01
C= 0.16E+19	10000.	0.230	0.137	0.304E-01	0.290E-01	*0.261E-01	*0.241E-01
	20000.	0.214	0.117	0.366E-01	0.359E-01	*0.326E-01	*0.300E-01
	30000.	0.206	0.109	0.426E-01	0.389E-01	0.356E-01	0.325E-01
	50000.	0.206	0.922E-01	0.484E-01	0.438E-01	0.391E-01	0.352E-01
Be II 3P-4D	2500.	0.726	-0.637E-01				
4362.1 A	5000.	0.620	-0.348E-01				
C= 0.48E+17	10000.	0.531	-0.668E-02				
	20000.	0.453	0.752E-02	*0.286	*0.277		
	30000.	0.414	0.515E-02	*0.329	*0.294		
	50000.	0.369	0.465E-02	*0.346	*0.306	*0.268	*0.290
Be II 3P-5D	2500.	0.834	-0.937E-01				
3047.5 A	5000.	0.757	-0.503E-01				
C= 0.13E+17	10000.	0.676	-0.899E-02				
	20000.	0.596	0.206E-01				
	30000.	0.550	0.135E-01				
	50000.	0.494	0.623E-02				
Be II 3D-4P	2500.	0.487	0.757E-01	0.279E-01	0.247E-01	*0.289E-01	*0.208E-01
4829.6 A	5000.	0.421	0.726E-01	0.431E-01	0.359E-01	*0.396E-01	*0.295E-01
C= 0.15E+19	10000.	0.378	0.683E-01	0.547E-01	0.478E-01	0.482E-01	0.400E-01
	20000.	0.348	0.590E-01	0.673E-01	0.587E-01	0.608E-01	0.496E-01
	30000.	0.333	0.556E-01	0.757E-01	0.642E-01	0.645E-01	0.525E-01
	50000.	0.316	0.478E-01	0.795E-01	0.679E-01	0.737E-01	0.594E-01

PERTURBER DENSITY = 0.1D+17(cm-3)

PERTURBERS ARE		ELECTRONS		PROTONS		IONIZED HELIUM	
TRANSITION	T(K)	WIDTH(A)	SHIFT(A)	WIDTH(A)	SHIFT(A)	WIDTH(A)	SHIFT(A)
Be II 3D-5P	2500.	0.467	0.128	*0.487E-01	*0.301E-01		
3234.5 A	5000.	0.424	0.114	*0.643E-01	*0.450E-01		
C= 0.35E+18	10000.	0.403	0.915E-01	*0.828E-01	*0.648E-01		
	20000.	0.387	0.818E-01	*0.916E-01	*0.780E-01	*0.848E-01	*0.632E-01
	30000.	0.378	0.726E-01	*0.969E-01	*0.887E-01	*0.832E-01	*0.703E-01
	50000.	0.364	0.589E-01	*0.106	*0.913E-01	*0.995E-01	*0.792E-01
Be II 3D-4F	2500.	0.524	0.667E-01				
4674.7 A	5000.	0.436	0.395E-01				
C= 0.56E+17	10000.	0.362	0.134E-01				
	20000.	0.299	-0.428E-02	*0.279	*-0.247		
	30000.	0.270	-0.216E-02	*0.310	*-0.279		
	50000.	0.237	-0.166E-02	*0.380	*-0.302	*0.272	*-0.249
Be II 3D-5F	2500.	0.904	0.519E-01				
3198.1 A	5000.	0.819	0.312E-01				
C= 0.16E+16	10000.	0.714	0.916E-02				
	20000.	0.609	-0.521E-02				
	30000.	0.551	-0.824E-02				
	50000.	0.482	-0.628E-02				
Be II 4S-5P	2500.	2.64	0.574	*0.247	*0.151		
7403.3 A	5000.	2.43	0.408	*0.324	*0.227		
C= 0.19E+19	10000.	2.30	0.277	*0.403	*0.327	*0.343	*0.263
	20000.	2.22	0.233	*0.470	*0.389	*0.430	*0.330
	30000.	2.19	0.197	*0.473	*0.426	*0.429	*0.335
	50000.	2.13	0.131	*0.562	*0.460	*0.503	*0.401
Be II 4P-5S	2500.	5.17	1.41	0.137	0.108	*0.149	*0.922E-01
11662.1 A	5000.	4.49	1.42	0.210	0.162	0.202	0.133
C= 0.90E+19	10000.	4.09	1.39	0.264	0.214	0.242	0.178
	20000.	3.92	1.20	0.319	0.260	0.293	0.219
	30000.	3.87	1.09	0.367	0.285	0.316	0.238
	50000.	3.85	0.966	0.388	0.317	0.325	0.259
Be II 4P-5D	2500.	8.97	-1.29				
9478.9 A	5000.	8.15	-0.742				
C= 0.12E+18	10000.	7.30	-0.327				
	20000.	6.49	0.284E-01				
	30000.	6.03	-0.479E-01				
	50000.	5.46	0.741E-02				
Be II 4D-5P	2500.	7.74	1.65				
10470.5 A	5000.	6.93	1.30				
C= 0.28E+18	10000.	6.37	0.950	*1.10	*-0.933		
	20000.	5.90	0.747	*1.41	*-1.16		
	30000.	5.64	0.677	*1.41	*-1.19		
	50000.	5.30	0.566	*1.68	*-1.41	*1.29	*-1.13

PERTURBER DENSITY = 0.1D+17(cm-3)

PERTURBERS ARE		ELECTRONS		PROTONS		IONIZED HELIUM	
TRANSITION	T(K)	WIDTH(A)	SHIFT(A)	WIDTH(A)	SHIFT(A)	WIDTH(A)	SHIFT(A)
Be II 4D-5F	2500.	11.4	0.687				
10098.4 A	5000.	10.3	0.369				
C= 0.16E+17	10000.	8.98	0.175E-01				
	20000.	7.71	-0.180				
	30000.	7.00	-0.191				
	50000.	6.14	-0.154				
Be II 4F-5D	2500.	10.5	-0.805				
10138.4 A	5000.	9.41	-0.471				
C= 0.14E+18	10000.	8.33	0.401E-01				
	20000.	7.31	0.380				
	30000.	6.72	0.247				
	50000.	6.01	0.248				
PERTURBER DENSITY = 0.1D+18(cm-3)							
Be II 2S-2P	2500.	0.126	-0.112E-01	0.336E-03	-0.217E-03	0.571E-03	-0.216E-03
3131.5 A	5000.	0.801E-01	-0.101E-01	0.985E-03	-0.605E-03	0.152E-02	-0.597E-03
C= 0.31E+21	10000.	0.573E-01	-0.497E-02	0.218E-02	-0.126E-02	0.292E-02	-0.118E-02
	20000.	0.445E-01	-0.499E-02	0.366E-02	-0.213E-02	0.433E-02	-0.188E-02
	30000.	0.405E-01	-0.395E-02	0.460E-02	-0.259E-02	0.508E-02	-0.229E-02
	50000.	0.384E-01	-0.482E-02	0.552E-02	-0.325E-02	0.571E-02	-0.274E-02
Be II 2S-3P	2500.	0.655E-01	0.412E-02	0.146E-02	0.115E-02	0.182E-02	0.102E-02
1036.3 A	5000.	0.555E-01	0.283E-02	0.299E-02	0.242E-02	0.330E-02	0.211E-02
C= 0.17E+19	10000.	0.478E-01	0.418E-02	0.477E-02	0.377E-02	0.457E-02	0.307E-02
	20000.	0.420E-01	0.414E-02	0.611E-02	0.502E-02	0.573E-02	0.423E-02
	30000.	0.392E-01	0.393E-02	0.679E-02	0.556E-02	0.636E-02	0.475E-02
	50000.	0.362E-01	0.400E-02	0.795E-02	0.643E-02	0.719E-02	0.554E-02
Be II 2S-4P	2500.	0.126	0.153E-01				
842.0 A	5000.	0.111	0.172E-01				
C= 0.47E+18	10000.	0.101	0.164E-01	*0.162E-01	*0.107E-01		
	20000.	0.948E-01	0.155E-01	*0.202E-01	*0.157E-01		
	30000.	0.915E-01	0.150E-01	*0.221E-01	*0.179E-01		
	50000.	0.872E-01	0.137E-01	*0.247E-01	*0.193E-01		
Be II 2S-5P	2500.	*0.245	*0.372E-01				
775.4 A	5000.	0.227	0.407E-01				
C= 0.20E+18	10000.	0.218	0.343E-01				
	20000.	0.212	0.400E-01				
	30000.	0.208	0.359E-01				
	50000.	0.201	0.320E-01				
Be II 2P-3S	2500.	0.187	0.816E-01	0.665E-03	0.159E-02	0.899E-03	0.146E-02
1776.2 A	5000.	0.133	0.621E-01	0.228E-02	0.366E-02	0.253E-02	0.317E-02
C= 0.26E+20	10000.	0.944E-01	0.481E-01	0.452E-02	0.570E-02	0.450E-02	0.495E-02
	20000.	0.723E-01	0.371E-01	0.729E-02	0.776E-02	0.651E-02	0.652E-02
	30000.	0.661E-01	0.333E-01	0.874E-02	0.867E-02	0.758E-02	0.735E-02
	50000.	0.605E-01	0.277E-01	0.105E-01	0.101E-01	0.903E-02	0.840E-02

PERTURBER DENSITY = 0.1D+18(cm-3)

PERTURBERS ARE		ELECTRONS		PROTONS		IONIZED HELIUM	
TRANSITION	T(K)	WIDTH(A)	SHIFT(A)	WIDTH(A)	SHIFT(A)	WIDTH(A)	SHIFT(A)
Be II 2P-4S	2500.	0.223	0.954E-01	*0.435E-02	*0.364E-02	*0.416E-02	*0.263E-02
1197.2 A	5000.	0.157	0.883E-01	*0.830E-02	*0.776E-02	*0.812E-02	*0.615E-02
C= 0.47E+19	10000.	0.118	0.722E-01	*0.127E-01	*0.111E-01	*0.112E-01	*0.908E-02
	20000.	0.100	0.642E-01	0.163E-01	0.155E-01	*0.144E-01	*0.131E-01
	30000.	0.950E-01	0.577E-01	0.193E-01	0.174E-01	*0.159E-01	*0.146E-01
	50000.	0.900E-01	0.488E-01	0.220E-01	0.197E-01	*0.181E-01	*0.164E-01
Be II 2P-5S	2500.	*0.340	*0.155				
1048.2 A	5000.	0.272	0.151				
C= 0.18E+19	10000.	0.220	0.141				
	20000.	0.200	0.122				
	30000.	0.190	0.117				
	50000.	0.190	0.991E-01	*0.531E-01	*0.465E-01		
Be II 2P-3D	2500.	0.167	0.105E-01	0.138E-02	-0.161E-02	0.175E-02	-0.143E-02
1512.4 A	5000.	0.123	0.809E-02	0.344E-02	-0.355E-02	0.359E-02	-0.299E-02
C= 0.36E+19	10000.	0.926E-01	0.396E-02	0.575E-02	-0.553E-02	0.581E-02	-0.467E-02
	20000.	0.708E-01	0.183E-02	0.810E-02	-0.736E-02	0.742E-02	-0.618E-02
	30000.	0.612E-01	0.102E-02	0.910E-02	-0.822E-02	0.826E-02	-0.689E-02
	50000.	0.532E-01	0.310E-03	0.108E-01	-0.964E-02	0.962E-02	-0.797E-02
Be II 2P-4D	2500.	0.342	-0.293E-01				
1143.0 A	5000.	0.308	-0.205E-01				
C= 0.33E+17	10000.	0.273	-0.118E-01				
	20000.	0.239	-0.454E-02				
	30000.	0.221	-0.865E-04				
	50000.	0.199	0.556E-02				
Be II 2P-5D	2500.	0.555	-0.794E-01				
1026.9 A	5000.	0.562	-0.579E-01				
C= 0.14E+17	10000.	0.548	-0.387E-01				
	20000.	0.515	-0.259E-01				
	30000.	0.489	-0.104E-01				
	50000.	0.451	0.795E-02				
Be II 3S-3P	2500.	13.7	-2.20	0.169	0.108	0.215	0.953E-01
12099.6 A	5000.	11.0	-1.66	0.345	0.237	0.388	0.200
C= 0.23E+21	10000.	8.81	-1.12	0.534	0.370	0.536	0.310
	20000.	7.56	-0.783	0.666	0.489	0.645	0.410
	30000.	7.15	-0.717	0.751	0.554	0.719	0.462
	50000.	6.72	-0.542	0.854	0.637	0.789	0.532
Be II 3S-4P	2500.	2.20	0.168				
3275.6 A	5000.	1.90	0.190				
C= 0.71E+19	10000.	1.69	0.166	*0.242	*0.159		
	20000.	1.57	0.151	*0.307	*0.233		
	30000.	1.51	0.148	*0.319	*0.263		
	50000.	1.45	0.136	*0.384	*0.290	*0.326	*0.258

PERTURBER DENSITY = 0.1D+18(cm-3)

PERTURBERS ARE		ELECTRONS		PROTONS		IONIZED HELIUM	
TRANSITION	T(K)	WIDTH(A)	SHIFT(A)	WIDTH(A)	SHIFT(A)	WIDTH(A)	SHIFT(A)
Be II 3S-5P	2500.	*2.57	*0.285				
2454.6 A	5000.	2.36	0.340				
C= 0.20E+19	10000.	2.25	0.311				
	20000.	2.18	0.345				
	30000.	2.14	0.350				
	50000.	2.08	0.277				
Be II 3P-4S	2500.	4.70	1.58	0.695E-01	0.573E-01	*0.737E-01	*0.441E-01
5272.1 A	5000.	3.60	1.50	0.133	0.118	*0.136	*0.978E-01
C= 0.43E+20	10000.	2.92	1.22	0.203	0.172	*0.186	*0.139
	20000.	2.68	1.08	0.261	0.238	*0.235	*0.195
	30000.	2.54	0.968	0.309	0.263	*0.266	*0.222
	50000.	2.44	0.811	0.336	0.302	*0.289	*0.253
Be II 3P-5S	2500.	*3.36	*1.44				
3242.7 A	5000.	2.65	1.49				
C= 0.16E+20	10000.	2.30	1.30				
	20000.	2.14	1.12				
	30000.	2.06	1.06	*0.428	*0.357		
	50000.	2.06	0.901	*0.484	*0.433		
Be II 3P-4D	2500.	5.44	-0.747				
4362.1 A	5000.	4.94	-0.507				
C= 0.48E+18	10000.	4.44	-0.334				
	20000.	3.92	-0.139				
	30000.	3.65	0.625E-02				
	50000.	3.31	-0.190E-01				
Be II 3P-5D	2500.	5.05	-0.793				
3047.5 A	5000.	5.14	-0.606				
C= 0.13E+18	10000.	5.02	-0.434				
	20000.	4.74	-0.295				
	30000.	4.51	-0.135				
	50000.	4.17	0.182E-01				
Be II 3D-4P	2500.	4.86	0.515				
4829.6 A	5000.	4.21	0.563				
C= 0.15E+20	10000.	3.77	0.564	*0.532	*0.366		
	20000.	3.48	0.543	*0.676	*0.540		
	30000.	3.33	0.550	*0.759	*0.608		
	50000.	3.16	0.470	*0.795	*0.671		
Be II 3D-5P	2500.	4.53	0.705				
3234.5 A	5000.	4.16	0.750				
C= 0.35E+19	10000.	3.97	0.619				
	20000.	3.83	0.702				
	30000.	3.75	0.709				
	50000.	3.62	0.568				

PERTURBER DENSITY = 0.1D+18(cm-3)

PERTURBERS ARE		ELECTRONS		PROTONS		IONIZED HELIUM	
TRANSITION	T(K)	WIDTH(A)	SHIFT(A)	WIDTH(A)	SHIFT(A)	WIDTH(A)	SHIFT(A)
Be II 3D-4F	2500.	3.74	0.846				
4674.7 A	5000.	3.33	0.583				
C= 0.56E+18	10000.	2.90	0.403				
	20000.	2.49	0.231				
	30000.	2.29	0.135				
	50000.	2.06	0.404E-01				
Be II 3D-5F	2500.	5.01	0.676				
3198.1 A	5000.	5.03	0.469				
C= 0.16E+17	10000.	4.81	0.339				
	20000.	4.42	0.193				
	30000.	4.14	0.623E-01				
	50000.	3.76	-0.515E-01				
PERTURBER DENSITY = 0.1D+19(cm-3)							
Be II 2S-2P	2500.	1.26	-0.105	0.163E-02	-0.649E-03	0.268E-02	-0.646E-03
3131.5 A	5000.	0.801	-0.967E-01	0.855E-02	-0.397E-02	0.129E-01	-0.390E-02
C= 0.31E+22	10000.	0.574	-0.465E-01	0.214E-01	-0.109E-01	0.284E-01	-0.101E-01
	20000.	0.444	-0.476E-01	0.364E-01	-0.197E-01	0.430E-01	-0.172E-01
	30000.	0.405	-0.386E-01	0.459E-01	-0.248E-01	0.507E-01	-0.219E-01
	50000.	0.384	-0.478E-01	0.552E-01	-0.320E-01	0.570E-01	-0.269E-01
Be II 2S-3P	2500.	0.649	-0.930E-03	*0.484E-02	*0.126E-02		
1036.3 A	5000.	0.553	0.408E-02	*0.228E-01	*0.989E-02		
C= 0.17E+20	10000.	0.477	0.261E-01	*0.460E-01	*0.262E-01		
	20000.	0.419	0.292E-01	*0.594E-01	*0.390E-01		
	30000.	0.392	0.298E-01	*0.686E-01	*0.484E-01		
	50000.	0.361	0.358E-01	*0.790E-01	*0.602E-01		
Be II 2S-4P	2500.	*1.25	*-0.102				
842.0 A	5000.	*1.02	*0.121E-01				
C= 0.47E+19	10000.	0.956	0.603E-01				
	20000.	0.909	0.735E-01				
	30000.	0.884	0.938E-01				
	50000.	0.849	0.107				
Be II 2S-5P	2500.						
775.4 A	5000.	*1.53	*-0.935E-01				
C= 0.20E+19	10000.	1.70	-0.131E-02				
	20000.	1.79	0.102				
	30000.	1.81	0.145				
	50000.	1.80	0.192				
Be II 2P-3S	2500.	1.87	0.772	0.462E-02	0.358E-02	*0.546E-02	*0.242E-02
1776.2 A	5000.	1.33	0.595	0.216E-01	0.197E-01	*0.233E-01	*0.149E-01
C= 0.26E+21	10000.	0.943	0.464	0.448E-01	0.434E-01	*0.442E-01	*0.358E-01
	20000.	0.722	0.358	0.736E-01	0.654E-01	*0.655E-01	*0.531E-01
	30000.	0.661	0.321	0.880E-01	0.781E-01	*0.773E-01	*0.646E-01
	50000.	0.605	0.269	0.106	0.967E-01	*0.910E-01	*0.788E-01

PERTURBER DENSITY = 0.1D+19(cm-3)

PERTURBERS ARE		ELECTRONS		PROTONS		IONIZED HELIUM	
TRANSITION	T(K)	WIDTH(A)	SHIFT(A)	WIDTH(A)	SHIFT(A)	WIDTH(A)	SHIFT(A)
Be II 2P-4S	2500.						
1197.2 A	5000.	*1.56	*0.780				
C= 0.47E+20	10000.	1.18	0.655				
	20000.	1.00	0.594				
	30000.	0.950	0.535				
	50000.	0.899	0.456				
Be II 2P-5S	2500.						
1048.2 A	5000.						
C= 0.18E+20	10000.	*2.19	*1.14				
	20000.	1.99	1.03				
	30000.	1.89	0.992				
	50000.	1.89	0.883				
Be II 2P-3D	2500.	1.66	0.157	*0.689E-02	*-0.306E-02	*0.588E-02	*-0.151E-02
1512.4 A	5000.	1.23	0.111	*0.297E-01	*-0.176E-01	*0.276E-01	*-0.121E-01
C= 0.36E+20	10000.	0.925	0.593E-01	*0.564E-01	*-0.406E-01	*0.561E-01	*-0.323E-01
	20000.	0.708	0.336E-01	*0.815E-01	*-0.604E-01	*0.728E-01	*-0.485E-01
	30000.	0.611	0.201E-01	*0.911E-01	*-0.726E-01	*0.830E-01	*-0.595E-01
	50000.	0.531	0.829E-02	*0.106	*-C.912E-01	*0.952E-01	*-0.745E-01
Be II 2P-4D	2500.						
1143.0 A	5000.	2.08	-0.304E-01				
C= 0.33E+18	10000.	2.00	-0.260E-01				
	20000.	1.86	-0.195E-01				
	30000.	1.77	-0.338E-01				
	50000.	1.65	-0.498E-02				
Be II 2P-5D	2500.						
1026.9 A	5000.	*3.13	*0.304E-01				
C= 0.14E+18	10000.	3.09	-0.172E-01				
	20000.	3.40	-0.785E-01				
	30000.	3.45	-0.796E-01				
	50000.	3.39	-0.728E-01				
Be II 3S-4P	2500.						
3275.6 A	5000.	*17.7	*-0.431				
C= 0.71E+20	10000.	16.0	0.149				
	20000.	15.1	0.323				
	30000.	14.6	0.661				
	50000.	14.1	0.918				

PERTURBER DENSITY = 0.1D+20(cm-3)

Be II 2S-2P	2500.						
3131.5 A	5000.	8.00	-0.858				
C= 0.31E+23	10000.	5.73	-0.387				
	20000.	4.44	-0.431	0.350	-0.160	*0.405	*-0.135
	30000.	4.05	-0.349	0.449	-0.213	*0.489	*-0.184
	50000.	3.84	-0.442	0.547	-0.288	*0.565	*-0.236

PERTURBER DENSITY = 0.1D+20(cm-3)

PERTURBERS ARE		ELECTRONS		PROTONS		IONIZED HELIUM	
TRANSITION	T(K)	WIDTH(A)	SHIFT(A)	WIDTH(A)	SHIFT(A)	WIDTH(A)	SHIFT(A)
Be II 2S-3P	2500.						
1036.3 A	5000.						
C= 0.17E+21	10000.	4.40	-0.226				
	20000.	3.91	-0.310E-01				
	30000.	3.70	0.262E-01				
	50000.	3.45	0.157				
Be II 2S-4P	2500.						
842.0 A	5000.						
C= 0.47E+20	10000.	*5.94	*-0.767				
	20000.	6.48	-0.322				
	30000.	6.73	-0.322E-01				
	50000.	6.88	0.129				
Be II 2P-3S	2500.						
1776.2 A	5000.	*13.2	*4.88				
C= 0.26E+22	10000.	9.42	4.03				
	20000.	7.22	3.19				
	30000.	6.61	2.91				
	50000.	6.05	2.46				
Be II 2P-4S	2500.						
1197.2 A	5000.						
C= 0.47E+21	10000.	*11.0	*4.02				
	20000.	9.67	4.31				
	30000.	9.24	4.07				
	50000.	8.80	3.56				
Be II 2P-5S	2500.						
1048.2 A	5000.						
C= 0.18E+21	10000.						
	20000.	*15.1	*4.56				
	30000.	*15.3	*5.32				
	50000.	16.3	5.23				
Be II 2P-3D	2500.						
1512.4 A	5000.	*10.7	*1.99				
C= 0.36E+21	10000.	8.51	1.20				
	20000.	6.68	0.735				
	30000.	5.81	0.538				
	50000.	5.09	0.373				

ТАБЕЛЕ ПАРАМЕТАРА ШТАРКОВОГ ШИРЕЊА ЛИНИЈА Be II ОД ЗНАЧАЈА У АСТРОФИЗИЦИ

М. С. Димитријевић[1] и S.Sahal–Bréchot[2]

[1]*Астрономска опсерваторија, Волгина 7, 11050 Београд, Југославија*
[2]*Laboratoire "Astrophysique, Atomes et Molécules" Département Atomes et Molécules en Astrophysique Unité associée au C.N.R.S. No 812 Observatoire de Paris-Meudon, 92190 Meudon, France*

УДК 52–355.3
Претходно саопштење

Користећи семикласичан прилаз, израчунате су ширине и помераји спектралних линија, проузроковани сударима са електронима, протонима и јонима хелијума, за 30 мултиплета јонизованог берилијума. Резултати су дати у функцији температуре и концентрације пертурбера.

Bull. Astron. Belgrade № 145 (1992), 81 – 99.

UDC 52-355.3
Preliminary report

STARK BROADENING PARAMETER TABLES FOR Ca II LINES OF ASTROPHYSICAL INTEREST

M. S. Dimitrijević[1], and S. Sahal–Bréchot[2]

[1] *Astronomical Observatory, Volgina 7, 11050 Beograd, Yugoslavia*
[2] *Laboratoire "Astrophysique, Atomes et Molécules" Département Atomes et Molécules en Astrophysique Unité associée au C.N.R.S. No 812 Observatoire de Paris–Meudon, 92190 Meudon, France*

(Received: October 21, 1991)

SUMMARY: Using a semiclassical approach, we have calculated electron–, proton–, and ionized helium–impact line widths and shifts for 28 Ca II multiplets as a function of temperature for perturber densities 10^{13} and 10^{16} – 10^{19}cm^{-3}.

1. INTRODUCTION

Calcium is one of the most abundant chemical elements in stellar plasmas. The well known resonance lines of Ca II are among the most important features in stellar spectra and are present in all spectra starting with B–type stars and reaching maximal intensity in the K0 spectral type. The knowledge of reliable Ca II Stark broadening parameters is of great importance for detailed investigation of stellar atmospheres. The astrophysical importance of Stark broadening data for the investigation of subphotospheric layers is discussed in Seaton (1987). Moreover, Ca II lines are of particular interest for the investigations of laboratory plasmas, since calcium is often present as an impurity. The present paper concerns singly ionized calcium : In order to provide reliable data for Ca II lines broadened by collisions with charged perturbers in stellar and laboratory plasmas, we have calculated electron–, proton–, and ionized helium–impact line widths and shifts for 28 Ca II multiplets, using the semiclassical–perturbation formalism (Sahal–Bréchot, 1969ab). The obtained results for perturber density of 10^{15}cm^{-3}, together with discussion, analysis and comparison with the existing experimental and theoretical data will be published in the principal article elsewhere (Dimitrijević, and Sahal–Bréchot, 1992). Since data are not linear with perturber density (N), due to the Debye screening effect, which is often important at high densities of interest for subphotospheric layers, we will present here the data for N = 10^{16} – 10^{19}cm^{-3}. Moreover, we also will present the data for N = 10^{13} cm^{-3} of special interest for stellar atmospheres.

2. RESULTS AND DISCUSSION

All details of the calculation procedure has been described in Dimitrijević, Sahal–Bréchot, Bommier (1991) and will not be repeated here. En-

ergy levels for Ca II lines have been taken from Bashkin and Stoner (1975). Oscillator strengths have been calculated using the method of Bates and Damgaard (1949) and tables of Oertel and Shomo (1968). For the transitions including higher atomic energy levels, the method described by Van Regemorter et al. (1979) has been used.

In addition to the electron–impact full half-widths and shifts, Stark broadening parameters due to proton–, and ionized helium–impact have been calculated. In such a way we provide Stark broadening data for all important charged perturbers in stellar plasma. Our results are shown in Table 1 for perturber densities 10^{13} and 10^{16} – 10^{19}cm^{-3} and temperatures of T = 5,000; 10,000; 20,000; 30,000; 50,000 and 100,000 K. We also specify a parameter c (Dimitrijević and Sahal–Bréchot, 1984) which gives an estimate for the maximum perturber density for which the line may be treated as isolated when it is divided by the electron–impact full width at half maximum.

For each value given in Table 1, the collision volume (V) multiplied by the perturber density (N) is much less than one and the impact approximation is valid (Sahal–Bréchot, 1969ab). Values for NV> 0.5 are not given in Table 1; values for 0.1< NV $\leq$ 0.5 are denoted by an asterisk. When the impact approximation is not valid, the ion broadening contribution may be estimated by using quasistatic formulae (cf. Sahal–Bréchot (1991) or Griem (1974)).

The analysis of present results and comparison with available experimental and theoretical data is given in Dimitrijević and Sahal – Bréchot (1992).

Acknowledgments – This work is a part of French–Yugoslav collaboration through the project "L'élargissement Stark des raies spectrales des plasmas astrophysiques et de laboratoire". It is also a part of the project "Physics and dynamics of celestial bodies", supported by RFN of Serbia.

REFERENCES

Bashkin, S., and Stoner, J. O. Jr.: 1975, *Atomic Energy Levels and Grotrian Diagrams*, **Vol. 1**, North Holland, Amsterdam.

Bates, D. R., and Damgaard, A.: 1949, *Trans. Roy. Soc. London*, Ser. A **242**, 101.

Dimitrijević, M. S., and Sahal–Bréchot, S.: 1984, *JQSRT*, **31**, 301.

Dimitrijević, M. S., and Sahal–Bréchot, S.: 1992, *JQSRT*,to be published.

Dimitrijević, M. S., Sahal–Bréchot, S., and Bommier, V.: 1991, *Astron. Astrophys. Suppl. Series.*, **89**, 581.

Griem, H. R.: 1974, *Spectral Line Broadening by Plasmas*, Academic Press, New York.

Oertel, G. K., and Shomo, L. P.: 1968, *Astrophys. J. Suppl. Series* , **16**, 175.

Sahal–Bréchot, S.: 1969a, *Astron. Astrophys.* , **1**, 91.

Sahal–Bréchot, S.: 1969b, *Astron. Astrophys.*, **2**, 322.

Sahal–Bréchot,S.: 1991, *Astron. Astrophys.*, **245**, 322.

Seaton, M. J.: 1987, *J. Phys. B* **20**, 6363.

Van Regemorter, H., Hoang Binh Dy, and Prud'homme, M.: 1979, *J. Phys. B* **12**, 1073.

Table 1. This table gives electron–, proton–, and ionized–helium– impact broadening parameters for Ca II lines, for perturber densities 10^{13} and 10^{16} – $10^{19} cm^{-3}$ and temperatures from 5,000 K to 100,000 K. Transitions and averaged wavelengths for the multiplet (in Å) are also given. By dividing c by the electron–impact full halfwidth, we obtain an estimate for the maximum perturber density for which the line may be treated as isolated and tabulated data may be used. The asterisk identifies cases for which the collision volume multiplied by the perturber density (the condition for validity of the impact approximation) lies between 0.1 and 0.5.

PERTURBER DENSITY = 0.1D+14(cm-3)

PERTURBERS ARE		ELECTRONS		PROTONS		IONIZED HELIUM	
TRANSITION	T(K)	WIDTH(A)	SHIFT(A)	WIDTH(A)	SHIFT(A)	WIDTH(A)	SHIFT(A)
CA II 3D-4P	5000.	0.134E-03	0.601E-05	0.404E-05	-0.765E-06	0.576E-05	-0.748E-06
8581.1 A	10000.	0.105E-03	0.298E-05	0.669E-05	-0.138E-05	0.834E-05	-0.128E-05
C= 0.86E+17	20000.	0.856E-04	0.229E-05	0.928E-05	-0.212E-05	0.101E-04	-0.185E-05
	30000.	0.776E-04	0.881E-06	0.101E-04	-0.258E-05	0.109E-04	-0.222E-05
	50000.	0.707E-04	0.748E-06	0.112E-04	-0.310E-05	0.118E-04	-0.255E-05
	100000.	0.643E-04	0.792E-06	0.125E-04	-0.374E-05	0.128E-04	-0.307E-05
CA II 3D-5P	5000.	0.303E-04	-0.387E-05	0.249E-05	-0.948E-06	0.291E-05	-0.820E-06
2132.3 A	10000.	0.241E-04	-0.235E-05	0.313E-05	-0.130E-05	0.332E-05	-0.108E-05
C= 0.17E+16	20000.	0.207E-04	-0.231E-05	0.360E-05	-0.157E-05	0.373E-05	-0.130E-05
	30000.	0.196E-04	-0.185E-05	0.390E-05	-0.175E-05	0.390E-05	-0.144E-05
	50000.	0.189E-04	-0.147E-05	0.410E-05	-0.199E-05	0.402E-05	-0.162E-05
	100000.	0.183E-04	-0.132E-05	0.431E-05	-0.225E-05	0.439E-05	-0.186E-05
CA II 3D-6P	5000.	0.413E-04	-0.140E-04	0.559E-05	-0.284E-05	0.586E-05	-0.232E-05
1644.1 A	10000.	0.358E-04	-0.107E-04	0.652E-05	-0.340E-05	0.667E-05	-0.280E-05
C= 0.48E+15	20000.	0.333E-04	-0.813E-05	0.732E-05	-0.404E-05	0.723E-05	-0.328E-05
	30000.	0.328E-04	-0.654E-05	0.757E-05	-0.439E-05	0.747E-05	-0.365E-05
	50000.	0.332E-04	-0.556E-05	0.806E-05	-0.481E-05	0.746E-05	-0.375E-05
	100000.	0.334E-04	-0.439E-05	0.885E-05	-0.558E-05	0.776E-05	-0.440E-05
CA II 3D-7P	5000.	0.721E-04	-0.317E-04	0.120E-04	-0.681E-05	0.121E-04	-0.560E-05
1474.4 A	10000.	0.645E-04	-0.266E-04	0.137E-04	-0.806E-05	0.135E-04	-0.670E-05
C= 0.21E+15	20000.	0.619E-04	-0.202E-04	0.149E-04	-0.935E-05	0.141E-04	-0.753E-05
	30000.	0.631E-04	-0.169E-04	0.161E-04	-0.103E-04	0.143E-04	-0.816E-05
	50000.	0.649E-04	-0.143E-04	0.161E-04	-0.106E-04	0.153E-04	-0.881E-05
	100000.	0.660E-04	-0.104E-04	0.173E-04	-0.118E-04	0.174E-04	-0.110E-04
CA II 3D-4F	5000.	0.174E-04	0.716E-05	0.133E-05	0.596E-06	0.160E-05	0.513E-06
1839.2 A	10000.	0.136E-04	0.550E-05	0.178E-05	0.825E-06	0.188E-05	0.695E-06
C= 0.16E+16	20000.	0.116E-04	0.430E-05	0.206E-05	0.101E-05	0.213E-05	0.831E-06
	30000.	0.112E-04	0.384E-05	0.223E-05	0.112E-05	0.225E-05	0.920E-06
	50000.	0.109E-04	0.323E-05	0.242E-05	0.127E-05	0.239E-05	0.103E-05
	100000.	0.109E-04	0.258E-05	0.266E-05	0.148E-05	0.249E-05	0.119E-05
CA II 3D-5F	5000.	0.784E-04	0.232E-04	0.145E-04	0.142E-04	0.125E-04	0.117E-04
1554.1 A	10000.	0.673E-04	0.198E-04	0.181E-04	0.167E-04	0.157E-04	0.132E-04
C= 0.31E+14	20000.	0.591E-04	0.159E-04	0.210E-04	0.192E-04	0.171E-04	0.153E-04
	30000.	0.552E-04	0.137E-04	0.242E-04	0.213E-04	0.190E-04	0.166E-04
	50000.	0.512E-04	0.115E-04	0.238E-04	0.224E-04	0.228E-04	0.173E-04
	100000.	0.463E-04	0.888E-05	0.340E-04	0.265E-04	0.221E-04	0.189E-04

PERTURBER DENSITY = 0.1D+14(cm-3)

PERTURBERS ARE		ELECTRONS		PROTONS		IONIZED HELIUM	
TRANSITION	T(K)	WIDTH(A)	SHIFT(A)	WIDTH(A)	SHIFT(A)	WIDTH(A)	SHIFT(A)
CA II 3D-6F	5000.	0.170E-03	0.574E-04	0.413E-04	0.373E-04	0.339E-04	0.304E-04
1433.3 A	10000.	0.154E-03	0.490E-04	0.466E-04	0.419E-04	0.379E-04	0.327E-04
C= 0.17E+14	20000.	0.139E-03	0.381E-04	0.551E-04	0.481E-04	0.415E-04	0.384E-04
	30000.	0.131E-03	0.329E-04	0.625E-04	0.532E-04	0.475E-04	0.412E-04
	50000.	0.122E-03	0.278E-04	0.692E-04	0.618E-04	0.543E-04	0.414E-04
	100000.	0.109E-03	0.197E-04	0.759E-04	0.660E-04	0.754E-04	0.486E-04
CA II 4S-4P	5000.	0.296E-04	-0.518E-05	0.108E-05	-0.375E-06	0.150E-05	-0.359E-06
3946.3 A	10000.	0.228E-04	-0.423E-05	0.174E-05	-0.634E-06	0.214E-05	-0.565E-06
C= 0.18E+17	20000.	0.188E-04	-0.327E-05	0.238E-05	-0.901E-06	0.255E-05	-0.776E-06
	30000.	0.177E-04	-0.278E-05	0.259E-05	-0.106E-05	0.275E-05	-0.871E-06
	50000.	0.171E-04	-0.257E-05	0.287E-05	-0.122E-05	0.301E-05	-0.999E-06
	100000.	0.166E-04	-0.214E-05	0.321E-05	-0.145E-05	0.317E-05	-0.119E-05
CA II 4S-5P	5000.	0.191E-04	-0.182E-05	0.157E-05	-0.590E-06	0.181E-05	-0.512E-06
1650.6 A	10000.	0.151E-04	-0.153E-05	0.195E-05	-0.811E-06	0.207E-05	-0.672E-06
C= 0.10E+16	20000.	0.129E-04	-0.166E-05	0.225E-05	-0.975E-06	0.232E-05	-0.809E-06
	30000.	0.122E-04	-0.144E-05	0.241E-05	-0.108E-05	0.242E-05	-0.900E-06
	50000.	0.118E-04	-0.129E-05	0.255E-05	-0.122E-05	0.253E-05	-0.985E-06
	100000.	0.115E-04	-0.118E-05	0.272E-05	-0.140E-05	0.274E-05	-0.115E-05
CA II 4S-6P	5000.	0.283E-04	-0.902E-05	0.377E-05	-0.190E-05	0.396E-05	-0.155E-05
1342.1 A	10000.	0.244E-04	-0.646E-05	0.439E-05	-0.228E-05	0.449E-05	-0.187E-05
C= 0.32E+15	20000.	0.226E-04	-0.541E-05	0.494E-05	-0.271E-05	0.486E-05	-0.220E-05
	30000.	0.222E-04	-0.458E-05	0.510E-05	-0.293E-05	0.502E-05	-0.244E-05
	50000.	0.225E-04	-0.398E-05	0.543E-05	-0.322E-05	0.501E-05	-0.251E-05
	100000.	0.227E-04	-0.309E-05	0.594E-05	-0.372E-05	0.525E-05	-0.292E-05
CA II 4S-7P	5000.	0.506E-04	-0.220E-04	0.834E-05	-0.472E-05	0.842E-05	-0.388E-05
1226.8 A	10000.	0.451E-04	-0.184E-04	0.950E-05	-0.558E-05	0.937E-05	-0.465E-05
C= 0.15E+15	20000.	0.432E-04	-0.142E-04	0.104E-04	-0.648E-05	0.979E-05	-0.522E-05
	30000.	0.440E-04	-0.119E-04	0.112E-04	-0.715E-05	0.998E-05	-0.566E-05
	50000.	0.452E-04	-0.101E-04	0.112E-04	-0.737E-05	0.106E-04	-0.610E-05
	100000.	0.460E-04	-0.744E-05	0.120E-04	-0.820E-05	0.121E-04	-0.765E-05
CA II 4P-5S	5000.	0.935E-04	0.385E-04	0.216E-05	0.298E-05	0.223E-05	0.259E-05
3727.6 A	10000.	0.671E-04	0.308E-04	0.364E-05	0.411E-05	0.356E-05	0.340E-05
C= 0.12E+17	20000.	0.510E-04	0.246E-04	0.506E-05	0.493E-05	0.456E-05	0.410E-05
	30000.	0.456E-04	0.229E-04	0.585E-05	0.549E-05	0.511E-05	0.455E-05
	50000.	0.421E-04	0.194E-04	0.700E-05	0.620E-05	0.600E-05	0.502E-05
	100000.	0.391E-04	0.150E-04	0.806E-05	0.708E-05	0.682E-05	0.585E-05
CA II 4P-4D	5000.	0.605E-04	0.275E-04	0.237E-05	0.231E-05	0.273E-05	0.201E-05
3173.5 A	10000.	0.457E-04	0.208E-04	0.370E-05	0.317E-05	0.363E-05	0.261E-05
C= 0.38E+16	20000.	0.368E-04	0.162E-04	0.468E-05	0.383E-05	0.440E-05	0.313E-05
	30000.	0.343E-04	0.143E-04	0.526E-05	0.422E-05	0.490E-05	0.348E-05
	50000.	0.320E-04	0.121E-04	0.594E-05	0.474E-05	0.539E-05	0.390E-05
	100000.	0.299E-04	0.940E-05	0.679E-05	0.552E-05	0.620E-05	0.454E-05

PERTURBER DENSITY = 0.1D+14(cm-3)

PERTURBERS ARE		ELECTRONS		PROTONS		IONIZED HELIUM	
TRANSITION	T(K)	WIDTH(A)	SHIFT(A)	WIDTH(A)	SHIFT(A)	WIDTH(A)	SHIFT(A)
CA II 4P-5D	5000.	0.588E-04	0.334E-04	0.581E-05	0.425E-05	0.582E-05	0.348E-05
2110.3 A	10000.	0.485E-04	0.272E-04	0.708E-05	0.509E-05	0.678E-05	0.417E-05
C= 0.79E+15	20000.	0.438E-04	0.220E-04	0.833E-05	0.609E-05	0.793E-05	0.503E-05
	30000.	0.423E-04	0.194E-04	0.920E-05	0.665E-05	0.821E-05	0.538E-05
	50000.	0.418E-04	0.164E-04	0.102E-04	0.743E-05	0.935E-05	0.599E-05
	100000.	0.413E-04	0.127E-04	0.106E-04	0.821E-05	0.951E-05	0.657E-05
CA II 4D-5P	5000.	0.645E-02	-0.251E-02	0.362E-03	-0.267E-03	0.407E-03	-0.233E-03
26778.0 A	10000.	0.504E-02	-0.191E-02	0.484E-03	-0.349E-03	0.485E-03	-0.288E-03
C= 0.27E+18	20000.	0.441E-02	-0.154E-02	0.586E-03	-0.418E-03	0.566E-03	-0.344E-03
	30000.	0.422E-02	-0.132E-02	0.656E-03	-0.467E-03	0.600E-03	-0.376E-03
	50000.	0.411E-02	-0.111E-02	0.709E-03	-0.515E-03	0.650E-03	-0.422E-03
	100000.	0.405E-02	-0.881E-03	0.815E-03	-0.606E-03	0.711E-03	-0.496E-03
CA II 4D-6P	5000.	0.551E-03	-0.218E-03	0.625E-04	-0.369E-04	0.646E-04	-0.302E-04
5662.9 A	10000.	0.471E-03	-0.174E-03	0.736E-04	-0.441E-04	0.732E-04	-0.361E-04
C= 0.57E+16	20000.	0.437E-03	-0.138E-03	0.858E-04	-0.529E-04	0.819E-04	-0.426E-04
	30000.	0.433E-03	-0.119E-03	0.912E-04	-0.585E-04	0.850E-04	-0.458E-04
	50000.	0.440E-03	-0.101E-03	0.946E-04	-0.626E-04	0.871E-04	-0.502E-04
	100000.	0.445E-03	-0.791E-04	0.106E-03	-0.723E-04	0.946E-04	-0.595E-04
CA II 4D-7P	5000.	0.571E-03	-0.253E-03	0.882E-04	-0.525E-04	0.888E-04	-0.430E-04
4055.2 A	10000.	0.513E-03	-0.217E-03	0.102E-03	-0.622E-04	0.994E-04	-0.520E-04
C= 0.16E+16	20000.	0.489E-03	-0.169E-03	0.111E-03	-0.720E-04	0.104E-03	-0.580E-04
	30000.	0.498E-03	-0.145E-03	0.120E-03	-0.791E-04	0.105E-03	-0.631E-04
	50000.	0.514E-03	-0.124E-03	0.122E-03	-0.833E-04	0.113E-03	-0.685E-04
	100000.	0.524E-03	-0.918E-04	0.130E-03	-0.928E-04	0.130E-03	-0.847E-04
CA II 4D-4F	5000.	0.407E-03	-0.141E-04	0.164E-04	-0.583E-05	0.203E-04	-0.539E-05
8923.7 A	10000.	0.350E-03	-0.127E-04	0.233E-04	-0.860E-05	0.257E-04	-0.755E-05
C= 0.30E+17	20000.	0.334E-03	-0.116E-04	0.278E-04	-0.116E-04	0.293E-04	-0.948E-05
	30000.	0.339E-03	-0.131E-04	0.301E-04	-0.129E-04	0.313E-04	-0.106E-04
	50000.	0.352E-03	-0.127E-04	0.330E-04	-0.146E-04	0.331E-04	-0.121E-04
	100000.	0.365E-03	-0.112E-04	0.359E-04	-0.173E-04	0.347E-04	-0.137E-04
CA II 4D-5F	5000.	0.744E-03	0.163E-03	0.131E-03	0.129E-03	0.112E-03	0.107E-03
4720.6 A	10000.	0.640E-03	0.136E-03	0.165E-03	0.153E-03	0.143E-03	0.121E-03
C= 0.29E+15	20000.	0.566E-03	0.111E-03	0.190E-03	0.175E-03	0.154E-03	0.140E-03
	30000.	0.534E-03	0.958E-04	0.217E-03	0.195E-03	0.171E-03	0.151E-03
	50000.	0.500E-03	0.784E-04	0.219E-03	0.205E-03	0.209E-03	0.159E-03
	100000.	0.457E-03	0.605E-04	0.307E-03	0.246E-03	0.206E-03	0.172E-03
CA II 4D-6F	5000.	0.118E-02	0.379E-03	0.282E-03	0.257E-03	0.232E-03	0.209E-03
3758.4 A	10000.	0.107E-02	0.317E-03	0.319E-03	0.288E-03	0.260E-03	0.225E-03
C= 0.12E+15	20000.	0.969E-03	0.243E-03	0.376E-03	0.330E-03	0.285E-03	0.263E-03
	30000.	0.916E-03	0.208E-03	0.428E-03	0.366E-03	0.325E-03	0.284E-03
	50000.	0.855E-03	0.175E-03	0.473E-03	0.425E-03	0.373E-03	0.285E-03
	100000.	0.770E-03	0.123E-03	0.519E-03	0.455E-03	0.517E-03	0.335E-03

PERTURBER DENSITY = 0.1D+14(cm-3)

PERTURBERS ARE		ELECTRONS		PROTONS		IONIZED HELIUM	
TRANSITION	T(K)	WIDTH(A)	SHIFT(A)	WIDTH(A)	SHIFT(A)	WIDTH(A)	SHIFT(A)
CA II 5S-5P	5000.	0.141E-02	-0.545E-03	0.872E-04	-0.507E-04	0.978E-04	-0.442E-04
11878.9 A	10000.	0.107E-02	-0.425E-03	0.111E-03	-0.666E-04	0.113E-03	-0.548E-04
C= 0.53E+17	20000.	0.903E-03	-0.339E-03	0.131E-03	-0.803E-04	0.130E-03	-0.661E-04
	30000.	0.857E-03	-0.296E-03	0.144E-03	-0.892E-04	0.136E-03	-0.716E-04
	50000.	0.834E-03	-0.250E-03	0.152E-03	-0.984E-04	0.144E-03	-0.800E-04
	100000.	0.824E-03	-0.195E-03	0.171E-03	-0.115E-03	0.154E-03	-0.931E-04
CA II 5S-6P	5000.	0.349E-03	-0.140E-03	0.426E-04	-0.229E-04	0.444E-04	-0.187E-04
4475.8 A	10000.	0.297E-03	-0.115E-03	0.496E-04	-0.274E-04	0.500E-04	-0.225E-04
C= 0.36E+16	20000.	0.274E-03	-0.907E-04	0.573E-04	-0.329E-04	0.551E-04	-0.264E-04
	30000.	0.272E-03	-0.793E-04	0.607E-04	-0.361E-04	0.569E-04	-0.285E-04
	50000.	0.277E-03	-0.675E-04	0.624E-04	-0.391E-04	0.581E-04	-0.309E-04
	100000.	0.282E-03	-0.526E-04	0.691E-04	-0.446E-04	0.630E-04	-0.368E-04
CA II 5S-7P	5000.	0.405E-03	-0.178E-03	0.646E-04	-0.370E-04	0.654E-04	-0.303E-04
3407.9 A	10000.	0.362E-03	-0.151E-03	0.743E-04	-0.439E-04	0.726E-04	-0.367E-04
C= 0.11E+16	20000.	0.345E-03	-0.121E-03	0.807E-04	-0.508E-04	0.762E-04	-0.408E-04
	30000.	0.352E-03	-0.104E-03	0.866E-04	-0.559E-04	0.769E-04	-0.444E-04
	50000.	0.364E-03	-0.884E-04	0.877E-04	-0.587E-04	0.817E-04	-0.483E-04
	100000.	0.372E-03	-0.663E-04	0.933E-04	-0.652E-04	0.946E-04	-0.598E-04
CA II 5P-5D	5000.	0.110E-02	0.509E-03	0.847E-04	0.710E-04	0.824E-04	0.579E-04
8235.7 A	10000.	0.897E-03	0.440E-03	0.105E-03	0.851E-04	0.996E-04	0.700E-04
C= 0.12E+17	20000.	0.813E-03	0.378E-03	0.127E-03	0.101E-03	0.115E-03	0.819E-04
	30000.	0.787E-03	0.330E-03	0.140E-03	0.110E-03	0.127E-03	0.914E-04
	50000.	0.779E-03	0.278E-03	0.154E-03	0.120E-03	0.132E-03	0.936E-04
	100000.	0.777E-03	0.216E-03	0.173E-03	0.139E-03	0.141E-03	0.110E-03
CA II 5D-6P	5000.	0.736E-01	-0.347E-01	0.654E-02	-0.511E-02	0.641E-02	-0.424E-02
56116.1 A	10000.	0.631E-01	-0.285E-01	0.808E-02	-0.619E-02	0.750E-02	-0.505E-02
C= 0.56E+18	20000.	0.589E-01	-0.240E-01	0.955E-02	-0.718E-02	0.885E-02	-0.593E-02
	30000.	0.577E-01	-0.215E-01	0.102E-01	-0.799E-02	0.894E-02	-0.627E-02
	50000.	0.587E-01	-0.181E-01	0.114E-01	-0.822E-02	0.102E-01	-0.709E-02
	100000.	0.594E-01	-0.141E-01	0.118E-01	-0.965E-02	0.114E-01	-0.775E-02
CA II 5D-7P	5000.	0.505E-02	-0.247E-02	0.671E-03	-0.458E-03	0.664E-03	-0.377E-03
11385.3 A	10000.	0.457E-02	-0.209E-02	0.794E-03	-0.544E-03	0.737E-03	-0.440E-03
C= 0.13E+17	20000.	0.442E-02	-0.176E-02	0.906E-03	-0.633E-03	0.804E-03	-0.507E-03
	30000.	0.449E-02	-0.153E-02	0.974E-03	-0.691E-03	0.895E-03	-0.574E-03
	50000.	0.465E-02	-0.130E-02	0.102E-02	-0.749E-03	0.859E-03	-0.592E-03
	100000.	0.473E-02	-0.980E-03	0.110E-02	-0.820E-03	0.108E-02	-0.720E-03
CA II 5D-5F	5000.	0.130E-01	0.823E-03	0.198E-02	0.198E-02	0.163E-02	0.162E-02
18843.3 A	10000.	0.112E-01	0.822E-03	0.248E-02	0.231E-02	0.212E-02	0.190E-02
C= 0.46E+16	20000.	0.102E-01	0.657E-03	0.287E-02	0.265E-02	0.232E-02	0.208E-02
	30000.	0.983E-02	0.552E-03	0.315E-02	0.300E-02	0.264E-02	0.234E-02
	50000.	0.942E-02	0.436E-03	0.341E-02	0.313E-02	0.314E-02	0.249E-02
	100000.	0.886E-02	0.314E-03	0.449E-02	0.384E-02	0.327E-02	0.260E-02

PERTURBER DENSITY = 0.1D+14(cm-3)

PERTURBERS ARE		ELECTRONS		PROTONS		IONIZED HELIUM	
TRANSITION	T(K)	WIDTH(A)	SHIFT(A)	WIDTH(A)	SHIFT(A)	WIDTH(A)	SHIFT(A)
CA II 5D-6F	5000.	0.748E-02	0.196E-02	0.169E-02	0.157E-02	0.140E-02	0.127E-02
9319.1 A	10000.	0.679E-02	0.160E-02	0.196E-02	0.175E-02	0.160E-02	0.136E-02
C= 0.71E+15	20000.	0.622E-02	0.121E-02	0.230E-02	0.202E-02	0.174E-02	0.160E-02
	30000.	0.593E-02	0.105E-02	0.261E-02	0.225E-02	0.192E-02	0.172E-02
	50000.	0.559E-02	0.863E-03	0.282E-02	0.258E-02	0.227E-02	0.175E-02
	100000.	0.510E-02	0.587E-03	0.308E-02	0.276E-02	0.311E-02	0.207E-02
PERTURBER DENSITY = 0.1D+17(cm-3)							
CA II 3D-4P	5000.	0.134	0.569E-02	0.403E-02	-0.724E-03	0.574E-02	-0.707E-03
8581.1 A	10000.	0.105	0.311E-02	0.669E-02	-0.137E-02	0.833E-02	-0.126E-02
C= 0.86E+20	20000.	0.856E-01	0.218E-02	0.928E-02	-0.212E-02	0.101E-01	-0.185E-02
	30000.	0.776E-01	0.895E-03	0.101E-01	-0.258E-02	0.109E-01	-0.222E-02
	50000.	0.707E-01	0.748E-03	0.112E-01	-0.310E-02	0.118E-01	-0.255E-02
	100000.	0.643E-01	0.792E-03	0.125E-01	-0.374E-02	0.128E-01	-0.307E-02
CA II 3D-5P	5000.	0.303E-01	-0.383E-02	0.248E-02	-0.879E-03	0.288E-02	-0.750E-03
2132.3 A	10000.	0.241E-01	-0.232E-02	0.312E-02	-0.128E-02	0.332E-02	-0.106E-02
C= 0.17D+19	20000.	0.207E-01	-0.230E-02	0.360E-02	-0.157E-02	0.373E-02	-0.130E-02
	30000.	0.196E-01	-0.184E-02	0.390E-02	-0.175E-02	0.390E-02	-0.144E-02
	50000.	0.189E-01	-0.147E-02	0.410E-02	-0.199E-02	0.402E-02	-0.162E-02
	100000.	0.183E-01	-0.132E-02	0.431E-02	-0.225E-02	0.439E-02	-0.186E-02
CA II 3D-6P	5000.	0.413E-01	-0.137E-01	0.555E-02	-0.251E-02	*0.574E-02	*-0.199E-02
1644.1 A	10000.	0.358E-01	-0.104E-01	0.651E-02	-0.328E-02	*0.665E-02	*-0.267E-02
C= 0.48D+18	20000.	0.333E-01	-0.810E-02	0.732E-02	-0.402E-02	*0.722E-02	*-0.326E-02
	30000.	0.329E-01	-0.652E-02	0.756E-02	-0.437E-02	0.746E-02	-0.364E-02
	50000.	0.332E-01	-0.553E-02	0.806E-02	-0.481E-02	0.746E-02	-0.375E-02
	100000.	0.334E-01	-0.439E-02	0.885E-02	-0.558E-02	0.776E-02	-0.440E-02
CA II 3D-7P	5000.	0.721E-01	-0.304E-01	*0.117E-01	*-0.560E-02		
1474.4 A	10000.	0.645E-01	-0.259E-01	*0.135E-01	*-0.762E-02		
C= 0.21D+18	20000.	0.619E-01	-0.199E-01	*0.149E-01	*-0.926E-02	*0.141E-01	*-0.744E-02
	30000.	0.631E-01	-0.168E-01	*0.161E-01	*-0.103E-01	*0.143E-01	*-0.809E-02
	50000.	0.649E-01	-0.142E-01	0.161E-01	-0.106E-01	*0.153E-01	*-0.881E-02
	100000.	0.660E-01	-0.104E-01	0.173E-01	-0.118E-01	*0.174E-01	*-0.110E-01
CA II 3D-4F	5000.	0.174E-01	0.712E-02	0.132E-02	0.554E-03	0.159E-02	0.471E-03
1839.2 A	10000.	0.136E-01	0.549E-02	0.178E-02	0.809E-03	0.188E-02	0.680E-03
C= 0.16D+19	20000.	0.116E-01	0.430E-02	0.206E-02	0.101E-02	0.213E-02	0.828E-03
	30000.	0.112E-01	0.384E-02	0.223E-02	0.112E-02	0.225E-02	0.918E-03
	50000.	0.109E-01	0.323E-02	0.242E-02	0.127E-02	0.239E-02	0.103E-02
	100000.	0.109E-01	0.258E-02	0.266E-02	0.148E-02	0.249E-02	0.119E-02
CA II 3D-5F	5000.	0.781E-01	0.194E-01	*0.143E-01	*0.109E-01		
1554.1 A	10000.	0.671E-01	0.184E-01	*0.180E-01	*0.155E-01		
C= 0.31D+17	20000.	0.589E-01	0.157E-01	*0.210E-01	*0.190E-01	*0.171E-01	*0.151E-01
	30000.	0.551E-01	0.136E-01	*0.242E-01	*0.211E-01	*0.189E-01	*0.165E-01
	50000.	0.511E-01	0.115E-01	*0.238E-01	*0.224E-01	*0.228E-01	*0.173E-01
	100000.	0.462E-01	0.888E-02	*0.340E-01	*0.265E-01	*0.221E-01	*0.189E-01

PERTURBER DENSITY = 0.1D+17(cm-3)

PERTURBERS ARE		ELECTRONS		PROTONS		IONIZED HELIUM	
TRANSITION	T(K)	WIDTH(A)	SHIFT(A)	WIDTH(A)	SHIFT(A)	WIDTH(A)	SHIFT(A)
CA II 3D-6F	5000.	0.166	0.408E-01				
1433.3 A	10000.	0.151	0.390E-01				
C= 0.17D+17	20000.	0.137	0.371E-01				
	30000.	0.129	0.320E-01				
	50000.	0.121	0.271E-01				
	100000.	0.108	0.197E-01				
CA II 4S-4P	5000.	0.296E-01	-0.516E-02	0.108E-02	-0.355E-03	0.150E-02	-0.338E-03
3946.3 A	10000.	0.228E-01	-0.422E-02	0.174E-02	-0.626E-03	0.214E-02	-0.557E-03
C= 0.18E+20	20000.	0.188E-01	-0.329E-02	0.238E-02	-0.900E-03	0.255E-02	-0.775E-03
	30000.	0.177E-01	-0.281E-02	0.259E-02	-0.106E-02	0.275E-02	-0.869E-03
	50000.	0.171E-01	-0.257E-02	0.287E-02	-0.122E-02	0.301E-02	-0.999E-03
	100000.	0.166E-01	-0.214E-02	0.321E-02	-0.145E-02	0.317E-02	-0.119E-02
CA II 4S-5P	5000.	0.191E-01	-0.184E-02	0.156E-02	-0.546E-03	0.180E-02	-0.468E-03
1650.6 A	10000.	0.151E-01	-0.150E-02	0.194E-02	-0.795E-03	0.207E-02	-0.656E-03
C= 0.10D+19	20000.	0.129E-01	-0.165E-02	0.225E-02	-0.973E-03	0.232E-02	-0.806E-03
	30000.	0.122E-01	-0.143E-02	0.241E-02	-0.108E-02	0.242E-02	-0.898E-03
	50000.	0.118E-01	-0.129E-02	0.255E-02	-0.122E-02	0.253E-02	-0.985E-03
	100000.	0.115E-01	-0.118E-02	0.272E-02	-0.140E-02	0.274E-02	-0.115E-02
CA II 4S-6P	5000.	0.283E-01	-0.880E-02	0.375E-02	-0.168E-02	*0.387E-02	*-0.133E-02
1342.1 A	10000.	0.244E-01	-0.635E-02	0.438E-02	-0.219E-02	*0.447E-02	*-0.179E-02
C= 0.32D+18	20000.	0.226E-01	-0.540E-02	0.494E-02	-0.269E-02	*0.486E-02	*-0.218E-02
	30000.	0.222E-01	-0.456E-02	0.510E-02	-0.292E-02	0.502E-02	-0.243E-02
	50000.	0.225E-01	-0.395E-02	0.543E-02	-0.322E-02	0.501E-02	-0.251E-02
	100000.	0.227E-01	-0.309E-02	0.594E-02	-0.372E-02	0.525E-02	-0.292E-02
CA II 4S-7P	5000.	0.506E-01	-0.211E-01	*0.812E-02	*-0.388E-02		
1226.8 A	10000.	0.451E-01	-0.179E-01	*0.940E-02	*-0.528E-02		
C= 0.15D+18	20000.	0.432E-01	-0.140E-01	*0.104E-01	*-0.642E-02	*0.978E-02	*-0.516E-02
	30000.	0.440E-01	-0.118E-01	*0.112E-01	*-0.711E-02	*0.997E-02	*-0.561E-02
	50000.	0.452E-01	-0.101E-01	0.112E-01	-0.737E-02	*0.106E-01	*-0.610E-02
	100000.	0.460E-01	-0.744E-02	0.120E-01	-0.820E-02	*0.121E-01	*-0.765E-02
CA II 4P-5S	5000.	0.934E-01	0.383E-01	0.216E-02	0.276E-02	0.222E-02	0.237E-02
3727.6 A	10000.	0.671E-01	0.307E-01	0.364E-02	0.402E-02	0.356E-02	0.332E-02
C= 0.12D+20	20000.	0.510E-01	0.246E-01	0.506E-02	0.492E-02	0.456E-02	0.408E-02
	30000.	0.456E-01	0.228E-01	0.585E-02	0.548E-02	0.511E-02	0.454E-02
	50000.	0.421E-01	0.194E-01	0.700E-02	0.620E-02	0.600E-02	0.502E-02
	100000.	0.391E-01	0.150E-01	0.806E-02	0.708E-02	0.682E-02	0.585E-02
CA II 4P-4D	5000.	0.605E-01	0.273E-01	0.237E-02	0.213E-02	0.271E-02	0.184E-02
3173.5 A	10000.	0.457E-01	0.207E-01	0.370E-02	0.311E-02	0.362E-02	0.254E-02
C= 0.38D+19	20000.	0.368E-01	0.162E-01	0.468E-02	0.381E-02	0.440E-02	0.312E-02
	30000.	0.343E-01	0.143E-01	0.526E-02	0.421E-02	0.490E-02	0.347E-02
	50000.	0.320E-01	0.121E-01	0.594E-02	0.474E-02	0.539E-02	0.390E-02
	100000.	0.299E-01	0.940E-02	0.679E-02	0.552E-02	0.620E-02	0.454E-02

PERTURBER DENSITY = 0.1D+17(cm-3)

PERTURBERS ARE		ELECTRONS		PROTONS		IONIZED HELIUM	
TRANSITION	T(K)	WIDTH(A)	SHIFT(A)	WIDTH(A)	SHIFT(A)	WIDTH(A)	SHIFT(A)
CA II 4P-5D	5000.	0.587E-01	0.329E-01	0.574E-02	0.375E-02	0.572E-02	0.300E-02
2110.3 A	10000.	0.485E-01	0.270E-01	0.707E-02	0.491E-02	0.676E-02	0.399E-02
C= 0.79D+18	20000.	0.438E-01	0.220E-01	0.833E-02	0.606E-02	0.793E-02	0.499E-02
	30000.	0.423E-01	0.194E-01	0.920E-02	0.662E-02	0.821E-02	0.535E-02
	50000.	0.418E-01	0.164E-01	0.102E-01	0.743E-02	0.935E-02	0.599E-02
	100000.	0.413E-01	0.127E-01	0.106E-01	0.821E-02	0.951E-02	0.657E-02
CA II 4D-5P	5000.	6.44	-2.49	0.359	-0.244	0.405	-0.210
26778.0 A	10000.	5.04	-1.89	0.484	-0.341	0.484	-0.280
C= 0.27D+21	20000.	4.41	-1.54	0.586	-0.417	0.566	-0.342
	30000.	4.22	-1.32	0.656	-0.465	0.600	-0.375
	50000.	4.11	-1.11	0.709	-0.515	0.650	-0.422
	100000.	4.05	-0.881	0.815	-0.606	0.711	-0.496
CA II 4D-6P	5000.	0.551	-0.214	0.617E-01	-0.324E-01	*0.632E-01	*-0.255E-01
5662.9 A	10000.	0.472	-0.172	0.735E-01	-0.425E-01	*0.728E-01	*-0.344E-01
C= 0.57D+19	20000.	0.437	-0.138	0.857E-01	-0.526E-01	0.818E-01	-0.423E-01
	30000.	0.433	-0.118	0.912E-01	-0.583E-01	0.850E-01	-0.455E-01
	50000.	0.440	-0.101	0.946E-01	-0.626E-01	0.871E-01	-0.502E-01
	100000.	0.445	-0.791E-01	0.106	-0.723E-01	0.946E-01	-0.595E-01
CA II 4D-7P	5000.	0.571	-0.243	*0.860E-01	-0.427E-01		
4055.2 A	10000.	0.513	-0.211	*0.101	*-0.586E-01		
C= 0.16D+19	20000.	0.489	-0.166	*0.111	*-0.713E-01	*0.104	*-0.573E-01
	30000.	0.499	-0.145	*0.120	*-0.786E-01	*0.105	*-0.626E-01
	50000.	0.514	-0.124	0.122	-0.833E-01	*0.113	*-0.685E-01
	100000.	0.524	-0.918E-01	0.130	-0.928E-01	*0.130	*-0.847E-01
CA II 4D-4F	5000.	0.407	-0.150E-01	0.164E-01	-0.547E-02	0.202E-01	-0.503E-02
8923.7 A	10000.	0.350	-0.122E-01	0.233E-01	-0.846E-02	0.257E-01	-0.742E-02
C= 0.30D+20	20000.	0.334	-0.114E-01	0.278E-01	-0.116E-01	0.293E-01	-0.945E-02
	30000.	0.339	-0.130E-01	0.301E-01	-0.129E-01	0.313E-01	-0.106E-01
	50000.	0.352	-0.127E-01	0.330E-01	-0.146E-01	0.331E-01	-0.121E-01
	100000.	0.365	-0.112E-01	0.359E-01	-0.173E-01	0.347E-01	-0.137E-01
CA II 4D-5F	5000.	0.742	0.133	*0.129	*0.991E-01		
4720.6 A	10000.	0.638	0.124	*0.162	*0.141		
C= 0.29D+18	20000.	0.565	0.108	*0.190	*0.173	*0.154	*0.138
	30000.	0.532	0.939E-01	*0.217	*0.193	*0.171	*0.149
	50000.	0.499	0.784E-01	*0.219	*0.205	*0.209	*0.159
	100000.	0.457	0.605E-01	*0.307	*0.246	*0.206	*0.172
CA II 4D-6F	5000.	1.16	0.267				
3758.4 A	10000.	1.05	0.249				
C= 0.12D+18	20000.	0.955	0.236				
	30000.	0.905	0.203				
	50000.	0.847	0.170				
	100000.	0.764	0.123				

PERTURBER DENSITY = 0.1D+17(cm-3)

PERTURBERS ARE		ELECTRONS		PROTONS		IONIZED HELIUM	
TRANSITION	T(K)	WIDTH(A)	SHIFT(A)	WIDTH(A)	SHIFT(A)	WIDTH(A)	SHIFT(A)
CA II 5S-5P	5000.	1.41	-0.540	0.865E-01	-0.464E-01	0.974E-01	-0.398E-01
11878.9 A	10000.	1.07	-0.423	0.110	-0.650E-01	0.113	-0.532E-01
C= 0.53D+20	20000.	0.903	-0.339	0.131	-0.800E-01	0.130	-0.658E-01
	30000.	0.857	-0.296	0.144	-0.889E-01	0.136	-0.713E-01
	50000.	0.834	-0.250	0.152	-0.984E-01	0.144	-0.800E-01
	100000.	0.824	-0.195	0.171	-0.115	0.154	-0.931E-01
CA II 5S-6P	5000.	0.349	-0.137	0.419E-01	-0.202E-01	*0.433E-01	*-0.158E-01
4475.8 A	10000.	0.297	-0.113	0.496E-01	-0.264E-01	*0.497E-01	*-0.214E-01
C= 0.36D+19	20000.	0.274	-0.904E-01	0.573E-01	-0.327E-01	*0.551E-01	*-0.263E-01
	30000.	0.272	-0.791E-01	0.606E-01	-0.359E-01	0.569E-01	-0.283E-01
	50000.	0.277	-0.675E-01	0.624E-01	-0.391E-01	0.581E-01	-0.309E-01
	100000.	0.282	-0.526E-01	0.691E-01	-0.446E-01	0.630E-01	-0.368E-01
CA II 5S-7P	5000.	0.405	-0.171	*0.629E-01	*-0.302E-01		
3407.9 A	10000.	0.362	-0.147	*0.736E-01	*-0.413E-01		
C= 0.11D+19	20000.	0.345	-0.119	*0.807E-01	*-0.503E-01	*0.761E-01	*-0.403E-01
	30000.	0.352	-0.104	*0.866E-01	*-0.555E-01	*0.768E-01	*-0.441E-01
	50000.	0.364	-0.881E-01	0.877E-01	-0.587E-01	*0.817E-01	*-0.483E-01
	100000.	0.372	-0.663E-01	0.933E-01	-0.652E-01	*0.946E-01	*-0.598E-01
CA II 5P-5D	5000.	1.10	0.501	0.843E-01	0.627E-01	0.821E-01	0.497E-01
8235.7 A	10000.	0.897	0.435	0.105	0.820E-01	0.993E-01	0.669E-01
C= 0.12D+20	20000.	0.813	0.377	0.127	0.101	0.115	0.813E-01
	30000.	0.787	0.330	0.140	0.109	0.127	0.910E-01
	50000.	0.779	0.278	0.154	0.120	0.132	0.936E-01
	100000.	0.777	0.216	0.173	0.139	0.141	0.110
CA II 5D-7P	5000.	5.05	-2.37	*0.664	*-0.368		
11385.3 A	10000.	4.57	-2.03	*0.795	*-0.511		
C= 0.13D+20	20000.	4.42	-1.74	*0.906	*-0.627	*0.803	*-0.501
	30000.	4.49	-1.53	*0.974	*-0.686	*0.896	*-0.570
	50000.	4.65	-1.30	1.02	-0.749	*0.859	*-0.592
	100000.	4.73	-0.980	1.10	-0.820	* 1.08	*-0.720
CA II 5D-5F	5000.	13.0	0.297	*1.94	*1.49		
18843.3 A	10000.	11.2	0.638	*2.50	*2.12		
C= 0.46D+19	20000.	10.2	0.624	*2.87	*2.62	*2.32	*2.05
	30000.	9.81	0.528	*3.15	*2.97	*2.64	*2.31
	50000.	9.41	0.436	*3.41	*3.13	*3.14	*2.49
	100000.	8.85	0.314	*4.49	*3.84	*3.27	*2.60
CA II 5D-6F	5000.	7.31	1.28				
9319.1 A	10000.	6.67	1.35				
C= 0.71D+18	20000.	6.14	1.16				
	30000.	5.86	1.01				
	50000.	5.54	0.863				
	100000.	5.06	0.587				

PERTURBER DENSITY = 0.1D+18(cm-3)

PERTURBERS ARE		ELECTRONS		PROTONS		IONIZED HELIUM	
TRANSITION	T(K)	WIDTH(A)	SHIFT(A)	WIDTH(A)	SHIFT(A)	WIDTH(A)	SHIFT(A)
CA II 3D-4P	5000.	1.34	0.595E-01	0.397E-01	-0.642E-02	0.562E-01	-0.625E-02
8581.1 A	10000.	1.05	0.308E-01	0.666E-01	-0.129E-01	0.828E-01	-0.119E-01
C= 0.86E+21	20000.	0.856	0.228E-01	0.927E-01	-0.209E-01	0.101	-0.182E-01
	30000.	0.776	0.913E-02	0.101	-0.255E-01	0.109	-0.220E-01
	50000.	0.707	0.736E-02	0.112	-0.309E-01	0.118	-0.254E-01
	100000.	0.643	0.792E-02	0.125	-0.374E-01	0.128	-0.307E-01
CA II 3D-5P	5000.	0.303	-0.363E-01	0.238E-01	-0.737E-02	*0.269E-01	*-0.607E-02
2132.3 A	10000.	0.241	-0.220E-01	0.308E-01	-0.115E-01	*0.323E-01	*-0.926E-02
C= 0.17E+20	20000.	0.207	-0.224E-01	0.359E-01	-0.152E-01	*0.371E-01	*-0.124E-01
	30000.	0.196	-0.182E-01	0.391E-01	-0.170E-01	*0.387E-01	*-0.139E-01
	50000.	0.189	-0.146E-01	0.410E-01	-0.198E-01	0.402E-01	-0.161E-01
	100000.	0.183	-0.132E-01	0.431E-01	-0.225E-01	0.439E-01	-0.186E-01
CA II 3D-6P	5000.	0.413	-0.129				
1644.1 A	10000.	0.358	-0.988E-01				
C= 0.48E+19	20000.	0.333	-0.783E-01	*0.730E-01	*-0.374E-01		
	30000.	0.328	-0.634E-01	*0.762E-01	*-0.415E-01		
	50000.	0.332	-0.552E-01	*0.806E-01	*-0.477E-01		
	100000.	0.334	-0.436E-01	*0.885E-01	*-0.558E-01	*0.776E-01	*-0.440E-01
CA II 3D-7P	5000.	0.721	-0.273				
1474.4 A	10000.	0.645	-0.237				
C= 0.21E+19	20000.	0.619	-0.184				
	30000.	0.631	-0.160				
	50000.	0.649	-0.141				
	100000.	0.660	-0.103				
CA II 3D-4F	5000.	0.174	0.702E-01	0.128E-01	0.469E-02	*0.151E-01	*0.385E-02
1839.2 A	10000.	0.136	0.540E-01	0.177E-01	0.729E-02	*0.184E-01	*0.602E-02
C= 0.16E+20	20000.	0.116	0.426E-01	0.206E-01	0.978E-02	*0.213E-01	*0.796E-02
	30000.	0.112	0.381E-01	0.223E-01	0.109E-01	0.223E-01	0.887E-02
	50000.	0.109	0.322E-01	0.242E-01	0.127E-01	0.239E-01	0.103E-01
	100000.	0.109	0.257E-01	0.266E-01	0.148E-01	0.249E-01	0.119E-01
CA II 3D-5F	5000.	0.705	0.116				
1554.1 A	10000.	0.621	0.118				
C= 0.31E+18	20000.	0.554	0.110				
	30000.	0.523	0.111				
	50000.	0.490	0.110				
	100000.	0.447	0.853E-01				
CA II 3D-6F	5000.	1.26	0.165				
1433.3 A	10000.	1.24	0.203				
C= 0.17E+18	20000.	1.19	0.202				
	30000.	1.15	0.229				
	50000.	1.09	0.256				
	100000.	1.00	0.182				

PERTURBER DENSITY = 0.1D+18

TRANSITION	T(K)	ELECTRONS WIDTH(A)	ELECTRONS SHIFT(A)	PROTONS WIDTH(A)	PROTONS SHIFT(A)	IONIZED HELIUM WIDTH(A)	IONIZED HELIUM SHIFT(A)
CA II 4S-4P	5000.	0.296	-0.507E-01	0.106E-01	-0.313E-02	0.146E-01	-0.297E-02
3946.3 A	10000.	0.228	-0.418E-01	0.173E-01	-0.588E-02	0.212E-01	-0.519E-02
C= 0.18E+21	20000.	0.188	-0.324E-01	0.238E-01	-0.884E-02	0.254E-01	-0.759E-02
	30000.	0.177	-0.275E-01	0.259E-01	-0.105E-01	0.275E-01	-0.856E-02
	50000.	0.171	-0.257E-01	0.287E-01	-0.121E-01	0.301E-01	-0.996E-02
	100000.	0.166	-0.214E-01	0.321E-01	-0.145E-01	0.317E-01	-0.119E-01
CA II 4S-5P	5000.	0.191	-0.168E-01	0.150E-01	-0.457E-02	*0.168E-01	*-0.378E-02
1650.6 A	10000.	0.151	-0.143E-01	0.192E-01	-0.713E-02	*0.201E-01	*-0.571E-02
C= 0.10E+20	20000.	0.129	-0.162E-01	0.224E-01	-0.938E-02	*0.230E-01	*-0.772E-02
	30000.	0.122	-0.142E-01	0.242E-01	-0.106E-01	*0.240E-01	*-0.865E-02
	50000.	0.118	-0.128E-01	0.254E-01	-0.121E-01	*0.253E-01	*-0.979E-02
	100000.	0.115	-0.118E-01	0.272E-01	-0.140E-01	0.274E-01	-0.115E-01
CA II 4S-6P	5000.	0.283	-0.825E-01				
1342.1 A	10000.	0.244	-0.593E-01				
C= 0.32E+19	20000.	0.226	-0.522E-01	*0.493E-01	*-0.251E-01		
	30000.	0.222	-0.442E-01	*0.515E-01	*-0.277E-01		
	50000.	0.225	-0.395E-01	*0.542E-01	*-0.319E-01		
	100000.	0.227	-0.306E-01	*0.594E-01	*-0.372E-01	*0.525E-01	*-0.292E-01
CA II 4S-7P	5000.	0.505	-0.189				
1226.8 A	10000.	0.451	-0.164				
C= 0.15E+19	20000.	0.432	-0.134				
	30000.	0.440	-0.113				
	50000.	0.452	-0.100				
	100000.	0.460	-0.736E-01				
CA II 4P-5S	5000.	0.935	0.377	0.214E-01	0.231E-01	0.218E-01	0.191E-01
3727.6 A	10000.	0.671	0.303	0.365E-01	0.361E-01	0.353E-01	0.289E-01
C= 0.12E+21	20000.	0.510	0.242	0.506E-01	0.475E-01	0.456E-01	0.391E-01
	30000.	0.455	0.227	0.584E-01	0.534E-01	0.511E-01	0.438E-01
	50000.	0.421	0.194	0.700E-01	0.617E-01	0.600E-01	0.499E-01
	100000.	0.391	0.150	0.806E-01	0.708E-01	0.682E-01	0.585E-01
CA II 4P-4D	5000.	0.605	0.269	0.233E-01	0.178E-01	0.264E-01	0.148E-01
3173.5 A	10000.	0.457	0.204	0.366E-01	0.277E-01	0.360E-01	0.222E-01
C= 0.38E+20	20000.	0.368	0.160	0.467E-01	0.368E-01	0.438E-01	0.298E-01
	30000.	0.343	0.142	0.526E-01	0.411E-01	0.488E-01	0.335E-01
	50000.	0.320	0.121	0.594E-01	0.472E-01	0.539E-01	0.387E-01
	100000.	0.299	0.939E-01	0.679E-01	0.552E-01	0.620E-01	0.454E-01
CA II 4P-5D	5000.	0.587	0.317	*0.549E-01	*0.280E-01		
2110.3 A	10000.	0.485	0.261	*0.695E-01	*0.405E-01		
C= 0.79E+19	20000.	0.438	0.213	*0.834E-01	*0.570E-01		
	30000.	0.423	0.191	*0.908E-01	*0.626E-01	*0.813E-01	*0.501E-01
	50000.	0.417	0.163	*0.102	*0.737E-01	*0.934E-01	*0.592E-01
	100000.	0.413	0.127	0.106	0.821E-01	*0.951E-01	*0.657E-01

PERTURBER DENSITY = 0.1D+18

TRANSITION	T(K)	ELECTRONS WIDTH(A)	ELECTRONS SHIFT(A)	PROTONS WIDTH(A)	PROTONS SHIFT(A)	IONIZED HELIUM WIDTH(A)	IONIZED HELIUM SHIFT(A)
CA II 4D-6P	5000.	5.51	-2.03				
5662.9 A	10000.	4.71	-1.63	*0.712	*-0.342		
C= 0.57E+20	20000.	4.37	-1.32	*0.855	*-0.493		
	30000.	4.33	-1.16	*0.905	*-0.552		
	50000.	4.40	-1.00	*0.946	*-0.620		
	100000.	4.45	-0.788	*1.06	*-0.723	*0.946	*-0.595
CA II 4D-7P	5000.	5.71	-2.19				
4055.2 A	10000.	5.13	-1.94				
C= 0.16E+20	20000.	4.89	-1.55				
	30000.	4.98	-1.38				
	50000.	5.14	-1.23				
	100000.	5.24	-0.909				
CA II 4D-4F	5000.	4.07	-0.132	0.160	-0.475E-01	0.194	-0.431E-01
8923.7 A	10000.	3.50	-0.120	0.231	-0.781E-01	0.253	-0.677E-01
C= 0.30E+21	20000.	3.34	-0.112	0.278	-0.113	0.292	-0.917E-01
	30000.	3.39	-0.130	0.300	-0.127	0.312	-0.103
	50000.	3.52	-0.127	0.330	-0.146	0.331	-0.121
	100000.	3.65	-0.112	0.359	-0.173	0.347	-0.137
CA II 4D-5F	5000.	6.72	0.579				
4720.6 A	10000.	5.91	0.651				
C= 0.29E+19	20000.	5.33	0.821				
	30000.	5.07	0.895				
	50000.	4.79	0.738				
	100000.	4.42	0.605				
CA II 4D-6F	5000.	8.79	0.985				
3758.4 A	10000.	8.68	1.24				
C= 0.12E+19	20000.	8.29	1.60				
	30000.	8.03	1.40				
	50000.	7.68	1.60				
	100000.	7.08	1.12				
CA II 5S-5P	5000.	14.1	-5.29	*0.835	*-0.375	*0.908	*-0.310
11878.9 A	10000.	10.7	-4.15	1.09	-0.566	*1.11	*-0.454
C= 0.53E+21	20000.	9.04	-3.34	1.30	-0.767	*1.29	*-0.624
	30000.	8.57	-2.93	1.43	-0.857	*1.36	*-0.680
	50000.	8.34	-2.49	1.52	-0.979	*1.44	*-0.795
	100000.	8.24	-1.95	1.71	-1.15	1.54	-0.931
CA II 5S-6P	5000.	3.49	-1.30				
4475.8 A	10000.	2.97	-1.08				
C= 0.36E+20	20000.	2.74	-0.868	*0.569	*-0.307		
	30000.	2.72	-0.773	*0.601	*-0.341		
	50000.	2.77	-0.672	*0.624	*-0.387		
	100000.	2.82	-0.523	*0.691	*-0.446	*0.630	*-0.368

PERTURBER DENSITY = 0.1D+18(cm-3)

PERTURBERS ARE		ELECTRONS		PROTONS		IONIZED HELIUM	
TRANSITION	T(K)	WIDTH(A)	SHIFT(A)	WIDTH(A)	SHIFT(A)	WIDTH(A)	SHIFT(A)
CA II 5S-7P	5000.	4.04	-1.54				
3407.9 A	10000.	3.62	-1.34				
C= 0.11E+20	20000.	3.45	-1.11				
	30000.	3.52	-0.997				
	50000.	3.64	-0.875				
	100000.	3.72	-0.655				
CA II 5P-5D	5000.	11.0	4.80	*0.806	*0.456		
8235.7 A	10000.	8.97	4.20	*1.03	*0.660		
C= 0.12E+21	20000.	8.13	3.66	*1.27	*0.937		
	30000.	7.87	3.25	*1.38	*1.04	*1.25	*0.855
	50000.	7.79	2.77	*1.54	*1.19	*1.32	*0.925
	100000.	7.77	2.15	*1.73	*1.39	*1.41	*1.10
PERTURBER DENSITY = 0.1D+19(cm-3)							
CA II 3D-4P	5000.	13.4	0.592	0.327	-0.420E-01	*0.428	*-0.403E-01
8581.1 A	10000.	10.5	0.323	0.644	-0.111	*0.785	*-0.101
C= 0.86E+22	20000.	8.56	0.248	0.918	-0.192	0.991	-0.165
	30000.	7.76	0.105	1.01	-0.243	1.08	-0.208
	50000.	7.07	0.857E-01	1.11	-0.303	1.18	-0.248
	100000.	6.43	0.813E-01	1.25	-0.372	1.28	-0.306
CA II 3D-5P	5000.	3.03	-0.303				
2132.3 A	10000.	2.41	-0.180				
C= 0.17E+21	20000.	2.07	-0.195				
	30000.	1.96	-0.158	*0.379	*-0.152		
	50000.	1.89	-0.134	*0.407	*-0.188		
	100000.	1.83	-0.131	*0.430	*-0.223		
CA II 3D-6P	5000.	*4.09	*-0.988				
1644.1 A	10000.	3.57	-0.794				
C= 0.48E+20	20000.	3.32	-0.628				
	30000.	3.28	-0.528				
	50000.	3.32	-0.499				
	100000.	3.34	-0.429				
CA II 3D-7P	5000.						
1474.4 A	10000.	*6.21	*-1.59				
C= 0.21E+20	20000.	6.05	-1.28				
	30000.	6.20	-1.11				
	50000.	6.41	-1.20				
	100000.	6.54	-1.00				
CA II 3D-4F	5000.	1.73	0.666	*0.822E-01	*0.238E-01		
1839.2 A	10000.	1.36	0.517	*0.161	*0.544E-01		
C= 0.16E+21	20000.	1.16	0.408	*0.200	*0.804E-01		
	30000.	1.12	0.367	*0.219	*0.972E-01		
	50000.	1.09	0.311	*0.241	*0.120		
	100000.	1.09	0.257	*0.265	*0.147	*0.249	*0.117

PERTURBER DENSITY = 0.1D+19(cm-3)

PERTURBERS ARE		ELECTRONS		PROTONS		IONIZED HELIUM	
TRANSITION	T(K)	WIDTH(A)	SHIFT(A)	WIDTH(A)	SHIFT(A)	WIDTH(A)	SHIFT(A)
CA II 3D-5F	5000.	4.28	0.411				
1554.1 A	10000.	4.37	0.563				
C= 0.31E+19	20000.	4.31	0.586				
	30000.	4.24	0.563				
	50000.	4.14	0.736				
	100000.	3.93	0.788				
CA II 3D-6F	5000.	*5.28	*0.225				
1433.3 A	10000.	*6.61	*0.700				
C= 0.17E+19	20000.	7.74	0.807				
	30000.	8.12	0.823				
	50000.	8.36	0.988				
	100000.	8.22	1.63				
CA II 4S-4P	5000.	2.96	-0.491	0.865E-01	-0.200E-01	*0.109	*-0.184E-01
3946.3 A	10000.	2.28	-0.408	0.167	-0.497E-01	*0.200	*-0.428E-01
C= 0.18E+22	20000.	1.88	-0.317	0.236	-0.800E-01	*0.248	*-0.671E-01
	30000.	1.77	-0.271	0.258	-0.991E-01	0.273	-0.794E-01
	50000.	1.71	-0.253	0.287	-0.118	0.300	-0.965E-01
	100000.	1.66	-0.213	0.321	-0.144	0.317	-0.119
CA II 4S-5P	5000.	1.91	-0.132				
1650.6 A	10000.	1.51	-0.119				
C= 0.10E+21	20000.	1.29	-0.142				
	30000.	1.22	-0.128				
	50000.	1.18	-0.122	*0.253	*-0.114		
	100000.	1.15	-0.116	*0.272	*-0.139		
CA II 4S-6P	5000.	*2.81	*-0.623				
1342.1 A	10000.	2.43	-0.464				
C= 0.32E+20	20000.	2.25	-0.420				
	30000.	2.22	-0.372				
	50000.	2.25	-0.358				
	100000.	2.26	-0.302				
CA II 4S-7P	5000.						
1226.8 A	10000.	*4.34	*-1.10				
C= 0.15E+20	20000.	4.22	-0.921				
	30000.	4.32	-0.846				
	50000.	4.47	-0.856				
	100000.	4.56	-0.716				
CA II 4P-5S	5000.	9.35	3.59	*0.187	*0.109	*0.167	*0.702E-01
3727.6 A	10000.	6.71	2.91	*0.356	*0.261	*0.340	*0.191
C=*0.12E+22	20000.	5.10	2.34	*0.504	*0.387	*0.447	*0.298
	30000.	4.56	2.19	*0.593	*0.476	*0.510	*0.372
	50000.	4.21	1.88	*0.708	*0.583	*0.592	*0.465
	100000.	3.91	1.47	*0.806	*0.702	*0.682	*0.579

PERTURBER DENSITY = 0.1D+19(cm-3)

PERTURBERS ARE		ELECTRONS		PROTONS		IONIZED HELIUM	
TRANSITION	T(K)	WIDTH(A)	SHIFT(A)	WIDTH(A)	SHIFT(A)	WIDTH(A)	SHIFT(A)
CA II 4P-4D	5000.	6.05	2.54	*0.179	*0.815E-01		
3173.5 A	10000.	4.57	1.94	*0.353	*0.201		
C=*0.38E+21	20000.	3.68	1.53	*0.462	*0.294		
	30000.	3.43	1.36	*0.521	*0.358		
	50000.	3.20	1.16	*0.590	*0.444	*0.540	*0.362
	100000.	2.99	0.934	*0.679	*0.547	*0.620	*0.449
CA II 4P-5D	5000.	*5.85	*2.75				
2110.3 A	10000.	4.84	2.34				
C= 0.79E+20	20000.	4.37	1.94				
	30000.	4.23	1.74				
	50000.	4.17	1.50				
	100000.	4.13	1.22				
PERTURBER DENSITY = 0.1D+20(cm-3)							
CA II 3D-4F	5000.	0.289E-01	-0.393E-02				
1839.2 A	10000.	13.6	4.32				
C= 0.16D+22	20000.	11.6	3.54				
	30000.	11.2	3.23				
	50000.	10.9	2.78				
	100000.	10.8	2.31				
CA II 4S-4P	5000.	*29.5	*-4.19	*0.193	*-0.432E-01		
3946.3 A	10000.	22.8	-3.68	*1.00	*-0.256		
C= 0.18E+23	20000.	18.8	-2.91	*2.14	*-0.597		
	30000.	17.7	-2.50	*2.41	*-0.800		
	50000.	17.1	-2.36	*2.79	*-1.01		
	100000.	16.6	-2.06	*3.18	*-1.37		
CA II 4S-5P	5000.	0.271E-01	0.162E-02				
1650.6 A	10000.	14.8	-0.234				
C= 0.10D+22	20000.	12.7	-0.821				
	30000.	12.1	-0.784				
	50000.	11.7	-0.790				
	100000.	11.5	-1.00				

ТАБЕЛЕ ПАРАМЕТАРА ШТАРКОВОГ ШИРЕЊА ЛИНИЈА Ca II ОД ЗНАЧАЈА У АСТРОФИЗИЦИ

М. С. Димитријевић[1] и S. Sahal–Bréchot[2]

[1]*Астрономска опсерваторија, Волгина 7, 11050 Београд, Југославија*
[2]*Laboratoire "Astrophysique, Atomes et Molécules" Département Atomes et Molécules en Astrophysique Unité associée au C.N.R.S. No 812 Observatoire de Paris–Meudon, 92190 Meudon, France*

УДК 52–355.3
Претходно саопштење

Користећи семикласичан прилаз, израчунате су ширине и помераји спектралних линија, проузроковани сударима са електронима, протонима и јонима хелијума, за 28 мултиплета јонизованог калцијума. Резултати су дати у функцији температуре и концентрације пертурбера.

Bull. Astron. Belgrade № 146 (1992), 105–114

UDC 52-355.3
Preliminary report

STARK BROADENING PARAMETER TABLES FOR LARGE QUANTUM NUMBER C IV UV LINES OF INTEREST FOR EXTREME ULTRAVIOLET EXPLORER MISSION

M. S. Dimitrijević[1], and S. Sahal – Bréchot[2]

[1] *Astronomical Observatory, Volgina 7, 11050 Beograd, Yugoslavia*

[2] *Laboratoire "Astrophysique, Atomes et Molécules" Département Atomes et Molécules en Astrophysique Unité associée au C.N.R.S. No 812 Observatoire de Paris–Meudon, 92190 Meudon, France*

(Received: April 17, 1992)

SUMMARY: Using a semiclassical approach, we have calculated electron-, proton-, and ionized helium–impact line widths and shifts for 20 large principal quantum number C IV UV multiplets as a function of temperature for perturber densities 10^{16}-10^{19}cm^{-3}.

1. INTRODUCTION

We have recently calculated, Stark broadening data for 108 C IV multiplets (Dimitrijević and Sahal-Bréchot 1991ab, 1992). However, in the case of far ultraviolet multiplets with large principal quantum number, only data for perturber density 10^{15}cm^{-3} have been provided (Dimitrijević and Sahal-Bréchot 1992, Table 2) . Stark broadening data in the far and extreme ultraviolet, for lines originating from transitions between energy levels with large principal quantum number and low lying levels will become important for astrophysics in the near future. The Extreme Ultraviolet Explorer (EUVE) mission will provide the all sky survey in the λ =70 - 700 Å range by four EUV telescopes in Earth orbit (Bowyer and Malina 1991). Since due to Debye screening Stark broadening data are not linear with density for higher densities, the principal aim of this paper is to complement available C IV Stark broadening data (Dimitrijević and Sahal-Bréchot 1992, Table 2) with the higher density values.

2. RESULTS AND DISCUSSION

By using the semiclassical-perturbation formalism (Sahal-Bréchot 1969ab), we have calculated electron-, proton-, and ionized helium-impact line widths and shifts for 20 large principal quantum number C IV UV multiplets . A summary of the formalism is given in Dimitrijević and Sahal-Bréchot (1991a), and analysis in Dimitrijević and Sahal-Bréchot (1992).

Energy levels for C IV lines have been taken from Bashkin and Stoner (1975). Oscillator strengths have been calculated by using the method of Bates and Damgaard (1949) and the tables of Oertel and Shomo (1968). For higher levels, the method

Table 1. This table shows electron-, proton-, and ionized- helium- impact broadening parameters for C IV UV lines of large principal quantum number, for perturber densities of 10^{17} - 10^{18} cm and temperatures from 20,000 to 200,000 K. Transitions and averaged wavelengths for the multiplet (in Å) are also given. By using c [see Eq. (5) in Dimitrijeviq et al, 1991a], we obtain an estimate for the maximum perturber density for which the line may be treated as isolated and tabulated data may be used. The asterisk identifies cases for which the collision volume multiplied by the perturber density (the condition for validity of the impact approximation) lies between 0.1 and 0.5.

PERTURBER DENSITY = 0.1D+17(cm-3)

PERTURBERS ARE		ELECTRONS		PROTONS		IONIZED HELIUM	
TRANSITION	T(K)	WIDTH(A)	SHIFT(A)	WIDTH(A)	SHIFT(A)	WIDTH(A)	SHIFT(A)
CIV 2S-6P	20000.	0.111E-02	0.956E-04	0.140E-03	0.129E-03	0.128E-03	0.108E-03
212.4 A	50000.	0.923E-03	0.924E-04	0.186E-03	0.169E-03	0.166E-03	0.139E-03
C= 0.27E+16	100000.	0.796E-03	0.768E-04	0.227E-03	0.193E-03	0.189E-03	0.160E-03
	200000.	0.672E-03	0.581E-04	0.270E-03	0.224E-03	0.218E-03	0.184E-03
CIV 2S-7P	20000.	0.193E-02	0.192E-03	*0.304E-03	*0.269E-03	*0.266E-03	*0.224E-03
206.6 A	50000.	0.166E-02	0.185E-03	*0.403E-03	*0.351E-03	*0.344E-03	*0.285E-03
C= 0.15E+16	100000.	0.145E-02	0.141E-03	0.453E-03	0.378E-03	*0.408E-03	*0.333E-03
	200000.	0.124E-02	0.112E-03	0.494E-03	0.445E-03	*0.479E-03	*0.366E-03
C IV 2P-6S	20000.	0.938E-03	0.336E-03	0.104E-03	0.113E-03	0.904E-04	0.949E-04
247.4 A	50000.	0.787E-03	0.258E-03	0.148E-03	0.147E-03	0.123E-03	0.123E-03
C= 0.12E+17	100000.	0.682E-03	0.212E-03	0.188E-03	0.175E-03	0.158E-03	0.142E-03
	200000.	0.582E-03	0.175E-03	0.223E-03	0.187E-03	0.188E-03	0.165E-03
C IV 2P-7S	20000.	0.159E-02	0.674E-03	0.223E-03	0.227E-03	*0.192E-03	*0.191E-03
239.1 A	50000.	0.138E-02	0.501E-03	0.313E-03	0.298E-03	0.258E-03	0.249E-03
C= 0.71E+16	100000.	0.123E-02	0.410E-03	0.372E-03	0.334E-03	0.336E-03	0.271E-03
	200000.	0.107E-02	0.320E-03	0.428E-03	0.386E-03	0.347E-03	0.307E-03
C IV 2P-8S	20000.	0.259E-02	0.117E-02	*0.432E-03	*0.423E-03	*0.371E-03	*0.344E-03
234.1 A	50000.	0.232E-02	0.883E-03	*0.565E-03	*0.534E-03	*0.478E-03	*0.447E-03
C= 0.45E+16	100000.	0.210E-02	0.715E-03	*0.649E-03	*0.616E-03	*0.564E-03	*0.483E-03
	200000.	0.184E-02	0.543E-03	0.816E-03	0.713E-03	*0.623E-03	*0.537E-03
C IV 2P-9S	20000.	0.408E-02	0.192E-02	*0.772E-03	*0.715E-03		
230.9 A	50000.	0.373E-02	0.149E-02	*0.996E-03	*0.907E-03		
C= 0.31E+16	100000.	0.342E-02	0.116E-02	*0.117E-02	*0.104E-02	*0.935E-03	*0.854E-03
	200000.	0.300E-02	0.878E-03	*0.126E-02	*0.116E-02	*0.123E-02	*0.104E-02
CIV 2P-6D	20000.	0.241E-02	0.713E-04				
245.8 A	50000.	0.187E-02	0.918E-04				
C= 0.19E+15	100000.	0.153E-02	0.695E-04	*0.188E-02	*0.162E-02		
	200000.	0.123E-02	0.390E-04	*0.218E-02	*0.205E-02		
CIV 2P-7D	20000.	0.421E-02	0.112E-03				
238.2 A	50000.	0.332E-02	0.162E-03				
C= 0.17E+15	100000.	0.274E-02	0.124E-03				
	200000.	0.221E-02	0.671E-04				
CIV 3S-6P	20000.	0.900E-02	0.724E-03	0.110E-02	0.101E-02	0.100E-02	0.847E-03
595.5 A	50000.	0.744E-02	0.699E-03	0.146E-02	0.133E-02	0.130E-02	0.109E-02
C= 0.21E+17	100000.	0.640E-02	0.572E-03	0.178E-02	0.151E-02	0.149E-02	0.125E-02
	200000.	0.540E-02	0.428E-03	0.213E-02	0.176E-02	0.170E-02	0.144E-02
CIV 3S-7P	20000.	0.140E-01	0.134E-02	*0.217E-02	*0.192E-02	*0.190E-02	*0.160E-02
552.2 A	50000.	0.120E-01	0.130E-02	*0.288E-02	*0.251E-02	*0.246E-02	*0.203E-02
C= 0.11E+17	100000.	0.105E-01	0.981E-03	0.325E-02	0.269E-02	*0.291E-02	*0.237E-02
	200000.	0.893E-02	0.773E-03	0.353E-02	0.318E-02	*0.342E-02	*0.261E-02

PERTURBER DENSITY = 0.1D+17(cm-3)

PERTURBERS ARE		ELECTRONS		PROTONS		IONIZED HELIUM	
TRANSITION	T(K)	WIDTH(A)	SHIFT(A)	WIDTH(A)	SHIFT(A)	WIDTH(A)	SHIFT(A)
C IV 3P-6S	20000.	0.730E-02	0.244E-02	0.760E-03	0.827E-03	0.664E-03	0.696E-03
672.4 A	50000.	0.611E-02	0.186E-02	0.109E-02	0.108E-02	0.912E-03	0.900E-03
C= 0.90E+17	100000.	0.530E-02	0.154E-02	0.137E-02	0.129E-02	0.117E-02	0.104E-02
	200000.	0.453E-02	0.127E-02	0.167E-02	0.137E-02	0.138E-02	0.121E-02
C IV 3P-7S	20000.	0.108E-01	0.441E-02	0.147E-02	0.150E-02	*0.126E-02	*0.126E-02
614.9 A	50000.	0.939E-02	0.328E-02	0.206E-02	0.197E-02	0.170E-02	0.164E-02
C= 0.47E+17	100000.	0.837E-02	0.269E-02	0.245E-02	0.221E-02	0.222E-02	0.179E-02
	200000.	0.725E-02	0.210E-02	0.282E-02	0.255E-02	0.230E-02	0.203E-02
C IV 3P-8S	20000.	0.164E-01	0.724E-02	*0.267E-02	*0.262E-02	*0.230E-02	*0.213E-02
582.8 A	50000.	0.146E-01	0.545E-02	*0.350E-02	*0.331E-02	*0.296E-02	*0.277E-02
C= 0.28E+17	100000.	0.132E-01	0.441E-02	0.401E-02	0.382E-02	*0.350E-02	*0.299E-02
	200000.	0.116E-01	0.335E-02	0.506E-02	0.442E-02	*0.385E-02	*0.333E-02
C IV 3P-9S	20000.	0.245E-01	0.114E-01	*0.459E-02	*0.425E-02		
562.9 A	50000.	0.224E-01	0.883E-02	*0.592E-02	*0.539E-02		
C= 0.18E+17	100000.	0.205E-01	0.686E-02	*0.698E-02	*0.619E-02	*0.555E-02	*0.507E-02
	200000.	0.180E-01	0.520E-02	*0.745E-02	*0.687E-02	*0.730E-02	*0.617E-02
CIV 3P-6D	20000.	0.178E-01	0.500E-03				
660.9 A	50000.	0.138E-01	0.639E-03				
C= 0.14E+16	100000.	0.113E-01	0.483E-03	*0.136E-01	*0.117E-01		
	200000.	0.905E-02	0.263E-03	*0.157E-01	*0.148E-01		
CIV 3P-7D	20000.	0.278E-01	0.720E-03				
608.9 A	50000.	0.219E-01	0.103E-02				
C= 0.11E+16	100000.	0.180E-01	0.794E-03				
	200000.	0.146E-01	0.422E-03				
CIV 3D-6P	20000.	0.117E-01	0.101E-02	0.145E-02	0.135E-02	0.132E-02	0.113E-02
685.4 A	50000.	0.971E-02	0.975E-03	0.194E-02	0.177E-02	0.172E-02	0.145E-02
C= 0.28E+17	100000.	0.837E-02	0.810E-03	0.235E-02	0.201E-02	0.196E-02	0.166E-02
	200000.	0.706E-02	0.615E-03	0.281E-02	0.234E-02	0.227E-02	0.192E-02
CIV 3D-7P	20000.	0.180E-01	0.179E-02	*0.282E-02	*0.249E-02	*0.246E-02	*0.208E-02
628.7 A	50000.	0.154E-01	0.172E-02	*0.373E-02	*0.326E-02	*0.318E-02	*0.264E-02
C= 0.14E+17	100000.	0.135E-01	0.132E-02	0.418E-02	0.350E-02	*0.378E-02	*0.309E-02
	200000.	0.115E-01	0.104E-02	0.456E-02	0.412E-02	*0.443E-02	*0.339E-02
CIV 3D-6F	20000.	0.186E-01	-0.228E-03				
682.5 A	50000.	0.148E-01	-0.215E-03				
C= 0.14E+15	100000.	0.120E-01	-0.201E-03				
	200000.	0.957E-02	-0.160E-03				
CIV 3D-7F	20000.	0.309E-01	-0.516E-03				
627.1 A	50000.	0.246E-01	-0.545E-03				
C= 0.76E+14	100000.	0.201E-01	-0.454E-03				
	200000.	0.160E-01	-0.310E-03				

PERTURBER DENSITY = 0.1D+18(cm-3)

PERTURBERS ARE		ELECTRONS		PROTONS		IONIZED HELIUM	
TRANSITION	T(K)	WIDTH(A)	SHIFT(A)	WIDTH(A)	SHIFT(A)	WIDTH(A)	SHIFT(A)
CIV 2S-6P	20000.	0.111E-01	0.706E-03	*0.139E-02	*0.107E-02		
212.4 A	50000.	0.923E-02	0.838E-03	*0.186E-02	*0.160E-02		
C= 0.27E+17	100000.	0.796E-02	0.751E-03	*0.227E-02	*0.191E-02		
	200000.	0.672E-02	0.581E-03	*0.270E-02	*0.224E-02	*0.218E-02	*0.184E-02
CIV 2S-7P	20000.	0.192E-01	0.114E-02				
206.6 A	50000.	0.165E-01	0.159E-02				
C= 0.15E+17	100000.	0.145E-01	0.137E-02				
	200000.	0.123E-01	0.112E-02				
C IV 2P-6S	20000.	0.938E-02	0.320E-02	*0.103E-02	*0.965E-03	*0.902E-03	*0.786E-03
247.4 A	50000.	0.786E-02	0.252E-02	*0.147E-02	*0.141E-02	*0.125E-02	*0.117E-02
C= 0.12E+18	100000.	0.682E-02	0.211E-02	*0.188E-02	*0.174E-02	*0.158E-02	*0.140E-02
	200000.	0.582E-02	0.174E-02	*0.223E-02	*0.187E-02	*0.188E-02	*0.165E-02
C IV 2P-7S	20000.	0.159E-01	0.626E-02				
239.1 A	50000.	0.138E-01	0.485E-02				
C= 0.71E+17	100000.	0.123E-01	0.408E-02	*0.372E-02	*0.331E-02		
	200000.	0.107E-01	0.318E-02	*0.428E-02	*0.386E-02		
C IV 2P-8S	20000.	0.259E-01	0.107E-01				
234.1 A	50000.	0.232E-01	0.841E-02				
C= 0.45E+17	100000.	0.210E-01	0.709E-02				
	200000.	0.184E-01	0.537E-02				
C IV 2P-9S	20000.	0.407E-01	0.168E-01				
230.9 A	50000.	0.372E-01	0.139E-01				
C= 0.31E+17	100000.	0.342E-01	0.115E-01				
	200000.	0.300E-01	0.865E-02				
CIV 2P-6D	20000.	0.202E-01	-0.773E-03				
245.8 A	50000.	0.163E-01	-0.326E-04				
C= 0.19E+16	100000.	0.136E-01	0.402E-03				
	200000.	0.111E-01	0.390E-03				
CIV 2P-7D	20000.	0.344E-01	-0.138E-02				
238.2 A	50000.	0.285E-01	-0.108E-03				
C= 0.17E+16	100000.	0.240E-01	0.686E-03				
	200000.	0.198E-01	0.671E-03				
CIV 3S-6P	20000.	0.900E-01	0.530E-02	*0.109E-01	*0.840E-02		
595.5 A	50000.	0.744E-01	0.632E-02	*0.146E-01	*0.125E-01		
C= 0.21E+18	100000.	0.640E-01	0.559E-02	*0.178E-01	*0.150E-01		
	200000.	0.540E-01	0.428E-02	*0.213E-01	*0.176E-01	*0.170E-01	*0.144E-01
CIV 3S-7P	20000.	0.139	0.783E-02				
552.2 A	50000.	0.120	0.111E-01				
C= 0.11E+18	100000.	0.105	0.948E-02				
	200000.	0.890E-01	0.773E-02				

PERTURBER DENSITY = 0.1D+18(cm-3)

PERTURBERS ARE		ELECTRONS		PROTONS		IONIZED HELIUM	
TRANSITION	T(K)	WIDTH(A)	SHIFT(A)	WIDTH(A)	SHIFT(A)	WIDTH(A)	SHIFT(A)
C IV 3P-6S	20000.	0.731E-01	0.232E-01	*0.756E-02	*0.709E-02	*0.663E-02	*0.577E-02
672.4 A	50000.	0.611E-01	0.182E-01	*0.108E-01	*0.104E-01	*0.919E-02	*0.857E-02
C= 0.90E+18	100000.	0.530E-01	0.153E-01	*0.137E-01	*0.128E-01	*0.117E-01	*0.104E-01
	200000.	0.453E-01	0.126E-01	*0.167E-01	*0.137E-01	*0.138E-01	*0.121E-01
C IV 3P-7S	20000.	0.108	0.409E-01				
614.9 A	50000.	0.939E-01	0.317E-01				
C= 0.47E+18	100000.	0.837E-01	0.267E-01	*0.245E-01	*0.219E-01		
	200000.	0.725E-01	0.208E-01	*0.282E-01	*0.255E-01		
C IV 3P-8S	20000.	0.164	0.659E-01				
582.8 A	50000.	0.146	0.518E-01				
C= 0.28E+18	100000.	0.132	0.437E-01				
	200000.	0.116	0.331E-01				
C IV 3P-9S	20000.	0.245	0.995E-01				
562.9 A	50000.	0.223	0.826E-01				
C= 0.18E+18	100000.	0.205	0.679E-01				
	200000.	0.180	0.512E-01				
CIV 3P-6D	20000.	0.150	-0.570E-02				
660.9 A	50000.	0.120	-0.468E-03				
C= 0.14E+17	100000.	0.100	0.271E-02				
	200000.	0.818E-01	0.263E-02				
CIV 3P-7D	20000.	0.228	-0.912E-02				
608.9 A	50000.	0.188	-0.900E-03				
C= 0.11E+17	100000.	0.159	0.431E-02				
	200000.	0.131	0.422E-02				
CIV 3D-6P	20000.	0.117	0.748E-02	*0.144E-01	*0.112E-01		
685.4 A	50000.	0.971E-01	0.886E-02	*0.193E-01	*0.167E-01		
C= 0.28E+18	100000.	0.837E-01	0.793E-02	*0.235E-01	*0.200E-01		
	200000.	0.706E-01	0.615E-02	*0.281E-01	*0.234E-01	*0.227E-01	*0.192E-01
CIV 3D-7P	20000.	0.179	0.106E-01				
628.7 A	50000.	0.154	0.148E-01				
C= 0.14E+18	100000.	0.135	0.128E-01				
	200000.	0.115	0.104E-01				
CIV 3D-6F	20000.	0.138	0.118E-02				
682.5 A	50000.	0.117	-0.199E-02				
C= 0.14E+16	100000.	0.985E-01	-0.278E-02				
	200000.	0.805E-01	-0.160E-02				
CIV 3D-7F	20000.	0.223	0.176E-02				
627.1 A	50000.	0.190	-0.440E-02				
C= 0.76E+15	100000.	0.161	-0.640E-02				
	200000.	0.133	-0.310E-02				

PERTURBER DENSITY = 0.1D+19(cm-3)

PERTURBERS ARE		ELECTRONS		PROTONS		IONIZED HELIUM	
TRANSITION	T(K)	WIDTH(A)	SHIFT(A)	WIDTH(A)	SHIFT(A)	WIDTH(A)	SHIFT(A)
CIV 2S-6P	20000.	0.106	0.267E-04				
212.4 A	50000.	0.893E-01	0.410E-02				
C= 0.27E+18	100000.	0.775E-01	0.543E-02				
	200000.	0.657E-01	0.542E-02				
CIV 2S-7P	20000.	0.168	-0.485E-02				
206.6 A	50000.	0.151	0.478E-02				
C= 0.15E+18	100000.	0.135	0.767E-02				
	200000.	0.116	0.998E-02				
C IV 2P-6S	20000.	0.937E-01	0.269E-01				
247.4 A	50000.	0.786E-01	0.222E-01				
C= 0.12E+19	100000.	0.682E-01	0.197E-01				
	200000.	0.582E-01	0.172E-01				
C IV 2P-7S	20000.	0.157	0.475E-01				
239.1 A	50000.	0.137	0.397E-01				
C= 0.71E+18	100000.	0.123	0.368E-01				
	200000.	0.106	0.312E-01				
C IV 2P-8S	20000.	*0.246	*0.697E-01				
234.1 A	50000.	0.224	0.625E-01				
C= 0.45E+18	100000.	0.205	0.607E-01				
	200000.	0.180	0.524E-01				
C IV 2P-9S	20000.	*0.353	*0.888E-01				
230.9 A	50000.	0.343	0.913E-01				
C= 0.31E+18	100000.	0.321	0.911E-01				
	200000.	0.286	0.834E-01				
CIV 2P-6D	20000.	0.151	-0.419E-02				
245.8 A	50000.	0.130	-0.343E-02				
C= 0.19E+17	100000.	0.112	-0.860E-03				
	200000.	0.944E-01	0.120E-02				
CIV 2P-7D	20000.	0.236	-0.351E-02				
238.2 A	50000.	0.215	-0.393E-02				
C= 0.17E+17	100000.	0.191	-0.445E-03				
	200000.	0.163	0.197E-02				
CIV 3S-6P	20000.	0.859	-0.221E-02				
595.5 A	50000.	0.720	0.296E-01				
C= 0.21E+19	100000.	0.624	0.395E-01				
	200000.	0.528	0.398E-01				
CIV 3S-7P	20000.	1.22	-0.374E-01				
552.2 A	50000.	1.10	0.317E-01				
C= 0.11E+19	100000.	0.977	0.520E-01				
	200000.	0.842	0.688E-01				

PERTURBER DENSITY = 0.1D+19(cm-3)

PERTURBERS ARE		ELECTRONS		PROTONS		IONIZED HELIUM	
TRANSITION	T(K)	WIDTH(A)	SHIFT(A)	WIDTH(A)	SHIFT(A)	WIDTH(A)	SHIFT(A)
C IV 3P-6S	20000.	0.730	0.195				
672.4 A	50000.	0.610	0.161				
C= 0.90E+19	100000.	0.530	0.143				
	200000.	0.453	0.125				
C IV 3P-7S	20000.	1.07	0.310				
614.9 A	50000.	0.931	0.259				
C= 0.47E+19	100000.	0.832	0.241				
	200000.	0.721	0.205				
C IV 3P-8S	20000.	*1.55	*0.429				
582.8 A	50000.	1.41	0.384				
C= 0.28E+19	100000.	1.29	0.374				
	200000.	1.13	0.323				
C IV 3P-9S	20000.	*2.13	*0.525				
562.9 A	50000.	2.06	0.540				
C= 0.18E+19	100000.	1.93	0.540				
	200000.	1.71	0.494				
CIV 3P-6D	20000.	1.12	-0.312E-01				
660.9 A	50000.	0.965	-0.270E-01				
C= 0.14E+18	100000.	0.833	-0.810E-02				
	200000.	0.698	0.685E-02				
CIV 3P-7D	20000.	1.57	-0.238E-01				
608.9 A	50000.	1.43	-0.275E-01				
C= 0.11E+18	100000.	1.27	-0.453E-02				
	200000.	1.08	0.113E-01				
CIV 3D-6P	20000.	1.11	0.129E-02				
685.4 A	50000.	0.940	0.439E-01				
C= 0.28E+19	100000.	0.815	0.575E-01				
	200000.	0.691	0.574E-01				
CIV 3D-7P	20000.	1.56	-0.439E-01				
628.7 A	50000.	1.41	0.453E-01				
C= 0.14E+19	100000.	1.26	0.719E-01				
	200000.	1.08	0.932E-01				
CIV 3D-6F	20000.	0.906	0.269E-01				
682.5 A	50000.	0.844	0.700E-02				
C= 0.14E+17	100000.	0.748	-0.101E-01				
	200000.	0.635	-0.198E-01				
CIV 3D-7F	20000.	1.38	0.418E-01				
627.1 A	50000.	1.32	0.810E-02				
C= 0.76E+16	100000.	1.19	-0.236E-01				
	200000.	1.02	-0.410E-01				

PERTURBER DENSITY = 0.1D+20(cm-3)

PERTURBERS ARE		ELECTRONS		PROTONS		IONIZED HELIUM	
TRANSITION	T(K)	WIDTH(A)	SHIFT(A)	WIDTH(A)	SHIFT(A)	WIDTH(A)	SHIFT(A)
CIV 2S-6P	20000.	*0.748	*-0.674E-01				
212.4 A	50000.	*0.707	*-0.188E-01				
C= 0.27E+19	100000.	0.649	-0.187E-02				
	200000.	0.570	0.202E-01				
CIV 2S-7P	20000.						
206.6 A	50000.	*1.02	*-0.291E-01				
C= 0.15E+19	100000.	*1.02	*-0.129E-01				
	200000.	0.931	0.324E-01				
C IV 2P-6S	20000.	*0.806	*0.881E-01				
247.4 A	50000.	0.728	0.114				
C= 0.12E+20	100000.	0.644	0.116				
	200000.	0.555	0.139				
C IV 2P-7S	20000.	*1.03	*0.700E-01				
239.1 A	50000.	1.11	0.139				
C= 0.71E+19	100000.	1.05	0.165				
	200000.	0.943	0.220				
C IV 2P-8S	20000.						
234.1 A	50000.	*1.47	*0.130				
C= 0.45E+19	100000.	1.55	0.195				
	200000.	1.45	0.317				
C IV 2P-9S	20000.						
230.9 A	50000.	*1.74	*0.121				
C= 0.31E+19	100000.	2.07	0.206				
	200000.	2.07	0.437				
CIV 2P-6D	20000.	*0.867	*0.532E-01				
245.8 A	50000.	0.867	0.124E-01				
C= 0.19E+18	100000.	0.813	0.164E-02				
	200000.	0.721	-0.648E-02				
CIV 2P-7D	20000.						
238.2 A	50000.	*1.26	*0.294E-01				
C= 0.17E+18	100000.	1.27	0.123E-01				
	200000.	1.17	-0.814E-02				
CIV 3S-6P	20000.	*6.16	*-0.549				
595.5 A	50000.	*5.74	*-0.170				
C= 0.21E+20	100000.	5.25	-0.433E-01				
	200000.	4.60	0.132				
CIV 3S-7P	20000.						
552.2 A	50000.	*7.48	*-0.229				
C= 0.11E+20	100000.	*7.38	*-0.118				
	200000.	6.75	0.207				

PERTURBER DENSITY = 0.1D+20(cm-3)

PERTURBERS ARE		ELECTRONS		PROTONS		IONIZED HELIUM	
TRANSITION	T(K)	WIDTH(A)	SHIFT(A)	WIDTH(A)	SHIFT(A)	WIDTH(A)	SHIFT(A)
C IV 3P-6S	20000.	*6.33	*0.625				
672.4 A	50000.	5.68	0.814				
C= 0.90E+20	100000.	5.02	0.836				
	200000.	4.33	1.01				
C IV 3P-7S	20000.	*7.10	*0.432				
614.9 A	50000.	7.58	0.892				
C= 0.47E+20	100000.	7.18	1.07				
	200000.	6.43	1.44				
C IV 3P-8S	20000.						
582.8 A	50000.	*9.35	*0.787				
C= 0.28E+20	100000.	9.77	1.19				
	200000.	9.18	1.95				
C IV 3P-9S	20000.						
562.9 A	50000.	*10.5	*0.704				
C= 0.18E+20	100000.	12.5	1.21				
	200000.	12.5	2.58				
CIV 3P-6D	20000.	*6.61	*0.386				
660.9 A	50000.	6.51	0.744E-01				
C= 0.14E+19	100000.	6.07	-0.183E-02				
	200000.	5.37	-0.635E-01				
CIV 3P-7D	20000.						
608.9 A	50000.	*8.47	*0.179				
C= 0.11E+19	100000.	8.44	0.684E-01				
	200000.	7.78	-0.672E-01				
CIV 3D-6P	20000.	*7.92	*-0.701				
685.4 A	50000.	*7.46	*-0.189				
C= 0.28E+20	100000.	6.84	-0.132E-01				
	200000.	6.00	0.219				
CIV 3D-7P	20000.						
628.7 A	50000.	*9.57	*-0.263				
C= 0.14E+20	100000.	9.47	-0.114				
	200000.	8.67	0.307				
CIV 3D-6F	20000.	*5.18	*0.187				
682.5 A	50000.	5.41	0.144				
C= 0.14E+18	100000.	5.18	0.127				
	200000.	4.67	0.411E-01				
CIV 3D-7F	20000.						
627.1 A	50000.	*7.71	*0.211				
C= 0.76E+17	100000.	7.75	0.158				
	200000.	7.21	0.246E-01				

described by Van Regemorter et al. (1979) has been used. In addition to electron-impact full halfwidths and shifts, Stark-broadening parameters due to proton-, and ionized helium- impacts have been calculated.

Our results for C IV UV multiplets of large principal quantum number are shown in Table 1, for perturber densities 10^{16} - 10^{19} cm and temperatures T = 20,000 - 200,000 K. We also specify a parameter c (Dimitrijević and Sahal-Bréchot 1984), which gives an estimate for the maximum perturber density for which the line may be treated as isolated when it is divided by the corresponding electron-impact full width at half maximum. For each value given in Table 1 , the collision volume (V) multiplied by the perturber density (N) is much less than one and the impact approximation is valid (Sahal-Bréchot, 1969ab). Values for NV > 0.5 are not given and values for $0.1 < NV \leq 0.5$ are denoted by an asterisk. When the impact approximation is not valid, the ion broadening contribution may be estimated by using quasistatic estimations (Sahal-Bréchot 1991 and Griem 1974). The accuracy of the results obtained decreases when broadening by ion interactions becomes important.

Acknowledgements - This work has been supported by the French C.N.R.S. and is a part of French-Yugoslav collaboration through the project "L'élargissement Stark des raies spéctrales des plasmas astrophysiques et de laboratoire". It is also a part of the project "Physics and Dynamics of Celestial Bodies" supported by Ministry for Science and Technology of Serbia.

REFERENCES

Bashkin,S., and Stoner,J.O.Jr.: 1975, *Atomic Energy Levels and Grotrian Diagrams*, Vol. 1, North Holland, Amsterdam.

Bates,D.R., and Damgaard,A.: 1949, *Trans. Roy. Soc. London*, Ser. **A 242**, 101.

Bowyer,S., and Malina, R.F.: 1991, *Proc.Int.Symp. "Evolution in Astrophysics"*, Toulouse 1990, ESA SP-310, 189.

Dimitrijević, M. S., and Sahal-Bréchot, S.: 1984, *JQSRT* **31**, 301.

Dimitrijević, M. S., Sahal-Bréchot, S., and Bommier, V.: 1991a, *Astron. Astrophys. Suppl. Series* **89**, 581.

Dimitrijević, M. S., Sahal-Bréchot, S., and Bommier, V.: 1991b, *Bull. Obs. Astron. Belgrade* **144**, 65.

Dimitrijević, M. S., and Sahal-Bréchot, S.: 1992, *Astron. Astrophys. Suppl. Series*, in press.

Griem,H.R.: 1974, *Spectral Line Broadening by Plasmas, Academic Press*, New York and London.

Oertel, G. K., and Shomo, L. P.: 1968, *Astrophys. J. Suppl.* **16**, 175.

Sahal-Bréchot,S.: 1969a, *Astron. Astrophys.* **1**, 91.

Sahal-Bréchot, S.: 1969b, *Astron. Astrophys.* **2**, 322.

Sahal-Bréchot, S.: 1991, *Astron. Astrophys.* **245**, 322.

Van Regemorter, H., Hoang Binh Dy, and Prud'homme, M.: 1979, *J. Phys. B* **12**, 1073.

ТАБЕЛЕ ПАРАМЕТАРА ШТАРКОВОГ ШИРЕЊА C IV UV МУЛТИПЛЕТА СА ВЕЛИКИМ ГЛАВНИМ КВАНТНИМ БРОЈЕМ ОД ЗНАЧАЈА ЗА EXTREME ULTRAVIOLET EXPLORER МИСИЈУ

М. С. Димитријевић[1] и S. Sahal-Bréchot[2]

[1]*Астрономска опсерваторија, Волгина 7, 11050 Београд, Југославија*
[2]*Laboratoire "Astrophysique, Atomes et Molécules" Département Atomes et Molécules en Astrophysique Unité associée au C.N.R.S. No 812 Observatoire de Paris-Meudon, 92190 Meudon, France*

УДК 52–355.3
Претходно саопштење

Користећи семикласичан прилаз, израчунате су ширине и помераји спектралних линија, проузроковани сударима са електронима, протонима и јонима хелијума, за 20 UV мултиплета са великим главним квантним бројем, троструко наелектрисаног јона угљеника. Резултати су дати у функцији температуре и концентрације пертурбера.

Bull. Astron. Belgrade № 146 (1992), 115–119

UDC 52–355.3
Preliminary report

INFLUENCE OF DIFFERENT COLLISIONAL PROCESSES ON THE STARK BROADENING WITHIN SPECTRAL SERIES: THE O VI CASE

Milan S. Dimitrijević

Astronomical Observatory, Volgina 7, 11050 Beograd, Yugoslavia

(Received: June 28, 1992)

SUMMARY: Using a semiclassical perturbation approach, behavior of Stark broadening parameters within spectral series has been investigated on the O VI case. The behavior of inelastic, elastic and strong collision contribution to line widths within a spectral series has been studied also.

1. INTRODUCTION

Stark broadening of strong multicharged ionic lines plays a non-negligible role in the calculation of the opacities, especially in the UV. Stark broadening data for these lines are very few numerous and many data are missing. The semiclassical-perturbation theory offers an interesting possibility for calculating numerous data, with an acceptable accuracy and without excessive computational time consuming. However, in the cases as e. g. stellar opacity calculations, when a lot of data are needed and where only a good average accuracy for a large set of lines is required, approximate methods are very useful. One such possibility provides knowledge about Stark broadening regularities and systematic trends (see e. g. Furić et al., 1991 and the references therein). In order to continue the investigation of systematic trends for Stark broadening parameters within spectral series (Dimitrijević and Sahal-Bréchot, 1984ab, 1985, 1987, 1990, 1992; Dimitrijević et al., 1991ab), the aim of this paper is to investigate Stark broadening parameter regularities within 2p - ns, 2s - np and ns - np (n = 3, 4, 5, 6) O VI spectral series, as well as the behavior of inelastic, elastic and strong collision contribution within the mentioned series.

2. RESULTS AND DISCUSSION

Using semiclassical-perturbation approach (Sahal-Bréchot, 1969 a b), inelastic, elastic and strong collision contribution to the Stark full half width (W) within 2p - ns, 2s - np and ns - np (n = 3, 4, 5, 6) O VI spectral series, has been calculated. Moreover, Stark broadening data from recently calculated comprehensive set of O VI Stark broadening parameters (Dimitrijević and Sahal-Bréchot, 1992) has also been used. In Figs. 1 and 2 the behavior of the electron and proton full halfwidths within the 2p $^2P^0$ - ns ^2S series are illustrated. We see the variation of the results for different plasma temperatures and different perturber type (electrons and protons). By inspecting the energy separation between the upper level and the principal perturbing levels (see the Grotrian diagrams in Bashkin and Stoner, 1975), we

find that this separation decreases gradually within a spectral series. This is the reason why we obtain a gradual change of Stark widths. In Figs. 3 and 4 we can see the same situation in the case of the shift. In Figs. 5 - 13 are presented inelastic, elastic and strong contribution to the electron-impact width for the case of 2p $^2P^0$ - ns ^2S O VI series as well as cases of 2s ^2S - np $^2P^0$, and ns ^2S - np $^2P^0$ series. We can see that inelastic and elastic contribution change very regularly in all cases examined. In the case of strong contribution there is a irregular jump for the highest member of 2p $^2P^0$ - ns ^2S series. This however, does not have signicant influence on the general behavior, due to the relatively small strong collision contribution for the case considered. Moreover, one must take into account that the strong collision contribution is one of the weakest points of the semiclassical theory. The demonstrated regular behavior might be used for the critical evaluation of existing resultsas well as for the interpolation of new data needed in astrophysics.

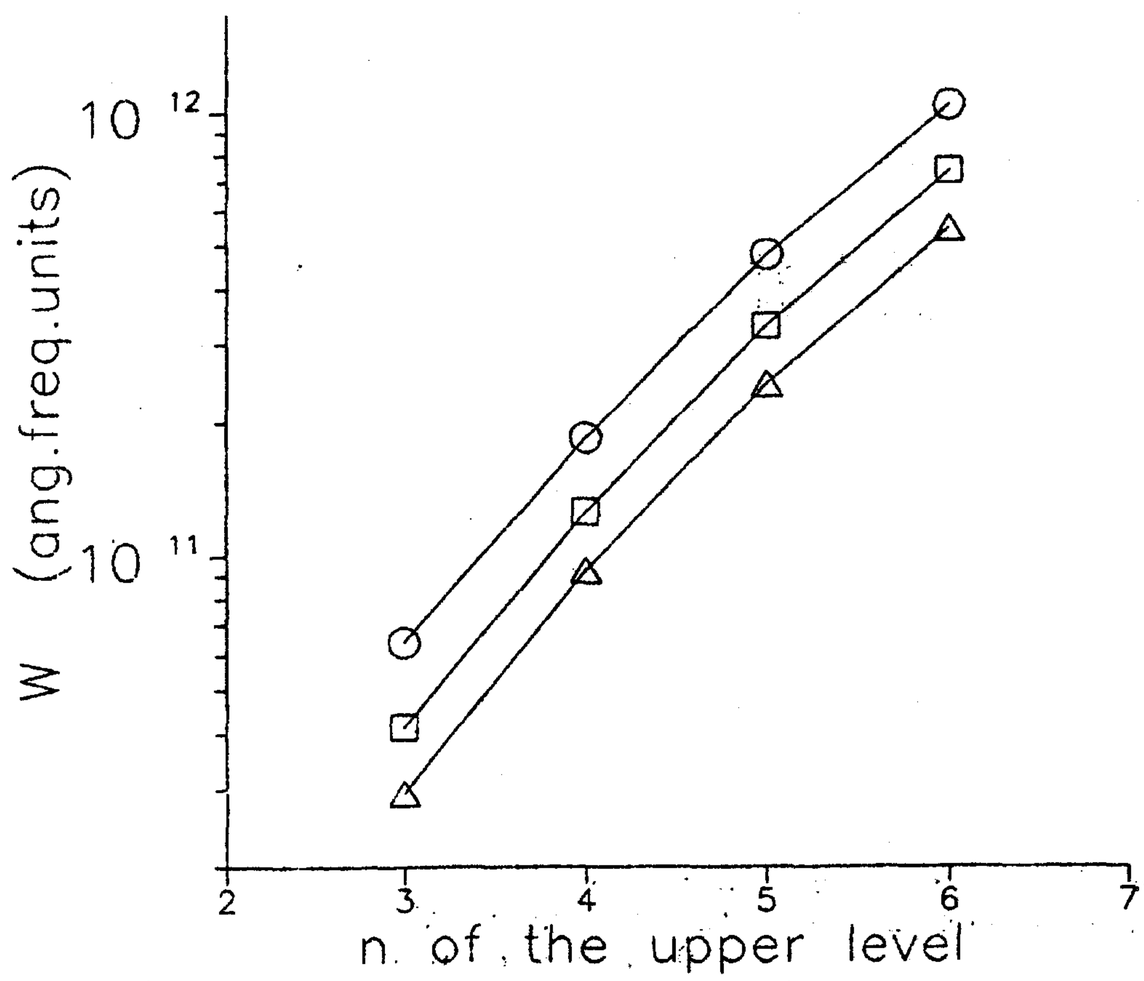

Fig. 1. Electron-impact widths (angular frequency units) along the O VI 2p $^2P^0$ - ns ^2S series as a function of n for T = 100,000 K (o); 300,000 K (□) and 800,000 K (△) at N = 10^{15} cm^{-3}.

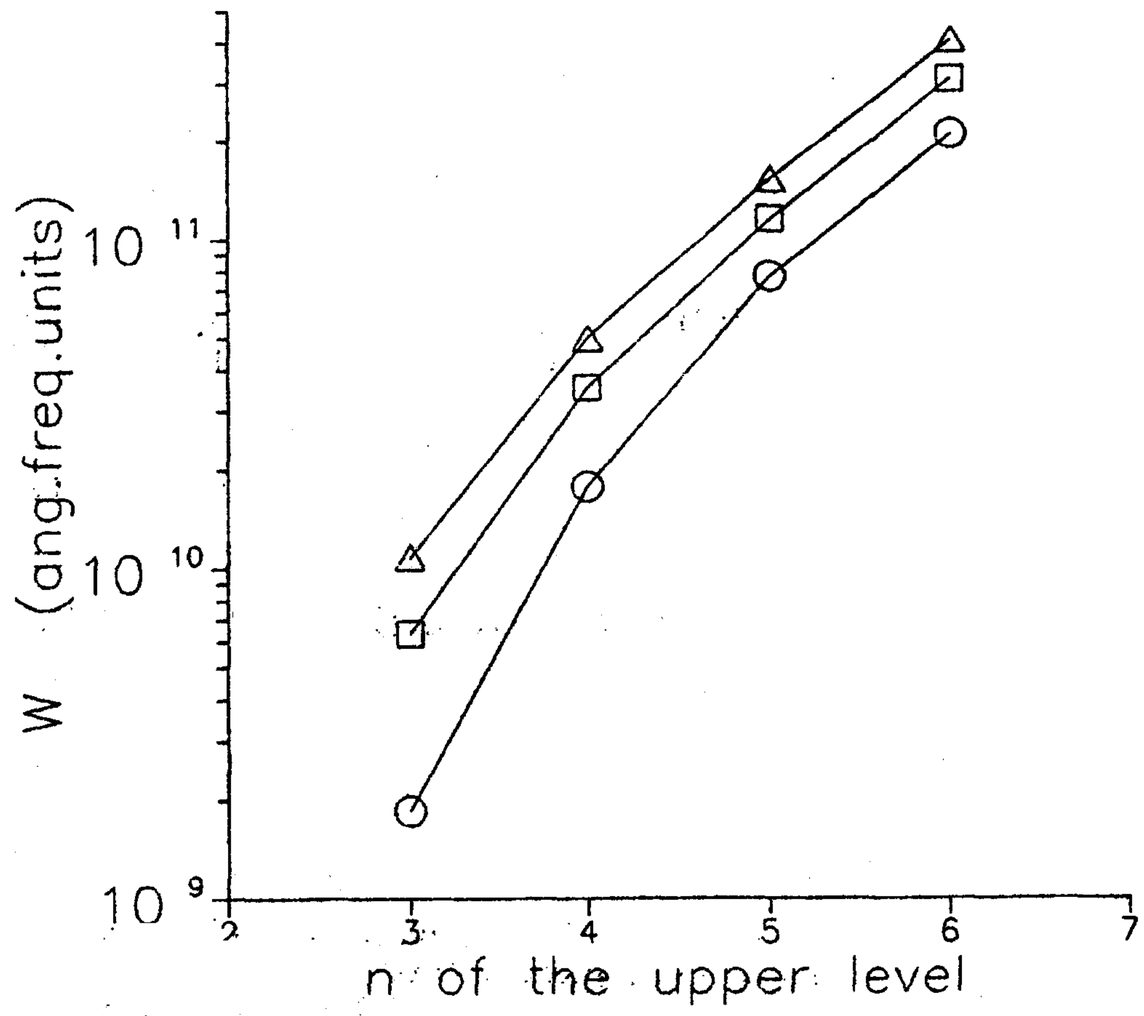

Fig. 2. As in Fig. 1 but for the proton-impact widths.

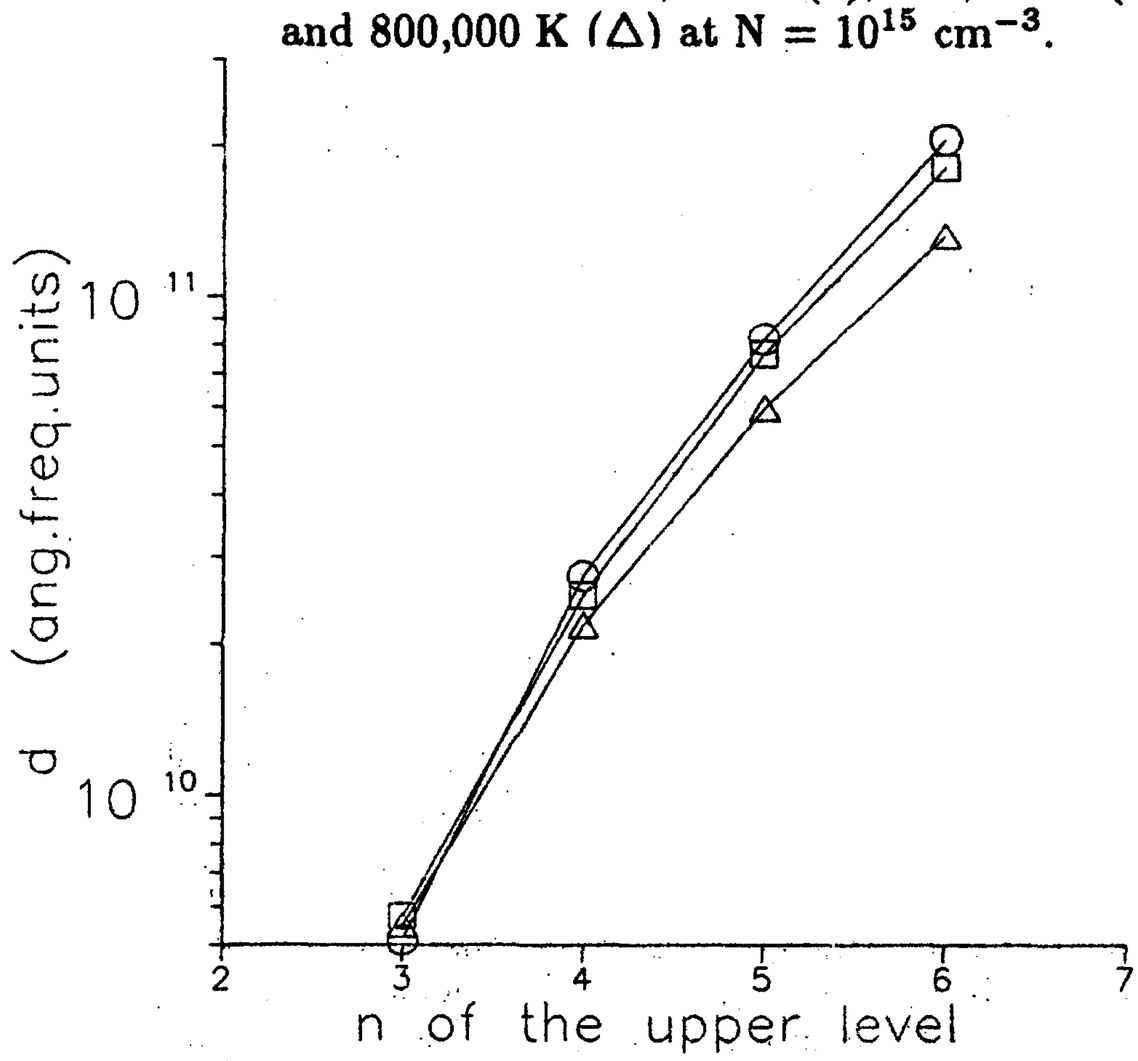

Fig. 3. As in Fig. 1 but for the electron-impact shifts.

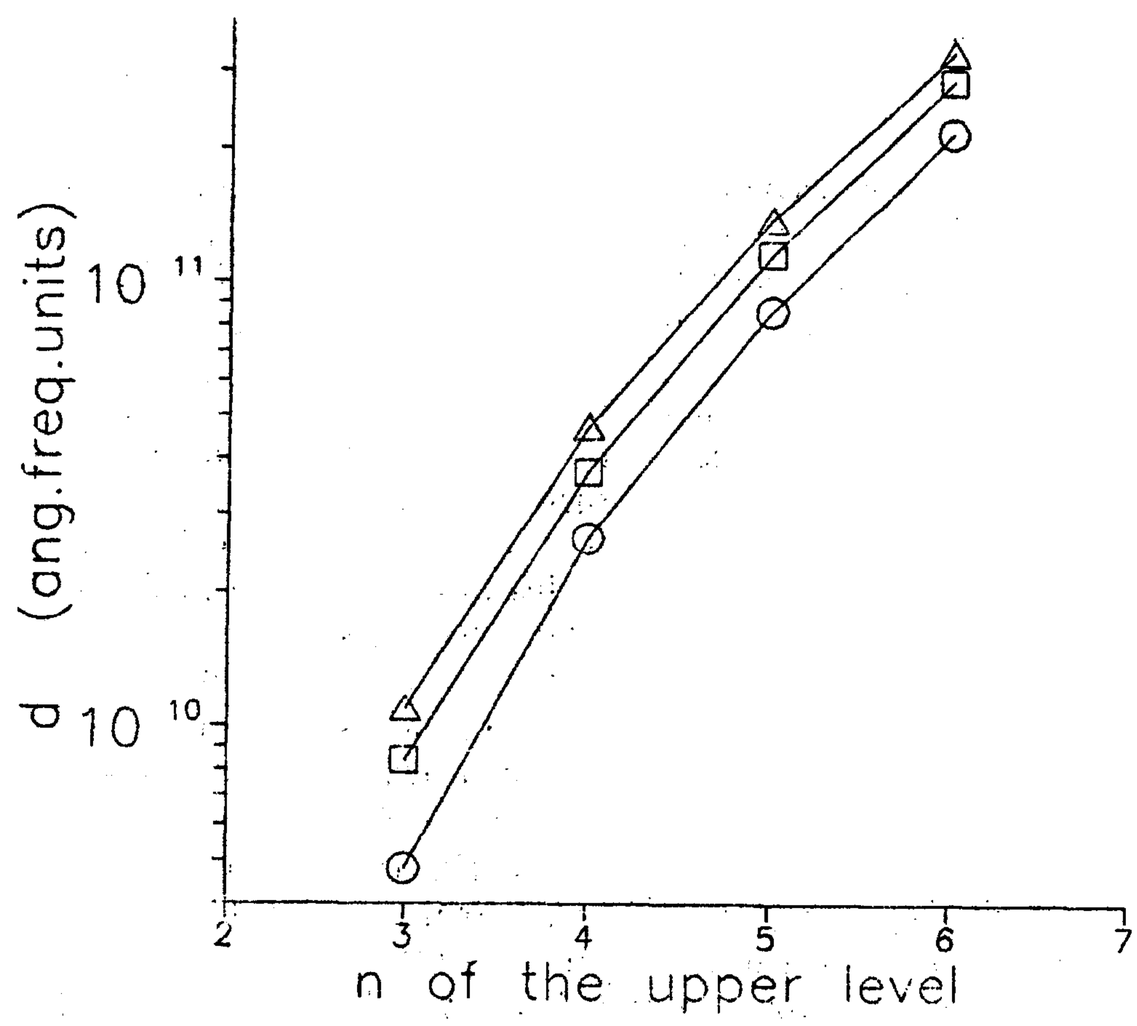

Fig. 4. As in Fig. 1 but for the proton-impact shifts.

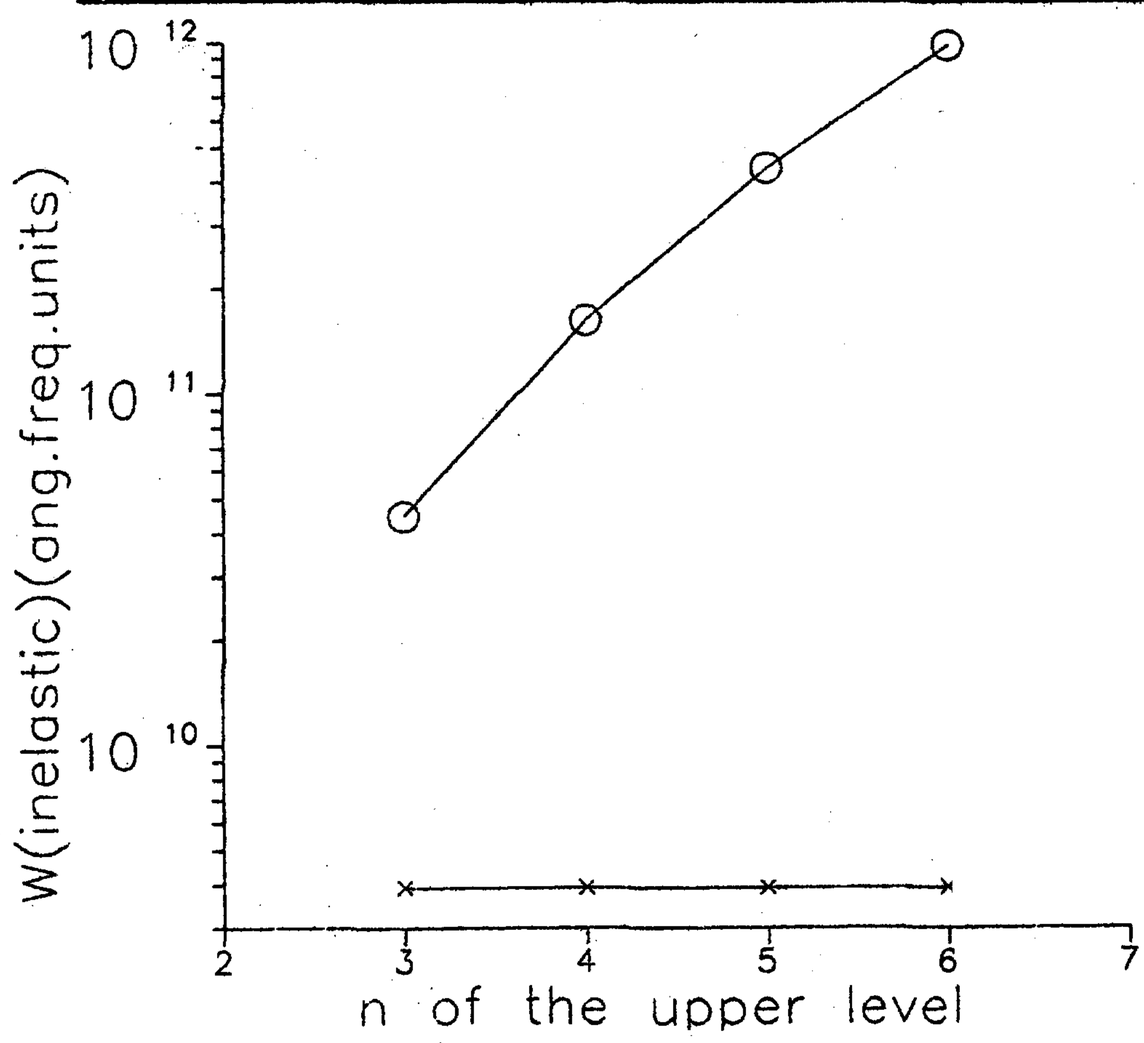

Fig. 5. As in Fig. 1 but for the inelastic collision contribution to the electron-impact widths. Here, (o) is for the upper level and (x) for the lower level $T = 100{,}000$ K.

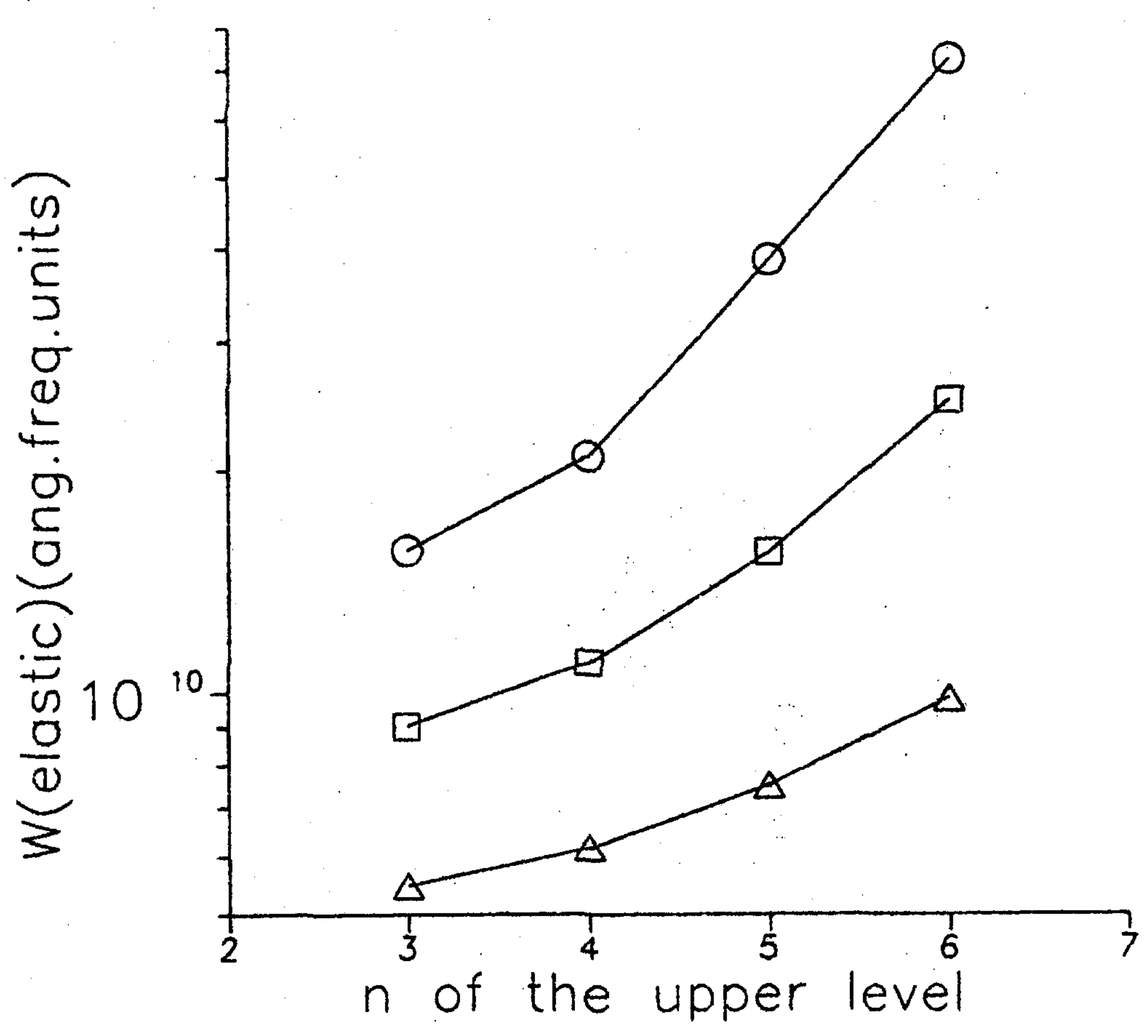

Fig. 6. As in Fig. 1 but for the elastic collision contribution to the electron-impact width.

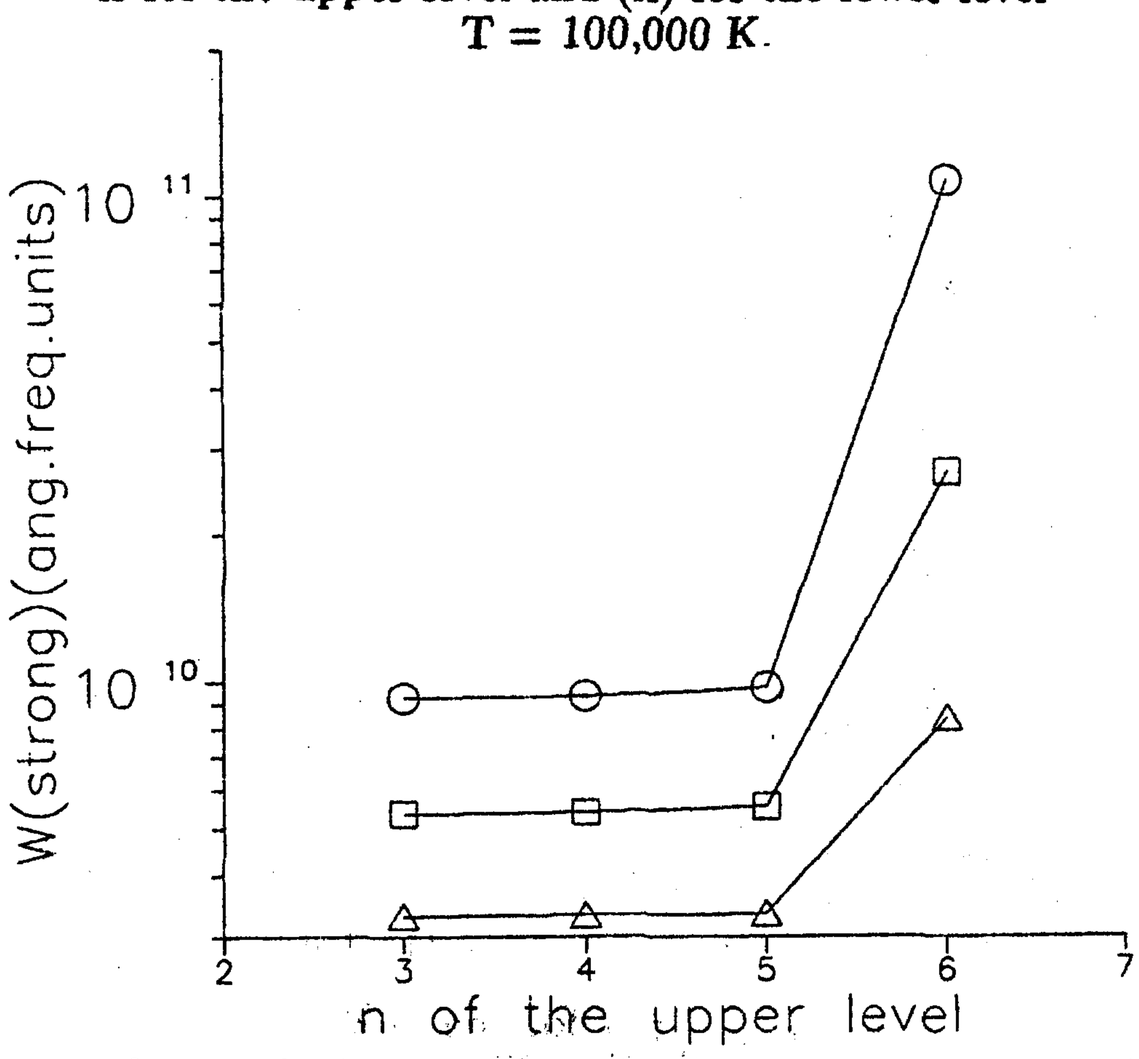

Fig. 7. As in Fig. 1 but for the strong collision contribution to the electron-impact width.

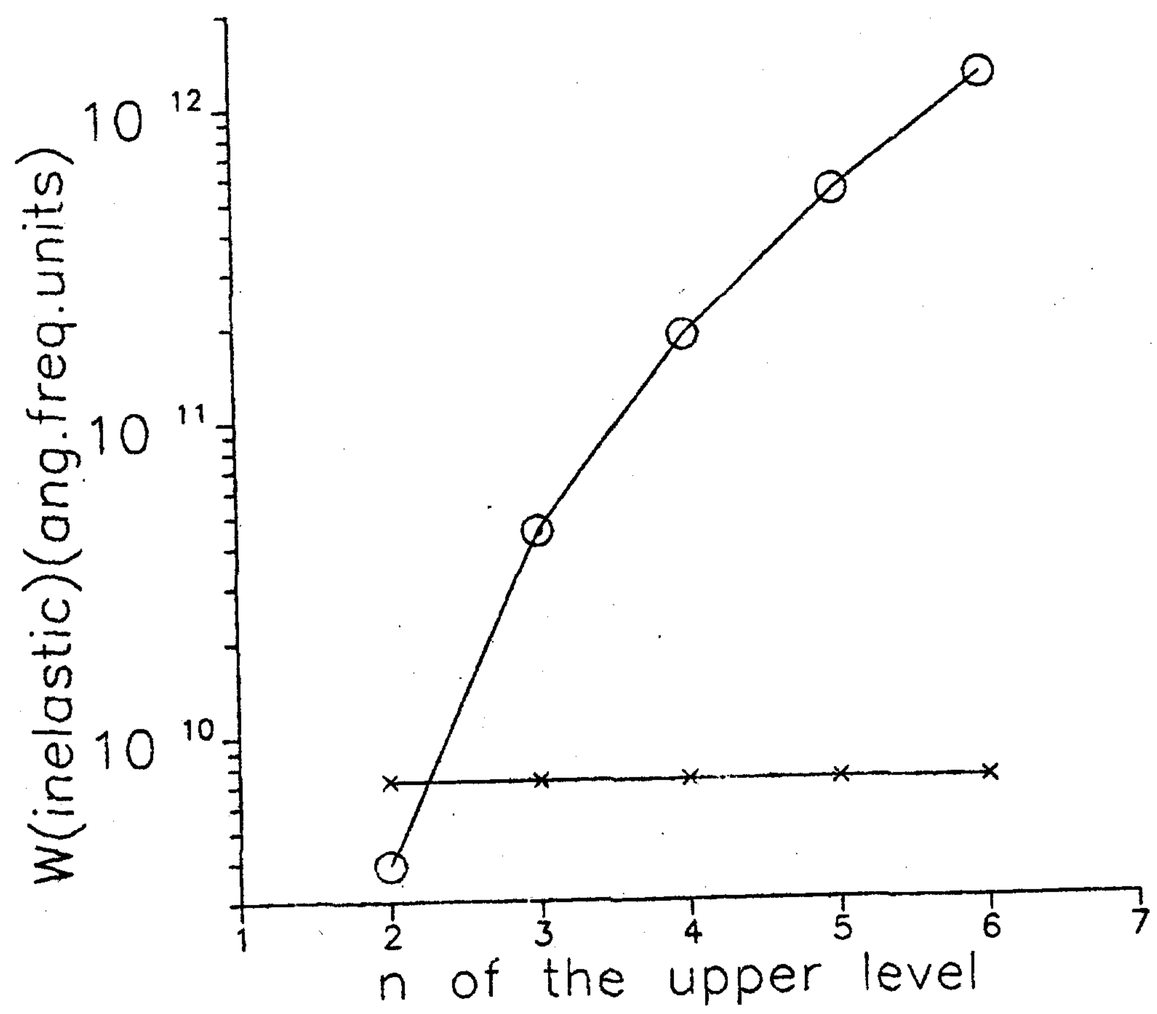

Fig. 8. As in Fig. 1 but for the O VI 2s ^2S - np $^2P^0$ series and for inelastic collision contribution to the electron-impact widths. Here, (o) is for the upper level and (x) for the lower level $T = 100{,}000$ K.

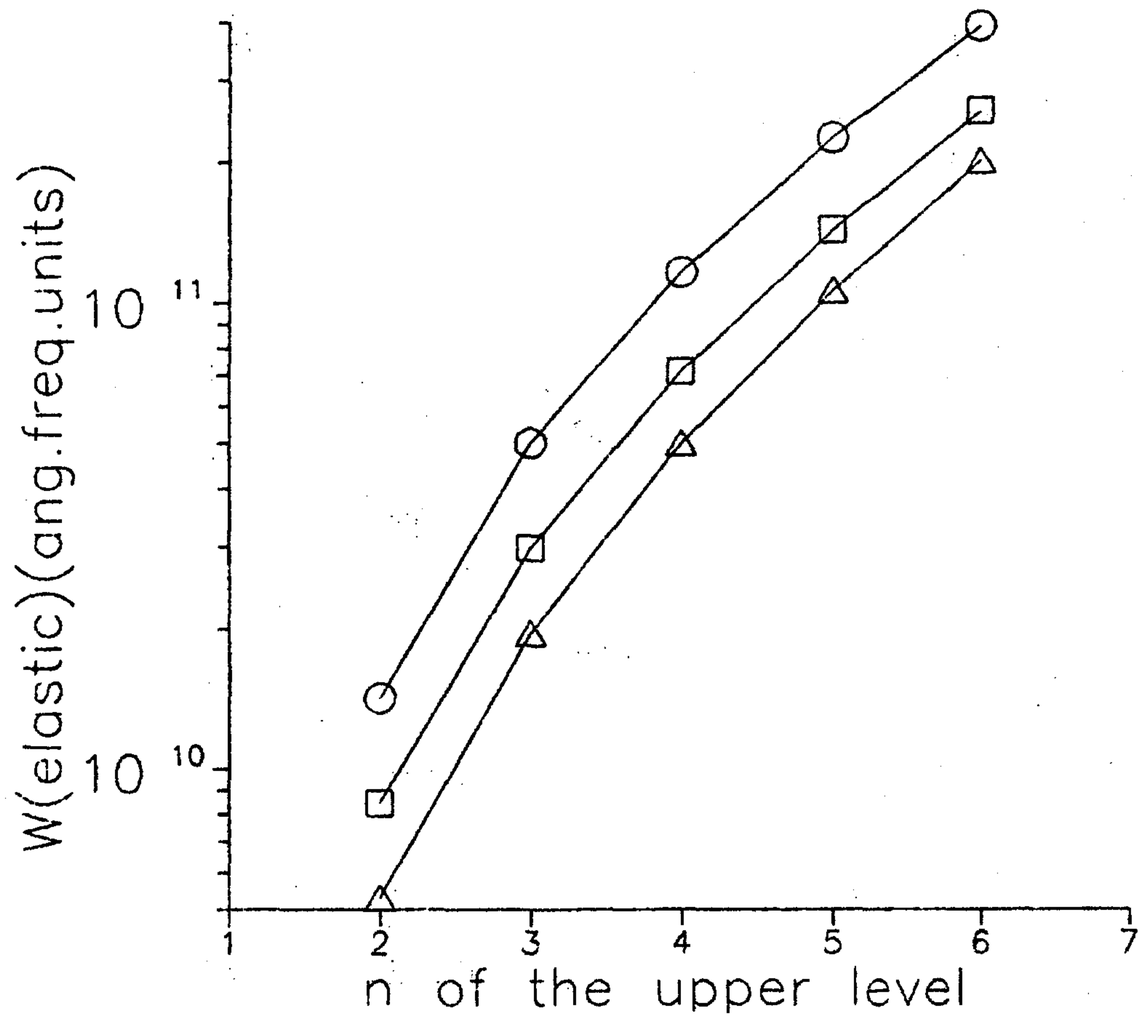

Fig. 9. As in Fig. 1 but for the the O VI 2s ^2S - np $^2P^0$ series and for the elastic collision contribution to the electron-impact width.

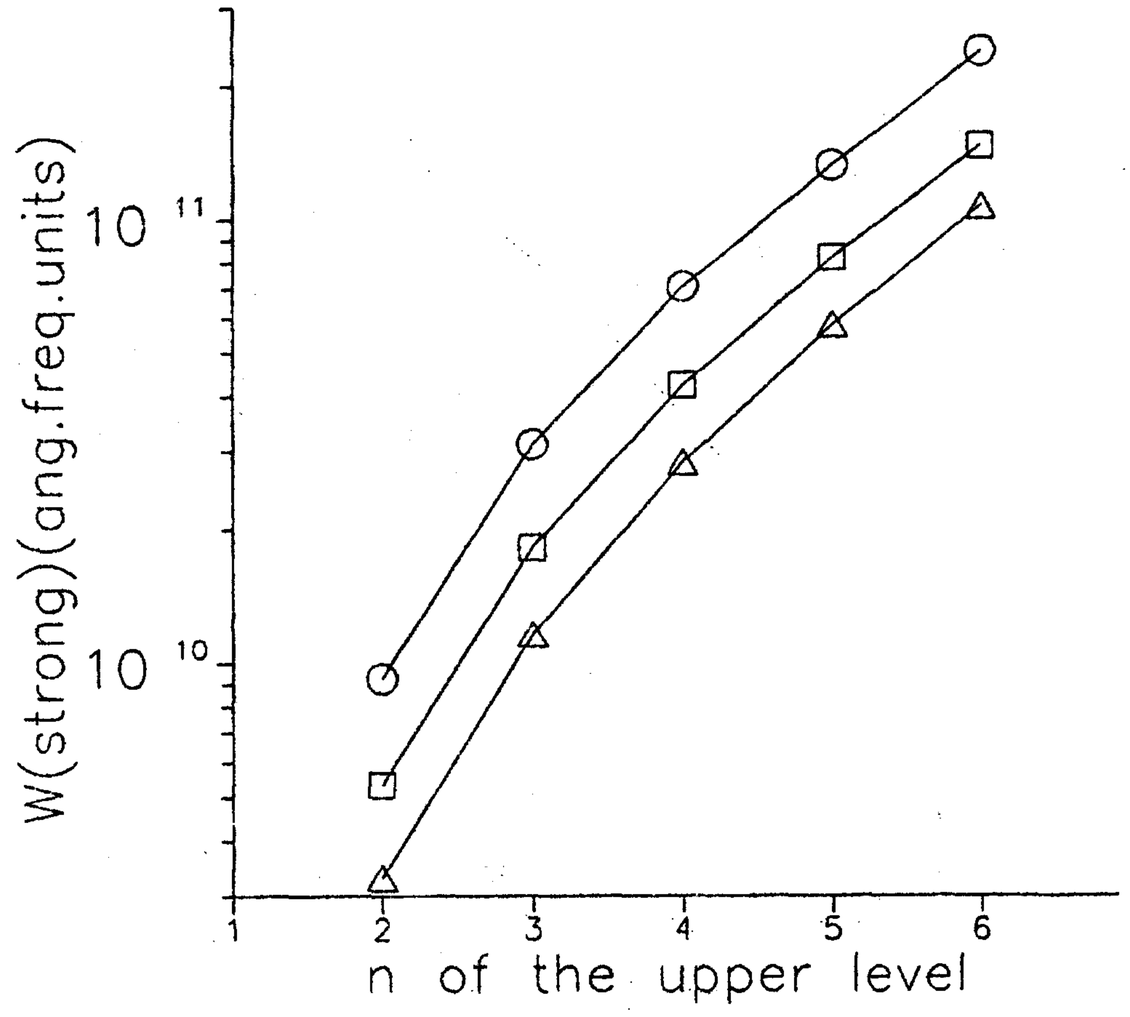

Fig. 10. As in Fig. 1 but for the O VI 2s ^2S - np $^2P^0$ series and for the strong collision contribution to the electron-impact width

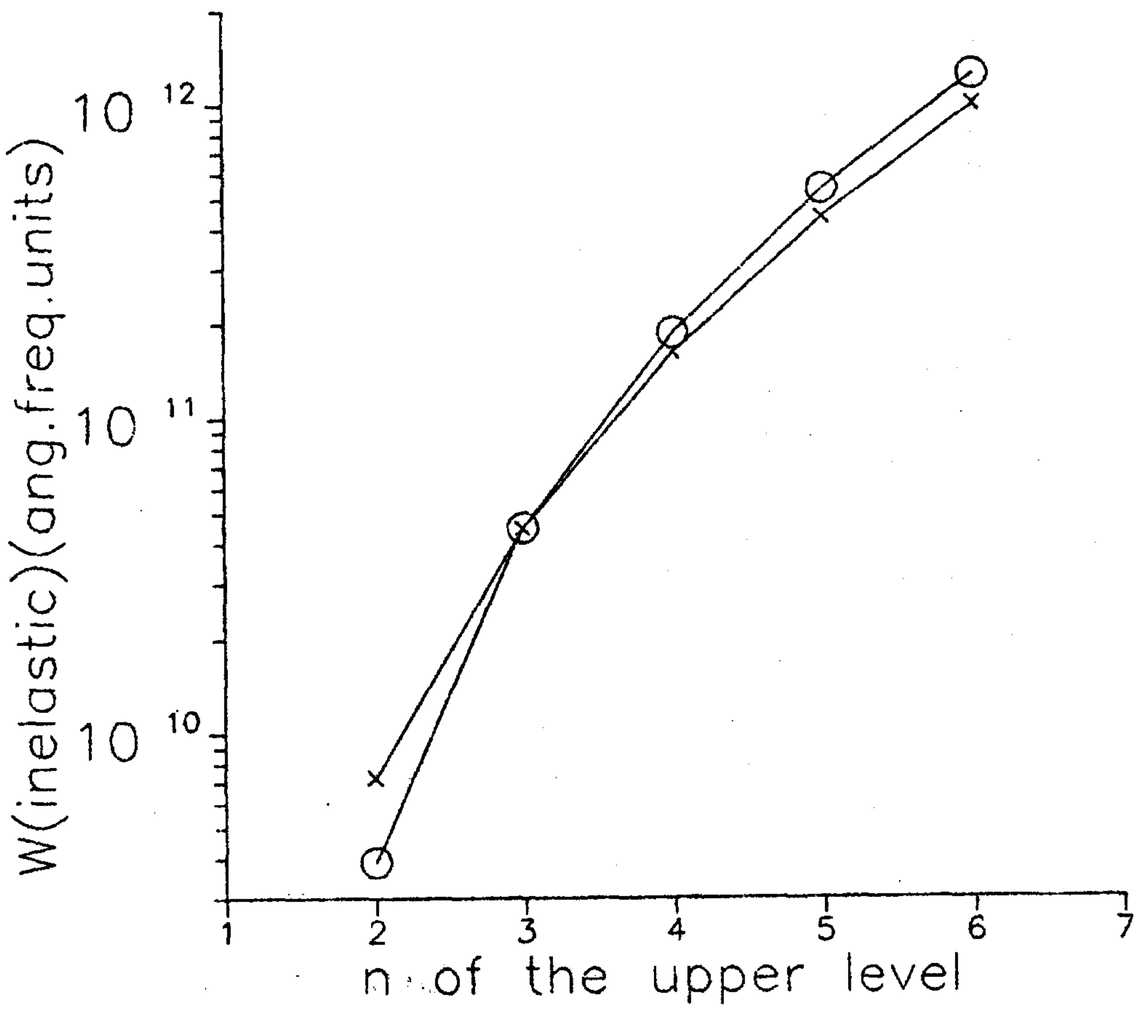

Fig. 11. As in Fig. 1 but for the O VI ns ^2S - np $^2P^0$ series and for inelastic collision contribution to the electron-impact widths Here, (o) is for the upper level and (x) for the lower level T = 100,000 K.

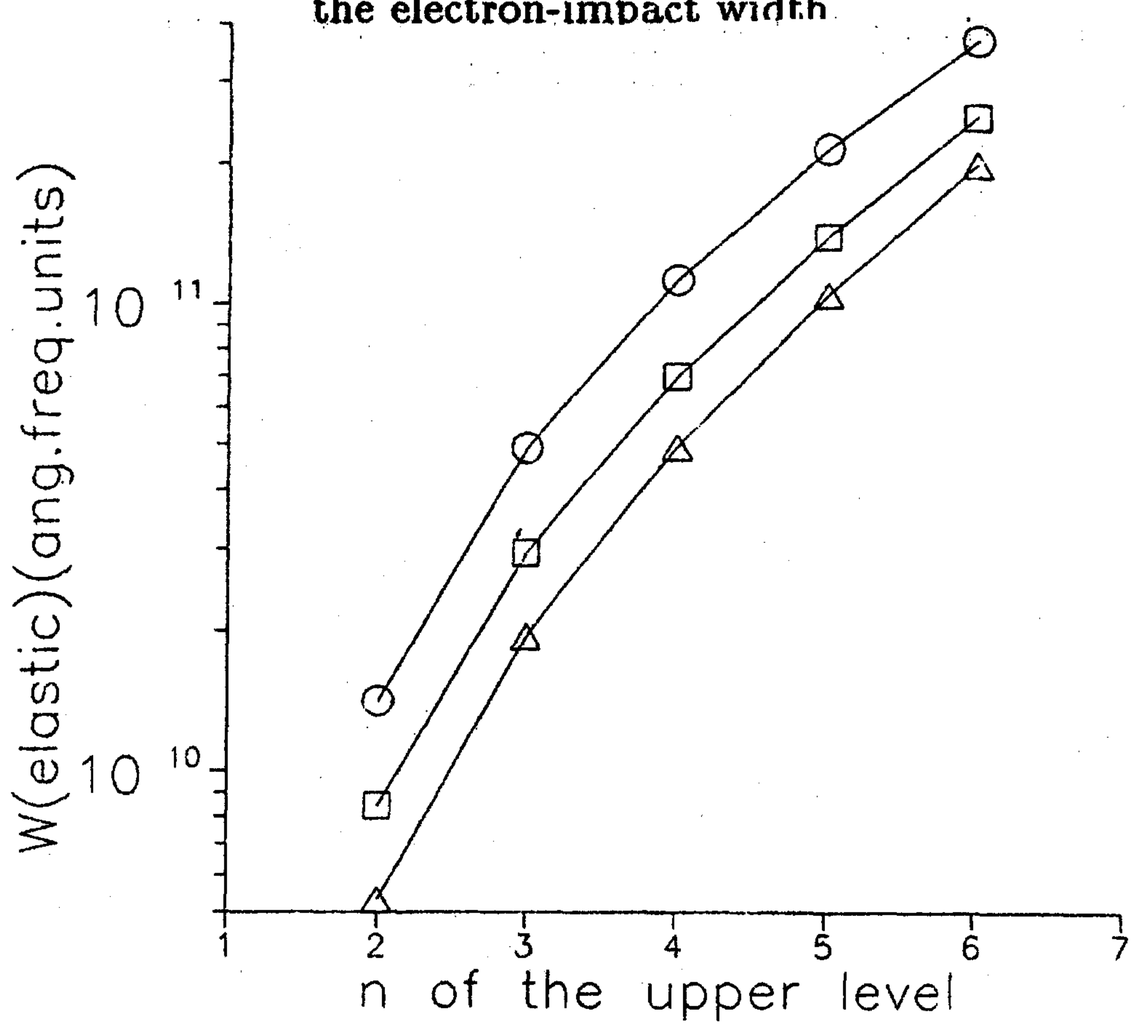

Fig. 12. As in Fig. 1 but for the O VI ns ^2S - np $^2P^0$ series and for the elastic collision contribution to the electron-impact width.

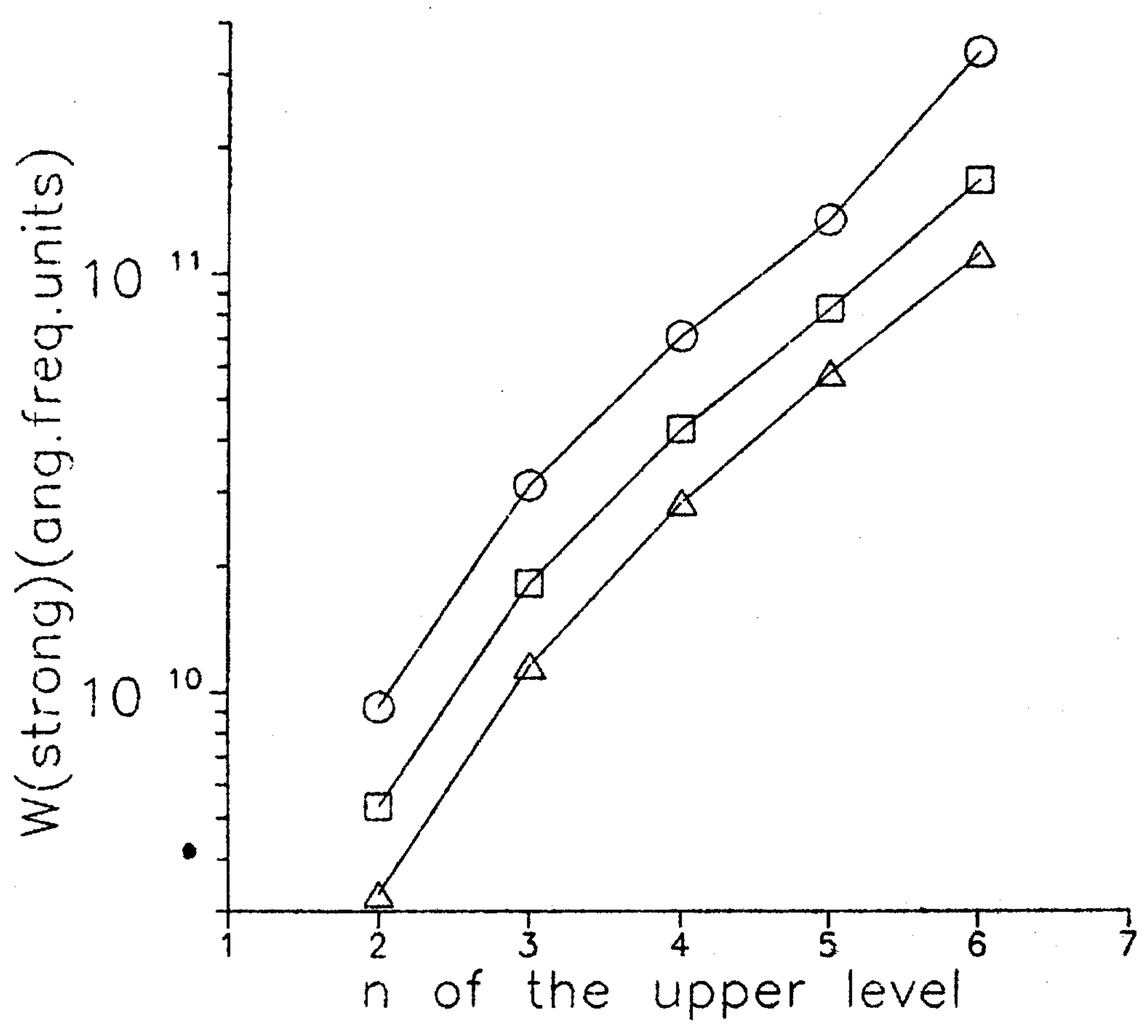

Fig. 13. As in Fig. 1 but for the the O VI ns^2 S - np $^2P^0$ series and for the strong collision contribution to the electron-impact width.

REFERENCES

Bashkin, S., and Stoner, J. O. Jr.: 1975, *Atomic Energy Levels and Grotrian Diagrams*, Vol. 1, North Holland, Amsterdam.

Dimitrijević, M. S., and Sahal-Bréchot, S.: 1984 a, *JQSRT* **31**, 301.

Dimitrijević, M. S., and Sahal-Bréchot, S.: 1984 b, *Astron. Astrophys.* **136**, 289.

Dimitrijević, M. S., and Sahal-Bréchot, S.: 1985, *JQSRT* **34**, 149.

Dimitrijević, M. S., and Sahal-Bréchot, S.: 1987, *JQSRT* **38**, 37.

Dimitrijević, M. S., and Sahal-Bréchot, S.: 1990, *Astron. Astrophys. Suppl. Series* **82**, 519.

Dimitrijević, M. S., and Sahal-Bréchot, S.: 1992, *Astron. Astrophys. Suppl. Series* **93**, 359.

Dimitrijević, M. S., Sahal-Bréchot, S. and Bommier, V.: 1991 a, *Astron. Astrophys. Suppl. Series* **89**, 581.

Dimitrijević, M. S., Sahal-Bréchot, S. and Bommier, V.: 1991 b, *Astron. Astrophys. Suppl. Series* **89**, 591.

Purić, J., Ćuk, M., Dimitrijević, M. S. and Lesage, A.: 1991, *Astrophys. J.* **382**, 353.

Sahal-Bréchot, S.: 1969 a, *Astron. Astrophys.* **1**, 91.

Sahal-Bréchot, S.: 1969 b, *Astron. Astrophys.* **2**, 322.

УТИЦАЈ РАЗЛИЧИТИХ СУДАРНИХ ПРОЦЕСА НА ШТАРКОВО ШИРЕЊЕ У СПЕКТРАЛНИМ СЕРИЈАМА: СЛУЧАЈ O VI

Милан С. Димитријевић

Астрономска опсерваторија, Волгина 7, 11050 Београд, Југославија

УДК 52-355.3
Претходно саопштење

Користећи семикласичан прилаз, истражено је понашање параметара Штарковог ширења у спектралним серијама на случају O VI. Такође је испитано понашање у спектралној серији утицаја нееластичних, еластичних и јаких судара на ширину спектралне линије.

Bull. Astron. Belgrade № 146 (1992), 73–81

UDC 52–355.3
Preliminary report

STARK BROADENING PARAMETER TABLES FOR Be I LINES OF ASTROPHYSICAL INTEREST

M. S. Dimitrijević[1], and S. Sahal-Bréchot[2]

[1] *Astronomical Observatory, Volgina 7, 11050 Beograd, Yugoslavia*

[2] *Laboratoire "Astrophysique, Atomes et Molécules"*
Département Atomes et Molécules en Astrophysique
Unité associée au C.N.R.S. No 812
Observatoire de Paris - Meudon, 92190 Meudon, France

(Received: July 14, 1992)

SUMMARY: Using a semiclassical approach, we have calculated electron–, proton–, and ionized helium–impact line widths and shifts for 19 Be I multiplets as a function of temperature for perturber densities 10^{16}–10^{19}cm^{-3}.

1. INTRODUCTION

As discussed in our article concerning Stark broadening parameters of Be II lines (Dimitrijević and Sahal–Bréchot, 1992 a), stark broadening data for beryllium lines are of interest in astrophysics since the surface content of Be provides informations on nucleogenesis, mixing between atmosphera and interior, the internal structure and evolution of a star (Boesgaard, 1988). Such data are of interest as well for the analysis and diagnostics of stellar and laboratory plasmas.

In order to provide reliable data for Be I lines broadened by collisions with charged perturbers in stellar and laboratory plasmas, we have calculated electron–, proton–, and ionized helium–impact line widths and shifts for 19 Be I multiplets, using the semiclassical–perturbation formalism (Sahal–Bréchot, 1969 a b). The obtained results for perturber density of 10^{15}cm^{-3}, together with discussion, analysis and comparison with existing theoretical data will be published in the principal article elsewhere (Dimitrijević, and Sahal–Bréchot, 1992b). Since data are not linear with perturber density (N), due to the Debye screening effect, we will present here the data for N $=10^{16}$– 10^{19}cm^{-3}.

2. RESULTS AND DISCUSSION

All details of the calculation procedure has been described in Dimitrijević and Sahal–Bréchot (1984) and will not be repeated here. Energy levels for Be II lines have been taken from Bashkin and Stoner (1975). Oscillator strengths have been calculated using the method of Bates and Damgaard (1949) and tables of Oertel and Shomo (1968). For the transitions including higher atomic energy levels,

Table 1. This table gives electron–, proton–, and ionized–helium– impact broadening parameters for Be I lines, for perturber densities $10^{16} - 10^{19}$ cm^{-3} and temperatures from 3,000 K to 50,000 K. Transitions and averaged wavelengths for the multiplet (in Å) are also given. By dividing c by the electron–impact full halfwidth, we obtain an estimate for the maximum perturber density for which the line may be treated as isolated and tabulated data may be used. The asterisk identifies cases for which the collision volume multiplied by the perturber density (the condition for validity of the impact approximation) lies between 0.1 and 0.5.

PERTURBER DENSITY= 0.1D+17(cm-3)

PERTURBERS ARE		ELECTRONS		PROTONS		IONIZED HELIUM	
TRANSITION	T(K)	WIDTH(A)	SHIFT(A)	WIDTH(A)	SHIFT(A)	WIDTH(A)	SHIFT(A)
2S - 2P	3000.	0.165E-02	0.955E-03	0.102E-02	0.254E-03	0.101E-02	0.209E-03
2349.3 A	5000.	0.184E-02	0.103E-02	0.102E-02	0.279E-03	0.101E-02	0.230E-03
C= 0.67E+19	10000.	0.201E-02	0.100E-02	0.103E-02	0.316E-03	0.102E-02	0.261E-03
	20000.	0.234E-02	0.820E-03	0.104E-02	0.356E-03	0.102E-02	0.295E-03
	30000.	0.267E-02	0.589E-03	0.104E-02	0.382E-03	0.103E-02	0.317E-03
	50000.	0.326E-02	0.325E-03	0.105E-02	0.417E-03	0.103E-02	0.345E-03
2S - 3P	3000.	0.792E-02	0.484E-02	0.310E-02	0.126E-02	0.300E-02	0.102E-02
1661.5 A	5000.	0.859E-02	0.549E-02	0.317E-02	0.141E-02	0.306E-02	0.115E-02
C= 0.12E+19	10000.	0.962E-02	0.628E-02	0.326E-02	0.163E-02	0.313E-02	0.134E-02
	20000.	0.109E-01	0.639E-02	0.338E-02	0.186E-02	0.321E-02	0.154E-02
	30000.	0.118E-01	0.610E-02	0.345E-02	0.201E-02	0.326E-02	0.166E-02
	50000.	0.131E-01	0.531E-02	0.357E-02	0.220E-02	0.334E-02	0.182E-02
2S - 4P	3000.	0.227E-01	0.127E-01	*0.871E-02	*0.300E-02		
1491.8 A	5000.	0.254E-01	0.144E-01	*0.898E-02	*0.348E-02	*0.865E-02	*0.280E-02
C= 0.39E+18	10000.	0.299E-01	0.165E-01	*0.926E-02	*0.412E-02	*0.893E-02	*0.335E-02
	20000.	0.357E-01	0.151E-01	0.955E-02	0.477E-02	*0.915E-02	*0.392E-02
	30000.	0.396E-01	0.140E-01	0.974E-02	0.517E-02	*0.929E-02	*0.426E-02
	50000.	0.447E-01	0.116E-01	0.100E-01	0.570E-02	0.948E-02	0.470E-02
2S - 5P	3000.	0.567E-01	0.291E-01				
1426.1 A	5000.	0.653E-01	0.319E-01				
C= 0.16E+18	10000.	0.798E-01	0.338E-01	*0.220E-01	*0.878E-02		
	20000.	0.976E-01	0.317E-01	*0.227E-01	*0.104E-01		
	30000.	0.109	0.276E-01	*0.232E-01	*0.114E-01	*0.222E-01	*0.930E-02
	50000.	0.122	0.229E-01	*0.238E-01	*0.126E-01	*0.226E-01	*0.104E-01
2S - 6P	3000.	0.124	0.524E-01				
1393.8 A	5000.	0.147	0.588E-01				
C= 0.83E+17	10000.	0.184	0.604E-01				
	20000.	0.228	0.543E-01				
	30000.	0.255	0.472E-01				
	50000.	0.282	0.383E-01				
3S - 3P	3000.	0.752	0.258	0.348	0.693E-01	0.344	0.566E-01
18148.6 A	5000.	0.825	0.274	0.350	0.770E-01	0.348	0.632E-01
C= 0.14E+21	10000.	1.05	0.220	0.352	0.880E-01	0.350	0.726E-01
	20000.	1.45	0.173	0.354	0.100	0.352	0.827E-01
	30000.	1.74	0.158	0.356	0.108	0.353	0.890E-01
	50000.	2.11	0.126	0.358	0.118	0.354	0.975E-01

PERTURBER DENSITY= 0.1D+17(cm-3)

PERTURBERS ARE		ELECTRONS		PROTONS		IONIZED HELIUM	
TRANSITION	T(K)	WIDTH(A)	SHIFT(A)	WIDTH(A)	SHIFT(A)	WIDTH(A)	SHIFT(A)
3S - 4P	3000.	0.657	0.353	*0.254	*0.818E-01		
8092.3 A	5000.	0.736	0.405	*0.261	*0.945E-01	*0.253	*0.762E-01
C= 0.11E+20	10000.	0.883	0.416	*0.268	*0.112	*0.260	*0.911E-01
	20000.	1.09	0.351	0.275	0.129	*0.265	*0.106
	30000.	1.24	0.303	0.280	0.140	*0.269	*0.115
	50000.	1.43	0.273	0.287	0.154	0.273	0.127
3S - 5P	3000.	1.17	0.579				
6475.3 A	5000.	1.35	0.666				
C= 0.33E+19	10000.	1.66	0.686	*0.452	*0.178		
	20000.	2.05	0.597	*0.467	*0.210		
	30000.	2.30	0.530	*0.475	*0.229	*0.456	*0.188
	50000.	2.59	0.454	*0.487	*0.255	*0.465	*0.209
3S - 6P	3000.	2.20	0.949				
5858.6 A	5000.	2.60	1.02				
C= 0.15E+19	10000.	3.27	1.09				
	20000.	4.07	0.916				
	30000.	4.55	0.784				
	50000.	5.05	0.661				
2P - 3S	3000.	0.130	0.929E-01	0.305E-01	0.246E-01	0.261E-01	0.200E-01
8256.3 A	5000.	0.145	0.105	0.329E-01	0.275E-01	0.280E-01	0.225E-01
C= 0.38E+20	10000.	0.162	0.123	0.365E-01	0.317E-01	0.309E-01	0.261E-01
	20000.	0.175	0.129	0.406E-01	0.361E-01	0.343E-01	0.298E-01
	30000.	0.186	0.126	0.433E-01	0.389E-01	0.364E-01	0.321E-01
	50000.	0.198	0.113	0.469E-01	0.426E-01	0.394E-01	0.353E-01
2P - 4S	3000.	0.203	0.148	*0.457E-01	*0.341E-01	*0.380E-01	*0.267E-01
4409.2 A	5000.	0.230	0.175	0.498E-01	0.400E-01	*0.414E-01	*0.320E-01
C= 0.35E+19	10000.	0.251	0.201	0.559E-01	0.478E-01	*0.464E-01	*0.388E-01
	20000.	0.262	0.198	0.627E-01	0.558E-01	0.521E-01	0.457E-01
	30000.	0.266	0.182	0.671E-01	0.606E-01	0.557E-01	0.498E-01
	50000.	0.281	0.155	0.731E-01	0.669E-01	0.607E-01	0.551E-01
3P - 4S	3000.	4.09	2.85	*0.923	*0.641	*0.789	*0.504
19770.7 A	5000.	4.54	3.34	0.995	0.750	*0.849	*0.601
C= 0.70E+20	10000.	5.00	3.40	1.10	0.895	*0.937	*0.728
	20000.	5.67	3.33	1.22	1.04	1.04	0.854
	30000.	6.12	2.94	1.30	1.13	1.10	0.930
	50000.	6.96	2.49	1.41	1.25	1.19	1.03
2P - 3D	3000.	0.853E-01	0.524E-01	0.287E-01	0.133E-01	*0.274E-01	*0.107E-01
4573.9 A	5000.	0.940E-01	0.594E-01	0.296E-01	0.150E-01	0.281E-01	0.122E-01
C= 0.55E+19	10000.	0.107	0.675E-01	0.308E-01	0.175E-01	0.290E-01	0.143E-01
	20000.	0.122	0.683E-01	0.323E-01	0.200E-01	0.301E-01	0.165E-01
	30000.	0.134	0.673E-01	0.333E-01	0.216E-01	0.308E-01	0.178E-01
	50000.	0.149	0.572E-01	0.347E-01	0.237E-01	0.319E-01	0.196E-01

PERTURBER DENSITY= 0.1D+17(cm-3)

PERTURBERS ARE		ELECTRONS		PROTONS		IONIZED HELIUM	
TRANSITION	T(K)	WIDTH(A)	SHIFT(A)	WIDTH(A)	SHIFT(A)	WIDTH(A)	SHIFT(A)
2P - 4D	3000.	0.217	-0.522E-01	*0.659E-01	-0.231E-01		
3814.5 A	5000.	0.251	-0.303E-01	*0.682E-01	-0.269E-01		
C= 0.79E+18	10000.	0.308	-0.733E-02	*0.706E-01	-0.321E-01	*0.678E-01	-0.261E-01
	20000.	0.364	0.121E-01	0.731E-01	-0.374E-01	*0.697E-01	-0.306E-01
	30000.	0.399	0.214E-01	0.747E-01	-0.405E-01	*0.708E-01	-0.333E-01
	50000.	0.439	0.229E-01	0.770E-01	-0.447E-01	*0.724E-01	-0.369E-01
3P - 3D	3000.	1.94	0.820	0.633	0.204	0.621	0.166
23579.5 A	5000.	2.14	0.866	0.642	0.229	0.629	0.187
C= 0.14E+21	10000.	2.72	0.850	0.654	0.264	0.638	0.217
	20000.	3.71	0.663	0.667	0.300	0.648	0.248
	30000.	4.44	0.558	0.677	0.324	0.654	0.267
	50000.	5.35	0.499	0.691	0.355	0.663	0.293
3P - 4D	3000.	2.05	-0.601	*0.576	*-0.230		
11636.7 A	5000.	2.34	-0.395	*0.598	*-0.270	*0.568	*-0.216
C= 0.73E+19	10000.	2.91	-0.242	*0.624	*-0.322	*0.591	*-0.262
	20000.	3.53	-0.134	0.653	-0.376	*0.612	*-0.308
	30000.	3.93	-0.908E-01	0.672	-0.408	*0.626	*-0.335
	50000.	4.40	0.295E-02	0.699	-0.450	0.645	-0.371
2P - 3S	3000.	0.142E-01	0.118E-01	0.369E-02	0.319E-02	0.307E-02	0.260E-02
3322.0 A	5000.	0.163E-01	0.133E-01	0.401E-02	0.356E-02	0.334E-02	0.292E-02
C= 0.75E+19	10000.	0.192E-01	0.157E-01	0.450E-02	0.408E-02	0.374E-02	0.336E-02
	20000.	0.211E-01	0.173E-01	0.504E-02	0.464E-02	0.419E-02	0.384E-02
	30000.	0.219E-01	0.175E-01	0.539E-02	0.500E-02	0.448E-02	0.413E-02
	50000.	0.229E-01	0.165E-01	0.587E-02	0.548E-02	0.488E-02	0.453E-02
3S - 3P	3000.	0.498	0.279	0.198	0.720E-01	0.193	0.586E-01
14648.5 A	5000.	0.545	0.283	0.201	0.805E-01	0.196	0.659E-01
C= 0.68E+20	10000.	0.678	0.212	0.205	0.925E-01	0.199	0.762E-01
	20000.	0.922	0.122	0.211	0.105	0.203	0.871E-01
	30000.	1.09	0.944E-01	0.215	0.114	0.205	0.938E-01
	50000.	1.29	0.553E-01	0.220	0.124	0.209	0.103
3S - 4P	3000.	0.644	0.444	*0.195	*0.939E-01		
6788.4 A	5000.	0.703	0.478	*0.205	*0.111	*0.189	*0.885E-01
C= 0.52E+19	10000.	0.803	0.456	*0.218	*0.134	*0.200	*0.108
	20000.	0.938	0.388	0.233	0.157	*0.211	*0.128
	30000.	1.05	0.339	0.242	0.170	*0.219	*0.140
	50000.	1.19	0.285	0.255	0.188	*0.229	*0.155

PERTURBER DENSITY= 0.1D+18(cm-3)

2S - 2P	3000.	0.165E-01	0.937E-02	0.100E-01	0.236E-02	0.985E-02	0.192E-02
2349.3 A	5000.	0.184E-01	0.101E-01	0.101E-01	0.265E-02	0.100E-01	0.217E-02
C= 0.67E+20	10000.	0.201E-01	0.991E-02	0.103E-01	0.306E-02	0.101E-01	0.252E-02
	20000.	0.234E-01	0.813E-02	0.104E-01	0.349E-02	0.102E-01	0.288E-02
	30000.	0.267E-01	0.584E-02	0.104E-01	0.376E-02	0.103E-01	0.311E-02
	50000.	0.326E-01	0.322E-02	0.105E-01	0.413E-02	0.103E-01	0.341E-02

PERTURBER DENSITY= 0.1D+18(cm-3)

PERTURBERS ARE		ELECTRONS		PROTONS		IONIZED HELIUM	
TRANSITION	T(K)	WIDTH(A)	SHIFT(A)	WIDTH(A)	SHIFT(A)	WIDTH(A)	SHIFT(A)
2S - 3P	3000.	0.792E-01	0.453E-01	*0.286E-01	*0.950E-02		
1661.5 A	5000.	0.859E-01	0.525E-01	*0.305E-01	*0.118E-01		
C= 0.12E+20	10000.	0.962E-01	0.611E-01	*0.322E-01	*0.146E-01	*0.306E-01	*0.117E-01
	20000.	0.109	0.628E-01	*0.336E-01	*0.174E-01	*0.318E-01	*0.142E-01
	30000.	0.118	0.603E-01	0.345E-01	0.191E-01	*0.325E-01	*0.156E-01
	50000.	0.131	0.528E-01	0.357E-01	0.213E-01	*0.333E-01	*0.175E-01
2S - 4P	3000.	0.226	0.113				
1491.8 A	5000.	0.254	0.133				
C= 0.39E+19	10000.	0.299	0.157				
	20000.	0.357	0.145				
	30000.	0.396	0.136				
	50000.	0.447	0.115	*0.998E-01	*0.534E-01		
2S - 5P	3000.	0.562	0.239				
1426.1 A	5000.	0.651	0.279				
C= 0.16E+19	10000.	0.797	0.310				
	20000.	0.975	0.296				
	30000.	1.09	0.261				
	50000.	1.22	0.223				
2S - 6P	3000.	*1.17	*0.382				
1393.8 A	5000.	*1.42	*0.478				
C= 0.83E+18	10000.	1.81	0.526				
	20000.	2.27	0.485				
	30000.	2.53	0.432				
	50000.	2.81	0.368				
3S - 3P	3000.	7.51	2.46	*3.20	*0.584		
18148.6 A	5000.	8.25	2.65	*3.37	*0.686		
C= 0.14E+22	10000.	10.5	2.15	*3.48	*0.821	*3.42	*0.666
	20000.	14.5	1.70	3.53	0.958	*3.49	*0.784
	30000.	17.4	1.58	3.55	1.04	*3.51	*0.855
	50000.	21.1	1.25	3.58	1.15	*3.53	*0.947
3S - 4P	3000.	6.55	3.15				
8092.3 A	5000.	7.35	3.76				
C= 0.11E+21	10000.	8.83	3.99				
	20000.	10.9	3.43				
	30000.	12.4	3.02				
	50000.	14.3	2.72	*2.86	*1.45		
3S - 5P	3000.	11.6	4.75				
6475.3 A	5000.	13.4	5.85				
C= 0.33E+20	10000.	16.6	6.38				
	20000.	20.5	5.77				
	30000.	23.0	5.13				
	50000.	25.9	4.51				

PERTURBER DENSITY= 0.1D+18(cm-3)

PERTURBERS ARE		ELECTRONS		PROTONS		IONIZED HELIUM	
TRANSITION	T(K)	WIDTH(A)	SHIFT(A)	WIDTH(A)	SHIFT(A)	WIDTH(A)	SHIFT(A)
2P - 3S	3000.	1.30	0.876	0.303	0.193	*0.257	*0.148
8256.3 A	5000.	1.45	1.01	0.328	0.235	*0.278	*0.185
C= 0.38E+21	10000.	1.62	1.20	0.365	0.288	0.309	0.232
	20000.	1.75	1.28	0.406	0.341	0.342	0.278
	30000.	1.86	1.25	0.433	0.372	0.364	0.305
	50000.	1.98	1.13	0.469	0.413	0.394	0.339
2P - 4S	3000.	2.03	1.28				
4409.2 A	5000.	2.30	1.60				
C= 0.35E+20	10000.	2.51	1.92				
	20000.	2.62	1.94	*0.627	*0.481		
	30000.	2.66	1.79	*0.671	*0.543		
	50000.	2.81	1.55	*0.731	*0.620		
2P - 3D	3000.	0.852	0.484	*0.262	*0.932E-01		
4573.9 A	5000.	0.940	0.564	*0.284	*0.120		
C= 0.55E+20	10000.	1.07	0.657	*0.304	*0.153	*0.283	*0.122
	20000.	1.22	0.675	*0.322	*0.185	*0.298	*0.150
	30000.	1.34	0.671	*0.332	*0.203	*0.307	*0.166
	50000.	1.49	0.571	0.347	0.227	*0.318	*0.186
2P - 4D	3000.	2.14	-0.385				
3814.5 A	5000.	2.49	-0.200				
C= 0.79E+19	10000.	3.07	-0.119E-01				
	20000.	3.64	0.147				
	30000.	3.98	0.218				
	50000.	4.39	0.233	*0.767	*0.416		
2P - 3S	3000.	0.142	0.112	0.368E-01	0.259E-01	*0.306E-01	*0.200E-01
3322.0 A	5000.	0.163	0.128	0.401E-01	0.309E-01	0.334E-01	0.245E-01
C= 0.75E+20	10000.	0.192	0.153	0.449E-01	0.375E-01	0.374E-01	0.303E-01
	20000	0.211	0.172	0.504E-01	0.441E-01	0.419E-01	0.360E-01
	30000	0.219	0.174	0.539E-01	0.481E-01	0.448E-01	0.394E-01
	50000	0.229	0.164	0.586E-01	0.532E-01	0.487E-01	0.438E-01
3S - 3P	3000.	4.98	2.66	*1.85	*0.573		
14648.5 A	5000.	5.45	2.72	*1.95	*0.691	*1.85	*0.545
C= 0.68E+21	10000.	6.78	2.04	*2.03	*0.845	*1.95	*0.681
	20000.	9.22	1.17	2.10	0.997	*2.02	*0.814
	30000.	10.9	0.919	2.14	1.09	*2.05	*0.892
	50000.	12.9	0.536	2.20	1.21	*2.09	*0.992
3S - 4P	3000.	6.42	3.82				
6788.4 A	5000.	7.03	4.30				
C= 0.52E+20	10000.	8.03	4.23				
	20000.	9.38	3.68				
	30000.	10.5	3.29				
	50000.	11.9	2.78				

PERTURBER DENSITY= 0.1D+19(cm-3)

PERTURBERS ARE		ELECTRONS		PROTONS		IONIZED HELIUM	
TRANSITION	T(K)	WIDTH(A)	SHIFT(A)	WIDTH(A)	SHIFT(A)	WIDTH(A)	SHIFT(A)
2S - 2P	3000.	0.165	0.883E-01	*0.863E-01	*0.181E-01	*0.749E-01	*0.136E-01
2349.3 A	5000.	0.184	0.970E-01	*0.949E-01	*0.222E-01	*0.889E-01	*0.174E-01
C= 0.67E+21	10000.	0.201	0.960E-01	*0.100	*0.276E-01	*0.974E-01	*0.221E-01
	20000.	0.234	0.789E-01	0.103	0.328E-01	*0.101	*0.267E-01
	30000.	0.267	0.565E-01	0.104	0.359E-01	*0.102	*0.293E-01
	50000.	0.326	0.310E-01	0.105	0.399E-01	0.103	0.327E-01
2S - 3P	3000.	0.784	0.355				
1661.5 A	5000.	0.856	0.449				
C= 0.12E+21	10000.	0.961	0.557				
	20000.	1.09	0.589				
	30000.	1.18	0.572				
	50000.	1.31	0.506				
2S - 4P	3000.	*2.10	*0.644				
1491.8 A	5000.	*2.47	*0.954				
C= 0.39E+20	10000.	2.96	1.30				
	20000.	3.55	1.27				
	30000.	3.95	1.21				
	50000.	4.46	1.04				
2S - 5P	3000.						
1426.1 A	5000.						
C= 0.16E+20	10000.	*6.94	*2.11				
	20000.	*9.06	*2.27				
	30000.	10.3	2.06				
	50000.	11.8	1.83				
2P - 3S	3000.	13.0	7.09				
8256.3 A	5000.	14.5	8.84				
C= 0.38E+22	10000.	16.2	11.1				
	20000.	17.5	12.5	*4.04	*2.77		
	30000.	18.6	12.2	*4.32	*3.20		
	50000.	19.8	11.2	*4.68	*3.72	*3.93	*2.99
2P - 3D	3000.	8.42	3.56				
4573.9 A	5000.	9.36	4.64				
C= 0.55E+21	10000.	10.7	5.98				
	20000.	12.2	6.50				
	30000.	13.4	6.48				
	50000.	14.9	5.67				
2P - 3S	3000.	1.42	0.934				
3322.0 A	5000.	1.63	1.14	*0.385	*0.163		
C= 0.75E+21	10000.	1.92	1.43	*0.446	*0.272		
	20000.	2.11	1.65	*0.503	*0.368	*0.418	*0.287
	30000.	2.18	1.71	*0.539	*0.421	*0.448	*0.334
	50000.	2.29	1.62	*0.586	*0.486	*0.487	*0.392

PERTURBER DENSITY= 0.1D+20(cm-3)

PERTURBERS ARE		ELECTRONS		PROTONS		IONIZED HELIUM	
TRANSITION	T(K)	WIDTH(A)	SHIFT(A)	WIDTH(A)	SHIFT(A)	WIDTH(A)	SHIFT(A)
2S - 2P	3000.	1.61	0.704				
2349.3 A	5000.	1.82	0.832				
C= 0.67E+22	10000.	2.00	0.862				
	20000.	2.34	0.722				
	30000.	2.66	0.510	*0.994	*0.303		
	50000.	3.26	0.266	*1.03	*0.356		

the method described by Van Regemorter et al. (1979) has been used.

Our results are shown in Table 1 for perturber densities $10^{16} - 10^{19}$ cm^{-3} and temperatures of T = 3,000; 5,000; 10,000; 20,000; 30,000 and 50,000 K. We also specify a parameter c (Dimitrijević and Sahal–Bréchot, 1984) which gives an estimate for the maximum perturber density for which the line may be treated as isolated when it is divided by the electron–impact full width at half maximum.

For each value given in Table 1, the collision volume (V) multiplied by the perturber density (N) is much less than one and the impact approximation is valid (Sahal–Bréchot, 1969 a b). Values for NV > 0.5 are not given in Table 1; values for $0.1 <$ NV ≤ 0.5 are denoted by an asterisk. When the impact approximation is not valid, the ion broadening contribution may be estimated by using quasistatic formulae (cf. Sahal–Bréchot (1991) or Griem (1974)).

The analysis of present results and comparison with available experimental and theoretical data is given in Dimitrijević and Sahal – Bréchot (1992b).

Acknowledgments – This work is a part of French–Yugoslav collaboration through the project "L'elargissement Stark des raies spectrales des plasmas astrophysiques et de laboratoire". It is also a part of the project "Physics and dynamics of celestial bodies", supported by Ministry for Science and Technology of Serbia.

REFERENCES

Bashkin, S., and Stoner, J. O. Jr.: 1975, *Atomic Energy Levels and Grotrian Diagrams*, Vol. **1**, North Holland, Amsterdam.

Bates, D. R., and Damgaard, A.: 1949, *Trans. Roy. Soc. London, Ser. A* **242**, 101.

Boesgaard, A. M.: 1988, *Vistas in Astronomy*, **31**, 167.

Dimitrijević, M. S., and Sahal–Bréchot, S.: 1984, *JQSRT*, **31**, 301.

Dimitrijević, M. S., and Sahal–Bréchot, S.: 1992 a, *JQSRT*, **48**, 397.

Dimitrijević, M. S., and Sahal–Bréchot, S.: 1992 b, *JQSRT*, to be published.

Griem, H. R.: 1974, *Spectral Line Broadening by Plasmas*, Academic Press, New York.

Oertel, G. K., and Shomo, L. P.: 1968, *Astrophys. J. Suppl. Series*, **16**, 175.

Sahal–Bréchot, S.: 1969 a, *Astron. Astrophys.* **1**, 91.

Sahal–Bréchot, S.: 1969b, *Astron. Astrophys.* **2**, 322.

Sahal–Bréchot, S.: 1991, *Astron. Astrophys.* **245**, 322.

Van Regemorter, H., Hoang Binh Dy, and Prud'homme, M.: 1979, *J. Phys.* B 12, 1073.

ТАБЕЛЕ ПАРАМЕТАРА ШТАРКОВОГ ШИРЕЊА ЛИНИЈА Be I ОД ЗНАЧАЈА У АСТРОФИЗИЦИ

М. С. Димитријевић[1] и S. Sahal-Bréchot[2]

[1]*Астрономска опсерваторија, Волгина 7, 11050 Београд, Југославија*

[2]*Laboratoire "Astrophysique, Atomes et Molécules"*
Département Atomes et Molécules en Astrophysique
Unité associée au C.N.R.S. No 812
Observatoire de Paris - Meudon, 92190 Meudon, France

УДК 52–355.3
Претходно саопштење

Користећи семикласичан прилаз, израчунате су ширине и помераји спектралних линија, проузроковани сударима са електронима, протонима и јонима хелијума, за 28 мултиплет неутралног берилијума. Резултати су дати у функцији температуре и концентрације пертурбера.

Bull. Astron. Belgrade № 146 (1992), 83–95

UDC 52–355.3
Preliminary report

STARK BROADENING PARAMETER TABLES FOR Al I LINES OF ASTROPHYSICAL INTEREST

M. S. Dimitrijević[1], and S. Sahal-Bréchot[2]

[1]*Astronomical Observatory, Volgina 7, 11050 Beograd, Yugoslavia*

[2]*Laboratoire "Astrophysique, Atomes et Molécules"*
Département Atomes et Molécules en Astrophysique
Unité associée au C.N.R.S. No 812
Observatoire de Paris - Meudon, 92190 Meudon, France

(Received: July 14, 1992)

SUMMARY: Using a semiclassical approach, we have calculated electron–, proton–, and ionized helium–impact line widths and shifts for 25 Al I multiplets as a function of temperature for perturber densities 10^{13}–10^{14}cm^{-3} and 10^{16}–10^{18}cm^{-3}.

1. INTRODUCTION

Astrophysical importance of neutral aluminium lines is due to its cosmical abundance and presence in solar (e. g. Goldberg, Muller, Aller, 1960) and stellar (e. g. Meril, 1956) spectra. Moreover, Al I lines are very important for spectral analysis of laboratory plasma as well. In order to provide reliable data for Al I lines broadened by collisions with charged perturbers in stellar and laboratory plasmas, we have calculated electron–, proton–, and ionized helium–impact line widths and shifts for 25 Al I multiplets, using the semiclassical–perturbation formalism (Sahal–Bréchot, 1969 a b). The obtained results for perturber density of 10^{15}cm^{-3}, together with discussion, analysis and comparison with existing theoretical data will be published in the principal article elsewhere (Dimitrijević, and Sahal–Bréchot, 1992). Since data are not linear with perturber density (N), due to the Debye screening effect, we will present here the data for N = 10^{13} – 10^{14}cm^{-3} of interest for stellar atmospheres and data for N =10^{16}–10^{19}cm^{-3}, of principal interest for subphotospheric plasma research and laboratory plasma.

2. RESULTS AND DISCUSSION

All details of the calculation procedure has been described in Dimitrijević and Sahal–Bréchot (1984) and will not be repeated here. Energy levels for Al I lines have been taken from Bashkin and Stoner (1975). Oscillator strengths have been calculated using the method of Bates and Damgaard (1949) and tables of Oertel and Shomo (1968). For the transitions including higher atomic energy levels, the method described by Van Regemorter et al.

Table 1. This table gives electron–, proton–, and ionized–helium– impact broadening parameters for Al I lines, for perturber densities $10^{13} - 10^{14}$ cm^{-3}; $10^{16} - 10^{19}$ cm^{-3} and temperatures from 3,000 K to 50,000 K. Transitions and averaged wavelengths for the multiplet (in Å) are also given. By dividing C by the electron–impact full halfwidth, we obtain an estimate for the maximum perturber density for which the line may be treated as isolated and tabulated data may be used. The asterisk identifies cases for which the collision volume multiplied by the perturber density (the condition for validity of the impact approximation) lies between 0.1 and 0.5.

PERTURBER DENSITY= 0.1D+14(cm-3)

PERTURBERS ARE		ELECTRONS		PROTONS		IONIZED HELIUM	
TRANSITION	T(K)	WIDTH(A)	SHIFT(A)	WIDTH(A)	SHIFT(A)	WIDTH(A)	SHIFT(A)
3D - 4P	3000.	0.364	-0.169	0.694E-01	-0.600E-01	0.584E-01	-0.484E-01
193106.1 A	5000.	0.382	-0.131	0.746E-01	-0.655E-01	0.624E-01	-0.529E-01
C= 0.19E+19	10000.	0.407	-0.862E-01	0.826E-01	-0.736E-01	0.686E-01	-0.595E-01
	20000.	0.404	-0.547E-01	0.917E-01	-0.827E-01	0.758E-01	-0.668E-01
	30000.	0.401	-0.363E-01	0.977E-01	-0.884E-01	0.804E-01	-0.715E-01
	50000.	0.400	-0.224E-01	0.106	-0.963E-01	0.868E-01	-0.778E-01
3D - 5P	3000.	0.188E-02	0.640E-03	0.615E-03	0.155E-03	0.611E-03	0.125E-03
12759.1 A	5000.	0.217E-02	0.774E-03	0.617E-03	0.169E-03	0.612E-03	0.136E-03
C= 0.84E+16	10000.	0.259E-02	0.854E-03	0.620E-03	0.190E-03	0.614E-03	0.153E-03
	20000.	0.307E-02	0.863E-03	0.626E-03	0.213E-03	0.617E-03	0.172E-03
	30000.	0.337E-02	0.764E-03	0.629E-03	0.228E-03	0.619E-03	0.184E-03
	50000.	0.375E-02	0.654E-03	0.635E-03	0.248E-03	0.623E-03	0.201E-03
3D - 6P	3000.	0.294E-02	0.179E-02	0.967E-03	0.467E-03	0.932E-03	0.377E-03
9174.6 A	5000.	0.331E-02	0.203E-02	0.987E-03	0.510E-03	0.944E-03	0.412E-03
C= 0.44E+16	10000.	0.388E-02	0.194E-02	0.102E-02	0.574E-03	0.965E-03	0.464E-03
	20000.	0.458E-02	0.176E-02	0.106E-02	0.646E-03	0.992E-03	0.521E-03
	30000.	0.507E-02	0.153E-02	0.109E-02	0.691E-03	0.101E-02	0.558E-03
	50000.	0.564E-02	0.128E-02	0.113E-02	0.753E-03	0.104E-02	0.608E-03
3D - 7P	3000.	0.610E-02	0.424E-02	0.181E-02	0.107E-02	0.169E-02	0.863E-03
8004.5 A	5000.	0.670E-02	0.446E-02	0.187E-02	0.118E-02	0.173E-02	0.947E-03
C= 0.27E+16	10000.	0.764E-02	0.439E-02	0.197E-02	0.133E-02	0.180E-02	0.107E-02
	20000.	0.882E-02	0.342E-02	0.209E-02	0.149E-02	0.188E-02	0.120E-02
	30000.	0.967E-02	0.280E-02	0.218E-02	0.160E-02	0.194E-02	0.129E-02
	50000.	0.105E-01	0.224E-02	0.229E-02	0.174E-02	0.203E-02	0.141E-02
4S - 4P	3000.	0.113E-02	-0.502E-03	0.268E-03	-0.205E-03	0.236E-03	-0.165E-03
13147.3 A	5000.	0.118E-02	-0.389E-03	0.284E-03	-0.223E-03	0.248E-03	-0.180E-03
C= 0.90E+16	10000.	0.127E-02	-0.299E-03	0.308E-03	-0.251E-03	0.266E-03	-0.203E-03
	20000.	0.134E-02	-0.225E-03	0.337E-03	-0.281E-03	0.287E-03	-0.228E-03
	30000.	0.140E-02	-0.175E-03	0.356E-03	-0.301E-03	0.301E-03	-0.243E-03
	50000.	0.149E-02	-0.131E-03	0.383E-03	-0.328E-03	0.321E-03	-0.265E-03
4S - 5P	3000.	0.435E-03	0.241E-03	0.185E-03	0.636E-04	0.182E-03	0.513E-04
6699.8 A	5000.	0.490E-03	0.276E-03	0.186E-03	0.693E-04	0.183E-03	0.560E-04
C= 0.78E+16	10000.	0.587E-03	0.268E-03	0.189E-03	0.779E-04	0.185E-03	0.629E-04
	20000.	0.724E-03	0.249E-03	0.193E-03	0.875E-04	0.187E-03	0.707E-04
	30000.	0.820E-03	0.214E-03	0.195E-03	0.936E-04	0.188E-03	0.756E-04
	50000.	0.947E-03	0.179E-03	0.199E-03	0.102E-03	0.191E-03	0.824E-04

PERTURBER DENSITY= 0.1D+14(cm-3)

PERTURBERS ARE		ELECTRONS		PROTONS		IONIZED HELIUM	
TRANSITION	T(K)	WIDTH(A)	SHIFT(A)	WIDTH(A)	SHIFT(A)	WIDTH(A)	SHIFT(A)
4S - 6P	3000.	0.103E-02	0.693E-03	0.365E-03	0.178E-03	0.352E-03	0.144E-03
5559.3 A	5000.	0.115E-02	0.760E-03	0.373E-03	0.194E-03	0.356E-03	0.157E-03
C= 0.26E+16	10000.	0.134E-02	0.763E-03	0.386E-03	0.219E-03	0.364E-03	0.177E-03
	20000.	0.160E-02	0.647E-03	0.402E-03	0.246E-03	0.375E-03	0.199E-03
	30000.	0.179E-02	0.572E-03	0.413E-03	0.263E-03	0.382E-03	0.213E-03
	50000.	0.201E-02	0.468E-03	0.430E-03	0.287E-03	0.393E-03	0.232E-03
4S - 7P	3000.	0.243E-02	0.170E-02	0.742E-03	0.440E-03	0.694E-03	0.354E-03
5106.9 A	5000.	0.267E-02	0.188E-02	0.768E-03	0.482E-03	0.711E-03	0.388E-03
C= 0.11E+16	10000.	0.304E-02	0.174E-02	0.809E-03	0.543E-03	0.739E-03	0.439E-03
	20000.	0.353E-02	0.141E-02	0.860E-03	0.612E-03	0.774E-03	0.494E-03
	30000.	0.388E-02	0.114E-02	0.893E-03	0.655E-03	0.798E-03	0.529E-03
	50000.	0.424E-02	0.889E-03	0.941E-03	0.714E-03	0.832E-03	0.577E-03
4P - 5S	3000.	0.542E-02	0.319E-02	0.101E-02	0.876E-03	0.853E-03	0.707E-03
21117.0 A	5000.	0.572E-02	0.331E-02	0.109E-02	0.956E-03	0.913E-03	0.772E-03
C= 0.23E+17	10000.	0.600E-02	0.336E-02	0.121E-02	0.107E-02	0.100E-02	0.868E-03
	20000.	0.640E-02	0.310E-02	0.134E-02	0.121E-02	0.111E-02	0.976E-03
	30000.	0.667E-02	0.267E-02	0.143E-02	0.129E-02	0.118E-02	0.104E-02
	50000.	0.729E-02	0.219E-02	0.154E-02	0.141E-02	0.127E-02	0.114E-02
4P - 4D	3000.	0.384E-02	0.225E-02	0.767E-03	0.618E-03	0.664E-03	0.499E-03
17929.8 A	5000.	0.405E-02	0.241E-02	0.817E-03	0.674E-03	0.702E-03	0.544E-03
C= 0.17E+17	10000.	0.425E-02	0.223E-02	0.895E-03	0.758E-03	0.761E-03	0.612E-03
	20000.	0.451E-02	0.198E-02	0.984E-03	0.851E-03	0.829E-03	0.688E-03
	30000.	0.474E-02	0.170E-02	0.104E-02	0.911E-03	0.874E-03	0.736E-03
	50000.	0.513E-02	0.138E-02	0.112E-02	0.992E-03	0.936E-03	0.802E-03
4P - 5D	3000.	0.236E-02	0.112E-02	0.598E-03	0.299E-03	0.574E-03	0.241E-03
10774.2 A	5000.	0.264E-02	0.126E-02	0.611E-03	0.326E-03	0.582E-03	0.263E-03
C= 0.60E+16	10000.	0.304E-02	0.119E-02	0.633E-03	0.367E-03	0.596E-03	0.296E-03
	20000.	0.354E-02	0.110E-02	0.661E-03	0.412E-03	0.614E-03	0.333E-03
	30000.	0.388E-02	0.962E-03	0.680E-03	0.441E-03	0.627E-03	0.356E-03
	50000.	0.432E-02	0.802E-03	0.708E-03	0.480E-03	0.646E-03	0.388E-03
4D - 5P	3000.	0.256E-01	0.431E-02	0.108E-01	0.149E-02	0.108E-01	0.120E-02
57393.7 A	5000.	0.315E-01	0.346E-02	0.108E-01	0.162E-02	0.108E-01	0.131E-02
C= 0.57E+18	10000.	0.443E-01	0.240E-02	0.108E-01	0.182E-02	0.108E-01	0.147E-02
	20000.	0.618E-01	0.207E-02	0.109E-01	0.205E-02	0.108E-01	0.165E-02
	30000.	0.729E-01	0.177E-02	0.109E-01	0.219E-02	0.108E-01	0.177E-02
	50000.	0.862E-01	0.148E-02	0.109E-01	0.238E-02	0.109E-01	0.193E-02
4D - 6P	3000.	0.140E-01	0.934E-02	0.471E-02	0.233E-02	0.452E-02	0.188E-02
20813.7 A	5000.	0.157E-01	0.926E-02	0.481E-02	0.254E-02	0.459E-02	0.205E-02
C= 0.36E+17	10000.	0.190E-01	0.925E-02	0.498E-02	0.286E-02	0.469E-02	0.231E-02
	20000.	0.234E-01	0.761E-02	0.520E-02	0.322E-02	0.483E-02	0.260E-02
	30000.	0.267E-01	0.634E-02	0.535E-02	0.344E-02	0.493E-02	0.278E-02
	50000.	0.304E-01	0.591E-02	0.556E-02	0.375E-02	0.508E-02	0.303E-02

PERTURBER DENSITY= 0.1D+14(cm-3)

PERTURBERS ARE		ELECTRONS		PROTONS		IONIZED HELIUM	
TRANSITION	T(K)	WIDTH(A)	SHIFT(A)	WIDTH(A)	SHIFT(A)	WIDTH(A)	SHIFT(A)
4D - 7P	3000.	0.227E-01	0.155E-01	0.674E-02	0.407E-02	0.628E-02	0.327E-02
15630.4 A	5000.	0.249E-01	0.166E-01	0.699E-02	0.446E-02	0.645E-02	0.359E-02
C= 0.10E+17	10000.	0.287E-01	0.158E-01	0.738E-02	0.502E-02	0.671E-02	0.406E-02
	20000.	0.337E-01	0.120E-01	0.785E-02	0.566E-02	0.704E-02	0.456E-02
	30000.	0.373E-01	0.949E-02	0.817E-02	0.606E-02	0.727E-02	0.489E-02
	50000.	0.410E-01	0.773E-02	0.862E-02	0.660E-02	0.759E-02	0.533E-02
5S - 5P	3000.	0.126E-01	0.858E-03	0.598E-02	0.533E-03	0.598E-02	0.431E-03
38697.4 A	5000.	0.152E-01	0.162E-03	0.598E-02	0.581E-03	0.598E-02	0.470E-03
C= 0.26E+18	10000.	0.211E-01	-0.275E-03	0.598E-02	0.652E-03	0.598E-02	0.527E-03
	20000.	0.294E-01	-0.659E-03	0.598E-02	0.732E-03	0.598E-02	0.592E-03
	30000.	0.347E-01	-0.536E-03	0.598E-02	0.783E-03	0.598E-02	0.633E-03
	50000.	0.412E-01	-0.427E-03	0.599E-02	0.853E-03	0.598E-02	0.689E-03
5S - 6P	3000.	0.102E-01	0.671E-02	0.365E-02	0.168E-02	0.353E-02	0.135E-02
17710.6 A	5000.	0.114E-01	0.661E-02	0.372E-02	0.183E-02	0.357E-02	0.148E-02
C= 0.26E+17	10000.	0.139E-01	0.651E-02	0.383E-02	0.206E-02	0.364E-02	0.166E-02
	20000.	0.172E-01	0.514E-02	0.397E-02	0.232E-02	0.373E-02	0.187E-02
	30000.	0.197E-01	0.441E-02	0.407E-02	0.248E-02	0.380E-02	0.200E-02
	50000.	0.224E-01	0.389E-02	0.421E-02	0.270E-02	0.389E-02	0.218E-02
5S - 7P	3000.	0.178E-01	0.121E-01	0.540E-02	0.317E-02	0.506E-02	0.255E-02
13813.0 A	5000.	0.195E-01	0.129E-01	0.559E-02	0.348E-02	0.518E-02	0.280E-02
C= 0.79E+16	10000.	0.225E-01	0.125E-01	0.588E-02	0.392E-02	0.538E-02	0.316E-02
	20000.	0.265E-01	0.930E-02	0.624E-02	0.441E-02	0.563E-02	0.356E-02
	30000.	0.293E-01	0.737E-02	0.648E-02	0.473E-02	0.580E-02	0.382E-02
	50000.	0.323E-01	0.593E-02	0.683E-02	0.515E-02	0.604E-02	0.416E-02
5P - 5D	3000.	0.375E-01	0.114E-01	0.113E-01	0.289E-02	0.112E-01	0.233E-02
50974.9 A	5000.	0.457E-01	0.120E-01	0.113E-01	0.315E-02	0.112E-01	0.255E-02
C= 0.24E+18	10000.	0.623E-01	0.102E-01	0.114E-01	0.354E-02	0.113E-01	0.286E-02
	20000.	0.853E-01	0.827E-02	0.115E-01	0.398E-02	0.113E-01	0.322E-02
	30000.	0.999E-01	0.785E-02	0.116E-01	0.426E-02	0.114E-01	0.344E-02
	50000.	0.117	0.667E-02	0.117E-01	0.464E-02	0.114E-01	0.375E-02
5D - 6P	3000.	0.282	0.160	0.805E-01	0.409E-01	0.771E-01	0.330E-01
90873.6 A	5000.	0.325	0.162	0.823E-01	0.446E-01	0.782E-01	0.360E-01
C= 0.69E+18	10000.	0.412	0.146	0.854E-01	0.502E-01	0.802E-01	0.405E-01
	20000.	0.538	0.116	0.893E-01	0.564E-01	0.828E-01	0.456E-01
	30000.	0.621	0.102	0.920E-01	0.604E-01	0.846E-01	0.488E-01
	50000.	0.712	0.867E-01	0.959E-01	0.658E-01	0.872E-01	0.532E-01
5D - 7P	3000.	0.132	0.862E-01	0.361E-01	0.226E-01	0.334E-01	0.182E-01
37123.9 A	5000.	0.145	0.900E-01	0.376E-01	0.248E-01	0.344E-01	0.200E-01
C= 0.57E+17	10000.	0.171	0.867E-01	0.398E-01	0.279E-01	0.360E-01	0.226E-01
	20000.	0.204	0.643E-01	0.425E-01	0.315E-01	0.379E-01	0.254E-01
	30000.	0.228	0.534E-01	0.444E-01	0.337E-01	0.392E-01	0.272E-01
	50000.	0.253	0.400E-01	0.469E-01	0.367E-01	0.411E-01	0.297E-01

PERTURBER DENSITY= 0.1D+15(cm-3)

PERTURBERS ARE		ELECTRONS		PROTONS		IONIZED HELIUM	
TRANSITION	T(K)	WIDTH(A)	SHIFT(A)	WIDTH(A)	SHIFT(A)	WIDTH(A)	SHIFT(A)
3P - 4S	3000.	0.210E-03	0.173E-03	0.526E-04	0.486E-04	0.428E-04	0.393E-04
3958.3 A	5000.	0.239E-03	0.194E-03	0.571E-04	0.531E-04	0.465E-04	0.428E-04
C= 0.12E+18	10000.	0.279E-03	0.232E-03	0.639E-04	0.597E-04	0.519E-04	0.482E-04
	20000.	0.310E-03	0.263E-03	0.716E-04	0.671E-04	0.581E-04	0.542E-04
	30000.	0.317E-03	0.251E-03	0.765E-04	0.718E-04	0.621E-04	0.580E-04
	50000.	0.341E-03	0.248E-03	0.832E-04	0.782E-04	0.675E-04	0.632E-04
3P - 5S	3000.	0.472E-03	0.352E-03	0.104E-03	0.964E-04	0.838E-04	0.776E-04
2659.2 A	5000.	0.528E-03	0.402E-03	0.113E-03	0.106E-03	0.912E-04	0.851E-04
C= 0.18E+17	10000.	0.584E-03	0.472E-03	0.127E-03	0.119E-03	0.102E-03	0.960E-04
	20000.	0.620E-03	0.457E-03	0.142E-03	0.134E-03	0.115E-03	0.108E-03
	30000.	0.650E-03	0.450E-03	0.152E-03	0.143E-03	0.123E-03	0.116E-03
	50000.	0.686E-03	0.388E-03	0.166E-03	0.156E-03	0.134E-03	0.126E-03
3P - 3D	3000.	0.392E-03	0.264E-03	0.102E-03	0.887E-04	0.852E-04	0.713E-04
3091.0 A	5000.	0.417E-03	0.243E-03	0.110E-03	0.969E-04	0.913E-04	0.782E-04
C= 0.49E+16	10000.	0.432E-03	0.216E-03	0.122E-03	0.109E-03	0.101E-03	0.880E-04
	20000.	0.420E-03	0.180E-03	0.136E-03	0.123E-03	0.111E-03	0.991E-04
	30000.	0.407E-03	0.160E-03	0.145E-03	0.131E-03	0.118E-03	0.106E-03
	50000.	0.390E-03	0.128E-03	0.157E-03	0.143E-03	0.128E-03	0.116E-03
3P - 4D	3000.	0.448E-03	0.328E-03	0.141E-03	0.888E-04	0.130E-03	0.714E-04
2601.0 A	5000.	0.500E-03	0.380E-03	0.146E-03	0.973E-04	0.134E-03	0.783E-04
C= 0.12E+17	10000.	0.558E-03	0.420E-03	0.155E-03	0.110E-03	0.140E-03	0.883E-04
	20000.	0.611E-03	0.416E-03	0.166E-03	0.123E-03	0.148E-03	0.995E-04
	30000.	0.642E-03	0.386E-03	0.173E-03	0.132E-03	0.153E-03	0.107E-03
	50000.	0.693E-03	0.327E-03	0.183E-03	0.144E-03	0.160E-03	0.116E-03
3P - 5D	3000.	0.853E-03	0.442E-03	0.303E-03	0.115E-03	0.297E-03	0.928E-04
2372.4 A	5000.	0.980E-03	0.492E-03	0.306E-03	0.127E-03	0.299E-03	0.102E-03
C= 0.52E+16	10000.	0.118E-02	0.540E-03	0.312E-03	0.143E-03	0.302E-03	0.115E-03
	20000.	0.142E-02	0.526E-03	0.320E-03	0.161E-03	0.307E-03	0.130E-03
	30000.	0.158E-02	0.485E-03	0.326E-03	0.172E-03	0.311E-03	0.139E-03
	50000.	0.177E-02	0.412E-03	0.334E-03	0.188E-03	0.316E-03	0.152E-03
3D - 4P	3000.	3.64	-1.69	0.694	-0.593	0.584	-0.477
193106.1 A	5000.	3.82	-1.31	0.746	-0.650	0.624	-0.523
C= 0.19E+20	10000.	4.07	-0.862	0.826	-0.732	0.686	-0.591
	20000.	4.04	-0.547	0.917	-0.824	0.758	-0.665
	30000.	4.01	-0.363	0.977	-0.883	0.804	-0.713
	50000.	4.00	-0.224	1.06	-0.962	0.868	-0.777
3D - 5P	3000.	0.188E-01	0.639E-02	0.614E-02	0.154E-02	0.611E-02	0.124E-02
12759.1 A	5000.	0.217E-01	0.773E-02	0.617E-02	0.168E-02	0.612E-02	0.136E-02
C= 0.84E+17	10000.	0.259E-01	0.854E-02	0.620E-02	0.189E-02	0.614E-02	0.153E-02
	20000.	0.307E-01	0.863E-02	0.626E-02	0.213E-02	0.617E-02	0.172E-02
	30000.	0.337E-01	0.764E-02	0.629E-02	0.228E-02	0.619E-02	0.184E-02
	50000.	0.375E-01	0.654E-02	0.635E-02	0.248E-02	0.623E-02	0.201E-02

PERTURBER DENSITY= 0.1D+15(cm-3)

PERTURBERS ARE		ELECTRONS		PROTONS		IONIZED HELIUM	
TRANSITION	T(K)	WIDTH(A)	SHIFT(A)	WIDTH(A)	SHIFT(A)	WIDTH(A)	SHIFT(A)
3D - 6P	3000.	0.294E-01	0.179E-01	0.967E-02	0.456E-02	0.930E-02	0.365E-02
9174.6 A	5000.	0.331E-01	0.203E-01	0.987E-02	0.501E-02	0.943E-02	0.403E-02
C= 0.44E+17	10000.	0.388E-01	0.194E-01	0.102E-01	0.569E-02	0.965E-02	0.458E-02
	20000.	0.458E-01	0.176E-01	0.106E-01	0.641E-02	0.992E-02	0.518E-02
	30000.	0.507E-01	0.153E-01	0.109E-01	0.688E-02	0.101E-01	0.555E-02
	50000.	0.564E-01	0.128E-01	0.113E-01	0.751E-02	0.104E-01	0.606E-02
3D - 7P	3000.	0.610E-01	0.421E-01	0.180E-01	0.103E-01	*0.168E-01	80.818E-02
8004.5 A	5000.	0.670E-01	0.445E-01	0.187E-01	0.114E-01	0.173E-01	0.911E-02
C= 0.27E+17	10000.	0.764E-01	0.439E-01	0.197E-01	0.130E-01	0.180E-01	0.104E-01
	20000.	0.882E-01	0.342E-01	0.209E-01	0.148E-01	0.188E-01	0.119E-01
	30000.	0.967E-01	0.280E-01	0.218E-01	0.159E-01	0.194E-01	0.128E-01
	50000.	0.105	0.224E-01	0.229E-01	0.173E-01	0.203E-01	0.140E-01
4S - 4P	3000.	0.113E-01	-0.502E-02	0.268E-02	-0.203E-02	0.236E-02	-0.163E-02
13147.3 A	5000.	0.118E-01	-0.389E-02	0.284E-02	-0.222E-02	0.248E-02	-0.179E-02
C= 0.90E+17	10000.	0.127E-01	-0.299E-02	0.308E-02	-0.250E-02	0.266E-02	-0.201E-02
	20000.	0.134E-01	-0.225E-02	0.337E-02	-0.281E-02	0.287E-02	-0.227E-02
	30000.	0.140E-01	-0.175E-02	0.356E-02	-0.301E-02	0.301E-02	-0.243E-02
	50000.	0.149E-01	-0.131E-02	0.383E-02	-0.328E-02	0.321E-02	-0.265E-02
4S - 5P	3000.	0.435E-02	0.241E-02	0.185E-02	0.628E-03	0.182E-02	0.505E-03
6699.8 A	5000.	0.490E-02	0.276E-02	0.186E-02	0.688E-03	0.183E-02	0.554E-03
C= 0.78E+17	10000.	0.587E-02	0.268E-02	0.189E-02	0.775E-03	0.185E-02	0.625E-03
	20000.	0.724E-02	0.249E-02	0.193E-02	0.872E-03	0.187E-02	0.704E-03
	30000.	0.820E-02	0.214E-02	0.195E-02	0.934E-03	0.188E-02	0.755E-03
	50000.	0.947E-02	0.179E-02	0.199E-02	0.102E-02	0.191E-02	0.823E-03
4S - 6P	3000.	0.103E-01	0.691E-02	0.365E-02	0.174E-02	0.351E-02	0.139E-02
5559.3 A	5000.	0.115E-01	0.759E-02	0.373E-02	0.191E-02	0.356E-02	0.153E-02
C= 0.26E+17	10000.	0.134E-01	0.763E-02	0.386E-02	0.217E-02	0.364E-02	0.174E-02
	20000.	0.160E-01	0.647E-02	0.402E-02	0.245E-02	0.375E-02	0.197E-02
	30000.	0.179E-01	0.572E-02	0.413E-02	0.262E-02	0.382E-02	0.211E-02
	50000.	0.201E-01	0.468E-02	0.430E-02	0.286E-02	0.393E-02	0.231E-02
4S - 7P	3000.	0.243E-01	0.168E-01	0.741E-02	0.421E-02	*0.692E-02	*0.335E-02
5106.9 A	5000.	0.267E-01	0.187E-01	0.767E-02	0.467E-02	0.710E-02	0.374E-02
C= 0.11E+17	10000.	0.304E-01	0.174E-01	0.809E-02	0.533E-02	0.739E-02	0.428E-02
	20000.	0.353E-01	0.140E-01	0.860E-02	0.605E-02	0.774E-02	0.487E-02
	30000.	0.388E-01	0.114E-01	0.893E-02	0.651E-02	0.798E-02	0.524E-02
	50000.	0.424E-01	0.889E-02	0.941E-02	0.710E-02	0.832E-02	0.573E-02
4P - 5S	3000.	0.542E-01	0.319E-01	0.101E-01	0.864E-02	0.853E-02	0.695E-02
21117.0 A	5000.	0.572E-01	0.331E-01	0.109E-01	0.948E-02	0.913E-02	0.763E-02
C= 0.23E+18	10000.	0.600E-01	0.336E-01	0.121E-01	0.107E-01	0.100E-01	0.862E-02
	20000.	0.640E-01	0.310E-01	0.134E-01	0.120E-01	0.111E-01	0.971E-02
	30000.	0.667E-01	0.267E-01	0.143E-01	0.129E-01	0.118E-01	0.104E-01
	50000.	0.729E-01	0.219E-01	0.154E-01	0.141E-01	0.127E-01	0.113E-01

PERTURBER DENSITY= 0.1D+15(cm-3)

PERTURBERS ARE		ELECTRONS		PROTONS		IONIZED HELIUM	
TRANSITION	T(K)	WIDTH(A)	SHIFT(A)	WIDTH(A)	SHIFT(A)	WIDTH(A)	SHIFT(A)
4P - 4D	3000.	0.384E-01	0.224E-01	0.767E-02	0.609E-02	0.664E-02	0.490E-02
17929.8 A	5000.	0.405E-01	0.241E-01	0.818E-02	0.668E-02	0.702E-02	0.538E-02
C= 0.17E+18	10000.	0.425E-01	0.223E-01	0.895E-02	0.753E-02	0.761E-02	0.608E-02
	20000.	0.451E-01	0.198E-01	0.984E-02	0.848E-02	0.829E-02	0.685E-02
	30000.	0.474E-01	0.170E-01	0.104E-01	0.909E-02	0.874E-02	0.734E-02
	50000.	0.513E-01	0.138E-01	0.112E-01	0.991E-02	0.936E-02	0.800E-02
4P - 5D	3000.	0.236E-01	0.112E-01	0.597E-02	0.294E-02	0.573E-02	0.236E-02
10774.2 A	5000.	0.264E-01	0.125E-01	0.611E-02	0.323E-02	0.582E-02	0.260E-02
C= 0.60E+17	10000.	0.304E-01	0.119E-01	0.633E-02	0.365E-02	0.596E-02	0.294E-02
	20000.	0.354E-01	0.110E-01	0.661E-02	0.410E-02	0.614E-02	0.331E-02
	30000.	0.388E-01	0.962E-02	0.680E-02	0.440E-02	0.627E-02	0.355E-02
	50000.	0.432E-01	0.802E-02	0.708E-02	0.480E-02	0.646E-02	0.387E-02
4D - 5P	3000.	0.256	0.431E-01	0.108	0.148E-01	0.108	0.120E-01
57393.7 A	5000.	0.315	0.346E-01	0.108	0.162E-01	0.108	0.130E-01
C= 0.57E+19	10000.	0.443	0.240E-01	0.108	0.182E-01	0.108	0.147E-01
	20000.	0.618	0.207E-01	0.109	0.204E-01	0.108	0.165E-01
	30000.	0.729	0.177E-01	0.109	0.219E-01	0.108	0.177E-01
	50000.	0.862	0.148E-01	0.109	0.238E-01	0.109	0.193E-01
4D - 6P	3000.	0.140	0.932E-01	0.470E-01	0.227E-01	0.452E-01	0.182E-01
20813.7 A	5000.	0.157	0.924E-01	0.481E-01	0.250E-01	0.458E-01	0.201E-01
C= 0.36E+18	10000.	0.190	0.925E-01	0.498E-01	0.283E-01	0.469E-01	0.228E-01
	20000.	0.234	0.761E-01	0.520E-01	0.320E-01	0.483E-01	0.258E-01
	30000.	0.267	0.634E-01	0.535E-01	0.343E-01	0.493E-01	0.277E-01
	50000.	0.304	0.591E-01	0.556E-01	0.374E-01	0.508E-01	0.302E-01
4D - 7P	3000.	0.227	0.154	0.673E-01	0.390E-01	*0.627E-01	*0.310E-01
15630.4 A	5000.	0.249	0.166	0.698E-01	0.432E-01	0.644E-01	0.346E-01
C= 0.10E+18	10000.	0.287	0.158	0.737E-01	0.493E-01	0.671E-01	0.396E-01
	20000.	0.337	0.120	0.785E-01	0.559E-01	0.704E-01	0.450E-01
	30000.	0.373	0.949E-01	0.817E-01	0.602E-01	0.727E-01	0.484E-01
	50000.	0.410	0.773E-01	0.862E-01	0.656E-01	0.759E-01	0.530E-01
5S - 5P	3000.	0.126	0.857E-02	0.597E-01	0.530E-02	0.597E-01	0.428E-02
38697.4 A	5000.	0.152	0.162E-02	0.598E-01	0.579E-02	0.597E-01	0.467E-02
C= 0.26E+19	10000.	0.211	-0.275E-02	0.598E-01	0.651E-02	0.598E-01	0.526E-02
	20000.	0.294	-0.659E-02	0.598E-01	0.732E-02	0.598E-01	0.591E-02
	30000.	0.347	-0.536E-02	0.598E-01	0.783E-02	0.598E-01	0.633E-02
	50000.	0.412	-0.427E-02	0.599E-01	0.853E-02	0.598E-01	0.689E-02
5S - 6P	3000.	0.102	0.670E-01	0.365E-01	0.164E-01	0.353E-01	0.131E-01
17710.6 A	5000.	0.114	0.659E-01	0.372E-01	0.180E-01	0.357E-01	0.145E-01
C= 0.26E+18	10000.	0.139	0.650E-01	0.383E-01	0.204E-01	0.364E-01	0.164E-01
	20000.	0.172	0.514E-01	0.397E-01	0.230E-01	0.373E-01	0.186E-01
	30000.	0.197	0.441E-01	0.407E-01	0.247E-01	0.380E-01	0.199E-01
	50000.	0.224	0.389E-01	0.421E-01	0.269E-01	0.389E-01	0.217E-01

PERTURBER DENSITY= 0.1D+15(cm-3)

PERTURBERS ARE		ELECTRONS		PROTONS		IONIZED HELIUM	
TRANSITION	T(K)	WIDTH(A)	SHIFT(A)	WIDTH(A)	SHIFT(A)	WIDTH(A)	SHIFT(A)
5S - 7P	3000.	0.178	0.120	0.539E-01	0.304E-01	*0.504E-01	*0.242E-01
13813.0 A	5000.	0.195	0.128	0.558E-01	0.337E-01	0.517E-01	0.270E-01
C= 0.79E+17	10000.	0.225	0.125	0.588E-01	0.385E-01	0.538E-01	0.309E-01
	20000.	0.265	0.929E-01	0.624E-01	0.436E-01	0.563E-01	0.351E-01
	30000.	0.293	0.737E-01	0.648E-01	0.470E-01	0.580E-01	0.378E-01
	50000.	0.323	0.593E-01	0.683E-01	0.512E-01	0.604E-01	0.413E-01
5P - 5D	3000.	0.375	0.114	0.113	0.286E-01	0.112	0.230E-01
50974.9 A	5000.	0.457	0.120	0.113	0.313E-01	0.112	0.253E-01
C= 0.24E+19	10000.	0.623	0.102	0.114	0.353E-01	0.113	0.285E-01
	20000.	0.853	0.827E-01	0.115	0.397E-01	0.113	0.321E-01
	30000.	0.999	0.785E-01	0.116	0.425E-01	0.114	0.343E-01
	50000.	1.17	0.667E-01	0.117	0.463E-01	0.114	0.374E-01
5D - 6P	3000.	2.82	1.60	0.804	0.399	0.770	0.320
90873.6 A	5000.	3.25	1.62	0.823	0.439	0.782	0.353
C= 0.69E+19	10000.	4.12	1.46	0.854	0.498	0.802	0.400
	20000.	5.38	1.16	0.893	0.561	0.828	0.453
	30000.	6.21	1.02	0.920	0.601	0.846	0.485
	50000.	7.12	0.867	0.959	0.656	0.872	0.530
5D - 7P	3000.	1.32	0.854	0.361	0.217	*0.333	*0.173
37123.9 A	5000.	1.45	0.896	0.375	0.240	0.344	0.192
C= 0.57E+18	10000.	1.71	0.867	0.398	0.274	0.359	0.220
	20000.	2.04	0.643	0.425	0.311	0.379	0.250
	30000.	2.28	0.534	0.443	0.335	0.392	0.269
	50000.	2.53	0.400	0.469	0.365	0.411	0.295

PERTURBER DENSITY= 0.1D+17(cm-3)

3P - 4S	3000.	0.209E-01	0.169E-01	0.525E-02	0.450E-02	0.428E-02	0.356E-02
3958.3 A	5000.	0.239E-01	0.191E-01	0.571E-02	0.503E-02	0.464E-02	0.400E-02
C= 0.12E+20	10000.	0.279E-01	0.231E-01	0.639E-02	0.577E-02	0.519E-02	0.462E-02
	20000.	0.310E-01	0.263E-01	0.716E-02	0.657E-02	0.581E-02	0.528E-02
	30000.	0.317E-01	0.250E-01	0.765E-02	0.707E-02	0.621E-02	0.569E-02
	50000.	0.341E-01	0.248E-01	0.832E-02	0.775E-02	0.675E-02	0.624E-02
3P - 5S	3000.	0.471E-01	0.337E-01	0.104E-01	0.813E-02	*0.837E-02	*0.625E-02
2659.2 A	5000.	0.528E-01	0.392E-01	0.113E-01	0.938E-02	0.912E-02	0.733E-02
C= 0.18E+19	10000.	0.585E-01	0.471E-01	0.127E-01	0.111E-01	0.102E-01	0.877E-02
	20000.	0.620E-01	0.454E-01	0.142E-01	0.128E-01	0.115E-01	0.102E-01
	30000.	0.650E-01	0.450E-01	0.152E-01	0.139E-01	0.123E-01	0.111E-01
	50000.	0.686E-01	0.388E-01	0.166E-01	0.153E-01	0.134E-01	0.123E-01
3P - 3D	3000.	0.392E-01	0.255E-01	0.102E-01	0.771E-02	0.848E-02	0.599E-02
3091.0 A	5000.	0.417E-01	0.236E-01	0.110E-01	0.880E-02	0.911E-02	0.692E-02
C= 0.49E+18	10000.	0.432E-01	0.213E-01	0.122E-01	0.103E-01	0.101E-01	0.818E-02
	20000.	0.420E-01	0.179E-01	0.135E-01	0.118E-01	0.111E-01	0.946E-02
	30000.	0.407E-01	0.160E-01	0.145E-01	0.128E-01	0.118E-01	0.103E-01
	50000.	0.390E-01	0.128E-01	0.157E-01	0.140E-01	0.128E-01	0.113E-01

PERTURBER DENSITY= 0.1D+17(cm-3)

PERTURBERS ARE		ELECTRONS		PROTONS		IONIZED HELIUM	
TRANSITION	T(K)	WIDTH(A)	SHIFT(A)	WIDTH(A)	SHIFT(A)	WIDTH(A)	SHIFT(A)
3P - 4D	3000.	0.448E-01	0.315E-01	*0.139E-01	*0.751E-02	*0.127E-01	*0.578E-02
2601.0 A	5000.	0.500E-01	0.375E-01	0.146E-01	0.865E-02	*0.132E-01	*0.677E-02
C= 0.12E+19	10000.	0.558E-01	0.416E-01	0.155E-01	0.102E-01	*0.140E-01	*0.809E-02
	20000.	0.611E-01	0.416E-01	0.166E-01	0.118E-01	0.147E-01	0.942E-02
	30000.	0.642E-01	0.386E-01	0.173E-01	0.128E-01	0.153E-01	0.102E-01
	50000.	0.693E-01	0.327E-01	0.183E-01	0.141E-01	0.160E-01	0.113E-01
3P - 5D	3000.	0.853E-01	0.428E-01	*0.290E-01	*0.931E-02		
2372.4 A	5000.	0.980E-01	0.477E-01	*0.300E-01	*0.109E-01		
C= 0.52E+18	10000.	0.118	0.534E-01	*0.310E-01	*0.130E-01	*0.298E-01	*0.103E-01
	20000.	0.142	0.525E-01	*0.319E-01	*0.152E-01	*0.306E-01	*0.121E-01
	30000.	0.158	0.484E-01	0.325E-01	0.165E-01	*0.310E-01	*0.132E-01
	50000.	0.177	0.412E-01	0.334E-01	0.182E-01	*0.315E-01	*0.146E-01
3D - 5P	3000.	1.88	0.621	*0.595	*0.134		
12759.1 A	5000.	2.17	0.760	*0.607	*0.152	*0.595	*0.120
C= 0.84E+19	10000.	2.59	0.849	*0.617	*0.178	*0.608	*0.142
	20000.	3.07	0.862	0.624	0.205	*0.615	*0.164
	30000.	3.37	0.763	0.629	0.222	*0.618	*0.178
	50000.	3.75	0.654	0.635	0.244	0.622	0.196
3D - 6P	3000.	2.94	1.64				
9174.6 A	5000.	3.31	1.94				
C= 0.44E+19	10000.	3.88	1.88				
	20000.	4.58	1.74	*1.06	*0.585		
	30000.	5.07	1.53	*1.09	*0.642		
	50000.	5.64	1.27	*1.13	*0.715	*1.04	*0.570
3D - 7P	3000.	6.09	3.65				
8004.5 A	5000.	6.69	4.02				
C= 0.27E+19	10000.	7.63	4.18				
	20000.	8.82	3.34				
	30000.	9.67	2.75				
	50000.	10.5	2.23				
4S - 4P	3000.	1.13	-0.473	0.266	-0.173	*0.233	*-0.134
13147.3 A	5000.	1.13	-0.372	0.283	-0.199	*0.246	*-0.156
C= 0.90E+19	10000.	1.27	-0.291	0.308	-0.233	0.265	-0.185
	20000.	1.34	-0.222	0.337	-0.269	0.287	-0.215
	30000.	1.40	-0.175	0.356	-0.291	0.301	-0.234
	50000.	1.49	-0.131	0.383	-0.321	0.321	-0.258
4S - 5P	3000.	0.435	0.231	*0.178	*0.528E-01		
6699.8 A	5000.	0.490	0.268	*0.183	*0.610E-01	*0.177	*0.477E-01
C= 0.78E+19	10000.	0.587	0.264	*0.188	*0.720E-01	*0.183	*0.571E-01
	20000.	0.724	0.247	0.192	0.834E-01	*0.186	*0.666E-01
	30000.	0.820	0.213	0.195	0.903E-01	*0.188	*0.723E-01
	50000.	0.947	0.179	0.199	0.994E-01	0.190	0.798E-01

PERTURBER DENSITY= 0.1D+17(cm-3)

PERTURBERS ARE		ELECTRONS		PROTONS		IONIZED HELIUM	
TRANSITION	T(K)	WIDTH(A)	SHIFT(A)	WIDTH(A)	SHIFT(A)	WIDTH(A)	SHIFT(A)
4S - 6P	3000.	1.03	0.636				
5559.3 A	5000.	1.15	0.717				
C= 0.26E+19	10000.	1.34	0.739				
	20000.	1.60	0.635	*0.400	*0.222		
	30000.	1.79	0.566	*0.412	*0.244		
	50000.	2.01	0.467	*0.429	*0.272		
4S - 7P	3000.	2.43	1.44				
5106.9 A	5000.	2.67	1.70				
C= 0.11E+19	10000.	3.04	1.62				
	20000.	3.53	1.35				
	30000.	3.88	1.11				
	50000.	4.24	0.882				
4P - 5S	3000.	5.42	3.04	*1.01	*0.702	*0.844	*0.533
21117.0 A	5000.	5.72	3.19	1.09	0.821	*0.908	*0.637
C= 0.23E+20	10000.	6.00	3.31	1.21	0.979	*1.00	*0.773
	20000.	6.40	3.09	1.34	1.14	1.11	0.908
	30000.	6.67	2.67	1.42	1.24	1.17	0.989
	50000.	7.29	2.19	1.54	1.37	1.27	1.10
4P - 4D	3000.	3.84	2.13	*0.761	*0.496	*0.653	*0.377
17929.8 A	5000.	4.05	2.33	0.815	0.580	*0.697	*0.450
C= 0.17E+20	10000.	4.25	2.19	0.894	0.691	*0.759	*0.545
	20000.	4.51	1.97	0.983	0.804	0.828	0.641
	30000.	4.74	1.69	1.04	0.873	0.873	0.698
	50000.	5.13	1.38	1.12	0.963	0.935	0.772
4P - 5D	3000.	2.36	1.06	*0.575	*0.231		
10774.2 A	5000.	2.64	1.21	*0.600	*0.273		
C= 0.60E+19	10000.	3.04	1.17	*0.629	*0.330	*0.589	*0.259
	20000.	3.54	1.10	*0.660	*0.386	*0.612	*0.307
	30000.	3.88	0.960	0.679	0.420	*0.625	*0.335
	50000.	4.32	0.800	0.708	0.464	*0.645	*0.372
PERTURBER DENSITY= 0.1D+18(cm-3)							
3P - 4S	3000.	0.209	0.160	0.524E-01	0.364E-01	*0.425E-01	*0.270E-01
3958.3 A	5000.	0.239	0.185	0.570E-01	0.436E-01	*0.463E-01	*0.334E-01
C= 0.12E+21	10000.	0.279	0.226	0.639E-01	0.530E-01	0.519E-01	0.415E-01
	20000.	0.310	0.262	0.716E-01	0.624E-01	0.581E-01	0.495E-01
	30000.	0.317	0.249	0.765E-01	0.679E-01	0.620E-01	0.542E-01
	50000.	0.341	0.247	0.832E-01	0.752E-01	0.674E-01	0.602E-01
3P - 5S	3000.	0.471	0.301				
2659.2 A	5000.	0.528	0.363	*0.112	*0.657E-01		
C= 0.18E+20	10000.	0.585	0.451	*0.126	*0.908E-01		
	20000.	0.620	0.447	*0.142	*0.114	*0.115	*0.882E-01
	30000.	0.650	0.448	*0.152	*0.127	*0.123	*0.996E-01
	50000.	0.686	0.388	*0.166	*0.144	*0.134	*0.114

PERTURBER DENSITY= 0.1D+18(cm-3)

PERTURBERS ARE		ELECTRONS		PROTONS		IONIZED HELIUM	
TRANSITION	T(K)	WIDTH(A)	SHIFT(A)	WIDTH(A)	SHIFT(A)	WIDTH(A)	SHIFT(A)
3P - 3D	3000.	0.391	0.225	*0.988E-01	*0.499E-01		
3091.0 A	5000.	0.416	0.213	*0.109	*0.668E-01		
C= 0.49E+19	10000.	0.431	0.197	*0.121	*0.879E-01	*0.100	*0.668E-01
	20000.	0.419	0.178	*0.135	*0.108	*0.111	*0.841E-01
	30000.	0.407	0.159	*0.144	*0.119	*0.118	*0.939E-01
	50000.	0.389	0.127	0.157	0.134	*0.128	*0.106
3P - 4D	3000.	0.447	0.282				
2601.0 A	5000.	0.500	0.348				
C= 0.12E+20	10000.	0.558	0.398	*0.152	*0.841E-01		
	20000.	0.611	0.406	*0.165	*0.105		
	30000.	0.642	0.381	*0.172	*0.117		
	50000.	0.693	0.325	*0.183	*0.133	*0.160	*0.105
4S - 4P	3000.	11.2	-3.98				
13147.3 A	5000.	11.7	-3.13	*2.75	*-1.44		
C= 0.90E+20	10000.	12.7	-2.57	*3.05	*-1.95		
	20000.	13.3	-2.08	*3.36	*-2.42	*2.85	*-1.88
	30000.	14.0	-1.64	*3.55	*-2.69	*3.00	*-2.11
	50000.	14.9	-1.29	*3.82	*-3.03	*3.21	*-2.40
4S - 5P	3000.	4.34	2.07				
6699.8 A	5000.	4.89	2.50				
C= 0.78E+20	10000.	5.87	2.51				
	20000.	7.24	2.39				
	30000.	8.20	2.09				
	50000.	9.47	1.76	*1.98	*0.936		
4S - 6P	3000.	*10.1	*4.96				
5559.3 A	5000.	11.4	6.09				
C= 0.26E+20	10000.	13.4	6.64				
	20000.	16.0	5.90				
	30000.	17.9	5.44				
	50000.	20.1	4.50				

PERTURBER DENSITY= 0.1D+19(cm-3)

3P - 4S	3000.	2.09	1.33				
3958.3 A	5000.	2.39	1.64	*0.545	*0.226		
C= 0.12E+22	10000.	2.79	2.11	*0.634	*0.381		
	20000.	3.10	2.50	*0.715	*0.518		
	30000.	3.17	2.41	*0.764	*0.594	*0.620	*0.456
	50000.	3.41	2.43	*0.832	*0.686	*0.674	*0.536
3P - 5S	3000.	*4.63	*1.83				
2659.2 A	5000.	*5.25	*2.72				
C= 0.18E+21	10000.	5.84	3.87				
	20000.	6.20	4.05				
	30000.	6.49	4.11				
	50000.	6.86	3.71				

PERTURBER DENSITY= 0.1D+19(cm-3)

PERTURBERS ARE		ELECTRONS		PROTONS		IONIZED HELIUM	
TRANSITION	T(K)	WIDTH(A)	SHIFT(A)	WIDTH(A)	SHIFT(A)	WIDTH(A)	SHIFT(A)
3P - 3D	3000.	3.39	1.37				
3091.0 A	5000.	3.74	1.45				
C= 0.49E+20	10000.	4.00	1.48				
	20000.	3.96	1.41				
	30000.	3.88	1.29				
	50000.	3.75	1.13				
3P - 4D	3000.	*4.36	*1.75				
2601.0 A	5000.	*4.95	*2.58				
C= 0.12E+21	10000.	5.56	3.39				
	20000.	6.10	3.71				
	30000.	6.41	3.51				
	50000.	6.92	3.11				

(1979) has been used.

Our results are shown in Table 1 for perturber densities $10^{13} - 10^{14}$ cm^{-3}; $10^{16} - 10^{19}$ cm^{-3} and temperatures of T = 3,000; 5,000; 10,000; 20,000; 30,000 and 50,000 K. We also specify a parameter C (Dimitrijević and Sahal–Bréchot, 1984) which gives an estimate for the maximum perturber density for which the line may be treated as isolated when it is divided by the electron–impact full width at half maximum.

For each value given in Table 1, the collision volume (V) multiplied by the perturber density (N) is much less than one and the impact approximation is valid (Sahal–Bréchot, 1969 a b). Values for NV > 0.5 are not given in Table 1; values for 0.1 < NV ≤ 0.5 are denoted by an asterisk. When the impact approximation is not valid, the ion broadening contribution may be estimated by using quasistatic formulae (cf. Sahal–Bréchot (1991) or Griem (1974)).

The analysis of present results and comparison with available experimental and theoretical data is given in Dimitrijević and Sahal – Bréchot (1992).

Acknowledgments – This work is a part of French–Yugoslav collaboration through the project "L' élargissement Stark des raies spectrales des plasmas astrophysiques et de laboratoire". It is also a part of the project "Physics and dynamics of celestial bodies", supported by Ministry for Science and Technology of Serbia.

REFERENCES

Bashkin, S., and Stoner, J. O. Jr.: 1975, *Atomic Energy Levels and Grotrian Diagrams*, Vol. 1, North Holland, Amsterdam.

Bates, D. R., and Damgaard, A.: 1949, *Trans. Roy. Soc.* London, Ser. **A 242**, 101.

Dimitrijević, M. S., and Sahal–Bréchot, S.: 1984, *JQSRT* **31**, 301.

Dimitrijević, M. S., and Sahal–Bréchot, S.: 1992, *JQSRT*, to be published.

Goldberg, L., Muller, E. A., and Aller, H.: 1960, *Astrophys. J. Suppl. Series* **5**, 1.

Griem, H. R.: 1974, *Spectral Line Broadening by Plasmas*, Academic Press, New York.

Meril, P. W.: 1956, *Lines of the Chemical Elements in Astronomical Spectra*, Carnegie Institution of Washington, Publ. G10, Washington D. C.

Oertel, G. K., and Shomo, L. P.: 1968, *Astrophys. J. Suppl. Series* **16**, 175.

Sahal–Bréchot, S.: 1969 a, *Astron. Astrophys.* **1**, 91.

Sahal–Bréchot, S.: 1969 b, *Astron. Astrophys.* **2**, 322.

Sahal–Bréchot, S.: 1991, *Astron. Astrophys.* **245**, 322.

Van Regemorter, H., Hoang Binh Dy, and Prud'homme, M.: 1979, *J. Phys.* B **12**, 1073.

ТАБЕЛЕ ПАРАМЕТАРА ШТАРКОВОГ ШИРЕЊА ЛИНИЈА Al I ОД ЗНАЧАЈА У АСТРОФИЗИЦИ

М. С. Димитријевић[1] и S. Sahal-Bréchot[2]

[1]*Астрономска опсерваторија, Волгина 7, 11050 Београд, Југославија*

[2]*Laboratoire "Astrophysique, Atomes et Molécules"*
Département Atomes et Molécules en Astrophysique
Unité associée au C.N.R.S. No 812
Observatoire de Paris - Meudon, 92190 Meudon, France

УДК 52–355.3
Претходно саопштење

Користећи семикласичан прилаз, израчунате су ширине и помераји спектралних линија, проузроковани сударима са електронима, протонима и јонима хелијума, за 25 мултиплета неутралног алуминијума. Резултати су дати у функцији температуре и концентрације пертурбера.

Bull. Astron. Belgrade № 146 (1992), 97–104

UDC 52–355.3
Preliminary report

STARK BROADENING PARAMETER TABLES FOR Rb I LINES

M. S. Dimitrijević[1], and S. Sahal-Bréchot[2]

[1]*Astronomical Observatory, Volgina 7, 11050 Beograd, Yugoslavia*

[2]*Laboratoire "Astrophysique, Atomes et Molécules"*
Département Atomes et Molécules en Astrophysique
Unité associée au C.N.R.S. No 812
Observatoire de Paris - Meudon, 92190 Meudon, France

(Received: September 9, 1992)

SUMMARY: Using a semiclassical approach, we have calculated electron–, proton–, and ionized argon–impact line widths and shifts for 24 Rb I multiplets as a function of temperature for perturber densities 10^{14} and 10^{16}–10^{18}cm^{-3}.

1. INTRODUCTION

Rubidium lines have been observed in Solar and stellar spectra (see e.g. Merrill, 1945; Davis, 1947) and consequently their Stark broadening parameters are of interest to astrophysicists. Neutral Rubidium Stark-broadening parameters are of interest for laboratory plasma spectroscopy as well, and have been investigated several times (Lakićević et al, 1975; Purić et al, 1977; Dimitrijević and Konjević, 1983).

In order to provide reliable data for Rb I lines broadened by collisions with charged perturbers in stellar and laboratory plasmas, we have calculated electron–, proton– (for stellar plasma research) and ionized argon– (for laboratory plasma investigations) impact line widths and shifts for 24 Rb I multiplets, using the semiclassical–perturbation formalism (Sahal–Bréchot, 1969ab). The obtained results for perturber density of 10^{15}cm^{-3}, together with discussion, analysis and comparison with existing theoretical and experimental data will be published in the principal article elsewhere (Dimitrijević, and Sahal–Bréchot, 1993). Since data are not linear with perturber density (N), due to the Debye screening effect, we will present here the data for N $=10^{14}$ and 10^{16}– 10^{18}cm^{-3}.

2. RESULTS AND DISCUSSION

All details of the calculation procedure has been described in Dimitrijević and Sahal–Bréchot (1984) and will not be repeated here. Energy levels for Be II lines have been taken from Moore (1971). Oscillator strengths have been calculated using the

Table 1. This table gives electron–, proton–, and ionized–argon– impact broadening parameters for Rb I lines, for perturber densities 10^{14} and $10^{16} - 10^{18}$ cm^{-3} and temperatures from 2,500 K to 50,000 K. Transitions and averaged wavelengths for the multiplet (in Å) are also given. By dividing c by the electron–impact full halfwidth, we obtain an estimate for the maximum perturber density for which the line may be treated as isolated and tabulated data may be used. The asterisk identifies cases for which the collision volume multiplied by the perturber density (the condition for validity of the impact approximation) lies between 0.1 and 0.5.

PERTURBER DENSITY= 0.1E+15 cm-3

PERTURBERS ARE:		ELECTRONS		PROTONS		IONIZED ARGON	
TRANSITION	T(K)	WIDTH(A)	SHIFT(A)	WIDTH(A)	SHIFT(A)	WIDTH(A)	SHIFT(A)
4D - 8P	2500.	0.708E-01	0.502E-01	0.203E-01	0.125E-01	*0.170E-01	*0.685E-02
9529.3 A	5000.	0.797E-01	0.569E-01	0.215E-01	0.144E-01	*0.175E-01	*0.804E-02
C= 0.39E+17	10000.	0.885E-01	0.564E-01	0.229E-01	0.164E-01	*0.181E-01	*0.928E-02
	20000.	0.988E-01	0.450E-01	0.246E-01	0.186E-01	0.188E-01	0.106E-01
	30000.	0.107	0.375E-01	0.257E-01	0.200E-01	0.192E-01	0.114E-01
	50000.	0.116	0.298E-01	0.273E-01	0.218E-01	0.199E-01	0.125E-01
5P - 6D	2500.	0.129E-01	0.856E-02	0.364E-02	0.218E-02	*0.314E-02	*0.122E-02
6276.9 A	5000.	0.149E-01	0.917E-02	0.383E-02	0.249E-02	0.321E-02	0.141E-02
C= 0.23E+17	10000.	0.175E-01	0.863E-02	0.406E-02	0.282E-02	0.329E-02	0.161E-02
	20000.	0.210E-01	0.712E-02	0.433E-02	0.318E-02	0.340E-02	0.182E-02
	30000.	0.230E-01	0.615E-02	0.452E-02	0.341E-02	0.347E-02	0.196E-02
	50000.	0.249E-01	0.494E-02	0.478E-02	0.372E-02	0.357E-02	0.214E-02
6S - 8P	2500.	0.822E-01	0.582E-01	0.239E-01	0.145E-01	*0.202E-01	*0.793E-02
10292.8 A	5000.	0.926E-01	0.650E-01	0.252E-01	0.166E-01	*0.207E-01	*0.931E-02
C= 0.46E+17	10000.	0.104	0.642E-01	0.268E-01	0.190E-01	*0.214E-01	*0.107E-01
	20000.	0.117	0.501E-01	0.288E-01	0.215E-01	0.221E-01	0.123E-01
	30000.	0.127	0.408E-01	0.301E-01	0.231E-01	0.226E-01	0.132E-01
	50000.	0.138	0.331E-01	0.319E-01	0.252E-01	0.234E-01	0.145E-01
6P - 6D	2500.	0.126	0.805E-01	0.341E-01	0.208E-01	0.292E-01	0.116E-01
20344.9 A	5000.	0.151	0.767E-01	0.359E-01	0.236E-01	0.299E-01	0.134E-01
C= 0.24E+18	10000.	0.186	0.643E-01	0.381E-01	0.268E-01	0.307E-01	0.153E-01
	20000.	0.238	0.481E-01	0.408E-01	0.302E-01	0.317E-01	0.173E-01
	30000.	0.267	0.434E-01	0.425E-01	0.324E-01	0.324E-01	0.187E-01
	50000.	0.293	0.321E-01	0.450E-01	0.354E-01	0.334E-01	0.204E-01
6D - 7P	2500.	4.12	0.253	1.03	-0.126	1.02	-0.718E-01
120891.2 A	5000.	6.09	0.605	1.03	-0.142	1.03	-0.815E-01
C= 0.86E+19	10000.	8.58	0.863	1.03	-0.160	1.03	-0.921E-01
	20000.	11.3	0.788	1.03	-0.180	1.03	-0.104
	30000.	12.9	0.775	1.03	-0.193	1.03	-0.111
	50000.	14.4	0.795	1.03	-0.212	1.03	-0.121
6D - 8P	2500.	5.73	3.60	1.38	0.852	*1.17	*0.470
86166.8 A	5000.	6.96	3.59	1.46	0.978	*1.20	*0.549
C= 0.32E+19	10000.	8.57	3.41	1.56	1.11	*1.24	*0.632
	20000.	10.6	2.54	1.67	1.26	1.28	0.720
	30000.	11.8	2.11	1.75	1.35	1.31	0.776
	50000.	12.9	1.68	1.86	1.48	1.36	0.850

PERTURBER DENSITY= 0.1E+15 cm-3

PERTURBERS ARE:		ELECTRONS		PROTONS		IONIZED ARGON	
TRANSITION	T(K)	WIDTH(A)	SHIFT(A)	WIDTH(A)	SHIFT(A)	WIDTH(A)	SHIFT(A)
7S - 7P	2500.	1.05	0.664	0.350	0.166	*0.325	*0.933E-01
64519.9 A	5000.	1.26	0.620	0.360	0.188	0.329	0.107
C= 0.34E+19	10000.	1.59	0.547	0.373	0.214	0.333	0.122
	20000.	2.08	0.430	0.390	0.241	0.338	0.138
	30000.	2.39	0.376	0.401	0.258	0.341	0.148
	50000.	2.71	0.310	0.417	0.281	0.347	0.162
7S - 8P	2500.	0.608	0.430	0.176	0.104	*0.151	*0.571E-01
28267.4 A	5000.	0.689	0.435	0.186	0.120	*0.155	*0.670E-01
C= 0.35E+18	10000.	0.798	0.413	0.197	0.136	*0.159	*0.773E-01
	20000.	0.941	0.310	0.211	0.155	0.164	0.882E-01
	30000.	1.05	0.239	0.220	0.166	0.168	0.950E-01
	50000.	1.15	0.198	0.232	0.181	0.173	0.104
7P - 8S	2500.	2.02	0.919	0.577	0.234	*0.551	*0.132
84354.7 A	5000.	2.79	0.917	0.589	0.265	0.555	0.151
C= 0.57E+19	10000.	3.95	0.776	0.604	0.300	0.559	0.172
	20000.	5.46	0.622	0.622	0.338	0.564	0.195
	30000.	6.33	0.558	0.636	0.363	0.568	0.209
	50000.	7.29	0.436	0.655	0.395	0.574	0.228
8S - 8P	2500.	10.8	6.40	3.17	1.63	*2.86	*0.902
124647.9 A	5000.	13.4	6.51	3.30	1.87	*2.91	*1.05
C= 0.67E+19	10000.	16.9	5.01	3.45	2.13	*2.96	*1.21
	20000.	22.0	3.70	3.63	2.41	3.03	1.38
	30000.	24.9	2.94	3.76	2.59	3.07	1.48
	50000.	27.7	1.81	3.94	2.83	3.14	1.63

PERTURBER DENSITY= 0.1E+17 cm-3

4D - 5P	2500.	0.367	0.122	0.122	0.309E-01	*0.117	*0.170E-01
15156.1 A	5000.	0.403	0.150	0.123	0.356E-01	*0.120	*0.199E-01
C= 0.10E+21	10000.	0.479	0.149	0.124	0.405E-01	0.121	0.230E-01
	20000.	0.616	0.143	0.126	0.460E-01	0.122	0.262E-01
	30000.	0.722	0.123	0.127	0.494E-01	0.122	0.283E-01
	50000.	0.872	0.102	0.128	0.539E-01	0.122	0.310E-01
4D - 6P	2500.	4.29	2.74	*1.31	*0.620		
22634.0 A	5000.	4.91	3.35	*1.39	*0.762		
C= 0.99E+20	10000.	5.51	3.56	1.47	0.903		
	20000.	6.29	3.44	1.56	1.05	*1.26	*0.581
	30000.	6.82	3.02	1.62	1.14	*1.28	*0.636
	50000.	7.68	2.57	1.71	1.25	*1.32	*0.707
4D - 7P	2500.	4.03	2.60				
11756.1 A	5000.	4.61	3.19				
C= 0.11E+20	10000.	5.13	3.19	*1.36	*0.811		
	20000.	5.73	3.00	*1.46	*0.973		
	30000.	6.20	2.70	*1.52	*1.07		
	50000.	6.82	2.19	*1.61	*1.19		

PERTURBER DENSITY= 0.1E+17 cm-3

PERTURBERS ARE:		ELECTRONS		PROTONS		IONIZED ARGON	
TRANSITION	T(K)	WIDTH(A)	SHIFT(A)	WIDTH(A)	SHIFT(A)	WIDTH(A)	SHIFT(A)
4D - 8P	2500.	7.07	4.25				
9529.3 A	5000.	7.96	5.18				
C= 0.39E+19	10000.	8.85	5.36				
	20000.	9.88	4.41				
	30000.	10.7	3.69				
	50000.	11.6	2.97				
5S - 6P	2500.	0.141	0.942E-01	*0.495E-01	*0.216E-01		
4206.4 A	5000.	0.162	0.113	*0.523E-01	*0.266E-01		
C= 0.34E+19	10000.	0.182	0.123	0.549E-01	0.315E-01		
	20000.	0.206	0.121	0.578E-01	0.366E-01	*0.483E-01	*0.203E-01
	30000.	0.222	0.106	0.598E-01	0.396E-01	*0.491E-01	*0.222E-01
	50000.	0.248	0.897E-01	0.626E-01	0.437E-01	*0.502E-01	*0.247E-01
5S - 7P	2500.	0.370	0.237				
3589.2 A	5000.	0.424	0.297				
C= 0.11E+19	10000.	0.472	0.298	*0.130	*0.757E-01		
	20000.	0.527	0.277	*0.139	*0.908E-01		
	30000.	0.568	0.240	*0.144	*0.997E-01		
	50000.	0.623	0.205	*0.152	*0.111		
5S - 8P	2500.	0.869	0.526				
3350.2 A	5000.	0.979	0.641				
C= 0.48E+18	10000.	1.09	0.663				
	20000.	1.21	0.548				
	30000.	1.31	0.463				
	50000.	1.42	0.372				
5P - 5D	2500.	0.620	0.398	*0.175	*0.859E-01		
7724.8 A	5000.	0.694	0.428	*0.187	*0.107		
C= 0.65E+19	10000.	0.806	0.413	0.199	0.128		
	20000.	0.977	0.331	0.213	0.148	*0.167	*0.819E-01
	30000.	1.09	0.291	0.222	0.161	*0.171	*0.899E-01
	50000.	1.21	0.258	0.235	0.178	*0.176	*0.100
5P - 6D	2500.	1.28	0.803				
6276.9 A	5000.	1.48	0.858				
C= 0.23E+19	10000.	1.75	0.831	*0.401	*0.239		
	20000.	2.10	0.655	*0.431	*0.287		
	30000.	2.31	0.575	*0.450	*0.316		
	50000.	2.52	0.459	*0.476	*0.352		
6S - 6P	2500.	5.27	3.03	*1.98	*0.708		
27474.6 A	5000.	6.04	3.22	*2.06	*0.858		
C= 0.15E+21	10000.	7.51	3.06	2.13	1.01		
	20000.	9.69	2.22	2.20	1.16	*1.98	*0.650
	30000.	11.3	1.89	2.25	1.26	*2.00	*0.709
	50000.	13.3	1.71	2.32	1.39	*2.02	*0.786

PERTURBER DENSITY= 0.1E+17 cm-3

PERTURBERS ARE:		ELECTRONS		PROTONS		IONIZED ARGON	
TRANSITION	T(K)	WIDTH(A)	SHIFT(A)	WIDTH(A)	SHIFT(A)	WIDTH(A)	SHIFT(A)
6S - 7P	2500.	4.77	3.05				
12940.3 A	5000.	5.46	3.62				
C= 0.14E+20	10000.	6.19	3.73	*1.65	*0.952		
	20000.	7.07	3.05	*1.77	*1.14		
	30000.	7.82	2.70	*1.84	*1.25		
	50000.	8.72	2.28	*1.94	*1.39		
6S - 8P	2500.	8.20	4.94				
10292.8 A	5000.	9.25	5.88				
C= 0.46E+19	10000.	10.3	6.05				
	20000.	11.7	4.86				
	30000.	12.7	3.98				
	50000.	13.8	3.30				
6P - 8S	2500.	12.8	8.11				
18962.7 A	5000.	14.4	9.96				
C= 0.29E+20	10000.	16.9	10.3	*3.30	*2.51		
	20000.	19.9	8.52	*3.68	*3.04		
	30000.	22.8	7.22	*3.93	*3.34		
	50000.	26.2	6.44	*4.27	*3.73		
6P - 6D	2500.	12.6	7.32				
20344.9 A	5000.	15.1	7.23				
C= 0.24E+20	10000.	18.6	6.25	*3.78	*2.31		
	20000.	23.8	4.78	*4.07	*2.76		
	30000.	26.7	4.32	*4.25	*3.03		
	50000.	29.3	3.20	*4.50	*3.37		
PERTURBER DENSITY= 0.1E+18 cm-3							
4D - 5P	2500.	3.67	1.17	*1.15	*0.264		
15156.1 A	5000.	4.03	1.47	1.21	0.324		
C= 0.10E+22	10000.	4.78	1.47	1.23	0.383		
	20000.	6.16	1.42	1.25	0.443	*1.20	*0.246
	30000.	7.22	1.23	1.26	0.480	*1.21	*0.269
	50000.	8.72	1.02	1.28	0.529	*1.22	*0.299
5S - 5P	2500.	0.722	0.422	*0.306	*0.922E-01		
7838.7 A	5000.	0.782	0.517	0.323	0.115		
C= 0.41E+21	10000.	0.877	0.527	0.333	0.138		
	20000.	1.09	0.457	0.343	0.160	*0.316	*0.883E-01
	30000.	1.26	0.377	0.349	0.174	*0.319	*0.970E-01
	50000.	1.54	0.297	0.358	0.192	*0.322	*0.108
5S - 6P	2500.	1.41	0.819				
4206.4 A	5000.	1.62	1.04				
C= 0.34E+20	10000.	1.82	1.17				
	20000.	2.06	1.17				
	30000.	2.22	1.03	*0.595	*0.361		
	50000.	2.48	0.884	*0.625	*0.409		

PERTURBER DENSITY= 0.1E+18 cm-3

PERTURBER SARE:		ELECTRONS		PROTONS		IONIZED ARGON	
TRANSITION	T(K)	WIDTH(A)	SHIFT(A)	WIDTH(A)	SHIFT(A)	WIDTH(A)	SHIFT(A)
5S - 7P	2500.	*3.66	*1.75				
3589.2 A	5000.	4.23	2.53				
C= 0.11E+20	10000.	4.72	2.67				
	20000.	5.26	2.56				
	30000.	5.68	2.26				
	50000.	6.23	1.98				
5S - 8P	2500.						
3350.2 A	5000.	*9.54	*4.66				
C= 0.48E+19	10000.	*10.7	*5.39				
	20000.	12.0	4.65				
	30000.	13.1	4.04				
	50000.	14.1	3.44				
5P - 6S	2500.	6.89	4.20	*1.55	*.728		
13556.7 A	5000.	7.92	5.32	*1.75	*1.06		
C= 0.67E+21	10000.	8.89	6.45	*1.93	*1.37		
	20000.	10.3	6.48	*2.14	*1.66		
	30000.	11.2	5.80	2.26	1.83		
	50000.	12.9	4.87	2.44	2.04	*1.57	*1.12
5P - 7S	2500.	7.48	4.15				
7377.7 A	5000.	8.59	5.46				
C= 0.84E+20	10000.	9.28	6.29				
	20000.	10.4	6.44				
	30000.	11.0	5.82				
	50000.	12.6	5.01	*2.61	*2.17		
5P - 8S	2500.	*14.0	*6.32				
6138.9 A	5000.	*16.4	*9.27				
C= 0.30E+20	10000.	17.1	9.99				
	20000.	19.1	9.85				
	30000.	21.0	8.97				
	50000.	23.8	7.50				
5P - 5D	2500.	6.19	3.42				
7724.8 A	5000.	6.94	3.88				
C= 0.65E+20	10000.	8.06	3.89				
	20000.	9.77	3.20				
	30000.	10.9	2.83	*2.21	*1.45		
	50000.	12.1	2.56	*2.35	*1.65		
5P - 6D	2500.	*12.6	*5.99				
6276.9 A	5000.	14.7	7.12				
C= 0.23E+20	10000.	17.4	7.29				
	20000.	21.0	6.19				
	30000.	23.1	5.46				
	50000.	25.2	4.53				

PERTURBER DENSITY= 0.1E+19 cm-3

PERTURBERS ARE:		ELECTRONS		PROTONS		IONIZED ARGON	
TRANSITION	T(K)	WIDTH(A)	SHIFT(A)	WIDTH(A)	SHIFT(A)	WIDTH(A)	SHIFT(A)
5S - 5P	2500.	7.17	3.61				
7838.7 A	5000.	7.81	4.75				
C= 0.41E+22	10000.	8.76	4.97				
	20000.	10.9	4.35	*3.35	*1.39		
	30000.	12.6	3.61	*3.45	*1.56		
	50000.	15.4	2.90	*3.56	*1.78		
5S - 6P	2500.	*13.2	*4.14				
4206.4 A	5000.	*16.0	*7.52				
C= 0.34E+21	10000.	18.1	9.68				
	20000.	20.6	10.3				
	30000.	22.2	9.29				
	50000.	24.7	8.39				

method of Bates and Damgaard (1949) and tables of Oertel and Shomo (1968). For the transitions including higher atomic energy levels, the method described by Van Regemorter et al. (1979) has been used.

Our results are shown in Table 1 for perturber densities 10^{14} and $10^{16} - 10^{18}$ cm^{-3} and temperatures of T = 2,500; 5,000; 10,000; 20,000; 30,000 and 50,000 K. We also specify a parameter c (Dimitrijević and Sahal–Bréchot, 1984) which gives an estimate for the maximum perturber density for which the line may be treated as isolated when it is divided by the electron–impact full width at half maximum. The presented data, together with the data published in the principal article (Dimitrijević and Sahal–Bréchot, 1993) enable a good interpolation for densities when a departure from the linear behaviour with N exists.

For each value given in Table 1, the collision volume (V) multiplied by the perturber density (N) is much less than one and the impact approximation is valid (Sahal–Bréchot, 1969 a b). Values for NV > 0.5 are not given in Table 1; values for $0.1 <$ NV ≤ 0.5 are denoted by an asterisk. When the impact approximation is not valid, the ion broadening contribution may be estimated by using quasistatic formulae (cf. Sahal–Bréchot (1991) or Griem (1974)).

The analysis of present results and comparison with available experimental and theoretical data is given in Dimitrijević and Sahal – Bréchot (1992 b).

Acknowledgments – This work is a part of French–Yugoslav collaboration through the project "L'elargissement Stark des raies spectrales des plasmas astrophysiques et de laboratoire". It is also a part of the project "Physics and dynamics of celestial bodies", supported by Ministry for Science and Technology of Serbia.

REFERENCES

Bates, D. R., and Damgaard, A.: 1949, *Trans. Roy. Soc. London, Ser.* **A 242**, 101.
Davis, D. N.: 1947, *Astrophys. J.* **106**, 28.
Dimitrijević, M. S., and Konjević, N.: 1983, *JQSRT* **30**, 45.
Dimitrijević, M. S., and Sahal–Bréchot, S.: 1984, *JQSRT* **31**, 301.
Dimitrijević, M. S., and Sahal–Bréchot, S.: 1993, *JQSRT*, to be published.
Griem, H. R.: 1974, *Spectral Line Broadening by Plasmas*, Academic Press, New York.
Lakićević, I., Purić, J. and Labat, J.: 1977, *Proc. of the XIII Int. Conf. Phen. Ioniz. Gases*, Part I, Physical Society of GDR, Berlin, p. 123.
Merrill, P. M.: 1956, *Lines of the Chemical Elements in Astronomical Spectra*, Carnegie Institution of Washington Publ. 610, Washington D. C.
Moore,C.: 1971, *Atomic Energy Levels III, NSRDS-NBS* **35** U. S. Govt. Printing Office, Washington D.C.
Oertel, G. K., and Shomo, L. P.: 1968, *Astrophys. J. Suppl. Series* **16**, 175.
Purić, J., Labat, J., Ćirković, Lj., Lakićević, I., and Djeniže, S.: 1977, *J. Phys* **B 10**, 2375.
Sahal–Bréchot, S.: 1969 a, *Astron. Astrophys.* **1**, 91.
Sahal–Bréchot, S.: 1969b, *Astron. Astrophys.* **2**, 322.
Sahal–Bréchot, S.: 1991, *Astron. Asirophys.* **245**, 322.
Van Regemorter, H., Hoang Binh Dy, and Prud'homme, M.: 1979, *J. Phys.* **B 12**, 1073.

ТАБЕЛЕ ПАРАМЕТАРА ШТАРКОВОГ ШИРЕЊА ЛИНИЈА Rb I

М. С. Димитријевић[1] и S. Sahal-Bréchot[2]

[1]*Астрономска опсерваторија, Волгина 7, 11050 Београд, Југославија*

[2]*Laboratoire "Astrophysique, Atomes et Molécules"*
Département Atomes et Molécules en Astrophysique
Unité associée au C.N.R.S. No 812
Observatoire de Paris - Meudon, 92190 Meudon, France

УДК 52–355.3
Претходно саопштење

Користећи семикласичан прилаз, израчунате су ширине и помераји спектралних линија, проузроковани сударима са електронима, протонима и јонима аргона, за 24 мултиплета неутралног рубидијума. Резултати су дати у функцији температуре и концентрације пертурбера.

Bull. Astron. Belgrade № 147 (1993), 35 – 40

UDC 52–355.3
Preliminary report

STARK BROADENING PARAMETER TABLES FOR Al III LINES

M. S. Dimitrijević[1], and S. Sahal–Bréchot[2]

[1]*Astronomical Observatory, Volgina 7, 11050 Beograd, Yugoslavia*

[2] *Laboratoire "Astrophysique, Atomes et Molécules" Département Atomes et Molécules en Astrophysique Unité associée au C. N. R. S. No 812 Observatoire de Paris–Meudon, 92190 Meudon, France*

(Received: October 12, 1992)

SUMMARY: Using a semiclassical approach, we have calculated electron–, proton–, and ionized helium–impact line widths and shifts for 13 Al III multiplets as a function of temperature for perturber densities 10^{17} - 10^{19} cm^{-3}.

1. INTRODUCTION

Absorption lines of Al III are very strong in hot star atmospheres (see e. g. Struve, 1930), where Stark broadening is the principal pressure broadening mechanisme. Moreover, results presented may be used for the diagnostic and modelling of an electrodynamic macro-particle accelerator arc plasma created by the evaporation of an Al-foil (see e. g. Rasheigh and Marshall, 1978; or Rolader and Batteh, 1989) and for spectroscopy of laboratory plasma (Davis and Morin, 1971).

In order to provide reliable data for Al III lines broadened by collisions with charged perturbers in stellar and laboratory plasmas, we have calculated recently electron–, proton– and ionized helium–impact line widths and shifts for 23 Al III multiplets, using the semiclassical–perturbation formalism (Sahal–Bréchot, 1969ab). The obtained results for perturber density of $10^{15} cm^{-3}$, together with discussion, analysis and comparison with existing theoretical and experimental data will be published in the principal article elsewhere (Dimitrijević, and Sahal–Bréchot, 1993). Since data are not linear with perturber density (N), due to the Debye screening effect, we will present here the data for N = 10^{17} – 10^{19} cm^{-3}, for 13 Al III multiplets. Additional data for 9 low lying multiplets for perturber densities of 10^{17} – 10^{20} cm^{-3} may be found in the article of Dimitrijević et al (1993) devoted to the diagnostic and modelling of an electrodynamic macro-particle accelerator arc plasma

2. RESULTS AND DISCUSSION

Energy levels for Al III lines have been taken from Bashkin and Stoner (1975). Oscillator strengths have been calculated by using the method of Bates and Damgaard (1949) and the tables of Oertel and Shomo (1968). For higher levels, the method described by Van Regemorter et al. (1979) has been

Table 1. This table gives electron–, proton–, and ionized–argon– impact broadening parameters for Al III lines, for perturber densities of 10^{17} - 10^{19} cm^{-3} and temperatures from 10,000 K to 500,000 K. Transitions and averaged wavelengths for the multiplet (in Å) are also given. By dividing c by the electron–impact full halfwidth, we obtain an estimate for the maximum perturber density for which the line may be treated as isolated and tabulated data may be used. The asterisk identifies cases for which the collision volume multiplied by the perturber density (the condition for validity of the impact approximation) lies between 0.1 and 0.5.

PERTURBER DENSITY = 0.1E+18 cm-3

PERTURBERS ARE:		ELECTRONS		PROTONS		IONIZED HELIUM	
TRANSITION	T(K)	WIDTH(A)	SHIFT(A)	WIDTH(A)	SHIFT(A)	WIDTH(A)	SHIFT(A)
ALIII 3S-5P	10000.	0.208E-01	0.131E-02	0.172E-02	0.154E-03	*0.207E-02	*0.142E-03
560.4 A	20000.	0.166E-01	0.843E-03	0.230E-02	0.268E-03	*0.248E-02	*0.229E-03
C= 0.25E+19	50000.	0.139E-01	0.797E-03	0.271E-02	0.421E-03	0.289E-02	0.345E-03
	100000.	0.128E-01	0.755E-03	0.297E-02	0.505E-03	0.304E-02	0.417E-03
	200000.	0.119E-01	0.651E-03	0.310E-02	0.601E-03	0.312E-02	0.489E-03
	500000.	0.106E-01	0.575E-03	0.317E-02	0.714E-03	0.318E-02	0.558E-03
ALIII 3P-5S	10000.	0.411E-01	0.200E-01	0.118E-02	0.176E-02	0.114E-02	0.147E-02
856.2 A	20000.	0.316E-01	0.148E-01	0.217E-02	0.268E-02	0.208E-02	0.221E-02
C= 0.57E+19	50000.	0.259E-01	0.112E-01	0.360E-02	0.368E-02	0.305E-02	0.304E-02
	100000.	0.230E-01	0.873E-02	0.455E-02	0.442E-02	0.382E-02	0.360E-02
	200000.	0.202E-01	0.696E-02	0.559E-02	0.508E-02	0.447E-02	0.417E-02
	500000.	0.169E-01	0.511E-02	0.690E-02	0.602E-02	0.515E-02	0.510E-02
ALIII 3P-5D	10000.	0.769E-01	0.135E-01	*0.732E-02	*0.563E-02		
740.5 A	20000.	0.661E-01	0.122E-01	*0.983E-02	*0.789E-02	*0.872E-02	*0.626E-02
C= 0.55E+18	50000.	0.560E-01	0.108E-01	*0.128E-01	*0.114E-01	*0.108E-01	*0.907E-02
	100000.	0.497E-01	0.926E-02	*0.157E-01	*0.131E-01	*0.138E-01	*0.106E-01
	200000.	0.436E-01	0.728E-02	0.168E-01	0.147E-01	*0.146E-01	*0.117E-01
	500000.	0.356E-01	0.532E-02	0.198E-01	0.187E-01	*0.185E-01	*0.131E-01
ALIII 3D-5P	10000.	0.169	0.653E-02	0.129E-01	0.120E-02	*0.157E-01	*0.111E-02
1600.0 A	20000.	0.135	0.609E-02	0.175E-01	0.210E-02	*0.188E-01	*0.180E-02
C= 0.20E+20	50000.	0.113	0.600E-02	0.206E-01	0.331E-02	0.219E-01	0.272E-02
	100000.	0.105	0.567E-02	0.226E-01	0.397E-02	0.232E-01	0.331E-02
	200000.	0.978E-01	0.495E-02	0.239E-01	0.475E-02	0.239E-01	0.389E-02
	500000.	0.871E-01	0.438E-02	0.249E-01	0.565E-02	0.244E-01	0.447E-02
ALIII 3D-5F	10000.	0.390	-0.157E-01				
1352.8 A	20000.	0.326	-0.835E-02				
C= 0.96E+17	50000.	0.259	0.534E-02				
	100000.	0.217	0.266E-02				
	200000.	0.180	0.276E-02				
	500000.	0.138	-0.123E-02				
ALIII 4S-5P	10000.	0.271	0.154E-02	0.200E-01	0.111E-03	*0.241E-01	*0.111E-03
1912.3 A	20000.	0.216	0.131E-03	0.267E-01	0.237E-03	*0.288E-01	*0.230E-03
C= 0.29E+20	50000.	0.183	0.746E-03	0.315E-01	0.508E-03	0.335E-01	0.456E-03
	100000.	0.171	0.184E-03	0.344E-01	0.727E-03	0.355E-01	0.630E-03
	200000.	0.159	0.117E-03	0.356E-01	0.924E-03	0.363E-01	0.770E-03
	500000.	0.141	0.938E-04	0.369E-01	0.118E-02	0.372E-01	0.974E-03
ALIII 4P-5S	10000.	0.907	0.335	0.300E-01	0.321E-01	0.318E-01	0.269E-01
3710.5 A	20000.	0.710	0.241	0.499E-01	0.489E-01	0.499E-01	0.405E-01
C= 0.11E+21	50000.	0.599	0.183	0.745E-01	0.676E-01	0.671E-01	0.556E-01
	100000.	0.549	0.144	0.926E-01	0.811E-01	0.807E-01	0.656E-01
	200000.	0.498	0.113	0.110	0.921E-01	0.912E-01	0.752E-01
	500000.	0.428	0.848E-01	0.129	0.111	0.100	0.910E-01

PERTURBER DENSITY = 0.1E+18 cm-3

PERTURBERS ARE:		ELECTRONS		PROTONS		IONIZED	HELIUM
TRANSITION	T(K)	WIDTH(A)	SHIFT(A)	WIDTH(A)	SHIFT(A)	WIDTH(A)	SHIFT(A)
ALIII 4P-5D	10000.	0.720	0.893E-01	*0.628E-01	*0.501E-01	*0.587E-01	*0.383E-01
2212.8 A	20000.	0.617	0.875E-01	*0.853E-01	*0.703E-01	*0.749E-01	*0.556E-01
C= 0.49E+19	50000.	0.524	0.880E-01	*0.111	*0.101	*0.943E-01	*0.805E-01
	100000.	0.468	0.752E-01	*0.138	*0.117	*0.119	*0.941E-01
	200000.	0.412	0.609E-01	0.148	0.131	*0.129	*0.104
	500000.	0.338	0.440E-01	0.173	0.167	*0.165	*0.117
ALIII 4D-5P	10000.	5.92	-0.115	0.287	-0.154	*0.340	*-0.129
7891.9 A	20000.	4.82	-0.166	0.414	-0.233	*0.426	*-0.193
C= 0.11E+21	50000.	4.06	-0.151	0.517	-0.321	0.512	-0.263
	100000.	3.72	-0.132	0.608	-0.385	0.566	-0.313
	200000.	3.38	-0.103	0.662	-0.439	0.618	-0.366
	500000.	2.91	-0.598E-01	0.735	-0.516	0.692	-0.445
ALIII 4D-5F	10000.	4.16	-0.223				
4151.2 A	20000.	3.47	-0.163				
C= 0.90E+18	50000.	2.78	-0.301E-01				
	100000.	2.34	-0.491E-01				
	200000.	1.95	-0.356E-01				
	500000.	1.50	-0.576E-01				
ALIII 4F-5D	10000.	3.69	0.537	*0.297	*0.241		
4702.6 A	20000.	3.11	0.451	*0.403	*0.336	*0.353	*0.271
C= 0.22E+20	50000.	2.59	0.444	*0.543	*0.490	*0.465	*0.401
	100000.	2.29	0.378	*0.639	*0.548	*0.565	*0.430
	200000.	1.99	0.305	0.722	0.633	*0.573	*0.503
	500000.	1.61	0.218	0.873	0.812	*0.745	*0.573
ALIII 5S-5P	10000.	14.4	-2.58	0.932	-0.346	*1.10	*-0.290
12786.7 A	20000.	11.9	-1.82	1.26	-0.528	*1.33	*-0.441
C= 0.13E+22	50000.	10.8	-1.40	1.53	-0.733	*1.58	*-0.608
	100000.	10.4	-1.22	1.71	-0.872	1.70	-0.708
	200000.	9.80	-1.03	1.87	-1.02	1.77	-0.816
	500000.	8.67	-0.765	2.02	-1.21	1.81	-0.962
ALIII 5P-5D	10000.	15.0	1.42	*1.16	*0.933	*1.09	*0.714
9597.1 A	20000.	12.9	1.45	*1.58	*1.31	*1.39	*1.03
C= 0.92E+20	50000.	11.3	1.48	*2.03	*1.87	*1.77	*1.50
	100000.	10.3	1.26	*2.52	*2.17	*2.23	*1.76
	200000.	9.29	1.01	2.72	2.41	*2.41	*1.96
	500000.	7.76	0.715	3.15	3.12	*3.04	*2.20

PERTURBER DENSITY = 0.1E+19 cm-3

ALIII 3S-5P	10000.	0.208	0.124E-01	*0.145E-01	*0.114E-02		
560.4 A	20000.	0.166	0.795E-02	*0.217E-01	*0.233E-02		
C= 0.25E+20	50000.	0.139	0.758E-02	*0.269E-01	*0.395E-02		
	100000.	0.128	0.751E-02	*0.298E-01	*0.494E-02		
	200000.	0.119	0.647E-02	*0.310E-01	*0.599E-02	*0.312E-01	*0.487E-02
	500000.	0.106	0.575E-02	0.317E-01	0.714E-02	*0.318E-01	*0.558E-02

PERTURBER DENSITY = 0.1E+19 cm-3

PERTURBERS ARE:		ELECTRONS		PROTONS		IONIZED	HELIUM
TRANSITION	T(K)	WIDTH(A)	SHIFT(A)	WIDTH(A)	SHIFT(A)	WIDTH(A)	SHIFT(A)
ALIII 3P-5S	10000.	0.411	0.192	*0.117E-01	*0.114E-01	*0.110E-01	*0.857E-02
856.2 A	20000.	0.316	0.142	*0.216E-01	*0.214E-01	*0.209E-01	*0.167E-01
C= 0.57E+20	50000.	0.259	0.108	*0.354E-01	*0.330E-01	*0.304E-01	*0.265E-01
	100000.	0.230	0.860E-01	*0.462E-01	*0.425E-01	*0.384E-01	*0.341E-01
	200000.	0.202	0.692E-01	*0.559E-01	*0.504E-01	*0.447E-01	*0.413E-01
	500000.	0.169	0.511E-01	0.690E-01	0.602E-01	*0.515E-01	*0.510E-01
ALIII 3P-5D	10000.	0.756	0.805E-01				
740.5 A	20000.	0.653	0.839E-01				
C= 0.55E+19	50000.	0.555	0.837E-01				
	100000.	0.494	0.825E-01				
	200000.	0.433	0.709E-01				
	500000.	0.354	0.532E-01				
ALIII 3D-5P	10000.	1.69	0.599E-01	*0.109	*0.888E-02		
1600.0 A	20000.	1.35	0.573E-01	*0.166	*0.183E-01		
C= 0.20E+21	50000.	1.13	0.569E-01	*0.204	*0.311E-01		
	100000.	1.05	0.563E-01	*0.226	*0.388E-01		
	200000.	0.978	0.492E-01	*0.238	*0.473E-01	*0.238	*0.387E-01
	500000.	0.871	0.438E-01	0.249	0.565E-01	*0.244	*0.447E-01
ALIII 3D-5F	10000.	3.09	-0.109				
1352.8 A	20000.	2.69	-0.943E-01				
C= 0.96E+18	50000.	2.23	-0.711E-01				
	100000.	1.92	-0.365E-01				
	200000.	1.62	-0.163E-02				
	500000.	1.27	-0.123E-01				
ALIII 4S-5P	10000.	2.71	0.139E-01	*0.168	*0.845E-03		
1912.3 A	20000.	2.16	0.168E-02	*0.253	*0.214E-02		
C= 0.29E+21	50000.	1.83	0.652E-02	*0.311	*0.491E-02		
	100000.	1.71	0.259E-02	*0.344	*0.719E-02		
	200000.	1.59	0.908E-03	*0.356	*0.923E-02	*0.363	*0.769E-02
	500000.	1.41	0.938E-03	0.369	0.118E-01	*0.372	*0.974E-02
ALIII 4P-5S	10000.	9.07	*3.19	*0.283	0.209	0.286	0.157
3710.5 A	20000.	7.10	*2.31	*0.489	0.391	0.487	0.308
C= 0.11E+22	50000.	5.99	*1.76	*0.729	0.597	0.662	0.482
	100000.	5.49	*1.42	*0.933	0.784	0.814	0.625
	200000.	4.98	*1.12	*1.10	0.915	0.912	0.747
	500000.	4.28	0.848	1.29	1.11	1.00	0.910
ALIII 4P-5D	10000.	7.08	0.408				
2212.8 A	20000.	6.10	0.540				
C= 0.49E+20	50000.	5.19	0.662				
	100000.	4.65	0.663				
	200000.	4.10	0.592				
	500000.	3.37	0.440				

PERTURBER DENSITY = 0.1E+20 cm-3

PERTURBERS ARE:		ELECTRONS		PROTONS		IONIZED	HELIUM
TRANSITION	T(K)	WIDTH(A)	SHIFT(A)	WIDTH(A)	SHIFT(A)	WIDTH(A)	SHIFT(A)
ALIII 3S-5P	10000.	*2.07	*0.105				
560.4 A	20000.	1.66	0.680E-01				
C= 0.25E+21	50000.	1.39	0.688E-01				
	100000.	1.28	0.696E-01				
	200000.	1.19	0.626E-01				
	500000.	1.06	0.570E-01				
ALIII 3P-5S	10000.	*4.10	*1.57				
856.2 A	20000.	3.15	1.21				
C= 0.57E+21	50000.	2.58	0.954				
	100000.	2.30	0.778				
	200000.	2.02	0.654				
	500000.	1.69	0.504				
ALIII 3P-5D	10000.	*5.71					
740.5 A	20000.	*5.30					
C= 0.55E+20	50000.	4.86	0.273				
	100000.	4.49	0.426				
	200000.	4.02	0.489				
	500000.	3.34	0.493				
ALIII 3D-5P	10000.	*16.8	*0.449				
1600.0 A	20000.	*13.5	*0.484				
C= 0.20E+22	50000.	11.3	0.515				
	100000.	10.5	0.521				
	200000.	9.78	0.476				
	500000.	8.71	0.434				

used.

Our results are shown in Table 1 for perturber densities of $10^{17} - 10^{19}$ cm^{-3} and temperatures of T = 10,000; 20,000; 50,000; 100,000; 200,000; and 500,000 K. We also specify a parameter c (Dimitrijević and Sahal–Bréchot, 1984) which gives an estimate for the maximum perturber density for which the line may be treated as isolated when it is divided by the electron–impact full width at half maximum. The presented data, together with the data for a perturber density of 10^{15} cm^{-3} published in the principal article (Dimitrijević and Sahal–Bréchot, 1993, where data for 23 Al III multiplets have been presented) and data for the 9 low lying multiplets, for perturber densities $10^{17} - 10^{20}$ cm^{-3} (Dimitrijević et al, 1993) enable in all cases of interest a good interpolation for densities when a departure from the linear behaviour with N exists.

For each value given in Table 1, the collision volume (V) multiplied by the perturber density (N) is much less than one and the impact approximation is valid (Sahal–Bréchot, 1969ab). Values for NV > 0.5 are not given in Table 1; values for 0.1 < NV ≤ 0.5 are denoted by an asterisk. When the impact approximation is not valid, the ion broadening contribution may be estimated by using quasistatic formulae (cf. Sahal–Bréchot (1991) or Griem (1974)).

The analysis of present results and comparison with available experimental and theoretical data is given in Dimitrijević and Sahal – Bréchot (1993).

Acknowledgments – This work is a part of French–Yugoslav collaboration through the project L'élargissement Stark des raies spectrales des plasmas astrophysiques et de laboratoire". It is also a part of the project "Physics and dynamics of celestial bodies", supported by Ministry for Science and Technology of Serbia.

REFERENCES

Bashkin, S., and Stoner, J. O. Jr.: 1975, Atomic Energy Levels and Grotrian Diagrams, Vol. 1, North Holland, Amsterdam.

Bates, D. R., and Damgaard, A.: 1949, Trans. Roy. Soc. London, Ser. A **242**, 101.

Davis, J., and Morin, S.: 1971, JQSRT **11**, 495.

Dimitrijević, M. S., Djurić, Z., and Mihajlov, A.: 1993, JQSRT, to be published.

Dimitrijević, M. S., and Sahal–Bréchot, S.: 1984, JQSRT 31, 301.

Dimitrijević, M. S., and Sahal–Bréchot, S.: 1993, Astron. Astrophys. Suppl. Series, to be published.

Griem, H. R.: 1974, Spectral Line Broadening by Plasmas, Academic Press, New York and London.

Oertel, G. K., and Shomo, L. P.: 1968, Astrophys. J. Suppl. Series 16, 175.

Rasheigh, S. C., and Marshall, R. A.: 1978, J. Appl. Phys. **49**, 2540.

Rolader, G. E., and Batteh, J. H.: 1989, IEEE Transactions on Plasma Sci. 17439.

Sahal–Bréchot, S.: 1969a, Astron. Astrophys. 1, 91.

Sahal–Bréchot, S.: 1969b, Astron. Astrophys. 2, 322.

Sahal–Bréchot, S.: 1991, Astron. Astrophys. 245, 322.

Struve, O.: 1930, Astrophys. J. **71**, 671.

Van Regemorter, H., Hoang Binh Dy, and Prud'homme, M.: 1979, J. Phys. B **12**, 1073.

ТАБЕЛЕ ПАРАМЕТАРА ШТАРКОВОГ ШИРЕЊА ЛИНИЈА Al III

М. С. Димитријевић[1] и S. Sahal-Bréchot[2]

[1]*Астрономска опсерваторија, Волгина 7, 11050 Београд, Југославија*

[2]*Laboratoire "Astrophysique, Atomes et Molécules" Département Atomes et Molécules en Astrophysique Unité associée au C. N. R. S. No 812 Observatoire de Paris-Meudon, 92190 Meudon, France*

УДК 52–355.3
Претходно саопштење

Користећи семикласичан прилаз, израчунате су ширине и помераји спектралних линија, проузроковани сударима са електронима, протонима и јонима хелијума, за 13 мултиплета Al III. Резултати су дати у функцији температуре и концентрације пертурбера.

Bull. Astron. Belgrade № 148 (1993), 21 – 28

UDC 52–355.3
Preliminary report

STARK BROADENING PARAMETER TABLES FOR Al XI AND Si XII LINES OF ASTROPHYSICAL INTEREST

M. S. Dimitrijević[1] and S. Sahal–Bréchot[2]

[1] *Astronomical Observatory, Volgina 7, 11050 Belgrade, Yugoslavia*

[2] *Laboratoire "Astrophysique, Atomes et Molécules"*
Département Atomes et Molécules en Astrophysique
Unité associée au C.N.R.S. No 812
Observatoire de Paris–Meudon, 92190 Meudon, France

(Received: October 20, 1993)

SUMMARY: Using a semiclassical approach, we have calculated electron–, proton–, and He III–impact line widths and shifts for 7 Al XI and 9 Si XII multiplets as a function of temperature and perturber density.

1. INTRODUCTION

Stark broadening parameters for spectral lines for ions within the lithium isoelectronic sequence have particular importance for the investigation of regularities and systematic trends, due to its simplicity (one optical electron) for theorethical research. Results of such investigations are of interest for acquisition of new data by interpolation and for critical evaluation of existing experimental and theoretical data, particularly in astrophysics. The astrophysical importance of multiply charged ion lines is increasing due to the developpement of UV astronomy from space and owing to the developpement of researches on the physics of stellar interiors (Seaton, 1987).

In order to investigate the behavior of Stark broadening parameters along an isoelectronic sequence as far as posible without the significant influence of relativistic effects, we have calculated electron–, proton–, and He III– impact line widths and shifts for 7 Al XI and 9 Si XII multiplets, by using the semiclassical-perturbation formalism (Sahal–Bréchot 1969ab). A summary of the formalism is given in Dimitrijević and Sahal–Bréchot (1991). Discussion and analysis of the obtained results, and all details of the calculations will be published in the principal article elsewhere (Dimitrijević, and Sahal–Bréchot, 1994). Since data are not linear with perturber density (N), due to the Debye screening effect, which is often important at high densities of interest for subphotospheric layers, we will present here the data for $N = 10^{18} - 10^{23}$ cm^{-3} and temperatures from 500,000 K up to 4,000,000 K.

Table 1. This table shows electron—, proton—, and He III— impact broadening parameters for Al XI and Si XII, for perturber densities of $10^{18} - 10^{23}$ cm^{-3} and temperatures from 500,000 to 4,000,000 K. Transitions and averaged wavelengths for the multiplet (in Å) are also given. By using c [see Eq. (5) in Dimitrijević et al, 1991a], we obtain an estimate for the maximum perturber density for which the line may be treated as isolated and tabulated data may be used. The asterisk identifies cases for which the collision volume multiplied by the perturber density (the condition for validity of the impact approximation) lies between 0.1 and 0.5. Table 1 is also available in electronic form: see the editorial in Astron.Astrophys. 1992, Vol. 266, No 2, page E1 or in Astron. Astrophys. Suppl. Series 1992, Vol. 96, No 3, and Dimitrijević and Sahal—Bréchot, 1994.

PERTURBER DENSITY = 0.1E+20 cm-3

PERTURBERS ARE:		ELECTRONS		PROTONS		He III	
TRANSITION	T(K)	WIDTH(A)	SHIFT(A)	WIDTH(A)	SHIFT(A)	WIDTH(A)	SHIFT(A)
Al XI 2S-3P	500000.	0.298E-03	0.306E-05	0.136E-04	0.194E-04	0.266E-04	0.381E-04
48.3 A	1000000.	0.223E-03	0.293E-05	0.254E-04	0.286E-04	0.504E-04	0.572E-04
C=0.43E+19	2000000.	0.169E-03	0.246E-05	0.405E-04	0.379E-04	0.810E-04	0.768E-04
	4000000.	0.131E-03	0.174E-05	0.510E-04	0.455E-04	0.103E-03	0.923E-04
Al XI 2P-5S	500000.	0.553E-03	0.954E-04	0.199E-03	0.218E-03	*0.398E-03	*0.413E-03
35.2 A	1000000.	0.446E-03	0.933E-04	0.264E-03	0.267E-03	*0.534E-03	*0.529E-03
C=0.12E+19	2000000.	0.360E-03	0.769E-04	0.333E-03	0.315E-03	*0.672E-03	*0.639E-03
	4000000.	0.287E-03	0.615E-04	0.392E-03	0.361E-03	*0.788E-03	*0.739E-03
Al XI 3P-4S	500000.	0.671E-02	0.583E-03	0.825E-03	0.119E-02	0.165E-02	0.232E-02
157.3 A	1000000.	0.524E-02	0.568E-03	0.137E-02	0.152E-02	0.280E-02	0.303E-02
C=0.45E+20	2000000.	0.414E-02	0.516E-03	0.182E-02	0.183E-02	0.373E-02	0.371E-02
	4000000.	0.330E-02	0.417E-03	0.228E-02	0.216E-02	0.463E-02	0.438E-02
Al XI 3P-5S	500000.	0.598E-02	0.832E-03	0.175E-02	0.192E-02	*0.355E-02	*0.363E-02
105.3 A	1000000.	0.477E-02	0.812E-03	0.234E-02	0.236E-02	*0.472E-02	*0.465E-02
C=0.11E+20	2000000.	0.382E-02	0.668E-03	0.294E-02	0.278E-02	*0.593E-02	*0.563E-02
	4000000.	0.304E-02	0.534E-03	0.348E-02	0.320E-02	*0.693E-02	*0.643E-02

PERTURBER DENSITY = 0.1E+21 cm-3

Al XI 2S-2P	500000.	0.105	-0.182E-02	0.560E-03	-0.205E-02	0.107E-02	-0.387E-02
554.4 A	1000000.	0.761E-01	-0.221E-02	0.187E-02	-0.400E-02	0.363E-02	-0.784E-02
C=0.55E+23	2000000.	0.557E-01	-0.220E-02	0.463E-02	-0.649E-02	0.915E-02	-0.130E-01
	4000000.	0.416E-01	-0.203E-02	0.795E-02	-0.903E-02	0.158E-01	-0.182E-01
Al XI 2S-3P	500000.	0.298E-02	0.218E-04	0.135E-03	0.184E-03	0.264E-03	0.345E-03
48.3 A	1000000.	0.223E-02	0.256E-04	0.254E-03	0.282E-03	0.504E-03	0.548E-03
C=0.43E+20	2000000.	0.169E-02	0.238E-04	0.405E-03	0.378E-03	0.810E-03	0.756E-03
	4000000.	0.131E-02	0.168E-04	0.510E-03	0.454E-03	0.103E-02	0.921E-03
Al XI 2P-3S	500000.	0.204E-02	0.171E-03	0.119E-03	0.281E-03	0.236E-03	0.528E-03
54.3 A	1000000.	0.155E-02	0.169E-03	0.274E-03	0.426E-03	0.550E-03	0.827E-03
C=0.15E+21	2000000.	0.121E-02	0.170E-03	0.493E-03	0.555E-03	0.990E-03	0.111E-02
	4000000.	0.949E-03	0.148E-03	0.650E-03	0.665E-03	0.132E-02	0.136E-02
Al XI 2P-4S	500000.	0.279E-02	0.341E-03	0.563E-03	0.760E-03		
39.6 A	1000000.	0.221E-02	0.363E-03	0.937E-03	0.102E-02		
C=0.33E+20	2000000.	0.177E-02	0.350E-03	0.124E-02	0.125E-02		
	4000000.	0.142E-02	0.282E-03	0.157E-02	0.148E-02		
Al XI 2P-5S	500000.	0.547E-02	0.687E-03	*0.200E-02	*0.189E-02		
35.2 A	1000000.	0.442E-02	0.812E-03	*0.264E-02	*0.256E-02		
C=0.12E+20	2000000.	0.357E-02	0.748E-03	*0.333E-02	*0.313E-02		
	4000000.	0.285E-02	0.599E-03	*0.392E-02	*0.359E-02		
Al XI 3P-4S	500000.	0.671E-01	0.501E-02	0.823E-02	0.109E-01	*0.165E-01	*0.200E-01
157.3 A	1000000.	0.524E-01	0.528E-02	0.137E-01	0.148E-01	*0.277E-01	*0.282E-01
C=0.45E+21	2000000.	0.414E-01	0.509E-02	0.182E-01	0.182E-01	*0.373E-01	*0.360E-01

PERTURBER DENSITY = 0.1E+21 cm-3

PERTURBERS ARE:		ELECTRONS		PROTONS		He III	
TRANSITION	T(K)	WIDTH(A)	SHIFT(A)	WIDTH(A)	SHIFT(A)	WIDTH(A)	SHIFT(A)
Al XI 3P-5S	500000.	0.592E-01	0.597E-02	*0.178E-01	*0.167E-01		
105.3 A	1000000.	0.473E-01	0.706E-02	*0.234E-01	*0.226E-01		
C=0.11E+21	2000000.	0.379E-01	0.649E-02	*0.294E-01	*0.277E-01		
	4000000.	0.302E-01	0.521E-02	*0.348E-01	*0.318E-01		
PERTURBER DENSITY = 0.1E+22 cm-3							
Al XI 2S-2P	500000.	1.05	-0.152E-01	0.555E-02	-0.182E-01	0.103E-01	-0.304E-01
554.4 A	1000000.	0.761	-0.202E-01	0.187E-01	-0.379E-01	0.361E-01	-0.710E-01
C=0.55E+24	2000000.	0.557	-0.211E-01	0.463E-01	-0.641E-01	0.913E-01	-0.125
	4000000.	0.416	-0.201E-01	0.795E-01	-0.902E-01	0.158	-0.180
Al XI 2S-3P	500000.	0.295E-01	-0.111E-03	0.134E-02	0.159E-02	*0.254E-02	*0.256E-02
48.3 A	1000000.	0.221E-01	0.253E-05	0.254E-02	0.259E-02	*0.498E-02	*0.469E-02
C=0.43E+21	2000000.	0.168E-01	0.132E-03	0.405E-02	0.369E-02	*0.809E-02	*0.703E-02
	4000000.	0.130E-01	0.154E-03	0.510E-02	0.453E-02	*0.103E-01	*0.894E-02
Al XI 2P-3S	500000.	0.204E-01	0.118E-02	0.119E-02	0.243E-02	*0.234E-02	*0.387E-02
54.3 A	1000000.	0.155E-01	0.131E-02	0.274E-02	0.391E-02	*0.548E-02	*0.703E-02
C=0.15E+22	2000000.	0.120E-01	0.154E-02	0.494E-02	0.540E-02	*0.994E-02	*0.103E-01
	4000000.	0.948E-02	0.146E-02	0.650E-02	0.663E-02	*0.132E-01	*0.131E-01
Al XI 2P-4S	500000.	0.268E-01	0.121E-02				
39.6 A	1000000.	0.214E-01	0.199E-02				
C=0.33E+21	2000000.	0.172E-01	0.282E-02				
	4000000.	0.138E-01	0.273E-02				
Al XI 2P-5S	500000.	0.461E-01	0.213E-04				
35.2 A	1000000.	0.385E-01	0.256E-02				
C=0.12E+21	2000000.	0.317E-01	0.484E-02				
	4000000.	0.257E-01	0.560E-02				
Al XI 3P-4S	500000.	0.651	0.190E-01				
157.3 A	1000000.	0.511	0.297E-01				
C=0.45E+22	2000000.	0.405	0.414E-01				
	4000000.	0.323	0.399E-01				
Al XI 3P-5S	500000.	0.514	0.160E-03				
105.3 A	1000000.	0.421	0.221E-01				
C=0.11E+22	2000000.	0.343	0.418E-01				
	4000000.	0.277	0.486E-01				
PERTURBER DENSITY = 0.1E+23 cm-3							
Al XI 2S-2P	500000.	10.5	-0.489E-01	0.501E-01	-0.119	0.795E-01	-0.137
554.4 A	1000000.	7.61	-0.136	0.186	-0.328	0.348	-0.526
C=0.55E+25	2000000.	5.57	-0.160	0.462	-0.594	*0.908	*-1.09
	4000000.	4.16	-0.180	0.794	-0.882	*1.57	*-1.68
Al XI 2S-3P	500000.	0.274	-0.254E-02	*0.118E-01	*0.921E-02		
48.3 A	1000000.	0.208	-0.161E-02	*0.248E-01	*0.205E-01		
C=0.43E+22	2000000.	0.159	-0.876E-03				
	4000000.	0.124	0.184E-04				

PERTURBER DENSITY = 0.1E+23 cm-3

PERTURBERS ARE:		ELECTRONS		PROTONS		He III	
TRANSITION	T(K)	WIDTH(A)	SHIFT(A)	WIDTH(A)	SHIFT(A)	WIDTH(A)	SHIFT(A)
Al XI 2P-3S	500000.	0.190	-0.413E-02	*0.115E-01	*0.138E-01		
54.3 A	1000000.	0.147	0.257E-02	*0.274E-01	*0.305E-01		
C=0.15E+23	2000000.	0.115	0.696E-02				
	4000000.	0.911E-01	0.109E-01				
Al XI 2P-4S	500000.	0.189	-0.205E-01				
39.6 A	1000000.	0.165	-0.446E-02				
C=0.33E+22	2000000.	0.140	0.509E-02				
	4000000.	0.116	0.151E-01				
Al XI 2P-5S	500000.	0.229	-0.398E-01				
35.2 A	1000000.	0.228	-0.126E-01				
C=0.12E+22	2000000.	0.210	0.129E-02				
	4000000.	0.183	0.244E-01				
Al XI 3P-4S	500000.	5.04	-0.301				
157.3 A	1000000.	4.19	-0.644E-01				
C=0.45E+23	2000000.	3.44	0.767E-01				
	4000000.	2.81	0.223				
Al XI 3P-5S	500000.	2.97	-0.346				
105.3 A	1000000.	2.75	-0.110				
C=0.11E+23	2000000.	2.43	0.990E-02				
	4000000.	2.08	0.212				

PERTURBER DENSITY = 0.1E+20 cm-3

PERTURBERS ARE:		ELECTRONS		PROTONS		He III	
TRANSITION	T(K)	WIDTH(A)	SHIFT(A)	WIDTH(A)	SHIFT(A)	WIDTH(A)	SHIFT(A)
Si XII 2S-3P	500000.	0.194E-03	0.162E-05	0.629E-05	0.101E-04	0.123E-04	0.198E-04
40.9 A	1000000.	0.144E-03	0.167E-05	0.134E-04	0.157E-04	0.266E-04	0.316E-04
C=0.34E+19	2000000.	0.108E-03	0.141E-05	0.218E-04	0.217E-04	0.433E-04	0.438E-04
	4000000.	0.833E-04	0.102E-05	0.287E-04	0.261E-04	0.582E-04	0.529E-04
Si XII 2P-4S	500000.	0.169E-03	0.226E-04	0.291E-04	0.468E-04	0.587E-04	0.911E-04
33.3 A	1000000.	0.133E-03	0.223E-04	0.541E-04	0.625E-04	0.109E-03	0.125E-03
C=0.25E+19	2000000.	0.107E-03	0.206E-04	0.722E-04	0.756E-04	0.147E-03	0.152E-03
	4000000.	0.856E-04	0.168E-04	0.916E-04	0.884E-04	0.187E-03	0.179E-03
Si XII 2P-5S	500000.	0.327E-03	0.532E-04	0.109E-03	0.127E-03	*0.220E-03	*0.243E-03
29.6 A	1000000.	0.263E-03	0.532E-04	0.147E-03	0.154E-03	*0.303E-03	*0.305E-03
C=0.97E+18	2000000.	0.213E-03	0.443E-04	0.192E-03	0.184E-03	*0.383E-03	*0.373E-03
	4000000.	0.170E-03	0.355E-04	0.235E-03	0.209E-03	*0.469E-03	*0.430E-03
Si XII 3P-4S	500000.	0.412E-02	0.329E-03	0.429E-03	0.672E-03	0.863E-03	0.131E-02
131.9 A	1000000.	0.320E-02	0.323E-03	0.788E-03	0.912E-03	0.158E-02	0.182E-02
C=0.36E+20	2000000.	0.252E-02	0.299E-03	0.105E-02	0.109E-02	0.216E-02	0.220E-02
	4000000.	0.200E-02	0.243E-03	0.137E-02	0.130E-02	0.273E-02	0.265E-02
Si XII 3P-5S	500000.	0.358E-02	0.464E-03	0.956E-03	0.111E-02	*0.193E-02	*0.214E-02
88.5 A	1000000.	0.285E-02	0.462E-03	0.130E-02	0.135E-02	*0.267E-02	*0.269E-02
C=0.87E+19	2000000.	0.228E-02	0.385E-03	0.168E-02	0.163E-02	*0.340E-02	*0.329E-02
	4000000.	0.181E-02	0.308E-03	0.205E-02	0.186E-02	*0.410E-02	*0.376E-02
Si XII 3P-3D	500000.	2.74	-0.582E-01	0.119	-0.251	0.236	-0.491
4880.8 A	1000000.	2.06	-0.565E-01	0.258	-0.369	0.515	-0.737
C=0.49E+23	2000000.	1.57	-0.488E-01	0.450	-0.485	0.910	-0.985
	4000000.	1.22	-0.350E-01	0.596	-0.585	1.19	-1.18

PERTURBER DENSITY = 0.1E+21 cm-3

Si XII 2S-2P	500000.	0.804E-01	-0.116E-02	0.258E-03	-0.119E-02	0.490E-03	-0.223E-02
504.6 A	1000000.	0.578E-01	-0.148E-02	0.907E-03	-0.239E-02	0.175E-02	-0.467E-02
C=0.50E+23	2000000.	0.420E-01	-0.144E-02	0.248E-02	-0.410E-02	0.487E-02	-0.819E-02
	4000000.	0.312E-01	-0.137E-02	0.477E-02	-0.589E-02	0.948E-02	-0.119E-01
Si XII 2S-3P	500000.	0.194E-02	0.110E-04	0.628E-04	0.954E-04	0.122E-03	0.179E-03
40.9 A	1000000.	0.144E-02	0.142E-04	0.134E-03	0.155E-03	0.267E-03	0.304E-03
C=0.34E+20	2000000.	0.108E-02	0.138E-04	0.218E-03	0.216E-03	0.433E-03	0.432E-03
	4000000.	0.833E-03	0.101E-04	0.287E-03	0.260E-03	0.582E-03	0.527E-03
Si XII 2P-3S	500000.	0.126E-02	0.939E-04	0.525E-04	0.146E-03	0.103E-03	0.274E-03
45.6 A	1000000.	0.956E-03	0.963E-04	0.143E-03	0.232E-03	0.288E-03	0.452E-03
C=0.11E+21	2000000.	0.737E-03	0.938E-04	0.258E-03	0.321E-03	0.519E-03	0.641E-03
	4000000.	0.577E-03	0.855E-04	0.364E-03	0.385E-03	0.743E-03	0.778E-03
Si XII 2P-4S	500000.	0.169E-02	0.188E-03	0.292E-03	0.431E-03	*0.588E-03	*0.780E-03
33.3 A	1000000.	0.134E-02	0.207E-03	0.541E-03	0.610E-03	*0.109E-02	*0.117E-02
C=0.25E+20	2000000.	0.107E-02	0.204E-03	0.722E-03	0.754E-03	*0.147E-02	*0.148E-02
	4000000.	0.856E-03	0.166E-03	0.916E-03	0.882E-03	*0.187E-02	*0.178E-02

PERTURBER DENSITY = 0.1E+21 cm-3

PERTURBERS ARE:		ELECTRONS		PROTONS		He III	
TRANSITION	T(K)	WIDTH(A)	SHIFT(A)	WIDTH(A)	SHIFT(A)	WIDTH(A)	SHIFT(A)
Si XII 2P-5S	500000.	0.325E-02	0.368E-03	*0.109E-02	*0.112E-02		
29.6 A	1000000.	0.262E-02	0.466E-03	*0.147E-02	*0.148E-02		
C=0.97E+19	2000000.	0.212E-02	0.435E-03	*0.192E-02	*0.184E-02		
	4000000.	0.169E-02	0.346E-03	*0.236E-02	*0.208E-02		
Si XII 3P-4S	500000.	0.412E-01	0.275E-02	0.430E-02	0.620E-02	*0.866E-02	*0.113E-01
131.9 A	1000000.	0.320E-01	0.300E-02	0.788E-02	0.891E-02	*0.158E-01	*0.170E-01
C=0.36E+21	2000000.	0.252E-01	0.296E-02	0.105E-01	0.109E-01	*0.216E-01	*0.214E-01
	4000000.	0.199E-01	0.241E-02	0.137E-01	0.130E-01	*0.273E-01	*0.264E-01
Si XII 3P-5S	500000.	0.356E-01	0.319E-02	*0.956E-02	*0.985E-02		
88.5 A	1000000.	0.283E-01	0.405E-02	*0.130E-01	*0.130E-01		
C=0.87E+20	2000000.	0.227E-01	0.377E-02	*0.168E-01	*0.162E-01		
	4000000.	0.180E-01	0.300E-02	*0.205E-01	*0.186E-01		
Si XII 2P-3D	500000.	0.135E-02	-0.131E-04	0.379E-04	-0.926E-04	0.733E-04	-0.174E-03
44.1 A	1000000.	0.987E-03	-0.131E-04	0.101E-03	-0.154E-03	0.199E-03	-0.302E-03
C=0.40E+20	2000000.	0.733E-03	-0.123E-04	0.177E-03	-0.216E-03	0.354E-03	-0.431E-03
	4000000.	0.554E-03	-0.584E-05	0.261E-03	-0.264E-03	0.529E-03	-0.534E-03
PERTURBER DENSITY = 0.1E+22 cm-3							
Si XII 2S-2P	500000.	0.804	-0.962E-02	0.255E-02	-0.104E-01	0.469E-02	-0.171E-01
504.6 A	1000000.	0.579	-0.134E-01	0.908E-02	-0.226E-01	0.175E-01	-0.421E-01
C=0.50E+24	2000000.	0.421	-0.139E-01	0.248E-01	-0.405E-01	0.485E-01	-0.787E-01
	4000000.	0.312	-0.136E-01	0.477E-01	-0.588E-01	0.949E-01	-0.117
Si XII 2S-3P	500000.	0.193E-01	-0.667E-04	0.621E-03	0.823E-03	*0.117E-02	*0.132E-02
40.9 A	1000000.	0.143E-01	0.653E-05	0.133E-02	0.143E-02	*0.263E-02	*0.262E-02
C=0.34E+21	2000000.	0.108E-01	0.814E-04	0.218E-02	0.211E-02	*0.432E-02	*0.403E-02
	4000000.	0.829E-02	0.909E-04	0.287E-02	0.260E-02	*0.581E-02	*0.513E-02
Si XII 2P-3S	500000.	0.126E-01	0.670E-03	0.525E-03	0.126E-02	0.103E-02	0.200E-02
45.6 A	1000000.	0.955E-02	0.754E-03	0.143E-02	0.213E-02	*0.287E-02	*0.387E-02
C=0.11E+22	2000000.	0.738E-02	0.858E-03	0.258E-02	0.313E-02	*0.520E-02	*0.596E-02
	4000000.	0.577E-02	0.846E-03	0.364E-02	0.384E-02	*0.744E-02	*0.756E-02
Si XII 2P-4S	500000.	0.164E-01	0.681E-03	*0.291E-02	*0.342E-02		
33.3 A	1000000.	0.130E-01	0.113E-02	*0.542E-02	*0.530E-02		
C=0.25E+21	2000000.	0.105E-01	0.166E-02	*0.722E-02	*0.719E-02		
	4000000.	0.838E-02	0.160E-02	*0.916E-02	*0.877E-02		
Si XII 2P-5S	500000.	0.280E-01	0.127E-05				
29.6 A	1000000.	0.233E-01	0.155E-02				
C=0.97E+20	2000000.	0.191E-01	0.289E-02				
	4000000.	0.155E-01	0.325E-02				
Si XII 3P-4S	500000.	0.402	0.107E-01	*0.428E-01	*0.494E-01		
131.9 A	1000000.	0.313	0.168E-01	*0.783E-01	*0.771E-01		
C=0.36E+22	2000000.	0.247	0.242E-01	*0.105	*0.104		
	4000000.	0.196	0.233E-01	*0.137	*0.129		

PERTURBER DENSITY = 0.1E+22 cm-3

PERTURBERS ARE:		ELECTRONS		PROTONS		He III	
TRANSITION	T(K)	WIDTH(A)	SHIFT(A)	WIDTH(A)	SHIFT(A)	WIDTH(A)	SHIFT(A)
Si XII 3P-5S	500000.	0.315	0.236E-04				
88.5 A	1000000.	0.257	0.134E-01				
C=0.87E+21	2000000.	0.208	0.250E-01				
	4000000.	0.167	0.282E-01				
Si XII 2P-3D	500000.	0.134E-01	0.240E-04	0.376E-03	-0.802E-03	0.716E-03	-0.129E-02
44.1 A	1000000.	0.980E-02	-0.428E-05	0.101E-02	-0.143E-02	*0.198E-02	-0.262E-02
C=0.40E+21	2000000.	0.728E-02	-0.689E-04	0.177E-02	-0.211E-02	*0.354E-02	-0.404E-02
	4000000.	0.551E-02	-0.508E-04	0.261E-02	-0.263E-02	*0.529E-02	-0.520E-02
PERTURBER DENSITY = 0.1E+23 cm-3							
Si XII 2S-2P	500000.	8.04	-0.298E-01	0.224E-01	-0.658E-01	0.336E-01	-0.697E-01
504.6 A	1000000.	5.78	-0.917E-01	0.897E-01	-0.194	0.167	-0.305
C=0.50E+25	2000000.	4.21	-0.106	0.249	-0.375	0.483	-0.685
	4000000.	3.12	-0.123	0.477	-0.576	0.945	-1.10
Si XII 2S-3P	500000.	0.181	-0.180E-02	*0.540E-02	*0.479E-02		
40.9 A	1000000.	0.136	-0.104E-02	*0.131E-01	*0.114E-01		
C=0.34E+22	2000000.	0.103	-0.540E-03	*0.217E-01	*0.184E-01		
	4000000.	0.797E-01	0.427E-04	*0.286E-01	*0.249E-01		
Si XII 2P-3S	500000.	0.119	-0.230E-02	0.510E-02	0.713E-02		
45.6 A	1000000.	0.916E-01	0.166E-02	*0.143E-01	*0.168E-01		
C=0.11E+23	2000000.	0.712E-01	0.393E-02	*0.260E-01	*0.271E-01		
	4000000.	0.559E-01	0.647E-02	*0.364E-01	*0.366E-01		
Si XII 2P-4S	500000.	0.118	-0.128E-01				
33.3 A	1000000.	0.102	-0.304E-02				
C=0.25E+22	2000000.	0.860E-01	0.301E-02				
	4000000.	0.710E-01	0.902E-02				
Si XII 2P-5S	500000.	0.146	-0.253E-01				
29.6 A	1000000.	0.143	-0.843E-02				
C=0.97E+21	2000000.	0.130	0.637E-03				
	4000000.	0.113	0.142E-01				
Si XII 3P-4S	500000.	3.18	-0.184				
131.9 A	1000000.	2.62	-0.432E-01				
C=0.36E+23	2000000.	2.13	0.456E-01				
	4000000.	1.73	0.133				
Si XII 3P-5S	500000.	1.90	-0.219				
88.5 A	1000000.	1.73	-0.732E-01				
C=0.87E+22	2000000.	1.51	0.494E-02				
	4000000.	1.28	0.123				
Si XII 2P-3D	500000.	0.127	0.246E-02	0.347E-02	-0.475E-02		
44.1 A	1000000.	0.938E-01	0.168E-02	*0.999E-02	-0.116E-01		
C=0.40E+22	2000000.	0.701E-01	0.101E-02	*0.176E-01	-0.185E-01		
	4000000.	0.532E-01	0.403E-03	*0.261E-01	-0.253E-01		

2. RESULTS AND DISCUSSION

Our results for 7 Al XI and 9 Si XII multiplets are shown in Table 1, for perturber densities 10^{18} – 10^{23} cm^{-3} and temperatures T = 500,000 - 4,000,000 K. We also specify a parameter c (Dimitrijević and Sahal–Bréchot 1984), which gives an estimate for the maximum perturber density for which the line may be treated as isolated when it is divided by the corresponding electron-impact full width at half maximum. For each value given in Tables 1 and 2, the collision volume (V) multiplied by the perturber density (N) is much less than one and the impact approximation is valid (Sahal–Bréchot, 1969ab). Values for NV > 0.5 are not given and values for 0.1 < NV ≤ 0.5 are denoted by an asterisk. When the impact approximation is not valid, the ion broadening contribution may be estimated by using quasistatic estimations (Sahal–Bréchot 1991 and Griem 1974). The accuracy of the results obtained decreases when broadening by ion interactions becomes important.

The analysis of present results is given in Dimitrijević and Sahal–Bréchot (1994).

Acknowledgements – This work is a part of French–Yugoslav collaboration through the project "L'elargissement Stark des raies spectrales des plasmas astrophysiques et de laboratoire", it is also a part of the project "Physics and dynamics of celestial bodies", supported by Ministry for Science and Technology of Serbia.

REFERENCES

Dimitrijević, M. S., and Sahal–Bréchot, S.: 1984, *JQSRT* **31**, 301.
Dimitrijević, M. S., and Sahal–Bréchot, S.: 1994, *Astron. Astrophys. Suppl. Series* in press.
Dimitrijević, M. S., Sahal–Bréchot, S., and Bommier, V.: 1991, *Astron. Astrophys. Suppl. Series.* **89**, 581.
Griem, H. R.: 1974, *Spectral Line Broadening by Plasmas*, Academic Press, New York.
Sahal–Bréchot, S.: 1969a, *Astron. Astrophys.* **1**, 91.
Sahal–Bréchot, S.: 1969b, *Astron. Astrophys.* **2**, 322.
Sahal–Bréchot, S.: 1991, *Astron. Astrophys.* **245**, 322.
Seaton, M. J.: 1987, *J. Phys.* B **20**, 6363.

ТАБЕЛЕ ПАРАМЕТАРА ШТАРКОВОГ ШИРЕЊА ЛИНИЈА Al XI и Si XII ОД ЗНАЧАЈА У АСТРОФИЗИЦИ

М. С. Димитријевић[1] и S. Sahal–Bréchot[2]

[1] *Астрономска опсерваторија, Волгина 7, 11050 Београд, Југославија*

[2] *Laboratoire "Astrophysique, Atomes et Molécules"*
Département Atomes et Molécules en Astrophysique
Unité associée au C.N.R.S. No 812
Observatoire de Paris-Meudon, 92190 Meudon, France

УДК 52–355.3
Претходно саопштење

Користећи семикласичан прилаз, израчунате су ширине и помераји спектралних линија, проузроковани сударима са електронима, протонима и He III, за 7 мултиплета Al XI и 9 мултиплета Si XII. Резултати су дати у функцији температуре и концентрације пертурбера.

Bull. Astron. Belgrade № 148 (1993), 29 – 42

UDC 52–355.3
Preliminary report

STARK BROADENING PARAMETER TABLES FOR Ne VIII AND Na IX LINES OF ASTROPHYSICAL INTEREST

M. S. Dimitrijević[1] and S. Sahal–Bréchot[2]

[1] *Astronomical Observatory, Volgina 7, 11050 Belgrade, Yugoslavia*

[2] *Laboratoire "Astrophysique, Atomes et Molécules"*
Département Atomes et Molécules en Astrophysique
Unité associée au C.N.R.S. No 812
Observatoire de Paris–Meudon, 92190 Meudon, France

(Received: November 1, 1993)

SUMMARY: Using a semiclassical approach, we have calculated electron–, proton–, and He III–impact line widths and shifts for 20 Ne VIII and 8 Na IX multiplets as a function of temperature and perturber density.

1. INTRODUCTION

In order to investigate the behavior of Stark broadening parameters along the lithium isoelectronic sequence as far as posible, we have calculated electron–, proton–, and He III– impact line widths and shifts for 20 Ne VIII and 8 Na IX multiplets, by using the semiclassical-perturbation formalism (Sahal–Bréchot 1969ab). A summary of the formalism is given in Dimitrijević and Sahal–Bréchot (1991). Discussion, analysis and comparison with the existing experimental and theoretical data, and all details of the calculations will be published in the principal article elsewhere (Dimitrijević, and Sahal–Bréchot, 1994). Since data are not linear with perturber density (N), due to the Debye screening effect, which is often important at high densities of interest for subphotospheric layers, we will present here the data for $N = 10^{16} - 10^{22}$ cm^{-3} and temperatures from 200,000 K up to 2,000,000 K.

2. RESULTS AND DISCUSSION

Our results for 20 Ne VIII and 8 Na IX multiplets are shown in Table 1, for perturber densities $10^{16} - 10^{22}$ cm^{-3} and temperatures T = 200,000 - 2,000,000 K. We also specify a parameter c (Dimitrijević & Sahal–Bréchot 1984), which gives an estimate for the maximum perturber density for which the line may be treated as isolated when it is divided by the corresponding electron-impact full width at *half maximum. For each value given in* Tables 1 and 2, the collision volume (V) multiplied by the perturber density (N) is much less than one and the impact approximation is valid (Sahal–Bréchot,

Table 1. This table shows electron—, proton—, and He III— impact broadening parameters for Ne VIII and Na IX, for perturber densities of 10^{16} – 10^{22} cm^{-3} and temperatures from 200,000 to 2,000,000 K. Transitions and averaged wavelengths for the multiplet (in Å) are also given. By using c [see Eq. (5) in Dimitrijević et al, 1991a], we obtain an estimate for the maximum perturber density for which the line may be treated as isolated and tabulated data may be used. The asterisk identifies cases for which the collision volume multiplied by the perturber density (the condition for validity of the impact approximation) lies between 0.1 and 0.5. Table 1 is also available in electronic form: see the editorial in Astron. Astrophys. 1992, Vol. 266, No 2, page E1 or in Astron. Astrophys. Suppl. Series 1992, Vol. 96, No 3, and Dimitrijević and Sahal—Bréchot, 1994.

PERTURBER DENSITY = 0.1E+17cm-3							
PERTURBERS ARE:		ELECTRONS		PROTONS		He III	
TRANSITION	T(K)	WIDTH(A)	SHIFT(A)	WIDTH(A)	SHIFT(A)	WIDTH(A)	SHIFT(A)
NeVIII 5S-5P	200000.	0.355	-0.210E-02	0.132	0.132	0.268	0.270
10427.5 A	500000.	0.263	-0.645E-02	0.185	0.160	0.371	0.336
C=0.54E+19	1000000.	0.211	-0.790E-02	0.198	0.184	0.409	0.367
	2000000.	0.169	-0.781E-02	0.221	0.219	0.444	0.434
PERTURBER DENSITY = 0.1E+18cm-3							
NeVIII 2S-4P	200000.	0.364E-04	0.127E-05	0.383E-05	0.437E-05	0.764E-05	0.887E-05
67.4 A	500000.	0.261E-04	0.117E-05	0.628E-05	0.589E-05	0.127E-04	0.120E-04
C=0.25E+17	1000000.	0.206E-04	0.908E-06	0.770E-05	0.703E-05	0.159E-04	0.142E-04
	2000000.	0.165E-04	0.724E-06	0.978E-05	0.823E-05	0.195E-04	0.169E-04
NeVIII 2S-5P	200000.	0.850E-04	0.584E-05	0.469E-04	0.478E-04	0.975E-04	0.967E-04
60.7 A	500000.	0.625E-04	0.415E-05	0.621E-04	0.582E-04	0.133E-03	0.117E-03
C=0.18E+16	1000000.	0.497E-04	0.288E-05	0.712E-04	0.663E-04	*0.149E-03	*0.136E-03
	2000000.	0.398E-04	0.180E-05	0.876E-04	0.790E-04	*0.170E-03	*0.164E-03
NeVIII 3S-4P	200000.	0.605E-03	0.106E-04	0.537E-04	0.600E-04	0.106E-03	0.122E-03
260.5 A	500000.	0.434E-03	0.895E-05	0.885E-04	0.814E-04	0.179E-03	0.167E-03
C=0.37E+18	1000000.	0.345E-03	0.538E-05	0.110E-03	0.968E-04	0.221E-03	0.198E-03
	2000000.	0.277E-03	0.335E-05	0.134E-03	0.116E-03	0.259E-03	0.234E-03
NeVIII 3S-5P	200000.	0.801E-03	0.489E-04	0.425E-03	0.432E-03	0.884E-03	0.875E-03
182.8 A	500000.	0.589E-03	0.334E-04	0.561E-03	0.527E-03	0.121E-02	0.106E-02
C=0.17E+17	1000000.	0.469E-03	0.221E-04	0.647E-03	0.600E-03	*0.135E-02	*0.124E-02
	2000000.	0.375E-03	0.126E-04	0.795E-03	0.713E-03	*0.153E-02	*0.148E-02
NeVIII 4S-5P	200000.	0.852E-02	0.304E-03	0.401E-02	0.404E-02	0.827E-02	0.823E-02
563.7 A	500000.	0.627E-02	0.170E-03	0.526E-02	0.488E-02	0.115E-01	0.996E-02
C=0.16E+18	1000000.	0.501E-02	0.734E-04	0.614E-02	0.562E-02	*0.124E-01	*0.115E-01
	2000000.	0.402E-02	0.132E-04	0.744E-02	0.679E-02	*0.138E-01	*0.138E-01
NeVIII 5S-5P	200000.	3.55	-0.235E-01	1.32	1.32	2.68	2.69
10427.5 A	500000.	2.63	-0.645E-01	1.85	1.60	3.71	3.35
C=0.54E+20	1000000.	2.11	-0.790E-01	1.98	1.84	*4.09	*3.67
	2000000.	1.69	-0.781E-01	2.21	2.19	*4.44	*4.34
NeVIII 2P-6S	200000.	0.104E-03	0.198E-04	0.324E-04	0.338E-04	0.660E-04	0.687E-04
62.6 A	500000.	0.786E-04	0.170E-04	0.446E-04	0.421E-04	0.903E-04	0.856E-04
C=0.13E+17	1000000.	0.632E-04	0.135E-04	0.533E-04	0.486E-04	0.105E-03	0.989E-04
	2000000.	0.502E-04	0.108E-04	0.593E-04	0.548E-04	0.123E-03	0.111E-03
NeVIII 5P-6S	200000.	0.760E-01	0.538E-02	0.114E-01	-0.114E-01	0.228E-01	-0.233E-01
1246.9 A	500000.	0.568E-01	0.497E-02	0.154E-01	-0.142E-01	0.319E-01	-0.296E-01
C=0.78E+18	1000000.	0.455E-01	0.412E-02	0.178E-01	-0.163E-01	0.372E-01	-0.331E-01
	2000000.	0.363E-01	0.351E-02	0.208E-01	-0.185E-01	0.430E-01	-0.383E-01
PERTURBER DENSITY = 0.1E+19cm-3							
NeVIII 2S-2P	200000.	0.432E-02	-0.729E-04	0.178E-04	-0.612E-04	0.334E-04	-0.120E-03
773.7 A	500000.	0.283E-02	-0.966E-04	0.794E-04	-0.140E-03	0.153E-03	-0.282E-03
C=0.77E+21	1000000.	0.208E-02	-0.984E-04	0.176E-03	-0.219E-03	0.350E-03	-0.444E-03
	2000000.	0.157E-02	-0.917E-04	0.289E-03	-0.300E-03	0.576E-03	-0.610E-03

PERTURBER DENSITY = 0.1E+19cm-3

PERTURBERS ARE:		ELECTRONS		PROTONS		He III	
TRANSITION	T(K)	WIDTH(A)	SHIFT(A)	WIDTH(A)	SHIFT(A)	WIDTH(A)	SHIFT(A)
NeVIII 2S-3P	200000.	0.215E-03	0.274E-05	0.772E-05	0.106E-04	0.150E-04	0.205E-04
88.1 A	500000.	0.147E-03	0.268E-05	0.173E-04	0.178E-04	0.343E-04	0.360E-04
C=0.98E+18	1000000.	0.113E-03	0.245E-05	0.250E-04	0.225E-04	0.504E-04	0.459E-04
	2000000.	0.889E-04	0.171E-05	0.318E-04	0.272E-04	0.634E-04	0.558E-04
NeVIII 2S-4P	200000.	0.364E-03	0.118E-04	0.383E-04	0.432E-04	0.764E-04	0.850E-04
67.4 A	500000.	0.261E-03	0.116E-04	0.628E-04	0.588E-04	0.127E-03	0.120E-03
C=0.29E+18	1000000.	0.206E-03	0.908E-05	0.770E-04	0.703E-04	0.159E-03	0.142E-03
	2000000.	0.165E-03	0.724E-05	0.978E-04	0.823E-04	0.195E-03	0.169E-03
NeVIII 2S-5P	200000.	0.831E-03	0.396E-04	*0.471E-03	*0.461E-03		
60.7 A	500000.	0.612E-03	0.384E-04	*0.621E-03	*0.579E-03		
C=0.18E+17	1000000.	0.488E-03	0.288E-04	*0.712E-03	*0.663E-03		
	2000000.	0.391E-03	0.180E-04	*0.876E-03	*0.790E-03		
NeVIII 3S-3P	200000.	0.304	-0.677E-02	0.597E-02	-0.154E-02	0.114E-01	-0.304E-02
2879.1 A	500000	0.212	-0.763E-02	0.120E-01	-0.351E-02	0.234E-01	-0.669E-02
C=0.10E+22	1000000.	0.166	-0.738E-02	0.165E-01	-0.485E-02	0.325E-01	-0.998E-02
	2000000.	0.132	-0.730E-02	0.189E-01	-0.646E-02	0.377E-01	-0.132E-01
NeVIII 3S-4P	200000.	0.605E-02	0.971E-04	0.537E-03	0.593E-03	0.106E-02	0.117E-02
260.5 A	500000.	0.434E-02	0.871E-04	0.885E-03	0.812E-03	0.179E-02	0.166E-02
C=0.37E+19	1000000.	0.345E-02	0.538E-04	0.110E-02	0.968E-03	0.221E-02	0.198E-02
	2000000.	0.277E-02	0.335E-04	0.134E-02	0.116E-02	0.259E-02	0.234E-02
NeVIII 3S-5P	200000.	0.784E-02	0.320E-03	*0.426E-02	*0.417E-02		
182.8 A	500000.	0.577E-02	0.306E-03	*0.561E-02	*0.524E-02		
C=0.17E+18	1000000.	0.461E-02	0.221E-03	*0.647E-02	*0.600E-02		
	2000000.	0.370E-02	0.126E-03	*0.795E-02	*0.713E-02		
NeVIII 4S-4P	200000.	5.75	-0.174	0.227	0.803E-01	0.445	0.159
6993.0 A	500000.	4.17	-0.164	0.342	0.132	0.679	0.268
C=0.27E+22	1000000.	3.33	-0.171	0.393	0.165	0.783	0.336
	2000000.	2.69	-0.140	0.446	0.197	0.885	0.403
NeVIII 4S-5P	200000.	0.835E-01	0.146E-02	*0.402E-01	*0.390E-01		
563.7 A	500000.	0.617E-01	0.144E-02	*0.526E-01	*0.485E-01		
C=0.16E+19	1000000.	0.493E-01	0.734E-03	*0.614E-01	*0.562E-01		
	2000000.	0.396E-01	0.132E-03	*0.744E-01	*0.679E-01		
NeVIII 2P-3S	200000.	0.173E-03	0.137E-04	0.627E-05	0.167E-04	0.124E-04	0.330E-04
103.0 A	500000.	0.121E-03	0.151E-04	0.188E-04	0.276E-04	0.378E-04	0.560E-04
C=0.37E+19	1000000.	0.943E-04	0.145E-04	0.311E-04	0.348E-04	0.631E-04	0.707E-04
	2000000.	0.748E-04	0.133E-04	0.413E-04	0.414E-04	0.840E-04	0.848E-04
NeVIII 2P-4S	200000.	0.250E-03	0.350E-04	0.317E-04	0.484E-04	0.632E-04	0.952E-04
74.6 A	500000.	0.183E-03	0.338E-04	0.614E-04	0.654E-04	0.124E-03	0.136E-03
C=0.80E+18	1000000.	0.147E-03	0.315E-04	0.795E-04	0.792E-04	0.160E-03	0.161E-03
	2000000.	0.118E-03	0.257E-04	0.992E-04	0.946E-04	0.191E-03	0.190E-03

PERTURBER DENSITY = 0.1E+19cm-3

PERTURBERS ARE:		ELECTRONS		PROTONS		He III	
TRANSITION	T(K)	WIDTH(A)	SHIFT(A)	WIDTH(A)	SHIFT(A)	WIDTH(A)	SHIFT(A)
NeVIII 2P-5S	200000.	0.458E-03	0.783E-04	0.893E-04	0.103E-03	0.179E-03	0.202E-03
66.3 A	500000.	0.340E-03	0.761E-04	0.132E-03	0.133E-03	0.267E-03	0.271E-03
C=0.42E+18	1000000.	0.275E-03	0.670E-04	0.165E-03	0.157E-03	0.337E-03	0.320E-03
	2000000.	0.223E-03	0.537E-04	0.194E-03	0.180E-03	*0.393E-03	*0.370E-03
NeVIII 2P-6S	200000.	0.104E-02	0.187E-03	0.324E-03	0.328E-03		
62.6 A	500000.	0.786E-03	0.168E-03	0.446E-03	0.419E-03		
C=0.13E+18	1000000.	0.632E-03	0.135E-03	0.553E-03	0.486E-03		
	2000000.	0.502E-03	0.108E-03	0.593E-03	0.548E-03		
NeVIII 3P-4S	200000.	0.581E-02	0.518E-03	0.467E-03	0.706E-03	0.933E-03	0.139E-02
298.6 A	500000.	0.419E-02	0.495E-03	0.897E-03	0.979E-03	0.183E-02	0.199E-02
C=0.11E+20	1000000.	0.334E-02	0.462E-03	0.118E-02	0.116E-02	0.240E-02	0.240E-02
	2000000.	0.268E-02	0.378E-03	0.144E-02	0.136E-02	0.299E-02	0.280E-02
NeVIII 3P-5S	200000.	0.491E-02	0.685E-03	0.783E-03	0.912E-03	0.158E-02	0.179E-02
198.9 A	500000.	0.361E-02	0.664E-03	0.117E-02	0.118E-02	0.237E-02	0.239E-02
C=0.38E+19	1000000.	0.291E-02	0.584E-03	0.147E-02	0.139E-02	0.297E-02	0.282E-02
	2000000.	0.235E-02	0.469E-03	0.174E-02	0.159E-02	0.353E-02	0.323E-02
NeVIII 3P-6S	200000.	0.815E-02	0.135E-02	0.235E-02	0.238E-02		
168.8 A	500000.	0.612E-02	0.121E-02	0.324E-02	0.304E-02		
C=0.91E+18	1000000.	0.491E-02	0.968E-03	0.386E-02	0.353E-02		
	2000000.	0.390E-02	0.775E-03	0.427E-02	0.396E-02		
NeVIII 4P-5S	200000.	0.746E-01	0.638E-02	0.677E-02	0.778E-02	0.136E-01	0.153E-01
651.4 A	500000.	0.549E-01	0.618E-02	0.101E-01	0.999E-02	0.209E-01	0.205E-01
C=0.23E+20	1000000.	0.442E-01	0.555E-02	0.123E-01	0.120E-01	0.256E-01	0.240E-01
	2000000.	0.358E-01	0.444E-02	0.155E-01	0.138E-01	0.307E-01	0.283E-01
NeVIII 4P-6S	200000.	0.571E-01	0.760E-02	0.135E-01	0.137E-01		
411.0 A	500000.	0.428E-01	0.679E-02	0.186E-01	0.175E-01		
C=0.54E+19	1000000.	0.343E-01	0.546E-02	0.216E-01	0.202E-01		
	2000000.	0.273E-01	0.436E-02	0.253E-01	0.226E-01		
NeVIII 5P-6S	200000.	0.752	0.574E-01	0.114	-0.111		
1246.9 A	500000.	0.563	0.503E-01	0.154	-0.142		
C=0.78E+19	1000000.	0.451	0.412E-01	0.178	-0.163		
	2000000.	0.360	0.351E-01	0.208	-0.185		

PERTURBER DENSITY = 0.1E+20cm-3

NeVIII 2S-2P	200000.	0.436E-01	-0.845E-03	0.178E-03	-0.592E-03	0.333E-03	-0.112E-02
773.7 A	500000.	0.283E-01	-0.951E-03	0.794E-03	-0.139E-02	0.153E-02	-0.278E-02
C=0.77E+22	1000000.	0.208E-01	-0.984E-03	0.176E-02	-0.218E-02	0.350E-02	-0.443E-02
	2000000.	0.157E-01	-0.917E-03	0.289E-02	-0.300E-02	0.576E-02	-0.610E-02
NeVIII 2S-3P	200000.	0.215E-02	0.250E-04	0.771E-04	0.102E-03	0.150E-03	0.192E-03
88.1 A	500000.	0.147E-02	0.248E-04	0.173E-03	0.176E-03	0.343E-03	0.353E-03
C=0.98E+19	1000000.	0.113E-02	0.240E-04	0.250E-03	0.224E-03	0.504E-03	0.458E-03
	2000000.	0.889E-03	0.171E-04	0.318E-03	0.272E-03	0.634E-03	0.557E-03

PERTURBER DENSITY = 0.1E+20cm-3

PERTURBERS ARE:		ELECTRONS		PROTONS		He III	
TRANSITION	T(K)	WIDTH(A)	SHIFT(A)	WIDTH(A)	SHIFT(A)	WIDTH(A)	SHIFT(A)
NeVIII 2S-4P	200000.	0.364E-02	0.955E-04	0.384E-03	0.407E-03	*0.757E-03	*0.746E-03
67.4 A	500000.	0.261E-02	0.106E-03	0.628E-03	0.577E-03	*0.127E-02	*0.115E-02
C=0.25E+19	1000000.	0.206E-02	0.883E-04	0.770E-03	0.701E-03	*0.159E-02	*0.1[illegible]
	2000000.	0.165E-02	0.724E-04	0.978E-03	0.823E-03	*0.195E-02	*0.1[illegible]
NeVIII 2S-5P	200000.	0.744E-02	-0.270E-04				
80.7 A	500000.	0.558E-02	0.130E-03				
C=0.18E+18	1000000.	0.450E-02	0.221E-03				
	2000000.	0.364E-02	0.180E-03				
NeVIII 3S-3P	200000.	3.04	-0.683E-01	0.596E-01	-0.149E-01	0.113	-0.282E-01
2879.1 A	500000.	2.12	-0.765E-01	0.120	-0.329E-01	0.234	0.[illegible]
C=0.17E+23	1000000.	1.66	-0.735E-01	0.165	-0.485E-01	0.325	0.[illegible]
	2000000.	1.32	-0.730E-01	0.189	-0.646E-01	0.377	-0.13[illegible]
NeVIII 3S-4P	200000.	0.606E-01	0.649E-03	0.536E-02	0.560E-02	*0.106E-01	*0.10[illegible]E-01
260.5 A	500000.	0.434E-01	0.735E-03	0.885E-02	0.798E-02	*0.179E-01	*0.160E-01
C=0.37E+20	1000000.	0.344E-01	0.508E-03	0.110E-01	0.966E-02	*0.221E-01	*0.197E-01
	2000000.	0.277E-01	0.335E-03	0.134E-01	0.116E-01	*0.259E-01	*0.233E-01
NeVIII 3S-5P	200000.	0.704E-01	-0.628E-03				
182.8 A	500000.	0.528E-01	0.764E-03				
C=0.17E+19	1000000.	0.420E-01	0.161E-02				
	2000000.	0.345E-01	0.126E-02				
NeVIII 4S-5P	200000.	0.760	-0.203E-01				
563.7 A	500000.	0.570	-0.678E-02				
C=0.16E+20	1000000.	0.460	0.171E-02				
	2000000.	0.373	0.132E-02				
NeVIII 2P-3S	200000.	0.174E-02	0.137E-03	0.625E-04	0.161E-03	0.124E-03	0.[illegible]E-05
103.0 A	500000.	0.121E-02	0.149E-03	0.188E-03	0.273E-03	0.3[illegible]E-03	0.549E-03
C=0.37E+20	1000000.	0.943E-03	0.144E-03	0.311E-03	0.346E-03	0.631E-03	0.705E-03
	2000000.	0.748E-03	0.133E-03	0.413E-03	0.414E-03	0.841E-03	0.847E-03
NeVIII 2P-4S	200000.	0.250E-02	0.323E-03	0.316E-03	0.457E-03	*0.632E-03	*0.638E-03
74.6 A	500000.	0.183E-02	0.324E-03	0.614E-03	0.652E-03	*0.124E-02	*0.131E-02
C=0.80E+19	1000000.	0.147E-02	0.313E-03	0.795E-03	0.789E-03	*0.160E-02	*0.161E-02
	2000000.	0.118E-02	0.257E-03	0.992E-03	0.946E-03	*0.191E-02	*0.190E-02
NeVIII 2P-5S	200000.	0.458E-02	0.700E-03	0.893E-03	0.954E-03		
66.3 A	500000.	0.340E-02	0.724E-03	*0.133E-02	*0.130E-02		
C=0.42E+19	1000000.	0.275E-02	0.664E-03	*0.165E-02	*0.157E-02		
	2000000.	0.223E-02	0.537E-03	*0.194E-02	*0.180E-02		
NeVIII 2P-6S	200000.	0.103E-01	0.137E-02				
62.6 A	500000.	0.779E-02	0.147E-02				
C=0.13E+19	1000000.	0.627E-02	0.131E-02				
	2000000.	0.498E-02	0.108E-02				

PERTURBER DENSITY = 0.1E+20cm-3

PERTURBERS ARE:		ELECTRONS		PROTONS		He III	
TRANSITION	T(K)	WIDTH(A)	SHIFT(A)	WIDTH(A)	SHIFT(A)	WIDTH(A)	SHIFT(A)
NeVIII 3P-4S	200000.	0.581E-01	0.477E-02	0.466E-02	0.667E-02	*0.930E-02	*0.122E-01
298.6 A	500000.	0.419E-01	0.477E-02	0.898E-02	0.962E-02	*0.183E-01	*0.192E-01
C=0.11E+21	1000000.	0.334E-01	0.460E-02	0.118E-01	0.116E-01	*0.240E-01	*0.239E-01
	2000000.	0.268E-01	0.378E-02	0.144E-01	0.136E-01	*0.299E-01	*0.279E-01
NeVIII 3P-5S	200000.	0.491E-01	0.611E-02	0.783E-02	0.842E-02		
198.9 A	500000.	0.361E-01	0.633E-02	*0.117E-01	*0.115E-01		
C=0.38E+20	1000000.	0.291E-01	0.578E-02	*0.147E-01	*0.138E-01		
	2000000.	0.235E-01	0.469E-02	*0.174E-01	*0.159E-01		
NeVIII 3P-6S	200000.	0.807E-01	0.986E-02				
168.8 A	500000.	0.607E-01	0.106E-01				
C=0.91E+19	1000000.	0.487E-01	0.939E-02				
	2000000.	0.388E-01	0.775E-02				
NeVIII 4P-5S	200000.	0.746	0.578E-01	0.677E-01	0.724E-01		
651.4 A	500000.	0.549	0.593E-01	0.101	0.974E-01		
C=0.23E+21	1000000.	0.442	0.551E-01	0.123	0.120		
	2000000.	0.358	0.444E-01	0.155	0.138		
NeVIII 4P-6S	200000.	0.566	0.554E-01				
411.0 A	500000.	0.425	0.594E-01				
C=0.54E+20	1000000.	0.341	0.529E-01				
	2000000.	0.272	0.436E-01				
NeVIII 5P-6S	200000.	7.11	0.555				
1246.9 A	500000.	5.37	0.528				
C=0.78E+20	1000000.	4.33	0.424				
	2000000.	3.47	0.351				

PERTURBER DENSITY = 0.1E+21cm-3

NeVIII 2S-2P	200000.	0.436	-0.735E-02	0.176E-02	-0.529E-02	0.324E-02	-0.909E-02
773.7 A	500000.	0.283	-0.914E-02	0.795E-02	-0.135E-01	0.153E-01	-0.259E-01
C=0.77E+23	1000000.	0.208	-0.955E-02	0.176E-01	-0.216E-01	0.350E-01	-0.436E-01
	2000000.	0.157	-0.914E-02	0.289E-01	-0.300E-01	0.576E-01	-0.609E-01
NeVIII 2S-3P	200000.	0.215E-01	0.836E-04	0.765E-03	0.893E-03	0.145E-02	0.150E-02
88.1 A	500000.	0.147E-01	0.157E-03	0.173E-02	0.168E-02	*0.341E-02	*0.316E-02
C=0.98E+20	1000000.	0.113E-01	0.201E-03	0.250E-02	0.220E-02	*0.503E-02	*0.442E-02
	2000000.	0.888E-02	0.163E-03	0.318E-02	0.271E-02	*0.634E-02	*0.555E-02
NeVIII 2S-4P	200000.	0.356E-01	0.124E-04	*0.377E-02	*0.328E-02		
67.4 A	500000.	0.256E-01	0.502E-03	*0.636E-02	*0.530E-02		
C=0.25E+20	1000000.	0.203E-01	0.608E-03	*0.762E-02	*0.674E-02		
	2000000.	0.163E-01	0.671E-03	*0.978E-02	*0.818E-02		
NeVIII 2S-5P	200000.	0.605E-01	-0.155E-02				
60.7 A	500000.	0.471E-01	-0.569E-03				
C=0.18E+19	1000000.	0.389E-01	0.376E-03				
	2000000.	0.321E-01	0.102E-02				

PERTURBER DENSITY = 0.10E+21cm-3

	PERTURBERS	ELECTRONS		PROTONS		He III	
TRANSITION	T(K)	WIDTH(A)	SHIFT(A)	WIDTH(A)	SHIFT(A)	WIDTH(A)	SHIFT(A)
NeVIII 3S-4P	200000.	0.595	-0.414E-02	*0.522E-01	*0.455E-01		
250.5 A	500000.	0.427	-0.279E-02	*0.381E-01	*0.734E-01		
C=0.57E+21	1000000.	0.340	0.181E-02	*0.111	*0.932E-01		
	2000000.	0.279	0.364E-02	*0.174	*0.115		
NeVIII 3S-5P	200000.	0.370	-0.172E-01				
182.8 A	500000.	0.290	-0.289E-02				
C=0.17E+20	1000000.	0.244	-0.428E-03				
	2000000.	0.306	0.563E-02				
NeVIII 4S-5P	200000.	5.40	-0.257				
563.7 A	500000.	4.99	-0.193				
C=0.16E+21	1000000.	4.08	-0.126				
	2000000.	3.36	-0.510E-01				
NeVIII 2P-3S	200000.	0.174E-01	0.112E-02	0.630E-03	0.141E-02	0.124E-02	[illegible]
103.0 A	500000.	0.123E-01	0.135E-02	0.188E-02	0.260E-02	*0.375E-02	[illegible]
C=0.37E+21	1000000.	0.943E-02	0.139E-02	0.311E-02	0.540E-02	*0.630E-02	[illegible]
	2000000.	0.743E-02	0.132E-02	0.413E-02	0.412E-02	*0.840E-02	[illegible]
NeVIII 2P-4S	200000.	0.249E-01	0.216E-02	*0.316E-02	*0.372E-02		
74.6 A	500000.	0.182E-01	0.264E-02	*0.605E-02	*0.600E-02		
C=0.80E+20	1000000.	0.146E-01	0.286E-02	*0.803E-02	*0.763E-02		
	2000000.	0.118E-01	0.252E-02	*0.992E-02	*0.941E-02		
NeVIII 2P-5S	200000.	0.450E-01	0.374E-02				
66.3 A	500000.	0.335E-01	0.542E-02				
C=0.42E+20	1000000.	0.272E-01	0.579E-02				
	2000000.	0.226E-01	0.521E-02				
NeVIII 2P-6S	200000.	0.866E-01	0.475E-03				
62.6 A	500000.	0.682E-01	0.635E-02				
C=0.13E+20	1000000.	0.559E-01	0.849E-02				
	2000000.	0.450E-01	0.986E-02				
NeVIII 3P-4S	200000.	0.579	0.326E-01	*0.465E-01	*0.545E-01		
298.6 A	500000.	0.418	0.391E-01	*0.906E-01	*0.883E-01		
C=0.11E+22	1000000.	0.333	0.421E-01	*0.117	*0.112		
	2000000.	0.267	0.372E-01	*0.144	*0.135		
NeVIII 3P-5S	200000.	0.404	0.327E-01				
198.9 A	500000.	0.357	0.474E-01				
C=0.38E+21	1000000.	0.305	0.506E-01				
	2000000.	0.273	0.455E-01				
NeVIII 3P-6S	200000.	0.667	0.276E-02				
158.8 A	500000.	0.536	0.451E-01				
C=0.91E+20	1000000.	0.438	0.506E-01				
	2000000.	0.353	0.407E-01				

PERTURBER DENSITY = 0.1E+21cm-3

PERTURBERS ARE:		ELECTRONS		PROTONS		He III	
TRANSITION	T(K)	WIDTH(A)	SHIFT(A)	WIDTH(A)	SHIFT(A)	WIDTH(A)	SHIFT(A)
NeVIII 4P-5S	200000.	7.31	0.353				
651.4 A	500000.	5.40	0.469				
C=0.23E+22	1000000.	4.36	0.495				
	2000000.	3.53	0.434				
NeVIII 4P-6S	200000.	4.93	0.176E-01				
411.0 A	500000.	3.81	0.252				
C=0.54E+21	1000000.	3.10	0.341				
	2000000.	2.50	0.398				
PERTURBER DENSITY = 0.1E+22cm-3							
NeVIII 2S-2P	200000.	4.36	-0.544E-01	0.163E-01	-0.372E-01	0.259E-01	-0.459E-01
773.7 A	500000.	2.83	-0.769E-01	0.788E-01	-0.122	0.151	-0.216
C=0.77E+24	1000000.	2.08	-0.870E-01	0.177	-0.208	0.348	-0.394
	2000000.	1.57	-0.865E-01	0.289	-0.296	0.576	-0.579
NeVIII 2S-3P	200000.	0.207	-0.290E-02	*0.697E-02	*0.576E-02		
88.1 A	500000.	0.143	-0.876E-03	*0.171E-01	*0.143E-01		
C=0.98E+21	1000000.	0.111	0.236E-03	*0.252E-01	*0.204E-01		
	2000000.	0.870E-01	0.665E-03	*0.318E-01	*0.262E-01		
NeVIII 2S-4P	200000.	*0.304	*-0.629E-02				
67.4 A	500000.	0.227	-0.123E-02				
C=0.25E+21	1000000.	0.183	0.561E-03				
	2000000.	0.149	0.272E-02				
NeVIII 2S-5P	200000.	*0.448	*0.334E-02				
60.7 A	500000.	0.366	-0.845E-03				
C=0.18E+20	1000000.	0.314	-0.946E-03				
	2000000.	0.268	0.101E-03				
NeVIII 3S-4P	200000.	*5.15	*-0.107				
260.5 A	500000.	3.84	-0.639E-01				
C=0.37E+22	1000000.	3.10	-0.496E-01				
	2000000.	2.53	-0.244E-01				
NeVIII 3S-5P	200000.	*4.36	*0.241E-01				
182.8 A	500000.	3.54	-0.300E-01				
C=0.17E+21	1000000.	3.02	-0.371E-01				
	2000000.	2.57	-0.311E-01				
NeVIII 2P-3S	200000.	0.172	0.295E-02	0.615E-02	0.895E-02		
103.0 A	500000.	0.120	0.847E-02	*0.189E-01	*0.219E-01		
C=0.37E+22	1000000.	0.937E-01	0.106E-01	*0.308E-01	*0.312E-01		
	2000000.	0.744E-01	0.117E-01	*0.412E-01	*0.399E-01		
NeVIII 2P-4S	200000.	0.219	-0.877E-02				
74.6 A	500000.	0.166	0.739E-02				
C=0.80E+21	1000000.	0.136	0.155E-01				
	2000000.	0.110	0.186E-01				

PERTURBER DENSITY = 0.1E+22cm-3

PERTURBERS ARE:		ELECTRONS		PROTONS		He III	
TRANSITION	T(K)	WIDTH(A)	SHIFT(A)	WIDTH(A)	SHIFT(A)	WIDTH(A)	SHIFT(A)
NeVIII 2P-5S	200000.	0.338	-0.328E-01				
66.3 A	500000.	0.276	0.773E-02				
C=0.42E+21	1000000.	0.232	0.244E-01				
	2000000.	0.192	0.335E-01				
NeVIII 2P-6S	200000.	0.417	-0.751E-01				
62.6 A	500000.	0.414	-0.157E-01				
C=0.13E+21	1000000.	0.375	0.129E-01				
	2000000.	0.322	0.439E-01				
NeVIII 3P-4S	200000.	5.22	-0.116				
298.6 A	500000.	3.89	0.117				
C=0.11E+23	1000000.	3.13	0.233				
	2000000.	2.53	0.277				
NeVIII 3P-5S	200000.	3.79	-0.285				
198.9 A	500000.	3.02	0.686E-01				
C=0.38E+22	1000000.	2.51	0.213				
	2000000.	2.07	0.293				
NeVIII 3P-6S	200000.	3.58	-0.538				
168.8 A	500000.	3.40	-0.115				
C=0.91E+21	1000000.	3.03	0.890E-01				
	2000000.	2.59	0.313				

PERTURBER DENSITY = 0.1E+23cm-3

NeVIII 2S-3P	200000.	*1.76	*-0.102E-01
88.1 A	500000.	1.26	-0.855E-02
C=0.98E+22	1000000.	0.996	-0.480E-02
	2000000.	0.796	-0.299E-02
NeVIII 2P-3S	200000.	1.36	-0.166
103.0 A	500000.	1.04	-0.386E-01
C=0.37E+23	1000000.	0.840	0.166E-01
	2000000.	0.678	0.536E-01
NeVIII 2P-4S	200000.	*1.02	*-0.304
74.6 A	500000.	1.01	-0.114
C=0.80E+22	1000000.	0.925	-0.164E-01
	2000000.	0.811	0.432E-01
NeVIII 2P-5S	200000.	*0.864	*-0.568
66.3 A	500000.	1.21	-0.221
C=0.42E+22	1000000.	1.26	-0.603E-01
	2000000.	1.20	0.572E-01

PERTURBER DENSITY = 0.1E+19 cm-3

PERTURBERS ARE:		ELECTRONS		PROTONS		He III	
TRANSITION	T(K)	WIDTH(A)	SHIFT(A)	WIDTH(A)	SHIFT(A)	WIDTH(A)	SHIFT(A)
Na IX 2P-5S	200000.	0.247E-03	0.384E-04	0.466E-04	0.604E-04	0.931E-04	0.117E-03
52.5 A	500000.	0.184E-03	0.375E-04	0.751E-04	0.784E-04	0.153E-03	0.159E-03
C=0.22E+18	1000000.	0.149E-03	0.330E-04	0.956E-04	0.922E-04	0.199E-03	0.188E-03
	2000000.	0.120E-03	0.264E-04	0.114E-03	0.107E-03	0.233E-03	0.215E-03
Na IX 3P-4S	200000.	0.298E-02	0.240E-03	0.190E-03	0.312E-03	0.380E-03	0.615E-03
235.6 A	500000.	0.212E-02	0.228E-03	0.407E-03	0.463E-03	0.817E-03	0.940E-03
C=0.79E+19	1000000.	0.168E-02	0.219E-03	0.539E-03	0.556E-03	0.110E-02	0.113E-02
	2000000.	0.134E-02	0.184E-03	0.682E-03	0.653E-03	0.142E-02	0.134E-02
Na IX 3P-5S	200000.	0.265E-02	0.336E-03	0.411E-03	0.534E-03	0.821E-03	0.104E-02
157.3 A	500000.	0.195E-02	0.327E-03	0.666E-03	0.693E-03	0.135E-02	0.141E-02
C=0.20E+19	1000000.	0.156E-02	0.288E-03	0.845E-03	0.814E-03	0.176E-02	0.167E-02
	2000000.	0.126E-02	0.230E-03	0.101E-02	0.940E-03	0.209E-02	0.189E-02

PERTURBER DENSITY = 0.1E+20 cm-3

Na IX 2S-2P	200000.	0.304E-01	-0.455E-03	0.641E-04	-0.285E-03	0.120E-03	-0.538E-03
684.8 A	500000.	0.196E-01	-0.513E-03	0.312E-03	-0.712E-03	0.599E-03	-0.142E-02
C=0.68E+22	1000000.	0.142E-01	-0.582E-03	0.812E-03	-0.121E-02	0.158E-02	-0.244E-02
	2000000.	0.106E-01	-0.550E-03	0.149E-02	-0.173E-02	0.296E-02	-0.350E-02
Na IX 2S-3P	200000.	0.120E-02	0.136E-04	0.273E-04	0.433E-04	0.525E-04	0.819E-04
70.6 A	500000.	0.812E-03	0.125E-04	0.725E-04	0.811E-04	0.144E-03	0.163E-03
C=0.71E+19	1000000.	0.618E-03	0.110E-04	0.117E-03	0.112E-03	0.235E-03	0.227E-03
	2000000.	0.479E-03	0.838E-05	0.151E-03	0.134E-03	0.307E-03	0.273E-03
Na IX 3S-3P	200000.	1.95	-0.306E-01	0.246E-01	-0.530E-02	0.467E-01	-0.100E-01
2500.6 A	500000.	1.34	-0.409E-01	0.591E-01	-0.130E-01	0.115	-0.259E-01
C=0.89E+22	1000000.	1.04	-0.412E-01	0.861E-01	-0.214E-01	0.169	-0.433E-01
	2000000.	0.816	-0.420E-01	0.105	-0.298E-01	0.209	-0.603E-01
Na IX 2P-3S	200000.	0.905E-03	0.568E-04	0.187E-04	0.655E-04	0.363E-04	0.124E-03
81.3 A	500000.	0.622E-03	0.671E-04	0.745E-04	0.120E-03	0.150E-03	0.241E-03
C=0.26E+20	1000000.	0.480E-03	0.664E-04	0.135E-03	0.165E-03	0.271E-03	0.334E-03
	2000000.	0.378E-03	0.633E-04	0.189E-03	0.199E-03	0.381E-03	0.401E-03
Na IX 2P-4S	200000.	0.126E-02	0.153E-03	0.129E-03	0.201E-03	*0.259E-03	*0.373E-03
59.0 A	500000.	0.913E-03	0.151E-03	0.276E-03	0.309E-03	*0.556E-03	*0.621E-03
C=0.57E+19	1000000.	0.730E-03	0.148E-03	0.367E-03	0.376E-03	0.753E-03	0.770E-03
	2000000.	0.588E-03	0.125E-03	0.445E-03	0.452E-03	0.931E-03	0.902E-03
Na IX 2P-5S	200000.	0.247E-02	0.336E-03	*0.466E-03	*0.549E-03		
52.5 A	500000.	0.184E-02	0.354E-03	*0.752E-03	*0.763E-03		
C=0.22E+19	1000000.	0.148E-02	0.325E-03	0.956E-03	0.918E-03		
	2000000.	0.120E-02	0.264E-03	0.114E-02	0.107E-02		
Na IX 3P-4S	200000.	0.298E-01	0.224E-02	0.191E-02	0.292E-02	0.379E-02	0.546E-02
235.6 A	500000.	0.212E-01	0.221E-02	0.406E-02	0.455E-02	0.817E-02	0.910E-02
C=0.79E+20	1000000.	0.168E-01	0.217E-02	0.539E-02	0.554E-02	*0.110E-01	*0.113E-01
	2000000.	0.134E-01	0.184E-02	0.682E-02	0.653E-02	*0.142E-01	*0.133E-01

PERTURBER DENSITY = 0.1E+20 cm-3

PERTURBERS ARE:		ELECTRONS		PROTONS		He III	
TRANSITION	T(K)	WIDTH(A)	SHIFT(A)	WIDTH(A)	SHIFT(A)	WIDTH(A)	SHIFT(A)
Na IX 3P-5S	200000.	0.265E-01	0.293E-02	*0.411E-02	*0.485E-02		
157.3 A	500000.	0.195E-01	0.309E-02	*0.666E-02	*0.674E-02		
C=0.20E+20	1000000.	0.156E-01	0.284E-02	0.845E-02	0.810E-02		
	2000000.	0.126E-01	0.230E-02	0.101E-01	0.940E-02		

PERTURBER DENSITY = 0.1E+21 cm-3

Na IX 2S-2P	200000.	0.304	0.361E-02	0.634E-03	-0.253E-02	0.116E-02	-0.423E-02
684.8 A	500000.	0.196	-0.502E-02	0.311E-02	-0.690E-02	0.596E-02	-0.131E-01
C=0.68E+23	1000000.	0.143	-0.574E-02	0.812E-02	-0.120E-01	0.158E-01	-0.236E-01
	2000000.	0.106	-0.548E-02	0.149E-01	-0.173E-01	0.296E-01	-0.349E-01
Na IX 2S-3P	200000.	0.120E-01	0.548E-04	0.271E-03	0.381E-03	0.507E-03	0.630E-03
70.6 A	500000.	0.812E-02	0.802E-04	0.726E-03	0.778E-03	0.144E-02	0.148E-02
C=0.71E+20	1000000.	0.617E-02	0.923E-04	0.117E-02	0.110E-02	*0.234E-02	*0.215E-02
	2000000.	0.479E-02	0.800E-04	0.151E-02	0.134E-02	*0.307E-02	*0.272E-02
Na IX 3S-3P	200000.	19.5	-0.310	0.243	-0.471E-01	0.466	-0.788E-01
2500.6 A	500000.	13.4	-0.420	0.590	-0.126	1.14	-0.240
C=0.89E+23	1000000.	10.4	-0.405	0.861	-0.212	1.69	-0.419
	2000000.	8.16	-0.421	1.05	-0.298	2.09	-0.602
Na IX 2P-3S	200000.	0.905E-02	0.452E-03	0.187E-03	0.575E-03	0.361E-03	0.950E-03
81.3 A	500000.	0.622E-02	0.621E-03	0.749E-03	0.114E-02	0.151E-02	0.219E-02
C=0.26E+21	1000000.	0.481E-02	0.632E-03	0.135E-02	0.162E-02	0.271E-02	0.318E-02
	2000000.	0.378E-02	0.628E-03	0.189E-02	0.198E-02	0.381E-02	0.400E-02
Na IX 2P-4S	200000.	0.126E-01	0.106E-02	*0.129E-02	*0.166E-02		
59.0 A	500000.	0.912E-02	0.124E-02	*0.276E-02	*0.286E-02		
C=0.57E+20	1000000.	0.729E-02	0.136E-02	*0.366E-02	*0.364E-02		
	2000000.	0.587E-02	0.123E-02	*0.445E-02	*0.450E-02		
Na IX 2P-5S	200000.	0.241E-01	0.146E-02				
52.5 A	500000.	0.180E-01	0.247E-02				
C=0.22E+20	1000000.	0.146E-01	0.275E-02				
	2000000.	0.118E-01	0.254E-02				
Na IX 3P-4S	200000.	0.297	0.158E-01	*0.190E-01	*0.244E-01		
235.6 A	500000.	0.212	0.183E-01	*0.407E-01	*0.422E-01		
C=0.79E+21	1000000.	0.168	0.200E-01	*0.540E-01	*0.538E-01		
	2000000.	0.134	0.180E-01	*0.682E-01	*0.650E-01		
Na IX 3P-5S	200000.	0.259	0.126E-01				
157.3 A	500000.	0.191	0.215E-01				
C=0.20E+21	1000000.	0.154	0.240E-01				
	2000000.	0.124	0.222E-01				

PERTURBER DENSITY = 0.1E+22 cm-3

Na IX 2S-2P	200000.	3.04	-0.211E-01	0.564E-02	-0.167E-01	0.864E-02	-0.192E-01
684.8 A	500000.	1.96	-0.421E-01	0.510E-01	-0.620E-01	0.586E-01	-0.108
C=0.68E+24	1000000.	1.43	-0.518E-01	0.810E-01	-0.115	0.157	-0.216
	2000000.	1.06	-0.527E-01	0.149	-0.170	0.296	-0.333

PERTURBER DENSITY = 0.1E+22 cm-3

PERTURBERS ARE:		ELECTRONS		PROTONS		He III	
TRANSITION	T(K)	WIDTH(A)	SHIFT(A)	WIDTH(A)	SHIFT(A)	WIDTH(A)	SHIFT(A)
Na IX 2S-3P	200000.	0.117	-0.137E-02	0.242E-02	0.240E-02	*0.372E-02	*0.251E-02
70.6 A	500000.	0.796E-01	-0.398E-03	*0.716E-02	*0.660E-02		
C=0.71E+21	1000000.	0.607E-01	0.779E-04	*0.117E-01	*0.102E-01		
	2000000.	0.471E-01	0.353E-03	*0.151E-01	*0.130E-01		
Na IX 2P-3S	200000.	0.901E-01	0.830E-03	0.183E-02	0.359E-02	*0.321E-02	*0.370E-02
81.3 A	500000.	0.620E-01	0.404E-02	0.746E-02	0.968E-02		
C=0.26E+22	1000000.	0.479E-01	0.497E-02	*0.135E-01	*0.150E-01		
	2000000.	0.377E-01	0.563E-02	*0.189E-01	*0.192E-01		
Na IX 2P-4S	200000.	0.114	-0.366E-02				
59.0 A	500000.	0.851E-01	0.375E-02				
C=0.57E+21	1000000.	0.689E-01	0.786E-02				
	2000000.	0.559E-01	0.940E-02				
Na IX 2P-5S	200000.	0.172	-0.202E-01				
52.5 A	500000.	0.143	0.726E-03				
C=0.22E+21	1000000.	0.121	0.981E-02				
	2000000.	0.101	0.152E-01				
Na IX 3P-4S	200000.	2.75	-0.458E-01				
235.6 A	500000.	2.01	0.592E-01				
C=0.79E+22	1000000.	1.60	0.118				
	2000000.	1.29	0.140				
Na IX 3P-5S	200000.	1.96	-0.176				
157.3 A	500000.	1.58	0.622E-02				
C=0.20E+22	1000000.	1.31	0.850E-01				
	2000000.	1.08	0.132				

PERTURBER DENSITY = 0.1E+23 cm-3

Na IX 2S-3P	200000.	*1.02	*-0.596E-02
70.6 A	500000.	0.717	-0.512E-02
C=0.71E+22	1000000.	0.556	-0.387E-02
	2000000.	0.437	-0.202E-02
Na IX 2P-3S	200000.	0.740	-0.850E-01
81.3 A	500000.	0.555	-0.180E-01
C=0.26E+23	1000000.	0.440	0.813E-02
	2000000.	0.351	0.279E-01
Na IX 2P-4S	200000.	0.573	-0.153
59.0 A	500000.	0.546	-0.612E-01
C=0.57E+22	1000000.	0.491	-0.901E-02
	2000000.	0.425	0.236E-01
Na IX 2P-5S	200000.	0.490	-0.264
52.5 A	500000.	0.638	-0.112
C=0.22E+22	1000000.	0.664	-0.373E-01
	2000000.	0.626	0.210E-01

PERTURBER DENSITY = 0.1E+23 cm-3

PERTURBERS ARE:		ELECTRONS		PROTONS		He III	
TRANSITION	T(K)	WIDTH(A)	SHIFT(A)	WIDTH(A)	SHIFT(A)	WIDTH(A)	SHIFT(A)
Na IX 3P-4S	200000.	*16.8	*-2.33				
235.6 A	500000.	14.3	-0.935				
C=0.79E+23	1000000.	12.3	-0.139				
	2000000.	10.4	0.350				
Na IX 3P-5S	200000.	*7.80	*-2.33				
157.3 A	500000.	8.24	-0.986				
C=0.20E+23	1000000.	7.96	-0.333				
	2000000.	7.23	0.178				

1969ab). Values for NV > 0.5 are not given and values for $0.1 < NV \leq 0.5$ are denoted by an asterisk. When the impact approximation is not valid, the ion broadening contribution may be estimated by using quasistatic estimations (Sahal–Bréchot 1991 and Griem 1974). The accuracy of the results obtained decreases when broadening by ion interactions becomes important.

The analysis of present results and comparison with available experimental and theoretical data is given in Dimitrijević and Sahal–Bréchot (1994).

Acknowledgements – This work is a part of French–Yugoslav collaboration through the project "L'elargissement Stark des raies spectrales des plasmas astrophysiques et de laboratoire", it is also a part of the project "Physics and dynamics of celestial bodies", supported by Ministry for Science and Technology of Serbia.

REFERENCES

Dimitrijević, M. S., and Sahal–Bréchot, S.: 1984, *JQSRT* **31**, 301.

Dimitrijević, M. S., and Sahal–Bréchot, S.: 1994, *Astron. Astrophys. Suppl. Series* in press.

Dimitrijević, M. S., Sahal–Bréchot, S., and Bommier, V.: 1991, *Astron. Astrophys. Suppl. Series.* **89**, 581.

Griem, H. R.: 1974, *Spectral Line Broadening by Plasmas*, Academic Press, New York.

Sahal–Bréchot, S.: 1969a, *Astron. Astrophys.* **1**, 91.

Sahal–Bréchot, S.: 1969b, *Astron. Astrophys.* **2**, 322.

Sahal–Bréchot, S.: 1991, *Astron. Astrophys.* **245**, 322.

ТАБЕЛЕ ПАРАМЕТАРА ШТАРКОВОГ ШИРЕЊА ЛИНИЈА Ne VIII и Na IX ОД ЗНАЧАЈА У АСТРОФИЗИЦИ

М. С. Димитријевић[1] и S. Sahal–Bréchot[2]

[1] *Астрономска опсерваторија, Волгина 7, 11050 Београд, Југославија*

[2] *Laboratoire "Astrophysique, Atomes et Molécules"*
Département Atomes et Molécules en Astrophysique
Unité associée au C.N.R.S. No 812
Observatoire de Paris-Meudon, 92190 Meudon, France

УДК 52–355.3
Претходно саопштење

Користећи семикласичан прилаз, израчунате су ширине и помераји спектралних линија, проузроковани сударима са електронима, протонима и He III, за 20 мултиплета Ne VIII и 8 мултиплета Na IX. Резултати су дати у функцији температуре и концентрације пертурбера.

Bull. Astron. Belgrade № 148 (1993), 65 – 69

UDC 52–355.3
Addendum

STARK BROADENING PARAMETER TABLES FOR Be I LINES OF ASTROPHYSICAL INTEREST

M. S. Dimitrijević[1] and S. Sahal–Bréchot[2]

[1] *Astronomical Observatory, Volgina 7, 11050 Belgrade, Yugoslavia*
[2] *Laboratoire "Astrophysique, Atomes et Molécules"*
Département Atomes et Molécules en Astrophysique
Unité associée au C.N.R.S. No 812
Observatoire de Paris–Meudon, 92190 Meudon, France

(Received: October 4, 1993)

(Addendum to the article published in Bull. Astron. Belgrade № 146 (1992) 73)

Table 1 is also available in electronic form: see the editorial in Astron.Astrophys. 1992, Vol. 266, No 2, page E1 or in Astron. Astrophys. Suppl. Series 1992, Vol. 96, No 3, and Dimitrijević, M. S., Sahal–Bréchot, S.: 1994, Astron. Astrophys. Suppl. Series, in press.

Addendum to the Table 1 for perturber density 10^{15} cm^{-3}. This addendum to the table 1 gives electron–, proton–, and ionized–helium– impact broadening parameters for Be I lines, for temperatures from 3,000 K to 50,000 K. Transitions and averaged wavelengths for the multiplet (in Å) are also given. By dividing c by the electron–impact full halfwidth, we obtain an estimate for the maximum perturber density for which the line may be treated as isolated and tabulated data may be used.

PERTURBER DENSITY = $1 \cdot 10^{15}$ cm^{-3}							
PERTURBERS ARE		ELECTRONS		PROTONS		IONIZED HELIUM	
TRANSITION	T [K]	WIDTH (Å)	SHIFT (Å)	WIDTH (Å)	SHIFT (Å)	WIDTH (Å)	SHIFT (Å)
2S - 2P	3000.	0.165E-03	0.961E-04	0.102E-03	0.259E-04	0.101E-03	0.215E-04
2349.3 Å	5000.	0.184E-03	0.103E-03	0.102E-03	0.283E-04	0.101E-03	0.235E-04
C= 0.67E+18	10000.	0.201E-03	0.100E-03	0.103E-03	0.319E-04	0.102E-03	0.264E-04
	20000.	0.234E-03	0.820E-04	0.104E-03	0.358E-04	0.102E-03	0.297E-04
	30000.	0.267E-03	0.589E-04	0.104E-03	0.384E-04	0.103E-03	0.318E-04
	50000.	0.326E-03	0.325E-04	0.105E-03	0.418E-04	0.103E-03	0.347E-04
2S - 3P	3000.	0.793E-03	0.494E-03	0.312E-03	0.135E-03	0.304E-03	0.112E-03
1661.5 Å	5000.	0.860E-03	0.556E-03	0.318E-03	0.149E-03	0.308E-03	0.123E-03
C= 0.12E+18	10000.	0.962E-03	0.633E-03	0.327E-03	0.169E-03	0.313E-03	0.140E-03
	20000.	0.109E-02	0.641E-03	0.338E-03	0.190E-03	0.321E-03	0.158E-03
	30000.	0.118E-02	0.612E-03	0.346E-03	0.204E-03	0.326E-03	0.169E-03
	50000.	0.131E-02	0.531E-03	0.357E-03	0.222E-03	0.334E-03	0.184E-03
2S - 4P	3000.	0.227E-02	0.132E-02	0.896E-03	0.346E-03	0.876E-03	0.283E-03
1491.8 Å	5000.	0.254E-02	0.148E-02	0.909E-03	0.383E-03	0.886E-03	0.315E-03
C= 0.39E+17	10000.	0.299E-02	0.166E-02	0.930E-03	0.437E-03	0.900E-03	0.361E-03
	20000.	0.357E-02	0.152E-02	0.957E-03	0.496E-03	0.918E-03	0.410E-03
	30000.	0.396E-02	0.140E-02	0.975E-03	0.533E-03	0.930E-03	0.441E-03
	50000.	0.447E-02	0.116E-02	0.100E-02	0.581E-03	0,948E-03	0.482E-03
2S - 5P	3000.	0.567E-02	0.306E-02	*0.215E-02	*0.750E-03	*0.210E-02	*0.610E-03
1426.1 Å	5000.	0.654E-02	0.331E-02	0.218E-02	0.840E-03	*0.213E-02	*0.687E-03
C= 0.16E+17	10000.	0.798E-02	0.345E-02	0.223E-02	0.967E-03	*0.217E-02	*0.796E-03
	20000.	0.976E-02	0.318E-02	0.228E-02	0.110E-02	0.220E-02	0.910E-03
	30000.	0.109E-01	0.277E-02	0.232E-02	0.119E-02	0.223E-02	0.981E-03
	50000.	0.122E-01	0.229E-02	0.238E-02	0.130E-02	0.227E-02	0.108E-02
2S - 6P	3000.	0.124E-01	0.568E-02	*0.442E-02	*0.136E-02		
1393.8 Å	5000.	0.147E-01	0.621E-02	*0.451E-02	*0.154E-02		
C= 0.83E+16	10000.	0.184E-01	0.623E-02	*0.460E-02	*0.180E-02	*0.449E-02	*0.147E-02
	20000.	0.228E-01	0.545E-02	0.469E-02	0.206E-02	*0.456E-02	*0.170E-02
	30000.	0.255E-01	0.472E-02	0.476E-02	0.223E-02	*0.460E-02	*0.184E-02
	50000.	0.282E-01	0.385E-02	0.485E-02	0.244E-02	*0.467E-02	*0.202E-02
3S - 3P	3000.	0.752E-01	0.261E-01	0.350E-01	0.727E-02	0.349E-01	0.601E-02
18148.6 Å	5000.	0.825E-01	0.275E-01	0.351E-01	0.798E-02	0.350E-01	0.659E-02
C= 0.14E+20	10000.	0.105	0.221E-01	0.353E-01	0.899E-02	0.351E-01	0.747E-02
	20000.	0.145	0.173E-01	0.355E-01	0.101E-01	0.352E-01	0.840E-02
	30000.	0.174	0.158E-01	0.356E-01	0.109E-01	0.353E-01	0.900E-02
	50000.	0.211	0.126E-01	0.358E-01	0.118E-01	0.354E-01	0.982E-02
3S - 4P	3000.	0.658E-01	0.365E-01	0.261E-01	0.937E-02	0.256E-01	0.768E-02
8092.3 Å	5000.	0.736E-01	0.414E-01	0.264E-01	0.104E-01	0.259E-01	0.854E-02
C= 0.11E+19	10000.	0.883E-01	0.421E-01	0.269E-01	0.118E-01	0.262E-01	0.976E-02
	20000.	0.109	0.352E-01	0.276E-01	0.134E-01	0.266E-01	0.111E-01
	30000.	0.124	0.304E-01	0.280E-01	0.144E-01	0.269E-01	0.119E-01
	50000.	0.143	0.273E-01	0.287E-01	0.157E-01	0.274E-01	0.130E-01

PERTURBER DENSITY = $1 \cdot 10^{18}$ cm^{-3}							
PERTURBERS ARE		ELECTRONS		PROTONS		IONIZED HELIUM	
TRANSITION	T [K]	WIDTH (Å)	SHIFT (Å)	WIDTH (Å)	SHIFT (Å)	WIDTH (Å)	SHIFT (Å)
3S - 5P	3000.	0.117	0.612E-01	*0.442E-01	*0.152E-01	*0.432E-01	*0.123E-01
6475.3 Å	5000.	0.135	0.690E-01	0.449E-01	0.170E-01	*0.439E-01	*0.139E-01
C= 0.33E+18	10000.	0.166	0.700E-01	0.458E-01	0.195E-01	*0.446E-01	*0.161E-01
	20000.	0.205	0.602E-01	0.469E-01	0.223E-01	0.453E-01	0.184E-01
	30000.	0.230	0.532E-01	0.476E-01	0.240E-01	0.458E-01	0.198E-01
	50000.	0.259	0.454E-01	0.487E-01	0.263E-01	0.466E-01	0.217E-01
3S - 6P	3000.	0.220	0.102	*0.781E-01	*0.239E-01		
5858.6 Å	5000.	0.260	0.108	*0.796E-01	*0.271E-01		
C= 0.15E+18	10000.	0.327	0.112	*0.811E-01	*0.315E-01	*0.793E-01	*0.258E-01
	20000.	0.407	0.929E-01	0.828E-01	0.362E-01	*0.805E-01	*0.298E-01
	30000.	0.455	0.792E-01	0.839E-01	0.390E-01	*0.813E-01	*0.322E-01
	50000.	0.505	0.662E-01	0.856E-01	0.429E-01	*0.824E-01	*0.354E-01
4S - 4P	3000.	3.26	-1.33	1.22	-0.337	1.20	-0.277
55885.6 Å	5000.	4.00	-1.48	1.22	-0.372	1.21	-0.307
C= 0.55E+20	10000.	5.45	-1.50	1.24	-0.423	1.22	-0.350
	20000.	7.33	-1.25	1.25	-0.480	1.23	-0.397
	30000.	8.53	-1.08	1.26	-0.515	1.24	-0.427
	50000.	9.93	-0.958	1.28	-0.562	1.25	-0.465
4S - 5P	3000.	1.08	0.408	*0.433	*0.111	*0.428	*0.908E-01
20512.1 Å	5000.	1.30	0.387	0.437	0.124	*0.432	*0.102
C= 0.34E+19	10000.	1.72	0.315	0.442	0.142	*0.436	*0.117
	20000.	2.28	0.234	0.447	0.162	0.440	0.134
	30000.	2.62	0.239	0.450	0.174	0.442	0.144
	50000.	2.99	0.170	0.456	0.191	0.445	0.158
4S - 6P	3000.	1.49	0.638	*0.535	*0.150		
15382.8 Å	5000.	1.78	0.633	*0.543	*0.170		
C= 0.10E+19	10000.	2.30	0.570	*0.553	*0.198	*0.542	*0.162
	20000.	2.94	0.418	0.562	0.226	*0.549	*0.187
	30000.	3.31	0.371	0.568	0.244	*0.554	*0.202
	50000.	3.70	0.292	0.577	0.268	*0.560	*0.222
2P - 3S	3000.	0.130E-01	0.946E-02	0.306E-02	0.262E-02	0.261E-02	0.216E-02
8256.3 Å	5000.	0.145E-01	0.107E-01	0.329E-02	0.288E-02	0.280E-02	0.238E-02
C= 0.38E+19	10000.	0.162E-01	0.124E-01	0.365E-02	0.326E-02	0.310E-02	0.270E-02
	20000.	0.175E-01	0.129E-01	0.406E-02	0.368E-02	0.343E-02	0.305E-02
	30000.	0.186E-01	0.126E-01	0.433E-02	0.394E-02	0.364E-02	0.327E-02
	50000.	0.198E-01	0.113E-01	0.469E-02	0.430E-02	0.394E-02	0.356E-02
2P - 4S	3000.	0.203E-01	0.155E-01	0.458E-02	0.404E-02	0.380E-02	0.330E-02
4409.2 Å	5000.	0.230E-01	0.179E-01	0.498E-02	0.449E-02	0.414E-02	0.368E-02
C= 0.35E+18	10000.	0.252E-01	0.202E-01	0.559E-02	0.513E-02	0.464E-02	0.423E-02
	20000.	0.262E-01	0.198E-01	0.628E-02	0.582E-02	0.521E-02	0.481E-02
	30000.	0.266E-01	0.182E-01	0.672E-02	0.627E-02	0.558E-02	0.518E-02
	50000.	0.281E-01	0.155E-01	0.731E-02	0.685E-02	0.607E-02	0.568E-02

PERTURBER DENSITY = $1 \cdot 10^{15}$ cm^{-3}							
PERTURBERS ARE		ELECTRONS		PROTONS		IONIZED HELIUM	
TRANSITION	T [K]	WIDTH (Å)	SHIFT (Å)	WIDTH (Å)	SHIFT (Å)	WIDTH (Å)	SHIFT (Å)
3P - 4S	3000.	0.409	0.296	0.927E-01	0.754E-01	0.796E-01	0.617E-01
19770.7 Å	5000.	0.454	0.342	0.997E-01	0.838E-01	0.852E-01	0.688E-01
C= 0.70E+19	10000.	0.501	0.345	0.110	0.957E-01	0.938E-01	0.789E-01
	20000.	0.567	0.335	0.122	0.109	0.104	0.898E-01
	30000.	0.612	0.294	0.130	0.117	0.110	0.967E-01
	50000.	0.696	0.250	0.141	0.128	0.119	0.106
2P - 3D	3000.	0.853E-02	0.537E-02	0.290E-02	0.145E-02	0.278E-02	0.120E-02
4573.9 Å	5000.	0.940E-02	0.603E-02	0.297E-02	0.160E-02	0.283E-02	0.132E-02
C= 0.55E+18	10000.	0.107E-01	0.681E-02	0.309E-02	0.182E-02	0.291E-02	0.150E-02
	20000.	0.122E-01	0.686E-02	0.323E-02	0.205E-02	0.301E-02	0.170E-02
	30000.	0.134E-01	0.673E-02	0.333E-02	0.220E-02	0.308E-02	0.182E-02
	50000.	0.149E-01	0.573E-02	0.347E-02	0.240E-02	0.319E-02	0.199E-02
2P - 4D	3000.	0.217E-01	-0.557E-02	0.681E-02	-0.270E-02	0.664E-02	-0.221E-02
3814.5 Å	5000.	0.251E-01	-0.333E-02	0.692E-02	-0.300E-02	0.673E-02	-0.247E-02
C= 0.79E+17	10000.	0.308E-01	-0.919E-03	0.710E-02	-0.343E-02	0.685E-02	-0.283E-02
	20000.	0.364E-01	0.113E-02	0.732E-02	-0.389E-02	0.699E-02	-0.322E-02
	30000.	0.399E-01	0.212E-02	0.748E-02	-0.419E-02	0.710E-02	-0.346E-02
	50000.	0.439E-01	0.228E-02	0.771E-02	-0.457E-02	0.725E-02	-0.379E-02
3P - 3D	3000.	0.194	0.835E-01	0.639E-01	0.218E-01	0.630E-01	0.180E-01
23579.5 Å	5000.	0.214	0.875E-01	0.645E-01	0.240E-01	0.634E-01	0.198E-01
C= 0.14E+20	10000.	0.272	0.850E-01	0.655E-01	0.272E-01	0.640E-01	0.225E-01
	20000.	0.371	0.663E-01	0.667E-01	0.306E-01	0.648E-01	0.254E-01
	30000.	0.444	0.559E-01	0.677E-01	0.328E-01	0.654E-01	0.272E-01
	50000.	0.535	0.499E-01	0.691E-01	0.358E-01	0.663E-01	0.297E-01
3P - 4D	3000.	0.205	-0.640E-01	0.593E-01	-0.272E-01	0.571E-01	-0.222E-01
11636.7 Å	5000.	0.234	-0.424E-01	0.606E-01	-0.302E-01	0.581E-01	-0.248E-01
C= 0.73E+18	10000.	0.290	-0.250E-01	0.627E-01	-0.345E-01	0.596E-01	-0.285E-01
	20000.	0.353	-0.136E-01	0.654E-01	-0.392E-01	0.614E-01	-0.324E-01
	30000.	0.393	-0.926E-02	0.672E-01	-0.422E-01	0.627E-01	-0.349E-01
	50000.	0.440	0.295E-03	0.699E-01	-0.461E-01	0.646E-01	-0.382E-01
4P - 4D	3000.	6.54	-3.29	1.52	-0.875	1.43	-0.714
57268.5 Å	5000.	7.32	-3.07	1.58	-0.975	1.47	-0.800
C= 0.18E+20	10000.	9.01	-2.59	1.67	-1.12	1.54	-0.921
	20000.	11.4	-2.07	1.78	-1.27	1.62	-1.05
	30000.	12.9	-1.78	1.86	-1.37	1.67	-1.13
	50000.	14.6	-1.40	1.96	-1.50	1.75	-1.24
3D - 4P	3000.	1.43	0.754	0.496	0.183	0.486	0.150
38367.2 Å	5000.	1.61	0.749	0.502	0.202	0.491	0.167
C= 0.26E+20	10000.	2.02	0.743	0.512	0.230	0.497	0.190
	20000.	2.61	0.579	0.525	0.261	0.506	0.216
	30000.	3.04	0.511	0.534	0.280	0.512	0.232
	50000.	3.56	0.468	0.548	0.306	0.521	0.254

PERTURBER DENSITY = $1 \cdot 10^{15}$ cm^{-3}							
PERTURBERS ARE		ELECTRONS		PROTONS		IONIZED HELIUM	
TRANSITION	T [K]	WIDTH (Å)	SHIFT (Å)	WIDTH (Å)	SHIFT (Å)	WIDTH (Å)	SHIFT (Å)
3D - 5P	3000.	0.858	0.449	*0.304	*0.108	*0.297	*0.381E-01
17568.0 Å	5000.	0.992	0.483	0.309	0.121	*0.301	*0.992E-01
C= 0.25E+19	10000.	1.23	0.490	0.315	0.139	0.306	0.115
	20000.	1.54	0.400	0.323	0.159	0.312	0.131
	30000.	1.74	0.360	0.329	0.171	0.315	0.141
	50000.	1.98	0.309	0.338	0.188	0.321	0.155
3D - 6P	3000.	1.20	0.538	*0.412	*0.129		
13665.3 Å	5000.	1.42	0.611	*0.419	*0.146		
C= 0.79E+18	10000.	1.79	0.595	*0.428	*0.170	*0.418	*0.139
	20000.	2.24	0.477	0.437	0.195	*0.424	*0.160
	30000.	2.50	0.409	0.443	0.210	*0.429	*0.173
	50000.	2.79	0.332	0.453	0.231	*0.435	*0.191
4D - 5P	3000.	20.9	9.91	5.20	2.47	*4.96	*2.01
74647.5 Å	5000.	23.9	10.6	5.34	2.78	*5.08	*2.27
C= 0.30E+20	10000.	29.4	10.6	5.57	3.21	5.24	2.64
	20000.	36.4	8.75	5.84	3.66	5.43	3.02
	30000.	41.1	7.31	6.02	3.95	5.57	3.26
	50000.	46.3	6.68	6.29	4.33	5.76	3.58
4D - 6P	3000.	8.35	3.68	*2.37	*0.855		
33724.2 Å	5000.	9.84	3.91	*2.43	*0.972	*2.35	*0.790
C= 0.48E+19	10000.	12.4	3.97	*2.49	*1.13	*2.41	*0.928
	20000.	15.3	3.19	2.57	1.30	*2.46	*1.07
	30000.	17.2	2.64	2.62	1.41	*2.49	*1.16
	50000.	19.1	2.31	2.69	1.54	2.54	1.28
2P - 3S	3000.	0.142E-02	0.120E-02	0.369E-03	0.338E-03	0.307E-03	0.279E-03
3322.0 Å	5000.	0.163E-02	0.134E-02	0.401E-03	0.370E-03	0.334E-03	0.306E-03
C= 0.75E+18	10000.	0.192E-02	0.157E-02	0.450E-03	0.419E-03	0.374E-03	0.347E-03
	20000.	0.211E-02	0.174E-02	0.504E-03	0.472E-03	0.419E-03	0.391E-03
	30000.	0.219E-02	0.175E-02	0.539E-03	0.506E-03	0.448E-03	0.419E-03
	50000.	0.229E-02	0.165E-02	0.587E-03	0.551E-03	0.488E-03	0.457E-03
3S - 3P	3000.	0.499E-01	0.285E-01	0.199E-01	0.766E-02	0.195E-01	0.632E-02
14643.5 Å	5000.	0.545E-01	0.286E-01	0.201E-01	0.841E-02	0.197E-01	0.695E-02
C= 0.68E+19	10000.	0.678E-01	0.214E-01	0.206E-01	0.953E-02	0.200E-01	0.788E-02
	20000.	0.922E-01	0.123E-01	0.211E-01	0.107E-01	0.203E-01	0.889E-02
	30000.	0.109	0.948E-02	0.215E-01	0.115E-01	0.206E-01	0.953E-02
	50000.	0.129	0.554E-02	0.220E-01	0.125E-01	0.209E-01	0.104E-01
3S - 4P	3000.	0.644E-01	0.464E-01	0.200E-01	0.113E-01	0.188E-01	0.925E-02
6788.4 Å	5000.	0.703E-01	0.493E-01	0.208E-01	0.126E-01	0.193E-01	0.104E-01
C= 0.52E+18	10000.	0.803E-01	0.467E-01	0.219E-01	0.145E-01	0.202E-01	0.119E-01
	20000.	0.938E-01	0.393E-01	0.233E-01	0.164E-01	0.212E-01	0.136E-01
	30000.	0.105	0.342E-01	0.242E-01	0.177E-01	0.219E-01	0.146E-01
	50000.	0.119	0.286E-01	0.255E-01	0.193E-01	0.229E-01	0.160E-01

Bull. Astron. Belgrade № 149 (1994), 31 – 84

UDC 52–355.3
Preliminary report

STARK BROADENING PARAMETER TABLES FOR Mg I LINES OF INTEREST FOR SOLAR AND STELLAR SPECTRA RESEARCH. I

M. S. Dimitrijević[1] and S. Sahal–Bréchot[2]

[1] *Astronomical Observatory, Volgina 7, 11050 Belgrade, Yugoslavia*

[2] *Laboratoire "Astrophysique, Atomes et Molécules"*
Département Atomes et Molécules en Astrophysique
Unité associée au C.N.R.S. No 812
Observatoire de Paris–Meudon, 92190 Meudon, France

(Received: May 6, 1994)

SUMMARY: Using a semiclassical approach, we have calculated electron–, proton–, and He II–impact line widths and shifts for 267 Mg I multiplets as a function of temperature and perturber density.

1. INTRODUCTION

Lines of neutral magnesium are present in the solar spectrum and the corresponding Stark broadening parameters are of interest for their analysis as well as for the diagnostic of solar plasma. Especially the infrared lines of Mg I have been observed in the solar spectrum at Kitt Peak and during the Atmos experiment on Spacelab (Brault and Noyes, 1983; Farmer and Norton, 1989; Jefferies, 1991). Due to the suitability of these lines for the solar atmosphere investigations (see e.g. Van Regemorter and Hoang-Binh 1993), and to the fact that with the increase of the principal quantum number increases the importance of the Stark broadening as well, the corresponding Stark widths and shifts are of importance for the structure of the solar atmosphere diagnostics. Moreover, Stark broadening parameters of the neutral magnesium lines are important for the diagnostics of laboratory plasmas as well. By using the semiclassical-perturbation formalism (Sahal–Bréchot, 1969ab) we have calculated electron-, proton-, and ionized helium-, -impact line widths and shifts for 267 Mg I multiplets, in order to continue our effort to provide to astrophysicists the needed Stark broadening data. In the second part of this article we will publish Stark broadening data for ionized magnesium-, ionized silicon-, and ionized iron-impacts with neutral magnesium in order to provide the data for all principal perturbers in the solar plasma. A summary of the formalism is given in Dimitrijević et al. (1991). Analysis of obtained results and all details of calculations will be published elsewhere (Dimitrijević and Sahal–Bréchot, 1994ab). Here, we present tables for solar and laboratory plasma diagnostic purposes.

Table 1. This table shows electron-, proton-, and He III- impact broadening parameters for Mg I for a perturber density of 10^{11} cm^{-3} and temperatures from 2,500 up to 50,000 K. Transitions and averaged wavelengths for the multiplet (in Å) are also given. By using c [see Eq. (5) in Dimitrijević et al, 1991a], we obtain an estimate for the maximum perturber density for which the line may be treated as isolated and tabulated data may be used. The asterisk identifies cases for which the collision volume multiplied by the perturber density (the condition for validity of the impact approximation) lies between 0.1 and 0.5. Table 1 is also available in electronic form: see the editorial in Astron. Astrophys. 1992, Vol. 266, No 2, page E1 or in Astron. Astrophys. Suppl. Series 1992, Vol. 96, No3, and Dimitrijević and Sahal-Bréchot, 1994a.

Perturber density = 1 x 10^{11} cm^{-3}

Transition	T(K)	Electrons Width (Å)	Electrons Shift (Å)	Protons Width (Å)	Protons Shift (Å)	Ionized helium Width (Å)	Ionized helium Shift (Å)
3S - 3P 2853.0 Å C= 0.69E+14	2500.	0.537E-07	0.408E-07	0.257E-07	0.116E-07	0.245E-07	0.734E-08
	5000.	0.630E-07	0.473E-07	0.263E-07	0.130E-07	0.247E-07	0.824E-08
	10000.	0.718E-07	0.549E-07	0.271E-07	0.146E-07	0.249E-07	0.924E-08
	20000.	0.804E-07	0.588E-07	0.281E-07	0.164E-07	0.253E-07	0.104E-07
	30000.	0.876E-07	0.604E-07	0.288E-07	0.175E-07	0.256E-07	0.111E-07
	50000.	0.974E-07	0.525E-07	0.298E-07	0.191E-07	0.259E-07	0.121E-07
3S - 4P 2026.5 Å C= 0.12E+14	2500.	0.163E-06	0.916E-07	0.688E-07	0.256E-07	0.669E-07	0.162E-07
	5000.	0.185E-06	0.109E-06	0.698E-07	0.287E-07	0.672E-07	0.182E-07
	10000.	0.211E-06	0.122E-06	0.711E-07	0.323E-07	0.676E-07	0.204E-07
	20000.	0.245E-06	0.127E-06	0.729E-07	0.362E-07	0.681E-07	0.229E-07
	30000.	0.268E-06	0.118E-06	0.741E-07	0.387E-07	0.685E-07	0.245E-07
	50000.	0.301E-06	0.102E-06	0.761E-07	0.422E-07	0.692E-07	0.267E-07
3S - 5P 1827.9 Å C= 0.49E+13	2500.	0.436E-06	0.263E-06	0.186E-06	0.710E-07	0.180E-06	0.449E-07
	5000.	0.510E-06	0.303E-06	0.189E-06	0.796E-07	0.181E-06	0.504E-07
	10000.	0.602E-06	0.333E-06	0.192E-06	0.894E-07	0.182E-06	0.566E-07
	20000.	0.723E-06	0.305E-06	0.197E-06	0.100E-06	0.184E-06	0.636E-07
	30000.	0.806E-06	0.278E-06	0.201E-06	0.107E-06	0.185E-06	0.680E-07
	50000.	0.914E-06	0.232E-06	0.206E-06	0.117E-06	0.187E-06	0.740E-07
3S - 6P 1747.8 Å C= 0.24E+13	2500.	0.107E-05	0.664E-06	0.430E-06	0.178E-06	0.413E-06	0.112E-06
	5000.	0.127E-05	0.751E-06	0.438E-06	0.199E-06	0.416E-06	0.126E-06
	10000.	0.152E-05	0.757E-06	0.449E-06	0.224E-06	0.419E-06	0.142E-06
	20000.	0.185E-05	0.674E-06	0.462E-06	0.251E-06	0.424E-06	0.159E-06
	30000.	0.208E-05	0.581E-06	0.472E-06	0.269E-06	0.427E-06	0.170E-06
	50000.	0.233E-05	0.478E-06	0.486E-06	0.293E-06	0.432E-06	0.185E-06
3S - 7P 1707.1 Å C= 0.13E+13	2500.	0.235E-05	0.147E-05	0.875E-06	0.388E-06	0.834E-06	0.246E-06
	5000.	0.279E-05	0.161E-05	0.895E-06	0.436E-06	0.840E-06	0.276E-06
	10000.	0.339E-05	0.154E-05	0.920E-06	0.489E-06	0.848E-06	0.310E-06
	20000.	0.416E-05	0.127E-05	0.953E-06	0.549E-06	0.860E-06	0.348E-06
	30000.	0.464E-05	0.108E-05	0.976E-06	0.587E-06	0.868E-06	0.372E-06
	50000.	0.516E-05	0.866E-06	0.101E-05	0.640E-06	0.881E-06	0.405E-06

Perturber density = 1 x 10^{11} cm^{-3}

Transition	T(K)	Electrons Width (Å)	Electrons Shift (Å)	Protons Width (Å)	Protons Shift (Å)	Ionized helium Width (Å)	Ionized helium Shift (Å)
3S - 8P 1683.4 Å C= 0.81E+12	2500.	0.464E-05	0.288E-05	0.161E-05	0.759E-06	0.152E-05	0.480E-06
	5000.	0.555E-05	0.301E-05	0.166E-05	0.853E-06	0.154E-05	0.540E-06
	10000.	0.677E-05	0.279E-05	0.171E-05	0.957E-06	0.156E-05	0.606E-06
	20000.	0.835E-05	0.215E-05	0.178E-05	0.107E-05	0.158E-05	0.680E-06
	30000.	0.928E-05	0.181E-05	0.183E-05	0.115E-05	0.160E-05	0.728E-06
	50000.	0.102E-04	0.141E-05	0.190E-05	0.125E-05	0.163E-05	0.793E-06
3S - 9P 1668.4 Å C= 0.53E+12	2500.	0.840E-05	0.513E-05	0.276E-05	0.136E-05	0.258E-05	0.859E-06
	5000.	0.101E-04	0.512E-05	0.284E-05	0.153E-05	0.261E-05	0.967E-06
	10000.	0.124E-04	0.449E-05	0.295E-05	0.172E-05	0.265E-05	0.109E-05
	20000.	0.154E-04	0.336E-05	0.308E-05	0.193E-05	0.270E-05	0.122E-05
	30000.	0.170E-04	0.278E-05	0.317E-05	0.206E-05	0.273E-05	0.131E-05
	50000.	0.184E-04	0.206E-05	0.330E-05	0.224E-05	0.279E-05	0.142E-05
4S - 4P 17112.5 Å C= 0.86E+15	2500.	0.111E-04	0.445E-05	0.478E-05	0.120E-05	0.473E-05	0.758E-06
	5000.	0.123E-04	0.492E-05	0.480E-05	0.134E-05	0.474E-05	0.850E-06
	10000.	0.148E-04	0.491E-05	0.483E-05	0.151E-05	0.475E-05	0.954E-06
	20000.	0.191E-04	0.374E-05	0.487E-05	0.169E-05	0.476E-05	0.107E-05
	30000.	0.225E-04	0.311E-05	0.491E-05	0.181E-05	0.477E-05	0.115E-05
	50000.	0.270E-04	0.273E-05	0.497E-05	0.197E-05	0.478E-05	0.125E-05
4S - 5P 8925.8 Å C= 0.12E+15	2500.	0.105E-04	0.607E-05	0.440E-05	0.161E-05	0.428E-05	0.102E-05
	5000.	0.122E-04	0.711E-05	0.446E-05	0.180E-05	0.430E-05	0.114E-05
	10000.	0.146E-04	0.718E-05	0.454E-05	0.202E-05	0.433E-05	0.128E-05
	20000.	0.179E-04	0.615E-05	0.465E-05	0.227E-05	0.436E-05	0.144E-05
	30000.	0.203E-04	0.527E-05	0.472E-05	0.243E-05	0.438E-05	0.154E-05
	50000.	0.234E-04	0.456E-05	0.483E-05	0.265E-05	0.442E-05	0.168E-05
4S - 6P 7292.9 Å C= 0.42E+14	2500.	0.188E-04	0.115E-04	0.747E-05	0.306E-05	0.719E-05	0.194E-05
	5000.	0.222E-04	0.129E-04	0.761E-05	0.343E-05	0.723E-05	0.217E-05
	10000.	0.268E-04	0.132E-04	0.779E-05	0.385E-05	0.729E-05	0.244E-05
	20000.	0.328E-04	0.110E-04	0.802E-05	0.432E-05	0.737E-05	0.274E-05
	30000.	0.369E-04	0.928E-05	0.819E-05	0.463E-05	0.743E-05	0.293E-05
	50000.	0.417E-04	0.791E-05	0.843E-05	0.504E-05	0.752E-05	0.319E-05
4S - 7P 6632.5 Å C= 0.20E+14	2500.	0.356E-04	0.223E-04	0.132E-04	0.584E-05	0.126E-04	0.370E-05
	5000.	0.423E-04	0.249E-04	0.135E-04	0.656E-05	0.127E-04	0.415E-05
	10000.	0.514E-04	0.229E-04	0.139E-04	0.736E-05	0.128E-04	0.466E-05
	20000.	0.632E-04	0.184E-04	0.144E-04	0.826E-05	0.130E-04	0.523E-05
	30000.	0.708E-04	0.156E-04	0.147E-04	0.884E-05	0.131E-04	0.560E-05
	50000.	0.788E-04	0.120E-04	0.152E-04	0.962E-05	0.133E-04	0.610E-05
4S - 8P 6289.3 Å C= 0.11E+14	2500.	0.648E-04	0.403E-04	0.225E-04	0.106E-04	0.213E-04	0.669E-05
	5000.	0.776E-04	0.424E-04	0.231E-04	0.119E-04	0.215E-04	0.752E-05
	10000.	0.947E-04	0.396E-04	0.239E-04	0.133E-04	0.217E-04	0.845E-05
	20000.	0.117E-03	0.295E-04	0.248E-04	0.150E-04	0.221E-04	0.949E-05
	30000.	0.130E-03	0.239E-04	0.255E-04	0.160E-04	0.223E-04	0.102E-04
	50000.	0.143E-03	0.180E-04	0.265E-04	0.174E-04	0.227E-04	0.111E-04

Perturber density = 1 x 10^{11} cm^{-3}

Transition	T(K)	Electrons Width (Å)	Electrons Shift (Å)	Protons Width (Å)	Protons Shift (Å)	Ionized helium Width (Å)	Ionized helium Shift (Å)
4S - 9P 6085.1 Å C= 0.71E+13	2500.	0.112E-03	0.691E-04	0.367E-04	0.181E-04	0.344E-04	0.114E-04
	5000.	0.135E-03	0.695E-04	0.378E-04	0.203E-04	0.347E-04	0.129E-04
	10000.	0.166E-03	0.617E-04	0.392E-04	0.228E-04	0.352E-04	0.144E-04
	20000.	0.205E-03	0.444E-04	0.409E-04	0.256E-04	0.359E-04	0.162E-04
	30000.	0.226E-03	0.351E-04	0.421E-04	0.274E-04	0.364E-04	0.174E-04
	50000.	0.246E-03	0.256E-04	0.439E-04	0.298E-04	0.371E-04	0.189E-04
5S - 5P 46508.0 Å C= 0.32E+16	2500.	0.242E-03	0.703E-04	0.116E-03	0.206E-04	0.115E-03	0.130E-04
	5000.	0.308E-03	0.550E-04	0.116E-03	0.231E-04	0.115E-03	0.146E-04
	10000.	0.425E-03	0.366E-04	0.116E-03	0.259E-04	0.115E-03	0.164E-04
	20000.	0.591E-03	0.283E-04	0.117E-03	0.291E-04	0.116E-03	0.184E-04
	30000.	0.696E-03	0.241E-04	0.117E-03	0.311E-04	0.116E-03	0.197E-04
	50000.	0.823E-03	0.191E-04	0.117E-03	0.339E-04	0.116E-03	0.215E-04
5S - 6P 21465.6 Å C= 0.37E+15	2500.	0.159E-03	0.954E-04	0.639E-04	0.240E-04	0.621E-04	0.152E-04
	5000.	0.190E-03	0.965E-04	0.648E-04	0.269E-04	0.623E-04	0.170E-04
	10000.	0.239E-03	0.900E-04	0.661E-04	0.302E-04	0.627E-04	0.191E-04
	20000.	0.306E-03	0.706E-04	0.677E-04	0.339E-04	0.632E-04	0.215E-04
	30000.	0.351E-03	0.608E-04	0.689E-04	0.362E-04	0.636E-04	0.230E-04
	50000.	0.402E-03	0.531E-04	0.706E-04	0.395E-04	0.642E-04	0.250E-04
5S - 7P 16600.7 Å C= 0.13E+15	2500.	0.222E-03	0.134E-03	0.823E-04	0.356E-04	0.787E-04	0.225E-04
	5000.	0.266E-03	0.144E-03	0.840E-04	0.400E-04	0.792E-04	0.253E-04
	10000.	0.328E-03	0.134E-03	0.863E-04	0.449E-04	0.800E-04	0.284E-04
	20000.	0.410E-03	0.999E-04	0.893E-04	0.504E-04	0.810E-04	0.319E-04
	30000.	0.463E-03	0.809E-04	0.913E-04	0.539E-04	0.818E-04	0.341E-04
	50000.	0.518E-03	0.660E-04	0.943E-04	0.587E-04	0.829E-04	0.372E-04
5S - 8P 14605.5 Å C= 0.61E+14	2500.	0.350E-03	0.214E-03	0.121E-03	0.565E-04	0.115E-03	0.358E-04
	5000.	0.420E-03	0.221E-03	0.124E-03	0.635E-04	0.116E-03	0.402E-04
	10000.	0.517E-03	0.199E-03	0.128E-03	0.713E-04	0.117E-03	0.452E-04
	20000.	0.643E-03	0.136E-03	0.133E-03	0.800E-04	0.119E-03	0.507E-04
	30000.	0.717E-03	0.110E-03	0.137E-03	0.856E-04	0.120E-03	0.542E-04
	50000.	0.790E-03	0.760E-04	0.142E-03	0.932E-04	0.122E-03	0.590E-04
5S - 9P 13549.7 Å C= 0.35E+14	2500.	0.556E-03	0.350E-03	0.182E-03	0.893E-04	0.170E-03	0.564E-04
	5000.	0.671E-03	0.338E-03	0.187E-03	0.100E-03	0.172E-03	0.635E-04
	10000.	0.828E-03	0.289E-03	0.194E-03	0.113E-03	0.175E-03	0.714E-04
	20000.	0.103E-02	0.186E-03	0.203E-03	0.127E-03	0.178E-03	0.801E-04
	30000.	0.114E-02	0.151E-03	0.208E-03	0.135E-03	0.180E-03	0.857E-04
	50000.	0.124E-02	0.899E-04	0.217E-03	0.147E-03	0.184E-03	0.933E-04
6S - 6P 97264.9 Å C= 0.75E+16	2500.	0.288E-02	0.487E-03	0.126E-02	0.203E-03	0.126E-02	0.128E-03
	5000.	0.398E-02	0.302E-03	0.127E-02	0.228E-03	0.126E-02	0.144E-03
	10000.	0.573E-02	0.226E-03	0.127E-02	0.255E-03	0.126E-02	0.162E-03
	20000.	0.791E-02	0.173E-03	0.127E-02	0.287E-03	0.126E-02	0.182E-03
	30000.	0.922E-02	0.108E-03	0.127E-02	0.307E-03	0.126E-02	0.194E-03
	50000.	0.107E-01	0.218E-04	0.128E-02	0.334E-03	0.126E-02	0.212E-03

Perturber density = 1 x 10^{11} cm^{-3}

Transition	T(K)	Electrons Width (Å)	Electrons Shift (Å)	Protons Width (Å)	Protons Shift (Å)	Ionized helium Width (Å)	Ionized helium Shift (Å)
6S - 7P 41782.3 Å C= 0.80E+15	2500.	0.136E-02	0.742E-03	0.511E-03	0.196E-03	0.496E-03	0.124E-03
	5000.	0.170E-02	0.757E-03	0.519E-03	0.220E-03	0.498E-03	0.140E-03
	10000.	0.220E-02	0.599E-03	0.530E-03	0.247E-03	0.501E-03	0.157E-03
	20000.	0.290E-02	0.464E-03	0.544E-03	0.278E-03	0.506E-03	0.176E-03
	30000.	0.330E-02	0.366E-03	0.554E-03	0.297E-03	0.509E-03	0.188E-03
	50000.	0.372E-02	0.230E-03	0.568E-03	0.324E-03	0.514E-03	0.205E-03
6S - 8P 31092.2 Å C= 0.28E+15	2500.	0.158E-02	0.952E-03	0.545E-03	0.245E-03	0.518E-03	0.155E-03
	5000.	0.193E-02	0.948E-03	0.558E-03	0.275E-03	0.522E-03	0.174E-03
	10000.	0.242E-02	0.719E-03	0.574E-03	0.309E-03	0.528E-03	0.196E-03
	20000.	0.308E-02	0.486E-03	0.595E-03	0.347E-03	0.535E-03	0.220E-03
	30000.	0.346E-02	0.373E-03	0.610E-03	0.371E-03	0.541E-03	0.235E-03
	50000.	0.383E-02	0.236E-03	0.632E-03	0.404E-03	0.549E-03	0.256E-03
6S - 9P 26668.4 Å C= 0.14E+15	2500.	0.215E-02	0.131E-02	0.701E-03	0.340E-03	0.659E-03	0.215E-03
	5000.	0.262E-02	0.123E-02	0.722E-03	0.382E-03	0.666E-03	0.242E-03
	10000.	0.327E-02	0.974E-03	0.747E-03	0.429E-03	0.675E-03	0.272E-03
	20000.	0.411E-02	0.614E-03	0.779E-03	0.482E-03	0.687E-03	0.305E-03
	30000.	0.455E-02	0.362E-03	0.802E-03	0.515E-03	0.695E-03	0.326E-03
	50000.	0.497E-02	0.250E-03	0.834E-03	0.561E-03	0.708E-03	0.355E-03
7S - 7P 175201.9 Å C= 0.14E+17	2500.	0.224E-01	0.228E-02	0.864E-02	0.138E-02	0.862E-02	0.872E-03
	5000.	0.324E-01	0.116E-02	0.865E-02	0.155E-02	0.862E-02	0.979E-03
	10000.	0.469E-01	0.617E-03	0.866E-02	0.173E-02	0.862E-02	0.110E-02
	20000.	0.638E-01	0.679E-04	0.868E-02	0.195E-02	0.863E-02	0.123E-02
	30000.	0.735E-01	-0.445E-03	0.870E-02	0.208E-02	0.863E-02	0.132E-02
	50000.	0.839E-01	-0.680E-03	0.873E-02	0.227E-02	0.864E-02	0.144E-02
7S - 8P 71754.0 Å C= 0.15E+16	2500.	0.812E-02	0.383E-02	0.283E-02	0.111E-02	0.274E-02	0.700E-03
	5000.	0.105E-01	0.356E-02	0.288E-02	0.124E-02	0.275E-02	0.787E-03
	10000.	0.141E-01	0.244E-02	0.294E-02	0.139E-02	0.277E-02	0.883E-03
	20000.	0.186E-01	0.145E-02	0.302E-02	0.157E-02	0.280E-02	0.991E-03
	30000.	0.210E-01	0.934E-03	0.307E-02	0.167E-02	0.282E-02	0.106E-02
	50000.	0.234E-01	0.480E-03	0.316E-02	0.182E-02	0.285E-02	0.115E-02
7S - 9P 51889.6 Å C= 0.51E+15	2500.	0.809E-02	0.437E-02	0.262E-02	0.121E-02	0.248E-02	0.767E-03
	5000.	0.101E-01	0.407E-02	0.269E-02	0.136E-02	0.251E-02	0.863E-03
	10000.	0.130E-01	0.249E-02	0.278E-02	0.153E-02	0.254E-02	0.969E-03
	20000.	0.167E-01	0.130E-02	0.288E-02	0.172E-02	0.257E-02	0.109E-02
	30000.	0.186E-01	0.923E-03	0.296E-02	0.184E-02	0.260E-02	0.116E-02
	50000.	0.204E-01	0.547E-03	0.307E-02	0.200E-02	0.265E-02	0.127E-02
8S - 8P 286049.4 Å C= 0.23E+17	2500.	0.128	0.971E-02	0.431E-01	0.712E-02	0.430E-01	0.451E-02
	5000.	0.189	0.482E-02	0.432E-01	0.799E-02	0.430E-01	0.506E-02
	10000.	0.272	0.401E-03	0.433E-01	0.897E-02	0.430E-01	0.568E-02
	20000.	0.365	-0.352E-02	0.434E-01	0.101E-01	0.431E-01	0.638E-02
	30000.	0.417	-0.380E-02	0.435E-01	0.108E-01	0.431E-01	0.682E-02
	50000.	0.468	-0.302E-02	0.436E-01	0.117E-01	0.431E-01	0.743E-02

Perturber density = 1 x 10^{11} cm^{-3}

Transition	T(K)	Electrons Width (Å)	Electrons Shift (Å)	Protons Width (Å)	Protons Shift (Å)	Ionized helium Width (Å)	Ionized helium Shift (Å)
8S - 9P 113236.2 Å C= 0.24E+16	2500.	0.381E-01	0.159E-01	0.121E-01	0.480E-02	0.117E-01	0.303E-02
	5000.	0.506E-01	0.105E-01	0.123E-01	0.539E-02	0.118E-01	0.341E-02
	10000.	0.694E-01	0.508E-02	0.126E-01	0.605E-02	0.119E-01	0.383E-02
	20000.	0.904E-01	0.269E-02	0.130E-01	0.679E-02	0.120E-01	0.430E-02
	30000.	0.101	0.165E-02	0.132E-01	0.726E-02	0.121E-01	0.460E-02
	50000.	0.112	0.398E-03	0.136E-01	0.791E-02	0.122E-01	0.501E-02
9S - 9P 435691.9 Å C= 0.36E+17	2500.	0.583	0.276E-01	0.172	0.294E-01	0.171	0.186E-01
	5000.	0.867	0.476E-02	0.172	0.330E-01	0.171	0.209E-01
	10000.	1.24	-0.711E-02	0.173	0.370E-01	0.172	0.235E-01
	20000.	1.64	-0.143E-01	0.173	0.416E-01	0.172	0.263E-01
	30000.	1.85	-0.114E-01	0.173	0.445E-01	0.172	0.282E-01
	50000.	2.05	-0.892E-02	0.174	0.484E-01	0.172	0.307E-01
3P - 4S 11832.0 Å C= 0.82E+15	2500.	0.253E-05	0.160E-05	0.598E-06	0.442E-06	0.483E-06	0.280E-06
	5000.	0.281E-05	0.192E-05	0.643E-06	0.496E-06	0.504E-06	0.314E-06
	10000.	0.306E-05	0.212E-05	0.696E-06	0.557E-06	0.530E-06	0.353E-06
	20000.	0.364E-05	0.213E-05	0.757E-06	0.626E-06	0.562E-06	0.396E-06
	30000.	0.403E-05	0.187E-05	0.798E-06	0.669E-06	0.583E-06	0.424E-06
	50000.	0.485E-05	0.156E-05	0.854E-06	0.729E-06	0.614E-06	0.462E-06
3P - 5S 5712.7 Å C= 0.70E+14	2500.	0.269E-05	0.196E-05	0.575E-06	0.538E-06	0.370E-06	0.340E-06
	5000.	0.311E-05	0.232E-05	0.644E-06	0.603E-06	0.413E-06	0.382E-06
	10000.	0.339E-05	0.254E-05	0.722E-06	0.677E-06	0.462E-06	0.429E-06
	20000.	0.381E-05	0.252E-05	0.809E-06	0.760E-06	0.517E-06	0.482E-06
	30000.	0.401E-05	0.225E-05	0.865E-06	0.813E-06	0.552E-06	0.515E-06
	50000.	0.456E-05	0.186E-05	0.941E-06	0.886E-06	0.600E-06	0.561E-06
3P - 6S 4731.4 Å C= 0.23E+14	2500.	0.556E-05	0.412E-05	0.116E-05	0.110E-05	0.737E-06	0.694E-06
	5000.	0.636E-05	0.467E-05	0.130E-05	0.123E-05	0.826E-06	0.779E-06
	10000.	0.695E-05	0.490E-05	0.146E-05	0.138E-05	0.927E-06	0.874E-06
	20000.	0.782E-05	0.464E-05	0.164E-05	0.155E-05	0.104E-05	0.982E-06
	30000.	0.848E-05	0.406E-05	0.176E-05	0.166E-05	0.111E-05	0.105E-05
	50000.	0.964E-05	0.338E-05	0.191E-05	0.181E-05	0.121E-05	0.114E-05
3P - 7S 4355.8 Å C= 0.11E+14	2500.	0.115E-04	0.829E-05	0.231E-05	0.218E-05	0.146E-05	0.138E-05
	5000.	0.131E-04	0.947E-05	0.260E-05	0.245E-05	0.164E-05	0.155E-05
	10000.	0.142E-04	0.915E-05	0.291E-05	0.275E-05	0.185E-05	0.174E-05
	20000.	0.162E-04	0.797E-05	0.327E-05	0.309E-05	0.207E-05	0.196E-05
	30000.	0.181E-04	0.667E-05	0.350E-05	0.330E-05	0.222E-05	0.209E-05
	50000.	0.204E-04	0.535E-05	0.381E-05	0.360E-05	0.241E-05	0.228E-05
3P - 8S 4166.3 Å C= 0.61E+13	2500.	0.215E-04	0.155E-04	0.429E-05	0.406E-05	0.272E-05	0.257E-05
	5000.	0.240E-04	0.169E-04	0.482E-05	0.456E-05	0.305E-05	0.288E-05
	10000.	0.279E-04	0.164E-04	0.541E-05	0.511E-05	0.343E-05	0.324E-05
	20000.	0.320E-04	0.126E-04	0.608E-05	0.574E-05	0.385E-05	0.364E-05
	30000.	0.359E-04	0.103E-04	0.650E-05	0.614E-05	0.412E-05	0.389E-05
	50000.	0.402E-04	0.800E-05	0.708E-05	0.669E-05	0.448E-05	0.424E-05

Perturber density = 1 x 10^{11} cm^{-3}

Transition	T(K)	Electrons Width (Å)	Electrons Shift (Å)	Protons Width (Å)	Protons Shift (Å)	Ionized helium Width (Å)	Ionized helium Shift (Å)
3P - 9S 4055.8 Å C= 0.38E+13	2500.	0.398E-04	0.273E-04	0.747E-05	0.705E-05	0.473E-05	0.446E-05
	5000.	0.422E-04	0.281E-04	0.839E-05	0.792E-05	0.531E-05	0.501E-05
	10000.	0.492E-04	0.260E-04	0.942E-05	0.890E-05	0.596E-05	0.563E-05
	20000.	0.593E-04	0.189E-04	0.106E-04	0.999E-05	0.669E-05	0.632E-05
	30000.	0.671E-04	0.152E-04	0.113E-04	0.107E-04	0.716E-05	0.677E-05
	50000.	0.726E-04	0.114E-04	0.123E-04	0.116E-04	0.780E-05	0.737E-05
3P -10S 3985.4 Å C= 0.25E+13	2500.	0.627E-04	0.439E-04	0.123E-04	0.116E-04	0.779E-05	0.732E-05
	5000.	0.751E-04	0.447E-04	0.138E-04	0.130E-04	0.874E-05	0.824E-05
	10000.	0.835E-04	0.386E-04	0.155E-04	0.146E-04	0.981E-05	0.926E-05
	20000.	0.103E-03	0.275E-04	0.174E-04	0.164E-04	0.110E-04	0.104E-04
	30000.	0.115E-03	0.212E-04	0.186E-04	0.176E-04	0.118E-04	0.111E-04
	50000.	0.124E-03	0.156E-04	0.203E-04	0.191E-04	0.128E-04	0.121E-04
4P - 5S 31155.6 Å C= 0.21E+16	2500.	0.829E-04	0.529E-04	0.203E-04	0.137E-04	0.173E-04	0.867E-05
	5000.	0.948E-04	0.613E-04	0.216E-04	0.154E-04	0.178E-04	0.974E-05
	10000.	0.111E-03	0.628E-04	0.231E-04	0.173E-04	0.185E-04	0.109E-04
	20000.	0.136E-03	0.541E-04	0.249E-04	0.194E-04	0.193E-04	0.123E-04
	30000.	0.157E-03	0.463E-04	0.260E-04	0.207E-04	0.199E-04	0.131E-04
	50000.	0.187E-03	0.406E-04	0.277E-04	0.226E-04	0.208E-04	0.143E-04
4P - 6S 14619.5 Å C= 0.22E+15	2500.	0.542E-04	0.385E-04	0.112E-04	0.102E-04	0.748E-05	0.645E-05
	5000.	0.619E-04	0.451E-04	0.125E-04	0.114E-04	0.824E-05	0.724E-05
	10000.	0.690E-04	0.456E-04	0.139E-04	0.128E-04	0.912E-05	0.812E-05
	20000.	0.793E-04	0.394E-04	0.155E-04	0.144E-04	0.101E-04	0.912E-05
	30000.	0.894E-04	0.351E-04	0.166E-04	0.154E-04	0.108E-04	0.975E-05
	50000.	0.103E-03	0.291E-04	0.180E-04	0.168E-04	0.116E-04	0.106E-04
4P - 7S 11543.6 Å C= 0.76E+14	2500.	0.808E-04	0.579E-04	0.162E-04	0.152E-04	0.104E-04	0.964E-05
	5000.	0.911E-04	0.657E-04	0.182E-04	0.171E-04	0.116E-04	0.108E-04
	10000.	0.102E-03	0.654E-04	0.204E-04	0.192E-04	0.130E-04	0.122E-04
	20000.	0.118E-03	0.523E-04	0.229E-04	0.215E-04	0.146E-04	0.136E-04
	30000.	0.133E-03	0.449E-04	0.245E-04	0.230E-04	0.156E-04	0.146E-04
	50000.	0.150E-03	0.347E-04	0.266E-04	0.251E-04	0.169E-04	0.159E-04
4P - 8S 10302.0 Å C= 0.37E+14	2500.	0.132E-03	0.936E-04	0.262E-04	0.247E-04	0.167E-04	0.156E-04
	5000.	0.147E-03	0.103E-03	0.294E-04	0.278E-04	0.187E-04	0.176E-04
	10000.	0.171E-03	0.988E-04	0.330E-04	0.312E-04	0.210E-04	0.198E-04
	20000.	0.199E-03	0.736E-04	0.371E-04	0.350E-04	0.235E-04	0.222E-04
	30000.	0.224E-03	0.584E-04	0.397E-04	0.374E-04	0.251E-04	0.237E-04
	50000.	0.251E-03	0.461E-04	0.432E-04	0.408E-04	0.274E-04	0.258E-04
4P - 9S 9652.1 Å C= 0.21E+14	2500.	0.226E-03	0.156E-03	0.423E-04	0.399E-04	0.268E-04	0.252E-04
	5000.	0.240E-03	0.159E-03	0.475E-04	0.448E-04	0.301E-04	0.284E-04
	10000.	0.279E-03	0.146E-03	0.533E-04	0.503E-04	0.338E-04	0.319E-04
	20000.	0.340E-03	0.104E-03	0.598E-04	0.565E-04	0.379E-04	0.358E-04
	30000.	0.380E-03	0.789E-04	0.640E-04	0.604E-04	0.405E-04	0.383E-04
	50000.	0.416E-03	0.601E-04	0.698E-04	0.658E-04	0.441E-04	0.417E-04

Perturber density = 1 x 10^{11} cm^{-3}

Transition	T(K)	Electrons Width (Å)	Electrons Shift (Å)	Protons Width (Å)	Protons Shift (Å)	Ionized helium Width (Å)	Ionized helium Shift (Å)
4P -10S 9262.2 Å C= 0.14E+14	2500.	0.339E-03	0.244E-03	0.664E-04	0.626E-04	0.421E-04	0.395E-04
	5000.	0.407E-03	0.245E-03	0.745E-04	0.704E-04	0.472E-04	0.445E-04
	10000.	0.452E-03	0.208E-03	0.836E-04	0.790E-04	0.530E-04	0.500E-04
	20000.	0.562E-03	0.143E-03	0.939E-04	0.887E-04	0.595E-04	0.562E-04
	30000.	0.623E-03	0.108E-03	0.101E-03	0.949E-04	0.636E-04	0.601E-04
	50000.	0.673E-03	0.766E-04	0.110E-03	0.103E-03	0.693E-04	0.654E-04
5P - 6S 67552.5 Å C= 0.47E+16	2500.	0.112E-02	0.706E-03	0.293E-03	0.179E-03	0.259E-03	0.114E-03
	5000.	0.135E-02	0.740E-03	0.308E-03	0.201E-03	0.265E-03	0.127E-03
	10000.	0.171E-02	0.740E-03	0.325E-03	0.226E-03	0.272E-03	0.143E-03
	20000.	0.223E-02	0.595E-03	0.347E-03	0.254E-03	0.282E-03	0.161E-03
	30000.	0.260E-02	0.515E-03	0.361E-03	0.271E-03	0.288E-03	0.172E-03
	50000.	0.303E-02	0.467E-03	0.381E-03	0.295E-03	0.298E-03	0.187E-03
5P - 7S 30276.2 Å C= 0.52E+15	2500.	0.550E-03	0.390E-03	0.114E-03	0.100E-03	0.800E-04	0.633E-04
	5000.	0.626E-03	0.412E-03	0.126E-03	0.112E-03	0.869E-04	0.711E-04
	10000.	0.750E-03	0.409E-03	0.140E-03	0.126E-03	0.950E-04	0.798E-04
	20000.	0.915E-03	0.321E-03	0.156E-03	0.141E-03	0.104E-03	0.896E-04
	30000.	0.105E-02	0.260E-03	0.166E-03	0.151E-03	0.110E-03	0.958E-04
	50000.	0.120E-02	0.227E-03	0.180E-03	0.165E-03	0.119E-03	0.104E-03
5P - 8S 23004.5 Å C= 0.19E+15	2500.	0.655E-03	0.460E-03	0.131E-03	0.121E-03	0.852E-04	0.768E-04
	5000.	0.736E-03	0.494E-03	0.146E-03	0.136E-03	0.947E-04	0.863E-04
	10000.	0.864E-03	0.461E-03	0.164E-03	0.153E-03	0.106E-03	0.970E-04
	20000.	0.106E-02	0.331E-03	0.184E-03	0.172E-03	0.118E-03	0.109E-03
	30000.	0.120E-02	0.261E-03	0.196E-03	0.184E-03	0.126E-03	0.116E-03
	50000.	0.134E-02	0.198E-03	0.214E-03	0.200E-03	0.136E-03	0.127E-03
5P - 9S 19997.7 Å C= 0.92E+14	2500.	0.921E-03	0.653E-03	0.181E-03	0.170E-03	0.116E-03	0.108E-03
	5000.	0.104E-02	0.663E-03	0.203E-03	0.191E-03	0.130E-03	0.121E-03
	10000.	0.121E-02	0.589E-03	0.228E-03	0.215E-03	0.145E-03	0.136E-03
	20000.	0.151E-02	0.383E-03	0.256E-03	0.241E-03	0.163E-03	0.153E-03
	30000.	0.169E-02	0.309E-03	0.274E-03	0.258E-03	0.174E-03	0.163E-03
	50000.	0.186E-02	0.195E-03	0.298E-03	0.281E-03	0.189E-03	0.178E-03
5P -10S 18393.5 Å C= 0.54E+14	2500.	0.137E-02	0.964E-03	0.262E-03	0.246E-03	0.166E-03	0.155E-03
	5000.	0.153E-02	0.963E-03	0.293E-03	0.277E-03	0.186E-03	0.175E-03
	10000.	0.180E-02	0.775E-03	0.329E-03	0.311E-03	0.209E-03	0.197E-03
	20000.	0.226E-02	0.477E-03	0.370E-03	0.349E-03	0.234E-03	0.221E-03
	30000.	0.253E-02	0.406E-03	0.396E-03	0.373E-03	0.251E-03	0.236E-03
	50000.	0.271E-02	0.208E-03	0.431E-03	0.406E-03	0.273E-03	0.257E-03
6P - 7S 125870.1 Å C= 0.90E+16	2500.	0.926E-02	0.537E-02	0.243E-02	0.136E-02	0.221E-02	0.860E-03
	5000.	0.118E-01	0.549E-02	0.253E-02	0.152E-02	0.224E-02	0.966E-03
	10000.	0.156E-01	0.457E-02	0.265E-02	0.171E-02	0.229E-02	0.108E-02
	20000.	0.210E-01	0.345E-02	0.280E-02	0.192E-02	0.235E-02	0.122E-02
	30000.	0.243E-01	0.317E-02	0.290E-02	0.206E-02	0.240E-02	0.130E-02
	50000.	0.278E-01	0.233E-02	0.304E-02	0.224E-02	0.246E-02	0.142E-02

STARK BROADENING PARAMETER TABLES FOR MG I LINES

Perturber density = 1 x 10^{11} cm^{-3}

Transition	T(K)	Electrons Width (Å)	Electrons Shift (Å)	Protons Width (Å)	Protons Shift (Å)	Ionized helium Width (Å)	Ionized helium Shift (Å)
6P - 8S 54391.3 Å C= 0.10E+16	2500.	0.366E-02	0.254E-02	0.757E-03	0.633E-03	0.554E-03	0.401E-03
	5000.	0.431E-02	0.239E-02	0.830E-03	0.711E-03	0.594E-03	0.450E-03
	10000.	0.528E-02	0.209E-02	0.914E-03	0.798E-03	0.641E-03	0.506E-03
	20000.	0.689E-02	0.143E-02	0.101E-02	0.896E-03	0.696E-03	0.567E-03
	30000.	0.787E-02	0.120E-02	0.107E-02	0.959E-03	0.732E-03	0.607E-03
	50000.	0.879E-02	0.803E-03	0.116E-02	0.104E-02	0.783E-03	0.661E-03
6P - 9S 40126.5 Å C= 0.37E+15	2500.	0.372E-02	0.263E-02	0.732E-03	0.667E-03	0.487E-03	0.422E-03
	5000.	0.430E-02	0.263E-02	0.816E-03	0.750E-03	0.537E-03	0.474E-03
	10000.	0.514E-02	0.207E-02	0.911E-03	0.842E-03	0.595E-03	0.533E-03
	20000.	0.661E-02	0.131E-02	0.102E-02	0.945E-03	0.661E-03	0.598E-03
	30000.	0.745E-02	0.105E-02	0.109E-02	0.101E-02	0.704E-03	0.640E-03
	50000.	0.818E-02	0.604E-03	0.118E-02	0.110E-02	0.762E-03	0.697E-03
6P -10S 34150.2 Å C= 0.19E+15	2500.	0.464E-02	0.326E-02	0.900E-03	0.838E-03	0.580E-03	0.530E-03
	5000.	0.537E-02	0.305E-02	0.101E-02	0.943E-03	0.647E-03	0.596E-03
	10000.	0.642E-02	0.242E-02	0.113E-02	0.106E-02	0.723E-03	0.670E-03
	20000.	0.818E-02	0.148E-02	0.127E-02	0.119E-02	0.808E-03	0.753E-03
	30000.	0.912E-02	0.110E-02	0.135E-02	0.127E-02	0.863E-03	0.805E-03
	50000.	0.988E-02	0.577E-03	0.147E-02	0.138E-02	0.938E-03	0.877E-03
7P - 8S 211286.9 Å C= 0.16E+17	2500.	0.546E-01	0.264E-01	0.139E-01	0.718E-02	0.129E-01	0.454E-02
	5000.	0.734E-01	0.260E-01	0.144E-01	0.806E-02	0.131E-01	0.510E-02
	10000.	0.101	0.189E-01	0.150E-01	0.905E-02	0.133E-01	0.573E-02
	20000.	0.136	0.135E-01	0.157E-01	0.102E-01	0.136E-01	0.643E-02
	30000.	0.155	0.104E-01	0.162E-01	0.109E-01	0.138E-01	0.688E-02
	50000.	0.176	0.649E-02	0.169E-01	0.118E-01	0.141E-01	0.749E-02
7P - 9S 88740.6 Å C= 0.18E+16	2500.	0.179E-01	0.112E-01	0.372E-02	0.298E-02	0.284E-02	0.188E-02
	5000.	0.225E-01	0.109E-01	0.405E-02	0.334E-02	0.301E-02	0.212E-02
	10000.	0.288E-01	0.730E-02	0.443E-02	0.375E-02	0.321E-02	0.238E-02
	20000.	0.380E-01	0.485E-02	0.487E-02	0.421E-02	0.345E-02	0.267E-02
	30000.	0.428E-01	0.314E-02	0.516E-02	0.451E-02	0.361E-02	0.285E-02
	50000.	0.475E-01	0.197E-02	0.556E-02	0.491E-02	0.384E-02	0.311E-02
7P -10S 63979.5 Å C= 0.65E+15	2500.	0.161E-01	0.106E-01	0.317E-02	0.283E-02	0.216E-02	0.179E-02
	5000.	0.197E-01	0.101E-01	0.352E-02	0.318E-02	0.237E-02	0.201E-02
	10000.	0.244E-01	0.640E-02	0.392E-02	0.357E-02	0.260E-02	0.226E-02
	20000.	0.317E-01	0.402E-02	0.437E-02	0.401E-02	0.288E-02	0.254E-02
	30000.	0.353E-01	0.227E-02	0.466E-02	0.429E-02	0.305E-02	0.272E-02
	50000.	0.386E-01	0.151E-02	0.506E-02	0.467E-02	0.329E-02	0.296E-02
8P - 9S 328947.4 Å C= 0.25E+17	2500.	0.257	0.106	0.618E-01	0.295E-01	0.583E-01	0.187E-01
	5000.	0.356	0.863E-01	0.635E-01	0.331E-01	0.588E-01	0.210E-01
	10000.	0.503	0.554E-01	0.657E-01	0.372E-01	0.596E-01	0.236E-01
	20000.	0.669	0.337E-01	0.684E-01	0.417E-01	0.606E-01	0.264E-01
	30000.	0.757	0.236E-01	0.703E-01	0.447E-01	0.613E-01	0.283E-01
	50000.	0.845	0.146E-01	0.731E-01	0.486E-01	0.624E-01	0.308E-01

Perturber density = 1 x 10^{11} cm^{-3}

Transition	T(K)	Electrons Width (Å)	Electrons Shift (Å)	Protons Width (Å)	Protons Shift (Å)	Ionized helium Width (Å)	Ionized helium Shift (Å)
8P -10S 135113.2 Å C= 0.29E+16	2500.	0.731E-01	0.390E-01	0.147E-01	0.113E-01	0.116E-01	0.712E-02
	5000.	0.938E-01	0.345E-01	0.159E-01	0.127E-01	0.122E-01	0.802E-02
	10000.	0.127	0.200E-01	0.173E-01	0.142E-01	0.129E-01	0.901E-02
	20000.	0.166	0.937E-02	0.189E-01	0.160E-01	0.138E-01	0.101E-01
	30000.	0.185	0.695E-02	0.200E-01	0.171E-01	0.143E-01	0.108E-01
	50000.	0.204	0.463E-02	0.215E-01	0.186E-01	0.152E-01	0.118E-01
9P -10S 484027.1 Å C= 0.37E+17	2500.	1.01	0.333	0.226	0.101	0.216	0.638E-01
	5000.	1.44	0.211	0.232	0.113	0.217	0.718E-01
	10000.	2.04	0.142	0.238	0.127	0.220	0.806E-01
	20000.	2.68	0.705E-01	0.247	0.143	0.223	0.905E-01
	30000.	3.01	0.504E-01	0.253	0.153	0.225	0.969E-01
	50000.	3.32	0.296E-01	0.262	0.167	0.228	0.105
3P - 3D 8809.2 Å C= 0.23E+15	2500.	0.105E-05	0.609E-06	0.511E-06	0.165E-06	0.501E-06	0.105E-06
	5000.	0.118E-05	0.595E-06	0.516E-06	0.185E-06	0.503E-06	0.117E-06
	10000.	0.141E-05	0.501E-06	0.523E-06	0.208E-06	0.505E-06	0.132E-06
	20000.	0.178E-05	0.330E-06	0.532E-06	0.233E-06	0.507E-06	0.148E-06
	30000.	0.206E-05	0.264E-06	0.539E-06	0.250E-06	0.509E-06	0.158E-06
	50000.	0.240E-05	0.192E-06	0.550E-06	0.272E-06	0.513E-06	0.172E-06
3P - 4D 5530.0 Å C= 0.47E+14	2500.	0.302E-05	0.221E-05	0.927E-06	0.600E-06	0.802E-06	0.380E-06
	5000.	0.346E-05	0.267E-05	0.979E-06	0.674E-06	0.824E-06	0.427E-06
	10000.	0.382E-05	0.261E-05	0.104E-05	0.756E-06	0.851E-06	0.479E-06
	20000.	0.424E-05	0.243E-05	0.112E-05	0.849E-06	0.886E-06	0.538E-06
	30000.	0.455E-05	0.207E-05	0.117E-05	0.908E-06	0.910E-06	0.575E-06
	50000.	0.504E-05	0.175E-05	0.124E-05	0.989E-06	0.945E-06	0.627E-06
3P - 5D 4704.3 Å C= 0.20E+14	2500.	0.617E-05	0.451E-05	0.187E-05	0.119E-05	0.163E-05	0.756E-06
	5000.	0.707E-05	0.528E-05	0.197E-05	0.134E-05	0.167E-05	0.849E-06
	10000.	0.789E-05	0.514E-05	0.210E-05	0.150E-05	0.172E-05	0.953E-06
	20000.	0.885E-05	0.471E-05	0.225E-05	0.169E-05	0.179E-05	0.107E-05
	30000.	0.964E-05	0.399E-05	0.235E-05	0.181E-05	0.184E-05	0.114E-05
	50000.	0.107E-04	0.338E-05	0.249E-05	0.197E-05	0.191E-05	0.125E-05
3P - 6D 4353.1 Å C= 0.10E+14	2500.	0.115E-04	0.813E-05	0.353E-05	0.214E-05	0.314E-05	0.135E-05
	5000.	0.132E-04	0.919E-05	0.371E-05	0.240E-05	0.321E-05	0.152E-05
	10000.	0.152E-04	0.911E-05	0.391E-05	0.269E-05	0.329E-05	0.170E-05
	20000.	0.178E-04	0.742E-05	0.417E-05	0.302E-05	0.340E-05	0.191E-05
	30000.	0.197E-04	0.624E-05	0.434E-05	0.323E-05	0.348E-05	0.205E-05
	50000.	0.217E-04	0.508E-05	0.460E-05	0.352E-05	0.359E-05	0.223E-05
3P - 7D 4168.5 Å C= 0.62E+13	2500.	0.200E-04	0.133E-04	0.620E-05	0.349E-05	0.564E-05	0.220E-05
	5000.	0.234E-04	0.143E-04	0.646E-05	0.391E-05	0.573E-05	0.248E-05
	10000.	0.280E-04	0.137E-04	0.677E-05	0.439E-05	0.585E-05	0.278E-05
	20000.	0.341E-04	0.105E-04	0.715E-05	0.493E-05	0.601E-05	0.312E-05
	30000.	0.379E-04	0.854E-05	0.742E-05	0.527E-05	0.613E-05	0.334E-05
	50000.	0.417E-04	0.670E-05	0.779E-05	0.574E-05	0.629E-05	0.364E-05

Perturber density = 1 x 10^{11} cm^{-3}

Transition	T(K)	Electrons Width (Å)	Electrons Shift (Å)	Protons Width (Å)	Protons Shift (Å)	Ionized helium Width (Å)	Ionized helium Shift (Å)
3P - 8D 4058.7 Å C= 0.40E+13	2500.	0.328E-04	0.199E-04	0.102E-04	0.525E-05	0.950E-05	0.332E-05
	5000.	0.399E-04	0.205E-04	0.106E-04	0.590E-05	0.961E-05	0.373E-05
	10000.	0.496E-04	0.186E-04	0.110E-04	0.662E-05	0.977E-05	0.419E-05
	20000.	0.619E-04	0.137E-04	0.115E-04	0.743E-05	0.997E-05	0.470E-05
	30000.	0.687E-04	0.109E-04	0.119E-04	0.795E-05	0.101E-04	0.503E-05
	50000.	0.752E-04	0.832E-05	0.124E-04	0.865E-05	0.103E-04	0.548E-05
3P - 9D 3987.9 Å C= 0.28E+13	2500.	0.518E-04	0.275E-04	0.160E-04	0.736E-05	0.151E-04	0.465E-05
	5000.	0.657E-04	0.273E-04	0.164E-04	0.827E-05	0.153E-04	0.523E-05
	10000.	0.847E-04	0.236E-04	0.169E-04	0.928E-05	0.155E-04	0.588E-05
	20000.	0.107E-03	0.172E-04	0.176E-04	0.104E-04	0.157E-04	0.660E-05
	30000.	0.118E-03	0.132E-04	0.180E-04	0.111E-04	0.159E-04	0.706E-05
	50000.	0.128E-03	0.990E-05	0.187E-04	0.121E-04	0.161E-04	0.769E-05
4P - 4D 26398.9 Å C= 0.11E+16	2500.	0.714E-04	0.456E-04	0.236E-04	0.122E-04	0.220E-04	0.772E-05
	5000.	0.812E-04	0.507E-04	0.244E-04	0.137E-04	0.222E-04	0.866E-05
	10000.	0.959E-04	0.502E-04	0.254E-04	0.154E-04	0.226E-04	0.972E-05
	20000.	0.115E-03	0.383E-04	0.266E-04	0.172E-04	0.231E-04	0.109E-04
	30000.	0.130E-03	0.330E-04	0.275E-04	0.184E-04	0.234E-04	0.117E-04
	50000.	0.149E-03	0.290E-04	0.287E-04	0.201E-04	0.239E-04	0.127E-04
4P - 5D 14364.2 Å C= 0.18E+15	2500.	0.588E-04	0.412E-04	0.178E-04	0.109E-04	0.158E-04	0.689E-05
	5000.	0.673E-04	0.473E-04	0.187E-04	0.122E-04	0.161E-04	0.773E-05
	10000.	0.764E-04	0.478E-04	0.198E-04	0.137E-04	0.166E-04	0.868E-05
	20000.	0.877E-04	0.389E-04	0.211E-04	0.154E-04	0.172E-04	0.974E-05
	30000.	0.972E-04	0.346E-04	0.220E-04	0.165E-04	0.176E-04	0.104E-04
	50000.	0.109E-03	0.278E-04	0.233E-04	0.179E-04	0.181E-04	0.113E-04
4P - 6D 11525.3 Å C= 0.73E+14	2500.	0.819E-04	0.565E-04	0.250E-04	0.149E-04	0.223E-04	0.940E-05
	5000.	0.940E-04	0.631E-04	0.261E-04	0.167E-04	0.228E-04	0.106E-04
	10000.	0.109E-03	0.625E-04	0.276E-04	0.187E-04	0.233E-04	0.119E-04
	20000.	0.128E-03	0.486E-04	0.293E-04	0.210E-04	0.241E-04	0.133E-04
	30000.	0.143E-03	0.416E-04	0.305E-04	0.225E-04	0.246E-04	0.142E-04
	50000.	0.158E-03	0.331E-04	0.323E-04	0.245E-04	0.254E-04	0.155E-04
4P - 7D 10315.2 Å C= 0.38E+14	2500.	0.123E-03	0.826E-04	0.382E-04	0.213E-04	0.348E-04	0.135E-04
	5000.	0.145E-03	0.868E-04	0.397E-04	0.239E-04	0.353E-04	0.151E-04
	10000.	0.173E-03	0.823E-04	0.416E-04	0.268E-04	0.360E-04	0.170E-04
	20000.	0.212E-03	0.608E-04	0.439E-04	0.301E-04	0.370E-04	0.191E-04
	30000.	0.236E-03	0.488E-04	0.455E-04	0.322E-04	0.377E-04	0.204E-04
	50000.	0.260E-03	0.382E-04	0.478E-04	0.351E-04	0.387E-04	0.222E-04
4P - 8D 9668.0 Å C= 0.23E+14	2500.	0.187E-03	0.113E-03	0.581E-04	0.297E-04	0.541E-04	0.188E-04
	5000.	0.227E-03	0.116E-03	0.600E-04	0.334E-04	0.547E-04	0.211E-04
	10000.	0.283E-03	0.104E-03	0.624E-04	0.375E-04	0.556E-04	0.237E-04
	20000.	0.354E-03	0.742E-04	0.654E-04	0.421E-04	0.567E-04	0.267E-04
	30000.	0.393E-03	0.574E-04	0.675E-04	0.450E-04	0.576E-04	0.285E-04
	50000.	0.431E-03	0.432E-04	0.704E-04	0.490E-04	0.588E-04	0.310E-04

Perturber density = 1 x 10^{11} cm^{-3}

Transition	T(K)	Electrons Width (Å)	Electrons Shift (Å)	Protons Width (Å)	Protons Shift (Å)	Ionized helium Width (Å)	Ionized helium Shift (Å)
4P - 9D 9275.9 Å C= 0.15E+14	2500.	0.281E-03	0.152E-03	0.866E-04	0.398E-04	0.821E-04	0.251E-04
	5000.	0.357E-03	0.148E-03	0.888E-04	0.447E-04	0.828E-04	0.283E-04
	10000.	0.460E-03	0.126E-03	0.916E-04	0.502E-04	0.838E-04	0.318E-04
	20000.	0.579E-03	0.877E-04	0.951E-04	0.563E-04	0.850E-04	0.357E-04
	30000.	0.641E-03	0.673E-04	0.975E-04	0.603E-04	0.860E-04	0.382E-04
	50000.	0.698E-03	0.473E-04	0.101E-03	0.656E-04	0.873E-04	0.416E-04
5P - 5D 62426.3 Å C= 0.35E+16	2500.	0.110E-02	0.698E-03	0.386E-03	0.175E-03	0.367E-03	0.111E-03
	5000.	0.131E-02	0.688E-03	0.395E-03	0.196E-03	0.370E-03	0.124E-03
	10000.	0.163E-02	0.665E-03	0.407E-03	0.220E-03	0.374E-03	0.139E-03
	20000.	0.208E-02	0.530E-03	0.422E-03	0.247E-03	0.379E-03	0.157E-03
	30000.	0.238E-02	0.462E-03	0.433E-03	0.264E-03	0.383E-03	0.167E-03
	50000.	0.271E-02	0.407E-03	0.450E-03	0.288E-03	0.389E-03	0.182E-03
5P - 6D 30150.2 Å C= 0.50E+15	2500.	0.564E-03	0.384E-03	0.178E-03	0.969E-04	0.163E-03	0.613E-04
	5000.	0.657E-03	0.393E-03	0.184E-03	0.109E-03	0.165E-03	0.689E-04
	10000.	0.790E-03	0.380E-03	0.193E-03	0.122E-03	0.168E-03	0.773E-04
	20000.	0.971E-03	0.292E-03	0.203E-03	0.137E-03	0.172E-03	0.868E-04
	30000.	0.110E-02	0.241E-03	0.211E-03	0.147E-03	0.175E-03	0.929E-04
	50000.	0.123E-02	0.204E-03	0.221E-03	0.160E-03	0.180E-03	0.101E-03
5P - 7D 23070.4 Å C= 0.19E+15	2500.	0.622E-03	0.394E-03	0.194E-03	0.104E-03	0.178E-03	0.660E-04
	5000.	0.736E-03	0.409E-03	0.201E-03	0.117E-03	0.181E-03	0.742E-04
	10000.	0.896E-03	0.376E-03	0.210E-03	0.131E-03	0.184E-03	0.833E-04
	20000.	0.111E-02	0.269E-03	0.221E-03	0.148E-03	0.188E-03	0.935E-04
	30000.	0.125E-02	0.213E-03	0.228E-03	0.158E-03	0.192E-03	0.100E-03
	50000.	0.139E-02	0.161E-03	0.239E-03	0.172E-03	0.196E-03	0.109E-03
5P - 8D 20066.3 Å C= 0.99E+14	2500.	0.811E-03	0.498E-03	0.253E-03	0.127E-03	0.236E-03	0.802E-04
	5000.	0.992E-03	0.480E-03	0.260E-03	0.142E-03	0.238E-03	0.902E-04
	10000.	0.124E-02	0.412E-03	0.270E-03	0.160E-03	0.242E-03	0.101E-03
	20000.	0.157E-02	0.273E-03	0.283E-03	0.180E-03	0.247E-03	0.114E-03
	30000.	0.175E-02	0.221E-03	0.291E-03	0.192E-03	0.250E-03	0.122E-03
	50000.	0.192E-02	0.142E-03	0.304E-03	0.209E-03	0.255E-03	0.132E-03
5P - 9D 18447.6 Å C= 0.59E+14	2500.	0.112E-02	0.610E-03	0.344E-03	0.156E-03	0.327E-03	0.989E-04
	5000.	0.142E-02	0.567E-03	0.353E-03	0.176E-03	0.330E-03	0.111E-03
	10000.	0.184E-02	0.462E-03	0.363E-03	0.197E-03	0.333E-03	0.125E-03
	20000.	0.233E-02	0.297E-03	0.377E-03	0.221E-03	0.338E-03	0.140E-03
	30000.	0.258E-02	0.240E-03	0.387E-03	0.237E-03	0.342E-03	0.150E-03
	50000.	0.282E-02	0.137E-03	0.401E-03	0.258E-03	0.347E-03	0.163E-03
6P - 6D 123719.5 Å C= 0.85E+16	2500.	0.941E-02	0.496E-02	0.349E-02	0.127E-02	0.339E-02	0.804E-03
	5000.	0.120E-01	0.493E-02	0.353E-02	0.142E-02	0.341E-02	0.902E-03
	10000.	0.159E-01	0.389E-02	0.360E-02	0.160E-02	0.343E-02	0.101E-02
	20000.	0.210E-01	0.297E-02	0.368E-02	0.180E-02	0.345E-02	0.114E-02
	30000.	0.241E-01	0.274E-02	0.375E-02	0.192E-02	0.347E-02	0.122E-02
	50000.	0.273E-01	0.185E-02	0.385E-02	0.209E-02	0.350E-02	0.132E-02

Perturber density = 1 x 10^{11} cm^{-3}

Transition	T(K)	Electrons Width (Å)	Electrons Shift (Å)	Protons Width (Å)	Protons Shift (Å)	Ionized helium Width (Å)	Ionized helium Shift (Å)
6P - 7D 54761.5 Å C= 0.11E+16	2500.	0.351E-02	0.208E-02	0.115E-02	0.537E-03	0.109E-02	0.340E-03
	5000.	0.435E-02	0.210E-02	0.118E-02	0.603E-03	0.110E-02	0.382E-03
	10000.	0.553E-02	0.164E-02	0.122E-02	0.677E-03	0.111E-02	0.429E-03
	20000.	0.717E-02	0.109E-02	0.127E-02	0.760E-03	0.113E-02	0.482E-03
	30000.	0.811E-02	0.942E-03	0.130E-02	0.813E-03	0.114E-02	0.515E-03
	50000.	0.905E-02	0.599E-03	0.135E-02	0.886E-03	0.116E-02	0.561E-03
6P - 8D 40403.6 Å C= 0.40E+15	2500.	0.331E-02	0.188E-02	0.105E-02	0.493E-03	0.991E-03	0.312E-03
	5000.	0.414E-02	0.186E-02	0.108E-02	0.554E-03	0.100E-02	0.350E-03
	10000.	0.532E-02	0.135E-02	0.111E-02	0.621E-03	0.101E-02	0.394E-03
	20000.	0.683E-02	0.900E-03	0.116E-02	0.698E-03	0.103E-02	0.442E-03
	30000.	0.766E-02	0.644E-03	0.119E-02	0.746E-03	0.104E-02	0.473E-03
	50000.	0.846E-02	0.408E-03	0.123E-02	0.813E-03	0.106E-02	0.515E-03
6P - 9D 34336.9 Å C= 0.21E+15	2500.	0.391E-02	0.197E-02	0.121E-02	0.529E-03	0.115E-02	0.334E-03
	5000.	0.503E-02	0.189E-02	0.124E-02	0.595E-03	0.116E-02	0.376E-03
	10000.	0.659E-02	0.130E-02	0.127E-02	0.668E-03	0.117E-02	0.423E-03
	20000.	0.841E-02	0.872E-03	0.131E-02	0.749E-03	0.119E-02	0.475E-03
	30000.	0.935E-02	0.546E-03	0.135E-02	0.802E-03	0.120E-02	0.508E-03
	50000.	0.102E-01	0.354E-03	0.139E-02	0.873E-03	0.122E-02	0.553E-03
7P - 7D 216985.6 Å C= 0.17E+17	2500.	0.569E-01	0.207E-01	0.214E-01	0.563E-02	0.212E-01	0.356E-02
	5000.	0.779E-01	0.175E-01	0.215E-01	0.631E-02	0.212E-01	0.400E-02
	10000.	0.109	0.114E-01	0.217E-01	0.709E-02	0.213E-01	0.449E-02
	20000.	0.145	0.858E-02	0.219E-01	0.796E-02	0.213E-01	0.504E-02
	30000.	0.165	0.584E-02	0.221E-01	0.851E-02	0.214E-01	0.539E-02
	50000.	0.185	0.331E-02	0.223E-01	0.927E-02	0.214E-01	0.587E-02
7P - 8D 90107.1 Å C= 0.20E+16	2500.	0.167E-01	0.750E-02	0.559E-02	0.210E-02	0.543E-02	0.133E-02
	5000.	0.221E-01	0.631E-02	0.567E-02	0.236E-02	0.545E-02	0.149E-02
	10000.	0.300E-01	0.407E-02	0.578E-02	0.264E-02	0.549E-02	0.168E-02
	20000.	0.394E-01	0.251E-02	0.592E-02	0.297E-02	0.553E-02	0.188E-02
	30000.	0.443E-01	0.169E-02	0.603E-02	0.318E-02	0.557E-02	0.201E-02
	50000.	0.493E-01	0.983E-03	0.618E-02	0.346E-02	0.562E-02	0.219E-02
7P - 9D 64637.9 Å C= 0.73E+15	2500.	0.141E-01	0.585E-02	0.443E-02	0.173E-02	0.428E-02	0.109E-02
	5000.	0.186E-01	0.486E-02	0.450E-02	0.194E-02	0.431E-02	0.123E-02
	10000.	0.251E-01	0.311E-02	0.460E-02	0.218E-02	0.434E-02	0.138E-02
	20000.	0.325E-01	0.166E-02	0.472E-02	0.245E-02	0.438E-02	0.155E-02
	30000.	0.363E-01	0.116E-02	0.481E-02	0.262E-02	0.441E-02	0.166E-02
	50000.	0.400E-01	0.714E-03	0.494E-02	0.285E-02	0.445E-02	0.181E-02
8P - 8D 348541.4 Å C= 0.30E+17	2500.	0.278	0.288E-01	0.100	0.145E-01	0.999E-01	0.919E-02
	5000.	0.401	0.180E-01	0.100	0.163E-01	0.999E-01	0.103E-01
	10000.	0.567	0.119E-01	0.100	0.183E-01	0.100	0.116E-01
	20000.	0.750	0.325E-02	0.101	0.205E-01	0.100	0.130E-01
	30000.	0.848	0.162E-02	0.101	0.220E-01	0.100	0.139E-01
	50000.	0.945	0.924E-03	0.101	0.239E-01	0.100	0.152E-01

Perturber density = 1 x 10^{11} cm^{-3}

Transition	T(K)	Electrons Width (Å)	Electrons Shift (Å)	Protons Width (Å)	Protons Shift (Å)	Ionized helium Width (Å)	Ionized helium Shift (Å)
8P - 9D 138083.4 Å C= 0.33E+16	2500.	0.675E-01	0.167E-01	0.220E-01	0.600E-02	0.218E-01	0.379E-02
	5000.	0.948E-01	0.910E-02	0.221E-01	0.673E-02	0.218E-01	0.426E-02
	10000.	0.133	0.631E-02	0.223E-01	0.756E-02	0.218E-01	0.479E-02
	20000.	0.173	0.218E-02	0.226E-01	0.849E-02	0.219E-01	0.537E-02
	30000.	0.194	0.135E-02	0.228E-01	0.908E-02	0.220E-01	0.575E-02
	50000.	0.214	0.741E-03	0.230E-01	0.989E-02	0.221E-01	0.626E-02
9P - 9D 524438.9 Å C= 0.48E+17	2500.	1.17	-0.965E-01	0.383	-0.247E-01	0.383	-0.156E-01
	5000.	1.71	-0.716E-01	0.383	-0.277E-01	0.383	-0.176E-01
	10000.	2.40	-0.531E-01	0.383	-0.311E-01	0.383	-0.197E-01
	20000.	3.14	-0.336E-01	0.383	-0.350E-01	0.383	-0.221E-01
	30000.	3.52	-0.218E-01	0.383	-0.374E-01	0.383	-0.237E-01
	50000.	3.88	-0.122E-01	0.383	-0.408E-01	0.383	-0.258E-01
3D - 4P 33972.8 Å C= 0.34E+16	2500.	0.462E-04	0.203E-04	0.207E-04	0.563E-05	0.205E-04	0.356E-05
	5000.	0.535E-04	0.242E-04	0.209E-04	0.632E-05	0.205E-04	0.400E-05
	10000.	0.642E-04	0.271E-04	0.210E-04	0.709E-05	0.206E-04	0.449E-05
	20000.	0.791E-04	0.262E-04	0.213E-04	0.796E-05	0.207E-04	0.504E-05
	30000.	0.893E-04	0.242E-04	0.215E-04	0.852E-05	0.207E-04	0.539E-05
	50000.	0.103E-03	0.200E-04	0.218E-04	0.927E-05	0.208E-04	0.587E-05
3D - 5P 12043.3 Å C= 0.21E+15	2500.	0.192E-04	0.113E-04	0.817E-05	0.298E-05	0.796E-05	0.189E-05
	5000.	0.225E-04	0.131E-04	0.828E-05	0.334E-05	0.799E-05	0.212E-05
	10000.	0.269E-04	0.134E-04	0.843E-05	0.375E-05	0.803E-05	0.238E-05
	20000.	0.328E-04	0.126E-04	0.862E-05	0.421E-05	0.809E-05	0.267E-05
	30000.	0.368E-04	0.110E-04	0.876E-05	0.451E-05	0.814E-05	0.285E-05
	50000.	0.420E-04	0.944E-05	0.897E-05	0.491E-05	0.821E-05	0.311E-05
3D - 6P 9249.1 Å C= 0.68E+14	2500.	0.303E-04	0.188E-04	0.121E-04	0.494E-05	0.116E-04	0.313E-05
	5000.	0.359E-04	0.208E-04	0.123E-04	0.554E-05	0.117E-04	0.351E-05
	10000.	0.432E-04	0.213E-04	0.126E-04	0.622E-05	0.118E-04	0.394E-05
	20000.	0.528E-04	0.185E-04	0.130E-04	0.698E-05	0.119E-04	0.442E-05
	30000.	0.593E-04	0.161E-04	0.132E-04	0.747E-05	0.120E-04	0.473E-05
	50000.	0.668E-04	0.135E-04	0.136E-04	0.814E-05	0.122E-04	0.515E-05
3D - 7P 8212.1 Å C= 0.31E+14	2500.	0.546E-04	0.342E-04	0.203E-04	0.896E-05	0.193E-04	0.567E-05
	5000.	0.650E-04	0.374E-04	0.207E-04	0.101E-04	0.195E-04	0.637E-05
	10000.	0.789E-04	0.361E-04	0.213E-04	0.113E-04	0.197E-04	0.715E-05
	20000.	0.969E-04	0.284E-04	0.221E-04	0.127E-04	0.199E-04	0.803E-05
	30000.	0.108E-03	0.237E-04	0.226E-04	0.136E-04	0.201E-04	0.859E-05
	50000.	0.121E-03	0.190E-04	0.234E-04	0.148E-04	0.204E-04	0.935E-05
3D - 8P 7692.3 Å C= 0.17E+14	2500.	0.970E-04	0.611E-04	0.337E-04	0.158E-04	0.319E-04	0.100E-04
	5000.	0.116E-03	0.632E-04	0.346E-04	0.178E-04	0.322E-04	0.113E-04
	10000.	0.142E-03	0.581E-04	0.358E-04	0.200E-04	0.325E-04	0.126E-04
	20000.	0.175E-03	0.425E-04	0.372E-04	0.224E-04	0.331E-04	0.142E-04
	30000.	0.195E-03	0.335E-04	0.382E-04	0.240E-04	0.335E-04	0.152E-04
	50000.	0.214E-03	0.257E-04	0.397E-04	0.261E-04	0.340E-04	0.165E-04

Perturber density = 1 x 10^{11} cm^{-3}

Transition	T(K)	Electrons Width (Å)	Electrons Shift (Å)	Protons Width (Å)	Protons Shift (Å)	Ionized helium Width (Å)	Ionized helium Shift (Å)
3D - 9P 7389.1 Å C= 0.10E+14	2500.	0.165E-03	0.101E-03	0.541E-04	0.267E-04	0.507E-04	0.169E-04
	5000.	0.199E-03	0.103E-03	0.558E-04	0.300E-04	0.513E-04	0.190E-04
	10000.	0.245E-03	0.886E-04	0.578E-04	0.336E-04	0.520E-04	0.213E-04
	20000.	0.303E-03	0.611E-04	0.604E-04	0.378E-04	0.529E-04	0.239E-04
	30000.	0.334E-03	0.469E-04	0.621E-04	0.404E-04	0.536E-04	0.256E-04
	50000.	0.362E-03	0.333E-04	0.647E-04	0.440E-04	0.547E-04	0.279E-04
4D - 5P 63619.7 Å C= 0.60E+16	2500.	0.473E-03	0.635E-04	0.249E-03	0.177E-04	0.249E-03	0.112E-04
	5000.	0.625E-03	0.638E-04	0.249E-03	0.199E-04	0.249E-03	0.126E-04
	10000.	0.870E-03	0.616E-04	0.249E-03	0.223E-04	0.249E-03	0.141E-04
	20000.	0.118E-02	0.558E-04	0.249E-03	0.251E-04	0.249E-03	0.159E-04
	30000.	0.138E-02	0.500E-04	0.249E-03	0.268E-04	0.249E-03	0.170E-04
	50000.	0.160E-02	0.418E-04	0.249E-03	0.292E-04	0.249E-03	0.185E-04
4D - 6P 24508.1 Å C= 0.48E+15	2500.	0.206E-03	0.121E-03	0.861E-04	0.301E-04	0.841E-04	0.191E-04
	5000.	0.251E-03	0.119E-03	0.872E-04	0.338E-04	0.844E-04	0.214E-04
	10000.	0.318E-03	0.116E-03	0.886E-04	0.379E-04	0.848E-04	0.240E-04
	20000.	0.408E-03	0.917E-04	0.904E-04	0.426E-04	0.854E-04	0.270E-04
	30000.	0.467E-03	0.867E-04	0.917E-04	0.455E-04	0.858E-04	0.288E-04
	50000.	0.530E-03	0.700E-04	0.937E-04	0.496E-04	0.865E-04	0.314E-04
4D - 7P 18363.7 Å C= 0.16E+15	2500.	0.272E-03	0.173E-03	0.102E-03	0.432E-04	0.977E-04	0.273E-04
	5000.	0.327E-03	0.180E-03	0.104E-03	0.485E-04	0.984E-04	0.307E-04
	10000.	0.405E-03	0.168E-03	0.107E-03	0.544E-04	0.992E-04	0.345E-04
	20000.	0.507E-03	0.131E-03	0.110E-03	0.611E-04	0.100E-03	0.387E-04
	30000.	0.571E-03	0.108E-03	0.113E-03	0.653E-04	0.101E-03	0.414E-04
	50000.	0.637E-03	0.806E-04	0.116E-03	0.711E-04	0.103E-03	0.451E-04
4D - 8P 15953.0 Å C= 0.73E+14	2500.	0.418E-03	0.254E-03	0.145E-03	0.673E-04	0.138E-03	0.425E-04
	5000.	0.503E-03	0.258E-03	0.149E-03	0.755E-04	0.139E-03	0.478E-04
	10000.	0.619E-03	0.227E-03	0.154E-03	0.848E-04	0.141E-03	0.537E-04
	20000.	0.771E-03	0.158E-03	0.160E-03	0.952E-04	0.143E-03	0.603E-04
	30000.	0.859E-03	0.121E-03	0.164E-03	0.102E-03	0.144E-03	0.645E-04
	50000.	0.945E-03	0.891E-04	0.170E-03	0.111E-03	0.147E-03	0.702E-04
4D - 9P 14701.7 Å C= 0.41E+14	2500.	0.654E-03	0.410E-03	0.215E-03	0.105E-03	0.201E-03	0.664E-04
	5000.	0.791E-03	0.379E-03	0.221E-03	0.118E-03	0.203E-03	0.747E-04
	10000.	0.978E-03	0.294E-03	0.229E-03	0.133E-03	0.206E-03	0.839E-04
	20000.	0.121E-02	0.170E-03	0.239E-03	0.149E-03	0.210E-03	0.942E-04
	30000.	0.134E-02	0.139E-03	0.246E-03	0.159E-03	0.213E-03	0.101E-03
	50000.	0.146E-02	0.986E-04	0.256E-03	0.173E-03	0.217E-03	0.110E-03
5D - 6P 110307.1 Å C= 0.97E+16	2500.	0.461E-02	0.211E-02	0.196E-02	0.574E-03	0.194E-02	0.364E-03
	5000.	0.609E-02	0.236E-02	0.198E-02	0.645E-03	0.194E-02	0.408E-03
	10000.	0.813E-02	0.251E-02	0.200E-02	0.724E-03	0.195E-02	0.458E-03
	20000.	0.106E-01	0.248E-02	0.202E-02	0.812E-03	0.195E-02	0.514E-03
	30000.	0.120E-01	0.238E-02	0.205E-02	0.869E-03	0.196E-02	0.550E-03
	50000.	0.135E-01	0.214E-02	0.208E-02	0.946E-03	0.197E-02	0.599E-03

Perturber density = 1 x 10^{11} cm^{-3}

Transition	T(K)	Electrons Width (Å)	Electrons Shift (Å)	Protons Width (Å)	Protons Shift (Å)	Ionized helium Width (Å)	Ionized helium Shift (Å)
5D - 7P 44018.0 Å C= 0.89E+15	2500.	0.151E-02	0.756E-03	0.598E-03	0.211E-03	0.583E-03	0.134E-03
	5000.	0.191E-02	0.784E-03	0.605E-03	0.237E-03	0.586E-03	0.150E-03
	10000.	0.248E-02	0.623E-03	0.615E-03	0.266E-03	0.589E-03	0.169E-03
	20000.	0.325E-02	0.506E-03	0.629E-03	0.299E-03	0.593E-03	0.189E-03
	30000.	0.370E-02	0.390E-03	0.638E-03	0.320E-03	0.596E-03	0.203E-03
	50000.	0.415E-02	0.243E-03	0.653E-03	0.348E-03	0.601E-03	0.221E-03
5D - 8P 32313.5 Å C= 0.30E+15	2500.	0.170E-02	0.103E-02	0.601E-03	0.263E-03	0.574E-03	0.166E-03
	5000.	0.209E-02	0.104E-02	0.614E-03	0.295E-03	0.578E-03	0.187E-03
	10000.	0.263E-02	0.761E-03	0.631E-03	0.331E-03	0.584E-03	0.210E-03
	20000.	0.335E-02	0.514E-03	0.653E-03	0.372E-03	0.591E-03	0.235E-03
	30000.	0.375E-02	0.400E-03	0.668E-03	0.397E-03	0.597E-03	0.252E-03
	50000.	0.414E-02	0.251E-03	0.691E-03	0.433E-03	0.605E-03	0.274E-03
5D - 9P 27561.9 Å C= 0.14E+15	2500.	0.230E-02	0.138E-02	0.757E-03	0.362E-03	0.713E-03	0.229E-03
	5000.	0.281E-02	0.125E-02	0.778E-03	0.407E-03	0.720E-03	0.257E-03
	10000.	0.351E-02	0.916E-03	0.805E-03	0.457E-03	0.729E-03	0.289E-03
	20000.	0.440E-02	0.512E-03	0.838E-03	0.513E-03	0.742E-03	0.325E-03
	30000.	0.487E-02	0.406E-03	0.862E-03	0.549E-03	0.751E-03	0.347E-03
	50000.	0.531E-02	0.265E-03	0.896E-03	0.597E-03	0.764E-03	0.378E-03
6D - 7P 179546.1 Å C= 0.15E+17	2500.	0.255E-01	0.373E-02	0.110E-01	0.157E-02	0.110E-01	0.992E-03
	5000.	0.358E-01	0.297E-02	0.110E-01	0.176E-02	0.110E-01	0.111E-02
	10000.	0.507E-01	0.203E-02	0.110E-01	0.197E-02	0.110E-01	0.125E-02
	20000.	0.680E-01	0.117E-02	0.111E-01	0.222E-02	0.110E-01	0.140E-02
	30000.	0.778E-01	0.601E-03	0.111E-01	0.237E-02	0.110E-01	0.150E-02
	50000.	0.882E-01	0.172E-03	0.111E-01	0.258E-02	0.110E-01	0.164E-02
6D - 8P 72472.2 Å C= 0.15E+16	2500.	0.848E-02	0.413E-02	0.311E-02	0.114E-02	0.302E-02	0.720E-03
	5000.	0.110E-01	0.380E-02	0.315E-02	0.128E-02	0.304E-02	0.809E-03
	10000.	0.146E-01	0.237E-02	0.321E-02	0.143E-02	0.305E-02	0.908E-03
	20000.	0.190E-01	0.165E-02	0.328E-02	0.161E-02	0.308E-02	0.102E-02
	30000.	0.214E-01	0.110E-02	0.334E-02	0.172E-02	0.309E-02	0.109E-02
	50000.	0.238E-01	0.599E-03	0.342E-02	0.188E-02	0.312E-02	0.119E-02
6D - 9P 52264.1 Å C= 0.52E+15	2500.	0.828E-02	0.446E-02	0.275E-02	0.123E-02	0.262E-02	0.780E-03
	5000.	0.104E-01	0.417E-02	0.281E-02	0.139E-02	0.264E-02	0.877E-03
	10000.	0.133E-01	0.259E-02	0.290E-02	0.156E-02	0.267E-02	0.986E-03
	20000.	0.170E-01	0.140E-02	0.301E-02	0.175E-02	0.270E-02	0.111E-02
	30000.	0.188E-01	0.101E-02	0.308E-02	0.187E-02	0.273E-02	0.118E-02
	50000.	0.206E-01	0.617E-03	0.319E-02	0.204E-02	0.277E-02	0.129E-02
7D - 8P 276227.8 Å C= 0.22E+17	2500.	0.131	0.316E-01	0.498E-01	0.102E-01	0.496E-01	0.645E-02
	5000.	0.184	0.226E-01	0.500E-01	0.114E-01	0.496E-01	0.725E-02
	10000.	0.259	0.152E-01	0.501E-01	0.128E-01	0.497E-01	0.814E-02
	20000.	0.342	0.814E-02	0.504E-01	0.144E-01	0.497E-01	0.913E-02
	30000.	0.388	0.506E-02	0.506E-01	0.154E-01	0.498E-01	0.977E-02
	50000.	0.434	0.268E-02	0.509E-01	0.168E-01	0.499E-01	0.106E-01

Perturber density = 1 x 10^{11} cm^{-3}

Transition	T(K)	Electrons Width (Å)	Electrons Shift (Å)	Protons Width (Å)	Protons Shift (Å)	Ionized helium Width (Å)	Ionized helium Shift (Å)
7D - 9P 111664.5 Å C= 0.24E+16	2500.	0.386E-01	0.167E-01	0.130E-01	0.497E-02	0.126E-01	0.314E-02
	5000.	0.506E-01	0.144E-01	0.132E-01	0.559E-02	0.126E-01	0.354E-02
	10000.	0.679E-01	0.844E-02	0.135E-01	0.627E-02	0.127E-01	0.397E-02
	20000.	0.879E-01	0.428E-02	0.138E-01	0.704E-02	0.128E-01	0.446E-02
	30000.	0.982E-01	0.292E-02	0.141E-01	0.753E-02	0.129E-01	0.477E-02
	50000.	0.108	0.179E-02	0.144E-01	0.820E-02	0.131E-01	0.520E-02
8D - 9P 405498.6 Å C= 0.31E+17	2500.	0.560	0.165	0.188	0.489E-01	0.187	0.309E-01
	5000.	0.782	0.118	0.189	0.549E-01	0.187	0.347E-01
	10000.	1.09	0.760E-01	0.191	0.616E-01	0.187	0.390E-01
	20000.	1.42	0.358E-01	0.193	0.691E-01	0.188	0.438E-01
	30000.	1.59	0.243E-01	0.194	0.740E-01	0.188	0.469E-01
	50000.	1.76	0.151E-01	0.196	0.806E-01	0.189	0.510E-01
3D - 4F 12087.2 Å C= 0.23E+15	2500.	0.935E-05	0.690E-06	0.391E-05	0.118E-06	0.391E-05	0.747E-07
	5000.	0.118E-04	0.163E-05	0.391E-05	0.133E-06	0.391E-05	0.839E-07
	10000.	0.152E-04	0.248E-05	0.391E-05	0.151E-06	0.391E-05	0.942E-07
	20000.	0.191E-04	0.299E-05	0.391E-05	0.165E-06	0.391E-05	0.106E-06
	30000.	0.215E-04	0.263E-05	0.391E-05	0.155E-06	0.391E-05	0.113E-06
	50000.	0.245E-04	0.217E-05	0.391E-05	0.147E-06	0.391E-05	0.123E-06
4D - 4F 64864.3 Å C= 0.65E+16	2500.	0.542E-03	-0.298E-03	0.169E-03	-0.802E-04	0.160E-03	-0.508E-04
	5000.	0.633E-03	-0.323E-03	0.174E-03	-0.900E-04	0.161E-03	-0.570E-04
	10000.	0.771E-03	-0.316E-03	0.180E-03	-0.101E-03	0.163E-03	-0.640E-04
	20000.	0.941E-03	-0.240E-03	0.187E-03	-0.113E-03	0.166E-03	-0.718E-04
	30000.	0.107E-02	-0.205E-03	0.192E-03	-0.121E-03	0.168E-03	-0.768E-04
	50000.	0.121E-02	-0.187E-03	0.199E-03	-0.132E-03	0.171E-03	-0.837E-04
4F - 5D 61272.6 Å C= 0.34E+16	2500.	0.116E-02	0.761E-03	0.337E-03	0.201E-03	0.301E-03	0.127E-03
	5000.	0.135E-02	0.874E-03	0.353E-03	0.226E-03	0.307E-03	0.143E-03
	10000.	0.156E-02	0.893E-03	0.372E-03	0.254E-03	0.315E-03	0.161E-03
	20000.	0.181E-02	0.746E-03	0.396E-03	0.285E-03	0.325E-03	0.180E-03
	30000.	0.201E-02	0.631E-03	0.412E-03	0.305E-03	0.332E-03	0.193E-03
	50000.	0.226E-02	0.568E-03	0.436E-03	0.332E-03	0.342E-03	0.210E-03
4F - 6D 29878.5 Å C= 0.49E+15	2500.	0.570E-03	0.386E-03	0.170E-03	0.100E-03	0.152E-03	0.636E-04
	5000.	0.661E-03	0.427E-03	0.178E-03	0.113E-03	0.155E-03	0.714E-04
	10000.	0.771E-03	0.427E-03	0.187E-03	0.127E-03	0.159E-03	0.801E-04
	20000.	0.912E-03	0.342E-03	0.199E-03	0.142E-03	0.164E-03	0.900E-04
	30000.	0.101E-02	0.279E-03	0.207E-03	0.152E-03	0.167E-03	0.962E-04
	50000.	0.113E-02	0.240E-03	0.219E-03	0.165E-03	0.172E-03	0.105E-03
4F - 7D 22911.0 Å C= 0.19E+15	2500.	0.620E-03	0.400E-03	0.189E-03	0.105E-03	0.172E-03	0.665E-04
	5000.	0.730E-03	0.429E-03	0.197E-03	0.118E-03	0.175E-03	0.748E-04
	10000.	0.877E-03	0.405E-03	0.206E-03	0.133E-03	0.179E-03	0.840E-04
	20000.	0.107E-02	0.295E-03	0.217E-03	0.149E-03	0.183E-03	0.943E-04
	30000.	0.120E-02	0.240E-03	0.225E-03	0.159E-03	0.187E-03	0.101E-03
	50000.	0.132E-02	0.183E-03	0.236E-03	0.173E-03	0.192E-03	0.110E-03

Perturber density = 1 x 10^{11} cm^{-3}

Transition	T(K)	Electrons Width (Å)	Electrons Shift (Å)	Protons Width (Å)	Protons Shift (Å)	Ionized helium Width (Å)	Ionized helium Shift (Å)
4F - 8D 19945.6 Å C= 0.98E+14	2500.	0.804E-03	0.492E-03	0.248E-03	0.127E-03	0.231E-03	0.801E-04
	5000.	0.980E-03	0.492E-03	0.256E-03	0.142E-03	0.233E-03	0.901E-04
	10000.	0.122E-02	0.434E-03	0.266E-03	0.160E-03	0.237E-03	0.101E-03
	20000.	0.153E-02	0.295E-03	0.279E-03	0.179E-03	0.242E-03	0.114E-03
	30000.	0.170E-02	0.247E-03	0.288E-03	0.192E-03	0.246E-03	0.122E-03
	50000.	0.186E-02	0.159E-03	0.300E-03	0.209E-03	0.251E-03	0.132E-03
4F - 9D 18345.5 Å C= 0.59E+14	2500.	0.111E-02	0.594E-03	0.339E-03	0.156E-03	0.322E-03	0.984E-04
	5000.	0.141E-02	0.575E-03	0.348E-03	0.175E-03	0.324E-03	0.111E-03
	10000.	0.181E-02	0.481E-03	0.359E-03	0.196E-03	0.328E-03	0.124E-03
	20000.	0.228E-02	0.315E-03	0.372E-03	0.220E-03	0.333E-03	0.140E-03
	30000.	0.253E-02	0.266E-03	0.382E-03	0.236E-03	0.337E-03	0.149E-03
	50000.	0.276E-02	0.152E-03	0.396E-03	0.257E-03	0.342E-03	0.163E-03
4F - 5G 38213.4 Å C= 0.13E+15	2500.	0.105E-02	-0.330E-03	0.236E-03	-0.206E-03	0.165E-03	-0.130E-03
	5000.	0.113E-02	-0.196E-03	0.263E-03	-0.231E-03	0.179E-03	-0.146E-03
	10000.	0.113E-02	-0.292E-04	0.295E-03	-0.259E-03	0.195E-03	-0.164E-03
	20000.	0.114E-02	0.264E-04	0.335E-03	-0.291E-03	0.215E-03	-0.184E-03
	30000.	0.114E-02	0.749E-04	0.364E-03	-0.311E-03	0.227E-03	-0.197E-03
	50000.	0.115E-02	0.835E-04	0.411E-03	-0.339E-03	0.244E-03	-0.215E-03
4F - 6G 25226.5 Å C= 0.52E+13	2500.	0.270E-02	0.153E-04	0.766E-03	0.684E-03	0.470E-03	0.432E-03
	5000.	0.266E-02	-0.272E-04	0.898E-03	0.769E-03	0.525E-03	0.486E-03
	10000.	0.250E-02	-0.570E-04	0.109E-02	0.867E-03	0.588E-03	0.547E-03
	20000.	0.228E-02	0.475E-05	0.135E-02	0.105E-02	0.659E-03	0.615E-03
	30000.	0.215E-02	0.424E-05	0.152E-02	0.109E-02	0.706E-03	0.658E-03
	50000.	0.199E-02	0.491E-04	0.169E-02	0.128E-02	0.772E-03	0.716E-03
4F - 7G 20936.4 Å C= 0.24E+13	2500.	0.477E-02	0.257E-03	0.150E-02	0.135E-02	0.923E-03	0.853E-03
	5000.	0.460E-02	0.485E-04	0.175E-02	0.152E-02	0.103E-02	0.961E-03
	10000.	0.428E-02	-0.105E-03	0.210E-02	0.171E-02	0.116E-02	0.108E-02
	20000.	0.385E-02	-0.296E-04	0.259E-02	0.196E-02	0.130E-02	0.122E-02
	30000.	0.360E-02	-0.263E-04	0.303E-02	0.215E-02	0.139E-02	0.130E-02
	50000.	0.328E-02	0.219E-04	0.335E-02	0.243E-02	0.152E-02	0.142E-02
4F - 8G 18855.7 Å C= 0.13E+13	2500.	0.795E-02	0.343E-03	0.265E-02	0.238E-02	0.162E-02	0.149E-02
	5000.	0.750E-02	-0.183E-03	0.308E-02	0.268E-02	0.182E-02	0.169E-02
	10000.	0.694E-02	-0.185E-03	0.369E-02	0.302E-02	0.204E-02	0.191E-02
	20000.	0.620E-02	-0.114E-03	0.455E-02	0.344E-02	0.229E-02	0.215E-02
	30000.	0.576E-02	-0.181E-03	0.515E-02	0.376E-02	0.245E-02	0.230E-02
	50000.	0.520E-02	-0.315E-04	0.589E-02	0.422E-02	0.268E-02	0.251E-02
5F - 6G 69625.8 Å C= 0.40E+14	2500.	0.240E-01	-0.168E-02	0.561E-02	0.498E-02	0.345E-02	0.314E-02
	5000.	0.237E-01	-0.157E-02	0.659E-02	0.560E-02	0.385E-02	0.354E-02
	10000.	0.227E-01	-0.149E-02	0.802E-02	0.632E-02	0.430E-02	0.398E-02
	20000.	0.209E-01	-0.809E-03	0.999E-02	0.729E-02	0.482E-02	0.447E-02
	30000.	0.198E-01	-0.122E-03	0.113E-01	0.816E-02	0.516E-02	0.479E-02
	50000.	0.185E-01	0.148E-03	0.126E-01	0.933E-02	0.564E-02	0.521E-02

Perturber density = 1 x 10^{11} cm^{-3}

Transition	T(K)	Electrons Width (Å)	Electrons Shift (Å)	Protons Width (Å)	Protons Shift (Å)	Ionized helium Width (Å)	Ionized helium Shift (Å)
5F - 7G 44473.3 Å C= 0.11E+14	2500.	0.230E-01	0.468E-03	0.673E-02	0.604E-02	0.413E-02	0.381E-02
	5000.	0.221E-01	-0.267E-03	0.784E-02	0.680E-02	0.462E-02	0.430E-02
	10000.	0.208E-01	-0.786E-03	0.941E-02	0.767E-02	0.518E-02	0.484E-02
	20000.	0.188E-01	-0.404E-03	0.116E-01	0.875E-02	0.582E-02	0.544E-02
	30000.	0.176E-01	-0.205E-03	0.132E-01	0.956E-02	0.623E-02	0.583E-02
	50000.	0.161E-01	0.324E-04	0.159E-01	0.110E-01	0.681E-02	0.635E-02
5F - 8G 36028.1 Å C= 0.48E+13	2500.	0.300E-01	0.153E-02	0.964E-02	0.866E-02	0.591E-02	0.543E-02
	5000.	0.283E-01	-0.801E-03	0.112E-01	0.975E-02	0.663E-02	0.616E-02
	10000.	0.263E-01	-0.867E-03	0.134E-01	0.110E-01	0.743E-02	0.694E-02
	20000.	0.236E-01	-0.580E-03	0.166E-01	0.125E-01	0.834E-02	0.781E-02
	30000.	0.219E-01	-0.688E-03	0.188E-01	0.137E-01	0.894E-02	0.837E-02
	50000.	0.199E-01	-0.133E-03	0.216E-01	0.157E-01	0.976E-02	0.912E-02
6F - 7G 113996.5 Å C= 0.70E+14	2500.	0.169	-0.972E-02	0.430E-01	0.385E-01	0.264E-01	0.243E-01
	5000.	0.163	-0.148E-01	0.501E-01	0.433E-01	0.295E-01	0.274E-01
	10000.	0.156	-0.970E-02	0.603E-01	0.488E-01	0.331E-01	0.308E-01
	20000.	0.143	-0.543E-02	0.748E-01	0.567E-01	0.371E-01	0.346E-01
	30000.	0.135	-0.352E-02	0.846E-01	0.611E-01	0.397E-01	0.371E-01
	50000.	0.124	-0.997E-03	0.957E-01	0.690E-01	0.434E-01	0.404E-01
5G - 6H 73776.2 Å C= 0.45E+14	2500.	0.193E-01	-0.981E-03	0.625E-02	-0.558E-02	0.382E-02	-0.353E-02
	5000.	0.177E-01	0.339E-03	0.732E-02	-0.628E-02	0.427E-02	-0.397E-02
	10000.	0.159E-01	0.748E-03	0.886E-02	-0.708E-02	0.479E-02	-0.447E-02
	20000.	0.144E-01	0.876E-03	0.110E-01	-0.814E-02	0.537E-02	-0.502E-02
	30000.	0.137E-01	0.791E-03	0.124E-01	-0.897E-02	0.575E-02	-0.537E-02
	50000.	0.128E-01	0.641E-03	0.139E-01	-0.102E-01	0.629E-02	-0.585E-02
6G - 7H 122295.7 Å C= 0.25E+14	2500.	0.275	-0.748E-02	0.602E-01	0.433E-01	0.292E-01	0.269E-01
	5000.	0.248	-0.128E-02	0.750E-01	0.510E-01	0.328E-01	0.303E-01
	10000.	0.216	0.154E-02	0.897E-01	0.566E-01	0.372E-01	0.341E-01
	20000.	0.186	0.245E-02	0.117	0.526E-01	0.430E-01	0.384E-01
	30000.	0.169	0.184E-02	0.134	0.421E-01	0.473E-01	0.414E-01
	50000.	0.150	0.138E-02	0.170	0.233E-01	0.529E-01	0.460E-01
6G - 7I 123290.9 Å C= 0.25E+14	2500.	0.150	0.165E-02	0.779E-01	-0.613E-01	0.415E-01	-0.384E-01
	5000.	0.129	0.522E-02	0.975E-01	-0.709E-01	0.466E-01	-0.434E-01
	10000.	0.109	0.547E-02	0.117	-0.839E-01	0.525E-01	-0.489E-01
	20000.	0.945E-01	0.292E-02	0.131	-0.946E-01	0.597E-01	-0.550E-01
	30000.	0.876E-01	0.327E-02	0.138	-0.906E-01	0.647E-01	-0.590E-01
	50000.	0.800E-01	0.206E-02	0.148	-0.880E-01	0.720E-01	-0.648E-01
4S - 4P 15036.2 Å C= 0.25E+14	2500.	0.405E-04	0.175E-04	0.114E-04	0.104E-04	0.741E-05	0.658E-05
	5000.	0.404E-04	0.134E-04	0.128E-04	0.117E-04	0.821E-05	0.738E-05
	10000.	0.386E-04	0.863E-05	0.146E-04	0.131E-04	0.913E-05	0.829E-05
	20000.	0.365E-04	0.449E-05	0.170E-04	0.147E-04	0.102E-04	0.930E-05
	30000.	0.353E-04	0.288E-05	0.187E-04	0.157E-04	0.108E-04	0.995E-05
	50000.	0.339E-04	0.104E-05	0.216E-04	0.172E-04	0.118E-04	0.108E-04

Perturber density = 1 x 10^{11} cm^{-3}

Transition	T(K)	Electrons Width (Å)	Electrons Shift (Å)	Protons Width (Å)	Protons Shift (Å)	Ionized helium Width (Å)	Ionized helium Shift (Å)
4S - 5P 7660.5 Å C= 0.35E+13	2500.	0.468E-04	-0.194E-04	0.124E-04	-0.114E-04	0.801E-05	-0.721E-05
	5000.	0.465E-04	-0.149E-04	0.140E-04	-0.128E-04	0.891E-05	-0.810E-05
	10000.	0.435E-04	-0.931E-05	0.159E-04	-0.144E-04	0.992E-05	-0.909E-05
	20000.	0.403E-04	-0.562E-05	0.184E-04	-0.161E-04	0.111E-04	-0.102E-04
	30000.	0.383E-04	-0.369E-05	0.202E-04	-0.172E-04	0.118E-04	-0.109E-04
	50000.	0.358E-04	-0.186E-05	0.232E-04	-0.188E-04	0.128E-04	-0.119E-04
4S - 6P 6320.7 Å C= 0.20E+13	2500.	0.739E-04	-0.360E-04	0.190E-04	-0.174E-04	0.124E-04	-0.110E-04
	5000.	0.765E-04	-0.264E-04	0.213E-04	-0.195E-04	0.138E-04	-0.123E-04
	10000.	0.737E-04	-0.179E-04	0.241E-04	-0.219E-04	0.153E-04	-0.139E-04
	20000.	0.696E-04	-0.104E-04	0.276E-04	-0.246E-04	0.170E-04	-0.156E-04
	30000.	0.669E-04	-0.677E-05	0.301E-04	-0.263E-04	0.181E-04	-0.167E-04
	50000.	0.631E-04	-0.328E-05	0.341E-04	-0.286E-04	0.197E-04	-0.181E-04
4S - 7P 5787.1 Å C= 0.12E+13	2500.	0.136E-03	-0.684E-04	0.351E-04	-0.321E-04	0.229E-04	-0.203E-04
	5000.	0.142E-03	-0.519E-04	0.394E-04	-0.361E-04	0.254E-04	-0.228E-04
	10000.	0.137E-03	-0.323E-04	0.446E-04	-0.405E-04	0.283E-04	-0.257E-04
	20000.	0.130E-03	-0.183E-04	0.510E-04	-0.455E-04	0.315E-04	-0.288E-04
	30000.	0.125E-03	-0.119E-04	0.556E-04	-0.487E-04	0.336E-04	-0.308E-04
	50000.	0.118E-03	-0.538E-05	0.630E-04	-0.530E-04	0.364E-04	-0.336E-04
4S - 8P 5511.1 Å C= 0.72E+12	2500.	0.245E-03	-0.115E-03	0.635E-04	-0.581E-04	0.413E-04	-0.367E-04
	5000.	0.254E-03	-0.853E-04	0.714E-04	-0.654E-04	0.459E-04	-0.413E-04
	10000.	0.247E-03	-0.599E-04	0.808E-04	-0.735E-04	0.511E-04	-0.465E-04
	20000.	0.234E-03	-0.299E-04	0.925E-04	-0.825E-04	0.569E-04	-0.522E-04
	30000.	0.225E-03	-0.194E-04	0.101E-03	-0.883E-04	0.607E-04	-0.559E-04
	50000.	0.212E-03	-0.102E-04	0.114E-03	-0.962E-04	0.659E-04	-0.609E-04
4S - 9P 5347.5 Å C= 0.48E+12	2500.	0.422E-03	-0.185E-03	0.110E-03	-0.101E-03	0.716E-04	-0.636E-04
	5000.	0.436E-03	-0.139E-03	0.124E-03	-0.114E-03	0.795E-04	-0.717E-04
	10000.	0.421E-03	-0.959E-04	0.141E-03	-0.128E-03	0.886E-04	-0.808E-04
	20000.	0.400E-03	-0.448E-04	0.161E-03	-0.144E-03	0.988E-04	-0.909E-04
	30000.	0.384E-03	-0.230E-04	0.177E-03	-0.154E-03	0.105E-03	-0.974E-04
	50000.	0.361E-03	-0.158E-04	0.201E-03	-0.168E-03	0.114E-03	-0.106E-03
5S - 5P 42035.5 Å C= 0.10E+15	2500.	0.146E-02	-0.631E-03	0.378E-03	-0.347E-03	0.244E-03	-0.220E-03
	5000.	0.146E-02	-0.504E-03	0.426E-03	-0.390E-03	0.271E-03	-0.247E-03
	10000.	0.139E-02	-0.316E-03	0.484E-03	-0.438E-03	0.302E-03	-0.277E-03
	20000.	0.132E-02	-0.211E-03	0.559E-03	-0.491E-03	0.337E-03	-0.311E-03
	30000.	0.127E-02	-0.160E-03	0.616E-03	-0.526E-03	0.360E-03	-0.333E-03
	50000.	0.122E-02	-0.969E-04	0.706E-03	-0.574E-03	0.391E-03	-0.363E-03
5S - 6P 19432.8 Å C= 0.19E+14	2500.	0.703E-03	-0.354E-03	0.180E-03	-0.165E-03	0.118E-03	-0.104E-03
	5000.	0.728E-03	-0.264E-03	0.202E-03	-0.185E-03	0.131E-03	-0.117E-03
	10000.	0.708E-03	-0.160E-03	0.229E-03	-0.208E-03	0.145E-03	-0.132E-03
	20000.	0.677E-03	-0.103E-03	0.262E-03	-0.233E-03	0.162E-03	-0.148E-03
	30000.	0.656E-03	-0.451E-04	0.286E-03	-0.249E-03	0.172E-03	-0.158E-03
	50000.	0.626E-03	-0.323E-04	0.324E-03	-0.272E-03	0.187E-03	-0.172E-03

Perturber density = 1 x 10^{11} cm^{-3}

Transition	T(K)	Electrons Width (Å)	Electrons Shift (Å)	Protons Width (Å)	Protons Shift (Å)	Ionized helium Width (Å)	Ionized helium Shift (Å)
5S - 7P 15140.4 Å C= 0.79E+13	2500.	0.935E-03	-0.465E-03	0.241E-03	-0.220E-03	0.157E-03	-0.139E-03
	5000.	0.973E-03	-0.340E-03	0.270E-03	-0.247E-03	0.174E-03	-0.156E-03
	10000.	0.947E-03	-0.229E-03	0.305E-03	-0.278E-03	0.194E-03	-0.176E-03
	20000.	0.903E-03	-0.119E-03	0.349E-03	-0.312E-03	0.216E-03	-0.198E-03
	30000.	0.873E-03	-0.402E-04	0.381E-03	-0.334E-03	0.230E-03	-0.211E-03
	50000.	0.827E-03	-0.293E-04	0.431E-03	-0.363E-03	0.249E-03	-0.230E-03
5S - 8P 13386.6 Å C= 0.42E+13	2500.	0.145E-02	-0.701E-03	0.375E-03	-0.343E-03	0.244E-03	-0.217E-03
	5000.	0.150E-02	-0.504E-03	0.421E-03	-0.386E-03	0.271E-03	-0.244E-03
	10000.	0.146E-02	-0.334E-03	0.477E-03	-0.434E-03	0.301E-03	-0.274E-03
	20000.	0.139E-02	-0.174E-03	0.546E-03	-0.487E-03	0.336E-03	-0.308E-03
	30000.	0.134E-02	-0.883E-04	0.596E-03	-0.521E-03	0.358E-03	-0.330E-03
	50000.	0.127E-02	-0.390E-04	0.676E-03	-0.568E-03	0.389E-03	-0.359E-03
5S - 9P 12460.3 Å C= 0.26E+13	2500.	0.229E-02	-0.110E-02	0.600E-03	-0.549E-03	0.389E-03	-0.345E-03
	5000.	0.237E-02	-0.752E-03	0.674E-03	-0.617E-03	0.432E-03	-0.390E-03
	10000.	0.229E-02	-0.488E-03	0.764E-03	-0.694E-03	0.481E-03	-0.439E-03
	20000.	0.218E-02	-0.235E-03	0.876E-03	-0.780E-03	0.537E-03	-0.494E-03
	30000.	0.210E-02	-0.142E-03	0.959E-03	-0.835E-03	0.572E-03	-0.529E-03
	50000.	0.197E-02	-0.579E-04	0.109E-02	-0.910E-03	0.621E-03	-0.576E-03
6S - 6P 88772.9 Å C= 0.39E+15	2500.	0.156E-01	-0.807E-02	0.382E-02	-0.349E-02	0.249E-02	-0.221E-02
	5000.	0.162E-01	-0.617E-02	0.429E-02	-0.393E-02	0.277E-02	-0.248E-02
	10000.	0.160E-01	-0.451E-02	0.485E-02	-0.441E-02	0.307E-02	-0.279E-02
	20000.	0.156E-01	-0.281E-02	0.554E-02	-0.495E-02	0.342E-02	-0.313E-02
	30000.	0.154E-01	-0.191E-02	0.605E-02	-0.529E-02	0.365E-02	-0.335E-02
	50000.	0.150E-01	-0.134E-02	0.685E-02	-0.576E-02	0.396E-02	-0.365E-02
6S - 7P 38679.2 Å C= 0.51E+14	2500.	0.620E-02	-0.317E-02	0.158E-02	-0.144E-02	0.103E-02	-0.911E-03
	5000.	0.646E-02	-0.214E-02	0.177E-02	-0.162E-02	0.114E-02	-0.103E-02
	10000.	0.637E-02	-0.120E-02	0.200E-02	-0.182E-02	0.127E-02	-0.115E-02
	20000.	0.615E-02	-0.537E-03	0.229E-02	-0.205E-02	0.141E-02	-0.130E-02
	30000.	0.600E-02	-0.474E-03	0.250E-02	-0.219E-02	0.151E-02	-0.139E-02
	50000.	0.576E-02	-0.230E-03	0.283E-02	-0.238E-02	0.164E-02	-0.151E-02
6S - 8P 28979.8 Å C= 0.20E+14	2500.	0.682E-02	-0.250E-02	0.176E-02	-0.161E-02	0.115E-02	-0.102E-02
	5000.	0.710E-02	-0.198E-02	0.198E-02	-0.181E-02	0.127E-02	-0.114E-02
	10000.	0.694E-02	-0.786E-03	0.224E-02	-0.204E-02	0.141E-02	-0.129E-02
	20000.	0.665E-02	-0.474E-03	0.256E-02	-0.229E-02	0.158E-02	-0.145E-02
	30000.	0.645E-02	-0.921E-04	0.280E-02	-0.245E-02	0.168E-02	-0.155E-02
	50000.	0.613E-02	-0.540E-04	0.317E-02	-0.266E-02	0.182E-02	-0.169E-02
6S - 9P 24962.4 Å C= 0.10E+14	2500.	0.923E-02	-0.409E-02	0.241E-02	-0.220E-02	0.156E-02	-0.139E-02
	5000.	0.956E-02	-0.235E-02	0.271E-02	-0.248E-02	0.173E-02	-0.156E-02
	10000.	0.927E-02	-0.176E-02	0.307E-02	-0.279E-02	0.193E-02	-0.176E-02
	20000.	0.885E-02	-0.503E-03	0.352E-02	-0.313E-02	0.216E-02	-0.198E-02
	30000.	0.854E-02	-0.405E-03	0.385E-02	-0.335E-02	0.230E-02	-0.212E-02
	50000.	0.806E-02	-0.308E-03	0.437E-02	-0.365E-02	0.250E-02	-0.231E-02

Perturber density = 1 x 10^{11} cm^{-3}

Transition	T(K)	Electrons Width (Å)	Electrons Shift (Å)	Protons Width (Å)	Protons Shift (Å)	Ionized helium Width (Å)	Ionized helium Shift (Å)
7S - 7P 160774.3 Å C= 0.89E+15	2500.	0.115	-0.605E-01	0.277E-01	-0.253E-01	0.180E-01	-0.160E-01
	5000.	0.119	-0.456E-01	0.311E-01	-0.285E-01	0.200E-01	-0.180E-01
	10000.	0.120	-0.322E-01	0.351E-01	-0.320E-01	0.223E-01	-0.202E-01
	20000.	0.118	-0.186E-01	0.401E-01	-0.359E-01	0.248E-01	-0.227E-01
	30000.	0.117	-0.123E-01	0.438E-01	-0.384E-01	0.264E-01	-0.243E-01
	50000.	0.114	-0.887E-02	0.495E-01	-0.418E-01	0.287E-01	-0.265E-01
7S - 8P 67235.9 Å C= 0.11E+15	2500.	0.376E-01	-0.181E-01	0.953E-02	-0.871E-02	0.620E-02	-0.550E-02
	5000.	0.392E-01	-0.118E-01	0.107E-01	-0.980E-02	0.688E-02	-0.619E-02
	10000.	0.388E-01	-0.758E-02	0.121E-01	-0.110E-01	0.766E-02	-0.697E-02
	20000.	0.378E-01	-0.399E-02	0.139E-01	-0.124E-01	0.853E-02	-0.784E-02
	30000.	0.369E-01	-0.234E-02	0.151E-01	-0.132E-01	0.910E-02	-0.839E-02
	50000.	0.355E-01	-0.160E-02	0.172E-01	-0.144E-01	0.987E-02	-0.914E-02
7S - 9P 48956.0 Å C= 0.40E+14	2500.	0.358E-01	-0.142E-01	0.928E-02	-0.849E-02	0.602E-02	-0.535E-02
	5000.	0.372E-01	-0.752E-02	0.104E-01	-0.955E-02	0.669E-02	-0.604E-02
	10000.	0.364E-01	-0.473E-02	0.118E-01	-0.107E-01	0.745E-02	-0.679E-02
	20000.	0.350E-01	-0.264E-02	0.136E-01	-0.121E-01	0.831E-02	-0.764E-02
	30000.	0.340E-01	-0.104E-02	0.148E-01	-0.129E-01	0.886E-02	-0.818E-02
	50000.	0.323E-01	-0.598E-03	0.169E-01	-0.141E-01	0.962E-02	-0.892E-02
8S - 8P 263144.0 Å C= 0.16E+16	2500.	0.613	-0.319	0.148	-0.135	0.961E-01	-0.855E-01
	5000.	0.641	-0.237	0.166	-0.152	0.107	-0.961E-01
	10000.	0.644	-0.156	0.188	-0.171	0.119	-0.108
	20000.	0.641	-0.815E-01	0.215	-0.192	0.132	-0.122
	30000.	0.636	-0.537E-01	0.235	-0.206	0.141	-0.130
	50000.	0.621	-0.374E-01	0.266	-0.224	0.153	-0.142
8S - 9P 106909.6 Å C= 0.19E+15	2500.	0.176	-0.839E-01	0.445E-01	-0.407E-01	0.288E-01	-0.256E-01
	5000.	0.183	-0.556E-01	0.500E-01	-0.458E-01	0.320E-01	-0.290E-01
	10000.	0.181	-0.341E-01	0.567E-01	-0.515E-01	0.357E-01	-0.326E-01
	20000.	0.177	-0.147E-01	0.650E-01	-0.579E-01	0.398E-01	-0.366E-01
	30000.	0.173	-0.106E-01	0.711E-01	-0.620E-01	0.425E-01	-0.392E-01
	50000.	0.167	-0.678E-02	0.808E-01	-0.675E-01	0.461E-01	-0.428E-01
9S - 9P 402074.7 Å C= 0.27E+16	2500.	2.63	-1.32	0.636	-0.583	0.412	-0.367
	5000.	2.75	-0.966	0.716	-0.656	0.458	-0.414
	10000.	2.77	-0.600	0.811	-0.738	0.511	-0.466
	20000.	2.77	-0.289	0.930	-0.829	0.570	-0.525
	30000.	2.74	-0.187	1.02	-0.887	0.608	-0.562
	50000.	2.68	-0.127	1.15	-0.967	0.660	-0.612
3P - 4S 5179.6 Å C= 0.18E+15	2500.	0.388E-06	0.316E-06	0.988E-07	0.899E-07	0.658E-07	0.570E-07
	5000.	0.460E-06	0.370E-06	0.110E-06	0.101E-06	0.726E-07	0.639E-07
	10000.	0.532E-06	0.438E-06	0.123E-06	0.113E-06	0.804E-07	0.718E-07
	20000.	0.582E-06	0.490E-06	0.137E-06	0.127E-06	0.892E-07	0.806E-07
	30000.	0.610E-06	0.480E-06	0.146E-06	0.136E-06	0.949E-07	0.862E-07
	50000.	0.649E-06	0.445E-06	0.159E-06	0.148E-06	0.103E-06	0.939E-07

Perturber density = 1 x 10^{11} cm^{-3}

Transition	T(K)	Electrons Width (Å)	Electrons Shift (Å)	Protons Width (Å)	Protons Shift (Å)	Ionized helium Width (Å)	Ionized helium Shift (Å)
3P - 5S 3335.4 Å C= 0.26E+14	2500.	0.809E-06	0.602E-06	0.178E-06	0.168E-06	0.113E-06	0.106E-06
	5000.	0.942E-06	0.714E-06	0.199E-06	0.188E-06	0.127E-06	0.119E-06
	10000.	0.104E-05	0.795E-06	0.224E-06	0.211E-06	0.142E-06	0.134E-06
	20000.	0.111E-05	0.817E-06	0.251E-06	0.237E-06	0.159E-06	0.150E-06
	30000.	0.118E-05	0.773E-06	0.269E-06	0.254E-06	0.170E-06	0.161E-06
	50000.	0.126E-05	0.652E-06	0.292E-06	0.276E-06	0.185E-06	0.175E-06
3P - 6S 2941.1 Å C= 0.97E+13	2500.	0.189E-05	0.138E-05	0.396E-06	0.374E-06	0.251E-06	0.237E-06
	5000.	0.217E-05	0.160E-05	0.445E-06	0.420E-06	0.282E-06	0.266E-06
	10000.	0.237E-05	0.171E-05	0.499E-06	0.472E-06	0.316E-06	0.299E-06
	20000.	0.267E-05	0.162E-05	0.561E-06	0.530E-06	0.355E-06	0.335E-06
	30000.	0.283E-05	0.143E-05	0.600E-06	0.567E-06	0.380E-06	0.359E-06
	50000.	0.318E-05	0.118E-05	0.653E-06	0.617E-06	0.414E-06	0.391E-06
3P - 7S 2780.5 Å C= 0.48E+13	2500.	0.400E-05	0.287E-05	0.812E-06	0.768E-06	0.515E-06	0.486E-06
	5000.	0.456E-05	0.330E-05	0.912E-06	0.862E-06	0.578E-06	0.546E-06
	10000.	0.509E-05	0.324E-05	0.102E-05	0.967E-06	0.648E-06	0.613E-06
	20000.	0.585E-05	0.284E-05	0.115E-05	0.109E-05	0.728E-06	0.688E-06
	30000.	0.649E-05	0.242E-05	0.123E-05	0.116E-05	0.778E-06	0.736E-06
	50000.	0.733E-05	0.198E-05	0.134E-05	0.126E-05	0.848E-06	0.801E-06
3P - 8S 2697.5 Å C= 0.28E+13	2500.	0.771E-05	0.541E-05	0.151E-05	0.143E-05	0.956E-06	0.902E-06
	5000.	0.878E-05	0.590E-05	0.169E-05	0.160E-05	0.107E-05	0.101E-05
	10000.	0.103E-04	0.566E-05	0.190E-05	0.180E-05	0.120E-05	0.114E-05
	20000.	0.120E-04	0.451E-05	0.213E-05	0.202E-05	0.135E-05	0.128E-05
	30000.	0.135E-04	0.377E-05	0.228E-05	0.216E-05	0.145E-05	0.137E-05
	50000.	0.151E-04	0.298E-05	0.249E-05	0.235E-05	0.157E-05	0.149E-05
3P - 9S 2648.4 Å C= 0.17E+13	2500.	0.136E-04	0.933E-05	0.261E-05	0.246E-05	0.165E-05	0.156E-05
	5000.	0.156E-04	0.968E-05	0.293E-05	0.277E-05	0.186E-05	0.175E-05
	10000.	0.187E-04	0.886E-05	0.329E-05	0.311E-05	0.208E-05	0.197E-05
	20000.	0.229E-04	0.671E-05	0.369E-05	0.349E-05	0.234E-05	0.221E-05
	30000.	0.257E-04	0.552E-05	0.395E-05	0.373E-05	0.250E-05	0.236E-05
	50000.	0.284E-04	0.414E-05	0.431E-05	0.406E-05	0.272E-05	0.257E-05
3P -10S 2616.9 Å C= 0.12E+13	2500.	0.224E-04	0.147E-04	0.416E-05	0.392E-05	0.263E-05	0.248E-05
	5000.	0.263E-04	0.146E-04	0.467E-05	0.441E-05	0.296E-05	0.279E-05
	10000.	0.322E-04	0.126E-04	0.524E-05	0.495E-05	0.332E-05	0.314E-05
	20000.	0.405E-04	0.924E-05	0.588E-05	0.556E-05	0.373E-05	0.352E-05
	30000.	0.452E-04	0.749E-05	0.630E-05	0.595E-05	0.399E-05	0.377E-05
	50000.	0.493E-04	0.533E-05	0.686E-05	0.648E-05	0.434E-05	0.410E-05
4P - 5S 24848.7 Å C= 0.67E+14	2500.	0.136E-03	-0.187E-04	0.277E-04	-0.251E-04	0.182E-04	-0.159E-04
	5000.	0.144E-03	0.224E-06	0.312E-04	-0.282E-04	0.201E-04	-0.178E-04
	10000.	0.147E-03	0.187E-04	0.357E-04	-0.316E-04	0.223E-04	-0.200E-04
	20000.	0.146E-03	0.265E-04	0.416E-04	-0.355E-04	0.248E-04	-0.225E-04
	30000.	0.145E-03	0.261E-04	0.462E-04	-0.380E-04	0.264E-04	-0.240E-04
	50000.	0.147E-03	0.247E-04	0.537E-04	-0.416E-04	0.286E-04	-0.262E-04

Perturber density = 1 x 10^{11} cm^{-3}

Transition	T(K)	Electrons Width (Å)	Electrons Shift (Å)	Protons Width (Å)	Protons Shift (Å)	Ionized helium Width (Å)	Ionized helium Shift (Å)
4P - 6S 12431.9 Å C= 0.17E+14	2500.	0.538E-04	0.141E-04	0.254E-05	-0.158E-05	0.212E-05	-0.100E-05
	5000.	0.608E-04	0.197E-04	0.282E-05	-0.178E-05	0.217E-05	-0.112E-05
	10000.	0.642E-04	0.232E-04	0.336E-05	-0.201E-05	0.225E-05	-0.126E-05
	20000.	0.679E-04	0.240E-04	0.434E-05	-0.235E-05	0.235E-05	-0.141E-05
	30000.	0.708E-04	0.213E-04	0.516E-05	-0.264E-05	0.242E-05	-0.151E-05
	50000.	0.763E-04	0.186E-04	0.633E-05	-0.310E-05	0.254E-05	-0.165E-05
4P - 7S 9992.8 Å C= 0.11E+14	2500.	0.642E-04	0.319E-04	0.822E-05	0.766E-05	0.525E-05	0.485E-05
	5000.	0.727E-04	0.382E-04	0.925E-05	0.860E-05	0.587E-05	0.545E-05
	10000.	0.798E-04	0.390E-04	0.105E-04	0.965E-05	0.656E-05	0.611E-05
	20000.	0.889E-04	0.334E-04	0.119E-04	0.108E-04	0.734E-05	0.686E-05
	30000.	0.970E-04	0.287E-04	0.129E-04	0.116E-04	0.785E-05	0.734E-05
	50000.	0.107E-03	0.236E-04	0.143E-04	0.126E-04	0.853E-05	0.799E-05
4P - 8S 8997.3 Å C= 0.88E+13	2500.	0.953E-04	0.566E-04	0.155E-04	0.146E-04	0.984E-05	0.924E-05
	5000.	0.108E-03	0.626E-04	0.175E-04	0.164E-04	0.110E-04	0.104E-04
	10000.	0.123E-03	0.604E-04	0.197E-04	0.184E-04	0.124E-04	0.117E-04
	20000.	0.144E-03	0.469E-04	0.222E-04	0.207E-04	0.139E-04	0.131E-04
	30000.	0.161E-03	0.388E-04	0.240E-04	0.221E-04	0.149E-04	0.140E-04
	50000.	0.178E-03	0.304E-04	0.264E-04	0.241E-04	0.162E-04	0.153E-04
4P - 9S 8473.8 Å C= 0.78E+13	2500.	0.148E-03	0.947E-04	0.259E-04	0.244E-04	0.164E-04	0.154E-04
	5000.	0.169E-03	0.991E-04	0.291E-04	0.274E-04	0.184E-04	0.174E-04
	10000.	0.201E-03	0.896E-04	0.327E-04	0.308E-04	0.207E-04	0.195E-04
	20000.	0.244E-03	0.653E-04	0.369E-04	0.346E-04	0.232E-04	0.219E-04
	30000.	0.272E-03	0.522E-04	0.396E-04	0.370E-04	0.248E-04	0.234E-04
	50000.	0.299E-03	0.393E-04	0.435E-04	0.403E-04	0.270E-04	0.255E-04
4P -10S 8159.6 Å C= 0.73E+13	2500.	0.226E-03	0.142E-03	0.398E-04	0.375E-04	0.252E-04	0.237E-04
	5000.	0.265E-03	0.142E-03	0.448E-04	0.422E-04	0.283E-04	0.267E-04
	10000.	0.322E-03	0.123E-03	0.503E-04	0.474E-04	0.318E-04	0.300E-04
	20000.	0.403E-03	0.878E-04	0.566E-04	0.532E-04	0.357E-04	0.337E-04
	30000.	0.448E-03	0.669E-04	0.607E-04	0.569E-04	0.382E-04	0.361E-04
	50000.	0.487E-03	0.488E-04	0.665E-04	0.620E-04	0.416E-04	0.393E-04
5P - 6S 60955.9 Å C= 0.22E+15	2500.	0.363E-02	0.184E-02	0.835E-03	0.770E-03	0.539E-03	0.487E-03
	5000.	0.368E-02	0.163E-02	0.942E-03	0.865E-03	0.599E-03	0.547E-03
	10000.	0.360E-02	0.131E-02	0.107E-02	0.970E-03	0.668E-03	0.615E-03
	20000.	0.352E-02	0.957E-03	0.123E-02	0.109E-02	0.746E-03	0.690E-03
	30000.	0.352E-02	0.776E-03	0.136E-02	0.117E-02	0.796E-03	0.738E-03
	50000.	0.352E-02	0.569E-03	0.155E-02	0.127E-02	0.865E-03	0.804E-03
5P - 7S 27747.6 Å C= 0.45E+14	2500.	0.991E-03	0.528E-03	0.198E-03	0.184E-03	0.127E-03	0.116E-03
	5000.	0.103E-02	0.515E-03	0.223E-03	0.206E-03	0.142E-03	0.131E-03
	10000.	0.105E-02	0.456E-03	0.254E-03	0.232E-03	0.158E-03	0.147E-03
	20000.	0.108E-02	0.338E-03	0.291E-03	0.260E-03	0.177E-03	0.165E-03
	30000.	0.113E-02	0.281E-03	0.319E-03	0.278E-03	0.189E-03	0.176E-03
	50000.	0.118E-02	0.209E-03	0.362E-03	0.303E-03	0.206E-03	0.192E-03

Perturber density = 1 x 10^{11} cm^{-3}

Transition	T(K)	Electrons Width (Å)	Electrons Shift (Å)	Protons Width (Å)	Protons Shift (Å)	Ionized helium Width (Å)	Ionized helium Shift (Å)
5P - 8S 21226.1 Å C= 0.27E+14	2500.	0.826E-03	0.463E-03	0.149E-03	0.139E-03	0.953E-04	0.881E-04
	5000.	0.881E-03	0.468E-03	0.168E-03	0.156E-03	0.107E-03	0.990E-04
	10000.	0.947E-03	0.424E-03	0.190E-03	0.176E-03	0.119E-03	0.111E-03
	20000.	0.104E-02	0.306E-03	0.218E-03	0.197E-03	0.133E-03	0.125E-03
	30000.	0.112E-02	0.243E-03	0.237E-03	0.211E-03	0.143E-03	0.134E-03
	50000.	0.120E-02	0.183E-03	0.266E-03	0.230E-03	0.155E-03	0.145E-03
5P - 9S 18525.9 Å C= 0.20E+14	2500.	0.936E-03	0.556E-03	0.162E-03	0.152E-03	0.103E-03	0.958E-04
	5000.	0.103E-02	0.549E-03	0.182E-03	0.170E-03	0.115E-03	0.108E-03
	10000.	0.116E-02	0.488E-03	0.206E-03	0.191E-03	0.129E-03	0.121E-03
	20000.	0.135E-02	0.340E-03	0.233E-03	0.215E-03	0.145E-03	0.136E-03
	30000.	0.148E-02	0.261E-03	0.253E-03	0.230E-03	0.155E-03	0.145E-03
	50000.	0.159E-02	0.191E-03	0.281E-03	0.250E-03	0.168E-03	0.158E-03
5P -10S 17087.6 Å C= 0.17E+14	2500.	0.119E-02	0.713E-03	0.201E-03	0.188E-03	0.127E-03	0.119E-03
	5000.	0.135E-02	0.702E-03	0.226E-03	0.212E-03	0.143E-03	0.134E-03
	10000.	0.158E-02	0.587E-03	0.254E-03	0.238E-03	0.160E-03	0.151E-03
	20000.	0.192E-02	0.395E-03	0.288E-03	0.267E-03	0.179E-03	0.169E-03
	30000.	0.211E-02	0.308E-03	0.310E-03	0.286E-03	0.192E-03	0.181E-03
	50000.	0.227E-02	0.204E-03	0.343E-03	0.311E-03	0.209E-03	0.197E-03
6P - 7S 119487.2 Å C= 0.71E+15	2500.	0.328E-01	0.178E-01	0.724E-02	0.664E-02	0.472E-02	0.420E-02
	5000.	0.342E-01	0.152E-01	0.813E-02	0.746E-02	0.524E-02	0.472E-02
	10000.	0.346E-01	0.122E-01	0.919E-02	0.838E-02	0.582E-02	0.531E-02
	20000.	0.349E-01	0.811E-02	0.105E-01	0.941E-02	0.649E-02	0.596E-02
	30000.	0.353E-01	0.613E-02	0.114E-01	0.101E-01	0.692E-02	0.637E-02
	50000.	0.355E-01	0.440E-02	0.129E-01	0.110E-01	0.751E-02	0.694E-02
6P - 8S 51435.3 Å C= 0.13E+15	2500.	0.756E-02	0.417E-02	0.149E-02	0.137E-02	0.963E-03	0.866E-03
	5000.	0.799E-02	0.381E-02	0.167E-02	0.154E-02	0.107E-02	0.974E-03
	10000.	0.837E-02	0.317E-02	0.189E-02	0.173E-02	0.119E-02	0.109E-02
	20000.	0.888E-02	0.212E-02	0.215E-02	0.194E-02	0.133E-02	0.123E-02
	30000.	0.925E-02	0.162E-02	0.234E-02	0.208E-02	0.142E-02	0.131E-02
	50000.	0.955E-02	0.111E-02	0.263E-02	0.226E-02	0.154E-02	0.143E-02
6P - 9S 38010.5 Å C= 0.72E+14	2500.	0.545E-02	0.307E-02	0.973E-03	0.903E-03	0.626E-03	0.570E-03
	5000.	0.589E-02	0.290E-02	0.109E-02	0.101E-02	0.698E-03	0.642E-03
	10000.	0.642E-02	0.240E-02	0.123E-02	0.114E-02	0.779E-03	0.721E-03
	20000.	0.721E-02	0.154E-02	0.140E-02	0.128E-02	0.871E-03	0.810E-03
	30000.	0.768E-02	0.123E-02	0.152E-02	0.137E-02	0.930E-03	0.867E-03
	50000.	0.806E-02	0.746E-03	0.170E-02	0.149E-02	0.101E-02	0.944E-03
6P -10S 32412.8 Å C= 0.53E+14	2500.	0.538E-02	0.299E-02	0.904E-03	0.843E-03	0.578E-03	0.532E-03
	5000.	0.602E-02	0.286E-02	0.102E-02	0.948E-03	0.646E-03	0.599E-03
	10000.	0.684E-02	0.233E-02	0.115E-02	0.106E-02	0.723E-03	0.674E-03
	20000.	0.804E-02	0.145E-02	0.130E-02	0.120E-02	0.809E-03	0.757E-03
	30000.	0.868E-02	0.116E-02	0.140E-02	0.128E-02	0.865E-03	0.810E-03
	50000.	0.918E-02	0.636E-03	0.156E-02	0.139E-02	0.940E-03	0.882E-03

Perturber density = 1 x 10^{11} cm^{-3}

Transition	T(K)	Electrons Width (Å)	Electrons Shift (Å)	Protons Width (Å)	Protons Shift (Å)	Ionized helium Width (Å)	Ionized helium Shift (Å)
7P - 8S 206062.4 Å C= 0.15E+16	2500.	0.212	0.115	0.471E-01	0.431E-01	0.306E-01	0.272E-01
	5000.	0.223	0.944E-01	0.529E-01	0.485E-01	0.340E-01	0.307E-01
	10000.	0.227	0.696E-01	0.597E-01	0.545E-01	0.378E-01	0.345E-01
	20000.	0.233	0.433E-01	0.682E-01	0.612E-01	0.422E-01	0.388E-01
	30000.	0.236	0.289E-01	0.744E-01	0.655E-01	0.450E-01	0.415E-01
	50000.	0.235	0.197E-01	0.840E-01	0.713E-01	0.488E-01	0.452E-01
7P - 9S 85327.9 Å C= 0.25E+15	2500.	0.432E-01	0.236E-01	0.867E-02	0.797E-02	0.562E-02	0.503E-02
	5000.	0.460E-01	0.204E-01	0.973E-02	0.896E-02	0.625E-02	0.566E-02
	10000.	0.484E-01	0.153E-01	0.110E-01	0.101E-01	0.696E-02	0.637E-02
	20000.	0.518E-01	0.945E-02	0.125E-01	0.113E-01	0.776E-02	0.716E-02
	30000.	0.537E-01	0.659E-02	0.137E-01	0.121E-01	0.828E-02	0.766E-02
	50000.	0.547E-01	0.404E-02	0.154E-01	0.132E-01	0.899E-02	0.834E-02
7P -10S 61489.3 Å C= 0.13E+15	2500.	0.276E-01	0.150E-01	0.505E-02	0.466E-02	0.326E-02	0.294E-02
	5000.	0.302E-01	0.136E-01	0.567E-02	0.524E-02	0.363E-02	0.331E-02
	10000.	0.330E-01	0.101E-01	0.641E-02	0.589E-02	0.405E-02	0.373E-02
	20000.	0.370E-01	0.609E-02	0.729E-02	0.662E-02	0.452E-02	0.419E-02
	30000.	0.390E-01	0.448E-02	0.792E-02	0.708E-02	0.483E-02	0.448E-02
	50000.	0.404E-01	0.242E-02	0.888E-02	0.771E-02	0.524E-02	0.488E-02
8P - 9S 326115.3 Å C= 0.25E+16	2500.	1.04	0.551	0.233	0.214	0.151	0.135
	5000.	1.10	0.440	0.262	0.241	0.168	0.152
	10000.	1.13	0.291	0.297	0.270	0.187	0.171
	20000.	1.16	0.167	0.339	0.304	0.209	0.192
	30000.	1.17	0.106	0.370	0.325	0.223	0.206
	50000.	1.16	0.689E-01	0.418	0.354	0.242	0.224
8P -10S 131407.8 Å C= 0.41E+15	2500.	0.193	0.102	0.398E-01	0.365E-01	0.257E-01	0.231E-01
	5000.	0.207	0.853E-01	0.447E-01	0.411E-01	0.286E-01	0.260E-01
	10000.	0.219	0.571E-01	0.505E-01	0.462E-01	0.319E-01	0.292E-01
	20000.	0.235	0.332E-01	0.577E-01	0.519E-01	0.356E-01	0.328E-01
	30000.	0.241	0.206E-01	0.629E-01	0.555E-01	0.380E-01	0.352E-01
	50000.	0.244	0.128E-01	0.710E-01	0.605E-01	0.412E-01	0.383E-01
9P -10S 486286.7 Å C= 0.39E+16	2500.	4.18	2.12	0.950	0.871	0.615	0.548
	5000.	4.42	1.63	1.07	0.980	0.684	0.619
	10000.	4.55	1.01	1.21	1.10	0.762	0.697
	20000.	4.69	0.508	1.39	1.24	0.850	0.784
	30000.	4.71	0.310	1.52	1.33	0.907	0.839
	50000.	4.66	0.214	1.72	1.44	0.985	0.915
3P - 3D 3836.4 Å C= 0.16E+13	2500.	0.192E-05	-0.627E-06	0.518E-06	-0.474E-06	0.332E-06	-0.301E-06
	5000.	0.182E-05	-0.402E-06	0.586E-06	-0.533E-06	0.370E-06	-0.337E-06
	10000.	0.168E-05	-0.172E-06	0.672E-06	-0.598E-06	0.412E-06	-0.379E-06
	20000.	0.151E-05	-0.445E-07	0.789E-06	-0.671E-06	0.460E-06	-0.425E-06
	30000.	0.141E-05	0.406E-07	0.880E-06	-0.719E-06	0.491E-06	-0.455E-06
	50000.	0.129E-05	0.706E-07	0.102E-05	-0.789E-06	0.533E-06	-0.495E-06

Perturber density = 1 x 10^{11} cm^{-3}

Transition	T(K)	Electrons Width (Å)	Electrons Shift (Å)	Protons Width (Å)	Protons Shift (Å)	Ionized helium Width (Å)	Ionized helium Shift (Å)
3P - 4D 3095.9 Å C= 0.57E+12	2500.	0.614E-05	0.340E-05	0.158E-05	0.146E-05	0.101E-05	0.922E-06
	5000.	0.599E-05	0.296E-05	0.179E-05	0.164E-05	0.113E-05	0.104E-05
	10000.	0.569E-05	0.233E-05	0.204E-05	0.184E-05	0.126E-05	0.116E-05
	20000.	0.534E-05	0.167E-05	0.236E-05	0.206E-05	0.141E-05	0.131E-05
	30000.	0.509E-05	0.137E-05	0.261E-05	0.221E-05	0.150E-05	0.140E-05
	50000.	0.473E-05	0.102E-05	0.301E-05	0.241E-05	0.163E-05	0.152E-05
3P - 5D 2850.8 Å C= 0.41E+12	2500.	0.137E-04	0.845E-05	0.327E-05	0.301E-05	0.212E-05	0.190E-05
	5000.	0.137E-04	0.736E-05	0.368E-05	0.338E-05	0.236E-05	0.214E-05
	10000.	0.134E-04	0.567E-05	0.417E-05	0.380E-05	0.263E-05	0.241E-05
	20000.	0.129E-04	0.415E-05	0.478E-05	0.426E-05	0.293E-05	0.270E-05
	30000.	0.125E-04	0.332E-05	0.522E-05	0.456E-05	0.313E-05	0.289E-05
	50000.	0.117E-04	0.228E-05	0.591E-05	0.497E-05	0.339E-05	0.315E-05
3P - 6D 2735.8 Å C= 0.26E+12	2500.	0.292E-04	0.184E-04	0.693E-05	0.638E-05	0.449E-05	0.403E-05
	5000.	0.292E-04	0.157E-04	0.780E-05	0.717E-05	0.499E-05	0.454E-05
	10000.	0.289E-04	0.117E-04	0.882E-05	0.806E-05	0.556E-05	0.510E-05
	20000.	0.280E-04	0.796E-05	0.101E-04	0.904E-05	0.621E-05	0.573E-05
	30000.	0.270E-04	0.639E-05	0.110E-04	0.968E-05	0.662E-05	0.613E-05
	50000.	0.254E-04	0.414E-05	0.124E-04	0.105E-04	0.719E-05	0.668E-05
3P - 7D 2671.8 Å C= 0.17E+12	2500.	0.567E-04	0.347E-04	0.135E-04	0.124E-04	0.873E-05	0.785E-05
	5000.	0.567E-04	0.279E-04	0.152E-04	0.140E-04	0.972E-05	0.884E-05
	10000.	0.562E-04	0.210E-04	0.172E-04	0.157E-04	0.108E-04	0.995E-05
	20000.	0.546E-04	0.138E-04	0.197E-04	0.177E-04	0.121E-04	0.112E-04
	30000.	0.525E-04	0.104E-04	0.215E-04	0.189E-04	0.129E-04	0.120E-04
	50000.	0.491E-04	0.657E-05	0.243E-04	0.206E-04	0.140E-04	0.130E-04
3P - 8D 2632.3 Å C= 0.12E+12	2500.	0.102E-03	0.610E-04	0.246E-04	0.226E-04	0.158E-04	0.142E-04
	5000.	0.102E-03	0.482E-04	0.277E-04	0.254E-04	0.176E-04	0.161E-04
	10000.	0.101E-03	0.328E-04	0.314E-04	0.286E-04	0.197E-04	0.181E-04
	20000.	0.978E-04	0.218E-04	0.359E-04	0.322E-04	0.220E-04	0.203E-04
	30000.	0.936E-04	0.154E-04	0.392E-04	0.344E-04	0.235E-04	0.218E-04
	50000.	0.873E-04	0.928E-05	0.444E-04	0.375E-04	0.255E-04	0.237E-04
3P - 9D 2606.0 Å C= 0.84E+11	2500.	0.170E-03	0.102E-03	0.414E-04	0.380E-04	0.266E-04	0.238E-04
	5000.	0.170E-03	0.794E-04	0.466E-04	0.428E-04	0.296E-04	0.270E-04
	10000.	0.169E-03	0.530E-04	0.528E-04	0.481E-04	0.331E-04	0.304E-04
	20000.	0.163E-03	0.316E-04	0.606E-04	0.541E-04	0.370E-04	0.342E-04
	30000.	0.155E-03	0.224E-04	0.662E-04	0.580E-04	0.395E-04	0.367E-04
	50000.	0.145E-03	0.133E-04	0.749E-04	0.632E-04	0.429E-04	0.400E-04
3P -10D 2587.8 Å C= 0.64E+11	2500.	0.267E-03	0.162E-03	0.656E-04	0.601E-04	0.420E-04	0.376E-04
	5000.	0.267E-03	0.126E-03	0.739E-04	0.678E-04	0.469E-04	0.427E-04
	10000.	0.266E-03	0.818E-04	0.838E-04	0.763E-04	0.524E-04	0.482E-04
	20000.	0.255E-03	0.462E-04	0.963E-04	0.859E-04	0.586E-04	0.543E-04
	30000.	0.243E-03	0.313E-04	0.105E-03	0.919E-04	0.626E-04	0.581E-04
	50000.	0.226E-03	0.190E-04	0.119E-03	0.100E-03	0.680E-04	0.634E-04

Perturber density = 1 x 10^{11} cm^{-3}

Transition	T(K)	Electrons Width (Å)	Electrons Shift (Å)	Protons Width (Å)	Protons Shift (Å)	Ionized helium Width (Å)	Ionized helium Shift (Å)
4P - 4D 15762.2 Å C= 0.15E+14	2500.	0.190E-03	0.714E-04	0.367E-04	0.334E-04	0.238E-04	0.211E-04
	5000.	0.189E-03	0.621E-04	0.415E-04	0.375E-04	0.263E-04	0.237E-04
	10000.	0.182E-03	0.487E-04	0.477E-04	0.421E-04	0.293E-04	0.266E-04
	20000.	0.172E-03	0.344E-04	0.561E-04	0.472E-04	0.326E-04	0.299E-04
	30000.	0.164E-03	0.273E-04	0.627E-04	0.506E-04	0.348E-04	0.320E-04
	50000.	0.153E-03	0.202E-04	0.734E-04	0.554E-04	0.378E-04	0.348E-04
4P - 5D 10964.6 Å C= 0.60E+13	2500.	0.217E-03	0.120E-03	0.472E-04	0.432E-04	0.306E-04	0.273E-04
	5000.	0.219E-03	0.106E-03	0.531E-04	0.486E-04	0.340E-04	0.307E-04
	10000.	0.215E-03	0.829E-04	0.602E-04	0.545E-04	0.379E-04	0.345E-04
	20000.	0.207E-03	0.580E-04	0.693E-04	0.612E-04	0.422E-04	0.388E-04
	30000.	0.200E-03	0.452E-04	0.760E-04	0.655E-04	0.450E-04	0.415E-04
	50000.	0.188E-03	0.309E-04	0.866E-04	0.713E-04	0.488E-04	0.452E-04
4P - 6D 9438.5 Å C= 0.31E+13	2500.	0.359E-03	0.218E-03	0.819E-04	0.753E-04	0.531E-04	0.476E-04
	5000.	0.360E-03	0.189E-03	0.922E-04	0.847E-04	0.590E-04	0.535E-04
	10000.	0.356E-03	0.144E-03	0.104E-03	0.951E-04	0.657E-04	0.602E-04
	20000.	0.346E-03	0.979E-04	0.120E-03	0.107E-03	0.733E-04	0.676E-04
	30000.	0.333E-03	0.735E-04	0.131E-03	0.114E-03	0.782E-04	0.723E-04
	50000.	0.312E-03	0.477E-04	0.148E-03	0.124E-03	0.849E-04	0.788E-04
4P - 7D 8717.8 Å C= 0.18E+13	2500.	0.613E-03	0.377E-03	0.144E-03	0.132E-03	0.928E-04	0.834E-04
	5000.	0.614E-03	0.320E-03	0.162E-03	0.149E-03	0.103E-03	0.939E-04
	10000.	0.609E-03	0.238E-03	0.183E-03	0.167E-03	0.115E-03	0.106E-03
	20000.	0.591E-03	0.157E-03	0.210E-03	0.188E-03	0.128E-03	0.119E-03
	30000.	0.568E-03	0.113E-03	0.229E-03	0.201E-03	0.137E-03	0.127E-03
	50000.	0.531E-03	0.700E-04	0.259E-03	0.219E-03	0.149E-03	0.138E-03
4P - 8D 8310.3 Å C= 0.12E+13	2500.	0.103E-02	0.626E-03	0.245E-03	0.225E-03	0.158E-03	0.142E-03
	5000.	0.102E-02	0.517E-03	0.276E-03	0.253E-03	0.176E-03	0.160E-03
	10000.	0.102E-02	0.370E-03	0.312E-03	0.285E-03	0.196E-03	0.180E-03
	20000.	0.984E-03	0.233E-03	0.358E-03	0.320E-03	0.219E-03	0.203E-03
	30000.	0.941E-03	0.165E-03	0.391E-03	0.343E-03	0.234E-03	0.217E-03
	50000.	0.878E-03	0.960E-04	0.443E-03	0.373E-03	0.254E-03	0.236E-03
4P - 9D 8054.4 Å C= 0.81E+12	2500.	0.163E-02	0.994E-03	0.395E-03	0.363E-03	0.254E-03	0.228E-03
	5000.	0.163E-02	0.802E-03	0.445E-03	0.408E-03	0.283E-03	0.258E-03
	10000.	0.163E-02	0.557E-03	0.504E-03	0.460E-03	0.316E-03	0.290E-03
	20000.	0.156E-02	0.342E-03	0.578E-03	0.517E-03	0.353E-03	0.327E-03
	30000.	0.149E-02	0.236E-03	0.632E-03	0.553E-03	0.377E-03	0.350E-03
	50000.	0.139E-02	0.131E-03	0.716E-03	0.603E-03	0.409E-03	0.382E-03
4P -10D 7882.4 Å C= 0.59E+12	2500.	0.249E-02	0.151E-02	0.609E-03	0.557E-03	0.390E-03	0.349E-03
	5000.	0.248E-02	0.120E-02	0.686E-03	0.629E-03	0.435E-03	0.396E-03
	10000.	0.248E-02	0.816E-03	0.778E-03	0.708E-03	0.486E-03	0.447E-03
	20000.	0.237E-02	0.490E-03	0.893E-03	0.796E-03	0.543E-03	0.503E-03
	30000.	0.226E-02	0.329E-03	0.977E-03	0.853E-03	0.580E-03	0.539E-03
	50000.	0.210E-02	0.179E-03	0.111E-02	0.930E-03	0.631E-03	0.588E-03

Perturber density = 1 x 10^{11} cm^{-3}

Transition	T(K)	Electrons Width (Å)	Electrons Shift (Å)	Protons Width (Å)	Protons Shift (Å)	Ionized helium Width (Å)	Ionized helium Shift (Å)
5P - 5D 36805.3 Å C= 0.68E+14	2500.	0.335E-02	0.179E-02	0.676E-03	0.621E-03	0.437E-03	0.393E-03
	5000.	0.332E-02	0.155E-02	0.762E-03	0.698E-03	0.486E-03	0.442E-03
	10000.	0.319E-02	0.118E-02	0.866E-03	0.784E-03	0.541E-03	0.497E-03
	20000.	0.303E-02	0.790E-03	0.998E-03	0.880E-03	0.604E-03	0.557E-03
	30000.	0.290E-02	0.597E-03	0.110E-02	0.941E-03	0.644E-03	0.596E-03
	50000.	0.271E-02	0.383E-03	0.125E-02	0.103E-02	0.699E-03	0.649E-03
5P - 6D 23857.5 Å C= 0.20E+14	2500.	0.268E-02	0.154E-02	0.565E-03	0.519E-03	0.365E-03	0.328E-03
	5000.	0.267E-02	0.135E-02	0.636E-03	0.584E-03	0.406E-03	0.369E-03
	10000.	0.260E-02	0.102E-02	0.722E-03	0.656E-03	0.453E-03	0.415E-03
	20000.	0.251E-02	0.678E-03	0.828E-03	0.737E-03	0.505E-03	0.467E-03
	30000.	0.240E-02	0.500E-03	0.906E-03	0.788E-03	0.539E-03	0.499E-03
	50000.	0.225E-02	0.311E-03	0.103E-02	0.858E-03	0.585E-03	0.544E-03
5P - 7D 19733.6 Å C= 0.92E+13	2500.	0.341E-02	0.204E-02	0.756E-03	0.695E-03	0.488E-03	0.439E-03
	5000.	0.340E-02	0.177E-02	0.851E-03	0.782E-03	0.543E-03	0.494E-03
	10000.	0.335E-02	0.130E-02	0.965E-03	0.879E-03	0.606E-03	0.556E-03
	20000.	0.324E-02	0.836E-03	0.111E-02	0.988E-03	0.676E-03	0.625E-03
	30000.	0.310E-02	0.608E-03	0.121E-02	0.106E-02	0.722E-03	0.669E-03
	50000.	0.289E-02	0.350E-03	0.137E-02	0.115E-02	0.784E-03	0.729E-03
5P - 8D 17762.3 Å C= 0.53E+13	2500.	0.491E-02	0.296E-02	0.113E-02	0.104E-02	0.728E-03	0.655E-03
	5000.	0.489E-02	0.249E-02	0.127E-02	0.117E-02	0.810E-03	0.738E-03
	10000.	0.484E-02	0.177E-02	0.144E-02	0.132E-02	0.904E-03	0.832E-03
	20000.	0.466E-02	0.110E-02	0.166E-02	0.148E-02	0.101E-02	0.935E-03
	30000.	0.446E-02	0.786E-03	0.181E-02	0.158E-02	0.108E-02	0.100E-02
	50000.	0.415E-02	0.416E-03	0.205E-02	0.172E-02	0.117E-02	0.109E-02
5P - 9D 16632.6 Å C= 0.34E+13	2500.	0.716E-02	0.433E-02	0.169E-02	0.155E-02	0.109E-02	0.976E-03
	5000.	0.714E-02	0.356E-02	0.191E-02	0.175E-02	0.121E-02	0.110E-02
	10000.	0.710E-02	0.248E-02	0.216E-02	0.197E-02	0.135E-02	0.124E-02
	20000.	0.681E-02	0.151E-02	0.248E-02	0.221E-02	0.151E-02	0.140E-02
	30000.	0.650E-02	0.105E-02	0.271E-02	0.237E-02	0.161E-02	0.150E-02
	50000.	0.605E-02	0.530E-03	0.307E-02	0.258E-02	0.175E-02	0.164E-02
5P -10D 15915.5 Å C= 0.24E+13	2500.	0.103E-01	0.624E-02	0.249E-02	0.228E-02	0.159E-02	0.143E-02
	5000.	0.103E-01	0.503E-02	0.280E-02	0.257E-02	0.178E-02	0.162E-02
	10000.	0.103E-01	0.345E-02	0.318E-02	0.289E-02	0.199E-02	0.183E-02
	20000.	0.981E-02	0.206E-02	0.365E-02	0.325E-02	0.222E-02	0.206E-02
	30000.	0.934E-02	0.140E-02	0.400E-02	0.348E-02	0.237E-02	0.220E-02
	50000.	0.868E-02	0.695E-03	0.453E-02	0.380E-02	0.258E-02	0.240E-02
6P - 6D 70197.1 Å C= 0.17E+15	2500.	0.285E-01	0.157E-01	0.562E-02	0.516E-02	0.364E-02	0.326E-02
	5000.	0.285E-01	0.135E-01	0.633E-02	0.580E-02	0.404E-02	0.367E-02
	10000.	0.278E-01	0.100E-01	0.717E-02	0.652E-02	0.451E-02	0.413E-02
	20000.	0.268E-01	0.635E-02	0.823E-02	0.732E-02	0.503E-02	0.464E-02
	30000.	0.257E-01	0.474E-02	0.900E-02	0.783E-02	0.536E-02	0.496E-02
	50000.	0.240E-01	0.259E-02	0.102E-01	0.853E-02	0.582E-02	0.540E-02

Perturber density = 1 x 10^{11} cm^{-3}

Transition	T(K)	Electrons Width (Å)	Electrons Shift (Å)	Protons Width (Å)	Protons Shift (Å)	Ionized helium Width (Å)	Ionized helium Shift (Å)
6P - 7D 43468.8 Å C= 0.45E+14	2500.	0.186E-01	0.107E-01	0.387E-02	0.356E-02	0.250E-02	0.225E-02
	5000.	0.186E-01	0.929E-02	0.436E-02	0.400E-02	0.278E-02	0.253E-02
	10000.	0.183E-01	0.672E-02	0.494E-02	0.450E-02	0.310E-02	0.285E-02
	20000.	0.177E-01	0.415E-02	0.567E-02	0.506E-02	0.346E-02	0.320E-02
	30000.	0.169E-01	0.309E-02	0.620E-02	0.541E-02	0.370E-02	0.343E-02
	50000.	0.158E-01	0.155E-02	0.702E-02	0.589E-02	0.401E-02	0.373E-02
6P - 8D 34929.6 Å C= 0.20E+14	2500.	0.203E-01	0.119E-01	0.447E-02	0.410E-02	0.288E-02	0.259E-02
	5000.	0.203E-01	0.101E-01	0.503E-02	0.462E-02	0.320E-02	0.292E-02
	10000.	0.200E-01	0.713E-02	0.571E-02	0.520E-02	0.358E-02	0.329E-02
	20000.	0.193E-01	0.430E-02	0.655E-02	0.584E-02	0.399E-02	0.370E-02
	30000.	0.184E-01	0.311E-02	0.716E-02	0.625E-02	0.426E-02	0.396E-02
	50000.	0.172E-01	0.146E-02	0.812E-02	0.681E-02	0.463E-02	0.431E-02
6P - 9D 30814.0 Å C= 0.12E+14	2500.	0.256E-01	0.152E-01	0.587E-02	0.539E-02	0.377E-02	0.338E-02
	5000.	0.256E-01	0.127E-01	0.661E-02	0.607E-02	0.420E-02	0.383E-02
	10000.	0.254E-01	0.875E-02	0.750E-02	0.683E-02	0.469E-02	0.431E-02
	20000.	0.244E-01	0.520E-02	0.861E-02	0.768E-02	0.524E-02	0.485E-02
	30000.	0.232E-01	0.365E-02	0.941E-02	0.822E-02	0.560E-02	0.520E-02
	50000.	0.216E-01	0.167E-02	0.107E-01	0.896E-02	0.608E-02	0.567E-02
6P -10D 28439.8 Å C= 0.77E+13	2500.	0.338E-01	0.202E-01	0.798E-02	0.730E-02	0.512E-02	0.458E-02
	5000.	0.338E-01	0.165E-01	0.899E-02	0.825E-02	0.571E-02	0.519E-02
	10000.	0.336E-01	0.113E-01	0.102E-01	0.928E-02	0.637E-02	0.587E-02
	20000.	0.322E-01	0.665E-02	0.117E-01	0.104E-01	0.713E-02	0.660E-02
	30000.	0.306E-01	0.455E-02	0.128E-01	0.112E-01	0.761E-02	0.707E-02
	50000.	0.285E-01	0.206E-02	0.146E-01	0.122E-01	0.827E-02	0.771E-02
7P - 7D 118821.3 Å C= 0.33E+15	2500.	0.171	0.933E-01	0.336E-01	0.309E-01	0.217E-01	0.195E-01
	5000.	0.171	0.802E-01	0.379E-01	0.347E-01	0.242E-01	0.219E-01
	10000.	0.168	0.566E-01	0.429E-01	0.391E-01	0.269E-01	0.247E-01
	20000.	0.162	0.344E-01	0.493E-01	0.439E-01	0.301E-01	0.278E-01
	30000.	0.155	0.247E-01	0.539E-01	0.469E-01	0.321E-01	0.297E-01
	50000.	0.145	0.114E-01	0.612E-01	0.511E-01	0.348E-01	0.324E-01
7P - 8D 71225.1 Å C= 0.85E+14	2500.	0.960E-01	0.542E-01	0.199E-01	0.183E-01	0.128E-01	0.115E-01
	5000.	0.959E-01	0.459E-01	0.224E-01	0.205E-01	0.143E-01	0.130E-01
	10000.	0.946E-01	0.317E-01	0.254E-01	0.231E-01	0.159E-01	0.146E-01
	20000.	0.910E-01	0.188E-01	0.292E-01	0.260E-01	0.178E-01	0.164E-01
	30000.	0.869E-01	0.131E-01	0.319E-01	0.278E-01	0.190E-01	0.176E-01
	50000.	0.809E-01	0.598E-02	0.362E-01	0.303E-01	0.206E-01	0.192E-01
7P - 9D 55979.1 Å C= 0.39E+14	2500.	0.918E-01	0.529E-01	0.200E-01	0.183E-01	0.128E-01	0.115E-01
	5000.	0.916E-01	0.441E-01	0.225E-01	0.207E-01	0.143E-01	0.130E-01
	10000.	0.908E-01	0.301E-01	0.255E-01	0.232E-01	0.160E-01	0.147E-01
	20000.	0.871E-01	0.179E-01	0.293E-01	0.261E-01	0.178E-01	0.165E-01
	30000.	0.830E-01	0.120E-01	0.321E-01	0.280E-01	0.191E-01	0.177E-01
	50000.	0.772E-01	0.544E-02	0.364E-01	0.305E-01	0.207E-01	0.193E-01

Perturber density = 1 x 10^{11} cm^{-3}

Transition	T(K)	Electrons Width (Å)	Electrons Shift (Å)	Protons Width (Å)	Protons Shift (Å)	Ionized helium Width (Å)	Ionized helium Shift (Å)
7P -10D 48607.4 Å C= 0.22E+14	2500.	0.104	0.613E-01	0.237E-01	0.217E-01	0.152E-01	0.136E-01
	5000.	0.104	0.500E-01	0.267E-01	0.245E-01	0.169E-01	0.154E-01
	10000.	0.104	0.339E-01	0.303E-01	0.275E-01	0.189E-01	0.174E-01
	20000.	0.990E-01	0.200E-01	0.348E-01	0.310E-01	0.211E-01	0.196E-01
	30000.	0.942E-01	0.133E-01	0.381E-01	0.332E-01	0.226E-01	0.210E-01
	50000.	0.875E-01	0.593E-02	0.433E-01	0.362E-01	0.245E-01	0.229E-01
8P - 8D 185635.5 Å C= 0.57E+15	2500.	0.791	0.426	0.157	0.144	0.101	0.904E-01
	5000.	0.791	0.355	0.177	0.162	0.112	0.102
	10000.	0.780	0.239	0.200	0.182	0.125	0.115
	20000.	0.747	0.143	0.230	0.205	0.140	0.129
	30000.	0.713	0.875E-01	0.252	0.219	0.149	0.139
	50000.	0.665	0.440E-01	0.287	0.239	0.162	0.151
8P - 9D 108569.4 Å C= 0.15E+15	2500.	0.394	0.218	0.811E-01	0.744E-01	0.521E-01	0.466E-01
	5000.	0.393	0.181	0.914E-01	0.837E-01	0.581E-01	0.529E-01
	10000.	0.389	0.121	0.104	0.943E-01	0.648E-01	0.595E-01
	20000.	0.372	0.724E-01	0.119	0.106	0.724E-01	0.670E-01
	30000.	0.354	0.435E-01	0.131	0.113	0.773E-01	0.718E-01
	50000.	0.330	0.217E-01	0.148	0.124	0.840E-01	0.783E-01
8P -10D 83893.3 Å C= 0.67E+14	2500.	0.340	0.194	0.734E-01	0.671E-01	0.471E-01	0.421E-01
	5000.	0.339	0.158	0.828E-01	0.758E-01	0.525E-01	0.477E-01
	10000.	0.337	0.106	0.940E-01	0.853E-01	0.586E-01	0.539E-01
	20000.	0.321	0.627E-01	0.108	0.960E-01	0.655E-01	0.607E-01
	30000.	0.306	0.387E-01	0.118	0.103	0.700E-01	0.650E-01
	50000.	0.284	0.183E-01	0.135	0.112	0.761E-01	0.709E-01
9P - 9D 273433.2 Å C= 0.93E+15	2500.	3.00	1.61	0.598	0.547	0.384	0.343
	5000.	2.99	1.29	0.674	0.616	0.428	0.389
	10000.	2.96	0.842	0.766	0.694	0.478	0.438
	20000.	2.82	0.503	0.881	0.781	0.534	0.493
	30000.	2.69	0.267	0.965	0.836	0.570	0.529
	50000.	2.50	0.153	1.10	0.911	0.619	0.576
9P -10D 157074.6 Å C= 0.23E+15	2500.	1.36	0.739	0.280	0.256	0.179	0.160
	5000.	1.36	0.601	0.316	0.289	0.200	0.182
	10000.	1.34	0.397	0.359	0.325	0.224	0.205
	20000.	1.28	0.237	0.413	0.366	0.250	0.231
	30000.	1.22	0.132	0.453	0.392	0.267	0.248
	50000.	1.13	0.694E-01	0.516	0.427	0.290	0.270
4P - 3D 917094.6 Å C= 0.92E+17	2500.	0.255	-0.105	0.580E-01	-0.530E-01	0.373E-01	-0.336E-01
	5000.	0.248	-0.791E-01	0.656E-01	-0.595E-01	0.415E-01	-0.377E-01
	10000.	0.228	-0.515E-01	0.752E-01	-0.668E-01	0.462E-01	-0.423E-01
	20000.	0.206	-0.325E-01	0.880E-01	-0.750E-01	0.516E-01	-0.475E-01
	30000.	0.193	-0.187E-01	0.978E-01	-0.802E-01	0.550E-01	-0.508E-01
	50000.	0.179	-0.117E-01	0.114	-0.875E-01	0.597E-01	-0.553E-01

Perturber density = 1 x 10^{11} cm^{-3}

Transition	T(K)	Electrons Width (Å)	Electrons Shift (Å)	Protons Width (Å)	Protons Shift (Å)	Ionized helium Width (Å)	Ionized helium Shift (Å)
3D - 5P 15887.5 Å C= 0.15E+14	2500.	0.227E-03	-0.744E-04	0.511E-04	-0.467E-04	0.331E-04	-0.295E-04
	5000.	0.225E-03	-0.539E-04	0.577E-04	-0.524E-04	0.368E-04	-0.332E-04
	10000.	0.211E-03	-0.308E-04	0.659E-04	-0.588E-04	0.409E-04	-0.373E-04
	20000.	0.194E-03	-0.141E-04	0.767E-04	-0.660E-04	0.456E-04	-0.418E-04
	30000.	0.183E-03	-0.103E-04	0.850E-04	-0.707E-04	0.486E-04	-0.448E-04
	50000.	0.170E-03	-0.141E-05	0.985E-04	-0.773E-04	0.527E-04	-0.487E-04
3D - 6P 11036.0 Å C= 0.61E+13	2500.	0.237E-03	-0.105E-03	0.572E-04	-0.522E-04	0.375E-04	-0.330E-04
	5000.	0.246E-03	-0.758E-04	0.643E-04	-0.586E-04	0.415E-04	-0.371E-04
	10000.	0.236E-03	-0.482E-04	0.728E-04	-0.658E-04	0.461E-04	-0.417E-04
	20000.	0.222E-03	-0.231E-04	0.835E-04	-0.739E-04	0.513E-04	-0.468E-04
	30000.	0.213E-03	-0.165E-04	0.914E-04	-0.790E-04	0.546E-04	-0.501E-04
	50000.	0.200E-03	-0.381E-05	0.104E-03	-0.861E-04	0.592E-04	-0.545E-04
3D - 7P 9505.6 Å C= 0.31E+13	2500.	0.376E-03	-0.179E-03	0.944E-04	-0.862E-04	0.617E-04	-0.545E-04
	5000.	0.392E-03	-0.130E-03	0.106E-03	-0.970E-04	0.684E-04	-0.613E-04
	10000.	0.379E-03	-0.800E-04	0.120E-03	-0.109E-03	0.760E-04	-0.689E-04
	20000.	0.359E-03	-0.422E-04	0.137E-03	-0.122E-03	0.846E-04	-0.775E-04
	30000.	0.345E-03	-0.273E-04	0.150E-03	-0.131E-03	0.902E-04	-0.829E-04
	50000.	0.325E-03	-0.862E-05	0.170E-03	-0.142E-03	0.978E-04	-0.902E-04
3D - 8P 8783.1 Å C= 0.18E+13	2500.	0.630E-03	-0.267E-03	0.161E-03	-0.147E-03	0.105E-03	-0.931E-04
	5000.	0.654E-03	-0.210E-03	0.181E-03	-0.166E-03	0.116E-03	-0.105E-03
	10000.	0.633E-03	-0.126E-03	0.205E-03	-0.186E-03	0.130E-03	-0.118E-03
	20000.	0.601E-03	-0.668E-04	0.235E-03	-0.209E-03	0.144E-03	-0.132E-03
	30000.	0.578E-03	-0.433E-04	0.257E-03	-0.224E-03	0.154E-03	-0.142E-03
	50000.	0.543E-03	-0.137E-04	0.291E-03	-0.244E-03	0.167E-03	-0.154E-03
3D - 9P 8374.6 Å C= 0.12E+13	2500.	0.104E-02	-0.486E-03	0.271E-03	-0.248E-03	0.175E-03	-0.156E-03
	5000.	0.108E-02	-0.332E-03	0.304E-03	-0.279E-03	0.195E-03	-0.176E-03
	10000.	0.104E-02	-0.184E-03	0.345E-03	-0.313E-03	0.217E-03	-0.198E-03
	20000.	0.987E-03	-0.983E-04	0.396E-03	-0.352E-03	0.242E-03	-0.223E-03
	30000.	0.948E-03	-0.647E-04	0.433E-03	-0.377E-03	0.258E-03	-0.239E-03
	50000.	0.889E-03	-0.184E-04	0.492E-03	-0.411E-03	0.281E-03	-0.260E-03
4D - 5P C= 0.17E+18	2500.	4.05	-1.87	0.860	-0.791	0.552	-0.500
	5000.	3.97	-1.49	0.973	-0.889	0.615	-0.563
	10000.	3.74	-1.06	1.11	-0.998	0.686	-0.632
	20000.	3.47	-0.674	1.29	-1.12	0.766	-0.709
	30000.	3.29	-0.487	1.43	-1.20	0.818	-0.759
	50000.	3.05	-0.301	1.65	-1.30	0.888	-0.826
4D - 6P 35385.7 Å C= 0.63E+14	2500.	0.306E-02	-0.146E-02	0.674E-03	-0.616E-03	0.438E-03	-0.389E-03
	5000.	0.310E-02	-0.107E-02	0.758E-03	-0.693E-03	0.486E-03	-0.438E-03
	10000.	0.300E-02	-0.692E-03	0.861E-03	-0.778E-03	0.541E-03	-0.492E-03
	20000.	0.282E-02	-0.391E-03	0.991E-03	-0.873E-03	0.603E-03	-0.553E-03
	30000.	0.270E-02	-0.259E-03	0.109E-02	-0.934E-03	0.643E-03	-0.592E-03
	50000.	0.253E-02	-0.138E-03	0.124E-02	-0.102E-02	0.697E-03	-0.644E-03

Perturber density = 1 x 10^{11} cm^{-3}

Transition	T(K)	Electrons Width (Å)	Electrons Shift (Å)	Protons Width (Å)	Protons Shift (Å)	Ionized helium Width (Å)	Ionized helium Shift (Å)
4D - 7P 23337.8 Å C= 0.19E+14	2500.	0.252E-02	-0.960E-03	0.595E-03	-0.543E-03	0.388E-03	-0.343E-03
	5000.	0.260E-02	-0.597E-03	0.669E-03	-0.611E-03	0.430E-03	-0.386E-03
	10000.	0.253E-02	-0.327E-03	0.758E-03	-0.687E-03	0.478E-03	-0.435E-03
	20000.	0.239E-02	-0.214E-03	0.869E-03	-0.771E-03	0.533E-03	-0.488E-03
	30000.	0.230E-02	-0.868E-04	0.951E-03	-0.825E-03	0.568E-03	-0.522E-03
	50000.	0.216E-02	-0.383E-04	0.108E-02	-0.897E-03	0.616E-03	-0.569E-03
4D - 8P 19416.7 Å C= 0.89E+13	2500.	0.324E-02	-0.140E-02	0.801E-03	-0.731E-03	0.521E-03	-0.462E-03
	5000.	0.336E-02	-0.802E-03	0.900E-03	-0.823E-03	0.578E-03	-0.520E-03
	10000.	0.326E-02	-0.343E-03	0.102E-02	-0.925E-03	0.643E-03	-0.585E-03
	20000.	0.309E-02	-0.204E-03	0.117E-02	-0.104E-02	0.717E-03	-0.658E-03
	30000.	0.297E-02	-0.117E-03	0.128E-02	-0.111E-02	0.764E-03	-0.704E-03
	50000.	0.280E-02	0.405E-05	0.145E-02	-0.121E-02	0.829E-03	-0.767E-03
4D - 9P 17526.8 Å C= 0.51E+13	2500.	0.470E-02	-0.220E-02	0.119E-02	-0.109E-02	0.773E-03	-0.687E-03
	5000.	0.485E-02	-0.145E-02	0.134E-02	-0.123E-02	0.860E-03	-0.776E-03
	10000.	0.469E-02	-0.748E-03	0.152E-02	-0.138E-02	0.957E-03	-0.873E-03
	20000.	0.445E-02	-0.191E-03	0.175E-02	-0.155E-02	0.107E-02	-0.982E-03
	30000.	0.427E-02	-0.198E-03	0.191E-02	-0.166E-02	0.114E-02	-0.105E-02
	50000.	0.401E-02	-0.930E-04	0.218E-02	-0.181E-02	0.124E-02	-0.115E-02
5D - 6P C= 0.20E+18	2500.	14.1	-7.31	2.79	-2.56	1.81	-1.62
	5000.	14.1	-6.15	3.14	-2.87	2.01	-1.82
	10000.	13.7	-4.46	3.56	-3.23	2.24	-2.04
	20000.	13.1	-2.84	4.09	-3.62	2.50	-2.30
	30000.	12.6	-2.05	4.48	-3.88	2.66	-2.46
	50000.	11.8	-1.17	5.09	-4.22	2.89	-2.67
5D - 7P 66273.4 Å C= 0.15E+15	2500.	0.250E-01	-0.128E-01	0.531E-02	-0.485E-02	0.345E-02	-0.307E-02
	5000.	0.254E-01	-0.100E-01	0.597E-02	-0.546E-02	0.383E-02	-0.345E-02
	10000.	0.249E-01	-0.683E-02	0.676E-02	-0.614E-02	0.427E-02	-0.388E-02
	20000.	0.237E-01	-0.403E-02	0.776E-02	-0.689E-02	0.475E-02	-0.436E-02
	30000.	0.228E-01	-0.260E-02	0.849E-02	-0.737E-02	0.507E-02	-0.467E-02
	50000.	0.214E-01	-0.142E-02	0.964E-02	-0.802E-02	0.550E-02	-0.508E-02
5D - 8P 42119.3 Å C= 0.42E+14	2500.	0.171E-01	-0.853E-02	0.392E-02	-0.358E-02	0.255E-02	-0.226E-02
	5000.	0.175E-01	-0.614E-02	0.441E-02	-0.403E-02	0.283E-02	-0.255E-02
	10000.	0.172E-01	-0.390E-02	0.499E-02	-0.453E-02	0.315E-02	-0.286E-02
	20000.	0.163E-01	-0.200E-02	0.573E-02	-0.509E-02	0.351E-02	-0.322E-02
	30000.	0.157E-01	-0.123E-02	0.627E-02	-0.544E-02	0.374E-02	-0.345E-02
	50000.	0.148E-01	-0.690E-03	0.712E-02	-0.593E-02	0.406E-02	-0.376E-02
5D - 9P 34134.8 Å C= 0.19E+14	2500.	0.189E-01	-0.894E-02	0.460E-02	-0.421E-02	0.298E-02	-0.265E-02
	5000.	0.194E-01	-0.594E-02	0.518E-02	-0.473E-02	0.331E-02	-0.299E-02
	10000.	0.190E-01	-0.335E-02	0.587E-02	-0.533E-02	0.369E-02	-0.337E-02
	20000.	0.180E-01	-0.160E-02	0.674E-02	-0.599E-02	0.412E-02	-0.379E-02
	30000.	0.173E-01	-0.105E-02	0.738E-02	-0.641E-02	0.439E-02	-0.406E-02
	50000.	0.162E-01	-0.481E-03	0.840E-02	-0.698E-02	0.477E-02	-0.442E-02

Perturber density = 1 x 10^{11} cm^{-3}

Transition	T(K)	Electrons Width (Å)	Electrons Shift (Å)	Protons Width (Å)	Protons Shift (Å)	Ionized helium Width (Å)	Ionized helium Shift (Å)
6D - 8P 111154.3 Å C= 0.29E+15	2500.	0.147	-0.754E-01	0.307E-01	-0.281E-01	0.199E-01	-0.177E-01
	5000.	0.149	-0.598E-01	0.345E-01	-0.316E-01	0.221E-01	-0.200E-01
	10000.	0.147	-0.401E-01	0.392E-01	-0.355E-01	0.246E-01	-0.225E-01
	20000.	0.140	-0.233E-01	0.449E-01	-0.399E-01	0.275E-01	-0.253E-01
	30000.	0.134	-0.146E-01	0.492E-01	-0.427E-01	0.293E-01	-0.270E-01
	50000.	0.126	-0.754E-02	0.559E-01	-0.465E-01	0.318E-01	-0.295E-01
6D - 9P 68728.5 Å C= 0.79E+14	2500.	0.873E-01	-0.434E-01	0.196E-01	-0.180E-01	0.127E-01	-0.113E-01
	5000.	0.888E-01	-0.321E-01	0.221E-01	-0.202E-01	0.141E-01	-0.128E-01
	10000.	0.872E-01	-0.204E-01	0.251E-01	-0.227E-01	0.157E-01	-0.144E-01
	20000.	0.829E-01	-0.107E-01	0.288E-01	-0.256E-01	0.176E-01	-0.162E-01
	30000.	0.796E-01	-0.638E-02	0.316E-01	-0.274E-01	0.187E-01	-0.173E-01
	50000.	0.747E-01	-0.362E-02	0.360E-01	-0.298E-01	0.203E-01	-0.189E-01
7D - 9P 172693.7 Å C= 0.50E+15	2500.	0.676	-0.342	0.140	-0.128	0.906E-01	-0.807E-01
	5000.	0.682	-0.270	0.158	-0.144	0.101	-0.912E-01
	10000.	0.671	-0.176	0.179	-0.162	0.112	-0.103
	20000.	0.639	-0.101	0.206	-0.183	0.125	-0.116
	30000.	0.612	-0.585E-01	0.226	-0.195	0.134	-0.124
	50000.	0.573	-0.317E-01	0.257	-0.213	0.145	-0.135
3D - 4F 14881.7 Å C= 0.24E+14	2500.	0.549E-04	-0.523E-05	0.699E-05	0.375E-05	0.632E-05	0.237E-05
	5000.	0.588E-04	-0.232E-05	0.739E-05	0.420E-05	0.641E-05	0.266E-05
	10000.	0.621E-04	-0.137E-06	0.805E-05	0.472E-05	0.654E-05	0.299E-05
	20000.	0.624E-04	0.104E-05	0.919E-05	0.533E-05	0.670E-05	0.336E-05
	30000.	0.622E-04	0.145E-05	0.102E-04	0.579E-05	0.682E-05	0.359E-05
	50000.	0.621E-04	0.921E-06	0.118E-04	0.663E-05	0.700E-05	0.391E-05
3D - 5F 10814.0 Å C= 0.10E+14	2500.	0.110E-03	0.165E-04	0.188E-04	0.157E-04	0.136E-04	0.991E-05
	5000.	0.124E-03	0.144E-04	0.208E-04	0.176E-04	0.146E-04	0.111E-04
	10000.	0.136E-03	0.101E-04	0.233E-04	0.197E-04	0.158E-04	0.125E-04
	20000.	0.139E-03	0.706E-05	0.267E-04	0.221E-04	0.171E-04	0.140E-04
	30000.	0.138E-03	0.537E-05	0.292E-04	0.237E-04	0.180E-04	0.150E-04
	50000.	0.134E-03	0.405E-05	0.335E-04	0.258E-04	0.193E-04	0.163E-04
3D - 6F 9417.7 Å C= 0.58E+13	2500.	0.195E-03	0.418E-04	0.347E-04	0.293E-04	0.248E-04	0.185E-04
	5000.	0.230E-03	0.349E-04	0.384E-04	0.330E-04	0.268E-04	0.209E-04
	10000.	0.258E-03	0.235E-04	0.429E-04	0.370E-04	0.290E-04	0.234E-04
	20000.	0.268E-03	0.150E-04	0.487E-04	0.415E-04	0.316E-04	0.263E-04
	30000.	0.267E-03	0.121E-04	0.530E-04	0.444E-04	0.333E-04	0.281E-04
	50000.	0.258E-03	0.755E-05	0.600E-04	0.484E-04	0.357E-04	0.306E-04
3D - 7F 8738.4 Å C= 0.40E+13	2500.	0.323E-03	0.772E-04	0.544E-04	0.452E-04	0.399E-04	0.286E-04
	5000.	0.396E-03	0.617E-04	0.597E-04	0.509E-04	0.427E-04	0.322E-04
	10000.	0.450E-03	0.459E-04	0.659E-04	0.571E-04	0.461E-04	0.362E-04
	20000.	0.474E-03	0.274E-04	0.732E-04	0.641E-04	0.500E-04	0.406E-04
	30000.	0.473E-03	0.206E-04	0.782E-04	0.685E-04	0.526E-04	0.434E-04
	50000.	0.459E-03	0.132E-04	0.857E-04	0.748E-04	0.562E-04	0.473E-04

Perturber density = 1×10^{11} cm^{-3}

Transition	T(K)	Electrons Width (Å)	Electrons Shift (Å)	Protons Width (Å)	Protons Shift (Å)	Ionized helium Width (Å)	Ionized helium Shift (Å)
3D - 8F 8348.4 Å C= 0.31E+13	2500.	0.511E-03	0.128E-03	0.746E-04	0.584E-04	0.578E-04	0.369E-04
	5000.	0.640E-03	0.105E-03	0.810E-04	0.656E-04	0.610E-04	0.415E-04
	10000.	0.735E-03	0.747E-04	0.886E-04	0.737E-04	0.648E-04	0.466E-04
	20000.	0.780E-03	0.471E-04	0.976E-04	0.827E-04	0.694E-04	0.524E-04
	30000.	0.781E-03	0.345E-04	0.104E-03	0.885E-04	0.725E-04	0.561E-04
	50000.	0.757E-03	0.213E-04	0.113E-03	0.964E-04	0.769E-04	0.611E-04
4D - 4F 206436.7 Å C= 0.25E+16	2500.	0.324E-01	-0.168E-01	0.738E-02	-0.674E-02	0.481E-02	-0.426E-02
	5000.	0.323E-01	-0.147E-01	0.832E-02	-0.757E-02	0.533E-02	-0.479E-02
	10000.	0.313E-01	-0.107E-01	0.947E-02	-0.849E-02	0.592E-02	-0.538E-02
	20000.	0.308E-01	-0.729E-02	0.110E-01	-0.953E-02	0.660E-02	-0.604E-02
	30000.	0.301E-01	-0.560E-02	0.121E-01	-0.102E-01	0.703E-02	-0.646E-02
	50000.	0.287E-01	-0.380E-02	0.139E-01	-0.111E-01	0.763E-02	-0.703E-02
4D - 5F 33200.8 Å C= 0.65E+14	2500.	0.149E-02	-0.230E-03	0.121E-03	-0.702E-04	0.106E-03	-0.444E-04
	5000.	0.166E-02	-0.231E-03	0.130E-03	-0.788E-04	0.108E-03	-0.499E-04
	10000.	0.176E-02	-0.180E-03	0.144E-03	-0.884E-04	0.111E-03	-0.560E-04
	20000.	0.179E-02	-0.161E-03	0.168E-03	-0.100E-03	0.114E-03	-0.629E-04
	30000.	0.175E-02	-0.120E-03	0.187E-03	-0.112E-03	0.117E-03	-0.673E-04
	50000.	0.168E-02	-0.735E-04	0.217E-03	-0.119E-03	0.121E-03	-0.732E-04
4D - 6F 22815.3 Å C= 0.31E+14	2500.	0.134E-02	0.826E-04	0.167E-03	0.130E-03	0.128E-03	0.824E-04
	5000.	0.156E-02	0.262E-04	0.183E-03	0.146E-03	0.135E-03	0.927E-04
	10000.	0.173E-02	-0.858E-05	0.205E-03	0.164E-03	0.144E-03	0.104E-03
	20000.	0.179E-02	-0.389E-04	0.234E-03	0.184E-03	0.154E-03	0.117E-03
	30000.	0.178E-02	-0.192E-04	0.258E-03	0.197E-03	0.161E-03	0.125E-03
	50000.	0.171E-02	-0.448E-05	0.299E-03	0.215E-03	0.171E-03	0.136E-03
4D - 7F 19199.5 Å C= 0.19E+14	2500.	0.169E-02	0.274E-03	0.244E-03	0.197E-03	0.184E-03	0.125E-03
	5000.	0.204E-02	0.188E-03	0.267E-03	0.222E-03	0.195E-03	0.140E-03
	10000.	0.232E-02	0.984E-04	0.295E-03	0.249E-03	0.209E-03	0.158E-03
	20000.	0.244E-02	0.637E-04	0.328E-03	0.279E-03	0.225E-03	0.177E-03
	30000.	0.243E-02	0.324E-04	0.352E-03	0.299E-03	0.236E-03	0.189E-03
	50000.	0.235E-02	0.281E-04	0.390E-03	0.325E-03	0.252E-03	0.206E-03
4D - 8F 17412.3 Å C= 0.13E+14	2500.	0.231E-02	0.461E-03	0.313E-03	0.239E-03	0.246E-03	0.151E-03
	5000.	0.288E-02	0.374E-03	0.339E-03	0.269E-03	0.259E-03	0.170E-03
	10000.	0.332E-02	0.243E-03	0.371E-03	0.302E-03	0.274E-03	0.191E-03
	20000.	0.352E-02	0.142E-03	0.409E-03	0.339E-03	0.292E-03	0.215E-03
	30000.	0.351E-02	0.720E-04	0.436E-03	0.363E-03	0.304E-03	0.230E-03
	50000.	0.341E-02	0.513E-04	0.477E-03	0.395E-03	0.322E-03	0.250E-03
5D - 5F 423764.7 Å C= 0.90E+16	2500.	0.426	-0.169	0.651E-01	-0.578E-01	0.439E-01	-0.365E-01
	5000.	0.458	-0.147	0.730E-01	-0.649E-01	0.481E-01	-0.411E-01
	10000.	0.470	-0.112	0.827E-01	-0.729E-01	0.530E-01	-0.462E-01
	20000.	0.473	-0.753E-01	0.954E-01	-0.818E-01	0.585E-01	-0.518E-01
	30000.	0.464	-0.571E-01	0.105	-0.875E-01	0.622E-01	-0.554E-01
	50000.	0.441	-0.381E-01	0.121	-0.954E-01	0.671E-01	-0.604E-01

Perturber density = 1 x 10^{11} cm^{-3}

Transition	T(K)	Electrons Width (Å)	Electrons Shift (Å)	Protons Width (Å)	Protons Shift (Å)	Ionized helium Width (Å)	Ionized helium Shift (Å)
5D - 6F 62227.0 Å C= 0.19E+15	2500.	0.133E-01	-0.220E-02	0.950E-03	-0.463E-03	0.876E-03	-0.293E-03
	5000.	0.154E-01	-0.229E-02	0.997E-03	-0.519E-03	0.886E-03	-0.329E-03
	10000.	0.167E-01	-0.172E-02	0.107E-02	-0.583E-03	0.898E-03	-0.369E-03
	20000.	0.172E-01	-0.126E-02	0.121E-02	-0.659E-03	0.915E-03	-0.415E-03
	30000.	0.170E-01	-0.102E-02	0.132E-02	-0.718E-03	0.927E-03	-0.444E-03
	50000.	0.163E-01	-0.580E-03	0.151E-02	-0.802E-03	0.946E-03	-0.483E-03
5D - 7F 41110.5 Å C= 0.85E+14	2500.	0.898E-02	-0.294E-03	0.904E-03	0.626E-03	0.752E-03	0.396E-03
	5000.	0.109E-01	-0.386E-03	0.969E-03	0.703E-03	0.778E-03	0.445E-03
	10000.	0.123E-01	-0.427E-03	0.105E-02	0.789E-03	0.811E-03	0.500E-03
	20000.	0.128E-01	-0.358E-03	0.117E-02	0.886E-03	0.852E-03	0.561E-03
	30000.	0.127E-01	-0.282E-03	0.126E-02	0.947E-03	0.881E-03	0.600E-03
	50000.	0.123E-01	-0.145E-03	0.141E-02	0.104E-02	0.921E-03	0.654E-03
5D - 8F 33703.2 Å C= 0.50E+14	2500.	0.930E-02	0.568E-03	0.106E-02	0.749E-03	0.879E-03	0.473E-03
	5000.	0.116E-01	0.382E-03	0.114E-02	0.842E-03	0.912E-03	0.533E-03
	10000.	0.134E-01	0.282E-05	0.124E-02	0.946E-03	0.953E-03	0.599E-03
	20000.	0.142E-01	0.748E-05	0.136E-02	0.106E-02	0.100E-02	0.673E-03
	30000.	0.142E-01	0.257E-04	0.145E-02	0.114E-02	0.104E-02	0.720E-03
	50000.	0.138E-01	-0.485E-04	0.159E-02	0.124E-02	0.109E-02	0.783E-03
6D - 6F 754944.9 Å C= 0.20E+17	2500.	3.19	-1.18	0.460	-0.407	0.312	-0.257
	5000.	3.51	-1.06	0.515	-0.457	0.341	-0.289
	10000.	3.69	-0.746	0.583	-0.514	0.375	-0.325
	20000.	3.74	-0.462	0.672	-0.577	0.414	-0.365
	30000.	3.67	-0.344	0.739	-0.617	0.440	-0.391
	50000.	3.49	-0.193	0.848	-0.673	0.474	-0.426
6D - 7F 104393.9 Å C= 0.37E+15	2500.	0.794E-01	-0.169E-01	0.718E-02	-0.528E-02	0.574E-02	-0.334E-02
	5000.	0.929E-01	-0.157E-01	0.779E-02	-0.594E-02	0.599E-02	-0.376E-02
	10000.	0.102	-0.109E-01	0.858E-02	-0.667E-02	0.631E-02	-0.422E-02
	20000.	0.106	-0.717E-02	0.967E-02	-0.748E-02	0.669E-02	-0.474E-02
	30000.	0.104	-0.516E-02	0.105E-01	-0.801E-02	0.695E-02	-0.507E-02
	50000.	0.999E-01	-0.273E-02	0.119E-01	-0.878E-02	0.732E-02	-0.552E-02
6D - 8F 67000.8 Å C= 0.15E+15	2500.	0.443E-01	-0.423E-02	0.326E-02	-0.401E-03	0.324E-02	-0.254E-03
	5000.	0.546E-01	-0.381E-02	0.329E-02	-0.453E-03	0.324E-02	-0.285E-03
	10000.	0.623E-01	-0.265E-02	0.335E-02	-0.482E-03	0.324E-02	-0.320E-03
	20000.	0.654E-01	-0.192E-02	0.347E-02	-0.405E-03	0.324E-02	-0.359E-03
	30000.	0.651E-01	-0.114E-02	0.360E-02	-0.327E-03	0.324E-02	-0.385E-03
	50000.	0.628E-01	-0.738E-03	0.385E-02	-0.203E-03	0.324E-02	-0.425E-03
7D - 7F C= 0.35E+17	2500.	16.7	-6.31	2.52	-2.24	1.69	-1.42
	5000.	18.6	-5.38	2.82	-2.53	1.86	-1.60
	10000.	19.8	-3.55	3.18	-2.84	2.05	-1.80
	20000.	20.1	-2.14	3.64	-3.19	2.27	-2.02
	30000.	19.7	-1.32	3.97	-3.41	2.41	-2.16
	50000.	18.7	-0.764	4.51	-3.72	2.60	-2.35

Perturber density = 1 x 10^{11} cm^{-3}

Transition	T(K)	Electrons Width (Å)	Electrons Shift (Å)	Protons Width (Å)	Protons Shift (Å)	Ionized helium Width (Å)	Ionized helium Shift (Å)
7D - 8F 162185.0 Å C= 0.62E+15	2500.	0.361	-0.924E-01	0.422E-01	-0.352E-01	0.306E-01	-0.222E-01
	5000.	0.422	-0.720E-01	0.467E-01	-0.396E-01	0.328E-01	-0.250E-01
	10000.	0.467	-0.425E-01	0.522E-01	-0.445E-01	0.355E-01	-0.281E-01
	20000.	0.483	-0.235E-01	0.593E-01	-0.499E-01	0.386E-01	-0.316E-01
	30000.	0.477	-0.159E-01	0.647E-01	-0.534E-01	0.406E-01	-0.338E-01
	50000.	0.457	-0.104E-01	0.733E-01	-0.583E-01	0.434E-01	-0.368E-01
4F - 5D 43637.8 Å C= 0.95E+14	2500.	0.344E-02	0.206E-02	0.777E-03	0.713E-03	0.506E-03	0.451E-03
	5000.	0.346E-02	0.183E-02	0.874E-03	0.801E-03	0.561E-03	0.507E-03
	10000.	0.341E-02	0.144E-02	0.989E-03	0.900E-03	0.625E-03	0.570E-03
	20000.	0.333E-02	0.958E-03	0.113E-02	0.101E-02	0.696E-03	0.640E-03
	30000.	0.325E-02	0.756E-03	0.124E-02	0.108E-02	0.742E-03	0.684E-03
	50000.	0.309E-02	0.479E-03	0.140E-02	0.118E-02	0.806E-03	0.745E-03
4F - 6D 26552.3 Å C= 0.24E+14	2500.	0.284E-02	0.177E-02	0.656E-03	0.603E-03	0.425E-03	0.381E-03
	5000.	0.285E-02	0.156E-02	0.737E-03	0.678E-03	0.473E-03	0.428E-03
	10000.	0.283E-02	0.121E-02	0.834E-03	0.761E-03	0.526E-03	0.482E-03
	20000.	0.276E-02	0.799E-03	0.954E-03	0.855E-03	0.587E-03	0.541E-03
	30000.	0.267E-02	0.598E-03	0.104E-02	0.914E-03	0.626E-03	0.579E-03
	50000.	0.252E-02	0.369E-03	0.118E-02	0.996E-03	0.680E-03	0.631E-03
4F - 7D 21542.0 Å C= 0.11E+14	2500.	0.374E-02	0.235E-02	0.880E-03	0.809E-03	0.569E-03	0.511E-03
	5000.	0.375E-02	0.205E-02	0.990E-03	0.911E-03	0.633E-03	0.575E-03
	10000.	0.373E-02	0.153E-02	0.112E-02	0.102E-02	0.706E-03	0.648E-03
	20000.	0.362E-02	0.966E-03	0.128E-02	0.115E-02	0.788E-03	0.728E-03
	30000.	0.349E-02	0.731E-03	0.140E-02	0.123E-02	0.841E-03	0.779E-03
	50000.	0.327E-02	0.387E-03	0.158E-02	0.134E-02	0.913E-03	0.849E-03
4F - 8D 19214.2 Å C= 0.62E+13	2500.	0.548E-02	0.342E-02	0.131E-02	0.120E-02	0.844E-03	0.759E-03
	5000.	0.547E-02	0.289E-02	0.148E-02	0.136E-02	0.940E-03	0.856E-03
	10000.	0.545E-02	0.209E-02	0.167E-02	0.153E-02	0.105E-02	0.964E-03
	20000.	0.527E-02	0.128E-02	0.192E-02	0.171E-02	0.117E-02	0.108E-02
	30000.	0.505E-02	0.965E-03	0.209E-02	0.183E-02	0.125E-02	0.116E-02
	50000.	0.472E-02	0.446E-03	0.237E-02	0.200E-02	0.136E-02	0.127E-02
4F - 9D 17899.1 Å C= 0.40E+13	2500.	0.806E-02	0.499E-02	0.195E-02	0.179E-02	0.125E-02	0.113E-02
	5000.	0.805E-02	0.412E-02	0.220E-02	0.202E-02	0.140E-02	0.127E-02
	10000.	0.804E-02	0.293E-02	0.249E-02	0.227E-02	0.156E-02	0.144E-02
	20000.	0.773E-02	0.175E-02	0.286E-02	0.255E-02	0.174E-02	0.162E-02
	30000.	0.738E-02	0.130E-02	0.312E-02	0.273E-02	0.186E-02	0.173E-02
	50000.	0.688E-02	0.573E-03	0.354E-02	0.298E-02	0.202E-02	0.189E-02
4F -10D 17071.3 Å C= 0.28E+13	2500.	0.117E-01	0.714E-02	0.286E-02	0.261E-02	0.183E-02	0.164E-02
	5000.	0.116E-01	0.579E-02	0.322E-02	0.295E-02	0.204E-02	0.186E-02
	10000.	0.116E-01	0.405E-02	0.365E-02	0.332E-02	0.228E-02	0.210E-02
	20000.	0.111E-01	0.241E-02	0.419E-02	0.374E-02	0.255E-02	0.236E-02
	30000.	0.106E-01	0.174E-02	0.458E-02	0.400E-02	0.272E-02	0.253E-02
	50000.	0.987E-02	0.771E-03	0.520E-02	0.436E-02	0.296E-02	0.276E-02

Perturber density = 1 x 10^{11} cm^{-3}

Transition	T(K)	Electrons Width (Å)	Electrons Shift (Å)	Protons Width (Å)	Protons Shift (Å)	Ionized helium Width (Å)	Ionized helium Shift (Å)
5F - 5D 423764.7 Å C= 0.90E+16	2500.	0.426	0.169	0.651E-01	0.578E-01	0.439E-01	0.365E-01
	5000.	0.458	0.147	0.730E-01	0.649E-01	0.481E-01	0.411E-01
	10000.	0.470	0.112	0.827E-01	0.729E-01	0.530E-01	0.462E-01
	20000.	0.473	0.753E-01	0.954E-01	0.818E-01	0.585E-01	0.518E-01
	30000.	0.464	0.571E-01	0.105	0.875E-01	0.622E-01	0.554E-01
	50000.	0.441	0.381E-01	0.121	0.954E-01	0.671E-01	0.604E-01
5F - 6D 80737.6 Å C= 0.22E+15	2500.	0.298E-01	0.156E-01	0.586E-02	0.535E-02	0.383E-02	0.338E-02
	5000.	0.311E-01	0.135E-01	0.659E-02	0.602E-02	0.424E-02	0.380E-02
	10000.	0.314E-01	0.101E-01	0.747E-02	0.676E-02	0.472E-02	0.428E-02
	20000.	0.311E-01	0.632E-02	0.857E-02	0.759E-02	0.525E-02	0.481E-02
	30000.	0.303E-01	0.470E-02	0.938E-02	0.812E-02	0.560E-02	0.514E-02
	50000.	0.287E-01	0.261E-02	0.107E-01	0.884E-02	0.607E-02	0.560E-02
5F - 7D 47292.1 Å C= 0.53E+14	2500.	0.192E-01	0.112E-01	0.420E-02	0.385E-02	0.272E-02	0.243E-02
	5000.	0.197E-01	0.957E-02	0.472E-02	0.433E-02	0.302E-02	0.274E-02
	10000.	0.198E-01	0.693E-02	0.535E-02	0.487E-02	0.336E-02	0.308E-02
	20000.	0.194E-01	0.419E-02	0.613E-02	0.547E-02	0.375E-02	0.346E-02
	30000.	0.187E-01	0.308E-02	0.670E-02	0.585E-02	0.400E-02	0.371E-02
	50000.	0.176E-01	0.149E-02	0.759E-02	0.637E-02	0.435E-02	0.403E-02
5F - 8D 37356.4 Å C= 0.23E+14	2500.	0.214E-01	0.129E-01	0.493E-02	0.453E-02	0.318E-02	0.285E-02
	5000.	0.217E-01	0.108E-01	0.555E-02	0.510E-02	0.354E-02	0.322E-02
	10000.	0.217E-01	0.759E-02	0.629E-02	0.574E-02	0.395E-02	0.363E-02
	20000.	0.211E-01	0.451E-02	0.722E-02	0.645E-02	0.441E-02	0.408E-02
	30000.	0.203E-01	0.303E-02	0.789E-02	0.690E-02	0.471E-02	0.437E-02
	50000.	0.190E-01	0.147E-02	0.894E-02	0.752E-02	0.511E-02	0.476E-02
5F - 9D 32687.2 Å C= 0.13E+14	2500.	0.274E-01	0.166E-01	0.650E-02	0.596E-02	0.417E-02	0.374E-02
	5000.	0.276E-01	0.136E-01	0.732E-02	0.672E-02	0.465E-02	0.424E-02
	10000.	0.277E-01	0.946E-02	0.830E-02	0.756E-02	0.519E-02	0.478E-02
	20000.	0.267E-01	0.560E-02	0.952E-02	0.850E-02	0.580E-02	0.537E-02
	30000.	0.255E-01	0.372E-02	0.104E-01	0.910E-02	0.620E-02	0.576E-02
	50000.	0.238E-01	0.171E-02	0.118E-01	0.992E-02	0.673E-02	0.627E-02
5F -10D 30028.0 Å C= 0.86E+13	2500.	0.366E-01	0.221E-01	0.883E-02	0.808E-02	0.566E-02	0.506E-02
	5000.	0.366E-01	0.178E-01	0.995E-02	0.913E-02	0.631E-02	0.574E-02
	10000.	0.367E-01	0.123E-01	0.113E-01	0.103E-01	0.705E-02	0.649E-02
	20000.	0.352E-01	0.717E-02	0.130E-01	0.115E-01	0.788E-02	0.730E-02
	30000.	0.336E-01	0.486E-02	0.142E-01	0.124E-01	0.842E-02	0.782E-02
	50000.	0.313E-01	0.210E-02	0.161E-01	0.135E-01	0.915E-02	0.853E-02
6F - 6D 754944.9 Å C= 0.20E+17	2500.	3.19	1.18	0.460	0.407	0.312	0.257
	5000.	3.51	1.06	0.515	0.457	0.341	0.289
	10000.	3.69	0.746	0.583	0.514	0.375	0.325
	20000.	3.74	0.462	0.672	0.577	0.414	0.365
	30000.	3.67	0.344	0.739	0.617	0.440	0.391
	50000.	3.49	0.193	0.848	0.673	0.474	0.426

Perturber density = 1 x 10^{11} cm^{-3}

Transition	T(K)	Electrons Width (Å)	Electrons Shift (Å)	Protons Width (Å)	Protons Shift (Å)	Ionized helium Width (Å)	Ionized helium Shift (Å)
6F - 7D 134502.6 Å C= 0.43E+15	2500.	0.174	0.851E-01	0.327E-01	0.298E-01	0.214E-01	0.188E-01
	5000.	0.184	0.732E-01	0.368E-01	0.336E-01	0.237E-01	0.212E-01
	10000.	0.189	0.505E-01	0.417E-01	0.377E-01	0.263E-01	0.239E-01
	20000.	0.189	0.307E-01	0.479E-01	0.424E-01	0.293E-01	0.268E-01
	30000.	0.184	0.197E-01	0.525E-01	0.453E-01	0.313E-01	0.287E-01
	50000.	0.173	0.109E-01	0.597E-01	0.494E-01	0.339E-01	0.313E-01
6F - 8D 76576.7 Å C= 0.98E+14	2500.	0.957E-01	0.526E-01	0.204E-01	0.187E-01	0.132E-01	0.118E-01
	5000.	0.993E-01	0.435E-01	0.230E-01	0.211E-01	0.147E-01	0.133E-01
	10000.	0.101	0.288E-01	0.261E-01	0.237E-01	0.164E-01	0.150E-01
	20000.	0.989E-01	0.174E-01	0.300E-01	0.267E-01	0.183E-01	0.169E-01
	30000.	0.955E-01	0.900E-02	0.328E-01	0.285E-01	0.195E-01	0.181E-01
	50000.	0.897E-01	0.584E-02	0.372E-01	0.311E-01	0.212E-01	0.197E-01
6F - 9D 59232.6 Å C= 0.44E+14	2500.	0.934E-01	0.540E-01	0.212E-01	0.194E-01	0.136E-01	0.122E-01
	5000.	0.955E-01	0.438E-01	0.239E-01	0.219E-01	0.152E-01	0.138E-01
	10000.	0.965E-01	0.289E-01	0.271E-01	0.246E-01	0.170E-01	0.156E-01
	20000.	0.936E-01	0.173E-01	0.311E-01	0.277E-01	0.189E-01	0.175E-01
	30000.	0.899E-01	0.841E-02	0.340E-01	0.297E-01	0.202E-01	0.188E-01
	50000.	0.841E-01	0.543E-02	0.386E-01	0.323E-01	0.220E-01	0.205E-01
6F -10D 51041.8 Å C= 0.25E+14	2500.	0.108	0.637E-01	0.254E-01	0.233E-01	0.163E-01	0.146E-01
	5000.	0.109	0.510E-01	0.287E-01	0.263E-01	0.182E-01	0.165E-01
	10000.	0.110	0.340E-01	0.325E-01	0.296E-01	0.203E-01	0.187E-01
	20000.	0.106	0.201E-01	0.374E-01	0.333E-01	0.227E-01	0.210E-01
	30000.	0.102	0.105E-01	0.409E-01	0.356E-01	0.242E-01	0.225E-01
	50000.	0.948E-01	0.597E-02	0.464E-01	0.388E-01	0.264E-01	0.246E-01
7F - 7D C= 0.35E+17	2500.	16.7	6.31	2.52	2.24	1.69	1.42
	5000.	18.6	5.38	2.82	2.53	1.86	1.60
	10000.	19.8	3.55	3.18	2.84	2.05	1.80
	20000.	20.1	2.14	3.64	3.19	2.27	2.02
	30000.	19.7	1.32	3.97	3.41	2.41	2.16
	50000.	18.7	0.764	4.51	3.72	2.60	2.35
7F - 8D 208146.9 Å C= 0.72E+15	2500.	0.778	0.368	0.147	0.134	0.959E-01	0.845E-01
	5000.	0.833	0.299	0.165	0.151	0.106	0.953E-01
	10000.	0.866	0.186	0.187	0.170	0.118	0.107
	20000.	0.863	0.106	0.215	0.191	0.132	0.121
	30000.	0.839	0.565E-01	0.235	0.204	0.141	0.129
	50000.	0.792	0.392E-01	0.266	0.223	0.152	0.141
7F - 9D 115900.4 Å C= 0.17E+15	2500.	0.379	0.201	0.802E-01	0.735E-01	0.518E-01	0.461E-01
	5000.	0.396	0.159	0.903E-01	0.827E-01	0.576E-01	0.522E-01
	10000.	0.407	0.978E-01	0.102	0.931E-01	0.643E-01	0.588E-01
	20000.	0.399	0.577E-01	0.117	0.105	0.717E-01	0.662E-01
	30000.	0.385	0.279E-01	0.128	0.112	0.766E-01	0.709E-01
	50000.	0.362	0.196E-01	0.145	0.122	0.832E-01	0.773E-01

Perturber density = 1 x 10^{11} cm^{-3}

Transition	T(K)	Electrons Width (Å)	Electrons Shift (Å)	Protons Width (Å)	Protons Shift (Å)	Ionized helium Width (Å)	Ionized helium Shift (Å)
7F -10D 88204.4 Å C= 0.74E+14	2500.	0.335	0.189	0.755E-01	0.690E-01	0.485E-01	0.433E-01
	5000.	0.345	0.148	0.850E-01	0.780E-01	0.541E-01	0.491E-01
	10000.	0.351	0.932E-01	0.965E-01	0.877E-01	0.604E-01	0.554E-01
	20000.	0.341	0.554E-01	0.111	0.987E-01	0.674E-01	0.624E-01
	30000.	0.327	0.261E-01	0.121	0.106	0.720E-01	0.668E-01
	50000.	0.306	0.172E-01	0.137	0.115	0.782E-01	0.729E-01
8F - 9D 304692.3 Å C= 0.12E+16	2500.	2.84	1.33	0.548	0.500	0.356	0.314
	5000.	3.06	1.01	0.617	0.562	0.396	0.355
	10000.	3.22	0.583	0.699	0.633	0.440	0.400
	20000.	3.20	0.231	0.801	0.712	0.491	0.450
	30000.	3.11	0.171	0.876	0.762	0.524	0.482
	50000.	2.94	0.125	0.993	0.831	0.568	0.525
8F -10D 166911.5 Å C= 0.26E+15	2500.	1.27	0.656	0.269	0.245	0.173	0.154
	5000.	1.33	0.496	0.303	0.277	0.193	0.174
	10000.	1.38	0.288	0.343	0.312	0.215	0.197
	20000.	1.35	0.151	0.394	0.351	0.240	0.222
	30000.	1.30	0.787E-01	0.431	0.375	0.256	0.237
	50000.	1.23	0.588E-01	0.489	0.409	0.279	0.259

Table 2. Same as in table 1 but for perturber densities 10^{16} - 10^{19} cm^{-3}

Perturber density = 1 x 10^{16} cm^{-3}

Transition	T(K)	Electrons Width (A)	Electrons Shift (A)	Protons Width (A)	Protons Shift (A)	Ionized helium Width (A)	Ionized helium Shift (A)
3S - 3P 2853.0 A C= 0.69E+19	2500.	0.537E-02	0.401E-02	0.257E-02	0.109E-02	0.242E-02	0.662E-03
	5000.	0.630E-02	0.470E-02	0.263E-02	0.125E-02	0.246E-02	0.774E-03
	10000.	0.718E-02	0.547E-02	0.271E-02	0.143E-02	0.249E-02	0.890E-03
	20000.	0.804E-02	0.587E-02	0.281E-02	0.162E-02	0.253E-02	0.101E-02
	30000.	0.876E-02	0.604E-02	0.288E-02	0.174E-02	0.255E-02	0.109E-02
	50000.	0.974E-02	0.524E-02	0.298E-02	0.190E-02	0.259E-02	0.120E-02
3S - 4P 2026.5 A C= 0.12E+19	2500.	0.163E-01	0.884E-02	0.676E-02	0.223E-02		
	5000.	0.185E-01	0.107E-01	0.694E-02	0.264E-02	*0.655E-02	*0.159E-02
	10000.	0.211E-01	0.121E-01	0.710E-02	0.306E-02	*0.670E-02	*0.188E-02
	20000.	0.245E-01	0.127E-01	0.728E-02	0.351E-02	*0.679E-02	*0.218E-02
	30000.	0.268E-01	0.118E-01	0.741E-02	0.378E-02	*0.684E-02	*0.236E-02
	50000.	0.301E-01	0.102E-01	0.760E-02	0.415E-02	0.691E-02	0.260E-02
3S - 5P 1827.9 A C= 0.49E+18	2500.	0.436E-01	0.247E-01	*0.175E-01	*0.539E-02		
	5000.	0.510E-01	0.293E-01	*0.185E-01	*0.676E-02		
	10000.	0.602E-01	0.332E-01	*0.191E-01	*0.810E-02		
	20000.	0.723E-01	0.302E-01	*0.197E-01	*0.945E-02		
	30000.	0.806E-01	0.277E-01	0.200E-01	0.103E-01		
	50000.	0.914E-01	0.232E-01	0.206E-01	0.113E-01	*0.186E-01	*0.703E-02
3S - 6P 1747.8 A C= 0.24E+18	2500.	0.107	0.595E-01				
	5000.	0.127	0.706E-01				
	10000.	0.152	0.734E-01				
	20000.	0.185	0.671E-01	*0.459E-01	*0.226E-01		
	30000.	0.208	0.578E-01	*0.470E-01	*0.249E-01		
	50000.	0.233	0.476E-01	*0.485E-01	*0.277E-01		
3S - 7P 1707.1 A C= 0.13E+18	2500.	*0.234	*0.124				
	5000.	0.279	0.148				
	10000.	0.338	0.146				
	20000.	0.416	0.126				
	30000.	0.464	0.107				
	50000.	0.516	0.860E-01				
3S - 8P 1683.4 A C= 0.81E+17	2500.	*0.461	*0.224				
	5000.	*0.553	*0.263				
	10000.	*0.676	*0.262				
	20000.	*0.835	*0.212				
	30000.	*0.928	*0.178				
	50000.	*1.02	*0.141				

Perturber density = 1 x 10^{16} cm^{-3}

Transition	T(K)	Electrons Width (A)	Electrons Shift (A)	Protons Width (A)	Protons Shift (A)	Ionized helium Width (A)	Ionized helium Shift (A)
3S - 9P 1668.4 A C= 0.53E+17	2500.						
	5000.						
	10000.	*1.24	*0.406				
	20000.	*1.54	*0.323				
	30000.	*1.69	*0.272				
	50000.	*1.84	*0.206				
4S - 4P 17112.5 A C= 0.86E+20	2500.	1.11	0.433	0.469	0.107		
	5000.	1.23	0.485	0.477	0.126	*0.462	*0.762E-01
	10000.	1.48	0.488	0.482	0.145	*0.470	*0.893E-01
	20000.	1.91	0.374	0.487	0.165	*0.474	*0.103
	30000.	2.25	0.311	0.491	0.178	*0.476	*0.111
	50000.	2.70	0.273	0.496	0.195	0.478	0.122
4S - 5P 8925.8 A C= 0.12E+20	2500.	1.05	0.571	*0.414	*0.123		
	5000.	1.22	0.688	*0.437	*0.154		
	10000.	1.46	0.707	*0.451	*0.184		
	20000.	1.79	0.611	*0.463	*0.214		
	30000.	2.03	0.525	0.471	0.233		
	50000.	2.34	0.455	0.483	0.257	*0.441	*0.159
4S - 6P 7292.9 A C= 0.42E+19	2500.	1.88	1.03				
	5000.	2.22	1.21				
	10000.	2.68	1.28				
	20000.	3.28	1.08	*0.797	*0.390		
	30000.	3.69	0.919	*0.816	*0.428		
	50000.	4.17	0.790	*0.842	*0.478		
4S - 7P 6632.5 A C= 0.20E+19	2500.	*3.55	*1.88				
	5000.	4.23	2.29				
	10000.	5.14	2.15				
	20000.	6.32	1.80				
	30000.	7.08	1.53				
	50000.	7.88	1.19				
4S - 8P 6289.3 A C= 0.11E+19	2500.	* 6.44	*3.12				
	5000.	* 7.74	*3.64				
	10000.	* 9.47	*3.61				
	20000*	11.7	*2.81				
	30000*	13.0	*2.30				
	50000*	14.3	*1.79				
3P - 4S 11832.0 A C= 0.82E+20	2500.	0.253	0.156	0.597E-01	0.402E-01	0.477E-01	0.239E-01
	5000.	0.281	0.191	0.642E-01	0.468E-01	0.502E-01	0.286E-01
	10000.	0.306	0.212	0.696E-01	0.538E-01	0.529E-01	0.333E-01
	20000.	0.364	0.213	0.757E-01	0.612E-01	0.562E-01	0.382E-01
	30000.	0.403	0.187	0.798E-01	0.659E-01	0.583E-01	0.413E-01
	50000.	0.485	0.156	0.854E-01	0.722E-01	0.614E-01	0.453E-01

Perturber density = 1 x 10^{16} cm^{-3}

Transition	T(K)	Electrons Width (A)	Electrons Shift (A)	Protons Width (A)	Protons Shift (A)	Ionized helium Width (A)	Ionized helium Shift (A)
3P - 5S 5712.7 A C= 0.70E+19	2500.	0.269	0.185	0.574E-01	0.424E-01	*0.367E-01	*0.226E-01
	5000.	0.310	0.226	0.644E-01	0.523E-01	*0.412E-01	*0.302E-01
	10000.	0.339	0.251	0.721E-01	0.621E-01	*0.461E-01	*0.372E-01
	20000.	0.381	0.251	0.809E-01	0.721E-01	*0.516E-01	*0.442E-01
	30000.	0.401	0.224	0.865E-01	0.782E-01	*0.552E-01	*0.483E-01
	50000.	0.456	0.186	0.941E-01	0.862E-01	*0.599E-01	*0.536E-01
3P - 6S 4731.4 A C= 0.23E+19	2500.	0.555	0.375	*0.115	*0.694E-01		
	5000.	0.636	0.441	*0.130	*0.947E-01		
	10000.	0.695	0.475	*0.146	*0.118		
	20000.	0.782	0.460	*0.164	*0.141		
	30000.	0.848	0.403	*0.176	*0.154		
	50000.	0.964	0.337	*0.191	*0.172	*0.121	*0.106
3P - 7S 4355.8 A C= 0.11E+19	2500.	1.15	0.709				
	5000.	1.31	0.871				
	10000.	1.42	0.867				
	20000.	1.62	0.783				
	30000.	1.81	0.657	*0.350	*0.295		
	50000.	2.04	0.531	*0.381	*0.333		
3P - 8S 4166.3 A C= 0.61E+18	2500.	*2.14	*1.23				
	5000.	*2.40	*1.48				
	10000.	*2.79	*1.52				
	20000.	3.20	1.20				
	30000.	3.59	1.00				
	50000.	4.02	0.798				
3P - 9S 4055.8 A C= 0.38E+18	2500.						
	5000.	*4.21	*2.30				
	10000.	*4.91	*2.31				
	20000.	*5.93	*1.76				
	30000.	*6.71	*1.47				
	50000.	*7.26	*1.13				
3P -10S 3985.4 A C= 0.25E+18	2500.						
	5000.						
	10000.						
	20000.						
	30000.	*11.4	*1.97				
	50000.	*12.3	*1.54				
4P - 5S 31155.6 A C= 0.21E+21	2500.	8.29	5.06	*2.00	*1.10		
	5000.	9.47	5.99	2.15	1.35	*1.74	*0.784
	10000.	11.1	6.24	2.30	1.59	*1.83	*0.959
	20000.	13.6	5.39	2.48	1.84	*1.93	*1.13
	30000.	15.7	4.62	2.60	2.00	*1.99	*1.24
	50000.	18.7	4.06	2.77	2.20	*2.07	*1.37

Perturber density = 1 x 10^{16} cm^{-3}

Transition	T(K)	Electrons Width (A)	Electrons Shift (A)	Protons Width (A)	Protons Shift (A)	Ionized helium Width (A)	Ionized helium Shift (A)
4P - 6S 14619.5 A C= 0.22E+20	2500.	5.41	3.50	*1.11	*0.650		
	5000.	6.19	4.29	*1.24	*0.883		
	10000.	6.90	4.45	*1.39	*1.10		
	20000.	7.93	3.90	*1.55	*1.31		
	30000.	8.94	3.49	*1.66	*1.44		
	50000.	10.3	2.91	*1.80	*1.60	*1.16	*0.981
4P - 7S 11543.6 A C= 0.76E+19	2500.	8.08	4.96				
	5000.	9.11	6.02				
	10000.	10.2	6.25				
	20000.	11.8	5.12				
	30000.	13.3	4.43	*2.45	*2.06		
	50000.	15.0	3.45	*2.66	*2.32		
3P - 3D 8809.2 A C= 0.23E+20	2500.	0.105	0.598E-01	0.507E-01	0.153E-01	*0.487E-01	*0.921E-02
	5000.	0.118	0.588E-01	0.515E-01	0.177E-01	0.498E-01	0.109E-01
	10000.	0.141	0.498E-01	0.522E-01	0.202E-01	0.503E-01	0.126E-01
	20000.	0.178	0.329E-01	0.532E-01	0.229E-01	0.507E-01	0.144E-01
	30000.	0.206	0.264E-01	0.539E-01	0.247E-01	0.509E-01	0.155E-01
	50000.	0.240	0.192E-01	0.550E-01	0.270E-01	0.512E-01	0.170E-01
3P - 4D 5530.0 A C= 0.47E+19	2500.	0.302	0.207	*0.906E-01	*0.461E-01		
	5000.	0.346	0.258	*0.972E-01	*0.576E-01		
	10000.	0.382	0.256	0.104	0.688E-01		
	20000.	0.424	0.242	0.112	0.801E-01	*0.882E-01	*0.489E-01
	30000.	0.455	0.206	0.117	0.870E-01	*0.908E-01	*0.536E-01
	50000.	0.504	0.175	0.124	0.960E-01	*0.944E-01	*0.596E-01
3P - 5D 4704.3 A C= 0.20E+19	2500.	0.616	0.407				
	5000.	0.707	0.500				
	10000.	0.789	0.497	*0.208	*0.128		
	20000.	0.885	0.464	*0.224	*0.153		
	30000.	0.964	0.395	*0.234	*0.168		
	50000.	1.07	0.337	*0.249	*0.187		
3P - 6D 4353.1 A C= 0.10E+19	2500.	1.15	0.697				
	5000.	1.32	0.844				
	10000.	1.52	0.872				
	20000.	1.78	0.725				
	30000.	1.97	0.615				
	50000.	2.17	0.508				
3P - 7D 4168.5 A C= 0.62E+18	2500.	*1.99	*1.07				
	5000.	*2.34	*1.27				
	10000.	*2.80	*1.28				
	20000.	3.41	1.01				
	30000.	3.79	0.834				
	50000.	4.17	0.668				

Perturber density = 1 x 10^{16} cm^{-3}

Transition	T(K)	Electrons Width (A)	Electrons Shift (A)	Protons Width (A)	Protons Shift (A)	Ionized helium Width (A)	Ionized helium Shift (A)
3P - 8D 4058.7 A C= 0.40E+18	2500.	*3.25	*1.50				
	5000.	*3.98	*1.73				
	10000.	*4.95	*1.69				
	20000.	*6.18	*1.30				
	30000.	*6.87	*1.05				
	50000.	*7.52	*0.828				
4P - 4D 26398.9 A C= 0.11E+21	2500.	7.14	4.31	*2.29	*0.953		
	5000.	8.12	4.92	*2.42	*1.18		
	10000.	9.59	4.93	2.53	1.40		
	20000.	11.5	3.79	2.66	1.63	*2.29	*0.999
	30000.	13.0	3.28	2.75	1.77	*2.33	*1.09
	50000.	14.9	2.90	2.87	1.95	*2.39	*1.21
4P - 5D 14364.2 A C= 0.18E+20	2500.	5.88	3.72				
	5000.	6.73	4.46				
	10000.	7.64	4.64	*1.96	*1.16		
	20000.	8.77	3.84	*2.10	*1.39		
	30000.	9.72	3.43	*2.19	*1.53		
	50000.	10.9	2.76	*2.33	*1.70		
4P - 6D 11525.3 A C= 0.73E+19	2500.	8.17	4.84				
	5000.	9.40	5.78				
	10000.	10.9	5.97				
	20000.	12.8	4.74				
	30000.	14.3	4.09				
	50000.	15.8	3.30				
3D - 4P 33972.8 A C= 0.34E+21	2500.	4.62	1.97	2.03	0.498		
	5000.	5.35	2.38	2.07	0.587	*2.00	*0.355
	10000.	6.42	2.70	2.10	0.678	*2.04	*0.417
	20000.	7.91	2.61	2.13	0.774	*2.06	*0.482
	30000.	8.93	2.42	2.15	0.834	*2.07	*0.522
	50000.	10.3	2.00	2.18	0.915	*2.08	*0.574
3D - 5P 12043.3 A C= 0.21E+20	2500.	1.92	1.07	*0.768	*0.227		
	5000.	2.25	1.28	*0.811	*0.285		
	10000.	2.69	1.34	*0.837	*0.340		
	20000.	3.28	1.26	*0.860	*0.397		
	30000.	3.68	1.10	0.875	0.431		
	50000.	4.20	0.944	0.897	0.476	*0.819	*0.290
3D - 6P 9249.1 A C= 0.68E+19	2500.	3.02	1.71				
	5000.	3.59	1.96				
	10000.	4.32	2.09				
	20000.	5.28	1.84	*1.29	*0.630		
	30000.	5.93	1.61	*1.32	*0.692		
	50000.	6.68	1.35	*1.36	*0.771		

Perturber density = 1 x 10^{16} cm^{-3}

Transition	T(K)	Electrons Width (A)	Electrons Shift (A)	Protons Width (A)	Protons Shift (A)	Ionized helium Width (A)	Ionized helium Shift (A)
3D - 7P 8212.1 A C= 0.31E+19	2500.	*5.44	*2.89				
	5000.	6.49	3.42				
	10000.	7.88	3.46				
	20000.	9.69	2.79				
	30000.	10.8	2.35				
	50000.	12.1	1.90				
3D - 8P 7692.3 A C= 0.17E+19	2500.	*9.64	*4.84				
	5000.	*11.6	*5.47				
	10000.	*14.2	*5.45				
	20000.	*17.5	*4.09				
	30000.	*19.5	*3.30				
	50000.	*21.4	*2.56				
4S - 5P 7660.5 A C= 0.35E+18	2500.	4.29	-1.13				
	5000.	4.37	-0.955				
	10000.	4.16	-0.657				
	20000.	3.89	-0.451				
	30000.	3.72	-0.301				
	50000.	3.50	-0.178				
4S - 6P 6320.7 A C= 0.20E+18	2500.	*6.28	*-1.73				
	5000.	*6.89	*-1.43				
	10000.	*6.84	*-1.12				
	20000.	6.59	-0.778				
	30000.	6.39	-0.508				
	50000.	6.07	-0.309				
4S - 7P 5787.1 A C= 0.12E+18	2500.						
	5000.						
	10000.	*11.7	*-1.60				
	20000.	*11.6	*-1.06				
	30000.	*11.4 *	-0.744				
	50000.	10.9	-0.477				
3P - 4S 5179.6 A C= 0.18E+20	2500.	0.388E-01	0.308E-01	0.987E-02	0.814E-02	0.657E-02	0.484E-02
	5000.	0.460E-01	0.365E-01	0.110E-01	0.950E-02	0.726E-02	0.579E-02
	10000.	0.532E-01	0.436E-01	0.123E-01	0.109E-01	0.804E-02	0.676E-02
	20000.	0.582E-01	0.490E-01	0.137E-01	0.124E-01	0.892E-02	0.777E-02
	30000.	0.610E-01	0.480E-01	0.146E-01	0.134E-01	0.949E-02	0.839E-02
	50000.	0.649E-01	0.445E-01	0.159E-01	0.147E-01	0.103E-01	0.921E-02
3P - 5S 3335.4 A C= 0.26E+19	2500.	0.808E-01	0.569E-01	0.177E-01	0.134E-01	*0.112E-01	*0.721E-02
	5000.	0.942E-01	0.693E-01	0.199E-01	0.164E-01	*0.126E-01	*0.951E-02
	10000.	0.104	0.782E-01	0.224E-01	0.194E-01	*0.142E-01	*0.117E-01
	20000.	0.111	0.816E-01	0.251E-01	0.225E-01	*0.159E-01	*0.138E-01
	30000.	0.118	0.772E-01	0.269E-01	0.244E-01	0.170E-01	0.151E-01
	50000.	0.126	0.651E-01	0.292E-01	0.269E-01	0.185E-01	0.168E-01

Perturber density = 1 x 10^{16} cm^{-3}

Transition	T(K)	Electrons Width (A)	Electrons Shift (A)	Protons Width (A)	Protons Shift (A)	Ionized helium Width (A)	Ionized helium Shift (A)
3P - 6S 2941.1 A C= 0.97E+18	2500.	0.189	0.125	*0.394E-01	*0.245E-01		
	5000.	0.217	0.152	*0.444E-01	*0.329E-01		
	10000.	0.237	0.167	*0.499E-01	*0.408E-01		
	20000.	0.267	0.162	*0.560E-01	*0.485E-01		
	30000.	0.283	0.142	*0.600E-01	*0.530E-01	*0.380E-01	*0.322E-01
	50000.	0.318	0.118	0.653E-01	0.589E-01	*0.413E-01	*0.363E-01
3P - 7S 2780.5 A C= 0.48E+18	2500.	0.400	0.248				
	5000.	0.456	0.308				
	10000.	0.509	0.311				
	20000.	0.585	0.283	*0.115	*0.945E-01		
	30000.	0.649	0.241	*0.123	*0.105		
	50000.	0.733	0.196	*0.134	*0.118		
3P - 8S 2697.5 A C= 0.28E+18	2500.	*0.770	*0.441				
	5000.	*0.878	*0.530				
	10000.	1.03	0.540				
	20000.	1.20	0.447				
	30000.	1.35	0.373				
	50000.	1.51	0.298				
3P - 9S 2648.4 A C= 0.17E+18	2500.	*1.36	*0.695				
	5000.	*1.56	*0.824				
	10000.	*1.87	*0.822				
	20000.	*2.29	*0.651				
	30000.	*2.57	*0.544				
	50000.	*2.84	*0.414				
3P -10S 2616.9 A C= 0.12E+18	2500.						
	5000.						
	10000.						
	20000.	*4.03	*0.881				
	30000.	*4.50	*0.749				
	50000.	*4.92	*0.533				
3P - 3D 3836.4 A C= 0.16E+18	2500.	0.189	-0.486E-01	*0.515E-01	*-0.333E-01		
	5000.	0.180	-0.310E-01	*0.585E-01	*-0.433E-01		
	10000.	0.167	-0.144E-01	*0.672E-01	*-0.528E-01		
	20000.	0.150	-0.249E-02	*0.789E-01	*-0.622E-01	*0.460E-01	*-0.376E-01
	30000.	0.140	0.445E-02	0.879E-01	-0.679E-01	*0.491E-01	*-0.415E-01
	50000.	0.128	0.732E-02	0.102	-0.759E-01	*0.533E-01	*-0.464E-01
3P - 4D 3095.9 A C= 0.57E+17	2500.	0.578	0.245				
	5000.	0.573	0.234				
	10000.	0.551	0.203				
	20000.	0.521	0.163				
	30000.	0.498	0.133				
	50000.	0.465	0.999E-01				

Perturber density = 1×10^{16} cm^{-3}

Transition	T(K)	Electrons Width (A)	Electrons Shift (A)	Protons Width (A)	Protons Shift (A)	Ionized helium Width (A)	Ionized helium Shift (A)
3P - 5D 2850.8 A C= 0.41E+17	2500.	*1.24	*0.548				
	5000.	*1.28	*0.560				
	10000.	*1.27	*0.492				
	20000.	1.25	0.390				
	30000.	1.21	0.321				
	50000.	1.14	0.228				
3P - 6D 2735.8 A C= 0.26E+17	2500.						
	5000.						
	10000.	*2.61	*0.910				
	20000.	*2.61	*0.737				
	30000.	*2.54	*0.602				
	50000.	2.41	0.414				
3D - 4F 14881.7 A C= 0.24E+19	2500.	5.45	-0.613	*0.680	*0.294		
	5000.	5.85	-0.279	*0.732	*0.364		
	10000.	6.19	-0.371E-01	0.802	0.432		
	20000.	6.23	0.968E-01	0.918	0.505	*0.667	*0.307
	30000.	6.21	0.143	1.02	0.556	*0.680	*0.336
	50000.	6.20	0.921E-01	1.18	0.647	*0.699	*0.373

Perturber density = 1 x 10^{17} cm^{-3}

Transition	T(K)	Electrons Width (Å)	Electrons Shift (Å)	Protons Width (Å)	Protons Shift (Å)	Ionized helium Width (Å)	Ionized helium Shift (Å)
3S - 3P 2853.0 Å C= 0.69E+20	2500.	0.537E-01	0.385E-01	0.249E-01	0.930E-02	*0.213E-01	*0.505E-02
	5000.	0.630E-01	0.458E-01	0.261E-01	0.114E-01	*0.235E-01	*0.662E-02
	10000.	0.718E-01	0.539E-01	0.270E-01	0.135E-01	*0.245E-01	*0.811E-02
	20000.	0.804E-01	0.582E-01	0.281E-01	0.156E-01	*0.252E-01	*0.958E-02
	30000.	0.876E-01	0.602E-01	0.288E-01	0.169E-01	0.255E-01	0.105E-01
	50000.	0.974E-01	0.524E-01	0.298E-01	0.186E-01	0.259E-01	0.116E-01
3S - 4P 2026.5 Å C= 0.12E+20	2500.	0.163	0.811E-01				
	5000.	0.185	0.102	*0.654E-01	*0.213E-01		
	10000.	0.211	0.117	*0.696E-01	*0.270E-01		
	20000.	0.245	0.124	*0.723E-01	*0.325E-01		
	30000.	0.268	0.116	*0.738E-01	*0.357E-01		
	50000.	0.301	0.101	*0.759E-01	*0.399E-01		
3S - 5P 1827.9 Å C= 0.49E+19	2500.	0.433	0.209				
	5000.	0.509	0.266				
	10000.	0.602	0.312				
	20000.	0.722	0.290				
	30000.	0.806	0.269				
	50000.	0.914	0.228				
3S - 6P 1747.8 Å C= 0.24E+19	2500.	*1.05	*0.435				
	5000.	*1.26	*0.593				
	10000.	*1.52	*0.654				
	20000.	*1.85	*0.615				
	30000.	*2.07	*0.543				
	50000.	*2.33	*0.461				
3S - 7P 1707.1 Å C= 0.13E+19	2500.						
	5000.						
	10000.						
	20000.						
	30000.	*4.61	*0.942				
	50000.	*5.14	*0.808				
3P - 4S 11832.0 Å C= 0.82E+21	2500.	2.53	1.48	*0.583	*0.312		
	5000.	2.81	1.85	0.638	0.405	*0.484	*0.222
	10000.	3.06	2.09	0.694	0.493	*0.523	*0.288
	20000.	3.64	2.12	0.757	0.580	*0.559	*0.351
	30000.	4.03	1.87	0.797	0.633	*0.582	*0.387
	50000.	4.85	1.56	0.854	0.701	0.613	0.433
3P - 5S 5712.7 Å C= 0.70E+20	2500.	2.69	1.60				
	5000.	3.10	2.08				
	10000.	3.39	2.38	*0.720	*0.497		
	20000.	3.81	2.44	*0.808	*0.633		
	30000.	4.01	2.21	*0.865	*0.710		
	50000.	4.56	1.85	*0.941	*0.806		

Perturber density = 1 x 10^{17} cm^{-3}

Transition	T(K)	Electrons Width (Å)	Electrons Shift (Å)	Protons Width (Å)	Protons Shift (Å)	Ionized helium Width (Å)	Ionized helium Shift (Å)
3P - 6S 4731.4 Å C= 0.23E+20	2500.	*5.53	*2.86				
	5000.	*6.35	*3.78				
	10000.	6.94	4.32				
	20000.	7.82	4.32				
	30000.	8.48	3.90				
	50000.	9.64	3.28				
3P - 7S 4355.8 Å C= 0.11E+20	2500.						
	5000.	*13.0	*6.69				
	10000.	*14.1	*7.29				
	20000.	*16.2	*6.99				
	30000.	*18.0	*6.17				
	50000.	*20.3	*5.02				
3P - 3D 8809.2 Å C= 0.23E+21	2500.	1.05	0.571	*0.474	*0.125		
	5000.	1.18	0.568	*0.503	*0.157		
	10000.	1.41	0.483	0.518	0.188		
	20000.	1.78	0.321	0.530	0.220	*0.501	*0.134
	30000.	2.06	0.259	0.538	0.239	*0.506	*0.147
	50000.	2.40	0.191	0.550	0.263	*0.511	*0.164
3P - 4D 5530.0 Å C= 0.47E+20	2500.	3.01	1.77				
	5000.	3.46	2.37				
	10000.	3.82	2.41				
	20000.	4.24	2.32				
	30000.	4.55	2.02	*1.16	*0.782		
	50000.	5.04	1.71	*1.24	*0.892		
3P - 5D 4704.3 Å C= 0.20E+20	2500.	*6.11	*3.05				
	5000.	*7.05	*4.27				
	10000.	*7.88	*4.47				
	20000.	8.85	4.34				
	30000.	9.64	3.81				
	50000.	10.7	3.26				
3P - 6D 4353.1 Å C= 0.10E+20	2500.						
	5000.						
	10000.	*15.1	*7.38				
	20000.	*17.7	*6.43				
	30000.	*19.6	*5.75				
	50000.	*21.7	*4.79				
3P - 4S 5179.6 Å C= 0.18E+21	2500.	0.388	0.289	0.980E-01	0.627E-01	*0.631E-01	*0.297E-01
	5000.	0.460	0.352	0.110	0.818E-01	*0.719E-01	*0.447E-01
	10000.	0.532	0.428	0.123	0.998E-01	*0.802E-01	*0.582E-01
	20000.	0.582	0.489	0.137	0.118	*0.891E-01	*0.710E-01
	30000.	0.610	0.479	0.146	0.128	*0.949E-01	*0.785E-01
	50000.	0.649	0.445	0.159	0.142	0.103	0.879E-01

Perturber density = 1×10^{17} cm^{-3}

Transition	T(K)	Electrons Width (Å)	Electrons Shift (Å)	Protons Width (Å)	Protons Shift (Å)	Ionized helium Width (Å)	Ionized helium Shift (Å)
3P - 5S 3335.4 Å C= 0.26E+20	2500.	0.808	0.495				
	5000.	0.942	0.640				
	10000.	1.04	0.745	*0.223	*0.157		
	20000.	1.11	0.795	*0.251	*0.199		
	30000.	1.18	0.762	*0.268	*0.223		
	50000.	1.26	0.649	*0.292	*0.252		
3P - 6S 2941.1 Å C= 0.97E+19	2500.	*1.88	*0.965				
	5000.	*2.17	*1.32				
	10000.	2.37	1.52				
	20000.	2.67	1.53				
	30000.	2.83	1.36				
	50000.	3.18	1.16				
3P - 7S 2780.5 Å C= 0.48E+19	2500.						
	5000.	*4.52	*2.43				
	10000.	*5.07	*2.65				
	20000.	*5.84	*2.54				
	30000.	*6.48	*2.21				
	50000.	*7.32	*1.88				
3P - 3D 3836.4 Å C= 0.16E+19	2500.	1.54	-0.224				
	5000.	1.57	-0.123				
	10000.	1.51	-0.148E-01				
	20000.	1.39	0.508E-01				
	30000.	1.31	0.574E-01				
	50000.	1.21	0.832E-01				
3P - 4D 3095.9 Å C= 0.57E+18	2500.	*3.72	*1.24				
	5000.	*4.31	*1.49				
	10000.	*4.50	*1.42				
	20000.	*4.50	*1.24				
	30000.	4.40	1.07				
	50000.	4.20	0.869				
3P - 5D 2850.8 Å C= 0.41E+18	2500.						
	5000.						
	10000.						
	20000.	*10.3	*2.56				
	30000.	*10.3	*2.27				
	50000.	*10.0	*1.86				

Perturber density = 1 x 10^{18} cm^{-3}

Transition	T(K)	Electrons Width (Å)	Electrons Shift (Å)	Protons Width (Å)	Protons Shift (Å)	Ionized helium Width (Å)	Ionized helium Shift (Å)
3S - 3P 2853.0 Å C= 0.69E+21	2500.	0.535	0.336	*0.176	*0.436E-01		
	5000.	0.629	0.423	*0.234	*0.788E-01		
	10000.	0.717	0.514	*0.261	*0.110		
	20000.	0.804	0.564	*0.278	*0.138		
	30000.	0.876	0.586	*0.286	*0.155		
	50000.	0.974	0.513	0.297	0.175		
3S - 4P 2026.5 Å C= 0.12E+21	2500.	*1.59	*0.578				
	5000.	1.83	0.852				
	10000.	2.11	1.05				
	20000.	2.45	1.16				
	30000.	2.68	1.09				
	50000.	3.01	0.964				
3S - 5P 1827.9 Å C= 0.49E+20	2500.						
	5000.	*4.84	*1.77				
	10000.	*5.90	*2.48				
	20000.	*7.15	*2.45				
	30000.	*8.00	*2.33				
	50000.	*9.09	*2.03				
3P - 3D 8809.2 Å C= 0.23E+22	2500.	10.4	4.82				
	5000.	11.8	5.06				
	10000.	14.1	4.41				
	20000.	17.8	2.95	*5.15	*1.89		
	30000.	20.6	2.46	*5.30	*2.14		
	50000.	24.0	1.80	*5.46	*2.44		
3P - 4S 5179.6 Å C= 0.18E+22	2500.	3.88	2.30				
	5000.	4.60	3.10				
	10000.	5.32	3.97	*1.21	*0.702		
	20000.	5.82	4.67	*1.37	*0.968		
	30000.	6.10	4.62	*1.46	*1.11		
	50000.	6.49	4.37	*1.59	*1.29		
3P - 5S 3335.4 Å C= 0.26E+21	2500.	*7.78	*2.53				
	5000.	*9.36	*4.69				
	10000.	*10.4	*6.23				
	20000.	11.1	7.09				
	30000.	11.8	6.99				
	50000.	12.6	6.18				
3P - 3D 3836.4 Å C= 0.16E+20	2500.	*6.26	*0.181				
	5000.	*8.92	*0.510				
	10000.	10.4	1.09				
	20000.	10.6	1.40				
	30000.	10.4	1.54				
	50000.	10.0	1.37				

Perturber density = 1×10^{19} cm^{-3}

		Electrons		Protons		Ionized helium	
Transition	T(K)	Width (Å)	Shift (Å)	Width (Å)	Shift (Å)	Width (Å)	Shift (Å)
3S - 3P	2500.	5.00	1.76				
2853.0 Å	5000.	6.20	3.09				
C= 0.69E+22	10000.	7.15	4.34				
	20000.	8.03	5.08				
	30000.	8.75	5.41				
	50000.	9.74	4.83				

2. RESULTS AND DISCUSSION

Our results for 267 Mg I multiplets are shown in Table 1, for a perturber density of 10^{11} cm^{-3} and temperatures T = 2,500 - 50,000 K. In Table 2, data for Mg I multiplets of interest for laboratory plasma diagnostic are shown for perturber densities $10^{16} - 10^{19}$ cm^{-3}. We also specify a parameter c (Dimitrijević and Sahal–Bréchot 1984), which gives an estimate for the maximum perturber density for which the line may be treated as isolated when it is divided by the corresponding electron-impact full width at half maximum. For each value given in Tables 1 and 2, the collision volume (V) multiplied by the perturber density (N) is much less than one and the impact approximation is valid (Sahal–Bréchot, 1969ab). Values for NV > 0.5 are not given and values for 0.1 < NV < 0.5 are denoted by an asterisk. When the impact approximation is not valid, the ion broadening contribution may be estimated by using quasistatic approach (Sahal–Bréchot 1991 and Griem 1974). The accuracy of the results obtained decreases when broadening by ion interactions becomes important.

The analysis of present results and comparison with available experimental and theoretical data will be published elsewhere. Dimitrijević and Sahal–Bréchot (1994ab).

Acknowledgements – This work is a part of the project "Physics and dynamics of celestial bodies", supported by Ministry of Science and Technology of Serbia.

REFERENCES

Brault, J., Noyes, R. W.: 1983, *Astrophys. J* **269**, L61.
Dimitrijević, M. S., and Sahal–Bréchot,S.: 1984, *JQSRT* **31**, 301.
Dimitrijević, M. S., and Sahal–Bréchot, S.: 1994a, *Astron. Astrophys. Suppl. Series*, submitted.
Dimitrijević, M. S., and Sahal–Bréchot, S.: 1994b, *Physica Scripta*, **49**, 661.
Dimitrijević, M. S., Sahal–Bréchot, S., and Bommier, V.: 1991, *Astron. Astrophys. Suppl. Series.* **89**, 581.
Farmer, C. B., Norton, R. H.: 1988, *A High Resolution Atlas of the Infrared Spectra of the Sun*, NASA Reference Publication 1, 1224.
Griem, H. R.: 1974, *Spectral Line Broadening by Plasmas*, Academic Press, New York.
Jefferies, J. T.: 1991, *Astrophys. J* **377**, 337.
Sahal–Bréchot, S.: 1969a, *Astron. Astrophys.* **1**, 91.
Sahal–Bréchot, S.: 1969b, *Astron. Astrophys.* **2**, 322.
Sahal–Bréchot, S.: 1991, *Astron. Astrophys.* **245**, 322.
Van Regemorter, H., Hoang Binh,D .: 1993, *Astron. Astrophys.* **277**, 623.

ТАБЕЛЕ ПАРАМЕТАРА ШТАРКОВОГ ШИРЕЊА ЛИНИЈА Mg I ОД ЗНАЧАЈА ЗА ПРОУЧАВАЊЕ СУНЧЕВОГ И ЗВЕЗДАНИХ СПЕКТАРА. I

М. С. Димитријевић[1] и S. Sahal–Bréchot[2]

[1] *Астрономска опсерваторија, Волгина 7, 11050 Београд, Југославија*

[2] *Laboratoire "Astrophysique, Atomes et Molécules"*
Département Atomes et Molécules en Astrophysique
Unité associée au C.N.R.S. No 812
Observatoire de Paris-Meudon, 92190 Meudon, France

УДК 52–355.3
Претходно саопштење

Користећи семикласичан прилаз, израчунате су ширине и помераји спектралних линија, проузроковани сударима са електронима, протонима и He II, за 267 мултиплета Mg I. Резултати су дати у функцији температуре и концентрације пертурбера.

Bull. Astron. Belgrade № 150 (1994), 121

UDC 52–355.3
Errata

STARK BROADENING PARAMETER TABLES FOR Mg I LINES OF INTEREST FOR SOLAR AND STELLAR SPECTRA RESEARCH. I

M. S. Dimitrijević[1] and S. Sahal–Bréchot[2]

[1] *Astronomical Observatory, Volgina 7, 11050 Belgrade, Yugoslavia*

[2] *Laboratoire "Astrophysique, Atomes et Molécules"*
Département Atomes et Molécules en Astrophysique
Unité associée au C.N.R.S. No 812
Observatoire de Paris–Meudon, 92190 Meudon, France

(Received: August 21, 1994)

(Correction of the article published in Bull. Astron. Belgrade № 149 (1994) 31)

The second perturber in Table 1 is not ionized helium but ionized argon. For the investigation of Mg I lines originating in solar photosphere, perturbation of the ionized helium is not significant. On the other hand, ionized argon-impact broadening is of importance for laboratory plasma diagnostics.

Bull. Astron. Belgrade № 150 (1994), 47 – 94

UDC 52–355.3
Preliminary report

STARK BROADENING PARAMETER TABLES FOR Mg I LINES OF INTEREST FOR SOLAR AND STELLAR SPECTRA RESEARCH. II

M. S. Dimitrijević[1] and S. Sahal–Bréchot[2]

[1] *Astronomical Observatory, Volgina 7, 11050 Belgrade, Yugoslavia*

[2] *Laboratoire "Astrophysique, Atomes et Molécules"*
Département Atomes et Molécules en Astrophysique
Unité associée au C.N.R.S. No 812
Observatoire de Paris–Meudon, 92190 Meudon, France

(Received: August 10, 1994)

SUMMARY: Using a semiclassical approach, we have calculated ionized magnesium–, ionized silicon–, and ionized iron–impact line widths and shifts for 270 Mg I multiplets as a function of temperature and perturber density.

1. INTRODUCTION

By using the semiclassical-perturbation formalism (Sahal–Bréchot, 1969ab) we have calculated and published in the previous article (Dimitrijević and Sahal–Bréchot, 1994a) electron-, proton-, and ionized argon-, -impact line widths and shifts for 267 Mg I multiplets, in order to continue our effort to provide to astrophysicists the needed Stark broadening data. Here are presented Stark broadening data for ionized magnesium-, ionized silicon-, and ionized iron-impacts with neutral magnesium for 270 Mg I multiplets, in order to provide the data for all principal perturbers in the solar plasma.

2. RESULTS AND DISCUSSION

A summary of the formalism is given in Dimitrijević et al. (1991) and all details of calculations in Dimitrijević and Sahal–Bréchot (1994ab). Our results for 270 Mg I multiplets are shown in Table 1, for a perturber density of 10^{11} cm^{-3} and temperatures T = 2,500 - 50,000 K. We also specify a parameter c (Dimitrijević and Sahal–Bréchot 1984), which gives an estimate for the maximum perturber density for which the line may be treated as isolated when it is divided by the corresponding electron-impact full width at half maximum.

Table 1. This table shows Mg II-, Si II-, and Fe II- impact broadening parameters for Mg I for a perturber density of 10^{11} cm^{-3} and temperatures from 2,500 up to 50,000 K. Transitions and averaged wavelengths for the multiplet (in Å) are also given. By using c [see Eq.(5) in Dimitrijević et al, 1991], we obtain an estimate for the maximum perturber density for which the line may be treated as isolated and tabulated data may be used. The asterisk identifies cases for which the collision volume multiplied by the perturber density (the condition for validity of the impact approximation) lies between 0.1 and 0.5. Table 1 is also available in electronic form: see the editorial in Astron.Astrophys. 1992, Vol. 266, No 2, page E1 or in Astron.Astrophys. Suppl. Series 1992, Vol. 96, No3, and Dimitrijević and Sahal-Bréchot, 1994.

Perturber density= 1 x 10^{+11} cm^{-3}

		Perturbers					
		Ionized silicon		Ionized iron		Ionized magnesium	
Transition	T(K)	Width (Å)	Shift (Å)	Width (Å)	Shift (Å)	Width (Å)	Shift (Å)
	2500.	0.245E-07	0.751E-08	0.245E-07	0.719E-08	0.245E-07	0.761E-08
3S - 3P	5000.	0.247E-07	0.843E-08	0.246E-07	0.807E-08	0.248E-07	0.854E-08
2853.0 Å	10000.	0.250E-07	0.946E-08	0.249E-07	0.906E-08	0.250E-07	0.958E-08
	20000.	0.254E-07	0.106E-07	0.252E-07	0.102E-07	0.254E-07	0.108E-07
C= 0.69E+14	30000.	0.257E-07	0.114E-07	0.255E-07	0.109E-07	0.257E-07	0.115E-07
	50000.	0.261E-07	0.124E-07	0.258E-07	0.118E-07	0.261E-07	0.125E-07
	2500.	0.669E-07	0.166E-07	0.669E-07	0.159E-07	0.670E-07	0.168E-07
3S - 4P	5000.	0.673E-07	0.186E-07	0.671E-07	0.178E-07	0.673E-07	0.189E-07
2026.5 Å	10000.	0.677E-07	0.209E-07	0.675E-07	0.200E-07	0.677E-07	0.212E-07
	20000.	0.683E-07	0.235E-07	0.680E-07	0.225E-07	0.683E-07	0.238E-07
C= 0.12E+14	30000.	0.687E-07	0.251E-07	0.684E-07	0.240E-07	0.688E-07	0.254E-07
	50000.	0.694E-07	0.274E-07	0.690E-07	0.262E-07	0.695E-07	0.277E-07
	2500.	0.180E-06	0.460E-07	0.180E-06	0.440E-07	0.180E-06	0.466E-07
3S - 5P	5000.	0.181E-06	0.516E-07	0.181E-06	0.494E-07	0.181E-06	0.523E-07
1827.9 Å	10000.	0.182E-06	0.580E-07	0.182E-06	0.555E-07	0.182E-06	0.587E-07
	20000.	0.184E-06	0.651E-07	0.183E-06	0.623E-07	0.184E-06	0.659E-07
C= 0.49E+13	30000.	0.185E-06	0.696E-07	0.184E-06	0.666E-07	0.186E-06	0.705E-07
	50000.	0.187E-06	0.758E-07	0.186E-06	0.725E-07	0.188E-06	0.767E-07
	2500.	0.414E-06	0.115E-06	0.413E-06	0.110E-06	0.414E-06	0.117E-06
3S - 6P	5000.	0.416E-06	0.129E-06	0.415E-06	0.124E-06	0.417E-06	0.131E-06
1747.8 Å	10000.	0.420E-06	0.145E-06	0.418E-06	0.139E-06	0.420E-06	0.147E-06
	20000.	0.425E-06	0.163E-06	0.423E-06	0.156E-06	0.426E-06	0.165E-06
C= 0.24E+13	30000.	0.429E-06	0.174E-06	0.426E-06	0.167E-06	0.429E-06	0.176E-06
	50000.	0.434E-06	0.190E-06	0.431E-06	0.182E-06	0.435E-06	0.192E-06
	2500.	0.835E-06	0.251E-06	0.833E-06	0.241E-06	0.835E-06	0.255E-06
3S - 7P	5000.	0.841E-06	0.283E-06	0.839E-06	0.270E-06	0.842E-06	0.286E-06
1707.1 Å	10000.	0.851E-06	0.317E-06	0.847E-06	0.303E-06	0.852E-06	0.321E-06
	20000.	0.863E-06	0.356E-06	0.858E-06	0.341E-06	0.864E-06	0.360E-06
C= 0.13E+13	30000.	0.872E-06	0.381E-06	0.866E-06	0.364E-06	0.874E-06	0.386E-06
	50000.	0.885E-06	0.415E-06	0.878E-06	0.397E-06	0.888E-06	0.420E-06

STARK BROADENING PARAMETER TABLES FOR MG I LINES

Perturber density= 1 x 10^{+11} cm^{-3}

		Perturbers					
		Ionized silicon		Ionized iron		Ionized magnesium	
Transition	T(K)	Width (Å)	Shift (Å)	Width (Å)	Shift (Å)	Width (Å)	Shift (Å)
	2500.	0.153E-05	0.491E-06	0.152E-05	0.470E-06	0.153E-05	0.498E-06
3S - 8P	5000.	0.154E-05	0.553E-06	0.154E-05	0.529E-06	0.154E-05	0.559E-06
1683.4 Å	10000.	0.156E-05	0.621E-06	0.155E-05	0.594E-06	0.156E-05	0.628E-06
	20000.	0.159E-05	0.697E-06	0.158E-05	0.667E-06	0.159E-05	0.705E-06
C= 0.81E+12	30000.	0.161E-05	0.745E-06	0.159E-05	0.713E-06	0.161E-05	0.755E-06
	50000.	0.164E-05	0.811E-06	0.162E-05	0.777E-06	0.164E-05	0.822E-06
	2500.	0.259E-05	0.880E-06	0.258E-05	0.842E-06	0.259E-05	0.891E-06
3S - 9P	5000.	0.262E-05	0.990E-06	0.261E-05	0.947E-06	0.262E-05	0.100E-05
1668.4 Å	10000.	0.266E-05	0.111E-05	0.264E-05	0.106E-05	0.266E-05	0.113E-05
	20000.	0.271E-05	0.125E-05	0.269E-05	0.120E-05	0.272E-05	0.126E-05
C= 0.53E+12	30000.	0.275E-05	0.134E-05	0.272E-05	0.128E-05	0.275E-05	0.135E-05
	50000.	0.280E-05	0.145E-05	0.277E-05	0.139E-05	0.281E-05	0.147E-05
	2500.	0.473E-05	0.775E-06	0.473E-05	0.742E-06	0.474E-05	0.785E-06
4S - 4P	5000.	0.474E-05	0.870E-06	0.474E-05	0.833E-06	0.474E-05	0.881E-06
17112.5 Å	10000.	0.475E-05	0.977E-06	0.475E-05	0.935E-06	0.475E-05	0.989E-06
	20000.	0.476E-05	0.110E-05	0.476E-05	0.105E-05	0.476E-05	0.111E-05
C= 0.86E+15	30000.	0.477E-05	0.117E-05	0.477E-05	0.112E-05	0.477E-05	0.119E-05
	50000.	0.479E-05	0.128E-05	0.478E-05	0.122E-05	0.479E-05	0.129E-05
	2500.	0.429E-05	0.104E-05	0.428E-05	0.997E-06	0.429E-05	0.105E-05
4S - 5P	5000.	0.431E-05	0.117E-05	0.430E-05	0.112E-05	0.431E-05	0.118E-05
8925.8 Å	10000.	0.433E-05	0.131E-05	0.432E-05	0.126E-05	0.434E-05	0.133E-05
	20000.	0.437E-05	0.147E-05	0.435E-05	0.141E-05	0.437E-05	0.149E-05
C= 0.12E+15	30000.	0.439E-05	0.158E-05	0.438E-05	0.151E-05	0.440E-05	0.160E-05
	50000.	0.443E-05	0.172E-05	0.441E-05	0.164E-05	0.444E-05	0.174E-05
	2500.	0.720E-05	0.198E-05	0.719E-05	0.190E-05	0.720E-05	0.201E-05
4S - 6P	5000.	0.724E-05	0.223E-05	0.723E-05	0.213E-05	0.725E-05	0.225E-05
7292.9 Å	10000.	0.731E-05	0.250E-05	0.728E-05	0.239E-05	0.731E-05	0.253E-05
	20000.	0.739E-05	0.280E-05	0.735E-05	0.268E-05	0.740E-05	0.284E-05
C= 0.42E+14	30000.	0.745E-05	0.300E-05	0.741E-05	0.287E-05	0.746E-05	0.304E-05
	50000.	0.754E-05	0.327E-05	0.749E-05	0.313E-05	0.756E-05	0.331E-05
	2500.	0.126E-04	0.378E-05	0.126E-04	0.362E-05	0.126E-04	0.383E-05
4S - 7P	5000.	0.127E-04	0.425E-05	0.127E-04	0.407E-05	0.127E-04	0.430E-05
6632.5 Å	10000.	0.128E-04	0.477E-05	0.128E-04	0.457E-05	0.129E-04	0.483E-05
	20000.	0.130E-04	0.536E-05	0.129E-04	0.513E-05	0.130E-04	0.542E-05
C= 0.20E+14	30000.	0.132E-04	0.573E-05	0.131E-04	0.548E-05	0.132E-04	0.580E-05
	50000.	0.134E-04	0.624E-05	0.132E-04	0.597E-05	0.134E-04	0.632E-05

Perturber density= 1 x 10^{+11} cm^{-3}

		Perturbers					
		Ionized silicon		Ionized iron		Ionized magnesium	
Transition	T(K)	Width (Å)	Shift (Å)	Width (Å)	Shift (Å)	Width (Å)	Shift (Å)
	2500.	0.213E-04	0.685E-05	0.212E-04	0.656E-05	0.213E-04	0.694E-05
4S - 8P	5000.	0.215E-04	0.770E-05	0.214E-04	0.737E-05	0.215E-04	0.780E-05
6289.3 Å	10000.	0.218E-04	0.865E-05	0.217E-04	0.828E-05	0.218E-04	0.876E-05
	20000.	0.222E-04	0.971E-05	0.220E-04	0.929E-05	0.222E-04	0.983E-05
C= 0.11E+14	30000.	0.224E-04	0.104E-04	0.223E-04	0.994E-05	0.225E-04	0.105E-04
	50000.	0.228E-04	0.113E-04	0.226E-04	0.108E-04	0.229E-04	0.115E-04
	2500.	0.344E-04	0.117E-04	0.343E-04	0.112E-04	0.345E-04	0.118E-04
4S - 9P	5000.	0.348E-04	0.132E-04	0.347E-04	0.126E-04	0.349E-04	0.133E-04
6085.1 Å	10000.	0.353E-04	0.148E-04	0.351E-04	0.142E-04	0.354E-04	0.150E-04
	20000.	0.360E-04	0.166E-04	0.358E-04	0.159E-04	0.361E-04	0.168E-04
C= 0.71E+13	30000.	0.365E-04	0.178E-04	0.362E-04	0.170E-04	0.366E-04	0.180E-04
	50000.	0.373E-04	0.193E-04	0.369E-04	0.185E-04	0.374E-04	0.196E-04
	2500.	0.115E-03	0.133E-04	0.115E-03	0.128E-04	0.115E-03	0.135E-04
5S - 5P	5000.	0.115E-03	0.150E-04	0.115E-03	0.143E-04	0.115E-03	0.151E-04
46508.0 Å	10000.	0.115E-03	0.168E-04	0.115E-03	0.161E-04	0.115E-03	0.170E-04
	20000.	0.116E-03	0.189E-04	0.115E-03	0.180E-04	0.116E-03	0.191E-04
C= 0.32E+16	30000.	0.116E-03	0.202E-04	0.116E-03	0.193E-04	0.116E-03	0.204E-04
	50000.	0.116E-03	0.220E-04	0.116E-03	0.210E-04	0.116E-03	0.222E-04
	2500.	0.621E-04	0.155E-04	0.620E-04	0.149E-04	0.621E-04	0.157E-04
5S - 6P	5000.	0.624E-04	0.174E-04	0.623E-04	0.167E-04	0.625E-04	0.176E-04
21465.6 Å	10000.	0.628E-04	0.196E-04	0.626E-04	0.187E-04	0.629E-04	0.198E-04
	20000.	0.634E-04	0.220E-04	0.631E-04	0.210E-04	0.634E-04	0.222E-04
C= 0.37E+15	30000.	0.638E-04	0.235E-04	0.635E-04	0.225E-04	0.639E-04	0.238E-04
	50000.	0.644E-04	0.256E-04	0.641E-04	0.245E-04	0.645E-04	0.259E-04
	2500.	0.788E-04	0.231E-04	0.786E-04	0.221E-04	0.789E-04	0.234E-04
5S - 7P	5000.	0.794E-04	0.259E-04	0.791E-04	0.248E-04	0.795E-04	0.262E-04
16600.7 Å	10000.	0.802E-04	0.291E-04	0.798E-04	0.278E-04	0.803E-04	0.295E-04
	20000.	0.813E-04	0.327E-04	0.808E-04	0.312E-04	0.814E-04	0.331E-04
C= 0.13E+15	30000.	0.820E-04	0.349E-04	0.815E-04	0.334E-04	0.822E-04	0.354E-04
	50000.	0.832E-04	0.380E-04	0.826E-04	0.364E-04	0.834E-04	0.385E-04
	2500.	0.115E-03	0.366E-04	0.114E-03	0.350E-04	0.115E-03	0.371E-04
5S - 8P	5000.	0.116E-03	0.412E-04	0.115E-03	0.394E-04	0.116E-03	0.417E-04
14605.5 Å	10000.	0.117E-03	0.462E-04	0.117E-03	0.442E-04	0.118E-03	0.468E-04
	20000.	0.119E-03	0.519E-04	0.119E-03	0.497E-04	0.120E-03	0.525E-04
C= 0.61E+14	30000.	0.121E-03	0.555E-04	0.120E-03	0.531E-04	0.121E-03	0.562E-04
	50000.	0.123E-03	0.604E-04	0.122E-03	0.578E-04	0.123E-03	0.612E-04

STARK BROADENING PARAMETER TABLES FOR MG I LINES

Perturber density= 1 x 10^{+11} cm^{-3}

		Perturbers					
		Ionized silicon		Ionized iron		Ionized magnesium	
Transition	T(K)	Width (Å)	Shift (Å)	Width (Å)	Shift (Å)	Width (Å)	Shift (Å)
	2500.	0.171E-03	0.578E-04	0.170E-03	0.553E-04	0.171E-03	0.585E-04
5S - 9P	5000.	0.173E-03	0.650E-04	0.172E-03	0.622E-04	0.173E-03	0.658E-04
13549.7 Å	10000.	0.175E-03	0.731E-04	0.174E-03	0.699E-04	0.175E-03	0.740E-04
	20000.	0.179E-03	0.820E-04	0.177E-03	0.785E-04	0.179E-03	0.830E-04
C= 0.35E+14	30000.	0.181E-03	0.878E-04	0.179E-03	0.840E-04	0.182E-03	0.889E-04
	50000.	0.185E-03	0.956E-04	0.183E-03	0.914E-04	0.185E-03	0.967E-04
	2500.	0.126E-02	0.131E-03	0.126E-02	0.126E-03	0.126E-02	0.133E-03
6S - 6P	5000.	0.126E-02	0.148E-03	0.126E-02	0.141E-03	0.126E-02	0.149E-03
97264.9 Å	10000.	0.126E-02	0.166E-03	0.126E-02	0.158E-03	0.126E-02	0.168E-03
	20000.	0.126E-02	0.186E-03	0.126E-02	0.178E-03	0.126E-02	0.188E-03
C= 0.75E+16	30000.	0.126E-02	0.199E-03	0.126E-02	0.190E-03	0.126E-02	0.201E-03
	50000.	0.127E-02	0.217E-03	0.126E-02	0.207E-03	0.127E-02	0.219E-03
	2500.	0.496E-03	0.127E-03	0.495E-03	0.122E-03	0.496E-03	0.129E-03
6S - 7P	5000.	0.499E-03	0.143E-03	0.498E-03	0.137E-03	0.499E-03	0.145E-03
41782.3 Å	10000.	0.502E-03	0.160E-03	0.501E-03	0.154E-03	0.502E-03	0.162E-03
	20000.	0.507E-03	0.180E-03	0.505E-03	0.172E-03	0.507E-03	0.182E-03
C= 0.80E+15	30000.	0.510E-03	0.193E-03	0.508E-03	0.184E-03	0.511E-03	0.195E-03
	50000.	0.516E-03	0.210E-03	0.513E-03	0.201E-03	0.517E-03	0.212E-03
	2500.	0.519E-03	0.159E-03	0.517E-03	0.152E-03	0.519E-03	0.161E-03
6S - 8P	5000.	0.523E-03	0.179E-03	0.521E-03	0.171E-03	0.524E-03	0.181E-03
31092.2 Å	10000.	0.529E-03	0.200E-03	0.527E-03	0.192E-03	0.530E-03	0.203E-03
	20000.	0.537E-03	0.225E-03	0.534E-03	0.215E-03	0.538E-03	0.228E-03
C= 0.28E+15	30000.	0.543E-03	0.241E-03	0.539E-03	0.230E-03	0.544E-03	0.244E-03
	50000.	0.552E-03	0.262E-03	0.547E-03	0.251E-03	0.553E-03	0.265E-03
	2500.	0.660E-03	0.220E-03	0.658E-03	0.211E-03	0.661E-03	0.223E-03
6S - 9P	5000.	0.667E-03	0.248E-03	0.664E-03	0.237E-03	0.668E-03	0.251E-03
26668.4 Å	10000.	0.677E-03	0.278E-03	0.673E-03	0.266E-03	0.678E-03	0.282E-03
	20000.	0.689E-03	0.312E-03	0.684E-03	0.299E-03	0.691E-03	0.316E-03
C= 0.14E+15	30000.	0.699E-03	0.334E-03	0.693E-03	0.320E-03	0.700E-03	0.338E-03
	50000.	0.712E-03	0.364E-03	0.705E-03	0.348E-03	0.715E-03	0.368E-03
	2500.	0.862E-02	0.893E-03	0.862E-02	0.854E-03	0.862E-02	0.904E-03
7S - 7P	5000.	0.862E-02	0.100E-02	0.862E-02	0.959E-03	0.862E-02	0.101E-02
175201.9 Å	10000.	0.862E-02	0.112E-02	0.862E-02	0.108E-02	0.863E-02	0.114E-02
	20000.	0.863E-02	0.126E-02	0.863E-02	0.121E-02	0.863E-02	0.128E-02
C= 0.14E+17	30000.	0.864E-02	0.135E-02	0.863E-02	0.129E-02	0.864E-02	0.137E-02
	50000.	0.864E-02	0.147E-02	0.864E-02	0.141E-02	0.864E-02	0.149E-02

Perturber density= 1 x 10^{+11} cm^{-3}

Transition	T(K)	Perturbers: Ionized silicon Width (Å)	Ionized silicon Shift (Å)	Ionized iron Width (Å)	Ionized iron Shift (Å)	Ionized magnesium Width (Å)	Ionized magnesium Shift (Å)
	2500.	0.274E-02	0.716E-03	0.274E-02	0.685E-03	0.274E-02	0.725E-03
7S - 8P	5000.	0.276E-02	0.805E-03	0.275E-02	0.771E-03	0.276E-02	0.815E-03
71754.0 Å	10000.	0.278E-02	0.904E-03	0.277E-02	0.865E-03	0.278E-02	0.915E-03
	20000.	0.280E-02	0.101E-02	0.279E-02	0.971E-03	0.281E-02	0.103E-02
C= 0.15E+16	30000.	0.282E-02	0.109E-02	0.281E-02	0.104E-02	0.283E-02	0.110E-02
	50000.	0.285E-02	0.118E-02	0.284E-02	0.113E-02	0.286E-02	0.120E-02
	2500.	0.249E-02	0.785E-03	0.248E-02	0.751E-03	0.249E-02	0.795E-03
7S - 9P	5000.	0.251E-02	0.883E-03	0.250E-02	0.845E-03	0.251E-02	0.894E-03
51889.6 Å	10000.	0.254E-02	0.992E-03	0.253E-02	0.950E-03	0.255E-02	0.100E-02
	20000.	0.258E-02	0.111E-02	0.257E-02	0.107E-02	0.259E-02	0.113E-02
C= 0.51E+15	30000.	0.261E-02	0.119E-02	0.259E-02	0.114E-02	0.262E-02	0.121E-02
	50000.	0.266E-02	0.130E-02	0.264E-02	0.124E-02	0.267E-02	0.131E-02
	2500.	0.430E-01	0.462E-02	0.430E-01	0.442E-02	0.430E-01	0.467E-02
8S - 8P	5000.	0.430E-01	0.518E-02	0.430E-01	0.496E-02	0.430E-01	0.525E-02
286049.4 Å	10000.	0.430E-01	0.582E-02	0.430E-01	0.557E-02	0.430E-01	0.589E-02
	20000.	0.431E-01	0.653E-02	0.431E-01	0.625E-02	0.431E-01	0.661E-02
C= 0.23E+17	30000.	0.431E-01	0.699E-02	0.431E-01	0.669E-02	0.431E-01	0.707E-02
	50000.	0.431E-01	0.761E-02	0.431E-01	0.728E-02	0.431E-01	0.770E-02
	2500.	0.117E-01	0.310E-02	0.117E-01	0.297E-02	0.117E-01	0.314E-02
8S - 9P	5000.	0.118E-01	0.349E-02	0.118E-01	0.334E-02	0.118E-01	0.353E-02
113236.2 Å	10000.	0.119E-01	0.392E-02	0.119E-01	0.375E-02	0.119E-01	0.397E-02
	20000.	0.120E-01	0.440E-02	0.120E-01	0.421E-02	0.120E-01	0.446E-02
C= 0.24E+16	30000.	0.121E-01	0.471E-02	0.120E-01	0.451E-02	0.121E-01	0.477E-02
	50000.	0.122E-01	0.513E-02	0.122E-01	0.491E-02	0.123E-01	0.519E-02
	2500.	0.171	0.190E-01	0.171	0.182E-01	0.171	0.193E-01
9S - 9P	5000.	0.172	0.214E-01	0.171	0.205E-01	0.172	0.217E-01
435691.9 Å	10000.	0.172	0.240E-01	0.172	0.230E-01	0.172	0.243E-01
	20000.	0.172	0.270E-01	0.172	0.258E-01	0.172	0.273E-01
C= 0.36E+17	30000.	0.172	0.288E-01	0.172	0.276E-01	0.172	0.292E-01
	50000.	0.172	0.314E-01	0.172	0.301E-01	0.172	0.318E-01
	2500.	0.487E-06	0.287E-06	0.480E-06	0.274E-06	0.489E-06	0.290E-06
3P - 4S	5000.	0.509E-06	0.322E-06	0.500E-06	0.308E-06	0.512E-06	0.326E-06
11832.0 Å	10000.	0.536E-06	0.361E-06	0.525E-06	0.346E-06	0.539E-06	0.366E-06
	20000.	0.569E-06	0.406E-06	0.556E-06	0.388E-06	0.573E-06	0.411E-06
C= 0.82E+15	30000.	0.591E-06	0.434E-06	0.577E-06	0.415E-06	0.596E-06	0.439E-06
	50000.	0.623E-06	0.472E-06	0.606E-06	0.452E-06	0.628E-06	0.478E-06

STARK BROADENING PARAMETER TABLES FOR MG I LINES

Perturber density= 1 x 10^{+11} cm^{-3}

		Perturbers					
		Ionized silicon		Ionized iron		Ionized magnesium	
Transition	T(K)	Width (Å)	Shift (Å)	Width (Å)	Shift (Å)	Width (Å)	Shift (Å)
	2500.	0.379E-06	0.349E-06	0.363E-06	0.334E-06	0.383E-06	0.353E-06
3P - 5S	5000.	0.423E-06	0.391E-06	0.405E-06	0.374E-06	0.428E-06	0.396E-06
5712.7 Å	10000.	0.472E-06	0.439E-06	0.453E-06	0.420E-06	0.478E-06	0.445E-06
	20000.	0.528E-06	0.493E-06	0.506E-06	0.472E-06	0.535E-06	0.499E-06
C= 0.70E+14	30000.	0.565E-06	0.527E-06	0.541E-06	0.505E-06	0.571E-06	0.534E-06
	50000.	0.614E-06	0.574E-06	0.588E-06	0.550E-06	0.621E-06	0.581E-06
	2500.	0.754E-06	0.710E-06	0.722E-06	0.680E-06	0.763E-06	0.719E-06
3P - 6S	5000.	0.846E-06	0.797E-06	0.810E-06	0.763E-06	0.856E-06	0.807E-06
4731.4 Å	10000.	0.949E-06	0.895E-06	0.908E-06	0.857E-06	0.961E-06	0.906E-06
	20000.	0.106E-05	0.100E-05	0.102E-05	0.962E-06	0.108E-05	0.102E-05
C= 0.23E+14	30000.	0.114E-05	0.107E-05	0.109E-05	0.103E-05	0.115E-05	0.109E-05
	50000.	0.124E-05	0.117E-05	0.119E-05	0.112E-05	0.126E-05	0.119E-05
	2500.	0.150E-05	0.142E-05	0.144E-05	0.135E-05	0.152E-05	0.143E-05
3P - 7S	5000.	0.168E-05	0.159E-05	0.161E-05	0.152E-05	0.170E-05	0.161E-05
4355.8 Å	10000.	0.189E-05	0.178E-05	0.181E-05	0.171E-05	0.191E-05	0.181E-05
	20000.	0.212E-05	0.200E-05	0.203E-05	0.192E-05	0.215E-05	0.203E-05
C= 0.11E+14	30000.	0.227E-05	0.214E-05	0.217E-05	0.205E-05	0.230E-05	0.217E-05
	50000.	0.247E-05	0.233E-05	0.236E-05	0.223E-05	0.250E-05	0.236E-05
	2500.	0.279E-05	0.263E-05	0.267E-05	0.251E-05	0.282E-05	0.266E-05
3P - 8S	5000.	0.313E-05	0.295E-05	0.299E-05	0.283E-05	0.317E-05	0.299E-05
4166.3 Å	10000.	0.351E-05	0.332E-05	0.336E-05	0.317E-05	0.355E-05	0.336E-05
	20000.	0.394E-05	0.372E-05	0.377E-05	0.356E-05	0.399E-05	0.377E-05
C= 0.61E+13	30000.	0.421E-05	0.398E-05	0.403E-05	0.381E-05	0.427E-05	0.403E-05
	50000.	0.459E-05	0.434E-05	0.439E-05	0.415E-05	0.465E-05	0.439E-05
	2500.	0.485E-05	0.456E-05	0.464E-05	0.437E-05	0.491E-05	0.462E-05
3P - 9S	5000.	0.544E-05	0.513E-05	0.520E-05	0.491E-05	0.551E-05	0.520E-05
4055.8 Å	10000.	0.610E-05	0.577E-05	0.584E-05	0.552E-05	0.618E-05	0.584E-05
	20000.	0.685E-05	0.647E-05	0.656E-05	0.620E-05	0.694E-05	0.656E-05
C= 0.38E+13	30000.	0.733E-05	0.693E-05	0.702E-05	0.663E-05	0.742E-05	0.701E-05
	50000.	0.798E-05	0.754E-05	0.764E-05	0.722E-05	0.808E-05	0.764E-05
	2500.	0.797E-05	0.750E-05	0.763E-05	0.717E-05	0.807E-05	0.759E-05
3P -10S	5000.	0.895E-05	0.844E-05	0.856E-05	0.807E-05	0.906E-05	0.854E-05
3985.4 Å	10000.	0.100E-04	0.948E-05	0.961E-05	0.908E-05	0.102E-04	0.960E-05
	20000.	0.113E-04	0.107E-04	0.108E-04	0.102E-04	0.114E-04	0.108E-04
C= 0.25E+13	30000.	0.121E-04	0.114E-04	0.115E-04	0.109E-04	0.122E-04	0.115E-04
	50000.	0.131E-04	0.124E-04	0.126E-04	0.119E-04	0.133E-04	0.126E-04

Perturber density= 1 x 10^{+11} cm^{-3}

		Perturbers					
		Ionized silicon		Ionized iron		Ionized magnesium	
Transition	T(K)	Width (Å)	Shift (Å)	Width (Å)	Shift (Å)	Width (Å)	Shift (Å)
	2500.	0.174E-04	0.888E-05	0.172E-04	0.850E-05	0.174E-04	0.899E-05
4P - 5S	5000.	0.179E-04	0.997E-05	0.177E-04	0.954E-05	0.180E-04	0.101E-04
31155.6 Å	10000.	0.186E-04	0.112E-04	0.184E-04	0.107E-04	0.187E-04	0.113E-04
	20000.	0.195E-04	0.126E-04	0.192E-04	0.120E-04	0.196E-04	0.127E-04
C= 0.21E+16	30000.	0.201E-04	0.134E-04	0.197E-04	0.129E-04	0.203E-04	0.136E-04
	50000.	0.210E-04	0.146E-04	0.205E-04	0.140E-04	0.211E-04	0.148E-04
	2500.	0.762E-05	0.660E-05	0.735E-05	0.631E-05	0.770E-05	0.668E-05
4P - 6S	5000.	0.841E-05	0.741E-05	0.810E-05	0.709E-05	0.850E-05	0.750E-05
14619.5 Å	10000.	0.931E-05	0.831E-05	0.896E-05	0.796E-05	0.942E-05	0.842E-05
	20000.	0.103E-04	0.933E-05	0.993E-05	0.893E-05	0.105E-04	0.945E-05
C= 0.22E+15	30000.	0.110E-04	0.998E-05	0.106E-04	0.956E-05	0.111E-04	0.101E-04
	50000.	0.119E-04	0.109E-04	0.114E-04	0.104E-04	0.120E-04	0.110E-04
	2500.	0.106E-04	0.987E-05	0.102E-04	0.944E-05	0.107E-04	0.999E-05
4P - 7S	5000.	0.119E-04	0.111E-04	0.114E-04	0.106E-04	0.120E-04	0.112E-04
11543.6 Å	10000.	0.133E-04	0.124E-04	0.127E-04	0.119E-04	0.135E-04	0.126E-04
	20000.	0.149E-04	0.140E-04	0.143E-04	0.134E-04	0.151E-04	0.141E-04
C= 0.76E+14	30000.	0.159E-04	0.149E-04	0.152E-04	0.143E-04	0.161E-04	0.151E-04
	50000.	0.173E-04	0.163E-04	0.166E-04	0.156E-04	0.175E-04	0.165E-04
	2500.	0.170E-04	0.160E-04	0.163E-04	0.153E-04	0.173E-04	0.162E-04
4P - 8S	5000.	0.191E-04	0.180E-04	0.183E-04	0.172E-04	0.194E-04	0.182E-04
10302.0 Å	10000.	0.214E-04	0.202E-04	0.205E-04	0.193E-04	0.217E-04	0.205E-04
	20000.	0.241E-04	0.227E-04	0.230E-04	0.217E-04	0.244E-04	0.230E-04
C= 0.37E+14	30000.	0.257E-04	0.243E-04	0.246E-04	0.232E-04	0.261E-04	0.246E-04
	50000.	0.280E-04	0.264E-04	0.268E-04	0.253E-04	0.284E-04	0.268E-04
	2500.	0.274E-04	0.258E-04	0.263E-04	0.247E-04	0.278E-04	0.261E-04
4P - 9S	5000.	0.308E-04	0.290E-04	0.295E-04	0.278E-04	0.312E-04	0.294E-04
9652.1 Å	10000.	0.346E-04	0.326E-04	0.331E-04	0.312E-04	0.350E-04	0.330E-04
	20000.	0.388E-04	0.366E-04	0.371E-04	0.351E-04	0.393E-04	0.371E-04
C= 0.21E+14	30000.	0.415E-04	0.392E-04	0.397E-04	0.375E-04	0.420E-04	0.397E-04
	50000.	0.452E-04	0.427E-04	0.432E-04	0.408E-04	0.457E-04	0.432E-04
	2500.	0.431E-04	0.405E-04	0.412E-04	0.387E-04	0.436E-04	0.410E-04
4P -10S	5000.	0.483E-04	0.455E-04	0.462E-04	0.436E-04	0.489E-04	0.461E-04
9262.2 Å	10000.	0.542E-04	0.512E-04	0.519E-04	0.490E-04	0.549E-04	0.518E-04
	20000.	0.609E-04	0.575E-04	0.583E-04	0.550E-04	0.616E-04	0.582E-04
C= 0.14E+14	30000.	0.651E-04	0.615E-04	0.623E-04	0.589E-04	0.659E-04	0.623E-04
	50000.	0.709E-04	0.670E-04	0.679E-04	0.641E-04	0.718E-04	0.678E-04

STARK BROADENING PARAMETER TABLES FOR MG I LINES

Perturber density= 1 x 10^{+11} cm^{-3}

		Perturbers					
		Ionized silicon		Ionized iron		Ionized magnesium	
Transition	T(K)	Width (Å)	Shift (Å)	Width (Å)	Shift (Å)	Width (Å)	Shift (Å)
	2500.	0.260E-03	0.116E-03	0.258E-03	0.111E-03	0.261E-03	0.118E-03
5P - 6S	5000.	0.266E-03	0.130E-03	0.264E-03	0.125E-03	0.267E-03	0.132E-03
67552.5 Å	10000.	0.274E-03	0.146E-03	0.271E-03	0.140E-03	0.275E-03	0.148E-03
	20000.	0.284E-03	0.164E-03	0.280E-03	0.157E-03	0.285E-03	0.166E-03
C= 0.47E+16	30000.	0.291E-03	0.176E-03	0.286E-03	0.168E-03	0.292E-03	0.178E-03
	50000.	0.301E-03	0.192E-03	0.296E-03	0.183E-03	0.303E-03	0.194E-03
	2500.	0.813E-04	0.648E-04	0.789E-04	0.620E-04	0.821E-04	0.656E-04
5P - 7S	5000.	0.885E-04	0.728E-04	0.856E-04	0.696E-04	0.893E-04	0.737E-04
30276.2 Å	10000.	0.967E-04	0.817E-04	0.935E-04	0.782E-04	0.977E-04	0.827E-04
	20000.	0.106E-03	0.917E-04	0.102E-03	0.877E-04	0.107E-03	0.928E-04
C= 0.52E+15	30000.	0.112E-03	0.981E-04	0.108E-03	0.939E-04	0.114E-03	0.993E-04
	50000.	0.121E-03	0.107E-03	0.117E-03	0.102E-03	0.122E-03	0.108E-03
	2500.	0.870E-04	0.786E-04	0.836E-04	0.752E-04	0.880E-04	0.796E-04
5P - 8S	5000.	0.968E-04	0.884E-04	0.930E-04	0.846E-04	0.980E-04	0.895E-04
23004.5 Å	10000.	0.108E-03	0.993E-04	0.104E-03	0.950E-04	0.109E-03	0.101E-03
	20000.	0.120E-03	0.111E-03	0.116E-03	0.107E-03	0.122E-03	0.113E-03
C= 0.19E+15	30000.	0.129E-03	0.119E-03	0.123E-03	0.114E-03	0.130E-03	0.121E-03
	50000.	0.140E-03	0.130E-03	0.134E-03	0.124E-03	0.141E-03	0.131E-03
	2500.	0.118E-03	0.110E-03	0.113E-03	0.105E-03	0.120E-03	0.112E-03
5P - 9S	5000.	0.133E-03	0.124E-03	0.127E-03	0.119E-03	0.134E-03	0.125E-03
19997.7 Å	10000.	0.149E-03	0.139E-03	0.142E-03	0.133E-03	0.150E-03	0.141E-03
	20000.	0.166E-03	0.156E-03	0.159E-03	0.150E-03	0.168E-03	0.158E-03
C= 0.92E+14	30000.	0.178E-03	0.167E-03	0.170E-03	0.160E-03	0.180E-03	0.169E-03
	50000.	0.194E-03	0.182E-03	0.185E-03	0.174E-03	0.196E-03	0.184E-03
	2500.	0.170E-03	0.159E-03	0.163E-03	0.152E-03	0.172E-03	0.161E-03
5P -10S	5000.	0.191E-03	0.179E-03	0.182E-03	0.171E-03	0.193E-03	0.181E-03
18393.5 Å	10000.	0.214E-03	0.201E-03	0.205E-03	0.193E-03	0.216E-03	0.204E-03
	20000.	0.240E-03	0.226E-03	0.230E-03	0.216E-03	0.243E-03	0.229E-03
C= 0.54E+14	30000.	0.257E-03	0.242E-03	0.246E-03	0.232E-03	0.260E-03	0.245E-03
	50000.	0.279E-03	0.263E-03	0.267E-03	0.252E-03	0.283E-03	0.267E-03
	2500.	0.222E-02	0.880E-03	0.220E-02	0.842E-03	0.222E-02	0.891E-03
6P - 7S	5000.	0.225E-02	0.988E-03	0.224E-02	0.946E-03	0.226E-02	0.100E-02
125870.1 Å	10000.	0.230E-02	0.111E-02	0.228E-02	0.106E-02	0.231E-02	0.112E-02
	20000.	0.237E-02	0.125E-02	0.234E-02	0.119E-02	0.238E-02	0.126E-02
C= 0.90E+16	30000.	0.241E-02	0.133E-02	0.238E-02	0.128E-02	0.242E-02	0.135E-02
	50000.	0.248E-02	0.145E-02	0.244E-02	0.139E-02	0.249E-02	0.147E-02

Perturber density= 1 x 10^{+11} cm^{-3}

		Perturbers					
		Ionized silicon		Ionized iron		Ionized magnesium	
Transition	T(K)	Width (Å)	Shift (Å)	Width (Å)	Shift (Å)	Width (Å)	Shift (Å)
	2500.	0.562E-03	0.410E-03	0.548E-03	0.392E-03	0.566E-03	0.415E-03
6P - 8S	5000.	0.603E-03	0.461E-03	0.587E-03	0.441E-03	0.608E-03	0.467E-03
54391.3 Å	10000.	0.652E-03	0.518E-03	0.632E-03	0.495E-03	0.657E-03	0.524E-03
	20000.	0.708E-03	0.581E-03	0.686E-03	0.556E-03	0.715E-03	0.588E-03
C= 0.10E+16	30000.	0.746E-03	0.622E-03	0.721E-03	0.595E-03	0.753E-03	0.629E-03
	50000.	0.797E-03	0.677E-03	0.770E-03	0.648E-03	0.805E-03	0.685E-03
	2500.	0.496E-03	0.432E-03	0.478E-03	0.413E-03	0.502E-03	0.437E-03
6P - 9S	5000.	0.549E-03	0.486E-03	0.528E-03	0.465E-03	0.555E-03	0.492E-03
40126.5 Å	10000.	0.608E-03	0.546E-03	0.584E-03	0.522E-03	0.615E-03	0.553E-03
	20000.	0.675E-03	0.613E-03	0.649E-03	0.586E-03	0.683E-03	0.620E-03
C= 0.37E+15	30000.	0.719E-03	0.655E-03	0.690E-03	0.627E-03	0.727E-03	0.664E-03
	50000.	0.779E-03	0.714E-03	0.747E-03	0.683E-03	0.788E-03	0.723E-03
	2500.	0.593E-03	0.542E-03	0.569E-03	0.519E-03	0.600E-03	0.549E-03
6P -10S	5000.	0.662E-03	0.610E-03	0.634E-03	0.584E-03	0.669E-03	0.618E-03
34150.2 Å	10000.	0.739E-03	0.686E-03	0.709E-03	0.656E-03	0.748E-03	0.695E-03
	20000.	0.827E-03	0.770E-03	0.792E-03	0.737E-03	0.837E-03	0.780E-03
C= 0.19E+15	30000.	0.883E-03	0.824E-03	0.846E-03	0.789E-03	0.894E-03	0.835E-03
	50000.	0.960E-03	0.898E-03	0.919E-03	0.859E-03	0.972E-03	0.909E-03
	2500.	0.130E-01	0.465E-02	0.129E-01	0.445E-02	0.130E-01	0.471E-02
7P - 8S	5000.	0.131E-01	0.522E-02	0.131E-01	0.500E-02	0.132E-01	0.529E-02
211286.9 Å	10000.	0.134E-01	0.586E-02	0.133E-01	0.561E-02	0.134E-01	0.594E-02
	20000.	0.137E-01	0.658E-02	0.135E-01	0.630E-02	0.137E-01	0.667E-02
C= 0.16E+17	30000.	0.139E-01	0.704E-02	0.137E-01	0.674E-02	0.139E-01	0.713E-02
	50000.	0.142E-01	0.767E-02	0.140E-01	0.734E-02	0.142E-01	0.777E-02
	2500.	0.287E-02	0.193E-02	0.281E-02	0.184E-02	0.289E-02	0.195E-02
7P - 9S	5000.	0.304E-02	0.217E-02	0.297E-02	0.207E-02	0.307E-02	0.219E-02
88740.6 Å	10000.	0.326E-02	0.243E-02	0.317E-02	0.233E-02	0.328E-02	0.246E-02
	20000.	0.351E-02	0.273E-02	0.341E-02	0.261E-02	0.354E-02	0.277E-02
C= 0.18E+16	30000.	0.367E-02	0.292E-02	0.356E-02	0.280E-02	0.370E-02	0.296E-02
	50000.	0.390E-02	0.318E-02	0.378E-02	0.305E-02	0.394E-02	0.322E-02
	2500.	0.220E-02	0.183E-02	0.213E-02	0.175E-02	0.222E-02	0.185E-02
7P -10S	5000.	0.241E-02	0.206E-02	0.233E-02	0.197E-02	0.244E-02	0.209E-02
63979.5 Å	10000.	0.266E-02	0.232E-02	0.256E-02	0.222E-02	0.268E-02	0.235E-02
	20000.	0.293E-02	0.260E-02	0.282E-02	0.249E-02	0.297E-02	0.263E-02
C= 0.65E+15	30000.	0.312E-02	0.278E-02	0.300E-02	0.266E-02	0.315E-02	0.282E-02
	50000.	0.336E-02	0.303E-02	0.323E-02	0.290E-02	0.340E-02	0.307E-02

STARK BROADENING PARAMETER TABLES FOR MG I LINES

Perturber density= 1 x 10^{+11} cm^{-3}

		Perturbers					
		Ionized silicon		Ionized iron		Ionized magnesium	
Transition	T(K)	Width (Å)	Shift (Å)	Width (Å)	Shift (Å)	Width (Å)	Shift (Å)
	2500.	0.584E-01	0.191E-01	0.582E-01	0.183E-01	0.584E-01	0.193E-01
8P - 9S	5000.	0.590E-01	0.215E-01	0.587E-01	0.205E-01	0.590E-01	0.217E-01
328947.4 Å	10000.	0.598E-01	0.241E-01	0.594E-01	0.231E-01	0.599E-01	0.244E-01
	20000.	0.608E-01	0.271E-01	0.604E-01	0.259E-01	0.610E-01	0.274E-01
C= 0.25E+17	30000.	0.616E-01	0.290E-01	0.611E-01	0.277E-01	0.617E-01	0.293E-01
	50000.	0.627E-01	0.315E-01	0.621E-01	0.302E-01	0.629E-01	0.319E-01
	2500.	0.117E-01	0.729E-02	0.115E-01	0.698E-02	0.118E-01	0.739E-02
8P -10S	5000.	0.123E-01	0.821E-02	0.121E-01	0.785E-02	0.124E-01	0.831E-02
135113.2 Å	10000.	0.131E-01	0.922E-02	0.128E-01	0.883E-02	0.132E-01	0.934E-02
	20000.	0.140E-01	0.104E-01	0.136E-01	0.991E-02	0.141E-01	0.105E-01
C= 0.29E+16	30000.	0.146E-01	0.111E-01	0.142E-01	0.106E-01	0.147E-01	0.112E-01
	50000.	0.154E-01	0.121E-01	0.150E-01	0.115E-01	0.155E-01	0.122E-01
	2500.	0.216	0.653E-01	0.215	0.625E-01	0.216	0.661E-01
9P -10S	5000.	0.218	0.735E-01	0.217	0.703E-01	0.218	0.744E-01
484027.1 Å	10000.	0.220	0.826E-01	0.219	0.790E-01	0.220	0.836E-01
	20000.	0.223	0.927E-01	0.222	0.887E-01	0.224	0.938E-01
C= 0.37E+17	30000.	0.226	0.992E-01	0.224	0.949E-01	0.226	0.100
	50000.	0.229	0.108	0.227	0.103	0.230	0.109
	2500.	0.502E-06	0.107E-06	0.501E-06	0.102E-06	0.502E-06	0.108E-06
3P - 3D	5000.	0.503E-06	0.120E-06	0.503E-06	0.115E-06	0.503E-06	0.122E-06
8809.2 Å	10000.	0.505E-06	0.135E-06	0.504E-06	0.129E-06	0.505E-06	0.137E-06
	20000.	0.508E-06	0.151E-06	0.507E-06	0.145E-06	0.508E-06	0.153E-06
C= 0.23E+15	30000.	0.510E-06	0.162E-06	0.509E-06	0.155E-06	0.511E-06	0.164E-06
	50000.	0.514E-06	0.176E-06	0.512E-06	0.169E-06	0.514E-06	0.179E-06
	2500.	0.806E-06	0.389E-06	0.799E-06	0.373E-06	0.808E-06	0.394E-06
3P - 4D	5000.	0.829E-06	0.437E-06	0.820E-06	0.418E-06	0.832E-06	0.442E-06
5530.0 Å	10000.	0.858E-06	0.490E-06	0.846E-06	0.469E-06	0.861E-06	0.497E-06
	20000.	0.894E-06	0.551E-06	0.879E-06	0.527E-06	0.899E-06	0.557E-06
C= 0.47E+14	30000.	0.919E-06	0.589E-06	0.903E-06	0.564E-06	0.924E-06	0.596E-06
	50000.	0.956E-06	0.641E-06	0.936E-06	0.614E-06	0.961E-06	0.649E-06
	2500.	0.164E-05	0.774E-06	0.162E-05	0.741E-06	0.164E-05	0.784E-06
3P - 5D	5000.	0.168E-05	0.869E-06	0.166E-05	0.832E-06	0.169E-05	0.880E-06
4704.3 Å	10000.	0.174E-05	0.976E-06	0.171E-05	0.934E-06	0.174E-05	0.988E-06
	20000.	0.181E-05	0.110E-05	0.178E-05	0.105E-05	0.182E-05	0.111E-05
C= 0.20E+14	30000.	0.186E-05	0.117E-05	0.182E-05	0.112E-05	0.187E-05	0.119E-05
	50000.	0.193E-05	0.128E-05	0.189E-05	0.122E-05	0.194E-05	0.129E-05

Perturber density= 1 x 10^{+11} cm^{-3}

		Perturbers					
		Ionized silicon		Ionized iron		Ionized magnesium	
Transition	T(K)	Width (Å)	Shift (Å)	Width (Å)	Shift (Å)	Width (Å)	Shift (Å)
	2500.	0.315E-05	0.138E-05	0.313E-05	0.132E-05	0.316E-05	0.140E-05
3P - 6D	5000.	0.322E-05	0.155E-05	0.319E-05	0.149E-05	0.323E-05	0.157E-05
4353.1 Å	10000.	0.331E-05	0.175E-05	0.328E-05	0.167E-05	0.332E-05	0.177E-05
	20000.	0.343E-05	0.196E-05	0.338E-05	0.187E-05	0.344E-05	0.198E-05
C= 0.10E+14	30000.	0.351E-05	0.210E-05	0.346E-05	0.201E-05	0.353E-05	0.212E-05
	50000.	0.363E-05	0.228E-05	0.356E-05	0.218E-05	0.365E-05	0.231E-05
	2500.	0.566E-05	0.226E-05	0.562E-05	0.216E-05	0.566E-05	0.229E-05
3P - 7D	5000.	0.575E-05	0.254E-05	0.571E-05	0.243E-05	0.577E-05	0.257E-05
4168.5 Å	10000.	0.588E-05	0.285E-05	0.583E-05	0.273E-05	0.590E-05	0.288E-05
	20000.	0.605E-05	0.320E-05	0.598E-05	0.306E-05	0.607E-05	0.324E-05
C= 0.62E+13	30000.	0.617E-05	0.342E-05	0.609E-05	0.327E-05	0.619E-05	0.346E-05
	50000.	0.634E-05	0.372E-05	0.625E-05	0.356E-05	0.637E-05	0.377E-05
	2500.	0.952E-05	0.340E-05	0.948E-05	0.325E-05	0.953E-05	0.344E-05
3P - 8D	5000.	0.964E-05	0.382E-05	0.959E-05	0.365E-05	0.965E-05	0.387E-05
4058.7 Å	10000.	0.980E-05	0.429E-05	0.973E-05	0.411E-05	0.982E-05	0.434E-05
	20000.	0.100E-04	0.482E-05	0.993E-05	0.461E-05	0.100E-04	0.488E-05
C= 0.40E+13	30000.	0.102E-04	0.515E-05	0.101E-04	0.493E-05	0.102E-04	0.522E-05
	50000.	0.104E-04	0.561E-05	0.103E-04	0.537E-05	0.104E-04	0.568E-05
	2500.	0.152E-04	0.476E-05	0.151E-04	0.455E-05	0.152E-04	0.482E-05
3P - 9D	5000.	0.153E-04	0.535E-05	0.153E-04	0.512E-05	0.153E-04	0.542E-05
3987.9 Å	10000.	0.155E-04	0.602E-05	0.154E-04	0.576E-05	0.155E-04	0.609E-05
	20000.	0.157E-04	0.675E-05	0.156E-04	0.646E-05	0.158E-04	0.684E-05
C= 0.28E+13	30000.	0.159E-04	0.723E-05	0.158E-04	0.692E-05	0.160E-04	0.732E-05
	50000.	0.162E-04	0.787E-05	0.161E-04	0.753E-05	0.162E-04	0.797E-05
	2500.	0.220E-04	0.790E-05	0.219E-04	0.756E-05	0.220E-04	0.800E-05
4P - 4D	5000.	0.223E-04	0.887E-05	0.222E-04	0.849E-05	0.223E-04	0.898E-05
26398.9 Å	10000.	0.227E-04	0.996E-05	0.225E-04	0.953E-05	0.227E-04	0.101E-04
	20000.	0.232E-04	0.112E-04	0.230E-04	0.107E-04	0.232E-04	0.113E-04
C= 0.11E+16	30000.	0.235E-04	0.120E-04	0.233E-04	0.114E-04	0.236E-04	0.121E-04
	50000.	0.241E-04	0.130E-04	0.238E-04	0.125E-04	0.242E-04	0.132E-04
	2500.	0.159E-04	0.705E-05	0.157E-04	0.675E-05	0.159E-04	0.714E-05
4P - 5D	5000.	0.162E-04	0.791E-05	0.161E-04	0.757E-05	0.163E-04	0.801E-05
14364.2 Å	10000.	0.167E-04	0.888E-05	0.165E-04	0.850E-05	0.167E-04	0.899E-05
	20000.	0.173E-04	0.997E-05	0.170E-04	0.954E-05	0.174E-04	0.101E-04
C= 0.18E+15	30000.	0.177E-04	0.107E-04	0.174E-04	0.102E-04	0.178E-04	0.108E-04
	50000.	0.183E-04	0.116E-04	0.180E-04	0.111E-04	0.184E-04	0.118E-04

STARK BROADENING PARAMETER TABLES FOR MG I LINES

Perturber density= 1 x 10^{+11} cm^{-3}

		Perturbers					
		Ionized silicon		Ionized iron		Ionized magnesium	
Transition	T(K)	Width (Å)	Shift (Å)	Width (Å)	Shift (Å)	Width (Å)	Shift (Å)
	2500.	0.224E-04	0.963E-05	0.223E-04	0.921E-05	0.224E-04	0.975E-05
4P - 6D	5000.	0.229E-04	0.108E-04	0.227E-04	0.103E-04	0.229E-04	0.109E-04
11525.3 Å	10000.	0.235E-04	0.121E-04	0.232E-04	0.116E-04	0.236E-04	0.123E-04
	20000.	0.243E-04	0.136E-04	0.239E-04	0.130E-04	0.244E-04	0.138E-04
C= 0.73E+14	30000.	0.248E-04	0.146E-04	0.244E-04	0.140E-04	0.249E-04	0.148E-04
	50000.	0.256E-04	0.159E-04	0.252E-04	0.152E-04	0.257E-04	0.161E-04
	2500.	0.349E-04	0.138E-04	0.347E-04	0.132E-04	0.349E-04	0.139E-04
4P - 7D	5000.	0.354E-04	0.155E-04	0.352E-04	0.148E-04	0.355E-04	0.157E-04
10315.2 Å	10000.	0.362E-04	0.174E-04	0.359E-04	0.166E-04	0.363E-04	0.176E-04
	20000.	0.372E-04	0.195E-04	0.368E-04	0.187E-04	0.373E-04	0.198E-04
C= 0.38E+14	30000.	0.379E-04	0.209E-04	0.375E-04	0.200E-04	0.381E-04	0.211E-04
	50000.	0.390E-04	0.227E-04	0.384E-04	0.218E-04	0.392E-04	0.230E-04
	2500.	0.542E-04	0.192E-04	0.540E-04	0.184E-04	0.542E-04	0.195E-04
4P - 8D	5000.	0.549E-04	0.216E-04	0.546E-04	0.207E-04	0.550E-04	0.219E-04
9668.0 Å	10000.	0.558E-04	0.243E-04	0.554E-04	0.233E-04	0.559E-04	0.246E-04
	20000.	0.570E-04	0.273E-04	0.565E-04	0.261E-04	0.572E-04	0.276E-04
C= 0.23E+14	30000.	0.579E-04	0.292E-04	0.573E-04	0.279E-04	0.581E-04	0.296E-04
	50000.	0.592E-04	0.318E-04	0.585E-04	0.304E-04	0.594E-04	0.322E-04
	2500.	0.822E-04	0.257E-04	0.820E-04	0.246E-04	0.823E-04	0.261E-04
4P - 9D	5000.	0.830E-04	0.289E-04	0.827E-04	0.277E-04	0.831E-04	0.293E-04
9275.9 Å	10000.	0.840E-04	0.325E-04	0.836E-04	0.311E-04	0.841E-04	0.329E-04
	20000.	0.853E-04	0.365E-04	0.848E-04	0.349E-04	0.855E-04	0.370E-04
C= 0.15E+14	30000.	0.863E-04	0.391E-04	0.857E-04	0.374E-04	0.865E-04	0.396E-04
	50000.	0.878E-04	0.425E-04	0.870E-04	0.407E-04	0.880E-04	0.431E-04
	2500.	0.367E-03	0.113E-03	0.366E-03	0.108E-03	0.368E-03	0.115E-03
5P - 5D	5000.	0.371E-03	0.127E-03	0.369E-03	0.122E-03	0.371E-03	0.129E-03
62426.3 Å	10000.	0.375E-03	0.143E-03	0.373E-03	0.137E-03	0.375E-03	0.145E-03
	20000.	0.381E-03	0.160E-03	0.378E-03	0.153E-03	0.381E-03	0.162E-03
C= 0.35E+16	30000.	0.385E-03	0.171E-03	0.382E-03	0.164E-03	0.386E-03	0.174E-03
	50000.	0.391E-03	0.187E-03	0.388E-03	0.179E-03	0.392E-03	0.189E-03
	2500.	0.163E-03	0.628E-04	0.162E-03	0.601E-04	0.163E-03	0.636E-04
5P - 6D	5000.	0.166E-03	0.705E-04	0.165E-03	0.675E-04	0.166E-03	0.714E-04
30150.2 Å	10000.	0.169E-03	0.792E-04	0.168E-03	0.758E-04	0.169E-03	0.802E-04
	20000.	0.173E-03	0.889E-04	0.172E-03	0.850E-04	0.174E-03	0.900E-04
C= 0.50E+15	30000.	0.177E-03	0.951E-04	0.175E-03	0.910E-04	0.177E-03	0.963E-04
	50000.	0.181E-03	0.104E-03	0.179E-03	0.991E-04	0.182E-03	0.105E-03

Perturber density= 1 x 10^{+11} cm^{-3}

		Perturbers					
		Ionized silicon		Ionized iron		Ionized magnesium	
Transition	T(K)	Width (Å)	Shift (Å)	Width (Å)	Shift (Å)	Width (Å)	Shift (Å)
	2500.	0.179E-03	0.676E-04	0.178E-03	0.647E-04	0.179E-03	0.684E-04
5P - 7D	5000.	0.181E-03	0.759E-04	0.180E-03	0.727E-04	0.182E-03	0.769E-04
23070.4 Å	10000.	0.185E-03	0.853E-04	0.183E-03	0.816E-04	0.185E-03	0.863E-04
	20000.	0.190E-03	0.957E-04	0.188E-03	0.916E-04	0.190E-03	0.969E-04
C= 0.19E+15	30000.	0.193E-03	0.102E-03	0.191E-03	0.980E-04	0.193E-03	0.104E-03
	50000.	0.198E-03	0.111E-03	0.195E-03	0.107E-03	0.199E-03	0.113E-03
	2500.	0.236E-03	0.821E-04	0.235E-03	0.786E-04	0.236E-03	0.831E-04
5P - 8D	5000.	0.239E-03	0.923E-04	0.238E-03	0.883E-04	0.239E-03	0.935E-04
20066.3 Å	10000.	0.243E-03	0.104E-03	0.241E-03	0.992E-04	0.243E-03	0.105E-03
	20000.	0.248E-03	0.116E-03	0.246E-03	0.111E-03	0.248E-03	0.118E-03
C= 0.99E+14	30000.	0.251E-03	0.125E-03	0.249E-03	0.119E-03	0.252E-03	0.126E-03
	50000.	0.257E-03	0.136E-03	0.254E-03	0.130E-03	0.258E-03	0.137E-03
	2500.	0.327E-03	0.101E-03	0.327E-03	0.968E-04	0.328E-03	0.102E-03
5P - 9D	5000.	0.330E-03	0.114E-03	0.329E-03	0.109E-03	0.331E-03	0.115E-03
18447.6 Å	10000.	0.334E-03	0.128E-03	0.333E-03	0.122E-03	0.335E-03	0.130E-03
	20000.	0.339E-03	0.144E-03	0.337E-03	0.137E-03	0.340E-03	0.145E-03
C= 0.59E+14	30000.	0.343E-03	0.154E-03	0.341E-03	0.147E-03	0.344E-03	0.156E-03
	50000.	0.349E-03	0.167E-03	0.346E-03	0.160E-03	0.350E-03	0.169E-03
	2500.	0.340E-02	0.823E-03	0.339E-02	0.787E-03	0.340E-02	0.833E-03
6P - 6D	5000.	0.341E-02	0.924E-03	0.341E-02	0.884E-03	0.341E-02	0.935E-03
123719.5 Å	10000.	0.343E-02	0.104E-02	0.342E-02	0.992E-03	0.343E-02	0.105E-02
	20000.	0.346E-02	0.116E-02	0.345E-02	0.111E-02	0.346E-02	0.118E-02
C= 0.85E+16	30000.	0.348E-02	0.125E-02	0.347E-02	0.119E-02	0.348E-02	0.126E-02
	50000.	0.351E-02	0.136E-02	0.349E-02	0.130E-02	0.352E-02	0.137E-02
	2500.	0.109E-02	0.348E-03	0.109E-02	0.333E-03	0.109E-02	0.352E-03
6P - 7D	5000.	0.110E-02	0.391E-03	0.110E-02	0.374E-03	0.110E-02	0.396E-03
54761.5 Å	10000.	0.112E-02	0.439E-03	0.111E-02	0.420E-03	0.112E-02	0.445E-03
	20000.	0.113E-02	0.493E-03	0.113E-02	0.472E-03	0.114E-02	0.499E-03
C= 0.11E+16	30000.	0.115E-02	0.527E-03	0.114E-02	0.505E-03	0.115E-02	0.534E-03
	50000.	0.117E-02	0.574E-03	0.116E-02	0.550E-03	0.117E-02	0.581E-03
	2500.	0.992E-03	0.319E-03	0.989E-03	0.305E-03	0.993E-03	0.323E-03
6P - 8D	5000.	0.100E-02	0.359E-03	0.998E-03	0.343E-03	0.100E-02	0.363E-03
40403.6 Å	10000.	0.101E-02	0.403E-03	0.101E-02	0.386E-03	0.102E-02	0.408E-03
	20000.	0.103E-02	0.452E-03	0.102E-02	0.433E-03	0.103E-02	0.458E-03
C= 0.40E+15	30000.	0.104E-02	0.484E-03	0.104E-02	0.463E-03	0.105E-02	0.490E-03
	50000.	0.106E-02	0.527E-03	0.105E-02	0.504E-03	0.107E-02	0.533E-03

Perturber density= 1 x 10^{+11} cm^{-3}

Transition	T(K)	Perturbers: Ionized silicon Width (Å)	Ionized silicon Shift (Å)	Ionized iron Width (Å)	Ionized iron Shift (Å)	Ionized magnesium Width (Å)	Ionized magnesium Shift (Å)
	2500.	0.116E-02	0.342E-03	0.115E-02	0.328E-03	0.116E-02	0.347E-03
6P - 9D	5000.	0.116E-02	0.385E-03	0.116E-02	0.369E-03	0.117E-02	0.390E-03
34336.9 Å	10000.	0.118E-02	0.433E-03	0.117E-02	0.414E-03	0.118E-02	0.438E-03
	20000.	0.119E-02	0.486E-03	0.119E-02	0.465E-03	0.119E-02	0.492E-03
C= 0.21E+15	30000.	0.120E-02	0.520E-03	0.120E-02	0.498E-03	0.121E-02	0.526E-03
	50000.	0.122E-02	0.566E-03	0.121E-02	0.542E-03	0.123E-02	0.573E-03
	2500.	0.212E-01	0.365E-02	0.212E-01	0.349E-02	0.212E-01	0.369E-02
7P - 7D	5000.	0.212E-01	0.409E-02	0.212E-01	0.392E-02	0.212E-01	0.415E-02
216985.6 Å	10000.	0.213E-01	0.460E-02	0.212E-01	0.440E-02	0.213E-01	0.465E-02
	20000.	0.213E-01	0.516E-02	0.213E-01	0.494E-02	0.213E-01	0.522E-02
C= 0.17E+17	30000.	0.214E-01	0.552E-02	0.214E-01	0.528E-02	0.214E-01	0.559E-02
	50000.	0.215E-01	0.601E-02	0.214E-01	0.575E-02	0.215E-01	0.608E-02
	2500.	0.543E-02	0.136E-02	0.542E-02	0.130E-02	0.543E-02	0.138E-02
7P - 8D	5000.	0.546E-02	0.153E-02	0.545E-02	0.146E-02	0.546E-02	0.155E-02
90107.1 Å	10000.	0.549E-02	0.171E-02	0.548E-02	0.164E-02	0.550E-02	0.174E-02
	20000.	0.554E-02	0.193E-02	0.552E-02	0.184E-02	0.555E-02	0.195E-02
C= 0.20E+16	30000.	0.558E-02	0.206E-02	0.555E-02	0.197E-02	0.559E-02	0.209E-02
	50000.	0.563E-02	0.224E-02	0.560E-02	0.215E-02	0.564E-02	0.227E-02
	2500.	0.429E-02	0.112E-02	0.428E-02	0.107E-02	0.429E-02	0.113E-02
7P - 9D	5000.	0.431E-02	0.126E-02	0.430E-02	0.120E-02	0.431E-02	0.127E-02
64637.9 Å	10000.	0.434E-02	0.141E-02	0.433E-02	0.135E-02	0.435E-02	0.143E-02
	20000.	0.439E-02	0.159E-02	0.437E-02	0.152E-02	0.439E-02	0.161E-02
C= 0.73E+15	30000.	0.442E-02	0.170E-02	0.440E-02	0.163E-02	0.443E-02	0.172E-02
	50000.	0.447E-02	0.185E-02	0.444E-02	0.177E-02	0.448E-02	0.187E-02
	2500.	0.999E-01	0.941E-02	0.999E-01	0.900E-02	0.999E-01	0.952E-02
8P - 8D	5000.	0.999E-01	0.106E-01	0.999E-01	0.101E-01	0.999E-01	0.107E-01
348541.4 Å	10000.	0.100	0.119E-01	0.100	0.114E-01	0.100	0.120E-01
	20000.	0.100	0.133E-01	0.100	0.127E-01	0.100	0.135E-01
C= 0.30E+17	30000.	0.100	0.142E-01	0.100	0.136E-01	0.100	0.144E-01
	50000.	0.100	0.155E-01	0.100	0.148E-01	0.100	0.157E-01
	2500.	0.218E-01	0.388E-02	0.218E-01	0.371E-02	0.218E-01	0.393E-02
8P - 9D	5000.	0.218E-01	0.436E-02	0.218E-01	0.418E-02	0.218E-01	0.442E-02
138083.4 Å	10000.	0.219E-01	0.490E-02	0.218E-01	0.469E-02	0.219E-01	0.496E-02
	20000.	0.219E-01	0.550E-02	0.219E-01	0.527E-02	0.219E-01	0.557E-02
C= 0.33E+16	30000.	0.220E-01	0.589E-02	0.220E-01	0.563E-02	0.220E-01	0.596E-02
	50000.	0.221E-01	0.641E-02	0.220E-01	0.613E-02	0.221E-01	0.649E-02

Perturber density= 1 x 10^{+11} cm^{-3}

		Perturbers					
		Ionized silicon		Ionized iron		Ionized magnesium	
Transition	T(K)	Width (Å)	Shift (Å)	Width (Å)	Shift (Å)	Width (Å)	Shift (Å)
	2500.	0.383	-0.160E-01	0.383	-0.153E-01	0.383	-0.162E-01
9P - 9D	5000.	0.383	-0.180E-01	0.383	-0.172E-01	0.383	-0.182E-01
524438.9 Å	10000.	0.383	-0.202E-01	0.383	-0.193E-01	0.383	-0.204E-01
	20000.	0.383	-0.227E-01	0.383	-0.217E-01	0.383	-0.229E-01
C= 0.48E+17	30000.	0.383	-0.242E-01	0.383	-0.232E-01	0.383	-0.245E-01
	50000.	0.383	-0.264E-01	0.383	-0.253E-01	0.383	-0.267E-01
	2500.	0.205E-04	0.365E-05	0.205E-04	0.349E-05	0.205E-04	0.369E-05
3D - 4P	5000.	0.206E-04	0.410E-05	0.205E-04	0.392E-05	0.206E-04	0.415E-05
33972.8 Å	10000.	0.206E-04	0.460E-05	0.206E-04	0.440E-05	0.206E-04	0.466E-05
	20000.	0.207E-04	0.516E-05	0.206E-04	0.494E-05	0.207E-04	0.523E-05
C= 0.34E+16	30000.	0.207E-04	0.552E-05	0.207E-04	0.528E-05	0.207E-04	0.559E-05
	50000.	0.208E-04	0.601E-05	0.208E-04	0.575E-05	0.208E-04	0.609E-05
	2500.	0.796E-05	0.193E-05	0.795E-05	0.185E-05	0.796E-05	0.196E-05
3D - 5P	5000.	0.800E-05	0.217E-05	0.798E-05	0.207E-05	0.800E-05	0.219E-05
12043.3 Å	10000.	0.804E-05	0.243E-05	0.802E-05	0.233E-05	0.805E-05	0.246E-05
	20000.	0.811E-05	0.273E-05	0.808E-05	0.261E-05	0.812E-05	0.277E-05
C= 0.21E+15	30000.	0.816E-05	0.292E-05	0.812E-05	0.280E-05	0.817E-05	0.296E-05
	50000.	0.823E-05	0.318E-05	0.819E-05	0.305E-05	0.824E-05	0.322E-05
	2500.	0.117E-04	0.320E-05	0.116E-04	0.306E-05	0.117E-04	0.324E-05
3D - 6P	5000.	0.117E-04	0.359E-05	0.117E-04	0.344E-05	0.117E-04	0.364E-05
9249.1 Å	10000.	0.118E-04	0.403E-05	0.118E-04	0.386E-05	0.118E-04	0.408E-05
	20000.	0.120E-04	0.453E-05	0.119E-04	0.433E-05	0.120E-04	0.458E-05
C= 0.68E+14	30000.	0.121E-04	0.484E-05	0.120E-04	0.464E-05	0.121E-04	0.490E-05
	50000.	0.122E-04	0.527E-05	0.121E-04	0.505E-05	0.122E-04	0.534E-05
	2500.	0.194E-04	0.581E-05	0.193E-04	0.556E-05	0.194E-04	0.588E-05
3D - 7P	5000.	0.195E-04	0.652E-05	0.195E-04	0.624E-05	0.195E-04	0.661E-05
8212.1 Å	10000.	0.197E-04	0.732E-05	0.196E-04	0.701E-05	0.198E-04	0.742E-05
	20000.	0.200E-04	0.822E-05	0.199E-04	0.787E-05	0.200E-04	0.832E-05
C= 0.31E+14	30000.	0.202E-04	0.880E-05	0.201E-04	0.842E-05	0.203E-04	0.890E-05
	50000.	0.205E-04	0.958E-05	0.204E-04	0.916E-05	0.206E-04	0.970E-05
	2500.	0.319E-04	0.103E-04	0.318E-04	0.981E-05	0.319E-04	0.104E-04
3D - 8P	5000.	0.322E-04	0.115E-04	0.321E-04	0.110E-04	0.323E-04	0.117E-04
7692.3 Å	10000.	0.326E-04	0.129E-04	0.325E-04	0.124E-04	0.327E-04	0.131E-04
	20000.	0.332E-04	0.145E-04	0.330E-04	0.139E-04	0.333E-04	0.147E-04
C= 0.17E+14	30000.	0.336E-04	0.155E-04	0.333E-04	0.149E-04	0.337E-04	0.157E-04
	50000.	0.342E-04	0.169E-04	0.339E-04	0.162E-04	0.343E-04	0.171E-04

Perturber density= 1 x 10^{+11} cm^{-3}

		Perturbers					
		Ionized silicon		Ionized iron		Ionized magnesium	
Transition	T(K)	Width (Å)	Shift (Å)	Width (Å)	Shift (Å)	Width (Å)	Shift (Å)
	2500.	0.508E-04	0.173E-04	0.506E-04	0.165E-04	0.509E-04	0.175E-04
3D - 9P	5000.	0.514E-04	0.194E-04	0.511E-04	0.186E-04	0.515E-04	0.197E-04
7389.1 Å	10000.	0.522E-04	0.218E-04	0.518E-04	0.209E-04	0.523E-04	0.221E-04
	20000.	0.532E-04	0.245E-04	0.528E-04	0.234E-04	0.533E-04	0.248E-04
C= 0.10E+14	30000.	0.539E-04	0.262E-04	0.534E-04	0.251E-04	0.541E-04	0.265E-04
	50000.	0.550E-04	0.285E-04	0.544E-04	0.273E-04	0.552E-04	0.289E-04
	2500.	0.249E-03	0.115E-04	0.249E-03	0.110E-04	0.249E-03	0.116E-04
4D - 5P	5000.	0.249E-03	0.129E-04	0.249E-03	0.123E-04	0.249E-03	0.131E-04
63619.7 Å	10000.	0.249E-03	0.145E-04	0.249E-03	0.139E-04	0.249E-03	0.147E-04
	20000.	0.249E-03	0.163E-04	0.249E-03	0.156E-04	0.249E-03	0.165E-04
C= 0.60E+16	30000.	0.249E-03	0.174E-04	0.249E-03	0.166E-04	0.249E-03	0.176E-04
	50000.	0.249E-03	0.189E-04	0.249E-03	0.181E-04	0.249E-03	0.192E-04
	2500.	0.842E-04	0.195E-04	0.841E-04	0.187E-04	0.842E-04	0.198E-04
4D - 6P	5000.	0.845E-04	0.219E-04	0.843E-04	0.210E-04	0.845E-04	0.222E-04
24508.1 Å	10000.	0.849E-04	0.246E-04	0.847E-04	0.235E-04	0.850E-04	0.249E-04
	20000.	0.855E-04	0.276E-04	0.853E-04	0.264E-04	0.856E-04	0.279E-04
C= 0.48E+15	30000.	0.860E-04	0.295E-04	0.857E-04	0.283E-04	0.861E-04	0.299E-04
	50000.	0.867E-04	0.321E-04	0.863E-04	0.308E-04	0.868E-04	0.325E-04
	2500.	0.979E-04	0.280E-04	0.976E-04	0.268E-04	0.979E-04	0.283E-04
4D - 7P	5000.	0.985E-04	0.314E-04	0.983E-04	0.301E-04	0.986E-04	0.318E-04
18363.7 Å	10000.	0.995E-04	0.353E-04	0.991E-04	0.338E-04	0.996E-04	0.357E-04
	20000.	0.101E-03	0.396E-04	0.100E-03	0.379E-04	0.101E-03	0.401E-04
C= 0.16E+15	30000.	0.102E-03	0.424E-04	0.101E-03	0.405E-04	0.102E-03	0.429E-04
	50000.	0.103E-03	0.461E-04	0.102E-03	0.441E-04	0.103E-03	0.467E-04
	2500.	0.138E-03	0.435E-04	0.138E-03	0.417E-04	0.138E-03	0.441E-04
4D - 8P	5000.	0.139E-03	0.490E-04	0.139E-03	0.468E-04	0.139E-03	0.496E-04
15953.0 Å	10000.	0.141E-03	0.550E-04	0.140E-03	0.526E-04	0.141E-03	0.557E-04
	20000.	0.143E-03	0.617E-04	0.142E-03	0.591E-04	0.144E-03	0.625E-04
C= 0.73E+14	30000.	0.145E-03	0.660E-04	0.144E-03	0.632E-04	0.145E-03	0.668E-04
	50000.	0.147E-03	0.719E-04	0.146E-03	0.688E-04	0.148E-03	0.728E-04
	2500.	0.202E-03	0.680E-04	0.201E-03	0.650E-04	0.202E-03	0.688E-04
4D - 9P	5000.	0.204E-03	0.764E-04	0.203E-03	0.731E-04	0.204E-03	0.774E-04
14701.7 Å	10000.	0.207E-03	0.859E-04	0.206E-03	0.822E-04	0.207E-03	0.870E-04
	20000.	0.211E-03	0.964E-04	0.209E-03	0.923E-04	0.211E-03	0.976E-04
C= 0.41E+14	30000.	0.214E-03	0.103E-03	0.212E-03	0.988E-04	0.214E-03	0.104E-03
	50000.	0.218E-03	0.112E-03	0.216E-03	0.108E-03	0.219E-03	0.114E-03

Perturber density= 1 x 10^{+11} cm^{-3}

		Perturbers					
		Ionized silicon		Ionized iron		Ionized magnesium	
Transition	T(K)	Width (Å)	Shift (Å)	Width (Å)	Shift (Å)	Width (Å)	Shift (Å)
	2500.	0.194E-02	0.372E-03	0.194E-02	0.356E-03	0.194E-02	0.377E-03
5D - 6P	5000.	0.194E-02	0.418E-03	0.194E-02	0.400E-03	0.194E-02	0.423E-03
110307.1 Å	10000.	0.195E-02	0.469E-03	0.194E-02	0.449E-03	0.195E-02	0.475E-03
	20000.	0.196E-02	0.527E-03	0.195E-02	0.504E-03	0.196E-02	0.533E-03
C= 0.97E+16	30000.	0.196E-02	0.563E-03	0.196E-02	0.539E-03	0.196E-02	0.571E-03
	50000.	0.197E-02	0.614E-03	0.197E-02	0.587E-03	0.197E-02	0.621E-03
	2500.	0.584E-03	0.137E-03	0.583E-03	0.131E-03	0.584E-03	0.139E-03
5D - 7P	5000.	0.586E-03	0.154E-03	0.585E-03	0.147E-03	0.586E-03	0.156E-03
44018.0 Å	10000.	0.589E-03	0.173E-03	0.588E-03	0.165E-03	0.590E-03	0.175E-03
	20000.	0.594E-03	0.194E-03	0.592E-03	0.185E-03	0.594E-03	0.196E-03
C= 0.89E+15	30000.	0.597E-03	0.207E-03	0.595E-03	0.198E-03	0.598E-03	0.210E-03
	50000.	0.602E-03	0.226E-03	0.599E-03	0.216E-03	0.603E-03	0.229E-03
	2500.	0.575E-03	0.170E-03	0.573E-03	0.163E-03	0.575E-03	0.172E-03
5D - 8P	5000.	0.579E-03	0.191E-03	0.577E-03	0.183E-03	0.580E-03	0.194E-03
32313.5 Å	10000.	0.585E-03	0.215E-03	0.583E-03	0.205E-03	0.586E-03	0.217E-03
	20000.	0.593E-03	0.241E-03	0.590E-03	0.231E-03	0.594E-03	0.244E-03
C= 0.30E+15	30000.	0.599E-03	0.258E-03	0.595E-03	0.247E-03	0.600E-03	0.261E-03
	50000.	0.608E-03	0.281E-03	0.603E-03	0.269E-03	0.609E-03	0.284E-03
	2500.	0.714E-03	0.234E-03	0.712E-03	0.224E-03	0.715E-03	0.237E-03
5D - 9P	5000.	0.722E-03	0.263E-03	0.718E-03	0.252E-03	0.722E-03	0.267E-03
27561.9 Å	10000.	0.731E-03	0.296E-03	0.727E-03	0.283E-03	0.733E-03	0.300E-03
	20000.	0.745E-03	0.332E-03	0.739E-03	0.318E-03	0.746E-03	0.337E-03
C= 0.14E+15	30000.	0.754E-03	0.356E-03	0.748E-03	0.340E-03	0.756E-03	0.360E-03
	50000.	0.768E-03	0.387E-03	0.761E-03	0.371E-03	0.771E-03	0.392E-03
	2500.	0.110E-01	0.102E-02	0.110E-01	0.972E-03	0.110E-01	0.103E-02
6D - 7P	5000.	0.110E-01	0.114E-02	0.110E-01	0.109E-02	0.110E-01	0.115E-02
179546.1 Å	10000.	0.110E-01	0.128E-02	0.110E-01	0.123E-02	0.110E-01	0.130E-02
	20000.	0.110E-01	0.144E-02	0.110E-01	0.138E-02	0.110E-01	0.145E-02
C= 0.15E+17	30000.	0.110E-01	0.154E-02	0.110E-01	0.147E-02	0.110E-01	0.156E-02
	50000.	0.110E-01	0.167E-02	0.110E-01	0.160E-02	0.110E-01	0.169E-02
	2500.	0.303E-02	0.737E-03	0.302E-02	0.705E-03	0.303E-02	0.746E-03
6D - 8P	5000.	0.304E-02	0.828E-03	0.303E-02	0.792E-03	0.304E-02	0.839E-03
72472.2 Å	10000.	0.306E-02	0.930E-03	0.305E-02	0.890E-03	0.306E-02	0.941E-03
	20000.	0.308E-02	0.104E-02	0.307E-02	0.999E-03	0.309E-02	0.106E-02
C= 0.15E+16	30000.	0.310E-02	0.112E-02	0.309E-02	0.107E-02	0.311E-02	0.113E-02
	50000.	0.313E-02	0.122E-02	0.311E-02	0.116E-02	0.314E-02	0.123E-02

Perturber density= 1 x 10^{+11} cm^{-3}

Transition	T(K)	Perturbers: Ionized silicon Width (Å)	Ionized silicon Shift (Å)	Ionized iron Width (Å)	Ionized iron Shift (Å)	Ionized magnesium Width (Å)	Ionized magnesium Shift (Å)
	2500.	0.262E-02	0.799E-03	0.261E-02	0.764E-03	0.262E-02	0.809E-03
6D - 9P	5000.	0.264E-02	0.898E-03	0.263E-02	0.860E-03	0.264E-02	0.910E-03
52264.1 Å	10000.	0.267E-02	0.101E-02	0.266E-02	0.966E-03	0.268E-02	0.102E-02
	20000.	0.271E-02	0.113E-02	0.270E-02	0.108E-02	0.272E-02	0.115E-02
C= 0.52E+15	30000.	0.274E-02	0.121E-02	0.272E-02	0.116E-02	0.275E-02	0.123E-02
	50000.	0.279E-02	0.132E-02	0.276E-02	0.126E-02	0.279E-02	0.134E-02
	2500.	0.496E-01	0.661E-02	0.496E-01	0.632E-02	0.496E-01	0.669E-02
7D - 8P	5000.	0.496E-01	0.742E-02	0.496E-01	0.710E-02	0.496E-01	0.751E-02
276227.8 Å	10000.	0.497E-01	0.833E-02	0.497E-01	0.797E-02	0.497E-01	0.844E-02
	20000.	0.498E-01	0.935E-02	0.497E-01	0.895E-02	0.498E-01	0.947E-02
C= 0.22E+17	30000.	0.498E-01	0.100E-01	0.498E-01	0.957E-02	0.498E-01	0.101E-01
	50000.	0.499E-01	0.109E-01	0.499E-01	0.104E-01	0.499E-01	0.110E-01
	2500.	0.126E-01	0.322E-02	0.126E-01	0.308E-02	0.126E-01	0.326E-02
7D - 9P	5000.	0.127E-01	0.362E-02	0.126E-01	0.346E-02	0.127E-01	0.367E-02
111664.5 Å	10000.	0.127E-01	0.407E-02	0.127E-01	0.389E-02	0.128E-01	0.412E-02
	20000.	0.129E-01	0.457E-02	0.128E-01	0.437E-02	0.129E-01	0.462E-02
C= 0.24E+16	30000.	0.130E-01	0.488E-02	0.129E-01	0.467E-02	0.130E-01	0.495E-02
	50000.	0.131E-01	0.532E-02	0.130E-01	0.509E-02	0.131E-01	0.539E-02
	2500.	0.187	0.316E-01	0.186	0.303E-01	0.187	0.320E-01
8D - 9P	5000.	0.187	0.356E-01	0.187	0.340E-01	0.187	0.360E-01
405498.6 Å	10000.	0.187	0.399E-01	0.187	0.382E-01	0.187	0.404E-01
	20000.	0.188	0.448E-01	0.188	0.429E-01	0.188	0.454E-01
C= 0.31E+17	30000.	0.188	0.480E-01	0.188	0.459E-01	0.188	0.486E-01
	50000.	0.189	0.522E-01	0.189	0.500E-01	0.189	0.529E-01
	2500.	0.391E-05	0.765E-07	0.391E-05	0.732E-07	0.391E-05	0.775E-07
3D - 4F	5000.	0.391E-05	0.859E-07	0.391E-05	0.822E-07	0.391E-05	0.870E-07
12087.2 Å	10000.	0.391E-05	0.964E-07	0.391E-05	0.923E-07	0.391E-05	0.976E-07
	20000.	0.391E-05	0.108E-06	0.391E-05	0.104E-06	0.391E-05	0.110E-06
C= 0.23E+15	30000.	0.391E-05	0.116E-06	0.391E-05	0.111E-06	0.391E-05	0.117E-06
	50000.	0.391E-05	0.126E-06	0.391E-05	0.121E-06	0.391E-05	0.128E-06
	2500.	0.160E-03	-0.520E-04	0.159E-03	-0.497E-04	0.160E-03	-0.526E-04
4D - 4F	5000.	0.161E-03	-0.583E-04	0.161E-03	-0.558E-04	0.162E-03	-0.591E-04
64864.3 Å	10000.	0.164E-03	-0.655E-04	0.163E-03	-0.627E-04	0.164E-03	-0.663E-04
	20000.	0.166E-03	-0.735E-04	0.165E-03	-0.703E-04	0.167E-03	-0.744E-04
C= 0.65E+16	30000.	0.169E-03	-0.786E-04	0.167E-03	-0.753E-04	0.169E-03	-0.796E-04
	50000.	0.172E-03	-0.856E-04	0.170E-03	-0.820E-04	0.172E-03	-0.867E-04

Perturber density= 1 x 10^{+11} cm^{-3}

		Perturbers					
		Ionized silicon		Ionized iron		Ionized magnesium	
Transition	T(K)	Width (Å)	Shift (Å)	Width (Å)	Shift (Å)	Width (Å)	Shift (Å)
	2500.	0.302E-03	0.131E-03	0.300E-03	0.125E-03	0.302E-03	0.132E-03
4F - 5D	5000.	0.308E-03	0.147E-03	0.305E-03	0.140E-03	0.309E-03	0.148E-03
61272.6 Å	10000.	0.316E-03	0.164E-03	0.313E-03	0.157E-03	0.317E-03	0.167E-03
	20000.	0.327E-03	0.185E-03	0.323E-03	0.177E-03	0.328E-03	0.187E-03
C= 0.34E+16	30000.	0.335E-03	0.197E-03	0.330E-03	0.189E-03	0.336E-03	0.200E-03
	50000.	0.346E-03	0.215E-03	0.340E-03	0.206E-03	0.347E-03	0.218E-03
	2500.	0.153E-03	0.651E-04	0.152E-03	0.623E-04	0.153E-03	0.659E-04
4F - 6D	5000.	0.156E-03	0.731E-04	0.154E-03	0.699E-04	0.156E-03	0.740E-04
29878.5 Å	10000.	0.160E-03	0.820E-04	0.158E-03	0.785E-04	0.160E-03	0.831E-04
	20000.	0.165E-03	0.921E-04	0.163E-03	0.881E-04	0.166E-03	0.932E-04
C= 0.49E+15	30000.	0.169E-03	0.985E-04	0.166E-03	0.943E-04	0.169E-03	0.997E-04
	50000.	0.174E-03	0.107E-03	0.171E-03	0.103E-03	0.175E-03	0.109E-03
	2500.	0.173E-03	0.681E-04	0.172E-03	0.652E-04	0.173E-03	0.690E-04
4F - 7D	5000.	0.176E-03	0.766E-04	0.175E-03	0.733E-04	0.176E-03	0.775E-04
22911.0 Å	10000.	0.180E-03	0.860E-04	0.178E-03	0.823E-04	0.180E-03	0.870E-04
	20000.	0.184E-03	0.965E-04	0.182E-03	0.923E-04	0.185E-03	0.977E-04
C= 0.19E+15	30000.	0.188E-03	0.103E-03	0.186E-03	0.988E-04	0.189E-03	0.105E-03
	50000.	0.193E-03	0.112E-03	0.190E-03	0.108E-03	0.194E-03	0.114E-03
	2500.	0.231E-03	0.820E-04	0.230E-03	0.785E-04	0.231E-03	0.830E-04
4F - 8D	5000.	0.234E-03	0.922E-04	0.233E-03	0.882E-04	0.234E-03	0.934E-04
19945.6 Å	10000.	0.238E-03	0.104E-03	0.236E-03	0.991E-04	0.239E-03	0.105E-03
	20000.	0.243E-03	0.116E-03	0.241E-03	0.111E-03	0.244E-03	0.118E-03
C= 0.98E+14	30000.	0.247E-03	0.124E-03	0.244E-03	0.119E-03	0.248E-03	0.126E-03
	50000.	0.252E-03	0.135E-03	0.249E-03	0.130E-03	0.253E-03	0.137E-03
	2500.	0.322E-03	0.101E-03	0.321E-03	0.964E-04	0.322E-03	0.102E-03
4F - 9D	5000.	0.325E-03	0.113E-03	0.324E-03	0.108E-03	0.325E-03	0.115E-03
18345.5 Å	10000.	0.329E-03	0.127E-03	0.327E-03	0.122E-03	0.329E-03	0.129E-03
	20000.	0.334E-03	0.143E-03	0.332E-03	0.137E-03	0.335E-03	0.145E-03
C= 0.59E+14	30000.	0.338E-03	0.153E-03	0.335E-03	0.146E-03	0.339E-03	0.155E-03
	50000.	0.344E-03	0.166E-03	0.341E-03	0.159E-03	0.345E-03	0.169E-03
	2500.	0.168E-03	-0.133E-03	0.163E-03	-0.127E-03	0.169E-03	-0.135E-03
4F - 5G	5000.	0.182E-03	-0.150E-03	0.176E-03	-0.143E-03	0.184E-03	-0.151E-03
38213.4 Å	10000.	0.199E-03	-0.168E-03	0.193E-03	-0.161E-03	0.201E-03	-0.170E-03
	20000.	0.219E-03	-0.189E-03	0.211E-03	-0.180E-03	0.221E-03	-0.191E-03
C= 0.13E+15	30000.	0.232E-03	-0.202E-03	0.224E-03	-0.193E-03	0.234E-03	-0.204E-03
	50000.	0.251E-03	-0.220E-03	0.241E-03	-0.210E-03	0.252E-03	-0.222E-03

Perturber density= 1 x 10^{+11} cm^{-3}

		Perturbers					
		Ionized silicon		Ionized iron		Ionized magnesium	
Transition	T(K)	Width (Å)	Shift (Å)	Width (Å)	Shift (Å)	Width (Å)	Shift (Å)
	2500.	0.482E-03	0.442E-03	0.461E-03	0.423E-03	0.486E-03	0.448E-03
4F - 6G	5000.	0.540E-03	0.498E-03	0.517E-03	0.476E-03	0.544E-03	0.504E-03
25226.5 Å	10000.	0.609E-03	0.560E-03	0.581E-03	0.536E-03	0.609E-03	0.567E-03
	20000.	0.691E-03	0.629E-03	0.658E-03	0.602E-03	0.683E-03	0.637E-03
C= 0.52E+13	30000.	0.748E-03	0.673E-03	0.710E-03	0.644E-03	0.733E-03	0.682E-03
	50000.	0.836E-03	0.733E-03	0.788E-03	0.701E-03	0.803E-03	0.742E-03
	2500.	0.946E-03	0.873E-03	0.906E-03	0.835E-03	0.956E-03	0.884E-03
4F - 7G	5000.	0.106E-02	0.984E-03	0.102E-02	0.941E-03	0.107E-02	0.997E-03
20936.4 Å	10000.	0.120E-02	0.111E-02	0.114E-02	0.106E-02	0.120E-02	0.112E-02
	20000.	0.136E-02	0.125E-02	0.129E-02	0.119E-02	0.135E-02	0.126E-02
C= 0.24E+13	30000.	0.147E-02	0.133E-02	0.139E-02	0.128E-02	0.144E-02	0.135E-02
	50000.	0.163E-02	0.145E-02	0.154E-02	0.139E-02	0.158E-02	0.147E-02
	2500.	0.167E-02	0.153E-02	0.159E-02	0.146E-02	0.168E-02	0.155E-02
4F - 8G	5000.	0.187E-02	0.173E-02	0.179E-02	0.166E-02	0.189E-02	0.175E-02
18855.7 Å	10000.	0.211E-02	0.195E-02	0.201E-02	0.187E-02	0.212E-02	0.198E-02
	20000.	0.239E-02	0.220E-02	0.228E-02	0.210E-02	0.238E-02	0.222E-02
C= 0.13E+13	30000.	0.259E-02	0.235E-02	0.246E-02	0.225E-02	0.255E-02	0.238E-02
	50000.	0.288E-02	0.256E-02	0.272E-02	0.245E-02	0.279E-02	0.260E-02
	2500.	0.353E-02	0.322E-02	0.339E-02	0.308E-02	0.356E-02	0.326E-02
5F - 6G	5000.	0.396E-02	0.362E-02	0.379E-02	0.347E-02	0.398E-02	0.367E-02
69625.8 Å	10000.	0.445E-02	0.408E-02	0.426E-02	0.390E-02	0.445E-02	0.413E-02
	20000.	0.506E-02	0.458E-02	0.481E-02	0.438E-02	0.500E-02	0.464E-02
C= 0.40E+14	30000.	0.548E-02	0.490E-02	0.520E-02	0.469E-02	0.535E-02	0.496E-02
	50000.	0.613E-02	0.533E-02	0.578E-02	0.510E-02	0.587E-02	0.540E-02
	2500.	0.424E-02	0.390E-02	0.406E-02	0.373E-02	0.428E-02	0.395E-02
5F - 7G	5000.	0.476E-02	0.440E-02	0.455E-02	0.421E-02	0.479E-02	0.446E-02
44473.3 Å	10000.	0.536E-02	0.496E-02	0.512E-02	0.474E-02	0.537E-02	0.502E-02
	20000.	0.608E-02	0.557E-02	0.579E-02	0.533E-02	0.603E-02	0.564E-02
C= 0.11E+14	30000.	0.657E-02	0.597E-02	0.624E-02	0.571E-02	0.646E-02	0.604E-02
	50000.	0.732E-02	0.650E-02	0.691E-02	0.622E-02	0.707E-02	0.658E-02
	2500.	0.606E-02	0.557E-02	0.580E-02	0.532E-02	0.612E-02	0.564E-02
5F - 8G	5000.	0.681E-02	0.631E-02	0.652E-02	0.603E-02	0.687E-02	0.639E-02
36028.1 Å	10000.	0.768E-02	0.710E-02	0.734E-02	0.680E-02	0.770E-02	0.719E-02
	20000.	0.871E-02	0.800E-02	0.830E-02	0.765E-02	0.865E-02	0.810E-02
C= 0.48E+13	30000.	0.942E-02	0.857E-02	0.895E-02	0.820E-02	0.927E-02	0.867E-02
	50000.	0.105E-01	0.934E-02	0.991E-02	0.893E-02	0.101E-01	0.945E-02

Perturber density= 1 x 10^{+11} cm^{-3}

Transition	T(K)	Perturbers: Ionized silicon Width (Å)	Ionized silicon Shift (Å)	Ionized iron Width (Å)	Ionized iron Shift (Å)	Ionized magnesium Width (Å)	Ionized magnesium Shift (Å)
6F - 7G	2500.	0.271E-01	0.249E-01	0.259E-01	0.238E-01	0.273E-01	0.252E-01
113996.5 Å	5000.	0.304E-01	0.280E-01	0.291E-01	0.268E-01	0.306E-01	0.284E-01
C= 0.70E+14	10000.	0.342E-01	0.315E-01	0.327E-01	0.302E-01	0.343E-01	0.319E-01
	20000.	0.388E-01	0.355E-01	0.369E-01	0.339E-01	0.385E-01	0.359E-01
	30000.	0.420E-01	0.380E-01	0.398E-01	0.363E-01	0.412E-01	0.385E-01
	50000.	0.467E-01	0.414E-01	0.441E-01	0.396E-01	0.451E-01	0.419E-01
5G - 6H	2500.	0.392E-02	-0.361E-02	0.375E-02	-0.346E-02	0.395E-02	-0.366E-02
73776.2 Å	5000.	0.440E-02	-0.407E-02	0.421E-02	-0.389E-02	0.443E-02	-0.412E-02
C= 0.45E+14	10000.	0.496E-02	-0.457E-02	0.473E-02	-0.438E-02	0.496E-02	-0.463E-02
	20000.	0.563E-02	-0.514E-02	0.536E-02	-0.492E-02	0.557E-02	-0.520E-02
	30000.	0.610E-02	-0.550E-02	0.579E-02	-0.526E-02	0.597E-02	-0.557E-02
	50000.	0.682E-02	-0.598E-02	0.643E-02	-0.573E-02	0.654E-02	-0.606E-02
6G - 7H	2500.	0.304E-01	0.275E-01	0.290E-01	0.263E-01	0.302E-01	0.279E-01
122295.7 Å	5000.	0.349E-01	0.310E-01	0.330E-01	0.296E-01	0.341E-01	0.314E-01
C= 0.25E+14	10000.	0.410E-01	0.349E-01	0.384E-01	0.334E-01	0.388E-01	0.353E-01
	20000.	0.503E-01	0.393E-01	0.463E-01	0.376E-01	0.446E-01	0.403E-01
	30000.	0.578E-01	0.425E-01	0.527E-01	0.404E-01	0.498E-01	0.432E-01
	50000.	0.691E-01	0.475E-01	0.629E-01	0.449E-01	0.552E-01	0.483E-01
6G - 7I	2500.	0.430E-01	-0.394E-01	0.410E-01	-0.376E-01	0.430E-01	-0.399E-01
123290.9 Å	5000.	0.489E-01	-0.445E-01	0.465E-01	-0.425E-01	0.483E-01	-0.450E-01
C= 0.25E+14	10000.	0.565E-01	-0.500E-01	0.534E-01	-0.479E-01	0.546E-01	-0.507E-01
	20000.	0.670E-01	-0.564E-01	0.626E-01	-0.539E-01	0.623E-01	-0.570E-01
	30000.	0.752E-01	-0.605E-01	0.697E-01	-0.577E-01	0.677E-01	-0.620E-01
	50000.	0.883E-01	-0.666E-01	0.812E-01	-0.633E-01	0.752E-01	-0.676E-01
4S - 4P	2500.	0.756E-05	0.673E-05	0.728E-05	0.644E-05	0.764E-05	0.682E-05
15036.2 Å	5000.	0.840E-05	0.756E-05	0.807E-05	0.723E-05	0.848E-05	0.765E-05
C= 0.25E+14	10000.	0.935E-05	0.848E-05	0.897E-05	0.812E-05	0.943E-05	0.859E-05
	20000.	0.104E-04	0.952E-05	0.100E-04	0.911E-05	0.105E-04	0.964E-05
	30000.	0.112E-04	0.102E-04	0.107E-04	0.975E-05	0.112E-04	0.103E-04
	50000.	0.122E-04	0.111E-04	0.116E-04	0.106E-04	0.122E-04	0.112E-04
4S - 5P	2500.	0.819E-05	-0.738E-05	0.787E-05	-0.706E-05	0.828E-05	-0.747E-05
7660.5 Å	5000.	0.911E-05	-0.829E-05	0.875E-05	-0.794E-05	0.921E-05	-0.840E-05
C= 0.35E+13	10000.	0.102E-04	-0.931E-05	0.975E-05	-0.891E-05	0.103E-04	-0.943E-05
	20000.	0.114E-04	-0.104E-04	0.109E-04	-0.100E-04	0.115E-04	-0.106E-04
	30000.	0.122E-04	-0.112E-04	0.116E-04	-0.107E-04	0.122E-04	-0.113E-04
	50000.	0.133E-04	-0.122E-04	0.127E-04	-0.117E-04	0.133E-04	-0.123E-04

Perturber density= 1 x 10^{+11} cm^{-3}

		Perturbers					
		Ionized silicon		Ionized iron		Ionized magnesium	
Transition	T(K)	Width (Å)	Shift (Å)	Width (Å)	Shift (Å)	Width (Å)	Shift (Å)
	2500.	0.127E-04	-0.112E-04	0.122E-04	-0.107E-04	0.128E-04	-0.114E-04
4S - 6P	5000.	0.141E-04	-0.126E-04	0.135E-04	-0.121E-04	0.142E-04	-0.128E-04
6320.7 Å	10000.	0.157E-04	-0.142E-04	0.150E-04	-0.136E-04	0.158E-04	-0.144E-04
	20000.	0.175E-04	-0.159E-04	0.167E-04	-0.153E-04	0.176E-04	-0.161E-04
C= 0.20E+13	30000.	0.186E-04	-0.171E-04	0.179E-04	-0.163E-04	0.188E-04	-0.173E-04
	50000.	0.203E-04	-0.186E-04	0.194E-04	-0.178E-04	0.204E-04	-0.188E-04
	2500.	0.234E-04	-0.208E-04	0.225E-04	-0.199E-04	0.237E-04	-0.210E-04
4S - 7P	5000.	0.260E-04	-0.234E-04	0.250E-04	-0.223E-04	0.263E-04	-0.237E-04
5787.1 Å	10000.	0.289E-04	-0.263E-04	0.278E-04	-0.251E-04	0.292E-04	-0.266E-04
	20000.	0.323E-04	-0.295E-04	0.310E-04	-0.282E-04	0.326E-04	-0.299E-04
C= 0.12E+13	30000.	0.345E-04	-0.316E-04	0.330E-04	-0.302E-04	0.347E-04	-0.320E-04
	50000.	0.375E-04	-0.344E-04	0.359E-04	-0.329E-04	0.377E-04	-0.348E-04
	2500.	0.422E-04	-0.375E-04	0.406E-04	-0.359E-04	0.427E-04	-0.380E-04
4S - 8P	5000.	0.469E-04	-0.423E-04	0.451E-04	-0.404E-04	0.474E-04	-0.428E-04
5511.1 Å	10000.	0.523E-04	-0.476E-04	0.502E-04	-0.455E-04	0.528E-04	-0.482E-04
	20000.	0.584E-04	-0.535E-04	0.559E-04	-0.512E-04	0.589E-04	-0.542E-04
C= 0.72E+12	30000.	0.623E-04	-0.573E-04	0.597E-04	-0.548E-04	0.628E-04	-0.580E-04
	50000.	0.679E-04	-0.623E-04	0.649E-04	-0.597E-04	0.682E-04	-0.631E-04
	2500.	0.731E-04	-0.651E-04	0.703E-04	-0.623E-04	0.739E-04	-0.660E-04
4S - 9P	5000.	0.813E-04	-0.734E-04	0.781E-04	-0.704E-04	0.822E-04	-0.744E-04
5347.5 Å	10000.	0.907E-04	-0.827E-04	0.870E-04	-0.792E-04	0.916E-04	-0.838E-04
	20000.	0.101E-03	-0.931E-04	0.971E-04	-0.891E-04	0.102E-03	-0.942E-04
C= 0.48E+12	30000.	0.108E-03	-0.997E-04	0.104E-03	-0.954E-04	0.109E-03	-0.101E-03
	50000.	0.118E-03	-0.109E-03	0.113E-03	-0.104E-03	0.118E-03	-0.110E-03
	2500.	0.249E-03	-0.225E-03	0.240E-03	-0.215E-03	0.252E-03	-0.228E-03
5S - 5P	5000.	0.278E-03	-0.253E-03	0.267E-03	-0.242E-03	0.281E-03	-0.256E-03
42035.5 Å	10000.	0.310E-03	-0.284E-03	0.297E-03	-0.272E-03	0.313E-03	-0.287E-03
	20000.	0.347E-03	-0.319E-03	0.332E-03	-0.305E-03	0.349E-03	-0.323E-03
C= 0.10E+15	30000.	0.371E-03	-0.341E-03	0.355E-03	-0.326E-03	0.373E-03	-0.345E-03
	50000.	0.404E-03	-0.371E-03	0.386E-03	-0.355E-03	0.405E-03	-0.376E-03
	2500.	0.120E-03	-0.107E-03	0.116E-03	-0.102E-03	0.122E-03	-0.108E-03
5S - 6P	5000.	0.133E-03	-0.120E-03	0.128E-03	-0.115E-03	0.135E-03	-0.121E-03
19432.8 Å	10000.	0.148E-03	-0.135E-03	0.143E-03	-0.129E-03	0.150E-03	-0.136E-03
	20000.	0.166E-03	-0.151E-03	0.159E-03	-0.145E-03	0.167E-03	-0.153E-03
C= 0.19E+14	30000.	0.177E-03	-0.162E-03	0.169E-03	-0.155E-03	0.178E-03	-0.164E-03
	50000.	0.192E-03	-0.176E-03	0.184E-03	-0.169E-03	0.193E-03	-0.178E-03

Perturber density= 1 x 10^{+11} cm^{-3}

Transition	T(K)	Perturbers: Ionized silicon Width (Å)	Ionized silicon Shift (Å)	Ionized iron Width (Å)	Ionized iron Shift (Å)	Ionized magnesium Width (Å)	Ionized magnesium Shift (Å)
	2500.	0.160E-03	-0.142E-03	0.154E-03	-0.136E-03	0.162E-03	-0.144E-03
5S - 7P	5000.	0.178E-03	-0.160E-03	0.171E-03	-0.153E-03	0.180E-03	-0.162E-03
15140.4 Å	10000.	0.198E-03	-0.180E-03	0.190E-03	-0.172E-03	0.200E-03	-0.182E-03
	20000.	0.221E-03	-0.202E-03	0.212E-03	-0.194E-03	0.223E-03	-0.205E-03
C= 0.79E+13	30000.	0.236E-03	-0.216E-03	0.226E-03	-0.207E-03	0.238E-03	-0.219E-03
	50000.	0.257E-03	-0.236E-03	0.246E-03	-0.226E-03	0.258E-03	-0.239E-03
	2500.	0.249E-03	-0.222E-03	0.240E-03	-0.212E-03	0.252E-03	-0.224E-03
5S - 8P	5000.	0.277E-03	-0.249E-03	0.266E-03	-0.239E-03	0.280E-03	-0.253E-03
13386.6 Å	10000.	0.309E-03	-0.281E-03	0.296E-03	-0.269E-03	0.312E-03	-0.284E-03
	20000.	0.344E-03	-0.316E-03	0.330E-03	-0.302E-03	0.348E-03	-0.320E-03
C= 0.42E+13	30000.	0.368E-03	-0.338E-03	0.352E-03	-0.323E-03	0.371E-03	-0.342E-03
	50000.	0.401E-03	-0.368E-03	0.383E-03	-0.352E-03	0.402E-03	-0.373E-03
	2500.	0.397E-03	-0.354E-03	0.382E-03	-0.338E-03	0.402E-03	-0.358E-03
5S - 9P	5000.	0.442E-03	-0.399E-03	0.424E-03	-0.382E-03	0.447E-03	-0.404E-03
12460.3 Å	10000.	0.493E-03	-0.449E-03	0.472E-03	-0.430E-03	0.498E-03	-0.455E-03
	20000.	0.550E-03	-0.505E-03	0.527E-03	-0.484E-03	0.555E-03	-0.512E-03
C= 0.26E+13	30000.	0.588E-03	-0.541E-03	0.563E-03	-0.518E-03	0.593E-03	-0.548E-03
	50000.	0.641E-03	-0.590E-03	0.613E-03	-0.564E-03	0.643E-03	-0.597E-03
	2500.	0.255E-02	-0.226E-02	0.245E-02	-0.216E-02	0.258E-02	-0.229E-02
6S - 6P	5000.	0.283E-02	-0.254E-02	0.272E-02	-0.243E-02	0.286E-02	-0.257E-02
88772.9 Å	10000.	0.315E-02	-0.286E-02	0.302E-02	-0.273E-02	0.318E-02	-0.289E-02
	20000.	0.351E-02	-0.321E-02	0.337E-02	-0.307E-02	0.354E-02	-0.325E-02
C= 0.39E+15	30000.	0.375E-02	-0.343E-02	0.359E-02	-0.328E-02	0.378E-02	-0.348E-02
	50000.	0.408E-02	-0.374E-02	0.390E-02	-0.358E-02	0.410E-02	-0.378E-02
	2500.	0.105E-02	-0.933E-03	0.101E-02	-0.892E-03	0.106E-02	-0.945E-03
6S - 7P	5000.	0.117E-02	-0.105E-02	0.112E-02	-0.100E-02	0.118E-02	-0.106E-02
38679.2 Å	10000.	0.130E-02	-0.118E-02	0.125E-02	-0.113E-02	0.131E-02	-0.120E-02
	20000.	0.145E-02	-0.133E-02	0.139E-02	-0.127E-02	0.146E-02	-0.134E-02
C= 0.51E+14	30000.	0.155E-02	-0.142E-02	0.148E-02	-0.136E-02	0.156E-02	-0.144E-02
	50000.	0.168E-02	-0.155E-02	0.161E-02	-0.148E-02	0.169E-02	-0.156E-02
	2500.	0.117E-02	-0.104E-02	0.112E-02	-0.996E-03	0.118E-02	-0.105E-02
6S - 8P	5000.	0.130E-02	-0.117E-02	0.125E-02	-0.112E-02	0.131E-02	-0.119E-02
28979.8 Å	10000.	0.145E-02	-0.132E-02	0.139E-02	-0.126E-02	0.146E-02	-0.133E-02
	20000.	0.162E-02	-0.148E-02	0.155E-02	-0.142E-02	0.163E-02	-0.150E-02
C= 0.20E+14	30000.	0.173E-02	-0.159E-02	0.165E-02	-0.152E-02	0.174E-02	-0.161E-02
	50000.	0.188E-02	-0.173E-02	0.180E-02	-0.165E-02	0.189E-02	-0.175E-02

Perturber density= 1 x 10^{+11} cm^{-3}

		Perturbers					
		Ionized silicon		Ionized iron		Ionized magnesium	
Transition	T(K)	Width (Å)	Shift (Å)	Width (Å)	Shift (Å)	Width (Å)	Shift (Å)
	2500.	0.159E-02	-0.142E-02	0.153E-02	-0.136E-02	0.161E-02	-0.144E-02
6S - 9P	5000.	0.177E-02	-0.160E-02	0.170E-02	-0.153E-02	0.179E-02	-0.162E-02
24962.4 Å	10000.	0.198E-02	-0.180E-02	0.190E-02	-0.173E-02	0.200E-02	-0.183E-02
	20000.	0.221E-02	-0.203E-02	0.212E-02	-0.194E-02	0.223E-02	-0.206E-02
C= 0.10E+14	30000.	0.236E-02	-0.217E-02	0.226E-02	-0.208E-02	0.238E-02	-0.220E-02
	50000.	0.257E-02	-0.237E-02	0.246E-02	-0.227E-02	0.258E-02	-0.240E-02
	2500.	0.184E-01	-0.164E-01	0.177E-01	-0.157E-01	0.186E-01	-0.166E-01
7S - 7P	5000.	0.205E-01	-0.184E-01	0.197E-01	-0.176E-01	0.207E-01	-0.187E-01
160774.3 Å	10000.	0.228E-01	-0.207E-01	0.219E-01	-0.198E-01	0.230E-01	-0.210E-01
	20000.	0.254E-01	-0.233E-01	0.244E-01	-0.223E-01	0.257E-01	-0.236E-01
C= 0.89E+15	30000.	0.271E-01	-0.249E-01	0.260E-01	-0.238E-01	0.274E-01	-0.252E-01
	50000.	0.295E-01	-0.271E-01	0.283E-01	-0.260E-01	0.297E-01	-0.275E-01
	2500.	0.633E-02	-0.563E-02	0.609E-02	-0.539E-02	0.640E-02	-0.570E-02
7S - 8P	5000.	0.703E-02	-0.634E-02	0.676E-02	-0.607E-02	0.711E-02	-0.642E-02
67235.9 Å	10000.	0.784E-02	-0.714E-02	0.752E-02	-0.683E-02	0.792E-02	-0.722E-02
	20000.	0.875E-02	-0.802E-02	0.839E-02	-0.768E-02	0.883E-02	-0.812E-02
C= 0.11E+15	30000.	0.935E-02	-0.859E-02	0.895E-02	-0.822E-02	0.942E-02	-0.870E-02
	50000.	0.102E-01	-0.935E-02	0.974E-02	-0.895E-02	0.102E-01	-0.947E-02
	2500.	0.615E-02	-0.547E-02	0.591E-02	-0.523E-02	0.621E-02	-0.554E-02
7S - 9P	5000.	0.684E-02	-0.617E-02	0.656E-02	-0.591E-02	0.691E-02	-0.625E-02
48956.0 Å	10000.	0.762E-02	-0.696E-02	0.731E-02	-0.665E-02	0.770E-02	-0.704E-02
	20000.	0.852E-02	-0.782E-02	0.817E-02	-0.749E-02	0.860E-02	-0.792E-02
C= 0.40E+14	30000.	0.911E-02	-0.838E-02	0.872E-02	-0.802E-02	0.917E-02	-0.848E-02
	50000.	0.992E-02	-0.913E-02	0.949E-02	-0.874E-02	0.996E-02	-0.924E-02
	2500.	0.982E-01	-0.874E-01	0.944E-01	-0.837E-01	0.992E-01	-0.885E-01
8S - 8P	5000.	0.109	-0.984E-01	0.105	-0.942E-01	0.110	-0.997E-01
263144.0 Å	10000.	0.122	-0.111	0.117	-0.106	0.123	-0.112
	20000.	0.136	-0.125	0.130	-0.119	0.137	-0.126
C= 0.16E+16	30000.	0.145	-0.133	0.139	-0.128	0.146	-0.135
	50000.	0.158	-0.145	0.151	-0.139	0.159	-0.147
	2500.	0.295E-01	-0.263E-01	0.283E-01	-0.251E-01	0.298E-01	-0.266E-01
8S - 9P	5000.	0.328E-01	-0.296E-01	0.315E-01	-0.284E-01	0.331E-01	-0.300E-01
106909.6 Å	10000.	0.365E-01	-0.334E-01	0.351E-01	-0.319E-01	0.369E-01	-0.338E-01
	20000.	0.408E-01	-0.375E-01	0.391E-01	-0.359E-01	0.412E-01	-0.380E-01
C= 0.19E+15	30000.	0.437E-01	-0.402E-01	0.418E-01	-0.384E-01	0.440E-01	-0.407E-01
	50000.	0.476E-01	-0.438E-01	0.455E-01	-0.419E-01	0.478E-01	-0.443E-01

Perturber density= 1 x 10^{+11} cm^{-3}

Transition	T(K)	Perturbers: Ionized silicon Width (Å)	Ionized silicon Shift (Å)	Ionized iron Width (Å)	Ionized iron Shift (Å)	Ionized magnesium Width (Å)	Ionized magnesium Shift (Å)
	2500.	0.421	-0.376	0.405	-0.359	0.426	-0.380
9S - 9P	5000.	0.469	-0.424	0.450	-0.406	0.474	-0.429
402074.7 Å	10000.	0.523	-0.477	0.501	-0.457	0.528	-0.483
	20000.	0.584	-0.537	0.560	-0.514	0.590	-0.544
C= 0.27E+16	30000.	0.624	-0.575	0.598	-0.550	0.629	-0.582
	50000.	0.680	-0.627	0.651	-0.600	0.683	-0.634
	2500.	0.671E-07	0.583E-07	0.647E-07	0.558E-07	0.679E-07	0.591E-07
3P - 4S	5000.	0.741E-07	0.655E-07	0.714E-07	0.626E-07	0.749E-07	0.663E-07
5179.6 Å	10000.	0.821E-07	0.735E-07	0.790E-07	0.703E-07	0.830E-07	0.744E-07
	20000.	0.912E-07	0.825E-07	0.876E-07	0.789E-07	0.922E-07	0.835E-07
C= 0.18E+15	30000.	0.970E-07	0.882E-07	0.932E-07	0.845E-07	0.981E-07	0.893E-07
	50000.	0.105E-06	0.961E-07	0.101E-06	0.920E-07	0.106E-06	0.973E-07
	2500.	0.116E-06	0.109E-06	0.111E-06	0.104E-06	0.117E-06	0.110E-06
3P - 5S	5000.	0.130E-06	0.122E-06	0.124E-06	0.117E-06	0.131E-06	0.124E-06
3335.4 Å	10000.	0.145E-06	0.137E-06	0.139E-06	0.131E-06	0.147E-06	0.139E-06
	20000.	0.163E-06	0.154E-06	0.156E-06	0.147E-06	0.165E-06	0.156E-06
C= 0.26E+14	30000.	0.174E-06	0.164E-06	0.167E-06	0.157E-06	0.177E-06	0.166E-06
	50000.	0.190E-06	0.179E-06	0.182E-06	0.171E-06	0.192E-06	0.181E-06
	2500.	0.257E-06	0.243E-06	0.246E-06	0.232E-06	0.260E-06	0.246E-06
3P - 6S	5000.	0.289E-06	0.273E-06	0.276E-06	0.261E-06	0.292E-06	0.276E-06
2941.1 Å	10000.	0.324E-06	0.306E-06	0.310E-06	0.293E-06	0.328E-06	0.310E-06
	20000.	0.363E-06	0.343E-06	0.348E-06	0.329E-06	0.368E-06	0.348E-06
C= 0.97E+13	30000.	0.389E-06	0.367E-06	0.372E-06	0.352E-06	0.394E-06	0.372E-06
	50000.	0.423E-06	0.400E-06	0.405E-06	0.383E-06	0.429E-06	0.405E-06
	2500.	0.527E-06	0.497E-06	0.504E-06	0.476E-06	0.533E-06	0.504E-06
3P - 7S	5000.	0.591E-06	0.559E-06	0.566E-06	0.535E-06	0.599E-06	0.566E-06
2780.5 Å	10000.	0.664E-06	0.627E-06	0.635E-06	0.600E-06	0.672E-06	0.635E-06
	20000.	0.745E-06	0.704E-06	0.713E-06	0.674E-06	0.754E-06	0.713E-06
C= 0.48E+13	30000.	0.797E-06	0.753E-06	0.763E-06	0.721E-06	0.807E-06	0.762E-06
	50000.	0.868E-06	0.820E-06	0.830E-06	0.785E-06	0.879E-06	0.830E-06
	2500.	0.978E-06	0.923E-06	0.936E-06	0.883E-06	0.991E-06	0.935E-06
3P - 8S	5000.	0.110E-05	0.104E-05	0.105E-05	0.993E-06	0.111E-05	0.105E-05
2697.5 Å	10000.	0.123E-05	0.116E-05	0.118E-05	0.111E-05	0.125E-05	0.118E-05
	20000.	0.138E-05	0.131E-05	0.132E-05	0.125E-05	0.140E-05	0.132E-05
C= 0.28E+13	30000.	0.148E-05	0.140E-05	0.142E-05	0.134E-05	0.150E-05	0.142E-05
	50000.	0.161E-05	0.152E-05	0.154E-05	0.146E-05	0.163E-05	0.154E-05

Perturber density= 1 x 10^{+11} cm^{-3}

		Perturbers					
		Ionized silicon		Ionized iron		Ionized magnesium	
Transition	T(K)	Width (Å)	Shift (Å)	Width (Å)	Shift (Å)	Width (Å)	Shift (Å)
	2500.	0.169E-05	0.160E-05	0.162E-05	0.153E-05	0.171E-05	0.162E-05
3P - 9S	5000.	0.190E-05	0.179E-05	0.182E-05	0.172E-05	0.192E-05	0.182E-05
2648.4 Å	10000.	0.213E-05	0.202E-05	0.204E-05	0.193E-05	0.216E-05	0.204E-05
	20000.	0.239E-05	0.226E-05	0.229E-05	0.216E-05	0.242E-05	0.229E-05
C= 0.17E+13	30000.	0.256E-05	0.242E-05	0.245E-05	0.232E-05	0.259E-05	0.245E-05
	50000.	0.279E-05	0.264E-05	0.267E-05	0.252E-05	0.282E-05	0.267E-05
	2500.	0.270E-05	0.254E-05	0.258E-05	0.243E-05	0.273E-05	0.257E-05
3P -10S	5000.	0.303E-05	0.286E-05	0.290E-05	0.273E-05	0.306E-05	0.289E-05
2616.9 Å	10000.	0.340E-05	0.321E-05	0.325E-05	0.307E-05	0.344E-05	0.325E-05
	20000.	0.381E-05	0.360E-05	0.365E-05	0.345E-05	0.386E-05	0.365E-05
C= 0.12E+13	30000.	0.408E-05	0.386E-05	0.391E-05	0.369E-05	0.413E-05	0.390E-05
	50000.	0.444E-05	0.420E-05	0.425E-05	0.402E-05	0.450E-05	0.425E-05
	2500.	0.186E-04	-0.163E-04	0.179E-04	-0.156E-04	0.187E-04	-0.165E-04
4P - 5S	5000.	0.205E-04	-0.183E-04	0.198E-04	-0.175E-04	0.207E-04	-0.185E-04
24848.7 Å	10000.	0.228E-04	-0.205E-04	0.219E-04	-0.196E-04	0.230E-04	-0.208E-04
	20000.	0.255E-04	-0.230E-04	0.244E-04	-0.220E-04	0.256E-04	-0.233E-04
C= 0.67E+14	30000.	0.272E-04	-0.246E-04	0.260E-04	-0.236E-04	0.273E-04	-0.249E-04
	50000.	0.296E-04	-0.268E-04	0.283E-04	-0.256E-04	0.296E-04	-0.271E-04
	2500.	0.213E-05	-0.102E-05	0.211E-05	-0.980E-06	0.213E-05	-0.104E-05
4P - 6S	5000.	0.219E-05	-0.115E-05	0.217E-05	-0.110E-05	0.219E-05	-0.116E-05
12431.9 Å	10000.	0.228E-05	-0.129E-05	0.224E-05	-0.123E-05	0.228E-05	-0.131E-05
	20000.	0.241E-05	-0.145E-05	0.235E-05	-0.139E-05	0.238E-05	-0.147E-05
C= 0.17E+14	30000.	0.251E-05	-0.155E-05	0.244E-05	-0.148E-05	0.247E-05	-0.157E-05
	50000.	0.268E-05	-0.169E-05	0.258E-05	-0.162E-05	0.260E-05	-0.171E-05
	2500.	0.537E-05	0.497E-05	0.515E-05	0.475E-05	0.544E-05	0.503E-05
4P - 7S	5000.	0.601E-05	0.557E-05	0.576E-05	0.533E-05	0.607E-05	0.564E-05
9992.8 Å	10000.	0.672E-05	0.626E-05	0.644E-05	0.599E-05	0.680E-05	0.633E-05
	20000.	0.754E-05	0.702E-05	0.721E-05	0.672E-05	0.761E-05	0.711E-05
C= 0.11E+14	30000.	0.806E-05	0.751E-05	0.772E-05	0.719E-05	0.813E-05	0.761E-05
	50000.	0.879E-05	0.818E-05	0.841E-05	0.783E-05	0.883E-05	0.828E-05
	2500.	0.101E-04	0.946E-05	0.964E-05	0.906E-05	0.102E-04	0.958E-05
4P - 8S	5000.	0.113E-04	0.106E-04	0.108E-04	0.102E-04	0.114E-04	0.108E-04
8997.3 Å	10000.	0.127E-04	0.119E-04	0.121E-04	0.114E-04	0.128E-04	0.121E-04
	20000.	0.142E-04	0.134E-04	0.136E-04	0.128E-04	0.144E-04	0.136E-04
C= 0.88E+13	30000.	0.152E-04	0.143E-04	0.146E-04	0.137E-04	0.154E-04	0.145E-04
	50000.	0.166E-04	0.156E-04	0.159E-04	0.149E-04	0.168E-04	0.158E-04

Perturber density= 1 x 10^{+11} cm^{-3}

		Perturbers					
		Ionized silicon		Ionized iron		Ionized magnesium	
Transition	T(K)	Width (Å)	Shift (Å)	Width (Å)	Shift (Å)	Width (Å)	Shift (Å)
	2500.	0.168E-04	0.158E-04	0.161E-04	0.151E-04	0.170E-04	0.160E-04
4P - 9S	5000.	0.188E-04	0.178E-04	0.180E-04	0.170E-04	0.191E-04	0.180E-04
8473.8 Å	10000.	0.211E-04	0.200E-04	0.202E-04	0.191E-04	0.214E-04	0.202E-04
	20000.	0.237E-04	0.224E-04	0.227E-04	0.214E-04	0.240E-04	0.227E-04
C= 0.78E+13	30000.	0.254E-04	0.240E-04	0.243E-04	0.229E-04	0.257E-04	0.243E-04
	50000.	0.277E-04	0.261E-04	0.265E-04	0.250E-04	0.280E-04	0.264E-04
	2500.	0.258E-04	0.243E-04	0.247E-04	0.232E-04	0.261E-04	0.246E-04
4P -10S	5000.	0.290E-04	0.273E-04	0.277E-04	0.262E-04	0.293E-04	0.277E-04
8159.6 Å	10000.	0.325E-04	0.307E-04	0.311E-04	0.294E-04	0.329E-04	0.311E-04
	20000.	0.365E-04	0.345E-04	0.350E-04	0.330E-04	0.370E-04	0.349E-04
C= 0.73E+13	30000.	0.391E-04	0.369E-04	0.374E-04	0.353E-04	0.396E-04	0.374E-04
	50000.	0.426E-04	0.402E-04	0.407E-04	0.385E-04	0.431E-04	0.407E-04
	2500.	0.551E-03	0.499E-03	0.529E-03	0.477E-03	0.557E-03	0.505E-03
5P - 6S	5000.	0.613E-03	0.560E-03	0.588E-03	0.536E-03	0.620E-03	0.567E-03
60955.9 Å	10000.	0.685E-03	0.629E-03	0.656E-03	0.602E-03	0.691E-03	0.637E-03
	20000.	0.766E-03	0.706E-03	0.734E-03	0.676E-03	0.772E-03	0.715E-03
C= 0.22E+15	30000.	0.819E-03	0.756E-03	0.784E-03	0.723E-03	0.824E-03	0.765E-03
	50000.	0.894E-03	0.823E-03	0.854E-03	0.787E-03	0.896E-03	0.833E-03
	2500.	0.130E-03	0.119E-03	0.125E-03	0.114E-03	0.132E-03	0.120E-03
5P - 7S	5000.	0.145E-03	0.134E-03	0.139E-03	0.128E-03	0.147E-03	0.135E-03
27747.6 Å	10000.	0.162E-03	0.150E-03	0.156E-03	0.144E-03	0.164E-03	0.152E-03
	20000.	0.182E-03	0.169E-03	0.174E-03	0.161E-03	0.183E-03	0.171E-03
C= 0.45E+14	30000.	0.195E-03	0.180E-03	0.186E-03	0.173E-03	0.196E-03	0.183E-03
	50000.	0.212E-03	0.196E-03	0.203E-03	0.188E-03	0.213E-03	0.199E-03
	2500.	0.975E-04	0.902E-04	0.934E-04	0.863E-04	0.986E-04	0.913E-04
5P - 8S	5000.	0.109E-03	0.101E-03	0.104E-03	0.970E-04	0.110E-03	0.103E-03
21226.1 Å	10000.	0.122E-03	0.114E-03	0.117E-03	0.109E-03	0.123E-03	0.115E-03
	20000.	0.137E-03	0.128E-03	0.131E-03	0.122E-03	0.138E-03	0.129E-03
C= 0.27E+14	30000.	0.147E-03	0.137E-03	0.140E-03	0.131E-03	0.148E-03	0.138E-03
	50000.	0.160E-03	0.149E-03	0.153E-03	0.143E-03	0.161E-03	0.151E-03
	2500.	0.105E-03	0.981E-04	0.101E-03	0.938E-04	0.106E-03	0.993E-04
5P - 9S	5000.	0.118E-03	0.110E-03	0.113E-03	0.106E-03	0.119E-03	0.112E-03
18525.9 Å	10000.	0.132E-03	0.124E-03	0.126E-03	0.119E-03	0.134E-03	0.125E-03
	20000.	0.148E-03	0.139E-03	0.142E-03	0.133E-03	0.150E-03	0.141E-03
C= 0.20E+14	30000.	0.159E-03	0.149E-03	0.152E-03	0.142E-03	0.160E-03	0.151E-03
	50000.	0.173E-03	0.162E-03	0.165E-03	0.155E-03	0.174E-03	0.164E-03

Perturber density= 1 x 10^{+11} cm^{-3}

		Perturbers					
		Ionized silicon		Ionized iron		Ionized magnesium	
Transition	T(K)	Width (Å)	Shift (Å)	Width (Å)	Shift (Å)	Width (Å)	Shift (Å)
	2500.	0.130E-03	0.122E-03	0.125E-03	0.117E-03	0.132E-03	0.123E-03
5P -10S	5000.	0.146E-03	0.137E-03	0.140E-03	0.131E-03	0.148E-03	0.139E-03
17087.6 Å	10000.	0.164E-03	0.154E-03	0.157E-03	0.148E-03	0.166E-03	0.156E-03
	20000.	0.184E-03	0.173E-03	0.176E-03	0.166E-03	0.186E-03	0.175E-03
C= 0.17E+14	30000.	0.197E-03	0.185E-03	0.188E-03	0.177E-03	0.199E-03	0.188E-03
	50000.	0.215E-03	0.202E-03	0.205E-03	0.193E-03	0.217E-03	0.204E-03
	2500.	0.482E-02	0.430E-02	0.463E-02	0.411E-02	0.487E-02	0.435E-02
6P - 7S	5000.	0.535E-02	0.483E-02	0.514E-02	0.463E-02	0.541E-02	0.490E-02
119487.2 Å	10000.	0.596E-02	0.543E-02	0.572E-02	0.520E-02	0.602E-02	0.550E-02
	20000.	0.665E-02	0.610E-02	0.638E-02	0.584E-02	0.671E-02	0.618E-02
C= 0.71E+15	30000.	0.711E-02	0.653E-02	0.681E-02	0.625E-02	0.716E-02	0.661E-02
	50000.	0.773E-02	0.711E-02	0.740E-02	0.680E-02	0.777E-02	0.719E-02
	2500.	0.984E-03	0.886E-03	0.945E-03	0.848E-03	0.995E-03	0.897E-03
6P - 8S	5000.	0.110E-02	0.997E-03	0.105E-02	0.954E-03	0.111E-02	0.101E-02
51435.3 Å	10000.	0.122E-02	0.112E-02	0.117E-02	0.107E-02	0.123E-02	0.113E-02
	20000.	0.136E-02	0.126E-02	0.131E-02	0.120E-02	0.138E-02	0.127E-02
C= 0.13E+15	30000.	0.146E-02	0.135E-02	0.140E-02	0.129E-02	0.147E-02	0.136E-02
	50000.	0.159E-02	0.147E-02	0.152E-02	0.140E-02	0.160E-02	0.148E-02
	2500.	0.640E-03	0.584E-03	0.614E-03	0.559E-03	0.647E-03	0.591E-03
6P - 9S	5000.	0.714E-03	0.657E-03	0.685E-03	0.629E-03	0.722E-03	0.665E-03
38010.5 Å	10000.	0.798E-03	0.739E-03	0.765E-03	0.707E-03	0.807E-03	0.748E-03
	20000.	0.893E-03	0.829E-03	0.856E-03	0.794E-03	0.902E-03	0.840E-03
C= 0.72E+14	30000.	0.955E-03	0.887E-03	0.914E-03	0.849E-03	0.963E-03	0.898E-03
	50000.	0.104E-02	0.966E-03	0.995E-03	0.925E-03	0.105E-02	0.978E-03
	2500.	0.591E-03	0.545E-03	0.566E-03	0.522E-03	0.598E-03	0.552E-03
6P -10S	5000.	0.661E-03	0.614E-03	0.633E-03	0.587E-03	0.669E-03	0.621E-03
32412.8 Å	10000.	0.740E-03	0.690E-03	0.709E-03	0.660E-03	0.748E-03	0.699E-03
	20000.	0.829E-03	0.775E-03	0.794E-03	0.742E-03	0.838E-03	0.785E-03
C= 0.53E+14	30000.	0.887E-03	0.829E-03	0.849E-03	0.794E-03	0.896E-03	0.840E-03
	50000.	0.966E-03	0.903E-03	0.924E-03	0.864E-03	0.974E-03	0.914E-03
	2500.	0.313E-01	0.279E-01	0.301E-01	0.267E-01	0.316E-01	0.282E-01
7P - 8S	5000.	0.348E-01	0.314E-01	0.334E-01	0.300E-01	0.352E-01	0.318E-01
206062.4 Å	10000.	0.387E-01	0.353E-01	0.372E-01	0.338E-01	0.391E-01	0.358E-01
	20000.	0.432E-01	0.397E-01	0.415E-01	0.380E-01	0.436E-01	0.402E-01
C= 0.15E+16	30000.	0.462E-01	0.425E-01	0.442E-01	0.406E-01	0.466E-01	0.430E-01
	50000.	0.503E-01	0.462E-01	0.481E-01	0.442E-01	0.505E-01	0.468E-01

Perturber density= 1 x 10^{+11} cm^{-3}

Transition	T(K)	Perturbers: Ionized silicon Width (Å)	Ionized silicon Shift (Å)	Ionized iron Width (Å)	Ionized iron Shift (Å)	Ionized magnesium Width (Å)	Ionized magnesium Shift (Å)
	2500.	0.574E-02	0.515E-02	0.552E-02	0.493E-02	0.581E-02	0.522E-02
7P - 9S	5000.	0.639E-02	0.580E-02	0.613E-02	0.555E-02	0.646E-02	0.587E-02
85327.9 Å	10000.	0.712E-02	0.652E-02	0.683E-02	0.624E-02	0.720E-02	0.660E-02
	20000.	0.796E-02	0.733E-02	0.763E-02	0.701E-02	0.803E-02	0.742E-02
C= 0.25E+15	30000.	0.850E-02	0.784E-02	0.814E-02	0.751E-02	0.857E-02	0.794E-02
	50000.	0.926E-02	0.854E-02	0.886E-02	0.817E-02	0.931E-02	0.865E-02
	2500.	0.333E-02	0.301E-02	0.320E-02	0.288E-02	0.337E-02	0.305E-02
7P -10S	5000.	0.371E-02	0.339E-02	0.356E-02	0.325E-02	0.375E-02	0.344E-02
61489.3 Å	10000.	0.414E-02	0.382E-02	0.397E-02	0.365E-02	0.419E-02	0.386E-02
	20000.	0.463E-02	0.429E-02	0.444E-02	0.411E-02	0.468E-02	0.434E-02
C= 0.13E+15	30000.	0.495E-02	0.459E-02	0.474E-02	0.439E-02	0.500E-02	0.465E-02
	50000.	0.539E-02	0.500E-02	0.516E-02	0.478E-02	0.543E-02	0.506E-02
	2500.	0.155	0.138	0.149	0.132	0.156	0.140
8P - 9S	5000.	0.172	0.156	0.165	0.149	0.174	0.158
326115.3 Å	10000.	0.192	0.175	0.184	0.168	0.194	0.177
	20000.	0.214	0.197	0.205	0.188	0.216	0.199
C= 0.25E+16	30000.	0.229	0.211	0.219	0.202	0.231	0.213
	50000.	0.249	0.230	0.239	0.220	0.251	0.232
	2500.	0.263E-01	0.236E-01	0.253E-01	0.226E-01	0.266E-01	0.239E-01
8P -10S	5000.	0.293E-01	0.266E-01	0.281E-01	0.254E-01	0.296E-01	0.269E-01
131407.8 Å	10000.	0.327E-01	0.299E-01	0.313E-01	0.286E-01	0.330E-01	0.303E-01
	20000.	0.365E-01	0.336E-01	0.350E-01	0.322E-01	0.369E-01	0.340E-01
C= 0.41E+15	30000.	0.390E-01	0.360E-01	0.374E-01	0.344E-01	0.393E-01	0.364E-01
	50000.	0.425E-01	0.392E-01	0.406E-01	0.375E-01	0.427E-01	0.397E-01
	2500.	0.628	0.561	0.604	0.537	0.635	0.568
9P -10S	5000.	0.699	0.633	0.671	0.606	0.707	0.641
486286.7 Å	10000.	0.780	0.713	0.748	0.682	0.788	0.722
	20000.	0.872	0.802	0.836	0.768	0.880	0.813
C= 0.39E+16	30000.	0.932	0.859	0.893	0.822	0.939	0.870
	50000.	1.02	0.936	0.972	0.896	1.02	0.948
	2500.	0.340E-06	-0.308E-06	0.326E-06	-0.294E-06	0.343E-06	-0.311E-06
3P - 3D	5000.	0.378E-06	-0.345E-06	0.363E-06	-0.330E-06	0.382E-06	-0.350E-06
3836.4 Å	10000.	0.423E-06	-0.388E-06	0.405E-06	-0.371E-06	0.426E-06	-0.392E-06
	20000.	0.474E-06	-0.435E-06	0.453E-06	-0.416E-06	0.476E-06	-0.441E-06
C= 0.16E+13	30000.	0.507E-06	-0.465E-06	0.485E-06	-0.445E-06	0.508E-06	-0.471E-06
	50000.	0.555E-06	-0.507E-06	0.530E-06	-0.485E-06	0.553E-06	-0.513E-06

Perturber density= 1 x 10^{+11} cm^{-3}

Transition	T(K)	Perturbers: Ionized silicon Width (Å)	Ionized silicon Shift (Å)	Ionized iron Width (Å)	Ionized iron Shift (Å)	Ionized magnesium Width (Å)	Ionized magnesium Shift (Å)
	2500.	0.104E-05	0.944E-06	0.996E-06	0.903E-06	0.105E-05	0.956E-06
3P - 4D	5000.	0.116E-05	0.106E-05	0.111E-05	0.102E-05	0.117E-05	0.107E-05
3095.9 Å	10000.	0.129E-05	0.119E-05	0.124E-05	0.114E-05	0.130E-05	0.121E-05
	20000.	0.145E-05	0.134E-05	0.139E-05	0.128E-05	0.146E-05	0.135E-05
C= 0.57E+12	30000.	0.155E-05	0.143E-05	0.148E-05	0.137E-05	0.156E-05	0.145E-05
	50000.	0.169E-05	0.156E-05	0.162E-05	0.149E-05	0.169E-05	0.158E-05
	2500.	0.217E-05	0.195E-05	0.208E-05	0.187E-05	0.219E-05	0.197E-05
3P - 5D	5000.	0.241E-05	0.219E-05	0.232E-05	0.210E-05	0.244E-05	0.222E-05
2850.8 Å	10000.	0.269E-05	0.246E-05	0.258E-05	0.236E-05	0.272E-05	0.249E-05
	20000.	0.301E-05	0.277E-05	0.288E-05	0.265E-05	0.303E-05	0.280E-05
C= 0.41E+12	30000.	0.321E-05	0.296E-05	0.308E-05	0.283E-05	0.324E-05	0.300E-05
	50000.	0.350E-05	0.322E-05	0.335E-05	0.308E-05	0.351E-05	0.326E-05
	2500.	0.459E-05	0.413E-05	0.441E-05	0.395E-05	0.464E-05	0.418E-05
3P - 6D	5000.	0.511E-05	0.464E-05	0.490E-05	0.444E-05	0.516E-05	0.470E-05
2735.8 Å	10000.	0.570E-05	0.522E-05	0.546E-05	0.500E-05	0.576E-05	0.529E-05
	20000.	0.637E-05	0.587E-05	0.610E-05	0.561E-05	0.642E-05	0.594E-05
C= 0.26E+12	30000.	0.680E-05	0.628E-05	0.652E-05	0.601E-05	0.686E-05	0.635E-05
	50000.	0.741E-05	0.683E-05	0.709E-05	0.654E-05	0.745E-05	0.692E-05
	2500.	0.893E-05	0.804E-05	0.857E-05	0.769E-05	0.903E-05	0.814E-05
3P - 7D	5000.	0.994E-05	0.905E-05	0.954E-05	0.866E-05	0.101E-04	0.917E-05
2671.8 Å	10000.	0.111E-04	0.102E-04	0.106E-04	0.975E-05	0.112E-04	0.103E-04
	20000.	0.124E-04	0.115E-04	0.119E-04	0.110E-04	0.125E-04	0.116E-04
C= 0.17E+12	30000.	0.133E-04	0.123E-04	0.127E-04	0.117E-04	0.134E-04	0.124E-04
	50000.	0.145E-04	0.134E-04	0.138E-04	0.128E-04	0.145E-04	0.135E-04
	2500.	0.162E-04	0.146E-04	0.155E-04	0.139E-04	0.164E-04	0.148E-04
3P - 8D	5000.	0.180E-04	0.164E-04	0.173E-04	0.157E-04	0.182E-04	0.167E-04
2632.3 Å	10000.	0.201E-04	0.185E-04	0.193E-04	0.177E-04	0.204E-04	0.188E-04
	20000.	0.226E-04	0.208E-04	0.216E-04	0.199E-04	0.228E-04	0.211E-04
C= 0.12E+12	30000.	0.241E-04	0.223E-04	0.231E-04	0.213E-04	0.243E-04	0.226E-04
	50000.	0.263E-04	0.243E-04	0.251E-04	0.233E-04	0.264E-04	0.246E-04
	2500.	0.272E-04	0.244E-04	0.261E-04	0.234E-04	0.275E-04	0.247E-04
3P - 9D	5000.	0.303E-04	0.277E-04	0.291E-04	0.265E-04	0.306E-04	0.280E-04
2606.0 Å	10000.	0.339E-04	0.311E-04	0.325E-04	0.298E-04	0.342E-04	0.315E-04
	20000.	0.379E-04	0.350E-04	0.363E-04	0.335E-04	0.383E-04	0.355E-04
C= 0.84E+11	30000.	0.406E-04	0.375E-04	0.388E-04	0.359E-04	0.409E-04	0.380E-04
	50000.	0.442E-04	0.409E-04	0.423E-04	0.392E-04	0.444E-04	0.414E-04

Perturber density= 1 x 10^{+11} cm^{-3}

		Perturbers					
		Ionized silicon		Ionized iron		Ionized magnesium	
Transition	T(K)	Width (Å)	Shift (Å)	Width (Å)	Shift (Å)	Width (Å)	Shift (Å)
	2500.	0.430E-04	0.386E-04	0.413E-04	0.369E-04	0.435E-04	0.391E-04
3P -10D	5000.	0.480E-04	0.437E-04	0.460E-04	0.418E-04	0.486E-04	0.443E-04
2587.8 Å	10000.	0.537E-04	0.493E-04	0.514E-04	0.472E-04	0.542E-04	0.500E-04
	20000.	0.601E-04	0.556E-04	0.576E-04	0.532E-04	0.607E-04	0.563E-04
C= 0.64E+11	30000.	0.643E-04	0.595E-04	0.616E-04	0.570E-04	0.648E-04	0.603E-04
	50000.	0.702E-04	0.649E-04	0.671E-04	0.621E-04	0.704E-04	0.657E-04
	2500.	0.243E-04	0.216E-04	0.233E-04	0.207E-04	0.245E-04	0.219E-04
4P - 4D	5000.	0.270E-04	0.243E-04	0.259E-04	0.233E-04	0.272E-04	0.246E-04
15762.2 Å	10000.	0.300E-04	0.273E-04	0.288E-04	0.261E-04	0.303E-04	0.276E-04
	20000.	0.336E-04	0.306E-04	0.322E-04	0.293E-04	0.338E-04	0.310E-04
C= 0.15E+14	30000.	0.360E-04	0.328E-04	0.344E-04	0.314E-04	0.360E-04	0.332E-04
	50000.	0.393E-04	0.357E-04	0.375E-04	0.341E-04	0.391E-04	0.361E-04
	2500.	0.313E-04	0.280E-04	0.301E-04	0.268E-04	0.316E-04	0.283E-04
4P - 5D	5000.	0.348E-04	0.315E-04	0.334E-04	0.301E-04	0.352E-04	0.319E-04
10964.6 Å	10000.	0.388E-04	0.354E-04	0.372E-04	0.338E-04	0.391E-04	0.358E-04
	20000.	0.433E-04	0.397E-04	0.415E-04	0.380E-04	0.437E-04	0.402E-04
C= 0.60E+13	30000.	0.463E-04	0.425E-04	0.443E-04	0.406E-04	0.466E-04	0.430E-04
	50000.	0.504E-04	0.462E-04	0.482E-04	0.442E-04	0.505E-04	0.468E-04
	2500.	0.542E-04	0.487E-04	0.521E-04	0.466E-04	0.548E-04	0.493E-04
4P - 6D	5000.	0.603E-04	0.548E-04	0.579E-04	0.524E-04	0.610E-04	0.555E-04
9438.5 Å	10000.	0.673E-04	0.616E-04	0.646E-04	0.590E-04	0.680E-04	0.624E-04
	20000.	0.752E-04	0.692E-04	0.721E-04	0.662E-04	0.759E-04	0.701E-04
C= 0.31E+13	30000.	0.804E-04	0.741E-04	0.770E-04	0.709E-04	0.810E-04	0.750E-04
	50000.	0.876E-04	0.806E-04	0.838E-04	0.772E-04	0.879E-04	0.817E-04
	2500.	0.948E-04	0.854E-04	0.910E-04	0.817E-04	0.959E-04	0.865E-04
4P - 7D	5000.	0.106E-03	0.961E-04	0.101E-03	0.919E-04	0.107E-03	0.973E-04
8717.8 Å	10000.	0.118E-03	0.108E-03	0.113E-03	0.103E-03	0.119E-03	0.110E-03
	20000.	0.132E-03	0.122E-03	0.126E-03	0.116E-03	0.133E-03	0.123E-03
C= 0.18E+13	30000.	0.141E-03	0.130E-03	0.135E-03	0.125E-03	0.142E-03	0.132E-03
	50000.	0.154E-03	0.142E-03	0.147E-03	0.136E-03	0.154E-03	0.143E-03
	2500.	0.161E-03	0.145E-03	0.155E-03	0.139E-03	0.163E-03	0.147E-03
4P - 8D	5000.	0.180E-03	0.164E-03	0.172E-03	0.157E-03	0.182E-03	0.166E-03
8310.3 Å	10000.	0.201E-03	0.184E-03	0.192E-03	0.176E-03	0.203E-03	0.187E-03
	20000.	0.225E-03	0.207E-03	0.215E-03	0.198E-03	0.227E-03	0.210E-03
C= 0.12E+13	30000.	0.240E-03	0.222E-03	0.230E-03	0.213E-03	0.242E-03	0.225E-03
	50000.	0.262E-03	0.242E-03	0.250E-03	0.232E-03	0.263E-03	0.245E-03

STARK BROADENING PARAMETER TABLES FOR MG I LINES

Perturber density= 1 x 10^{+11} cm^{-3}

		Perturbers					
		Ionized silicon		Ionized iron		Ionized magnesium	
Transition	T(K)	Width (Å)	Shift (Å)	Width (Å)	Shift (Å)	Width (Å)	Shift (Å)
	2500.	0.259E-03	0.233E-03	0.249E-03	0.223E-03	0.262E-03	0.236E-03
4P - 9D	5000.	0.289E-03	0.264E-03	0.277E-03	0.253E-03	0.293E-03	0.267E-03
8054.4 Å	10000.	0.323E-03	0.297E-03	0.310E-03	0.284E-03	0.327E-03	0.301E-03
	20000.	0.362E-03	0.335E-03	0.347E-03	0.320E-03	0.365E-03	0.339E-03
C= 0.81E+12	30000.	0.387E-03	0.358E-03	0.371E-03	0.343E-03	0.390E-03	0.363E-03
	50000.	0.422E-03	0.391E-03	0.404E-03	0.374E-03	0.424E-03	0.396E-03
	2500.	0.399E-03	0.358E-03	0.383E-03	0.342E-03	0.403E-03	0.362E-03
4P -10D	5000.	0.445E-03	0.406E-03	0.427E-03	0.388E-03	0.450E-03	0.411E-03
7882.4 Å	10000.	0.498E-03	0.458E-03	0.477E-03	0.438E-03	0.503E-03	0.463E-03
	20000.	0.558E-03	0.515E-03	0.534E-03	0.493E-03	0.563E-03	0.522E-03
C= 0.59E+12	30000.	0.597E-03	0.552E-03	0.571E-03	0.528E-03	0.601E-03	0.559E-03
	50000.	0.651E-03	0.602E-03	0.622E-03	0.576E-03	0.653E-03	0.610E-03
	2500.	0.446E-03	0.402E-03	0.429E-03	0.385E-03	0.451E-03	0.407E-03
5P - 5D	5000.	0.497E-03	0.452E-03	0.477E-03	0.433E-03	0.502E-03	0.458E-03
36805.3 Å	10000.	0.554E-03	0.508E-03	0.532E-03	0.486E-03	0.560E-03	0.515E-03
	20000.	0.620E-03	0.571E-03	0.594E-03	0.546E-03	0.625E-03	0.578E-03
C= 0.68E+14	30000.	0.663E-03	0.611E-03	0.635E-03	0.584E-03	0.667E-03	0.618E-03
	50000.	0.723E-03	0.665E-03	0.692E-03	0.636E-03	0.724E-03	0.673E-03
	2500.	0.373E-03	0.336E-03	0.359E-03	0.321E-03	0.377E-03	0.340E-03
5P - 6D	5000.	0.416E-03	0.378E-03	0.399E-03	0.362E-03	0.420E-03	0.383E-03
23857.5 Å	10000.	0.464E-03	0.425E-03	0.445E-03	0.407E-03	0.468E-03	0.430E-03
	20000.	0.519E-03	0.478E-03	0.497E-03	0.457E-03	0.523E-03	0.484E-03
C= 0.20E+14	30000.	0.554E-03	0.511E-03	0.531E-03	0.489E-03	0.558E-03	0.517E-03
	50000.	0.604E-03	0.556E-03	0.578E-03	0.533E-03	0.606E-03	0.563E-03
	2500.	0.499E-03	0.449E-03	0.479E-03	0.430E-03	0.504E-03	0.455E-03
5P - 7D	5000.	0.556E-03	0.506E-03	0.533E-03	0.484E-03	0.562E-03	0.512E-03
19733.6 Å	10000.	0.620E-03	0.569E-03	0.595E-03	0.545E-03	0.627E-03	0.576E-03
	20000.	0.694E-03	0.640E-03	0.665E-03	0.612E-03	0.700E-03	0.648E-03
C= 0.92E+13	30000.	0.742E-03	0.685E-03	0.710E-03	0.656E-03	0.747E-03	0.694E-03
	50000.	0.809E-03	0.746E-03	0.773E-03	0.714E-03	0.812E-03	0.755E-03
	2500.	0.744E-03	0.670E-03	0.714E-03	0.641E-03	0.752E-03	0.679E-03
5P - 8D	5000.	0.829E-03	0.756E-03	0.795E-03	0.723E-03	0.838E-03	0.765E-03
17762.3 Å	10000.	0.926E-03	0.851E-03	0.888E-03	0.815E-03	0.936E-03	0.862E-03
	20000.	0.104E-02	0.958E-03	0.993E-03	0.916E-03	0.105E-02	0.970E-03
C= 0.53E+13	30000.	0.111E-02	0.103E-02	0.106E-02	0.981E-03	0.112E-02	0.104E-02
	50000.	0.121E-02	0.112E-02	0.116E-02	0.107E-02	0.121E-02	0.113E-02

Perturber density= 1 x 10^{+11} cm^{-3}

Transition	T(K)	Perturbers: Ionized silicon Width (Å)	Ionized silicon Shift (Å)	Ionized iron Width (Å)	Ionized iron Shift (Å)	Ionized magnesium Width (Å)	Ionized magnesium Shift (Å)
	2500.	0.111E-02	0.999E-03	0.107E-02	0.955E-03	0.112E-02	0.101E-02
5P - 9D	5000.	0.124E-02	0.113E-02	0.119E-02	0.108E-02	0.125E-02	0.115E-02
16632.6 Å	10000.	0.139E-02	0.127E-02	0.133E-02	0.122E-02	0.140E-02	0.129E-02
	20000.	0.155E-02	0.143E-02	0.149E-02	0.137E-02	0.157E-02	0.145E-02
C= 0.34E+13	30000.	0.166E-02	0.154E-02	0.159E-02	0.147E-02	0.167E-02	0.155E-02
	50000.	0.181E-02	0.167E-02	0.173E-02	0.160E-02	0.182E-02	0.169E-02
	2500.	0.163E-02	0.146E-02	0.156E-02	0.140E-02	0.165E-02	0.148E-02
5P -10D	5000.	0.182E-02	0.166E-02	0.175E-02	0.158E-02	0.184E-02	0.168E-02
15915.5 Å	10000.	0.203E-02	0.187E-02	0.195E-02	0.179E-02	0.206E-02	0.189E-02
	20000.	0.228E-02	0.211E-02	0.218E-02	0.201E-02	0.230E-02	0.213E-02
C= 0.24E+13	30000.	0.244E-02	0.226E-02	0.233E-02	0.216E-02	0.246E-02	0.228E-02
	50000.	0.266E-02	0.246E-02	0.254E-02	0.235E-02	0.267E-02	0.249E-02
	2500.	0.372E-02	0.334E-02	0.357E-02	0.319E-02	0.376E-02	0.338E-02
6P - 6D	5000.	0.414E-02	0.376E-02	0.397E-02	0.359E-02	0.418E-02	0.380E-02
70197.1 Å	10000.	0.461E-02	0.422E-02	0.443E-02	0.404E-02	0.466E-02	0.428E-02
	20000.	0.516E-02	0.475E-02	0.494E-02	0.454E-02	0.520E-02	0.481E-02
C= 0.17E+15	30000.	0.551E-02	0.508E-02	0.528E-02	0.486E-02	0.555E-02	0.514E-02
	50000.	0.601E-02	0.553E-02	0.575E-02	0.529E-02	0.603E-02	0.560E-02
	2500.	0.256E-02	0.230E-02	0.245E-02	0.220E-02	0.258E-02	0.233E-02
6P - 7D	5000.	0.285E-02	0.259E-02	0.273E-02	0.248E-02	0.288E-02	0.262E-02
43468.8 Å	10000.	0.318E-02	0.291E-02	0.305E-02	0.279E-02	0.321E-02	0.295E-02
	20000.	0.355E-02	0.328E-02	0.340E-02	0.314E-02	0.358E-02	0.332E-02
C= 0.45E+14	30000.	0.380E-02	0.351E-02	0.364E-02	0.336E-02	0.383E-02	0.355E-02
	50000.	0.414E-02	0.382E-02	0.396E-02	0.366E-02	0.416E-02	0.387E-02
	2500.	0.294E-02	0.265E-02	0.282E-02	0.253E-02	0.297E-02	0.268E-02
6P - 8D	5000.	0.328E-02	0.299E-02	0.315E-02	0.286E-02	0.332E-02	0.303E-02
34929.6 Å	10000.	0.366E-02	0.336E-02	0.351E-02	0.322E-02	0.370E-02	0.341E-02
	20000.	0.410E-02	0.379E-02	0.393E-02	0.362E-02	0.414E-02	0.383E-02
C= 0.20E+14	30000.	0.438E-02	0.405E-02	0.420E-02	0.388E-02	0.442E-02	0.410E-02
	50000.	0.478E-02	0.442E-02	0.457E-02	0.423E-02	0.480E-02	0.447E-02
	2500.	0.385E-02	0.346E-02	0.370E-02	0.331E-02	0.390E-02	0.351E-02
6P - 9D	5000.	0.430E-02	0.392E-02	0.412E-02	0.375E-02	0.435E-02	0.397E-02
30814.0 Å	10000.	0.480E-02	0.442E-02	0.460E-02	0.422E-02	0.485E-02	0.447E-02
	20000.	0.538E-02	0.497E-02	0.515E-02	0.475E-02	0.543E-02	0.503E-02
C= 0.12E+14	30000.	0.575E-02	0.532E-02	0.551E-02	0.509E-02	0.579E-02	0.539E-02
	50000.	0.628E-02	0.580E-02	0.600E-02	0.555E-02	0.630E-02	0.587E-02

Perturber density= 1 x 10^{+11} cm^{-3}

		Perturbers					
		Ionized silicon		Ionized iron		Ionized magnesium	
Transition	T(K)	Width (Å)	Shift (Å)	Width (Å)	Shift (Å)	Width (Å)	Shift (Å)
	2500.	0.523E-02	0.469E-02	0.502E-02	0.448E-02	0.529E-02	0.475E-02
6P -10D	5000.	0.584E-02	0.532E-02	0.560E-02	0.509E-02	0.591E-02	0.539E-02
28439.8 Å	10000.	0.653E-02	0.600E-02	0.626E-02	0.575E-02	0.660E-02	0.608E-02
	20000.	0.732E-02	0.676E-02	0.700E-02	0.647E-02	0.738E-02	0.684E-02
C= 0.77E+13	30000.	0.783E-02	0.724E-02	0.749E-02	0.693E-02	0.788E-02	0.733E-02
	50000.	0.854E-02	0.789E-02	0.816E-02	0.755E-02	0.857E-02	0.799E-02
	2500.	0.222E-01	0.200E-01	0.213E-01	0.191E-01	0.225E-01	0.202E-01
7P - 7D	5000.	0.247E-01	0.225E-01	0.237E-01	0.215E-01	0.250E-01	0.228E-01
118821.3 Å	10000.	0.276E-01	0.253E-01	0.265E-01	0.242E-01	0.279E-01	0.256E-01
	20000.	0.309E-01	0.284E-01	0.296E-01	0.272E-01	0.311E-01	0.288E-01
C= 0.33E+15	30000.	0.330E-01	0.304E-01	0.316E-01	0.291E-01	0.332E-01	0.308E-01
	50000.	0.360E-01	0.331E-01	0.344E-01	0.317E-01	0.361E-01	0.336E-01
	2500.	0.131E-01	0.118E-01	0.126E-01	0.113E-01	0.132E-01	0.119E-01
7P - 8D	5000.	0.146E-01	0.133E-01	0.140E-01	0.127E-01	0.147E-01	0.134E-01
71225.1 Å	10000.	0.163E-01	0.150E-01	0.156E-01	0.143E-01	0.165E-01	0.151E-01
	20000.	0.182E-01	0.168E-01	0.175E-01	0.161E-01	0.184E-01	0.170E-01
C= 0.85E+14	30000.	0.195E-01	0.180E-01	0.187E-01	0.172E-01	0.196E-01	0.182E-01
	50000.	0.213E-01	0.196E-01	0.203E-01	0.188E-01	0.213E-01	0.199E-01
	2500.	0.131E-01	0.118E-01	0.126E-01	0.113E-01	0.133E-01	0.119E-01
7P - 9D	5000.	0.146E-01	0.133E-01	0.140E-01	0.128E-01	0.148E-01	0.135E-01
55979.1 Å	10000.	0.164E-01	0.150E-01	0.157E-01	0.144E-01	0.165E-01	0.152E-01
	20000.	0.183E-01	0.169E-01	0.175E-01	0.162E-01	0.185E-01	0.171E-01
C= 0.39E+14	30000.	0.196E-01	0.181E-01	0.188E-01	0.173E-01	0.197E-01	0.184E-01
	50000.	0.214E-01	0.198E-01	0.204E-01	0.189E-01	0.214E-01	0.200E-01
	2500.	0.155E-01	0.139E-01	0.149E-01	0.133E-01	0.157E-01	0.141E-01
7P -10D	5000.	0.173E-01	0.158E-01	0.166E-01	0.151E-01	0.175E-01	0.160E-01
48607.4 Å	10000.	0.194E-01	0.178E-01	0.186E-01	0.170E-01	0.196E-01	0.180E-01
	20000.	0.217E-01	0.200E-01	0.208E-01	0.192E-01	0.219E-01	0.203E-01
C= 0.22E+14	30000.	0.232E-01	0.215E-01	0.222E-01	0.206E-01	0.234E-01	0.218E-01
	50000.	0.253E-01	0.234E-01	0.242E-01	0.224E-01	0.254E-01	0.237E-01
	2500.	0.103	0.926E-01	0.991E-01	0.885E-01	0.104	0.938E-01
8P - 8D	5000.	0.115	0.105	0.110	0.100	0.116	0.106
185635.5 Å	10000.	0.128	0.118	0.123	0.113	0.130	0.119
	20000.	0.144	0.133	0.138	0.127	0.145	0.134
C= 0.57E+15	30000.	0.154	0.142	0.147	0.136	0.155	0.144
	50000.	0.168	0.155	0.160	0.148	0.168	0.157

Perturber density= 1 x 10^{+11} cm^{-3}

Transition	T(K)	Perturbers: Ionized silicon Width (Å)	Ionized silicon Shift (Å)	Ionized iron Width (Å)	Ionized iron Shift (Å)	Ionized magnesium Width (Å)	Ionized magnesium Shift (Å)
8P - 9D	2500.	0.533E-01	0.478E-01	0.511E-01	0.457E-01	0.539E-01	0.484E-01
108569.4 Å	5000.	0.594E-01	0.541E-01	0.570E-01	0.518E-01	0.601E-01	0.548E-01
C= 0.15E+15	10000.	0.664E-01	0.610E-01	0.636E-01	0.583E-01	0.671E-01	0.617E-01
	20000.	0.744E-01	0.686E-01	0.712E-01	0.657E-01	0.750E-01	0.695E-01
	30000.	0.796E-01	0.735E-01	0.761E-01	0.703E-01	0.801E-01	0.744E-01
	50000.	0.868E-01	0.801E-01	0.830E-01	0.767E-01	0.870E-01	0.811E-01
8P -10D	2500.	0.481E-01	0.431E-01	0.462E-01	0.412E-01	0.487E-01	0.436E-01
83893.3 Å	5000.	0.537E-01	0.489E-01	0.515E-01	0.467E-01	0.543E-01	0.495E-01
C= 0.67E+14	10000.	0.601E-01	0.552E-01	0.576E-01	0.528E-01	0.607E-01	0.559E-01
	20000.	0.673E-01	0.621E-01	0.644E-01	0.594E-01	0.679E-01	0.629E-01
	30000.	0.720E-01	0.666E-01	0.689E-01	0.637E-01	0.725E-01	0.674E-01
	50000.	0.786E-01	0.726E-01	0.751E-01	0.694E-01	0.788E-01	0.735E-01
9P - 9D	2500.	0.393	0.351	0.377	0.336	0.397	0.356
273433.2 Å	5000.	0.438	0.398	0.420	0.381	0.443	0.403
C= 0.93E+15	10000.	0.489	0.449	0.469	0.429	0.494	0.454
	20000.	0.548	0.505	0.525	0.483	0.552	0.512
	30000.	0.586	0.541	0.561	0.518	0.590	0.548
	50000.	0.640	0.590	0.611	0.565	0.641	0.598
9P -10D	2500.	0.184	0.164	0.176	0.157	0.186	0.166
157074.6 Å	5000.	0.205	0.186	0.197	0.178	0.207	0.189
C= 0.23E+15	10000.	0.229	0.210	0.220	0.201	0.231	0.213
	20000.	0.257	0.237	0.246	0.227	0.259	0.240
	30000.	0.275	0.254	0.263	0.243	0.276	0.257
	50000.	0.300	0.277	0.286	0.265	0.300	0.280
4P - 3D	2500.	0.382E-01	-0.344E-01	0.367E-01	-0.329E-01	0.386E-01	-0.348E-01
917094.6 Å	5000.	0.425E-01	-0.386E-01	0.408E-01	-0.369E-01	0.429E-01	-0.391E-01
C= 0.92E+17	10000.	0.474E-01	-0.433E-01	0.454E-01	-0.415E-01	0.478E-01	-0.439E-01
	20000.	0.531E-01	-0.486E-01	0.508E-01	-0.465E-01	0.533E-01	-0.492E-01
	30000.	0.568E-01	-0.520E-01	0.544E-01	-0.498E-01	0.569E-01	-0.527E-01
	50000.	0.622E-01	-0.566E-01	0.593E-01	-0.542E-01	0.618E-01	-0.573E-01
3D - 5P	2500.	0.338E-04	-0.302E-04	0.325E-04	-0.289E-04	0.342E-04	-0.306E-04
15887.5 Å	5000.	0.376E-04	-0.340E-04	0.361E-04	-0.325E-04	0.380E-04	-0.344E-04
C= 0.15E+14	10000.	0.419E-04	-0.382E-04	0.402E-04	-0.365E-04	0.423E-04	-0.386E-04
	20000.	0.469E-04	-0.428E-04	0.449E-04	-0.410E-04	0.472E-04	-0.434E-04
	30000.	0.501E-04	-0.458E-04	0.480E-04	-0.439E-04	0.503E-04	-0.464E-04
	50000.	0.547E-04	-0.499E-04	0.523E-04	-0.477E-04	0.546E-04	-0.505E-04

Perturber density= 1 x 10^{+11} cm^{-3}

Transition	T(K)	Perturbers: Ionized silicon Width (Å)	Ionized silicon Shift (Å)	Ionized iron Width (Å)	Ionized iron Shift (Å)	Ionized magnesium Width (Å)	Ionized magnesium Shift (Å)
	2500.	0.382E-04	-0.338E-04	0.368E-04	-0.323E-04	0.387E-04	-0.342E-04
3D - 6P	5000.	0.424E-04	-0.380E-04	0.408E-04	-0.363E-04	0.429E-04	-0.385E-04
11036.0 Å	10000.	0.472E-04	-0.427E-04	0.453E-04	-0.408E-04	0.476E-04	-0.432E-04
	20000.	0.526E-04	-0.479E-04	0.504E-04	-0.458E-04	0.530E-04	-0.485E-04
C= 0.61E+13	30000.	0.561E-04	-0.513E-04	0.538E-04	-0.491E-04	0.565E-04	-0.519E-04
	50000.	0.611E-04	-0.558E-04	0.585E-04	-0.534E-04	0.613E-04	-0.565E-04
	2500.	0.630E-04	-0.558E-04	0.606E-04	-0.533E-04	0.637E-04	-0.565E-04
3D - 7P	5000.	0.699E-04	-0.628E-04	0.672E-04	-0.600E-04	0.706E-04	-0.635E-04
9505.6 Å	10000.	0.778E-04	-0.706E-04	0.747E-04	-0.675E-04	0.786E-04	-0.715E-04
	20000.	0.868E-04	-0.793E-04	0.832E-04	-0.759E-04	0.875E-04	-0.803E-04
C= 0.31E+13	30000.	0.927E-04	-0.848E-04	0.888E-04	-0.812E-04	0.933E-04	-0.859E-04
	50000.	0.101E-03	-0.924E-04	0.965E-04	-0.884E-04	0.101E-03	-0.935E-04
	2500.	0.107E-03	-0.952E-04	0.103E-03	-0.912E-04	0.108E-03	-0.964E-04
3D - 8P	5000.	0.119E-03	-0.107E-03	0.114E-03	-0.103E-03	0.120E-03	-0.109E-03
8783.1 Å	10000.	0.133E-03	-0.121E-03	0.127E-03	-0.115E-03	0.134E-03	-0.122E-03
	20000.	0.148E-03	-0.136E-03	0.142E-03	-0.130E-03	0.149E-03	-0.137E-03
C= 0.18E+13	30000.	0.158E-03	-0.145E-03	0.151E-03	-0.139E-03	0.159E-03	-0.147E-03
	50000.	0.172E-03	-0.158E-03	0.165E-03	-0.151E-03	0.173E-03	-0.160E-03
	2500.	0.179E-03	-0.160E-03	0.172E-03	-0.153E-03	0.181E-03	-0.162E-03
3D - 9P	5000.	0.199E-03	-0.180E-03	0.191E-03	-0.172E-03	0.202E-03	-0.182E-03
8374.6 Å	10000.	0.222E-03	-0.203E-03	0.213E-03	-0.194E-03	0.225E-03	-0.205E-03
	20000.	0.249E-03	-0.228E-03	0.238E-03	-0.218E-03	0.251E-03	-0.231E-03
C= 0.12E+13	30000.	0.266E-03	-0.244E-03	0.254E-03	-0.234E-03	0.267E-03	-0.247E-03
	50000.	0.289E-03	-0.266E-03	0.277E-03	-0.255E-03	0.290E-03	-0.270E-03
	2500.	0.565	-0.512	0.542	-0.490	0.571	-0.519
4D - 5P	5000.	0.630	-0.576	0.604	-0.551	0.636	-0.583
	10000.	0.703	-0.647	0.674	-0.619	0.710	-0.655
C= 0.17E+18	20000.	0.788	-0.726	0.754	-0.695	0.793	-0.735
	30000.	0.844	-0.777	0.807	-0.743	0.847	-0.787
	50000.	0.922	-0.846	0.880	-0.809	0.920	-0.856
	2500.	0.448E-03	-0.399E-03	0.431E-03	-0.382E-03	0.453E-03	-0.404E-03
4D - 6P	5000.	0.497E-03	-0.449E-03	0.478E-03	-0.429E-03	0.503E-03	-0.454E-03
35385.7 Å	10000.	0.554E-03	-0.504E-03	0.531E-03	-0.482E-03	0.559E-03	-0.510E-03
	20000.	0.619E-03	-0.566E-03	0.593E-03	-0.542E-03	0.623E-03	-0.573E-03
C= 0.63E+14	30000.	0.661E-03	-0.606E-03	0.633E-03	-0.579E-03	0.665E-03	-0.613E-03
	50000.	0.720E-03	-0.659E-03	0.689E-03	-0.631E-03	0.721E-03	-0.668E-03

Perturber density= 1 x 10^{+11} cm^{-3}

		Perturbers					
		Ionized silicon		Ionized iron		Ionized magnesium	
Transition	T(K)	Width (Å)	Shift (Å)	Width (Å)	Shift (Å)	Width (Å)	Shift (Å)
	2500.	0.396E-03	-0.351E-03	0.381E-03	-0.336E-03	0.400E-03	-0.356E-03
4D - 7P	5000.	0.440E-03	-0.396E-03	0.422E-03	-0.378E-03	0.444E-03	-0.401E-03
23337.8 Å	10000.	0.490E-03	-0.445E-03	0.470E-03	-0.426E-03	0.494E-03	-0.450E-03
	20000.	0.547E-03	-0.500E-03	0.524E-03	-0.478E-03	0.551E-03	-0.506E-03
C= 0.19E+14	30000.	0.584E-03	-0.535E-03	0.559E-03	-0.512E-03	0.588E-03	-0.542E-03
	50000.	0.636E-03	-0.582E-03	0.608E-03	-0.557E-03	0.638E-03	-0.590E-03
	2500.	0.532E-03	-0.473E-03	0.511E-03	-0.453E-03	0.538E-03	-0.479E-03
4D - 8P	5000.	0.591E-03	-0.532E-03	0.568E-03	-0.509E-03	0.597E-03	-0.539E-03
19416.7 Å	10000.	0.658E-03	-0.599E-03	0.632E-03	-0.573E-03	0.665E-03	-0.607E-03
	20000.	0.735E-03	-0.674E-03	0.705E-03	-0.645E-03	0.742E-03	-0.682E-03
C= 0.89E+13	30000.	0.786E-03	-0.721E-03	0.752E-03	-0.690E-03	0.791E-03	-0.730E-03
	50000.	0.855E-03	-0.785E-03	0.818E-03	-0.752E-03	0.859E-03	-0.795E-03
	2500.	0.790E-03	-0.704E-03	0.759E-03	-0.673E-03	0.799E-03	-0.713E-03
4D - 9P	5000.	0.879E-03	-0.794E-03	0.844E-03	-0.760E-03	0.889E-03	-0.804E-03
17526.8 Å	10000.	0.980E-03	-0.894E-03	0.940E-03	-0.855E-03	0.990E-03	-0.905E-03
	20000.	0.110E-02	-0.101E-02	0.105E-02	-0.962E-03	0.111E-02	-0.102E-02
C= 0.51E+13	30000.	0.117E-02	-0.108E-02	0.112E-02	-0.103E-02	0.118E-02	-0.109E-02
	50000.	0.128E-02	-0.117E-02	0.122E-02	-0.112E-02	0.128E-02	-0.119E-02
	2500.	1.85	-1.65	1.78	-1.58	1.87	-1.68
	5000.	2.06	-1.86	1.98	-1.78	2.08	-1.88
5D - 6P	10000.	2.29	-2.09	2.20	-2.00	2.32	-2.12
C= 0.20E+18	20000.	2.56	-2.35	2.45	-2.25	2.58	-2.38
	30000.	2.74	-2.51	2.62	-2.41	2.75	-2.55
	50000.	2.98	-2.74	2.85	-2.62	2.99	-2.77
	2500.	0.353E-02	-0.314E-02	0.339E-02	-0.300E-02	0.357E-02	-0.318E-02
5D - 7P	5000.	0.392E-02	-0.353E-02	0.377E-02	-0.338E-02	0.396E-02	-0.358E-02
66273.4 Å	10000.	0.437E-02	-0.397E-02	0.419E-02	-0.380E-02	0.441E-02	-0.402E-02
	20000.	0.488E-02	-0.447E-02	0.467E-02	-0.427E-02	0.492E-02	-0.452E-02
C= 0.15E+15	30000.	0.521E-02	-0.478E-02	0.499E-02	-0.457E-02	0.524E-02	-0.484E-02
	50000.	0.567E-02	-0.520E-02	0.543E-02	-0.498E-02	0.569E-02	-0.527E-02
	2500.	0.260E-02	-0.232E-02	0.250E-02	-0.222E-02	0.263E-02	-0.234E-02
5D - 8P	5000.	0.289E-02	-0.261E-02	0.278E-02	-0.249E-02	0.292E-02	-0.264E-02
42119.3 Å	10000.	0.322E-02	-0.293E-02	0.309E-02	-0.281E-02	0.325E-02	-0.297E-02
	20000.	0.360E-02	-0.330E-02	0.345E-02	-0.316E-02	0.363E-02	-0.334E-02
C= 0.42E+14	30000.	0.384E-02	-0.353E-02	0.368E-02	-0.338E-02	0.387E-02	-0.357E-02
	50000.	0.419E-02	-0.384E-02	0.401E-02	-0.368E-02	0.420E-02	-0.389E-02

Perturber density= 1 x 10^{+11} cm^{-3}

		Perturbers					
		Ionized silicon		Ionized iron		Ionized magnesium	
Transition	T(K)	Width (Å)	Shift (Å)	Width (Å)	Shift (Å)	Width (Å)	Shift (Å)
	2500.	0.305E-02	-0.271E-02	0.293E-02	-0.259E-02	0.308E-02	-0.275E-02
5D - 9P	5000.	0.339E-02	-0.306E-02	0.325E-02	-0.293E-02	0.343E-02	-0.310E-02
34134.8 Å	10000.	0.378E-02	-0.345E-02	0.362E-02	-0.330E-02	0.382E-02	-0.349E-02
	20000.	0.422E-02	-0.388E-02	0.405E-02	-0.371E-02	0.426E-02	-0.393E-02
C= 0.19E+14	30000.	0.451E-02	-0.415E-02	0.432E-02	-0.397E-02	0.455E-02	-0.420E-02
	50000.	0.492E-02	-0.452E-02	0.470E-02	-0.433E-02	0.494E-02	-0.458E-02
	2500.	8.81	-7.87	8.46	-7.54	8.90	-7.97
	5000.	9.79	-8.87	9.40	-8.48	9.90	-8.98
6D - 7P	10000.	10.9	-9.97	10.5	-9.54	11.0	-10.1
C= 0.29E+18	20000.	12.2	-11.2	11.7	-10.7	12.3	-11.4
	30000.	13.0	-12.0	12.5	-11.5	13.1	-12.1
	50000.	14.2	-13.1	13.6	-12.5	14.3	-13.2
	2500.	0.203E-01	-0.182E-01	0.195E-01	-0.174E-01	0.206E-01	-0.184E-01
6D - 8P	5000.	0.226E-01	-0.204E-01	0.217E-01	-0.196E-01	0.229E-01	-0.207E-01
111154.3 Å	10000.	0.252E-01	-0.230E-01	0.242E-01	-0.220E-01	0.255E-01	-0.233E-01
	20000.	0.282E-01	-0.259E-01	0.270E-01	-0.247E-01	0.284E-01	-0.262E-01
C= 0.29E+15	30000.	0.301E-01	-0.277E-01	0.288E-01	-0.265E-01	0.303E-01	-0.280E-01
	50000.	0.328E-01	-0.302E-01	0.314E-01	-0.289E-01	0.329E-01	-0.305E-01
	2500.	0.130E-01	-0.116E-01	0.125E-01	-0.111E-01	0.131E-01	-0.117E-01
6D - 9P	5000.	0.145E-01	-0.131E-01	0.139E-01	-0.125E-01	0.146E-01	-0.132E-01
68728.5 Å	10000.	0.161E-01	-0.147E-01	0.155E-01	-0.141E-01	0.163E-01	-0.149E-01
	20000.	0.180E-01	-0.166E-01	0.173E-01	-0.158E-01	0.182E-01	-0.168E-01
C= 0.79E+14	30000.	0.193E-01	-0.177E-01	0.185E-01	-0.170E-01	0.194E-01	-0.180E-01
	50000.	0.210E-01	-0.193E-01	0.201E-01	-0.185E-01	0.211E-01	-0.196E-01
	2500.	0.926E-01	-0.826E-01	0.889E-01	-0.790E-01	0.936E-01	-0.837E-01
7D - 9P	5000.	0.103	-0.934E-01	0.989E-01	-0.893E-01	0.104	-0.945E-01
172693.7 Å	10000.	0.115	-0.105	0.110	-0.101	0.116	-0.106
	20000.	0.129	-0.118	0.123	-0.113	0.130	-0.120
C= 0.50E+15	30000.	0.138	-0.127	0.132	-0.121	0.138	-0.128
	50000.	0.150	-0.138	0.143	-0.132	0.150	-0.140
	2500.	0.634E-05	0.243E-05	0.631E-05	0.232E-05	0.635E-05	0.246E-05
3D - 4F	5000.	0.644E-05	0.273E-05	0.640E-05	0.261E-05	0.645E-05	0.276E-05
14881.7 Å	10000.	0.659E-05	0.306E-05	0.653E-05	0.293E-05	0.658E-05	0.310E-05
	20000.	0.678E-05	0.343E-05	0.670E-05	0.329E-05	0.676E-05	0.348E-05
C= 0.24E+14	30000.	0.694E-05	0.368E-05	0.683E-05	0.352E-05	0.689E-05	0.372E-05
	50000.	0.719E-05	0.400E-05	0.705E-05	0.383E-05	0.708E-05	0.405E-05

Perturber density= 1 x 10^{+11} cm^{-3}

		Perturbers					
		Ionized silicon		Ionized iron		Ionized magnesium	
Transition	T(K)	Width (Å)	Shift (Å)	Width (Å)	Shift (Å)	Width (Å)	Shift (Å)
	2500.	0.138E-04	0.101E-04	0.135E-04	0.971E-05	0.139E-04	0.103E-04
3D - 5F	5000.	0.148E-04	0.114E-04	0.144E-04	0.109E-04	0.149E-04	0.115E-04
10814.0 Å	10000.	0.160E-04	0.128E-04	0.156E-04	0.122E-04	0.162E-04	0.130E-04
	20000.	0.175E-04	0.144E-04	0.169E-04	0.137E-04	0.176E-04	0.145E-04
C= 0.10E+14	30000.	0.184E-04	0.154E-04	0.178E-04	0.147E-04	0.186E-04	0.156E-04
	50000.	0.197E-04	0.167E-04	0.190E-04	0.160E-04	0.199E-04	0.169E-04
	2500.	0.252E-04	0.190E-04	0.245E-04	0.182E-04	0.254E-04	0.192E-04
3D - 6F	5000.	0.272E-04	0.214E-04	0.264E-04	0.204E-04	0.274E-04	0.216E-04
9417.7 Å	10000.	0.295E-04	0.240E-04	0.286E-04	0.230E-04	0.298E-04	0.243E-04
	20000.	0.322E-04	0.269E-04	0.311E-04	0.258E-04	0.325E-04	0.273E-04
C= 0.58E+13	30000.	0.340E-04	0.288E-04	0.328E-04	0.276E-04	0.343E-04	0.292E-04
	50000.	0.365E-04	0.314E-04	0.352E-04	0.300E-04	0.368E-04	0.318E-04
	2500.	0.405E-04	0.293E-04	0.395E-04	0.280E-04	0.407E-04	0.296E-04
3D - 7F	5000.	0.434E-04	0.329E-04	0.422E-04	0.315E-04	0.437E-04	0.333E-04
8738.4 Å	10000.	0.468E-04	0.370E-04	0.455E-04	0.354E-04	0.472E-04	0.375E-04
	20000.	0.509E-04	0.416E-04	0.493E-04	0.398E-04	0.514E-04	0.421E-04
C= 0.40E+13	30000.	0.536E-04	0.445E-04	0.518E-04	0.426E-04	0.541E-04	0.450E-04
	50000.	0.573E-04	0.484E-04	0.553E-04	0.463E-04	0.578E-04	0.490E-04
	2500.	0.584E-04	0.377E-04	0.573E-04	0.361E-04	0.587E-04	0.382E-04
3D - 8F	5000.	0.617E-04	0.425E-04	0.604E-04	0.406E-04	0.621E-04	0.430E-04
8348.4 Å	10000.	0.657E-04	0.478E-04	0.641E-04	0.457E-04	0.662E-04	0.484E-04
	20000.	0.705E-04	0.536E-04	0.686E-04	0.513E-04	0.710E-04	0.543E-04
C= 0.31E+13	30000.	0.737E-04	0.574E-04	0.716E-04	0.549E-04	0.743E-04	0.581E-04
	50000.	0.782E-04	0.625E-04	0.758E-04	0.598E-04	0.788E-04	0.633E-04
	2500.	0.491E-02	-0.437E-02	0.472E-02	-0.418E-02	0.496E-02	-0.442E-02
4D - 4F	5000.	0.545E-02	-0.491E-02	0.524E-02	-0.469E-02	0.551E-02	-0.497E-02
206436.7 Å	10000.	0.607E-02	-0.551E-02	0.582E-02	-0.527E-02	0.612E-02	-0.558E-02
	20000.	0.678E-02	-0.618E-02	0.650E-02	-0.591E-02	0.682E-02	-0.626E-02
C= 0.25E+16	30000.	0.724E-02	-0.661E-02	0.694E-02	-0.633E-02	0.728E-02	-0.670E-02
	50000.	0.790E-02	-0.720E-02	0.755E-02	-0.689E-02	0.790E-02	-0.729E-02
	2500.	0.106E-03	-0.455E-04	0.106E-03	-0.435E-04	0.107E-03	-0.461E-04
4D - 5F	5000.	0.109E-03	-0.511E-04	0.108E-03	-0.489E-04	0.109E-03	-0.517E-04
33200.8 Å	10000.	0.112E-03	-0.573E-04	0.111E-03	-0.549E-04	0.112E-03	-0.580E-04
	20000.	0.116E-03	-0.644E-04	0.114E-03	-0.616E-04	0.116E-03	-0.652E-04
C= 0.65E+14	30000.	0.119E-03	-0.688E-04	0.117E-03	-0.659E-04	0.118E-03	-0.697E-04
	50000.	0.124E-03	-0.750E-04	0.121E-03	-0.717E-04	0.122E-03	-0.759E-04

Perturber density= 1 x 10^{+11} cm^{-3}

Transition	T(K)	Perturbers: Ionized silicon Width (Å)	Ionized silicon Shift (Å)	Ionized iron Width (Å)	Ionized iron Shift (Å)	Ionized magnesium Width (Å)	Ionized magnesium Shift (Å)
	2500.	0.129E-03	0.844E-04	0.127E-03	0.807E-04	0.130E-03	0.855E-04
4D - 6F	5000.	0.137E-03	0.949E-04	0.134E-03	0.908E-04	0.137E-03	0.961E-04
22815.3 Å	10000.	0.146E-03	0.107E-03	0.142E-03	0.102E-03	0.147E-03	0.108E-03
	20000.	0.157E-03	0.120E-03	0.152E-03	0.114E-03	0.157E-03	0.121E-03
C= 0.31E+14	30000.	0.164E-03	0.128E-03	0.159E-03	0.122E-03	0.165E-03	0.130E-03
	50000.	0.175E-03	0.139E-03	0.169E-03	0.133E-03	0.175E-03	0.141E-03
	2500.	0.186E-03	0.128E-03	0.182E-03	0.122E-03	0.187E-03	0.129E-03
4D - 7F	5000.	0.198E-03	0.144E-03	0.193E-03	0.137E-03	0.199E-03	0.145E-03
19199.5 Å	10000.	0.212E-03	0.161E-03	0.206E-03	0.154E-03	0.214E-03	0.163E-03
	20000.	0.229E-03	0.181E-03	0.223E-03	0.173E-03	0.231E-03	0.183E-03
C= 0.19E+14	30000.	0.241E-03	0.194E-03	0.233E-03	0.185E-03	0.242E-03	0.196E-03
	50000.	0.257E-03	0.211E-03	0.248E-03	0.202E-03	0.258E-03	0.214E-03
	2500.	0.249E-03	0.155E-03	0.244E-03	0.148E-03	0.250E-03	0.157E-03
4D - 8F	5000.	0.262E-03	0.174E-03	0.256E-03	0.167E-03	0.263E-03	0.176E-03
17412.3 Å	10000.	0.277E-03	0.196E-03	0.271E-03	0.187E-03	0.279E-03	0.198E-03
	20000.	0.297E-03	0.220E-03	0.289E-03	0.211E-03	0.299E-03	0.223E-03
C= 0.13E+14	30000.	0.309E-03	0.235E-03	0.301E-03	0.225E-03	0.311E-03	0.238E-03
	50000.	0.328E-03	0.256E-03	0.318E-03	0.245E-03	0.330E-03	0.260E-03
	2500.	0.447E-01	-0.374E-01	0.432E-01	-0.358E-01	0.452E-01	-0.379E-01
5D - 5F	5000.	0.491E-01	-0.421E-01	0.474E-01	-0.402E-01	0.496E-01	-0.426E-01
423764.7 Å	10000.	0.542E-01	-0.472E-01	0.521E-01	-0.452E-01	0.546E-01	-0.478E-01
	20000.	0.600E-01	-0.530E-01	0.577E-01	-0.508E-01	0.604E-01	-0.537E-01
C= 0.90E+16	30000.	0.638E-01	-0.567E-01	0.613E-01	-0.543E-01	0.642E-01	-0.575E-01
	50000.	0.692E-01	-0.618E-01	0.663E-01	-0.591E-01	0.693E-01	-0.626E-01
	2500.	0.878E-03	-0.300E-03	0.875E-03	-0.287E-03	0.879E-03	-0.304E-03
5D - 6F	5000.	0.889E-03	-0.337E-03	0.884E-03	-0.322E-03	0.889E-03	-0.341E-03
62227.0 Å	10000.	0.903E-03	-0.378E-03	0.897E-03	-0.362E-03	0.903E-03	-0.383E-03
	20000.	0.924E-03	-0.424E-03	0.915E-03	-0.406E-03	0.921E-03	-0.430E-03
C= 0.19E+15	30000.	0.939E-03	-0.454E-03	0.929E-03	-0.435E-03	0.935E-03	-0.460E-03
	50000.	0.965E-03	-0.494E-03	0.951E-03	-0.473E-03	0.954E-03	-0.501E-03
	2500.	0.757E-03	0.405E-03	0.748E-03	0.388E-03	0.759E-03	0.410E-03
5D - 7F	5000.	0.785E-03	0.455E-03	0.773E-03	0.436E-03	0.788E-03	0.461E-03
41110.5 Å	10000.	0.820E-03	0.512E-03	0.806E-03	0.490E-03	0.823E-03	0.518E-03
	20000.	0.864E-03	0.574E-03	0.846E-03	0.550E-03	0.867E-03	0.582E-03
C= 0.85E+14	30000.	0.894E-03	0.615E-03	0.874E-03	0.588E-03	0.897E-03	0.622E-03
	50000.	0.939E-03	0.669E-03	0.915E-03	0.640E-03	0.940E-03	0.678E-03

Perturber density= 1 x 10^{+11} cm^{-3}

Transition	T(K)	Perturbers: Ionized silicon Width (Å)	Ionized silicon Shift (Å)	Ionized iron Width (Å)	Ionized iron Shift (Å)	Ionized magnesium Width (Å)	Ionized magnesium Shift (Å)
	2500.	0.885E-03	0.485E-03	0.874E-03	0.464E-03	0.889E-03	0.491E-03
5D - 8F	5000.	0.920E-03	0.545E-03	0.906E-03	0.522E-03	0.924E-03	0.552E-03
33703.2 Å	10000.	0.963E-03	0.613E-03	0.945E-03	0.587E-03	0.967E-03	0.621E-03
	20000.	0.102E-02	0.688E-03	0.994E-03	0.659E-03	0.102E-02	0.697E-03
C= 0.50E+14	30000.	0.105E-02	0.737E-03	0.103E-02	0.705E-03	0.106E-02	0.746E-03
	50000.	0.111E-02	0.802E-03	0.108E-02	0.768E-03	0.111E-02	0.812E-03
	2500.	0.317	-0.263	0.307	-0.252	0.320	-0.267
6D - 6F	5000.	0.348	-0.296	0.336	-0.283	0.351	-0.300
754944.9 Å	10000.	0.383	-0.333	0.369	-0.319	0.387	-0.337
	20000.	0.424	-0.374	0.408	-0.358	0.427	-0.379
C= 0.20E+17	30000.	0.451	-0.400	0.433	-0.383	0.454	-0.405
	50000.	0.489	-0.436	0.469	-0.417	0.490	-0.441
	2500.	0.579E-02	-0.342E-02	0.570E-02	-0.327E-02	0.581E-02	-0.346E-02
6D - 7F	5000.	0.606E-02	-0.385E-02	0.595E-02	-0.368E-02	0.609E-02	-0.389E-02
104393.9 Å	10000.	0.639E-02	-0.432E-02	0.626E-02	-0.414E-02	0.642E-02	-0.438E-02
	20000.	0.681E-02	-0.485E-02	0.664E-02	-0.464E-02	0.683E-02	-0.491E-02
C= 0.37E+15	30000.	0.709E-02	-0.519E-02	0.690E-02	-0.497E-02	0.710E-02	-0.526E-02
	50000.	0.751E-02	-0.565E-02	0.729E-02	-0.541E-02	0.749E-02	-0.572E-02
	2500.	0.324E-02	-0.260E-03	0.324E-02	-0.249E-03	0.324E-02	-0.263E-03
6D - 8F	5000.	0.324E-02	-0.292E-03	0.324E-02	-0.279E-03	0.324E-02	-0.295E-03
67000.8 Å	10000.	0.324E-02	-0.327E-03	0.324E-02	-0.313E-03	0.324E-02	-0.331E-03
	20000.	0.325E-02	-0.367E-03	0.325E-02	-0.352E-03	0.324E-02	-0.372E-03
C= 0.15E+15	30000.	0.326E-02	-0.393E-03	0.325E-02	-0.376E-03	0.324E-02	-0.398E-03
	50000.	0.327E-02	-0.427E-03	0.326E-02	-0.410E-03	0.324E-02	-0.432E-03
	2500.	1.73	-1.45	1.67	-1.39	1.74	-1.47
7D - 7F	5000.	1.90	-1.63	1.83	-1.56	1.92	-1.65
	10000.	2.10	-1.84	2.02	-1.76	2.12	-1.86
	20000.	2.32	-2.07	2.23	-1.98	2.34	-2.09
C= 0.35E+17	30000.	2.47	-2.21	2.38	-2.12	2.49	-2.24
	50000.	2.68	-2.41	2.57	-2.31	2.69	-2.44
	2500.	0.310E-01	-0.227E-01	0.302E-01	-0.217E-01	0.313E-01	-0.230E-01
7D - 8F	5000.	0.334E-01	-0.256E-01	0.324E-01	-0.245E-01	0.336E-01	-0.259E-01
162185.0 Å	10000.	0.361E-01	-0.288E-01	0.350E-01	-0.275E-01	0.364E-01	-0.292E-01
	20000.	0.394E-01	-0.324E-01	0.381E-01	-0.310E-01	0.396E-01	-0.328E-01
C= 0.62E+15	30000.	0.416E-01	-0.346E-01	0.401E-01	-0.331E-01	0.418E-01	-0.351E-01
	50000.	0.447E-01	-0.377E-01	0.430E-01	-0.361E-01	0.447E-01	-0.382E-01

Perturber density= 1 x 10^{+11} cm^{-3}

Transition	T(K)	Perturbers: Ionized silicon Width (Å)	Ionized silicon Shift (Å)	Ionized iron Width (Å)	Ionized iron Shift (Å)	Ionized magnesium Width (Å)	Ionized magnesium Shift (Å)
	2500.	7.66	-6.55	7.38	-6.26	7.74	-6.63
8D - 8F	5000.	8.45	-7.38	8.14	-7.06	8.54	-7.47
	10000.	9.36	-8.31	9.00	-7.95	9.45	-8.42
	20000.	10.4	-9.35	9.99	-8.94	10.5	-9.47
C= 0.57E+17	30000.	11.1	-10.0	10.6	-9.58	11.2	-10.1
	50000.	12.1	-10.9	11.5	-10.4	12.1	-11.0
	2500.	0.517E-03	0.462E-03	0.497E-03	0.442E-03	0.522E-03	0.467E-03
4F - 5D	5000.	0.574E-03	0.519E-03	0.551E-03	0.497E-03	0.580E-03	0.526E-03
43637.8 Å	10000.	0.639E-03	0.583E-03	0.614E-03	0.558E-03	0.646E-03	0.591E-03
	20000.	0.714E-03	0.655E-03	0.684E-03	0.627E-03	0.720E-03	0.663E-03
C= 0.95E+14	30000.	0.763E-03	0.701E-03	0.731E-03	0.670E-03	0.768E-03	0.709E-03
	50000.	0.831E-03	0.763E-03	0.795E-03	0.730E-03	0.834E-03	0.772E-03
	2500.	0.434E-03	0.390E-03	0.417E-03	0.373E-03	0.439E-03	0.395E-03
4F - 6D	5000.	0.483E-03	0.439E-03	0.464E-03	0.420E-03	0.489E-03	0.444E-03
26552.3 Å	10000.	0.539E-03	0.493E-03	0.517E-03	0.472E-03	0.544E-03	0.499E-03
	20000.	0.602E-03	0.554E-03	0.577E-03	0.530E-03	0.608E-03	0.561E-03
C= 0.24E+14	30000.	0.643E-03	0.593E-03	0.616E-03	0.567E-03	0.648E-03	0.600E-03
	50000.	0.701E-03	0.646E-03	0.670E-03	0.618E-03	0.704E-03	0.654E-03
	2500.	0.581E-03	0.523E-03	0.558E-03	0.501E-03	0.588E-03	0.530E-03
4F - 7D	5000.	0.647E-03	0.589E-03	0.621E-03	0.564E-03	0.655E-03	0.597E-03
21542.0 Å	10000.	0.722E-03	0.663E-03	0.693E-03	0.634E-03	0.730E-03	0.671E-03
	20000.	0.808E-03	0.745E-03	0.774E-03	0.713E-03	0.815E-03	0.755E-03
C= 0.11E+14	30000.	0.864E-03	0.798E-03	0.827E-03	0.763E-03	0.870E-03	0.808E-03
	50000.	0.941E-03	0.869E-03	0.900E-03	0.831E-03	0.945E-03	0.880E-03
	2500.	0.863E-03	0.777E-03	0.828E-03	0.743E-03	0.872E-03	0.787E-03
4F - 8D	5000.	0.962E-03	0.877E-03	0.922E-03	0.839E-03	0.972E-03	0.888E-03
19214.2 Å	10000.	0.107E-02	0.987E-03	0.103E-02	0.945E-03	0.109E-02	0.100E-02
	20000.	0.120E-02	0.111E-02	0.115E-02	0.106E-02	0.121E-02	0.112E-02
C= 0.62E+13	30000.	0.129E-02	0.119E-02	0.123E-02	0.114E-02	0.130E-02	0.120E-02
	50000.	0.140E-02	0.130E-02	0.134E-02	0.124E-02	0.141E-02	0.131E-02
	2500.	0.128E-02	0.115E-02	0.123E-02	0.110E-02	0.130E-02	0.117E-02
4F - 9D	5000.	0.143E-02	0.131E-02	0.137E-02	0.125E-02	0.145E-02	0.132E-02
17899.1 Å	10000.	0.160E-02	0.147E-02	0.153E-02	0.141E-02	0.161E-02	0.149E-02
	20000.	0.179E-02	0.165E-02	0.171E-02	0.158E-02	0.181E-02	0.167E-02
C= 0.40E+13	30000.	0.191E-02	0.177E-02	0.183E-02	0.169E-02	0.193E-02	0.179E-02
	50000.	0.209E-02	0.193E-02	0.200E-02	0.185E-02	0.210E-02	0.195E-02

Perturber density= 1 x 10^{+11} cm^{-3}

Transition	T(K)	Perturbers: Ionized silicon Width (Å)	Ionized silicon Shift (Å)	Ionized iron Width (Å)	Ionized iron Shift (Å)	Ionized magnesium Width (Å)	Ionized magnesium Shift (Å)
	2500.	0.187E-02	0.168E-02	0.180E-02	0.160E-02	0.189E-02	0.170E-02
4F -10D	5000.	0.209E-02	0.190E-02	0.200E-02	0.182E-02	0.211E-02	0.193E-02
17071.3 Å	10000.	0.234E-02	0.215E-02	0.224E-02	0.206E-02	0.236E-02	0.217E-02
	20000.	0.262E-02	0.242E-02	0.251E-02	0.231E-02	0.264E-02	0.245E-02
C= 0.28E+13	30000.	0.280E-02	0.259E-02	0.268E-02	0.248E-02	0.282E-02	0.262E-02
	50000.	0.305E-02	0.283E-02	0.292E-02	0.270E-02	0.307E-02	0.286E-02
	2500.	0.447E-01	0.374E-01	0.432E-01	0.358E-01	0.452E-01	0.379E-01
5F - 5D	5000.	0.491E-01	0.421E-01	0.474E-01	0.402E-01	0.496E-01	0.426E-01
423764.7 Å	10000.	0.542E-01	0.472E-01	0.521E-01	0.452E-01	0.546E-01	0.478E-01
	20000.	0.600E-01	0.530E-01	0.577E-01	0.508E-01	0.604E-01	0.537E-01
C= 0.90E+16	30000.	0.638E-01	0.567E-01	0.613E-01	0.543E-01	0.642E-01	0.575E-01
	50000.	0.692E-01	0.618E-01	0.663E-01	0.591E-01	0.693E-01	0.626E-01
	2500.	0.391E-02	0.346E-02	0.376E-02	0.331E-02	0.395E-02	0.350E-02
5F - 6D	5000.	0.434E-02	0.390E-02	0.417E-02	0.373E-02	0.438E-02	0.394E-02
80737.6 Å	10000.	0.483E-02	0.438E-02	0.463E-02	0.419E-02	0.488E-02	0.443E-02
	20000.	0.539E-02	0.492E-02	0.516E-02	0.471E-02	0.543E-02	0.498E-02
C= 0.22E+15	30000.	0.575E-02	0.526E-02	0.551E-02	0.504E-02	0.579E-02	0.533E-02
	50000.	0.626E-02	0.573E-02	0.599E-02	0.549E-02	0.628E-02	0.580E-02
	2500.	0.277E-02	0.249E-02	0.267E-02	0.238E-02	0.281E-02	0.252E-02
5F - 7D	5000.	0.309E-02	0.280E-02	0.296E-02	0.268E-02	0.312E-02	0.284E-02
47292.1 Å	10000.	0.344E-02	0.315E-02	0.330E-02	0.302E-02	0.348E-02	0.319E-02
	20000.	0.385E-02	0.354E-02	0.369E-02	0.339E-02	0.388E-02	0.359E-02
C= 0.53E+14	30000.	0.411E-02	0.379E-02	0.394E-02	0.363E-02	0.415E-02	0.384E-02
	50000.	0.448E-02	0.413E-02	0.429E-02	0.395E-02	0.450E-02	0.418E-02
	2500.	0.325E-02	0.292E-02	0.312E-02	0.280E-02	0.329E-02	0.296E-02
5F - 8D	5000.	0.362E-02	0.330E-02	0.347E-02	0.315E-02	0.366E-02	0.334E-02
37356.4 Å	10000.	0.404E-02	0.371E-02	0.388E-02	0.355E-02	0.409E-02	0.376E-02
	20000.	0.452E-02	0.418E-02	0.433E-02	0.400E-02	0.456E-02	0.423E-02
C= 0.23E+14	30000.	0.484E-02	0.447E-02	0.463E-02	0.428E-02	0.487E-02	0.453E-02
	50000.	0.527E-02	0.487E-02	0.504E-02	0.466E-02	0.529E-02	0.493E-02
	2500.	0.427E-02	0.383E-02	0.410E-02	0.367E-02	0.432E-02	0.388E-02
5F - 9D	5000.	0.476E-02	0.434E-02	0.457E-02	0.415E-02	0.481E-02	0.440E-02
32687.2 Å	10000.	0.532E-02	0.489E-02	0.510E-02	0.468E-02	0.537E-02	0.495E-02
	20000.	0.596E-02	0.550E-02	0.570E-02	0.526E-02	0.601E-02	0.557E-02
C= 0.13E+14	30000.	0.637E-02	0.589E-02	0.610E-02	0.564E-02	0.642E-02	0.597E-02
	50000.	0.695E-02	0.642E-02	0.664E-02	0.615E-02	0.697E-02	0.650E-02

Perturber density= 1 x 10^{+11} cm^{-3}

		Perturbers					
		Ionized silicon		Ionized iron		Ionized magnesium	
Transition	T(K)	Width (Å)	Shift (Å)	Width (Å)	Shift (Å)	Width (Å)	Shift (Å)
	2500.	0.579E-02	0.519E-02	0.555E-02	0.496E-02	0.585E-02	0.525E-02
5F -10D	5000.	0.646E-02	0.588E-02	0.620E-02	0.562E-02	0.653E-02	0.596E-02
30028.0 Å	10000.	0.722E-02	0.664E-02	0.692E-02	0.636E-02	0.730E-02	0.672E-02
	20000.	0.809E-02	0.747E-02	0.775E-02	0.715E-02	0.816E-02	0.757E-02
C= 0.86E+13	30000.	0.866E-02	0.801E-02	0.828E-02	0.766E-02	0.872E-02	0.811E-02
	50000.	0.944E-02	0.873E-02	0.903E-02	0.835E-02	0.948E-02	0.884E-02
	2500.	0.317	0.263	0.307	0.252	0.320	0.267
6F - 6D	5000.	0.348	0.296	0.336	0.283	0.351	0.300
754944.9 Å	10000.	0.383	0.333	0.369	0.319	0.387	0.337
	20000.	0.424	0.374	0.408	0.358	0.427	0.379
C= 0.20E+17	30000.	0.451	0.400	0.433	0.383	0.454	0.405
	50000.	0.489	0.436	0.469	0.417	0.490	0.441
	2500.	0.218E-01	0.193E-01	0.210E-01	0.184E-01	0.221E-01	0.195E-01
6F - 7D	5000.	0.242E-01	0.217E-01	0.233E-01	0.208E-01	0.245E-01	0.220E-01
134502.6 Å	10000.	0.270E-01	0.244E-01	0.259E-01	0.234E-01	0.272E-01	0.247E-01
	20000.	0.301E-01	0.275E-01	0.288E-01	0.263E-01	0.303E-01	0.278E-01
C= 0.43E+15	30000.	0.321E-01	0.294E-01	0.308E-01	0.281E-01	0.323E-01	0.298E-01
	50000.	0.349E-01	0.320E-01	0.334E-01	0.306E-01	0.351E-01	0.324E-01
	2500.	0.135E-01	0.121E-01	0.130E-01	0.116E-01	0.136E-01	0.122E-01
6F - 8D	5000.	0.150E-01	0.136E-01	0.144E-01	0.130E-01	0.152E-01	0.138E-01
76576.7 Å	10000.	0.168E-01	0.153E-01	0.161E-01	0.147E-01	0.169E-01	0.155E-01
	20000.	0.188E-01	0.173E-01	0.180E-01	0.165E-01	0.189E-01	0.175E-01
C= 0.98E+14	30000.	0.200E-01	0.185E-01	0.192E-01	0.177E-01	0.202E-01	0.187E-01
	50000.	0.218E-01	0.201E-01	0.209E-01	0.193E-01	0.219E-01	0.204E-01
	2500.	0.139E-01	0.125E-01	0.134E-01	0.120E-01	0.141E-01	0.127E-01
6F - 9D	5000.	0.155E-01	0.142E-01	0.149E-01	0.135E-01	0.157E-01	0.143E-01
59232.6 Å	10000.	0.174E-01	0.159E-01	0.166E-01	0.153E-01	0.175E-01	0.161E-01
	20000.	0.194E-01	0.179E-01	0.186E-01	0.172E-01	0.196E-01	0.182E-01
C= 0.44E+14	30000.	0.208E-01	0.192E-01	0.199E-01	0.184E-01	0.209E-01	0.195E-01
	50000.	0.227E-01	0.209E-01	0.217E-01	0.200E-01	0.228E-01	0.212E-01
	2500.	0.167E-01	0.149E-01	0.160E-01	0.143E-01	0.169E-01	0.151E-01
6F -10D	5000.	0.186E-01	0.169E-01	0.179E-01	0.162E-01	0.188E-01	0.172E-01
51041.8 Å	10000.	0.208E-01	0.191E-01	0.199E-01	0.183E-01	0.210E-01	0.193E-01
	20000.	0.233E-01	0.215E-01	0.223E-01	0.206E-01	0.235E-01	0.218E-01
C= 0.25E+14	30000.	0.249E-01	0.231E-01	0.239E-01	0.221E-01	0.251E-01	0.233E-01
	50000.	0.272E-01	0.251E-01	0.260E-01	0.241E-01	0.273E-01	0.255E-01

Perturber density= $1 \times 10^{+11}$ cm^{-3}

Transition	T(K)	Perturbers: Ionized silicon Width (Å)	Ionized silicon Shift (Å)	Ionized iron Width (Å)	Ionized iron Shift (Å)	Ionized magnesium Width (Å)	Ionized magnesium Shift (Å)
7F - 7D	2500.	1.73	1.45	1.67	1.39	1.74	1.47
	5000.	1.90	1.63	1.83	1.56	1.92	1.65
	10000.	2.10	1.84	2.02	1.76	2.12	1.86
	20000.	2.32	2.07	2.23	1.98	2.34	2.09
C= 0.35E+17	30000.	2.47	2.21	2.38	2.12	2.49	2.24
	50000.	2.68	2.41	2.57	2.31	2.69	2.44
7F - 8D	2500.	0.979E-01	0.866E-01	0.942E-01	0.828E-01	0.990E-01	0.877E-01
	5000.	0.109	0.976E-01	0.104	0.933E-01	0.110	0.988E-01
208146.9 Å	10000.	0.121	0.110	0.116	0.105	0.122	0.111
	20000.	0.135	0.124	0.130	0.118	0.136	0.125
C= 0.72E+15	30000.	0.144	0.132	0.138	0.127	0.145	0.134
	50000.	0.157	0.144	0.150	0.138	0.158	0.146
7F - 9D	2500.	0.529E-01	0.472E-01	0.508E-01	0.452E-01	0.535E-01	0.478E-01
	5000.	0.590E-01	0.535E-01	0.566E-01	0.511E-01	0.596E-01	0.542E-01
115900.4 Å	10000.	0.658E-01	0.602E-01	0.631E-01	0.576E-01	0.665E-01	0.610E-01
	20000.	0.736E-01	0.678E-01	0.705E-01	0.648E-01	0.743E-01	0.686E-01
C= 0.17E+15	30000.	0.787E-01	0.726E-01	0.754E-01	0.694E-01	0.793E-01	0.735E-01
	50000.	0.858E-01	0.791E-01	0.820E-01	0.757E-01	0.861E-01	0.801E-01
7F -10D	2500.	0.496E-01	0.443E-01	0.476E-01	0.424E-01	0.502E-01	0.449E-01
	5000.	0.553E-01	0.503E-01	0.531E-01	0.480E-01	0.559E-01	0.509E-01
88204.4 Å	10000.	0.618E-01	0.567E-01	0.593E-01	0.543E-01	0.625E-01	0.574E-01
	20000.	0.692E-01	0.638E-01	0.663E-01	0.611E-01	0.698E-01	0.646E-01
C= 0.74E+14	30000.	0.741E-01	0.684E-01	0.709E-01	0.655E-01	0.746E-01	0.693E-01
	50000.	0.808E-01	0.746E-01	0.772E-01	0.714E-01	0.810E-01	0.755E-01
8F - 8D	2500.	7.66	6.55	7.38	6.26	7.74	6.63
	5000.	8.45	7.38	8.14	7.06	8.54	7.47
	10000.	9.36	8.31	9.00	7.95	9.45	8.42
	20000.	10.4	9.35	9.99	8.94	10.5	9.47
C= 0.57E+17	30000.	11.1	10.0	10.6	9.58	11.2	10.1
	50000.	12.1	10.9	11.5	10.4	12.1	11.0
8F - 9D	2500.	0.364	0.321	0.350	0.307	0.368	0.325
	5000.	0.405	0.364	0.389	0.348	0.409	0.368
304692.3 Å	10000.	0.451	0.409	0.433	0.392	0.455	0.415
	20000.	0.504	0.461	0.483	0.441	0.508	0.467
C= 0.12E+16	30000.	0.538	0.494	0.515	0.472	0.542	0.500
	50000.	0.586	0.538	0.561	0.515	0.588	0.545

Perturber density= $1 \times 10^{+11}$ cm^{-3}

		Perturbers					
		Ionized silicon		Ionized iron		Ionized magnesium	
Transition	T(K)	Width (Å)	Shift (Å)	Width (Å)	Shift (Å)	Width (Å)	Shift (Å)
	2500.	0.177	0.157	0.170	0.151	0.179	0.159
8F -10D	5000.	0.197	0.179	0.189	0.171	0.200	0.181
166911.5 Å	10000.	0.220	0.201	0.211	0.193	0.223	0.204
	20000.	0.247	0.227	0.236	0.217	0.249	0.230
C= 0.26E+15	30000.	0.264	0.243	0.252	0.233	0.266	0.246
	50000.	0.288	0.265	0.275	0.254	0.288	0.268

For each value given in Table 1, the collision volume (V) multiplied by the perturber density (N) is much less than one and the impact approximation is valid (Sahal–Bréchot, 1969ab). Values for NV > 0.5 are not given and values for 0.1 < NV < 0.5 are denoted by an asterisk. When the impact approximation is not valid, the ion broadening contribution may be estimated by using quasistatic approach (Sahal–Bréchot 1991 and Griem 1974). The accuracy of the results obtained decreases when broadening by ion interactions becomes important.

Acknowledgements – This work is a part of the project "Physics and dynamics of celestial bodies", supported by Ministry of Science and Technology of Serbia.

REFERENCES

Dimitrijević, M. S., and Sahal–Bréchot,S.: 1984, *JQSRT* **31**, 301.

Dimitrijević, M. S., and Sahal–Bréchot,S.: 1994a, *Bull. Astron. Belgrade* **149**, 31.

Dimitrijević, M. S., and Sahal–Bréchot, S.: 1994b, *Astron. Astrophys. Suppl. Series*, submitted.

Dimitrijević, M. S., Sahal–Bréchot, S., and Bommier, V.: 1991, *Astron. Astrophys. Suppl. Series.* **89**, 581.

Griem, H. R.: 1974, *Spectral Line Broadening by Plasmas*, Academic Press, New York.

Sahal–Bréchot, S.: 1969a, *Astron. Astrophys.* **1**, 91.

Sahal–Bréchot, S.: 1969b, *Astron. Astrophys.* **2**, 322.

Sahal–Bréchot, S.: 1991, *Astron. Astrophys.* **245**, 322.

ТАБЕЛЕ ПАРАМЕТАРА ШТАРКОВОГ ШИРЕЊА ЛИНИЈА Mg I ОД ЗНАЧАЈА ЗА ПРОУЧАВАЊЕ СУНЧЕВОГ И ЗВЕЗДАНИХ СПЕКТАРА. II

М. С. Димитријевић[1] и S. Sahal–Bréchot[2]

[1] *Астрономска опсерваторија, Волгина 7, 11050 Београд, Југославија*

[2] *Laboratoire "Astrophysique, Atomes et Molécules"*
Département Atomes et Molécules en Astrophysique
Unité associée au C.N.R.S. No 812
Observatoire de Paris-Meudon, 92190 Meudon, France

УДК 52–355.3
Претходно саопштење

Користећи семикласичан прилаз, израчунате су ширине и помераји спектралних линија, проузроковани сударима са Mg II, Si II и Fe II, за 270 мултиплета Mg I. Резултати су дати у функцији температуре и концентрације пертурбера.

Bull. Astron. Belgrade № 150 (1994), 95 – 108

UDC 52–355.3
Preliminary report

STARK BROADENING PARAMETER TABLES FOR O IV AND O V LINES OF ASTROPHYSICAL IMPORTANCE

M. S. Dimitrijević[1] and S. Sahal–Bréchot[2]

[1] *Astronomical Observatory, Volgina 7, 11050 Belgrade, Yugoslavia*

[2] *Laboratoire "Astrophysique, Atomes et Molécules"*
Département Atomes et Molécules en Astrophysique
Unité associée au C.N.R.S. No 812
Observatoire de Paris–Meudon, 92190 Meudon, France

(Received: August 12, 1994)

SUMMARY: Using a semiclassical approach, we have calculated electron–, proton–, and He III–impact line widths and shifts for 5 O IV and 19 O V multiplets as a function of temperature and perturber density.

1. INTRODUCTION

Due to its high cosmical abundance oxygen lines are of particular interest for the analysis of stellar spectra. In order to provide to astrophysicists the needed Stark broadening data, we have calculated within the semiclassical-perturbation formalism (Sahal–Bréchot, 1969ab) electron-, proton-, and He III-, -impact line widths and shifts for 5 O IV and 19 O V multiplets, in order to continue our effort to provide to astrophysicists the needed Stark broadening data.

2. RESULTS AND DISCUSSION

Analysis of obtained results and all details of calculations as well as the comparison with availlable experimental data will be published elsewhere (Dimitrijević and Sahal–Bréchot, 1994). Here, we present tables of Stark broadening parameters for solar and laboratory plasma diagnostic purposes. Our results for 5 O IV and 19 O V multiplets are shown in Table 1, for perturber densities $10^{17} - 10^{22}$ cm^{-3} and temperatures T = 20,000 – 1,000,000 K. We also specify a parameter c (Dimitrijević and Sahal–Bréchot

Table 1. This table shows electron-, proton-, and He III- impact broadening parameters for O IV and O V, for perturber densities of 10^{17} - 10^{22} cm^{-3} and temperatures from 200,000 to 2,000,000 K. Transitions and averaged wavelengths for the multiplet (in Å) are also given. By using c [see Eq. (5) in Dimitrijević et al, 1991], we obtain an estimate for the maximum perturber density for which the line may be treated as isolated and tabulated data may be used. The asterisk identifies cases for which the collision volume multiplied by the perturber density (the condition for validity of the impact approximation) lies between 0.1 and 0.5. Table 1 is also available in electronic form: see the editorial in Astron.Astrophys. 1992, Vol. 266, No 2, page E1 or in Astron.Astrophys. Suppl. Series 1992, Vol. 96, No3, and Dimitrijević and Sahal-Brechot, 1994.

		Perturbers					
		Electrons		Protons		He III	
Transition	T(K)	Width (Å)	Shift (Å)	Width (Å)	Shift (Å)	Width (Å)	Shift (Å)
Perturber density = $1 \times 10^{+17}$ cm^{-3}							
O IV 2P 3S 279.9 Å C= 0.26E+19	20000.	0.609E-03	0.158E-04	0.995E-06	0.858E-05	0.186E-05	0.161E-04
	50000.	0.362E-03	0.330E-04	0.736E-05	0.192E-04	0.146E-04	0.378E-04
	100000.	0.266E-03	0.358E-04	0.176E-04	0.282E-04	0.356E-04	0.568E-04
	200000.	0.205E-03	0.383E-04	0.323E-04	0.373E-04	0.655E-04	0.764E-04
O IV 2P 3D 238.5 Å C= 0.17E+19	20000.	0.477E-03	-0.138E-04	0.345E-05	-0.124E-05	0.637E-05	-0.233E-05
	50000.	0.303E-03	-0.198E-05	0.997E-05	-0.317E-05	0.190E-04	-0.624E-05
	100000.	0.221E-03	0.814E-06	0.163E-04	-0.547E-05	0.319E-04	-0.110E-04
	200000.	0.167E-03	0.343E-06	0.227E-04	-0.792E-05	0.447E-04	-0.161E-04
O IV 3S 3P 3066.4 Å C= 0.28E+21	20000.	0.155	-0.141E-02	0.110E-02	-0.613E-03	0.203E-02	-0.115E-02
	50000.	0.991E-01	-0.237E-02	0.289E-02	-0.145E-02	0.554E-02	-0.286E-02
	100000.	0.741E-01	-0.233E-02	0.444E-02	-0.224E-02	0.865E-02	-0.453E-02
	200000.	0.578E-01	-0.270E-02	0.584E-02	-0.308E-02	0.116E-01	-0.628E-02
O IV 3P 3D 3410.9 Å C= 0.34E+21	20000.	0.162	-0.244E-02	0.964E-03	-0.780E-03	0.178E-02	-0.146E-02
	50000.	0.106	-0.205E-02	0.274E-02	-0.184E-02	0.525E-02	-0.363E-02
	100000.	0.784E-01	-0.211E-02	0.441E-02	-0.283E-02	0.864E-02	-0.572E-02
	200000.	0.607E-01	-0.220E-02	0.617E-02	-0.389E-02	0.123E-01	-0.794E-02
O IV 3D 4F 1067.8 Å C= 0.30E+19	20000.	0.306E-01	-0.666E-03	0.745E-03	-0.123E-02	0.144E-02	-0.229E-02
	50000.	0.208E-01	-0.539E-03	0.177E-02	-0.209E-02	0.350E-02	-0.409E-02
	100000.	0.160E-01	-0.572E-03	0.269E-02	-0.261E-02	0.530E-02	-0.526E-02
	200000.	0.129E-01	-0.336E-03	0.350E-02	-0.313E-02	0.680E-02	-0.638E-02
Perturber density = $1 \times 10^{+18}$ cm^{-3}							
O IV 2P 3S 279.9 Å C= 0.26E+20	20000.	0.609E-02	0.435E-04	0.988E-05	0.744E-04	0.184E-04	0.119E-03
	50000.	0.363E-02	0.333E-03	0.738E-04	0.184E-03	0.145E-03	0.345E-03
	100000.	0.266E-02	0.354E-03	0.176E-03	0.278E-03	0.356E-03	0.544E-03
	200000.	0.205E-02	0.378E-03	0.323E-03	0.372E-03	0.654E-03	0.752E-03
O IV 2P 3D 238.5 Å C= 0.17E+20	20000.	0.476E-02	-0.215E-03	0.339E-04	-0.108E-04	0.597E-04	-0.174E-04
	50000.	0.302E-02	-0.129E-04	0.995E-04	-0.306E-04	0.189E-03	-0.576E-04
	100000.	0.221E-02	0.734E-05	0.163E-03	-0.541E-04	0.318E-03	-0.106E-03
	200000.	0.167E-02	0.289E-05	0.227E-03	-0.791E-04	0.447E-03	-0.159E-03

STARK BROADENING PARAMETER TABLES FOR O IV AND O V LINES

Transition	T(K)	Electrons Width (Å)	Electrons Shift (Å)	Perturbers Protons Width (Å)	Perturbers Protons Shift (Å)	Perturbers He III Width (Å)	Perturbers He III Shift (Å)
O IV 3S 3P 3066.4 Å C= 0.28E+22	20000.	1.55	-0.875E-02	0.108E-01	-0.532E-02	0.190E-01	-0.855E-02
	50000.	0.991	-0.236E-01	0.288E-01	-0.139E-01	0.549E-01	-0.262E-01
	100000.	0.741	-0.231E-01	0.444E-01	-0.221E-01	0.863E-01	-0.437E-01
	200000.	0.578	-0.267E-01	0.584E-01	-0.308E-01	0.116	-0.620E-01
O IV 3P 3D 3410.9 Å C= 0.34E+22	20000.	1.62	-0.261E-01	0.948E-02	-0.677E-02	0.167E-01	-0.109E-01
	50000.	1.06	-0.199E-01	0.273E-01	-0.177E-01	0.520E-01	-0.333E-01
	100000.	0.784	-0.209E-01	0.441E-01	-0.279E-01	0.862E-01	-0.552E-01
	200000.	0.607	-0.217E-01	0.617E-01	-0.388E-01	0.123	-0.783E-01
O IV 3D 4F 1067.8 Å C= 0.30E+20	20000.	0.306	-0.447E-02	0.738E-02	-0.103E-01	*0.138E-01	-0.156E-01
	50000.	0.208	-0.377E-02	0.178E-01	-0.195E-01	*0.348E-01	-0.350E-01
	100000.	0.160	-0.449E-02	0.269E-01	-0.254E-01	*0.530E-01	-0.484E-01
	200000.	0.129	-0.247E-02	0.350E-01	-0.312E-01	0.680E-01	-0.618E-01
Perturber density = $1 \times 10^{+19}$ cm^{-3}							
O IV 2P 3S 279.9 Å C= 0.26E+21	20000.	0.618E-01	-0.207E-03	0.961E-04	0.454E-03	0.159E-03	0.428E-03
	50000.	0.362E-01	0.305E-02	0.736E-03	0.159E-02	0.145E-02	0.260E-02
	100000.	0.266E-01	0.335E-02	0.176E-02	0.257E-02	0.356E-02	0.470E-02
	200000.	0.205E-01	0.364E-02	0.323E-02	0.363E-02	0.654E-02	0.702E-02
O IV 2P 3D 238.5 Å C= 0.17E+21	20000.	0.477E-01	-0.218E-02	0.283E-03	-0.667E-04	0.352E-03	-0.645E-04
	50000.	0.302E-01	-0.104E-03	0.980E-03	-0.270E-03	0.179E-02	-0.455E-03
	100000.	0.221E-01	0.938E-04	0.163E-02	-0.511E-03	0.313E-02	-0.957E-03
	200000.	0.167E-01	0.473E-04	0.227E-02	-0.779E-03	0.445E-02	-0.152E-02
O IV 3S 3P 3066.4 Å C= 0.28E+23	20000.	15.4	-0.453E-01	0.894E-01	-0.327E-01	*0.110	-0.313E-01
	50000.	9.91	-0.216	0.283	-0.122	*0.517	-0.203
	100000.	7.41	-0.218	0.441	-0.206	*0.847	-0.385
	200000.	5.78	-0.257	0.583	-0.301	*1.16	-0.584
O IV 3P 3D 3410.9 Å C= 0.34E+23	20000.	16.2	-0.218	0.792E-01	-0.416E-01	*0.995E-01	-0.398E-01
	50000.	10.6	-0.177	0.269	-0.154	*0.494	-0.257
	100000.	7.84	-0.192	0.439	-0.260	*0.848	-0.485
	200000.	6.07	-0.205	0.616	-0.380	*1.22	-0.738
O IV 3D 4F 1067.8 Å C= 0.30E+21	20000.	*3.01	*0.517E-01	*0.647E-01	-0.522E-01		
	50000.	2.05	0.161E-01	*0.175	-0.151		
	100000.	1.59	-0.823E-02	*0.267	-0.218		
	200000.	1.28	0.235E-02	*0.350	-0.296		
Perturber density = $1 \times 10^{+20}$ cm^{-3}							
O IV 2P 3S 279.9 Å C= 0.26E+22	20000.	*0.613	-0.218E-01	*0.663E-03	*0.938E-03		
	50000.	0.363	0.207E-01	*0.716E-02	*0.954E-02		
	100000.	0.266	0.271E-01	*0.175E-01	*0.205E-01		
	200000.	0.205	0.321E-01	*0.322E-01	*0.316E-01		

Transition	T(K)	Perturbers: Electrons Width (Å)	Electrons Shift (Å)	Protons Width (Å)	Protons Shift (Å)	He III Width (Å)	He III Shift (Å)
O IV 2P 3D 238.5 Å C=0.17E+22	20000.	*0.477	-0.177E-01	*0.109E-02	-0.152E-03		
	50000.	0.302	0.421E-03	*0.828E-02	-0.179E-02		
	100000.	0.221	0.188E-02	*0.158E-01	-0.437E-02		
	200000.	0.167	0.114E-02	*0.224E-01	-0.711E-02		
Perturber density = 1 x 10^{+21} cm^{-3}							
O IV 2P 3S 279.9 Å C= 0.26E+23	20000.						
	50000.	*3.45	-0.224				
	100000.	*2.61	*0.289E-01				
	200000.	2.02	0.165				
O IV 2P 3D 238.5 Å C= 0.17E+23	20000.						
	50000.						
	100000.	*2.18	*0.561E-01				
	200000.	1.66	0.354E-01				
Perturber density = 1 x 10^{+17} cm^{-3}							
O V 2S-2P 629.7 Å C= 0.63E+20	40000.	0.810E-03	0.189E-04	0.123E-05	-0.199E-05	0.226E-05	-0.385E-05
	100000.	0.516E-03	-0.999E-05	0.477E-05	-0.506E-05	0.888E-05	-0.101E-04
	200000.	0.369E-03	-0.987E-05	0.113E-04	-0.947E-05	0.215E-04	-0.190E-04
	500000.	0.245E-03	-0.129E-04	0.230E-04	-0.168E-04	0.451E-04	-0.343E-04
O V 2P 3S 248.5 Å C= 0.12E+19	40000.	0.375E-03	0.152E-04	0.327E-05	0.138E-04	0.627E-05	0.267E-04
	100000.	0.250E-03	0.260E-04	0.153E-04	0.258E-04	0.306E-04	0.522E-04
	200000.	0.191E-03	0.263E-04	0.275E-04	0.356E-04	0.549E-04	0.725E-04
	500000.	0.138E-03	0.250E-04	0.447E-04	0.455E-04	0.893E-04	0.928E-04
O V 2P 4S 174.6 Å C= 0.19E+18	40000.	0.631E-03	0.645E-04	0.349E-04	0.557E-04	0.703E-04	0.108E-03
	100000.	0.445E-03	0.723E-04	0.738E-04	0.832E-04	0.150E-03	0.168E-03
	200000.	0.352E-03	0.699E-04	0.986E-04	0.100E-03	0.199E-03	0.205E-03
	500000.	0.264E-03	0.614E-04	0.135E-03	0.124E-03	0.269E-03	0.256E-03
O V 2P 3D 220.4 Å C= 0.15E+19	40000.	0.257E-03	-0.932E-05	0.224E-05	-0.147E-05	0.417E-05	-0.283E-05
	100000.	0.166E-03	-0.775E-06	0.637E-05	-0.347E-05	0.122E-04	-0.694E-05
	200000.	0.122E-03	-0.170E-05	0.103E-04	-0.555E-05	0.202E-04	-0.113E-04
	500000.	0.864E-04	-0.198E-07	0.152E-04	-0.834E-05	0.301E-04	-0.170E-04
O V 2P 4D 170.2 Å C= 0.10E+18	40000.	0.657E-03	0.105E-04	0.224E-04	0.234E-04	0.432E-04	0.454E-04
	100000.	0.463E-03	0.120E-04	0.431E-04	0.379E-04	0.846E-04	0.762E-04
	200000.	0.366E-03	0.127E-04	0.581E-04	0.464E-04	0.113E-03	0.951E-04
	500000.	0.276E-03	0.989E-05	0.814E-04	0.586E-04	0.147E-03	0.119E-03
O V 3D 4F 728.7 Å C= 0.19E+19	40000.	0.810E-02	-0.165E-03	0.271E-03	-0.446E-03	0.521E-03	-0.863E-03
	100000.	0.555E-02	-0.152E-03	0.623E-03	-0.717E-03	0.123E-02	-0.144E-02
	200000.	0.433E-02	-0.974E-04	0.929E-03	-0.875E-03	0.180E-02	-0.179E-02
	500000.	0.327E-02	-0.535E-04	0.134E-02	-0.110E-02	0.244E-02	-0.226E-02

STARK BROADENING PARAMETER TABLES FOR O IV AND O V LINES

Transition	T(K)	Perturbers: Electrons Width (Å)	Electrons Shift (Å)	Protons Width (Å)	Protons Shift (Å)	He III Width (Å)	He III Shift (Å)
O V 3D 5F 509.4 Å C= 0.14E+18	40000.	0.160E-01	-0.119E-02	0.363E-02	-0.358E-02		
	100000.	0.119E-01	-0.114E-02	0.528E-02	-0.489E-02	*0.102E-01	-0.967E-02
	200000.	0.959E-02	-0.889E-03	0.701E-02	-0.566E-02	*0.129E-01	-0.116E-01
	500000.	0.722E-02	-0.656E-03	0.939E-02	-0.670E-02	*0.160E-01	-0.137E-01
O V 2P 3S 215.2 Å C= 0.17E+19	40000.	0.222E-03	0.690E-05	0.935E-06	0.564E-05	0.177E-05	0.109E-04
	100000.	0.144E-03	0.130E-04	0.552E-05	0.116E-04	0.107E-04	0.234E-04
	200000.	0.108E-03	0.163E-04	0.112E-04	0.162E-04	0.225E-04	0.331E-04
	500000.	0.779E-04	0.151E-04	0.205E-04	0.216E-04	0.416E-04	0.444E-04
O V 2P 4S 156.2 Å C= 0.33E+18	40000.	0.370E-03	0.346E-04	0.110E-04	0.231E-04	0.213E-04	0.449E-04
	100000.	0.253E-03	0.445E-04	0.275E-04	0.367E-04	0.553E-04	0.738E-04
	200000.	0.199E-03	0.416E-04	0.417E-04	0.443E-04	0.849E-04	0.910E-04
	500000.	0.149E-03	0.387E-04	0.585E-04	0.557E-04	0.117E-03	0.116E-03
O V 3P 4S 716.3 Å C= 0.69E+19	40000.	0.107E-01	0.679E-03	0.237E-03	0.456E-03	0.458E-03	0.883E-03
	100000.	0.736E-02	0.849E-03	0.574E-03	0.728E-03	0.115E-02	0.147E-02
	200000.	0.577E-02	0.803E-03	0.855E-03	0.885E-03	0.175E-02	0.182E-02
	500000.	0.433E-02	0.742E-03	0.119E-02	0.113E-02	0.237E-02	0.228E-02
O V 3S 3P 2784.8 Å C= 0.14E+21	40000.	0.852E-01	-0.101E-02	0.812E-03	-0.259E-03	0.152E-02	-0.501E-03
	100000.	0.567E-01	-0.100E-02	0.198E-02	-0.609E-03	0.380E-02	-0.122E-02
	200000.	0.431E-01	-0.170E-02	0.291E-02	-0.963E-03	0.566E-02	-0.196E-02
	500000.	0.315E-01	-0.148E-02	0.388E-02	-0.143E-02	0.750E-02	-0.293E-02
O V 2P 3D 192.9 Å C= 0.67E+18	40000.	0.187E-03	-0.824E-05	0.158E-05	-0.230E-05	0.294E-05	-0.445E-05
	100000.	0.121E-03	-0.214E-05	0.493E-05	-0.507E-05	0.948E-05	-0.102E-04
	200000.	0.897E-04	-0.191E-05	0.847E-05	-0.747E-05	0.166E-04	-0.152E-04
	500000.	0.634E-04	-0.933E-06	0.137E-04	-0.106E-04	0.267E-04	-0.217E-04
O V 2P 4D 151.5 Å C= 0.12E+18	40000.	0.497E-03	0.150E-05	0.126E-04	0.451E-05	0.240E-04	0.873E-05
	100000.	0.348E-03	0.498E-05	0.227E-04	0.865E-05	0.439E-04	0.175E-04
	200000.	0.273E-03	0.521E-05	0.292E-04	0.119E-04	0.564E-04	0.243E-04
	500000.	0.206E-03	0.506E-05	0.378E-04	0.153E-04	0.684E-04	0.313E-04
O V 3P 3D 5591.4 Å C= 0.56E+21	40000.	0.282	-0.697E-02	0.278E-02	-0.464E-02	0.523E-02	-0.899E-02
	100000.	0.189	-0.644E-02	0.829E-02	-0.930E-02	0.162E-01	-0.187E-01
	200000.	0.143	-0.566E-02	0.135E-01	-0.129E-01	0.265E-01	-0.263E-01
	500000.	0.105	-0.499E-02	0.204E-01	-0.169E-01	0.396E-01	-0.346E-01
O V 3P 4D 627.5 Å C= 0.21E+19	40000.	0.955E-02	0.185E-04	0.169E-03	0.443E-04	0.321E-03	0.859E-04
	100000.	0.669E-02	0.258E-04	0.312E-03	0.924E-04	0.602E-03	0.185E-03
	200000.	0.527E-02	0.377E-04	0.417E-03	0.130E-03	0.800E-03	0.264E-03
	500000.	0.397E-02	0.337E-04	0.548E-03	0.174E-03	0.959E-03	0.356E-03

Transition	T(K)	Perturbers: Electrons Width (Å)	Electrons Shift (Å)	Protons Width (Å)	Protons Shift (Å)	He III Width (Å)	He III Shift (Å)
O V 3D 4F 681.3 Å C= 0.25E+19	40000.	0.671E-02	-0.904E-04	0.159E-03	-0.242E-03	0.306E-03	-0.469E-03
	100000.	0.458E-02	-0.832E-04	0.373E-03	-0.412E-03	0.737E-03	-0.829E-03
	200000.	0.355E-02	-0.510E-04	0.563E-03	-0.519E-03	0.111E-02	-0.106E-02
	500000.	0.268E-02	-0.289E-04	0.811E-03	-0.663E-03	0.153E-02	-0.136E-02
O V 3D 5F 481.1 Å C= 0.52E+17	40000.	0.134E-01	-0.887E-03	*0.393E-02	-0.360E-02		
	100000.	0.996E-02	-0.825E-03	*0.599E-02	-0.487E-02		
	200000.	0.803E-02	-0.729E-03	0.803E-02	-0.567E-02	*0.130E-01	-0.116E-01
	500000.	0.608E-02	-0.529E-03	0.115E-01	-0.680E-02	*0.165E-01	-0.141E-01
O V 4D 4F 18849.4 Å C= 0.19E+22	40000.	9.26	-0.166	0.156	-0.256	0.300	-0.495
	100000.	6.55	-0.161	0.364	-0.419	0.713	-0.841
	200000.	5.21	-0.138	0.551	-0.517	1.07	-1.06
	500000.	3.98	-0.109	0.830	-0.651	1.46	-1.35
O V 4D 5F 1506.7 Å C= 0.51E+18	40000.	0.153	-0.935E-02	*0.385E-01	-0.354E-01		
	100000.	0.113	-0.873E-02	*0.586E-01	-0.479E-01		
	200000.	0.917E-01	-0.778E-02	0.788E-01	-0.560E-01	*0.127	*-0.114
	500000.	0.695E-01	-0.575E-02	0.114	-0.669E-01	*0.163	*-0.139
Perturber density = 1 x 10^{+18} cm^{-3}							
O V 2S-2P 629.7 Å C= 0.63E+21	40000.	0.812E-02	0.154E-03	0.122E-04	-0.186E-04	0.223E-04	-0.338E-04
	100000.	0.516E-02	-0.107E-03	0.477E-04	-0.501E-04	0.887E-04	-0.974E-04
	200000.	0.369E-02	-0.101E-03	0.113E-03	-0.946E-04	0.215E-03	-0.189E-03
	500000.	0.245E-02	-0.129E-03	0.230E-03	-0.168E-03	0.451E-03	-0.343E-03
O V 2P 3S 248.5 Å C= 0.12E+20	40000.	0.377E-02	0.157E-03	0.327E-04	0.128E-03	0.626E-04	0.232E-03
	100000.	0.250E-02	0.255E-03	0.153E-03	0.254E-03	0.306E-03	0.497E-03
	200000.	0.191E-02	0.259E-03	0.275E-03	0.355E-03	0.549E-03	0.712E-03
	500000.	0.138E-02	0.250E-03	0.447E-03	0.454E-03	0.893E-03	0.925E-03
O V 2P 4S 174.6 Å C= 0.19E+19	40000.	0.633E-02	0.592E-03	0.349E-03	0.498E-03	*0.701E-03	*0.874E-03
	100000.	0.445E-02	0.685E-03	0.738E-03	0.807E-03	*0.150E-02	*0.153E-02
	200000.	0.352E-02	0.674E-03	0.986E-03	0.100E-02	*0.199E-02	*0.198E-02
	500000.	0.264E-02	0.612E-03	0.135E-02	0.124E-02	*0.269E-02	*0.254E-02
O V 2P 3D 220.4 Å C= 0.15E+20	40000.	0.256E-02	-0.813E-04	0.223E-04	-0.136E-04	0.411E-04	-0.248E-04
	100000.	0.166E-02	-0.391E-05	0.637E-04	-0.343E-04	0.122E-03	-0.670E-04
	200000.	0.122E-02	-0.162E-04	0.103E-03	-0.555E-04	0.202E-03	-0.111E-03
	500000.	0.864E-03	-0.162E-06	0.152E-03	-0.833E-04	0.301E-03	-0.170E-03
O V 2P 4D 170.2 Å C= 0.10E+19	40000.	0.657E-02	0.919E-04	0.223E-03	0.214E-03	0.425E-03	0.384E-03
	100000.	0.463E-02	0.107E-03	0.430E-03	0.370E-03	0.845E-03	0.714E-03
	200000.	0.366E-02	0.118E-03	0.581E-03	0.463E-03	0.113E-02	0.927E-03
	500000.	0.276E-02	0.982E-04	0.814E-03	0.585E-03	0.147E-02	0.119E-02

Transition	T(K)	Perturbers: Electrons Width (Å)	Electrons Shift (Å)	Protons Width (Å)	Protons Shift (Å)	He III Width (Å)	He III Shift (Å)
O V 3D 4F 728.7 Å C= 0.19E+20	40000.	0.810E-01	-0.123E-02	0.270E-02	-0.407E-02	0.517E-02	-0.729E-02
	100000.	0.555E-01	-0.123E-02	0.622E-02	-0.700E-02	0.123E-01	-0.135E-01
	200000.	0.433E-01	-0.830E-03	0.929E-02	-0.873E-02	0.180E-01	-0.175E-01
	500000.	0.327E-01	-0.522E-03	0.134E-01	-0.110E-01	0.244E-01	-0.225E-01
O V 3D 5F 509.4 Å C= 0.14E+19	40000.	0.154	-0.356E-02				
	100000.	0.116	-0.599E-02				
	200000.	0.934E-01	-0.514E-02				
	500000.	0.706E-01	-0.627E-02				
O V 2P 3S 215.2 Å C= 0.17E+20	40000.	0.223E-02	0.758E-04	0.938E-05	0.523E-04	0.177E-04	0.953E-04
	100000.	0.144E-02	0.130E-03	0.552E-04	0.115E-03	0.108E-03	0.224E-03
	200000.	0.108E-02	0.161E-03	0.112E-03	0.162E-03	0.225E-03	0.326E-03
	500000.	0.779E-03	0.151E-03	0.205E-03	0.215E-03	0.416E-03	0.443E-03
O V 2P 4S 156.2 Å C= 0.33E+19	40000.	0.372E-02	0.331E-03	0.109E-03	0.211E-03	0.213E-03	0.378E-03
	100000.	0.253E-02	0.432E-03	0.275E-03	0.359E-03	0.553E-03	0.689E-03
	200000.	0.199E-02	0.407E-03	0.417E-03	0.442E-03	0.849E-03	0.885E-03
	500000.	0.149E-02	0.386E-03	0.585E-03	0.556E-03	0.117E-02	0.116E-02
O V 3P 4S 716.3 Å C= 0.69E+20	40000.	0.107	0.646E-02	0.236E-02	0.415E-02	0.457E-02	0.745E-02
	100000.	0.736E-01	0.821E-02	0.573E-02	0.711E-02	0.115E-01	0.137E-01
	200000.	0.577E-01	0.784E-02	0.855E-02	0.883E-02	0.175E-01	0.177E-01
	500000.	0.433E-01	0.741E-02	0.119E-01	0.113E-01	0.237E-01	0.227E-01
O V 3S 3P 2784.8 Å C= 0.14E+22	40000.	0.852	-0.104E-01	0.808E-02	-0.241E-02	0.150E-01	-0.439E-02
	100000.	0.567	-0.100E-01	0.198E-01	-0.601E-02	0.379E-01	-0.117E-01
	200000.	0.431	-0.170E-01	0.291E-01	-0.962E-02	0.566E-01	-0.193E-01
	500000.	0.315	-0.148E-01	0.388E-01	-0.143E-01	0.750E-01	-0.293E-01
O V 2P 3D 192.9 Å C= 0.67E+19	40000.	0.187E-02	-0.720E-04	0.157E-04	-0.214E-04	0.290E-04	-0.390E-04
	100000.	0.121E-02	-0.182E-04	0.493E-04	-0.500E-04	0.948E-04	-0.978E-04
	200000.	0.897E-03	-0.181E-04	0.847E-04	-0.746E-04	0.166E-03	-0.150E-03
	500000.	0.634E-03	-0.927E-05	0.137E-03	-0.106E-03	0.267E-03	-0.216E-03
O V 2P 4D 151.5 Å C= 0.12E+19	40000.	0.497E-02	0.180E-04	0.125E-03	0.417E-04	0.235E-03	0.759E-04
	100000.	0.348E-02	0.492E-04	0.227E-03	0.851E-04	0.437E-03	0.167E-03
	200000.	0.273E-02	0.500E-04	0.291E-03	0.119E-03	0.564E-03	0.239E-03
	500000.	0.206E-02	0.505E-04	0.378E-03	0.153E-03	0.684E-03	0.312E-03
O V 3P 3D 5591.4 Å C= 0.56E+22	40000.	2.82	-0.648E-01	0.277E-01	-0.430E-01	0.517E-01	-0.784E-01
	100000.	1.89	-0.617E-01	0.829E-01	-0.916E-01	0.162	-0.179
	200000.	1.43	-0.549E-01	0.135	-0.129	0.265	-0.259
	500000.	1.05	-0.498E-01	0.204	-0.169	0.396	-0.345

Transition	T(K)	Perturbers: Electrons Width (Å)	Electrons Shift (Å)	Protons Width (Å)	Protons Shift (Å)	He III Width (Å)	He III Shift (Å)
O V 3P 4D 627.5 Å C= 0.21E+20	40000.	0.955E-01	0.196E-03	0.168E-02	0.412E-03	0.315E-02	0.750E-03
	100000.	0.669E-01	0.248E-03	0.311E-02	0.910E-03	0.600E-02	0.178E-02
	200000.	0.527E-01	0.352E-03	0.417E-02	0.130E-02	0.800E-02	0.261E-02
	500000.	0.397E-01	0.336E-03	0.548E-02	0.174E-02	0.959E-02	0.356E-02
O V 3D 4F 681.3 Å C= 0.25E+20	40000.	0.672E-01	-0.676E-03	0.158E-02	-0.222E-02	0.304E-02	-0.401E-02
	100000.	0.458E-01	-0.675E-03	0.373E-02	-0.404E-02	0.736E-02	-0.782E-02
	200000.	0.355E-01	-0.450E-03	0.563E-02	-0.517E-02	0.111E-01	-0.104E-01
	500000.	0.268E-01	-0.282E-03	0.811E-02	-0.662E-02	0.153E-01	-0.135E-01
O V 3D 5F 481.1 Å C= 0.52E+18	40000.	0.126	-0.329E-02				
	100000.	0.944E-01	-0.445E-02				
	200000.	0.767E-01	-0.444E-02				
	500000.	0.585E-01	-0.496E-02				
O V 4D 4F 18849.4 Å C= 0.19E+23	40000.	92.6	-1.44	1.55	-2.34	2.98	-4.19
	100000.	65.5	-1.45	3.63	-4.10	7.13	-7.89
	200000.	52.1	-1.29	5.51	-5.16	10.7	-10.3
	500000.	39.8	-1.09	8.30	-6.50	14.6	-13.5
O V 4D 5F 1506.7 Å C= 0.51E+19	40000.	1.44	-0.384E-01				
	100000.	1.08	-0.498E-01				
	200000.	0.881	-0.496E-01				
	500000.	0.673	-0.542E-01				
Perturber density = $1 \times 10^{+19}$ cm^{-3}							
O V 2S-2P 629.7 Å C= 0.63E+22	100000.	0.516E-01	-0.102E-02	0.475E-03	-0.470E-03	0.878E-03	-0.869E-03
	200000.	0.369E-01	-0.997E-03	0.113E-02	-0.933E-03	0.215E-02	-0.180E-02
	500000.	0.245E-01	-0.129E-02	0.230E-02	-0.168E-02	0.452E-02	-0.340E-02
	800000.	0.203E-01	-0.119E-02	0.303E-02	-0.211E-02	0.601E-02	-0.429E-02
O V 2P 3S 248.5 Å C= 0.12E+21	100000.	0.250E-01	0.234E-02	0.153E-02	0.231E-02	0.306E-02	0.420E-02
	200000.	0.191E-01	0.244E-02	0.275E-02	0.345E-02	0.547E-02	0.648E-02
	500000.	0.138E-01	0.240E-02	0.447E-02	0.453E-02	0.894E-02	0.902E-02
	800000.	0.119E-01	0.234E-02	0.527E-02	0.507E-02	0.105E-01	0.104E-01
O V 2P 4S 174.6 Å C= 0.19E+20	100000.	0.445E-01	0.560E-02	*0.739E-02	*0.673E-02		
	200000.	0.351E-01	0.580E-02	*0.986E-02	*0.944E-02		
	500000.	0.264E-01	0.549E-02	*0.135E-01	*0.123E-01		
	800000.	0.228E-01	0.503E-02	*0.154E-01	*0.137E-01		
O V 2P 3D 220.4 Å C= 0.15E+21	100000.	0.166E-01	-0.272E-04	0.634E-03	-0.320E-03	0.120E-02	-0.592E-03
	200000.	0.122E-01	-0.148E-03	0.103E-02	-0.545E-03	0.201E-02	-0.105E-02
	500000.	0.864E-02	0.103E-04	0.152E-02	-0.832E-03	0.301E-02	-0.168E-02
	800000.	0.742E-02	-0.203E-04	0.172E-02	-0.942E-03	0.337E-02	-0.193E-02

Transition	T(K)	Electrons Width (Å)	Electrons Shift (Å)	Perturbers Protons Width (Å)	Perturbers Protons Shift (Å)	He III Width (Å)	He III Shift (Å)
O V 2P 4D 170.2 Å C= 0.10E+20	100000.	0.462E-01	0.614E-03	*0.426E-02	*0.324E-02		
	200000.	0.365E-01	0.844E-03	*0.580E-02	*0.444E-02		
	500000.	0.275E-01	0.754E-03	*0.814E-02	*0.583E-02		
	800000.	0.240E-01	0.780E-03	*0.965E-02	*0.639E-02		
O V 3D 4F 728.7 Å C= 0.19E+21	100000.	0.554	-0.374E-02	0.618E-01	-0.612E-01		
	200000.	0.432	-0.180E-02	0.929E-01	-0.836E-01		
	500000.	0.326	-0.916E-03	0.134	-0.110		
	800000.	0.286	0.433E-03	0.163	-0.120		
O V 3D 5F 509.4 Å C= 0.14E+20	100000.	0.975	0.142E-01				
	200000.	0.811	0.698E-02				
	500000.	0.629	-0.726E-02				
	800000.	0.551	-0.172E-01				
O V 2P 3S 215.2 Å C= 0.17E+21	100000.	0.144E-01	0.121E-02	0.553E-03	0.106E-02	0.107E-02	0.193E-02
	200000.	0.108E-01	0.156E-02	0.112E-02	0.158E-02	0.226E-02	0.300E-02
	500000.	0.779E-02	0.147E-02	0.205E-02	0.215E-02	0.415E-02	0.433E-02
	800000.	0.670E-02	0.143E-02	0.243E-02	0.245E-02	0.492E-02	0.498E-02
O V 2P 4S 156.2 Å C= 0.33E+20	100000.	0.253E-01	0.389E-02	0.274E-02	0.312E-02		
	200000.	0.199E-01	0.376E-02	0.417E-02	0.423E-02		
	500000.	0.149E-01	0.365E-02	0.585E-02	0.554E-02		
	800000.	0.130E-01	0.338E-02	0.673E-02	0.622E-02		
O V 3P 4S 716.3 Å C= 0.69E+21	100000.	0.736	0.739E-01	0.574E-01	0.622E-01		
	200000.	0.577	0.723E-01	0.855E-01	0.845E-01		
	500000.	0.433	0.700E-01	0.119	0.112		
	800000.	0.377	0.647E-01	0.137	0.122		
O V 3S 3P 2784.8 Å C= 0.14E+23	100000.	5.67	-0.967E-01	0.197	-0.561E-01	0.373	-0.104
	200000.	4.31	-0.168	0.291	-0.945E-01	0.563	-0.182
	500000.	3.15	-0.146	0.388	-0.143	0.749	-0.288
	800000.	2.73	-0.144	0.437	-0.161	0.819	-0.331
O V 2P 3D 192.9 Å C= 0.67E+20	100000.	0.121E-01	-0.157E-03	0.491E-03	-0.464E-03	0.937E-03	-0.855E-03
	200000.	0.897E-02	-0.157E-03	0.847E-03	-0.731E-03	0.166E-02	-0.140E-02
	500000.	0.634E-02	-0.761E-04	0.137E-02	-0.105E-02	0.267E-02	-0.212E-02
	800000.	0.543E-02	-0.846E-04	0.162E-02	-0.120E-02	0.309E-02	-0.245E-02
O V 2P 4D 151.5 Å C= 0.12E+20	100000.	0.347E-01	0.414E-03	0.224E-02	0.777E-03	*0.424E-02	*0.142E-02
	200000.	0.273E-01	0.451E-03	0.291E-02	0.116E-02	*0.559E-02	*0.218E-02
	500000.	0.206E-01	0.470E-03	0.378E-02	0.152E-02	*0.684E-02	*0.304E-02
	800000.	0.179E-01	0.462E-03	0.436E-02	0.171E-02	*0.746E-02	*0.353E-02

Transition	T(K)	Perturbers: Electrons Width (Å)	Electrons Shift (Å)	Protons Width (Å)	Protons Shift (Å)	He III Width (Å)	He III Shift (Å)
O V 3P 4D 627.5 Å C= 0.21E+21	100000.	0.668	0.172E-02	0.309E-01	0.840E-02	*0.583E-01	*0.154E-01
	200000.	0.526	0.305E-02	0.416E-01	0.127E-01	*0.792E-01	*0.240E-01
	500000.	0.396	0.300E-02	0.548E-01	0.173E-01	*0.958E-01	*0.348E-01
	800000.	0.346	0.310E-02	0.647E-01	0.196E-01	*0.104	*0.401E-01
O V 3D 4F 681.3 Å C= 0.25E+21	100000.	0.457	-0.249E-02	0.371E-01	-0.359E-01	*0.726E-01	-0.632E-01
	200000.	0.355	-0.125E-02	0.563E-01	-0.499E-01	*0.111	-0.913E-01
	500000.	0.268	-0.695E-03	0.811E-01	-0.660E-01	*0.153	-0.131
	800000.	0.235	0.762E-03	0.989E-01	-0.740E-01	*0.173	-0.150
O V 3D 5F 481.1 Å C= 0.52E+19	100000.	0.829	-0.379E-02				
	200000.	0.687	-0.104E-01				
	500000.	0.534	-0.130E-01				
	800000.	0.469	-0.187E-01				
O V 4D 5F 1506.7 Å C= 0.51E+20	100000.	9.68	-0.894E-01				
	200000.	8.02	-0.157				
	500000.	6.23	-0.179				
	800000.	5.46	-0.234				
Perturber density = $1 \times 10^{+20}$ cm^{-3}							
O V 2S-2P 629.7 Å C= 0.63E+23	100000.	0.516	-0.925E-02	0.465E-02	-0.397E-02	0.797E-02	-0.604E-02
	200000.	0.369	-0.927E-02	0.112E-01	-0.864E-02	0.212E-01	-0.158E-01
	500000.	0.245	-0.125E-01	0.230E-01	-0.166E-01	0.451E-01	-0.325E-01
	800000.	0.203	-0.116E-01	0.303E-01	-0.211E-01	0.601E-01	-0.421E-01
O V 2P 3S 248.5 Å C= 0.12E+22	100000.	0.250	0.161E-01	*0.152E-01	*0.177E-01		
	200000.	0.191	0.195E-01	*0.274E-01	*0.295E-01		
	500000.	0.138	0.208E-01	*0.447E-01	*0.434E-01		
	800000.	0.119	0.211E-01	*0.527E-01	*0.504E-01		
O V 2P 4S 174.6 Å C= 0.19E+21	100000.	*0.420	*0.130E-01				
	200000.	0.336	0.291E-01				
	500000.	0.254	0.361E-01				
	800000.	0.221	0.360E-01				
O V 2P 3D 220.4 Å C= 0.15E+22	100000.	0.166	0.409E-03	0.615E-02	-0.266E-02	*0.104E-01	-0.396E-02
	200000.	0.122	-0.996E-03	0.102E-01	-0.495E-02	*0.195E-01	-0.890E-02
	500000.	0.864E-01	0.434E-03	0.152E-01	-0.813E-02	*0.299E-01	-0.157E-01
	800000.	0.742E-01	0.241E-05	0.172E-01	-0.939E-02	*0.336E-01	-0.186E-01
O V 2P 4D 170.2 Å C= 0.10E+21	100000.	*0.434	*-0.299E-02				
	200000.	0.347	0.216E-02				
	500000.	0.264	0.314E-02				
	800000.	0.231	0.392E-02				

Transition	T(K)	Electrons Width (Å)	Electrons Shift (Å)	Perturbers Protons Width (Å)	Perturbers Protons Shift (Å)	Perturbers He III Width (Å)	Perturbers He III Shift (Å)
O V 3D 4F 728.7 Å C= 0.19E+22	100000.	5.21	0.178				
	200000.	4.12	0.128				
	500000.	3.14	0.897E-01				
	800000.	2.77	0.860E-01				
O V 3D 5F 509.4 Å C= 0.14E+21	100000.	*6.85	*0.414				
	200000.	*6.05	*0.311				
	500000.	5.01	0.169				
	800000.	4.50	0.107				
O V 2P 3S 215.2 Å C= 0.17E+22	100000.	0.144	0.941E-02	0.551E-02	0.842E-02		
	200000.	0.108	0.136E-01	0.112E-01	0.138E-01		
	500000.	0.779E-01	0.134E-01	0.204E-01	0.207E-01		
	800000.	0.670E-01	0.134E-01	0.243E-01	0.244E-01		
O V 2P 4S 156.2 Å C= 0.33E+21	100000.	0.251	0.239E-01				
	200000.	0.198	0.275E-01				
	500000.	0.148	0.299E-01				
	800000.	0.129	0.291E-01				
O V 3P 4S 716.3 Å C= 0.69E+22	100000.	*7.32	*0.448				
	200000.	5.75	0.527				
	500000.	4.31	0.572				
	800000.	3.76	0.555				
O V 2P 3D 192.9 Å C= 0.67E+21	100000.	0.121	-0.424E-03	0.479E-02	-0.379E-02	*0.832E-02	-0.545E-02
	200000.	0.897E-01	-0.801E-03	0.840E-02	-0.650E-02	*0.162E-01	-0.114E-01
	500000.	0.633E-01	-0.250E-03	0.137E-01	-0.102E-01	*0.266E-01	-0.195E-01
	800000.	0.543E-01	-0.494E-03	0.162E-01	-0.120E-01	*0.308E-01	-0.235E-01
O V 2P 4D 151.5 Å C= 0.12E+21	100000.	*0.332	*0.232E-02				
	200000.	0.263	0.333E-02				
	500000.	0.200	0.387E-02	*0.377E-01	*0.146E-01		
	800000.	0.175	0.390E-02	*0.436E-01	*0.170E-01		
O V 3P 4D 627.5 Å C= 0.21E+22	100000.	*6.41	*0.426E-02	*0.289	*0.672E-01		
	200000.	5.09	0.223E-01	*0.406	*0.111		
	500000.	3.86	0.234E-01	*0.546	*0.167		
	800000.	3.38	0.243E-01	*0.646	*0.195		
O V 3D 4F 681.3 Å C= 0.25E+22	100000.	4.44	0.112				
	200000.	3.46	0.785E-01				
	500000.	2.63	0.530E-01				
	800000.	2.31	0.553E-01				

Transition	T(K)	Perturbers: Electrons Width (Å)	Electrons Shift (Å)	Protons Width (Å)	Protons Shift (Å)	He III Width (Å)	He III Shift (Å)
O V 3D 5F 481.1 Å C= 0.52E+20	100000.	*6.33	*0.327				
	200000.	*5.50	*0.186				
	500000.	4.48	0.959E-01				
	800000.	4.01	0.537E-01				
Perturber density = $1 \times 10^{+21}$ cm^{-3}							
O V 2S-2P 629.7 Å C= 0.63E+24	100000.	5.16	-0.605E-01	0.378E-01	-0.226E-01	*0.380E-01	-0.176E-01
	200000.	3.69	-0.717E-01	0.109	-0.704E-01	*0.181	*-0.998E-01
	500000.	2.45	-0.112	0.229	-0.152	*0.442	*-0.277
	800000.	2.03	-0.105	0.302	-0.200	*0.597	*-0.377
O V 2P 3S 248.5 Å C= 0.12E+23	100000.	*2.31	*-0.989E-01				
	200000.	1.81	0.295E-01				
	500000.	1.33	0.112				
	800000.	1.15	0.130				
O V 2P 4S 174.6 Å C= 0.19E+22	100000.						
	200000.	*2.32	*-0.147				
	500000.	*1.95	*0.714E-01				
	800000.	1.74	0.108				
O V 2P 3D 220.4 Å C= 0.15E+23	100000.	*1.64	*0.337E-01	*0.447E-01	-0.141E-01		
	200000.	1.22	0.791E-02	*0.953E-01	-0.376E-01		
	500000.	0.860	0.148E-01	*0.150	-0.710E-01		
	800000.	0.739	0.871E-02	*0.170	-0.861E-01		
O V 2P 4D 170.2 Å C= 0.10E+22	100000.						
	200000.						
	500000.	*2.20	*0.304E-01				
	800000.	*1.97	*0.318E-01				
O V 2P 3S 215.2 Å C= 0.17E+23	100000.	*1.42	*-0.139E-01				
	200000.	1.07	0.699E-01				
	500000.	0.773	0.948E-01				
	800000.	0.665	0.101				
O V 2P 4S 156.2 Å C= 0.33E+22	100000.						
	200000.	*1.69	-0.188E-01				
	500000.	*1.32	*0.125				
	800000.	1.17	0.143				
O V 2P 3D 192.9 Å C= 0.67E+22	100000.	*1.17	*0.364E-01				
	200000.	0.874	0.179E-01				
	500000.	0.621	0.124E-01				
	800000.	0.533	0.780E-02	*0.163	*-0.107		

Transition	T(K)	Electrons Width (Å)	Electrons Shift (Å)	Perturbers Protons Width (Å)	Perturbers Protons Shift (Å)	Perturbers He III Width (Å)	Perturbers He III Shift (Å)
O V 2P 4D 151.5 Å C= 0.12E+22	100000.						
	200000.	*2.06	*0.252E-01				
	500000.	*1.67	*0.331E-01				
	800000.	*1.49	*0.336E-01				
Perturber density = 1 x 10^{+22} cm^{-3}							
O V 2P 3S 248.5 Å C= 0.12E+24	100000.						
	200000.	*11.6	*-1.94				
	500000.	*9.85	-0.432				
	800000.	*8.89	*0.642E-01				
O V 2P 3D 220.4 Å C= 0.15E+24	100000.						
	200000.						
	500000.	*8.03	*0.331				
	800000.	*6.97	*0.235				
O V 2P 3S 215.2 Å C= 0.17E+24	100000.						
	200000.	*8.06	*-1.03				
	500000.	*6.52	-0.785E-01				
	800000.	*5.75	*0.220				
O V 2P 3D 192.9 Å C= 0.67E+23	100000.						
	200000.	*7.44	*0.333				
	500000.	*5.52	*0.277				
	800000.	*4.81	*0.204				

1984), which gives an estimate for the maximum perturber density for which the line may be treated as isolated when it is divided by the corresponding full width at half maximum. For each value given in Table 1, the collision volume (V) multiplied by the perturber density (N) is much less than one and the impact approximation is valid (Sahal–Bréchot, 1969ab). Values for NV > 0.5 are not given and values for 0.1 < NV < 0.5 are denoted by an asterisk. When the impact approximation is not valid, the ion broadening contribution may be estimated by using quasistatic approach (Sahal–Bréchot 1991 and Griem 1974). The accuracy of the results obtained decreases when broadening by ion interactions becomes important.

The analysis of present results and comparison with available experimental and theoretical data will be published elsewhere (Dimitrijević and Sahal–Bréchot, 1994).

Acknowledgements – This work is a part of the project "Physics and dynamics of celestial bodies", supported by Ministry of Science and Technology of Serbia.

REFERENCES

Dimitrijević, M. S., and Sahal–Bréchot,S.: 1984, *JQSRT* **31**, 301.

Dimitrijević, M. S., and Sahal–Bréchot, S.: 1994, *Astron. Astrophys. Suppl. Series*, submitted.

Griem, H. R.: 1974, *Spectral Line Broadening by Plasmas*, Academic Press, New York.

Sahal–Bréchot, S.: 1969a, *Astron. Astrophys.* **1**, 91.

Sahal–Bréchot, S.: 1969b, *Astron. Astrophys.* **2**, 322.

Sahal–Bréchot, S.: 1991, *Astron. Astrophys.* **245**, 322.

ТАБЕЛЕ ПАРАМЕТАРА ШТАРКОВОГ ШИРЕЊА АСТРОФИЗИЧКИ ЗНАЧАЈНИХ ЛИНИЈА O IV И O V

М. С. Димитријевић[1] и S. Sahal–Bréchot[2]

[1] *Астрономска опсерваторија, Волгина 7, 11050 Београд, Југославија*

[2] *Laboratoire "Astrophysique, Atomes et Molécules"*
Département Atomes et Molécules en Astrophysique
Unité associée au C.N.R.S. No 812
Observatoire de Paris-Meudon, 92190 Meudon, France

УДК 52–355.3
Претходно саопштење

Користећи семикласичан прилаз, израчунате су ширине и помераји спектралних линија, проузроковани сударима са електронима, протонима и He III, за 5 мултиплета O IV и 19 мултиплета O V. Резултати су дати у функцији температуре и концентрације пертурбера.

Bull. Astron. Belgrade № 151 (1995), 101 – 114

UDC 52–355.3
Preliminary report

STARK BROADENING PARAMETER TABLES FOR Mg II

M. S. Dimitrijević[1] and S. Sahal–Bréchot[2]

[1] *Astronomical Observatory, Volgina 7, 11050 Belgrade, Yugoslavia*

[2] *Laboratoire "Astrophysique, Atomes et Molécules"*
Département Atomes et Molécules en Astrophysique
Unité associée au C.N.R.S. No 812
Observatoire de Paris–Meudon, 92190 Meudon, France

(Received: January 10, 1995)

SUMMARY: Using a semiclassical approach, we have calculated electron–, proton–, and ionised helium–impact line widths and shifts for 52 Mg II multiplets as a function of temperature and perturber density.

1. INTRODUCTION

Due to the cosmical abundance of magnesium and its ionization potential value, Mg II lines are present in solar and stellar spectra and the corresponding Stark broadening data are of interest for their analysis. In order to provide to astrophysicists the needed Stark broadening data, we have calculated within the semiclassical-perturbation formalism (Sahal–Bréchot, 1969ab) electron-, proton-, and ionized helium-impact line widths and shifts for 52 Mg II multiplets.

2. RESULTS AND DISCUSSION

Analysis of obtained results and all details of calculations as well as the comparison with availlable experimental data will be published elsewhere (Dimitrijević and Sahal–Bréchot, 1995). Here, we present only tables of Stark broadening parameters for astrophysical and laboratory plasma diagnostic purposes. Our results for 52 Mg II multiplets are shown in Table 1, for perturber densities of 10^{16}–10^{19} cm^{-3} and temperatures T = 5,000 – 150,000 K. We also specify a parameter c (Dimitrijević and

Table 1. This table shows electron-, proton-, and He II- impact broadening parameters for Mg II, for perturber densities of 10^{16} – 10^{19} cm^{-3} and temperatures from 5,000 up to 150,000 K. Transitions and averaged wavelengths for the multiplet (in Å) are also given. By using c [see Eq. (5) in Dimitrijević et *al.*, 1991], we obtain an estimate for the maximum perturber density for which the line may be treated as isolated and tabulated data may be used. The asterisk identifies cases for which the collision volume multiplied by the perturber density (the condition for validity of the impact approximation) lies between 0.1 and 0.5.

PERTURBER DENSITY = 1xE+16cm-3

TRANSITION	T(K)	ELECTRONS WIDTH(A)	ELECTRONS SHIFT(A)	PROTONS WIDTH(A)	PROTONS SHIFT(A)	IONIZED HELIUM WIDTH(A)	IONIZED HELIUM SHIFT(A)
Mg II 3s-3p	5000.	0.173E-01	-0.312E-04	0.263E-03	-0.641E-05	0.388E-03	-0.641E-05
2798.7 A	10000.	0.126E-01	-0.382E-04	0.475E-03	-0.133E-04	0.592E-03	-0.132E-04
C= 0.27E+20	20000.	0.911E-02	-0.443E-04	0.679E-03	-0.256E-04	0.773E-03	-0.244E-04
	50000.	0.651E-02	-0.493E-04	0.846E-03	-0.487E-04	0.906E-03	-0.421E-04
	100000.	0.559E-02	-0.541E-04	0.944E-03	-0.670E-04	0.990E-03	-0.564E-04
	150000.	0.525E-02	-0.513E-04	0.988E-03	-0.751E-04	0.101E-02	-0.628E-04
Mg II 3s-4p	5000.	0.726E-02	0.627E-03	0.565E-03	0.317E-04	0.691E-03	0.304E-04
1240.1 A	10000.	0.561E-02	0.391E-03	0.751E-03	0.563E-04	0.812E-03	0.509E-04
C= 0.14E+19	20000.	0.460E-02	0.286E-03	0.851E-03	0.818E-04	0.910E-03	0.713E-04
	50000.	0.416E-02	0.249E-03	0.968E-03	0.112E-03	0.993E-03	0.927E-04
	100000.	0.410E-02	0.204E-03	0.101E-02	0.134E-03	0.103E-02	0.110E-03
	150000.	0.405E-02	0.179E-03	0.103E-02	0.148E-03	0.103E-02	0.120E-03
Mg II 3s-5p	5000.	0.103E-01	0.868E-03	0.156E-02	-0.941E-04*	0.167E-02	-0.851E-04
1026.0 A	10000.	0.861E-02	0.661E-03	0.178E-02	-0.143E-03	0.190E-02	-0.125E-03
C= 0.44E+18	20000.	0.795E-02	0.446E-03	0.198E-02	-0.188E-03	0.204E-02	-0.157E-03
	50000.	0.822E-02	0.336E-03	0.210E-02	-0.240E-03	0.214E-02	-0.198E-03
	100000.	0.860E-02	0.226E-03	0.216E-02	-0.282E-03	0.218E-02	-0.228E-03
	150000.	0.867E-02	0.220E-03	0.219E-02	-0.305E-03	0.220E-02	-0.248E-03
Mg II 3s-6p	5000.	0.165E-01	-0.839E-03*	0.345E-02	-0.564E-03		
946.7 A	10000.	0.151E-01	-0.642E-03*	0.392E-02	-0.747E-03*	0.406E-02	-0.613E-03
C= 0.20E+18	20000.	0.153E-01	-0.456E-03	0.417E-02	-0.916E-03*	0.424E-02	-0.753E-03
	50000.	0.171E-01	-0.206E-03	0.436E-02	-0.113E-02*	0.439E-02	-0.916E-03
	100000.	0.184E-01	-0.137E-03	0.441E-02	-0.131E-02	0.443E-02	-0.103E-02
	150000.	0.186E-01	-0.832E-04	0.442E-02	-0.138E-02	0.444E-02	-0.113E-02
Mg II 3s-7p	5000.	0.282E-01	-0.554E-02				
907.4 A	10000.	0.271E-01	-0.426E-02*	0.764E-02	-0.204E-02		
C= 0.11E+18	20000.	0.289E-01	-0.273E-02*	0.803E-02	-0.251E-02		
	50000.	0.338E-01	-0.215E-02*	0.847E-02	-0.298E-02*	0.834E-02	-0.246E-02
	100000.	0.365E-01	-0.127E-02	0.888E-02	-0.345E-02*	0.836E-02	-0.289E-02
	150000.	0.369E-01	-0.106E-02	0.879E-02	-0.365E-02*	0.807E-02	-0.295E-02
Mg II 4s-4p	5000,	0.514	-0.124	0.318E-01	-0.904E-02	0.386E-01	-0.804E-02
9229.4 A	10000.	0.393	-0.917E-01	0.426E-01	-0.135E-01	0.456E-01	-0.117E-01
C= 0.78E+20	20000.	0.327	-0.670E-01	0.487E-01	-0.174E-01	0.514E-01	-0.145E-01
	50000.	0.313	-0.501E-01	0.564E-01	-0.222E-01	0.563E-01	-0.183E-01
	100000.	0.318	-0.397E-01	0.592E-01	-0.261E-01	0.596E-01	-0.210E-01
	150000.	0.318	-0.353E-01	0.626E-01	-0.278E-01	0.611E-01	-0.227E-01
Mg II 4s-5p	5000.	0.136	-0.101E-01	0.194E-01	-0.242E-02*	0.208E-01	-0.207E-02
3615.4 A	10000.	0.114	-0.806E-02	0.222E-01	-0.352E-02	0.236E-01	-0.295E-02
C= 0.54E+19	20000.	0.107	-0.696E-02	0.247E-01	-0.435E-02	0.254E-01	-0.359E-02
	50000.	0.113	-0.566E-02	0.262E-01	-0.554E-02	0.267E-01	-0.452E-02
	100000.	0.120	-0.521E-02	0.272E-01	-0.635E-02	0.270E-01	-0.509E-02
	150000.	0.121	-0.418E-02	0.269E-01	-0.678E-02	0.271E-01	-0.560E-02
Mg II 4s-6p	5000.	0.150	-0.996E-02*	0.301E-01	-0.534E-02		
2791.6 A	10000.	0.136	-0.125E-01*	0.342E-01	-0.700E-02*	0.353E-01	-0.576E-02
C= 0.17E+19	20000.	0.138	-0.830E-02	0.365E-01	-0.864E-02*	0.371E-01	-0.707E-02
	50000.	0.155	-0.816E-02	0.376E-01	-0.105E-01*	0.386E-01	-0.850E-02
	100000.	0.168	-0.606E-02	0.390E-01	-0.119E-01	0.381E-01	-0.968E-02
	150000.	0.170	-0.511E-02	0.397E-01	-0.128E-01	0.393E-01	-0.102E-01

PERTURBER DENSITY = 1xE+16cm-3

TRANSITION	T(K)	ELECTRONS WIDTH(A)	ELECTRONS SHIFT(A)	PROTONS WIDTH(A)	PROTONS SHIFT(A)	IONIZED HELIUM WIDTH(A)	IONIZED HELIUM SHIFT(A)
Mg II 4s-7p	5000.	0.216	-0.387E-01				
2475.2 A	10000.	0.206	-0.322E-01	*0.571E-01	-0.155E-01		
C= 0.80E+18	20000.	0.219	-0.263E-01	*0.597E-01	-0.189E-01		
	50000.	0.257	-0.197E-01	*0.633E-01	-0.227E-01	*0.620E-01	-0.186E-01
	100000.	0.278	-0.136E-01	0.654E-01	-0.259E-01	*0.631E-01	-0.218E-01
	150000.	0.281	-0.114E-01	0.646E-01	-0.274E-01	*0.606E-01	-0.226E-01
Mg II 5s-5p	5000.	6.74	-2.40	0.713	-0.278	*0.750	*-0.231
21395.8 A	10000.	5.46	-2.01	0.828	-0.368	0.859	-0.302
C= 0.19E+21	20000.	5.21	-1.76	0.943	-0.449	0.937	-0.372
	50000.	5.49	-1.29	1.05	-0.552	1.02	-0.457
	100000.	5.84	-1.03	1.12	-0.638	1.06	-0.506
	150000.	5.88	-0.888	1.15	-0.670	1.10	-0.551
Mg II 5s-6p	5000.	1.30	-0.418	*0.237	*-0.593E-01		
7790.1 A	10000.	1.20	-0.350	*0.269	*-0.776E-01	*0.277	*-0.639E-01
C= 0.13E+20	20000.	1.23	-0.275	0.288	-0.952E-01	*0.291	*-0.788E-01
	50000.	1.40	-0.204	0.301	-0.117	*0.297	*-0.954E-01
	100000.	1.51	-0.158	0.313	-0.131	0.315	-0.103
	150000.	1.53	-0.137	0.327	-0.144	0.312	-0.120
Mg II 5s-7p	5000.	1.20	-0.331				
5741.8 A	10000.	1.17	-0.286	*0.308	*-0.918E-01		
C= 0.43E+19	20000.	1.25	-0.228	*0.326	*-0.112		
	50000.	1.48	-0.178	*0.343	*-0.138	*0.334	*-0.108
	100000.	1.61	-0.133	0.348	-0.149	*0.344	*-0.123
	150000.	1.62	-0.113	0.356	-0.159	*0.335	*-0.128
Mg II 6s-7p	5000.	9.10	-3.75				
14265.8 A	10000.	8.73	-3.18	* 1.97	*-0.754		
C= 0.27E+20	20000.	9.24	-2.79	* 2.09	*-0.915		
	50000.	10.8	-2.04	* 2.28	* -1.12	* 2.10	*-0.889
	100000.	11.7	-1.58	* 2.40	* -1.29	* 2.19	*-0.984
	150000.	11.8	-1.32	2.49	-1.36	* 2.34	* -1.13
Mg II 3p-4s	5000.	0.419E-01	0.173E-01	0.672E-03	0.104E-02	0.781E-03	0.913E-03
2934.7 A	10000.	0.295E-01	0.133E-01	0.125E-02	0.154E-02	0.129E-02	0.133E-02
C= 0.93E+19	20000.	0.214E-01	0.991E-02	0.193E-02	0.196E-02	0.175E-02	0.163E-02
	50000.	0.177E-01	0.746E-02	0.270E-02	0.251E-02	0.233E-02	0.205E-02
	100000.	0.163E-01	0.583E-02	0.321E-02	0.290E-02	0.281E-02	0.240E-02
	150000.	0.158E-01	0.509E-02	0.368E-02	0.319E-02	0.309E-02	0.261E-02
Mg II 3p-5s	5000.	0.326E-01	0.154E-01	0.134E-02	0.173E-02	0.133E-02	0.146E-02
1752.5 A	10000.	0.234E-01	0.145E-01	0.217E-02	0.231E-02	0.189E-02	0.190E-02
C= 0.14E+19	20000.	0.199E-01	0.121E-01	0.282E-02	0.282E-02	0.241E-02	0.232E-02
	50000.	0.175E-01	0.978E-02	0.371E-02	0.345E-02	0.298E-02	0.284E-02
	100000.	0.173E-01	0.772E-02	0.427E-02	0.393E-02	0.370E-02	0.325E-02
	150000.	0.169E-01	0.674E-02	0.470E-02	0.428E-02	0.397E-02	0.354E-02
Mg II 3p-6s	5000.	0.463E-01	0.249E-01	0.360E-02	0.343E-02	*0.315E-02	*0.274E-02
1482.2 A	10000.	0.387E-01	0.230E-01	0.475E-02	0.462E-02	0.400E-02	0.377E-02
C= 0.53E+18	20000.	0.324E-01	0.209E-01	0.615E-02	0.566E-02	0.504E-02	0.466E-02
	50000.	0.322E-01	0.162E-01	0.778E-02	0.673E-02	0.617E-02	0.546E-02
	100000.	0.317E-01	0.135E-01	0.842E-02	0.776E-02	0.688E-02	0.600E-02
	150000.	0.312E-01	0.114E-01	0.989E-02	0.834E-02	0.742E-02	0.667E-02
Mg II 3p-7s	5000.	0.737E-01	0.420E-01	*0.781E-02	*0.642E-02	*0.670E-02	*0.502E-02
1368.9 A	10000.	0.628E-01	0.428E-01	*0.980E-02	*0.902E-02	*0.825E-02	*0.728E-02
C= 0.27E+18	20000.	0.564E-01	0.367E-01	*0.124E-01	*0.110E-01	*0.985E-02	*0.897E-02
	50000.	0.593E-01	0.297E-01	0.146E-01	0.132E-01	*0.122E-01	*0.110E-01
	100000.	0.599E-01	0.232E-01	0.178E-01	0.148E-01	*0.141E-01	*0.123E-01
	150000.	0.589E-01	0.194E-01	0.168E-01	0.158E-01	*0.163E-01	*0.127E-01
Mg II 4p-5s	5000.	0.775	0.331	0.408E-01	0.375E-01	0.429E-01	0.316E-01
8230.0 A	10000.	0.578	0.305	0.575E-01	0.502E-01	0.536E-01	0.413E-01
C= 0.32E+20	20000.	0.513	0.252	0.714E-01	0.614E-01	0.648E-01	0.505E-01
	50000.	0.488	0.201	0.898E-01	0.748E-01	0.758E-01	0.611E-01
	100000.	0.502	0.157	0.101	0.851E-01	0.896E-01	0.712E-01
	150000.	0.497	0.137	0.111	0.928E-01	0.959E-01	0.766E-01

PERTURBER DENSITY = 1xE+16cm-3

TRANSITION	T(K)	ELECTRONS WIDTH(A)	ELECTRONS SHIFT(A)	PROTONS WIDTH(A)	PROTONS SHIFT(A)	IONIZED HELIUM WIDTH(A)	IONIZED HELIUM SHIFT(A)
Mg II 4p-6s	5000.	0.431	0.224	0.333E-01	0.306E-01	*0.296E-01	*0.245E-01
4433.2 A	10000.	0.363	0.205	0.435E-01	0.412E-01	0.372E-01	0.336E-01
C= 0.48E+19	20000.	0.311	0.184	0.560E-01	0.506E-01	0.462E-01	0.416E-01
	50000.	0.311	0.146	0.705E-01	0.601E-01	0.563E-01	0.486E-01
	100000.	0.318	0.117	0.757E-01	0.695E-01	0.627E-01	0.534E-01
	150000.	0.315	0.993E-01	0.894E-01	0.746E-01	0.671E-01	0.594E-01
Mg II 4p-7s	5000.	0.506	0.282	*0.529E-01	0.432E-01	*0.455E-01	*0.338E-01
3553.1 A	10000.	0.434	0.287	*0.663E-01	*0.607E-01	*0.560E-01	*0.490E-01
C= 0.18E+19	20000.	0.394	0.246	*0.838E-01	*0.744E-01	*0.668E-01	*0.603E-01
	50000.	0.419	0.198	0.984E-01	0.890E-01	*0.820E-01	*0.739E-01
	100000.	0.425	0.154	0.120	0.995E-01	*0.946E-01	*0.829E-01
	150000.	0.421	0.129	0.113	0.106	*0.110	*0.856E-01
Mg II 5p-6s	5000.	7.55	3.48	0.676	0.483	*0.645	*0.386
17444.6 A	10000.	6.53	3.16	0.833	0.649	*0.777	*0.532
C= 0.74E+20	20000.	5.93	2.83	1.01	0.791	*0.897	*0.650
	50000.	6.32	2.17	1.21	0.945	1.03	0.768
	100000.	6.56	1.80	1.31	1.10	1.08	0.843
	150000.	6.55	1.51	1.49	1.16	1.19	0.942
Mg II 5p-7s	5000.	3.35	1.75	*0.348	*0.268	*0.306	*0.209
8833.9 A	10000.	2.93	1.78	*0.433	*0.378	*0.370	*0.305
C= 0.11E+20	20000.	2.72	1.52	*0.538	*0.460	*0.437	*0.376
	50000.	2.96	1.17	0.629	0.553	*0.531	*0.458
	100000.	3.05	0.950	0.758	0.614	*0.610	*0.510
	150000.	3.03	0.793	0.716	0.660	*0.694	*0.526
Mg II 3p-3d	5000.	0.267E-01	0.444E-02	0.997E-03	0.331E-03	0.127E-02	0.306E-03
2796.3 A	10000.	0.199E-01	0.321E-02	0.149E-02	0.545E-03	0.174E-02	0.470E-03
C= 0.72E+19	20000.	0.151E-01	0.217E-02	0.187E-02	0.759E-03	0.199E-02	0.638E-03
	50000.	0.120E-01	0.186E-02	0.225E-02	0.980E-03	0.231E-02	0.809E-03
	100000.	0.109E-01	0.149E-02	0.248E-02	0.117E-02	0.244E-02	0.957E-03
	150000.	0.105E-01	0.132E-02	0.260E-02	0.127E-02	0.251E-02	0.103E-02
Mg II 3p-4d	5000.	0.423E-01	0.143E-01	0.462E-02	0.399E-02	*0.423E-02	*0.323E-02
1736.7 A	10000.	0.356E-01	0.114E-01	0.598E-02	0.532E-02	0.527E-02	0.437E-02
C= 0.15E+18	20000.	0.312E-01	0.959E-02	0.751E-02	0.657E-02	0.643E-02	0.535E-02
	50000.	0.272E-01	0.710E-02	0.948E-02	0.787E-02	0.774E-02	0.656E-02
	100000.	0.246E-01	0.556E-02	0.113E-01	0.885E-02	0.919E-02	0.711E-02
	150000.	0.231E-01	0.480E-02	0.110E-01	0.945E-02	0.945E-02	0.761E-02
Mg II 3p-5d	5000.	0.780E-01	0.324E-01	*0.127E-01	*0.929E-02		
1477.3 A	10000.	0.713E-01	0.269E-01	*0.159E-01	*0.133E-01		
C= 0.59E+17	20000.	0.662E-01	0.224E-01	*0.197E-01	*0.165E-01	*0.163E-01	*0.134E-01
	50000.	0.599E-01	0.163E-01	*0.236E-01	*0.192E-01	*0.194E-01	*0.153E-01
	100000.	0.547E-01	0.130E-01	*0.273E-01	*0.217E-01	*0.195E-01	*0.175E-01
	150000.	0.511E-01	0.108E-01	*0.317E-01	*0.245E-01	*0.222E-01	*0.185E-01
Mg II 3p-6d	5000.	0.146	0.644E-01				
1366.7 A	10000.	0.139	0.548E-01				
C= 0.30E+17	20000.	0.132	0.440E-01				
	50000.	0.121	0.329E-01				
	100000.	0.111	0.257E-01	*0.624E-01	*0.459E-01		
	150000.	0.103	0.213E-01	*0.724E-01	*0.551E-01		
Mg II 3p-7d	5000.	*0.260	*0.112				
1307.8 A	10000.	0.253	0.964E-01				
C= 0.18E+17	20000.	0.242	0.755E-01				
	50000.	0.224	0.591E-01				
	100000.	0.205	0.460E-01				
	150000.	0.191	0.379E-01				
Mg II 4p-4d	5000.	0.951	0.271	0.101	0.820E-01	*0.942E-01	*0.663E-01
7892.1 A	10000.	0.807	0.213	0.129	0.110	0.116	0.898E-01
C= 0.30E+19	20000.	0.718	0.176	0.160	0.135	0.139	0.110
	50000.	0.649	0.131	0.200	0.162	0.166	0.135
	100000.	0.607	0.103	0.236	0.182	0.194	0.146
	150000.	0.578	0.898E-01	0.232	0.194	0.200	0.156

PERTURBER DENSITY = 1xE+16cm-3

TRANSITION	T(K)	ELECTRONS WIDTH(A)	ELECTRONS SHIFT(A)	PROTONS WIDTH(A)	PROTONS SHIFT(A)	IONIZED HELIUM WIDTH(A)	IONIZED HELIUM SHIFT(A)
Mg II 4p-5d	5000.	0.708	0.285	*0.113	*0.819E-01		
4389.8 A	10000.	0.648	0.234	*0.142	*0.118		
C= 0.52E+18	20000.	0.604	0.196	*0.175	*0.145	*0.144	*0.118
	50000.	0.553	0.140	*0.209	*0.169	*0.172	*0.135
	100000.	0.511	0.111	*0.242	*0.192	*0.172	*0.154
	150000.	0.480	0.932E-01	*0.280	*0.216	*0.196	*0.163
Mg II 4p-6d	5000.	0.991	0.431				
3538.4 A	10000.	0.943	0.366				
C= 0.20E+18	20000.	0.895	0.298				
	50000.	0.828	0.218				
	100000.	0.761	0.170	*0.419	*0.307		
	150000.	0.711	0.141	*0.485	*0.369		
Mg II 4p-7d	5000.	*1.53	*0.659				
3168.8 A	10000.	1.49	0.566				
C= 0.10E+18	20000.	1.43	0.454				
	50000.	1.33	0.345				
	100000.	1.22	0.268				
	150000.	1.13	0.222				
Mg II 5p-5d	5000.	11.3	4.30	* 1.72	* 1.20		
16791.0 A	10000.	10.4	3.46	* 2.14	* 1.73		
C= 0.76E+19	20000.	9.84	2.89	* 2.63	* 2.13	* 2.19	* 1.74
	50000.	9.31	2.04	* 3.10	* 2.48	* 2.56	* 1.98
	100000.	8.83	1.62	* 3.58	* 2.81	* 2.60	* 2.28
	150000.	8.41	1.34	* 4.17	* 3.17	* 2.93	* 2.40
Mg II 5p-6d	5000.	6.27	2.67				
8743.8 A	10000.	5.98	2.26				
C= 0.12E+19	20000.	5.71	1.83				
	50000.	5.36	1.33				
	100000.	5.00	1.04	* 2.56	* 1.88		
	150000.	4.70	0.858	* 2.97	* 2.26		
Mg II 5p-7d	5000.*	7.16	* 3.04				
6787.6 A	10000.	6.98	2.61				
C= 0.48E+18	20000.	6.70	2.09				
	50000.	6.28	1.58				
	100000.	5.79	1.23				
	150000.	5.41	1.02				
Mg II 3d-4p	5000.	0.620	-0.970E-03	0.513E-01	-0.277E-02	0.620E-01	-0.264E-02
10931.0 A	10000.	0.487	-0.404E-02	0.665E-01	-0.488E-02	0.719E-01	-0.436E-02
C= 0.11E+21	20000.	0.411	-0.767E-02	0.753E-01	-0.701E-02	0.804E-01	-0.607E-02
	50000.	0.382	-0.426E-02	0.850E-01	-0.949E-02	0.873E-01	-0.783E-02
	100000.	0.382	-0.451E-02	0.885E-01	-0.113E-01	0.892E-01	-0.935E-02
	150000.	0.380	-0.526E-02	0.897E-01	-0.125E-01	0.912E-01	-0.102E-01
Mg II 3d-5p	5000.	0.151	-0.342E-04	0.226E-01	-0.180E-02	*0.243E-01	-0.157E-02
3850.2 A	10000.	0.126	-0.682E-03	0.258E-01	-0.265E-02	0.275E-01	-0.229E-02
C= 0.62E+19	20000.	0.117	-0.144E-03	0.286E-01	-0.338E-02	0.295E-01	-0.281E-02
	50000.	0.122	-0.238E-03	0.304E-01	-0.433E-02	0.307E-01	-0.353E-02
	100000.	0.128	-0.361E-03	0.311E-01	-0.499E-02	0.316E-01	-0.413E-02
	150000.	0.129	0.471E-03	0.316E-01	-0.549E-02	0.318E-01	-0.448E-02
Mg II 3d-6p	5000.	0.162	-0.956E-02	*0.334E-01	-0.554E-02		
2929.5 A	10000.	0.148	-0.948E-02	*0.379E-01	-0.733E-02	*0.393E-01	-0.601E-02
C= 0.19E+19	20000.	0.150	-0.696E-02	0.405E-01	-0.897E-02	*0.411E-01	-0.740E-02
	50000.	0.168	-0.450E-02	0.421E-01	-0.109E-01	*0.426E-01	-0.891E-02
	100000.	0.180	-0.330E-02	0.427E-01	-0.128E-01	0.424E-01	-0.100E-01
	150000.	0.182	-0.236E-02	0.433E-01	-0.136E-01	0.432E-01	-0.109E-01
Mg II 3d-7p	5000.	0.232	-0.434E-01				
2583.0 A	10000.	0.223	-0.324E-01	*0.623E-01	-0.166E-01		
C= 0.87E+18	20000.	0.237	-0.230E-01	*0.654E-01	-0.204E-01		
	50000.	0.277	-0.179E-01	*0.690E-01	-0.243E-01	*0.679E-01	-0.199E-01
	100000.	0.299	-0.119E-01	0.720E-01	-0.279E-01	*0.684E-01	-0.236E-01
	150000.	0.302	-0.979E-02	0.709E-01	-0.296E-01	*0.658E-01	-0.241E-01

PERTURBER DENSITY = 1xE+16cm-3

TRANSITION	T(K)	ELECTRONS WIDTH(A)	ELECTRONS SHIFT(A)	PROTONS WIDTH(A)	PROTONS SHIFT(A)	IONIZED HELIUM WIDTH(A)	IONIZED HELIUM SHIFT(A)
Mg II 4d-5p	5000.	11.3	-2.39	1.29	-0.781	* 1.28	*-0.632
24076.0 A	10000.	9.77	-1.72	1.57	-1.05	* 1.50	*-0.856
C= 0.28E+20	20000.	9.02	-1.52	1.84	-1.28	* 1.71	* -1.05
	50000.	8.77	-1.12	2.16	-1.53	1.97	-1.28
	100000.	8.65	-0.914	2.50	-1.74	2.13	-1.39
	150000.	8.44	-0.777	2.46	-1.90	2.17	-1.49
Mg II 4d-6p	5000.	1.85	-0.342	*0.283	*-0.106		
8119.2 A	10000.	1.68	-0.284	*0.329	*-0.142	*0.330	*-0.116
C= 0.32E+19	20000.	1.64	-0.226	*0.356	*-0.173	*0.346	*-0.142
	50000.	1.73	-0.168	0.392	-0.207	*0.364	*-0.167
	100000.	1.79	-0.129	0.426	-0.240	0.372	-0.186
	150000.	1.78	-0.111	0.451	-0.254	0.402	-0.206
Mg II 4d-7p	5000.	1.56	-0.344				
5918.7 A	10000.	1.47	-0.289	*0.342	*-0.120		
C= 0.17E+19	20000.	1.51	-0.226	*0.363	*-0.147		
	50000.	1.69	-0.169	*0.390	*-0.173	*0.373	*-0.141
	100000.	1.78	-0.121	0.393	-0.195	*0.377	*-0.157
	150000.	1.79	-0.101	0.430	-0.214	*0.415	*-0.180
Mg II 5d-7p	5000.	14.1	-4.72				
14734.8 A	10000.	13.3	-3.86				
C= 0.59E+19	20000.	13.4	-3.03	* 2.98	*-1.90		
	50000.	14.2	-2.25	* 3.36	*-2.31		
	100000.	14.5	-1.66	* 3.77	*-2.60	* 3.38	*-2.19
	150000.	14.2	-1.36	* 4.31	*-2.75	* 3.11	*-2.14
Mg II 3d-4f	5000.	0.269	-0.658E-02	0.214E-01	-0.194E-01	0.197E-01	-0.154E-01
4482.7 A	10000.	0.213	-0.863E-02	0.282E-01	-0.254E-01	0.250E-01	-0.209E-01
C= 0.98E+18	20000.	0.173	-0.111E-01	0.354E-01	-0.313E-01	0.306E-01	-0.258E-01
	50000.	0.144	-0.831E-02	0.463E-01	-0.382E-01	0.378E-01	-0.313E-01
	100000.	0.128	-0.639E-02	0.544E-01	-0.432E-01	0.416E-01	-0.335E-01
	150000.	0.120	-0.521E-02	0.609E-01	-0.466E-01	0.470E-01	-0.390E-01
Mg II 3d-5f	5000.	0.569	-0.371E-01				
3105.8 A	10000.	0.497	-0.230E-01				
C= 0.15E+17	20000.	0.432	-0.160E-01				
	50000.	0.356	-0.518E-02				
	100000.	0.303	-0.754E-03				
	150000.	0.273	-0.224E-02				
Mg II 3d-6f	5000.	*0.954	*-0.892E-01				
2661.6 A	10000.	0.881	-0.583E-01				
C= 0.69E+16	20000.	0.793	-0.372E-01				
	50000.	0.668	-0.170E-01				
	100000.	0.570	-0.360E-02				
	150000.	0.513	-0.101E-01				
Mg II 3d-7f	5000.	* 1.46	*-0.164				
2450.4 A	10000.	* 1.42	*-0.110				
C= 0.38E+16	20000.	* 1.32	*-0.762E-01				
	50000.	1.14	-0.456E-01				
	100000.	0.978	-0.199E-01				
	150000.	0.882	-0.295E-01				
Mg II 4d-5f	5000.	6.28	-0.655				
9634.8 A	10000.	5.51	-0.517				
C= 0.15E+18	20000.	4.83	-0.378				
	50000.	4.05	-0.163				
	100000.	3.49	-0.154				
	150000.	3.17	-0.127				
Mg II 4d-6f	5000.	* 5.77	*-0.611				
6348.6 A	10000.	5.32	-0.459				
C= 0.39E+17	20000.	4.80	-0.311				
	50000.	4.06	-0.558E-01				
	100000.	3.49	-0.861E-01				
	150000.	3.15	-0.695E-01				

PERTURBER DENSITY = 1xE+16cm-3

TRANSITION	T(K)	ELECTRONS WIDTH(A)	ELECTRONS SHIFT(A)	PROTONS WIDTH(A)	PROTONS SHIFT(A)	IONIZED HELIUM WIDTH(A)	IONIZED HELIUM SHIFT(A)
Mg II 4d-7f	5000.*	6.96	*-0.814				
5265.7 A	10000.*	6.76	*-0.602				
C= 0.18E+17	20000.*	6.30	*-0.413				
	50000.	5.43	-0.528E-01				
	100000.	4.68	-0.137				
	150000.	4.23	-0.969E-01				
Mg II 4f-5d	5000.	4.78	1.75	*0.682	*0.488		
10394.8 A	10000.	4.29	1.42	*0.848	*0.708		
C= 0.29E+19	20000.	3.92	1.17	* 1.01	*0.846	*0.848	*0.688
	50000.	3.52	0.827	* 1.15	* 1.02	*0.981	*0.808
	100000.	3.20	0.655	* 1.43	* 1.16	* 1.05	*0.950
	150000.	2.98	0.544	* 1.65	* 1.23	* 1.17	*0.968
Mg II 4f-6d	5000.	3.81	1.59				
6622.0 A	10000.	3.57	1.34				
C= 0.71E+18	20000.	3.35	1.08				
	50000.	3.07	0.783				
	100000.	2.80	0.611				
	150000.	2.61	0.504	* 1.77	* 1.30		
Mg II 4f-7d	5000.*	4.75	* 1.99				
5435.6 A	10000.*	4.58	* 1.70				
C= 0.31E+18	20000.	4.36	1.36				
	50000.	4.03	1.03				
	100000.	3.67	0.799				
	150000.	3.42	0.660				

PERTURBER DENSITY = 1xE+17cm-3

Mg II 3s-3p	5000.	0.173	-0.337E-03	0.260E-02	-0.569E-04	0.380E-02	-0.569E-04
2798.7 A	10000.	0.126	-0.392E-03	0.473E-02	-0.127E-03	0.588E-02	-0.126E-03
C= 0.27E+21	20000.	0.911E-01	-0.443E-03	0.678E-02	-0.254E-03	0.772E-02	-0.242E-03
	50000.	0.651E-01	-0.481E-03	0.846E-02	-0.486E-03	0.906E-02	-0.420E-03
	100000.	0.559E-01	-0.541E-03	0.944E-02	-0.670E-03	0.990E-02	-0.564E-03
	150000.	0.525E-01	-0.513E-03	0.988E-02	-0.751E-03	0.101E-01	-0.628E-03
Mg II 3s-4p	5000.	0.726E-01	0.620E-02	0.546E-02	0.280E-03	*0.654E-02	*0.267E-03
1240.1 A	10000.	0.561E-01	0.387E-02	0.743E-02	0.530E-03	*0.796E-02	*0.475E-03
C= 0.14E+20	20000.	0.460E-01	0.282E-02	0.849E-02	0.804E-03	0.906E-02	0.699E-03
	50000.	0.416E-01	0.249E-02	0.968E-02	0.112E-02	0.993E-02	0.925E-03
	100000.	0.410E-01	0.204E-02	0.101E-01	0.134E-02	0.103E-01	0.110E-02
	150000.	0.405E-01	0.179E-02	0.103E-01	0.148E-02	0.103E-01	0.120E-02
Mg II 3s-5p	5000.	0.103	0.880E-02	*0.144E-01	-0.812E-03		
1026.0 A	10000.	0.861E-01	0.667E-02	*0.173E-01	-0.131E-02		
C= 0.44E+19	20000.	0.795E-01	0.452E-02	*0.196E-01	-0.183E-02		
	50000.	0.822E-01	0.342E-02	*0.210E-01	-0.239E-02	*0.213E-01	-0.197E-02
	100000.	0.860E-01	0.226E-02	0.216E-01	-0.282E-02	*0.218E-01	-0.228E-02
	150000.	0.867E-01	0.220E-02	0.219E-01	-0.305E-02	*0.220E-01	-0.248E-02
Mg II 3s-6p	5000.	0.165	-0.685E-02				
946.7 A	10000.	0.151	-0.533E-02				
C= 0.20E+19	20000.	0.153	-0.392E-02				
	50000.	0.171	-0.160E-02	*0.436E-01	-0.112E-01		
	100000.	0.184	-0.113E-02	*0.441E-01	-0.131E-01		
	150000.	0.186	-0.798E-03	*0.442E-01	-0.138E-01		
Mg II 3s-7p	5000.*	0.282	*-0.484E-01				
907.4 A	10000.	0.271	-0.376E-01				
C= 0.11E+19	20000.	0.289	-0.238E-01				
	50000.	0.338	-0.194E-01				
	100000.	0.365	-0.117E-01				
	150000.	0.369	-0.104E-01				
Mg II 4s-4p	5000.	5.14	-1.22	0.307	-0.777E-01	*0.366	*-0.677E-01
9229.4 A	10000.	3.93	-0.906	0.421	-0.124	*0.447	*-0.105
C= 0.78E+21	20000.	3.27	-0.661	0.486	-0.169	*0.512	*-0.140
	50000.	3.13	-0.496	0.564	-0.222	0.563	-0.182
	100000.	3.18	-0.394	0.592	-0.261	0.596	-0.210
	150000.	3.18	-0.353	0.626	-0.278	0.611	-0.227

PERTURBER DENSITY = 1xE+17cm-3

PERTURBERS ARE:		ELECTRONS		PROTONS		IONIZED HELIUM	
TRANSITION	T(K)	WIDTH(A)	SHIFT(A)	WIDTH(A)	SHIFT(A)	WIDTH(A)	SHIFT(A)
Mg II 4s-5p	5000.	1.36	-0.968E-01	*0.179	*-0.204E-01		
3615.4 A	10000.	1.14	-0.770E-01	*0.215	*-0.317E-01		
C= 0.54E+20	20000.	1.07	-0.668E-01	*0.245	*-0.420E-01		
	50000.	1.13	-0.560E-01	*0.262	*-0.551E-01	*0.266	*-0.450E-01
	100000.	1.20	-0.520E-01	0.272	-0.635E-01	*0.270	*-0.509E-01
	150000.	1.21	-0.417E-01	0.269	-0.678E-01	*0.271	*-0.560E-01
Mg II 4s-6p	5000.	1.50	-0.851E-01				
2791.6 A	10000.	1.36	-0.114				
C= 0.17E+20	20000.	1.38	-0.755E-01				
	50000.	1.55	-0.788E-01	*0.375	*-0.104		
	100000.	1.68	-0.600E-01	*0.390	*-0.119		
	150000.	1.70	-0.506E-01	*0.397	*-0.128		
Mg II 4s-7p	5000.*	2.15	*-0.334				
2475.2 A	10000.*	2.06	*-0.285				
C= 0.80E+19	20000.	2.19	-0.234				
	50000.	2.57	-0.185				
	100000.	2.78	-0.134				
	150000.	2.81	-0.112				
Mg II 5s-6p	5000.	13.0	-3.98				
7790.1 A	10000.	12.0	-3.37				
C= 0.13E+21	20000.	12.3	-2.66				
	50000.	14.0	-1.98	* 3.00	*-1.16		
	100000.	15.1	-1.56	* 3.13	*-1.31		
	150000.	15.3	-1.36	* 3.27	*-1.44		
Mg II 5s-7p	5000.*	12.0	*-2.97				
5741.8 A	10000.*	11.6	*-2.63				
C= 0.43E+20	20000.	12.5	-2.12				
	50000.	14.8	-1.69				
	100000.	16.1	-1.29				
	150000.	16.2	-1.12				
Mg II 3p-4s	5000.	0.419	0.172	0.667E-02	0.894E-02	0.773E-02	0.764E-02
2934.7 A	10000.	0.295	0.132	0.125E-01	0.140E-01	0.129E-01	0.119E-01
C= 0.93E+20	20000.	0.214	0.983E-01	0.193E-01	0.191E-01	0.175E-01	0.157E-01
	50000.	0.177	0.740E-01	0.270E-01	0.250E-01	0.233E-01	0.204E-01
	100000.	0.163	0.581E-01	0.321E-01	0.290E-01	0.281E-01	0.240E-01
	150000.	0.158	0.509E-01	0.368E-01	0.319E-01	0.309E-01	0.261E-01
Mg II 3p-5s	5000.	0.326	0.150	0.134E-01	0.135E-01	*0.133E-01	*0.107E-01
1752.5 A	10000.	0.234	0.142	0.217E-01	0.196E-01	*0.189E-01	*0.155E-01
C= 0.14E+20	20000.	0.199	0.119	0.282E-01	0.267E-01	*0.242E-01	*0.218E-01
	50000.	0.175	0.965E-01	0.372E-01	0.343E-01	*0.298E-01	*0.281E-01
	100000.	0.173	0.766E-01	0.427E-01	0.393E-01	0.370E-01	0.325E-01
	150000.	0.169	0.673E-01	0.470E-01	0.428E-01	0.397E-01	0.354E-01
Mg II 3p-6s	5000.	0.463	0.235	*0.355E-01	*0.220E-01		
1482.2 A	10000.	0.387	0.220	*0.471E-01	*0.351E-01		
C= 0.53E+19	20000.	0.324	0.202	*0.614E-01	*0.522E-01		
	50000.	0.322	0.158	*0.778E-01	*0.665E-01		
	100000.	0.317	0.133	*0.842E-01	*0.776E-01	*0.688E-01	*0.600E-01
	150000.	0.312	0.114	*0.989E-01	*0.834E-01	*0.742E-01	*0.667E-01
Mg II 3p-7s	5000.*	0.736	*0.378				
1368.9 A	10000.*	0.628	*0.399				
C= 0.27E+19	20000.	0.564	0.347				
	50000.	0.593	0.285				
	100000.	0.599	0.226				
	150000.	0.589	0.193				
Mg II 4p-5s	5000.	7.75	3.21	*0.401	*0.293	*0.412	*0.233
8230.0 A	10000.	5.77	2.99	*0.572	*0.427	*0.531	*0.338
C= 0.32E+21	20000.	5.13	2.47	0.714	0.583	*0.649	*0.475
	50000.	4.88	1.98	0.898	0.742	*0.758	*0.606
	100000.	5.02	1.55	1.01	0.851	*0.896	*0.712
	150000.	4.97	1.37	1.11	0.928	0.959	0.766

PERTURBER DENSITY = 1xE+17cm-3

TRANSITION	T(K)	ELECTRONS WIDTH(A)	ELECTRONS SHIFT(A)	PROTONS WIDTH(A)	PROTONS SHIFT(A)	IONIZED HELIUM WIDTH(A)	IONIZED HELIUM SHIFT(A)
Mg II 4p-6s	5000.	4.31	2.11				
4433.2 A	10000.	3.63	1.96	*0.430	*0.313		
C= 0.48E+20	20000.	3.11	1.78	*0.559	*0.466		
	50000.	3.10	1.43	*0.705	*0.594		
	100000.	3.18	1.15	*0.757	*0.695	*0.627	*0.534
	150000.	3.15	0.990	*0.894	*0.746	*0.671	*0.594
Mg II 4p-7s	5000.*	5.06	* 2.54				
3553.1 A	10000.*	4.34	* 2.68				
C= 0.18E+20	20000.	3.93	2.32				
	50000.	4.19	1.90				
	100000.	4.25	1.50				
	150000.	4.21	1.28				
Mg II 3p-3d	5000.	0.267	0.440E-01	0.976E-02	0.291E-02	0.123E-01	0.265E-02
2796.3 A	10000.	0.199	0.318E-01	0.148E-01	0.508E-02	0.172E-01	0.433E-02
C= 0.72E+20	20000.	0.151	0.214E-01	0.187E-01	0.743E-02	0.198E-01	0.622E-02
	50000.	0.120	0.185E-01	0.225E-01	0.977E-02	0.231E-01	0.806E-02
	100000.	0.109	0.149E-01	0.248E-01	0.117E-01	0.244E-01	0.957E-02
	150000.	0.105	0.132E-01	0.260E-01	0.127E-01	0.251E-01	0.103E-01
Mg II 3p-4d	5000.	0.422	0.127	*0.451E-01	*0.268E-01		
1736.7 A	10000.	0.356	0.103	*0.592E-01	*0.414E-01		
C= 0.15E+19	20000.	0.312	0.877E-01	*0.751E-01	*0.607E-01		
	50000.	0.271	0.686E-01	*0.948E-01	*0.778E-01	*0.774E-01	*0.647E-01
	100000.	0.246	0.533E-01	*0.113	*0.885E-01	*0.919E-01	*0.711E-01
	150000.	0.231	0.477E-01	*0.110	*0.945E-01	*0.945E-01	*0.761E-01
Mg II 3p-5d	5000.*	0.756	*0.247				
1477.3 A	10000.	0.697	0.216				
C= 0.59E+18	20000.	0.651	0.188				
	50000.	0.592	0.152				
	100000.	0.542	0.119				
	150000.	0.507	0.107				
Mg II 3p-6d	5000.*	1.28	*0.401				
1366.7 A	10000.*	1.27	*0.383				
C= 0.30E+18	20000.*	1.24	*0.325				
	50000.	1.16	0.288				
	100000.	1.07	0.219				
	150000.	1.00	0.207				
Mg II 3p-7d	5000.						
1307.8 A	10000.						
C= 0.18E+18	20000.*	2.10	*0.484				
	50000.*	2.05	*0.484				
	100000.*	1.91	*0.357				
	150000.	1.79	0.363				
Mg II 4p-4d	5000.	9.49	2.37	*0.974	*0.552		
7892.1 A	10000.	8.06	1.90	* 1.27	*0.852		
C= 0.30E+20	20000.	7.17	1.59	* 1.60	* 1.25		
	50000.	6.48	1.24	* 2.00	* 1.60	* 1.65	* 1.33
	100000.	6.07	1.02	* 2.36	* 1.82	* 1.94	* 1.46
	150000.	5.77	0.891	* 2.32	* 1.94	* 2.00	* 1.56
Mg II 4p-5d	5000.*	6.87	* 2.17				
4389.8 A	10000.	6.34	1.88				
C= 0.52E+19	20000.	5.95	1.62				
	50000.	5.47	1.30				
	100000.	5.07	1.09				
	150000.	4.77	0.918				
Mg II 4p-6d	5000.						
3538.4 A	10000.*	8.64	* 2.56				
C= 0.20E+19	20000.*	8.41	* 2.16				
	50000.	7.94	1.91				
	100000.	7.37	1.66				
	150000.	6.91	1.37				

PERTURBER DENSITY = 1xE+17cm-3

TRANSITION	T(K)	ELECTRONS WIDTH(A)	ELECTRONS SHIFT(A)	PROTONS WIDTH(A)	PROTONS SHIFT(A)	IONIZED HELIUM WIDTH(A)	IONIZED HELIUM SHIFT(A)
Mg II 4p-7d	5000.						
3168.8 A	10000.						
C= 0.10E+19	20000.*	12.4	* 2.83				
	50000.*	12.1	* 2.82				
	100000.*	11.4	* 2.56				
	150000.	10.7	2.12				
Mg II 3d-4p	5000.	6.20	-0.343E-02	0.494	-0.244E-01	*0.584	*-0.232E-01
10931.0 A	10000.	4.87	-0.349E-01	0.657	-0.458E-01	*0.704	*-0.406E-01
C= 0.11E+22	20000.	4.11	-0.754E-01	0.751	-0.688E-01	*0.800	*-0.594E-01
	50000.	3.82	-0.420E-01	0.850	-0.947E-01	0.872	-0.781E-01
	100000.	3.82	-0.450E-01	0.885	-0.113	0.892	-0.935E-01
	150000.	3.80	-0.525E-01	0.897	-0.125	0.912	-0.102
Mg II 3d-5p	5000.	1.51	0.183E-02	*0.208	*-0.154E-01		
3850.2 A	10000.	1.26	-0.441E-02	*0.251	*-0.242E-01		
C= 0.62E+20	20000.	1.17	0.101E-02	*0.284	*-0.329E-01		
	50000.	1.22	-0.190E-02	*0.304	*-0.431E-01	*0.307	*-0.352E-01
	100000.	1.28	-0.353E-02	0.311	-0.499E-01	*0.316	*-0.413E-01
	150000.	1.29	0.481E-02	0.316	-0.549E-01	*0.318	*-0.448E-01
Mg II 3d-6p	5000.	1.62	-0.796E-01				
2929.5 A	10000.	1.48	-0.842E-01				
C= 0.19E+20	20000.	1.50	-0.626E-01				
	50000.	1.67	-0.405E-01	*0.420	*-0.108		
	100000.	1.80	-0.326E-01	*0.427	*-0.128		
	150000.	1.82	-0.231E-01	*0.433	*-0.136		
Mg II 3d-7p	5000.*	2.32	*-0.376				
2583.0 A	10000.*	2.23	*-0.284				
C= 0.87E+19	20000.	2.37	-0.199				
	50000.	2.77	-0.171				
	100000.	2.99	-0.118				
	150000.	3.02	-0.967E-01				
Mg II 4d-6p	5000.*	18.5	* -2.95				
8119.2 A	10000.	16.8	-2.51				
C= 0.32E+20	20000.	16.4	-2.02				
	50000.	17.3	-1.59				
	100000.	17.9	-1.28	* 4.26	*-2.40		
	150000.	17.7	-1.09	* 4.51	*-2.54		
Mg II 4d-7p	5000.*	15.6	*-2.94				
5918.7 A	10000.*	14.6	*-2.55				
C= 0.17E+20	20000.	15.0	-2.04				
	50000.	16.9	-1.59				
	100000.	17.8	-1.19				
	150000.	17.8	-0.992				
Mg II 3d-4f	5000.	2.68	0.312E-02	*0.210	*-0.141		
4482.7 A	10000.	2.12	-0.395E-01	*0.279	*-0.206		
C= 0.98E+19	20000.	1.73	-0.771E-01	*0.355	*-0.293	*0.305	*-0.237
	50000.	1.44	-0.699E-01	*0.463	*-0.378	*0.378	*-0.309
	100000.	1.28	-0.622E-01	*0.544	*-0.432	*0.416	*-0.335
	150000.	1.19	-0.500E-01	0.609	-0.466	*0.470	*-0.390
Mg II 3d-5f	5000.*	4.29	*-0.292				
3105.8 A	10000.*	3.98	*-0.202				
C= 0.15E+18	20000.	3.62	-0.176				
	50000.	3.12	-0.691E-01				
	100000.	2.72	-0.246E-01				
	150000.	2.48	-0.361E-01				
Mg II 3d-6f	5000.						
2661.6 A	10000.*	6.21	*-0.364				
C= 0.69E+17	20000.*	6.09	*-0.281				
	50000.*	5.51	*-0.145				
	100000.	4.88	-0.548E-01				
	150000.	4.46	-0.117				

PERTURBER DENSITY = 1xE+17cm-3

TRANSITION	T(K)	ELECTRONS WIDTH(A)	ELECTRONS SHIFT(A)	PROTONS WIDTH(A)	PROTONS SHIFT(A)	IONIZED HELIUM WIDTH(A)	IONIZED HELIUM SHIFT(A)
Mg II 3d-7f	5000.						
2450.4 A	10000.						
C= 0.38E+17	20000.						
	50000.*	8.88	*-0.301				
	100000.*	8.02	*-0.193				
	150000.	7.38	-0.290				

PERTURBER DENSITY = 1xE+18cm-3

TRANSITION	T(K)	ELECTRONS WIDTH(A)	ELECTRONS SHIFT(A)	PROTONS WIDTH(A)	PROTONS SHIFT(A)	IONIZED HELIUM WIDTH(A)	IONIZED HELIUM SHIFT(A)
Mg II 3s-3p	5000.	1.73	-0.308E-02	0.218E-01	-0.376E-03	0.302E-01	-0.376E-03
2798.7 A	10000.	1.26	-0.365E-02	0.460E-01	-0.111E-02	0.563E-01	-0.110E-02
C= 0.27E+22	20000.	0.911	-0.434E-02	0.672E-01	-0.239E-02	0.761E-01	-0.227E-02
	50000.	0.651	-0.474E-02	0.845E-01	-0.481E-02	0.904E-01	-0.415E-02
	100000.	0.559	-0.535E-02	0.944E-01	-0.669E-02	0.989E-01	-0.563E-02
	150000.	0.525	-0.511E-02	0.988E-01	-0.750E-02	0.101	-0.627E-02
Mg II 3s-4p	5000.	0.726	0.604E-01*	0.351E-01*	0.180E-02		
1240.1 A	10000.	0.561	0.378E-01*	0.678E-01*	0.449E-02		
C= 0.14E+21	20000.	0.460	0.274E-01*	0.820E-01*	0.729E-02		
	50000.	0.416	0.244E-01*	0.963E-01*	0.109E-01		
	100000.	0.410	0.201E-01*	0.101	*0.133E-01*	0.103	*0.110E-01
	150000.	0.405	0.177E-01*	0.103	*0.147E-01*	0.103	*0.120E-01
Mg II 3s-5p	5000.*	1.02	*0.938E-01				
1026.0 A	10000.*	0.860	*0.706E-01				
C= 0.44E+20	20000.	0.795	0.479E-01				
	50000.	0.822	0.358E-01				
	100000.	0.860	0.238E-01				
	150000.	0.867	0.226E-01				
Mg II 3s-6p	5000.						
946.7 A	10000.*	1.50	*-0.158E-01				
C= 0.20E+20	20000.*	1.52	*-0.139E-01				
	50000.*	1.71	*-0.435E-03				
	100000.	1.84	-0.774E-03				
	150000.	1.86	-0.204E-02				
Mg II 3s-7p	5000.						
907.4 A	10000.						
C= 0.11E+20	20000.						
	50000.*	3.35	*-0.118				
	100000.*	3.64	*-0.656E-01				
	150000.*	3.68	*-0.766E-01				
Mg II 4s-5p	5000.*	13.6	*-0.805				
3615.4 A	10000.*	11.4	*-0.669				
C= 0.54E+21	20000.	10.6	-0.592				
	50000.	11.3	-0.512				
	100000.	12.0	-0.483				
	150000.	12.1	-0.399				
Mg II 4s-6p	5000.						
2791.6 A	10000.*	13.5	*-0.782				
C= 0.17E+21	20000.*	13.7	*-0.513				
	50000.*	15.5	*-0.617				
	100000.	16.8	-0.482				
	150000.	17.0	-0.450				
Mg II 3p-4s	5000.	4.19	1.65	0.603E-01	0.490E-01*	0.656E-01*	0.361E-01
2934.7 A	10000.	2.95	1.28	0.123	0.108	*0.125	*0.866E-01
C= 0.93E+21	20000.	2.14	0.956	0.192	0.160	*0.175	*0.128
	50000.	1.77	0.724	0.270	0.239	*0.233	*0.193
	100000.	1.63	0.569	0.321	0.288	*0.281	*0.238
	150000.	1.58	0.503	0.368	0.317	*0.309	*0.259
Mg II 3p-5s	5000.*	3.26	* 1.34				
1752.5 A	10000.*	2.34	* 1.32				
C= 0.14E+21	20000.	1.99	1.12				
	50000.	1.75	0.921				
	100000.	1.73	0.735	*0.426	*0.387		
	150000.	1.69	0.656	*0.470	*0.423		

PERTURBER DENSITY = 1xE+18cm-3

TRANSITION	T(K)	ELECTRONS WIDTH(A)	ELECTRONS SHIFT(A)	PROTONS WIDTH(A)	PROTONS SHIFT(A)	IONIZED HELIUM WIDTH(A)	IONIZED HELIUM SHIFT(A)
Mg II 3p-6s	5000.						
1482.2 A	10000.*	3.86	* 1.86				
C= 0.53E+20	20000.*	3.24	* 1.79				
	50000.	3.22	1.43				
	100000.	3.17	1.23				
	150000.	3.11	1.08				
Mg II 3p-7s	5000.						
1368.9 A	10000.						
C= 0.27E+20	20000.						
	50000.*	5.89	* 2.42				
	100000.*	5.96	* 1.97				
	150000.*	5.87	* 1.76				
Mg II 3p-3d	5000.	2.67	0.423	*0.762E-01	*0.180E-01	*0.830E-01	*0.155E-01
2796.3 A	10000.	1.99	0.307	*0.141	*0.418E-01	*0.159	*0.344E-01
C= 0.72E+21	20000.	1.51	0.206	0.184	0.659E-01	*0.193	*0.540E-01
	50000.	1.20	0.180	0.224	0.946E-01	*0.230	*0.775E-01
	100000.	1.09	0.145	0.248	0.117	*0.244	*0.951E-01
	150000.	1.05	0.130	0.260	0.127	0.251	0.102
Mg II 3p-4d	5000.*	3.76	*0.737				
1736.7 A	10000.*	3.30	*0.684				
C= 0.15E+20	20000.	2.95	0.641				
	50000.	2.61	0.509				
	100000.	2.39	0.425				
	150000.	2.25	0.414				
Mg II 3p-5d	5000.						
1477.3 A	10000.						
C= 0.59E+19	20000.*	5.39	* 1.09				
	50000.*	5.23	*0.876				
	100000.*	4.94	*0.792				
	150000.	4.68	0.812				
Mg II 3p-6d	5000.						
1366.7 A	10000.						
C= 0.30E+19	20000.						
	50000.						
	100000.*	9.08	* 1.24				
	150000.*	8.69	* 1.37				
Mg II 3d-6p	5000.						
2929.5 A	10000.*	14.7	*-0.471				
C= 0.19E+21	20000.*	14.9	*-0.379				
	50000.*	16.7	*-0.250				
	100000.	18.0	-0.203				
	150000.	18.2	-0.173				
Mg II 3d-4f	5000.*	24.5	* 2.19				
4482.7 A	10000.*	19.9	* 1.03				
C= 0.98E+20	20000.	16.5	0.191				
	50000.	13.9	0.240E-01				
	100000.	12.4	-0.988E-01				
	150000.	11.7	-0.240				

PERTURBER DENSITY = 1xE+19cm-3

TRANSITION	T(K)	ELECTRONS WIDTH(A)	ELECTRONS SHIFT(A)	PROTONS WIDTH(A)	PROTONS SHIFT(A)	IONIZED HELIUM WIDTH(A)	IONIZED HELIUM SHIFT(A)
Mg II 3s-3p	5000.*	17.3	*-0.192E-01	*0.705E-01	-0.105E-02		
2798.7 A	10000.*	12.6	*-0.298E-01	*0.319	*-0.697E-02		
C= 0.27E+23	20000.	9.11	-0.392E-01	*0.627	*-0.204E-01		
	50000.	6.51	-0.451E-01	*0.831	*-0.451E-01	*0.877	*-0.386E-01
	100000.	5.59	-0.516E-01	*0.940	*-0.657E-01	*0.982	*-0.550E-01
	150000.	5.25	-0.495E-01	0.988	-0.748E-01	1.01	-0.625E-01
Mg II 3s-4p	5000.						
1240.1 A	10000.*	5.59	*0.347				
C= 0.14E+22	20000.*	4.59	*0.254				
	50000.	4.16	0.228				
	100000.	4.10	0.189				
	150000.	4.05	0.170				

PERTURBER DENSITY = 1xE+19cm-3

PERTURBERS ARE:		ELECTRONS		PROTONS		IONIZED HELIUM	
TRANSITION	T(K)	WIDTH(A)	SHIFT(A)	WIDTH(A)	SHIFT(A)	WIDTH(A)	SHIFT(A)
Mg II 3s-5p	5000.						
1026.0 A	10000.						
C= 0.44E+21	20000.						
	50000.*	8.16	*0.421				
	100000.*	8.56	*0.283				
	150000.*	8.64	*0.258				
Mg II 3p-3d	5000.						
2796.3 A	10000.*	19.8	* 2.69				
C= 0.72E+22	20000.*	15.1	* 1.81				
	50000.	12.0	1.64				
	100000.	10.9	1.34	* 2.47	* 1.10		
	150000.	10.5	1.21	* 2.59	* 1.26		

Sahal–Bréchot 1984), which gives an estimate for the maximum perturber density for which the line may be treated as isolated when it is divided by the corresponding full width at half maximum. For each value given in Table 1, the collision volume (V) multiplied by the perturber density (N) is much less than one and the impact approximation is valid (Sahal–Bréchot, 1969ab). Values for NV > 0.5 are not given and values for 0.1 < NV ≤ 0.5 are denoted by an asterisk. When the impact approximation is not valid, the ion broadening contribution may be estimated by using quasistatic approach (Sahal–Bréchot 1991 and Griem 1974). The accuracy of the results obtained decreases when broadening by ion interactions becomes important.

The analysis of present results and comparison with available theoretical data will be published elsewhere (Dimitrijević and Sahal–Bréchot, 1995).

Acknowledgements – This work is a part of the project "Physics and dynamics of celestial bodies", supported by Ministry of Science and Technology of Serbia.

REFERENCES

Dimitrijević, M. S., and Sahal–Bréchot, S.: 1984, *JQSRT*, **31**, 301.

Dimitrijević, M. S., and Sahal–Bréchot, S.: 1995, *Physica Scripta*, submitted.

Griem, H. R.: 1974, *Spectral Line Broadening by Plasmas*, Academic Press, New York.

Sahal–Bréchot, S.: 1969a, *Astron. Astrophys.* **1**, 91.

Sahal–Bréchot, S.: 1969b, *Astron. Astrophys.* **2**, 322.

Sahal–Bréchot, S.: 1991, *Astron. Astrophys.* **245**, 322.

ТАБЕЛЕ ПАРАМЕТАРА ШТАРКОВОГ ШИРЕЊА Mg II

М. С. Димитријевић[1] и S. Sahal–Bréchot[2]

[1] *Астрономска опсерваторија, Волгина 7, 11050 Београд, Југославија*

[2] *Laboratoire "Astrophysique, Atomes et Molécules"*
Département Atomes et Molécules en Astrophysique
Unité associée au C.N.R.S. No 812
Observatoire de Paris-Meudon, 92190 Meudon, France

УДК 52–355.3
Претходно саопштење

Користећи семикласичан прилаз, израчунате су ширине и помераји спектралних линија, проузроковани сударима са електронима, протонима и јонизованим хелијумом, за 52 мултиплета Mg II. Резултати су дати у функцији температуре и концентрације пертурбера.

Bull. Astron. Belgrade № 151 (1995), 115 – 126

UDC 52–355.3
Preliminary report

STARK BROADENING PARAMETER TABLES FOR Li II

M. S. Dimitrijević[1] and S. Sahal–Bréchot[2]

[1] *Astronomical Observatory, Volgina 7, 11050 Belgrade, Yugoslavia*

[2] *Laboratoire "Astrophysique, Atomes et Molécules"*
Département Atomes et Molécules en Astrophysique
Unité associée au C.N.R.S. No 812
Observatoire de Paris–Meudon, 92190 Meudon, France

(Received: October 20, 1994)

SUMMARY: Using a semiclassical approach, we have calculated electron–, proton–, and ionised helium–impact line widths and shifts for 37 Li II multiplets as a function of temperature and perturber density.

1. INTRODUCTION

Since the He-like Li II spectrum is particularly suitable for theoretical research, the corresponding Stark broadening parameters are of importance for the consideration of Stark broadening theory as well as for the examination of regularities and systematic trends within the astrophysically important helium isoelectronic sequence. In order to provide to astrophysicists the needed Stark broadening data, we have calculated within the semiclassical-perturbation formalism (Sahal–Bréchot, 1969ab) electron-, proton-, and ionized helium-impact line widths and shifts for 37 Li II multiplets.

2. RESULTS AND DISCUSSION

Analysis of obtained results and all details of calculations as well as the comparison with availlable experimental data will be published elsewhere (Dimitrijević and Sahal–Bréchot, 1995). Here, we present only tables of Stark broadening parameters for astrophysical and laboratory plasma diagnostic purposes. Our results for 37 Li II multiplets are shown in Table 1, for perturber densities 10^{11} (of interest for infrared spectroscopy) and 10^{15}– 10^{20} cm^{-3} (the data for 10^{17} cm^{-3} will be published in Dimitrijević and Sahal–Bréchot, 1995) and temperatures T = 5,000 – 40,000 K. We also specify a parameter c (Dimitri-

Table 1. This table shows electron-, proton-, and He II- impact broadening parameters for Li II, for perturber densities of 10^{11} (of interest for infrared spectroscopy) and $10^{15} - 10^{20}$ cm^{-3} and temperatures from 5,000 up to 40,000 K. Transitions and averaged wavelengths for the multiplet (in Å) are also given. By using c [see Eq. (5) in Dimitrijević et *al.*, 1991], we obtain an estimate for the maximum perturber density for which the line may be treated as isolated and tabulated data may be used. The asterisk identifies cases for which the collision volume multiplied by the perturber density (the condition for validity of the impact approximation) lies between 0.1 and 0.5.

		ELECTRONS		PROTONS		IONIZED HELIUM	
TRANSITION	T(K)	WIDTH(A)	SHIFT(A)	WIDTH(A)	SHIFT(A)	WIDTH(A)	SHIFT(A)
PERTURBER DENSITY = 0.1E+12cm-3							
Li II 3D- 3P	5000.	0.550E-02	-0.108E-02	0.471E-03	-0.527E-03	0.947E-03	-0.110E-02
	10000.	0.446E-02	-0.902E-03	0.632E-03	-0.630E-03	0.131E-02	-0.132E-02
C= 0.21E+17	20000.	0.373E-02	-0.783E-03	0.801E-03	-0.751E-03	0.164E-02	-0.157E-02
	40000.	0.319E-02	-0.640E-03	0.100E-02	-0.865E-03	0.200E-02	-0.182E-02
Li II 4S- 6P	5000.	0.276E-04	0.578E-05	0.443E-05	0.383E-05	0.907E-05	0.804E-05
5655.7 A	10000.	0.279E-04	0.447E-05	0.523E-05	0.443E-05	0.110E-04	0.934E-05
C= 0.68E+13	20000.	0.283E-04	0.348E-05	0.590E-05	0.510E-05	0.125E-04	0.105E-04
	40000.	0.279E-04	0.245E-05	0.739E-05	0.582E-05	0.144E-04	0.123E-04
Li II 4P- 4D	5000.	0.829E-02	-0.188E-03	0.194E-02	0.181E-02	0.379E-02	0.378E-02
	10000.	0.727E-02	-0.176E-03	0.250E-02	0.208E-02	0.482E-02	0.443E-02
C= 0.56E+15	20000.	0.643E-02	-0.148E-03	0.334E-02	0.239E-02	0.561E-02	0.502E-02
	40000.	0.572E-02	-0.188E-03	0.397E-02	0.272E-02	0.683E-02	0.563E-02
PERTURBER DENSITY = 0.1E+16cm-3							
Li II 1S- 3P	5000.	0.282E-04	-0.408E-05	0.230E-05	-0.272E-05	0.460E-05	-0.544E-05
178.0 A	10000.	0.228E-04	-0.315E-05	0.333E-05	-0.334E-05	0.689E-05	-0.690E-05
C= 0.15E+15	20000.	0.190E-04	-0.287E-05	0.424E-05	-0.399E-05	0.867E-05	-0.836E-05
	40000.	0.161E-04	-0.227E-05	0.531E-05	-0.471E-05	0.109E-04	-0.970E-05
Li II 1S- 4P	5000.	0.841E-04	-0.223E-04	0.132E-04	-0.128E-04*	0.273E-04	-0.247E-04
171.6 A	10000.	0.730E-04	-0.183E-04	0.167E-04	-0.156E-04*	0.345E-04	-0.319E-04
C= 0.59E+14	20000.	0.643E-04	-0.146E-04	0.209E-04	-0.183E-04	0.417E-04	-0.378E-04
	40000.	0.568E-04	-0.114E-04	0.245E-04	-0.204E-04	0.511E-04	-0.434E-04
Li II 1S- 5P	5000.	0.191E-03	-0.671E-04*	0.387E-04	-0.351E-04		
168.7 A	10000.	0.174E-03	-0.546E-04	0.485E-04	-0.421E-04		
C= 0.34E+14	20000.	0.159E-03	-0.425E-04	0.585E-04	-0.496E-04*	0.112E-03	-0.101E-03
	40000.	0.144E-03	-0.329E-04	0.682E-04	-0.542E-04*	0.136E-03	-0.117E-03
Li II 2S- 2P	5000.	0.237E-01	-0.154E-02	0.170E-03	-0.319E-03	0.306E-03	-0.632E-03
9584.1 A	10000.	0.169E-01	-0.137E-02	0.405E-03	-0.525E-03	0.773E-03	-0.107E-02
C= 0.96E+19	20000.	0.125E-01	-0.114E-02	0.679E-03	-0.731E-03	0.134E-02	-0.151E-02
	40000.	0.974E-02	-0.123E-02	0.974E-03	-0.909E-03	0.198E-02	-0.190E-02
Li II 2S- 3P	5000.	0.197E-02	-0.330E-03	0.148E-03	-0.176E-03	0.297E-03	-0.351E-03
1420.9 A	10000.	0.158E-02	-0.254E-03	0.214E-03	-0.215E-03	0.445E-03	-0.445E-03
C= 0.97E+16	20000.	0.131E-02	-0.215E-03	0.273E-03	-0.257E-03	0.558E-03	-0.539E-03
	40000.	0.112E-02	-0.185E-03	0.348E-03	-0.303E-03	0.699E-03	-0.625E-03

PERTURBER DENSITY = 0.1E+16cm-3

TRANSITION	T(K)	ELECTRONS WIDTH(A)	ELECTRONS SHIFT(A)	PROTONS WIDTH(A)	PROTONS SHIFT(A)	IONIZED HELIUM WIDTH(A)	IONIZED HELIUM SHIFT(A)
Li II 2S- 4P	5000.	0.352E-02	-0.903E-03	0.536E-03	-0.520E-03*	0.111E-02	-0.100E-02
1093.4 A	10000.	0.304E-02	-0.733E-03	0.677E-03	-0.633E-03*	0.140E-02	-0.130E-02
C= 0.24E+16	20000.	0.267E-02	-0.626E-03	0.853E-03	-0.742E-03	0.170E-02	-0.154E-02
	40000.	0.236E-02	-0.474E-03	0.995E-03	-0.831E-03	0.208E-02	-0.177E-02
Li II 2S- 5P	5000.	0.663E-02	-0.227E-02	0.133E-02	-0.120E-02		
987.6 A	10000.	0.603E-02	-0.183E-02	0.166E-02	-0.144E-02		
C= 0.12E+16	20000.	0.550E-02	-0.148E-02	0.201E-02	-0.170E-02*	0.382E-02	-0.347E-02
	40000.	0.496E-02	-0.112E-02	0.234E-02	-0.186E-02*	0.464E-02	-0.401E-02
Li II 3S- 3P	5000.	1.48	-0.507	0.106	-0.121	0.213	-0.242
33614.6 A	10000.	1.20	-0.390	0.146	-0.148	0.300	-0.303
C= 0.54E+19	20000.	1.04	-0.317	0.185	-0.176	0.378	-0.370
	40000.	0.915	-0.250	0.231	-0.205	0.476	-0.425
Li II 3S- 4P	5000.	0.544E-01	-0.178E-01	0.791E-02	-0.771E-02*	0.164E-01	-0.149E-01
4157.6 A	10000.	0.477E-01	-0.145E-01	0.999E-02	-0.940E-02*	0.207E-01	-0.192E-01
C= 0.34E+17	20000.	0.427E-01	-0.117E-01	0.127E-01	-0.109E-01	0.252E-01	-0.229E-01
	40000.	0.383E-01	-0.915E-02	0.147E-01	-0.122E-01	0.307E-01	-0.257E-01
Li II 3S- 5P	5000.	0.607E-01	-0.221E-01*	0.120E-01	-0.108E-01		
2953.6 A	10000.	0.556E-01	-0.182E-01	0.148E-01	-0.130E-01		
C= 0.11E+17	20000.	0.510E-01	-0.143E-01	0.181E-01	-0.152E-01*	0.343E-01	-0.313E-01
	40000.	0.464E-01	-0.112E-01	0.210E-01	-0.166E-01*	0.416E-01	-0.362E-01
Li II 2P- 3S	5000.	0.188E-02	0.841E-03	0.749E-04	0.118E-03	0.152E-03	0.236E-03
1755.3 A	10000.	0.147E-02	0.655E-03	0.138E-03	0.157E-03	0.281E-03	0.326E-03
C= 0.92E+17	20000.	0.127E-02	0.536E-03	0.185E-03	0.189E-03	0.381E-03	0.394E-03
	40000.	0.114E-02	0.424E-03	0.233E-03	0.225E-03	0.488E-03	0.470E-03
Li II 2P- 3D	5000.	0.171E-02	0.412E-03	0.118E-03	0.156E-03	0.235E-03	0.313E-03
1681.7 A	10000.	0.133E-02	0.334E-03	0.187E-03	0.198E-03	0.387E-03	0.409E-03
C= 0.14E+17	20000.	0.107E-02	0.271E-03	0.248E-03	0.239E-03	0.507E-03	0.500E-03
	40000.	0.877E-03	0.214E-03	0.320E-03	0.278E-03	0.628E-03	0.596E-03
Li II 3D- 4P	5000.	0.699E-01	-0.180E-01	0.101E-01	-0.975E-02*	0.208E-01	-0.188E-01
4639.0 A	10000.	0.601E-01	-0.146E-01	0.126E-01	-0.119E-01*	0.264E-01	-0.243E-01
C= 0.43E+17	20000.	0.526E-01	-0.124E-01	0.159E-01	-0.136E-01	0.318E-01	-0.288E-01
	40000.	0.463E-01	-0.954E-02	0.185E-01	-0.153E-01	0.381E-01	-0.322E-01
Li II 3D- 5P	5000.	0.722E-01	-0.250E-01*	0.140E-01	-0.126E-01		
3188.6 A	10000.	0.654E-01	-0.204E-01	0.172E-01	-0.152E-01		
C= 0.12E+17	20000.	0.594E-01	-0.160E-01	0.212E-01	-0.177E-01*	0.402E-01	-0.367E-01
	40000.	0.535E-01	-0.125E-01	0.245E-01	-0.195E-01*	0.489E-01	-0.425E-01
Li II 2S- 3P	5000.	0.780E-03	0.282E-04	0.363E-04	0.341E-04	0.709E-04	0.689E-04
1198.1 A	10000.	0.667E-03	0.489E-04	0.563E-04	0.474E-04	0.111E-03	0.974E-04
C= 0.25E+17	20000.	0.590E-03	0.407E-04	0.709E-04	0.570E-04	0.143E-03	0.120E-03
	40000.	0.533E-03	0.378E-04	0.860E-04	0.679E-04	0.177E-03	0.144E-03

PERTURBER DENSITY = 0.1E+16cm-3

TRANSITION	T(K)	ELECTRONS WIDTH(A)	ELECTRONS SHIFT(A)	PROTONS WIDTH(A)	PROTONS SHIFT(A)	IONIZED HELIUM WIDTH(A)	IONIZED HELIUM SHIFT(A)
Li II 2S- 4P	5000.	0.134E-02	0.257E-03	0.146E-03	0.129E-03	0.296E-03	0.258E-03
944.7 A	10000.	0.127E-02	0.215E-03	0.183E-03	0.157E-03	0.375E-03	0.323E-03
C= 0.65E+16	20000.	0.121E-02	0.185E-03	0.226E-03	0.187E-03	0.459E-03	0.390E-03
	40000.	0.116E-02	0.163E-03	0.261E-03	0.212E-03	0.551E-03	0.457E-03
Li II 2S- 5P	5000.	0.273E-02	0.669E-03	0.408E-03	0.347E-03	*0.839E-03	*0.668E-03
861.3 A	10000.	0.269E-02	0.560E-03	0.501E-03	0.427E-03	*0.103E-02	*0.854E-03
C= 0.27E+16	20000.	0.268E-02	0.504E-03	0.586E-03	0.486E-03	*0.121E-02	*0.103E-02
	40000.	0.262E-02	0.391E-03	0.657E-03	0.551E-03	0.138E-02	0.116E-02
Li II 2S- 6P	5000.	0.534E-02	0.151E-02	*0.953E-03	*0.786E-03		
822.2 A	10000.	0.541E-02	0.120E-02	0.113E-02	0.957E-03		
C= 0.14E+16	20000.	0.550E-02	0.104E-02	0.130E-02	0.112E-02	*0.270E-02	*0.228E-02
	40000.	0.539E-02	0.781E-03	0.159E-02	0.124E-02	*0.319E-02	*0.267E-02
Li II 3S- 3P	5000.	0.354	-0.723E-01	0.867E-02	0.502E-03	0.162E-01	0.987E-03
21066.8 A	10000.	0.290	-0.479E-01	0.123E-01	0.912E-03	0.234E-01	0.185E-02
C= 0.77E+19	20000.	0.264	-0.381E-01	0.146E-01	0.139E-02	0.285E-01	0.289E-02
	40000.	0.245	-0.298E-01	0.166E-01	0.191E-02	0.322E-01	0.398E-02
Li II 3S- 4P	5000.	0.240E-01	0.223E-02	0.212E-02	0.184E-02	0.430E-02	0.368E-02
3685.8 A	10000.	0.219E-01	0.184E-02	0.266E-02	0.225E-02	0.543E-02	0.461E-02
C= 0.99E+17	20000.	0.209E-01	0.149E-02	0.322E-02	0.267E-02	0.670E-02	0.565E-02
	40000.	0.201E-01	0.136E-02	0.383E-02	0.303E-02	0.777E-02	0.647E-02
Li II 3S- 5P	5000.	0.279E-01	0.475E-02	0.389E-02	0.331E-02	*0.803E-02	*0.641E-02
2675.3 A	10000.	0.272E-01	0.420E-02	0.477E-02	0.407E-02	*0.991E-02	*0.818E-02
C= 0.26E+17	20000.	0.270E-01	0.391E-02	0.559E-02	0.462E-02	*0.115E-01	*0.978E-02
	40000.	0.265E-01	0.301E-02	0.629E-02	0.526E-02	0.133E-01	0.110E-01
Li II 3S- 6P	5000.	0.439E-01	0.114E-01	*0.765E-02	*0.630E-02		
2330.6 A	10000.	0.443E-01	0.878E-02	0.905E-02	0.767E-02		
C= 0.12E+17	20000.	0.450E-01	0.789E-02	0.104E-01	0.895E-02	*0.215E-01	*0.182E-01
	40000.	0.442E-01	0.576E-02	0.127E-01	0.991E-02	*0.254E-01	*0.214E-01
Li II 4S- 4P	5000.	6.43	-1.16	0.287	0.124	0.554	0.247
52504.5 A	10000.	6.09	-0.950	0.339	0.160	0.672	0.332
C= 0.20E+20	20000.	5.85	-0.838	0.392	0.193	0.776	0.404
	40000.	5.70	-0.634	0.438	0.228	0.865	0.481
Li II 4S- 5P	5000.	0.305	0.226E-01	0.341E-01	0.283E-01	*0.698E-01	*0.547E-01
8228.6 A	10000.	0.297	0.162E-01	0.420E-01	0.347E-01	*0.854E-01	*0.706E-01
C= 0.25E+18	20000.	0.295	0.122E-01	0.487E-01	0.403E-01	*0.102	*0.833E-01
	40000.	0.291	0.830E-02	0.560E-01	0.451E-01	0.120	0.980E-01
Li II 4S- 6P	5000.	0.276	0.538E-01	*0.444E-01	*0.363E-01		
5655.7 A	10000.	0.279	0.423E-01	0.522E-01	0.439E-01		
C= 0.68E+17	20000.	0.283	0.337E-01	0.590E-01	0.510E-01	*0.125	*0.104
	40000.	0.279	0.244E-01	0.739E-01	0.582E-01	*0.144	*0.123

PERTURBER DENSITY = 0.1E+16cm-3

TRANSITION	T(K)	ELECTRONS WIDTH(A)	ELECTRONS SHIFT(A)	PROTONS WIDTH(A)	PROTONS SHIFT(A)	IONIZED HELIUM WIDTH(A)	IONIZED HELIUM SHIFT(A)
Li II 2P- 3S	5000.	0.137E-02	0.640E-03	0.396E-04	0.657E-04	0.786E-04	0.133E-03
1653.1 A	10000.	0.101E-02	0.483E-03	0.710E-04	0.913E-04	0.143E-03	0.188E-03
C= 0.13E+18	20000.	0.844E-03	0.396E-03	0.104E-03	0.110E-03	0.217E-03	0.231E-03
	40000.	0.749E-03	0.312E-03	0.132E-03	0.131E-03	0.279E-03	0.276E-03
Li II 2P- 4S	5000.	0.168E-02	0.113E-02	0.144E-03	0.168E-03	0.292E-03	0.337E-03
1166.6 A	10000.	0.143E-02	0.931E-03	0.197E-03	0.205E-03	0.410E-03	0.421E-03
C= 0.26E+17	20000.	0.129E-02	0.749E-03	0.253E-03	0.245E-03	0.516E-03	0.512E-03
	40000.	0.122E-02	0.597E-03	0.303E-03	0.281E-03	0.649E-03	0.595E-03
Li II 3P- 4S	5000.	0.341E-01	0.184E-01	0.235E-02	0.269E-02	0.471E-02	0.538E-02
4882.8 A	10000.	0.304E-01	0.150E-01	0.323E-02	0.327E-02	0.667E-02	0.674E-02
C= 0.42E+18	20000.	0.286E-01	0.120E-01	0.408E-02	0.391E-02	0.855E-02	0.819E-02
	40000.	0.275E-01	0.944E-02	0.500E-02	0.447E-02	0.103E-01	0.947E-02
Li II 2P- 3D	5000.	0.123E-02	0.775E-04	0.357E-04	-0.392E-04	0.683E-04	-0.786E-04
1493.0 A	10000.	0.926E-03	0.422E-04	0.577E-04	-0.550E-04	0.112E-03	-0.112E-03
C= 0.39E+17	20000.	0.709E-03	0.227E-04	0.783E-04	-0.678E-04	0.158E-03	-0.142E-03
	40000.	0.565E-03	0.106E-04	0.976E-04	-0.809E-04	0.197E-03	-0.169E-03
Li II 2P- 4D	5000.	0.415E-02	0.147E-03	0.136E-02	0.121E-02*	0.267E-02*	0.226E-02
1131.9 A	10000.	0.345E-02	0.156E-03	0.176E-02	0.149E-02*	0.343E-02*	0.292E-02
C= 0.38E+15	20000.	0.288E-02	0.157E-03	0.230E-02	0.167E-02*	0.402E-02*	0.362E-02
	40000.	0.242E-02	0.123E-03	0.281E-02	0.195E-02*	0.475E-02*	0.391E-02
Li II 3P- 3D	5000.	2.74	-0.164	0.123	-0.120	0.239	-0.239
57388.8 A	10000.	2.26	-0.183	0.186	-0.160	0.376	-0.333
C= 0.57E+20	20000.	1.95	-0.153	0.232	-0.193	0.473	-0.404
	40000.	1.72	-0.136	0.282	-0.229	0.581	-0.485
Li II 3P- 4D	5000.	0.656E-01	0.568E-03	0.198E-01	0.176E-01*	0.390E-01*	0.328E-01
4326.7 A	10000.	0.554E-01	0.702E-03	0.255E-01	0.217E-01*	0.501E-01*	0.425E-01
C= 0.55E+16	20000.	0.470E-01	0.131E-02	0.336E-01	0.244E-01*	0.584E-01*	0.526E-01
	40000.	0.401E-01	0.887E-03	0.409E-01	0.283E-01*	0.695E-01*	0.573E-01
Li II 3D- 4P	5000.	0.407E-01	0.715E-02	0.401E-02	0.353E-02	0.819E-02	0.707E-02
4844.4 A	10000.	0.376E-01	0.618E-02	0.503E-02	0.433E-02	0.104E-01	0.893E-02
C= 0.17E+18	20000.	0.356E-01	0.511E-02	0.617E-02	0.515E-02	0.126E-01	0.108E-01
	40000.	0.338E-01	0.457E-02	0.702E-02	0.586E-02	0.150E-01	0.123E-01
Li II 3D- 5P	5000.	0.407E-01	0.998E-02	0.582E-02	0.493E-02*	0.119E-01*	0.947E-02
3237.3 A	10000.	0.397E-01	0.825E-02	0.716E-02	0.607E-02*	0.147E-01*	0.122E-01
C= 0.39E+17	20000.	0.394E-01	0.728E-02	0.839E-02	0.693E-02*	0.173E-01*	0.147E-01
	40000.	0.384E-01	0.565E-02	0.934E-02	0.787E-02	0.196E-01	0.166E-01
Li II 3D- 6P	5000.	0.611E-01	0.163E-01*	0.107E-01*	0.878E-02		
2745.8 A	10000.	0.616E-01	0.138E-01	0.127E-01	0.107E-01		
C= 0.16E+17	20000.	0.624E-01	0.118E-01	0.145E-01	0.125E-01*	0.303E-01*	0.254E-01
	40000.	0.611E-01	0.885E-02	0.178E-01	0.138E-01*	0.356E-01*	0.298E-01

PERTURBER DENSITY = 0.1E+17cm-3

TRANSITION	T(K)	ELECTRONS WIDTH(A)	ELECTRONS SHIFT(A)	PROTONS WIDTH(A)	PROTONS SHIFT(A)	IONIZED HELIUM WIDTH(A)	IONIZED HELIUM SHIFT(A)
Li II 1S- 3P	5000.	0.282E-03	-0.386E-04	0.229E-04	-0.247E-04	0.460E-04	-0.457E-04
178.0 A	10000.	0.228E-03	-0.299E-04	0.333E-04	-0.323E-04	0.693E-04	-0.632E-04
C= 0.15E+16	20000.	0.190E-03	-0.275E-04	0.424E-04	-0.397E-04	0.868E-04	-0.808E-04
	40000.	0.161E-03	-0.221E-04	0.531E-04	-0.469E-04	0.109E-03	-0.964E-04
Li II 1S- 4P	5000.	0.841E-03	-0.202E-03*	0.132E-03	-0.105E-03		
171.6 A	10000.	0.730E-03	-0.167E-03*	0.166E-03	-0.146E-03		
C= 0.59E+15	20000.	0.643E-03	-0.136E-03*	0.209E-03	-0.181E-03		
	40000.	0.568E-03	-0.109E-03*	0.245E-03	-0.203E-03		
Li II 1S- 5P	5000.	0.190E-02	-0.570E-03				
168.7 A	10000.	0.173E-02	-0.474E-03				
C= 0.34E+15	20000.	0.158E-02	-0.378E-03				
	40000.	0.143E-02	-0.307E-03				
Li II 2S- 2P	5000.	0.237	-0.145E-01	0.170E-02	-0.305E-02	0.304E-02	-0.579E-02
9584.1 A	10000.	0.169	-0.139E-01	0.405E-02	-0.519E-02	0.772E-02	-0.104E-01
C= 0.96E+20	20000.	0.125	-0.114E-01	0.679E-02	-0.730E-02	0.134E-01	-0.149E-01
	40000.	0.974E-01	-0.123E-01	0.974E-02	-0.908E-02	0.198E-01	-0.189E-01
Li II 2S- 3P	5000.	0.197E-01	-0.315E-02	0.148E-02	-0.160E-02	0.297E-02	-0.294E-02
1420.9 A	10000.	0.158E-01	-0.243E-02	0.214E-02	-0.208E-02	0.447E-02	-0.406E-02
C= 0.97E+17	20000.	0.131E-01	-0.207E-02	0.273E-02	-0.256E-02	0.560E-02	-0.521E-02
	40000.	0.112E-01	-0.181E-02	0.348E-02	-0.302E-02	0.699E-02	-0.621E-02
Li II 2S- 4P	5000.	0.352E-01	-0.814E-02*	0.537E-02	-0.425E-02		
1093.4 A	10000.	0.304E-01	-0.668E-02*	0.674E-02	-0.594E-02		
C= 0.24E+17	20000.	0.267E-01	-0.577E-02*	0.853E-02	-0.735E-02		
	40000.	0.236E-01	-0.454E-02*	0.997E-02	-0.826E-02		
Li II 2S- 5P	5000.	0.659E-01	-0.192E-01				
987.6 A	10000.	0.600E-01	-0.158E-01				
C= 0.12E+17	20000.	0.547E-01	-0.129E-01				
	40000.	0.495E-01	-0.105E-01				
Li II 3S- 3P	5000.	14.8	-4.96	1.06	-1.09	* 2.11	-2.00
33614.6 A	10000.	12.0	-3.82	1.46	-1.43	* 2.99	-2.75
C= 0.54E+20	20000.	10.4	-3.12	1.85	-1.75	* 3.80	-3.56
	40000.	9.15	-2.47	2.31	-2.04	4.76	-4.22
Li II 3S- 4P	5000.	0.544	-0.165	*0.791E-01	-0.628E-01		
4157.6 A	10000.	0.477	-0.136	*0.999E-01	-0.884E-01		
C= 0.34E+18	20000.	0.426	-0.111	*0.127	-0.107		
	40000.	0.383	-0.885E-01	*0.147	-0.121		
Li II 3S- 5P	5000.	0.603	-0.190				
2953.6 A	10000.	0.553	-0.160				
C= 0.11E+18	20000.	0.508	-0.129				
	40000.	0.463	-0.105				

PERTURBER DENSITY = 0.1E+17cm-3

TRANSITION	T(K)	ELECTRONS WIDTH(A)	ELECTRONS SHIFT(A)	PROTONS WIDTH(A)	PROTONS SHIFT(A)	IONIZED HELIUM WIDTH(A)	IONIZED HELIUM SHIFT(A)
Li II 2P- 3S	5000.	0.188E-01	0.835E-02	0.750E-03	0.110E-02	0.153E-02	0.205E-02
1755.3 A	10000.	0.147E-01	0.651E-02	0.138E-02	0.153E-02	0.281E-02	0.305E-02
C= 0.92E+18	20000.	0.127E-01	0.533E-02	0.185E-02	0.188E-02	0.381E-02	0.384E-02
	40000.	0.114E-01	0.422E-02	0.233E-02	0.224E-02	0.488E-02	0.468E-02
Li II 2P- 3D	5000.	0.171E-01	0.399E-02	0.117E-02	0.143E-02	0.235E-02	0.269E-02
1681.7 A	10000.	0.133E-01	0.326E-02	0.187E-02	0.193E-02	0.388E-02	0.379E-02
C= 0.14E+18	20000.	0.107E-01	0.265E-02	0.248E-02	0.238E-02	0.506E-02	0.486E-02
	40000.	0.877E-02	0.211E-02	0.320E-02	0.278E-02	0.628E-02	0.594E-02
Li II 3D- 4P	5000.	0.699	-0.164	*0.100	-0.793E-01		
4639.0 A	10000.	0.601	-0.134	*0.127	-0.112		
C= 0.43E+18	20000.	0.526	-0.116	*0.159	-0.134		
	40000.	0.463	-0.915E-01	*0.185	-0.152		
Li II 3D- 5P	5000.	0.718	-0.213				
3188.6 A	10000.	0.651	-0.178				
C= 0.12E+18	20000.	0.592	-0.140				
	40000.	0.534	-0.117				
Li II 2S- 3P	5000.	0.780E-02	0.285E-03	0.362E-03	0.319E-03	0.705E-03	0.613E-03
1198.1 A	10000.	0.666E-02	0.480E-03	0.563E-03	0.465E-03	0.111E-02	0.923E-03
C= 0.25E+18	20000.	0.590E-02	0.395E-03	0.709E-03	0.569E-03	0.143E-02	0.117E-02
	40000.	0.533E-02	0.373E-03	0.860E-03	0.678E-03	0.177E-02	0.143E-02
Li II 2S- 4P	5000.	0.134E-01	0.244E-02	0.145E-02	0.114E-02	*0.291E-02	*0.206E-02
944.7 A	10000.	0.127E-01	0.205E-02	0.182E-02	0.151E-02	*0.375E-02	*0.288E-02
C= 0.65E+17	20000.	0.121E-01	0.179E-02	0.226E-02	0.186E-02	*0.457E-02	*0.371E-02
	40000.	0.116E-01	0.160E-02	0.261E-02	0.211E-02	*0.551E-02	*0.454E-02
Li II 2S- 5P	5000.	0.273E-01	0.610E-02	*0.403E-02	*0.282E-02		
861.3 A	10000.	0.269E-01	0.518E-02	*0.500E-02	*0.398E-02		
C= 0.27E+17	20000.	0.268E-01	0.476E-02	*0.586E-02	*0.480E-02		
	40000.	0.262E-01	0.377E-02	*0.657E-02	*0.548E-02		
Li II 2S- 6P	5000.	0.533E-01	0.131E-01				
822.2 A	10000.	0.541E-01	0.105E-01				
C= 0.14E+17	20000.	0.549E-01	0.943E-02				
	40000.	0.539E-01	0.732E-02				
Li II 3S- 3P	5000.	3.54	-0.722	0.864E-01	0.480E-02	0.160	0.908E-02
21066.8 A	10000.	2.90	-0.481	0.123	0.903E-02	0.234	0.179E-01
C= 0.77E+20	20000.	2.63	-0.382	0.146	0.139E-01	0.285	0.287E-01
	40000.	2.45	-0.297	0.166	0.191E-01	0.322	0.398E-01
Li II 3S- 4P	5000.	0.240	0.205E-01	0.210E-01	0.163E-01	*0.423E-01	*0.297E-01
3685.8 A	10000.	0.219	0.171E-01	0.266E-01	0.217E-01	*0.538E-01	*0.413E-01
C= 0.99E+18	20000.	0.209	0.138E-01	0.322E-01	0.266E-01	*0.672E-01	*0.543E-01
	40000.	0.201	0.132E-01	0.383E-01	0.302E-01	*0.777E-01	*0.643E-01

PERTURBER DENSITY = 0.1E+17cm-3

TRANSITION	T(K)	ELECTRONS WIDTH(A)	ELECTRONS SHIFT(A)	PROTONS WIDTH(A)	PROTONS SHIFT(A)	IONIZED HELIUM WIDTH(A)	IONIZED HELIUM SHIFT(A)
LI II 3S- 5P	5000.	0.279	0.417E-01	*0.383E-01	*0.269E-01		
2675.3 A	10000.	0.272	0.375E-01	*0.477E-01	*0.381E-01		
C= 0.26E+18	20000.	0.270	0.359E-01	*0.559E-01	*0.457E-01		
	40000.	0.265	0.287E-01	*0.629E-01	*0.522E-01		
LI II 3S- 6P	5000.	0.438	0.974E-01				
2330.6 A	10000.	0.443	0.755E-01				
C= 0.12E+18	20000.	0.450	0.695E-01				
	40000.	0.442	0.536E-01				
LI II 4S- 5P	5000.	3.05	0.179	*0.336	*0.232		
8228.6 A	10000.	2.97	0.129	*0.418	*0.325		
C= 0.25E+19	20000.	2.95	0.100	*0.487	*0.399		
	40000.	2.91	0.726E-01	*0.560	*0.448		
LI II 4S- 6P	5000.	2.75	0.441				
5655.7 A	10000.	2.78	0.353				
C= 0.68E+18	20000.	2.83	0.293				
	40000.	2.79	0.222				
LI II 2P- 3S	5000.	0.137E-01	0.636E-02	0.396E-03	0.614E-03	0.786E-03	0.118E-02
1653.1 A	10000.	0.101E-01	0.480E-02	0.711E-03	0.896E-03	0.143E-02	0.178E-02
C= 0.13E+19	20000.	0.844E-02	0.394E-02	0.104E-02	0.109E-02	0.217E-02	0.225E-02
	40000.	0.749E-02	0.311E-02	0.132E-02	0.130E-02	0.279E-02	0.275E-02
LI II 2P- 4S	5000.	0.168E-01	0.112E-01	0.144E-02	0.150E-02	*0.292E-02	*0.275E-02
1166.6 A	10000.	0.143E-01	0.922E-02	0.197E-02	0.197E-02	*0.412E-02	*0.381E-02
C= 0.26E+18	20000.	0.129E-01	0.740E-02	0.253E-02	0.244E-02	*0.520E-02	*0.491E-02
	40000.	0.122E-01	0.594E-02	0.304E-02	0.280E-02	*0.649E-02	*0.591E-02
LI II 3P- 4S	5000.	0.341	0.181	0.235E-01	0.241E-01	*0.472E-01	*0.442E-01
4882.8 A	10000.	0.304	0.148	0.323E-01	0.316E-01	*0.671E-01	*0.607E-01
C= 0.42E+19	20000.	0.286	0.119	0.408E-01	0.389E-01	*0.853E-01	*0.784E-01
	40000.	0.275	0.939E-01	0.501E-01	0.445E-01	0.103	0.941E-01
LI II 2P- 3D	5000.	0.124E-01	0.799E-03	0.357E-03	-0.369E-03	0.679E-03	-0.706E-03
1493.0 A	10000.	0.926E-02	0.429E-03	0.577E-03	-0.540E-03	0.112E-02	-0.107E-02
C= 0.39E+18	20000.	0.709E-02	0.237E-03	0.783E-03	-0.677E-03	0.159E-02	-0.139E-02
	40000.	0.565E-02	0.112E-03	0.976E-03	-0.808E-03	0.197E-02	-0.169E-02
LI II 2P- 4D	5000.	0.383E-01	-0.660E-03				
1131.9 A	10000.	0.323E-01	-0.608E-04				
C= 0.38E+16	20000.	0.273E-01	0.374E-03				
	40000.	0.231E-01	0.561E-03	*0.281E-01	*0.193E-01		
LI II 3P- 4D	5000.	0.610	-0.257E-01				
4326.7 A	10000.	0.521	-0.164E-01				
C= 0.55E+17	20000.	0.447	-0.807E-02				
	40000.	0.385	-0.877E-03	*0.410	*0.281		

PERTURBER DENSITY = 0.1E+17cm-3

TRANSITION	T(K)	ELECTRONS WIDTH(A)	ELECTRONS SHIFT(A)	PROTONS WIDTH(A)	PROTONS SHIFT(A)	IONIZED HELIUM WIDTH(A)	IONIZED HELIUM SHIFT(A)
Li II 3D- 4P	5000.	0.407	0.676E-01	0.398E-01	0.311E-01	*0.806E-01	*0.563E-01
4844.4 A	10000.	0.376	0.591E-01	0.503E-01	0.416E-01	*0.103	*0.793E-01
C= 0.17E+19	20000.	0.356	0.492E-01	0.617E-01	0.512E-01	*0.126	*0.103
	40000.	0.338	0.448E-01	0.702E-01	0.584E-01	*0.150	*0.122
Li II 3D- 5P	5000.	0.407	0.913E-01	*0.579E-01	*0.403E-01		
3237.3 A	10000.	0.397	0.763E-01	*0.712E-01	*0.566E-01		
C= 0.39E+18	20000.	0.394	0.687E-01	*0.839E-01	*0.685E-01		
	40000.	0.384	0.545E-01	*0.935E-01	*0.783E-01		
Li II 3D- 6P	5000.	0.610	0.140				
2745.8 A	10000.	0.616	0.121				
C= 0.16E+18	20000.	0.624	0.107				
	40000.	0.611	0.829E-01				
Li II 4D- 5P	5000.	6.79	1.05				
10503.5 A	10000.	6.37	0.844				
C= 0.33E+18	20000.	6.04	0.695	* 1.60	-1.07		
	40000.	5.66	0.537	* 2.08	-1.22		
Li II 4D- 6P	5000.	4.53	0.867				
6644.8 A	10000.	4.45	0.724	*0.469	*0.236		
C= 0.13E+18	20000.	4.40	0.625	*0.586	*0.284		
	40000.	4.22	0.473	*0.739	*0.324		

PERTURBER DENSITY = 0.1E+19cm-3

TRANSITION	T(K)	ELECTRONS WIDTH(A)	ELECTRONS SHIFT(A)	PROTONS WIDTH(A)	PROTONS SHIFT(A)	IONIZED HELIUM WIDTH(A)	IONIZED HELIUM SHIFT(A)
Li II 1S- 2P	5000.	0.557E-02	0.407E-03	0.434E-04	-0.141E-04	0.586E-04	-0.162E-04
199.3 A	10000.	0.395E-02	0.407E-03	0.104E-03	-0.390E-04	0.180E-03	-0.633E-04
C= 0.41E+19	20000.	0.286E-02	0.279E-03	0.171E-03	-0.718E-04	0.322E-03	-0.135E-03
	40000.	0.211E-02	0.178E-03	0.237E-03	-0.107E-03	0.463E-03	-0.210E-03
Li II 1S- 3P	5000.	*0.259E-01	-0.622E-03				
178.0 A	10000.	0.215E-01	-0.853E-03				
C= 0.15E+18	20000.	0.181E-01	-0.127E-02				
	40000.	0.155E-01	-0.115E-02				
Li II 1S- 4P	5000.						
171.6 A	10000.	*0.536E-01	-0.311E-02				
C= 0.59E+17	20000.	*0.515E-01	-0.381E-02				
	40000.	*0.480E-01	-0.372E-02				
Li II 2S- 2P	5000.	23.7	-1.26	0.152	-0.169	*0.224	-0.183
9584.1 A	10000.	16.9	-1.25	0.399	-0.406	*0.731	-0.632
C= 0.96E+22	20000.	12.5	-1.04	0.678	-0.642	* 1.32	-1.16
	40000.	9.74	-1.16	0.973	-0.875	* 1.97	-1.68
Li II 2S- 3P	5000.	*1.82	-0.105				
1420.9 A	10000.	*1.50	-0.105				
C= 0.97E+19	20000.	1.26	-0.111				
	40000.	1.08	-0.113				

PERTURBER DENSITY = 0.1E+19cm-3

TRANSITION	T(K)	ELECTRONS WIDTH(A)	ELECTRONS SHIFT(A)	PROTONS WIDTH(A)	PROTONS SHIFT(A)	IONIZED HELIUM WIDTH(A)	IONIZED HELIUM SHIFT(A)
Li II 2S- 4P	5000.						
1093.4 A	10000.*	2.25	-0.114				
C= 0.24E+19	20000.*	2.15	-0.180				
	40000.*	2.00	-0.161				
Li II 2P- 3S	5000.	*1.88	*0.720	*0.652E-01	*0.322E-01		
1755.3 A	10000.	1.47	0.575	*0.136	*0.878E-01		
C= 0.92E+20	20000.	1.27	0.481	*0.184	*0.138		
	40000.	1.14	0.385	*0.234	*0.206		
Li II 2P- 3D	5000.*	1.60	0.237				
1681.7 A	10000.	1.27	0.219				
C= 0.14E+20	20000.	1.02	0.191				
	40000.	0.846	0.158				
Li II 2S- 2P	5000.	6.23	-0.431	0.288E-01	-0.269E-01	0.407E-01	-0.304E-01
5486.1 A	10000.	4.41	-0.255	0.754E-01	-0.682E-01	0.134	-0.109
C= 0.55E+22	20000.	3.19	-0.220	0.134	-0.113	0.257	-0.209
	40000.	2.40	-0.239	0.202	-0.164	0.407	-0.323
Li II 2S- 3P	5000.*	0.779	-0.124E-02*	0.272E-01*	0.122E-01		
1198.1 A	10000.	0.666	0.285E-01*	0.535E-01*	0.300E-01		
C= 0.25E+20	20000.	0.590	0.261E-01*	0.693E-01*	0.438E-01		
	40000.	0.532	0.277E-01*	0.858E-01*	0.631E-01		
Li II 2S- 4P	5000.*	1.26	*0.369E-01				
944.7 A	10000.*	1.21	*0.711E-01				
C= 0.65E+19	20000.*	1.17	*0.847E-01				
	40000.	1.14	0.933E-01				
Li II 2P- 3S	5000.	1.37	0.580	*0.368E-01	*0.234E-01		
1653.1 A	10000.	1.01	0.444	*0.706E-01	*0.576E-01		
C= 0.13E+21	20000.	0.844	0.369	*0.103	*0.846E-01		
	40000.	0.749	0.294	*0.132	*0.121		
Li II 2P- 4S	5000.*	1.67	*0.875				
1166.6 A	10000.*	1.43	*0.764				
C= 0.26E+20	20000.	1.29	0.633				
	40000.	1.21	0.516				
Li II 2P- 3D	5000.*	1.23	*0.112	*0.292E-01	-0.161E-01		
1493.0 A	10000.	0.925	0.633E-01*	0.556E-01	-0.366E-01		
C= 0.39E+20	20000.	0.708	0.378E-01*	0.776E-01	-0.541E-01		
	40000.	0.564	0.213E-01*	0.974E-01	-0.758E-01		
Li II 2P- 4D	5000.						
1131.9 A	10000.*	1.97	-0.362E-01				
C= 0.38E+18	20000.*	1.83	-0.240E-01				
	40000.	1.67	-0.257E-01				

PERTURBER DENSITY = 0.1E+20cm-3

TRANSITION	T(K)	ELECTRONS WIDTH(A)	ELECTRONS SHIFT(A)	PROTONS WIDTH(A)	PROTONS SHIFT(A)	IONIZED HELIUM WIDTH(A)	IONIZED HELIUM SHIFT(A)
Li II 1S- 2P	5000.	0.556E-01	0.438E-02	0.179E-03	-0.382E-04*	0.469E-04	-0.100E-04
199.3 A	10000.	0.395E-01	0.433E-02	0.807E-03	-0.233E-03*	0.913E-03	-0.222E-03
C= 0.41E+20	20000.	0.286E-01	0.296E-02	0.163E-02	-0.587E-03*	0.270E-02	-0.875E-03
	40000.	0.211E-01	0.189E-02	0.233E-02	-0.943E-03*	0.442E-02	-0.168E-02
Li II 2P- 3D	5000.						
1681.7 A	10000.						
C= 0.14E+21	20000.*	8.33	* 1.18				
	40000.	7.19	1.05				
Li II 2S- 3P	5000.						
1198.1 A	10000.*	6.27	-0.219				
C= 0.25E+21	20000.*	5.59	-0.670E-01				
	40000.*	5.12	0.577E-01				
Li II 2P- 3S	5000.						
1653.1 A	10000.*	9.99	* 3.40				
C= 0.13E+22	20000.*	8.39	* 3.03				
	40000.	7.46	2.49				
Li II 2P- 3D	5000.						
1493.0 A	10000.*	8.66	* 1.18				
C= 0.39E+21	20000.*	6.77	*0.730				
	40000.	5.45	0.448				

PERTURBER DENSITY = 0.1E+21cm-3

Li II 1S- 2P	5000.		
199.3 A	10000.*	0.382	*0.558E-01
C= 0.41E+21	20000.*	0.282	*0.364E-01
	40000.	0.209	0.232E-01

jević and Sahal–Bréchot 1984), which gives an estimate for the maximum perturber density for which the line may be treated as isolated when it is divided by the corresponding full width at half maximum. For each value given in Table 1, the collision volume (V) multiplied by the perturber density (N) is much less than one and the impact approximation is valid (Sahal–Bréchot, 1969ab). Values for NV > 0.5 are not given and values for 0.1 < NV ≤ 0.5 are denoted by an asterisk. When the impact approximation is not valid, the ion broadening contribution may be estimated by using quasistatic approach (Sahal–Bréchot 1991 and Griem 1974). The accuracy of the results obtained decreases when broadening by ion interactions becomes important.

The analysis of present results and comparison with available theoretical data will be published elsewhere (Dimitrijević and Sahal–Bréchot, 1995).

Acknowledgements – This work is a part of the project "Physics and dynamics of celestial bodies", supported by Ministry of Science and Technology of Serbia.

REFERENCES

Dimitrijević, M. S., and Sahal–Bréchot, S.: 1984, *JQSRT*, **31**, 301.

Dimitrijević, M. S., and Sahal–Bréchot, S.: 1995, *Physica Scripta*, submitted.

Griem, H. R.: 1974, *Spectral Line Broadening by Plasmas*, Academic Press, New York.

Sahal–Bréchot, S.: 1969a, *Astron. Astrophys.* **1**, 91.

Sahal–Bréchot, S.: 1969b, *Astron. Astrophys.* **2**, 322.

Sahal–Bréchot, S.: 1991, *Astron. Astrophys.* **245**, 322.

ТАБЕЛЕ ПАРАМЕТАРА ШТАРКОВОГ ШИРЕЊА Li II

М. С. Димитријевић[1] и S. Sahal–Bréchot[2]

[1] *Астрономска опсерваторија, Волгина 7, 11050 Београд, Југославија*

[2] *Laboratoire "Astrophysique, Atomes et Molécules"*
Département Atomes et Molécules en Astrophysique
Unité associée au C.N.R.S. No 812
Observatoire de Paris-Meudon, 92190 Meudon, France

УДК 52–355.3
Претходно саопштење

Користећи семикласичан прилаз, израчунате су ширине и помераји спектралних линија, проузроковани сударима са електронима, протонима и јонизованим хелијумом, за 37 мултиплета Li II. Резултати су дати у функцији температуре и концентрације пертурбера.

Bull. Astron. Belgrade № 152 (1995), 99 – 129

UDC 52–355.3
Preliminary report

STARK BROADENING PARAMETER TABLES FOR C V AND P V

M. S. Dimitrijević[1] and S. Sahal–Bréchot[2]

[1] *Astronomical Observatory, Volgina 7, 11050 Belgrade, Yugoslavia*

[2] *Laboratoire "Astrophysique, Atomes et Molécules"*
Département Atomes et Molécules en Astrophysique
Unité associée au C.N.R.S. No 812
Observatoire de Paris–Meudon, 92190 Meudon, France

(Received: October 20, 1994)

SUMMARY: Using a semiclassical approach, we have calculated electron–, proton–, and He III–impact line widths and shifts for for 25 C V and 51 P V multiplets as a function of temperature and perturber density.

1. INTRODUCTION

Spectral lines of neutral and ionized carbon are of particular astrophysical interest, since such lines are present in stellar atmospheres. Stark broadening parameters for these lines are needed especially for hot and dense stellar plasma analysis. A good example are PG 1159 pre-white dwarfs with effective temperature 100,000 - 140,000 K where carbon and helium are the dominant constituents (C/He = 0.5, Werner *et al.* 1991). Other astrophysical applications have been pointed out in more detail in Dimitrijević *et al.* 1991). Stark broadening of C V lines are as well of interest for the diagnostic of laser-produced plasma and for the research of regularities and systematic trends. For such research are of interest P V lines as well. Recently e.g., estimates of the Stark widths for P V 4s-4p and 4p-4d transitions have been performed within a study on Stark broadening regularities within successive ionization stages of phosphorus (Srećković *et al.* 1990). Such investigations are of astrophysical importance since they provide a tool for a simple interpolation and prediction of new data needed in astrophysics.

In order to provide to astrophysicists the needed Stark broadening data, we have calculated within the semiclassical-perturbation formalism (Sahal-Bréchot, 1969ab) electron-, proton-, and He III-impact line widths and shifts for 25 C V and 51 P V multiplets.

2. RESULTS AND DISCUSSION

Analysis of obtained results and all details of calculations as well as the comparison with availlable experimental data will be published elsewhere (Dimitrijević and Sahal–Bréchot, 1995). Here, we present only tables of Stark broadening parameters for astrophysical and laboratory plasma diagnostic

Table 1. This table shows electron-, proton-, and He III- impact broadening parameters for C V and P V, for perturber densities of 10^{17} – 10^{22} cm^{-3} and temperatures from 50,000 up to 1,000,000 K. Transitions and averaged wavelengths for the multiplet (in Å) are also given. By using c [see Eq. (5) in Dimitrijević *et al.*, 1991], we obtain an estimate for the maximum perturber density for which the line may be treated as isolated and tabulated data may be used. The asterisk identifies cases for which the collision volume multiplied by the perturber density (the condition for validity of the impact approximation) lies between 0.1 and 0.5.

PERTURBER DENSITY = 1xE+17cm-3

PERTURBERS ARE: TRANSITION	T(K)	ELECTRONS WIDTH(Å)	ELECTRONS SHIFT(Å)	PROTONS WIDTH(Å)	PROTONS SHIFT(Å)	He III WIDTH(Å)	He III SHIFT(Å)
C V 1S 2P	50000.	0.297E-05	-0.126E-06	0.121E-07	-0.203E-07	0.218E-07	-0.396E-07
40.3 Å	100000.	0.211E-05	-0.483E-07	0.333E-07	-0.402E-07	0.614E-07	-0.801E-07
C= 0.47E+17	150000.	0.174E-05	-0.196E-07	0.558E-07	-0.574E-07	0.105E-06	-0.116E-06
	200000.	0.152E-05	-0.163E-07	0.748E-07	-0.710E-07	0.142E-06	-0.144E-06
	300000.	0.127E-05	-0.117E-07	0.108E-06	-0.929E-07	0.209E-06	-0.189E-06
	500000.	0.102E-05	-0.115E-07	0.151E-06	-0.119E-06	0.290E-06	-0.243E-06
C V 2S 2P	50000.	0.343E-01	-0.114E-02	0.153E-03	-0.686E-03	0.280E-03	-0.134E-02
3478.6 Å	100000.	0.249E-01	-0.108E-02	0.550E-03	-0.125E-02	0.105E-02	-0.250E-02
C= 0.35E+21	150000.	0.208E-01	-0.120E-02	0.967E-03	-0.165E-02	0.186E-02	-0.336E-02
	200000.	0.185E-01	-0.121E-02	0.133E-02	-0.190E-02	0.264E-02	-0.389E-02
	300000.	0.156E-01	-0.114E-02	0.181E-02	-0.231E-02	0.361E-02	-0.473E-02
	500000.	0.129E-01	-0.111E-02	0.269E-02	-0.276E-02	0.533E-02	-0.570E-02
C V 2P 3S	50000.	0.609E-03	0.516E-04	0.258E-04	0.539E-04	0.499E-04	0.106E-03
272.2 Å	100000.	0.463E-03	0.567E-04	0.521E-04	0.760E-04	0.105E-03	0.154E-03
C= 0.61E+18	150000.	0.400E-03	0.560E-04	0.750E-04	0.886E-04	0.151E-03	0.182E-03
	200000.	0.362E-03	0.547E-04	0.863E-04	0.950E-04	0.175E-03	0.195E-03
	300000.	0.316E-03	0.533E-04	0.104E-03	0.106E-03	0.209E-03	0.218E-03
	500000.	0.269E-03	0.503E-04	0.127E-03	0.121E-03	0.253E-03	0.250E-03
C V 2P 3D	50000.	0.459E-03	0.238E-04	0.318E-04	0.568E-04	0.610E-04	0.112E-03
267.6 Å	100000.	0.345E-03	0.263E-04	0.621E-04	0.800E-04	0.118E-03	0.161E-03
C= 0.13E+18	150000.	0.294E-03	0.270E-04	0.903E-04	0.921E-04	0.167E-03	0.190E-03
	200000.	0.264E-03	0.249E-04	0.105E-03	0.994E-04	0.190E-03	0.204E-03
	300000.	0.227E-03	0.238E-04	0.130E-03	0.111E-03	0.228E-03	0.227E-03
	500000.	0.191E-03	0.223E-04	0.167E-03	0.127E-03	0.274E-03	0.260E-03
C V 2S 2P	50000.	0.131E-01	-0.255E-03	0.412E-04	-0.173E-03	0.750E-04	-0.337E-03
2274.6 Å	100000.	0.939E-02	-0.317E-03	0.142E-03	-0.328E-03	0.265E-03	-0.655E-03
C= 0.23E+21	150000.	0.780E-02	-0.364E-03	0.248E-03	-0.441E-03	0.480E-03	-0.892E-03
	200000.	0.688E-02	-0.386E-03	0.364E-03	-0.533E-03	0.709E-03	-0.109E-02
	300000.	0.580E-02	-0.386E-03	0.501E-03	-0.643E-03	0.995E-03	-0.131E-02
	500000.	0.473E-02	-0.374E-03	0.763E-03	-0.809E-03	0.150E-02	-0.166E-02
C V 2S 3P	50000.	0.506E-03	0.680E-05	0.118E-04	0.148E-04	0.224E-04	0.291E-04
227.2 Å	100000.	0.380E-03	0.617E-05	0.226E-04	0.228E-04	0.443E-04	0.463E-04
C= 0.30E+18	150000.	0.325E-03	0.665E-05	0.299E-04	0.277E-04	0.582E-04	0.568E-04
	200000.	0.293E-03	0.575E-05	0.364E-04	0.313E-04	0.706E-04	0.643E-04
	300000.	0.254E-03	0.594E-05	0.431E-04	0.348E-04	0.821E-04	0.714E-04
	500000.	0.214E-03	0.515E-05	0.531E-04	0.398E-04	0.975E-04	0.823E-04
C V 2S 4P	50000.	0.900E-03	0.279E-04	0.610E-04	0.679E-04	0.119E-03	0.132E-03
173.3 Å	100000.	0.703E-03	0.303E-04	0.935E-04	0.876E-04	0.188E-03	0.178E-03
C= 0.73E+17	150000.	0.614E-03	0.301E-04	0.111E-03	0.984E-04	0.217E-03	0.202E-03
	200000.	0.559E-03	0.291E-04	0.123E-03	0.105E-03	0.240E-03	0.218E-03
	300000.	0.492E-03	0.255E-04	0.145E-03	0.117E-03	0.269E-03	0.240E-03
	500000.	0.421E-03	0.213E-04	0.174E-03	0.131E-03	0.314E-03	0.270E-03
C V 2S 5P	50000.	0.182E-02	0.818E-04	0.200E-03	0.188E-03	*0.404E-03	*0.363E-03
156.2 Å	100000.	0.146E-02	0.821E-04	0.260E-03	0.232E-03	*0.517E-03	*0.465E-03
C= 0.31E+17	150000.	0.128E-02	0.773E-04	0.298E-03	0.259E-03	*0.588E-03	*0.531E-03
	200000.	0.118E-02	0.700E-04	0.336E-03	0.276E-03	*0.642E-03	*0.565E-03
	300000.	0.104E-02	0.625E-04	0.382E-03	0.297E-03	*0.722E-03	*0.618E-03
	500000.	0.891E-03	0.537E-04	0.451E-03	0.330E-03	*0.795E-03	*0.679E-03

PERTURBER DENSITY = 1xE+17cm-3

PERTURBERS ARE:		ELECTRONS		PROTONS		He III	
TRANSITION	T(K)	WIDTH(Å)	SHIFT(Å)	WIDTH(Å)	SHIFT(Å)	WIDTH(Å)	SHIFT(Å)
C V 3S 3P	50000.	1.02	-0.230E-01	0.150E-01	-0.165E-01	0.284E-01	-0.323E-01
8434.5 Å	100000.	0.777	-0.337E-01	0.287E-01	-0.261E-01	0.559E-01	-0.529E-01
C= 0.42E+21	150000.	0.670	-0.306E-01	0.377E-01	-0.317E-01	0.725E-01	-0.647E-01
	200000.	0.605	-0.311E-01	0.455E-01	-0.360E-01	0.867E-01	-0.738E-01
	300000.	0.529	-0.299E-01	0.546E-01	-0.403E-01	0.102	-0.832E-01
	500000.	0.449	-0.299E-01	0.689E-01	-0.464E-01	0.120	-0.957E-01
C V 3S 4P	50000.	0.156E-01	0.214E-03	0.831E-03	0.897E-03	0.162E-02	0.175E-02
672.1 Å	100000.	0.122E-01	0.187E-03	0.130E-02	0.118E-02	0.259E-02	0.240E-02
C= 0.11E+19	150000.	0.106E-01	0.200E-03	0.152E-02	0.132E-02	0.299E-02	0.272E-02
	200000.	0.969E-02	0.190E-03	0.169E-02	0.142E-02	0.330E-02	0.294E-02
	300000.	0.854E-02	0.142E-03	0.198E-02	0.158E-02	0.376E-02	0.326E-02
	500000.	0.731E-02	0.846E-04	0.242E-02	0.177E-02	0.426E-02	0.364E-02
C V 3S 5P	50000.	0.176E-01	0.644E-03	0.180E-02	0.169E-02	*0.363E-02	*0.326E-02
472.2 Å	100000.	0.141E-01	0.616E-03	0.235E-02	0.209E-02	*0.465E-02	*0.417E-02
C= 0.28E+18	150000.	0.124E-01	0.581E-03	0.268E-02	0.231E-02	*0.526E-02	*0.474E-02
	200000.	0.114E-01	0.517E-03	0.300E-02	0.248E-02	*0.582E-02	*0.509E-02
	300000.	0.101E-01	0.451E-03	0.344E-02	0.267E-02	*0.649E-02	*0.560E-02
	500000.	0.862E-02	0.375E-03	0.406E-02	0.298E-02	*0.720E-02	*0.610E-02
C V 4S 4P	50000.	21.0	-0.799	0.543	-0.343	1.05	-0.677
20755.5 Å	100000.	16.5	-0.722	0.813	-0.483	1.55	-0.974
C= 0.10E+22	150000.	14.4	-0.703	0.944	-0.556	1.76	-1.15
	200000.	13.2	-0.686	1.06	-0.601	1.92	-1.23
	300000.	11.7	-0.715	1.25	-0.669	2.13	-1.37
	500000.	9.99	-0.638	1.58	-0.765	2.41	-1.57
C V 4S 5P	50000.	0.203	0.124E-02	0.154E-01	0.140E-01	*0.308E-01	*0.271E-01
1475.1 Å	100000.	0.162	0.149E-02	0.199E-01	0.171E-01	*0.394E-01	*0.344E-01
C= 0.27E+19	150000.	0.143	0.116E-02	0.230E-01	0.191E-01	*0.446E-01	*0.392E-01
	200000.	0.131	0.668E-03	0.255E-01	0.203E-01	*0.492E-01	*0.423E-01
	300000.	0.116	0.112E-03	0.294E-01	0.219E-01	*0.545E-01	*0.459E-01
	500000.	0.994E-01	0.264E-04	0.346E-01	0.242E-01	0.609E-01	0.498E-01
C V 2P 3S	50000.	0.491E-03	0.346E-04	0.135E-04	0.340E-04	0.263E-04	0.666E-04
260.2 Å	100000.	0.367E-03	0.445E-04	0.312E-04	0.496E-04	0.627E-04	0.999E-04
C= 0.80E+18	150000.	0.316E-03	0.428E-04	0.456E-04	0.595E-04	0.912E-04	0.122E-03
	200000.	0.285E-03	0.423E-04	0.569E-04	0.641E-04	0.116E-03	0.133E-03
	300000.	0.247E-03	0.413E-04	0.683E-04	0.715E-04	0.139E-03	0.147E-03
	500000.	0.209E-03	0.402E-04	0.833E-04	0.814E-04	0.168E-03	0.168E-03
C V 2P 4S	50000.	0.784E-03	0.104E-03	0.674E-04	0.976E-04	0.136E-03	0.191E-03
189.3 Å	100000.	0.609E-03	0.993E-04	0.112E-03	0.124E-03	0.229E-03	0.251E-03
C= 0.17E+18	150000.	0.531E-03	0.976E-04	0.134E-03	0.139E-03	0.274E-03	0.287E-03
	200000.	0.484E-03	0.949E-04	0.148E-03	0.149E-03	0.305E-03	0.307E-03
	300000.	0.426E-03	0.929E-04	0.171E-03	0.166E-03	0.345E-03	0.342E-03
	500000.	0.364E-03	0.812E-04	0.203E-03	0.186E-03	0.404E-03	0.376E-03
C V 2P 5S	50000.	0.159E-02	0.243E-03	0.229E-03	0.249E-03	*0.471E-03	*0.477E-03
168.4 Å	100000.	0.126E-02	0.236E-03	0.307E-03	0.307E-03	*0.617E-03	*0.616E-03
C= 0.68E+17	150000.	0.111E-02	0.235E-03	0.350E-03	0.341E-03	*0.721E-03	*0.700E-03
	200000.	0.101E-02	0.225E-03	0.391E-03	0.366E-03	*0.778E-03	*0.747E-03
	300000.	0.896E-03	0.203E-03	0.444E-03	0.398E-03	*0.878E-03	*0.811E-03
	500000.	0.763E-03	0.172E-03	0.519E-03	0.439E-03	*0.971E-03	*0.895E-03
C V 3P 4S	50000.	0.165E-01	0.153E-02	0.103E-02	0.148E-02	0.206E-02	0.289E-02
756.9 Å	100000.	0.128E-01	0.148E-02	0.171E-02	0.188E-02	0.352E-02	0.381E-02
C= 0.28E+19	150000.	0.112E-01	0.144E-02	0.207E-02	0.211E-02	0.417E-02	0.434E-02
	200000.	0.102E-01	0.141E-02	0.229E-02	0.226E-02	0.463E-02	0.468E-02
	300000.	0.895E-02	0.137E-02	0.268E-02	0.252E-02	0.530E-02	0.515E-02
	500000.	0.765E-02	0.120E-02	0.317E-02	0.277E-02	0.635E-02	0.576E-02

PERTURBER DENSITY = 1xE+17cm-3

PERTURBERS ARE: TRANSITION	T(K)	ELECTRONS WIDTH(Å)	ELECTRONS SHIFT(Å)	PROTONS WIDTH(Å)	PROTONS SHIFT(Å)	He III WIDTH(Å)	He III SHIFT(Å)
C V 3P 5S	50000.	0.160E-01	0.213E-02	0.205E-02	0.222E-02	*0.421E-02	*0.427E-02
506.3 Å	100000.	0.127E-01	0.208E-02	0.274E- 02	0.276E-02	*0.554E-02	*0.549E-02
C= 0.62E+18	150000.	0.112E-01	0.206E-02	0.312E-02	0.305E-02	*0.646E-02	*0.628E-02
	200000.	0.102E-01	0.198E-02	0.349E-02	0.328E-02	*0.699E-02	*0.668E-02
	300000.	0.904E-02	0.179E-02	0.393E-02	0.356E-02	*0.785E-02	*0.726E-02
	500000.	0.771E-02	0.151E-02	0.469E-02	0.394E-02	*0.876E-02	*0.801E-02
C V 4P 5S	50000.	0.223	0.202E-01	0.199E-01	0.212E-01	*0.406E-01	*0.409E-01
1651.0 Å	100000.	0.178	0.196E-01	0.264E-01	0.263E-01	*0.533E-01	*0.525E-01
C= 0.66E+19	150000.	0.157	0.195E-01	0.305E-01	0.293E-01	*0.614E-01	*0.598E-01
	200000.	0.144	0.187E-01	0.345E-01	0.311E-01	*0.673E-01	*0.639E-01
	300000.	0.127	0.170E-01	0.391E-01	0.334E-01	*0.765E-01	*0.695E-01
	500000.	0.109	0.144E-01	0.461E-01	0.370E-01	0.848E-01	0.766E-01
C V 2P 3D	50000.	0.370E-03	-0.976E-05	0.890E-05	-0.162E-04	0.169E-04	-0.318E-04
248.7 Å	100000.	0.272E-03	-0.608E-05	0.200E-04	-0.252E-04	0.394E-04	-0.513E-04
C= 0.36E+18	150000.	0.230E-03	-0.515E-05	0.271E-04	-0.307E-04	0.528E-04	-0.628E-04
	200000.	0.205E-03	-0.556E-05	0.340E-04	-0.348E-04	0.654E-04	-0.712E-04
	300000.	0.176E-03	-0.473E-05	0.423E-04	-0.386E-04	0.811E-04	-0.795E-04
	500000.	0.147E-03	-0.248E-05	0.534E-04	-0.445E-04	0.987E-04	-0.915E-04
C V 2P 4D	50000.	0.101E-02	0.175E-05	0.546E-03	0.455E-03	*0.918E-03	*0.862E-03
186.7 Å	100000.	0.798E-03	0.348E-05	0.783E-03	0.564E-03	*0.121E-02	*0.112E-02
C= 0.51E+16	150000.	0.698E-03	0.830E-05	0.966E-03	0.616E-03	*0.140E-02	*0.127E-02
	200000.	0.636E-03	0.752E-05	0.109E-02	0.647E-03	*0.158E-02	*0.136E-02
	300000.	0.557E-03	0.127E-04	0.129E-02	0.725E-03	*0.173E-02	*0.145E-02
	500000.	0.471E-03	0.945E-05	0.157E-02	0.777E-03	*0.213E-02	*0.166E-02
C V 3D 4P	50000.	0.185E-01	0.662E-03	0.127E-02	0.140E-02	0.249E-02	0.274E-02
763.1 Å	100000.	0.145E-01	0.680E-03	0.192E-02	0.180E-02	0.385E-02	0.364E-02
C= 0.14E+19	150000.	0.126E-01	0.674E-03	0.227E-02	0.201E-02	0.446E-02	0.415E-02
	200000.	0.115E-01	0.660E-03	0.253E-02	0.217E-02	0.493E-02	0.446E-02
	300000.	0.102E-01	0.583E-03	0.294E-02	0.239E-02	0.563E-02	0.498E-02
	500000.	0.869E-02	0.478E-03	0.360E-02	0.265E-02	0.650E-02	0.556E-02
C V 3D 5P	50000.	0.203E-01	0.945E-03	0.220E-02	0.207E-02	*0.445E-02	*0.399E-02
515.4 Å	100000.	0.162E-01	0.936E-03	0.288E-02	0.256E-02	*0.569E-02	*0.512E-02
C= 0.33E+18	150000.	0.143E-01	0.882E-03	0.331E-02	0.286E-02	*0.649E-02	*0.584E-02
	200000.	0.131E-01	0.805E-03	0.371E-02	0.303E-02	*0.705E-02	*0.623E-02
	300000.	0.116E-01	0.720E-03	0.416E-02	0.326E-02	*0.790E-02	*0.679E-02
	500000.	0.993E-02	0.615E-03	0.493E-02	0.362E-02	*0.868E-02	*0.748E-02
C V 4D 5P	50000.	0.260	0.913E-02	0.323E-01	-0.228E-01	*0.503E-01	-0.437E-01
1651.4 Å	100000.	0.210	0.906E-02	0.489E-01	-0.282E-01	*0.664E-01	-0.562E-01
C= 0.40E+18	150000.	0.185	0.818E-02	0.610E-01	-0.310E-01	*0.771E-01	-0.646E-01
	200000.	0.170	0.744E-02	0.701E-01	-0.333E-01	*0.874E-01	-0.687E-01
	300000.	0.150	0.619E-02	0.847E-01	-0.361E-01	*0.999E-01	-0.736E-01
	500000.	0.129	0.546E-02	0.104	-0.404E-01	*0.120	-0.818E-01
C V 3D 4F	50000.	0.107E-01	-0.157E-03	0.711E-02	-0.605E-02	*0.118E-01	-0.114E-01
748.4 Å	100000.	0.837E-02	-0.133E-03	0.105E-01	-0.742E-02	*0.160E-01	-0.149E-01
C= 0.82E+17	150000.	0.728E-02	-0.194E-03	0.128E-01	-0.819E-02	*0.188E-01	-0.169E-01
	200000.	0.661E-02	-0.126E-03	0.147E-01	-0.872E-02	*0.205E-01	-0.180E-01
	300000.	0.579E-02	-0.130E-03	0.175E-01	-0.943E-02	*0.236E-01	-0.195E-01
	500000.	0.493E-02	-0.815E-04	0.201E-01	-0.103E-01	*0.283E-01	-0.212E-01
PERTURBER DENSITY = 1xE+18cm-3							
C V 1S 2P	50000.	0.297E-04	-0.168E-05	0.120E-06	-0.192E-06	0.216E-06	-0.359E-06
40.3 Å	100000.	0.211E-04	-0.283E-06	0.333E-06	-0.398E-06	0.613E-06	-0.775E-06
C= 0.47E+18	150000.	0.174E-04	-0.206E-06	0.558E-06	-0.570E-06	0.105E-05	-0.114E-05
	200000.	0.152E-04	-0.175E-06	0.748E-06	-0.709E-06	0.142E-05	-0.142E-05
	300000.	0.127E-04	-0.119E-06	0.108E-05	-0.929E-06	0.209E-05	-0.189E-05
	500000.	0.102E-04	-0.114E-06	0.151E-05	-0.119E-05	0.290E-05	-0.243E-05

PERTURBER DENSITY = 1xE+18cm-3

PERTURBERS ARE:		ELECTRONS		PROTONS		He III	
TRANSITION	T(K)	WIDTH(Å)	SHIFT(Å)	WIDTH(Å)	SHIFT(Å)	WIDTH(Å)	SHIFT(Å)
C V 2S 2P	50000.	0.343	-0.113E-01	0.153E-02	-0.647E-02	0.279E-02	-0.121E-01
3478.6 Å	100000.	0.249	-0.104E-01	0.550E-02	-0.123E-01	0.105E-01	-0.241E-01
C= 0.35E+22	150000.	0.209	-0.119E-01	0.967E-02	-0.164E-01	0.186E-01	-0.330E-01
	200000.	0.185	-0.120E-01	0.133E-01	-0.190E-01	0.264E-01	-0.385E-01
	300000.	0.156	-0.114E-01	0.181E-01	-0.231E-01	0.361E-01	-0.472E-01
	500000.	0.129	-0.111E-01	0.269E-01	-0.276E-01	0.533E-01	-0.570E-01
C V 2P 3S	50000.	0.608E-02	0.472E-03	0.258E-03	0.501E-03	0.500E-03	0.930E-03
272.2 Å	100000.	0.463E-02	0.541E-03	0.521E-03	0.744E-03	0.105E-02	0.145E-02
C= 0.61E+19	150000.	0.400E-02	0.538E-03	0.750E-03	0.872E-03	0.151E-02	0.177E-02
	200000.	0.362E-02	0.531E-03	0.863E-03	0.948E-03	0.175E-02	0.191E-02
	300000.	0.316E-02	0.524E-03	0.104E-02	0.106E-02	0.209E-02	0.218E-02
	500000.	0.269E-02	0.502E-03	0.127E-02	0.121E-02	0.253E-02	0.249E-02
C V 2P 3D	50000.	0.459E-02	0.189E-03	0.318E-03	0.527E-03	0.609E-03	0.979E-03
267.6 Å	100000.	0.345E-02	0.237E-03	0.621E-03	0.782E-03	0.118E-02	0.151E-02
C= 0.13E+19	150000.	0.294E-02	0.244E-03	0.902E-03	0.906E-03	0.167E-02	0.184E-02
	200000.	0.263E-02	0.232E-03	0.105E-02	0.992E-03	0.190E-02	0.199E-02
	300000.	0.227E-02	0.227E-03	0.130E-02	0.110E-02	0.228E-02	0.227E-02
	500000.	0.190E-02	0.221E-03	0.167E-02	0.127E-02	0.274E-02	0.259E-02
C V 2S 2P	50000.	0.131	-0.199E-02	0.411E-03	-0.163E-02	0.746E-03	-0.305E-02
2274.6 Å	100000.	0.939E-01	-0.318E-02	0.142E-02	-0.324E-02	0.265E-02	-0.632E-02
C= 0.23E+22	150000.	0.781E-01	-0.360E-02	0.248E-02	-0.438E-02	0.480E-02	-0.879E-02
	200000.	0.688E-01	-0.385E-02	0.364E-02	-0.532E-02	0.709E-02	-0.107E-01
	300000.	0.580E-01	-0.385E-02	0.501E-02	-0.643E-02	0.995E-02	-0.131E-01
	500000.	0.473E-01	-0.373E-02	0.763E-02	-0.809E-02	0.150E-01	-0.166E-01
C V 2S 3P	50000.	0.506E-02	0.533E-04	0.117E-03	0.139E-03	0.222E-03	0.260E-03
227.2 Å	100000.	0.380E-02	0.572E-04	0.226E-03	0.224E-03	0.442E-03	0.441E-03
C= 0.30E+19	150000.	0.325E-02	0.611E-04	0.299E-03	0.274E-03	0.582E-03	0.555E-03
	200000.	0.293E-02	0.542E-04	0.364E-03	0.313E-03	0.706E-03	0.632E-03
	300000.	0.254E-02	0.568E-04	0.431E-03	0.347E-03	0.821E-03	0.712E-03
	500000.	0.214E-02	0.512E-04	0.531E-03	0.397E-03	0.975E-03	0.821E-03
C V 2S 4P	50000.	0.900E-02	0.218E-03	0.608E-03	0.614E-03	*0.118E-02	*0.110E-02
173.3 Å	100000.	0.703E-02	0.258E-03	0.935E-03	0.848E-03	*0.187E-02	*0.162E-02
C= 0.73E+18	150000.	0.614E-02	0.261E-03	0.111E-02	0.962E-03	*0.217E-02	*0.193E-02
	200000.	0.559E-02	0.262E-03	0.123E-02	0.105E-02	*0.240E-02	*0.211E-02
	300000.	0.492E-02	0.239E-03	0.145E-02	0.117E-02	*0.269E-02	*0.239E-02
	500000.	0.421E-02	0.210E-03	0.174E-02	0.131E-02	*0.314E-02	*0.269E-02
C V 2S 5P	50000.	0.181E-01	0.542E-03	*0.198E-02	*0.160E-02		
156.2 Å	100000.	0.145E-01	0.619E-03	*0.260E-02	*0.221E-02		
C= 0.31E+18	150000.	0.128E-01	0.592E-03	*0.299E-02	*0.250E-02		
	200000.	0.117E-01	0.569E-03	*0.336E-02	*0.275E-02		
	300000.	0.104E-01	0.551E-03	*0.382E-02	*0.295E-02		
	500000.	0.890E-02	0.528E-03	*0.451E-02	*0.328E-02		
C V 3S 3P	50000.	10.2	-0.219	0.150	-0.155	0.281	-0.289
8434.5 Å	100000.	7.77	-0.330	0.287	-0.257	0.558	-0.505
C= 0.42E+22	150000.	6.70	-0.301	0.377	-0.314	0.725	-0.633
	200000.	6.05	-0.306	0.455	-0.359	0.867	-0.727
	300000.	5.29	-0.297	0.546	-0.402	1.02	-0.830
	500000.	4.49	-0.299	0.689	-0.463	1.20	-0.954
C V 3S 4P	50000.	0.156	0.141E-02	0.829E-02	0.814E-02	*0.161E-01	*0.147E-01
672.1 Å	100000.	0.122	0.128E-02	0.130E-01	0.115E-01	*0.258E-01	*0.220E-01
C= 0.11E+20	150000.	0.106	0.147E-02	0.152E-01	0.129E-01	*0.299E-01	*0.261E-01
	200000.	0.969E-01	0.152E-02	0.169E-01	0.141E-01	*0.330E-01	*0.284E-01
	300000.	0.854E-01	0.122E-02	0.198E-01	0.157E-01	*0.376E-01	*0.324E-01
	500000.	0.731E-01	0.817E-03	0.242E-01	0.177E-01	*0.426E-01	*0.363E-01

PERTURBER DENSITY = 1xE+18cm-3

PERTURBERS ARE: TRANSITION	T(K)	ELECTRONS WIDTH(Å)	ELECTRONS SHIFT(Å)	PROTONS WIDTH(Å)	PROTONS SHIFT(Å)	He III WIDTH(Å)	He III SHIFT(Å)
C V 3S 5P	50000.	0.176	0.400E-02	*0.179E-01	*0.143E-01		
472.2 Å	100000.	0.141	0.437E-02	*0.235E-01	*0.198E-01		
C= 0.28E+19	150000.	0.124	0.419E-02	*0.268E-01	*0.223E-01		
	200000.	0.114	0.400E-02	*0.300E-01	*0.247E-01		
	300000.	0.100	0.386E-02	*0.344E-01	*0.266E-01		
	500000.	0.861E-01	0.366E-02	*0.406E-01	*0.296E-01		
C V 4S 5P	50000.	2.02	-0.649E-02	*0.154	*0.121		
1475.1 Å	100000.	1.62	0.848E-03	*0.199	*0.163		
C= 0.27E+20	150000.	1.43	-0.106E-02	*0.230	*0.184		
	200000.	1.31	-0.247E-02	*0.255	*0.202		
	300000.	1.16	-0.400E-02	*0.294	*0.218		
	500000.	0.992	-0.411E-03	*0.346	*0.241		
C V 2P 3S	50000.	0.490E-02	0.311E-03	0.135E-03	0.317E-03	0.264E-03	0.588E-03
260.2 Å	100000.	0.367E-02	0.432E-03	0.312E-03	0.487E-03	0.627E-03	0.945E-03
C= 0.80E+19	150000.	0.316E-02	0.415E-03	0.457E-03	0.587E-03	0.912E-03	0.119E-02
	200000.	0.285E-02	0.414E-03	0.569E-03	0.640E-03	0.116E-02	0.130E-02
	300000.	0.247E-02	0.408E-03	0.683E-03	0.714E-03	0.139E-02	0.147E-02
	500000.	0.209E-02	0.401E-03	0.833E-03	0.813E-03	0.168E-02	0.168E-02
C V 2P 4S	50000.	0.783E-02	0.938E-03	0.674E-03	0.877E-03	*0.135E-02	*0.157E-02
189.3 Å	100000.	0.609E-02	0.928E-03	0.112E-02	0.120E-02	*0.229E-02	*0.227E-02
C= 0.17E+19	150000.	0.531E-02	0.918E-03	0.134E-02	0.136E-02	*0.274E-02	*0.273E-02
	200000.	0.484E-02	0.908E-03	0.148E-02	0.149E-02	*0.305E-02	*0.295E-02
	300000.	0.426E-02	0.904E-03	0.171E-02	0.165E-02	*0.345E-02	*0.340E-02
	500000.	0.364E-02	0.809E-03	0.203E-02	0.185E-02	*0.404E-02	*0.374E-02
C V 2P 5S	50000.	0.159E-01	0.206E-02	*0.228E-02	*0.209E-02		
168.4 Å	100000.	0.126E-01	0.209E-02	*0.307E-02	*0.291E-02		
C= 0.68E+18	150000.	0.111E-01	0.211E-02	*0.350E-02	*0.328E-02		
	200000.	0.101E-01	0.208E-02	*0.391E-02	*0.364E-02		
	300000.	0.896E-02	0.194E-02	*0.444E-02	*0.395E-02		
	500000.	0.763E-02	0.171E-02	*0.519E-02	*0.437E-02		
C V 3P 4S	50000.	0.165	0.140E-01	0.103E-01	0.133E-01	*0.206E-01	*0.239E-01
756.9 Å	100000.	0.128	0.138E-01	0.171E-01	0.182E-01	*0.351E-01	*0.346E-01
C= 0.28E+20	150000.	0.112	0.135E-01	0.207E-01	0.206E-01	*0.417E-01	*0.414E-01
	200000.	0.102	0.134E-01	0.229E-01	0.226E-01	*0.463E-01	*0.451E-01
	300000.	0.895E-01	0.134E-01	0.268E-01	0.251E-01	*0.530E-01	*0.512E-01
	500000.	0.765E-01	0.119E-01	0.317E-01	0.277E-01	*0.635E-01	*0.573E-01
C V 3P 5S	50000.	0.160	0.181E-01	*0.205E-01	*0.187E-01		
506.3 Å	100000.	0.127	0.184E-01	*0.274E-01	*0.261E-01		
C= 0.62E+19	150000.	0.112	0.185E-01	*0.312E-01	*0.294E-01		
	200000.	0.102	0.183E-01	*0.349E-01	*0.326E-01		
	300000.	0.904E-01	0.170E-01	*0.393E-01	*0.353E-01		
	500000.	0.771E-01	0.150E-01	*0.469E-01	*0.392E-01		
C V 4P 5S	50000.	2.23	0.173	*0.198	*0.180		
1651.0 Å	100000.	1.78	0.174	*0.264	*0.249		
C= 0.66E+20	150000.	1.57	0.176	*0.306	*0.283		
	200000.	1.44	0.173	*0.345	*0.309		
	300000.	1.27	0.162	*0.391	*0.332		
	500000.	1.09	0.143	*0.461	*0.369		
C V 2P 3D	50000.	0.369E-02	-0.104E-03	0.889E-04	-0.152E-03	0.168E-03	-0.284E-03
248.7 Å	100000.	0.272E-02	-0.503E-04	0.200E-03	-0.248E-03	0.393E-03	-0.489E-03
C= 0.36E+19	150000.	0.230E-02	-0.464E-04	0.271E-03	-0.304E-03	0.528E-03	-0.615E-03
	200000.	0.205E-02	-0.506E-04	0.340E-03	-0.347E-03	0.654E-03	-0.700E-03
	300000.	0.176E-02	-0.450E-04	0.423E-03	-0.385E-03	0.811E-03	-0.793E-03
	500000.	0.147E-02	-0.245E-04	0.534E-03	-0.444E-03	0.987E-03	-0.913E-03

PERTURBER DENSITY = 1xE+18cm-3

PERTURBERS ARE: TRANSITION	T(K)	ELECTRONS WIDTH(Å)	ELECTRONS SHIFT(Å)	PROTONS WIDTH(Å)	PROTONS SHIFT(Å)	He III WIDTH(Å)	He III SHIFT(Å)
C V 2P 4D	50000.	0.920E-02	-0.246E-03				
186.7 Å	100000.	0.738E-02	-0.175E-03				
C= 0.51E+17	150000.	0.650E-02	-0.152E-03				
	200000.	0.594E-02	-0.108E-03				
	300000.	0.523E-02	-0.187E-04				
	500000.	0.445E-02	0.643E-04				
C V 3D 4P	50000.	0.185	0.544E-02	0.126E-01	0.126E-01	*0.247E-01	*0.227E-01
763.1 Å	100000.	0.145	0.583E-02	0.192E-01	0.174E-01	*0.383E-01	*0.331E-01
C= 0.14E+20	150000.	0.126	0.589E-02	0.227E-01	0.197E-01	*0.446E-01	*0.397E-01
	200000.	0.115	0.599E-02	0.253E-01	0.216E-01	*0.493E-01	*0.430E-01
	300000.	0.102	0.550E-02	0.294E-01	0.238E-01	*0.563E-01	*0.495E-01
	500000.	0.869E-01	0.473E-02	0.360E-01	0.265E-01	*0.650E-01	*0.553E-01
C V 3D 5P	50000.	0.202	0.644E-02	*0.219E-01	*0.176E-01		
515.4 Å	100000.	0.162	0.712E-02	*0.287E-01	*0.243E-01		
C= 0.33E+19	150000.	0.143	0.682E-02	*0.333E-01	*0.276E-01		
	200000.	0.131	0.661E-02	*0.371E-01	*0.301E-01		
	300000.	0.116	0.639E-02	*0.416E-01	*0.324E-01		
	500000.	0.992E-01	0.604E-02	*0.493E-01	*0.360E-01		
C V 4D 5P	50000.	2.53	0.808E-01				
1651.4 Å	100000.	2.05	0.845E-01				
C= 0.40E+19	150000.	1.81	0.799E-01				
	200000.	1.66	0.740E-01				
	300000.	1.47	0.651E-01				
	500000.	1.26	0.559E-01				
C V 3D 4F	50000.	0.972E-01	0.201E-02				
748.4 Å	100000.	0.769E-01	0.152E-02				
C= 0.82E+18	150000.	0.672E-01	0.111E-02				
	200000.	0.613E-01	0.105E-02				
	300000.	0.540E-01	0.534E-03				
	500000.	0.462E-01	-0.447E-03	*0.201	*-0.102		

PERTURBER DENSITY = 1xE+19cm-3

C V 1S 2P	50000.	0.297E-03	-0.128E-04	0.118E-05	-0.166E-05	0.202E-05	-0.261E-05
40.3 Å	100000.	0.211E-03	-0.335E-05	0.332E-05	-0.373E-05	0.607E-05	-0.690E-05
C= 0.47E+19	150000.	0.174E-03	-0.189E-05	0.557E-05	-0.553E-05	0.104E-04	-0.106E-04
	200000.	0.152E-03	-0.139E-05	0.748E-05	-0.699E-05	0.142E-04	-0.135E-04
	300000.	0.127E-03	-0.993E-06	0.108E-04	-0.920E-05	0.209E-04	-0.183E-04
	500000.	0.102E-03	-0.108E-05	0.151E-04	-0.119E-04	0.290E-04	-0.240E-04
C V 2S 2P	50000.	3.43	-0.101	0.151E-01	-0.556E-01	0.268E-01	-0.877E-01
3478.6 Å	100000.	2.49	-0.971E-01	0.550E-01	-0.115	0.105	-0.212
C= 0.35E+23	150000.	2.09	-0.112	0.966E-01	-0.158	0.186	-0.303
	200000.	1.85	-0.114	0.133	-0.186	0.264	-0.360
	300000.	1.56	-0.108	0.181	-0.228	0.361	-0.452
	500000.	1.29	-0.107	0.269	-0.276	0.532	-0.560
C V 2P 3S	50000.	0.608E-01	0.361E-02	0.258E-02	0.409E-02	*0.492E-02	*0.599E-02
272.2 Å	100000.	0.463E-01	0.462E-02	0.520E-02	0.659E-02	*0.105E-01	*0.116E-01
C= 0.61E+20	150000.	0.400E-01	0.473E-02	0.750E-02	0.813E-02	*0.151E-01	*0.149E-01
	200000.	0.362E-01	0.471E-02	0.863E-02	0.912E-02	*0.174E-01	*0.167E-01
	300000.	0.316E-01	0.472E-02	0.104E-01	0.103E-01	*0.210E-01	*0.197E-01
	500000.	0.269E-01	0.463E-02	0.127E-01	0.120E-01	*0.251E-01	*0.240E-01
C V 2P 3D	50000.	0.451E-01	0.694E-03	0.316E-02	0.429E-02	*0.592E-02	*0.622E-02
267.6 Å	100000.	0.339E-01	0.151E-02	0.619E-02	0.691E-02	*0.118E-01	*0.120E-01
C= 0.13E+20	150000.	0.290E-01	0.173E-02	0.902E-02	0.843E-02	*0.167E-01	*0.154E-01
	200000.	0.260E-01	0.167E-02	0.105E-01	0.954E-02	*0.190E-01	*0.173E-01
	300000.	0.224E-01	0.169E-02	0.130E-01	0.107E-01	*0.228E-01	*0.206E-01
	500000.	0.188E-01	0.176E-02	0.167E-01	0.126E-01	*0.272E-01	*0.248E-01

PERTURBER DENSITY = 1xE+19cm-3

PERTURBERS ARE:		ELECTRONS		PROTONS		He III	
TRANSITION	T(K)	WIDTH(Å)	SHIFT(Å)	WIDTH(Å)	SHIFT(Å)	WIDTH(Å)	SHIFT(Å)
C V 2S 2P	50000.	1.31	-0.218E-01	0.407E-02	-0.141E-01	0.706E-02	-0.222E-01
2274.6 Å	100000.	0.939	-0.297E-01	0.142E-01	-0.303E-01	0.264E-01	-0.560E-01
C= 0.23E+23	150000.	0.781	-0.342E-01	0.248E-01	-0.423E-01	0.478E-01	-0.809E-01
	200000.	0.688	-0.373E-01	0.364E-01	-0.523E-01	0.709E-01	-0.101
	300000.	0.580	-0.370E-01	0.500E-01	-0.635E-01	0.995E-01	-0.126
	500000.	0.473	-0.365E-01	0.763E-01	-0.808E-01	0.151	-0.164
C V 2S 3P	50000.	0.506E-01	0.281E-03	0.115E-02	0.117E-02	*0.207E-02	*0.180E-02
227.2 Å	100000.	0.380E-01	0.374E-03	0.224E-02	0.204E-02	*0.436E-02	*0.372E-02
C= 0.30E+20	150000.	0.325E-01	0.441E-03	0.299E-02	0.260E-02	*0.579E-02	*0.489E-02
	200000.	0.293E-01	0.391E-03	0.364E-02	0.304E-02	*0.705E-02	*0.575E-02
	300000.	0.254E-01	0.443E-03	0.431E-02	0.340E-02	*0.826E-02	*0.667E-02
	500000.	0.214E-01	0.415E-03	0.531E-02	0.396E-02	*0.974E-02	*0.800E-02
C V 2S 4P	50000.	0.887E-01	0.692E-04	*0.593E-02	*0.459E-02		
173.3 Å	100000.	0.694E-01	0.112E-02	*0.928E-02	*0.705E-02		
C= 0.73E+19	150000.	0.607E-01	0.146E-02	*0.111E-01	*0.865E-02		
	200000.	0.554E-01	0.156E-02	*0.123E-01	*0.990E-02		
	300000.	0.488E-01	0.144E-02	*0.145E-01	*0.112E-01		
	500000.	0.417E-01	0.136E-02	*0.174E-01	*0.130E-01		
C V 2S 5P	50000.	*0.168	*-0.151E-02				
156.2 Å	100000.	*0.137	*0.149E-02				
C= 0.31E+19	150000.	0.121	0.200E-02				
	200000.	0.112	0.212E-02				
	300000.	0.991E-01	0.209E-02				
	500000.	0.854E-01	0.248E-02				
C V 3S 4P	50000.	1.54	-0.138E-01	*0.807E-01	*0.615E-01		
672.1 Å	100000.	1.20	-0.610E-02	*0.129	*0.963E-01		
C= 0.11E+21	150000.	1.05	-0.641E-04	*0.152	*0.116		
	200000.	0.961	0.144E-02	*0.169	*0.134		
	300000.	0.847	-0.144E-03	*0.199	*0.151		
	500000.	0.725	-0.150E-02	*0.242	*0.176		
C V 3S 5P	50000.	* 1.64	*-0.213E-01				
472.2 Å	100000.	* 1.33	*0.218E-02				
C= 0.28E+20	150000.	1.18	0.729E-02				
	200000.	1.08	0.845E-02				
	300000.	0.961	0.828E-02				
	500000.	0.828	0.118E-01				
C V 4S 5P	50000.	* 19.1	*-0.496				
1475.1 Å	100000.	* 15.4	*-0.284				
C= 0.27E+21	150000.	* 13.7	*-0.252				
	200000.	12.5	-0.250				
	300000.	11.1	-0.262				
	500000.	9.60	-0.190				
C V 2P 3S	50000.	0.490E-01	0.254E-02	0.134E-02	0.263E-02	*0.260E-02	*0.391E-02
260.2 Å	100000.	0.367E-01	0.384E-02	0.313E-02	0.436E-02	*0.627E-02	*0.774E-02
C= 0.80E+20	150000.	0.316E-01	0.376E-02	0.456E-02	0.552E-02	*0.911E-02	*0.102E-01
	200000.	0.285E-01	0.379E-02	0.569E-02	0.618E-02	*0.115E-01	*0.115E-01
	300000.	0.247E-01	0.377E-02	0.684E-02	0.696E-02	*0.140E-01	*0.135E-01
	500000.	0.209E-01	0.378E-02	0.833E-02	0.810E-02	*0.168E-01	*0.163E-01
C V 2P 4S	50000.	0.781E-01	0.631E-02	*0.671E-02	*0.641E-02		
189.3 Å	100000.	0.608E-01	0.717E-02	*0.112E-01	*0.984E-02		
C= 0.17E+20	150000.	0.530E-01	0.739E-02	*0.135E-01	*0.120E-01		
	200000.	0.483E-01	0.753E-02	*0.148E-01	*0.140E-01		
	300000.	0.425E-01	0.767E-02	*0.172E-01	*0.158E-01		
	500000.	0.363E-01	0.704E-02	*0.203E-01	*0.184E-01		

PERTURBER DENSITY = 1xE+19cm-3

PERTURBERS ARE: TRANSITION	T(K)	ELECTRONS WIDTH(Å)	ELECTRONS SHIFT(Å)	PROTONS WIDTH(Å)	PROTONS SHIFT(Å)	He III WIDTH(Å)	He III SHIFT(Å)
C V 2P 5S	50000.	*0.154	*0.786E-02				
168.4 Å	100000.	0.123	0.122E-01				
C= 0.68E+19	150000.	0.108	0.141E-01				
	200000.	0.990E-01	0.144E-01				
	300000.	0.877E-01	0.137E-01				
	500000.	0.748E-01	0.127E-01				
C V 3P 4S	50000.	1.64	0.935E-01	*0.102	*0.978E-01		
756.9 Å	100000.	1.28	0.106	*0.171	*0.150		
C= 0.28E+21	150000.	1.11	0.109	*0.206	*0.183		
	200000.	1.02	0.112	*0.229	*0.212		
	300000.	0.893	0.113	*0.267	*0.240		
	500000.	0.764	0.104	*0.317	*0.275		
C V 3P 5S	50000.	* 1.56	*0.669E-01				
506.3 Å	100000.	1.24	0.106				
C= 0.62E+20	150000.	1.09	0.123				
	200000.	1.00	0.126				
	300000.	0.887	0.120				
	500000.	0.757	0.111				
C V 4P 5S	50000.	* 21.7	*0.696				
1651.0 Å	100000.	* 17.4	* 1.04				
C= 0.66E+21	150000.	15.3	1.19				
	200000.	14.1	1.21				
	300000.	12.5	1.16				
	500000.	10.7	1.07				
C V 2P 3D	50000.	0.369E-01	-0.594E-03	0.877E-03	-0.128E-02	*0.160E-02	-0.198E-02
248.7 Å	100000.	0.272E-01	-0.303E-03	0.199E-02	-0.226E-02	*0.390E-02	-0.414E-02
C= 0.36E+20	150000.	0.230E-01	-0.290E-03	0.271E-02	-0.288E-02	*0.526E-02	-0.543E-02
	200000.	0.205E-01	-0.350E-03	0.340E-02	-0.338E-02	*0.653E-02	-0.636E-02
	300000.	0.176E-01	-0.320E-03	0.423E-02	-0.377E-02	*0.813E-02	-0.742E-02
	500000.	0.147E-01	-0.138E-03	0.534E-02	-0.443E-02	*0.987E-02	-0.890E-02
C V 2P 4D	50000.	0.785E-01	-0.155E-02				
186.7 Å	100000.	0.642E-01	-0.143E-02				
C= 0.51E+18	150000.	0.572E-01	-0.144E-02				
	200000.	0.526E-01	-0.123E-02				
	300000.	0.468E-01	-0.932E-03				
	500000.	0.402E-01	-0.733E-03				
C V 3D 4P	50000.	1.83	0.943E-02	*0.123	*0.940E-01		
763.1 Å	100000.	1.43	0.279E-01	*0.191	*0.144		
C= 0.14E+21	150000.	1.25	0.349E-01	*0.228	*0.175		
	200000.	1.14	0.377E-01	*0.253	*0.203		
	300000.	1.01	0.352E-01	*0.293	*0.227		
	500000.	0.862	0.318E-01	*0.360	*0.263		
C V 3D 5P	50000.	* 1.88	*-0.127E-01				
515.4 Å	100000.	* 1.52	*0.190E-01				
C= 0.33E+20	150000.	1.35	0.247E-01				
	200000.	1.24	0.265E-01				
	300000.	1.11	0.260E-01				
	500000.	0.952	0.294E-01				
C V 4D 5P	50000.	* 22.8	*-0.359E-01				
1651.4 Å	100000.	* 18.8	*0.293				
C= 0.40E+20	150000.	* 16.8	*0.354				
	200000.	15.5	0.353				
	300000.	13.8	0.326				
	500000.	11.9	0.353				

PERTURBER DENSITY = 1xE+18cm-3

PERTURBERS ARE: TRANSITION	T(K)	ELECTRONS WIDTH(Å)	ELECTRONS SHIFT(Å)	PROTONS WIDTH(Å)	PROTONS SHIFT(Å)	He III WIDTH(Å)	He III SHIFT(Å)
C V 3D 4F	50000.	0.827	0.293E-01				
748.4 Å	100000.	0.665	0.245E-01				
C= 0.82E+19	150000.	0.588	0.206E-01				
	200000.	0.540	0.220E-01				
	300000.	0.480	0.223E-01				
	500000.	0.416	0.179E-01				
PERTURBER DENSITY = 1xE+20cm-3							
C V 1S 2P	50000.	0.297E-02	-0.121E-03	0.990E-05	-0.997E-05	0.112E-04	-0.871E-05
40.3 Å	100000.	0.211E-02	-0.277E-04	0.325E-04	-0.314E-04	0.552E-04	-0.477E-04
C= 0.47E+20	200000.	0.152E-02	-0.916E-05	0.744E-04	-0.643E-04	0.140E-03	-0.118E-03
	300000.	0.127E-02	-0.595E-05	0.108E-03	-0.881E-04	0.207E-03	-0.167E-03
	500000.	0.102E-02	-0.696E-05	0.151E-03	-0.117E-03	0.290E-03	-0.228E-03
	1000000.	0.779E-03	-0.696E-07	0.213E-03	-0.151E-03	0.399E-03	-0.306E-03
C V 2P 3S	50000.	*0.590	*-0.883E-02				
272.2 Å	100000.	0.453	0.179E-01				
C= 0.61E+21	200000.	0.356	0.280E-01				
	300000.	0.311	0.319E-01				
	500000.	0.265	0.339E-01				
	1000000.	0.213	0.309E-01	*0.166	*0.139		
C V 2P 3D	50000.	0.402	-0.108E-01				
267.6 Å	100000.	0.309	0.195E-02				
C= 0.13E+21	200000.	0.240	0.711E-02				
	300000.	0.208	0.899E-02				
	500000.	0.176	0.108E-01				
	1000000.	0.143	0.112E-01				
C V 2S 2P	50000.	13.1	-0.107	0.354E-01	-0.842E-01	0.446E-01	-0.727E-01
2274.6 Å	100000.	9.39	-0.232	0.140	-0.252	0.248	-0.377
C= 0.23E+24	200000.	6.88	-0.327	0.363	-0.476	0.703	-0.864
	300000.	5.80	-0.334	0.500	-0.602	0.992	-1.12
	500000.	4.73	-0.335	0.763	-0.790	1.50	-1.54
	1000000.	3.69	-0.321	1.06	-0.971	2.07	-1.94
C V 2S 3P	50000.	*0.492	*-0.700E-02	*0.947E-02	*0.627E-02		
227.2 Å	100000.	0.372	-0.264E-02	*0.217E-01	*0.155E-01		
C= 0.30E+21	200000.	0.288	-0.355E-03	*0.361E-01	*0.259E-01		
	300000.	0.250	0.994E-03	*0.430E-01	*0.308E-01		
	500000.	0.211	0.136E-02	*0.531E-01	*0.379E-01		
	1000000.	0.170	0.122E-02	*0.712E-01	*0.470E-01		
C V 2S 4P	50000.						
173.3 Å	100000.	*0.607	*-0.831E-02				
C= 0.73E+20	200000.	*0.497	*0.783E-03				
	300000.	0.442	0.217E-02				
	500000.	0.382	0.311E-02				
	1000000.	0.315	0.597E-02				
C V 2S 5P	50000.						
156.2 Å	100000.						
C= 0.31E+20	200000.	*0.883	*-0.225E-02				
	300000.	*0.805	*0.146E-02				
	500000.	*0.711	*0.555E-02				
	1000000.	0.597	0.111E-01				
C V 3S 4P	50000.						
672.1 Å	100000.	* 10.7	*-0.249				
C= 0.11E+22	200000.	* 8.74	*-0.137				
	300000.	7.78	-0.128				
	500000.	6.72	-0.127				
	1000000.	5.53	-0.681E-01				

PERTURBER DENSITY = 1xE+20cm-3

PERTURBERS ARE: TRANSITION	T(K)	ELECTRONS WIDTH(Å)	ELECTRONS SHIFT(Å)	PROTONS WIDTH(Å)	PROTONS SHIFT(Å)	He III WIDTH(Å)	He III SHIFT(Å)
C V 3S 5P	50000.						
472.2 Å	100000.						
C= 0.28E+21	200000.	* 8.69	*-0.945E-01				
	300000.	* 7.90	*-0.662E-01				
	500000.	* 6.97	*-0.354E-01				
	1000000.	5.85	0.231E-01				
C V 2P 3S	50000.	0.486	-0.126E-02	*0.127E-01	*0.129E-01		
260.2 Å	100000.	0.365	0.217E-01	*0.311E-01	*0.317E-01		
C= 0.80E+21	200000.	0.283	0.267E-01	*0.570E-01	*0.506E-01		
	300000.	0.246	0.285E-01	*0.679E-01	*0.619E-01		
	500000.	0.208	0.305E-01	*0.833E-01	*0.768E-01		
	1000000.	0.168	0.279E-01	*0.108	*0.949E-01		
C V 2P 4S	50000.	*0.681	*-0.375E-01				
189.3 Å	100000.	*0.553	*0.615E-02				
C= 0.17E+21	200000.	0.448	0.315E-01				
	300000.	0.397	0.408E-01				
	500000.	0.342	0.414E-01				
	1000000.	0.277	0.397E-01				
C V 2P 5S	50000.						
168.4 Å	100000.						
C= 0.68E+20	200000.	*0.791	*0.299E-01				
	300000.	*0.718	*0.429E-01				
	500000.	0.627	0.480E-01				
	1000000.	0.513	0.587E-01				
C V 3P 4S	50000.						
756.9 Å	100000.	* 11.8	*0.932E-01				
C= 0.28E+22	200000.	* 9.53	*0.467				
	300000.	8.44	0.601				
	500000.	7.26	0.608				
	1000000.	5.90	0.586				
C V 3P 5S	50000.						
506.3 Å	100000.						
C= 0.62E+21	200000.	* 8.19	*0.252				
	300000.	* 7.41	*0.363				
	500000.	* 6.46	*0.409				
	1000000.	5.29	0.508				
C V 2P 3D	50000.	0.359	0.486E-02	*0.764E-02	-0.697E-02		
248.7 Å	100000.	0.266	0.402E-02	*0.195E-01	-0.174E-01		
C= 0.36E+21	200000.	0.202	0.121E-02	*0.337E-01	-0.288E-01		
	300000.	0.173	0.626E-03	*0.422E-01	-0.343E-01		
	500000.	0.145	0.170E-02	*0.534E-01	-0.424E-01		
	1000000.	0.117	0.134E-02	*0.719E-01	-0.522E-01		
C V 2P 4D	50000.	*0.591	*0.216E-01				
186.7 Å	100000.	*0.504	*0.994E-02				
C= 0.51E+19	200000.	0.428	0.299E-02				
	300000.	0.387	0.282E-02				
	500000.	0.340	0.212E-02				
	1000000.	0.283	0.385E-03				
C V 3D 4P	50000.						
763.1 Å	100000.	* 12.5	*-0.173				
C= 0.14E+22	200000.	* 10.3	*0.407E-01				
	300000.	9.16	0.739E-01				
	500000.	7.93	0.820E-01				
	1000000.	6.54	0.139				

PERTURBER DENSITY = 1xE+20cm-3

PERTURBERS ARE: TRANSITION	T(K)	ELECTRONS WIDTH(Å)	ELECTRONS SHIFT(Å)	PROTONS WIDTH(Å)	PROTONS SHIFT(Å)	He III WIDTH(Å)	He III SHIFT(Å)
C V 3D 5P	50000.						
515.4 Å	100000.						
C= 0.33E+21	200000.	* 9.89	*-0.130E-01				
	300000.	* 9.01	*0.303E-01				
	500000.	* 7.96	*0.703E-01				
	1000000.	6.69	0.131				
C V 3D 4F	50000.	* 6.93	*0.124				
748.4 Å	100000.	5.60	0.157				
C= 0.82E+20	200000.	4.62	0.185				
	300000.	4.16	0.200				
	500000.	3.66	0.171				
	1000000.	3.09	0.165				
PERTURBER DENSITY = 1x+21cm-3							
C V 1S 2P	50000.						
40.3 Å	100000.	0.210E-01	0.571E-04	0.265E-03	-0.177E-03	*0.263E-03	-0.132E-03
C= 0.47E+21	200000.	0.152E-01	0.958E-04	0.720E-03	-0.514E-03	*0.118E-02	-0.708E-03
	300000.	0.126E-01	0.908E-04	0.107E-02	-0.759E-03	*0.198E-02	-0.126E-02
	500000.	0.102E-01	0.417E-04	0.150E-02	-0.106E-02	*0.284E-02	-0.190E-02
	1000000.	0.777E-02	0.811E-04	0.213E-02	-0.146E-02	*0.397E-02	-0.279E-02
C V 2P 3S	50000.						
272.2 Å	100000.	* 3.41	*-0.362				
C= 0.61E+22	200000.	* 2.90	*-0.980E-01				
	300000.	2.61	0.704E-02				
	500000.	2.27	0.997E-01				
	1000000.	1.87	0.127				
C V 2P 3D	50000.						
267.6 Å	100000.	* 2.62	*-0.416E-01				
C= 0.13E+22	200000.	2.06	0.941E-02				
	300000.	1.80	0.356E-01				
	500000.	1.55	0.636E-01				
	1000000.	1.28	0.702E-01				
C V 2S 3P	50000.						
227.2 Å	100000.	* 3.13	*-0.423E-01				
C= 0.30E+22	200000.	* 2.52	*-0.262E-01				
	300000.	* 2.22	*-0.147E-01				
	500000.	1.91	-0.723E-02				
	1000000.	1.56	-0.564E-02				
C V 2S 4P	50000.						
173.3 Å	100000.						
C= 0.73E+21	200000.						
	300000.	* 3.27	*-0.414E-02				
	500000.	* 2.96	*0.585E-02				
	1000000.	* 2.54	*0.246E-01				
C V 2P 3S	50000.						
260.2 Å	100000.	* 3.04	*-0.231				
C= 0.80E+22	200000.	* 2.49	*-0.335E-01				
	300000.	2.20	0.475E-01				
	500000.	1.89	0.125				
	1000000.	1.54	0.143				
C V 2P 4S	50000.						
189.3 Å	100000.						
C= 0.17E+22	200000.	* 2.87	*-0.218				
	300000.	* 2.72	*-0.489E-01				
	500000.	* 2.48	*0.541E-01				
	1000000.	* 2.12	*0.107				

PERTURBERS ARE:		ELECTRONS		PROTONS		He III	
TRANSITION	T(K)	WIDTH(Å)	SHIFT(Å)	WIDTH(Å)	SHIFT(Å)	WIDTH(Å)	SHIFT(Å)
PERTURBER DENSITY = 1xE+21cm-3							
C V 2P 3D	50000.						
248.7 Å	100000.	* 2.35	*0.114				
C= 0.36E+22	200000.	1.82	0.708E-01				
	300000.	1.58	0.575E-01				
	500000.	1.34	0.572E-01				
	1000000.	1.09	0.454E-01				
C V 2P 4D	50000.						
186.7 Å	100000.						
C= 0.51E+20	200000.	* 3.04	*0.113				
	300000.	* 2.83	*0.102				
	500000.	* 2.58	*0.808E-01				
	1000000.	2.24	0.620E-01				
PERTURBER DENSITY = 1xE+22							
C V 1S 2P	50000.						
40.3 Å	100000.						
C= 0.47E+22	200000.	*0.142	*0.441E-02				
	300000.	0.120	0.385E-02				
	500000.	0.970E-01	0.264E-02				
	1000000.	0.747E-01	0.237E-02				
PERTURBER DENSITY = 1xE+17cm-3							
P V 3S 3P	50000.	0.626E-02	-0.594E-04	0.633E-04	-0.266E-04	0.122E-03	-0.519E-04
1121.8 Å	100000.	0.447E-02	-0.762E-04	0.136E-03	-0.516E-04	0.266E-03	-0.103E-03
C= 0.11E+21	150000.	0.371E-02	-0.584E-04	0.190E-03	-0.713E-04	0.373E-03	-0.143E-03
	200000.	0.328E-02	-0.729E-04	0.224E-03	-0.875E-04	0.443E-03	-0.176E-03
	300000.	0.278E-02	-0.871E-04	0.278E-03	-0.108E-03	0.550E-03	-0.219E-03
	500000.	0.232E-02	-0.764E-04	0.329E-03	-0.139E-03	0.657E-03	-0.280E-03
P V 3S 4P	50000.	0.139E-02	0.178E-04	0.619E-04	0.890E-05	0.121E-03	0.174E-04
328.6 Å	100000.	0.103E-02	0.166E-04	0.923E-04	0.156E-04	0.182E-03	0.310E-04
C= 0.34E+19	150000.	0.877E-03	0.202E-04	0.110E-03	0.201E-04	0.218E-03	0.406E-04
	200000.	0.792E-03	0.224E-04	0.117E-03	0.228E-04	0.233E-03	0.460E-04
	300000.	0.693E-03	0.220E-04	0.127E-03	0.277E-04	0.252E-03	0.561E-04
	500000.	0.598E-03	0.206E-04	0.138E-03	0.321E-04	0.275E-03	0.649E-04
P V 3S 5P	50000.	0.175E-02	0.497E-04	0.158E-03	0.299E-04	0.310E-03	0.583E-04
255.6 Å	100000.	0.140E-02	0.570E-04	0.200E-03	0.439E-04	0.399E-03	0.875E-04
C= 0.95E+18	150000.	0.125E-02	0.646E-04	0.217E-03	0.529E-04	0.432E-03	0.107E-03
	200000.	0.116E-02	0.584E-04	0.228E-03	0.574E-04	0.453E-03	0.116E-03
	300000.	0.105E-02	0.566E-04	0.243E-03	0.638E-04	0.484E-03	0.130E-03
	500000.	0.934E-03	0.528E-04	0.258E-03	0.728E-04	0.514E-03	0.148E-03
P V 3S 6P	50000.	0.282E-02	0.104E-03	0.356E-03	0.694E-04	*0.705E-03	*0.135E-03
229.8 Å	100000.	0.238E-02	0.137E-03	0.404E-03	0.961E-04	*0.804E-03	*0.192E-03
C= 0.42E+18	150000.	0.217E-02	0.124E-03	0.433E-03	0.107E-03	*0.863E-03	*0.216E-03
	200000.	0.204E-02	0.122E-03	0.452E-03	0.115E-03	0.902E-03	0.234E-03
	300000.	0.187E-02	0.117E-03	0.471E-03	0.128E-03	0.938E-03	0.259E-03
	500000.	0.170E-02	0.114E-03	0.492E-03	0.145E-03	0.974E-03	0.293E-03
P V 4S 4P	50000.	0.170	-0.412E-02	0.600E-02	-0.260E-02	0.117E-01	-0.508E-02
3185.6 Å	100000.	0.127	-0.405E-02	0.908E-02	-0.405E-02	0.179E-01	-0.812E-02
C= 0.32E+21	150000.	0.110	-0.481E-02	0.109E-01	-0.493E-02	0.217E-01	-0.996E-02
	200000.	0.997E-01	-0.485E-02	0.117E-01	-0.558E-02	0.233E-01	-0.113E-01
	300000.	0.882E-01	-0.432E-02	0.128E-01	-0.619E-02	0.255E-01	-0.125E-01
	500000.	0.767E-01	-0.423E-02	0.142E-01	-0.714E-02	0.283E-01	-0.144E-01
P V 4S 5P	50000.	0.217E-01	0.112E-03	0.172E-02	0.122E-03	0.337E-02	0.238E-03
845.8 Å	100000.	0.174E-01	0.218E-03	0.218E-02	0.200E-03	0.433E-02	0.400E-03
C= 0.10E+20	150000.	0.156E-01	0.228E-03	0.235E-02	0.242E-03	0.468E-02	0.487E-03
	200000.	0.144E-01	0.142E-03	0.246E-02	0.279E-03	0.491E-02	0.562E-03
	300000.	0.131E-01	0.164E-03	0.262E-02	0.320E-03	0.523E-02	0.650E-03
	500000.	0.117E-01	0.142E-03	0.278E-02	0.367E-03	0.553E-02	0.740E-03

PERTURBER DENSITY = 1xE+17cm-3

PERTURBERS ARE: TRANSITION	T(K)	ELECTRONS WIDTH(Å)	ELECTRONS SHIFT(Å)	PROTONS WIDTH(Å)	PROTONS SHIFT(Å)	He III WIDTH(Å)	He III SHIFT(Å)
P V 4S 6P	50000.	0.218E-01	0.471E-03	0.256E-02	0.428E-03	*0.506E-02	*0.833E-03
616.8 Å	100000.	0.183E-01	0.753E-03	0.290E-02	0.597E-03	*0.577E-02	*0.119E-02
C= 0.30E+19	150000.	0.166E-01	0.617E-03	0.310E-02	0.662E-03	*0.618E-02	*0.134E-02
	200000.	0.156E-01	0.605E-03	0.324E-02	0.718E-03	0.646E-02	0.145E-02
	300000.	0.144E-01	0.591E-03	0.337E-02	0.796E-03	0.671E-02	0.162E-02
	500000.	0.130E-01	0.586E-03	0.349E-02	0.906E-03	0.694E-02	0.182E-02
P V 5S 5P	50000.	1.88	-0.715E-01	0.121	-0.588E-01	0.238	-0.114
6872.7 Å	100000.	1.53	-0.866E-01	0.156	-0.817E-01	0.311	-0.163
C= 0.69E+21	150000.	1.38	-0.805E-01	0.171	-0.906E-01	0.343	-0.183
	200000.	1.28	-0.819E-01	0.182	-0.983E-01	0.365	-0.199
	300000.	1.16	-0.783E-01	0.199	-0.109	0.398	-0.221
	500000.	1.04	-0.767E-01	0.215	-0.123	0.431	-0.251
P V 5S 6P	50000.	0.193	-0.123E-02	0.196E-01	-0.105E-02	*0.388E-01	-0.204E-02
1710.8 Å	100000.	0.163	-0.425E-03	0.222E-01	-0.157E-02	*0.441E-01	-0.313E-02
C= 0.23E+20	150000.	0.149	-0.116E-02	0.237E-01	-0.192E-02	*0.472E-01	-0.387E-02
	200000.	0.140	-0.995E-03	0.247E-01	-0.212E-02	0.492E-01	-0.429E-02
	300000.	0.129	-0.968E-03	0.257E-01	-0.236E-02	0.511E-01	-0.477E-02
	500000.	0.116	-0.815E-03	0.266E-01	-0.269E-02	0.527E-01	-0.546E-02
P V 6S 6P	50000.	13.5	-0.860	1.18	-0.629	* 2.34	*-1.21
12638.2 Å	100000.	11.6	-0.803	1.38	-0.780	* 2.76	*-1.54
C= 0.13E+22	150000.	10.6	-0.804	1.51	-0.869	* 3.01	*-1.75
	200000.	10.0	-0.771	1.60	-0.933	* 3.22	*-1.89
	300000.	9.25	-0.751	1.69	-1.02	3.38	-2.06
	500000.	8.34	-0.669	1.84	-1.13	3.63	-2.31
P V 3P 4S	50000.	0.276E-02	0.194E-03	0.441E-04	0.100E-03	0.869E-04	0.195E-03
544.0 Å	100000.	0.203E-02	0.187E-03	0.103E-03	0.150E-03	0.207E-03	0.301E-03
C= 0.93E+19	150000.	0.173E-02	0.213E-03	0.142E-03	0.184E-03	0.284E-03	0.371E-03
	200000.	0.155E-02	0.223E-03	0.182E-03	0.205E-03	0.363E-03	0.415E-03
	300000.	0.136E-02	0.209E-03	0.219E-03	0.228E-03	0.440E-03	0.461E-03
	500000.	0.116E-02	0.199E-03	0.263E-03	0.259E-03	0.536E-03	0.526E-03
P V 3P 5S	50000.	0.251E-02	0.320E-03	0.117E-03	0.185E-03	0.235E-03	0.358E-03
347.8 Å	100000.	0.194E-02	0.355E-03	0.214E-03	0.253E-03	0.428E-03	0.505E-03
C= 0.18E+19	150000.	0.169E-02	0.345E-03	0.261E-03	0.282E-03	0.523E-03	0.571E-03
	200000.	0.155E-02	0.335E-03	0.292E-03	0.304E-03	0.591E-03	0.613E-03
	300000.	0.137E-02	0.320E-03	0.334E-03	0.336E-03	0.685E-03	0.681E-03
	500000.	0.118E-02	0.304E-03	0.400E-03	0.382E-03	0.792E-03	0.772E-03
P V 3P 6S	50000.	0.382E-02	0.758E-03	0.326E-03	0.407E-03	0.650E-03	0.780E-03
295.8 Å	100000.	0.311E-02	0.732E-03	0.468E-03	0.499E-03	0.951E-03	0.983E-03
C= 0.69E+18	150000.	0.277E-02	0.690E-03	0.542E-03	0.555E-03	0.110E-02	0.112E-02
	200000.	0.254E-02	0.659E-03	0.601E-03	0.601E-03	0.120E-02	0.121E-02
	300000.	0.227E-02	0.625E-03	0.691E-03	0.647E-03	0.141E-02	0.131E-02
	500000.	0.198E-02	0.569E-03	0.790E-03	0.712E-03	0.159E-02	0.145E-02
P V 3P 7S	50000.	0.614E-02	0.188E-02	0.735E-03	0.790E-03	*0.148E-02	*0.148E-02
272.9 Å	100000.	0.524E-02	0.158E-02	0.965E-03	0.967E-03	*0.195E-02	*0.190E-02
C= 0.36E+18	150000.	0.471E-02	0.140E-02	0.109E-02	0.107E-02	*0.222E-02	*0.215E-02
	200000.	0.438E-02	0.130E-02	0.121E-02	0.114E-02	*0.245E-02	*0.230E-02
	300000.	0.396E-02	0.122E-02	0.139E-02	0.123E-02	*0.278E-02	*0.252E-02
	500000.	0.349E-02	0.103E-02	0.149E-02	0.135E-02	*0.302E-02	*0.274E-02
P V 4P 5S	50000.	0.522E-01	0.427E-02	0.222E-02	0.283E-02	0.444E-02	0.548E-02
1383.2 Å	100000.	0.406E-01	0.500E-02	0.376E-02	0.388E-02	0.755E-02	0.775E-02
C= 0.28E+20	150000.	0.356E-01	0.487E-02	0.444E-02	0.433E-02	0.895E-02	0.874E-02
	200000.	0.327E-01	0.469E-02	0.491E-02	0.464E-02	0.995E-02	0.941E-02
	300000.	0.292E-01	0.447E-02	0.564E-02	0.516E-02	0.112E-01	0.105E-01
	500000.	0.255E-01	0.430E-02	0.647E-02	0.584E-02	0.131E-01	0.118E-01

PERTURBER DENSITY = 1xE+17cm-3

PERTURBERS ARE: TRANSITION	T(K)	ELECTRONS WIDTH(Å)	ELECTRONS SHIFT(Å)	PROTONS WIDTH(Å)	PROTONS SHIFT(Å)	He III WIDTH(Å)	He III SHIFT(Å)
P V 4P 6S	50000.	0.326E-01	0.531E-02	0.253E-02	0.306E-02	0.504E-02	0.586E-02
814.1 Å	100000.	0.265E-01	0.523E-02	0.358E-02	0.375E-02	0.729E-02	0.739E-02
C= 0.52E+19	150000.	0.237E-01	0.496E-02	0.414E-02	0.417E-02	0.843E-02	0.841E-02
	200000.	0.219E-01	0.473E-02	0.455E-02	0.452E-02	0.918E-02	0.905E-02
	300000.	0.197E-01	0.451E-02	0.527E-02	0.488E-02	0.108E-01	0.987E-02
	500000.	0.173E-01	0.411E-02	0.606E-02	0.536E-02	0.121E-01	0.109E-01
P V 4P 7S	50000.	0.383E-01	0.103E-01	0.433E-02	0.463E-02	*0.872E-02	*0.865E-02
661.1 Å	100000.	0.326E-01	0.886E-02	0.568E-02	0.567E-02	*0.115E-01	*0.111E-01
C= 0.21E+19	150000.	0.294E-01	0.801E-02	0.642E-02	0.627E-02	*0.131E-01	*0.126E-01
	200000.	0.274E-01	0.719E-02	0.711E-02	0.666E-02	*0.144E-01	*0.134E-01
	300000.	0.248E-01	0.681E-02	0.816E-02	0.719E-02	*0.163E-01	*0.147E-01
	500000.	0.220E-01	0.582E-02	0.873E-02	0.789E-02	*0.176E-01	*0.161E-01
P V 5P 6S	50000.	0.463	0.531E-01	0.349E-01	0.344E-01	0.696E-01	0.660E-01
2778.6 Å	100000.	0.388	0.533E-01	0.462E-01	0.422E-01	0.930E-01	0.835E-01
C= 0.61E+20	150000.	0.353	0.502E-01	0.526E-01	0.469E-01	0.106	0.946E-01
	200000.	0.329	0.488E-01	0.568E-01	0.504E-01	0.116	0.102
	300000.	0.299	0.468E-01	0.655E-01	0.550E-01	0.132	0.113
	500000.	0.267	0.429E-01	0.726E-01	0.605E-01	0.149	0.123
P V 5P 7S	50000.	0.234	0.490E-01	0.245E-01	0.252E-01	*0.491E-01	*0.472E-01
1552.6 Å	100000.	0.202	0.445E-01	0.319E-01	0.310E-01	*0.643E-01	*0.606E-01
C= 0.11E+20	150000.	0.185	0.391E-01	0.361E-01	0.342E-01	*0.735E-01	*0.688E-01
	200000.	0.173	0.372E-01	0.399E-01	0.364E-01	*0.810E-01	*0.738E-01
	300000.	0.158	0.355E-01	0.452E-01	0.395E-01	*0.895E-01	*0.807E-01
	500000.	0.141	0.304E-01	0.488E-01	0.429E-01	*0.968E-01	*0.871E-01
P V 6P 7S	50000.	2.83	0.415	0.276	0.241	*0.548	*0.448
4877.0 Å	100000.	2.50	0.360	0.344	0.296	*0.698	*0.582
C= 0.11E+21	150000.	2.30	0.344	0.387	0.325	*0.787	*0.661
	200000.	2.18	0.328	0.420	0.349	*0.832	*0.705
	300000.	2.01	0.316	0.462	0.382	*0.910	*0.766
	500000.	1.81	0.266	0.496	0.410	* 1.01	*0.830
P V 3P 3D	50000.	0.434E-02	-0.481E-05	0.885E-04	-0.146E-05	0.171E-03	-0.285E-05
869.1 Å	100000.	0.311E-02	-0.138E-05	0.168E-03	-0.295E-05	0.328E-03	-0.586E-05
C= 0.67E+20	150000.	0.259E-02	-0.392E-05	0.214E-03	-0.441E-05	0.422E-03	-0.881E-05
	200000.	0.229E-02	-0.398E-05	0.248E-03	-0.580E-05	0.488E-03	-0.116E-04
	300000.	0.195E-02	-0.526E-05	0.292E-03	-0.831E-05	0.579E-03	-0.167E-04
	500000.	0.163E-02	-0.412E-05	0.322E-03	-0.121E-04	0.641E-03	-0.243E-04
P V 3P 4D	50000.	0.252E-02	0.947E-04	0.130E-03	0.114E-03	0.257E-03	0.222E-03
390.2 Å	100000.	0.191E-02	0.102E-03	0.201E-03	0.161E-03	0.398E-03	0.320E-03
C= 0.11E+19	150000.	0.165E-02	0.950E-04	0.240E-03	0.186E-03	0.479E-03	0.376E-03
	200000.	0.150E-02	0.941E-04	0.264E-03	0.200E-03	0.524E-03	0.404E-03
	300000.	0.132E-02	0.953E-04	0.297E-03	0.223E-03	0.588E-03	0.450E-03
	500000.	0.114E-02	0.839E-04	0.345E-03	0.253E-03	0.672E-03	0.513E-03
P V 3P 5D	50000.	0.385E-02	0.278E-03	0.363E-03	0.316E-03	0.719E-03	0.606E-03
311.0 Å	100000.	0.310E-02	0.247E-03	0.481E-03	0.396E-03	0.966E-03	0.786E-03
C= 0.37E+18	150000.	0.274E-02	0.244E-03	0.544E-03	0.439E-03	0.109E-02	0.892E-03
	200000.	0.253E-02	0.247E-03	0.597E-03	0.475E-03	0.117E-02	0.958E-03
	300000.	0.227E-02	0.230E-03	0.673E-03	0.524E-03	0.132E-02	0.106E-02
	500000.	0.199E-02	0.194E-03	0.754E-03	0.577E-03	0.147E-02	0.117E-02
P V 3P 6D	50000.	0.659E-02	0.572E-03	0.833E-03	0.694E-03	*0.167E-02	*0.130E-02
280.3 Å	100000.	0.549E-02	0.540E-03	0.104E-02	0.855E-03	*0.210E-02	*0.168E-02
C= 0.18E+18	150000.	0.494E-02	0.552E-03	0.118E-02	0.951E-03	*0.233E-02	*0.192E-02
	200000.	0.460E-02	0.520E-03	0.130E-02	0.102E-02	*0.254E-02	*0.206E-02
	300000.	0.416E-02	0.464E-03	0.140E-02	0.109E-02	*0.278E-02	*0.224E-02
	500000.	0.368E-02	0.379E-03	0.163E-02	0.121E-02	*0.310E-02	*0.248E-02

PERTURBER DENSITY = 1xE+17cm-3

PERTURBERS ARE: TRANSITION	T(K)	ELECTRONS WIDTH(Å)	ELECTRONS SHIFT(Å)	PROTONS WIDTH(Å)	PROTONS SHIFT(Å)	He III WIDTH(Å)	He III SHIFT(Å)
P V 3P 7D	50000.	0.109E-01	0.108E-02	*0.170E-02	*0.137E-02		
264.7 Å	100000.	0.936E-02	0.109E-02	*0.211E-02	*0.170E-02		
C= 0.10E+18	150000.	0.857E-02	0.105E-02	*0.234E-02	*0.186E-02		
	200000.	0.804E-02	0.954E-03	0.245E-02	0.196E-02		
	300000.	0.734E-02	0.834E-03	0.263E-02	0.213E-02		
	500000.	0.651E-02	0.698E-03	0.297E-02	0.231E-02	*0.582E-02	*0.468E-02
P V 4P 4D	50000.	0.131	0.244E-02	0.705E-02	0.405E-02	0.139E-01	0.789E-02
2436.0 Å	100000.	0.100E+00	0.270E-02	0.102E-01	0.572E-02	0.203E-01	0.114E-01
C= 0.43E+20	150000.	0.869E-01	0.232E-02	0.114E-01	0.669E-02	0.228E-01	0.135E-01
	200000.	0.792E-01	0.209E-02	0.124E-01	0.718E-02	0.246E-01	0.145E-01
	300000.	0.703E-01	0.209E-02	0.137E-01	0.802E-02	0.269E-01	0.162E-01
	500000.	0.613E-01	0.178E-02	0.155E-01	0.909E-02	0.300E-01	0.185E-01
P V 4P 5D	50000.	0.394E-01	0.235E-02	0.349E-02	0.285E-02	0.692E-02	0.547E-02
940.9 Å	100000.	0.315E-01	0.206E-02	0.455E-02	0.358E-02	0.913E-02	0.711E-02
C= 0.34E+19	150000.	0.280E-01	0.202E-02	0.514E-02	0.398E-02	0.102E-01	0.806E-02
	200000.	0.258E-01	0.202E-02	0.559E-02	0.430E-02	0.110E-01	0.863E-02
	300000.	0.232E-01	0.186E-02	0.628E-02	0.475E-02	0.122E-01	0.958E-02
	500000.	0.204E-01	0.156E-02	0.700E-02	0.521E-02	0.135E-01	0.106E-01
P V 4P 6D	50000.	0.441E-01	0.352E-02	0.535E-02	0.439E-02	*0.107E-01	*0.825E-02
706.8 Å	100000.	0.366E-01	0.332E-02	0.666E-02	0.542E-02	*0.134E-01	*0.107E-01
C= 0.11E+19	150000.	0.329E-01	0.339E-02	0.757E-02	0.604E-02	*0.149E-01	*0.122E-01
	200000.	0.306E-01	0.317E-02	0.829E-02	0.646E-02	*0.162E-01	*0.131E-01
	300000.	0.277E-01	0.281E-02	0.895E-02	0.691E-02	*0.178E-01	*0.142E-01
	500000.	0.245E-01	0.228E-02	0.104E-01	0.768E-02	*0.198E-01	*0.157E-01
P V 4P 7D	50000.	0.603E-01	0.573E-02	*0.921E-02	*0.742E-02		
615.1 Å	100000.	0.518E-01	0.580E-02	*0.114E-01	*0.920E-02		
C= 0.54E+18	150000.	0.474E-01	0.555E-02	*0.127E-01	*0.100E-01		
	200000.	0.445E-01	0.505E-02	0.132E-01	0.106E-01		
	300000.	0.406E-01	0.440E-02	0.143E-01	0.115E-01		
	500000.	0.360E-01	0.367E-02	0.160E-01	0.124E-01	*0.314E-01	*0.252E-01
P V 5P 5D	50000.	1.45	0.555E-01	0.130	0.800E-01	*0.258	*0.154
5143.7 Å	100000.	1.19	0.432E-01	0.159	0.101	0.317	0.201
C= 0.10E+21	150000.	1.07	0.396E-01	0.176	0.113	0.348	0.227
	200000.	0.996	0.425E-01	0.188	0.121	0.374	0.245
	300000.	0.903	0.382E-01	0.206	0.134	0.404	0.269
	500000.	0.803	0.302E-01	0.227	0.147	0.443	0.300
P V 5P 6D	50000.	0.326	0.217E-01	0.376E-01	0.291E-01	*0.750E-01	*0.546E-01
1830.1 Å	100000.	0.273	0.199E-01	0.462E-01	0.359E-01	*0.932E-01	*0.708E-01
C= 0.75E+19	150000.	0.247	0.201E-01	0.519E-01	0.400E-01	*0.103	*0.804E-01
	200000.	0.231	0.190E-01	0.565E-01	0.428E-01	*0.111	*0.866E-01
	300000.	0.210	0.166E-01	0.622E-01	0.463E-01	*0.120	*0.936E-01
	500000.	0.187	0.132E-01	0.703E-01	0.510E-01	*0.135	*0.105
P V 5P 7D	50000.	0.293	0.254E-01	*0.430E-01	*0.340E-01		
1320.3 Å	100000.	0.252	0.255E-01	*0.531E-01	*0.423E-01		
C= 0.25E+19	150000.	0.231	0.242E-01	*0.587E-01	*0.461E-01		
	200000.	0.217	0.221E-01	*0.615E-01	*0.485E-01		
	300000.	0.199	0.191E-01	0.660E-01	0.526E-01		
	500000.	0.177	0.158E-01	0.743E-01	0.567E-01	*0.144	*0.115
P V 6P 6D	50000.	10.3	0.470	1.13	0.722	* 2.25	* 1.36
9310.3 Å	100000.	8.81	0.370	1.36	0.895	* 2.69	* 1.76
C= 0.20E+21	150000.	8.04	0.406	1.48	0.985	* 2.96	* 1.99
	200000.	7.54	0.371	1.59	1.07	* 3.09	* 2.13
	300000.	6.90	0.316	1.71	1.15	* 3.30	* 2.31
	500000.	6.18	0.226	1.92	1.29	* 3.57	* 2.58

PERTURBER DENSITY = 1xE+17cm-3

PERTURBERS ARE:		ELECTRONS		PROTONS		He III	
TRANSITION	T(K)	WIDTH(Å)	SHIFT(Å)	WIDTH(Å)	SHIFT(Å)	WIDTH(Å)	SHIFT(Å)
P V 6P 7D	50000.	1.86	0.133	*0.254	*0.190		
3140.9 Å	100000.	1.61	0.128	*0.310	*0.237		
C= 0.14E+20	150000.	1.48	0.124	*0.339	*0.257		
	200000.	1.40	0.111	*0.357	*0.272		
	300000.	1.28	0.951E-01	0.383	0.293		
	500000.	1.14	0.764E-01	0.432	0.317	*0.837	*0.646
P V 3D 4P	50000.	0.130E-01	0.222E-03	0.635E-03	0.103E-03	0.124E-02	0.202E-03
998.5 Å	100000.	0.964E-02	0.218E-03	0.938E-03	0.178E-03	0.185E-02	0.355E-03
C= 0.31E+20	150000.	0.823E-02	0.239E-03	0.111E-02	0.224E-03	0.220E-02	0.452E-03
	200000.	0.743E-02	0.271E-03	0.117E-02	0.257E-03	0.233E-02	0.518E-03
	300000.	0.652E-02	0.280E-03	0.127E-02	0.308E-03	0.252E-02	0.622E-03
	500000.	0.564E-02	0.257E-03	0.138E-02	0.354E-03	0.275E-02	0.715E-03
P V 3D 5P	50000.	0.764E-02	0.239E-03	0.708E-03	0.136E-03	0.139E-02	0.264E-03
534.8 Å	100000.	0.615E-02	0.271E-03	0.895E-03	0.199E-03	0.178E-02	0.396E-03
C= 0.42E+19	150000.	0.549E-02	0.300E-03	0.968E-03	0.239E-03	0.193E-02	0.482E-03
	200000.	0.508E-02	0.275E-03	0.102E-02	0.258E-03	0.203E-02	0.523E-03
	300000.	0.460E-02	0.271E-03	0.108E-02	0.288E-03	0.216E-02	0.582E-03
	500000.	0.410E-02	0.251E-03	0.115E-02	0.329E-03	0.229E-02	0.664E-03
P V 3D 6P	50000.	0.100E-01	0.389E-03	0.127E-02	0.249E-03	*0.252E-02	*0.483E-03
433.1 Å	100000.	0.845E-02	0.505E-03	0.145E-02	0.344E-03	*0.288E-02	*0.686E-03
C= 0.15E+19	150000.	0.771E-02	0.453E-03	0.155E-02	0.382E-03	*0.309E-02	*0.773E-03
	200000.	0.724E-02	0.449E-03	0.162E-02	0.413E-03	0.323E-02	0.835E-03
	300000.	0.666E-02	0.430E-03	0.168E-02	0.457E-03	0.336E-02	0.925E-03
	500000.	0.603E-02	0.418E-03	0.176E-02	0.520E-03	0.349E-02	0.105E-02
P V 4D 5P	50000.	0.165	0.806E-03	0.134E-01	-0.166E-02	0.264E-01	-0.324E-02
2183.7 Å	100000.	0.133	0.123E-02	0.166E-01	-0.249E-02	0.329E-01	-0.497E-02
C= 0.34E+20	150000.	0.119	0.194E-02	0.179E-01	-0.304E-02	0.356E-01	-0.613E-02
	200000.	0.110	0.157E-02	0.188E-01	-0.337E-02	0.373E-01	-0.684E-02
	300000.	0.995E-01	0.147E-02	0.201E-01	-0.375E-02	0.398E-01	-0.760E-02
	500000.	0.885E-01	0.151E-02	0.213E-01	-0.429E-02	0.419E-01	-0.865E-02
P V 4D 6P	50000.	0.756E-01	0.166E-02	0.870E-02	0.985E-03	*0.172E-01	*0.192E-02
1114.9 Å	100000.	0.635E-01	0.245E-02	0.986E-02	0.139E-02	*0.196E-01	*0.276E-02
C= 0.89E+19	150000.	0.578E-01	0.217E-02	0.105E-01	0.159E-02	*0.210E-01	*0.322E-02
	200000.	0.542E-01	0.217E-02	0.110E-01	0.172E-02	0.219E-01	0.348E-02
	300000.	0.498E-01	0.205E-02	0.114E-01	0.192E-02	0.227E-01	0.386E-02
	500000.	0.450E-01	0.207E-02	0.119E-01	0.218E-02	0.234E-01	0.441E-02
P V 5D 6P	50000.	1.33	-0.166E-01	0.135	-0.404E-01	*0.268	*-0.780E-01
4088.1 Å	100000.	1.12	0.867E-03	0.155	-0.517E-01	*0.308	*-0.103
C= 0.64E+20	150000.	1.02	-0.298E-02	0.166	-0.581E-01	*0.330	*-0.117
	200000.	0.957	-0.344E-02	0.174	-0.625E-01	*0.345	*-0.126
	300000.	0.877	-0.189E-02	0.182	-0.691E-01	0.358	-0.139
	500000.	0.789	0.340E-02	0.193	-0.760E-01	0.373	-0.155
P V 3D 4F	50000.	0.601E-02	-0.125E-03	0.261E-03	-0.228E-03	0.511E-03	-0.444E-03
673.9 Å	100000.	0.448E-02	-0.109E-03	0.418E-03	-0.333E-03	0.827E-03	-0.663E-03
C= 0.33E+19	150000.	0.383E-02	-0.110E-03	0.522E-03	-0.398E-03	0.104E-02	-0.803E-03
	200000.	0.346E-02	-0.829E-04	0.570E-03	-0.428E-03	0.113E-02	-0.867E-03
	300000.	0.303E-02	-0.640E-04	0.654E-03	-0.477E-03	0.128E-02	-0.967E-03
	500000.	0.261E-02	-0.635E-04	0.764E-03	-0.546E-03	0.147E-02	-0.110E-02
P V 3D 5F	50000.	0.116E-01	0.126E-03	0.385E-02	0.349E-02		
475.6 Å	100000.	0.923E-02	0.106E-03	0.535E-02	0.434E-02		
C= 0.50E+17	150000.	0.813E-02	0.158E-03	0.654E-02	0.469E-02		
	200000.	0.743E-02	0.140E-03	0.739E-02	0.494E-02	*0.115E-01	*0.101E-01
	300000.	0.657E-02	0.144E-03	0.857E-02	0.539E-02	*0.127E-01	*0.108E-01
	500000.	0.563E-02	0.112E-03	0.103E-01	0.594E-02	*0.142E-01	*0.120E-01

PERTURBER DENSITY = 1xE+17cm-3

PERTURBERS ARE: TRANSITION	T(K)	ELECTRONS WIDTH(Å)	ELECTRONS SHIFT(Å)	PROTONS WIDTH(Å)	PROTONS SHIFT(Å)	He III WIDTH(Å)	He III SHIFT(Å)
P V 3D 6F	50000.	0.221E-01	0.136E-03				
410.0 Å	100000.	0.179E-01	0.163E-03				
C= 0.24E+17	150000.	0.158E-01	0.328E-03	*0.147E-01	*0.103E-01		
	200000.	0.144E-01	0.262E-03	*0.164E-01	*0.109E-01		
	300000.	0.127E-01	0.390E-03	*0.187E-01	*0.118E-01		
	500000.	0.109E-01	0.287E-03	*0.222E-01	*0.127E-01		
P V 4D 5F	50000.	0.124	-0.169E-03	0.354E-01	0.319E-01		
1447.9 Å	100000.	0.991E-01	-0.430E-03	0.492E-01	0.395E-01		
C= 0.46E+18	150000.	0.874E-01	0.142E-03	0.604E-01	0.428E-01		
	200000.	0.801E-01	-0.131E-04	0.686E-01	0.455E-01	*0.105	*0.925E-01
	300000.	0.709E-01	0.684E-05	0.791E-01	0.491E-01	*0.116	*0.992E-01
	500000.	0.611E-01	-0.133E-03	0.951E-01	0.541E-01	*0.131	*0.109
P V 4D 6F	50000.	0.132	0.162E-03				
973.8 Å	100000.	0.106	0.280E-03				
C= 0.13E+18	150000.	0.940E-01	0.125E-02	*0.829E-01	*0.581E-01		
	200000.	0.861E-01	0.882E-03	*0.922E-01	*0.615E-01		
	300000.	0.762E-01	0.160E-02	*0.106	*0.664E-01		
	500000.	0.652E-01	0.109E-02	*0.125	*0.711E-01		
P V 5D 6F	50000.	1.13	-0.149E-01				
2670.0 Å	100000.	0.916	-0.114E-01				
C= 0.10E+19	150000.	0.812	-0.417E-02	*0.628	*0.430		
	200000.	0.745	-0.716E-02	*0.692	*0.454		
	300000.	0.661	-0.453E-03	*0.803	*0.492		
	500000.	0.569	-0.219E-02	*0.948	*0.529		
P V 4F 5D	50000.	0.134	0.939E-02	0.120E-01	0.104E-01	0.239E-01	0.200E-01
1722.9 Å	100000.	0.108	0.830E-02	0.158E-01	0.130E-01	0.317E-01	0.258E-01
C= 0.11E+20	150000.	0.954E-01	0.823E-02	0.178E-01	0.144E-01	0.354E-01	0.291E-01
	200000.	0.879E-01	0.813E-02	0.196E-01	0.155E-01	0.385E-01	0.313E-01
	300000.	0.788E-01	0.749E-02	0.219E-01	0.171E-01	0.430E-01	0.344E-01
	500000.	0.692E-01	0.640E-02	0.254E-01	0.190E-01	0.480E-01	0.386E-01
P V 4F 6D	50000.	0.102	0.871E-02	0.125E-01	0.103E-01	*0.248E-01	*0.193E-01
1072.4 Å	100000.	0.850E-01	0.818E-02	0.155E-01	0.128E-01	*0.310E-01	*0.249E-01
C= 0.26E+19	150000.	0.765E-01	0.836E-02	0.174E-01	0.141E-01	*0.349E-01	*0.286E-01
	200000.	0.711E-01	0.782E-02	0.193E-01	0.150E-01	*0.379E-01	*0.307E-01
	300000.	0.644E-01	0.696E-02	0.208E-01	0.162E-01	*0.417E-01	*0.331E-01
	500000.	0.569E-01	0.571E-02	0.240E-01	0.178E-01	*0.465E-01	*0.367E-01
P V 4F 7D	50000.	0.122	0.120E-01	*0.187E-01	*0.151E-01		
874.6 Å	100000.	0.105	0.121E-01	*0.232E-01	*0.187E-01		
C= 0.11E+19	150000.	0.963E-01	0.116E-01	*0.258E-01	*0.203E-01		
	200000.	0.903E-01	0.106E-01	0.269E-01	0.215E-01		
	300000.	0.823E-01	0.922E-02	0.290E-01	0.235E-01		
	500000.	0.731E-01	0.773E-02	0.330E-01	0.255E-01	*0.638E-01	*0.511E-01
P V 5F 6D	50000.	1.24	0.686E-01	0.143	-0.103	*0.249	*-0.192
3187.7 Å	100000.	1.03	0.651E-01	0.199	-0.127	*0.317	*-0.249
C= 0.22E+19	150000.	0.924	0.643E-01	0.240	-0.140	*0.360	*-0.284
	200000.	0.857	0.610E-01	0.275	-0.149	*0.385	*-0.303
	300000.	0.771	0.536E-01	0.330	-0.164	*0.429	*-0.329
	500000.	0.676	0.440E-01	0.399	-0.177	*0.489	*-0.356
P V 5F 7D	50000.	0.700	0.542E-01	*0.668E-01	*0.303E-01		
1905.9 Å	100000.	0.597	0.549E-01	0.862E-01	0.376E-01		
C= 0.80E+18	150000.	0.544	0.517E-01	0.100	0.414E-01	*0.153	*0.836E-01
	200000.	0.509	0.473E-01	0.112	0.448E-01	*0.161	*0.896E-01
	300000.	0.462	0.410E-01	0.130	0.484E-01	*0.172	*0.971E-01
	500000.	0.408	0.344E-01	0.160	0.541E-01	*0.194	*0.109

PERTURBER DENSITY = 1xE+18cm-3

PERTURBERS ARE:		ELECTRONS		PROTONS		He III	
TRANSITION	T(K)	WIDTH(Å)	SHIFT(Å)	WIDTH(Å)	SHIFT(Å)	WIDTH(Å)	SHIFT(Å)
P V 3S 3P	50000.	0.626E-01	-0.595E-03	0.631E-03	-0.252E-03	0.121E-02	-0.469E-03
1121.8 Å	100000.	0.447E-01	-0.742E-03	0.136E-02	-0.510E-03	0.265E-02	-0.992E-03
C= 0.11E+22	150000.	0.371E-01	-0.587E-03	0.190E-02	-0.708E-03	0.373E-02	-0.141E-02
	200000.	0.328E-01	-0.711E-03	0.224E-02	-0.874E-03	0.443E-02	-0.174E-02
	300000.	0.278E-01	-0.872E-03	0.278E-02	-0.108E-02	0.550E-02	-0.218E-02
	500000.	0.232E-01	-0.763E-03	0.329E-02	-0.138E-02	0.657E-02	-0.279E-02
P V 3S 4P	50000.	0.139E-01	0.176E-03	0.616E-03	0.839E-04	0.119E-02	0.156E-03
328.6 Å	100000.	0.103E-01	0.164E-03	0.923E-03	0.154E-03	0.181E-02	0.299E-03
C= 0.34E+20	150000.	0.877E-02	0.199E-03	0.110E-02	0.200E-03	0.218E-02	0.399E-03
	200000.	0.792E-02	0.223E-03	0.117E-02	0.228E-03	0.233E-02	0.454E-03
	300000.	0.693E-02	0.220E-03	0.127E-02	0.277E-03	0.252E-02	0.560E-03
	500000.	0.598E-02	0.206E-03	0.138E-02	0.320E-03	0.275E-02	0.647E-03
P V 3S 5P	50000.	0.175E-01	0.478E-03	0.157E-02	0.279E-03	*0.301E-02	*0.515E-03
255.6 Å	100000.	0.140E-01	0.555E-03	0.200E-02	0.431E-03	*0.396E-02	*0.828E-03
C= 0.95E+19	150000.	0.125E-01	0.636E-03	0.217E-02	0.522E-03	*0.431E-02	*0.104E-02
	200000.	0.116E-01	0.577E-03	0.228E-02	0.573E-03	*0.453E-02	*0.114E-02
	300000.	0.105E-01	0.561E-03	0.243E-02	0.637E-03	*0.484E-02	*0.129E-02
	500000.	0.934E-02	0.527E-03	0.258E-02	0.727E-03	*0.514E-02	*0.148E-02
P V 3S 6P	50000.	0.282E-01	0.975E-03	*0.351E-02	*0.635E-03		
229.8 Å	100000.	0.238E-01	0.133E-02	*0.403E-02	*0.937E-03		
C= 0.42E+19	150000.	0.217E-01	0.120E-02	*0.432E-02	*0.105E-02		
	200000.	0.204E-01	0.120E-02	*0.452E-02	*0.115E-02		
	300000.	0.187E-01	0.115E-02	0.471E-02	0.127E-02		
	500000.	0.170E-01	0.114E-02	0.492E-02	0.145E-02		
P V 4S 4P	50000.	1.70	-0.397E-01	0.598E-01	-0.244E-01	0.116	-0.453E-01
3185.6 Å	100000.	1.27	-0.393E-01	0.907E-01	-0.399E-01	0.178	-0.773E-01
C= 0.32E+22	150000.	1.10	-0.479E-01	0.109	-0.488E-01	0.217	-0.974E-01
	200000.	0.997	-0.480E-01	0.117	-0.557E-01	0.233	-0.111
	300000.	0.882	-0.429E-01	0.128	-0.618E-01	0.255	-0.125
	500000.	0.767	-0.422E-01	0.142	-0.714E-01	0.283	-0.144
P V 4S 5P	50000.	0.217	0.104E-02	0.170E-01	0.115E-02	*0.328E-01	*0.213E-02
845.8 Å	100000.	0.174	0.211E-02	0.217E-01	0.197E-02	*0.430E-01	*0.383E-02
C= 0.10E+21	150000.	0.156	0.221E-02	0.235E-01	0.240E-02	*0.467E-01	*0.478E-02
	200000.	0.144	0.139E-02	0.246E-01	0.278E-02	*0.490E-01	*0.553E-02
	300000.	0.131	0.162E-02	0.262E-01	0.320E-02	*0.522E-01	*0.649E-02
	500000.	0.117	0.141E-02	0.278E-01	0.366E-02	*0.553E-01	*0.739E-02
P V 4S 6P	50000.	0.218	0.432E-02	*0.252E-01	*0.393E-02		
616.8 Å	100000.	0.183	0.729E-02	*0.289E-01	*0.582E-02		
C= 0.30E+20	150000.	0.166	0.593E-02	*0.310E-01	*0.650E-02		
	200000.	0.156	0.587E-02	*0.324E-01	*0.716E-02		
	300000.	0.144	0.584E-02	0.337E-01	0.793E-02		
	500000.	0.130	0.585E-02	0.349E-01	0.904E-02	*0.694E-01	*0.182E-01
P V 5S 5P	50000.	18.8	-0.667	1.20	-0.539	* 2.32	-0.977
6872.7 Å	100000.	15.3	-0.835	1.56	-0.797	* 3.09	-1.51
C= 0.69E+22	150000.	13.8	-0.778	1.71	-0.890	* 3.42	-1.77
	200000.	12.8	-0.798	1.82	-0.981	* 3.65	-1.93
	300000.	11.6	-0.772	1.99	-1.09	* 3.98	-2.20
	500000.	10.4	-0.765	2.15	-1.23	* 4.31	-2.50
P V 5S 6P	50000.	1.93	-0.121E-01	*0.193	-0.980E-02		
1710.8 Å	100000.	1.63	-0.384E-02	*0.221	-0.154E-01		
C= 0.23E+21	150000.	1.49	-0.115E-01	*0.237	-0.189E-01		
	200000.	1.40	-0.983E-02	*0.247	-0.212E-01		
	300000.	1.29	-0.945E-02	0.257	-0.236E-01		
	500000.	1.16	-0.813E-02	0.266	-0.269E-01	*0.526	-0.545E-01

PERTURBER DENSITY = 1xE+18cm-3

PERTURBERS ARE: TRANSITION	T(K)	ELECTRONS WIDTH(Å)	ELECTRONS SHIFT(Å)	PROTONS WIDTH(Å)	PROTONS SHIFT(Å)	He III WIDTH(Å)	He III SHIFT(Å)
P V 3P 4S	50000.	0.277E-01	0.189E-02	0.442E-03	0.937E-03	0.867E-03	0.173E-02
544.0 Å	100000.	0.203E-01	0.183E-02	0.103E-02	0.148E-02	0.207E-02	0.286E-02
C= 0.93E+20	150000.	0.173E-01	0.212E-02	0.142E-02	0.182E-02	0.284E-02	0.362E-02
	200000.	0.155E-01	0.221E-02	0.182E-02	0.204E-02	0.363E-02	0.407E-02
	300000.	0.136E-01	0.208E-02	0.219E-02	0.227E-02	0.440E-02	0.460E-02
	500000.	0.116E-01	0.199E-02	0.263E-02	0.259E-02	0.536E-02	0.525E-02
P V 3P 5S	50000.	0.251E-01	0.305E-02	0.116E-02	0.169E-02	*0.234E-02	*0.303E-02
347.8 Å	100000.	0.194E-01	0.344E-02	0.214E-02	0.247E-02	*0.429E-02	*0.466E-02
C= 0.18E+20	150000.	0.169E-01	0.337E-02	0.261E-02	0.276E-02	*0.523E-02	*0.549E-02
	200000.	0.155E-01	0.328E-02	0.292E-02	0.303E-02	*0.591E-02	*0.594E-02
	300000.	0.137E-01	0.316E-02	0.334E-02	0.335E-02	*0.686E-02	*0.678E-02
	500000.	0.118E-01	0.304E-02	0.400E-02	0.381E-02	*0.792E-02	*0.769E-02
P V 3P 6S	50000.	0.382E-01	0.711E-02	0.325E-02	0.359E-02		
295.8 Å	100000.	0.311E-01	0.699E-02	0.468E-02	0.479E-02		
C= 0.69E+19	150000.	0.277E-01	0.661E-02	0.542E-02	0.538E-02		
	200000.	0.254E-01	0.638E-02	0.601E-02	0.598E-02		
	300000.	0.227E-01	0.614E-02	0.691E-02	0.644E-02		
	500000.	0.198E-01	0.567E-02	0.790E-02	0.709E-02	*0.159E-01	*0.145E-01
P V 3P 7S	50000.	0.614E-01	0.175E-01	*0.741E-02	*0.655E-02		
272.9 Å	100000.	0.524E-01	0.149E-01	*0.965E-02	*0.911E-02		
C= 0.36E+19	150000.	0.471E-01	0.132E-01	*0.109E-01	*0.102E-01		
	200000.	0.438E-01	0.124E-01	*0.121E-01	*0.113E-01		
	300000.	0.396E-01	0.118E-01	*0.139E-01	*0.122E-01		
	500000.	0.349E-01	0.103E-01	*0.149E-01	*0.134E-01		
P V 4P 5S	50000.	0.522	0.403E-01	0.221E-01	0.258E-01	*0.440E-01	*0.464E-01
1383.2 Å	100000.	0.406	0.483E-01	0.376E-01	0.378E-01	*0.754E-01	*0.716E-01
C= 0.28E+21	150000.	0.356	0.474E-01	0.445E-01	0.424E-01	*0.895E-01	*0.840E-01
	200000.	0.327	0.458E-01	0.491E-01	0.463E-01	*0.995E-01	*0.911E-01
	300000.	0.292	0.442E-01	0.564E-01	0.514E-01	*0.112	*0.104
	500000.	0.255	0.429E-01	0.647E-01	0.583E-01	*0.131	*0.117
P V 4P 6S	50000.	0.326	0.496E-01	*0.252E-01	*0.270E-01		
814.1 Å	100000.	0.265	0.498E-01	*0.358E-01	*0.359E-01		
C= 0.52E+20	150000.	0.237	0.475E-01	0.414E-01	0.404E-01		
	200000.	0.219	0.457E-01	0.455E-01	0.450E-01		
	300000.	0.197	0.442E-01	0.527E-01	0.486E-01		
	500000.	0.173	0.410E-01	0.606E-01	0.535E-01	*0.121	*0.108
P V 4P 7S	50000.	0.383	0.956E-01	*0.436E-01	*0.384E-01		
661.1 Å	100000.	0.326	0.832E-01	*0.568E-01	*0.534E-01		
C= 0.21E+20	150000.	0.294	0.756E-01	*0.640E-01	*0.597E-01		
	200000.	0.274	0.685E-01	*0.711E-01	*0.662E-01		
	300000.	0.248	0.662E-01	*0.816E-01	*0.713E-01		
	500000.	0.220	0.579E-01	*0.873E-01	*0.785E-01		
P V 5P 6S	50000.	4.63	0.491	*0.347	*0.303		
2778.6 Å	100000.	3.88	0.506	*0.461	*0.404		
C= 0.61E+21	150000.	3.53	0.478	*0.525	*0.455		
	200000.	3.29	0.471	0.568	0.502		
	300000.	2.99	0.459	0.655	0.548		
	500000.	2.67	0.428	0.726	0.603		
P V 5P 7S	50000.	2.34	0.450	*0.245	*0.210		
1552.6 Å	100000.	2.02	0.416	*0.319	*0.292		
C= 0.11E+21	150000.	1.85	0.366	*0.361	*0.326		
	200000.	1.73	0.354	*0.399	*0.362		
	300000.	1.58	0.344	*0.452	*0.392		
	500000.	1.41	0.302	*0.488	*0.427		

PERTURBER DENSITY = 1xE+18cm-3

PERTURBERS ARE:		ELECTRONS		PROTONS		He III	
TRANSITION	T(K)	WIDTH(Å)	SHIFT(Å)	WIDTH(Å)	SHIFT(Å)	WIDTH(Å)	SHIFT(Å)
P V 3P 3D	50000.	0.434E-01	-0.340E-04	0.883E-03	-0.138E-04	0.169E-02	-0.258E-04
869.1 Å	100000.	0.311E-01	-0.290E-04	0.168E-02	-0.292E-04	0.328E-02	-0.567E-04
C= 0.67E+21	150000.	0.259E-01	-0.320E-04	0.214E-02	-0.438E-04	0.422E-02	-0.870E-04
	200000.	0.229E-01	-0.276E-04	0.248E-02	-0.580E-04	0.488E-02	-0.115E-03
	300000.	0.195E-01	-0.558E-04	0.292E-02	-0.831E-04	0.579E-02	-0.167E-03
	500000.	0.163E-01	-0.412E-04	0.322E-02	-0.121E-03	0.641E-02	-0.243E-03
P V 3P 4D	50000.	0.252E-01	0.867E-03	0.130E-02	0.106E-02	0.253E-02	0.194E-02
390.2 Å	100000.	0.191E-01	0.963E-03	0.201E-02	0.157E-02	0.397E-02	0.300E-02
C= 0.11E+20	150000.	0.165E-01	0.901E-03	0.240E-02	0.183E-02	0.478E-02	0.365E-02
	200000.	0.150E-01	0.903E-03	0.264E-02	0.200E-02	0.524E-02	0.395E-02
	300000.	0.132E-01	0.933E-03	0.297E-02	0.222E-02	0.588E-02	0.449E-02
	500000.	0.114E-01	0.836E-03	0.345E-02	0.253E-02	0.672E-02	0.512E-02
P V 3P 5D	50000.	0.385E-01	0.247E-02	0.361E-02	0.283E-02		
311.0 Å	100000.	0.310E-01	0.224E-02	0.481E-02	0.382E-02		
C= 0.37E+19	150000.	0.274E-01	0.224E-02	0.544E-02	0.427E-02		
	200000.	0.253E-01	0.233E-02	0.597E-02	0.473E-02		
	300000.	0.227E-01	0.221E-02	0.673E-02	0.522E-02	*0.132E-01	*0.106E-01
	500000.	0.199E-01	0.193E-02	0.754E-02	0.576E-02	*0.147E-01	*0.117E-01
P V 3P 6D	50000.	0.659E-01	0.471E-02	*0.825E-02	*0.583E-02		
280.3 Å	100000.	0.549E-01	0.462E-02	*0.104E-01	*0.809E-02		
C= 0.18E+19	150000.	0.494E-01	0.484E-02	*0.118E-01	*0.912E-02		
	200000.	0.460E-01	0.472E-02	*0.130E-01	*0.101E-01		
	300000.	0.416E-01	0.436E-02	*0.140E-01	*0.108E-01		
	500000.	0.367E-01	0.375E-02	*0.163E-01	*0.120E-01		
P V 3P 7D	50000.	0.108	0.783E-02				
264.7 Å	100000.	0.934E-01	0.870E-02				
C= 0.10E+19	150000.	0.856E-01	0.847E-02				
	200000.	0.803E-01	0.812E-02				
	300000.	0.733E-01	0.754E-02				
	500000.	0.650E-01	0.687E-02				
P V 4P 4D	50000.	1.31	0.214E-01	0.702E-01	0.376E-01	*0.137	*0.691E-01
2436.0 Å	100000.	1.000	0.250E-01	0.102	0.560E-01	*0.202	*0.107
C= 0.43E+21	150000.	0.869	0.214E-01	0.114	0.659E-01	*0.227	*0.132
	200000.	0.792	0.196E-01	0.124	0.716E-01	*0.246	*0.142
	300000.	0.703	0.202E-01	0.137	0.800E-01	0.269	0.161
	500000.	0.613	0.177E-01	0.155	0.908E-01	0.300	0.184
P V 4P 5D	50000.	0.394	0.207E-01	*0.348E-01	*0.255E-01		
940.9 Å	100000.	0.315	0.186E-01	0.455E-01	0.345E-01		
C= 0.34E+20	150000.	0.280	0.184E-01	0.513E-01	0.387E-01		
	200000.	0.258	0.190E-01	0.559E-01	0.428E-01		
	300000.	0.232	0.178E-01	0.628E-01	0.473E-01	*0.122	*0.953E-01
	500000.	0.204	0.154E-01	0.700E-01	0.519E-01	*0.135	*0.105
P V 4P 6D	50000.	0.441	0.287E-01	*0.530E-01	*0.370E-01		
706.8 Å	100000.	0.366	0.282E-01	*0.664E-01	*0.512E-01		
C= 0.11E+20	150000.	0.329	0.296E-01	*0.757E-01	*0.579E-01		
	200000.	0.306	0.287E-01	*0.829E-01	*0.642E-01		
	300000.	0.277	0.263E-01	*0.895E-01	*0.686E-01		
	500000.	0.245	0.226E-01	*0.104	*0.765E-01		
P V 4P 7D	50000.	0.601	0.413E-01				
615.1 Å	100000.	0.517	0.461E-01				
C= 0.54E+19	150000.	0.473	0.448E-01				
	200000.	0.444	0.428E-01				
	300000.	0.405	0.397E-01				
	500000.	0.360	0.361E-01				

PERTURBER DENSITY = 1xE+18cm-3

PERTURBERS ARE: TRANSITION	T(K)	ELECTRONS WIDTH(Å)	ELECTRONS SHIFT(Å)	PROTONS WIDTH(Å)	PROTONS SHIFT(Å)	He III WIDTH(Å)	He III SHIFT(Å)
P V 5P 5D	50000.	14.5	0.477	* 1.29	*0.715	-	
5143.7 Å	100000.	11.9	0.375	* 1.59	*0.977		
C= 0.10E+22	150000.	10.7	0.345	* 1.75	* 1.10		
	200000.	9.96	0.390	1.88	1.20		
	300000.	9.03	0.361	2.06	1.33		
	500000.	8.03	0.299	2.27	1.46	* 4.43	* 2.99
P V 5P 6D	50000.	3.26	0.175	*0.371	*0.244		
1830.1 Å	100000.	2.73	0.166	*0.461	*0.339		
C= 0.75E+20	150000.	2.47	0.172	*0.520	*0.384		
	200000.	2.31	0.170	*0.564	*0.425		
	300000.	2.10	0.155	*0.622	*0.460		
	500000.	1.87	0.131	*0.703	*0.508		
P V 5P 7D	50000.	* 2.92	*0.180				
1320.3 Å	100000.	2.52	0.200				
C= 0.25E+20	150000.	2.31	0.193				
	200000.	2.17	0.186				
	300000.	1.98	0.171				
	500000.	1.77	0.156				
P V 6P 7D	50000.	* 18.5	*0.926				
3140.9 Å	100000.	16.1	0.974				
C= 0.14E+21	150000.	14.8	0.968				
	200000.	13.9	0.917				
	300000.	12.8	0.841				
	500000.	11.4	0.749				
P V 3D 4P	50000.	0.130	0.218E-02	0.633E-02	0.976E-03	0.122E-01	0.182E-02
998.5 Å	100000.	0.964E-01	0.217E-02	0.938E-02	0.176E-02	0.184E-01	0.341E-02
C= 0.31E+21	150000.	0.823E-01	0.236E-02	0.111E-01	0.222E-02	0.219E-01	0.443E-02
	200000.	0.743E-01	0.267E-02	0.117E-01	0.257E-02	0.233E-01	0.511E-02
	300000.	0.652E-01	0.280E-02	0.127E-01	0.307E-02	0.252E-01	0.621E-02
	500000.	0.564E-01	0.257E-02	0.138E-01	0.353E-02	0.275E-01	0.714E-02
P V 3D 5P	50000.	0.764E-01	0.231E-02	0.702E-02	0.127E-02	*0.135E-01	*0.234E-02
534.8 Å	100000.	0.615E-01	0.264E-02	0.894E-02	0.195E-02	*0.177E-01	*0.375E-02
C= 0.42E+20	150000.	0.549E-01	0.295E-02	0.967E-02	0.236E-02	*0.192E-01	*0.469E-02
	200000.	0.508E-01	0.272E-02	0.102E-01	0.257E-02	*0.202E-01	*0.513E-02
	300000.	0.460E-01	0.269E-02	0.108E-01	0.287E-02	*0.216E-01	*0.580E-02
	500000.	0.410E-01	0.250E-02	0.115E-01	0.328E-02	*0.229E-01	*0.662E-02
P V 3D 6P	50000.	0.100	0.366E-02	*0.126E-01	*0.228E-02		
433.1 Å	100000.	0.845E-01	0.491E-02	*0.144E-01	*0.335E-02		
C= 0.15E+20	150000.	0.771E-01	0.440E-02	*0.155E-01	*0.375E-02		
	200000.	0.724E-01	0.439E-02	*0.162E-01	*0.411E-02		
	300000.	0.666E-01	0.426E-02	0.168E-01	0.456E-02		
	500000.	0.603E-01	0.417E-02	0.176E-01	0.519E-02		
P V 4D 5P	50000.	1.65	0.915E-02	0.133	-0.155E-01	*0.256	-0.287E-01
2183.7 Å	100000.	1.33	0.128E-01	0.165	-0.244E-01	*0.327	-0.472E-01
C= 0.34E+21	150000.	1.19	0.202E-01	0.179	-0.301E-01	*0.355	-0.599E-01
	200000.	1.10	0.163E-01	0.188	-0.337E-01	*0.373	-0.671E-01
	300000.	0.995	0.149E-01	0.201	-0.375E-01	*0.398	-0.759E-01
	500000.	0.885	0.152E-01	0.213	-0.428E-01	*0.419	-0.862E-01
P V 4D 6P	50000.	0.756	0.157E-01	*0.858E-01	*0.913E-02		
1114.9 Å	100000.	0.635	0.240E-01	*0.983E-01	*0.136E-01		
C= 0.89E+20	150000.	0.578	0.212E-01	*0.105	*0.156E-01		
	200000.	0.542	0.213E-01	*0.110	*0.172E-01		
	300000.	0.498	0.203E-01	0.114	0.191E-01		
	500000.	0.450	0.207E-01	0.119	0.218E-01		

PERTURBER DENSITY = 1xE+18cm-3

PERTURBERS ARE: TRANSITION	T(K)	ELECTRONS WIDTH(Å)	ELECTRONS SHIFT(Å)	PROTONS WIDTH(Å)	PROTONS SHIFT(Å)	He III WIDTH(Å)	He III SHIFT(Å)
P V 5D 6P	50000.	13.3	-0.132	* 1.33	-0.364		
4088.1 Å	100000.	11.2	0.357E-01	* 1.54	-0.501		
C= 0.64E+21	150000.	10.2	-0.668E-02	* 1.66	-0.567		
	200000.	9.57	-0.191E-01	* 1.74	-0.623		
	300000.	8.77	-0.827E-02	1.82	-0.689		
	500000.	7.89	0.353E-01	1.93	-0.758		
P V 3D 4F	50000.	0.601E-01	-0.108E-02	0.260E-02	-0.213E-02	0.506E-02	-0.392E-02
673.9 Å	100000.	0.448E-01	-0.962E-03	0.418E-02	-0.326E-02	0.826E-02	-0.626E-02
C= 0.33E+20	150000.	0.383E-01	-0.103E-02	0.522E-02	-0.392E-02	0.104E-01	-0.782E-02
	200000.	0.346E-01	-0.789E-03	0.570E-02	-0.427E-02	0.113E-01	-0.848E-02
	300000.	0.303E-01	-0.595E-03	0.654E-02	-0.476E-02	0.128E-01	-0.964E-02
	500000.	0.261E-01	-0.629E-03	0.764E-02	-0.545E-02	0.147E-01	-0.110E-01
P V 3D 5F	50000.	0.108	-0.231E-02				
475.6 Å	100000.	0.870E-01	-0.169E-02				
C= 0.50E+18	150000.	0.769E-01	-0.123E-02				
	200000.	0.706E-01	-0.809E-03				
	300000.	0.626E-01	-0.101E-03				
	500000.	0.540E-01	0.831E-03				
P V 3D 6F	50000.	0.195	-0.624E-02				
410.0 Å	100000.	0.160	-0.468E-02				
C= 0.24E+18	150000.	0.143	-0.376E-02				
	200000.	0.131	-0.282E-02				
	300000.	0.117	-0.527E-03				
	500000.	0.101	0.195E-02				
P V 4D 5F	50000.	1.17	-0.336E-01				
1447.9 Å	100000.	0.941	-0.291E-01				
C= 0.46E+19	150000.	0.834	-0.240E-01				
	200000.	0.766	-0.200E-01				
	300000.	0.681	-0.140E-01				
	500000.	0.589	-0.394E-02				
P V 4D 6F	50000.	1.17	-0.407E-01				
973.8 Å	100000.	0.962	-0.325E-01				
C= 0.13E+19	150000.	0.857	-0.269E-01				
	200000.	0.789	-0.216E-01				
	300000.	0.703	-0.887E-02				
	500000.	0.606	0.573E-02				
P V 5D 6F	50000.	10.2	-0.449				
2670.0 Å	100000.	8.38	-0.365				
C= 0.10E+20	150000.	7.49	-0.325				
	200000.	6.91	-0.292				
	300000.	6.17	-0.186				
	500000.	5.35	-0.602E-01				
P V 4F 5D	50000.	1.34	0.831E-01	*0.119	*0.926E-01		
1722.9 Å	100000.	1.08	0.751E-01	0.158	0.125		
C= 0.11E+21	150000.	0.954	0.756E-01	0.178	0.140		
	200000.	0.879	0.767E-01	0.196	0.155		
	300000.	0.788	0.720E-01	0.219	0.170		
	500000.	0.692	0.636E-01	0.254	0.190	*0.479	*0.384
P V 4F 6D	50000.	1.02	0.718E-01	*0.123	*0.867E-01		
1072.4 Å	100000.	0.850	0.701E-01	*0.155	*0.121		
C= 0.26E+20	150000.	0.765	0.734E-01	*0.174	*0.135		
	200000.	0.711	0.711E-01	*0.193	*0.149		
	300000.	0.644	0.654E-01	*0.208	*0.161		
	500000.	0.568	0.566E-01	*0.240	*0.177		

PERTURBER DENSITY = 1xE+18cm-3

PERTURBERS ARE:		ELECTRONS		PROTONS		He III	
TRANSITION	T(K)	WIDTH(Å)	SHIFT(Å)	WIDTH(Å)	SHIFT(Å)	WIDTH(Å)	SHIFT(Å)
P V 4F 7D	50000.	1.22	0.874E-01				
874.6 Å	100000.	1.05	0.966E-01				
C= 0.11E+20	150000.	0.961	0.942E-01				
	200000.	0.901	0.901E-01				
	300000.	0.822	0.834E-01				
	500000.	0.730	0.761E-01				
P V 5F 6D	50000.	12.1	0.715				
3187.7 Å	100000.	10.1	0.674				
C= 0.22E+20	150000.	9.05	0.682				
	200000.	8.40	0.647				
	300000.	7.58	0.569				
	500000.	6.65	0.448				
P V 5F 7D	50000.	* 6.86	*0.444				
1905.9 Å	100000.	5.88	0.479				
C= 0.80E+19	150000.	5.37	0.459				
	200000.	5.02	0.435				
	300000.	4.57	0.393				
	500000.	4.04	0.343				
PERTURBER DENSITY = 1xE+19cm-3							
P V 3S 3P	50000.	0.626	-0.583E-02	0.620E-02	-0.217E-02	0.112E-01	-0.342E-02
1121.8 Å	100000.	0.447	-0.713E-02	0.136E-01	-0.477E-02	0.262E-01	-0.881E-02
C= 0.11E+23	150000.	0.371	-0.564E-02	0.190E-01	-0.686E-02	0.371E-01	-0.131E-01
	200000.	0.328	-0.697E-02	0.224E-01	-0.860E-02	0.441E-01	-0.165E-01
	300000.	0.278	-0.846E-02	0.278E-01	-0.107E-01	0.549E-01	-0.211E-01
	500000.	0.232	-0.750E-02	0.329E-01	-0.138E-01	0.656E-01	-0.276E-01
P V 3S 4P	50000.	0.139	0.161E-02	0.598E-02	0.719E-03	*0.105E-01	*0.113E-02
328.6 Å	100000.	0.103	0.155E-02	0.914E-02	0.142E-02	*0.175E-01	*0.261E-02
C= 0.34E+21	150000.	0.877E-01	0.191E-02	0.110E-01	0.192E-02	*0.214E-01	*0.362E-02
	200000.	0.792E-01	0.218E-02	0.117E-01	0.223E-02	*0.231E-01	*0.422E-02
	300000.	0.693E-01	0.212E-02	0.127E-01	0.273E-02	*0.251E-01	*0.534E-02
	500000.	0.598E-01	0.201E-02	0.138E-01	0.320E-02	*0.274E-01	*0.636E-02
P V 3S 5P	50000.	0.175	0.422E-02	*0.148E-01	*0.232E-02		
255.6 Å	100000.	0.140	0.516E-02	*0.196E-01	*0.387E-02		
C= 0.95E+20	150000.	0.125	0.598E-02	*0.215E-01	*0.491E-02		
	200000.	0.116	0.548E-02	*0.227E-01	*0.554E-02		
	300000.	0.105	0.533E-02	*0.243E-01	*0.622E-02		
	500000.	0.934E-01	0.508E-02	*0.258E-01	*0.725E-02		
P V 3S 6P	50000.	*0.282	*0.806E-02				
229.8 Å	100000.	0.238	0.121E-01				
C= 0.42E+20	150000.	0.217	0.111E-01				
	200000.	0.204	0.111E-01				
	300000.	0.187	0.107E-01				
	500000.	0.170	0.108E-01				
P V 4S 4P	50000.	17.0	-0.353	0.580	-0.206	* 1.02	*-0.315
3185.6 Å	100000.	12.7	-0.360	0.899	-0.363	* 1.73	*-0.654
C= 0.32E+23	150000.	11.0	-0.445	1.09	-0.463	* 2.13	*-0.858
	200000.	9.97	-0.454	1.16	-0.543	* 2.31	* -1.01
	300000.	8.82	-0.408	1.28	-0.606	* 2.53	* -1.17
	500000.	7.67	-0.406	1.42	-0.712	* 2.82	* -1.40
P V 4S 5P	50000.	2.17	0.840E-02	*0.161	*0.976E-02		
845.8 Å	100000.	1.74	0.197E-01	*0.213	*0.181E-01		
C= 0.10E+22	150000.	1.56	0.208E-01	*0.233	*0.228E-01		
	200000.	1.44	0.128E-01	*0.245	*0.272E-01		
	300000.	1.31	0.151E-01	*0.262	*0.315E-01		
	500000.	1.17	0.134E-01	*0.277	*0.366E-01		

PERTURBER DENSITY = 1xE+19cm-3

PERTURBERS ARE: TRANSITION	T(K)	ELECTRONS WIDTH(Å)	ELECTRONS SHIFT(Å)	PROTONS WIDTH(Å)	PROTONS SHIFT(Å)	He III WIDTH(Å)	He III SHIFT(Å)
P V 4S 6P	50000.	* 2.17	*0.332E-01				
616.8 Å	100000.	1.82	0.657E-01				
C= 0.30E+21	150000.	1.66	0.542E-01				
	200000.	1.56	0.537E-01				
	300000.	1.44	0.536E-01				
	500000.	1.30	0.549E-01				
P V 5S 6P	50000.	* 19.3	*-0.991E-01				
1710.8 Å	100000.	* 16.3	*-0.273E-01				
C= 0.23E+22	150000.	14.9	-0.972E-01				
	200000.	14.0	-0.871E-01				
	300000.	12.9	-0.850E-01				
	500000.	11.6	-0.748E-01				
P V 3P 4S	50000.	0.277	0.171E-01	0.438E-02	0.784E-02	*0.840E-02	*0.118E-01
544.0 Å	100000.	0.203	0.170E-01	0.103E-01	0.134E-01	*0.206E-01	*0.237E-01
C= 0.93E+21	150000.	0.173	0.199E-01	0.142E-01	0.172E-01	*0.284E-01	*0.316E-01
	200000.	0.155	0.211E-01	0.181E-01	0.198E-01	*0.364E-01	*0.366E-01
	300000.	0.136	0.199E-01	0.219E-01	0.222E-01	*0.437E-01	*0.425E-01
	500000.	0.116	0.192E-01	0.263E-01	0.258E-01	0.536E-01	0.510E-01
P V 3P 5S	50000.	0.251	0.256E-01	*0.116E-01	*0.130E-01		
347.8 Å	100000.	0.194	0.311E-01	*0.214E-01	*0.210E-01		
C= 0.18E+21	150000.	0.169	0.308E-01	*0.262E-01	*0.252E-01		
	200000.	0.155	0.304E-01	*0.292E-01	*0.287E-01		
	300000.	0.137	0.294E-01	*0.334E-01	*0.323E-01		
	500000.	0.118	0.287E-01	*0.400E-01	*0.380E-01		
P V 3P 6S	50000.	*0.382	*0.561E-01				
295.8 Å	100000.	0.311	0.597E-01				
C= 0.69E+20	150000.	0.277	0.578E-01				
	200000.	0.254	0.561E-01				
	300000.	0.226	0.548E-01				
	500000.	0.198	0.516E-01				
P V 3P 7S	50000.	*0.610	*0.132				
272.9 Å	100000.	*0.522	*0.120				
C= 0.36E+20	150000.	*0.469	*0.107				
	200000.	0.437	0.103				
	300000.	0.395	0.993E-01				
	500000.	0.349	0.885E-01				
P V 4P 5S	50000.	5.22	0.330	*0.218	*0.199		
1383.2 Å	100000.	4.06	0.433	*0.375	*0.324		
C= 0.28E+22	150000.	3.56	0.431	*0.442	*0.387		
	200000.	3.27	0.421	*0.490	*0.440		
	300000.	2.92	0.408	*0.564	*0.496		
	500000.	2.55	0.404	*0.647	*0.580		
P V 4P 6S	50000.	* 3.26	*0.383				
814.1 Å	100000.	2.65	0.422				
C= 0.52E+21	150000.	2.37	0.412				
	200000.	2.19	0.400				
	300000.	1.96	0.393				
	500000.	1.73	0.372				
P V 4P 7S	50000.	* 3.81	*0.705				
661.1 Å	100000.	* 3.24	*0.662				
C= 0.21E+21	150000.	* 2.93	*0.612				
	200000.	2.73	0.561				
	300000.	2.47	0.552				
	500000.	2.19	0.495				

PERTURBER DENSITY = 1xE+19cm-3

PERTURBERS ARE: TRANSITION	T(K)	ELECTRONS WIDTH(Å)	ELECTRONS SHIFT(Å)	PROTONS WIDTH(Å)	PROTONS SHIFT(Å)	He III WIDTH(Å)	He III SHIFT(Å)
P V 3P 3D	50000.	0.434	-0.393E-03	0.865E-02	-0.119E-03	0.155E-01	-0.188E-03
869.1 Å	100000.	0.311	-0.253E-03	0.167E-01	-0.274E-03	0.322E-01	-0.507E-03
C= 0.67E+22	150000.	0.259	-0.322E-03	0.214E-01	-0.426E-03	0.418E-01	-0.812E-03
	200000.	0.229	-0.238E-03	0.248E-01	-0.572E-03	0.485E-01	-0.110E-02
	300000.	0.195	-0.529E-03	0.292E-01	-0.824E-03	0.578E-01	-0.162E-02
	500000.	0.163	-0.414E-03	0.322E-01	-0.121E-02	0.640E-01	-0.242E-02
P V 3P 4D	50000.	0.252	0.618E-02	*0.126E-01	*0.863E-02		
390.2 Å	100000.	0.191	0.792E-02	*0.199E-01	*0.139E-01		
C= 0.11E+21	150000.	0.165	0.759E-02	*0.239E-01	*0.170E-01		
	200000.	0.150	0.775E-02	*0.264E-01	*0.192E-01		
	300000.	0.132	0.823E-02	0.297E-01	0.216E-01		
	500000.	0.114	0.750E-02	0.345E-01	0.252E-01		
P V 3P 5D	50000.	*0.383	*0.136E-01				
311.0 Å	100000.	0.308	0.150E-01				
C= 0.37E+20	150000.	0.274	0.163E-01				
	200000.	0.252	0.178E-01				
	300000.	0.226	0.173E-01				
	500000.	0.198	0.157E-01				
P V 3P 6D	50000.	*0.641	*0.110E-01				
280.3 Å	100000.	*0.537	*0.217E-01				
C= 0.18E+20	150000.	*0.485	*0.286E-01				
	200000.	0.452	0.292E-01				
	300000.	0.410	0.276E-01				
	500000.	0.362	0.250E-01				
P V 3P 7D	50000.						
264.7 Å	100000.	*0.876	*0.273E-01				
C= 0.10E+20	150000.	*0.809	*0.359E-01				
	200000.	*0.763	*0.367E-01				
	300000.	*0.700	*0.342E-01				
	500000.	0.625	0.357E-01				
P V 4P 4D	50000.	13.1	0.126	*0.676	*0.308		
2436.0 Å	100000.	10.00	0.190	* 1.01	*0.496		
C= 0.43E+22	150000.	8.68	0.164	* 1.14	*0.615		
	200000.	7.92	0.149	* 1.24	*0.690		
	300000.	7.02	0.164	* 1.37	*0.778		
	500000.	6.13	0.147	* 1.55	*0.904		
P V 4P 5D	50000.	* 3.92	*0.107				
940.9 Å	100000.	3.14	0.119				
C= 0.34E+21	150000.	2.79	0.129				
	200000.	2.57	0.140				
	300000.	2.31	0.135				
	500000.	2.03	0.121				
P V 4P 6D	50000.	* 4.29	*0.589E-01				
706.8 Å	100000.	* 3.58	*0.127				
C= 0.11E+21	150000.	* 3.23	*0.170				
	200000.	3.01	0.173				
	300000.	2.73	0.162				
	500000.	2.42	0.147				
P V 4P 7D	50000.						
615.1 Å	100000.	* 4.85	*0.139				
C= 0.54E+20	150000.	* 4.48	*0.185				
	200000.	* 4.22	*0.188				
	300000.	* 3.88	*0.174				
	500000.	3.46	0.183				

PERTURBER DENSITY = 1xE+19cm-3

PERTURBERS ARE: TRANSITION	T(K)	ELECTRONS WIDTH(Å)	ELECTRONS SHIFT(Å)	PROTONS WIDTH(Å)	PROTONS SHIFT(Å)	He III WIDTH(Å)	He III SHIFT(Å)
P V 3D 4P	50000.	1.30	0.205E-01	0.613E-01	0.834E-02		
998.5 Å	100000.	0.964	0.205E-01	0.928E-01	0.163E-01		
C= 0.31E+22	150000.	0.823	0.227E-01	0.110	0.212E-01	*0.215	*0.401E-01
	200000.	0.743	0.261E-01	0.117	0.251E-01	*0.230	*0.474E-01
	300000.	0.652	0.271E-01	0.126	0.303E-01	*0.251	*0.590E-01
	500000.	0.564	0.251E-01	0.138	0.353E-01	*0.274	*0.700E-01
P V 3D 5P	50000.	0.764	0.206E-01	*0.662E-01	*0.105E-01		
534.8 Å	100000.	0.615	0.246E-01	*0.874E-01	*0.175E-01		
C= 0.42E+21	150000.	0.549	0.278E-01	*0.958E-01	*0.222E-01		
	200000.	0.508	0.258E-01	*0.101	*0.249E-01		
	300000.	0.460	0.256E-01	*0.108	*0.280E-01		
	500000.	0.410	0.241E-01	*0.115	*0.327E-01		
P V 3D 6P	50000.	* 1.00	*0.306E-01				
433.1 Å	100000.	0.845	0.447E-01				
C= 0.15E+21	150000.	0.771	0.407E-01				
	200000.	0.724	0.408E-01				
	300000.	0.666	0.397E-01				
	500000.	0.603	0.396E-01				
P V 4D 5P	50000.	* 16.5	*0.129				
2183.7 Å	100000.	13.3	0.152				
C= 0.34E+22	150000.	11.9	0.218	* 1.77	*-0.284		
	200000.	11.0	0.182	* 1.87	*-0.327		
	300000.	9.95	0.162	* 2.01	*-0.367		
	500000.	8.85	0.163	* 2.13	*-0.427		
P V 4D 6P	50000.	* 7.55	*0.138				
1114.9 Å	100000.	* 6.35	*0.225				
C= 0.89E+21	150000.	5.78	0.202				
	200000.	5.42	0.203				
	300000.	4.98	0.193				
	500000.	4.50	0.199				
P V 3D 4F	50000.	0.601	-0.591E-02	0.254E-01	-0.176E-01		
673.9 Å	100000.	0.448	-0.644E-02	0.415E-01	-0.292E-01		
C= 0.33E+21	150000.	0.383	-0.756E-02	0.521E-01	-0.369E-01		
	200000.	0.346	-0.540E-02	0.570E-01	-0.413E-01	*0.112	*-0.750E-01
	300000.	0.303	-0.390E-02	0.653E-01	-0.464E-01	*0.128	*-0.885E-01
	500000.	0.261	-0.468E-02	0.764E-01	-0.543E-01	*0.146	*-0.106
P V 3D 5F	50000.	*0.925	*-0.277E-01				
475.6 Å	100000.	0.763	-0.234E-01				
C= 0.50E+19	150000.	0.683	-0,191E-01				
	200000.	0.631	-0.170E-01				
	300000.	0.566	-0.156E-01				
	500000.	0.493	-0.113E-01				
P V 3D 6F	50000.	* 1.54	*-0.388E-01				
410.0 Å	100000.	* 1.32	*-0.383E-01				
C= 0.24E+19	150000.	* 1.19	*-0.362E-01				
	200000.	1.11	-0.338E-01				
	300000.	1.00	-0.282E-01				
	500000.	0.881	-0.221E-01				
P V 4D 5F	50000.	* 10.3	*-0.345				
1447.9 Å	100000.	8.42	-0.328				
C= 0.46E+20	150000.	7.53	-0.283				
	200000.	6.97	-0.265				
	300000.	6.25	-0.260				
	500000.	5.46	-0.209				

PERTURBER DENSITY = 1xE+19cm-3

PERTURBERS ARE: TRANSITION	T(K)	ELECTRONS WIDTH(Å)	ELECTRONS SHIFT(Å)	PROTONS WIDTH(Å)	PROTONS SHIFT(Å)	He III WIDTH(Å)	He III SHIFT(Å)
P V 4D 6F	50000.	* 9.42	*-0.259				
973.8 Å	100000.	* 8.00	*-0.266				
C= 0.13E+20	150000.	* 7.25	*-0.252				
	200000.	* 6.76	*-0.239				
	300000.	6.10	-0.211				
	500000.	5.35	-0.172				
P V 4F 5D	50000.	* 13.4	*0.459				
1722.9 Å	100000.	10.7	0.504				
C= 0.11E+22	150000.	9.51	0.550				
	200000.	8.77	0.584				
	300000.	7.86	0.560				
	500000.	6.91	0.512				
P V 4F 6D	50000.	* 9.98	*0.177				
1072.4 Å	100000.	* 8.32	*0.335				
C= 0.26E+21	150000.	* 7.51	*0.438				
	200000.	6.99	0.442				
	300000.	6.34	0.414				
	500000.	5.61	0.378				
P V 4F 7D	50000.						
874.6 Å	100000.	* 9.86	*0.309				
C= 0.11E+21	150000.	* 9.10	*0.405				
	200000.	* 8.58	*0.410				
	300000.	* 7.87	*0.381				
	500000.	7.02	0.398				

PERTURBER DENSITY = 1xE+20cm-3

P V 3S 3P	50000.	6.26	-0.428E-01	0.507E-01	-0.130E-01	*0.566E-01	-0.113E-01
1121.8 Å	100000.	4.47	-0.610E-01	0.132	-0.400E-01	*0.228	-0.600E-01
C= 0.11E+24	200000.	3.28	-0.627E-01	0.222	-0.788E-01	*0.429	-0.142
	300000.	2.78	-0.797E-01	0.277	-0.102	*0.541	
-0.190							
	500000.	2.32	-0.704E-01	0.329	-0.136	*0.653	
-0.260							
	1000000.	1.87	-0.721E-01	0.380	-0.170	*0.757	-0.336
P V 3S 4P	50000.	* 1.39	*0.106E-01				
328.6 Å	100000.	1.03	0.121E-01				
C= 0.34E+22	200000.	0.792	0.195E-01				
	300000.	0.693	0.193E-01	*0.125	*0.256E-01		
	500000.	0.598	0.185E-01	*0.137	*0.311E-01		
	1000000.	0.503	0.187E-01	*0.150	*0.383E-01		
P V 3S 5P	50000.						
255.6 Å	100000.	* 1.40	*0.381E-01				
C= 0.95E+21	200000.	* 1.16	*0.457E-01				
	300000.	1.05	0.464E-01				
	500000.	0.932	0.449E-01				
	1000000.	0.808	0.451E-01				
P V 3S 6P	50000.						
229.8 Å	100000.						
C= 0.42E+21	200000.	* 2.00	*0.824E-01				
	300000.	* 1.85	*0.829E-01				
	500000.	* 1.67	*0.891E-01				
	1000000.	1.47	0.806E-01				
P V 3P 4S	50000.	* 2.76	*0.103	*0.399E-01	*0.409E-01		
544.0 Å	100000.	2.03	0.127	*0.102	*0.100		
C= 0.93E+22	200000.	1.55	0.181	*0.180	*0.167		
	300000.	1.36	0.176	*0.220	*0.201		
	500000.	1.16	0.172	*0.263	*0.246		
	1000000.	0.957	0.171	*0.331	*0.303		

PERTURBER DENSITY = 1xE+20cm-3

PERTURBERS ARE: TRANSITION	T(K)	ELECTRONS WIDTH(Å)	ELECTRONS SHIFT(Å)	PROTONS WIDTH(Å)	PROTONS SHIFT(Å)	He III WIDTH(Å)	He III SHIFT(Å)
P V 3P 5S	50000.	* 2.49	*0.677E-01				
347.8 Å	100000.	* 1.93	*0.194				
C= 0.18E+22	200000.	1.54	0.225				
	300000.	1.36	0.229				
	500000.	1.18	0.236				
	1000000.	0.985	0.216				
P V 3P 6S	50000.						
295.8 Å	100000.						
C= 0.69E+21	200000.	* 2.45	*0.317				
	300000.	* 2.19	*0.352				
	500000.	1.93	0.359				
	1000000.	1.61	0.320				
P V 3P 7S	50000.						
272.9 Å	100000.						
C= 0.36E+21	200000.						
	300000.	* 3.54	*0.503				
	500000.	* 3.17	*0.488				
	1000000.	* 2.69	*0.436				
P V 3P 3D	50000.	4.34	-0.292E-02	0.690E-01	-0.718E-03		
869.1 Å	100000.	3.11	-0.212E-02	0.161	-0.232E-02		
C= 0.67E+23	200000.	2.29	-0.206E-02	0.244	-0.532E-02		
	300000.	1.95	-0.502E-02	0.291	-0.797E-02		
	500000.	1.63	-0.382E-02	0.322	-0.120E-01	*0.635	*-0.233E-01
	1000000.	1.34	-0.293E-02	0.362	-0.174E-01	*0.719	*-0.347E-01
P V 3P 4D	50000.	* 2.46	*-0.332E-01				
390.2 Å	100000.	* 1.88	*0.188E-01				
C= 0.11E+22	200000.	1.48	0.368E-01				
	300000.	1.30	0.495E-01				
	500000.	1.13	0.489E-01				
	1000000.	0.943	0.444E-01				
P V 3P 5D	50000.						
311.0 Å	100000.	* 2.84	*-0.473E-01				
C= 0.37E+21	200000.	* 2.36	*0.442E-01				
	300000.	* 2.14	*0.628E-01				
	500000.	1.89	0.661E-01				
	1000000.	1.61	0.705E-01				
P V 3P 6D	50000.						
280.3 Å	100000.						
C= 0.18E+21	200000.						
	300000.	* 3.59	*0.419E-01				
	500000.	* 3.24	*0.510E-01				
	1000000.	* 2.80	*0.947E-01				
P V 3D 4P	50000.	* 13.0	*0.140				
998.5 Å	100000.	9.64	0.166				
C= 0.31E+23	200000.	7.43	0.233				
	300000.	6.52	0.249	* 1.25	*0.282		
	500000.	5.64	0.232	* 1.37	*0.342		
	1000000.	4.77	0.234	* 1.50	*0.419		
P V 3D 5P	50000.						
534.8 Å	100000.	* 6.14	*0.185				
C= 0.42E+22	200000.	* 5.07	*0.217				
	300000.	4.59	0.224				
	500000.	4.10	0.215				
	1000000.	3.56	0.215				

PERTURBER DENSITY = 1xE+20cm-3

PERTURBERS ARE:		ELECTRONS		PROTONS		He III	
TRANSITION	T(K)	WIDTH(Å)	SHIFT(Å)	WIDTH(Å)	SHIFT(Å)	WIDTH(Å)	SHIFT(Å)
P V 3D 6P	50000.						
433.1 Å	100000.						
C= 0.15E+22	200000.	* 7.11	*0.305				
	300000.	* 6.56	*0.309				
	500000.	* 5.95	*0.329				
	1000000.	5.23	0.298				
P V 3D 4F	50000.	* 5.88	*0.121				
673.9 Å	100000.	4.42	0.496E-01				
C= 0.33E+22	200000.	3.42	0.227E-01				
	300000.	2.99	0.220E-01				
	500000.	2.58	0.271E-02				
	1000000.	2.16	0.115E-01	*0.933	*-0.632		
P V 3D 5F	50000.						
475.6 Å	100000.	* 6.10	*0.634E-01				
C= 0.50E+20	200000.	* 5.23	*0.552E-02				
	300000.	* 4.77	*-0.208E-01				
	500000.	4.24	-0.177E-01				
	1000000.	3.61	-0.139E-01				
P V 3D 6F	50000.						
410.0 Å	100000.						
C= 0.24E+20	200000.						
	300000.	* 7.68	*0.245E-01				
	500000.	* 6.97	*0.179E-01				
	1000000.	* 6.02	*-0.324E-01				

purposes. Our results for 25 C V and 51 P V multiplets are shown in Table 1, for perturber densities 10^{17}– 10^{22} cm^{-3} and temperatures T = 50,000 – 1,000,000 K. We also specify a parameter c (Dimitrijević and Sahal–Bréchot 1984), which gives an estimate for the maximum perturber density for which the line may be treated as isolated when it is divided by the corresponding full width at half maximum. For each value given in Table 1, the collision volume (V) multiplied by the perturber density (N) is much less than one and the impact approximation is valid (Sahal–Bréchot, 1969ab). Values for NV > 0.5 are not given and values for 0.1 < NV < 0.5 are denoted by an asterisk. When the impact approximation is not valid, the ion broadening contribution may be estimated by using quasistatic approach (Sahal–Bréchot 1991 and Griem 1974). The accuracy of the results obtained decreases when broadening by ion interactions becomes important.

The analysis of present results and comparison with available theoretical data will be published elsewhere (Dimitrijević and Sahal–Bréchot, 1995).

Acknowledgements – This work is a part of the project "Physics and dynamics of celestial bodies", supported by Ministry of Science and Technology of Serbia.

REFERENCES

Dimitrijević, M. S. and Sahal–Bréchot, S.: 1984, *JQSRT*, **31**, 301.
Dimitrijević, M. S. and Sahal–Bréchot, S.: 1995, *Astron. Astrophys. Suppl. Series*, submitted.
Dimitrijević, M. S., Sahal–Bréchot, S. and Bommier, V.: 1991, *Astron. Astrophys. Suppl. Series* **89**, 581.
Griem, H. R.: 1974, *Spectral Line Broadening by Plasmas*, Academic Press, New York.
Sahal–Bréchot, S.: 1969a, *Astron. Astrophys.* **1**, 91.
Sahal–Bréchot, S.: 1969b, *Astron. Astrophys.* **2**, 322.
Sahal–Bréchot, S.: 1991, *Astron. Astrophys.* **245**, 322.
Srećković, A., Djeniže, S., Labat, J., Platiša, M., Purić, J.: 1990, *Fizika* **22**, 583.
Werner, K., Heber, U., Hunger, K.: 1991, *Astron. Astrophys.* **244**, 437.

ТАБЕЛЕ ПАРАМЕТАРА ШТАРКОВОГ ШИРЕЊА C V И P V

М. С. Димитријевић[1] и S. Sahal–Bréchot[2]

[1] *Астрономска опсерваторија, Волгина 7, 11050 Београд, Југославија*

[2] *Laboratoire "Astrophysique, Atomes et Molécules"*
Département Atomes et Molécules en Astrophysique
Unité associée au C.N.R.S. No 812
Observatoire de Paris-Meudon, 92190 Meudon, France

УДК 52–355.3
Претходно саопштење

Користећи семикласичан прилаз, израчунате су ширине и помераји спектралних линија, проузроковани сударима са електронима, протонима и јонизованим хелијумом, за 25 мултиплета C V и 51 мултиплет P V. Резултати су дати у функцији температуре и концентрације пертурбера.

2000BaltA...9..595M

Baltic Astronomy, vol. 9, 595–598, 2000

BELDATA – THE DATABASE OF BELGRADE ASTRONOMICAL OBSERVATORY

N. Milovanović, L. Č. Popović and M. S. Dimitrijević

Astronomical Observatory, Volgina 7, 11000 Belgrade, Yugoslavia

Received September 10, 2000.

Abstract. The Belgrade Astronomical Database (BELDATA) is an Internet-based database designed to contain Stark broadening parameters, spectra of active galactic nuclei, catalogs of observations done at the Belgrade Observatory and abstracts of papers published in the publications of the observatory.

Key words: astronomical databases – atomic data: Stark broadening

1. INTRODUCTION

In the last decade the scientific community has extensively used the advantages of Internet communication, as an easy and fast access to large amount of data around the world. Various types of data are now on Internet databases: catalogues, papers, abstracts, atomic data, observation material, etc. In order to enable to the astronomical community to use the results produced at Astronomical Observatory, a concept of database which will hold the work of our fellows has been developed. Software and hardware support of the database are constantly updated, in order to provide to Internet users and administrators of BELDATA a convenient service (Popović et al. 1999, 2000, Milovanović et al. 2000)

Four main data sets will be held at BELDATA: Stark broadening parameters, spectra of active galactic nuclei, observational catalogues made at the Belgrade Astronomical Observatory, as well as abstracts and full papers from the Serbian Astronomical Journal and Publications of the Belgrade Astronomical Observatory.

© Teorines fizikos ir astronomijos institutas • Provided by the NASA Astrophysics Data System

2000BaltA...9..595M

Up to now, we have been working on the main parts of BELDATA: the software installation and the core data set for Stark broadening parameters.

2. STARK BROADENING PARAMETERS DATABASE

In early-type stars like B and A stars and white dwarfs, the Stark broadening is the main pressure broadening mechanism, and the corresponding Stark broadening parameters are of interest for a number of investigations related to stellar opacities, stellar atmosphere modeling and investigations, abundance determinations, interpretation and modeling of stellar spectra, investigation and modeling of subphotospheric layers and laboratory plasma research.

In a series of papers, large scale calculations of Stark broadening parameters for a number of spectral lines of various emitters performed at the Belgrade Observatory have been published. Our calculations have been performed within the semiclassical (SC) perturbation formalism (Sahal-Bréchot 1969a,b) for transitions when a sufficiently complete set of reliable atomic data exists and within the modified semiempirical approach (MSE) (Dimitrijević & Konjević 1980, Dimitrijević & Kršljanin 1986) if there is no sufficiently complete set of reliable atomic energy levels for a full semiclassical calculation.

Table 1. Example of input and output query form for Stark broadening parameter database.

Input query		Output data
Element	Zr	
Ionization stage	II	
Electron density (m^{-3})	10^{23}	$w=0.333\cdot10^{-2}$ nm
Wavelength (nm)	193.85	
Temperature (K)	30000	

Stark broadening parameters will be presented as widths and shifts as a function of temperature and electron density for a particular atom or ion and for a particular spectral line or multiplet. These parameters are calculated using the SC or MSE formalism. Users can access the database by filling an Internet-based query form specifying element, ionization stage, electron density, transition wavelength

© Teorines fizikos ir astronomijos institutas • Provided by the NASA Astrophysics Data System

2000BaltA...9..595M

and temperature. A simple input query form and output data for Stark widths are shown in Table 1.

Users will have the possibility to choose specific temperature and wavelengths or to choose a range of these two parameters e.g. for wavelengths 190–200 nm. The output will show Stark broadening parameters for transitions which exist in the database between 190 nm and 200 nm.

Besides Stark broadening parameters, BELDATA will hold all papers and abstracts concerning Stark broadening produced at the Astronomical Observatory in PDF format.

3. DATABASE OF SPECTRA OF ACTIVE GALACTIC NUCLEI

The spectral lines, mainly Hα and Hβ of 3C390.3, 3C120, Akn 120, III Zw 2 and Mkn 817 observed at the Crimean Astrophysical Observatory by K. K. Chuvaev will be included in BELDATA in FITS format.

4. OBSERVATIONS MADE AT THE BELGRADE OBSERVATORY

Observational and compiled catalogues made at the Belgrade Observatory will be included in BELDATA in various formats.

(1) A catalogue of declinations of the latitude program stars,

(2) A catalogue of NPZT program stars,

(3) Belgrade catalogue of double stars,

(4) A catalogue of positions of 290 stars situated in the vicinity of radio sources,

(5) A catalogue of positions of 223 Ondrejov PZT stars observed at the Belgrade Observatory,

(6) A position catalogue of 146 HLS stars and 78 radio stars observed with the Belgrade meridian circle,

(7) A position catalogue of 351 stars situated in the vicinity of radio sources observed with the Belgrade meridian circle,

(8) The First general catalogue of double star observations made in Belgrade in 1951–1971,

(9) A catalogue of declinations of 307 bright stars in the zone +30° to +90°,

© Teorines fizikos ir astronomijos institutas • Provided by the NASA Astrophysics Data System

2000BaltA...9..595M

(10) Declinations and proper motions of the stars of the International Latitude Service on the basis of meridian catalogue from 1929–1972,

(11) A compiled catalogue of latitude stars,

(12) A preliminary compilation of DS-program star positions.

5. ABSTRACTS OF PAPERS

Also, the BELDATA database will contain abstracts and, in the future, articles published in the Serbian Astronomical Journal and the Publications of the Astronomical Observatory of Belgrade. The Serbian Astronomical Journal was founded in 1936 under the name of Bulletin de l'Observatoire Astronomique de Belgrade. Since No. 145 in 1992, after the merging with the Publications of Department of Astronomy founded in 1969, the journal has the title Bulletin Astronomique de Belgrade and under the title Serbian Astronomical Journal; the journal is being published starting with No. 157 in 1998. The Publications of the Astronomical Observatory of Belgrade were founded in 1947. Collaboration with other Internet databases will be established, e.g., with the Vienna Atomic Line Database (Kupka et al. 1999).

The Internet address of the Database of the Belgrade Astronomical Observatory is http://www.aob.bg.ac.yu/BELDATA.

REFERENCES

Dimitrijević M. S., Konjević N. 1980, JQSRT, 24, 451

Dimitrijević M. S., Kršljanin V. 1986, A&A, 165, 269

Kupka F., Piskunov N. E., Ryabchikova T. A., Stempeles H. C., Weiss W. W. 1999, A&AS, 138, 119

Milovanović N., Popović L. Č., Dimitrijević M. S. 2000, Publ. Astron. Obs. Belgrade, 68, 117

Popović L. Č., Dimitrijević M. S., Milovanović N. 1999, Publ. Astron. Obs. Belgrade, 65, 225

Popović L. Č., Dimitrijević M. S., Milovanović N., Trajković N. 2000, in *Proceedings of the 3rd Yugoslav Conference on Spectral Line Shapes*, in press

Sahal-Bréchot S. 1969a, A&A, 1, 91

Sahal-Bréchot S. 1969b, A&A, 2, 322

© Teorines fizikos ir astronomijos institutas • Provided by the NASA Astrophysics Data System

2000BaltA...9..656P

Baltic Astronomy, vol. 9, 656–657, 2000

THE IMPORTANCE OF ELECTRON-IMPACT BROADENING IN HOT STAR ATMOSPHERES: THE CASE OF Zr II AND Zr III LINES

L. Č. Popović, N. Milovanović and M. S. Dimitrijević

Astronomical Observatory, Volgina 7, 11000 Belgrade, Yugoslavia

Received September 10, 2000.

Key words: atomic data – atomic processes – stars: early-type

In the atmospheres of early-type stars the main pressure broadening mechanism of spectral lines is the electron-impact broadening (Popović et al. 1999). Abundance anomalies are present in 10–20% of A- and B-type stars (so-called CP stars). Zirconium is usually overabundant in HgMn star atmospheres. HgMn star χ Lupi is characterized by the so-called "zirconium conflict", i.e. the fact that the zirconium abundance determination from Zr II lines is different than from Zr III lines (Sikström et al. 1999).

Using the Modified Semiempirical Method (MSE, Dimitrijević & Konjević 1980, Dimitrijević & Kršljanin 1986) we have calculated Stark broadening widths of two Zr II and two Zr III spectral lines. We calculated Stark widths of Zr II 232.47 nm, Zr II 193.85 nm, Zr III 194.105 nm and Zr III 194.023 nm spectral lines. We have synthesized the line profiles using the SYNTH code (Piskunov 1992) and ATLAS9 program (Kurucz 1993) for a stellar atmosphere which is similar to the atmosphere of χ Lupi (Leckrone 1999). In Table 1 the ratios of equivalent widths (EW) with and without Stark broadening effect as a function of abundance are given.

© Teorines fizikos ir astronomijos institutas • Provided by the NASA Astrophysics Data System

2000BaltA...9..656P

Table 1. The ratio of EWs for two Zr II and two Zr III spectral lines calculated with Stark broadening effect (EW_{st}) and without it (EW_0) as a function of zirconium abundance.

$\log(N_{Zr}/N_H)$ λ (nm) =	Zr II 232.47	Zr II 138.85	Zr III 194.023	Zr III 194.105
−6.0	1.062	1.073	1.172	1.211
−6.5	1.032	1.038	1.099	1.136
−7.0	1.017	1.019	1.049	1.073
−7.5	1.009	1.010	1.023	1.035

As one can see from Table 1, the Stark broadening effect is more important for higher zirconium abundance. The EW increases with abundance in all considered cases, but EW for Zr III is more sensitive to the zirconium abundance change than for Zr II lines. It may cause the errors of about 20% in zirconium abundance determination (Popović et al. 2000).

REFERENCES

Dimitrijević M. S., Konjević N. 1980, JQSRT, 24, 541

Dimitrijević M. S., Kršljanin V. 1986, A&A, 165, 269

Kurucz R. L. 1993, *Model Atmosphere Program ATLAS9*, published on CDROM13

Leckrone D. S., Proffitt C. R., Wahlgren G. M., Johansson S. G., Brege T. 1999, AJ, 115, 1454

Piskunov N.E. 1992, in *Stellar Magnetism*, eds. Yu. V. Glagolevskij & I. I. Romanyuk, Nauka Publishers, St. Petersburg, p. 92

Popović L.Č., Dimitrijević M. S., Ryabchikova T. 1999, A&A, 350, 719

Popović L.Č., Milovanović N., Dimitrijević M. S. 2000, A&AS, accepted

Sikström C.M., Lundberg H., Wahlgren G. M., Li Y. S., Lyngå C., Johansson S., Leckrone D. S. 1999, A&A, 343, 297

© Teorines fizikos ir astronomijos institutas • Provided by the NASA Astrophysics Data System

2000BaltA...9..662T

Baltic Astronomy, vol. 9, 662–663, 2000

STARK BROADENING OF HEAVY ELEMENT SPECTRAL LINES IN HOT STARS: Au II, Co II, Ti II AND Co III

D. Tankosić, L. Č. Popović and M. S. Dimitrijević

Astronomical Observatory, Volgina 7, 11000 Belgrade, Yugoslavia

Received October 3, 1994.

Key words: atomic processes – line profiles – stars: early-type

Spectral lines of heavy elements are present in hot star spectra, e.g. in the spectra of CP stars. Moreover, in hot star atmospheres, the Stark broadening is the main pressure broadening mechanism (Dimitrijević 1989). This mechanism is important in modeling and investigation of subphotospheric layers. Also, the Stark broadening parameters for spectral lines of many elements are of interest in modeling the atmospheres of hot stars, including the Hg-Mn stars.

The Stark broadening data for Au II λ = 174.048 nm, Co II λ = 230.785 nm, Ti II λ = 376.132 nm and 27 Co III spectral lines (from a^6D -z^6D^o and a^6D -z^6F^o Co III multiplets), as a function of temperature, have been calculated by using the modified semiempirical approach (Dimitrijevič & Konjevič 1980). Table 1 presents, as an example, the Stark broadening data for the 4s^{6}D$_{1/2}$-4p^{6}D$^o_{1/2}$ Co III spectral line.

Also, considering that Au II λ = 174.048 nm, Co II λ = 230.785 nm and Ti II λ = 376.132 nm lines have been used for gold, cobalt and titanium abundance determination (see e.g. Fuhrmann 1988 for gold, Smith and Dworetsky 1993 for cobalt and Guthrie 1987 for titanium) in HgMn-type stars, we have tested the influence of the Stark broadening mechanism on the widths of these lines for an A-type atmosphere, as well as for DA and DB white dwarfs. This has been done with the help of Kurucz's model atmosphere (Kurucz 1979) of an A-type star ($T_{\rm eff}$ = 10 000 K, log g = 4), and with Wickramasinghe's models of DA ($T_{\rm eff}$ = 10 000 K, log g = 6) and DB ($T_{\rm eff}$ = 15 000 K, log g = 7) white dwarf atmospheres

© Teorines fizikos ir astronomijos institutas • Provided by the NASA Astrophysics Data System

2000BaltA...9..662T

Table 1. Stark broadening parameters for the $4s^6D_{1/2}$-$4p^6D^o_{1/2}$ Co III spectral line, for an electron density of $10^{23}m^{-3}$, as a function of temperature.

Transition	T(K)	W(nm)	d(nm)
	10000	0.323E-02	–0.294E-03
	20000	0.225E-02	–0.211E-03
$4s^6D_{1/2}$-$4p^6D^o_{1/2}$	30000	0.182E-02	–0.174E-03
λ=194.87 nm	50000	0.140E-02	–0.132E-03
	100000	0.101E-02	–0.882E-04
	150000	0.882E-03	–0.726E-04

(Wickramasinghe 1972). We found that there are conditions where the Stark broadening is the principal broadening mechanism influencing the line shape formation and that it should be taken into account when modeling stellar atmospheres.

REFERENCES

Dimitrijević M. S. 1989, Bull. Obs. Astron. Belgrade, No. 140, 111

Dimitrijević M. S., Konjević N. 1980, JQSRT, 24, 451

Guthrie B. N. G. 1987, *Elemental Abundance Analyses*, Institut d'Astronomie de l'Université de Lausanne, Chavannes-des-Bois, Switzerland, p. 64

Fuhrmann K. 1988, in *A Decade of UV Astronomy with the IUE Satellite*, eds. N. Longdon & E. J. Rolfe, ESA-SP 281, Vol.1, p. 405

Kurucz R. L. 1979, ApJS, 120, 373

Wickramasinghe D. T. 1972, Mem. Roy. Astron. Soc., 76, 129

© Teorines fizikos ir astronomijos institutas • Provided by the NASA Astrophysics Data System

Baltic Astronomy, vol. 21, 349–355, 2012

VAMDC: THE INFRASTRUCTURE

Pierre Le Sidaner[1], Tatiana Ryabchikova[2], and the VAMDC Collaboration

[1] *Division Informatique de l'Observatoire, VO-Paris Data Centre, UMS2201 CNRS/INSU, Observatoire de Paris,*
5 Place Janssen, 92195 Meudon Cedex, France; pierre.lesidaner@obspm.fr

[2] *Institute for Astronomy of the Russian Academy of Sciences,*
48, Pyatnitskaya Str., Moscow 119017, Russian Federation; ryabchik@inasan.ru

Received: 2012 February 13; accepted: 2012 May 18

Abstract. The Virtual Atomic and Molecular Data Centre (VAMDC; `http://www.vamdc.eu`) is a European-Union-funded collaboration between several groups involved in the generation, evaluation, and use of atomic and molecular data. VAMDC aims at building a secure, documented, flexible and interoperable *e*-Science environment-based interface to existing atomic and molecular databases. The global infrastructure of this project uses technologies derived from the International Virtual Observatory Alliance (IVOA). The infrastructure, as well as the first database prototypes will be described.

Key words: astronomical databases: virtual observatory tools – physical data and processes: atomic data, molecular data

1. INTRODUCTION

VAMDC is an initiative funded by the EU. In this paper we will describe the infrastructure built to create a complete Virtual Observatory dedicated to Atomic and Molecular Data (Dubernet et al. 2010). This project takes advantage of the experience acquired in astronomy by the IVOA. The Virtual Observatory infrastructure and technologies were used to obtain some important results in Galactic (Zolotukhin & Chilingarian 2011; Zolotukhin, this meeting) and extragalactic astrophysics (Padovani et al. 2004; Chilingarian et al. 2009; Chilingarian, this meeting). We will present different elements required to develop this infrastructure.

The Virtual Observatory is an architecture made of components usually hidden from the end users but necessary to allow them to reach and automatically compare data coming from various sources. We will describe the following components:

• The Data Model that provides a complete and shared descriptions of all data sources;

• The Data Access Layer which allows to query all resources of all data providers in a standard way;

• The data exchange format allowing to retrieve data and metadata in a standardized way;

• The registry: as the core of the information system, it centralizes all the

data services compliant with VAMDC and contains a first level of content and capability description.

2. THE VAMDC INFRASTRUCTURE

Further information on the VAMDC infrastructure is available on the project web site available at `http://www.vamdc.eu` and updated regularly.

2.1. The data model

The standard model for the data exchange within VAMDC is a modified version of the International Atomic Energy Agency's XML Schema for Atoms, Molecules and Solids (XSAMS), commonly referred to as VAMDC-XSAMS. The overall structure of the schema consists of specifying physical processes in terms of physical states. Physical states of atoms, molecules, ions, elementary particles and solids are indeed described as unambiguously as possible. States can be specified with any number of levels of detail and in different coupling schemes. Processes between states can be described using a reference to an initial and a final state, as well as a process type. The numerical data for processes can be tabulated, or presented in terms of parameters for a fitting procedure with provision for specifying the exact nature of the fitting function. Different types of differential cross sections as well as total cross sections can be accommodated. Finally, since the origin and history of the data are necessary for data quality assessment purposes, the schema requires strict requirements on the traceability of the data, with the mandatory inclusion of information on the data sources and methods used to generate specific sets of data.

2.2. The data access layer

The protocol used to access the data is TAP-VAMDC, based on the IVOA Table Access Protocol (TAP), a protocol designed to access tabular data and catalogues. This very generic protocol is designed for accessing relational databases. It supports different query languages (Astronomical Data Query Language (ADQL), Parameter Query Language (PQL) etc.). VAMDC defines a specific query language VSS1 (VAMDC SQL Sub-set) directly derived from a subset of SQL92. The service returns results in the VAMDC-XSAMS format. TAP is implemented over the HTTP protocol using standard HTTP GET and POST requests and conventions. As of now, TAP-VAMDC implements only the synchronous mode of TAP.

A TAP-VAMDC query looks like :
http://MyURLService.com/tap/sync/&
REQUEST=doQuery&
LANG=VSS1&
FORMAT=XSAMS&
QUERY=SELECT+*+WHERE+RadTransWavelengthExperimentalValue+

Metadata access

As the query language is directly derived from SQL, the queries can be easily constructed by a user familiar with this language. The query parameters are related to the database content. A specific syntax provides access to them and presents them in a standard way. Within the IVOA, this is known as VOSI (Virtual Observatory Support Interface). VOSI provides all the metadata information for

a given service such as: (1) the availability URL to inform about the service availability status; (2) a capability describing the functional capability of the service (TAP and query languages supported, web interface service, Common Executive Architecture for numerical codes etc.) with the specific access URLs provided for each feature; (3) a table giving the structure of the data table in the databases and containing the names of data tables, primary keys, foreign keys etc.

Standardized data output format for exchange

By default, the output of the TAP-VAMDC service is provided in the VAMDC-XSAMS compatible form. The description of the service output capability is presented in VOSI.

2.3. Registry

The VAMDC registry uses the International Virtual Observatory (IVOA) registry technology. The registry is the core of the information system. It consists of a database holding metadata that describes all the VAMDC resources, and a web service. The IVOA registry defines interfaces on how to query and share resources. The software is developed in a way that conforms to standard interfaces in order to allow scientific programs to access particular resources. A resource in this context is represented in XML form and is stored in the registry. A resource may describe anything about an observatory, a particular instrument, another registry, and services such as catalogue or table services or cone searches. Extensions can be added if necessary and this functionality is made available for VAMDC. As of now, in the case of VAMDC a resource in the registry can be :

- a collection of A-M data;
- a web service giving access to the data;
- a scientific code to run on A-M data;
- a service to run a code on a computational grid;
- an organization.

The access protocol to query the registry, the XML description of a resource and the data exchange format are fully described in the VAMDC documentation.

2.4. VAMDC interface and tools

End users can take advantage of the web interface to discover services, perform a query to access data and retrieve the results from a different data service in a common format. The information retrieved is sufficiently self-described to allow cross correlation.

Figure 1 shows the current interface to access VAMDC data. A standard web interface contains a simple graphical view to define and filter the type of data requested by the user.

VAMDC offers a client prototype for the cross-federation and cross-matching of spectroscopic and collisional data.

There are also tools to help publishing data, aimed at the data providers. Two software packages are already available with documentation and tutorials describing how to install and use them: (1) a package based on the DJANGO CMS; and (2) a package implemented in JAVA over TOMCAT.

Fig. 1. The VAMDC Web portal

2.5. VAMDC infrastructure maintenance and control

As a Virtual Observatory is a complex set of tools and services distributed all over the world, and which have to be available and fully compliant to the standards, we needed to develop a set of tools to ensure the reliability of the whole system. We monitor all registered services using NAGIOS (The Industry Standard In IT Infrastructure Monitoring). A validator has been developed to ensure the compliance of services to the standards.

3. VAMDC FOR ASTROPHYSICS

VAMDC is an ongoing project that is due by the end of 2012. Detailed description of VAMDC, its structure and purposes is given by Dubernet et al. (2010). 22 Atomic and Molecular databases are a part of the VAMDC consortium. Originally, all of them were created for some special field of scientific (mostly astronomical and atmospheric) research, which specified their individual structure and content. At present, 14 databases are prepared in the VAMDC-XSAMS format and their A&M data are available to the end user through the User Portal (http://portal.vamdc.eu/vamdc-portal-level-2/). A short description of some of these databases is given below.

3.1. Atomic line and processes databases

VALD contains over 150 line lists, 1.1 million atomic lines for detailed spectral analysis and over 50 million lines for opacity calculations (predicted lines) provided by all major spectroscopy centers across the world. Diatomic molecules data (TiO)

are currently included. It was created in 1995 for precisely modeling the spectra and the atmospheric structure of stars hotter that the Sun, including magnetic CP stars. It contains radiative data for 84 elements up to $Z = 92$ (U) in the first 6 ionization stages.

CHIANTI is a database for the analysis of optically thin collisionally-ionized plasmas. It is the preferred reference database in solar physics. It contains wavelengths and radiative data and rates for electron and proton collisions for highly charged ions with $Z \leq 30$ (up to Zn).

TIPTOPbase (with OPserver) contains radiative atomic data, photoionization cross-sections and electron impact excitation cross-sections on elements with $Z \leq 28$ (up to Ni). It is used for mean opacity calculations in stellar modeling and in NLTE line formation calculations.

Spectr-W^3 contains experimental and calculated data on wavelengths, energy levels, ionization potentials, transition probabilities for $\sim$ 450000 atomic lines. The most complete data is available for highly charged ions.

3.2. Molecular line and processes databases

HITRAN – HIgh-resolution TRANsmission molecular absorption database is the largest database for atmospheric research and planetology. The line-by-line portion of HITRAN contains spectroscopic parameters for 42 molecules. It also provides absorption cross-section parameters and aerosol indices of refraction. In total, HITRAN currently contains data for about 2×10^6 individual transitions.

CDMS (Cologne Database for Molecular Spectroscopy) provides recommended values of transition frequencies and intensities for molecules. It is used for studying the terrestrial atmosphere in the 0−340 cm^{-1} wavenumber range. CDMS is cross correlated with its US counterpart, the JPL sub-millimeter catalogue, which is now a member of the VAMDC consortium as well.

BASECOL provides excitation rate coefficients for ro-vibrational excitation of molecules by electrons, He and H_2. BASECOL is mainly used for the study of interstellar and circumstellar media as well as cometary atmospheres.

CDCD (Carbon Dioxide Spectroscopic Databank) contains calculated spectral line parameters for 7 isotopologues of carbon dioxide in the 5−12784 cm^{-1} wavenumber range.

S&MPO (Spectroscopy & Molecular Properties of Ozone), a database which contains well-established data on spectral line parameters for the ozone molecule (experimental UV cross-sections, for example).

UMIST, a database for astrochemistry which provides a fundamental set of reaction-rate data and related software for use in chemical kinetic modeling of astronomical regions (star formation regions, for example).

Why do we need a unique interface to all these DB's? Let us consider a couple of examples from astrospectroscopy.

In solar-like stars and cooler objects, the emerged line radiation consists of millions of atomic and molecular lines. Molecular lines appear as blends to the atomic lines in the visible spectral region. Figure 2 represents a part of the solar spectrum in the region of the famous Mg I triplet at 5167–83 Å. Atomic-line data from VALD describes the observed spectrum fairly well; however, for a full description, we need data for C_2 molecule transitions (contour lines) that may be extracted from molecular databases like HITRAN, together with the VALD data.

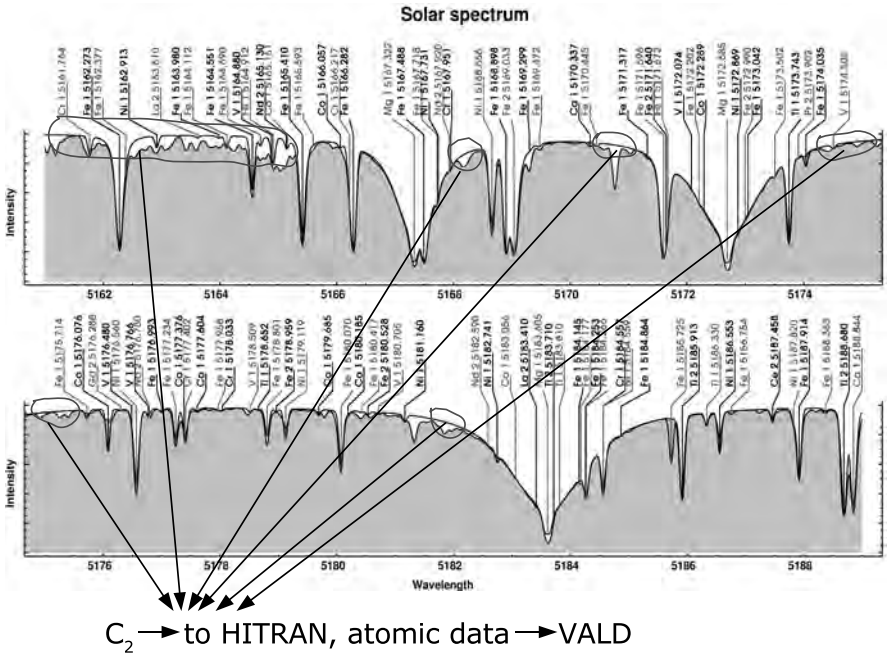

Fig. 2. The observed solar spectrum in the region of the 5167–83 Å Mg I triplet (shadowed area). Synthetic spectrum calculations with atomic lines only are shown by full line. Spectral regions with molecular C_2 lines are indicated by contour lines.

Ground-based spectroscopic observations in the near ultraviolet region are now available with modern CCD cameras, extending up to $\sim$3000 Å. However, proper continuum fits in the 3000–3400 Å range, so spectral analysis requires knowledge of the ozone molecule absorption in the Earth's atmosphere. Figure 3 demonstrates that all depressions seen in a non-normalized stellar spectrum have roughly the same shape as broad features in the ozone absorption curve taken from the S&MPO database. Thus, one cannot make a proper analysis of the atomic spectrum in the near UV without taking into account ozone absorption.

4. CONCLUSIONS

We have presented how the infrastructure of VAMDC has been designed with the aim of being a Virtual Observatory. This short presentation can be completed by the project documentation already available on the web site of VAMDC.

VAMDC is a virtual Observatory for Atomic and Molecular data that takes advantage of the work already done in the IVOA. It is a European program in development within the FP7 framework. However, VAMDC is already able to deliver results. Users who wish to test the system in the present status, before the end of the project, are welcome to contact the PI (Marie-Lise Dubernet). A contact form is available on the project web site.

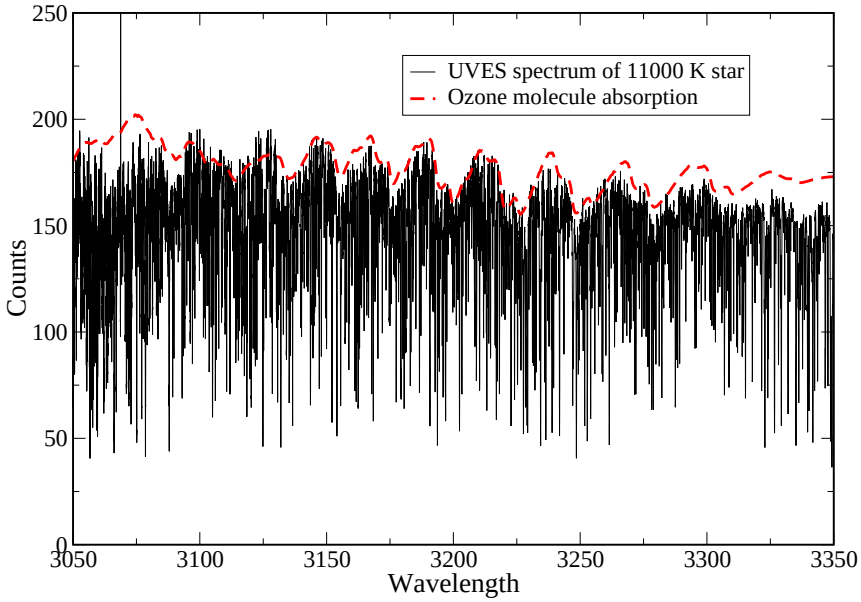

Fig. 3. The non-normalized spectrum of an 11 000 K star in the near ultraviolet range as observed with the UVES spectrograph. Depressions due to ozone molecule absorption (red dashed line) are clearly seen.

ACKNOWLEDGMENTS. The authors are grateful to the VAMDC Team for their help and to the IVOA for its work reused in the VAMDC project. VAMDC is funded under the "Combination of Collaborative Projects and Coordination and Support Actions" Funding Scheme of The Seventh Framework Program. Call topic: INFRA-2008-1.2.2 Scientific Data Infrastructure. Grant Agreement number: 239108.

REFERENCES

Chilingarian I. et al. 2009, Science, 326, 1379
Dubernet M. L., Boudon V., Culhane J. L. et al. 2010, JQSRT, 111, 2151
Padovani P. et al. 2004, A&A, 424, 545
Zolotukhin I., Chilingarian I. 2011, A&A, 526, A84

Baltic Astronomy, vol. 20, 448–452, 2011

THE COMPLEX BROAD ABSORPTION LINE PROFILES IN A SAMPLE OF QSO SPECTRA

E. Lyratzi[1,2], E. Danezis[1], L. Č. Popović[3], A. Antoniou[1,4], M. S. Dimitrijević[3,5] and D. Stathopoulos[1,2]

[1] *University of Athens, Faculty of Physics Department of Astrophysics, Astronomy and Mechanics, Panepistimioupoli, Zographou 157 84, Athens, Greece*

[2] *Eugenides Foundation, 387 Sygrou Av., 17564, Athens, Greece*

[3] *Astronomical Observatory of Belgrade, Volgina 7, 11160 Belgrade, Serbia*

[4] *University of Peloponnese, Faculty of Science and Technology, Department of Telecommunications Science and Technology, Karaiskakis Str. 22100 Tripolis, Greece*

[5] *Laboratoire d' Étude du Rayonnement et de la Matiére en Astrophysique, Observatoire de Paris-Meudon, UMR CNRS 8112, Bâtiment 18, 5 Place Jules Janssen, F-92195 Meudon Cedex, France*

Received: 2011 August 8; accepted: 2011 August 15

Abstract. Most of the Broad Absorption Lines (BALs) in quasars show very complex profiles. An idea to explain these profiles is that the dynamical systems of broad line regions are not homogeneous but consist of a number of dense regions or ion populations with different physical parameters. This approach is used to study the ultraviolet C IV resonance lines in the spectra of a group of high ionization BAL quasars, using the Gauss-Rotation model.

Key words: quasars: absorption lines

1. INTRODUCTION

Approximately 10% of all quasars exhibit broad, blue-shifted absorption lines. The outflow velocity of the regions producing these lines can reach (0.1–0.2) c. Usually, in their spectra we observe the lines of atoms with high ionization, such as C IV at $\lambda = 1549$ Å, Si IV at $\lambda = 1397$ Å, N V at $\lambda = 1240$ Å and Lyα. In some cases, low ionization lines, such as Mg II at $\lambda = 2798$ Å and Al III at $\lambda = 1857$ Å, also exhibit broad absorption lines (see, e.g., Hamann et al. 1993; Crenshaw et al. 2003). These Broad Absorption Lines (BALs) have different shapes; some types of these objects may also have differences in their continua (Reichard et al. 2003).

The spectra of the BAL quasars usually are interpreted as a combination of (1) a broad-band continuum arising from the central engine, (2) broad emission lines coming from the broad emission line regions (usually designated as BLRs or BELRs), emerging near the quasar center, and (3) superposed broad absorption lines, originating in a separate outlying region, so called Broad Absorption Line Region (BALR) (see also Lyratzi et al. 2009). However, it is also possible, that

both the emission and absorption lines originate in the same line-forming region (Branch et al. 2002).

An important question is: what is the physical connection between the standard BLRs and BALRs? It is known that at least a part of BLRs originate in the wind outflowing from the accretion disks (see Murray & Chiang 1998; Popović et al. 2004).

Another question is: where are BALRs placed with respect to the quasar centers and BLRs? To answer this question, one should investigate kinematical properties of the emission and absorption lines.

Disk wind models (Murray & Chiang 1998; Proga et al. 2000; Williams et al. 1999) explain many properties of BAL quasars, but it is unclear if they can explain the full range of BAL profiles and column densities. BALs are caused by outflowing gas intrinsic to the quasar, and are not produced by galaxies along the line of sight (as is the case for most narrow-absorption systems).

Determining whether a quasar contains a BALR is a complicated task. The standard method is to calculate the 'balnicity' index (BI), defined by Weymann et al. (1991).

Here we present some ideas directed to explain the complex structure of BALs in quasars and investigate the ultraviolet C IV resonance lines in the spectra of a group of high ionization BAL (Hi-BAL) quasars using the Gauss-Rotation model (GR model).

2. THE MULTI-STRUCTURE OF BALs

Most of BALs in quasars exhibit very complex profiles. This means that we cannot fit them with a known physical distribution. An idea is that the dynamical systems of BLRs are not homogeneous but consist of a number of dense regions or ion populations with different physical parameters.

Each of these dense regions gives an independent classical absorption line. If the source regions rotate with a large velocity and move radially with lower velocities, the produced lines have large widths and small shifts. As a result, they are blended among themselves as well as with the main spectral lines forming a complicated profiles. A similar model is used to explain the complex profiles of broad lines in the spectra of hot emission-line stars (Danezis et al. 2006, 2007; Lyratzi et al. 2009). Based on this idea, we study BALs by the ultraviolet C IV resonance lines in the spectra of 30 Hi-BAL QSOs using the GR model (Danezis et al. 2006, 2007; Lyratzi et al. 2009).

We assume that broad emission and absorption line regions are composed of a number of successive independent absorbing/emitting density layers of matter originating in the disk wind. The absorbing regions have three apparent velocities (projected on the line-of-sight of an observer): radial velocity (V_{rad}) of the BALR, random velocity of the ions (V_{rand}) in the BALR and the rotational velocity (V_{rot}) of the BALR.

3. DATA AND SPECTRAL ANALYSIS

In order to study the C IV resonance lines (1548.187 and 1550.772 Å) we apply the GR model to the spectra of 30 Broad Absorption Line Quasars (BAL QSOs) taken from the Sloan Digital Sky Survey (SDSS) Data Release 7. The SDSS imaging survey uses a wide-field multi-CCD camera (Gunn et al. 1998). The

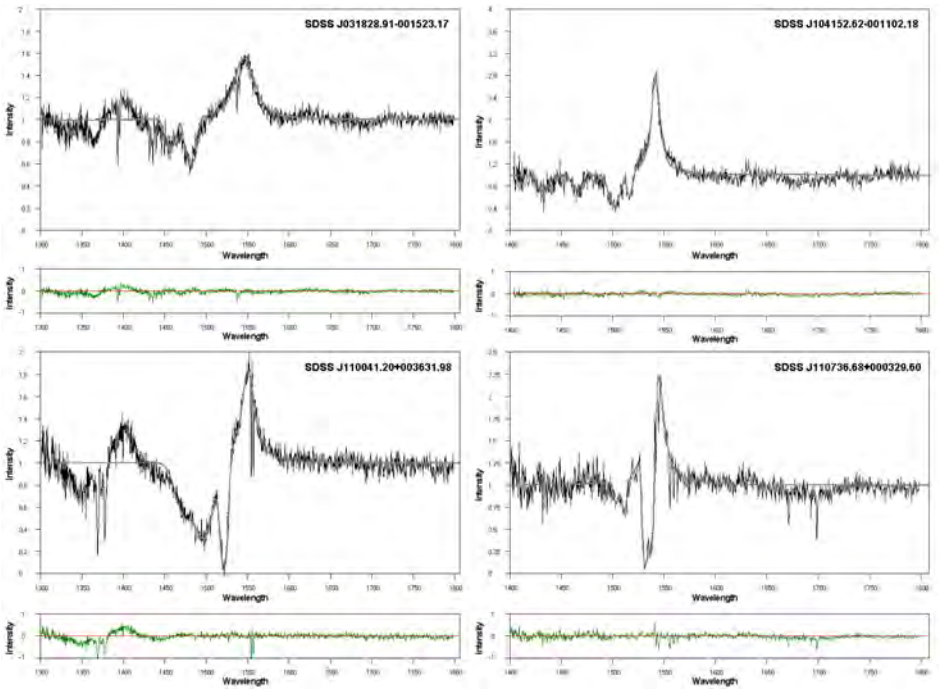

Fig. 1. Four examples of the fitted spectra. Black lines show the observed spectra and grey lines – theoretical line profiles given by the GR model. The lower panels show differences between the observed spectra and the corresponding theoretical profiles.

spectra cover the optical range 3800–9200 Å at a resolution of 1800–2100.

In Figure 1 we give some examples of the fitted spectra. The black line corresponds to the observed spectra and the grey line corresponds to the theoretical line profiles given by the GR model. The lower lines present the residuals, i.e., the differences between the observed spectrum and the theoretical profile.

We studied all the absorption lines that follow the first Balnicity Index criterion, i.e. the lines that are located between 3000 and 25 000 km/s blueward of the C IV emission, what means that these lines come from the studied BAL quasars. Then, from all these lines we accepted as BALs only those which follow the rest Balnicity Index criteria, i.e., the absorption lines are at least 2000 km/s broad and for them the absorption falls at least 10% below the continuum. We found that 25 of the 30 quasars of our sample have broad absorption lines.

4. RESULTS AND CONCLUSIONS

Using the GR model, we were able to fit the complex profiles of the studied C IV lines with 1 to 5 absorption components. For them we calculated the values of the kinematical parameters (rotational, radial and random velocities), as well as the column density and the absorbed energy. The calculated values of kinematical parameters only, are given in Tables 1 and 2.

It seems that the dynamical systems of BLRs are not homogeneous but consist of a number of density regions or ion populations with different physical parameters. Each one of these density regions gives us an independent classical absorption

Table 1. Radial velocities (km/s).

Object name (SDSS)	V_{rad1}	V_{rad2}	V_{rad3}	V_{rad4}	V_{rad5}
J001025.90+005447.6	–15092	–10642			
J001438.28-010750.1	–17026				
J001502.26+001212.4	–19348				
J002127.88+010420.1	–14624				
J003551.98+005726.4				–6192	
J004041.39-005537.3	–17220				
J004118.59+001742.4	–13931		–7740		
J004323.43-001552.4	–20896	–12770			
J004732.73+002111.3	–17414				
J005355.15-000309.3	–17026	–11609			
J005419.99+002727.9	–17607		–8513		
J010241.04-004208.9	–17414	–11802			–4063
J010336.40-005508.7	–17800				–4063
J011227.60-011221.7	–21283	–16446	–8513	–6385	
J015024.44+004432.99			–7546		–3483
J015048.83+004126.29	–18381				
J021327.25-001446.92				–5321	–3096
J023908.99-002121.42	–17414		–8513		
J025747.75-000502.91			–7352		
J031828.91-001523.17	–17994	–13157			
J102517.58+003422.17	–17994				
J104109.86+001051.76			–9867		
J104152.62-001102.18	–22637	–16059	–9287		
J104841.03+000042.81	–19348				
J110041.20+003631.98	–14704	–10061		–5417	
Mean	–17757	–12818	–8416	–5829	–3676

line.

As we can see in Tables 1 and 2, the GR model is able to reproduce accurately the complex profiles of Hi-BAL QSOs and to calculate a group of physical parameters of the corresponding BALRs.

The absorption lines which follow the BI criteria satisfy the following conclusions: (1) their radial velocities are between -3676 ± 410 km/s and -17757 ± 2171 km/s; (2) their random velocities are between 1117 ± 302 km/s and 2952 ± 1704 km/s; (3) the column density of all the absorption components of both doublet lines is almost the same, with the mean value $-3.35 \times 10^{-10} \pm 0.24 \times 10^{-10}$ cm^{-2}; (4) the absorbed energy is -5.52 ± 1.32 eV for $\lambda\,1548.187$ Å and -4.79 ± 1.26 eV for $\lambda\,1550.772$ Å.

ACKNOWLEDGMENTS. This research project is in progress at the University of Athens, Department of Astrophysics, Astronomy and Mechanics; we are thankful to the Special Account for Research Grants for the financial support.
This work was also supported by the Ministry of Science and Technological Development of Serbia through the projects "Influence of coalitional processes on astrophysical plasma line shapes" and "Astrophysical spectroscopy of extragalactic objects". We also acknowledge the use of the data from the SDSS and SDSS-II surveys.

Table 2. Rotational and random velocities (km/s).

Object name (SDSS)	$V_{\rm rot1}$	$V_{\rm rot2}$	$V_{\rm rot3}$	$V_{\rm rot4}$	$V_{\rm rot5}$	$V_{\rm rand1}$	$V_{\rm rand2}$	$V_{\rm rand3}$	$V_{\rm rand4}$	$V_{\rm rand5}$
J001025.90+005447.6	600	600				1596	1368			
J001438.28-010750.1	100					6155				
J001502.26+001212.4	100					6155				
J002127.88+010420.1	100					6155				
J003551.98+005726.4				100					787	
J004041.39-005537.3	3000					4559				
J004118.59+001742.4	100		100			2508		1824		
J004323.43-001552.4	3000	3000				2736	2736			
J004732.73+002111.3	100					4332				
J005355.15-000309.3	100	100				912	912			
J005419.99+002727.9	3000		550			2280		2052		
J010241.04-004208.9	50	50			50	1824	1824			798
J010336.40-005508.7	100				100	3420				1596
J011227.60-011221.7	550	550	550	550		1596	1254	912	798	
J015024.44+004432.99			1500		2200			1368		1140
J015048.83+004126.29	50					4104				
J021327.25-001446.92				100	100				912	935
J023908.99-002121.42	30		30			2280		2280		
J025747.75-000502.91			100					2280		
J031828.91-001523.17	2000	2000				456	570			
J102517.58+003422.17	50					2508				
J104109.86+001051.76			100					798		
J104152.62-001102.18	50	50	50			1140	1140	1140		
J104841.03+000042.81	50					2052				
J110041.20+003631.98	50	70		50		2280	2280		912	
Mean	1830	1538	550	550		2952	1510	1582	852	1117

REFERENCES

Branch D., Leighly K. M., Thomas R. C., Baron E. 2002, ApJ, 578, L37
Crenshaw M. D., Kraemer S. B., George I. M. 2003, ARA&A, 41, 117
Danezis E., Popović L. Č., Lyratzi E., Dimitrijević M. S. 2006, AIPC, 876, 373
Danezis. E, Nikolaidis D., Lyratzi E. et al. 2007, PASJ, 59, 827
Gunn J. E., Carr M., Rockosi C. et al. 1998, AJ, 116, 3040
Hamann F., Korista K. T., Morris S. L. 1993, ApJ, 415, 541
Lyratzi E., Popović L. Č., Danezis E. et al. 2009, NewAR, 53, 179
Murray N., Chiang J. 1998, ApJ, 494, 125
Popović L. Č., Mediavilla E., Bon E., Ilić D. 2004, A&A, 423, 909
Proga D., Stone J. M., Kallman T. R. 2000, ApJ, 543, 686
Reichard T. A., Richards G. T., Hall P. B. et al. 2003, AJ, 126, 2594
Weymann R. J., Morris S. L., Foltz C. B., Hewett P. C. 1991, ApJ, 373, 23
Williams R. J. R., Baker A. C., Perry J. J. 1999, MNRAS, 310, 913

Baltic Astronomy, vol. 20, 495–502, 2011

STARK BROADENING AND WHITE DWARFS

Milan S. Dimitrijević[1,2], Andjelka Kovačević[3], Zoran Simić[1] and Sylvie Sahal-Bréchot[2]

[1] *Astronomical Observatory, Volgina 7, 11060 Belgrade 38, Serbia; mdimitrijevic@aob.bg.ac.rs, zsimic@aob.bg.ac.rs*

[2] *Observatoire de Paris, LERMA, 5 Place Jules Janssen, 92190 Meudon, France; sylvie.sahal-brechot@obspm.fr*

[3] *Department of Astronomy, Faculty of Mathematics, University of Belgrade, Studentski Trg 16, 11000 Belgrade, Serbia; andjelka@matf.bg.ac.rs*

Received: 2011 August 8; accepted: 2011 August 15

Abstract. White dwarf and pre-white dwarfs are the best types of stars for the application of Stark broadening research results in astrophysics, since in the atmospheres of these stars physical conditions are very favorable for this line broadening mechanism – in hot hydrogen-deficient white dwarfs and pre-white dwarfs $T_{\rm eff}$ = 75 000–180 000 K and $\log g$ = 5.5–8 [cgs]. Even for much cooler DA and DB white dwarfs with typical effective temperatures of 10 000 K–20 000 K, Stark broadening is usually the dominant broadening mechanism. In this review, Stark broadening in white dwarf spectra is considered, and the attention is drawn to the STARK-B database (http://stark-b.obspm.fr/), containing the parameters needed for analysis and synthesis of white dwarf spectra, as well as for the collective efforts to develop the Virtual Atomic and Molecular Data Center.

Key words: stars: white dwarfs – Stark broadening, line profiles – databases

1. INTRODUCTION

Stellar spectroscopy is a powerful tool for investigation of stellar plasma – the temperatures in particular atmospheric layers, their chemical composition, as well as the surface gravity, spectral type and effective temperature of the star. For such purposes, in a number of cases, the influence of collisions with charged particles on emitting/absorbing atoms and ions is important in astrophysical plasmas, which results in the Stark broadening of spectral lines.

Physical conditions in the astrophysical plasmas are exceptionally different, so the Stark broadening is of interest in extreme conditions – from interstellar molecular clouds, where typical electron temperatures are $\sim$30 K or smaller and typical electron densities N_e = 2–15 cm^{-3} (see e.g. Dimitrijević 2010), to the temperatures 10^6–10^7 K and electron densities 10^{22}–10^{24} cm^{-3}. Especially favorable conditions for the Stark broadening are white dwarf and pre-white-dwarf atmo-

spheres, where this broadening mechanism is usually dominant in comparison with the concurrent one – thermal Doppler broadening.

In this work, we will consider Stark broadening in white dwarf spectra and the corresponding results obtained by members of the Group for Astrophysical Spectroscopy at the Belgrade Astronomical Observatory, and their partners from France, Tunisia, Russia and Canada. Also, the attention will be drawn to the STARK-B database (http://stark-b.obspm.fr/), containing Stark broadening parameters needed for white dwarf spectra analysis and synthesis, as well as to the new collective effort to develop Virtual Atomic and Molecular Data Center (VAMDC - http://vamdc.org/ – Dubernet et al. 2010, Rixon et al. 2011).

2. STELLAR PLASMA RESEARCH AND STARK BROADENING

As an example of the application of Stark broadening for astrophysical plasma research, we will draw attention that line profiles enter the modeling of stellar atmospheric layers when we determine quantities such as the absorption coefficient and the optical depth τ_ν. Let us take the direction of gravity as z-direction, dealing with a stellar atmosphere. If the atmosphere is in macroscopic mechanical equilibrium, with ρ is denoted gas density, the optical depth is

$$\tau_\nu = \int_z^\infty \kappa_\nu \rho dz, \tag{1}$$

$$\kappa_\nu = N(A,i)\phi_\nu \frac{\pi e^2}{mc} f_{ij}, \tag{2}$$

where κ_ν is the absorption coefficient at a frequency ν, $N(A,i)$ is the volume density of radiators in the state i, f_{ij} is the absorption oscillator strength, m is the electron mass and ϕ_ν is spectral line profile.

Stark broadening may be also important for radiative transfer and opacity calculations, abundances, surface gravity and chemical composition determination, spectra analysis, interpretation and synthesis and astrophysical plasma modeling. In the following, we will give several examples of the investigations of Stark broadening in stellar plasma, performed in the Group for Astrophysical Spectroscopy at the Belgrade Astronomical Observatory.

In a number of papers, the influence of Stark broadening on Au II (Popović et al. 1999b), Zr II and Zr III (Popović et al. 2001a), Nd II (Popović et al. 2001b), Co III (Tankosić et al. 2003), Ge I (Dimitrijević et al. 2003a), Si I (Dimitrijević et al. 2003b), Ga I (Dimitrijević et al. 2004), Cd I (Simić et al. 2005), Cr II (Dimitrijević et al. 2007) and Te I (Simić et al. 2009) spectral lines was considered in the spectra of chemically peculiar A-type stars, and in each case deeper atmospheric layers are found where the contribution of this broadening mechanism is dominant or could not be neglected in comparison with the Doppler broadening. In order to provide the corresponding Stark broadening data for rare-earth peak in elemental abundances distribution, Popović et al. (1999a) considered the influence of collisions with charged particles on rare earth ion lines in Ap star atmospheres (La II, La III, Eu II and Eu III) and found that the errors in equivalent width synthesis and corresponding abundance determination may be important and should be taken into account.

In order to demonstrate the influence of Stark broadening in atmospheres of hot stars, Figure 1 shows the Stark widths for Te I 6s $^5S^o$ – 7p ^5P (5125.2 Å)

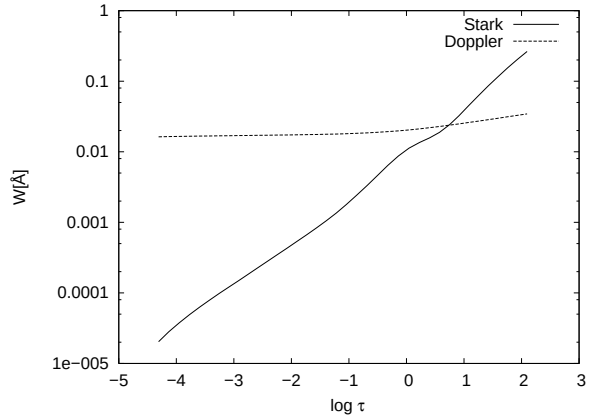

Fig. 1. Thermal Doppler and Stark widths for Te I 6s $^5S^o$ – 7p ^5P (5125.2 Å) multiplet as functions of Rosseland optical depth for an A-type star ($T_{\rm eff}$ = 10 000 K, log g = 4.5).

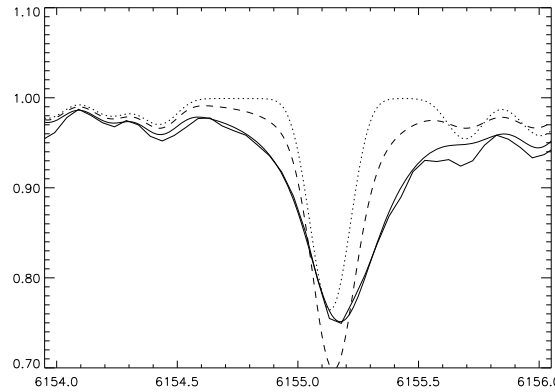

Fig. 2. A comparison between the observed Si I, 6155 Å line profile in the spectrum of Ap star 10 Aql (thick line) and synthetic spectra calculated with Stark widths and shifts from Table 1 in Dimitrijević et al. (2003b) and Si abundance stratification (thin line), with the same Stark parameters but for homogeneous Si distribution (dashed line), and with Stark width calculated by approximation formulae for the same stratification (dotted line).

multiplet (Simić et al. 2009), compared with the thermal Doppler widths for a model ($T_{\rm eff}$ = 10 000 K, log g = 4.5) of A-type star atmosphere (Kurucz 1979). Namely thermal Doppler broadening in stellar atmospheres is not a negligible broadening mechanism, and the comparison of the Stark and thermal Doppler widths may give an estimate on the importance of this effect. We note, however, that due to differences in the Gauss distribution function for the Doppler profile and the Lorentz distribution for Stark, even when the Stark width is smaller, this broadening mechanism may be significant in line widths. One can see in Figure 1, that in deeper atmospheric layers the Stark broadening mechanism becomes first comparable and than dominates in comparison with the thermal Doppler broadening.

The influence of Stark broadening and stratification on neutral silicon lines in the spectra of normal late A star HD 32115 and Ap stars HD 122970 and 10 Aql was investigated in Dimitrijević et al. (2003b). It was demonstrated that the synthetic profile of $\lambda = 6155.13$ Å Si I line fits much better to the observed one when Stark broadening is included.

3. WHITE DWARFS

From the aspect of the Stark broadening in stellar plasmas, white dwarfs are of particular interest. The first white dwarf, 40 Eridani, was discovered by W. Herschel on 1783 March 31. The second was Sirius B, the existence of which was predicted by Bessel in 1844; it was discovered by Alvan Graham Clarck in 1862. In 1950 one hundred of these stars were known, in 1999 – about 2000, and in the Sloan Digital Sky Survey more than 9000 white dwarfs are discovered.

Traditional division of white dwarfs is into hydrogen-rich (DA) and helium-rich (DB), where 'D' denotes degenerate objects. Due to gravitational separation in the absence of macroscopic motions like stellar wind or convection, the most abundant elements dominate by several orders of magnitude (Koester 2010), with rare exceptions. While the heavier elements diffuse downward, the lightest ones rest floating on the top of the atmosphere. The origin of H-deficient stars is the late helium shell flash in which white dwarf or post Asymptotic Giant Branch (AGB) star reignites helium shell burning, eliminating the rest of hydrogen in this violent event. Post AGB stars are also of great interest from the point of view of need and applicability of the Stark broadening data. Namely, AGB are stars which have terminated hydrogen and helium but not carbon burning. They form a sequence of bright red giants – AGB, and they are more luminous than the red giant branch stars, which have electron-degenerate helium cores. We note that AGB is often divided in AGB stars with carbon-oxygen cores and Super AGB (SAGB) stars with heavier elements in the cores.

White dwarfs of DA and DB types have effective temperatures between around 10 000 K and 40 000 K, so that the Stark broadening is important in analysis and modeling of their atmospheres and spectra. When the effective temperature of a cooling white dwarf becomes so low that neither helium nor hydrogen lines are present, the spectrum becomes only continuum (DC type). If in the spectra of hydrogen-rich or helium-rich atmospheres lines of various metals (but not carbon lines which will be discussed later) are seen, white dwarfs belong to DZ, DAZ or DBZ types. Such metals are considered to be accreted from outside, from interstellar matter or from some tidally disrupted asteroid (Koester 2010).

The non-DA white dwarfs are most interesting from the point of view of Stark broadening of non-hydrogen lines. They are divided to the following types: (1) DO, with 40 000 K $< T_{\rm eff} <$ 100 000 K (120 000 K according to Dreizler & Werner 1996) with the He II lines and the effective Stark broadening (Hamdi et al. 2008), (2) DB, with 12 000 K $< T_{\rm eff} <$ 40 000 K with He I lines, and (3) DQ, with 4000 K $< T_{\rm eff} <$ 12 000 K, with C lines and C_2 Swan band in the spectrum. It is assumed that carbon in the DQ white dwarfs is extracted from deeper layers by the growing convective zone (Koester 2010).

McGraw et al. (1979) discovered the first object of a new class of hot hydrogen-deficient degenerate stars, PG 1159-035. In the atmospheres of PG 1159 stars, a mixture of helium, carbon and oxygen is present. Most likely, they experienced a

very late thermal pulse which eliminated the rest of hydrogen, mixed helium with carbon, oxygen and other elements from the envelope and returned them back from white dwarf phase to the post-AGB phase. PG 1195 objects are very interesting for applications of results of Stark broadening investigations (Werner et al. 1991), with effective temperatures ranging from $T_{\rm eff} = 100\,000$ K to 140 000 K. They have high surface gravity ($\log g = 7$), and their photospheres are dominated by helium and carbon with a significant amount of oxygen (C/He = 0.5 and O/He = 0.13) (Werner et al. 1991). Their spectra, strongly influenced by Stark broadening, are dominated by He II, C IV, O VI and N V lines.

Nugent et al. (1983) discovered a faint blue star of the PG 1195 type, H 1504+65, which is not only hydrogen-, but also helium-deficient, with the atmosphere of carbon and oxygen in equal amounts. This is the hottest known star with $T_{\rm eff}$ of $170\,000 \pm 20\,000$ K, or a 'bare core of the former AGB star', according to Werner & Wolff (1999).

The need for abundant and reliable Stark broadening data for a number of trace elements, was highly stimulated by the Far Ultraviolet Spectroscopic Explorer satellite (FUSE), which provided astronomers with a great number of high resolution spectra of hot evolved stars within the wavelength range 907–1187 Å. Fontaine et al. (2008) note that FUSE range includes 'high density of transitions associated with numerous ionization levels of several elements such as: C, N, O, Si, S, P, Cl, Ne, Ar, V, Mn, Cr, Fe, Co, Ni, Ge, As, Se, Zr, Te, I and Pb among others.' For analysis and synthesis of spectra and modeling of atmospheres of hot white dwarfs, PG 1159 stars, hot B subdwarfs, post Asymptotic Giant Branch (AGB) objects such as Central Stars of Planetary Nebulae (CSPN), observed by FUSE, accurate Strak broadening data for great number of spectral lines of various atoms and their ions are needed. However, as it was pointed out in Rauch et al. (2007), line broadening data for many species and their ions are missing in the literature. Moreover, some existing data are provided within insufficient temperature and density ranges, and the extrapolation to the plasma conditions in line forming regions introduces additional errors.

A new type of hot DQ white dwarfs with $T_{\rm eff} = 18\,000$–$24\,000$ K and carbon-rich atmospheres, has been discovered recently by Dufour et al. (2007, 2008), enabling them to propose an evolutionary sequence of white dwarfs from H 1504+65 and PG 1195 objects to hot DO, DB and DQ types. In the newly discovered class of hot DQ white dwarfs, hydrogen and helium are absent; their spectra are dominated by the C II lines, while O II lines are also present (Dufour 2011). For the investigation and modeling of these stars, and in order to understand their origin and evolution, the accurate determination of surface gravity is essential. However, the interpretation and analysis of these new objects was humped by the lack of the corresponding Stark broadening data.

Members of the Group for Astrophysical Spectroscopy considered the influence of Stark broadening for DA, DB and DO white dwarf atmospheres (Popović et al. 1999b; Tankosić et al. 2003; Milovanović et al. 2004; Simić et al. 2006; Hamdi et al. 2008) and found that for these stars Stark broadening is dominant in practically all atmospheric layers.

As an example, Simić et al. (2006) considered the influence of Stark broadening on Cu III, Zn III and Se III spectral lines in DB white dwarf atmospheres for 4s ^{2}F – 4p ^{2}G^o (λ = 1774.4 Å), 4s ^{3}D – 4p ^{3}P^o (λ=1667.9 Å) and 4p5s ^{3}P^o - 5p ^{3}D (λ = 3815.5 Å) by using the corresponding model with $T_{\rm eff} = 15\,000$ K and $\log g =$

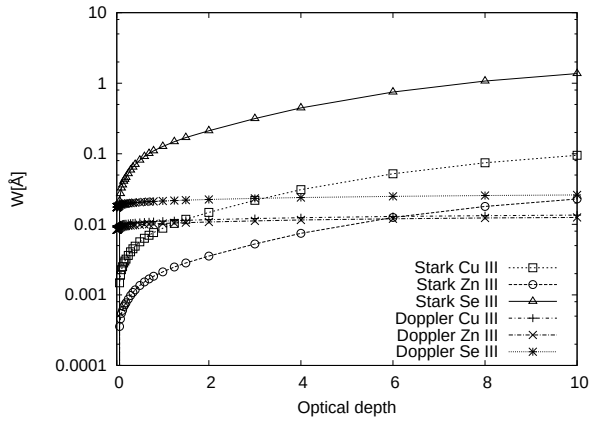

Fig. 3. Thermal Doppler and Stark widths for Cu III 4s ^{2}F – 4p ^{2}G^o (λ = 1774.4 Å), Zn III 4s ^{3}D – 4p ^{3}P^o (λ = 1667.9 Å) and Se III 4p5s ^{3}P^o – 5p ^{3}D (λ = 3815.5 Å) spectral lines for a model of the DB white dwarf atmosphere with $T_{\rm eff}$ = 15 000 K and $\log g$ = 7, as a function of the optical depth τ_{5150}.

7 (Wickramasinghe 1972). For this analysis, optical depth points at the standard wavelength λ_s = 5150 Å (τ_{5150}) are used as in Wickramasinghe (1972). One can see in Figure 3 that the thermal Doppler broadening has a much less importance in comparison with the Stark broadening mechanism. Comparing Figures 1 and 3 one can see that the importance of Stark broadening is much greater for DB white dwarf atmospheres than for A-type stars. This is the consequence of larger electron densities due to larger $\log g$ and $T_{\rm eff}$, so that electron-impacts producing Stark broadening are more effective.

For example, Figure 4 shows that the Stark width of the Se III 3815.5 Å line is larger than the Doppler width even by two orders of magnitude within the range of optical depths considered.

Hamdi et al. (2008) considered the broadening on Si VI lines in DO white dwarf spectra for $50\,000 \leq T_{\rm eff} \leq 100000$ K and for $6 \leq \log g \leq 9$ atmosphere models. They found that the influence of Stark broadening increases with $\log g$ and is dominant in broad regions of the considered DO atmospheres.

Currently, within a wide international collaboration (Canada, France, Tunisia, Serbia), the work on the Stark broadening of carbon and oxygen lines in hot DQ spectra (Dufour et al. 2011) is in progress.

Reliable Stark broadening data for white dwarf research may be found in the STARK-B database (http://stark-b.obspm.fr), dedicated for modeling of stellar atmospheres, analysis and synthesis of stellar spectra, as well as for laboratory plasma research, inertial fusion plasma, laser development and investigations of plasmas in various technologies. This database enters also in the European FP7 project 'Virtual Atomic and Molecular Data Centre' (VAMDC, P.I. Marie Lise Dubernet) with the following aims: (i) to build a secure, flexible and interoperable e-science environment based interface to the existing atomic and molecular databases; (ii) to coordinate groups involved in the generation, evaluation and use of atomic and molecular data, and (iii) to provide a forum for training of potential users (Dubernet et al. 2010; Rixon et al. 2011).

In future, a mirror site will be a part of the Serbian Virtual Observatory

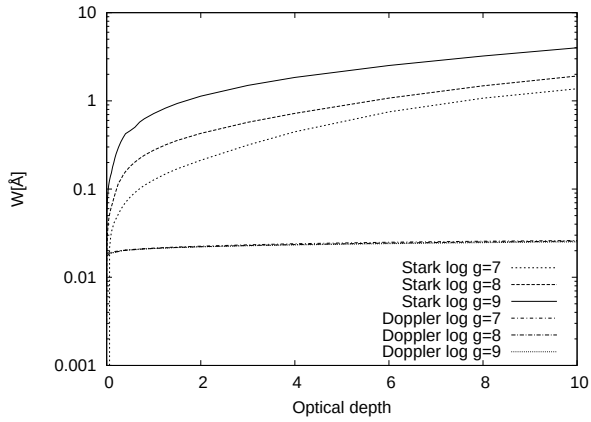

Fig. 4. Thermal Doppler and Stark widths for Se III spectral line 5s $^3P^o$ – 5p ^3D (λ = 3815.5 Å) for a model of the DB white dwarf atmosphere with $T_{\rm eff}$ = 15 000 K and $7 \leq \log g \leq 9$, as a function of the optical depth τ_{5150}.

(SerVO, http://www.servo.aob.rs/∼darko, P.I. Darko Jevremović). The main goal of the SerVO is to place the data, obtained by Serbian astronomers, into the VO with a compatible format, in particular the digitized photographic plates from the Belgrade Astronomical Observatory archive, in order to make them accessible to scientific community, as well as to provide astronomers in Serbia with VO tools for their research (Jevremović et al. 2009)

ACKNOWLEDGMENTS. This work was supported by VAMDC, funded under the 'Combination of Collaborative Projects and Coordination and Support Actions' Funding Scheme of the 7th Framework Program, grant agreement No. 239108. The authors are also grateful for the support provided by the Ministry of Education and Science of the Republic of Serbia through project No. 176002 'Influence of collisional processes on astrophysical plasma spectra', and No. III-44002 'Astroinformatics: Application of IT in astronomy and related disciplines'.

REFERENCES

Dimitrijević M. S. 2010, Mem. Soc. Astron. Ital., 75, 282
Dimitrijević M. S., Dačić M., Cvetković, Z. Simić Z. 2004, A&A, 425, 1147
Dimitrijević M. S., Jovanović P., Simić Z. 2003a, A&A, 410, 735
Dimitrijević M. S., Ryabchikova T., Popović L. Č. et al. 2003b, A&A, 404, 1099
Dimitrijević M. S., Ryabchikova T., Simić Z. et al. 2007, A&A, 469, 681
Dreizler S., Werner K. 1996, A&A, 314, 217
Dubernet M. L., Boudon V., Culhane J. L. et al. 2010, JQSRT, 111, 2151
Dufour P., Ben Nessib N., Sahal-Bréchot S., Dimitrijević M. S. 2011, Baltic Astronomy, 20, 511 (this issue)
Dufour P., Fontaine G., Liebert J. et al. 2008, ApJ, 683, 978
Dufour P., Liebert J., Fontaine G., Behara N. 2007, Nature, 450, 522
Fontaine M., Chayer P., Oliveira C. M. et al. 2008, ApJ, 678, 394
Hamdi R., Ben Nessib N., Milovanović N. et al. 2008, MNRAS, 387, 871

Jevremović D., Dimitrijević M. S., Popović L. Č. et al. 2009, New Astron. Rev., 53, 222

Koester D. 2010, Mem. Soc. Astron. Ital., 81, 921

Kurucz R. L. 1979, ApJS, 40, 1

McGraw J. T., Starrfield S., Liebert J., Green R. F. 1979, in *White Dwarfs and Variable Degenerate Stars*, IAU Coll. 53, eds. H. M. van Horn & V. Weidemann, Univ. of Rochester, p. 377

Milovanović N., Dimitrijević M. S., Popović L. Č., Simić Z. 2004, A&A, 417, 375

Nugent J. J., Jensen K. A., Nousek J. A. et al. 1983, ApJS, 51, 1

Popović L.Č., Dimitrijević M. S., Ryabchikova T. 1999a, A&A, 350, 719

Popović L.Č., Dimitrijević M. S., Tankosić D. 1999b, A&AS, 139, 617

Popović L.Č ., Milovanović N., Dimitrijević M. S., 2001a, A&A, 365, 656

Popović L.Č ., Simić S., Milovanović N., Dimitrijević M. S. 2001b, ApJS, 135, 109

Rauch T., Ziegler M., Werner K. et al. 2007, A&A, 470, 317

Rixon G., Dubernet M. L., Piskunov N. et al. 2011, AIP Conf. Proc., 1344, 107

Simić Z., Dimitrijević M. S., Kovačević A. 2009, New Astron. Rev., 53, 246

Simić Z., Dimitrijević M. S., Milovanović N., Sahal-Bréchot S. 2005, A&A, 441, 391

Simić Z., Dimitrijević M. S., Popović L.Č., Dačić M. 2006, New Astron., 12, 187

Tankosić D., Popović L. Č., Dimitrijević M. S. 2003, A&A, 399, 795

Werner K., Heber U., Hunger R. 1991, A&A, 244, 437

Werner K., Wolff B. 1999, A&A, 347, L9

Wickramasinghe D. T. 1972, Mem. Roy. Astron. Soc., 76, 129

Baltic Astronomy, vol. 20, 503–510, 2011

VAMDC AS A RESOURCE FOR ATOMIC AND MOLECULAR DATA AND THE NEW RELEASE OF VALD

F. Kupka[1] and the VAMDC Collaboration (P.I. M.-L. Dubernet)[2,3]

[1] *Faculty of Mathematics, University of Vienna, Nordbergstraße 15, A-1090 Vienna, Austria; Friedrich.Kupka@univie.ac.at*

[2] *LPMAA, UMR7092 CNRS/INP, Université Pierre et Marie Curie, France; Marie-Lise.Dubernet-Tuckey@upmc.fr*

[3] *LUTH, UMR8102 CNRS/INSU, Obsérvatoire de Paris, France*

Received: 2011 August 8; accepted: 2011 August 15

Abstract. The Virtual Atomic and Molecular Data Centre (VAMDC) is an EU-FP7 project devoted to build a common electronic infrastructure for the exchange and distribution of atomic and molecular data. Within VAMDC scientists from many different disciplines in atomic and molecular physics collaborate with users of their data and also with scientists and engineers from the information and communication technology community. In this presentation an overview of the current status of VAMDC and its capabilities are provided. In the second part of the presentation I will focus on one of the databases which have become part of the VAMDC platform, the Vienna Atomic Line Data Base (VALD). VALD has developed into a well-known resource of atomic data for spectroscopy particularly in astrophysics. A new release, VALD-3, will provide numerous improvements over its predecessor. This particularly relates to the data contents where new sets of atomic data for both precision spectroscopy (i.e., with data for observed energy levels) as well as opacity calculations (i.e., with data involving predicted energy levels) have been included. Data for selected diatomic molecules have been added and a new system for data distribution and data referencing provides more convenience in using the third release of VALD.

Key words: databases: catalogs – atomic data – molecular data

1. INTRODUCTION

The Virtual Atomic and Molecular Data Centre (VAMDC) has been founded to develop an interoperable electronic infrastructure for the exchange of atomic and molecular data. It unites 15 administrative partners who represent 24 teams from six European Union member states (Austria, France, Germany, Italy, Sweden, United Kingdom) as well as the Russian Federation, Serbia and Venezuela. Scientists from a wide variety of disciplines in atomic and molecular physics are involved in VAMDC as well as scientists and engineers from information and communication technology. Since many partners of VAMDC have already developed

specialized databases in their own field and many of them maintain a close connection to both data producer and data user communities, these resources were a natural asset of VAMDC from its very beginning.

The key difference of VAMDC to the databases provided by any of its contributors is that the newly developed electronic infrastructure allows access to each of these data resources through a single portal. The effort required by users in finding and retrieving data can thus be minimized, while the datasets themselves become available to a much wider community.

One of the databases integrated into the VAMDC framework is VALD, the Vienna Atomic Line Data Base (Piskunov et al. 1995; Kupka et al. 1999; Ryabchikova et al. 1999; Heiter et al. 2008). Developed and maintained at three of the VAMDC partner institutions, VALD has served as one of the databases selected for prototype implementations of VAMDC. The data collection available at VALD has been greatly enhanced as a result of very close collaboration with the data producers. Through the development of VAMDC a new functionality has been added. This new release, denoted VALD-3, has now reached a state of development which soon will permit its official distribution to the user community.

In the following section, the main concepts and capabilities of VAMDC are described. Its current status and further development plans are then reviewed. Finally, the most important improvements of VALD-3 over previous releases are briefly described. A final section summarizes these developments and looks forward to new releases of VAMDC.

2. CONCEPTS AND CAPABILITIES OF VAMDC

Atomic and molecular data have been collected and assessed in various databases which underpin a wide range of physics in applied research and industrial development. Many of them have been built to serve specific needs. VALD is one such examples with its own advantages, special tools and limitations. Heterogeneous data sets have been collected in different formats and with a varied degree of completeness. Specialized extraction tools exist for most of the databases, which often significantly contribute to their popularity. However, this development has also created problems: data often exist in duplicated form, sometimes also within a database, which requires non-trivial selection criteria when using them. Moreover, different user interfaces have to be handled each time a different database is being accessed. Thus access may be restricted and the available data may be fragmentary as a result of the collection process.

The main outcome expected from the VAMDC project is to

- develop and extend standards for interoperability of resources on atomic and molecular data;
- implement its concepts for the selected databases;
- allow easy access to numerous data resources;
- query of those resources with dedicated protocols and query languages;
- allow asynchronous transfer of large amounts of data;
- create a safe environment for publishing the latest sets of atomic and molecular data;
- link data producers more closely with data users.

The key benefits expected from using VAMDC are the possibilities to

- find any type of atomic and molecular data with a single click;

- have uniform access to the published data;
- allow cross-matching of different data sets;
- allow wide access to the latest published data.

The clientele of VAMDC includes people working in the fields of astrophysics, astronomy, planetary science, atmospheric science, fusion science, plasma science, radiation sciences and in the application of such research in e.g. industrial development, for instance, in the lighting industry.

The data exchange with databases that are part of VAMDC is organized through a web-based transport protocol. A user interface and an automatic interface are supported. This also allows access of the data through procedures developed for the international virtual observatory (Quinn et al. 2004). Publishing tools of data producers can access the system in a similar fashion. Mirroring and synchronization of the capabilities developed within VAMDC ensures a highly reliable service. This is backed up by an archiving strategy for long-term preservation of the distributed contents.

The transport protocol of VAMDC handles database queries for the status and data content (registry update), the query and data transfer between the user and the VAMDC portal as well as between specific databases and the portal. The transport protocol is self-descriptive (XML description of the data sent including units, formats etc. based on an extension of the XSAMS data format of Dubernet et al. 2009). It is also efficient for large data sets through using compressed binary tables. The interface to each database is fully compatible with the VAMDC transport on the outside (i.e., how the data resource is seen by a VAMDC user), but tuned to the specific database on the inside (i.e., how VAMDC sees a data resource). Functionalities of this interface include converting incoming queries to the internal query format and converting the database extraction to the transport-compatible VAMDC output format. Further capabilities are the ability to respond to VAMDC-specific queries such as registry updates (to keep track of which resources are available at what location) and collecting accounting information.

For a more detailed discussion of the scope of the VAMDC project the reader is referred to Dubernet et al. (2010) and to http://www.vamdc.eu/.

3. STATUS AND DEVELOPMENT OF VAMDC

An overview on the 'Level 1 Release' of VAMDC has been provided by Rixon et al. (2011). Achievements during this period included first prototypes of the protocol and XSAMS data model which were used to develop and provide archive-data services for a small selection of databases: VALD (Piskunov et al. 1995; Kupka et al. 1999; Ryabchikova et al. 1999; Heiter et al. 2008), XstarDB (Bautista & Kallman 2001), BASECOL (Dubernet et al. 2006) and CDMS (Müller et al. 2005).

Subsequently, protocols and data models have been further refined and a test web-site has been set up with a registry browser which enables users to access data contents from a much larger number of databases. In Table 1 we list the databases included in the Level 2 release of VAMDC which are accessible through the registry browser at the time of writing this paper and further databases for which access is just being prepared. All of them are expected to be available upon completion of the Level 2 release. Work on further databases is in progress.

Detailed references concerning these databases can be found in Dubernet et

Table 1. Databases accessible through the VAMDC Level 2 Release registry browser. Further information include the VAMDC node hosting the database, and its availability (all databases including those in preparation (in prep.) will become accessible at the most recent portal level). References to the original description are listed in column 5.

Database	Node	Status	Portal	Reference
BASECOL	LPMAA	available	Level 2	Dubernet et al. 2006
CDMS	Köln	available	Level 2	Müller et al. 2005
CDSD	IAO (LTS) Russia	available	Level 2	Perevalov & Tashkun 2008
CHIANTI	Cambridge / MSSL	available	Level 2	Dere et al. 2009
Ethylen	Reims	available	Level 2	see S&MPO and vadmc.eu
HITRAN	UCL	available	Level 2	Rothman et al. 2009
UDfA (UMIST)	Manchester / QUB (Belfast)	available	Level 2	Woodall et al. 2007
VALD	Uppsala University (mirror)	available	Level 2	see text
GhoSST	Grenoble	available	Level 1	Schmitt et al. 2009
Lund data	Uppsala University	available	Level 1	various
Methane lines	Dijon	available	Level 1	see S&MPO and vadmc.eu
S&MPO	Reims	available	Level 1	Mikhailenko et al.
Spectr-W^3	RFNC–VNIITF	available	Level 1	Faenov et al. 2002
KIDA	Bordeaux	in prep.		kida.obs.u-bordeaux1.fr
Stark-B	Paris-Meudon	in prep.		Jevremović et al. 2009
TipTopBase	IVIC / Cambridge	in prep.		Cunto et al. 1993

al. (2010), on the VAMDC website (http://www.vamdc.eu/), the Wiki page of VAMDC (http://voparis-twiki.obspm.fr/twiki/bin/view/VAMDC/WebHome) and the VAMDC newsletter available through these resources. After the Level 2 release a larger user community will be invited to test the VAMDC portal and its capabilities and the feedback will be used to improve the final release.

4. IMPROVEMENTS IN VALD-3

VALD was created by an international team of researchers (Piskunov et al. 1995; Kupka et al. 1999; Ryabchikova et al. 1999; Heiter et al. 2008). A lot of its early development occurred during small workshops at the Institute for Astronomy at the University of Vienna which became the site of the main server with mirror sites of the database installed at Uppsala University and the Institute of Astronomy of the Russian Academy of Sciences in Moscow. Today most of the software development and work on integrating molecular data into VALD is performed at Uppsala University. Most of the atomic data collection and systematic testing of the data distributed through VALD occurs at the Institute of Astronomy of the Russian Academy of Sciences in Moscow.

Ahead of the VALD-3 release, the database contains over 160 line lists and over 66 million atomic lines provided by all major spectroscopy centres across the world. The mirror sites in Vienna, Uppsala and Moscow serve nearly 1500 users from more than 50 countries. On average 30 requests are being processed per day.

VALD was designed to compile accurate and complete line lists for stellar atmospheres and spectroscopy. Line lists included within it are evaluated to provide a ranking which is used to prefer in the case of duplicated entries one set of data over another. The database was designed to be expandable with respect to data and content to allow simple access through customized extraction software, fast access to individual data entries, and allow either an overview of parameters from different sources or, as an alternative choice, extract sets of the best available data according to data ranking lists and compile data references for citing original

sources.

To this end before adding a data set to the database the data have to be converted first into a standard format with units which are commonly used in astrophysics. Multiple extraction layers within VALD allow accessing and merging of the data and prepare output for different applications. Requests can be posed as e-mails or issued through a web interface. Originally data were sent back only by e-mail, although as part of VALD-3 a possibility for downloading much larger responses to user requests will be offered (internally, data output can simply be streamed into files or standard text input interfaces).

Several quantities must be known about a line when adding its data to VALD: central wavelength, species identifier, $\log(gf)$, and energies as well as total angular momentum quantum numbers of lower and upper levels of the transition. These are the most crucial data for calculating absorption lines (in local thermal equilibrium) and they are also used for deciding on how to merge line lists from different sources. Lines are considered to be identical, if they originate from the same species, have identical total angular momentum quantum numbers for both levels and differ by less than a threshold with respect to wavelength and energy of both levels.

Further data entries which can be added for a spectral line included within the VALD database are Landé-factors of both energy levels, damping constants for natural line broadening as well as quadratic Stark effect and Van-der-Waals broadening, term designations and information on accuracy or comments on multiplets, as well as some multipurpose flags.

For spectral lines where both energy levels are experimentally known the mandatory data entries are usually sufficient to uniquely distinguish them and avoid erroneous identification of duplicates. Since lines with at least one predicted energy level have a very low ranking, such data will be rejected, when misidentified with a spectral line with observed energy levels, which results in the worst case in not putting out a (usually very weak) predicted line. No false information can be generated this way in an entry put out as a response to a request to the database. Such a potential loss only affects statistical opacity calculations for model atmospheres, since for precision spectroscopy data with even just one predicted energy level is useless because of an unacceptable uncertainty in wavelength of the transition. It is important to note here that also term designations may be uncertain for some spectral lines and that their notation can be incoherent among different sources. Hence, using them as an additional criterion for line identification was not an option when VALD was originally created. The introduction of such a consistent notation for the line data stored is still an ongoing project.

The ranking provided by the VALD team uses quality determinations based on error estimates from original sources, comparisons with existing alternative sources, and applications in astrophysics (user feedback). A re-ranking is possible and has occurred on several occasions. General guidelines for this process are that experimental data are preferred over calculations (with few exceptions) and data with individual error estimates are considered more reliable. Line lists from homogeneous sources with high accuracy data are given priority over sources which are inhomogeneous or have low quality data. To add flexibility to this process users can change the ranking for the merging process.

While the first two releases of VALD, dating from 1995 and 1999 (with a subsequent number of data updates) were accomplished by a rather small team of researchers, the VALD-3 release is now being prepared by a much larger group

which is a consortium of scientists from different institutions. Already the core group working in Uppsala, Moscow and Vienna is twice as large and includes U. Heiter, N. Piskunov, H.C. Stempels as well as P. Barklem and O. Kochukhov at Uppsala University, R. Kildiyarova, Yu. Pakhomov and T. Ryabchikova at Institute of Astronomy in Moscow, with both sides supported by further researchers working primarily on VAMDC, and F. Kupka, T. Rank-Lüftinger, W.W. Weiss at University of Vienna, where further researchers have contributed to earlier stages of VALD-3 (L. Fossati, N. Nesvacil, M. Obbrugger, Ch. Stütz). There is also a very close collaboration with many of the leading data producers in the area of interest for VALD. This originally included the spectroscopy group at the University of Wisconsin headed by J. E. Lawler and E. A. Den Hartog, the spectroscopy group at Lund University (H. Nilsson et al.), the Dream Database team (Biémont et al. 1999), as well as B. Plez at the Université de Montpellier and R. L. Kurucz at CfA in Harvard, the team of J.S. Sobeck et al. at the University of Texas at Austin, and the team at Imperial College London, headed by J. C. Pickering and R. J. Blackwell-Whitehead. The list of data provides is still growing at this point.

In VALD-3, data are still sorted as a function of wavelength and still stored in a special compressed format allowing semi-direct access to individual entries. The data stored therein still contains for each spectral line a species description, wavelength (inside the database consistently in Å for *vacuum conditions*), energies of lower and upper levels (*now in* cm^{-1}), total angular momentum quantum number, oscillator strength in the form of $\log gf$, Landé-factors of both energy levels, damping constants, but also more information on the *accuracy of* $\log gf$, and in addition to the data reference, a *full designation of level and term name*.

Publishing a new dataset in VALD-3 still means adding a new data file to the existing set, while data description continues to be stored in various support files (i.e., a list of species, and a configuration file which stores ranks for every field in each file to allow merging data from different sources). An important change is that references for each data set are now provided in BibTeX format. Indeed, the origin of each entry is now accessible even for merged line lists such as BELLHEAVY (cf. Kurucz 1992).

In addition to many smaller new lists the New Kurucz Calculations (2006–2010) for Fe-peak elements have been included into the data. All these additions allow much more accurate matching of absorption line spectra of various types of stars. The model-based selection of lines within VALD, a very popular tool among users, has also been improved to make estimates of the contribution to opacities and predictions of the line strength more accurate and convenient.

5. OUTLOOK AND CONCLUSIONS

In spite of its improvements the upcoming VALD-3 release is subject to a number of restrictions: the range of ionization stages is limited (neutral up to 8 times ionized) and only simple molecules will be included in VALD-3 (basically diatomics: TiO, CO, CN, CH, C_2, FeH). Generally missing data include collisional transition probabilities and advanced broadening approximations, among others. Since the VALD consortium has neither the personnel nor the expertise to fix these deficiencies, even frequent VALD users may sometimes want to look for alternatives. One possible solution is to access the VAMDC data resources.

With its very wide range of atomic and molecular databases VAMDC can offer a common access portal to a large variety of data collections through platform

and database independent methods. It thus can provide benefits for both current users of the databases participating in VAMDC and to novice users searching for information on atomic and molecular data who will no longer have to learn how to use a multitude of interfaces.

A number of conferences will provide opportunities for testing VAMDC and also offer tutorials on how to use its capabilities. The third annual VAMDC Conference which will take place in Vienna, Austria, on 2012 February 21–24 (see http://www.vamdc.eu/) is one such opportunity, as is the VAMDC Regional Workshop and School in Atomic and Molecular Data, which is to take place in Belgrade, Serbia, on 2012 June 7–9 (http://poincare.matf.bg.ac.rs/~andjelka/VAMDC/). It is hoped that in the future VAMDC will become the reference location in the internet where to look for atomic and molecular data.

ACKNOWLEDGMENTS. F. Kupka would like to express his gratitude to the LOC of the 8th SCSLSA for financial support as well as the Austrian FWF for funding through project P21742-N16. The help and suggestions of U. Heiter and N. Mason who carefully proofread this manuscript are greatly appreciated. This work has been presented as part of the VAMDC collaboration. VAMDC is funded under the 'Combination of Collaborative Projects and Coordination and Support Actions' Funding Scheme of the Seventh Framework Program. Call topic: INFRA-2008-1.2.2 Scientific Data Infrastructure. Grant Agreement number: 239108.

REFERENCES

Bautista M. A., Kallman T. R. 2001, ApJS, 134, 139

Biémont E., Palmeri P., Quinet P. 1999, Ap&SS, 269, 635

Cunto W., Mendoza C., Ochsenbein F., Zeippen C. 1993, A&A, 275, L5

Dere K. P., Landi E., Young P. R. et al. 2009, A&A, 498, 915

Dubernet M. L., Grosjean A., Flower D. et al. 2006, J. Plasma Research, 7, 356

Dubernet M. L., Humbert D., Clark R. E. H. et al. 2009, XSAMS: XML schema for Atomic, Molecular and Solid Data, http://www-amdis.iaea.org/xml/, Version 0.1

Dubernet M. L., Boudon V., Culhane J. L. et al. 2010, JQSRT, 111, 2151

Faenov A. Y., Magunov A. I., Pikuz T. A. et al. 2002, AIP Conf. Proc., 636, 253

Heiter U., Barklem P., Fossati L. et al. 2008, *VALD – an Atomic and Molecular Database for Astrophysics*, Journal of Physics, Conf. Ser., 130, 1

Jevremović D., Dimitrijević M. S., Popović L.Č et al. 2009, New Astron. Rev., 53, 222

Kupka F., Piskunov N., Ryabchikova T. A. et al. 1999, A&AS, 138, 119

Kurucz R. L. 1992, Rev. Mex. A&A, 23, 45

Mikhailenko S., Barbe A., Babikov Y., Tyuterev V. G. http://smpo.iao.ru/

Müller H. S. P., Schlöder F., Stutzki J., Winnewisser G. 2005, J. Mol. Struct., 742, 215

Perevalov V. I., Tashkun S. A. 2008, *Carbon Dioxide Spectroscopic Databank: Updated and Enlarged Version for Atmospheric Applications*, in 10th HITRAN Database Conference, Cambridge University Press

Piskunov N. E., Kupka F., Ryabchikova T. A. et al. 1995, A&AS, 112, 525

Quinn P., Barnes D., Csabai I. et al. 2004, *The International Virtual Observatory Alliance: Recent Technical Developments and the Road Ahead*, SPIE, 5493, 137

Rixon G., Dubernet M. L., Piskunov N. et al. 2011, in *7th International Conference on Atomic and Molecular Data and Their Applications*, AIP Conf. Proc., 1344, 107

Rothman L. S., Gordon I. E., Barbe A. et al. 2009, JQSRT, 110, 533

Ryabchikova T. A., Piskunov N. E., Stempels H. C. et al. 1999, in *Proc. of the 6th Int. Coll. on Atomic Spectra and Oscillator Strengths*, Phys. Scripta, T83, 162

Schmitt B. P., Volcke E., Quirico O. et al. 2009, *The Grenoble Astrophysics and Planetology Solid Spectroscopy and Thermodynamics Database Service*, http://ghosst.obs.ujf-grenoble.fr/

Woodall J., Agúndez M., Markwick-Kemper A. J., Millar T. J. 2007, A&A, 466, 1197

Baltic Astronomy, vol. 20, 511–515, 2011

STARK BROADENING OF CARBON AND OXYGEN LINES IN HOT DQ WHITE DWARF STARS: RECENT RESULTS AND APPLICATIONS

P. Dufour[1], N. Ben Nessib[2], S. Sahal-Bréchot[3] and M. S. Dimitrijević[3,4]

[1] *Département de Physique, Université de Montréal, Montréal, H3C 3J7, Canada; dufourpa@astro.umontreal.ca*

[2] *INSAT (National Institute of Applied Sciences and Technology), University of Carthage, Tunis, Tunisia; nebil.bennessib@planet.tn*

[3] *Observatoire de Paris, LERMA, CNRS, UMR 8112, 5 Place Jules Janssen, 92190 Meudon, France; sylvie.sahal-brechot@obspm.fr*

[4] *Astronomical Observatory, Volgina, 7, 11060 Belgrade 38, Serbia; mdimitrijevic@aob.bg.ac.rs*

Received: 2011 August 8; accepted: 2011 August 15

Abstract. White dwarf stars are traditionally found to have surface compositions made primarily of hydrogen or helium. However, a new family has recently been uncovered, the so-called hot DQ white dwarfs, which have surface compositions dominated by carbon and oxygen with little or no trace of hydrogen and helium (Dufour et al. 2007, 2008, 2010). Deriving precise atmospheric parameters for these objects (such as the effective temperature and the surface gravity) requires detailed modeling of spectral line profiles. Stark broadening parameters are of crucial importance in that context. We present preliminary results from our new generation of model atmospheres including the latest Stark broadening calculations for C II lines and discuss the implications as well as future work that remains to be done.

Key words: stars: white dwarfs, fundamental parameters, Stark broadening

1. INTRODUCTION

A new spectral class of white dwarf stars with surface compositions dominated by carbon and oxygen, the hot DQs, has recently been discovered (Dufour et al. 2007). The first generation of model atmospheres used to analyze these stars revealed that they were both hydrogen and helium deficient and that all of them are clustered in a very narrow range of effective temperatures between 18 000 and 23 000 K (Dufour et al. 2008). Follow-up high signal-to-noise spectroscopic observations of these rare white dwarfs using the MMT (6.5 m) and the Keck (10 m) telescopes also revealed Zeeman splitted line profiles in more than half of these stars, indicating the presence of strong surface magnetic fields in the mega Gauss range (Dufour et al. 2009, 2010). Luminosity variations have also been observed in five of the 14 known hot DQ white dwarfs (Montgomery et al. 2008; Barlow

et al. 2008; Dunlap et al. 2010; Dufour et al. 2011), opening up a new window through which one may study these stars by means of asteroseismology.

One of our main challenges is now to successfully explain and understand the extraordinary properties and characteristics of these stars, as well as the place they occupy in stellar evolution. In order to achieve this, atmospheric parameters (effective temperatures, surface gravities, surface chemical compositions, etc.) must be determined accurately. Of particular importance is a better determination of the surface gravity since this would severely constrain the mass of the progenitors via the initial-to-final mass relationship. For example, an extremely high surface gravity may indicate that these white dwarf stars have evolved from some of the most massive stars on the main sequence that do not explode as supernovae. As such, they could have cores made of elements much heavier than carbon and oxygen.

In the context of carbon/oxygen dominated atmosphere, it is very important to have good Stark broadening damping constants in order to derive meaningful atmospheric parameters from line profiles. However, Stark damping constants for all of the hundreds of C II lines, from UV to optical, observed in hot DQ white dwarfs, are not readily available from the literature (for example, only a few lines can be found in Griem 1974, Goly and Weniger 1982, Djenize et al. 1988, Blagojevic et al. 1999, Sreckovic et al. 2000, Mahmoudi et al. 2004 and many other references, clearly insufficient for our needs). Moreover, since the first detailed analysis of hot DQ white dwarfs presented in Dufour et al. (2007, 2008) were based on low signal-to-noise ratio SDSS observations, the first generation of hot DQ model atmospheres were built simply using the standard approximation (see Castelli 2005): $\gamma_s/N_e = 10^{-8} n_{\rm eff}^5$ where γ_s is the Stark width of the line in angular frequency units and $n_{\rm eff}$ is the effective quantum number (Kurucz line list also gives damping constants for a few C II lines, but these values are listed only for a single temperature of 10 000 K and are based on questionable approximations as well). While this approximation, which is loosely a fit by Peytremann (1972) to detailed calculations by Sahal-Bréchot & Segre (1971), was enough to reveal the basic properties of hot DQ stars. However, this method is not appropriate for a precise determination of atmospheric parameters, especially the surface gravity from the high S/N spectroscopic data now available.

In order to go beyond these limitations from the input data in our stellar modeling, we calculated widths and shifts for all the isolated lines of the C II ion due to electron collisions, recalculated model atmosphere grids for hot DQs and refitted the C II line profiles appropriately.

2. CALCULATIONS AND RESULTS

Stark broadening parameters were determined within the semi-classical perturbation method for 1002 C II lines between $\sim$400 and 10 000 Å in the VALD database (see Larbi-Terzi et al. 2010, Sahal-Bréchot 2010 and Sahal-Bréchot et al. 2011). The calculations were performed for an electron density of 10^{17} cm^{-3} and temperatures between 5000 K and 100 000 K. In order to facilitate the inclusion of all these calculations in our stellar atmosphere code, we fitted, for each C II line, a smooth function of the form $\log(w) = D_1 + D_2\ log(T) + D_3\ (log(T))^2$, where w is the FWHM width in angstroms. The D_i for each line can easily be implemented into our line list in order to get the correct width for the temperature and electron density at each depth of a given model atmosphere. It is noted that the

Table 1. Stark widths for the strong C II 4267 line ($N_e = 10^{17}$ cm^{-3}).

T (K)	Width (Å)
5000	2.08
10 000	1.67
20 000	1.37
30 000	1.26
50 000	1.16

new Stark widths calculated here are significantly different than those obtained from the above approximation. Moreover, we now explicitly take into account the variation of the width with the temperature in the model atmosphere calculations, a variation that is not simply proportional to $T^{-1/2}$, the expected dependency according to simple classical calculations (Table 1 shows, for example, the result of the new Stark broadening calculations for the strong C II 4267 line). The widths are scaled linearly with electron density, a reasonable approximation that is valid for the densities of interest here (electron densities of the order of $N_e \sim 10^{18}$ cm^{-3} are reached only in the deepest layers where $\tau_R > 10$).

Using these state-of-the-art Stark broadening parameters for C II lines, we next computed a new model atmosphere grid for hot DQ stars. This new generation of model atmosphere also includes several improvements over those presented in Dufour et al. (2008). The numerous modifications made to our code will be reported in details in a forthcoming publication. Our grid covers a range from $T_{\rm eff} = 16\,000$ to $25\,000$ K in steps of 1000 K, from $\log g = 7.5$ to 10.0, in steps of 0.5 dex, and from $\log({\rm C/H}) = +3.0$ to 0.0, in steps of 1.0 dex. This grid has been calculated with a fixed value of C/O = 1.0 for this exploratory study, a value appropriate for SDSS J1153+0056 according to a preliminary inquiry. Proper navigation in the C/O dimension will be done in due time.

We first focus on the simpler objects which do not show signs of magnetic line splitting (limits of about 300–400 kG given the spectral resolution of our observations). Our spectroscopic fitting procedure relies on the standard nonlinear least-squares method of Levenberg-Marquardt, and is similar to that described in Dufour et al. (2008). Figure 1 shows an example of our best fit solution for SDSS J1153+0056. We refrain, however, from giving final atmospheric parameters at this point since, in this preliminary study, we calculated only one grid with a fixed oxygen abundance. Moreover, new oxygen line Stark width calculations, which are currently underway, will also need to be included to replace the approximation used in our grid. As a consequence, it is expected that the atmospheric parameters that we derive here will change slightly when all the correct ingredients are put together and the parameter space explored appropriately.

Nevertheless, we can already notice significant improvements in the quality of our fits compared to our first generation of models (see Fig. 2 of Dufour et al. 2009, for example). Quantitatively, we also observe significant difference between the parameters determined in Dufour et al. (2008) and those found with our new model atmosphere grid. For egzample, we find surface gravities much higher than $\log g \sim 8$ reported in Dufour et al. (2008), with our values in the vicinity of $\log g \sim 9$. Such differences are due to a combination of several factors: better S/N ratio spectroscopic observations, improved continuum opacities, new Stark

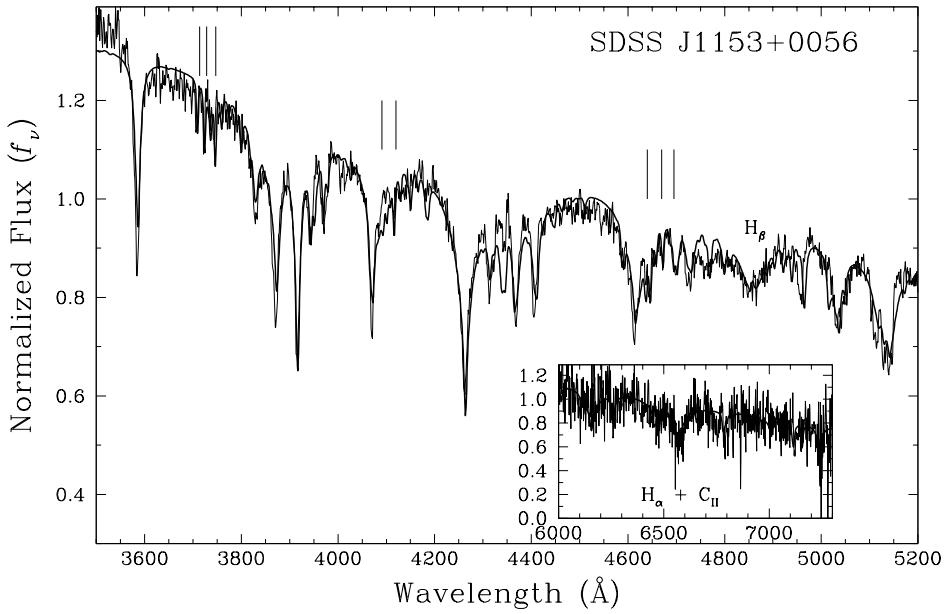

Fig. 1. Fit of a model to the carbon lines for the hot DQ SDSS J1153+0056. Oxygen lines, which are not fitted, are indicated by tick marks. The thick line is the best solution obtained by fitting the optical (MMT) data. The insert shows the Hα region (SDSS spectroscopic observations). The C/O ratio is fixed to 1 in this preliminary analysis. This represent a significant improvement over the 'first generation' fits of Dufour et al. (2009, see their Fig. 2).

broadening parameters and the presence of large amount of oxygen that was previously unnoticed. It thus appear that hot DQ stars are among the most massive white dwarfs known. Unfortunately, as noted above, there are still more calculations that remain to be completed before we can provide a better quantitative assessment of this affirmation. We must, however, remain cautious about such interpretation since it is possible that the line profile appears broader as a result of unresolved components of lines slightly split by a weak magnetic field. Further high resolution spectropolarimetric observations, which we hope to obtain soon, should alleviate this issue.

3. CONCLUSIONS

A new generation of model atmospheres, including state-of-the-art C II Stark broadening data, is used for a detailed modeling of hot DQ white dwarfs. The new Stark broadening data calculated specifically for this work will soon be available in the STARK-B database (http://stark-b.obspm.fr/).

Fits of the modeled line profiles to high *S/N* spectroscopic data yield atmospheric parameters that are significantly different from those presented in Dufour et al. (2008). As a consequence, it is now believed that the hot DQ stars might be among the most massive isolated white dwarfs that can be formed by standard stellar evolutionary channels. However, further calculations are still required before more precise atmospheric parameters can be published with confidence. For

instance, O I, O II and C I Stark broadening data also need to be incorporated in our model atmosphere calculations.

Future work will also focus on modeling of the UV region (spectroscopic data from HST/COS are now available for 5 hot DQs, see Dufour et al. (2010). For such hot stars, most of the flux is emitted in that part of the electromagnetic spectrum. Furthermore, model atmospheres including magnetic fields with different geometry will need to be developed for the analysis of the majority of hot DQs. As the spectroscopic modeling of the hot DQ stars gains in maturity, and more accurate atmospheric parameters become available, a better understanding of the origin and evolution of these strange stars should soon emerge.

ACKNOWLEDGMENTS. P.D. is CRAQ postdoctoral fellow. This work was supported in part by the NSERC of Canada and FQRNT Québec. It is also supported in part by the project 176002 of the Ministry of Education and Science of Serbia, by the bilateral cooperation agreement between Tunisia (DGRS) and France (CNRS) (project code 09/R 13.03, No. 22637), by the Paris Observatory and by the Programme National de Physique Stellaire (INSU-CNRS).

REFERENCES

Barlow B. N., Dunlap B. H., Rosen R., Clemens J. C. 2008, ApJ, 688, 95

Blagojević B., Popović M. V., Konjević N. 1999, Physica Scripta, 59, 374

Castelli F. 2005, Mem. Soc. Astron. Ital. Suppl., 8, 44

Djenize S., Srecković A., Milosavljević M., Labat O., Platisa M. 1988, Z. f. Phys. D, 9, 129

Dufour P., Liebert J., Fontaine G., Behara N. 2007, Nature, 450, 522

Dufour P., Fontaine G., Liebert J., Schmidt G. D., Behara N. 2008, ApJ, 683, 978

Dufour P., Liebert J., Swift B. et al. 2009, J. Phys. Conf. Ser., 172, 012012

Dufour P., Fontaine G., Bergeron P. et al. 2010, *17th European White Dwarf Workshop*, AIP Conf. Proc., 1273, 64

Dufour P., Béland S., Fontaine G. et al. 2011, ApJ, 733, 19

Dunlap B. H., Barlow B. N., Clemens J. C. 2010, ApJ, 720, 159

Goly A., Weniger S. 1982, JQSRT, 28, 389

Griem H. R, 1974, *Spectral Line Broadening by Plasmas*, Academic Press

Larbi-Terzi N., Sahal-Bréchot S., Ben Nessib N., Dimitrijević M. S. 2010, *17th European White Dwarf Workshop*, AIP Conf. Proc., 1273, 428

Mahmoudi W. F., Ben Nessib B., Sahal-Bréchot S. 2004, Physica Scripta, 70, 142

Montgomery M. H., Williams K. A., winget D. E. et al. 2008, ApJ, 678, 51

Peytremann E. 1972, A&A, 17, 76

Sahal-Bréchot S. 2010, J. Phys. Conf. Ser., 257, 012028

Sahal-Bréchot S., Dimitrijević M. S., Ben Nessib N. 2011, Baltic Astronomy, 20, 523 (this issue)

Sahal-Bréchot S., Segre E. R. A. 1971, A&A, 13, 161

Sreckovic A., Drincić V., Bukvić S., Djenize S. 2000, J. Phys. B, 33, 4873

Baltic Astronomy, vol. 20, 523–530, 2011

COMPARISONS AND COMMENTS ON ELECTRON AND ION IMPACT PROFILES OF SPECTRAL LINES

Sylvie Sahal-Bréchot[1], Milan S. Dimitrijević[2,1], Nebil Ben Nessib[3]

[1] *Paris Observatory, LERMA CNRS UMR 8112, UPMC, 5 Place Jules Janssen, 92190 Meudon, France; sylvie.sahal-brechot@obspm.fr*

[2] *Astronomical Observatory, Volgina 7, 11060 Belgrade 38, Serbia; mdimitrijevic@aob.bg.ac.rs.*

[3] *National Institute of Applied Sciences and Technology, University of Carthage, Tunis, Tunisia; nebil.bennessib@planet.tn*

Received: 2011 August 8; accepted: 2011 August 15

Abstract. Stark broadening theory is currently operated for calculating widths and shifts of spectral lines that are needed for spectroscopic diagnostics and modeling in astrophysics, laboratory and technological plasmas. We have calculated a great number of data, obtained through the impact semiclassical perturbation theory: tables have been published for neutral atom and ion emitters, and typical temperatures, electron and ion densities. They are currently implemented in the STARK-B database which participates in the European effort within the Virtual Atomic and Molecular Data Centre. Despite of that, a great number of data are still missing and their orders of magnitude would be welcome. In the present paper, we will revisit and compare a great number of the impact Stark widths and shifts, by considering their semiclassical perturbation expressions. We will also provide fitting formulae which are essential for the modeling codes of stellar atmospheres and envelopes.

Key words: atomic data – atomic processes – line: profiles – astronomical databases

1. INTRODUCTION

Pressure broadening of spectral lines arises when an atom, ion or molecule which emits or absorbs light in a gas or a plasma, is perturbed by its interactions with the other particles of the medium. In the present paper, we will consider atom or ion emitters and electron and ion colliders. This so-called Stark broadening has been extensively investigated for about 50 years. The results are now currently used for spectroscopic diagnostics and modeling. In astrophysics, with the increasing sensitivity of observations and spectral resolution in all domains of wavelengths, from far UV to infrared, it has become possible to develop realistic models of interiors and atmospheres of stars and interpret their evolution and the creation of elements through nuclear reactions. This requires the knowledge of numerous profiles, especially for trace elements, which are used as useful probes

for abundance determinations. For white dwarfs in particular, Stark broadening is the dominant line broadening process. Hence, calculations based on a simple but enough accurate and fast method, are useful for obtaining numerous results. Ab initio calculations are a growing domain of development. Nowadays, the access to such data via an on-line database becomes crucial. This is the object of STARK-B (Sahal-Bréchot et al. 2008), which is a collaborative project between the Paris Observatory and the Astronomical Observatory of Belgrade. This database contains calculated widths and shifts of isolated lines of atoms and ions due to electron and ion collisions. It is devoted to modeling and spectroscopic diagnostics of stellar atmospheres and envelopes. In addition, it is relevant to laboratory plasmas, laser equipments and technological plasmas. It is a part of the Virtual Atomic and Molecular Data Centre (VAMDC, Dubernet et al. 2010; Rixon et al. 2010), which is a collaboration between groups involved in the generation and use of atomic and molecular data, funded by the European Union.

In the present paper, we will briefly recall the important points of the theory. Then we will revisit the orders of magnitudes and trends of the widths and shifts in the impact approximation for electron and ion colliders. This is useful for providing interpolation or extrapolation formulae for missing data, since it is impossible to calculate all the data necessary to the modeling. We will also provide fitting formulae, which are essential for the modeling codes of stellar atmospheres and stellar envelopes. The coefficients of our proposed fitting formulae will be implemented in STARK-B.

2. REMIND OF THE IMPACT LINE BROADENING FOR ISOLATED LINES

Stark broadening theory in the impact approximation is based on the founding papers by Baranger (1958a,b,c). The impact approximation is the first basic one: ρ being a typical impact parameter and v the relative velocity. The duration of a collision or collision time $\tau = \rho/v$ must be much smaller than the mean interval between two collisions which is of the order of the inverse of the line width w (in angular frequency units). So the collisions between the radiating atom (or ion) act in dependently and are additive. It is quite always valid for electron collisions and is generally valid for collisions with positive ions in the conditions of stellar atmospheres (Sahal-Bréchot 1969a,b). The second basic approximation is the complete collision approximation: the radiating atom has no time to emit (or absorb) a photon during the collision process. In other words, the collision time τ must be very much smaller than the time interval be tween two emissions (or absorptions) of photons. The latter is of the order of the inverse of the detuning $\Delta\omega$. So, in the far wings, the atom can emit photons before the perturber has any time to move, and thus the process becomes quasistatic. In the line center, the impact approximation and the complete collision approximation are together valid, and the line broadening theory becomes an application of the theory of collisions between the radiating atom and the surrounding perturbers.

Then we will limit our study to the case of isolated lines: the levels of the $i-f$ transition broadened by collisions do not overlap with the neighbouring perturbing levels which are likely to modify the broadening by introducing optical coherences. So we will consider in the present paper neither hydrogen nor hydrogenic ionic lines, nor some specific helium lines and nor some lines arising from Rydberg levels.

This leads to a Lorentz line profile characterized by a width w (full half-width at half-maximum) and a shift d which depend on the physical conditions of the

medium (temperature T and density N of the perturbers). Owing to the impact approximation, w and d are proportional to the density. The width of the $i-f$ line can be expressed as a sum over the inelastic cross-sections $\sigma_{ii'}(v)$ and $\sigma_{ff'}(v)$ (i' and f' are the so-called perturbing levels) and over an elastic contribution $\sigma_{el}(v)$ that are integrated over the Maxwell distribution of velocities $f(v)$. The shift can be expressed in terms of another elastic contribution, cf. Baranger (1958c).

In addition, the Debye screening effect which can be important at high densities must be taken into account. This decreases w and d which are thus not proportional to the density.

Finally, we will remark that the fine and hyperfine structure can be neglected during collisions with electrons. This is due to the fact that the electron spin of the atom has no time to rotate (Larmor precession) during the collision time τ, because the relative velocity atom-perturber v is large. Consequently, but only in LS coupling, the widths and shifts due to electron collisions are equal for the different lines of a multiplet. Departures from LS coupling can be important for heavy atoms or for highly charged ions and then the fine structure widths and shifts can be different. For collisions with ions, the relative velocity is smaller, and the preceding condition is not completely fulfilled for the electronic spin, but the widths and shifts of the fine structure line are not very different. In fact, the hyperfine structure is always negligible during the collisions. However, if the fine structure (or hyperfine structure) splitting is not negligible, the components must be added (taking into account their shift and their relative intensities) for obtaining the global profile. This is the case of the hyperfine Mn II lines (Popović et al. 2008) and of the fine hydrogen Balmer lines (Stehlé 1985).

3. THE SEMICLASSICAL-PERTURBATION THEORY-SCP

Most of our calculations have been performed with the semi-classical-perturbation method (SCP) developed by Sahal-Bréchot (1969a,b) and further papers: Sahal-Bréchot (1974) for complex atoms, Fleurier et al. (1977) for inclusion of Feshbach resonances in elastic cross-sections of radiating ions, and by Mahmoudi et al. (2009) for very complex atoms. The numerical codes have been updated and operated by Dimitrijević & Sahal-Bréchot (1984) and then by many further papers. The accuracy is about 20% for the widths but less for the shifts, due to oscillations in the integration over the impact parameters in the neighbourhood of the cut-off region. Other methods are briefly reminded by Sahal-Bréchot (2010).

We now focus on the physical quantities that enter the expressions of w and d. This permits to understand their behaviours and trends as functions of atomic structure (oscillator strengths $f_{ii'}$, $f_{ff'}$, energy levels E_i, $E_{i'}$, E_f, $E_{f'}$), temperature T, charges of the radiating ion Z_A and perturber Z_P, reduced mass atom-perturber μ. The incoming perturber moves along a straight path (neutral radiating atom) or a hyperbola for a radiating ion (Sahal-Bréchot 1969a,b). We refer to Sahal-Bréchot (1969a,b) for all the required formulae which will not be recalled here. We will only have a look on the results. We will focus on widths because shifts are often less accurate. First, we consider the role of collision strengths.

We begin by lines of neutral atoms on the example of Mg I lines (Dimitrijević & Sahal-Bréchot 1996 and STARK-B). Figure 1 shows the width of Mg I $3s^1S-3p^1P^o$ as a function of the temperature T in K, for an electronic density of 10^{12} cm^{-3}. The difference of energy between the initial (or final) level and the closest perturbing level is $\Delta E_{\min} = 8451.64$ cm^{-1}, and $\Delta E_{\min}/kT = 1.2$ at 5000 K. Rather distant

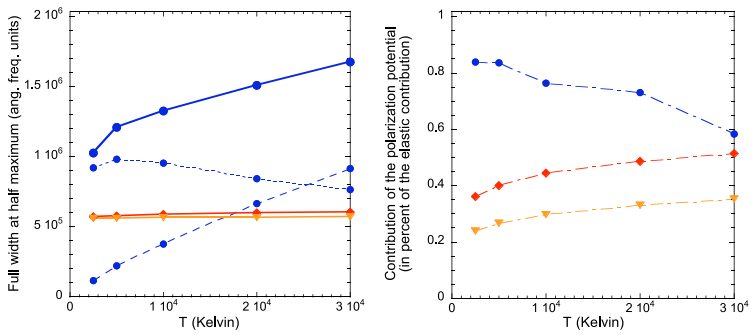

Fig. 1. Mg I $3s^1S - 3p^1P^o$. Left panel: the line widths w in angular frequency units as a function of the temperature T in K, the electronic density is 10^{12} cm^{-3}. Full lines are for total widths, dotted lines for elastic contributions, dashed lines for inelastic contributions, circles for electrons, diamonds for protons, triangles for a soup of ions. Right panel: contribution of the polarization potential, in percent of the elastic contribution.

levels are involved, hence at those temperatures inelastic collisions are completely negligible for impact ions. Elastic collisions are mostly due to the quadrupolar potential (cf. right panel of Figure 1), and since the quadrupolar contribution does not depend on the reduced mass, this explains why the width due to impact proton and the soup of ions (same charge as that of protons) are equal.

Table 1 shows the increasing contribution of impact ions when higher levels are involved. It displays the ratio of the width due to electron collisions to the width due to Fe II collisions as a function of T for Mg I $n+1, l+1-n, l$, with $l = n$. The width due to impact ions becomes higher than that due to impact electrons.

Table 1. Mg I $n+1, l+1-n, l$, with $l = n$: the ratio of the widths due to electron collisions to the width due to Fe II collisions as a function of T (in 10^3 K). $N = 10^{10}$ cm^{-3}.

T (10^3 K)	$6h-5g$	$7i-6h$	$8j-7i$	$9k-8j$	$10l-9k$
2.5	5.08	3.59	2.30	1.440	0.720
4.5	4.35	2.80	1.71	0.998	0.474
6.0	3.97	2.48	1.45	0.800	0.400

Figure 2 shows the details of the contributions for two lines : Mg I $5g^1G - 6h^1H^o$, where the closest perturbing level is such as $\Delta E_{\min} = 89.04$ cm^{-1}, and Mg I $9k - 10l$, where $\Delta E_{\min} = 0.04$ cm^{-1}. The inelastic contribution of impact ions increases, and the contribution of the quadrupole term becomes negligible: it is less than 4% for electrons and less than 1% for ions.

Then we consider the case of ion lines on the example of the Li-like Al XI ion (Dimitrijević & Sahal-Bréchot 1994 and STARK-B). We begin with the case of the resonance line $2s-2p$ (Figure 3), $\Delta E_{\min} = 1.8446\ 10^6$ cm^{-1}, and $\Delta E_{\min}/kT = 2.6$ at 5 10^5 K. Coulomb repulsion is high for colliding ions, and their contributions are less than 10%. The quadrupole part of the elastic contribution is predominant. Proton contribution is higher than He III contribution at high temperatures, ow-

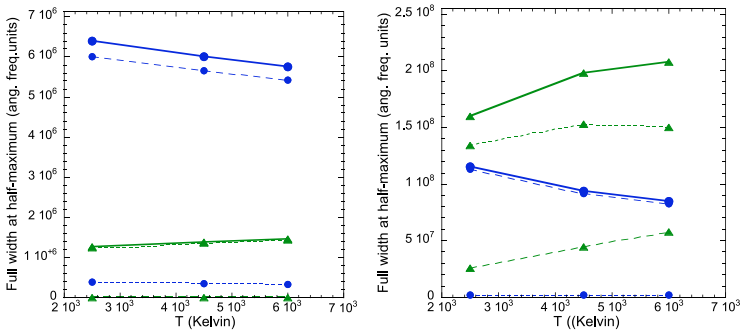

Fig. 2. Left panel: Mg I $5g^1G-6h^1H^o$. Right panel: Mg I $9k-10l$. The line widths w in angular frequency units as a function of the temperature T in K, the electronic density is 10^{10} cm^{-3}. Full lines are for total widths, dashed lines for inelastic contributions, dotted lines for elastic contributions, circles for electrons; triangles for Fe II ions.

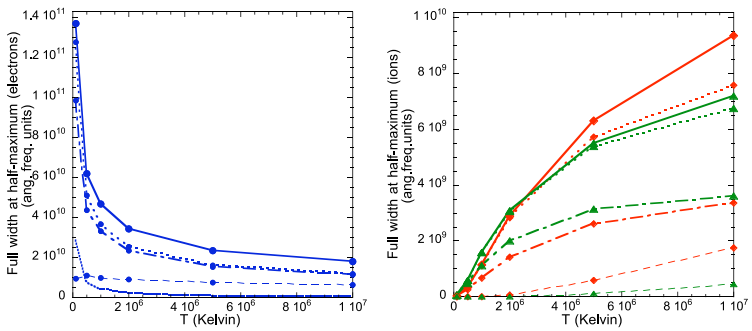

Fig. 3. Al XI $2s^2S-2p^2P^o$. The line widths w are in angular frequency units, $N=10^{18}$ cm^{-3}. Full lines are for total widths, dashed lines for inelastic contribution,: dotted lines for elastic contributions; dot-dashed lines for quadrupole contribution, dotted lines without circles for Feshbach resonances, circles for electrons, diamonds for protons, triangles for He III ions. Left panel is for impact electrons, right panel – for impact ions.

ing to the decrease of the Coulomb repulsion. For elastic electron collisions, the quadrupole part is dominant, but Feshbach resonances are important at low temperatures. The case of the $2p-5s$ line is completely different, because the $5s$ level is rather close to the $5p$ one: $\Delta E_{\min}/kT = 1.39\ 10^{-2}$ at $5\ 10^5$ K. So the Coulomb repulsion is rather small for colliding ions, and the ionic width increases and becomes higher than the one due to electrons. The highest contribution is due to He III. This is due to the charge- and the reduced mass- effect. This is shown in Figure 4. The polarization potential prevails for elastic collisions because the involved levels are high.

This study explains why the widths due to impact ions of Cr I lines (Dimitrijević et al. 2005) are larger than the widths due to electrons: there are perturbing levels that are very close to the upper ones (4.26 and 14.14 cm^{-1}). This abnormal situation is due to configuration interaction effects.

Concerning the behaviour with the charge of the perturber, the widths and the shifts increase linearly with Z_P (e.g., Dimitrijević 1999), as expected by the SCP formulae.

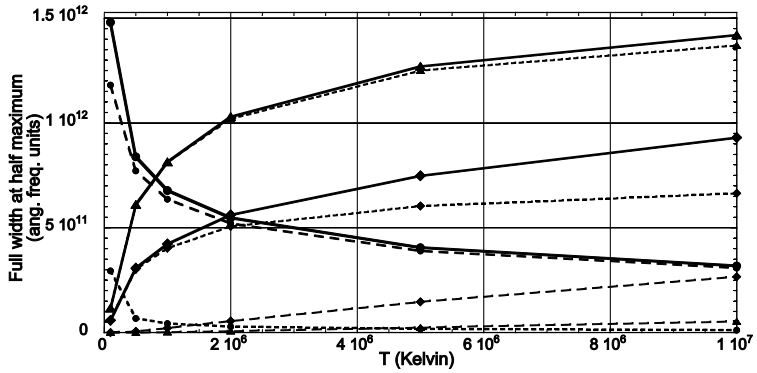

Fig. 4. Al XI $2p^2S - 5s^2P^o$. The line widths w are in angular frequency units, $N = 10^{18}$ cm^{-3}. Full lines are for total widths, dashed lines for inelastic contributions, dotted lines for elastic contributions, circles for electrons, diamonds for protons, triangles for He III ions.

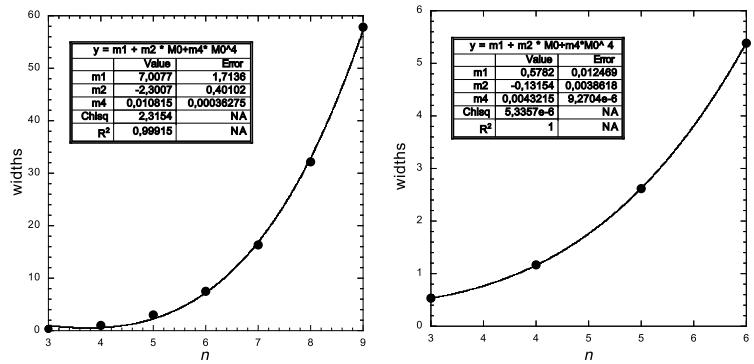

Fig. 5. Behaviour of the principal quantum number n for line widths of the series $3s - np$ (arbitrary units). Dots are results of the calculations. Full line: least squares polynomial fitting (4th order), M0= n. The coefficients of the fitting, χ^2 and the correlation factor R^2, are given in the insert. Left panel is for Na I, right panel – for Li II.

Second, we consider the effect of atomic structure and the charge of the radiating ion Z_A. It is expected than the width increases as n^4 when the principal quantum number n increases. This is shown in Figure 5.

The widths are predicted to vary as $Z_{\rm eff}^{-2}$, with $Z_{\rm eff} = Z_A + 1$. Fig. 20 of Elabidi et al. (2009) shows a -1.84 slope for the $3s - 3p$ transitions from C IV to P XIII.

Now let we look at the influence of the chosen atomic structure for the SCP calculations. Larbi-Terzi et al. (2009), on the example of the widths of the C II $3d-nf$ series, have shown that the differences in the results are very weak (less than 1%) when the Coulomb approximation with quantum defect (Bates & Damgaard 1949) oscillator strengths are used, compared to the TOPBASE R-matrix calculations (Cunto et al. 1973). In fact, C II is a simple atom and a simple atomic structure is sufficient. However, when highly charged ions or moderately charged ions like Si V (Ben Nessib et al. 2004) or Ne V (Hamdi et al. 2007) are concerned, the choice of a good atomic structure becomes important. For these two ions, the difference

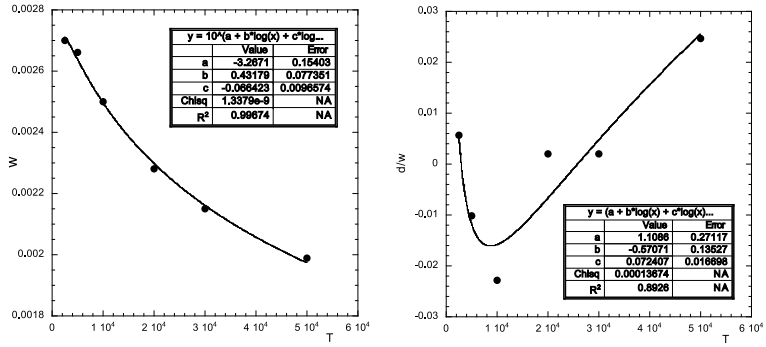

Fig. 6. Example of fitting corresponding to Equation (1) for Mg I $4f^1F^o - 6g^1G$ at 10^{11} cm^{-3}. Left panel is the line width, right panel is the shift/width, the x-axis is the temperature in K. Dots are the results of the SCP calculations; electron collisions. Fitting is shown as the full line. The fitting coefficients (a, b, c), χ^2 and R^2 are given in the insert.

can attain 25–30% between the Bates & Damgaard approximation and the more sophisticated method SUPERSTRUCTURE (Nussbaumer & Storey 1978).

Finally, the behaviour of the fine structure widths of a multiplet are not very sensitive to the fine structure splitting: for the $3s - 3p$ multiplets of the Li-like series, the ratio of the widths of the two components attains 1.12 only for P XIII (Elabidi et al. 2009). This is quite negligible by looking at the accuracy of the calculations.

4. FITTING FORMULAE AS THE FUNCTIONS OF TEMPERATURE

The theory and the SCP formulae show that the widths vary as $T^{-1/2}$ at low temperature and as $\log(T)/T^{1/2}$ at high temperatures (e.g., see Elabidi et al. 2009). But this is not sufficient for the users. Astrophysics need fitting formulae and coefficients as functions of temperature for each line. In fact, such fitting coefficients are easier to enter the computing codes than tables providing widths and shifts for a set of temperatures. So, for the astrophysical needs, we have obtained a simple but accurate fitting formula based on the least-squares method. It is logarithmic + second degree polynomial:

$$\begin{aligned} \log(w) &= a_0 + a_1 \log(T) + a_2 \left[\log(T)\right]^2 , \\ d/w &= b_0 + b_1 \log(T) + b_2 \left[\log(T)\right]^2 . \end{aligned} \tag{1}$$

Another fitting formula, $w = C + AT^B$, was proposed by Dimitrijević et al. (2007). The present one is more accurate, due to the second degree term of the expansion. However, none of them have a real physical sense.

Figure 6 shows an example of such fitting for Mg I $4f^1F^o - 6g^1G$ at 10^{11} cm^{-3} (Dimitrijević & Sahal-Bréchot 1996, and other related papers cited in STARK-B). The fit is excellent for the width, but not so good for the shift: this happens due to the fact that the accuracy of the shift calculation can be low at small shifts. This bad shift example has been deliberately chosen for testing the accuracy of the fitting formula.

The present coefficients will be placed at STARK-B in a near future under the form of complementary tables for each line.

5. CONCLUSION

We hope that the present study will help the users to interpret the results of SCP calculations, to obtain interpolated and extrapolated data that are absent in the STARK-B tables, and to include the provided fitting coefficients into their modeling codes for stellar atmospheres and interiors.

ACKNOWLEDGMENTS. A part of this work was supported by VAMDC. VAMDC is funded under the 7th Framework Program, grant agreement No. 239108. This work was also supported by the cooperation agreement between Tunisia (DGRS) and France (CNRS) (project code 09/R 13.03, No. 22637), by the Programme National de Physique Stellaire (INSU-CNRS), by the Paris Observatory and by the project No. 176002 of the Ministry of Education and Science of Serbia.

REFERENCES

Baranger M. 1958a, Phys. Rev., 111, 481
Baranger M. 1958b, Phys. Rev., 111, 494
Baranger M. 1958c, Phys. Rev., 112, 885
Bates D. R., Damgaard A. 1949, Phil. Trans. R. Soc. London A, 242, 101
Ben Nessib N., Dimitrijević M. S., Sahal-Bréchot S. 2004, A&A, 423, 397
Cunto W., Mendoza C., Ochsenbein F., Zeippen C. J. 1993, A&A, 275, L5
Dimitrijević M. S., Sahal-Bréchot S. 1984, JQSRT, 31, 301
Dimitrijević M. S., Sahal-Bréchot S. 1994, A&AS, 105, 245
Dimitrijević M. S., Sahal-Bréchot S. 1996, A&AS, 117, 127
Dimitrijević M. S. 1999, Serbian AJ, 159, 65
Dimitrijević M. S., Ryabchikova T., Popović L. Č. et al. 2005, A&A, 435, 1191
Dimitrijević M. S., Ryabchikova T., Simić Z. et al. 2007, A&A, 469, 681
Dubernet M. L., Boudon V., Culhane J. L. et al. 2010, JQSRT, 111, 2151; http://www.vamdc.eu
Elabidi H., Ben Nessib N., Sahal-Bréchot S. 2009, EPJD, 54, 51
Fleurier C., Sahal-Bréchot S., Chapelle J. 1977, JQSRT, 17, 5954
Hamdi R., Ben Nessib N., Dimitrijević M. S., Sahal-Bréchot S. 2007, ApJS, 170, 243
Larbi-Terzi N., Sahal-Bréchot S., Ben Nessib N. et al. 2010 AIP Conf. Proc., 1273, 428
Nussbaumer H., Storey J. P. 1978, A&A, 64, 139
Mahmoudi W., Ben Nessib N., Sahal-Bréchot S. 2008, EPJD, 47, 7
Popović L. Č. , Dimitrijević M. S., Simić Z. et al. 2008, New Astronomy, 13, 85
Rixon G., Dubernet M. L., Piskunov N. et al. 2010, AIP Conf. Proc., 1344, 107
Sahal-Bréchot S. 1969a, A&A, 1, 91
Sahal-Bréchot S. 1969b, A&A, 2, 322
Sahal-Bréchot S. 1974, A&A, 35, 319
Sahal-Bréchot S. 2010, J. Phys. Conf. Ser., 257, 012028
Sahal-Bréchot S., Dimitrijević M. S., Moreau N. 2008, http://stark-b.obspm.fr
Stehlé C. 1985, J. Phys. B, At. Mol. Phys., 18, L43

Baltic Astronomy, vol. 20, 548–551, 2011

A STATISTICAL STUDY OF THE Si IV RESONANCE LINE PARAMETERS IN 19 Be STARS

A. Antoniou[1,2], E. Danezis[1], E. Lyratzi[1,3], D. Stathopoulos[1,3] and M. S. Dimitrijević[4,5]

[1] *University of Athens, Faculty of Physics, Department of Astrophysics, Astronomy and Mechanics, Panepistimioupoli, Zographou 15784, Athens, Greece*

[2] *University of Peloponnese, Faculty of Science and Technology, Department of Telecommunication Science and Technology, Karaiskakis Str., 22100, Tripolis, Greece*

[3] *Eugenides Foundation, 387 Sygrou Av., 17564, Athens, Greece*

[4] *Astronomical Observatory of Belgrade, Volgina 7, 11160, Belgrade, Serbia*

[5] *Observatoire de Paris-Meudon, 5 Place Jules Janssen, F-92195 Meudon Cedex, France*

Received: 2011 August 8; accepted: 2011 August 15

Abstract. Using the GR model, we analyze the ultraviolet Si IV resonance lines in the spectra of 19 Be stars of different spectral subtypes, in order to detect the presence of absorption components and to analyze their characteristics. From this analysis we can calculate the values of a group of physical parameters, such as the apparent rotational and radial velocities, the random velocities of the ion thermal motions, as well as the absorbed energy and the logarithm of the column density of the independent regions of matter which produce the main and the satellite components of the studied spectral lines.

Key words: stars: Be – techniques: spectroscopic – ultraviolet: Si IV resonance lines

1. INTRODUCTION

The ultraviolet resonance lines of Si IV at 1393.755 and 1402.77 Å have peculiar profiles in the spactra of Be-type stars, which indicate a multicomponent nature of their origin. This doublet is usually a strong feature in the spectra of early-type stars and is a useful tool for the study of the structure of stellar atmospheres. Many researchers have studied the existence of absorption components, which accompany the Si IV resonance lines in the spectra of Be-type stars and which are of circumstellar or interstellar origin (e.g., Underhill 1975; Snow et al. 1979; Sapar & Sapar 1992). Lyratzi et al. (2006), applying the model proposed by Danezis et al. (2003), investigated the presence of absorption components in the vicinity of the Si IV resonance lines in 68 Be-type stars and their kinematical characteristics.

In this paper, using the new Gauss-Rotation model (Danezis et al. 2007),

Table 1. Kinematical parameters for the studied Be stars (in km/s) determined from the two Si/,IV resonance lines (1 and 2).

Star	Spectral type	$V_{\rm rad1}$	$V_{\rm rad2}$	$V_{\rm rot1}$	$V_{\rm rot2}$	$V_{\rm rand1}$	$V_{\rm rand2}$
HD 53367	B0 IVe	–22		180		51	
HD 44458	B1 Vpe	10	–18	128	140	57	66
HD 58343	B2 Vne	–32	–22	118	128	44	38
HD 45910	B2 IIIe	–65	–69	200	180	26	26
HD 41335	B2 Vne	–5	–7	113	100	64	53
HD 52721	B2 Vne	–30	–25	183	173	25	25
HD 37202	B2 IVp	–73	–71	170	190	25	25
HD 32991	B2 Ve	21	26	127	140	28	25
HD 58050	B2 Ve	9	9	150	142	38	25
HD 37490	B3 IIIe	–43	–43	125	100	53	51
HD 25940	B3 Ve	–40	–42	193	175	38	25
HD 183362	B3 Ve	–10	–11	158	140	51	51
HD 67888	B4 IIIpe	22		100		48	
HD 89884	B5 IIIe	–48	–56	117	115	42	51
HD 23480	B6 IVe	–11	–15	103	100	39	38
HD 192044	B7 Ve	–18	–16	160	150	38	35
HD 29866	B8 IVne	–43	–43	100	95	38	31
HD 199218	B8 IVnne	–18	–12	95	90	36	33
HD 50138	B9 e	19	18	133	130	34	25
Mean		–20±28	–23±28	140±34	135±32	41±11	37±13

Table 2. Absorbed energy (in eV) and logarithm of the column density in one or two absorption components of the Si IV resonance lines.

		λ 1392.755 Å				λ 1402.772Å			
Star	Spectral type	$E_{\rm ab1}$	$E_{\rm ab2}$	log $CD1$	log $CD2$	$E_{\rm ab1}$	$E_{\rm ab2}$	log $CD1$	log $CD2$
HD 53367	B0 IVe	0.18		11.47		0.15		11.37	
HD 44458	B1 Vpe	0.76	0.57	11.28	10.30	0.61	0.45	11.18	10.20
HD 58343	B2 Vne	0.35	0.39	10.86	10.24	0.28	0.31	10.76	10.14
HD 45910	B2 IIIe	0.79	0.51	11.65	11.65	0.63	0.41	11.55	11.55
HD 41335	B2 Vne	0.67	0.61	11.23	11.23	0.54	0.49	11.13	11.13
HD 52721	B2 Vne	0.50	0.58	11.09	10.13	0.40	0.46	11.00	10.04
HD 37202	B2 IVp	0.67	0.57	11.22	10.70	0.54	0.46	11.13	10.61
HD 32991	B2 Ve	0.30	0.19	10.88	10.25	0.24	0.15	10.78	10.15
HD 58050	B2 Ve	0.54	0.58	11.13	10.73	0.43	0.46	11.04	10.64
HD 37490	B3 IIIe	0.65	0.62	11.21	10.11	0.52	0.50	11.11	10.01
HD 25940	B3 Ve	0.28	0.24	10.85	10.85	0.23	0.20	10.75	10.75
HD 183362	B3 Ve	0.66	0.56	11.27	9.97	0.52	0.45	11.17	9.87
HD 67888	B4 IIIpe	0.56		11.15		0.45		11.05	
HD 89884	B5 IIIe	0.36	0.37	10.95	11.49	0.28	0.30	10.85	11.40
HD 23480	B6 IVe	0.29	0.28	10.67	10.93	0.23	0.23	10.58	10.83
HD 192044	B7 Ve	0.26	0.22	10.81	10.08	0.21	0.20	10.71	9.99
HD 29866	B8 IVne	0.24	0.15	10.77	10.12	0.19	0.12	10.68	10.03
HD 199218	B8 IVnne	0.24	0.15	10.78	10.22	0.20	0.12	10.68	10.12
HD 50138	B9e	0.45	0.40	11.38	10.58	0.36	0.32	11.28	10.48
Mean		0.46	0.41	11.09	10.56	0.37	0.33	10.99	10.47
St. dev.		0.20	0.17	0.27	0.52	0.16	0.14	0.27	0.52

we analyze the Si IV resonance lines in the spectra of 19 Be stars of different spectral subtypes. For this we calculate the models for grids of different physical parameters: the apparent rotational and radial velocities, the random velocities of

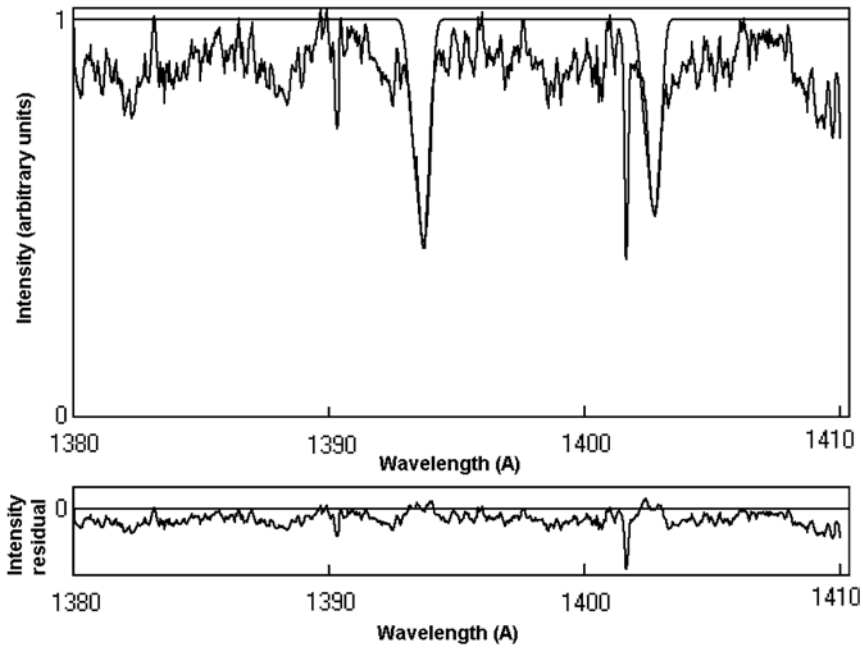

Fig. 1. The region around the Si IV resonance lines at 1393.755 and 1402.778 Å in the spectrum of HD 29866 fitted to the synthetic line profiles of the model. Each of the Si IV lines consists of two components. The graph below shows the differences between the observed and the model line profiles.

the thermal motions of ions, as well as the absorbed energy and the the column density of the distinct regions in the atmosphere and above it, which produce the main and the satellite components of the studied spectral lines.

2. RESULTS

The spectrograms of 19 Be-stars, listed in Table 1, have been obtained with the IUE satellite short wavelength range camera (SWP) at high resolution (0.1 to 0.3 Å). Table 1 also gives the values of the kinematical parameters measured for the two Si IV lines: the apparent radial velocities (columns 3 and 4), rotational velocities (columns 5 and 6) and the random velocities of the thermal motions of ions in one or two satellite absorption components (columns 7 and 8). In Table 2 we give the values of the absorbed energy (columns 3–4 and 7–8) and the logarithms of column density (columns 5–6 and 9–10) for the same absorption components.

In Figure 1, we present the spectrum of a B2 Ve star HD 29866 in the vicinity of the Si IV doublet and the best fit of these lines to a model. The best fit has been obtained with two absorption components. The graph below shows the differences between the observed and the model line profiles.

We conclude that the values of the parameters of a set of Be stars calculated using the new GR model (Danezis et al. 2007) are in agreement with the values of the parameters calculated earlier by Lyratzi et al. (2006).

ACKNOWLEDGMENTS. This research project is progressing at the University of Athens, Department of Astrophysics, Astronomy and Mechanics, under the financial support of the Special Account for Research Grants. This work also was supported by Ministry of Science Technological Development of Serbia through the projects "Influence of coalitional processes on astrophysical plasma line shapes" and "Astrophysical spectroscopy of extragalactic objects".

REFERENCES

Danezis E., Nikolaidis D., Lyratzi E. et al. 2003, Ap&SS, 284, 1119
Danezis E., Nikolaidis D., Lyratzi E. et al. 2007, PASJ, 59, 827
Lyratzi E., Danezis E., Antoniou A. 2006, XXVIth IAU General Assembly, Prague
Sapar L., Sapar A. 1992, Baltic Astronomy, 1, 37
Snow T. P., Mathieu R. D., Peters G. J. 1979, ApJS, 39, 359
Underhill A. B. 1975, AJ, 199, 691

Baltic Astronomy, vol. 20, 552–557, 2011

AB INITIO DETERMINATION OF ATOMIC STRUCTURE AND STARK BROADENING PARAMETERS: Pb IV AND RECENT RESULTS

R. Hamdi[1], N. Ben Nessib[1], M. S. Dimitrijević[2,3] and S. Sahal-Bréchot[3]

[1] *Groupe de Recherche en Physique Atomique et Astrophysique, Institut National des Sciences Appliquées et de Technologie, Université de Carthage, Tunisia; hamdi.rafik@gmail.com*

[2] *Astronomical Observatory, Volgina 7, 11160 Belgrade 74, Serbia; mdimitrijevic@aob.bg.ac.rs*

[3] *Observatoire de Paris-Meudon, 92195 Meudon, France; sylvie.sahal-brechot@obspm.fr*

Received: 2011 August 8; accepted: 2011 August 15

Abstract. We present a review of our previous ab initio calculations of Stark broadening parameters using semi-classical perturbation method for the calculation of Stark widths and shifts, and the SUPERSTRUCURE (SST) code for the determination of atomic structure. SST code takes into account the configuration interactions and relativistic effects. New results are also presented for some spectral lines of Pb IV. Energy levels and oscillator strengths are calculated using Hartree-Fock relativistic approach, and the Stark broadening parameters are determined using a semiclassical perturbation approach.

Key words: atomic data – atomic processes – lines: formation

1. INTRODUCTION

In atomic structure study, ab initio calculation of energy levels and radiative parameters can be made, when no other data are taken from other sources, i.e., no semi-empirical adjustment of any parameter. Many methods can be used, as for example, Hartree-Fock with relativistic corrections of Cowan (1981), a scaled Thomas-Fermi-Dirac statistical potential employed in SST code (Eissner et al. 1974) and fully relativistic calculation based on multiconfiguration Dirac-Fock method employed in GRASP code (Grant et al. 1980).

Energy levels and oscillator strengths are the main input data for the Stark broadening parameter determination. Ab initio calculation of Stark broadening parameters can be made when the needed set of energy levels and oscillator strengths are determined during the calculation, not taken from other sources.

The lack of atomic data makes Stark broadening determination impossible, especially when we use the semiclassical perturbation method (Sahal-Bréchot 1969a,b). Indeed, this method needs a large set of energy levels and oscillator strengths com-

paring with other methods such as the modified semi-empirical approach (Dimitrijević & Konjević 1980). Therefore, ab initio determination of Stark widths and shifts is of great interest for ions for which the set of atomic data is not complete. This method allows us to treat a large number of ions and transitions, thereby, we contribute to the creation of a database as the STARK-B containing the calculated widths and shifts of isolated lines due to electron and ion collisions. This database is devoted for modeling and spectroscopic diagnostics of stellar atmospheres and envelopes.

In our previous work (Ben Nessib et al. 2004; Hamdi et al. 2007; Hamdi et al. 2010), we have performed ab initio calculation of Stark broadening parameters for Si V, Ne V and Ca V ions. Energy levels and oscillator strengths are determined using the SST code, and Stark widths and shifts are calculated using the semi-classical perturbation approach. All these results are reviewed in this paper. New results are also presented for spectral lines of triply ionized lead (Pb IV). Atomic data are determined using Hartree-Fock with relativistic correction method, and the Stark broadening parameters are calculated using the semi-classical perturbation method. Pb IV lines are of interest for modeling of hot star atmospheres, since Pb IV is characterized by a strong resonance line and it is a candidate for spectroscopic detection in DA white dwarfs (Vennes et al. 2005). The Pb IV resonance line is also detected in the photospheres of subdwarfs (O'Toole 2004).

2. AB INITIO DETERMINATION OF ATOMIC DATA

2.1. The SUPERSTRUCTURE code

The SST code was originally realized by Eissner et al. (1974). The wave functions are of configuration mixing type, and each configuration is expanded in terms of slater states. The radial functions P_{nl} are calculated in the scaled Thomas-Fermi statistical potential $V(\lambda_l)$ such that all P_{nl} of the same l are calculated in the same potential. The SST code was modified by Nussbaumer & Storey (1978) so that each P_{nl} is calculated in the separate potential $V(\lambda_{nl})$. Parameters λ_{nl} are determined variationally by optimizing the weighted sum of energy terms. Relativistic corrections are introduced by means of Breit-Pauli approximation in intermediate coupling. The Breit-Pauli Hamiltonian H_{BP} can be written

$$H_{BP} = H_{nr} + H_{rc}. \tag{1}$$

Here H_{nr} is the non relativistic Hamiltonian and H_{rc} is a sum of relativistic correction operators. H_{rc} contains the one electron operators for the mass correction, the Darwin contact term, the spin-orbit interaction in the field of the nucleus and two electron operators for spin-orbit, spin-other orbit and spin-spin interactions.

2.2. The Cowan code

For theoretical calculations of atomic parameters needed for spectral line calculations, we can use the Cowan code (Cowan 1981) structure package for atomic calculations. The Cowan code consists of the following three programs:

1. RCN calculates the single configuration radial wave functions. In RCN, there is a choice of four approximations to the true Hartree-Fock method, namely, Hartree (H), Hartree-Fock-Slater (HFS), Hartree plus statistical exchange (HX) and Hartree-Slater (HS). HX is the normal option since it is most efficient in computations.

2. RCN2 calculates the multiple-configuration radial integrals, dipole integrals and Bessel integrals.

3. RCG calculates the angular factors, radiative data and collision strengths.

For the electric dipole transition, total transition probability from a state $\gamma' J' M'$ to all states M of the level γJ is given by (Cowan 1981):

$$A = \frac{64\pi^4 e^2 a_0^2 \sigma^3}{3h(2J'+1)} \mathbf{S}, \tag{2}$$

where $\sigma = \frac{|E(\gamma') - E(\gamma)|}{hc}$, c is the light velocity, h is Plank's constant, e is elementary charge, a_0 is the Bohr radius and $\mathbf{S}$ is the dipole line strength defined as :

$$\mathbf{S} = \left| \left\langle \gamma J \left\| \mathbf{P}^{(1)} \right\| \gamma' J' \right\rangle \right|^2, \tag{3}$$

where $\mathbf{P}^{(1)}$ is the classical dipole moment of the atom measured in units of $-ea_0$. The weighted oscillator strength is given by :

$$gf = \frac{8\pi^2 mca_0^2 \sigma}{3h} \mathbf{S}. \tag{4}$$

In order to calculate gf, the corresponding value of the line strength must be computed. The wavefunction $|\gamma J\rangle$ is expanded in terms of a suitable set of the basis functions $|\beta J\rangle$.

$$|\gamma J\rangle = \sum_{\beta} Y^{\gamma}_{\beta J} |\beta J\rangle \tag{5}$$

3. AB INITIO DETERMINATION OF STARK BROADENING PARAMETERS

Using the calculated set of atomic data and the semiclassical perturbation (SCP) method (Sahal-Bréchot 1969a,b) for the determination of Stark broadening parameters, ab initio Stark widths and shifts can be obtained.

In the SCP approach, the full width at half maximum (W) can be expressed in terms of inelastic cross-section and elastic processes as

$$W = N \int v f(v) dv \left(\sum_{i' \neq i} \sigma_{ii'}(v) + \sum_{f' \neq f} \sigma_{ff'}(v) + \sigma_{el}(v) \right),$$

where N is the density of colliding perturber, $f(v)$ is the Maxwell distribution of the relative atom-perturber velocity v, $\sigma_{ii'}$ and $\sigma_{ff'}$ are the inelastic cross-sections between the initial level i (resp. f final level) and the perturbing levels i' (resp. f') of $i - f$ transition. $\sigma_{el}(v)$ represents the contribution of elastic collisions and include Feshbach resonances when ion-electron [...???] are studied.

In Ben Nessib et al. (2004), ab initio Stark broadening parameters were obtained for 16 multiplet of Si V. The energy levels and oscillator strengths were calculated using the SST code (Eissner et al. 1974). Scaling parameters λ_l were obtained by self-consistent energy minimization procedure on all term energies of the eleven configurations: $2s^2 2p^6$, $2s^2 2p^5\ 3\ell$, $2s\ 2p^6\ 3\ell$, $2s^2 2p$Results were obtained

for collisions with electrons and compared with the values calculated with Bates & Damgaard (1949) approximation oscillator strengths. The broadening parameters for proton, ionized helium and Si II were also given.

In Hamdi et al. (2007), Stark broadening parameters were calculated for 26 multiplets of Ne V. Atomic data were carried out using the SST code. The adopted atomic model includes 17 configurations: $2s^22p^2$, $2s\ 2p^3$, $2p^4$, $2s^22p\ 3\ell$, $2s\ 2p^2\ 3\ell$, $2s^22p\ 4\ell$, $2s\ 2p^2\ 4\ell$ ($\ell \leq n-1$). The results are given for broadening by electron, proton and singly and doubly charged helium ion collisions. Comparison between the Stark widths obtained using the SST oscillator strengths and the Bates and Damgaard approximation oscillator strengths show that the difference is tolerable. The set of oscillator strength obtained using Bates and Damgaard approximation may then be useful for the Stark broadening calculations when more reliable data are not available. The Stark width for $3s\ ^3P^\circ - 3p\ ^3D$ was compared with theoretical and experimental results from Uzelac et al. (1993). We have found the best agreement with the measured width.

Ab initio SCP Stark broadening parameters were also calculated for Ca V lines (Hamdi et al. 2010). The needed set of atomic data was obtained using the SST code and 12 configurations of the atomic model. Such data may be of astrophysical interest, since calcium in different ionization stages is observed in the atmospheres of white dwarfs.

Triply ionized lead Pb IV belongs to gold isoelectronic sequence, its ground state configuration is $4f^{14}5d^{10}6s$. This is an interesting isoelectronic sequence with filled subshells and a single electron in the outer shell. This ion is characterized by a strong resonance line, and it is a candidate for spectroscopic detection in hot DA white dwarfs (Vennes et al. 2005). O'Toole (2004) reported the discovery of strong photospheric resonance lines of several heavy elements in the UV spectra of more than two dozen sdB and sdOB stars at temperatures ranging from 22 000 K to 40 000 K. Among these lines, several correspond to Pb IV ones. Pb IV 1313.1 Å resonance line was detected by Proffitt et al. (2001) in the main-sequence B star AV 304.

Using the SCP approach, ab initio Stark broadening parameters are determined for 11 transitions of Pb IV of the type $5d^{10}nl - 5d^{10}n'l'$. The energy levels and oscillator strengths were carried out in the Hatree-Fock relativistic (HFR) approach using the Cowan code. We adopt an atomic model including 43 configurations: $5d^96s^2$, $5d^96p^2$, $5d^{10}ns$ ($6\leq n \leq 11$), $5d^{10}nd$ ($6\leq n \leq 11$), $5d^{10}ng$ ($5\leq n \leq 11$), $5d^96s7s$, $5d^96s6d$ (even parity) and $5d^{10}np$ ($6\leq n \leq 11$), $5d^{10}nf$ ($5\leq n \leq 11$), $5d^{10}nh$ ($6\leq n \leq 11$), $5d^96s6p$ (odd parity).

Stark widths and shifts are shown in Table 1 for the perturber density $N=10^{17}$ cm^{-3} and temperatures from 20 000 K up to 400 000 K for collisions with electrons, protons and singly charged helium. Such temperatures are of interest for modeling of sdB, sdBO and hot white dwarf atmospheres. We also specify a parameter C (Dimitrijević & Sahal-Bréchot 1984), which gives an estimate for the maximal perturber density for which the line may be treated as isolated. For each value given in Table 1, the collision volume V multiplied by the perturber density N is much less than 1, and the impact approximation is valid.

ACKNOWLEDGMENTS. This work is a part of the Project 146001, "Influence of collisional processes on astrophysical plasma lineshapes" supported by the Ministry of Science and Technological Development of Serbia.

Table 1. This table gives electron, proton and singly-charged helium impact broadening parameters for Pb IV lines, for a perturber density of 10^{17} cm^{-3} and temperatures in the range of 20 000 to 400 000 K. Transitions, wavelengths (in Å) and the parameter C are also given. This parameter when divided to the corresponding Stark width gives an estimate for the maximal perturber density for which the line may be treated as isolated. W_e is the electron-impact full Stark width at half maximum, d_e is the electron-impact Stark shift, W_{H^+} is the proton-impact full Stark width at half maximum, d_{H^+} is the proton-impact Stark shift, W_{He^+} is the singly charged helium-impact full Stark width at half maximum, d_{He^+} is the singly charged helium-impact Stark shift.

Transition	$T(kK)$	W_e	d_e	W_{H^+}	d_{H^+}	W_{He^+}	d_{He^+}
	20	0.66E-02	-0.85E-04	0.31E-03	-0.24E-04	0.39E-03	-0.23E-04
$6s\ ^2S_{1/2} -\ 8p\ ^2P_{3/2}$	30	0.58E-02	-0.39E-04	0.39E-03	-0.34E-04	0.47E-03	-0.32E-04
$\lambda = 385,5$ Å	50	0.51E-02	-0.53E-04	0.48E-03	-0.51E-04	0.52E-03	-0.45E-04
C= 0.20E+19	100	0.45E-02	-0.32E-04	0.55E-03	-0.72E-04	0.59E-03	-0.62E-04
	200	0.41E-02	-0.29E-04	0.61E-03	-0.91E-04	0.64E-03	-0.75E-04
	400	0.37E-02	-0.35E-04	0.65E-03	-0.11E-03	0.66E-03	-0.89E-04
	20	0.71E-02	-0.11E-03	0.30E-03	-0.88E-04	0.38E-03	-0.81E-04
$6s\ ^2S_{1/2} -\ 8p\ ^2P_{1/2}$	30	0.62E-02	-0.42E-04	0.37E-03	-0.12E-03	0.45E-03	-0.10E-03
389.9 Å	50	0.54E-02	-0.12E-03	0.47E-03	-0.16E-03	0.51E-03	-0.14E-03
C= 0.17E+19	100	0.47E-02	-0.80E-04	0.55E-03	-0.21E-03	0.58E-03	-0.17E-03
	200	0.42E-02	-0.67E-04	0.62E-03	-0.25E-03	0.63E-03	-0.21E-03
	400	0.38E-02	-0.72E-04	0.67E-03	-0.30E-03	0.66E-03	-0.24E-03
	20	0.52-E02	-0.13E-03	0.14E-03	-0.28E-05	0.20E-03	-0.28E-05
	30	0.44E-02	-0.82E-04	0.19E-03	-0.44E-05	0.25E-03	-0.43E-05
$6s\ ^2S_{1/2} -\ 7p\ ^2P_{3/2}$	50	0.36E-02	-0.48E-04	0.25E-03	-0.73E-05	0.31E-03	-0.71E-05
474.4 Å	100	0.29E-02	-0.53E-04	0.33E-03	-0.13E-04	0.36E-03	-0.12E-04
C= 0.67E+19	200	0.23E-02	-0.35E-04	0.38E-03	-0.20E-04	0.40E-03	-0.17E-04
	400	0.20E-02	-0.39E-04	0.41E-03	-0.27E-04	0.43E-03	-0.22E-0
	20	0.55E-02	-0.99E-04	0.13E-03	-0.11E-04	0.19E-03	-0.11E-04
$6s\ ^2S_{1/2} -\ 7p\ ^2P_{1/2}$	30	0.47E-02	-0.74E-04	0.18E-03	-0.16E-04	0.24E-03	-0.16E-04
484.8 Å	50	0.38E-02	-0.11E-04	0.24E-03	-0.26E-04	0.30E-03	-0.24E-04
C= 0.60E+19	100	0.30E-02	-0.46E-04	0.32E-03	-0.41E-04	0.35E-03	-0.35E-04
	200	0.25E-02	-0.11E-04	0.36E-03	-0.57E-04	0.39E-03	-0.48E-04
	400	0.21E-02	-0.24E-04	0.41E-03	-0.71E-04	0.42E-03	-0.57E-04
	20	0.15E-01	0.16E-02	0.80E-03	0.70E-03	0.92E-03	0.60E-03
$6p\ ^2P_{1/2} -\ 8d\ ^2D_{3/2}$	30	0.13E-01	0.14E-02	0.11E-02	0.89E-03	0.11E-02	0.74E-03
500.8 Å	50	0.11E-01	0.16E-02	0.13E-02	0.11E-02	0.13E-02	0.88E-03
C= 0.15E+19	100	0.99E-02	0.14E-02	0.16E-02	0.13E-02	0.15E-02	0.11E-02
	200	0.85E-02	0.13E-02	0.20E-02	0.16E-02	0.17E-02	0.13E-02
	400	0.73E-02	0.11E-02	0.23E-02	0.18E-02	0.20E-02	0.14E-02
	20	0.212E-01	0.62E-02	0.13E-02	0.13E-02	0.14E-02	0.11E-02
$6p\ ^2P_{3/2} -\ 8d\ ^2D_{5/2}$	30	0.19E-01	0.53E-02	0.17E-02	0.16E-02	0.17E-02	0.13E-02
552.1 Å	50	0.17E-01	0.46E-02	0.22E-02	0.19E-02	0.19E-02	0.16E-02
C= 0.19E+19	100	0.16E-01	0.37E-02	0.27E-02	0.24E-02	0.24E-02	0.19E-02
	200	0.15E-01	0.31E-02	0.33E-02	0.28E-02	0.27E-02	0.22E-02
	400	0.14E-01	0.27E-02	0.38E-02	0.32E-02	0.33E-02	0.25E-02
	20	0.18E-01	0.20E-02	0.97E-03	0.85E-03	0.11E-02	0.73E-03
$6p\ ^2P_{3/2} -\ 8d\ ^2D_{3/2}$	30	0.16E-01	0.17E-02	0.13E-02	0.11E-02	0.13E-02	0.90E-03
553.0 A	50	0.14E-01	0.20E-02	0.16E-02	0.13E-02	0.15E-02	0.11E-02
C= 0.18E+19	100	0.12E-01	0.17E-02	0.20E-02	0.16E-02	0.18E-02	0.13E-02
	200	0.10E-01	0.16E-02	0.24E-02	0.19E-02	0.21E-02	0.15E-02
	400	0.89E-02	0.14E-02	0.28E-02	0.22E-02	0.24E-02	0.18E-02

Table 1. Continued

Transition	$T(kK)$	W_e	d_e	W_{H+}	d_{H+}	W_{He+}	d_{He+}
	20	0.14E-01	0.17E-02	0.42E-03	0.42E-03	0.51E-03	0.37E-03
$6p\ ^2P_{1/2} -\ 7d\ ^2D_{3/2}$	30	0.12E-01	0.13E-02	0.57E-03	0.53E-03	0.65E-03	0.46E-03
592.7 Å	50	0.99E-02	0.12E-02	0.80E-03	0.70E-03	0.81E-03	0.58E-03
C= 0.17E+19	100	0.85E-02	0.12E-02	0.10E-02	0.87E-03	0.99E-03	0.71E-03
	200	0.74E-02	0.11E-02	0.13E-02	0.10E-02	0.12E-02	0.84E-03
	400	0.64E-02	0.10E-02	0.16E-02	0.12E-02	0.13E-02	0.97E-03
	20	0.12E-01	0.32E-02	0.27E-03	0.51E-03	0.29E-03	0.44E-03
$6p\ ^2P_{1/2} -\ 8s\ ^2S_{1/2}$	30	0.11E-01	0.28E-02	0.42E-03	0.64E-03	0.41E-03	0.55E-03
594.7 Å	50	0.93E-02	0.21E-02	0.66E-03	0.84E-03	0.62E-03	0.68E-03
C= 0.21E+19	100	0.81E-02	0.19E-02	0.97E-03	0.10E-02	0.82E-03	0.84E-03
	200	0.70E-02	0.16E-02	0.12E-02	0.12E-02	0.10E-02	0.99E-03
	400	0.61E-02	0.13E-02	0.16E-02	0.14E-02	0.12E-02	0.11E-02
	20	0.16E-01	0.21E-02	0.55E-03	0.55E-03	0.66E-03	0.47E-03
$6p\ ^2P_{3/2} -\ 7d\ ^2D_{5/2}$	30	0.14E-01	0.16E-02	0.73E-03	0.69E-03	0.85E-03	0.60E-03
663.4 Å	50	0.12E-01	0.15E-02	0.10E-02	0.91E-03	0.10E-02	0.75E-03
C= 0.56E+19	100	0.11E-01	0.16E-02	0.14E-02	0.11E-02	0.13E-02	0.91E-03
	200	0.92E-02	0.14E-02	0.16E-02	0.13E-02	0.15E-02	0.11E-02
	400	0.80E-02	0.13E-02	0.19E-02	0.15E-02	0.17E-02	0.13E-02
	20	0.17E-01	0.21E-02	0.54E-03	0.53E-03	0.65E-03	0.46E-03
$6p\ ^2P_{3/2} -\ 7d\ ^2D_{3/2}$	30	0.15E-01	0.15E-02	0.72E-03	0.67E-03	0.84E-03	0.59E-03
667.0 Å	50	0.13E-01	0.14E-02	0.10E-02	0.89E-03	0.10E-02	0.73E-03
C= 0.21E+19	100	0.11E-01	0.15E-02	0.13E-02	0.11E-02	0.13E-02	0.89E-03
	200	0.93E-02	0.14E-02	0.16E-02	0.13E-02	0.15E-02	0.11E-02
	400	0.81E-02	0.12E-02	0.20E-02	0.15E-02	0.17E-02	0.12E-02

REFERENCES

Bates D. R., Damgaard A. 1949, Philos. Trans. R. Soc. London A, 242, 101

Ben Nessib N., Dimitrijević M. S., Sahal-Bréchot S. 2004, A&A, 423, 397

Cowan R. D., 1981, *The Theory of Atomic Structure and Spectra*, Univ. California Press, Berkeley

Dimitrijević M. S., Konjević N. 1980, JQSRT, 24, 451

Dimitrijević M. S., Sahal-Bréchot S. 1984, JQSRT, 31, 301

Eissner W., Jones M., Nussbaumer H. 1974, Comput. Phys. Commun., 8, 270

Grant I. P., Mc Kenzie B. J., Norrington P. H. et al. 1980, Comput. Phys. Commun., 21, 233

Hamdi R., Ben Nessib N., Dimitrijević M. S.,Sahal-Bréchot S. 2007, ApJ, 170, 243

Hamdi R., Ben Nessib N., Dimitrijević M. S., Sahal-Bréchot S. 2010, Mem. Soc. Astron. Ital. Suppl., 15, 148

Nussbaumer H., Storey P. J. 1978, A&A, 64, 139

O'Toole S. J. 2004, A&A, 423, L25

Proffitt C. R., Sansonetti C. J., Reader J. 2001, ApJ, 557, 320

Sahal-Bréchot S. 1969a, A&A, 1, 91

Sahal-Bréchot S. 1969b, A&A, 2, 322

Uzelac N. I., Glenzer S., Konjevic B. et al. 1993, Phys. Rev. E, 47, 3623

Vennes S., Chayer P., Dupuis J. 2005, ApJ, 622, L121

Baltic Astronomy, vol. 20, 566–571, 2011

THE INFLUENCE OF CHEMI-IONIZATION AND RECOMBINATION PROCESSES ON SPECTRAL LINE SHAPES IN STELLAR ATMOSPHERES

Anatolij A. Mihajlov[1,2], Ljubinko M. Ignjatović[1,2], Vladimir A. Srećković[1,2] and Milan S. Dimitrijević[2,3,4]

[1] *Institute of Physics, University of Belgrade, P.O. Box 57, 11001 Belgrade, Serbia*
[2] *Isaac Newton Institute of Chile, Yugoslavia Branch, Volgina 7, 11060 Belgrade, Serbia*
[3] *Astronomical Observatory, Volgina 7, 11060 Belgrade, Serbia*
[4] *Observatoire de Paris, 92195 Meudon Cedex, France*

Received: 2011 August 8; accepted: 2011 August 15

Abstract. The chemi-ionization processes in atom – Rydberg atom collisions, as well as the corresponding chemi-recombination processes are considered as factors of influence on the atom exited-state populations in weakly ionized layers of stellar atmospheres. The presented results are related to the photospheres of the Sun and some M red dwarfs, as well as weakly ionized layers of DB white dwarf atmospheres. It has been found that the mentioned chemi-ionization and recombination processes dominate over the concurrent electron-atom and electron-ion ionization and recombination processes in all parts of the considered stellar atmospheres. The obtained results demonstrate the fact that the considered processes must have significant influence on the optical properties of stellar atmospheres. It is shown that these processes and their importance for non-local thermodynamic equilibrium (non-LTE) modeling of the solar atmospheres should be investigated further.

Key words: stars: atomic processes

1. INTRODUCTION

Chemi-ionization processes in principle include the processes of associative ionization

$$A^*(n) + X \Rightarrow AX^+ + e, \tag{1}$$

as well as the processes of Penning ionization

$$A^*(n) + X \Rightarrow A + X^+ + e, \tag{2}$$

where A, X and X^+ are atoms and the atomic ions in their ground states, A*(n) – atom in a highly excited (Rydberg) state with the principal quantum number $n \gg 1$, and AX^+ is the corresponding molecular ion in its ground electronic state.

It is customary that in the case $A = X$ chemi-ionization processes are treated as symmetric, and in the case $A \neq X$ – as non-symmetric. Concerning Penning-ionization processes let us draw attention to the fact that for all the processes which can be described by the scheme (2), only those are treated as chemi-ionization which go on in a similar way as the associative-ionization processes (1). Here, all chemi-ionization processes are treated on the basis of dipole resonant mechanism, which was introduced in the considerations in Smirnov & Mihajlov (1971) and was described in details in Ignjatović & Mihajlov (2005) and Ignjatović et al. (2008). The symmetric $A = X$ chemi-ionization processes

$$A^*(n) + A \Rightarrow A_2^+ + e, \tag{3}$$

$$A^*(n) + A \Rightarrow A + A^+ + e, \tag{4}$$

and the corresponding inverse recombination processes,

$$A_2^+ + e \Rightarrow A^*(n) + A, \tag{5}$$

$$A + A^+ + e \Rightarrow A^*(n) + A, \tag{6}$$

where $A = H(1s)$ or $He(1s^2)$, were theoretically considered by Mihajlov et al. (1996, 1997b) as factors of influence on the populations of excited atoms in the weakly ionized hydrogen and helium plasmas. It means that the efficiency of these processes had to be compared with the efficiency of the processes

$$A^*(n) + e \Rightarrow A^+ + 2e, \tag{7}$$

$$A^+ + 2e \Rightarrow A^*(n) + e, \tag{8}$$

$$A^+ + e \Rightarrow A^*(n) + \varepsilon_\lambda, \tag{9}$$

where $A = H(1s)$ or $He(1s^2)$ and ε_λ is the energy of a photon with wavelength λ. For the considered conditions in Mihajlov et al. (1996, 1997b) the rate coefficients for all chemi-ionization and chemi-recombination processes (3)-(6) were determined. It was found that under the mentioned conditions these processes in the region $n \leq 10$ are dominant or at least comparable with the concurrent electron-atom and electron-ion processes (from the aspect of their influence on excited-atom populations) when the ionization degree of the considered plasma is $\leq 10^{-3}$.

These results, as well as the experience gained earlier with radiation ion-atom processes (Mihajlov & Dimitrijevic 1986, 1992, etc.), have suggested the idea that the chemi-ionization processes (3), (4) and the chemi-recombination processes (5), (6) should be of considerable interest **from the aspect of their influence on excited-atom populations** for the weakly ionized layers of stellar atmospheres. This was proven at a qualitative level for the hydrogen case (solar photosphere) in Mihajlov et al. (1997a), and for the helium case (atmospheres of DB white dwarfs with $T_{\rm eff} = 12\,000 \div 18\,000K$) in Mihajlov et al. (2003a).

Then, the influence of the chemi-ionization processes (3), (4) and the chemi-recombination processes (5), (6) with $A = H$ on the excited hydrogen atom populations was examined in much more detail in Mihajlov et al. (2003b), where these processes were included ab initio in a non-LTE modeling of an M red dwarf atmosphere with the effective temperature $T_{\rm eff} = 3800$ K, using PHOENIX code (see

Baron & Hauschildt 1998). A fact was established that including even the chemi-ionization and recombination only for $4 \leq n \leq 8$, generates significant changes (by up to 50%), at least in the populations of hydrogen-atom excited states with $2 \leq n \leq 20$.

Later, again using the PHOENIX code for the case of the atmosphere of the same red dwarf, the influence was examined of the processes (3-6) with $n \leq 10$ on the free electron density and the profiles of hydrogen atom spectral lines. It was established that if all these processes (with $n \geq 2$) are included, a significant change (somewhere up to 2–3 times) for the free electron density, N_e, is generated and, as one of further consequences, significant changes in the hydrogen line profiles take place.

In this paper, one of our main aims is to draw attention to the importance of all processes (1) – (4) with A = H for non-LTE modeling of the solar atmosphere. For this purpose, it should be demonstrated that in the solar photosphere the efficiency of these processes is greater than, or at least comparable to, the efficiency of processes (7) – (9) with A = H within those ranges of values of $n \geq 2$ and temperature T which are relevant to the chosen solar atmosphere model. However, until now, only for chemi-recombination processes (3) and (4) was qualitatively shown that for $4 \leq n \leq 8$ their efficiency is comparable to the efficiency of the concurrent processes (8) and (9) in a part of the solar photosphere (see Mihajlov et al. 1997a).

Besides the mentioned, the fact that the processes (1) – (4) can be important for the solar photosphere is supported by the results obtained in Mihajlov et al. (2003a, 2007) in connection with an M red dwarf atmosphere ($T_{\rm eff} = 3800$ K).

2. THE RATE COEFFICIENTS OF THE CHEMI-IONIZATION AND RECOMBINATION PROCESSES

The corresponding partial rate coefficients of the chemi-ionization processes (3) and (4) are denoted here with $K_{ci}^{(a,b)}(n;T)$, where T is the temperature of the considered plasma, and the partial rate coefficients of the inverse chemi-recombination processes (5) and (6) – with $K_{cr}^{(a,b)}(n;T)$. Under the conditions which exist in the solar atmosphere, we can determine the rate coefficients $K_{cr}^{(a,b)}(n;T)$ over the rate coefficients $K_{ci}^{(a,b)}(n;T)$ from the principle of the thermodynamical balance for processes (3), (4), (5) and (6) in the form

$$K_{ci}^{(a,b)} \cdot N_n N_1 = K_{cr}^{(a,b)}(n,T) \cdot N_1 N_{ai} N_e, \tag{10}$$

where N_1 and N_n denote the densities of ground- and excited-state hydrogen atoms respectively. Using these partial rate coefficients we will determine the total ones, namely,

$$K_{ci,cr}(n,T) = K_{ci,cr}^{(a)}(n,T) + K_{ci,cr}^{(b)}(n,T), \tag{11}$$

which characterizes the efficiency of the considered chemi-ionization and chemi-recombination processes together.

Here we will consider processes (3) – (6) with A = H within the regions $n \geq 5$ and $2 \leq n \leq 4$ separately. The reason for it is the behavior of the adiabatic potential curves of atom-atom systems $H^*(n) + H(1s)$. Namely, in the first region the atom-atom curves lie above the adiabatic curve of the ion-ion system $H^+ +$

$H^-(1s^2)$ for any R, and the dipole resonant mechanism can be applied for $n \geq 5$ without any exceptions. Consequently, for $n \geq 5$ we will determine the rate coefficients of these processes following the previous papers (Mihajlov et al. 1997a, 2003a,b, 2007).

However, in the region $n \leq 4$ there are points where the atom-atom curves cross the ion-ion one and application of this mechanism generates some errors (see Janev & Mihajlov 1979).

Due to this fact and the mentioned errors, we use here semi-empirical rate coefficients $K^{(a)}_{cr,ci}(n = 3, T)$ and $K^{(a)}_{cr,ci}(n = 4, T)$, which are obtained on the bases of the data from Janev et al. (1987). For relatively minor chemi-ionization and recombination processes with $n = 2$ we use here rate coefficients $K^{(a)}_{ci}(n = 2, T)$ and $K^{(a)}_{cr}(n = 2, T)$, which are 10–30 percent greater than the corresponding coefficients obtained using the data from Janev et al. (1987), in accordance with the calculated results from Urbain et al. (1991) and Rawlings et al. (1993). It gives a possibility to compensate the decrease of the rate coefficients $K^{(a)}_{ci}(n \geq 5, T)$ and $K^{(a)}_{cr}(n \geq 5, T)$ in comparison with the corresponding ones obtained using Janev et al. (1987), due to the fact that here, unlike Janev et al. (1987), the decay of the considered system's initial electronic state has been taken into account.

3. RESULTS AND DISCUSSION

In accordance with the aim of this work we consider here model C of solar atmosphere from Vernazza et al. (1981). Namely, this is a non-LTE model which is still actual (see Stix 2002), and it is only for this model that all the quantities necessary for our calculations are available in tabular form as functions of height (h) in solar photosphere.

Let $I_{ci}(n, T)$, $I_{cr}(n, T)$ be the total chemi-ionization and chemi-recombination fluxes caused by the processes (3,4) and (5,6), i.e.,

$$I_{ci}(n, T) = K_{ci}(n, T) \cdot N_n N_1, \qquad I_{cr}(n, T) = K_{cr}(n, T) \cdot N_1 N_i N_e, \tag{12}$$

and $I_{i;ea}(n, T)$, $I_{r;eei}(n, T)$ and $I_{r;ph}(n, T)$ be the fluxes caused by ionization and recombination processes (7), (8) and (9), i.e.

$$\begin{aligned} I_{i;ea}(n, T) = K_{ea}(n, T) \cdot N_n N_e, \quad I_{r;eei}(n, T) &= K_{eei}(n, T) \cdot N_i N_e N_e, \\ I_{r;ph}(n, T) &= K_{ph}(n, T) \cdot N_i N_e, \end{aligned} \tag{13}$$

where N_1, N_n, N_i, and N_e are, respectively, the densities of the ground and excited states of a hydrogen atom, of ion H^+, and of free electron in the considered plasma with given T.

Using these expressions, we will first calculate quantities $F_{i,ea}(n, T)$ given by

$$F_{i,ea}(n, T) = \frac{I_{ci}(n, T)}{I_{i;ea}(n, T)} = \frac{K_{ci}(n, T)}{K_{ea}(n, T)} \cdot N_1 N_e, \tag{14}$$

which characterize the relative efficiency of partial chemi-ionization processes (3) and (4) together and the impact electron-atom ionization (7) in the considered plasma. The impact ionization rate coefficients $K_{ea}(n, T)$ are taken from Vriens & Smeets (1980). In Figure the behavior of the quantities $F_{i,ea}(n, T)$ for $2 \leq n \leq 8$

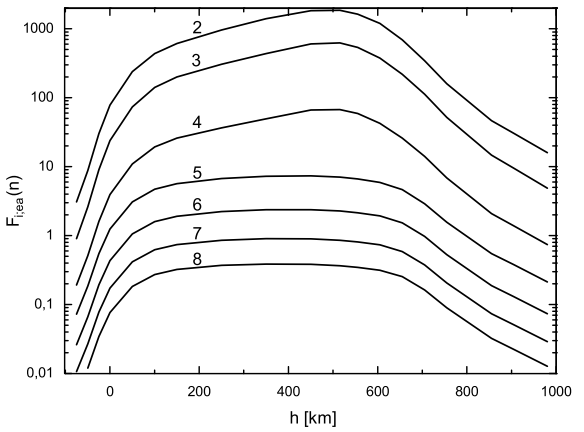

Fig. 1. Behavior of the quantity $F_{i;ea}^{(ab)}(n)$ given by Eq. (14), as a function of height h.

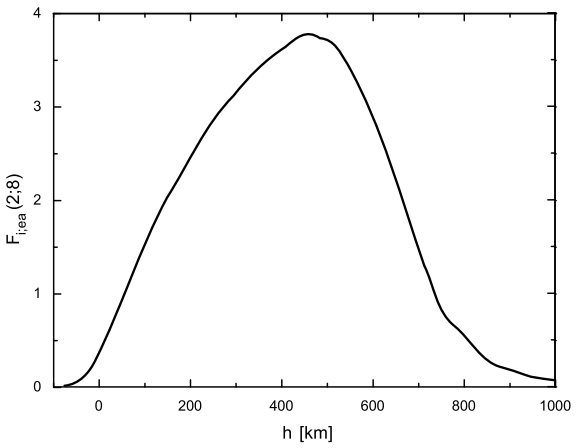

Fig. 2. Behavior of the quantity $F_{i;ea}(2;8)$ given by Eq. (15), as a function of height h.

as functions of height h is shown. One can see that the efficiency of the considered chemi-ionization processes in comparison with the electron-atom impact ionization is dominant for $2 \leq n \leq 6$ and becomes comparable for $n = 7$ and 8.

Then, in order to compare the relative influence of the chemi-ionization processes (3) and (4) together to that of the impact electron-atom ionization process (7) on the whole block of the excited hydrogen atom states with $2 \leq n \leq 8$, we will calculate quantity $F_{i,ea;2-8}(T)$, given by

$$F_{i,ea;2-8}(T) = \frac{\sum\limits_{n=2}^{8} I_{ci}(n,T)}{\sum\limits_{n=2}^{8} I_{i;ea}(n,T)} = \frac{\sum\limits_{n=2}^{8} K_{ci}(n,T) \cdot N_n}{\sum\limits_{n=2}^{8} K_{ea}(n,T) \cdot N_n} \cdot N_1 N_e, \tag{15}$$

which can reflect the influence of the existing populations of excited hydrogen atom states within a non-LTE model of solar atmosphere. In Figure the behavior

of the quantity $F_{i,ea;2-8}(T)$ as functions of height h is shown. As one can see, the real influence of the chemi-ionization processes on the total populations of states with $2 \leq n \leq 8$ remains dominant with respect to the concurrent electron-atom impact ionization processes almost in the whole photosphere (50 km $\leq h \leq$ 750 km).

Finally, we compared the relative influence of the chemi-recombination processes (5) and (6) together and total influence of the electron – electron – H^+ recombination process (8) and photo-recombination electron – H^+ process (9) on the same block of excited hydrogen atom states with $2 \leq n \leq 8$. It was confirmed a domination of the chemi-recombination processes with $2 \leq n \leq 8$ over the mentioned concurrent processes in a significant part of the photosphere (50 km $\leq h \leq$ 600 km).

The obtained results demonstrate the fact that the considered chemi-ionization and recombiontion processes must have a very significant influence on the optical properties of the solar photosphere in comparison to the concurrent electron-atom impact ionization and electron-ion recombination processes. Thus it is shown that the importance of these processes for non-LTE modeling of solar atmosphere should be necessarily investigated.

ACKNOWLEDGMENTS. This work was supported by the Ministry of Science and Technological Development of Serbia as a part of the projects 176002 and III4402.

REFERENCES

Baron E., Hauschildt P. H. 1998, ApJ, 495, 370
Ignjatović L. M., Mihajlov A. A. 2005, Phys. Rev. A., 72, 022715
Ignjatović L. M., Mihajlov A. A., Klyucharev A. N. 2008, J. Phys.B, Atomic Molecular Physics, 41, 025203
Janev R. K., Langer W. D., Evans Jr. K., Post Jr. D. E. 1987, *Elementary Processes in Hydrogen-Helium Plasmas*, Springer-Verlag
Janev R. K., Mihajlov A. A. 1979, Phys. Rev. A., 20, 1890
Mihajlov A. A., Dimitrijević M. S. 1986, A&A, 155, 319
Mihajlov A. A., Dimitrijević M. S. 1992, A&A, 256, 305
Mihajlov A. A., Dimitrijević M. S., Djurić Z. 1996, Physica Scripta, 53, 159
Mihajlov A. A., Djurić Z., Dimitrijević M. S., Ljepojević N. N. 1997b, Physica Scripta, 56, 631
Mihajlov A. A., Ignjatović L. M., Vasilijević M. M., Dimitrijević M. S. 1997a, A&A, 324, 1206
Mihajlov A. A., Ignjatović L. M., Dimitrijević M. S., Djurić Z. 2003a, ApJS, 147, 369
Mihajlov A. A., Jevremović D., Hauschildt P. et al. 2003b, A&A, 403, 787
Mihajlov A. A., Jevremović D., Hauschildt P. et al. 2007, A&A, 471, 671
Mihajlov A. A., Ljepojević N. N., Dimitrijević M. S. 1992, J.Phys.B, Atomic Molecular Physics, 25, 5121
Rawlings J., Drew J., Barlow M. 1993, MNRAS, 265, 968
Smirnov V. M., Mihajlov A. A. 1971, Optika i Spektroskopiya, 30, 984
Stix M. 2002, *The Sun*, Sect. 4.3. Atmospheric Models, Springer Verlag
Urbain X., Cornet A., Brouillard F. et al. 1991, Phys. Rev. Lett., 66, 1685
Vernazza J., Avrett E., Loser R. 1981, ApJS, 45, 635
Vriens L., Smeets A. H. M. 1980, Phys. Rev. A, 22, 940

Baltic Astronomy, vol. 20, 576–579, 2011

STARK BROADENING OF SEVERAL Ar I SPECTRAL LINES IN THE VISIBLE SPECTRUM

Milan S. Dimitrijević[1,2], Andjelka Kovačević[3], Zoran Simić[1] and Sylvie Sahal-Bréchot[2]

[1] *Astronomical Observatory, Volgina 7, 11060 Belgrade 38, Serbia; mdimitrijevic@aob.bg.ac.rs, zsimic@aob.bg.ac.rs*

[2] *Observatoire de Paris, LERMA, 5 Place Jules Janssen, F-92190 Meudon, France; sylvie.sahal-brechot@obspm.fr*

[3] *Department of Astronomy, Faculty of Mathematics, University of Belgrade, Studentski Trg 16, 11000 Belgrade, Serbia; andjelka@matf.bg.ac.rs*

Received: 2011 August 8; accepted: 2011 August 15

Abstract. In order to complete data on Stark broadening parameters for Ar I line in the visible spectrum, we determined Stark widths and shifts due to electron, proton and ionized helium impacts, for nine lines (4191.0, 4259.4, 5912.1, 6043.2, 6045.0, 6752.9, 7503.9, 7514.6, 7724.2 Å), using jK coupling and semiclassical-perturbation theory. The obtained results will enter the STARK-B database, which is a part of the Virtual Atomic and Molecular Data Center.

Key words: physical data and processes: Stark broadening, line profiles, databases

1. INTRODUCTION

Argon spectral lines, which are useful not only for laboratory and technological plasmas but also were observed in stellar atmospheres, are of particular interest, especially in the visible spectrum. Stark broadening parameters of spectral lines are of interest for diagnostics, modeling and investigations of various plasmas in laboratory, technology, fusion research, laser designing, as well as for analysis, interpretation and synthesis of Ar I lines in stellar spectra.

As the continuation of our previous work on the theoretical determination of Stark broadening of Ar I lines (Dimitrijević et al. 2003, 2007; Milosavljević et al. 2003; Christova et al. 2010), and in order to supplement the STARK-B database (http://stark-b.obspm.fr/), a part of Virtual Atomic and Molecular Data Center (VAMDC - http://vamdc.org/, Dubernet et al. 2010; Rixon et al. 2011), we determined here Stark widths and shifts for nine lines at 4191.0, 4259.4, 5912.1, 6043.2, 6045.0, 6752.9, 7503.9, 7514.6, 7724.2 Å due to electron, proton and ionized helium impacts, using the jK coupling and semiclassical-perturbation theory (Sahal-Bréchot 1969a,b, 1974; Dimitrijević & Sahal-Bréchot 1984).

Table 1. Stark full widths at half intensity maximum (W) and shifts (d) due to electron, proton and ionized helium impacts for Ar I, for a perturber density of 10^{16} cm^{-3}. The quantity C (given in Å cm^{-3}), when divided by the corresponding perturber width, gives an estimate for the maximum perturber density for which tabulated data may be used. The validity of the impact approximation has been estimated by checking if the collision volume (V) multiplied by the perturber density (N) is much less than one (Sahal-Bréchot 1969a,b). Asterisk denotes the values where $0.1 < NV \leq 0.5$.

		Electrons		Protons		Ionized helium	
Transition	T (K)	W (Å)	d (Å)	W (Å)	d (Å)	W (Å)	d (Å)
Ar I 4s-4p	2500	0.0761	0.0512	0.0333	0.0129	0.0322	0.0101
$[3/2]_1 - [1/2]_0$	5000	0.0851	0.0620	0.0341	0.0149	0.0329	0.0118
7514.6 Å	10 000	0.0967	0.0610	0.0350	0.0171	0.0335	0.0136
C = 0.27E+20	20 000	0.119	0.0586	0.0361	0.0195	0.0342	0.0156
	30 000	0.135	0.0484	0.0369	0.0209	0.0347	0.0168
	50 000	0.162	0.0389	0.0380	0.0229	0.0354	0.0184
Ar I 4s′-4p′	2500	0.0740	0.0464	0.0336	0.0121	0.0328	0.00951
$[1/2]_1 - [1/2]_0$	5000	0.0820	0.0578	0.0343	0.0140	0.0334	0.0111
7503.9 Å	10 000	0.0929	0.0586	0.0351	0.0160	0.0339	0.0128
C = 0.35E+20	20 000	0.115	0.0569	0.0360	0.0182	0.0345	0.0146
	30 000	0.131	0.0481	0.0367	0.0196	0.0349	0.0157
	50 000	0.157	0.0385	0.0377	0.0215	0.0355	0.0172
Ar I 4s′-4p′	2500	0.0665	0.0379	0.0307	0.00961	0.0301	0.00759
$[1/2]_0 - [1/2]_1$	5000	0.0713	0.0458	0.0312	0.0111	0.0305	0.00882
7724.2 Å	10 000	0.0795	0.0442	0.0316	0.0127	0.0309	0.0101
C = 0.44E+20	20 000	0.0990	0.0412	0.0322	0.0144	0.0312	0.0115
	30 000	0.115	0.0342	0.0327	0.0155	0.0315	0.0124
	50 000	0.141	0.0272	0.0333	0.0169	0.0319	0.0136
Ar I 4s′-5p′	2500	0.142	0.0941	*0.0524	*0.0218	*0.0488	*0.0164
$[1/2]_1 - [1/2]_0$	5000	0.164	0.113	*0.0552	*0.0268	*0.0517	*0.0207
4259.4 Å	10 000	0.186	0.128	0.0577	0.0317	*0.0538	*0.0249
C = 0.39E+19	20 000	0.212	0.125	0.0605	0.0367	*0.0558	*0.0292
	30 000	0.229	0.109	0.0624	0.0398	0.0571	0.0317
	50 000	0.257	0.0908	0.0651	0.0439	0.0589	0.0350
Ar I 4s′-5p′	2500	0.117	0.0793	*0.0451	*0.0176	*0.0424	*0.0134
$[1/2]_0 - [3/2]_1$	5000	0.134	0.0893	*0.0470	*0.0214	*0.0446	*0.0166
4191.0 Å	10 000	0.153	0.0997	0.0488	0.0252	*0.0461	*0.0198
C = 0.40E+19	20 000	0.177	0.0962	0.0509	0.0291	*0.0475	*0.0231
	30 000	0.194	0.0837	0.0522	0.0315	0.0484	0.0251
	50 000	0.220	0.0695	0.0542	0.0346	0.0497	0.0277
Ar I 4p-4d	2500	0.443	0.271	*0.135	*0.0591	*0.124	*0.0443
$[1/2]_1 - [3/2]_2$	5000	0.505	0.315	*0.142	*0.0730	*0.132	*0.0565
6752.9 Å	10 000	0.585	0.315	0.150	0.0867	*0.138	*0.0681
C = 0.60E+19	20 000	0.697	0.276	0.158	0.101	*0.144	*0.0798
	30 000	0.773	0.241	0.163	0.109	0.148	0.0868
	50 000	0.862	0.202	0.171	0.120	0.153	0.0960

Table 1. Continued

Transition	T (K)	Electrons		Protons		Ionized helium	
		W (Å)	d (Å)	W (Å)	d (Å)	W (Å)	d (Å)
Ar I 4p-4d′	2500	0.650	0.430	*0.162	*0.0856		
$[1/2]_1 - [3/2]_1$	5000	0.721	0.495	*0.178	*0.112		
5912.1 Å	10 000	0.778	0.485	*0.194	*0.138	*0.167	*0.107
$C = 0.22$E+19	20 000	0.843	0.432	*0.212	*0.163	*0.181	*0.128
	30 000	0.887	0.382	*0.224	*0.178	*0.190	*0.141
	50 000	0.937	0.309	0.240	0.197	*0.202	*0.157
Ar I 4p-5d	2500	1.76	1.07				
$[5/2]_2 - [7/2]_3$	5000	1.91	0.919				
6043.2 Å	10 000	2.24	0.667				
$C = 0.11$E+19	20 000	2.53	0.504				
	30 000	2.60	0.376	*0.636	*0.487		
	50 000	2.67	0.213	*0.690	*0.547		
Ar I 4p′-6d	2500	* 4.89	* 2.86				
$[3/2]_2 - [5/2]_3$	5000	* 5.31	* 3.14				
6045.0 Å	10 000	* 5.73	* 3.01				
$C = 0.80$E+18	20 000	6.32	2.36				
	30 000	6.61	1.92				
	50 000	6.78	1.48				

2. RESULTS AND DISCUSSION

Stark broadening parameters for nine Ar I lines have been determined within the semiclassical perturbation formalism, discussed in detail in Sahal-Bréchot (1969a,b). The optimization and updates can be found in e.g. Sahal-Bréchot (1974), Dimitrijević & Sahal-Bréchot (1984). Energy levels have been taken from Bashkin & Stoner (1978). The obtained results for electron, proton and ionized helium impact widths (FWHM) and shifts are shown in Table 1, for a perturber density of 10^{16} cm^{-3} and temperatures between 2500 and 50 000 K. For perturber densities lower than tabulated, Stark broadening parameters may be scaled linearly.

For each value given in Table 1, the collision volume (V) multiplied by the perturber density (N) is much less than one, and the impact approximation is valid (Sahal-Bréchot 1969a). When the impact approximation is not valid, the ion broadening contribution may be estimated by using quasistatic approach (Griem 1974 or Sahal-Bréchot 1991). In the region between where neither of these two approximations is valid, a unified type theory should be used.

The accuracy of the results obtained decreases when broadening by ion interactions becomes important.

For extrapolation of values from Table 1 towards higher electron densities, the results start to deviate from linear behavior due to Debye screening. This effect is more important for the shift than for the width and could be taken into account by the approximative method described in Griem (1974).

The obtained results will enter the STARK-B database (http://stark-b.obs

pm.fr/), which is a part of Virtual Atomic and Molecular Data Center (VAMDC – http://vamdc.org/, Dubernet et al. 2010; Rixon et al. 2011). supported by EU in the framework of the FP7 "Research Infrastructures – INFRA-2008-1.2.2 – Scientific Data Infrastructures" initiative, with the aim to build an interoperable e-Infrastructure for the exchange of atomic and molecular data.

ACKNOWLEDGMENTS. This work has been supported by VAMDC, funded under the "Combination of Collaborative Projects and Coordination and Support Actions" Funding Scheme of The 7th Framework Program; call topic: INFRA-2008-1.2.2 Scientific Data Infrastructure, grant No. 239108. The authors are also grateful for the support provided by the Ministry of Education and Science of Republic of Serbia through project 176002 "Influence of collisional processes on astrophysical plasma spectra".

REFERENCES

Bashkin S., Stoner Jr. J. J. 1978, *Atomic Energy Levels and Grotrian Diagrams*, Vol. 2, North Holland, Amsterdam

Christova M., Dimitrijević M. S., Kovačević A. 2010, J. Phys. Conf. Ser., 207, 012024

Dimitrijević M. S., Christova M., Sahal-Bréchot S. 2007, Physica Scripta, 75, 809

Dimitrijević M. S., Skuljan Lj., Djeniže S. 2003, Physica Scripta, 66, 77

Dimitrijević M. S., Sahal-Bréchot S. 1984, JQSRT, 31, 301

Dubernet M. L. et al. 2010, JQSRT, 111, 2151

Griem H. R. 1974, *Spectral Line Broadening by Plasmas*, Academic Press, New York

Milosavljević V., Dimitrijević M. S., Djeniže S. 2003, High Temp. Material Processes, 7, 525

Rixon G., Dubernet M. L., Piskunov N. et al. 2011, AIP Conf. Proc., 1344, 107

Sahal-Bréchot S. 1969a, A&A, 1, 91

Sahal-Bréchot S. 1969b, A&A, 2, 322

Sahal-Bréchot S. 1974, A&A, 35, 321

Sahal-Bréchot S. 1991, A&A, 245, 322

Baltic Astronomy, vol. 20, 580–586, 2011

STARK BROADENING OF SEVERAL Ne II, Ne III AND O III SPECTRAL LINES FOR THE STARK-B DATABASE

Milan S. Dimitrijević[1,2], Andjelka Kovačević[3], Zoran Simić[1] and Sylvie Sahal-Bréchot[2]

[1] *Astronomical Observatory, Volgina 7, 11060 Belgrade 38, Serbia; mdimitrijevic@aob.bg.ac.rs, zsimic@aob.bg.ac.rs*

[2] *Observatoire de Paris, LERMA, 5 Place Jules Janssen, F-92190 Meudon, France; sylvie.sahal-brechot@obspm.fr*

[3] *Department of Astronomy, Faculty of Mathematics, University of Belgrade, Studentski Trg 16, 11000 Belgrade, Serbia; andjelka@matf.bg.ac.rs*

Received: 2011 August 8; accepted: 2011 August 15

Abstract. In order to complete Stark broadening data for Ne II, and O III lines, needed for analysis of stellar atmospheres, we determined, within the semiclassical perturbation method, the missing Stark broadening parameters for the broadening by collisions with protons and ionized helium, for 15 Ne II and 5 O III multiplets. Also, electron, proton and ionized helium impact broadening parameters for an important Ne II multiplet in the visible part of the spectrum and for three Ne III multiplets were calculated. The obtained data will be included in the STARK-B database, which is a part of the Virtual Atomic and Molecular Data Center.

Key words: physical data and processes: Stark broadening, line profiles, databases

1. INTRODUCTION

The data on Stark broadening of spectral lines are of interest for diagnostics, modeling and investigations of stellar atmospheres and other various plasmas in astrophysics, laboratory, technology and fusion research. Such data obtained by us using a semiclassical perturbation method, are organized in the STARK-B database (http://stark-b.obspm.fr/), a part of the Virtual Atomic and Molecular Data Center (VAMDC – http://vamdc.org/, Dubernet et al. 2010; Rixon et al. 2011), supported by EU in the framework of the FP7 Research Infrastructures-INFRA-2008-1.2.2-Scientific Data Infrastructures initiative.

Table 1. Stark full widths at half intensity maximum (W) and shifts (d) due to electron, proton and ionized helium impacts for Ne II, for a perturber density of 10^{17} cm^{-3}. The quantity C (given in Å cm^{-3}), when divided by the corresponding perturber width, gives an estimate for the maximum perturber density for which tabulated data may be used.

		Electrons		Protons		Ionized helium	
Transition	T (K)	W (Å)	d (Å)	W (Å)	d (Å)	W (Å)	d (Å)
Ne II	5000	0.376	0.0257	0.0151	0.273E-02	0.0188	0.256E-02
3292.1 Å	10 000	0.281	0.0149	0.0224	0.502E-02	0.0259	0.437E-02
C = 0.11E+21	20 000	0.214	0.0133	0.0277	0.741E-02	0.0297	0.641E-02
$3p^2D^\circ$-$3d^2P$	30 000	0.190	0.0141	0.0300	0.869E-02	0.0318	0.716E-02
	50 000	0.171	0.0147	0.0328	0.100E-01	0.0341	0.836E-02
	100 000	0.157	0.0127	0.0356	0.120E-01	0.0357	0.998E-02

Table 2. Stark broadening parameters for Ne II multiplets for a perturber density of 10^{17} cm^{-3}. Designations are the same as in Table 1.

		Protons		Ionized helium	
Transition	T (K)	W (Å)	d (Å)	W (Å)	d (Å)
Ne II	5000	0.152E-01	0.276E-02	0.190E-01	0.260E-02
3375.6 Å	10 000	0.227E-01	0.510E-02	0.264E-01	0.445E-02
C = 0.13E+21	20 000	0.282E-01	0.755E-02	0.303E-01	0.653E-02
$3p^2D^\circ$-$3d^2F$	30 000	0.305E-01	0.888E-02	0.324E-01	0.729E-02
	50 000	0.333E-01	0.102E-01	0.348E-01	0.853E-02
	100 000	0.363E-01	0.122E-01	0.365E-01	0.101E-01
Ne II	5000	0.498E-02	-0.512E-03	0.716E-02	-0.508E-03
3572.1 Å	10 000	0.886E-02	-0.109E-02	0.109E-01	-0.104E-02
C = 0.36E+21	20 000	0.126E-01	-0.193E-02	0.140E-01	-0.172E-02
$3s'^2D$-$3p'^2F^\circ$	30 000	0.141E-01	-0.236E-02	0.152E-01	-0.209E-02
	50 000	0.154E-01	-0.304E-02	0.165E-01	-0.257E-02
	100 000	0.173E-01	-0.371E-02	0.179E-01	-0.308E-02
Ne II	5000	0.475E-02	-0.200E-03	0.678E-02	-0.199E-03
3337.8 Å	10 000	0.832E-02	-0.439E-03	0.102E-01	-0.428E-03
C = 0.33E+21	20 000	0.117E-01	-0.824E-03	0.130E-01	-0.765E-03
$3s'^2D$-$3p'^2P^\circ$	30 000	0.130E-01	-0.109E-02	0.140E-01	-0.958E-03
	50 000	0.142E-01	-0.141E-02	0.152E-01	-0.123E-02
	100 000	0.159E-01	-0.182E-02	0.165E-01	-0.152E-02
Ne II	5000	0.146E-01	0.221E-02	0.184E-01	0.211E-02
3422.7 Å	10 000	0.219E-01	0.417E-02	0.257E-01	0.374E-02
C = 0.14E+21	20 000	0.274E-01	0.632E-02	0.295E-01	0.549E-02
$3p'^2P$-$3d'^2P^\circ$	30 000	0.297E-01	0.754E-02	0.316E-01	0.623E-02
	50 000	0.324E-01	0.876E-02	0.340E-01	0.726E-02
	100 000	0.353E-01	0.104E-01	0.357E-01	0.867E-02

Table 2. Continued

Transition	T (K)	Protons		Ionized helium	
		W (Å)	d (Å)	W (Å)	d (Å)
Ne II	5000	0.106E-01	0.195E-02	0.136E-01	0.185E-02
3040.1 Å	10 000	0.161E-01	0.364E-02	0.191E-01	0.323E-02
C = 0.11E+21	20 000	0.205E-01	0.546E-02	0.220E-01	0.472E-02
$3p^4P^\circ$-$3d^4D$	30 000	0.222E-01	0.647E-02	0.236E-01	0.532E-02
	50 000	0.243E-01	0.749E-02	0.254E-01	0.621E-02
	100 000	0.265E-01	0.892E-02	0.268E-01	0.745E-02
Ne II	5000	0.134E-01	0.207E-02	0.170E-01	0.198E-02
3352.6 Å	10 000	0.202E-01	0.392E-02	0.238E-01	0.352E-02
C = 0.13E+21	20 000	0.255E-01	0.594E-02	0.274E-01	0.517E-02
$3p^4D^\circ$-$3d^4D$	30 000	0.276E-01	0.711E-02	0.294E-01	0.587E-02
	50 000	0.301E-01	0.825E-02	0.317E-01	0.685E-02
	100 000	0.329E-01	0.987E-02	0.333E-01	0.815E-02
Ne II	5000	0.153E-01	0.289E-02	0.192E-01	0.271E-02
3421.5 Å	10 000	0.229E-01	0.532E-02	0.267E-01	0.463E-02
C = 0.13E+21	20 000	0.285E-01	0.786E-02	0.306E-01	0.680E-02
$3p^2D^\circ$-$3d^4F$	30 000	0.309E-01	0.923E-02	0.328E-01	0.759E-02
	50 000	0.338E-01	0.106E-01	0.353E-01	0.888E-02
	100 000	0.368E-01	0.127E-01	0.370E-01	0.105E-01
Ne II	5000	0.171E-01	0.281E-02	0.212E-01	0.265E-02
3473.1 Å	10 000	0.254E-01	0.521E-02	0.292E-01	0.456E-02
C = 0.13E+21	20 000	0.312E-01	0.773E-02	0.335E-01	0.668E-02
$3p^2S^\circ$-$3d^2P$	30 000	0.337E-01	0.911E-02	0.359E-01	0.749E-02
	50 000	0.368E-01	0.105E-01	0.385E-01	0.872E-02
	100 000	0.398E-01	0.126E-01	0.402E-01	0.103E-01
Ne II	5000	0.192E-01	0.281E-02	0.238E-01	0.267E-02
3651.8 Å	10 000	0.285E-01	0.526E-02	0.328E-01	0.466E-02
C = 0.14E+21	20 000	0.349E-01	0.788E-02	0.375E-01	0.681E-02
$3p^2P^\circ$-$3d^2P$	30 000	0.377E-01	0.934E-02	0.401E-01	0.767E-02
	50 000	0.411E-01	0.108E-01	0.430E-01	0.896E-02
	100 000	0.443E-01	0.129E-01	0.450E-01	0.108E-01
Ne II	5000	0.152E-01	0.313E-02	0.190E-01	0.291E-02
3352.6 Å	10 000	0.227E-01	0.567E-02	0.263E-01	0.491E-02
C = 0.11E+21	20 000	0.282E-01	0.836E-02	0.302E-01	0.717E-02
$3p^2D^\circ$-$3d^4P$	30 000	0.306E-01	0.970E-02	0.324E-01	0.801E-02
	50 000	0.334E-01	0.112E-01	0.348E-01	0.930E-02
	100 000	0.362E-01	0.135E-01	0.364E-01	0.110E-01

Table 2. Continued

Transition	T (K)	Protons		Ionized helium	
		W (Å)	d (Å)	W (Å)	d (Å)
Ne II	5000	0.131E-01	0.154E-01	0.141E-01	0.129E-01
3412.3 Å	10 000	0.229E-01	0.241E-01	0.234E-01	0.202E-01
C = 0.10E+21	20 000	0.339E-01	0.323E-01	0.305E-01	0.267E-01
$3p^2P^\circ$-$4s^2P$	30 000	0.393E-01	0.362E-01	0.347E-01	0.299E-01
	50 000	0.462E-01	0.418E-01	0.405E-01	0.346E-01
	100 000	0.549E-01	0.486E-01	0.470E-01	0.403E-01
Ne II	5000	0.152E-01	0.190E-02	0.192E-01	0.182E-02
3432.3 Å	10 000	0.228E-01	0.362E-02	0.266E-01	0.329E-02
C = 0.14E+21	20 000	0.284E-01	0.555E-02	0.305E-01	0.485E-02
$3p^2D^\circ$-$3d^2D$	30 000	0.307E-01	0.670E-02	0.327E-01	0.559E-02
	50 000	0.334E-01	0.780E-02	0.351E-01	0.650E-02
	100 000	0.361E-01	0.934E-02	0.366E-01	0.778E-02
Ne II	5000	0.176E-01	0.163E-02	0.221E-01	0.157E-02
3650.0 Å	10 000	0.263E-01	0.317E-02	0.306E-01	0.293E-02
C = 0.16E+21	20 000	0.325E-01	0.494E-02	0.351E-01	0.437E-02
$3p^4S^\circ$-$3d^2D$	30 000	0.351E-01	0.608E-02	0.375E-01	0.517E-02
	50 000	0.382E-01	0.713E-02	0.403E-01	0.596E-02
	100 000	0.412E-01	0.862E-02	0.422E-01	0.716E-02
Ne II	5000	0.177E-01	0.277E-02	0.221E-01	0.263E-02
3637.8 Å	10 000	0.264E-01	0.519E-02	0.306E-01	0.460E-02
C = 0.15E+21	20 000	0.327E-01	0.778E-02	0.351E-01	0.672E-02
$3p^4S^\circ$-$3d^4F$	30 000	0.353E-01	0.921E-02	0.376E-01	0.757E-02
	50 000	0.386E-01	0.107E-01	0.404E-01	0.884E-02
	100 000	0.418E-01	0.127E-01	0.423E-01	0.106E-01
Ne II	5000	0.179E-01	0.578E-02	0.220E-01	0.527E-02
3560.0 Å	10 000	0.268E-01	0.982E-02	0.306E-01	0.852E-02
C = 0.12E+21	20 000	0.334E-01	0.144E-01	0.353E-01	0.119E-01
$3p^4S^\circ$-$3d^4P$	30 000	0.364E-01	0.161E-01	0.379E-01	0.133E-01
	50 000	0.402E-01	0.187E-01	0.411E-01	0.155E-01
	100 000	0.444E-01	0.223E-01	0.435E-01	0.183E-01

In Djeniže et al. (2002) and Milosavljević et al. (2001) we determined Stark broadening parameters due to collisions with electrons for 15 Ne II and 3 Ne III, and in Srećković et al. (2001) electron-impact widths for 5 O III multiplets. However, for stellar atmospheres research, Stark broadening data due to collisions with the principal ionic perturbers, protons and ionized helium, are also useful. In order to complete data to be included in the STARK-B database, we determined here these additional data. Also, we determined within the semiclassical perturbation method electron, proton and ionized helium impact broadening parameters for the

Table 3. Stark broadening parameters for Ne III multiplets for a perturber density of 10^{17} cm^{-3}. Designations are the same as in Table 1.

Transition	T (K)	Electrons W (Å)	Electrons d (Å)	Protons W (Å)	Protons d (Å)	Ionized helium W (Å)	Ionized helium d (Å)
Ne III	20 000	0.0931	-0.00108	0.00182	-0.478E-03	0.00256	-0.464E-03
2611.8 Å	50 000	0.0603	-0.00117	0.00340	-0.102E-02	0.00412	-0.912E-03
C = 0.25E+21	100 000	0.0458	-0.00157	0.00451	-0.145E-02	0.00482	-0.126E-02
$3s'^3D^\circ$-$3p'^3F$	200 000	0.0368	-0.00143	0.00515	-0.183E-02	0.00542	-0.153E-02
	300 000	0.0331	-0.00144	0.00553	-0.205E-02	0.00573	-0.170E-02
	500 000	0.0294	-0.00136	0.00597	-0.233E-02	0.00595	-0.193E-02
Ne III	20 000	0.0771	-0.207E-02	0.00290	-0.477E-04	0.00376	-0.476E-04
2265.1 Å	50 000	0.0515	-0.106E-03	0.00482	-0.120E-03	0.00544	-0.116E-03
C = 0.18E+21	100 000	0.0398	-0.133E-03	0.00571	-0.206E-03	0.00615	-0.189E-03
$3p'^3F$-$3d'^3F^\circ$	200 000	0.0325	-0.717E-04	0.00643	-0.299E-03	0.00681	-0.263E-03
	300 000	0.0296	-0.974E-04	0.00680	-0.361E-03	0.00702	-0.303E-03
	500 000	0.0267	-0.890E-04	0.00707	-0.416E-03	0.00723	-0.346E-03
Ne III	20 000	0.0666	-0.254E-04	0.00249	0.306E-04	0.00323	0.306E-04
2092.4 Å	50 000	0.0443	0.554E-04	0.00414	0.775E-04	0.00466	0.753E-04
C = 0.15E+21	100 000	0.0342	0.833E-04	0.00490	0.136E-03	0.00527	0.127E-03
$3p'^3D$-$3d'^3D^\circ$	200 000	0.0280	0.120E-03	0.00551	0.203E-03	0.00584	0.180E-03
	300 000	0.0254	0.983E-04	0.00583	0.248E-03	0.00601	0.212E-03
	500 000	0.0230	0.988E-04	0.00605	0.289E-03	0.00619	0.242E-03

important Ne II $2s^22p^4(^3P)3p^2D^\circ$ – $2s^22p^4(^3P)3d^2P$ multiplet in the visible part of the spectrum, and the missing data for three O III multiplets.

2. RESULTS AND DISCUSSION

Stark broadening parameters have been determined within the semiclassical perturbation formalism, discussed in detail in Sahal-Bréchot (1969a,b). The optimization and updates can be found, e.g., in Sahal-Bréchot (1974), Dimitrijević & Sahal-Bréchot (1984). All details of the calculation are in Djeniže et al. (2002) for Ne II and Ne III and in Srećković et al. (2001) for O III, and will not be repeated here. Obtained results for electron, proton and ionized helium impact broadening parameters for Ne II, Ne III are presented in Tables 1–3. Table 4 contains the corresponding results for O III. Results are obtained for a perturber density of 10^{17} cm^{-3}.

3. CONCLUSION

Using the semiclassical perturbation theory and the corresponding computer code, we determined Stark broadening parameters due to collisions with protons and helium ions for 15 Ne II and 5 O III multiplets, needed for stellar plasma research, missing in Djeniže et al. (2002), Milosavljević et al. (2001) and Srećković et al. (2001), where only electron-impact broadening data are given. The missing data are also needed for the STARK-B database (http://stark-b.obspm.fr), containing Stark broadening parameters for modeling stellar atmospheres, for stellar spectra analysis and synthesis, for the laboratory plasma, inertial fusion plasma, laser development and plasmas in technology investigations. It is a part of Virtual

Table 4. Stark broadening parameters for O III multiplets. for a perturber density of 10^{17} cm^{-3}. Designations are the same as in Table 1.

		Protons		Ionized helium	
Transition	T (K)	W (Å)	d (Å)	W (Å)	d (Å)
O III	20 000	0.504E-02	-0.213E-02	0.685E-02	-0.201E-02
3763.4 Å	50 000	0.921E-02	-0.406E-02	0.107E-01	-0.356E-02
C = 0.38E+21	100 000	0.118E-01	-0.560E-02	0.124E-01	-0.469E-02
$3p^3D$-$3s^3P^\circ$	200 000	0.137E-01-	0.674E-02	0.141E-01	-0.564E-02
	300 000	0.148E-01	-0.746E-02	0.148E-01	-0.624E-02
	500 000	0.161E-01	-0.847E-02	0.156E-01	-0.700E-02
O III	20 000	0.424E-02	-0.148E-02	0.572E-02	-0.141E-02
3327.6 Å	50 000	0.761E-02	-0.289E-02	0.884E-02	-0.251E-02
C = 0.29E+21	100 000	0.958E-02	-0.397E-02	0.102E-01	-0.336E-02
$3p^3S$-$3s^3P^\circ$	200 000	0.110E-01	-0.483E-02	0.115E-01	-0.402E-02
	300 000	0.119E-01	-0.537E-02	0.120E-01	-0.445E-02
	500 000	0.127E-01	-0.612E-02	0.125E-01	-0.503E-02
O III	20 000	0.417E-02	-0.723E-03	0.552E-02	-0.700E-03
2984.7 Å	50 000	0.719E-02	-0.152E-02	0.823E-02	-0.134E-02
C = 0.16E+21	100 000	0.871E-02	-0.212E-02	0.934E-02	-0.185E-02
$3p^1D$-$3s^1P^\circ$	200 000	0.990E-02	-0.267E-02	0.104E-01	-0.223E-02
	300 000	0.106E-01	-0.298E-02	0.108E-01	-0.249E-02
	500 000	0.113E-01	-0.338E-02	0.112E-01	-0.280E-02
O III	20 000	0.747E-02	-0.366E-02	0.982E-02	-0.340E-02
4082.2 Å	50 000	0.133E-01	-0.656E-02	0.150E-01	-0.583E-02
C = 0.22E+21	100 000	0.166E-01	-0.886E-02	0.173E-01	-0.733E-02
$3p'^3D$-$3s'^3P^\circ$	200 000	0.195E-01	-0.106E-01	0.196E-01	-0.881E-02
	300 000	0.213E-01	-0.117E-01	0.207E-01	-0.980E-02
	500 000	0.234E-01	-0.133E-01	0.217E-01	-0.108E-01
O III	20 000	0.131E-01	-0.336E-02	0.162E-01	-0.313E-02
4110.8 Å	50 000	0.208E-01	-0.610E-02	0.226E-01	-0.543E-02
C = 0.38E+21	100 000	0.243E-01	-0.832E-02	0.257E-01	-0.688E-02
$3d'^5P$-$3p'^5S^\circ$	200 000	0.275E-01	-0.997E-02	0.284E-01	-0.831E-02
	300 000	0.291E-01	-0.110E-01	0.293E-01	-0.914E-02
	500 000	0.307E-01	-0.124E-01	0.304E-01	-0.102E-01

Atomic and Molecular Data Center – VAMDC, an European FP7 project (P.I. Marie Lise Dubernet, Dubernetet et al. 2010; Rixon et al. 2010) with the aims: (1) to build a secure, flexible and interoperable e-science environment based interface to the existing atomic and molecular databases; (2) to coordinate groups involved in the generation, evaluation and use of atomic and molecular data, and (3) to provide a forum for training of potential users.

Also, we determined electron, proton and ionized helium impact broadening parameters for the important Ne II $2s^22p^4(^3P)3p^2D^\circ$ - $2s^22p^4(^3P)3d^2P$ multiplet in the visible part of the spectrum, and for 3 O III multiplets.

Due to high abundance of neon and oxygen in stellar atmospheres, we hope

that the obtained results will be of interest for interpretation and synthesis of stellar spectra and for a number of other investigations in astrophysics, physics and plasma technologies.

ACKNOWLEDGMENTS. This work has been supported by VAMDC, funded under the "Combination of Collaborative Projects and Coordination and Support Actions" Funding Scheme of The 7th Framework Program; call topic: INFRA-2008-1.2.2 Scientific Data Infrastructure, grant agreement No. 239108. The authors are also grateful for the support provided by the Ministry Education and Science of Republic of Serbia through project 176002 "Influence of collision processes on astrophysical plasma spectra".

REFERENCES

Djeniže S., Milosavljević V., Dimitrijević M. S. 2002, A&A, 382, 359
Dimitrijević M. S., Sahal-Bréchot S. 1984, JQSRT, 31, 301
Dubernet M. L. et al. 2010, JQSRT, 111, 2151
Milosavljević V., Dimitrijević M. S., Djeniže S. 2001, ApJS, 135, 115
Rixon G., Dubernet M. L., Piskunov N. et al. 2011, AIP Conf. Proc., 1344, 107
Sahal-Bréchot S. 1969a, A&A, 1, 91
Sahal-Bréchot S. 1969b, A&A, 2, 322
Sahal-Bréchot S. 1974, A&A, 35, 321
Srećković V., Dimitrijević M. S., Djeniže S. 2001, A&A, 371, 354

Baltic Astronomy, vol. 20, 613–617, 2011

STARK BROADENING OF In III LINES IN ASTROPHYSICAL AND LABORATORY PLASMA

Z. Simić[1], M. S. Dimitrijević[1], A. Kovačević[2] and S. Sahal-Bréchot[3]

[1] *Astronomical Observatory, Volgina 7, 11060 Belgrade, Serbia; zsimic@aob.bg.ac.rs; mdimitrijevic@aob.bg.ac.rs*

[2] *Department for Astronomy, Faculty for Mathematics, University of Belgrade, Studentski Trg 16, 11000 Belgrade, Serbia; andjelka@matf.bg.ac.rs*

[3] *Observatoire de Paris, 92195 Meudon Cedex, France; sylvie.sahal-brechot@obspm.fr*

Received: 2011 August 8; accepted: 2011 August 15

Abstract. Besides the need of Stark broadening parameters for a number of problems in physics and plasma technology, in hot star atmospheres the conditions exist where Stark widths are comparable and even larger than the thermal Doppler widths. Using the semiclassical perturbation method we investigated here the influence of collisions with charged particles for In III spectral lines. We determined a number of Stark broadening parameters important for the investigation of plasmas in the atmospheres of A-type stars and white dwarfs. Also, we have compared the obtained results with existing experimental data. The results will be included in the STARK-B database, the Virtual Atomic and Molecular Data Center and the Serbian Virtual Observatory.

Key words: stars: atmospheres, spectral lines, Stark broadening

1. INTRODUCTION

Stark broadening parameters of indium spectral lines are of interest for a number of problems in astrophysics, physics and plasma technology. For example indium is identified in the spectrum of HD 110066, an A-type chemically peculiar star (Cowley et al. 1974).

Dimitrijević & Sahal-Bréchot (1999) determined, using semiclassical perturbation theory (Sahal-Bréchot 1969a,b) Stark broadening parameters due to collisions with electrons, protons and helium ions of 20 In III multiplets, for the effective temperatures from 20 000 K to 50 000 K. Djeniže et al. (2006) obtained experimentally Stark widths for sixteen In III spectral lines at a temperature of 13 000 K, without citation of Dimitrijević & Sahal-Bréchot (1999).

In order to make a better comparison with their experimental results and to provide the data of interest for hot stellar plasma research, we recalculated Stark broadening parameters for ten In III spectral lines using the semiclassical perturbation method (Sahal-Bréchot 1969ab) within four previously considered multiplets (Dimitrijević & Sahal-Bréchot 1999), for which the experimental data (Djeniže et al. 2006) exist. Differently with the previous work, we calculated

the data for each line separately, and we increased the temperature range from 20 000–50 000 K to 10 000–100 000 K, to cover the temperature of the experimental investigation. The obtained results are used to investigate the influence of Stark broadening of the In III lines in the A-type stellar atmospheres.

2. RESULTS AND DISCUSSION

The calculations have been performed within the semiclassical perturbation formalism, developed and discussed in detail in Sahal-Bréchot (1969a,b). This formalism, as well as the corresponding computer code, have been optimized and updated several times (e.g., see Sahal-Bréchot 1974; Dimitrijević & Sahal-Bréchot 1984; Dimitrijević et al. 1991, and the review by Dimitrijević 1996). The needed atomic energy levels for Stark broadening calculations were taken from Bhatia (1978).

Table 1 shows the Stark broadening parameters for electron, proton and helium impacts (full widths at half intesity maximum, FWHM, and shifts) for ten In III lines, obtained by using the semiclassical perturbation method for a perturber density of 10^{17} cm^{-3} and temperatures from 10 000 K to 10 0000 K. The quantity C (given in Å cm^{-3}), when divided by the corresponding FWHM, gives an estimate for the maximum perturber density for which tabulated data may be used.

In Table 2 we show a comparison between the experimental (Djeniže et al. 2006) and our theoretical results for Stark line widths. One can see a large disagreement between both results. Ratio of experimental and theoretical widths changes from 0.25 to 0.52, i.e., the experimental widths are two to four times smaller than theoretical. A new experimental determination of Stark widths for In III spectral lines would be important.

In order to investigate the influence of Stark broadening mechanism for the In III lines in stellar plasma conditions, we calculated Stark widths for the Kurucz's (1979) model of the A-type atmosphere with $T_{\rm eff} = 10\,000$ K and $\log g = 4.5$) and compared them with the Doppler broadening (see Figure 1). We found that the photospheric layers exist where the Doppler and Stark widths are comparable and even where the Stark width is dominant.

Additionally, we compared the thermal (Doppler) and total Stark widths and the contribution of other collisional processes for the In III 6199.3 Å line for the same model atmosphere. The contribution of elastic collisions is leading in the total Stark widths (see Figure 2). The strong collisions, inelastic collisions inducing transition from or to upper atomic energy levels and inelasic collisions for lower levels are less important.

The obtained Stark broadening parameters will supplement the STARK-B database (http://stark-b.obspm.fr), dedicated for modeling of stellar atmospheres, analysis and synthesis of stellar spectra, as well as for investigations of laboratory plasma, inertial fusion plasma, laser development and for plasmas in technology. This database is a part of a FP7 project "Virtual Atomic and Molecular Data Center" – VAMDC (P.I. Marie Lise Dubernet) with the following aims: (i) to build a secure, flexible and interoperable e-science environment based interface to the existing Atomic and Molecular databases; (ii) to coordinate groups involved in the generation, evaluation and use of atomic and molecular data, and (iii) to provide a forum for training of potential users (Dubernet et al. 2010; Rixon et al. 2011).

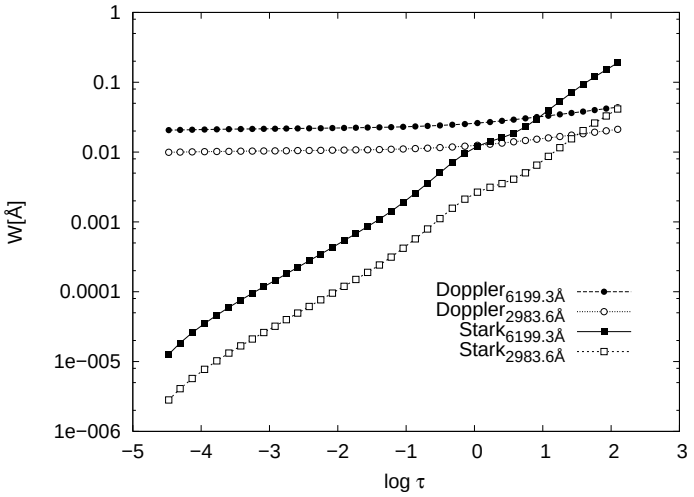

Fig. 1. The Doppler and Stark widths for two In III lines at 2983.6 and 6199.3 Å as functions of the Rosseland optical depth for an A-type star ($T_{\rm eff}$ = 10 000 K, $\log g$ = 4.5). One can see that the Stark broadening mechanism is absolutely dominant in comparison with the thermal Doppler mechanism in deeper layers of the stellar atmosphere ($\log \tau > 1.0$).

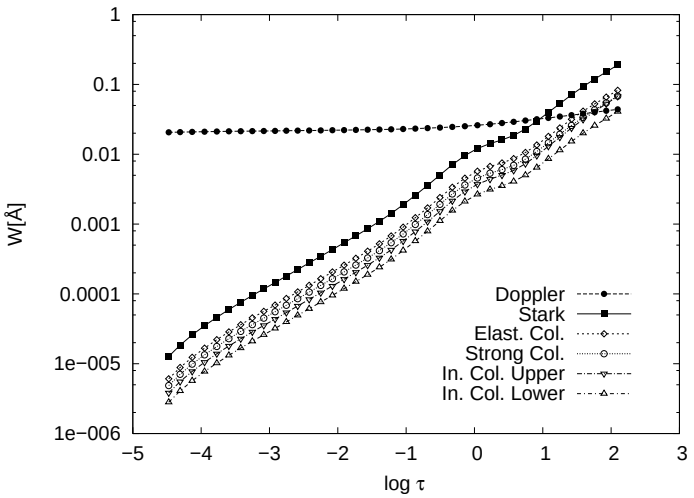

Fig. 2. The thermal (Doppler) and total Stark line widths and the contribution of other collisional processes to the total Stark width for the In III 6199.3 Å line as a function of the Rosseland optical depth for a model atmosphere of A-type star ($T_{\rm eff}$ = 10 000 K, $\log g$ = 4.5).

ACKNOWLEDGMENTS. This work has been supported by VAMDC, funded under the "Combination of Collaborative Projects and Coordination and Support Actions" funding scheme of the 7th Framework program, INFRA-2008-1.2.2 Scientific Data Infrastructure, grant agreement No. 239108. The authors are also

grateful for the support provided by Ministry of Education and Science of Republic of Serbia through projects 176002 "Influence of collisional processes on astrophysical plasma spectra" and III44002 "Astroinformatics: its application in astronomy and related disciplines".

REFERENCES

Bhatia K. S. 1978, J. Phys. B, 11, 2421
Cowley C. R., Hartoog M. R., Cowley A. P. 1974, ApJ, 194, 343
Dimitrijević M. S. 1996, Zh. Priklad. Spektrosk., 63, 810
Dimitrijević M. S., Sahal-Bréchot S. 1984, JQSRT, 31, 301
Dimitrijević M. S., Sahal-Bréchot S., Bomier V. 1991, A&AS, 89, 581
Dimitrijević M. S., Sahal-Bréchot S. 1999, Journal of Applied Spectroscopy, 66, 868
Djeniže S., Bukvić S., Srećković A., Nikolić Z. 2006, Spectrochimica Acta, Part B, 61, 588
Dubernet M. L., Boudon V., Culhane J. L. et al. 2010, JQSRT, 111, 2151
Kurucz R. L. 1979, ApJS, 40, 1
Rixon G., Dubernet M. L., Piskunov N. et al. 2011, AIP Conf. Proc., 1344, 107
Sahal-Bréchot S. 1969a, A&A, 1, 91
Sahal-Bréchot S. 1969b, A&A, 2, 322
Sahal-Bréchot S. 1974, A&A, 35, 321

Table 1. Stark broadening parameters: widths (FWHM) and shifts for the In III spectral lines obtained within semiclasical approach for a perturber density of 10^{17} cm^{-3} and the temperatures from 10 000 K to 100 000 K.

Transition	T (K)	W_{e^-} (Å)	d_{e^-} (Å)	W_{p^+} (Å)	d_{p^+} (Å)	W_{He^+} (Å)	d_{He^+} (Å)
	10 000	0.358	0.637E-02	0.118E-01	0.244E-02	0.158E-01	0.232E-02
In III	13 000	0.319	0.698E-02	0.144E-01	0.317E-02	0.181E-01	0.291E-02
5d $^2D_{3/2}$ – 4f $^2F^o_{5/2}$	20000	0.268	0.632E-02	0.181E-01	0.451E-02	0.222E-01	0.401E-02
2983.6 Å	30 000	0.231	0.608E-02	0.220E-01	0.575E-02	0.242E-01	0.500E-02
C = 0.77E+20	50 000	0.197	0.680E-02	0.248E-01	0.747E-02	0.267E-01	0.626E-02
	100 000	0.167	0.636E-02	0.282E-01	0.921E-02	0.297E-01	0.748E-02
	10 000	0.365	0.638E-02	0.120E-01	0.244E-02	0.161E-01	0.232E-02
In III	13 000	0.326	0.695E-02	0.147E-01	0.316E-02	0.185E-01	0.291E-02
5d $^2D_{5/2}$ – 4f $^2F^o_{5/2}$	20 000	0.273	0.626E-02	0.185E-01	0.450E-02	0.226E-01	0.401E-02
3009.7 Å	30 000	0.236	0.602E-02	0.225E-01	0.575E-02	0.247E-01	0.500E-02
C = 0.79E+20	50 000	0.201	0.672E-02	0.252E-01	0.747E-02	0.272E-01	0.627E-02
	100 000	0.170	0.627E-02	0.287E-01	0.921E-02	0.303E-01	0.751E-02
	10 000	0.365	0.639E-02	0.120E-01	0.244E-02	0.161E-01	0.233E-02
In III	13 000	0.326	0.696E-02	0.147E-01	0.317E-02	0.184E-01	0.291E-02
5d $^2D_{5/2}$ – 4f $^2F^o_{7/2}$	20 000	0.273	0.628E-02	0.185E-01	0.451E-02	0.226E-01	0.402E-02
3008.9 Å	30 000	0.236	0.604E-02	0.225E-01	0.576E-02	0.247E-01	0.501E-02
C = 0.78E+20	50 000	0.201	0.674E-02	0.252E-01	0.749E-02	0.272E-01	0.628E-02
	100 000	0.170	0.629E-02	0.287E-01	0.923E-02	0.303E-01	0.753E-02
	10 000	1.26	-0.112	0.426E-01	-0.133E-01	0.554E-01	-0.122E-01
In III	13 000	1.12	-0.701E-01	0.516E-01	-0.167E-01	0.640E-01	-0.153E-01
6s $^2S_{1/2}$ – 6p $^2P^o_{1/2}$	20 000	0.946	-0.710E-01	0.649E-01	-0.231E-01	0.774E-01	-0.196E-01
5250.3 Å	30 000	0.824	-0.599E-01	0.782E-01	-0.287E-01	0.841E-01	-0.248E-01
C= 0.48E+21	50 000	0.721	-0.635E-01	0.876E-01	-0.363E-01	0.929E-01	-0.294E-01
	100 000	0.626	-0.622E-01	0.100	-0.436E-01	0.103	-0.355E-01

Table 1. Continued

Transition	T (K)	W_{e^-} (Å)	d_{e^-} (Å)	W_{p^+} (Å)	d_{p^+} (Å)	W_{He^+} (Å)	d_{He^+} (Å)
	10 000	1.49	-0.158	0.472E-01	-0.177E-01	0.616E-01	-0.161E-01
In III	13 000	1.33	-0.135	0.575E-01	-0.221E-01	0.711E-01	-0.201E-01
6s $^2S_{1/2}$ – 6p $^2P^o_{3/2}$	20 000	1.12	-0.118	0.727E-01	-0.303E-01	0.867E-01	-0.258E-01
5646.9 Å	30 000	0.967	-0.867E-01	0.883E-01	-0.378E-01	0.944E-01	-0.324E-01
C = 0.51E+21	50 000	0.842	-0.888E-01	0.996E-01	-0.470E-01	0.105	-0.381E-01
	100 000	0.726	-0.852E-01	0.115	-0.563E-01	0.117	-0.459E-01
	10 000	1.09	0.461	0.386E-01	0.389E-01	0.418E-01	0.324E-01
In III	13 000	0.996	0.408	0.454E-01	0.455E-01	0.502E-01	0.387E-01
6p $^2P^o_{1/2}$ – 7s $^2S_{1/2}$	20 000	0.860	0.338	0.630E-01	0.591E-01	0.625E-01	0.481E-01
4024.8 Å	30 000	0.785	0.285	0.763E-01	0.689E-01	0.711E-01	0.564E-01
C = 0.13E+21	50 000	0.728	0.251	0.918E-01	0.816E-01	0.825E-01	0.667E-01
	100 000	0.666	0.196	0.114	0.976E-01	0.982E-01	0.777E-01
	10 000	1.19	0.491	0.435E-01	0.426E-01	0.474E-01	0.354E-01
In III	13 000	1.09	0.434	0.511E-01	0.498E-01	0.568E-01	0.424E-01
6p $^2P^o_{3/2}$ – 7s $^2S_{1/2}$	20 000	0.942	0.358	0.705E-01	0.648E-01	0.703E-01	0.528E-01
4253.8 Å	30 000	0.864	0.302	0.853E-01	0.757E-01	0.799E-01	0.619E-01
C = 0.15E+21	50 000	0.804	0.267	0.102	0.896E-01	0.920E-01	0.729E-01
	100 000	0.741	0.208	0.126	0.108	0.110	0.852E-01
	10 000	1.62	-0.358E-01	0.681E-01	-0.112E-01	0.876E-01	-0.106E-01
In III	13 000	1.45	-0.365E-01	0.811E-01	-0.145E-01	0.101	-0.133E-01
5d $^2D_{3/2}$ – 6p $^2P^o_{1/2}$	20000	1.23	-0.426E-01	0.102	-0.206E-01	0.120	-0.182E-01
6199.3 Å	30 000	1.06	-0.372E-01	0.120	-0.261E-01	0.130	-0.228E-01
C = 0.61E+21	50 000	0.916	-0.456E-01	0.133	-0.339E-01	0.142	-0.283E-01
	100 000	0.781	-0.449E-01	0.149	-0.416E-01	0.157	-0.339E-01
	10 000	1.35	-0.173E-01	0.604E-01	-0.685E-02	0.774E-01	-0.658E-02
In III	13 000	1.21	-0.169E-01	0.716E-01	-0.896E-02	0.895E-01	-0.836E-02
5d $^2D_{3/2}$ – 6p $^2P^o_{3/2}$	20 000	1.03	-0.233E-01	0.895E-01	-0.129E-01	0.105	-0.117E-01
5724.6 Å	30 000	0.896	-0.210E-01	0.105	-0.170E-01	0.114	-0.145E-01
C = 0.56E+21	50 000	0.776	-0.271E-01	0.116	-0.219E-01	0.125	-0.187E-01
	100 000	0.666	-0.269E-01	0.130	-0.275E-01	0.137	-0.225E-01
	10 000	1.40	-0.187E-01	0.626E-01	-0.728E-02	0.801E-01	-0.698E-02
In III	13 000	1.26	-0.182E-01	0.741E-01	-0.951E-02	0.927E-01	-0.885E-02
5d $^2D_{5/2}$ – 6p $^2P^o_{3/2}$	20 000	1.07	-0.248E-01	0.928E-01	-0.136E-01	0.109	-0.124E-01
5821.2 Å	30 000	0.929	-0.224E-01	0.109	-0.180E-01	0.118	-0.154E-01
C = 0.57E+21	50 000	0.805	-0.288E-01	0.120	-0.231E-01	0.129	-0.198E-01
	100 000	0.692	-0.287E-01	0.135	-0.290E-01	0.142	-0.237E-01

Table 2. Comparison between the experimental W_m and theoretical W_{th} results.

Transition	λ_m (Å)	W_m (Å)	$\frac{W_m}{W_{th}}$
5d $^2D_{3/2}$ – 4f $^2F^o_{5/2}$	2982.8	0.240	0.51
5d $^2D_{5/2}$ – 4f $^2F^o_{5/2}$	3008.1	0.250	0.52
5d $^2D_{5/2}$ – 4f $^2F^o_{7/2}$	3008.8	0.210	0.44
6s $^2S_{1/2}$ – 6p $^2P^o_{1/2}$	5248.8	0.717	0.43
6s $^2S_{1/2}$ – 6p $^2P^o_{3/2}$	5645.2	0.520	0.27
6p $^2P^o_{1/2}$ – 7s $^2S_{1/2}$	4023.8	0.545	0.37
6p $^2P^o_{3/2}$ – 7s $^2S_{1/2}$	4252.7	0.480	0.30
5d $^2D_{3/2}$ – 6p $^2P^o_{1/2}$	6197.7	0.800	0.37
5d $^2D_{3/2}$ – 6p $^2P^o_{3/2}$	5723.2	0.450	0.25
5d $^2D_{5/2}$ – 6p $^2P^o_{3/2}$	5819.5	0.520	0.28

Baltic Astronomy, vol. 20, 620, 2011

ON THE GAS TEMPERATURE DETERMINATION FROM VAN DER WAALS BROADENING IN ARGON – NEON MICROWAVE PLASMAS

José Muñoz[1,2], Milan S. Dimitrijević[3,4] and M. D. Calzada[1]

[1] *Grupo de Espectroscopía de Plasma, Córdoba University, Edificio Einstein, Campus de Rabanales, E-14071, Córdoba, Spain; md.calzada@uco.es*

[2] *Département de Physique, Université de Montréal, C.P. 6128, Succ. Centre-ville, Montréal, Québec, Canada*

[3] *Astronomical Observatory, Volgina 7, 11060 Belgrade 38, Serbia; mdimitrijevic@aob.bg.ac.rs*

[4] *Observatoire de Paris, LERMA, 5 Place Jules Janssen, F-92190, Meudon, France*

Received: 2011 August 8; accepted: 2011 August 15

Abstract. Recently we proposed a method to determine the gas temperature using the van der Waals broadening of atomic spectral lines for atmospheric pressure Ar-He plasma. Here our investigations are continued by studying the influence of Ar*-Ne interactions in order to enlarge the applicability of the proposed method for the determination of gas temperature in argon – neon mixtures. The Ar I 425.9 nm line is found to be suitable for the gas temperature determination.

Key words: microwave discharges, gas temperature, Ar-Ne plasma, line broadening: van der Waals

Bull. Astron. Belgrade № 148 (1993), 29 – 42

UDC 52-355.3
Preliminary report

STARK BROADENING PARAMETER TABLES FOR Ne VIII AND Na IX LINES OF ASTROPHYSICAL INTEREST

M. S. Dimitrijević[1] and S. Sahal–Bréchot[2]

[1] *Astronomical Observatory, Volgina 7, 11050 Belgrade, Yugoslavia*

[2] *Laboratoire "Astrophysique, Atomes et Molécules"*
Département Atomes et Molécules en Astrophysique
Unité associée au C.N.R.S. No 812
Observatoire de Paris–Meudon, 92190 Meudon, France

(Received: November 1, 1993)

SUMMARY: Using a semiclassical approach, we have calculated electron–, proton–, and He III–impact line widths and shifts for 20 Ne VIII and 8 Na IX multiplets as a function of temperature and perturber density.

1. INTRODUCTION

In order to investigate the behavior of Stark broadening parameters along the lithium isoelectronic sequence as far as posible, we have calculated electron–, proton–, and He III– impact line widths and shifts for 20 Ne VIII and 8 Na IX multiplets, by using the semiclassical-perturbation formalism (Sahal–Bréchot 1969ab). A summary of the formalism is given in Dimitrijević and Sahal–Bréchot (1991). Discussion, analysis and comparison with the existing experimental and theoretical data, and all details of the calculations will be published in the principal article elsewhere (Dimitrijević, and Sahal–Bréchot, 1994). Since data are not linear with perturber density (N), due to the Debye screening effect, which is often important at high densities of interest for subphotospheric layers, we will present here the data for N = 10^{16} – 10^{22} cm^{-3} and temperatures from 200,000 K up to 2,000,000 K.

2. RESULTS AND DISCUSSION

Our results for 20 Ne VIII and 8 Na IX multiplets are shown in Table 1, for perturber densities 10^{16} – 10^{22} cm^{-3} and temperatures T = 200,000 - 2,000,000 K. We also specify a parameter c (Dimitrijević & Sahal–Bréchot 1984), which gives an estimate for the maximum perturber density for which the line may be treated as isolated when it is divided by the corresponding electron-impact full width at half maximum. For each value given in Tables 1 and 2, the collision volume (V) multiplied by the perturber density (N) is much less than one and the impact approximation is valid (Sahal–Bréchot,

Table 1. This table shows electron—, proton—, and He III— impact broadening parameters for Ne VIII and Na IX, for perturber densities of $10^{16} - 10^{22}$ cm^{-3} and temperatures from 200,000 to 2,000,000 K. Transitions and averaged wavelengths for the multiplet (in Å) are also given. By using c [see Eq. (5) in Dimitrijević et al, 1991a], we obtain an estimate for the maximum perturber density for which the line may be treated as isolated and tabulated data may be used. The asterisk identifies cases for which the collision volume multiplied by the perturber density (the condition for validity of the impact approximation) lies between 0.1 and 0.5. Table 1 is also available in electronic form: see the editorial in Astron. Astrophys. 1992, Vol. 266, No 2, page E1 or in Astron. Astrophys. Suppl. Series 1992, Vol. 96, No 3, and Dimitrijević and Sahal—Bréchot, 1994.

PERTURBER DENSITY = 0.1E+17cm-3							
PERTURBERS ARE:		ELECTRONS		PROTONS		He III	
TRANSITION	T(K)	WIDTH(A)	SHIFT(A)	WIDTH(A)	SHIFT(A)	WIDTH(A)	SHIFT(A)
NeVIII 5S-5P	200000.	0.355	-0.210E-02	0.132	0.132	0.268	0.270
10427.5 A	500000.	0.263	-0.645E-02	0.185	0.160	0.371	0.336
C=0.54E+19	1000000.	0.211	-0.790E-02	0.198	0.184	0.409	0.367
	2000000.	0.169	-0.781E-02	0.221	0.219	0.444	0.434
PERTURBER DENSITY = 0.1E+18cm-3							
NeVIII 2S-4P	200000.	0.364E-04	0.127E-05	0.383E-05	0.437E-05	0.764E-05	0.887E-05
67.4 A	500000.	0.261E-04	0.117E-05	0.628E-05	0.589E-05	0.127E-04	0.120E-04
C=0.25E+17	1000000.	0.206E-04	0.908E-06	0.770E-05	0.703E-05	0.159E-04	0.142E-04
	2000000.	0.165E-04	0.724E-06	0.978E-05	0.823E-05	0.195E-04	0.169E-04
NeVIII 2S-5P	200000.	0.850E-04	0.584E-05	0.469E-04	0.478E-04	0.975E-04	0.967E-04
60.7 A	500000.	0.625E-04	0.415E-05	0.621E-04	0.582E-04	0.133E-03	0.117E-03
C=0.18E+16	1000000.	0.497E-04	0.288E-05	0.712E-04	0.663E-04	*0.149E-03	*0.136E-03
	2000000.	0.398E-04	0.180E-05	0.876E-04	0.790E-04	*0.170E-03	*0.164E-03
NeVIII 3S-4P	200000.	0.605E-03	0.106E-04	0.537E-04	0.600E-04	0.106E-03	0.122E-03
260.5 A	500000.	0.434E-03	0.895E-05	0.885E-04	0.814E-04	0.179E-03	0.167E-03
C=0.37E+18	1000000.	0.345E-03	0.538E-05	0.110E-03	0.968E-04	0.221E-03	0.198E-03
	2000000.	0.277E-03	0.335E-05	0.134E-03	0.116E-03	0.259E-03	0.234E-03
NeVIII 3S-5P	200000.	0.801E-03	0.489E-04	0.425E-03	0.432E-03	0.884E-03	0.875E-03
182.8 A	500000.	0.589E-03	0.334E-04	0.561E-03	0.527E-03	0.121E-02	0.106E-02
C=0.17E+17	1000000.	0.469E-03	0.221E-04	0.647E-03	0.600E-03	*0.135E-02	*0.124E-02
	2000000.	0.375E-03	0.126E-04	0.795E-03	0.713E-03	*0.153E-02	*0.148E-02
NeVIII 4S-5P	200000.	0.852E-02	0.304E-03	0.401E-02	0.404E-02	0.827E-02	0.823E-02
563.7 A	500000.	0.627E-02	0.170E-03	0.526E-02	0.488E-02	0.115E-01	0.996E-02
C=0.16E+18	1000000.	0.501E-02	0.734E-04	0.614E-02	0.562E-02	*0.124E-01	*0.115E-01
	2000000.	0.402E-02	0.132E-04	0.744E-02	0.679E-02	*0.138E-01	*0.138E-01
NeVIII 5S-5P	200000.	3.55	-0.235E-01	1.32	1.32	2.68	2.69
10427.5 A	500000.	2.63	-0.645E-01	1.85	1.60	3.71	3.35
C=0.54E+20	1000000.	2.11	-0.790E-01	1.98	1.84	*4.09	*3.67
	2000000.	1.69	-0.781E-01	2.21	2.19	*4.44	*4.34
NeVIII 2P-6S	200000.	0.104E-03	0.198E-04	0.324E-04	0.338E-04	0.660E-04	0.687E-04
62.6 A	500000.	0.786E-04	0.170E-04	0.446E-04	0.421E-04	0.903E-04	0.856E-04
C=0.13E+17	1000000.	0.632E-04	0.135E-04	0.533E-04	0.486E-04	0.105E-03	0.989E-04
	2000000.	0.502E-04	0.108E-04	0.593E-04	0.548E-04	0.123E-03	0.111E-03
NeVIII 5P-6S	200000.	0.760E-01	0.538E-02	0.114E-01	-0.114E-01	0.228E-01	-0.233E-01
1246.9 A	500000.	0.568E-01	0.497E-02	0.154E-01	-0.142E-01	0.319E-01	-0.296E-01
C=0.78E+18	1000000.	0.455E-01	0.412E-02	0.178E-01	-0.163E-01	0.372E-01	-0.331E-01
	2000000.	0.363E-01	0.351E-02	0.208E-01	-0.185E-01	0.430E-01	-0.383E-01
PERTURBER DENSITY = 0.1E+19cm-3							
NeVIII 2S-2P	200000.	0.432E-02	-0.729E-04	0.178E-04	-0.612E-04	0.334E-04	-0.120E-03
773.7 A	500000.	0.283E-02	-0.966E-04	0.794E-04	-0.140E-03	0.153E-03	-0.282E-03
C=0.77E+21	1000000.	0.208E-02	-0.984E-04	0.176E-03	-0.219E-03	0.350E-03	-0.444E-03
	2000000.	0.157E-02	-0.917E-04	0.289E-03	-0.300E-03	0.576E-03	-0.610E-03

PERTURBER DENSITY = 0.1E+19cm-3

PERTURBERS ARE:		ELECTRONS		PROTONS		He III	
TRANSITION	T(K)	WIDTH(A)	SHIFT(A)	WIDTH(A)	SHIFT(A)	WIDTH(A)	SHIFT(A)
NeVIII 2S-3P	200000.	0.215E-03	0.274E-05	0.772E-05	0.106E-04	0.150E-04	0.209E-04
88.1 A	500000.	0.147E-03	0.268E-05	0.173E-04	0.178E-04	0.343E-04	0.360E-04
C=0.98E+18	1000000.	0.113E-03	0.245E-05	0.250E-04	0.225E-04	0.504E-04	0.459E-04
	2000000.	0.889E-04	0.171E-05	0.318E-04	0.272E-04	0.634E-04	0.558E-04
NeVIII 2S-4P	200000.	0.364E-03	0.118E-04	0.383E-04	0.432E-04	0.764E-04	0.850E-04
67.4 A	500000.	0.261E-03	0.116E-04	0.628E-04	0.588E-04	0.127E-03	0.120E-03
C=0.25E+18	1000000.	0.206E-03	0.908E-05	0.770E-04	0.703E-04	0.159E-03	0.142E-03
	2000000.	0.165E-03	0.724E-05	0.978E-04	0.823E-04	0.195E-03	0.169E-03
NeVIII 2S-5P	200000.	0.831E-03	0.396E-04	*0.471E-03	*0.461E-03		
60.7 A	500000.	0.612E-03	0.384E-04	*0.621E-03	*0.579E-03		
C=0.18E+17	1000000.	0.488E-03	0.288E-04	*0.712E-03	*0.663E-03		
	2000000.	0.391E-03	0.180E-04	*0.876E-03	*0.790E-03		
NeVIII 3S-3P	200000.	0.304	-0.677E-02	0.597E-02	-0.154E-02	0.114E-01	-0.304E-02
2879.1 A	500000.	0.212	-0.763E-02	0.120E-01	-0.331E-02	0.234E-01	-0.668E-02
C=0.10E+22	1000000.	0.166	-0.738E-02	0.165E-01	-0.485E-02	0.325E-01	-0.983E-02
	2000000.	0.132	-0.730E-02	0.189E-01	-0.646E-02	0.377E-01	-0.132E-01
NeVIII 3S-4P	200000.	0.605E-02	0.971E-04	0.537E-03	0.593E-03	0.106E-02	0.117E-02
260.5 A	500000.	0.434E-02	0.871E-04	0.885E-03	0.812E-03	0.179E-02	0.166E-02
C=0.37E+19	1000000.	0.345E-02	0.538E-04	0.110E-02	0.968E-03	0.221E-02	0.198E-02
	2000000.	0.277E-02	0.335E-04	0.134E-02	0.116E-02	0.259E-02	0.234E-02
NeVIII 3S-5P	200000.	0.784E-02	0.320E-03	*0.426E-02	*0.417E-02		
182.8 A	500000.	0.577E-02	0.306E-03	*0.561E-02	*0.524E-02		
C=0.17E+18	1000000.	0.461E-02	0.221E-03	*0.647E-02	*0.600E-02		
	2000000.	0.370E-02	0.126E-03	*0.795E-02	*0.713E-02		
NeVIII 4S-4P	200000.	5.75	-0.174	0.227	0.803E-01	0.445	0.159
6993.0 A	500000.	4.17	-0.164	0.342	0.132	0.679	0.268
C=0.27E+22	1000000.	3.33	-0.171	0.393	0.165	0.783	0.336
	2000000.	2.69	-0.140	0.446	0.197	0.885	0.403
NeVIII 4S-5P	200000.	0.835E-01	0.146E-02	*0.402E-01	*0.390E-01		
563.7 A	500000.	0.617E-01	0.144E-02	*0.526E-01	*0.485E-01		
C=0.16E+19	1000000.	0.493E-01	0.734E-03	*0.614E-01	*0.562E-01		
	2000000.	0.396E-01	0.132E-03	*0.744E-01	*0.679E-01		
NeVIII 2P-3S	200000.	0.173E-03	0.137E-04	0.627E-05	0.167E-04	0.124E-04	0.330E-04
103.0 A	500000.	0.121E-03	0.151E-04	0.188E-04	0.276E-04	0.378E-04	0.560E-04
C=0.37E+19	1000000.	0.943E-04	0.145E-04	0.311E-04	0.346E-04	0.631E-04	0.707E-04
	2000000.	0.748E-04	0.133E-04	0.413E-04	0.414E-04	0.840E-04	0.848E-04
NeVIII 2P-4S	200000.	0.250E-03	0.350E-04	0.317E-04	0.484E-04	0.632E-04	0.952E-04
74.6 A	500000.	0.183E-03	0.338E-04	0.614E-04	0.664E-04	0.124E-03	0.136E-03
C=0.80E+18	1000000.	0.147E-03	0.315E-04	0.795E-04	0.792E-04	0.160E-03	0.161E-03
	2000000.	0.118E-03	0.257E-04	0.992E-04	0.946E-04	0.191E-03	0.190E-03

PERTURBER DENSITY = 0.1E+19cm-3

PERTURBERS ARE:		ELECTRONS		PROTONS		He III	
TRANSITION	T(K)	WIDTH(A)	SHIFT(A)	WIDTH(A)	SHIFT(A)	WIDTH(A)	SHIFT(A)
NeVIII 2P-5S	200000.	0.458E-03	0.783E-04	0.893E-04	0.103E-03	0.179E-03	0.202E-03
66.3 A	500000.	0.340E-03	0.761E-04	0.132E-03	0.133E-03	0.267E-03	0.271E-03
C=0.42E+18	1000000.	0.275E-03	0.670E-04	0.165E-03	0.157E-03	0.337E-03	0.320E-03
	2000000.	0.223E-03	0.537E-04	0.194E-03	0.180E-03	*0.393E-03	*0.370E-03
NeVIII 2P-6S	200000.	0.104E-02	0.187E-03	0.324E-03	0.328E-03		
62.6 A	500000.	0.786E-03	0.168E-03	0.446E-03	0.419E-03		
C=0.13E+18	1000000.	0.632E-03	0.135E-03	0.533E-03	0.486E-03		
	2000000.	0.502E-03	0.108E-03	0.593E-03	0.548E-03		
NeVIII 3P-4S	200000.	0.581E-02	0.518E-03	0.467E-03	0.706E-03	0.933E-03	0.139E-02
298.6 A	500000.	0.419E-02	0.495E-03	0.897E-03	0.979E-03	0.183E-02	0.199E-02
C=0.11E+20	1000000.	0.334E-02	0.462E-03	0.118E-02	0.116E-02	0.240E-02	0.240E-02
	2000000.	0.268E-02	0.378E-03	0.144E-02	0.136E-02	0.299E-02	0.280E-02
NeVIII 3P-5S	200000.	0.491E-02	0.685E-03	0.783E-03	0.912E-03	0.158E-02	0.179E-02
198.9 A	500000.	0.361E-02	0.664E-03	0.117E-02	0.118E-02	0.237E-02	0.239E-02
C=0.38E+19	1000000.	0.291E-02	0.584E-03	0.147E-02	0.139E-02	0.297E-02	0.282E-02
	2000000.	0.235E-02	0.469E-03	0.174E-02	0.159E-02	0.353E-02	0.323E-02
NeVIII 3P-6S	200000.	0.815E-02	0.135E-02	0.235E-02	0.238E-02		
168.8 A	500000.	0.612E-02	0.121E-02	0.324E-02	0.304E-02		
C=0.91E+18	1000000.	0.491E-02	0.968E-03	0.386E-02	0.353E-02		
	2000000.	0.390E-02	0.775E-03	0.427E-02	0.396E-02		
NeVIII 4P-5S	200000.	0.746E-01	0.638E-02	0.677E-02	0.778E-02	0.136E-01	0.153E-01
651.4 A	500000.	0.549E-01	0.618E-02	0.101E-01	0.999E-02	0.209E-01	0.205E-01
C=0.23E+20	1000000.	0.442E-01	0.555E-02	0.123E-01	0.120E-01	0.256E-01	0.240E-01
	2000000.	0.358E-01	0.444E-02	0.155E-01	0.138E-01	0.307E-01	0.283E-01
NeVIII 4P-6S	200000.	0.571E-01	0.760E-02	0.135E-01	0.137E-01		
411.0 A	500000.	0.428E-01	0.679E-02	0.186E-01	0.175E-01		
C=0.54E+19	1000000.	0.343E-01	0.546E-02	0.216E-01	0.202E-01		
	2000000.	0.273E-01	0.436E-02	0.253E-01	0.226E-01		
NeVIII 5P-6S	200000.	0.752	0.574E-01	0.114	-0.111		
1246.9 A	500000.	0.563	0.503E-01	0.154	-0.142		
C=0.78E+19	1000000.	0.451	0.412E-01	0.178	-0.163		
	2000000.	0.360	0.351E-01	0.208	-0.185		

PERTURBER DENSITY = 0.1E+20cm-3

NeVIII 2S-2P	200000.	0.436E-01	-0.845E-03	0.178E-03	-0.592E-03	0.333E-03	-0.112E-02
773.7 A	500000.	0.283E-01	-0.951E-03	0.794E-03	-0.139E-02	0.153E-02	-0.278E-02
C=0.77E+22	1000000.	0.208E-01	-0.984E-03	0.176E-02	-0.218E-02	0.350E-02	-0.443E-02
	2000000.	0.157E-01	-0.917E-03	0.289E-02	-0.300E-02	0.576E-02	-0.610E-02
NeVIII 2S-3P	200000.	0.215E-02	0.250E-04	0.771E-04	0.102E-03	0.150E-03	0.192E-03
88.1 A	500000.	0.147E-02	0.248E-04	0.173E-03	0.176E-03	0.343E-03	0.353E-03
C=0.98E+19	1000000.	0.113E-02	0.240E-04	0.250E-03	0.224E-03	0.504E-03	0.458E-03
	2000000.	0.889E-03	0.171E-04	0.318E-03	0.272E-03	0.634E-03	0.557E-03

PERTURBER DENSITY = 0.1E+19cm-3

PERTURBERS ARE:		ELECTRONS		PROTONS		He III	
TRANSITION	T(K)	WIDTH(A)	SHIFT(A)	WIDTH(A)	SHIFT(A)	WIDTH(A)	SHIFT(A)
NeVIII 2S-3P	200000.	0.215E-03	0.274E-05	0.772E-05	0.106E-04	0.150E-04	0.209E-04
88.1 A	500000.	0.147E-03	0.268E-05	0.173E-04	0.178E-04	0.343E-04	0.360E-04
C=0.98E+18	1000000.	0.113E-03	0.245E-05	0.250E-04	0.225E-04	0.504E-04	0.459E-04
	2000000.	0.889E-04	0.171E-05	0.318E-04	0.272E-04	0.634E-04	0.558E-04
NeVIII 2S-4P	200000.	0.364E-03	0.118E-04	0.383E-04	0.432E-04	0.764E-04	0.850E-04
67.4 A	500000.	0.261E-03	0.116E-04	0.628E-04	0.588E-04	0.127E-03	0.120E-03
C=0.25E+18	1000000.	0.206E-03	0.908E-05	0.770E-04	0.703E-04	0.159E-03	0.142E-03
	2000000.	0.165E-03	0.724E-05	0.978E-04	0.823E-04	0.195E-03	0.169E-03
NeVIII 2S-5P	200000.	0.831E-03	0.396E-04	*0.471E-03	*0.461E-03		
60.7 A	500000.	0.612E-03	0.384E-04	*0.621E-03	*0.579E-03		
C=0.18E+17	1000000.	0.488E-03	0.288E-04	*0.712E-03	*0.663E-03		
	2000000.	0.391E-03	0.180E-04	*0.876E-03	*0.790E-03		
NeVIII 3S-3P	200000.	0.304	-0.677E-02	0.597E-02	-0.154E-02	0.114E-01	-0.304E-02
2879.1 A	500000.	0.212	-0.763E-02	0.120E-01	-0.331E-02	0.234E-01	-0.668E-02
C=0.10E+22	1000000.	0.166	-0.738E-02	0.165E-01	-0.485E-02	0.325E-01	-0.983E-02
	2000000.	0.132	-0.730E-02	0.189E-01	-0.646E-02	0.377E-01	-0.132E-01
NeVIII 3S-4P	200000.	0.605E-02	0.971E-04	0.537E-03	0.593E-03	0.106E-02	0.117E-02
260.5 A	500000.	0.434E-02	0.871E-04	0.885E-03	0.812E-03	0.179E-02	0.166E-02
C=0.37E+19	1000000.	0.345E-02	0.538E-04	0.110E-02	0.968E-03	0.221E-02	0.198E-02
	2000000.	0.277E-02	0.335E-04	0.134E-02	0.116E-02	0.259E-02	0.234E-02
NeVIII 3S-5P	200000.	0.784E-02	0.320E-03	*0.426E-02	*0.417E-02		
182.8 A	500000.	0.577E-02	0.306E-03	*0.561E-02	*0.524E-02		
C=0.17E+18	1000000.	0.461E-02	0.221E-03	*0.647E-02	*0.600E-02		
	2000000.	0.370E-02	0.126E-03	*0.795E-02	*0.713E-02		
NeVIII 4S-4P	200000.	5.75	-0.174	0.227	0.803E-01	0.445	0.159
6993.0 A	500000.	4.17	-0.164	0.342	0.132	0.679	0.268
C=0.27E+22	1000000.	3.33	-0.171	0.393	0.165	0.783	0.336
	2000000.	2.69	-0.140	0.446	0.197	0.885	0.403
NeVIII 4S-5P	200000.	0.835E-01	0.146E-02	*0.402E-01	*0.390E-01		
563.7 A	500000.	0.617E-01	0.144E-02	*0.526E-01	*0.485E-01		
C=0.16E+19	1000000.	0.493E-01	0.734E-03	*0.614E-01	*0.562E-01		
	2000000.	0.396E-01	0.132E-03	*0.744E-01	*0.679E-01		
NeVIII 2P-3S	200000.	0.173E-03	0.137E-04	0.627E-05	0.167E-04	0.124E-04	0.330E-04
103.0 A	500000.	0.121E-03	0.151E-04	0.188E-04	0.276E-04	0.378E-04	0.560E-04
C=0.37E+19	1000000.	0.943E-04	0.145E-04	0.311E-04	0.346E-04	0.631E-04	0.707E-04
	2000000.	0.748E-04	0.133E-04	0.413E-04	0.414E-04	0.840E-04	0.848E-04
NeVIII 2P-4S	200000.	0.250E-03	0.350E-04	0.317E-04	0.484E-04	0.632E-04	0.952E-04
74.6 A	500000.	0.183E-03	0.338E-04	0.614E-04	0.664E-04	0.124E-03	0.136E-03
C=0.80E+18	1000000.	0.147E-03	0.315E-04	0.795E-04	0.792E-04	0.160E-03	0.161E-03
	2000000.	0.118E-03	0.257E-04	0.992E-04	0.946E-04	0.191E-03	0.190E-03

PERTURBER DENSITY = 0.1E+20cm-3

PERTURBERS ARE:		ELECTRONS		PROTONS		He III	
TRANSITION	T(K)	WIDTH(A)	SHIFT(A)	WIDTH(A)	SHIFT(A)	WIDTH(A)	SHIFT(A)
NeVIII 2S-4P	200000.	0.364E-02	0.955E-04	0.384E-03	0.407E-03	*0.757E-03	*0.746E-03
67.4 A	500000.	0.261E-02	0.106E-03	0.628E-03	0.577E-03	*0.127E-02	*0.115E-02
C=0.25E+19	1000000.	0.206E-02	0.883E-04	0.770E-03	0.701E-03	*0.159E-02	*0.141E-02
	2000000.	0.165E-02	0.724E-04	0.978E-03	0.823E-03	*0.195E-02	*0.168E-02
NeVIII 2S-5P	200000.	0.744E-02	-0.270E-04				
60.7 A	500000.	0.558E-02	0.130E-03				
C=0.18E+18	1000000.	0.450E-02	0.221E-03				
	2000000.	0.364E-02	0.180E-03				
NeVIII 3S-3P	200000.	3.04	-0.683E-01	0.596E-01	-0.149E-01	0.113	-0.282E-01
2879.1 A	500000.	2.12	-0.765E-01	0.120	-0.329E-01	0.234	-0.659E-01
C=0.10E+23	1000000.	1.66	-0.735E-01	0.165	-0.485E-01	0.325	-0.981E-01
	2000000.	1.32	-0.730E-01	0.189	-0.646E-01	0.377	-0.132
NeVIII 3S-4P	200000.	0.605E-01	0.649E-03	0.536E-02	0.560E-02	*0.106E-01	*0.103E-01
260.5 A	500000.	0.434E-01	0.735E-03	0.885E-02	0.798E-02	*0.179E-01	*0.160E-01
C=0.37E+20	1000000.	0.344E-01	0.508E-03	0.110E-01	0.966E-02	*0.221E-01	*0.197E-01
	2000000.	0.277E-01	0.335E-03	0.134E-01	0.116E-01	*0.259E-01	*0.233E-01
NeVIII 3S-5P	200000.	0.704E-01	-0.628E-03				
182.8 A	500000.	0.528E-01	0.764E-03				
C=0.17E+19	1000000.	0.426E-01	0.161E-02				
	2000000.	0.345E-01	0.126E-02				
NeVIII 4S-5P	200000.	0.760	-0.203E-01				
563.7 A	500000.	0.570	-0.678E-02				
C=0.16E+20	1000000.	0.460	0.171E-02				
	2000000.	0.373	0.132E-02				
NeVIII 2P-3S	200000.	0.174E-02	0.137E-03	0.625E-04	0.161E-03	0.124E-03	0.303E-03
103.0 A	500000.	0.121E-02	0.149E-03	0.188E-03	0.273E-03	0.378E-03	0.549E-03
C=0.37E+20	1000000.	0.943E-03	0.144E-03	0.311E-03	0.346E-03	0.631E-03	0.705E-03
	2000000.	0.748E-03	0.133E-03	0.413E-03	0.414E-03	0.841E-03	0.847E-03
NeVIII 2P-4S	200000.	0.250E-02	0.323E-03	0.316E-03	0.457E-03	*0.632E-03	*0.838E-03
74.6 A	500000.	0.183E-02	0.324E-03	0.614E-03	0.652E-03	*0.124E-02	*0.131E-02
C=0.80E+19	1000000.	0.147E-02	0.313E-03	0.795E-03	0.789E-03	*0.160E-02	*0.161E-02
	2000000.	0.118E-02	0.257E-03	0.992E-03	0.946E-03	*0.191E-02	*0.190E-02
NeVIII 2P-5S	200000.	0.458E-02	0.700E-03	0.893E-03	0.954E-03		
66.3 A	500000.	0.340E-02	0.724E-03	*0.133E-02	*0.130E-02		
C=0.42E+19	1000000.	0.275E-02	0.664E-03	*0.165E-02	*0.157E-02		
	2000000.	0.223E-02	0.537E-03	*0.194E-02	*0.180E-02		
NeVIII 2P-6S	200000.	0.103E-01	0.137E-02				
62.6 A	500000.	0.779E-02	0.147E-02				
C=0.13E+19	1000000.	0.627E-02	0.131E-02				
	2000000.	0.498E-02	0.108E-02				

PERTURBER DENSITY = 0.1E+20cm-3

PERTURBERS ARE: TRANSITION	T(K)	ELECTRONS WIDTH(A)	ELECTRONS SHIFT(A)	PROTONS WIDTH(A)	PROTONS SHIFT(A)	He III WIDTH(A)	He III SHIFT(A)
NeVIII 3P-4S	200000.	0.581E-01	0.477E-02	0.466E-02	0.667E-02	*0.930E-02	*0.122E-01
298.6 A	500000.	0.419E-01	0.477E-02	0.898E-02	0.962E-02	*0.183E-01	*0.192E-01
C=0.11E+21	1000000.	0.334E-01	0.460E-02	0.118E-01	0.116E-01	*0.240E-01	*0.239E-01
	2000000.	0.268E-01	0.378E-02	0.144E-01	0.136E-01	*0.299E-01	*0.279E-01
NeVIII 3P-5S	200000.	0.491E-01	0.611E-02	0.783E-02	0.842E-02		
198.9 A	500000.	0.361E-01	0.633E-02	*0.117E-01	*0.115E-01		
C=0.38E+20	1000000.	0.291E-01	0.578E-02	*0.147E-01	*0.138E-01		
	2000000.	0.235E-01	0.469E-02	*0.174E-01	*0.159E-01		
NeVIII 3P-6S	200000.	0.807E-01	0.986E-02				
168.8 A	500000.	0.607E-01	0.106E-01				
C=0.91E+19	1000000.	0.487E-01	0.939E-02				
	2000000.	0.388E-01	0.775E-02				
NeVIII 4P-5S	200000.	0.746	0.578E-01	0.677E-01	0.724E-01		
651.4 A	500000.	0.549	0.593E-01	0.101	0.974E-01		
C=0.23E+21	1000000.	0.442	0.551E-01	0.123	0.120		
	2000000.	0.358	0.444E-01	0.155	0.138		
NeVIII 4P-6S	200000.	0.566	0.554E-01				
411.0 A	500000.	0.425	0.594E-01				
C=0.54E+20	1000000.	0.341	0.529E-01				
	2000000.	0.272	0.436E-01				
NeVIII 5P-6S	200000.	7.11	0.555				
1246.9 A	500000.	5.37	0.528				
C=0.78E+20	1000000.	4.33	0.424				
	2000000.	3.47	0.351				

PERTURBER DENSITY = 0.1E+21cm-3

NeVIII 2S-2P	200000.	0.436	-0.735E-02	0.176E-02	-0.529E-02	0.324E-02	-0.909E-02
773.7 A	500000.	0.283	-0.914E-02	0.795E-02	-0.135E-01	0.153E-01	-0.259E-01
C=0.77E+23	1000000.	0.208	-0.955E-02	0.176E-01	-0.216E-01	0.350E-01	-0.436E-01
	2000000.	0.157	-0.914E-02	0.289E-01	-0.300E-01	0.576E-01	-0.609E-01
NeVIII 2S-3P	200000.	0.215E-01	0.836E-04	0.765E-03	0.893E-03	0.145E-02	0.150E-02
88.1 A	500000.	0.147E-01	0.157E-03	0.173E-02	0.168E-02	*0.341E-02	*0.316E-02
C=0.98E+20	1000000.	0.113E-01	0.201E-03	0.250E-02	0.220E-02	*0.503E-02	*0.442E-02
	2000000.	0.888E-02	0.163E-03	0.318E-02	0.271E-02	*0.634E-02	*0.555E-02
NeVIII 2S-4P	200000.	0.356E-01	0.124E-04	*0.377E-02	*0.328E-02		
67.4 A	500000.	0.256E-01	0.502E-03	*0.636E-02	*0.530E-02		
C=0.25E+20	1000000.	0.203E-01	0.608E-03	*0.762E-02	*0.674E-02		
	2000000.	0.163E-01	0.671E-03	*0.978E-02	*0.818E-02		
NeVIII 2S-5P	200000.	0.605E-01	-0.155E-02				
60.7 A	500000.	0.471E-01	-0.569E-03				
C=0.18E+19	1000000.	0.389E-01	0.376E-03				
	2000000.	0.321E-01	0.102E-02				

PERTURBER DENSITY = 0.1E+21cm-3

PERTURBERS ARE:		ELECTRONS		PROTONS		He III	
TRANSITION	T(K)	WIDTH(A)	SHIFT(A)	WIDTH(A)	SHIFT(A)	WIDTH(A)	SHIFT(A)
NeVIII 3S-4P	200000.	0.593	-0.614E-02	*0.529E-01	*0.455E-01		
260.5 A	500000.	0.427	-0.979E-04	*0.881E-01	*0.734E-01		
C=0.37E+21	1000000.	0.340	0.131E-02	*0.111	*0.932E-01		
	2000000.	0.273	0.264E-02	*0.134	*0.115		
NeVIII 3S-5P	200000.	0.579	-0.172E-01				
182.8 A	500000.	0.450	-0.889E-02				
C=0.17E+20	1000000.	0.371	-0.422E-03				
	2000000.	0.306	0.563E-02				
NeVIII 4S-5P	200000.	6.40	-0.253				
563.7 A	500000.	4.95	-0.195				
C=0.16E+21	1000000.	4.08	-0.126				
	2000000.	3.36	-0.510E-01				
NeVIII 2P-3S	200000.	0.174E-01	0.112E-02	0.630E-03	0.141E-02	0.124E-02	0.235E-02
103.0 A	500000.	0.121E-01	0.135E-02	0.188E-02	0.260E-02	*0.375E-02	*0.489E-02
C=0.37E+21	1000000.	0.943E-02	0.139E-02	0.311E-02	0.340E-02	*0.630E-02	*0.680E-02
	2000000.	0.748E-02	0.132E-02	0.413E-02	0.412E-02	*0.840E-02	*0.843E-02
NeVIII 2P-4S	200000.	0.249E-01	0.216E-02	*0.316E-02	*0.372E-02		
74.6 A	500000.	0.182E-01	0.264E-02	*0.605E-02	*0.600E-02		
C=0.80E+20	1000000.	0.146E-01	0.286E-02	*0.803E-02	*0.763E-02		
	2000000.	0.118E-01	0.252E-02	*0.992E-02	*0.941E-02		
NeVIII 2P-5S	200000.	0.450E-01	0.374E-02				
66.3 A	500000.	0.335E-01	0.542E-02				
C=0.42E+20	1000000.	0.272E-01	0.579E-02				
	2000000.	0.220E-01	0.521E-02				
NeVIII 2P-6S	200000.	0.866E-01	0.475E-03				
62.6 A	500000.	0.682E-01	0.635E-02				
C=0.13E+20	1000000.	0.559E-01	0.849E-02				
	2000000.	0.450E-01	0.986E-02				
NeVIII 3P-4S	200000.	0.579	0.326E-01	*0.465E-01	*0.545E-01		
298.6 A	500000.	0.418	0.391E-01	*0.906E-01	*0.883E-01		
C=0.11E+22	1000000.	0.333	0.421E-01	*0.117	*0.112		
	2000000.	0.267	0.372E-01	*0.144	*0.135		
NeVIII 3P-5S	200000.	0.484	0.327E-01				
198.9 A	500000.	0.357	0.474E-01				
C=0.38E+21	1000000.	0.288	0.504E-01				
	2000000.	0.233	0.455E-01				
NeVIII 3P-6S	200000.	0.687	0.278E-02				
168.8 A	500000.	0.536	0.451E-01				
C=0.91E+20	1000000.	0.438	0.606E-01				
	2000000.	0.353	0.707E-01				

PERTURBER DENSITY = 0.1E+21cm-3

PERTURBERS ARE:		ELECTRONS		PROTONS		He III	
TRANSITION	T(K)	WIDTH(A)	SHIFT(A)	WIDTH(A)	SHIFT(A)	WIDTH(A)	SHIFT(A)
NeVIII 4P-5S	200000.	7.31	0.353				
651.4 A	500000.	5.40	0.469				
C=0.23E+22	1000000.	4.36	0.495				
	2000000.	3.53	0.434				
NeVIII 4P-6S	200000.	4.93	0.176E-01				
411.0 A	500000.	3.81	0.252				
C=0.54E+21	1000000.	3.10	0.341				
	2000000.	2.50	0.398				
PERTURBER DENSITY = 0.1E+22cm-3							
NeVIII 2S-2P	200000.	4.36	-0.544E-01	0.163E-01	-0.372E-01	0.259E-01	-0.459E-01
773.7 A	500000.	2.83	-0.769E-01	0.788E-01	-0.122	0.151	-0.216
C=0.77E+24	1000000.	2.08	-0.870E-01	0.177	-0.208	0.348	-0.394
	2000000.	1.57	-0.865E-01	0.289	-0.296	0.576	-0.579
NeVIII 2S-3P	200000.	0.207	-0.290E-02	*0.697E-02	*0.576E-02		
88.1 A	500000.	0.143	-0.876E-03	*0.171E-01	*0.143E-01		
C=0.98E+21	1000000.	0.111	0.236E-03	*0.252E-01	*0.204E-01		
	2000000.	0.870E-01	0.665E-03	*0.318E-01	*0.262E-01		
NeVIII 2S-4P	200000.	*0.304	*-0.629E-02				
67.4 A	500000.	0.227	-0.123E-02				
C=0.25E+21	1000000.	0.183	0.561E-03				
	2000000.	0.149	0.272E-02				
NeVIII 2S-5P	200000.	*0.448	*0.334E-02				
60.7 A	500000.	0.366	-0.845E-03				
C=0.18E+20	1000000.	0.314	-0.946E-03				
	2000000.	0.268	0.101E-03				
NeVIII 3S-4P	200000.	*5.15	*-0.107				
260.5 A	500000.	3.84	-0.639E-01				
C=0.37E+22	1000000.	3.10	-0.496E-01				
	2000000.	2.53	-0.244E-01				
NeVIII 3S-5P	200000.	*4.36	*0.241E-01				
182.8 A	500000.	3.54	-0.300E-01				
C=0.17E+21	1000000.	3.02	-0.371E-01				
	2000000.	2.57	-0.311E-01				
NeVIII 2P-3S	200000.	0.172	0.295E-02	0.615E-02	0.895E-02		
103.0 A	500000.	0.120	0.847E-02	*0.189E-01	*0.219E-01		
C=0.37E+22	1000000.	0.937E-01	0.106E-01	*0.308E-01	*0.312E-01		
	2000000.	0.744E-01	0.117E-01	*0.412E-01	*0.399E-01		
NeVIII 2P-4S	200000.	0.219	-0.877E-02				
74.6 A	500000.	0.166	0.739E-02				
C=0.80E+21	1000000.	0.136	0.155E-01				
	2000000.	0.110	0.186E-01				

PERTURBER DENSITY = 0.1E+22cm-3

PERTURBERS ARE:		ELECTRONS		PROTONS		He III	
TRANSITION	T(K)	WIDTH(A)	SHIFT(A)	WIDTH(A)	SHIFT(A)	WIDTH(A)	SHIFT(A)
NeVIII 2P-5S	200000.	0.338	-0.328E-01				
66.3 A	500000.	0.276	0.773E-02				
C=0.42E+21	1000000.	0.232	0.244E-01				
	2000000.	0.192	0.335E-01				
NeVIII 2P-6S	200000.	0.417	-0.751E-01				
62.6 A	500000.	0.414	-0.157E-01				
C=0.13E+21	1000000.	0.375	0.129E-01				
	2000000.	0.322	0.439E-01				
NeVIII 3P-4S	200000.	5.22	-0.116				
298.6 A	500000.	3.89	0.117				
C=0.11E+23	1000000.	3.13	0.233				
	2000000.	2.53	0.277				
NeVIII 3P-5S	200000.	3.79	-0.285				
198.9 A	500000.	3.02	0.686E-01				
C=0.38E+22	1000000.	2.51	0.213				
	2000000.	2.07	0.293				
NeVIII 3P-6S	200000.	3.58	-0.538				
168.8 A	500000.	3.40	-0.115				
C=0.91E+21	1000000.	3.03	0.890E-01				
	2000000.	2.59	0.313				

PERTURBER DENSITY = 0.1E+23cm-3

NeVIII 2S-3P	200000.	*1.76	*-0.102E-01
88.1 A	500000.	1.26	-0.855E-02
C=0.98E+22	1000000.	0.996	-0.480E-02
	2000000.	0.796	-0.299E-02
NeVIII 2P-3S	200000.	1.36	-0.166
103.0 A	500000.	1.04	-0.386E-01
C=0.37E+23	1000000.	0.840	0.166E-01
	2000000.	0.678	0.536E-01
NeVIII 2P-4S	200000.	*1.02	*-0.304
74.6 A	500000.	1.01	-0.114
C=0.80E+22	1000000.	0.925	-0.164E-01
	2000000.	0.811	0.432E-01
NeVIII 2P-5S	200000.	*0.864	*-0.568
66.3 A	500000.	1.21	-0.221
C=0.42E+22	1000000.	1.26	-0.603E-01
	2000000.	1.20	0.572E-01

PERTURBER DENSITY = 0.1E+19 cm-3

PERTURBERS ARE:		ELECTRONS		PROTONS		He III	
TRANSITION	T(K)	WIDTH(A)	SHIFT(A)	WIDTH(A)	SHIFT(A)	WIDTH(A)	SHIFT(A)
Na IX 2P-5S	200000.	0.247E-03	0.384E-04	0.466E-04	0.604E-04	0.931E-04	0.117E-03
52.5 A	500000.	0.184E-03	0.375E-04	0.751E-04	0.784E-04	0.153E-03	0.159E-03
C=0.22E+18	1000000.	0.149E-03	0.330E-04	0.956E-04	0.922E-04	0.199E-03	0.188E-03
	2000000.	0.120E-03	0.264E-04	0.114E-03	0.107E-03	0.233E-03	0.215E-03
Na IX 3P-4S	200000.	0.298E-02	0.240E-03	0.190E-03	0.312E-03	0.380E-03	0.615E-03
235.6 A	500000.	0.212E-02	0.228E-03	0.407E-03	0.463E-03	0.817E-03	0.940E-03
C=0.79E+19	1000000.	0.168E-02	0.219E-03	0.539E-03	0.556E-03	0.110E-02	0.113E-02
	2000000.	0.134E-02	0.184E-03	0.682E-03	0.653E-03	0.142E-02	0.134E-02
Na IX 3P-5S	200000.	0.265E-02	0.336E-03	0.411E-03	0.534E-03	0.821E-03	0.104E-02
157.3 A	500000.	0.195E-02	0.327E-03	0.666E-03	0.693E-03	0.135E-02	0.141E-02
C=0.20E+19	1000000.	0.156E-02	0.288E-03	0.845E-03	0.814E-03	0.176E-02	0.167E-02
	2000000.	0.126E-02	0.230E-03	0.101E-02	0.940E-03	0.209E-02	0.189E-02
PERTURBER DENSITY = 0.1E+20 cm-3							
Na IX 2S-2P	200000.	0.304E-01	-0.455E-03	0.641E-04	-0.285E-03	0.120E-03	-0.538E-03
684.8 A	500000.	0.196E-01	-0.513E-03	0.312E-03	-0.712E-03	0.599E-03	-0.142E-02
C=0.68E+22	1000000.	0.142E-01	-0.582E-03	0.812E-03	-0.121E-02	0.158E-02	-0.244E-02
	2000000.	0.106E-01	-0.550E-03	0.149E-02	-0.173E-02	0.296E-02	-0.350E-02
Na IX 2S-3P	200000.	0.120E-02	0.136E-04	0.273E-04	0.433E-04	0.525E-04	0.819E-04
70.6 A	500000.	0.812E-03	0.125E-04	0.725E-04	0.811E-04	0.144E-03	0.163E-03
C=0.71E+19	1000000.	0.618E-03	0.110E-04	0.117E-03	0.112E-03	0.235E-03	0.227E-03
	2000000.	0.479E-03	0.838E-05	0.151E-03	0.134E-03	0.307E-03	0.273E-03
Na IX 3S-3P	200000.	1.95	-0.306E-01	0.246E-01	-0.530E-02	0.467E-01	-0.100E-01
2500.6 A	500000.	1.34	-0.409E-01	0.591E-01	-0.130E-01	0.115	-0.259E-01
C=0.89E+22	1000000.	1.04	-0.412E-01	0.861E-01	-0.214E-01	0.169	-0.433E-01
	2000000.	0.816	-0.420E-01	0.105	-0.298E-01	0.209	-0.603E-01
Na IX 2P-3S	200000.	0.905E-03	0.568E-04	0.187E-04	0.655E-04	0.363E-04	0.124E-03
81.3 A	500000.	0.622E-03	0.671E-04	0.745E-04	0.120E-03	0.150E-03	0.241E-03
C=0.26E+20	1000000.	0.480E-03	0.664E-04	0.135E-03	0.165E-03	0.271E-03	0.334E-03
	2000000.	0.378E-03	0.633E-04	0.189E-03	0.199E-03	0.381E-03	0.401E-03
Na IX 2P-4S	200000.	0.126E-02	0.153E-03	0.129E-03	0.201E-03	*0.259E-03	*0.373E-03
59.0 A	500000.	0.913E-03	0.151E-03	0.276E-03	0.309E-03	*0.556E-03	*0.621E-03
C=0.57E+19	1000000.	0.730E-03	0.148E-03	0.367E-03	0.376E-03	0.753E-03	0.770E-03
	2000000.	0.588E-03	0.125E-03	0.445E-03	0.452E-03	0.931E-03	0.902E-03
Na IX 2P-5S	200000.	0.247E-02	0.336E-03	*0.466E-03	*0.549E-03		
52.5 A	500000.	0.184E-02	0.354E-03	*0.752E-03	*0.763E-03		
C=0.22E+19	1000000.	0.148E-02	0.325E-03	0.956E-03	0.918E-03		
	2000000.	0.120E-02	0.264E-03	0.114E-02	0.107E-02		
Na IX 3P-4S	200000.	0.298E-01	0.224E-02	0.191E-02	0.292E-02	0.379E-02	0.546E-02
235.6 A	500000.	0.212E-01	0.221E-02	0.406E-02	0.455E-02	0.817E-02	0.910E-02
C=0.79E+20	1000000.	0.168E-01	0.217E-02	0.539E-02	0.554E-02	*0.110E-01	*0.113E-01
	2000000.	0.134E-01	0.184E-02	0.682E-02	0.653E-02	*0.142E-01	*0.133E-01

PERTURBER DENSITY = 0.1E+20 cm-3

PERTURBERS ARE:		ELECTRONS		PROTONS		He III	
TRANSITION	T(K)	WIDTH(A)	SHIFT(A)	WIDTH(A)	SHIFT(A)	WIDTH(A)	SHIFT(A)
Na IX 3P-5S	200000.	0.265E-01	0.293E-02	*0.411E-02	*0.485E-02		
157.3 A	500000.	0.195E-01	0.309E-02	*0.666E-02	*0.674E-02		
C=0.20E+20	1000000.	0.156E-01	0.284E-02	0.845E-02	0.810E-02		
	2000000.	0.126E-01	0.230E-02	0.101E-01	0.940E-02		
PERTURBER DENSITY = 0.1E+21 cm-3							
Na IX 2S-2P	200000.	0.304	-0.361E-02	0.634E-03	-0.253E-02	0.116E-02	-0.423E-02
684.8 A	500000.	0.196	-0.502E-02	0.311E-02	-0.690E-02	0.596E-02	-0.131E-01
C=0.68E+23	1000000.	0.143	-0.574E-02	0.812E-02	-0.120E-01	0.158E-01	-0.236E-01
	2000000.	0.106	-0.548E-02	0.149E-01	-0.173E-01	0.296E-01	-0.349E-01
Na IX 2S-3P	200000.	0.120E-01	0.548E-04	0.271E-03	0.381E-03	0.507E-03	0.630E-03
70.6 A	500000.	0.812E-02	0.802E-04	0.726E-03	0.776E-03	0.144E-02	0.146E-02
C=0.71E+20	1000000.	0.617E-02	0.923E-04	0.117E-02	0.110E-02	*0.234E-02	*0.215E-02
	2000000.	0.479E-02	0.800E-04	0.151E-02	0.134E-02	*0.307E-02	*0.272E-02
Na IX 3S-3P	200000.	19.5	-0.310	0.243	-0.471E-01	0.446	-0.788E-01
2500.6 A	500000.	13.4	-0.420	0.590	-0.126	1.14	-0.240
C=0.89E+23	1000000.	10.4	-0.405	0.861	-0.212	1.69	-0.419
	2000000.	8.16	-0.421	1.05	-0.298	2.09	-0.602
Na IX 2P-3S	200000.	0.905E-02	0.452E-03	0.187E-03	0.575E-03	0.361E-03	0.950E-03
81.3 A	500000.	0.622E-02	0.621E-03	0.749E-03	0.114E-02	0.151E-02	0.215E-02
C=0.26E+21	1000000.	0.481E-02	0.632E-03	0.135E-02	0.162E-02	0.271E-02	0.316E-02
	2000000.	0.378E-02	0.628E-03	0.189E-02	0.198E-02	0.381E-02	0.400E-02
Na IX 2P-4S	200000.	0.126E-01	0.106E-02	*0.129E-02	*0.166E-02		
59.0 A	500000.	0.912E-02	0.124E-02	*0.276E-02	*0.286E-02		
C=0.57E+20	1000000.	0.729E-02	0.136E-02	*0.366E-02	*0.364E-02		
	2000000.	0.587E-02	0.123E-02	*0.445E-02	*0.450E-02		
Na IX 2P-5S	200000.	0.241E-01	0.146E-02				
52.5 A	500000.	0.180E-01	0.247E-02				
C=0.22E+20	1000000.	0.146E-01	0.275E-02				
	2000000.	0.118E-01	0.254E-02				
Na IX 3P-4S	200000.	0.297	0.158E-01	*0.190E-01	*0.244E-01		
235.6 A	500000.	0.212	0.183E-01	*0.407E-01	*0.422E-01		
C=0.79E+21	1000000.	0.168	0.200E-01	*0.540E-01	*0.538E-01		
	2000000.	0.134	0.180E-01	*0.682E-01	*0.650E-01		
Na IX 3P-5S	200000.	0.259	0.126E-01				
157.3 A	500000.	0.191	0.215E-01				
C=0.20E+21	1000000.	0.154	0.240E-01				
	2000000.	0.124	0.222E-01				
PERTURBER DENSITY = 0.1E+22 cm-3							
Na IX 2S-2P	200000.	3.04	-0.211E-01	0.564E-02	-0.167E-01	0.864E-02	-0.192E-01
684.8 A	500000.	1.96	-0.421E-01	0.310E-01	-0.620E-01	0.586E-01	-0.108
C=0.68E+24	1000000.	1.43	-0.518E-01	0.810E-01	-0.115	0.157	-0.216
	2000000.	1.06	-0.527E-01	0.149	-0.170	0.296	-0.333

PERTURBER DENSITY = 0.1E+22 cm-3

PERTURBERS ARE:		ELECTRONS		PROTONS		He III	
TRANSITION	T(K)	WIDTH(A)	SHIFT(A)	WIDTH(A)	SHIFT(A)	WIDTH(A)	SHIFT(A)
Na IX 2S-3P	200000.	0.117	-0.137E-02	0.242E-02	0.240E-02	*0.372E-02	*0.251E-02
70.6 A	500000.	0.796E-01	-0.398E-03	*0.716E-02	*0.660E-02		
C=0.71E+21	1000000.	0.607E-01	0.779E-04	*0.117E-01	*0.102E-01		
	2000000.	0.471E-01	0.353E-03	*0.151E-01	*0.130E-01		
Na IX 2P-3S	200000.	0.901E-01	0.830E-03	0.183E-02	0.359E-02	*0.321E-02	*0.370E-02
81.3 A	500000.	0.620E-01	0.404E-02	0.746E-02	0.968E-02		
C=0.26E+22	1000000.	0.479E-01	0.497E-02	*0.135E-01	*0.150E-01		
	2000000.	0.377E-01	0.563E-02	*0.189E-01	*0.192E-01		
Na IX 2P-4S	200000.	0.114	-0.366E-02				
59.0 A	500000.	0.851E-01	0.375E-02				
C=0.57E+21	1000000.	0.689E-01	0.786E-02				
	2000000.	0.559E-01	0.940E-02				
Na IX 2P-5S	200000.	0.172	-0.202E-01				
52.5 A	500000.	0.143	0.726E-03				
C=0.22E+21	1000000.	0.121	0.981E-02				
	2000000.	0.101	0.152E-01				
Na IX 3P-4S	200000.	2.75	-0.458E-01				
235.6 A	500000.	2.01	0.592E-01				
C=0.79E+22	1000000.	1.60	0.118				
	2000000.	1.29	0.140				
Na IX 3P-5S	200000.	1.96	-0.176				
157.3 A	500000.	1.58	0.622E-02				
C=0.20E+22	1000000.	1.31	0.850E-01				
	2000000.	1.08	0.132				

PERTURBER DENSITY = 0.1E+23 cm-3

Na IX 2S-3P	200000.	*1.02	*-0.596E-02
70.6 A	500000.	0.717	-0.512E-02
C=0.71E+22	1000000.	0.556	-0.387E-02
	2000000.	0.437	-0.202E-02
Na IX 2P-3S	200000.	0.740	-0.850E-01
81.3 A	500000.	0.555	-0.180E-01
C=0.26E+23	1000000.	0.440	0.813E-02
	2000000.	0.351	0.279E-01
Na IX 2P-4S	200000.	0.573	-0.153
59.0 A	500000.	0.546	-0.612E-01
C=0.57E+22	1000000.	0.491	-0.901E-02
	2000000.	0.425	0.236E-01
Na IX 2P-5S	200000.	0.490	-0.264
52.5 A	500000.	0.638	-0.112
C=0.22E+22	1000000.	0.664	-0.373E-01
	2000000.	0.626	0.210E-01

PERTURBER DENSITY = 0.1E+23 cm-3

PERTURBERS ARE:		ELECTRONS		PROTONS		He III	
TRANSITION	T(K)	WIDTH(A)	SHIFT(A)	WIDTH(A)	SHIFT(A)	WIDTH(A)	SHIFT(A)
Na IX 3P-4S	200000.	*16.8	*-2.33				
235.6 A	500000.	14.3	-0.935				
C=0.79E+23	1000000.	12.3	-0.139				
	2000000.	10.4	0.350				
Na IX 3P-5S	200000.	*7.80	*-2.33				
157.3 A	500000.	8.24	-0.986				
C=0.20E+23	1000000.	7.96	-0.333				
	2000000.	7.23	0.178				

1969ab). Values for NV > 0.5 are not given and values for 0.1 < NV ≤ 0.5 are denoted by an asterisk. When the impact approximation is not valid, the ion broadening contribution may be estimated by using quasistatic estimations (Sahal–Bréchot 1991 and Griem 1974). The accuracy of the results obtained decreases when broadening by ion interactions becomes important.

The analysis of present results and comparison with available experimental and theoretical data is given in Dimitrijević and Sahal–Bréchot (1994).

Acknowledgements – This work is a part of French–Yugoslav collaboration through the project "L'elargissement Stark des raies spectrales des plasmas astrophysiques et de laboratoire", it is also a part of the project "Physics and dynamics of celestial bodies", supported by Ministry for Science and Technology of Serbia.

REFERENCES

Dimitrijević, M. S., and Sahal–Bréchot, S.: 1984, *JQSRT* **31**, 301.

Dimitrijević, M. S., and Sahal–Bréchot, S.: 1994, *Astron. Astrophys. Suppl. Series* in press.

Dimitrijević, M. S., Sahal–Bréchot, S., and Bommier, V.: 1991, *Astron. Astrophys. Suppl. Series.* **89**, 581.

Griem, H. R.: 1974, *Spectral Line Broadening by Plasmas*, Academic Press, New York.

Sahal–Bréchot, S.: 1969a, *Astron. Astrophys.* **1**, 91.

Sahal–Bréchot, S.: 1969b, *Astron. Astrophys.* **2**, 322.

Sahal–Bréchot, S.: 1991, *Astron. Astrophys.* **245**, 322.

ТАБЕЛЕ ПАРАМЕТАРА ШТАРКОВОГ ШИРЕЊА ЛИНИЈА Ne VIII и Na IX ОД ЗНАЧАЈА У АСТРОФИЗИЦИ

М. С. Димитријевић[1] и S. Sahal–Bréchot[2]

[1] *Астрономска опсерваторија, Волгина 7, 11050 Београд, Југославија*

[2] *Laboratoire "Astrophysique, Atomes et Molécules"*
Département Atomes et Molécules en Astrophysique
Unité associée au C.N.R.S. No 812
Observatoire de Paris-Meudon, 92190 Meudon, France

УДК 52–355.3
Претходно саопштење

Користећи семикласичан прилаз, израчунате су ширине и помераји спектралних линија, проузроковани сударима са електронима, протонима и He III, за 20 мултиплета Ne VIII и 8 мултиплета Na IX. Резултати су дати у функцији температуре и концентрације пертурбера.

Six calendar systems in the European history from 18th to 20th Century

Efstratios Theodossiou[1], Vassilios N. Manimanis[1], and Milan S. Dimitrijević[2]

[1] Department of Astrophysics, Astronomy and Mechanics Physics Faculty, University of Athens-Zografos 157 84

[2] Astronomical Observatory, Volgina 7, 11060 Belgrade, Serbia

etheodos@phys.uoa.gr

mdimitrijevic@aob.bg.ac.rs

Abstract. The following calendar systems, introduced in Europe from 18th to 20th century, which were in use in Europe for a shorter or longer period by a larger or smaller community, were reviewed and discussed: The French Revolutionary Calendar, the Theosebic calendar invented by Th. Kairis, the Revolutionary Calendar of the Soviet Union (or 'Bolshevik calendar'), the fascist calendar in Italy and the calendar of the Metaxas dictatorship in Greece before World War II. Also the unique of them which is still in use, the New Rectified Julian calendar of the Orthodox Church, adopted according to proposition of Milutin Milanković on the Congress of Orthodox Churches in 1923 in Constantinople, is presented and discussed. At the end, difficulties to introduce a new calendar are discussed as well.

Key words: Calendars: French Revolutionary, Theosebic, Italian fascist, of I. Metaxas, Bol'shevik's, New Rectified Julian

Introduction

In the history of calendar reforms the Julian calendar that prevailed for at least 16 centuries was gradually replaced by the Gregorian one, from 1582 onwards. The Gregorian calendar was necessary, because it corrected the Julian one and returned the vernal equinox in its true astronomical date; however, it did not change the months, or the days of the week (their number and names): it just changed the way of calculation of the leap years. After these two calendars, five other political calendar systems and one ecclesiastic were introduced in Europe, but none of political ones prevailed beyond its limited (in time and place) political environment. In this work the following such unsuccessful calendars are reviewed: The French Revolutionary Calendar, the Theosebic calendar invented by Th. Kairis, the Revolutionary Calendar of the Soviet Union (or 'Bolshevik calendar'), the fascist calendar in Italy and the calendar of the Metaxas dictatorship in Greece before World War II. Also the unique of them which is still in use, the New Rectified Julian calendar of the Orthodox Church is presented and discussed.

Essentially, with the exception of the French Revolutionary Calendar (*Le Calendrier Républicain*), which is well-known and studied in the international bibliography, our effort is centered at the other 5 calendar systems, which are much less known, especially the three of them: the Theosebic calendar, the fascist calendar in Italy and the calendar of the Metaxas dictatorship in Greece (1936-1940). At the end, difficulties to introduce a new calendar are discussed as well.

1 The French Revolutionary Calendar

After the Gregorian calendar, the next step of a calendar reform was taken in France, after the French Revolution of 1789, which resulted in the abolishment of monarchy and the declaration of Democracy. The French revolutionaries, after breaking the bonds of the monarchy wanted to break also their links with the religious-papal (as they perceived it) calendar, by reintroducing its primal basis, the ancient Egyptian calendar. For this reason, they wanted to create a calendar similar with one that would lead to the complete decoupling of Church and the State. The first attacks against the Gregorian calendar, accompanied by the respective calendar propositions for its reformation, took place during the years 1785 to 1788.

The times were ripe, after the fall of Bastille in July 14, 1789, for the French revolutionaries to ask with considerable intensity for a new calendar, having as its starting point the first year of Democracy. So in 1793 the National Assembly entrusted Charles Gilbert Romme, president of the public education committee, with the calendar reform. He in turn assigned to the famous mathematicians Joseph-Louis Lagrange and Gaspar Monge the task to work on the technicalities of the issue. The results of the studies of the two mathematicians were submitted to National Assembly in September 1793 and were accepted immediately. At the same time it was decided that this new calendar system would be applied soon. Indeed, the *Calendrier Républicain de la Rèvolution de 1789*, as it was called, was accepted by the National Assembly on October 5, 1793 and was voted on December 4, 1793. As the starting point of its chronology was set a date of the recent past, namely the September 22, 1792, known in the new calendar as 1 Vendèmiaire, the date of the abolishment of monarchy and the declaration of democracy, which accidentally coincided with the astronomical autumnal (fall) equinox. So the New Year's Day of the 'revolutionary' civil year was the autumnal equinox of each tropical year, with the chronology starting on September 22, 1792 or 1 Vendèmiaire of the Year 1.

The year of this 'democratic' calendar consisted of 12 months of 30 days each, followed by an extra 5 or 6 supplementary days (*jours complémentaires*), which, added at the end of the 12th month, that is between the respective dates 17 and 22 September, were completing the total number of the days of the year. Thus, the total number of the days of the year was again 365 or 366 for leap years, keeping the tradition of the Julian calendar and its evolution, the Gregorian calendar.

The day-and-night time interval, from one midnight to the next, was divided into 10 hours and the 1/100 of such an hour was defined as the 'decimal minute'. I.e. the French democrats abolished the hexadecimal system in time keeping and established the simpler decimal one (each minute had also 100 seconds). The weeks, because they were related to the Jewish calendar, and thus they had been adopted in interconnection with Religion, were abandoned and each month was divided into three *décades*. The names of the days of the week were also abolished and the ten days of each 10-day span were just called with their order: first, second, third,..., tenth day (*primidi, duodi, tridi, quartidi, quintidi, sextidi, septidi, octidi, nonidi, décadi*). The last day of each *décade*, the *décadi*, was a day of rest, dedicated to the worship of

the Supreme Being. The names of the months had the same ending for each three-month group and they were inspired by nature. They were invented by the member of the National Assembly, poet Philippe Fabre d'Eglantine (1750-1794). This poet and playwright had won (with his work *Étude de la nature*, 1783) in 1783 the first prize in Toulouse's flower festival; the prize was a golden wild rose, which is called *eglantine* in French, and he adopted this word as his nickname, with which he is known in history. Philippe Fabre was a member of Danton's group, and when his friend lost his political power, he was accused of corruption because he had been involved in the scandalous dissolution of the Society of Indies. For this reason he was beheaded together with Danton and his followers on April 5, 1794.

The democratic calendar was permeated by an anti-Christian, rationalistic and nature-loving spirit. The poetic names of the months of the year, together with their meaning and the correlation with our months are as follows (Flammarion, 1955, p. 28):

Table I: The French Revolutionary Calendar

Season	Month	Meaning	Correlation
Fall	Vendèmiaire	Vintager	Sept. 22 - Oct. 21
	Brumaire	Foggy	Oct. 22 - Nov. 20
	Frimaire	Chilly	Nov. 21 - Dec. 20
Winter	Nivôse	Snowy	Dec. 21 - Jan. 19
	Pluviôse	Rainy	Jan. 20 - Feb. 18
	Ventôse	Windy	Feb. 19 - March 20
Spring	Germinal	Of the sprouts	March 21 - April 19
	Floréal	Flowery	April 20 - May 19
	Prairial	Grassy	May 20 - June 18
Summer	Messidor	Harvester	June 19 - July 18
	Thermidor	Heat-giver	July 19 - Aug. 17
	Fructidor	Fruit-giver	Aug. 18 - Sept. 16
	Jour de la Vertu	Day of Virtue	Sept. 17
	Jour du Génie	Day of Engineering	Sept. 18
	Jour du Travail	Day of Work	Sept. 19
	Jour de l' Opinion	Day of Opinion	Sept. 20
	Jour des Récompenses	Day of Rewards	Sept. 21
	Jour de la Révolution	Day of Revolution	
		(Only in leap years)	Sept.22

These Gregorian dates vary slightly because of leap years. Moreover, due to incompatibility of Articles III (Every year begins in the midnight of the day of autumnal equinox for Paris observatory) and X (...The fourth year of a *Franciade* is *Sextile*) of *Décret de la Convention nationale sur l'ère, le commencement et l'organisation de l'année, et sur les noms des jours et des mois*, the calendar is not applicable after the year XVIII, since an additional leap day for compatibility with tropical year is not needed for the Year XIX (the fourth year of Franciade) but for Year XX (the fifth year of Franciade). Consequently, exist different systems for the conversion after the year XVIII and the corresponding dates are slightly different for different systems.

The five or six supplementary days were initially called *Sans Culottides*, to honor the revolutionaries who didn't wear the expensive trousers (culottes)

of the aristocrats but long hairy pants instead. The French who were using the calendar were saying: the first Sans Culottide, the second Sans Culottide, etc. (*la première sans culottide, la seconde sans culottide*, etc.). The collective name 'supplementary days' (*jours complémentaires*) was given to the Sans Culottides on 7 Fructidor of the Year III, i.e. on August 24, 1795.

The names of the saints associated with each date of the year in the Christian calendars were replaced by names of trees, plants, flowers, fruits and grains, since this calendar was designed to be free of Christian nomenclature (Renouard, A.A., 1822).

The supplementary days, between 17th and 22nd September of the Gregorian calendar, were dedicated: to Virtue (*la Fête de la Vertu*), Engineering (*la Fête du Génie*), to Work (*la Fête du Travail*), to Opinion (*la Fête de l' Opinion*), and to Rewards (*la Fête des Récompenses*).

The Day of the Opinion was especially important for its singular character: on this date, every citizen had the right to freely express his opinion. At a collective level, the citizens were judging publicly, albeit figuratively, all public servants for their deeds. During this day, any kind of satire was permitted, along with cartoons, satirical songs and many other smart jokes, which were freely aimed towards those in power. It was then up to those in power to disprove through its Virtue these humoristic accusations. For this reason, this day was also considered to be dedicated to Actions and Virtue. The sixth supplementary day added in the leap years was dedicated to the celebration of the Revolution (*la Fête de la Rèvolution*). The first leap year of the new calendar was decided to be the Year III. The four-year period between two successive Days of the Revolution was called *Franciade*.

The wonderful French invention of calling the democratic calendar's months with names corresponding closely to the real climate of France was ridiculed by the British (then adversaries of the French) with the following parody:

Fall: *wheezy, sneezy, freezy*
Winter: *slippy, drippy, nippy*
Spring: *showery, flowery, bowery*
Summer: *hoppy, croppy, poppy*
(Wilson P.W., 1937, p. 154). For Summer somewhere is given and: *Wheatty, Heaty, Sweety* (The Historical Maritime Society, Nelson and His Navy - Revolutionary Calendar, http://www.hms.org.uk/nelsonsnavyrevcalend.htm,

This rather poetic calendar was functional and efficient for France; however, it was disadvantageous for the working class, as it contained only one day of rest every ten days and not one in seven, as it used to be. Its other major weakness had to do with the fact that it was a calendar of limited use, since it was used only in France, and thus isolated it calendarly, administratively, economically and in international relations issues from the rest European countries.

For these reasons, but mainly for political purposes Napoleon the Great agreed with the Pope in 1801 to restore Sunday in the calendar, as well as the major Christian holidays: Christmas and the Easter. Finally, in 1806 the French Revolutionary Calendar was abolished with the decree of 22 Fructidor XIII signed by Napoleon and France adopted again the Gregorian calendar on

Fig. 1. Colored drawing from 19th century. The person on the right side is wearing short trousers of aristocrats - culottes.

11 Nivôse XIV that is in Gregorian date January 1st, 1806. The Revolutionary Calendar had a short life, less than 13.5 years. However, some decades later, an attempt was made to restore it, which is described below.

In 1870, emperor Napoleon III (1808-1873) lost a war with the Prussians he was responsible for. This defeat had as a result the abdication of the emperor on September 4, 1870 and the declaration of the Second Republic. However, the Prussians advanced and occupied a part of Paris. The end of the war came on March 1st, 1871, when Thierry's government signed the capitulation with the invaders.

The defeat and the humiliating terms of the treaty had as a result a new revolution in Paris, on March 18, 1871. The people of Paris installed in the Town Hall a communal administration, which passed in history under the

Fig. 2. French Revolutionary calendar by Louis-Philibert Debucourt 1755-1832.

name "Paris Commune". The revolutionary commission that was formed organized the city's defense. And one of its first actions was the revival of the Revolutionary Calendar, the *Calendrier Républicain de la Rèvolution*, on May 10, 1871, which corresponded to the 18 Floréal of the Year 79. The 'Government of National Salvation' as Thierry's government was known, found refuge in Versailles. It managed to summon 100,000 men and with this army it attacked Paris. After a couple of weeks of battles, in which more than 20,000 people died, the governmental army crushed the revolutionaries in the end of May 1871, aided by the Prussians.

The quick end of this popular uprising brought once again the abolishment of the Revolutionary-Democratic Calendar, this time forever, on May 28, 1871. So, the Commune in Paris restored French Revolutionary Calendar just for a brief period (Wilson, P.W., 1937, p. 155 & p. 334).

Nevertheless, even today the French astronomical almanacs, as a tribute towards the First French Republic, give along with the other calendars (Gregorian, Julian, Islamic, Jewish and Coptic) the date correlation of the Rev-

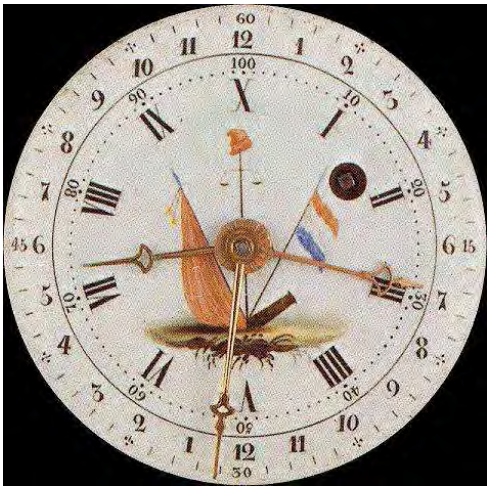

Fig. 3. French republican clock with combined decimal (inside) and traditional (outside)hour-plate.

olutionary Calendar, which in 2009 is at its 217th Year (the first of January 2010 corresponded to 12 Nivôse 218).

2 The Theosebic calendar

The abolishment of the French Revolutionary-Democratic calendar discouraged other regimes from adopting some novel calendar system. Yet, the French calendar inspired the Greek priest and scholar Theophilos Kairis to invent his own 'Theosebic calendar' who was also destined not to prevail at any place. This was a variant of the French Revolutionary calendar, but under a religious cover.

The monk and priest Theophilos Kairis (1784-1853), a thinker and scholar from the island of Andros, who participated in the Greek War of Independence of 1821, and is considered as one of the major 'Teachers of the Nation', had studied in the universities of Pisa and Paris. He was the creator of a cult, 'Theosebism', and for this reason he was persecuted and he died in prison. His original philosophical system was echoing the ideas of Theosophy, positivism and mysticism.

Theophilos Kairis, influenced by the Western Christian-social philosophy, was searching for the 'golden analogy' among religious faith, scientific knowledge and social justice. He did not accept the Christian chronology and, inspired by the French Revolutionary calendar (*Calendrier Républicain de la Rèvolution de 1789*), he proposed the abandonment of the week and the division of each month in three ten-day intervals: "Twelve '30-day' months in three groups of 10 days each (Theophilos Kairis, Code 53).

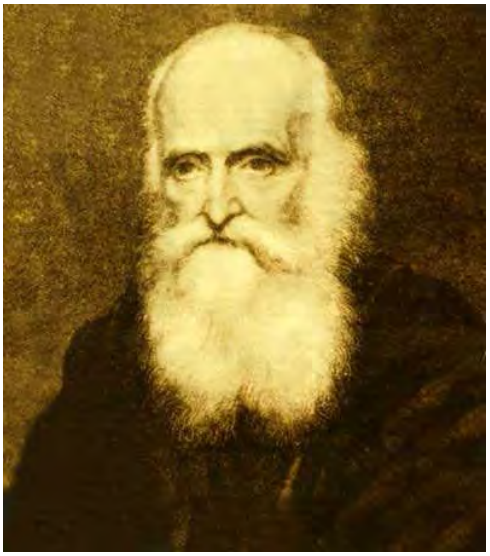

Fig. 4. Theophilos Kairis.

He also changed the names of the months, into the following ones (Theodossiou, E., & Danezis, E., 2000, pp. 337-338):

Table II: Month names in the Theosebic calendar, their meaning and equivalence

	Name	Meaning	Correlation*
1	Theosebius	Pius (of respect to God)	11/23 Sept.- 10/22 Oct.
2	Sopharetus	Wise and virtuous (of Wisdom and Virtue)	11/23 Oct.- 10/22 Nov.
3	Dicaeos	Righteous (Just)	11/23 Nov.- 9/21 Dec.
4	Hagios	Holy	10/22 Dec.- 8/20 Jan.
5	Agathius	Good (Benevolent)	9/21 Jan.- 7/19 Feb.
6	Sthenius	Courageous (of Power)	8/20 Feb.- 9/21 March
7	Agapius	Beloved (of Love)	10/22 Mar.- 8/20 April
8	Charisius	Graceful (of Grace)	9/21 April- 8/20 May
9	Macrothymus	Forbearing	9/21 May- 7/19 June
10	Aeonius	Eternal (Perpetual)	8/20 June- 7/19 July
11	Entheus	Divine ('God-in-it')	8/20 July- 6/18 Aug.
12	Sosius	Savior (of Salvation)	7/19 Aug.- 5/17 Sept.

* The first date is according to Julian calendar and the second according to Gregorian one, with a difference of 12 days as was in 19th century. For conversion of dates from 20th and 21st century one should take into account that the difference increased to 13 days. As in the case of French Revolutionary

Calendar, dates slightly vary due to leap years (We note that in Portaz (1935, p. 220) Gregorian dates are erroneously increased for one since was taken the difference of 13 days as in 20th century).

The five or six days added for the completion of the tropical year were the dates 18 to 22 September of the Gregorian calendar.

Theophilos Kairis knew that from an astronomical point of view there is no special significance in setting the start of the year on January 1st and that all ancient calendars were starting their year at one of the 4 characteristic points of the solar apparent orbit, which are:

a) The two equinoxes - the vernal on March 21 and the autumnal on September 23 - and

b) The solstices - the summer on June 22 and the winter on December 22.

The calendar system of Kairis, known as the 'Theosebic calendar' had also as its New Year's Day the autumnal equinox. The first year of the Theosebic chronology began on September 23, 1800 (Gregorian calendar). Actually, he chose as the start of his calendar system the autumnal equinox, which used to occur on September 11/23 (the first date refers to the Julian and the second date to the Gregorian calendar, which then had a difference of 12 days between them), like the ancient Greek calendars of the Dorians and the Macedonians. The Dorian (Spartan) calendar started on the first new moon after the autumnal equinox, in the month Panamos, and the Macedonian calendar started in the holy month Dios. But also his calendar model, the French Revolutionary-Democratic calendar, started at the autumnal equinox (September 22 or equivalently 1st Vendèmiaire of 1792 (Theodossiou & Danezis 2000, p. 338).

Correspondingly, the first year of the Theosebic chronology started on September 11 / 23 (when that year occurred autumnal equinox) of 1800 AD and ended on September 10 / 22 of 1801 AD. As we already noted, the Theosebic year had 12 months of 30 days each (12 x 30 = 360), so that 5 days remained (or 6 for the leap years) for the completion of the solar year of 365 (or 366) days. These extra days, as in the ancient Greek calendars, were called "induced days" and were inserted at the end of the Theosebic year, i.e. before the $11^{th}/23^{th}$ of September of the "Christian" calendars (Julian and Gregorian).

Similarly, as in the ancient Greek calendars, each month was divided into 10-day spans (decans); the first decan of each month was called "starting decan of the month", the second one "middle decan of the month" and the third one "decan of leaving or ending month", or "the decan after the twenty" (Theodossiou & Danezis 1996, vol. I, pp. 360-364).

The specialist on Kairis late scholar Demetrios I. Polemis, director of the Kairian Library in Andros, edited the correspondence of Theophilos Kairis, which was published in three volumes. He divides these three volumes of letters into three periods. The first volume contains the letters up to the closure of the Orphanage (1839), the second volume contains the letters of the period of his persecution and exile up to his return to Greece (1844) and the third one contains letters written in Andros to various receivers until the scholar's death in 1853 (D. Polemis, vol. I, p. 22). In the second volume's introduction Polemis reports that a detailed description of the Theosebic

calendar exists in the work *Epitome of the Theosebic teaching and ethics* (London 1852, pp. 102-104) by Kairis. Also, as far as the decans are concerned, Polemis writes the following:

"The decan is divided into ten days, the day into ten hours, the hour into 100 first minutes and the minute into 100 seconds. The days of the decan are named First, Second,... ..., Tenth or Holy". As Kairis writes, "the age of the Theosebists" begins "from the first year of the nineteenth century of the Christians and it is divided into five-year **entheades***". Therefore, the first year of the Theosebic chronology started on September 11 / 23, 1800* [the first year of 19th Century is not 1800 but 1801 - Remark of authors], *and ended on September 10 / 22, 1801. The days of September 6 to 10, 1801, were the* **Epacts** *(induced days).*

A complete Theosebic chronology is exposed in the letter No. 220: "33, or 9th of the entheas 9, to 3rd, the 1st of the middle [decan of] Sopharetus". The year 33 began on September 11 / 23 of 1842 AD, while the 8th entheas was completed on September 10 / 22, 1840 and the next day started the ninth entheas, of which the third year was 1842-1843. Sopharetus is the second month of the Theosebic calendar (October 11 / 23 to November 9 / 21). Therefore, the first of the middle decan of this month is the October 21st / November 2nd 1842.

Kairis and the followers of his sect were using tables of corresponding dates of the two calendars (Theosebic and Christian), some of which have been preserved.") (Polemis, Introduction, vol. II, pp. 12-13).

Kairis considered the year 1801 'as the year 1' in his Theosebian calendar, essentially a covert variation of the French revolutionary calendar cloaked in religion and, being the after-clap of a calendar that did not survive, Kairis's calendar was also still-born.

Table III: The "Times" of the day in the Theosebic calendar

Ecclesiastical "Hours"	Kairian "Times"
Matins	Time of prayer
Hours	Time of studying and reading
Evensong	Time of own profession
Compline	Time of charity work
Midnight	Time of irrevocable comfort (repose)

The nineteenth century is the first century of the Kairian measuring of time. In his calendar he used the ancient Greek numbering; so in the year $\mu\lambda$ of the Kairian chronology (corresponding to 1852) the "Compendium of Theosebian Doctrine and Ethics" was published in London. In this book, the doctrinal background of Theosebism and the Kairian calendar are described in detail. According to his ecclesiastical calendar, Kairis divided the 'night and day' -and not 'day and night'- into five periods "Times" of two hours (ten hours in total divided in 100 minutes and each minute in 100 seconds - Portaz, 1935, p. 220).

In his calendar, Kairis abolishes all Christian feasts (those of Jesus Christ, of the Holy Mother, of Saints, etc.). He also replaces Sunday -the day of the

Lord- with the 'Tithe' (the tenth day), i.e. since he does not accept the divine nature of Jesus Christ he abolishes also the day devoted to Him.

According to the principles of Theosebism, the believers, the God-pious people, were gathering at the middle of the four seasons of the year, beginning at the corresponding autumnal middle, celebrating the following: Entheogona, Entheagona, Entheobia and Entheondia.

All these -untranslatable- terms were invented by Kairis. Their meanings are difficult even in Greek and each one includes the word God (Theo, in Greek).

We conclude that Kairis created his calendar with the new chronology in order to use it in the religion or sect he introduced, in the ritual of which he adds new prayers, new hymns and a new worship, thus creating his own special theoretical and worshipping ritual, written in the ancient Dorian dialect.

Indeed, Kairis, among other things, being an admirer of the ancient Greek spirit, formulated in the ancient Doric dialect of the Greek language a fully operational hymnbook. He called the corresponding workers 'God's ministers' (Theagi). These Theagi or Hieragoi (Holy priests) were classified into five orders: Deans, Readers, Hymnodists, Preachers and Ministers.

Of course, this calendar, unknown to the international literature as far as we know, was never put in real use and became extinct with the death of its inventor, together with the Theosebism cult (Theodossiou et al., 2007, p. 117).

3 The Revolutionary Calendar of the Soviet Union ('Bolshevik calendar')

The last major attempt for a calendar reform took place in 1929 by the government of the Soviet Union (USSR), which adopted the Revolutionary calendar (or 'Bolshevik calendar').

To begin with, in 1918, the government formed after the October Revolution replaced the Julian calendar with the Gregorian one, thus actually harmonizing Russia with Western Europe from a calendar point of view; this is why the celebration of the anniversary of the 'October Revolution' was taking place on November 7 in the Soviet Union. However, the Russian Orthodox Church never accepted the Gregorian calendar.

Different, much more radical change occurred in 1929. The idea was to abolish Sunday as a rest day and to introduce a continuous production week (nepereryvka). So in production, from the autumn of 1929 until near the end of 1931, in parallel with Gregorian one, was introduced the calendar divided into 72 five-day weeks (=360 days), three of which were split into two partial weeks by five days of national holidays, but holidays were not a part of the week so that each split week still had also five days. Each day of the five-day week (pyatidnevka) was labeled by either one of five different colors or with a Roman numeral from I to V or with the the names The First (pervyj), The Second (vtoroj), The Third (tretij), The Fourth (chetvertyj) and the Fifth (pyatyj). In fact, each worker obtained a color or a number to identify his or her day of rest, so that every day, 80% of each factory's staff worked, while 20% were resting.

ТАБЕЛЬ-КАЛЕНДАРЬ НА 1931 ГОД.

	ЯНВАРЬ							ФЕВРАЛЬ							МАРТ							АПРЕЛЬ						
I день	1	6	11	16	21	27		1	6	11	16	21	26			3	8	13	18	23	28		2	7	12	17	22	27
II день	2	7	12	17	23	28		2	7	12	17	22	27			4	9	14	19	24	29		3	8	13	18	23	28
III день	3	8	13	18	24	29		3	8	13	18	23	28			5	10	15	20	25	30		4	9	14	19	24	29
IV день	4	9	14	19	25	30		4	9	14	19	24			1	6	11	16	21	26	31		5	10	15	20	25	30
V день	5	10	15	20	26	31		5	10	15	20	25			2	7	12	17	22	27		1	6	11	16	21	26	

	МАЙ							ИЮНЬ							ИЮЛЬ							АВГУСТ						
I день		4	9	14	19	24	29		3	8	13	18	23	28		3	8	13	18	23	28		2	7	12	17	22	27
II день		5	10	15	20	25	30		4	9	14	19	24	29		4	9	14	19	24	29		3	8	13	18	23	28
III день		6	11	16	21	26	31		5	10	15	20	25	30		5	10	15	20	25	30		4	9	14	19	24	29
IV день		7	12	17	22	27		1	6	11	16	21	26		1	6	11	16	21	26	31		5	10	15	20	25	30
V день	3	8	13	18	23	28		2	7	12	17	22	27		2	7	12	17	22	27		1	6	11	16	21	26	31

	СЕНТЯБРЬ							ОКТЯБРЬ							НОЯБРЬ							ДЕКАБРЬ						
I день	1	6	11	16	21	26		1	6	11	16	21	26	31		5	12	17	22	27			2	7	12	17	22	27
II день	2	7	12	17	22	27		2	7	12	17	22	27		1	6	13	18	23	28			3	8	13	18	23	28
III день	3	8	13	18	23	28		3	8	13	18	23	28		2	9	14	19	24	29			4	9	14	19	24	29
IV день	4	9	14	19	24	29		4	9	14	19	24	29		3	10	15	20	25	30			5	10	15	20	25	30
V день	5	10	15	20	25	30		5	10	15	20	25	30		4	11	16	21	26			1	6	11	16	21	26	31

ЯНВАРЬ. 22 — день 9 янв. 1905 г. и памяти вождя пролетар. В. И. Ленина.
МАЙ. 1-2 дни Интернац. **НОЯБРЬ 7-8** — дни праздн. Пролетарск. революции.

Fig. 5. Schema of Soviet pocket calendar for 1931. On Gregorian calendar are denoted days of five days continuous production week. Five non-working days, January 22 Day of memory on 9 January 1905, and Lenin, May 1-2, Days of International and November 7-8, Days of Proletarian Revolution are excluded (http://ru.wikipedia.org/wiki/Файл:Soviet_calendar_1931_pocket_2.jpg)

In 1930 was proposed the Soviet Revolutionary Calendar with 12 months of 30 days and five national holidays, not belonging to any month. It was rejected and never introduced but in many western sources is erroneously stated that the 72 five day weeks were organized in 12 months of 30 days, for example in Parry Albert (1940, "The Soviet calendar", *Journal of Calendar Reform* **10**, p. 68).

However, the attempt to change the week was unsuccessful, and on November 21st, Sovet Narodnykh Komissarov (Sovnarkom) SSSR replaced the five-day intervals with six-day intervals (shestidnevka), so that the year of 360 days consisted of 60 such intervals. This week was not with continuous production, but 6, 12, 18, 24, and 30 day of a month were the days of rest. At the end of February the last day was the day of rest or it was the 1st of March. In months with 31 days, the work on this day was assumed as a surplus and paid additionally. But neither system could take roots in the people's conscience. Therefore, in 1940 the Soviet government restored the use of the initial Gregorian calendar in factories and enterprises and the ancient seven-day week, with its Saturdays and Sundays. It is interesting as well that in addition to the Gregorian years, in some cases an additional date was given as e.g. in Fig. 6: *Twenty first year of the Socialist Revolution*, where

Fig. 6. From Soviet calendar for 1937 Translation of calendar page: Twenty first year of the Socialist Revolution / 1937 DECEMBER 1937 / 12 / sixth day of the six-day week / Day of elections to the Supreme Soviet of the USSR (http://ru.wikipedia.org/wiki/Файл::Revolution_kalendar.jpg)

this chronology was counted from the 7th November 1917. This was present until the disintegration of Soviet Union in 1991 (see e.g. Shcherbinin 2008, p. 58).

The Revolutionary Calendar of the Soviet Union ('Bolshevik calendar') is described in detail in our published paper: Theodossiou, E., Manimanis, V. N. and Danezis, E, 2002, "The Russians Calendars after the Christianization of the country", *JAAT* **21**, No. 1-3, June, pp. 149-153.

4 The Fascist calendar of Mussolini

The so-called 'Fascist calendar' appeared (and ended) in fascist Italy. However, it was not really a different calendar, but merely the setting of a new start for chronology, after the famous 'March towards Rome' of the 'black-shirted' fascists, on October 28, 1922, which brought Mussolini on power.

Actually, according to Marla Stone: *Using the French example, fascism retroactively restarted the calendar in 1927, making 28 October 1922, the first day of the first year of the new calendar I.I.I. Fascism declared it would re-*

Fig. 7. Plate at the Stock exchange in Milano with date according to fascist calendar. Photo of Giovanni Dall'Orto.

place old allegiances and collective history. In this way, 'fascistization' was inextricably bound to 'nationalization' (1993, p. 230).

So, the Fascist calendar started on 28 October 1922. The date in the Fascist Era was written in Roman numerals. Thus, beginning in November, the year 1922-1923 was set as fascist year I (or year I *"di era fascista"* - of the Fascist Age). This year was written in Italian diaries *together* with the normal year A.D.: next to the Christian year there was a Roman numeral indicating the corresponding fascist year. For example, the day of Italy's war declaration against Greece was written as: 28 October 1940 - XIX (the number 19 written as a Roman numeral).

According to Mark Antliff: *The most dramatic instance of such social engineering was the 'superimposition over the Gregorian Calendar' of a fascist time frame, in which 1922 became 'Year I' of the fascist era, signaling a regenerative break from the plutocratic decadence of the immediate past. The new calendar was then punctuated with certain days of national celebration, each with a 'two fold mythical significance'. Thus March 23, Youth Day, commemorated the founding of Fasci; April 21, Labour Day, the founding of Rome; May 24, Empire Day, the entry of Italy into the First World War; September 20, Italian Unity, the incorporation of Rome into the Kingdom of Italy; October 28, the fascist Revolution, the March of Rome... In this way ordinary Italians were encouraged to experience the unfolding of time as a phenomenon*

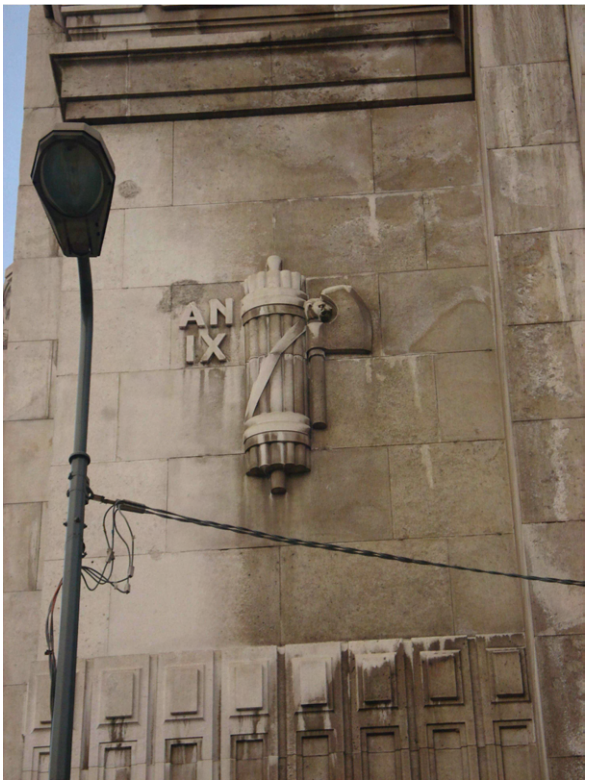

Fig. 8. Year IX of fascist era on the Milano central railway station. Photo of Giovanni Dall'Orto.

with a transcendental core on a par with metaphysical reality which underlay Christianity (2004, pp. 149-150).

The year 1922 (October) to 1923 was considered the fascist year 1 - with Latin digits: I. It was part of a date that was functioning in parallel with the Gregorian calendar in all fascist documents and other printed material. For example, the first of May of 1934 AD was accompanied by the fascist year XII, while December 25, 1938, was accompanied by the fascist year XVII, since December is after October and thus the fascist year had changed. As it should be expected, the overthrowing of the fascist regime in Italy brought with it the abolishment of this trivial calendar change.

5 The calendar of Metaxas dictatorship in Greece

It is interesting to note that Mussolini's chronology was imitated in Greece by the Ioannis Metaxas dictatorship (1936-1940), considering in turn 1936, the year of its start, as 'year A'', written with Greek numeral. In all official

papers of the Greek dictatorship there were two chronologies: the Christian year AD and the corresponding year of the dictatorship. For example, the day of Italy's war declaration against Greece was written as: 28 October 1940 - year E'.

ΠΡΩΤΗ ΔΙΑΣΚΕΨΙΣ

ΠΡΑΚΤΙΚΑ ΣΥΝΕΔΡΙΑΣΕΩΝ

Fig. 9. The proceedings of the First Conference of Regional Administrators of the National Youth Organization of 1939, where the year Delta (Δ') of the Metaxas dictatorship appears.

Needless to say, this way of year enumeration died together with the respective regimes. Moreover, this action of the dictatorship is virtually unknown to modern Greek society. It is not mentioned and has not been recorded anywhere, with the exception of certain official documents and state archives from that period, such as the proceedings of the First Conference of Regional Administrators of the National Youth Organization of 1939, year Delta (Δ'), from where we learned about it.

6 The New Rectified Julian calendar of the Orthodox Churches

Patriarch Meletios IV (1922-1923), head of the Orthodox Churches, convened an Ecumenical Congress in Constantinople in May 1923, where one of the principal topics of discussion was the reform of the Julian calendar. In the Serbian delegation were Gavrilo Dožić and Milutin Milanković. At that time, Dožić was the Metropolitan of Crna Gora and Primorje (Montenegro and the Littoral), and later become Patriarch of the Serbian Orthodox Church. Milutin Milanković (Dalj, May 28, 1879-Belgrade, December 12, 1958) is worldwide known for his groundbreaking work on the causal relationship of solar heating to the phenomenon of the occurrence of the Ice Ages in Europe during

the Quaternary Period. He developed an astronomical theory for the evolution of planetary climates and explained the phenomenon of the Earth's Ice Ages and polar motion.

Milutin Milanković, was the vice president of the Serbian Academy of Sciences and Arts and director of the Belgrade Astronomical Observatory (1948-1951). To honor to his scientific achievements in astronomy, a crater on the far side of the Moon (coordinates $+170^o$, $+77^o$) was given his name at the 14th I.A.U. General Assembly in Brighton in 1970. His name was also given to a crater on Mars (coordinates $+147^o$, $+55^o$) at the 15th I.A.U. General Assembly in Sidney in 1973. In 1982, a small planet, discovered in 1930 by Milorad Protić and Pero Djurković and provisionally designated 1936 GA, received its permanent name: 1605 Milanković (Dimitrijević, 2002).

At the Ecumenical Congress representatives of Serbian and Romanian Orthodox Churches submitted two elaborate propositions (detailed description of the calendar reform and of the Pan Orthodox Congress in Constantinople is given in Milanković 1923, 1995, 1997, see also Dimitrijević 2002, Dimitrijević, Theodossiou 2002, Dimitrijević, Theodossiou, Mantarakis, 2008). The proposition of Serbian delegation, formulated by Maksim Trpković, was to introduce the intercalation rule that the secular years in centuries which when divided by 9 have remainders of 0 or 4 will be leap years. Consequently, 7 days will be omitted from 9 centuries, and the calendar will be closer to the tropical year than the Gregorian one, where the intercalation rule is that leap years are only secular years where the number of centuries is divisible by four. Moreover, the vernal equinox will always fall on March 21 or very close to it.

The Romanian delegation consisted of Archimandrite Julius Scriban and Senator Dragici. They came with the following proposal for calendar reform (Milanković 1923, 1997, Trajkovska, Ninković 2008): Each year is to have 364 days (exactly 52 weeks) so that every date has a fixed day in the week. March, June, September and December have 31 days, and other months 30 days. An additional week is added every 5 years between June 31 and July 1, whose number of days corrects the difference with the tropical year. The first day of Easter is fixed at April 29, and all other holidays become fixed. This proposition was presented to the Congress by Senator Dragici, but he told to Milanković that the author was actually baron Gustav Bedeus from Sibiu, who was not an Orthodox Christian so that it is not convenient to put his name on the proposal. However, according to investigations of Trajkovska and Ninković (2008), "A Resolution Concept for Conference of the Calendar of Orthodox Churches in Constantinople on May 1, 1923", published in German by Bedeus in *Siebenbuergisch-Deutschen Tagesblatt* (Daily of Germans from Siebenburger - Seven towns or Transilvania in Romanian) differs from the proposition of Senator Dragici.

Congress rejected both propositions. The Serbian, authored by Trpković, since the year 2000 would not be a leap one as in the Gregorian calendar, and after only 77 years a difference of one day between the Gregorian and New Rectified Julian calendars would appear. The Congress concluded that the better solution is to delete thirteen days in Julian calendar in order to put it into line with Gregorian one, until 2100, when the one-day difference would appear.

Milutin Milanković obtained the task to develop a new proposal. He concluded that the wish of the majority of participants was that calendar of the Eastern Orthodox Church should not be identical with the Gregorian one, but that the two should parallel one another as far as possible. Consequently, instead to try to fix the date of the vernal equinox to March 21st, as in the Trpković's proposal, he tried to obtain the longest possible consonance of the two calendars. He elaborated a new intercalation rule, that secular years are leap years only provided that the number of centuries they belong to, when divided by 9 yields the remainder 2 or 6. In such a way the new calendar is more precise than the Gregorian one but consistent with it up to 2800, i.e. for 877 years after the Ecumenical Congress in Constantinople. Another advantage is that New Rectified Julian calendar of Orthodox Church will be in better agreement with nature than Gregorian calendar. A disagreement of one day with the tropical year will accumulate after almost 30,000 years!

Milanković presented to the Congress his new proposal signed by him and Gavrilo Dožić, as the new proposition of the Serbian Orthodox Church, on the session of May 23, 1923. In his historic speech to the Congress, he told the delegates that if they only adopted to delete 13 days from Julian calendar, the Orthodox Church would be in an inferior position in any future discussion on the calendar question. With the proposition of the Serbian delegation, the Orthodox Church could confidently enter into any negotiation on the calendar question with Western Churches since they would have the most precise and most scientific calendar in the Christian world. He underlined also that with such a decision, the Orthodox Church would not be accepting the calendar of the Roman-Catholic Church, but would be obtaining a better one.

Also at the Congress, Anthimos Metropolitan of Viziys proposed to determine the exact date of Easter by astronomical methods with the help of Observatories and Universities in Athens, Belgrade, Bucharest and Pulkovo.

Milutin Milanković formulated the final version of the calendar reform that was adopted by the Congress, and signed on June 8th, 1923, by Patriarch Meletios IV, Metropolitan of Kyzikos, Kalinikos, Archbishop of North America, Alexander, Metropolitan of Montenegro and Littoral Gavrilo Dožić, Metropolitan of Nicaea, Vasilios, Metropolitan of Durachion, Jakub, Archimandrite Julius Scriban, and Professors E. Antoniadis and Milutin Milanković.

The date of the official inception of the New Julian calendar was originally set for October 1st, 1923, which will become October 14th, in order to omit the 13 days of difference between Julian calendar and Tropical year. This was the date when the calendar reform would be introduced in the Ecumenical Patriarchate and in the Greek Churches, but without the part concerning the Easter determination, where the old Julian calendar was retained, until all Orthodox Churches introduce the reform. Today, Patriarchates of Constantinople, Alexandria and Antioch, Churches of Greece, Cyprus, Romania, Poland, Finland, Bulgaria (from 1968) and Orthodox Church in America (September 1, 1983, see e.g. http://www.holy-trinity.org/modern/calen2.html) use the "New", "Revised" or "Rectified" Julian calendar. On the other hand, the Patriarchate of Jerusalem, and Churches of Russia and Serbia, along with the monasteries on Mt. Athos, all continue to adhere to the Julian or Old Calendar (see e.g. http://www.yalchicago.org/paschacalculation.html).

7 Conclusions

From these six calendar systems that were devised from the late 18th to the middle of the 20th century, survived up to now only New Julian calendar of Orthodox Churches. This should be expected, since history History has shown that calendar changes are accepted with great difficulty by the people, who do not want to change calendar they are used to and the social and religious habits that are associated with it. Even in the case of New Julian Calendar, which dates are at that moment identical with Gregorian one, and only dates of movable eclesiastic feasts are changed, the great resistance against it exist. In Orthodox Churches which accepted it, sects of Old calendarians, refusing its usage, were created.

From these 6 calendar systems, which were devised centuries after the Gregorian calendar, the most discussed about in the international literature is the French Revolutionary Calendar (*Le Calendrier Républicain*), since it is associated with the famous French Revolution of 1789, which still moves and influences European thought.

About New Julian Calendar was also written, in particular in Orthodox sources. Then comes the Revolutionary Calendar of the Soviet Union ('Bolshevik calendar'), interwoven with a special period of the Soviet history, while the Theosebic calendar of Th. Kairis is totally unknown internationally, since only a few scholars or astronomers know about it in Greece.

Mussolini's Fascist calendar is mentioned in the international literature, but both it and the totally unheard of calendar of Metaxas dictatorship in Greece are not separate calendar systems; they are rather a parallel writing of the years next to the Gregorian calendar date that denoted the length of these dictatorships, while in the case of Mussolini's Fascist calendar some important holidays are also mentioned. They essentially represented, as professor Sterios Fassoulakis of the University of Athens writes, calendar systems of political ideology (Istorica, 2001).

These cases strengthen the conclusion that it is difficult for a calendar reform to prevail or even to survive for long. If they are not accepted by several states, Church or some organization existing in a number of different communities, the end of regime which implemented them is usually also the end of such calendar systems

Acknowledgements

This study formed part of the research at the University of Athens, Department of Astrophysics Astronomy and Mechanics, and we are grateful to the University of Athens for financial support through the Special Account for Research Grants. It is also supported by the Ministry of Science and Technological Development of Serbia through the project III44002.

References

Antliff Mark: 2004, Fascism, modernism and modernity, in R. Griffin & M. Feldman (Ed.), *Fascism: Critical concepts in Political Science.* Routledge, New York, pp. 149-150.

Dimitrijević, M. S.: 2002, Milutin Milanković (1879-1958) and his contribution to European astronomy, *Astronomische Nachrichten*, **323**, 570-573.
Dimitrijević, M. S., Theodossiou, E.: 2002, The calendar of the Greek Orthodox Church, *Astronomical and Astrophysical Transactions*, **21**, 145-148.
Dimitrijević, M. S., Theodossiou, E. Th., Mantarakis, P. Z.: 2008, Milutin Milanković and the reform of the Julian Calendar in 1923, *J. Astron. History and Heritage*, **11**, 50-54.
Fassoulakis Sterios: 2001, Calendars of political ideology, *Istorika*, **64**, January 4, 2001, 48-49.
Flammarion Camille: 1955, *Astronomie Populaire*, Édition Entièrement Refaite, G.C. Flammarion, Paris.
Le Calendrier Républicain: 1994, Bureau des Longitudes, Paris, p. 19.
Milanković, M.: 1923, *The reform of the Julian Calendar*, Serbian Royal Academy of Sciences and Arts, Special editions No 47, Natural and Mathematical Sciences No 11 [in Serbian].
Milanković, M.: 1997, *Memories, experiences, cognition*, Selected works of Milutin Milanković, No 7, Zavod za udžbenike i nastavna sredstva, Beograd [in Serbian].
Milanković, V.: 1995, *Milutin Milanković 1879-1958*, European Geophysical Society, Katlenburg - Lindau.
Parry Albert: 1940, The Soviet calendar, *Journal of Calendar Reform* **10**, p. 68.
Polemis, D. P.: 1994-1996, *Allilografia Theofilou Kairi*, 3 volumes, Kairios Vivliothiki Publ., Andros [in Greek].
Portaz Maximine: 1935, *Essai critique sur Theóphilos Kaíris*, Paquet, Lyon, p. 220.
Renouard, Antoine Augustin: 1822, *Manuel pour la concordance des calendriers républicain et grégorien: ou, Recueil complet de tous les annuaires depuis la première année républicaine* (2 ed.).
Shcherbinin, A. I.: 2008, "The red day in the calendar": The formation of the political time perception matrix in Russia, p. 58 [in Russian], *Vestnik Tomskogo Gosudarstvennogo Universiteta, Filosofiya, Sociologiya, Politologiya*, No 2(3), pp. 52-69.
Stone Marla: 1993, Staging Fascism: The Exbition of the Fascist Revolution, *Journal of Contemporary History*, **28**, No. 2. April, by Sage Publications, Ltd.
Theodossiou, E. and Danezis, E.: 1996, *The Odyssey of the Calendars*, Diavlos Publications, Athens [in Greek].
Theodossiou, E. and Danezis, E.: 2000, *In the traces of ICHTYS: Astronomy, History and Philosophy*, Diavlos Publications, Athens [in Greek].
Theodossiou, E., Manimanis, V. N. and Danezis, E.: 2002, The Russian Calendars after the Christianization of the country, *Journal of the Astronomical and Astrophysical Transactions*, **21**, pp. 149-153.
Theodossiou, E., Grammenos, Th. and Manimanis, V. N.: 2004, Theophilos Kairis: The Creator and Initiator of Theosebism in Greece, *The European Legacy*, **9**, pp. 783-797.
Theodossiou, E., Danezis, E, Katsiotis, M. and Mantarakis, P.: 2007, Theophilos Kairis: The Initiator of Theosevism in Greece, *Aeropos*, February, September-October, **75**, pp. 104-117 [in Greek].
Theophilos Kairis, Code 53, Library of the Historical and Theological Society, as in Issue 65 the text 'Correspondence of months' [s.d.].
Trajkovska, V., Ninković, S.: 2008, On a resolution concept concerning the calendar reform submitted to Pan-Orthodox Congress in Constantinople in 1923, *Publ. Astron. Obs. Belgrade*, **85**, pp. 189-194.
Wilson P. W.: 1937, *The Romance of the calendars*, W.W. Norton, New York.

The heliocentric system from the Orphic Hymns and the Pythagoreans to emperor Julian

Efstratios Theodossiou[1], Aris Dacanalis[1],
Milan S. Dimitrijević, Petros Mantarakis[3]
[1] Department of Astrophysics, Astronomy and Mechanics Physics Faculty, University of Athens-Zografos 157 84
[2] Astronomical Observatory, Volgina 7, 11060 Belgrade, Serbia
[3] 322127 Needles, Street, Chatsworth, California 91311, USA
etheodos@phys.uoa.gr
mdimitrijevic@aob.bg.ac.yu
zanispetros@socal.rr.com
(Research report. Accepted on 21.10.2008)

Abstract. The evolution of the heliocentric theory in the antiquity has been analyzed, from the first seeds in the Orphic Hymns to the emperor Julian, also called "the Apostate" in the 4th century A.D. In particular the Orphic Hymns, views of Pythagoreans, as well as the heliocentric ideas of Philolaus of Croton, Icetas, Ecphantus, Heraclides of Pontos, Anaximander, Seleucus of Seleucia, Aristarchus of Samos and Emperor Julian were analyzed.
Key words: Heliocentric system, Orphic Hymns, Pythagoreans, Philolaus, Anaximander, Aristarchus, Emperor Julian

Хелиоцентричната система от орфическите химни и питагорейците до император Юлиан

Е. Теодосиу, А. Даканалис, М. Димитрийевич, Р. Мантаракис

Проследено е развитието на хелиоцентричната теория в античността, от орфическипе химни до император Юлиан, наричан в IV в сл.н.е. още "изменникът". Анализирани са, в частност, орфическите химни, възгледите на питагорейците, както и хелиоцентричните идеи на Филолаус от Кротон, Икетас, Екфантус, Хераклидес от Понтос, Анаксимандер, Селеукус от Селеуциа, Аристархус от Самос и император Юлиан.

Introduction

Ever since early antiquity, philosophers and astronomers had been preoccupied with the question concerning which of the heavenly bodies occupied the center of the known world. The geocentric system, in accordance with its egocentric formulation, placed our small planet in the center of the world, a notion that seemed to fit the egocentric minds of the wise. Enjoying the favor of the majority of the philosophers and astronomers, it dominated for centuries. However, there were also opposite views in favor of the heliocentric theory. Indeed, even before Aristarchus the Samian, seeds of the heliocentric theory can be traced back to the Orphic Hymns and in the teachings of Anaximander and the Pythagoreans. Later on Aristarchus the Samian founded the heliocentric theory, which unfortunately did not prevail, unlike its geocentric adversary which gained wide recognition, initially due to the weight of Aristotle's views, and later on due to those of the great astronomer Claudius Ptolemy (2nd century A.D.).

Yet the heliocentric system had not been entirely forsaken. During the 4th century A.D., emperor Julian -also called "the Apostate"-, the last emperor of the first Byzantine dynasty, became a fervent supporter. Julian held the Earth as a planet which, like all other planets, went around the sun in a circular orbit. Thus, Aristarchus' theory had not been forgotten during the first centuries A.D., but even enjoyed advocacy.

1 Orphic Hymns

The ancient teachings of Orpheus are considered to be the first mystic Greek religion, with poems and hymns of great beauty. The Orphic Hymns consist of 87 hexametric poems or 1200 verses in total, which have reached us under the title "*Hymns of Orpheus to Musaeus*".

The hymns contain a breadth of astronomical information, partly obscured by the use of a strongly poetic language, as well as interesting ideas for the creation and the supreme being. This last piece of information tells us that the hymns belong to a monotheistic cult, since the creation of the Universe is ascribed to a single supreme force. We also come across the interesting notions of Chaos and the cosmic egg, which led to the creation of "Phanes", he who is radiant and existent.

From eyes obscure thou wip'st the gloom of night, all-spreading splendour,
pure and holy light. Hence Phanes call'd, the glory of the sky,
on waving pinions thro' the world you fly.
[V. TO PROTOGONUS, *The Fumigation from Myrrh*, verse 15
(see e.g. *Orphic Hymns* sine datum, or *Orphicorum Fragmenta*, 1922)]

Nearly all of the ancient Greek sages and writers drew inspiration from themes found in the Orphic Hymns, and were thus influenced while formulating their unique theories and teachings.

Let it be noted that in the Orphic Hymns, "Chaos" stands for what nowadays we would call space, "Gaia" for the earth-mother (and not the planet) whereas "Eros" (love), stands for the creational force. In the same hymn, we find a praise to Chaos which spans the aether, and was born from the cosmic egg:

O Mighty first-begotten [Protogonos], hear my pray'r, two-fold, egg-born, and
wand'ring thro' the aether...
[V. TO PROTOGONUS, *The Fumigation from Myrrh*, verse 1]

Let it also be noted that during the Homeric times, the Earth was perceived as a circular flat disk which was surrounded by a vast circular river, the Ocean. This notion is made evident in the following verse:

Old Ocean [Okeanos] too reveres thy high command, whose liquid arms
begirt the solid land.
[X. TO PAN, *The Fumigation from Various Odors*, verse 15]

Fig. 1. Phanes: God of light, truth and justice. Here he appears to be surrounded by an elliptical (egg-shaped) ecliptic with the zodiacal signs of the four basic elements. Above and below him are the two halves of the cosmic egg, and between them, lies a flaming Phanes, winged just like the creative Eros. In his right hand he holds thunder (like Zeus does) and a scepter in his left, signifying his kingly place on the world. The curled snake on him symbolizes the Earth, the cup stands for water, the wings for air and the torch for fire. Its legs are shaped like a fork, just like those of the god Pan.

The hymns mention Heaven being the ruler of the world, revolving around the Earth:

Great Heav'n [Ouranos], whose mighty frame no respite knows... Hear, world ruler,..., forever whirling as a sphere around this earth
[III. TO HEAVEN: *The Fumigation from Frankincense*, verse 1]

Fig. 2. The Homeric Universe: In the Universe of Homer's times, the mountains can be seen to rise over the surface of the great disk of the Earth, the Ocean spreading around them, while the center is dominated by Mount Olympus which rises up to heaven. In its highest peak, the all-seeing Zeus is seated, supervising both immortal gods and mortal men, sometimes rewarding and sometimes punishing them. Beyond Olympus spreads Heaven, supported by the pillars of Atlas. In heaven we can locate the Moon, the stars and the constellations. In particular, in this figure we can distinguish -but not referred by Homer- the constellations of Hydra, Corvus, Crater, Cancer, Leo, Gemini, Taurus as well as the Pleiades open cluster (as cited in D. Cotsakis, 1976, p. 18)

Another verse suggests that the origins of the heliocentric system seem to be located in the Orphic Hymns, as has been previously stressed by Constantinos Chassapis (1967), the late Greek astronomer, and Maria Papathanassiou (1978, 1980), assistant professor in the Mathematics Faculty at the University of Athens:

Hear golden Titan! Glowing like gold, you who strides above, oh heavenly light...
... you who combines the epochs ... You are the world ruler...
With your golden lyre, draw on the harmonious path of the world...
... [you] who wanders through fire and moves around in a circle
[VIII. *To the Sun*, verse 2]

The phrase "[you who attracts] *draw on the harmonious path of the world*" is striking since this could be a spermatic idea of the harmonious movement of the planets around the Sun, a notion which was commonly used during at least the first five (perhaps more) centuries B.C. If the planets are to be included in the notion of the world, then the golden Sun could be seen as

the attractive center of their harmonious orbits. One may therefore make the assumption that the seeds of a heliocentric theory can be traced in the Orphic Hymns.

Furthermore, on hymn (34): To Apollo, we find the following:

Loxias, the pure! . . . You mixed in equal parts winter and summer. . .
[XXXIV. *To Apollo*, verse 6,. . . and 20]

Thus, the "Loxias" Sun (meaning "tilted") mixed the components of the year and divided it in two equal parts, the summer and the winter. This is a very important astronomical detail which has drawn some attention from the astronomical community, because it has been linked to the dating of the Orphic Hymns. If one were to view this information literally, he would look back in time when the summer and winter were of exactly equal length. This would place the Orphic Hymns -more or less- near the following dates: 1841 B.C. and 1366 B.C. (Chassapis, 1967 and Papathanassiou, 2003). This view however, requires the assumption that ancient Greece possessed very capable astronomers in early antiquity, an idea with little evidence to support it.

Another excerpt which, although referring to Hestia, seems to add to the heliocentric aspect of the hymns, is Hymn (84) [To Hestia]

You who occupies the center of the home of the greatest and eternal fire.
[LXXXIV. To Hestia, verse 2]

In *Orphicorum Fragmenta* a fragment tell us about the rotation of the Earth. This fragment says that Musaeus knew the path of the star and the movement of the sphere around the Earth, as this round Earth revolves in equal time period around its axis (Fr. 247 v. 24-26, pp. 261-262).

2 The Pythagoreans

Pythagoras founded his School at Croton in lower Italy, in c.540 B.C. He and his followers held the view that the most important cosmological principle were the numbers. In a way they were not mistaken, since it is in numbers that today's scientific thought is focused, for numbers identify with mathematical harmony and, without them, science would have never existed in the first place.

The Pythagorean School placed the foundations for the philosophy of mathematics as well as for physics, by relating order and the harmony of sound to the harmony of the Universe.

Virtually all of the students of Pythagoras were trained in astronomy, but their studies of the motion and the distances of the planets were carried out with a rather mystical approach. They believed in mystical and sacred relations between the numbers and the phenomena that they describe. In the Pythagorean view, the planetary distances were analogous to a heavenly musical harmony, which was created by harmonious sounds. They believed that this harmony was constantly created, being an eternal expression -of the highest order- of the unique divine harmony.

The Pythagoreans would have been delighted to see ideas very similar to their own, used in contemporary science. For example, modern String theory holds that everything on a microscopic level is a combination of vibrating strings. The Pythagoreans, developers of the "music and harmony of the spheres", would have seen particles as microscopic strings whose rhythmical vibrations create other particles, i.e. "the musical notes". These notes, in turn, create the music of the heavenly spheres. Thus though their eyes, our whole world would seem like a musical symphony, composed with these notes.

Pythagoras' School was a brotherhood, most likely in an almost religious sense, had various degrees of initiation, and may have been founded after the manner of the Orphic communities. Its contribution to geometry, music, arithmetic and astronomy was integral for the evolution of scientific thought. Through geometry, as well as the harmony of sound and numbers, the Pythagoreans developed the notion of perfection in the Universe, and coined an appropriate word to describe it: "Cosmos". This name is derived either from the word "cosmo" which means "to orderly arrange" or from the world "cosmema" which means "jewel" (ornament). Pythagoras himself appears to be the first to use the word "Cosmos", according to the doxographer Aetius: "*Pythagoras was the first to name the place of all things Cosmos, due to its orderly nature*" [Aetius, *De Vestutis Placitis*, II, 1, 1 (D. 327, 8)]

The Pythagorean School held that the essence of all things was the "number", a rather abstract notion, which could not be perceived through one's senses, but only through intellect. In this manner, the philosophers of this school equated infinity with those material elements which could not be subject to measurement or definition. They introduced the notion of "matter", which was perceived as an element that resisted every definition of its ontological and moral imperfection.

Some elements of the Pythagorean cosmology have reached us through one of Aristotle's books, namely *Metaphysics*. According to the Pythagoreans, the Cosmos was created after the "One" initially came into being. The "one" -or "en" in Greek- served as the first principle, attracted the "infinite" (apeiron) to its own self, and bestowed on it with the "limit" (peras). These last two notions, the "limit" and the "infinite" have no clear meaning, but it has been speculated that they could be referring to the prime and even numbers.

Aristotle also mentions the following: "*The elements of number, according to them, are the Even and the Odd. Of these the former is limited and the latter unlimited; Unity consists of both (since it is both odd and even) [note of trans: either because by addition it makes odd numbers even and even numbers odd (Alexander, Theo Smyrnaeus) or because it was regarded as the principle of both odd and even numbers (Heath)]. Number is derived from Unity; and numbers, as we have said, compose the whole sensible universe*" [Aristotle, *Metaphysics*, A5, 986, 15]

Aristotle provides us with a further comment on the Pythagorean ideas: "*It is absurd also, or rather it is one of the impossibilities of this theory, to introduce generation of things which are eternal. There is no reason to doubt whether the Pythagoreans do or do not introduce it; for they clearly state that when the One had been constituted -whether out of planes of superficies or seed or of something that they cannot explain- immediately the nearest part of the Infinite began to be drawn in and limited by the Limit [note of trans:*

if numbers are eternal, it is absurd that they should be generated]. [Aristotle, *Metaphysics*, 1091a, 14].

Another cosmological notion that the Pythagorean School of thought held was that the Creation began from a unique single point, which continuously expanded to infinity. It is evident that the Pythagoreans believed that the Universe evolved from a spherically expanding infinitesimal core. This idea once again, has been shared by some astronomers, who believe in a static spherical universe whose existence began from an initial point.

Another idea that Pythagoras believed in was that the Earth was spherical and immobile in the center of the Cosmos, which was spherical as well. "*..the water, earth and air; these elements interchange and turn into one another completely and combine to produce a universe animate, intelligent, spherical, with the earth at its center, the earth itself too being spherical and inhabited round about*" [Diogenes Laertius, *Lives of Eminent Philosophers*, VIII, 25, 8-10].

Many Pythagoreans held an identical view of a spherical Earth, placed in the center of the world, *without being supported by anything.* This was a novel idea in its time, and is demonstrative of a clear progress when compared to assumptions that were previously held by other Greek philosophers.

According to the late professor of astronomy, Demetrios Kotsakis, "Pythagoras was the first who taught that the apparent motion of the sun on the celestial sphere from the east to the west, could be analyzed in to two distinct motions: One daily from East to West, parallel to the equator, and one yearly from West to East on the ecliptic" (Kotsakis, 1976, p. 28).

In the 6tth century B.C., some students and followers of Pythagoras, and most importantly Philolaus of Croton, Heraclides of Pontus, Ecphantus of Syracuse as well as others, believed in a "pyrocentric" theory. This means that they accepted that the element of fire was the "first principle" of the Cosmos. They believed that after the Creation, the element of fire accumulated in the center of the Cosmos and its attraction to its neighboring parts was part of the creation, formation and formulation of the various bodies that made up the spherical Universe.

2.1 The ideas of Philolaus of Croton

Philolaus of Croton (450-500 B.C.), spread the pythagorean ideas concerning the "first principle", by organizing and writing a synopsis of pythagorean philosophy. It appears that he was the principle creator of the philosophical notions of the "limit", the "infinite" and the harmony between the two, which, according to his views, was achieved due to the "number". He believed that the Cosmos is unique and began its creation from the center, which was occupied by fire. There, he placed the "Anticthon", (or Counter-earth - a hypothetical invisible Earth), the Earth, the Moon, the Sun, the five planets known at the time (Mercury, Venus, Mars, Jupiter and Saturn), and the sphere of the fixed stars. Thus, ten heavenly bodies "danced" around the central fire, a number which the Pythagoreans held as sacred. It has been speculated that the Anticthon was introduced exactly for this reason, namely to raise the number of the celestial bodies to the sacred number ten.

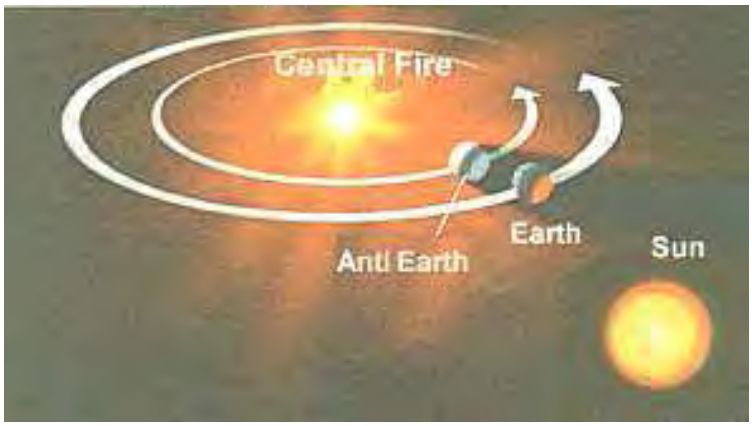

Fig. 3. Pythagorean Universe

It is told that Philolaus of Croton, along with Archippus, Lysis and few others, survived the revolt against the Pythagoreans in Croton, which was instigated by Cylon, an ex student of Pythagoras, who had been sent off from the school for failing to comply with its principles. It is certain that the teachings of Pythagoras and his students, their innovative theories, their mysticism, as well as their aristocratic political tendencies caused the violent reaction of their democratic adversaries, who either killed or exiled many of them: "*Cylon of Croton... and those allied with him, hunted (killed) the Pythagoreans down to the man.* (Iamblichus *Vita Pythagorii* (V.P.) 248-249 ff).

Following this course of events, Philolaus left Croton and based himself in Thebes, where he taught Pythagorean philosophy and wrote the books *Bachae* and *On Nature* A, B and C (Cosmos, Nature and Soul respectively). An extant fragment from his first book reads: "*The world is uniform, it began its creation from the center, and from the center it expanded uniformly upwards and downwards, keeping equal distances from the center*" (Diels and Kranz, 1996, *Die Fragmente der Vorsokratiker*).

Several sources provide information on some of his cosmological thoughts: *The initial One, the beginning of the creation of the Universe, is called Hestia* [*On Nature*, fragment 7, Stobaei *Eclogae* I 21, 8 (p. 189, 17 W)].

Diogenes Laertius mentions: *According to Demetrius, in his work "on men of the same name", Philolaus was the first to publish pythagorean treatises, to which he gave the title "On Nature", beginning as follows: Nature in the ordered universe was composed of unlimited and limiting elements, and so was the whole universe and all that is therein* [Diogenes Laertius, *Lives of Eminent Philosophers*, 85 (A1 I 398, 20)].

The doxographer Aetius (Aet. I 3, 10), informs us (citing Theophrastus) of the following: *Philolaus believes that there is fire around the center of the Universe, which he calls "hestia of all" and "house of Zeus", "mother*

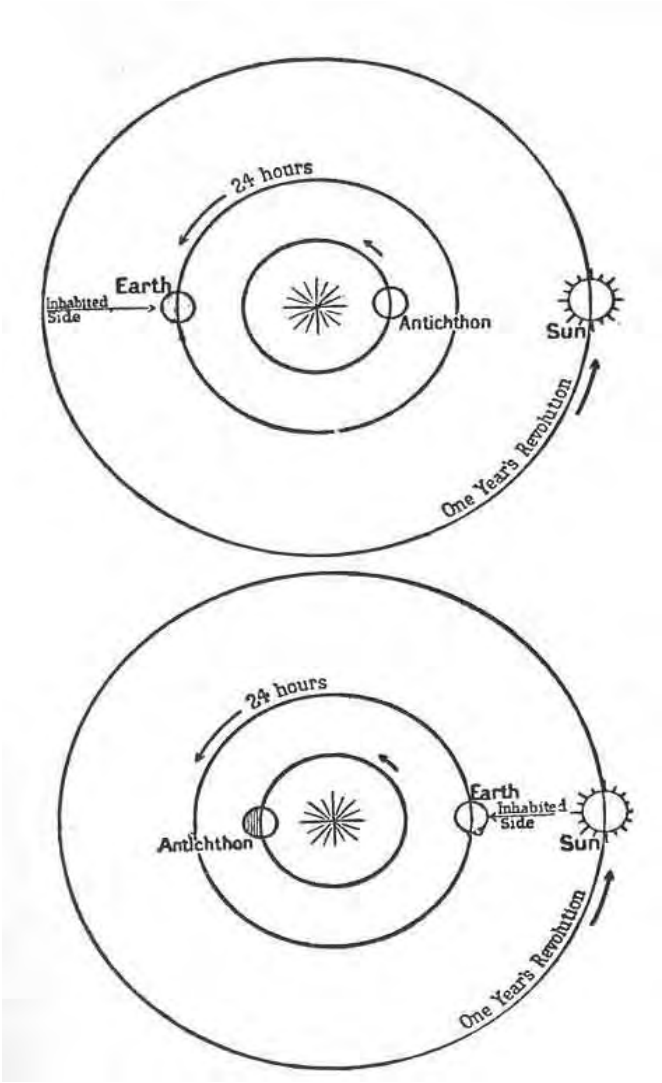

Fig. 4. Antichthon: The hypothetical invisible Earth, which according to the Pythagoreans occupied the antipodes of the Earth.

of the Gods", "altar, constraint and measure of nature". There is another fire which dwells in the outer region of the Universe. The center, he says, came first by nature, and around it dance ten heavenly bodies: The sphere of

fixed stars, then the five planets, then the Sun, then the Moon, followed by the Earth and Anticthon, and after all these the fire of "hestia", which lies around the center. The outer region, which surrounds the whole Universe, is a place where the elements are in their pure state, unmixed, and that place he calls "Olympus". All that lies beneath Olympus, namely the part where the five planets along with the Sun and the Moon lie, he calls "cosmos", while the area beneath those, the sublunar space ... he calls "heaven". Wisdom is relevant with the order which holds in the heavenly bodes, while virtue is relevant with the disorder of the things which are subject to birth. The first is perfect while the second is imperfect. [Aet. *De Vestutis Placitis*, II 7, 7 (D. 336, vermutlich Theophrast. im Poseidonios-Excerpt)].

The above are mentioned once again by Aetius: *The Pythagorean Philolaus places the fire in the center (for it is the Universe's focal point), secondly he places the Anticthon, then, our habitat, the Earth comes third, placed opposite [from the Antictchon] and moving in a circle, that being the reason for the beings of the Anticthon being invisible to the beings of the Earth. The ruling power of the Universe lies in the central fire, which God placed, like a keel, to base the foundation of the sphere that makes up the world".* [Aet. III 11, 3 (D. 337 from Theophrastus)].

¿From all of the above we can sum up that, according to Philolaus, everything in "Olympus" and the "Cosmos" never changed, while in the areas up to the Moon, every being gifted with life was born, changed and finally died. The Earth and all the other planets were rotating around Hestia with the same direction but at different levels and with different speeds. Hestia was invisible because it shed its light to the antipodes of the Earth, which were impossible to get to. The Sun did not have its own light, but accepted and accumulated the sun of Hestia.

Philolaus, through his questioning of the traditional geocentric cosmology, set the foreground for Aristarchus' heliocentric theory, which would clearly dispute the central role of our small planet in the Universe. Even though he did not specifically place the Sun in the center, the idea of the "central fire" certainly served as a basis for the heliocentric theory. Stavros Plakides (1983-1990), a late Greek professor of Astronomy at the University of Athens, speculated that Philolaus, after having experienced the violence in southern Italy, avoided placing the Sun in the center of the Universe. Fear for his life may have been the motive for adopting the milder approach of placing the "central fire" instead (Plakides, 1974).

Diogenes Laertius, an important source from which we draw the views of Philolaus, mentions that opinions were divided as to who claimed first that the Earth is indeed moving: *It is told that he [Philolaus] was the first to claim that the Earth moves in a circle, while others ascribe it to Icetas of Syracuse* [Diog. Laert. *Lives of Eminent Philosophers* VIII, 84, 85)].

Aetius, another source, informs us that concerning the motion of the Earth Philolaus taught the following: *Others believe that the Earth is immobile. Philolaus on the contrary, believes that the earth is moving in a circle around the fire, tracing a tilted circle, just like the Sun and the Moon does* [Aet. *De Vestutis Placitis* III, 13, 1. 2. (D 378)]. Therefore, Philolaus came at a disagreement with his master, and taught that the earth was not immobile in the center of the world, but was circling the "Central Fire".

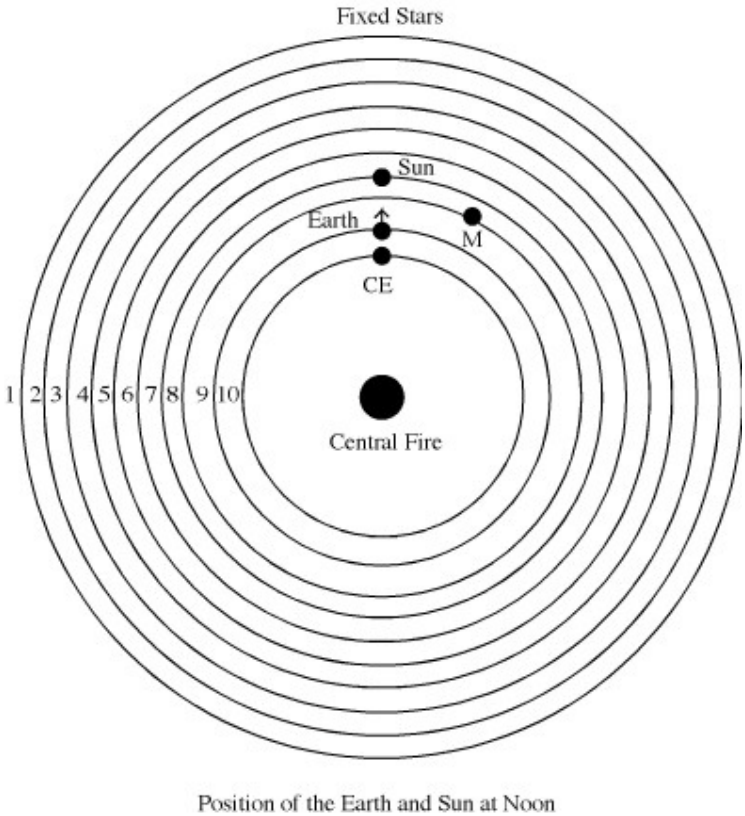

Fig. 5. The world view of Philolaus. In the world view of Philolaus, the center is occupied by the Central Fire, Anticthon (Counter-Earth, CE),The Earth, the Moon (M), the Sun, and beyond those lie the spheres of the five planets and that of the fixed stars. The crystalline spheres around the Central Fire are 10 (= 1+2+3+4), equal to the sum of the first four numbers.

Diogenes Laertius also informs us that Plato bought a copy of the work of Philolaus for the -astronomical at its time- price of 100 mnae: *Some authorites, amongst them Satyrus, say that he wrote to Dion in Sicily instructing him to purchase three Pythagorean books from Philolaus for 100 mnae* [Diog. Laertius, *Lives of Eminent Philosophers*, III 9].

Plato, according to Plutarch, studied the work of Philolaus carefully, and after careful reading, nearing the end of his days -as the story goes by- was convinced that the Earth is indeed moving around the Sun: *As Theophrastus informs us, Plato, near the end of his days had regrets for his older opinion, by which he unfittingly placed the Earth at the center of the Universe* [*Platonicae Quaestiones* H1 915, vol. XIII1, 76-78]. The study of Philolaus may have

been the reason for another change in the views of Plato: In *Republic* he identifies the celestial equator with the ecliptic, an idea which he turns from in Timaeus.

Aristotle, in his book *On the Heavens (De Caelo)*, provided us with some commentary on a few pythagorean views: *These affirm that the center is occupied by fire and that the Earth is one of the stars, and creates night and day as it travels in a circle about the center* [Aristotle, *On the Heavens* B, 13, 293a, 21-23]. Also, *The Pythagoreans make a further point. Because the most important part of the Universe -which is the center- ought more than any to be guarded, they call the fire which occupies this place the Watch-tower of Zeus, as if it were the center in an unambiguous sense, being at the same time the geometrical center and the natural center of the thing itself... For this reason there is no need for them to be alarmed about the universe, nor to call in a guard for its mathematical center; they ought rather to consider what sort of thing the true center is, and what is its natural place* [Aristotle, *On the Heavens* B, 13, 293b, 1-10].

The late professor of Astronomy at the University of Athens Demetrios Cotsakis (1976) mentions that the creation of the world-view which Philolaus describes was indeed revolutionary for the scientific thought of the time. He specifically mentions the views of the Italian astronomer Giovanni Schiaparelli (1835-1910), who wrote, as cited in Cotsakis (1976), the following, concerning the views of the Pythagoreans and the system proposed by Philolaus: *The system of Philolaus was not a fruit of some restless imagination, but came through the torque and pull of one who sets the outcomes of observation in accordance with a predetermined principle, which exists above the nature of things... Appreciating this, and combining it to the fundamental theorems of the Pythagorean Philosophy, the system of Philolaus naturally appears as one of the most wonderful creations of human genius. His critics are incapable of appreciating the power of research, which was necessary, in order to unify the ideas of the roundness of the Earth, its levitation in space, and its motion. Indeed, without these ideas, there would have been no Copernicus, neither Kepler, nor Galileo or Newton* [Cotsakis, 1976, p. 30].

2.2 The views of Icetas, Ecphantus and Heraclides of Pontus

Beyond the theories of Philolaus of Croton, there were other students of Pythagoras which put forward novel ideas, like Icetas and Ecphantus of Syracuse as well as Heraclides of Pontus.

Icetas of Syracuse claimed that the Heaven, the Sun, the Moon and the stars were immobile, and the only thing that moved was the Earth. Concerning his views, Cicero mentions the following: *As Theophrastus says, Icetas of Syracuse was of the opinion that the heaven, the Sun, the moon and the stars (i.e. the planets) and all that is high above are immobile, and nothing in the world is moving, apart from the Earth. But as it rotates around its axis with the greatest possible speed, its motion causes all these phenomena to appear, which would have appeared were the Earth immobile and heaven rotated instead of it* [Cicero, *Academica priora* II, xxxix, 123].

It appears that this theory was embraced by both Ecphantus and Heraclides as well, both of which believed that the Earth moves rotating in space, just like a wheel does around its axis.

Therefore, the students of Pythagoras were the ones to reduce our planet to its real place and motions, while at the same time holding a pyrocentric planetary theory, which certainly assisted Aristarchus of Samos (310-230 B.C) to formulate his novel heliocentric theory.

According to Hippolytus, the Pythagorean Ecphantus appears to have also followed an "atomic theory" of Pythagorean inspiration, by "giving body" to units, which were directed and governed by some divine force, "nous" (the mind). He also mentions that Ecphantus believed that the Earth spins around its axis with an eastern direction, but does not change its place in space. [Hippolytus *Refutationis Omnium Haeresium* I 15 (D. 566W. 28)]. These last two pieces of information are also mentioned by the doxographer Aetius, who finds Heraclides in agreement with Ecphantus. [Aet. *De Vetustis Placitis*, III, 13, 3 (D. 378)].

Heraclides in particular appears to have modified the atomic theory of Leucippus and Democritus, proposing that the first material elements were molecules and not atoms. According to him, the universe was composed of small material molecules which did not share any connection.

3 The views of other Philosophers

3.1 Anaximander and Seleucus

So far we have mentioned the views of the Pythagoreans concerning the motion of the Earth. However, even before the Pythagoreans, during the 6th century B.C., the great philosopher Anaximander, was most likely the first Greek astronomer to talk about the motion of our planet around the center of the world, which may have been the Sun. He also discovered other fundamental astronomical facts, like the "detachment" of the Earth, and its axial rotation. This information can be found in the work "*Expositio rerum mathematicarum ad legendum Platonem utilium*" of Theon Smyrnaus (70-135 B.C.), who lived during the reign of emperor Adrian (Theon of Smyrna, 1979).

Anaximander's views were adopted by later philosophers like Empedocles of Agrigentum (490-430 B.C.), Parmenides of Elea (early 5th century B.C.), Aristarchus of Samos, Cleomedes (2nd or 3rd century B.C.) and several Pythagoreans.

Another philosopher, which name is Seleucus of Seleucia (c. 2nd century B.C.), was an astronomer of the hellenistic period from Anatolia, who supported a heliocentric theory of his own. Fragments of his work are found in the works of Plutarch, Strabo, Aetius and Hippolytus. Hippolytus informs us that the Earth was indeed moving, and that the Moon played a part in its axial rotation as well as in its orbit around the Sun. [*Philosophoumena*, Book C, 897C, 14-16]. The same source also informs us that he believed that the Cosmos was infinite [*Philosophoumena*, Book ?, 886C, 6].

Plutarch mentions a few of his other astronomical ideas [*Platonicae Quaestiones* H1 915, vol. XIII1, 76-78]; unfortunately, all of the work of Seleucus was lost and we have no knowledge of his heliocentric theory.

3.2 Aristarchus of Samos

After the Pythagoreans, appeared the great astronomer Aristarchus of Samos (310-230 B.C.), the foremost introducer of the heliocentric theory as we know from the book of Archimedes *Arenarius* [I 4-6 (3, 180-182), manuscript 2, Cod. Laurent. Gr. 28]. Plutarch, also, writes about the heliocentric theory of Aristarchus of Samos [*De placitis philosophorum* II, 24 (7, 355a)].

Aristarchus' hypothesis was original and quite bold for its time. For this reason Plutarch mentions that he was accused of atheism [*De facie in orbe lunae*, 923A (15, vol. XII, p. 54)]. Aristarchus, according to Aetius was helped to escape in Alexandria by his teacher Straton of Lampsacus (Aetius, *Placitorum Compositione* book 7, 313b, 16-17).

It is apparent that apart from the fervent geocentrists, there were several Greek thinkers whose philosophical thoughts disputed the validity of the geocentric system.

Unfortunately, overcoming the objections of the heliocentrists, the geocentric system, as was formulated by Claudius Ptolemy (2nd century A.D.), reigned for centuries, seconded by the weight of the views of Aristotle, whose work was held as indisputable during the Dark Ages.

4 Emperor Julian

Yet faith in the heliocentric system had not been forsaken. During the 4th century A.D. emperor Julian (336-363 A.D.) studied with care the works of the ancient Greek philosophers, which he held in deep respect. His studies took place in the philosophical schools of Athens. Enchanted by the beauty of the ancient Greek spirit, he wished to revitalize it. He believed that the Earth's world order was influenced by a heavenly and divine hierarchy, in which everything originated from the unique God, the illuminating Sun.

He was interested in philosophy as well as astronomy, and rose as a fervent supporter of the heliocentric system. In his book *Hymn to King Helios* dedicated to Sallust (*Hymn to the king Sun dedicated to Sallust*), he writes: *For that the planets dance about him as their king, in certain intervals, fired in relation to him, and revolve in a circle with perfect accord, making certain halts, and pursuing to and from their orbit, as those who are learned in the study of the spheres call their visible motions; and that the light of the moon waxes and wanes varying in proportion to its distance from the Sun, is I think, clear to all* [*Hymn to King Helios dedicated to Sallust*, 135b, 1-6].

Therefore, Julian held the Earth as a planet, which revolved in a circular orbit around the Sun. The Earth is moving, and along with it the other planets in circular orbits around the Sun, in determined intervals i.e. constant distances. The above clearly show that the theory of Aristarchus hadn't been forgotten, but during the 4th century A.D. enjoyed advocacy.

Conclusion

Beyond the sperms of the heliocentric theory that we saw in the Orphic Hymns, several scholars of Ancient Greece supported this "heretical" for its time view. Its main introducers were the Pythagorean philosophers Philolaus, Icetas, Ecphantus, Heraclides and foremost Aristarchus of Samos, who gave the Sun its rightful place in the Pythagorean "central fire".

The heliocentric theory did not prevail, and instead, the geocentric model, elaborated by the great astronomer Claudius Ptolemy, reigned for centuries in the West, since the undisputed Aristotle was in agreement with it.

Yet the heliocentric theory had not perished, since in the 4th century A.D. the Emperor Julian, a believer in the divinity of the Sun, became a fervent supporter. In the end, the heliocentric system faded away until the 16th century when the great Polish clergyman and astronomer Mikolaj Kopernik (Nicolaus Copernicus 1473-1543 A.D.), brought it back to light (Copernicus, 1995). The hypotheses of Aristarchus of Samos and the preparation of the Pythagoreans were the foundations for the great Polish astronomer's thoughts.

References

Aetius, 1879 (reprinted 1965), Placitorum Compositione (De Vetustis Placitis). Vol. IV 9, 8. in Diels Hermann: Doxographi Graeci. Berolini. Apud Walter De Gruyter et Socios, Editio Quarta.

Archimedes, 1972, Arenarius in Opera Omnia, Bibliotheca Scriptorum Graecorum et Romanorum Teubneriana. Ed. I. L. Heiberg, vol. II corrigenda Adiecit E. S. Stamatis. Stutgardiae in Aedibus MCMLXXII.

Aristotle, 1956, The Metaphysics. Vol. I-IX, The Loeb Classical Library, Book XVII with an English Translation by H. Rackham. London: William Heinemann Ltd. Cambridge, Massachusetts: Harvard University Press.

Aristotle, 1953, On the Heavens (De Caelo). The Loeb Classical Library, with an English Translation by W.K.C. Guthrie. M. A. London. William Heinemann Ltd. Cambridge, Massachussets, Harvard University Press, MCMLIII (First printed 1933, reprinted 1936, 1947, 1953, 1956).

Chassapis Constantinos, 1967, The Greek Astronomy of the 2nd millennium B.C. according the Orphic Hymns. PhD. Thesis, University of Athens [self edited], Athens [in Greek].

Cicero, 1961, Academica Priora, with an English Translation by H. Rackham, M.A. The Loeb Classical Library. London. William Heinemann LtD. Cambridge, Massachussetes, Harvard University Press. MCMLXI (First printed 1933, reprinted 1951, 1956, 1961).

Cicero Marcus Tullius, 1984, Academica. Publ. Lubrecht & Cramer, Ltd. October.

Copernicus Nicolaus, 1995, De Revolutionibus Orbium Coelestium, libri VI. On the Revolution of Heavenly Spheres. Trans. By Charles Glenn Wallis. Prometheus Books, October 1995.

Cotsakis Demetrios, 1976, The pioneers of Science and the creation of the World. Ed. Zoe, Athens.

Diels Herman, 1996, Die Fragmente der Vorsokratiker, Herausgegeben von Walther Kranz. Ester und Zweiter Band, Weidmann, Zurich.

Diogenes Laertius, 1925, Lives of Eminent Philosophers, vol. II, IX 34-35, pp. 3, 441-445. Heinemann, London. The Loeb Classical Library; English translation by R.D. Hicks, revised and reprint 1959.

Hippolytus,1857-1866, A Refutation of All Heresies: Refutationis Omnium Haeresium (Filosofoumena). Patrologia Greca (P.G.) 16, In Origenes, Liber VII, 404-405, 339. Typographi Brepols Editores Pontificii, Parisiis.

Iamblichus, 1965, Vita Pythagorii (V.P.) Life of Pythagoras, with the English translation by Thomas Taylor in 1881, J. M. Watkins, 1965, p. 248-249ff.

Iuliani Imperatoris, 1875, Vol I. Oratio IV (To King Helios), 143 B. 146 D., Lipsiae Teubner.
Julian the Emperor 1954, The works of the emperor Julian, The Orations of Julian, IV. Hymn to king Helios dedicated to Sallust. The Loeb Classical Library. Trans. By Wilmer Cave Wright, Ph.D., William Heinemann Ltd. Cambridge, Massachusetts, Harvard University Press MCMLIV (First printed 1923, reprinted 1930, 1954).
Orphic Hymns, sine datum, Ed. Ideotheatro, Athens [in Greek].
Orphicorum Fragmenta, 1922, Ed. O. Kern, Weidmann.
Papathanassiou Maria, 1978, Cosmological and cosmogonical aspects in Greece during 2nd millennium B.C. PhD. Thesis, University of Athens [self edited], Athens [in Greek].
Papathanassiou Maria, 1980, Aristarchus the Samian, Mathematical Review 20, Editions of the Hellenic Mathematical Society, p. 91-120 [in Greek].
Papathanassiou Maria, 2003, Primordial astronomical learning. Elefterotypia-Historica, Athens, January 2, 2003, p. 6-12 [in Greek].
Petrides, S., 2002, The Orphic Hymns, Astronomy in the Age of Ice [self edited], Athens [in Greek].
Plakides Stavros, 1974, The Geocentric and the Heliocentric Theory. Parnassos 16, Athens [in Greek].
Plutarch Chaeronsis, 1841, Scripta Moralia. Graece et Latine. Tomus Secundus. De placitis Philosophorum Libri quinque. Parisiis. Editore Ambrosio Firmin Didot MDCCCXLI.
Stobaei Ioanni Eclogae, sine datum, Wachsmuth Dox. 336 B 20-337 B 10 and Bibliotheca of the ancient Greek writers, Ed. Georgiades, Athens.
Theonis Smyrnaei, 1878, Philos. Platonici. Ed. Hiller. Lipsiae 1878, p. 198, 14-19.
Theon of Smyrna, 1979, Mathematics useful for understanding Plato or Pythagorean Arithmetic, Music, Astronomy, Spiritual Disciplines. Trans. by Christos Toulis, Wizards Bookshelf.

The cosmology of Democritus

E. Danezis[1], E. Theodossiou[1], M. S. Dimitrijević[2],
A. Dacanalis[1], Ch. Katsavrias[1]
[1] University of Athens, School of Physics, Department of Astrophysics, Astronomy and Mechanics, GR 157 84 Zografos, Athens, Greece
[2] Astronomical Observatory of Belgrade, Volgina 7, Belgrade, Serbia
edanezis@phys.uoa.gr
(Research report; Accepted on 10.12.2009)

Abstract. Cosmological views of Democritus have been analyzed.
Key words: Democritus, Cosmology, Atomic Theory, Inflation Theory

Космологията на Демокрит

Е.Данезис, Е.Теодосиу, М.С.Димитрийевич, А.Даканалис, Х.Катсавриас

Анализиран е космологичният светоглед на Демокрит.

1 Introduction

Democritus is one of the most famous natural philosophers of ancient Greece – especially for his theory on the atoms. Information about Democritus is supplied by the doxographer Diogenes Laertius (3rd century A.D.), who reports:

Democritus was the son of Hegesistratus, though some say of Athenocritus, and others again of Damasippus. He was a native of Abdera or, according to some, of Miletus. He was a pupil of certain Magians and Chaldaeans... Afterwards he met Leucippus and, according to some, Anaxagoras, being forty years younger than the latter... As Apollodorus writes in his "Chronika", he should have been born during the eightieth Olympiad (460-457 B.C.), while according to Thrasylos in his work with the title "The ones before reading the books by Democritus"; he was born in the third year of the seventy-seventh Olympiad (470-469 B.C.) being (as he says) one year younger than Socrates... According to Demetrius in his book Men of the Same Name and Antisthenes in his Successions of Philosophers, he travelled into Egypt to learn geometry from the priests, and he also went into Persia to visit the Chaldaeans as well as to the Red Sea. Some say that he was associated with the Gymnosophists in India and went to Aethiopia. (Diogenes Laertius, 1925: 443-445).

Also the geographer Strabo writes:

And if one must believe Poseidonius, the ancient dogma about atoms originated with Mochus, a Sidonian, born before the Trojan times. (Strabo, 1967: 271).

Additionally Sextus Empiricus reports:

And Democritus and Epicurus, atoms, unless one should regard this opinion as more ancient and –as the Stoic Poseidonius asserted– derived from a certain Phoenician called Mochus. (Sextus Empiricus, 1968: 175).

Finally Diogenes Laertius writes that:

There are some who say that the study of philosophy had its beginning among the barbarians. They urge that the Persians have had their Magi, the Babylonians or Assyrians their Chaldaeans, and the Indians their Gymnosophists... Also they say that Mochus was a Phoenician, Zamolxis a Thracian, and Atlas a Libyan. (Diogenes Laertius, 1925: 3).

From the above ancient Greek texts we can conclude that Democritus had received a variety of studies. Thus, his philosophy –including the part of natural philosophy– was influenced with the beliefs of the places he had visited.

2 Some interesting views

Democritean view about 'time' may be seen from the following citation of Sextus Empiricus:

It seems, too, that there is ascribed to the physicists Epicurus and Democritus a conception of time such as this – Time is a day-like and a night-like phantasm. (Sextus Empiricus, 1968: 301).

It is interesting that the time as perceived by Democritus and ordinary people is what we call today 'Newtonian time', measured with our clocks and calendars, constitutes only the projection of the Riemannian relativistic dimension 'time' inside and over an Euclidean space or a Minkowski space, i.e. a ghost of what is time in reality. As Albert Einstein writes:

For us, the sworn in physicists, the distinction between past, presence and future is only an illusion, even if it is so persistent. [A letter of A. Einstein to the family of his dead friend Michel Besso on March 21st 1955 – as cited in *Le Temps* by Étienne Klein (1995: 38)].

Another interesting question considered by Democritus, was the problem of the structure of our Galaxy. Democritus, according to Achilles Tatius (4th century A.D.), believed that:

Others say that the Galaxy consists of very small and dense stars, that to us appear united due to the large distance from heaven to Earth, as an object powdered with many grains of salt. (Achilles Tatius, 1898: 55).

Intuitively he assumed that the nature of the Milky Way is similar to the observational fact obtained by Galileo Galilei 1610 A.D., when, turning his small telescope towards it, he realized –as he reports in his book *Nuncius Sidereus* (1610)–, that:

Est enim GALAXIA nihil aliud, quam innumerarum Stellarum coacervatim consitarum congeries (in latin) or La GALASSIA infatti non e altro che un ammasso di innumerabili stele disseminate a mucchi (in italian in *Avviso astronomico*, 1610), that is in English translation: In fact the Galaxy consists of a mass of innumerable stars, being placed one close to the other by swarms.

Democritus also tried to understand the way our senses work. According to the doxographer Aetius (1879: IV 8, 10.*A*.), as it is translated in Kirk's et al. book:

Leucippus, Democritus and Epicurus say that the perception and thought arise when images enter from outside, neither occurs to anybody without an image impinging. (Kirk G.S. et al., 1983: 428).

As we realize from the above passage, Democritus considers that the senses are just the result being caused when 'images', radiations as we could say today, of external origin (from the field of the real world of thinking) stimulate the organs of our senses. The result of these stimuli (the senses) does not, according to Democritus, consists an objective reality. As has already been mentioned, Charles Muses and Arthur M. Young in their book *Consciousness and Reality*: *The Human Pivot Point* state:

All the objects we can observe are three-dimensional images formed by waves stationary or moving under the influence of electromagnetic and nuclear processes. All the objects of the world are three-dimensional images formed electromagnetically, images of a super hologram, if you wish. (Muses, C. and Young, M.A., 1972: 33).

In addition, we note the views of Democritus on the equality of action and reaction. As Aristotle states:

Democritus, however, in disagreement with all other philosophers, held a view peculiar to himself. For he says that action and reaction are the same and alike, for (he declares) it is not possible for things which are 'other' and different to be affected by one another, but even if two things which are 'other' do act in any way upon one another, this occurs to them not in as much as they are 'other', but because some identical property belongs to them both. (Aristotle, 1965: 229).

The definition of action – reaction is: "For two interactive bodies, the force from the first one is equal with the opposite of the force from the other" (Alonso / Finn, 1980: 180).

3 The terminology in the texts of Democritus

The most important thing, when we want to analyze the views which are mentioned at the ancient texts from the modern point of view, is to study in detail the meaning of the terms that appears. Simplicius (*Phys.* 28, 4. *Λ*) according to Kirk et al. (1983), reports that:

He posited (Leucippus) innumerable elements in perpetual motion –namely the atoms– and held that the number of their shapes was infinite, on the ground that there was no reason why any atom should be of one shape rather than another, for he observed too that coming-into-being and change are incessant in the world. Further he held that not being exists as well as being, and the two are equally the causes of thing coming-into-being. The nature of atoms he supposed to compact and full, that, he said, was being, and it moved in the void, which he called not being and held to exist no less than being. In the same way his associate Democritus of Abdera posited as principles the full and the void (Kirk G.S. et al., 1983: 416).

Or in another translation

Leucippus... posited the atoms as unlimited and ever moving elements and an unlimited multitude of shapes among them on the grounds that they are no more like this than like that since he observed that coming to be and change are unceasing in things that are. Further, he posited that what is, is no more than what is not, and both are equally causes of what comes to be. For supposing the substance of atoms to be compact and full, he said it is 'being' and that is moves in the void, which he called 'not being' and which he declares is not less than what is. His associate Democritus of Abdera likewise posited the full and the void as principles, of which he calls the former 'being' and the latter 'not being' (Simpl. *Commentary on Aristotle's Physics* 28. 4).

Most probably, as the previous thesis evidences, Democritus had moreover understood that the field where our senses operate is but a subjective arbitrary division our senses create out of the space of not-being ($\mu\eta \quad o\nu$ = mi on), in order to perceive as sensed beings some interpretations (projections) of the properties of the not-beings. This view is supported by the fact that Democritus believed, as we will see, that one (out of many) sensed world is created when in the total 'void' space of the Universe ($\mu\eta \quad o\nu$ = mi on), is formed a partial 'great void' (a section of a more general space of the Universe), within which many bodies concentrate (Diogenes Laertius, 1925: 441-443).

Also Simplicius, according to Kirk et al. (1983), reports that:

Democritus... calls space by these names –the void, nothing, and the infinite– while each individual atom he calls – thing [nothing without not], the compact, and being (Aristotle on Democritus, quoted by Simplicius 294, 33, Kirk et al., 1983: 414).

It appears that Democritus describes the '$\tau o\pi o\varsigma$ = topos', i.e. what we call today 'mathematical space', using the words void ($\kappa\varepsilon\nu o\nu$ = kenon), nothing ($o\upsilon\delta\varepsilon\nu$ = ouden) or infinite ($\alpha\pi\varepsilon\iota\rho o\nu$ = apeiron). The void for him coincides with the notion of not being. The not being according to Democritus (quotation 2) has an existence in no way inferior to that of the sensed being, since it also possesses a nature and substance of its own.

Similarly he calls the being, full ($\pi\lambda\eta\rho\varepsilon\varsigma$), identifying it with the notion of atoms, thus calling the being, compact ($\nu\alpha\sigma\tau o\nu$ = naston) and not ($\delta\varepsilon\nu$ = den). The Greek word '$\delta\varepsilon\nu$ =den' means, in exact English translation, 'not'. These words, if used alone, have no meaning both in Greek and English. They simply declare the denial of the fact that follows.

As a conclusion, Democritus was supporting that only the atoms and the void are true, the *being* and the *not being*, and these cannot be understood with our senses. Everything else, everything we can see, hear or touch, is a very small piece of the real world –creation of our senses– composed by these *"first elements"*.

According to Aetius:

Others say that the sensed are physical, but Leucippus and Democritus that we think them as such, from our personal opinion and our impressions. Nothing is true or perceivable, except from the first elements, the atoms and the void. For only these exist physically, and all the rest happen from differences in position, in class and in shape (Aetius, 1879: IV 9, 8).

Or another passage with the same meaning:

Leucippus and his associate Democritus declare the full and the empty [void] to be the elements, calling the former 'what is' and the other 'what is not'. Of these the one, 'what is' is full and solid, the other, 'what is not', is empty [void] and rare. (This is why they say that what is, is no more than what is not, because the 'void' is no less than the body is). These are the material causes of existing things (Aristotle, 1956: 31).

According to the famous physicist and astronomer John Archibald Wheeler: The notions of time and space do not represent the nature of reality, but the images of the human cognition (1968: 243).

This view is in agreement with the thoughts of the ancient Hindu philosophers (it has already been reported that Democritus had traveled to India and studied there), as the former Greek ambassador in India and writer D.C. Velissaropoulos reports in his book *The History of Indian Philosophy.* In this book writes that for this topic they believed that:

The feeling of the existence of separate and specific tangible objects, instead of the realization of the real continuous flow, is the result of imaginary and arbitrary divisions of the continuous and permanent flow of becoming (1975: 283).

In the text of Democritean cosmology that follows, some words appear with a specific meaning, which we must make clear. In the texts of the Loeb's

Classical Library there is the phrase *'vast empty space'* but the exact translation of the phrase that Democritus uses is *'great void = megala kena = μεγαλα κενα'* (Democritus is not referring to the space which is empty of matter). Also, the phrase *'light ones'* is been used but the exact translation is *'thin'* (not by the ordinary meaning). This word describes a variety of bodies similar to each other. We point out that the Greek word for thin is also *'lepton'* (λεπτον = lepton).

4 The cosmology of Democritus

In further we will analyze and comment the cosmological views of Democritus and earlier of Leucippus. Let us see what Diogenes Laertius writes about the views of Leucippus, which had been also accepted by Democritus:

> *[Leucippus believed that] the worlds are formed when atoms fall into the void and are antangled with one another, and from their motion as they increase in bulk arises the substance of the stars... This is how the worlds are formed. In a given section many atoms of all manner of shapes are carried from the unlimited into the vast empty space (great void). These collect together and form a single vortex (whirl), in which they jostle against each other and, circling around in every possible way, separate off, by like atoms joining like. And the atoms being so numerous that thy can no longer revolve in equilibrium, the light ones pass into the empty space (great void) outside, as if they were being winnowed, the remainder keep together and, becoming entangled, go in their circuit together, and form a primary spherical system. This parts off like shell (a thin material membrane is detached), enclosing within it atoms of all kinds, and, as these are whirled round by virtue of the resistance of the centre, the enclosing shell becomes thinner, the adjacent atoms continually combining when they touch the vortex (whirl). And again, even the outer shell grows larger by the influx of atoms from outside, and, asit is carried round in the vortex (whirl), adds to it self-whatever atoms it touches. And of these some portions are locked together and form a mass, at first damp and miry, but, when they have dried and revolve with the universal vortex (whirl), they afterwards take fire and form the substances of the stars* (Diogenes Laertius, 1925: 441-443).

The above text is the exact translation from the Loeb Classical Library translation in which an important matter appears. We have used translations from both Loeb Classical Library and G.S. Kirk et al. (1983) book and it seems that they use different words to describe the very same thing. Anyway, in order to avoid the possibility someone to misunderstand the meanings of Democritus, we must make clear that the void (in this case the great void) is not the empty space but a substance as real as the atoms and more full than the materials. As a result, we found out more suitable the (word) 'void', and not 'empty space', which we will use from now on. Similarly we use the word 'whirl' instead of 'vortex'.

With this quotation as a basis, the main steps of the cosmic creation, according to Leucippus and Democritus were the following:

4.1 In the beginning there was the full and the void

Prior to the events described in the previous quotation, as already has been mentioned, initially there was the total creation (not being = void = infinity), inside which were floating the atoms (being). The system (being + not being) was beyond the perceptual capabilities of the human senses, since (as already has been mentioned) the atomic philosophers were supposing that: The full and the void, i.e. the atoms and space, are true and objective realities outside of the field of the human senses (Aetius, 1879: IV 9, 8 and Democritus, 2002: 13).

As can be seen, with the unified system [full + void] (= atoms + space) Democritus replaces a previous Greek prehistoric system, that of the Orphic Chaos and Erebos, without -of course- suggesting the identification of the respective partial components of the system.

4.2 Creation of the 'great voids'

As Diogenes Laertius reports: In a given section many atoms of all manner of shapes are carried from the unlimited into the vast empty space (great void) (Diogenes Laertius, 1925: 441).

In this phase, in the frame of the total original space of the Universe (not being = void = infinity) many partial 'great voids' (megala kena = $\mu\varepsilon\gamma\alpha\lambda\alpha \quad \kappa\varepsilon\nu\alpha$), i.e. smaller sub-spaces of the total space, are created.

It is an interesting fact that Democritus seems to be especially intrigued about the 'cause' (the great voids) that, as we shall see, forced the atoms to accumulate into small regions, and not about the cause that created the great voids themselves. For this reason he fashions the notion of the partial voids-spaces as the cause for the subsequent accumulation of the atoms, but without explaining the physical process of their formation.

4.3 Local collapse of 'atoms' in the 'great voids', formation of the 'whirl'

As Diogenes Laertius reports: *In a given section many atoms of all manner of shapes are carried from the unlimited into the vast empty space (great void).* These collect together and form a single vortex (whirl), in which they jostle against each other. (Diogenes Laertius, 1925: 441).

In this phase, non-perceivable parts of the being (atoms), originated from the total non-perceivable creation of the Universe (infinity + atoms = void + full = not being +being), tend to occupy the created 'great voids', generating for each one of them a corresponding 'whirl' ($\delta\iota\nu\eta$=dini). With the entry of atoms inside the sub-spaces of the 'great voids' are created the perceivable through the senses 'worlds', perhaps infinite in number and contained in the total non-perceivable set 'being + not being' (atoms + void = Universe).

Also in the case of Democritean Cosmology the material is being led from the funnel of the whirl to the edge of the cord, since, as we shall see the final result of the whirl is a sphere of limited dimensions. At this point it should be emphasized that Democritus and the other presocratic philosophers knew

very well, as we shall see, the natural phenomenon of the whirl. This leads to the conclusion that by the term Democritus refers to the specific and known phenomenon of the whirl. Let be noted that in a common natural whirl in general we can distinguish two regions, the funnel and its narrower and tighter ending, similar to a twisted cord.

All the previous thoughts, as in the Cosmology of Alcman (Danezis et al., 1999: 125-130), lead us to the conclusion that, if we want to describe using modern scientific terminology the views of Leucippus and Democritus in respect to what existed before the perceivable Universe was created and to how we were led to the starting point of the cosmic creation, a convenient possibility might be the creation of the Universe through a white hole. The difference between the cosmological system of Alcman and the one of Leucippus / Democritus is that the atomic philosophers, being experts on the scientific knowledge of their time, expose in greater detail their views attaching to them a series of scientific (for their era) explanations. The notion of whirl in particular renders the cord of Alcman easier to understand, while the spherical condensation of 'not thin' materials makes more concrete the notion of the Alcmanian '$\tau\varepsilon\kappa\mu\omega\rho$ = tekmor'.

The coincidence of the views of Leucippus and Democritus about the creation of the Universe with those of Alcman leads to questions, such as whether the atomic philosophers knew the Alcmanian Cosmology and, moreover, whether their views consist the lost or destroyed continuation of the text of Alcman, where he continued the exposition of his cosmological proposal.

In the context of Democritean Cosmology appears, with a physical etiology (explanation), the idea of the existence of many perceivable worlds like ours within the frames of the created 'great voids'. The idea of the existence of many 'worlds' inside successive 'heavens' consists an older presocratic view. But the complete physical explanation and description of a Universe including an infinite number of perceivable worlds was given by the atomic philosophers and in particular Democritus.

Hippolytus, according to Kirk et al. (1983), refers that:

Democritus holds the same view as Leucippus about the elements, full and void... he spoke as if the things that are were in constant motion in the void, and there are innumerable worlds, which differ in size. In some worlds there is no sun and moon, in others they are larger than in our world, and in others more numerous. The intervals between the worlds are unequal, in some parts there are more worlds, in others fewer, some are increasing, some at their height, some decreasing, in some parts they are arising, in others failing. They are destroyed by collision one with another. There are some worlds devoid of living creatures or plants or any moisture (Hippolytus, 1857-1866: I, 13, 2, Kirk G.S. et al. 1983: 418).

In this passage, as in several previous ones, one can clearly discern the view that the natural laws can be different in the various worlds and hence totally different events can be generated.

But let us see what the modern cosmological theories have to say about the existence of many worlds. According to the inflation cosmological proposal of A. Guth and A. Linde, in the original non-Euclidean, hence non-perceivable, Universe there was two known scalar fields: The 'inflation field'

and the 'Higgs field'. The inflation field and the associated phenomena are the reason for the expansion of space (void, not being), while the Higgs field is responsible for the kind of natural laws establishing themselves inside the expanding space. These two fields, as it has been proved, exist everywhere in the Universe, and their presence is betrayed from their influence on the elementary particles.

However, the scalar fields are not constant and, as proved by quantum physics, undergo unexpected fluctuations and variations. If the fluctuations cause a large increase in the intensity of the inflation field, then in this region the Universe begins to expand much faster, creating a bubble (generation of a great void). This effect can be produced continuously in different regions of the original non-perceivable Universe (creation of an infinite number of great voids). This implies that if we conceive the Universe as a homogeneous bubble, every new perturbation in it will create a new bubble of the universe (great void). In this way Andrei Linde (1989, 1990, 1994) and Alan Guth (1984, 1988, 1989, 1998) answered the question that Leucippus and Democritus could not answer: How the great voids are created.

As mentioned by the astronomer Martin Clatton Brok as cited by M. Talbot:

By its own definition the word Universe includes everything. Therefore it is preferable to speak about many worlds, imagining that the Universe branches out to an infinite number of these. We know of only one such world. There are open and closed worlds. There are some fully structured and some chaotic. In some of them life never appears. In some others it exists, but in an elementary form. Finally, in a very few worlds life thrives (Talbot, M., 1993: 39).

The bubble spaces are initially limited by irregular limits that continually smooth down, and tend to expand with velocities approaching the speed of light. Later on, the limits of the bubbles can possibly shrink with much lower velocities. On this basis, the Big Bang theory describes the creation of just one bubble, inside which we find ourselves, and not of the total Universe of the infinite bubbles.

It should be noted that, if in the original non-perceivable Universe there were a set of specific natural laws, the Higgs field would have changed it in the produced bubbles (great voids). This means that every bubble (great void) will eventually have its own set of natural laws.

It should be mentioned that Linde's model is an elaboration of the inflation theory, which predicts the existence of a Universe with many bubbles in space-time, perhaps ruled by different natural laws.

In 1982 American physicists Andreas Albrecht and Paul J. Steinhardt (1982: 1220) announced similar results. It is interesting to note that the views of the Universe that Leucippus and Democritus pioneered have an advantage that are somewhat compatible with the cosmological views of contemporary science.

4.4 Formation of spherical system of perceivable matter with simultaneous ejection of material in the external void

According to Diogenes Laertius:

And the atoms being so numerous that they can no longer revolve in equilibrium, the light ones pass into the empty space (great void) outside, as if they were being winnowed, the remainder keep together and, becoming entangled, go in their circuit together, and form a primary spherical system (Diogenes Laertius, 1925: 441).

Due to the rotating 'whirl', there is first a separation of the 'similar' from the 'dissimilar'. Next the rotation ceases and a system is created consisting of 'thin bodies' 'leptons' (not small in dimensions, nor atoms) that advance towards the external void (space) as if being hurled, while the rest, the 'non-thin' (thick = hadra), remain united and becoming entangled approach each other and form initially a spherical system. We must emphasize that the Greek word for thin is 'lepton = $\lambda\varepsilon\pi\tau o\nu$' as the word leptons that describes a certain category of particles and the word for not thin, 'hadron = $\alpha\delta\rho o\nu$' as the word hadrons.

It is interesting to note that the new term 'thin bodies' is used in order to set these bodies apart from all the others that have already been mentioned.

The hurling and the expansion of the 'thin' material according to Leucippus and Democritus is not a result of the explosion of the spherical system formed by the 'non-thin' materials, but instead they occur together with the creation of the spherical condensation, as a result of events taking place at the edge of the 'whirl', since there the 'similar' have separated from the 'dissimilar' and equilibrated, and the bodies cannot rotate anymore.

Consequently, Leucippus and Democritus support that from a mixture of 'thin' and 'non-thin' bodies (leptons + hadrons) that is in equilibrium and does not rotate, the hurling of the thin ones towards the exterior creates an opposite motion, a contraction, of the 'non-thin' ones, that tend to form a small but dense spherical structure of matter.

As it is evident from the respective quotation, at the end of the whirl, where it meets the great void, there is a limited in space, momentarily non-rotating and in equilibrium, spherical condensation of 'non-thin' (not small in dimensions or atoms) material. The sphere occupies a very small space of the 'great void', because how else could be the described 'thin' material hurled into the external space if the initial sphere occupied this space? It is interesting that at the limits of the whirl, towards the region of the 'great void', and before the formation of the spherical condensation, the material of the non-perceivable Universe (space + atoms) consists of an 'exotic' for our senses 'matter', indescribable by the atomic philosophers, that later on it separates into two constituents, the 'thin' and the 'non-thin' (thick = hadra), which in a later phase were to form the 'matter' that is known today to our senses, according to the atomic philosophers.

4.5 Formation of a thin membrane onset of a rotational motion of the universe

According to Diogenes Laertius:

This parts off like shell (thin membrane), enclosing within it atoms of all kinds, and, as these are whirled round by virtue of the resistance of the centre, the enclosing shell becomes thinner, the adjacent atoms continually combining when they touch the vortex (whirl). And again, even the outer shell grows larger by the influx of atoms from outside, and, as it is carried round in the vortex (whirl), adds to it self what ever atoms it touches. (Diogenes Laertius, 1925: 441-443).

At this stage, from the central spherical condensation of 'non-thin' (hadrons) material detaches a membrane, i.e. a thin shell of 'non-thin' matter. This membrane starts rotating, while material from it is carried towards the central spherical condensation 'due to the whirl'. But which whirl? The original 'whirl' was carrying material from the non-perceivable Universe of the 'being' + 'not being' to the world of the 'great void', that is the spherical accumulation of 'non-thin' material we mentioned. On the contrary, the whirl referred here leads from the 'world' of the 'great void' to the original spherical accumulation of 'non-thin'. This means that the whirl mentioned here is of opposite direction in respect to the first. In other words, the atomic philosophers propose a cosmological system of two whirls of opposite polarity [(+) and (-)]. The first evolves outside the world of the 'great void' and the second inside. But both lead to a common region, which forms the beginning and the end of the world of the 'great void'.

5 Conclusions

If we summarize the views of Leucippus and Democritus about the structuring of the Universe using the corresponding modern scientific terminology, we can generally discern two periods:

1. The process before the creation of the spherical condensation and of the great voids, when the Universe [being + not being = void + atoms] consisted a non-perceivable entity (logos), a situation that Hesiod describes as Chaos and Erebus: 'From Chaos came forth Erebus and black Night' (*Theogony*, 1914: 123).

2. The process after the creation of the great voids and of the spherical condensation, which is interesting to analyze by phases:

a. Originally there is an initial spheroidal condensation in a small space of a very large quantity of 'thin' and 'non-thin' material. The violent hurling of the "thin" material forces as a reaction the "non-thin" material to contract and to rotate violently.

b. The violent contraction of a very large mass of material creates internal energetic processes that generate and propagate outwards a shock wave, resulting to the ejection through an explosion of a large quantity of matter from the surface of the spherical condensation, i.e. of a material membrane

that starts to rotate rapidly. It is interesting to note the similarities of these processes with the processes when a star reaches the evolutionary phase of a nova or of a supernova. The violent ejection of material from the surface during this stellar phase, forces its central regions to contract violently, a process that leads the star to become, according to its mass, a white dwarf, a neutron star, or a black hole.

c. After the ejection of the membrane's material, the remaining spherical condensation, which should be enormous (the entire mass of the local Universe), continues to contract as a reaction, which has similarities with the creation a black hole in modern science. The material of the membrane of the surface layers that had been ejected revolves now around some kind of modern black hole as some kind of modern accretion disk, being led towards the singularity of the black hole, using modern terms.

This discussion leads to the conclusion that, back in the 5th century B.C., Leucippus and Democritus had formulated a very pioneering view about the creation and evolution of the Universe, which involves many, intuitively developed, ideas which are not incompatible with modern science.

References

Achilles Tatius, 1898, *Aratos phenomena*, from Achilles, 24, ed. E. Maas, *Commentariorum in Aratum reliquiae*, Berlin, pp. 27-75 [about Galaxy].

Aetius, 1879, *Aetii De Placitorum Compositione* (*De Vestutis Placitis*). Diels, H., *Doxographi Graeci. Editio Quarta.* Walter De Gruyter et Socios, Berolini (reprinted 1965), vol. IV 9, 8.

Albrecht A. and Steinhardt P. J., 1982, Cosmology for Grand Unified Theories with Radiatively Induced Symmetry Breaking. *Phys. Rev. Lett.* 48, pp. 1220-1223.

Alonso / Finn, 1980, *Fundamental University Physics*, vol. I, Addison- Wesley Publishing Company. (in Greek translation by prof. L. K. Resvanis and T. A. Filippas), p. 180.

Aristotle, 1956, *The Metaphysics.* Heinemann, London (The Loeb Classical Library; English translation by H. Rackham), vol. I-IX, Book I, IV 9, 31.

Aristotle, 1965. *Coming to be and passing away.* Heinemann, London (The Loeb Classical Library; English translation by E. S. Forster), vol. I 7, 323b, 10, p. 229.

Danezis, E., Theodossiou E. et al., 1999, A presocratic Cosmological Proposal, *Journal of History and Heritage of Astronomy*, 2(2): 125-130.

Democritus, 2002, in Presocratic Philosophers, Ed. Kaktos Athens 2002 [in Greek], p. 13.

Diogenes Laertius, 1925. *Lives of Eminent Philosophers.* Heinemann, London (The Loeb Classical Library; English translation by R. D. Hicks, revised and reprint 1959), vol. II, IX 34-35, pp. 3, 441-445.

Galileo Galilei, 1610. *Nuncius Sidereus*, (in Latin) – 1610. *Avisso astronomico* (in Italian): [http://www.liberliber.it/biblioteca/g/galilei/sidereus_nuncius/html/index.htm].

Guth, A. H. and Steinhardt, P. J., May 1984, The Inflationary universe. *Scientific American*, 250: 90-102.

Guth, A. H. and Steinhardt, P. J., 1988, The Inflationary Universe. In *The New Physics*, ed. by Paul Davies. New York. Cambridge University Press.

Guth, A. H., 1989, *The birth of the Cosmos.* In Origins and Extinctions, ed. by D. E. Osterbrock and P. H. Raven. New Haven, Conn., Yale University Press.

Guth, A. H., 1998, *The Inflationary Universe: The Quest for a New Theory of Cosmic Origins*, Perseus Publishing, U.S.A.

Hesiod, 1914, *Theogony*, Harvard University Press, London (English translation by Hugh G. Evelyn-White), line 123.

Hippolytus, *Kata pason ton aireseon eleghos* or*A Refutation of All Heresies*, *Refutationis Omnium Haeresium*, 1857-1866 I, 13, 2 (*Filosofoumena*). Patrologia Greca (P.G.) 16, In Origenes, Liber VII, 404-405, 339. Typographi Brepols Editores Pontificii, Parisiis.

Kirk G. S., Raven J. E. and Schofield, M., 1983. *The Presocratic Philosophers: A Critical History with a selection of Texts*, 2nd edition, Cambridge University Press, pp. 414, 416, 418, 428.

Klein Étienne, 1995, *Le Temps*. Dominos, Flammarion, Paris, p. 38.

Linde, A., 1989, *Particle Physics and Inflationary Cosmology*, Gordon and Breach. New York.

Linde, A., 1990, *Inflation and Quantum Cosmology-A collection of reprints*. Academic Press. New York.

Linde, A., November 1994, 1972, The Self-Reproducing Inflationary Universe. *Scientific American*, vol. 271, no. 5, p. 32.

Muses Charles and Young Arthur M., *Consciousness and Reality*: *The Human Pivot Point*. Outerbridge and Lazard Inc., N.Y., p. 33.

Sextus Empiricus,*Against the physicists*, 1968, (The Loeb Classical Library; English translation by R. G. Bury). vol. III, I 363, p. 175, vol. III, II 181, p. 301.

Simplicius, *Simplicii in Aristotelis Physicorum* (*Commentary on Aristotle's Physics*), MDCCCLXXXII (1882), Libros quattuor priores Commentaria. Editit Hermannus Diels. Berolini Typis and Impensis G. Reimeri.

Simplicius, *Simplicii in Aristotelis De Caelo* (*Commentary on Aristotle's On the Heavens*). Priores Commentaria, MDCCCLXXXII (1882), Edit, Hermannus Diels, Berolini, Typis et Impensis G. Reimeri, 294, 33.

Strabo, 1967, *Geography*. Heinemann, London (The Loeb Classical Library; English translation by H. L. Jones), vol. VII, XVI 757, p. 271.

Talbot, M., 1993, *Mysticism and the New Physics*, Ed. Arkana, Ontario, Canada. (In Greek translation *Chronos*, Publ. Iamvlichos, Athens, 1993), p. 39.

Velissaropoulos, D. C., 1975, *The history of Indian Philosophy*. Ed. Dodoni, Athens, p. 238. [in Greek].

Wheeler, J. A., 1968, *Superspace and the nature of Quantum geometrodynamics*, in Batelle Rencontres / DeWitt, Cecile M. (ed.). 1967, Lectures in mathematics and physics, W. A. Benjamin, N.Y., pp. 242-307.

The pyramids of Greece – ancient meridian observatories?

Efstratios Theodossiou[1], Vassilios N. Manimanis[1],
Milan S. Dimitrijević[2], and Marco Katsiotis[3]
[1] Department of Astrophysics, Astronomy and Mechanics Physics Faculty, University of Athens-Zografos 157 84
[2] Astronomical Observatory, Volgina 7, 11060 Belgrade, Serbia
[3] National Technical University of Athens, Polytechniopoli Zographou, Athens, Greece
etheodos@phys.uoa.gr
mdimitrijevic@aob.bg.ac.rs markos@central.ntua.gr
(Research report. Accepted on 21.12.2011)

Abstract. Pyramids, "Dragon Houses" ("Drakospita") and megalithic structures in general create always a special interest. We postulate that, as happens with the Drakospita of Euboea, the pyramid-like structures of Argolis (Eastern Peloponnese) were constructed by the Dryops. It is known that, in addition to Euboea and some Cyclades islands, this prehellenic people had also settled in Argolis, where they founded the city of Asine. We also propose that the pyramids of Argolis and in particular the pyramid of Hellinikon village were very likely, besides being a burial monument or guard house, might be served also for astronomical observations.
Key words: Archaeoastronomy, Greek pyramids, Hellinikon, Drakospita, Dryops

Пирамидите на Гърция – древни меридианни обсерватории

Ефстратиос Теодосиу, Василиос Н. Маниманис,
Милан С. Димитрийевич, Марко Кациотис

Пирамидите, "драконовите домове" ("дракоспити") и мегалитните структури предизвикват винаги специален интерес. Ние приемаме, че както при дракоспита на остров Еубоеа, пирамидовидните структури в Арголис (Източен Пелопонес) са били построени от Дриопите. Известно е, че освен в Еубоеа и някои от Цикладските острави, този пред-елински народ е пребивавал и в Арголис, където е основал град Азин. Ние предполагаме че пирамидите в Арголис, и в частност пирамидата в селището Хелиникон, без да са погребални монументи или охранителни постройки, са твърде подобни помежду си и са могли да служат и за астрономически наблюдения.

Introduction

The existence of pyramids, or rather pyramid-like buildings, in Greece has not been widely known, as most people, even most researchers worldwide know only of the Egyptian pyramids. Yet, it seems that there are several ancient pyramid-like buildings in southern Greece, the most impressive of which is the structure near the village Hellinikon in Argolis (Eastern Peloponnese). Some of these buildings have suffered major and irreparable damages, as their large stones were used through the centuries as raw material for the construction of other buildings, such as churches, or even for the production of lime in limekilns.

In the literature for this topic, the following pyramids are mentioned in Greece (Lazos, 1995):

Table I

	Name	Locality	Remarks
1.	Hellinikon	Hellinikon and Kephalari	The best-preserved one
2.	Ligourio	Epidaurus	Only its base exists
3.	Dalamanara	Epidaurus	Only traces remain
4.	Kambia = tower for fire-signaling	Nea Epidaurus	Preserved to some height
5.	Sikyon (?)	Corinthia (?)	Only traces remain (?)
6.	Viglafia	Neapoli (Laconia)	Only its base exists
7.	Amfio	near Thebes (Thiva)	scalar

In addition to the above, two other singular structures have been referred to as pyramid-like buildings: the cone-like pyramid in Khania (Crete), and the Rock Pyramid forming the peak of Mt. Taygetos; however, the latter is just the natural peak of the mountain, the tallest in Peloponnese (2,407 m). Prof. I. Liritzis (1995 & 1997), assiduous researcher of such ancient megalithic structures, supports the view that there are over 20 ancient Greek pyramids; they refer to pyramid-like structures in Astros (in Kynouria, to the south of Argolis), in Neochori of Phthiotida (they even date it in 11,000 BC), in Agios Andreas of Mt. Parnassos, in Vathy (of Avlis, in northern Boeotia), and in other places.

From all the above structures, only the Hellinikon pyramid to the south-eastern edge of Argive plain is preserved in a relatively good condition. For some of these structures, the data used in this study come from descriptions and references by ancient travelers, for example the description and comments of Pausanias (1985) for the Hellinikon pyramid, or from foreign travelers of the 19th century AD (Blouet A. and Ravoisié, A., 1831, Curtius, E.R., 1851).

1 References, studies and excavations

Although the pyramid-like buildings of Argolis stand out due to their form and shape, the references to them, even from Greek antiquity, are rather scarce.

Only the Greek traveler and geographer Pausanias (1985), writing in the 2^{nd}nd century AD, mentions the Hellinikon pyramid in his *Corinthiaka* (2, 25, 7):

"Traveling from Argus to the region of Epidaurus, there is a building to the right that resembles very much a pyramid and bears relief carved shields of the shape of the Argolic shields. In this place Proetus had battled with Acrisius for the throne and they say that the battle ended without a winner; for this reason they were later reconciled, as none could achieve a decisive victory. It is said that this was the first time that men and armies equipped with shields clashed; for those that fell in this battle from both armies, since they were compatriots and even relatives, a common tomb was built in that place."

Thus, according to Pausanias, the pyramid was a common tomb, built most probably by Proetus and Acrisius for the soldiers who died in a battle

between them; a battle in which soldiers used shields for the first time. This reference to mythical figures (Proetus, Acrisius) indicates that the building was considered to be very old.

Fig. 1. The Hellinikon pyramid. Prof. E. Theodossiou (left) and the physicist N. Saridakis (right)

Pausanias also mentions (*Corinthiaka* 2, 24, 7) that in adjacent areas there were some polyandria (mass tombs) of the Argives killed in the battle against the Spartans that was held in Hysiae (an acropolis next to the modern village Akhladocampos) in 669 BC:

"And polyandria exist here for Argives who won in a battle against the Lacedaemonians near Hysiae" (*Corinthiaka* 2, 24, 7).

So the ancient author considered the 'pyramid' as one of these burial monuments. Other researchers have suggested different possible uses (Lord, 1939, pp. 78-84).

The pyramids found in Greece are the only cases of pyramidal architecture in the broader European region. The shape of the pyramid-like buildings, their static and architecture, probably classify some of them in the pre-Pelasgic period (Lazos, 1987 & 1995). However, in a country rich in archaeological findings the ruins of these structures did not attract the interest of researchers. Thus, their study is almost nonexistent and a mystery surrounds them due to lack of adequate knowledge. There is still a chance that some reference could still be discovered in Byzantine texts. Currently, the next known reference to the 'Greek pyramids' after Pausanias (2nd century

AD) is from the first decade of 19th century. William Martin Leake toured Peloponnese in 1806, when Greece was still under the Ottoman rule, and he mentions the Hellinikon pyramid, which he visited on March 14, 1806, in his book *Travels on the Moréa* (vol. II, pp. 340, 344). In it, he gives two drawings, front view and top view of the buildings.

Fig. 2. The entrance of the Hellinikon pyramid with the eastern side. The entrance is next to the SE corner. The width of the entrance is 1.35 m, while its top consists of two converging stones that form a large capital Greek letter Λ.

In 1829 the French Scientific Mission in Moreas (Peloponnese) studied the two pyramids (in villages Hellinikon and Ligourio) and published the results in 1831 - in the three tomes of Abel Blouet and Ravoisié, Amable: *Expedition Scientifique de Morée*, vol. II, 107.

In 1901, Th. Wiegand conducted a preliminary excavation (the first one, 1901, pp. 241-246) of the Hellinikon pyramid. Wiegand removed all the fill from the floor of the pyramid, while the first Greek scientist who studied it was the archaeologist Apostolos S. Arvanitopoulos in 1916 (pp.72-99). Apostolos Arvanitopoulos believes that the monument dates to the Mycenean era (1600 BC-1100 BC), while the archaeologist Christos Tsountas (1857-1934),

the founder of Greek prehistoric archaeology, believes it is from the 6th century BC (1893).

More excavations followed in the Hellinikon pyramid by R. Ehrich and Mrs. Ann Hoskin-Ehrich, on August 1937, of the American School of Classic Studies and Archaeology in Athens, while at about the same time R. Scranton (1938) was excavating the Ligourio pyramid. Louis Lord, then director of the American School of Classic Studies in Athens, edited the report (1938, pp. 481-527) of these excavations based on the conclusions of the three archaeologists mentioned above, while he subsequently researched himself and discovered several buildings in Argolis, mainly square archaic towers, which were most probably the *polyandria* of Pausanias (Lord, 1939, pp. 78-84). Amongst the findings in the pyramid of Hellinikon were a big pithos, the floor of the long corridor and the room, re-carved from repairs entrance door and parts of the wall, infill from earlier excavations, some ceramics of Protohelladic II period (2800-2500 BC), also room foundations and mortals from later uses of the pyramid, as well as mixture disturb sediments with ceramics of classical period, such as lamps, house ware and few coarse shards of doubtful age and some roman lamps. The infill at the floor varies between 20-60 cm (Lord, 1938, pp. 508-538).

Louis Lord considers that the pyramids were not tombs, because their doors were opening from inside; nor were they towers for fire-signaling, as they were not built in elevated positions with a view. Lord believes they were posts capable of housing a guard of a few men, which could control the road to Tegea. However, he stresses that the peculiar pyramid-like construction is a fact that remains unexplained (1938). There wasn't a reason to build this form of structure for this purpose, as an outpost with a small wall would be the normal thing to do. What could be the purpose of these singular, pyramid-like constructions? Also, Lord supports the idea that the pyramid was from the early Hellenistic era, more specifically late 4^{th}th century BC.

The topic appeared to close from an archaeological point of view, as the American archaeologists had done a good job. The German archaeologist S. Oppermann, with a relative publication in German (1971, pp. 45-52), made known the two pyramids, in Hellinikon and Ligourio, to a wider German-speaking public, without adding something to the topic from a research point of view.

After about 15 years followed the researcher and author Christos Lazos, with two publications on Greek pyramids (1984, 1987), and an article by Helena Fracchia of the University of Toronto (1985, pp. 683-689), in 1986 Professor I. Liritzis published his book *Archaeometry - Methods of dating in archaeology*, and in 1994 the civil engineer V. Katsiadramis made a static study of the two pyramids and the corresponding figures (1994, pp. 9215-9236). In 1994 appear a paper by Professor Ioannis Liritzis and another one by the academician Theocharis *et al.* (1994, pp. 399-405) and the two books, again by archaeometrist Professor Ioannis Liritzis (1995) and by author C. Lazos (1995), which exhaust the topic from the descriptive point of view. Finally, Professor Ioannis Liritzis, in 1997, published an article about the mystery of these pyramids and similarly Professor Theodore Spiropoulos (2003).

In practical, the real research work on the Greek pyramids started under the supervision of the archaeometrist Professor Ioannis Liritzis and his group. The dating of the pyramid was approached through five sub-projects:

1) Geophysical prospection inside and around the two main pyramids at Hellenikon and Ligourio, where buried monuments were discovered (Theocharis *et. al.*, 1997, pp. 593-618).

2) The results of the above team directed the archaeological excavations carried out by archaeologist A. Sampson (1996, pp. 56-61) and archaeologists of the Archaeological Museum of Nauplion (Pikoulas, 1996, pp. 60-63; Piteros, 1995, pp. 11-13, and Piteros, 1998, pp. 344-394). Amongst the new findings were foundations of rooms, ceramics of Classical, Hellenistic, Roman and Protochristian periods, and Protohelladic II in the exterior foundations of Hellenikon pyramid above the bedrock. A comparative study of masonries was also made (Liritzis, 1995 & 1997, pp. 32-34).

3) Astronomical orientation of the long entrance corridor was found related to the rise of Orion's belt occurring in *circa* 2000-2400 BC (Liritzis, 1998, pp. 10-21).

4) The dating of some parts of the over lied large megalithic blocks in the wall, with the novel thermoluminescence dating method of rock surfaces. Sampling was chosen for their firmness and lack of sun exposure of internal contact surfaces, by removing a few milligrams of powder from pieces in firm contact. Seven pieces gave an age range of *circa* 2000-2500 BC. Liritzis, 1994a, pp. 603-604; 1994b, 361-366; Theocharis *et al.* 1994, 399-405), while two ceramic shards of non-diagnostic typology one from Hellenikon and one from Ligourio pyramids dated by TL (ThermoLuminescence) and OSL (Optically Stimulated Luminescence) gave concordant ages of 3000±250 BC and 660±200 BC respectively (Liritzis *et al.*, 1994, pp. 189-198). The novel dating method has been well published by the initiator and others Liritzis *et al.* 1997, pp. 479-496); Liritzis and Galloway, 1999, pp. 361-368; Habermann, 2000, pp. 847-851; Greilich *et al.* 2005, pp. 645-665; Morgenstein *et al.* 2003, pp. 503-518; Liritzis and Vafiadou, 2005, pp. 25-38).

5) The mythological genealogy of Argolid has been cautiously interpreted. It involves Inachus and his deluge and his descendants of Proetus and Acrissius that according to ancient traveler Pausanias (2nd c. AD) they fought for domination but had a draw and erected Hellenikon pyramid, shown to be at c. 2800 BC (Zangger, 1993; Liritzis and Raftopoulou, 1999, pp. 87-99)

2 The use of the pyramids

Pausanias, as is evident from his text, acknowledges that the purpose served by the pyramids had been forgotten in his age (*circa* 150 AD) and for this reason he writes about what the people were 'saying' about it, mentioning the hypotheses of being tombs and small military outposts.

The construction of these buildings, their dimensions and inclination, being added to the fact that no tomb-associated findings (such as bones or death ornaments) were found, lead to the conclusion that these structures were rather a kind of small fort or an observatory (Kalleyia, 1995).

The pyramids are dated by some archaeologists (Leake, 1846; Lord, 1938; Fracchia, 1985; Piteros, 1998), based on their wall structure, in the 4th century BC; the same archaeologists consider that they indicate the relations between Egypt and Argos, a tradition reinforced by the mission of 3000 Argive mercenaries in Egypt in 349 BC.

However, the Greek pyramids seem to have no relation to Egyptian ones (interior plan, masonry, slope, size), though there were trade contacts between the people of SE Mediterranean evidenced at least by the early presence of Minoans, Myceneans and later on Greek colonizations, in the West, Asia Minor and the Levant and Egypt, e.g. Tel Kabri, Avaris, Meggido etc. (Barbara and Wolf-Dietrich Neimeier, 1997, pp. 763-802).

Leake (1846, pp. 334-483), Vischer Wilhelm (1857, pp. 325-328) and others support the burial monuments theory, which is rejected by Wiegand (1901, pp. 241-246), who suggests that they can't be tombs because of the mortar used in their construction, a material hinting for him a building date in the 1st century BC. Other researchers, though, suggest that the mortar probably does not belong to the original building but to a posterior conservation work.

The Egyptian pyramids were Pharaohs' burial monuments, but they also served for astronomical purposes: Cheops Pyramid was a huge meridian instrument, the largest ever constructed, while its main passage's direction was towards the pole star of its age, Thuban or Alpha Draconis (α Dra).

Helena Fracchia (1985) supports the view that the Argolis pyramids were erected for the defense of the region, as fortifications incorporated into some large farms, as she believes from her research of ancient farms in Attica.

Civil engineer V. Katsiadramis (1994), after his static study of the whole Hellinikon monument, draws the conclusion that this building was in its initial form most probably a truncated pyramid 3.60 m high. He suggests that it was never complete up to its projected summit with stones or a roof of some kind, not being an Egypt-like, mathematical pyramid. He adds that the truncated pyramid shape *'is a very ancient worshipping tradition in Greece... ...this exact shape of the Elliniko building was intentionally chosen, as it combined static and aesthetic requirements with the Greek worshipping tradition'* (Katsiadramis, 1994). He, thus, considers a worshipping use for the building; in his view, it was a roofless sanctuary.

The Argolis pyramids continue to attract the interest of researchers. Professor I. Liritzis in his book (1995) argues that their megaliths were used as construction materials for churches and for lime production, in order to explain the reason for the disappearance of the Astros, Sikyon and Viglafia pyramids, which were reported by foreign travelers in early 19th century. C. Lazos, an author specialized in the research and recording of the feats of ancient Greek technology, in his book Pyramids of Greece (1995), provides a complete list of the Greek pyramid-like structures.

Our team visited the Hellinikon and Lygourio pyramids and photographed them; the architect, Marcos Katsiotis measured the dimensions of the Hellinikon pyramid and drew the top view, a section and perspective drawing of this pyramid, which is the best preserved one. But, finally, we used the drawings made by the civil engineer Vassilios Katsiadramis, which exist in the current Bibliography (1994, p. 9222).

3 The Hellinikon pyramid

The Hellinikon pyramid is located 5 to 6 km to the southeastern edge of the plain of Argolid, in the direction of the ancient road to Arcadia, between the villages Hellinikon and Kefalari, where the Erasinos River sources are (nowadays Kephalari). This is the best preserved pyramid (Fig. 1).

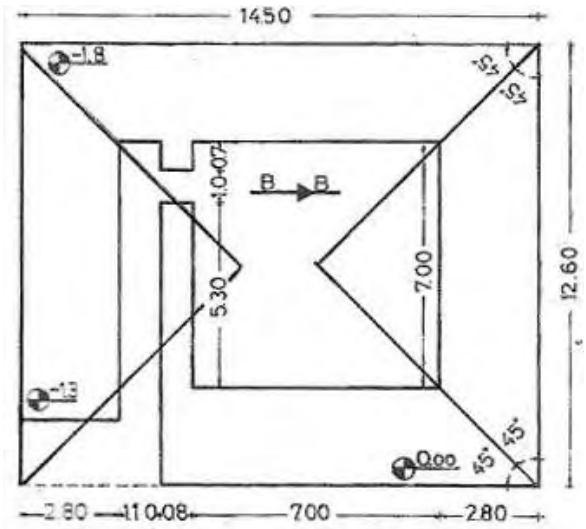

Fig. 3. Perspective drawing of the truncated pyramid of Hellinikon, made by civil engineer Vassilios Katsiadramis (1994, p. 9222).

However, archaeometric measurements based on optical thermoluminescence conducted by prof. I. Liritzis at the Nuclear Dating Laboratory of the University of Edinburgh and at the Archaeometry Laboratory of Democritos Center (Theocharis *et al.* 1995) showed that at least the Hellinikon pyramid is much older: *circa* 2700 BC. The optical thermoluminescence method is based on laser technology that can be applied on stones from walls; unfortunately, this method, used by Liritzis since 1986, although it is theoretically accepted, had not yet been fully calibrated in that time (1995) and doubts can be raised about this dating. At this point, if one remembers the geographer and traveler Pausanias, who gives a hint for this monument about being built in the Mycenaic period, one could find most probable this period as being in the middle of the two datings mentioned above: from 1600 to 1100 BC.

The dimensions of the Hellinikon pyramid are 14.50 x 12.60 x 10.80 x 10.60 m. Many researchers have wondered whether there is any relationship with the Egyptian pyramids, for example a correlation in their dating. Traditional archaeological research, as we saw, dated these structures in the 4th century BC, a much more recent date than the dates of the Egyptian pyramids.

Lois Lord (1938) dated both Hellinikon and Ligourio in the dawn of the Hellenistic period, i.e. in the end of 4th century BC. The Greek archaeologists E. Spathari, Chr. Piteros and G.A. Pikoulas also suggested (Chr. Piteros,

1995; G.A. Pikoulas, 1996) that both pyramids were built in late 4th century BC and that they were guardhouses or outposts. Th. Wiegand (1901) dated the Hellinikon pyramid in 1st century BC. However, these datings must not create a bias toward a more recent period, as archaeologist and Professor of Prehistoric Archaeology at the University of Athens Theodore Spiropoulos (1981), who discovered a pyramid in the shape of the Ampheio hill in Thebes, dates it *circa* 2500 BC.

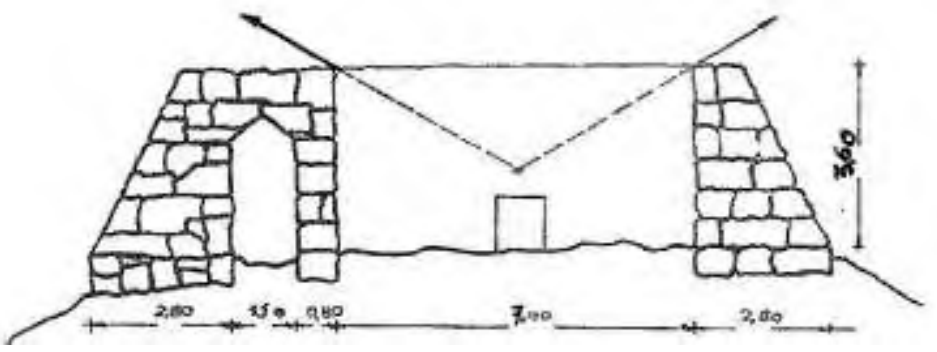

Fig. 4. Drawing of the truncated pyramid of Hellinikon, made by the civil engineer Vassilios Katsiadramis (1994, p. 9222).

4 The Ligourio pyramid

The Ligourio pyramid is located in the foot of Mt. Arachnaeo, to the left side of the road leading from Argos to Epidaurus, 1.5 km West of the village of Ligourio. Its dimensions are approximately 14 (north side) x 12 x 12 x 12 m. Pausanias does not mention this pyramid at all and the first reference to it comes from the "French Scientific Mission in Moreas" (Blouet, A. and Ravoisié, A., 1831). In the years that passed since the early 19th century the pyramid, made of sandstone blocks, deteriorated to the point it is now almost leveled. Only a couple of building stones have remained in their original positions; the rest were used for the construction of other buildings in Ligourio, while some stones are incorporated in the Byzantine church of Agia Marina (St. Marina).

The first excavations in the region were conducted by the American School of Classic Studies of Athens, from 9 to 18 December 1936 and later from 1 to 9 August 1937.

Among the findings of the 1937 excavation, led by R. Scranton (1938, 7.4, pp. 528-538), was a stone axe (*keltis*) dated in the Neolithic Age, that is prior to 3000 BC, a most intriguing fact that created certain connotations. Scranton writes that *"the keltis, an isolated prehistoric artifact, does not prove the existence of a Neolithic settlement at the site. It was probably just transported there from a distant place as something curious"*.

However, some researchers are skeptic about this view: How is it possible for the Neolithic axe to have been preserved at a different site for 2500 years,

to have been transported as something curious to the Ligourio pyramid in the 4th century BC and subsequently preserved at its new position for another 2300 years? It is a difficult question.

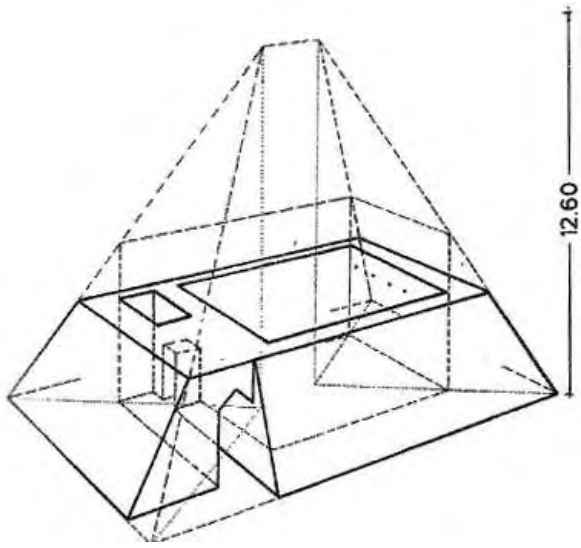

Fig. 5. Drawing of the truncated pyramid of Hellinikon, made by the civil engineer Vassilios Katsiadramis (1994, p. 9222).

Nevertheless, most researchers date the Ligourio pyramid along with the Hellinikon pyramid, around the 4th century BC.

Fig. 6. The Ligourio pyramid, as imaged by the *French Scientific Mission in Moreas* (Expedition Scientifique de Morée, 1831).

In 1995 academician Petros Theocharis and his colleagues announced that the optical thermoluminescence method gives an age for the Ligourio pyramid of 4100 ± 600 years, that is it was built *circa* 2100 BC or about 600 years 'younger' than the Hellinikon pyramid as dated with the same method, although as far as it can be discerned the two pyramids are very similar. The same researchers supported the view that both theses pyramids were astronomical observatories!

On the contrary, archaeologist Christos Piteros, curator of antiquities in Nafplio, supports (1995) a dating of the pyramids in the 4th century BC - definitively no older than 450 BC. As for their purpose, he believes that they were fortified out-posts-military observatories. Piteros is especially critical against the views of Theocharis *et al.* (1995). He strongly argues that their views are misleading(!), since they reject consolidated views of archaeologists simply based on a 'magical unproved physical method for a purely archaeological issue'.

The archaeologists excavators are reserved to accept without doubts the Classical or Hellenistic age, while A. Sampson (1996, pp. 56-61) supports such a younger age but his reserve to reject an earlier age is apparent.

So, up to now, there is no satisfying explanation of the reason behind the construction of several reported small sized pyramids in Greece and about the choice of their shape as a message tower or else. To summarize, the following views have been supported about the Greek pyramids:

a) Purpose

1. Burial monuments - polyandria (Pausanias, 2nd century AD; Leake, 1846; Vischer, 1857).

2. A 'tomb identifier', indicating the existence of an important person's tomb at a nearby site (hill), or even under it (Arvanitopoulos, 1916).

3. Fortified military outposts-guardhouses (Lord, 1938 & 1939; Wiegand, 1901; Fracchia, 1985; Spathari-Piteros-Pikoulas, 1995 & 1996).

4. Towers for fire -or smoke- signaling (Curtius, 1851).

5. Astronomical observatories - with an evident astronomical orientation, after a relative study (Theocharis e*t al.*, 1994 & 1997; Kalleyia, 1995; Theodossiou *et al.*, 2002).

6. Sanctuaries (Katsiadramis, 1994).

b) Dating

1. 1600 to 1100 BC (Pausanias, 2nd century AD; Arvanitopoulos, 1916).

2. 6th century BC (Tsountas, 1893; Curtius, 1851).

3. 4th century BC (Leake, 1846; Lord, 1938 & 1939; Fracchia, 1985; Spathari-Piteros-Pikoulas, 1995 & 1996).

4. 1st century BC (Wiegand, 1901).

5. 2100 BC for the Ligourio pyramid and 2730 BC for the Hellinikon pyramid (Theocharis *et al.*, 1994 & 1997).

5 Conclusion

When excavations were made around the Greek pyramids in the early 1900s, pottery fragments from the 4th century BC were found, and it was presumed that the pyramids were also constructed then; that is, about the time of Alexander the Great. Recent dating of crystals from internal surfaces of the limestone blocks using thermoluminescence puts the construction times back two millennia. The Hellenikon pyramid dates to 2730 B.C.; the Ligourio, to 2100 BC. This means that the Greek pyramids were built in roughly the same time frame as the Egyptian pyramids (Hammond, 1997).

Why would the ancient Greeks want to build miniature pyramids? The classical scholar Pausanias wrote in the 2nd century AD that the Hellenikon pyramid was a cenotaph for the dead fallen in a fratricidal battle 4,000 years ago. Nobody believed his story until now (Corliss, 1998).

The date and the purpose of even the two main Greek pyramids are not known with any certainty. What it can be said is that these are carved and not scalar; moreover they also differ from the Egyptian ones in the slope inclination.

Archaeologists suggest that the Hellinikon pyramid can't be a building of the 3rd millennium BC; it must have been constructed at least after 2100 BC. The later corollary follows from a finding of the excavation conducted for the Academy of Athens' research: a proto-Hellenic ditch in the foundations of the building. The proto-Hellenic period conventionally ends in circa 2100 BC, therefore archaeologists conclude that the pyramid was built definitely after 2100 BC.

Archaeologists also stress that not even one ceramic fragment was discovered in the pyramid sites dated from the two subsequent periods, the meso-Hellenic and the Mycenaean period. If the pyramid was indeed a 3rd-millenium construction, then the lack of ceramics would be a unique case.

The vast majority of archaeologists support the view that the pyramids are buildings of the 4th century BC.

The disagreement among the experts extends to the purpose these structures served. Our team expresses its agreement with professor Theocharis and his colleagues that the Greek pyramids could have an astronomical significance, probably in addition with their use as burial monuments or military outposts. We have also propose that the pyramids of Argolis and in particular the pyramid of Hellinikon village were very likely, besides being a burial monument or guard house, one of the first meridian observatories (Theodossiou et al., 2002).

To support this view there is the case of another Greek megalithic structure, the 'Drakospito' (= dragon house) on top of Mt. Oche, which was studied by our team and was shown to have an ancient Sirius-rise astronomical orientation (Theodossiou et al. 2009). Besides, several astronomical connotations have been proved in the case of the Egyptian pyramids.

For the Greek pyramids, the case is still open. We believe that a coordinated effort of archaeologists, historians, astronomers, architects and archaeometrists is needed in order to reach definite conclusions as far as the use of the pyramid-like structures in Greece is concerned.

Acknowledgements

This study formed part of the research at the University of Athens, Department of Astrophysics Astronomy and Mechanics, and we are grateful to the University of Athens for financial support through the Special Account for Research Grants. It is also supported by the Ministry for Education and Science of Serbia through the project III 44002.

References

Arvanitopoulos, A.S.: 1916, "Research in Argolis during the year 1916", *Proceedings of the Archaeological Society of Athens* [in Greek].

Blouet, Abel and Ravoisié, Amable: 1831, *Expédition scientifique de Morée, ordonnée par le Gouvernement Francais. Architecture, Sculptures, Inscriptions et Vues du Péloponèse, des Cyclades et de l'Attique*, Firmin Didot, (3 volumes), Paris. [in French].

Corliss, W. R.: 1998, *Science Frontiers*, **116**, March-April (on-line reference).

Curtius, E. R.: 1851, *Peloponnesos, eine historisch-geographische Beschreibung der Halbinsel*, band II. Elibron Classics [in German].

Fracchia, H.: 1985, "The Peloponnesian Pyramids Reconsidered", *American Journal of Archaeology*, 89.

Greilich, S., Glasmacher, G. A., Wagner, G. A.: 2005, "Optical dating of granitic stone surfaces", *Archaeometry*, **47**, no. 3.

Habermann, J., Schilles, T., Kalchgruber, R., Wagner, G. A.: 2000, "Steps towards surface dating using luminescence", *Radiation Measurements*, 32.

Hammond, Norman: 1997, "Did the Early Greeks Simply Copy the Pyramids of Egypt?", *London Times*, August 1.

Kalleyia, A.: 1995, in *Papyros-Larousse-Britannica Encyclopaedia*, vol. **33**, p. 73 [in Greek].

Katsiadramis, V.: 1994, "The ancient pyramid-like structures of Hellinikon and Ligourio in Argos - A technical and archaeological study", *Davlos*, 156 [in Greek].

Lazos, C.: 1984, "The pyramids of Argolis", *Istoria Ikonografimeni*, 189 (March), [in Greek].

Lazos, C.: 1987, "The pyramids of Argolis", *Anexigito*, 33 (May) [in Greek].

Lazos, C.: 1995, *Pyramids in Greece*, Athens, Aeolos Publ. [in Greek].

Leake, W. M.: 1846, *Peloponnesiaca: Supplement to Travels on the Moréa*, vol. II. J. Rodwell, London.

Liritzis, I.: 1986, *Archaeometry - Methods of dating in archaeology*, Kardamitsas publ., Athens [in Greek].

Liritzis, I.: 1994a, "A new dating method by thermoluminescence of carved megalithic stone building", *Comptes Rendus* (Academie des Sciences), **319**, serie II, Paris.

Liritzis, I.: 1994b, "Archaeometry: Dating the past", *EKISTICS*, **368**, 364.

Liritzis, I., Galloway R. B. and Theocaris P.: 1994, "Thermoluminescence dating of ceramics revisited: Optical stimulated luminesccence of quartz single aliquot with green light emitting diodes", *J. Radioanal. Nucl. Chem. Letters*, **188** (3).

Liritzis, I.: 1995, *The mystery of the Hellenic pyramids*, Academy of Delphic Studies Publ. [in Greek].

Liritzis, I.: 1997, "The mystery of the Hellenic pyramids", *AELLO* (Yacht Club of Greece) 9, Athens [in Greek].

Liritzis, I., Guilbert, P., Foti, F., Schoerer, M.: 1997, "The Temple of Apollo (Delphi) strengthens new thermoluminescence dating method", *Geoarchaeology International*, **12**, no. 5.

Liritzis I.: 1998, "Bronze Age Greek Pyramids and Orion's belt", *Griffith Observer*, **63**, n. 10.

Liritzis, I. and Raftopoulou, M.: 1999, "Argolid: connection of prehistoric legends with geoenvironmental and archaeological evidence", *TUBA-AR*, II.

Liritzis, I. and Galloway, R. B.: 1999, "Dating implications from solar bleaching of thermoluminescente of ancient marble", *J. Radioanal. Nucl. Chem.*, **241**, 2.

Liritzis, I. and Vafiadou, A.: 2005, "Dating by luminescence of ancient megalithic masonry", *Mediterranean Archaeology & Archaeometry*, **5**, no.1.

Lord, E. L.: 1938, "The Pyramids of Argolis", *Hesperia*, **7** (vii), no. 4.
Lord, E. L.: 1939, "Watchtowers and Forteresses in Argolis", *American Journal of Archaeology*, **43** (January-March).
Lord, E. L., Frantz, M. A., Roebuck, C.: 1941, "Blockhouses in the Argolid", *Hesperia*, **10**, No. 2 (April - June), pp. 93-112.
Morgenstein, M. E, Luo, S., Ku, T. L. and Feathers, J.: 2003, "Uranium series and luminescence dating of volcanic lithic artefacts", *Archaeometry*, 45.
Neimeier, Barbara and Wolf-Dietrich: 1997, "Aegean Frescoes in Syria-Palestine: Alalakh and Tel Kabri", *Proceedings of the 1st International Congress of Minoan Paintings*, vol.II, Thera Foundation.
Oppermann, S.: 1971, "Pyramiden in Griechenland", *Antike Welt*, 2.
Pausanias, *Corinthiaka-Laconika*, 2, 24, 7 and 2, 25, 7 (in: *Pausanias' Guide to Ancient Greece*, 1985, translated by Christian Habicht, Berkeley Univiversity Press, Berkeley, U.S.A.).
Pikoulas, G. A.: 1996, "The 'pyramids' of Argolis", *Archaiologia and Tehnes*, **59** [in Greek].
Piteros, Chr.: 1995, "The so-called 'pyramids' of Argolis: Myth or reality?", *Anagennisi*, issue no. 327 (March) [in Greek].
Piteros, Chr.: 1998 (year of published), "The pyramids of Argolis", *Proceedings of the 5th International Conference of Pelloponesian Studies*, vol. III, p. 370. Argos-Nauplion, September 6-10 1995, Athens [in Greek].
Sampson, A.: 1996, "The pyramids of Argolid and their meaning", *Archaeology*, **57** [in Greek].
Scranton, R.: 1938, "The pottery from the Pyramids", *Hesperia* **7.4**, pp. 528-538.
Spiropoulos, Th.: 1981, *Study of the Site of the Amphion in Thebes*, Sparta [in Greek].
Spiropoulos, Th.: 2003, "The big Hellenic pyramid", *Trito Mati*, pp.34-47.
Theocharis, P., Liritzis, I., Galloway, R. B.: 1994, "Dating of two Hellenic pyramids by a novel application of thermoluminescence", *Jour. of Archaeol. Sci.* 24.
Theocharis, P., Liritzis, I., Lagios, E. and Sampson A.: 1997. "Geophysical prospection and archaeological test excavation and dating in two Hellenic pyramids", *Surveys in Geophysics*, 17.
Theodossiou, E., Niarchos, P. G. and Manimanis, V. N.: 2002, "Are the unknown Greek Pyramids old Observatories?", *Xth SEAC-2002 Conference: "Cultural Context from Archaeoastronomical Data and the Echoes of the Cosmic Catastrophic Events"*, Tartu, 27 August - 1 September.
Theodossiou, E., Manimanis, V. N., Katsiotis, M., Papanikolaou, D.: 2009, "Study and Orientation of the Oche 'Dragon House' in Euboea, Greece", *Journal of Astronomical History and Heritage* (JAH2), **12**, no. 2 (July), 151-156.
Tsountas Christos: 1893, *Mycenae and mycenaean civilization*, Estia Publ., Athens.
Vischer, W.: 1857, *Erinnerungen und Eindrücke aus Griechenland*, Basel.
Wiegand Th.: 1901, "Die pyramide von Kenchreai", *Athen. Mitteilungen* (des Deutschen Archeologischen Instituts. Athenische Abteilung, Athen), **xxvi** [in German].
Zangger, E.: 1993, *Argolis I: The geoarchaeology of the Argolid*, Deutsches Archaologisches Institut, Athen.

The heliocentric system from the Orphic Hymns and the Pythagoreans to emperor Julian

Efstratios Theodossiou[1], Aris Dacanalis[1],
Milan S. Dimitrijević, Petros Mantarakis[3]
[1] Department of Astrophysics, Astronomy and Mechanics Physics Faculty, University of Athens-Zografos 157 84
[2] Astronomical Observatory, Volgina 7, 11060 Belgrade, Serbia
[3] 322127 Needles, Street, Chatsworth, California 91311, USA
etheodos@phys.uoa.gr
mdimitrijevic@aob.bg.ac.yu
zanispetros@socal.rr.com
(Research report. Accepted on 21.10.2008)

Abstract. The evolution of the heliocentric theory in the antiquity has been analyzed, from the first seeds in the Orphic Hymns to the emperor Julian, also called "the Apostate" in the 4th century A.D. In particular the Orphic Hymns, views of Pythagoreans, as well as the heliocentric ideas of Philolaus of Croton, Icetas, Ecphantus, Heraclides of Pontos, Anaximander, Seleucus of Seleucia, Aristarchus of Samos and Emperor Julian were analyzed.
Key words: Heliocentric system, Orphic Hymns, Pythagoreans, Philolaus, Anaximander, Aristarchus, Emperor Julian

Хелиоцентричната система от орфическите химни и питагорейците до император Юлиан

Е. Теодосиу, А. Даканалис, М. Димитрийевич, Р. Мантаракис

Проследено е развитието на хелиоцентричната теория в античността, от орфическипе химни до император Юлиан, наричан в IV в сл.н.е. още "изменникът". Анализирани са, в частност, орфическите химни, възгледите на питагорейците, както и хелиоцентричните идеи на Филолаус от Кротон, Икетас, Екфантус, Хераклидес от Понтос, Анаксимандер, Селеукус от Селеуциа, Аристархус от Самос и император Юлиан.

Introduction

Ever since early antiquity, philosophers and astronomers had been preoccupied with the question concerning which of the heavenly bodies occupied the center of the known world. The geocentric system, in accordance with its egocentric formulation, placed our small planet in the center of the world, a notion that seemed to fit the egocentric minds of the wise. Enjoying the favor of the majority of the philosophers and astronomers, it dominated for centuries. However, there were also opposite views in favor of the heliocentric theory. Indeed, even before Aristarchus the Samian, seeds of the heliocentric theory can be traced back to the Orphic Hymns and in the teachings of Anaximander and the Pythagoreans. Later on Aristarchus the Samian founded the heliocentric theory, which unfortunately did not prevail, unlike its geocentric adversary which gained wide recognition, initially due to the weight of Aristotle's views, and later on due to those of the great astronomer Claudius Ptolemy (2nd century A.D.).

Yet the heliocentric system had not been entirely forsaken. During the 4th century A.D., emperor Julian -also called "the Apostate"-, the last emperor of the first Byzantine dynasty, became a fervent supporter. Julian held the Earth as a planet which, like all other planets, went around the sun in a circular orbit. Thus, Aristarchus' theory had not been forgotten during the first centuries A.D., but even enjoyed advocacy.

1 Orphic Hymns

The ancient teachings of Orpheus are considered to be the first mystic Greek religion, with poems and hymns of great beauty. The Orphic Hymns consist of 87 hexametric poems or 1200 verses in total, which have reached us under the title "*Hymns of Orpheus to Musaeus*".

The hymns contain a breadth of astronomical information, partly obscured by the use of a strongly poetic language, as well as interesting ideas for the creation and the supreme being. This last piece of information tells us that the hymns belong to a monotheistic cult, since the creation of the Universe is ascribed to a single supreme force. We also come across the interesting notions of Chaos and the cosmic egg, which led to the creation of "Phanes", he who is radiant and existent.

From eyes obscure thou wip'st the gloom of night, all-spreading splendour,
pure and holy light. Hence Phanes call'd, the glory of the sky,
on waving pinions thro' the world you fly.
[V. TO PROTOGONUS, *The Fumigation from Myrrh*, verse 15
(see e.g. *Orphic Hymns* sine datum, or *Orphicorum Fragmenta*, 1922)]

Nearly all of the ancient Greek sages and writers drew inspiration from themes found in the Orphic Hymns, and were thus influenced while formulating their unique theories and teachings.

Let it be noted that in the Orphic Hymns, "Chaos" stands for what nowadays we would call space, "Gaia" for the earth-mother (and not the planet) whereas "Eros" (love), stands for the creational force. In the same hymn, we find a praise to Chaos which spans the aether, and was born from the cosmic egg:

O Mighty first-begotten [Protogonos], hear my pray'r, two-fold, egg-born, and
wand'ring thro' the aether...
[V. TO PROTOGONUS, *The Fumigation from Myrrh*, verse 1]

Let it also be noted that during the Homeric times, the Earth was perceived as a circular flat disk which was surrounded by a vast circular river, the Ocean. This notion is made evident in the following verse:

Old Ocean [Okeanos] too reveres thy high command, whose liquid arms
begirt the solid land.
[X. TO PAN, *The Fumigation from Various Odors*, verse 15]

Fig. 1. Phanes: God of light, truth and justice. Here he appears to be surrounded by an elliptical (egg-shaped) ecliptic with the zodiacal signs of the four basic elements. Above and below him are the two halves of the cosmic egg, and between them, lies a flaming Phanes, winged just like the creative Eros. In his right hand he holds thunder (like Zeus does) and a scepter in his left, signifying his kingly place on the world. The curled snake on him symbolizes the Earth, the cup stands for water, the wings for air and the torch for fire. Its legs are shaped like a fork, just like those of the god Pan.

The hymns mention Heaven being the ruler of the world, revolving around the Earth:

Great Heav'n [Ouranos], whose mighty frame no respite knows... Hear, world ruler,..., forever whirling as a sphere around this earth
[III. TO HEAVEN: *The Fumigation from Frankincense*, verse 1]

Fig. 2. The Homeric Universe: In the Universe of Homer's times, the mountains can be seen to rise over the surface of the great disk of the Earth, the Ocean spreading around them, while the center is dominated by Mount Olympus which rises up to heaven. In its highest peak, the all-seeing Zeus is seated, supervising both immortal gods and mortal men, sometimes rewarding and sometimes punishing them. Beyond Olympus spreads Heaven, supported by the pillars of Atlas. In heaven we can locate the Moon, the stars and the constellations. In particular, in this figure we can distinguish -but not referred by Homer- the constellations of Hydra, Corvus, Crater, Cancer, Leo, Gemini, Taurus as well as the Pleiades open cluster (as cited in D. Cotsakis, 1976, p. 18)

Another verse suggests that the origins of the heliocentric system seem to be located in the Orphic Hymns, as has been previously stressed by Constantinos Chassapis (1967), the late Greek astronomer, and Maria Papathanassiou (1978, 1980), assistant professor in the Mathematics Faculty at the University of Athens:

Hear golden Titan! Glowing like gold, you who strides above, oh heavenly light...
... you who combines the epochs ... You are the world ruler...
With your golden lyre, draw on the harmonious path of the world...
... [you] who wanders through fire and moves around in a circle
[VIII. *To the Sun*, verse 2]

The phrase "[you who attracts] *draw on the harmonious path of the world*" is striking since this could be a spermatic idea of the harmonious movement of the planets around the Sun, a notion which was commonly used during at least the first five (perhaps more) centuries B.C. If the planets are to be included in the notion of the world, then the golden Sun could be seen as

the attractive center of their harmonious orbits. One may therefore make the assumption that the seeds of a heliocentric theory can be traced in the Orphic Hymns.

Furthermore, on hymn (34): To Apollo, we find the following:

Loxias, the pure! . . . You mixed in equal parts winter and summer. . .
[XXXIV. *To Apollo*, verse 6,. . . and 20]

Thus, the "Loxias" Sun (meaning "tilted") mixed the components of the year and divided it in two equal parts, the summer and the winter. This is a very important astronomical detail which has drawn some attention from the astronomical community, because it has been linked to the dating of the Orphic Hymns. If one were to view this information literally, he would look back in time when the summer and winter were of exactly equal length. This would place the Orphic Hymns -more or less- near the following dates: 1841 B.C. and 1366 B.C. (Chassapis, 1967 and Papathanassiou, 2003). This view however, requires the assumption that ancient Greece possessed very capable astronomers in early antiquity, an idea with little evidence to support it.

Another excerpt which, although referring to Hestia, seems to add to the heliocentric aspect of the hymns, is Hymn (84) [To Hestia]

You who occupies the center of the home of the greatest and eternal fire.
[LXXXIV. To Hestia, verse 2]

In *Orphicorum Fragmenta* a fragment tell us about the rotation of the Earth. This fragment says that Musaeus knew the path of the star and the movement of the sphere around the Earth, as this round Earth revolves in equal time period around its axis (Fr. 247 v. 24-26, pp. 261-262).

2 The Pythagoreans

Pythagoras founded his School at Croton in lower Italy, in c.540 B.C. He and his followers held the view that the most important cosmological principle were the numbers. In a way they were not mistaken, since it is in numbers that today's scientific thought is focused, for numbers identify with mathematical harmony and, without them, science would have never existed in the first place.

The Pythagorean School placed the foundations for the philosophy of mathematics as well as for physics, by relating order and the harmony of sound to the harmony of the Universe.

Virtually all of the students of Pythagoras were trained in astronomy, but their studies of the motion and the distances of the planets were carried out with a rather mystical approach. They believed in mystical and sacred relations between the numbers and the phenomena that they describe. In the Pythagorean view, the planetary distances were analogous to a heavenly musical harmony, which was created by harmonious sounds. They believed that this harmony was constantly created, being an eternal expression -of the highest order- of the unique divine harmony.

The Pythagoreans would have been delighted to see ideas very similar to their own, used in contemporary science. For example, modern String theory holds that everything on a microscopic level is a combination of vibrating strings. The Pythagoreans, developers of the "music and harmony of the spheres", would have seen particles as microscopic strings whose rhythmical vibrations create other particles, i.e. "the musical notes". These notes, in turn, create the music of the heavenly spheres. Thus though their eyes, our whole world would seem like a musical symphony, composed with these notes.

Pythagoras' School was a brotherhood, most likely in an almost religious sense, had various degrees of initiation, and may have been founded after the manner of the Orphic communities. Its contribution to geometry, music, arithmetic and astronomy was integral for the evolution of scientific thought. Through geometry, as well as the harmony of sound and numbers, the Pythagoreans developed the notion of perfection in the Universe, and coined an appropriate word to describe it: "Cosmos". This name is derived either from the word "cosmo" which means "to orderly arrange" or from the world "cosmema" which means "jewel" (ornament). Pythagoras himself appears to be the first to use the word "Cosmos", according to the doxographer Aetius: "*Pythagoras was the first to name the place of all things Cosmos, due to its orderly nature*" [Aetius, *De Vestutis Placitis*, II, 1, 1 (D. 327, 8)]

The Pythagorean School held that the essence of all things was the "number", a rather abstract notion, which could not be perceived through one's senses, but only through intellect. In this manner, the philosophers of this school equated infinity with those material elements which could not be subject to measurement or definition. They introduced the notion of "matter", which was perceived as an element that resisted every definition of its ontological and moral imperfection.

Some elements of the Pythagorean cosmology have reached us through one of Aristotle's books, namely *Metaphysics*. According to the Pythagoreans, the Cosmos was created after the "One" initially came into being. The "one" -or "en" in Greek- served as the first principle, attracted the "infinite" (apeiron) to its own self, and bestowed on it with the "limit" (peras). These last two notions, the "limit" and the "infinite" have no clear meaning, but it has been speculated that they could be referring to the prime and even numbers.

Aristotle also mentions the following: "*The elements of number, according to them, are the Even and the Odd. Of these the former is limited and the latter unlimited; Unity consists of both (since it is both odd and even) [note of trans: either because by addition it makes odd numbers even and even numbers odd (Alexander, Theo Smyrnaeus) or because it was regarded as the principle of both odd and even numbers (Heath)]. Number is derived from Unity; and numbers, as we have said, compose the whole sensible universe*" [Aristotle, *Metaphysics*, A5, 986, 15]

Aristotle provides us with a further comment on the Pythagorean ideas: "*It is absurd also, or rather it is one of the impossibilities of this theory, to introduce generation of things which are eternal. There is no reason to doubt whether the Pythagoreans do or do not introduce it; for they clearly state that when the One had been constituted -whether out of planes of superficies or seed or of something that they cannot explain- immediately the nearest part of the Infinite began to be drawn in and limited by the Limit [note of trans:*

if numbers are eternal, it is absurd that they should be generated]. [Aristotle, *Metaphysics*, 1091a, 14].

Another cosmological notion that the Pythagorean School of thought held was that the Creation began from a unique single point, which continuously expanded to infinity. It is evident that the Pythagoreans believed that the Universe evolved from a spherically expanding infinitesimal core. This idea once again, has been shared by some astronomers, who believe in a static spherical universe whose existence began from an initial point.

Another idea that Pythagoras believed in was that the Earth was spherical and immobile in the center of the Cosmos, which was spherical as well. "*..the water, earth and air; these elements interchange and turn into one another completely and combine to produce a universe animate, intelligent, spherical, with the earth at its center, the earth itself too being spherical and inhabited round about*" [Diogenes Laertius, *Lives of Eminent Philosophers*, VIII, 25, 8-10].

Many Pythagoreans held an identical view of a spherical Earth, placed in the center of the world, *without being supported by anything.* This was a novel idea in its time, and is demonstrative of a clear progress when compared to assumptions that were previously held by other Greek philosophers.

According to the late professor of astronomy, Demetrios Kotsakis, "Pythagoras was the first who taught that the apparent motion of the sun on the celestial sphere from the east to the west, could be analyzed in to two distinct motions: One daily from East to West, parallel to the equator, and one yearly from West to East on the ecliptic" (Kotsakis, 1976, p. 28).

In the 6tth century B.C., some students and followers of Pythagoras, and most importantly Philolaus of Croton, Heraclides of Pontus, Ecphantus of Syracuse as well as others, believed in a "pyrocentric" theory. This means that they accepted that the element of fire was the "first principle" of the Cosmos. They believed that after the Creation, the element of fire accumulated in the center of the Cosmos and its attraction to its neighboring parts was part of the creation, formation and formulation of the various bodies that made up the spherical Universe.

2.1 The ideas of Philolaus of Croton

Philolaus of Croton (450-500 B.C.), spread the pythagorean ideas concerning the "first principle", by organizing and writing a synopsis of pythagorean philosophy. It appears that he was the principle creator of the philosophical notions of the "limit", the "infinite" and the harmony between the two, which, according to his views, was achieved due to the "number". He believed that the Cosmos is unique and began its creation from the center, which was occupied by fire. There, he placed the "Anticthon", (or Counter-earth - a hypothetical invisible Earth), the Earth, the Moon, the Sun, the five planets known at the time (Mercury, Venus, Mars, Jupiter and Saturn), and the sphere of the fixed stars. Thus, ten heavenly bodies "danced" around the central fire, a number which the Pythagoreans held as sacred. It has been speculated that the Anticthon was introduced exactly for this reason, namely to raise the number of the celestial bodies to the sacred number ten.

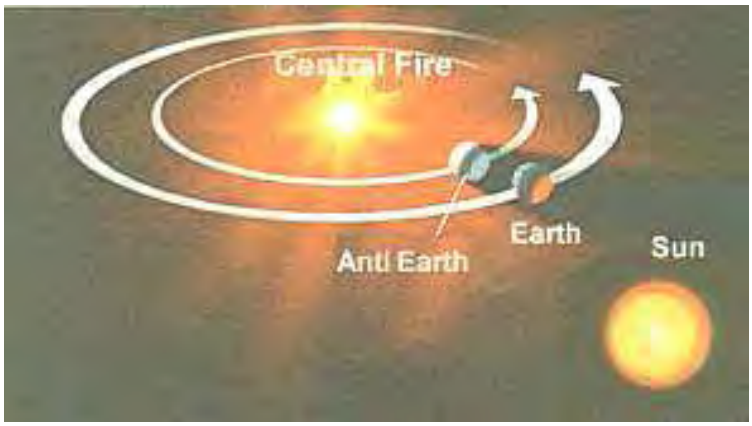

Fig. 3. Pythagorean Universe

It is told that Philolaus of Croton, along with Archippus, Lysis and few others, survived the revolt against the Pythagoreans in Croton, which was instigated by Cylon, an ex student of Pythagoras, who had been sent off from the school for failing to comply with its principles. It is certain that the teachings of Pythagoras and his students, their innovative theories, their mysticism, as well as their aristocratic political tendencies caused the violent reaction of their democratic adversaries, who either killed or exiled many of them: "*Cylon of Croton... and those allied with him, hunted (killed) the Pythagoreans down to the man.* (Iamblichus *Vita Pythagorii* (V.P.) 248-249 ff).

Following this course of events, Philolaus left Croton and based himself in Thebes, where he taught Pythagorean philosophy and wrote the books *Bachae* and *On Nature* A, B and C (Cosmos, Nature and Soul respectively). An extant fragment from his first book reads: "*The world is uniform, it began its creation from the center, and from the center it expanded uniformly upwards and downwards, keeping equal distances from the center*" (Diels and Kranz, 1996, *Die Fragmente der Vorsokratiker*).

Several sources provide information on some of his cosmological thoughts: *The initial One, the beginning of the creation of the Universe, is called Hestia* [*On Nature*, fragment 7, Stobaei *Eclogae* I 21, 8 (p. 189, 17 W)].

Diogenes Laertius mentions: *According to Demetrius, in his work "on men of the same name", Philolaus was the first to publish pythagorean treatises, to which he gave the title "On Nature", beginning as follows: Nature in the ordered universe was composed of unlimited and limiting elements, and so was the whole universe and all that is therein* [Diogenes Laertius, *Lives of Eminent Philosophers*, 85 (A1 I 398, 20)].

The doxographer Aetius (Aet. I 3, 10), informs us (citing Theophrastus) of the following: *Philolaus believes that there is fire around the center of the Universe, which he calls "hestia of all" and "house of Zeus", "mother*

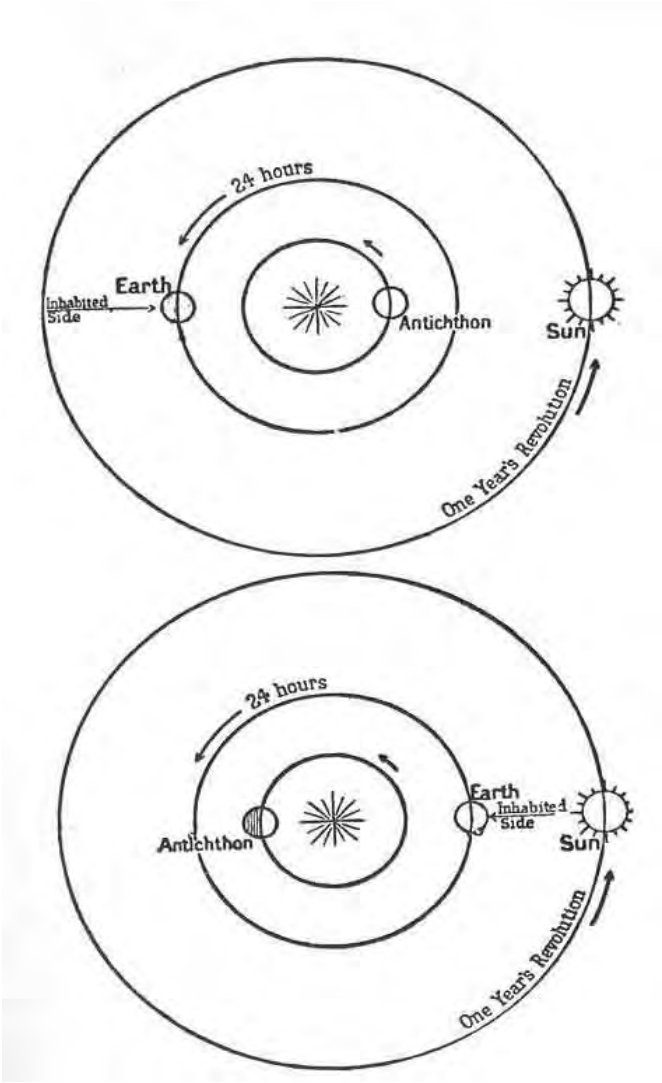

Fig. 4. Antichthon: The hypothetical invisible Earth, which according to the Pythagoreans occupied the antipodes of the Earth.

of the Gods", "altar, constraint and measure of nature". There is another fire which dwells in the outer region of the Universe. The center, he says, came first by nature, and around it dance ten heavenly bodies: The sphere of

fixed stars, then the five planets, then the Sun, then the Moon, followed by the Earth and Anticthon, and after all these the fire of "hestia", which lies around the center. The outer region, which surrounds the whole Universe, is a place where the elements are in their pure state, unmixed, and that place he calls "Olympus". All that lies beneath Olympus, namely the part where the five planets along with the Sun and the Moon lie, he calls "cosmos", while the area beneath those, the sublunar space ... he calls "heaven". Wisdom is relevant with the order which holds in the heavenly bodes, while virtue is relevant with the disorder of the things which are subject to birth. The first is perfect while the second is imperfect. [Aet. *De Vestutis Placitis*, II 7, 7 (D. 336, vermutlich Theophrast. im Poseidonios-Excerpt)].

The above are mentioned once again by Aetius: *The Pythagorean Philolaus places the fire in the center (for it is the Universe's focal point), secondly he places the Anticthon, then, our habitat, the Earth comes third, placed opposite [from the Antictchon] and moving in a circle, that being the reason for the beings of the Anticthon being invisible to the beings of the Earth. The ruling power of the Universe lies in the central fire, which God placed, like a keel, to base the foundation of the sphere that makes up the world".* [Aet. III 11, 3 (D. 337 from Theophrastus)].

¿From all of the above we can sum up that, according to Philolaus, everything in "Olympus" and the "Cosmos" never changed, while in the areas up to the Moon, every being gifted with life was born, changed and finally died. The Earth and all the other planets were rotating around Hestia with the same direction but at different levels and with different speeds. Hestia was invisible because it shed its light to the antipodes of the Earth, which were impossible to get to. The Sun did not have its own light, but accepted and accumulated the sun of Hestia.

Philolaus, through his questioning of the traditional geocentric cosmology, set the foreground for Aristarchus' heliocentric theory, which would clearly dispute the central role of our small planet in the Universe. Even though he did not specifically place the Sun in the center, the idea of the "central fire" certainly served as a basis for the heliocentric theory. Stavros Plakides (1983-1990), a late Greek professor of Astronomy at the University of Athens, speculated that Philolaus, after having experienced the violence in southern Italy, avoided placing the Sun in the center of the Universe. Fear for his life may have been the motive for adopting the milder approach of placing the "central fire" instead (Plakides, 1974).

Diogenes Laertius, an important source from which we draw the views of Philolaus, mentions that opinions were divided as to who claimed first that the Earth is indeed moving: *It is told that he [Philolaus] was the first to claim that the Earth moves in a circle, while others ascribe it to Icetas of Syracuse* [Diog. Laert. *Lives of Eminent Philosophers* VIII, 84, 85)].

Aetius, another source, informs us that concerning the motion of the Earth Philolaus taught the following: *Others believe that the Earth is immobile. Philolaus on the contrary, believes that the earth is moving in a circle around the fire, tracing a tilted circle, just like the Sun and the Moon does* [Aet. *De Vestutis Placitis* III, 13, 1. 2. (D 378)]. Therefore, Philolaus came at a disagreement with his master, and taught that the earth was not immobile in the center of the world, but was circling the "Central Fire".

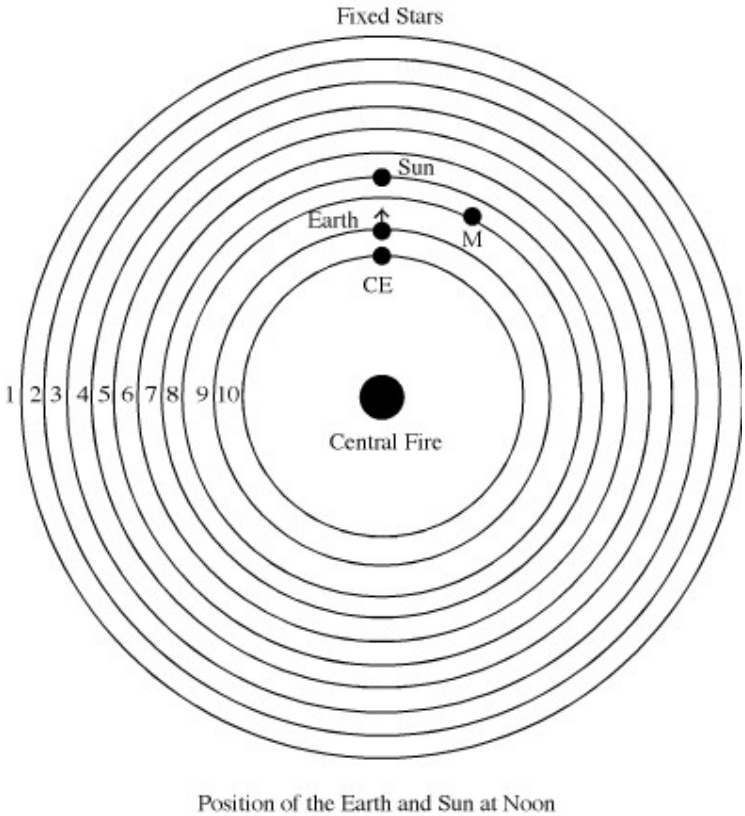

Fig. 5. The world view of Philolaus. In the world view of Philolaus, the center is occupied by the Central Fire, Anticthon (Counter-Earth, CE),The Earth, the Moon (M), the Sun, and beyond those lie the spheres of the five planets and that of the fixed stars. The crystalline spheres around the Central Fire are 10 (= 1+2+3+4), equal to the sum of the first four numbers.

Diogenes Laertius also informs us that Plato bought a copy of the work of Philolaus for the -astronomical at its time- price of 100 mnae: *Some authorites, amongst them Satyrus, say that he wrote to Dion in Sicily instructing him to purchase three Pythagorean books from Philolaus for 100 mnae* [Diog. Laertius, *Lives of Eminent Philosophers*, III 9].

Plato, according to Plutarch, studied the work of Philolaus carefully, and after careful reading, nearing the end of his days -as the story goes by- was convinced that the Earth is indeed moving around the Sun: *As Theophrastus informs us, Plato, near the end of his days had regrets for his older opinion, by which he unfittingly placed the Earth at the center of the Universe* [*Platonicae Quaestiones* H1 915, vol. XIII1, 76-78]. The study of Philolaus may have

been the reason for another change in the views of Plato: In *Republic* he identifies the celestial equator with the ecliptic, an idea which he turns from in Timaeus.

Aristotle, in his book *On the Heavens (De Caelo)*, provided us with some commentary on a few pythagorean views: *These affirm that the center is occupied by fire and that the Earth is one of the stars, and creates night and day as it travels in a circle about the center* [Aristotle, *On the Heavens* B, 13, 293a, 21-23]. Also, *The Pythagoreans make a further point. Because the most important part of the Universe -which is the center- ought more than any to be guarded, they call the fire which occupies this place the Watch-tower of Zeus, as if it were the center in an unambiguous sense, being at the same time the geometrical center and the natural center of the thing itself... For this reason there is no need for them to be alarmed about the universe, nor to call in a guard for its mathematical center; they ought rather to consider what sort of thing the true center is, and what is its natural place* [Aristotle, *On the Heavens* B, 13, 293b, 1-10].

The late professor of Astronomy at the University of Athens Demetrios Cotsakis (1976) mentions that the creation of the world-view which Philolaus describes was indeed revolutionary for the scientific thought of the time. He specifically mentions the views of the Italian astronomer Giovanni Schiaparelli (1835-1910), who wrote, as cited in Cotsakis (1976), the following, concerning the views of the Pythagoreans and the system proposed by Philolaus: *The system of Philolaus was not a fruit of some restless imagination, but came through the torque and pull of one who sets the outcomes of observation in accordance with a predetermined principle, which exists above the nature of things... Appreciating this, and combining it to the fundamental theorems of the Pythagorean Philosophy, the system of Philolaus naturally appears as one of the most wonderful creations of human genius. His critics are incapable of appreciating the power of research, which was necessary, in order to unify the ideas of the roundness of the Earth, its levitation in space, and its motion. Indeed, without these ideas, there would have been no Copernicus, neither Kepler, nor Galileo or Newton* [Cotsakis, 1976, p. 30].

2.2 The views of Icetas, Ecphantus and Heraclides of Pontus

Beyond the theories of Philolaus of Croton, there were other students of Pythagoras which put forward novel ideas, like Icetas and Ecphantus of Syracuse as well as Heraclides of Pontus.

Icetas of Syracuse claimed that the Heaven, the Sun, the Moon and the stars were immobile, and the only thing that moved was the Earth. Concerning his views, Cicero mentions the following: *As Theophrastus says, Icetas of Syracuse was of the opinion that the heaven, the Sun, the moon and the stars (i.e. the planets) and all that is high above are immobile, and nothing in the world is moving, apart from the Earth. But as it rotates around its axis with the greatest possible speed, its motion causes all these phenomena to appear, which would have appeared were the Earth immobile and heaven rotated instead of it* [Cicero, *Academica priora* II, xxxix, 123].

It appears that this theory was embraced by both Ecphantus and Heraclides as well, both of which believed that the Earth moves rotating in space, just like a wheel does around its axis.

Therefore, the students of Pythagoras were the ones to reduce our planet to its real place and motions, while at the same time holding a pyrocentric planetary theory, which certainly assisted Aristarchus of Samos (310-230 B.C) to formulate his novel heliocentric theory.

According to Hippolytus, the Pythagorean Ecphantus appears to have also followed an "atomic theory" of Pythagorean inspiration, by "giving body" to units, which were directed and governed by some divine force, "nous" (the mind). He also mentions that Ecphantus believed that the Earth spins around its axis with an eastern direction, but does not change its place in space. [Hippolytus *Refutationis Omnium Haeresium* I 15 (D. 566W. 28)]. These last two pieces of information are also mentioned by the doxographer Aetius, who finds Heraclides in agreement with Ecphantus. [Aet. *De Vetustis Placitis*, III, 13, 3 (D. 378)].

Heraclides in particular appears to have modified the atomic theory of Leucippus and Democritus, proposing that the first material elements were molecules and not atoms. According to him, the universe was composed of small material molecules which did not share any connection.

3 The views of other Philosophers

3.1 Anaximander and Seleucus

So far we have mentioned the views of the Pythagoreans concerning the motion of the Earth. However, even before the Pythagoreans, during the 6th century B.C., the great philosopher Anaximander, was most likely the first Greek astronomer to talk about the motion of our planet around the center of the world, which may have been the Sun. He also discovered other fundamental astronomical facts, like the "detachment" of the Earth, and its axial rotation. This information can be found in the work "*Expositio rerum mathematicarum ad legendum Platonem utilium*" of Theon Smyrnaus (70-135 B.C.), who lived during the reign of emperor Adrian (Theon of Smyrna, 1979).

Anaximander's views were adopted by later philosophers like Empedocles of Agrigentum (490-430 B.C.), Parmenides of Elea (early 5th century B.C.), Aristarchus of Samos, Cleomedes (2nd or 3rd century B.C.) and several Pythagoreans.

Another philosopher, which name is Seleucus of Seleucia (c. 2nd century B.C.), was an astronomer of the hellenistic period from Anatolia, who supported a heliocentric theory of his own. Fragments of his work are found in the works of Plutarch, Strabo, Aetius and Hippolytus. Hippolytus informs us that the Earth was indeed moving, and that the Moon played a part in its axial rotation as well as in its orbit around the Sun. [*Philosophoumena*, Book C, 897C, 14-16]. The same source also informs us that he believed that the Cosmos was infinite [*Philosophoumena*, Book ?, 886C, 6].

Plutarch mentions a few of his other astronomical ideas [*Platonicae Quaestiones* H1 915, vol. XIII1, 76-78]; unfortunately, all of the work of Seleucus was lost and we have no knowledge of his heliocentric theory.

3.2 Aristarchus of Samos

After the Pythagoreans, appeared the great astronomer Aristarchus of Samos (310-230 B.C.), the foremost introducer of the heliocentric theory as we know from the book of Archimedes *Arenarius* [I 4-6 (3, 180-182), manuscript 2, Cod. Laurent. Gr. 28]. Plutarch, also, writes about the heliocentric theory of Aristarchus of Samos [*De placitis philosophorum* II, 24 (7, 355a)].

Aristarchus' hypothesis was original and quite bold for its time. For this reason Plutarch mentions that he was accused of atheism [*De facie in orbe lunae*, 923A (15, vol. XII, p. 54)]. Aristarchus, according to Aetius was helped to escape in Alexandria by his teacher Straton of Lampsacus (Aetius, *Placitorum Compositione* book 7, 313b, 16-17).

It is apparent that apart from the fervent geocentrists, there were several Greek thinkers whose philosophical thoughts disputed the validity of the geocentric system.

Unfortunately, overcoming the objections of the heliocentrists, the geocentric system, as was formulated by Claudius Ptolemy (2nd century A.D.), reigned for centuries, seconded by the weight of the views of Aristotle, whose work was held as indisputable during the Dark Ages.

4 Emperor Julian

Yet faith in the heliocentric system had not been forsaken. During the 4th century A.D. emperor Julian (336-363 A.D.) studied with care the works of the ancient Greek philosophers, which he held in deep respect. His studies took place in the philosophical schools of Athens. Enchanted by the beauty of the ancient Greek spirit, he wished to revitalize it. He believed that the Earth's world order was influenced by a heavenly and divine hierarchy, in which everything originated from the unique God, the illuminating Sun.

He was interested in philosophy as well as astronomy, and rose as a fervent supporter of the heliocentric system. In his book *Hymn to King Helios* dedicated to Sallust (*Hymn to the king Sun dedicated to Sallust*), he writes: *For that the planets dance about him as their king, in certain intervals, fired in relation to him, and revolve in a circle with perfect accord, making certain halts, and pursuing to and from their orbit, as those who are learned in the study of the spheres call their visible motions; and that the light of the moon waxes and wanes varying in proportion to its distance from the Sun, is I think, clear to all* [*Hymn to King Helios dedicated to Sallust*, 135b, 1-6].

Therefore, Julian held the Earth as a planet, which revolved in a circular orbit around the Sun. The Earth is moving, and along with it the other planets in circular orbits around the Sun, in determined intervals i.e. constant distances. The above clearly show that the theory of Aristarchus hadn't been forgotten, but during the 4th century A.D. enjoyed advocacy.

Conclusion

Beyond the sperms of the heliocentric theory that we saw in the Orphic Hymns, several scholars of Ancient Greece supported this "heretical" for its time view. Its main introducers were the Pythagorean philosophers Philolaus, Icetas, Ecphantus, Heraclides and foremost Aristarchus of Samos, who gave the Sun its rightful place in the Pythagorean "central fire".

The heliocentric theory did not prevail, and instead, the geocentric model, elaborated by the great astronomer Claudius Ptolemy, reigned for centuries in the West, since the undisputed Aristotle was in agreement with it.

Yet the heliocentric theory had not perished, since in the 4th century A.D. the Emperor Julian, a believer in the divinity of the Sun, became a fervent supporter. In the end, the heliocentric system faded away until the 16th century when the great Polish clergyman and astronomer Mikolaj Kopernik (Nicolaus Copernicus 1473-1543 A.D.), brought it back to light (Copernicus, 1995). The hypotheses of Aristarchus of Samos and the preparation of the Pythagoreans were the foundations for the great Polish astronomer's thoughts.

References

Aetius, 1879 (reprinted 1965), Placitorum Compositione (De Vetustis Placitis). Vol. IV 9, 8. in Diels Hermann: Doxographi Graeci. Berolini. Apud Walter De Gruyter et Socios, Editio Quarta.

Archimedes, 1972, Arenarius in Opera Omnia, Bibliotheca Scriptorum Graecorum et Romanorum Teubneriana. Ed. I. L. Heiberg, vol. II corrigenda Adiecit E. S. Stamatis. Stutgardiae in Aedibus MCMLXXII.

Aristotle, 1956, The Metaphysics. Vol. I-IX, The Loeb Classical Library, Book XVII with an English Translation by H. Rackham. London: William Heinemann Ltd. Cambridge, Massachusetts: Harvard University Press.

Aristotle, 1953, On the Heavens (De Caelo). The Loeb Classical Library, with an English Translation by W.K.C. Guthrie. M. A. London. William Heinemann Ltd. Cambridge, Massachussets, Harvard University Press, MCMLIII (First printed 1933, reprinted 1936, 1947, 1953, 1956).

Chassapis Constantinos, 1967, The Greek Astronomy of the 2nd millennium B.C. according the Orphic Hymns. PhD. Thesis, University of Athens [self edited], Athens [in Greek].

Cicero, 1961, Academica Priora, with an English Translation by H. Rackham, M.A. The Loeb Classical Library. London. William Heinemann LtD. Cambridge, Massachussetes, Harvard University Press. MCMLXI (First printed 1933, reprinted 1951, 1956, 1961).

Cicero Marcus Tullius, 1984, Academica. Publ. Lubrecht & Cramer, Ltd. October.

Copernicus Nicolaus, 1995, De Revolutionibus Orbium Coelestium, libri VI. On the Revolution of Heavenly Spheres. Trans. By Charles Glenn Wallis. Prometheus Books, October 1995.

Cotsakis Demetrios, 1976, The pioneers of Science and the creation of the World. Ed. Zoe, Athens.

Diels Herman, 1996, Die Fragmente der Vorsokratiker, Herausgegeben von Walther Kranz. Ester und Zweiter Band, Weidmann, Zurich.

Diogenes Laertius, 1925, Lives of Eminent Philosophers, vol. II, IX 34-35, pp. 3, 441-445. Heinemann, London. The Loeb Classical Library; English translation by R.D. Hicks, revised and reprint 1959.

Hippolytus,1857-1866, A Refutation of All Heresies: Refutationis Omnium Haeresium (Filosofoumena). Patrologia Greca (P.G.) 16, In Origenes, Liber VII, 404-405, 339. Typographi Brepols Editores Pontificii, Parisiis.

Iamblichus, 1965, Vita Pythagorii (V.P.) Life of Pythagoras, with the English translation by Thomas Taylor in 1881, J. M. Watkins, 1965, p. 248-249ff.

Iuliani Imperatoris, 1875, Vol I. Oratio IV (To King Helios), 143 B. 146 D., Lipsiae Teubner.
Julian the Emperor 1954, The works of the emperor Julian, The Orations of Julian, IV. Hymn to king Helios dedicated to Sallust. The Loeb Classical Library. Trans. By Wilmer Cave Wright, Ph.D., William Heinemann Ltd. Cambridge, Massachusetts, Harvard University Press MCMLIV (First printed 1923, reprinted 1930, 1954).
Orphic Hymns, sine datum, Ed. Ideotheatro, Athens [in Greek].
Orphicorum Fragmenta, 1922, Ed. O. Kern, Weidmann.
Papathanassiou Maria, 1978, Cosmological and cosmogonical aspects in Greece during 2nd millennium B.C. PhD. Thesis, University of Athens [self edited], Athens [in Greek].
Papathanassiou Maria, 1980, Aristarchus the Samian, Mathematical Review 20, Editions of the Hellenic Mathematical Society, p. 91-120 [in Greek].
Papathanassiou Maria, 2003, Primordial astronomical learning. Elefterotypia-Historica, Athens, January 2, 2003, p. 6-12 [in Greek].
Petrides, S., 2002, The Orphic Hymns, Astronomy in the Age of Ice [self edited], Athens [in Greek].
Plakides Stavros, 1974, The Geocentric and the Heliocentric Theory. Parnassos 16, Athens [in Greek].
Plutarch Chaeronsis, 1841, Scripta Moralia. Graece et Latine. Tomus Secundus. De placitis Philosophorum Libri quinque. Parisiis. Editore Ambrosio Firmin Didot MDCCCXLI.
Stobaei Ioanni Eclogae, sine datum, Wachsmuth Dox. 336 B 20-337 B 10 and Bibliotheca of the ancient Greek writers, Ed. Georgiades, Athens.
Theonis Smyrnaei, 1878, Philos. Platonici. Ed. Hiller. Lipsiae 1878, p. 198, 14-19.
Theon of Smyrna, 1979, Mathematics useful for understanding Plato or Pythagorean Arithmetic, Music, Astronomy, Spiritual Disciplines. Trans. by Christos Toulis, Wizards Bookshelf.

The heliocentric system from the Orphic Hymns and the Pythagoreans to emperor Julian

Efstratios Theodossiou[1], Aris Dacanalis[1], Milan S. Dimitrijević[2], and Petros Mantarakis[3]

[1] Department of Astrophysics, Astronomy and Mechanics Physics Faculty - University of Athens-Zografos 157 84

[2] Astronomical Observatory, Volgina 7, 11060 Belgrade, Serbia

[3] 322127 Needles, Street, Chatsworth, California 91311, USA

etheodos@phys.uoa.gr

mdimitrijevic@aob.bg.ac.yu

zanispetros@socal.rr.com

(Research report)

Abstract. The evolution of the heliocentric theory in the antiquity has been analyzed, from the first seeds in the Orphic Hymns to the emperor Julian, also called "the Apostate" in the 4th century A.D. In particular the Orphic Hymns, views of Pythagoreans, the heliocentric ideas of Philolaus of Croton, Icetas, Ecphantus, Heraclides of Pontos, Anaximander, Seleucus of Seleucia, Aristarchus of Samos and Emperor Julian were analyzed.

Key words: Heliocentric system, Orphic Hymns, Pythagoreans, Philolaus, Anaximander, Aristarchus, Emperor Julian

Introduction

Ever since early antiquity, philosophers and astronomers had been preoccupied with the question concerning which of the heavenly bodies occupied the center of the known world. The geocentric system, in accordance with its egocentric formulation, placed our small planet in the center of the world, a notion that seemed to fit the egocentric minds of the wise. Enjoying the favor of the majority of the philosophers and astronomers, it dominated for centuries. However, there were also opposite views in favor of the heliocentric theory. Indeed, even before Aristarchus the Samian, seeds of the heliocentric theory can be traced back to the Orphic Hymns and in the teachings of Anaximander and the Pythagoreans. Later on Aristarchus the Samian founded the heliocentric theory, which unfortunately did not prevail, unlike its geocentric adversary which gained wide recognition, initially due to the weight of Aristotle's views, and later on due to those of the great astronomer Claudius Ptolemy (2nd century A.D.).

Yet the heliocentric system had not been entirely forsaken. During the 4th century A.D., emperor Julian -also called "the Apostate"-, the last emperor of the first Byzantine dynasty, became a fervent supporter. Julian held the Earth as a planet which, like all other planets, went around the sun in a circular orbit. Thus, Aristarchus' theory had not been forgotten during the first centuries A.D., but even enjoyed advocacy.

1 Orphic Hymns

The ancient teachings of Orpheus are considered to be the first mystic Greek religion, with poems and hymns of great beauty. The Orphic Hymns consist of 87 hexametric poems or 1200 verses in total, which have reached us under the title "*Hymns of Orpheus to Musaeus*".

The hymns contain a breadth of astronomical information, partly obscured by the use of a strongly poetic language, as well as interesting ideas for the creation and the supreme being. This last piece of information tells us that the hymns belong to a monotheistic cult, since the creation of the Universe is ascribed to a single supreme force. We also come across the interesting notions of Chaos and the cosmic egg, which led to the creation of "Phanes", he who is radiant and existent.

From eyes obscure thou wip'st the gloom of night, all-spreading splendour, pure and holy light. Hence Phanes call'd, the glory of the sky, on waving pinions thro' the world you fly.
[V. TO PROTOGONUS, *The Fumigation from Myrrh*, verse 15
(see e.g.*Orphic Hymns* sine datum, or *Orphicorum Fragmenta*, 1922)]

Nearly all of the ancient Greek sages and writers drew inspiration from themes found in the Orphic Hymns, and were thus influenced while formulating their unique theories and teachings.

Let it be noted that in the Orphic Hymns, "Chaos" stands for what nowadays we would call space, "Gaia" for the earth-mother (and not the planet) whereas "Eros" (love), stands for the creational force. In the same hymn, we find a praise to Chaos which spans the aether, and was born from the cosmic egg:

O Mighty first-begotten [Protogonos], hear my pray'r, two-fold, egg-born, and wand'ring thro' the aether...
[V. TO PROTOGONUS, *The Fumigation from Myrrh*, verse 1]

Let it also be noted that during the Homeric times, the Earth was perceived as a circular flat disk which was surrounded by a vast circular river, the Ocean. This notion is made evident in the following verse:

Old Ocean [Okeanos] too reveres thy high command, whose liquid arms begirt the solid land.
[X. TO PAN, *The Fumigation from Various Odors*, verse 15]

The hymns mention Heaven being the ruler of the world, revolving around the Earth:

Great Heav'n [Ouranos], whose mighty frame no respite knows... Hear, world ruler,..., forever whirling as a sphere around this earth
[III. TO HEAVEN: *The Fumigation from Frankincense*, verse 1]

Another verse suggests that the origins of the heliocentric system seem to be located in the Orphic Hymns, as has been previously stressed by Constantinos Chassapis (1967), the late Greek astronomer, and Maria Papathanassiou (1978, 1980), assistant professor in the Mathematics Faculty at the University of Athens:

Hear golden Titan! Glowing like gold, you who strides above, oh heavenly light...
...you who combines the epochs ... You are the world ruler...

Fig. 1. Phanes: God of light, truth and justice. Here he appears to be surrounded by an elliptical (egg-shaped) ecliptic with the zodiacal signs of the four basic elements. Above and below him are the two halves of the cosmic egg, and between them, lies a flaming Phanes, winged just like the creative Eros. In his right hand he holds thunder (like Zeus does) and a scepter in his left, signifying his kingly place on the world. The curled snake on him symbolizes the Earth, the cup stands for water, the wings for air and the torch for fire. Its legs are shaped like a fork, just like those of the god Pan.

With your golden lyre, draw on the harmonious path of the world...
... [you] who wanders through fire and moves around in a circle
[VIII. *To the Sun*, verse 2]

The phrase "[you who attracts] *draw on the harmonious path of the world*" is striking since this could be a spermatic idea of the harmonious movement of

Fig. 2. The Homeric Universe: In the Universe of Homer's times, the mountains can be seen to rise over the surface of the great disk of the Earth, the Ocean spreading around them, while the center is dominated by Mount Olympus which rises up to heaven. In its highest peak, the all-seeing Zeus is seated, supervising both immortal gods and mortal men, sometimes rewarding and sometimes punishing them. Beyond Olympus spreads Heaven, supported by the pillars of Atlas. In heaven we can locate the Moon, the stars and the constellations. In particular, in this figure we can distinguish -but not referred by Homer- the constellations of Hydra, Corvus, Crater, Cancer, Leo, Gemini, Taurus as well as the Pleiades open cluster (as cited in D. Cotsakis, 1976, p. 18)

the planets around the Sun, a notion which was commonly used during at least the first five (perhaps more) centuries B.C. If the planets are to be included in the notion of the world, then the golden Sun could be seen as the attractive center of their harmonious orbits. One may therefore make the assumption that the seeds of a heliocentric theory can be traced in the Orphic Hymns.

Furthermore, on hymn (34): To Apollo, we find the following:

Loxias, the pure! . . . You mixed in equal parts winter and summer. . .
[XXXIV. *To Apollo*, verse 6,. . . and 20]

Thus, the "Loxias" Sun (meaning "tilted") mixed the components of the year and divided it in two equal parts, the summer and the winter. This is a very important astronomical detail which has drawn some attention from the astronomical community, because it has been linked to the dating of the Orphic Hymns. If one were to view this information literally, he would look back in time when the summer and winter were of exactly equal length. This would place the Orphic Hymns -more or less- near the following dates: 1841 B.C. and 1366 B.C. (Chassapis, 1967 and Papathanassiou, 2003). This view

however, requires the assumption that ancient Greece possessed very capable astronomers in early antiquity, an idea with little evidence to support it.

Another excerpt which, although referring to Hestia, seems to add to the heliocentric aspect of the hymns, is Hymn (84) [To Hestia]

You who occupies the center of the home of the greatest and eternal fire.
[LXXXIV. To Hestia, verse 2]

In *Orphicorum Fragmenta* a fragment tell us about the rotation of the Earth. This fragment says that Musaeus knew the path of the star and the movement of the sphere around the Earth, as this round Earth revolves in equal time period around its axis (Fr. 247 v. 24-26, pp. 261-262).

2 The Pythagoreans

Pythagoras founded his School at Croton in lower Italy, in c.540 B.C. He and his followers held the view that the most important cosmological principle were the numbers. In a way they were not mistaken, since it is in numbers that today's scientific thought is focused, for numbers identify with mathematical harmony and, without them, science would have never existed in the first place.

The Pythagorean School placed the foundations for the philosophy of mathematics as well as for physics, by relating order and the harmony of sound to the harmony of the Universe.

Virtually all of the students of Pythagoras were trained in astronomy, but their studies of the motion and the distances of the planets were carried out with a rather mystical approach. They believed in mystical and sacred relations between the numbers and the phenomena that they describe. In the Pythagorean view, the planetary distances were analogous to a heavenly musical harmony, which was created by harmonious sounds. They believed that this harmony was constantly created, being an eternal expression -of the highest order- of the unique divine harmony.

The Pythagoreans would have been delighted to see ideas very similar to their own, used in contemporary science. For example, modern String theory holds that everything on a microscopic level is a combination of vibrating strings. The Pythagoreans, developers of the "music and harmony of the spheres", would have seen particles as microscopic strings whose rhythmical vibrations create other particles, i.e. "the musical notes". These notes, in turn, create the music of the heavenly spheres. Thus though their eyes, our whole world would seem like a musical symphony, composed with these notes.

Pythagoras' School was a brotherhood, most likely in an almost religious sense, had various degrees of initiation, and may have been founded after the manner of the Orphic communities. Its contribution to geometry, music, arithmetic and astronomy was integral for the evolution of scientific thought. Through geometry, as well as the harmony of sound and numbers, the Pythagoreans developed the notion of perfection in the Universe, and coined an appropriate word to describe it: "Cosmos". This name is derived either from the word "cosmo" which means "to orderly arrange" or from the world "cosmema" which means "jewel" (ornament). Pythagoras himself appears to be the first to use the word "Cosmos", according to the doxographer Aetius: "*Pythagoras was the*

first to name the place of all things Cosmos, due to its orderly nature" [Aetius, *De Vestutis Placitis*, II, 1, 1 (D. 327, 8)]

The Pythagorean School held that the essence of all things was the "number", a rather abstract notion, which could not be perceived through one's senses, but only through intellect. In this manner, the philosophers of this school equated infinity with those material elements which could not be subject to measurement or definition. They introduced the notion of "matter", which was perceived as an element that resisted every definition of its ontological and moral imperfection.

Some elements of the Pythagorean cosmology have reached us through one of Aristotle's books, namely *Metaphysics*. According to the Pythagoreans, the Cosmos was created after the "One" initially came into being. The "one" -or "en" in Greek- served as the first principle, attracted the "infinite" (apeiron) to its own self, and bestowed on it with the "limit" (peras). These last two notions, the "limit" and the "infinite" have no clear meaning, but it has been speculated that they could be referring to the prime and even numbers.

Aristotle also mentions the following: "*The elements of number, according to them, are the Even and the Odd. Of these the former is limited and the latter unlimited; Unity consists of both (since it is both odd and even) [note of trans: either because by addition it makes odd numbers even and even numbers odd (Alexander, Theo Smyrnaeus) or because it was regarded as the principle of both odd and even numbers (Heath)]. Number is derived from Unity; and numbers, as we have said, compose the whole sensible universe*" [Aristotle, *Metaphysics*, A5, 986, 15]

Aristotle provides us with a further comment on the Pythagorean ideas: "*It is absurd also, or rather it is one of the impossibilities of this theory, to introduce generation of things which are eternal. There is no reason to doubt whether the Pythagoreans do or do not introduce it; for they clearly state that when the One had been constituted -whether out of planes of superficies or seed or of something that they cannot explain- immediately the nearest part of the Infinite began to be drawn in and limited by the Limit [note of trans: if numbers are eternal, it is absurd that they should be generated]*. [Aristotle, *Metaphysics*, 1091a, 14].

Another cosmological notion that the Pythagorean School of thought held was that the Creation began from a unique single point, which continuously expanded to infinity. It is evident that the Pythagoreans believed that the Universe evolved from a spherically expanding infinitesimal core. This idea once again, has been shared by some astronomers, who believe in a static spherical universe whose existence began from an initial point.

Another idea that Pythagoras believed in was that the Earth was spherical and immobile in the center of the Cosmos, which was spherical as well. "*..the water, earth and air; these elements interchange and turn into one another completely and combine to produce a universe animate, intelligent, spherical, with the earth at its center, the earth itself too being spherical and inhabited round about*" [Diogenes Laertius, *Lives of Eminent Philosophers*, VIII, 25, 8-10].

Many Pythagoreans held an identical view of a spherical Earth, placed in the center of the world, *without being supported by anything*. This was a novel

idea in its time, and is demonstrative of a clear progress when compared to assumptions that were previously held by other Greek philosophers.

According to the late professor of astronomy, Demetrios Kotsakis, "Pythagoras was the first who taught that the apparent motion of the sun on the celestial sphere from the east to the west, could be analyzed in to two distinct motions: One daily from East to West, parallel to the equator, and one yearly from West to East on the ecliptic" (Kotsakis, 1976, p. 28).

In the 6tth century B.C., some students and followers of Pythagoras, and most importantly Philolaus of Croton, Heraclides of Pontus, Ecphantus of Syracuse as well as others, believed in a "pyrocentric" theory. This means that they accepted that the element of fire was the "first principle" of the Cosmos. They believed that after the Creation, the element of fire accumulated in the center of the Cosmos and its attraction to its neighboring parts was part of the creation, formation and formulation of the various bodies that made up the spherical Universe.

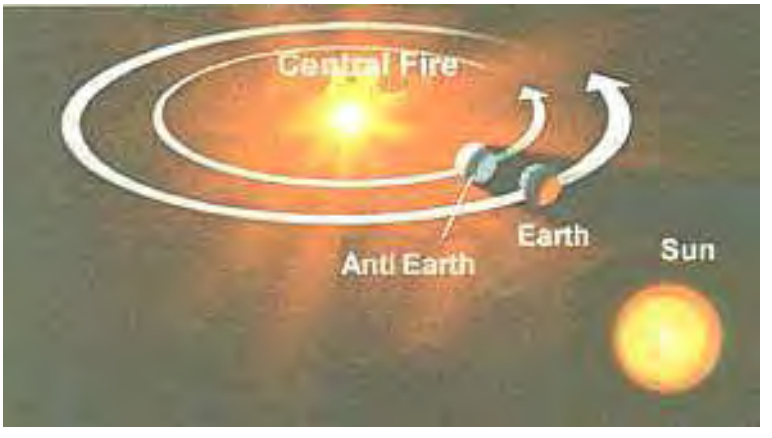

Fig. 3. Pythagorean Universe

2.1 The ideas of Philolaus of Croton

Philolaus of Croton (450-500 B.C.), spread the pythagorean ideas concerning the "first principle", by organizing and writing a synopsis of pythagorean philosophy. It appears that he was the principle creator of the philosophical notions of the "limit", the "infinite" and the harmony between the two, which, according to his views, was achieved due to the "number". He believed that the Cosmos is unique and began its creation from the center, which was occupied by fire. There, he placed the "Anticthon", (or Counter-earth - a hypothetical invisible Earth), the Earth, the Moon, the Sun, the five planets known at the time (Mercury, Venus, Mars, Jupiter and Saturn), and the sphere of the fixed stars. Thus, ten heavenly bodies "danced" around the central fire, a number

which the Pythagoreans held as sacred. It has been speculated that the Anticthon was introduced exactly for this reason, namely to raise the number of the celestial bodies to the sacred number ten.

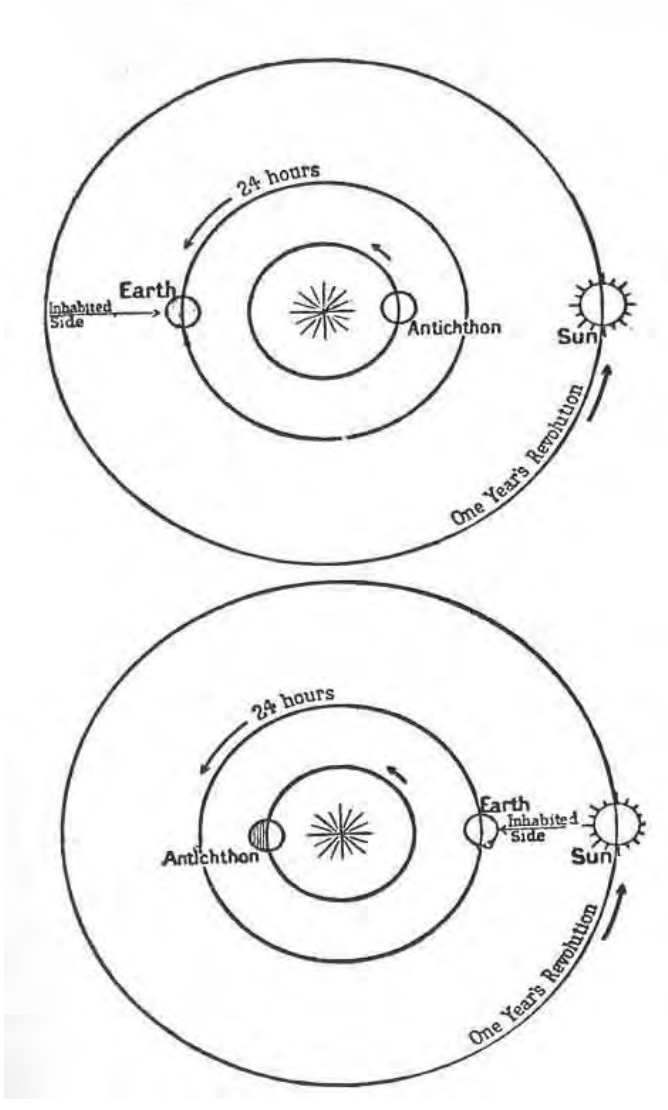

Fig. 4. Antichthon: The hypothetical invisible Earth, which according to the Pythagoreans occupied the antipodes of the Earth.

It is told that Philolaus of Croton, along with Archippus, Lysis and few others, survived the revolt against the Pythagoreans in Croton, which was instigated by Cylon, an ex student of Pythagoras, who had been sent off from the school for failing to comply with its principles. It is certain that the teachings of Pythagoras and his students, their innovative theories, their mysticism, as well as their aristocratic political tendencies caused the violent reaction of their democratic adversaries, who either killed or exiled many of them: "*Cylon of Croton... and those allied with him, hunted (killed) the Pythagoreans down to the man.* (Iamblichus *Vita Pythagorii* (V.P.) 248-249 ff).

Following this course of events, Philolaus left Croton and based himself in Thebes, where he taught Pythagorean philosophy and wrote the books *Bachae* and *On Nature* A, B and C (Cosmos, Nature and Soul respectively). An extant fragment from his first book reads: "*The world is uniform, it began its creation from the center, and from the center it expanded uniformly upwards and downwards, keeping equal distances from the center*" (Diels and Kranz, 1996, *Die Fragmente der Vorsokratiker*).

Several sources provide information on some of his cosmological thoughts: *The initial One, the beginning of the creation of the Universe, is called Hestia* [*On Nature*, fragment 7, Stobaei *Eclogae* I 21, 8 (p. 189, 17 W)].

Diogenes Laertius mentions: *According to Demetrius, in his work "on men of the same name", Philolaus was the first to publish pythagorean treatises, to which he gave the title "On Nature", beginning as follows: Nature in the ordered universe was composed of unlimited and limiting elements, and so was the whole universe and all that is therein* [Diogenes Laertius, *Lives of Eminent Philosophers*, 85 (A1 I 398, 20)].

The doxographer Aetius (Aet. I 3, 10), informs us (citing Theophrastus) of the following: *Philolaus believes that there is fire around the center of the Universe, which he calls "hestia of all" and "house of Zeus", "mother of the Gods", "altar, constraint and measure of nature". There is another fire which dwells in the outer region of the Universe. The center, he says, came first by nature, and around it dance ten heavenly bodies: The sphere of fixed stars, then the five planets, then the Sun, then the Moon, followed by the Earth and Anticthon, and after all these the fire of "hestia", which lies around the center. The outer region, which surrounds the whole Universe, is a place where the elements are in their pure state, unmixed, and that place he calls "Olympus". All that lies beneath Olympus, namely the part where the five planets along with the Sun and the Moon lie, he calls "cosmos", while the area beneath those, the sublunar space ...he calls "heaven". Wisdom is relevant with the order which holds in the heavenly bodes, while virtue is relevant with the disorder of the things which are subject to birth. The first is perfect while the second is imperfect.* [Aet. *De Vestutis Placitis*, II 7, 7 (D. 336, vermutlich Theophrast. im Poseidonios-Excerpt)].

The above are mentioned once again by Aetius: *The Pythagorean Philolaus places the fire in the center (for it is the Universe's focal point), secondly he places the Anticthon, then, our habitat, the Earth comes third, placed opposite [from the Antictchon] and moving in a circle, that being the reason for the beings of the Anticthon being invisible to the beings of the Earth. The ruling power of the Universe lies in the central fire, which God placed, like a keel, to base the foundation of the sphere that makes up the world".* [Aet. III 11, 3 (D. 337 from Theophrastus)].

>From all of the above we can sum up that, according to Philolaus, everything in "Olympus" and the "Cosmos" never changed, while in the areas up to the Moon, every being gifted with life was born, changed and finally died. The Earth and all the other planets were rotating around Hestia with the same direction but at different levels and with different speeds. Hestia was invisible because it shed its light to the antipodes of the Earth, which were impossible to get to. The Sun did not have its own light, but accepted and accumulated the sun of Hestia.

Philolaus, through his questioning of the traditional geocentric cosmology, set the foreground for Aristarchus' heliocentric theory, which would clearly dispute the central role of our small planet in the Universe. Even though he did not specifically place the Sun in the center, the idea of the "central fire" certainly served as a basis for the heliocentric theory. Stavros Plakides (1983-1990), a late Greek professor of Astronomy at the University of Athens, speculated that Philolaus, after having experienced the violence in southern Italy, avoided placing the Sun in the center of the Universe. Fear for his life may have been the motive for adopting the milder approach of placing the "central fire" instead (Plakides, 1974).

Diogenes Laertius, an important source from which we draw the views of Philolaus, mentions that opinions were divided as to who claimed first that the Earth is indeed moving: *It is told that he [Philolaus] was the first to claim that the Earth moves in a circle, while others ascribe it to Icetas of Syracuse* [Diog. Laert. *Lives of Eminent Philosophers* VIII, 84, 85)].

Aetius, another source, informs us that concerning the motion of the Earth Philolaus taught the following: *Others believe that the Earth is immobile. Philolaus on the contrary, believes that the earth is moving in a circle around the fire, tracing a tilted circle, just like the Sun and the Moon does* [Aet. *De Vestutis Placitis* III, 13, 1. 2. (D 378)]. Therefore, Philolaus came at a disagreement with his master, and taught that the earth was not immobile in the center of the world, but was circling the "Central Fire".

Diogenes Laertius also informs us that Plato bought a copy of the work of Philolaus for the -astronomical at its time- price of 100 mnae: *Some authorites, amongst them Satyrus, say that he wrote to Dion in Sicily instructing him to purchase three Pythagorean books from Philolaus for 100 mnae* [Diog. Laertius, *Lives of Eminent Philosophers*, III 9].

Plato, according to Plutarch, studied the work of Philolaus carefully, and after careful reading, nearing the end of his days -as the story goes by- was convinced that the Earth is indeed moving around the Sun: *As Theophrastus informs us, Plato, near the end of his days had regrets for his older opinion, by which he unfittingly placed the Earth at the center of the Universe* [*Platonicae Quaestiones* H1 915, vol. XIII1, 76-78]. The study of Philolaus may have been the reason for another change in the views of Plato: In *Republic* he identifies the celestial equator with the ecliptic, an idea which he turns from in Timaeus.

Aristotle, in his book *On the Heavens (De Caelo)*, provided us with some commentary on a few pythagorean views: *These affirm that the center is occupied by fire and that the Earth is one of the stars, and creates night and day as it travels in a circle about the center* [Aristotle, *On the Heavens* B, 13, 293a, 21-23]. Also, *The Pythagoreans make a further point. Because the most important part of the Universe -which is the center- ought more than any to be guarded, they call the fire which occupies this place the Watch-tower of Zeus,*

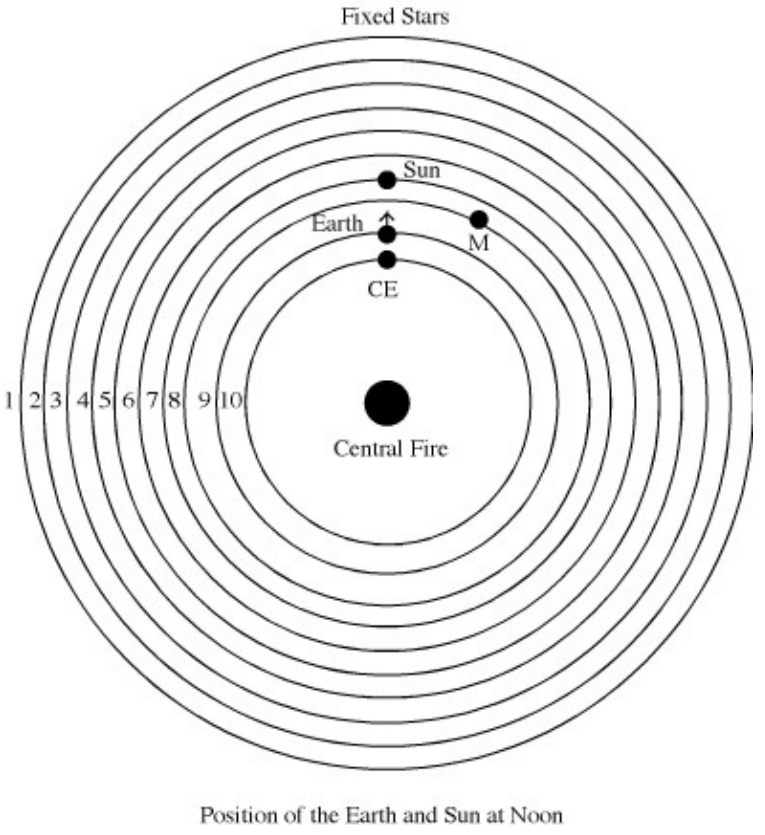

Fig. 5. The world view of Philolaus. In the world view of Philolaus, the center is occupied by the Central Fire, Anticthon (Counter-Earth, CE),The Earth, the Moon (M), the Sun, and beyond those lie the spheres of the five planets and that of the fixed stars. The crystalline spheres around the Central Fire are 10 (= 1+2+3+4), equal to the sum of the first four numbers.

as if it were the center in an unambiguous sense, being at the same time the geometrical center and the natural center of the thing itself... For this reason there is no need for them to be alarmed about the universe, nor to call in a guard for its mathematical center; they ought rather to consider what sort of thing the true center is, and what is its natural place [Aristotle, *On the Heavens* B, 13, 293b, 1-10].

The late professor of Astronomy at the University of Athens Demetrios Cotsakis (1976) mentions that the creation of the world-view which Philolaus describes was indeed revolutionary for the scientific thought of the time. He specifically mentions the views of the Italian astronomer Giovanni Schiaparelli (1835-1910), who wrote, as cited in Cotsakis (1976), the following, concern-

ing the views of the Pythagoreans and the system proposed by Philolaus: *The system of Philolaus was not a fruit of some restless imagination, but came through the torque and pull of one who sets the outcomes of observation in accordance with a predetermined principle, which exists above the nature of things... Appreciating this, and combining it to the fundamental theorems of the Pythagorean Philosophy, the system of Philolaus naturally appears as one of the most wonderful creations of human genius. His critics are incapable of appreciating the power of research, which was necessary, in order to unify the ideas of the roundness of the Earth, its levitation in space, and its motion. Indeed, without these ideas, there would have been no Copernicus, neither Kepler, nor Galileo or Newton* [Cotsakis, 1976, p. 30].

2.2 The views of Icetas, Ecphantus and Heraclides of Pontus

Beyond the theories of Philolaus of Croton, there were other students of Pythagoras which put forward novel ideas, like Icetas and Ecphantus of Syracuse as well as Heraclides of Pontus.

Icetas of Syracuse claimed that the Heaven, the Sun, the Moon and the stars were immobile, and the only thing that moved was the Earth. Concerning his views, Cicero mentions the following: *As Theophrastus says, Icetas of Syracuse was of the opinion that the heaven, the Sun, the moon and the stars (i.e. the planets) and all that is high above are immobile, and nothing in the world is moving, apart from the Earth. But as it rotates around its axis with the greatest possible speed, its motion causes all these phenomena to appear, which would have appeared were the Earth immobile and heaven rotated instead of it* [Cicero, *Academica priora* II, xxxix, 123].

It appears that this theory was embraced by both Ecphantus and Heraclides as well, both of which believed that the Earth moves rotating in space, just like a wheel does around its axis.

Therefore, the students of Pythagoras were the ones to reduce our planet to its real place and motions, while at the same time holding a pyrocentric planetary theory, which certainly assisted Aristarchus of Samos (310-230 B.C) to formulate his novel heliocentric theory.

According to Hippolytus, the Pythagorean Ecphantus appears to have also followed an "atomic theory" of Pythagorean inspiration, by "giving body" to units, which were directed and governed by some divine force, "nous" (the mind). He also mentions that Ecphantus believed that the Earth spins around its axis with an eastern direction, but does not change its place in space. [Hippolytus *Refutationis Omnium Haeresium* I 15 (D. 566W. 28)]. These last two pieces of information are also mentioned by the doxographer Aetius, who finds Heraclides in agreement with Ecphantus. [Aet. *De Vetustis Placitis*, III, 13, 3 (D. 378)].

Heraclides in particular appears to have modified the atomic theory of Leucippus and Democritus, proposing that the first material elements were molecules and not atoms. According to him, the universe was composed of small material molecules which did not share any connection.

3 The views of other Philosophers

3.1 Anaximander and Seleucus

So far we have mentioned the views of the Pythagoreans concerning the motion of the Earth. However, even before the Pythagoreans, during the 6th century B.C., the great philosopher Anaximander, was most likely the first Greek astronomer to talk about the motion of our planet around the center of the world, which may have been the Sun. He also discovered other fundamental astronomical facts, like the "detachment" of the Earth, and its axial rotation. This information can be found in the work "*Expositio rerum mathematicarum ad legendum Platonem utilium*" of Theon Smyrnaus (70-135 B.C.), who lived during the reign of emperor Adrian (Theon of Smyrna, 1979).

Anaximander's views were adopted by later philosophers like Empedocles of Agrigentum (490-430 B.C.), Parmenides of Elea (early 5th century B.C.), Aristarchus of Samos, Cleomedes (2nd or 3rd century B.C.) and several Pythagoreans.

Another philosopher, which name is Seleucus of Seleucia (c. 2nd century B.C.), was an astronomer of the hellenistic period from Anatolia, who supported a heliocentric theory of his own. Fragments of his work are found in the works of Plutarch, Strabo, Aetius and Hippolytus. Hippolytus informs us that the Earth was indeed moving, and that the Moon played a part in its axial rotation as well as in its orbit around the Sun. [*Philosophoumena*, Book C, 897C, 14-16]. The same source also informs us that he believed that the Cosmos was infinite [*Philosophoumena*, Book ?, 886C, 6].

Plutarch mentions a few of his other astronomical ideas [*Platonicae Quaestiones* H1 915, vol. XIII1, 76-78]; unfortunately, all of the work of Seleucus was lost and we have no knowledge of his heliocentric theory.

3.2 Aristarchus of Samos

After the Pythagoreans, appeared the great astronomer Aristarchus of Samos (310-230 B.C.), the foremost introducer of the heliocentric theory as we know from the book of Archimedes *Arenarius* [I 4-6 (3, 180-182), manuscript 2, Cod. Laurent. Gr. 28]. Plutarch, also, writes about the heliocentric theory of Aristarchus of Samos [*De placitis philosophorum* II, 24 (7, 355a)].

Aristarchus' hypothesis was original and quite bold for its time. For this reason Plutarch mentions that he was accused of atheism [*De facie in orbe lunae*, 923A (15, vol. XII, p. 54)]. Aristarchus, according to Aetius was helped to escape in Alexandria by his teacher Straton of Lampsacus (Aetius, *Placitorum Compositione* book 7, 313b, 16-17).

It is apparent that apart from the fervent geocentrists, there were several Greek thinkers whose philosophical thoughts disputed the validity of the geocentric system.

Unfortunately, overcoming the objections of the heliocentrists, the geocentric system, as was formulated by Claudius Ptolemy (2nd century A.D.), reigned for centuries, seconded by the weight of the views of Aristotle, whose work was held as indisputable during the Dark Ages.

4 Emperor Julian

Yet faith in the heliocentric system had not been forsaken. During the 4th century A.D. emperor Julian (336-363 A.D.) studied with care the works of the ancient Greek philosophers, which he held in deep respect. His studies took place in the philosophical schools of Athens. Enchanted by the beauty of the ancient Greek spirit, he wished to revitalize it. He believed that the Earth's world order was influenced by a heavenly and divine hierarchy, in which everything originated from the unique God, the illuminating Sun.

He was interested in philosophy as well as astronomy, and rose as a fervent supporter of the heliocentric system. In his book *Hymn to King Helios* dedicated to Sallust (*Hymn to the king Sun dedicated to Sallust*), he writes: *For that the planets dance about him as their king, in certain intervals, fired in relation to him, and revolve in a circle with perfect accord, making certain halts, and pursuing to and from their orbit, as those who are learned in the study of the spheres call their visible motions; and that the light of the moon waxes and wanes varying in proportion to its distance from the Sun, is I think, clear to all* [*Hymn to King Helios dedicated to Sallust*, 135b, 1-6].

Therefore, Julian held the Earth as a planet, which revolved in a circular orbit around the Sun. The Earth is moving, and along with it the other planets in circular orbits around the Sun, in determined intervals i.e. constant distances. The above clearly show that the theory of Aristarchus hadn't been forgotten, but during the 4th century A.D. enjoyed advocacy.

Conclusion

Beyond the sperms of the heliocentric theory that we saw in the Orphic Hymns, several scholars of Ancient Greece supported this "heretical" for its time view. Its main introducers were the Pythagorean philosophers Philolaus, Icetas, Ecphantus, Heraclides and foremost Aristarchus of Samos, who gave the Sun its rightful place in the Pythagorean "central fire".

The heliocentric theory did not prevail, and instead, the geocentric model, elaborated by the great astronomer Claudius Ptolemy, reigned for centuries in the West, since the undisputed Aristotle was in agreement with it.

Yet the heliocentric theory had not perished, since in the 4th century A.D. the Emperor Julian, a believer in the divinity of the Sun, became a fervent supporter. In the end, the heliocentric system faded away until the 16th century when the great Polish clergyman and astronomer Mikolaj Kopernik (Nicolaus Copernicus 1473-1543 A.D.), brought it back to light (Copernicus, 1995). The hypotheses of Aristarchus of Samos and the preparation of the Pythagoreans were the foundations for the great Polish astronomer's thoughts.

References

Aetius, 1879 (reprinted 1965), Placitorum Compositione (De Vetustis Placitis). Vol. IV 9, 8. in Diels Hermann: Doxographi Graeci. Berolini. Apud Walter De Gruyter et Socios, Editio Quarta.

Archimedes, 1972, Arenarius in Opera Omnia, Bibliotheca Scriptorum Graecorum et Romanorum Teubneriana. Ed. I. L. Heiberg, vol. II corrigenda Adiecit E. S. Stamatis. Stutgardiae in Aedibus MCMLXXII.

Aristotle, 1956, The Metaphysics. Vol. I-IX, The Loeb Classical Library, Book XVII with an English Translation by H. Rackham. London: William Heinemann Ltd. Cambridge, Massachusetts: Harvard University Press.
Aristotle, 1953, On the Heavens (De Caelo). The Loeb Classical Library, with an English Translation by W.K.C. Guthrie. M. A. London. William Heinemann Ltd. Cambridge, Massachussets, Harvard University Press, MCMLIII (First printed 1933, reprinted 1936, 1947, 1953, 1956).
Chassapis Constantinos, 1967, The Greek Astronomy of the 2nd millennium B.C. according the Orphic Hymns. PhD. Thesis, University of Athens [self edited], Athens [in Greek].
Cicero, 1961, Academica Priora, with an English Translation by H. Rackham, M.A. The Loeb Classical Library. London. William Heinemann LtD. Cambridge, Massachussetes, Harvard University Press. MCMLXI (First printed 1933, reprinted 1951, 1956, 1961).
Cicero Marcus Tullius, 1984, Academica. Publ. Lubrecht & Cramer, Ltd. October.
Copernicus Nicolaus, 1995, De Revolutionibus Orbium Coelestium, libri VI. On the Revolution of Heavenly Spheres. Trans. By Charles Glenn Wallis. Prometheus Books, October 1995.
Cotsakis Demetrios, 1976, The pioneers of Science and the creation of the World. Ed. Zoe, Athens.
Diels Herman, 1996, Die Fragmente der Vorsokratiker, Herausgegeben von Walther Kranz. Ester und Zweiter Band, Weidmann, Zьrich.
Diogenes Laertius, 1925, Lives of Eminent Philosophers, vol. II, IX 34-35, pp. 3, 441-445. Heinemann, London. The Loeb Classical Library; English translation by R.D. Hicks, revised and reprint 1959.
Hippolytus,1857-1866, A Refutation of All Heresies: Refutationis Omnium Haeresium (Filosofoumena). Patrologia Greca (P.G.) 16, In Origenes, Liber VII, 404-405, 339. Typographi Brepols Editores Pontificii, Parisiis.
Iamblichus, 1965, Vita Pythagorii (V.P.) Life of Pythagoras, with the English translation by Thomas Taylor in 1881, J. M. Watkins, 1965, p. 248-249ff.
Iuliani Imperatoris, 1875, Vol I. Oratio IV (To King Helios), 143 B. 146 D., Lipsiae Teubner.
Julian the Emperor 1954, The works of the emperor Julian, The Orations of Julian, IV. Hymn to king Helios dedicated to Sallust. The Loeb Classical Library. Trans. By Wilmer Cave Wright, Ph.D., William Heinemann Ltd. Cambridge, Massachusetts, Harvard University Press MCMLIV (First printed 1923, reprinted 1930, 1954).
Orphic Hymns, sine datum, Ed. Ideotheatro, Athens [in Greek].
Orphicorum Fragmenta, 1922, Ed. O. Kern, Weidmann.
Papathanassiou Maria, 1978, Cosmological and cosmogonical aspects in Greece during 2nd millennium B.C. PhD. Thesis, University of Athens [self edited], Athens [in Greek].
Papathanassiou Maria, 1980, Aristarchus the Samian, Mathematical Review 20, Editions of the Hellenic Mathematical Society, p. 91-120 [in Greek].
Papathanassiou Maria, 2003, Primordial astronomical learning. Elefterotypia-Historica, Athens, January 2, 2003, p. 6-12 [in Greek].
Petrides, S., 2002, The Orphic Hymns, Astronomy in the Age of Ice [self edited], Athens [in Greek].
Plakides Stavros, 1974, The Geocentric and the Heliocentric Theory. Parnassos 16, Athens [in Greek].
Plutarch Chaeronsis, 1841, Scripta Moralia. Graece et Latine. Tomus Secundus. De placitis Philosophorum Libri quinque. Parisiis. Editore Ambrosio Firmin Didot MDCCCXLI.
Stobaei Ioanni Eclogae, sine datum, Wachsmuth Dox. 336 B 20-337 B 10 and Bibliotheca of the ancient Greek writers, Ed. Georgiades, Athens.
Theonis Smyrnaei, 1878, Philos. Platonici. Ed. Hiller. Lipsiae 1878, p. 198, 14-19.
Theon of Smyrna, 1979, Mathematics useful for understanding Plato or Pythagorean Arithmetic, Music, Astronomy, Spiritual Disciplines. Trans. by Christos Toulis, Wizards Bookshelf.

Six calendar systems in the European history from 18th to 20th Century

Efstratios Theodossiou[1], Vassilios N. Manimanis[1], Milan S. Dimitrijević[2]
[1] Department of Astrophysics, Astronomy and Mechanics Physics Faculty, University of Athens-Zografos 157 84
[2] Astronomical Observatory, Volgina 7, 11060 Belgrade, Serbia
etheodos@phys.uoa.gr
mdimitrijevic@aob.bg.ac.rs
(Research report. Accepted on 30.04.2011)

Abstract. The following calendar systems, introduced in Europe from 18th to 20th century, which were in use for a shorter or longer period by a larger or smaller community, were reviewed and discussed: The French Revolutionary Calendar, the Theosebic calendar invented by Theophilos Kairis, the Revolutionary Calendar of the Soviet Union (or 'Bolshevik calendar'), the Fascist calendar in Italy and the calendar of the Metaxas dictatorship in Greece before World War II. Also the unique of them, which is still in use, the New Rectified Julian calendar of the Orthodox Church, adopted according to proposition of Milutin Milanković on the Congress of Orthodox Churches in 1923 in Constantinople, is presented and discussed. At the end, difficulties to introduce a new calendar are discussed as well.
Key words: Calendars: French Revolutionary, Theosebic, Italian fascist, of I. Metaxas, Bol'shevik's, New Rectified Julian

Шест календарни системи в европейската история от XVIII до XX век

Ефстатиос Теодосиу, Василиос Маниманис, Милан Димитрийевич

Радгладани са и са обсъдени следните календарни системи, въвеждани в Европа от от XVII до XX век и използвани дълго или кратко от големи или малки общества: Френският революционен календар,Теосебичният календар, измислен от Теофилос Кайрис, Революционният календар на Съветския Съюз (Болшевишкият календар), Фашисткият календар в Италия и календарът на Метакса-диктатурата в Гърция преди Втората световна война. Представен и обсъден е също така и единственият такъв календар, който все още се използва, Новият ректифициран юлиански календар на Източно-православната църква, възприет по предложение на Милутин Миланкович на конгрес на Източно-православната църква през 1923 г в Истанбул. Накрая са дискутирани и трудностите пред въвеждането на нов календар.

Introduction

In the history of calendar reforms the Julian calendar that prevailed for at least 16 centuries was gradually replaced by the Gregorian one, from 1582 onwards. The Gregorian calendar was necessary, because it corrected the Julian one and returned the vernal equinox in its true astronomical date; however, it did not change the months, or the days of the week (their number and names): it just changed the way of calculation of the leap years. After these two calendars, five other political calendar systems and one ecclesiastic were introduced in Europe, but none of political ones prevailed beyond its limited

(in time and place) political environment. In this work the following such unsuccessful calendars are reviewed: The French Revolutionary Calendar, the Theosebic calendar invented by Th. Kairis, the Revolutionary Calendar of the Soviet Union (or 'Bolshevik calendar'), the fascist calendar in Italy and the calendar of the Metaxas dictatorship in Greece before World War II. Also the unique of them which is still in use, the New Rectified Julian calendar of the Orthodox Church is presented and discussed.

Essentially, with the exception of the French Revolutionary Calendar (*Le Calendrier Républicain*), which is well-known and studied in the international bibliography, our effort is centered at the other 5 calendar systems, which are much less known, especially the three of them: the Theosebic calendar, the fascist calendar in Italy and the calendar of the Metaxas dictatorship in Greece (1936-1940). At the end, difficulties to introduce a new calendar are discussed as well.

1 The French Revolutionary Calendar

After the Gregorian calendar, the next step of a calendar reform was taken in France, after the French Revolution of 1789, which resulted in the abolishment of monarchy and the declaration of Democracy. The French revolutionaries, after breaking the bonds of the monarchy wanted to break also their links with the religious-papal (as they perceived it) calendar, by reintroducing its primal basis, the ancient Egyptian calendar. For this reason, they wanted to create a calendar similar with one that would lead to the complete decoupling of Church and the State. The first attacks against the Gregorian calendar, accompanied by the respective calendar propositions for its reformation, took place during the years 1785 to 1788.

The times were ripe, after the fall of Bastille in July 14, 1789, for the French revolutionaries to ask with considerable intensity for a new calendar, having as its starting point the first year of Democracy. So in 1793 the National Assembly entrusted Charles Gilbert Romme, president of the public education committee, with the calendar reform. He in turn assigned to the famous mathematicians Joseph-Louis Lagrange and Gaspar Monge the task to work on the technicalities of the issue. The results of the studies of the two mathematicians were submitted to National Assembly in September 1793 and were accepted immediately. At the same time it was decided that this new calendar system would be applied soon. Indeed, the *Calendrier Républicain de la Rèvolution de 1789*, as it was called, was accepted by the National Assembly on October 5, 1793 and was voted on December 4, 1793. As the starting point of its chronology was set a date of the recent past, namely the September 22, 1792, known in the new calendar as 1 Vendèmiaire, the date of the abolishment of monarchy and the declaration of democracy, which accidentally coincided with the astronomical autumnal (fall) equinox. So the New Year's Day of the 'revolutionary' civil year was the autumnal equinox of each tropical year, with the chronology starting on September 22, 1792 or 1 Vendèmiaire of the Year 1.

The year of this 'democratic' calendar consisted of 12 months of 30 days each, followed by an extra 5 or 6 supplementary days (*jours complémentaires*), which, added at the end of the 12th month, that is between the respective

dates 17 and 22 September, were completing the total number of the days of the year. Thus, the total number of the days of the year was again 365 or 366 for leap years, keeping the tradition of the Julian calendar and its evolution, the Gregorian calendar.

The day-and-night time interval, from one midnight to the next, was divided into 10 hours and the 1/100 of such an hour was defined as the 'decimal minute'. I.e. the French democrats abolished the hexadecimal system in time keeping and established the simpler decimal one (each minute had also 100 seconds). The weeks, because they were related to the Jewish calendar, and thus they had been adopted in interconnection with Religion, were abandoned and each month was divided into three *décades*. The names of the days of the week were also abolished and the ten days of each 10-day span were just called with their order: first, second, third,..., tenth day (*primidi, duodi, tridi, quartidi, quintidi, sextidi, septidi, octidi, nonidi, décadi*). The last day of each *décade*, the *décadi*, was a day of rest, dedicated to the worship of the Supreme Being. The names of the months had the same ending for each three-month group and they were inspired by nature. They were invented by the member of the National Assembly, poet Philippe Fabre d'Eglantine (1750-1794). This poet and playwright had won (with his work *Étude de la nature*, 1783) in 1783 the first prize in Toulouse's flower festival; the prize was a golden wild rose, which is called *eglantine* in French, and he adopted this word as his nickname, with which he is known in history. Philippe Fabre was a member of Danton's group, and when his friend lost his political power, he was accused of corruption because he had been involved in the scandalous dissolution of the Society of Indies. For this reason he was beheaded together with Danton and his followers on April 5, 1794.

The democratic calendar was permeated by an anti-Christian, rationalistic and nature-loving spirit. The poetic names of the months of the year, together with their meaning and the correlation with our months are as follows (Flammarion, 1955, p. 28):

These Gregorian dates vary slightly because of leap years. Moreover, due to incompatibility of Articles III (Every year begins in the midnight of the day of autumnal equinox for Paris observatory) and X (...The fourth year of a *Franciade* is *Sextile*) of *Décret de la Convention nationale sur l'ère, le commencement et l'organisation de l'année, et sur les noms des jours et des mois*, the calendar is not applicable after the year XVIII, since an additional leap day for compatibility with tropical year is not needed for the Year XIX (the fourth year of Franciade) but for Year XX (the fifth year of Franciade). Consequently, exist different systems for the conversion after the year XVIII and the corresponding dates are slightly different for different systems.

The five or six supplementary days were initially called *Sans Culottides*, to honor the revolutionaries who didn't wear the expensive trousers (culottes) of the aristocrats but long hairy pants instead. The French who were using the calendar were saying: the first Sans Culottide, the second Sans Culottide, etc. (*la première sans culottide, la seconde sans culottide*, etc.). The collective name 'supplementary days' (*jours complémentaires*) was given to the Sans Culottides on 7 Fructidor of the Year III, i.e. on August 24, 1795.

Table I: The French Revolutionary Calendar

Season	Month	Meaning	Correlation
Fall	Vendèmiaire	Vintager	Sept. 22 - Oct. 21
	Brumaire	Foggy	Oct. 22 - Nov. 20
	Frimaire	Chilly	Nov. 21 - Dec. 20
Winter	Nivôse	Snowy	Dec. 21 - Jan. 19
	Pluviôse	Rainy	Jan. 20 - Feb. 18
	Ventôse	Windy	Feb. 19 - March 20
Spring	Germinal	Of the sprouts	March 21 - April 19
	Floréal	Flowery	April 20 - May 19
	Prairial	Grassy	May 20 - June 18
Summer	Messidor	Harvester	June 19 - July 18
	Thermidor	Heat-giver	July 19 - Aug. 17
	Fructidor	Fruit-giver	Aug. 18 - Sept. 16
	Jour de la Vertu	Day of Virtue	Sept. 17
	Jour du Génie	Day of Engineering	Sept. 18
	Jour du Travail	Day of Work	Sept. 19
	Jour de l' Opinion	Day of Opinion	Sept. 20
	Jour des Récompenses	Day of Rewards	Sept. 21
	Jour de la Révolution	Day of Revolution	
		(Only in leap years)	Sept.22

The names of the saints associated with each date of the year in the Christian calendars were replaced by names of trees, plants, flowers, fruits and grains, since this calendar was designed to be free of Christian nomenclature (Renouard, A.A., 1822).

The supplementary days, between 17th and 22nd September of the Gregorian calendar, were dedicated: to Virtue (*la Fête de la Vertu*), Engineering (*la Fête du Génie*), to Work (*la Fête du Travail*), to Opinion (*la Fête de l' Opinion*), and to Rewards (*la Fête des Récompenses*).

The Day of the Opinion was especially important for its singular character: on this date, every citizen had the right to freely express his opinion. At a collective level, the citizens were judging publicly, albeit figuratively, all public servants for their deeds. During this day, any kind of satire was permitted, along with cartoons, satirical songs and many other smart jokes, which were freely aimed towards those in power. It was then up to those in power to disprove through its Virtue these humoristic accusations. For this reason, this day was also considered to be dedicated to Actions and Virtue. The sixth supplementary day added in the leap years was dedicated to the celebration of the Revolution (*la Fête de la Rèvolution*). The first leap year of the new calendar was decided to be the Year III. The four-year period between two successive Days of the Revolution was called *Franciade*.

The wonderful French invention of calling the democratic calendar's months with names corresponding closely to the real climate of France was ridiculed by the British (then adversaries of the French) with the following parody:

Fall: *wheezy, sneezy, freezy*
Winter: *slippy, drippy, nippy*
Spring: *showery, flowery, bowery*
Summer: *hoppy, croppy, poppy*

Fig. 1. Colored drawing from 19th century. The person on the right side is wearing short trousers of aristocrats - culottes.

(Wilson P.W., 1937, p. 154). For Summer somewhere is given and: *Wheatty, Heaty, Sweety* (The Historical Maritime Society, Nelson and His Navy - Revolu-tionary Calendar, http://www.hms.org.uk/nelsonsnavyrevcalend.htm,

This rather poetic calendar was functional and efficient for France; however, it was disadvantageous for the working class, as it contained only one day of rest every ten days and not one in seven, as it used to be. Its other major weakness had to do with the fact that it was a calendar of limited use, since it was used only in France, and thus isolated it calendarly, administratively, economically and in international relations issues from the rest European countries.

Fig. 2. French Revolutionary calendar by Louis-Philibert Debucourt 1755-1832.

For these reasons, but mainly for political purposes Napoleon the Great agreed with the Pope in 1801 to restore Sunday in the calendar, as well as the major Christian holidays: Christmas and the Easter. Finally, in 1806 the French Revolutionary Calendar was abolished with the decree of 22 Fructidor XIII signed by Napoleon and France adopted again the Gregorian calendar on 11 Nivôse XIV that is in Gregorian date January 1st, 1806. The Revolutionary Calendar had a short life, less than 13.5 years. However, some decades later, an attempt was made to restore it, which is described below.

In 1870, emperor Napoleon III (1808-1873) lost a war with the Prussians he was responsible for. This defeat had as a result the abdication of the emperor on September 4, 1870 and the declaration of the Second Republic. However, the Prussians advanced and occupied a part of Paris. The end of

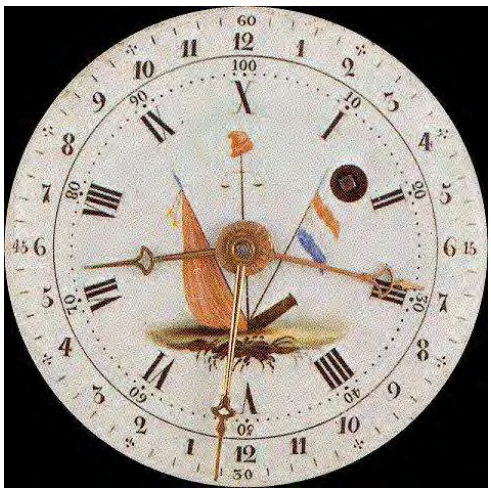

Fig. 3. French republican clock with combined decimal (inside) and traditional (outside)hour-plate.

the war came on March 1st, 1871, when Thierry's government signed the capitulation with the invaders.

The defeat and the humiliating terms of the treaty had as a result a new revolution in Paris, on March 18, 1871. The people of Paris installed in the Town Hall a communal administration, which passed in history under the name "Paris Commune". The revolutionary commission that was formed organized the city's defense. And one of its first actions was the revival of the Revolutionary Calendar, the *Calendrier Républicain de la Rèvolution*, on May 10, 1871, which corresponded to the 18 Floréal of the Year 79. The 'Government of National Salvation' as Thierry's government was known, found refuge in Versailles. It managed to summon 100,000 men and with this army it attacked Paris. After a couple of weeks of battles, in which more than 20,000 people died, the governmental army crushed the revolutionaries in the end of May 1871, aided by the Prussians.

The quick end of this popular uprising brought once again the abolishment of the Revolutionary-Democratic Calendar, this time forever, on May 28, 1871. So, the Commune in Paris restored French Revolutionary Calendar just for a brief period (Wilson, P.W., 1937, p. 155 & p. 334).

Nevertheless, even today the French astronomical almanacs, as a tribute towards the First French Republic, give along with the other calendars (Grego-rian, Julian, Islamic, Jewish and Coptic) the date correlation of the Revolutio-nary Calendar, which in 2009 is at its 217th Year (the first of January 2010 corresponded to 12 Nivôse 218).

2 The Theosebic calendar

The abolishment of the French Revolutionary-Democratic calendar discouraged other regimes from adopting some novel calendar system. Yet, the French calendar inspired the Greek priest and scholar Theophilos Kairis to invent his own 'Theosebic calendar' who was also destined not to prevail at any place. This was a variant of the French Revolutionary calendar, but under a religious cover.

The monk and priest Theophilos Kairis (1784-1853), a thinker and scholar from the island of Andros, who participated in the Greek War of Independence of 1821, and is considered as one of the major 'Teachers of the Nation', had studied in the universities of Pisa and Paris. He was the creator of a cult, 'Theosebism', and for this reason he was persecuted and he died in prison. His original philosophical system was echoing the ideas of Theosophy, positivism and mysticism.

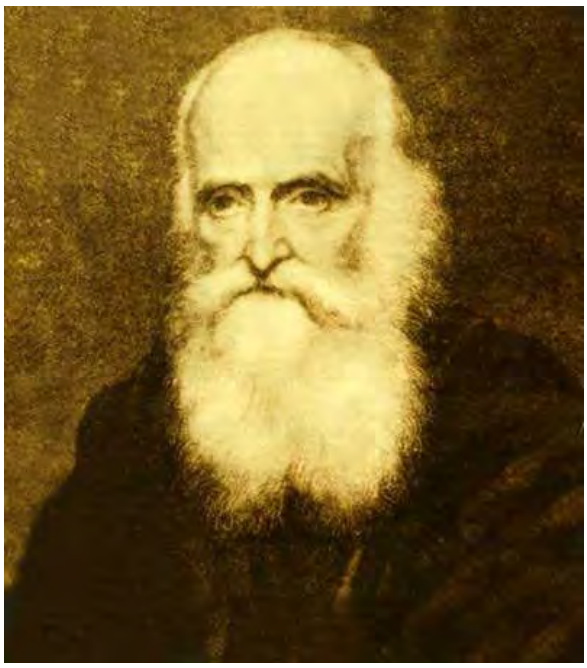

Fig. 4. Theophilos Kairis.

Theophilos Kairis, influenced by the Western Christian-social philosophy, was searching for the 'golden analogy' among religious faith, scientific knowledge and social justice. He did not accept the Christian chronology and, inspired by the French Revolutionary calendar (*Calendrier Républicain de la*

Rèvolution de 1789), he proposed the abandonment of the week and the division of each month in three ten-day intervals: "Twelve '30-day' months in three groups of 10 days each (Theophilos Kairis, Code 53).

He also changed the names of the months, into the following ones (Theodossiou, E., & Danezis, E., 2000, pp. 337-338):

Table II: Month names in the Theosebic calendar, their meaning and equivalence

	Name	Meaning	Correlation*
1	Theosebius	Pius (of respect to God)	11/23 Sept.- 10/22 Oct.
2	Sopharetus	Wise and virtuous (of Wisdom and Virtue)	11/23 Oct.- 10/22 Nov.
3	Dicaeos	Righteous (Just)	11/23 Nov.- 9/21 Dec.
4	Hagios	Holy	10/22 Dec.- 8/20 Jan.
5	Agathius	Good (Benevolent)	9/21 Jan.- 7/19 Feb.
6	Sthenius	Courageous (of Power)	8/20 Feb.- 9/21 March
7	Agapius	Beloved (of Love)	10/22 Mar.- 8/20 April
8	Charisius	Graceful (of Grace)	9/21 April- 8/20 May
9	Macrothymus	Forbearing	9/21 May- 7/19 June
10	Aeonius	Eternal (Perpetual)	8/20 June- 7/19 July
11	Entheus	Divine ('God-in-it')	8/20 July- 6/18 Aug.
12	Sosius	Savior (of Salvation)	7/19 Aug.- 5/17 Sept.

* The first date is according to Julian calendar and the second according to Gregorian one, with a difference of 12 days as was in 19th century. For conversion of dates from 20th and 21st century one should take into account that the difference increased to 13 days. As in the case of French Revolutionary Calendar, dates slightly vary due to leap years (We note that in Portaz (1935, p. 220) Gregorian dates are erroneously increased for one since was taken the difference of 13 days as in 20th century).

The five or six days added for the completion of the tropical year were the dates 18 to 22 September of the Gregorian calendar.

Theophilos Kairis knew that from an astronomical point of view there is no special significance in setting the start of the year on January 1st and that all ancient calendars were starting their year at one of the 4 characteristic points of the solar apparent orbit, which are:

a) The two equinoxes - the vernal on March 21 and the autumnal on September 23 - and

b) The solstices - the summer on June 22 and the winter on December 22.

The calendar system of Kairis, known as the 'Theosebic calendar' had also as its New Year's Day the autumnal equinox. The first year of the Theosebic chronology began on September 23, 1800 (Gregorian calendar). Actually, he chose as the start of his calendar system the autumnal equinox, which used to occur on September 11/23 (the first date refers to the Julian and the second date to the Gregorian calendar, which then had a difference of 12 days between them), like the ancient Greek calendars of the Dorians and

the Macedonians. The Dorian (Spartan) calendar started on the first new moon after the autumnal equinox, in the month Panamos, and the Macedonian calendar started in the holy month Dios. But also his calendar model, the French Revolutionary-Democratic calendar, started at the autumnal equinox (September 22 or equivalently 1st Vendèmiaire of 1792 (Theodossiou & Danezis 2000, p. 338).

Correspondingly, the first year of the Theosebic chronology started on September 11 / 23 (when that year occurred autumnal equinox) of 1800 AD and ended on September 10 / 22 of 1801 AD. As we already noted, the Theosebic year had 12 months of 30 days each (12 x 30 = 360), so that 5 days remained (or 6 for the leap years) for the completion of the solar year of 365 (or 366) days. These extra days, as in the ancient Greek calendars, were called "induced days" and were inserted at the end of the Theosebic year, i.e. before the $11^{th}/23^{th}$ of September of the "Christian" calendars (Julian and Gregorian).

Similarly, as in the ancient Greek calendars, each month was divided into 10-day spans (decans); the first decan of each month was called "starting decan of the month", the second one "middle decan of the month" and the third one "decan of leaving or ending month", or "the decan after the twenty" (Theodossiou & Danezis 1996, vol. I, pp. 360-364).

The specialist on Kairis late scholar Demetrios I. Polemis, director of the Kairian Library in Andros, edited the correspondence of Theophilos Kairis, which was published in three volumes. He divides these three volumes of letters into three periods. The first volume contains the letters up to the closure of the Orphanage (1839), the second volume contains the letters of the period of his persecution and exile up to his return to Greece (1844) and the third one contains letters written in Andros to various receivers until the scholar's death in 1853 (D. Polemis, vol. I, p. 22). In the second volume's introduction Polemis reports that a detailed description of the Theosebic calendar exists in the work *Epitome of the Theosebic teaching and ethics* (London 1852, pp. 102-104) by Kairis. Also, as far as the decans are concerned, Polemis writes the following:

"The decan is divided into ten days, the day into ten hours, the hour into 100 first minutes and the minute into 100 seconds. The days of the decan are named First, Second,... ..., Tenth or Holy". As Kairis writes, "the age of the Theosebists" begins "from the first year of the nineteenth century of the Christians and it is divided into five-year **entheades***". Therefore, the first year of the Theosebic chronology started on September 11 / 23, 1800* [the first year of 19th Century is not 1800 but 1801 - Remark of authors], *and ended on September 10 / 22, 1801. The days of September 6 to 10, 1801, were the* **Epacts** *(induced days).*

A complete Theosebic chronology is exposed in the letter No. 220: "33, or 9th of the entheas 9, to 3rd, the 1st of the middle [decan of] Sopharetus". The year 33 began on September 11 / 23 of 1842 AD, while the 8th entheas was completed on September 10 / 22, 1840 and the next day started the ninth entheas, of which the third year was 1842-1843. Sopharetus is the second month of the Theosebic calendar (October 11 / 23 to November 9 / 21). Therefore,

the first of the middle decan of this month is the October 21st / November 2nd 1842.

Kairis and the followers of his sect were using tables of corresponding dates of the two calendars (Theosebic and Christian), some of which have been preserved.") (Polemis, Introduction, vol. II, pp. 12-13).

Kairis considered the year 1801 'as the year 1' in his Theosebian calendar, essentially a covert variation of the French revolutionary calendar cloaked in religion and, being the after-clap of a calendar that did not survive, Kairis's calendar was also still-born.

Table III: The "Times" of the day in the Theosebic calendar

Ecclesiastical "Hours"	Kairian "Times"
Matins	Time of prayer
Hours	Time of studying and reading
Evensong	Time of own profession
Compline	Time of charity work
Midnight	Time of irrevocable comfort (repose)

The nineteenth century is the first century of the Kairian measuring of time. In his calendar he used the ancient Greek numbering; so in the year $\mu\lambda$ of the Kairian chronology (corresponding to 1852) the "Compendium of Theosebian Doctrine and Ethics" was published in London. In this book, the doctrinal background of Theosebism and the Kairian calendar are described in detail. According to his ecclesiastical calendar, Kairis divided the 'night and day' -and not 'day and night'- into five periods "Times" of two hours (ten hours in total divided in 100 minutes and each minute in 100 seconds - Portaz, 1935, p. 220).

In his calendar, Kairis abolishes all Christian feasts (those of Jesus Christ, of the Holy Mother, of Saints, etc.). He also replaces Sunday -the day of the Lord- with the 'Tithe' (the tenth day), i.e. since he does not accept the divine nature of Jesus Christ he abolishes also the day devoted to Him.

According to the principles of Theosebism, the believers, the God-pious people, were gathering at the middle of the four seasons of the year, beginning at the corresponding autumnal middle, celebrating the following: Entheogona, Entheagona, Entheobia and Entheondia.

All these -untranslatable- terms were invented by Kairis. Their meanings are difficult even in Greek and each one includes the word God (Theo, in Greek).

We conclude that Kairis created his calendar with the new chronology in order to use it in the religion or sect he introduced, in the ritual of which he adds new prayers, new hymns and a new worship, thus creating his own special theoretical and worshipping ritual, written in the ancient Dorian dialect.

Indeed, Kairis, among other things, being an admirer of the ancient Greek spirit, formulated in the ancient Doric dialect of the Greek language a fully operational hymnbook. He called the corresponding workers 'God's ministers' (Theagi). These Theagi or Hieragoi (Holy priests) were classified into five orders: Deans, Readers, Hymnodists, Preachers and Ministers.

Of course, this calendar, unknown to the international literature as far as we know, was never put in real use and became extinct with the death of its inventor, together with the Theosebism cult (Theodossiou et al., 2007, p. 117).

3 The Revolutionary Calendar of the Soviet Union ('Bolshevik calendar')

The last major attempt for a calendar reform took place in 1929 by the government of the Soviet Union (USSR), which adopted the Revolutionary calendar (or 'Bolshevik calendar').

To begin with, in 1918, the government formed after the October Revolution replaced the Julian calendar with the Gregorian one, thus actually harmonizing Russia with Western Europe from a calendar point of view; this is why the celebration of the anniversary of the 'October Revolution' was taking place on November 7 in the Soviet Union. However, the Russian Orthodox Church never accepted the Gregorian calendar.

ТАБЕЛЬ-КАЛЕНДАРЬ НА 1931 ГОД.

	ЯНВАРЬ							ФЕВРАЛЬ							МАРТ							АПРЕЛЬ						
I день	1	6	11	16	21	27		1	6	11	16	21	26			3	8	13	18	23	28		2	7	12	17	22	27
II день	2	7	12	17	23	28		2	7	12	17	22	27			4	9	14	19	24	29		3	8	13	18	23	28
III день	3	8	13	18	24	29		3	8	13	18	23	28			5	10	15	20	25	30		4	9	14	19	24	29
IV день	4	9	14	19	25	30		4	9	14	19	24			1	6	11	16	21	26	31		5	10	15	20	25	30
V день	5	10	15	20	26	31		5	10	15	20	25			2	7	12	17	22	27		1	6	11	16	21	26	

	МАЙ							ИЮНЬ							ИЮЛЬ							АВГУСТ						
I день		4	9	14	19	24	29		3	8	13	18	23	28		3	8	13	18	23	28		2	7	12	17	22	27
II день		5	10	15	20	25	30		4	9	14	19	24	29		4	9	14	19	24	29		3	8	13	18	23	28
III день		6	11	16	21	26	31		5	10	15	20	25	30		5	10	15	20	25	30		4	9	14	19	24	29
IV день		7	12	17	22	27		1	6	11	16	21	26		1	6	11	16	21	26	31		5	10	15	20	25	30
V день	3	8	13	18	23	28		2	7	12	17	22	27		2	7	12	17	22	27		1	6	11	16	21	26	31

	СЕНТЯБРЬ							ОКТЯБРЬ							НОЯБРЬ							ДЕКАБРЬ						
I день	1	6	11	16	21	26		1	6	11	16	21	26	31		5	12	17	22	27			2	7	12	17	22	27
II день	2	7	12	17	22	27		2	7	12	17	22	27		1	6	13	18	23	28			3	8	13	18	23	28
III день	3	8	13	18	23	28		3	8	13	18	23	28		2	9	14	19	24	29			4	9	14	19	24	29
IV день	4	9	14	19	24	29		4	9	14	19	24	29		3	10	15	20	25	30			5	10	15	20	25	30
V день	5	10	15	20	25	30		5	10	15	20	25	30		4	11	16	21	26			1	6	11	16	21	26	31

ЯНВАРЬ. 22 — день 9 янв. 1905 г. и памяти вождя пролетар. В. И. Ленина.
МАЙ. 1-2 дни Интернац. **НОЯБРЬ 7-8** — дни праздн. Пролетарск. революции.

Fig. 5. Schema of Soviet pocket calendar for 1931. On Gregorian calendar are denoted days of five days continuous production week. Five non-working days, January 22 Day of memory on 9 January 1905, and Lenin, May 1-2, Days of International and November 7-8, Days of Proletarian Revolution are excluded (http://ru.wikipedia.org/wiki/Файл:Soviet_calendar_1931_pocket_2.jpg)

Different, much more radical change occurred in 1929. The idea was to abolish Sunday as a rest day and to introduce a continuous production week (nepereryvka). So in production, from the autumn of 1929 until near the end of 1931, in parallel with Gregorian one, was introduced the calendar divided into 72 five-day weeks (=360 days), three of which were split into two partial weeks by five days of national holidays, but holidays were not a part of the week so that each split week still had also five days. Each day of the five-day week (pyatidnevka) was labeled by either one of five different colors or with a Roman numeral from I to V or with the the names The First (pervyj), The Second (vtoroj), The Third (tretij), The Fourth (chetvertyj) and the Fifth (pyatyj). In fact, each worker obtained a color or a number to identify his or her day of rest, so that every day, 80% of each factory's staff worked, while 20% were resting.

In 1930 was proposed the Soviet Revolutionary Calendar with 12 months of 30 days and five national holidays, not belonging to any month. It was rejected and never introduced but in many western sources is erroneously stated that the 72 five day weeks were organized in 12 months of 30 days, for example in Parry Albert (1940, "The Soviet calendar", *Journal of Calendar Reform* **10**, p. 68).

However, the attempt to change the week was unsuccessful, and on November 21st, Sovet Narodnykh Komissarov (Sovnarkom) SSSR replaced the five-day intervals with six-day intervals (shestidnevka), so that the year of 360 days consisted of 60 such intervals. This week was not with continuous production, but 6, 12, 18, 24, and 30 day of a month were the days of rest. At the end of February the last day was the day of rest or it was the 1st of March. In months with 31 days, the work on this day was assumed as a surplus and paid additionally. But neither system could take roots in the people's conscience. Therefore, in 1940 the Soviet government restored the use of the initial Gregorian calendar in factories and enterprises and the ancient seven-day week, with its Saturdays and Sundays. It is interesting as well that in addition to the Gregorian years, in some cases an additional date was given as e.g. in Fig. 6: *Twenty first year of the Socialist Revolution*, where this chronology was counted from the 7th November 1917. This was present until the disintegration of Soviet Union in 1991 (see e.g. Shcherbinin 2008, p. 58).

The Revolutionary Calendar of the Soviet Union ('Bolshevik calendar') is described in detail in our published paper: Theodossiou, E., Manimanis, V. N. and Danezis, E, 2002, "The Russians Calendars after the Christianization of the country", *JAAT* **21**, No. 1-3, June, pp. 149-153.

4 The Fascist calendar of Mussolini

The so-called 'Fascist calendar' appeared (and ended) in fascist Italy. However, it was not really a different calendar, but merely the setting of a new start for chronology, after the famous 'March towards Rome' of the 'black-shirted' fascists, on October 28, 1922, which brought Mussolini on power.

Actually, according to Marla Stone: *Using the French example, fascism retroactively restarted the calendar in 1927, making 28 October 1922, the first*

Fig. 6. From Soviet calendar for 1937 Translation of calendar page: Twenty first year of the Socialist Revolution / 1937 DECEMBER 1937 / 12 / sixth day of the six-day week / Day of elections to the Supreme Soviet of the USSR (http://ru.wikipedia.org/wiki/Файл::Revolution_kalendar.jpg)

day of the first year of the new calendar I.I.I. Fascism declared it would replace old allegiances and collective history. In this way, 'fascistization' was inextricably bound to 'nationalization' (1993, p. 230).

So, the Fascist calendar started on 28 October 1922. The date in the Fascist Era was written in Roman numerals. Thus, beginning in November, the year 1922-1923 was set as fascist year I (or year I *"di era fascista"* - of the Fascist Age). This year was written in Italian diaries *together* with the normal year A.D.: next to the Christian year there was a Roman numeral indicating

Fig. 7. Plate at the Stock exchange in Milano with date according to fascist calendar. Photo of Giovanni Dall'Orto.

the corresponding fascist year. For example, the day of Italy's war declaration against Greece was written as: 28 October 1940 - XIX (the number 19 written as a Roman numeral).

According to Mark Antliff: *The most dramatic instance of such social engineering was the 'superimposition over the Gregorian Calendar' of a fascist time frame, in which 1922 became 'Year I' of the fascist era, signaling a regenerative break from the plutocratic decadence of the immediate past. The new calendar was then punctuated with certain days of national celebration, each with a 'two fold mythical significance'. Thus March 23, Youth Day, commemorated the founding of Fasci; April 21, Labour Day, the founding of Rome; May 24, Empire Day, the entry of Italy into the First World War; September 20, Italian Unity, the incorporation of Rome into the Kingdom of Italy; October 28, the fascist Revolution, the March of Rome... In this way ordinary Italians were encouraged to experience the unfolding of time as a phenomenon with a transcendental core on a par with metaphysical reality which underlay Christianity* (2004, pp. 149-150).

The year 1922 (October) to 1923 was considered the fascist year 1 - with Latin digits: I. It was part of a date that was functioning in parallel with the Gregorian calendar in all fascist documents and other printed material. For example, the first of May of 1934 AD was accompanied by the fascist year XII, while December 25, 1938, was accompanied by the fascist year XVII,

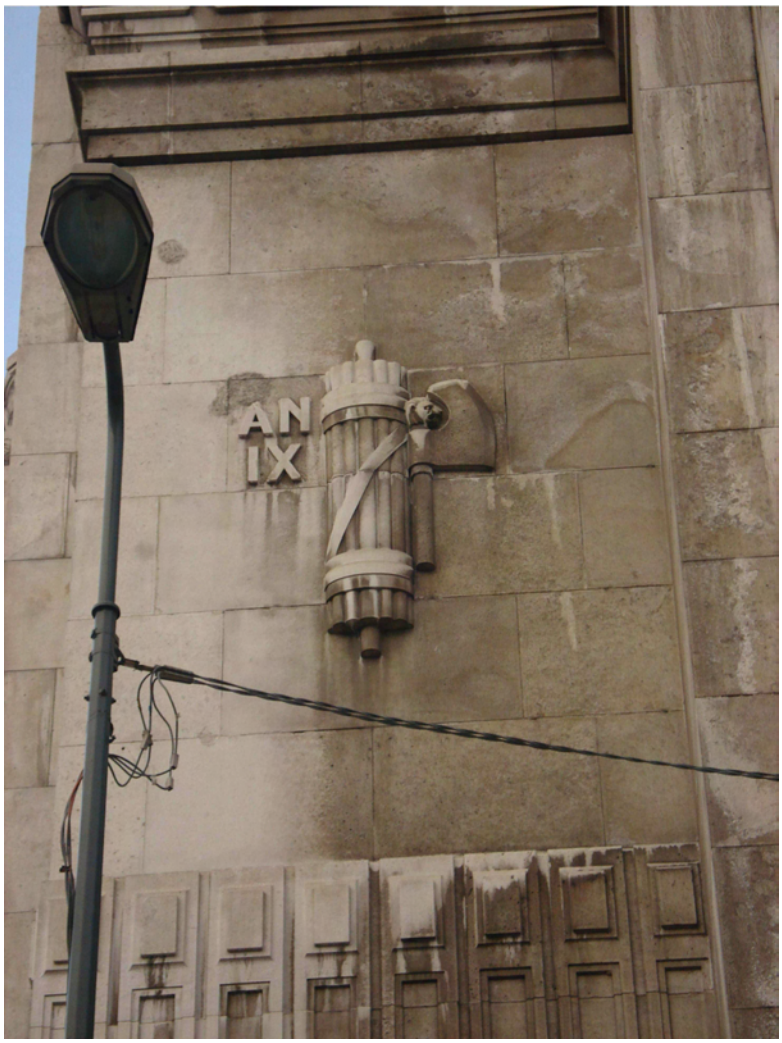

Fig. 8. Year IX of fascist era on the Milano central railway station. Photo of Giovanni Dall'Orto.

since December is after October and thus the fascist year had changed. As it should be expected, the overthrowing of the fascist regime in Italy brought with it the abolishment of this trivial calendar change.

5 The calendar of Metaxas dictatorship in Greece

It is interesting to note that Mussolini's chronology was imitated in Greece by the Ioannis Metaxas dictatorship (1936-1940), considering in turn 1936,

the year of its start, as 'year A'', written with Greek numeral. In all official papers of the Greek dictatorship there were two chronologies: the Christian year AD and the corresponding year of the dictatorship. For example, the day of Italy's war declaration against Greece was written as: 28 October 1940 - year E'.

ΠΡΩΤΗ ΔΙΑΣΚΕΨΙΣ

ΠΡΑΚΤΙΚΑ ΣΥΝΕΔΡΙΑΣΕΩΝ

Fig. 9. The proceedings of the First Conference of Regional Administrators of the National Youth Organization of 1939, where the year Delta (Δ') of the Metaxas dictatorship appears.

Needless to say, this way of year enumeration died together with the respective regimes. Moreover, this action of the dictatorship is virtually unknown to modern Greek society. It is not mentioned and has not been recorded anywhere, with the exception of certain official documents and state archives from that period, such as the proceedings of the First Conference of Regional Administrators of the National Youth Organization of 1939, year Delta (Δ'), from where we learned about it.

6 The New Rectified Julian calendar of the Orthodox Churches

Patriarch Meletios IV (1922-1923), head of the Orthodox Churches, convened an Ecumenical Congress in Constantinople in May 1923, where one of the principal topics of discussion was the reform of the Julian calendar. In the Serbian delegation were Gavrilo Dožić and Milutin Milanković. At that time, Dožić was the Metropolitan of Crna Gora and Primorje (Montenegro and the Littoral), and later become Patriarch of the Serbian Orthodox Church. Milutin Milanković (Dalj, May 28, 1879-Belgrade, December 12, 1958) is worldwide known for his groundbreaking work on the causal relationship of solar heating to the phenomenon of the occurrence of the Ice Ages in Europe during the Quaternary Period. He developed an astronomical theory for the evolution of planetary climates and explained the phenomenon of the Earth's Ice Ages and polar motion.

Milutin Milanković, was the vice president of the Serbian Academy of Sciences and Arts and director of the Belgrade Astronomical Observatory (1948-1951). To honor to his scientific achievements in astronomy, a crater on the far side of the Moon (coordinates $+170^o$, $+77^o$) was given his name at the 14th I.A.U. General Assembly in Brighton in 1970. His name was also given to a crater on Mars (coordinates $+147^o$, $+55^o$) at the 15th I.A.U. General Assembly in Sidney in 1973. In 1982, a small planet, discovered in 1930 by Milorad Protić and Pero Djurković and provisionally designated 1936 GA, received its permanent name: 1605 Milanković (Dimitrijević, 2002).

At the Ecumenical Congress representatives of Serbian and Romanian Orthodox Churches submitted two elaborate propositions (detailed description of the calendar reform and of the Pan Orthodox Congress in Constantinople is given in Milanković 1923, 1995, 1997, see also Dimitrijević 2002, Dimitrijević, Theodossiou 2002, Dimitrijević, Theodossiou, Mantarakis, 2008). The propo-sition of Serbian delegation, formulated by Maksim Trpković, was to introduce the intercalation rule that the secular years in centuries which when divided by 9 have remainders of 0 or 4 will be leap years. Consequently, 7 days will be omitted from 9 centuries, and the calendar will be closer to the tropical year than the Gregorian one, where the intercalation rule is that leap years are only secular years where the number of centuries is divisible by four. Moreover, the vernal equinox will always fall on March 21 or very close to it.

The Romanian delegation consisted of Archimandrite Julius Scriban and Senator Dragici. They came with the following proposal for calendar reform (Milanković 1923, 1997, Trajkovska, Ninković 2008): Each year is to have 364 days (exactly 52 weeks) so that every date has a fixed day in the week. March, June, September and December have 31 days, and other months 30 days. An additional week is added every 5 years between June 31 and July 1, whose number of days corrects the difference with the tropical year. The first day of Easter is fixed at April 29, and all other holidays become fixed. This proposition was presented to the Congress by Senator Dragici, but he told to Milanković that the author was actually baron Gustav Bedeus from Sibiu, who was not an Orthodox Christian so that it is not convenient to put his name on the proposal. However, according to investigations of Trajkovska and Ninković (2008), "A Resolution Concept for Conference of the Calendar of

Orthodox Churches in Constantinople on May 1, 1923", published in German by Bedeus in *Siebenbuergisch-Deutschen Tagesblatt* (Daily of Germans from Siebenburger - Seven towns or Transilvania in Romanian) differs from the proposition of Senator Dragici.

Congress rejected both propositions. The Serbian, authored by Trpković, since the year 2000 would not be a leap one as in the Gregorian calendar, and after only 77 years a difference of one day between the Gregorian and New Rectified Julian calendars would appear. The Congress concluded that the better solution is to delete thirteen days in Julian calendar in order to put it into line with Gregorian one, until 2100, when the one-day difference would appear.

Milutin Milanković obtained the task to develop a new proposal. He concluded that the wish of the majority of participants was that calendar of the Eastern Orthodox Church should not be identical with the Gregorian one, but that the two should parallel one another as far as possible. Consequently, instead to try to fix the date of the vernal equinox to March 21st, as in the Trpković's proposal, he tried to obtain the longest possible consonance of the two calendars. He elaborated a new intercalation rule, that secular years are leap years only provided that the number of centuries they belong to, when divided by 9 yields the remainder 2 or 6. In such a way the new calendar is more precise than the Gregorian one but consistent with it up to 2800, i.e. for 877 years after the Ecumenical Congress in Constantinople. Another advantage is that New Rectified Julian calendar of Orthodox Church will be in better agreement with nature than Gregorian calendar. A disagreement of one day with the tropical year will accumulate after almost 30,000 years!

Milanković presented to the Congress his new proposal signed by him and Gavrilo Dožić, as the new proposition of the Serbian Orthodox Church, on the session of May 23, 1923. In his historic speech to the Congress, he told the delegates that if they only adopted to delete 13 days from Julian calendar, the Orthodox Church would be in an inferior position in any future discussion on the calendar question. With the proposition of the Serbian delegation, the Orthodox Church could confidently enter into any negotiation on the calendar question with Western Churches since they would have the most precise and most scientific calendar in the Christian world. He underlined also that with such a decision, the Orthodox Church would not be accepting the calendar of the Roman-Catholic Church, but would be obtaining a better one.

Also at the Congress, Anthimos Metropolitan of Viziys proposed to determine the exact date of Easter by astronomical methods with the help of Observatories and Universities in Athens, Belgrade, Bucharest and Pulkovo.

Milutin Milanković formulated the final version of the calendar reform that was adopted by the Congress, and signed on June 8th, 1923, by Patriarch Meletios IV, Metropolitan of Kyzikos, Kalinikos, Archbishop of North America, Alexander, Metropolitan of Montenegro and Littoral Gavrilo Dožić, Metropo-litan of Nicaea, Vasilios, Metropolitan of Durachion, Jakub, Archimandrite Julius Scriban, and Professors E. Antoniadis and Milutin Milanković.

The date of the official inception of the New Julian calendar was originally set for October 1st, 1923, which will become October 14th, in order to omit the 13 days of difference between Julian calendar and Tropical year. This was the date when the calendar reform would be introduced in the Ecumenical Patri-

archate and in the Greek Churches, but without the part concerning the Easter determination, where the old Julian calendar was retained, until all Orthodox Churches introduce the reform. Today, Patriarchates of Constanti-nople, Alexandria and Antioch, Churches of Greece, Cyprus, Romania, Poland, Finland, Bulgaria (from 1968) and Orthodox Church in America (September 1, 1983, see e.g. http://www.holy-trinity.org/modern/calen2.html) use the "New", "Revised" or "Rectified" Julian calendar. On the other hand, the Patriarchate of Jerusalem, and Churches of Russia and Serbia, along with the monasteries on Mt. Athos, all continue to adhere to the Julian or Old Calendar (see e.g. http://www.yalchicago.org/paschacalculation.html).

7 Conclusions

From these six calendar systems that were devised from the late 18th to the middle of the 20th century, survived up to now only New Julian calendar of Orthodox Churches. This should be expected, since history History has shown that calendar changes are accepted with great difficulty by the people, who do not want to change calendar they are used to and the social and religious habits that are associated with it. Even in the case of New Julian Calendar, which dates are at that moment identical with Gregorian one, and only dates of movable eclesiastic feasts are changed, the great resistance against it exist. In Orthodox Churches which accepted it, sects of Old calendarians, refusing its usage, were created.

From these 6 calendar systems, which were devised centuries after the Gregorian calendar, the most discussed about in the international literature is the French Revolutionary Calendar (*Le Calendrier Républicain*), since it is associated with the famous French Revolution of 1789, which still moves and influences European thought.

About New Julian Calendar was also written, in particular in Orthodox sources. Then comes the Revolutionary Calendar of the Soviet Union ('Bolshevik calendar'), interwoven with a special period of the Soviet history, while the Theosebic calendar of Th. Kairis is totally unknown internationally, since only a few scholars or astronomers know about it in Greece.

Mussolini's Fascist calendar is mentioned in the international literature, but both it and the totally unheard of calendar of Metaxas dictatorship in Greece are not separate calendar systems; they are rather a parallel writing of the years next to the Gregorian calendar date that denoted the length of these dictatorships, while in the case of Mussolini's Fascist calendar some important holidays are also mentioned. They essentially represented, as professor Sterios Fassoulakis of the University of Athens writes, calendar systems of political ideology (Istorica, 2001).

These cases strengthen the conclusion that it is difficult for a calendar reform to prevail or even to survive for long. If they are not accepted by several states, Church or some organization existing in a number of different communities, the end of regime which implemented them is usually also the end of such calendar systems

Acknowledgements

This study formed part of the research at the University of Athens, Department of Astrophysics Astronomy and Mechanics, and we are grateful to the University of Athens for financial support through the Special Account for Research Grants. It is also supported by the Ministry of Science and Technological Development of Serbia through the project III44002.

References

Antliff Mark: 2004, Fascism, modernism and modernity, in R. Griffin & M. Feldman (Ed.), *Fascism: Critical concepts in Political Science*. Routledge, New York, pp. 149-150.

Dimitrijević, M. S.: 2002, Milutin Milanković (1879-1958) and his contribution to European astronomy, *Astronomische Nachrichten*, **323**, 570-573.

Dimitrijević, M. S., Theodossiou, E.: 2002, The calendar of the Greek Orthodox Church, *Astronomical and Astrophysical Transactions*, **21**, 145-148.

Dimitrijević, M. S., Theodossiou, E. Th., Mantarakis, P. Z.: 2008, Milutin Milanković and the reform of the Julian Calendar in 1923, *J. Astron. History and Heritage*, **11**, 50-54.

Fassoulakis Sterios: 2001, Calendars of political ideology, *Istorika*, **64**, January 4, 2001, 48-49.

Flammarion Camille: 1955, *Astronomie Populaire*, Édition Entièrement Refaite, G.C. Flammarion, Paris.

Le Calendrier Républicain: 1994, Bureau des Longitudes, Paris, p. 19.

Milanković, M.: 1923, *The reform of the Julian Calendar*, Serbian Royal Academy of Sciences and Arts, Special editions No 47, Natural and Mathematical Sciences No 11 [in Serbian].

Milanković, M.: 1997, *Memories, experiences, cognition*, Selected works of Milutin Milanković, No 7, Zavod za udžbenike i nastavna sredstva, Beograd [in Serbian].

Milanković, V.: 1995, *Milutin Milanković 1879-1958*, European Geophysical Society, Katlenburg - Lindau.

Parry Albert: 1940, The Soviet calendar, *Journal of Calendar Reform* **10**, p. 68.

Polemis, D. P.: 1994-1996, *Allilografia Theofilou Kairi*, 3 volumes, Kairios Vivliothiki Publ., Andros [in Greek].

Portaz Maximine: 1935, *Essai critique sur Theóphilos Kaíris*, Paquet, Lyon, p. 220.

Renouard, Antoine Augustin: 1822, *Manuel pour la concordance des calendriers républicain et grégorien: ou, Recueil complet de tous les annuaires depuis la première année républicaine* (2 ed.).

Shcherbinin, A. I.: 2008, "The red day in the calendar": The formation of the political time perception matrix in Russia, p. 58 [in Russian], *Vestnik Tomskogo Gosudarstvennogo Universiteta, Filosofiya, Sociologiya, Politologiya*, No 2(3), pp. 52-69.

Stone Marla: 1993, Staging Fascism: The Exbition of the Fascist Revolution, *Journal of Contemporary History*, **28**, No. 2. April, by Sage Publications, Ltd.

Theodossiou, E. and Danezis, E.: 1996, *The Odyssey of the Calendars*, Diavlos Publications, Athens [in Greek].

Theodossiou, E. and Danezis, E.: 2000, *In the traces of ICHTYS: Astronomy, History and Philosophy*, Diavlos Publications, Athens [in Greek].

Theodossiou, E., Manimanis, V. N. and Danezis, E.: 2002, The Russian Calendars after the Christianization of the country, *Journal of the Astronomical and Astrophysical Transactions*, **21**, pp. 149-153.

Theodossiou, E., Grammenos, Th. and Manimanis, V. N.: 2004, Theophilos Kairis: The Creator and Initiator of Theosebism in Greece, *The European Legacy*, **9**, pp. 783-797.

Theodossiou, E., Danezis, E, Katsiotis, M. and Mantarakis, P.: 2007, Theophilos Kairis: The Initiator of Theosevism in Greece, *Aeropos*, February, September-October, **75**, pp. 104-117 [in Greek].

Theophilos Kairis, Code 53, Library of the Historical and Theological Society, as in Issue 65 the text 'Correspondence of months' [s.d.].

Trajkovska, V., Ninković, S.: 2008, On a resolution concept concerning the calendar reform submitted to Pan-Orthodox Congress in Constantinople in 1923, *Publ. Astron. Obs. Belgrade*, **85**, pp. 189-194.

Wilson P. W.: 1937, *The Romance of the calendars*, W.W. Norton, New York.

The pyramids of Greece: Ancient meridian observatories?

Efstratios Theodossiou[1],Vassilios N. Manimanis[1],
Milan S. Dimitrijević[2], Marco Katsiotis[3]
[1] Department of Astrophysics, Astronomy and Mechanics Physics Faculty,
University of Athens-Zografos 157 84, Athens
[2] Astronomical Observatory, Volgina 7, 11060 Belgrade
[3] National Technical University of Athens, Polytechniopoli Zographou, Athens
etheodos@phys.uoa.gr
mdimitrijevic@aob.bg.ac.rs markos@central.ntua.gr
(Research report. Accepted on 21.12.2011)

Abstract. Pyramids, "Dragon Houses" ("Drakospita") and megalithic structures in general create always a special interest. We postulate that, as happens with the Drakospita of Euboea, the pyramid-like structures of Argolis (Eastern Peloponnese) were constructed by the Dryops. It is known that, in addition to Euboea and some Cyclades islands, this prehellenic people had also settled in Argolis, where they founded the city of Asine. We also propose that the pyramids of Argolis and in particular the pyramid of Hellinikon village were very likely, besides being a burial monument or guard house, might be served also for astronomical observations.
Key words: Archaeoastronomy, Greek pyramids, Hellinikon, Drakospita, Dryops

Пирамидите на Гърция – древни меридианни обсерватории?

Ефстратиос Теодосиу, Василиос Н. Маниманис,
Милан С. Димитрийевич, Марко Кациотис

Пирамидите, "драконовите домове" ("дракоспити") и мегалитните структури предизвикват винаги специален интерес. Ние приемаме, че както при дракоспита на остров Еубоеа, пирамидовидните структури в Арголис (Източен Пелопонес) са били построени от Дриопите. Известно е, че освен в Еубоеа и някои от Цикладските острави, този пред-елински народ е пребивавал и в Арголис, където е основал град Азин. Ние предполагаме че пирамидите в Арголис, и в частност пирамидата в селището Хелиникон, без да са погребални монументи или охранителни постройки, са твърде подобни помежду си и са могли да служат и за астрономически наблюдения.

Introduction

The existence of pyramids, or rather pyramid-like buildings, in Greece has not been widely known, as most people, even most researchers worldwide know only of the Egyptian pyramids. Yet, it seems that there are several ancient pyramid-like buildings in southern Greece, the most impressive of which is the structure near the village Hellinikon in Argolis (Eastern Peloponnese). Some of these buildings have suffered major and irreparable damages, as their large stones were used through the centuries as raw material for the construction of other buildings, such as churches, or even for the production of lime in limekilns.

In the literature for this topic, the following pyramids are mentioned in Greece (Lazos, 1995):

Table I

	Name	Locality	Remarks
1.	Hellinikon	Hellinikon and Kephalari	The best-preserved one
2.	Ligourio	Epidaurus	Only its base exists
3.	Dalamanara	Epidaurus	Only traces remain
4.	Kambia = tower for fire-signaling	Nea Epidaurus	Preserved to some height
5.	Sikyon (?)	Corinthia (?)	Only traces remain (?)
6.	Viglafia	Neapoli (Laconia)	Only its base exists
7.	Amfio	near Thebes (Thiva)	scalar

In addition to the above, two other singular structures have been referred to as pyramid-like buildings: the cone-like pyramid in Khania (Crete), and the Rock Pyramid forming the peak of Mt. Taygetos; however, the latter is just the natural peak of the mountain, the tallest in Peloponnese (2,407 m). Prof. I. Liritzis (1995 & 1997), assiduous researcher of such ancient megalithic structures, supports the view that there are over 20 ancient Greek pyramids; they refer to pyramid-like structures in Astros (in Kynouria, to the south of Argolis), in Neochori of Phthiotida (they even date it in 11,000 BC), in Agios Andreas of Mt. Parnassos, in Vathy (of Avlis, in northern Boeotia), and in other places.

From all the above structures, only the Hellinikon pyramid to the south-eastern edge of Argive plain is preserved in a relatively good condition. For some of these structures, the data used in this study come from descriptions and references by ancient travelers, for example the description and comments of Pausanias (1985) for the Hellinikon pyramid, or from foreign travelers of the 19th century AD (Blouet A. and Ravoisié, A., 1831, Curtius, E.R., 1851).

1 References, studies and excavations

Although the pyramid-like buildings of Argolis stand out due to their form and shape, the references to them, even from Greek antiquity, are rather scarce.

Only the Greek traveler and geographer Pausanias (1985), writing in the 2^{nd}nd century AD, mentions the Hellinikon pyramid in his *Corinthiaka* (2, 25, 7):

"Traveling from Argus to the region of Epidaurus, there is a building to the right that resembles very much a pyramid and bears relief carved shields of the shape of the Argolic shields. In this place Proetus had battled with Acrisius for the throne and they say that the battle ended without a winner; for this reason they were later reconciled, as none could achieve a decisive victory. It is said that this was the first time that men and armies equipped with shields clashed; for those that fell in this battle from both armies, since they were compatriots and even relatives, a common tomb was built in that place."

Thus, according to Pausanias, the pyramid was a common tomb, built most probably by Proetus and Acrisius for the soldiers who died in a battle

between them; a battle in which soldiers used shields for the first time. This reference to mythical figures (Proetus, Acrisius) indicates that the building was considered to be very old.

Fig. 1. The Hellinikon pyramid. Prof. E. Theodossiou (left) and the physicist N. Saridakis (right)

Pausanias also mentions (*Corinthiaka* 2, 24, 7) that in adjacent areas there were some polyandria (mass tombs) of the Argives killed in the battle against the Spartans that was held in Hysiae (an acropolis next to the modern village Akhladocampos) in 669 BC:

"And polyandria exist here for Argives who won in a battle against the Lacedaemonians near Hysiae" (*Corinthiaka* 2, 24, 7).

So the ancient author considered the 'pyramid' as one of these burial monuments. Other researchers have suggested different possible uses (Lord, 1939, pp. 78-84).

The pyramids found in Greece are the only cases of pyramidal architecture in the broader European region. The shape of the pyramid-like buildings, their static and architecture, probably classify some of them in the pre-Pelasgic period (Lazos, 1987 & 1995). However, in a country rich in archaeological findings the ruins of these structures did not attract the interest of researchers. Thus, their study is almost nonexistent and a mystery surrounds them due to lack of adequate knowledge. There is still a chance that some reference could still be discovered in Byzantine texts. Currently, the next known reference to the 'Greek pyramids' after Pausanias (2nd century

AD) is from the first decade of 19th century. William Martin Leake toured Peloponnese in 1806, when Greece was still under the Ottoman rule, and he mentions the Hellinikon pyramid, which he visited on March 14, 1806, in his book *Travels on the Moréa* (vol. II, pp. 340, 344). In it, he gives two drawings, front view and top view of the buildings.

Fig. 2. The entrance of the Hellinikon pyramid with the eastern side. The entrance is next to the SE corner. The width of the entrance is 1.35 m, while its top consists of two converging stones that form a large capital Greek letter Λ.

In 1829 the French Scientific Mission in Moreas (Peloponnese) studied the two pyramids (in villages Hellinikon and Ligourio) and published the results in 1831 - in the three tomes of Abel Blouet and Ravoisié, Amable: *Expedition Scientifique de Morée*, vol. II, 107.

In 1901, Th. Wiegand conducted a preliminary excavation (the first one, 1901, pp. 241-246) of the Hellinikon pyramid. Wiegand removed all the fill from the floor of the pyramid, while the first Greek scientist who studied it was the archaeologist Apostolos S. Arvanitopoulos in 1916 (pp.72-99). Apostolos Arvanitopoulos believes that the monument dates to the Mycenean era (1600 BC-1100 BC), while the archaeologist Christos Tsountas (1857-1934),

the founder of Greek prehistoric archaeology, believes it is from the 6th century BC (1893).

More excavations followed in the Hellinikon pyramid by R. Ehrich and Mrs. Ann Hoskin-Ehrich, on August 1937, of the American School of Classic Studies and Archaeology in Athens, while at about the same time R. Scranton (1938) was excavating the Ligourio pyramid. Louis Lord, then director of the American School of Classic Studies in Athens, edited the report (1938, pp. 481-527) of these excavations based on the conclusions of the three archaeologists mentioned above, while he subsequently researched himself and discovered several buildings in Argolis, mainly square archaic towers, which were most probably the *polyandria* of Pausanias (Lord, 1939, pp. 78-84). Amongst the findings in the pyramid of Hellinikon were a big pithos, the floor of the long corridor and the room, re-carved from repairs entrance door and parts of the wall, infill from earlier excavations, some ceramics of Protohelladic II period (2800-2500 BC), also room foundations and mortals from later uses of the pyramid, as well as mixture disturb sediments with ceramics of classical period, such as lamps, house ware and few coarse shards of doubtful age and some roman lamps. The infill at the floor varies between 20-60 cm (Lord, 1938, pp. 508-538).

Louis Lord considers that the pyramids were not tombs, because their doors were opening from inside; nor were they towers for fire-signaling, as they were not built in elevated positions with a view. Lord believes they were posts capable of housing a guard of a few men, which could control the road to Tegea. However, he stresses that the peculiar pyramid-like construction is a fact that remains unexplained (1938). There wasn't a reason to build this form of structure for this purpose, as an outpost with a small wall would be the normal thing to do. What could be the purpose of these singular, pyramid-like constructions? Also, Lord supports the idea that the pyramid was from the early Hellenistic era, more specifically late 4^{th}th century BC.

The topic appeared to close from an archaeological point of view, as the American archaeologists had done a good job. The German archaeologist S. Oppermann, with a relative publication in German (1971, pp. 45-52), made known the two pyramids, in Hellinikon and Ligourio, to a wider German-speaking public, without adding something to the topic from a research point of view.

After about 15 years followed the researcher and author Christos Lazos, with two publications on Greek pyramids (1984, 1987), and an article by Helena Fracchia of the University of Toronto (1985, pp. 683-689), in 1986 Professor I. Liritzis published his book *Archaeometry - Methods of dating in archaeology*, and in 1994 the civil engineer V. Katsiadramis made a static study of the two pyramids and the corresponding figures (1994, pp. 9215-9236). In 1994 appear a paper by Professor Ioannis Liritzis and another one by the academician Theocharis *et al.* (1994, pp. 399-405) and the two books, again by archaeometrist Professor Ioannis Liritzis (1995) and by author C. Lazos (1995), which exhaust the topic from the descriptive point of view. Finally, Professor Ioannis Liritzis, in 1997, published an article about the mystery of these pyramids and similarly Professor Theodore Spiropoulos (2003).

In practical, the real research work on the Greek pyramids started under the supervision of the archaeometrist Professor Ioannis Liritzis and his group. The dating of the pyramid was approached through five sub-projects:

1) Geophysical prospection inside and around the two main pyramids at Hellenikon and Ligourio, where buried monuments were discovered (Theocharis *et. al.*, 1997, pp. 593-618).

2) The results of the above team directed the archaeological excavations carried out by archaeologist A. Sampson (1996, pp. 56-61) and archaeologists of the Archaeological Museum of Nauplion (Pikoulas, 1996, pp. 60-63; Piteros, 1995, pp. 11-13, and Piteros, 1998, pp. 344-394). Amongst the new findings were foundations of rooms, ceramics of Classical, Hellenistic, Roman and Protochristian periods, and Protohelladic II in the exterior foundations of Hellenikon pyramid above the bedrock. A comparative study of masonries was also made (Liritzis, 1995 & 1997, pp. 32-34).

3) Astronomical orientation of the long entrance corridor was found related to the rise of Orion's belt occurring in *circa* 2000-2400 BC (Liritzis, 1998, pp. 10-21).

4) The dating of some parts of the over lied large megalithic blocks in the wall, with the novel thermoluminescence dating method of rock surfaces. Sampling was chosen for their firmness and lack of sun exposure of internal contact surfaces, by removing a few milligrams of powder from pieces in firm contact. Seven pieces gave an age range of *circa* 2000-2500 BC. Liritzis, 1994a, pp. 603-604; 1994b, 361-366; Theocharis *et al.* 1994, 399-405), while two ceramic shards of non-diagnostic typology one from Hellenikon and one from Ligourio pyramids dated by TL (ThermoLuminescence) and OSL (Optically Stimulated Luminescence) gave concordant ages of 3000±250 BC and 660±200 BC respectively (Liritzis *et al.*, 1994, pp. 189-198). The novel dating method has been well published by the initiator and others Liritzis *et al.* 1997, pp. 479-496); Liritzis and Galloway, 1999, pp. 361-368; Habermann, 2000, pp. 847-851; Greilich *et al.* 2005, pp. 645-665; Morgenstein *et al.* 2003, pp. 503-518; Liritzis and Vafiadou, 2005, pp. 25-38).

5) The mythological genealogy of Argolid has been cautiously interpreted. It involves Inachus and his deluge and his descendants of Proetus and Acrissius that according to ancient traveler Pausanias (2nd c. AD) they fought for domination but had a draw and erected Hellenikon pyramid, shown to be at c. 2800 BC (Zangger, 1993; Liritzis and Raftopoulou, 1999, pp. 87-99)

2 The use of the pyramids

Pausanias, as is evident from his text, acknowledges that the purpose served by the pyramids had been forgotten in his age (*circa* 150 AD) and for this reason he writes about what the people were 'saying' about it, mentioning the hypotheses of being tombs and small military outposts.

The construction of these buildings, their dimensions and inclination, being added to the fact that no tomb-associated findings (such as bones or death ornaments) were found, lead to the conclusion that these structures were rather a kind of small fort or an observatory (Kalleyia, 1995).

The pyramids are dated by some archaeologists (Leake, 1846; Lord, 1938; Fracchia, 1985; Piteros, 1998), based on their wall structure, in the 4th century BC; the same archaeologists consider that they indicate the relations between Egypt and Argos, a tradition reinforced by the mission of 3000 Argive mercenaries in Egypt in 349 BC.

However, the Greek pyramids seem to have no relation to Egyptian ones (interior plan, masonry, slope, size), though there were trade contacts between the people of SE Mediterranean evidenced at least by the early presence of Minoans, Myceneans and later on Greek colonizations, in the West, Asia Minor and the Levant and Egypt, e.g. Tel Kabri, Avaris, Meggido etc. (Barbara and Wolf-Dietrich Neimeier, 1997, pp. 763-802).

Leake (1846, pp. 334-483), Vischer Wilhelm (1857, pp. 325-328) and others support the burial monuments theory, which is rejected by Wiegand (1901, pp. 241-246), who suggests that they can't be tombs because of the mortar used in their construction, a material hinting for him a building date in the 1st century BC. Other researchers, though, suggest that the mortar probably does not belong to the original building but to a posterior conservation work.

The Egyptian pyramids were Pharaohs' burial monuments, but they also served for astronomical purposes: Cheops Pyramid was a huge meridian instrument, the largest ever constructed, while its main passage's direction was towards the pole star of its age, Thuban or Alpha Draconis (α Dra).

Helena Fracchia (1985) supports the view that the Argolis pyramids were erected for the defense of the region, as fortifications incorporated into some large farms, as she believes from her research of ancient farms in Attica.

Civil engineer V. Katsiadramis (1994), after his static study of the whole Hellinikon monument, draws the conclusion that this building was in its initial form most probably a truncated pyramid 3.60 m high. He suggests that it was never complete up to its projected summit with stones or a roof of some kind, not being an Egypt-like, mathematical pyramid. He adds that the truncated pyramid shape *'is a very ancient worshipping tradition in Greece... ...this exact shape of the Elliniko building was intentionally chosen, as it combined static and aesthetic requirements with the Greek worshipping tradition'* (Katsiadramis, 1994). He, thus, considers a worshipping use for the building; in his view, it was a roofless sanctuary.

The Argolis pyramids continue to attract the interest of researchers. Professor I. Liritzis in his book (1995) argues that their megaliths were used as construction materials for churches and for lime production, in order to explain the reason for the disappearance of the Astros, Sikyon and Viglafia pyramids, which were reported by foreign travelers in early 19th century. C. Lazos, an author specialized in the research and recording of the feats of ancient Greek technology, in his book Pyramids of Greece (1995), provides a complete list of the Greek pyramid-like structures.

Our team visited the Hellinikon and Lygourio pyramids and photographed them; the architect, Marcos Katsiotis measured the dimensions of the Hellinikon pyramid and drew the top view, a section and perspective drawing of this pyramid, which is the best preserved one. But, finally, we used the drawings made by the civil engineer Vassilios Katsiadramis, which exist in the current Bibliography (1994, p. 9222).

3 The Hellinikon pyramid

The Hellinikon pyramid is located 5 to 6 km to the southeastern edge of the plain of Argolid, in the direction of the ancient road to Arcadia, between the villages Hellinikon and Kefalari, where the Erasinos River sources are (nowadays Kephalari). This is the best preserved pyramid (Fig. 1).

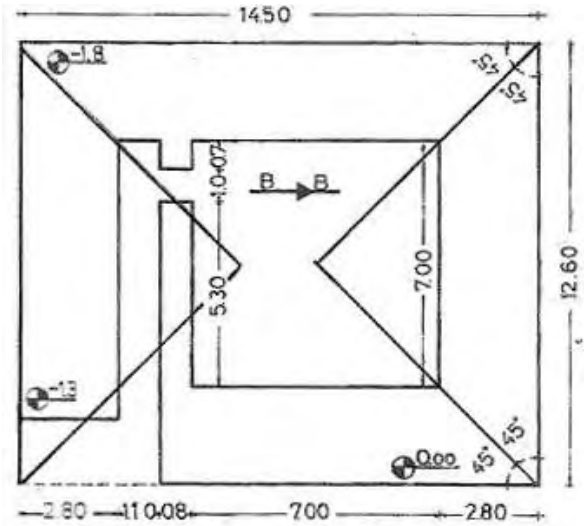

Fig. 3. Perspective drawing of the truncated pyramid of Hellinikon, made by civil engineer Vassilios Katsiadramis (1994, p. 9222).

However, archaeometric measurements based on optical thermoluminescence conducted by prof. I. Liritzis at the Nuclear Dating Laboratory of the University of Edinburgh and at the Archaeometry Laboratory of Democritos Center (Theocharis *et al.* 1995) showed that at least the Hellinikon pyramid is much older: *circa* 2700 BC. The optical thermoluminescence method is based on laser technology that can be applied on stones from walls; unfortunately, this method, used by Liritzis since 1986, although it is theoretically accepted, had not yet been fully calibrated in that time (1995) and doubts can be raised about this dating. At this point, if one remembers the geographer and traveler Pausanias, who gives a hint for this monument about being built in the Mycenaic period, one could find most probable this period as being in the middle of the two datings mentioned above: from 1600 to 1100 BC.

The dimensions of the Hellinikon pyramid are 14.50 x 12.60 x 10.80 x 10.60 m. Many researchers have wondered whether there is any relationship with the Egyptian pyramids, for example a correlation in their dating. Traditional archaeological research, as we saw, dated these structures in the 4th century BC, a much more recent date than the dates of the Egyptian pyramids.

Lois Lord (1938) dated both Hellinikon and Ligourio in the dawn of the Hellenistic period, i.e. in the end of 4th century BC. The Greek archaeologists E. Spathari, Chr. Piteros and G.A. Pikoulas also suggested (Chr. Piteros,

1995; G.A. Pikoulas, 1996) that both pyramids were built in late 4th century BC and that they were guardhouses or outposts. Th. Wiegand (1901) dated the Hellinikon pyramid in 1st century BC. However, these datings must not create a bias toward a more recent period, as archaeologist and Professor of Prehistoric Archaeology at the University of Athens Theodore Spiropoulos (1981), who discovered a pyramid in the shape of the Ampheio hill in Thebes, dates it *circa* 2500 BC.

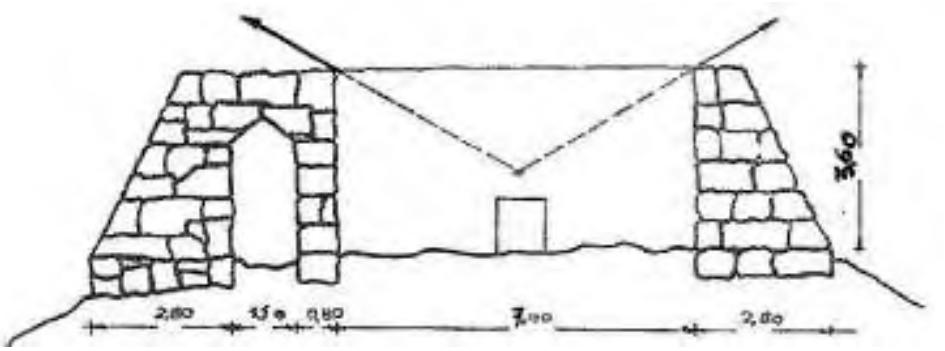

Fig. 4. Drawing of the truncated pyramid of Hellinikon, made by the civil engineer Vassilios Katsiadramis (1994, p. 9222).

4 The Ligourio pyramid

The Ligourio pyramid is located in the foot of Mt. Arachnaeo, to the left side of the road leading from Argos to Epidaurus, 1.5 km West of the village of Ligourio. Its dimensions are approximately 14 (north side) x 12 x 12 x 12 m. Pausanias does not mention this pyramid at all and the first reference to it comes from the "French Scientific Mission in Moreas" (Blouet, A. and Ravoisié, A., 1831). In the years that passed since the early 19th century the pyramid, made of sandstone blocks, deteriorated to the point it is now almost leveled. Only a couple of building stones have remained in their original positions; the rest were used for the construction of other buildings in Ligourio, while some stones are incorporated in the Byzantine church of Agia Marina (St. Marina).

The first excavations in the region were conducted by the American School of Classic Studies of Athens, from 9 to 18 December 1936 and later from 1 to 9 August 1937.

Among the findings of the 1937 excavation, led by R. Scranton (1938, 7.4, pp. 528-538), was a stone axe (*keltis*) dated in the Neolithic Age, that is prior to 3000 BC, a most intriguing fact that created certain connotations. Scranton writes that *"the keltis, an isolated prehistoric artifact, does not prove the existence of a Neolithic settlement at the site. It was probably just transported there from a distant place as something curious"*.

However, some researchers are skeptic about this view: How is it possible for the Neolithic axe to have been preserved at a different site for 2500 years,

to have been transported as something curious to the Ligourio pyramid in the 4th century BC and subsequently preserved at its new position for another 2300 years? It is a difficult question.

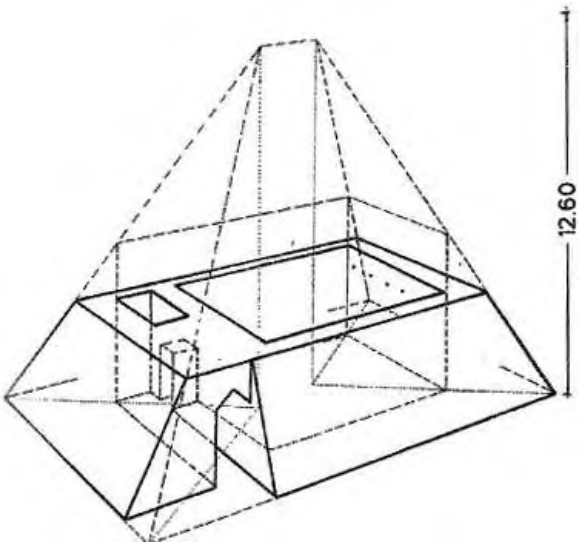

Fig. 5. Drawing of the truncated pyramid of Hellinikon, made by the civil engineer Vassilios Katsiadramis (1994, p. 9222).

Nevertheless, most researchers date the Ligourio pyramid along with the Hellinikon pyramid, around the 4th century BC.

Fig. 6. The Ligourio pyramid, as imaged by the *French Scientific Mission in Moreas* (Expedition Scientifique de Morée, 1831).

In 1995 academician Petros Theocharis and his colleagues announced that the optical thermoluminescence method gives an age for the Ligourio pyramid of 4100 ± 600 years, that is it was built *circa* 2100 BC or about 600 years 'younger' than the Hellinikon pyramid as dated with the same method, although as far as it can be discerned the two pyramids are very similar. The same researchers supported the view that both theses pyramids were astronomical observatories!

On the contrary, archaeologist Christos Piteros, curator of antiquities in Nafplio, supports (1995) a dating of the pyramids in the 4th century BC - definitively no older than 450 BC. As for their purpose, he believes that they were fortified out-posts-military observatories. Piteros is especially critical against the views of Theocharis *et al.* (1995). He strongly argues that their views are misleading(!), since they reject consolidated views of archaeologists simply based on a 'magical unproved physical method for a purely archaeological issue'.

The archaeologists excavators are reserved to accept without doubts the Classical or Hellenistic age, while A. Sampson (1996, pp. 56-61) supports such a younger age but his reserve to reject an earlier age is apparent.

So, up to now, there is no satisfying explanation of the reason behind the construction of several reported small sized pyramids in Greece and about the choice of their shape as a message tower or else. To summarize, the following views have been supported about the Greek pyramids:

a) Purpose

1. Burial monuments - polyandria (Pausanias, 2nd century AD; Leake, 1846; Vischer, 1857).

2. A 'tomb identifier', indicating the existence of an important person's tomb at a nearby site (hill), or even under it (Arvanitopoulos, 1916).

3. Fortified military outposts-guardhouses (Lord, 1938 & 1939; Wiegand, 1901; Fracchia, 1985; Spathari-Piteros-Pikoulas, 1995 & 1996).

4. Towers for fire -or smoke- signaling (Curtius, 1851).

5. Astronomical observatories - with an evident astronomical orientation, after a relative study (Theocharis e*t al.*, 1994 & 1997; Kalleyia, 1995; Theodossiou *et al.*, 2002).

6. Sanctuaries (Katsiadramis, 1994).

b) Dating

1. 1600 to 1100 BC (Pausanias, 2nd century AD; Arvanitopoulos, 1916).

2. 6th century BC (Tsountas, 1893; Curtius, 1851).

3. 4th century BC (Leake, 1846; Lord, 1938 & 1939; Fracchia, 1985; Spathari-Piteros-Pikoulas, 1995 & 1996).

4. 1st century BC (Wiegand, 1901).

5. 2100 BC for the Ligourio pyramid and 2730 BC for the Hellinikon pyramid (Theocharis *et al.*, 1994 & 1997).

5 Conclusion

When excavations were made around the Greek pyramids in the early 1900s, pottery fragments from the 4th century BC were found, and it was presumed that the pyramids were also constructed then; that is, about the time of Alexander the Great. Recent dating of crystals from internal surfaces of the limestone blocks using thermoluminescence puts the construction times back two millennia. The Hellenikon pyramid dates to 2730 B.C.; the Ligourio, to 2100 BC. This means that the Greek pyramids were built in roughly the same time frame as the Egyptian pyramids (Hammond, 1997).

Why would the ancient Greeks want to build miniature pyramids? The classical scholar Pausanias wrote in the 2nd century AD that the Hellenikon pyramid was a cenotaph for the dead fallen in a fratricidal battle 4,000 years ago. Nobody believed his story until now (Corliss, 1998).

The date and the purpose of even the two main Greek pyramids are not known with any certainty. What it can be said is that these are carved and not scalar; moreover they also differ from the Egyptian ones in the slope inclination.

Archaeologists suggest that the Hellinikon pyramid can't be a building of the 3rd millennium BC; it must have been constructed at least after 2100 BC. The later corollary follows from a finding of the excavation conducted for the Academy of Athens' research: a proto-Hellenic ditch in the foundations of the building. The proto-Hellenic period conventionally ends in circa 2100 BC, therefore archaeologists conclude that the pyramid was built definitely after 2100 BC.

Archaeologists also stress that not even one ceramic fragment was discovered in the pyramid sites dated from the two subsequent periods, the meso-Hellenic and the Mycenaean period. If the pyramid was indeed a 3rd-millenium construction, then the lack of ceramics would be a unique case.

The vast majority of archaeologists support the view that the pyramids are buildings of the 4th century BC.

The disagreement among the experts extends to the purpose these structures served. Our team expresses its agreement with professor Theocharis and his colleagues that the Greek pyramids could have an astronomical significance, probably in addition with their use as burial monuments or military outposts. We have also propose that the pyramids of Argolis and in particular the pyramid of Hellinikon village were very likely, besides being a burial monument or guard house, one of the first meridian observatories (Theodossiou et al., 2002).

To support this view there is the case of another Greek megalithic structure, the 'Drakospito' (= dragon house) on top of Mt. Oche, which was studied by our team and was shown to have an ancient Sirius-rise astronomical orientation (Theodossiou et al. 2009). Besides, several astronomical connotations have been proved in the case of the Egyptian pyramids.

For the Greek pyramids, the case is still open. We believe that a coordinated effort of archaeologists, historians, astronomers, architects and archaeometrists is needed in order to reach definite conclusions as far as the use of the pyramid-like structures in Greece is concerned.

Acknowledgements

This study formed part of the research at the University of Athens, Department of Astrophysics Astronomy and Mechanics, and we are grateful to the University of Athens for financial support through the Special Account for Research Grants. It is also supported by the Ministry for Education and Science of Serbia through the project III 44002.

References

Arvanitopoulos, A.S.: 1916, "Research in Argolis during the year 1916", *Proceedings of the Archaeological Society of Athens* [in Greek].

Blouet, Abel and Ravoisié, Amable: 1831, *Expédition scientifique de Morée, ordonnée par le Gouvernement Francais. Architecture, Sculptures, Inscriptions et Vues du Péloponèse, des Cyclades et de l'Attique*, Firmin Didot, (3 volumes), Paris. [in French].

Corliss, W. R.: 1998, *Science Frontiers*, **116**, March-April (on-line reference).

Curtius, E. R.: 1851, *Peloponnesos, eine historisch-geographische Beschreibung der Halbinsel*, band II. Elibron Classics [in German].

Fracchia, H.: 1985, "The Peloponnesian Pyramids Reconsidered", *American Journal of Archaeology*, 89.

Greilich, S., Glasmacher, G. A., Wagner, G. A.: 2005, "Optical dating of granitic stone surfaces", *Archaeometry*, **47**, no. 3.

Habermann, J., Schilles, T., Kalchgruber, R., Wagner, G. A.: 2000, "Steps towards surface dating using luminescence", *Radiation Measurements*, 32.

Hammond, Norman: 1997, "Did the Early Greeks Simply Copy the Pyramids of Egypt?", *London Times*, August 1.

Kalleyia, A.: 1995, in *Papyros-Larousse-Britannica Encyclopaedia*, vol. **33**, p. 73 [in Greek].

Katsiadramis, V.: 1994, "The ancient pyramid-like structures of Hellinikon and Ligourio in Argos - A technical and archaeological study", *Davlos*, 156 [in Greek].

Lazos, C.: 1984, "The pyramids of Argolis", *Istoria Ikonografimeni*, 189 (March), [in Greek].

Lazos, C.: 1987, "The pyramids of Argolis", *Anexigito*, 33 (May) [in Greek].

Lazos, C.: 1995, *Pyramids in Greece*, Athens, Aeolos Publ. [in Greek].

Leake, W. M.: 1846, *Peloponnesiaca: Supplement to Travels on the Moréa*, vol. II. J. Rodwell, London.

Liritzis, I.: 1986, *Archaeometry - Methods of dating in archaeology*, Kardamitsas publ., Athens [in Greek].

Liritzis, I.: 1994a, "A new dating method by thermoluminescence of carved megalithic stone building", *Comptes Rendus* (Academie des Sciences), **319**, serie II, Paris.

Liritzis, I.: 1994b, "Archaeometry: Dating the past", *EKISTICS*, **368**, 364.

Liritzis, I., Galloway R. B. and Theocaris P.: 1994, "Thermoluminescence dating of ceramics revisited: Optical stimulated luminesccence of quartz single aliquot with green light emitting diodes", *J. Radioanal. Nucl. Chem. Letters*, **188** (3).

Liritzis, I.: 1995, *The mystery of the Hellenic pyramids*, Academy of Delphic Studies Publ. [in Greek].

Liritzis, I.: 1997, "The mystery of the Hellenic pyramids", *AELLO* (Yacht Club of Greece) 9, Athens [in Greek].

Liritzis, I., Guilbert, P., Foti, F., Schoerer, M.: 1997, "The Temple of Apollo (Delphi) strengthens new thermoluminescence dating method", *Geoarchaeology International*, **12**, no. 5.

Liritzis I.: 1998, "Bronze Age Greek Pyramids and Orion's belt", *Griffith Observer*, **63**, n. 10.

Liritzis, I. and Raftopoulou, M.: 1999, "Argolid: connection of prehistoric legends with geoenvironmental and archaeological evidence", *TUBA-AR*, II.

Liritzis, I. and Galloway, R. B.: 1999, "Dating implications from solar bleaching of thermoluminescente of ancient marble", *J. Radioanal. Nucl. Chem.*, **241**, 2.

Liritzis, I. and Vafiadou, A.: 2005, "Dating by luminescence of ancient megalithic masonry", *Mediterranean Archaeology & Archaeometry*, **5**, no.1.

Lord, E. L.: 1938, "The Pyramids of Argolis", *Hesperia*, **7** (vii), no. 4.
Lord, E. L.: 1939, "Watchtowers and Forteresses in Argolis", *American Journal of Archaeology*, **43** (January-March).
Lord, E. L., Frantz, M. A., Roebuck, C.: 1941, "Blockhouses in the Argolid", *Hesperia*, **10**, No. 2 (April - June), pp. 93-112.
Morgenstein, M. E, Luo, S., Ku, T. L. and Feathers, J.: 2003, "Uranium series and luminescence dating of volcanic lithic artefacts", *Archaeometry*, 45.
Neimeier, Barbara and Wolf-Dietrich: 1997, "Aegean Frescoes in Syria-Palestine: Alalakh and Tel Kabri", *Proceedings of the 1st International Congress of Minoan Paintings*, vol.II, Thera Foundation.
Oppermann, S.: 1971, "Pyramiden in Griechenland", *Antike Welt*, 2.
Pausanias, *Corinthiaka-Laconika*, 2, 24, 7 and 2, 25, 7 (in: *Pausanias' Guide to Ancient Greece*, 1985, translated by Christian Habicht, Berkeley Univiversity Press, Berkeley, U.S.A.).
Pikoulas, G. A.: 1996, "The 'pyramids' of Argolis", *Archaiologia and Tehnes*, **59** [in Greek].
Piteros, Chr.: 1995, "The so-called 'pyramids' of Argolis: Myth or reality?", *Anagennisi*, issue no. 327 (March) [in Greek].
Piteros, Chr.: 1998 (year of published), "The pyramids of Argolis", *Proceedings of the 5th International Conference of Pelloponesian Studies*, vol. III, p. 370. Argos-Nauplion, September 6-10 1995, Athens [in Greek].
Sampson, A.: 1996, "The pyramids of Argolid and their meaning", *Archaeology*, **57** [in Greek].
Scranton, R.: 1938, "The pottery from the Pyramids", *Hesperia* **7.4**, pp. 528-538.
Spiropoulos, Th.: 1981, *Study of the Site of the Amphion in Thebes*, Sparta [in Greek].
Spiropoulos, Th.: 2003, "The big Hellenic pyramid", *Trito Mati*, pp.34-47.
Theocharis, P., Liritzis, I., Galloway, R. B.: 1994, "Dating of two Hellenic pyramids by a novel application of thermoluminescence", *Jour. of Archaeol. Sci.* 24.
Theocharis, P., Liritzis, I., Lagios, E. and Sampson A.: 1997. "Geophysical prospection and archaeological test excavation and dating in two Hellenic pyramids", *Surveys in Geophysics*, 17.
Theodossiou, E., Niarchos, P. G. and Manimanis, V. N.: 2002, "Are the unknown Greek Pyramids old Observatories?", *Xth SEAC-2002 Conference: "Cultural Context from Archaeoastronomical Data and the Echoes of the Cosmic Catastrophic Events"*, Tartu, 27 August - 1 September.
Theodossiou, E., Manimanis, V. N., Katsiotis, M., Papanikolaou, D.: 2009, "Study and Orientation of the Oche 'Dragon House' in Euboea, Greece", *Journal of Astronomical History and Heritage* (JAH2), **12**, no. 2 (July), 151-156.
Tsountas Christos: 1893, *Mycenae and mycenaean civilization*, Estia Publ., Athens.
Vischer, W.: 1857, *Erinnerungen und Eindrücke aus Griechenland*, Basel.
Wiegand Th.: 1901, "Die pyramide von Kenchreai", *Athen. Mitteilungen* (des Deutschen Archeologischen Instituts. Athenische Abteilung, Athen), **xxvi** [in German].
Zangger, E.: 1993, *Argolis I: The geoarchaeology of the Argolid*, Deutsches Archaologisches Institut, Athen.

Gaia, Helios, Selene and Ouranos: the three principal celestial bodies and the sky in the ancient Greek cosmogony

Efstratios Theodossiou[1], Vassilios N. Manimanis[1],
Milan S. Dimitrijević[2], Petros Mantarakis[3]
[1] Department of Astrophysics, Astronomy and Mechanics Physics Faculty, University of Athens-Zografos 157 84
[2] Astronomical Observatory, Volgina 7, 11060 Belgrade, Serbia
[3] 322127 Needles, Street, Chatsworth, California 91311, USA
etheodos@phys.uoa.gr
mdimitrijevic@aob.bg.ac.rs
zanispetros@socal.rr.com
(Research report. Accepted on 21.09.2010)

Abstract. In this article we consider the role of the three principal celestial bodies, the Earth (Gaia), the Sun (Helios) and the Moon (Selene), as well as the Sky (Ouranos) in the ancient Greek cosmogony. This is done by the analysis of antique Greek texts like *Orphic Hymns* and the literary remains of the writers and philosophers like Aeschylus, (Pseudo) Apollodorus, Apollonius Rhodius, Aristotle, Euripides, Hesiod, Homer, Hyginus, Nonnus, Pausanias, Pindar and Sophocles, as well as by the analysis of texts of Roman writers like Cicero, Ovid and Pliny.
Key words: Gaia, Mother Earth, Helios, Sun, Ouranos, Sky, Selene, Moon

Гея, Хелиос, Селена и Уран – трите главни небесни тела и небето в древно-гръцката космогония

Е. Теодосиу, В. Н. Маниманис, М. С. Димитрийевич, П. Мантаракис

В тази статия ние разглеждаме ролята на трите главни небесни тела – Земята (Гея), Слънцето (Хелиос) и Луната (Селена), както и Небето (Уран) в древно-гръцката космогония. Това е направено чрез анализ на антични гръцки текстове като Орфеевите химни и литературното наследство на писатели и философи като Есхилус, (Псевдо) Аполодорус, Аполониус Родиус, Аристотел, Еврипид, Хесиод, Омир, Хигинус, Нонус, Паусаниас, Пиндер и Софокъл, както и анализ на текстове на римски писатели като Цицерон, Овидий и Плиний.

1.Introduction

Our aim here is to analyze, on the basis of ancient Greek and Roman texts, the role of the three principal celestial bodies, the Earth (Gaia), the Sun (Helios) and the Moon (Selene) as well as the Sky (Ouranos) in ancient Greek cosmogony.

Since the remotest antiquity, human beings worshipped the divine couple of goddess Gaia (Gaea, Earth) and god Ouranos (Uranus, Sky), the primal pair. Hesiod's *Theogony* (1914) begins with Gaia and concludes with the polytheistic reign of the Olympians. The genesis of the elements of nature and the genesis of personified gods behaving like humans proceed in parallel: "in the beginning the gods and Gaia were born" (*Theog.*, 105). Gaia's mate, Ouranos, surrounds her and fertilizes her.

In juxtaposition with Gaia, who is the deification of our planet, Mother Earth is the deification of the ground, whose products support human existence, and which gives the space where they are born, they live and they die.

Beyond the cosmic duo of deities, Ouranos and Gaia / Mother Earth, humans worshipped the light-giver and life-giver Helios (Sun), the source of every life form on Earth. For all people, in all regions of the Earth, the Sun, Sky and Earth are the eternal witnesses of human acts and the natural avengers of the violations of the laws. From the age of the emergence of Greek philosophy comes the theory that the solar rays that fell on the wet Mother Earth created the first living creatures, while mythographers consider as progenitors of all things the Sun and Mother Earth.

The Moon gave primal units for the measurement of time: the definition of the lunar (synodic) month and of the week; its role is therefore crucial in the invention of the first calendars, which served as the foundation for all ancient religions.

In this paper, we will consider and analyze the role of Gaia/Mother Earth, Ouranos, Helios and Selene in ancient Greek mythological Cosmogony.

2. Gaia

According to the cosmogony of the Orphics, Gaia (*Gaea*) pre-existed, along with Chaos and Eros-Phanes, during the Creation of the Universe. These three cosmic beings were born from the cosmic egg, which in turn either originated *ex nihilo* or was produced by Nyx (the Night).

Gaia, one of the primal deities, is a cosmogonical symbol of the material aspect of the Universe, and not just of the earth as a ground (Demetrakos, *Mega Lexikon*, 1964, vol. 3, p. 1534). Chaos symbolizes the space of the Universe and Eros symbolizes the motive and world-creating power that unifies and transforms the Universe.

In the oldest Orphic cosmogony Gaia is born with the intervention ('energy') of this cosmogonic Eros, who "*put together everything*" (*Orphic Fragm.* Kern, 1922, 1). In the later version of Orphic cosmogony Gaia and the Sky (Ouranos, Uranus) are formed from the two halves of the huge cosmic egg born by the timeless Chronos (Time) (*Orphic Fragm.* Kern, 1922, 57).

In Hesiod's *Theogony* (1914), the primal entity of the Universe is Chaos: "... *first Chaos was created*" (*Theog.* 116), which was a formless mass without any structure; an abyss or an 'undecorated' space. After the creation of Chaos, Erevos (= Darkness) and Nyx (= Night) were born; Nyx gave birth to Ether and Hemera (= Day).

Subsequently, the 'broad-chested Gaia', as Hesiod characterizes her, one of the three primeval elements of the Universe -along with Chaos and Eros-, gives birth to Ouranos, Pontos (= sea) and the mountains (*Theog.* 123+).

Another version identifies Chaos with Ouranos proper, thus defining Gaia and Ouranos as the first cosmic-divine couple of Creation. Ancient Greeks begin the genesis of gods and of nature with a feminine entity, Gaia, which appears after Chaos and before Eros. Gaia is both the natural element that

produces and supports the world, and the Mother Earth, with the birth of Ouranos, of the Ocean and other aquatic deities.

Initially, the divine reproduction is asexual, i.e. the fertility of Gaia is not associated with any god. In a second stage, however, Gaia appears to mate with her first-born son Ouranos (*Theog.* 147), while she had produced him without the intervention of a masculine entity. Ouranos (Uranus) was the most appropriate of all mates, as he was surrounding her totally and he was destined to be the abode of the gods. In this way, Gaia and the Sky formed the first divine couple. Whenever Night was succeeding Day, Ouranos was uniting himself with his own mother. Gaia was being fertilized by his raindrops as by sperm, so she gave birth to many children (*Homeric Hymns*, 1914, 30, 17 and *Theog.* 127): Six Titans (the Ocean, Creius, Hyperion, Japetus, Coeus and Cronus), six Titanids (Theia, Rhea, Themis, Mnemosyne, Phoebe and Tethys), three Cyclops (Arges and Steropes = lightning, Vrontes = thunder) and the three Hecatonchires, huge creatures with 100 hands each: Vriareos (= powerful), Gyes (= giant) and Cottus (= angry).

Uranus started to worry because of the number and the steadily growing power of his children; he feared that some day they would push him aside. Therefore, he imprisoned them in Tartara, a dark and cold place in the depths of the earth. Gaia, displeased by Uranus' violent behavior against their children and by his violent daily embracing, produced a hard scythe from her interior and gave it to her sons, asking them to mutilate their father, thus depriving him of his reproductive power. Cronus (*Kronos*), the youngest of all Titans, decided to punish his divine father himself, and all his half-brothers and half-sisters except Ocean agreed with that. When night fell, Uranus, full of passion, spread his vast body over Gaia and then Cronus, seizing the opportunity, cut off the genitals of his father using Gaia's scythe. From the droplets of blood that fell on earth from the wound, other creatures were born: the three Furies (Alycto = the non-stopping chaser of the guilty ones, Tissiphone = the punisher of murder, and Megaera = the malevolent), the Giants (Enceladus, Porphyrion, Pállas, Polybiotes, Ephialtes, Clytios, Hippolytus, Eurytus, Gration, Agrios, Theon, Alcyoneus, Athos, Vesvicus and Echion) and the Meliades Nymphs, spirits of hatred and violence (*Theog.* 182+). Finally, from the seminal foam and the god's sperm that fell into the sea, emerged Aphrodite on a seashore of Cyprus (*Theog.* 187-206).

Uranus understood the betrayal and realized that he had lost his power: wounded and having lost his reproductive ability (and hence his divine power), he retired high on the celestial vault, where he stayed forever, uttering a curse against Cronus: to also loose his power by his own offspring.

In Homer, the powerful and primeval Gaia is mentioned as overseer of the oaths: she is invoked, along with Uranus and the holy water of Styx, by goddess Hera when she swears (Homer, 1924, *Iliad.* XV 36-38). Homeric heroes, such as Agamemnon, also invoke Gaia in their oaths, along with Zeus, Helios and the Furies (*Iliad* XIX 258-265). Menelaus, before his duel with Paris, asks to validate the oaths of their agreement by sacrificing two lambs, one white and one black, to Helios (the Sun) and Gaia, respectively (*Iliad* III 103+).

Finally, there is a version according to which Gaia, after the 'abdication' of Uranus, joined Ocean and gave birth to gods and goddesses of the waters. However, Gaia and Uranus are not considered just the parents of the gods, but also the parents of humans, as the Homeric Hymn to Gaia, 'the mother of gods', mentions: "*Praise to me the mother of the gods and of all people*" (*Homeric Hymns*, 1914).

Gaia is seldom depicted in a whole-body representation in art. Usually the goddess is shown from waist up, a fact hinting that the rest of her body is the ground or soil, that is the earth itself, whose deification she was.

3. Ouranos (Uranus)

Uranus, whose name comes from the Greek words *oros* and *ano* (Demetrakos, *Mega Lexikon*, 1964, vol. 10, p. 5289), that is who is above the mountains (Aristotle, *On the Heavens* (*De Caelo*) 400a, 7), was in Greek mythology the personification of the celestial vault or dome, of the primeval cosmogonic force. He was the sovereign of the first generation of beings on Earth. For this reason, Uranus plays an important role in Hesiod's *Theogony*, while according to pseudo-Apollodorus: "*Uranus was the first to rule the entire world*" (*The Library (Bibliotheca)*, 1921, A, 1, 1).

In the Orphic tradition Uranus is mentioned as son of Nyx (the Night) and brother of Gaia, while elsewhere he appears as son of Ether and Gaia or Nyx. In either case, Uranus belongs to the first generation of beings, the oldest of gods and of the elements of nature. According to Hesiod, in the prevailing version, he was the first born son of Gaia, who conceived him when she was sleeping next to Eros, without fertilization, "*to surround her and to be an eternal and safe abode of gods*" (*Theog.* 486). Uranus is the first masculine element, the father of gods in Greek mythology.

We already mentioned how Uranus lost his power and retired on the celestial vault, where he stayed forever. So the word *ouranos* in Greek means the sky or celestial vault, where stars and all celestial bodies are positioned and move: the firmament, stretching from zenith to the horizon, regarded as a hemisphere placed above the surface of the earth and supported on it along the horizon line by columns (*Iliad* VI 108). On *ouranos* all celestial phenomena take place. According to Homer, the stars are attached to it and move along with it: the celestial vault is the one that rotates incessantly (*Iliad* XVII 425). Of course, today we know that this perception is totally wrong: the 'sky' in that sense does not exist.

After taking power, Cronus released all his half-brothers and half-sisters from Tartara. The Cyclops and Hecatonchires, however, started after a while to lay claims upon his power and they became dangerous. Therefore, Cronus threw them again into Tartara and he put a terrible monster, Campe (= caterpillar) to guard them. This period is the second generation of immortal deities, where Cronus reigns with his wife Rhea and Titans impose his power in the world. Yet, the increasing cruelty and injustice of Cronus, who was devouring his own children in order to avoid being dethroned himself, finally led Gaia to help Zeus (the Greek analog of Roman Jupiter) against the Titans, giving him a potion that would force Cronus to disgorge the baby gods he had

devoured. It should be noticed here that the primal Gaia still influences the course of the world, appearing at certain crucial moments to give a solution.

Zeus, after being advised by Gaia, also released the Cyclops and Hecatonchires. The three Cyclops, with their awesome weapons, the lightning and the thunder, and the three Hecatonchires with their 300 hands in total, managed to obtain a decisive victory against the Titans on Mountain Othrys. The Titans were defeated and were thrown deep in the earth, in Tartara, where the Hecatonchires guard them.

According to professor of Geology at the University of Athens Mariolakos Elias: *"The end of the Titans means i) a relative abatement of earthquakes and volcanic activity, and ii) the end of the direct and decisive influence of the natural environment in the life of prehistoric humans. It is the period when the food-gatherers and hunters are turned into farmers and animal breeders* (Mariolakos, E., 2009, *Geomythotopoi*, p. 5).

It should be added that ancient Greek art did not treat the myth of Uranus as a subject; nevertheless, in the Vatican Museums there is an ancient depiction of him on the chariot of Helios (the Sun god).

According to an alternative Greek tradition, probably even older than the prevailing myth, initially Uranus and Gaia were very close. But due to the frequent infidelities and illegitimate children from other females, Gaia as Earth finally detached herself from him and agreed to meet him only in certain time periods. From an astronomical point of view, this tradition is an excellent attempt to explain the cycle of the year's seasons and the place of the Earth in the Universe, as the other mates and children of Uranus were the other moving planets and the stars of the celestial vault (*Helios Encyclopaedia*, 1957, vol. 4, p. 920).

There are also other traditions about Gaia, such as the one mentioned by Diodorus of Sicily (1935), in which Gaia was a beautiful mortal woman, under the name of Titaia. She was loved by Uranus and they had 18 children, named 'Titans' after their mother. As Titaia was a wise and prudent woman, having offered many services to humans, after her death humans deified her and gave her the name of Mother Earth.

4. Mother Earth

A special and important place in worship was held by Mother Earth, the universal mother and supreme goddess, called for this reason by Greeks *Hypertatan Gan*. This worship, however, was addressed to Earth not as a celestial body, neither as a personified deity with a human appearance, but rather as earth-chthon, as a part of nature with its soil, ground and underground, which feeds and sustains humans. Man is 'accused' by tragic poet Sophocles (5th century BC) as the one being that dares to disturb the supreme goddess, since he doesn't hesitate to hurt her by "*ploughing it with his plough, incessantly furrowing her year after year*" (Sophocles, 1994, *Antigone*, Vol. II., verse 330+).

Regarding earth-nature as the omnipotent goddess Mother Earth must have begun in the age when the first agricultural societies and their festivals developed, festivals full of mysticism for the primeval cycle of life (sprouting -

Fig. 1. At the period of Emperor August (1st century AD) people were picturing the Earth as a sweet mother with two children in her lap, inside a flowery natural environment. Later on, Pliny the Elder in his *Naturalis Historia* stressed some ominous points: he wrote that we humans excavate Earth's bowels by digging mining holes upon which we live; we wonder when gaps open or the ground shakes, as if these signs were not the expression of wrath of the holy mother. Inside dark corridors we search for treasures, as if the soil on the surface of the ground were not generous and rich enough.

fruit bearing - maturing - decay - seed - seeding - 'rebirth'). However, starting from prehistoric times, it can be said that the first humans, from the moment they started to observe life on Earth they understood that both they and the rest of animal and plant life were attached to the triptych life-reproduction-death. The survival of humans depended on earth's vegetation, as they and the animals they were hunting were being fed by the gifts of nature (Eliade, 1978).

The primitive humans, by carefully observing the life cycle of plants, the seeding of Mother Earth and subsequent sprouting aided by rain from Uranus, discovered the corresponding cycle of animal sexual reproduction.. Therefore, it was concluded that Earth was alive and in order to give birth 'she' needed to come into contact with the masculine entity. For this reason, humans personified Earth as a feminine entity, while the fertilizing masculine entity was the sky with the rain, or some large river, such as the divine Nile in Egypt (the ancient Egyptian religion is the only one in the world in which the Sky is personified as a female deity, Nout, see Theodossiou 2007, p. 28).

The Mother Earth (Terra Mater), due to the vague character of her worship, is sometimes identified in Greek literature as Rhea, Hestia, Hera, but mostly as Demeter, whose own name comes from Ge-meter = Earth-mother, denoting the womb that encloses the seeds. Indeed, the worship of Gaia as Mother Earth goddess diminishes over time, without disappearing completely, and is replaced by the better-defined worship of Demeter as the goddess of agriculture; Gaia's role is thus reduced to the dream-giving, story-telling, and to the feeding of plants and children.

The miraculous divine union of Uranus-Sky and Earth, out of which gods, humans, and all living things are born, is reflected in the cry of Eleusis Mysteries '*hye, Kye*'; with this cry the mysts were calling the Sky to pour his fertilizing rain, so that the earth (here personified as Demeter) could use her womb to produce all kinds of offspring.

As opposed to Gaia, which is the deification of our world-planet, Mother Earth is essentially the deification of soil-ground, whose products sustain humans and which gives them the space on which they are born, live and die.

The presence of Gaia as a primeval element-material and deity is apparent in the founding of the first oracle, which catered only to the gods. Later on, identified with Mother Earth, established her oracle in Delphi; this is why she is also called 'protomantis' = first foreteller (Aeschylus, 1989, *Eumenides, Pythias* 2). The Dodone oracle was also dedicated to Gaia; there she was worshipped together with Zeus as "fruit-giver and mother" (Pausanias, 1935, *Phocis* 12, 10).

Finally, Pliny the Elder in his *Naturalis Historia* (1971) wrote that the Sky belongs to the gods, but the Earth belongs to the human race. The Earth welcomes us when we are born, it gives us food to grow and it receives us in her lap when we die. This earth suffers from human actions that destroy its surface and cut into its body as men search for gold, silver, copper and lead; men open wells into its depth in quest for precious gems and excavate its bowels. (Pantermalis, *Ancient Greek mines*, 1995, p. 42).

Finally, the questions about Earth, as they were summarized by Aristotle (*On the Heavens* 1956, II 293a, 15+), were culminating with the question of the place of Earth in the Universe, of its exact shape and of its size.

5. The Couple of Sky and Earth

As a corollary, it can be said that in Greek cosmogony, as in the creation myths of the other Indoeuropean people, the great creation activity taking place continuously in nature is exemplified in the following simple picture: One divine couple, the first of creation, gave and still gives birth to all beings. The fertilizing 'father', in this case Uranus, and the conceiving 'mother', in this case Gaia, who also feeds her children.

This first divine couple is united by Eros, and in the erotic-cosmogonic symbolism the Sky-Uranus embraces and fertilizes Earth-Gaia through the rain. Their union is presented as an omnipotent reproductive ability, which multiplied the number of gods, a fact praised by Orpheus (Proclus in *Tim.* 3, 1820, p. 137, 11) as creation of the primeval Chaos (or Erevos) and of the Day (*Orphic Hymns* IV: *Incense to Uranus*, and XXVI: *Incense to Earth*).

Besides, this same symbolism is hidden in the union of Semele (who personifies Earth) and Zeus, the celestial god who fertilizes his beloved woman with lightning, the harbinger of rain. 'Earthly' Danae is fertilized in the same way, by the 'celestial' Zeus transformed into golden rain. Metaphorically, the celestial god, with his beneficiary waters, softens the parched womb of the earth for the development of life.

Since Mother Earth and Uranus were the progenitors of life, humans (who depended on earth's vegetation) had to either pacify or challenge god Uranus to copulate more frequently with Mother Earth for richer production.

This cosmogonic theme of the primeval couple of Sky and Earth is found not only in ancient Greece, but in almost all ancient civilizations. According to some scientific evidence, many prehistoric societies were matriarchic ('matriarchy' in *The New Encyclopaedia Britannica*, 2007)

The first human societies were intimately aware of nature. They believed that humans, animals, plants, rocks and minerals, all were the descendants of Mother Earth; therefore, everything had a soul and any living creature had the same rights on life.

At the dawn of history human societies respected the other life forms because they knew that their differences were just morphological. People believed that rain was the intercourse of Sky and Earth (the masculine and the feminine). They knew that everything depended on this event, including the survival of the other forms of life on the land.

For pre-Socratic Greek natural philosophers, however, it should be added that Earth and the Sky were regarded as a continuous body, united at the ends of the horizon.

Earth of the Homeric Universe was a circular flat disk surrounded by a huge circular river, the Ocean, a model first appearing in the *Orphic Hymn* 'X. TO PAN, *The Fumigation from Various Odors*', verse 15: "*Old Ocean too reveres thy high command, whose liquid arms begirt the solid land.*" This mythical 'river' is different from the seas: it is something that defines the boundaries of the terrestrial world. Above all, Ocean is the primal and original creative element, the starting point of all things (*Iliad*, XIV 246). This mythical 'river' has no sources, nor estuary, it is 'apsorroos', i.e. cyclically moving or backward-flowing. Its current goes back to where it started in a ceaseless and eternal flux. This Ocean supports the sky, which is above Earth's circular disk as a huge vault.

In the *Orphic Hymns*, the Sky is mentioned as the sovereign of the World, surrounding the Earth as a sphere; it is the abode of the gods and rotates like a spinning-top; personified, he guards everything, not just in his place, but also on Earth: "*Uranus ruler of the world, spinning like a sphere around Gaia, house of the blessed gods, moving with whirlings, guard of everything on both sky and earth" (Orphic Hymns)* IV, *Incense to Uranus*).

On the other hand, the Sky was for ancient Greeks a metallic vault made of copper or iron, held up there by very tall columns or, according to another view, by some giant. Homer combines these two views by having Atlas supporting the columns (Homer, 1919, *Odyssey* i 53-54). Hesiod in *Theogony* (1914, 517e) writes that Zeus was the one who had assigned this duty to Atlas. So the sky for them was made of a solid metallic material, called 'polychalcus', that is 'of much copper' (*Iliad* V 504, *Odyssey* ii 458, iii 2, *Iliad* XVI

364, XIX 351), 'copper' (*Iliad* XVII 424-425) and 'iron' (*Odyssey* xv 329 and xvii 565).

The space between sky and Earth, according to the view recorded by Homer, was filled at first by the dense air: aer (*Iliad* XIV 288). Over this layer and towards the direction of the sky there was the clean and transparent 'ether', lighter than the air. Above the ether was the 'polychalcus' sky.

Of course, one should not assume that the Homeric sky was a barren metallic dome; it was, as Homer sings, full of life, the life of the stars that decorate it: he calls the sky 'full of stars' ('asteroeis') (*Iliad* VI 108, XV 371) and star-decorated (*Odyssey* ix 534-535). On this celestial dome, Helios, the god of the Sun, travels on its path, so he is described with the adjective 'uranodromos', that is 'sky-running' (*Odyssey* i 7-9).

6. The Sun and the Sun-god Helios

From prehistoric times, humans admired the starry night sky, with its thousands of naked-eye stars twinkling on its vault. But their joy was greatest at dawn, "the rosy-fingered Eos" (Hesiod, 2006, *Works and Days*, 609), when the diffuse sunlight gradually prevailed over the darkness of the fearful night. They naturally worshipped the light-giving Sun, since they realized that everything on earth owed its existence and life to the influence of its rays.

According to archaeologist Chr. G. Doumas: *"The word 'als' in Homer means the sea when observed from the land. The presence of this root in tablets of Linear B writings as component of other words indicates a long-standing use, during which it evolved into a versatile noun of the third declension that easily makes compounds with other roots... the fact that with the original root so many and various needs of the Greek language, e.g. alios / helios [= sun], shows both the close relationship of the aegean society with the sea and the strong influence of the liquid element upon the history and the culture of that age."* (Doumas, 2010, *The ancient monuments of the names*, p. 16).

"Indeed, from 'als' (genitive form: alos) came the adjective 'alios', which, even though it is recognized as the doric type of 'helios' = sun, it essentially means the one that is related to the sea... The depiction of the Sun on the proto-Cycladic pan-shaped vessels of the 3rd millenium BC is probably an indication of the importance assigned to it by the Cycladians of that period. The islanders of the Aegean Sea and the inhabitants of the eastern shores of the Greek peninsula see every morning the Sun rising from the sea" (Doumas, 2008, *The aligenes Aegean Sun, p.15), as described in the first verses of Rhapsody iii of the Odyssey: "When the Sun, leaving the lake, ascended towards the all-copper sky to shine on both immortals and the mortal people of the life-giving earth... ".*

The Sun is the 'radiating one', the 'fiery one' and as such it symbolized the celestial representation of the universal father, being essentially the representative of God's spirit (Demetrakos, 1964, vol. 7, p. 3250). The Sun's appearance in the morning, its culmination at noon and its majestic disappearance for the night (or during the eclipses) influenced much human thought. Darkness falling every evening after sunset filled the soul of the primitive human with stressful questions. With time, the savants of the society assigned to

the Sun supernatural divine properties, since as a god 'he' could appear or disappear at will, both daily and during the much more rare eclipses.

All ancient people worshipped the light- and life-giving Sun. The Sun was Samas of the Assurians, Bel of the Semites, Bel-Marduk of the Babylonians, El or Outou of the Sumerians, Baal of the Phoenicians and Chananeans, Moloch of the Ammonites, Chimoch of the Moabites, Ammun-Ra of the Egyptians, Surya of the Indians, Mithra of the Persians, Indi of the Inka, Tonatiuch of the Aztecs, Sol of the Romans, Swarog or Yarila of Slavic tribes, Belenos of the Celts, Helios and Phoebos-Apollo (the symbol of sunlight) of the Greeks. The worship of the Sun god was universal and prevalent, since for ancient humans the Sun was the source of life, light and warmth, a guarantee of the celestial order of the hours of the day and the seasons of the year, a creative force for nature and, more mundanely, an aid for orientation. Besides, the Sophoclean phrase *"everybody adores the rotating solar orb"* (Achilles Tatius, 1917, frag. 672 Nauk2), is true for all ages (Sophocles, 1892, *Trachiniae*, 738, 2).

7. The Sun-Helios in Greek mythology

In Homer's *Iliad* and *Odyssey* (ca 8th century BC) the external aspect of the bright appearance of the Sun is especially stressed along with the notions associated with sunrise and sunset. According to Hesiod, the Sun-god, Helios, was the son of Titans Hyperion and Theia (*Theog.*, 371-372), or of Hyperion and Euryphaessa (*Homeric Hymn to Helios* 31, 2), while his sisters were Selene (the Moon goddess) and Eos (the personification of dawn). Pindar celebrates Theia as the mother of Helios in his 5th *Isthmian Ode* (1997):

"Mother of the Sun, Theia of many names, for your sake men honor gold as more powerful than anything else; and through the value you bestow on them, o queen, ships contending on... "

As Titans, Theia and Hyperion (= he who hovers above earth) belong to the same generation as Cronus; all of them were children of Gaia and Uranus (Patsi-Garin, 1969).

Homer, calling Helios 'Hyperionides' (*Odyssey* xii 176), stresses his concrete bond with life, as since their birth, humans behold the solar 'augeae' (daybreaks): they live *"under the stars of the sky and the light of the Sun"* (*Iliad* IV 45), rejoicing when they see *"the bright light of the Sun"* (*Iliad* V 120). Eventually, when a person dies "he abandons the light of the Sun" (*Iliad* XIX 2).

The Sun for Homer is the god who *"sees everything and hears everything"* (*Iliad* III 277). This characteristic of Helios is stressed by the adjectives 'panoptes' (Aeschylus, 1983, *Prometheus Bound* 91), 'the overseer of everything' (Aeschylus, 1984, *The Libation Bearers*, 982-986), 'the prevailing one by sight' (Sophocles, 1892, *Trachiniae*,101) and many other references of the ancient Greek tragic poets, who stress that these 'over-seeing' abilities of the Sun render him a guarantor of the keeping of oaths; always Helios was a

witness of truth (*Homeric Hymn* 3, 381, Sophocles: *Oedipus Tyrannus* 660), *"index of justice, guardian of oath keeping, eye of justice"* (*Orph. Hymn* 16).

In Greek mythology in general, Helios is presented as the god who travels around Earth and watches the administration of justice shedding light on good and evil (Segal, C.P., 1992, pp. 3-29, McCarthy, D.J., 1978, p. 185, West, M.L., 1997, p. 20). Helios was considered a very important god, and Homer reports that sacrifices were offered to Gaia and Helios (*Iliad* III 104, 276). As far as his other attributes are concerned, Helios was worshipped in Corinth (Pausanias, 1918, *Corinth* Book II, 3:2, 4:6 and 5:1) as god of storms, thunderstorms and other sky forces.

Additionally, it has been suggested that the 'Horse monument' (Pausanias, 1935, Book III 20, 9) with the seven *"columns... ... who they say are statues of the planets"*, was a part of the worship of Helios. Also, in Hermione there was a temple dedicated to Helios (Pausanias, 1935, Vol. II, 34, 10). Indeed, in the Christian church of Taxiarches was found a part of a circular altar of the 3rd century AD with the following inscription: *"To Helios the king god, to Hyperion altar... "* (Jameson, M. and Runnels C.N., 1959, p. 15).

The special place of Helios with respect to the Olympian gods (although Helios is a celestial and not one of the 12 Olympian gods), is connected with his importance for the life of the Olympians. Diodorus (1935, *Bibl. Histor.* V 71) writes that Zeus before the battle with the Giants sacrifices to Helios, Uranus and Gaia. This is why Aeschylus refers to Helios as 'the overseer of everything' (Aeschylus, 1989, *Eumenides*).

From about the 5th century BC and after, Helios loses its status as a distinct deity and begins to mingle with Apollo, the Olympian god of sunlight. After the battle with Giants, Helios was identified with Zeus, who, as a celestial and Olympian god relative to the celestial light included the divine substance of Helios. However the gradual increase in Zeus' strengths forced the Helios part out of his substance which Apollo then usurped to become a deity with many of the characteristics of a pure Sun god. The identification of Helios with Phoebus-Apollo (phoebus = shining) is traced throughout the whole ancient Greek literature after Parmenides and Empedocles (Diels, 1996, *Vorsokratiker*, I2 108, 29.157, 10 and DK -Diels-Kranz, 1996, 28 A 20, 31 A 23), up to Plutarch and Crates Ascondes of Thebes.

Eratosthenes reports this identification of Helios with Apollo (Spandagos, 2002, 24) writing that Aeschylus suggests in one of his works that Orpheus identified Helios with Apollo and placed him at the center of his worship, refusing to offer honors to Dionysus. Similarly, in *Saturnalia* by Macrobius (1969), it is written characteristically: *'Item Orpheus Liberum atque Solem unum esse deum eundemque demonstrans de ornatu vestituque eius in sacris Liberalibus ita scribit'* (*Saturnalia* 1.18.22, frag. 238).

Nevertheless, although this Helios-Apollo identification began at least since the 5th century BC, it was not widely accepted until centuries later.

According to Homer, Helios started his trip every dawn from the eastern ocean or from Ethiopia, the land of the 'sun-burned people' (*Odyssey* I 24-26); he crossed the sky with his winged four-horse chariot, pulled by four beautiful fire-breathing white horses: Eous, Aethiops, Bronte and Sterope (Hyginus, 1933, *Fabulae* 183):

"Eous; by him the sky is turned. Aethiops, as if flaming, parches the grain. These trace-horses are male. The female are yoke-bearers: Bronte, whom we call Thunder, Sterope, whom we call Lightning"

These equine names allude to the power of the God, the succession of the celestial phenomena and the maturing of the fruits. Other authors report other names for the Sun's horses: Lampon, Aethops, Aethon and Flegon (Gelling & Davidson, 1969, p. 14+; Glob 1974, pp. 99-103, and Green 1991, pp. 64-66, p. 114+). Every evening, Helios completed his journey and then rested in the West, in the land of Hesperides.

The notion of the 'flaming' or 'fiery' nature of Helios is very common among the Greek tragic poets: *"baked by the fire of the sun"* (Aeschylus, 1983, *Prometheus Bound* 22), *"High o'er the earth, at whose ethereal fire. . . "* (Euripides: *Ion* 34), *"Hot flame of the King"* (Euripides, 1996, *Phaethon* 776). Euripides describes sunrise as follows: *"Now flames this radiant chariot of the sun / high o'er the earth, at whose ethereal fire / the stars into the sacred night retreat"* (Euripides, 2004, *Ion* 82-84). This description has often been compared with a depiction of Helios on a Greek vase of the 5th century BC that is kept in the British Museum; there, Helios is depicted with a ray-surrounded head, riding a winged four-horse chariot, rising from the sea, in which child-like apparitions swim, denoting the stars that go to hide.

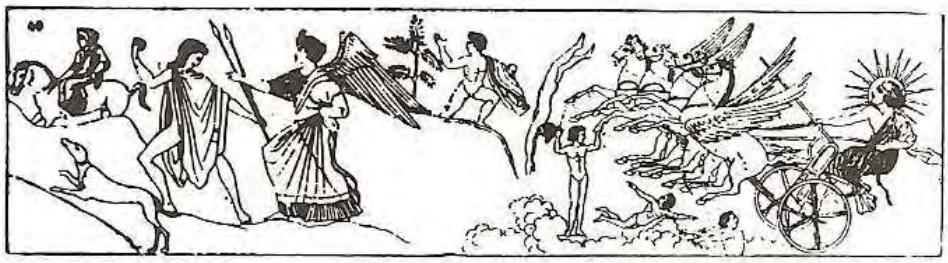

Fig. 2. At the period of Emperor August (Ink drawing: The rise of the Sun with his 4-horse chariot. The vanishing stars of the night are depicted as children sinking in the sea (Greek vase, 435 BC - British Museum).

The Sun, completing his daily (diurnal) course on the celestial vault, rested every night on a golden bed made by the hammer of the god Hephaestos (Vulcan), in order to shine again the following day over the world.

Helios had many sons and daughters. With Oceanid Perseis they had three children: Circe, Passiphae and Aeëtes (Apollonius, 1962, *Argonautica* 3, 1, 2 and Homer: *Odyssey* XII 3). Circe was famous for her magical powers and for her love for Ulysses (*Theogony*, 1914, 957). Passiphae, wife of king Minos of Crete, is identified with the Moon and considered the primeval deity of light, as her name states (passiphaessa = apparent to all). It was due to Passiphae

that the worship of Helios was widely practiced in Crete, where he was adored under the form of a bull (Bekker, 1814-1821, *Anecd. Gr.* 344, 10). The myth of Passiphae falling in love with a bull (the zodiacal constellation Taurus = the Bull) reflects a very ancient tradition, according to which the bull-shaped sun-god and the cow-shaped moon-goddess were united with a holy wedding.

In another myth, Aeëtes was king of Aea, who refused to give the Golden Fleece (a symbol of sunlight) to Jason and the Argonauts.

Helios had two other daughters, Phaethusa and Lampetie, and a son, Phaethon, with Clymene.. Once, Phaethon got permission from his father to cross the sky with his chariot. However, when Phaethon saw the huge constellation Scorpius (the scorpion) he became freightened and lost control of his father's chariot. Its horses bolted and the chariot started to go up and down, threatening the Earth with destruction. Then Zeus saved the world by killing Phaethon with one of his thunderbolts. Phaethon's body fell on the bank of the river Eridanus. His sisters, the Heliads, who mourned him, were transformed into poplars, the holy trees of the god Helios, and their tears became amber.

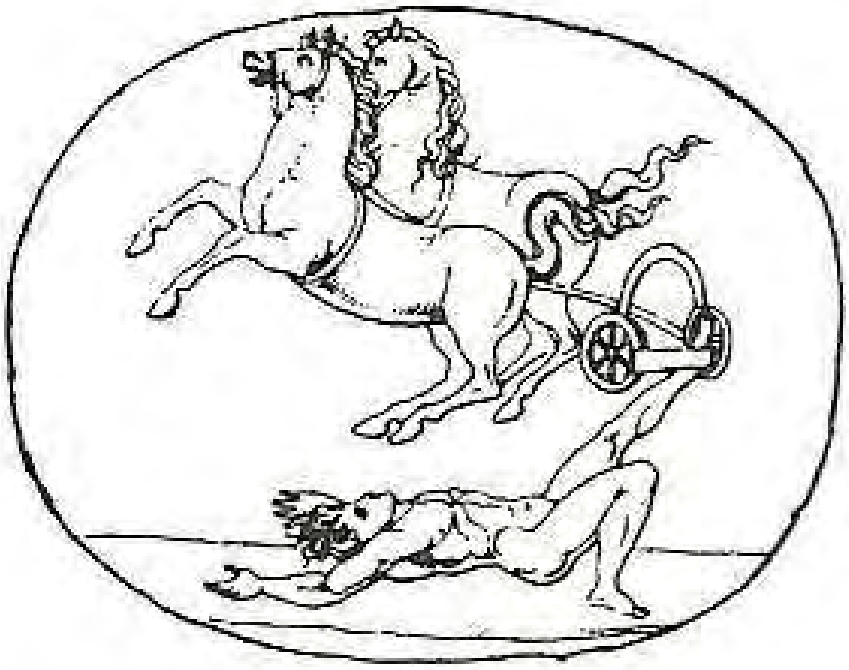

Fig. 3. Ink drawing: The fall of Phaethon.

'Phaethon' was also a name given to of Helios himself because of its radiant light (*Iliad* XI 730, *Odyssey* v 479, xi 15, *Homeric Hymn* 31.2). In his *Theogony* (1914), Hesiod writes of Phaethon and Hyperion as 'substances' of god Helios (*Theog.* 987 and Nagy, 1990, p. 235). Additionally, Phaethon is mentioned by both Nonnus (1940, *Dionysiaka* 38.167) and Ovid (1857, *Metamorph.* 2007, 1.747-79: *Phaethon's parentage, struggle with Epaphos* and 2.42: *Phaethon and his father*).

Helios, according to Greek mythology, also had numerous other affairs with other women; subsequently, he had many other sons and daughters, collectively known in ancient Greek literature as Heliades.

A famous center of Helios worship was Rhodes; as Pindar (1997) reports (*Olymp. Ode* 7, 69), the whole island belonged to him. The famous Colossus was a giant statue of Helios (this statue was one of the 'seven wonders' of the ancient world), an artwork by Rhodian sculptor Chares from Lindos (Pliny, 1971, *Historia Naturalis* 34.63), a student of Lysippus (3rd cent. BC). Every four years a Sun festival was celebrated on the island, called Ali(ei)a or Helieia (Nilsson, 1906, p. 427), during which they offered to Helios a four-horse chariot thrown into the sea. Helios stayed in Rhodes with Nymph Rhodos, a daughter of Aphrodite, and together they had seven sons, named: Ochimos, Cercaphus, Actis, Macar, Candalus, Triopes and Tenages, and their wisdom is exalted by Pindar (1997, *Olymp. Ode* 7, 72-75).

In Greek art the personification of the sun is often depicted as a young man bearing a radiant wreath and a tunic, standing upon a four-horse chariot, as on the metope of the Hellenistic temple of goddess Athena in Ilion (Troy).

Of more astronomical interest is a statue of Helios in the Vatican. He is depicted as a young man bearing a radiant wreath, and has an extra feature: a wide belt with the symbols of the zodiac.

Moreover, there is the tradition, mentioned among others by Homer (*Odyssey* xii 127), that in Trinacria island (Sicily),Helios had seven herds of cattle and seven herds of sheep, each having fifty animals. They grazed steadily every day, never getting more or less. According to the explanation given by Aristotle, the lunar year consisted of 50 weeks, each having 7 days and 7 nights; therefore the 50 times 7 cattle and the 50 times 7 sheep were denoting the 350 days and 350 nights, respectively, which make the lunar year used by ancient Greeks according to the original calculations (Theodossiou & Danezis, 1995, p. 315).

The worship of the Sun-god was universal, while very ancient practices originating in it, such as the orientation of temples of several religions towards the East, were kept until our days in the conscience of people.

8. Selene, The Moon

According to Hesiod's *Theogony*, Selene was the daughter of Hyperion and Theia, and sister of Eos (the Dawn) and of Helios, who illuminates her eternally due to their relation as half-brothers. The word *selene* comes from *selas* = light (Demetrakos *Mega Lexikon*, 1964, vol. 13, p. 6489). In Greek mythology Selene or Selana (Pindar, *Olymp. Ode* 10, 75) is the first and only lunar deity, at least in pre-classic and classic poetry, also called by the adjectives

Fig. 4. An ink drawing of the metope of the temple of Athena in Ilion (Troy) with a relief depiction of ray-headed Helios standing on his chariot, most probably based on an older work by Lysippus (Staatliche Museen, Berlin

Aegle, Passiphae, Mene, Titanis (as daughter of two Titans) and Phoebe as sister of Phoebos-Helios. As Greek mythology evolved, other goddesses were correlated with the Moon: Hecate, Artemis and Hera.

Selene is usually imaged as a feminine form bearing a crescent as crown, riding a horse or a chariot with two winged horses (diphros). Sometimes she is described as leading a herd of cattle so that her crescent-shaped crown resembles a bull's horns. Her brother Helios rides a four-horse chariot, while Selene rides a two-horse chariot; her two horses have one of their sides white

and the other black, a metaphor meaning that only the one side of the Moon's surface is illuminated by sunlight.

According to various local traditions Selene had one daughter with Aer (air), called Drosos (the morning Dew). In the Attica tradition she gave birth to Pandia, daughter of Zeus (*pan* + *dia* = all-godly), worshipped along with her mother in the Pandion festival. In an Arcadian tradition the Moon was a lover of god Pan and she was worshipped in common with him on Arcadian Mt Lykaio. In Elis and Karia they believed that Selene was in love with a mortal man, Endymion, whom she met every night on Mt Latmos, and had 50 daughters with him, as many as the lunar months of an Olympiad.

In a tradition of late antiquity mentioned by Quintus Smyrnaeus (*Fall of Troy*, 1913, 10. 334 ff), Selene also had a love affair with her brother Helios. The oldest known depiction of Helios in a Greek sculpture is on the eastern gable of the Parthenon, where the birth of goddess Athena is imaged. Helios and Selene also framed the composition of the birth of Aphrodite on the throne of the statue of Zeus in Olympia (Pausanias, 1935, Vol. II, Elis 1, Book 5, 11, 8) and a similar depiction is alluded to by the 'sunset' mentioned by Pausanias on the gable of the temple of Delphi (Pausanias, 1935, *Phocis*, Vol. IV, Book X 19, 4: *The temple at Delphi*).

Selene was worshipped throughout Greece, but especially in Peloponnese. It is known from the history of the Persian Wars that the Spartans, in order to start a military campaign took seriously into consideration the lunar phases. Near the city of Thalames there was a well-known oracle of Selene, where the ephoroi of Sparta stayed overnight asking her advice; a local spring was named after her (Pausanias, 1935, *Laconica*, Vol. II, Book 3, 26, 1).

The pair Helios-Selene was finally correlated with the pair of Olympians Apollo-Artemis, to which similar characteristics were attributed, along with the same symbols: for Selene these were silver, the bull horns and the crescent.

At a symbolic level, the Moon is the feminine component of the creation of the World and the entrance (due to its 'secret' appearance at night) towards the apocryphal nature of humanity and of the Universe, i.e. towards what remains inexpressible from the usual observation of nature. The Moon is the luminous image of cyclical time; representative of the constant flux of everything. The infinite new moons symbolize the infinite time moments of any end that signals a new beginning.

Selene is a chthonic (earth) deity in the antithesis sun-earth, light-darkness. On the other side, Selene is the goddess with the white arms that drives away the darkness of night when it is full. The rosy-fingered Eos (dawn), Selene's sister, brings the first light of the new day. Hecate, the three-form chthonic deity, is another expression of her; Ores, the Hours or the year's seasons, are considered her daughters. Another metaphor of the Moon is a huge luminous *clepsydra*, a water-clock, filled during its waxing phases and emptying during its waning phases. It gave the definite measure of time with the succession of its phases.

The ancient Greek tragic poets presented Selene-Moon as a very beautiful young woman before which all the other stars paled, when its silvery figure appears on the celestial dome.

9. Conclusions

Since the most ancient times, humans worshipped the primal divine couple, goddess Gaia and god Uranus, who were the ancestors of the other gods that gave their names to the planets of the Solar System. Hesiod's *Theogony* starts with goddess Gaia and ends to the polytheistic reign of the Olympian gods.

Uranus surrounds Gaia and fertilizes her. In juxtaposition with goddess Gaia, a deification of our planet, Mother Earth is essentially the deification of ground and soil, whose products sustain humans and offer them the space on which they live and die. The birth of the nature's elements comes in parallel with the birth of gods, who metaphorically behave as people. Cronus symbolizes Time, Rhea the flux and Hera (an anagram of Aer) air along with all the variations of weather.

The light-giving Helios, the Sun, is the source of every life form on Earth. For all people on Earth the Sky, the Sun, the Earth and the Moon (especially the full moon at night) seemed as appropriate eternal witnesses of human acts and the natural avengers of cheatings. On the other hand, the rays of the Sun falling on Mother Earth after the rain-sperm of the Sky created the first living creatures.

Of astronomical importance is the Celestial Dome, where in daytime reigns the all-seeing Helios, and at night the stars and the pale figure of Selene-Moon are observed.

The Moon was the origin, in remote antiquity, of the definition of the month and the week, and of the creation of the first (lunar) calendars; its role was crucial for the invention of the religious calendrical systems of the ancient people, which survive even today in the Islamic world and in the determination of the date of the Christian and Jewish Easter.

References

Achilles Tatius, 1917, with an English trans. by S. Gaselle, Heinemann, London & G.P. Putnam's Son, New York.

Aeschylus, 1989, Eumenides. Ed. Alan H. Sommerstein, Cambridge University Press, Cambridge.

Aeschylus, 1983, Prometheus bound, Greek and Latin Classics. Ed. Mark Griffith, Cambridge University Press. Cambridge.

Aeschylus, 1984, The Oresteia: Agamemnon, The Libation Bearers, The Eumenides. Ed. and Intr. by W.B. Stanford, trans. by Robert Fagles, Penguin Press. New York.

(Pseudo)Apollodorus, 1921, The Library I (Bibliotheca), trans. by J.G. Frazer. Vol I Books 1-3.9, Vol. II, Book 3.10-to end. Epitome. The Loeb Classical Library, Harvard University Press, No. 122, Heinemann, London (reprint 1995).

Apollonius Rhodius, 1962, Argonautica, trans. by R.C. Seaton, The Loeb Classical Library, Harvard University Press, Heinemann, London.

Aristotle, 1956, On the Heavens (De Caelo), trans. by W.K.C. Guthrie, The Loeb Classical Library; Harvard University Press, Heinemann. London. (reprinted 1936, 1947, 1953, 1956).

Bekker, A.I. (ed.), 1814-1821, Anecdota Graeca, 3 vols., Berolini.

Demetrakos, D., 1964, Mega Lexikon olis tis ellinikis Glossis, Publ. Ch. Tegopoulos - B. Asimakopoulos, Athens [in Greek].

Diels, H., 1996, Die Fragmente der Vorsokratiker, Herausgegeben von Walter Kranz. Erster Band - Zweiter Band, Weidmann, Zьrich.

Diodorus Siculus, 1935, Bibliotheca Historica. Library of History (Books III - VIII), trans. by C. H. Oldfather, The Loeb Classical Library Volumes 303 and 340. Harvard University Press. Heinemann. London.

Doumas, Ch.G., 2008, "The aligenes Aegean Sun" in: Kathimerini - Technes & Grammata, December 7, Athens [in Greek].
Doumas, Ch.G., 2010, "The ancient monuments of the names" in: Kathimerini - Technes & Grammata, February 14, Athens [in Greek].
Eliade, M., 1978, A History of Religious Ideas, vol. I, From the Stone Age to the Eleusinian Mysteries, trans. by W. Trask, IL: University of Chicago Press. Chicago.
Euripides, 2004, Ion, transl. by Robert Potter, ebooks@Adelaida, on line: http://classics.mit.edu/Euripides/ion.html.
Euripides, 1996, Phaethon, Ekdoseis tou 21ou, Athens [in Greek].
Gelling, P. and Davidson, H.E., 1969, The Chariot of the Sun, Dent. London.
Glob, P.V., 1974, The Mound People, Faber. London.
Green, M., 1991, The Sun-Gods of Ancient Europe, B.T. Batsford, London. Helios Encyclopaedia, 1957, Edition of Helios, Athens [in Greek].
Hesiod, 1914, The Homeric Hymns and Homerica (Theogony), trans. by H.G. Evelyn-White. The Loeb Classical Library, Heinemann, London (reprinted 1954).
Hesiod, 2006, Volume I, Theogony. Works and Days. Testimonia. Ed. & trans. by Glenn W. Most. The Loeb Classical Library, No. 57N, Heinemann, London.
Homer, 1924, The Iliad, trans. by A.T. Murray. The Loeb Classical Library, Heinemann. London (reprinted 1954).
Homer, 1919, The Odyssey, trans. by A.T. Murray, revised by G.E. Dimock. The Loeb Classical Library, Heinemann. London (reprinted 1995).
Homeric Hymns, 1914, by Hugh G. Evelyn-White, Cambridge, M.A., Harvard University Press. Heinemann. London.
Hyginus, 1993, Fabulae. Editio altera. Ed. Marshall, P.K. (corrected ed. 2002), K.G. Saur, Munich.
Jameson, M.H. and Runnels C.N., 1959, A Greek countryside: the southern Argolid from prehistory to present day. Stanford University Press, Stanford, California (repr. 1994).
Kern, O., 1922, Orphicorum Fragmenta, Weidmann. Berlin.
Macrobius, 1969, Saturnalia, trans. by Percival Vaughan Davies, Columbia University Press. New York.
Mariolakos, Elias (ed.), 2009, Geomythotopoi - Geomythological courses of Phthiotis, Publ. of the Local Union of Boroughs and Communes (TEDK) of Phthiotis Prefecture [in Greek].
McCarthy, D.J., 1978, Treaty and Covenant 2, Pontifical Biblical Institute, Rome.
Nagy, G., 1990, Greek Mythology and Poetics, Ithaca. London. Neoteron Encyclopedicon Lexicon Iliou, 1957, vol. 4, Ilios Publications, Athens [in Greek].
Nilsson, M.P., 1906, Griechische Feste von religiцser Bedeutung mit AusschluЯ der Attischen, B.G. Teubner, Leipzig.
Nonnus, Dionysiaca, 1940, Vol. I, Books 1-15, trans. by W.H.D. Rouse. The Loeb Classical Library No. 344. Heinemann. London.
Orphic Hymns, 1997, Ideotheatro Publications-R. Anastasakis, Athens [in Greek].
Ovid, 1857, The Metamorphoses, trans. by Nathan Covington Brooks, 5th ed., A.S. Barnes & Co., Cincinnati; H.W. Derby & Co., New York.
Pantermalis, D., 1995, "Ancient Greek mines", in Kathimerini, April 9, Athens [in Greek].
Patsi-Garin, E., 1969, Epitomo Lexikon Ellinikis Mythologias. Editions Hari Patsi, Athens [in Greek].
Pausanias, 1918, Description of Greece, Books I & II. Attica and Corinth, Edit. & trans. by W.H.S. Jones, The Loeb Classical Library, Heinemann. London.
Pausanias, Description of Greece, 1935, Vol. IV. Arcadia, Boeotia, Phocis and Ozolian Locri, Books 8.22-10, trans. by W.H.S. Jones. The Loeb Classical Library No. 297. Heinemann, London.
Pausanias, 1935, Description of Greece, Volume II (Laconia, Messenia, Elis 1) Books 3-5, trans. by W.H.S. Jones and H. A. Ormerod. The Loeb Classical Library No. 188. Heinemann, London.
Pindar, 1997, Nemean Odes, Isthmian Odes, Fragments. Edit. & trans. by W.H. Race, The Loeb Classical Library No. 485. Heinemann, London.
Pindar, Olympian Odes, trans. by T.K. Hubbard, via the Perseus Project at Tufts University.
Pindar, 1997, Olympian Odes, Pythian Odes. Edit. & trans. by W.H. Race, The Loeb Classical Library No. 56. Heinemann, London.

Pliny, 1971, Natural History (Historia Naturalis), trans. by H. Rackham, The Loeb Classical Library. Harvard University Press. Heinemann, London.
Proclus, 1820, The commentaries on the Timaeus of Plato, 5 Books. Edit. & trans. in English by Thomas Taylor, London.
Quintus Smyrnaeus, 1913, The Fall of Troy. Trans. by A.S. Way. The Loeb Classical Library Vol. 19. Heinemann, London.
Segal, C.P., 1992, "Divine Justice in the Odyssey: Poseidon, Cyclops and Helios", American Journal of Philology (AJP) 113, pp. 3-29.
Sophocles, 1994, Vol. I. Ajax. Electra. Oedipus Tyrannus. Edit. & trans. by W.H.S. Jones, The Loeb Classical Library No. 20. Harvard University Press. Heinemann, London.
Sophocles, 1994, Vol. II. Antigone. The women of Trachis. Philoctetes. Oedipus at Colonus. Edit. & trans. by W.H.S. Jones, The Loeb Classical Library No. 21. Harvard University Press. Heinemann, London.
Sophocles, 1892, Trachiniae, Ed. & trans. by R.C. Jebb, Cambridge University Press, Cambridge [on line: trachiniae.10.zip].
Spandagos, E., 2002, Catasterismoi of Eratosthenes of Cyrene, Aithra publ., Athens [in Greek].
The New Encycloaedia Britannica On line: http://www.britannica.com/, entry: matriarchy.
Theodossiou, E., 2007, The dethronement of the Earth - The dispute between geocentric and heliocentric systems, Diavlos Publ., Athens [in Greek].
Theodossiou, E. and Danezis, E., 1995, The Odyssey of the Calendars - vol. I: Searching for the roots of Knowledge, Diavlos Publ., Athens [in Greek].
West, M.L., 1997, The East face of the Helicon: West Asiatic Elements in Greek Poetry and Myth. Clarendon Press. Oxford.

Gaia, Helios, Selene and Ouranos: the three principal celestial bodies and the sky in the ancient Greek cosmogony

Efstratios Theodossiou[1], Vassilios N. Manimanis[1],
Milan S. Dimitrijević[2], Petros Mantarakis[3]
[1] Department of Astrophysics, Astronomy and Mechanics Physics Faculty, University of Athens-Zografos 157 84
[2] Astronomical Observatory, Volgina 7, 11060 Belgrade, Serbia
[3] 322127 Needles, Street, Chatsworth, California 91311, USA
etheodos@phys.uoa.gr
mdimitrijevic@aob.bg.ac.rs
zanispetros@socal.rr.com
(Research report. Accepted on 21.09.2010)

Abstract. In this article we consider the role of the three principal celestial bodies, the Earth (Gaia), the Sun (Helios) and the Moon (Selene), as well as the Sky (Ouranos) in the ancient Greek cosmogony. This is done by the analysis of antique Greek texts like *Orphic Hymns* and the literary remains of the writers and philosophers like Aeschylus, (Pseudo) Apollodorus, Apollonius Rhodius, Aristotle, Euripides, Hesiod, Homer, Hyginus, Nonnus, Pausanias, Pindar and Sophocles, as well as by the analysis of texts of Roman writers like Cicero, Ovid and Pliny.
Key words: Gaia, Mother Earth, Helios, Sun, Ouranos, Sky, Selene, Moon

Гея, Хелиос, Селена и Уран – трите главни небесни тела и небето в древно-гръцката космогония

Е. Теодосиу, В. Н. Маниманис, М. С. Димитрийевич, П. Мантаракис

В тази статия ние разглеждаме ролята на трите главни небесни тела – Земята (Гея), Слънцето (Хелиос) и Луната (Селена), както и Небето (Уран) в древно-гръцката космогония. Това е направено чрез анализ на антични гръцки текстове като Орфеевите химни и литературното наследство на писатели и философи като Есхилус, (Псевдо) Аполодорус, Аполониус Родиус, Аристотел, Еврипид, Хесиод, Омир, Хигинус, Нонус, Паусаниас, Пиндер и Софокъл, както и анализ на текстове на римски посатели като Цицерон, Овидий и Плиний.

1.Introduction

Our aim here is to analyze, on the basis of ancient Greek and Roman texts, the role of the three principal celestial bodies, the Earth (Gaia), the Sun (Helios) and the Moon (Selene) as well as the Sky (Ouranos) in ancient Greek cosmogony.

Since the remotest antiquity, human beings worshipped the divine couple of goddess Gaia (Gaea, Earth) and god Ouranos (Uranus, Sky), the primal pair. Hesiod's *Theogony* (1914) begins with Gaia and concludes with the polytheistic reign of the Olympians. The genesis of the elements of nature and the genesis of personified gods behaving like humans proceed in parallel: "in the beginning the gods and Gaia were born" (*Theog.*, 105). Gaia's mate, Ouranos, surrounds her and fertilizes her.

In juxtaposition with Gaia, who is the deification of our planet, Mother Earth is the deification of the ground, whose products support human existence, and which gives the space where they are born, they live and they die.

Beyond the cosmic duo of deities, Ouranos and Gaia / Mother Earth, humans worshipped the light-giver and life-giver Helios (Sun), the source of every life form on Earth. For all people, in all regions of the Earth, the Sun, Sky and Earth are the eternal witnesses of human acts and the natural avengers of the violations of the laws. From the age of the emergence of Greek philosophy comes the theory that the solar rays that fell on the wet Mother Earth created the first living creatures, while mythographers consider as progenitors of all things the Sun and Mother Earth.

The Moon gave primal units for the measurement of time: the definition of the lunar (synodic) month and of the week; its role is therefore crucial in the invention of the first calendars, which served as the foundation for all ancient religions.

In this paper, we will consider and analyze the role of Gaia/Mother Earth, Ouranos, Helios and Selene in ancient Greek mythological Cosmogony.

2. Gaia

According to the cosmogony of the Orphics, Gaia (*Gaea*) pre-existed, along with Chaos and Eros-Phanes, during the Creation of the Universe. These three cosmic beings were born from the cosmic egg, which in turn either originated *ex nihilo* or was produced by Nyx (the Night).

Gaia, one of the primal deities, is a cosmogonical symbol of the material aspect of the Universe, and not just of the earth as a ground (Demetrakos, *Mega Lexikon*, 1964, vol. 3, p. 1534). Chaos symbolizes the space of the Universe and Eros symbolizes the motive and world-creating power that unifies and transforms the Universe.

In the oldest Orphic cosmogony Gaia is born with the intervention ('energy') of this cosmogonic Eros, who "*put together everything*" (*Orphic Fragm.* Kern, 1922, 1). In the later version of Orphic cosmogony Gaia and the Sky (Ouranos, Uranus) are formed from the two halves of the huge cosmic egg born by the timeless Chronos (Time) (*Orphic Fragm.* Kern, 1922, 57).

In Hesiod's *Theogony* (1914), the primal entity of the Universe is Chaos: "... *first Chaos was created*" (*Theog.* 116), which was a formless mass without any structure; an abyss or an 'undecorated' space. After the creation of Chaos, Erevos (= Darkness) and Nyx (= Night) were born; Nyx gave birth to Ether and Hemera (= Day).

Subsequently, the 'broad-chested Gaia', as Hesiod characterizes her, one of the three primeval elements of the Universe -along with Chaos and Eros-, gives birth to Ouranos, Pontos (= sea) and the mountains (*Theog.* 123+).

Another version identifies Chaos with Ouranos proper, thus defining Gaia and Ouranos as the first cosmic-divine couple of Creation. Ancient Greeks begin the genesis of gods and of nature with a feminine entity, Gaia, which appears after Chaos and before Eros. Gaia is both the natural element that

produces and supports the world, and the Mother Earth, with the birth of Ouranos, of the Ocean and other aquatic deities.

Initially, the divine reproduction is asexual, i.e. the fertility of Gaia is not associated with any god. In a second stage, however, Gaia appears to mate with her first-born son Ouranos (*Theog.* 147), while she had produced him without the intervention of a masculine entity. Ouranos (Uranus) was the most appropriate of all mates, as he was surrounding her totally and he was destined to be the abode of the gods. In this way, Gaia and the Sky formed the first divine couple. Whenever Night was succeeding Day, Ouranos was uniting himself with his own mother. Gaia was being fertilized by his raindrops as by sperm, so she gave birth to many children (*Homeric Hymns*, 1914, 30, 17 and *Theog.* 127): Six Titans (the Ocean, Creius, Hyperion, Japetus, Coeus and Cronus), six Titanids (Theia, Rhea, Themis, Mnemosyne, Phoebe and Tethys), three Cyclops (Arges and Steropes = lightning, Vrontes = thunder) and the three Hecatonchires, huge creatures with 100 hands each: Vriareos (= powerful), Gyes (= giant) and Cottus (= angry).

Uranus started to worry because of the number and the steadily growing power of his children; he feared that some day they would push him aside. Therefore, he imprisoned them in Tartara, a dark and cold place in the depths of the earth. Gaia, displeased by Uranus' violent behavior against their children and by his violent daily embracing, produced a hard scythe from her interior and gave it to her sons, asking them to mutilate their father, thus depriving him of his reproductive power. Cronus (*Kronos*), the youngest of all Titans, decided to punish his divine father himself, and all his half-brothers and half-sisters except Ocean agreed with that. When night fell, Uranus, full of passion, spread his vast body over Gaia and then Cronus, seizing the opportunity, cut off the genitals of his father using Gaia's scythe. From the droplets of blood that fell on earth from the wound, other creatures were born: the three Furies (Alycto = the non-stopping chaser of the guilty ones, Tissiphone = the punisher of murder, and Megaera = the malevolent), the Giants (Enceladus, Porphyrion, Pállas, Polybiotes, Ephialtes, Clytios, Hippolytus, Eurytus, Gration, Agrios, Theon, Alcyoneus, Athos, Vesvicus and Echion) and the Meliades Nymphs, spirits of hatred and violence (*Theog.* 182+). Finally, from the seminal foam and the god's sperm that fell into the sea, emerged Aphrodite on a seashore of Cyprus (*Theog.* 187-206).

Uranus understood the betrayal and realized that he had lost his power: wounded and having lost his reproductive ability (and hence his divine power), he retired high on the celestial vault, where he stayed forever, uttering a curse against Cronus: to also loose his power by his own offspring.

In Homer, the powerful and primeval Gaia is mentioned as overseer of the oaths: she is invoked, along with Uranus and the holy water of Styx, by goddess Hera when she swears (Homer, 1924, *Iliad.* XV 36-38). Homeric heroes, such as Agamemnon, also invoke Gaia in their oaths, along with Zeus, Helios and the Furies (*Iliad* XIX 258-265). Menelaus, before his duel with Paris, asks to validate the oaths of their agreement by sacrificing two lambs, one white and one black, to Helios (the Sun) and Gaia, respectively (*Iliad* III 103+).

Finally, there is a version according to which Gaia, after the 'abdication' of Uranus, joined Ocean and gave birth to gods and goddesses of the waters. However, Gaia and Uranus are not considered just the parents of the gods, but also the parents of humans, as the Homeric Hymn to Gaia, 'the mother of gods', mentions: "*Praise to me the mother of the gods and of all people*" (*Homeric Hymns*, 1914).

Gaia is seldom depicted in a whole-body representation in art. Usually the goddess is shown from waist up, a fact hinting that the rest of her body is the ground or soil, that is the earth itself, whose deification she was.

3. Ouranos (Uranus)

Uranus, whose name comes from the Greek words *oros* and *ano* (Demetrakos, *Mega Lexikon*, 1964, vol. 10, p. 5289), that is who is above the mountains (Aristotle, *On the Heavens* (*De Caelo*) 400a, 7), was in Greek mythology the personification of the celestial vault or dome, of the primeval cosmogonic force. He was the sovereign of the first generation of beings on Earth. For this reason, Uranus plays an important role in Hesiod's *Theogony*, while according to pseudo-Apollodorus: "*Uranus was the first to rule the entire world*" (*The Library (Bibliotheca)*, 1921, A, 1, 1).

In the Orphic tradition Uranus is mentioned as son of Nyx (the Night) and brother of Gaia, while elsewhere he appears as son of Ether and Gaia or Nyx. In either case, Uranus belongs to the first generation of beings, the oldest of gods and of the elements of nature. According to Hesiod, in the prevailing version, he was the first born son of Gaia, who conceived him when she was sleeping next to Eros, without fertilization, "*to surround her and to be an eternal and safe abode of gods*" (*Theog.* 486). Uranus is the first masculine element, the father of gods in Greek mythology.

We already mentioned how Uranus lost his power and retired on the celestial vault, where he stayed forever. So the word *ouranos* in Greek means the sky or celestial vault, where stars and all celestial bodies are positioned and move: the firmament, stretching from zenith to the horizon, regarded as a hemisphere placed above the surface of the earth and supported on it along the horizon line by columns (*Iliad* VI 108). On *ouranos* all celestial phenomena take place. According to Homer, the stars are attached to it and move along with it: the celestial vault is the one that rotates incessantly (*Iliad* XVII 425). Of course, today we know that this perception is totally wrong: the 'sky' in that sense does not exist.

After taking power, Cronus released all his half-brothers and half-sisters from Tartara. The Cyclops and Hecatonchires, however, started after a while to lay claims upon his power and they became dangerous. Therefore, Cronus threw them again into Tartara and he put a terrible monster, Campe (= caterpillar) to guard them. This period is the second generation of immortal deities, where Cronus reigns with his wife Rhea and Titans impose his power in the world. Yet, the increasing cruelty and injustice of Cronus, who was devouring his own children in order to avoid being dethroned himself, finally led Gaia to help Zeus (the Greek analog of Roman Jupiter) against the Titans, giving him a potion that would force Cronus to disgorge the baby gods he had

devoured. It should be noticed here that the primal Gaia still influences the course of the world, appearing at certain crucial moments to give a solution.

Zeus, after being advised by Gaia, also released the Cyclops and Hecatonchires. The three Cyclops, with their awesome weapons, the lightning and the thunder, and the three Hecatonchires with their 300 hands in total, managed to obtain a decisive victory against the Titans on Mountain Othrys. The Titans were defeated and were thrown deep in the earth, in Tartara, where the Hecatonchires guard them.

According to professor of Geology at the University of Athens Mariolakos Elias: *"The end of the Titans means i) a relative abatement of earthquakes and volcanic activity, and ii) the end of the direct and decisive influence of the natural environment in the life of prehistoric humans. It is the period when the food-gatherers and hunters are turned into farmers and animal breeders* (Mariolakos, E., 2009, *Geomythotopoi*, p. 5).

It should be added that ancient Greek art did not treat the myth of Uranus as a subject; nevertheless, in the Vatican Museums there is an ancient depiction of him on the chariot of Helios (the Sun god).

According to an alternative Greek tradition, probably even older than the prevailing myth, initially Uranus and Gaia were very close. But due to the frequent infidelities and illegitimate children from other females, Gaia as Earth finally detached herself from him and agreed to meet him only in certain time periods. From an astronomical point of view, this tradition is an excellent attempt to explain the cycle of the year's seasons and the place of the Earth in the Universe, as the other mates and children of Uranus were the other moving planets and the stars of the celestial vault (*Helios Encyclopaedia*, 1957, vol. 4, p. 920).

There are also other traditions about Gaia, such as the one mentioned by Diodorus of Sicily (1935), in which Gaia was a beautiful mortal woman, under the name of Titaia. She was loved by Uranus and they had 18 children, named 'Titans' after their mother. As Titaia was a wise and prudent woman, having offered many services to humans, after her death humans deified her and gave her the name of Mother Earth.

4. Mother Earth

A special and important place in worship was held by Mother Earth, the universal mother and supreme goddess, called for this reason by Greeks *Hypertatan Gan*. This worship, however, was addressed to Earth not as a celestial body, neither as a personified deity with a human appearance, but rather as earth-chthon, as a part of nature with its soil, ground and underground, which feeds and sustains humans. Man is 'accused' by tragic poet Sophocles (5th century BC) as the one being that dares to disturb the supreme goddess, since he doesn't hesitate to hurt her by "*ploughing it with his plough, incessantly furrowing her year after year*" (Sophocles, 1994, *Antigone*, Vol. II., verse 330+).

Regarding earth-nature as the omnipotent goddess Mother Earth must have begun in the age when the first agricultural societies and their festivals developed, festivals full of mysticism for the primeval cycle of life (sprouting -

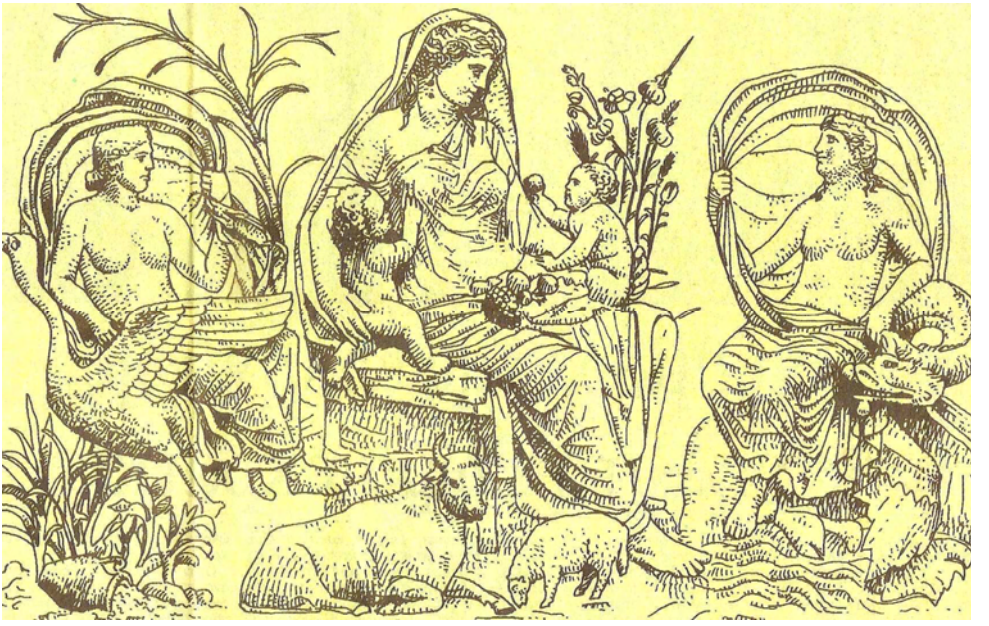

Fig. 1. At the period of Emperor August (1st century AD) people were picturing the Earth as a sweet mother with two children in her lap, inside a flowery natural environment. Later on, Pliny the Elder in his *Naturalis Historia* stressed some ominous points: he wrote that we humans excavate Earth's bowels by digging mining holes upon which we live; we wonder when gaps open or the ground shakes, as if these signs were not the expression of wrath of the holy mother. Inside dark corridors we search for treasures, as if the soil on the surface of the ground were not generous and rich enough.

fruit bearing - maturing - decay - seed - seeding - 'rebirth'). However, starting from prehistoric times, it can be said that the first humans, from the moment they started to observe life on Earth they understood that both they and the rest of animal and plant life were attached to the triptych life-reproduction-death. The survival of humans depended on earth's vegetation, as they and the animals they were hunting were being fed by the gifts of nature (Eliade, 1978).

The primitive humans, by carefully observing the life cycle of plants, the seeding of Mother Earth and subsequent sprouting aided by rain from Uranus, discovered the corresponding cycle of animal sexual reproduction.. Therefore, it was concluded that Earth was alive and in order to give birth 'she' needed to come into contact with the masculine entity. For this reason, humans personified Earth as a feminine entity, while the fertilizing masculine entity was the sky with the rain, or some large river, such as the divine Nile in Egypt (the ancient Egyptian religion is the only one in the world in which the Sky is personified as a female deity, Nout, see Theodossiou 2007, p. 28).

The Mother Earth (Terra Mater), due to the vague character of her worship, is sometimes identified in Greek literature as Rhea, Hestia, Hera, but mostly as Demeter, whose own name comes from Ge-meter = Earth-mother, denoting the womb that encloses the seeds. Indeed, the worship of Gaia as Mother Earth goddess diminishes over time, without disappearing completely, and is replaced by the better-defined worship of Demeter as the goddess of agriculture; Gaia's role is thus reduced to the dream-giving, story-telling, and to the feeding of plants and children.

The miraculous divine union of Uranus-Sky and Earth, out of which gods, humans, and all living things are born, is reflected in the cry of Eleusis Mysteries '*hye, Kye*'; with this cry the mysts were calling the Sky to pour his fertilizing rain, so that the earth (here personified as Demeter) could use her womb to produce all kinds of offspring.

As opposed to Gaia, which is the deification of our world-planet, Mother Earth is essentially the deification of soil-ground, whose products sustain humans and which gives them the space on which they are born, live and die.

The presence of Gaia as a primeval element-material and deity is apparent in the founding of the first oracle, which catered only to the gods. Later on, identified with Mother Earth, established her oracle in Delphi; this is why she is also called 'protomantis' = first foreteller (Aeschylus, 1989, *Eumenides, Pythias* 2). The Dodone oracle was also dedicated to Gaia; there she was worshipped together with Zeus as "fruit-giver and mother" (Pausanias, 1935, *Phocis* 12, 10).

Finally, Pliny the Elder in his *Naturalis Historia* (1971) wrote that the Sky belongs to the gods, but the Earth belongs to the human race. The Earth welcomes us when we are born, it gives us food to grow and it receives us in her lap when we die. This earth suffers from human actions that destroy its surface and cut into its body as men search for gold, silver, copper and lead; men open wells into its depth in quest for precious gems and excavate its bowels. (Pantermalis, *Ancient Greek mines*, 1995, p. 42).

Finally, the questions about Earth, as they were summarized by Aristotle (*On the Heavens* 1956, II 293a, 15+), were culminating with the question of the place of Earth in the Universe, of its exact shape and of its size.

5. The Couple of Sky and Earth

As a corollary, it can be said that in Greek cosmogony, as in the creation myths of the other Indoeuropean people, the great creation activity taking place continuously in nature is exemplified in the following simple picture: One divine couple, the first of creation, gave and still gives birth to all beings. The fertilizing 'father', in this case Uranus, and the conceiving 'mother', in this case Gaia, who also feeds her children.

This first divine couple is united by Eros, and in the erotic-cosmogonic symbolism the Sky-Uranus embraces and fertilizes Earth-Gaia through the rain. Their union is presented as an omnipotent reproductive ability, which multiplied the number of gods, a fact praised by Orpheus (Proclus in *Tim.* 3, 1820, p. 137, 11) as creation of the primeval Chaos (or Erevos) and of the Day (*Orphic Hymns* IV: *Incense to Uranus*, and XXVI: *Incense to Earth*).

Besides, this same symbolism is hidden in the union of Semele (who personifies Earth) and Zeus, the celestial god who fertilizes his beloved woman with lightning, the harbinger of rain. 'Earthly' Danae is fertilized in the same way, by the 'celestial' Zeus transformed into golden rain. Metaphorically, the celestial god, with his beneficiary waters, softens the parched womb of the earth for the development of life.

Since Mother Earth and Uranus were the progenitors of life, humans (who depended on earth's vegetation) had to either pacify or challenge god Uranus to copulate more frequently with Mother Earth for richer production.

This cosmogonic theme of the primeval couple of Sky and Earth is found not only in ancient Greece, but in almost all ancient civilizations. According to some scientific evidence, many prehistoric societies were matriarchic ('matriarchy' in *The New Encyclopaedia Britannica*, 2007)

The first human societies were intimately aware of nature. They believed that humans, animals, plants, rocks and minerals, all were the descendants of Mother Earth; therefore, everything had a soul and any living creature had the same rights on life.

At the dawn of history human societies respected the other life forms because they knew that their differences were just morphological. People believed that rain was the intercourse of Sky and Earth (the masculine and the feminine). They knew that everything depended on this event, including the survival of the other forms of life on the land.

For pre-Socratic Greek natural philosophers, however, it should be added that Earth and the Sky were regarded as a continuous body, united at the ends of the horizon.

Earth of the Homeric Universe was a circular flat disk surrounded by a huge circular river, the Ocean, a model first appearing in the *Orphic Hymn* 'X. TO PAN, *The Fumigation from Various Odors*', verse 15: "*Old Ocean too reveres thy high command, whose liquid arms begirt the solid land.*" This mythical 'river' is different from the seas: it is something that defines the boundaries of the terrestrial world. Above all, Ocean is the primal and original creative element, the starting point of all things (*Iliad*, XIV 246). This mythical 'river' has no sources, nor estuary, it is 'apsorroos', i.e. cyclically moving or backward-flowing. Its current goes back to where it started in a ceaseless and eternal flux. This Ocean supports the sky, which is above Earth's circular disk as a huge vault.

In the *Orphic Hymns*, the Sky is mentioned as the sovereign of the World, surrounding the Earth as a sphere; it is the abode of the gods and rotates like a spinning-top; personified, he guards everything, not just in his place, but also on Earth: "*Uranus ruler of the world, spinning like a sphere around Gaia, house of the blessed gods, moving with whirlings, guard of everything on both sky and earth" (Orphic Hymns)* IV, *Incense to Uranus*).

On the other hand, the Sky was for ancient Greeks a metallic vault made of copper or iron, held up there by very tall columns or, according to another view, by some giant. Homer combines these two views by having Atlas supporting the columns (Homer, 1919, *Odyssey* i 53-54). Hesiod in *Theogony* (1914, 517e) writes that Zeus was the one who had assigned this duty to Atlas. So the sky for them was made of a solid metallic material, called 'polychalcus', that is 'of much copper' (*Iliad* V 504, *Odyssey* ii 458, iii 2, *Iliad* XVI

364, XIX 351), 'copper' (*Iliad* XVII 424-425) and 'iron' (*Odyssey* xv 329 and xvii 565).

The space between sky and Earth, according to the view recorded by Homer, was filled at first by the dense air: aer (*Iliad* XIV 288). Over this layer and towards the direction of the sky there was the clean and transparent 'ether', lighter than the air. Above the ether was the 'polychalcus' sky.

Of course, one should not assume that the Homeric sky was a barren metallic dome; it was, as Homer sings, full of life, the life of the stars that decorate it: he calls the sky 'full of stars' ('asteroeis') (*Iliad* VI 108, XV 371) and star-decorated (*Odyssey* ix 534-535). On this celestial dome, Helios, the god of the Sun, travels on its path, so he is described with the adjective 'uranodromos', that is 'sky-running' (*Odyssey* i 7-9).

6. The Sun and the Sun-god Helios

From prehistoric times, humans admired the starry night sky, with its thousands of naked-eye stars twinkling on its vault. But their joy was greatest at dawn, "the rosy-fingered Eos" (Hesiod, 2006, *Works and Days*, 609), when the diffuse sunlight gradually prevailed over the darkness of the fearful night. They naturally worshipped the light-giving Sun, since they realized that everything on earth owed its existence and life to the influence of its rays.

According to archaeologist Chr. G. Doumas: *"The word 'als' in Homer means the sea when observed from the land. The presence of this root in tablets of Linear B writings as component of other words indicates a long-standing use, during which it evolved into a versatile noun of the third declension that easily makes compounds with other roots... the fact that with the original root so many and various needs of the Greek language, e.g. alios / helios [= sun], shows both the close relationship of the aegean society with the sea and the strong influence of the liquid element upon the history and the culture of that age."* (Doumas, 2010, *The ancient monuments of the names*, p. 16).

"Indeed, from 'als' (genitive form: alos) came the adjective 'alios', which, even though it is recognized as the doric type of 'helios' = sun, it essentially means the one that is related to the sea... The depiction of the Sun on the proto-Cycladic pan-shaped vessels of the 3rd millenium BC is probably an indication of the importance assigned to it by the Cycladians of that period. The islanders of the Aegean Sea and the inhabitants of the eastern shores of the Greek peninsula see every morning the Sun rising from the sea" (Doumas, 2008, *The aligenes Aegean Sun, p.15), as described in the first verses of Rhapsody iii of the Odyssey: "When the Sun, leaving the lake, ascended towards the all-copper sky to shine on both immortals and the mortal people of the life-giving earth... ".*

The Sun is the 'radiating one', the 'fiery one' and as such it symbolized the celestial representation of the universal father, being essentially the representative of God's spirit (Demetrakos, 1964, vol. 7, p. 3250). The Sun's appearance in the morning, its culmination at noon and its majestic disappearance for the night (or during the eclipses) influenced much human thought. Darkness falling every evening after sunset filled the soul of the primitive human with stressful questions. With time, the savants of the society assigned to

the Sun supernatural divine properties, since as a god 'he' could appear or disappear at will, both daily and during the much more rare eclipses.

All ancient people worshipped the light- and life-giving Sun. The Sun was Samas of the Assurians, Bel of the Semites, Bel-Marduk of the Babylonians, El or Outou of the Sumerians, Baal of the Phoenicians and Chananeans, Moloch of the Ammonites, Chimoch of the Moabites, Ammun-Ra of the Egyptians, Surya of the Indians, Mithra of the Persians, Indi of the Inka, Tonatiuch of the Aztecs, Sol of the Romans, Swarog or Yarila of Slavic tribes, Belenos of the Celts, Helios and Phoebos-Apollo (the symbol of sunlight) of the Greeks. The worship of the Sun god was universal and prevalent, since for ancient humans the Sun was the source of life, light and warmth, a guarantee of the celestial order of the hours of the day and the seasons of the year, a creative force for nature and, more mundanely, an aid for orientation. Besides, the Sophoclean phrase *"everybody adores the rotating solar orb"* (Achilles Tatius, 1917, frag. 672 Nauk2), is true for all ages (Sophocles, 1892, *Trachiniae*, 738, 2).

7. The Sun-Helios in Greek mythology

In Homer's *Iliad* and *Odyssey* (ca 8th century BC) the external aspect of the bright appearance of the Sun is especially stressed along with the notions associated with sunrise and sunset. According to Hesiod, the Sun-god, Helios, was the son of Titans Hyperion and Theia (*Theog.*, 371-372), or of Hyperion and Euryphaessa (*Homeric Hymn to Helios* 31, 2), while his sisters were Selene (the Moon goddess) and Eos (the personification of dawn). Pindar celebrates Theia as the mother of Helios in his 5th *Isthmian Ode* (1997):

"Mother of the Sun, Theia of many names, for your sake men honor gold as more powerful than anything else; and through the value you bestow on them, o queen, ships contending on... "

As Titans, Theia and Hyperion (= he who hovers above earth) belong to the same generation as Cronus; all of them were children of Gaia and Uranus (Patsi-Garin, 1969).

Homer, calling Helios 'Hyperionides' (*Odyssey* xii 176), stresses his concrete bond with life, as since their birth, humans behold the solar 'augeae' (daybreaks): they live *"under the stars of the sky and the light of the Sun"* (*Iliad* IV 45), rejoicing when they see *"the bright light of the Sun"* (*Iliad* V 120). Eventually, when a person dies "he abandons the light of the Sun" (*Iliad* XIX 2).

The Sun for Homer is the god who *"sees everything and hears everything"* (*Iliad* III 277). This characteristic of Helios is stressed by the adjectives 'panoptes' (Aeschylus, 1983, *Prometheus Bound* 91), 'the overseer of everything' (Aeschylus, 1984, *The Libation Bearers*, 982-986), 'the prevailing one by sight' (Sophocles, 1892, *Trachiniae*,101) and many other references of the ancient Greek tragic poets, who stress that these 'over-seeing' abilities of the Sun render him a guarantor of the keeping of oaths; always Helios was a

witness of truth (*Homeric Hymn* 3, 381, Sophocles: *Oedipus Tyrannus* 660), *"index of justice, guardian of oath keeping, eye of justice"* (*Orph. Hymn* 16).

In Greek mythology in general, Helios is presented as the god who travels around Earth and watches the administration of justice shedding light on good and evil (Segal, C.P., 1992, pp. 3-29, McCarthy, D.J., 1978, p. 185, West, M.L., 1997, p. 20). Helios was considered a very important god, and Homer reports that sacrifices were offered to Gaia and Helios (*Iliad* III 104, 276). As far as his other attributes are concerned, Helios was worshipped in Corinth (Pausanias, 1918, *Corinth* Book II, 3:2, 4:6 and 5:1) as god of storms, thunderstorms and other sky forces.

Additionally, it has been suggested that the 'Horse monument' (Pausanias, 1935, Book III 20, 9) with the seven *"columns... ... who they say are statues of the planets"*, was a part of the worship of Helios. Also, in Hermione there was a temple dedicated to Helios (Pausanias, 1935, Vol. II, 34, 10). Indeed, in the Christian church of Taxiarches was found a part of a circular altar of the 3rd century AD with the following inscription: *"To Helios the king god, to Hyperion altar... "* (Jameson, M. and Runnels C.N., 1959, p. 15).

The special place of Helios with respect to the Olympian gods (although Helios is a celestial and not one of the 12 Olympian gods), is connected with his importance for the life of the Olympians. Diodorus (1935, *Bibl. Histor.* V 71) writes that Zeus before the battle with the Giants sacrifices to Helios, Uranus and Gaia. This is why Aeschylus refers to Helios as 'the overseer of everything' (Aeschylus, 1989, *Eumenides*).

From about the 5th century BC and after, Helios loses its status as a distinct deity and begins to mingle with Apollo, the Olympian god of sunlight. After the battle with Giants, Helios was identified with Zeus, who, as a celestial and Olympian god relative to the celestial light included the divine substance of Helios. However the gradual increase in Zeus' strengths forced the Helios part out of his substance which Apollo then usurped to become a deity with many of the characteristics of a pure Sun god. The identification of Helios with Phoebus-Apollo (phoebus = shining) is traced throughout the whole ancient Greek literature after Parmenides and Empedocles (Diels, 1996, *Vorsokratiker*, I2 108, 29.157, 10 and DK -Diels-Kranz, 1996, 28 A 20, 31 A 23), up to Plutarch and Crates Ascondes of Thebes.

Eratosthenes reports this identification of Helios with Apollo (Spandagos, 2002, 24) writing that Aeschylus suggests in one of his works that Orpheus identified Helios with Apollo and placed him at the center of his worship, refusing to offer honors to Dionysus. Similarly, in *Saturnalia* by Macrobius (1969), it is written characteristically: *'Item Orpheus Liberum atque Solem unum esse deum eundemque demonstrans de ornatu vestituque eius in sacris Liberalibus ita scribit'* (*Saturnalia* 1.18.22, frag. 238).

Nevertheless, although this Helios-Apollo identification began at least since the 5th century BC, it was not widely accepted until centuries later.

According to Homer, Helios started his trip every dawn from the eastern ocean or from Ethiopia, the land of the 'sun-burned people' (*Odyssey* I 24-26); he crossed the sky with his winged four-horse chariot, pulled by four beautiful fire-breathing white horses: Eous, Aethiops, Bronte and Sterope (Hyginus, 1933, *Fabulae* 183):

"Eous; by him the sky is turned. Aethiops, as if flaming, parches the grain. These trace-horses are male. The female are yoke-bearers: Bronte, whom we call Thunder, Sterope, whom we call Lightning"

These equine names allude to the power of the God, the succession of the celestial phenomena and the maturing of the fruits. Other authors report other names for the Sun's horses: Lampon, Aethops, Aethon and Flegon (Gelling & Davidson, 1969, p. 14+; Glob 1974, pp. 99-103, and Green 1991, pp. 64-66, p. 114+). Every evening, Helios completed his journey and then rested in the West, in the land of Hesperides.

The notion of the 'flaming' or 'fiery' nature of Helios is very common among the Greek tragic poets: *"baked by the fire of the sun"* (Aeschylus, 1983, *Prometheus Bound* 22), *"High o'er the earth, at whose ethereal fire. . . "* (Euripides: *Ion* 34), *"Hot flame of the King"* (Euripides, 1996, *Phaethon* 776). Euripides describes sunrise as follows: *"Now flames this radiant chariot of the sun / high o'er the earth, at whose ethereal fire / the stars into the sacred night retreat"* (Euripides, 2004, *Ion* 82-84). This description has often been compared with a depiction of Helios on a Greek vase of the 5th century BC that is kept in the British Museum; there, Helios is depicted with a ray-surrounded head, riding a winged four-horse chariot, rising from the sea, in which child-like apparitions swim, denoting the stars that go to hide.

Fig. 2. At the period of Emperor August (Ink drawing: The rise of the Sun with his 4-horse chariot. The vanishing stars of the night are depicted as children sinking in the sea (Greek vase, 435 BC - British Museum).

The Sun, completing his daily (diurnal) course on the celestial vault, rested every night on a golden bed made by the hammer of the god Hephaestos (Vulcan), in order to shine again the following day over the world.

Helios had many sons and daughters. With Oceanid Perseis they had three children: Circe, Passiphae and Aeëtes (Apollonius, 1962, *Argonautica* 3, 1, 2 and Homer: *Odyssey* XII 3). Circe was famous for her magical powers and for her love for Ulysses (*Theogony*, 1914, 957). Passiphae, wife of king Minos of Crete, is identified with the Moon and considered the primeval deity of light, as her name states (passiphaessa = apparent to all). It was due to Passiphae

that the worship of Helios was widely practiced in Crete, where he was adored under the form of a bull (Bekker, 1814-1821, *Anecd. Gr.* 344, 10). The myth of Passiphae falling in love with a bull (the zodiacal constellation Taurus = the Bull) reflects a very ancient tradition, according to which the bull-shaped sun-god and the cow-shaped moon-goddess were united with a holy wedding.

In another myth, Aeëtes was king of Aea, who refused to give the Golden Fleece (a symbol of sunlight) to Jason and the Argonauts.

Helios had two other daughters, Phaethusa and Lampetie, and a son, Phaethon, with Clymene.. Once, Phaethon got permission from his father to cross the sky with his chariot. However, when Phaethon saw the huge constellation Scorpius (the scorpion) he became freightened and lost control of his father's chariot. Its horses bolted and the chariot started to go up and down, threatening the Earth with destruction. Then Zeus saved the world by killing Phaethon with one of his thunderbolts. Phaethon's body fell on the bank of the river Eridanus. His sisters, the Heliads, who mourned him, were transformed into poplars, the holy trees of the god Helios, and their tears became amber.

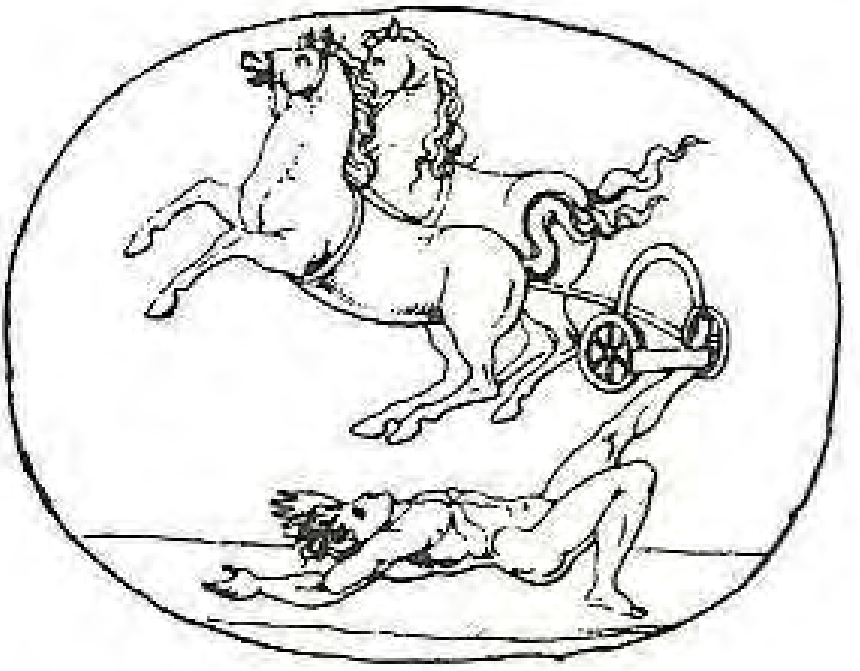

Fig. 3. Ink drawing: The fall of Phaethon.

'Phaethon' was also a name given to of Helios himself because of its radiant light (*Iliad* XI 730, *Odyssey* v 479, xi 15, *Homeric Hymn* 31.2). In his *Theogony* (1914), Hesiod writes of Phaethon and Hyperion as 'substances' of god Helios (*Theog.* 987 and Nagy, 1990, p. 235). Additionally, Phaethon is mentioned by both Nonnus (1940, *Dionysiaka* 38.167) and Ovid (1857, *Metamorph.* 2007, 1.747-79: *Phaethon's parentage, struggle with Epaphos* and 2.42: *Phaethon and his father*).

Helios, according to Greek mythology, also had numerous other affairs with other women; subsequently, he had many other sons and daughters, collectively known in ancient Greek literature as Heliades.

A famous center of Helios worship was Rhodes; as Pindar (1997) reports (*Olymp. Ode* 7, 69), the whole island belonged to him. The famous Colossus was a giant statue of Helios (this statue was one of the 'seven wonders' of the ancient world), an artwork by Rhodian sculptor Chares from Lindos (Pliny, 1971, *Historia Naturalis* 34.63), a student of Lysippus (3rd cent. BC). Every four years a Sun festival was celebrated on the island, called Ali(ei)a or Helieia (Nilsson, 1906, p. 427), during which they offered to Helios a four-horse chariot thrown into the sea. Helios stayed in Rhodes with Nymph Rhodos, a daughter of Aphrodite, and together they had seven sons, named: Ochimos, Cercaphus, Actis, Macar, Candalus, Triopes and Tenages, and their wisdom is exalted by Pindar (1997, *Olymp. Ode* 7, 72-75).

In Greek art the personification of the sun is often depicted as a young man bearing a radiant wreath and a tunic, standing upon a four-horse chariot, as on the metope of the Hellenistic temple of goddess Athena in Ilion (Troy).

Of more astronomical interest is a statue of Helios in the Vatican. He is depicted as a young man bearing a radiant wreath, and has an extra feature: a wide belt with the symbols of the zodiac.

Moreover, there is the tradition, mentioned among others by Homer (*Odyssey* xii 127), that in Trinacria island (Sicily),Helios had seven herds of cattle and seven herds of sheep, each having fifty animals. They grazed steadily every day, never getting more or less. According to the explanation given by Aristotle, the lunar year consisted of 50 weeks, each having 7 days and 7 nights; therefore the 50 times 7 cattle and the 50 times 7 sheep were denoting the 350 days and 350 nights, respectively, which make the lunar year used by ancient Greeks according to the original calculations (Theodossiou & Danezis, 1995, p. 315).

The worship of the Sun-god was universal, while very ancient practices originating in it, such as the orientation of temples of several religions towards the East, were kept until our days in the conscience of people.

8. Selene, The Moon

According to Hesiod's *Theogony*, Selene was the daughter of Hyperion and Theia, and sister of Eos (the Dawn) and of Helios, who illuminates her eternally due to their relation as half-brothers. The word *selene* comes from *selas* = light (Demetrakos *Mega Lexikon*, 1964, vol. 13, p. 6489). In Greek mythology Selene or Selana (Pindar, *Olymp. Ode* 10, 75) is the first and only lunar deity, at least in pre-classic and classic poetry, also called by the adjectives

Fig. 4. An ink drawing of the metope of the temple of Athena in Ilion (Troy) with a relief depiction of ray-headed Helios standing on his chariot, most probably based on an older work by Lysippus (Staatliche Museen, Berlin

Aegle, Passiphae, Mene, Titanis (as daughter of two Titans) and Phoebe as sister of Phoebos-Helios. As Greek mythology evolved, other goddesses were correlated with the Moon: Hecate, Artemis and Hera.

Selene is usually imaged as a feminine form bearing a crescent as crown, riding a horse or a chariot with two winged horses (diphros). Sometimes she is described as leading a herd of cattle so that her crescent-shaped crown resembles a bull's horns. Her brother Helios rides a four-horse chariot, while Selene rides a two-horse chariot; her two horses have one of their sides white

and the other black, a metaphor meaning that only the one side of the Moon's surface is illuminated by sunlight.

According to various local traditions Selene had one daughter with Aer (air), called Drosos (the morning Dew). In the Attica tradition she gave birth to Pandia, daughter of Zeus (*pan* + *dia* = all-godly), worshipped along with her mother in the Pandion festival. In an Arcadian tradition the Moon was a lover of god Pan and she was worshipped in common with him on Arcadian Mt Lykaio. In Elis and Karia they believed that Selene was in love with a mortal man, Endymion, whom she met every night on Mt Latmos, and had 50 daughters with him, as many as the lunar months of an Olympiad.

In a tradition of late antiquity mentioned by Quintus Smyrnaeus (*Fall of Troy*, 1913, 10. 334 ff), Selene also had a love affair with her brother Helios. The oldest known depiction of Helios in a Greek sculpture is on the eastern gable of the Parthenon, where the birth of goddess Athena is imaged. Helios and Selene also framed the composition of the birth of Aphrodite on the throne of the statue of Zeus in Olympia (Pausanias, 1935, Vol. II, Elis 1, Book 5, 11, 8) and a similar depiction is alluded to by the 'sunset' mentioned by Pausanias on the gable of the temple of Delphi (Pausanias, 1935, *Phocis*, Vol. IV, Book X 19, 4: *The temple at Delphi*).

Selene was worshipped throughout Greece, but especially in Peloponnese. It is known from the history of the Persian Wars that the Spartans, in order to start a military campaign took seriously into consideration the lunar phases. Near the city of Thalames there was a well-known oracle of Selene, where the ephoroi of Sparta stayed overnight asking her advice; a local spring was named after her (Pausanias, 1935, *Laconica*, Vol. II, Book 3, 26, 1).

The pair Helios-Selene was finally correlated with the pair of Olympians Apollo-Artemis, to which similar characteristics were attributed, along with the same symbols: for Selene these were silver, the bull horns and the crescent.

At a symbolic level, the Moon is the feminine component of the creation of the World and the entrance (due to its 'secret' appearance at night) towards the apocryphal nature of humanity and of the Universe, i.e. towards what remains inexpressible from the usual observation of nature. The Moon is the luminous image of cyclical time; representative of the constant flux of everything. The infinite new moons symbolize the infinite time moments of any end that signals a new beginning.

Selene is a chthonic (earth) deity in the antithesis sun-earth, light-darkness. On the other side, Selene is the goddess with the white arms that drives away the darkness of night when it is full. The rosy-fingered Eos (dawn), Selene's sister, brings the first light of the new day. Hecate, the three-form chthonic deity, is another expression of her; Ores, the Hours or the year's seasons, are considered her daughters. Another metaphor of the Moon is a huge luminous *clepsydra*, a water-clock, filled during its waxing phases and emptying during its waning phases. It gave the definite measure of time with the succession of its phases.

The ancient Greek tragic poets presented Selene-Moon as a very beautiful young woman before which all the other stars paled, when its silvery figure appears on the celestial dome.

9. Conclusions

Since the most ancient times, humans worshipped the primal divine couple, goddess Gaia and god Uranus, who were the ancestors of the other gods that gave their names to the planets of the Solar System. Hesiod's *Theogony* starts with goddess Gaia and ends to the polytheistic reign of the Olympian gods.

Uranus surrounds Gaia and fertilizes her. In juxtaposition with goddess Gaia, a deification of our planet, Mother Earth is essentially the deification of ground and soil, whose products sustain humans and offer them the space on which they live and die. The birth of the nature's elements comes in parallel with the birth of gods, who metaphorically behave as people. Cronus symbolizes Time, Rhea the flux and Hera (an anagram of Aer) air along with all the variations of weather.

The light-giving Helios, the Sun, is the source of every life form on Earth. For all people on Earth the Sky, the Sun, the Earth and the Moon (especially the full moon at night) seemed as appropriate eternal witnesses of human acts and the natural avengers of cheatings. On the other hand, the rays of the Sun falling on Mother Earth after the rain-sperm of the Sky created the first living creatures.

Of astronomical importance is the Celestial Dome, where in daytime reigns the all-seeing Helios, and at night the stars and the pale figure of Selene-Moon are observed.

The Moon was the origin, in remote antiquity, of the definition of the month and the week, and of the creation of the first (lunar) calendars; its role was crucial for the invention of the religious calendrical systems of the ancient people, which survive even today in the Islamic world and in the determination of the date of the Christian and Jewish Easter.

References

Achilles Tatius, 1917, with an English trans. by S. Gaselle, Heinemann, London & G.P. Putnam's Son, New York.

Aeschylus, 1989, Eumenides. Ed. Alan H. Sommerstein, Cambridge University Press, Cambridge.

Aeschylus, 1983, Prometheus bound, Greek and Latin Classics. Ed. Mark Griffith, Cambridge University Press. Cambridge.

Aeschylus, 1984, The Oresteia: Agamemnon, The Libation Bearers, The Eumenides. Ed. and Intr. by W.B. Stanford, trans. by Robert Fagles, Penguin Press. New York.

(Pseudo)Apollodorus, 1921, The Library I (Bibliotheca), trans. by J.G. Frazer. Vol I Books 1-3.9, Vol. II, Book 3.10-to end. Epitome. The Loeb Classical Library, Harvard University Press, No. 122, Heinemann, London (reprint 1995).

Apollonius Rhodius, 1962, Argonautica, trans. by R.C. Seaton, The Loeb Classical Library, Harvard University Press, Heinemann, London.

Aristotle, 1956, On the Heavens (De Caelo), trans. by W.K.C. Guthrie, The Loeb Classical Library; Harvard University Press, Heinemann. London. (reprinted 1936, 1947, 1953, 1956).

Bekker, A.I. (ed.), 1814-1821, Anecdota Graeca, 3 vols., Berolini.

Demetrakos, D., 1964, Mega Lexikon olis tis ellinikis Glossis, Publ. Ch. Tegopoulos - B. Asimakopoulos, Athens [in Greek].

Diels, H., 1996, Die Fragmente der Vorsokratiker, Herausgegeben von Walter Kranz. Erster Band - Zweiter Band, Weidmann, Zьrich.

Diodorus Siculus, 1935, Bibliotheca Historica. Library of History (Books III - VIII), trans. by C. H. Oldfather, The Loeb Classical Library Volumes 303 and 340. Harvard University Press. Heinemann. London.

Doumas, Ch.G., 2008, "The aligenes Aegean Sun" in: Kathimerini - Technes & Grammata, December 7, Athens [in Greek].
Doumas, Ch.G., 2010, "The ancient monuments of the names" in: Kathimerini - Technes & Grammata, February 14, Athens [in Greek].
Eliade, M., 1978, A History of Religious Ideas, vol. I, From the Stone Age to the Eleusinian Mysteries, trans. by W. Trask, IL: University of Chicago Press. Chicago.
Euripides, 2004, Ion, transl. by Robert Potter, ebooks@Adelaida, on line: http://classics.mit.edu/Euripides/ion.html.
Euripides, 1996, Phaethon, Ekdoseis tou 21ou, Athens [in Greek].
Gelling, P. and Davidson, H.E., 1969, The Chariot of the Sun, Dent. London.
Glob, P.V., 1974, The Mound People, Faber. London.
Green, M., 1991, The Sun-Gods of Ancient Europe, B.T. Batsford, London. Helios Encyclopaedia, 1957, Edition of Helios, Athens [in Greek].
Hesiod, 1914, The Homeric Hymns and Homerica (Theogony), trans. by H.G. Evelyn-White. The Loeb Classical Library, Heinemann, London (reprinted 1954).
Hesiod, 2006, Volume I, Theogony. Works and Days. Testimonia. Ed. & trans. by Glenn W. Most. The Loeb Classical Library, No. 57N, Heinemann, London.
Homer, 1924, The Iliad, trans. by A.T. Murray. The Loeb Classical Library, Heinemann. London (reprinted 1954).
Homer, 1919, The Odyssey, trans. by A.T. Murray, revised by G.E. Dimock. The Loeb Classical Library, Heinemann. London (reprinted 1995).
Homeric Hymns, 1914, by Hugh G. Evelyn-White, Cambridge, M.A., Harvard University Press. Heinemann. London.
Hyginus, 1993, Fabulae. Editio altera. Ed. Marshall, P.K. (corrected ed. 2002), K.G. Saur, Munich.
Jameson, M.H. and Runnels C.N., 1959, A Greek countryside: the southern Argolid from prehistory to present day. Stanford University Press, Stanford, California (repr. 1994).
Kern, O., 1922, Orphicorum Fragmenta, Weidmann. Berlin.
Macrobius, 1969, Saturnalia, trans. by Percival Vaughan Davies, Columbia University Press. New York.
Mariolakos, Elias (ed.), 2009, Geomythotopoi - Geomythological courses of Phthiotis, Publ. of the Local Union of Boroughs and Communes (TEDK) of Phthiotis Prefecture [in Greek].
McCarthy, D.J., 1978, Treaty and Covenant 2, Pontifical Biblical Institute, Rome.
Nagy, G., 1990, Greek Mythology and Poetics, Ithaca. London. Neoteron Encyclopedicon Lexicon Iliou, 1957, vol. 4, Ilios Publications, Athens [in Greek].
Nilsson, M.P., 1906, Griechische Feste von religiцser Bedeutung mit AusschluЯ der Attischen, B.G. Teubner, Leipzig.
Nonnus, Dionysiaca, 1940, Vol. I, Books 1-15, trans. by W.H.D. Rouse. The Loeb Classical Library No. 344. Heinemann. London.
Orphic Hymns, 1997, Ideotheatro Publications-R. Anastasakis, Athens [in Greek].
Ovid, 1857, The Metamorphoses, trans. by Nathan Covington Brooks, 5th ed., A.S. Barnes & Co., Cincinnati; H.W. Derby & Co., New York.
Pantermalis, D., 1995, "Ancient Greek mines", in Kathimerini, April 9, Athens [in Greek].
Patsi-Garin, E., 1969, Epitomo Lexikon Ellinikis Mythologias. Editions Hari Patsi, Athens [in Greek].
Pausanias, 1918, Description of Greece, Books I & II. Attica and Corinth, Edit. & trans. by W.H.S. Jones, The Loeb Classical Library, Heinemann. London.
Pausanias, Description of Greece, 1935, Vol. IV. Arcadia, Boeotia, Phocis and Ozolian Locri, Books 8.22-10, trans. by W.H.S. Jones. The Loeb Classical Library No. 297. Heinemann, London.
Pausanias, 1935, Description of Greece, Volume II (Laconia, Messenia, Elis 1) Books 3-5, trans. by W.H.S. Jones and H. A. Ormerod. The Loeb Classical Library No. 188. Heinemann, London.
Pindar, 1997, Nemean Odes, Isthmian Odes, Fragments. Edit. & trans. by W.H. Race, The Loeb Classical Library No. 485. Heinemann, London.
Pindar, Olympian Odes, trans. by T.K. Hubbard, via the Perseus Project at Tufts University.
Pindar, 1997, Olympian Odes, Pythian Odes. Edit. & trans. by W.H. Race, The Loeb Classical Library No. 56. Heinemann, London.

Pliny, 1971, Natural History (Historia Naturalis), trans. by H. Rackham, The Loeb Classical Library. Harvard University Press. Heinemann, London.
Proclus, 1820, The commentaries on the Timaeus of Plato, 5 Books. Edit. & trans. in English by Thomas Taylor, London.
Quintus Smyrnaeus, 1913, The Fall of Troy. Trans. by A.S. Way. The Loeb Classical Library Vol. 19. Heinemann, London.
Segal, C.P., 1992, "Divine Justice in the Odyssey: Poseidon, Cyclops and Helios", American Journal of Philology (AJP) 113, pp. 3-29.
Sophocles, 1994, Vol. I. Ajax. Electra. Oedipus Tyrannus. Edit. & trans. by W.H.S. Jones, The Loeb Classical Library No. 20. Harvard University Press. Heinemann, London.
Sophocles, 1994, Vol. II. Antigone. The women of Trachis. Philoctetes. Oedipus at Colonus. Edit. & trans. by W.H.S. Jones, The Loeb Classical Library No. 21. Harvard University Press. Heinemann, London.
Sophocles, 1892, Trachiniae, Ed. & trans. by R.C. Jebb, Cambridge University Press, Cambridge [on line: trachiniae.10.zip].
Spandagos, E., 2002, Catasterismoi of Eratosthenes of Cyrene, Aithra publ., Athens [in Greek].
The New Encycloaedia Britannica On line: http://www.britannica.com/, entry: matriarchy.
Theodossiou, E., 2007, The dethronement of the Earth - The dispute between geocentric and heliocentric systems, Diavlos Publ., Athens [in Greek].
Theodossiou, E. and Danezis, E., 1995, The Odyssey of the Calendars - vol. I: Searching for the roots of Knowledge, Diavlos Publ., Athens [in Greek].
West, M.L., 1997, The East face of the Helicon: West Asiatic Elements in Greek Poetry and Myth. Clarendon Press. Oxford.

Bull. Astron. Belgrade № 153 (1996), 89 – 100

UDC 52–355.3
Preliminary report

STARK BROADENING PARAMETER TABLES FOR Sr I

M. S. Dimitrijević[1] and S. Sahal–Bréchot[2]

[1] *Astronomical Observatory, Volgina 7, 11050 Belgrade, Yugoslavia*

[2] *Laboratoire "Astrophysique, Atomes et Molécules"*
Département Atomes et Molécules en Astrophysique
Unité associée au C.N.R.S. No 812
Observatoire de Paris–Meudon, 92190 Meudon, France

(Received: February 15, 1996)

SUMMARY: Using a semiclassical approach, we have calculated electron–, proton–, and ionized helium–impact line widths and shifts for 33 Sr I multiplets as a function of temperature and perturber density.

1. INTRODUCTION

Strontium lines are present in solar and stellar spectra (see e.g. Komarov and Basak, 1993). They are also of interest since Sr is one of thermonuclear s - processes product in stars and its overabundance is observed in metal deficient barium stars (Šleivyté and Bartkevičius, 1995). In order to provide to astrophysicists the needed Stark broadening data, we have calculated within the semiclassical-perturbation formalism (Sahal–Bréchot, 1969ab) electron-, proton-, and ionized helium-impact line widths and shifts for 33 Sr I multiplets.

2. RESULTS AND DISCUSSION

We will publish elsewhere the analysis of obtained results and all details of calculations (Dimitrijević and Sahal–Bréchot, 1996). Here, we present only tables of Stark broadening parameters for astrophysical and laboratory plasma diagnostic purposes. Our results for 33 Sr I multiplets are shown in Table 1, for perturber densities 10^{13} cm^{-3} (for stellar plasma research) and 10^{15}– 10^{18} cm^{-3} (for laboratory plasma research) and temperatures T = 2,500 – 50,000 K. We also specify a parameter c (Dimitrijević and Sahal–Bréchot 1984), which gives an estimate

Table 1. This table shows electron-, proton-, and He II- impact broadening parameters for Sr I, for perturber densities of 10^{13} cm^{-3} and 10^{15}– 10^{18} cm^{-3} and temperatures from 2,500 up to 50,000 K. Transitions and averaged wavelengths for the multiplet (in Å) are also given. By using c [see Eq. (5) in Dimitrijević et *al.*, 1991], we obtain an estimate for the maximum perturber density for which the line may be treated as isolated and tabulated data may be used. The asterisk identifies cases for which the collision volume multiplied by the perturber density (the condition for validity of the impact approximation) lies between 0.1 and 0.5.

PERTURBER DENSITY= 1.E+13cm-3

PERTURBERS ARE:		ELECTRONS		PROTONS		IONIZED HELIUM	
TRANSITION	T(K)	WIDTH(Å)	SHIFT(Å)	WIDTH(Å)	SHIFT(Å)	WIDTH(Å)	SHIFT(Å)
7S - 7P	2500.	2.23	-1.41	0.440	-0.357	0.376	-0.284
216052.7Å	5000.	2.62	-1.39	0.481	-0.402	0.407	-0.321
C= 0.22E+19	10000.	3.03	-1.09	0.530	-0.453	0.442	-0.361
	20000.	3.61	-0.854	0.587	-0.509	0.484	-0.407
	30000.	3.85	-0.706	0.626	-0.545	0.511	-0.436
	50000.	4.00	-0.532	0.681	-0.594	0.548	-0.475
5P - 8S	2500.	0.450E-02	0.325E-02	0.988E-03	0.905E-03	0.789E-03	0.718E-03
5166.9Å	5000.	0.462E-02	0.302E-02	0.111E-02	0.103E-02	0.885E-03	0.818E-03
C= 0.32E+15	10000.	0.472E-02	0.238E-02	0.125E-02	0.116E-02	0.994E-03	0.928E-03
	20000.	0.466E-02	0.180E-02	0.142E-02	0.131E-02	0.112E-02	0.105E-02
	30000.	0.450E-02	0.142E-02	0.152E-02	0.141E-02	0.119E-02	0.112E-02
	50000.	0.427E-02	0.977E-03	0.168E-02	0.153E-02	0.130E-02	0.122E-02
6P - 8S	2500.	0.349E-01	0.244E-01	0.759E-02	0.695E-02	0.606E-02	0.551E-02
14380.1Å	5000.	0.363E-01	0.215E-01	0.854E-02	0.789E-02	0.680E-02	0.628E-02
C= 0.25E+16	10000.	0.378E-01	0.157E-01	0.961E-02	0.894E-02	0.764E-02	0.712E-02
	20000.	0.380E-01	0.111E-01	0.109E-01	0.101E-01	0.857E-02	0.803E-02
	30000.	0.369E-01	0.868E-02	0.117E-01	0.108E-01	0.917E-02	0.861E-02
	50000.	0.352E-01	0.524E-02	0.129E-01	0.118E-01	0.999E-02	0.940E-02
7P - 8S	2500.	0.378	0.259	0.805E-01	0.732E-01	0.646E-01	0.581E-01
46607.0Å	5000.	0.399	0.234	0.905E-01	0.832E-01	0.723E-01	0.662E-01
C= 0.26E+17	10000.	0.425	0.172	0.102	0.942E-01	0.810E-01	0.750E-01
	20000.	0.445	0.111	0.115	0.106	0.908E-01	0.846E-01
	30000.	0.441	0.866E-01	0.124	0.114	0.971E-01	0.908E-01
	50000.	0.429	0.465E-01	0.137	0.124	0.106	0.990E-01
5P - 6D	2500.	0.123E-02	-0.696E-03	0.283E-03	-0.231E-03	0.241E-03	-0.184E-03
5544.9Å	5000.	0.129E-02	-0.549E-03	0.311E-03	-0.260E-03	0.261E-03	-0.208E-03
C= 0.60E+15	10000.	0.141E-02	-0.356E-03	0.343E-03	-0.293E-03	0.284E-03	-0.234E-03
	20000.	0.150E-02	-0.207E-03	0.383E-03	-0.330E-03	0.311E-03	-0.264E-03
	30000.	0.154E-02	-0.130E-03	0.410E-03	-0.353E-03	0.329E-03	-0.282E-03
	50000.	0.158E-02	-0.672E-04	0.451E-03	-0.385E-03	0.353E-03	-0.308E-03
5P - 7D	2500.	0.124E-02	-0.632E-03	0.351E-03	-0.200E-03	0.330E-03	-0.159E-03
4966.9Å	5000.	0.142E-02	-0.506E-03	0.366E-03	-0.225E-03	0.340E-03	-0.180E-03
C= 0.77E+15	10000.	0.176E-02	-0.323E-03	0.386E-03	-0.254E-03	0.352E-03	-0.203E-03
	20000.	0.213E-02	-0.184E-03	0.411E-03	-0.285E-03	0.367E-03	-0.228E-03
	30000.	0.231E-02	-0.119E-03	0.428E-03	-0.306E-03	0.378E-03	-0.244E-03
	50000.	0.252E-02	-0.395E-04	0.454E-03	-0.333E-03	0.393E-03	-0.266E-03
5P - 8D	2500.	0.236E-02	-0.973E-03	0.645E-03	-0.364E-03	0.607E-03	-0.289E-03
4689.9Å	5000.	0.295E-02	-0.636E-03	0.673E-03	-0.412E-03	0.625E-03	-0.328E-03
C= 0.40E+15	10000.	0.372E-02	-0.387E-03	0.708E-03	-0.465E-03	0.647E-03	-0.371E-03
	20000.	0.440E-02	-0.169E-03	0.750E-03	-0.523E-03	0.675E-03	-0.418E-03
	30000.	0.477E-02	-0.772E-04	0.779E-03	-0.560E-03	0.695E-03	-0.448E-03
	50000.	0.510E-02	0.247E-04	0.821E-03	-0.611E-03	0.723E-03	-0.488E-03
6P - 6D	2500.	0.147E-01	-0.844E-02	0.316E-02	-0.258E-02	0.269E-02	-0.205E-02
17747.3Å	5000.	0.159E-01	-0.743E-02	0.347E-02	-0.290E-02	0.292E-02	-0.232E-02
C= 0.61E+16	10000.	0.172E-01	-0.522E-02	0.383E-02	-0.327E-02	0.317E-02	-0.261E-02
	20000.	0.187E-01	-0.348E-02	0.427E-02	-0.368E-02	0.348E-02	-0.294E-02
	30000.	0.191E-01	-0.230E-02	0.458E-02	-0.394E-02	0.367E-02	-0.315E-02
	50000.	0.195E-01	-0.141E-02	0.504E-02	-0.429E-02	0.394E-02	-0.343E-02

PERTURBER DENSITY= 1.E+13cm-3

PERTURBERS ARE:		ELECTRONS		PROTONS		IONIZED HELIUM	
TRANSITION	T(K)	WIDTH(Å)	SHIFT(Å)	WIDTH(Å)	SHIFT(Å)	WIDTH(Å)	SHIFT(Å)
6P - 7D	2500.	0.937E-02	-0.517E-02	0.249E-02	-0.146E-02	0.232E-02	-0.116E-02
12931.2Å	5000.	0.109E-01	-0.427E-02	0.260E-02	-0.165E-02	0.240E-02	-0.132E-02
C= 0.52E+16	10000.	0.133E-01	-0.280E-02	0.275E-02	-0.186E-02	0.249E-02	-0.148E-02
	20000.	0.161E-01	-0.175E-02	0.294E-02	-0.209E-02	0.261E-02	-0.167E-02
	30000.	0.174E-01	-0.120E-02	0.307E-02	-0.224E-02	0.269E-02	-0.179E-02
	50000.	0.188E-01	-0.582E-03	0.327E-02	-0.244E-02	0.281E-02	-0.195E-02
6P - 8D	2500.	0.141E-01	-0.593E-02	0.375E-02	-0.213E-02	0.351E-02	-0.170E-02
11207.7Å	5000.	0.176E-01	-0.379E-02	0.391E-02	-0.242E-02	0.362E-02	-0.193E-02
C= 0.23E+16	10000.	0.222E-01	-0.247E-02	0.412E-02	-0.273E-02	0.376E-02	-0.218E-02
	20000.	0.263E-01	-0.691E-03	0.437E-02	-0.307E-02	0.392E-02	-0.245E-02
	30000.	0.285E-01	-0.206E-03	0.454E-02	-0.329E-02	0.404E-02	-0.263E-02
	50000.	0.304E-01	0.392E-03	0.479E-02	-0.358E-02	0.421E-02	-0.286E-02
7P - 7D	2500.	0.754E-01	-0.357E-01	0.185E-01	-0.994E-02	0.176E-01	-0.791E-02
34190.4Å	5000.	0.907E-01	-0.340E-01	0.192E-01	-0.112E-01	0.180E-01	-0.896E-02
C= 0.37E+17	10000.	0.112	-0.253E-01	0.202E-01	-0.126E-01	0.186E-01	-0.101E-01
	20000.	0.137	-0.196E-01	0.213E-01	-0.142E-01	0.193E-01	-0.114E-01
	30000.	0.150	-0.156E-01	0.222E-01	-0.152E-01	0.198E-01	-0.122E-01
	50000.	0.162	-0.108E-01	0.235E-01	-0.166E-01	0.205E-01	-0.133E-01
7P - 8D	2500.	0.704E-01	-0.280E-01	0.180E-01	-0.994E-02	0.170E-01	-0.790E-02
24307.2Å	5000.	0.888E-01	-0.202E-01	0.188E-01	-0.113E-01	0.175E-01	-0.897E-02
C= 0.11E+17	10000.	0.113	-0.153E-01	0.197E-01	-0.127E-01	0.181E-01	-0.101E-01
	20000.	0.136	-0.798E-02	0.208E-01	-0.143E-01	0.188E-01	-0.114E-01
	30000.	0.148	-0.549E-02	0.216E-01	-0.153E-01	0.193E-01	-0.122E-01
	50000.	0.158	-0.147E-02	0.228E-01	-0.167E-01	0.201E-01	-0.133E-01
5D - 6P	2500.	0.420	0.245	0.880E-01	0.667E-01	0.773E-01	0.532E-01
158972.4Å	5000.	0.460	0.236	0.952E-01	0.751E-01	0.823E-01	0.599E-01
C= 0.16E+19	10000.	0.489	0.175	0.104	0.844E-01	0.884E-01	0.674E-01
	20000.	0.531	0.136	0.114	0.949E-01	0.955E-01	0.758E-01
	30000.	0.540	0.114	0.121	0.102	0.100	0.812E-01
	50000.	0.540	0.834E-01	0.132	0.111	0.107	0.884E-01
6D - 7P	2500.	0.834	0.410	0.161	0.116	0.143	0.926E-01
121034.6Å	5000.	0.946	0.378	0.174	0.131	0.152	0.105
C= 0.28E+18	10000.	1.06	0.316	0.189	0.148	0.162	0.118
	20000.	1.19	0.225	0.207	0.166	0.174	0.133
	30000.	1.26	0.195	0.220	0.178	0.182	0.142
	50000.	1.31	0.155	0.241	0.194	0.193	0.155
6P - 5D	2500.	0.956E-01	-0.577E-01	0.232E-01	-0.146E-01	0.214E-01	-0.116E-01
90508.4Å	5000.	0.106	-0.542E-01	0.244E-01	-0.164E-01	0.222E-01	-0.131E-01
C= 0.91E+18	10000.	0.118	-0.478E-01	0.259E-01	-0.184E-01	0.233E-01	-0.147E-01
	20000.	0.136	-0.350E-01	0.278E-01	-0.207E-01	0.245E-01	-0.166E-01
	30000.	0.148	-0.298E-01	0.291E-01	-0.222E-01	0.254E-01	-0.177E-01
	50000.	0.156	-0.253E-01	0.309E-01	-0.241E-01	0.266E-01	-0.193E-01
4D - 7P	2500.	0.113E-02	0.818E-03	0.269E-03	0.222E-03	0.227E-03	0.177E-03
4719.6Å	5000.	0.119E-02	0.794E-03	0.295E-03	0.251E-03	0.247E-03	0.200E-03
C= 0.56E+15	10000.	0.125E-02	0.675E-03	0.326E-03	0.283E-03	0.270E-03	0.226E-03
	20000.	0.130E-02	0.515E-03	0.363E-03	0.318E-03	0.296E-03	0.254E-03
	30000.	0.130E-02	0.421E-03	0.387E-03	0.341E-03	0.314E-03	0.272E-03
	50000.	0.128E-02	0.311E-03	0.423E-03	0.371E-03	0.337E-03	0.297E-03
5D - 7P	2500.	0.279E-01	0.190E-01	0.631E-02	0.518E-02	0.536E-02	0.412E-02
22664.1Å	5000.	0.298E-01	0.183E-01	0.692E-02	0.585E-02	0.581E-02	0.467E-02
C= 0.13E+17	10000.	0.316E-01	0.156E-01	0.764E-02	0.659E-02	0.634E-02	0.526E-02
	20000.	0.331E-01	0.114E-01	0.849E-02	0.741E-02	0.695E-02	0.592E-02
	30000.	0.336E-01	0.924E-02	0.906E-02	0.794E-02	0.735E-02	0.634E-02
	50000.	0.337E-01	0.689E-02	0.990E-02	0.865E-02	0.790E-02	0.691E-02

PERTURBER DENSITY= 1.E+15cm-3

PERTURBERS ARE:		ELECTRONS		PROTONS		IONIZED HELIUM	
TRANSITION	T(K)	WIDTH(Å)	SHIFT(Å)	WIDTH(Å)	SHIFT(Å)	WIDTH(Å)	SHIFT(Å)
5S - 5P	2500.	0.227E-02	0.326E-04	0.780E-03	-0.119E-03	0.778E-03	-0.944E-04
4608.6Å	5000.	0.229E-02	0.267E-03	0.782E-03	-0.133E-03	0.779E-03	-0.107E-03
C= 0.33E+18	10000.	0.236E-02	0.419E-03	0.785E-03	-0.150E-03	0.780E-03	-0.120E-03
	20000.	0.258E-02	0.504E-03	0.791E-03	-0.175E-03	0.781E-03	-0.135E-03
	30000.	0.279E-02	0.430E-03	0.797E-03	-0.181E-03	0.781E-03	-0.145E-03
	50000.	0.316E-02	0.337E-03	0.809E-03	-0.197E-03	0.782E-03	-0.158E-03
5S - 6P	2500.	0.828E-02	0.623E-02	0.228E-02	0.160E-02	0.200E-02	0.125E-02
2932.7Å	5000.	0.901E-02	0.608E-02	0.246E-02	0.185E-02	0.213E-02	0.146E-02
C= 0.54E+17	10000.	0.983E-02	0.473E-02	0.268E-02	0.211E-02	0.229E-02	0.168E-02
	20000.	0.108E-01	0.365E-02	0.294E-02	0.240E-02	0.247E-02	0.191E-02
	30000.	0.111E-01	0.316E-02	0.311E-02	0.258E-02	0.259E-02	0.206E-02
	50000.	0.112E-01	0.238E-02	0.337E-02	0.282E-02	0.276E-02	0.225E-02
5S - 7P	2500.	0.146E-01	0.421E-02	0.350E-02	0.921E-03	*0.345E-02	*0.724E-03
2570.2Å	5000.	0.183E-01	0.573E-02	0.354E-02	0.106E-02	0.349E-02	0.839E-03
C= 0.31E+17	10000.	0.220E-01	0.673E-02	0.358E-02	0.121E-02	0.351E-02	0.960E-03
	20000.	0.252E-01	0.667E-02	0.365E-02	0.137E-02	0.354E-02	0.109E-02
	30000.	0.268E-01	0.603E-02	0.370E-02	0.148E-02	0.356E-02	0.117E-02
	50000.	0.283E-01	0.515E-02	0.378E-02	0.161E-02	0.359E-02	0.128E-02
6S - 6P	2500.	0.750	0.417	0.193	0.127	0.174	0.995E-01
28517.3Å	5000.	0.896	0.280	0.207	0.146	0.183	0.116
C= 0.51E+19	10000.	1.12	0.148	0.223	0.167	0.194	0.132
	20000.	1.28	0.592E-01	0.243	0.189	0.208	0.151
	30000.	1.35	0.625E-02	0.256	0.204	0.216	0.162
	50000.	1.42	-0.203E-01	0.276	0.222	0.229	0.178
6S - 7P	2500.	0.312	0.810E-01	0.758E-01	0.149E-01	*0.751E-01	*0.117E-01
12026.3Å	5000.	0.393	0.105	0.764E-01	0.171E-01	0.758E-01	0.135E-01
C= 0.67E+18	10000.	0.482	0.118	0.770E-01	0.194E-01	0.762E-01	0.154E-01
	20000.	0.572	0.974E-01	0.778E-01	0.220E-01	0.765E-01	0.175E-01
	30000.	0.623	0.910E-01	0.786E-01	0.237E-01	0.766E-01	0.188E-01
	50000.	0.672	0.876E-01	0.799E-01	0.262E-01	0.769E-01	0.205E-01
5P - 6S	2500.	0.538E-01	0.355E-01	0.113E-01	0.948E-02	0.935E-02	0.749E-02
11244.4Å	5000.	0.608E-01	0.423E-01	0.125E-01	0.108E-01	0.103E-01	0.860E-02
C= 0.20E+19	10000.	0.663E-01	0.486E-01	0.139E-01	0.123E-01	0.114E-01	0.979E-02
	20000.	0.707E-01	0.491E-01	0.155E-01	0.139E-01	0.126E-01	0.111E-01
	30000.	0.734E-01	0.452E-01	0.165E-01	0.149E-01	0.134E-01	0.119E-01
	50000.	0.790E-01	0.375E-01	0.179E-01	0.163E-01	0.144E-01	0.130E-01
5P - 7S	2500.	0.149	0.107	*0.308E-01	*0.247E-01	*0.246E-01	*0.189E-01
5971.7Å	5000.	0.161	0.118	0.346E-01	0.296E-01	*0.276E-01	*0.230E-01
C= 0.17E+18	10000.	0.166	0.114	0.389E-01	0.345E-01	*0.310E-01	*0.272E-01
	20000.	0.170	0.969E-01	0.438E-01	0.397E-01	0.348E-01	0.314E-01
	30000.	0.172	0.828E-01	0.470E-01	0.428E-01	0.373E-01	0.340E-01
	50000.	0.172	0.666E-01	0.515E-01	0.471E-01	0.406E-01	0.374E-01
5P - 8S	2500.	0.450	0.299				
5166.9Å	5000.	0.462	0.287				
C= 0.32E+17	10000.	0.472	0.236	*0.125	*0.103		
	20000.	0.466	0.179	*0.141	*0.122		
	30000.	0.450	0.142	*0.152	*0.133		
	50000.	0.427	0.977E-01	*0.168	*0.147	*0.130	*0.117
6P - 7S	2500.	2.23	1.45	0.427	0.339	*0.344	*0.260
23011.7Å	5000.	2.55	1.56	0.478	0.405	*0.385	*0.316
C= 0.25E+19	10000.	2.79	1.51	0.536	0.471	0.430	0.371
	20000.	3.00	1.28	0.603	0.541	0.481	0.428
	30000.	3.09	1.11	0.647	0.584	0.514	0.464
	50000.	3.12	0.900	0.710	0.641	0.558	0.510

PERTURBER DENSITY= 1.E+15cm-3

PERTURBERS ARE:		ELECTRONS		PROTONS		IONIZED HELIUM	
TRANSITION	T(K)	WIDTH(Å)	SHIFT(Å)	WIDTH(Å)	SHIFT(Å)	WIDTH(Å)	SHIFT(Å)
6P - 8S	2500.	3.49	2.27				
14380.1Å	5000.	3.63	2.08				
C= 0.25E+18	10000.	3.78	1.56	*0.961	*0.792		
	20000.	3.80	1.10	* 1.09	*0.935		
	30000.	3.69	0.861	* 1.17	* 1.02		
	50000.	3.52	0.524	* 1.29	* 1.13	*0.998	*0.895
5P - 5D	2500.	0.498E-01	-0.233E-01	0.107E-01	-0.717E-02	0.958E-02	-0.564E-02
7675.2Å	5000.	0.516E-01	-0.162E-01	0.115E-01	-0.824E-02	0.101E-01	-0.652E-02
C= 0.37E+18	10000.	0.564E-01	-0.988E-02	0.124E-01	-0.939E-02	0.107E-01	-0.746E-02
	20000.	0.582E-01	-0.530E-02	0.135E-01	-0.106E-01	0.115E-01	-0.847E-02
	30000.	0.590E-01	-0.366E-02	0.143E-01	-0.114E-01	0.120E-01	-0.911E-02
	50000.	0.600E-01	-0.242E-02	0.155E-01	-0.125E-01	0.127E-01	-0.996E-02
5P - 6D	2500.	0.123	-0.666E-01	*0.282E-01	-0.200E-01	*0.239E-01	-0.153E-01
5544.9Å	5000.	0.129	-0.531E-01	0.310E-01	-0.239E-01	*0.260E-01	-0.186E-01
C= 0.60E+17	10000.	0.141	-0.350E-01	0.343E-01	-0.278E-01	*0.284E-01	-0.219E-01
	20000.	0.150	-0.206E-01	0.383E-01	-0.319E-01	0.311E-01	-0.253E-01
	30000.	0.154	-0.129E-01	0.410E-01	-0.344E-01	0.329E-01	-0.273E-01
	50000.	0.158	-0.668E-02	0.451E-01	-0.378E-01	0.353E-01	-0.301E-01
5P - 7D	2500.	0.124	-0.605E-01	*0.347E-01	-0.172E-01		
4966.9Å	5000.	0.142	-0.490E-01	*0.365E-01	-0.206E-01	*0.337E-01	-0.160E-01
C= 0.77E+17	10000.	0.176	-0.317E-01	0.385E-01	-0.240E-01	*0.351E-01	-0.189E-01
	20000.	0.213	-0.183E-01	0.410E-01	-0.276E-01	*0.367E-01	-0.218E-01
	30000.	0.231	-0.118E-01	0.428E-01	-0.298E-01	*0.378E-01	-0.236E-01
	50000.	0.252	-0.390E-02	0.454E-01	-0.327E-01	0.393E-01	-0.260E-01
5P - 8D	2500.	0.236	-0.910E-01				
4689.9Å	5000.	0.295	-0.594E-01	*0.667E-01	-0.360E-01		
C= 0.40E+17	10000.	0.372	-0.382E-01	*0.706E-01	-0.428E-01		
	20000.	0.440	-0.166E-01	*0.749E-01	-0.497E-01	*0.674E-01	-0.392E-01
	30000.	0.477	-0.750E-02	*0.778E-01	-0.539E-01	*0.694E-01	-0.427E-01
	50000.	0.510	0.247E-02	0.820E-01	-0.595E-01	*0.722E-01	-0.472E-01
6P - 6D	2500.	1.47	-0.809	*0.315	-0.221	*0.267	-0.169
17747.3Å	5000.	1.59	-0.721	0.347	-0.265	*0.291	-0.206
C= 0.61E+18	10000.	1.72	-0.511	0.383	-0.309	*0.317	-0.243
	20000.	1.87	-0.345	0.427	-0.355	0.347	-0.281
	30000.	1.91	-0.229	0.458	-0.384	0.367	-0.304
	50000.	1.95	-0.140	0.504	-0.421	0.394	-0.335
6P - 7D	2500.	0.937	-0.497	*0.245	-0.125		
12931.2Å	5000.	1.09	-0.415	*0.259	-0.150	*0.238	- 0.117
C= 0.52E+18	10000.	1.33	-0.275	0.275	-0.175	*0.248	-0.138
	20000.	1.61	-0.175	0.294	-0.201	*0.261	-0.159
	30000.	1.74	-0.119	0.307	-0.218	*0.269	-0.173
	50000.	1.88	-0.579E-01	0.327	- 0.239	0.281	-0.190
6P - 8D	2500.	1.41	-0.557				
11207.7Å	5000.	1.76	-0.363	*0.388	-0.211		
C= 0.23E+18	10000.	2.22	-0.237	*0.410	-0.251		
	20000.	2.63	-0.674E-01	*0.436	-0.292	*0.391	-0.230
	30000.	2.85	-0.193E-01	*0.454	-0.316	*0.403	-0.250
	50000.	3.04	0.399E-01	*0.479	-0.349	*0.420	- 0.277
7P - 7D	2500.	7.54	-3.50	* 1.82	-0.852		
34190.4Å	5000.	9.07	-3.36	* 1.91	-1.02	* 1.78	-0.795
C= 0.37E+19	10000.	11.2	-2.52	* 2.01	-1.19	* 1.85	-0.938
	20000.	13.7	-1.96	2.13	-1.37	* 1.92	-1.09
	30000.	15.0	-1.56	2.22	-1.48	* 1.97	-1.18
	50000.	16.2	-1.08	2.35	-1.63	2.05	-1.29

PERTURBER DENSITY= 1.E+15cm-3

PERTURBERS ARE:		ELECTRONS		PROTONS		IONIZED HELIUM	
TRANSITION	T(K)	WIDTH(Å)	SHIFT(Å)	WIDTH(Å)	SHIFT(Å)	WIDTH(Å)	SHIFT(Å)
7P - 8D	2500.	7.04	-2.63				
24307.2Å	5000.	8.88	-1.95	* 1.86	-0.983		
C= 0.11E+19	10000.	11.3	-1.51	* 1.96	-1.17		
	20000.	13.6	- 0.791	* 2.08	-1.36	* 1.88	-1.07
	30000.	14.8	- 0.549	* 2.16	-1.47	* 1.93	-1.17
	50000.	15.8	- 0.147	* 2.28	-1.62	* 2.01	-1.29
4D - 5P	2500.	0.535	-0.197E-01	0.161	-0.337E-01	0.160	-0.268E-01
64566.9Å	5000.	0.590	0.310E-01	0.162	-0.380E-01	0.161	-0.304E-01
C= 0.65E+20	10000.	0.637	0.970E-01	0.163	-0.428E-01	0.161	-0.342E-01
	20000.	0.669	0.154	0.166	-0.482E-01	0.161	-0.385E-01
	30000.	0.684	0.174	0.168	-0.516E-01	0.162	-0.412E-01
	50000.	0.702	0.179	0.173	-0.562E-01	0.162	-0.449E-01
4D - 6P	2500.	0.502E-01	0.371E-01	0.136E-01	0.954E-02	0.120E-01	0.747E-02
7169.1Å	5000.	0.551E-01	0.365E-01	0.147E-01	0.110E-01	0.128E-01	0.870E-02
C= 0.32E+18	10000.	0.603E-01	0.292E-01	0.160E-01	0.126E-01	0.137E-01	0.100E-01
	20000.	0.660E-01	0.234E-01	0.176E-01	0.143E-01	0.148E-01	0.114E-01
	30000.	0.673E-01	0.209E-01	0.186E-01	0.154E-01	0.155E-01	0.123E-01
	50000.	0.675E-01	0.160E-01	0.202E-01	0.168E-01	0.165E-01	0.134E-01
4D - 7P	2500.	0.631E-01	0.180E-01	0.151E-01	0.395E-02	*0.149E-01	*0.310E-02
5331.3Å	5000.	0.796E-01	0.244E-01	0.152E-01	0.454E-02	0.150E-01	0.360E-02
C= 0.13E+18	10000.	0.954E-01	0.287E-01	0.154E-01	0.518E-02	0.152E-01	0.412E-02
	20000.	0.109	0.288E-01	0.157E-01	0.588E-02	0.153E-01	0.468E-02
	30000.	0.116	0.281E-01	0.159E-01	0.632E-02	0.153E-01	0.503E-02
	50000.	0.122	0.242E-01	0.163E-01	0.691E-02	0.155E-01	0.551E-02
5D - 7P	2500.	1.63	0.531	0.330	0.117	*0.321	*0.916E-01
23926.8Å	5000.	1.99	0.680	0.337	0.136	0.327	0.107
C= 0.26E+19	10000.	2.33	0.675	0.345	0.155	0.332	0.123
	20000.	2.62	0.656	0.357	0.176	0.337	0.140
	30000.	2.77	0.588	0.366	0.190	0.341	0.151
	50000.	2.91	0.515	0.380	0.207	0.347	0.165
6D - 7P	2500.	83.4	39.6	* 16.0	* 10.0	* 14.1	* 7.66
121034.6Å	5000.	94.6	37.2	17.3	12.0	* 15.1	* 9.33
C= 0.28E+20	10000.	106.	31.4	18.8	14.0	* 16.1	* 11.0
	20000.	119.	22.4	20.7	16.1	17.4	12.7
	30000.	126.	19.5	22.0	17.3	18.2	13.8
	50000.	131.	15.5	24.1	19.0	19.3	15.1
5P - 4D	2500.	0.358E-01	-0.166E-01	0.172E-01	-0.461E-02	0.170E-01	-0.367E-02
28160.1Å	5000.	0.353E-01	-0.185E-01	0.173E-01	-0.519E-02	0.171E-01	-0.415E-02
C= 0.28E+20	10000.	0.364E-01	-0.204E-01	0.174E-01	-0.584E-02	0.172E-01	-0.466E-02
	20000.	0.382E-01	-0.217E-01	0.177E-01	-0.657E-02	0.173E-01	-0.525E-02
	30000.	0.395E-01	-0.216E-01	0.179E-01	-0.703E-02	0.174E-01	-0.562E-02
	50000.	0.415E-01	-0.205E-01	0.182E-01	-0.766E-02	0.175E-01	-0.613E-02
5P - 5D	2500.	0.130E-01	-0.392E-02	0.347E-02	-0.145E-02	0.336E-02	-0.115E-02
4919.5Å	5000.	0.152E-01	-0.178E-02	0.355E-02	-0.165E-02	0.341E-02	-0.131E-02
C= 0.27E+18	10000.	0.182E-01	0.304E-04	0.365E-02	-0.188E-02	0.347E-02	-0.149E-02
	20000.	0.204E-01	0.177E-02	0.379E-02	-0.212E-02	0.355E-02	-0.169E-02
	30000.	0.217E-01	0.263E-02	0.390E-02	-0.227E-02	0.361E-02	-0.181E-02
	50000.	0.230E-01	0.248E-02	0.407E-02	-0.248E-02	0.369E-02	-0.198E-02
6P - 5D	2500.	9.56	-5.69	2.31	-1.36	2.13	-1.07
90508.4Å	5000.	10.6	-5.36	2.44	-1.57	2.22	-1.24
C= 0.91E+20	10000.	11.8	-4.76	2.59	-1.80	2.32	-1.43
	20000.	13.6	-3.50	2.78	-2.04	0.45	-1.62
	30000.	14.8	-2.98	2.91	-2.19	2.54	-1.75
	50000.	15.6	-2.53	3.09	-2.40	2.66	-1.91

PERTURBER DENSITY= 1.E+15cm-3

PERTURBERS ARE: TRANSITION	T(K)	ELECTRONS WIDTH(Å)	ELECTRONS SHIFT(Å)	PROTONS WIDTH(Å)	PROTONS SHIFT(Å)	IONIZED HELIUM WIDTH(Å)	IONIZED HELIUM SHIFT(Å)
4D - 6P	2500.	0.322E-01	0.233E-01	0.917E-02	0.587E-02	0.830E-02	0.461E-02
6381.2Å	5000.	0.356E-01	0.258E-01	0.976E-02	0.676E-02	0.872E-02	0.535E-02
C= 0.45E+18	10000.	0.385E-01	0.255E-01	0.105E-01	0.771E-02	0.921E-02	0.612E-02
	20000.	0.416E-01	0.225E-01	0.113E-01	0.875E-02	0.980E-02	0.696E-02
	30000.	0.436E-01	0.203E-01	0.118E-01	0.941E-02	0.102E-01	0.749E-02
	50000.	0.455E-01	0.170E-01	0.126E-01	0.103E-01	0.108E-01	0.820E-02
4D - 7P	2500.	0.113	0.785E-01	*0.267E-01	*0.188E-01	*0.225E-01	*0.143E-01
4719.6Å	5000.	0.119	0.776E-01	*0.295E-01	*0.227E-01	*0.246E-01	*0.176E-01
C= 0.56E+17	10000.	0.125	0.668E-01	0.326E-01	0.266E-01	*0.270E-01	*0.209E-01
	20000.	0.130	0.514E-01	0.362E-01	0.306E-01	*0.296E-01	*0.242E-01
	30000.	0.130	0.420E-01	0.387E-01	0.331E-01	0.313E-01	0.262E-01
	50000.	0.128	0.310E-01	0.423E-01	0.364E-01	0.337E-01	0.289E-01
5D - 7P	2500.	2.79	1.83	*0.628	*0.437	*0.530	*0.332
22664.1Å	5000.	2.98	1.79	*0.691	*0.528	*0.579	*0.409
C= 0.13E+19	10000.	3.16	1.55	0.764	0.619	*0.633	*0.486
	20000.	3.31	1.14	0.849	0.713	*0.695	*0.564
	30000.	3.36	0.922	0.906	0.771	0.735	0.611
	50000.	3.37	0.689	0.990	0.847	0.790	0.673

PERTURBER DENSITY= 1.E+16cm-3

5S - 5P	2500.	0.227E-01	0.374E-03	0.777E-02	-0.115E-02	0.772E-02	-0.910E-03
4608.6Å	5000.	0.229E-01	0.269E-02	0.781E-02	-0.131E-02	0.777E-02	-0.104E-02
C= 0.33E+19	10000.	0.236E-01	0.419E-02	0.785E-02	-0.149E-02	0.779E-02	-0.118E-02
	20000.	0.258E-01	0.505E-02	0.791E-02	-0.174E-02	0.780E-02	-0.134E-02
	30000.	0.279E-01	0.430E-02	0.797E-02	-0.180E-02	0.781E-02	-0.144E-02
	50000.	0.316E-01	0.337E-02	0.808E-02	-0.196E-02	0.782E-02	-0.157E-02
5S - 6P	2500.	0.827E-01	0.595E-01	*0.225E-01	*0.132E-01	*0.194E-01	*0.972E-02
2932.7Å	5000.	0.901E-01	0.589E-01	*0.245E-01	*0.165E-01	*0.211E-01	*0.126E-01
C= 0.54E+18	10000.	0.983E-01	0.462E-01	0.267E-01	0.197E-01	*0.228E-01	*0.154E-01
	20000.	0.108	0.362E-01	0.294E-01	0.230E-01	*0.247E-01	*0.181E-01
	30000.	0.111	0.316E-01	0.311E-01	0.250E-01	0.259E-01	0.197E-01
	50000.	0.112	0.238E-01	0.337E-01	0.276E-01	0.276E-01	0.219E-01
5S - 7P	2500.	0.146	0.407E-01	*0.331E-01	*0.783E-02		
2570.2Å	5000.	0.183	0.564E-01	*0.347E-01	*0.963E-02		
C= 0.31E+18	10000.	0.220	0.667E-01	*0.356E-01	*0.114E-01	*0.347E-01	*0.891E-02
	20000.	0.252	0.666E-01	*0.364E-01	*0.132E-01	*0.352E-01	*0.104E-01
	30000.	0.268	0.603E-01	0.369E-01	0.143E-01	*0.355E-01	*0.113E-01
	50000.	0.283	0.515E-01	0.378E-01	0.158E-01	*0.358E-01	*0.125E-01
6S - 6P	2500.	7.50	3.98	* 1.91	* 1.07	* 1.68	*0.794
28517.3Å	5000.	8.96	2.66	2.06	1.32	* 1.81	* 1.01
C= 0.51E+20	10000.	11.2	1.40	2.23	1.57	* 1.94	* 1.22
	20000.	12.8	0.552	2.42	1.82	2.07	1.44
	30000.	13.5	0.550E-01	2.56	1.97	2.16	1.56
	50000.	14.2	-0.209	2.76	2.18	2.29	1.73
6S - 7P	2500.	3.12	0.789	*0.716	*0.130		
12026.3Å	5000.	3.93	1.04	*0.749	*0.157		
C= 0.67E+19	10000.	4.82	1.18	*0.765	*0.185	*0.752	*0.145
	20000.	5.72	0.973	*0.776	*0.213	*0.761	*0.168
	30000.	6.23	0.910	0.785	0.231	*0.764	*0.182
	50000.	6.72	0.876	0.798	0.257	*0.768	*0.201
5P - 6S	2500.	0.538	0.344	0.113	0.847E-01	0.931E-01	0.648E-01
11244.4Å	5000.	0.608	0.416	0.125	0.101	0.103	0.788E-01
C= 0.20E+20	10000.	0.663	0.484	0.139	0.118	0.113	0.928E-01
	20000.	0.707	0.491	0.155	0.135	0.126	0.107
	30000.	0.734	0.452	0.165	0.146	0.133	0.116
	50000.	0.790	0.375	0.179	0.161	0.144	0.128

PERTURBER DENSITY= 1.E+16cm-3

PERTURBERS ARE: TRANSITION	T(K)	ELECTRONS WIDTH(Å)	ELECTRONS SHIFT(Å)	PROTONS WIDTH(Å)	PROTONS SHIFT(Å)	IONIZED HELIUM WIDTH(Å)	IONIZED HELIUM SHIFT(Å)
5P - 7S	2500.	1.49	0.970				
5971.7Å	5000.	1.61	1.11				
C= 0.17E+19	10000.	1.66	1.10				
	20000.	1.70	0.960	*0.438	*0.363		
	30000.	1.72	0.825	*0.470	*0.401		
	50000.	1.72	0.663	*0.515	*0.449	*0.406	*0.353
5P - 8S	2500.	* 4.40	* 2.30				
5166.9Å	5000.	* 4.55	* 2.38				
C= 0.32E+18	10000.	* 4.67	* 2.10				
	20000.	4.63	1.71				
	30000.	4.47	1.39				
	50000.	4.25	0.977				
5P - 5D	2500.	0.497	-0.223	0.106	-0.618E-01	*0.936E-01	-0.465E-01
7675.2Å	5000.	0.516	-0.155	0.114	-0.754E-01	*0.100	-0.582E-01
C= 0.37E+19	10000.	0.564	-0.954E-01	0.124	-0.889E-01	0.107	-0.696E-01
	20000.	0.582	-0.526E-01	0.135	-0.103	0.115	-0.812E-01
	30000.	0.590	-0.363E-01	0.143	-0.111	0.120	-0.881E-01
	50000.	0.600	-0.239E-01	0.155	-0.122	0.127	-0.973E-01
5P - 6D	2500.	1.22	-0.589				
5544.9Å	5000.	1.29	-0.480				
C= 0.60E+18	10000.	1.41	-0.330				
	20000.	1.50	-0.202	*0.382	-0.293		
	30000.	1.54	-0.126	*0.410	-0.323		
	50000.	1.57	-0.646E-01	*0.451	-0.361	*0.353	-0.284
5P - 7D	2500.	1.24	-0.537				
4966.9Å	5000.	1.42	-0.444				
C= 0.77E+18	10000.	1.76	-0.292				
	20000.	2.13	-0.180				
	30000.	2.31	-0.115	*0.427	-0.278		
	50000.	2.52	-0.371E-01	*0.454	-0.312		
5P - 8D	2500.	* 2.34	-0.717				
4689.9Å	5000.	* 2.94	-0.461				
C= 0.40E+18	10000.	* 3.71	-0.314				
	20000.	4.40	-0.146				
	30000.	4.76	-0.684E-01				
	50000.	5.10	0.247E-01				
6P - 6D	2500.	14.7	-7.20				
17747.3Å	5000.	15.9	-6.60				
C= 0.61E+19	10000.	17.2	-4.74				
	20000.	18.7	-3.29	* 4.27	-3.25		
	30000.	19.1	-2.26	* 4.57	-3.59		
	50000.	19.5	-1.38	* 5.03	-4.02		
6P - 7D	2500.	9.36	-4.48				
12931.2Å	5000.	10.9	-3.85				
C= 0.52E+19	10000.	13.3	-2.62				
	20000.	16.1	-1.72				
	30000.	17.4	-1.18				
	50000.	18.8	-0.565	* 3.26	-2.28		
4D - 5P	2500.	5.35	-0.182	1.60	-0.326	1.59	-0.257
64566.9Å	5000.	5.90	0.318	1.62	-0.372	1.60	-0.295
C= 0.65E+21	10000.	6.37	0.975	1.63	-0.423	1.61	-0.336
	20000.	6.69	1.55	1.66	-0.479	1.61	-0.381
	30000.	6.84	1.74	1.68	-0.513	1.62	-0.409
	50000.	7.02	1.79	1.73	-0.559	1.62	-0.447

PERTURBER DENSITY= 1.E+16cm-3

PERTURBERS ARE:		ELECTRONS		PROTONS		IONIZED HELIUM	
TRANSITION	T(K)	WIDTH(Å)	SHIFT(Å)	WIDTH(Å)	SHIFT(Å)	WIDTH(Å)	SHIFT(Å)
4D - 6P	2500.	0.502	0.355	*0.134	*0.787E-01	*0.116	*0.580E-01
7169.1Å	5000.	0.551	0.354	*0.146	*0.984E-01	*0.126	*0.752E-01
C= 0.32E+19	10000.	0.603	0.286	0.160	0.118	*0.136	*0.916E-01
	20000.	0.660	0.232	0.176	0.137	*0.148	*0.108
	30000.	0.673	0.209	0.186	0.149	0.155	0.118
	50000.	0.675	0.160	0.202	0.164	0.165	0.130
4D - 7P	2500.	0.631	0.174	*0.143	*0.336E-01		
5331.3Å	5000.	0.796	0.240	*0.150	*0.413E-01		
C= 0.13E+19	10000.	0.954	0.285	*0.153	*0.489E-01	*0.149	*0.382E-01
	20000.	1.09	0.287	*0.157	*0.567E-01	*0.152	*0.447E-01
	30000.	1.16	0.280	0.159	0.614E-01	*0.153	*0.486E-01
	50000.	1.22	0.242	0.163	0.678E-01	*0.154	*0.537E-01
5P - 4D	2500.	0.358	-0.165	0.171	-0.447E-01	0.170	-0.354E-01
28160.1Å	5000.	0.353	-0.184	0.173	-0.510E-01	0.171	-0.405E-01
C= 0.28E+21	10000.	0.364	-0.203	0.174	-0.578E-01	0.172	-0.460E-01
	20000.	0.382	-0.217	0.177	-0.653E-01	0.173	-0.521E-01
	30000.	0.395	-0.216	0.179	-0.700E-01	0.174	-0.558E-01
	50000.	0.415	-0.205	0.182	-0.764E-01	0.175	-0.610E-01
5P - 5D	2500.	0.130	-0.388E-01	0.342E-01	-0.131E-01	*0.327E-01	-0.101E-01
4919.5Å	5000.	0.152	-0.171E-01	0.353E-01	-0.156E-01	*0.338E-01	-0.122E-01
C= 0.27E+19	10000.	0.182	0.790E-03	0.364E-01	-0.181E-01	0.346E-01	-0.142E-01
	20000.	0.204	0.179E-01	0.379E-01	-0.207E-01	0.355E-01	-0.164E-01
	30000.	0.217	0.263E-01	0.390E-01	-0.223E-01	0.360E-01	-0.177E-01
	50000.	0.230	0.248E-01	0.407E-01	-0.245E-01	0.369E-01	-0.195E-01
4D - 6P	2500.	0.322	0.224	*0.904E-01	*0.498E-01	*0.805E-01	*0.372E-01
6381.2Å	5000.	0.356	0.251	0.971E-01	0.613E-01	*0.863E-01	*0.472E-01
C= 0.45E+19	10000.	0.385	0.251	0.104	0.727E-01	*0.918E-01	*0.568E-01
	20000.	0.416	0.223	0.113	0.843E-01	0.979E-01	0.664E-01
	30000.	0.436	0.203	0.118	0.913E-01	0.102	0.723E-01
	50000.	0.455	0.170	0.126	0.101	0.108	0.799E-01
4D - 7P	2500.	1.13	0.700				
4719.6Å	5000.	1.19	0.717				
C= 0.56E+18	10000.	1.25	0.636				
	20000.	1.30	0.500				
	30000.	1.30	0.417	*0.387	*0.307		
	50000.	1.28	0.308	*0.423	*0.345		

PERTURBER DENSITY= 1. E+17cm-3

5S - 5P	2500.	0.227	0.460E-02	0.747E-01	-0.105E-01	*0.714E-01	-0.807E-02
4608.6Å	5000.	0.229	0.276E-01	0.770E-01	-0.124E-01	*0.756E-01	-0.969E-02
C= 0.33E+20	10000.	0.236	0.425E-01	0.781E-01	-0.143E-01	0.771E-01	-0.113E-01
	20000.	0.258	0.508E-01	0.790E-01	-0.170E-01	0.778E-01	-0.130E-01
	30000.	0.279	0.431E-01	0.796E-01	-0.177E-01	0.780E-01	-0.141E-01
	50000.	0.316	0.337E-01	0.808E-01	-0.194E-01	0.782E-01	-0.154E-01
5S - 6P	2500.	0.825	0.502				
2932.7Å	5000.	0.900	0.524				
C= 0.54E+19	10000.	0.982	0.415				
	20000.	1.08	0.329				
	30000.	1.11	0.294	*0.311	*0.224		
	50000.	1.12	0.229	*0.337	*0.256		
5S - 7P	2500.	* 1.43	*0.372				
2570.2Å	5000.	* 1.82	*0.539				
C= 0.31E+19	10000.	2.19	0.650				
	20000.	2.52	0.654				
	30000.	2.68	0.595				
	50000.	2.83	0.511				

PERTURBER DENSITY= 1. E+17cm-3

PERTURBERS ARE:		ELECTRONS		PROTONS		IONIZED HELIUM	
TRANSITION	T(K)	WIDTH(Å)	SHIFT(Å)	WIDTH(Å)	SHIFT(Å)	WIDTH(Å)	SHIFT(Å)
5P - 6S	2500.	5.38	3.12	* 1.09	*0.528		
11244.4Å	5000.	6.08	3.93	* 1.24	*0.787	* 1.01	*0.563
C= 0.20E+21	10000.	6.63	4.67	* 1.38	* 1.02	* 1.13	*0.769
	20000.	7.06	4.81	* 1.54	* 1.24	* 1.25	*0.960
	30000.	7.33	4.47	1.65	1.37	* 1.33	* 1.07
	50000.	7.90	3.74	1.79	1.53	* 1.44	* 1.21
5P - 7S	2500.	* 14.5	* 6.47				
5971.7Å	5000.	* 15.9	* 8.85				
C= 0.17E+20	10000.	* 16.5	* 9.42				
	20000.	* 16.9	* 8.65				
	30000.	17.1	7.78				
	50000.	17.1	6.35				
5P - 5D	2500.	4.96	-1.90				
7675.2Å	5000.	5.15	-1.31				
C= 0.37E+20	10000.	5.63	-0.792	* 1.22	-0.732		
	20000.	5.82	-0.431	* 1.35	-0.917		
	30000.	5.89	-0.318	* 1.43	-1.02		
	50000.	6.00	-0.230	* 1.55	-1.15	* 1.27	-0.903
5P - 6D	2500.	* 10.6	-3.38				
5544.9Å	5000.	* 11.8	-3.02				
C= 0.60E+19	10000.	* 13.4	-2.00				
	20000.	* 14.5	-1.29				
	30000.	15.0	-0.903				
	50000.	15.4	-0.576				
5P - 7D	2500.	* 11.3	-2.99				
4966.9Å	5000.	* 13.5	-2.75				
C= 0.77E+19	10000.	* 17.2	-1.75				
	20000.	* 21.0	-1.07				
	30000.	* 22.9	-0.813				
	50000.	* 25.0	-0.165				
4D - 6P	2500.	5.00	2.99				
7169.1Å	5000.	5.50	3.15				
C= 0.32E+20	10000.	6.02	2.63				
	20000.	6.60	2.22				
	30000.	6.72	2.01	* 1.86	* 1.34		
	50000.	6.75	1.59	* 2.01	* 1.53		
4D - 7P	2500.	* 6.20	* 1.59				
5331.3Å	5000.	* 7.89	* 2.29				
C= 0.13E+20	10000.	* 9.50	* 2.77				
	20000.	10.9	2.84				
	30000.	11.6	2.78				
	50000.	12.2	2.41				
5P - 4D	2500.	3.58	-1.61	1.68	-0.406	* 1.62	-0.313
28160.1Å	5000.	3.53	-1.81	1.71	-0.481	1.68	-0.376
C= 0.28E+22	10000.	3.64	-2.01	1.74	-0.557	1.71	-0.440
	20000.	3.82	-2.15	1.77	-0.638	1.72	- 0.506
	30000.	3.95	-2.16	1.79	-0.688	1.73	- 0.546
	50000.	4.15	-2.04	1.82	-0.755	1.75	- 0.601
5P - 5D	2500.	1.29	-0.343				
4919.5Å	5000.	1.52	-0.139	*0.336	-0.125		
C= 0.27E+20	10000.	1.82	0.300E-01	*0.359	-0.159		
	20000.	2.04	0.187	*0.377	-0.192	*0.351	-0.149
	30000.	2.17	0.265	*0.389	-0.211	*0.358	-0.165
	50000.	2.30	0.250	0.406	-0.235	*0.368	-0.185

PERTURBER DENSITY= 1. E+17cm-3

PERTURBERS ARE:		ELECTRONS		PROTONS		IONIZED HELIUM	
TRANSITION	T(K)	WIDTH(Å)	SHIFT(Å)	WIDTH(Å)	SHIFT(Å)	WIDTH(Å)	SHIFT(Å)
4D - 6P	2500.	3.21	1.96				
6381.2Å	5000.	3.56	2.31				
C= 0.45E+20	10000.	3.85	2.39				
	20000.	4.16	2.18	* 1.12	*0.743		
	30000.	4.36	1.98	* 1.18	*0.832		
	50000.	4.55	1.69	* 1.26	*0.943		
4D - 7P	2500.	* 10.2	* 4.13				
4719.6Å	5000.	* 11.2	* 5.19				
C= 0.56E+19	10000.	* 12.0	* 5.13				
	20000.	* 12.6	* 4.48				
	30000.	12.7	3.80				
	50000.	12.6	3.00				

PERTURBER DENSITY= 1. E+18cm-3

5S - 5P	2500.	2.21	0.858E-01	*0.482	-0.722E-01		
4608.6Å	5000.	2.28	0.304	*0.666	-0.101		
C= 0.33E+21	10000.	2.36	0.446	*0.744	-0.127		
	20000.	2.58	0.521	*0.777	-0.153		
	30000.	2.79	0.441	*0.789	-0.167	*0.766	-0.131
	50000.	3.16	0.342	*0.805	-0.187	*0.775	-0.147
5S - 6P	2500.	* 6.37	* 2.03				
2932.7Å	5000.	* 7.84	* 3.10				
C= 0.54E+20	10000.	* 9.00	* 2.64				
	20000.	* 10.2	* 2.24				
	30000.	10.6	2.05				
	50000.	10.8	1.66				

for the maximum perturber density for which the line may be treated as isolated when it is divided by the corresponding full width at half maximum. For each value given in Table 1, the collision volume (V) multiplied by the perturber density (N) is much less than one and the impact approximation is valid (Sahal–Bréchot, 1969ab). Values for NV > 0.5 are not given and values for 0.1 < NV < 0.5 are denoted by an asterisk. When the impact approximation is not valid, the ion broadening contribution may be estimated by using quasistatic approach (Sahal–Bréchot 1991 and Griem 1974). The accuracy of the results obtained decreases when broadening by ion interactions becomes important.

The analysis of present results and comparison with available theoretical data will be published elsewhere (Dimitrijević and Sahal–Bréchot, 1996).

Acknowledgements – This work is a part of the project "Astrometrical, Astrodynamical and Astrophysical Researches", supported by Ministry of Science and Technology of Serbia.

REFERENCES

Dimitrijević, M. S., and Sahal–Bréchot,S.: 1984, *JQSRT* **31**, 301.

Dimitrijević, M. S., and Sahal–Bréchot, S.: 1996, *Astron. Astrophys. Suppl. Series, submitted.*

Griem, H. R.: 1974, *Spectral Line Broadening by Plasmas*, Academic Press, New York.

Komarov, N.S., and Basak, N.Yu.: 1993, Astron. Zh. **70**, 111.

Sahal–Bréchot, S.: 1969a, *Astron. Astrophys.* **1**, 91.

Sahal–Bréchot, S.: 1969b, *Astron. Astrophys.* **2**, 322.

Sahal–Bréchot, S.: 1991, *Astron. Astrophys.* **245**, 322.

Šleivyté, J., Bartkevičius, A.: 1995, *Vilniaus Astronomijos Observatorijos Biuletenis* **85**, 3. **1**, 91.

ТАБЕЛЕ ПАРАМЕТАРА ШТАРКОВОГ ШИРЕЊА Sr I

М. С. Димитријевић[1] и S. Sahal–Bréchot[2]

[1] *Астрономска опсерваторија, Волгина 7, 11050 Београд, Југославија*

[2] *Laboratoire "Astrophysique, Atomes et Molécules"*
Département Atomes et Molécules en Astrophysique
Unité associée au C.N.R.S. No 812
Observatoire de Paris-Meudon, 92190 Meudon, France

УДК 52–355.3
Претходно саопштење

Користећи семикласичан прилаз, израчунате су ширине и помераји спектралних линија, проузроковани сударима са електронима, протонима и јонизованим хелијумом, за 33 мултиплета Sr I. Резултати су дати у функцији температуре и концентрације пертурбера.

Bull. Obs. Astron. Belgrade, N° 139 (1988) UDC 535.338.334:539.186.24:533.9 82.5

COMPARISON BETWEEN DIFFERENT APPROXIMATE APPROACHES FOR THE CALCULATION OF STARK WIDTHS OF DOUBLY – AND TRIPLY–CHARGED ION LINES OF ASTROPHYSICAL IMPORTANCE

Milan S. Dimitrijević

Astronomical Observatory, Volgina 7, 11050 Beograd, Yugoslavia

(Received: May 20, 1988)

SUMMARY: Stark widths of spectral lines from 127 astrophysically important multiplets of doubly – and triply–charged ions were calculated by means of the Griem's (1968) semiempirical method, Griem's simplified semiclassical method (1974), and a modified version of this latter method (Dimitrijević and Konjević, 1980). Obtained results were compared with those (Dimitrijević, 1988a) derived by using the modified semiempirical method (Dimitrijević and Konjević, 1980).

1. INTRODUCTION

In atmospheres of 0, B and A type stars, and of white dwarfs, where a large number of singly and multiply charged ion lines has been observed (see e. g. Peytremann, 1972, or Lanz et al, 1982), Stark broadening is the dominant pressure broadening mechanism. Even in atmospheres of cooler stars, like our Sun, Stark broadening may be important in line wings or for higher spectral series members (Vince et al, 1985a). Moreover, Stark effect is one of the causes of the stellar spectral line aymmetries (Vince et al, 1985b).

Refined quantum mechanical or semiclassical theories, requiring knowledge of a lot of the atomic data, and time consuming computer codes, are not suitable for large scale calculations when high accuracy of each particular line is not so important and only a reasonable, average accuracy for a number of lines is required. For such purposes, an effort has been made to develop simple approximate formulae with good average accuracy (see e.g. Griem, 1968, Griem, 1974, Hey and Bryan, 1977, Dimitrijević and Konjević, 1980, 1981, 1986, 1987, Dimitrijević and Kršljanin, 1986, Seaton, 1987).

A convenient method for Stark broadening calculations of ion lines, when more sophysticated theories are not needed or not applicable, might be the modified semiempirical approach (Dimitrijević and Konjević, 1980, 1981a, 1987; Dimitrijević and Kršljanin, 1986). This method has been tested several times (Dimitrijević and Konjević, 1981a, b, c; Dimitrijević, 1982a, c, 1983, 1988b, Konjević et al, 1984; Lanz et al, 1988, El–Farra and Hughes, 1983, Ackermann et al, 1985) and on the average it gives a satisfactory agreement with experiments. Recently, the modified semiempirical approach was applied to the Stark broadening of spectral lines from 127 astrophysicaly important multiplets of doubly and triply charged ions (Dimitrijević, 1988a). In this paper calculations for the same 127 multiplets were performed, but using Griem's (1968) semiempirical method, Griem's symplified semiclassical method (1974), and a modified version (Dimitrijević and Konjević, 1980) of this latter one in order to compare the simple approaches to the Stark broadening determination and to provide new data needed in astrophysics.

2. THEORY

According to the Griem's (1968) semiempirical approach, full half–width (FWHM) W of an isolated ion line, is given by the following expression:

$$W = N\frac{8\pi}{3}\frac{\hbar^2}{m^2}\left(\frac{2m}{\pi kT}\right)^{1/2}\frac{\pi}{\sqrt{3}}\left[\sum_{i'}\mathbf{R}^2_{i'i}g\left(\frac{E}{\Delta E_{ii}}\right)+\right.$$

$$\left.+\sum_{f'}\mathbf{R}^2_{f'f}g\left(\frac{E}{\Delta E_{f'f}}\right)\right] \qquad (1)$$

Here, i, f and i', f' denote initial and final energy level, as well as their perturbing levels, respectively, $\mathbf{R}^2_{j'j}$ (in units of the Bohr radius a_0) is the square of the coordinate operator matrix element summed over all components of the operator, the magnetic substates of total angular momentum J', and averaged over the magnetic substates of J. $E = 3kT/2$ is the energy of the perturbing electron and $\Delta E_{j'j} = |E_{j'} - E_j$ is the energy difference between levels j' and j; g (x) = 0.20 for $x \leqslant 2$ and g (x) = 0.24, 0.33, 0.56, 0.98 1.33 for x = = 3, 5, 10, 30 and 100.

If the nearest perturbing level in Eq. (1) is so far from E_i or E_f that the condition $E/\Delta E_{j'j} \lesssim 2$ is satisfied, g becomes a constant (Griem, 1968). Then, the summation in Eq. (1) can be performed straightforwardly, leading to considerable simplification of the

Table 1. Table lists electron impact ful half widths of isolated lines from beryllium through argon at an electron density of 1×10^{17} cm^{-3}, and electron temperature from 10000 to 160000 K. Transitions and averaged wavelength for the multiplet (in Angstrom units) are also given. Under W_{SEM} and W_{SE} are given the modified semiempirical results (Dimitrijević, 1988a), and semiempirical results calculated here by using Eq. (2). W_{GM} are semiclassical results obtained by using Eqs. (4–9) with 1.4 instead of 5–4.5/Z on the r.h. s of Eq. (5), and W_G are results obtained by using Eqs. (4–9). The value for $3kT/2\Delta E$ represents the ratio of the thermal electron energy at 10000 K to the energy difference to the nearest perturbing level.

Element/Transition	T(K)	W_{SEM}(Å)	W_{SE}(Å)	W_{GM}(Å)	W_G(Å)
BE III $2s^1S-2p^1P^o$	10000	0.227	0.128	0.197	0.282
	20000	0.160	0.904-1	0.155	0.210
λ=6141.0	40000	0.117	0.711-1	0.131	0.165
$3kT/2\Delta E$=0.64	80000	0.947-1		0.117	0.136
	160000	0.843-1		0.108	0.118
BE III $2s^3S-2p^3P^o$	10000	0.701-1	0.402-1	0.617-1	0.874-1
	20000	0.496-1	0.284-1	0.471-1	0.644-1
λ=3721.8	40000	0.351-1	0.201-1	0.383-1	0.493-1
$3kT/2\Delta E$=0.39	80000	0.263-1	0.175-1	0.333-1	0.399-1
	160000	0.221-1		0.304-1	0.342-1
BE III $2p^1P^o-3d^1D$	10000	0.883-2		0.112-1	0.126-1
	20000	0.732-2		0.931-1	0.101-1
λ=746.2	40000	0.599-2		0.797-2	0.836-2
$3kT/2\Delta E$=12	80000	0.591-2		0.698-2	0.717-2
	160000	0.481-2		0.625-2	0.633-2
BE III $2p^3P^o-3d^3D$	10000	0.559-2		0.809-2	0.945-2
	20000	0.449-2		0.650-2	0.731-2
λ=675.6	40000	0.370-2		0.548-2	0.594-2
$3kT/2\Delta E$=3.4	80000	0.309-2		0.482-2	0.506-2
	160000	0.312-2		0.439-2	0.451-2
B III $2s^2S-2p^2P^o$	10000	0.191-1	0.115-1	0.176-1	0.244-1
	20000	0.135-1	0.815-2	0.131-1	0.178-1
λ=2066.3	40000	0.953-2	0.576-2	0.103-1	0.134-1
$3kT/2\Delta E$=0.22	80000	0.674-2	0.408-2	0.867-2	0.106-1
	160000	0.516-2		0.778-2	0.892-2
B III $2p^2P^o-3d^2D$	10000	0.558-2		0.811-2	0.946-2
	20000	0.449-2		0.650-2	0.732-2
λ=677.1	40000	0.370-2		0.547-2	0.594-2
$3kT/2\Delta E$=3.3	80000	0.308-2		0.480-2	0.505-2
	160000	0.310-2		0.437-2	0.450-2

Table 1 (Continued)

Element/Transition	T(K)	W_{SEM}(Å)	W_{SE}(Å)	W_{GM}(Å)	W_G(Å)
B III $4p^2P^o-5d^2D$	10000	10.1		6.72	7.74
	20000	8.46		6.08	6.62
λ =4243.6	40000	6.92		5.39	5.66
3kT/2ΔE=390.	80000	5.84		4.66	4.79
	160000	4.83		3.96	4.02
B III $4d^2D-5f^2F^o$	10000	12.9		7.62	8.15
	20000	10.0		6.76	7.00
λ =4487.5	40000	8.01		5.86	5.96
3kT/2ΔE=1000.	80000	6.46		4.96	5.01
	160000	5.20		4.15	4.17
B IV $2s^3S-2p^3P^o$	10000	0.269-1	0.136-1	0.201-1	0.316-1
	20000	0.190-1	0.958-2	0.150-1	0.228-1
λ =2823.4	40000	0.134-1	0.678-2	0.117-1	0.169-1
3kT/2ΔE=0.29	80000	0.966-2	0.513-2	0.986-2	0.131-1
	160000	0.767-2		0.886-2	0.107-1
B IV $2s^3S-3p^3P^o$	10000	0.665-3	0.353-3	0.729-3	0.963-3
	20000	0.496-3		0.587-3	0.734-3
λ =344.2	40000	0.403-3		0.502-3	0.589-3
3kT/2ΔE=2.1	80000	0.343-3		0.449-3	0.497-3
	160000	0.295-3		0.412-3	0.436-3
C III $2p^3P^o-3s^3S$	10000	0.344-2	0.184-2	0.314-2	0.463-2
mult. 5UV	20000	0.243-2	0.130-2	0.244-2	0.344-2
λ =538.2	40000	0.172-2	0.920-3	0.203-2	0.267-2
3kT/2ΔE=0.48	80000	0.139-2		0.180-2	0.218-2
	160000	0.121-2		0.167-2	0.189-2
C III $2p^3P^o-3d^3D$	10000	0.199-2	0.128-2	0.306-2	0.357-2
mult. 6UV	20000	0.141-2	0.907-3	0.236-2	0.269-2
λ =459.6	40000	0.109-2		0.193-2	0.213-2
3kT/2ΔE=1.0	80000	0.891-3		0.167-2	0.178-2
	160000	0.748-3		0.153-2	0.159-2

Table 1 (Continued)

Element/Transition	T(K)	W_{SEM}(Å)	W_{SE}(Å)	W_{GM}(Å)	W_G(Å)
C III $3s^3S-3p^3P^o$	10000	0.523	0.263	0.410	0.642
mult. 1	20000	0.370	0.187	0.329	0.482
λ =4648.8	40000	0.274		0.283	0.379
3kT/2ΔE=1.0	80000	0.229		0.256	0.313
	160000	0.203		0.239	0.271
C III $3s^1P^o-3p^1D$	10000	0.486	0.230	0.377	0.589
mult. 7	20000	0.346	0.167	0.314	0.451
λ =4326.0	40000	0.280		0.281	0.363
3kT/2ΔE=1.1	80000	0.249		0.260	0.307
	160000	0.223		0.243	0.268
C III $3p^1P^o-3d^1D$	10000	0.736	0.410	0.716	0.991
mult. 2	20000	0.521	0.290	0.564	0.745
λ =5696.0	40000	0.384		0.474	0.588
3kT/2ΔE=0.89	80000	0.315		0.422	0.489
	160000	0.279		0.390	0.427
C III $3p^1P^o-4d^1D$	10000	0.185		0.180	0.233
	20000	0.160		0.158	0.189
λ =1531.8	40000	0.139		0.142	0.159
3kT/2ΔE=6.9	80000	0.125		0.128	0.137
	160000	0.115		0.115	0.120
C III $3d^1D-4f^1F^o$	10000	0.184		0.258	0.294
	20000	0.147		0.209	0.231
λ =2162.9	40000	0.120		0.177	0.190
3kT/2ΔE=6.9	80000	0.106		0.156	0.162
	160000	0.964-1		0.141	0.145
C III $4p^3P^o-5d^3D$	10000	3.33		2.83	3.80
mult. 10	20000	2.95		2.54	3.10
λ =3609.3	40000	2.64		2.31	2.62
3kT/2ΔE=8.3	80000	2.26		2.08	2.24
	160000	2.04		1.86	1.94

Table 1 (Continued)

Element/Transition	T(K)	W_{SEM}(Å)	W_{SE}(Å)	W_{GM}(Å)	W_G(Å)
C III $4f\,^1F^o-5g\,^1G$	10000	1.53		2.42	2.68
	20000	1.26		1.97	2.12
λ =4187.0	40000	1.07		1.67	1.76
3kT/2ΔE=77	80000	1.02		1.47	1.51
	160000	0.981		1.34	1.36
C IV $2s^2S-2p^2P^o$	10000	0.728-2	0.383-2	0.570-2	0.873-2
mult. 1UV	20000	0.515-2	0.271-2	0.417-2	0.627-2
λ =1549.1	40000	0.364-2	0.192-2	0.318-2	0.460-2
3kT/2ΔE=0.16	80000	0.258-2	0.135-2	0.257-2	0.350-2
	160000	0.187-2	0.107-2	0.224-2	0.281-2
C IV $2s^2S-4p^2P^o$	10000	0.295-2		0.232-2	0.354-2
mult. 3UV	20000	0.250-2		0.202-2	0.277-2
λ =244.9	40000	0.218-2		0.183-2	0.227-2
3kT/2ΔE=5.2	80000	0.188-2		0.169-2	0.193-2
	160000	0.176-2		0.156-2	0.168-2
C IV $2p^2P^o-3s^2S$	10000	0.227-2	0.949-3	0.164-2	0.278-2
mult. 6UV	20000	0.161-2	0.671-3	0.128-2	0.204-2
λ =419.6	40000	0.116-2	0.509-3	0.107-2	0.156-2
3kT/2ΔE=0.61	80000	0.936-3		0.954-3	0.125-2
	160000	0.829-3		0.896-3	0.107-2
C IV $2p^2P^o-3d^2D$	10000	0.106-2		0.139-2	0.173-2
	20000	0.811-3		0.108-2	0.129-2
λ =384.1	40000	0.656-3		0.886-3	0.101-2
3kT/2ΔE=2.2	80000	0.538-3		0.769-3	0.842-3
	160000	0.440-3		0.702-3	0.740-3
C IV $2p^2P^o-4d^2D$	10000	0.598-2		0.449-2	0.536-2
mult. 9UV	20000	0.503-2		0.397-2	0.445-2
λ=289.2	40000	0.416-2		0.352-2	0.377-2
3kT/2ΔE=110.	80000	0.338-2		0.309-2	0.321-2
	160000	0.286-2		0.270-2	0.276-2

Table 1 (Continued)

Element/Transition	T(K)	W_{SEM}(Å)	W_{SE}(Å)	W_{GM}(Å)	W_G(Å)
C IV $3s^2S-3p^2P^o$	10000	0.776	0.320	0.495	0.880
mult. 1	20000	0.571		0.402	0.656
λ=5804.9	40000	0.440		0.352	0.511
3kT/2ΔE=2.2	80000	0.368		0.325	0.419
	160000	0.325		0.307	0.359
C IV $4d^2D-5f^2F^o$	10000	2.16		1.24	1.38
mult. 14UV	20000	1.75		1.12	1.18
λ=2524.4	40000	1.40		0.983	1.01
3kT/2ΔE=1000.	80000	1.11		0.847	0.860
	160000	0.889		0.719	0.724
N III $2p^2P^o-3s^2S$	10000	0.202-2	0.108-2	0.185-2	0.272-2
mult. 4UV	20000	0.143-2	0.801-3	0.143-2	0.201-2
λ=452.1	40000	0.101-2		0.118-2	0.155-2
3kT/2ΔE=1.1	80000	0.783-3		0.104-2	0.127-2
	160000	0.681-3		0.959-3	0.109-2
N III $2p^2P^o-3d^2D$	10000	0.130-2	0.832-3	0.200-2	0.235-2
mult. 5UV	20000	0.922-3	0.588-3	0.152-2	0.175-2
λ=374.4	40000	0.652-3	0.416-3	0.121-2	0.137-2
3kT/2ΔE=0.48	80000	0.501-3		0.104-2	0.113-2
	160000	0.413-3		0.947-3	0.100-2
N III $3s^4P^o-3p^4D$	10000	1.30		2.34	2.47
mult. 3	20000	1.09		1.94	2.02
λ=4517.3	40000	0.967		1.65	1.70
3kT/2ΔE=6.6	80000	0.968		1.44	1.46
	160000	0.946		1.29	1.30
N III $3s^4P^o-3p^4P$	10000	0.399	0.121	0.188	0.292
mult. 5	20000	0.167	0.853-1	0.149	0.218
λ=3367.3	40000	0.121		0.127	0.170
3kT/2ΔE=0.81	80000	0.984-1		0.114	0.140
	160000	0.863-1		0.106	0.121

Table 1 (Continued)

Element/Transition	T(K)	W_{SEM}(Å)	W_{SE}(Å)	W_{GM}(Å)	W_G(Å)
N III $3p^2P^o-3d^2D$	10000	0.415	0.236	0.413	0.565
mult. 2	20000	0.294	0.167	0.319	0.421
λ =4640.6	40000	0.208	0.118	0.263	0.328
3kT/2ΔE=0.48	80000	0.163		0.230	0.270
	160000	0.139		0.212	0.235
N III $3p^4D-3d^4F^o$	10000	0.435	0.241	0.430	0.588
mult. 9	20000	0.307	0.171	0.333	0.439
λ =4864.9	40000	0.218	0.121	0.275	0.342
3kT/2ΔE=0.51	80000	0.173		0.241	0.282
	160000	0.147		0.222	0.245
N III $3d^4P^o-4f^4D$	10000	0.171		0.246	0.285
mult. 29UV	20000	0.141		0.200	0.223
λ =2063.8	40000	0.116		0.169	0.183
3kT/2ΔE=5.0	80000	0.976-1		0.149	0.156
	160000	0.944-1		0.136	0.140
N IV $2p^1P^o-3d^1D$	10000	0.780-3	0.459-3	0.999-3	0.127-2
mult. 10UV	20000	0.552-3	0.324-3	0.746-3	0.928-3
λ =335.0	40000	0.390-3	0.229-3	0.585-3	0.705-3
3kT/2ΔE=0.42	80000	0.290-3	0.206-3	0.491-3	0.567-3
	160000	0.232-3	0.226-3	0.445-3	0.490-3
N IV $2p^3P^o-3d^3D$	10000	0.471-3	0.284-3	0.649-3	0.795-3
mult. 5UV	20000	0.333-3	0.201-3	0.490-3	0.587-3
λ =283.5	40000	0.244-3	0.166-3	0.389-3	0.450-3
3kT/2ΔE=0.74	80000	0.194-3		0.330-3	0.367-3
	160000	0.160-3		0.300-3	0.320-3
N IV $3s^3S-3p^3P^o$	10000	0.213	0.906-1	0.135	0.242
mult. 1	20000	0.151	0.641-1	0.105	0.177
λ =3480.8	40000	0.108	0.499-1	0.869-1	0.134
3kT/2ΔE=0.74	80000	0.837-1		0.776-1	0.107
	160000	0.715-1		0.728-1	0.898-1

Table 1 (Continued)

Element/Transition	T(K)	W_{SEM}(Å)	W_{SE}(Å)	W_{GM}(Å)	W_G(Å)
N IV $3p^3P^o-3d^3D$	10000	0.735	0.353	0.588	0.904
mult. 4	20000	0.520	0.250	0.454	0.666
λ=7117.0	40000	0.379	0.211	0.373	0.509
3kT/2ΔE=0.74	80000	0.304		0.329	0.411
	160000	0.259		0.305	0.352
O III $3s^3P^o-3p^3D$	10000	0.230	0.122	0.183	0.283
mult. 2	20000	0.163	0.863-1	0.142	0.209
λ=3762.3	40000	0.115	0.641-1	0.118	0.161
3kT/2ΔE=0.63	80000	0.866-1		0.104	0.131
	160000	0.742-1		0.967-1	0.112
O III $3s^3P^o-3p^3S$	10000	0.185	0.981-1	0.148	0.229
mult. 3	20000	0.131	0.694-1	0.115	0.169
λ=3326.6	40000	0.925-1	0.514-1	0.952-1	0.130
3kT/2ΔE=0.63	80000	0.697-1		0.844-1	0.106
	160000	0.598-1		0.782-1	0.908-1
O III $3s^3P^o-3p^3P$	10000	0.158	0.839-1	0.127	0.197
mult. 4	20000	0.112	0.594-1	0.985-1	0.146
λ=3041.5	40000	0.792-1	0.440-1	0.821-1	0.112
3kT/2ΔE=0.63	80000	0.600-1		0.728-1	0.912-1
	160000	0.515-1		0.675-1	0.782-1
O III $3s^5P-3p^5D^o$	10000	0.223	0.118	0.177	0.275
mult. 21	20000	0.158	0.836-1	0.138	0.203
λ=3706.1	40000	0.112	0.591-1	0.114	0.157
3kT/2ΔE=0.39	80000	0.841-1	0.513-1	0.101	0.127
	160000	0.722-1		0.939-1	0.109
O III $3s^5P-3p^5S^o$	10000	0.126	0.673-1	0.103	0.158
mult. 22UV	20000	0.891-1	0.476-1	0.796-1	0.117
λ=2678.2	40000	0.630-1	0.337-1	0.660-1	0.901-1
3kT/2ΔE=0.46	80000	0.479-1		0.585-1	0.732-1
	160000	0.410-1		0.542-1	0.628-1

Table 1 (Continued)

Element/Transition	T(K)	W_{SEM}(Å)	W_{SE}(Å)	W_{GM}(Å)	W_G(Å)
O III $3p^3S-3d^3P^o$	10000	0.171	0.103	0.181	0.241
mult. 12	20000	0.121	0.726-1	0.138	0.179
λ =3127.3	40000	0.854-1	0.514-1	0.112	0.138
3kT/2ΔE=0.36	80000	0.626-1	0.417-1	0.966-1	0.113
	160000	0.515-1		0.885-1	0.984-1
O III $3p^3P-3d^3D^o$	10000	0.245	0.144	0.252	0.339
mult. 14	20000	0.173	0.102	0.193	0.252
λ =3712.5	40000	0.122	0.719-1	0.157	0.195
3kT/2ΔE=0.39	80000	0.907-1	0.625-1	0.136	0.160
	160000	0.753-1		0.125	0.139
O III $3p^3D-3d^3F^o$	10000	0.178	0.103	0.186	0.249
mult. 8	20000	0.126	0.728-1	0.142	0.185
λ =3265.9	40000	0.891-1	0.515-1	0.116	0.143
3kT/2ΔE=0.43	80000	0.668-1		0.101	0.117
	160000	0.556-1		0.922-1	0.102
O III $3p^5D^o-3d^5F$	10000	0.196	0.113	0.204	0.273
mult. 25	20000	0.139	0.800-1	0.156	0.202
λ =3453.0	40000	0.982-1	0.566-1	0.126	0.157
3kT/2ΔE=0.39	80000	0.727-1	0.480-1	0.109	0.128
	160000	0.601-1		0.100	0.111
O III $3d^3P^o-4p^3S$	10000	0.321	0.171	0.300	0.437
mult. 20UV	20000	0.227	0.121	0.240	0.330
λ =2601.6	40000	0.175		0.203	0.260
3kT/2ΔE=0.95	80000	0.150		0.181	0.215
	160000	0.137		0.167	0.187
O III $3d^1F^o-4p^1D$	10000	0.356	0.179	0.333	0.483
mult. 21UV	20000	0.262	0.148	0.272	0.369
λ =2558.1	40000	0.215		0.236	0.295
3kT/2ΔE=1.5	80000	0.189		0.213	0.247
	160000	0.173		0.196	0.215

Table 1 (Continued)

Element/Transition	T(K)	W_{SEM}(Å)	W_{SE}(Å)	W_{GM}(Å)	W_G(Å)
O IV $2p^2P^o-3s^2S$	10000	0.596-3	0.270-3	0.453-3	0.746-3
mult. 4UV	20000	0.421-3	0.191-3	0.342-3	0.543-3
λ=279.8	40000	0.298-3	0.135-3	0.273-3	0.406-3
3kT/2ΔE=0.32	80000	0.217-3	0.105-3	0.235-3	0.319-3
	160000	0.176-3		0.216-3	0.266-3
O IV $2p^2P^o-3d^2D$	10000	0.330-3	0.195-3	0.451-3	0.556-3
mult. 5UV	20000	0.233-3	0.138-3	0.336-3	0.408-3
λ=238.5	40000	0.165-3	0.973-4	0.262-3	0.310-3
3kT/2ΔE=0.36	80000	0.120-3	0.792-4	0.219-3	0.249-3
	160000	0.948-4		0.197-3	0.215-3
O IV $3s^4P^o-3p^4D$	10000	0.168	0.721-1	0.106	0.190
mult. 3	20000	0.119	0.510-1	0.812-1	0.139
λ=3374.3	40000	0.838-1	0.360-1	0.663-1	0.104
3kT/2ΔE=0.39	80000	0.622-1	0.294-1	0.583-1	0.820-1
	160000	0.520-1		0.544-1	0.684-1
O IV $3p^4P-3d^4D^o$	10000	0.310	0.152	0.252	0.385
mult. 9	20000	0.219	0.107	0.192	0.282
λ=4792.5	40000	0.155	0.758-1	0.154	0.213
3kT/2ΔE=0.50	80000	0.119		0.133	0.170
	160000	0.983-1		0.123	0.144
O IV $3p^2D-3d^2D^o$	10000	0.400	0.193	0.323	0.495
mult. 11	20000	0.283	0.137	0.246	0.363
λ=5339.5	40000	0.202	0.101	0.200	0.276
3kT/2ΔE=0.56	80000	0.156		0.174	0.221
	160000	0.132		0.161	0.188
F III $3s^4P_6-3p^4P^o_6$	10000	0.119	0.660-1	0.975-1	0.148
	20000	0.839-1	0.467-1	0.748-1	0.109
λ=2916.3	40000	0.593-1	0.330-1	0.612-1	0.837-1
3kT/2ΔE=0.33	80000	0.431-1	0.258-1	0.535-1	0.676-1
	160000	0.355-1		0.493-1	0.576-1

Table 1 (Continued)

Element/Transition	T(K)	W_{SEM}(Å)	W_{SE}(Å)	W_{GM}(Å)	W_G(Å)
F III $3s^4P-3p^4D^o$	10000	0.134	0.743-1	0.110	0.167
mult. 1	20000	0.949-1	0.525-1	0.842-1	0.123
λ=3124.4	40000	0.671-1	0.371-1	0.689-1	0.944-1
3kT/2ΔE=0.33	80000	0.489-1	0.294-1	0.603-1	0.761-1
	160000	0.403-1	0.318-1	0.556-1	0.649-1
F III $3s^2P_4-3p^2P^o_4$	10000	0.130	0.684-1	0.105	0.162
	20000	0.918-1	0.483-1	0.822-1	0.120
λ=2811.4	40000	0.652-1	0.346-1	0.686-1	0.929-1
3kT/2ΔE=0.53	80000	0.505-1		0.611-1	0.759-1
	160000	0.436-1		0.567-1	0.653-1
F III $3s^2P-3p^2D^o$	10000	0.160	0.843-1	0.129	0.198
mult. 2	20000	0.113	0.596-1	0.101	0.147
λ=3176.9	40000	0.803-1	0.426-1	0.840-1	0.114
3kT/2ΔE=0.53	80000	0.622-1		0.748-1	0.929-1
	160000	0.534-1		0.694-1	0.799-1
F III $3p'^2D^o-3d'^2D$	10000	0.128	0.776-1	0.138	0.182
	20000	0.903-1	0.548-1	0.105	0.135
λ=2788.1	40000	0.638-1	0.388-1	0.846-1	0.104
3kT/2ΔE=0.33	80000	0.463-1	0.306-1	0.729-1	0.835-1
	160000	0.373-1		0.666-1	0.741-1
NE III $3s^3S^o-3p^3P$	10000	0.965-1	0.540-1	0.800-1	0.121
mult. 12UV	20000	0.683-1	0.382-1	0.612-1	0.892-1
λ=2678.2	40000	0.483-1	0.270-1	0.498-1	0.682-1
3kT/2ΔE=0.32	80000	0.348-1	0.200-1	0.434-1	0.549-1
	160000	0.285-1	0.212-1	0.399-1	0.468-1
NE III $3s^5S^o-3p^5P$	10000	0.820-1	0.479-1	0.695-1	0.104
mult. 11UV	20000	0.580-1	0.339-1	0.529-1	0.765-1
λ=2592.3	40000	0.410-1	0.240-1	0.427-1	0.583-1
3kT/2ΔE=0.27	80000	0.292-1	0.175-1	0.370-1	0.467-1
	160000	0.235-1		0.339-1	0.397-1

Table 1 (Continued)

Element/Transition	T(K)	W_{SEM}(Å)	W_{SE}(Å)	W_{GM}(Å)	W_G(Å)
NE III $3s'^3D^o-3p'^3F$	10000	0.832-1	0.474-1	0.697-1	0.105
	20000	0.588-1	0.335-1	0.532-1	0.771-1
λ=2612.4	40000	0.416-1	0.237-1	0.431-1	0.588-1
3kT/2ΔE=0.29	80000	0.298-1	0.176-1	0.374-1	0.472-1
	160000	0.241-1		0.343-1	0.402-1
NE III $3p^3P-3d^3D^o$	10000	0.540-1	0.280-1	0.598-1	0.761-1
	20000	0.382-1	0.198-1	0.450-1	0.561-1
λ=2413.0	40000	0.270-1	0.140-1	0.356-1	0.429-1
3kT/2ΔE= 0.28	80000	0.192-1	0.102-1	0.302-1	0.348-1
	160000	0.150-1		0.273-1	0.300-1
NE III $3p'^3D-3d'^3D^o$	10000	0.625-1	0.395-1	0.722-1	0.928-1
	20000	0.442-1	0.279-1	0.546-1	0.687-1
λ=2091.7	40000	0.312-1	0.197-1	0.436-1	0.530-1
3kT/2ΔE= 0.29	80000	0.223-1	0.147-1	0.373-1	0.432-1
	160000	0.175-1	0.156-1	0.340-1	0.376-1
NE III $3p^5P_7-3d^5D^o_9$	10000	0.685-1	0.452-1	0.803-1	0.103
	20000	0.484-1	0.319-1	0.606-1	0.760-1
λ=2163.8	40000	0.342-1	0.226-1	0.483-1	0.586-1
3kT/2ΔE=0.27	80000	0.243-1	0.162-1	0.412-1	0.477-1
	160000	0.189-1		0.375-1	0.415-1
NE IV $3s^4P-3p^4D^o$	10000	0.608-1	0.281-1	0.404-1	0.703-1
	20000	0.430-1	0.199-1	0.303-1	0.509-1
λ=2361.5	40000	0.304-1	0.141-1	0.240-1	0.378-1
3kT/2ΔE=0.25	80000	0.215-1	0.994-2	0.204-1	0.293-1
	160000	0.169-1		0.187-1	0.241-1
NE IV $3s'^2D-3p'^2F^o$	10000	0.588-1	0.270-1	0.390-1	0.679-1
	20000	0.416-1	0.191-1	0.292-1	0.492-1
λ=2289.1	40000	0.294-1	0.135-1	0.231-1	0.366-1
3kT/2ΔE=0.39	80000	0.208-1	0.106-1	0.197-1	0.284-1
	160000	0.163-1		0.180-1	0.233-1

Table 1 (Continued)

Element/Transition	T(K)	W_{SEM}(Å)	W_{SE}(Å)	W_{GM}(Å)	W_G(Å)
NA III $3s^4P-3p^4P^o$	10000	0.667-1	0.390-1	0.570-1	0.846-1
	20000	0.472-1	0.276-1	0.432-1	0.621-1
λ=2515.6	40000	0.333-1	0.195-1	0.348-1	0.472-1
3kT/2ΔE=0.26	80000	0.237-1	0.141-1	0.300-1	0.378-1
	160000	0.189-1		0.274-1	0.321-1
NA III $3s^4P-3p^4D^o$	10000	0.545-1	0.319-1	0.469-1	0.695-1
	20000	0.385-1	0.226-1	0.355-1	0.510-1
λ=2232.5	40000	0.272-1	0.159-1	0.286-1	0.388-1
3kT/2ΔE=0.26	80000	0.193-1	0.114-1	0.246-1	0.311-1
	160000	0.154-1		0.225-1	0.264-1
NA III $3s^4P-3p^4S^o$	10000	0.441-1	0.260-1	0.384-1	0.568-1
	20000	0.311-1	0.184-1	0.291-1	0.417-1
λ=1971.5	40000	0.220-1	0.130-1	0.234-1	0.317-1
3kT/2ΔE=0.26	80000	0.156-1	0.928-2	0.201-1	0.254-1
	160000	0.124-1		0.184-1	0.216-1
NA III $3s^2P-3p^2D^o$	10000	0.689-1	0.408-1	0.591-1	0.879-1
	20000	0.487-1	0.289-1	0.449-1	0.645-1
λ=2458.9	40000	0.345-1	0.204-1	0.361-1	0.491-1
3kT/2ΔE=0.26	80000	0.244-1	0.146-1	0.311-1	0.393-1
	160000	0.195-1		0.285-1	0.334-1
NA III $3s^2P-3p^2P^o$	10000	0.593-1	0.351-1	0.512-1	0.760-1
	20000	0.419-1	0.248-1	0.388-1	0.558-1
λ=2247.4	40000	0.296-1	0.176-1	0.312-1	0.424-1
3kT/2ΔE=0.26	80000	0.210-1	0.125-1	0.269-1	0.340-1
	160000	0.168-1		0.246-1	0.289-1
NA III $3p^2D^o-3d^2F$	10000	0.558-1	0.377-1	0.672-1	0.851-1
	20000	0.394-1	0.266-1	0.507-1	0.630-1
λ=1995.9	40000	0.279-1	0.188-1	0.403-1	0.485-1
3kT/2ΔE=0.26	80000	0.197-1	0.134-1	0.342-1	0.395-1
	160000	0.152-1	0.130-1	0.311-1	0.344-1

Table 1 (Continued)

Element/Transition	T(K)	W_{SEM}(Å)	W_{SE}(Å)	W_{GM}(Å)	W_G(Å)
NA III $3p^4P^o-3d^4D$	10000	0.447-1	0.293-1	0.540-1	0.681-1
	20000	0.316-1	0.207-1	0.407-1	0.503-1
λ=1852.0	40000	0.223-1	0.146-1	0.323-1	0.387-1
3kT/2ΔE=0.26	80000	0.158-1	0.104-1	0.274-1	0.315-1
	160000	0.121-1	0.103-1	0.249-1	0.274-1
NA III $3p^4D^o-3d^4F$	10000	0.514-1	0.343-1	0.620-1	0.784-1
	20000	0.363-1	0.243-1	0.467-1	0.579-1
λ=1947.1	40000	0.257-1	0.172-1	0.370-1	0.446-1
3kT/2ΔE=0.23	80000	0.182-1	0.121-1	0.314-1	0.363-1
	160000	0.139-1	0.114-1	0.286-1	0.316-1
MG IV $3s^4P-3p^4S^o$	10000	0.199-1	0.969-2	0.140-1	0.236-1
	20000	0.140-1	0.685-2	0.104-1	0.170-1
λ=1477.8	40000	0.993-2	0.484-2	0.810-2	0.126-1
3kT/2ΔE=0.20	80000	0.702-2	0.342-2	0.678-2	0.972-2
	160000	0.520-2	0.284-2	0.612-2	0.795-2
MG IV $3s^4P-3p^4P^o$	10000	0.314-1	0.152-1	0.217-1	0.368-1
	20000	0.222-1	0.107-1	0.161-1	0.266-1
λ=1911.5	40000	0.157-1	0.758-2	0.126-1	0.197-1
3kT/2ΔE=0.20	80000	0.111-1	0.536-2	0.106-1	0.152-1
	160000	0.828-2	0.477-2	0.953-2	0.124-1
MG IV $3s^4P_6-3p^4D^o_8$	10000	0.249-1	0.120-1	0.174-1	0.294-1
	20000	0.176-1	0.852-2	0.129-1	0.212-1
λ=1683.0	40000	0.125.1	0.602-2	0.101-1	0.157-1
3kT/2ΔE=0.20	80000	0.882-2	0.426-2	0.842-2	0.121-1
	160000	0.654-2	0.362-2	0.760-2	0.988-2
MG IV $3p^4S^o_4-4d^4P_6$	10000	0.238-1	0.133-1	0.230-1	0.324-1
	20000	0.169-1	0.941-2	0.170-1	0.236-1
λ=1548.1	40000	0.119-1	0.665-2	0.132-1	0.176-1
3kT/2ΔE=0.16	80000	0.843-2	0.470-2	0.109-1	0.138-1
	160000	0.611-2	0.371-2	0.975-2	0.116-1

Table 1 (Continued)

Element/Transition	T(K)	W_{SEM}(Å)	W_{SE}(Å)	W_{GM}(Å)	W_G(Å)
AL III $3s^2S-3p^2P^o$	10000	0.303-1	0.193-1	0.277-1	0.398-1
mult. 1UV	20000	0.214-1	0.136-1	0.208-1	0.291-1
λ=1857.4	40000	0.151-1	0.963-2	0.165-1	0.220-1
3kT/2ΔE=0.19	80000	0.107-1	0.681-2	0.140-1	0.175-1
	160000	0.801-2	0.592-2	0.126-1	0.148-1
AL III $3s^2S-4p^2P^o$	10000	0.136-1	0.837-2	0.138-1	0.199-1
mult. 2UV	20000	0.964-2	0.592-2	0.107-1	0.148-1
λ=696.0	40000	0.688-2	0.446-2	0.886-2	0.115-1
3kT/2ΔE=0.60	80000	0.549-2		0.777-2	0.940-2
	160000	0.494-2		0.718-2	0.815-2
AL III $3s^2S-5p^2P^o$	10000	0.238-1	0.145-1	0.254-1	0.361-1
mult. 3UV	20000	0.172-1	0.115-1	0.204-1	0.274-1
λ=560.4	40000	0.142-1		0.173-1	0.217-1
3kT/2ΔE=1.3	80000	0.130-1		0.154-1	0.180-1
	160000	0.122-1		0.141-1	0.157-1
AL III $3p^2P^o-3d^2D$	10000	0.316-1	0.230-1	0.415-1	0.509-1
	20000	0.224-1	0.163-1	0.312-1	0.376-1
λ=1609.9	40000	0.158-1	0.115-1	0.246-1	0.290-1
3kT/2ΔE=0.38	80000	0.112-1	0.919-2	0.208-1	0.236-1
	160000	0.825-2	0.974-2	0.188-1	0.206-1
AL III $3d^2D-4f^2F^o$	10000	0.148		0.214	0.244
	20000	0.121		0.173	0.191
λ=1935.9	40000	0.998-1		0.147	0.157
3kT/2ΔE=5.7	80000	0.833-1		0.129	0.134
	160000	0.798-1		0.117	0.120
AL III $4s^2S-4p^2P^o$	10000	1.48	0.859	1.20	1.87
mult. 2	20000	1.04	0.607	0.951	1.40
λ=5705.9	40000	0.751	0.462	0.805	1.09
3kT/2ΔE=0.60	80000	0.616		0.720	0.895
	160000	0.569		0.666	0.768

Table 1 (Continued)

Element/Transition	T(K)	W_{SEM}(Å)	W_{SE}(Å)	W_{GM}(Å)	W_G(Å)
AL III $4p^2P^o-4d^2D$	10000	1.45		1.37	1.90
mult. 3	20000	1.14		1.14	1.47
λ=4523.2	40000	0.909		0.983	1.19
3kT/2ΔE=5.7	80000	0.764		0.876	1.00
	160000	0.727		0.797	0.867
AL III $4d^2D-6f^2F^o$	10000	6.51		4.82	5.40
	20000	5.48		4.27	4.58
λ=2762.8	40000	4.35		3.72	3.87
3kT/2ΔE=320.	80000	3.69		3.18	3.25
	160000	3.09		2.70	2.73
AL III $4f^2F^o-5d^2D$	10000	4.42		4.14	5.25
mult. 6	20000	3.77		3.60	4.25
λ=4701.6	40000	3.23		3.18	3.56
3kT/2ΔE=10.	80000	2.80		2.83	3.03
	160000	2.56		2.52	2.63
AL III $4f^2F^o-6g^2G$	10000	4.04		3.69	3.87
	20000	3.32		3.14	3.23
λ=2907.0	40000	2.77		2.67	2.71
3kT/2ΔE=1700.	80000	2.34		2.26	2.28
	160000	1.97		1.94	1.94
SI III $3p^3P^o-3d^3D$	10000	0.894-2	0.761-2	0.148-1	0.165-1
mult. 5UV	20000	0.632-2	0.538-2	0.110-1	0.122-1
λ=1111.6	40000	0.447-2	0.380-2	0.856-2	0.938-2
3kT/2ΔE=0.32	80000	0.316-2	0.290-2	0.713-2	0.767-2
	160000	0.223-2		0.641-2	0.676-2
SI III $3p^3P^o-4s^3S$	10000	0.175-1	0.109-1	0.165-1	0.242-1
mult. 6UV	20000	0.124-1	0.772-2	0.129-1	0.180-1
λ=996.1	40000	0.876-2	0.546-2	0.106-1	0.139-1
3kT/2ΔE=0.48	80000	0.702-2		0.936-2	0.114-1
	160000	0.613-2		0.865-2	0.983-2

Table 1 (Continued)

Element/Transition	T(K)	W_{SEM}(Å)	W_{SE}(Å)	W_{GM}(Å)	W_G(Å)
SI III $4s^3S-4p^3P^o$	10000	0.728	0.438	0.604	0.932
mult. 2	20000	0.514	0.310	0.473	0.693
λ=4560.1	40000	0.364	0.219	0.395	0.538
3kT/2ΔE=0.48	80000	0.289		0.350	0.438
	160000	0.257		0.324	0.376
SI III $4p^3P^o-4d^3D$	10000	0.762	0.456	0.746	1.06
mult. 5	20000	0.546	0.347	0.590	0.800
λ=3801.4	40000	0.411		0.496	0.630
3kT/2ΔE=1.3	80000	0.342		0.438	0.520
	160000	0.316		0.403	0.451
SI III $4p^3P^o-5s^3S$	10000	0.793	0.438	0.680	1.04
mult. 6	20000	0.571	0.326	0.555	0.792
λ=3237.8	40000	0.458		0.481	0.628
3kT/2ΔE=1.2	80000	0.411		0.433	0.521
	160000	0.379		0.399	0.449
SI IV $3s^2S-3p^2P^o$	10000	0.141-1	0.733-2	0.104-1	0.170-1
mult. 1UV	20000	0.995-2	0.518-2	0.764-2	0.122-1
λ=1396.7	40000	0.703-2	0.366-2	0.588-2	0.902-2
3kT/2ΔE=0.15	80000	0.497-2	0.259-2	0.484-2	0.691-2
	160000	0.356-2	0.195-2	0.431-2	0.561-2
SI IV $3p^2P^o-3d^2D$	10000	0.109-1	0.659-2	0.116-1	0.156-1
mult. 3UV	20000	0.768-2	0.466-2	0.856-2	0.114-1
λ=1126.4	40000	0.543-2	0.329-2	0.659-2	0.851-2
3kT/2ΔE=0.18	80000	0.384-2	0.233-2	0.541-2	0.670-2
	160000	0.273-2	0.186-2	0.482-2	0.564-2
SI IV $4s^2S-4p^2P^o$	10000	0.605	0.281	0.388	0.700
mult. 1	20000	0.428	0.199	0.298	0.512
λ=4097.9	40000	0.302	0.140	0.245	0.386
3kT/2ΔE=0.43	80000	0.230		0.216	0.305
	160000	0.196		0.201	0.255

Table 1 (Continued)

Element/Transition	T(K)	W_{SEM}(Å)	W_{SE}(Å)	W_{GM}(Å)	W_G(Å)
SI IV $4p^2P^o-4d^2D$	10000	0.467	0.233	0.355	0.576
mult. 2	20000	0.346		0.281	0.429
λ=3160.3	40000	0.267		0.237	0.332
3kT/2ΔE=2.5	80000	0.213		0.211	0.270
	160000	0.180		0.195	0.230
SI IV $4d^2D-5p^2P^o$	10000	1.19	0.576	0.866	1.46
mult. 3	20000	0.866		0.692	1.09
λ=3766.0	40000	0.675		0.589	0.841
3kT/2ΔE=2.5	80000	0.568		0.529	0.683
	160000	0.507		0.491	0.581
SI IV $5p^2P^o-6s^2S$	10000	3.37	1.46	2.29	4.03
mult. 4	20000	2.55	1.27	1.89	3.03
λ=4323.5	40000	2.14		1.66	2.37
3kT/2ΔE=1.7	80000	1.89		1.51	1.93
	160000	1.71		1.40	1.64
SI IV $5d^2D-6f^2F^o$	10000	8.51		6.03	7.67
mult. 5	20000	7.23		5.39	6.34
λ=4212.4	40000	6.08		4.80	5.32
3kT/2ΔE=140.	80000	4.92		4.22	4.49
	160000	4.20		3.66	3.80
P III $3d^2D-4p^2P^o$	10000	0.343	0.242	0.367	0.492
mult. 1	20000	0.242	0.171	0.280	0.365
λ=4066.2	40000	0.171	0.121	0.226	0.282
3kT/2ΔE=0.44	80000	0.128		0.195	0.230
	160000	0.106		0.178	0.200
P III $4s^2S-4p^2P^o$	10000	0.531	0.326	0.446	0.682
mult. 3	20000	0.375	0.230	0.347	0.507
λ=4230.4	40000	0.265	0.163	0.289	0.392
3kT/2ΔE=0.44	80000	0.206		0.255	0.319
	160000	0.180		0.236	0.274

Table 1 (Continued)

Element/Transition	T(K)	W_{SEM}(Å)	W_{SE}(Å)	W_{GM}(Å)	W_G(Å)
P III $4s^4P^o-4p^4P$	10000	0.462		0.388	0.594
mult. 9	20000	0.327		0.301	0.441
λ=3943.5	40000	0.231		0.250	0.341
3kT/2ΔE=8.9	80000	0.176		0.220	0.277
	160000	0.154		0.204	0.237
P IV $3p^3P^o-3d^3D$	10000	0.350-2	0.260-2	0.477-2	0.573-2
mult. 3UV	20000	0.248-2	0.184-2	0.350-2	0.417-2
λ=826.3	40000	0.175-2	0.130-2	0.267-2	0.313-2
3kT/2ΔE=0.15	80000	0.124-2	0.920-2	0.216-2	0.248-2
	160000	0.876-3	0.690-3	0.190-2	0.211-2
P IV $4s^3S-4p^3P^o$	10000	0.330	0.158	0.216	0.385
mult. 1	20000	0.233	0.112	0.165	0.281
λ=3355.9	40000	0.165	0.790-1	0.134	0.211
3kT/2ΔE=0.35	80000	0.121	0.648-1	0.117	0.166
	160000	0.100		0.108	0.138
P IV $4s^1S-4p^1P^o$	10000	0.565	0.264	0.363	0.653
mult. 2	20000	0.399	0.186	0.279	0.477
λ=4249.6	40000	0.282	0.132	0.229	0.360
3kT/2ΔE=0.44	80000	0.215		0.202	0.285
	160000	0.183		0.188	0.238
S III $3d^3P_o-4p^3P$	10000	0.202	0.135	0.216	0.289
mult. 2	20000	0.143	0.954-1	0.164	0.214
λ=3346.2	40000	0.101	0.675-1	0.132	0.165
3kT/2ΔE=0.41	80000	0.745-1		0.114	0.134
	160000	0.609-1		0.104	0.116
S III $3d^3P^o-4p^3S$	10000	0.193	0.128	0.205	0.275
mult. 3	20000	0.136	0.904-1	0.156	0.203
λ=3233.4	40000	0.963-1	0.640-1	0.126	0.157
3kT/2ΔE=0.40	80000	0.708-1		0.108	0.128
	160000	0.580-1		0.983-1	0.110

Table 1 (Continued)

Element/Transition	T(K)	W_{SEM}(Å)	W_{SE}(Å)	W_{GM}(Å)	W_G(Å)
S III $3d^3D^o-4p^3P$	10000	0.284	0.193	0.302	0.404
mult. 8	20000	0.201	0.137	0.230	0.299
λ=3950.5	40000	0.142	0.966-1	0.185	0.231
3kT/2ΔE=0.46	80000	0.104		0.159	0.188
	160000	0.853-1		0.145	0.163
S III $4s^3P^o-4p^3D$	10000	0.472	0.277	0.388	0.598
mult. 4	20000	0.334	0.196	0.303	0.444
λ=4287.1	40000	0.236	0.139	0.252	0.343
3kT/2ΔE=0.46	80000	0.183		0.223	0.280
	160000	0.159		0.207	0.240
S III $4s^3P^o-4p^3S$	10000	0.364	0.214	0.302	0.465
mult. 6	20000	0.258	0.152	0.235	0.345
λ=3692.3	40000	0.182	0.107	0.195	0.266
3kT/2ΔE=0.45	80000	0.140		0.173	0.217
	160000	0.121		0.160	0.186
S III $4s^3P^o-4p^3P$	10000	0.389	0.229	0.322	0.495
mult. 5	20000	0.275	0.162	0.251	0.368
λ=3840.0	40000	0.194	0.115	0.208	0.284
3kT/2ΔE=0.45	80000	0.150		0.184	0.231
	160000	0.130		0.171	0.198
S III $4p^3P-4d^3D^o$	10000	0.248	0.212	0.308	0.396
mult. 18UV	20000	0.175	0.150	0.236	0.296
λ=2961.0	40000	0.124	0.106	0.191	0.230
3kT/2ΔE=0.41	80000	0.909-1		0.165	0.190
	160000	0.814-1		0.151	0.166
S III $4p^3D-4d^3P^o$	10000	0.207	0.178	0.261	0.335
mult. 16UV	20000	0.147	0.126	0.200	0.250
λ=2740.6	40000	0.104	0.892-1	0.162	0.195
3kT/2ΔE=0.46	80000	0.765-1		0.140	0.161
	160000	0.686-1		0.128	0.141

Table 1 (Continued)

Element/Transition	T(K)	W_{SEM}(Å)	W_{SE}(Å)	W_{GM}(Å)	W_G(Å)
S III $4p^3D-4d^3F^o$	10000	0.222	0.189	0.277	0.356
mult. 15UV	20000	0.157	0.134	0.212	0.266
λ=2865.7	40000	0.111	0.945-1	0.172	0.207
3kT/2ΔE= 0.46	80000	0.819-1		0.148	0.170
	160000	0.729-1		0.136	0.150
S III $4p^3P-5s^3P^o$	10000	0.129	0.230	0.225	0.268
mult. 19UV	20000	0.914-1	0.163	0.171	0.200
λ=2677.0	40000	0.646-1	0.115	0.138	0.157
3kT/2ΔE=0.41	80000	0.479-1		0.119	0.131
	160000	0.431-1		0.110	0.117
S III $4p^3D-5s^3P^o$	10000	0.107	0.197	0.193	0.228
mult. 17UV	20000	0.756-1	0.139	0.147	0.170
λ=2495.6	40000	0.534-1	0.985-1	0.118	0.134
3kT/2ΔE=0.46	80000	0.400-1		0.102	0.111
	160000	0.360-1		0.942-1	0.999-1
S IV $3p^2P^o-4s^2S$	10000	0.396-2	0.202-2	0.306-2	0.503-2
	20000	0.280-2	0.143-2	0.231-2	0.366-2
λ=553.1	40000	0.198-2	0.101-2	0.185-2	0.275-2
3kT/2ΔE=0.32	80000	0.144-2	0.784-3	0.159-2	0.217-2
	160000	0.118-2	0.798-3	0.147-2	0.181-2
S IV $4s^2S-4p^2P^o$	10000	0.245	0.118	0.162	0.287
mult. 1	20000	0.173	0.838-1	0.123	0.209
λ=3104.1	40000	0.122	0.592-1	0.991-1	0.156
3kT/2ΔE=0.35	80000	0.886-1	0.476-1	0.861-1	0.123
	160000	0.723-1		0.796-1	0.102
CL III $3d^4P-4p^4P^o$	10000	0.257	0.175	0.178	0.367
mult. 7	20000	0.182	0.123	0.211	0.271
λ=4045.8	40000	0.129	0.873-1	0.169	0.209
3kT/2ΔE=0.47	80000	0.931-1		0.144	0.170
	160000	0.744-1		0.131	0.147

Table 1 (Continued)

Element/Transition	T(K)	W_{SEM}(Å)	W_{SE}(Å)	W_{GM}(Å)	W_G(Å)
CL III $3d^4F-4p^4D^o$	10000	0.452-1	0.296-1	0.514-1	0.669-1
mult. 7UV	20000	0.320-1	0.209-1	0.390-1	0.495-1
λ=1825.7	40000	0.226-1	0.148-1	0.312-1	0.381-1
3kT/2ΔE=0.47	80000	0.165-1	0.141-1	0.267-1	0.310-1
	160000	0.134-1	0.156-1	0.243-1	0.269-1
CL III $4s^4P-4p^4D^o$	10000	0.284	0.171	0.238	0.363
mult. 1	20000	0.201	0.121	0.184	0.268
λ=3629.0	40000	0.142	0.855-1	0.151	0.206
3kT/2ΔE=0.47	80000	0.106		0.133	0.167
	160000	0.898-1		0.123	0.143
CL III $4s^4P-4p^4P^o$	10000	0.246	0.148	0.207	0.315
mult. 2	20000	0.174	0.104	0.160	0.233
λ=3330.9	40000	0.123	0.739-1	0.132	0.179
3kT/2ΔE=0.42	80000	0.912-1		0.116	0.145
	160000	0.773-1		0.107	0.124
CL III $4s^4P-4p^4S^o$	10000	0.226	0.135	0.190	0.290
mult. 3	20000	0.160	0.956-1	0.147	0.214
λ=3160.1	40000	0.113	0.676-1	0.121	0.165
3kT/2ΔE=0.40	80000	0.836-1		0.106	0.134
	160000	0.707-1		0.980-1	0.114
CL III $4s^2P-4p^2D^o$	10000	0.314	0.194	0.266	0.404
mult. 5	20000	0.222	0.137	0.206	0.299
λ=3739.4	40000	0.157	0.982-1	0.170	0.231
3kT/2ΔE=0.53	80000	0.118		0.149	0.187
	160000	0.101		0.138	0.160
CL III $4s^2P-4p^2P^o$	10000	0.243	0.157	0.212	0.318
mult. 6	20000	0.172	0.111	0.164	0.236
λ=3300.9	40000	0.121	0.784-1	0.135	0.182
3kT/2ΔE=0.45	80000	0.903-1		0.118	0.147
	160000	0.768-1		0.109	0.126

Table 1 (Continued)

Element/Transition	T(K)	W_{SEM}(Å)	W_{SE}(Å)	W_{GM}(Å)	W_G(Å)
CL III $4s'^2D-4p'^2F^o$	10000	0.271	0.165	0.229	0.348
mult. 10	20000	0.192	0.117	0.177	0.257
λ=3543.8	40000	0.136	0.859-1	0.145	0.198
3kT/2ΔE=0.59	80000	0.100		0.128	0.160
	160000	0.852-1		0.118	0.137
CL III $4s'^2D-4p'^2D^o$	10000	0.252	0.153	0.213	0.324
mult. 11	20000	0.178	0.108	0.165	0.240
λ=3394.2	40000	0.126	0.785-1	0.135	0.184
3kT/2ΔE=0.55	80000	0.933-1		0.119	0.149
	160000	0.790-1		0.110	0.128
CL III $4s'^2D-4p'^2P^o$	10000	0.204	0.123	0.173	0.263
mult. 11UV	20000	0.144	0.871-1	0.134	0.195
λ=2975.4	40000	0.102	0.616-1	0.110	0.150
3kT/2ΔE=0.45	80000	0.752-1		0.963-1	0.121
	160000	0.634-1		0.889-1	0.104
CL III $4p^2D^o-4d^2F$	10000	0.164	0.149	0.217	0.273
mult. 18UV	20000	0.116	0.106	0.166	0.204
λ=2581.6	40000	0.820-1	0.754-1	0.133	0.159
3kT/2ΔE=0.53	80000	0.593-1		0.115	0.131
	160000	0.527-1		0.105	0.115
CL III $4p^2D^o-4d^2D$	10000	0.135	0.132	0.190	0.235
mult. 19UV	20000	0.952-1	0.936-1	0.145	0.175
λ=2324.3	40000	0.673-1	0.667-1	0.117	0.137
3kT/2ΔE=0.53	80000	0.489-1		0.100	0.113
	160000	0.441-1		0.921-1	0.100
CL III $4p^4P^o-4d^4D$	10000	0.174	0.151	0.222	0.283
mult. 16UV	20000	0.123	0.107	0.170	0.211
λ=2668.2	40000	0.872-1	0.754-1	0.137	0.164
3kT/2ΔE=0.42	80000	0.628-1		0.117	0.135
	160000	0.548-1		0.108	0.118

Table 1 (Continued)

Element/Transition	T(K)	W_{SEM}(Å)	W_{SE}(Å)	W_{GM}(Å)	W_G(Å)
CL III $4p^4S^o-4d^4P$	10000	0.182	0.160	0.233	0.296
mult. 20UV	20000	0.129	0.113	0.178	0.221
λ=2700.2	40000	0.909-1	0.798-1	0.143	0.172
3kT/2ΔE=0.40	80000	0.654-1	0.633-1	0.123	0.141
	160000	0.572-1		0.113	0.124
CL III $4p^4P^o-5s^4P$	10000	0.888-1	0.167	0.163	0.191
mult. 17UV	20000	0.628-1	0.118	0.124	0.143
λ=2416.9	40000	0.444-1	0.836-1	0.991-1	0.111
3kT/2ΔE=0.42	80000	0.321-1	0.649-1	0.849-1	0.927-1
	160000	0.283-1	0.707-1	0.784-1	0.831-1
CL III $4p^4D^o-5s^4P$	10000	0.779-1	0.147	0.145	0.169
mult. 15UV	20000	0.551-1	0.104	0.110	0.126
λ=2281.0	40000	0.390-1	0.736-1	0.879-1	0.987-1
3kT/2ΔE=0.47	80000	0.283-1	0.585-1	0.754-1	0.822-1
	160000	0.251-1	0.636-1	0.697-1	0.738-1
CL IV $4s^3P^o-4p^3D$	10000	0.162	0.991-1	0.122	0.200
	20000	0.114	0.701-1	0.924-1	0.146
λ=3082.2	40000	0.808-1	0.496-1	0.743-1	0.110
3kT/2ΔE=0.32	80000	0.589-1	0.391-1	0.643-1	0.870-1
	160000	0.479-1		0.549-1	0.731-1
CL IV $4s^3P^o-4p^3P$	10000	0.131	0.819-1	0.100	0.164
	20000	0.924-1	0.579-1	0.760-1	0.119
λ=2767.6	40000	0.653-1	0.409-1	0.609-1	0.899-1
3kT/2ΔE=0.32	80000	0.474-1	0.314-1	0.526-1	0.710-1
	160000	0.384-1		0.486-1	0.597-1
A III $3d^5D^o_9-4p^5P_7$	10000	0.342-1	0.222-1	0.394-1	0.508-1
mult. 6UV	20000	0.242-1	0.157-1	0.298-1	0.376-1
λ=1669.7	40000	0.171-1	0.111-1	0.237-1	0.289-1
3kT/2ΔE=0.34	80000	0.123-1	0.883-1	0.202-1	0.235-1
	160000	0.986-2		0.184-1	0.203-1

Table 1 (Continued)

Element/Transition	T(K)	W_{SEM}(Å)	W_{SE}(Å)	W_{GM}(Å)	W_G(Å)
A III $3d'^3D^o-4p'^3D$	10000	0.911-1	0.623-1	0.104	0.134
mult. 9UV	20000	0.644-1	0.440-1	0.789-1	0.990-1
λ=2690.3	40000	0.456-1	0.311-1	0.630-1	0.763-1
3kT/2ΔE=0.36	80000	0.330-1	0.254-1	0.537-1	0.621-1
	160000	0.265-1	0.284-1	0.488-1	0.539-1
A III $3d''^3P^o-4p''^3P$	10000	0.164	0.114	0.183	0.238
mult. 6	20000	0.116	0.806-1	0.139	0.176
λ=3432.6	40000	0.822-1	0.570-1	0.110	0.135
3kT/2ΔE=0.42	80000	0.587-1		0.938-1	0.110
	160000	0.461-1		0.851-1	0.949-1
A III $4s^5S^o-4p^5P$	10000	0.208	0.128	0.178	0.268
mult. 1	20000	0.147	0.906-1	0.137	0.198
λ=3296.6	40000	0.104	0.641-1	0.112	0.152
3kT/2ΔE=0.35	80000	0.763-1	0.522-1	0.978-1	0.123
	160000	0.637-1	0.578-1	0.902-1	0.105
A III $4s'^3D^o-4p'^3D$	10000	0.238	0.144	0.200	0.304
mult. 2	20000	0.168	0.102	0.155	0.225
λ=3492.1	40000	0.119	0.720-1	0.127	0.173
3kT/2ΔE=0.37	80000	0.877-1	0.603-1	0.111	0.140
	160000	0.741-1		0.103	0.120
A III $4s'^3D^o-4p'^3F$	10000	0.221	0.134	0.187	0.283
mult. 3	20000	0.156	0.946-1	0.144	0.209
λ=3344.8	40000	0.110	0.669-1	0.118	0.161
3kT/2ΔE=0.37	80000	0.814-1	0.553-1	0.104	0.130
	160000	0.685-1		0.956-1	0.111
A IV $4s^4P-4p^4D^o$	10000	0.117	0.716-1	0.888-1	0.145
mult. 4UV	20000	0.829-1	0.506-1	0.670-1	0.106
λ=2810.9	40000	0.586-1	0.358-1	0.536-1	0.795-1
3kT/2ΔE=0.29	80000	0.422-1	0.271-1	0.461-1	0.626-1
	160000	0.340-1		0.425-1	0.525-1

Table 1 (Continued)

Element/Transition	T(K)	W_{SEM}(Å)	W_{SE}(Å)	W_{GM}(Å)	W_G(Å)
A IV $4s^4P-4p^4P^o$	10000	0.102	0.631-1	0.781-1	0.127
mult. 5UV	20000	0.721-1	0.446-1	0.589-1	0.926-1
λ=2617.5	40000	0.510-1	0.315-1	0.470-1	0.696-1
3kT/2ΔE=0.29	80000	0.366-1	0.234-1	0.404-1	0.548-1
	160000	0.294-1		0.372-1	0.459-1
A IV $4s^2P-4p^2D^o$	10000	0.133	0.813-1	0.101	0.165
mult. 2	20000	0.943-1	0.575-1	0.761-1	0.120
λ=2925.4	40000	0.667-1	0.407-1	0.610-1	0.905-1
3kT/2ΔE=0.31	80000	0.482-1	0.313-1	0.526-1	0.714-1
	160000	0.389-1		0.485-1	0.599-1
A IV $4s'^2D-4p'^2F^o$	10000	0.114	0.701-1	0.868-1	0.142
mult. 6UV	20000	0.806-1	0.496-1	0.654-1	0.103
λ=2769.2	40000	0.570-1	0.350-1	0.523-1	0.775-1
3kT/2ΔE=0.29	80000	0.410-1	0.263-1	0.449-1	0.610-1
	160000	0.330-1		0.414-1	0.511-1

relation. The line width (FWHM) in Å units then becomes

$$W(\mathring{A}) = 0.4430 \cdot 10^{-8} \frac{\lambda^2(\mathrm{cm})N(\mathrm{cm}^{-3})}{T^{1/2}} (\mathbf{R}_{ii}^2 + \mathbf{R}_{ff}^2), \tag{2}$$

$$\mathbf{R}_{jj}^2 = \sum_{j'} \mathbf{R}_{j'j}^2 \simeq \frac{1}{2}\left(\frac{n_j}{Z}\right)^2 [5n_j^2 + 1 - 3l_j(l_j+1)], \tag{3}$$

where n_j is the effective principal, and l_j the orbital angular momentum quantum numbers, while (Z−1) is the ionic charge.

Within more refined, simple semiclassical approach (Griem, 1974) the Stark width is given by

$$\begin{aligned} W = N\frac{8\pi}{3}\frac{\hbar^2}{m^2}\int_0^\infty \frac{f(v)}{v}\,dv \Bigg\{ \Bigg[\left(\mathbf{R}^2 \ln\frac{\epsilon_{\max}}{\epsilon_{\min}}\right)_{l_i,l_i+1} + \\ \left(\mathbf{R}^2 \ln\frac{\epsilon_{\max}}{\epsilon_{\min}}\right)_{l_i,l_i-1} + \left(\mathbf{R}^2 \ln\frac{\epsilon_{\max}}{\epsilon_{\min}}\right)_{l_{i'},l_{i'}+1} + \\ + \left(\mathbf{R}^2 \ln\frac{\epsilon_{\max}}{\epsilon_{\min}}\right)_{l_{i'},l_{i'}-1} \Bigg]_{\Delta n=0} \sum_{i'} (\mathbf{R}_{i'i}^2)_{\Delta n\neq 0} \left(\ln\frac{\epsilon_{\max}}{\epsilon_{\min}}\right)_{n_i,n_i+1} \\ + \sum_{f'} (\mathbf{R}_{f'f}^2)_{\Delta n\neq 0} \left(\ln\frac{\epsilon_{\max}}{\epsilon_{\min}}\right)_{n_f,n_f+1} \Bigg\} + W_c. \end{aligned} \tag{4}$$

For $\Delta n = 0$,

$$\left(\ln\frac{\epsilon_{\max}}{\epsilon_{\min}}\right)_{l,l'} = \ln\left\{5 - \frac{4.5}{\sqrt{Z}} + \xi_{l,l'}^{-1}\left[1 + \frac{mv^2 n_l^2}{2E_H Z(Z-1)}\right]^{-1}\right\}, \tag{5}$$

$$\xi_{l,l'} = \frac{(Z-1)e^2\omega_c}{mv^3}, \tag{6}$$

$$\omega_c = \max\{|\omega_{l,l'}|, \omega_P, \omega_F, \Delta\omega_i\}. \tag{7}$$

$$\mathbf{R}_{l,l'}^2 \simeq \left(\frac{3n}{2Z}\right)^2 \frac{\max(l,l')}{2l+1}[n^2 - \max^2(l,l')]\phi^2, \tag{8}$$

$$\sum_{j'} (\mathbf{R}_{jj'}^2)_{\Delta n\neq 0} \simeq \left(\frac{3n_j}{2Z}\right)^2 \frac{1}{9}(n_j^2 + 3l_j^2 + 3l_j + 11). \tag{9}$$

Here, ϵ is the eccentricity of the hyperbolic perturber path, $\omega_{l,l'}$ is the frequency separation between l, l' levels, $\omega_p = (4\pi Ne^2/m)^{1/2}$ is the plasma frequency, ω_F is the fine structure splitting and $\Delta\omega_i$ is the ion splitting. The cases where the one–electron model (i. e. only one energy level for each nl electons) assumed in Eq. (4) is not satisfied, are analyzed in detail by Dimitrijević (1982b). For example for a multiplet as a whole,

$R^2_{j'j}$ should be multiplied by R^2_{mult} $(2l + 1)/(2L + 1)$. The multiplet factor R^2_{mult} can be found in Tables of Shore and Menzel (1965). E_H is the hydrogen ionization energy, the residual ionic charge is denoted by Z, while ϕ^2 is the Bates–Damgaard (1949) factor (Tabulated e. g. in Oertel and Shomo, 1968).

For the transitions with $\Delta n \neq 0$, in Eq. (4), $5 - (4.5/\sqrt{Z})$ must be replaced by 1.4, the value which corresponds to the Gaunt factor 0.2 for energies up to about three times the threshold energy. Furthermore, since the $n \rightarrow n + 1$ transitions dominate between all $\Delta n \neq 0$ contributions, one should take

$$\hbar\,\omega_c \approx 2Z^2 E_H/n^3 .$$

In Eq. (4), W_c is the line width induced by strong collisions and higher multipole interactions (Griem, 1974), i. e.

$$W_c = 2\pi N\left(\frac{2m}{\pi kT}\right)^{1/2}\left(\frac{\hbar}{mZ}\right)^2 n_i^4\left[1+\frac{kT}{E_H\left(1+\frac{kT}{E_H}+\frac{Z^2}{n_i^4}\right)}\right] \tag{10}$$

In order to compensate for the overestimation of the line width, since the possible cancelation of elastic contributions to the width was ignored, Dimitrijević and Konjević (1980) proposed that 1.4 instead of $5 - 4.5/Z$ have to be used on the r. h. s. of Eq. (5), on the basis of the following argument: below the inelastic transition threshold, the elastic contribution is taken into account twice, via the strong collision correction and via the extrapolated Gaunt factor. At higher temperatures, the difference between these two versions of Eq. (4) is small, well within theoretical uncertainties for this relation.

3. RESULTS

The results of electron-impact line calculations (FWHM) for the prominent isolated lines of Be III through Ar III and B IV through Ar IV are given in Table 1. Besides the modified semiempirical widths (W_{SEM}) (Dimitrijević, 1988a), present calculations according to Griem's (1968) semiempirical approach were also shown (W_{SE}) in the cases when the condition $3kT/2\Delta E_{jj'} \lesssim 2$ is satisfied. Under W_G are given present simple semiclassical results obtained by using the method proposed by Griem (1974) (Eq. (4)), and under W_{GM} widths obtained by using the same method, but with modified Gaunt factor treshold value for the $\Delta n = 0$ transitions.

For evaluation of the radial integrals, Coulomb approximation (Bates and Damgaard, 1949; Oertel and Shomo, 1968) has been used. Cases with an initial atomic state with equivalent electrons were avoided, when possible. If not, corresponding coefficients of fractional parentage (Shore and Menzel, 1965) are included.

All four methods are compared with available experimental values by Dimitrijević and Konjević (1980). The average values of the ratios of measured to calculated widths are as follows: for doubly-charged ions, $R_{SEM} = 1.06 \pm 0.32$; $R_{SE} = 1.53 \pm 0.46$; $R_{GM} = 0.96 \pm 0.24$; $R_G = 0.72 \pm 0.19$; for triply-charged ions: $R_{SEM} = 0.91 \pm 0.42$; $R_{SE} = 1.56 \pm 0.85$; $R_{GM} = 1.08 \pm 0.41$ and $R_G = 0.72 \pm 0.32$. We can conclude that modified semiempirical method and the modified simple semiclassical method (Dimitrijević and Konjević, 1980) compare best with the experimental data. Hence, we expect that both methods, and especially the simpler, modified semiempirical one, may be quite useful for astrophysical purpose.

ACKNOWLEDGEMENT

This work has been supported by Republic Association for Science in Serbia through the project "Physics and Motions of Celestial Bodies and Artificial Satelites.

REFERENCES

Ackermann, U., Finken, K. H, and Musielok, J.: 1985, *Phys, Rev.* A, **31**, 2597.
Bates, D. R., and Damgaard, A.: 1949, *Phil. Trans. Roy. Soc. London,* Ser. A, **242**, 101.
Dimitrijević, M. S.: 1982a, in *Sun and Planetary System,* eds. W. Fricke, G. Teleki, D. Reidel P. C., Dordrecht, 101.
Dimitrijević, M. S.: 1982b, *Astron. Astrpohys.* **112**, 251.
Dimitrijević, M. S.: 1982c, in *The Physics of Ionized Gases* (Inv. Lectures of SPIG–82), ed. G. Pichler, Inst. Phys. University Zagreb, 397.
Dimitrijević, M. S.: 1983, *Astron. Astrophys.* **127**, 68.
Dimitrijević, M. S.: 1988a, *Astron. Astrpohys. Suppl.* to be published.
Dimitrijević, M. S.: 1988b, in *Physics of Formation of Fe II Lines Outside LTE,* ed R. Viotti, A. Vittone, M. Friedjung, D. Reidel P. C., Dordrecht, 211.
Dimitrijević, M. S. and Konjević, N.: 1978, *J. Quant, Spectrosc. Radiat. Transfer,* **20**, 223.
Dimitrijević, M. S. and Konjević, N.: 1980, *J. Quant, Spectrosc. Radiat. Transfer,* **24**, 451.
Dimitrijević, M. S. and Konjević, N.: 1981a, in *Spectral Line Shapes,* ed B, Wende, W. de Gruyter, Berlin, New York, 211.
Dimitrijević, M. S. and Konjević, N.: 1981b, *Astron. Astrophys.* **102**, 93.

Dimitrijević, M. S. and Konjević, N.: 1981c, *J. Quant. Spectrosc. Radiat. Transfer,* **25**, 387.
Dimitrijević, M. S., Feautrier, N., Sahal–Brechot, S.: 1981, *J. Phys. B* **14**, 2559.
Dimtrijević, M. S. and Kršljanin, V.: 1986, *Astron.Astrophys.* **165**, 269.
Dimitrijević, M. S. and Konjević, N.: 1986, *Astron. Astrophys.* **163**, 297.
Dimitrijević, M. S. and Konjević, N.: 1987, *Astron. Astrpohys.* **172**, 345.
El–Farra, M. A., Hughes, T. P.: 1983, *J. Quant. Spectrosc. Radiat. Transfer* 30, 335.
Griem, H. R.: 1964, *Plasma Spectroscopy,* Chap. 4, Mc-Graw--Hill, New York.
Griem, H. R.: 1968, *Phys. Rev.* **165**, 258.
Griem, H. R.: 1974, *Spectral Line Broadening by Plasmas,* Academic Press, New York.
Griem, H. R., Baranger, M., Kolb, A. C., Oertel, G. K.: 1962, *Phys. Rev.* **125**, 177.
Hey, J. D. and Bryan, R. J.: 1977, *J. Quant. Spectrosc. Radiat. Transfer* **17**, 221.
Konjević, N., Dimitrijević, M. S. and Wiese, W. L.: 1984, *J. Phys. Chem. Ref. Data* **13**, 649.
Lanz, T., Dimitrijević, M. S. and Artru, M. C.: 1988, *Astron. Astrophys.* **192**, 249.
Oertel, G. K. and Shomo, L. P.: 1968, *Astrophys. J. Suppl.Series* **16**, 175.
Peytremann, E.: 1972, *Astron. Astrophys.* **17**, 76.
Seaton, M. J.: 1987, *J. Phys.* B **20**, 6431.
Shore, B. W. and Menzel, D. H.: 1965, *Astrophys. J. Suppl. Series* **12**, 187.
Vince, I., Dimitrijević, M. S. and Kršljanin, V.: 1985a, in *Spectral Line Shapes III,* ed. F. Rostas, W. de Gruyter, Berlin, New York, 649.
Vince, I., Dimitrijević, M. S. and Kršljanin, V.: 1985b, in *Progress in Stellar Spectral Line Formation Theory,* eds. J. E. Beckman, L. Crivellari, D. Reidel, Dordrecht, Boston, Lancaster, 373.

Bull. Obs. Astron. Belgrade, N° 139 (1988) UDC 52

II WORKSHOP: ASTROPHYSICS IN YUGOSLAVIA

Milan S. Dimitrijević

Astronomical Observatory, Volgina 7, 11050 Belgrade, Yugoslavia

(Received: June 6, 1988)

After the first meeting of Yugoslav astrophysicists held from 13 to 14 february 1986. in Ljubljana, II workshop: Astrophysics in Yugoslavia was held from 8 to 10 September 1987 in National Library in Belgrade, during the celebration of the centenary of Belgrade astronomical observatory. About fifty astrophysicists from Belgrade, Zagreb, Ljubljana, Sarajevo, Novi Sad, France, the USSR and Hungary attended the meeting, presenting 36 communications from all domains of astrophysics.

The first session of this meeting was devoted to stars and galaxies, and was opened by the talk of J. Arsenijević *Be stars, a challenge to observers and theoreticians.* The main historical steps in the investigation of Be stars with emission lines and the achievements of the Belgrade program of long-term polarimetric study of Be stars, which started in 1974, were reviewed. Observational results in the confrontation with the theoretical interpretations, from Struve's hypothesis to the contemporary empirical Be stars models were also presented and discussed.

B. Balazs spoke on the influence of the angular velocity of spiral arms and the spatial distribution of galactic civilizations. He assumed that the case of mankind is about average and, that the longevity of a civilization might be limited with high probability by catastrophic events treatening during the crossing of the galactic arms. He concluded that intelligent life is presumably concentrated on a belt in the Galaxy which is a narrow annulus including the galactic orbit of our Sun. Consequently, from a heliocentric point of view, the distribution of our potential extraterestrial partners is highly anizotropic.

S. Ninković discussed the role of some special types of stars in contemporary galactic astronomy and T. Zwitter informed the conference on the recent investigations of SS 433 object. Finaly, I. Vince and M. S. Dimitrijević presented the results of their examinations of C IV line profiles in white dwarfs.

The afternoon session started with the talk on cosmic synchrotron radiation by J. Milogradov-Turin and was devoted to the theoretical investigations in astrpohysics. A number of communications (B. S. Milić) *Quasi-perpendicular ion-cyclotron instability in plasmas containing ion with two temperatures;* S. R. Krstić, B. S. Milić: *Landau damping of the transverse electromagnetic waves in multi-special plasmas with polarizable heavy paricles;* A. A. Mihajlov, M. S. Dimitrijević: *Influence of ion-atom impact complexes on different processes in low temperature weakly ionized plasmas;* V. Vitel, M. Skowronek, M. S. Dimitrijević, M. M. Popović: *Electron impact broadening along homologous sequence of noble gases)* was devoted to the theoretical investigations of different processes in solar and stellar plasmas. In two papers (J. Vranješ: *Influence of radiative processes on gravitational instability in homogeneous magnetized fluid,* and B. Gaković, V. Čadež: *Resonant excitation of MHD surface waves by streaming fluid)* MHD investigations of astrophysical interest were given. O. Atanacković-Vukmanović and E. Simonneau presented an approximative solution in the frame of the kinetic non-LTE approach of Ly alfa line transfer in chromospheric conditions. Finally, I. Lukačević discussed some metric properties of Rosen's *bimetric gravitation theory,* and Logunov's *relativistic gravitation theory.*

Morning session of 9. September was devoted to the Sun and started by the talk of M. Karabin on variations in Solar constant followed by the report on spectral analysis of a white light flare by P. Sotirovski, with particular emphasis on the Stark effect and the continuum emission.

The need for various research programs at Belgrade equatorial solar spectrograph motivated the construction of a manual solar spectrum scanner described by A. Kubičela, I. Vince and S. Jankov. N. K. Todorović and S. Todorović discussed the 22 year cycle of sunspots and, J. Arsenijević, M. Karabin, A. Kubičela and I. Vince informed on the beginning of a study of long-term changes of selected Fraunhofer spectral lines. The measurements of the depth, half-width and equivalent width of some selected lines, have been started at Belgrade astronomical observatory with the Solar spectrograph and its new scanner. The program is aimed to last at least trough one 11-year cycle.

The afternoon session started with the paper on the influence of Stark broadening on equivalent widths of Si II visible lines in stellar atmospheres by T. Lanz, M. S. Dimitrijević and M. C. Artru. S. Jankov presented two papers: *Constrained deconvolution and indirect stellar imaging from spectroscopic and photometric observations.* An investigation of the formation of O I lines observed in the infrared spectrum of γ Cas, was reported by M. S. Dimitrijević, N. Feautrier and S. Sahal-Bréchot. In the communication: *Close binary systems with accretion disk,* G. Đurašević discussed the possibility to

determine parameters of close binary systems with accretion disk, from the curve of luminosity analysis. The system's model, giving the synthetic curve of luminosity has been made and the inverse problem method was presented, too. In two contributions: *The chemical composition of the Galileian satellites* by V. Čelebonović, it was shown that the theory proposed by Savić and Kašanin can be used in studies of planetary satellites, and that it seems reasonable to attempt using it in studies of asteroids.

The last day of the conference was dominated by contributions to practical astrophysics, amateur's reports and contributions dealing with educational side of astrophysics and astrophysics in literature. After the contributions: *Astrophysics in the nineteenth century serbian literature* by N. Janković and: *On the astronomy text books and their representation of contemporary science* by V. Vujnović, J. Francisti spoke on developement of amateur radioastronomy for improvement of activity of astronomical societies and people's observatories.

In a series of communications (A. Tomić, M. Vuletić, S. Marković: *Some characteristics of the sky brightness in Belgrade;* A. Tomić, Lj. Jovanović: *On the photographic observation of double stars,* A. Tomić, Z. Glišić, M. Muminović, M. Stupar: *On the photographic determination of Lunar librations;* A. Tomić, M. Muminović, M. Stupar; *The limiting stellar magnitude of the Sarajevo sky atlas;* A. Dolžan: *Photoelectric photometry of eclipsing binary stars;* A. Dolžan: *Photography of Supernova 1987a*) various aspects of practical astrophysics and amateur's observations were examined.

During the round table discussion, it was decided that the next meeting of Yugoslav astrophysicists would be organized in 1989 by Hvar observatory, since National conference of Yugoslav astronomers would be held in Sarajevo 1988.

The number of contributions presented during this conference on various topics of astrophysics, short time after the first astrophysical meeting in Ljubljana, give evidence of developement of astrophysical investigations in Yugoslavia.

Bull. Obs. Astron. Belgrade N° 140 (1989), 111–116.

UDC 52–355.3
Review paper

STARK BROADENING IN ASTROPHYSICS

Milan S.Dimitrijević

Astronomical Observatory, Volgina 7, 11050 Beograd, Yugoslavia

(Received: October 26, 1988)

SUMMARY: The importance of Stark broadening in astrophysics is briefly reviewed. A short review of results of Yugoslav research workers on this field is also presented.

1. INTRODUCTION

As the typical information in astronomy is obtained by analyzing the radiation, the understanding of astrophysical spectral line shapes is of great importance. Spectral line shapes are an important research field particularly in special laboratories and institutions found in order to provide basic physical data to astronomers, e.g. JILA (Joint Institute for Laboratory Astrophysics) in Boulder Colorado. Stark and other broadening mechanisms of lines in astrophysical spectra are also investigated within the comission 14 of the IAU for fundamental spectroscopic data.

Spectral line shapes enter the analysis of a stellar spectrum essentially in two ways:

a) Selected lines from which we may derrive information about stellar parameters require reliable line shape theory and data of high accuracy for the contribution of the main broadening mechanism.

b) For the bulk of ($\gtrsim 10^6$) lines, as well as for smaller contributions to the main broadening mechanisms, broadening parameters of only modest accuracy are sufficient. Such lines only add together to the total absorption coefficient, which determines the atmospheric stratification, and we need only the good average accuracy while the accuracy for a particular line is not so important.

Stellar spectroscopy depends on very extensive list of elements and line transitions with their atomic and line broadening parameters. It is difficult to state in general terms which are the relevant transitions since the atmospheric composition of a star is not known a priori, and many interesting groups of stars exist with very peculiar abundances as compared to the Sun.

The interest for a very extensive list of line broadening data is stimulated also by spectroscopy from space. After the launch of Copernicus in 1972, it became possible to study the ultraviolet spectra of the brighter stars at very high spectral resolution. These studies were extended to considerably fainter objects with the launch of the International Ultraviolet Explorer (IUE) on January 26, 1978. A number of projects to follow up the achievements made in the space spectroscopy have been discussed The most advanced project is the Space Telescope (ST), a 2.4 m telescope (f/24) for studies at ultraviolet and optical wavelength. Using space spectroscopy, an extensive amount of spectroscopic information over large spectral regions of all kind of celestial objects has been and will be collected, stimulating spectral–line–shape research.

2. STARK BROADENING IN ASTROPHYSICS

Among the various pressure broadening mechanism, broadening due to interaction between emitter and charged particles (Stark broadening) is dominant in several cases. The relevant physical parameters for stellar plasma are most conveniently expressed in terms of the Hertzsprung–Russel diagram in which luminosity is plotted against effective surface temperature (figure 1). For $T_{eff} \geqslant 10^4$ K, hydrogen, the main constituent of a stellar astmosphera is mainly ionized, electron pressure, total pressure and the main collisional broadening mechanism for spectral lines is the interatomic Stark effect. We can see in Fig. 1 that this is the case for white dwarfs and hot stars of O, B and A0 type. Even in cooler stars atmospherae as e.g. Solar one Stark broadening may be important in some cases. In figure 2 is presented temperature as a function of height in the Solar atmosphera according to VAL model (Vernaza et al, 1981) as well as regions of formation of a number of Solar lines. We can see that far line wings of e.g. H_α line are formed in deeper atmospheric layers where the electron concentration is sufficiently high and Stark broadening contribution is not a priori negligible. On the other hand, the influence of Stark broadening within a spectral series increases with the increase of the principal quantum number of the upper level (Dimitrijević, Sahal–Bréchot, 1984ab; 1985) and Stark broadening contribution may become significant in the Solar spectrum (Vince et al. 1985abc).

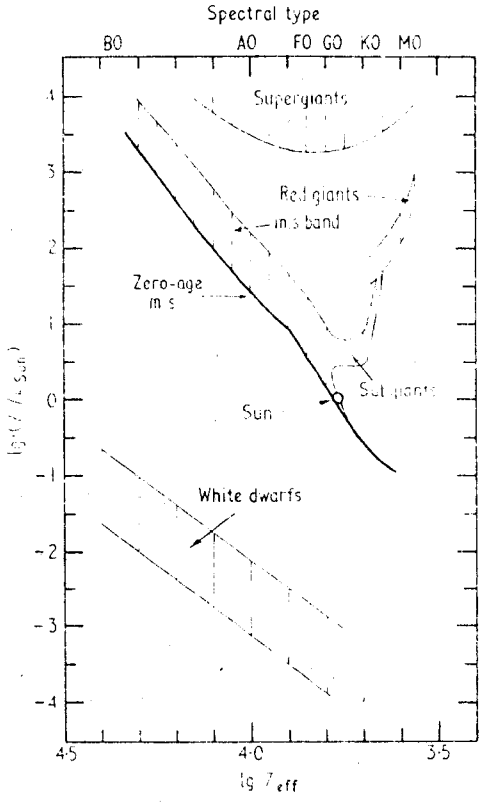

Figure 1. Schematic Hertzsprung–Russell diagram: m.s., main sequence.

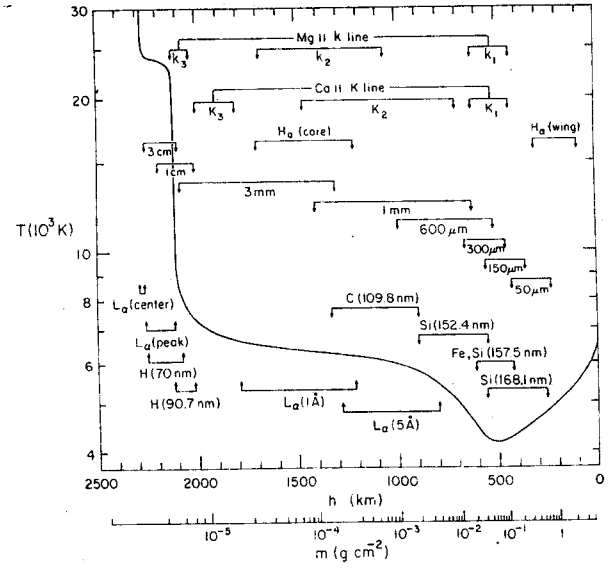

Figure 2. The average quiet–Sun temperature distribution derived from the EUV continuum, the Lα line, and other observations. The approximate depths where the various continua and lines originate are indicated.

Another case where the Stark broadening is the dominant pressure broadening mechanism are radio recombination lines from interstellar clouds of ionized and neutral hydrogen. The range of principal quantum numbers over which radio recombination lines have been observed is $56 \leqslant n \leqslant 253$ which corresponds in frequency to a range from 37.5 to 0.40 GHz. In such atoms the optical electron is far from the nucleus and very sensitive to the weak electric field fluctuations. The Stark broadening is the main collisional broadening mechanism in this case.

For example Stark broadening has been detected in the radio frequency recombination lines emitted by the emission nebula W51 (Lang and Willson, 1978). In figure 3 are given observed linewidths $\Delta\nu_L$, plotted as a function of principal quantum number, n. The solid curves illustrate the convolution of Stark and Doppler broadening for different values of electron density, N_e. The dashed lines correspond to $N_e = 10^3 \cdot cm^{-3}$ and Stark broadening which varies as $n^{4.0}$ and $n^{5.0}$. Under the assumption that the Stark broadening varies as $n^{4.4}$, these data indicate that $N_e = 10^{3.0 \pm 0.1}$ cm^{-3}.

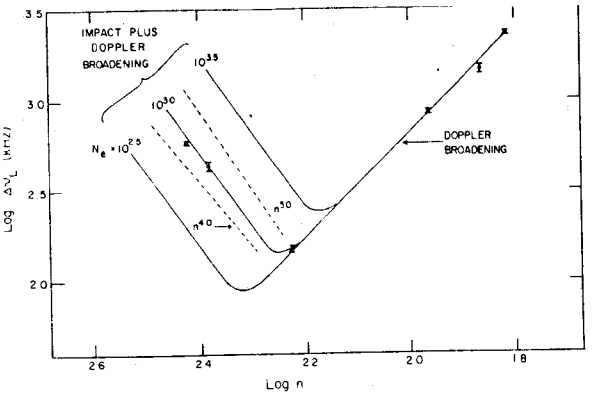

Figure 3. Observed linewidths in the emission nebula W51 compared with calculations (see the text) (Lang and Willson, 1978).

Appart the investigation of profiles of radio recombination lines from molecular and ionized hydrogen regions, typical astrophysical problems where pressure broadening is important may be devided in following categories :

a) Understanding of qualitative effects that one can see on spectrograms.

b) Determination of temperature (T) and electron concentration (N_e) of an astrophysical plasma and surface gravity in stars.

c) Determination of abundances of elements from profiles or equivalent widths of absorption lines.

d) Radiative transfer through astrophysical plasmas.

Table 1: Number of articles, authors and articles in international journals, published by Yugoslav research workers in the period 1962–1985

Year	Number of articles published	Number of authors	Number of articles in international journals
1962	1	1	1
1963	0	0	0
1964	2	2	0
1965	1	1	1
1966	0	0	0
1967	0	0	0
1968	2	4	1
1969	4	4	0
1970	15	13	4
1971	11	9	4
1972	10	11	4
1973	10	13	3
1974	16	16	4
1975	14	15	5
1976	23	16	4
1977	13	14	7
1978	23	16	8
1979	17	14	7
1980	30	19	6
1981	26	17	4
1982	46	19	9
1983	31	19	10
1984	41	22	13
1985	35	21	7
Total	371		102

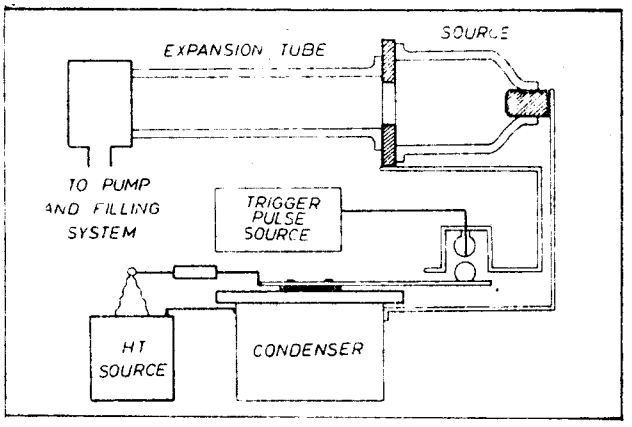

Figure 8. The palsma source of Josephson type.

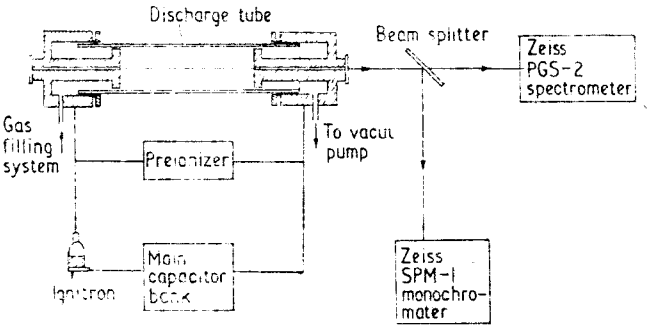

Figure 9. Pulsed arc

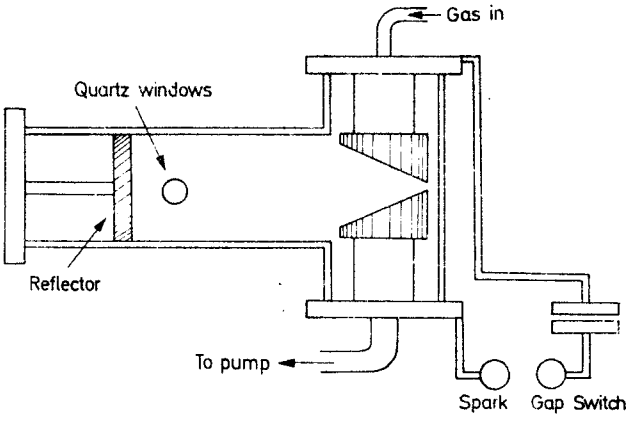

Figure 10. Electromagnetically driven T tube.

plasmas with $N_e = 2 \times 10^{13} - 4 \times 10^{17}$ cm^{-3} and T=2 x 10^3 – 6 x 10^4 K. In Yugoslav laboratories, Stark line widths are measured for 352 lines for 58 different kinds of emitters. Stark shifts for lines of non hydrogenic emitters are measured for 187 lines and 33 different emitters. The plasma sources were: a) The source of Josephson type (Figure 8) (e.g. J.Purić et al, 1970). Here, a condenser battery was discharged via a triggered spark gap. The discharge between the ring and cylindrical electrode in the source is pinched, causing the shock wave to propagate along the expansion tube; b) Pulsed arc (figure 9) (e g. Konjević et al, 1971) and very similar Z pinch; c) Electromagnetically driven T–tube (figure 10 (Konjević et al, 1970) and d) Wall stabilized arc (figure 11) (Đurović, 1979). We can see in figure 11 that the arc channel was formed by a series of water cooled coopper discs with a central hole. The end parts of the arc chamber were closed by two brass discs in each of which there was a centrally bored hole for end–on plasma observations.

Theoretical research of Stark broadening was performed using quantum mechanical (the first strong coupling calculation for a non–hydrogenic neutral atom line, Li I 2s–2p, Dimitrijević et al. 1981) and semiclassical (BrI, CdI, GeI, HgI, PbI, RbI, SnI, ZnI, FI, OII, TiII, MnII, ArIII, ClIII, SiIII, SIII, NIII, CIII, OIII, ArIV, SiIV, CIV, NIV, SIV etc, see e.g. Dimitrijević, 1982 and references therein) approaches. Also, approximative approaches useful for large scale calculations or quick estimates, have been investigated. The modified semi-

Observed spectral lines may be used also for determining the electron temperature and the concentration in astrophysical sources. Especially Balmer line profiles are a powerful diagnostic tool in studying stellar atmospheres. In cooler stars, such as the Sun, the line intensity is a good measure of the effective temperature. as can be seen from Fig. 7, line widths of higher members of the Balmer sequence are very sensitive to the change of electron density. In atmospheres of O and B stars, and also of some white dwarfs and A0 type stars ($T_{eff} \geqslant 10^4$ K) hydrogen is mainly ionized and the main collisional broadening mechanism for spectral lines is the impact broadening by electrons (Stark broadening). In such case the atmospheric pressure P is proportional to the electron concentration N_e at a fixed temperature. From the hydrostatic equation we can now deduce the surface gravity g. Total pressure P is given by $P \cong g^k$ (the coefficient k is different for different particles).

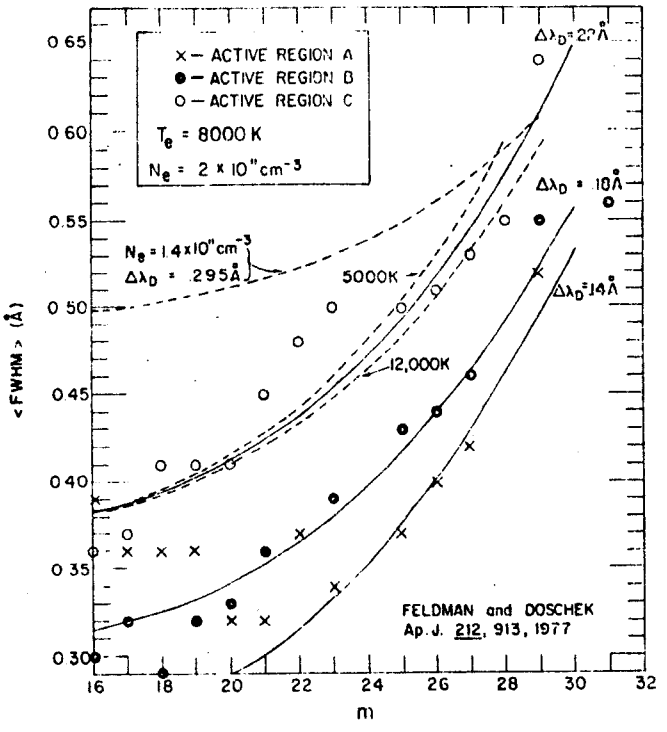

Figure 7. Stark broadening of high member series lines at 2" above the limb over active regions. The density of 2 x 10^{11} cm^{-3} is an average of the actual values. The dashed curve with a density of 1.4 x 10^{11} cm^{-3} is fitted to the data at m = 29.

The important problem for which we need good pressure broadening data is that of determining abundances of elements from equivalent widths (W) of absorption lines. If the line is very weak, the problem is quite straightforward, since W (in wavelength units) is proportional to the abundance ratio of the element to hydrogen, multiplied by the oscillator strength of the transition

$$\left(\frac{W}{\lambda}\right)_{weak} = X \equiv \frac{N_M}{N_H} f\lambda \int_0^\infty \phi(\tau)d\tau$$

where $\phi(\tau)$ is a contribution function depending on the structure of the stellar atmosphere and the relevant states of excitation and ionization and τ is the optical depth in the continuum. If the line is not weak, the situation is much more complicated. The relationship between X and (W/λ) is described by the curve of growth, whose shape depends on the amount of line broadening due to both Doppler and pressure effects. The curve has three main branches:

Linear (unsaturated): $(W/\lambda) = X$

Flat (saturated): $(W/\lambda) \cong 3v_D/c$

Damping branch: $(W/\lambda) = (\lambda X\gamma/\pi c)^{1/2}$

Here, γ is damping (pressure broadening) constant and v_D the velocity corresponding to the given Doppler width.

Pressure broadening data are also required for the estimation of the radiative transfer through the stellar plasma In this case data for a great number of lines are often needed. For such large scale calculations high accuracy of every particular value is not so important. In such cases, tedious calculations can be avoided if one uses simple, approximative formulae with good average accuracy (for Stark broadening see e.g. Dimitrijević (1982) and references therein).

3. LINE SHAPES INVESTIGATIONS IN YUGOSLAVIA 1962–1985

Since the first article on this topic (Vujnović et al., 1962) 371 publications concerning line shapes investigations have been published by 68 Yugoslav authors. The number of published articles, authors and, articles published in international journals are given in Table 1 for every year. We can see that 113 articles are published in international journals during the considered period. Also, 12 theses for Mr.Sc. degree and 9 doctoral theses have been done. Among the published articles, 15 are in Astronomy and Astrophysics and 1 in Astrophysical Journal.

Up to date, a large experimental work on Stark broadening for nonhydrogenic emitters has been done in the world and in Yugoslavia, in laboratory

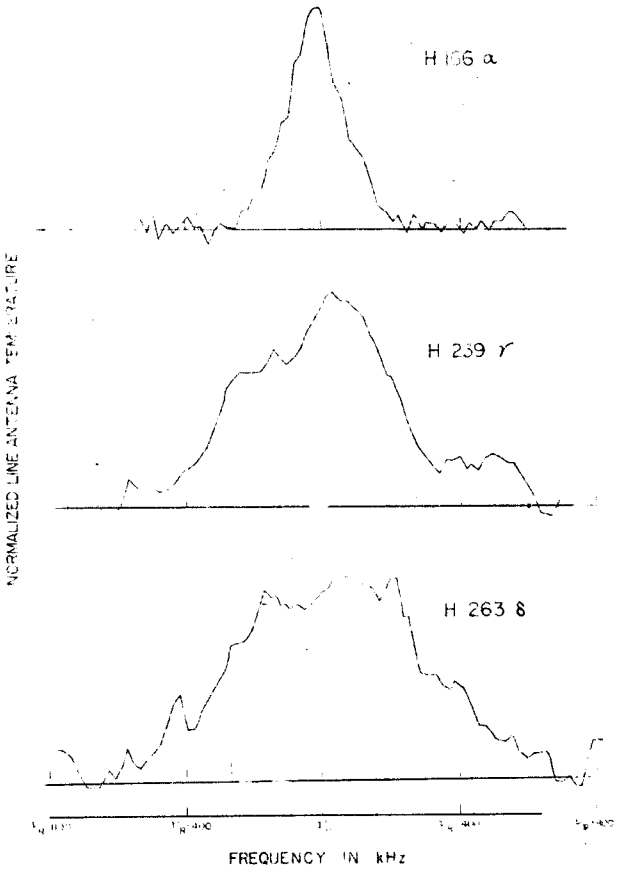

Figure 4. Observed Stark andDoppler broadened profiles in the emission nebula W 51 (Lang and Willson, 1978).

In order to explain astrophysical spectra, the knowledge about the pressure broadening is often needed. An example is the Stark shift in the spectra of white dwarfs which made difficulties in the interpretation of the Einstein shift, determined using helium lines (Wiese and Kelleher, 1971)

As another example one can mention the Solar limb effect. Careful measurements of the Fraunhofer lines show a small but systematic red shift across the Solar disk (as compared with their wevelength at the center) reaching a maximum on the limb. Appart from radial current hypothesis for explanation of this effect (see e.g. Hart, 1974) there are attempts to explain it partially or completely as a consequence of collisions between the absorbing atoms and surrounding particles (see e.g. Hart 1974 or Vince et al. 1985c). Calculations (Vince et al 1985c) of linewidths and relative line shifts across the Solar disk for Na I 3p–6s line are presented in figures 5 and 6. Relative lineshifts are compared also with simple radial current theory predictions (Hart, 1974). As an illustration, in figure 6 are given averaged observations for Fe I 525.02 nm line (Labonte and Howard, 1982). We can notice that Stark broadening contribution is not negligible.

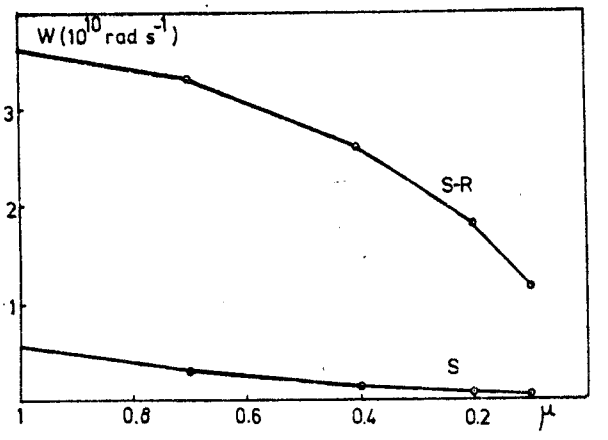

Figure 5. The full halfwidth for Na I 3p–6s line due to collisions with neutral (S–R) and charged particles (S) as a function of the heliocentric angle ($\mu = \cos\theta$).

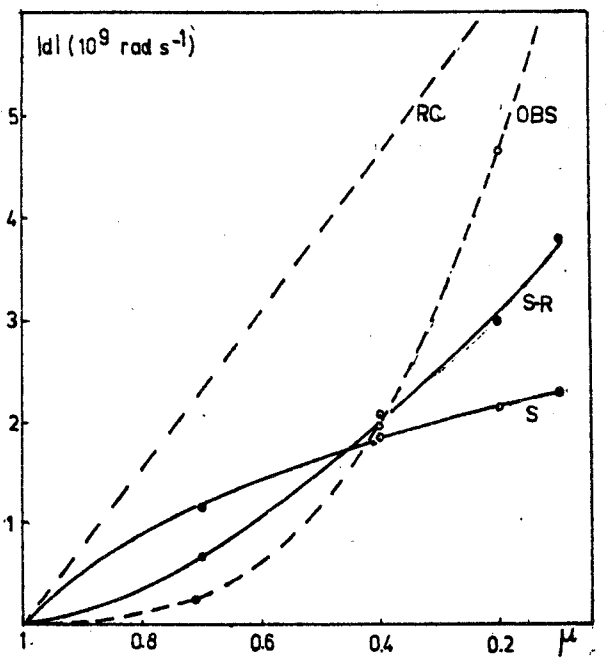

Figure 6. Relative Na I 3p–6s line shifts (shift at the Solar disk centre is taken as zero) as a function of the heliocentric angle ($\mu = \cos\theta$) of observed points; RC – the shift according to the radial current hypothesis (see e.g. Hart, 1974); OBS – averaged observation for Fe I 525.02 nm line (Labonte and Howard, 1982); S–R – Relative shift due to Na–H collisions using Smirnov–Roueff potential; S– Relative shift due to collisions with charged particles.

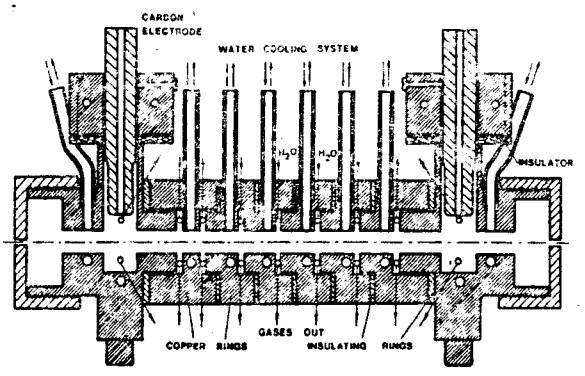

Figure 11. Wall stabilized arc.

empirical approach for ion lines is formulated (Dimitrijević and Konjević, 1981; 1977; Dimitrijević and Kršljanin, 1986) as well as an approximative approach for neutral atom lines (Dimitrijević, and Konjević, 1986).

When reliable data do not exist, knowledge about regularities and systematic trends of Stark broadening parameters offer an additional possibility for estimation or critical evaluation of Stark broadening data. The first paper on this topic is published by Purić and Ćirković (1973) and up to date a lot of work is done by Yugoslav authors. Stark broadening parameters regularities and similarities of lines within a multiplet, supermultiplet, transition arry, spectral series, izoelectronic sequences and for homologous emitters have been investigated (see e.g. review article: Konjević and Dimitrijević (1981) and references therein).

Critical reviews of existing experimental data for neutral (Konjević and Roberts, 1976; Konjević et al. 1984a) and ion (Konjević and Wiese, 1976; Konjević et al. 1984b) lines Stark broadening parameters and tables for doubly and triply charged ion line widths (Dimitrijević, 1988) may also be useful in astrophysics as sources of basic data.

ACKNOWLEDGEMENT

This work has been supported by Republic Association for Science in Serbia through the project „Physics and Motions of Celestial Bodies and Artificial Satellites".

REFERENCES

Dimitrijević, M.S.: 1982a, *Astron. Astrophys.* **112**, 251.

Dimitrijević, M.S.: 1982b, in *The Physics of Ionized Gases*, ed G.Pichler, Inst. Phys. University, Zagreb, 397.

Dimitrijević, M.S.: 1988, *Astron, Astrophys. Suppl. Ser.*, **76**, 53.

Dimitrijević, M.S, Feautrier, N. and Sahal–Bréchot,S.: 1981, *J. Phys.* B. **14**, 2559.

Dimitrijević, M.S. and Konjević, N.: 1981a, *J. Quant. Spectrosc. Radiative Transfer* **24**, 451.

Dimitrijević, M.S., and Konjević, N.: 1987, *Astron. Astrophys.*, **172**, 345.

Dimitrijević, M.S. and Konjević, N. : 1986 *Astron. Astrophys.*, **163**, 297.

Dimitrijević, M.S. and Kršljanin, V.: 1986, *Astron. Astrophys.*, **165**, 269.

Dimitrijević, M.S. and Sahal–Bréchot, S.: 1984a, *J. Quant. Spectrosc. Radiat. Transfer*, **31**, 301.

Dimitrijević, M.S. and Sahal–Bréchot, S.: 1984b, *Astron. Astrophys.* **136**, 289.

Dimitrijević, M.S. and Sahal–Bréchot, S.: 1985 *J.Quant. Spectrosc. Radiat. Transfer* **34**, 149.

Djurović, S.: 1979, *Rev. Research Fac. Sci. Univ. Novi Sad*, **9**, 307.

Feldman, U. and Doschek, G.A.: 1977, *Astrophys. J.* **212**, 913.

Hart, M.H.: 1974, *Astrophys. J.*: **187**, 393.

Konjević, N. and Dimitrijević, M.S.: 1981, in *Spectral Line Shapes I* ed. B.Wende, W. de Gruyter, Berlin, New York, 241.

Konjević, N., Dimitrijević, M.S. and Wiese, W.L.: 1984a, *J. Phys. Chem. Ref. Data* **13**, 619.

Konjević, N., Dimitrijević, M.S. and Wiese, W.L.: 1984b, *J. Phys. Chem. Ref. Data* **13**, 649.

Konjević, N., Labat. J., Ćirković, Lj. and Purić, J.: 1970, *Z. Physik* **235**, 35.

Konjević, N., Platiša, M. and Purić, J.: 1971, *J. Phys.* B. **4**, 1541.

Konjević, N. and Roberts, J.R.: 1976, *J.Phys. Chem. Ref. Data* **5**, 209.

Konjević, N. and Wiese, W.L.: 1976, *J. Phys. Chem. Ref. Data* **5**, 259.

Labonte, B.J. and Howard, D.R.: 1982, *Solar Phys.* **80**, 361.

Lang, K.R. and Willson, R.F.: 1978, *Mon. Not. Roy, Astr. Soc.* **183**, 5p.

Purić, J.M. and Ćirković, Lj.M.: 1973, *XI Int. Conf. Phen. Ioniz. Gases*, Prag 398.

Purić, J., Labat, J., Ćirković, Lj. and Konjević, N.: 1970, *Fizika* **2**, 67.

Vernazza, J.E., Avrett, E.H. and Loeser, R.: 1981 *Astrophys. J. Suppl. Series* **45**, 635.

Vince, I. and Dimitrijević, M.S.: 1985a, *Publ. Obs. Astron. de Belgrade* No. 33, 15.

Vince, I., Dimitrijević, M.S. and Kršljanin, V.: 1985b, in *Spectral Line Shapes III*, ed. F.Rostas, W. de Gruyter, Berlin, New York, 649.

Vince, I., Dimitrijević, M.S. and Kršljanin, V.: 1985c, in *Progress in Stellar Spectral Line Formation Theory*, eds. J. Beckman and L. Crivelari, D. Reidel, Dordrecht, Boston, Lancaster, 373.

Vujnović, V., Harrison, J.A. and Crags, J.D.: 1962, *Proc. Phys. Soc.* (London) **80**, 516.

Wiese, W.L. and Kelleher, D.E.: 1971, *Astrophys. J.* **166**, L59.

ASTRONOMICAL INSTITUTE
SLOVAK ACADEMY OF SCIENCES

*

CHEMICALLY PECULIAR AND MAGNETIC STARS

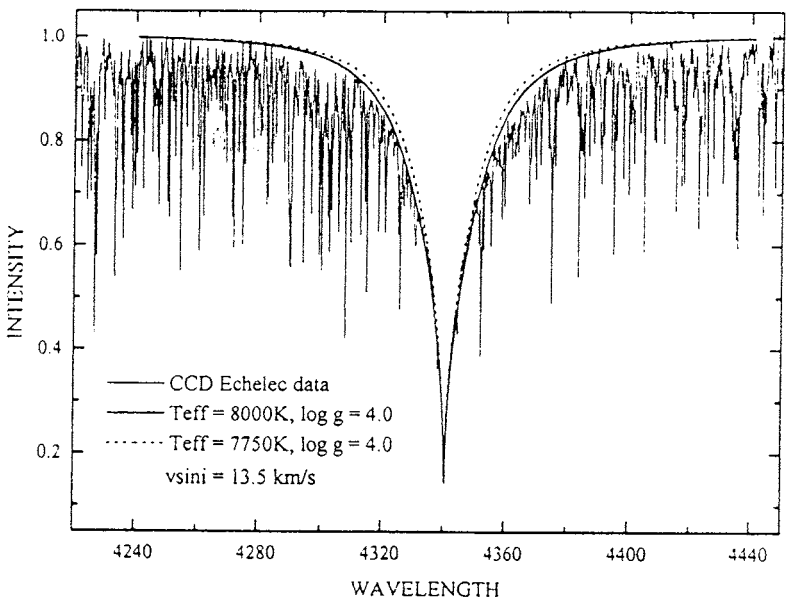

The H_γ profile of α Circinis

*

Tatranská Lomnica, 1994

THE INFLUENCE OF ION-ATOM RADIATIVE COLLISIONS TO THE OPACITY IN HELIUM RICH DB WHITE DWARFS

A.A. MIHAJLOV[1,2], M.S. DIMITRIJEVIĆ[2], Lj.M. IGNjATOVIĆ[1]

[1] *Institute of Physics, P.O.Box 57, 11001 Beograd, Yugoslavia*

[2] *Astronomical Observatory, Volgina 7, 11050 Beograd, Yugoslavia*

Received: November, 1993

Abstract. We investigate the influence to the continuous optical spectrum of the helium rich DB white dwarf atmosphere of radiative processes due to $He^+(1s) - He(1s^2)$ collisions. We show that these ion-atom radiative collision processes are of importance at certain layers of the investigated white dwarf atmosphere, and the corresponding contributions to the optical depth and continuous opacity are not negligible.

Key words: white dwarfs – radiation mechanisms

1. Introduction

It was shown (Mihajlov & Dimitrijević, 1986, 1992) that the contribution of radiative collision processes during $H^+ + H(1s)$- and $He^+(1s) + He(1s^2)$-collisions to the solar- and certain white dwarf- opacities is comparable to the contribution of the known processes of H_2^+ and He_2^+ molecular ion photodissotiation. Moreover, it was found that $H^+ + H(1s)$ radiative collision processes are of significance for particular Solar atmosphere layers, in spite of the fact that they occure in the presence of the very intensive processe of H^- ion photocreation (Mihajlov et al., 1993).

Since there is not a stable negative atomic ion for helium (Massey, 1976), the influence of the $He^+(1s) + He(1s^2)$ radiative collision processes is expected to be more significant for relatively low temperature ($T < 20000K$) helium plasma than for the corresponding hydrogen case. Consequently we will investigate here in detail the contribution of these processes to the DB white dwarf atmosphere continuous spectra, within the semiclassical approach (Mihajlov & Popović, 1981; Mihajlov & Dimitrijević, 1992).

Chemically Peculiar & Magnetic Stars, 1994, 149– 154.
J. Zverko & J. Žižňovský (eds.)

2. Radiative processes

The following ion-atom radiative collision processes will be considered

$$He^+(1s) + He(1s^2) \Longleftrightarrow \epsilon_\lambda + He_2^+, \tag{1}$$

$$He^+(1s) + He(1s^2) \Longleftrightarrow \epsilon_\lambda + \begin{cases} He^+(1s) + He(1s^2) \\ He(1s^2) + He^+(1s) \end{cases} \tag{2}$$

where $\epsilon_\lambda = 2\pi\hbar c/\lambda$ is the energy of photon with the wavelength λ in the optical spectral range ($350nm \leq \lambda \leq 800nm$).

The contribution of processes (1) to the white dwarf continuous spectra will be compared here with the contribution of the following known radiative processes:

i) free-free radiative transitions during free electron scattering on helium atom:

$$He(1s^2) + e \Longleftrightarrow \epsilon_\lambda + He(1s^2) + e; \tag{3}$$

ii) free-free and free-bound radiative transitions during free electron scattering on positive ions:

$$A^+ + e \Longleftrightarrow \epsilon_\lambda + \begin{cases} A^+ + e \\ A^* \end{cases} \tag{4}$$

where A^* is an atom in an excited state. We use A in Eq.(3) since besides He, the presence of H and other atoms will be taken into account (see Koester, 1980).

The semiclassical theory of the reaction (1) has been given by Drukarev & Mihajlov (1974); Mihajlov & Popović (1981); Mihajlov & Dimitrijević (1986). Electron-atom process (2) have been studied by e.g. Firsov & Chibisov (1960) and Bell et al. (1982). The electron-ion processes (3) have been treated by e.g. Menzel (1962) and Sobelman (1979).

As a characteristic of the considered processes influence we will use the corresponding spectral emissivity. The spectral emissivity corresponding to reactions (1a) and (1b) together is:

$$\varepsilon_{ia}(\lambda) = S_{ia}^{He}(\lambda) N(He^+) N(He) \tag{5}$$

where $N(He^+)$ and $N(He)$ are the number density of the ion $He^+(1s)$ and the atom $He(1s^2)$ respectively, and $S_{ia}^{He}(\lambda)$ is the emission spectral coefficient characterizing the total contribution of both photoemissive channels. It is given in analytical form by Mihajlov & Popović (1981).

For processes (2) and (3) we have respectively:

$$\varepsilon_{ea}(\lambda) = S_{ea}^{He,ff}(\lambda) N(He) N_e, \tag{6}$$

$$\varepsilon_{ei}(\lambda) = \sum S_{ei}^{A}(\lambda) N(A^+) N_e \tag{7}$$

where N_e is the electronic density and the summation has to be performed over different atom kinds. The spectral coefficient $S_{ea}^{He,ff}(\lambda)$ for free-free transitions due to electron-atom scattering, will be determined with the help of Bell et al. (1982) results, and $S_{ei}^{A}(\lambda)$ is given analytically by Sobelman (1979).

We also define the quantities:

$$F_{ea}^{ff}(\lambda) = \frac{\varepsilon_{ia}(\lambda)}{\varepsilon_{ea}^{ff}(\lambda)} \tag{8}$$

$$F_{ei}(\lambda) = \frac{\varepsilon_{ia}(\lambda)}{\varepsilon_{ei}(\lambda)} \tag{9}$$

characterizing relative contribution of the process (1) in comparison with processes (2) and (3) respectively. We note that in the case of local thermal equilibrium, these quantities are also the ratios of the adequatly defined absorption coefficients. For reactions (1), (2) and (3) corresponding absorption coefficients have been derrived in Mihajlov & Dimitrijević (1992), Bell et al. (1982) and Sobelman (1979).

3. Basic relations

Following Mihajlov & Popović (1981), $S_{ia}^{He}(\lambda)$ for a given plasma temperature T may be expressed as:

$$S_{ia}^{He}(\lambda,T) = 4.777\cdot 10^{-34}\frac{C(R_\lambda)(R_\lambda/a_0)^4}{1.345\cdot(1-0.362\cdot a_0/R_\lambda)}\left(\frac{\varepsilon_\lambda}{2Ry}\right)^5 \exp\left[\frac{-U_2(R_\lambda)}{kT}\right], \tag{10}$$

$$C(R_\lambda) = \left[\frac{2D_{1,2}(R_\lambda)}{eR_\lambda}\right]^2 \cdot \frac{1.345\cdot(1-0.362\cdot a_0/R_\lambda)}{\gamma(R_\lambda)}, \tag{11}$$

$$\gamma(R_\lambda) = \left|\frac{d\ln[E_{12}(R)/2Ry]}{d(R/a_0)}\right|_{R=R_\lambda}, \tag{12}$$

$$E_{12}(R) = U_2(R) - U_1(R), \tag{13}$$

where R is the internuclear distance in the $He^+ + He$ system, $U_1(R)$ and $U_2(R)$ - adiabatic terms of the ground ($1\Sigma_u$) and the first excited ($1\Sigma_g$) electronic states of ion He_2^+ and $D_{12}(R)$ - modulus of dipole matrix element (between these states). Finally, R_λ is the root of the equation:

$$E_{12}(R) = \epsilon_\lambda \tag{14}$$

The values of R_λ are tabulated in Mihajlov & Dimitrijević (1992) and $U_{1,2}$ molecular terms are given in Gupta & Madsen (1967). For the λ range considered we will approximate $D_{1,2}(R)$ to be $eR/2$ as in Mihajlov & Dimitrijević (1992). In the corresponding R_λ range we have that the factor $C(R_\lambda) \simeq 1$

With numerical coefficients given in Eqs.(6), the spectral coefficient $S_{ia}^{He}(\lambda)$ is expressed in $[cm^3 Js^{-1} nm^{-1}]$ units.

Table 1. Temperature T, and factors η_{ei} and η_{ea} defined by Eq. (11) for DB white dwarf model with $\log g = 8.00$ and $T_{eff} = 12000$ K (Koester, 1980).

$\log\tau$	T [K]	η_{ei}	η_{ea}
-5.60	8119.	.2928E+04	.3851E-01
-4.80	8053.	.2135E+04	.1820E-01
-4.00	7967.	.1432E+04	.8154E-02
-3.60	7942.	.1198E+04	.5734E-02
-2.80	8024.	.1179E+04	.4471E-02
-2.00	8474.	.2981E+04	.1156E-01
-1.20	9896.	.2493E+05	.2030E+00
-1.00	10554.	.2766E+05	.3970E+00
-.50	11832.	.1719E+05	.7696E+00
.00	12969.	.7665E+04	.9148E+00
.40	13900.	.3834E+04	.9480E+00
.80	14807.	.1793E+04	.8704E+00
1.00	15412.	.1442E+04	.9757E+00
1.50	16821.	.6621E+03	.9799E+00
2.00	18302.	.2902E+03	.8932E+00
2.75	21039.	.1154E+03	.9473E+00

4. Results and discussion

We now apply the described method to the DB white dwarf atmosphere using one of models of Koester (1980) (the $\log g = 8$ and $T_{eff} = 12000\ K$ case in Table 1).

We will take into account that in the investigated DB white dwarf atmosphere the $N(He) : N(H) : N(\text{metals})$ abundance ratios are $10^5 : 1 : 1.5$ (Bues, 1970). Consequently, it is justified to take the electron-ion emissivity $\varepsilon_{ei}(\lambda)$, defined by Eq. (4c) as

$$\varepsilon_{ei}(\lambda) = \chi_{ei}^{He} S_{ei}^{He}(\lambda) N_i N_e \tag{15}$$

where N_i is the positiv atomic ion total density, $S_{ei}^{He}(\lambda)$ electron-ion spectral coefficient characterizing the pure helium plasma, and with the help of the coefficient χ_{ei}^{He} one takes into account the real plasma composition. It has the same role as the Biberman-Norman factor for hydrogen plasma and here it is close to one.

Taking into account Eq.(5) as well as Eqs.(4b,9) we will represent quantities $F_{ei}(\lambda)$ and $F_{ea}^{ff}(\lambda)$ as:

$$F_{ei}(\lambda) = f_{ei} \frac{S_{ia}^{He}(\lambda)}{S_{ei}^{He}(\lambda)} \eta_{ei}, \qquad F_{ea}^{ff}(\lambda) = \frac{S_{ia}^{He}(\lambda)}{S_{ea}^{He,ff}(\lambda)} \eta_{ea}, \tag{16}$$

where $f^{ei} = 1/\chi_{ei}^{He}$ and

$$\eta_{ea} = \frac{N(He^+)}{N_e}, \qquad \eta_{ei} = \frac{N(He^+)N(He)}{N_e N_i} = \eta_{ea}\frac{N(He)}{N_i}. \tag{17}$$

The factor η_{ei} and η_{ea} values, determining regions (with $\eta_{ea} \approx 1$ and $\eta_{ei} \gg 1$) where investigated processes may be of interest, are presented in Table 1 as functions of $\log\tau$, where τ is Rosseland optical depth taken from Koester (1980).

The comparison of (1) and (2) processes contribution is presented in Fig. 1 where the behavior of the quantity $F_{ea}^{ff}(\lambda)$ is shown.

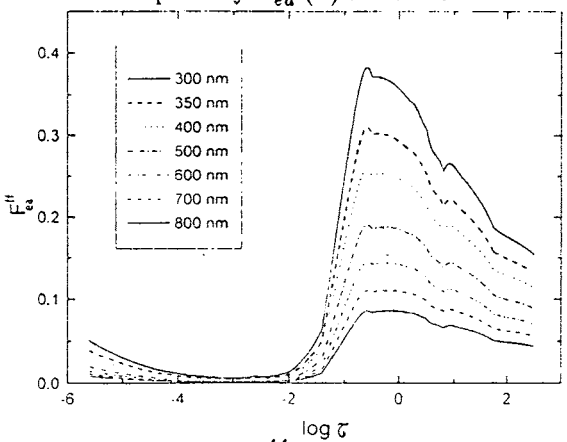

Figure 1. The behavior of parameter $F_{ea}^{ff}(\lambda)$, within the 350 nm $\leq \lambda \leq$ 800 nm range, as a function of Rosseland optical depth logarithm.

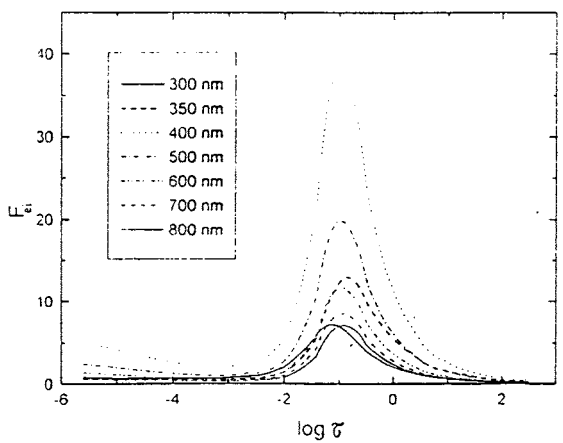

Figure 2. The behavior of parameter $F_{ei}(\lambda)$, within the 350 nm $\leq \lambda \leq$ 800 nm range, as a function of Rosseland optical depth logarithm.

We can see that $F_{ea}^{ff}(\lambda)$ increases fast with the temperature increases in the 8000 K $< T <$ 10000 K range, reaches a maximum and after them decreases

1994cpms.conf..146P

ON STARK BROADENING OF HEAVY ION LINES IN SPECTRA OF CP STARS: Sb II LINES

L. Č. POPOVIĆ, M. S. DIMITRIJEVIĆ

Astronomical Observatory, Volgina 7, Belgrade, Yugoslavia

Received: November 30, 1993

Abstract. We present here Stark broadening data for three Sb II multiplets as a function of temperature. Stark broadening data have been calculated within the modified semi–empirical approach for electron density of 10^{23} m^{-3}. The Stark width data for Sb II multiplets are compared with corresponding thermal Doppler widths for typical plasma condition within CP stars (e.g. A_m) layers where Sb II lines are formed. Our results show that Stark width for higher multiplets may be even more important than the thermal Doppler one.

Key words: stars: chemically peculiar – atomic data

1. Introduction

Strong absorption heavy ion lines have been observed in spectra of CP stars, as e.g. Sb II spectral line (λ = 143.65 nm) in spectra of HR 7775 and ι CrB (Hg-Mn) stars (Jacobs & Dworetsky, 1982). Since the electron density in layers where the Sb II lines are formed is $10^{20} - 10^{21}$ m^{-3} it is of interest to provide the corresponding Stark broadening data wich might be of significance for the analysis of stellar spectra.

In this paper we present our calculations of the corresponding Stark widths and shifts with the modified semiempirical approach (Dimitrijević & Konjević, 1980).

2. Results and discussion

For the Stark broadening data calculation the modified semiempirical approach (Dimitrijević & Konjević, 1980, Dimitrijević & Kršljanin, 1986) has been used. The oscillator strengths needed for calculation have been taken from Wiese & Martin (1980) and Gruzdev (1968). The needed atomic energy levels have been taken from Moore (1971). The deparature from LS coupling has been taken into account (see Dimitrijević & Popović, 1993) as well.

In Table 1. we have compared Stark ($w_{\rm St}$) and thermal Doppler ($w_{\rm Dopp}$) full widths for three multiplets for typical conditions in A type star layers where Sb II lines are formed. As one can see from Table 1. Stark widths in the case

Chemically Peculiar & Magnetic Stars, 1994, 146– 148.
J. Zverko & J. Žižňovský (eds.)

© Astronomical Institute of the Slovak Academy of Sciences • Provided by the NASA Astrophysics Data System

1994cpms.conf..146P

Table 1. Comparison of Stark and thermal Doppler full widths for Sb II multiplets for $T = 10\,000$ K and the electron density of 10^{21} m^{-3}.

Transition	$w_{\rm St}$ (nm)	$w_{\rm Dopp}$ (nm)
$6s^3P_1^0 - 6p^3D_2$	.111E-02	.234E-02
$\lambda = 600.5$ nm		
$6s^3P_2^0 - 6p^3P_1$	.448E-02	.361E-02
$\lambda = 927.8$ nm		
$6s^3P_2^0 - 6p^3S_1$	.202E-02	.220E-02
$\lambda = 564.1$ nm		

of considered multiplets may be even larger than widths due to the thermal Doppler effect. This may be expected in the case of transitions involving higher principal quantum number. In such cases due to the weaker influence of the core on the optical electron, which is more sensitive to the weak electron field, Stark broadening may be important even in the atmospheres of cooler stars as e.g. the Sun (Vince *et al.*, 1985).

Table 2. Stark full widths (w) and shifts (d) of Sb II spectral lines as a function of temperature. The electron density is 10^{23} m^{-3}.

Transition	T(K)	w (nm)	d (nm)
	5000.	.160	-.539E-01
	10000.	.111	-.399E-01
$6s^3P_1^0 - 6p^3D_2$	20000.	.809E-01	-.315E-01
$\lambda = 600.5$ nm	30000.	.717E-01	-.291E-01
	40000.	.685E-01	-.280E-01
	50000.	.676E-01	-.263E-01
	5000.	.637	-.339
	10000.	.448	-.256
$6s^3P_2^0 - 6p^3P_1$	20000.	.334	-.211
$\lambda = 927.8$ nm	30000.	.300	-.215
	40000.	.286	-.221
	50000.	.281	-.229
	5000.	.271	-.929E-01
	10000.	.202	-.631E-01
$6s^3P_2^0 - 6p^3S_1$	20000.	.162	-.336E-01
$\lambda = 564.1$ nm	30000.	.160	-.224E-01
	40000.	.157	-.214E-01
	50000.	.153	-.219E-01

In Table 2. we present Stark full width (w) and shift (d) for three multiplets, calculated by using the modified semiempiricial approach (Dimitrijević & Kon-

© Astronomical Institute of the Slovak Academy of Sciences • Provided by the NASA Astrophysics Data System

1994cpms.conf..146P

Table 3. Comparison of experimental (Purić *et al.*, 1985) and theoretical results. The electron density is 10^{23} m^{-3}.

Transition	λ (nm)	T (1000 K)	w_{exp}/w_{MSE}	d_{exp}/d_{MSE}
$6s^3P_1^0 - 5p^3D_2$	603.5	16	2.0	1.3
		20	1.8	1.0

jević, 1980, Dimitrijević & Kršljanin, 1986) for electron density of 10^{23} m^{-3} and temperatures from 5000 to 50000 K.

In Table 3. our results have been compared with available experimental data (Purić *et al.*, 1985). We can see that shifts are in better agreement with our calculations than the widths.

References

Dimitrijević M. S., Konjević N. P: 1980, *J. Quant. Spectroscopy and Rad. Transfer*, **24**, 451

Dimitrijević M. S., Kršljanin V.: 1986, *Astron. Astrophys.* **165**, 269

Dimitrijević M. S., Popović L. Č.: 1993, *Astron. Astrophys., Suppl. Ser.* , in press

Gruzdev P. F., 1968, *Opt. Spectr.*, **25**, 3

Jacobs J. M., Dworetsky M. M.: 1982, *Nature* **299**, 535

Moore C. E.: 1971, *Atomic Enegy levels*, Vol. III, USDC/NBS, Washington D. C.

Purić J., Ćuk M., Lakićević I. S.: 1985, *Phys. Rev. A*, **32**, 1106

Vince I., Dimitrijević M. S., Kršljanin V.: 1985, in *Progres in Stellar Spectral Line Formation Theory*, eds.: J. Beckman, L. Crivellari, D. Reidel, Dordrecht, 373

Wiese W. L., Martin G. A.: 1980, *Wavelengths and Transition Probabilities for Atoms and Atomic Ions*, Part II, USDC/NBS, Washington D. C.

© Astronomical Institute of the Slovak Academy of Sciences • Provided by the NASA Astrophysics Data System

Astronomy in Serbia

Milan S. Dimitrijević
Astronomical Observatory, Volgina 7,11050 Belgrade, Yugoslavia
mdimitrijevic@aob.bg.ac.yu

Abstract

A review of professional and amateur astronomy in Serbia is given.

1 Belgrade Astronomical Observatory

The principal astronomical institution in Serbia is the Belgrade Astronomical Observatory, one of the oldest scientific organizations and the only autonomous astronomical institute in Yugoslavia. Its past development forms an important part of the history of science and culture in these regions. The decree of its founding conjointly with the Meteorological Observatory was signed on 20 March (7 April) 1887 by the Minister of Education and Church Affaires of Kingdom of Serbia Milan Kujundžić on the initiative of Milan Nedeljković (Belgrade 27. Sept. 1857 - Belgrade 27 Dec. 1950), a professor of the Grand School (Belgrade University). Nedeljković was appointed first director of the newly founded Observatory.

On 1 May 1871 Nedeljković started his activity at the provisory Observatory in the rented Geizler family's house. Here the Observatory was operating until 1 May 1891, when it was moved into its own building constructed meanwhile - the one in which at present is Meteorological Observatory in the Karadjordje Park. In the minor museum section of this building there is, since the celebration of the Observatory's centenary in 1987, a room dedicated to the origins of astronomical science in Yugoslavia.

Nedeljković was at the head of the Observatory from 26 March (7 April) 1887 until 30 January 1924. A break took place only between 5 July 1899 and 31 October 1900, when he was sent into retirement for political reasons, in connection with the Ivanjdan attempt on King Milan, which was exploited by King Alexander for settling accounts with his political opponents. Nedeljković's place was filled during this period by Djordje Stanojević (Negotin, 7 April 1858 - Paris 24 Dec. 1921), the first Serbian astrophysicist, later on the rector of Belgrade University. Dj. Stanojević was a great popularizer of astronomy and science in general; he was the driving force in the introduction of electrical light in Belgrade, Užice, Čačak, Leskovac... He was the builder of the first hydroelectric power station in Serbia, a pioneer of industry of refrigerating appliances, the initiator of setting up a committee for cooling problems and of forming an international organization for cooling technique in Paris in 1903. He was also the pioneer of the color photography in Serbia.

Apart from its importance for astronomy and meteorology, the newly built Observatory, headed by Nedeljković, was a cradle of the seismic and geomagnetic researches in Serbia. Nedeljković borrowed the instruments for geomagnetic measurements from Tege Miklosh Konkoly, the founder of the Budapest Astronomical Observatory, and took care of building an earth-magnetism pavilion. Thanks to Konkoly, Nedeljković acquired in 1903 also a seismograph, installed next year in a special pavilion. The observations were carried out regularly and for these purposes the construction of what at present is the Seismological Institute was executed in 1906. This activity was taken over by Nedeljković's assistant Jelenko Mihailović (Vrbica, 11 Jan. 1869 - Belgrade 10 Oct. 1958) who worked at the Observatory since 1896.

During the Austro-Hungarian occupation of Serbia in World War I, the Observatory was administered by Victor Konrad from Vienna. During their flight from Serbia the Austrians took away or destroyed all the instruments. However, thanks to his extraordinary and professional skill Nedeljković contrived to acquire in Germany after the war, on account of war reparations, a number of instruments appertaining equipment for the new Observatory.

The instruments procured by Nedeljković constitute still practically the only observing basis of the Observatory, although some of them were taken away by the Germans during the World War II, two were ceded to each Ljubljana and Zagreb Universities (Djurković 1968), some of the smaller ones being left unmounted.

Currently mounted in appropriate pavilions are the following instruments procured by Nedeljković:

1. Large Refractor - ZEISS 650/10550mm equatorial;
2. Solar spectrograph (monochromatic) LITTROW, 9000 mm/100.000 developed by adapting to the ZEISS 200/3020 mm equatorial two astro cameras TESSAR and PETZVAL 160/800 mm;
3. Large Transit Instrument ASKANIA 190/2578 mm;
4. Large Vertical Circle ASKANIA 190/2578 mm;
5. Astrograph ZEISS 160/800 mm;
6. Photovisual Refractor ZEISS 135/1000 mm and 125/1000 mm;
7. Transit Instrument BAMBERG 100/1000 mm;
8. Zenith-telescope ASKANIA 110/1287 mm;

Large Meridian Circle ASKANIA 190/2578 mm burnt up on 11th of May 1999 during NATO air attack.

As Nedeljković was struggling for the new Observatory at which the acquired instruments were to be mounted and regular astronomical observations started, he suddenly was sent into retirement on 30 Jan. 1924. By ruling of the Faculty Council the Observatory was divided into two separate institutions: Astronomical Observatory and Meteorological Observatory of Belgrade University.

At the head of the Astronomical Observatory was appointed in 1925 Vojislav V. Mišković (Fužine 18 Jan. 1892 - Belgrade 25 Nov. 1976), at the time already

a well established astronomer engaged at Nice Observatory, France. He began his astronomical studies in Budapest and Göttingen before the World War I. On his demobilization at the end of 1918 from the Serbian Army, in which he served as a volunteer, he was sent to France to complete his studies. He graduated in 1919 and was appointed assistant at the Marseille Observatory. Since 1922 he was engaged as an astronomer at the Nice Observatory, receiving his doctor's degree in 1924 at the Montpellier University. In 1925 he won French Academy Prize for his studies in stellar statistics. In the period 1919-1925 he published a score of papers in the French scientific journals, treating the observation of the minor planets and comets and the determination of their orbits. He came to Belgrade in 1926 taking, in addition to the Astronomical Observatory, charge of the newly established Chair of Theoretical and Practical Astronomy at the Faculty of Philosophy, whereat he was elected associated professor. In 1929 he was elected corresponding member of the Serbian Royal Academy and in 1939 its full member. He directed the Observatory's activity to a considerable degree toward mathematical and numerical works, which yielded valuable results. Of importance are numerical works connected with the Mathematical Climatology of M. Milanković as well as with Mišković's own Precession Tables.

In 1929 Mišković succeeded in getting funds for the constructions of a new, modern, observatory, at 6 km distance southeast from the city's centre, occupying a 4.5 ha area at 253 m high hill Veliki Vračar, named since, along with the entire surrounding part of Belgrade, Zvezdara (=concerned with stars).

Exceptional and highly valued complex constituting the Astronomical Observatory was drawn up by Jan Dubovi, a member of GAMP (Group of Modern Outlook Architects) founded in 1928. It is thanks to this very achievement that Dubovi was conferred a doctor of science degree in Prague. The construction works were carried out in 1930 to 1932, the instruments being mounted during the following two years.

Mišković started also publishing the scientific periodical Mémoires de l'Obs. Astr. Belgrade (issued five volumes for: 1932, 1933, 1936, 1938 and 1949), Annuaire de l'Obs. Astr. Belgrade (six volumes for 1929 through 1934) containing sidereal time, short-period nutation terms, the mean and apparent places of 189 stars, newly discovered minor planets and directions for use. Nautički godišnjak (Nautical Almanac) for years 1934 through 1941) for navigation purposes in the Navy and Godišnjak Našeg Neba (Almanac of our Sky) an astronomical calendar in Serbian, issued in the years 1930 to 1941 and 1948 to 1952 (the 1948 issue was edited by F. Dominko and the issues for 1949, 1950 and 1951 by B. Popović.

In 1936 Mišković, assisted by Milorad Protić, organized the Minor Planets and Sun Observation Service. In the same year P. Djurković discovered at the Uccle Observatory, Belgium, a minor planet, subsequently named 1605 Milanković and M. Protić, at the Belgrade Observatory, discovered the minor planet 1564 Serbia, which marked the opening of a long series of 43 minor planets discovered by the Belgrade astronomers. Protić alone, in the period 1936-1956, made 33 discoveries. Of the 43 minor planets owing their discovery to Belgrade astronomers, 12 have obtained by the IAU permanent names, three of the discoveries having later been ascribed to other authors.

Besides Serbia, using his author's right, Protić gave the following names to the minor planets he discovered: 1507 Beograd, 1550 Tito, 1554 Yugoslavia, 1675 Simonida, 1724 Vladimir (after his grandson), 2244 Tesla and 2348 Mišković. P. Djurković discovered in the period 1936-1941, 5 minor planets, one of them - Zvezdara- named by him using his discover's prerogative. In 1980 Z. Knežević discovered on the photo-plates taken according to his instructions at Piszkesteto Observatory, Hungary, four minor planets, one of which having obtained the name 3276 Paolicchi, after one of his colleagues in Italy. In 1991, as a mark of honour, a minor planet was given the name 3900 Knežević - after our fellow. Another minor planet connected with the Belgrade Observatory is that named 1555 Dejan, after P. Djurković's son.

In 1936 Mišković started issuing Bulletin de l'Observatoire astronomique de Belgrade, a scientific periodical which from No. 145 for 1992 on appears under the name Bulletin astronomique de Belgrade, and from the number 157 for 1998 under the name Serbian astronomical Journal. This periodical's editors have been: V. V. Mišković (1936-1940, 1943 – 1948 and 1952-1956), M. Protić (1941-1942, 1955-1960 and 1971-1975), B. Popović (1950), V. Oskanjan (1964), P. Djurković (1964-1970), M. Mijatov (Nos. 127-131 in 1976-1981), D. Zulević (Nos. 132-133, in 1982-1983), Dj. Teleki (Nos. 134-136 in 1984-1986) and M. S. Dimitrijević (No. 137 in 1987 successively up to date).

Since July 1941 at the Observatory were quartered German military. The Wehrmacht brought along profs. Grotrian and Kippenheur from Potsdam, the two having inscribed the Observatory's instruments as German property, dispatching to Germany the spectroheliograph and the comet searcher. On the terraces of the Observaroty's edifice and on the water storage building pillboxes were erected for directing the flak, while the library was turned into officers mess. In the course of the liberation fightings in 1944 particularly heavy damages were inflicted on the main edifice, the water storage building and on "Large Refractor" pavilion. The Observatory's reconstruction was undertaken immediately after the war. Mišković remained its director until March 1946 when he submitted his resignation, accepted not before May 1948.

In 1945 P. Djurković started and edited the professional periodical Astonomska i Meteorološka Saopštenja (Astronomical and Meteorological Reports), published by the Observatory up to 1950 (seven issues in all). In 1947 Observatory started the series Publikacije Astronomske Opservatorije u Beogradu (Publications of Astronomical Observatory). Its editors in chief were: V. Oskanjan (No. 10), P. Djurković (Nos. 12-16), M. Protić (Nos. 17-19, 20-21) Dj. Teleki (Nos. 20, 26, 32, 34 and 35), M. Mijatov (Nos. 24, 25, 27-31), G. Popović (No. 33) and M. S. Dimitrijević (Nos. 36-69).

Up to 1 July the Observatory was, as it was before the war, under the Belgrade University. From that date on, up to 18 Dec. 1950. it is under the jurisdiction of the Serbian Academy of Sciences and thereafter, under the Committee for Scientific Institutions, University and Schools for Higher Education of SR Serbia. This status was kept until 27 March 1954, when the Observatory became institution with independent financing at the Executive Council of SR Serbia. On 9 Aug. 1985 the Observatory obtained the status of autonomous scientific research institute with the Executive Council of the Assembly of SR

Serbia as its founder, its name changed into Astronomical Observatory - Institute for Astronomical Researches. At the time it was financed by the Republic Community of Sciences of SR Serbia. After Community's dissolution it is being financed by the Republic Fund for Science of Serbia through the scientific project "Physics and Motion of Celestial Bodies and Artificial Earth's Satellites" (1985-1990). Leading the Project were: Dj. Teleki (1985-1987), A. Kubičela (1987-1989) and M. Dimitrijević (1990). In the period 1991-1995 the Project is named "Physics and Motion of Celestial Bodies" and was led by M. Dimitrijević (1991-1993) and Z. Knežević (1993-1996). For the period 1996-2000 the project is named "Astronomical, Astrodynamical and Astrophysical Researches", being led by Z. Knežević. The Time and Latitude Services are financed directly from the budget of SR Serbia. On 12 May 1992 the Observatory became a scientific institute financed through the mentioned scientific project at the Republic Ministry for Science and Technology, its founder being the Government of Republic Serbia. On 20 Dec. 1994 the Observatory was re-registrated as a scientific institute, resuming its old name.

When in May 1948 V. Mišković's resignation was accepted, to the post of Observatory's director was appointed academician Milutin Milanković (Dalj 28 May 1879 - Belgrade 12 Dec. 1958) who went down in history of science by his having explained the ice ages phenomenon through the slow changes in the Earth's insolation in consequence of the Earth's axis inclination and its motion around Sun, undergoing changes produced by various influences. Milanković elucidated also the history of the climate of Earth and other planets, being the originator of the mathematical theory of the Earth's poles motion. The Observatory's direction was entrusted to the Observatory's Council, at the head of which was the director and Council's president M. Milanković, with members Anton Bilimović, V. Mišković and Pavle Savić (Popović 1951). Milanković held this post till 26 June 1951.

In 1951 P. Djurković organized the Double Star Service. Within this Service, subsequently named Group, were discovered over 200 new double and multiple stars, the bulk of the which is due to Georgije Popović, working in this Group since 1960, being at its head since 1976.

In this same year the Variable Stars Service was organized by Vasilije Oskanjan. In this he was joined by Alexander Kubičela and Jelisaveta Arsenijević (at the Obsevatory since 1956) whereby an impetuous development of the astrophysical researches took place later directed toward stellar and solar physics and astronomical spectroscopy. Initially it was the photometry of eruptive stars which was pursued. Since 1959, after Oskanjan's return from his specialization in the Soviet Union, it was the work in the field of polarimetry of eruptive stars that was taken up. Formally, the Astrophysical Group was founded in 1960. In 1969 and 1970 working in the Group was Trajče Angelov. In 1972 the Group was joined by Ištvan Vince, in 1980 by Gojko Djurašević, in 1983 by Slobodan Jankov, in 1984 by Milan Dimitrijević, in 1985 - 1996 by Vladimir Kršljanin, in 1989-1996 by Olga Atanacković-Vukmanović (at the Observatory since 1982 first in the Absolute Declinations Group), in 1991 by Sanja Erkapić and Snežana Marković, in 1992 by Luka Popović, in 1994 by Darko Jevremović and in 1995 by Silvana Nikolic. Since 15 February 1997 the Group was joined

by Milan Ćirković, since 1st January of 1998 by Dragana Tankosić and Nataša Trajković (since 14 November 1998 Nataša Stanić), since 15 April 1998 up to 1 November 1999 by Desanka Šulić, since 1 January 1999 by Edi Bon, since 20 January 1999 by Nenad Milovanović and since 1 December 1999 by Oliver Vince.

From 26 June 1951 to March 1954 the Observatory's director is again V. Mišković. After he went into retirement the Observatory was headed by M. Protić in the capacity of deputy director and from 21 Nov. 1956 to 21 Nov. 1960 as a director.

After M. Protić at the head of the Observatory was Vasilije Oskanjan, first as acting director since 1960, then in 1964-1965 as the director. Following him, from July 1965 to 1970, the director was Pero Djurković. After him in the period 1971-1975 at the head of Observatory is again M. Protić. Since 1975, first as acting director and from 13 July 1977 to Sept 1981 as the director was M. Mijatov (Belgrade 3 July 1933 - Belgrade 19 Nov 1996). The director's post from 1982 to 1989 was held by Miodrag Mitrović, in 1990-1993 by Ištvan Vince and from 21 Nov 1994 on, by Milan Dimitrijević.

In 1986, on the part of the Assembly of SR Serbia and Republic Executive Council, the project was adopted and funds allocated for the building of an astrophysical observing station at Rgaj mountain near Prokuplje. Due to the investments in the Republic having meanwhile been suspended, the project has not been realized yet.

In 1987, in the presence of a number of statesmen and eminent guests from the country and abroad, the centenary of the Observatory's founding was solemnly celebrated in the hall of the Assembly of Serbia. On the occasion of this jubilee three international and one Yugoslav scientific conferences were held: IAU Colloquium 100 "Fundamental Astrometry" (8-11 Nov. - Chairman SOC H. Eichorn, Gainsville, USA), International Symposium on Astronomical Refraction in memory of Dj. Teleki, former President of IAU Working Group on Astronomical Refraction (3-4 Nov., Chairman SOC V. Milovanović), Second International Symposium on Catastrophic Collisions of the Small Sollar System Bodies (8-11 Nov., Chairman SOC V. Zappala, Italy) and Second Workshop "Astrophysics in Yugoslavia" (8-10 Nov Chairman SOC M. Dimitrijević). During these festivities a minor museum was opened in the old Observatory's building in Karadjordje Park, one of its rooms being dedicated to the development of the Astronomical Observatory.

In 1994 there took place a reorganization of the Observatory's inner structure, resulting in the establishment of : Department of Astrophysics, Department of Dynamical Astronomy and Department of Astrometry. Since 15 February 1997, Department of Astrometry was joined by Nataša Popović and since 20 May 1998 by Predrag Jovanović (working since 1 January 1996 in Time keeping and geographic coordinates determination service).

In 1995 the Observatory participated in the organization of the International Russian - Yugoslav Conference "Newcomb and Fundamental Astrometry" in St. Petersburg, of the First Hungarian-Yugoslav Conference in Baja and the First Romanian-Yugoslav Round Table on collaboration in astronomy in Temishoara; it organized the First Yugoslav Conference on Spectral Line Shapes in Krivaja.

In 1996 the Observatory organized the Second Yugoslav-Romanian Round Table on collaboration in astronomy in Belgrade and the Astrophysics Section at the 18th Summer School and International Symposium on the Physics and Ionized Gases in Kotor. The Observatory participated in the organization of the First Belaruss-Yugoslav Conference on Physics and Dynamics of Laboratory and Astrophysical Plasma in Minsk. The Observatory's fellows presented their results at 13 international and 6 national conferences. They published 129 bibliographic items of which 16 in the international leading journals. It published 4 volumes of Publ. Astron. Obs. Belgrade and 2 Nos. of its periodical Bull. Aston. Belgrade.

In 1997 the Observatory organized in the framework of celebration of its 110th anniversary the scientific conference "Development of Astronomy among Serbs". It took part also in the organization of the Third Romanian-Yugoslav Round Table on Cooperation in Astronomy in Kluj-Napoca, as well as in the Second Yugoslav Conference on Spectral Line Shapes in Bela Crkva. It fellows presented their results at 13 international and 4 national conferences. They published 152 bibliographic items, 11 of which in international journals of the highest standing.

During 1998, 154 bibliographic items have been published, with 19 among them in international scientific journals of the highest standing. Five invited lectures and progress reports have been given by fellows of Observatory at international conferences and one at national one. Four reviews and monographic texts in national publications have been published. Observatory's fellows have participated in works of 16 Scientific conferences abroad (28 participations by 19 fellows) and six conferences in Yugoslavia (61 participation by 28 fellows). Organized by the Observatory were IV Yugoslav - Romanian Astronomical Meeting, Belgrade, 5-8.05.1998; I Bulgarian - Serbian Astronomical Seminar, Belogradchik, 6-7.08 1998 and II Yugoslav - Belarussian Symposium on Physics and Diagnostics of Laboratory and Astrophysical Plasmas, Zlatibor, 5-6.09.1998. It issued four publications of the series Publ. Astron. Obs. Belgrade and two Nos. of its periodical Bull. Astron. Belgrade. As from 1998 Astronomical Observatory has an internet connection available from each personal computer on Observatory with Windows 95 installed.

During 1999, in spite of NATO air attacks on Yugoslavia and the destruction of the Big meridian circle, 112 bibliographic items have been published, 23 among them in international scientific journals of the highest standing. Six invited lectures have been given by Observatory's fellows at international conferences and five at national ones. Moreover, two Ph. D and one M. Sc Thesis have been published. Numbers 159 and 160 of the Observatory's publication Serbian Astronomical Journal, as well as Nos. 63, 64, 65 and 66 of the Publications of the Astronomical Observatory of Belgrade have been issued. These publications are regularly sent to 136 institutions and libraries in 45 countries and to 15 institutions and libraries within Yugoslavia. Observatory's fellows have participated in works of 8 scientific conferences abroad (9 participations by 6 fellows) and three conferences in Yugoslavia (35 participation by 22 fellows).

During 1999, Belgrade observatory organized or took part in the organi-

zation of the following conferences: III Yugoslav Conference on Spectral Line Shapes, Brankovac (Fruška gora), 4-6.10.1999; XII National Conference of Yugoslav Astronomers and International Workshop on the Development of Astronomical Databases, Belgrade, 19-21.11. 1999 and Symposium Milanković - juče, danas, sutra (Symposium Milanković - yesterday, today, tomorrow), Belgrade, 25-26.11. 1999.

Besides numerous newspaper articles and radio and TV emissions Observatory's fellows authored, explaining particularly the 11th August 1999 total Solar eclipse, they gave 48 lectures on astronomical subjects outside our institution contributing to the cultural life in our country. Moreover 4 lectures have been given at the Astronomical Observatory itself.

I note as well that Serbian Astronomical Journal is available on www through the Astrophysical Data System (ADS), thanks to the courtesy of the System's holders. The www address is: http://adswww.harvard.edu.BOBeo. During 1999, the web site of the Belgrade astronomical observatory has been made and the corresponding www address is: http://www.aob.bg.ac.yu. Moreover the database BELDATA has started to develop and it is available through internet with the address: http://www.aob.bg.ac.yu/BELDATA.

Currently there are 40 employees at the Observatory 32 of them are astronomers.

In the course of its history the Belgrade Astronomical Observatory grew to an institution of great importance in the history of science and culture of the Serbian people, not only in the field of astronomy but also in meteorology, seismology and geomagnetics. Linked to this institution are the names of the famous personalities in the history of science who contributed to the Observatory, and the scientific achievements of Serbian astronomers in general, having earned esteem in the international scientific community as well as to the young having a good perspective, in our country too, in engaging in this beautiful and challenging science, in an ambience enabling them to achieve results of the highest value.

2 University teaching of astronomy in Serbia after the Second world war

Beside Astronomical Observatory, there is in Belgrade also the Chair of Astronomy at the Faculty of Mathematics. As the Faculty of Sciences separated from the Philosophical Faculty in 1947, the Chair of Celestial Mechanics and Astronomy was formed, having shortly thereafter changed its name into Chair of Mechanics and Astronomy. The splitting up of this Chair into the Chair of Mechanics and the Chair of Astronomy began in 1960, being completed in 1962. The reorganization of the Faculty of Sciences in 1971 entailed the Chair of Astronomy becoming the Institute of Astronomy. In 1995 there took place the division of the Faculty of Sciences into several faculties. As the Faculty of Mathematics there remained the Chair of Astronomy which re-took, in the new organization, its old name.

In 1961 two study groups were formed - one for Astronomy, the other for

Astrophysics. Currently, there are at the Chair of Astronomy 12 full time astronomers and one engaged at one third-time basis, teaching fifteen subjects. The names of the Chair's fellows, the subjects they are lecturing on, as well as their electronic addresses are given in Appendix.

Beside Belgrade, Astronomy is taught at University in Novi Sad, Niš and Kragujevac. At the Faculty of Sciences of the Novi Sad University there is, since 1986, in 8th semester, the subject "Astrophysics and Astronomy", involving twice a week lectures and twice a week exercises. The subject is obligatory for students wishing to teach Physics in the secondary schools while being optional for students of Applied Physics.

At the Faculty of Philosophy of the Niš University in the study group for Physics, within the specialized training in General Physics, since the school year 1990/91 until 1993/94 there was taught twice a week in the 7th and 8th semesters, the subject Fundamentals of Astrophysics. The subject was thereafter dropped for two years from the curriculum, to be again taught within the 7th semester twice a week. In addition, there is in the study group for chemistry a Chair for Geo- and Cosmochemistry, occupying itself with the study of meteors and meteorites.

At the Faculty of Sciences of the Kragujevac University there has been introduced in the school year 1998/99 the subject Astrophysics and Astronomy in the 6th semester of the specialized training of the Group for Physics, with twice a week teaching and twice a week exercises.

3 Amateur astronomical societies

In addition to professional Astronomy, well developed in Serbia is also the amateur Astronomy. The largest and the oldest organization of amateur-astronomers is the Astronomical Society "Rudjer Bošković" in Belgrade (Kalemegdan, Gornji Grad 16, 11000 Belgrade), which in the course of 65 years of its existence was spreading astronomical knowledge in our country. The founding meeting was held on 22 April 1934. The first Society's President was Djordje Nikolić (1934-1936) and the second Vojin Djuričić (1936-1941), the governor of the State Mortgage Bank.

After the War, on 9 December 1951 was held the founding meeting of the Belgrade Astronomical Club "Rudjer Bošković" (as component part of the Association of students of the Natural-Mathematical Faculty (PMF)), Dr Radovan Danić being elect its President. Considering that already in 1952 there were in the Club 64 members, the majority of whom were not associated with the PMF, the Club Administrative Committee took decision on 23 March 1952, the Club to be re-registered into Astronomical Society "Rudjer Bošković". The founding meeting of the Society was held on 18 May 1952, Radovan Danić having been elected its President (1952-1966). Following him the Society' Presidents have been: Branislav Ševarlić (1966-1970), Pero Djurković (1970-1972), Nenad Janković (1972-1974), Božidar Popović (1974-1979), Zoran Knežević (1979-1982) and Milan S. Dimitrijević (1982-).

In 1953 the Society, jointly with the Aeronautical Association of Yugoslavia,

started publishing the periodical for astronomy and aeronautics (currently for astronomy) "Vasiona" (Universe). The periodical's editors in chief were: Nenad Dj. Janković (1953-1972), Pero Djurković (1973-1974), Jelena Milogradov-Turin (1975-1982), Branislav Ševarlić (1983-1984) and Milan S. Dimitrijević (1985-).

Thanks to the exertion of Pero Djurković and Radovan Danić with the authorities concerned, the Society obtained for itself the permises? in the Despot Tower at Kalemegdan where, on 20 December 1964 was solemnly opened the People's Observatory, whose regular activity started in June 1965. The Society managed also to procure a Zeiss planetarium, which was installed in an old spacious steam bath-house - Turkish Hamam - in the Kalemegdan Donji Grad. The Planetarium started operating in 1969, being formally opened on 17 February 1970.

The founding meeting of the Astronomical Society "Novi Sad", ADNOS (Jaroslav Francisti, Astronomska Opservatorija, Petrovaradinska tvrdjava, 21000 Novi Sad), took place on 4 March 1974. In 1976 the Society bought telescopes 20T Observatory 108/1600 mm and 10K 80/1200 mm and 14T 60/900 mm, of the American firm TASCO, and in 1991 purchased the reflector type telescopes Meade 200/1500 mm and 102/1000 mm. In 1989 the adaptation of the Astronomical Observatory at the Petrovaradin Fortress was completed while in 1996 the premises for the planetarium were secured and its adaptation is now finished. The Society's President in the period 1974-1980 was Živojin Ćulum, in the period 1980-1984 Božidar Jovanović, 1984-1998 Djura Paunić, from 1998 - up to 1 September 2000 Svetislav Krstić, and from 1 September 2000 the President is Dragoslav Petrović.

At Petnica near Valjevo the organization of the Young Researchers of Serbia is building the House of Young Researchers. This institution, initially of a recreative character, became the Research Station Petnica (Istraživačka stanica Petnica, Petnica, 14000 Valjevo). The first programmes were carried out in 1982, the first seminar in Astronomy in 1983 in preparation for going out for Rgaj Mountain, where astroclimatic explorations were conducted. In 1968 was obtained a Celestron telescope of Schmidt-Cassegrain type, objective diameter 20 cm. Later on were purchased Celestron, opening 102 cm, as well as a reflector of 33 cm opening, manufactured by Aljoša Jovanović. The heads of the seminar were Darko Jevremović, Silvana Nikolić, Samir Salim and Nikola Božinović, the duty being currently discharged by Oliver Vince.

In Valjevo, within the framework of the Society of researchers "Vladimir Mandić - Manda", founded on 16 February 1969, there is active also the Astronomical Group founded in 1972 (Nikola Božić, Birčaninova 68, p. fah 118, 14000 Valjevo).

In Kragujevac, on the roof of the Institute of Physics of the Faculty of Sciences, there is the Belerofont Observatory (Vukota Babović, Institut za fiziku PMF, Sestre Janjić 4, Kragujevac), opened on 20 February 1986. It disposes of a telescope Meniscus Cassegrain Spiegel 130/2250 mm.

In Niš, at the close of the sixties and the start of the seventies, there was operating a branch of the Astronomical Society "Rudjer Bošković, while at the Faculty of Philosophy there existed in the period 1876-1980 the "Astro-

Geophysical Society". In the year 1996 there was founded Astronomical Society "Alpha" (Dragan Ž. Gajić, Filozofski fakultet, Studijska grupa za Fiziku, p. fah 91, 18001 Niš). The first Society's President was Zoran Sekulić, while from March 1997 on, the President is Dragan Ž. Gajić.

In 1996 Zrenjanin too got an organization of amateur astronomers, Astronomical Society "Milutin Milanković" (Miša Bradić, Zrenjaninska gimnazija, Gimnazijska 2, 23000 Zrenjanin).

The amateur astronomers societies greatly contributed to the spreading of astronomical knowledge in our midst and to keeping step with the latest astronomical achievements and discoveries, the creating a more suitable climate for the development of Astronomy in Serbia.

References

[1] Babović Vukota: 1997, Multidisciplinarnost u razvoju Belerofonta, u Razvoj astronomije kod Srba, eds. M. S. Dimitrijević, J. Milogradov-Turin, L.Č. Popović, Publ. Astron. Obs. Belgrade, **56**, 95.

[2] Dimitrijević Milan S.: 1996, Beogradska Astronomska opservatorija u 1995, Belgrade Astronomical observatory in 1995, Publ. Obs. Astron. Belgrade, **52**.

[3] Dimitrijević Milan S.: 1997, 110 godina Astronomske opservatorije, u: Razvoj astronomije kod Srba, eds. M. S. Dimitrijević, J. Milogradov-Turin, L.Č. Popović, Publ. Astron. Obs. Belgrade, **56**, 9.

[4] Dimitrijević Milan S.: 1997, Beogradska Astronomska opservatorija u 1996, Belgrade Astronomical observatory in 1996, Publ. Astron. Obs. Belgrade, **55**.

[5] Dimitrijević Milan S.: 1998, Beogradska Astronomska opservatorija u 1997, Belgrade Astronomical observatory in 1997, Publ. Astron. Obs. Belgrade, **59**.

[6] Dimitrijević Milan S.: 1998, Belgrade Astronomical observatory, Proc. 4th Yugoslav-Romanian Astronomical Meeting, eds. M. S. Dimitrijević, L. Č. Popović, Publ. Astron. Obs. Belgrade, **60**, 162.

[7] Dimitrijević Milan S.: 1999, Beogradska Astronomska opservatorija u 1998, Belgrade Astronomical observatory in 1998, Publ. Astron. Obs. Belgrade, **63**.

[8] Dimitrijević Milan S.: 1998, Astronomija u Srbiji, Proc. I Bulgarian - Yugoslav Astronomical Meeting, eds. M. S. Dimitrijević, L. Č. Popović, M. Tsvetkov, Publ. Astron. Obs. Belgrade, **64**, 19.

[9] Djokić Milorad: 1989, Arhivska gradja o Opservatoriji Velike škole i Univerziteta u Beogradu u vremenu od 1887. do 1924. godine, u: Sto godina Astronomske opservatorije u Beogradu, Publ. Obs. Astron. Belgrade, **36**, 177.

[10] Djurković Pero: 1968, Sedamdeset pet godina rada Astronomske opservatorije u Beogradu, Publ. Obs. Astron. Belgrade, **12**, 15.

[11] Djurković P.: 1969, Rapport sur l'activité de l'Observatoire Astronomique de Belgrade de 1966 á 1969, Bull. Obs. Astron. Belgrade **XXII**, No 2, 143.

[12] Djurković P.: 1970, Rapport sur l'activité de l'Observatoire Astronomique de Belgrade en 1970, Bull. Obs. Astron. Belgrade **124**, 195.

[13] Francisti Jaroslav: 1997, Astronomsko društvo "Novi sad" - ADNOS, u Razvoj astronomije kod Srba, eds. M. S. Dimitrijević, J. Milogradov-Turin, L.Č. Popović, Publ. Astron. Obs. Belgrade, **56**, 91.

[14] Gajić Dragan Ž.: 1997, Astronomija i astrofizika na Univerzitetu u Nišu, u: Razvoj astronomije kod Srba, eds. M. S. Dimitrijević, J. Milogradov-Turin, L.Č. Popović, Publ. Astron. Obs. Belgrade, **56**, 109.

[15] Janković, Nenad Dj.: 1984, Zapisi i sećanja na Astronomsko društvo, Publ. Astron. Društva "Rudjer Bošković", No. 3.

[16] Janković Dj. Nenad: 1989, Milan Nedeljković, profesor Velike škole i osnivač njene Opservatorije, u: Sto godina Astronomske opservatorije u Beogradu, Publ. Obs. Astron. Belgrade, **36**, 107.

[17] Jeličić, Milan: 1984, Pedest godina Astronomskog društva "Rudjer Bošković", Vasiona, XXXII, No 1, 1.

[18] Michkovitch V.V.: 1930, Rapport annuel sur l'état et les travaux de l'Observatoire Astronomique de Belgrade pour l'année 1929, Annuaire pour l'an 1930, 125.

[19] Michkovitch V.V.: 1931, Rapport annuel sur l'état et les travaux de l'Observatoire Astronomique de Belgrade pour l'année 1930, Annuaire pour l'an 1931, 133.

[20] Michkovitch V.V.: 1932, Rapport annuel pour l'année 1931 sur l'état et les travaux de l'Observatoire Astronomique de l'Université de Belgrade, Mémoires I, 38.

[21] Michkovitch V.V.: 1941, Services et travaux d'observations en 1939 á l'Observatoire Astronomique de l'Université de Belgrade, Bull. Obs. Astron. Belgrade **V**, No 1-2, 1.

[22] Michkovitch V.V.: 1950, Services et travaux d'observations en 1940 á l'Observatoire Astronomique de l'Université de Belgrade, Bull. Obs. Astron. Belgrade **VI**, No 1-2, 1.

[23] Michkovitch V.V.: 1952, Rapport annuel présenté à l'Academie des sciences Serbe, sur l'état et l'activité de l'Observatoire en 1951, Bull. Obs. Astron. Belgrade **XVI**, No 1-4, 1.

[24] Milogradov - Turin J.: 1996, Astronomy education in FR Yugoslavia 1993 - 1996, Publ. Astron. Obs. Belgrade, **54**, 165.

[25] Milogradov - Turin J.: 1997, Jedan prilog istoriji Katedre za astronomiju Univerziteta u Beogradu, u Razvoj astronomije kod Srba, eds. M. S. Dimitrijević, J. Milogradov-Turin, L.Č. Popović, Publ. Astron. Obs. Belgrade, **56**, 65.

[26] Milogradov - Turin, J.: 1998, Chair of Astronomy of the University of Belgrade, Proc. 4th Yugoslav-Romanian Astronomical Meeting, eds. M. S. Dimitrijević, L. Č. Popović, Publ. Astron. Obs. Belgrade, **60**, 193.

[27] Milogradov - Turin, J.: 1999, Astronomy Education in FR Yugoslavia 1996 - 1999, Proc. XII Nat. Conf. Yug. Astronomers and Int. Workshop on the Development of Astronomical Databases, eds. L. Č. Popović, M. Dačić, Publ. Astron. Obs. Belgrade, **65**, 185.

[28] Naumovski Krste, Bradić Miša: 1997, Astronomsko društvo u Zrenjaninu, u: Razvoj astronomije kod Srba, eds. M. S. Dimitrijević, J. Milogradov-Turin, L.Č. Popović, Publ. Astron. Obs. Belgrade, **56**, 115.

[29] Nedeljković Milan: 1904, Izveštaj Opservatorije Velike škole i njenih meteoroloških stacija, 1899-1903, Državna štamparija, Beograd.

[30] Nedeljković Milan: 1905, Izveštaj Opservatorije i Meteoroloških stacija, 1904, Državna štamparija, Beograd.

[31] Nedeljković Milan: 1907, Izveštaj Opservatorije i Meteoroloških stacija, 1905-1906, Štamparija Davidović, Beograd.

[32] Nedeljković Milan: 1908, Izveštaj Opservatorije i Meteoroloških stacija, 1907, Državna štamparija, Beograd.

[33] Nedeljković Milan: 1909, Izveštaj Opservatorije i Meteoroloških stacija, 1908-1909, Državna štamparija, Beograd.

[34] Nedeljković Milan: 1910, Izveštaj Opservatorije i Meteoroloških stacija, 1910, Državna štamparija, Beograd.

[35] Nedeljković Milan: 1914, Izveštaj Opservatorije i Meteoroloških stacija, 1911-1912, Merkur, Beograd.

[36] Nedeljković Milan: 1923, Izveštaj Opservatorije, za 1919-1920, 1922 i 1923, Beogradska opservatorija, Beograd.

[37] Nedeljković Milan: 1925, Izveštaj Opservatorije, za 1924, Beogradska opservatorija, Beograd.

[38] Popović B.: 1950, Services et travaux d'observations en 1949 á l'Observatoire astronomique de l'Université de Belgrade, Bull. Obs. Astron. Belgrade **XIV- 1949**, VII.

[39] Popović B.: 1951, Rapport annuel sur l'état et l'activité de l'Observatoire astronomique de Belgrade en 1950, Bull. Obs. Astron. Belgrade **XV - 1950**, VII.

[40] Popović, L. Č.: 1997, Razvoj i aktivnosti Astronomskog društva "Rudjer Bošković", u Razvoj astronomije kod Srba, eds. M. S. Dimitrijević, J. Milogradov-Turin, L.Č. Popović, Publ. Astron. Obs. Belgrade, **56**, 77.

[41] Popović, Luka Č.: 1999, Amaterska astronomija u Jugoslaviji, Proc. I Bulgarian - Yugoslav Astronomical Meeting, eds. M. S. Dimitrijević, L. Č. Popović, M. Tsvetkov, Publ. Astron. Obs. Belgrade, **64**, 89.

[42] Protić, M.: 1975, Izveštaj o radu Astronomske opservatorije u Beogradu tokom 1973. godine, Publ. Obs. Astron. Belgrade, **20**, 231.

[43] Protitch M.: 1950, Services et travaux d'observations en 1941 á l'Observatoire astronomique de l'Université de Belgrade, Bull. Obs. Astron. Belgrade **VII - 1942**, 1.

[44] Protitch M.: 1956, Rapport annuel sur l'état et les travaux de l'Observatoire en 1955, Bull. Obs. Astron. Belgrade **XX**, No 3-4, 16.

[45] Protitch M.: 1960, Rapport annuel sur l'état et les travaux de l'Observatoire en 1959, Bull. Obs. Astron. Belgrade **XXIV**, No 3-4, 42.

[46] Salim Samir: 1997, Astronomija u Istraživačkoj stanici Petnica, u: Razvoj astronomije kod Srba, eds. M. S. Dimitrijević, J. Milogradov-Turin, L.Č. Popović, Publ. Astron. Obs. Belgrade, **56**, 101.

[47] Sekulić Miodrag: 1997, Astronomsko društvo "Alfa" - Niš, u: Razvoj astronomije kod Srba, eds. M. S. Dimitrijević, J. Milogradov-Turin, L.Č. Popović, Publ. Astron. Obs. Belgrade, **56**, 111.

[48] Simovljević Jovan: 1987, Astronomija, Četrdeset godina Prirodno - Matematičkog fakulteta u Beogradu, Beograd, 166.

[49] Stanojević M. Djordje: 1905b, Beogradska opservatorija i njen izveštaj za 1899 - 1903. god., str. 32, Beograd.